Patai Series:
The Chemistry of Functional Groups

Series Editor: Zvi Rappoport

Volume Editors: Zvi Rappoport and Ilan Marek

The Chemistry of Organolithium Compounds

Part 1

R-Li

Patai Series online:
http://www3.interscience.wiley.com/bookfinder.html

WILEY

An Interscience®
Publication

The chemistry of
organolithium compounds

Patai Series: The Chemistry of Functional Groups

A series of advanced treatises founded by Professor Saul Patai and under the general editorship of Professor Zvi Rappoport

The **Patai Series** publishes comprehensive reviews on all aspects of specific functional groups. Each volume contains outstanding surveys on theoretical and computational aspects, NMR, MS, other spectroscopical methods and analytical chemistry, structural aspects, thermochemistry, photochemistry, synthetic approaches and strategies, synthetic uses and applications in chemical and pharmaceutical industries, biological, biochemical and environmental aspects.
To date, over 100 volumes have been published in the series.

Recently Published Titles

The chemistry of the Cyclopropyl Group (Volume 2)
The chemistry of the Hydrazo, Azo and Azoxy Groups (Volume 2, 2 parts)
The chemistry of Double-Bonded Functional Groups (Volume 3, 2 parts)
The chemistry of Organophosphorus Compounds (Volume 4)
The chemistry of Halides, Pseudo-Halides and Azides (Volume 2, 2 parts)
The chemistry of the Amino, Nitro and Nitroso Groups (2 volumes, 2 parts)
The chemistry of Dienes and Polyenes (2 volumes)
The chemistry of Organic Derivatives of Gold and Silver
The chemistry of Organic Silicon Compounds (2 volumes, 4 parts)
The chemistry of Organic Germanium, Tin and Lead Compounds (Volume 2, 2 parts)
The chemistry of Phenols (2 parts)
The chemistry of Organolithium Compounds (2 parts)

Forthcoming Titles

The chemistry of Cyclobutanes
The chemistry of Peroxides (Volume 2)

The Patai Series Online

The **Patai Series** is now available in electronic format on Wiley InterScience. All new titles will be published online and a growing list of older titles will be added every year. It is the ultimate goal that all titles published in the **Patai Series** will be available in electronic format.
For more information see the **Patai Series Online** website:

www.interscience.wiley.com/bookfinder.html

R—Li

The chemistry of
organolithium compounds
Part 1

Edited by

ZVI RAPPOPORT
The Hebrew University, Jerusalem

ILAN MAREK
Technion-Israel Institute of Technology, Haifa

2004

John Wiley & Sons, Ltd

An Interscience® Publication

The chemistry of
organolithium compounds
Part 2

Edited by

ZVI RAPPOPORT
The Hebrew University, Jerusalem

ILAN MAREK
Technion-Israel Institute of Technology, Haifa

2004

John Wiley & Sons, Ltd

An Interscience® Publication

John Wiley & Sons Ltd, The Atrium, Southern Gate, Chichester,
West Sussex PO19 8SQ, England

Telephone (+44) 1243 779777

Email (for orders and customer service enquiries): cs-books@wiley.co.uk
Visit our Home Page on www.wileyeurope.com or www.wiley.com

Other Wiley Editorial Offices

John Wiley & Sons Inc., 111 River Street, Hoboken, NJ 07030, USA

Jossey-Bass, 989 Market Street, San Francisco, CA 94103-1741, USA

Wiley-VCH Verlag GmbH, Boschstr. 12, D-69469 Weinheim, Germany

John Wiley & Sons Australia Ltd, 33 Park Road, Milton, Queensland 4064, Australia

John Wiley & Sons (Asia) Pte Ltd, 2 Clementi Loop #02-01, Jin Xing Distripark, Singapore 129809

John Wiley & Sons Canada Ltd, 22 Worcester Road, Etobicoke, Ontario, Canada M9W 1L1

Wiley also publishes its books in a variety of electronic formats. Some content that appears
in print may not be available in electronic books.

Library of Congress Cataloging-in-Publication Data

The chemistry of organolithium compounds / edited by Zvi Rappoport, Ilan Marek.
p. cm.—(Chemistry of functional groups)
Includes bibliographical references and index.
ISBN 0-470-84339-X (cloth : alk. paper)
1. Organolithium compounds. I. Rappoport, Zvi. II. Marek, Ilan. III. Series.

QD412.L5 C48 2004
547′.05381–dc22

2003021758

British Library Cataloguing in Publication Data

A catalogue record for this book is available from the British Library

ISBN 0-470-84339-X

Typeset in 9/10pt Times by Laserwords Private Limited, Chennai, India
Printed and bound in India by Thompson Press, Faridabad
This book is printed on acid-free paper responsibly manufactured from sustainable forestry
in which at least two trees are planted for each one used for paper production.

Dedicated to

Eitan, Alon and **Naomi**

and

Haya, Efraim and **Rivka**

Contributing authors

Manfred Braun	Institut für Organische Chemie und Makromolekulare Chemie, Universität Düsseldorf, D-40225 Düsseldorf, Germany
Marvin Charton	Chemistry Department, School of Liberal Arts and Sciences, Pratt Institute, Brooklyn, NewYork 11205, USA
Fabrice Chemla	Laboratoire de Chimie Organique, Université Pierre et Marie Curie, Tour 44-45 2ème étage, Bte 183, 4 Place Jussieu, 75252 Paris Cedex 05, France
Guido Christoph	Organisch-Chemisches Institut der Westfälischen Wilhelms-Universität Münster, Corrensstr. 40, D-48149 Münster, Germany
Jonathan Clayden	Department of Chemistry, University of Manchester, Oxford Road, Manchester, M13 9PL, UK
Iain Coldham	School of Chemistry, University of Exeter, Stocker Road, Exeter, EX4 4QD, UK
Chagit Denekamp	Department of Chemistry, Technion–Israel Institute of Technology, Technion City, 32000 Haifa, Israel
Robert E. Gawley	Department of Chemistry and Biochemistry, University of Arkansas, Fayetteville, AR 72701, USA
G. Gopakumar	School of Chemistry, University of Hyderabad, Gachibowli, Hyderabad 500 046, Andhra Pradesh, India
Harald Günther	University of Siegen, Fachbereich 8, OCII, D-57068 Siegen, Germany
Dieter Hoppe	Organisch-Chemisches Institut der Westfälischen Wilhelms-Universität Münster, Corrensstr. 40, D-48149 Münster, Germany
Eluvathingal D. Jemmis	School of Chemistry, University of Hyderabad, Gachibowli, Hyderabad 500 046, Andhra Pradesh, India
Dan Johnels	Department of Chemistry/Organic Chemistry, Umeå University, SE-901 87 Umeå, Sweden
Wolfgang Kiefer	Institut für Physikalische Chemie, Universität Würzburg, Am Hubland, D-97074 Würzburg, Germany
Frédéric Leroux	Laboratoire de stéréochimie, Université Louis Pasteur (ECPM), 25 rue Becquerel, F-67087 Strasbourg, France

Joel F. Liebman	Department of Chemistry and Biochemistry, University of Maryland, Baltimore County, 1000 Hilltop Circle, Baltimore, Maryland 21250, USA
Ilan Marek	Department of Chemistry and Institute of Catalysis, Science and Technology, Technion-Israel Institute of Technology, Technion City, 32000 Haifa, Israel
I. Pavel	Institut für Physikalische Chemie, Universität Würzburg, Am Hubland, D-97074 Würzburg, Germany
Daniel Schildbach	Institut für Anorganische Chemie, Universität Würzburg, Am Hubland, D-97074 Würzburg, Germany
Manfred Schlosser	Institute of Molecular and Biological Chemistry, Swiss Federal Institute of Technology, CH-1015, Lausanne, Switzerland
Suzanne W. Slayden	Department of Chemistry, George Mason University, 4400 University Drive, Fairfax, Virginia 22030, USA
Dietmar Stalke	Institut für Anorganische Chemie, Universität Würzburg, Am Hubland, D-97074 Würzburg, Germany
Thomas Stey	Institut für Anorganische Chemie, Universität Würzburg, Am Hubland, D-97074 Würzburg, Germany
Carsten Strohmann	Institut für Anorganische Chemie, Universität Würzburg, Am Hubland, D-97074 Würzburg, Germany
K. Tomioka	Graduate School of Pharmaceutical Sciences, Kyoto University, Yoshida, Sakyo-ku, Kyoto 606–8501, Japan
Katsuhiko Tomooka	Department of Applied Chemistry, Tokyo Institute of Technology, Meguro-ku, Tokyo 152–8552, Japan
Emmanuel Vrancken	Laboratoire de Chimie Organique, Université Pierre et Marie Curie, Tour 44-45 2ème étage, Bte 183, 4 Place Jussieu, F-75252 Paris Cedex 05, France
K. Yamada	Graduate School of Pharmaceutical Science, Kyoto University, Yoshida, Sakyo-ku, Kyoto 606–8501, Japan
Hiroshi Yamataka	Institute of Scientific and Industrial Research, Osaka University, Ibaraki, Osaka 567–0047, Japan
Miguel Yus	Departamento de Química Orgánica, Facultad de Ciencias, Universidad de Alicante, Apdo. 99, 03080 Alicante, Spain
Jacob Zabicky	Institutes for Applied Research, Ben-Gurion University of the Negev, P. O. Box 653, Beer-Sheva 84105, Israel
Elinor Zohar	Department of Chemistry and Institute of Catalysis, Science and Technology, Technion—Israel Institute of Technology, Technion City, 32000 Haifa, Israel

Foreword

This is another volume in 'The Chemistry of Functional Groups' series which deals with organometallic derivatives. We have assembled the remarkable recent achievements in the synthesis, structure, synthetic uses and spectroscopy of organic lithium derivatives which are in daily use in the organic chemist's laboratory.

The two parts of the present volume contain 18 chapters written by experts from 10 countries. They include chapters on new developments, since Sapse and Schleyer's *Lithium chemistry* published in 1995, dealing with theoretical aspects, structural chemistry, thermochemistry, various spectroscopic characteristics such as solid state NMR and vibrational spectroscopy, and gas phase chemistry, of organolithium compounds. Mechanistically oriented chapters deal with directing and activating effects of organolithium derivatives and the mechanism of their additions to double bonds. There are chapters on analysis, as well as on rearrangements of organolithium compounds and on specific classes such as polylithium compounds, lithium carbenoids and α-amino-organolithiums.

Several chapters deal with the synthesis of and the synthetic applications of organolithium compounds such as orthometallation, arene catalysed lithiation, addition to carbon–carbon double bonds, their reaction with oxiranes, and asymmetric deprotonation with lithium (-)-sparteine. We gratefully acknowledge the contributions of all the authors of these chapters.

Three promised chapters on the dynamic behaviour of organolithium compounds, on chiral alkyllithium amides in asymmetric synthesis and on the intramolecular carbolithiation reaction were not delivered. Although some material related to the first of these two chapters appear partially in other chapters, we hope that the missing chapters will appear in a future volume.

The literature coverage is mostly up to mid or late 2002, and several chapters contain references from 2003.

We will be grateful to readers who draw our attention to any mistakes in the present volume, or to omissions and new topics which deserve to be included in a future volume on organolithium compounds.

Jerusalem and Haifa
September 2003

ZVI RAPPOPORT
ILAN MAREK

The Chemistry of Functional Groups
Preface to the series

The series 'The Chemistry of Functional Groups' was originally planned to cover in each volume all aspects of the chemistry of one of the important functional groups in organic chemistry. The emphasis is laid on the preparation, properties and reactions of the functional group treated and on the effects which it exerts both in the immediate vicinity of the group in question and in the whole molecule.

A voluntary restriction on the treatment of the various functional groups in these volumes is that material included in easily and generally available secondary or tertiary sources, such as Chemical Reviews, Quarterly Reviews, Organic Reactions, various 'Advances' and 'Progress' series and in textbooks (i.e. in books which are usually found in the chemical libraries of most universities and research institutes), should not, as a rule, be repeated in detail, unless it is necessary for the balanced treatment of the topic. Therefore each of the authors is asked not to give an encyclopaedic coverage of his subject, but to concentrate on the most important recent developments and mainly on material that has not been adequately covered by reviews or other secondary sources by the time of writing of the chapter, and to address himself to a reader who is assumed to be at a fairly advanced postgraduate level.

It is realized that no plan can be devised for a volume that would give a complete coverage of the field with no overlap between chapters, while at the same time preserving the readability of the text. The Editors set themselves the goal of attaining reasonable coverage with moderate overlap, with a minimum of cross-references between the chapters. In this manner, sufficient freedom is given to the authors to produce readable quasi-monographic chapters.

The general plan of each volume includes the following main sections:

(a) An introductory chapter deals with the general and theoretical aspects of the group.

(b) Chapters discuss the characterization and characteristics of the functional groups, i.e. qualitative and quantitative methods of determination including chemical and physical methods, MS, UV, IR, NMR, ESR and PES—as well as activating and directive effects exerted by the group, and its basicity, acidity and complex-forming ability.

(c) One or more chapters deal with the formation of the functional group in question, either from other groups already present in the molecule or by introducing the new group directly or indirectly. This is usually followed by a description of the synthetic uses of the group, including its reactions, transformations and rearrangements.

(d) Additional chapters deal with special topics such as electrochemistry, photochemistry, radiation chemistry, thermochemistry, syntheses and uses of isotopically labelled compounds, as well as with biochemistry, pharmacology and toxicology. Whenever applicable, unique chapters relevant only to single functional groups are also included (e.g. 'Polyethers', 'Tetraaminoethylenes' or 'Siloxanes').

This plan entails that the breadth, depth and thought-provoking nature of each chapter will differ with the views and inclinations of the authors and the presentation will necessarily be somewhat uneven. Moreover, a serious problem is caused by authors who deliver their manuscript late or not at all. In order to overcome this problem at least to some extent, some volumes may be published without giving consideration to the originally planned logical order of the chapters.

Since the beginning of the Series in 1964, two main developments have occurred. The first of these is the publication of supplementary volumes which contain material relating to several kindred functional groups (Supplements A, B, C, D, E, F and S). The second ramification is the publication of a series of 'Updates', which contain in each volume selected and related chapters, reprinted in the original form in which they were published, together with an extensive updating of the subjects, if possible, by the authors of the original chapters. A complete list of all above mentioned volumes is available from the publisher. Unfortunately, the publication of the 'Updates' has been discontinued for economic reasons.

Advice or criticism regarding the plan and execution of this series will be welcomed by the Editors.

The publication of this series would never have been started, let alone continued, without the support of many persons in Israel and overseas, including colleagues, friends and family. The efficient and patient co-operation of staff-members of the publisher also rendered us invaluable aid. Our sincere thanks are due to all of them.

The Hebrew University SAUL PATAI
Jerusalem, Israel ZVI RAPPOPORT

Sadly, Saul Patai who founded 'The Chemistry of Functional Groups' series died in 1998, just after we started to work on the 100th volume of the series. As a long-term collaborator and co-editor of many volumes of the series, I undertook the editorship and I plan to continue editing the series along the same lines that served for the preceeding volumes. I hope that the continuing series will be a living memorial to its founder.

The Hebrew University ZVI RAPPOPORT
Jerusalem, Israel
May 2000

Contents

List of abbreviations used

Ac	acetyl (MeCO)
acac	acetylacetone
Ad	adamantyl
AIBN	azoisobutyronitrile
Alk	alkyl
All	allyl
An	anisyl
Ar	aryl
Bn	benzyl
Bz	benzoyl (C_6H_5CO)
Bu	butyl (C_4H_9)
CD	circular dichroism
CI	chemical ionization
CIDNP	chemically induced dynamic nuclear polarization
CNDO	complete neglect of differential overlap
Cp	η^5-cyclopentadienyl
Cp^*	η^5-pentamethylcyclopentadienyl
DABCO	1,4-diazabicyclo[2.2.2]octane
DBN	1,5-diazabicyclo[4.3.0]non-5-ene
DBU	1,8-diazabicyclo[5.4.0]undec-7-ene
DIBAH	diisobutylaluminium hydride
DME	1,2-dimethoxyethane
DMF	*N,N*-dimethylformamide
DMSO	dimethyl sulphoxide
ee	enantiomeric excess
EI	electron impact
ESCA	electron spectroscopy for chemical analysis
ESR	electron spin resonance
Et	ethyl
eV	electron volt

Fc	ferrocenyl
FD	field desorption
FI	field ionization
FT	Fourier transform
Fu	furyl(OC_4H_3)
GLC	gas liquid chromatography
Hex	hexyl (C_6H_{13})
c-Hex	cyclohexyl (c-C_6H_{11})
HMPA	hexamethylphosphortriamide
HOMO	highest occupied molecular orbital
HPLC	high performance liquid chromatography
i-	iso
ICR	ion cyclotron resonance
Ip	ionization potential
IR	infrared
LAH	lithium aluminium hydride
LCAO	linear combination of atomic orbitals
LDA	lithium diisopropylamide
LUMO	lowest unoccupied molecular orbital
M	metal
M	parent molecule
MCPBA	*m*-chloroperbenzoic acid
Me	methyl
MNDO	modified neglect of diatomic overlap
MS	mass spectrum
n	normal
Naph	naphthyl
NBS	*N*-bromosuccinimide
NCS	*N*-chlorosuccinimide
NMR	nuclear magnetic resonance
Pen	pentyl (C_5H_{11})
Ph	phenyl
Pip	piperidyl($C_5H_{10}N$)
ppm	parts per million
Pr	propyl (C_3H_7)
PTC	phase transfer catalysis or phase transfer conditions
Py, Pyr	pyridyl (C_5H_4N)

R	any radical
RT	room temperature
s-	secondary
SET	single electron transfer
SOMO	singly occupied molecular orbital
t-	tertiary
TCNE	tetracyanoethylene
TFA	trifluoroacetic acid
THF	tetrahydrofuran
Thi	thienyl (SC_4H_3)
TLC	thin layer chromatography
TMEDA	tetramethylethylene diamine
TMS	trimethylsilyl or tetramethylsilane
Tol	tolyl (MeC_6H_4)
Tos or Ts	tosyl (*p*-toluenesulphonyl)
Trityl	triphenylmethyl (Ph_3C)
Xyl	xylyl($Me_2C_6H_3$)

In addition, entries in the ‘List of Radical Names’ in *IUPAC Nomenclature of Organic Chemistry*, 1979 Edition, Pergamon Press, Oxford, 1979, p. 305–322, will also be used in their unabbreviated forms, both in the text and in formulae instead of explicitly drawn structures.

CHAPTER **1**

Theoretical studies in organolithium chemistry

ELUVATHINGAL D. JEMMIS and G. GOPAKUMAR

School of Chemistry, University of Hyderabad, Gachibowli, Hyderabad 500 046,
Andhra Pradesh, India
e-mail: jemmis@uohyd.ernet.in

I. INTRODUCTION

With their versatile structure, bonding and reactions, organolithium compounds continue to fascinate chemists. Tremendous progress has been made in each of these areas during the last few years. Theoretical studies have played an important role in these developments. Several reviews had appeared on the contribution of theoretical methods in organolithium compounds[1,2]. Wave-function-based quantum mechanical methods at various levels continue to be used in these studies; theoretical studies based on Density Functional Theory

---

The Chemistry of Organolithium Compounds. Edited by Z. Rappoport and I. Marek
ISBN: 0-470-84339-X

(DFT) have also become popular in recent years. A major review on theoretical studies in organolithium compounds was published in 1995 by Streitwieser, Bachrach and Schleyer[2]. We concentrate here on publications that have appeared since then. During these years considerable progress has been made in the application of theoretical methods to the chemistry of organolithium compounds at various levels of sophistication depending on the problem. Attempts have been made to further delineate the nature of C−Li bonding. Semiempirical calculations with the inclusion of solvent effects through various approximations have been used to study larger systems. Reactions have been modeled in the gas phase. Mechanistic details of several reactions have been studied theoretically. We discuss the developments in the nature of the C−Li bonding first. Theoretical studies on the structure and energetics, reactions and some applications involving NMR parameters are discussed in subsequent sections.

II. THE NATURE OF THE C−Li BOND

The nature of C−Li bond is still a dilemma for chemists due to the unusual behavior of the bond in different compounds. Although the electronegativity difference suggests the carbon−lithium bond to be essentially ionic, the solubility of some organolithium compounds in nonpolar solvents such as benzene makes the problem more complex[3]. The nature of the C−Li bond is different from those of the heavier analogs of alkali−metal organic complexes; C−Na to C−Cs bonds are acknowledged to be even more ionic than the C−Li bond. It was therefore felt that a certain percentage of covalent character may be associated with the C−Li bond[3]. But recent studies and developments of methodologies for the analysis of wave functions and charge distributions suggest a much higher polarity to the bond. In 1995, Streitwieser, Bachrach and Schleyer[2]suggested: 'The carbon lithium bond in theory and in chemical properties can be modeled as an essentially ionic bond'. They described a number of examples, which support the ionic behavior of the carbon−lithium bond.

Later, Koizumi and Kikuchi[4] used *ab initio* calculations of NMR spin−spin coupling constants in monomeric methyllithium, *tert*-butyllithium and methyllithium oligomers using self-consistent perturbation theory to probe the nature of C−Li bonding. Their studies suggested that solvation affects the nature of the C−Li bond and reduces the $^1J_{\mathrm{CLi}}$ value significantly. The calculations were also carried out using a truncated basis set (the MIDI-4 basis set for lithium which includes only the 1s function and corresponds to lithium cation), which models a purely ionic C−Li bond. The calculated coupling constants were in excellent agreement with experimental data, suggesting the importance of the ionic character of the C−Li bond in alkyllithiums. The calculated $^1J_{\mathrm{CLi}}$ value of methyllithium, 44.0 Hz, is found to be very close to that calculated for methyllithium with three solvating ligands. This result, which strongly suggests the ionic nature of the C−Li bond in methyllithium, does not change with the addition of ligands. The difference between the $^1J_{\mathrm{CLi}}$ values calculated by two different types of basis set for methyllithium tetramer is much smaller than that in monomeric methyllithium. This trend is in accordance with the observation that the coupling constants in methyllithium tetramer are independent of solvent. Comparing the coupling constants of the ring structures **1a, 1b** and **1c** (Figure 1) with the tetrahedral structure **1d** (staggered and eclipsed form) implies that $^1J_{\mathrm{CLi}}$ depends on the state of aggregation rather than on the degree of aggregation. More clearly, $^1J_{\mathrm{CLi}}$ in methyllithium varies nearly inversely with the number of lithium atoms, which are bonded directly to the carbon atom. The implications are that the ionic nature of the monomeric MeLi increases on solvation and the tetrameric MeLi has more ionic C−Li bonding. In addition, further solvation is not desirable as the bridging nature of tetramer provides the effect of solvation.

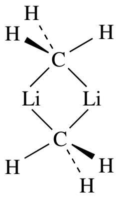

20.9 Hz
(1a)

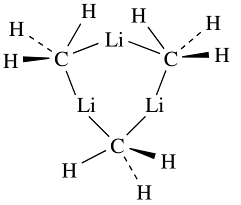

24.1 Hz
(1b)

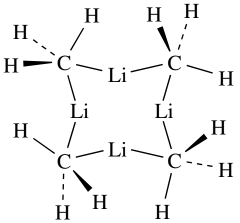

24.6 Hz
(1c)

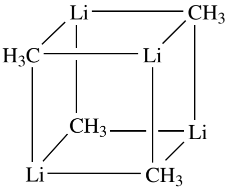

Staggered 12.5 Hz and eclipsed 14.0 Hz
(1d)

FIGURE 1. The ring structures of the dimer (**1a**), trimer (**1b**) and tetramer (**1c**) of CH_3Li and a perspective representation of the tetrahedral structure (**1d**) of the latter. The calculated coupling constants are given below each structure. Reprinted with permission from Reference 4. Copyright 1995 American Chemical Society

In 1996, Bickelhaupt and coworkers investigated CH_3Li, $(CH_3Li)_2$ and $(CH_3Li)_4$ using Density Functional Theory (DFT) and conventional *ab initio* Molecular Orbital Theory (MOT)[5]. This study highlighted the important role of a small covalent component in the polar C−Li bond, especially in the methyllithium tetramer. It was suggested that the lithium outer 2p orbital serves only as 'superposition functions', helping to describe the carbanion, and does not play any part in covalent interaction. However, there appears to be a small contribution from the inner parts of the Li 2p orbital. Streitwieser and coworkers[6] showed that calculations using a truncated basis set on lithium with only s-type basis functions yield essentially the same result (including the energetic ordering of isomers) as calculated using the full basis sets. They concluded that the bonding is governed by electrostatic interactions. The extended 6-31+G* basis set used in the evaluation of aggregation energies was expected to minimize the basis set superposition error as suggested by Bickelhaupt and coworkers[5]. The result showed that the oligomerization energies ($\Delta E_{\text{oligo}} + \Delta \text{ZPE}$) calculated with truncated basis set are up to 20% lower than those obtained using the full 6-31+G* basis. This indicated that the bonding mechanism is more complicated than suggested by the purely electrostatic model.

Charges on lithium calculated using the Voronoi Deformation Density (VDD) decrease from 0.38 via 0.26 to 0.13e along CH_3Li, $(CH_3Li)_2$, $(CH_3Li)_4$ showing that the shift of electron density from lithium to methyl decreases upon oligomerization[5]. Similarly, Hirshfeld lithium charges decrease from +0.49 via 0.42 down to +0.30e along the same series of methyl lithium oligomers (Table 1). The fragment molecular orbital analysis shows $(CH_3^\bullet)_n$ and $(Li^\bullet)_n$ fragments to have triplet and quintet electronic structures in $(CH_3Li)_2$ and $(CH_3Li)_4$, respectively. Thus the interacting fragments are two singly occupied molecular orbitals (SOMO_{low} and $\text{SOMO}_{\text{high}}$) in each $(CH_3^\bullet)_n$ and $(Li^\bullet)_n$. The

TABLE 1. The charges of Li in CH_3Li and its oligomers. Reproduced with permission from Ref. 5

Method	CH_3Li	$(CH_3Li)_2$	$(CH_3Li)_4$
Voronoi deformation density (VDD)	0.38	0.26	0.13
Hirshfeld	0.49	0.42	0.30

above trend of decrease in electron density transfer from lithium is in accordance with the increasing population of the $(Li^\bullet)_n$ fragment orbitals $SOMO_{low}$ and $SOMO_{high}$ from $(CH_3Li)_2$ [$SOMO_{low} = 0.57$ and $SOMO_{high} = 0.63$] to $(CH_3Li)_4$ [$SOMO_{low} = 0.91$ and $SOMO_{high} = 0.85$]. This is indicative of the increasing importance of a covalent component in the carbon–lithium bond. Also, the carbon–lithium bond is much less ionic according to Hirshfeld[5] (50–30%) than according to NPA charges (90%). These factors suggest that the degree of ionicity of a bond obtained on the basis of atomic charges should not be regarded as an absolute quantity, rather it will be more meaningful to consider trends in atomic charges across a series of molecules using the same method. Even though Bickelhaupt[5] emphasized the importance of covalent contributions to the C−Li bonding, the results imply the ‘dual nature’ of the C−Li bond. It can be concluded that the appearance of a covalent or ionic aspect depends strongly on the physical and chemical context.

From their analysis of the conformational energies of pentadienyl anion and the pentadienyl metal compounds, Pratt and Streitwieser[7] in 2000 pointed out that the stabilization of the planar forms of the organometallic structures results from both conjugation and electrostatic attraction between the negative carbons and the alkali metal cations. To determine the relative magnitude of these effects, the reaction energies were determined for hypothetical reaction, shown in Scheme 1 where M represents any alkali metal.

SCHEME 1

The reaction energies for the formation of pentadienyllithium are found to be much greater than those for pentadienyl sodium, which indicate a greater electrostatic attraction for the shorter Li−C bond. The calculated regional charges for the pentadienyllithiums (HF/6-311+G*) indicate that the most positive charge is concentrated on lithium and the most negative charge is concentrated on the carbon atom coordinated to the lithium. These results imply an ionic nature of the C−Li bond in pentadienyllithium. However, the larger magnitude of electrostatic interaction may be due to the shorter distance of the C−Li bond, and not necessarily to a larger charge separation. In other words, it is possible that the charge on lithium may be less than that on sodium in the corresponding sodium derivative and yet the electrostatic interaction may be larger in the former due to the shorter distance.

Density functional theory calculations on methyllithium, *tert*-butyllithium and phenyllithium oligomers by Kwon, Sevin and McKee support the ionic character of the C−Li bond[8]. Their calculations of carbon lithium Natural Population Analysis (NPA) charges and dipole moments for CH_3Li, *t*-BuLi and Ph-Li oligomers (Table 2) indicate the ionic behavior of the C−Li bond. Comparison of the charges of various oligomers suggests that charges of lithium and carbon atoms are almost independent of the size of oligomers. There are minor variations in the charge of the Li on going from CH_3Li via *t*-BuLi and PhLi, implying that there are changes in the nature of C−Li bonding as a function of the organic group. Thus it is not correct to say that all C−Li bonds are 100% ionic. There are minor variations.

TABLE 2. The charges on Li and, C coordinated to the Li and the dipole moments for a series of MeLi, *t*-BuLi and PhLi oligomers. Reproduced with permission from Ref. 8

	NPA charge[a]		Dipole moment[b]
	Li	C	
MeLi (monomer)	0.83	−1.48	5.51
Me_2Li_2	0.87	−1.53	0
Me_3Li_3	0.84	−1.51	0
Me_4Li_4	0.86	−1.51	0
t-BuLi	0.81	−0.59	6.23
t-Bu_2Li_2	0.87	−0.71	0
t-Bu_3Li_3	0.82	−0.69	0
t-Bu_4Li_4	0.85	−0.74	0
PhLi (monomer)	0.87[c]	−0.64[c]	6.61
Ph_4Li_4	0.85[c]	−0.69[c]	0

[a] At the B3LYP/6-31+G* level where diffuse functions have been omitted from lithium atoms.

[b] At the B3LYP/6-31+G* level.

[c] At the B3LYP/6-31+G* level where diffuse functions have been omitted from lithium atoms and carbon atoms not coordinated to the lithium face.

Ponec and coworkers[9] reconsidered the conventional concept of C−Li bond in CH_3Li and CLi_6. Their calculations were based on two recently proposed methodologies: the Atoms in Molecule (AIM) generalized population analysis and Fermi hole analysis. These results support the ionic nature of C−Li bonding in CH_3Li, but in CLi_6 a different description than the one published earlier[2] is suggested. The bonding description of CLi_6 proposed by Schleyer and coworkers in 1995 involves a C^{4-} ion surrounded by $Li_6{}^{4+}$ in an octahedral fashion (Figure 2). The two electrons in the lithium cluster are placed in an orbital, which is completely symmetric, being a Li−Li bonding orbital among all lithium atoms, with a small contribution from the carbon 2s orbital. This extra electron pair was considered as a part of the Li···Li bonding interactions. According to Ponec

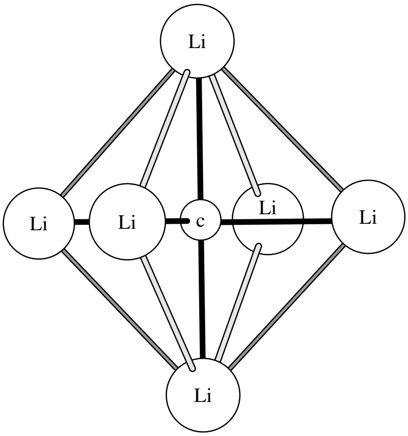

FIGURE 2. Optimized structure of CLi_6 at HF/6-31G*. Reproduced by permission of J. Wiley & Sons from A. M. Sapse and P. v. R. Schleyer (Eds.), *Lithium Chemistry. A Theoretical and Experimental Overview,* J. Wiley & Sons, New York, 1995

and coworkers the AIM analysis suggests that this electron pair is also shared between the carbon and lithiums and the contributions of C and Li are roughly equal to 1.2 and 0.8*e*, respectively. Although the oxidation state of the central carbon is indeed close to the NPA estimate (−IV), the interactions between the central atom and the surrounding cage need not be purely ionic as expected so far. This is supported by the result of generalized population analysis, which detects the presence of 3-center bonding interactions in Li−C−Li fragments as seen from the values of the corresponding indices, such as the C $\cdots$ Li cage interactions. The Li $\cdots$ Li bond indices drop from 0.167 (Mulliken-like analysis) to 0.020 (AIM generalized value), correlating the conclusions above.

Thus it is evident from all these studies that the nature of the C−Li bond varies from compound to compound; hence any generalization of the nature of bonding is to be taken cautiously. As Schleyer and Streitwieser have discussed in the past, the C−Li bond is essentially ionic; however, the covalent components cannot be neglected[5]. The unusual behavior of the C−Li bond has been a subject of discussion from the initial years of applying theoretical methods, and the debate continues in an interesting manner due to the developments of new theoretical methodologies. In fact, we support the implications of Bickelhaupt that there is a covalent contribution to the C−Li bonding, however small this turns out to be in specific examples[5].

III. STRUCTURE AND ENERGY

Theoretical studies of the structure of organolithium compounds continue to attract much attention for several reasons. Often, it is not possible to obtain detailed structural information from experiments. Experimental realization of a single crystal, which is good enough for X-ray diffraction studies, is not always easy. Even when such detailed information about the structure is available, theoretical studies provide an electronic structural description that helps one proceed further. The theoretical results depend on the level of theory used. This often results in the re-examination of structures studied earlier using lower levels of theory. Many of the structures that were thought to be minima were found to have several imaginary frequencies at more sophisticated levels of theory. Schleyer and coworkers in 1995 discussed a large number of compounds and their optimized structures. We consider here results that have appeared since then. Optimized structures and the factors affecting the stability are discussed below. The last ten years have witnessed a revolution in modeling solvent effects. Several theoretical studies incorporating the effect of solvents are known and we first discuss this aspect of structural studies.

A. Effect of Solvation

The structures of organolithium compounds are affected by solvation. For example, Sorger, Schleyer and Stalke have shown that the solid-state cisoid dimeric structure of 3,3-dimethyl-2-(trimethylsilyl)cyclopropenyllithium-tetramethylenediamine does not persist in solution; it is monomeric in THF solution[10]. In 1996, Weiss and coworkers studied the effect of specific and nonspecific solvations by THF on methyl isobutyrate aggregates[11]. This study shows that the solvent influences the stability of the dimer to a higher extent than that of the tetramer. In total disagreement with earlier experimental results, *ab initio* MO calculations (gas-phase studies) at the MP2/SVD//SCF/SVD, SCF/SVD//SCF/SVD and SCF/TZD//SCF/SVD (split valence basis sets augmented with one d-polarization function for carbon and oxygen, for Li augmented with one p-polarization function and a double-ζ basis set for hydrogen; this is referred to as SVD; the Karlsruhe TZP basis sets for Li, O and C, and for hydrogen the same DZ basis set as for the structure optimization have been used, is referred to as TZD) levels for the energies of dimer and cubic tetramer, suggest that the tetramer is more stable than the dimer. But the results of solvent effects, using the semiempirical MNDO and PM3 methods, predict the dimer to be more stable[11]. Clearly, more careful investigation is required here before definite conclusions can be drawn. The general indication is that the dimers are more strongly affected by solvation than the tetramers.

Since several aspects of the regio- and stereoselectivity of lithium enolates involves the characteristics of their aggregation, the effect of solvation on the structure and aggregation of lithium enolates plays an important role in the mechanistic study. In 1997, Abbotto, Streitwieser and Schleyer investigated theoretically by using *ab initio* and semiempirical MO methods the effect of ether solvent on the aggregation of lithium enolates[12]. This study shows that solvation has a critical role in determining the relative energies of the aggregated species. π-Interaction between lithium and the enolate double bond is another factor that helps to determine the relative stabilities of the isomers and the degree of solvation. The cubic tetramer is stable because of the electrostatic stabilization of the aggregation, but the monomeric species is important in the equilibrium owing to its high solvation energies. In contrast, the dimer, and to a greater extent the trimer, is less important. The tendency of lithium cation to reach tetracoordination is shown to be less significant than commonly believed. Jackman and Lange studied the aggregation and reactivity of lithium enolates using ^{6}Li and ^{13}C NMR spectroscopy and suggested that the parent lithium enolate of acetaldehyde exists exclusively as a tetramer in THF solution[13]. Selection of water as a solvent molecule in the study of the solvation effect is less effective due to the property of water to form hydrogen bonds. In their study Abbotto and coworkers abandoned THF as the solvent due to its large size and took dimethyl ether as a realistic coordinating solvent[12].

The effect of solvation in CH_2=CHOLi was studied in detail. Earlier studies at the B3LYP/6-31+G* level suggested that the lowest energy minima correspond to isolated bridged lithium enolate **2a**, rather than the open-chain structure **2b**; this is attributed to the interaction of the lithium cation with the enolate anion (Figure 3).

The main consequences of the solvation are found to be the increment in bond lengths between the enolate oxygen atom and the lithium in the mono and the disolvated (**3a**) enolates, together with the increment in the Li−Osolvent bond. However, the trend continues up to trisolvated species **3b** (Figure 4), where the Li−O distance is found to be less than that in isolated species. These characteristics of larger Li−dimethyl ether distance (due to the steric hindrance) and the absence of coordination to the double bonds suggest an ionic interaction of Li with enolate oxygen.

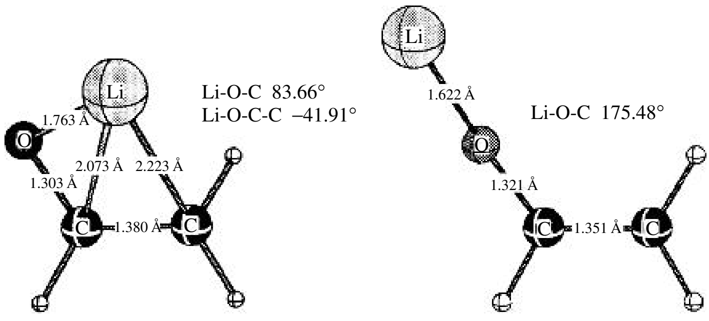

(2a) **(2b)**

FIGURE 3. Optimized structures of monomer CH_2=CHOLi as obtained from B3LYP/6-31+G* calculations. Reprinted with permission from Reference 12. Copyright 1997 American Chemical Society

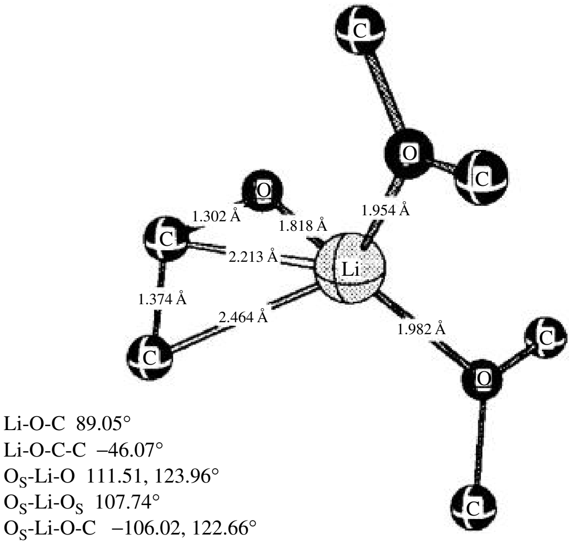

Li-O-C 89.05°
Li-O-C-C −46.07°
O_S-Li-O 111.51, 123.96°
O_S-Li-O_S 107.74°
O_S-Li-O-C −106.02, 122.66°

(B3LYP)
(6–31 + G*)
(3a)

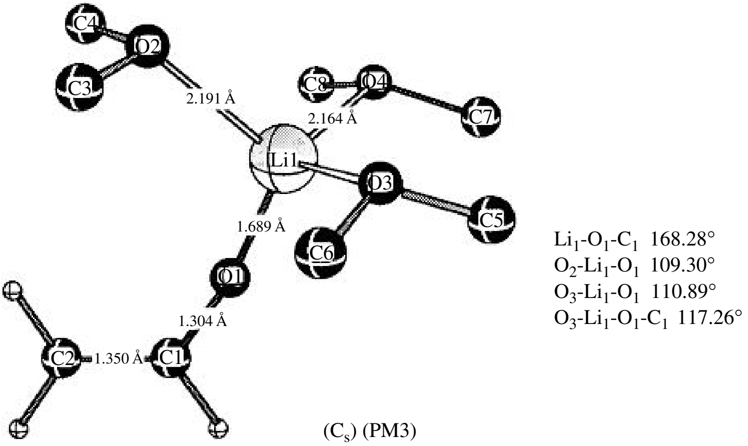

Li_1-O_1-C_1 168.28°
O_2-Li_1-O_1 109.30°
O_3-Li_1-O_1 110.89°
O_3-Li_1-O_1-C_1 117.26°

(C_s) (PM3)
(6–31 + G*)
(3b)

FIGURE 4. Optimized structures of $CH_2{=}CHOLi(Me_2O)_2$ (**3a**) as obtained from B3LYP/6-31+G* calculations (**3b**) and $CH_2{=}CHOLi(Me_2O)_3$ as obtained from PM3 calculations. Reprinted with permission from Reference 12. Copyright 1997 American Chemical Society

The geometries for the dimeric isomers are also optimized at the B3LYP/6-31+G* level. The results were compared with Hartree–Fock and PM3 results. The stable dimers **4a, 4b** and **4c** are found to have C_1 symmetry (Figure 5).

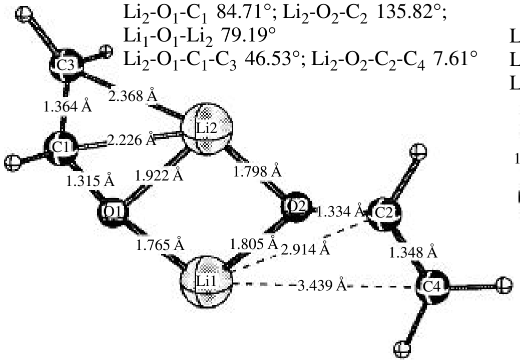

Li_2-O_1-C_1 84.71°; Li_2-O_2-C_2 135.82°;
Li_1-O_1-Li_2 79.19°
Li_2-O_1-C_1-C_3 46.53°; Li_2-O_2-C_2-C_4 7.61°

(C_1) (B3LYP)
(4a)

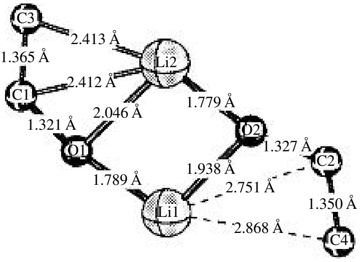

Li_2-O_1-C_1 88.82°; Li_2-O_2-C_2 113.49°;
Li_1-O_1-Li_2 79.21°
Li_2-O_1-C_1-C_3 38.98°; Li_2-O_2-C_2-C_4 −0.88°

(C_1) (PM3)
(4b)

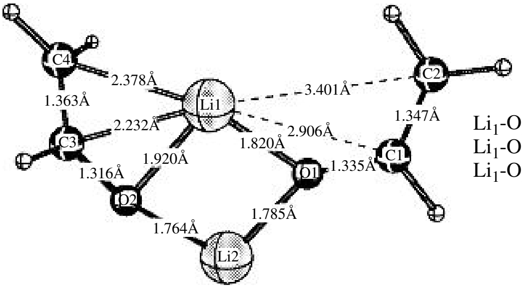

Li_1-O_2-C_3 85.05°; Li_1-O_1-C_1 133.60°;
Li_1-O_2-Li_2 79.14°
Li_1-O_2-C_3-C_4 46.62°; Li_1-O_1-C_1-C_2 4.13°

(C_1) (B3LYP)
(4c)

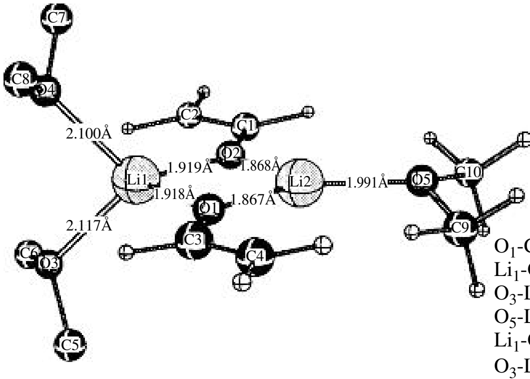

O_1-C_3 1.32 Å; C_3-C_4 1.35 Å
Li_1-O_1-C_3 130.97°; O_2-Li_1-O_1 85.94°
O_3-Li_1-O_1 118.20°; O_4-Li_1-O_3 91.07°
O_5-Li_2-O_1 137.72°
Li_1-O_1-C_2-C_4 −176.65°;
O_3-Li_1-O_1-C_3 −52.59°

(C_1) (PM3)
(4d)

FIGURE 5. **4a–4c** are optimized structures of dimers $(CH_2{=}CHOLi)_2$ as obtained from B3LYP/6-31+G* and PM3 calculations. Hydrogen atoms are omitted in PM3. Structure **4d** represents the optimized structure of the complex of the dimer $(CH_2{=}CHOLi)_2$ with three molecules of Me_2O at the PM3 level. Reprinted with permission from Reference 12. Copyright 1997 American Chemical Society

The relatively high stability of the three isomers **4a, 4b** and **4c** is attributed to the stabilizing interaction between lithium cation and enolate double bond. Comparison of the energy of monomer, dimer and trimer systems, with and without π-coordination (as in **2a** vs **2b** in Figure 3) indicated the π-coordination energy to be 0.5–2.6 kcal mol^{-1}. It is found that for the trisolvated monomer **3b** (and for other aggregates) π-coordination disappears on solvation (Figure 4). Thus π-coordination is also a decisive factor in determining the most favorable degree of solvation. Abbotto and coworkers concluded that if the negative entropic contribution relative to the third solvation process of monomeric CH_2=CHOLi is assumed to be about 5–10 eu, the small negative enthalpy suggests that this step has a positive ΔG at room temperature. Thus it is clear that tetracoordination of the lithium center is not necessarily a thermodynamically favored process; less solvated species with coordinated lithium may well be more stable. If we consider the solvation enthalpies and entropies, the most stable solvated species are the disolvated monomer **4a**, the trisolvated dimer **4d**, the trisolvated trimer **5a** and the tetrasolvated tetramer **5b** (Figures 5–6). The association energies among these solvated species are monomer/dimer −14.9, monomer/trimer −11.6 and monomer/tetramer −17.2 kcal mol^{-1} (per mol of monomeric unit). Comparison of these values with the corresponding energies without solvation of −26.0, −33.5 and −35.3 kcal mol^{-1} (which are increasing in the order monomer/dimer < monomer/trimer < monomer/tetramer) suggests a different order with the monomer/dimer equilibrium being the least favored.

The calculations of the natural charge populations of selected B3LYP/6-31+G* optimized structures, using the two different basis sets 6-31+G* and 6-311+G**, reveal the increase of negative charge on the oxygen, and a decrease on the carbons on aggregation (Table 3). The results are rationalized as follows. Compared to the monomer, each oxygen of the dimer is close to two positively charged lithium centers and, as a consequence of its higher effective electronegativity, it removes more charge from the double bond. The increase in the charge on oxygen is about the same as the decrease in C_β charge. In the dimer in which the π-coordination is absent, the lithium atom carries more positive charge. Hence the oxygen of the bridged unit is effectively less electronegative and less charge is withdrawn from the α-carbon. This fact suggests that the π-coordination between the enolate double bond and the lithium cation increases the negative charge by about 0.1 electron at the β-position. The lack of significant difference observed between the carbon of the bridged unit in **4a** in Figure 5 and the corresponding position of the C_{2h} isomer (Figure 7) suggests that the π-delocalization from oxygen to the double bond is not important and that the polarization mechanism controls charge redistribution in lithium enolates. This is also reflected in the identical distances of O−C and C−C bonds[12] in the unbridged enolate unit of C_1 isomer (Figure 5) and in the C_{2h} isomer **6** (Figure 7).

The decrease in the negative charge on C_β on going from monomer to higher aggregates implies the opposite behavior in the solvated monomers. The reverse behavior is due to the bonding of lithium to more oxygens on solvation. Thus the solvation limits its effect on charge redistribution primarily to the lithium cation, and the populations on the enolate moiety are relatively unaffected by solvent contribution.

B. Stability due to Sulfur

The high nucleophilicity of heterosubstituted allyllithium compounds makes them attractive reagents in synthetic organic chemistry. Structural studies of these compounds give a fundamental understanding about the control of the regioselectivity. Often, these studies are difficult due to the tendency of the compounds to form complex fluxional aggregates in solution. Piffl and coworkers have studied the dependency of the oxidation state of sulfur on the structure and electronic properties of the heterosubstituted

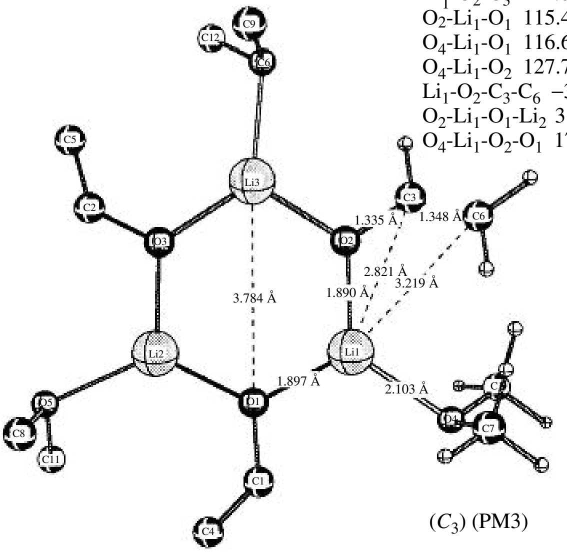

Li_1-O_2-C_3 121.04°
O_2-Li_1-O_1 115.44°
O_4-Li_1-O_1 116.63°
O_4-Li_1-O_2 127.70°
Li_1-O_2-C_3-C_6 −38.67°
O_2-Li_1-O_1-Li_2 3.15°
O_4-Li_1-O_2-O_1 174.24°

(C_3) (PM3)

(5a)

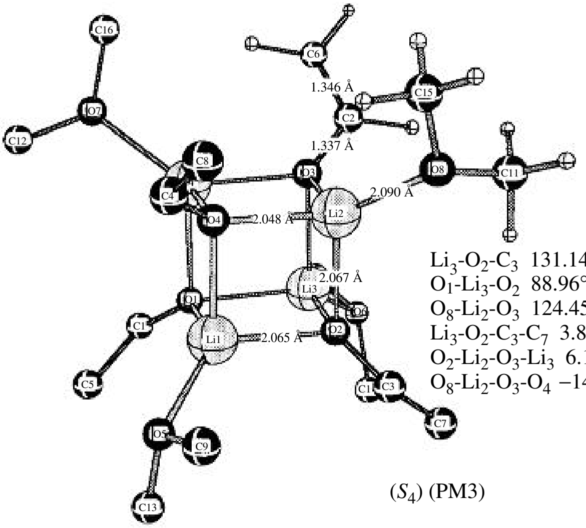

Li_3-O_2-C_3 131.14°; O_2-Li_3-O_3 90.54°
O_1-Li_3-O_2 88.96°; O_8-Li_2-O_2 119.91°
O_8-Li_2-O_3 124.45°; O_8-Li_2-O_4 131.43°
Li_3-O_2-C_3-C_7 3.81°; O_1-Li_1-O_2-Li_3 1.63°;
O_2-Li_2-O_3-Li_3 6.10°; C_2-O_3-Li_2-Li_3 −128.28°
O_8-Li_2-O_3-O_4 −142.20°; O_8-Li_2-O_2-Li_3 −129.75°

(S_4) (PM3)

(5b)

FIGURE 6. Optimized structures of trimer ($CH_2{=}CHOLi$) (**5a**) complex with three molecules of Me_2O from PM3 computations and of the Cubic tetrasolvated tetramer $(CH_2{=}CHOLi)_4(Me_2O)_4$ (**5b**) obtained at the PM3 level. Reprinted with permission from Reference 12. Copyright 1997 American Chemical Society

TABLE 3. The natural charge population in monomeric and aggregated structures of $CH_2{=}CHOLi$ and corresponding solvated forms using method A (B3LYP/6-31+G*//6-31+G*) and method B (B3LYP/6-311+G**//6-31+G*) calculations

Species	Method	Li	O	C_α (CH)	C_β (CH_2)
$CH_2{=}CHOLi$ (C_i)	A	+0.926	−0.887	+0.158 (0.036)	−0.820 (−0.375)
	B	+0.923	−0.884	+0.912 (0.330)	−0.758 (−0.369)
$CH_2{=}CHOLi(Me_2O)$ C_1	A	+0.889	−0.882	+0.161 (0.331)	−0.803 (−0.367)
	B	+0.888	−0.881	+0.194 (0.324)	−0.742 (−0.360)
$CH_2{=}CHOLi(Me_2O)_2$ (C_1)	A	+0.873	−0.891	+0.159 (0.318)	−0.765 (−0.346)
	B	+0.868	−0.891	+0.192 (0.313)	−0.706 (−0.340)
$(CH_2{=}CHOLi)_2$ (C_1)					
unit 1[a]	A	+0.913	−0.998	+0.160 (0.348)	−0.725 (−0.273)
unit 1[b]	B	+0.913	−1.002	+0.195 (0.343)	−0.660 (−0.267)
unit 2[a]	A	+0.943	−1.059	+0.160 (0.330)	−0.625 (−0.203)
unit 2[b]	B	+0.950	−1.068	+0.196 (0.327)	−0.564 (−0.199)
$(CH_2{=}CHOLi)_2$ (C_{2h})[c]	A	+0.948	−1.087	+0.148 (0.322)	−0.615 (−0.182)
$(CH_2{=}CHOLi)_3$ (C_1)	A	+0.921	−1.015	+0.145 (0.332)	−0.688 (−0.238)
	B	+0.921	−1.019	+0.181 (0.329)	−0.624 (−0.233)

[a] Bridged (Li-π-interaction) unit of the dimer.

[b] Non-bridged unit of the dimer.

[c] Plane corresponding to the moiety Li—O—Li—O is perpendicular to the plane of the carbon atoms.

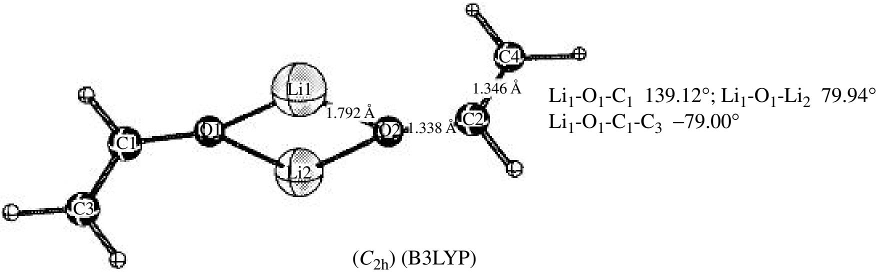

(6)

FIGURE 7. Optimized structures of dimer $(CH_2{=}CHOLi)_2$ (**6**) as obtained from B3LYP/6-31+G* calculations. Reprinted with permission from Reference 12. Copyright 1997 American Chemical Society

allyllithium compounds[14]. They combined *ab initio* calculations with experimental NMR and cryoscopic investigations, which gave insight to the structural assignments as suggested by Weston and Ahlbrecht in 1999[15]. The stability of the *endo* conformation over the *exo* (called the ‘*cis*-effect’) is observed both experimentally and theoretically for all lithiated compounds during the studies. Successive coordination of THF molecules to lithium and re-optimization of the two nearly isoenergetic *endo* conformers for 1-thiophenylallyllithium **7a** and **7b** (Figure 8) shows that specific solvation has a strong influence on the structure and electronic properties of the anionic substrate.

Increasing the solvation causes the C_γ—Li contact to be gradually given up whereas the electrostatic contact of the lithium to the α-carbon is maintained. However, the estimation of the solvation number in the solid state shows the presence of two THF molecules per lithium. This study suggests that specific solvation increases the ability of the sulfur group to localize the negative charge on the α-carbon atom (α-heteroatom stabilization).

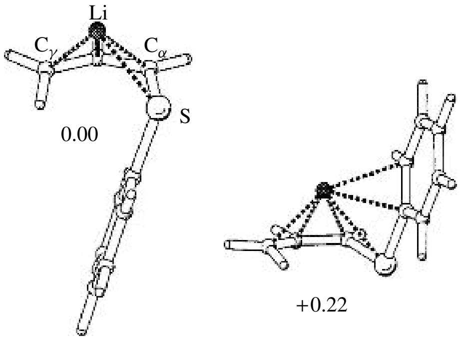

(7a) **(7b)**

FIGURE 8. Energetically stable *endo* conformations found for 1-thiophenylallyllithium at the B3LYP/6-31+G* level of theory. Energy difference in kcal mol^{-1}. Reprinted with permission from Reference 14. Copyright 2000 American Chemical Society

Close examination of various B3LYP/6-31+G* optimized geometries of all the three isomers of sulfoxy-substituted allyllithium suggests the minimum energy structures as **8a** and **8b** (Figure 9). The relative stabilities of these structures are attributed to the additional electrostatic interaction due to the presence of extra Li−O contact.

Although in structure **8c** the allyl system is decoupled, the structure shows surprising stability (only 2.2 kcal mol^{-1} above global minimum) due to the presence of Li−O contact. The calculations on the solvated structure lead to the conclusion that the presence of Li−O contact reduces the number of THF molecules bound to lithium as compared to the thiophenyl compound. This is supported by experimental results, which suggests the presence of two THF molecules per allyllithium unit in the solid state. The cation decoupled solvated allyl system **9a** is only 1.7 kcal mol^{-1} less stable than **9b** (Figure 10) even though specific solvation stabilizes conformer **8c** more than **8a**. The calculated solvation energies indicate that conformer **8a** is only 0.5 kcal mol^{-1} more stable than **8c**, indicating the presence of both conformers in the solution. The conformational equilibrium

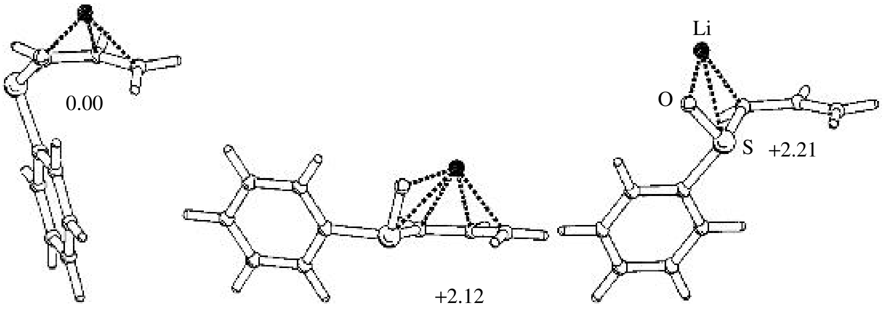

(8a) **(8b)** **(8c)**

FIGURE 9. Energetically stable *endo* conformers found for sulfoxides of 1-thiophenylallyllithium at the B3LYP/6-31+G* level of theory. Energy difference in kcal mol^{-1}. Reprinted with permission from Reference 14. Copyright 2000 American Chemical Society

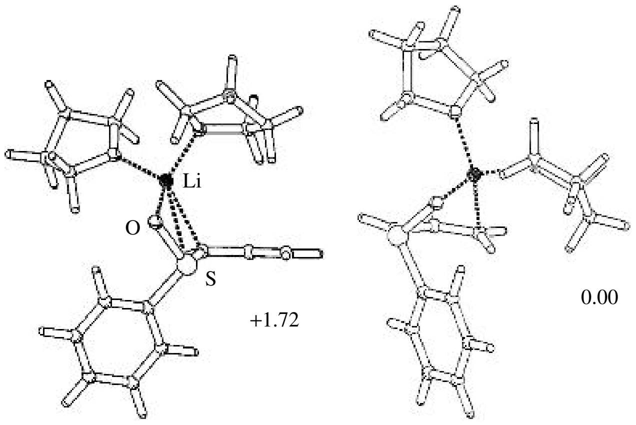

(9a) **(9b)**

FIGURE 10. Energetically stable solvated conformers found for sulfoxides of 1-thiophenylallyllithium at the B3LYP/6-31+G* computations. Energy difference in kcal mol^{-1}. Reprinted with permission from Reference 14. Copyright 2000 American Chemical Society

was not found in the NMR timescale since warming the solution caused a slight broadening of the signals observed in the ^{1}H and ^{13}C NMR spectra; the solution decomposes, however, before coalescence is observed.

The presence of two chelating oxygen atoms in 1-(phenyl)sulfonylallyllithium enables the lithium to form a very stable intramolecular O−Li−O scissor contact ion pair, at least in the solid state. Thus, among all the heteroatom-substituted allyllithium compounds, the lithium is bonded not only to the heteroatom but also to the allylic backbone. Recent investigations of the structure of lithiated allylic norbornyl sulfones showed that, in addition to the *exo–endo* equilibrium, there is also a monomer–dimer aggregational equilibrium present in THF solution, which occur rapidly on the NMR timescale. Knowledge of the solution structure of these three types of lithiated compounds enabled Piffl and coworkers to develop a reliable model system for the calculation of heterocumulene fixation. New developments in this area will help direct experimental investigations[14].

C. Lithium Amides

Though many lithium amides have no formal Li−C bonds, they are included here as honorary organolithium compounds because the lithium amides are used extensively in organic synthesis. The interest in aminolithium complexes is in their use as non-nucleophilic Brönsted–Lowry bases in organic synthesis and in their applications as anionic transfer reagents for the preparation of other main group and transition metal amides. In addition to the *ab initio* molecular orbital calculations on the association of solvent-free and solvated $LiNH_2$, the theories concerning autocomplexation of these species have considerable interest. In 1995, Gardiner and Raston reported a model *ab initio* theoretical study of (*E*)-4-lithio-1,4-diazabut-1-ene focusing on the energetics of association to the possible diastereomers arising from amido nitrogen bridging[16]. The *ab initio* theoretical studies dealt with the aggregation of Lewis base functionalized derivatives, which are very few in number. Their study used a 3-21G* basis set. The fully

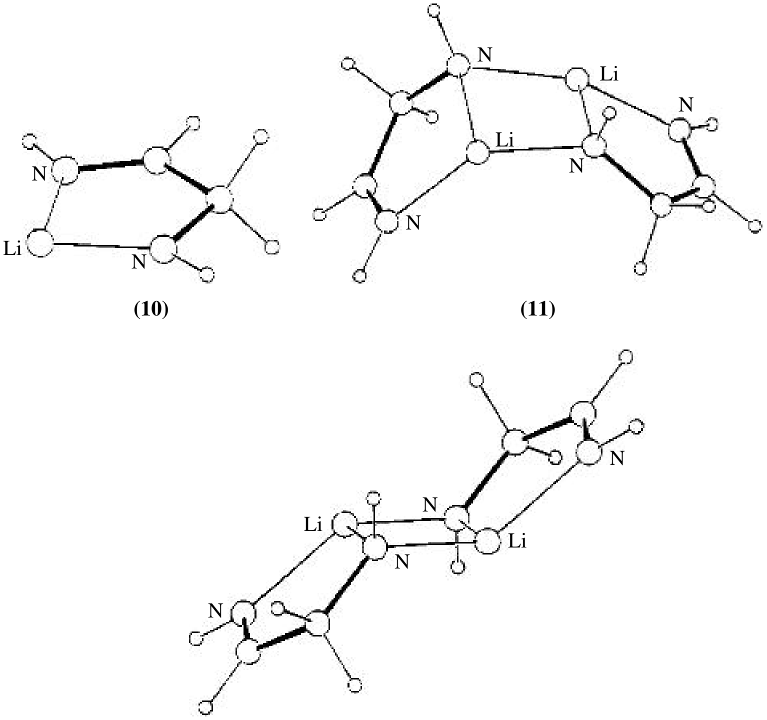

(10) **(11)**

(12)

FIGURE 11. Optimized geometries for minima located using the 3-21G* basis set for [LiN(H)CH$_2$CHNH] (**10**), [*cis*-{Li[μ-N(H)CH$_2$CHNH]}$_2$] **11** and [*trans*-{Li[μ-N(H)CH$_2$CHNH]}$_2$] (**12**). Reprinted with permission from Reference 16a. Copyright 1995 American Chemical Society

optimized structures of [LiN(H)CH$_2$CHNH], [*cis*-{Li[μ-N(H)CH$_2$CHNH]}$_2$] and [*trans*-{Li[μ-N(H)CH$_2$CHNH]}$_2$] with C_s symmetry for monomer **10**, C_i for centrosymmetric dimer **11** and C_2 for symmetric dimer **12** are represented in Figure 11.

The minimum energy structure corresponding to the monomer **10** has C_s symmetry. The Li−N bond distance in this highly electron-deficient complex, as expected, is much shorter than typically observed. The calculations suggest the dimeric species to have structures with C_i and C_2 symmetry (**11** and **12**). The amido nitrogen atoms in the dimers are sp^3 hybridized[16a], which introduce stepped and concaved secondary structures into the three edge-fused rings of the C_i and C_2 symmetric dimers. The formation of C_i and C_2 dimers gives stabilization energies of 31.9 and 32.0 kcal mol^{-1}, respectively.

Even though *ab initio* molecular orbital calculations on unsolvated and solvated model compounds of lithium amides suggest the formation of polymeric/cyclic oligomeric aggregates featuring Li$_n$N$_n$ ladder core, a shortage of direct experimental evidence makes the evaluation of the reliability of the study difficult. The only structurally characterized polymeric lithium amide in the solid state, {Li(μ-N(Pr-*i*)$_2$)}$_n$ has a coiled linear Li$_n$N$_n$ framework. Gardiner and Raston also reported the synthesis of the lithium amides **14–16** by lithiation of *N*,*N*′-di-*tert*-butylethylenediamine **13** by alkyllithium species (Figure 12) together with *ab initio* molecular orbital calculations, in order to monitor the energetics of

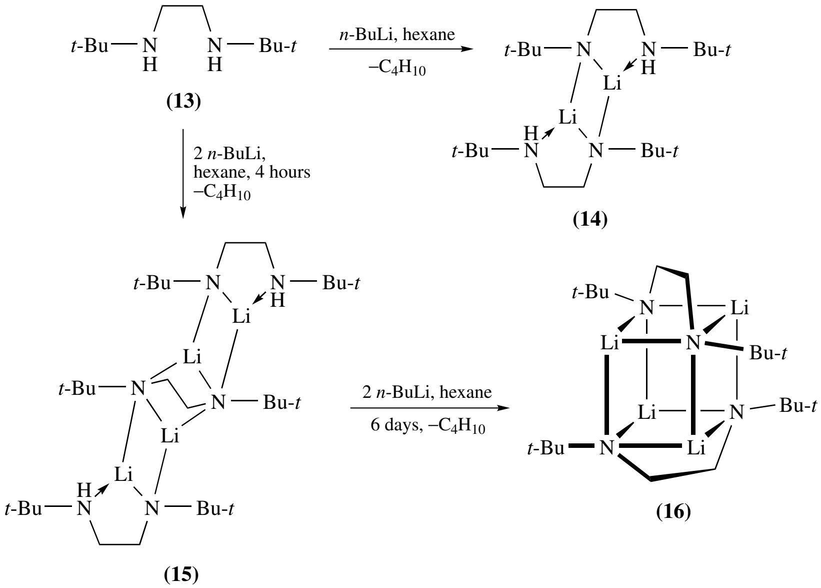

FIGURE 12. Synthesis of the lithium amides **14–16** produced by the lithiation of *N*,*N*′-di-*tert*-butylethylenediamine. Reprinted with permission from Reference 16b. Copyright 1996 American Chemical Society

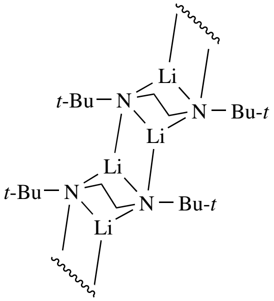

(16a)

aggregation[16a]. The calculations indeed proved the polymeric ladders **16a** as energetically favored over stacked dimers. The aggregates of various oligomeric/polymeric form in *N*,*N*′-dilithium ethylenediamide complexes were optimized using basis sets ranging from STO-3G, 3-21G*, to 6-31G*. The association energies and optimized structures (Figure 13) are discussed below.

The above data indicate that the association energy for dimerization of stacked dimeric species **G** is -26.3 (-29.2) kcal mol^{-1} (energies at the 6-31G* and 3-21G* level of theory). The energies for the polymerization of the species **C** and **F** are -40.4 (-47.0) kcal mol^{-1} and -40.6 (-46.1) kcal mol^{-1}, respectively. This calculated energy of aggregation suggests the formation of a polymeric ladder as more favorable than the stacked dimer. In the experiment, it is seen that the stacked dimer crystallizes only on rapid cooling

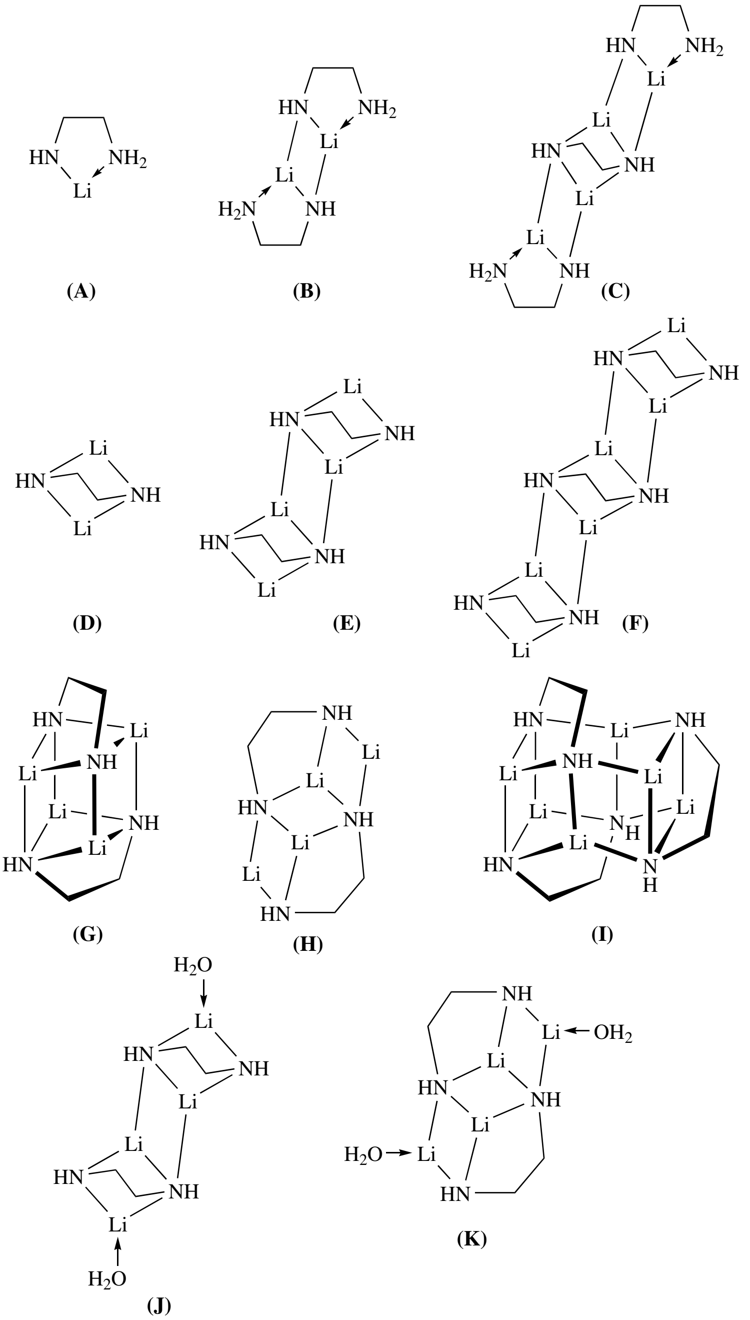
(A) (B) (C) (D) (E) (F) (G) (H) (I) (J) (K)

FIGURE 13. The aggregates of various oligomeric/polymeric form in N,N'-dilithiumethylenediamide complexes were optimized using minimal basis sets ranging from STO-3G, 3-21G*, to 6-31G*. Reprinted with permission from Reference 16b. Copyright 1996 American Chemical Society

of solutions but the polymeric ladder form precipitates from solution over time as the most stable form. This was found to be in good agreement with theoretical calculations.

The centrosymmetric four-ring ethylene edge-bridged ladder structure of $[\{Li_2[N(2,6\text{-}i\text{-}Pr_2C_6H_3)CH_2]_2\}_2]$ is 16.7 (19.8) kcal mol^{-1} higher in energy than the polymeric ethylene face-bridging ladder. This energy difference, close to that of the ladder and stacked dimer difference, can be attributed to the influence of the steric effect due to the highly hindered aryl group. Comparison of the unsolvated ladders **E** and **H** with ladders bearing a single molecule of water on each terminal lithium atom, **J** and **K**, shows an energy difference of 5.0 (4.6) and 3.8(3.1) kcal mol^{-1}, which favors the ethylene edge-bridged ladders (per monomeric unit), (**H**-**E**)/2 and (**K**-**J**)/2. According to the authors this preference is due to the relief of steric strain in the 'Li_2N_2 double bridged' butterfly shaped Li_2N_2 ring.

D. Oligomerization and Aggregation

The questions of oligomerization and aggregation of organolithium compounds appear wherever these reagents are discussed. We have already given several examples in the context of solvation. In view of the great insights it provides to the structure and energies, we give here definite examples not discussed earlier. While the literature in this area is not as extensive as those of lithium amides, there are several interesting theoretical studies.

An *ab initio* study on the 'superbasic reagents' formed by transmetalation reaction is performed using mixed alkali–metal dimers[17]. Comparison of the structure and energies of the resulting dimeric aggregates suggests that mixed aggregates are more stable than other possible combinations (Figure 14a). The stability of mixed metal dimers is attributed to a combination of high LiX/LiO bond strengths and the decrease of the metal–metal repulsions, even though the latter is considered to be a main factor in mixed dimers involving heavier alkali metals (Rb, Cs). The relative energies for dimethyl ether solvated mixtures compared to the uncomplexed species and computational results on the intermolecular exchange reactions are illustrated in Figure 14b. The final energies are obtained by single point calculations using B3LYP density functional theory on RHF optimized geometries. Although mixed aggregates may well exist in superbasic mixtures, their enhanced reactivity is yet to be explained.

E. Examples of Other Organolithium Compounds

Goldfuss, Schleyer and Hampel studied in 1996 the interactions of alkali–metal ions with cyclopropyl groups and correlated them with experimental results from X-ray crystal structure of $[Li{-}O{-}C(Me)\text{-}(c\text{-}Pr)_2]_6$ **17a** (Figure 15)[18]. This work explained the bonding in terms of edge-coordinated cyclopropyllithium arrangements. The geometries of the lithium-bonded cyclopropyl groups obtained from the X-ray crystal structure studies and from theoretical studies at the B3LYP/6-311+G** level are comparable. The geometries **17b–f** obtained from the calculations are given in Figure 15. The coordination energies and natural charges of protonated lithium-complexed hydrocarbons are listed in Table 4. The results indicate the exceptional stability of edge complex **17d** in comparison to corner transition structure **17c** and face isomer **17e**. The C–C bent bonds of cyclopropane **17b** give rise to areas of negative electrostatic potential outside the ring; this favors the Li^+ edge coordination of **17b** over **17c** (corner coordination). Above the ring plane the positively charged H atoms provide three electrostatic potential minima, surrounding a lower positive area. This explains the 'meta'-stable Li^+ position in **17e**.

In 1997, Jemmis, Schleyer and coworkers studied the structure and energetics of lithiated cyclopropenyl cation and their acyclic isomers using *ab initio* MO (HF/6-31G*) and density functional theory (DFT, B3LYP/6-31G*) methods[19]. Successive lithiation results in

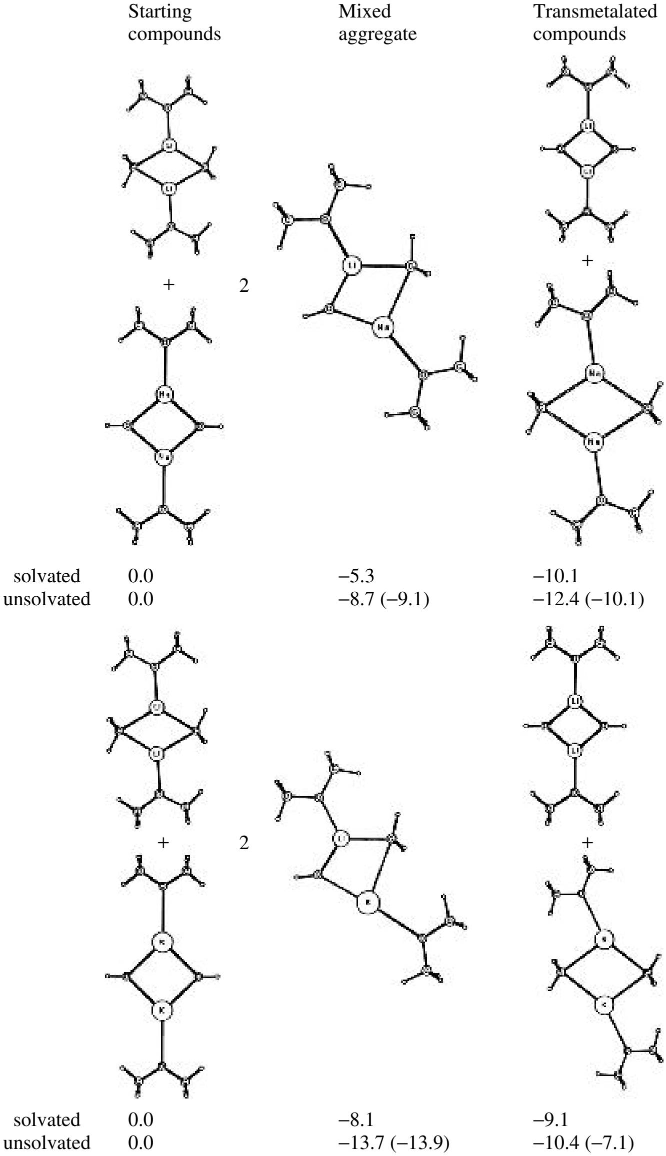

	Starting compounds	Mixed aggregate	Transmetalated compounds
solvated	0.0	−5.3	−10.1
unsolvated	0.0	−8.7 (−9.1)	−12.4 (−10.1)

	Starting compounds	Mixed aggregate	Transmetalated compounds
solvated	0.0	−8.1	−9.1
unsolvated	0.0	−13.7 (−13.9)	−10.4 (−7.1)

FIGURE 14a. Relative energies for dimethyl ether solvated mixtures [$(MOH)_2$ /$(LiCH_3)_2$; M = Na, K] compared to the uncomplexed species at B3LYP basis D //RHF basis A. (D //MP2(full) basis B energies for the unsolvated equilibria are given in parentheses.) Basis A: Li, Na, H, C, N, O, F (6-31+G*) K, Rb, Cs: 9VE-ECP MWB 6s6p1d/4s4p1d; basis B: Li, Na, H, C, N, O, F (6-31++G**), K, Rb, Cs: 9VE-ECP MWB 6s6p2d/5s5p2d; basis D: Li, Na, H, C, O (6-311+G*), K: 9VE-ECP MWB 6s6p2d/5s5p2d. Reprinted with permission from Reference 17. Copyright 1996 American Chemical Society

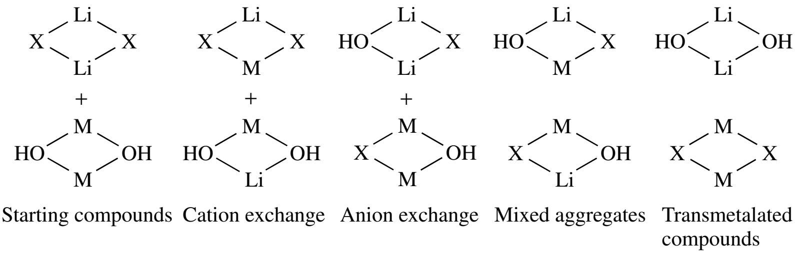

$E_{\text{rel}} = 0.0$

M = Li				
X = H	0.0	−2.6	−2.6	0.0
X = CH_3	0.0	−3.4	−3.4	0.0
X = NH_2	0.0	−2.0	−2.0	0.0
X = OH	0.0	0.0	0.0	0.0
X = F	0.0	−0.8	−0.8	0.0
M = Na				
X = H	−10.2	−10.5	−11.9	−16.8
X = CH_3	−6.3	−7.3	−9.1	−10.1
X = NH_2	−2.9	−2.6	−4.3	−2.6
X = OH	−2.0	0.0	−2.0	0.0
X = F	−4.0	−1.8	−4.8	−2.6
M = K				
X = H	−14.4	−9.5	−16.0	−14.1
X = CH_3	−11.8	−5.8	−13.9	−7.1
X = NH_2	−6.5	−0.9	−8.2	0.6
X = OH	−6.8	0.0	−6.8	0.0
X = F	−11.2	−3.8	−12.2	−6.5
M = Rb				
X = H	−17.6	−10.6	−19.0	−16.9
X = CH_3	−15.1	−6.8	−17.2	−9.3
X = NH_2	−8.1	−0.7	−9.8	1.0
X = OH	−8.6	0.0	−8.6	0.0
X = F	−13.6	−4.2	−14.5	−7.4
M = Cs				
X = H	−18.7	−10.0	−19.8	−16.4
X = CH_3	−16.9	−6.7	−18.9	−9.4
X = NH_2	−8.5	0.1	−9.9	2.5
X = OH	−9.5	0.0	−9.5	0.0
X = F	−14.7	−4.6	−15.6	−8.2

FIGURE 14b. Summary of computational results on intermolecular exchange reactions at MP2(full) (+ΔZPE) (kcal mol^{-1}). Reprinted with permission from Reference 17. Copyright 1996 American Chemical Society

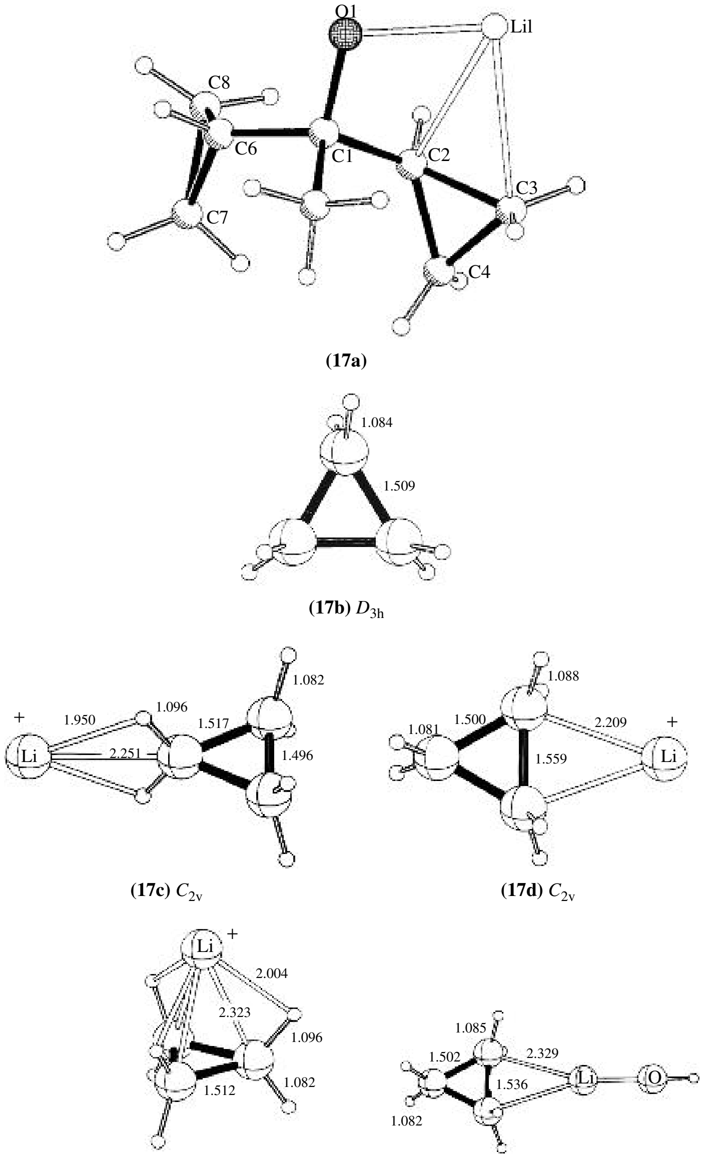

(17a)

(17b) $D_{3\mathrm{h}}$

(17c) $C_{2\mathrm{v}}$

(17d) $C_{2\mathrm{v}}$

(17e) $C_{3\mathrm{v}}$

(17f) $C_{2\mathrm{v}}$

FIGURE 15. Asymmetric unit in the X-ray crystal structure of $[\mathrm{Li{-}O{-}C(Me)\text{-}(}c\mathrm{\text{-}Pr)_2]_6}$ **17a**, cyclopropane **17b** (D_{3h}); **17c–f** are optimized geometries of $\mathrm{Li^+}$ and LiOH cyclopropane complexes (C_{2v}, C_{2v}, C_{3v}, C_{2v} respectively) at RB3LYP/6-311+G** (C, H, O), /6-31G* (Li) level. Bond distances are given in angstroms. Reprinted with permission from Reference 18. Copyright 1996 American Chemical Society

TABLE 4. Coordination energies and natural charges of protonated lithium-complexed hydrocarbons[a] illustrated in Figure 15. Reproduced with permission from Reference 18. Copyright 1996 American Chemical Society

	PG(NIMAG)[b]	*E* coord (kcal mol^{-1})[c]	qH$^+$ or qLi$^+$ (au)[d]
17c	C_{2v} (1)	13.18	+0.985
17d	C_{2v} (0)	22.91	+0.982
17e	C_{3v} (0)	11.63	+0.974
17f	C_{2v} (0)	8.86	+0.953

[a] B3LYP/6-311+G** (C,H,O), /6-31G* (Li) optimized geometries.

[b] Point group and number of imaginary frequencies, obtained from B3LYP frequency calculations.

[c] H$^+$ or Li$^+$ coordination energies *E* coord (ZPE corrected) of the protonated or Li$^+$-complexed species.

[d] Natural charges of coordinated H$^+$ or Li$^+$.

$C_3H_2Li^+$, $C_3HLi_2{}^+$ and $C_3Li_3{}^+$ with lithiation energy of 67.0, 48.2 and 40.5 kcal mol^{-1}, respectively (equations 1, 2 and 3). The fall-off in this lithium-substituted cyclopropenium ion is somewhat less than that along CH_2Li^+, $CHLi_2{}^+$, and $CLi_3{}^+$ series. This study showed the elongation of adjacent C−C bonds when both Li and NH_2 substituents are used; this is attributed to hyperconjugation and π-delocalization. The results suggest that one NH_2 and two Li substituents should be more stabilizing than two NH_2 and one Li substituents.

$$c\text{-}C_3H_3{}^+ + CH_3Li \longrightarrow c\text{-}C_3H_2Li^+ + CH_4 \qquad \Delta H = -67.0\ \text{kcal mol}^{-1} \quad (1)$$

$$c\text{-}C_3H_2Li^+ + CH_3Li \longrightarrow c\text{-}C_3HLi_2{}^+ + CH_4 \qquad \Delta H = -48.2\ \text{kcal mol}^{-1} \quad (2)$$

$$c\text{-}C_3HLi_2{}^+ + CH_3Li \longrightarrow c\text{-}C_3Li_3{}^+ + CH_4 \qquad \Delta H = -40.5\ \text{kcal mol}^{-1} \quad (3)$$

Improvements of the theoretical methodologies during the past few years have resulted in valuable corrections in the proposed structures. The availability of accurate structural and energetic data has encouraged detailed mechanistic studies of the reactions of organolithium compounds. These are discussed in the next section.

IV. THEORETICAL STUDIES INVOLVING REACTIONS OF ORGANOLITHIUM COMPOUNDS

Many reactions exhibited by organolithium compounds are studied theoretically. The structure, energy and bonding discussed above have direct consequences in determining the reaction paths. The large variety of the reactions of organolithium compounds studied theoretically are discussed below.

A. Regioselectivity in Addition

Regioselectivity of a reaction is important in synthetic organic chemistry. Although experimental results suggest an overview concerning the regioselectivity of the lithium metallation reaction, detailed theoretical studies were unavailable until recently. Application of the theoretical methodologies to various regioselectivity problems will be useful in predicting the result of a reaction. In 1995, Opitz and coworkers conducted a theoretical survey on the lithiation reaction of lithium methyl 1-naphthylcarbamate·$2H_2O$, lithium methyl 2-naphthylcarbamate·$2H_2O$ and lithium 1,2,3,4-tetrahydroisoquinoline carbamate·$2H_2O$ based on MO theory[20]. The theoretical results using PM3 and MNDO approximations correlate well with experiments. Comparison of the calculated energy of various transition state structures indicates the favored reaction path. The usefulness of semiempirical calculations for the investigation of the regioselectivity of lithiation reaction for molecules in which the carbon center has the same type of hybridization is very clear from this study.

Canepa and Tonachini investigated the addition reaction of formaldehyde with (1,1-difluoroallyl)lithium and (1,1-dichloro)allyllithium and -potassium (and the corresponding free anions) at HF and MP2 levels of theory[21]. It is found that the α-attack pathway (Scheme 2) is sharply preferred in 1,1-difluoroallyllithium, in the free anion and in 1,1-dichloroallylpotassium. In contrast, for (1,1-dichloroallyl)lithium the transition state energies for both the α- and γ-pathways are nearly the same, and the γ-attack pathway (Figure 16 and Table 5) is slightly preferred. Their calculations indicate that varying substituents on the electrophilic carbon could modulate the regioselectivity. These results are in good agreement with experiments.

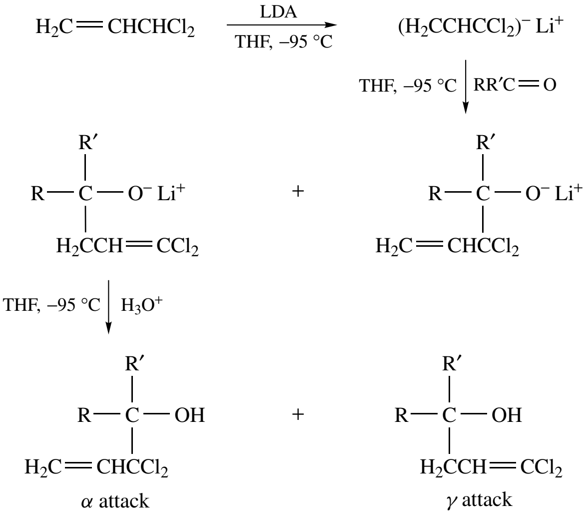

SCHEME 2. The α- and γ-selectivity in the addition reaction of carbonyl electrophiles to *gem*-dichloroallyl anion

The theoretical study of Saa and coworkers on the stereochemical puzzle of Birch and vinylogous Birch reductive cleavage (BICLE and VIBICLE) of unsaturated benzyl ethers throws some light on the mechanistic path[22]. Their work, involving the theoretical analysis of these complex reactions using a simplified model for contact, solvent separated and isolated ion pairs, is the first one in which calculations predict the existence of haptomers in anion radicals. Alternative routes for the vinylogous Birch reductive cleavage of cinnamyl ether (**18**) and Birch reductive cleavage of methyl phenylpropenyl ether (**19**) promoted by lithium naphthalenide is examined (Figures 17a and 17b) in order to understand the mechanistic details.

The MNDO structures of intermediates and transition states for the cleavage of benzyl and cinnamyl ethers through anion-radical routes and dianion routes involving CIPs (contact ion pairs) and IIPs (isolated nonsolvated ion pairs) are given in Figure 18.

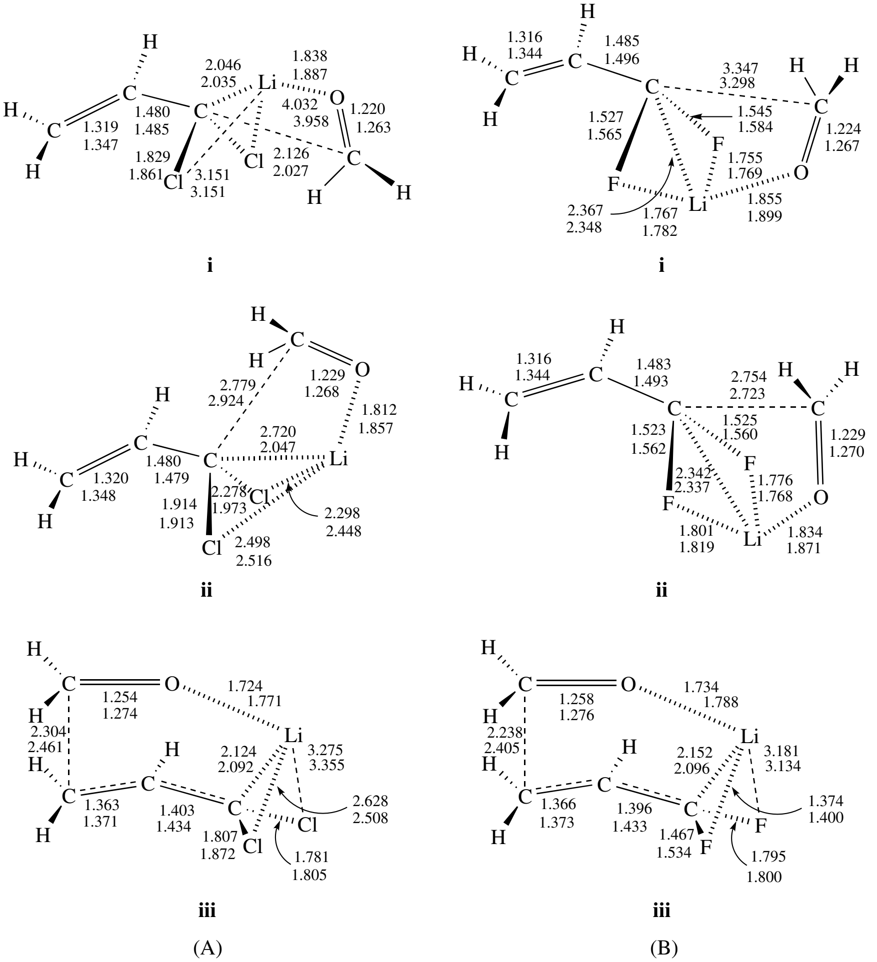

FIGURE 16. Structures involved in the addition of allyllithium reagents to formaldehyde. A(i) The σ-complex between formaldehyde and (1,1-dichloroallyl)lithium; A(ii) the α-attack transition structure; A(iii) the γ-attack transition structure. B(i) The σ-complex between formaldehyde and (1,1-difluoroallyl)lithium; B(ii) the α-attack transition structure; B(iii) the γ-attack transition structure. Interatomic distances are in angstroms, angles in degrees (top figures: HF; bottom: MP2). Reprinted with permission from Reference 21. Copyright 1996 American Chemical Society

Based on their study, Saa and coworkers[22] suggested the lower energy cleavage routes as those involving contact ion pair, in which an important role is played by the lithium counterion, by assisting the leaving group through a spin β-elimination pathway. Transition states TS **A** and TS **B** in Figure 18a clearly illustrate this assertion. The lithium-promoted cleavage of phenylpropenyl derivatives (BICLE) is a stepwise process involving transient radical anion/cation species (Figure 18a). But the lowest energy route for cleavage of cinnamyl derivatives (VIBICLE), also stepwise, is that of the dianion/dication

TABLE 5. (1,1-Dichloroallyl)lithium and (1,1-difluoroallyl)lithium. Total[a] and relative[b] energies of the important structures. Reproduced with permission from Reference 21. Copyright 1996 American Chemical Society

Structure in Figure 16		MP2/3-21G*[c]		RHF/3-21G*[c]	
		E	ΔE	E	ΔE
		(1,1-Dichloroallyl)lithium			
σ-Complex	A(i)	−1150.94546	0.0	−1150.15497	0.0
α T.S	A(ii)	−1150.93094	9.1	−1150.13734	11.1
γ T.S	A(iii)	−1150.93765	4.9	−1150.14091	8.8
α Product	—	−1150.98167	−22.7	−1150.19049	−22.3
γ Product	—	−1150.97565	−18.9	−1150.18671	−19.9
		(1,1-Difluoroallyl)lithium			
σ-Complex	B(i)	−433.91239	0.0	−433.17589	0.0
α T.S	B(ii)	−433.90641	3.8	−433.16996	3.7
γ T.S	B(iii)	−4333.88817	15.2	−433.14354	20.3
α Product	—	−433.95507	−26.8	−433.22434	−30.4
γ Product	—	−433.94525	−20.6	−433.21046	−21.7

[a] In hartees.

[b] In kcal mol^{-1}.

[c] Level of theory at which the geometries of the critical points are optimized.

species as seen in transition structures TSC and TSD (Figure 18b). There are two competing diastereomeric transition states for the latter due to the existence of a chiral plane, but only one for the former, which does not have a chiral plane. This is responsible for the puzzling stereochemistry observed for BICLE and VIBICLE reactions.

In 1998, Kubota, Nakamura and coworkers studied the addition of substituted (alkoxy)allyllithium and zinc reagents to cyclopropenone acetal[23]. They found that the regioselectivity of the (alkoxy)allyllithiation is dependent on the substituent, while the diastereoselectivity remains constantly high (>97%). This is supported by their theoretical study (at the B3LYP/6-31G* level, Scheme 3) which reveals that a (hydroxy)allyllithium species of π-allylmetal nature can react with cyclopropene via two $[2 + 2]$-type four-centered transition states of similar energies leading to α- and γ-adducts.

Tomioka and coworkers studied recently the effect of the electronic and steric factors in α,β-unsaturated imines required for high 1,2- and 1,4-regioselectivity[24] (Figure 19). The 1,4- and 1,2-addition reactions of organolithium reagents with enaldimines depend on the nature of imines. Besides experimental investigation, they found that calculations using MOPAC (PM3, precise mode) and *ab initio* calculations at the HF/STO-3G level are comparable. The study reveals that the relative magnitude of the LUMO coefficient is one of the essential factors governing the substituent-dependent regioselectivity of the ambident enimines. An electron-withdrawing aryl group can increase the C_2 LUMO coefficient and direct the 1,2-selective addition reaction. Hence, the LUMO coefficient as well as steric control would become an essential methodology for designing a selective reaction.

B. Self-condensation Reaction

Self-condensations are another set of important reactions of organolithium compounds. Tamao and Kawachi had reported that [(*tert*-butoxy diphenyl)silyl]lithium (**20**) exhibited ambiphilic character, and underwent a self-condensation reaction to give a [2-(*tert*-butoxy)disilynyl]lithium derivative in THF as shown in Scheme 4, and also a nucleophilic substitution reaction with n-butyllithium[25].

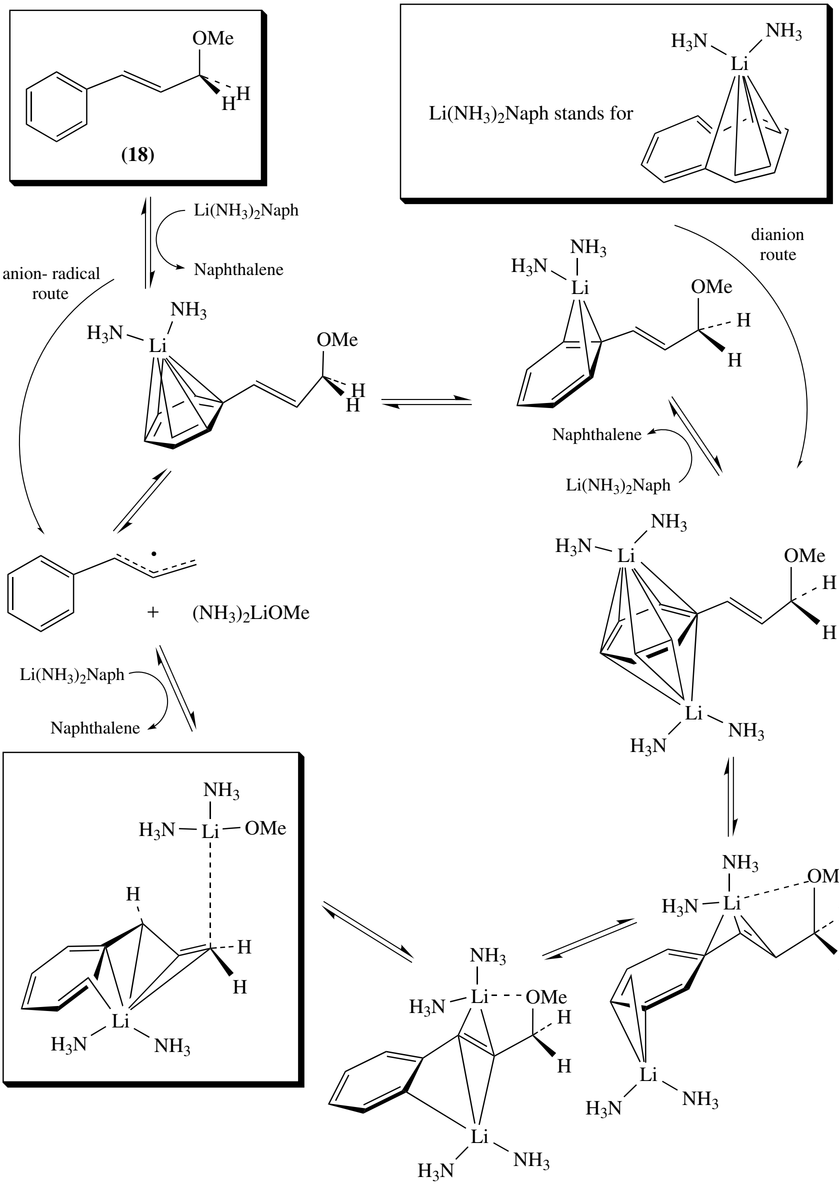

FIGURE 17a. Alternative routes for vinylogous birch reductive cleavage of cinnamyl ether promoted by lithium naphthalenide. Reprinted with permission from Reference 22. Copyright 1996 American Chemical Society

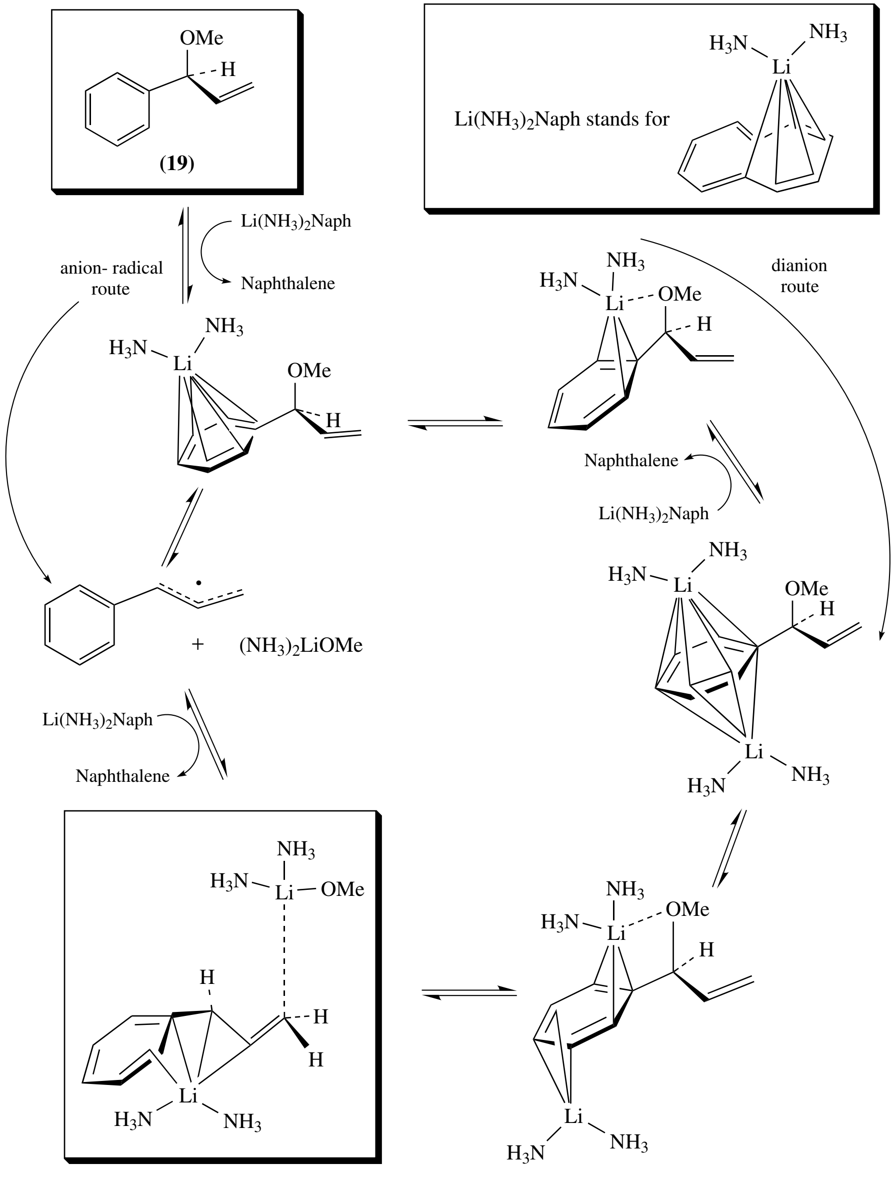

FIGURE 17b. Alternative routes for Birch reductive cleavage of methyl phenylpropenyl ether promoted by lithium naphthalenide. Reprinted with permission from Reference 22. Copyright 1996 American Chemical Society

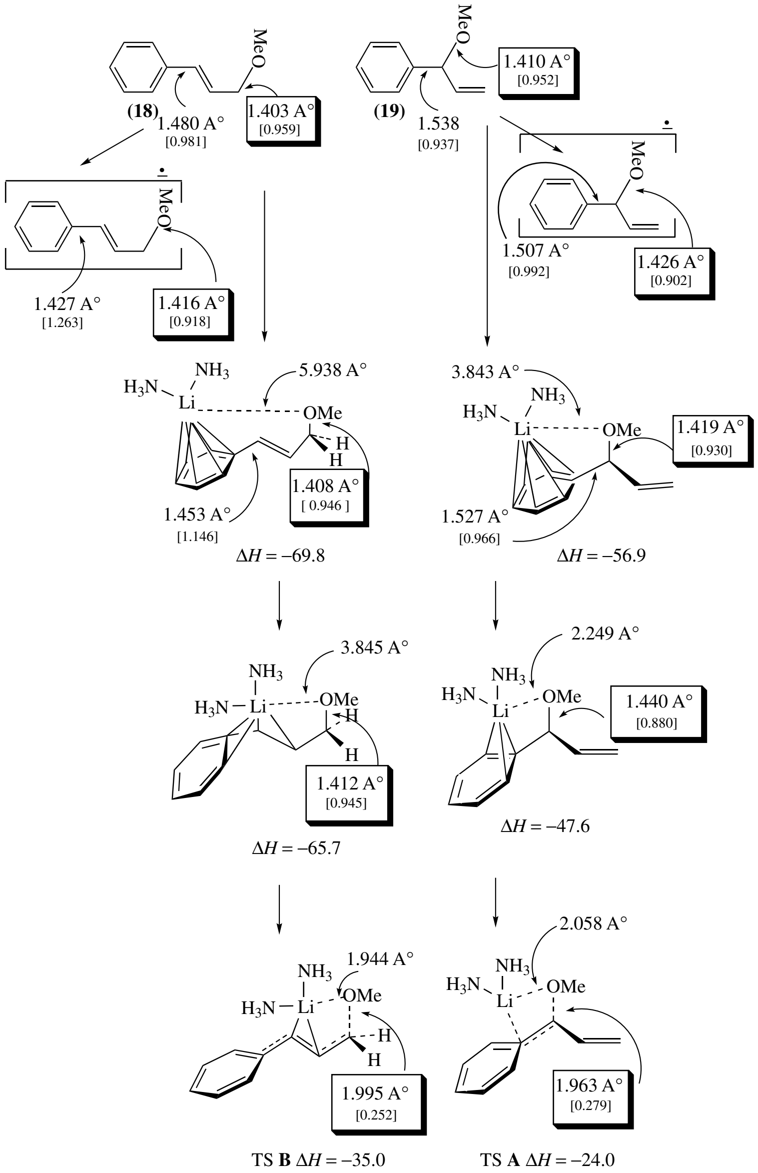

FIGURE 18a. MNDO-determined structures of intermediates and transition states for the cleavage of cinnamyl and phenylpropenyl ethers **18** and **19**, through anion-radical routes involving contact ion pairs (CIP) and isolated ion pairs (IIP). All energies are in kcal mol^{-1}. Geometrical features relevant to haptomeric activation are shown: (1) C−OMe bond length and bond order (in brackets), (2) Li−OMe distance and (3) enthalpy of formation. Reprinted with permission from Reference 22. Copyright 1996 American Chemical Society

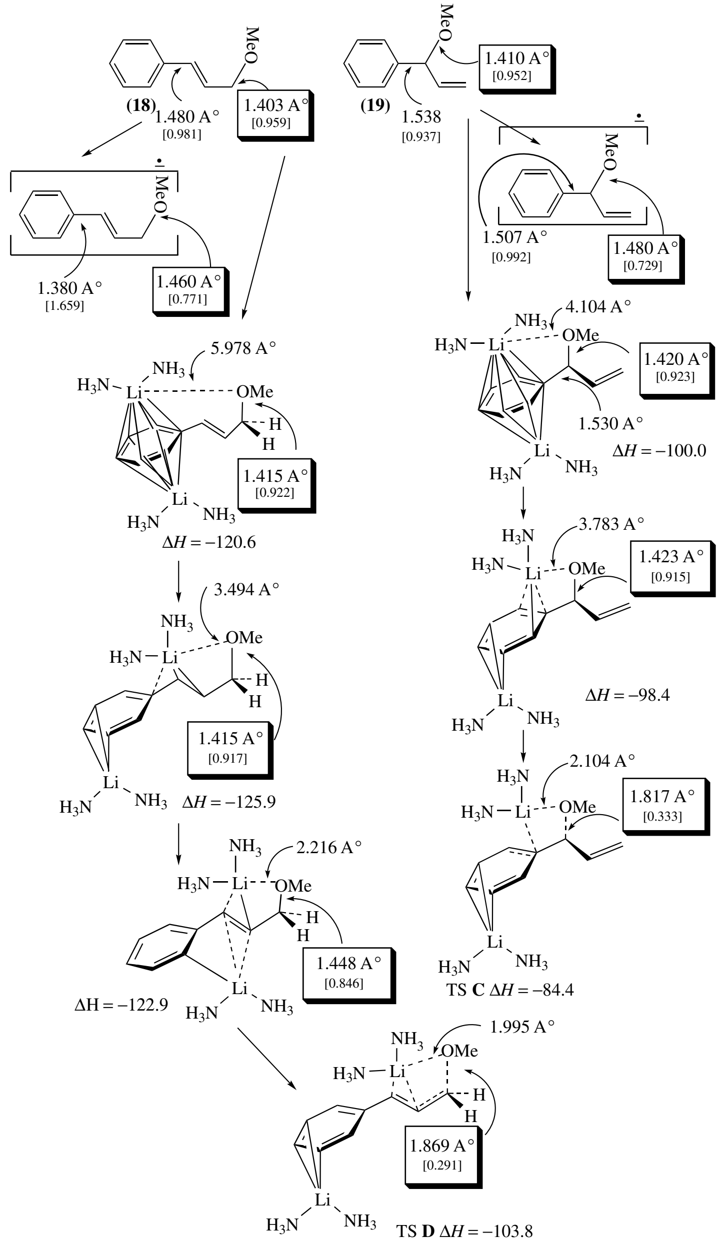

FIGURE 18b. MNDO-determined structures of intermediates and transition states for the cleavage of cinnamyl and phenylpropenyl ethers **18** and **19**, through dianion-radical routes involving contact ion pairs (CIP) and isolated ion pairs (IIP). All energies are in kcal mol^{-1}. Geometrical features relevant to haptomeric activation are shown: (1) C−OMe bond length and bond order (in brackets), (2) Li−OMe distance and (3) enthalpy of formation. Reprinted with permission from Reference 22. Copyright 1996 American Chemical Society

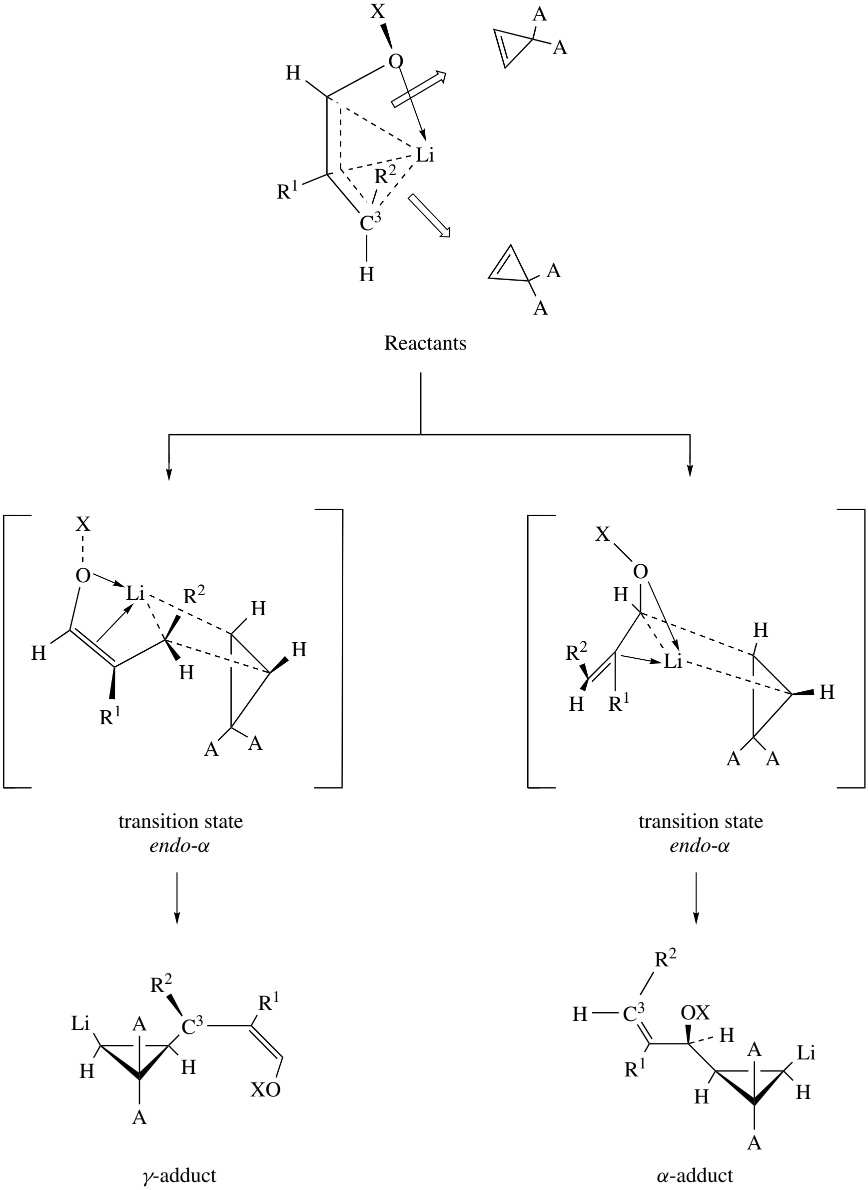

A = alkoxy in experiments.
A = H in calculations.

SCHEME 3. (Alkoxy)allylmetalation of cyclopropene, the four-centered transition states leading to both α-adduct and γ-adduct are shown.

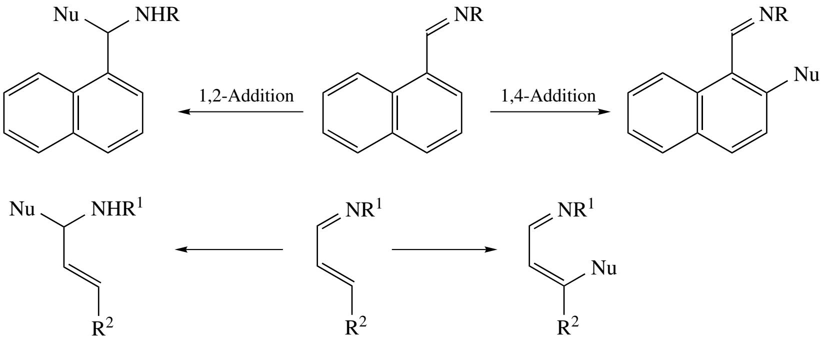

FIGURE 19. Scheme showing 1,2- and 1,4-selective addition reactions of NuLi (Nu = Ph, Bu) followed by work-up. Reprinted with permission from Reference 24. Copyright 2001 American Chemical Society

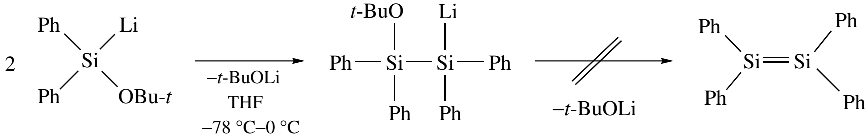

(20) **(21)**

SCHEME 4. Self-condensation reaction of [(*tert*-butoxydiphenyl)silyl]lithium (**20**) to give [2-(*tert*-butoxy)disilanyl]lithium derivative **21**

In this case the self-condensation product undergoes no β-elimination, perhaps due to the low stability of the corresponding elimination product, disilene. Tanaka and coworkers studied theoretically the self-condensation reaction of lithium (alkoxy)silylenoid[26] and provided a new reaction mode of silicon–silicon bond formation. A possible mechanism for this reaction involves the direct condensation of two molecules in which one functions as a nucleophile and the other as an electrophile. Although (t-BuO)Ph_2SiLi was used experimentally, (MeO)H_2SiLi was used as a model to make the calculation feasible. Various geometries are optimized at HF/6-31G* level of theory and single-point energies at the optimized stationary points were calculated at the MP2/6-31G** level. Stable geometries of (MeO)H_2SiLi **22** (**I–VI**) and its bis (**23**) and tris (**24**) solvated compounds are reproduced in Figure 20.

In order to undergo self-condensation, the two reactant molecules should approach each other to form a Si–Si bond. The geometries of the intermediate, the transition structure and the product are shown in Figure 21.

The potential-energy profile of the self-condensation reaction is given in Figure 22. The small activation energy of 0.9 kcal mol^{-1} agrees with the experimental result that the compound undergoes a self-condensation reaction at low temperatures. The product is 24.8 kcal mol^{-1} more favorable than the reactants. The transition state is formed at the Si–Si distance of 2.62 Å in which one silicon center has become nucleophilic and the other electrophilic. The lithium-assisted ionization of the Si–O bond lowers the energy of the σ^*(Si–O) in the electrophilic part. The interaction between the HOMO in the nucleophilic part and the backside lobe of the σ^*(Si–O) orbital in the electrophilic part leads to the formation of the Si–Si bond and breaking of the Si–O bond (Figure 23).

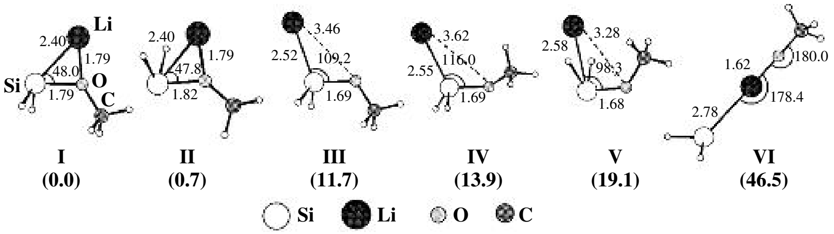

(22)

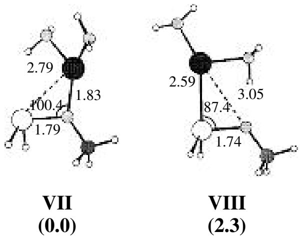

(23)

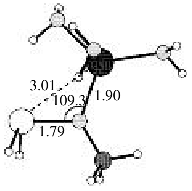

(24)

FIGURE 20. Optimized geometries and relative energies (kcal mol^{-1}) for (MeO)H$_2$SiLi (**22**), (MeO)H$_2$SiLi(H$_2$O)$_2$ (**23**) at MP2//HF/6-31G** and optimized geometry for (MeO)H$_2$SiLi(H$_2$O)$_3$ (**24**) at HF/6-31G**. Bond lengths are in angstroms, bond angles in degrees. Reprinted with permission from Reference 26. Copyright 1998 American Chemical Society

The study also suggests that the reaction proceeds via S$_N$2-type displacement with retention of configuration of the silicon in the nucleophilic part but with inversion of configuration of the silicon in the electrophilic part. However, the final products, [2-(alkoxy)disilanyl]lithium and lithium methoxide, were in good agreement with experimental results. The verification of the stereochemistry is of future interest.

C. Lithium Organocuprate Clusters

The reactions of organocuprate reagents are of great importance owing to their synthetic utilities. The nature of the reacting species and their mechanism was a mystery until 1960. It was after the work of House in 1960, who demonstrated that the reactive species in organocopper reactions is a species having R$_2$CuLi stoichiometry, that the study emerged in new directions.

Experimental evidence indicates that cuprates in solution exist largely as dimer (R$_2$CuLi)$_2$ (**25**), which is found as the reactive species in conjugate addition. The kinetic results were consistent with the participation of the dimer (R$_2$CuLi)$_2$/enone complex **26** (Figure 24) in the C−C bond-forming process of the conjugate addition. Relatively unreactive α, β-unsaturated ketones, esters and nitriles were also found to form complexes represented by **26** in Figure 24.

Since NMR studies suggest a $C_\alpha - C_\beta$ double bond in **26** to be significantly weak, a better representation of the cuprate/enone complex is as a cupriocyclopropene **27**, which is represented in the reaction shown in Figure 25. However, the indispensability of the dimeric cluster in the crucial C−C bond-forming step is not clearly understood.

In 1997, the work of Nakamura, Mon and Morokuma demonstrated the important roles of the cluster structure and the cooperation of different metals therein[27]. They determined

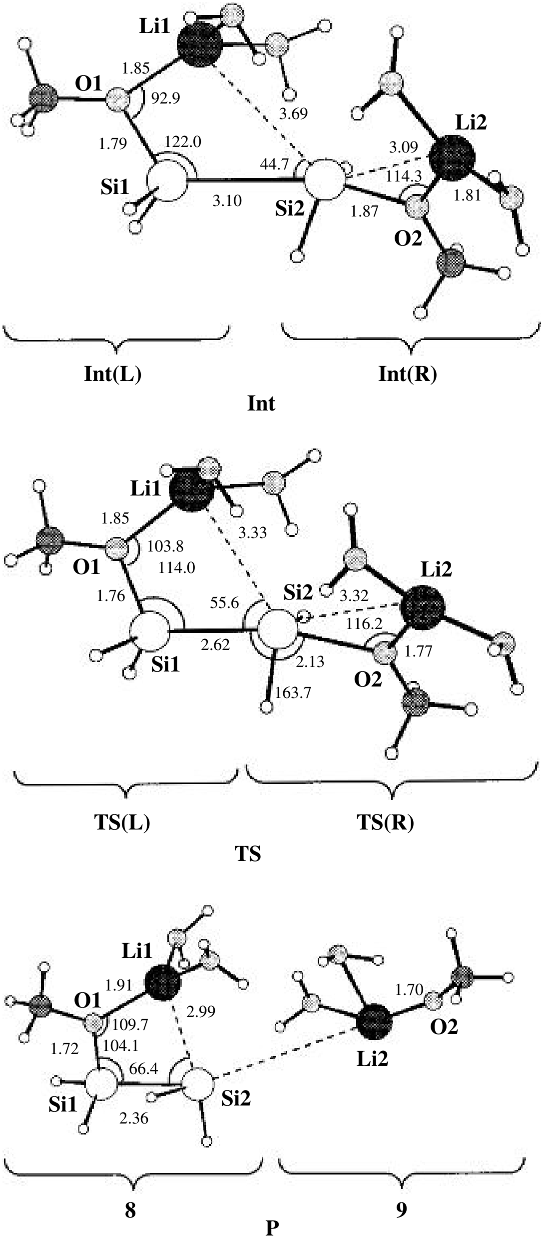

FIGURE 21. Optimized geometries for reactive intermediate (**Int**), transition state (**TS**) and product (**P**) at MP2//HF/6-31G** for the self-condensation reaction of lithium(alkoxy)silylenoid. Bond lengths are in angstroms, and bond angles in degrees. Reprinted with permission from Reference 26. Copyright 1998 American Chemical Society

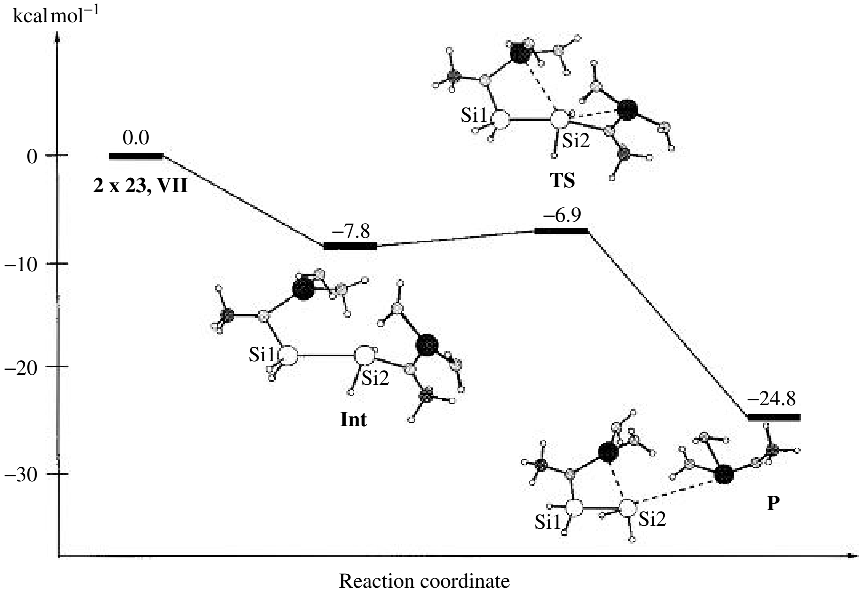

FIGURE 22. Potential-energy profile for the self-condensation reaction of lithium(alkoxy)silylenoid **23, VII** (see Figure 20) at MP2//HF/6-31G**. Reprinted with permission from Reference 26. Copyright 1998 American Chemical Society

the structures of the intermediates and the transition states on the potential-energy surface of the reaction pathway for transfer of a methyl group of a cuprate cluster $(Me_2CuLi)_2$ to acrolein in the conjugate addition, using DFT calculations. At the stage of crucial C−C bond formation, intrinsic reaction coordinate (IRC) analysis was also performed. The study demonstrated a rotational pathway for the dimer which undergoes the conjugate addition, and cooperation of lithium and copper atoms in order to facilitate the reaction. A number of complexes that exist before the transition state of irreversible C−C bond formation as well as a series of structural rearrangements involved in the conjugate addition are shown in Figure 26. The two Lewis acidic lithium atoms in the cluster cooperatively assist the electron transfer process. Electron transfer from the cuprate moiety to the substrate triggers the cluster opening. This study reveals the important role of the cations in organocuprate clusters for the C−C bond-forming reaction. These theoretical calculations also suggest the importance of solvation in the C−C bond-forming stage of carbocupration and the conjugate addition.

Nakamura and coworkers extended their work on organocuprate clusters by studying its effects on acetylene[27]. In 1997, they illustrated the 1,2-addition of cuprates to acetylene and discussed computational studies on the conjugate addition of bis-, tris- and tetrametallic cuprate clusters to acrolein. In the cluster reaction of $Me_2CuLi.LiCl$, the lithium atom in the cluster stabilizes the developing negative charge on the acetylene moiety and assists the electron flow from the copper atom. Experimental results imply that the solvation of lithium atom with a crown ether, which separates the lithium cation from the cluster, affects the carbocupration reaction. Excellent correlation between the theoretical and experimental results suggests the cooperative functions of lithium and copper atoms in the cuprate reactions.

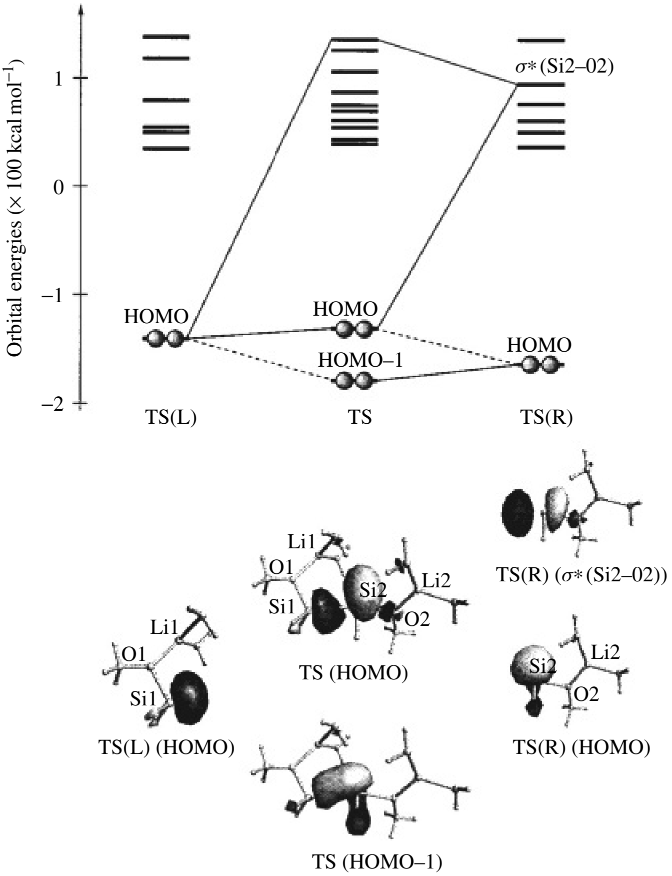

FIGURE 23. Molecular orbital analysis of the **TS** of the dimerization of lithium(alkoxy)silylenoid. Orbital correlation energy diagram (above) and molecular orbitals of HOMO (**TS, TS**(**L**) and **TS**(**R**)), HOMO-1 (**TS**) and σ^*-(Si2-O2) (**TS**(**R**)) (below). Reprinted with permission from Reference 26. Copyright 1998 American Chemical Society

D. Organolithium Compounds Involving Aldehydes and Ketones

Though lithium enolates are important reagents in their versatile synthetic utility, the property of aggregation makes it difficult to understand the mechanism of their reactions. The carbonyl carbon kinetic isotope effect (KIE) and the substituent effect were measured in 1997 for the reaction of lithium pinacolone enolate ($CH_2{=}C(OLi)C(CH_3)_3$) with benzaldehyde by Yamataka, Tsuno and coworkers[28]. The results were compared with those for other lithium reagents such as MeLi, PhLi and $CH_2{=}CHCH_2Li$. *Ab initio* MO calculations at HF/6-31+G* were carried out to estimate the equilibrium isotopic effect (IE) on the addition to benzaldehyde. Two general mechanisms were analyzed for carbonyl addition reaction using model compounds: the polar addition mechanism (PL) and the electron transfer (ET)–radical coupling (RC) sequence (Figure 27).

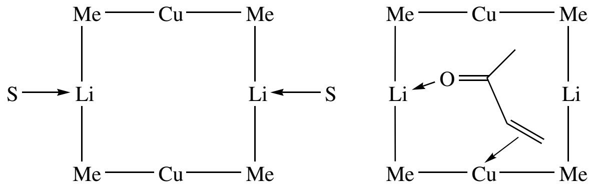

(25)
S = Solvent or enone
dimeric $(Me_2CuLi)_2$

(26)
complex

FIGURE 24. Structures of the cyclic solvated dimer (**25**) of Me_2CuLi and of the dimer $(Me_2CuLi)_2$/enone complex (**26**). Reprinted with permission from Reference 27. Copyright 1997 American Chemical Society

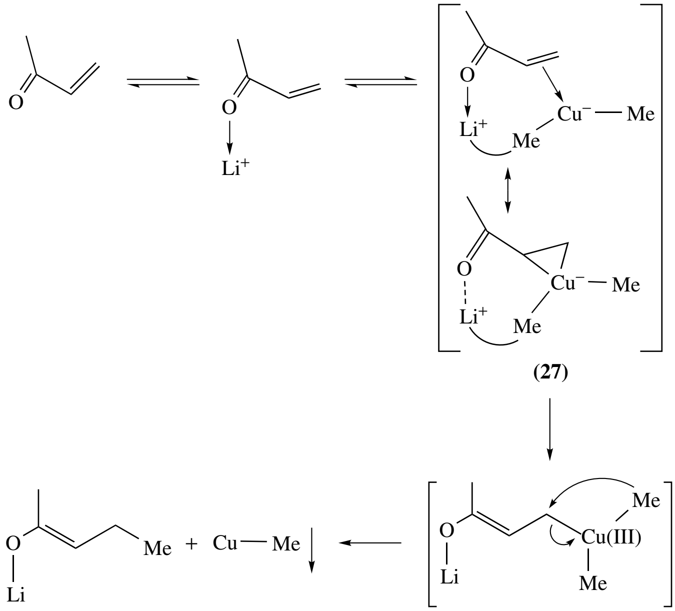

FIGURE 25. Reaction pathway of conjugate addition occurring via the formation of cupriocyclopropane **27** (a donation/back-donation complex). Reprinted with permission from Reference 27. Copyright 1997 American Chemical Society

In this study, benzaldehyde and benzaldehyde-methyllithium adduct were fully optimized at HF/6-31G* and their vibrational frequencies were calculated. The authors used MeLi instead of lithium pinacolone enolate, since it was assumed that the equilibrium IEs are not much different for the MeLi addition and lithium enolate addition. Dehalogenation and enone-isomerization probe experiments detected no evidence of a single electron transfer to occur during the course of the reaction. The primary carbonyl carbon kinetic isotope effects and chemical probe experiments led them to conclude that the reaction of lithium pinacolone enolate with benzaldehyde proceeds via a polar mechanism.

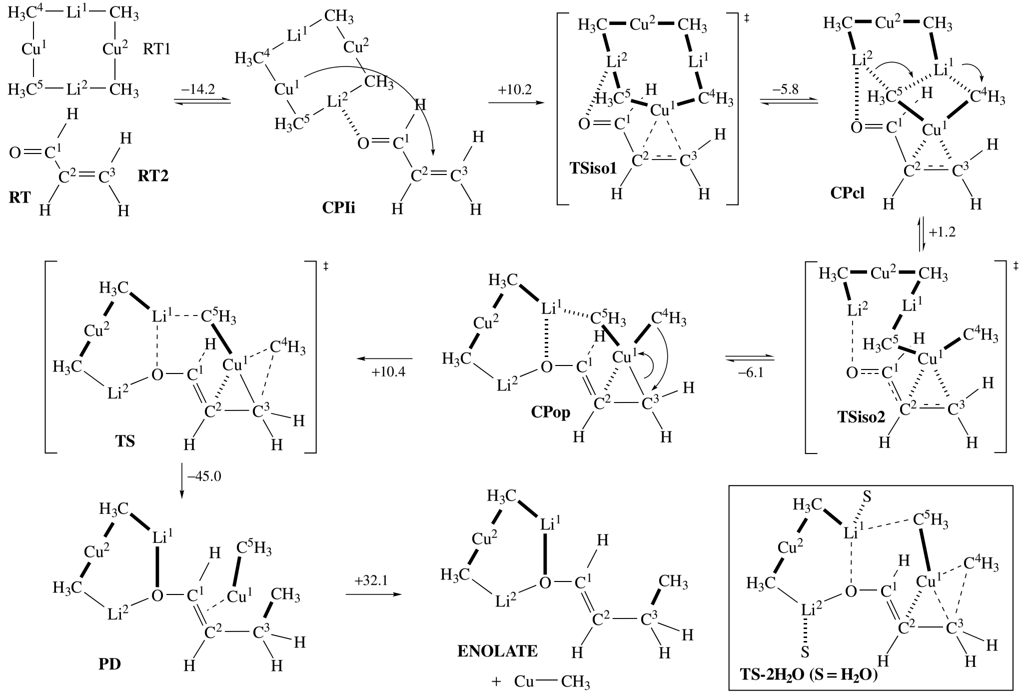

FIGURE 26. The reaction pathway of the conjugate addition of $(Me_2CuLi)_2$ to acrolein. Approximate stereochemistry is implied by the use of bold lines. Dative bonds are depicted by a thick dotted line and forming/cleaving forming bonds by a broken line. Note, however, that this distinction could be oversimplified and may be misleading. **RT1**—$(Me_2CuLi)_2$; **RT2**—acrolein; **CPli**—lithium complex formed by coordination of **RT2** to Li atom of **RT1; CPcl**—complex formed by isomerization of **CPli** via transition state **TSiso1; CPop**- Copper π-complex which is in equilibrium with **CPcl** via transition state **TSiso2; PD**—product complex formed from **CPop** via transition state **TS** by following intrinsic reaction pathway. The energy changes are in kcal mol^{-1} at the B3LYP/631A//B3LYP/631A (which consists of the Ahlrichs all-electron SVP basis set for Cu and 6-31G(d) for the rest) and are given above the arrows. Reprinted with permission from Reference 27. Copyright 1997 American Chemical Society

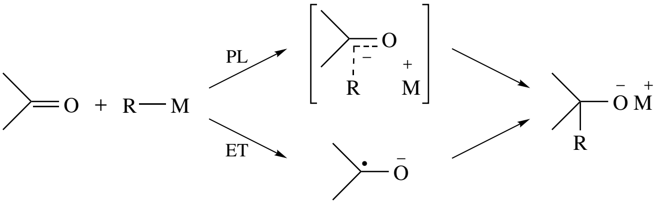

FIGURE 27. The polar addition mechanism and electron transfer–radical coupling sequence in the addition of lithium pinacolone enolate to benzaldehyde. Reprinted with permission from Reference 28. Copyright 1997 American Chemical Society

In 1998, Hasanayn and Streitwieser reported the kinetics and isotope effects of the Aldol–Tishchenko reaction[29]. They studied the reaction between lithium enolates of isobutyrophenone and two molecule of benzaldehyde, which results in the formation of a 1,3-diol monoester after protonation (Figure 28). They analyzed several aspects of this mechanism experimentally. *Ab initio* molecular orbital calculations on models are used to study the equilibrium and transition state structures. The spectroscopic properties of the lithium enolate of *p*-(phenylsulfonyl) isobutyrophenone (LiSIBP) have allowed kinetic study of the reaction. The computed equilibrium and transition state structures for the compounds in the sequence of reactions in Figure 28 are given along with the computed reaction barriers and energy in Figure 29 and Table 6.

The excellent agreement with the experimental and calculated isotope effect (calculated for formaldehyde, 3.22, and for acetaldehyde, 3.3; experimental value 2.9) supports the computational approach. This suggests that the computed transition structure for hydride transfer in the reaction of the lithium enolate of acetone with acetaldehyde (Figure 30) is realistic.

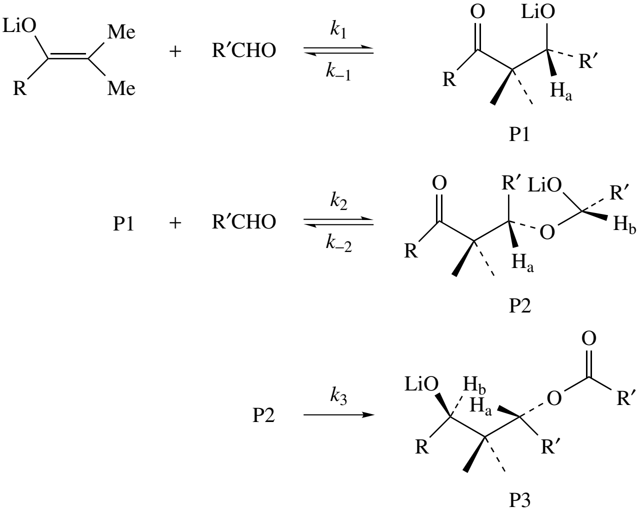

FIGURE 28. Reaction sequence for formation of a diol monoester from the reaction between a lithium enolate and two aldehyde molecules. Reprinted with permission from Reference 29. Copyright 1998 American Chemical Society

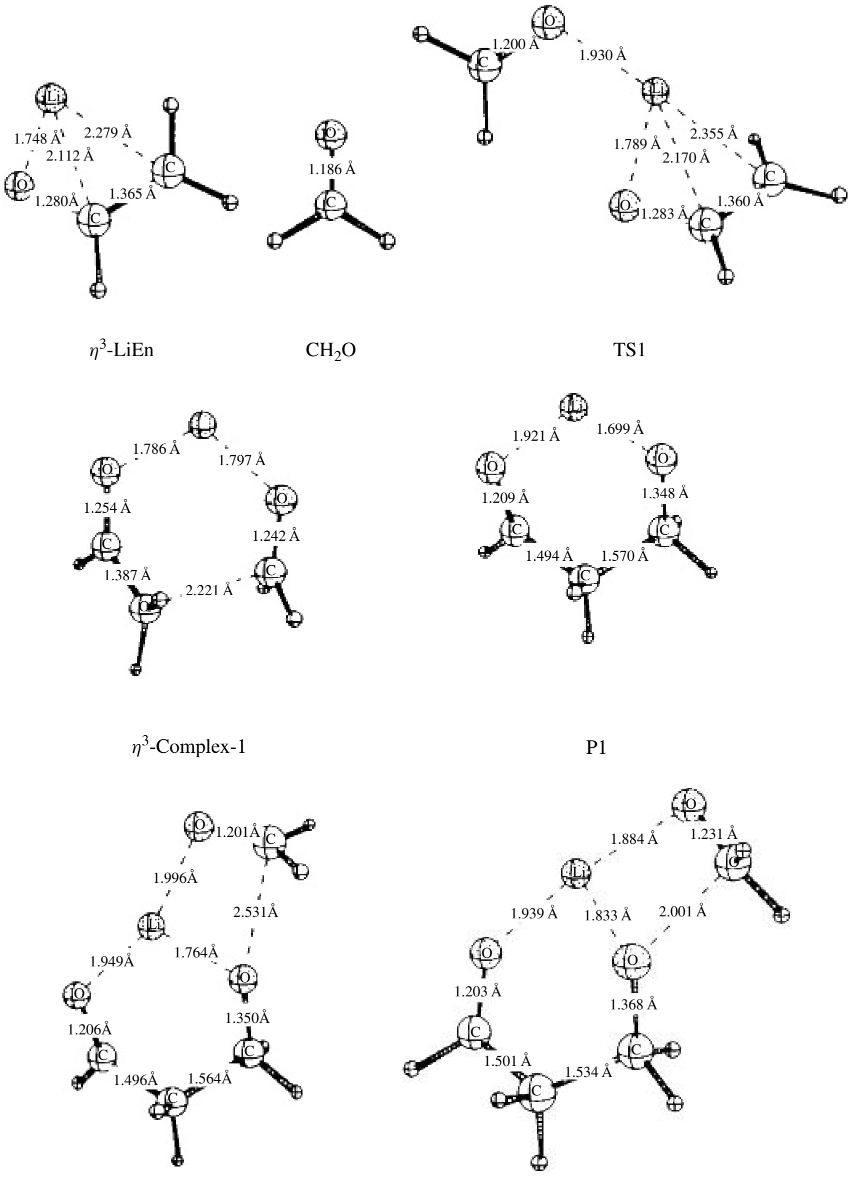

η^3-LiEn CH$_2$O TS1

η^3-Complex-1 P1

Complex-2 TS2

FIGURE 29. Optimized geometries for the reactants, transition structures and products in the sequence of reactions between the lithium enolate (LiEn) derived from acetaldehyde and formaldehyde. The total reaction sequence is: LiEn+CH$_2$O→complex-1→TS1→P1→complex-2→TS2→P2 (Figure 28)→TS3 (Figure 30)→P3 (Figure 28). Theoretical calculations were carried out at the HF/6-311++G* level. Reprinted with permission from Reference 29. Copyright 1998 American Chemical Society

TABLE 6. Computed reaction and activation energies and corresponding isotope effects for the sequence of reactions between lithium vinyloxide (LiEn) and formaldehyde and between the lithium enolate of acetone ($AcCH_2Li$) and acetaldehyde. Reproduced with permission from Reference 29. Copyright 1998 American Chemical Society

Reaction	ΔE^a	ΔZPE^b	$\Delta\Delta ZPE^c$	MMI^d	EXC^d	EXP^d	Isotope effect^{e,f}
$LiEn + CH_2O \rightarrow$ complex-1	−18.4	1.625	0.122	1.35	0.83	0.82	$EIE_{com-1} = 0.92$
$LiEn + CH_2O \rightarrow$ TS1	−12.2	2.379	0.225	1.35	0.91	0.68	$KIE_1 = 0.84$
$LiEn + CH_2O \rightarrow$ P1	−26.8	4.135	0.256	1.34	0.94	0.65	$EIE_1 = 0.82$
$P1 + CH_2O \rightarrow$ complex-2	−13.8	1.280	0.085	1.36	0.80	0.87	$EIE_{com-2} = 0.95$
$P1 + CH_2O \rightarrow$ TS2	−11.1	2.205	0.225	1.37	0.85	0.68	$KIE_2 = 0.79$
$P1 + CH_2O \rightarrow$ P2	−14.1	4.070	0.293	1.37	0.92	0.61	$EIE_2 = 0.77$
P2 → P3	25.1	−1.152	−0.654	1.01	1.06	3.01	$KIE_3 = 3.22$
LiAc + MeCHO → TS1-Me	−3.0	0.315	−0.033	0.99	1.00	1.06	$EIE_3 = 1.05$
LiAc + MeCHO → TS1-Me	−9.0	1.872	0.175	1.15	0.98	0.74	$KIE_{1-Me} = 0.84$
LiAc + MeCHO → P1-Me	−24.5	3.654	0.187	1.15	1.00	0.73	$EIE_{1-Me} = 0.84$
P1-Me + MeCHO → P2-Me	−10.2	3.348	0.240	1.16	1.00	0.67	$EIE_{2-Me} = 0.78$
P2Me → TS3-Me	27.9	−1.584	−0.702	1.00	1.02	3.27	$KIE_{3-Me} = 3.33$

[a] Energies are given in $kcal\,mol^{-1}$ and corrected for ΔZPE (scaled by a factor of 0.9).

[b] $\Delta ZPE = ZPE_{product} - \Sigma\ (ZPE)_{reactants}$; or $ZPE_{TS} - \Sigma\ (ZPE)_{reactants}$ (protio species).

[c] $\Delta\Delta ZPE = \Delta ZPE_H - \Delta ZPE_D$; ΔZPE_D corresponds to the terms for the reactions of monodeuteriated aldehydes.

[d] Terms defined by IE = MMI x EXC x EXP (IE is the Isotopic exchange equilibrium, MMI is the mass moment of inertia term representing the rotational and translational partition function ratios, EXC is the vibrational excitation term and EXP is the exponential zero point energy).

[e] Isotope effects were computed at 25 °C. The symmetry term due to $CH_2O/CHDO$ has not been accounted for in the calculation, since this is unique to formaldehyde. EIE is the equilibrium isotope effect and KIE is the Kinetic isotope effect.

[f] The two hydrogens of formaldehyde become inequivalent in their action products. Similar isotope effects are obtained when either of the two hydrogens is deuteriated.

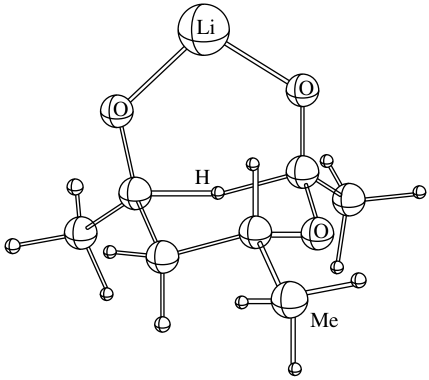

FIGURE 30. Computed transition structure (TS3-Me) for hydride transfer in the reaction of the lithium enolate of acetone with acetaldehyde. The methyl substituent is equatorial. Reprinted with permission from Reference 29. Copyright 1998 American Chemical Society

The computed transition state also rationalizes the observed stereochemistry. For the current reactions, a transition structure represented in Figure 31 appears to be appropriate. This structure indicates that the three substituents R and R′ are all equatorial and give rise to the *anti* product. The corresponding *syn* product would require a highly strained structure in which one R′ group is axial.

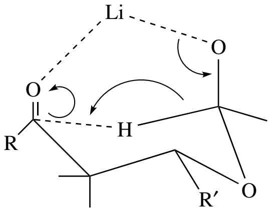

FIGURE 31. Another representation of the transition structure for hydride transfer in the reaction of the lithium enolate of acetone with acetaldehyde. R = R′ = Me. Reprinted with permission from Reference 29. Copyright 1998 American Chemical Society

E. Other Reactions

Besides the reactions discussed earlier for organolithium compounds, there are several specific reactions which have been studied theoretically. A brief description of some of them is given below.

Romesberg and Collum studied the lithium-amide-mediated metallations of ketones and the corresponding *N*-alkylimines, through semiempirical MNDO calculations[30]. The study suggests that the relative stabilities of the transition state structures for two or more competing reaction pathways are not regulated by their geometries, but depend more precisely on the effect of substituents and solvents. In 1998, Johansson, Tegenfeldt and Lindgren attempted to model the lithium ion transport along a polyethyleneoxide (PEO) chain[31]. They used the PEO oligomer diglyme ($CH_3(CH_2CH_2O)_2CH_3$) as the model system. The results obtained using HF/6-31G** and MP2/6-311+G** were compared with the NMR data for the activation energies of conformational transformations in complexed PEO. A transport path of Li^+ along a single PEO chain involving tetradentate and tridentate coordination with small energy difference has been calculated.

In the same year, Schleyer and coworkers came up with a revolutionary observation regarding the anionic $(3 + 2)$ cycloaddition of allyl, 2-borylallyl- and 2-azaallyllithium to ethylene[32]. Their study used B3LYP/6-311+G** and MP2(fc)6-31+G* computations. The study revealed that the concerted $4\pi_s + 2\pi_s$ mechanism as expected from the Woodward–Hoffmann rules is less favorable than the two-step pathway for the cycloadditions of ethylene to the allyl, 2-borylallyl and 2-azaallyl anion and their lithiated counterparts. The work was also in excellent agreement with that of Sauers in 1996[33]. A suggestion for the unfavorability of the concerted cycloaddition mechanism has been made in terms of molecular polarizability anisotropy of the reactants, which is illustrated in Figure 32 and Table 7. The diagonal elements of the polarizability tensors (α_{xx}, α_{yy} and α_{zz}) define the molecular polarizabilities along the x, y and z axes and measure the ease and direction in which the electrons in a molecule are shifted by an external magnetic field. Experimental data are only available for ethylene.

The electrostatic interaction of ethylene and the allylic compounds is more favorable energetically for the stepwise than for the concerted cycloaddition mechanism.

Campos, Sampedro and Rodriguez studied theoretically in 1998[34] the competition of the concerted and stepwise mechanism of hydrogen migration and lithium iodide α-elimination in the trihydrate 1-iodo-1-lithioethene **28**. Since the lithiated derivative of 1-iodoethane readily decomposes to ethylene, experimental techniques are found to be of less use. Their *ab initio* theoretical calculations indicate that the preferred mechanism is the concerted rather than stepwise pathway as illustrated in Figure 33. Their studies also suggest that 1-iodo-1-thioethene prefers to be a monomer in THF and the activation barriers for the *cis* and *trans* hydrogen migration are nearly the same.

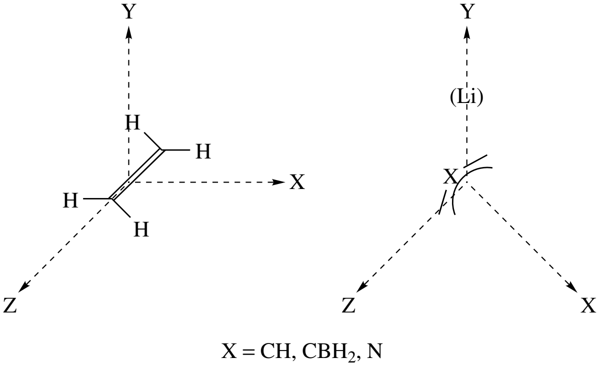

FIGURE 32. Diagonal elements of the polarizability tensors of ethylene and the allylic compounds (cf. Table 7). Reprinted with permission from Reference 32. Copyright 1998 American Chemical Society

TABLE 7. The polarizability tensors of ethylene, allyl anions and allyl lithiums. Reproduced with permission from Reference 32. Copyright 1998 American Chemical Society

Compound	α_{xx}	α_{yy}	α_{zz}
Ethylene	24.91	22.68	36.22
Allyl anion	48.65	89.51	111.42
Allyllithium	50.73	50.31	81.56
2-Borylallyl anion	80.26	86.12	134.73
2-Borylallyllithium	71.44	59.22	95.69
2-Azaallyl anion	51.35	75.06	113.26
2-Azaallyllithium	42.53	49.77	83.34

V. APPLICATIONS IN SPECTROSCOPY

In addition to the structural characterization, several dynamic processes involving organolithium reagents are monitored by various spectroscopic methods. Theoretical studies have helped enormously in these studies. Many of these applications have already been discussed. A few additional results are added here. Experimentally observed and theoretically calculated ^{13}C and ^{1}H NMR shifts suggest some insights into the mechanism of the reactions. Wave functions obtained at the RHF/6-31+G* level of theory were used with the new method IGAIM (Individual Gauges for Atoms In Molecules) developed by Keith and Bader in the calculation of ^{13}C and ^{1}H NMR chemical shifts[35]. Werstiuk and Ma supported the usefulness of this method in 1996 during their study of ^{13}C and ^{1}H chemical shift calculations on unsaturated hydrocarbons and organolithium compounds[36]. The ionic nature of the C−Li bond is supported by theoretical calculation of the NMR spin−spin coupling constant by Koizumi and Kikuchi in 1995[4]. The implications of their study and conclusion on the mostly ionic nature of the C−Li bond in alkyllithiums are supported by experiment. The usefulness of HOESY experiment in the description of initial state geometries of organolithium complexes is also supported by crystallographic and computational results of Hilmersson and coworkers[37]. This study suggests the importance of theory in extracting maximum information from an experimental technique.

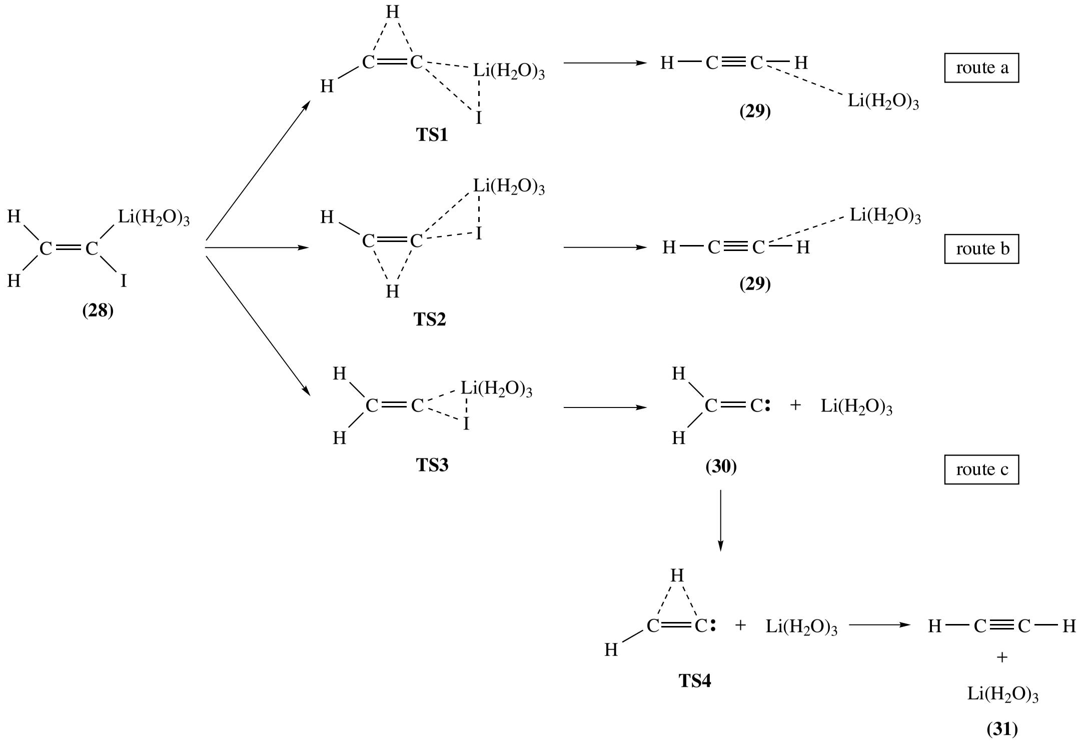

FIGURE 33. Hydrogen migration and lithium iodide α-elimination in 1-iodo-1-lithioethene trihydrate **28** **a**: The concerted pathway involving migration of the hydrogen with a *cis* relationship to the lithium atom together with a simultaneous loss of lithium iodide through transition state **TS1** to yield acetylene **29**. **b**: The concerted pathway involving the migration of the hydrogen with a *trans* relationship to the lithium atom through transition state **TS2** giving the acetylene **29**. **c**: The stepwise route involving the formation of carbene **30** through transition state **TS3** and finally giving acetylene **31** via **TS4**. Reprinted with permission from Reference 34. Copyright 1998 American Chemical Society

VI. CONCLUSIONS

It is clear from the above survey that theoretical approaches contribute enormously in the study of structure, bonding, energetics and reactions of organolithium compounds. Major advances have been made in understanding the nature of the C−Li bond during the last six years. A predominantly ionic bond with a definite, though small and varying covalent contribution is perhaps a description that reflects the emerging trends. Theoretical studies of various reactions gave a clear answer to many questions, which were unanswered in the past. The developments in software and hardware have enabled theoretical studies on systems that were considered beyond reach just a few years ago. Theoretical calculations in conjunction with spectroscopic measurements are of great importance in many applications. Further developments of sophisticated methodologies and more powerful computers will lead to yet deeper understanding of the chemistry of organolithium compounds through theoretical studies.

VII. REFERENCES

1. C. Lambert and P. v. R. Schleyer, in *Carbanionen Methoden der Organischen Chemie* (Ed. M. Hanack), Houben-Weyl, Brand E 19d, Thieme; Stuttgart, 1993; C. Lambert and P. v. R. Schleyer, *Angew. Chem.*, **106**, 1187 (1994). *Angew. Chem., Int. Ed. Engl.*, **33**, 1129 (1994).
2. A. Streitwieser, S. M. Bachrach and P. v. R. Schleyer, in *Lithium Chemistry. A Theoretical and Experimental Overview* (Eds. A. M. Sapse and P. v. R. Schleyer), Wiley, New York, 1995.
3. H. F. Ebel, *Tetrahedron*, **21**, 699 (1965); G. E. Coatis, M. L. H. Green and K. Wade, *Organometallic Compounds*, Vol. 1. 3rd edn., Methuen, London, 1967, p. 32; D. R. Armstrong and P. G. Perkins, *Coord. Chem. Rev.*, **38**, 139 (1981).
4. T. Koizumi and O. Kikuchi, *Organometallics*, **14**, 987 (1995).
5. F. M. Bickelhaupt, N. J. R. v. E. Hommes, C. F. Guerra and E. J. Baerends, *Organometallics*, **15**, 2923 (1996).
6. D. Kost, J. Klein, A. Streitwieser and G. W. Schriver, *Proc. Natl. Acad. Sci. U.S.A.*, **79**, 3922 (1982).
7. L. M. Pratt and A. Streitwieser, *J. Org. Chem.*, **65**, 290 (2000).
8. O. Kwon, F. Sevin and M. L. McKee, *J. Phys. Chem. A*, **105**, 913 (2001).
9. R. Ponec, J. Roithova, X. Girones, L. Lain, A. Torre and R. Bochicchio, *J. Phys. Chem. A*, **106**, 1019 (2002).
10. K. Sorger, P. v. R. Schleyer and D. Stalke, *J. Am. Chem. Soc.*, **118**, 1086 (1996).
11. H. Weiss, A. V. Yakimansky and A. H. E. Muller, *J. Am. Chem. Soc.*, **118**, 8897 (1996).
12. A. Abbotto, A. Streitwieser and P. v. R. Schleyer, *J. Am. Chem. Soc.*, **119**, 11255 (1997).
13. L. M. Jackman and B. C. Lange, *Tetrahedron*, **33**, 2737 (1977).
14. M. Piffl, J. Weston, W. Gunther and E. Anders, *J. Org. Chem.*, **65**, 5942 (2000).
15. J. Weston and H. Ahlbrecht, *Tetrahedron*, **55**, 2289 (1999).
16. M. G. Gardiner and C. L. Raston, (a) *Inorg. Chem.*, **34**, 4206 (1995); (b) *Inorg. Chem.*, **35**, 4047 (1996).
17. T. Kremer, S. Harder, M. Junge and P. v. R. Schleyer, *Organometallics*, **15**, 585 (1996).
18. B. Goldfuss, P. v. R. Schleyer and F. Hampel, *J. Am. Chem. Soc.*, **118**, 12183 (1996).
19. E. D. Jemmis, G. Subramanian, A. J. Kos and P. v. R. Schleyer, *J. Am. Chem. Soc.*, **119**, 9504 (1997).
20. A. Opitz, R. Koch, A. R. Katritzky, W. Q. Fan and E. Anders, *J. Org. Chem.*, **60**, 3743 (1995).
21. C. Canepa and G. Tonachini, *J. Org. Chem.*, **61**, 7066 (1996).
22. J. M. Saa, P. Ballester, P. M. Deya, M. Capo and X. Garcias, *J. Org. Chem.*, **61**, 1035 (1996).
23. K. Kubota, S. Mori, M. Nakamura and E. Nakamura, *J. Am. Chem. Soc.*, **120**, 13334 (1998).
24. K. Tomioka, Y. Shioya, Y. Nagaoka and K. I. Yamada, *J. Org. Chem.*, **66**, 7051 (2001).
25. K. Tamao and A. Kawachi, *Angew. Chem., Int. Ed. Engl.*, **34**, 818 (1995).
26. Y. Tanaka, M. Hada, A. Kawachi, K. Tamao and H. Nakatsuji, *Organometallics*, **17**, 4573 (1998).
27. E. Nakamura, S. Mori and K. Morokuma, *J. Am. Chem. Soc.*, **119**, 4900 (1997).

28. H. Yamataka, D. Sasaki, Y. Kuwatani, M. Mishima and Y. Tsuno, *J. Am. Chem. Soc.*, **119**, 9975 (1997).
29. F. A. Hasanayn and A. Streitwieser, *J. Org. Chem.*, **63**, 2954 (1998).
30. F. E. Romesberg and D. B. Collum, *J. Am. Chem. Soc.*, **117**, 2166 (1995).
31. P. Johansson, J. Tegenfeldt and J. Lindgren, *J. Phys. Chem. A*, **102**, 4660 (1998).
32. F. Neumann, C. Lambert and P. v. R. Schleyer, *J. Am. Chem. Soc.*, **120**, 3357 (1998).
33. R. R. Sauers, *Tetrahedron Lett.*, **37**, 7679 (1996).
34. P. J. Campos, D. Sampedro and M. A. Rodriguez, *Organometallics*, **17**, 5390 (1998).
35. T. A. Keith and R. F. W. Bader, *Chem. Phys. Lett.*, **1**, 194 (1992).
36. N. H. Werstiuk and J. Ma, *Can. J. Chem.*, **74**, 875 (1996).
37. G. Hilmersson, P. I. Arvidsson, O. Davidsson and M. Hakansson, *J. Am. Chem. Soc.*, **120**, 8143 (1998).

CHAPTER 2

Lead structures in lithium organic chemistry

THOMAS STEY and DIETMAR STALKE

Institut für Anorganische Chemie der Bayerischen Julius-Maximilians Universität Würzburg, Am Hubland, 97074 Würzburg, Germany
Fax: +49-931-888-4619; e-mail: dstalke@chemie.uni-wuerzburg.de

---

The Chemistry of Organolithium Compounds. Edited by Z. Rappoport and I. Marek
ISBN: 0-470-84339-X

I. INTRODUCTION

Structures of lithium organics can basically be approached either by diffraction, spectroscopic or by computational methods. This chapter is almost exclusively concerned with structures derived from experimental methods, either from powder diffraction techniques or from single crystal structure determination. In the class of s-block metal organics the lithium compounds are by far the most elaborated subset. In the current Cambridge Crystallographic Database 778 structures containing a Li−C bond are filed[1,2]. Second is the Mg−C bond with 274 structures, yet again confirming the diagonal relationship between lithium and magnesium. It seems worth mentioning that there are more potassium organic structures (235) than sodium organics (197, see Figure 1). Cesium (57) and rubidium (31) are far less employed in metal organic compounds.

The plain numbers already document the outstanding role of the lithium organics, even ahead of the about 20 years older Grignard reagents[3,4]. After the first landmark

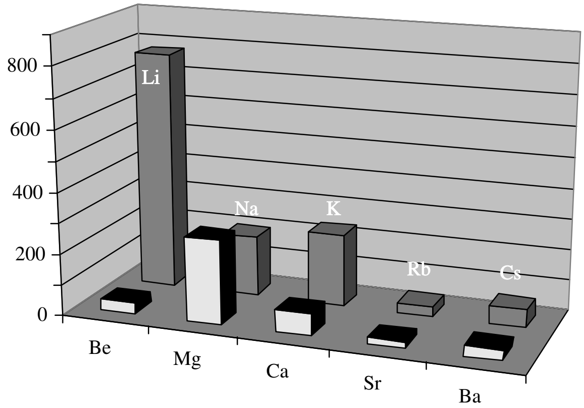

FIGURE 1. Number of structures containing M−C bonds in the current CSD, M = s-block metal

synthesis by Schlenk and Holtz[5] it took 46 years until the first structure of a lithium organic compound was published. Dietrich determined the structure of soluble ethyllithium from single crystals[6] in 1963 and just shortly afterwards the structure of insoluble methyllithium was published by Lucken and Weiss from powder data[7]. As the structure determination techniques improved over the years, both the textbook structures of $[\mathrm{EtLi}]_4$[8] and $[\mathrm{MeLi}]_4$[9, 10] were re-determined various times. It took another 15 years until the first increase in the amount of lithium organic structures was detectable in the mid-80s (from the previously one or two each year to 31 in 1984; Figure 2a). As most lithium organics are notoriously pyrophoric and thermally unstable, this is most probably due to the developments in low temperature data collection techniques in the early 80s[11–14]. The second increase in the mid-90s is due to the improvements in cryo techniques enabling maintenance of a cold chain all the way from the synthesis to the end of the data collection, hence cryo crystal application[15–17]. The third increase coincides with the area detector technology, i.e. the Charge Coupled Device (CCD)[18], following the serial scintillation detectors. The parallel detection of a magnitude of Bragg reflections increased the amount of structures per time eminently. The total number of Li−C structures increases almost exponentially. In the year 2010 one can expect about 1600 lithium organic structures (Figure 2b).

The 778 present lithium organic structures in the CSD[1] contain 3228 Li−C contacts. This means that every lithium atom either forms a multiple contact to the related carbanion or that most of the structures dimerize around the metal or both. On average, every lithium shows four Li−C contacts and certainly it is not just coincidence that this number is identical to the favorite coordination number of lithium in a molecular environment.

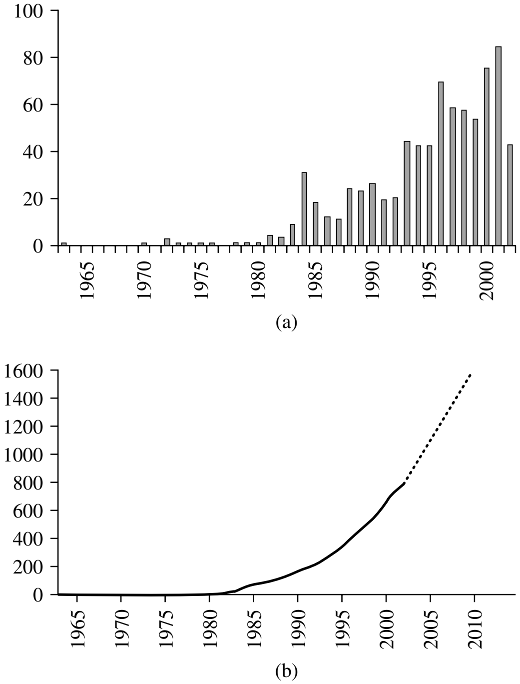

FIGURE 2. (a) Number of lithium organic structures per year and (b) total amount over the years

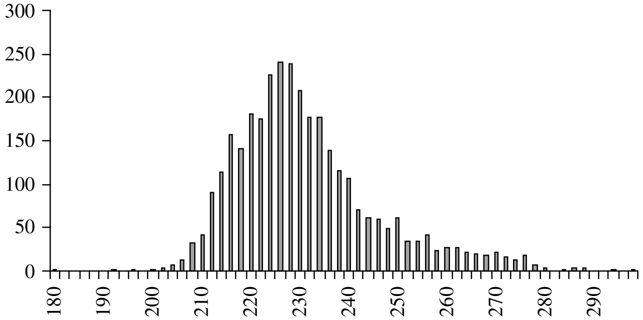

FIGURE 3. Number of Li−C bonds above Li−C distances in pm

The mean Li−C bond length is 230 pm with a minimum of 180 pm and a maximum of 300 pm (see Figure 3).

However, rather than discussing bond distances in detail, with this chapter we try to elucidate some basic lead structure forming principles in lithium organics. Aggregation and deaggregation phenomena will be discussed throughout this chapter. Basically, deaggregation is achieved by addition of neutral Lewis donor-bases, by inter- or intramolecular side-arm donation or by salt co-complexation. Synthetically, deaggregation is most important as in most cases the monomer is believed to be the rate-determining species. This chapter will outline the basic building principles of the molecular architectures of lithium organics.

Of course, it is not without precedence as there are already various reviews and textbooks in the area. Most closely related to this work are the reviews by Setzer and Schleyer[19] and by Weiss[20]. A textbook edited by Sapse and Schleyer contains chapters on various topics of lithium chemistry[21]. Three reviews by Stalke[22], Harder[23] and by Jutzi and Burford[24] concentrate on cyclopentadienyl organometallic derivatives, containing also the s-block derivatives. Two reviews deal with the heavier alkali metal organics, the first written by Schade and Schleyer[25], the second by Smith[26]. There are several chapters on lithium organics within more general metal organic publications[27, 28].

II. DELTAHEDRAL $[RLi]_4$ TETRAMERS AND $[RLi]_6$ HEXAMERS

One of the most efficient structure building principles in lithium organic chemistry is the Li_3 triangle μ_3-capped by a carbanionic C_α atom. This structural motif can further be aggregated to build deltahedral metal cores. The Li_4 tetrahedron is found in various lithium organic tetramers while the Li_6 octahedron is present in many hexamers (Figure 4).

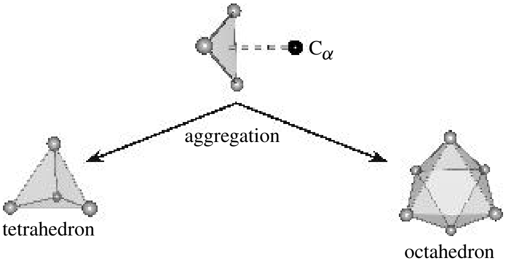

FIGURE 4. Aggregation of the μ_3-C_α capped Li_3 triangle to give deltahedral metal cores

The nature of the Li–C bond was an issue of constant debate, oscillating between predominantly ionic[29] and mainly covalent[30]. Currently, the Li–C bond is commonly considered basically ionic. However, the presence of a direct Li–Li metal bond has never been assumed in the tetrameric or hexameric aggregates. If there is any covalent contribution the Li_3C_α moieties are believed to be held together by a 4c2e bond. Hence the lines between lithium atoms in this chapter are purely of topological nature and do not suggest any 2c2e bonding between the metals. Most phenomena in lithium organic structural chemistry can reasonably be explained by electrostatics and simple point charges.

Figure 5 explains the virtual metamorphosis of the cubic $[LiF]_\infty$ salt structure to the lithium organic $[RLi]_4$ tetramer. From the infinite $[AB]_\infty$ lithium fluoride salt structure (gray spheres for Li^+ and black spheres for F^-) in (a), a single Li_4F_4 cube is highlighted (b) and extruded (c). A cube can always be described as two interpenetrating tetrahedra. This becomes evident by connecting the lithium metal atoms topologically (d) and already gives the Li_4 metal core known from the lithium organic tetramers. Switching the fluorides to carbon and connecting them to the center of each Li_3 face (e) gives the leading building block of lithium organics in the solid-state (f). This suggests that the infinite lithium halide salts and the tetrameric molecular metal organic aggregates share the

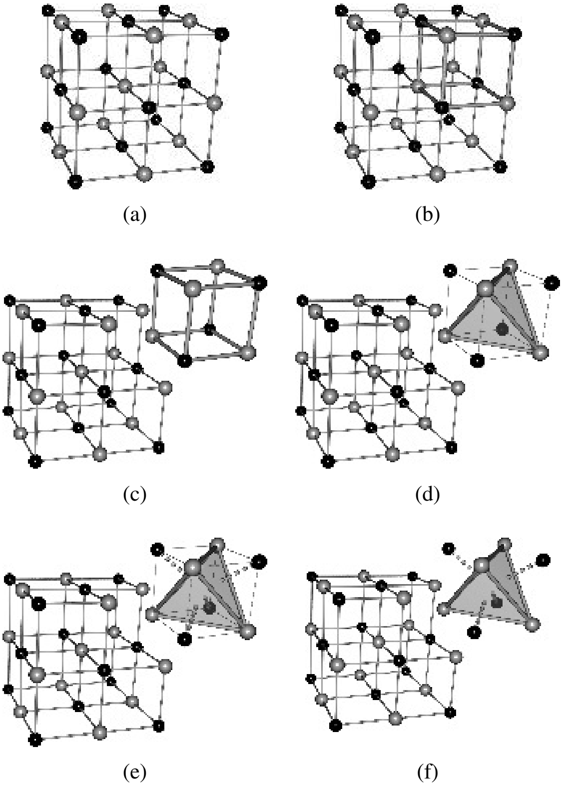

FIGURE 5. Virtual metamorphosis of the $[LiF]_\infty$ salt to the molecular $[RLi]_4$ tetramer

same ionic building principles. Even the Li···Li distances fit reasonably well. While they are 284 pm in $[LiF]_\infty$, they cover the range from 241 to 259 pm in the $[RLi]_4$ tetramers. We leave it to the reader's imagination to 'morph' a $[RLi]_6$ hexamer by an analogous procedure from the $[LiF]_\infty$ salt.

A. Donor-base-free Deltahedra

Tetrameric $[MeLi]_4$[9] (**1**), $[EtLi]_4$[8] (**2**) and $[t\text{-BuLi}]_4$[31] (**3**) are white pyrophoric powders. While methyllithium is soluble only in polar solvents like diethyl ether, the two others are soluble even in non-polar hydrocarbons like hexane. In non-donating solvent the tetrameric aggregation is retained. Each of the four Li_3 triangles is μ_3-capped by a C_α atom above the center of the equilateral metal triangle. Even in the solid-state none of the three tetramers adopts ideal T_d symmetry (Figure 6).

However, the crystallographically independent Li···Li distances of the individual tetramers are similar within the estimated standard deviations (esd). They decrease from 256 pm in $[MeLi]_4$ (**1**) to 253 pm in $[EtLi]_4$ (**2**) and 241 pm in $[t\text{-BuLi}]_4$[31] (**3**). Interestingly, the $Li{-}C_\alpha$ bond lengths are almost invariant at 226±2 pm and close to the mean Li−C bond distance of 230 pm from the CCDC[1]. In addition, $[EtLi]_4$ and $[t\text{-BuLi}]_4$ display relatively short $Li\cdots C_\beta$ distances. In the latter they are only 10 pm longer than the $Li{-}C_\alpha$ bonds (Table 1).

In both carbanions the methyl groups are arranged in close proximity to a lithium cation. Each *t*-Bu group in $[t\text{-BuLi}]_4$ is arranged ecliptically relative to the Li_3 triangle, although *a priori* a staggered conformation might be assumed sterically more favorable. Certainly, this arrangement provides some extra charge density from the C_β atom to the lithium cation and hydrophilic shielding of the electropositive metal core. In the solid-state

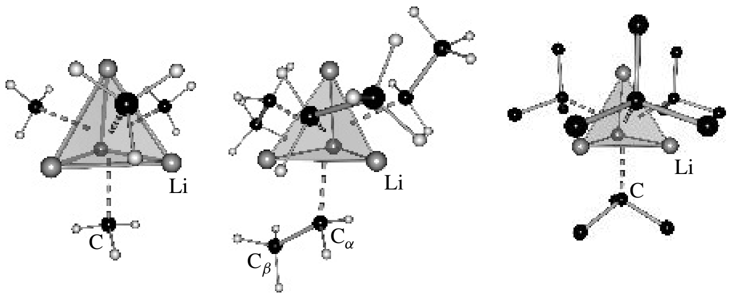

$[MeLi]_4$ (**1**) $[EtLi]_4$ (**2**) $[t\text{-BuLi}]_4$ (**3**)

FIGURE 6. Solid-state structures of the basic $[RLi]_4$ tetramers $[MeLi]_4$ (**1**), $[EtLi]_4$ (**2**) and $[t\text{-BuLi}]_4$ (**3**)

TABLE 1. Donor-base-free tetrameric lithium organics

Compound		Li···Li	$Li{-}C_\alpha$	$Li\cdots C_\beta$	CCDC code	Reference
$[MeLi]_4$	**1**	259	226	236[a]	METHLI01	10
$[EtLi]_4$	**2**	253	228	250	ETHYLI	8
$[t\text{-BuLi}]_4$	**3**	241	225	237	SUHBIG	31

[a] Distance of the methanide carbon atom to the *apical* lithium atom of an adjacent tetramer.

structure of $[MeLi]_4$ (**1**), this long-range interaction is arranged by the methyl group of an adjacent tetramer. Each *apical* lithium cation points towards the 'back side' of a μ_3-coordinated methanide of the neighboring tetramer. Along the room diagonal of the cubic body-centered unit cell this gives a rod-like arrangement of tilted tetrahedra leaving each carbon atom coordinated to four lithium cations (Figure 7a). Since not only the *apical* lithium cation points towards a nearby methanide group but also the *basal* lithium atoms, the sum of all long-range interactions give the unit cell with a tetramer in the center and the centroid of a tetramer at each corner (Figure 7b). The related $Li\cdots$'C_β' distances (236 pm) are only 10 pm longer than the $Li-C_\alpha$ bonds. Their considerable contribution to the overall lattice energy leaves $[MeLi]_{4,\infty}$ insoluble in non-donating solvents. The 'back-site' coordination, however, makes the methanide in methyl lithium an exceptional strong base, not accomplished by any other binary lithium organic. The solvation energy gained by donor-base addition (e.g. THF) and deaggregation is lost in the overall reactivity. Once the long-range interactions are cleaved, methyl lithium loses parts of its reactivity (*vide infra*).

The short $Li\cdots C_\beta$ interactions in $[EtLi]_4$, and $[t\text{-}BuLi]_4$ classify them as metal organic molecules rather than infinite solid-state aggregates. They provide solubility even in non-polar hydrocarbons. The decreasing $Li\cdots Li$ distances from methyl via ethyl to *t*-butyl lithium display the increasing electron-releasing capability of the carbanions along this line. The *t*-butyl group provides so much charge to the single lithium cations that they can get closer than in methyl lithium with a considerably higher positive charge and higher repulsion. All structurally determined binary hexamers, $[n\text{-}BuLi]_6$[31] (**4**), $[i\text{-}PrLi]_6$[32] (**5**), $[c\text{-}PenLi]_6$[33] (**6**), $[c\text{-}HexLi]_6$[34] (**7**), $[c\text{-}PrH(Me)_4CH_2Li]_6$[35] (**8**), $[(t\text{-}Bu)_2C_6H_3Li]_6$[36] (**9**) and $[Me_3SiCH_2Li]_6$[37] (**10**) are readily soluble in non-polar hydrocarbons. In the Li_6 octahedra only six of the eight present Li_3 triangles are μ_3-capped by C_α atoms. The two remaining uncapped are arranged opposite. The six carbanions form a 'paddle-wheel' along the non-crystallographic three-fold axis through the mid-point of these uncapped triangles. This structural motif is most obvious with the cyclic carbanions in **6** and **7** (Figure 8).

Due to the missing binding carbanions, the related $Li\cdots Li$ distances in the unoccupied Li_3 triangles are considerably longer (294–318 pm; Table 2) than those in the tetrahedra

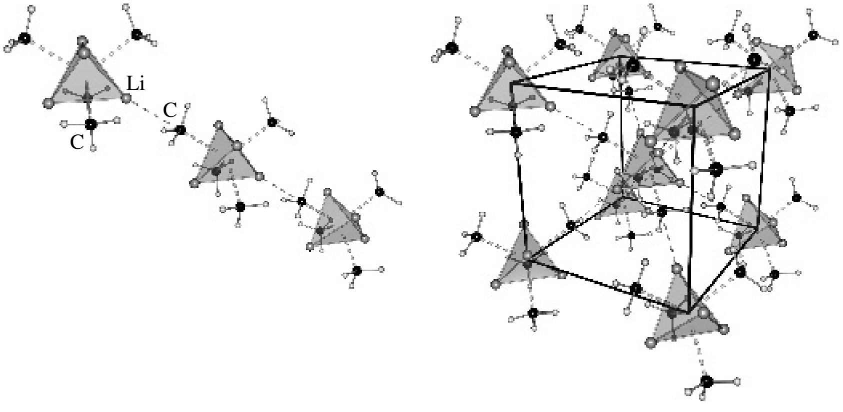

(a) (b)

FIGURE 7. Polymeric solid-state structure of $[MeLi]_4$ (**1**); arrangement of three tetrahedra along the room diagonal of the unit cell illustrating the $Li_3-C\cdots Li$ long-range interactions (a) and the unit cell content (b)

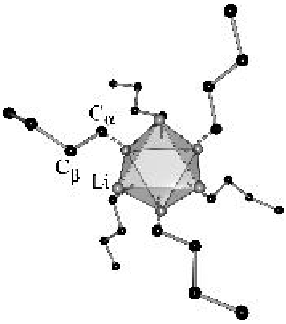

[n-BuLi]$_6$
(4)

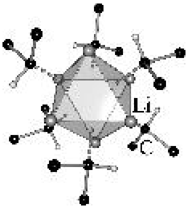

[i-PrLi]$_6$
(5)

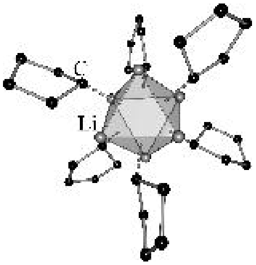

[c-PenLi]$_6$
(6)

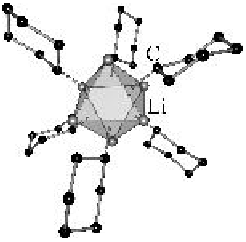

[c-HexLi]$_6$
(7)

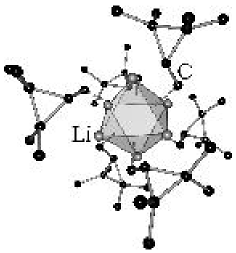

[c-PrH(Me)$_4$CH$_2$Li]$_6$
(8)

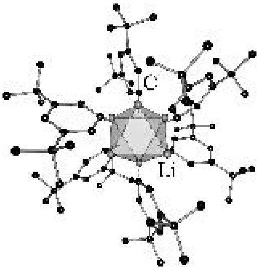

[(t-Bu)$_2$C$_6$H$_3$Li]$_6$
(9)

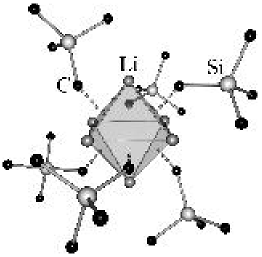

[Me$_3$SiCH$_2$Li]$_6$
(10)

FIGURE 8. Solid-state structures of donor-base-free [RLi]$_6$ hexamers

of **1**–**3** (241–259 pm). Only these unoccupied Li$_3$ sites form equilateral metal triangles. The six μ_3-C$_\alpha$-capped form isosceles with the long Li···Li distance as hypotenuse. On average, the short Li···Li distances in the hexamers match those of the tetramers (Table 2). The carbanionic C$_\alpha$ atom is considerably shifted towards the mid-point of the

TABLE 2. Donor-base-free hexameric lithium organics

Compound		Li···Li	Li—C_α	Li···C_β	CCDC code	Reference
[*n*-BuLi]$_6$	**4**	243 (294)[a]	216 (227)	229	SUHBEC	31
[*i*-PrLi]$_6$	**5**	240 (296)	218 (231)	231	POBLAT	32
[*c*-PenLi]$_6$	**6**	241 (296)	218 (228)	235		33
[*c*-HexLi]$_6$	**7**	240 (297)	218 (230)	249	CHXYLI	34
[*c*-PrH(Me)$_4$CH$_2$Li]$_6$	**8**	246 (297)	214 (230)	274	COHKIT	35
[(*t*-Bu)$_2$C$_6$H$_3$Li]$_6$	**9**	251 (314)	215 (221)		RIZXON	36
[Me$_3$SiCH$_2$Li]$_6$	**10**	246 (318)	219 (227)	267[b]	JAFMUY	37

[a] Values in brackets represent the Li···Li distances in the unoccupied Li_3 triangles.
[b] Distance of a methyl carbon atom of the trimethylsilyl group (C_γ) to the next lithium atom of the hexamer.

longer Li···Li distance. Hence, two shorter Li—C_α bonds to the two lithium atoms at the hypotenuse are found (214–219 pm). The longer bond is formed to the lithium atom at the *apex* (227–231 pm; Table 2).

In **9**, the metalated ring carbon atom is shifted towards one lithium atom of the long Li···Li distance and the *apical*. Like the tetramers, all structures **4–10** except **9** display short Li···C_β distances. In [*i*-PrLi]$_6$ (**5**), this distance is as short as the long Li—C_α bond (231 pm), while in **4**, **6** and **7** they are only marginally longer. In **8**, C_β and C_γ are equally involved in charge transfer to the lithium cations. Although there is no C_α atom in the hexameric structure of lithiated tetrakis(trimethyl)silane [Me$_3$SiCH$_2$Li]$_6$ (**10**), the secondary electron donation is achieved by the methyl group in the γ-position relative to the metalated carbon atom.

B. Donor-base-coordinated Deltahedra

Addition of neutral Lewis-bases like diethyl ether (Et_2O), tetrahydrofuran (THF), dimethoxy methane (DME), tetramethylethylene diamine (TMEDA), pentamethyldiethylene triamine (PMDETA) or various crown ethers (12-crown-4), commonly referred to as donor-bases, to aggregated lithium organics normally decreases their degree of aggregation. Multiple Li—C_α and additional Li···C_β interactions are partly substituted by N or O→Li donor bonds. This deaggregation commonly furnishes magnitudes of increased reactivity because the rate determining step is normally the reaction of the monomer[38, 39]. With insoluble polymeric [MeLi]$_{4,\infty}$ (**1**), deaggregation used to be difficult. In all structurally characterized methyllithium donor-base adducts the tetrameric aggregation of the starting material is retained in the solid-state products. While [(THF)LiMe]$_4$[40] (**11**) consists of molecules, [(TMEDA)$_2$(LiMe)$_4$]$_\infty$[41] (**12**) and [(DEM)$_{1.5}$(LiMe)$_4$]$_\infty$[42] (**13**) still adopt polymeric architectures. **11** and **12** do not exhibit any Li···C long-range interactions. Like in **1**, each Li_3 triangle is μ_3-capped by a C_α methanide atom but, different from the donor-base-free starting material, each lithium atom is *apically* coordinated by the heteroatom of the donor-base. The monodentate THF terminates the coordination of [(THF)LiMe]$_4$ (**11**) to molecules (Figure 9a), while the (*N*,*N*)-chelating TMEDA in [(TMEDA)$_2$(LiMe)$_4$]$_\infty$ (**12**) further links the tetramers as the nitrogen atoms coordinate lithium atoms of two adjacent tetramers (Figure 9b). Addition of THF to [MeLi]$_{4,\infty}$ (**1**) at low temperature yields molecular [(THF)LiMe]$_4$ (**11**), but the reactivity suffers considerably[40]. It is decreased by the solvation energy $\Delta H_{\text{solv.}}$, which was experimentally determined to be 30–40 kJ mol^{-1}. As far as the activation of the methanide group is concerned, the long-range Li_3—CH_3···Li interactions seem to be vital. Addition of TMEDA even to diethyl ether solutions of methyllithium causes precipitation of a white product which was determined to be [(TMEDA)$_2$(LiMe)$_4$]$_\infty$ (**12**). Hence the donor-base would not enhance the reactivity but causes substraction from the reaction equilibrium. Obviously, the bite of TMEDA is flexible enough to tolerate the most dense arrangement of the lithium organic tetramers in the lattice without any space for additional solvent, emphasizing precipitation. In diethoxymethane (DEM) both oxygen donor atoms are so close to each other that the bite is suitable neither to coordinate the same lithium atom nor to tolerate closest cubic packing of the $[MeLi]_4$ tetramers. In the solid-state structure of $[(DEM)_{1.5}(LiMe)_4]_\infty$ (**13**), straight polymeric rods of Li_4 tetrahedra are formed by face-to-vertex bridging methanide groups along a three-fold axis (Figure 9c). This basic polymeric arrangement is emulating the solid-state structure of parent $[(MeLi)_4]_\infty$ along the body diagonal of the cubic body-centered cell (see also Figure 7a).

In **13** only one methyl group is exposed to intertetrameric long-range Li···C interactions. The remaining three methyl groups cap a single Li_3 face, each without further coordination. The three lithium atoms of the Li_3 *basal* face are coordinated to a single

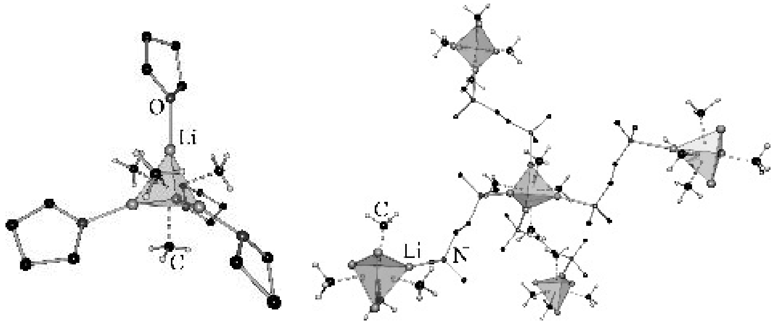

(a) $[(THF)LiMe]_4$ **(11)**

(b) $[(TMEDA)_2(LiMe)_4]_\infty$ **(12)**

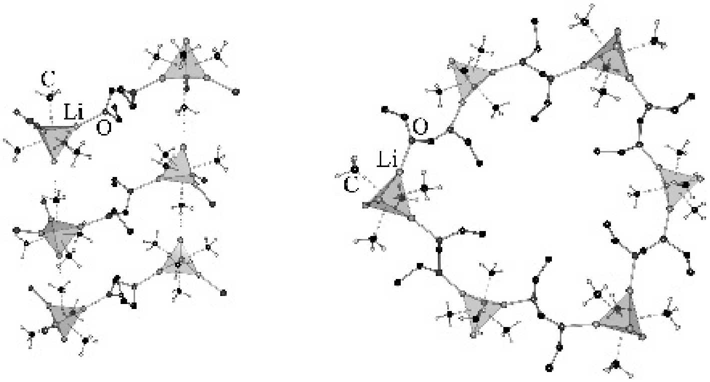

(c)

(d)

$[(DEM)_{1.5}(LiMe)_4]_\infty$ **(13)**

FIGURE 9. Solid-state structures of donor-base-coordinated $[MeLi]_4$ tetramers

oxygen atom of the DEM donor each. The second provides linkage to another $[(MeLi)_4]_\infty$ rod (Figure 9c). Space group symmetry constitutes a hexagonal channel along the six rods of a more than 720 pm light diameter (Figure 9d). These channels can easily accommodate various solvents as the lipophilic ethyl groups of the DEM molecules coat the walls to the inside. DEM yields the nanoporous structure of **13** with solvent-filled channels, reminiscent of the ice structure, to improve solubility and decrease chemical hazards of a pyrophorus material in a solvent with a very low flame point like diethyl ether.

In all three structurally known binary lithium *n*-butanide donor-base adducts **14**–**16** the parent hexamer $[n\text{-BuLi}]_6$[31] (**4**) is deaggregated to a tetramer. While $[(THF)LiBu\text{-}n]_4$[43] (**14**) is molecular in the solid-state, $[(DME)_2(LiBu\text{-}n)_4]_\infty$[43] (**15**) and $[(TMEDA)(LiBu\text{-}n)_4]_\infty$[43,44] (**16**) aggregate by bridging (O,O)- or (N,N)-chelating donor bases. Like in **11**, each Li_3 triangle in **14** is μ_3-capped by a C_α butanide atom. In addition, each lithium atom is *apically* coordinated by the THF oxygen atom (Figure 10a). **15** is more reminiscent of **12**, while **16** builds ribbon-like polymers (Figure 10b). The *n*-hexyl carbanionic C_α atom in $[(THF)LiCH_2CH_2Bu\text{-}t]_4$[45] (**17**), the vinyl in $[(THF)LiC(H){=}CH_2]_4$[46] (**18**), the phenyl *ipso*-C in $[(Et_2O)LiPh]_4$[47] (**19**) and $[(Me_2S)LiPh]_4$[48] (**20**), as well as the ethynyl group in $[(THF)LiC{\equiv}CBu\text{-}t]_4$[49] (**21**) and in $[(TMHDA)_2(LiC{\equiv}CPh)_4]_\infty$[50] (**22**) (TMHDA = $Me_2N(CH_2)_6NMe_2$) μ_3-cap a Li_3 triangle in the tetrameric aggregates. **17**–**21** form molecular structures like **11** and **14** (Figures 9a and 10a, respectively), while **22** is a donor-base-bridged polymer like **12** and **13**.

On average, the metal–metal distances in the donor-base-coordinated tetrahedra **11** to **22** are about 10 pm longer than the short Li···Li distances in the octahedra of the hexamers (Table 3). However, the found distances that range from 250 to 272 pm are always considerably smaller than the long Li···Li distances in the hexamers of just below 300 pm. It is interesting to note that the sp^2 C_α atoms in $[(THF)LiC(H){=}CH_2]_4$ (**18**) and $[(Et_2O)LiPh]_4$ (**19**), as well as the sp C_α atoms in $[(THF)LiC{\equiv}CBu\text{-}t]_4$ (**21**) and $[(TMHDA)_2(LiC{\equiv}CPh)_4]_\infty$ (**22**), cause the longest Li···Li distances in that series (260 in **18**, 264 in **19**, 268 in **21** and 272 pm in **22**). Apparently, in contrast to sp^3 carbon atoms they are less efficient electron density donors and cause more positive charge to be accumulated at the metal core. This is further substantiated by the fact that with the phenylethynyl substituent in **22** the Li···Li distance is the widest because the electron density is delocalized to the aromatic substituent. This is precluded with the *t*-butylethynyl carbanion in **21**. The result is a stronger repulsion of the lithium cations. The carbanionic

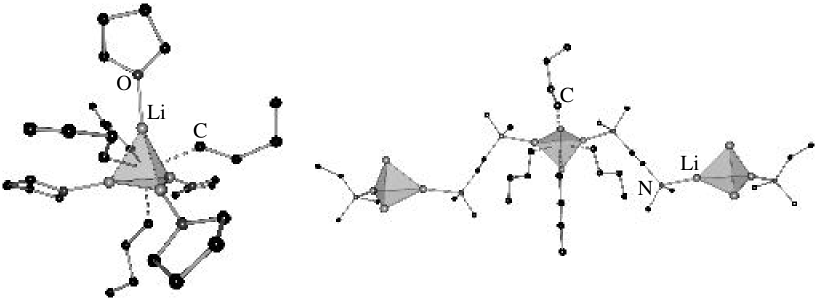

(a)

$[(THF)LiBu\text{-}n]_4$

(14)

(b)

$[(TMEDA)(LiBu\text{-}n)_4]_\infty$

(16)

FIGURE 10. Solid-state structures of donor-base-coordinated $[n\text{-BuLi}]_4$ tetramers

TABLE 3. Donor-base-coordinated deltahedra

Compound		Li···Li	Li−C_α	Li−O, *N*	CCDC code	Reference
$[(THF)LiMe]_4$	**11**	251	224	196	LAMNIW	40
$[(TMEDA)_2(LiMe)_4]_\infty$	**12**	257	226	*221*	MELIME	41
$[(DEM)_{1.5}(LiMe)_4]_\infty$	**13**	254	226	199	QOSLOZ	42
$[(THF)LiBu\text{-}n]_4$	**14**	254	224	197	WAFJES	43
$[(DME)_2(LiBu\text{-}n)_4]_\infty$	**15**	252	227	201	WAFJIW	43
$[(TMEDA)(LiBu\text{-}n)_4]_\infty$	**16**	248	225	*213*	WAFJOC	43, 44
$[(THF)LiCH_2CH_2Bu\text{-}t]_4$	**17**	250	226	195	RIFJUL	45
$[(THF)LiC(H){=}CH_2]_4$	**18**	260	225	197	PAFCEE	46
$[(Et_2O)LiPh]_4$	**19**	264	232	205	CALKOP	47
$[(Me_2S)LiPh]_4$	**20**	257	226	260[b]	SIMRUB	48
$[(THF)LiC{\equiv}CBu\text{-}t]_4$	**21**	268	220	196	GIFHEI	49
$[(TMHDA)_2(LiC{\equiv}CPh)_4]_\infty$[a]	**22**	272	220	*211*	CAMNEJ	50

[a] TMHDA = $Me_2N(CH_2)_6NMe_2$.
[b] S→Li donor bond.

charge seems to be delocalized in the C=C double or C≡C triple bond rather than being transferred to the metals. The remarkably short Li−C_α bonds of 220 pm in **21** and **22** compared to the average 225 pm in this class of compounds (Table 3) does not necessarily reflect strong bonding but might be attributed to the on average 8 pm smaller radius of a sp carbon atom compared to a sp^3 carbon atom[51]. The most obvious fact in the geometrical features of **11** to **22** is the absence of any Li···C_β interactions. This secondary electron donation of the carbanion via the C_β is substituted by the heteroatom of the donor-base. The found N→Li donor bond lengths of average 215 pm and O→Li of average 200 pm are typical. Note that the Li−N bonds in lithium amide stacks and ladders are on average more than 15 pm shorter[52–55]. Li−O bonds in LiOR species (R = alkyl, aryl, silyl) are on average even 20 pm shorter than O→Li donor bonds[56, 57].

C. Donor-base-induced Dimers and Monomers

Electron donation of Lewis basic donor molecules, like ethers or amines to the electropositive lithium metal, causes the lithium organic aggregates to reduce in size. The *n*-BuLi hexamer[31] **4** shrinks to a donor-base-coordinated tetramer in **14** to **16**[43, 44]. Unfortunately, with $[MeLi]_4$[10] (**1**), this strategy does not seem to be successful. All known solvates of methyllithium retain the tetrameric aggregation (**11**–**13**)[40–42]. Obviously, there are other requisites needed to get monomeric methyllithium (*vide infra*). While addition of TMEDA to methyllithium causes precipitation[41], the addition to *n*-BuLi generates donor-base-bridged tetramers **14**–**16** (Figure 10) and even dimers. In $[(TMEDA)LiBu\text{-}n)]_2$[43] (**23**), a Li_2C_2 four-membered ring is assembled as each C_α binds to both lithium atoms. The preferred four-fold coordination of lithium is reached by the two nitrogen atoms of the chelating TMEDA coordinating to the same lithium atom (Figure 11). In diethyl ether the *t*-BuLi tetramers[31] are deaggregated to give dimers of the composition $[(Et_2O)LiBu\text{-}t]_2$[31] (**24**). Like in **23**, in **24** a Li_2C_2 four-membered ring is formed but the coordination number of the lithium atom is only three, as each metal is coordinated by just one diethyl ether molecule. It is important to note that dimeric *t*-BuLi in diethyl ether is only stable at temperatures below −80 °C, because at higher temperatures the ether cleavage reaction generates explosive reaction mixtures[16, 17, 58]. Both Li_2C_2 rings in **23** and **24** are bent along the transannular C···C line because, e.g. in $[(Et_2O)LiBu\text{-}t]_2$ (**24**), the six methyl groups and the two lithium atoms along that vector need to

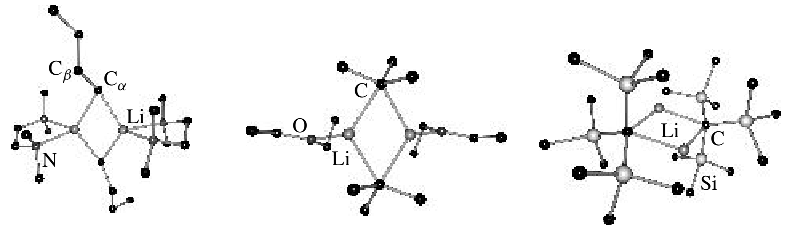

$[(TMEDA)(LiBu\text{-}n)]_2$
(23)

$[(Et_2O)LiBu\text{-}t]_2$
(24)

$[LiC(SiMe_3)_3]_2$
(26)

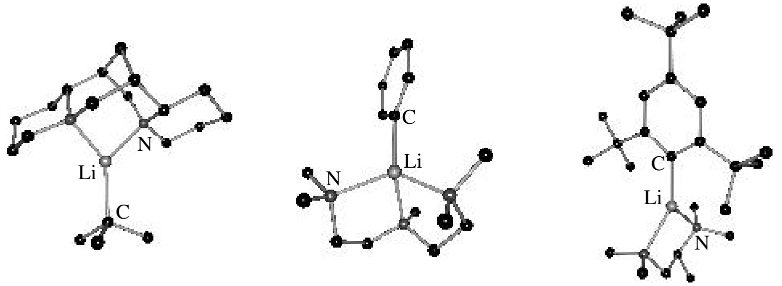

[{(−)-sparteine}LiBu-*t*]
(27)

[(PMDETA)LiPh]
(28)

[(TMEDA)LiMes*]
(29)

FIGURE 11. Solid-state structures of donor-base-coordinated dimers and monomers

be accommodated in a staggered arrangement. This can only be reached in a non-planar four-membered ring. While Et_2O and Me_2S in $[(Et_2O)LiPh]_4$[47] (**19**) and $[(Me_2S)LiPh]_4$[48] (**20**) coordinate the *apical* lithium atoms in the tetrahedral tetramers, addition of the chelating diamine TMEDA results in the formation of the dimer $[(TMEDA)LiPh]_2$[59] (**25**). The carbanions are almost orthogonal aligned to the Li_2C_2 four-membered ring. $[LiC(SiMe_3)_3]_2$[60] (**26**) is a paradigmatic example that even $Li\cdots C_\gamma$ distances can be as important as E→Li donor bonds (E = O, N): **26** is a dimer with a Li_2C_2 four-membered ring not coordinating any donor solvent. The methyl C_γ atoms are so close to the lithium (average 250 compared to 267 pm in $[Me_3SiCH_2Li]_6$[37], (**10**)) that they either shield the metal perfectly or supply sufficient electron density. Addition of the enantiomeric pure chiral donor-base (−)-sparteine to a *t*-BuLi solution at −78 °C gives crystals of monomeric [{(−)-sparteine}LiBu-*t*][61] (**27**) at −30 °C. It is the to-date only known enantiomerically pure complex of a basic lithium organic. Like in [(PMDETA)LiPh][62] (**28**), it is the bulk of the donor ligand that prevents this lithium organic from aggregation. In [(TMEDA)LiMes*][63] (**29**) (Mes* = (2, 4, 6-tri-*t*-butyl)phenyl), this is precluded by the bulk of the carbanion. In monomeric phenyl and supermesityl lithium (**28** and **29**, respectively) the metal atom is in the mean plane of the C_6 perimeter and additionally chelated by the PMDETA and TMEDA donor-base, respectively.

Compared to the deltahedra, the $Li\cdots Li$ distances across the Li_2C_2 rings in **23** to **26** are shorter. The four-membered rings are elongated along the $C\cdots C$ vector (C−Li−C 110.7°, Li−C−Li 63.6° in **24**) bringing the lithium atoms in close transannular proximity. The $Li{-}C_\alpha$ distances in the non-silylated compounds **23** to **25, 27** and **28** scale nicely to the charge at the lithium atoms. In the dimers $[(TMEDA)(LiBu\text{-}n)]_2$[43] (**23**), $[(Et_2O)LiBu\text{-}t]_2$[31] (**24**) and $[(TMEDA)LiPh]_2$[59] (**25**), these bonds are longer due to the steric repulsion. The by 4 pm shorter bond in **24** compared to **23** is explained by the two N donor atoms in the

TABLE 4. Donor-base-induced dimers and monomers of basic lithium organics

Compound		Li···Li	Li−C_α	Li−O, *N*	CCDC code	Reference
[(TMEDA)(LiBu-*n*)]$_2$	**23**	236	222	*221*	WAFJAO	43
[(Et_2O)LiBu-*t*]$_2$	**24**	230	218	194	SUHBOM	31
[(TMEDA)LiPh]$_2$	**25**	249	224	*219*	PHENLI	59
[LiC($SiMe_3$)$_3$]$_2$	**26**	235	230	250 (C_γ)	KIRPEG	60
[{(−)-sparteine}LiBu-*t*]	**27**		211	*206*		61
[(PMDETA)LiPh]	**28**		214	*214*	DANKUY	62
[(TMEDA)LiMes*][a]	**29**		212	*217*	VAPHUP	63

[a] Mes* = (2,4,6-tri-*t*-butyl)phenyl, $C_6H_2(Bu\text{-}t)_3$.

first, rather than the single oxygen atom in the latter. In **24** the Li−C contact needs to be closer, even against stronger steric repulsion of the *t*-Bu group, compared with the *n*-Bu substituent as electrostatics are more pronounced because the lithium atom in **24** is more positive by getting less charge donated. In [{(−)-sparteine}LiBu-*t*][61] (**27**), the lithium gets about the same electron density donated as in **23** (two nitrogen atoms) but it has not to be shared between two carbanions. Hence, the Li−C distance of 211 pm in **27** falls at the short end of the range covered in the CCDC (see Figure 2). Although the sparteine donor provides considerable steric bulk to prevent further aggregation, there is enough room at the other hemisphere of the metal to get close to the *tert* carbanionic atom (Table 4). At first sight the 214 pm in [(PMDETA)LiPh] (**28**) seems to be only marginally longer, but one has to take into account the by 4 pm reduced radius of the sp^2 carbon atom in **28** compared to the sp^3 carbon atom in **27**. Hence, the Li−C_α distance of 212 pm in [(TMEDA)LiMes*][63] (**29**) seems much more reasonable than the 180 pm found in donor-base-free monomeric [LiMes*] co-crystallized with a molybdenum phosphide complex[64]. The N→Li and O→Li donor bond lengths in **23, 24, 28** and **29** are typical but the N→Li distance of 206 pm in **27** is remarkably short. The relatively long Li−C_α bond in [LiC($SiMe_3$)$_3$]$_2$ (**26**) of 230 pm rather suits the distances found in donor-base-coordinated tetramers (Table 3). This seems to be a shape effect of the pocket provided by the adjacent γ-methyl groups, hence an equilibrium of the σ-bond density and the secondary electron density donated by the methyl groups.

III. LITHIUM ORGANICS WITH CYCLIC CARBANIONS

While the previous section was predominantly concerned with lithium alkyls, this one will elucidate the lead structures of lithium organics with cyclic C_n anions. The C_3 perimeter of the cyclopropanyl anion is only used scarcely in lithium organic structural chemistry and the cyclopropenyl carbanions have only recently been conceived in dilithiated species. The same is valid for the C_4 perimeter. Dimetalated cyclobutadienyl has just been introduced to lithium chemistry. Lithium organics with a C_5 perimeter are certainly the most elaborated class of compounds in this context. Lithium cyclopentadienyl derivatives are one of the most applied starting materials in metal organic synthesis. They are compounds *par excellence* to generate a huge variety of sandwich or half-sandwich d-block metal organics via transmetalation or salt elimination reactions. The indenyl and fluorenyl substituents contain, apart from the C_5 perimeter, either one or two anellated six-membered carbon rings. In addition to the likely η^5-bonding mode, they supply the feasible η^6-coordination mode. The most important class of lithium organics with a C_6 perimeter are the phenyllithium derivatives. They support σ- as well as π-bonding up to η^6-coordination. Examples of lithium organics containing a C_7 or larger perimeter are scarce.

A. C_3 and C_4 Perimeter

Cyclopropane and -propene exhibit a remarkable chemical applicability, predominantly due to their steric strain. The acidity of cyclopropene is comparable to that of acetylene[65]. *Ab initio* studies suggested that upon lithiation the bond lengths in the metalated species should differ considerably compared to the starting material[66]. The vicinal formal $C_\alpha-C_\gamma$ single bond was computed to be much longer than in parent cyclopropene (157 vs. 151 pm), while the $C_\gamma-C_\beta$ distal bond shortens to 146 pm. Moreover, the unsolvated cyclopropenyl lithium dimer was calculated to have two planar tetracoordinated $R^1R^2CLi_2$ fragments (on average 45 $kJ\,mol^{-1}$ lower in energy than the perpendicular tetrahedral carbon atom)[67].

The preference of the planar dimer is due to attractive electrostatic $Li^+\cdots C_\gamma{}^{\delta-}$ interactions, which are considerably reduced in the orthogonal dimer. In terms of natural charges (C_α: −0.57; C_β: −0.26; C_γ: −0.66) the C_γ carbon atom seems at least as attractive as the C_α[68] in the in-plane dimer. However, the solvated lithium cyclopropenyl $[(TMEDA)LiC_3(Me)_2SiMe_3]_2$[69] (**30**) adopts the orthogonal form with a tetrahedral tetracoordinated ring carbon atom. Again, the secondary electron density donation via the anionic periphery is substituted by a donor-base-coordination. Hence, the steric requirements force the compound into the orthogonal arrangement as electrostatics are satisfied by the donor-base (Figure 12). The predicted distortion of the C_3 perimeter, however, could be confirmed by experiment: the vicinal $C_\alpha-C_\gamma$ bond was found to be widened to 156.1 pm, while the $C_\gamma-C_\beta$ distal bond is shortened to 148.9 pm[69]. The same is valid for the dilithiated derivatives $[(THF)Li_2C_3(Me)_2Si(NBu\text{-}t)Me_2]_2$[70] (**31**), $[(THF)_2Li_2C_3(Me)_2C(O)Bu\text{-}t_2]_2$[71] (**32**) and $[(TMEDA)Li_2C_3(Me)_2C(O)Bu\text{-}t_2]_2$[70] (**33**). On average, the vicinal $C_\alpha-C_\gamma$ bond in the C_3 perimeter of **30**–**33** is 148.6, the $C_\gamma-C_\beta$ distal bond 157.0 and the formal $C_\alpha{=}C_\beta$ double bond 134.1 pm long. The latter three complexes show ladder-type dimerization known from lithium amides[54] (Figure 12). The tetracoordinated $R^1R^2CLi_2$ fragments show a high degree of planarization, promoted by lithium alkoxide and amide side-arm donation. In **31** this not only leaves the C_α in an almost planar environment, but also the C_β atom next to the lithiated site. In addition to the t-BuN^- donation, the partial $C_\alpha{=}C_\beta$ double bond serves as electron donor to the metal. The short Li−C distances are found in the plane of the C_3 anion (213–218 pm) and the longer ones provide dimerization (Table 5).

In none of the known tricyclic carbanions is the metal haptotropic π-coordinated on top of the ring. Obviously, the ring is too small to suit even the small lithium cation.

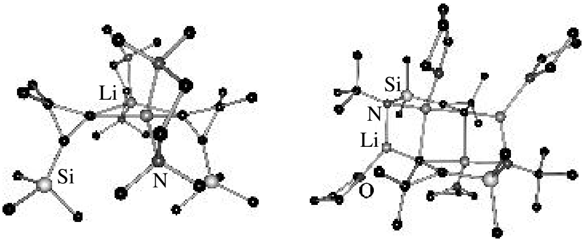

$[(TMEDA)LiC_3(Me)_2SiMe_3]_2$ **(30)**

$[(THF)Li_2C_3(Me)_2Si(NBu\text{-}t)Me_2]_2$ **(31)**

FIGURE 12. Solid-state structures of monolithium and dilithium cyclopropenyl dimers. While in-plane dimerization is hampered by the donor-base in **30,** side-arm donation promotes a planar $R^1R^2CLi_2$-fragment in **31**

TABLE 5. Lithium organics with a cyclic C_3 anion

Compound		Li···Li	Li–C_α	Li–O, *N*	CCDC code	Reference
$[(TMEDA)LiC_3(Me)_2SiMe_3]_2$	**30**	247	221	*216*	ZOTGIY	69
$[(THF)Li_2C_3(Me)_2Si(NBu\text{-}t)Me_2]_2$	**31**	264	218/232[a]	198/*203*	TIMCUN	70
$[(THF)_2Li_2C_3(Me)_2C(O)Bu\text{-}t_2]_2$	**32**	267	213	194/202[c]	ZIHJAB	71
$[(TMEDA)Li_2C_3(Me)_2C(O)Bu\text{-}t_2]_2$	**33**	225	214/337[b]	192/*232*	TIMCOH	70

[a] First number refers to lithium atoms in-plane, second to out-of-plane atoms relative to the C_3 perimeter.
[b] First number σ-bonded, second η^2-coordinated lithium atoms.
[c] First number THF, second alkoxy side-arm donor bond.

Furthermore, η-coordination is precluded by the substituents at the sp^3 carbon atom shielding the top and the bottom of the C_3 perimeter. With the $C_4R_4{}^{2-}$ and the $C_5R_5{}^-$ perimeter this is quite different. The substituents are in-plane with the ring or can at least be arranged to give access to the planar carbanionic core. Though the substituents at the cyclobutadienediide need to be sterically demanding, there seems to be enough room at the C_4 core and even in the ligand periphery for the lithium atom to decide in a haptotropic search for a η^2- or η^4-coordination. In all known $C_4R_4{}^{2-}$ structures the C_4 center is μ_2-bridging the two lithium metals on top and underneath. In this arrangement, often referred to as 'inverted sandwich complex' or 'inverted metallocene', both metals can be shifted from the center to the periphery in accord with the electron density distribution and steric requirements. In the benzocyclobutadienediide $[\{(TMEDA)Li\}_2C_4(Ph)_2C_4H_4]$[72] (**34**), the electron density is partially delocalized to the anellated benzene ring. This leaves the common C_4- and C_6-bond non-attractive for both electropositive lithium atoms, although one might anticipate the lithium atoms to be shifted away from the η^2-position close to the phenyl groups to minimize steric interaction (Figure 13). In the isomorphous $[\{(DME)Li\}_2C_4(Ph)_2(SiMe_2)_2C_2H_4]$[73] (**35**), only the donor-base in **34** is switched to DME and the anellated benzene ring is replaced by a non-planar cyclic $(SiMe_2)_2C_2H_4$ chain. Hence two silyl substituents supply charge density to the $C_4{}^{2-}$ center. This makes all four carbon atoms equally attractive for the metal and η^4-coordination for both metal atoms is observed (Figure 13).

The Li–C distances seem to be directly correlated to the amount of silyl groups bonded to the ring. In **34** there is none and the η^2-coordination is relatively unattractive, resulting in a long $Li{-}C_{2(\text{center})}$ distance of 204 pm (Table 6). In **35** with two silyl groups the $Li{-}C_{4(\text{center})}$ distance is only 196 pm. Addition of two more silyl groups

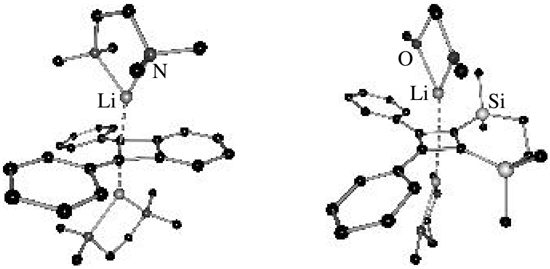

$[\{(TMEDA)Li\}_2C_4(Ph)_2C_4H_4]$ $[\{(DME)Li\}_2C_4(Ph)_2(SiMe_2)_2C_2H_4]$

(34) **(35)**

FIGURE 13. Solid-state structures of dilithium cyclobutadienediide C_4 perimeters

TABLE 6. Dilithium organics with a cyclic C_4 anion

Compound		η^n $n=$	Li···C_n n(center)	Li−O, N	CCDC code	Reference
$[\{(TMEDA)Li\}_2C_4(Ph)_2C_4H_4]$	**34**	2	204	*205*	DOBRUH01	72
$[\{(DME)Li\}_2C_4(Ph)_2(SiMe_2)_2C_2H_4]$	**35**	4	196	205	GUNJII	73
$[\{(DME)Li\}_2C_4(SiMe_3)_4]$	**36**	4	191	208	QIZTEY	74
$[\{(DME)Li\}_2C_4\{C_2(SiMe_2)_6(CH_2)_3\}]$	**37**	4/2	222/209	200/396	ROLJUX	75

in the per-silylated $C_4(SiMe_3)_4{}^{2-}$ anion in $[\{(DME)Li\}_2C_4(SiMe_3)_4]$[74] (**36**) causes the Li−$C_{4(center)}$ distance further to decrease to 191 pm. In the heavily substituted $[\{(DME)Li\}_2C_4\{C_2(SiMe_2)_6(CH_2)_3\}]$[75] (**37**), there are only two silyl groups directly bonded to the C_4 perimeter. The two remaining adjacent positions are occupied by sp^2 hybridized carbon atoms. Those peripheral partial C−C multiple bonds are equally attractive for the lithium metal. From the charge density point of view the electrostatic surface of the dianion seems not accentuated and spread out. One lithium atom can be regarded to be η^4-coordinated to the core (Li−$C_{4(center)}$ 222 pm), while the second is more η^2-coordinated to the peripheral exocyclic C−C multiple bond (Li−$C_{2(center)}$ 209 pm).

B. C_5 Perimeter

The physical properties of parent lithium cyclopentadienyl are those of a typical salt[22−24]. Like $[MeLi]_4$ (**1**), it is insoluble in hydrocarbons, has a high melting point and a low volatility. Developments in powder diffraction techniques[76, 77] just recently enabled the structure determination of $[CpLi]_\infty$[78] (**38**).

Many lithium organic structures can be rationalized as molecular fractions from polymeric lithium cyclopentadienyl (a in Figure 14): a single lithium atom and two rings give the smallest possible metallocene[79], the lithocene sandwich anion, (b), two solvated lithium atoms and a single ring give the inverted sandwich cation, (c), and solvated lithium plus ring in the ratio 1:1 give monomeric lithium cyclopentadienyl, (d). Less important to d-block organometallic chemistry, but nevertheless structurally interesting, are the lithium indenyl and fluorenyl derivatives as they supply an additionally potential η^6-coordination site. In dilithium structures with fused C_5 and C_6 rings this alternative is particularly interesting.

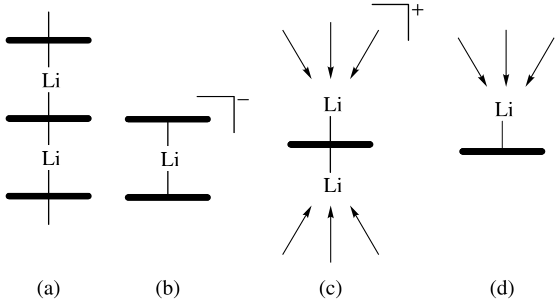

FIGURE 14. Fractions from the $[CpLi]_\infty$ polymer (a), a single lithium atom and two rings give the lithocene sandwich anion (b), two solvated lithium atoms and a single ring give the inverted sandwich cation (c) and solvated lithium plus ring in the ratio 1:1 give monomeric lithium cyclopentadienyl (d)

1. Polymeric lithium cyclopentadienyl derivatives

In polymeric $[\mathrm{CpLi}]_\infty$[78] (**38**), each metal is η^5-sandwiched by two ecliptically arranged Cp rings, hence a $[\mathrm{Cp_2Li}]^-$ section shows local D_{5h} symmetry at the lithium atom. The straight single CpLi rods are 'zipped' together as each Cp of one rod interlocks to the metal site of the neighboring strand (Figure 15). This dense packing is unique among the other polymeric Cp derivatives. Although they also feature infinite (η^5-Cp)$-$Li$-$(η^5-Cp) aggregation, the substituents at the C_5 skeleton prevent interlocking. In $[\mathrm{LiC_5H_4SiMe_3}]_\infty$[80] (**39**), an almost straight CpLi rod is formed (Cp$-$Li$-$Cp 175°) but the silyl groups shield the core in a helical fashion. As a consequence monosilylated Cp-lithium is much better soluble in hydrocarbons than **38**. As the substituents at the Cp ligand get larger, the Cp$-$Li$-$Cp angle more and more deviates from 180°. The menthyl groups in $[\mathrm{LiC_5H_4Men}]_\infty$[81] (**40**) are also helically arranged but require much more room causing a Cp$-$Li$-$Cp angle of 166° (Figure 15). To avoid that bending the even bulkier groups in

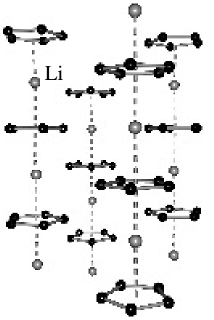

$[\mathrm{CpLi}]_\infty$

(38)

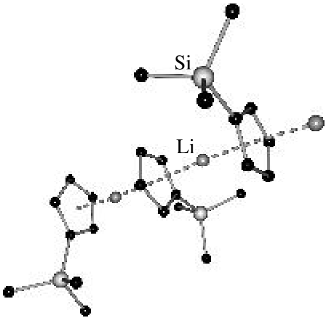

$[\mathrm{LiC_5H_4SiMe_3}]_\infty$

(39)

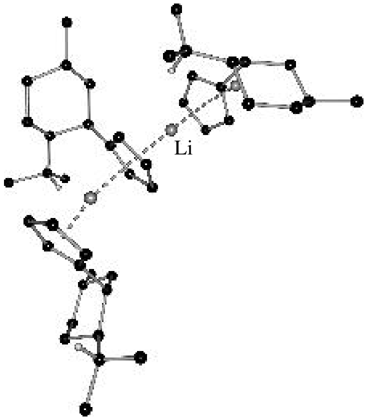

$[\mathrm{LiC_5H_4Men}]_\infty$

(40)

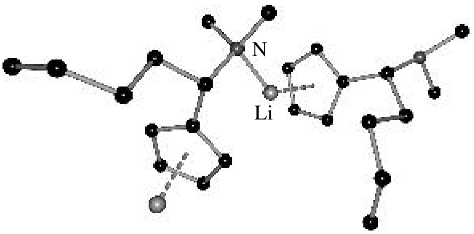

$[\mathrm{LiC_5H_4CH}(n\text{-Bu})\mathrm{NMe_2}]_\infty$

(42)

FIGURE 15. Solid-state structures of polymeric lithium cyclopentadienyl derivatives

$[LiC_5H_4SiMe_2Fl]_\infty$[82] (**41**) (Fl = fluorenyl, ($C_{13}H_9$)) are adjusted in a zigzag mode at both sides of the CpLi strand. In the $[Cp_2Li]^-$ section this causes local D_{5d} symmetry at the lithium atom as the Cp rings are forced in a staggered orientation. Ring substitution with Lewis-basic groups, like Me_2N capable of side-arm donation, can break the infinite CpLi strand as one Cp–Li interaction might be substituted by a N→Li donor bond. In polymeric $[LiC_5H_4CH\text{-}(n\text{-}Bu)NMe_2]_\infty$[83] (**42**), each lithium atom is only η^5-coordinated by a single Cp ligand, while the second coordination site is occupied by the side-arm amino nitrogen atom (Figure 15). Polymeric aggregation is accomplished via the side-arm. Similar structures show the polymers of $[LiC_5H_4CH(Ph)NMe_2]_\infty$[83] (**43**), $[LiC_5H_4CH(Tol)NMe_2]_\infty$[83] (**44**) and $[(THF)LiC_5H_4CH(C_2Me)NMe_2]_\infty$[83] (**45**). The structure of **44** exhibits two different lithium environments: an η^5/η^5- and an η^2/η^5-coordination. The propynyl substituent in **45** leaves enough room for the additional coordination of a donating THF molecule without changing the overall aggregation.

In the polymeric lithium cyclopentadienyl derivatives the Li–ring center distances cover the range of 185 to 201 pm (Table 7). These distances are predominantly determined by the charge concentration in the rings, at the lithium atoms and the steric demand and shielding of the substituents at the rings. The higher the charge in the ring, the smaller the Li–ring center distance is with a given fixed charge at the lithium atom. Obviously, this electrostatic attraction is counterbalanced by bulky ligands. The bigger they are, the more they prevent the metal from reaching the center of the ring. In the currently discussed compounds each lithium atom is coordinated by two Cp anions and each Cp by two lithium cations. Thus, in any compound with a non-one-to-one anion/cation relation, like the lithocene anion (Figure 14b) and the inverted sandwich cation (Figure 14c), one might expect longer average distances. Ecliptic D_{5h} or staggered D_{5d} arrangement of the rings has only marginal impact. As the ring–ring distance of about 400 pm is well above the layer distance in graphite of 335 pm, there is enough room for the ring to 'rotate' on the metal. Interestingly, the ecliptic distance of 197 pm in $[CpLi]_\infty$ (**38**) is still marginally longer than the staggered distance of 196 pm in heavily substituted $[LiC_5H_4SiMe_2Fl]_\infty$ (**41**). At first sight the Li–ring center distance gets simultaneously smaller with decreasing N→Li distances (i.e. rising efficiency of donor bonding) like in **43** via **42** to **44** (Table 7). In **45**, however, the lithium atom is donated by a nitrogen and an oxygen atom but the Li–ring center distance is only 201 pm. Presumably, the propynyl substituent in-plane to the Cp ring couples into the aromatic system and leaves it less attractive to the lithium atom.

TABLE 7. Polymeric lithium cyclopentadienyl derivatives

Compound		η^n $n=$	$Li\cdots C_n$ n(center)	Li–O, *N*	CCDC code	Reference
$[CpLi]_\infty$[a]	**38**	5	197		NIBSEW	78
$[LiC_5H_4SiMe_3]_\infty$	**39**	5	197		PAPYOU	80
$[LiC_5H_4Men]_\infty$[b]	**40**	5	201		NUPYEC	81
$[LiC_5H_4SiMe_2Fl]_\infty$[c]	**41**	5	196		UDIZUC	82
$[LiC_5H_4CH(n\text{-}Bu)NMe_2]_\infty$	**42**	5	192	*211*	BESQAR	83
$[LiC_5H_4CH(Ph)NMe_2]_\infty$	**43**	5/2	198/224	*241*	BESQUL	83
$[LiC_5H_4CH(Tol)NMe_2]_\infty$	**44**	5	185	*203*	BERHOV	83
$[(THF)LiC_5H_4CH(C_2Me)NMe_2]_\infty$	**45**	5	201	202, *218*	BEQWUP	83

[a] Cp = cyclopentadienyl (C_5H_5).
[b] Men = menthyl ($c\text{-}C_6H_9(Me)Pr\text{-}i$).
[c] Fl = fluorenyl ($C_{13}H_9$).

2. Molecular fractions of polymeric lithium cyclopentadienyl derivatives

$[(C_6D_6)Li_2(C_5Bn_5)_2]$[84] (**46**) is a cut from the polymeric CpLi rod made up from two subunits. Deaggregation is provided by the demanding substituents and η^2-coordination of a C_6D_6 solvent molecule (Figure 16). One lithium cation is sandwiched by the two perbenzylated Cp rings in an η^5-fashion. All ten benzyl groups are oriented *exo* relative to that metal. Hence, one C_5Bn_5 ligand offers lipophilicity and the other the basket for the second lithium atom. This basket in the contact ion pair (CIP) is closed by the η^2-coordinated deuteriobenzene molecule. The smallest possible metallocene, the lithocene anion $[Cp_2Li]^-$ [85] (**47**), crystallizes as a solvent-separated ion pair (SSIP) with $[Ph_4P]^+$ as the cation. Although the anisotropic displacement parameters indicate some disorder, local D_{5d} symmetry describes the anion best. The staggered conformation of both rings in $[(i\text{-dicp})_2Li]^-$ (**48**) (i-diCp = isodicyclopentadienyl, $C_{10}H_{11}$)[86] is induced by the *anti*-orientation of the bicycles to avoid steric strain (Figure 16). The cation in this SSIP is $[(12\text{-crown-}4)_2Li]^+$. The anion $[(t\text{-}BuC_5H_4)_2Li]^-$ [87] (**49**) in $[Me_2Ph_2P][(t\text{-}BuC_5H_4)_2Li]$ shows a ring-twist of just about 90° rather than 180° in the latter. The inverted sandwich complexes contain a single Cp ligand coordinated on both sides with a metal each (Figure 14c). Either they are cations or contain a second deprotonated center in the side-arm. The cation $[(TMEDA)_2Li_2C_5H_4Me]^+$ [88] (**50**) can be regarded to be the prototype of an inverted sandwich in a SSIP. The C_5 perimeter is η^5-coordinated above and below by a (TMEDA)Li unit. The same structural motif is present in $[(TMEDA)_2Li_2C_5H_4C(Me)_2PPh]$[89] (**51**), however the ligand is a dianion. In addition to the $C_5H_4R^-$ site there is the R_2P^- site. The side-arm contains a divalent P(III) center. The phosphorus atom donates to the upper lithium atom, indicated by the inclination of the TMEDA chelate away from the P atom (Figure 16). The P donation in **50** is substituted by an azaallyl η^3-coordination in $[(TMEDA)Li_4\{C_5H_4Si(Me)_2NC(Bu\text{-}t)CHSiMe_3\}_2]$[90] (**52**). Two lithium atoms are η^5/η^3-sandwiched, one is nitrogen di-coordinated and the fourth coordinates in a (TMEDA)Li unit on top of a η^5/η^3-sandwich to give the Li−Cp−Li motif. This inverted sandwich motif does not have to consist of two lithium metals. In [(PMDETA)LiCpTlCp][91] (**53**), the second metal is a thallium(I) atom (Figure 16). Both metals coordinate in the η^5-mode to one common Cp ligand. While the $Li{-}Cp_{(center)}{-}Tl$ angle is almost straight (176°), the $Cp_{(center)}{-}Tl{-}Cp_{(center)}$ angle indicates a bend at the thallium atom (153°). The latter is almost identical to that in the bis(cyclopentadienyl) thallate(I) anion $[Cp_2Tl]^-$ [91] (157°). In $[(PMDETA)LiCp_2Sn\{N(SiMe_3)_2\}]$[92] (**54**), a lithium and a tin(II) atom share a single Cp ring. The angle $Li{-}Cp_{(center)}{-}Sn$ of 163° indicates considerable bending at the common Cp ligand. $[(THF)_2Li_3\{(C_5Me)_4Si(Me)_2(o\text{-}C_2B_{10}H_{10})\}_2]^-$ [93] (**55**) is a remarkable example of an inverted triple-decker anion. The cation in the SSIP is $[(THF)_4Li]^+$. In the center of the anion a single lithium cation is sandwiched by two staggered $C_5Me_4R^-$ rings. They need to be staggered as the bulky substituents have to avoid steric interaction. On top and below that lithocene motif an additional lithium cation is η^5-coordinated to each ring. Furthermore, this is bonded to the deprotonated carbon atom of the *o*-carboranate in the side-arm and a THF donor molecule. The $Li{-}C_5{-}Li{-}C_5{-}Li$ core is almost linear (Figure 16).

On average, the $Li\cdots C_{5(center)}$ distances in the lithocene derivatives and the inverted sandwich complexes are marginally longer because two anions compete for one lithium cation or *vice versa*. As opposed to the polymeric lithium cyclopentadienyl derivatives, here the charge relation is 2:1. While the distance is an average 191 pm in $[(C_6D_6)Li_2(C_5Bn_5)_2]$ (**46**), a 1:1 fraction of polymeric CpLi matches the distances found in the polymers (see Tables 7 and 8). The related distances in $[Cp_2Li]^-$ (**47**) and $[(i\text{-diCp})_2Li]^-$ (**48**) are with 201 pm marginally longer than in $[CpLi]_\infty$[78] (**38**), with 197 pm. In the symmetrically inverted sandwich cation $[(TMEDA)_2Li_2C_5H_4Me]^+$ (**50**), the $Li\cdots C_{5(center)}$ distances are 200 pm. They can significantly be varied by other

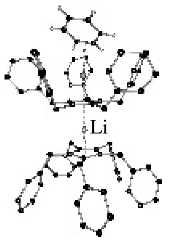

$[(C_6D_6)Li_2(C_5Bn_5)_2]$

(46)

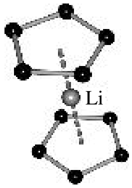

$[Cp_2Li]^-$

(47)

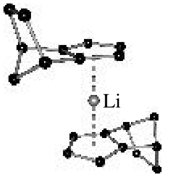

$[(i\text{-dicp})_2Li]^-$

(48)

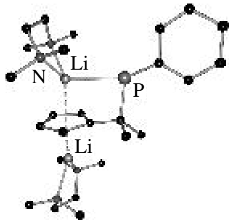

$[(TMEDA)_2Li_2C_5H_4C(Me)_2PPh]$

(51)

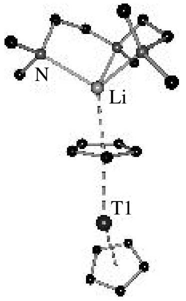

$[(PMDETA)LiCpTlCp]$

(53)

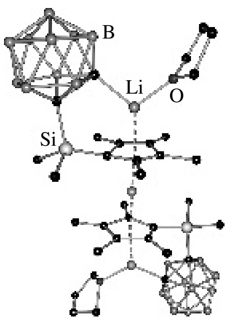

$[(THF)_2Li_3\{(C_5Me_4)Si(Me)_2\text{-}(o\text{-}C_2B_{10}H_{10})\}_2]^-$

(55)

FIGURE 16. Molecular fractions of polymeric lithium cyclopentadienyl derivatives in the solid-state. The cations of the lithocene anions **47** and **48** (Ph_4P^+ and $[(12\text{-crown-}4)_2Li]^+$, respectively) have been omitted for clarity. With **55** the cation is $[(THF)_4Li]^+$. All three are solvent-separated ion pairs.

TABLE 8. Molecular fractions of polymeric lithium cyclopentadienyl derivatives

Compound		η^n $n=$	Li···C_n n(center)	Li–O, N	CCDC code	Reference
$[(C_6D_6)Li_2(C_5Bn_5)_2]$	**46**	5/2	191/248		RAQWUB	84
Lithocenes						
$[Cp_2Li]^{-a}$	**47**	5	201		HESJIY	85
$[(i\text{-diCp})_2Li]^{-b}$	**48**	5	201		YEHTOU	86
$[(t\text{-BuC}_5H_4)_2Li]$-	**49**	5	199		RAZPOX	87
Inverted Sandwiches						
$[(TMEDA)_2Li_2C_5H_4Me]^+$	**50**	5	200	*209*	KANNAO	88
$[(TMEDA)_2Li_2C_5H_4C(Me)_2PPh]$	**51**	5	194/214	208/214	XALMAY	89
$[(TMEDA)Li_4\{C_5H_4Si(Me)_2NC(Bu\text{-}t)\text{-}CHSiMe_3\}_2]$	**52**	5/3	200/195	*210*	NECSAP	90
$[(PMDETA)LiCpTlCp]$	**53**	5	223	*223*	SUMSIC	91
$[(PMDETA)LiCp_2Sn\{N(SiMe_3)_2\}]$	**54**	5	225	*222*	PESVUE	92
$[(THF)_2Li_3\{(C_5Me_4)Si(Me)_2\text{-}(o\text{-}C_2B_{10}H_{10})\}_2]^-$	**55**	5/1	193/205	198	QOMCOK	93

[a] Cp = cyclopentadienyl (C_5H_5).

[b] i-diCp = isodicyclopentadienyl ($C_{10}H_{11}$).

donor atoms. In [(TMEDA)$_2$Li$_2$C$_5$H$_4$C(Me)$_2$PPh] (**51**), the two (TMEDA)Li$\cdots$ring center distances are 194 and 214 pm. The second is longer since the related lithium cation gets additional charge density from the phosphorus donor atom in the side-arm. Thus, the other lithium atom can get closer to receive more charge from the ring. This shift of the metal relative to a fixed Cp environment can be studied in the mixed metal species [(PMDETA)LiCpTlCp] (**53**) and [(PMDETA)LiCp$_2$Sn{N(SiMe$_3$)$_2$}] (**54**).

The long additional (PMDETA)Li$\cdots$Cp contact of average 224 pm causes the related Cp$\cdots$M contact to elongate (285 vs. 261 pm in **53** with $M = Tl$ and 283 vs. 257 pm in **54** with $M = Sn$). The inverse sandwiched ring can supply less charge density to the heavy p-block metal. It is interesting to note that the sum of all distances is constant. Elongation is compensated by shortening and *vice versa*. In [Cp$_2$Tl]$^-$ both ring center−Tl distances are 272 pm. Thus, the sum of 544 pm is almost identical to that in **53** (546 pm). The same phenomenon has been described in main group chemistry: either a sulfur[94] or a phosphorus[95] atom centrally bonded to three or four nitrogen atoms shows the same sum of S−N or P−N bond distances. Even this covalent bonding is dominated by electrostatics and not by hypervalent multiple bonding[96]. The flexible response of the ring center−Li distances to the charge density requirements is documented in the alternating distances in the inverted triple-decker anion **55**. A short distance of 193 pm at one side of the ring is always combined with a longer one of 205 pm at the other side, thus the sum is constantly 398 pm (Table 8). This matches almost perfectly the sum in the lithocenes [Cp$_2$Li]$^-$ (**47**) and [(*i*-diCp)$_2$Li]$^-$ (**48**) of 402 pm.

3. Monomeric lithium cyclopentadienyl derivatives

In most monomeric CpLi derivatives the metal is η^5-coordinated to the cyclopentadienyl ligand. The second hemisphere of the metal is shielded by donor-bases. The chelating amine TMEDA seems an excellent choice as it provides the appropriate bulk and donor capacity to break up the polymeric aggregation of CpLi discussed previously. As can be seen from the series [(TMEDA)LiC$_5$H$_4$Me][97] (**56**), [(TMEDA)LiC$_5$H$_4$(C$_3$H$_5$)][98] (**57**), [(TMEDA)LiC$_5$H$_3$(Bu-*t*)$_2$][99] (**58**), [(TMEDA)LiC$_5$H$_4$Men][81] (**59**) and [(TMEDA)Li (*i*-diCp)][86] (**60**), there is still enough room for increasingly bulky substituents at the C$_5$ perimeter. Sterically demanding substituents are located at the opposite side of the metal atom. In the menthyl substituent of **59** the methyl group is at the same side as the (TMEDA)Li group, while the larger *i*-Pr group is placed at the opposite side. The same is valid for the arrangement of the CH$_2$/(CH)$_2$ bridges in the isodicyclopentadienyl ligand of **60**. The first faces the metal and the sterically more demanding (CH)$_2$ bridge points away from the metal. This was already observed in the lithocene [(*i*-diCp)$_2$Li]$^-$ (**47**). The Lewis basicity of TMEDA is obviously high enough to supply adequate charge density: the lone-pair at the phosphorus(III) center in the side-arm of [(TMEDA)LiC$_5$H$_4$C(Me)$_2$PMe$_2$][98] (**61**) and [(TMEDA)LiC$_5$H$_4$C(Me)$_2$PPh$_2$][98] (**62**) is not donating to the metal but twisted to the other side of the ring to minimize steric interaction. However, the number of donating atoms to the lithium atom above the C$_5$ ring is not limited to two. In [(12-crown-4)LiCp][100] (**63**), all four oxygen atoms of the crown ether molecule in the upper hemisphere bind to the metal. Although not all four Li−O distances are equally long (214 to 243 pm) this clearly proves that coordination numbers of five (1 Cp and 4 O) are feasible (Figure 17). The crown can even be fixed as a side-arm in a Cp *ansa* cryptand fashion to the C$_5$ perimeter. In [LiC$_5$H$_4$(CH$_2$)$_2${*c*-N$_3$(C$_2$H$_4$)$_3$}(Pr-*i*)$_2$][101] (**64**), the triazacyclononanyl crown is fixed with a dimethylene *ansa* bridge to the Cp ring. This gives enough reach to locate the lithium atom coordinated to all three nitrogen atoms in an η^5-position above the Cp ring (Figure 17). In [LiC$_5$(Me)$_4$Si(Me)$_2${*c*-N$_3$(C$_2$H$_4$)$_3$}(Pr-*i*)$_2$][102] (**65**), the single dimethylsilyl *ansa* function is too short and the lithium atom can just

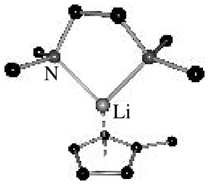

$[(TMEDA)LiC_5H_4Me]$

(56)

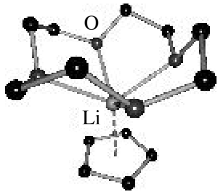

[(12-crown-4)LiCp]

(63)

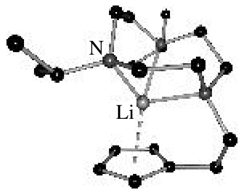

$[LiC_5H_4(CH_2)_2\{c\text{-}N_3(C_2H_4)_3\}\text{-}(Pr\text{-}i)_2]$

(64)

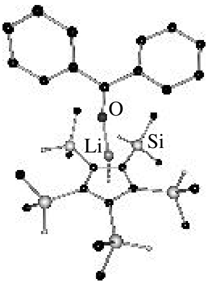

$[(Ph_2CO)LiC_5\{SiHMe_2\}_5]$

(71)

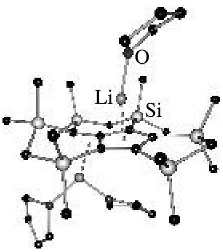

$[(THF)_3Li_2C_5\{C(SiMe_2)_6(CH_2)_3\}]$

(72)

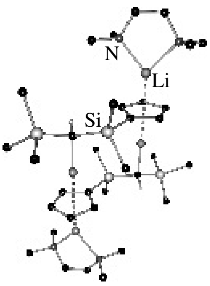

$[(TMEDA)Li_2C_5H_4Si(Me)_2\text{-}CHSiMe_3]_2$

(75)

FIGURE 17. Donor-base-coordinated monomeric lithium cyclopentadienyl derivatives in the solid-state

reach an η^2-position above a bond in the substituted Cp ring. It is interesting to note that the metal prefers the coordination to the nitrogen atoms of the cryptand rather than the η^5-position.

Silylation of the Cp ring provides much more solubility in hydrocarbons, both to the starting material of CpLi and to the organometallic targets. This permits synthetic access to metal complexes via homogeneous phase. The volatility of the silylated products is comparable to that of the hydrogen substituted. This feature makes them versatile starting materials in d-block chemistry[24, 103]. One Li···Cp ring center contact in polymeric $[LiC_5H_4SiMe_3]_\infty$[80] (**39**) is substituted by the donor base TMEDA in $[(TMEDA)LiC_5H_4SiMe_3]$[104] (**66**).

The higher the silylation degree of the ring gets, the smaller the donor-base can be. In the trisilylated C_5 perimeter in $[(THF)LiC_5H_2(SiMe_3)_3]$[105] (**67**) and $[(QUIN)LiC_5H_2(SiMe_3)_3]$[106] (**68**), even the single donor atom of THF or quinuclidine is sufficient to get monomeric lithium cyclopentadienyl derivatives. In $[(TMEDA)LiC_5H_2(SiMe_3)_3]$[106] (**69**), both nitrogen atoms of the chelating amine coordinate to the lithium, while in $[(PMDETA)LiC_5H_2(SiMe_3)_3]$[107] (**70**), only two nitrogen atoms of the tripodal triamine coordinate. Reduction of the trimethylsilyl group to the dimethylsilyl group enables pentasilylation of the C_5 perimeter. In $[(Ph_2CO)LiC_5\{SiHMe_2\}_5]$[108] (**71**), benzophenone is the donor-base (Figure 17, Table 9).

In dilithiated polycyclic $[(THF)_3Li_2C_5\{C(SiMe_2)_6(CH_2)_3\}]$[109] (**72**), one (THF)Li-group is η^5-coordinated to the central C_5 ring, while a second $(THF)_2$Li-group is η^3-coordinated

TABLE 9. Monomeric lithium cyclopentadienyl derivatives

Compound		η^n $n=$	Li···C_n n(center)	Li−O, N	CCDC code	Reference
$[(TMEDA)LiC_5H_4Me]$	**56**	5	192	*213*	SIJNII	97
$[(TMEDA)LiC_5H_4(C_3H_5)]$	**57**	5	194	*212*	QAKPIB	98
$[(TMEDA)LiC_5H_3(Bu\text{-}t)_2]$	**58**	5	195	*220*	GISCEQ	99
$[(TMEDA)LiC_5H_4Men]$[a]	**59**	5	191	*216*	NUPYIG	81
$[(TMEDA)Li(i\text{-diCp})]$[b]	**60**	5	191	*215*	YEHTIO	86
$[(TMEDA)LiC_5H_4C(Me)_2PMe_2]$	**61**	5	192	*214*	QAKPOH	98
$[(TMEDA)LiC_5H_4C(Me)_2PPh_2]$	**62**	5	192	*213*	QAKPEX	98
[(12-crown-4)LiCp][c]	**63**	5	206	226	VITKAK	100
$[LiC_5H_4(CH_2)_2\{c\text{-}N_3(C_2H_4)_3\}(Pr\text{-}i)_2]$	**64**	5	210	*217*	IBAXIS	101
$[LiC_5(Me)_4Si(Me)_2\{c\text{-}N_3(C_2H_4)_3\}(Pr\text{-}i)_2]$	**65**	2	220	*217*	VIQGAD	102
Lithium Derivatives of Silylated Cyclopentadienyl						
$[(TMEDA)LiC_5H_4SiMe_3]$	**66**	5	193	*213*	CEZTIK	104
$[(THF)LiC_5H_2(SiMe_3)_3]$	**67**	5	179	188	SEBHUC	105
$[(QUIN)LiC_5H_2(SiMe_3)_3]$[d]	**68**	5	178	*201*	DECPOQ	106
$[(TMEDA)LiC_5H_2(SiMe_3)_3]$	**69**	5	198	*219*	COJRUO10	106
$[(PMDETA)LiC_5H_2(SiMe_3)_3]$	**70**	5	198	*220*	COJROI	107
$[(Ph_2CO)LiC_5\{SiHMe_2\}_5]$	**71**	5	182	182	PAVMEE	108
$[(THF)_3Li_2C_5\{C(SiMe_2)_6(CH_2)_3\}]$	**72**	5/3	180/216	187/194[e]	GAKQIS	109
$[(TMEDA)LiC_5H_3(SiMe_2)]_2$	**73**	5/5	197	*220*	KIXMIN	110
$[(THF)_3Li_2\{C_5H(Pr\text{-}i)_2\}\{C_5H_2(Men)\}\text{-}(SiMe_2)_2]$[a]	**74**	5/5	177/195	188/201[e]	DAHQAE	111
$[(TMEDA)Li_2C_5H_4Si(Me)_2CHSiMe_3]_2$	**75**	5/1	194/208	196	NECRUI	90

[a] Men = menthyl ($c\text{-}C_6H_9(Me)Pr\text{-}i$).
[b] i-dicp = isodicyclopentadienyl ($C_{10}H_{11}$).
[c] Cp = cyclopentadienyl (C_5H_5).
[d] QUIN = quinuclidine ($N(CH_2)_6CH$).
[e] Distances of the THF mono-/di-coordination.

to the other side employing a ring C−C bond and an exocyclic formal C=C double bond (Figure 17). In the dilithiated compounds $[(TMEDA)LiC_5H_3(SiMe_2)]_2$[110] (**73**) and $[(THF)_3Li_2\{C_5H(Pr\text{-}i)_2\}\{C_5H_2(Men)\}(SiMe_2)_2]$[111] (**74**), both five-membered rings are η^5-coordinated. The dimeric dilithium complex $[(TMEDA)Li_2C_5H_4Si(Me)_2CHSiMe_3]_2$[90] (**75**) resembles the structural features of an inverted sandwich complex. While the silylated Cp ring is η^5-coordinated by a (TMEDA)Li unit on top, it is coordinated underneath by another lithium atom σ-bonded to a metalated carbon atom of the side-arm. The dimer is generated by a center of inversion (Figure 17).

4. Lithium indenyl derivatives

In the presented lithium indenyl (InLi) derivatives the donor-base-free or -coordinated lithium metal is always coordinated to the five-membered ring rather than to the six-membered. This demonstrates the preference of the metal for the smaller ring. The structure of polymeric $[InLi]_\infty$[112] (**76**) is reminiscent of that of polymeric $[CpLi]_\infty$[78] (**38**). Each metal is η^5-sandwiched by two ecliptically arranged indenyl rings. Interestingly, the fused benzene rings are located at the same side of the single InLi strand, although steric considerations may suggest a helical or zigzag arrangement of the anellated rings. The straight InLi strands are ‘zipped’ together as each In of one rod interlocks to the metal site of the neighboring rod (Figure 18). Ring substitution of the C_5 perimeter

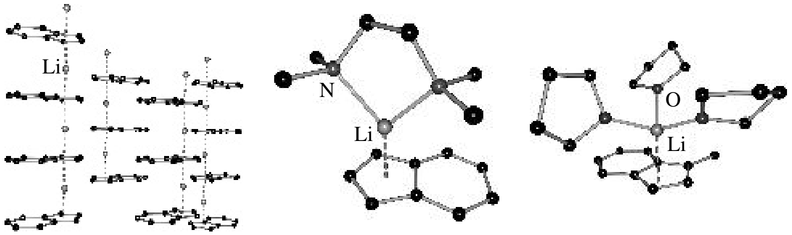

$[InLi]_\infty$ **(76)** $[(TMEDA)LiIn]$ **(78)** $[(THF)_3LiC_9H_6Me]$ **(79)**

FIGURE 18. Structures of lithium indenyl derivatives in the solid-state

like in $[LiC_9H_6N(Et)CH_2(C_3H_5)]_\infty$[113] (**77**) causes bending of the $C_{5(center)}\cdots Li\cdots C_{5(center)}$ angle at the lithium atom (167°) and helical arrangement of the substituents along the $[Li{-}C_5{-}Li{-}C_5]_\infty$ core.

Like in the cyclopentadienyl derivatives, addition of donor-bases facilitates deaggregation of the infinite solid-state structures. In monomeric $[(TMEDA)LiIn]$[114] (**78**), the (TMEDA)Li unit is η^5-coordinated to the five-membered ring while in $[(THF)_3LiC_9H_6Me]$[115] (**79**), the $(THF)_3Li$-fragment is only η^3-coordinated opposite to the 1-methylindenyl ring position (Figure 18). However, in 1-borylindenyl $[c\text{-}(MeNCH_2)_3LiC_9H_6B(NMe_2)_2]$[116] (**80**), η^5-coordination is achieved despite about the same substitution pattern.

On average, the $Li\cdots C_{5(center)}$ distances in the lithium indenyl derivatives are closer to the related distances in polymeric lithium cyclopentadienyl species than to those of monomeric CpLi molecules. Different to the Cp derivatives the negative charge is additionally delocalized in the fused benzene ring. This leaves the C_5 perimeter less attractive for the lithium cation. In donor-base-coordinated lithium indenyl monomers the $Li\cdots$ ring center distance gets longer compared to the polymers. A donor-base-coordinated lithium cation seems to be less polarizing and the charge density of the carbanions vanishes to the benzene ring (Table 10).

5. Dilithium organics with fused C_5 and C_6 perimeters

Dianions of anellated rings can either be generated by deprotonation of the hydrocarbons or by two-fold electron transfer[38]. Both five-membered rings in the pentalene dianion in $[(DME)_2Li_2(C_8H_6)]$[117] (**81**) are η^5-coordinated at both sides by the metal in

TABLE 10. Lithium indenyl derivatives

Compound		η^n $n=$	$Li\cdots C_n$ n(center)	Li–O, *N*	CCDC code	Reference
$[InLi]_\infty$[a]	**76**	5	198		XACROI	112
$[LiC_9H_6N(Et)CH_2(C_3H_5)]_\infty$	**77**	5	196		QAQZAJ	113
$[(TMEDA)LiIn]$[a]	**78**	5	200	*210*	INDYLI	114
$[(THF)_3LiC_9H_6Me]$	**79**	3	232	196	SUPYEH	115
$[c\text{-}(MeNCH_2)_3LiC_9H_6B(NMe_2)_2]$	**80**	5	195	*222*	GOSNIL	116

[a] In = indenyl (C_9H_7).

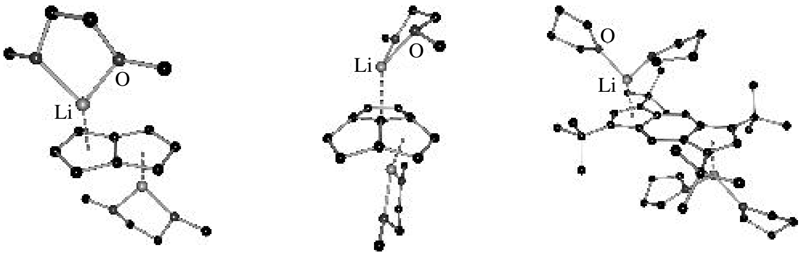

$[(DME)_2Li_2(C_8H_6)]$ **(81)**   1/2 $[(DME)_2Li_2(C_{10}H_6)]_2$ **(82)** $[(THF)_4Li_2\{C_{12}H_4(Bu\text{-}t)_4\}]$ **(83)**

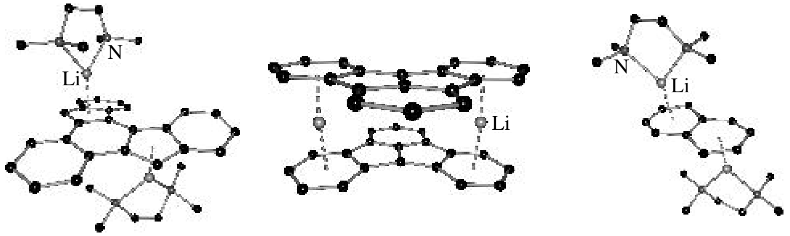

$[(TMEDA)_2Li_2(C_{24}H_{14})]$ **(85)** $[Li(C_{19}H_{11})]_2$ **(86)** $[(TMEDA)_2Li_2(C_{10}H_8)]$ **(87)**

FIGURE 19. Solid-state structures of dilithium organics with fused C_5 and C_6 perimeters

the (DME)Li moieties (Figure 19). Three fused five-membered rings in the acepentalene $C_{10}H_6$ give the smallest curved subunit of the smallest possible fullerene C_{20}. Because of the considerable strain the hydrocarbon $C_{10}H_6$ was predicted to be a triplet diradical in the ground state[118]. It can be stabilized by generating the closed-shell dianion. $[(DME)_2Li_2(C_{10}H_6)]_2$[119] (**82**) is a dimer consisting of two bowl-shaped $C_{10}H_6$ dianions facing each other with their convex site. Two (DME)Li units are connected by mutual μ_2-DME/Li coordination and sandwiched by the bottom of the bowls. The other two (DME)Li moieties are coordinated to the inside of the bowl. All lithium–ring contacts are η^5-coordinations. Thus, only four of the six present C_5 perimeters in the dimer are metal coordinated. Surprisingly, this induces no geometrical asymmetries in the $C_{10}H_6$ skeleton. The bonding parameters in the non-coordinated rings are virtually the same as the others. The three central C−C bonds are 140 pm long and of about the same length as the three (H)C−C(H) bonds (141 pm). The six C−C(H) bonds, however, are on average 5 pm longer (146 pm). The dilithium tribenzacepentalene, $[(DME)_3Li]_2[C_{22}H_{12}]$, forms an SSIP even in the solid-state with a layered structure. There is no Li−C contact between the dianions arranged in layers and the solvent encapsulated lithium cations in the adjacent layer[120]. This again supports the hypothesis deduced from the comparison of cyclopentadienyl and indenyl: fused aromatic rings deplete the charge density in the five-membered ring and leave it less attractive for the electropositive metal. In the CIP $[(DME)_2Li_2(C_{10}H_6)]_2$[119] (**82**), the bowl-shaped dianion is still attractive for the metal but in the tribenzacepentalene dianion in $[(DME)_3Li]_2[C_{22}H_{12}]$[120] the lithium cation prefers additional solvent coordination.

The dianions in $[(THF)_4Li_2\{C_{12}H_4(Bu\text{-}t)_4\}]$[121] (**83**), $[(Et_2O)_4Li_2\{C_{12}H_4(Bu\text{-}t)_4\}]$[121] (**84**), $[(TMEDA)_2Li_2(C_{24}H_{14})]$[122] (**85**) and $[Li(C_{19}H_{11})]_2$[123] (**86**) offer a potential η^6- next to the η^5-coordination site. Amazingly, both **83** and **84** crystallize in the same asymmetric unit. Both the two $(THF)_2Li$- and the two $(Et_2O)_2Li$ units coordinate η^5 to both five-membered rings of the same dianion. They emulate the coordination mode of the pentalene dianion in **81**, solemnly with an inserted six-membered ring in the common edge of the latter. In $[(TMEDA)_2Li_2(C_{24}H_{14})]$ (**85**), the two $(TMEDA)_2Li$ moieties picked the two five-membered rings and leave none of the four C_6 perimeters coordinated. In $[Li(C_{19}H_{11})]_2$ (**86**), however, both lithium cations are sandwiched between the six-membered rings (Figure 19). Apparently, the two anellated C_5 perimeters are too close to accommodate two metals at the same side of the dianion. To gain some space and to reduce electrostatic repulsion the cations are shifted to the C_6 rings towards the periphery. There is still a considerable ring center–Li–ring center bent to the outside. $[(TMEDA)_2Li_2(C_{10}H_8)]$[124] (**87**) is a fundamental structure as it reveals that the addition of two electrons to an otherwise planar aromatic hydrocarbon like naphthalene causes severe puckering of the anion, although that would not cause the metal to leave the η^6-coordination site. Obviously there is no charge accumulation involved that distinguishes one site from the others.

The $Li \cdots C_{5(\text{center})}$ distances in the dilithium organics with fused C_5 and C_6 perimeters in the dianions of **81** to **85** match those already discussed in this chapter. The found 189 pm in $[(DME)_2Li_2(C_8H_6)]$ (**81**), are shorter than the distances in $[(DME)_2Li_2(C_{10}H_6)]_2$ (**82**), of 199 and 204 pm, respectively. This is mainly because of the curve shape of the latter anion. In the planar pentalenediide both (DME)Li units got free access to both sides. In the curved acepentanlenediide even the access to the inside of the bowl is more shielded and the distance is elongated by 10 pm (Table 11). The approach to the bottom of the bowl is even more difficult because of the dimeric $(DME)_2Li_2$ moiety. **83** and **84** allow the direct comparison of a $(THF)_2Li$ and a $(Et_2O)_2Li$ moiety in contact with the same anion in the same crystal. The higher polarity of THF (1.75 μ[D]) relative to Et_2O (1.15 μ[D]) causes shorter Li–O distances (197 and 205 pm, respectively; Table 11) and longer Li–ring center distances. Apparently, the less polar diethyl ether provides more charge density to the metal because the ring contact to the cation seems to be less important. However, steric considerations might play an important role. The Li–ring distances in the η^6-coordination of $[Li(C_{19}H_{11})]_2$ (**86**) and $[(TMEDA)_2Li_2(C_{10}H_8)]$ (**87**) are in the range of the already discussed metal–η^5-distances. Although the move from η^5 to η^3 causes an average elongation of 35 pm (see **72** in Table 9 and **79** in Table 10), the shift from η^5 to η^6 does not lead to significant changes.

6. Lithium fluorenyl derivatives

The structure of dimeric donor-base-free lithium fluorenyl $[FlLi]_2$[125] (**88**) is reminiscent of $[Li(C_{19}H_{11})]_2$[123] (**86**), because in both structures the two present lithium cations are

TABLE 11. Dilithium organics with fused C_5 and C_6 perimeters in the dianion

Compound		η^n $n=$	$Li \cdots C_n$ n(center)	Li–O, *N*	CCDC code	Reference
$[(DME)_2Li_2(C_8H_6)]$	**81**	5	189	201	DANPOX	117
$[(DME)_2Li_2(C_{10}H_6)]_2$	**82**	5	199/204	203/212	WABPEV	119
$[(THF)_4Li_2\{C_{12}H_4(Bu\text{-}t)_4\}]$	**83**	5	195	197	NEXMAE	121
$[(Et_2O)_4Li_2\{C_{12}H_4(Bu\text{-}t)_4\}]$	**84**	5	200	205	NEXMAE	121
$[(TMEDA)_2Li_2(C_{24}H_{14})]$	**85**	5	199	*212*	KIZPUE	122
$[Li(C_{19}H_{11})]_2$	**86**	6	195		INFLLI10	123
$[(TMEDA)_2Li_2(C_{10}H_8)]$	**87**	6	197	*211*	NAPLIM	124

sandwiched between the six-membered rings. Both $C_{6(center)}-Li-C_{6(center)}$ angles of 174° in the first and 175° in the latter indicate that the metal atoms are marginally displaced to the outside of the anion. The different Li···Li distances of 586 pm in **86** and 435 pm in **88** do not cause different angles at the lithium atoms (see Figures 19 and 20). In dilithium difluorenyl $[(TMEDA)_2Li_2(diFl)]$[126] (**89**), the two best planes of the $C_{13}H_8$ units, connected in the 9-position, intersect at an angle of 51.4° and both (TMEDA)Li units bridge the central C−C bond. In the polymeric structure of $[(THF)Li_2(C_{13}H_8)]_\infty$[127] (**90**), a μ-bridging oxygen atom of the donor-base THF and the deprotonated 9-carbon atoms of the fluorenyl dianion form a kite-shaped Li_2CO four-membered ring with the THF and the fluorenyl almost orthogonal to that ring. Those arrays are alternately turned by 180° in the Li_2CO ring plane and stacked to infinite sheets with coplanar fluorenyl substituents and THF molecules. In addition to the C9 and O contact each lithium atom is η^3-coordinated by the fluorenyl involving C9 (Figure 20). In the polymeric diethyl ether solvate $[(Et_2O)LiFl]_\infty$[128] (**91**), this η^3-coordination is replaced by μ-η^1/η^1-bonding of C9. This carbon atom is coordinated by a lithium atom at each side. Each three-fold coordinated metal binds two C9-atoms and a single diethyl ether molecule. Thus, the planes of the fluorenyl anions intersect at an angle of about 120°. Further addition of diethyl ether to that polymeric structure yields molecular monomers in $[(Et_2O)_2LiFl]$[129] (**92**). Again, the lithium atom is three-fold coordinated by a fluorenyl carbanion in the η^2-bonding mode and two diethyl ether molecules. Two molecules of the donor-base quinuclidine shift the lithium atom in the monomer $[(QUIN)_2LiFl]$[130] (**93**) to the η^1/C9-position. Similar to the lithium cyclopentadienyl derivatives, an intramolecular donor-base function can be integrated in a side-arm in the 9-position. In the structural analogs $[(Et_2O)LiC_{13}H_8(CH_2)_2NMe_2]$[131] (**94**)

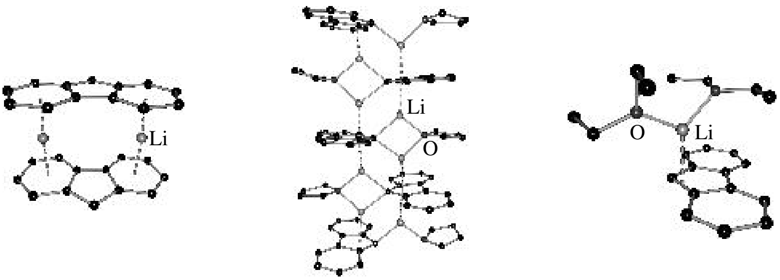

$[FlLi]_2$ **(88)** $[(THF)Li_2(C_{13}H_8)]_\infty$ **(90)** $[(Et_2O)_2LiFl]$ **(92)**

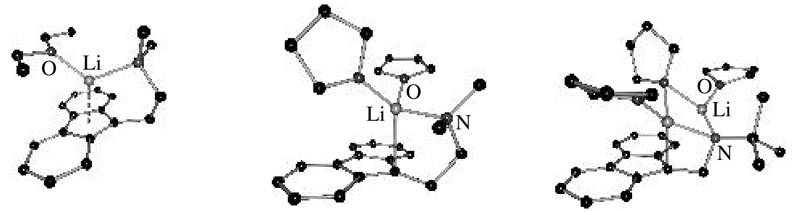

$[(Et_2O)LiC_{13}H_8(CH_2)_2NMe_2]$ **(94)** $[(THF)_2LiC_{13}H_8(CH_2)_2NMe_2]$ **(95)** $[(THF)_3Li_2C_{13}H_8(CH_2)NBu\text{-}t]$ **(98)**

FIGURE 20. Solid-state structures of lithium fluorenyl derivatives

and $[(\mathrm{THF})_2\mathrm{LiC}_{13}\mathrm{H}_8(\mathrm{CH}_2)_2\mathrm{NMe}_2]$[131] (**95**), a dimethylene(dimethylamino) side-arm coordinates the lithium atom via the nitrogen atom. In addition, one diethyl ether molecule and two THF molecules are coordinated to the lithium atom in the first and in the latter. While the three-fold coordinated lithium atom in **94** needs full charge density supply of the five-membered ring in the η^5-position, the donation of two THF molecules in **95** facilitates ring slippage to the η^1/C9-position. The same ring slippage is observed by keeping the donor solvent constant but varying the substituents at the side-arm donor atom.

The otherwise identical complexes $[(\mathrm{THF})\mathrm{LiC}_{13}\mathrm{H}_8(\mathrm{CH}_2)\mathrm{Si}(\mathrm{Me})_2\mathrm{NHPr}\text{-}i]$[132] (**96**) and $[(\mathrm{THF})\mathrm{LiC}_{13}\mathrm{H}_8(\mathrm{CH}_2)\mathrm{Si}(\mathrm{Me})_2\mathrm{NHBu}\text{-}t]$[133] (**97**) just vary in the substituents at the N donor atom. The less electron-releasing *i*-Pr group causes full η^5-coordination and the more electron-releasing *t*-Bu substituent allows relaxation of the side-arm and ring slippage to the η^3-position. The side-arm in the dimetalated compound $[(\mathrm{THF})_3\mathrm{Li}_2\mathrm{C}_{13}\mathrm{H}_8(\mathrm{CH}_2)\mathrm{NBu}\text{-}t]$[128] (**98**) is too short to promote η^5-bonding (Table 12). Both lithium atoms are bridged by the amido N-atom but only one is η^1-coordinated to the fluorenyl carbon atom C9. The metals are terminally donated by a THF molecule each and μ-bridged by a common THF donor-base (Figure 20). The single lithium atom in the $[(\mathrm{THF})\mathrm{Li}(\mathrm{C}_{13}\mathrm{H}_8\mathrm{BNMe}_2)_2]^-$-anion[134] (**99**) is sandwiched in an *ansa*-fluorenyl fashion. The *ansa*-connection of the two fluorenyl carbanions is provided by the diboranyl bridge and the metal is bis-η^1-coordinated by the two C9 carbon atoms. A single THF molecule completes the planar three-fold coordination.

The average lithium–ring center distance in the fluorenyl derivatives is at the long end of the range already discussed. The mutual η^6-coordination in dimeric $[\mathrm{FlLi}]_2$ (**88**) gives the shortest distance of the presented compounds (199 pm). The η^5-coordination results in longer distances of about 216–217 pm in **94** and **96**. The η^1-metal contact to the carbon atom in the 9-position gives the longest distances of 231 pm on average (221 pm in **99** to 239 pm in **95**). The ring slippage from the η^5-position to the η^3-coordination in **94** and **95**, respectively, results in an elongation by 22 pm from 217 pm in the first to 239 in the latter. The move from η^5 to η^3 causes an elongation of just 3 pm in **97** as compared

TABLE 12. Lithium fluorenyl derivatives

Compound		η^n $n=$	Li···C_n n(center)	Li–O, *N*	CCDC code	Reference
$[\mathrm{FlLi}]_2$[a]	**88**	6	199		GITNEC	125
Donor-base-coordinated Lithium Fluorenyl Derivatives						
$[(\mathrm{TMEDA})_2\mathrm{Li}_2(\mathrm{diFl})]$[b]	**89**	μ_2/η^2	229	*207*	BFLULI	126
$[(\mathrm{THF})\mathrm{Li}_2(\mathrm{C}_{13}\mathrm{H}_8)]_\infty$[a]	**90**	3/1	214/217	202	VACHIR	127
$[(\mathrm{Et}_2\mathrm{O})\mathrm{LiFl}]_\infty$[a]	**91**	1	225	194	NUWDEO	128
$[(\mathrm{Et}_2\mathrm{O})_2\mathrm{LiFl}]$[a]	**92**	2	217	190	SANNUQ	129
$[(\mathrm{QUIN})_2\mathrm{LiFl}]$[a,c]	**93**	1	233	*203*	FULIAO10	130
Side-arm-coordinated Lithium Fluorenyl Derivatives						
$[(\mathrm{Et}_2\mathrm{O})\mathrm{LiC}_{13}\mathrm{H}_8(\mathrm{CH}_2)_2\mathrm{NMe}_2]$	**94**	5	217	189/*208*	RAWYET	131
$[(\mathrm{THF})_2\mathrm{LiC}_{13}\mathrm{H}_8(\mathrm{CH}_2)_2\mathrm{NMe}_2]$	**95**	1	239	193/*206*	RAWYIX	131
$[(\mathrm{THF})\mathrm{LiC}_{13}\mathrm{H}_8(\mathrm{CH}_2)\mathrm{Si}(\mathrm{Me})_2\mathrm{NHPr}\text{-}i]$	**96**	5	216	189/*215*	NONQUC	132
$[(\mathrm{THF})\mathrm{LiC}_{13}\mathrm{H}_8(\mathrm{CH}_2)\mathrm{Si}(\mathrm{Me})_2\mathrm{NHBu}\text{-}t]$	**97**	3	219	185/*216*	ZUTJED	133
$[(\mathrm{THF})_3\mathrm{Li}_2\mathrm{C}_{13}\mathrm{H}_8(\mathrm{CH}_2)\mathrm{NBu}\text{-}t]$	**98**	1	237	192/206[d]	NUWDIS	128
$[(\mathrm{THF})\mathrm{Li}(\mathrm{C}_{13}\mathrm{H}_8\mathrm{BNMe}_2)_2]^-$	**99**	1	221	183	YELDAU	134

[a] Fl = fluorenyl ($\mathrm{C}_{13}\mathrm{H}_9$).

[b] diFl = difluorenyl ($\mathrm{C}_{26}\mathrm{H}_{16}$).

[c] QUIN = quinuclidine ($\mathrm{N}(\mathrm{CH}_2)_6\mathrm{CH}$).

[d] Terminal/μ_2-THF.

to **96**. However, the polymeric structure of $[(THF)Li_2(C_{13}H_8)]_\infty$ (**90**) is a convincing example that the coordination mode is not necessarily correlated to the distance: the η^3-coordination in **90** gives rise to a distance of 214 pm, thus even shorter than in the related η^5-bonding modes in this class of compounds. The two Li−C9 σ-bonds of average 217 pm are comparably short (Table 12). This is even more remarkable, as one has to consider that a single fluorenyl dianion in **90** is coordinated by four lithium cations. This competitive 2:1 ratio of charges normally results in longer distances.

C. C_6 and C_7 Perimeter

In the lithium aryls two of the already introduced structure building principles are combined: (i) the haptotropic η^6-coordination of the lithium cation to the π charge density of the aromatic carbanion and (ii) the Li_2C_2 four-membered ring discussed with donor-base-induced dimer formation. On addition of donor bases or implementation of donating side-arms it is the π-bonding that is given up first. It is the predetermined breaking point of the infinite solid-state structure if molecular fractions are cut out in the deaggregation process. The structure of donor-base-free phenyllithium $[PhLi]_\infty$[135] (**100**) recently determined by Rietveld refinement from high-resolution synchrotron X-ray powder data shows both bonding principles in a most lucid way (Figure 21). Two metalated *ipso*-carbon atoms of the phenyl groups form together with the lithium atoms a Li_2C_2 four-membered ring. Both planes of the C_6 perimeters are perpendicular to that ring (90.1°), thus none of the lithium atoms is in the plane of the carbanion. Those σ-bonded $[PhLi]_2$ dimers are π-stacked to give access to the C_6 perimeter of the adjacent

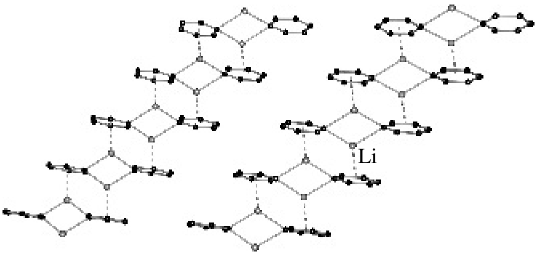

$[PhLi]_\infty$

(100)

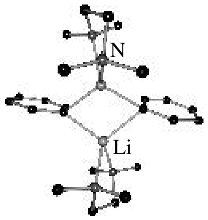

$[(TMEDA)LiPh]_2$

(25)

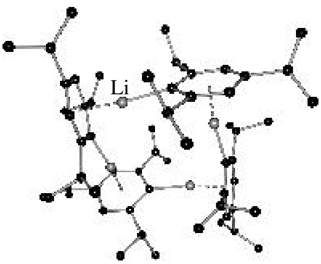

$[LiTip]_4$

(101)

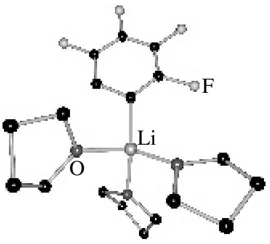

$[(THF)_3LiC_6HF_4]$

(105)

FIGURE 21. Solid-state structures of lithium phenyl derivatives

dimer to each lithium atom. The resulting infinite $[PhLi]_{2,\infty}$ bands of dimers are aligned along the crystallographic *b*-axis. In the TMEDA solvate $[(TMEDA)LiPh]_2$[59] (**25**), the Li_2C_2 four-membered ring from the polymeric structure in **100** is retained, while the π-bonding is substituted by (*N*,*N*)-chelation (Figure 21). Although the out-of-plane σ-bonding within a Li_2C_2 four-membered ring is common with lithium aryls, there are examples of in-plane σ-bonding like in the tetramer $[LiTip]_4$[136] (**101**) (Tip = 2,4,6-tri-*i*-propylphenyl). Each Li−C bond points towards the ring center of the next perpendicular molecule. Four moieties arrange in a circle. The steric bulk of the Tip substituent cannot serve as a reason why the Li_2C_2 four-membered ring is not built in **101** because it is found in the diethyl ether solvate $[(Et_2O)LiTip]_2$[137] (**102**). The steric strain is only liable for the three-fold coordination of the lithium atoms. The *o*-*i*-Pr groups shield the lithium atoms sufficiently and there is room for just one single Et_2O molecule coordinated to each metal. Steric reduction of the *ortho*-substituents like in $[(THF)_2LiMes]_2$[138] (**103**) (Mes = 2,4,6-trimethylphenyl) provides access for a second donor-base molecule. Structures of supermesityllithium are only known from co-crystallizing with other products.

In $[(LiMes^*)(LiPHMes^*)]_2$ (Mes* = 2, 4, 6-tri-*t*-butylphenyl)[139] (**104**), the structure formation principle of $[LiTip]_4$ (**101**) is present: the Li−C bond points towards the phosphorus atom of the adjacent phosphanide anion. The second lithium atom at the phosphorus atom is η^6-coordinated by the C_6 perimeter of the LiMes*. In light of this aggregation principle the synthesis, isolation and structural characterization of the monomer $[(THF)_3LiC_6HF_4]$[140] (**105**) is even more remarkable, because it is both kinetically and thermodynamically unstable. THF solvated monomers of lithium organics are particularly thermally unstable and have very low melting points. Furthermore, fluorinated lithium organics tend to be explosive as the formation of lithium fluoride is the thermodynamically favorite reaction path. In the structure of $[(THF)_3LiC_6HF_4]$ (**105**), the lithium atom is almost perfectly located in the plane of the C_6 perimeter but not exactly at the C−C−C bisection. It is slightly displaced towards the hydrogen rather than towards the fluorine atom (Figure 21). In the non-conjugated benzene dianion in $[(THF)_2Li_2C_6(SiMe_3)_6]$[141] (**106**), the C_6 perimeter is bent considerably along a transannular C···C vector and the two (THF)Li units are η^4-coordinated to the same side. In $[(DME)Li_2C_6H_2(SiMe_3)_4]$[142] (**107**), the ring is puckered and the two (DME)Li moieties are η^6-coordinated to both sides of the ring. Although the 8π electron rings in **106** and **107** have to be regarded as antiaromatic and heavily substituted, they are very attractive to the lithium cations. The (donor-base)Li···C(η^n) center distances of 184 pm in the former and 188 pm in the latter are remarkably short.

1. Lithium terphenyl derivatives

In terphenyl substituents both *ortho*-positions of a phenyl ring are substituted by aryl groups and provide excellent shielding of the ring *ipso*-position. Lithium terphenyl derivatives recently came to the focus of research[143] as they facilitate the synthesis of molecules with elements in either unusual oxidation states or bonding modes[144]. The spherical dimer $[LiC_6H_3Mes_2]_2$[136] (**108**) consists of two moieties organized like the two units of a tennis ball separated by the rubber imprint. The two lithium atoms of the Li_2C_2 four-membered ring form the metal core of the sphere (Figure 22). If a tennis ball is cut along the imprint, the two units are pulled apart from each other, one is turned relative to the other by 90°, shifted aside and put together again, one gets the structure of $[LiC_6H_3Dip_2]_2$[145] (**109**) (Dip = 2,6-di-*i*-propylphenyl). The σ-bonded lithium cations are located in the plane of the central phenyl ring and in addition η^6-coordinated by one Dip substituent of the second molecule. This last π-coordination can even be passed over to a benzene molecule. If the Dip substituents are replaced by Tip groups the ligand reaches even further out. The ends

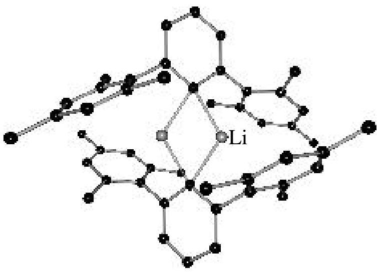

$[LiC_6H_3Mes_2]_2$

(108)

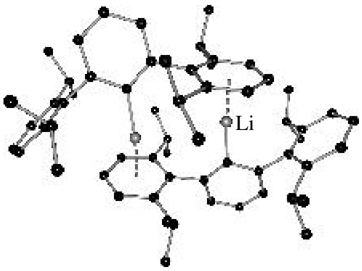

$[LiC_6H_3Dip_2]_2$

(109)

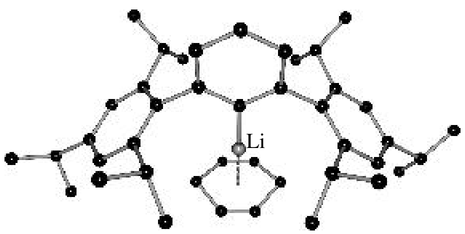

$[(C_6H_6)LiC_6H_3Tip_2]$

(110)

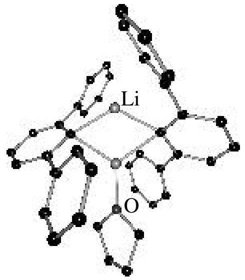

$[(THF)(LiC_6H_3Ph_2)_2]$

(111)

FIGURE 22. Solid-state structures of lithium terphenyl derivatives

of the single tennis ball unit are elongated by another p-i-Pr group. Now even the smaller benzene molecule can serve as a cap to the σ-bonded metal in $[(C_6H_6)LiC_6H_3Tip_2]^{145}$ (**110**). If the substituents at the terphenyl ligand are not so bulky and allow almost in-plane orientation relative to the central phenyl group, the tennis ball units around the Li_2 core get more slim and let a polar donor-base molecule slip in to coordinate the core. In $[(THF)(LiC_6H_3Ph_2)_2]^{146}$ (**111**), a single THF molecule is coordinated to just one lithium atom of the dinuclear metal core (Figure 22). In $[(Et_2O)LiC_6H_3Tip_2]^{147}$ (**112**), the i-Pr substituents at the peripheral phenyl groups force them to align almost orthogonal relative to the central ring plane. The π-coordination of the benzene molecule in **110** is now substituted by a single diethyl ether molecule. As the terphenyl ligand gets smaller in $[(Et_2O)_2LiC_6H_3Ph_2]^{148}$ (**113**), the wider coordination site can accommodate two diethyl ether molecules. Substitution of the central ring in the 4-position additionally to the 2- and 6-position like in $[(Et_2O)_2LiC_6H_2Ph_3]^{149}$ (**114**) does not change this motif. Exclusive substitution of the peripheral rings in the 4-position, even with potentially donating methoxy side-arms, does not cause changes either: the lithium atom in $[(Et_2O)_2LiC_6H_3(C_6H_4OMe)_2]^{150}$ (**115**) is bonded to the *ipso*-carbon atom of the central ring and to two diethyl ether molecules. Even naphthyl substituents in the 2- and 6-position of the central phenyl ring in $[(THF)_2LiC_6H_3Naph_2]^{146}$ (**116**) leave a groove big enough to slot in two THF molecules coordinated to the lithium cation.

The average Li−C(σ) bond lengths in the lithium aryls span a range of 26 pm (202 to 228 pm) but the $Li\cdots C(\eta^6)$ distances cover 42 pm (183 to 225 pm, Table 13).

TABLE 13. Lithium phenyl derivatives

Compound		η^n $n=$	Li–C η^6/σ	Li–O, N	Li···Li	CCDC code	Reference
$[PhLi]_\infty$	**100**	6/1	225/228		239	PUDLUV	135
$[LiTip]_4$[a]	**101**	6/1	186/212			LEFSEU	136
$[(Et_2O)LiTip]_2$[a]	**102**	1	223	193	242	GABHIA	137
$[(THF)_2LiMes]_2$[b]	**103**	1	228	204	249	GAFCAR	138
$[(LiMes^*)(LiPHMes^*)]_2$[c]	**104**	6/1	183/209	*247(P)*		VULPUN	139
$[(THF)_3LiC_6HF_4]$	**105**	1	214	196		ZELDUP	140
$[(THF)_2Li_2C_6(SiMe_3)_6]$	**106**	4	184	199		KINFUI	141
$[(DME)Li_2C_6H_2(SiMe_3)_4]$	**107**	6	188	199		KODBOU	142
Lithium Terphenyl Derivatives							
$[LiC_6H_3Mes_2]_2$[b]	**108**	1	216		227	LEFSIY	136
$[LiC_6H_3Dip_2]_2$[d]	**109**	6/1	201/207			TOPSUM	145
$[(C_6H_6)LiC_6H_3Tip_2]$[a]	**110**	6/1	194/203			TOPSOG	145
$[(THF)(LiC_6H_3Ph_2)_2]$	**111**	1	212/223[f]	186	228	XELSIQ	146
$[(Et_2O)LiC_6H_3Tip_2]$[a]	**112**	1	202	185		ZUJVOP	147
$[(Et_2O)_2LiC_6H_3Ph_2]$	**113**	1	211	194		HOPTUB	148
$[(Et_2O)_2LiC_6H_2Ph_3]$	**114**	1	208	196		KIYSIU	149
$[(Et_2O)_2LiC_6H_3(C_6H_4OMe)_2]$	**115**	1	213	195		QASKUQ	150
$[(THF)_2LiC_6H_3Naph_2]$[e]	**116**	1	208	190		XELSOW	146

[a] Tip = 2,4,6-tri-*i*-propylphenyl, $C_6H_2(Pr\text{-}i)_3$.
[b] Mes = 2,4,6-trimethylphenyl, $C_6H_2Me_3$.
[c] Mes* = 2,4,6-tri-*t*-butylphenyl, $C_6H_2(Bu\text{-}t)_3$.
[d] Dip = 2,6-di-*i*-propylphenyl, $C_6H_3(Pr\text{-}i)_2$.
[e] Naph = naphthyl, $C_{10}H_7$.
[f] Di/tricoordinated lithium–C(σ) bonds.

This already indicates that the latter are more easily influenced by marginal changes in the metal coordination. Obviously, the weak interactions respond first to solid-state structural variations and can be fine-tuned to electronic requirements. It is important to recognize that Li···C(η^n) interaction like any other bonding force is an infinite *continuum* without a determined limit. The frontiers are open and η^n-coordination naturally is a point of constant debate[23]. They may be regarded as important to organometallic chemistry as the hydrogen bond to life science. In polymeric $[PhLi]_\infty$[135] (**100**), the Li–C(σ) bond distances of 224 and 232 pm are in the same region as the Li···C_6 ring center distances (average 228 pm) indicating their mutual importance. Within every dimer there are four Li–C bonds and to every dimer four Li···C_6 ring interactions, respectively. Both distances get considerably shorter in $[LiTip]_4$[136] (**101**), because each lithium cation contacts only two carbanions as opposed to three in the latter example (Table 13). The close Li···C_6 ring center contact of 186 pm in **101** and the even closer one in $[(LiMes^*)(LiPHMes^*)]_2$[139] (**104**) (183 pm) is a strong argument against the tired out 'steric hindrance reasoning'. The two most heavily substituted phenyl rings provide the shortest Li···C_6 ring center distances, while their Li–C(σ) bonds are of common length. On average, the Li–C(σ) bond length of an *ipso*-aryl carbon atom to a single lithium atom in the ring plane is 209 pm. In a Li_2C_2 four-membered ring they are on average 13 pm longer. The σ-bond density needs to be shared between two metals in a four-membered ring. In most structures of lithium aryls with a Li_2C_2 four-membered ring the Li–C bonds are not equally long. In $[(TMEDA)LiPh]_2$ (**25**), they differ by 7 pm (221 vs. 228 pm), 8 pm (224 vs. 232 pm) in $[PhLi]_\infty$ (**100**), 5 pm (220 vs. 225 pm) in $[(Et_2O)LiTip]_2$ (**102**) and by 11 pm (212 vs. 223 pm) in $[(THF)(LiC_6H_3Ph_2)_2]$ (**111**). Additionally, the two C_6 planes are not located at the bisection of the Li–C–Li angle but lean simultaneously against each lithium cation. This causes one lithium to be located closer to the best plane of the carbanion, while the second is further off (77 out-of-plane vs. 164 pm in **25**, 102 vs. 137 pm in **100**, 40 vs. 185 pm in **102** and 21 vs. 153 pm in **111**). The shorter bond is always found towards the more in-plane lithium atom, while the longer involves the out-of-plane lithium cation. The first participates more in the directed sp^2 charge density of the *ipso*-carbon atom, while the second more in the diffuse π-ring charge density at the metalated carbon atom. However, on average the Li–C bonds in the Li_2C_2 four-membered rings are shorter than in the tetramers and longer than in the monomers (e.g. 232 pm in $[Et_2OLiPh]_4$ (**19**), 226 pm in $[(TMEDA)LiPh]_2$ (**25**) and 214 pm in [(PMDETA)LiPh] (**28**)). This is commonly explained by a 4c2e bond in the tetramers, a 3c2e bond in the dimers and a 2c2e bond in the monomers[135].

2. Side-arm coordination in lithium aryls

The merely shielding function or weak η^6-coordination of the peripheral aryl groups in the terphenyls can be replaced by Lewis-basic heteroatoms in side-arms bonded in one or both *ortho*-positions to the lithiated benzene ring. If the donor atom is attractive to the metal and in the right proximity, this usually generates single or dual side-arm coordinated lithium organics. In the first there is still room for donor solvent coordination but in the second class there is hardly any solvent required to give soluble molecules. In both cases the dimer with a central Li_2C_2 four-membered ring is the favorite state of aggregation.

A single methoxy group in the *ortho*-position to the *ipso*-carbon atom in $[(TMEDA)\{(LiC_6H_4OMe)_4\}_2]$[151] (**117**), however, causes a completely different and rather atypical structure: it refers back to the building principle of the donor-base-coordinated deltahedra discussed in Section II.B. Seven of the eight present C_α carbon atoms cap a Li_3 face of the tetramers, while their methoxy oxygen atoms coordinate an *apical* position. A single TMEDA molecule connects the two tetramers *N*-coordinating to different molecules. The lithium atoms show rather asymmetrical coordination. In one tetrameric unit one metal is non-, the second mono- and the third tri-coordinated by the methoxy groups. In the second deltahedron a single carbanion is located above the metal edge. The deprotonated carbon atom and the donating oxygen atom coordinate the metals of that edge. One of the remaining two *apexes* is coordinated by one, the other by two oxygen atoms (Figure 23). The methoxy oxygen atoms are partially able to replace the diethyl ether molecules in $[(Et_2O)LiPh]_4$[47] (**19**) with gross structure retention. With the *t*-BuS group this idea seems not to work. Although the lithium atoms in $[(Me_2S)LiPh]_4$[48] (**20**) are S-coordinated by solvent molecules, the pendent side-arms in $[(TMEDA)LiC_6H_4SBu\text{-}t]_\infty$[152] (**118**) are not involved in donation and the Li_2C_2 four-membered rings are merely linked via TMEDA molecules leaving the lithium atom tri-coordinated.

The vast majority of the structures in this class of compounds form dimers. In the centrosymmetrical species the metals and their coordination sphere are generated via a center of inversion in the middle of the Li···Li vector. As a consequence both metals show the same coordination number. $[(THF)LiC_6H_4(c\text{-}NC_4H_8NMe)]_2$[153] (**119**) belongs to this group of dimers. Another type is rather common: both lithium atoms are located at a two-fold axis. One lithium atom is coordinated by both side-arms and the other by donor solvent molecules. In $[(TMEDA)\{LiC_6H_4(CH_2NMe_2)\}_2]$[154] (**120**), both lithium atoms show their favorite four-fold coordination as the (*N*, *N*)-chelating TMEDA molecule provides two nitrogen donor atoms, but they might also differ in coordination number. In $[(Et_2O)\{LiC_6H_2(Me)_2(CH_2NMe_2)\}_2]$[155] (**121**), a single Et_2O molecule is coordinated exclusively to one metal. Since this is a member of the Li_2C_2 ring it remains tri-coordinated, while the second is bonded to both side-arms and four-fold coordinated

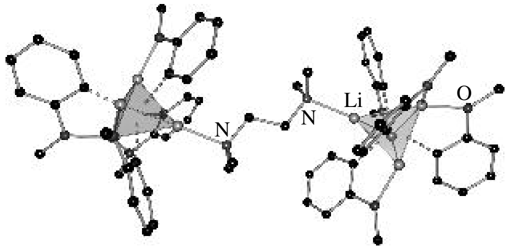

[(TMEDA){(LiC$_6$H$_4$OMe)$_4$}$_2$]

(117)

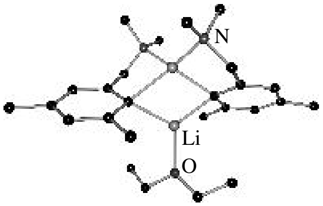

[(Et$_2$O){LiC$_6$H$_2$(Me)$_2$(CH$_2$NMe$_2$)}$_2$]

(121)

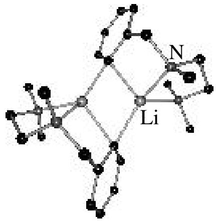

[LiC$_6$H$_4${CH$_2$N(Me)(CH$_2$)$_2$NMe$_2$}]$_2$

(123)

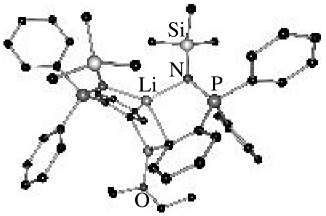

[(Et$_2$O){LiC$_6$H$_4$P(Ph)$_2$NSiMe$_3$}$_2$]

(127)

FIGURE 23. Solid-state structures of lithium phenyl derivatives with single donating side-arm coordination

(Figure 23). Substitution of the aminomethyl by a hydrazinyl side-arm in [(TMEDA) {LiC$_6$H$_4$N(Me)NMe$_2$}]^{155} (**122**) furnishes virtually the same result. Extension of the side-arm and addition of another donor center allows total wrap-up of the metal without the aid of any additional donor molecule. The complex [LiC$_6$H$_4${(CH$_2$N(Me)(CH$_2$)$_2$NMe$_2$}]$_2$^{156} (**123**) already contains an inbuilt TMEDA molecule (Figure 23). The side-arm in [(Et$_2$O)-LiC$_6$H$_4$C(O)N(Pr-*i*)$_2$]$_2$^{157} (**124**) offers the choice of *i*-Pr$_2$N or C=O donation. Obviously, the latter is more attractive as both lithium atoms in the centrosymmetric dimer are O-donated. The amino nitrogen atom shows planar environment. This does not necessarily imply that the lithium atom always picks the harder donor because the steric demand almost discriminates the nitrogen atom. Softer centers are very well suitable for side-arm donation. The (dimethylamino)methyl side-arm might be replaced by a (dimethylphosphino)methyl group to give [(Et$_2$O)LiC$_6$H$_4$(CH$_2$PMe$_2$)]$_2$^{158} (**125**), with Li−P donor bonds. The phosphorus atom in the Ph$_2$P unit of *ortho*-metalated triphenylphosphane [(Et$_2$O)-LiC$_6$H$_4$PPh$_2$]$_2$^{159} (**126**) might not reach the lithium atom because the bite is too restricted. If a potential donor center is added to the phosphorus atom this accesses the metal. In [(Et$_2$O){LiC$_6$H$_4$P(Ph)$_2$NSiMe$_3$}$_2$]^{160} (**127**), the methylene linker of the classic Me$_2$NCH$_2$ side-arm is substituted by a Ph$_2$P group and the donor is the P=NSiMe$_3$ imino nitrogen atom. In the resulting dimer one lithium atom is four-fold coordinated by the two carbon atoms and both imino side-arms, while the second bounds a diethyl ether molecule in addition to the two carbon atoms (Figure 23).

In dual side-arm coordinating complexes, no solvent is required to fill the sphere of the metal atom as both donor atoms are involved in metal donation. The effect of the length of the side-arm can be studied in detail in the structural series of [LiC$_6$H$_3$(NMe$_2$)$_2$]$_3$^{161} (**128**), [LiC$_6$H$_3$(NMe$_2$)(CH$_2$NMe$_2$)]$_2$^{162} (**129**) and [LiC$_6$H$_3$(CH$_2$NEt$_2$)$_2$]$_2$^{163} (**130**). In the first the donor atoms are directly bonded to the ring and hardly reach for the lithium atoms in the common dimeric arrangement with a Li_2C_2 four-membered ring with the usual acute Li−C−Li angle. The way out is the formation of a trimer with long distances between the lithium atoms (308 vs. 243 pm usually in this class of dimers) to facilitate wide Li−C−Li angles and dual N-coordination (Figure 24). Elongation of only one side-arm in **129** already generates the dimer, although the shorter reach of the Me_2N compared to the Me_2NCH_2 side-arm causes a considerable bend of the ring towards the involved metal. The bend is relaxed when both side-arms are elongated in **130** and the usual dimer with dual side-arm coordination and the acute angle at the C(*ipso*) carbon atom in the Li_2C_2 four-membered ring is facilitated. This predominant structural class is further substantiated by the complexes of $[LiC_6H(CH_2NMe_2)_4]_2$[164] (**131**), $[LiC_6H_2(Ph)(CH_2NMe_2)_2]_2$[165] (**132**) and $[LiC_6H_3\{CH(Me)NMe_2\}_2]_2$[166] (**133**). They all feature the Li_2C_2 four-membered ring with the acute Li−C−Li angle. Neither substitution of the *meta*-positions with further side-arms (**131**) nor of the *para*-position with a phenyl group (**132**) nor of the methylene linker with a methyl group (**133**) will alter the structural type. Even the N donor atoms in the Me_2NCH_2 side-arms can be substituted by the much softer phosphorus atoms. The structure of $[LiC_6H_3(CH_2PMe_2)_2]_2$[167] (**134**) shows the same dimer but with four Li−P rather than Li−N contacts. Even Li−F can be utilized for the side-arm coordination with retention of this dimeric lead structure. The lithium atoms in thermally unstable

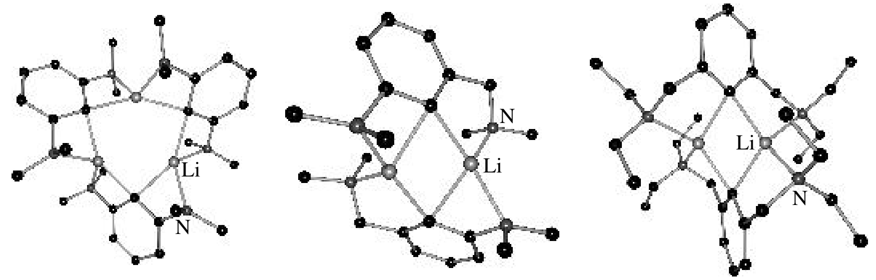

$[LiC_6H_3(NMe_2)_2]_3$ **(128)** $[LiC_6H_3(NMe_2)(CH_2NMe_2)]_2$ **(129)** $[LiC_6H_3(CH_2NEt_2)_2]_2$ **(130)**

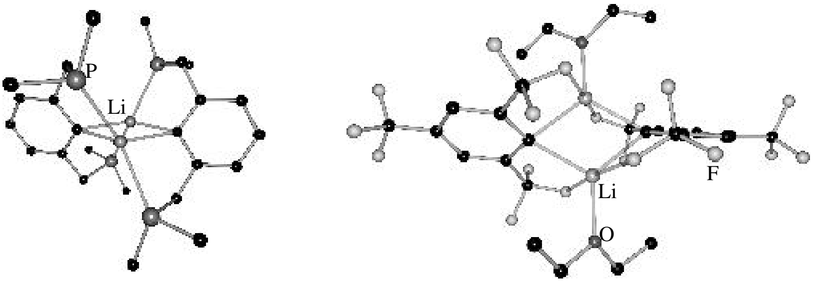

$[LiC_6H_3(CH_2PMe_2)_2]_2$ **(134)** $[(Et_2O)LiC_6H_2(CF_3)_3]_2$ **(135)**

FIGURE 24. Solid-state structures of lithium phenyl derivatives with dual donating side-arm coordination

$[(Et_2O)LiC_6H_2(CF_3)_3]_2$[168] (**135**) are side-arm coordinated by a single fluorine atom of the F_3C groups in the *ortho*-ring positions (Figure 24). The additional diethyl ether coordination at each metal is required because a fluorine atom does not supply the same steric shield as a Me_2N or Me_2P group. The Li−F contacts already indicate the favorite reaction channel to form lithium fluoride and explain why **135** is reasonably explosive at ambient temperatures. In this light it is even more remarkable that no Li−F contacts were detected in $[(THF)_3LiC_6HF_4]$[140] (**105**). Like the directly ring-bonded Me_2N groups, the fluorine atom is relatively hard to reach for the lithium atom. Even against entropy the coordination of three THF molecules is favored relative to potential Li−F contacts.

On average, the Li−C distances in lithium phenyl derivatives with donating side-arm coordination are longer than in other lithium aryls (222 vs. 214 pm). Here $Li\cdots C(\eta^n)$ contacts cannot be detected because the lithium cation prefers intramolecular side-arm coordination rather than intermolecular π-interactions. This is reflected by the longer Li−C bonds: in the competition for the charge density the side-arm donor is a more serious rival to the anionic carbon atom than the soft and easy to polarize π-density. The directed charge of the close-by donors makes the carbon atoms more dispensable for the lithium cation. The $E\rightarrow Li$ ($E = N, O$) bond lengths involving the side-arm donor centers do not differ significantly from those of Lewis-basic solvent molecules (Table 14). It is interesting to note that the phosphane $P\rightarrow Li$ donor bond is about 20 pm longer than the phosphanide P−Li bond (e.g. 262 pm in **125** and 266 pm in **134** compared to 247 pm in the lithium supermesitylphosphanide in **104**). An analogous observation in the systems amine/amide and ether/alkoxide has been discussed in Section II.B.

TABLE 14. Lithium phenyl derivatives with donating side-arm coordination

Compound		Li−C	Li−O, *N* (*P*) or (*F*)	Li···Li	CCDC code	Reference
Single Side-arm Coordination						
$[(TMEDA)\{(LiC_6H_4OMe)_4\}_2]$	**117**	230	195, *214*	264	GANBAY	151
$[(TMEDA)LiC_6H_4SBu\text{-}t]_\infty$	**118**	222	*216*	246	FOWDEA	152
$[(THF)LiC_6H_4(c\text{-}NC_4H_8NMe)]_2$	**119**	221	194, *206*	242	LEDQUG	153
$[(TMEDA)\{LiC_6H_4(CH_2NMe_2)\}_2]$	**120**	217[a]/224	207[a]/217	246	TEQPEK	154
$[(Et_2O)\{LiC_6H_2(Me)_2(CH_2NMe_2)\}_2]$	**121**	224[a]/216	196, *206*	237	RISPOY	155
$[(TMEDA)\{LiC_6H_4N(Me)NMe_2\}]$	**122**	211[a]/228	207[a]/217	239	RISPUE	155
$[LiC_6H_4\{CH_2N(Me)(CH_2)_2NMe_2\}]_2$	**123**	223	*214*	244	POMLAE	156
$[(Et_2O)LiC_6H_4C(O)N(Pr\text{-}i)_2]_2$	**124**	224	194[a]/204	248	QOGBAP	157
$[(Et_2O)LiC_6H_4(CH_2PMe_2)]_2$	**125**	222	195,262(*P*)	241	QODTUY	158
$[(Et_2O)LiC_6H_4PPh_2]_2$	**126**	220	191	243	KOPCOH	159
$[(Et_2O)\{LiC_6H_4P(Ph)_2NSiMe_3\}_2]$	**127**	230[a]/213	190, *203*	240	SUPTAY	160
Dual Side-arm Coordination						
$[LiC_6H_3(NMe_2)_2]_3$	**128**	217	*212*	308	KARMUL	161
$[LiC_6H_3(NMe_2)(CH_2NMe_2)]_2$	**129**	222	*207*	248	JUKDAU	162
$[LiC_6H_3(CH_2NEt_2)_2]_2$	**130**	223	*217*	248	REDNOD	163
$[LiC_6H(CH_2NMe_2)_4]_2$	**131**	221	*211*	240	FISWEJ	164
$[LiC_6H_2(Ph)(CH_2NMe_2)_2]_2$	**132**	219	*213*	242	NAMBUY	165
$[LiC_6H_3\{CH(Me)NMe_2\}_2]_2$	**133**	224	*212*	248	POYBUA	166
$[LiC_6H_3(CH_2PMe_2)_2]_2$	**134**	225	266(*P*)	240	YESVEX	167
$[(Et_2O)LiC_6H_2(CF_3)_3]_2$	**135**	226	197,225(*F*)	255	JEJDIL	168

[a] Distances at the side-arm coordinated lithium atom.

Although shorter Li−F distances were detected in molecular lithium fluorosilylamides (190 pm in $[LiFSi(Bu\text{-}t)_2NBu\text{-}t]_2$[169], 185 and 209 pm in $[(THF)LiFSi(Bu\text{-}t)_2N\,Bu\text{-}t]_2$[170]) and -phosphanides (190 pm in $[(THF)_2LiFSi(Bu\text{-}t)_2PPh]$[171]), the distances in **135** of 225 pm on average are comparable to those found in $[(THF)_2LiFN(C_6F_5)SiBu\text{-}t_2]$[172] (227 and 239 pm) and in $[(THF)_2Li\{FSi(Bu\text{-}t)_2\}N]$[173] (212 and 220 pm). There can be no doubt about the contribution of this interaction to the stabilization of the dimer in $[(Et_2O)LiC_6H_2(CF_3)_3]_2$[168] **135**. The acute angle at the *ipso*-carbon atom brings the two lithium atoms in close proximity.

The average Li· · ·Li distance in the dimers is 244 pm, thus matching the related distance in the donor-base-free tetramers and the shorter Li· · ·Li distances of the donor-base-free hexamers (see Tables 1, 2 and 14). This proves that there is no substantial difference between the formation of dimers, tetramers or hexamers.

3. Lithium naphthyl derivatives

In principle, the lithium naphthyl derivatives do not differ from their C_6 aryl analogs. $[(TMEDA)LiNaph]_2$[174] (**136**) is reminiscent of $[(TMEDA)LiPh]_2$[59] (**25**) (see Figures 21 and 25). Both form dimers with a Li_2C_2 four-membered ring. Intramolecular side-arm coordination can be employed by introduction of a donor center in the 8-position of the naphthyl C_{10} ring. This position gives about the same distances to the lithium cation in the 1-position as the Me_2NCH_2 group in the *ortho*-position in lithium aryls. However, there is an important difference: the donor-base in the 8-position will force the lithium cation into the plane of the anion. This can be seen with $[(THF)C_{10}H_6OMe]_2$[175] (**137**) (Figure 25). The metal is (C, O) chelated in the C_{10} plane. The deprotonated carbon atom of a second moiety provides the dimeric link. A single THF molecule is coordinated to complete the coordination sphere of the metal. All main geometrical features are similar to those already discussed (Table 15). $[(THF)LiC_{10}H_6NMe_2]_2$[176] (**138**) shows virtually the same structure, although the lithium is further dislocated from the best plane of the anion. The most pronounced displacement from that plane exhibits $[(THF)LiC_{10}H_6C(O)N(Pr\text{-}i)_2]_2$[157] (**139**) as a rotation about the C8−C(O)N(Pr-*i*)$_2$ bond removes the donating oxygen and, as a consequence, the lithium atom out of the plane.

4. Non-planar carbanions with a C_6 perimeter and the C_7 perimeter

Naturally, the concept of intramolecular coordination in lithium chemistry via side-arm complexation is not limited to aromatic planar aryls. Like the metalation of cyclohexane

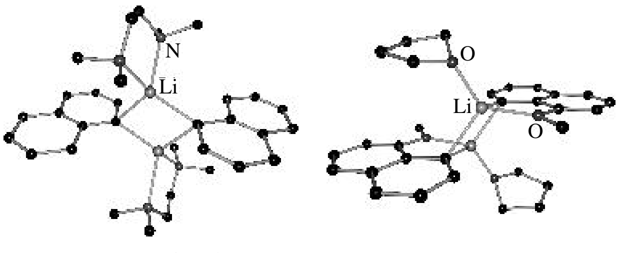

$[(TMEDA)LiNaph]_2$

(136)

$[(THF)C_{10}H_6OMe]_2$

(137)

FIGURE 25. Solid-state structures of lithium naphthyl derivatives

TABLE 15. Lithium naphthyl derivatives

Compound		Li−C	Li−O, *N*	Li···Li	CCDC code	Reference
[(TMEDA)LiNaph]$_2$[a]	**136**	223	*226*	257	HIGQUJ	174
[(THF)C$_{10}$H$_6$OMe]$_2$	**137**	220	202[b]/195	239	QESQUA	175
[(THF)LiC$_{10}$H$_6$NMe$_2$]$_2$	**138**	221	193, *210*	234	QOYZOT	176
[(THF)LiC$_{10}$H$_6$C(O)N(Pr-*i*)$_2$]$_2$	**139**	228	197[b]/197	262	QOGBET	157

[a] Naph = naphthyl, $C_{10}H_7$.

[b] Distance of the oxygen atom in the side-arm.

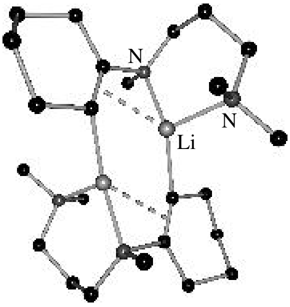

[LiC$_6$H$_8$N(Me)(CH$_2$)$_3$NMe$_2$]$_2$

(140)

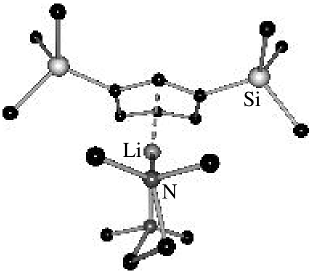

[(TMEDA)Li-*c*-C$_6$H$_7$(SiMe$_3$)$_2$]

(141)

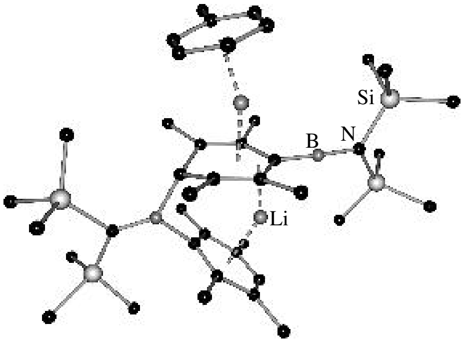

[(C$_7$H$_8$)Li$_2$-*c*-(C$_6$Me$_4$){BN(SiMe$_3$)$_2$}$_2$C$_6$HMe$_4$]

(142)

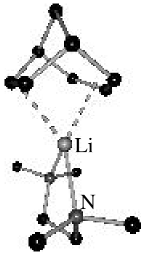

[(TMEDA)Li-*bicyclo*-C$_8$H$_9$]

(143)

FIGURE 26. Solid-state structures of lithium organics with a non-planar C_6 perimeter and a C_7 perimeter

to give [*c*-HexLi]$_6$[34] (**7**), metalation of cyclohexene is feasible. [LiC$_6$H$_8$N(Me)(CH$_2$)$_3$-NMe$_2$]$_2$[177] (**140**) contains a bifunctional long side-arm. It is flexible enough to keep the metal in the plane of the C_4 moiety. In-plane coordination yields η^2-coordination to the formal C=C double bond while σ-bonding is generated via dimerization. An almost planar $Li_2C_4N_2$ eight-membered ring is built (Figure 26). In the merely disilylated cyclohexenyl derivative [(TMEDA)Li-*c*-C$_6$H$_7$(SiMe$_3$)$_2$][178] (**141**), the (TMEDA)Li unit is out-of-plane

TABLE 16. Lithium organics with a non-planar C_6 perimeter or a C_7 perimeter in the anion

Compound		η^n $n=$	Li···C_n n(center)	Li−N	CCDC code	Reference
$[LiC_6H_8N(Me)(CH_2)_3NMe_2]_2$	**140**	2/1	220/220	*207*	CIYDUJ	177
$[(TMEDA)Li\text{-}c\text{-}C_6H_7(SiMe_3)_2]$	**141**	3	207	*213*	GOTDIC	178
$[(C_7H_8)Li_2\text{-}c\text{-}(C_6Me_4)\text{-}\{BN(SiMe_3)_2\}_2C_6HMe_4]$	**142**	6/5/2	194/185/215 213 (sol.)		SIKBAP	179
C_7 Perimeter						
$[(TMEDA)Li\text{-}bicyclo\text{-}C_8H_9]$	**143**	3/2	215/232	*218*	FAGCAR	180

η^3-coordinated to the anion. Diborylidenation of the C_6 perimeter provides access to the cyclohexadienylidene dianion in $[(C_7H_8)Li_2\text{-}c\text{-}(C_6Me_4)\{BN(SiMe_3)_2\}_2C_6HMe_4]$[179] (**142**). The two lithium atoms are sandwiched in different ways: the first is reminiscent of the metal in *ansa*-metallocenes[79], although the ligands consist of six-membered rings, the second to bind metal arene complexes. The first is sandwiched between the boron bonded aromatic C_6Me_4H and the puckered $C_6Me_5H_2$ substituents with an η^6-coordination to the first (Li···$C_{6(center)}$ 194 pm) and an η^3-contact to the latter (Li···$C_{3(center)}$ 215 pm). The *ansa*-link is provided from a boron atom. The second is sandwiched by the η^5-bonded puckered ring (Li···$C_{5(center)}$ 185 pm) and an η^6-bonded toluene molecule (Li···$C_{6(center)}$ 213 pm, Figure 26 and Table 16).

The bicyclooctadienyl ligand in $[(TMEDA)Li\text{-}bicyclo\text{-}C_8H_9]$[180] (**143**) is coordinated to the (TMEDA)Li unit via an η^3-coordination of the allyl residue and an η^2 side-on coordination of the double bond (Figure 26). The first contact is 215 pm, while the distance of 232 pm to the center of the double bond is considerably longer (Table 16).

D. Lithium Organics with Heterocyclic Perimeters

Starting from the $C_5R_5^-$ cyclopentadienyl anion containing 6 electrons in the aromatic ring, one CR ring member can isoelectronically be replaced either by a ER_2 ring member (E = B, Al, Ga, In), a E′R ring member (E′ = Si, Ge, Sn, Pb) or a divalent group 15 element E″ (E″ = N, P, As, Sb, Bi). Replacement by a ER group or by a divalent group 14 element E′ will increase the charge of the ring to two. Replacement by a E″R group or a group 16 element reduces the charge to zero. To generate an anion those rings usually have to be deprotonated.

1. Containing a group 13 element

All of the group 13 elements containing heterocycles presented here enclose charge-increasing BR groups in a five- or six-membered ring. As the BR group contributes one electron less than the CR group the $C_5H_5^-$ is converted to a dianion in the replacement of CR by BR. The aromatic neutral C_6R_6 perimeter is converted to a $C_5BR_6^-$ monoanion. The charge-increasing BR group is either substituted with an organic group (R = alkyl or aryl) or an amino substituent ($R = NR_2$). Thus, the structure of $[(TMEDA)_2Li_2C_8H_6B(NEt_2)]$[181] (**144**) is reminiscent of monomeric lithium indenyl [(TMEDA)LiIn][114] (**78**) (see Figure 18), but the planar C_8H_6B dianion is η^5-coordinated by two (TMEDA)Li moieties above and below the five-membered C_4B ring like in the inverted sandwich cation $[(TMEDA)_2Li_2C_5H_4Me]^+$ [88] (**50**). The amino substituent at the boron atom can be employed in side-arm donation as can be seen in the structure of $[(TMEDA)Li_2C_4H_4B(NEt_2)]_2$[182] (**145**). It goes back to the structure of $[(TMEDA)_2Li_2C_5H_4C(Me)_2PPh]$[89] (**51**), where one charge is located in the Cp ring and the second at the divalent phosphorus(III) atom (see Figures 16 and 27). In **145**, the structural motif is the inverted sandwich of a single hetero-Cp ring with two lithium cations above and below. One of the metal cations is coordinated to the donor-base TMEDA, the second by the Et_2N substituent at the boron atom of the other molecule in the dimer (Figure 27). Replacement of two CR ring members by charge-increasing BR groups generates a trianon. In $[(Et_2O)_2Li_3C_3B_2(Me)_2(C_6HMe_4)_2\{C(SiMe_3)_2\}]$[183] (**146**), two lithium cations are η^5/η^5-coordinated to the C_3B_2 five-membered ring. One is additionally bonding a single diethyl ether molecule and the second is coordinated by the carbon atom of a remote trimethylsilyl group akin to the Li$-$C$_\beta$ interactions already discussed in Section II.A. The third lithium cation in a $(Et_2O)Li$ moiety slots in between two *ipso*-carbon atoms of the B-bonded Mes groups in an η^2-bonding mode above the B$-$B ring bond (Figure 27). $[(Et_2O)_2Li_2C_{12}BH_5(Me)_3Mes]$[184] (**147**) features the 9-position of the fluorenyl anion $C_{13}H_9^-$ substituted by a charge-increasing BR group. Rather than in the structure of $[(THF)Li_2(C_{13}H_8)]_\infty$[127] (**90**) (see Figure 20), containing the fluorenyl dianion,

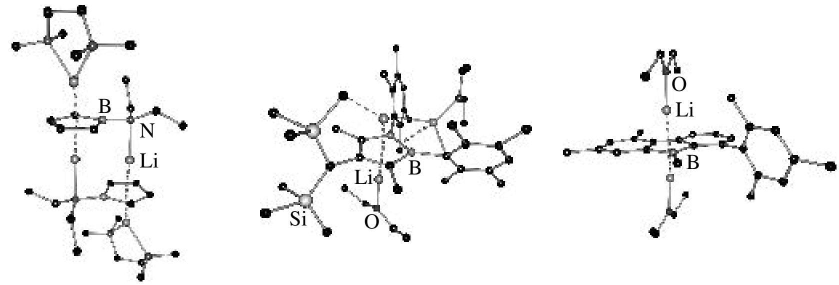

$[(TMEDA)Li_2C_4H_4B\text{-}(NEt_2)]_2$

(145)

$[(Et_2O)_2Li_3C_3B_2(Me)_2(C_6HMe_4)_2\{C(SiMe_3)_2\}]$

(146)

$[(Et_2O)_2Li_2C_{12}BH_5(Me)_3Mes]$

(147)

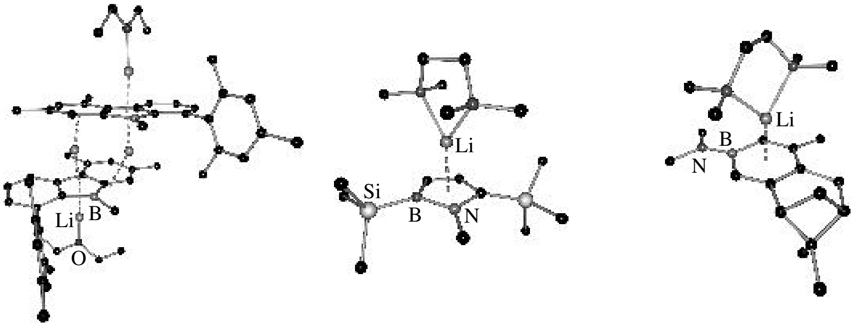

$[(Et_2O)_2Li_2C_{12}BH_5(Me)_3Mes]_2$

(148)

$[(TMEDA)LiC_3BNH_2\text{-}(Me)(SiMe_3)_2]$

(149)

$[(TMEDA)LiC_9BH_7\text{-}(NMe_2)(Me)CMe_2]$

(152)

FIGURE 27. Solid-state structures of lithium organics with heterocyclic perimeters containing boron as a group 13 element

in the boron derivative (**147**), both $(Et_2O)Li$ units are η^5/η^5-coordinated to the central C_4B five-membered ring. In fluorenyl derivatives this is only facilitated by side-arm donation (e.g. in **94**).

The structure of **147**, however, can be regarded as the diethyl ether induced deaggregation product of dimeric $[(Et_2O)_2Li_2C_{12}BH_5(Me)_3Mes]_2$[184] (**148**). Aggregation occurs via dual sandwiching of two lithium cations already discussed in $[FlLi]_2$[125] (**88**). However, while η^6/η^6-coordination was found in the latter, in **148** η^5/η^5-coordination is predominant. The first is interchelated in the η^5/η^6-mode between the dianions, the second in the η^5/η^3-fashion, involving the outer BC_2 moiety of one dianion. The two remaining $(Et_2O)Li$ units both coordinate η^5 above and below the dimer (Figure 27). Hence, four of the six present metal–ring interactions are η^5-interactions. In $[(TMEDA)LiC_3BNH_2(Me)(SiMe_3)_2]$[185] (**149**), two CR ring members in Cp are either replaced by a charge-increasing BR group and a charge-decreasing NR group leaving the central C_3BN ring monoanionic. The structure resembles the geometrical features of the silylated Cp derivatives $[(TMEDA)LiC_5H_4SiMe_3]$[104] (**66**) and $[(TMEDA)LiC_5H_2(SiMe_3)_3]$[106] (**69**). The (TMEDA)Li unit in all three examples is η^5-coordinated to the ring. The same is valid in $[(TMEDA)LiC_2B_2NH_3(Bu\text{-}t)_3]$[186] (**150**). Three CR ring members in Cp were either replaced by a charge-increasing BR group, charge-precise BR_2 group and charge-decreasing NR group leaving the C_2B_2N four-membered ring anionic. As opposed to the last example with the ring-bonded atoms almost in the plane of the anion, now the ring is considerably puckered and the *tert*-carbon atom of the B(H)Bu-*t* unit is considerably displaced from that plane. $[(TMEDA)LiC_9BH_7N(Pr\text{-}i)_2]$[187] (**151**) and $[(TMEDA)LiC_9BH_7(NMe_2)(Me)CMe_2]$[188] (**152**) contain a charge-increasing BR group in an otherwise neutral C_6R_6 six-membered ring. Unlike the six-membered rings of the $C_{10}H_8{}^{2-}$ dianion in $[(TMEDA)_2Li_2(C_{10}H_8)]$[124] (**87**), the C_5B rings in both heterocyclic structures are almost ideally planar and rather symmetrically η^5-coordinated. The $Li\cdots C_5$ ring center distances towards the polyanions in **144** to **148** (Table 17) are on average considerably shorter than the related distances in the inverted sandwich structures of Section III.B.2 (Table 8). Two (donor-base)Li units do not need to compete for the single charge of a single C_5 perimeter. The related distances towards the heterocyclic monoanions in **149** and **150** compare very well to those of substituted monomeric Cp derivatives (Table 9). The different distances in both compounds (196 pm in **149** and 206 pm in **150**) reflect the increasing steric shielding of **150** vs. **149**, but also the higher charge concentration in the five-membered ring of $[(TMEDA)LiC_3BNH_2(Me)(SiMe_3)_2]$ (**149**). The two trimethylsilyl groups are more electron-releasing than the three *t*-Bu groups in **150**. The $Li\cdots C_6$ ring center distances in **151** and **152** of 197 and 190 pm, respectively, match the related distances in $[(TMEDA)_2Li_2(C_{10}H_8)]$[124] (**87**) and in substituted phenyl derivatives (see Tables 11, 13 and 17). A typical $Li\cdots B$ distance of an η^5-coordinated (donor-base)Li unit can be found in **144** (235 pm) and **147** (224 pm). However, those distances span a relatively wide range of 222 pm (donor-base-free lithium cation to the trianion of **146**) to 271 pm (peripheral η^3-coordinated lithium cation in **148**, Table 17).

2. Containing a heavier group 14 element

In the lithium organics with heterocyclic perimeters containing a heavier group 14 element discussed here, one CR ring member of the cyclopentadienyl $C_5R_5{}^-$ is charge-increasingly replaced by the group 14 metal silicon or germanium. Hence, the $C_5{}^-$ monoanionic perimeter is converted into a C_4Si^{2-} or C_4Ge^{2-} perimeter coordinated to two lithium cations. In the structure of $[(THF)_5Li_2C_4SiPh_4]$[189] (**153**), one $(THF)_3Li$ unit

TABLE 17. Lithium organics with heterocyclic perimeters containing boron as a group 13 element

Compound		η^n $n=$	Li···Ar (center)	Li···B, *N*	CCDC code	Reference
$[(TMEDA)_2Li_2C_8H_6B(NEt_2)]$	**144**	5	193	235	PELGES	181
$[(TMEDA)Li_2C_4H_4B(NEt_2)]_2$	**145**	5	180/187[a]	228/234[a]	SIJWIR	182
$[(Et_2O)_2Li_3C_3B_2(Me)_2(C_6HMe_4)_2\text{-}\{C(SiMe_3)_2\}]$	**146**	5/5/2	170/178/210	229[b]/222/227[c]	CINCAD	183
$[(Et_2O)_2Li_2C_{12}BH_5(Me)_3Mes]$[d]	**147**	5	179	224	TIZXIJ	184
$[(Et_2O)_2Li_2C_{12}BH_5(Me)_3Mes]_2$[d]	**148**	6/5/3	196/188/216	227–271	TIZXOP	184
$[(TMEDA)LiC_3BNH_2(Me)\text{-}(SiMe_3)_2]$	**149**	5	196	238/226	VADLIV	185
$[(TMEDA)LiC_2B_2NH_3(Bu\text{-}t)_3]$	**150**	5	206	268/231/*228*	ZUFZIJ	186
$[(TMEDA)LiC_9BH_7N(Pr\text{-}i)_2]$	**151**	6	197	259	DOBJAF	187
$[(TMEDA)LiC_9BH_7(NMe_2)\text{-}(Me)CMe_2]$	**152**	6	190	248	SEQTUD	188

[a] Terminal (TMEDA)Li moiety.
[b] Terminal η^5 $(Et_2O)Li$ moiety.
[c] η^2 $(Et_2O)Li$ moiety.
[d] Mes = (2,4,6-trimethyl)phenyl, $C_6H_2Me_3$.

is terminally σ-bonded to the silicon atom in the ring, while one $(THF)_2Li$ moiety is π-bonded in the η^5-coordination mode to the five-membered ring (Figure 28). The Li···C_4Si ring center distance of 197 pm (Table 18) matches analogous distances in lithium cyclopentadienyl derivatives (see Table 8). The Li−Si σ-bond length of 267 pm matches distances found in lithium silanides (e.g. 264 and 267 pm in $[(THF)_3LiSi(SiMe_3)_3]$[190] and 256 pm in dilithium silandiides[191]). In the first of the heavier homologues $[(dioxane)_4Li_2C_4GePh_4]_\infty$[189] (**154**) and $[(dioxane)_3Li_2C_4GePh_4]_\infty$[189] (**155**), a $(dioxane)_3Li$ unit is σ-bonded to the germanium atom in the ring and a $(dioxane)_2Li$ moiety is η^5-bonded to the five-membered ring. In the latter both $(dioxane)_2Li$-motifs adopt the η^5-coordination. Further aggregation in both structures is achieved by dioxane bridging. The Li···C_4Ge ring center distances of 197 pm are identical to that of the silicon derivative **153**. The Li−Ge σ-bond length of 261 pm differs not significantly from the values found in $[(THF)_3LiGe(SiMe_3)_3]$[192] with 267 pm and in $[(PMDETA)LiGe(SiMe_3)_3]$[192] with 265 pm.

Each C_4Ge^{2-} ring in the polymeric structure of $[(TMEDA)Li_2C_4GeEt_4]_\infty$[193] (**156**) is coordinated by three lithium cations. A (TMEDA)Li unit is terminally η^5-bonded (189 pm) and one lithium cation is Li−Ge σ-bonded (269 pm). The latter is η^5-located above the ring of the adjacent anion (198 pm; Figure 28, Table 18). In $[(TMEDA)_2Li_2C_8GeH_4Ph_2]$[194] (**157**), both (TMEDA)Li moieties are η^5-located above and below the ring (206 pm). In the most remarkable structure of $[(TMEDA)(THF)Li_2(C_4GeEt_4)_3]$[195] (**158**), one lithium cation is sandwiched by two C_4Ge^- rings, connected by a third C_4Ge heterocycle to give a Ge_3 chain. The Li···C_4Ge ring center distances of 192 and 205 pm frame the 201 pm found in $[Cp_2Li]^-$ [85] (**47**). The germanium atom in the ring with the longer Li ring center distance is additionally σ-bonded to a (TMEDA/THF)Li moiety (Li−Ge bond length 272 pm). This decreases the charge density in the ring and leaves it less attractive to the sandwiched metal.

3. Containing a group 15 element

One CR ring member in the $C_5R_5^-$ cyclopentadienyl anion can be replaced isoelectronically charge precise by a divalent group 15 element E (E = N, P, As, Sb, Bi).

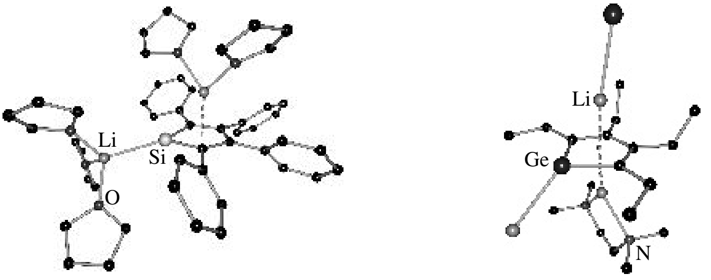

[(THF)$_5$Li$_2$C$_4$SiPh$_4$]

(153)

[(TMEDA)Li$_2$C$_4$GeEt$_4$]$_\infty$

(156)

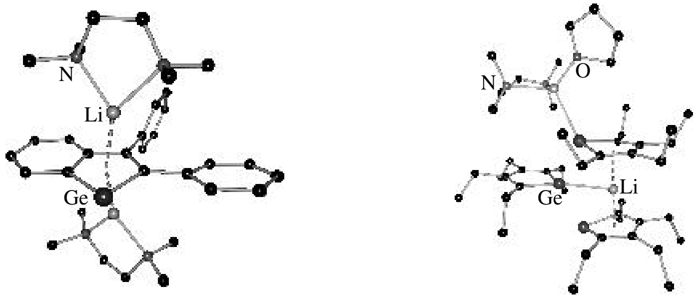

[(TMEDA)$_2$Li$_2$C$_8$GeH$_4$Ph$_2$]

(157)

[(TMEDA)(THF)Li$_2$(C$_4$GeEt$_4$)$_3$]

(158)

FIGURE 28. Solid-state structures of lithium organics with heterocyclic perimeters containing a heavier group 14 element

TABLE 18. Lithium organics with heterocyclic perimeters containing heavier group 14 elements

Compound		η^n $n=$	Li···Ar (center)	Li···Si, *Ge*	CCDC code	Reference
[(THF)$_5$Li$_2$C$_4$SiPh$_4$]	**153**	5	197	260/267(σ)	ZUBWOI	189
[(dioxane)$_4$Li$_2$C$_4$GePh$_4$]$_\infty$	**154**	5	197	264/261(σ)	NACTOA	189
[(dioxane)$_3$Li$_2$C$_4$GePh$_4$]$_\infty$	**155**	5	197	*271*	NACTIU	189
[(TMEDA)Li$_2$C$_4$GeEt$_4$]$_\infty$	**156**	5	189^a/198^b	268^a/258^b/269(σ)	WOKYOK	193
[(TMEDA)$_2$Li$_2$C$_8$GeH$_4$Ph$_2$]	**157**	5	206	*271*	QINTIQ	194
[(TMEDA)(THF)Li$_2$(C$_4$GeEt$_4$)$_3$]	**158**	5/1	192/205	273/272(σ)	ZOHWUO	195

[a] (TMEDA)Li moiety.
[b] Ge-bonded η^5-distance.

Replacement by a ER group will decrease the charge of the ring to give heterocycles like pyrroles, indoles or phospholes. To generate carbanions of the latter they usually need to be metalated in the 2-position, next to the heteroatom. Upon donor-base addition, those derivatives give rise to a Li$_2$C$_2$ four-membered ring already discussed in Section II.C. The shape of the Li$_2$C$_2$ ring is reminiscent of the geometrical features presented with the lithium phenyl derivatives in Section III.C. Two examples of this class of compounds are $[(TMEDA)LiC_4NH_3Ph]_2$[196] (**159**) and $[(THF)_2LiC_8NH_4(Me)I]_2$[197] (**160**). $[(THF)LiC_4NH_2(c\text{-}C_6H_{10})]_4$[198] (**161**) can be regarded as a tetrakis-lithium calix(4)pyrrole with the four pyrrole rings connected via the same carbon atom of four cyclohexyl rings (Figure 29). The pyrrole rings are not arranged in-plane like in haem systems but oriented almost orthogonal in a cyclic zigzag fashion. This facilitates joint σ-N and η^5-coordination of the (THF)Li unit to the heteroaromatic ring. The almost identical distances of 204 pm for the first and 206 pm for the second interaction substantiate their mutual importance as a structure-determining contribution already discussed with the lithium phenyl derivatives in Section III.C. In the monomeric lithium phospholyl complex $[(TMEDA)LiC_4PMe_4]$[199] (**162**), the (TMEDA)Li-building block is η^5-coordinated to the C_4P^- perimeter (Figure 29). The $Li\cdots\eta^5$ ring center distance of 204 pm is marginally longer than the distances found in lithium cyclopentadienyl derivatives (see Tables 9 and 19) but compares well to the related values in $[(toluene)LiC_3P_2(Bu\text{-}t)_3LiSi(SiMe_3)_3]$[200] (**163**). The central $C_3P_2{}^-$ ring is η^5-coordinated by a $(Me_3Si)_3SiLi$ moiety (202 pm) and a (toluene)Li unit (199 pm).

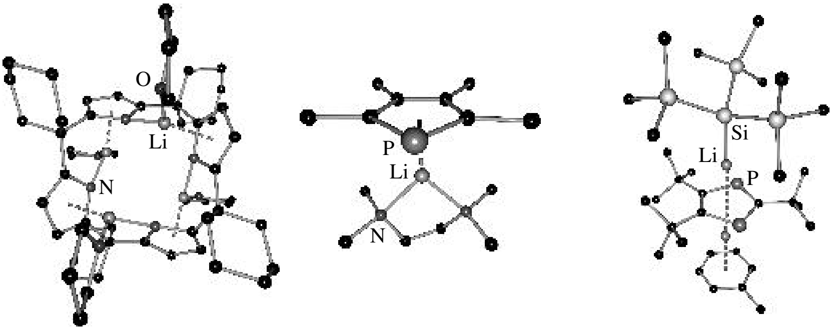

$[(THF)LiC_4NH_2(c\text{-}C_6H_{10})]_4$ **(161)**

$[(TMEDA)LiC_4PMe_4]$ **(162)**

$[(toluene)LiC_3P_2(Bu\text{-}t)_3LiSi(SiMe_3)_3]$ **(163)**

FIGURE 29. Solid-state structures of lithium organics with heterocyclic perimeters containing a group 15 element

TABLE 19. Lithium organics with heterocyclic perimeters containing group 15 elements

Compound		η^n $n=$	Li···Ar (center)	Li···E E = N, *P*, As	CCDC code	Reference
$[(TMEDA)LiC_4NH_3Ph]_2$	**159**	1	219		FATPEV	196
$[(THF)_2LiC_8NH_4(Me)I]_2$	**160**	1	224		HAJHEF	197
$[(THF)LiC_4NH_2(c\text{-}C_6H_{10})]_4$	**161**	5	206	239/204(σ)	QOVGUD	198
$[(TMEDA)LiC_4PMe_4]$	**162**	5	204	*253*	JAZNAZ	199
$[(toluene)LiC_3P_2(Bu\text{-}t)_3\text{-}LiSi(SiMe_3)_3]$	**163**	5	199[a]/202[b]	257[b]/251[c]	TECTUQ	200
$[(TMEDA)LiC_4AsMe_4]$	**164**	5	207	260	JOCSEZ	201

[a] η^6-Coordinated toluene.

[b] $(Me_3Si)_3SiLi$ moiety.

[c] (Toluene)Li moiety.

As expected, the Li−Si bond in **163** is considerably shorter than in $[(THF)_3LiSi(SiMe_3)_3]$[190] (252 vs. 264 pm in the latter) because the diphospholyl ring supplies not as much charge density as three THF donor-base molecules. The distance of the lithium cation to the ring center of the toluene molecule is 218 pm, significantly longer than the distance of the lithium cation to the benzene center in $[(C_6H_6)LiC_6H_3Tip_2]$[145] (**110**) of 194 pm. Apparently, the diphospholyl ring supplies more charge density than the σ-bonded sp^2 hybridized carbon atom in **110**. The lithium arsolyl complex $[(TMEDA)LiC_4AsMe_4]$[201] (**164**) is isostructural to **162** (Figure 29).

4. Containing a group 16 element

Replacement of a single CR ring member in the $C_5R_5^-$ cyclopentadienyl anion by a group 16 element reduces the charge of the ring to zero and gives heterocycles like thiophene, selenophene or benzothiophene. They need to be metalated to generate carbanions. Lithium methylthiophenyl $[(Et_2O)LiC_4SH_2Me]_4$[202] (**165**) forms a solvated tetrahedron reminiscent of the molecular architectures discussed in Section II.B. The deprotonated carbon atoms in the 2-position cap a Li_3 face of the tetramer each (Figure 30). Every ring-sulfur atom points towards an *apical* lithium cation, donating charge density like the $Li\cdots C_\beta$ interactions discussed earlier. The average $Li\cdots Li$ distances of 273 pm fall at the long end of the range covered by the donor-base-coordinated tetrahedra (see Tables 3 and 20). Like in $[(THF)LiC{\equiv}CBu\text{-}t]_4$[49] (**21**) and $[(TMHDA)_2LiC{\equiv}CPh]_\infty$[50] (**22**), the charge of the carbanions is delocalized from the C_α and therefore not as distinctly supplied to the metal core as with sp^3 hybridized carbanions. Thus, the positive charge at the lithium cations is higher, resulting in stronger repulsion.

With chelating donor bases $[(TMEDA)LiC_4SH_3]_2$[203] (**166**) and $[(TMEDA)LiC_8SH_5]_2$[204] (**167**), adopt the dimeric structure with a Li_2C_2 four-membered ring known from lithium phenyl derivatives discussed in Section III.C. Even another analogy is present: the side-arm coordination concept can successfully be transferred for the heterocyclic carbanions. The well-known (dimethylamino)methyl side-arm occurs in the thiophenyl derivative $[(TMEDA)Li_2\{C_4SH_2(CH_2NMe_2)\}_2]$[205] (**168**), equally to the phenyl derivative $[(Et_2O)\{LiC_6H_2(Me)_2(CH_2NMe_2)\}_2]$ (**121**), to give a dimer with a lithium exclusively side-arm and donor-base-coordinated, respectively (see Figures 23 and 30). The related distances are very similar (see Tables 14 and 20).

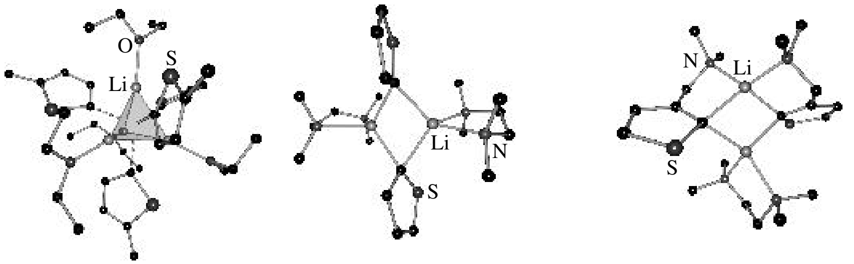

$[(Et_2O)LiC_4SH_2Me]_4$ **(165)**

$[(TMEDA)LiC_4SH_3]_2$ **(166)**

$[(TMEDA)Li_2\{C_4SH_2(CH_2NMe_2)\}_2]$ **(168)**

FIGURE 30. Solid-state structures of lithium organics with heterocyclic perimeters containing sulfur as a group 16 element

TABLE 20. Lithium organics with heterocyclic perimeters containing group 16 elements

Compound		Li···Ar (Center)	Li−O, *N*	Li···Li	CCDC code	Reference
$[(Et_2O)LiC_4SH_2Me]_4$	**165**	226/229	202, 300(*S*)[a]	273	HIGTEW	202
$[(TMEDA)LiC_4SH_3]_2$	**166**	221	*216*	258	JUJXER	203
$[(TMEDA)LiC_8SH_5]_2$	**167**	221	*216*	264	KASHIV	204
$[(TMEDA)Li_2\{C_4SH_2$-$(CH_2NMe_2)\}_2]$	**168**	217[b]/221	206[b]/213	251	LEDSES	205

[a] Sulfur as the analogue to C_β.
[b] Side-arm coordinated lithium atom.

IV. ALKYLLITHIUMS

A. R_3C-Metalated Derivatives

As deprotonation and C−C bond formation reagents, lithium organic compounds ousted the Grignard reagents from their leading position a long time ago. There are various reasons for their triumphant advance. *In situ* generation of lithium organics is straightforward and involves normally just commercially available products like *n*-BuLi, *t*-BuLi, MeLi or *i*-Pr_2NLi (LDA). Compared to the Grignard reagents the temperature window for the reaction is wider. Normally, just cooling to dry ice temperatures and warming to room temperature is sufficient. Compared to that it seems much more difficult to explore the various reaction pathways involved in the Schlenk equilibrium of the Grignard reagents and find the right conditions. In general, lithium organics are soluble even in non-polar hydrocarbons once they are coordinated by donor bases. This facilitates reactions in homogeneous phase.

Although the regioselectivity of lithium organics is very good already, the improvement of their conformational stability at the metalated stereogenic center is currently a flourishing area of research[206].

1. Alkyl-, aryl- and silyl-substituted lithium organics

The field of R_3C lithium organic structures is wide and we will concentrate on those with alkyl-, aryl- and silyl-substituted anions. Heteroatom-substituted lithium organics will just be mentioned briefly.

The structures of the basic allyllithium derivatives $[(PMDETA)LiC_3H_5]$[207] (**169**) and $[(TMEDA)LiC_3H_3(SiMe_3)_2]$[208] (**170**) already exhibit one of the major problems in lithium organic stereochemistry: although anticipated with the allyl systems, lithium organics also tend to generate a planar environment at the central metalated carbon atom. Stereoinformation is lost as the access of the electrophile in solution is equally likely from both sides of the carbanion, provided that the complex is a solvent-separated ion pair in solution. In donating solvents epimerization is promoted. In the solid-state, however, one side of the allyl anion is η^3-coordinated to the lithium metal (Figure 31). In d-block metal allyls this bonding mode is frequently found. Even against steric considerations the $Li\cdots\eta^3$ center distance in the silylated derivative (**170**) is much shorter than in the hydrogen derivative (195 vs. 220 pm; Table 21). Again, this shows the predominant electron-releasing ability of silyl groups and proves higher charge concentration in the C_3-backbone of **170** compared to **169**. In $[(TMEDA)_2Li_2C(Ph)(Bu\text{-}n)CHPh]$[209] (**171**), both adjacent carbanionic centers show planar environment and the (TMEDA)Li moieties are η^4-coordinated to both sides of the dianion, employing the deprotonated carbon atoms, the phenyl *ipso*-

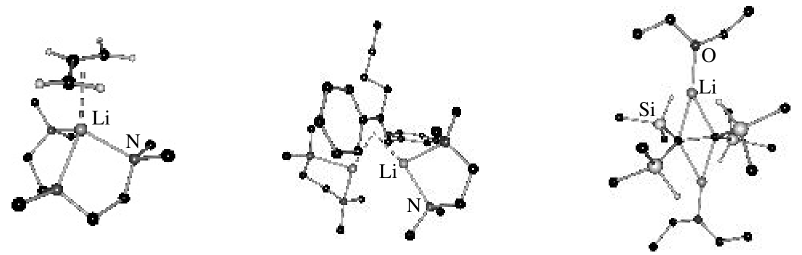

[(PMDETA)LiC$_3$H$_5$] **(169)** [(TMEDA)$_2$Li$_2$C(Ph)(Bu-*n*)CHPh] **(171)** [(Et$_2$O)$_2$Li$_2${C(SiHMe$_2$)$_2$}$_2$] **(174)**

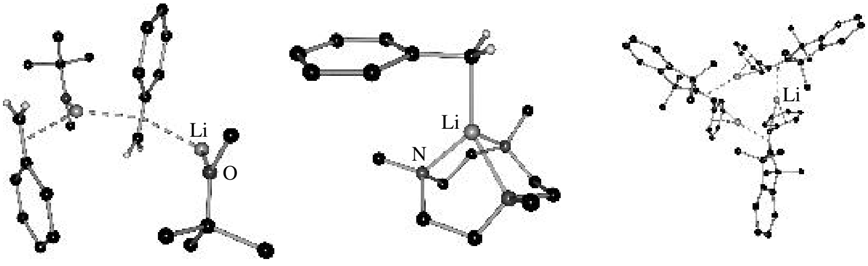

[{*t*-Bu(Me)O}LiBn]$_\infty$ **(177)** [(PMDETA)LiBn] **(178)** [LiCH(Ph)(C$_9$H$_4$Me$_4$)]$_3$ **(186)**

FIGURE 31. Solid-state structures of lithium organics with alkyl-, aryl- and silyl-substituted lithium organics

TABLE 21. R$_3$C-metalated species (R = alkyl, aryl, silyl)

Compound		η	Li–C	Li–O, *N*	CCDC code	Reference
[(PMDETA)LiC$_3$H$_5$]	**169**	3	220	*217*	FOBHAF	207
[(TMEDA)LiC$_3$H$_3$(SiMe$_3$)$_2$]	**170**	3	195	*208*	SUCKAC	208
[(TMEDA)$_2$Li$_2$C(Ph)(Bu-*n*)CHPh]	**171**	4/4	201	*215*	GINVEE	209
[(DME)$_2$Li$_2$C(Ph)(SiMe$_3$)C(SiMe$_3$)$_2$]	**172**	6/3	185/194	206[a]/196	KUWWAA	210
[(THF)$_2$Li$_2${*c*-C(SiMe$_2$)$_2$(CH$_2$)$_2$}$_2$]	**173**		206	187	YOSTAB	211
[(Et$_2$O)$_2$Li$_2${C(SiHMe$_2$)$_2$}$_2$]	**174**		213	191	NIHDOX	212
[(THF)$_2$Li$_2${C(SiMe$_3$)$_2$}$_2$]	**175**		211	185	JAMSEV	213

[a] η^6-Coordinated (TMEDA)Li moiety.

and the *ortho*-atom (Figure 31). The Li$\cdots\eta^4$ center distance of 201 pm (Table 21) is comparable to those distances in lithium organics with cyclic C$_4$ perimeters discussed in Section III.A. It is interesting to note that the phenyl ring not involved in conjugation aligns almost perpendicular to the η^4-coordinated array. Like the latter, the structure of [(DME)$_2$Li$_2$C(Ph)(SiMe$_3$)C(SiMe$_3$)$_2$][210] (**172**) contains two adjacent deprotonated carbon atoms. The first is dual, the second single-silylated. Hence, one can anticipate that both carbon atoms are sufficiently electron-rich.

However, the indication of charge accumulation is only marginal, because both C$_\alpha$ carbon atoms show virtually planar environments. By inspection of the metal coordination it becomes obvious where the charge is located. One (TMEDA)Li unit is η^6-coordinated to the neighboring phenyl group (185 pm) and the second η^3-bonded (194 pm, Table 21) involving both carbanionic centers and the *ipso*-carbon atom of the phenyl ring. Hence, via conjugation the charge density at the carbanionic C atoms is depleted and transferred to the phenyl ring which gets attractive for both lithium cations. Tetrasubstituted silicon atoms adjacent to the carbanionic centers preclude conjugation. Thus, both lithium atoms in $[(THF)_2Li_2\{c\text{-}C(SiMe_2)_2(CH_2)_2\}_2]$[211] (**173**), $[(Et_2O)_2Li_2\{C(SiHMe_2)_2\}_2]$[212] (**174**) and $[(THF)_2Li_2\{C(SiMe_3)_2\}_2]$[213] (**175**) are coordinated to the two negatively charged carbon atoms in the 1,2-dianions (Figure 31). The charge is not engaged in multiple bonding because the central C−C bond is considerably longer than the standard $C(sp^3)-C(sp^3)$ bond length.

The delocalization of charge in correlation to the donor-base and the aggregation can be studied in the series of benzyllithium derivatives $[(THF)_2LiBn]_\infty$[214] (**176**), $[\{t\text{-}Bu(Me)O\}LiBn]_\infty$[215] (**177**) and [(PMDETA)LiBn][216] (**178**). Two diethyl ether molecules donating to the lithium atom cause metal contact at both sides of the carbanion. In the resulting polymer the phenyl groups point in opposite directions. The donor-base *t*-BuOMe in **177** causes a shift of the metal into an η^2-position towards the *ipso*-carbon atom, but changes neither the aggregation (Figure 31) nor the $H_2C-C(ipso)$ bond length (142 pm in **176** and 141 pm in **177**). It is only the use of the donor-base PMDETA to give monomeric **178**. As anticipated, the Li−C bond gets shorter (Table 22). The charge concentration at the terminal carbon atom elongates the $H_2C-C(ipso)$ bond to 150 pm in **178** and the hydrogen atoms are not located in the mean plane of the carbanion. However, the metalated carbon should not be regarded as sp^3 hybridized, because the C−C−Li angle is almost 90° indicating some π-interaction. In the metalated tetramethylbiphenyl $[(PMDETA)LiCH_2(C_{12}H_6)Me_3]$[217] (**179**), this interaction can be ruled out, because the $(ipso)C-CH_2-Li$ angle is closer to the anticipated ideal tetrahedral angle. In dilithiated 2,2′-dimethylbiphenyl $[(TMEDA)Li_2(CH_2)_2(C_{12}H_8)]_\infty$[218] (**180**), the bidentate donor-base TMEDA causes the polymeric aggregation at each metalated group akin to **176** and **177**. In dimetalated 1,1′-dimethylnaphthyl $[(TMEDA)_2Li_2(CH_2)_2(C_{10}H_6)_2]$[217] (**181**), one (TMEDA)Li unit is fixed to both H_2C groups (Li−C 213 and 223 pm, respectively), while the second is 'back-side' coordinated to the H_2CLi unit (236 pm), like the already discussed 'long-range' interaction in the solid-state structure of $[MeLi]_{4,\infty}^{10}$ (**1**).

In the dimeric dilithium terphenyl complex $[(Et_2O)_2Li_4C_6H_3\{(C_6H_3(Me)Bu\text{-}t)(C_6H_3(CH_2)Bu\text{-}t)\}_2]$[219] (**182**), the lithium atoms are employed in the benzylic η^3-coordination although there are plenty of C_6 perimeters close-by. The charge is definitely concentrated at the H_2C group because the carbon atom bridges two lithium atoms each (221 and 216 pm; Table 22).

TABLE 22. $H_2(Ar)C$-metalated species

Compound		Li−C	Li−O, *N*	CCDC code	Reference
$H_2(Ar)C-Li$					
$[(THF)_2LiBn]_\infty$	**176**	233	198	WALQEF	214
$[\{t\text{-}Bu(Me)O\}LiBn]_\infty$	**177**	225	193	ZUZTAP	215
[(PMDETA)LiBn]	**178**	215	*210*	IGOFAL	216
$[(PMDETA)LiCH_2(C_{12}H_6)Me_3]$	**179**	214	*212*	GIMPIB	217
$[(TMEDA)Li_2(CH_2)_2(C_{12}H_8)]_\infty$	**180**	230	*216*	CEVZAE	218
$[(TMEDA)_2Li_2(CH_2)_2(C_{10}H_6)_2]$	**181**	213[a]/223[a]/236[b]	225[a]/207[b]	GIMPOH	217
$[(Et_2O)_2Li_4C_6H_3\{(C_6H_3(Me)Bu\text{-}t)\text{-}(C_6H_3(CH_2)Bu\text{-}t)\}_2]$	**182**	221[c]/216[c]/206	191	MOBRAW	219

[a] (TMEDA)Li unit coordinated to both H_2C-groups.

[b] (TMEDA)Li unit 'back-side' coordinated just to one H_2C-group.

[c] σ-Bonded Li.

As pointed out earlier, the substitution with silyl groups increases the charge density and makes the carbanion more attractive for the lithium cation even against steric strain. In lithium (trimethylsilyl)benzylide $[(TMEDA)LiCH(Ph)SiMe_3]$[220] (**183**), only the bidentate donor-base TMEDA is required to get the monomeric complex (PMDETA in **178**). The $Li\cdots C_{3(center)}$ distance is 14 pm shorter than in $[\{t\text{-}Bu(Me)O\}LiBn]_\infty$ (**177**) (Table 23). In dilithiated $[(TMEDA)_2Li_2\{(CH(SiMe_3))_2C_6H_4\}]$[221] (**184**) and $[(TMEDA)_2Li_2\{(CH(SiMe_3))_2C_{12}H_8\}]$[218] (**185**), the disilylated analog to **180**, the charge is localized at the metalated benzylic carbon atom. Neither aggregation nor additional η^3-coordination is found in their structures. In $[LiCH(Ph)(C_9H_4Me_4)]_3$[222] (**186**), an indanylidene substituent is bonded to the benzylic carbon atom instead of a silyl group. Now the formal double bond and the η^3-moiety of the benzyl are providing the link in the trimer (Figure 31).

2. Heteroaryl-substituted lithium organics

The delocalization of the charge density can be promoted considerably if heteroaryl substituents like 2-pyridyl (Py) are connected directly to the metalated carbon atom. This virtually converts the carbanion to an amide and employs the concept of the side-arm donation, discussed in Section III.C.2. The methylpicolyl anion in the dimer $[(TMEDA)LiCH_2(C_5NH_3Me)]_2$[223] (**187**) is mutually $H_2C{-}Li$- and $(Py)N{\rightarrow}Li$-coordinated (Figure 32). This explains the rather long Li−C bonds of 235 pm. Instead, the Li−N bond distances of 208 pm are half-way between those found in donor-base complexes and lithium amides[52–55]. The hydrogen atoms at the picolytic carbon atom indicate planar environment although the lithium atom is not shifted to the η^3-position. This is achieved when the donor-base is changed to diethyl ether and the deprotonated carbon atom is silylated in $[(Et_2O)LiCH(SiMe_3)Py]_2$[224] (**188**). The complex dimerizes via mutual η^3-sandwiching of the diethyl ether coordinated lithium cation. The Li···azaallyl center distance of 205 pm (Table 24) already indicates strong interaction, but is even shortened when a molecule of the starting material is employed as a donor-base to the metalated species in $[\{(Me_3Si)_2CHPy\}LiC(SiMe_3)_2Py]$[224] (**189**). Here the Li···azaallyl center distance is just 192 pm and the $(Py)N{\rightarrow}Li$ donor bond length 201 pm. Addition of TMEDA gives $[(TMEDA)LiC(SiMe_3)_2Py]$[224] (**190**), with retention of the $Li\cdots\eta^3$-azaallyl interaction. In $[(PMDETA)LiCH(SiMe_3)(C_5NH_3Me)]$[225] (**191**), exclusively a $(Py)N{\rightarrow}Li$ donor bond (205 pm) is observed (Figure 32). The C-bonded hydrogen atom and the silicon atom at the carbanionic atom are located in the plane of the pyridyl ring. The structure emulates all geometric features of an amide.

Charge delocalization can also be promoted by multiple aryl substitution at the metalated carbon atom. A lucid example is the Ph_3C^- trityl anion. The central carbon atoms in $[(TMEDA)LiCPh_3]$[226] (**192**) and $[(Et_2O)_2LiCPh_3]$[137] (**193**) show almost ideal planar environment. The three phenyl groups cannot all be arranged in a coplanar fashion due to

TABLE 23. H(R)(Ar)C-metalated species

Compound		Li−C	Li−N	CCDC code	Reference
H(R)(Ar)C−Li					
$[(TMEDA)LiCH(Ph)SiMe_3]$	**183**	211	205	JILPUP	220
$[(TMEDA)_2Li_2\{(CH(SiMe_3))_2C_6H_4\}]$	**184**	214	206	DAZSOM	221
$[(TMEDA)_2Li_2\{(CH(SiMe_3))_2C_{12}H_8\}]$	**185**	220	207	CEVZEI	218
$[LiCH(Ph)(C_9H_4Me_4)]_3$	**186**	213[a]/237		VULSOK	219

[a] σ-Bonded Li.

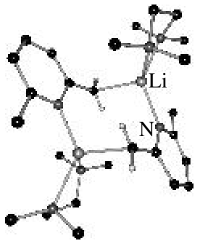

[(TMEDA)LiCH$_2$(C$_5$NH$_3$Me)]$_2$

(187)

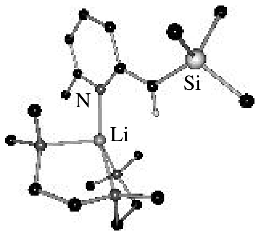

[(PMDETA)LiCH(SiMe$_3$)(C$_5$NH$_3$Me)]

(191)

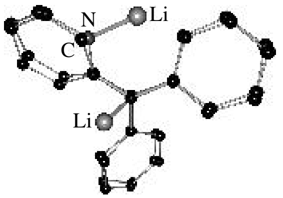

Superposition-plot of the Ph$_3$C- and Ph$_2$PyC-anions in **193** and **194**

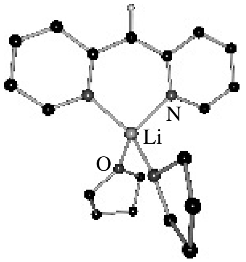

[(THF)$_2$LiCHPy$_2$]

(196)

FIGURE 32. Solid-state structures of lithium organics with heteroaryl-substituted lithium organics

TABLE 24. Heteroaryl-substituted lithium organics

Compound		η	Li−C	Li−O, *N*	CCDC code	Reference
[(TMEDA)LiCH$_2$(C$_5$NH$_3$Me)]$_2$	**187**		235	*208*/224^a	CUPVAK	223
[(Et$_2$O)LiCH(SiMe$_3$)Py]$_2$^{b}	**188**	3	205	191, *204*	COXTOY	224
[{(Me$_3$Si)$_2$CHPy}LiC(SiMe$_3$)$_2$Py]^b	**189**	3	192	*201*	COXTEO	224
[(TMEDA)LiC(SiMe$_3$)$_2$Py]^b	**190**	3	205	*211*	COXTIS	224
[(PMDETA)LiCH(SiMe$_3$)(C$_5$NH$_3$Me)]	**191**			205^c/218	XETLIR	225
[(TMEDA)LiCPh$_3$]	**192**		223	*208*	TPMLIE	226
[(Et$_2$O)$_2$LiCPh$_3$]	**193**		231	193	GABHEW	137
[(Et$_2$O)$_2$LiCPh$_2$Py]^b	**194**		326^d/245^e	*197*	YANREK	228
[(H$_2$CPy$_2$)LiCHPy$_2$]	**195**			197^f/206	YIFJEC	229
[(THF)$_2$LiCHPy$_2$]	**196**			198, *197*	SUMSOI	230

[a] (TMEDA)Li unit.

[b] Py = 2-pyridyl, C$_5$NH$_4$.

[c] Ring-N-bonded (PMDETA)Li moiety.

[d] Li···C distance to the central carbon atom.

[e] Next non-bonded distance to the carbon atom of an *ortho*-CH-group.

[f] Average Li−N distance in the anion.

steric hindrance of the *ortho*-hydrogen atoms. The 'windmill' conformation is a reasonable compromise between steric strain and total conjugation. Although this conformation is virtually the same in all alkali metal trityl complexes, only lithium coordinates the central carbon atom (Li−C 223 pm in **192** and 231 pm in **193**).

With increasing mass, the heavier metals become more and more shifted to the center of a single phenyl ring[227]. Subtraction of the lithium from the central carbon atom is facilitated by introduction of a single pyridyl ring instead of a phenyl. Like in the examples just discussed, the lithium cation in $[(\mathrm{Et_2O})_2\mathrm{LiCPh_2Py}]$[228] (**194**) is coordinated to the ring nitrogen atom ((Py)N→Li 197 pm). The Li−C distance to the central carbon atom of 326 pm is too long to be considered an interaction. The closest Li$\cdots$C distance of 245 pm is found to the *ortho*-CH group opposite the ring nitrogen atom. Certainly, this is just caused by steric strain. A superposition plot of the $\mathrm{Ph_3C}$ and $\mathrm{Ph_2PyC}$ anions in **193** and **194** elucidates the totally different positions of the metal cations relative to the anions (Figure 32). Likewise, the lithium cations in the dipyridylmethyl structures of $[(\mathrm{H_2CPy_2})\mathrm{LiCHPy_2}]$[229] (**195**) and $[(\mathrm{THF})_2\mathrm{LiCHPy_2}]$[230] (**196**) exhibit no Li−C contact at all. Lithium is exclusively coordinated to both ring nitrogen atoms of the anion. The pyridyl rings are arranged coplanar, indicating total conjugation. As anticipated, the (Py)N→Li donor bonds from the starting material in **195**, that serves as a donor-base, are about 10 pm longer than the (Py)N→Li donor bonds from the anion (197 *vs*. 206 pm; Table 24). As suggested by **195** and **196**, the dipyridylmethyl anion attained the right shape and coordination facility to generate lithium lithiates.

3. Lithiates

Two anions coordinated to a single lithium cation in a solvent-separated ion pair (SSIP) generates a lithiate. Although the name might suggest negative charge at the lithium, it is important to note that the lithium cation remains electropositive. It is just part of a complex anion. Replacement of the $\mathrm{H_2CPy_2}$ donor molecule in $[(\mathrm{H_2CPy_2})\mathrm{LiCHPy_2}]$[229] (**195**) and the two THF molecules in $[(\mathrm{THF})_2\mathrm{LiCHPy_2}]$[230] (**196**) by another N-coordinated chelating $\mathrm{Py_2C}$ anion will give rise to a lithium-containing anion. The related SSIPs are $[\mathrm{Li(12\text{-}crown\text{-}4)_2}]\ [\mathrm{Li(CHPy_2)_2}]^{-}$ [230] (**197**) and $[(\mathrm{THF})_6\mathrm{Na}]\ [\mathrm{Li(CHPy_2)_2}]^{-}$ [230] (**198**). Because of the highly solvated sodium cation, the latter sodium lithiate is thermally instable (Figure 33). The Li−N distances are not different from the related distances in the previous section. Firstly synthesized, however, were the lithium lithiates by employment of the bulky tris(trimethylsilyl)methyl $(\mathrm{Me_3Si})_3\mathrm{C}$ anion. Two of them coordinate linearly a single lithium cation (Figure 33).

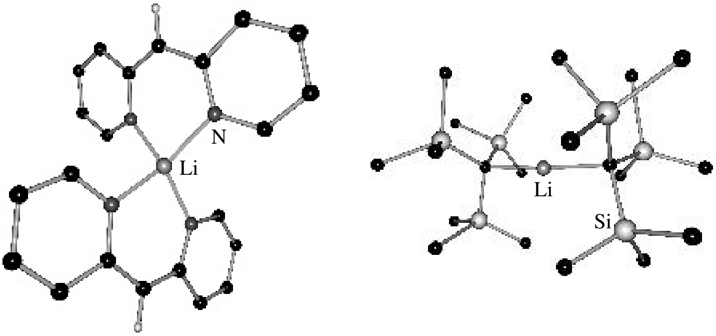

The lithiate anion from the SSIP $[(\mathrm{THF})_6\mathrm{Na}]\ [\mathrm{Li(CHPy_2)_2}]$

(197)

The lithiate anion from the SSIP $[(\mathrm{TMEDA})_2\mathrm{Li}]\ [\mathrm{Li\{C(SiMe_3)_3\}_2}]$

(201)

FIGURE 33. Solid-state structures of lithium lithiate anions

The SSIPs are [(THF)$_4$Li] [Li{C(SiMe$_3$)$_3$}$_2$]^{231} (**199**), [{(PMDETA)Li}$_2$Cl] [Li{C(SiMe$_3$)$_3$}$_2$]^{232} (**200**), [(TMEDA)$_2$Li] [Li{C(SiMe$_3$)$_3$}$_2$]^{233} (**201**) and [(THF)$_3$Li] [Li{C(SiMe$_3$)$_3$}$_2$]^{234} (**202**). The most common cation in this class of compounds is the single lithium cation chelated by two TMEDA molecules like in [(TMEDA)$_2$Li] [Li{C(SiMe$_3$)$_2$Si(Me)$_2$Ph)}]$^{-\ 235}$ (**203**) and [(TMEDA)$_2$Li] [Li{C(SiMe$_3$)$_2$Si(Me)$_2$CH$_2$}$_2$]$^{-\ 236}$ (**204**). The Li−C bond lengths in the latter lithiates span the relatively narrow range from 212 pm to 219 pm (Table 25).

4. Enantiomerically pure lithium organics

As pointed out earlier, the improvement of the conformational stability at the metalated stereogenic center in lithium organics is currently a flourishing area of research^{206}. The determination and retention of the absolute configuration of the metalated carbon center is of vital interest for the development of new stereoselective synthetic strategies. However, to date there are only a few enantiomerically pure lithium organics investigated in the solid-state. In [((−)-sparteine)LiCH(SiMe$_3$)Py]^{237} (**205**), [((−)-sparteine)LiC$_9$H$_6$Bu-*n*]^{238} (**206**) and [((−)-sparteine)LiC$_3$H$_3$Ph$_2$]^{239} (**207**), chirality is just induced by employment of the enantiomerically pure donor-base (−)-sparteine. Although they contain a prochiral trigonal planar metalated carbon atom in their *meso*-forms, they crystallize in chiral space groups (Table 26). In **205**, the ((−)-sparteine)Li unit coordinates in the η^3-mode to the azaallyl system (197 pm). In **206**, it η^3-coordinates the five-membered ring of the 1-butyl-substituted indenyl substituent. Due to the two donor atoms, the Li$\cdots$ring center distance of 211 pm falls at the long end of the range of equivalent values in lithium indenyl derivatives discussed in Section III.B.4 (see Tables 26 and 10). The Li$\cdots\eta^3$ center distance of 205 pm in **207** is longer than that of **205** because a C$_3$ moiety is less attractive than a C$_2$N backbone. The structures of [((−)-sparteine)LiC$_3$H$_3$(SiMe$_3$) {OC(O)N (Pr-*i*)$_2$}]^{240} (**208**), [((−)-sparteine)LiC$_3$H$_3$(Ph)N{C(O)OBu-*t*)}C$_6$H$_4$OMe]^{241} (**209**) and [((−)-sparteine)LiCH(Ph)N(Me)C(O)Bu-*t*]^{242} (**210**) already highlight a successful strategy to get conformational stability at the stereogenic carbon atom in the solid-state: a carbonyl side-arm is employed to coordinate the metal and to fix it at one side of the RC* center. The metalated carbon atom shows a considerable pyramidal environment in **208** (Li−C 221 pm; Figure 34; Table 26) but the ((−)-sparteine)Li moiety is η^3-coordinated (236 pm) to the anion in **209**. The Li−C distance to the central carbon atom of the RR'HC*-anion in

TABLE 25. Lithiates

Compound		Li−C	Li−O, *N*	CCDC code	Reference
[Li(CHPy$_2$)$_2$]$^{-a}$	**197**		237^a, 201	SUMSUO	230
[Li(CHPy$_2$)$_2$]$^{-b}$	**198**		*200*	SUMTAV	230
[Li{C(SiMe$_3$)$_3$}$_2$]$^{-c}$	**199**	217	189	BUTXUJ	231
[Li{C(SiMe$_3$)$_3$}$_2$]$^{-d}$	**200**	212	*218*	DONYAG	232
[Li{C(SiMe$_3$)$_3$}$_2$]$^{-e}$	**201**	216	195	PEYLIO	233
[Li{C(SiMe$_3$)$_3$}$_2$]$^{-f}$	**202**	217	*209*	LONYES	234
[Li{C(SiMe$_3$)$_2$Si(Me)$_2$Ph)}]$^{-e}$	**203**	219	*213*	ICUNID	235
[Li{C(SiMe$_3$)$_2$Si(Me)$_2$CH$_2$}$_2$]$^{-e}$	**204**	216	*212*	ZIWZUA10	236

[a] [Li(12-crown-4)$_2$]$^+$ is the cation.
[b] [(THF)$_6$Na]$^+$ is the cation.
[c] [(THF)$_4$Li]$^+$ is the cation.
[d] [{(PMDETA)Li}$_2$Cl]$^+$ is the cation.
[e] [(TMEDA)$_2$Li]$^+$ is the cation.
[f] [(THF)$_3$Li]$^+$ is the cation.

TABLE 26. Enantiomerically pure lithium organics

Compound		η	Li–C	Li–O, *N*	space group	CCDC code	Reference
[((−)-sparteine)LiCH($SiMe_3$)Py]	**205**	3	197	*200*	$P2_12_12_1$	SEWMEM	237
[((−)-sparteine)LiC_9H_6Bu-*n*]	**206**	5	211	*212*	$P2_12_12_1$	SUPYIL	238
[((−)-sparteine)Li$C_3H_3Ph_2$]	**207**	3	205	*201*	P1	WUKPOH	239
[((−)-sparteine)LiC_3H_3($SiMe_3$) {OC(O)N(Pr-*i*)$_2$}]	**208**		221	190, *205*	P1	SIZBUY	240
[((−)-sparteine)LiC_3H_3(Ph)-N{C(O)OBu-*t*)}C_6H_4OMe]	**209**	3	236	192, *212*	$P2_12_12_1$	JANKAK	241
[((−)-sparteine)LiCH(Ph)-N(Me)C(O)Bu-*t*]	**210**		215	189, *206*	$P2_12_12_1$	HAJHAB	242
[LiC_2H_2(Ph){C(Ph)-pyrrolidine-CH_2OMe}]$_2$	**211**		240	187, *213*	$P2_12_12_1$	SIKBUJ	243
[(DABCO)LiCH(Ph)Si(Me)$_2$-CH_2-pyrrolidine-CH_2OMe]	**212**		228	200, *212*	$P2_1$		244
[LiCH(Ph)Si(Me)$_2$$CH_2$-pyrrolidine-$CH_2OMe_2$]$_\infty$	**213**	2	227[a]/248	195, *218*	$P3_2$	AGILEH	245
[(TMEDA){LiCH(Ph)Si(Me)$_2$-CH_2-pyrrolidine-CH_2OMe}$_2$]	**214**	3	240	200, *218*	$P2_12_12_1$		244

[a] σ-Bonded.

210 is only 215 pm. A much more capable side-arm to fix the conformation at the metalated stereogenic center is the pyrrolidine-N,O substituent, because it got two donor atoms to coordinate the lithium cation. The dimer [LiC_2H_2(Ph){C(Ph)-pyrrolidine-CH_2OMe}]$_2$[243] (**211**) crystallizes in the chiral space group $P2_12_12_1$. The efficiency of this substituent can even be improved when it is connected via a Me_2Si group to the stereogenic center. The silicon atom provides the necessary charge density to the carbanionic center and prevents conjugation. The (DABCO)Li moiety is only enantioselectively coordinated to one side of the benzyl anion in [(DABCO)LiCH(Ph)Si(Me)$_2$$CH_2$-pyrrolidine-$CH_2$OMe][244] (**212**), although the Li−C bond of 228 pm is fairly long (Figure 34). The enantioselectivity seems to be quite invariant towards donor-base addition, because the donor-base-free product [LiCH(Ph)Si(Me)$_2$$CH_2$-pyrrolidine-$CH_2OMe_2$]$_\infty$[245] (**213**) and the TMEDA-bridged molecules in [(TMEDA){LiCH(Ph)Si(Me)$_2$$CH_2$-pyrrolidine-$CH_2$OMe}$_2$][244] (**214**) show the same conformational stability in the solid-state. **213** crystallizes in the space group $P3_2$ with a helical arrangement employing an additional η^2-contact to the C_3 perimeter of the benzyl anion.

5. Silyl-substituted lithium organics

The electron-releasing facility and the steric bulk of bis- or tris(trimethylsilyl)methyl was employed successfully in various areas of organometallic chemistry[246–248]. The silyl groups supply the metalated carbon atom with sufficient charge density. The polymeric structure of [LiCH($SiMe_3$)$_2$]$_\infty$[249] (**215**) is a rare example of two-fold coordinated lithium in a polymeric strand (Figure 35). The silyl groups supply enough solubility despite the fact that no donor-base is coordinated to the lithium. The Li−C distance of 219 pm is only marginally elongated, although two lithium cations compete for the charge density of a single (Me_3Si)$_2$CH anion (Table 27). In the monomeric PMDETA complex [(PMDETA)LiCH($SiMe_3$)$_2$][250] (**216**), the bond is shortened by only 6 pm. The shape of the anion can easily be modified by introducing various substituents apart from methyl. The

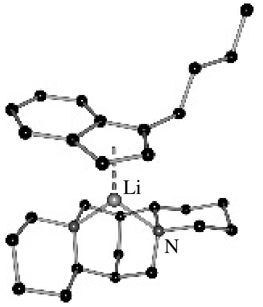

[((−)-sparteine)LiC_9H_6Bu-*n*]

(206)

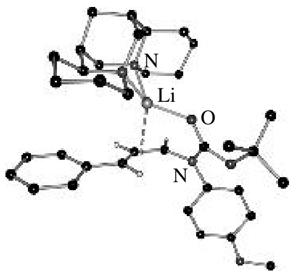

[((−)-sparteine)LiC_3H_3(Ph)-N{C(O)OBu-*t*)}C_6H_4OMe]

(209)

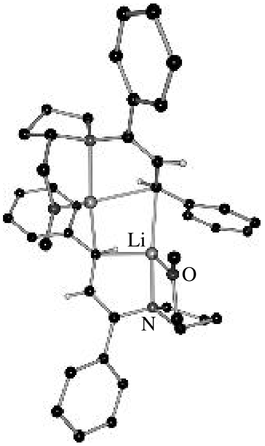

[LiC_2H_2(Ph){C(Ph)-pyrrolidine-CH_2OMe}]$_2$

(211)

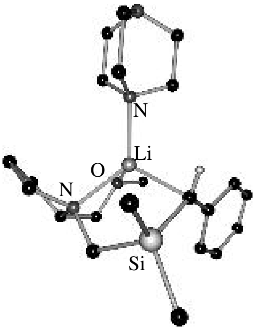

[(DABCO)LiCH(Ph)Si(Me_2)CH_2-pyrrolidine-CH_2OMe]

(212)

FIGURE 34. Solid-state structures of enantiomerically pure lithium organics

$(PhMe_2Si)_2CH$ anion in $[LiCH(Si(Me)_2Ph)_2]_2$[251] (**217**) seems to be a remarkable example, since it emulates the features discussed with the terphenyl ligands (see Figures 22 and 35) in Section III.C.1. The dimer consists of two moieties organized like the two units of a tennis ball, separated by the rubber imprint and shielding the metal core to the outside. From merely steric considerations one might expect the phenyl groups to point away from the lithium atoms at the metalated carbon atom, but from the discussion of weak interactions it is clear that even the relatively hard lithium cation requires metal π-contacts. However, total encapsulation of the lithium metal with three silicon-bonded phenyl groups is not accomplished in $[(THF)LiC(Si(Me)_2Ph)_3]$[252] (**218**). Only two phenyl groups face the metal, while the third points away in the other direction. The lithium is just coordinated to a single THF donor-base molecule. The bis(trimethylsilyl) ketone in $[\{(Me_3Si)_2CO\}LiC(SiMe_3)_3]$[234] (**219**) seems to be a very original donor, because once it is coordinated to the $(Me_3Si)_3CLi$ anion it leaves the lithium cation

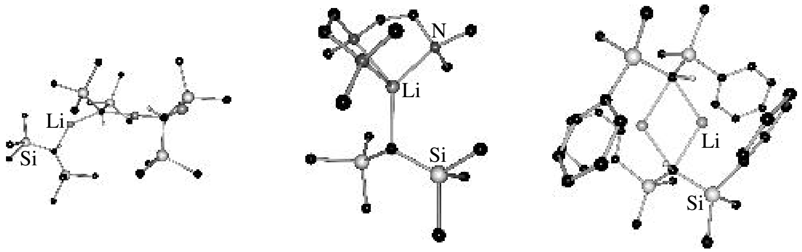

$[LiCH(SiMe_3)_2]_\infty$ **(215)**

$[(PMDETA)LiCH(SiMe_3)_2]$ **(216)**

$[LiCH(Si(Me)_2Ph)_2]_2$ **(217)**

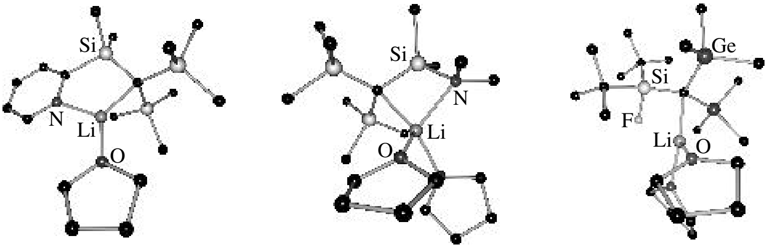

$[(THF)LiC(SiMe_3)_2$-$Si(Me)_2Py]$ **(220)**

$[(THF)_2LiC(SiMe_3)_2$-$Si(Me)_2NMe_2]$ **(221)**

$[(THF)_2LiC(GeMe_3)_2$-$\{Si(Bu\text{-}t)_2F\}]$ **(223)**

FIGURE 35. Solid-state structures of lithium organics with silyl-substituted lithium organics

TABLE 27. Silyl-substituted lithium organics

Compound		Li−C	Li−O, *N*	CCDC code	Reference
$[LiCH(SiMe_3)_2]_\infty$	**215**	219		CIMVUP	249
$[(PMDETA)LiCH(SiMe_3)_2]$	**216**	213	225	BIYXOW	250
$[LiCH(Si(Me)_2Ph)_2]_2$	**217**	219		NOXLIV	251
$[(THF)LiC(Si(Me)_2Ph)_3]$	**218**	212	185	CATZAY	252
$[\{(Me_3Si)_2CO\}LiC(SiMe_3)_3]$	**219**	213	184	LONYIW	234
$[(THF)LiC(SiMe_3)_2Si(Me)_2Py]$	**220**	214	187, *204*	XARZUL	253
$[(THF)_2LiC(SiMe_3)_2Si(Me)_2NMe_2]$	**221**	229	198, *216*	HOPPOR	254
$[(PMDETA)LiCH(SiMe_3)(PMe_2)]$	**222**	221	*220*	JEBGEC	255
$[(THF)_2LiC(GeMe_3)_2\{Si(Bu\text{-}t)_2F\}]$	**223**	222	196	TATFAV	256

two-fold coordinated. Of course, modifications of the periphery of the trisilylmethyl anion allows introduction of side-arm coordinating groups. In $[(THF)LiC(SiMe_3)_2Si(Me)_2Py]^{253}$ (**220**), the intramolecular (Py)N→Li donation discussed in Section IV.A.2. is applied to silylated anions. The lithium cation is in-plane coordinated by the ring-nitrogen atom (Figure 35). A dimethylamino side-arm coordinates as well as can be seen in the complex $[(THF)_2LiC(SiMe_3)_2Si(Me)_2NMe_2]^{254}$ (**221**). In the latter the N→Li donor bond is longer (216 vs. 204 pm in the first; Table 27) because the bite is more limited. The dimethylphosphane side-arm in $[(PMDETA)LiCH(SiMe_3)(PMe_2)]^{255}$ (**222**) shows no coordination to the metal, probably because of the tridentate donor-base PMDETA. In the last example presented here, a potential fluorine side-arm is in close proximity to the lithium atom in $[(THF)_2LiC(GeMe_3)_2\{Si(Bu\text{-}t)_2F\}]$[256] (**223**), but the distance of 333 pm is too long to be considered an interaction.

6. Heteroatom-substituted lithium organics

Obviously, the structures of heteroatom-substituted lithium organics would fill another chapter of this book. The building principles of the enolates[57] and enamines are most interesting, but as they predominantly build Li−O and Li−N rings, stacks and cages and hardly show any Li−C bond, they were not regarded as an issue in this chapter. Nevertheless, there are still lots of interesting compounds with a heteroatom next to a lithiated carbon atom. In $[(THF)_3Li_2(CH_2NPh_2)_2]$[257] (**224**), a Li_2C_2 four-membered ring similar to those discussed in Section III.C without any contact of the metal to the nitrogen atom is formed (Figure 36). Similarly, the metalated phosphane $[(TMEDA)LiCH_2PPh_2]$[258] (**225**) gives a monomer with a lithium cation exclusively bonded to the metalated H_2C group and no P→Li donor bond. The same phosphanide crystallizes even with the same donor-base in a different space group to give a cyclic dimer with Li−C *and* P→Li bonds in $[(TMEDA)LiCH_2PPh_2]_2$[259] (**226**) (Figure 36). The same phenomenon was observed with metalated sulfur organic compounds. $[(TMEDA)LiCH_2SMe]_2$[260] (**227**) forms Li_2C_2 four-membered rings without any S→Li bonds. In $[(THF)LiCH_2SMe]_\infty$[261] (**228**), they are further aggregated via $C_2S_2Li_2$ six-membered rings with S→Li donor bonds already detected in $[(TMEDA)LiCH_2SPh]_2$[260] (**229**). As anticipated, the donor-base PMDETA generates a monomer with no lithium−sulfur contact in $[(PMDETA)LiCH_2SPh]$[262] (**230**).

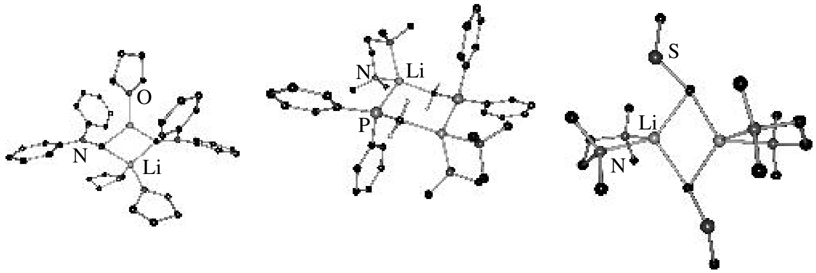

$[(THF)_3Li_2(CH_2NPh_2)_2]$ **(224)** $[(TMEDA)LiCH_2PPh_2]_2$ **(226)** $[(TMEDA)LiCH_2SMe]_2$ **(227)**

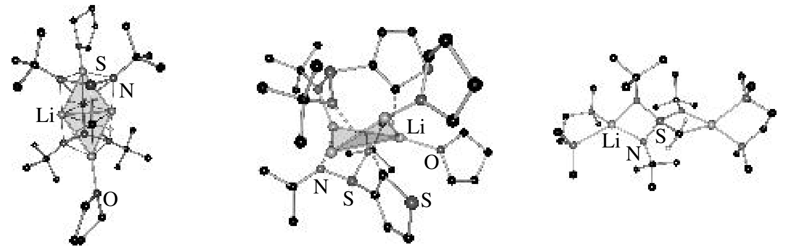

$[(THF)Li_2CH_2S(NBu\text{-}t)_2]_2$ **(231)** $[(THF)Li_2(C_4SH_2)S(NBu\text{-}t)_2]_2$ **(234)** $[(TMEDA)_2Li_2CH_2S(NBu\text{-}t)_3]$ **(235)**

FIGURE 36. Solid-state structures of heteroatom-substituted lithium organics

The dianionic methylene diimidosulfites $CR_2S(NR)_2{}^{2-}$ can be regarded to be the carba/imido analogues of $SO_3{}^{2-}$. Thus, they are sulfur(IV) ylides. Like Wittig ylides, they might be employed in C-C coupling reactions. The structures of $[(THF)Li_2CH_2S(NBu\text{-}t)_2]_2$[263] (**231**), $[(Et_2O)Li_2CH_2S(NSiMe_3)(NBu\text{-}t)]_2$[264] (**232**) and $[(THF)Li_2C(Et)(Me)S(NBu\text{-}t)_2]_2$[263] (**233**) reveal two distorted $SN_2C_2Li_3$ cubes with a common C_2Li_2 face (Figure 36). Like in the basic lithium organics discussed in Section II, a Li_3 triangle is formed at the diagonal cut of each cube. This metal triangle is μ_3-bridged by a carbanionic R_2C group. The average Li−C bonds (Table 28) are about 10 pm longer than the related distances in the donor-base-coordinated tetrahedra (Table 3), because the tripodal $S(CR_2)(NR)_2{}^{2-}$ dianion governs the correlated Li···Li distances. $[(THF)Li_2(C_4SH_2)S(NBu\text{-}t)_2]_2$[264] (**234**) is the first example of a dianionic S(VI)-β-ylide. The structure differs considerably from the face-connected cubes of the sulfur(IV)-α-ylides **231** to **233**. Both tripodal $S(CR_2)(NR)_2{}^{2-}$ dianions face each other with their concave sites in a staggered conformation. The metal core consists of two edge-connected Li_3 triangles resulting from a Li_4 tetrahedron with a broken edge. Both triangles are μ_3-capped by a metalated thiophenyl carbon atom (Figure 36). $[(TMEDA)_2Li_2CH_2S(NBu\text{-}t)_3]$[265] (**235**) is the first structurally characterized dianionic sulfur(VI)-ylide. The sulfur atom shows a distorted tetrahedral geometry bonding three imido groups and one methylene moiety (Figure 36). The two lithium atoms bridge two opposite edges of the SN_3C tetrahedron. The Li−C bond length shows the typical value of 213 pm. The most remarkable structural feature involves the bonding and orientation of the CH_2 group. The S−C bond length of 173 pm is short compared to the average value in the $H_3CS(NBu\text{-}t)_3{}^-$ anion of 179 pm. However, this bond shortening upon deprotonation should not be attributed to S=C double bonding in the sulfur ylenic mesomeric form[266].

TABLE 28. Heteroatom-substituted lithium organics

Compound		Li−C	Li−O, *N*	Li···Li	CCDC code	Reference
$[(THF)_3Li_2(CH_2NPh_2)_2]$	**224**	217[a]/224[b]	194[a]/198[b]	242	SUQRIF	257
$[(TMEDA)LiCH_2PPh_2]$	**225**	215	*214*		KAYFIZ	258
$[(TMEDA)LiCH_2PPh_2]_2$	**226**	217	*214*		RIFKAS	259
$[(TMEDA)LiCH_2SMe]_2$	**227**	224	*215*	246	CEPLEO	260
$[(THF)LiCH_2SMe]_\infty$	**228**	224	198	250	RURKUK	261
$[(TMEDA)LiCH_2SPh]_2$	**229**	213	*214*	374	CEPLAK	260
$[(PMDETA)LiCH_2SPh]$	**230**	215	*213*		WIZGER	262
$[(THF)Li_2CH_2S(NBu\text{-}t)_2]_2$	**231**	178[c]	194, 155[d]	265	QUCWAM	263
$[(Et_2O)Li_2CH_2S(NSiMe_3)\text{-}(NBu\text{-}t)]_2$	**232**	197[d,e]	196, 155[d]	266	IHUYAL	264
$[(THF)Li_2C(Et)(Me)S(NBu\text{-}t)_2]_2$	**233**	199[d,e]	201, 130[d]	265	QUCVUF	263
$[(THF)Li_2(C_4SH_2)S(NBu\text{-}t)_2]_2$	**234**	168[d,e]/174[d]	196, 130[d] and 155[d]/191	254 to 339	IHUXUE	264
$[(TMEDA)_2Li_2CH_2S(NBu\text{-}t)_3]$	**235**	213	*197/222*[f]		NEVKUU	265

[a] (THF)Li moiety.
[b] $(THF)_2Li$ unit.
[c] μ_3-Coordinated.
[d] μ_2-Coordinated.
[e] Central Li···Li vector.
[f] TMEDA nitrogen atom.

B. R_2C- and RC-Metalated Derivatives

In this section we present lithiated R_2C and RC species, hence lithium organics in which only two substituents or one group is bonded to the metalated center. Thus, normally there is a high degree of delocalization of the charge density along a conjugated system. Like the cyclic delocalized anions, this species contain various attractive coordination sites for the lithium cation. $[(Et_2O)LiC(CH_2)C_6H_3Me_2]_2$[267] (**236**) and $[(t\text{-BuOMe})LiC(CH_2)C_6H_3Me_2]_2$[267] (**237**) provide a C=C double bond and a C_6 perimeter next to the metalated carbon atom, but the lithium cation is exclusively coordinated to the C_α atom. Both structures show a Li_2C_2 four-membered ring with a pendent C=C double bond. Obviously, *t*-BuOMe is a better donor-base than Et_2O, because in **237** shorter Li−O and longer Li−C bonds are found compared to **236**. In the dimetalated butadiene derivatives $[(TMEDA)_2Li_2C_4(Me)_2(SiMe_3)_2]$[268] (**238**) and $[(DME)_2Li_2C_4Ph_4]$[269] (**239**), exclusively the deprotonated carbon atoms show Li−C contacts. Both (donor-base)Li moieties bridge the 1- and 4-position of the dianion (Figure 37). As opposed to $[(Et_2O)_2LiC(Ph)CCPh_2]$[270] (**240**), the extended π-system is not involved in metal coordination. In the latter the $(Et_2O)_2Li$ residue is η^3-coordinated above the center of an almost linear C_3 chain (Figure 37). Introduction of an methoxy side-arm shifts the lithium atom from the middle position to the terminal position of the C_3 chain in $[(Et_2O)LiC(CCPh_2)C_6H_4OMe]$[270] (**241**). A particularly interesting molecule is $[(THF)_2Li_2C_4(Bu\text{-}t)_2]_2$[271] (**242**): the conjugated system is extended to four carbon atoms. Two linear C_4 units can arrange parallel because the terminal *t*-Bu substituents are bent to the outside. The C_4 rods are connected by four lithium atoms. Two (THF)Li moieties bridge the aligned anions via σ-bonds (average Li−C 217 pm) and two bridge the rods via mutual π-bonding above and below the terminal C=C double bond, respectively (Figure 37). Heteroatom substitution at a dimetalated carbon center normally precludes conjugation and promotes charge accumulation. $[Li_2C\{P(Ph)_2NSiMe_3\}_2]_2$[272, 273] (**243** and **244**) is a rare example of 1,1′-dianion and the structure was independently determined twice. The two C-bonded phosphorus atoms concentrate the charge at the carbanionic center. The two imino side-arms arrange the four lithium atoms in the dimer to give a Li_4 four-membered ring. The four edges are μ_2-N-bridged. The $C\cdots Li_4$ ring center distance of 168 pm in **243** and 167 pm in **244** is remarkably short (Table 29).

Two RC-metalated compounds were discussed earlier in Section II.B, because $[(THF)LiC{\equiv}CBu\text{-}t]_4$[49] (**21**) and $[(TMHDA)_2(LiC{\equiv}CPh)_4]_\infty$[50] (**22**) form donor-base-coordinated tetramers. In dimeric $[(TMPDA)LiC{\equiv}CPh]_2$[274] (**245**), a Li_2C_2 four-membered

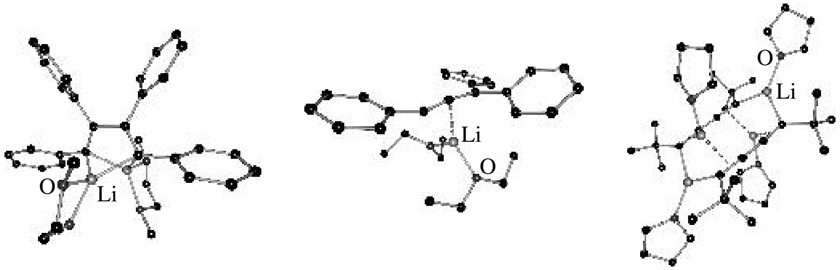

$[(DME)_2Li_2C_4Ph_4]$ **(239)** $[(Et_2O)_2LiC(Ph)CCPh_2]$ **(240)** $[(THF)_2Li_2C_4(Bu\text{-}t)_2]_2$ **(242)**

FIGURE 37. Solid-state structures of lithiated R_2C and RC species

TABLE 29. Lithiated R_2C and RC species

Compound		Li–C	Li–O, *N*	CCDC code	Reference
Lithiated R_2C species					
$[(Et_2O)LiC(CH_2)C_6H_3Me_2]_2$	**236**	217	192	REMHIA	267
$[(t\text{-BuOMe})LiC(CH_2)C_6H_3Me_2]_2$	**237**	220	190	REMHOG	267
$[(TMEDA)_2Li_2C_4(Me)_2(SiMe_3)_2]$	**238**	216	*220*	PETVOZ	268
$[(DME)_2Li_2C_4Ph_4]$	**239**	216	201	POJNIL	269
$[(Et_2O)_2LiC(Ph)CCPh_2]$	**240**	210	191	YOZJUS	270
$[(Et_2O)LiC(CCPh_2)C_6H_4OMe]$	**241**	225	196	YOZKAZ	270
$[(THF)_2Li_2C_4(Bu\text{-}t)_2]_2$	**242**	211[a]/217[b]	191[a]/195[b]	DANTAN	271
$[Li_2C\{P(Ph)_2NSiMe_3\}_2]_2$	**243**	167[c]	*210*	GOQXEP	272
$[Li_2C\{P(Ph)_2NSiMe_3\}_2]_2$	**244**	168[c]	*211*	GUBVOO	273
Lithiated RC species					
$[(TMPDA)LiC{\equiv}CPh]_2$	**245**	215	*212*	CIGXUL	274
$[\{(PMDETA,THF)Li\}_2C{\equiv}N][CuBu\text{-}t_2]$	**246**	210	202, *210/229*	NUTBIN	275
$[LiC_2Si(Me)_2C_6H_4OMe]_6$	**247**	224, 213/221	217	RICCIP	276

[a] η^2-Coordinated.

[b] σ-Coordinated.

[c] $C\cdots Li_4$ center distance.

ring is built without any further interaction of the cation to the phenylethynyl π-electron system. In the cation of the remarkable SSIP of $[\{(PMDETA,THF)Li\}_2C{\equiv}N][CuBu\text{-}t_2]$[275] (**246**), a cyanide anion is mutually C- and N-coordinated by a (PMDETA,THF)Li unit each to give an almost linear LiCNLi arrangement. The anion is reminiscent of the lithiates discussed in Section IV.A.3. The single Cu(I) cation is linearly coordinated by two t-Bu groups. The hexamer $[LiC_2Si(Me)_2C_6H_4OMe]_6$[276] (**247**) is generated along a crystallographic axis. The terminal carbon atom of the Si–C≡C unit μ_2-bridges two lithium atoms of which one is O-side-arm-coordinated and the second η^2-coordinated by the formal carbon triple bond. These few structural examples already prove that multiple bonds are attractive to lithium coordination.

V. CO-COMPLEXATION OF BASIC LITHIUM ORGANICS

As pointed out on various occasions in the course of this chapter, it is a major goal to deaggregate lithium organics to enhance their reactivity. This has to be done in a most controlled way to tune the reactivity to the required target system. Not always is the more reactive RLi necessarily the better RLi. The fine-tuning should provide some additional features like enantioselectivity, discrimination of specific functional groups against others, or enable definite reaction conditions like polar or non-polar solvents, higher or lower reaction temperatures, etc. Starting originally from a laboratory curiosity, today it is a flourishing area of research to generate tuned lithium organics like BuLi sponges or nanoporous lithium organic solid-state materials from the basic starting materials. By inspection of the solid-state structures of those products, it is obvious that those basic lithium organics seem to remember their 'structural past' and superimpose their 'structural memory' on the new products. Comparison of the changes and quantification of the effects enables firm judgment on the frequently quoted structure–reactivity relationship. This will be elucidated in the following section.

A. Release of the $Li_3\cdots C$ Motif

If the substituent and the donor-base provide the right steric and electronic profile, even monomers of basic lithium organics can be stabilized. In just very few cases is this accomplished by the release of the leading structural motif of the C_α-μ_3-capped Li_3 triangle. As one might anticipate, substituted lithium aryl derivatives discussed in Section C are a good choice to enable co-complexation of basic lithium organics, as they provide the whole range of Li—C σ- *and* π-interactions. The two terphenyl units in $[LiC_6H_3Dip_2]_2$[145] (**109**) accommodate two lithium cations in the inner metal core via metal π-interactions. In $[(C_6H_6)LiC_6H_3Tip_2]$[145] (**110**), just a π-bonded benzene molecule is required as a donor-base (Figure 22). Due to the possible integration of two metals and the need for only weak donor bases, it seems not surprising that $LiC_6H_4Tip_2$ co-complexes one equivalent of *t*-BuLi in $[Li_2(Bu\text{-}t)C_6H_3Tip_2])$[219] (**248**) (Figure 38). Compared to benzene, the butanide anion is a far better donor.

The structure of $[Li_2(Bu\text{-}n)Mes^*]_2$[136] (**249**) is a co-complex of *n*-BuLi and Mes*Li in a dimer. One lithium cation is σ-bonded to the alkyl and the aryl carbanion, emulating the structures of the lithiates discussed in Section IV.A.3. The second is bonded to the alkyl carbon atom and η^6-coordinated to the C_6 perimeter like in $[LiTip]_4$[136] (**101**) (Figure 21). At the methyl group lithiated trimethyltriazacyclononane co-complexes an equivalent of *t*-BuLi in the dimeric complex $[Li_2(Bu\text{-}t)CH_2{-}c\text{-}N_3(Me_2)(C_2H_4)_3]_2$[216] (**250**). The cyclic tripodal donor attained the right additional coordination site to (*N*, *N*, *N*)-accommodate the second lithium atom from the basic lithium organic. The butanide anion bridges the N-coordinated and the C-bonded lithium atom of the metalated methyl group to give a C_2Li_2N five-membered ring. These three examples document that lots of coordination abilities have to coincide to generate monomeric basic lithium organics. In most cases, under less ideal conditions, the 'structural memory' of the basic lithium organics is active and generates at least a single Li_3 triangle.

B. Retention of the $Li_3\cdots C$ Motif

In the isomorphous structures of $[Li_3(Bu\text{-}n)\{N(Pr\text{-}i)CH(Pr\text{-}i)CH_2OMe\}_2]$[277] (**251**), $[Li_3(Bu\text{-}s)\{N(Pr\text{-}i)CH(Pr\text{-}i)CH_2OMe\}_2]$[277] (**252**) and $[Li_3(Bu\text{-}t)\{N(Pr\text{-}i)CH(Pr\text{-}i)\text{-}CH_2OMe\}_2]$[277] (**253**), an equivalent of *n*-BuLi, *s*-Buli and *t*-BuLi, respectively, is co-complexed to two equivalents of an enantiomerically pure amide with a methoxy side-arm. The molecules crystallize in chiral space groups and are made up from a Li_3 triangle, which is not μ_3-capped from the carbanionic C_α atom. This is located almost ideally in the plane of the metal triangle, μ_2-bridging one Li···Li side. The two remaining sides are also μ_2-bridged by the amide nitrogen atoms. The two lithium corners, adjacent to the carbanion, are additionally coordinated by the side-arm (Figure 38). The structure of $[Li_6(Bu\text{-}t)_2\{C(Et)_2C_4NH_2)\}_4]$[278] (**254**) shows a calix(4)pyrrole reminiscent of $[(THF)LiC_4NH_2(c\text{-}C_6H_{10})]_4$[198] (**161**), presented in Section III.D.3. The two Li cations

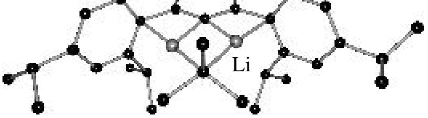

FIGURE 38. Solid-state structure of $[Li_2(Bu\text{-}t)C_6H_3Tip_2]$ (**248**)

at each side of **161** host another one from *t*-BuLi to build a Li_3 triangle above and below the macrocycle. One corner of the metal triangle is (N, N)-chelated by two pyrrole nitrogen atoms, while the remaining two are η^5-coordinated by the two other pyrrole rings. Like in the solid-state structure of $[t\text{-BuLi}]_4$[31] (**3**), the Li_3 site is μ_3-capped by the C_α carbon atom of the anion (Figure 39). As both capped faces are arranged staggered, the Li_6 moiety can be regarded as a Li_6 octahedron sliced perpendicular to the axis by a macrocycle.

In the dimer $[Li_2(Bu\text{-}n)\{CH_2Si(Ph)_2CH_2N(CH_2)_2OMe\}_2]_2$[279] (**255**), two edge-sharing Li_3 triangles are assembled. Each is μ_3-capped by the C_α carbon atom of the *n*-butyl anion like in the solid-state structure of $[n\text{-BuLi}]_6$[31] (**4**). One lithium cation is (N, N)-chelated by the side-arm and the remaining edges are μ_2-O and -C_α bridged. $[Li_2(Bu\text{-}n)CH(SiMe_3)\{C_6H(Me)_2(CH_2NMe_2)_2\}]_2$[280] (**256**) exhibits a similar arrangement. Again, the Li_3 triangles are capped by a *n*-butyl anion. As opposed to **255**, the anionic carbon atom of the ligand is not bridging a $Li\cdots Li$ edge, but coordinated to a corner. The ligand side-arms prefer likewise the terminal metal contact. Two fused Li_3 triangles can be found in $[Li_2(Bu\text{-}n)\{C_6H_3(CH(Et)NMe_2)_2\}]_2$[281] (**257**) as well. In the dimer two equivalents of *n*-BuLi are complexed. As the metalated *ipso*-C of the ring is almost located in the

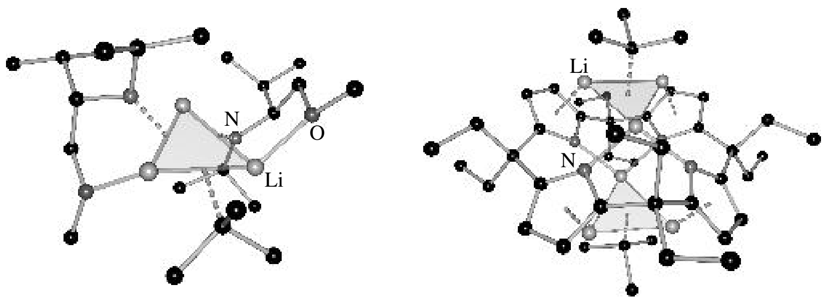

$[Li_3(Bu\text{-}t)\{N(Pr\text{-}i)CH(Pr\text{-}i)CH_2OMe\}_2]$

(253)

$[Li_6(Bu\text{-}t)_2\{C(Et_2)C_4NH_2)\}_4]$

(254)

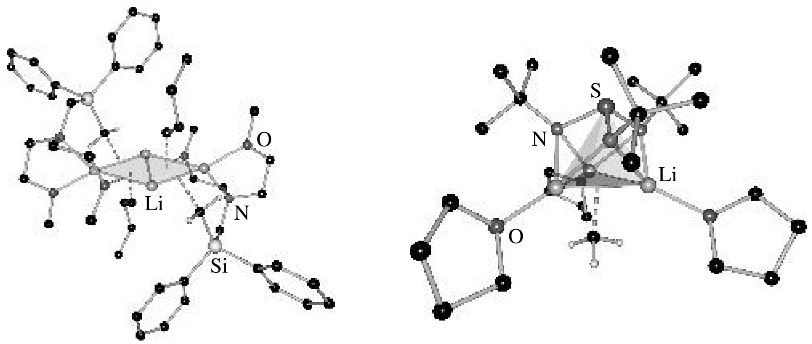

$[Li_2(Bu\text{-}n)\{CH_2Si(Ph)_2CH_2N(CH_2)_2OMe\}_2]_2$

(255)

$[(THF)_3Li_3Me\{(t\text{-BuN})_3S\}]$

(258)

FIGURE 39. Solid-state structures of lithium organic co-complexes that show retention of the $Li_3\cdots C$ motif

plane of the Li_4 area and the side-arms coordinate the involved lithium cations, the C_α atom is considerably displaced from the center of the metal triangle. In $[(THF)_3Li_3Me\{(t\text{-}BuN)_3S\}]$[282] (**258**), one equivalent of MeLi is co-complexed. The structure shows a triimidosulfite coordinated to three lithium atoms μ_2-arranged at every SN_2 bisection to form a Li_3 triangle known from the basic lithium organics. The upper triangle face is shielded by the triimidosulfite substituting the top $(THF)LiMe_3{}^{2-}$ site in the tetrahedron of $[(THF)LiMe]_4$[40] (**11**), while the lower face is capped by the methanide anion. The sulfur atom occupies the site of the *apical* lithium atom mimicking the tetrahedron of the starting material (Figure 39).

C. Retention of the Deltahedron

The first class of co-complexes is generated from chiral alkoxides with a methoxy side-arm. The method takes advantage of the fact that lithium alkoxides predominantly aggregate to give $[LiOR]_4$ cubes. However, with the employed bulky substituent there is not enough room to accommodate four alkoxides in a cube, the more they attain donating side-arms. Obviously, it is just possible to arrange three alkoxides close together. The missing lithium atom to occupy the four vertices in the Li_4O_4 cube is recruited from *n*-BuLi. This is promoted by the fact that there is just enough room to fit in the *n*-butyl anion. In the first example, in the structure of $[Li_4(Bu\text{-}n)(C_{17}H_{23}O_2)_3]$[283] (**259**), four lithium atoms organize to build a tetrahedron and three oxygen atoms of the alkoxide ligands μ_3-cap three faces. This would be equivalent to a Li_4O_4 cube with a missing O-vertex. This missing vertex is occupied by the C_α atom of the butyl anion. It μ_3-caps the otherwise unoccupied Li_3 triangle. The metal atoms of this triangle are additionally donated by the three methoxy side-arms. $Li\cdots C_\beta$ interactions are not required. $[Li_4(Bu\text{-}n)_2\{C_{17}H_{22}O_2(Bu\text{-}t)\}_2]$[284] (**260**), $[Li_4(Bu\text{-}n)_2\{C_{17}H_{22}O_2(Si(Me)_2Bu\text{-}t)\}_2]$[284] (**261**) and $[Li_4(Bu\text{-}n)_2\{C_{17}H_{22}O_2(SiMe_3)\}_2]$[284] (**262**) are constructed by the same principle plan, although they got even bulkier alkoxide ligands and thus only two can organize around a virtual Li_4O_4 cube. As a consequence they include two equivalents *n*-BuLi in their molecular architecture. All six C_α atoms of the butyl anions in **260**, **261** and **262** μ_3-cap their Li_3 face. At first sight, the structure of $[(Et_2O)_4Li_7(Bu\text{-}n)_2\{N(Ph)C_6H_4\}_2(NPh_2)]$[285] (**263**) looks very complex and incomprehensible (Figure 40). However, application of the lead building principles in lithium organics and lithium amides immediately clarifies the architecture: the main building blocks are seven lithium cations, three diphenylamides and two *n*-butyl anions. Thus, at first sight there are two negative charges missing. Fortunately, four of the seven lithium atoms organize to form a tetrahedron. As anticipated, the two butyl anions μ_3-cap two Li_3 faces. The three amides take the remaining three lithium anions to form a lithium amide ladder structure[52–55]. However, that ladder is connected via μ_3-capping of two Li_3 faces by *ortho*-phenyl carbon atoms discussed with the structure of $[(t\text{-}Bu)_2C_6H_3Li]_6$[36] (**9**) in Section II.A. Thus, two phenyl groups at the ends of the lithium amide ladder are *ortho*-metalated and provide the missing negative charges. This example impressively documents that the Li_3 formation principle of lithium organics and the lithium amide stacking and laddering principle interact at mutual benefit. While the related complexes **256** and **257** from the previous section just support Li_3 triangles, in $[Li_2(Bu\text{-}n)CH_2\{C_6H(Me)_2(CH_2NMe_2)_2\}]_2$[286] (**264**), the tetrahedron is retained. Two benzylic C_α anions μ_3-cap two Li_3 faces and the remaining two are capped by the butyl anions. A particularly remarkable example for co-complexation of basic lithium organics with retention of the deltahedron is provided in $[Li_8(Bu\text{-}n)_4(OBu\text{-}t)_4]$[287] (**265**). The complex can be rationalized as ‘on his way’ to mix the $[LiOR]_4$ cube with the $[LiR]_4$ tetrahedron. Although rather distorted, one Li_4 tetrahedron stays intact in the structure. Two faces are butyl-capped and two are BuO-capped. In the second, one edge of the tetrahedron is already broken on its way to reorganization. While the butyl groups are still

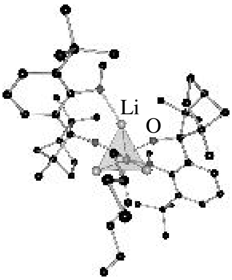

$[Li_4(Bu\text{-}n)_2\{C_{17}H_{22}O_2(Bu\text{-}t)\}_2]$

(260)

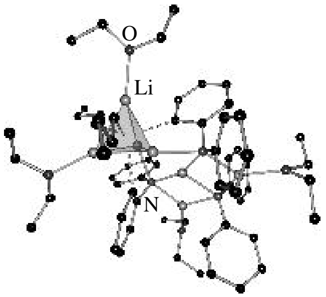

$[(Et_2O)_4Li_7(Bu\text{-}n)_2\{N(Ph)C_6H_4\}_2(NPh_2)]$

(263)

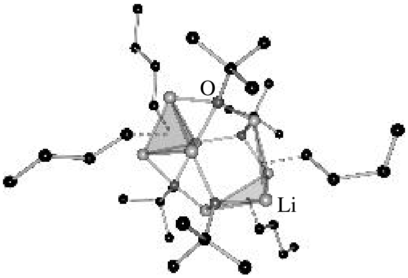

$[Li_8(Bu\text{-}n)_4(OBu\text{-}t)_4]$

(265)

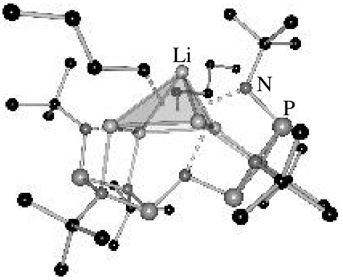

$[Li_5(Bu\text{-}n)_2N\{(PNBu\text{-}t)_2NBu\text{-}t\}_2]$

(266)

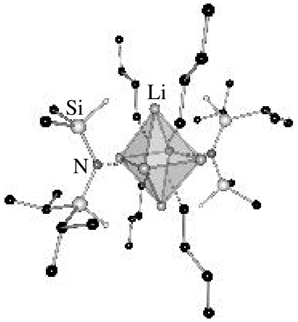

$[Li_6(Bu\text{-}n)_4\{N(SiHMe_2)(SiH(Pr\text{-}i)_2)\}_2]$

(270)

FIGURE 40. Solid-state structures of lithium organic co-complexes that show retention of the deltahedron

μ_3-capping, the BuO groups are shifted towards the edges of the Li_3 triangles. However, whether the molecule is on its way to organize to a mixed $[Li_4Bu_2(OR)_2]$ aggregate or to disintegrate any further remains open by just looking at that structure, although the analogy with **259** to **261** suggests the first.

$[Li_5(Bu\text{-}n)_2N\{(PNBu\text{-}t)_2NBu\text{-}t\}_2]$[288] (**266**) provides an appropriate link from the retention of the tetrahedron to the retention of the octahedron, because the hemispherical trianionic PN ligand promotes the generation of a distorted square-pyramidal Li_5 metal core in the cradle. The two additional metal cations derive from co-coordination of two equivalents n-BuLi. The Li_4 face is assembled via dual μ_2-bridging of the opposite edges by the terminal and the central amide nitrogen atoms. The second terminal amide μ_3-caps a Li_3 face in the radial direction of the ligand. The lateral Li_3 faces are occupied by the butyl anions. As anticipated from the structures of basic lithium organics, the unoccupied Li_3 face shows the widest Li$\cdots$Li distances.

Obviously, the co-complexation of basic lithium organics with lithium alkoxides is not limited to tetrahedra. In $[Li_6(Bu\text{-}n)_4(C_{18}H_{25}O_2)_2]$[289] (**267**), two of the previously discussed alkoxide ligands μ_3-cap two opposite sides of the Li_6 octahedron. The other four are capped by the butyl anions. In $[(Et_2O)Li_6\{Bu\text{-}n\}_2\{CH(Me)(C_6H_2(Bu\text{-}t)_2O)_2\}_2]$[290] (**268**), four Li_3 triangles are capped by the oxygen atoms of the bis(alkoxide) ligands. The remaining two accommodate the two butyl anions. The tripodal monoanionic $OC(CH_2PMe_2)_3$ ligands in $[Li_6(Bu\text{-}n)_4\{OC(CH_2PMe_2)_3\}_2]$[291] (**269**) facilitate the pre-organization of a Li_3 triangle by the phosphorus donor side-arms. The anionic oxygen atom is in the right position to μ_3-cap that metal triangle. Arrangement at opposite sides of the octahedron leaves four faces vacant for butyl coordination. The structure of $[Li_6(Bu\text{-}n)_4\{N(SiH\,Me_2)(SiH(Pr\text{-}i)_2)\}_2]$[292] (**270**) shows a combination of the μ_3-capping from the butyl groups and μ_2-bridging already discussed in the amide **266**. The bis(silylamide) in **270** bridges two opposite Li$\cdots$Li vectors in the equatorial position of the octahedron.

D. Correlation of the Structure Formation Principles

Looking at the discussed complexes containing basic lithium organics, it might be most striking that the vast majority of those complexes are donor-base-free compounds, thus members of the class of lithium organics with which this chapter started. Normally, donor bases are employed to deaggregate basic oligomeric lithium organics. However, solid-state structural information on donor-base-stabilized monomers or even dimers are scarce (see Section II.C, Table 4). In this chapter we presented one structure with a single MeLi moiety (**258**[282]), two structures with a single n-BuLi unit (**251**[277], **259**[283]) and two structures with a unique t-BuLi molecule (**248**[219], **253**[277]). This suggests that co-complexation of basic lithium organics seems to be the more promising approach to deaggregation than merely donor-base addition. The tools to model the appropriate environment for the required aggregate are much more sophisticated than working merely on a collection of solvents. The combination of both methods will give great impetus to the field. Molecular pre-organization is likely to supply the right cavities, suitable coordination sites and the right mix of weak and strong molecular interactions, like σ-bonds, donor bonds of readily modified Lewis bases, π-bonds, Li$\cdots C_\beta$ interaction, stereogenic fixation via side-arm donation etc. None of the previously discussed classes of compounds showed such a tremendous diversity in interactions (Table 30). We have just started to understand and utilize the structure formation principles and there is still a lot to learn.

VI. CONCLUSION

To uncover new reaction pathways towards unprecedented target materials, the understanding of structure formation principles is important. One of the lead structural principles in lithium organic chemistry is the μ_3-capping of the metalated carbon atom C_α to a lithium triangle. This motif can further aggregate to form deltahedra. The tetrahedra and octahedra can either be free of solvent or be coordinated by Lewis-basic donor molecules

TABLE 30. Complexes containing basic lithium organics

Compound		Li–C	Li–O, *N*	Li···Li	CCDC code	Reference
$[Li_2(Bu\text{-}t)C_6H_3Tip_2]$	**248**	210[a]/217[b]/230[c]		223	MOBREA	219
$[Li_2(Bu\text{-}n)Mes^*]_2$	**249**	188[d]/205[e]/214[f]/206[b]			LEFSOE	136
$[Li_2(Bu\text{-}t)CH_2\text{-}c\text{-}N_3(Me_2)(C_2H_4)_3]_2$	**250**	221[a]/222[g]	*209*	245	IGODUD	216
$[Li_3(Bu\text{-}n)\{N(Pr\text{-}i)CH(Pr\text{-}i)CH_2OMe\}_2]$	**251**	159[h]/249[j]	192,*141*[h]	280/278[i]	NUVXEH	277
$[Li_3(Bu\text{-}s)\{N(Pr\text{-}i)CH(Pr\text{-}i)CH_2OMe\}_2]$	**252**	159[h]/235[j]/251[j]	193,*142*[h]	277/280[i]	NUVXIL	277
$[Li_3(Bu\text{-}t)\{N(Pr\text{-}i)CH(Pr\text{-}i)CH_2OMe\}_2]$	**253**	169[h]	198,*143*[h]	277/284[i]	NUVXOR	277
$[Li_6(Bu\text{-}t)_2\{C(Et)_2C_4NH_2)\}_4]$	**254**	158[k]/185[l]	*202*	267	ZALCOE	278
$[Li_2(Bu\text{-}n)\{CH_2Si(Ph)_2CH_2N(CH_2)_2OMe\}_2]_2$	**255**	170[k]/260[h, j]/191[m]	174[h]/204, 220	248-280	RAHLUH	279
$[Li_2(Bu\text{-}n)CH(SiMe_3)\{C_6H(Me)_2(CH_2NMe_2)_2\}]_2$	**256**	155[k]/215[a]	*209*	253/335	NOYKOB	280
$[Li_2(Bu\text{-}n)\{C_6H_3(CH(Et)NMe_2)_2\}]_2$	**257**	219[a]/223[b]	*205*	241/268	POYBOU	281
$[(THF)_3Li_3Me\{(t\text{-}BuN)_3S\}]$	**258**	172[k]	199,*206*	263	QOSLUF	282
$[Li_4(Bu\text{-}n)(C_{17}H_{23}O_2)_3]$	**259**	169[k]/278[j]	130[k]/200	247	XAWGOR	283
$[Li_4(Bu\text{-}n)_2\{C_{17}H_{22}O_2(Bu\text{-}t)\}_2]$	**260**	179[k]/268[j]	126[k]/194	248	TIGMOL	284
$[Li_4(Bu\text{-}n)_2\{C_{17}H_{22}O_2(Si(Me)_2Bu\text{-}t)\}_2]$	**261**	175[k]/237[j]	127[k]/195	234[n]/248	TIGNAY	284
$[Li_4(Bu\text{-}n)_2\{C_{17}H_{22}O_2(SiMe_3)\}_2]$	**262**	178[k]/237[a, j]	123[k]/196	249	LOVLAJ	284
$[(Et_2O)_4Li_7(Bu\text{-}n)_2\{N(Ph)C_6H_4\}_2(NPh_2)]$	**263**	166[a, k]/183[b, k]/263[a, j]/194[b, j]	203,*204*	249[a, i]/268[b, i]/263	RETBEX	285
$[Li_2(Bu\text{-}n)CH_2C_6H(Me)_2(CH_2NMe_2)_2]_2$	**264**	168[a]/178[o]	*208*	257	YIJFIG	286
$[Li_8(Bu\text{-}n)_4(OBu\text{-}t)_4]$	**265**	158[k, p]/163[k, q]/235[j]	187	242-368[p]/242-291[q]	TABSIY	287
$[Li_5(Bu\text{-}n)_2N\{(PNBu\text{-}t)_2NBu\text{-}t\}_2]$	**266**	155[k]/234-246[j]	*146*[h]*/162*[k]*/176*[h]	271[r]/269[s]-301	QIDNIA	288
$[Li_6(Bu\text{-}n)_4(C_{18}H_{25}O_2)_2]$	**267**	154[k]/259[j]/268[t]	115[k]/193	244/317 289[u]/331[v]	TIGMIF	289
$[(Et_2O)Li_6\{Bu\text{-}n\}_2\{CH(Me)(C_6H_2(Bu\text{-}t)_2O)_2\}_2]$	**268**	151[k]/235[j]/271[j]	109[k]/206	251/325	NENMEY	290
$[Li_6(Bu\text{-}n)_4\{OC(CH_2PMe_2)_3\}_2]$	**269**	159[k]/228[h, j] and 254[h, j]	110[k]	250/310	QOZHAO	291
$[Li_6(Bu\text{-}n)_4\{N(SiHMe_2)(SiH(Pr\text{-}i)_2)\}_2]$	**270**	152[k]/242[j]	*143*[h]	252[s]/285[n]	XINSUI	292

[a] Alkyl-coordinated. [b] Aryl-C σ-coordinated. [c] Coordinated by peripheral aryl-C. [d] η^6-coordinated. [e] Alkyl-Li bond (Li additionally η^6-coordinated). [f] Alkyl-Li bond (Li additionally aryl-C_σ-coordinated). [g] Li-C_{crypt}. [h] μ_2-coordinated. [i] C-bridged Li···Li vector. [j] Li···C_β. [k] μ_3-coordinated. [l] η^5-coordinated. [m] Li-CH_2SiR_3 bond. [n] Both Li atoms C_β-coordinated. [o] Aryl-substituted alkyl C-Li bond. [p] Within intact tetrahedron. [q] Within 'broken' tetrahedron. [r] Within Li_3 center coordinated Li_3 triangle. [s] N-bridged Li···Li vector. [t] Li···Li vector coordinated by two C_β atoms. [u] Oxygen atom caps adjacent Li_3 triangle. [v] C_α caps adjacent Li_3 triangle.

at their metal vertices. Among these interactions the $Li\cdots C_\beta$ contact seems to play an important role. Normally, the coordination of donor molecules supplies charge density to the cationic lithium metal and the bond towards the carbanion becomes less attractive. The second important structure formation principle is the additional favor of the lithium cation for delocalized π-systems. The η^5-coordination is particularly important. If there is the choice of a C_5 perimeter in competition with any other ring, the lithium coordinates the first. Aryl carbanions hardly ever get η^6-coordinated. In this case, the lithium cation prefers the σ-bond to the carbanion in a Li_2C_2 four-membered ring, still in demand of easy-to-polarize charge density. One of the most fruitful chemical concepts during the last years was the intramolecular side-arm coordination, not only to deaggregate basic lithium organics but also to keep the metal in a fixed position relative to the carbanion. Certainly, this approach is in its importance comparable to the application of phosphanes in transition metal chemistry. Introduction of heteroatoms near the metalated carbon atom alters the charge density at the carbanion considerably. Nitrogen substitution depletes the electron density at the carbanionic center and it might rather mimic the coordinational behavior of an amide. Silyl substitution increases the charge density at the carbanion and the Li−C bonds get shorter, even against steric strain. A most interesting and promising area of research is the co-complexation of basic lithium organics with various metal organics. Other structure formation principles, like the lithium amide ring stacking and laddering principle and the formation of lithium alkoxides, start to get involved in this process. A blend of today's donor-base application, side-arm donation and co-complexation will further improve the stereogenic stability of chiral lithium organics. We have just started to elaborate the structure–reactivity relation. No doubt, the insight in structure-determining factors will further unearth new reaction pathways and will provide access to unprecedented molecules and materials.

VII. ACKNOWLEDGMENT

The authors thank the Deutsche Forschungsgemeinschaft, the Fonds der Chemischen Industrie and Chemetall, Frankfurt, for continuous financial support. Without the marvelous help of S. Deuerlein, V. Duchnik, N. Kocher, D. Leusser and A. Murso during the writing of this chapter, it would not have materialized.

VIII. REFERENCES

1. Cambridge Structural Database, release 5.24, April 2003.
2. F. H. Allen, *Acta Crystallogr., Sect. B*, **58**, 380 (2002).
3. P. Barbier, *Compt. Rend.*, **128**, 110 (1899).
4. V. Grignard, *Compt. Rend.*, **130**, 1322 (1900).
5. W. Schlenk and J. Holtz, *Ber. Dtsch. Chem. Ges.*, **50**, 262 (1917).
6. H. Dietrich, *Acta Crystallogr.*, **16**, 681 (1963).
7. E. A. C. Lucken and E. Weiss, *J. Organomet. Chem.*, **2**, 197 (1964).
8. H. Dietrich, *J. Organomet. Chem.*, **205**, 291 (1981).
9. E. Weiss and G. Henken, *J. Organomet. Chem.*, **21**, 265 (1970).
10. E. Weiss, T. Lambertsen, B. Schubert, J. K. Cockcroft and A. Wiedenmann, *Chem. Ber.*, **123**, 79 (1990).
11. R. Rudman, *Low Temperature X-Ray Diffraction: Apparatus and Techniques*, Plenum, New York, 1976.
12. M. Veith and H. Bärninghausen, *Acta Crystallogr., Sect. B*, **30**, 1806 (1974).
13. D. Seebach, R. Amstutz, T. Laube, W. B. Schweizer and J. D. Dunitz, *J. Am. Chem. Soc.*, **107**, 5403 (1985).
14. R. Boese and D. Bläser, *J. Appl. Crystallogr.*, **22**, 394 (1989).

15. H. Hope, *Acta Crystallogr., Sect. B*, **44**, 22 (1988).
16. T. Kottke and D. Stalke, *J. Appl. Crystallogr.*, **26**, 615 (1993).
17. D. Stalke, *Chem. Soc. Rev.*, **27**, 171 (1998).
18. W. Phillips, M. Stanton, D. O'Mara, Y. Li, I. Naday and E. Westbrook, *Proc. SPIE-Int. Soc. Opt. Eng.*, **2009**, 133 (1993).
19. W. N. Setzer and P. v. R. Schleyer, *Adv. Organomet. Chem.*, **24**, 353 (1985).
20. E. Weiss, *Angew. Chem., Int. Ed. Engl.*, **32**, 1501 (1993).
21. A.-M. Sapse and P. v. R. Schleyer (Eds.), *Lithium Chemistry: A Theoretical and Experimental Overview*, Wiley, New York, 1994.
22. D. Stalke, *Angew. Chem., Int. Ed. Engl.*, **33**, 2168 (1994).
23. S. Harder, *Coord. Chem. Rev.*, **176**, 17 (1998).
24. P. Jutzi and N. Burford, *Chem. Rev.*, **99**, 969 (1999).
25. C. Schade and P. v. R. Schleyer, *Adv. Organomet. Chem.*, **27**, 169 (1987).
26. J. D. Smith, *Adv. Organomet. Chem.*, **43**, 267 (1999).
27. J. L. Wardell, N. A. Bell and W. E. Lindsell, *Comprehensive Organometallic Chemistry II*, C.E. Housecroft (Ed.), Vol. 1, Pergamon Press, New York, 1995, p. 1.
28. I. Haiduc and F. T. Edelmann, *Supramolecular Organometallic Chemistry*, Wiley-VCH, Weinheim, 1999, 471 pp.
29. A. Streitwieser, Jr., J. E. Williams, Jr. and J. M. McKelvey, *J. Am. Chem. Soc.*, **98**, 4778 (1976).
30. E. Kaufmann, K. Raghavachari, A. E. Reed and P. v. R. Schleyer, *Organometallics*, **7**, 1597 (1988).
31. T. Kottke and D. Stalke, *Angew. Chem., Int. Ed. Engl.*, **32**, 580 (1993).
32. U. Siemeling, T. Redecker, B. Neumann and H.-G. Stammler, *J. Am. Chem. Soc.*, **116**, 5507 (1994).
33. D. Hoffmann, P. v. R. Schleyer and D. Stalke, unpublished results.
34. R. Zerger, W. Rhine and G. Stucky, *J. Am. Chem. Soc.*, **106**, 6048 (1974).
35. A. Maercker, M. Bsata, W. Buchmeier and B. Engelen, *Chem. Ber.*, **117**, 2547 (1984).
36. R. J. Wehmschulte and P. P. Power, *J. Am. Chem. Soc.*, **119**, 2847 (1997).
37. B. Teclé, A. F. M. M. Rahman and J. P. Oliver, *J. Organomet. Chem.*, **317**, 267 (1986).
38. M. Schlosser, 'Organoalkali Reagents', in *Organometallics in Synthesis, A Manual* (Ed. M. Schlosser), Wiley, New York, 2002.
39. F. Totter and P. Rittmeyer, 'Organolithium Compounds—Industrial Applications and Handling', in *Organometallics in Synthesis, A Manual* (Ed. M. Schlosser), Wiley, New York, 2002.
40. C. A. Ogle, B. K. Huckabee, H. C. Johnson IV, P. F. Sims, S. D. Winslow and A. A. Pinkerton, *Organometallics*, **12**, 1960 (1993).
41. H. Köster, D. Thoennes and E. Weiss, *J. Organomet. Chem.*, **160**, 1 (1978).
42. B. Walfort, L. Lameyer, W. Weiss, R. Herbst-Irmer, R. Bertermann, J. Rocha and D. Stalke, *Chem. Eur. J.*, **7**, 1417 (2001).
43. M. A. Nichols and P. G. Williard, *J. Am. Chem. Soc.*, **115**, 1568 (1993).
44. N. D. R. Barnett, R. E. Mulvey, W. Clegg and P. A. O'Neil, *J. Am. Chem. Soc.*, **115**, 1573 (1993).
45. T. Kottke, R. J. Lagow, D. Hoffmann and R. D. Thomas, *Organometallics*, **16**, 789 (1997).
46. W. Bauer and F. Hampel, *J. Chem. Soc., Chem. Commun.*, 903 (1992).
47. H. Hope and P. P. Power, *J. Am. Chem. Soc.*, **105**, 5320 (1983).
48. M. M. Olmstead and P. P. Power, *J. Am. Chem. Soc.*, **112**, 8008 (1990).
49. M. Geissler, J. Kopf, B. Schubert, E. Weiss, W. Neugebauer and P. v. R. Schleyer, *Angew. Chem., Int. Ed. Engl.*, **26**, 587 (1987).
50. B. Schubert and E. Weiss, *Angew. Chem., Int. Ed. Engl.*, **22**, 496 (1983).
51. P. Rademacher, *Strukturen Organischer Moleküle*, VCH, Weinheim, 1987.
52. K. Gregory, P. v. R. Schleyer and R. Snaith, *Adv. Inorg. Chem.*, **37**, 47 (1991).
53. R. E. Mulvey, *Chem. Soc. Rev.*, **20**, 167 (1991).
54. R. E. Mulvey, *Chem. Soc. Rev.*, **27**, 339 (1998).
55. A. Downard and T. Chivers, *Eur. J. Inorg. Chem.*, 2193 (2001).
56. F. Pauer and P. P. Power, in *Lithium Chemistry: A Theoretical and Experimental Overview*, (Eds. A.-M. Sapse and P. v. R. Schleyer), Chap. 9, Wiley, New York, 1994.
57. D. Seebach, *Angew. Chem., Int. Ed. Engl.*, **27**, 1624 (1988).

58. B. Walfort, S. K. Pandey and D. Stalke, *Chem. Commun.*, 1640 (2001).
59. D. Thoennes and E. Weiss, *Chem. Ber.*, **111**, 3157 (1978).
60. W. Hiller, M. Layh and W. Uhl, *Angew. Chem., Int. Ed. Engl.*, **30**, 324 (1991).
61. C. Strohmann, T. Seibel and K. Strohfeldt, *Angew. Chem., Int. Ed.*, **42**, 4531 (2003).
62. U. Schümann, J. Kopf and E. Weiss, *Angew. Chem., Int. Ed. Engl.*, **24**, 215 (1985).
63. T. Maetzke and D. Seebach, *Helv. Chim. Acta*, **72**, 624 (1989).
64. E. Hey-Hawkins and K. Fromm, *Polyhedron*, **14**, 2027 (1995).
65. B. Halton and M. G. Banwell, in *The Chemistry of the Cyclopropyl Group*, Part 2 (Ed. Z. Rappoport), Wiley, New York, 1987, p. 1223.
66. E. D. Jemmis, J. Chandrasekhar and P. v. R. Schleyer, *J. Am. Chem. Soc.*, **101**, 2848 (1979).
67. A. Streitwieser, S. M. Bachrach, A. Dorigo and P. v. R. Schleyer, in *Lithium Chemistry: A Theoretical and Experimental Overview* (Eds. A.-M. Sapse and P. v. R. Schleyer), Chap. 1, Wiley, New York, 1994.
68. A. E. Reed, L. A. Curtiss and F. Weinhold, *Chem. Rev.*, **88**, 889 (1988).
69. K. Sorger, P. v. R. Schleyer and D. Stalke, *J. Am. Chem. Soc.*, **118**, 1086 (1996).
70. K. Sorger, P. v. R. Schleyer, R. Fleischer and D. Stalke, *J. Am. Chem. Soc.*, **118**, 6924 (1996).
71. K. Sorger, P. v. R.Schleyer and D. Stalke, *J. Chem. Soc., Chem. Commun.*, 2279 (1995).
72. G. Boche, H. Etzrodt, W. Massa and G. Baum, *Angew. Chem., Int. Ed. Engl.*, **24**, 863 (1985).
73. T. Matsuo, T. Mizue and A. Sekiguchi, *Chem. Lett.*, 896 (2000).
74. A. Sekiguchi, T. Matsuo and H. Watanabe, *J. Am. Chem. Soc.*, **122**, 5652 (2000).
75. A. Sekiguchi, T. Matsuo, K. Ebata and K. Sakurai, *Chem. Lett.*, 1133 (1996).
76. R. E. Dinnebier, *Mat. Sci. Forum*, 321 (2000).
77. D. M. K. Harris, M. Tremayne and B. M. Kariuki, *Angew. Chem., Int. Ed.*, **40**, 1626 (2001).
78. R. E. Dinnebier, U. Behrens and F. Olbrich, *Organometallics*, **16**, 3855 (1997).
79. N. J. Long, *Metallocenes: An Introduction to Sandwich Complexes*, Blackwell Science, Oxford, London, 1998.
80. W. J. Evans, T. J. Boyle and J. W. Ziller, *Organometallics*, **11**, 3903 (1992).
81. W.-P. Leung, F.-Q. Song, F. Xue and T. C. W. Mak, *J. Chem. Soc., Dalton Trans.*, 4307 (1997).
82. W. Nie, C. Qian and J. Sun, *Organometallics*, **20**, 5780 (2001).
83. K. Kunz, J. Pflug, A. Bertuleit, R. Fröhlich, E. Wegelius, G. Erker and E.-U. Würthwein, *Organometallics*, **19**, 4208 (2000).
84. C. Dohmeier, E. Baum, A. Ecker, R. Köppe and H. Schnöckel, *Organometallics*, **15**, 4702 (1996).
85. S. Harder and M. H. Prosenc, *Angew. Chem., Int. Ed. Engl.*, **33**, 1744 (1994).
86. F. Zaegel, J. C. Gallucci, P. Meunier, B. Gautheron, M. R. Sivik and L. A. Paquette, *J. Am. Chem. Soc.*, **116**, 6466 (1994).
87. W.-K. Wong, L. Zhang, W.-T. Wong, F. Xue and T. C. W. Mak, *Polyhedron*, **15**, 4593 (1996).
88. S. D. Stults, R. A. Andersen and A. Zalkin, *J. Am. Chem. Soc.*, **111**, 4507 (1989).
89. U. J. Bildmann and G. Müller, *Z. Naturforsch., Teil B*, **55**, 895 (2000).
90. P. B. Hitchcock, J. Hu and M. F. Lappert, *Chem. Commun.*, 143 (1998).
91. D. R. Armstrong, R. Herbst-Irmer, A. Kuhn, D. Moncrieff, M. A. Paver, C. A. Russell, D. Stalke, A. Steiner and D. S. Wright, *Angew. Chem., Int. Ed. Engl.*, **32**, 1774 (1993).
92. M. A. Paver, C. A. Russell, D. Stalke and D. S. Wright, *J. Chem. Soc., Chem. Commun.*, 1349 (1993).
93. G. Zi, Q. Yang, T. C. W. Mak and Z. Xie, *Organometallics*, **20**, 2359 (2001).
94. B. Walfort, A. P. Leedham, C. A. Russell and D. Stalke, *Inorg. Chem.*, **40**, 5668 (2001).
95. A. Steiner, S. Zacchini and P. I. Richards, *Coord. Chem. Rev.*, **227**, 193 (2002).
96. D. Leusser, B. Walfort and D. Stalke, *Angew. Chem., Int. Ed.*, **41**, 2079 (2002).
97. A. Hammel, W. Schwarz and J. Weidlein, *Acta Crystallogr., Sect. C*, **46**, 2337 (1990).
98. U. J. Bildmann, M. Winkler and G. Müller, *Z. Naturforsch., Teil B*, **55**, 1005 (2000).
99. M. A. Edelman, P. B. Hitchcock, M. F. Lappert, D.-S. Liu and S. Tian, *J. Organomet. Chem.*, **550**, 397 (1998).
100. H. Chen, P. Jutzi, W. Leffers, M. M. Olmstead and P. P. Power, *Organometallics*, **10**, 1282 (1991).
101. B. Qian, L. M. Henling and J. C. Peters, *Organometallics*, **19**, 2805 (2000).
102. G. R. Giesbrecht, A. Gebauer, A. Shafir and J. Arnold, *J. Chem. Soc., Dalton Trans.*, 4018 (2000).

103. P. Jutzi, *Pure Appl. Chem.* **62**, 1035 (1990).
104. M. F. Lappert, A. Singh, L. M. Engelhardt and A. H. White, *J. Organomet.Chem.*, **262**, 271 (1984).
105. P. Jutzi, W. Leffers, S. Pohl and W. Saak, *Chem. Ber.*, **122**, 1449 (1989).
106. P. Jutzi, E. Schlüter, S. Pohl and W. Saak, *Chem. Ber.*, **118**, 1959 (1985).
107. P. Jutzi, E. Schlüter, C. Krüger and S. Pohl, *Angew. Chem., Int. Ed. Engl.*, **22**, 994 (1983).
108. A. Sekiguchi, Y. Sugai, K. Ebata, C. Kabuto and H. Sakurai, *J. Am. Chem. Soc.*, **115**, 1144 (1993).
109. T. Matsuo, A. Sekiguchi, M. Ichinohe, K. Ebata and H. Sakurai, *Organometallics*, **17**, 3143 (1998).
110. J. Hiermeier, F. H. Köhler and G. Müller, *Organometallics*, **10**, 1787 (1991).
111. D. Veghini, L. M. Henling, T. J. Burkhardt and J. E. Bercaw, *J. Am. Chem. Soc.*, **121**, 564 (1999).
112. R. E. Dinnebier, S. Neander, U. Behrens and F. Olbrich, *Organometallics*, **18**, 2915 (1999).
113. J.-L. Fauré, G. Erker, R. Fröhlich and K. Bergander, *Eur. J. Inorg. Chem.*, 2603 (2000).
114. W. E. Rhine and G. D. Stucky, *J. Am. Chem. Soc.*, **97**, 737 (1975).
115. I. Hoppe, M. Marsch, K. Harms, G. Boche and D. Hoppe, *Angew. Chem., Int. Ed. Engl.*, **34**, 2158 (1995).
116. G. E. Herberich, E. Barday and A. Fischer, *J. Organomet. Chem.*, **567**, 127 (1998).
117. J. J. Stezowski, H. Hoier, D. Wilhelm, T. Clark and P. v. R. Schleyer, *J. Chem. Soc., Chem. Commun.*, 1263 (1985).
118. A. Streitwieser, *Molecular Orbital Theory for Organic Chemists*, Wiley, New York, 1961.
119. R. Haag, R. Fleischer, D. Stalke and A. de Meijere, *Angew. Chem., Int. Ed. Engl.*, **34**, 1492 (1995).
120. R. Haag, B. Ohlhorst, M. Noltemeyer, R. Fleischer, D. Stalke, A. Schuster, D. Kuck and A. de Meijere, *J. Am. Chem. Soc.*, **117**, 10474 (1995).
121. D. R. Cary, J. C. Green and D. O'Hare, *Angew. Chem., Int. Ed. Engl.*, **36**, 2618 (1997).
122. W. J. Youngs, A. Djebli and C. A. Tessier, *Organometallics*, **10**, 2089 (1991).
123. D. Bladauski, W. Broser, H.-J. Hecht, D. Rewicki and H. Dietrich, *Chem. Ber.*, **112**, 1380 (1979).
124. J. J. Brooks, W. Rhine and G. D. Stucky, *J. Am. Chem. Soc.*, **94**, 7346 (1972).
125. C. Üffing, R. Köppe and H. Schnöckel, *Organometallics*, **17**, 3512 (1998).
126. M. Walczak and G. D. Stucky, *J. Organomet. Chem.*, **97**, 313 (1975).
127. G. Linti, A. Rodig and H. Pritzkow, *Angew. Chem., Int. Ed.*, **41**, 4503 (2002).
128. M. Könemann, G. Erker, R. Fröhlich and E.-U. Würthwein, *J. Am. Chem. Soc.*, **119**, 11155 (1997).
129. M. Håkansson, C.-H. Ottosson, A. Boman and D. Johnels, *Organometallics*, **17**, 1208 (1998).
130. J. J. Brooks, W. Rhine and G. D. Stucky, *J. Am. Chem. Soc.*, **94**, 7339 (1972).
131. R. D. Culp and A. H. Cowley, *Organometallics*, **15**, 5380 (1996).
132. H. V. R. Dias and Z. Wang, *J. Organomet. Chem.*, **539**, 77 (1997).
133. H. V. R. Dias, Z. Wang and S. G. Bott, *J. Organomet. Chem.*, **508**, 91 (1996).
134. R. Littger, N. Metzler, H. Nöth and M. Wagner, *Chem. Ber.*, **127**, 1901 (1994).
135. R. E. Dinnebier, U. Behrens and F. Olbrich, *J. Am. Chem. Soc.*, **120**, 1430 (1998).
136. K. Ruhlandt-Senge, J. J. Ellison, R. J. Wehmschulte, F. Pauer and P. P. Power, *J. Am. Chem. Soc.*, **115**, 11353 (1993).
137. R. A. Bartlett, H. V. R. Dias and P. P. Power, *J. Organomet. Chem.*, **341**, 1 (1988).
138. M. A. Beno, H. Hope, M. M. Olmstead and P. P. Power, *Organometallics*, **4**, 2117 (1985).
139. S. Kurz and E. Hey-Hawkins, *Organometallics*, **11**, 2729 (1992).
140. T. Kottke, K. Sung and R. J. Lagow, *Angew. Chem., Int. Ed. Engl.*, **34**, 1517 (1995).
141. A. Sekiguchi, K. Ebata, C. Kabuto and H. Sakurai, *J. Am. Chem. Soc.*, **113**, 1464 (1991).
142. A. Sekiguchi, K. Ebata, C. Kabuto and H. Sakurai, *J. Am. Chem. Soc.*, **113**, 7081 (1991).
143. B. Twanley, S. T. Haubrich and P. P. Power, *Adv. Organomet. Chem.*, **44**, 1 (1999).
144. P. P. Power, *Struct. Bonding*, **103**, 57 (2002).
145. B. Schiemenz and P. P. Power, *Angew. Chem., Int. Ed. Engl.*, **35**, 2150 (1996).
146. G. W. Rabe, R. D. Sommer and A. L. Rheingold, *Organometallics*, **19**, 5537 (2000).
147. B. Schiemenz and P. P. Power, *Organometallics*, **15**, 958 (1996).
148. R. C. Crittendon, B. C. Beck, J. Su, X.-W. Li and G. H. Robinson, *Organometallics*, **18**, 156 (1999).

149. M. M. Olmstead and P. P. Power, *J. Organomet. Chem.*, **408**, 1 (1991).
150. G. L. Wegner, R. J. F. Berger, A. Schier and H. Schmidbaur, *Z. Naturforsch., Teil B*, **55**, 995 (2000).
151. S. Harder, J. Boersma, L. Brandsma and J. A. Kanters, *J. Organomet. Chem.*, **339**, 7 (1988).
152. S. Harder, L. Brandsma, J. A. Kanters and A. J. M. Duisenberg, *Acta Crystallogr., Sect. C*, **43**, 1535 (1987).
153. A. L. Spek, M. T. Lakin and R. den Besten, Private Commun. to the CCDC (1999).
154. H. J. Reich and B. O. Gudmundsson, *J. Am. Chem. Soc.*, **118**, 6074 (1996).
155. J. Belzner, D. Schär, U. Dehnert and M. Noltemeyer, *Organometallics*, **16**, 285 (1997).
156. M. H. P. Rietveld, I. C. M. Wehman-Ooyevaar, G. M. Kapteijn, D. M. Grove, W. J. J. Smeets, H. Kooijman, A. L. Spek and G. van Koten, *Organometallics*, **13**, 3782 (1994).
157. J. Clayden, R. P. Davies, M. A. Hendy, R. Snaith and A. E. H. Wheatley, *Angew. Chem., Int. Ed.*, **40**, 1238 (2001).
158. G. Müller, H.-P. Abicht, M. Waldkircher, J. Lachmann, M. Lutz and M. Winkler, *J. Organomet. Chem.*, **622**, 121 (2001).
159. S. Harder, L. Brandsma, J. A. Kanters, A. Duisenberg and J. H. van Lenthe, *J. Organomet. Chem.*, **420**, 143 (1991).
160. A. Steiner and D. Stalke, *Angew. Chem., Int. Ed. Engl.*, **34**, 1752 (1995).
161. S. Harder, J. Boersma, L. Brandsma, J. A. Kanters, W. Bauer and P. v. R. Schleyer, *Organometallics*, **8**, 1696 (1989).
162. A. L. Spek and N. Veldman, Private Commun. to the CCDC (1999).
163. R. Schlengermann, J. Sieler, S. Jelonek and E. Hey-Hawkins, *Chem. Commun.*, 197 (1997).
164. W. J. J. Smeets, A. L. Spek, A. A. H. van dear Zeijden and G. van Koten, *Acta Crystallogr., Sect. C*, **43**, 1429 (1987).
165. P. Steenwinkel, S. L. James, D. M. Grove, N. Veldman, A. L. Spek and G. van Koten, *Chem. Eur. J.*, **2**, 1440 (1996).
166. J. G. Donkervoort, J. L. Vicario, E. Rijnberg, J. T. B. H. Jastrzebski, H. Kooijman, A. L. Spek and G. van Koten, *J. Organomet. Chem.*, **550**, 463 (1998).
167. A. Pape, M. Lutz and G. Müller, *Angew. Chem., Int. Ed. Engl.*, **33**, 2281 (1994).
168. D. Stalke and K. H. Whitmire, *Chem. Commun.*, 833 (1990).
169. D. Stalke, N. Keweloh, U. Klingebiel, M. Noltemeyer and G. M. Sheldrick, *Z. Naturforsch., Teil B*, **42**, 1237 (1987).
170. D. Stalke, U. Klingebiel and G. M. Sheldrick, *J. Organomet. Chem.*, **344**, 37 (1988).
171. D. Stalke, M. Meyer, M. Andrianarison, M. Noltemeyer and G. M. Sheldrick, *J. Organomet. Chem.*, **366**, C15 (1989).
172. D. Stalke, U. Klingebiel and G. M. Sheldrick, *Chem. Ber.*, **121**, 1457 (1988).
173. U. Pieper, S. Walter, U. Klingebiel and D. Stalke, *Angew. Chem., Int. Ed. Engl.*, **29**, 209 (1990).
174. A. L. Spek, Private Commun. to the CCDC (1999).
175. J. Betz, F. Hampel and W. Bauer, *Org. Lett.*, **2**, 3805 (2000).
176. J. Betz, F. Hampel and W. Bauer, *J. Chem. Soc., Dalton Trans.*, 1876 (2001).
177. R. L. Polt, G. Stork, G. B. Carpenter and P. G. Williard, *J. Am. Chem. Soc.*, **106**, 4276 (1984).
178. P. B. Hitchcock, M. F. Lappert, W.-P. Leung, D.-S. Liu, T. C. W. Mak and Z.-X. Wang, *J. Chem. Soc., Dalton Trans.*, 1257 (1999).
179. M. Pilz, J. Allwohn, P. Willershausen, W. Massa and A. Berndt, *Angew. Chem., Int. Ed. Engl.*, **29**, 1030 (1990).
180. N. Hertkorn, F. H. Köhler, G. Müller and G. Reber, *Angew. Chem., Int. Ed. Engl.*, **25**, 468 (1986).
181. G. E. Herberich, U. Eigendorf and U. Englert, *Chem. Ber.*, **126**, 1397 (1993).
182. G. E. Herberich, M. Hostalek, R. Laven and R. Boese, *Angew. Chem., Int. Ed. Engl.*, **29**, 317 (1990).
183. D. Scheschkewitz, M. Menzel, M. Hofmann, P. v. R. Schleyer, G. Geiseler, W. Massa, K. Harms and A. Berndt, *Angew. Chem., Int. Ed.*, **38**, 2936 (1999).
184. W. J. Grigsby and P. P. Power, *J. Am. Chem. Soc.*, **118**, 7981 (1996).
185. G. Schmid, D. Zaika, J. Lehr, N. Augart and R. Boese, *Chem. Ber.*, **121**, 1873 (1988).
186. S. Luckert, U. Englert and P. Paetzold, *Chem. Ber.*, **129**, 361 (1996).
187. P. Paetzold, N. Finke, P. Wennek, G. Schmid and R. Boese, *Z. Naturforsch., Teil B*, **41**, 167 (1986).

188. G. E. Herberich, B. Ganter and M. Pons, *Organometallics*, **17**, 1254 (1998).
189. R. West, H. Sohn, U. Bankwitz, J. Calabrese, Y. Apeloig and T. Mueller, *J. Am. Chem. Soc.*, **117**, 11608 (1995).
190. A. Heine, R. Herbst-Irmer, G. M. Sheldrick and D. Stalke, *Inorg. Chem.*, **32**, 2694 (1993).
191. J. Belzner, U. Dehnert and D. Stalke, *Angew. Chem., Int. Ed. Engl.*, **33**, 2450 (1994).
192. S. Freitag, R. Herbst-Irmer, L. Lameyer and D. Stalke, *Organometallics*, **15**, 2839 (1996).
193. S.-B. Choi, P. Boudjouk and J.-H. Hong, *Organometallics*, **18**, 2919 (1999).
194. S.-B. Choi, P. Boudjouk and K. Qin, *Organometallics*, **19**, 1806 (2000).
195. J.-H. Hong, Y. Pan and P. Boudjouk, *Angew. Chem., Int. Ed. Engl.*, **35**, 186 (1996).
196. W. Bauer, G. Müller, R. Pi and P. v. R. Schleyer, *Angew. Chem., Int. Ed. Engl.*, **25**, 1103 (1986).
197. G. Boche, M. Marsch, J. Harbach, K. Harms, B. Ledig, F. Schubert, J. C. W. Lohrenz and H. Ahlbrecht, *Chem. Ber.*, **126**, 1887 (1993).
198. J. Guan, T. Dubé, S. Gambarotta and G. P. A. Yap, *Organometallics*, **19**, 4820 (2000).
199. T. Douglas and K. H. Theopold, *Angew. Chem., Int. Ed. Engl.*, **28**, 1367 (1989).
200. R. Ficker, W. Hiller, M. Bohringer and G. Becker, *Z. Kristallogr.*, **211**, 341 (1996).
201. S. C. Sendlinger, B. S. Haggerty, A. L. Rheingold and K. H. Theopold, *Chem. Ber.*, **124**, 2453 (1991).
202. D. R. Powell, W. L. Whipple and H. J. Reich, *Acta Crystallogr., Sect. C*, **52**, 1346 (1996).
203. A. L. Spek and W. J. J. Smeets, Private Commun. to the CCDC (1999).
204. S. Harder, J. Boersma, L. Brandsma, J. A. Kanters, W. Bauer, R. Pi, P. v. R. Schleyer, H. Schöllhorn and U. Thewalt, *Organometallics*, **8**, 1688 (1989).
205. A. L. Spek, M. T. Lakin and R. den Besten, Private Commun. to the CCDC (1999).
206. A. Basu and S. Thayumanavan, *Angew. Chem., Int. Ed.*, **41**, 716 (2002)
207. U. Schümann, E. Weiss, H. Dietrich and W. Mahdi, *J. Organomet. Chem.*, **322**, 299 (1987).
208. G. Boche, G. Fraenkel, J. Cabral, K. Harms, N. J. R. Van Eikema Hommes and P. v. R. Schleyer, *J. Am. Chem. Soc.*, **114**, 1562 (1992).
209. W. Bauer, M. Feigel, G. Müller and P. v. R. Schleyer, *J. Am. Chem. Soc.*, **110**, 6033 (1988).
210. A. Sekiguchi, T. Nakanishi, C. Kabuto and H. Sakurai, *Chem. Lett.*, 867 (1992).
211. A. Sekiguchi, M. Ichinohe, C. Kabuto and H. Sakurai, *Organometallics*, **14**, 1092 (1995).
212. A. Sekiguchi, M. Ichinohe, M. Takahashi, C. Kabuto and H. Sakurai, *Angew. Chem., Int. Ed. Engl.*, **36**, 1533 (1997).
213. A. Sekiguchi, T. Nakanishi, C. Kabuto and H. Sakurai, *J. Am. Chem. Soc.*, **111**, 3748 (1989).
214. M. Hage, C. A. Ogle, T. L. Rathman and J. L. Hubbard, *Main Group Metal Chem.*, **21**, 777 (1998).
215. G. Müller, M. Lutz and M. Waldkircher, *Acta Crystallogr., Sect. C*, **52**, 1182 (1996).
216. J. Arnold, V. Knapp, J. A. R. Schmidt and A. Shafir, *J. Chem. Soc., Dalton Trans.*, 3273 (2002).
217. L. M. Engelhardt, W.-P. Leung, C. L. Raston, G. Salem, P. Twiss and A. H. White, *J. Chem. Soc., Dalton Trans.*, 2403 (1988).
218. L. M. Engelhardt, W.-P. Leung, C. L. Raston, P. Twiss and A. H. White, *J. Chem. Soc., Dalton Trans.*, 321 (1984).
219. N. J. Hardman, B. Twamley, M. Stender, R. Baldwin, S. Hino, B. Schiemenz, S. M. Kauzlarich and P. P. Power, *J. Organomet. Chem.*, **643**, 461 (2002).
220. W. Zarges, M. Marsch, K. Harms, W. Koch, G. Frenking and G. Boche, *Chem. Ber.*, **124**, 543 (1991).
221. L. M. Engelhardt, W.-P. Leung, C. L. Raston and A. H. White, *J. Chem. Soc., Dalton Trans.*, 337 (1985).
222. R. Knorr, T. P. Hoang, H. Nöth and G. Linti, *Organometallics*, **11**, 2669 (1992).
223. P. v. R. Schleyer, R. Hacker, H. Dietrich and W. Mahdi, *J. Chem. Soc., Chem. Commun.*, 622 (1985).
224. D. Colgan, R. I. Papasergio, C. L. Raston and A. H. White, *J. Chem. Soc., Chem. Commun.*, 1708 (1984).
225. P. C. Andrews, D. R. Armstrong, C. L. Raston, B. A. Roberts, B. W. Skelton and A. H. White, *J. Chem. Soc., Dalton Trans.*, 996 (2001).
226. J. J. Brooks and G. D. Stucky, *J. Am. Chem. Soc.*, **94**, 7333 (1972).
227. D. Hoffmann, W. Bauer, P. v. R. Schleyer, U. Pieper and D. Stalke, *Organometallics*, **12**, 1193 (1993).

228. U. Pieper and D. Stalke, *Organometallics*, **12**, 1201 (1993).
229. H. Gornitzka and D. Stalke, *Organometallics*, **13**, 4398 (1994).
230. H. Gornitzka and D. Stalke, *Angew. Chem., Int. Ed. Engl.*, **33**, 693 (1994).
231. C. Eaborn, P. B. Hitchcock, J. D. Smith and A. C. Sullivan, *J. Chem. Soc., Chem. Commun.*, 827 (1983).
232. N. H. Buttrus, C. Eaborn, P. B. Hitchcock, J. D. Smith, J. G. Stamper and A. C. Sullivan, *J. Chem. Soc., Chem. Commun.*, 969 (1986).
233. A. G. Avent, C. Eaborn, P. B. Hitchcock, G. A. Lawless, P. D. Lickiss, M. Mallien, J. D. Smith, A. D. Webb and B. Wrackmeyer, *J. Chem. Soc., Dalton Trans.*, 3259 (1993).
234. T. Viefhaus, A. Walz, M. Niemeyer, W. Schwarz and J. Weidlein, *Z. Anorg. Allg. Chem.*, **626**, 2040 (2000).
235. S. S. Al-Juaid, A. G. Avent, C. Eaborn, S. M. El-Hamruni, S. A. Hawkes, M. S. Hill, M. Hopman, P. B. Hitchcock and J. D. Smith, *J. Organomet. Chem.*, **631**, 76 (2001).
236. C. Eaborn, P. B. Hitchcock, K. Izod and J. D. Smith, *Organometallics*, **15**, 1651 (1996).
237. R. I. Papasergio, B. W. Skelton, P. Twiss, A. H. White and C. L. Raston, *J. Chem. Soc., Dalton Trans.*, 1161 (1990).
238. I. Hoppe, M. Marsch, K. Harms, G. Boche and D. Hoppe, *Angew. Chem., Int. Ed. Engl.*, **34**, 2158 (1995).
239. F. Marr, R. Fröhlich and D. Hoppe, *Tetrahedron: Asymmetry*, **13**, 2587, (2002).
240. M. Marsch, K. Harms, O. Zschage, D. Hoppe and G. Boche, *Angew. Chem., Int. Ed. Engl.*, **30**, 321 (1991).
241. D. J. Pippel, G. A. Weisenburger, S. R. Wilson and P. Beak, *Angew. Chem., Int. Ed.*, **37**, 2522 (1998).
242. G. Boche, M. Marsch, J. Harbach, K. Harms, B. Ledig, F. Schubert, J. C. W. Lohrenz and H. Ahlbrecht, *Chem. Ber.*, **126**, 1887 (1993).
243. H. Ahlbrecht, G. Boche, K. Harms, M. Marsch and H. Sommer, *Chem. Ber.*, **123**, 1853 (1990).
244. C. Strohmann, D. H. M.Buchold, T. Seibel, K. Wild and D. Schildbach, *Eur. J. Inorg. Chem.*, 3453 (2003).
245. C. Strohmann, K. Lehmen, K. Wild and D. Schildbach, *Organometallics*, **21**, 3079 (2002).
246. C. Eaborn and J. D. Smith, *J. Chem. Soc., Dalton Trans.*, **10**, 1541 (2001).
247. M. F. Lappert, *J. Organomet. Chem*, **600**, 144 (2000).
248. N. Wiberg, *Coord. Chem. Rev.*, **163**, 217 (1997).
249. J. L. Atwood, T. Fjeldberg, M. F. Lappert, N. T. Luong-Thi, R. Shakir and A. J. Thorne, *Chem. Commun.*, 1163 (1984).
250. M. F. Lappert, L. M. Engelhardt, C. L. Raston and A. H. White, *J. Chem. Soc., Chem. Commun.*, 1323 (1982).
251. C. Eaborn, W. Clegg, P. B. Hitchcock, M. Hopman, K. Izod, P. N. O'Shaughnessy and J. D. Smith, *Organometallics*, **16**, 4728 (1997).
252. C. Eaborn, P. B. Hitchcock, J. D. Smith and A. C. Sullivan, *J. Chem. Soc., Chem. Commun.*, 1390 (1983).
253. S. S. Al-Juaid, C. Eaborn, P. B. Hitchcock, M. S. Hill and J. D. Smith, *Organometallics*, **19**, 3224 (2000).
254. S. S. Al-Juaid, C. Eaborn, S. M. El-Hamruni, P. B. Hitchcock and J. D. Smith, *Organometallics*, **18**, 45 (1999).
255. H. H. Karsch, K. Zellner, P. Mikulcik, J. Lachmann and G. Müller, *Organometallics*, **9**, 190 (1990).
256. N. Wiberg, H.-S. Hwang-Park, P. Mikulcik and G. Müller, *J. Organomet. Chem.*, **511**, 239 (1996).
257. F. Becke, F. W. Heinemann, T. Rüffer, P. Wiegeleben, R. Boese, D. Bläser and D. Steinborn, *J. Organomet. Chem.*, **548**, 205 (1997).
258. G. Fraenkel, W. R. Winchester and P. G. Williard, *Organometallics*, **8**, 2308 (1989).
259. S. Blaurock, O. Kühl and E. Hey-Hawkins, *Organometallics*, **16**, 807 (1997).
260. R. Amstutz, T. Laube, W. B. Schweizer, D. Seebach and J. D. Dunitz, *Helv. Chim. Acta*, **67**, 224 (1984).
261. F. Becke, F. W. Heinemann and D. Steinborn, *Organometallics*, **16**, 2736 (1997).
262. T. Rüffer, C. Bruhn, A. H. Maulitz, D. Ströhl and D. Steinborn, *Organometallics*, **19**, 2829 (2000).
263. B. Walfort, R. Bertermann and D. Stalke, *Chem. Eur. J.*, **7**, 1424 (2001).

264. C. Selinka and D. Stalke, *Z. Naturforsch., Teil B*, **58**, 291 (2003).
265. B. Walfort and D. Stalke, *Angew. Chem., Int. Ed.*, **40**, 3846 (2001).
266. B. Walfort, A. P. Leedham, C. A. Russell and D. Stalke, *Inorg. Chem.*, **40**, 5668 (2001).
267. R. Knorr, C. Behringer, H. Nöth, M. Schmidt, E. Lattke and E. Rapple, *Chem. Ber.*, **130**, 585 (1997).
268. A. J. Ashe III, J. W. Kampf and P. M. Savla, *Organometallics*, **12**, 3350 (1993).
269. F. Pauer and P. P. Power, *J. Organomet. Chem.*, **474**, 27 (1994).
270. P. Dem'yanov, G. Boche, M. Marsch, K. Harms, G. Fyodorova and V. Petrosyan, *Justus Liebigs Ann. Chem.*, 457 (1995).
271. W. Neugebauer, G. A. P. Geiger, A. J. Kos, J. J. Stezowski and P. v. R. Schleyer, *Chem. Ber.*, **118**, 1504 (1985).
272. A. Kasani, R. P. Kamalesh Babu, R. McDonald and R. G. Cavell, *Angew. Chem., Int. Ed.*, **38**, 1483 (1999).
273. C. M. Ong and D. W. Stephan, *J. Am. Chem. Soc.*, **121**, 2939 (1999).
274. B. Schubert and E. Weiss, *Chem. Ber.*, **116**, 3212 (1983).
275. G. Boche, F. Bosold, M. Marsch and K. Harms, *Angew. Chem., Int. Ed.*, **37**, 1684 (1998).
276. B. Goldfuss, P. v. R. Schleyer and F. Hampel, *J. Am. Chem. Soc.*, **119**, 1072 (1997).
277. P. G. Williard and C. Sun, *J. Am. Chem. Soc.*, **119**, 11693 (1997).
278. J. Jubb, P. Berno, S. Hao and S. Gambarotta, *Inorg. Chem.*, **34**, 3563 (1995).
279. C. Strohmann and B. C. Abele, *Organometallics*, **19**, 4173 (2000).
280. P. Wijkens, J. T. B. H. Jastrzebski, N. Veldman, A. L. Spek and G. van Koten, *Chem. Commun.*, 2143 (1997).
281. J. G. Donkervoort, J. L. Vicario, E. Rijnberg, J. T. B. H. Jastrzebski, H. Kooijman, A. L. Spek and G. van Koten, *J. Organomet. Chem.*, **550**, 463 (1998).
282. B. Walfort, L. Lameyer, W. Weiss, R. Herbst-Irmer, R. Bertermann, J. Rocha and D. Stalke, *Chem. Eur. J.*, **7**, 1417 (2001).
283. B. Goldfuss, S. I. Khan and K. N. Houk, *Organometallics*, **18**, 2927 (1999).
284. B. Goldfuss, M. Steigelmann, F. Rominger and H. Urtel, *Chem. Eur. J.*, **7**, 4456 (2001).
285. R. P. Davies, P. R. Raithby and R. Snaith, *Angew. Chem., Int. Ed. Engl.*, **36**, 1215 (1997).
286. P. Wijkens, E. M. van Koten, M. D. Janssen, J. T. B. H. Jastrzebski, A. L. Spek and G. van Koten, *Angew. Chem., Int. Ed. Engl.*, **34**, 219 (1995).
287. M. Marsch, K. Harms, L. Lochmann and G. Boche, *Angew. Chem., Int. Ed. Engl.*, **29**, 308 (1990).
288. M. A. Beswick, B. R. Elvidge, N. Feeder, S. J. Kidd and D. S. Wright, *Chem. Commun.*, 379 (2001).
289. B. Goldfuss, M. Steigelmann and F. Rominger, *Angew. Chem., Int. Ed.*, **39**, 4133 (2000).
290. B.-T. Ko and C.-C. Lin, *J. Am. Chem. Soc.*, **123**, 7973 (2001).
291. A. Feustel and G. Müller, *Chem. Commun.*, 1024 (2001).
292. J. Schneider, E. Popowski and H. Reinke, *Z. Anorg. Allg. Chem.*, **628**, 719 (2002).

CHAPTER 3

Thermochemistry of organolithium compounds

SUZANNE W. SLAYDEN

Department of Chemistry, George Mason University, 4400 University Drive, Fairfax, Virginia 22030, USA
Fax: (+1)703-993-1055; e-mail: sslayden@gmu.edu

and

JOEL F. LIEBMAN

Department of Chemistry and Biochemistry, University of Maryland, Baltimore County, 1000 Hilltop Circle, Baltimore, Maryland 21250, USA
Fax: (+1)410-455-2608; e-mail: jliebman@umbc.edu

The Chemistry of Organolithium Compounds. Edited by Z. Rappoport and I. Marek
ISBN: 0-470-84339-X

I. INTRODUCTION: SCOPE AND DEFINITIONS

A. Thermochemistry

The current chapter is primarily devoted to the relatively restricted property, the 'molar standard enthalpy of formation', $\Delta_f H_m{}^\circ$, often called the 'heat of formation', ΔH_f or $\Delta H_f{}^\circ$. This chapter foregoes discussion of other thermochemical properties such as entropy, heat capacity or excess enthalpy. We will only tangentially discuss bond dissociation energies (e.g. of the C−Li bond), Gibbs energy, and complexation and clustering energies (e.g. oligomerization enthalpies). Temperature and pressure are assumed to be 25 °C ('298 K') and 1 atmosphere or the nearly equal 1 bar (101,325 or 100,000 Pa), respectively. The energy units are kJ mol^{-1}, where 4.184 kJ is defined to equal 1 kcal. The relationships between enthalpies of formation in the solid (s), liquid (lq) and gaseous (g) phases are expressed in terms of enthalpies of vaporization (vap), sublimation (sub) and fusion (fus) (equations 1–3).

$$\Delta_{vap} H = \Delta_f H_m{}^\circ(g) - \Delta_f H_m{}^\circ(lq) \tag{1}$$

$$\Delta_{sub} H = \Delta_f H_m{}^\circ(g) - \Delta_f H_m{}^\circ(s) \tag{2}$$

$$\Delta_{fus} H = \Delta_f H_m{}^\circ(lq) - \Delta_f H_m{}^\circ(s) \tag{3}$$

In attempting a systematic analysis of related organolithium species, it would be advantageous to consider all of them in at least one common phase. Our preference is for the gas phase where intermolecular interactions are usually absent, although this may not hold true for organolithium species. Unfortunately, most of the desired phase change enthalpies for organolithiums are not found in the experimental literature. However, where the species of interest is a liquid, we can employ the published 'CHLP protocol' for the estimation of the enthalpy of vaporization[1].

$$\Delta_{vap} H = 4.7\tilde{n}_c + 1.3n_Q + 3.0 + b \tag{4}$$

where $\tilde{n}_c$ and n_Q are the number of non-quaternary and quaternary carbons, respectively, and b is a substituent-dependent parameter.

The only measured enthalpy of vaporization[2] is for n-butyl lithium, 107.1 ± 2.9 kJ mol^{-1}, from which the constant b(Li) in equation 4 is derived as 85 kJ mol^{-1}. This is a 'hefty' value compared to $b(\mathrm{OH}) = 29$, $b(-\mathrm{S(O)_2}-) = 53$ and $b(\mathrm{Cl}) = 11$ kJ mol^{-1}. However, the oligomeric states of the organolithium liquid and gas phases are not known with certainty. This is reminiscent of problems for hydrogen-bonded species such as carboxylic acids and hydrogen fluoride.

B. Nature and Nomenclature of Lithium-Containing Species of Interest

Unlike our earlier review on the thermochemistry of lithium compounds[3], we limit our attention to compounds containing a C−Li bond and therefore discuss only alkyl and aryl lithiums and a few of their derivatives. We will not discuss species with Li bonds to any other element and so avoid any thermochemical investigation of alkoxides, carboxylates or halides. Whichever lithiated species are chosen, they are not likely to be monomeric. Lithium compounds, from the very smallest to quite large, are known to associate in solution, in the condensed phases and even in the gas phase, most typically as dimers, tetramers or hexamers[4].

There are multiple systems for naming organolithium compounds. In one, C_6H_5Li is named phenyl lithium and n-C_4H_9Li is n-butyl lithium. In another, these species are named lithiobenzene and 1-lithiobutane, respectively, when the lithium atom is regarded as a substituent on the hydrocarbon parent. A third nomenclature approach assumes these species are ionic salts, e.g. the above two compounds are called lithium phenylide and lithium butylide. We will bypass any questions of aggregation by referring to these compounds by their monomeric names (e.g. phenyl lithium and not dimeric phenyl lithium, phenyl lithium dimer nor diphenyl dilithium), and where monomeric species are actually meant, we will make this explicit.

C. Sources of Data

Thermochemical investigations of reactive, often flammable, organolithium compounds have been difficult, rare and sometimes suspect. Combustion calorimetrists, used to working with well-defined materials and well-defined processes, have generally avoided organometallic compounds. Consequently, most experimental enthalpy data for such compounds were determined from reaction-solution calorimetry[5,6]. A serious source of error in most of these studies is the lack of enthalpy of formation or of solution data for some of the reaction species and thus the necessity for making assumptions and estimations. Phase-change enthalpies are notably missing.

Experimental enthalpies of formation for twelve alkyl- and aryl-lithium reagents were derived by Holm[7] from the enthalpies of reaction 5 in which the organolithium reagents were dissolved or suspended in ether or in petroleum ether.

$$\mathrm{RLi(soln/susp)} + \mathrm{HBr(soln)} \longrightarrow \mathrm{LiBr(s)} + \mathrm{RH(g/soln)} \tag{5}$$

Although Holm calculated the enthalpies of formation of RLi, no details are given regarding the enthalpies of solution used to derive the enthalpies of formation of the condensed-phase compounds. The reaction enthalpy values appearing in the Sussex-NPL Tables[8] are recalculations of Holm's data that most likely incorporate corrections to the enthalpies of solution of RH in the calorimetric mixture. The most recent review of organometallic thermochemistry by Martinho Simões is part of the NIST Standard Reference Data Program online database[9]. Again, Holm's original data have been recalculated, this time on the basis of a single set of ancillary data used for the entire database. The recalculated data are nearly the same as the original, except for isopropyl lithium for which the recalculated values are inexplicably nearly 18 $\mathrm{kJ\,mol^{-1}}$ more negative. The data appear in Table 1. Generally, we will use the average or 'consensus' value for a particular species.

Frequently, comparisons will be made between the organolithium and the corresponding compound wherein Li is replaced by H. Unreferenced enthalpies of formation for these and any other organic species in the current chapter are taken from the now 'classic' thermochemical archive by Pedley and his coworkers[12]. These thermochemical numbers are usually for comparatively simple and well-understood species where we benefit from the data evaluation performed by these authors, rather than using the

TABLE 1. Enthalpies of formation of lithium compounds (kJ mol^{-1})

Compound	ΔH°_f(lq/s)	Reference	ΔH°_f(g)
LiMe, s	-74.9	7	
	-71.1 ± 2.1	8	
	-72.0 ± 2.1	9	
LiEt, s	-55.2	7	61.5[a]
	-53.0 ± 2.2	8, 9	63.7 ± 2.2[a]
	-58.7 ± 5.4	5, 6, 9	58.0 ± 5.5[a]
Li allyl, s	-5.9	7	
	-5.0 ± 2.2	8	
	-3.8 ± 3.2	9	
Li(*i*-Pr), lq	-57.7	7	
	-74.5 ± 2.1	8	
	-75.7 ± 2.1	9	
Li(*n*-Bu), lq	-109.2	7	-2.1[b]
	-108.7 ± 2.1	8	-1.6[b]
	-109.5 ± 3.2	9	-2.4 ± 4.3[b]
Li(*sec*-Bu), lq	-87.9	7	
	-87.4 ± 2.1	8	
	-88.2 ± 3.2	9	
Li(*tert*-Bu), lq	-92.0	7	
	-91.1 ± 2.1	8	
	-92.5 ± 2.4	9	
LiPh, s	51.5	7	
	51.4 ± 2.1	8	
	50.4 ± 2.1	9	
$\mathrm{LiCH_2Ph}$, s	17.6	7	
	17.4 ± 2.1	8	
	16.7 ± 2.1	9	
$\mathrm{Li(C_6H_4Me}$-$p)$, s	5.9	7	
	5.7 ± 2.1	8	
	5.0 ± 2.1	9	
$\mathrm{Li(C_6H_4Cl}$-$p)$, s	7.5	7	
	7.6 ± 2.2	8	
	6.7 ± 2.4	9	
Li cyclopentadienide, s	-76.5 ± 2.9	10(a)	
$\mathrm{Li_2}$ cyclooctatetraenide, s	-140.9 ± 8.5	10(b)	
	-142 ± 13	9	
$\mathrm{Li_2C_2}$, s	-67.7 ± 4.3	11	

[a] The enthalpy of formation of the gas was derived from the enthalpy of formation of the solid and the enthalpy of sublimation, 116.7 ± 0.8 kJ mol^{-1}, from Reference 2.

[b] The enthalpy of formation of the gas was derived from the enthalpy of formation of the liquid and the enthalpy of vaporization, 107.1 ± 2.9 kJ mol^{-1}, from Reference 5.

raw, but much more complete, set of data found in the recent, evolving, on-line NIST WebBook database[13]. A major conceptual problem in using the currently available thermochemical data is ambiguity as to what phase many of the starting materials and products are in. For example, in the absence of enthalpy of solution data, it is not obvious whether to consider the non-organolithium species, i.e. the related hydrocarbon species, as liquids or gases. Our assumption is to consider the species as they would be found under the reaction conditions if they were pure substances and therefore to assume that these enthalpies of solution cancel. The value accepted for the enthalpy of formation of gaseous monoatomic lithium is the 'JANAF'[14] recommended value, 159.3 ± 1.0 kJ mol^{-1}.

II. ISOMERIC AND HOMOLOGOUS ALKYL LITHIUM SERIES

We would like to begin by discussing a homologous series of organolithiums, perhaps the *n*-alkyl lithiums, and the linear correlation of their enthalpies of formation with the number of carbon atoms. Such correlations are well-established for other functional group homologous series[6] The slope of the regression line for the gaseous *n*-alkanes (n-R$-$(CH$_2$)$_x$$-$H), -20.6 kJ mol^{-1}, and the similar values of the slopes for other n-R$-$(CH$_2$)$_x$$-$Z series, is often called the 'universal methylene increment'[6]. However, there are enthalpy of formation values for only two gaseous *n*-alkyl lithiums, ethyl and *n*-butyl lithium. The slope of the line for their enthalpies of formation vs. the number of carbon atoms is *ca* -32 kJ mol^{-1}, rather larger than the universal methylene increment. A rough estimate of the enthalpy of formation of gaseous *n*-propyl lithium interpolated from the ethyl and *n*-butyl homologs is *ca* 29 kJ mol^{-1}. The ethyl and *n*-propyl liquid enthalpies of formation calculated from equation 4 and the experimental or derived gaseous enthalpies of formation are *ca* -36 and -73 kJ mol^{-1}, respectively. The methylene increment is *ca* -36, again about 10 kJ mol^{-1} more negative than for the liquid *n*-alkanes.

The enthalpy of formation of solid methyl lithium is *ca* 17 kJ mol^{-1} more negative than for solid ethyl lithium. In *n*-RZ series where Z is more electronegative than carbon, the methyl derivative, R$=$CH$_3$, exhibits a positive deviation from the otherwise straight line established by the other members of the series. For electropositive Z$=$H, and boron- and aluminum-containing substituents, just as with lithium, the experimental methyl deviations are in the opposite direction. The magnitude of the gaseous methyl deviations can be correlated to the electronegativity of Z[15]. The enthalpy of formation of monomeric gaseous methyl lithium has been calculated as 122 kJ mol^{-1} using the experimental enthalpy of formation values for $CH_3^\bullet$ and $Li^\bullet$[16].

The secondary isopropyl and *sec*-butyl lithium compounds, for which there are liquid-phase enthalpy of formation values, are two in a homologous series. Their enthalpy of formation difference, representing one methylene group, is *ca* -13 or -30 kJ mol^{-1} depending on which enthalpy of formation is chosen for isopropyl lithium. By comparison, the methylene increment for liquid-phase 2-methylalkanes is *ca* -25 kJ mol^{-1}.

In isomeric alkanes substituted with an electronegative atom such as *n*-, *sec*- and *tert*-butyl bromide, alkyl group branching at the carbon bonded to the substituent atom increases the thermodynamic stability in both the liquid and gaseous phases. The increasing stability parallels the alkyl group carbocation stability. It might be expected that a substituent atom which is more electropositive than carbon, such as lithium, would reverse the stability trend. Among the isomeric *n*-, *sec*- and *tert*-butyl lithium, all as liquids, *n*-butyl lithium is indeed the most stable, but within the uncertainty intervals, the enthalpies of formation of *sec*- and *tert*-butyl lithium are equal. Whether this equality arises because of experimental error, substituent electronic effects on carbanions or steric effects on solvation or aggregation, is not known.

The enthalpy of isomerization of the primary *n*-butyl lithium to *sec*-butyl lithium is *ca* $+21$ kJ mol^{-1}. From the two different enthalpies of formation of isopropyl lithium and the previously derived liquid-phase enthalpy of formation of *n*-propyl lithium, the isomerization enthalpy is either *ca* $+15$ kJ mol^{-1} or nearly zero. Considering both this result and the one earlier that also compares the two different enthalpy of formation values for isopropyl lithium, the value from Reference 7, -57.7 kJ mol^{-1}, seems more plausible.

III. COMPARISON OF ORGANOLITHIUMS AND GRIGNARD REAGENTS

Organolithiums and Grignard reagents are two key classes of carbanion-like organometallics. In addition to the organolithiums, Holm determined the enthalpies

TABLE 2. Enthalpies of formation of organomagnesium bromides and organic bromides (kJ mol^{-1})

R	RMgBr(soln)[a]	RBr(lq)[b]
Me	−331.8	−59.4 ± 1.2
Vinyl	−264.4	—
Et	−323.0	−90.1 ± 2.8
Allyl	−265.7	12.2 ± 3.6
n-Pr	−360.7	−121.8 ± 3.0
i-Pr	−339.7	−130.5 ± 2.6
n-Bu	−378.2	−143.8 ± 1.3
i-Bu	−391.6	−160.2[17]
sec-Bu	−368.2	−154.8 ± 1.2
tert-Bu	−370.7	−163.8 ± 1.9
n-Pentyl	−406.7	−170.2 ± 1.5
1-Ethylpropyl	−389.9	—
n-Hexyl	−427.6	−194.2 ± 1.6
n-Heptyl	−452.3	−218.4 ± 1.6
n-Octyl	−478.6	−245.1 ± 2.3
Cyclopropyl	−211.3	—
Cyclobutyl	−229.7	—
Cyclopentyl	−336.8	—
Cyclohexyl	−380.3	—
Cycloheptyl	−379.5	—
Cyclooctyl	−395.4	—
Ph	−208.4	60.9 ± 4.1
Bz	−252.3	16.0 ± 2.7
p-Tol	−244.8	12.1[17]
p-ClC_6H_4	−251.5	28.5[17]

[a] All values are from Reference 17. The experimental uncertainties are ±2.2 kJ mol^{-1}.

[b] All values are from Reference 12 unless otherwise stated.

of formation of a collection of organomagnesium bromides[17] by direct-reaction static calorimetry in diethyl ether. Some of the data from the study are in Table 2.

There are seven species with *n*-alkyl groups and three with *sec*-alkyl groups with which to derive methylene increments by a least-squares analysis for the Grignards. For the solution-phase species, the *n*-alkyl series methylene increment is -25.0 ± 0.8 kJ mol^{-1} and the *sec*-alkyl series increment is -25.1 ± 2.0 kJ mol^{-1}. These values are reasonable and nearly the same as their liquid-phase alkane counterparts. Consistent with the deviation of methyl lithium, the methyl magnesium bromide enthalpy of formation is more negative than that for ethyl magnesium bromide. The enthalpies of formation of methyl derivatives bonded to electronegative atoms are typically less negative than those of the ethyl derivatives. In the isomeric butyl series, the most stable is the isobutyl magnesium bromide in which there is a branched alkyl group (stabilizing, generally) and the electropositive magnesium bonded to a primary carbon. The other three isomers exhibit the same behavior as their lithium counterparts: *n*-butyl is most stable and the *sec*-butyl and *tert*-butyl are of comparable stability.

There is a variation in the differences between the enthalpies of formation of RMgBr(soln) and RLi, depending on the class of hydrocarbon substituent. For the sole example, or the average of multiple examples, the enthalpy of formation differences between the organolithium and the corresponding solution-phase Grignard are methyl (259), primary (268), secondary/tertiary (280) and aryl (256) kJ mol^{-1}. Generally, the solution Grignard species has an enthalpy of formation some 267 ± 10 kJ mol^{-1} more negative than the corresponding condensed-phase organolithium[7]; more precisely, for the linear equation 6

$$\Delta_f H^\circ{}_m(\mathrm{RLi}) = m\Delta_f H^\circ{}_m(\mathrm{RMgBr}) + b \tag{6}$$

the regression analysis values are 0.87 ± 0.04 for the slope, m, and 228 ± 11.3 kJ mol^{-1} for the intercept, b. The squared correlation coefficient, r^2, is 0.98. From these constants, the enthalpy of formation of n-propyl lithium is −86 kJ mol^{-1}, presumably as the liquid. This value is compatible with the measured enthalpy of formation of liquid n-butyl lithium where the methylene increment is *ca* −23 kJ mol^{-1}. It is also compatible with the earlier derived value of −73 kJ mol^{-1} from Section II. The estimated enthalpies of formation of the cycloalkyl lithiums, C_3–C_8, are: 44, 28, −65, −103, −102 and −116 kJ mol^{-1}, respectively.

There is also a variation in the differences between the enthalpies of formation of RMgBr(soln) and RBr(lq), depending on the class of hydrocarbon substituent. For the sole example, or the average of multiple examples, the enthalpy of formation differences between the solution-phase Grignard and the corresponding liquid-phase alkyl bromide are methyl (272), primary (234), secondary (211) and tertiary (207) kJ mol^{-1}. Omitting the data for R=Me because of the methyl deviation of methyl bromide, and including data for the allyl and aromatic magnesium bromides, the regression analysis for the linear equation 7

$$\Delta_f H^\circ{}_m(\mathrm{RBr}) = m\Delta_f H^\circ{}_m(\mathrm{RMgBr}) + b \tag{7}$$

yields the constants $m = 1.20$, $b = 310$ and $r^2 = 0.97$. We could derive a linear equation describing the relationship between organic bromides and organolithiums. However, the only other monobromo compounds for which there are liquid enthalpy of formation measurements are n-alkyl bromides. Since they form a homologous series, with a constant methylene increment, we can expect to learn nothing new regarding enthalpies of formation of substituted lithium compounds from this approach.

IV. PROTODELITHIATION REACTIONS

A. Protodelithiation with HBr

All of the thermochemical investigations of both organolithiums and Grignard reagents by Holm[7, 17] discussed in the previous section involved measurements of the enthalpy of protodelithiation by HBr in ether or petroleum ether. Of all the protodelithiation studies to be discussed in this chapter, these are the only ones that include determination of organolithium enthalpies of formation. Using one of these as a benchmark species, we can calculate enthalpies of formation of other organolithiums by combining their measured protodelithiation enthalpies if we assume that all solvation and aggregation energies and other terms cancel, that is, for a given Z and given reaction conditions, these additional terms are plausibly assumed to be independent of R.

More explicitly, from the measured enthalpy of the protodelithiation reaction for the benchmark organolithium, RLi (equation 8), we subtract the protodelithiation enthalpy of some other organolithium, R′Li (equation 9), under the same reaction conditions to result in the enthalpy of the formal, generally hypothetical reaction 10.

$$\mathrm{RLi} + \mathrm{HZ} \longrightarrow \mathrm{RH} + \mathrm{LiZ} \tag{8}$$

$$\mathrm{R'Li} + \mathrm{HZ} \longrightarrow \mathrm{R'H} + \mathrm{LiZ} \tag{9}$$

$$\mathrm{RLi} + \mathrm{R'H} \longrightarrow \mathrm{R'Li} + \mathrm{RH} \tag{10}$$

From the known, or estimated, enthalpies of formation of RLi, RH and R′H we derive the enthalpy of formation of the R′Li of direct interest. Again, we will use the average enthalpy of formation where there are more than one listed for a species in Table 1.

B. Protodelithiation with Ethanol

Brubaker and Beak[18] used ethanol in diethyl ether as the proton source and reaction medium, and found reaction enthalpies of reaction 9 (as monomers) for $R' =$ allyl, -212.0 ± 5.4; *E*-1-propenyl, -217.5 ± 2.1; 2-propenyl, -279.1 ± 10.5; phenyl, -246.9 ± 3.3; ethyl, -270.3 ± 5.4 kJ mol^{-1}. The first three organolithiums generate the same product, propene, upon protodelithiation. Within our assumptions above, the difference between the enthalpies of protodelithiation therefore equals the difference between the enthalpies of formation of these species. The large difference of *ca* 60 kJ mol^{-1} between the *E*-1- and 2-propenyl isomers is partly ascribed by the original authors to decomposition of 2-propenyl lithium during the enthalpy measurement. It is not surprising that the allyl species is the most stable. In addition to the stabilization from π-electron delocalization, the allyl anion presumably offers all three carbons for coordination with the lithium cation[4]. The authors cautioned against comparing the propenyl and allyl lithiums because of their great variation in structure and aggregation: while the 1-propenyl lithium is tetrameric, the allyl lithium's aggregation of between two and ten varies with concentration.

From equation 10 with phenyl lithium as the benchmark species, RLi, and the hydrocarbon compounds, R′H, in their reference gaseous states, the derived enthalpies of formation of allyl, *E*-1-propenyl, 2-propenyl and ethyl lithium, are -12.8, -7.3, 54.3 and -58.3 kJ mol^{-1}, respectively. The first and last of these are remarkably consistent with the values in Table 1.

C. Protodelithiation with 2-Butanol

Geurink and Klumpp[19] used 2-butanol as the proton source in benzene solvent. They found an exothermic protodelithiation of -221 ± 4 kJ mol^{-1} for *n*-butyl lithium and -240 ± 5 kJ mol^{-1} for the isomeric *sec*-butyl lithium to form the same *n*-butane product. The difference between the protodelithiation enthalpies is 19 ± 6 kJ mol^{-1}, the same as the difference between the enthalpies of formation of the two alkyl lithiums. From Table 1, the difference is *ca* 21 kJ mol^{-1}, in complete agreement.

The protodelithiation enthalpy of *n*-propyl lithium is very nearly the same as for the *n*-butyl species, -219 ± 2 kJ mol^{-1}. From reaction 10 with *n*-butyl lithium as the benchmark species and the enthalpies of formation of the hydrocarbons in their gaseous reference states, the enthalpy of formation of *n*-propyl lithium is calculated as *ca* -91 kJ mol^{-1}, a value consistent with that of -86 kJ mol^{-1} derived from *n*-PrMgBr in an earlier section. If the reference state of *n*-butane is taken as the liquid instead, the enthalpy of formation of *n*-propyl lithium is *ca* -70 kJ mol^{-1}, a value consistent with another previous derivation of *ca* -73 kJ mol^{-1}. At least with respect to consistency with the enthalpies of formation in Table 1, the best reference state for ethane and propene is the gas; it is not yet clear which is better for butane.

These authors also investigated 2-norbornyl lithium and found a protodelithiation enthalpy of -222 ± 5 kJ mol^{-1}. They asserted that the norbornyl lithium was present in an *exo/endo* ratio of essentially 1:1. Equating Gibbs energy and enthalpy differences (*vida infra*), we will assume there is a negligible difference between the enthalpies of formation of the isomeric norbornyl lithiums. From equation 10 with *n*-butyl lithium as the benchmark species, and with norbornane in its solid reference state and *n*-butane in its liquid reference state, the enthalpy of formation of 2-norbornyl lithium is *ca* −57 kJ mol^{-1}. For *n*-butane in its gaseous reference state, the enthalpy of formation is *ca* −78 kJ mol^{-1}. We might have expected the protodelithiation enthalpy of the secondary norbornyl lithium to be more negative than it is and to resemble the reaction enthalpy of *sec*-butyl lithium instead of *n*-butyl lithium. The results seem to suggest that norbornyl lithium, and so the norbornyl anion, is relatively stabilized. From Reference[17] the exothermicities of the reaction of the Grignards with HBr are: Et, −290.8; *n*-Bu, −288.6; *i*-Pr, −301.2 cyclobutyl, −289.1; cyclopentyl, −291.6; cyclohexyl, −298.7 kJ mol^{-1}. In that the angle strain of the bicyclic norbornyl is between that of cyclobutyl and cyclopentyl[20], the protodelithiation enthalpies of primary and these cyclic secondary derivatives are similar in both the organolithium and Grignard series.

D. Protodelithiation with Isopropyl Alcohol

Arnett and Moe studied the protodelithiation of organolithiums with isopropyl alcohol in hexane/ether mixtures[21]. These authors found protodelithiation enthalpies for *n*- and *sec*-butyl lithium of −209.2 ± 4.2 and −220.9 ± 2.9, respectively. The difference between their enthalpies of reaction, and so of the enthalpies of formation of the two organolithiums, is 11.7 ± 5.1 kJ mol^{-1}, about half the difference between these species as found in Table 1. The protodelithiation enthalpy of *tert*-butyl lithium is −237.7 ± 7.5 kJ mol^{-1}. From equation 10 with *n*-butyl lithium as the benchmark species, and the butane hydrocarbons in their liquid reference states, the derived enthalpy of formation of *tert*-butyl lithium is −87.5 kJ mol^{-1}, in good agreement with that found before by Holm[7].

We note two more measurements by Arnett and Moe: methyl lithium, −174.1 ± 2.9, and phenyl lithium, −177.0 ± 1.3 kJ mol^{-1}. Both values are considerably smaller than those of the butyl lithiums documenting the reverse stabilization pattern of organolithiums over that of hydrocarbons substituted with more electronegative elements. From equation 10 with phenyl lithium as the benchmark species, and benzene in its liquid reference state and methane in its gaseous reference state, the derived enthalpy of formation of methyl lithium is −75.2 kJ mol^{-1}, in good agreement with that found by Holm[7]. In summary, all of the protodelithiation enthalpies except for *sec*-butyl lithium are consistent with those found in other sources. The deprotonating power of alkyl lithiums increases in the order methyl < primary < secondary < tertiary, and aryl lithiums are less basic than alkyl lithiums.

V. ARYL HALOGEN–LITHIUM EXCHANGE REACTIONS

In principle, each of the above protodelithiation reactions is in equilibrium. It is clear that, in practice, they are not. The protonating species, HBr, isopropanol and 2-butanol, are simply too acidic for the reaction to be reversible. Although the hydrogen/lithium exchange equilibria cannot be studied in both directions, halogen/lithium exchange reactions with aryl substituents evidently are true equilibrium processes. Winkler and Winkler[22] studied reaction 11 (among others), in either diethyl ether or in THF at 25 °C.

$$p\text{-TolBr} + \text{PhLi} \rightleftharpoons p\text{-TolLi} + \text{PhBr} \qquad (11)$$

For the equation as written, $K_{\text{obsd}} = 0.56 \pm 0.04$ (ether) and $K_{\text{obsd}} = 0.40 \pm 0.03$ (THF) where equilibrium was approached from both sides and in varying concentrations. A van't Hoff plot of results at other temperatures led to $\Delta H^{\circ}_{277} = 0.71 \pm 0.20$ kJ mol^{-1}

(ether) and $\Delta H^{\circ}_{277} = 0.04 \pm 0.54$ kJ mol^{-1} (THF). The entropy change was also small for the structurally similar reactants and products: $\Delta S^{\circ}_{277} = -2.59 \pm 0.63$J mol^{-1} deg^{-1} (ether) and $\Delta S^{\circ}_{277} = -7.74 \pm 1.97$J mol^{-1} deg^{-1} (THF). Because the enthalpy change for the reaction is essentially equal to 0, the difference between the enthalpies of formation of the two aryl bromides is the same as the difference (with opposite sign) between the enthalpies of formation of the two aryl lithiums. The difference between the two bromides is *ca* 49 kJ mol^{-1}, in spectacular agreement with the 46 kJ mol^{-1} difference found for the two lithiums by Holm[7].

Because the free energy of the aryl halide/lithium exchange equilibrium is essentially equal to the enthalpy change of the reaction, we consider other reactions from the same source of the general type (equation 11),

$$\text{ArBr} + \text{PhLi} \rightleftharpoons \text{ArLi} + \text{PhBr} \tag{12}$$

We will explicitly ignore entropy and any other temperature-related phenomena and use the simplified expression given by equation 13,

$$\Delta H_r = -RT \ln K = -2.303RT \log K \tag{13}$$

Usable equilibrium constants were obtained only for Ar = p-CH_3, m-CH_3 (i.e. p-Tol and m-Tol) and p-Ph and were reported for approach to equilibrium from both the left and right sides of the equation with equimolar concentrations of reactants. The averaged K_{obsd} values are 0.64, 0.86 and 3.78, respectively. The corresponding values of ΔH_r estimated from equation 13 are 1.1, 0.37 and −3.3 kJ mol^{-1}. From equation 11, the enthalpy of formation of p-tolyl lithium is calculated to be *ca* 3 kJ mol^{-1} where the enthalpy of formation of p-tolyl bromide is 12.1 kJ mol^{-1}, as suggested in Reference[7]. The enthalpy of formation value for p-tolyl lithium derived here is nearly identical to that in Table 1. Unfortunately, there is no measured enthalpy of formation of m-tolyl bromide. However, the difference between the enthalpies of formation of phenyl bromide and phenyl lithium (9.8 kJ mol^{-1}) must be about the same as the difference between the enthalpies of formation of the m-tolyl bromide and the m-tolyl lithium when the reaction is thermoneutral for equation 12.

Acknowledging complications in the measurement and concomitant analysis of the calorimetry of organic bromides[23], we nevertheless accept the enthalpy of formation for p-bromobiphenyl (115.1 kJ mol^{-1}) calculated from the reported enthalpy of combustion of the solid suggested in Reference[24]. From the enthalpies of formation of p-BrC_6H_4Ph, PhLi and PhBr, and the enthalpy of reaction, slightly more exothermic than the others, the enthalpy of formation of 102.4 kJ mol^{-1} for p-lithiobiphenyl is derived. If only the p-bromobiphenyl were a liquid, we could compare this value to that obtained from equations 6 and 7.

Halogen–lithium interchange equilibria were measured for several organolithium/organic iodide pairs such that $K_{\text{obsd}} > 1$[25]. Generally, the effect on the equilibrium of the solvent differences between ethyl ether and 40% ether–60% pentane or the temperature differences between −70 °C and −23 °C on the equilibrium were not large. All of the equilibrium constants were converted to log K constants for reactions of the various organolithiums with standard phenyl iodide (equation 14).

$$\text{PhI} + \text{RLi} \rightleftharpoons \text{PhLi} + \text{RI} \tag{14}$$

At a temperature of −70 °C in a 40:60 ethyl ether/pentane medium, the observed values of log K are: vinyl, -2.41 ± 0.02; cyclopropyl, 0.98 ± 0.02; Et, 3.50 ± 0.04; n-Pr, 3.88 ± 0.09; i-Bu, 4.59 ± 0.06; neopentyl, 5.46 ± 0.06; cyclobutyl, 6.14 ± 0.07 and cyclopentyl, 6.90 ± 0.10. Continuing to assume that Gibbs energies and enthalpies are essentially equal, the above reaction is endothermic by 14 kJ mol^{-1} for R = vinyl. However, it is exothermic for the other R groups: cyclopropyl, −6; ethyl, −20; propyl, −22; isobutyl, −26; neopentyl, −31; cyclobutyl, −35 and cyclopentyl, −39 kJ mol^{-1}. The values are in the order expected for carbanion stability.

Unfortunately, we lack measured enthalpy of formation values for most organic iodides of interest here except for ethyl, *n*-propyl and phenyl iodides. From equation 14 and with phenyl iodide in its reference liquid state and with ethyl and propyl iodides in their reference gaseous states, the enthalpies of formation of ethyl lithium and of *n*-propyl lithium are calculated to be *ca* −54 and −74 kJ mol^{-1}, respectively. The former value is the same as those from Table 1 and the latter is compatible with one of the other values for *n*-propyl lithium derived in earlier sections.

VI. OXYGENATED ORGANOLITHIUMS: INTRAMOLECULAR COMPLEXATION AND ENTHALPIES OF FORMATION

A. Aliphatic Ethers

Geurink and Klumpp[19] measured the protodelithiation enthalpies of 3-lithiopropyl methyl ether, 3-lithiobutyl methyl ether, 5-lithiopentyl methyl ether and 7-*syn*-methoxy-2-*exo*-lithionorbornane in the same study that was discussed in an earlier section for the non-oxygenated compounds *n*-propyl lithium, *n*-butyl lithium, *sec*-butyl lithium and 2-norbornyl lithium. The reaction enthalpies for the oxygen-containing lithium species with *sec*-butyl alcohol in benzene were −190 ± 2, −199 ± 4, −190 ± 3 and −199 ± 2 kJ mol^{-1}, respectively, where all of the lithiated ethers purportedly exist as tetrameric species.

The enthalpies of the formal exchange reaction 15 between corresponding oxygenated and deoxygenated species

$$\mathrm{MeO(CH_2)}_{n+1}\mathrm{R} + \mathrm{H(CH_2)}_n\mathrm{CHRLi} \longrightarrow \mathrm{MeO(CH_2)}_n\mathrm{CHRLi} + \mathrm{H(CH_2)}_{n+1}\mathrm{R} \quad (15)$$

are −29 ± 3 kJ mol^{-1} for $n = 2$, R=H; −41 ± 6 kJ mol^{-1} for $n = 2$, R=Me and −30 ± 5 kJ mol^{-1} for $n = 4$, R=H, where the average of the protodelithiation enthalpies for *n*-PrLi and *n*-BuLi are used for the unmeasured *n*-pentyl lithium protodelithiation enthalpy. The exchange enthalpy for the norbornyl derivative is −23 ± 5 kJ mol^{-1}. The largest exothermicity is for the *sec*-butyl system, where all the lithiated species are tetrameric and the favorable exchange reaction enthalpy was attributed to non-sterically hindered intramolecular complexation of the 3-lithiobutyl methyl ether. The smaller exothermicity for the likewise secondary norbornyl system could be due to steric crowding of the intramolecular complex in the tetrameric cluster as suggested by the original authors, or perhaps to complications in the measurement of the protodelithiation of the 1:1 mixture of *exo*- and *endo*-2-lithionorbornane. The enthalpically less favorable exchange reactions for the primary alkyl systems were partly due to the enthalpy of deaggregation from a hexameric alkyl lithium to a tetrameric methoxy alkyl lithium[19]. Assuming that the enthalpy of the protodelithiation reaction would be essentially the same as for the other primary alkyl systems if the protodelithiation enthalpy of *n*-pentyl lithium were available, it is noteworthy that the intramolecular complexation strength is the same for both the 5-membered cycle of 3-lithiopropyl methyl ether and the 7-membered cycle of 5-lithiopentyl methyl ether. Although the 5- and 7-membered carbocycles, cyclopentane and cycloheptane, have very similar strain energies[20], this finding is nonetheless a surprise since most chelates (and other intramolecular metallic complexes) contain either 5- or 6-membered rings.

The derived enthalpies of formation of the *n*-propyl and *sec*-butyl lithiated methoxy ethers are -260 and -275 kJ mol^{-1}, respectively, from equation 16, the enthalpies of protodelithiation, the enthalpy of formation of *n*-butyl lithium from Table 1 and of liquid *n*-butane, and the measured enthalpies of formation of methyl *n*-propyl ether (lq, -266.0 ± 7 kJ mol^{-1}) and *n*-butyl methyl ether (lq, -290.6 ± 1 kJ mol^{-1}).

$$\mathrm{MeO(CH_2)_{\mathit{n}+1}R} + n\text{-BuLi} \longrightarrow \mathrm{MeO(CH_2)_{\mathit{n}}CHRLi} + n\text{-BuH} \qquad (16)$$

The enthalpy of formation of methyl *n*-pentyl ether is unavailable from experiment, but a value of -316 kJ mol^{-1} is obtained from the linear regression analysis of the known enthalpies of formation of methyl *n*-alkyl ethers vs. the number of carbon atoms in the ethers[26]. The methylene increment of -25.3 kJ mol^{-1} for this homologous ether series is nearly identical to the methylene increment for *n*-alkanes. Because the experimental protodelithiation enthalpies for the two primary lithio ethers are identical, the methylene increment in that homologous series as calculated here is necessarily identical to that of the homologous methoxy ethers. As calculated from the methylene increment or from equation 16, the enthalpy of formation of 5-lithiopentyl methyl ether is *ca* -309 kJ mol^{-1}.

If the enthalpy of formation of 4-lithiobutyl methyl ether is interpolated between the values for the lithiopropyl and the lithiopentyl ethers to be -285 kJ mol^{-1}, then the enthalpy of isomerization to the less stable 3-lithiobutyl methyl ether is $+10$ kJ mol^{-1}, which is about half that of isomerization of *n*-butyl lithium to *sec*-butyl lithium ($+21.3$ kJ mol^{-1}). However, a linear interpolation assumes the same strain energy for the 6-membered 4-lithiobutyl ether as for the above 5- and 7-membered ω-lithioalkyl methyl ethers. If it is less strained, then the isomerization enthalpy would be larger. How much of the isomerization enthalpy difference is due to other differences, such as intramolecular complexation and/or aggregation among the various species, is not known. Unfortunately, there is no enthalpy of formation measurement for the delithiated 7-methoxynorbornane.

B. Aryl Ethers

Beak and Siegel[27] studied the protodelithiation of the lithioanisole isomers by ethanol in di-*n*-butyl ether solution. As are phenyl lithium in diethyl ether solution and *o*-lithioanisole in dibutyl ether solution, the *p*- and *m*-lithioanisoles also were presumed to be predominately dimeric in the di-*n*-butyl ether solution. As dimers, the *o*-isomer is some 35 kJ mol^{-1} more stable than the nearly isoenergetic *m*- and *p*-isomers, consistent with intramolecular association between the lithium and oxygen. That the inductive effect is small in comparison with association is shown by the nearly identical enthalpies of protodelithiation of the *p*- and *m*-lithioanisoles.

Klumpp and Sinnige[28] proceeded similarly, using *sec*-butyl alcohol to protodelithiate the anisoles and other lithiated aryl ethers in di-*n*-butyl ether. The protodelithiation enthalpies for all the lithiated aryl ethers, as monomers, from the latter study are listed in Table 3. The reaction enthalpies for the *o*- and *p*-lithioanisoles are *ca* 20 kJ mol^{-1} more negative from Reference[28] compared to the ones from Reference[27], presumably due to differences in the reaction media. From the exchange reaction, equation 17, and the enthalpies of formation of phenyl lithium, benzene and the relevant aryl ether, the enthalpies of formation of the lithiated aryl ethers can be derived. The calculated values are shown in Table 3.

$$\mathrm{PhLi + ROArH} \longrightarrow \mathrm{PhH + ROArLi} \qquad \mathrm{R = Me, Ph} \qquad (17)$$

Interestingly, the protodelithiation enthalpy of 2-lithio-1,3-dimethoxybenzene is very nearly the same as that for the single methoxy species *o*-lithioanisole. If the stabilization of lithium by an *ortho* ether group is due mainly to intramolecular complexation or

TABLE 3. Enthalpies of protodelithiation[28] and calculated enthalpies of formation of lithioaryl ethers

Lithium compound	ΔH(protodelithiation) (kJ mol^{-1})	Calculated ΔH_f (kJ mol^{-1})
Lithiobenzene (phenyl lithium)	-174 ± 2	51.5 (from Table 1)[a]
o-Lithioanisole	-137 ± 2	-149 ± 3[b]
p-Lithioanisole	-152 ± 3	-134 ± 4[b]
2-Lithio-1,3-dimethoxybenzene	-136 ± 3	-318 ± 5[c]
o-Lithiophenyl phenyl ether	-147 ± 4	-62 ± 5[d]
p-Lithiophenyl phenyl ether	-165 ± 3	-44 ± 5[d]
1-Lithiodibenzofuran	-139 ± 3	106 ± 8[e]
2-Lithio-1-methoxynaphthalene	-150 ± 4	
4-Lithio-1-methoxynaphthalene	-170 ± 5	
8-Lithio-1-methoxynaphthalene	-142 ± 5	

[a] The enthalpy of formation of benzene (lq) is 49.0 ± 0.6 kJ mol^{-1} from Reference 12.
[b] The enthalpy of formation of anisole (lq) is -114.8 ± 0.8 kJ mol^{-1} from Reference 12.
[c] The enthalpy of formation of *m*-dimethoxybenzene (s) is -283.3 ± 1.9 kJ mol^{-1} from Reference 29.
[d] The enthalpy of formation of diphenyl ether (s) is -32.1 ± 1.5 kJ mol^{-1} from Reference 12.
[e] The enthalpy of formation of dibenzofuran (lq) is -29.0 ± 4.8 kJ mol^{-1} from Reference 30.

chelation, then it is likely that the phenoxy is less stabilizing than methoxy because in aryl ethers, less basic than their aliphatic counterparts, the oxygen electrons are delocalized into the substituted phenyl ring via resonance and so the relatively positive oxygen is a poorer electron donor for chelation. However, the protodelithiation enthalpy of 1-lithiodibenzofuran with its phenoxy-like substituent *ortho* to the lithium is very nearly the same as for *o*-lithioanisole. Consideration of the experimental error bars shows that the differences are quite small.

The protodelithiation enthalpies of the 2- and 4-lithio-1-methoxynaphthalenes are *ca* 15 kJ mol^{-1} more exothermic than for their *o*- and *p*-lithiomethoxybenzene counterparts. The enthalpy of formation difference between 1- and 2-methoxynaphthalene in the solid phase is calculated (using estimation approaches of Reference 31) to be less than 1 kJ mol^{-1}, indicating virtually no destabilization of the 1-isomer due to repulsion with the (8-) *peri* hydrogen. That the 2-lithio-1-methoxynaphthalene would be destabilized relative to the corresponding benzene analog is apparent: if the oxygen is coordinated to the lithium, the methyl substituent must be oriented toward the *peri* hydrogen, or if the *peri* repulsion is avoided, the intramolecular association between the oxygen and lithium is reduced. The protodelithiation enthalpy for the internally complexing 8-lithio species is similar to that for the other complexed lithioethers, and relative to the 4-lithio-1-methoxynaphthalene, suggestive of considerable $O \cdots Li$ stabilization. However, it remains enigmatic why the protodelithiation enthalpy value for the 4-lithio species is so much larger than that for *p*-lithioanisole. There would not seem to be that much *peri* repulsion between the Li and the (5-) hydrogen or between the methoxy and the (8-) hydrogen. Lacking the enthalpy of formation of 1-methoxynaphthalene thwarts our efforts in deriving the enthalpy of formation of either lithio-1-methoxynaphthalene.

VII. PERLITHIOCARBONS AND LITHIATED AROMATIC ANIONS

A. Perlithiocarbons

Many perlithiocarbon species have been reported but the thermochemistry of only two have been studied, C_2Li_2 and CLi_4. The enthalpy of formation of the former, dilithium acetylenide (lithium carbide), is recommended[11] to be −67.7 ± 4.3 kJ mol^{-1}. The enthalpy of formation of solid acetylene may be deduced to be *ca* 205 kJ mol^{-1}, found by arithmetically combining its archival gas-phase enthalpy of formation, 228.2 ± 0.7, and a consensus value[32] of its temperature-uncorrected enthalpy of sublimation, *ca* 23 kJ mol^{-1}. Thus, the enthalpy of the formal protodelithiation reaction (corresponding to a simple Li/H exchange reaction) is +273 kJ mol^{-1} or some +136 kJ mol^{-1} per lithium. This is in stark contrast to alkyl lithiums for which the formal protodelithiation enthalpies are exothermic, or to aryl lithiums where the formal reactions are nearly thermoneutral. Then again, if we view Li_2C_2 as a solid salt, considerable stabilization is expected. The enthalpy of formation of solid Li_2O is over 300 kJ mol^{-1} more negative than that of liquid H_2O, its conjugate acid, and Li_2S and Li_2Se are over 400 kJ mol^{-1} more negative than gaseous H_2S and H_2Se, the corresponding conjugate acids[14, 33].

The enthalpy of atomization of CLi_4 was shown[11] to be 1219 ± 31 kJ mol^{-1} at 1065 K. How do we derive the value at 298 K and thereby derive an enthalpy of formation at 298 K? Linearly interpolating between 1000 K and 1100K (from Reference 14), the enthalpies of formation of atomic C and Li are 719.4 and 150.2 kJ mol^{-1}, respectively, and so the enthalpy of formation of CLi_4 at 1065 K is 101 ± 31 kJ mol^{-1}. The enthalpies of formation of gaseous Li_2O and LiF at 298 K are −166.9 kJ mol^{-1} and −340.1 kJ mol^{-1}, respectively[14]. Interpolating between 1000 K and 1100 K[14], the enthalpies of formation at 1065 K are −185.5 kJ mol^{-1} for Li_2O and −352.3 kJ mol^{-1} for LiF. The enthalpy of formation differences between the two temperatures are thus *ca* 19 and 12 kJ mol^{-1} for these two substances, or roughly 10 kJ mol^{-1} per lithium. Very roughly then, the enthalpy of formation for CLi_4 at 1065 K is *ca* 40 kJ mol^{-1} more negative than at 298 K, corresponding to a value of *ca* 140 kJ mol^{-1} for the desired enthalpy of formation of solid CLi_4.

The related hydrogen-containing species, gaseous CH_4, NH_3, H_2O and HF, show an enthalpy of formation difference of only *ca* 3 kJ mol^{-1} per hydrogen at the two temperatures. We thus conclude that CLi_4 has a more positive enthalpy of formation than CH_4(−74.4 ± 0.4 kJ mol^{-1}) by 214 kJ mol^{-1} or *ca* 54 kJ mol^{-1} per lithium. This is in comparison to *ca* 40–60 kJ mol^{-1} per lithium in alkyl species and the effectively no difference in the aryl species. We thus find that even though we might have expected CLi_4 to be considerably destabilized as would be expected from electrostatic repulsion of the positive lithiums and the general instability of anions with multiple negative charges, no such destabilization was found. $C^{-4}(Li^+)_4$ is an inadequate description of CLi_4.

B. Lithium Cyclopentadienide and Lithium Cyclooctatetraenide

Lithium cyclopentadienide (s), LiCp, may be formally protodelithiated to cyclopentadiene (lq) by a simple Li/H exchange with an accompanying reaction enthalpy of 182.4 kJ mol^{-1}. The large endothermicity is not unexpected for the nominally aromatic cyclopentadienyl anion. By comparison, for formal protodelithiation of solid LiOH to liquid H_2O is 199.1 kJ mol^{-1}.

We close this chapter by considering solid (di)lithium cyclooctatetraenide, Li_2cot. The two choices for the protodelithiated product are 1,3,5- and 1,3,6-cyclooctatriene. Gas-phase equilibrium studies[34] suggest the former is the more stable isomer by 13.6 kJ mol^{-1}. From the enthalpy of formation of the latter olefin[35], 196.3 kJ mol^{-1}, the enthalpy of formation of the former is 182.7 kJ mol^{-1}. Applying the CHLP protocol[1] to estimate the enthalpy of vaporization results in an enthalpy of formation of 142 kJ mol^{-1} for liquid 1,3,5-cyclooctatriene. This corresponds to a Li/H exchange enthalpy of 284 kJ mol^{-1} or some 142 kJ mol^{-1} per lithium. This considerable stabilization, while less than for LiCp, is comparable to that found in the other dilithium species, C_2Li_2.

VIII. ACKNOWLEDGMENT

We wish to thank Torkil Holm for helpful personal communications as well as significant contributions to the literature.

IX. REFERENCES AND NOTES

1. J. S. Chickos, D. G. Hesse, J. F. Liebman and S. Y. Panshin, *J. Org. Chem.*, **53**, 3424 (1988); J. S. Chickos, D. G. Hesse and J. F. Liebman, *J. Org. Chem.*, **54**, 5250 (1989).
2. Yu. A. Lebedev, E. A. Miroschnichenko and A. M. Chaikin, *Dokl. Akad. Nauk SSSR*, **145**, 1288 (1962); *Chem. Abstr.*, **58**, 2906n (1962).
3. J. F. Liebman, J. A. Martinho Simões and S. W. Slayden, in *Lithium Chemistry: A Theoretical and Experimental Overview* (Eds. A.-M. Sapse and P. v. R. Schleyer), chap. 6, Wiley, New York, 1995.
4. A-M. Sapse, D. C. Jain and K. Raghavachari, in *Lithium Chemistry: A Theoretical and Experimental Overview* (Eds. A.-M. Sapse and P. v. R. Schleyer), chap. 3, Wiley, New York, 1995.
5. G. Pilcher and H. A. Skinner, in *The Chemistry of the Metal–Carbon Bond* (Eds. F. R. Hartley and S. Patai), Wiley, New York, 1982.
6. J. D. Cox and G. Pilcher, *Thermochemistry of Organic and Organometallic Compounds*, Academic Press, London, 1970.
7. T. Holm, *J. Organomet. Chem.*, **77**, 27 (1974).
8. J. B. Pedley and J. Rylance, *Sussex N.P.L. Computer Analyzed Thermochemical Data: Organic and Organometallic Compounds*, University of Sussex, Brighton, 1977. Although this is the older edition of the compendium by the first-named author, these values do not appear in the later 1986 volume.
9. J. A. Martinho Simões, 'Organometallic thermochemistry data', in *NIST Chemistry WebBook, NIST Standard Reference Database Number 69* (Eds. P. J. Linstrom and W. G. Mallard), July 2001, National Institute of Standards and Technology, Gaithersburg, MD 20899 (http://webbook.nist.gov).
10. (a). J. P. Leal, V. Cachata and A. Carvalho, *Eur. J. Inorg. Chem.*, 1587 (2001).
    (b). G. R. Stevenson and J. Valentin, *J. Phys. Chem.*, **82**, 498 (1978).
11. H. Kudo, *Chem. Lett.*, 1611 (1989).
12. J. B. Pedley, R. D. Naylor and S. P. Kirby, *Thermochemical Data of Organic Compounds*, 2nd edn., Chapman & Hall, New York, 1986.
13. H. Y. Afeefy, J. F. Liebman and S. E. Stein, 'Neutral thermochemical data', in *NIST Chemistry WebBook, NIST Standard Reference Database Number 69* (Eds. P. J. Linstrom and W. G. Mallard), July 2001, National Institute of Standards and Technology, Gaithersburg, MD 20899 (http://webbook.nist.gov).
14. M. W. Chase, Jr., *NIST-JANAF Thermochemical Tables*, 4th edn., *J. Phys. Chem. Ref. Data Monograph 9* (1998).
15. J. F. Liebman, J. A. Martinho Simões and S. W. Slayden, *Struct. Chem.*, **6**, 65 (1995).
16. F. M. Bickelhaupt, N. J. R. v. Eikema Hommes, C. F. Guerra and E. J. Baerends, *Organometallics*, **15**, 2923 (1996).
17. T. Holm, *J. Chem. Soc., Perkin Trans. 2*, 464 (1981); T. Holm, *J. Organomet. Chem.*, **56**, 87 (1973).
18. G. R. Brubaker and P. Beak, *J. Organomet. Chem.*, **136**, 147 (1977).
19. P. J. A. Geurink and G. W. Klumpp, *J. Am. Chem. Soc.*, **108**, 538 (1986).
20. See, for example, A. Greenberg and J. F. Liebman, *Strained Organic Molecules*, Academic Press, New York. 1978.
21. E. M. Arnett and K. D. Moe, *J. Am. Chem. Soc.*, **113**, 7068 (1991).
22. H. J. S. Winkler and H. Winkler, *J. Am. Chem. Soc.*, **88**, 964 (1966).
23. S. W. Slayden, J. F. Liebman and W. G. Mallard, 'Thermochemistry of halogenated organic compounds', in *The Chemistry of Functional Groups, Supplement D2: The Chemistry of Organic*

Halides, Pseudohalides and Azides (Eds. S. Patai and Z. Rappoport), Wiley, Chichester, 1995, p. 361.

24. L. Brull, *Gazz. Chim. Ital.*, **65**, 19 (1935); *Chem. Abstr.*, **28**, 35897 (1935).
25. D. E. Applequist and D. F. O'Brien, *J. Am. Chem. Soc.*, **85**, 743 (1963).
26. S. W. Slayden and J. F. Liebman, 'Thermochemistry of ethers, alcohols, arenols, enols and peroxides', in *The Chemistry of Functional Groups, Supplement E: The Chemistry of Hydroxyl, Ether and Peroxide Groups, Vol. 2* (Ed. S. Patai), Wiley, Chichester, 1993.
27. P. Beak and B. Siegel, *J. Am. Chem. Soc.*, **96**, 6803 (1974).
28. G. Klumpp and M. J. Sinnige, *Tetrahedron Lett.*, **27**, 2247 (1986).
29. M. A. R. Matos, M. S. Miranda and V. M. F. Morais, *J. Phys. Chem. A*, **104**, 9260 (2000).
30. R. Sabbah, *Bull. Soc. Chim. Fr.*, **128**, 350 (1991).
31. S. W. Slayden and J. F. Liebman, 'Thermochemistry of phenols', in *The Chemistry of Phenols* (Ed. Z. Rappoport), Wiley, Chichester, 2003.
32. J. S. Chickos and W. E. Acree, Jr., *J. Phys. Chem. Ref. Data*, **31**, 537 (2002).
33. D. D. Wagman, W. H. Evans, V. B. Parker, R. H. Schumm, I. Halow, S. M. Bailey, K. L. Churney and R. L. Nuttall, 'The NBS tables of chemical thermodynamic properties: Selected values for inorganic and C_1 and C_2 organic substances in SI units', *J. Phys. Chem. Ref. Data* **11**, 1982 Supplement No. 2.
34. J. M. Greathead and S. W. Orchard, *Int. J. Chem. Kinet.*, **15**, 1069 (1983).
35. R. B. Turner, B. J. Mallon, M. Tichy, W. v. E. Doering, W. R. Roth and G. Schroder, *J. Am. Chem. Soc.*, **95**, 8605 (1973); R. B. Turner, W. R. Meador, W. v. E. Doering, L. H. Knox, J. R. Mayer and D. W. Wiley, *J. Am. Chem. Soc.*, **79**, 4127 (1957).

CHAPTER **4**

Solid state NMR spectroscopy in organolithium chemistry

DAN JOHNELS

Department of Chemistry/Organic Chemistry, Umeå University, SE-901 87 Umeå, Sweden. Fax: +46 90 138885; e-mail: Dan.Johnels@chem.umu.se

and

HARALD GÜNTHER

University of Siegen, Fachbereich 8, OCII, D-57068 Siegen, Germany. Fax: +49 −271 740 2512; e-mail: guenmr@chemie.uni-siegen.de

---

The Chemistry of Organolithium Compounds. Edited by Z. Rappoport and I. Marek
© 2004 John Wiley & Sons, Ltd. ISBN: 0-470-84339-X

I. INTRODUCTION

A. General Aspects of Organolithium Compounds

The alkali metal lithium is present as a constituent in a number of important contexts, such as inorganic salts, glassy materials, solid electrolytes, lithium containing batteries, lithium intercalation carbonaceous materials and in sedatives. In many of these areas solid state NMR spectroscopy plays an important role in the characterization of the materials. This review is, however, restricted to the application of solid state NMR to organolithium complexes including lithium amides and phenolates, an area of organometallic chemistry which is closely related to the progress made in organic synthesis. Thus, organolithium compounds constitute a commonly used and very important class of organometallic reagents, as evident from this volume. They have been successfully used in organic and organometallic chemistry for nearly a century[1], but much is still unknown about the structure and reactivity of these systems.

The interaction between the carbon and lithium atom in these species was unclear at first. For example, the solubility of organolithium compounds in non-polar solvents seemed to indicate a covalent interaction. However, more recent results clearly demonstrate that the interaction is chiefly of an ionic nature[2]. This fact also explains the prevalent aggregation of organolithium compounds, where monomers can be considered as dipoles, dimers as quadrupoles, tetramers as octapoles etc.[3,4], stabilized by Coulomb interactions (Figure 1). It is convenient to indicate the aggregation and solvation as $\text{Li}_x\text{A}_x\text{S}_y$, where x indicates the size of the aggregate built up of lithium cations (Li) and relevant anions (A), and y indicates the number of solvent or ligand molecules (S) present in the complex.

In the solid state, the degree of aggregation depends largely upon the steric requirements of the anion and the complexing ability and steric factors of the ligands, as well as on its denticity. Polydentate ligands tend to produce smaller aggregates or monomers. In solution, experimental conditions such as temperature and concentration play an additional, but equally important role.

The aggregation phenomena are important as it is generally recognized that the degree of aggregation and complexation has a strong influence on the reactivity and selectivity of the complexes. Consequently, it is of general interest to understand the structures of these reagents in order to optimize the reaction conditions under which they are used[5−17]. These aspects are treated in other parts of this volume.

Investigations by various experimental techniques have been prompted by the structural diversity of organolithium complexes. The methods used range from

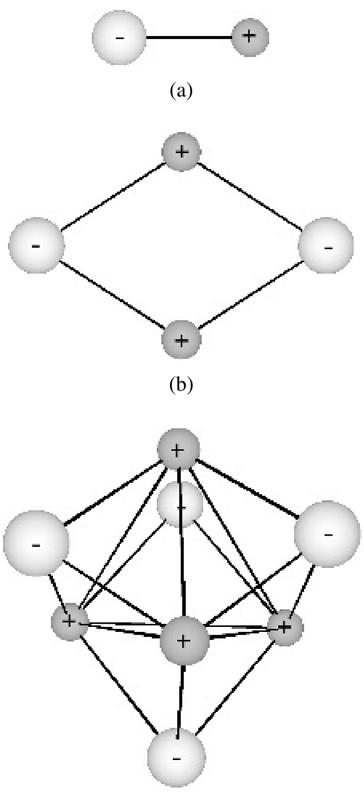

(a)

(b)

(c)

FIGURE 1. Organolithium aggregates described as interacting negatively charged carbon and positively charged lithium ions: (a) monomers viewed as dipoles, (b) dimers as quadrupoles and (c) tetramers as octapoles

colligative measurements[18], different spectroscopic methods, mainly NMR spectroscopy in solution[19–26] to X-ray crystallography in the solid state[27–31]. In addition, there have been a number of theoretical investigations in which the structures of a variety of organolithium compounds were studied[2, 32, 33].

As for NMR, it is of historical interest that already in 1936 an attempt was made to utilize the magnetic properties of ^{7}Li to detect the phenomenon later to be called nuclear magnetic resonance[34]. However, the effort was not met with success, probably due to saturation of the signal. Already in the beginning of the 1960s the possibility of observing the NMR active lithium nucleus in organolithium complexes was utilized and solution NMR spectroscopy was applied to the field of organolithium chemistry[35–37]. ^{1}H and ^{13}C chemical shifts were used to determine the charge distribution, aggregation, solvation, or the position of the equilibrium between contact ion pairs (CIP) and solvent-separated ion pairs (SSIP) of such complexes[19–26]. ^{13}C$-$^{1}H coupling constants were used to deduce the hybridization of the lithium bearing carbon[38] and ^{13}C$-$$^{6/7}$Li couplings were employed to gain direct information about the degree of aggregation.[39–41] Scalar couplings to ^{31}P in hexamethylphosphorous triamide (HMPA) have improved our understanding of solvation phenomena[17, 42–44]. In the area of lithium amides, couplings between $^{6/7}$Li and ^{15}N have played an important role in understanding the chemistry of such N-lithiated species.[13, 45, 46] Dynamic aspects have been investigated by variable temperature studies combined with lineshape analysis.[19, 47–51] Dipolar interactions have been used in one- and two-dimensional ^{6}Li,^{1}H heteronuclear Overhauser effect spectroscopy (HOESY) to deduce the location of the lithium cation relative to the anion[23, 52–57]. In a few applications diffusion investigations have been conducted to obtain further information about aggregation phenomena[58–60].

With respect to structural investigations of organolithium compounds, one relevant question to answer is whether the solid structures of organolithium complexes, as determined by X-ray crystallography, are suitable models for the structures present in solution. One way to relate the information gathered by X-ray crystallography to the solution structure is to compare data from solution NMR with those from solid state NMR. Moreover, solid state NMR spectroscopy will enable the study of, for example, polylithiated systems[61], which are difficult to study in solution due to limited solubility and, for the same reason, difficult to obtain as single crystals suitable for X-ray determinations. As shown below, solid state NMR investigations can also give direct structural information regarding geometry and interatomic distances and, as an important advantage over X-ray investigations, NMR parameters are sensitive to dynamic phenomena.

B. General Aspects of Solid State NMR

In the early days of NMR, wideline spectra of solids defied a straightforward interpretation and this area remained for a long time a domain of solid state physics. It was only after considerable progress had been made through the introduction of line narrowing and other techniques that chemical applications of solid state NMR came into reach. Over the years, and with the advent of the Fourier transform technique, methods have been developed that circumvent the complications introduced by various factors into solid state NMR spectra. Among these, the most important is without doubt magic angle spinning (MAS), but sensitivity enhancement by cross-polarization (CP, Hartmann–Hahn experiments), high power decoupling and pulse NMR are equally indispensable. Thus, high-resolution solid state NMR spectra can today be obtained routinely and their interpretation and analysis yields important parameters for structural research[62]. As it turns out, wideline or static spectra as well as MAS spectra for many nuclei are easily obtained and analysed and in the present context those of ^{13}C and both lithium isotopes, ^{6}Li and ^{7}Li, are of particular relevance. In the following, we shall show examples of several solid state NMR techniques.

The complications that arise in solid state NMR spectra as compared to NMR spectra in solution are the consequence of the fixed orientation of the sample relative to the external magnetic field B_0. Mainly three interactions are responsible for the enormous line-broadening that can be observed for solid powder samples. These are (1) the shielding or chemical shift, including the chemical shift or shielding anisotropy CSA or $\Delta\sigma$ ($\boldsymbol{H}_{\mathrm{CSA}}$), (2) homo- and/or heteronuclear dipole–dipole coupling ($\boldsymbol{H}_{\mathrm{DD}}$) and (3) in addition, for nuclei with spin $>1/2$, the quadrupolar interactions ($\boldsymbol{H}_{\mathrm{Q}}$).

The total Hamilton operator for solid state NMR, including the Zeeman term ($\boldsymbol{H}_0$), is given in equation (1):

$$\boldsymbol{H} = \boldsymbol{H}_0 + \boldsymbol{H}_{\mathrm{CSA}} + \boldsymbol{H}_{\mathrm{DD}} + \boldsymbol{H}_{\mathrm{Q}} \qquad (1)$$

Theory[63, 64] shows that the lineshape contribution of these factors is characterized by an angle dependence of the type $(3\cos^2\theta - 1)$, where θ is the angle between the principal tensor axis of the respective interaction and the direction of B_0. At the angle $\theta = 54.7^\circ$ this term is equal to zero and the interaction vanishes; this angle is thus called the *magic angle*. In solution, as a consequence of molecular motion, θ is averaged over all possible values and the direct lineshape contribution of the interactions (1)–(3) vanishes on the NMR time scale. They only contribute to relaxation.

The expressions for the various parts of the Hamiltonian (equation 1) are well documented[62–64] and for our purpose and the following discussion it suffices to summarize the results for axially symmetric situations in angular frequency units with the equations 2–6, where $\boldsymbol{\sigma}_{iso}$ and $\Delta\boldsymbol{\sigma}$ are the isotropic part of the shielding tensor and the shielding anisotropy, respectively, D is the dipole coupling, eq or V is the electric field gradient at the nucleus, eQ is the nuclear quadrupole moment and the other symbols have their usual meaning:

$$\boldsymbol{H}_0 = -\gamma B_0 \boldsymbol{I}_z \tag{2}$$

$$\boldsymbol{H}_{CSA} = -\gamma B_0 \boldsymbol{I}_z[\sigma_{iso} + \Delta\sigma \tfrac{1}{2}(3\cos^2\theta - 1)] \tag{3}$$

where $\sigma_{iso} = \frac{1}{3}(\sigma_{11} + \sigma_{22} + \sigma_{33})$ and $\Delta\sigma = \sigma_{iso} - \sigma_{33}$,

$$\boldsymbol{H}_{\mathrm{DD}} = -D(3\cos^2\theta - 1)\boldsymbol{I}_z\boldsymbol{S}_z \quad \text{(heteronuclear)} \tag{4}$$

where $D = (\mu_0/4\pi)\gamma_I\gamma_S\hbar/r_{IS}{}^3$,

$$\boldsymbol{H}_{\mathrm{DD}} = -D\tfrac{1}{2}(3\cos^2\theta - 1)[3\boldsymbol{I}_{1z}\boldsymbol{I}_{2z} - (\mathbf{I}_1\mathbf{I}_2)] \quad \text{(homonuclear)} \tag{5}$$

$$\boldsymbol{H}_{\mathrm{Q}} = (eQ\,eq_{zz}/th)\tfrac{1}{2}(3\cos^2\theta - 1)(3\boldsymbol{I}_z^2 - \mathbf{I}^2)/4I(2I - 1) \tag{6}$$

According to the properties of the nuclei of interest, the individual contributions of the factors (1)–(3) discussed above to the solid state NMR lineshape differ considerably. In the case of spin-1/2 nuclei, quadrupolar interactions are absent, but many of these nuclei are abundant and strong homonuclear dipole–dipole couplings dominate the linewidth. A typical example for this situation is the proton. In the spectra of rare spin-1/2 nuclei, on the other hand, homonuclear interactions are absent and heteronuclear interactions may be eliminated if appropriate decoupling techniques are used. If sensitivity problems can be overcome, these nuclei are thus favourable candidates for solid state NMR. A typical example for this situation is carbon-13, where the lineshape is dominated by the CSA term. On the other hand, abundant spin-1/2 nuclei may be isolated from each other as a consequence of the chemical structure so that homonuclear dipole–dipole coupling, which depends on the distance factor $1/r^3$, vanishes. This situation is often met for phosphorous-31 in organophosphorous compounds. Finally, for the large group of quadrupolar nuclei with $I > 1/2$ the magnitude of the quadrupolar constant, Q, and the spin quantum number are factors that govern the degree of complexity introduced by quadrupolar interactions. In general, it is true that the larger the quadrupole moment, the larger the observed effect. In addition, there is a difference between nuclei with half-integer and integer spin quantum number, where second-order effects complicate the spectra in the former case. Typical powder patterns calculated for spin-1 (^{6}Li) and spin-3/2 (^{7}Li) nuclei with dominating quadrupolar interaction are shown in Figure 2.

In the present context, solid state NMR spectra of ^{13}C and the lithium nuclides ^{6}Li and ^{7}Li are of relevance and specific aspects of these techniques are discussed in the following sections.

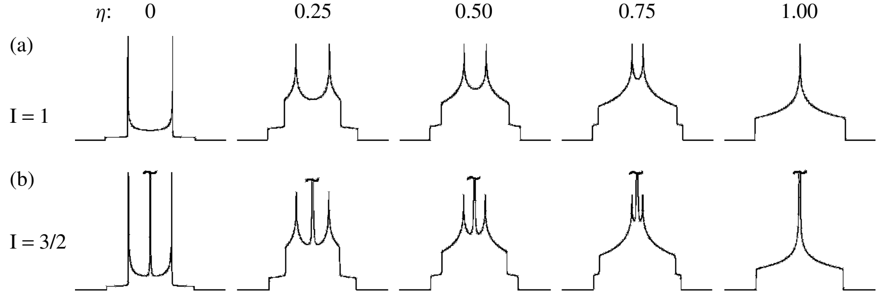

FIGURE 2. Calculated powder patterns for spin-1 (a) and spin-3/2 (b) nuclei with a dominating quadrupolar interaction (QUASAR[65] simulation); η is the asymmetry parameter of the quadrupolar interaction (equation (9))

1. ^{13}C solid state NMR

For this spin-1/2 nucleus shielding effects and heteronuclear dipole–dipole coupling are important. In **solution** only the isotropic chemical shift will be observed, as the molecules tumble rapidly on the NMR time scale. In the **solid state**, however, all possible orientations of the molecules relative to the magnetic field will be present, unless a single crystalline sample is used. This will result in broad signals, as the chemical shift is a tensor property. The line shape of the observed signal depends on the CSA and its asymmetry. The CSA of carbon atoms varies between *ca* 20 ppm up to *ca* 450 ppm in extreme cases, such as the charged carbon of the *t*-butyl cation[66]. In cases where the samples only give rise to one signal, the CSA can be very informative as it depends on the electron distribution about the nucleus. However, in samples containing many different nuclei, the CSA will lead to severe signal overlap. One experimental technique to deal with this line broadening is to exploit the angular dependence of the chemical shift interaction as in the MAS technique, where only the isotropic shift remains if the rotation rate is fast relative to the CSA. Under favourable conditions, linewidths of a few Hz can be obtained using this method. The CSA will appear as a pattern of spinning sidebands if the rotation speed is slow in comparison to the magnitude of the CSA. This opens up the possibility to determine the CSA even for samples giving rise to several signals by the analysis of the intensity of the spinning sidebands[67]. For chemical shift measurement, line-overlap can be avoided using special techniques which allow sideband suppression, such as TOSS[68, 69] or SELTICS[70]. The methylene resonance of adamantane at 38.4 ppm relative to the ^{13}C resonance of TMS is usually used as external reference. In general, the ^{13}C chemical shifts of the organic moiety are the same in the solid and in solution if the structures are identical.

The line will also broaden due to dipolar interactions to neighbouring magnetically active nuclei, typically protons. This broadening can to a certain extent be reduced by proton decoupling. As the dipolar interaction is much larger than the scalar coupling, the decoupling field has to be quite strong. The dipolar interaction has an angular dependence such that it vanishes at the magic angle (equations 4 and 5), an additional advantage of MAS. Of course, due to the low natural abundance of ^{13}C, homonuclear ^{13}C couplings are absent in solid state spectra.

The third technique generally utilized in ^{13}C solid state NMR spectroscopy is to improve the signal amplitude by magnetization transfer from ^{1}H to ^{13}C by cross-polarization. The combination of these methods is called CP/MAS[65, 70].

2. $^{6/7}$Li solid state NMR

Turning now to lithium, we have two nuclides available for NMR measurements: ^{6}Li and ^{7}Li. Both are quadrupolar nuclei with spin quantum number I of 1 and 3/2, respectively. The natural abundance of ^{7}Li (92.6%) provides enough NMR sensitivity for direct measurements, but also ^{6}Li (7.4%) can easily be observed without enrichment. However, isotopic enrichment poses no practical problem and is advantageous if sensitivity is important, as for measurements of spin–spin coupling constants in solution and of quadrupole coupling constants in the solid state.

In solid state NMR it turns out that, contrary to the situation described for ^{13}C, $^{6/7}$Li spectra are affected by all three factors discussed above, albeit with varying importance. The lineshapes of $^{6/7}$Li solid state NMR spectra obtained from different species may thus be quite different, as Figure 3 demonstrates with three examples.

a. Chemical shifts. The chemical shift range of $^{6/7}$Li is relatively small, normally *ca* 5 ppm, due to a near-cancellation of the diamagnetic term and the relatively small paramagnetic shielding term. ^{7}Li has a larger spectral dispersion than ^{6}Li as the gyromagnetic ratio is larger, but this advantage is often cancelled by a larger linewidth.

The chemical shift in **solution** is affected by factors such as solvent effects, viscosity, temperature and concentration. These effects are often of the same order as the shift changes induced due to structural effects[73, 74] (Table 1). This often limits the structural information that can be gained from the $^{6/7}$Li chemical shift. In cases when the lithium cation experiences the ring current of delocalized anions[75] the shift range is expanded considerably[76, 77]. As seen in Table 2, a change in solvent can induce large chemical shift changes if the equilibrium between the CIP and the SSIP is affected. For example, the ^{7}Li chemical shift of fluorenyllithium is −6.95 ppm when the CIP dominates in diethyl ether (DEE) and the lithium cation experiences the effect of the ring current of the delocalized anion, and −2.08 ppm when SSIP is dominating in tetrahydrofuran (THF) and the lithium cation is mostly interacting with the solvent[76].

The chemical shift is measured relative to a reference compound, for example LiBr in THF or H_2O. Due to the common dynamic processes observed between organolithium complexes, an external reference is often used. One problem is that there is not a single reference compound in general use, but different external references are employed. Thus, chemical shifts reported in different investigations must be compared with caution.

In the **solid state** the situation for ^{7}Li can be further complicated due to second-order effects as the nucleus has a spin quantum number of $I = 3/2$. The magnitude of this effect depends on the Larmor frequency and the size of the quadrupolar interaction, but is often relatively small, up to *ca* 1 ppm. Since the chemical shift range of lithium is so small, however, this effect can be significant in special cases. In order to correct for this second-order quadrupolar interaction, the quadrupolar coupling constant has to be measured. A straightforward way to circumvent this complication is to use ^{6}Li NMR for shift determinations because second-order effects are absent for spin-1 nuclei and the primary isotope effect on the shielding constant can be neglected. In addition, the smaller linewidth of ^{6}Li spectra is advantageous for the resolution of overlapping resonance lines[79].

The magnitude of the chemical shift anisotropy depends on the bonding situation and the nucleus gyromagnetic ratio. Since the bonds formed by lithium in organolithium compounds or other lithiated systems are mainly ionic, the anisotropy of the lithium chemical shift is generally small. It is more pronounced for ^{7}Li than for ^{6}Li. ^{7}Li spectra are dominated by the quadrupolar effect and the CSA contribution to the ^{7}Li lineshape is often negligible. Exceptions are compounds with poly-hapto bound lithium, such as

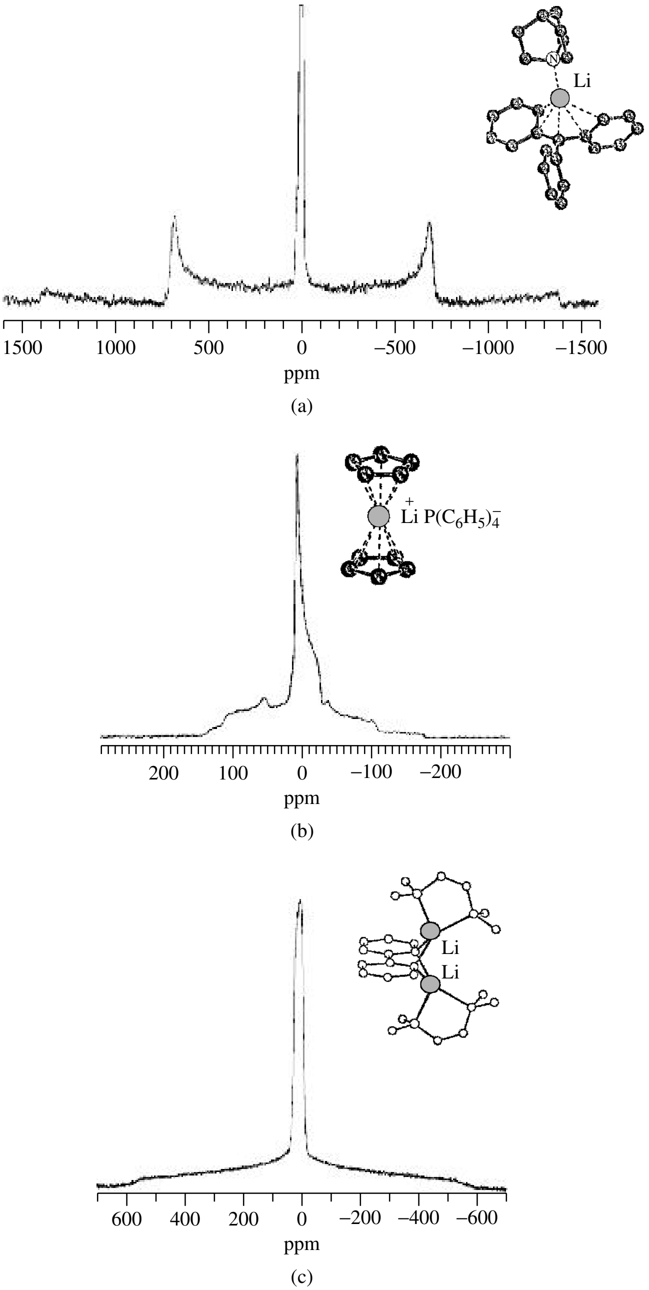

FIGURE 3. Lineshapes for static solid state ^{7}Li NMR spectra of: (a) triphenylmethyllithiumquinuclidine, dominating quadrupolar interaction; (b) lithiocene•P(C_6H_5)$_4$, dominating chemical shift anisotropy; (c) *o*,*o*′-dilithium diphenyl•(TMEDA)$_2$, strong homonuclear ^{7}Li,^{7}Li dipolar coupling[72]

TABLE 1a. ^{7}Li chemical shifts[a] of inorganic lithium salts in various solvents[74]

Solvent	δ (ppm)
Pyridine	+2.54
Acetone	+1.34
DMF	+0.45
Methanol	−0.54
THF	−0.60
DMSO	−1.01
Acetonitrile	−2.80

[a] The scale is changed to correspond to modern convention.

TABLE 1b. ^{7}Li chemical shifts, in ppm[a], of selected organolithium compounds in various solvents[73]

System[b]	Cyclopentane	Benzene	DEE[c]
EtLi	1.55	1.25	0.80
n-BuLi	1.55	1.50	0.75
BzLi	−0.45	0.15	−0.15

[a] Chemical shift, in ppm, as read out of the figure in the original paper; the scale is changed to correspond to modern convention.
[b] Et = ethyl, *n*-Bu = *n*-butyl, Bz = benzyl.
[c] DEE = diethyl ether.

TABLE 2. ^{7}Li chemical shifts, in ppm[a], of some selected delocalized organolithium complexes in various solvents[b 78]

System	Solvent[c]		
	DEE	THF	DME
Cyclopentadienyllithium	−8.86	−8.37	−8.67
Indenyllithium	−8.99	−6.12	−3.11
Fluorenyllithium	−6.95	−2.08	−3.06

[a] Chemical shift, in ppm, relative to external 1.0 M aqueous LiCl; the scale is changed to correspond to modern convention.
[b] For a more complete list see References 24 and 25.
[c] DEE = diethyl ether, THF = tetrahydrofuran, DME = dimethoxyethane.

various lithium salts of anions of cyclic π-systems, where a strong ring current effect is observed for the Li nuclei[76, 77]. A typical case where the shift anisotropy dominates the lineshape is lithiocene, as demonstrated in Figure 3b.

b. Dipole couplings. Heteronuclear dipolar coupling of $^{6/7}$Li in organolithium compounds is generally present to protons and gives rise to pronounced line broadening. It is normally eliminated by high-power decoupling. In these cases, the sensitivity of the $^{6/7}$Li signals may also be enhanced by cross-polarization[80–82]. However, the heteronuclear dipolar interaction can be used to advantage as it depends on the distance between the coupled nuclei.

In **solution**, dipole–dipole interactions constitute a relaxation mechanism, and the dipolar relaxation which is the basis for the well-known nuclear Overhauser effect (NOE), mostly used in the homonuclear $^1H,^1H$ case. The 2D HOESY method between ^1H and ^6Li has been used to obtain structural information of many organolithium systems in solution[52,53,55,56,83–89] and this field was reviewed in 1995[23]. ^6Li is commonly used as the relaxation is dominated by the dipole–dipole mechanism and the relaxation time is relatively long. Knowledge of the proximity of the lithium cation relative to protons in the substrate is used to derive information about the structure and aggregation of organolithium systems in solution. In a few cases quantitative investigations have been made[88–90]. An average error of the lithium position of *ca* 0.2 Å was reported.

In the **solid state**, the dipolar interaction is suppressed by MAS. If suitably placed rotor synchronized pulses are applied, however, the dipolar interaction is active under MAS conditions. This fact has been used to measure atomic distances in solids with the Rotational Echo Double Resonance (REDOR) experiment, introduced by Guillion and Schaefer for heteronuclear spin-1/2 systems in 1989[91]. In the REDOR experiment, the heteronuclear dipolar coupling leads to a dephasing of the observed signal, in addition to the normal T_2 relaxation. A function of both T_2 relaxation and dipolar dephasing is fitted to the observed signal decay, giving the dipolar coupling constant as one of the parameters. An experiment without the rotor synchronized pulses is conducted in order to estimate the T_2 relaxation time. The obtained dipolar coupling constant is directly related to the distance separating the two interacting nuclei according to equation 7,

$$r_{IS} = \sqrt[3]{\frac{\mu_0}{4\pi}\frac{\gamma_I\gamma_S\hbar}{D}} \tag{7}$$

where r_{IS} is the distance separating nuclei $\boldsymbol{I}$ and $\boldsymbol{S}$, D is the dipolar coupling constant in rad s^{-1} and the other symbols have their usual meaning. The determination of the dipolar couplings thus gives direct quantitative structural information.

An example of a spin-1/2 and spin-1 pair, i.e. ^{13}C and ^2H in enriched DL-[2-^2H,3-^{13}C] alanine was later studied by the REDOR technique[92], proving the applicability of the method in these cases as well. Another spin-1/2 and spin-1 pair of interest in the present context is ^{13}C–^6Li. In Figure 4, the dipolar coupling between ^6Li and ^{13}C is given as a function of the carbon–lithium distance. It is clear from this graph that distances up to *ca* 4 Å can be measured by this method and successful applications of the REDOR technique for the measurement of C–Li distances have been reported (see Section II.D).

Homonuclear lithium–lithium dipolar coupling, on the other hand, is expected for situations where two or more lithium nuclei exist and a short distance allows effective interactions such as in aggregates. Since this effect between quadrupolar nuclei cannot be eliminated by the MAS technique, considerable line broadening may result (Figure 3c). An interesting approach to solving this problem is ^6Li or ^7Li decoupling in a sample enriched with the appropriate isotope. The undesired homonuclear coupling is thereby transformed into a heteronuclear coupling which allows double resonance experiments. This technique is promising as recent experiments show, where the ^7Li linewidth could be considerably reduced (Figure 5)[93, 94]. ^6Li decoupling experiments were first performed in a study of methyllithium and dilithio methane by Yannoni, Lagow and coworkers[95, 96]. Here, the resulting ^{13}C resonance was extremely broad. By a combination of ^6Li isotope enriched material and simultaneous ^1H and ^6Li high-power decoupling the half-width of the line was reduced to 80 Hz (Figure 6). This is still much wider than commonly observed in ^{13}C solid state NMR spectroscopy under MAS conditions.

c. Quadrupolar interactions. The lithium nucleus has yet another very useful NMR property, i.e. an electric quadrupole moment, as both ^6Li and ^7Li have a spin quantum

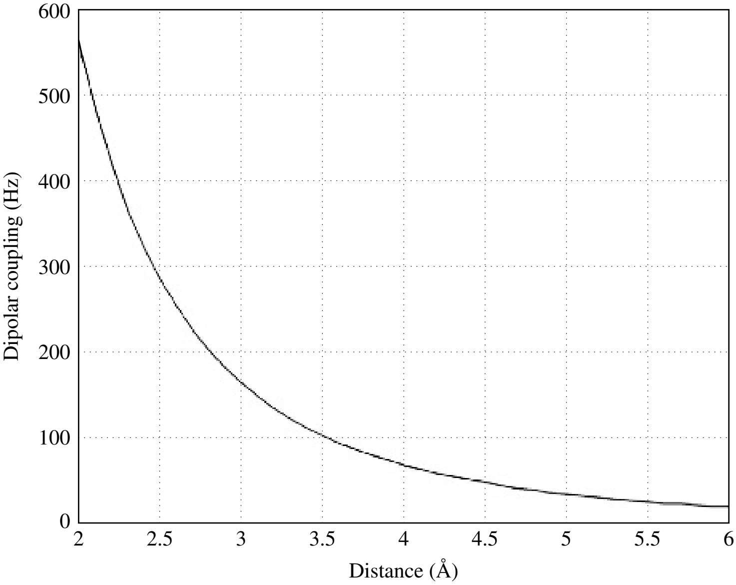

FIGURE 4. The ^{6}Li–^{13}C dipolar coupling as a function of the Li–C distance

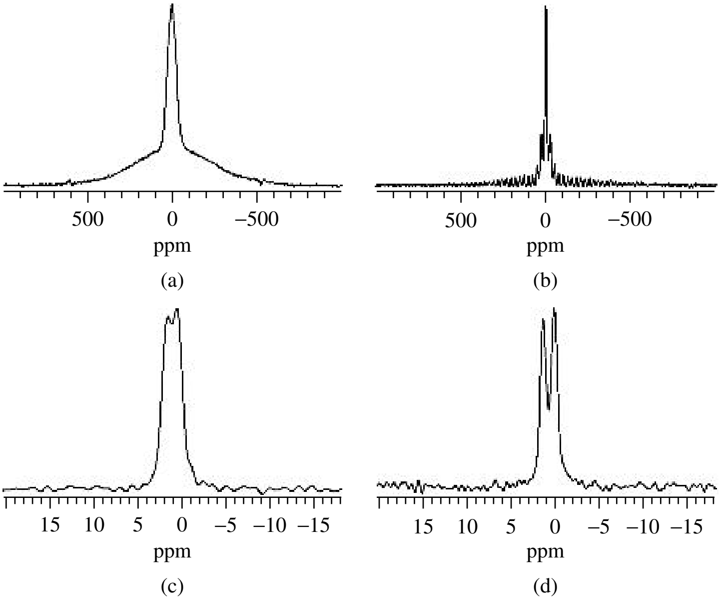

FIGURE 5. Reduction in linewidth in the ^{7}Li solid state NMR spectrum of the dimer of (*E*)-2-lithio-1-phenyl-1-(*o*-lithiophenyl)pent-1-ene (90% ^{6}Li) by various techniques: (a) static ^{7}Li{^{1}H} spectrum, halfwidth 6.3 kHz; (b) ^{7}Li{^{1}H} CP/MAS spectrum, rotational frequency 3 kHz; (c) central transition in the ^{7}Li{^{1}H} CP/MAS spectrum, halfwidth 130 Hz; (d) central transition in the ^{7}Li{^{1}H} CP/MAS spectrum with additional ^{6}Li decoupling. The two ^{7}Li resonances are separated by 1.25 ppm; lineshape analysis yields half-widths of 92 and 81 Hz, respectively[93, 94]

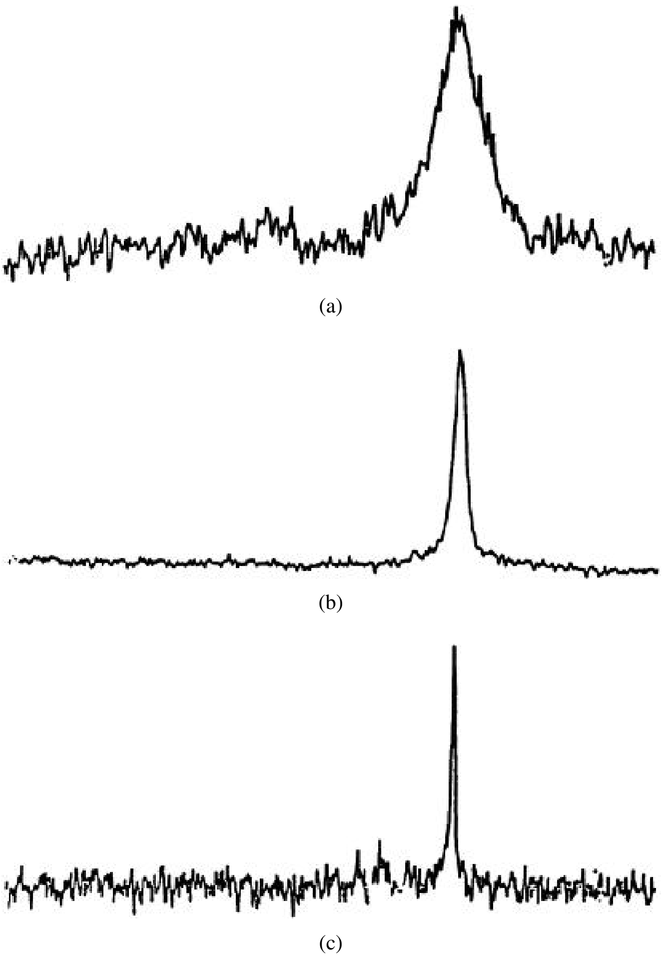

FIGURE 6. The first (proton decoupled) ^{13}C CP/MAS NMR spectrum of an organolithium spectrum, methyllithium at −150 °C: (a) CH$_3^7$Li, (b) CH$_3^6$Li, (c) CH$_3^6$Li with both ^{1}H and ^{6}Li high-power decoupling. Reprinted with permission from Reference 95. Copyright 1984 American Chemical Society

number $\boldsymbol{I} > 1/2$. The resulting quadrupole coupling constant, χ, is related to the electric field gradient at the nucleus and thus to the bonding situation of the lithium cation. For an atom at a site of cubic symmetry, for example in a spherical, tetrahedral or octahedral environment, the quadrupolar coupling constant is expected to vanish. Any deviation from this situation, however, leads to observable quadrupolar coupling constants. The relation is expressed according to equation 8

$$\chi = eQeq_{zz}/h \tag{8}$$

where χ (in Hz) is the quadrupole coupling constant elementary charge, eQ the nuclear quadrupole and eq_{zz} the largest principal component of the electric field gradient tensor at the nucleus Planck's. The electric quadrupole moments of ^{6}Li and ^{7}Li are relatively small, ^{6}Li actually has the smallest of all quadrupolar nuclei ($Q = -8.2 \times 10^{-4}$ [barn] for ^{6}Li and -4.0×10^{-2} [barn] for ^{7}Li)[24].

In addition, the asymmetry parameter of the quadrupolar coupling, η, is defined in equation 9

$$\eta = (q_{xx} - q_{yy})/q_{zz} \tag{9}$$

η is zero for axial symmetry ($q_{xx} = q_{yy}$) and close to 1 if $q_{xx} \gg q_{yy}$ holds.

The theoretical background for the quadrupole coupling constant was developed already in the 1950s[97, 98]. Direct calculation of quadrupolar coupling constants is still not straightforward and depends heavily on the basis set used[99–103]. The quadrupolar coupling constant is thus mainly used as an empirical parameter. Nevertheless, experimental trends can be reproduced quite well with available theoretical methods as shown in Section II.F.

Experimentally, χ values for gaseous lithium halides were determined as early as 1949 by molecular beam resonance experiments[104–106]. In solution, the quadrupolar interaction of ethyllithium and of *t*-butyllithium were investigated in 1964[107]. It was found that tetrameric and hexameric aggregates have different interactions. In the solid state χ of tetrameric methyl- and ethyllithium was determined in 1965 and 1966[108, 109], and for lithium formate in 1972[110]. However, it was not until Jackman started his investigations of lithium enolates and phenoxides in solution that the quadrupolar interaction was used in a systematic fashion to obtain structural information[111].

In **solution**, the quadrupolar coupling constant is not measured directly. Instead, the quadrupolar splitting constant is obtained from relaxation time measurements. The QSC is related to χ according to equation 10:

$$\mathrm{QSC} = \chi\sqrt{1 + \frac{\eta^2}{3}} \tag{10}$$

However, certain assumptions must be made in order to derive the QSC. First, it is often assumed that the relaxation of ^{7}Li is totally dominated by the quadrupole mechanism, i.e. $T_1 = T_1^Q$. If the relaxation of ^{6}Li is measured on the same sample, relaxation contributions from other mechanisms can be eliminated[112]. T_1^Q is related to QSC by equation 11[111]:

$$\frac{1}{T_1^Q} = \frac{2\pi^2}{5}(\mathrm{QSC})^2\tau_C \tag{11}$$

where τ_C is the rotational correlation time. This quantity has to be estimated, normally from ^{13}C relaxation time measurements, assuming that the relaxation is dominated by the dipole–dipole mechanism, and that the C—H vector under consideration does not experience any extra local dynamic process, i.e. internal rotation within the aggregate.

In the **solid state**, however, the quadrupolar coupling constant can be obtained directly from the spectrum without the above-mentioned assumptions. The coupling constants, which range from about 10 to 600 kHz for ^{7}Li depending on the structure, can be measured having the sample either static in the magnetic field or under MAS conditions. If the sample is static in the magnetic field and a suitable single crystal is at hand, the χ and η values, as well as the direction of the principal components of the electric field gradient tensor relative to the molecular framework can be determined. This is rarely the case for organolithium complexes, but has been realized for inorganic lithium salts[113–115]. Normally, having a microcrystalline or a powdered sample, only χ and η can be determined from the resulting powder pattern and not the orientation of the tensor. A quadrupolar echo sequence is used to measure the fast decaying signal[116–118]. As shown in Figures 2b

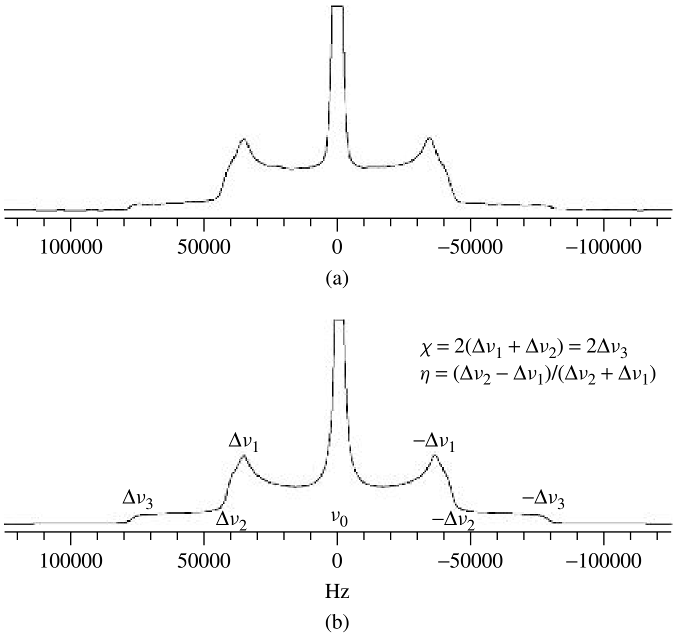

FIGURE 7. (a) Experimental[122] and (b) WINFIT[123] simulated static ^{7}Li solid state NMR spectrum of the TMEDA complex of trimethylsilylcyclopentadienyllithium. The χ and η values are 156 kHz and 0.1, respectively. The small effect of CSA was neglected in the simulation. In (b), the singularities are indicated together with the relation of these to the χ and η values[119]

and 7, the powder spectrum is a Pake doublet overlaid by the central 1/2 to $-1/2$ transition for an $I = 3/2$ nucleus.

When a powdered sample is rotated about the magic angle, a number of spinning sidebands are obtained, separated by the spinning speed (Figure 8). These are distributed over an area determined mainly by the strength of the quadrupolar interaction. The central transition is not affected by the quadrupolar interaction to first order. The other transitions are affected by this interaction, and the degeneracy of the transitions vanishes. In Figures 7 and 8 it is indicated how the singularities at $\Delta\nu_1$, $\Delta\nu_2$ and $\Delta\nu_3$ are related to the χ and η values. A straightforward direct analysis is possible on the basis of equations 12 and 13, which hold for static as well as for MAS spectra of spin-3/2 nuclei[119, 120].

$$\chi = 2(\Delta\nu_1 + \Delta\nu_2) = 2\Delta\nu_3 \tag{12}$$

$$\eta = (\Delta\nu_2 - \Delta\nu_1)/(\Delta\nu_2 + \Delta\nu_1) = 1 - 2\Delta\nu_1/\Delta\nu_3 \tag{13}$$

However, $\chi(^7\text{Li})$ and $\eta(^7\text{Li})$ are mostly derived by spectral simulation, as shown in Figures 7b and 8b. Various programmes are available for this purpose[121].

As a consequence of the small quadrupole moment of ^{6}Li, the quadrupolar interaction in solid state NMR spectra is much smaller for ^{6}Li than for ^{7}Li. This has been used to advantage for the determination of the ^{6}Li chemical shift anisotropy from the ^{6}Li static solid state powder spectrum of 2,4,6-tris(isopropyl)phenyllithium (see below)[125]. Applying MAS up to 10 kHz, the CSA contributions to the lineshape can be completely eliminated in most ^{6}Li spectra of organolithium compounds. If the measurement of the quadrupolar

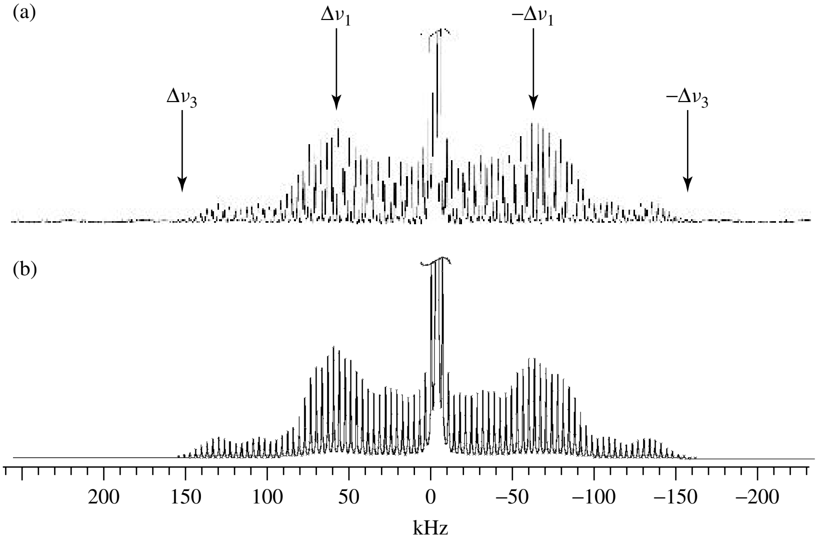

FIGURE 8. 116.589 MHz ^{7}Li MAS spectrum of $[((H_3C)_3Si)_2NLi{\cdot}OEt_2]_2$; rotational frequency 3.5 kHz; 5000 transients; (a) experimental[124]; (b) QUASAR[65] simulation with $\chi = 298$ kHz, $\eta = 0.2$, $\Delta\sigma = -42$ ppm, $\eta(\text{CSA}) = 1.0$, exponential line-broadening 320 Hz. During the simulation the χ and η values are optimized together with the CSA and residual ^{7}Li–^{7}Li dipolar couplings. In case of small quadrupolar coupling constants (<20 kHz), few sidebands are generated and $\eta(^7\text{Li})$ is less well defined. In these cases additional static spectra have to be measured

coupling constant is of interest, the use of ^{7}Li is thus advantageous. The second-order quadrupolar effect is usually very small and chemical shift data obtained from ^{6}Li and ^{7}Li MAS spectra of organolithium compounds are often identical within experimental error.

Finally, an important experimental aspect of solid state NMR studies of organolithium compounds is the stability of the air- and moisture-sensitive samples during the NMR measurements. Sample cells, usually rotors used for MAS and static spectra, have to be filled and sealed under argon in a glove-box or an equivalent device. Kel-F plastic caps are in general tight enough to guarantee stable conditions, but specially designed rotor inserts[126] have also been used[127].

It has been found that the ^{7}Li quadrupole parameters $\chi(^7\text{Li})$ and $\eta(^7\text{Li})$ are sensitive probes of solid state structures of organolithium compounds, for example with respect to aggregate size, solvation, ion pair structure and the X–Li–X structural angle. These results will be discussed in the following sections.

II. APPLICATIONS

A. ^{13}C Chemical Shifts in Solid Organolithium Complexes

It was not until the study of methyllithium and dilithiomethane by Yannoni, Lagow and coworkers that solid state ^{13}C CP/MAS NMR was applied to organolithium systems (Figure 6)[95,96]. However, as mentioned above, heteronuclear dipolar ^{7}Li,^{13}C coupling unfortunately complicated the observation of the single ^{13}C resonance in this particular case, even if ^{6}Li decoupling in a ^{6}Li-enriched compound was used. The need for triple resonance MAS probes, uncommon at that time, further deterred investigations of organolithium systems by solid state NMR spectroscopy. Today, this situation has changed because later studies showed that dipolar $^{6/7}$Li,^{13}C coupling is not important in most cases and high-resolution solid state ^{13}C NMR spectra can be observed for the great majority of organolithium systems without this complication. In fact, it has been found that data for the solid sample and the species in solution agree closely if the structure is retained. One point particular to solid state NMR should, however, be kept in mind when solid state ^{13}C NMR spectra are interpreted: the number of signals may be larger than expected on the basis of a given structure if time-averaging by dynamic processes in the solid structure is slowed down and/or non-equivalent molecules exist in the unit cell of the solid.

In a first application of general interest, fluorenyllithium complexes (**1**, Scheme 1) were studied by ^{13}C solid state NMR spectroscopy[128]. One reason for the choice of this system was that the results from the X-ray investigation presented at that time and solution NMR investigations were in conflict. The bis-quinuclidine complexes investigated in the solid state by X-ray analysis show that the lithium cation is asymmetrically positioned relative to the carbon framework of the anion, mainly interacting in a η^3 fashion with carbons C-1, C-9a and C-9 (Figure 9)[129].

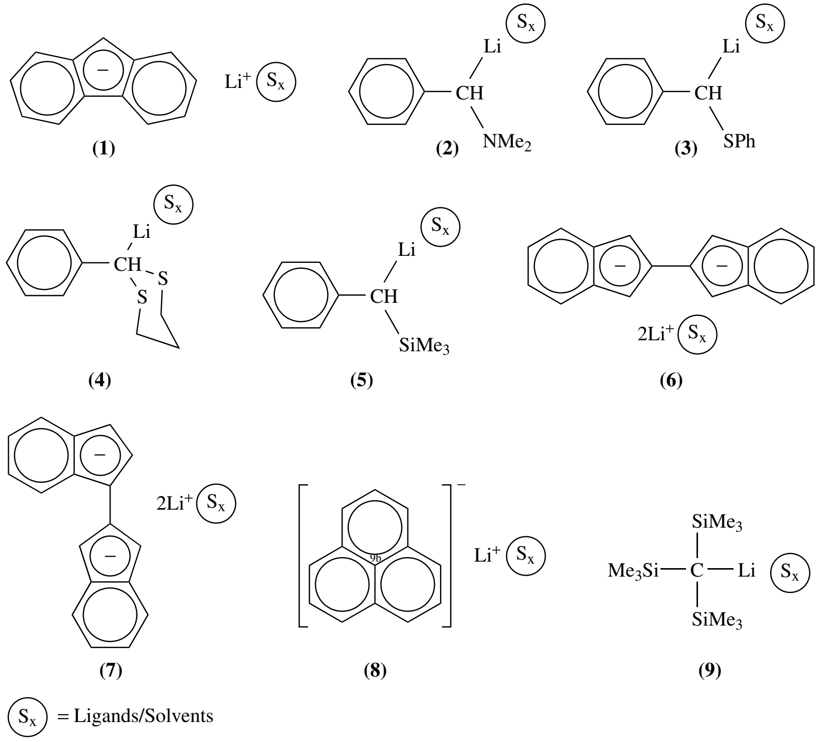

SCHEME 1

In solution, NMR investigations of fluorenyl complexes give rise to only seven ^{13}C signals, either due to a symmetric position of the lithium cation relative to the carbanion framework or to fast exchange on the NMR time scale under the experimental

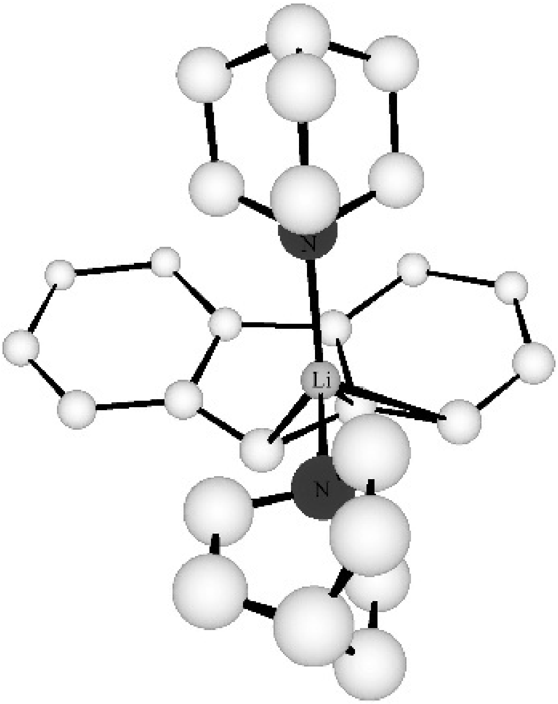

FIGURE 9. The X-ray structure of the bis-quinuclidine complex of fluorenyllithium; the lithium cation interacts in an unsymmetrical η^3 fashion with the anion[129]

conditions[130, 131]. Furthermore, as these complexes are monomeric, dipolar couplings to more than one lithium cation, as observed in the methyllithium complexes mentioned earlier, can be neglected.

As seen in Figure 10a, the ^{13}C CP/MAS NMR spectrum of the quinuclidine complex shows the expected asymmetry (for instance, different signals for C-8a and C-9a) due to the asymmetric position of the lithium cation relative to the carbon framework in accordance with the X-ray investigation[129]. The observed linewidths are not exceptionally large, and only small effects on the linewidths were observed when ^{7}Li was substituted by ^{6}Li, as shown in Figure 10b.

Other fluorenyllithium complexes were investigated as well. As is evident from Figure 11, the quinuclidine and DEE complexes give rise to asymmetric structures. However, the spectra of both the tetramethyl-ethylenediamine (TMEDA) and the THF complex indicate symmetric structures as for example shown by the lack of splitting of the C-8a, C-9a signals. Again, this apparent symmetry could be due to rapid exchange even in the solid state. To investigate this further, a variable temperature study of the TMEDA complex was undertaken. The signals of the fluorenyl system were unaffected by lowering the temperature down to −60 °C[128]. However, the broad signal from the TMEDA ligand observed at ambient temperature was resolved into three signals, due to a dynamic process of the ligand. This dynamic process has been indicated for several TMEDA complexes as large thermal anisotropy parameters of the ligand atoms in the pertinent X-ray structure and was later investigated in detail for several organolithium

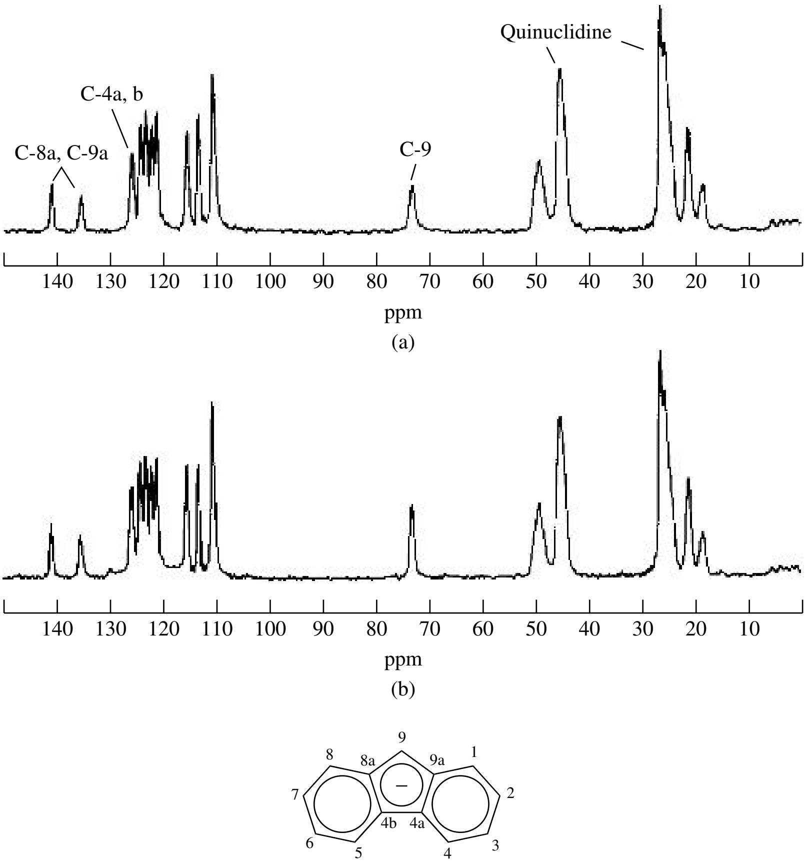

FIGURE 10. ^{13}C CP/MAS NMR spectra of the bis-quinuclidine complex of fluorenyllithium: (a) ^{7}Li isotopomer and (b) ^{6}Li isotopomer. Reprinted in part with permission from Reference 128. Copyright 1990 American Chemical Society

TMEDA complexes using solid state ^{13}C and ^{15}N variable temperature (VT) CP/MAS NMR spectroscopy (see Section II.E)[132].

The conclusion from the NMR study was that ^{13}C spectra of high resolution can be obtained from these monomeric complexes and, more importantly, that the position of the lithium cation relative to the fluorenyl system depends on the ligand/solvent. This indicates that the potential energy surface is rather flat, as predicted by simple theoretical investigations[133–135] and later confirmed by a more stringent theoretical treatment[136].

Another system that has been investigated by ^{13}C CP/MAS NMR spectroscopy as a function of different ligands is α-(dimethylamino)benzyllithium (**2**, Scheme 1)[137]. The DEE complex was proven to exist in the solid state as an η^3 coordinated dimer[138]. All the studied complexes are of an η^3 type according to comparison to solution NMR data. However, the actual structure varies as reflected by the shift difference between the two *ortho*-carbons. This difference ranges from 4.4 ppm for the N, N, N', N', N''-pentamethyldiethylenetriamine (PMDTA) complex to 20.3 ppm for the TMEDA complex.

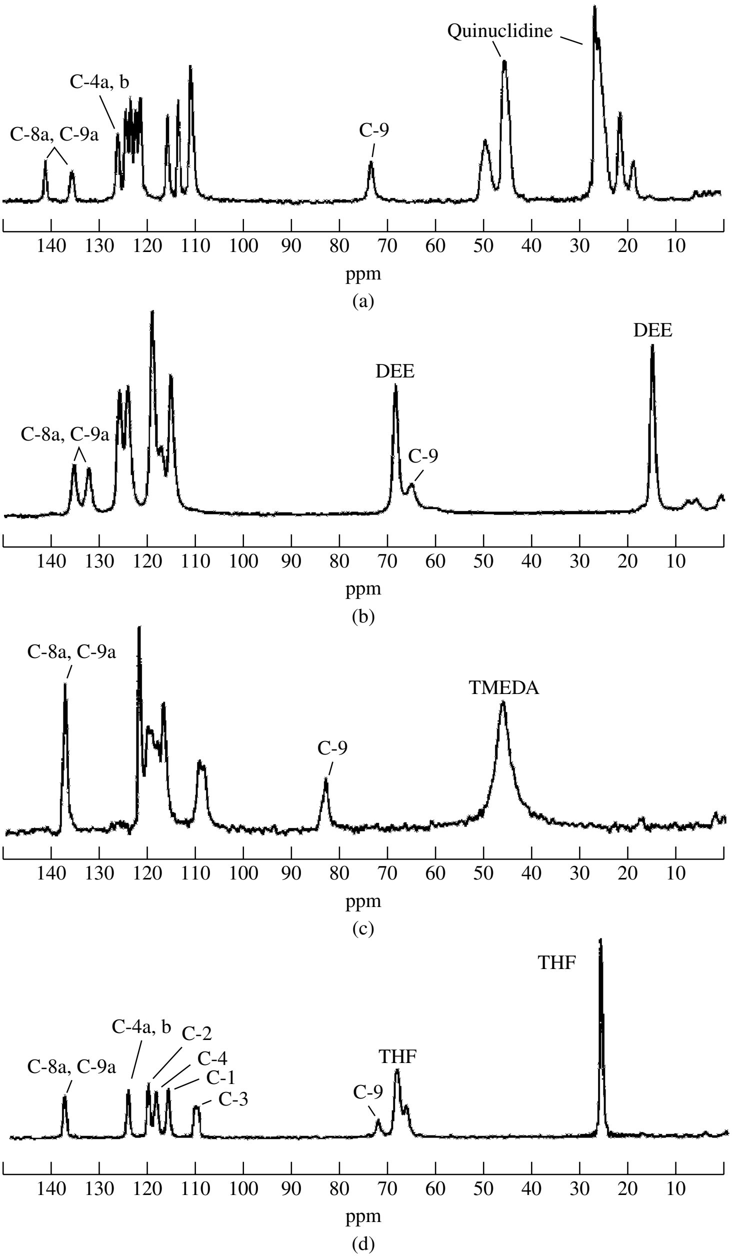

FIGURE 11. ^{13}C CP/MAS NMR spectra of fluorenyllithium complexes: (a) Quinuclidine complex, (b) DEE complex, (c) TMEDA complex and (d) THF complex. Reprinted with permission from Reference 128. Copyright 1990 American Chemical Society

In a study of related benzyllithium systems (**3**–**5**, Scheme 1) it was found that characteristic differences in ^{13}C chemical shifts are observed for CIP and SSIP structures[139]. While in the CIP structure the negative charge is stabilized at C_α by the C_α–Li contact, the SSIP structure allows a more effective delocalization of charge into the benzene ring by separating the lithium cation from C_α. This leads to ^{13}C shielding for the *ortho*- and *para*-positions. For example, the complexes of α-(phenylthio)benzyllithium (**3**) with one and two moles of 12-crown-4 exist as CIP and SSIP structures, respectively (see Section II.C.5), and exhibit $\Delta\delta(^{13}C)$ values of -5.5 ppm for the *ortho*-carbons and -5.6 ppm for the *para*-carbon in going from the CIP to the SSIP. At the same time, a high-frequency shift (deshielding) of $+9.9$ ppm is found for C_α as a consequence of reduced charge density and a hybridization change towards sp^2. It is interesting to note that the ^{13}C data of the mono-crown ether complex in THF solution are nearly identical with those of the solid state SSIP structure obtained with two moles of crown ether indicating the same structural motif, i.e. solvent separated ion pairs. Furthermore, in the solid the rotation of the phenyl ring around the C_α–C-1 bond is slow on the NMR time scale and two signals are observed for the *ortho*- and *meta*-carbons.

A number of phenyllithium complexes have also been investigated by solid state ^{13}C CP/MAS NMR spectroscopy[150]. This choice stems from the fact that phenyllithium is one of the best characterized organolithium systems. A number of different aggregates of various solvating ligands, i.e. monomers, dimers and tetramers, have been investigated in the solid state by X-ray crystallography and in solution by NMR spectroscopy[17, 41, 42, 140–149]. More than 50 entries of lithiated benzene derivatives are found in a search of the Cambridge Structural Database (version 5.23 April 2002), restricting the search to complexes where lithium is the sole metal.

In the solid state NMR study, uncomplexed phenyllithium, assumed to be a tetramer, as well as the TMEDA complexed dimer and the PMDTA complexed monomer were investigated. Both ^{7}Li and ^{6}Li isotopes were used in the preparations. The ^{13}C spectra of the complexes are presented in Figure 12. It is evident that the substitution of ^{7}Li with ^{6}Li has profound effects on the linewidths, especially of the *ipso*-carbon at *ca* 180 ppm in the aggregated uncomplexed system (Figure 12a and 12b, respectively). This is in accordance with the previously mentioned study of methyllithium. However, even the other positions are affected by the dipolar couplings to the four quadrupolar lithium cations, but to a lesser extent due to the larger C–Li distances.

The same effect is noted for the dimer in Figure 12c and 12d, but it is attenuated because the *ipso*-carbon is only coupled to two lithium cations. The lineshape of the TMEDA ligand indicates that, again, a dynamic process occurs. This complex was included in the investigation of dynamic processes previously alluded to and discussed below in Section II.E[132].

In the monomer the *ipso*-carbon signal of the ^{7}Li isotopomer is split into a quartet, typical for a scalar coupling to one lithium cation of spin $I = 3/2$ (Figure 12e). However, closer inspection of the signal reveals that the splitting is not symmetric. The origin of this asymmetry is the combination of scalar and dipolar couplings. The magnitude of the coupling constant is in the expected range for a monomeric organolithium complex[41, 145]. The coupling to ^{6}Li is, however, not resolved due to the smaller coupling constant. A similar splitting was later observed in a multinuclear solid state NMR investigation of the 2,4,6-tri(isopropyl)phenyllithium, indicating an interaction between the *ipso*-carbon of this complex with one lithium cation[125]. This complex will be further discussed below.

In Table 3, the observed ^{13}C chemical shifts obtained in the solid state are compared to the shifts in solution. It is evident that the agreement between shifts in the solid state and solution is relatively good. The largest discrepancy is observed for the *ipso*-carbon in the uncomplexed phenyllithium tetramer model and the tetramer in solution measured

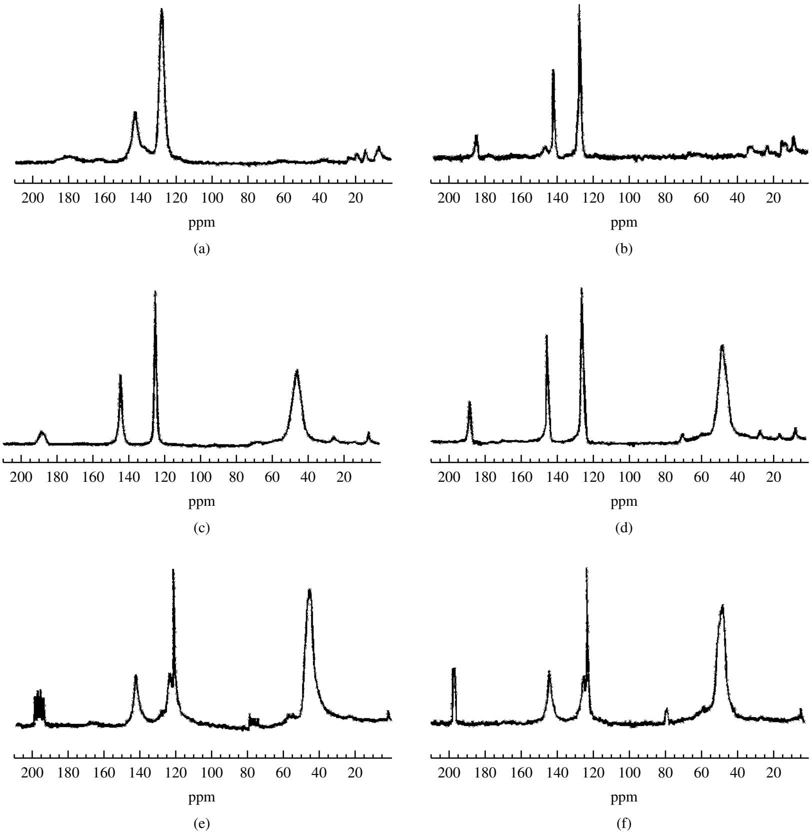

FIGURE 12. ^{13}C CP/MAS NMR spectra of the ^{7}Li (a, c, d) and ^{6}Li (b, d, f) isotopomers of phenyllithium; (a, b) uncomplexed phenyllithium, (c, d) with TMEDA as ligand and (e, f) with PMDTA as ligand, respectively. Reproduced with permission of Elsevier Science from Reference 150

in 1:2 DEE−cyclohexane. The complex in solution is without doubt solvated by DEE, a fact that explains the observed difference.

The general conclusion from this investigation is that even aggregated organolithium species can be studied by solid state ^{13}C NMR spectroscopy, and that these complexes seem to retain the solid state structure in solution.

In another solid state NMR study a tetrameric aggregate of phenyllithium, prepared from ^{13}C enriched [1-^{13}C]bromobenzene and [^{6}Li]*n*-butyllithium in benzene, was investigated in order to increase understanding of the origin of the observed ^{13}C NMR chemical shifts[151]. The naïve presumption would be that the *ipso*-carbon should be shielded relative to the corresponding neutral system, due to the increased electron density in the organolithium system, as is observed in aliphatic complexes. However, the *ipso*-carbon is deshielded on substitution of hydrogen with lithium. This was known from solution data and explained as due to a small ΔE term in the paramagnetic contribution to the shielding constant in the Ramsey equation[151, 152] as a consequence of the electron pair in the sp^2 hybrid orbital of the C−Li bond[141, 152]. In the solid state study, the possibility to recover the shift tensors

TABLE 3. ^{13}C NMR chemical shifts, in ppm[a], of phenyllithium aggregates in the solid state and in solution[150]

Isotopomer	Aggregate	*ipso*	*ortho*	*meta*	*para*
Solid state					
^{7}Li	uncomplexed	180[b]	143.3	128.3[c]	128.3[c]
^{7}Li	dimer	189.1	144.6	124.8[c]	124.8[c]
^{7}Li	monomer	197.5	143.7	124.6	122.0
^{6}Li	uncomplexed	186.3	142.5	127.5[c]	127.5[c]
^{6}Li	dimer	188.6	144.8	124.9[c]	124.9[c]
^{6}Li	monomer	197.9	143.8	124.5	122.0
Solution					
^{7}Li[d]	tetramer	176.2	142.9	127.9	127.1
^{6}Li[e]	dimer	188.5	144.6	124.8	123.2
^{6}Li[e]	monomer	196.7	143.4	124.8	120.9

[a] Relative to adamantane used as external reference.

[b] Broad signal.

[c] Signals not resolved.

[d] 6 M in DEE, 26 °C.[144]

[e] 0.26 M in THF, −103 °C.[145]

from the spinning sideband pattern was used, and the results were compared with results of theoretical IGLO calculations. These calculations give the shift tensor as the result. In earlier studies the tensors were disregarded and the results compared to solution NMR data, where just the isotropic shift is measured[153].

The studied powdered material did not allow the experimental determination of the orientation of the tensors relative to the molecular framework. The combination of the experimental data with the calculated data, however, allowed the alignment of the tensors. Agreement between the experimental and theoretical data was good, even though by today's standard the calculation was conducted at a low level. The theoretical results explained the observed deshielding by comparison to the chemical shift tensor in benzene. The largest change occurs in the tensor component perpendicular to the C−H and C−Li bonds and in the plane of the phenyl group in the two systems. This component is deshielded about 180 ppm in the latter case, overcompensating the shielding effect due to the increased electron density. This change was again explained as an effect on the ΔE term in addition to an increased $1/r^3$ value for the C−Li bond, resulting in a larger σ^{p} contribution in the Ramsey equation[151, 152].

In a study of 2,2′- and 1,2′-biindenyl dilithium (**6, 7**, Scheme 1), ^{13}C solid state NMR investigations were used, in combination with solution NMR studies and calculations, to obtain information about the existence of so-called 'triplet structures'[53]. Triplet structures are alkali metal complexes of dianions that arrange in a structure akin to dimers in Figure 1b and were found by X-ray crystallography for the TMEDA complex of the dilithium salt of 9,9′-bifluorene (Figure 13)[154]. This kind of structure has been proposed to account for the unexpected small difference in the first and second pK_{a} value in some systems, where ΔpK_{a} is found to be less than 1 pK_{a} unit[4].

The chemical shifts obtained in solution under different experimental conditions were compared to the shifts of the TMEDA complexes in the solid state. For **6**, all data indicate a triplet structure of the CIP. The most compelling evidence for the triplet structure is the polarization of charge towards the two bridging carbons under CIP conditions. However, for **7**, the charge distribution differs under CIP conditions in solution and in the solid state, as reflected by the chemical shifts. In solution, the shift data indicate again a triplet structure. In the solid state, however, the cations are not located at the bridging carbons, but shifted towards the five-membered ring systems.

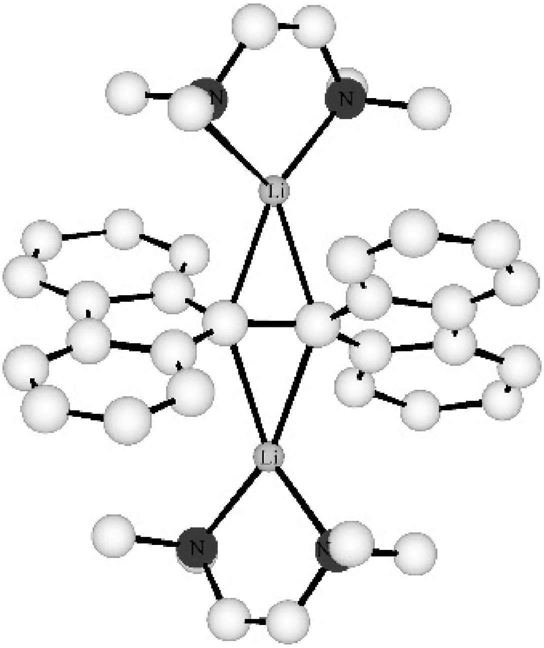

FIGURE 13. X-ray structure of the TMEDA complex of the dilithium salt of 9,9′-bifluorene[154], where a triplet structure is evident

^{13}C solid state NMR spectroscopy was also used in combination with solution NMR and semi-empirical calculations to investigate the electronic and ring current structure of phenalenyl ions (**8**, Scheme 1)[155]. The solid state spectrum of the DEE complex of phenalenyllithium correlates closely to the solution spectrum using DEE as solvent. It was proposed that the lithium cation was positioned over the central C-9b carbon in the CIP structure in solution as well as in the solid state. This arrangement was also favoured in the MNDO calculations when the lithium cation was treated as a sparkle.

The TMEDA and THF complexes of the very sterically crowded methyllithium derivative tris(trimethylsilyl)methyllithium (**9**, Scheme 1) were studied by multinuclear solid state NMR spectroscopy in combination with solution NMR spectroscopy and X-ray crystallography to reveal the structure and dynamic behaviour of the complexes[80]. In the solid state, this complex crystallizes as an *ate*-complex, with one lithium cation interacting with two substituted methyl anions while the other lithium cation is complexed by two TMEDA ligands. In solution, the *ate*-complex is partly transformed into solvated monomers or aggregates, depending on the experimental conditions.

B. $^{6/7}Li$ Chemical Shifts in Solid Organolithium Complexes

1. Lithium complexes of localized anions

A number of different phenyllithium aggregates of known solid state structure (**10**–**24**) have been investigated (Scheme 2). The ^{7}Li chemical shifts of these systems are summarized in Table 4. The data for the first 15 complexes vary in a narrow range

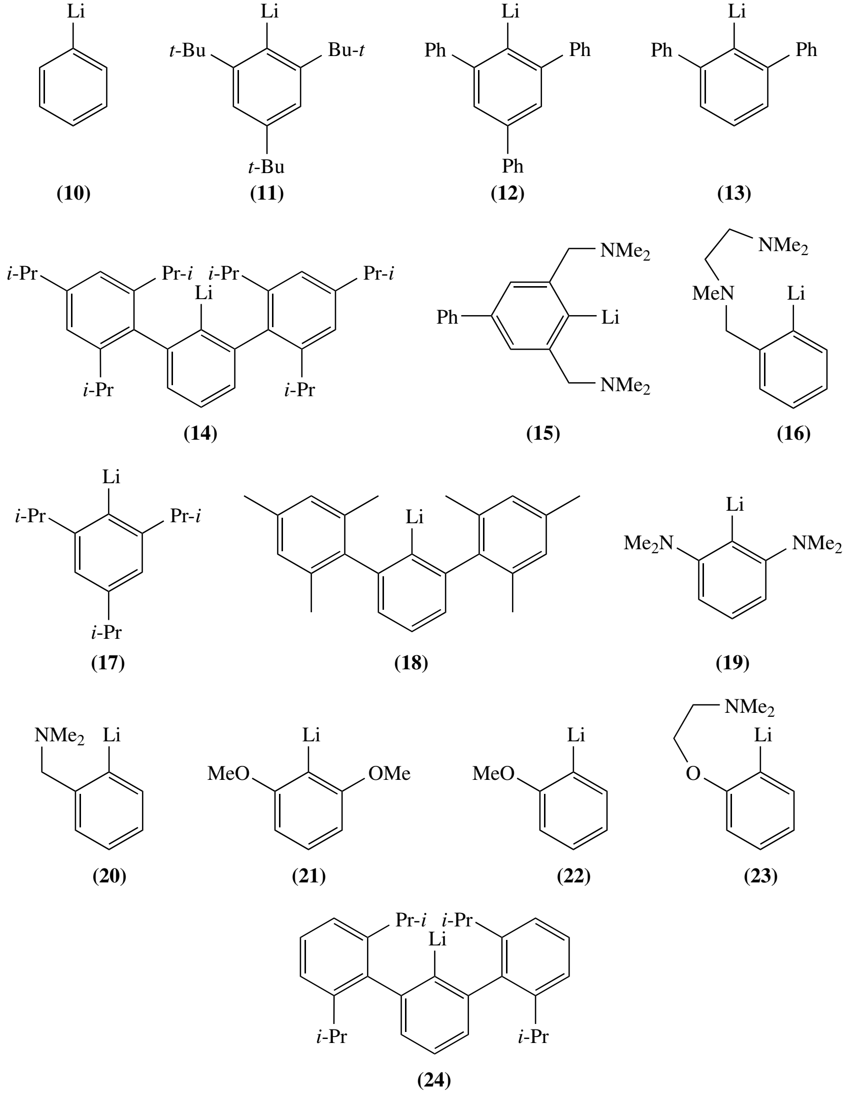

SCHEME 2

of −0.8 to 2.0 ppm without any clear dependence on either aggregation or complexation. The only deviations are found for the last two entries, where the chemical shifts are −4.6 and −4.7 ppm, respectively. The reason for this difference is that the lithium cation is complexed in a η^6 fashion by a π-system of a benzene or phenyl ring, thus experiencing a diatropic ring current.

For SSIP structures, a typical shift value of −2.4 ppm is found when the lithium cation is complexed by, for example, two 12-crown-4 molecules. This was shown recently for a

TABLE 4. ^{7}Li solid state NMR chemical shifts for various aryllithium complexes[156]

No	Aggregation state	Aryl system[a]	Ligand	Donor atom	δ^b/ (ppm)
1	$LiAS_3$	**10**	PMDTA	N	2.0
2	$LiAS_2$	**11**	MeTMEDA	N	1.4
3	$LiAS_2$	**12**	DEE	O	−0.8
4	$LiAS_2$	**13**	DEE	O	0.7
5	LiAS	**14**	DEE	O	1.5
6	$Li_2A_2S_4$	**15**	Internal[c]	N	0.8
7	$Li_2A_2S_4$	**10**	TMEDA	N	1.2
8	$Li_2A_2S_4$	**16**	Internal[c]	N	1.7
9	$Li_2A_2S_2$	**17**	DEE	O	1.2
10	Li_2A_2	**18**	—	—	0.8
11	$Li_3A_3S_6$	**19**	Internal[c]	N	0.9
12	$Li_4A_4S_4$	**20**	Internal[c]	N	0.4
13	$Li_4A_4S_8$	**21**	Internal[c]	O	0.3
14	$Li_4A_4S_4$	**22**	Internal[c]	O	0.3
15	$Li_4A_4S_8$	**23**	Internal[c]	N,O	0.2
16	LiAS	**14**	Benzene	C/η^6	−4.6
17	$Li_2A_2S_2$	**24**	Internal[c]	C/η^6	−4.7

[a] See Scheme 2.
[b] Relative to external 1.0 M aqueous LiCl.
[c] The cation is complexed to a substituent on the aryl system.

number of lithium cuprates[157] (see Section II.C.5) and has also been observed for some complexes of delocalized organolithium systems (see below)[122, 158].

Recently, a study of methyllithium complexes was presented where solid state NMR was used in combination with X-ray crystallography and solution NMR spectroscopy[159]. The aim of this study was to find suitable ligands to increase the solubility and reactivity of methyllithium. The use of diethoxymethane (DEM) or triazasulphite dianion was proposed. Using DEM as ligand, polymeric rods are formed in the solid state, $[(MeLi)_4(DEM)_{1.5}]_\infty$. These rods form channels which can accommodate solvent molecules, thereby increasing the solubility. ^{7}Li multiple quantum MAS (MQMAS)[160] NMR investigations were used in order to resolve two signals in the ratio 1:3 at 1.0 and 2.1 ppm, respectively (relative to saturated aqueous LiCl). These signals were assigned to the lithium situated on the rod axis and to the three lithium cations perpendicular to the three-fold axis of the rod. An equilibrium between monomers, oligomers and polymers was indicated by the NMR spectrum in solution. The addition of a dilithium triazasulphite increased the solubility of methyllithium by the formation of a monomeric complex. In the ^{7}Li MQMAS experiment, two signals were revealed at 1.55 and 2.75 ppm with a ratio of 1:2, presumably due to the slightly different carbon−lithium distances in the crystal[159].

2. Lithium complexes of delocalized anions

One of the most thoroughly investigated delocalized organolithium system is that of complexes of substituted cyclopentadienyl (Cp*) lithium. In the solid state, these compounds have been shown by X-ray crystallography to adopt at least six different structure types depending on substitution and the choice of ligand, as shown in Scheme 3: CIP (**A**), SSIP (**B**), sandwich structures (**C**), inverted sandwich structures (**D**), super-sandwich structures (**E**) and higher polymeric species (**F**)[161, 162]. A number of these systems were selected and studied by ^{7}Li solid state NMR spectroscopy[158]. The ^{7}Li chemical shifts of the investigated complexes are reported in Table 5 together with the substitution pattern

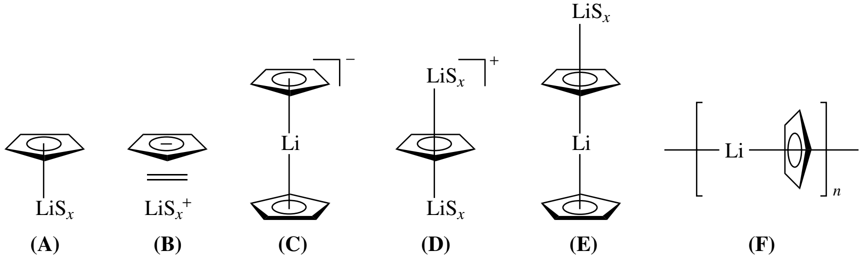

SCHEME 3. Structures of cyclopentadienyllithium systems

of the cyclopentadienyl system. As mentioned, the chemical shift of the lithium cation is markedly affected if it experiences the ring current effect of a delocalized system as shown for the CIP complexes, entries 1–13 in Table 5. The chemical shift varies in a range from −7.1 to −9.1 ppm for these complexes. There seems to be a weak trend in this series of compounds, i.e. lithium cations interacting with oxygen rather than nitrogen ligands are slightly more shielded.

Larger effects are observed when the type of complex is changed. In the sole investigated SSIP a ^{7}Li chemical shift of −2.4 ppm was observed (Table 5, entry 14), well outside the range of the different investigated CIP complexes. The lithium cation is interacting with two 12-crown-4 ligands in this complex, and does not experience the effect of the ring current of the cyclopentadienyl anion.

TABLE 5. Solid state ^{7}Li NMR chemical shifts of selected Cp*Li complexes[158]

Entry	System[a]	Type according to Scheme 3	Structure	Ligand	Ligation No.[b]	δ^c(ppm)
1	Me-Cp	**A**	CIP	TMEDA	2 (N)	−7.1
2	TMS-Cp	**A**	CIP	TMEDA	2 (N)	−7.5
3	tris-TMS-Cp	**A**	CIP	TMEDA	2 (N)	−7.5
4	bis-TMS-Cp	**A**	CIP	TMEDA	2 (N)	−7.8
5	tris-TMS-Cp	**A**	CIP	PMDTA	2 (N)	−7.5
6	bis-TMS-Cp	**A**	CIP	TMPDA	2 (N)	−8.9
7	tris-TMS-Cp	**A**	CIP	TMPDA	2 (N)	−7.7
8	tris-TMS-Cp	**A**	CIP	Quinuclidine	1 (N)	−7.7
9	tris-TMS-Cp	**A**	CIP	THF	1 (O)	−9.1
10	bis-TMS-Cp	**A**	CIP	DME	2 (O)	−8.4
11	tris-TMS-Cp	**A**	CIP	DME	2 (O)	−8.3
12	tris-TMS-Cp	**A**	CIP	Diglyme	2 (O)	−8.8
13	Cp	**A**	CIP	12-crown-4	4 (O)	−7.3
14	tris-TMS-Cp	**B**	SSIP	12-crown-4	8 (O)	−2.4
15	Cp	**C**	Sandwich	PPh_4^+	η^{10}	−12.9
16	Cp	**C**	Sandwich	Diglyme	η^{10}	−12.4 −1.6
17	bis-TMS-Cp	**C**	Sandwich	Diglyme	η^{10}	−12.2 −2.0
18	Cp	**F**	Polymer	—	η^{10}	−13.1

[a] Me = methyl, TMS = trimethylsilyl.

[b] Number (and type) of donor atom.

[c] Corrected for second order quadrupolar interactions, relative to 1.0 M aqueous LiCl.

One sandwich complex of known solid state structure was studied as well. The chemical shift of the lithium cation is −12.9 ppm, again well outside the range of the other CIP complexes, due to the effect of the ring current from two cyclopentadienyl units (entry 15). A tetraphenyl phosphonium cation was used as the counterion in the preparation of the solid material. Based on these findings two additional complexes were assigned the sandwich type structure, i.e. two diglyme coordinated systems. The ^{7}Li MAS spectrum consists of two lithium signals, as the counterion in these cases is a solvent separated lithium cation (entries 16 and 17). Finally, a cyclopentadienyllithium polymer was investigated. The chemical shift clearly falls in the range of cations experiencing ring currents from two cyclopentadienyl systems (entry 18).

Results for other delocalized systems which have been investigated, such as indenyl and fluorenyllithium complexes, are summarized in Table 6. In the case of fluorenyllithium, it is known from the ^{13}C solid state studies mentioned that the position of the lithium cation relative to the carbon framework of the anion varies, depending on the ligand used. In the structurally known bis-quinuclidine system, a ^{7}Li chemical shift of −1.8 ppm was obtained. The lithium cation is interacting with the anion in a η^3 fashion. The cation is occupying a position where the shielding and deshielding effects of the ring current of the fluorenyl anion cancel each other.

In the DEE complex a chemical shift of −5.6 indicates that the ring current has a much more profound effect in this complex. However, the solid state structure was not known at that time. In the TMEDA complex, the lithium cation is postulated to be positioned above the central five-membered ring, and the ^{7}Li chemical shift is −7.5 ppm, i.e. in the range of CIPs of cyclopentadienyllithium. In the THF complex, a shift of −2.6 ppm was observed. Again, no effect from the ring current is observed. However, based on the quadrupolar interaction this system was assigned as an SSIP, as discussed below.

Two other complexes of known solid state structure have been included: the SSIP of the dianion of ethylene-bisfluorenyllithium[163] and the CIP TMEDA complex of indenyllithium[164]. The observed chemical shifts were in accordance with expectations i.e. −1.8 ppm for the SSIP complex and −7.9 ppm for the CIP complex.

From these investigations it is clear that the ^{7}Li chemical shift gives a clear indication of the lithium cation position when there are direct effects from ring currents in delocalized anions. However, as shown for the quinuclidine CIP and THF SSIP fluorenyllithium complexes, the correct assignment cannot be reached solely based on the chemical shifts. Furthermore, there is no clear-cut information about solvation to be gained from the chemical shifts. As we discuss in the following Section, the quadrupolar interaction is much more sensitive to these effects. In order to obtain maximal structural information from ^{7}Li NMR spectroscopy, the chemical shift should be determined and used in combination with the quadrupolar coupling constant.

TABLE 6. Solid state ^{7}Li chemical shifts of different delocalized organolithium complexes.[122]

No.	System	Ligand	Structure	δ^a (ppm)
1	Fluorenyl	Quinuclidine	CIP	−1.8
2	Fluorenyl	DEE	CIP	−5.6
3	Fluorenyl	TMEDA	CIP	−7.5
4	Fluorenyl	THF	SSIP	−2.6
5	Ethylene-bisfluorenyl	THF	SSIP	−1.8
6	Indenyl	TMEDA	CIP	−7.9

[a] Relative to 1.0 M aqueous LiCl.

C. Lithium Quadrupolar Interactions

1. Applications of the quadrupolar splitting constants in solution

Jackman and Szeverenyi were the first to systematically correlate the quadrupolar interaction with molecular structure, i.e. with the aggregation of lithium enolates[111]. They noted that a tetrameric aggregate had a smaller QSC than a dimeric aggregate, *ca* 135 kHz compared to an estimate of 230 kHz for the dimer. The QSC of the tetramer was shown to be of the same magnitude in three different ethereal solvents.

In a later study, substituted lithium phenolates were investigated in different solvents[165]. Here, the lithium phenolates were shown to exist as monomers, dimers and tetramers, depending on the solvent and substitution pattern. It was found that the different aggregates have different QSC ranges, where the QSC is smaller for higher aggregates. It was also noted that the QSC value depends to some extent on the solvent, especially on the type of coordinating atom, i.e. O *vs.* N in ethers and amines, respectively.

Wen and Grutzner used, among other NMR parameters, the QSC of the lithium enolate of acetaldehyde to deduce that it exists as tetramers of different solvation in THF and THF/*n*-hexane solvent systems[166]. However, the most thorough study of ^{7}Li QSC and the most interesting in the present context was reported by Jackman and coworkers in 1987[167]. The effects on the QSC values of both aggregation and solvation in a number of organolithium systems was studied in this paper, i.e. different arylamides, phenolates, enolates, substituted phenyllithium complexes and lithium phenylacetylide.

It was again found that aggregates of different sizes have QSC values in different ranges, higher aggregates having lower QSC values. In general, tetrameric aggregates of the $Li_4A_4S_4$ type show QSC values between 50 to 100 kHz, with small effects due to the type of anion. Lower solvation and reduced symmetry results in higher QSC values. Dimeric aggregates of the $Li_2A_2S_4$ type show QSC in a range between 150 to 160 kHz. For the lithium arylamides it was shown that solvation has a significant effect on the QSC. The QSC was found to be 151 kHz for a $Li_2A_2S_4$ system and 317 kHz for a $Li_2A_2S_2$ system. Monomers of the type $LiAS_3$ have QSC values in the range of 210 kHz, and desolvation to $LiAS_2$ increases the QSC to more than 350 kHz.

Finally, in another study the QSC of fluorenyllithium in different solvents was investigated, an investigation that will be further discussed below[112].

2. Localized anions

In order to explore the quadrupolar parameter further, and to test the validity of the assumptions used when determining QSC values in solution and to investigate if solid state aggregates are relevant models for the aggregates in solution, a ^{7}Li solid state NMR study of phenyllithium complexes was conducted[150]. Three different aggregates of phenyllithium had been structurally determined by X-ray crystallography, i.e. a $Li_4A_4S_4$ DEE complex[168], the $Li_2A_2S_4$ TMEDA complex[169] and the $LiAS_3$ PMDTA complex[170]. However, the diethyl ether complex proved to be unstable under the experimental conditions, so the internally coordinated 2-[(dimethylamino)methyl]phenyllithium was used instead as an $Li_4A_4S_4$ model[171]. The X-ray structures of these investigated aggregates are shown in Figure 14. The slight deviation from tetrahedral coordination of lithium in this $Li_4A_4S_4$ complex is expected to increase the χ value, as noted already in solution. The results, reported in Table 7 entries 1, 5 and 9, supported the earlier conclusions that different aggregates have different χ-value ranges, a fact also observed for a series of $Li[BH_4]$ complexes where the number of donor atoms around the lithium varied (Table 7, entries 15–18)[127].

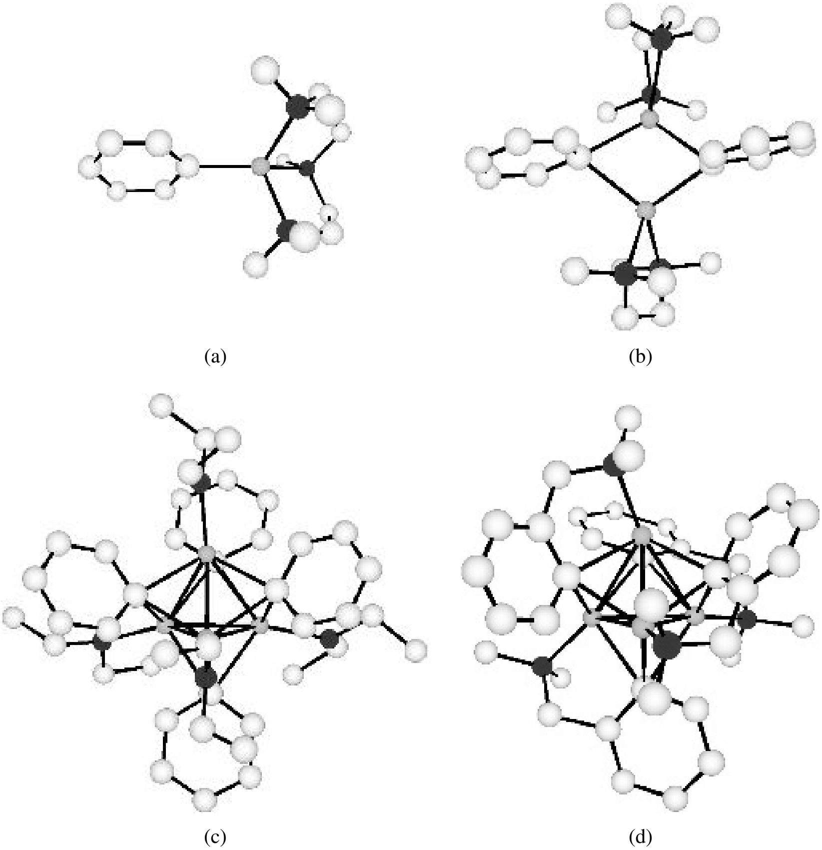

FIGURE 14. (a) The monomeric PMDTA complex of phenyllithium[170]. (b) The dimeric TMEDA complex of phenyllithium[169]. (c) The tetrameric DEE complex of phenyllithium[168]. (d) The internally coordinated tetramer of 2-[(dimethylamino)methyl]phenyllithium[171]

With the aim to obtain additional benchmark values, a larger number of substituted phenyllithium complexes with known solid state structures were included in this study[156]. They range from monomers of different solvation, over dimers and one trimer to different tetramers. The investigated aryl systems are shown in Scheme 2 and the obtained χ values are reported in Table 7.

a. Monomers. Six different monomers were investigated ranging from $LiAS_3$ to LiAS. It was again noted that the χ value is very sensitive to the solvation, increasing from 260 kHz for a $LiAS_3$ system to 400 for a $LiAS_2$ system when complexed with amines (entries 1 and 2, respectively). Changing from amines to ethers reduces the χ value significantly from 400 kHz for the amine to *ca* 310 kHz for two different $LiAS_2$-type DEE complexes (entries 2 and 3). Reducing solvation, i.e. going from $LiAS_2$ to LiAS, increases the χ value from *ca* 310 kHz to 475 kHz for yet another DEE complex (entries 3 and 4).

TABLE 7. ^{7}Li quadrupolar coupling and splitting constants of substituted aryllithium[150,156] and $[LiBH_4]_n$ complexes[127]

Entry	Complex type	No. of studied complexes	Aryl system[a]	Ligand	Donor atom	χ-value (kHz)	QSC solid (kHz)	QSC solution (kHz)
1	$LiAS_3$	1	**10**	PMDTA	N	260		
2	$LiAS_2$	1	**11**	MeTMEDA[b]	N	400		
3	$LiAS_2$	2	**12, 13**	DEE	O	308–310		
4	LiAS	1	**14**	DEE	O	475		
5	$Li_2A_2S_4$	3	**10, 15, 16**	Internal[c] or TMEDA	N	147,138, 171	161	162[d]
6	$Li_2A_2S_2$	1	**17**	DEE	O	303		
7	Li_2A_2	1	**18**	None	—	200		
8	$Li_3A_2S_6$	1	**19**	Internal	N	141		
9	$Li_4A_4S_4$	1	**20**	Internal	N	112	117	116
10	$Li_4A_4S_8$	1	**21**	Internal	O	83	85	82
11	$Li_4A_4S_4$	1	**22**	Internal	O	142		
12	$Li_4A_4S_8$	1	**23**	Internal	N,O	138		
13	LiAS	1	**14**	Benzene	π-system, C	334		
14	$Li_2A_2S_2$	1	**24**	Internal	π-system, C	336		
15	$Li[BH_4]_2$	1	—	$TMEDA_2$	N	$\geqslant$145		
16	$Li[BH_4]$	1	—	PMDTA	N	124		
17	$Li[BH_4]$	1	—	Pyr_4	N	34		
18	$Li[BH_4]$	1	—	$HMPTA_4$	N	11		

[a] See Scheme 2.

[b] *N*,*N*,*N*′,*N*′-tetramethyl-1,2-propanediamine.

[c] The cation is complexed to a substituent on the aryl system.

[d] The QSC value in solution is measured in THF as solvent, thus the coordinating atom is O rather than N; see text.

b. Dimers. For a number of amine complexed dimers of the $Li_2A_2S_4$ type the χ values range from 138 kHz to 171 kHz, substantially smaller χ values than for the monomers, entry 5. The surroundings of the lithium cations deviate from a tetrahedral arrangement to different extents, as do the bond lengths, which affect the observed χ values to some degree. One $Li_2A_2S_2$ system was also included in the study, a DEE complex of 2,4,6-tri-isopropylphenyllithium[172], entry 6. This complex was incorrectly assumed to be a $Li_2A_2S_4$ system in the ^7Li NMR study[156].

One dimer of the unsolvated Li_2A_2 type was included in the study and the χ value was found to be 200 kHz, entry 7.

c. Trimers. In a few rare cases trimers have been reported. One example was included in the mentioned study, a $Li_3A_3S_6$ system[173]. The χ value of 141 kHz falls in the range of $Li_2A_2S_4$-type dimers, entry 8. Inspecting the local environment of a lithium cation, it is surrounded by two anions and two ligands as in $Li_2A_2S_4$ dimers. The angles and distances differ, however, but the net effect is obviously that the ranges for the χ values overlap.

d. Tetramers. Apart from the mentioned $Li_4A_4S_4$ system (entry 9), a tetrameric $Li_4A_4S_8$ system was studied with oxygen as coordinating atom (Table 7, entry 10). The χ value is smaller than for the $Li_4A_4S_4$ system, possibly as a result of both increased solvation and a change in ligating atom.

For an additional $Li_4A_4S_4$ tetramer, the internally coordinated 2-methoxyphenyllithium, the four lithium cations have different environments according to X-ray crystallography[174]. One of the lithium cations is coordinated to two oxygens, two lithiums are coordinated to one oxygen each and one lithium cation is not coordinated by any Lewis base at all. The experimental ^7Li NMR spectra, however, give just one signal with a χ value of 142 kHz, entry 11. The reason for this is probably that this compound can form polymorphic crystals, where the actual structure depends on the experimental conditions. Further experiments are needed to determine the structure of this complex. Polymorphism has been observed in several cases, for example 2,4,6-tri-isopropylphenyllithium (**17**), where a disolvated dimer is obtained from DEE[172] and a monosolvated monomer when crystallized from benzene[175]. This latter structure is of a relatively new type, where the lithium cation is interacting in a η^6 fashion with the aromatic system, as discussed in the next section.

In yet another investigated $Li_4A_4S_8$-type complex, the lithium cation is coordinated by one N and one O atom. This leads to an increased χ value due to the different donicities of nitrogen and oxygen, i.e. 138 kHz, entry 12. This is in the range found for dimeric species.

e. π-Solvated lithium cations. In a few recent cases, the lithium cation behaves akin to transition metals and is interacting in a η^6 fashion with an aromatic system, a behaviour that has recently been investigated theoretically by Tacke[176].

The χ value of the η^6 coordinated 2,6-bis(2,4,6-tri-isopropylphenyl)phenyllithium complex (**14**) and a related dimeric structure of 2,6-bis-(2,6-di-isopropylphenyl)phenyllithium (**24**) have been determined as well. The lithium cations are in similar environments in these two systems regardless of the aggregation state, as seen in Figure 15. In the dimer, the lithium cation is not coordinated to an external ligand but coordinated to an aromatic ring in the neighbouring molecule. The values are 334 and 336 kHz for the monomer and dimer, respectively (Table 7, entries 13 and 14). This is in the range of disolvated monomers. The ^7Li chemical shift, however, differentiates this type of complex from the

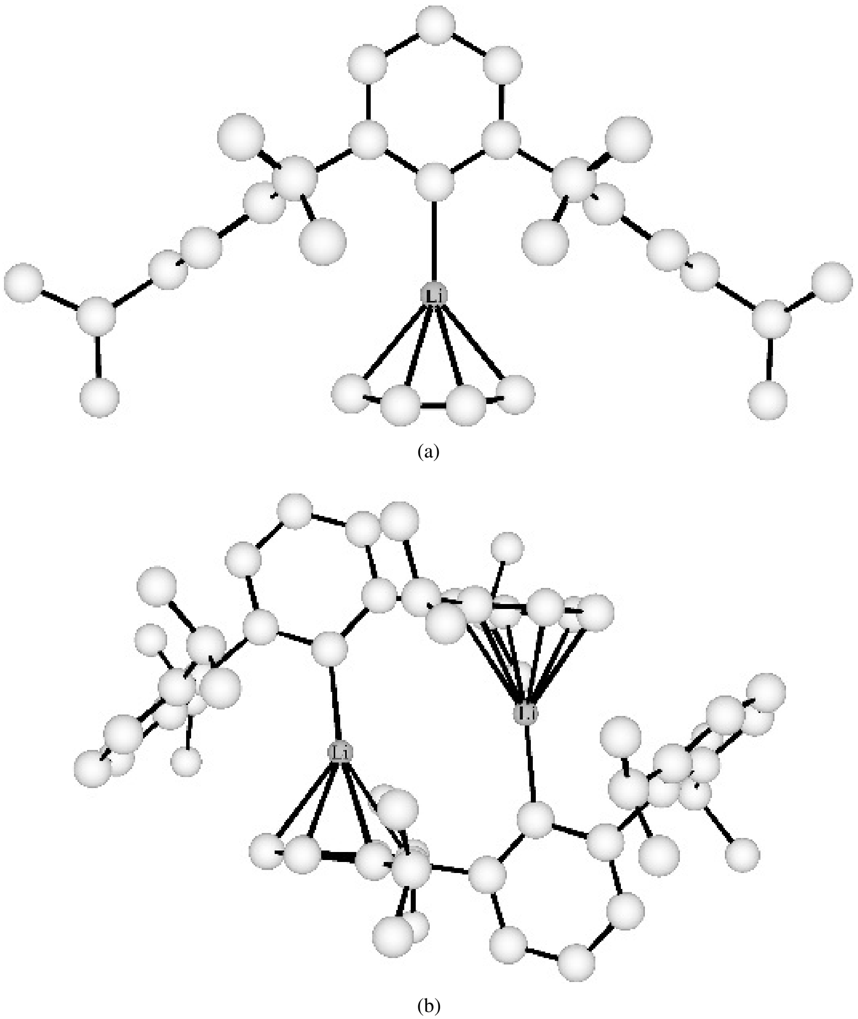

FIGURE 15. (a) X-ray structure of the π-complexed lithium in the monomeric benzene complex of 2,6-bis(2,4,6-tri-isopropylphenyl)phenyllithium[177]. (b) X-ray structure of the π-complexed lithium in the dimeric 2,6-bis(2,6-di-isopropylphenyl)phenyllithium[177]. It is evident from the Figure that the local environments around the lithium cations are similar

other aggregates, as mentioned in Section II.B.1. The ^{7}Li chemical shift in these η^6 complexes are -4.6 and -4.7 ppm due to the effect of the ring current, whereas it is between -1 and 3 ppm for the other complexes (Table 4).

A system that displays polymorphism is the aforementioned 2,4,6-tri-isopropylphenyllithium (**17**). It crystallized as a $Li_2A_2S_2$ system from DEE[172], but as an η^6 cyclic tetramer from non-coordinating solvents[175]. Furthermore, a combined solid state ^{6}Li and ^{7}Li NMR study indicates a third type of complex, notwithstanding the attempt to prepare the mentioned $Li_2A_2S_2$ DEE complex[125]. From ^{13}C CP/MAS experiments, however, it was clear that the prepared complex did not contain any DEE. Thus it must be some other type of structure. The ^6Li χ value was determined to be 6.63 kHz, which translates to 324 kHz for ^7Li, due to the 48.9 times larger nuclear quadrupole moment for ^7Li. This agrees well with the χ value obtained from a ^7Li powder spectrum, i.e. 320 kHz. However, when determining χ values from ^6Li, the resulting spectrum is affected profoundly by other interactions as well. For example, the CSA has to be considered. The observed χ value would fit a η^6-type complex, nevertheless the chemical shift is not in the expected negative range but rather $+0.7$ ppm relative to aqueous LiCl[82, 125]. Furthermore, the *ipso*-carbon shows the typical splitting pattern for a carbon interacting with a single ^7Li, i.e. a quartet with a splitting of *ca* 40 Hz. An *ab initio* calculation was performed on an unsolvated monomeric unsubstituted phenyllithium system, giving a χ value of 360 kHz. Based on these findings the author proposed that the structure of the investigated system is that of an unsolvated monomer, LiA[125]. However, we believe that most probably this study dealt with the tetramer,[175] a structure not considered by the author.

f. Comparisons of ^7Li QSC and χ values in aryllithium complexes. The QSC values determined in solution can be compared with QSC values in the solid which are derived from the measured quadrupole parameters according to equation 10. For three complexes, a $Li_2A_2S_4$ dimer, a $Li_4A_4S_4$ tetramer and a $Li_4A_4S_8$ tetramer, QSC values have earlier been determined in solution (Table 7, entries 5, 9 and 10, respectively)[167]. For 2-[(dimethylamino)methyl]phenyllithium (**20**), a $Li_4A_4S_4$ tetramer, the QSC values are 116 kHz and 117 kHz in solution and in the solid, respectively. These values agree within experimental error, even if the compound investigated in solution was the 4-methyl isomer, which was used due to solubility problems with the parent compound. Thus, for these compounds, the same structure exists in solution and in the solid state.

2,6-Dimethoxyphenyllithium (**21**) is an internally coordinated $Li_4A_4S_8$ system. The QSC value is 85 kHz in the solid state and 82 kHz in solution[167], again virtually identical.

For the investigated unsubstituted phenyllithium (**10**) dimers, the measured QSC values are 161 and 162 kHz, respectively. However, the solid material is a TMEDA complex whereas the solution data are obtained in neat THF[167]. This difference in ligating atom is expected to affect the quadrupolar interaction to some extent. The reason for the similarity in χ value for the dimers could be fortuitous, and due to fast exchange between complexes of different solvation in solution. It should be mentioned that the measured QSC value represents a weighted average of the different aggregates and solvates present under the experimental conditions if they are in an equilibrium that is fast on the NMR timescale. This is most probably also the explanation for the large χ value noted for the diethyl ether solvated phenyllithium dimer, i.e. 250 kHz[167]. This high value indicates a substantial amount of a $Li_2A_2S_2$ complex in solution.

Knowing that a change in the local structure around the lithium cation changes the χ value significantly, the conclusion from these data is that, for the internally complexed aggregates, the solid state structure is indeed a good model for the structure in solution. However, for the complexes that are externally solvated, dynamic processes in solution, such as an equilibrium between complexes of different solvation or even aggregation states, change the observed QSC values from the benchmark values obtained in the solid state.

From these studies of aryllithium complexes, it can further be concluded that the quadrupolar interaction is a very sensitive indicator of the type of aggregation and solvation state. In certain cases the χ-value ranges overlap, but additional investigations can often easily clarify the ambiguity, such as the ligand/metal ratio. The latter can, for example, be determined by a solution ^1H NMR spectrum of the solid material in a suitable solvent.

g. Quadrupolar interactions in lithium phenolates. For lithium phenolates it was found that ^{13}C NMR chemical shifts in solution and in the solid state are not always applicable for the differentiation between aggregates of different size[178]. Instead, a better discrimination is possible on the basis of the observed ^{7}Li QSC values.

When determining QSC values of dimeric lithium phenolates in solution, the value has to be corrected for anisotropic rotational diffusion as the complexes have an oblate, non-spherical shape[179]. The $Li_2A_2S_2$ complex of 2,6-di-*t*-butylphenolate has a ^{7}Li QSC value of *ca* 280 kHz in a number of different solvents. The 2,6-dimethylphenolate system is present as an $Li_2A_2S_4$ complex in THF and apparently as an $Li_2A_2S_2$ complex in DEE. These complexes have QSC values of 170 and 270 kHz in the two solvents, respectively.

The QSC value of the lithium phenolate tetramer in THF solution is between 40 and 46 kHz at -67 and $+30\,^\circ$C, respectively[178]. For other tetramers the QSC ranges from 35 to 57 kHz, depending on substitution pattern and solvent. It was observed that the magnitude of the observed QSC values correlates with the Lewis basicity of the solvent.

Lithium phenolate is present as a mixture of tetramers and hexamers in 1,3-dioxolane solution. Crystallization of lithium phenolate from THF yields an $Li_6A_6S_6$ aggregate, as determined by X-ray crystallography, although the predominant aggregate in solution is the tetramer[178]. In the solid state the measured χ value is 67 kHz with a η value of 0.77, which translates to a QSC value of 73 kHz. This agrees with the QSC value of 72 kHz measured for the hexamer in dioxolane solution.

Again, the sensitivity of the quadrupolar interaction to both aggregation and solvation is proven.

3. Delocalized anions

The π-type interaction to a lithium cation was proposed in the 1960s for delocalized carbanions. The basis for this was the observation of high-field ^{7}Li chemical shifts[76–78,180] As mentioned earlier, (Sections I.B.2.a and II.B.2), the chemical shift is strongly affected by the ring current of delocalized carbanions.

The effect of structure and solvation on the ^{7}Li quadrupolar interaction was studied for a relatively large number of cyclopentadienyllithium derivatives[158] of known solid state structure[161, 162]. As mentioned above, these complexes have been shown to form several types of structures (Scheme 3)[161, 162]. Again, the factors determining the structure are the steric requirements of the substituents and ligands. For solubility reasons, most of the complexes studied by X-ray crystallography are substituted, often with large trimethylsilyl substituents.

The results from this study are summarized in Table 8. The lithium cation is interacting with the Cp* systems in a more or less symmetric η^5 manner in the CIP complexes. The remaining coordination sites of the lithium cation are occupied by Lewis bases. In entry 1, a single quinuclidine molecule acts as ligand. The resulting χ value is 172 kHz. Increasing the solvation of the lithium cation by addition of a bidentate ligand reduces the χ value to *ca* 155 kHz (entry 2). The magnitude of the reduction is smaller than observed for the previously discussed aryllithium complexes. Three different bidentate nitrogen-based ligands were studied, among them PMDTA. This potential terdentate ligand was shown by X-ray crystallography to interact with only two of the nitrogens[181]. With a χ value of 157 kHz, this complex falls nicely in the expected range of 150–158 kHz for a bidentate nitrogen ligand. Changing the complexing atom to oxygen reduces the χ value by approximately 50 kHz compared with the nitrogen-containing analogues (entries 3 and 4). The magnitude of the reduction is again smaller than for localized carbanions. Once more, a potential terdentate ligand, diglyme, only interacts with two of the three oxygens. This fact has earlier been noted in solution as well[182].

TABLE 8. ^{7}Li quardupolar coupling constants of delocalized organolithium complexes[122,158]

Entry	System	Structure[a]	No. of studied complexes	Ligand	No. and type of donor atom(s)	χ value (kHz)
1	Cp*[b]	CIP (**A**)	1	Quinuclidine	1, N	172
2	Cp*	CIP (**A**)	7	TMEDA, PMDTA, TMPDA[c]	2, N	150–158
3	Cp*	CIP (**A**)	1	THF	1, O	125
4	Cp*	CIP (**A**)	3	DME, Diglyme	2, O	94–98
5	Cp*	CIP (**A**)	1	12-Crown-4	4, O	21
6	Cp*	SSIP (**B**)	1	12-Crown-4	8, O	39
7	Cp*	Sandwich (**C**)	3	None	η^{10}, C	26–45
8	Cp*	Polymer (**F**)	1	None	η^{10}, C	$\leqslant 5$
9	Indenyl	CIP	1	TMEDA	2, N	163
10	Fluorenyl	CIP	1	TMEDA	2, N	179
11	Fluorenyl	CIP	1	Quinuclidine	2, N	262
12	Fluorenyl	CIP	1	DEE	2, O	188
13	Fluorenyl	SSIP	1	THF	4, O	27

[a] See Scheme 3.
[b] Cyclopentadienyl anion with or without substituents; for details, see Reference 158.
[c] *N*,*N*,*N*′,*N*′-Tetramethyl-1,3-propanediamine.

Increasing the coordination number of the ligand further reduces the χ value even more as seen in entry 5. In this complex 12-crown-4 was used as ligand. Introduction of a TMS group on the cyclopentadienyl anion leads to a SSIP when 12-crown-4 was used as a ligand. As expected, the observed χ value is small (entry 6).

Three sandwich-type structures were examined, one of which had been investigated by X-ray crystallography[183]. In that case the counterion was a tetraphenyl phosphonium cation, consequently only one ^{7}Li signal was observed. In the other two proposed sandwich structures, diglyme was used as ligand. Now two ^{7}Li signals are observed, with different chemical shifts. In spite of the spectral overlap in the static spectrum, both χ values can be extracted by spectral simulation with χ values of 51 and 26 kHz and $\eta = 0.17$ and 0.21, respectively, as shown in Figure 16. The 26 kHz peak is assigned to the high-field signal, i.e. the lithium within the sandwich, as this gives a better fit to the experimental spectrum (entry 7).

A polymeric material, the polymer of the parent compound, was included in the study[184]. The χ value is of so small a magnitude that it cannot be determined from the static spectrum (entry 8). The quadrupolar interaction was investigated using MAS in order to measure the χ value. Furthermore, when the quadrupolar interaction is of this small size, other interactions have to be considered as well, such as the CSA and dipolar effect from other adjacent lithium cations.

Other delocalized anions have been investigated as well, such as complexes of indenyl and fluorenyllithium[122]. These data are also included in Table 8. The sole investigated indenyllithium system was the TMEDA complex. It is known from X-ray crystallography that the lithium cation is located above the five-membered ring and that the TMEDA binds in a bidentate fashion[164]. The χ value is somewhat larger than for the corresponding cyclopentadienyllithium complexes (entry 9).

As discussed earlier, the structures of fluorenyllithium complexes were not known from crystallographic studies, except for the bisquinuclidine complex, when the NMR study was started. The TMEDA complex was suggested to be a symmetric structure with the lithium cation positioned above the central five-membered ring based on ^{13}C and ^{7}Li chemical shifts. The observed χ value supports this proposal, as it falls nicely in the trend observed for the Cp* and indenyl systems (entry 10). In the quinuclidine complex, the lithium is removed from the centre of the carbon framework and is interacting in an η^3 fashion[129] (Figure 9). This is reflected in the quadrupolar interaction as well, because the χ value is increased in a profound way (entry 11). The DEE complex is again asymmetric, as pointed out earlier. The χ value is reduced compared to the quinuclidine complex (entry 12). The assignment of this type of structure was, however, not straightforward. In order to resolve this uncertainty, single crystals were grown and the solid state structure was determined by X-ray crystallography[185] As it turned out, the lithium cation interacts in an η^2 fashion with the carbanion in this system (Figure 17). This is one example where solid state NMR spectroscopy has served as a means for selection of suitable candidates for X-ray crystallography.

The THF complex of fluorenyllithium is according to the small χ value an SSIP-type structure (entry 13). The polymorphism of fluorenyllithium is in accordance with theoretical investigations which show that the global minimum of monomeric unsolvated fluorenyllithium is a structure where the lithium cation is interacting in an η^5 fashion with the central five-membered ring[134–136,185,186]. However, the potential-energy surface above the delocalized anionic systems is rather flat, leading to the presence of other local minima. Thus, the effect of crystal packing and steric effects could have an impact on the overall structure of complexes of delocalized anions. In one paper, the effect of DEE solvation of fluorenyllithium was investigated theoretically[185]. The conclusion was that, for this system, intramolecular steric effects determine the preferred structure. However, a polymeric DEE complex of fluorenyllithium was obtained under different experimental conditions[187].

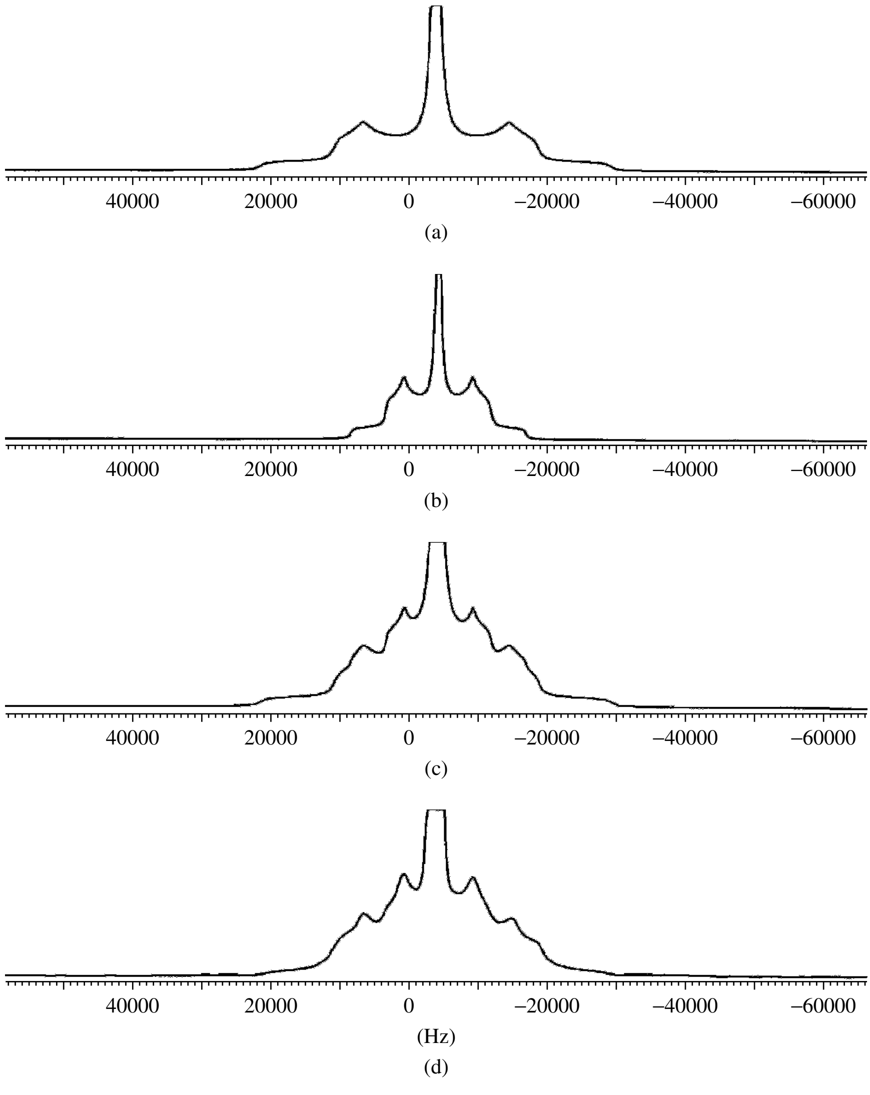

FIGURE 16. (a–c) Simulated and (d) experimental static ^{7}Li NMR spectrum of the diglyme complex of cyclopentadienyllithium at 38.92 MHz. Reproduced with permission of John Wiley & Sons Ltd. from Reference 158

Without solvation, fluorenyllithium has been shown to crystallize as a dimeric sandwich structure where the lithium cations interact with the fluorenyl units in η^6 fashions[188].

Finally, we mention that the variation in quadrupolar interactions of different lithium cations was used to resolve three different lithium environments in the solid state by a ^{7}Li quadrupole nutation MAS NMR experiment[189] of a sulphinamidinolithium complex[190]. The investigated 12-crown-4 complex of *N*, *N*′-bis(trimethylsilyl)benzenesulphinamidino

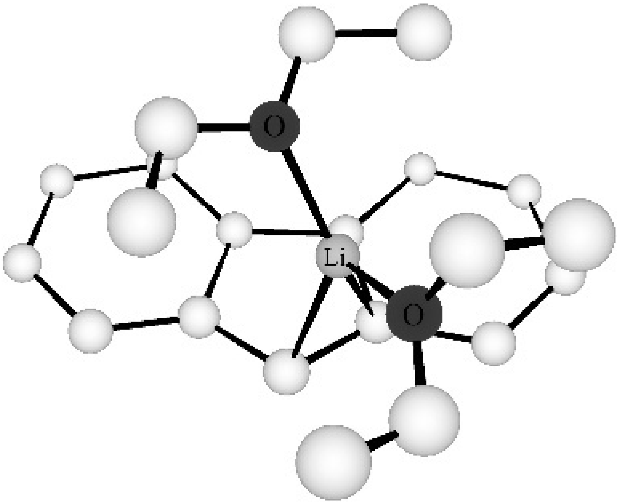

FIGURE 17. X-ray structure of the DEE complex of fluorenyllithium[185]

lithium crystallizes as a complex solvent separated ion pair. One lithium is interacting with two anions, giving an *ate* complex; the other is complexed by two 12-crown-4 ligands. These crystals undergo a phase transition at room temperature into what was proposed to be a CIP structure. A co-mixture of these two forms explains the three resonances observed in the room-temperature solid state ^{7}Li NMR spectrum. However, the magnitudes of the χ values were not determined in this study, but only used qualitatively to distinguish different lithium sites. In toluene solution, however, only one resonance, assigned to a CIP structure, is observed in the ^{7}Li NMR spectrum even at low temperatures.

a. Comparisons of ^{7}Li QSC and χ values in delocalized anions. The equilibrium between CIP and SSIP structures of fluorenyllithium has been thoroughly investigated **in solution** by several methods[130, 131, 191–194]. In one study the QSC values of fluorenyllithium were investigated in several solvents[112]. In that study, the contribution of the quadrupolar relaxation mechanism of ^{7}Li was determined by the measurement of ^{6}Li relaxation in the same sample, thus correcting the ^{7}Li relaxation for the dipole–dipole and CSA mechanisms. This correction is of most importance in THF, where it is known that the SSIP dominates the ion-pair equilibrium. Due to the small QSC of the SSIP, other relaxation mechanisms can make significant contributions to the observed relaxation. The measured QSC in THF varies between 22 kHz at −70 °C and 58 kHz at 60 °C. The measured QSC is a weighted average of the different ion pairs present in solution. These QSC values reflect the larger amount of CIP at higher temperature. The corresponding value in the solid SSIP THF complex is 29 kHz[122].

In the more sterically hindered ether, 2-methyltetrahydrofuran (MTHF), the change in QSC is larger, varying from 60 kHz at −70 °C to 180 kHz at 60 °C. This is in accordance with a larger amount of CIP already at −70 °C compared to THF solution, as also shown earlier by other methods[130]. In DEE, the QSC value varies between 220 kHz at −20 °C and 150 kHz at 56 °C. In this case, the QSC value decreases at higher temperatures. This effect is not fully understood, but aggregation phenomena were suggested as an explanation[112]. The QSC values observed in solution are of the same magnitude as that observed in the solid state, i.e. 190 kHz.

4. Dependence of $\chi(^7Li)$ on the structural X–Li–X angle (X = N, C)

An investigation of lithium diisopropyl amide (LDA) by solid state NMR[124] led to the observation of dramatic differences between the spectra of the solid polymer and the complex crystallized from THF. ^{7}Li as well as ^{13}C and ^{15}N MAS spectra showed large sideband patterns in the former case and only a few sidebands in the latter. For both materials X-ray data are available and establish a helix structure for the polymeric material, which is insoluble in hydrocarbon or ethereal solvents, and a dimer structure of the THF complex (**25**, **26**, Scheme 4). The obvious difference between both structures, apart from the solvent coordination in the THF complex, is the magnitude of the structural N-Li-N angle, which is close to 180° in the first case and close to 90° in the second (176° and 107°, respectively). Thus, a large difference for the electric field gradient around the Li cation is expected for the different bonding situations.

In order to test this hypothesis, a set of lithium amides with varying N-Li-N angle was investigated (**25**–**29**, Scheme 4). The results (Table 9) established a linear relation which describes the dependence of $\chi(^7\text{Li})$ on the N-Li-N angle for two-coordinated lithium cations (equations 14 and 15):

$$\chi(^7\text{Li}) = (4.1 \pm 0.5)\angle\text{N-Li-N} - (110.8 \pm 69.0) \tag{14}$$

or

$$\angle\text{N-Li-N} = (0.24 \pm 0.03)\chi(^7\text{Li}) + (27.2 \pm 17.0) \tag{15}$$

On this basis, information about the aggregation state and the solid state structure of lithium amides becomes available. A similar relationship is known for $\chi(^{17}\text{O})$ and the Si-O-Si angle in silicates[195].

Later, this type of investigation was extended to lithiated carbon compounds in order to reveal a possible relationship between $\chi(^7\text{Li})$ and the structural C–Li–C angle[196]. Again, a set of systems was selected where structural data were available from X-ray investigations (compounds **30**–**35**, Scheme 5). The data (Table 9) yielded equations 16 and 17.

$$\chi(^7\text{Li}) = (3.9 \pm 0.4)\angle(\text{C–Li–C}) - (215.2 \pm 55.6) \tag{16}$$

or

$$\angle(\text{C–Li–C}) = (0.25 \pm 0.03)\chi(^7\text{Li}) + (58.8 \pm 8.6) \tag{17}$$

A graphical representation of both $\angle$X–Li–X/$\chi(^7\text{Li})$ relations is given in Figure 18. It was argued that the fact that carbon and nitrogen systems display practically the same slope means that the angular dependence is governed primarily by geometrical factors and $\chi(^7\text{Li})$ is mainly determined by electrostatic interactions. This supports the ionic nature of both the C–Li and the N–Li bonds. The different magnitude of the $\chi(^7\text{Li})$ values in both series, on the other hand, can be attributed to the different charge separation in these bonds. According to a straightforward consideration of the electronegativities for nitrogen and carbon, the N–Li bond should be more polar than the C–Li bond, a result also found by calculations[206]. Atomic charge densities obtained from *ab initio* calculations for simple model systems further supported this conclusion. The calculated charge separation in the N–Li bond was in all cases larger than in the C–Li bond of the corresponding system. Since $\chi(^7\text{Li})$ is proportional to the z-component of the electric field gradient at the Li nucleus, the more polar bond is expected to yield the larger χ value.

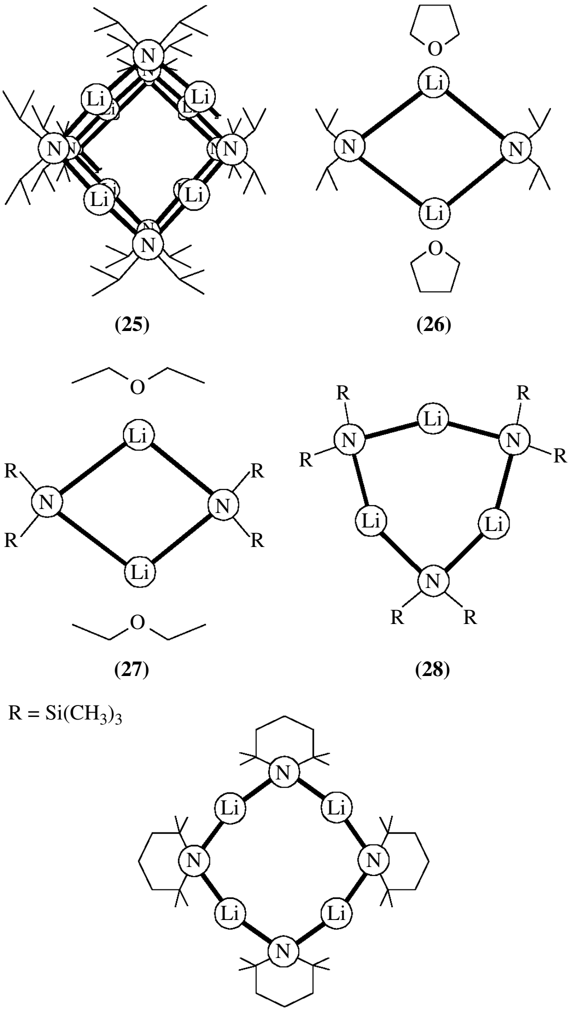

(25) **(26)** **(27)** **(28)**

R = Si(CH_3)$_3$

(29)

SCHEME 4. Structures of lithium amides with different N-Li-N angles

This aspect is further supported by observations made for the dimers of phenyllithium systems **10**, **17** and **31** (Scheme 6)[207, 208]. The quadrupolar coupling constants in this series increase as shown in Scheme 6, while the C−Li−C angle is not much changed. The same is true for the C−Li distances. A reasonable explanation for the observed trend is found if one considers the inductive effect of the alkyl groups in **17** and **31**, which should increase the charge density at the lithiated carbon. This is borne out by calculations, which show that the charge difference in the C−Li bond increases in going from **10** over **31** to **17**. In addition, the change in $\Delta\rho$ is proportional to the change in $\chi(^7\text{Li})$.

TABLE 9. ^{7}Li quadrupole parameters for **25**–**35** (Schemes 4 and 5) from solid state NMR and X–Li–X angles (deg) from X-ray data[124, 196]

Compound	X	Structure	∠X–Li–X	χ (kHz)/η	References for X-ray data
Helix polymer **25**	N	Helix	176	610/0.1	197
Cyclic oligomers					
29	N	Tetramer	169	600/0.0	198
28	N	Trimer	147	456/0.1	199, 200
26	N	Dimer	107	360/0.6	201
27	N	Dimer	105	298/0.2	198
30	C	Dimer	106	156/0.81	169
31	C	Dimer	114	264/0.74	202
32	C	Dimer	118	252/1.00	203
33	C	Tetramer	143	334/0.09	204
34	C	*ate*-Complex	174	460/0.06	80
		$Li^+(TMEDA)_2$	—	126/0.73	
35	C	*ate*-Complex	180	478/0.12	205
		$Li^+(THF)_4$	—	19/0.05	

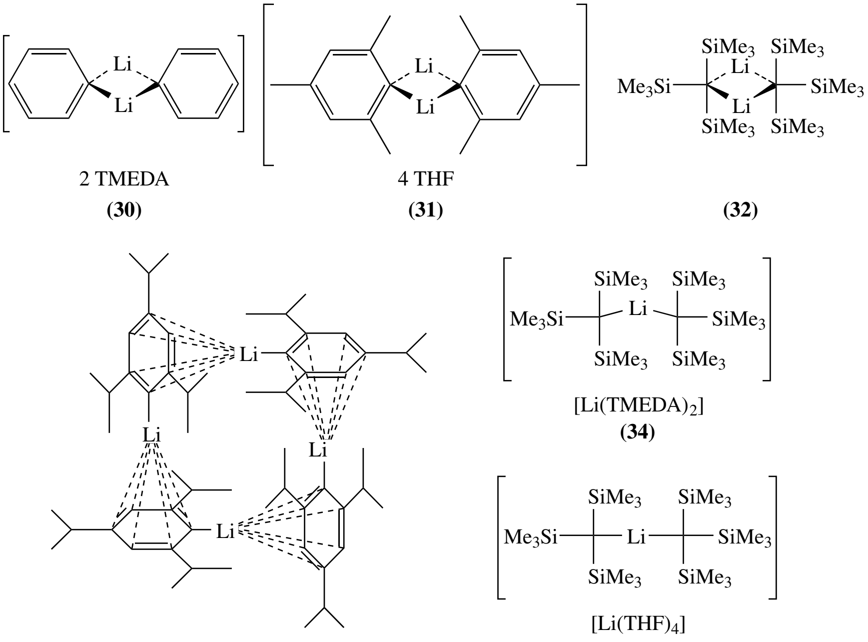

(30) **(31)** **(32)**

(33) **(34)** **(35)**

SCHEME 5. Structures of organolithium compounds with different C–Li–C angles

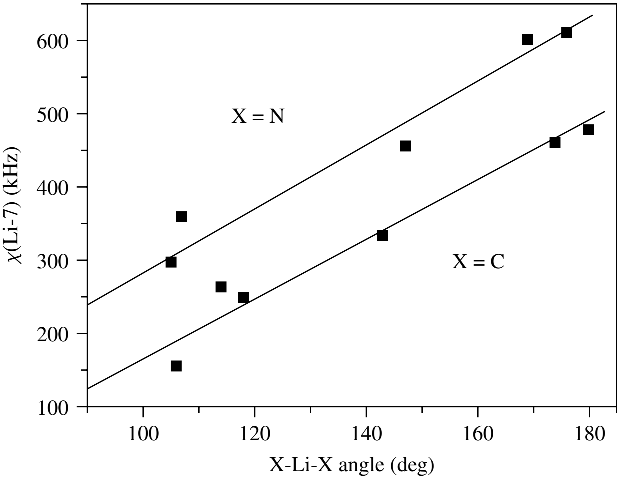

FIGURE 18. $\chi(^{7}\text{Li})$ vs. the X–Li–X angle in lithium amides (X = N) and organolithium compounds (X = C)

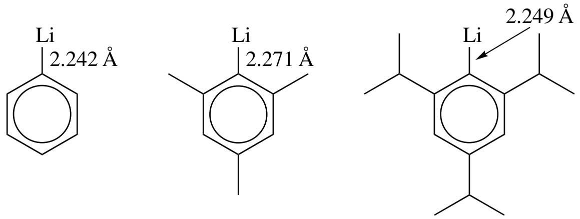

(10) **(31)** **(17)**

$\chi(^7\text{Li})$ (kHz)	234	264	308
α	117°	114°	114°
$\Delta\rho$	1.996	2.203	2.489

SCHEME 6. $\chi(^7\text{Li})$ (in kHz) and charge separation in the C−Li bond of phenyllithium systems: ligand-free (phenyllithium)$_2$[209], (mesityllithium)$_2$(THF)$_2$[202], (2,4,6-tri-isopropylphenyllithium)$_2$ (DEE)$_2$[172]; C−Li−C angle α from X-ray investigations of the dimers; charge separation $\Delta\rho$ for the C−Li bond from HF/6-311G** calculations[210]

Finally, the asymmetry parameter of the quadrupolar interaction, $\eta(^7\text{Li})$, also correlates with the C−Li−C angle in the series of compounds studied (equation 18).

$$\eta(^7\text{Li}) = 1 + \cos\angle(\text{C} - \text{Li} - \text{C}) \tag{18}$$

This fact parallels observations made for ^{17}O in silicate glasses and agrees with the results of *ab initio* calculations[211,212].

5. CIP vs. SSIP: The quadrupolar coupling constant as a new indicator of structure

An aspect of general interest in organometallic chemistry is the equilibrium between contact and solvent-separated ion pairs, because metal cations which are surrounded by an individual solvent cage are expected to show different reactivity towards basic centres than those closely attached to carbanions or amines[213,214]. At the same time, the anionic centre is less shielded in an SSIP than in a CIP and thus expected to be more reactive. In solution, the differentiation by NMR methods between both structural motifs relies in most cases on chemical shift interpretations and, if possible, on heteronuclear Overhauser (NOE) measurements. The latter method is especially powerful in the case of lithium organic compounds, where ^{1}H,^{6}Li or even ^{1}H,^{7}Li NOE can be detected by one- and two-dimensional experiments[23].

Numerous X-ray investigations have unravelled the solid state structure of contact and solvent-separated ion pairs[27–31]. It was therefore considered to be of interest to evaluate also the potential of solid state NMR as a tool for the investigation of this structural problem. In addition to the study of chemical shifts discussed above (Section II.B), the quadrupole coupling constant of the nuclide ^{7}Li, $\chi(^7\text{Li})$, was expected to be an ideal sensor for the bonding situation around the lithium cation because, due to its dependence on the electric field gradient, the quadrupolar interaction for this spin-3/2 nucleus is strongly influenced by local symmetry, as exemplified in Section II.C.3. This is also shown with some model calculations in Section II.F.

These aspects have been investigated for a number of substituted benzyllithium systems—α-(phenylthio)benzyllithium (**3**), α-phenyl-α-lithiodithiane (**4**) and α-trimethylsilyl

TABLE 10. Solid state $^{6/7}$Li NMR data for **3**–**5**[a] with various ligands obtained from the analysis of the ^{7}Li MAS spectra[139]

	3				**4**			**5**		
Ligand	3 THF	PMDTA	12-crown-4	2(12-crown-4)	THF	PMDTA	2(12-crown-4)	TMEDA	PMDTA	2(12-crown-4)
$\delta(^{6}\text{Li})^{b}$ (ppm)	0.20	0.43	−0.27	−2.32	0.3	−0.18	−2.4	1.39	0.45	−2.34
$\delta(^{7}\text{Li})^{b}$ (ppm)	0.2	0.8	−0.30	−2.1	0.68	−0.16	−2.44	0.38	0.49	−2.0
$\chi(^{7}\text{Li})$ (kHz)	132	105	110	30	160	128	24	274	128	28
$\eta_Q(^{7}\text{Li})$	0.82	0.95	0.22	0.20	1.0	0.875	0.45	0.75	0.98	0.01
CSA(^{7}Li) (ppm)	−20	−35	−2.5	−5	−35	—	+10	−20	−30	−10
d^{c}/Hz	800	750	500	0	0	—	800	1000	800	0

[a] See Scheme 1.

[b] Chemical shift from ^{6}Li or ^{7}Li MAS spectra.

[c] Residual homonuclear dipolar ^{7}Li,^{7}Li coupling.

benzyllithium (**5**) (cf. Scheme 1), where different complexing agents were used for stabilization[139]. It was shown that $\chi(^7\mathrm{Li})$ values > 80 kHz are observed for all CIP structures, while the SSIP structures, where the lithium cation is separated from the carbanionic centre by double complexation with 12-crown-4, have $\chi(^7\mathrm{Li})$ values < 50 kHz (Table 10). As discussed above (Section II.A), the different structures are also revealed by characteristic changes in the ^{13}C and $^{6/7}$Li chemical shifts.

An interesting case is **3**•12-crown-4, where an SSIP structure was proposed in THF solution on the basis of NMR results[54]. Here, the solvent THF may provide suitable additional ligand molecules which assist the separation of the lithium cation by the added crown ether. In the solid, these auxiliary reagents are not available and a CIP structure, characterized by a $\chi(^7\mathrm{Li})$ value of 110 kHz, results.

Independent support for the low $\chi(^7\mathrm{Li})$ values typical for SSIP structures was recently obtained from a study of lithium cuprates, where several X-ray structures are available (Table 11). Lithium(12-crown-4)$_2$dimethyl and diphenyl cuprate (**36**, **37**) and lithium(THF)$_4$ tris(trimethylsilyl)cuprate (**38**) (Scheme 7) have been investigated with respect to the quadrupolar coupling constant $\chi(^7\mathrm{Li})$ and the asymmetry parameter $\eta(^7\mathrm{Li})$ (Table 11)[157, 215]. The $\chi(^7\mathrm{Li})$ values range from 18 to 30 kHz and confirm the small magnitude of this parameter for the symmetric environment of a solvent-separated lithium cation. Again, typical $\delta(^7\mathrm{Li})$ values around -2.5 ppm relative to LiBr/H$_2$O were observed (cf. Section II.B.2). The $\chi(^7\mathrm{Li})$ value for the THF-separated lithium cation in **38** is in close agreement with the value found for the same structural moiety in **35** (Table 9). It is interesting to note that the TMEDA-separated lithium cation in **34** gives rise to a much larger $\chi(^7\mathrm{Li})$ value (126 kHz, Table 9), which is already in the range of CIP structures. The lower symmetry in the case of **34** is also indicated by the difference found for the asymmetry parameters $\eta(^7\mathrm{Li})$: 0.73 for Li$^+$(TMEDA)$_2$ vs. 0.05 for Li$^+$(THF)$_4$. The lithium environment in Li$^+$(THF)$_4$ is thus close to tetrahedral.

The ability of the crown ether ligand, 12-crown-4, to separate the lithium cation from the organic moiety, thus stabilizing the SSIP structure, was also observed in the study dealing with cyclopentadienyllithium systems[158]. As described in Section II.C.3, SSIP structures of these compounds are characterized by low $\chi(^7\mathrm{Li})$ values. However, it is important to realize that the variation found for $\chi(^7\mathrm{Li})$ is basically caused by the local symmetry around the lithium cation and other highly symmetric situations will also lead to small $\chi(^7\mathrm{Li})$ values. Examples are the sandwich compounds mentioned in Section II.C.3. It is thus necessary to consider also $^{6/7}$Li and ^{13}C chemical shift data in order to classify a certain complex as SSIP or CIP.

The potential of $\chi(^7\mathrm{Li})$ for structural studies is further demonstrated by results obtained for dianions of substituted ethenes. Reduction of (*Z*)-1,2-bis(trimethylsilyl)-1-phenylethene with lithium in THF led to the formation of a dimer which in solution shows two distinct ^{6}Li resonances at 0.37 and -1.20 ppm relative to 0.1 M LiBr[217]. The structure derived from NMR studies in THF solution (**39**, Scheme 7) contains one lithium cation in close contact to the organic moiety and the other one, at high field, at a larger distance and presumably surrounded by solvent molecules. In the solid, two ^{7}Li resonances separated by 1.85 ppm are found, which yield $\chi(^7\mathrm{Li})$ values of 180 and 30 kHz for the low- and high-field MAS sideband pattern, respectively, thus supporting the CIP structural motif for the lithium cation that gives rise to the low-field resonance and the SSIP structural motif for that which resonates at higher field.

A similar result is obtained for the dianion of (*E*)-1,2-diphenyl-1,2-bis(trimethylsilyl)-ethene which in solution shows ^{6}Li resonances at -0.8 and -3.8 ppm respectively[218]. The ^{7}Li MAS NMR spectrum of the solid displays the superposition of two sideband patterns separated by 2.5 ppm which yield quadrupole parameters $\chi(^7\mathrm{Li})$ of 135 and 32 kHz with $\eta(^7\mathrm{Li})$ values of 0.27 and 0.80, respectively (Figure 19)[219]. Here, the lithium

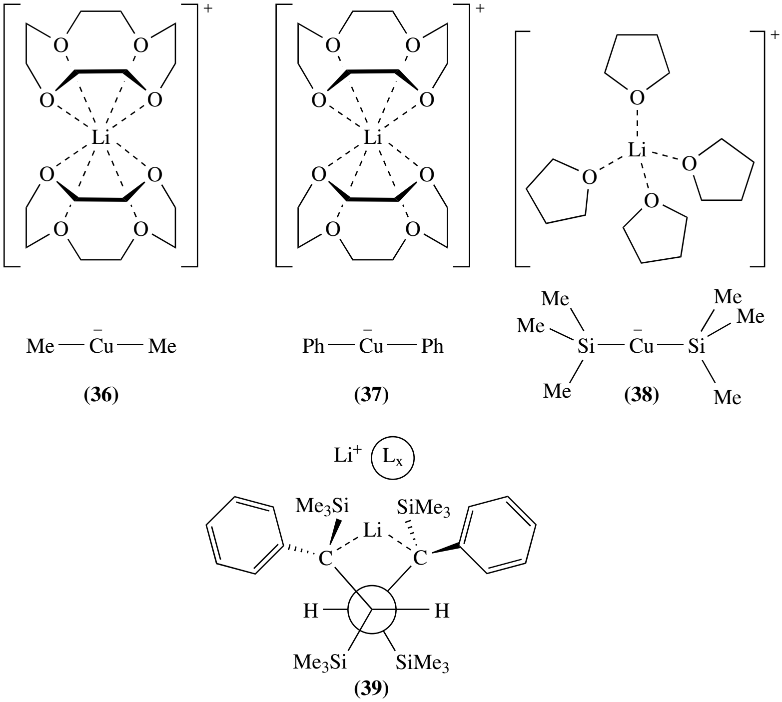

SCHEME 7. Structures of lithium cuprates and the Schlenck dimer formed by Li reduction of 1,2-bis(trimethylsilyl)-1-phenylethene

TABLE 11. ^{7}Li NMR quadrupole parameters $\chi(^{7}\mathrm{Li})$ and $\eta(^{7}\mathrm{Li})$ for cuprates **36**–**38**, see Scheme 7[215]

Compound	χ(kHz)	η	$\delta(^{7}\mathrm{Li})/(^{6}\mathrm{Li})$(ppm)	Reference for X-ray data
36	23	0.50	−2.3/−2.1	216
37	30	0.45	−2.9/−2.8	216
38	18	0.25	−1.8/−1.8	205

cation giving rise to the high-field resonance has the larger quadrupole coupling, in line with the stronger interaction with the phenyl rings deduced from the solution studies.

D. ^{6}Li–^{13}C Dipole Couplings

As mentioned in Sections I.B.2.b and II.A, the dipolar coupling between ^{7}Li–^{13}C may complicate solid state NMR spectra of organolithium compounds and its elimination is often desirable. On the other hand, dipolar coupling constants are related to atomic distances and their determination can yield important structural information. It is therefore of general interest that the REDOR technique, briefly described in Section I.B.2.b, provides a means to determine these parameters.

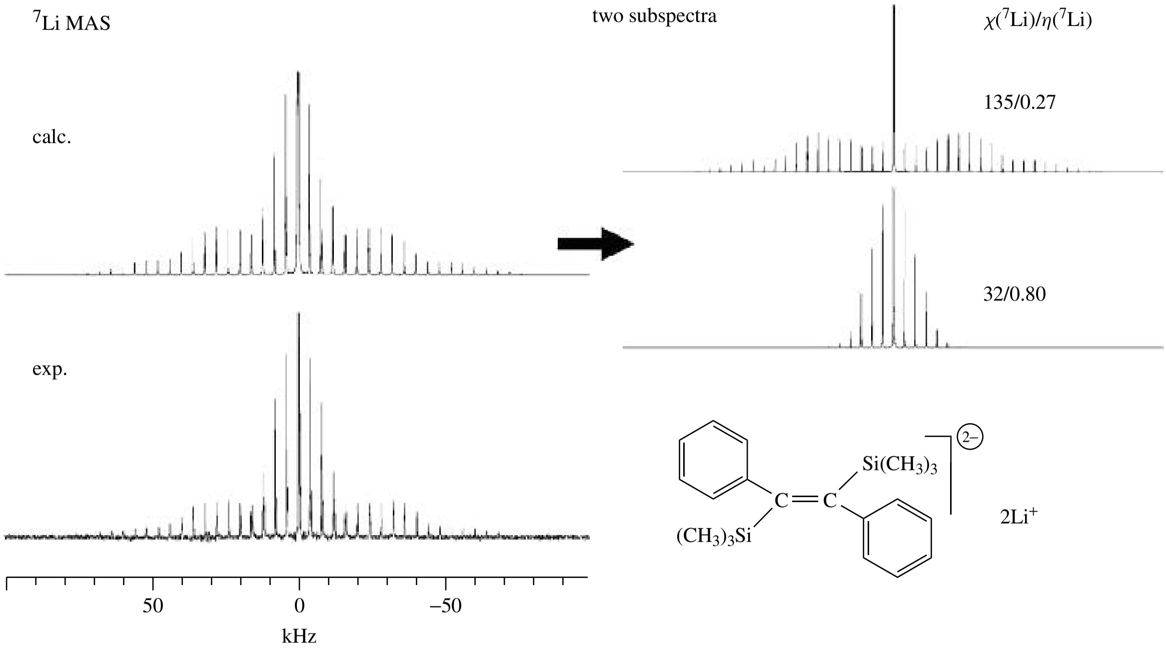

FIGURE 19. Solid state ^{7}Li MAS spectrum of the dianion formed by Li reduction of (*E*)-1,2-diphenyl-1,2-bis(trimethylsilyl)ethene[219]

In our context, especially C–Li distances are of interest. A first successful ^{6}Li–^{13}C REDOR study was undertaken in order to establish the structure of the previously discussed TMEDA complex of fluorenyllithium[220], prepared from ^{6}Li-enriched *n*-butyllithium and fluorene with ^{13}C at natural abundance. The REDOR pulse sequence used is depicted in Figure 20. The number of rotor cycles is increased in a symmetric fashion about the central ^{13}C π-pulse in order to increase the dephasing time.

The resulting ^{13}C spectrum consists of five peaks from the aromatic anion that can be partly assigned based on the solution NMR spectrum[130] (Figure 21). The limited resolution

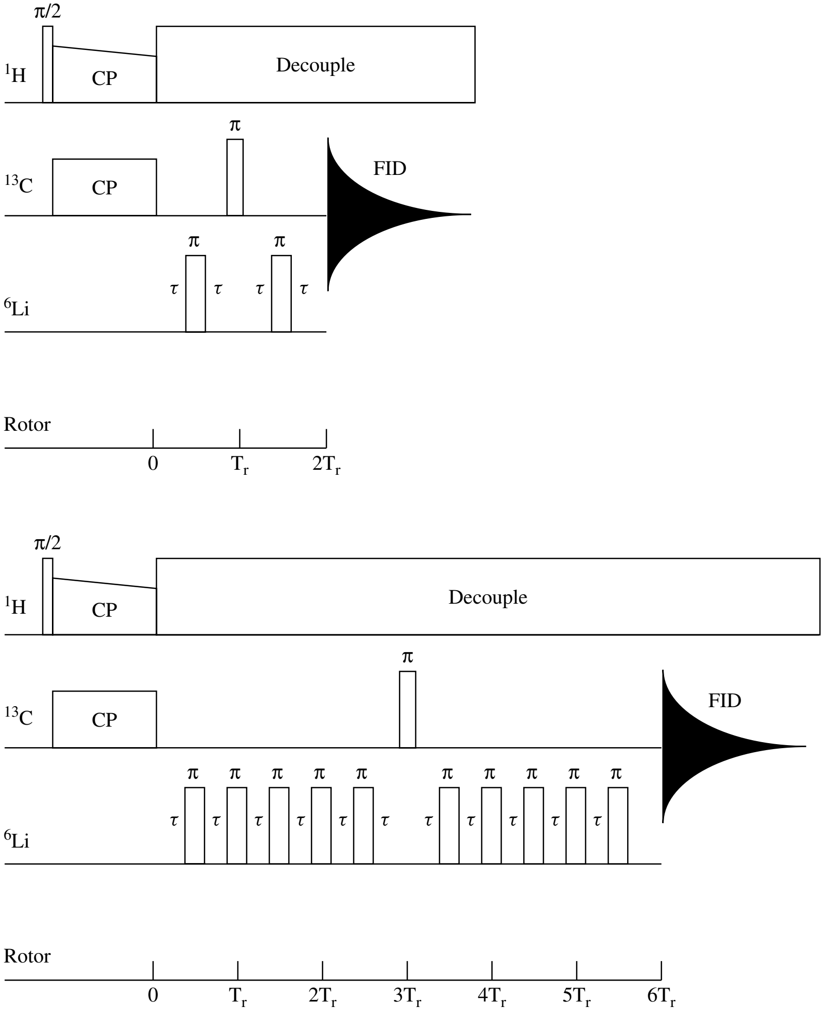

FIGURE 20. The first two experiments in the REDOR pulse sequence, where the dephasing delay is increased by adding more rotor periods and ^{6}Li π-pulses symmetrically around the ^{13}C π-pulse. Reproduced with permission of Blackwell Publishing from Reference 221

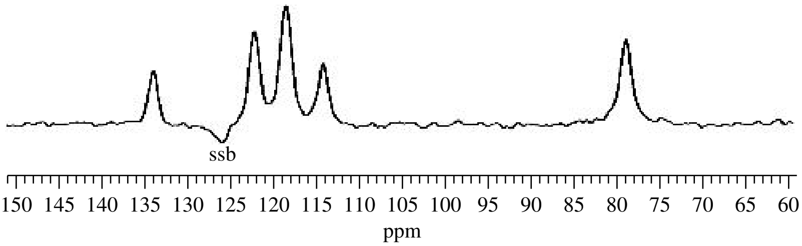

FIGURE 21. ^{13}C MAS spectrum of the TMEDA complex of fluorenyllithium. ssb = spinning sideband. Reprinted with permission from Reference 220. Copyright 1997 American Chemical Society

of the ^{13}C spectrum results in overlapping signals at 119 and 122 ppm, respectively. The signals show different decaying behaviour. The signal decay as a function of dephasing time for the signals at 78 and 114 ppm are shown in Figure 22. In Figure 22a, unfilled symbols, the typical undulation of a signal dominated by the dipolar dephasing is noted. In Figure 22b, a signal with a smaller dipolar contribution is shown. The dipolar coupling of the assigned signal at 134 ppm was also determined. The obtained parameters are reported in Table 12. From the distance information it is possible to locate the position of the lithium cation relative to the fluorenyl framework. The optimized structure is presented in Figure 23. The position was determined with a precision better than 0.2 Å. Compared to X-ray crystallography of small molecules, this is a relatively large error. However, the precision is certainly good enough to select one out of several possible positions of the lithium cation.

In the study the REDOR transform was applied to the peaks from overlapping signals[222, 223]. This transform can deconvolute different dipolar couplings under favourable circumstances. When applied to the signal at 119 ppm, the transform gives rise to two peaks at 130 and 300 Hz, respectively (Figure 24). This indicates that this signal originates from two carbons with large differences in the carbon–lithium distance. The signal at 122 ppm only gives rise to one signal after the REDOR transform at about 100 Hz. The conclusion is that the difference in the carbon–lithium distance is too small for the REDOR transform to resolve.

With the lithium position determined, it is now possible to calculate the lithium–carbon distances to the remaining carbon atoms. Based on these results, the complete assignment of the ^{13}C spectrum can be made, as shown in Table 12.

Another ^{6}Li–^{13}C REDOR study was recently reported[221]. The aim of this study was to compare the structure from a REDOR experiment with the results from X-ray crystallography. The TMEDA complex of indenyllithium was selected as test system for this comparison. The X-ray structure of this complex was determined already in 1975[164]. The lithium is positioned above the five-membered ring interacting with the carbanion in a slightly asymmetric η^5 fashion. The difference in carbon–lithium distance is minute, less than 0.004 Å, and is well below the resolution of the REDOR experiment. However, the ligand is also asymmetrically positioned relative to the carbon framework. This leads to a splitting of some of the signals in the ^{13}C NMR spectrum. The signals were assigned by comparing with solution NMR data[130]. The obtained dipolar couplings and the resulting carbon–lithium distances are reported in Table 13 together with the average distances from the X-ray study. As is evident from Table 13, the REDOR method systematically overestimates the Li–C distances by *ca* 0.1 Å on the average (r_{REDOR} vs $r_{\text{X-ray}}$). The error gets larger, however, for longer distances, i.e. smaller dipolar couplings, due to the inherent difficulty in accurately determining small dipolar coupling constants.

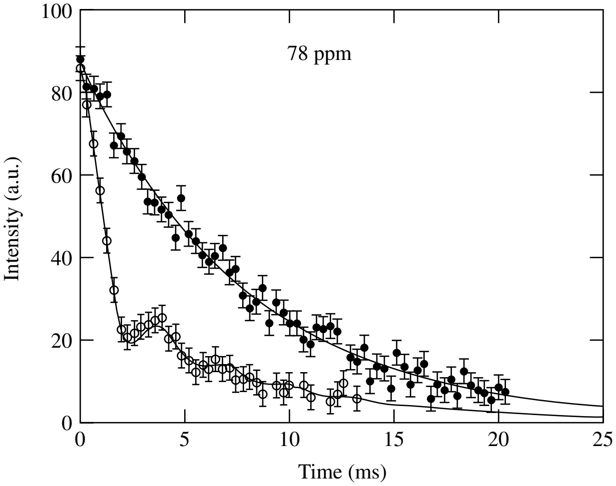

(a)

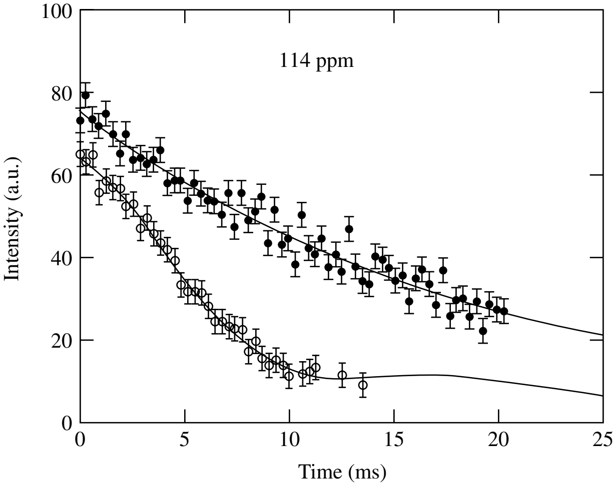

(b)

FIGURE 22. Best fits to the signal decays of the ^{13}C signals at (a) 78 ppm and (b) 114 ppm. Filled symbols, experiment without ^6Li π-pulses, giving an estimate of the T_2 relaxation time. Unfilled symbols, experiment with ^6Li π-pulses. Reprinted with permission from Reference 220. Copyright 1997 American Chemical Society

To locate the lithium cation, the distances based on dipolar couplings larger than 100 Hz were used. The result is shown in Figure 25, where the darker lithium cation corresponds to the position according to X-ray crystallography and the lighter grey cation corresponds to the position according to REDOR. The difference between the Li positions according to X-ray and REDOR is *ca* 0.15 Å.

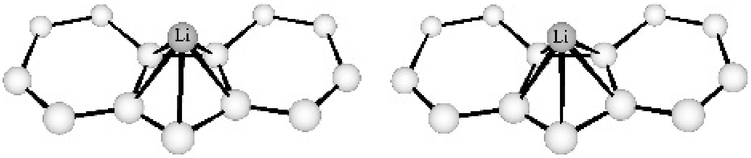

FIGURE 23. Stereoview of the position of the lithium cation relative to the fluorenyl system in the TMEDA complex of fluorenyllithium as determined by REDOR NMR spectroscopy

TABLE 12. ^{6}Li$-$^{13}C dipolar couplings and calculated Li$-$C distances between the indicated carbon atoms and the Li cation in the TMEDA complex of fluorenyllithium based on the dipolar coupling and on the structure optimization[220]

Carbon	d^a (Hz)	r_{REDOR} (Å)	$r_{\text{optimized}}$ (Å)	δ (ppm)
9	354 ± 33	2.32 ± 0.07	2.34	78
9a	271 ± 54	2.54 ± 0.17	2.39	134
3	71 ± 12	3.97 ± 0.22	4.10	114
1			3.31	119
2			4.05	122
4			3.44	122
4a			2.48	119

$^a d = D/2\pi$.

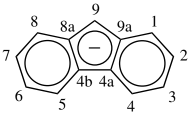

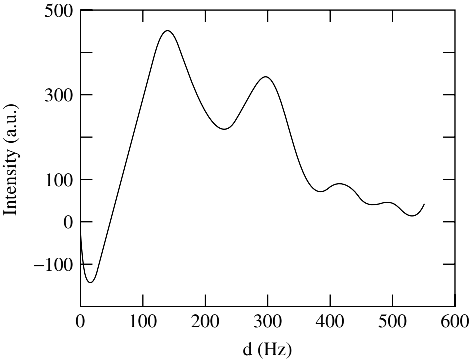

FIGURE 24. REDOR transform of the decay of the peak at 119 ppm clearly indicating two overlapping signals of different dipolar couplings. Reprinted in part with permission from Reference[220]. Copyright 1997 American Chemical Society

The observed difference between the REDOR lithium position and the position according to X-ray crystallography can be explained by dynamic effects, and from instrumental imperfections. A recent theoretical investigation shows that NMR and X-ray distances are expected to differ to some degree[224]. Dynamic processes have different influences on X-ray and REDOR, especially at higher temperatures. In this system the TMEDA ligand is

TABLE 13. $^{6}Li-^{13}C$ dipolar couplings and calculated Li–C distances between the indicated carbon atoms and the Li cation in the TMEDA complex of indenyllithium according to REDOR and X-ray crystallography[221]

Carbon	δ (ppm)	d^a (Hz)	r_{REDOR} (Å)	$r_{\text{optimized}}$ (Å)	$r_{\text{X-ray}}$ (Å)
1,3	92	310 ± 13	2.43 ± 0.03	2.43	2.31
2	115	324 ± 15	2.39 ± 0.06	2.39	2.28
3a,7a	127	281 ± 18	2.51 ± 0.06	2.51	2.38
4,7	121, 122	$87 \pm 6{,}93 \pm 6$	3.63 ± 0.07, 3.71 ± 0.09	3.46	3.35
5,6	117	50 ± 2	4.46 ± 0.06	4.18	4.08

[a] $d = D/2\pi$.

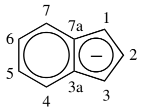

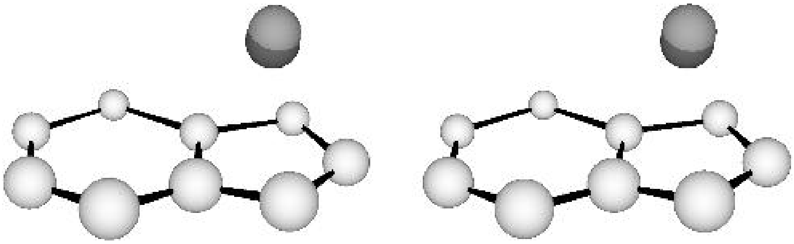

FIGURE 25. Stereoview of the position of the lithium cation relative to the indenyl system in the TMEDA complex as determined by REDOR NMR spectroscopy (light grey) and X-ray crystallography (dark grey). Reproduced by permission of Blackwell Publishing from Reference 221

likely to be involved in dynamic processes, similar to those investigated in detail in some related organolithium complexes[132]. This dynamic process could change the position of the lithium cation to an extent that affects the observed dipolar coupling, as mentioned in the next section.

In conclusion, the investigations presented show that the $^{6}Li-^{13}C$ REDOR technique can be a valuable tool for the structural characterization of organolithium complexes. Contrary to X-ray, there is no need for single crystals. Although the carbon–lithium distances are to some extent overestimated by the REDOR technique, the precision is sufficient to discriminate between various possible lithium positions in the complexes.

One problem with the REDOR method and other similar solid state NMR techniques is that unambiguous results only can be obtained when the spin system is based on isolated spin pairs, as shown in a recent publication[225]. This means that the prevalent aggregates found in organolithium complexes cannot be studied by these methods. However, a recent 3D TEDOR study of uniformly $^{13}C-^{15}N$ labelled peptides gives some hope, provided that the interacting nuclei have different chemical shifts[226].

E. Dynamic NMR of Solid Organolithium Compounds

A unique feature of NMR is its sensitivity for dynamic processes. Using different techniques, from the well-known lineshape analysis to the application of relaxation time measurements, the correlation times of dynamic processes which can be studied span a

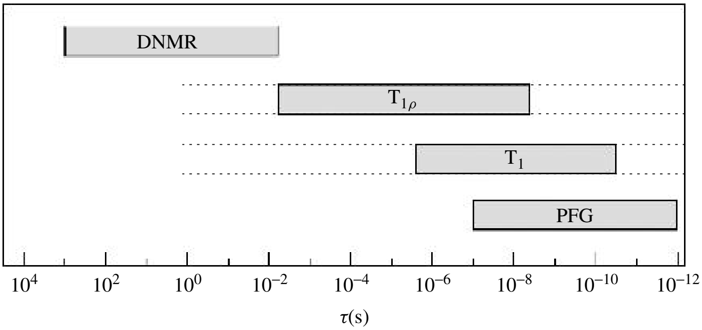

FIGURE 26. NMR methods and correlation times for dynamic processes

range of several orders of magnitude (Figure 26). This applies to high-resolution NMR in the liquid phase as well as to investigations of solids by solid state NMR techniques.

Molecular motion in solids has been the object of many studies in the field of physical chemistry of polymers[63], but dynamic processes in molecular crystals of organic and inorganic compounds are less well investigated. In fact, the average chemist is not aware of the fact that processes like internal rotation or ring inversion proceed in solids quite often with barriers which are not very different from those found for these types of internal motion in the liquid state. Thus, for the equatorial → axial ring inversion of fluorocyclohexane values of 42.4 and 43.9 kJ mol^{-1} have been measured in the liquid[227] and the solid[228], respectively. The familiar thermal ellipsoids of individual atoms obtained from X-ray studies are qualitative indicators of molecular motion in the crystal, but a more quantitative study of such processes is only possible after appropriate solid state NMR techniques are applied.

In the case of organolithium compounds, besides internal rotations or conformational changes in the carbanionic moiety, dynamic processes associated with the ligands are of particular interest because, in solution, such processes might affect the reactivity of these systems. Since dynamic processes which, for example, involve the cleavage of dative bonds are absent in the solid, the situation in the solid is in many cases easier to analyse than the analogous process in the liquid because *inter*molecular exchange is not encountered. On the other hand, solid state NMR spectra are sensitive for solid–solid phase transitions caused by a change of the crystallographic modification and/or the chemical structure. This well-known phenomenon is used to calibrate the temperature in the rotor of MAS experiments[229, 230].

In many cases the temperature dependence of the quadrupolar coupling constant is an indicator of dynamic processes, because the symmetry around the lithium cation is affected by motions which are fast on the NMR time scale. If the rate of these processes exceeds $1/\chi$, the effective symmetry around the lithium cation increases and a decrease in $\chi(^7\text{Li})$ results. In ^{7}Li MAS spectra, a broadening of the satellite transitions can be observed which eventually disappear completely if the rate of the dynamic process comes in the order of the quadrupole frequency[231]. This behaviour was observed for the THF solvated dimer of bis(trimethylsilylamido)lithium, where the ^{7}Li MAS spectrum at 353 K shows only the central transition and the sidebands caused by CSA and homonuclear ^{7}Li–^{7}Li dipole coupling (Figure 27)[93, 94]. The simulation of the high-temperature spectrum yielded −20 ppm and 1300 Hz for these quantities, respectively. The dipole coupling agrees closely with the theoretical value of 1319 Hz calculated from the Li–Li distance of 2.4 Å, which was determined by an X-ray study.

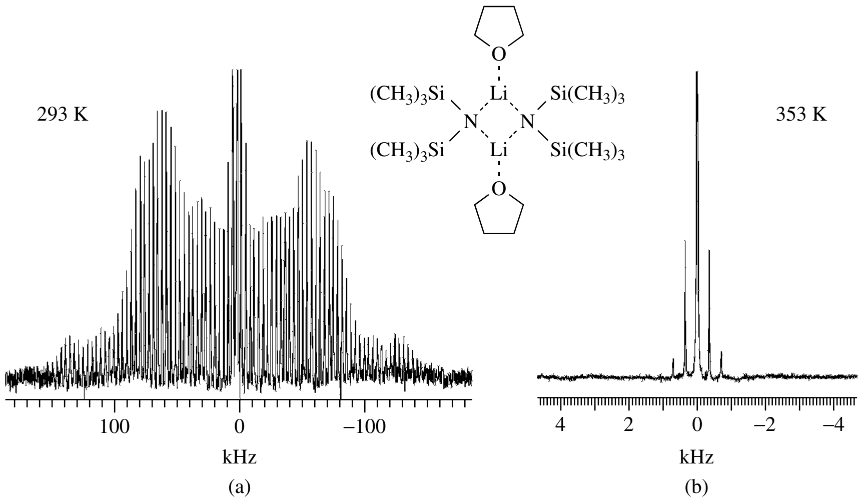

FIGURE 27. ^{7}Li{^{1}H} CP/MAS spectrum of bis(trimethylsilylamido)lithium(THF)$_2$ at different temperatures[93, 94]

In a variable temperature study of the TMEDA complex of trimethylsilylcyclopentadienyllithium, Pietrass and Burkert observed that the χ value decreases linearly with increasing temperature, from *ca* 190 kHz at *ca* 200 K to *ca* 165 kHz at 340 K[232]. The slightly higher value at ambient temperature than that reported in Table 8, entry 2, could be due to the assumption of a zero asymmetry parameter in the variable temperature study. The effects of the temperature on χ values of inorganic salts have been investigated in some instances as well[233, 234]. For example, for lithium di(t-butoxydimethylsilyl)amide, (t-BuOSiMe$_2$)$_2$NLi, a change of χ(^{7}Li) from 100 kHz at 273 K to 88 kHz at 383 K was associated with a phase transition from monoclinic to tetrahedral[235].

In a recent investigation of the t-butyllithium tetramer, the temperature dependence of the χ(^{7}Li) was used to demonstrate the exchange of ligands in the solid state[236]. At temperatures below 150 K, the χ value is 100 kHz. At higher temperatures it becomes smaller and is <5 kHz at 293 K. This process was proposed to be an *intra*-aggregate exchange of the lithium ions between the different tetrahedral sites. ^{7}Li T_1 relaxation time measurements were used to establish a phase transition and to determine the rate constant for this dynamic process in both phases. Extrapolation to RT indicates an exchange rate of 8.5×10^8 s^{-1}.

In another study[93, 94], a sudden spectral change and a reduction in χ(^{7}Li) from 360 kHz at 213 K to 85 kHz at RT was observed for the LDA–THF complex (**26**, Scheme 4, Table 9) between 282 and 286 K. Again, this result can be associated with dynamic processes which involve, according to ^{13}C and ^{2}H NMR investigations of partially deuteriated species, the THF ligands.

A prominent feature of many organolithium compounds is complexation by TMEDA ligands. The resulting heterocyclic five-membered ring has, according to X-ray investigations[169], a twist conformation. Two dynamic processes (Scheme 8) can be expected in this system: ring inversion A $\rightleftharpoons$ B and, presumably with a higher activation barrier, rotation by 180° (C $\rightleftharpoons$ D).

The ring inversion of the TMEDA–Li metallacycle often results in a broadening and disappearance of the ^{13}C resonance of the methylene groups caused by the phenomenon

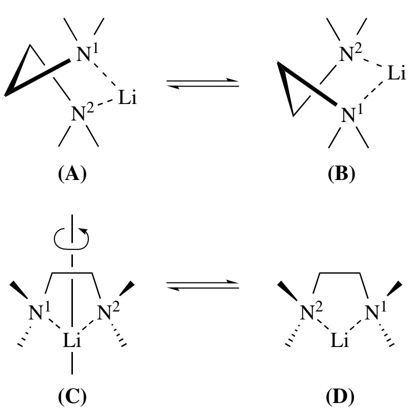

SCHEME 8. Dynamic processes for the Li-TMEDA metallacycle: ring inversion (A $\rightleftharpoons$ B) and rotation by 180° (π-flip, C $\rightleftharpoons$ D)

of *dipolar broadening*[237]. It occurs if the power of the proton decoupler field B_2 matches the exchange rate between non-equivalent positions. At the point of largest linewidth, the condition $\gamma B_2 = 1/\tau_c$ holds and the exchange rate $k = 1/\tau_c$ can be determined if the power of the decoupling field is known.

Solid state NMR investigations of the phenyllithium (**10**) dimer, $[\text{Li(TMEDA)}\mu\text{-}C_6H_5]_2$, revealed on the basis of temperature-dependent lineshape analyses of the ^{13}C and ^{15}N spectra dynamic processes characterized by barriers $\Delta G^{\ddagger}(326)$ of 40 and 68 kJ mol^{-1}, respectively[132]. These were assigned to the ring inversion process and the 180° ring flip, respectively. Again, a temperature-dependent $\chi(^7\text{Li})$ was observed, with values of 146 and 90 kHz at 297 and 340 K, respectively. For the 180° ring flip in the dilithiumnaphthalenediide(TMEDA)$_2$ complex a barrier of $\Delta G^{\ddagger}(317) = 64$ kJ mol^{-1} was found on the basis of ^{15}N lineshape measurements and a two-dimensional ^{15}N EXSY spectrum (Figure 28) measured with a modified $90° - t_1 - 90° - t_M - 90°$, FID($t_2$) pulse sequence, where the first 90° pulse is replaced by a CP sequence[238].

The rotation of the TMEDA rings on the two sides of the naphthalenediide moiety is uncorrelated, as shown by the temperature-independent ^{13}C spectrum. A 180° ring flip with a similar barrier, $\Delta G^{\ddagger}(293) = 65.9 \pm 11.4$ kJ mol^{-1}, was also observed for the Li–TMEDA ring in pyrrolidinatolithium(TMEDA), $[c\text{-}(CH_2)_4\text{NLi})_2\text{(TMEDA)}]_2$[124].

Temperature-dependent lineshape changes were observed in an early study of the fluorenyllithium(TMEDA) complex[128]. A detailed study by ^{13}C lineshape analysis, which was also applied to the TMEDA complex of 2,3-benzofluorenyllithium(TMEDA) (Figure 29)[72], yielded barriers $\Delta G^{\ddagger}(298)$ of 44.4 and 41.9 kJ mol^{-1} for the 180° ring flip in these systems, respectively[215]. A second dynamic process, which was detected via the temperature dependence of $T_{1\rho}$, the spin–lattice relaxation time in the rotating frame, is characterized by barriers of 35.1 and 37.6 kJ mol^{-1}, respectively, and may be ascribed to the ring inversion process. For the fluorenyl complex, a barrier $\Delta G^{\ddagger}$ (298) of 15.9 kJ mol^{-1} for the methyl rotation in the TMEDA ligand was determined from temperature-dependent ^{2}H NMR spectra of the deuteriated system.

Finally, an interesting temperature effect was observed in the spectra of α-(phenylthio)benzyllithium•3THF (**3**, Scheme 1)[239]. Differences exist in the ^{13}C and ^{7}Li CP/MAS spectra observed at 293 and 208 K, respectively, which indicate a phase transition. This was confirmed by differential scanning calorimetry (DSC), which yielded a transition temperature of 204–212 K. The most characteristic NMR parameters of the

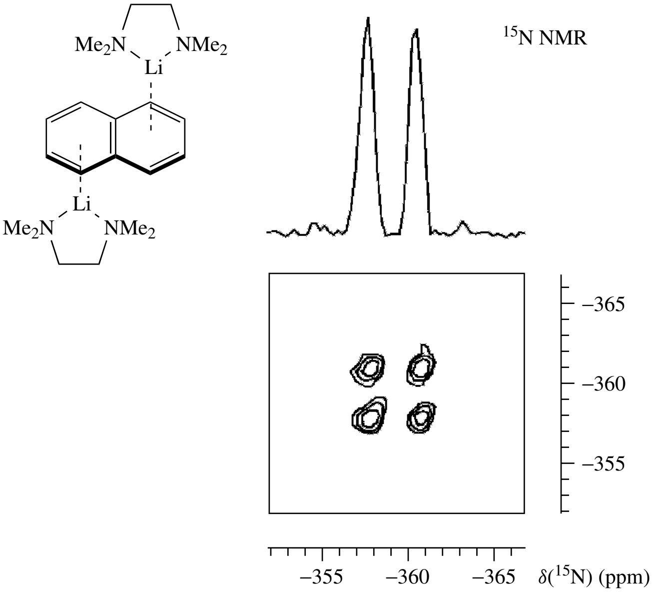

FIGURE 28. Two-dimensional natural abundance ^{15}N solid-state EXSY spectrum of the dilithium-naphthalenediide(TMEDA)$_2$ complex at 292 K[132]

high- and low-temperature modification are collected in Table 14. In going from 293 to 208 K, deshielding of C_α and the *ipso*-carbons C-1 and C-7 is observed, while the *para*-carbon C-6 is more shielded. There is apparently less charge on C_α in the low-temperature structure. At the same time the lithium resonance is shielded, presumably due to a higher electron density. With less negative charge on C_α and less positive charge on the lithium, the C_α−Li bond in the low-temperature structure is thus less polar than in the high-temperature structure. This conclusion is supported by the difference in the quadrupole parameters. The more polar C_α−Li bond in the high-temperature modification yields a larger field gradient and $\chi(^7\mathrm{Li})$ increases. The increase in the asymmetry parameter, $\eta(^7\mathrm{Li})$, on the other hand, indicates an increasing difference between the transverse components of the field gradient, q_{xx} and q_{yy} (cf. equation 9), which may be related to a stronger C_α−S interaction, as reflected by the shielding of C-7. The origin of these changes is not known, but changes in the Li−O distances to the THF ligands or in the C−Li distance could be important. Since the ^{13}C chemical shifts measured in solution at RT and at 193 K[88] are identical within experimental error with the low-temperature solid NMR data, the low temperature structure is also present in solution. In line with this interpretation is the fact that the high-temperature solid state NMR data do not match the RT solution state NMR data. Finally, the X-ray structure determined at 220 K,[240] just above the phase transition temperature, must correspond to the high-temperature solid state modification and thus does not represent the solution-state structure.

F. Calculations of ^{7}Li Quadrupole Parameters

The possibility to calculate $\chi(^7\mathrm{Li})$ and $\eta(^7\mathrm{Li})$ parameters for a given structure is an important aspect for the interpretation of the experimental data. A number of theoretical

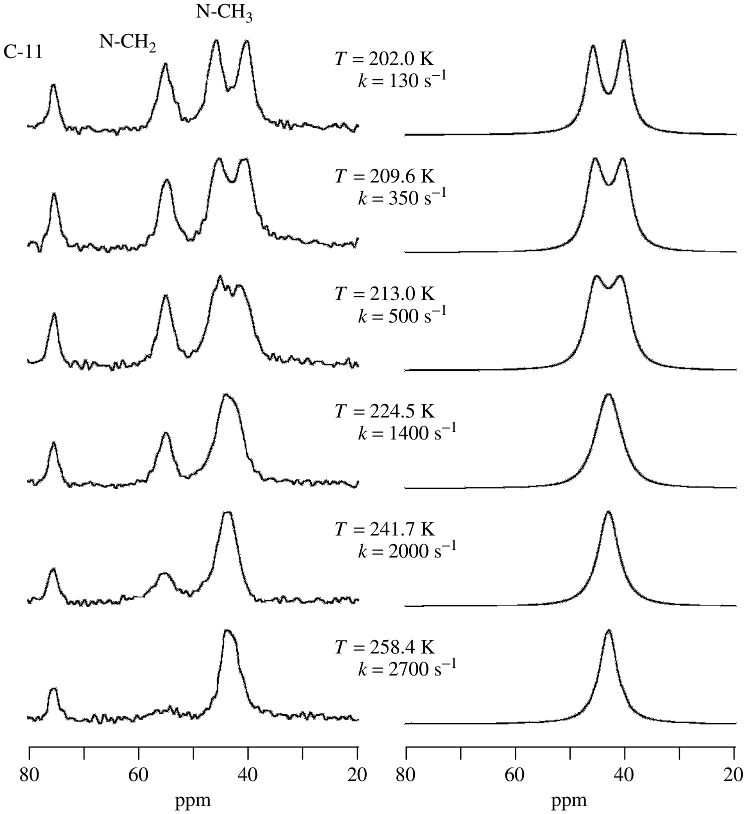

FIGURE 29. Experimental (left) and calculated (right) ^{13}C CP/MAS partial spectra of 2,3-benzofluorenyllithium(TMEDA) showing the lineshape changes for the methyl resonances[215]

TABLE 14. Characteristic solid state ^{13}C NMR parameters for the high- and low-temperature modification of α-(phenylthio)benzyllithium·**3**THF (**3**)[239]

NMR parameter	High temperature form	low temperature form	Difference
δ (^{13}C$_\alpha$)(ppm)	31.3	35.3	−4.0
δ (^{13}C-6)(ppm)	113.8	110.6	3.2
δ (^{13}C-1)(ppm)	153.6	156.2	−2.6
δ (^{13}C-7)(ppm)	144.0	151.3	−7.3
δ (^{7}Li)(ppm)	0.2	−0.5	0.7
χ(^{7}Li)(kHz)	132	80	52
η_Q(^{7}Li)	0.82	0.29	0.53

approaches are available which allow the calculation of the electric field gradient of an atom and thus open the way to the calculation of both χ(^{7}Li) and η(^{7}Li).

The simplest approach is to apply a point charge model (PCM). It is based on the physical definitions of electrical quantities, where a charge q at a distance r from the origin contributes to the components of the electric field gradient according to equation 19[241],

$$V_{i,j} = \frac{q}{4\pi\varepsilon_0}\left(\frac{3x_i x_j}{r^5} - \delta_{ij}\frac{1}{r^3}\right) \tag{19}$$

The electric field gradient at an ion in an ionic compound is then given as the sum of contributions from individual components surrounding this ion (equation 20),

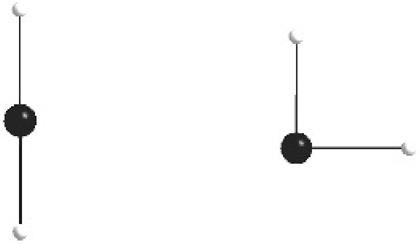

A; linear B; 90° angle

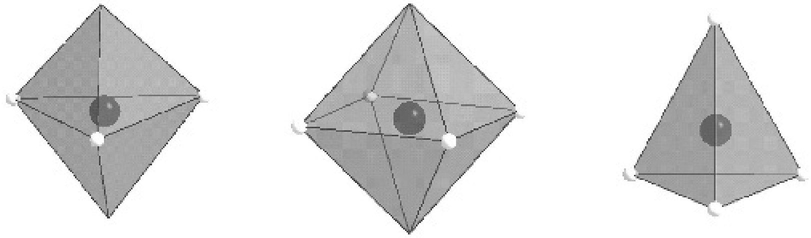

C; trigonal planar D; tetragonal planar E; trigonal pyramidal

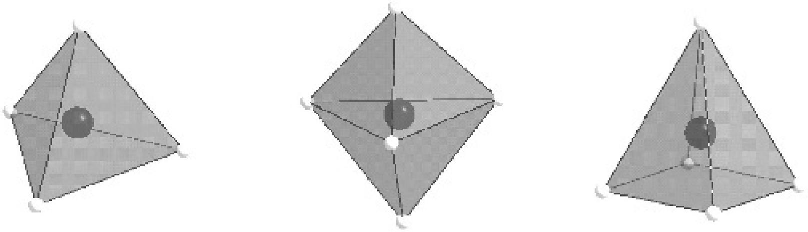

F; tetrahedral G; trigonal bipyramidal H; quadratic pyramidal

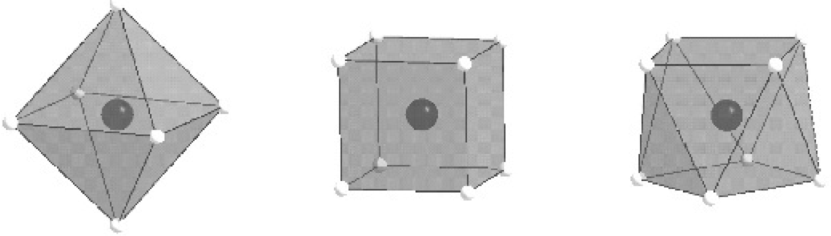

I; octahedral J; cube K; quadratic antiprisma

SCHEME 9. Models for ligand spheres around a lithium cation

$$V_{i,j} = \frac{e}{4\pi\varepsilon_0} \sum_k \frac{Z_k}{r_k^5} \begin{pmatrix} 3x_k^2 - r^2 & 3x_k y_k & 3x_k z_k \\ 3x_k y_k & 3y_k^2 - r^2 & 3y_k z_k \\ 3x_k z_k & 3y_k z_k & 3z_k^2 - r^2 \end{pmatrix} \tag{20}$$

where Z_k is the partial charge of the k-th atom. The inclusion of orbital terms has improved this essentially electrostatic model[242], but its success for complicated structures is still limited. However, in the case of organolithium compounds where the most important C−Li interaction is highly ionic, even this simple approach can yield results which reflect experimental trends. An example is the model calculation of $\chi(^7\text{Li})$ for a number of geometrical arrangements of ligands around a lithium cation as shown in Scheme 9. Using an arbitrary distance of 2.0 Å and point charges of −1, the results (Table 15) give a clear indication about the relative magnitude of $\chi(^7\text{Li})$ to be expected in real structures of related geometry.

As a refinement, the bonding geometry can be taken from results of an X-ray analysis of the structure of interest and the atomic charges may be calculated on this basis by a standard quantum-chemical program. Alternatively, the geometry can be optimized by calculations. The distances and charges derived in either way are then used as input parameters for the PCM calculations. For example, geometry and atomic charges for the structures shown in Scheme 10, which represent situations encountered for lithium cations in solvent-separated ion pairs, were obtained from structures which were geometry-optimized by *ab initio* calculations of the HF/6−31G* type using the program SPARTAN[210]. The quadrupole parameters derived on the basis of PCM calculations are collected in Table 16. Alternatively, the electric field gradient at the lithium cation of interest can be calculated on the basis of an optimized geometry by the program GAMESS[243]. These results are also given in Table 16. In general, the $\chi(^7\text{Li})$ values are better reproduced than the $\eta(^7\text{Li})$ values and the results obtained by GAMESS are closer to the experimental values than those of the PCM calculations in the case of the highly symmetric systems $[\text{Li(THF)}_4]^+$ and $[\text{Li(12-crown-4)}_2]^+$.

Finally, more sophisticated quantum-chemical programs like WIEN95[244] or the well-known program GAUSSIAN98[245] allow the calculation of the electric field gradient and the quadrupole parameters, but involving more computer time. Results obtained on this basis for a number of systems are collected in Table 17[125, 236, 246]. They compare quite well with the experimental data, except for the polymeric structure of lithiumdiisopropylamide (**25**, Scheme 4). In this helical structure the ionic centres of several monomer units are in close proximity. The resulting perturbations of the electric field gradient are not reproduced by the calculations, which were based on only two monomer units.

TABLE 15. PCM calculations for model systems of Scheme 9[239]

Point charges	Geometry	$V_{yy} - V_{xx}^a$	V_{zz}(a.u.)	$\chi(^7\text{Li})$(kHz)
2	A	0	0.5349	517
2	B	0	0.2674	258
3	C	0	0.4012	388
4	D	0	0.5349	517
4	E	0	0.1337	129
4	F	0	0	0
5	G	0	0.1337	129
5	H	0	0.1337	129
6	I	0	0	0
8	J	0	0	0
8	K	0	0	0

[a] Consequently, $\eta_Q(^7\text{Li}) = 0$ in all cases (cf. equation 9).

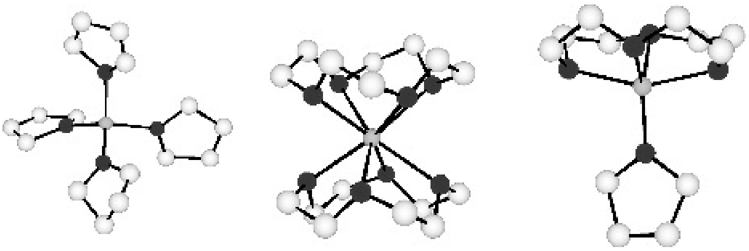

$[Li(THF)_4]^+$ $[Li(12\text{-crown-}4)_2]^+$ $[Li(12\text{-crown-}4)(THF)]^+$

FIGURE 10. Examples for solvent-separated lithium cations

TABLE 16. Calculated and experimental quadrupole parameters for the solvent-separated-lithium cation in selected complexes (Schemes 1, 5, 7 and 10)[239]

Compound	CN(Li)[a]	$\chi(^7Li)$(kHz)			$\eta_Q(^7Li)$		
		calc.[b]		exp./compound	calc.[b]		exp.
$[Li(THF)_4]^+$	4	28	15	19/**35**	0.12	0.3	0.05
				18/**38**			0.25
$[Li(12\text{-crown-}4)_2]^+$	8	15	35	30/**3**	0.26	0.0	0.20
				24/**4**			0.45
				28/**5**			0.01
				23/**36**			0.50
				30/**37**			0.45
$[Li(12\text{-crown-}4)(THF)]^+$	5	71	53	110/**3**	0.24	0.75	0.22

[a] Coordination number.

[b] Left entry PCM calculations, right entry GAMESS[243] results.

TABLE 17. ^7Li quadrupole NMR parameters calculated by high-level *ab initio* methods of selected compounds (Schemes 1, 4, 5 and 6)[125,236,239,246]

Compound	Theoretical method[a]	$\chi(^7Li)$(kHz)		$\eta(^7Li)$	
		calc.	exp.	calc.	exp.
$[C_6H_5Li]_2$, **10**	**a**	223	234	0.05	0.45
35	**a**	465	478	0.29	0.12
27	**a**	286	298	0.16	0.18
25	**a**	898	610	0.02	0.07
5·TMEDA	**b**	288	274	0.31	0.75
5·PMDTA	**b**	153	128	0.66	0.98
$[(CH_3)_3CLi]_4$[b]	**b**	150	100[c]	—	—
17[d]	**c**	320	360	—	—

[a] **a**: hydrogens were added to the X-ray heavy atom structure and geometry-optimized with the program SPARTAN; this geometry was then used for 6-311G**6d10f calculations of the electric field gradient by the program GAUSSIAN98; **b**: geometry-optimized DFT B3LYP calculations using GAUSSIAN98; **c**. GAUSSIAN92 with MP2/6-31G** basis set.

[b] Reference 236.

[c] At 150 K.

[d] Reference 125.

III. CONCLUSIONS

The results collected in this review clearly demonstrate the potential of solid state NMR for structural studies in the field of organolithium compounds. ^{13}C as well as $^{6/7}$Li spectra provide parameters that correlate with various structural features like aggregation, solvation, structural angles and distances, as well as dynamic processes. For ^{13}C the information comes primarily from the chemical shifts, while for $^{6/7}$Li in addition the quadrupolar interactions are valuable sources of information. NMR and X-ray investigations nicely complement each other. While X-ray diffraction is unsurpassed in the determination of the complete geometry of a complex, NMR yields information about the charge distribution and dynamic processes. Solid state NMR spectroscopy is furthermore indispensible in cases where only microcrystalline powders are available which prevent X-ray measurements. Calculations by theoretical methods allow predictions of solid state NMR parameters which can be used to differentiate between several alternatives available for a given structure. With the ongoing progress in NMR instrumentation and methodology, solid state NMR investigations of organolithium systems hold promise also for the future.

IV. ACKNOWLEDGEMENTS

As far as our own contributions are concerned, we thank our coworkers Anders Andersson, Wolfgang Baumann, Arne Boman, Ulf Edlund, the late Arnd Focke, Michael Hartung, Heike Hausmann, Steffen Jost, Martin Kühnen, Yuri Oprunenko and Iugman Sethson for their enthusiasm and experimental skill. D. J. acknowledges financial support from the Swedish Science Research Council and Umeå University. H. G. thanks Jean-Pierre Amoureux and Christian Fernandéz for permission to use their program QUASAR and gratefully acknowledges a spectrometer grant from the Volkswagenstiftung and financial support from the Deutsche Forschungsgemeinschaft and the Fonds der Chemischen Industrie, Frankfurt.

V. REFERENCES

1. W. Schlenk and J. Holtz, *Chem. Ber.*, **50**, 262 (1917).
2. A. Steitwieser, S. M. Bachrach, A. Dorigo and P. v. R. Schleyer, in *Lithium Chemistry* (Eds. A.-M. Sapse and P. v. R. Schleyer), Wiley Interscience, New York, 1995.
3. A. Streitwieser, Jr., *J. Organomet. Chem.*, **156**, 1 (1978).
4. A. Streitwieser, Jr., *Acc. Chem. Res.*, **17**, 353 (1984).
5. B. J. Wakefield, in *Organolithium Methods*, Academic Press, London, 1988.
6. M. Schlosser, in *Organometallics in Synthesis: A Manual* (Ed. M. Schlosser), Wiley, Chichester, 1994.
7. P. J. Cox and N. S. Simpkins, *Tetrahedron: Asymmetry*, **2**, 1 (1991).
8. K. Koga, *Pure Appl. Chem.*, **66**, 1487 (1994).
9. P. Beak, D. R. Anderson, M. D. Curtis, J. M. Laumer, D. J. Pippel and G. A. Weisenburger, *Acc. Chem. Res.*, **33**, 715 (2000).
10. P. Beak, A. Basu, D. J. Gallagher, Y. S. Park and S. Thayumanavan, *Acc. Chem. Res.*, **29**, 552 (1996).
11. D. Hoppe and T. Hense, *Angew. Chem., Int. Ed. Engl.*, **36**, 2283 (1997).
12. A. Basu and S. Thayumanavan, *Angew. Chem., Int. Ed.*, **41**, 717 (2002).
13. B. L. Lucht and D. B. Collum, *Acc. Chem. Res.*, **32**, 1035 (1999).
14. A. Streitwieser, S. S. W. Leung and Y.-J. Kim, *Org. Lett.*, **1**, 145 (1999).
15. A. Streitwieser, E. Juaristi, Y.-J. Kim and J. K. Pugh, *Org. Lett.*, **2**, 3739 (2000).
16. A. Streitwieser, Y.-J. Kim and D. Z.-R. Wang, *Org. Lett.*, **3**, 2599 (2001).
17. H. J. Reich, D. P. Green, M. A. Medina, W. S. Goldenberg, B. O. Gudmundsson, R. R. Dykstra and N. H. Phillips, *J. Am. Chem. Soc.*, **120**, 7201 (1998).
18. W. Bauer and D. Seebach, *Helv. Chim. Acta*, **67**, 1972 (1984).

19. G. Fraenkel, H. Hsu and B. M. Su, in *Lithium: Curr. Appl. Sci., Med. Technol.*, (Ed. R. O. Bach), Wiley, New York, 1985.
20. H. Günther, D. Moskau, P. Bast and D. Schmalz, *Angew. Chem., Int. Ed. Engl.*, **26**, 1212 (1987).
21. R. D. Thomas, in *Isot. Phys. Biomed. Sci.*, Vol. 2, (Eds. E. Buncel and J. R. Jones), Elsevier, Amsterdam, 1991.
22. W. Bauer and P. v. R. Schleyer, *Adv. Carbanion Chem.*, **1**, 89 (1992).
23. W. Bauer, in *Lithium Chemistry* (Eds. A.-M. Sapse and P. v. R. Schleyer), Wiley Interscience, New York, 1995.
24. H. Günther, in *Encyclopedia of Nuclear Magnetic Resonance*, Vol. 5 (Eds. D. M. Grant and R. K. Harris), Wiley, Chichester, 1996.
25. H. Günther, in *Advanced Applications of NMR to Organometallic Chemistry* (Eds. M. Gielen, R. Willem and B. Wrackmeyer), Wiley, Chichester, 1996.
26. H. Günther, *J. Braz. Chem. Soc.*, **10**, 241 (1999).
27. W. N. Setzer and P. v. R. Schleyer, *Adv. Organomet. Chem.*, **24**, 353 (1985).
28. D. Seebach, *Angew. Chem., Int. Ed. Engl.*, **27**, 1624 (1988).
29. E. Weiss, *Angew. Chem., Int. Ed. Engl.*, **32**, 1501 (1993).
30. G. Boche, J. C. W. Lohrenz and A. Opel, in *Lithium Chemistry*, (Eds. A.-M. Sapse and P. v. R. Schleyer), Wiley Interscience, New York, 1995.
31. F. Pauer and P. P. Power, in *Lithium Chemistry* (Eds. A.-M. Sapse and P. v. R. Schleyer), Wiley Interscience, New York, 1995.
32. C. Lambert and P. v. R. Schleyer, *Angew. Chem., Int. Ed. Engl.*, **33**, 1129 (1994).
33. A.-M. Sapse, D. C. Jain and K. Raghavachari, in *Lithium Chemistry* (Eds. A.-M. Sapse and P. v. R. Schleyer), Wiley Interscience, New York, 1995.
34. C. J. Gorter, *Physica*, **3**, 995 (1936).
35. C. S. Johnson, Jr., M. A. Weiner, J. S. Waugh and D. Seyferth, *J. Am. Chem. Soc.*, **83**, 1306 (1961).
36. T. L. Brown, D. W. Dickerhoof and D. A. Bafus, *J. Am. Chem. Soc.*, **84**, 1371 (1962).
37. M. A. Weiner and R. West, *J. Am. Chem. Soc.*, **85**, 485 (1963).
38. R. Waack, M. A. Doran, E. B. Baker and G. A. Olah, *J. Am. Chem. Soc.*, **88**, 1272 (1966).
39. L. D. McKeever, R. Waack, M. A. Doran and E. B. Baker, *J. Am. Chem. Soc.*, **90**, 3244 (1968).
40. G. Fraenkel, A. M. Fraenkel, M. J. Geckle and F. Schloss, *J. Am. Chem. Soc.*, **101**, 4745 (1979).
41. D. Seebach, R. Hässig and J. Gabriel, *Helv. Chim. Acta*, **66**, 308 (1983).
42. H. J. Reich and D. P. Green, *J. Am. Chem. Soc.*, **111**, 8729 (1989).
43. H. J. Reich and J. P. Borst, *J. Am. Chem. Soc.*, **113**, 1835 (1991).
44. H. J. Reich, J. P. Borst, R. R. Dykstra and P. D. Green, *J. Am. Chem. Soc.*, **115**, 8728 (1993).
45. D. B. Collum, *Acc. Chem. Res.*, **25**, 448 (1992).
46. D. B. Collum, *Acc. Chem. Res.*, **26**, 227 (1993).
47. T. L. Brown, *Acc. Chem. Res.*, **1**, 23 (1968).
48. G. Fraenkel, A. Chow and W. R. Winchester, *J. Am. Chem. Soc.*, **112**, 6190 (1990).
49. G. Fraenkel and K. V. Martin, *J. Am. Chem. Soc.*, **117**, 10336 (1995).
50. G. Fraenkel, J. H. Duncan, K. Martin and J. H. Wang, *J. Am. Chem. Soc.*, **121**, 10538 (1999).
51. G. Fraenkel and F. Y. Qiu, *J. Am. Chem. Soc.*, **122**, 12806 (2000).
52. D. Hoffmann, W. Bauer and P. v. R. Schleyer, *J. Chem. Soc., Chem. Commun.*, 208 (1990).
53. I. Sethson, D. Johnels, T. Lejon, U. Edlund, B. Wind, A. Sygula and P. W. Rabideau, *J. Am. Chem. Soc.*, **114**, 953 (1992).
54. S. Schade and G. Boche, *J. Organomet. Chem.*, **550**, 359 (1998).
55. G. Hilmersson and B. Malmros, *Chem.-Eur. J.*, **7**, 337 (2001).
56. R. M. Gschwind, P. R. Rajamohanan, M. John and G. Boche, *Organometallics*, **19**, 2868 (2000).
57. H. J. Gais, G. Hellmann, H. Günther, F. Lopez, H. J. Lindner and S. Braun, *Angew. Chem., Int. Ed. Engl.*, **28**, 1025 (1989).
58. Y. Cohen and A. Ayalon, *Angew. Chem., Int. Ed. Engl.*, **34**, 816 (1995).
59. R. E. Hoffman, E. Shabtai, M. Rabinovitz, V. S. Iyer, K. Müllen, A. K. Rai, E. Bayrd and L. T. Scott, *J. Chem. Soc.,Perkin Trans. 2*, 1659 (1998).
60. I. Keresztes and P. G. Williard, *J. Am. Chem. Soc.*, **122**, 10228 (2000).

61. A. Maercker, in *Lithium Chemistry* (Eds. A.-M. Sapse and P. v. R. Schleyer), Wiley Interscience, New York, 1995.
62. D. D. Laws, H.-M. L. Bitter and A. Jerschow, *Angew. Chem., Int. Ed.*, **41**, 3096 (2002).
63. K. Schmidt-Rohr and W. Spiess, in *Multidimensional Solid State NMR and Polymers*, Academic Press, London, 1994.
64. M. J. Duer, in *Solid State NMR Spectroscopy, Principles and Applications* (Ed. M. J. Duer), Blackwell Science, Oxford, 2001.
65. J. P. Amoureux and C. Fernandez, *QUASAR—Solid-State NMR Simulation for Quadrupolar Nuclei*, Lille, 1996.
66. C. S. Yannoni, *Acc. Chem. Res.*, **15**, 201 (1982).
67. J. Herzfeld and A. E. Berger, *J. Chem. Phys.*, **73**, 6021 (1980).
68. W. T. Dixon, *J. Chem. Phys.*, **77**, 1800 (1982).
69. W. T. Dixon, J. Schaefer, M. D. Sefcik, E. O. Stejskal and R. A. McKay, *J. Magn. Reson.*, **49**, 341 (1982).
70. J. Hong and G. S. Harbison, *J. Magn. Reson., Ser. A*, **105**, 128 (1993).
71. J. Schaefer, E. O. Stejskal and R. Buchdahl, *Macromolecules*, **8**, 291 (1975).
72. A. Focke, S. Jost and H. Günther, unpublished results.
73. P. A. Scherr, R. J. Hogan and J. P. Oliver, *J. Am. Chem. Soc.*, **96**, 6055 (1974).
74. Y. M. Cahen, P. R. Handy, E. T. Roach and A. I. Popov, *J. Phys. Chem.*, **79**, 80 (1975).
75. J. Gomes and R. B. Mallion, *Chem. Rev.*, **101**, 1349 (2001).
76. R. H. Cox, H. W. Terry, Jr. and L. W. Harrison, *J. Am. Chem. Soc.*, **93**, 3297 (1971).
77. J. A. Dixon, P. A. Gwinner and D. C. Lini, *J. Am. Chem. Soc.*, **87**, 1379 (1965).
78. R. H. Cox and H. W. Terry, Jr., *J. Magn. Reson.*, **14**, 317 (1974).
79. S. P. Bond, A. Gelder, J. Homer, W. R. McWhinnie and M. C. Perry, *J. Mater. Chem.*, **1**, 327 (1991).
80. A. G. Avent, C. Eaborn, P. B. Hitchcock, G. A. Lawless, P. D. Lickiss, M. Mallien, J. D. Smith, A. D. Webb and B. Wrackmeyer, *J. Chem. Soc., Dalton Trans.*, 3259 (1993).
81. R. K. Harris and A. P. Minoja, *Magn. Reson. Chem.*, **33**, 152 (1995).
82. G. H. Penner and J. Hutzal, *Magn. Reson. Chem.*, **35**, 222 (1997).
83. W. Bauer, G. Muller, R. Pi and P. v. R. Schleyer, *Angew. Chem., Int. Ed. Engl.*, **25**, 1103 (1986).
84. W. Bauer, T. Clark and P. v. R. Schleyer, *J. Am. Chem. Soc.*, **109**, 970 (1987).
85. M. Eiermann and K. Hafner, *J. Am. Chem. Soc.*, **114**, 135 (1992).
86. S. Berger and F. Muller, *Chem. Ber.*, **128**, 799 (1995).
87. L. Glendenning, N. Bampos and L. D. Field, *Bull. Chem. Soc. Jpn.*, **69**, 2025 (1996).
88. S. Schade and G. Boche, *J. Organomet. Chem.*, **550**, 381 (1998).
89. G. Hilmersson, P. I. Arvidsson, Ö. Davidsson and M. Håkansson, *J. Am. Chem. Soc.*, **120**, 8143 (1998).
90. W. Bauer and F. Hampel, *J. Chem. Soc., Chem. Commun.*, 903 (1992).
91. T. Gullion and J. Schaefer, *J. Magn. Reson.*, **81**, 196 (1989).
92. A. Schmidt, R. A. McKay and J. Schaefer, *J. Magn. Reson.*, **96**, 644 (1992).
93. M. Hartung, Ph.D. Thesis, University of Siegen, 1999.
94. H. Günther and M. Hartung, unpublished results.
95. J. A. Gurak, J. W. Chinn, Jr., R. J. Lagow, H. Steinfink and C. S. Yannoni, *Inorg. Chem.*, **23**, 3717 (1984).
96. J. A. Gurak, J. W. Chinn, Jr., R. J. Lagow, R. D. Kendrick and C. S. Yannoni, *Inorg. Chim. Acta*, **96**, L75 (1985).
97. M. H. Cohen and F. Reif, *Solid State Physics*, **5**, 321 (1957).
98. A. D. Buckingham, *Quart. Rev.*, **13**, 183 (1959).
99. A. Lal, V. Keshari and P. Chandra, *J. Mol. Struct.*, **192**, 263 (1989).
100. S. Gerber and H. Huber, *J. Phys. Chem.*, **93**, 545 (1989).
101. M. H. Palmer and J. A. Blair-Fish, *Z. Naturforsch., A*, **49**, 137 (1994).
102. G. B. Bacskay and A. D. Buckingham, *Mol. Phys.*, **91**, 391 (1997).
103. B. K. Lee, J. M. Stout and C. E. Dykstra, *J. Mol. Struct. (THEOCHEM)*, **400**, 57 (1997).
104. P. Kusch, *Phys. Rev.*, **76**, 138 (1949).
105. P. Kusch, *Phys. Rev.*, **75**, 887 (1949).
106. P. Kusch and A. K. Mann, *Phys. Rev.*, **76**, 707 (1949).
107. T. L. Brown and J. A. Ladd, *J. Organomet. Chem.*, **2**, 373 (1964).

108. E. A. C. Lucken, *J. Organometal. Chem.*, **4**, 252 (1965).
109. R. A. Bernheim, I. L. Adler, B. J. Lavery, D. C. Lini, B. A. Scott and J. A. Dixon, *J. Chem. Phys.*, **45**, 3442 (1966).
110. S. V. Bhat, K. Muthukrishnan, J. Ramakrishna and R. Srinivasan, *Phys. Status Solidi A*, **11**, K109 (1972).
111. L. M. Jackman and N. M. Szeverenyi, *J. Am. Chem. Soc.*, **99**, 4954 (1977).
112. I. Sethson, B. Eliasson and U. Edlund, *Magn. Reson. Chem.*, **29**, 1012 (1991).
113. K. Differt and R. Messer, *J. Phys. C*, **13**, 717 (1980).
114. A. R. Lim, S. H. Choh and S. Y. Jeong, *J. Phys. Cond. Matter*, **8**, 4597 (1996).
115. E. V. Charnaya, V. S. Kasperovich and M. G. Shelyapina, *Ferroelectrics*, **208**, 225 (1998).
116. J. H. Davis, K. R. Jeffrey, M. Bloom, M. I. Valic and T. P. Higgs, *Chem. Phys. Lett.*, **42**, 390 (1976).
117. P. P. Man, *Mol. Phys.*, **69**, 337 (1990).
118. P. R. Bodart, J.-P. Amoureux, Y. Dumazy and R. Lefort, *Mol. Phys.*, **98**, 1545 (2000).
119. J. F. Hon and P. J. Bray, *Phys. Rev.*, **110**, 624 (1958).
120. J. P. Amoureux, C. Fernandez and P. Granger, *NATO ASI Ser., Ser. C*, **322**, 409 (1990).
121. D. Massiot, F. Fayon, M. Capron, I. King, S. Le Calve, B. Alonso, J. O. Durand, B. Bujoli, Z. H. Gan and G. Hoatson, *Magn. Reson. Chem.*, **40**, 70 (2002).
122. D. Johnels, A. Andersson, A. Boman and U. Edlund, *Magn. Reson. Chem.*, **34**, 908 (1996).
123. 'Win-Fit #961107', Bruker-Franzen Analytik GmbH, Bremen, 1996.
124. M. Hartung, H. Günther, J.-P. Amoureux and C. Fernandéz, *Magn. Reson. Chem.*, **36**, S61 (1998).
125. G. H. Penner, *Chem. Phys. Lett.*, **261**, 665 (1996).
126. L. H. Merwin, A. Sebald, J. E. Espidel and R. K. Harris, *J. Magn. Reson.*, **84**, 367 (1989).
127. J. E. Espidel, R. K. Harris and K. Wade, *Magn. Reson. Chem.*, **32**, 166 (1994).
128. D. Johnels and U. Edlund, *J. Am. Chem. Soc.*, **112**, 1647 (1990).
129. J. J. Brooks, W. Rhine and G. D. Stucky, *J. Am. Chem. Soc.*, **94**, 7339 (1972).
130. U. Edlund, *Org. Magn. Reson.*, **12**, 661 (1979).
131. D. H. O'Brien, C. R. Russell and A. J. Hart, *J. Am. Chem. Soc.*, **101**, 633 (1979).
132. W. Baumann, Y. Oprunenko and H. Günther, *Z. Naturforsch., A*, **50**, 429 (1995).
133. R. J. Bushby and A. S. Patterson, *J. Organomet. Chem.*, **132**, 163 (1977).
134. R. J. Bushby, H. L. Steel and M. P. Tytko, *J. Chem. Soc., Perkin Trans. 2*, 1155 (1990).
135. R. J. Bushby and M. P. Tytko, *J. Organomet. Chem.*, **270**, 265 (1984).
136. H. Jiao, P. v. R. Schleyer, Y. Mo, M. A. McAllister and T. T. Tidwell, *J. Am. Chem. Soc.*, **119**, 7075 (1997).
137. H. Ahlbrecht, J. Harbach, H. O. Kalinowski, A. Lang and G. Maier, *Chem. Ber.-Recl.*, **130**, 683 (1997).
138. G. Boche, M. Marsch, J. Harbach, K. Harms, B. Ledig, F. Schubert, J. C. W. Lohrenz and H. Ahlbrecht, *Chem. Ber.-Recl.*, **126**, 1887 (1993).
139. M. Kühnen, H. Günther, J. P. Amoureux and C. Fernandéz, *Magn. Reson. Chem.*, **40**, 24 (2002).
140. G. E. Hartwell and A. Allerhand, *J. Am. Chem. Soc.*, **93**, 4415 (1971).
141. A. J. Jones, D. M. Grant, J. G. Russell and G. Fraenkel, *J. Phys. Chem.*, **73**, 1624 (1969).
142. G. Fraenkel, S. Subramanian and A. Chow, *J. Am. Chem. Soc.*, **117**, 6300 (1995).
143. F. W. Wehrli, *Org. Magn. Reson.*, **11**, 106 (1978).
144. L. M. Jackman and L. M. Scarmoutzos, *J. Am. Chem. Soc.*, **106**, 4627 (1984).
145. W. Bauer, W. R. Winchester and P. v. R. Schleyer, *Organometallics*, **6**, 2371 (1987).
146. E. Wehman, J. T. B. H. Jastrzebski, J. M. Ernsting, D. M. Grove and G. v. Koten, *J. Organomet. Chem.*, **353**, 133 (1988).
147. H. J. Reich, D. P. Green and N. H. Phillips, *J. Am. Chem. Soc.*, **113**, 1414 (1991).
148. H. J. Reich, W. S. Goldenberg, A. W. Sanders and C. C. Tschucke, *Org. Lett.*, **3**, 33 (2001).
149. O. Eppers and H. Günther, *Helv. Chim. Acta*, **75**, 2553 (1992).
150. D. Johnels and U. Edlund, *J. Organomet. Chem.*, **393**, C35 (1990).
151. S. Berger, U. Fleischer, C. Geletneky and J. C. W. Lohrenz, *Chem. Ber.*, **128**, 1183 (1995).
152. J. B. Grutzner, in *Recent Advances in Organic NMR Spectroscopy* (Eds. R. Rittner and J. B. Lambert), Norell Press, Landsville, 1987.

153. M. Buehl, N. J. R. v. Eikema Hommes, P. v. R. Schleyer, U. Fleischer and W. Kutzelnigg, *J. Am. Chem. Soc.*, **113**, 2459 (1991).
154. M. Walczak and G. D. Stucky, *J. Organomet. Chem.*, **97**, 313 (1975).
155. I. Sethson, D. Johnels, U. Edlund and A. Sygula, *J. Chem. Soc., Perkin Trans. 2*, 1339 (1990).
156. A. Boman and D. Johnels, *Magn. Reson. Chem.*, **38**, 853 (2000).
157. S. Jost and H. Günther, unpublished results.
158. D. Johnels, A. Boman and U. Edlund, *Magn. Reson. Chem.*, **36**, S151 (1998).
159. B. Walfort, L. Lameyer, W. Weiss, R. Herbst-Irmer, R. Bertermann, J. Rocha and D. Stalke, *Chem.-Eur. J.*, **7**, 1417 (2001).
160. A. Medek, J. S. Harwood and L. Frydman, *J. Am. Chem. Soc.*, **117**, 12779 (1995).
161. S. Harder, *Coord. Chem. Rev.*, **176**, 17 (1998).
162. P. Jutzi and N. Burford, *Chem. Rev.*, **99**, 969 (1999).
163. B. Becker, V. Enkelmann and K. Müllen, *Angew. Chem., Int. Ed. Engl.*, **28**, 458 (1989).
164. W. E. Rhine and G. D. Stucky, *J. Am. Chem. Soc.*, **97**, 737 (1975).
165. L. M. Jackman and C. W. DeBrosse, *J. Am. Chem. Soc.*, **105**, 4177 (1983).
166. J. Q. Wen and J. B. Grutzner, *J. Org. Chem.*, **51**, 4220 (1986).
167. L. M. Jackman, L. M. Scarmoutzos and C. W. DeBrosse, *J. Am. Chem. Soc.*, **109**, 5355 (1987).
168. H. Hope and P. P. Power, *J. Am. Chem. Soc.*, **105**, 5320 (1983).
169. D. Thoennes and E. Weiss, *Chem. Ber.*, **111**, 3157 (1978).
170. U. Schümann, J. Kopf and E. Weiss, *Angew. Chem.*, **97**, 222 (1985).
171. J. T. B. H. Jastrzebski, G. v. Koten, M. Konijn and C. H. Stam, *J. Am. Chem. Soc.*, **104**, 5490 (1982).
172. R. A. Bartlett, H. V. R. Dias and P. P. Power, *J. Organomet. Chem.*, **341**, 1 (1988).
173. S. Harder, J. Boersma, L. Brandsma, J. A. Kanters, W. Bauer and P. v. R. Schleyer, *Organometallics*, **8**, 1696 (1989).
174. S. Harder, J. Boersma, L. Brandsma, G. P. M. Vanmier and J. A. Kanters, *J. Organomet. Chem.*, **364**, 1 (1989).
175. K. Ruhlandtsenge, J. J. Ellison, R. J. Wehmschulte, F. Pauer and P. P. Power, *J. Am. Chem. Soc.*, **115**, 11353 (1993).
176. M. Tacke, *Eur. J. Inorg. Chem.*, 537 (1998).
177. B. Schiemenz and P. P. Power, *Angew. Chem., Int. Ed. Engl.*, **35**, 2150 (1996).
178. L. M. Jackman, D. Cizmeciyan, P. G. Williard and M. A. Nichols, *J. Am. Chem. Soc.*, **115**, 6262 (1993).
179. L. M. Jackman and D. Cizmeciyan, *Magn. Reson. Chem.*, **34**, 14 (1996).
180. M. M. Exner, R. Waack and E. C. Steiner, *J. Am. Chem. Soc.*, **95**, 7009 (1973).
181. P. Jutzi, E. Schlueter, C. Krueger and S. Pohl, *Angew. Chem.*, **95**, 1015 (1983).
182. P. Jutzi, W. Leffers, S. Pohl and W. Saak, *Chem. Ber.*, **122**, 1449 (1989).
183. S. Harder and M. H. Prosenc, *Angew. Chem., Int. Ed. Engl.*, **33**, 1744 (1994).
184. R. E. Dinnebier, U. Behrens and F. Olbrich, *Organometallics*, **16**, 3855 (1997).
185. M. Håkansson, C.-H. Ottosson, A. Boman and D. Johnels, *Organometallics*, **17**, 1208 (1998).
186. K. B. Lipkowitz, C. Uhegbu, A. M. Naylor and R. Vance, *J. Comput. Chem.*, **6**, 662 (1985).
187. M. Könemann, G. Erker, R. Fröhlich and E. U. Würthwein, *J. Am. Chem. Soc.*, **119**, 11155 (1997).
188. C. Üffing, R. Köppe and H. Schnöckel, *Organometallics*, **17**, 3512 (1998).
189. A. Samoson and E. Lippmaa, *J. Magn. Reson.*, **79**, 255 (1988).
190. F. Pauer, J. Rocha and D. Stalke, *J. Chem. Soc., Chem. Commun.*, 1477 (1991).
191. T. E. Hogen-Esch and J. Smid, *J. Am. Chem. Soc.*, **88**, 307 (1966).
192. T. E. Hogen-Esch and J. Smid, *J. Am. Chem. Soc.*, **88**, 318 (1966).
193. R. H. Cox, *J. Phys. Chem.*, **73**, 2649 (1969).
194. M. Szwarc and J. Jagur-Grodzinski, in *Ions and Ion Pairs in Organic Reactions*, Vol. 2 (Ed. M. Szwarc), Wiley Interscience, New York, 1974.
195. P. J. Grandinetti, J. H. Baltisberger, I. Farnan, J. F. Stebbins, U. Werner and A. Pines, *J. Phys. Chem.*, **99**, 12341 (1995).
196. A. Pepels, H. Günther, J. P. Amoureux and C. Fernandéz, *J. Am. Chem. Soc.*, **122**, 9858 (2000).
197. N. D. R. Barnett, R. E. Mulvey, W. Clegg and P. A. O' Neil, *J. Am. Chem. Soc.*, **113**, 8187 (1991).

198. M. F. Lappert, M. J. Slade, A. Singh, J. L. Atwood, R. D. Rogers and R. Shakir, *J. Am. Chem. Soc.*, **105**, 302 (1983).
199. D. Mootz, A. Zinnius and B. Böttcher, *Angew. Chem., Int. Ed. Engl.*, **8**, 378 (1969).
200. R. D. Rogers, J. L. Atwood and R. Grüning, *J. Organomet. Chem.*, **157**, 229 (1978).
201. P. G. Williard and J. M. Salvino, *J. Org. Chem.*, **58**, 1 (1993).
202. M. A. Beno, H. Hope, M. M. Olmstead and P. P. Power, *Organometallics*, **4**, 2117 (1985).
203. W. Hiller, M. Layh and W. Uhl, *Angew. Chem., Int. Ed. Engl.*, **30**, 324 (1991).
204. K. Ruhlandt-Senge, J. J. Ellison, R. J. Wehmschulte, F. Pauer and P. P. Power, *J. Am. Chem. Soc.*, **115**, 11353 (1993).
205. C. Eaborn, P. B. Hitchcock, J. D. Smith and A. C. Sullivan, *J. Chem. Soc., Chem. Commun.*, 827 (1983).
206. C. Lambert, M. Kaupp and P. v. R. Schleyer, *Organometallics*, **12**, 853 (1993).
207. A. Pepels and H. Günther, unpublished results.
208. A. Pepels, Ph.D. Thesis, University of Siegen, 2001
209. R. E. Dinnebier, U. Behrens and F. Olbrich, *J. Am. Chem. Soc.*, **120**, 1430 (1998).
210. 'PC SPARTAN Pro', Wavefunction Inc., Irvine, 2000.
211. I. Farnan, P. J. Grandinetti, J. H. Baltisberger, J. F. Stebbins, U. Werner, M. A. Eastman and A. Pines, *Nature*, **358**, 31 (1992).
212. J. A. Tossell and P. Lazzeretti, *Phys. Chem. Miner.*, **15**, 564 (1988).
213. Y. Marcus, *Ion Solvation*, Wiley, Chichester, 1985.
214. G. Boche, *Angew. Chem., Int. Ed. Engl.*, **31**, 731 (1992).
215. S. Jost, Ph.D. Thesis, University of Siegen, 2002.
216. H. Hope, M. M. Olmstead, P. P. Power, J. Sandell and X. Xu, *J. Am. Chem. Soc.*, **107**, 4337 (1985).
217. B. Böhler, D. Hüls and H. Günther, *Tetrahedron Lett.*, **37**, 8719 (1996).
218. A. Fürstner, G. Seidel, H. E. Mons and R. Mynott, *Eur. J. Inorg. Chem.*, 1771 (1998).
219. R. He and H. Günther, unpublished results.
220. P.-O. Quist, H. Förster and D. Johnels, *J. Am. Chem. Soc.*, **119**, 5390 (1997).
221. A. Boman, U. Edlund, H. Förster and D. Johnels, *Acta Chem. Scand.*, **53**, 699 (1999).
222. K. T. Mueller, T. P. Jarvie, D. J. Aurentz and B. W. Roberts, *Chem. Phys. Lett.*, **242**, 535 (1995).
223. K. T. Mueller, T. P. Jarvie, D. J. Aurentz and B. W. Roberts, *Chem. Phys. Lett.*, **254**, 281 (1996).
224. Y. Ishii, T. Terao and S. Hayashi, *J. Chem. Phys.*, **107**, 2760 (1997).
225. C. A. Fyfe and A. R. Lewis, *J. Phys. Chem. B*, **104**, 48 (2000).
226. C. P. Jaroniec, C. Filip and R. G. Griffin, *J. Am. Chem. Soc.*, **124**, 10728 (2002).
227. F. A. Bovey, E. W. Anderson, F. P. Hood and R. L. Kornegay, *J. Chem. Phys.*, **40**, 3099 (1964).
228. R. E. Wasylishen, *Can. J. Chem.*, **64**, 2094 (1986).
229. J. F. Haw, R. A. Crook and R. C. Crosby, *J. Magn. Reson.*, **66**, 551 (1986).
230. F. G. Riddell, R. A. Spark and G. V. Günther, *Magn. Reson. Chem.*, **34**, 824 (1996).
231. J. H. Kristensen, H. Bildsoe, H. J. Jakobsen and N. C. Nielsen, *J. Magn. Reson.*, **100**, 437 (1992).
232. T. Pietrass and P. K. Burkert, *Z. Naturforsch., B*, **48**, 1555 (1993).
233. T. Pietrass, P. K. Burkert and H. H. Karsch, *Z. Naturforsch., A*, **47**, 117 (1992).
234. T. Pietrass and P. K. Burkert, *Magn. Reson. Chem.*, **31**, 709 (1993).
235. M. Veith, M. Zimmer, K. Fries, J. BohnleinMaus and V. Huch, *Angew. Chem., Int. Ed. Engl.*, **35**, 1529 (1996).
236. G. H. Penner and Y. C. P. Chang, *J. Chem. Soc., Chem. Commun.*, 1803 (2000).
237. W. P. Rothwell and J. S. Waugh, *J. Chem. Phys.*, **74**, 2721 (1981).
238. J. M. Twyman and C. M. Dobson, *Magn. Reson. Chem.*, **28**, 163 (1990).
239. M. Kühnen and H. Günther, unpublished results.
240. W. Zarges, M. Marsch, K. Harms, W. Koch, G. Frenking and G. Boche, *Chem. Ber.*, **124**, 543 (1991).
241. A. Abragam, *Principles of Nuclear Magnetism*, Oxford University Press, London, 1961, p. 165.
242. C. H. Townes and B. P. Dailey, *J. Chem. Phys.*, **17**, 782 (1949).

243. M. W. Schmidt, K. K. Baldridge, J. A. Boatz, S. T. Elbert, M. S. Gordon, J. H. Jensen, S. Koseki, N. Matsunaga, K. A. Nguyen, S. J. Su, T. L. Windus, M. Dupuis and J. A. Montgomery, *J. Comput. Chem.*, **14**, 1347 (1993).

244. P. Blaha, K. Schwarz and P. Sorantin, *Comput. Phys. Commun.*, **59**, 399 (1990).

245. M. J. Frisch, G. W. Trucks, H. B. Schlegel, G. E. Scuseria, M. A. Robb, J. R. Cheeseman, V. G. Zakrzewski, J. A. Montgomery, R. E. Stratmann, J. C. Burant, S. Dapprich, J. M. Millam, A. D. Daniels, K. N. Kudin, M. C. Strain, O. Farkas, J. Tomasi, V. Barone, M. Cossi, R. Cammi, B. Mennucci, C. Pomelli, C. Adamo, S. Clifford, J. Ochterski, G. A. Petersson, P. Y. Ayala, Q. Cui, K. Morokuma, D. K. Malick, A. D. Rabuck, K. Raghavachari, B. Foresman, J. Cioslowski, J. V. Ortiz, A. G. Baboul, B. B. Stefanov, G. Liu, A. Liashenko, P. Piskorz, I. Komaromi, R. Gomperts, R. L. Martin, D. J. Fox, T. Keith, M. A. Al-Laham, C. Y. Peng, A. Nanayakkara, C. Gonzales, M. Challacombe, P. M. W. Gill, B. Johnson, W. Chen, M. W. Wong, J. L. Andres, C. Gonzales, M. Head-Gordon, E. S. Replogle and J. A. Pople, ‘Gaussian98’, Gaussian Inc., Pittsburgh, 1998.

246. A. Pepels, M. Kühnen, H. Günther, J. E. Niu-Schwarz, H. J. Fan and W. H. E. Schwarz, unpublished results.

CHAPTER **5**

Gas phase chemistry of organolithium compounds

CHAGIT DENEKAMP

Department of Chemistry, Technion–Israel Institute of Technology, Technion City,
32000 Haifa, Israel
Fax: +972-4-8293751; e-mail: chchagit@tx.technion.ac.il

I. INTRODUCTION

The study of the interactions between organic compounds and alkali–metal cations, in the gas phase, is related to many topics such as ion solvation, catalysis and molecular recognition. Furthermore, mass spectrometry has been used for the analyses of organolithium compounds and supramolecular assemblies that contain lithium cations. Alkali cationization is an important ionization technique, implemented for the analyses of a wide range of organic compounds. Finally, gas-phase studies are also useful for the quantitative determination of lithium cation affinity. The interaction between lithium cation and organic substances is thus related to different aspects of gas-phase chemistry and mass spectrometry.

The Chemistry of Organolithium Compounds. Edited by Z. Rappoport and I. Marek
ISBN: 0-470-84339-X

II. DETERMINATION OF ORGANOLITHIUM COMPLEXES

A. Alkyllithium

Alkyllithium compounds form clusters containing multicentered bonds not only in the solid state and in solution but also in the gas phase. The C−Li bond is largely ionic in nature, dominated by electrostatic interactions[1]. This leads to structures where the lithium bridges anionic centers. A typical number of lithium atoms in an alkyllithium cluster is 2, 4 or 6, however in certain cases larger or odd membered aggregates have also been observed. Gas-phase experiments on alkyllithium compounds were performed by Berkowitz and coworkers in 1961[2]. They have investigated the vapor of ethyllithium using electron-impact mass spectrometry (EIMS) with the aid of a double-chambered, separately heated Knudsen cell. Mass peaks corresponding to $Li_nR_{n-1}^+ (R = \text{ethyl}; n = 1–6)$ were observed, RLi_2^+ and $R_3Li_4^+$ being the most abundant ions in the spectrum. The high abundance of RLi_2^+ was attributed to the fragmentation of the tetramer $R_3Li_4^+$. Peaks corresponding to $Li_6R_5^+$ and $Li_4R_3^+$ had appearance potentials that were 3–4 eV lower than any of the other $Li_nR_{n-1}^+$ peaks and were thus assumed to be parent ions. The results show that ions of the hexamer and the tetramer that are predominant species in ethyllithium vapor decompose into smaller $Li_{n-x}R_{n-x-1}^+$ ions, where x is an even integer. Methyllithium, the simplest metal–alkyl compound, has also been the subject of theoretical and experimental investigations concerning the nature of its structure and bonding. The electron-impact mass spectrum of methyllithium has been obtained by using flash-vaporization mass spectroscopy[3]. Positive ions corresponding to the lithiated species $(CH_3)_3Li_4^+$, $(CH_3)_2Li_3^+$ and $CH_3Li_2^+$ were observed. The authors conclude that the largest clusters in methyllithium vapor are tetramers[3].

The gas-phase structure of t-BuLi has also been probed by McLean and coworkers using photoionization mass spectrometry[4]. At room temperature, they detected only tetramers and determined the ionization potential of $(t\text{-BuLi})_4$ to be 6.2 eV. Other ions were detected above 8 eV with general formulae $R_nLi_4^+ (n = 1–3)$ and $RLi_2^+ (R = t\text{-Bu})$. Both $R_3Li_4^+$ and RLi_2^+ had also been observed by Brown and coworkers in the EI spectra of t-BuLi vapor, while $R_2Li_4^+$ and RLi_4^+ had not[5].

$$Li_4(t\text{-Bu})_4 + h\nu \longrightarrow Li_4(t\text{-Bu})_4{}^* \longrightarrow Li_4(t\text{-Bu})_3^+ + C_4H_9 + e^-$$

Plavšić, Srzić and Klasinc performed a detailed electron impact mass spectrometric investigation of alkyllithium compounds[6]. They have concluded that MeLi, i-PrLi, s-BuLi and t-BuLi consist of tetrameric clusters only, while n-PrLi, n-BuLi and i-BuLi form mixtures of tetramers and hexamers, in the gas phase. Fast atom bombardment (FAB) mass spectrometry was used by Abdul-Sada, Greenway and Seddon to show that the extent of aggregation of t-BuLi is tetrameric while n-BuLi is hexameric (Table 1)[7]. Nevertheless, for both alkyllithium compounds the ion corresponding to $(RLi)Li^+$ is the most abundant in the spectrum, as also shown in other studies of alkyllithium vapor.

More recently, Szepes and coworkers investigated the electronic structure of some alkyllithium clusters by photoelectron spectroscopy[8]. In their study two distinct types of spectra have been observed. This is explained by the different degree of association of the compounds in the gas phase, as determined by the steric demands of the alkyl substituents. Thus, i-PrLi, s-BuLi and t-BuLi form tetramers while EtLi, n-PrLi, n-BuLi and i-BuLi are mixtures of tetrameric and hexameric clusters, in the gas phase[8]. Lagow and coworkers showed that the vapor species observed for polylithium compounds include $(CH_2Li_2)_n^+ (n = 1–6)$, $(CLi_4)_n^+ (n = 1–5)$ and $(C_3Li_4)_n^+ (n = 1–3)$. They also showed that polylithium compounds undergo rearrangements at high temperature and the following thermal stability series has been established from this work: $CLi_4 < C_2Li_4 < C_3Li_4 < C_2Li_2$[9–11].

TABLE 1. Assignment of the FAB mass spectra of *n*-BuLi and *t*-BuLi in Nujol[7] (RA = relative abundance)

m/*z*	Ion	RA (%), R = *n*-Bu	RA (%), R = *t*-Bu
391	$[(RLi)_6Li]^+$	8	—
327	$[(RLi)_5Li]^+$	8	—
263	$[(RLi)_4Li]^+$	7	1
199	$[(RLi)_3Li]^+$	35	75
135	$[(RLi)_2Li]^+$	14	8
71	$[(RLi)\ Li]^+$	100	100

B. Organic Functionalized Lithium Salts

Mass spectra were also recorded for lithium *t*-butoxide and lithiomethyltrimethylsilane[12]. It was demonstrated that lithium *t*-butoxide is a hexamer in the vapor phase, while lithiomethyltrimethylsilane has a nearly 100% tetrameric composition at 100 °C. Further on, the association of $LiB(CH_3)_4$ in the gas phase was examined by Stucky and coworkers, using EIMS[13,14]. They found that at an ionization potential of 18 eV and a temperature of 150 °C, the two most intense peaks in the mass spectrum correspond to $LiB(CH_3)_3{}^+$ and $B(CH_3)_2{}^+$. At 25 eV additional peaks, corresponding to $LiB(CH_3)_4{}^+$ and $B(CH_3)_3{}^+$, can be identified and at 70 eV and 90 °C the highest mass value detected corresponds to the tetrameric species $Li_4B_4(CH_3)_{15}{}^+$, indicating that $LiB(CH_3)_4$ is also associated in the gas phase[13,14].

Thus, it might be said that in the gas phase, alkyllithium polyhedra of high stability are the hexamer and the tetramer and that the dimer, considerably higher in energy, is the next most stable species.

The development of electrospray ionization (ESI) enabled multiply charged ions, solvated ions, and metal-coordinated species to be formed in the gas phase. Recently, Kass and coworkers showed that collision-induced dissociation (CID) of RCO_2Li containing ions (e.g. **1**) leads to the loss of carbon dioxide and the attachment of Li to R (Scheme 1)[15]. This is an exceptionally stable alkyl lithium compound that could be synthesized, in the gas phase, under relatively mild conditions.

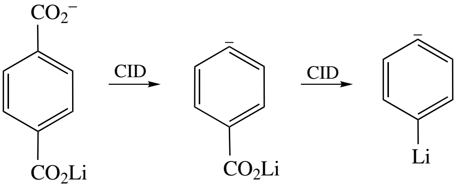

(1)

SCHEME 1

High-level *ab initio* calculations indicate that thermodynamic deprotonation of phenyllithium will produce a bridged *ortho* dianion that is remarkably stable. The deprotonation energy of phenyllithium is predicted to be only 389.5 kcal mol^{-1}, or about 10 kcal mol^{-1} less than that for benzene. The relative energies of the isomers of these salts are based on interplay of competing effects, namely coulombic repulsion of the dianions and electrostatic stabilization of the ion triplet[15]. Ions corresponding to $C_6H_4Li_2{}^+$ have been observed by electrospray mass spectrometry, thereby confirming their stability (Figure 1).

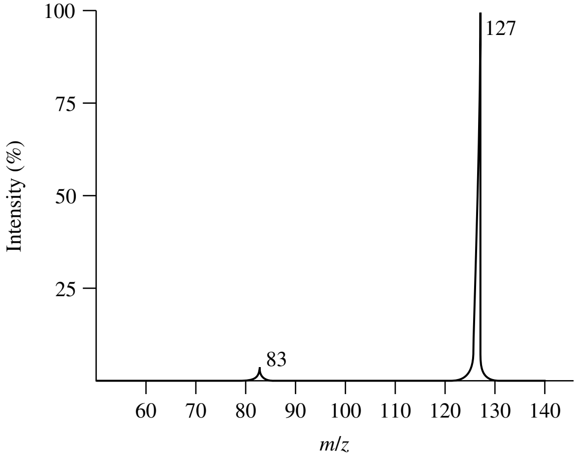

FIGURE 1. CID spectrum of $LiC_6H_4CO_2^-$ (*m/z* 127). The fragment ion at *m/z* 83 corresponds to $C_6H_5Li^-$. Reproduced with permission from Ref. 15

III. LITHIUM CATION AFFINITY

Gas phase experiments utilizing various mass spectral techniques were used in order to determine the lithium cation affinity (LCA) of substances and it has been shown that molecular binding energies of Li^+ are substantial even for hydrocarbons. For example, the LCA of cyclohexane is 24 kcal mol^{-1} and 37 kcal mol^{-1} for benzene[16]. LCA of alkenes, like proton affinity (PA), increases with methyl substituent at a double bond (isobutene > propene) and the trend of LCA values in *n*-bases is the same as for PA as well, that is $Me_2O > MeOH > H_2O$ and $Me_3N > NH_3$. The nature of the proton–base bond is very different than the lithium–base bond[17, 18]. The proton adds to the base forming a polar sigma bond with a partial positive charge of 0.35 electronic units or less at the hydrogen atom itself. In contrast, the bonds formed with Li^+ are ionic and the lithium bares a major part of the positive charge, i.e. 0.8 electronic units or more[17,18].

In addition to the different nature in binding between proton and lithium cations that result in the significantly lower LCA values when compared with the corresponding PA values[19], lithium shows a chelation effect in its binding, as will be discussed shortly. Li ion solvation has been quantitatively defined by gas-phase studies. Some of these studies offer a relative LCA scale using various experimental techniques. Frequently cited is the work of Dzidic and Kebarle[20], who measured the binding energies of Li^+ to multiple H_2O ligands. Until recently, the reference point used to provide absolute LCA values was the LCA of water that was measured in this study [$\text{LCA}(H_2O) = 34.0\ \text{kcal mol}^{-1}$)][20]. The $Li^+{-}OH_2$ bond energy was extrapolated from measurements made for larger $Li^+{-}(H_2O)_n$ clusters. Lithium water clusters have also been studied experimentally and theoretically by others[21–24], and recently Rodgers and Armentrout reported the first direct measurement of the $Li^+{-}OH_2$ bond energy as well as the dissociation energy for $Li^+{-}(H_2O)_n$ clusters ($n = 1{-}6$)[25], using kinetic energy-dependent CID experiments in a guided ion-beam mass spectrometer. Table 2 summarized the bond enthalpies that were measured in this work and those measured by Dzidic and Kebarle[20]. The $Li^+{-}OH_2$ dissociation energy reported by Rodgers and Armentrout is 1.2 kcal mol^{-1} lower (32.8 kcal mol^{-1}) than the value

TABLE 2. Bond dissociation enthalpies of $Li(H_2O)_n$, $n = 1-6$, at 298 K

Species	$\Delta H_{298}{}^a$ (kcal mol^{-1})	$\Delta H_{298}{}^b$ (kcal mol^{-1})
$Li(H_2O)^+$	32.8	34.0
$Li(H_2O)_2{}^+$	27.3	25.8
$Li(H_2O)_3{}^+$	22.5	20.7
$Li(H_2O)_4{}^+$	17.0	16.4
$Li(H_2O)_5{}^+$	14.4	13.9
$Li(H_2O)_6{}^+$	15.1	12.1

[a] Reference 25.
[b] Reference 20.

reported by Kebarle and Dzidic. This implies that the absolute values of all lithium ion affinity scales that are anchored to the LCA of water should be slightly revised.

Armentrout and Rogers also suggest more suitable anchor points for the LCA scale, e.g. the lithium cation bond energies to methanol or dimethyl ether. They further examined the kinetic energy dependences of the CID of $Li^+{-}ROH$ with Xe[26] and reported that the dominant dissociation process in all cases is the loss of alcohol. The thresholds for $Li^+{-}ROH$ dissociations were determined and converted to enthalpies and free energies at 298 and 373 K for comparison with previous equilibrium data on these systems. LCA values at 298 K for a series of alcohols are summarized in Table 3. The experimental results are compared with enthalpies of H^+ binding (PA) at 298 K (Figure 2) and a linear correlation between the LCA and the PA is found.

Since many of the LCA values are measured by comparison methods, a reliable reference point to which all data are anchored is important. For example, Woodin and Beauchamp measured LCAs for several compounds[27]. They report that the LCA of MeOH is 38.1 kcal mol^{-1}, 1.0 kcal mol^{-1} higher than the LCA of methanol reported by Rodgers and Armentrout[26]. Both investigators used the dissociation of $Li^+{-}OH_2$ as a reference point and the 1.2 kcal mol^{-1} correction that was lately introduced for this value can account for the discrepancy.

Cole and coworkers[28] studied mixtures of LiCl and equimolar quantities of MeOH, EtOH and *n*-PrOH with electrospray ionization (ESI) and showed that the tendency for lithium binding to an alcohol follows the order *n*-PrOH > EtOH > MeOH. They point out that different effects can provide an explanation for this trend, such as polarizability, inductive effect and size effect. However, literature reports of Taft and coworkers indicate that the polarizability effect is likely to predominate in the gas phase[29]. ESI mass spectra obtained from solutions of LiCl in dimethylformamide (DMF), dimethylacetamide (DMAc) and dimethylpropionamide (DMP) show that DMP has the greatest tendency to form lithium cationized adducts followed by DMAc, which is situated well above DMF (Figure 3). These experimental trends have been correlated to calculated differences in electrostatic charges and binding energies of the homologous amides. Calculations indicate an increased inductive effect on part of the longer alkyl groups attached to the carbonyl

TABLE 3. LCA values, in kcal mol^{-1} [26]

MeOH	EtOH	*n*-PrOH	*i*-PrOH
37.5	39.6	41.3	41.8
n-BuOH	*i*-BuOH	*s*-BuOH	*t*-BuOH
41.0	40.9	42.2	43.1

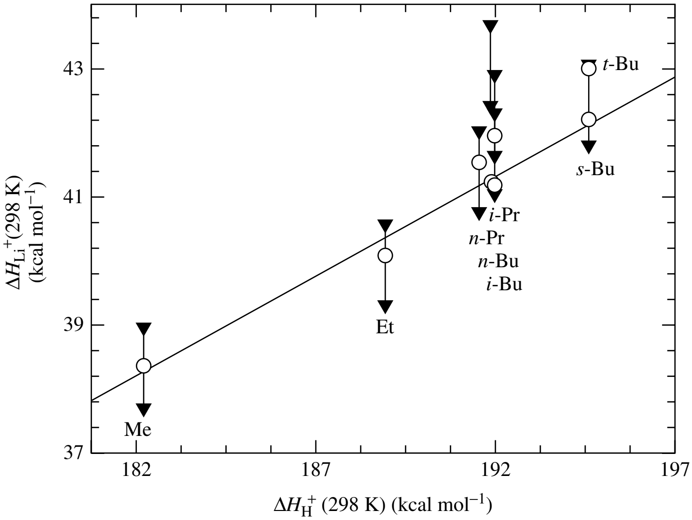

FIGURE 2. LCA vs PA at 298 K (in kcal mol^{-1})[26]. Open circles show CID results from Reference 26 and inverted triangles show a range of values measured with an FT-ICR and cited in Reference 26

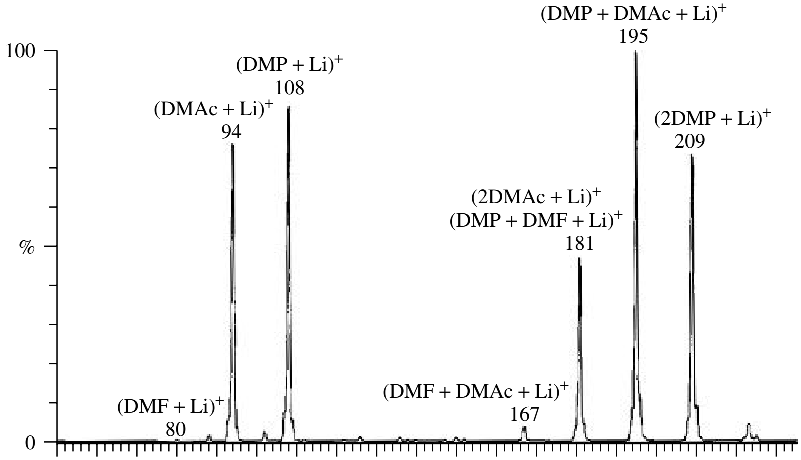

FIGURE 3. ESI mass spectra of 0.4 M LiCl in an equimolar mixture of DMF, DMAc and DMP. Reproduced with permission from Ref. 28

carbon in comparison with DMF that may result in higher LCA. In addition, the larger lithiated amides also have increased abilities to dissipate internal energy and are therefore more stable[28].

Gal and coworkers measured relative LCAs for amides of the structure RC(O)NRR′ (R, R′ = H, Me)[30] using the kinetic method[31]. From this work, the effect of methyl substituent at the amide nitrogen and the alpha carbon can be derived (Table 4).

TABLE 4. LCB values, in kcal mol^{-1} [30]

$HCONH_2$	$HCONHCH_3$	$HCON(CH_3)_2$
37.5	39.6	41.5
CH_3CONH_2	$CH_3CONHCH_3$	$CH_3CON(CH_3)_2$
39.9	41.4	43.0

The same group studied the lithium cation basicities of a series of compounds of the general formula $R^1R^2R^3PO$, i.e. phosphine oxides, phosphinates, phosphonates and phosphates, by using Fourier Transform Ion Cyclotron Resonance (FTICR) mass spectrometry. A summary of their results is shown in Figure 4[32]. The effect of methyl substitution on LCA as well as the correlation between LCA and PA was also investigated by Taft, Yáñez and coworkers on a series of methyldiazoles with an FTICR mass spectrometer[33]. They showed that methyl substituent effects on Li binding energies are practically additive.

The most comprehensive study of lithium cation basicities for organic bases was conducted by Taft, Gal and coworkers[18, 34], who investigated the effect of molecular structure on the gas-phase cation and proton basicities. Taft's LCA scale[18] was revised and extended[34], and the lithium cation basicity scale now includes over 200 compounds. In the same work the correlations between gas-phase basicities toward lithium cation (LCB) and proton (GB) were examined. Good correlations are obtained provided that separate lines are drawn for homogeneous families and the differences in slopes are traced back to the different sensitivities to structural effects. Large deviations are explained by either a different attachment center for Li^+ and H^+ or a chelation effect toward Li^+. Figure 5 describes three types of interactions that involve chelation of a lithium cation.

Earlier comparisons[18] of experimental basicities toward H^+ and Li^+ have led to the conclusion that there is no precise general correlation between LCBs and GBs, especially when diverse families of compounds with different functional groups are included (Figure 6).

However, closer examination of data reveals that the correlations for the families with the same basicity center are much better and even more so for subfamilies where the basicity center is the same functional group (i.e. nitrogen in cyano group, oxygen in carbonyl group etc.). All oxygen bases that were investigated exhibit fair correlation between GB and LCB[34]. For alkyl-substituted alcohols a significant deviation from a linear relationship between LCB and GB values is evident for methoxy-, fluorine-, chlorine- and phenyl-substituted compounds such as $CH_3OCH_2CH_2OH$ (LCB deviates from the correlation line by 11.7 kcal mol^{-1}), CF_3CH_2OH (deviation of 2.4 kcal mol^{-1}), CCl_3CH_2OH (deviation of 2.1 kcal mol^{-1}) and $PhCH_2OH$ (deviation of 3.4 kcal mol^{-1}), which form bidentate ring structures with the Li^+ cation, but not with a proton (Figure 5). Reasonably satisfactory correlation is observed for all carbonyl compounds (including aldehydes, ketones, esters, amides, carboxylic acids etc.). Here one point, corresponding to $(CF_3CO)_2NH$, deviated strongly from the regression line (by 6.2 kcal mol^{-1}) as this compound is assumed to exist in the gas phase in the enol form (compound **5** in Figure 7).

Significant deviations toward decreased stabilities of Li^+ complexes from a linear relationship between LCB and GB values also appear for several fluorine-substituted compounds while reasonably good correlation is observed for the S=O (sulfoxides and sulfones) and P=O bases. Within the class of oxygen bases the ethers give the worst correlation between basicities. This is because the lithium adducts are much more prone to bidentate chelate ethers as is evident by the enhanced stabilities of Li^+ complexes of methoxy- and fluorine-substituted ethers. Their LCBs are therefore significantly higher than predicted from the linear relationship between LCB and GB values for unsubstituted

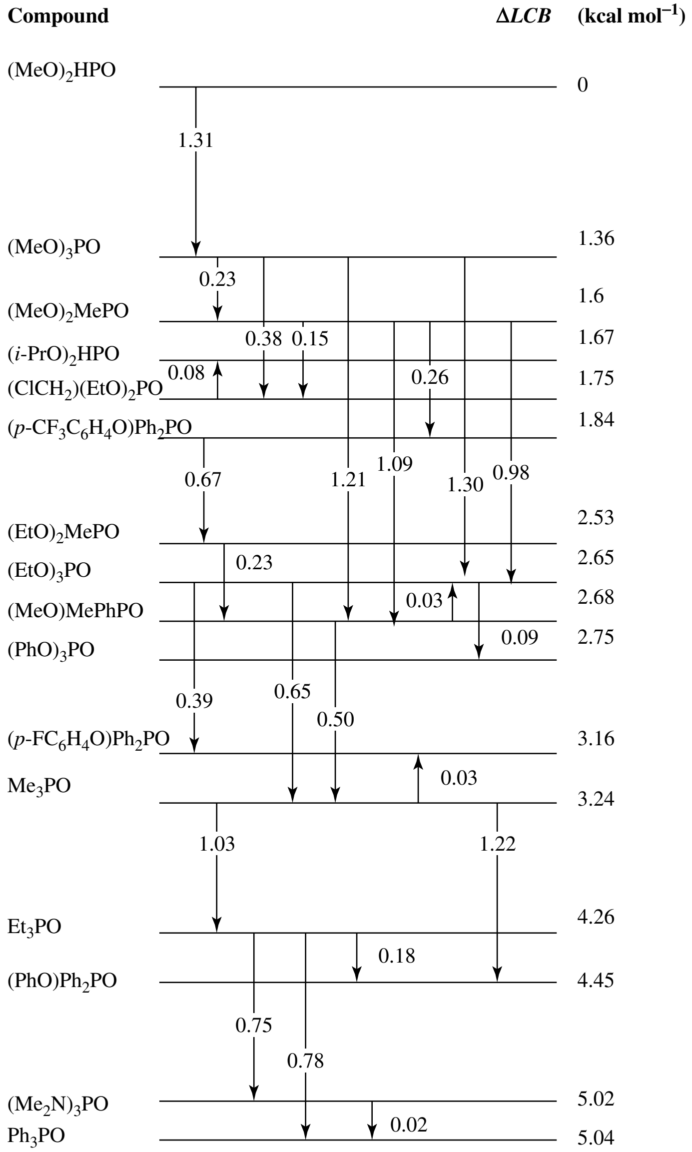

FIGURE 4. LCB of phosphoryl compounds, measured with an FT-ICR mass spectrometer. ΔLCB values referred to $(CH_3O)_2HPO$[32]

alkyl ethers [for $(CH_3OCH_2)_2$ by 9.3 kcal mol^{-1}, for $(CF_3CH_2)_2O$ by 8.3 kcal mol^{-1}, for $CF_3CH_2OCH_3$ by 4.4 kcal mol^{-1} and for $(CF_3)_2CHOCH_3$ by 4.3 kcal mol^{-1}].

The N bases have the worst correlation. However, within the subfamilies, the correlations between LCB and GB are better. Thus cyanides exhibit good correlation between LCB

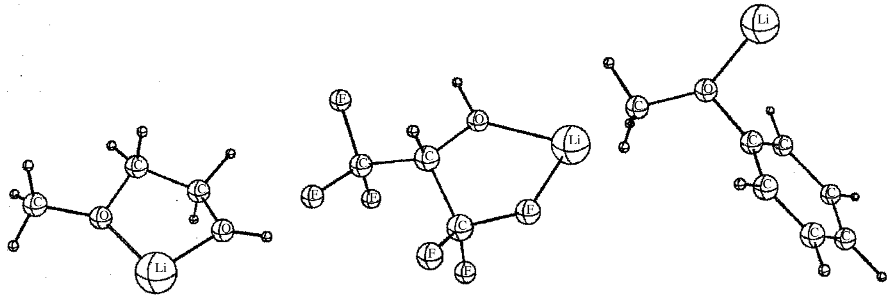

(2) **(3)** **(4)**

FIGURE 5. Different types of chelation in Li^+ cation complexation: (a) true chelation in a polyfunctional compound (e.g. $CH_3OCH_2CH_2OH{-}Li^+$, **2**); (b) formation of nonclassical chelates involving fluorine or chlorine atoms (e.g. $(CF_3)_2CHOH{-}Li^+$, **3**); (c) unexpected 'chelate structures' (e.g. $PhOCH_3{-}Li^+$, **4**). Reproduced with permission from Ref. 34

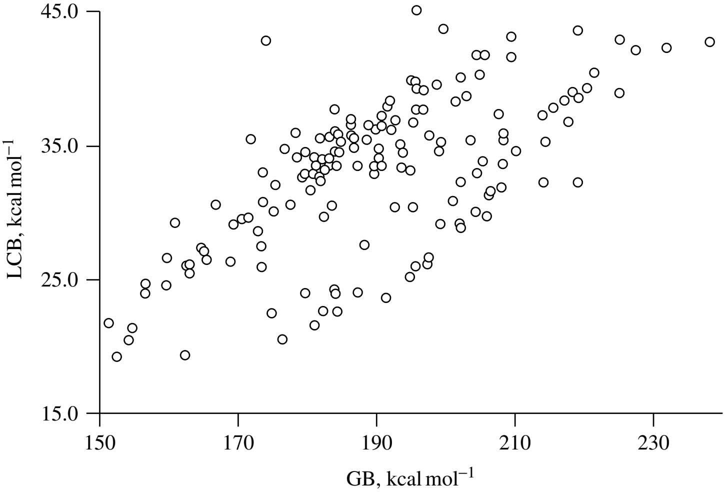

FIGURE 6. Correlation between experimental LCBs and gas-phase basicities towards the proton (GB). Reproduced with permission from Ref. 34

and GB, and when bidentate compounds are excluded the correlation for cyclic amines improves considerably as well.

LCA toward amino acids and nucleic bases has also been measured. Wesdemiotis and Cerda[35] measured the alkali metal ion affinities of nucleobases in the gas phase from the dissociation of metal ion-bound heterodimers [nucleobase + B]M^+, in which B represents a reference base of known affinity and M is an alkali metal. By assessing the dimer decomposition for two different internal energies, entropy is deconvoluted from enthalpy and LCA values are obtained. For guanine, cytosine, adenine, thymine and uracil, the corresponding Li^+–nucleobase bond energies are as follows: 57.2, 55.5, 54.1,

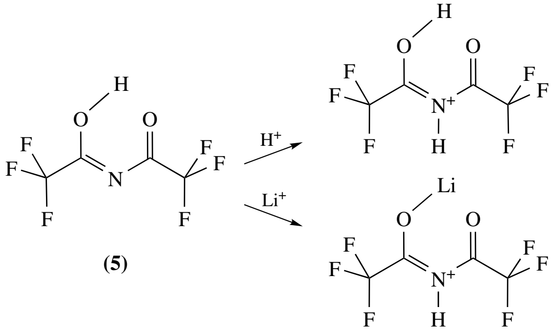

FIGURE 7. Differences in the mechanism of protonation and lithium cation addition to $(CF_3CO)_2NH$ (**5**) as seen by DFT calculations[34]: proton adds directly to the nitrogen atom in the enol form while lithium displaces H^+ at the oxygen atom and the displaced proton moves to the nitrogen. Reproduced with permission from Ref. 34

51.4 and 50.5 kcal mol^{-1}. The magnitude of the operating entropy effects gives information on the structures of both the metal ion-bound dimers and the metalated nucleobase monomers. It is found that Li^+, Na^+ and K^+ bind very similarly to the nucleobases. Specifically for [Gly + adenine]Li^+ heterodimer, it is suggested that binding to lithium restricts more rotations in the amino acid than in the nucleobase. As a consequence, there is less entropy gain upon the formation of [Gly]Li^+ + adenine than upon the formation of Gly + [adenine]Li^+, resulting in a negative $\Delta(\Delta S^\circ Li^+)$ quantity. A net entropy loss would increase the apparent LCA of adenine upon collision activation. Wesdemiotis and Cerda[35] also propose structures for [NB]Li^+ (Scheme 2).

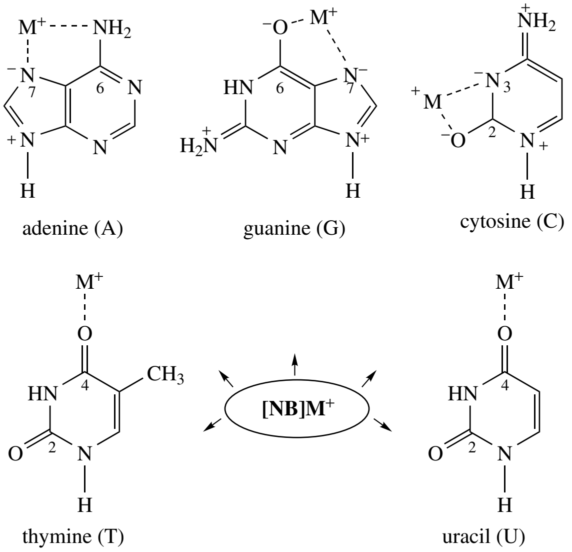

SCHEME 2. Structures for lithium (M) cationized nucleobases[35]

A parallel investigation on the binding of alkali metal cations to nucleobases, employing guided ion beam mass spectrometry, has recently been reported by Rodgers and Armentrout[36, 37].

IV. HOST–GUEST INTERACTION AND SUPRAMOLECULAR ASSEMBLIES

Ion-crown ether complexes are of the simplest molecular recognition systems studied in the gas phase. The selective binding involved in host–guest complexation requires an optimum structure for each substrate prior to possible bonding interactions. Gas-phase media provide an optimum environment to study the intrinsic behaviors of alkali metal–crown ether interactions without the interference of solvent effect. Complexation of alkali metal cations with macrocyclic ligands was initially studied by Johnstone and coworkers using fast-atom-bombardment mass spectrometry, in glycerol. They found that the abundances of gas-phase ions corresponding to metal cation–ligand complexes reflect the calculated concentrations of these complexes in solution[38, 39]. Dearden and coworkers showed the specific binding of lithium cation to 12-Crown-4 using laser desorption techniques (Table 5)[40].

Maleknia and Brodbelt generated ion complexes of crown ethers with different alkali metals by liquid secondary ion mass spectrometry (LSIMS) and used the kinetic method to estimate relative affinities of crown ethers for alkali metal ions. This study determines qualitatively size selectivity of crown ethers in a solvent-free environment[41]. Crown ether selective cation complexation with alkali metal ions has also been established using ESI. For example, it has been shown that crown ether acetals of structures **6a–6d** (Figure 8) tend to preferentially bind smaller ions as compared with the corresponding simple crown ethers possessing the same number of ring oxygen atoms. This is probably the result of ring-contracted deformation and hydrophobic effects of the diphenyl groups[42].

Lariat ethers of structure **8** were found to be selective toward Li^+ ion and the lariat crown ether–Li^+ complexes are more stable than the corresponding complexes with Na^+ or K^+, in methanol. Nevertheless, experiments conducted in aqueous solution showed that Na^+ had a better complexation ability than the other two alkali metal cations. Hence, selective complexation of lariat crown ethers with cations changes with the solvent system; this may be due in part to the difference in solvation between solvent and cation (Figure 9)[43].

ESI has been used to study the effect of the basicities of the side arms on the abilities of these lariat ethers to extract metal ions from solution. A series of compounds of structure **9** were studied and the authors conclude that the lariat ether with the least basic side arm binds best to the smaller cations (Table 6). Specifically for Li^+, it was found that it is best bound to the lariat ether with the ester side arm. It is proposed that electrostatic repulsion of the lariat ether side arm and the electron-rich π cloud of the adjacent aromatic ring play a dominant role in determining cation selectivities. The least basic side arm has lower electron density and thus these compounds have smaller cavity sizes and are more selective for smaller ions[44].

TABLE 5. Observed alkali cation bound dimers of crown ether. Reproduced with permission from Ref. 40

Cation	$(12\text{-Crown-4})_2M^+$	$(15\text{-Crown-5})_2M^+$	$(18\text{-Crown-6})_2M^+$
Li^+	yes	no	no
Na^+	yes	yes	no
K^+	yes	yes	no
Rb^+	yes	yes	yes
Cs^+	yes	yes	yes

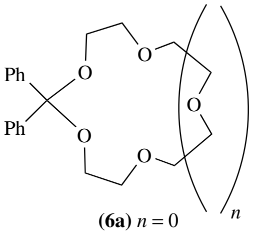

(6a) $n = 0$
(6b) $n = 1$
(6c) $n = 2$
(6d) $n = 3$

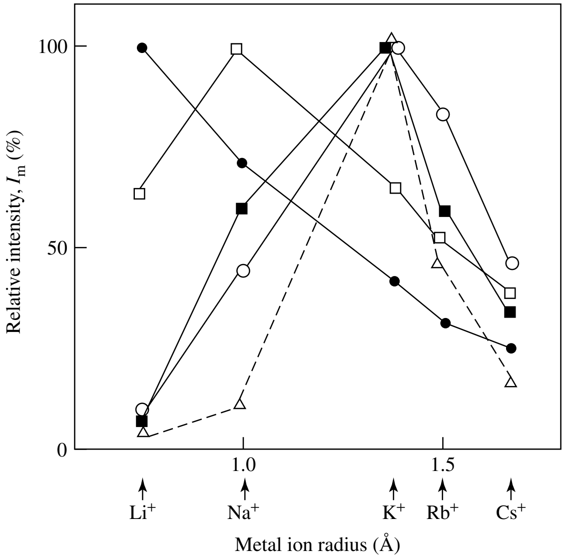

FIGURE 8. Relative intensities of ions corresponding to alkali cationized crown ethers **6a** (●), **6b** (□), **6c** (■), **6d** (○) and benzo-18-crown-6, **7** (△). Reproduced with permission from Ref. 42

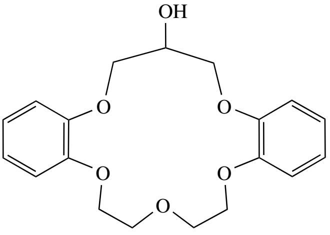

(8)

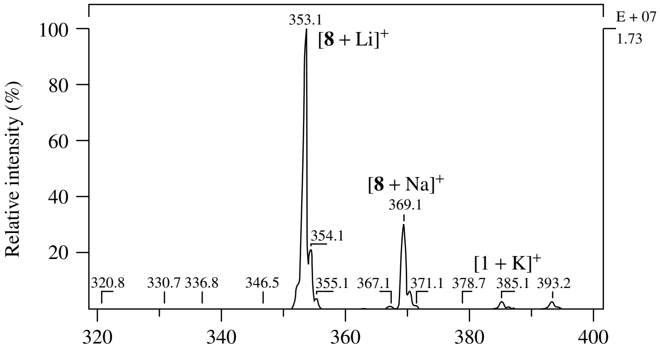

FIGURE 9. ESI mass spectrum of compound **8** with LiCl[43]

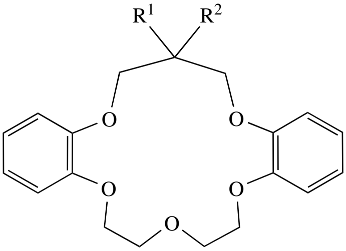

(9)

	R^1	R^2
9a	H	H
9b	H	OCH_3
9c	C_3H_7	OCH_3
9d	H	OCH_2CO_2H
9e	C_3H_7	OCH_2CO_2H
9f	H	$OCH_2CO_2C_2H_5$
9g	C_3H_7	$OCH_2CO_2C_2H_5$
9h	H	$OCH_2CON(CH_3)_2$
9i	C_3H_7	$OCH_2CON(CH_3)_2$
9j	H	OCH_2CONH_2
9k	C_3H_7	OCH_2CONH_2

TABLE 6. Alkali metal selectivities of lariat ethers **9a–9k** measured by ESI in chloroform–methanol (1:19). Reproduced with permission from Ref. 44

Lariat ether (LE)	% $[LE + Li]^+$	% $[LE + Na]^+$	% $[LE + K]^+$
9a	7	54	39
9b	4	40	56
9c	5	37	58
9d	0	79	22
9e	0	87	13
9f	60	40	0
9g	77	22	1
9h	0	60	40
9i	0	84	16
9j	0	73	26
9k	0	80	20

A class of crown spirobenzopyrans **10** exhibit thermally irreversible photochromism only in the presence of alkali-metal cations (Scheme 3). The favored complexation between **10** and lithium cation was thus revealed by the effect of lithium salt on the electronic absorption spectra of **10**. Lithium complexation was also corroborated on the basis of FAB mass experiments. Before addition of LiI to **10**, ion peaks for MH^+, $[M + Na]^+$ and $[M + K]^+$ were detected; after the addition the signals decreased, while a peak for $[M + Li]^+$ appeared (Figure 10)[45].

Carbohydrates show a considerable affinity toward alkali cations, which are frequently used for their mass spectral analyses. Lithium cation exhibits specific affinity toward glucose, as has been detected by electrospray ionization mass spectrometry. The experimental results were found to be consistent with the *ab initio* theoretical calculations and confirm the following order of stability of the M^+–glucose complexes: $[gl\text{-}Li]^+ > [gl\text{-}Na]^+ > [gl\text{-}K]^+$[46].

Another class of lithium cationized species that were generated and studied are polyglycols. Backbones or molecular chains of functional polyglycols are often difficult to dissociate in tandem mass spectrometers using low energy CID[47,48]. Apparently, Li^+ can

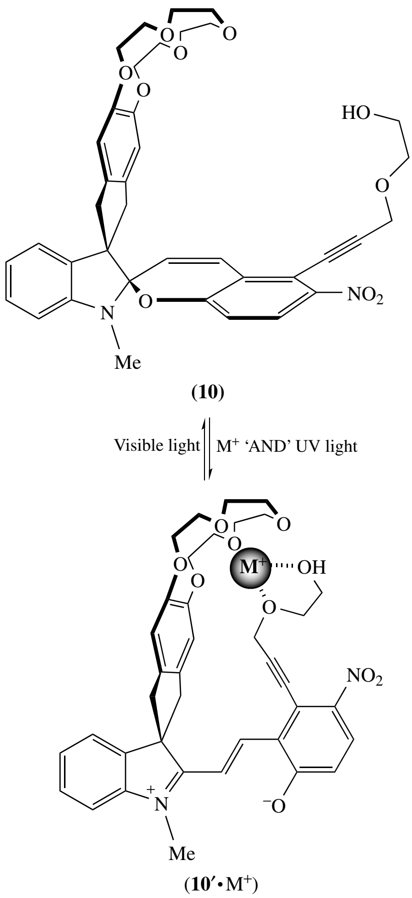

SCHEME 3. Isomerization of spirobenzopyran **10** to colored merocyanine **10′•M**$^+$ is induced by recognition of alkali metal cations as well as by UV irradiation[45]

catalyze these processes and provide informative MSMS spectra under the same conditions. The observation of more intense low mass fragment ions generated using Li^+ compared to other metal ions was attributed to the fact that the lowest energy conformer of $[PEG + Li]^+$ requires less oxygen atoms. Since lithium polyglycol adduct ions can be readily fragmented, it opens the possibility of using conventional and readily available low energy CID tandem MS to study polyglycol structures[48]. Wesdemiotis and coworkers report that the lithium and sodium ion complexes of the polyglycol-derived radicals ($R^\bullet$) $H(OCH_2CH_2)_nO(CH_2)_m{}^\bullet$ are produced in the gas phase by FAB ionization and their structures and unimolecular decompositions were investigated by tandem mass spectrometry. Molecular orbital calculations show that the $[R^\bullet + X]^+$ ions ($X = Li$, Na) carry their positive charge and unpaired electron at distinct centers. These dystonic $[R^\bullet + X]^+$ ions undergo typical radical site decompositions. Although these reactions are induced by the unpaired electron, the metal ion is not just a spectator. The presence of alkali cations

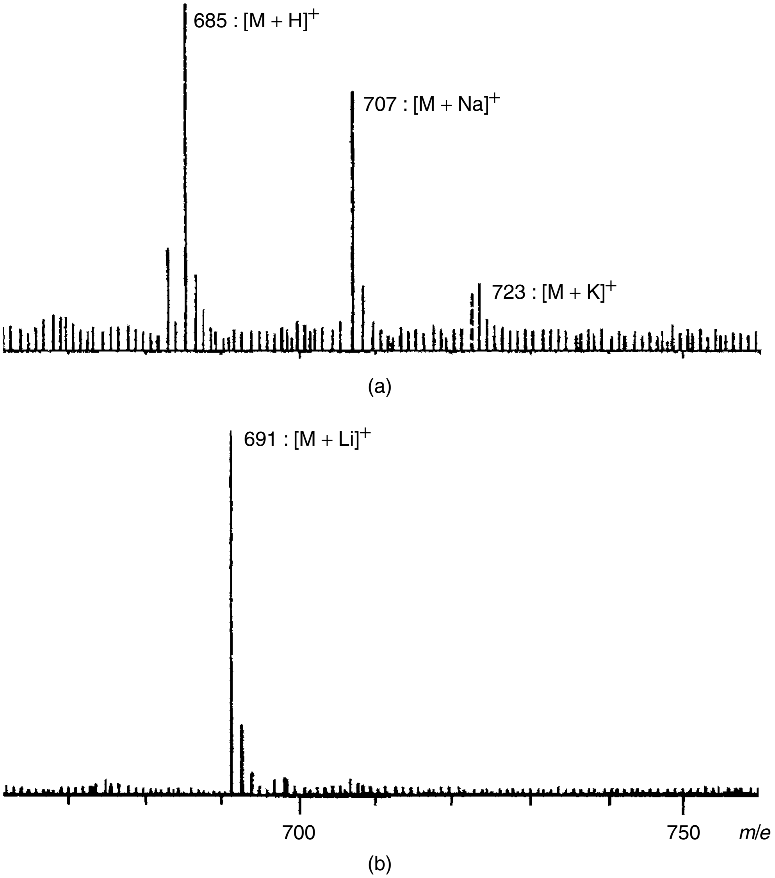

FIGURE 10. FAB mass spectra of **10** (a) before and (b) after addition of LiI. Reproduced with permission from Ref. 45

influences these reactions either by preventing bond rotations in R• (through coordination), allowing for the formation of intermediary metal ion-bound heterodimer complexes, or influencing the energetics of the radical site decompositions (Scheme 4)[48].

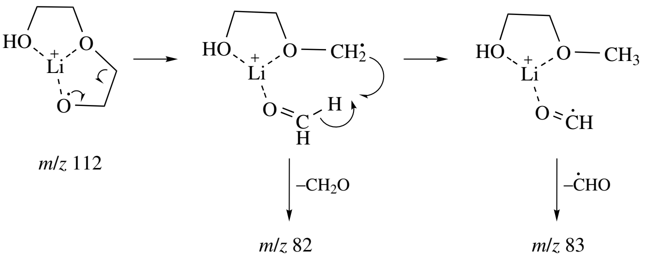

SCHEME 4. Lithium cation mediated fragmentations in cationized PEG production[48]

V. CATIONIZATION MASS SPECTROMETRY

Experimental and theoretical aspects of cationization mass spectrometry have recently been reviewed[49, 50]. Alkali ion attachment (cationization) of organic molecules occurs in the gas phase near the surface, giving rise to cationized molecular ions under the conditions of ESI, FAB, matrix assisted laser desorption ionization (MALDI) and other ionization techniques. There have been numerous studies that include the analyses of organic compounds using alkali ion cationization. Alkali cation salts are either present or being added to the organic mixture under study, to facilitate metal cationization for the characterization of organic molecules. Many studies also include CID of biologically important molecules such as fatty acids and sugars[51–53]. Metal cationized closed-shell ions having highly localized charge sites were found to undergo charge-remote fragmentations (CRF) giving straightforward structural information[53]. Specifically, lithium cationization followed by CID has been extremely useful in the location of double bonds in fatty acids, esters and alcohols[54, 55].

As stated above, the presence and nature of the alkali cation can affect the fragmentation behavior and regularity. Lithium cationized molecules sometimes exhibit very different fragmentation behavior than the protonated analogs and provide complementary structural information. For example, the product ion formation characteristics of the four diastereomeric benzo[*ghi*]fluoranthene tetraols was studied using MALDI ionization with post-source decay (PSD) activation. The protonated molecules of all four isomers are unstable and lose water readily, therefore no MH^+ ions are present in the spectra. However, all four diastereomeric tetraols form product ions by the losses of one and/or two water molecules in varying proportions when lithium-cationized molecule ions are selected for PSD product ion analysis. The differences in the PSD spectra of these four Li^+-cationized molecules are rationalized in terms of 1,2-water elimination which involves the loss of a hydrogen atom and hydroxyl group that are *cis* with respect to each other on adjacent carbons (Scheme 5)[56].

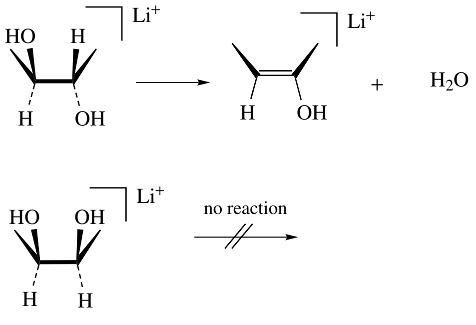

SCHEME 5. *Syn*-elimination of water in lithium cationized diols[56]

Specific interactions between organic substances and alkali metals may dominate the fragmentation behavior. It was shown that lithium and sodium cationized fatty acid esters show a remarkably different behavior upon high energy CID[57]. Accordingly, lithium cationized *n*-butyl oleate **11** exhibits excessive loss of butene (Figure 11a) while the corresponding ion in the CID spectrum of the sodium cationized analog is very low (Figure 11b).

Lithium and silver cationized loganin, *epi*-loganin and ketologanin also fragment differently, as has been shown by Madhusudanan and coworkers[58]. They also compared

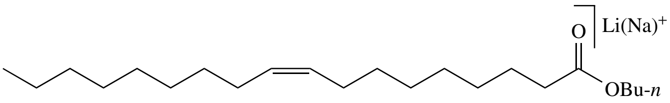

(11)

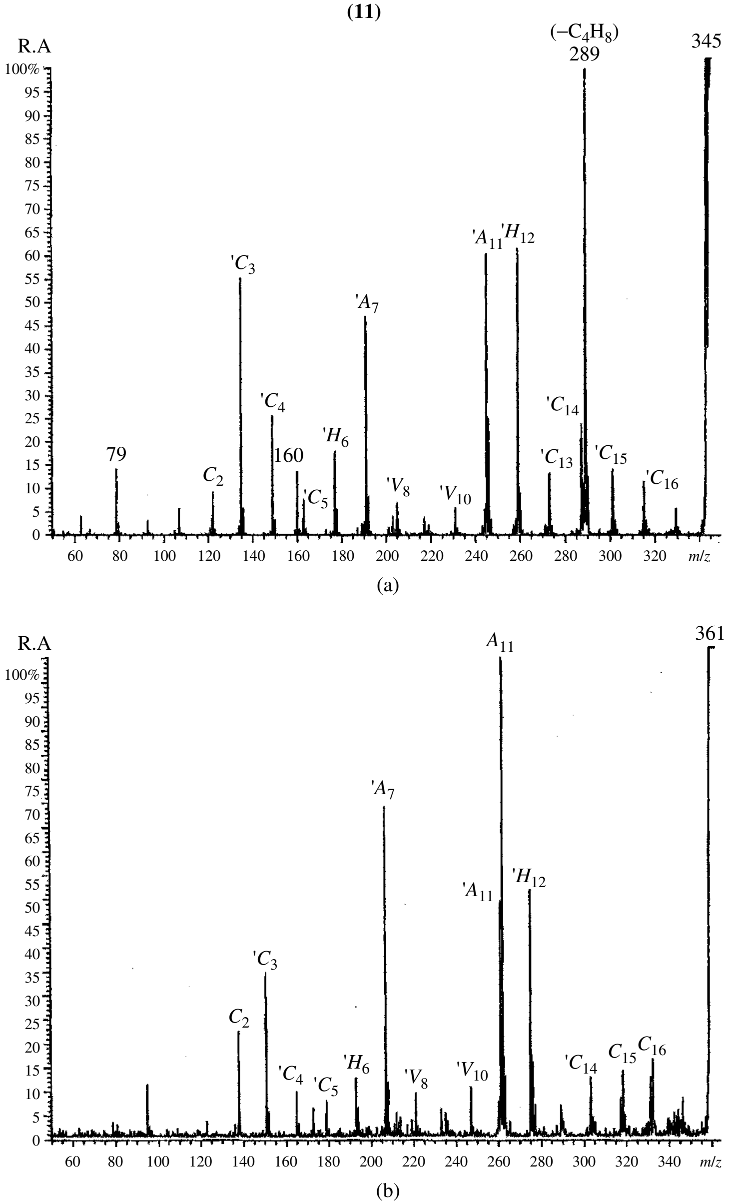

(a)

(b)

FIGURE 11. High-energy CID of lithium (a) and sodium (b) cationized n-butyl oleate[58]

the CID spectra of ammonium cationized loganic acid **12** with those of metal cationized species and found that glycosidic cleavage and ring cleavages of aglycone and sugar moieties are the major fragmentation pathways observed for $[M + NH_4]^+$ (Figure 12) while lithium adducts show fragmentation characteristic of both the aglycone and the sugar moieties[59]. Glycosidic cleavage results in the $[\text{Aglycone} + \text{Li}]^+$ ion which further loses H_2O (Scheme 6). There are also peaks corresponding to eliminations of CO_2 from $[\text{Aglycone} + \text{Li}]^+$ and $[\text{Aglycone} + \text{Li} - H_2O]^+$, respectively. Elimination of CO_2 is characteristic of the fragmentation of lithiated species and is not observed in the case of $[M + NH_4]^+$ ions (Scheme 6)[60].

Another characteristic of the CID behavior of lithium containing cationized loganic acid is the retro Diels–Alder (RDA) reaction that affords several possible fragmentation products. These so-called cross ring cleavages are very useful in the structure determination of various compounds and are typically present in the CID spectra of alkali cationized ions of several groups of compounds (Schemes 7 and 8)[59, 61].

In some cases lithium cationization is particularly useful, since the resulting $[M + Li]^+$ ions give rise to informative CID spectra. Liu and coworkers used electrospray ionization and MS^n experiments for the structural analysis of ginsenosides[62]. They find that $[M + Li]^+$ ions afford much more abundant fragment ions than the corresponding $[M + Na]^+$ and MH^+ precursors. The fragmentation pathways of $[M + Li]^+$ are

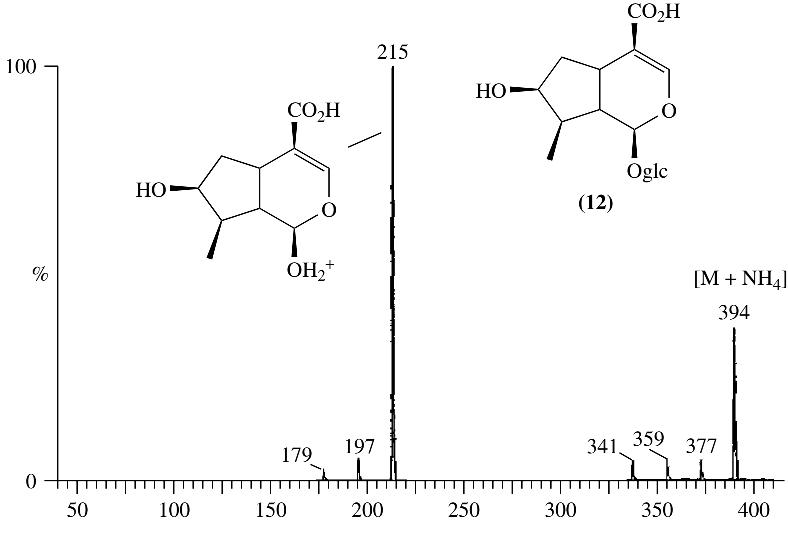

FIGURE 12. Decomposition of the $[M + NH_4]^+$ ion of **12**[59]

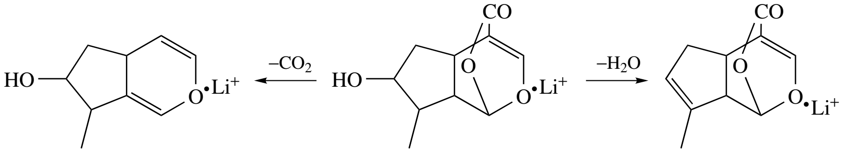

SCHEME 6. Typical lithium-cation induced fragmentations in the CID spectra of lithiated loganin: loss of water and CO_2[60]

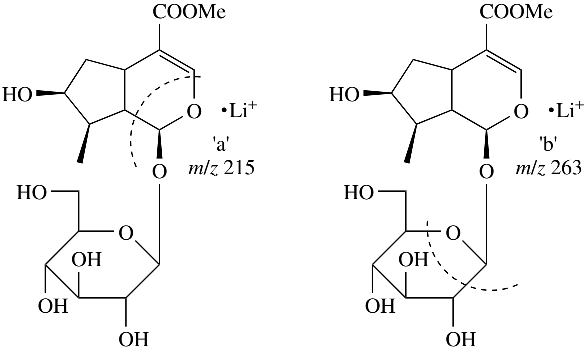

SCHEME 7. Fragmentation characteristic of the substituents present in either aglycone or sugar parts of the molecule[59]

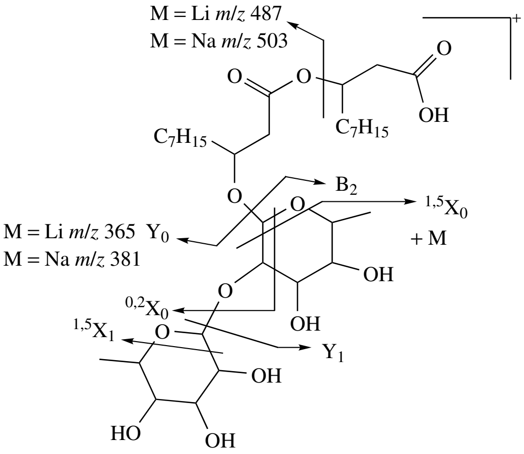

SCHEME 8. The fragmentation routes of Rha-Rha-C_{10}-C_{10} (Rha = Rhamnosyl) $[M + Na]^+$ and $[M + Li]^+$ precursor ions during high-energy CID[61]

similar to those of the corresponding $[M + Na]^+$ precursors, except for the higher efficiency of glycosidic bond cleavage and cross ring cleavages at the disaccharide moieties. Gross and coworkers examined the high-energy CID spectra of a series of oxofatty acids[63]. It is clearly demonstrated that cationization affords efficient and informative fragmentation upon high-energy CID (Figure 13). The CID spectra of the MH^+ ion of 10-oxohexadecanoic acid (**13**) and the corresponding $[M + Li]^+$ and $[M - H + 2Li]^+$ ions are very different. The CID of the MH^+ ion is not distinctive and does not allow the detection of the oxo group position as it mainly consists of the $[MH - H_2O]^+$ ion. Loss of water is also observed in the CID spectra of $[M + Li]^+$. However, the $[M - H + 2Li]^+$ ion affords the so-called charge remote fragmentation series of ions, that allow the positioning of the oxo group in the alkyl chain while loss of water is suppressed because the OH group is replaced by OLi (Figure 13).

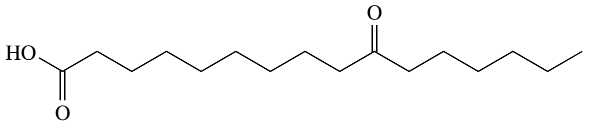

(13)

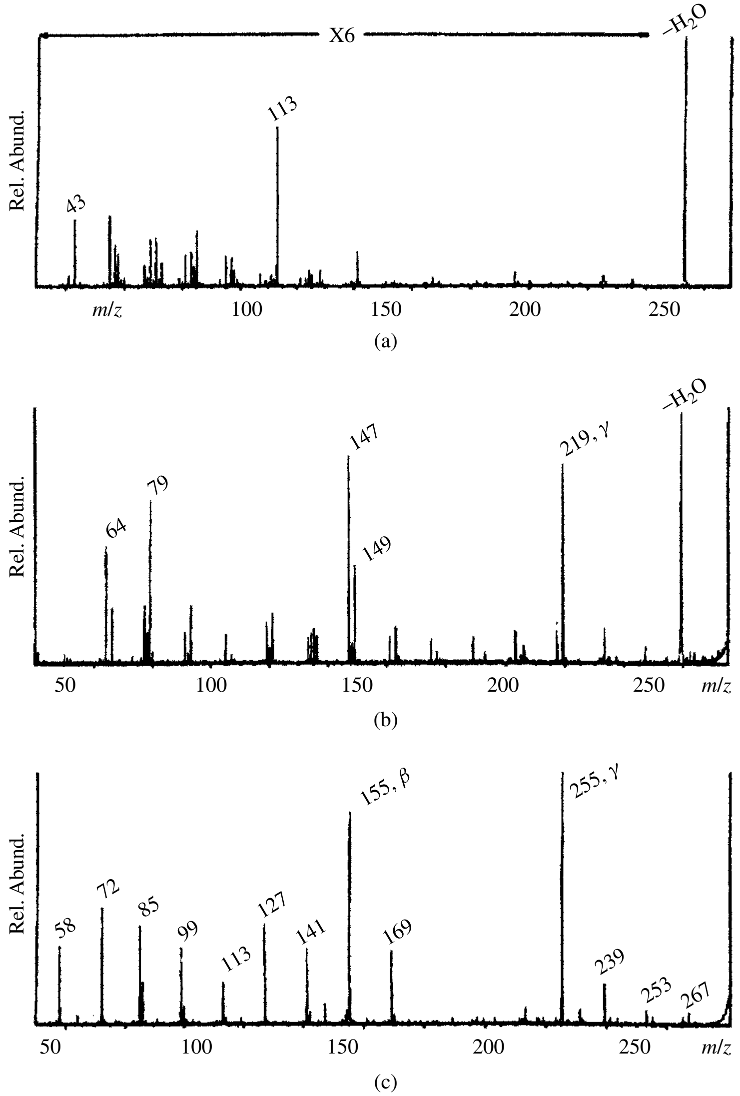

FIGURE 13. High-energy CID spectra of (a) MH$^+$, (b) $[M + Li]^+$ and (c) $[M - H + 2Li]^+$ ions of 10-oxohexadecanoic acid **13**. Reproduced with permission from Ref. 63

Fujii developed a method for detecting radical species in the gas phase with the use of lithium ion attachment to chemical species. Li ions have been chosen as reactant ions, because the affinity of the species is highest among all the alkali metal ions. The author also explored some of the unique properties of Li ion attachment in mass spectrometry. This technique provides mass spectra of quasi-molecular $[R + Li]^+$ ions formed by lithium-ion attachment to the radical species under high pressure[49, 64].

VI. ACKNOWLEDGMENT

The author thanks the Israel National Science Foundation for financial support.

VII. REFERENCES

1. O. Kwon, F. Sevin and L. McKee, *J. Phys. Chem. A*, **105**, 913 (2001).
2. J. Berkowitz, D. A. Bafus and T. L. Brown, *J. Phys. Chem.*, **65**, 1380 (1961).
3. J. W. Chinn, Jr. and R. J. Lagow, *Organometallics*, **3**, 75 (1984).
4. W. McClean, P. T. Murray, T. Baer and R. C. Jarnagin, *J. Chem. Phys.*, **69**, 2715 (1978).
5. M. Y. Darensbourg, B. Y. Kimura, G. E. Hartwell and T. L. Brown, *J. Am. Chem. Soc.*, **92**, 1236 (1970).
6. D. Plavšić, D. Srzić and L. Klasinc, *J. Phys. Chem.*, **90**, 2075 (1986).
7. A. K. Abdul-Sada, A. M. Greenway and K. R. Seddon, *J. Organomet. Chem.*, **375**, C17 (1989).
8. G. Tarczay, G. Vass, G. Magyarfalvi and L. Szepes, *Organometallics*, **19**, 3925 (2000).
9. L. A. Shimp, J. A. Morrison, J. A. Gurak, J. W. Chinn, Jr. and R. J. Lagow, *J. Am. Chem. Soc.*, **103**, 5951 (1981).
10. J. A. Gurak, J. W. Chinn, Jr. and R. J. Lagow, *J. Am. Chem. Soc.* **104**, 2637 (1982).
11. F. J. Landro, J. A. Gurak, J. W. Chinn, Jr. and R. J. Lagow, *J. Organomet. Chem.*, **249**, 1 (1983).
12. G. E. Hartwell and T. L. Brown, *Inorg. Chem.*, **5**, 1257 (1966).
13. D. Groves, W. Rhine and G. D. Stucky, *J. Am. Chem. Soc.*, **93**, 1553 (1971).
14. W. E. Rhine, G. Stucky and S. W. Peterson, *J. Am. Chem. Soc.*, **97**, 6401 (1975).
15. S. M. Bachrach, M. Hare and S. R. Kass, *J. Am. Chem. Soc.*, **120**, 12646 (1998).
16. R. H. Staley and J. L. Beauchamp, *J. Am. Chem. Soc.*, **97**, 5920 (1975).
17. R. L. Woodin, F. A. Houle and W. A. Goddard III, *Chem. Phys.*, **14**, 461 (1976).
18. R. W. Taft, F. Anvia, J.-F. Gal, S. Walsh, M. Capon, M. C. Holmes, K. Hosn, G. Oloumi, R. Vasanwala and S. Yazdani, *Pure Appl. Chem.*, **62**, 17 (1990).
19. E. P. Hunter and S. G. Lias, *J. Phys. Chem. Ref. Data*, **27**, 413 (1998); NIST WebBook, http://webbook.nist.gov.
20. I. Dzidic and P. Kebarle, *J. Phys. Chem.*, **74**, 1466 (1970).
21. E. Clementi and H. Popkie, *J. Chem. Phys.*, **57**, 1077 (1972).
22. H. Kistenmacher, H. Popkie and E. Clementi, *J. Chem. Phys.*, **59**, 5842 (1973).
23. H. Kistenmacher, H. Popkie and E. Clementi, *J. Chem. Phys.*, **61**, 799 (1974).
24. D. Feller, E. D. Glendening, R. A. Kendall and K. A. Peterson, *J. Chem. Phys.*, **100**, 4981 (1994).
25. M. T. Rodgers and P. B. Armentrout, *J. Phys. Chem. A*, **101**, 1238 (1997).
26. M. T. Rodgers and P. B. Armentrout, *J. Phys. Chem. A*, **101**, 2614 (1997).
27. R. L. Woodin and J. L. Beauchamp, *J. Am. Chem. Soc.*, **100**, 501 (1978).
28. A. M. Striegel, P. Piotrowiak, S. M. Boue and R. B. Cole, *J. Am. Soc. Mass Spectrom.*, **10**, 254 (1999).
29. R. W. Taft, M. Taagepera, J. L. M. Abboud, J. F. Wolf, D. J. DeFrees, W. J. Hehre, J. E. Bartmess and R. T. McIver, *J. Am. Chem. Soc.*, **100**, 7765 (1978).
30. M. Herreros, J.-F. Gal, P.-C. Maria and M. Decouzon, *Eur. J. Mass Spectrom.*, **5**, 259 (1999).
31. R. G. Cooks, J. S. Patrick, T. Kotiaho and S. A. McLucky, *Mass Spectrom. Rev.*, **13**, 287 (1994).
32. E. Buncel, A. Chen, M. Decouzon, S. A. Fancy, J.-F. Gal, M. Herreros and P.-C. Maria, *J. Mass Spectrom.*, **33**, 757 (1998).

33. M. Alcami, O. Mo, M. F. Yáñez and R. W. Taft, *J. Phys. Chem.*, **94**, 4796 (1990).
34. P. Burk, I. A. Koppel, I. Koppel, R. Kurg, J.-F. Gal, P.-C. Maria, M. Herreros, R. Notario, J.-L. Abboud, F. Anvia and R. W. Taft, *J. Phys. Chem. A*, **104**, 2824 (2000).
35. B. A. Cerda and C. Wesdemiotis, *J. Am. Chem. Soc.*, **118**, 11884 (1996).
36. M. T. Rodgers and P. B. Armentrout, *Proceedings of the 44th ASMS Conference on Mass Spectrometry and Allied Topics*, May 12–16, 1996, Portland, OR, p. 88.
37. M. T. Rodgers and P. B Armentrout, *J. Am. Chem. Soc.*, **122**, 8548 (2000).
38. R. A. W. Johnstone and M. E. Rose, *J. Chem. Soc., Chem. Commun.*, 1268 (1983).
39. R. A. Johnstone, I. A. S. Lewis and M. E. Rose, *Tetrahedron*, **39**, 1597 (1983).
40. H. Zhang, I.-H. Chu, S. Leming and D. V. Dearden, *J. Am. Chem. Soc.*, **113**, 7416 (1991).
41. S. Maleknia and J. Brodbelt, *J. Am. Chem. Soc.*, **114**, 4295 (1992).
42. T. Oshima, F. Matsuda, K. Fukushima, H. Tamura, G. Matsubayashi and R. Arakawa, *J. Chem. Soc., Perkin Trans. 2*, 145 (1998).
43. D.-S. Young, H.-Y. Hung and L. K. Liu, *J. Mass Spectrom.*, **32**, 432 (1997).
44. E. C. Kempen and J. S. Brodbelt, *Anal. Chem.*, **71**, 5493 (1999).
45. M. Inouye, K. Akamatsu and H. Nakazumi, *J. Am. Chem. Soc.*, **119**, 9160 (1997).
46. E. Botek, J. L. Debrun, B. Hakim and L. Morin-Allory, *Rapid Commun. Mass Spectrom.*, **15**, 273 (2001).
47. R. Chen and L. Li, *J. Am. Soc. Mass Spectrom.*, **12**, 832 (2001).
48. J. Wu, M. J. Polce and C. Wesdemiotis, *J. Am. Chem. Soc.*, **122**, 12786 (2000).
49. T. Fujii, *Mass Spectrom. Rev.*, **19**, 111 (2000).
50. M. T. Rodgers and P. B. Armentrout, *Mass Spectrom. Rev.*, **19**, 215 (2000).
51. L. M. Teesch and J. Adams, *Org. Mass Spectrom.*, **27**, 931 (1992).
52. M. Takayama, *New Advances in Analytical Chemistry*, P2/31 (2000). Harwood Academic Publisher, Amsterdam.
53. M. L. Gross, *Int. J. Mass Spectrom.*, **200**, 611 (2000).
54. M. Claeys, L. Nizigiyimana, H. Van den Heuvel and P. J. Derrick, *Rapid Commun. Mass Spectrom.*, **10**, 770 (1996).
55. J. Adams and M. L. Gross, *J. Am. Chem. Soc.*, **108**, 6915 (1986).
56. D. M. Huffer, H.-F. Chang, B. P. Cho, L. K. Zhang and M. P. Chiarelli, *J. Am. Soc. Mass Spectrom.*, **12**, 376 (2001).
57. M. Claeys, L. Nizigiyimana, H. Van Den Heuvel, I. Vedernikova and A. Haemers, *J. Mass Spectrom.*, **33**, 631 (1998).
58. K. P. Madhusudanan, K. Raj and A. P. Bhaduri, *J. Mass Spectrom.*, **35**, 901 (2000).
59. K. P. Madhusudanan, V. T. M. Shefali, K. Raj and A. P. Bhaduri, *J. Mass Spectrom.*, **35**, 321 (2000).
60. K. P. Madhusudanan, K. Raj and A. P. Bhaduri, *Rapid Commun. Mass Spectrom.*, **14**, 885 (2000).
61. C. Denekamp, M. Claeys and G. Pocsfalvi, *Rapid Commun. Mass Spectrom.*, **14**, 794 (2000).
62. M. Cui, F. Song, Z. Liu and S. Liu, *Rapid Commun. Mass Spectrom.*, **15**, 586 (2001).
63. C. Cheng, D. Giblin and M. L. Gross, *J. Am. Soc. Mass Spectrom.*, **9**, 216 (1998).
64. T. Fujii, M. Ogura and H. Jimba, *Anal. Chem.*, **61**, 1026 (1989).

CHAPTER 6

Vibrational spectroscopy of organolithium compounds

I. PAVEL and W. KIEFER

Institut für Physikalische Chemie, Universität Würzburg, Am Hubland, D-97074 Würzburg, Germany
Fax: +49(0)931 888 6332; e-mail: wolfgang.kiefer@mail.uni-wuerzburg.de

and

D. STALKE

Institut für Anorganische Chemie, Universität Würzburg, Am Hubland, D-97074 Würzburg, Germany
Fax: +49(0)931 888 4619; e-mail: dstalke@chemie.uni-wuerzburg.de

---

The Chemistry of Organolithium Compounds. Edited by Z. Rappoport and I. Marek
ISBN: 0-470-84339-X

I. INTRODUCTION

The most straightforward way of observing vibrational transitions of molecules is through absorption of infrared (IR) radiation. The interaction of matter with electromagnetic radiation is subject to selection rules and hence not all vibrations may give rise to absorption bands in the IR spectrum. The prerequisite of IR activity is the change in dipole moment of the molecule during a given normal mode of vibration. Because of this the stretching vibration of a homonuclear diatomic molecule (such as H_2, O_2 etc.) or the totally symmetrical vibrations of larger molecules having a centre of symmetry, as well as any other vibrations which do not generate a vibrating electric dipole, are IR inactive. In order to detect such vibrations, it is necessary to consider the inelastic scattering of light, a phenomenon that is referred to as Raman scattering. This is governed by different selection rules compared to the absorption of light. A given normal vibration of a molecule may appear in the Raman spectrum if at least one component of the polarizability tensor changes during this vibration[1–6]. However, the distinct advantage of Raman to IR is that in Raman, there is little or no sample preparation, and the ability to use glass optics and work in aqueous media. Samples can therefore often be examined in the form in which they are submitted, and the samples can usually be returned unaffected after the measurements. Further, low wavenumber measurements are possible and hence signals can be observed easily below 100 cm^{-1}. Thus, IR and Raman spectroscopy are powerful complementary tools for obtaining precise and detailed information about the structure of organolithium compounds, particularly since lasers have been developed in optical spectroscopy[1–6].

However, the high frequency of the laser irradiation in the visible region may lead to photochemical reactions in the laser focus. Besides, fluorescence can often cover the whole Raman spectrum. Such problems can be avoided by using an excitation wavelength in the near-infrared (NIR) region, e.g. with an Nd:YAG laser operating at 1064 nm. Deficits arising from the ν^4 dependence of the Raman intensity and the lower sensitivity of NIR detectors are compensated by the Fourier-Transform (FT) technique, which is widespread in IR spectroscopy[1,4].

In modern chemistry, the IR or Raman spectroscopy in combination with the matrix isolation technique has been frequently used to clear up the reaction mechanism of several compounds and to characterise the products[7–9]. One of the first matrix reaction techniques for alkali metal reactions was developed by Andrews and Pimentel[10]. The experimental goal is to bring lithium atoms and reactive molecules together long enough for primary reactions to take place and then to quickly trap the products in the grid of a solid and inert host material at low temperature for spectroscopic study. For matrix materials often-rare gases and pure nitrogen are used. In this way inter- and intramolecular interactions can be prevented[7–10].

Spectroscopic methods such as IR and Raman have proven to be exceptionally powerful methods for solving many chemistry problems[1–10]. However, the vibrational assignment, as well as the understanding of the relationship between the observed spectral features and molecular structure or reactivity of the sample, can be very difficult. Theoretical methods can certainly assist to obtain a deeper understanding of the vibrational spectra of new compounds. These are the well-established force field calculations, semi-empirical and *ab initio* methods[1].

II. LITHIUM COMPLEXES OF SATURATED HYDROCARBONS

A. The Methyl- and Ethyllithium Compounds

Early spectroscopic investigations on such organolithium compounds concerned the IR spectra of methyl- and ethyllithium in the 700–4000 cm^{-1} spectral region[11–16]. The first two groups of workers involved in these investigations came to different conclusions.

The first study belongs to Brown and Rogers[11], who measured the IR spectra of methyl- and ethyllithium as Nujol mulls, and of ethyllithium in benzene solution, and assigned the bands observed at 880 and 925 cm^{-1} to the C−Li stretching vibrational modes of the monomeric and polymeric species, respectively.

Shortly after, Rodionov and coworkers studied the IR spectra of methyl- and ethyllithium in the vapour phase[12–14] as well as a great variety of organolithium compounds as solids and in solution[15,16]. They completely based their interpretation on the vibrational assignment proposed for CH_3Li, which was assumed to be monomeric in the vapour phase and to have C_{3n} symmetry[12–14]. Accordingly, the peak at 1050 cm^{-1}, which was not taken into consideration by Brown and coworkers, was ascribed to the C−Li fundamental stretching mode in all organolithium compounds, while the bands in the 850–930 cm^{-1} spectral region were attributed to the C−Li vibrational modes of various polymers.

The disagreement between the two groups of researchers was later solved by an infrared study of West and Glaze[17] on methyl- and ethyllithium as mulls in dry white petroleum oil. To eliminate complications from C−H bands in the mulling agent, methyllithium was also measured as mulls in perfluoro-kerosene. Additionally, ethyllithium was examined at various concentrations in benzene solution and as vapour. They extended the spectral region to 300 cm^{-1} and used lithium and hydrogen isotopes to clear up the previous assignments.

In the C−H stretching region, methyllithium present two peaks at 2840 and 2780 cm^{-1}, which shift to 2150 and 2027 cm^{-1} upon deuterium substitution (Table 1). Accordingly, they have been ascribed to symmetrical and asymmetrical C−H stretching motions and their appearance at much lower wavenumbers was attributed to a multicentre Li−C−Li bonding[11], such as in polymeric dimethylberyllium[18,19] and dimeric aluminium trialkyls[20,21]. The absence of the bands in the usual C−H stretching region, as the earlier investigators reported it[11], show that free CH_3 groups are not present in methyllithium (Figure 1)[22]. The methyl groups cap the Li_3 faces.

TABLE 1. Infrared absorption bands (cm^{-1}) observed for some alkyllithium compounds

Methyllithium				Ethyllithium	
$CH_3{}^6Li$	$CH_3{}^7Li$	$CD_3{}^6Li$	$CD_3{}^7Li$	$C_2H_5{}^6Li$	$C_2H_5{}^7Li$
				2940^{a,b}	2940^{a,b}
2840	2840	2150	2150	2840^{a,b}	2840^{a,b}
2780	2780	2027	2027	2760^{a,b}	2760^{a,b}
1480	1480	1100	1100	1450^{a}	1450^{a}
1427	1427	1043	1043		
				1383^{a,b}	1383^{a,b}
1096	1096	827	827	1098^{a,b}	1098^{a,b}
1061	1061	815	815	1050^{a,b}	1050^{a,b}
(1025)	(1025)				
(923)	(923)	(923)	(923)	945^{a,b}	945^{a,b}
(900)	(900)	(900)	(900)	920^{b}	920^{b}
(867)	(867)			877^{a,b}	877^{a,b}
517	514	455	436	570^{b}	566^{b}
				565^{a}	535^{a}
446	417	348	336	496^{a}	465^{a}
				362^{a}	340^{a}

[a] Bands observed in mulls[17].

[b] Bands observed in the vapour[17].

Reprinted with permission from Reference 17. Copyright 1961 American Chemical Society.

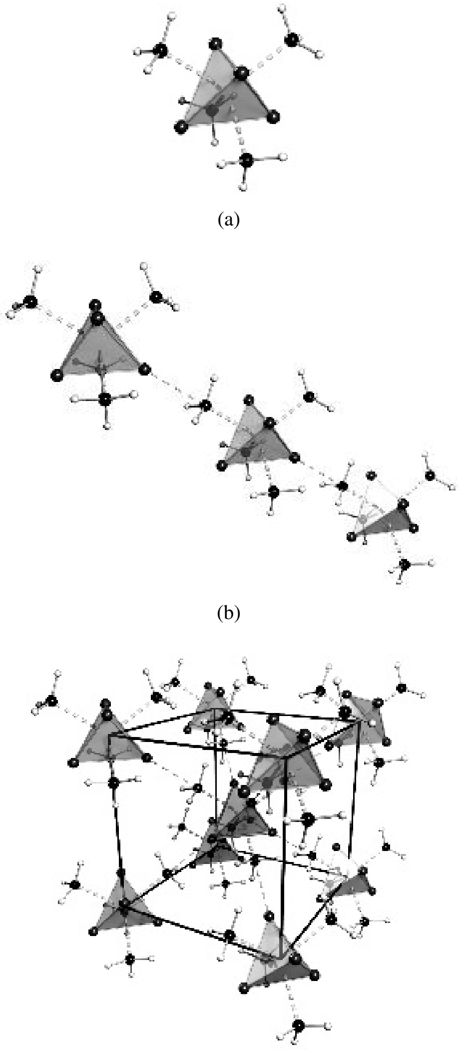

(a)

(b)

(c)

FIGURE 1. Solid-state structure of: (a) $[(H_3CLi)_4]$, (b) $[\{(H_3CLi)_4\}_3]$ and (c) $[\{(H_3CLi)_4\}_\infty]$. Reproduced with permission from Ref. 24

Two bands were observed for ethyllithium in the C−H stretching region at unusual low wavenumbers (2840 and 2760 cm^{-1}), as for methyllithium. Besides, a new band at 2940 cm^{-1} was found in the proper C−H stretching vibrational region of the terminal CH_3 group, not influenced by multicentre bonding. The symmetrical stretching motion of the CH_3 group should occur near 2870 cm^{-1} [23] and so probably overlaps with and contributes to the CH_2 stretching band at 2840 cm^{-1}, whose value is lowered by electrostatic interaction.

The IR spectra of methyllithium exhibited two C−H bending vibrational modes at 1480 and 1427 cm^{-1}. Their assignment was again substantiated by significant isotopic shifts to 1100 and 1043 cm^{-1} in the deuterium compound (Table 1). Only one weak band was observed for ethyllithium in the C−H deformation region at 1450 cm^{-1}. Moreover, a new sharp peak was detected at 1385 cm^{-1} and ascribed to the C−H symmetrical bending mode of CH_3. Its absence in the IR spectrum of methyllithium is a further indication that free methyl groups exist only in ethyllithium.

The bands at 1096 and 1091 cm^{-1}, which were attributed by Rodionov and coworkers to symmetrical and asymmetrical Li−C stretching modes in methyllithium[12–16], did not shift on ^{6}Li substitution (Table 1). Therefore, they cannot represent modes of vibration involving carbon and lithium to any significant extent. West and Glaze[17] assigned them to C−H rocking or deformation. Similar peaks were found at 1098 and 1050 cm^{-1} for ethyllithium and ascribed to C−H deformations.

All of the modes discussed above present important shifts upon deuterium substitution (Table 1). Consequently, the authors came to the conclusion that they mainly involved motions of hydrogen atoms. The isotopic ratios ($\nu_H/\nu_D = 1.30$ to 1.36)[17] are in this case comparable to those for the hydrogenic stretching and deformations modes found in methyl chloride ($\nu_H/\nu_D = 1.31$ to 1.37)[24].

As we have already mentioned, both earlier groups of scientists assigned the signals between 950 and 870 cm^{-1} to C−Li stretching bands in polymeric species of methyl- and ethyllithium, respectively. West and Glaze[17] noticed that their intensities strongly depended on the method of preparation of methyl- or ethyllithium or they were entirely absent. Therefore, these bands must be due to some impurities present in variable amounts in most methyl- and ethyllithium preparations. From their position in the IR spectra of methyllithium it seems possible that C−O vibrations of oxidation products are responsible for these peaks. In the vapour spectra of ethyllithium they may also be due to skeletal deformations in the C_2H_5 groups[17,23]. Anyway, these modes were not shifted upon hydrogen or lithium isotopic substitution (Table 1).

Bands, which do shift upon lithium substitution, were found in both compounds below 600 cm^{-1}. The two absorption bands observed near 500 cm^{-1} in methyllithium appeared at much higher wavenumbers in the corresponding ^{6}Li compound. Most of the shifts observed upon ^{6}Li substitution (Table 1) are smaller than the characteristic shifts for harmonic C−Li bonds (about 26 cm^{-1} for bands near 500 cm^{-1})[25], as expected since they represent complex vibrational modes. Furthermore, all of these signals are significantly shifted upon deuterium substitution, which indicates that they involve the motion of hydrogen as well as lithium (Table 1)[17].

Therefore, the appearance of the C−Li bands at unexpected low wavenumbers and their behaviour upon isotopic substitution demonstrate that these bands represent complex modes of vibration in polymeric molecules rather than simple C−Li stretching motions (Figure 1)[22]. It is well known that organolithium compounds are strongly associated in solution[11,26,27]. Furthermore, the C−Li bands occurred in the mulls and solution spectra of ethyllithium at similar positions to those in the vapour spectra, namely in the region from 570 to 340 cm^{-1} (Table 1)[17]. In benzene solution the bands were found at 560 and 398 cm^{-1} for $C_2H_5{}^{6}Li$ and at 538 and 382 cm^{-1} for $C_2H_5{}^{7}Li$. This seems to confirm the previous finding of Berkowitz and coworkers that ethyllithium is polymeric even in the vapour phase[28].

In their papers Rodionov and coworkers described the polymerization of organolithium compounds in terms of the formation of ‘lithium bonds’ (Scheme 1), analogous to hydrogen bonds, which brought about cyclic or linear association of these compounds in solution[12–16]. However, the strong association of alkyllithium compounds, persisting even in the vapour phase, indicates that their association takes place through the formation of multicentre bonds like in polymeric dimethylberyllium and the dimeric aluminium trialkyls (Figure 1)[11, 17–22]. A few years later, the multicentre Li–C–Li bonding was proved by the X-ray studies on methyllithium of Weiss and coworkers[29, 30]. Afterwards, the crystal structure of deuteriated methyllithium was refined by neutron powder diffraction at 1.5 and 290 K[31]. At both temperatures a cubic body-centred arrangement of $(LiCD_3)_4$ units (T_d symmetry) was found. In agreement with the first X-ray investigations (290 K), each tetramer contains a distorted cubic Li_4C_4 core with pyramidal methyl groups in staggered positions with respect to the adjacent Li_3 unit (Figure 1). So the intermolecular interactions between the tetrahedra could be related to the physical properties of methyl- and ethyllithium.

$$\cdots\mathrm{Li}\!-\!\mathrm{C}\cdots\mathrm{Li}\!-\!\mathrm{C}\cdots\mathrm{Li}\!-\!\mathrm{C}\cdots$$

SCHEME 1

B. The *t*-Butyllithium Compound

Polymerization in electrostatic systems like the ones mentioned above is sterically inhibited by alkyl substitution at the α-carbon[20, 21], which must assume a coordination number greater than 4. Coates and Glockling have treated this inhibition of polymerization in terms of decreased electronegative character of the branched alkyl groups[32]. Therefore, stimulated by the idea that *t*-alkyllithium compounds may exist as low polymers or even as monomeric molecules, Weiner and coworkers[33] and Kottke and Stalke[34] have isolated *t*-butyllithium as a pure substance for the first time and characterised it by spectroscopic methods[33] and X-ray diffraction[34]. The colourless crystalline solid was found to be tetrameric over a range of concentrations in both benzene and hexane[33, 34].

The observed IR and Raman bands for $t\text{-}C_4H_9{}^7Li$ and its isotopic species, $t\text{-}C_4H_9{}^6Li$, are summarized in Table 2. As for methyl- and ethyllithium[17], a pair of bands was observed in the C–H stretching region of *t*-butyllithium. However, their appearance at unusually low wavenumbers could not be explained in this case by the influence of multicentre bonding on the character of the α-carbon–hydrogen bond, since the corresponding carbon atoms in *t*-butyllithium had no attached hydrogen atoms. So the assignment of these bands remained unequivocal.

According to the literature[35–38], the peaks at 1450, 1375, 1210, 1130, 1000, 925 and 780 cm^{-1} were attributed to various vibrational modes of the *t*-butyl moiety[33]. Upon Li^6 substitution, the bands were retrieved at the same position in the IR and Raman spectra, which substantiated the proposed assignment (Table 2).

As expected[17], bands which do shift upon lithium isotopic substitution were found below 625 cm^{-1} (Table 2) and their appearance at such low wavenumbers is consistent with their assignment to complex vibrations of the tetrameric molecules.

In the Raman spectrum of *t*-butyllithium-7, only the strongly polarized band at 521 cm^{-1} shifts significantly upon Li^6 substitution (563 cm^{-1}) (Table 2). It was assigned to a totally symmetrical C–Li stretching mode. The peak at 525 cm^{-1} in the IR spectrum was attributed to an impurity, because it exhibited widely variable intensity in various determinations and disappeared in one spectrum[33].

Two general types of structures have been considered for the tetrameric molecules of *t*-butyllithium. The first structure is an eight-membered cycle, in which ordinary three-centre electrostatic interaction is present, involving two lithium atoms and one carbon. The highest possible symmetry would be that of regular puckered crown form, in which the eight atoms in the ring constitute a C_{4v} point group. The second structure is that of a cube, in which lithium atoms at alternate corners have been pushed in along the three-fold

TABLE 2. IR and Raman wavenumbers (cm^{-1}) observed for t-butyllithium

t-$C_4H_9{}^6Li$				t-$C_4H_9{}^7Li$			
Raman[a]		IR		Raman[a]		IR	
Benzene	Nujol	Benzene	Vapour	Benzene	Nujol	Benzene	Vapour
2833				2835			
	2810	2805			2810	2805	
2781 (dp)			2780	2782 (dp)			2780
2755				2757			
	2730	2725			2730	2725	
2692 (p)				2692 (p)			
2603 (p)				2603 (p)			
1474 (dp)				1475 (dp)			
		1455				1455	
1436 (dp)				1433 (dp)			
1385 (dp)		1375		1385 (dp)		1375	
1360 (dp)	1350	1355		1360 (dp)	1350	1355	
	1210	1215	1210		1210	1215	1210
1129 (p)	1130	1130	1130	1130 (p)	1130	1130	1130
	995	990	980		995	990	980
929 (a)	930	930	925	933 (a)	930	930	925
773 (dp)	775	780		774 (dp)	775	780	
	608				580		
563 (p)				521 (p)			
	538	(533)			522	(525)	
	500	496			480	480	
463 (p)				467 (p)			
	429	429			415	420	
383 (dp)	386	384		388 (dp)	385	384	

[a] p—polarized, dp—depolarized, a—possibly due to a benzene vibration[33].

Reprinted with permission from Reference 33. Copyright 1962 American Chemical Society.

axes (Figure 2). The lithium and α-carbon atoms make up the framework of a structure of T_d symmetry[33].

While both types of structures are equally consistent with the IR spectral pattern, the Raman spectra of t-butyllithium-6 and -7 allows distinguishing between the two models. The totally symmetric C−Li stretching mode at 525 cm^{-1} was used as diagnostic band, because it should be IR-active in structures of C_{4v} or lower symmetry and IR-inactive in structures of symmetry class T_d[39]. As we have already mentioned, none of the IR bands in this spectral region exhibits such a significant shift on ^6Li substitution to be assigned to a totally symmetrical C−Li mode. Therefore, the tetrahedral structure is favoured[33]. The proposed structure, similar to that found by Rundle and Sturdivant for the tetramer of tetramethylplatinum[40], has *four-centre* bonds, each involving three lithium atoms and the sp^3 orbital of one of the α-carbon atoms, and was later confirmed by one of our X-ray studies (Figure 2)[34].

C. Complex Formation between Ethyl- and *t*-Butyllithium

The complex formation between ethyl and t-butyllithium in benzene was later investigated by Weiner and West[41] by spectroscopic methods. The new organolithium compounds differ from any pure component, but contain both types of alkyl groups bonded to lithium.

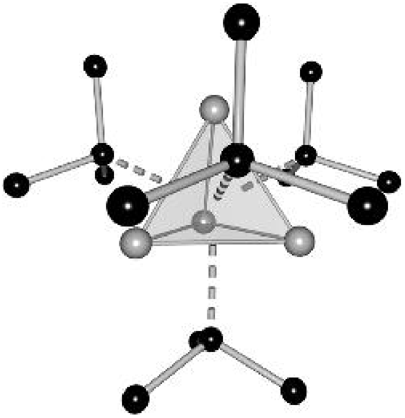

FIGURE 2. Solid-state structure of *t*-butyllithium. Reproduced with permission from Ref. 34. Copyright 1993 Wiley-VCH

It was already established that pure ethyl-[11, 17] and *t*-butyllithium[33] exist as six- and four-fold polymers, respectively, in benzene solution. Apparently, C−Li bond cleavage takes place in this solvent leading to an exchange of alkyl groups between polymeric organolithium molecules when both compounds are present. The products are believed to be electron-deficient polymers of the type $(\text{EtLi})_n(t\text{-BuLi})_{m-n}$, where m is a small number such as 4 or 6[41].

The IR spectrum of a benzene solution containing a 1:1 mixture of Et^7Li and $t\text{-Bu}^7\text{Li}$ presents a strong broad band centred around 500 cm^{-1}, not found in the IR spectra of any of the components. As we have already shown in this chapter, ethyl-[17] and *t*-butyllithium[33] have in benzene solutions strong absorption bands at 538 and 480 cm^{-1}, respectively, which were attributed to C−Li modes. A closer examination of the IR spectra of Et^7Li and *t*-BuLi showed that the band at 500 cm^{-1} could not result from an overlapping of the bands of the components. Moreover, in a 1:1 solution of Et^6Li and $t\text{-Bu}^7\text{Li}$ it shifted to 514 cm^{-1}. So the peak at 500 cm^{-1} was assigned to C−Li framework vibrations in one or more new organolithium species containing both ethyl and *t*-butyl groups.

III. LITHIUM COMPLEXES OF UNSATURATED HYDROCARBONS

A. The $\text{Li(C}_2\text{H}_2)_{1,2}$ and $\text{Li}_2\text{C}_2\text{H}_2$ Compounds

The possible complexation between lithium atoms and different π systems of unsaturated hydrocarbon compounds has stimulated various theoretical and experimental research on lithiocarbon species[42−50]. One of the first experimental studies is that of Manceron and Andrews[47] concerning the simultaneous matrix deposition of lithium atoms and acetylene molecules at high dilution in argon on a CsI window maintained at 15 K, which led to the appearance of new IR bands attributable to different species. The absorptions could be correlated to four different species, $\text{Li(C}_2\text{H}_2)_{1,2}$, $\text{Li}_2\text{C}_2\text{H}_2$ and $(\text{Li}_2\text{C}_2\text{H}_2)'$, by means of concentration effects in either lithium or acetylene and UV-VIS irradiation. Moreover, the IR spectra of these new compounds and their deuteriated species provided new information about their structure and bonding situation (Figures 3 and 4).

The authors established that the main reaction product has a LiC_2H_2 stoichiometry and ascribed six of the observed fundamentals to this species (Table 3)[47]. The presence of only

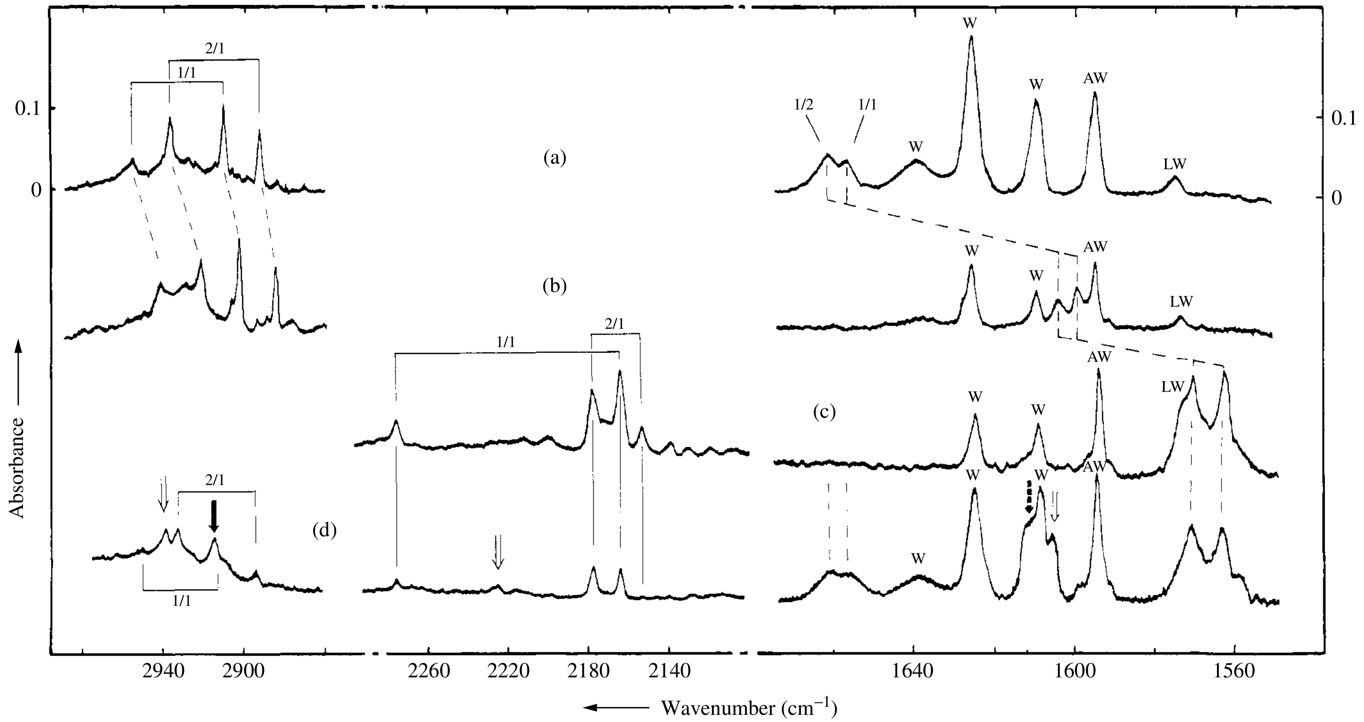

FIGURE 3. Infrared spectra recorded after deposition of Li atoms with various acetylene isotopic molecules in an argon matrix. The total concentration of acetylene in the argon matrix ($C_2H_2/Ar = 1/800$) and the lithium effusion rate (temperature *ca* 395 °C) were kept constant: (a) Li + C_2H_2; (b) Li + $^{13}C_2H_2$; (c) Li + C_2D_2; (d) Li + C_2H_2 (10%), C_2D_2 (50%), CHD (40%). W designates bands due to water impurity, AW those due to acetylene complexed water and LW those due to lithium complexed water. The open arrows indicate new signals assigned to the 1/1 and 2/1 complexes, respectively, and the dotted arrow shows the band assigned to the 1/2 complex. Reprinted with permission from Reference 47. Copyright 1985 American Chemical Society

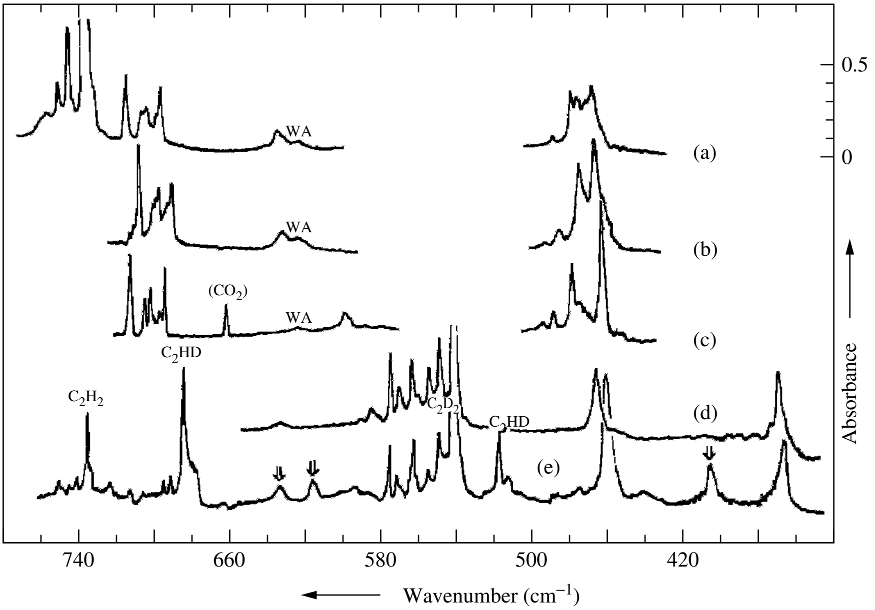

FIGURE 4. Infrared spectra recorded after deposition of Li atoms with various acetylene isotopic molecules in an argon matrix. Total concentration of acetylene in the argon matrix ($C_2H_2/Ar = 1/800$) was kept constant: (a) $^6Li + C_2H_2$; (b) $^6Li + {}^{13}C_2H_2$; (c) $^7Li + C_2H_2$; (d) $^6Li + C_2D_2$; (e) $^7Li + C_2H_2$ (10%), C_2D_2 (50%) and C_2HD (40%). The open arrows designate absorptions of the LiC_2HD species. Reprinted with permission from Reference 47. Copyright 1985 American Chemical Society

one signal in each C−H and C−D stretching region of LiC_2HD (the open arrows marked 1/1 in Figure 3) shows that the two C−H bonds in LiC_2H_2 are chemically equivalent. The existence of an ethyl radical-like adduct is ruled out, because it would have led to two sets of bands for each isotopomer (Scheme 2)[47,50]. Thus, the two signals observed for LiC_2H_2 in the C−H stretching region at 2953 and 2908 cm^{-1} were attributed to symmetrical and asymmetrical motions (Table 3). It should be mentioned that they are significantly shifted to lower wavenumbers in comparison with the corresponding modes of free acetylene (3374 and 3290 cm^{-1}), which indicates a substantial rehybridization of the acetylene unit. In addition, after $^{12}C/^{13}C$ isotopic substitution the two signals at 2908 cm^{-1} and 2953 cm^{-1} were detected at 14 and 7.5 cm^{-1}, respectively, lower [the open arrows marked 1/1 in Figure 3(a) and (b)]. This demonstrates that the stretching motion at 2908 cm^{-1} is coupled with another motion of the same symmetry, namely the C=C stretching. Therefore, the symmetrical C−H vibrational mode appears at a higher wavenumber than the asymmetrical one (Table 3).

SCHEME 2

TABLE 3. Infrared absorption bands (cm^{-1}) observed in isotopic lithium atom–acetylene matrix reactions[47]

$^6Li/C_2H_2$	$^6Li/C_2D_2$	$^7Li/C_2D_2$	$^7Li/C_2H_2$	$^6Li/^{13}C_2H_2$	LiC_2HD		Vibrational assignment[c]	
					^6Li	^7Li		
2953	2272	2272	2953	2939	2930 (CH)	2930 (CH)	ν_{sym} (CH)	LiC_2H_2
2908	2161	2161	2908	2900	2222 (CD)	2222 (CD)	ν_{asym} (CH)	
1655[a]	1561	1561	1655[a]	1597	1605[a]	1605[a]	ν (CC)	
715	577	577	714	708			i.p. δ_{asym} (CH)	
635	635[a]	[a]	601	632	645[b]	617	ν_{sym} (LiC)	
					632	632	δ_{sym} (CH)	
480	368	367	479	478	407	405	o.p. δ_{asym} (CH)	
2885[b]	2139[b]	2139[b]	2885[b]				ν_{asym} (CH)[b]	$Li(C_2H_2)_2$
1660	1569	1569	1660	1604			ν (CC)	
707	573	573	707	698			i.p. δ_{asym} (CH)	
703			703					
490	371[a]	370[a]	475[a]				o.p. δ_{asym} (CH)	
477[a]								
2936	2176	2176	2936	2919		2912 (CH)	ν_{sym} (CH)	$Li_2C_2H_2$
2890	2152	2152	2890	2883		2215[b] (CD)	ν_{asym} (CH)	
697	566	566	696	691			i.p. δ_{asym} (CH)	
1100	1098	1092	1093	1100		1092		$(Li_2C_2H_2)'$
933	930	926	929	944				
927	927		919	930		919		
918	917	919	915	924		915		
469	466	460	463	469		460		

[a] Overlapping makes measurement inaccurate.

[b] Tentative assignment.

[c] sym—symmetrical; asym—asymmetrical; i.p.—in-plane; o.p.—out-of-plane.

Reprinted with permission from Reference 47. Copyright 1985 American Chemical Society.

Structurally, the equivalence of the two C−H oscillators in LiC_2H_2 means that the new molecule kept at least a two-fold symmetry axis, or a symmetry plane bisecting or including the CC bond. Strictly speaking, the structures in Scheme 3 are consistent with this experimental fact[47].

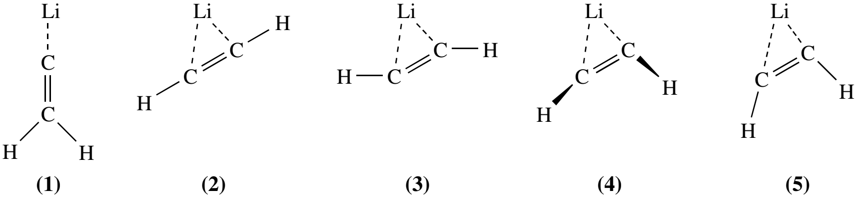

SCHEME 3

If we accept structure **1** (Scheme 3) as possible, the position of the two CH motions, the symmetrical mode above the asymmetrical mode, would not be in accord with all data of comparable structures. Moreover, the two bending motions observed at 714 and 480 cm^{-1} are very unlikely due to a rocking or wagging motion of the CH_2 group. Hence, structure **1** can be ruled out.

Models **2** and **3** (Scheme 3) have the major disadvantage of not predicting an active symmetrical C−H stretching mode without involving a fluctuation of electron density between the π system and lithium, which is determined by a change in the C−H distance or the partial C−C stretching character of the C−H symmetrical stretching. This seems unlikely since the symmetrical C−H stretching mode is more intense than the C−C stretching mode. Besides, structure **2** (Scheme 3) would not have any direct lithium contribution in the hydrogen bending modes.

Unfortunately, the only available theoretical study on lithium−acetylene species is that of Apeloig and coworkers on dilithioethylene[42], in which the most stable isomer of $Li_2C_2H_2$ was found to have a C_{2v} geometry with two lithium atoms bridging the C−C bond and the C_2H_2 group in a *cis* planar position. This seems to indicate structure **5** more probable than structure **4**. Consequently, the structure, which meets best all conditions, is **5** (Scheme 3)[47].

Further, the normal coordinate analysis using a harmonic model together with the isotopic data reinforced the conclusion that structural model **5** has a C_{2v} symmetry with the lithium atom bridging the π system and *cis* C−H groups with CCH and CLiC bond angles of $140 \pm 10°$ and $40 \pm 5°$, respectively[47]. As expected, the C−C bond is clearly the most affected by metal complexation. The F_{CC} force constant decreased by 40% from 16 to about 10.5 mdyne $Å^{-1}$ [47]. The considerable weakening of the C−C bond was experimentally demonstrated by the position of the C−C stretching mode at 1655 cm^{-1}, which is near the value for ethylene, probably due to electron density sharing between the π system of C_2H_2 and lithium rather than a valence electron transfer from lithium into an antibonding π^* orbital of C_2H_2.

A closer examination of the IR spectra in Figures 3 and 4 shows that all four peaks attributed to $Li(C_2H_2)_2$ motions are very little shifted in comparison with the corresponding modes of the LiC_2H_2 species (Table 3). Additionally, the experiments concentrated in both C_2H_2 or C_2D_2 did not lead to any new signal, which indicates that the two C_2H_2 groups are inequivalent in the $Li(C_2H_2)_2$ species. It seems that the structure of $Li(C_2H_2)_2$ is analogous to a LiC_2H_2 complex 'solvated' by another acetylene molecule[47], like in the acetylene dimer, where one acetylene molecule is hydrogen bonded to the π system of another molecule[51,52]. A decrease in the acidity of the C−H bond in the LiC_2H_2 unit indicates the solvating acetylene molecule as proton donor. This was experimentally proved by the presence of only one signal in the C−H stretching region, which is not significantly shifted from the corresponding one in LiC_2H_2 (Table 3). The bending modes observed for the $Li(C_2H_2)_2$ system present a similar behaviour (Table 3). All this rules out the possible decoupling of the two CH oscillators in the LiC_2H_2 unit. In good agreement with the trend observed for the acetylene dimer[51, 52], the C−C stretching mode at 1662 cm^{-1} is also selectively shifted compared to the other motions of the same $Li(C_2H_2)_2$ compound (Table 3).

Three fundamentals have been observed and assigned for the $Li_2C_2H_2$ species (Table 3). Experiments performed with the mixed Li_2C_2HD species showed that the two CH stretching modes keep their symmetrical and asymmetrical character, but the symmetrical motion is much weaker coupled with the C−C stretch (Table 3, the open arrows marked 2/1 in Figure 3). This can be due to a smaller CCH angle and/or the appearance of the ν (CC) mode at lower wavenumbers[47]. So the intensity ratio between the symmetrical and asymmetrical stretching modes ($I\nu_s/I\nu_a = 1.8 \pm 0.3$) calculated in the very crude model of the bond dipole moment[53, 54] allowed the estimation of the mentioned angle ($127 \pm 2°$)[47].

The $(Li_2C_2H_2)^{/}$ species showed a behaviour strictly parallel to that of the $Li_2C_2H_2$ complex, but upon UV-VIS irradiation the $(Li_2C_2H_2)^{/}$ compound did not dissociate. However, a different stoichiometry could not be excluded based on a similar Li/C_2H_2 ratio.

B. The $Li(C_2H_4)_{1,2,3}$ and $Li_2C_2H_4$ Compounds

The next logical step in the investigation of lithium atom interaction with unsaturated hydrocarbons would be the reaction with ethylene. An early theoretical study predicted that this reaction was unlikely to give anything else than an ethyl radical-like adduct[55]. Moreover, the potential energy surface of 1,2-dilithioethane has been the subject of a thorough investigation but has never been confronted with experimental data[43, 45]. That is why Manceron and Andrews carried out an IR study on the products of lithium atom matrix reactions with ethylene molecules trapped in solid argon and solid ethylene[48]. They found that the chemistry of lithium atoms with ethylene was surprisingly richer than that with acetylene. At least eight different species were evidenced, which demonstrated different Li/C_2H_4 stoichiometries. Four of these, namely $Li(C_2H_4)_{1,2,3}$ and $Li_2C_2H_4$, contained only lithium and ethylene, whereas all others contained in addition nitrogen and will be discussed in the following section.

As for LiC_2H_2, the authors have shown spectroscopically by using partial asymmetrical deuteriation $[Li_n(CH_2CD_2)_m]$ that lithium bridged symmetrically the carbon−carbon bond[48, 50]. Possible structures for the $Li(C_2H_4)_n$, $n = 1$, 2, and 3 complexes are depicted in Scheme 4.

The bridging position was further confirmed by the $^6Li/^7Li$ or $^{12}C/^{13}C$ isotopic shifts of the $Li{-}C_2H_4$ symmetrical stretching mode at 400 cm^{-1}, which were too large and too small, respectively, for a simple C−Li oscillator[48].

The $Li(C_2H_4)_{1,2,3}$ species have strong IR bands in the C=C and CH_2 scissoring spectral range, showing important shifts upon H/D substitution and insignificant or nonexistent shifts upon $^6Li/^7Li$ substitution. On the contrary, in the lower spectral region, the observed shifts are more substantial upon $^6Li/^7Li$ substitution.

The vibrational spectrum of LiC_2H_4 presents some striking similarities to that of ethylene bonded to other metals[48, 56, 57]. The C−C stretching and in-phase CH_2 scissoring modes were found to be very strongly IR-activated. The other symmetrical vibrations, CH_2 wagging and Li−C stretching motions, were detected at about 700 and 300 cm^{-1} [48, 50].

In order to give a more quantitative view of the relative perturbation of each vibrator (C=C stretching and CH_2 scissoring), the authors performed calculations for this complex based on simplified harmonic models involving mechanical couplings between the C=C

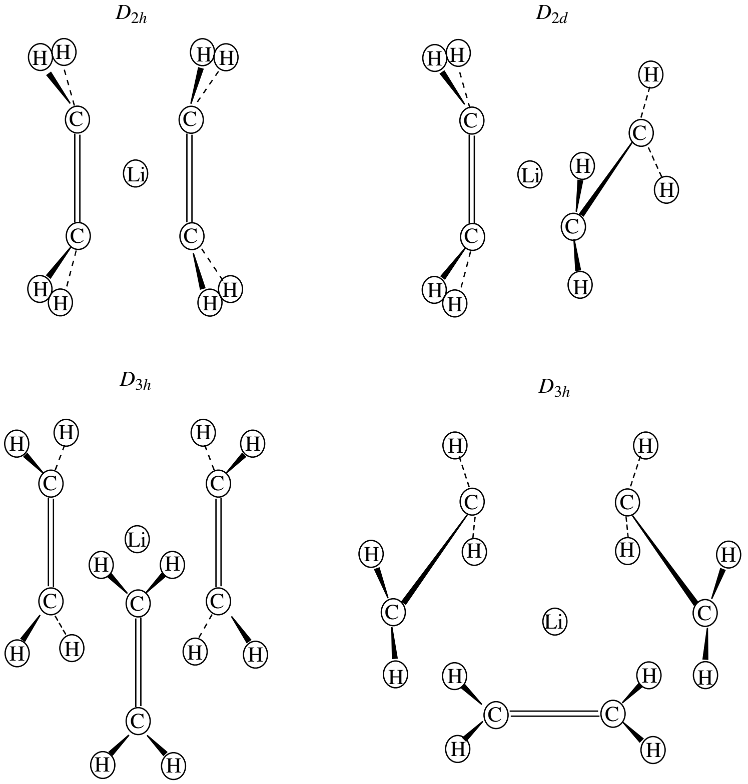

SCHEME 4

stretching and CH_2 bending oscillators. The C=C bond with a force constant lowered by about 30% was found to be the most affected by the complexation. This led to a R_{CC} internuclear distance of about 140 pm[48, 50]. The perturbation on the CH_2 bond angle deformation was only 6%.

The normal coordinate analysis also allowed the authors to quantify the relative weakness of the metal–carbon force constant in comparison with other metal–ethylene complexes (0.33 vs 0.58 mdyne Å^{-1})[48, 50].

Upon ^{6}Li/^{7}Li substitution a small shift was noticed for the modes involving the C−C coordinate. This seems to indicate a vibrational coupling between the C−C and C−Li motions, but an analysis of the IR intensities showed that the main contribution to the IR activity comes from the carbon–carbon oscillator itself. That is, the fluctuation of the C−C distance results in a very large variation of the overall dipole moment of the LiC_2H_4 complex, in the direction of the metal, perpendicular to the C−C bond itself. Therefore, this fluctuation has a large influence on the amount of possible charge transfer between the ligand and metal atom, which is also probably the cause of the vibrational coupling between ν(CC) and $\nu_s(LiC_2)$. That is, it is not necessary to invoke large puckering distortion of the ethylene group to explain the large IR intensification of the C−C coordinate[48, 50].

For di- and triethylene lithium the use of isotopic mixtures enabled the authors to show that the $Li(C_2H_4)(C_2D_4)$ and $Li(C_2H_4)_2(C_2D_4)$ species have only one isotopomer and therefore two and three equivalent ligand molecules (Scheme 4).

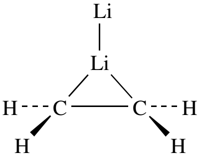

SCHEME 5

It was found that ethylene molecules do not vibrate independently of one another when they are bonded on the same lithium atom. The appearance of all in-phase C−C motions at higher wavenumbers than the out-of-phase ones indicates that stretching of one of the C−C bonds within a complex favours the shortening of the others. This was further substantiated by the calculated decrease in the F_{CC} force constant on going from C_2H_4 to LiC_2H_4 (−30%), $Li(C_2H_4)_2$ (−21%) and then to $Li(C_2H_4)_3$ (−16%)[48, 50].

For the fourth species, $Li_2C_2H_4$, the lithium atoms are not equivalent and at least one of them bridges the C−C bond. Such a structure with no inversion centre is presented in Scheme 5.

The C−C bond was found to be slightly more perturbed than in the monolithium species (i.e., LiC_2H_4) and the Li−C interactions somewhat more rigid. The normal coordinate analysis showed that such a model is capable of satisfactorily reproducing the measured isotopic shifts on the observed 12 fundamentals. However, the very important Li−Li vibration, which could prove the proposed geometry, was not detected in the expected far-infrared spectral region[48, 50].

The *ab initio* study performed by Kos and coworkers on the isomers of 1,2 dilithioethane[43] led to more symmetrical structures and did not consider the one pointed out by the experimental investigations of Manceron and Andrews[48, 50]. They showed that this structure might be only an energy subminimum kinetically stabilized in their experimental conditions by a sizeable barrier to rearrangement. However, the fact that addition of a second metal atom takes place rather on the first metal centre than on the other side of the C−C bond may also indicate why an α,β-dilithioalkane reagent has not been synthesized so far[48, 54].

C. Ternary $Li/C_2H_4/N_2$ Complexes

As could already be noted from the previous paragraph, complexes of Li with alkenes have the ability to fix one or several nitrogen molecules[48−50]. To explore this unique property among the unsaturated hydrocarbon series, Manceron and coworkers extended their studies to lithium−ethylene−nitrogen complexes[49]. During the condensation of lithium atoms with ethylene and nitrogen molecules a series of $Li(C_2H_4)_x(N_2)_y$ mixed complexes were produced spontaneously even in inert rare-gas matrices. Their IR spectra are characterised by very intense N≡N stretching bands in the 2300−2220 cm^{-1} spectral range and mixed C=C stretching and CH_2 deformation modes similar to those of $Li(C_2H_2)_n$ species with $n = 1{-}3$[49, 50]. A detailed spectral analysis of these regions and observations throughout various experimental conditions and clear-cut isotopic patterns allowed the authors to determine the stoichiometry of almost all species.

The $Li(C_2H_4)(N_2)_y$ compounds with $y = 1{-}3$ were very unstable and required large excesses of nitrogen to be observed. As discussed above, the authors showed that the

$Li(C_2H_4)_3$ species represents the highest possible level of aggregation and the most stable compounds in the $Li + C_2H_4$ system. Hence, the existence of a tetracoordinated form was at first sight surprising. But nitrogen is not as bulky as ethylene and could be bonded differently to the metal centre (especially in an end-on configuration), which would allow one to reach tetracoordination. The characteristic N≡N stretching modes (2275–2195 cm^{-1}) were detected at about 100 cm^{-1} higher than those in transition metal complexes. Therefore, the lithium–nitrogen interaction in these compounds is weaker than that in transition metal nitrogen complexes. This is further substantiated by the very small perturbations of the LiC_2H_4 subunit with respect to uncoordinated LiC_2H_4[48–50].

It was found that the stability of the mixed complexes increased considerably with the number of ethylene ligands. More exactly, the $Li(C_2H_4)_2(N_2)$ complex was stable up to the temperature at which the rare-gas matrix sublimed. It was identified and described as a $Li(C_2H_4)_2$ complex with two equivalent ethylene ligands, slightly perturbed by the addition of a N_2 molecule (Scheme 6)[49, 50]. The comparison of the IR spectrum of $Li(C_2H_4)_2(N_2)$ with those of $Li(C_2H_4)_2$ and $Li(C_2H_4)_3$ indicated the presence of a new weak peak at 1273 cm^{-1}, which was identified at 1386 cm^{-1} for the (C_2D_4) species (Table 4). In a partial force field model it was attributed to the symmetric motion at 1258 cm^{-1}, which should not be IR-active for a D_{2h} symmetry, but should occur in the IR spectrum of the structure of C_{2v} symmetry. In order to check this statement and obtain a more qualitative comparison with the $Li(C_2H_4)_n$, $n = 1–3$ compounds, the authors undertook calculations of the vibrational fundamentals based on simplified harmonic models involving the C=C stretching and CH_2 bond angle deformations of the ethylene subunits, as for the $Li(C_2H_4)_n$ species. The calculated modes for the $Li(C_2H_4)_2(N_2)$ compound with a C_{2v} structure showed acceptable agreement with the experimental values (Scheme 6). A value of $140 \pm 15°$ for the angle θ between the ethylene ligand axes could then be determined from the relative intensity ratios of the A_1 and B_2 symmetry motions of the coupled ethylene submolecules. However, the experimental data could not provide a definitive determination of the binding arrangement of N_2. The very large IR activation of the N≡N stretching mode suggested a maximal asymmetry between the two ends of the molecule, and therefore an end-on configuration[49, 50].

The fifth product was detected at high lithium concentrations. Its IR spectrum presented a N=N stretching mode at 1795 cm^{-1}, characteristic of the $Li^+ N_2^-$ ion pair with side-on bonding of the lithium atom and equivalent nitrogen atoms. However, this species was *not* observed in solid argon without ethylene *having been added* to the sample[49, 50].

TABLE 4. Comparison between observed and calculated wavenumbers (cm^{-1}) for $Li(C_2H_4)(N_2)$ using a 6 × 6 harmonic model including the C=C stretch and two CH_2 bond angle deformations of the ethylene subunits[49]

Mode	C_{2v}	$Li(C_2H_4)_2(N_2)$		$Li(^{13}C_2H_4)_2(N_2)$		$Li(C_2D_4)_2(N_2)$	
		ν_{obs}	ν_{calc}	ν_{obs}	ν_{calc}	ν_{obs}	ν_{calc}
ν_1	A_1		1485		1461	1383	1386
ν_2	B_2	1479	1481	1462	1460	1339	1342
ν_3	$A_2{}^a$		1443		1437		1076
ν_4	$B_1{}^b$		1443		1437		1076
ν_5	A_1	1273	1258		1229		953
ν_6	B_2	1200	1201	1175	1171	941	939

[a] IR active.

[b] Close to parent ν_{12} absorption.

Reprinted with permission from Reference 49. Copyright 1986 American Chemical Society.

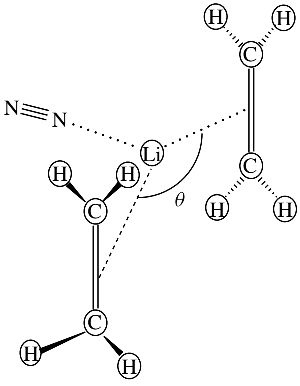

SCHEME 6

It is clear from these experiments that the presence of ethylene catalyses the fixation of nitrogen in lithium complexes. This assisted complexation was also observed with methyl-substituted ethylene and butadiene. It is a characteristic property of lithium–alkene complexes, as experiments performed with other lithium complexes have so far not yielded such ternary complexes. If one can easily anticipate that the fractional positive charge on the lithium in LiC_2H_4 and $Li(C_2H_4)_2$ facilitates the coordination of N_2 with, presumably, a σ-donation to lithium, and possibly, to a weaker extent, p-donation from the metal, it is difficult to rationalize why LiC_2H_2 and LiC_2H_4 behave so differently with respect to nitrogen, for instance.

D. Carbonyl- and Arenelithium Complexes

The most important application of organolithium reagents is their nucleophilic addition to carbonyl compounds. One of the simplest cases would be the reaction with the molecule CO itself, whose products are stable at room temperature. Recently, it was shown that a variety of RLi species are able to react with CO or t-BuNC[58] in a newly developed liquid xenon (LXe) cell[59]. LXe was used as reaction medium because it suppresses electron-transfer reactions, which are known to complicate the reaction[60]. In this way the carbonyllithium and acyllithium compounds, as well as the corresponding isolobal isonitrile products, could be characterised by IR spectroscopy for the first time.

In a first experiment a pressure of 2 bar of CO at $-100\,^{\circ}$C was applied to a saturated solution of n-BuLi in liquid xenon. Surprisingly, no free CO was detected, but a stretching vibrational mode of the carbonyl adduct of the lithium alkyl[61, 62] was observed at 2047 cm^{-1} (triple-bonded CO group). Warming up to $-30\,^{\circ}$C led to the appearance of a new ν(CO) peak at 1635 cm^{-1} (double-bonded CO group), while the IR band of the carbonyl adduct vanished. The new absorption was therefore attributed to the acyllithium compound, which also decomposed at slightly higher temperature ($-20\,^{\circ}$C) (equation 1)[58].

$$n\text{-BuLi} + \text{CO} \xrightarrow[-100\,^{\circ}\text{C}]{\text{LXe}} [n\text{-BuLi}\text{—CO}] \xrightarrow[-30\,^{\circ}\text{C}]{\text{LXe}} [n\text{-Bu—C(O)Li}] \qquad (1)$$

While in the following experiments with PhLi the corresponding carbonyllithium compound with an absorption band at 2047 cm^{-1} could be reproduced, no complexation of CO was detected with sterically hindered t-BuLi. The PhLi adduct decomposed during heating, but noticeable amounts of acyllithium species could not be found under these reaction conditions.

For further investigations *t*-BuNC, which is isolobal to CO, was used. With PhLi and *t*-BuLi, the characteristic vibrational mode of the lithium isonitrile adduct (2135 cm^{-1}) was observed at a lower wavenumber than that of the free isonitrile (2179 cm^{-1}). Unfortunately, *n*-BuLi did not undergo complexation. As indicated by the C=N stretching vibrational mode at 1510 cm^{-1}, only *t*-BuLi−CN−R reacted further to afford the lithiated Schiff base up to −20 °C (equation 2)[58].

$$t\text{-BuLi} + \text{R—NC} \xrightarrow[-100\ ^{\circ}\text{C}]{\text{LXe}} [t\text{-BuLi—CN—R}] \xrightarrow[-20\ ^{\circ}\text{C}]{\text{LXe}} [t\text{-Bu(Li)C}{=}\text{NR}] \qquad (2)$$

Only the most reactive organolithium compound, e.g. *t*-BuLi, is able to attack the carbon−nitrogen triple bond at temperatures below −20 °C. For the other less reactive species, namely PhLi and *n*-BuLi, higher temperatures in ordinary solvents like pentane would be more appropriate to synthesize their lithiated Schiff bases. However, for their detection IR spectroscopy seems to be unsuitable, since the relevant C=N stretching mode will be hidden by strong CH deformation modes of the solvent.

For a precise determination of the structures, *ab initio* calculations on the energies of formation and characteristic harmonic wavenumbers have been performed at the HF and MP2/6-31G(d,p) level of theory with the Gaussian 92 program for the species of interest[58, 63]. The *ab initio* calculated energies and harmonic vibrational wavenumbers are given in Table 5.

The addition and insertion of one molecule of CO into the lithium−hydrogen bond of the $(\text{LiH})_4$ model compound turned out to be a slightly endothermic partial reaction (23 kJ mol^{-1}) (Table 5)[58], which is hard to believe in light of the successful experiment in LXe. Using $(\text{LiMe})_4$ as substitute it was shown that the reaction is actually exothermic

TABLE 5. *Ab initio* calculated energies (Joule)[a] and harmonic vibrational wavenumbers (cm^{-1}) of the species of interest[58,63]

Species	Electronic energy (10^{-18}J)	Zero-point energy (10^{-21}J)	ν(CO)/ν(CN) (cm^{-1})
	HF	HF	HF
CO	−451.5	24.4	2171
Li_4H_4	−140.1	128.6	
$\text{Li}_4\text{H}_4\text{CO}$	−631.7	159.1	2207
$\text{Li}_4\text{H}_3\text{(COH)}$	−631.7	183.5	1441
	MP2	HF	HF
CO	−492.7	20.9	2118
$\text{Li}_4\text{Me}_4\text{CO}$	−1316.7	682.7	2475
$\text{Li}_4\text{Me}_3\text{(COMe)}$	−1316.8	706.7	1626
	HF	HF	HF
CNH	−404.8	74.1	2054
$\text{Li}_4\text{H}_4\text{CNH}$	−545.1	210.1	2108
$\text{Li}_4\text{H}_3\text{(CHNH)}$	−545.2	245.6	1426
	MP2	HF	
$\text{Li}^+ \cdot \text{PhH}$	−1041.1	480.0	
$\text{LiH} \cdot \text{PhH}$	−1044.3	492.2	
$\text{LiMe} \cdot \text{PhH}$	−1215.2	627.8	
$\text{LiPh} \cdot \text{PhH}$	−2048.6	889.8	

[a] Reaction enthalpies were determined at 0 K and corrected by the zero-point vibrational energy. Wavenumbers were scaled with a factor of 0.89.

Reprinted with permission from Reference 63.

(-32.6 kJ mol^{-1}) (Table 5) and that the wrong sign of the enthalpy in the first case is due to the inadequate $(LiH)_4$ model.

This addition led to a linear LiCO substructure with a relative long Li$-$C distance of 234.0 pm. The d(Li$-$C) in tetrameric methyllithium was theoretically determined to be 221.0 pm[63]. However, the calculated geometry of Li_4Me_3CO did not point out backbonding to CO, as it was also indicated by the CO stretching mode, which was determined at much higher wavenumber (2475 cm^{-1}) than for free carbon monoxide (2118 cm^{-1}) (Table 5)[63]. The second possible isomer presenting likewise linear CO substructure is higher in energy. The insertion of carbon monoxide into the lithium$-$carbon bond is now exothermic (-17.6 kJ mol^{-1}) and the resulting acetyl group coordinates with its carbon atom to a lithium atom [d(LiC) = 210.8 pm] and with the oxygen atom to two lithium atoms of a lithium tetrahedron face [d(LiO) = 196.9 pm]. This coordination in a μ_3 fashion favours the exothermic reaction pathway for the insertion. Figure 5 illustrates the results at the MP2/6-31G(d,p) level of theory of the above-mentioned reaction steps.

In this second case, the results of the calculations were in good agreement with the experimental data[63]. The organolithium compound with the RC=O coordinated in the proposed μ_3 fashion may now explain the significant shift of the carbonyl stretching mode from 2047 cm^{-1} in n-BuLi$-$CO to 1635 cm^{-1} in n-Bu$-$C(O)Li (equation 1).

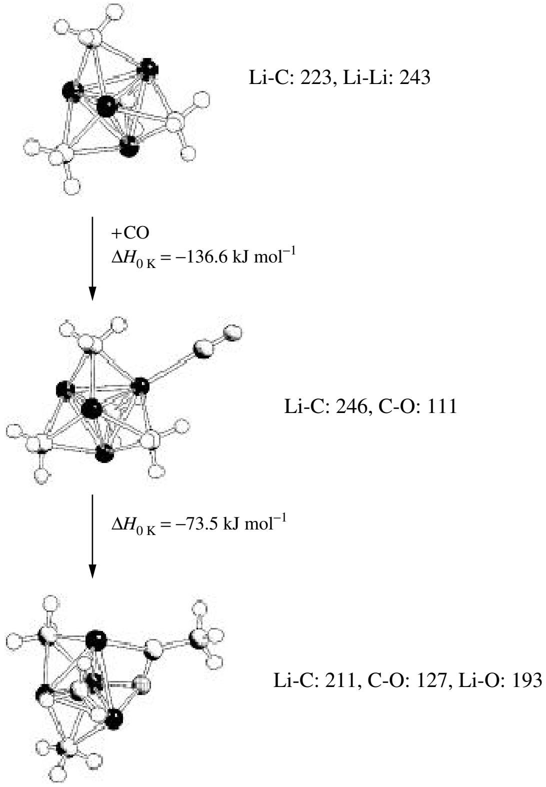

FIGURE 5. MP2/6-31G(d,p) optimized geometries of Li_4Me_4, Li_4Me_4CO, and $Li_4Me_3(COMe)$. The selected bond lengths are in pm. Reprinted with permission from Reference 63

Further investigations regarded the isonitrile reaction (equation 2). Addition of HNC to $(LiH)_4$ is accompanied by an energy release of 46 $kJ\,mol^{-1}$, and a long lithium–carbon bond is formed (225 pm). The resulting adduct Li_4H_4CNH has a linear LiCNH unit and displays C_{3v} symmetry. The calculated CN stretching mode at 2108 cm^{-1} differs only by 27 cm^{-1} from the experimental value. The second step of the reaction involved insertion into the lithium–hydrogen bond again. This partial reaction is exothermic (-54 $kJ\,mol^{-1}$) and a similar product with C_s symmetry was found. The HCNH group coordinates to all three lithium atoms in a lithium tetrahedron face. The lithium–carbon distance of 213 pm is identical with the one found in $Li_4H_3(COH)$. The CN stretching mode was again underestimated (1426 cm^{-1}) in comparison with the experimental value (1510 cm^{-1}).

As carbonyl complexes, arene organometallic fragments were believed to be an exclusive area of transition metals due to their ability of backbonding to these ligands. But recently, crystals of $(2,4,6\text{-}i\text{-}Pr_3C_6H_2)_2C_6H_3Li$ were obtained from benzene/hexane solution as monomers with the lithium centre coordinated at the benzene molecule[64]. Unfortunately, X-ray crystallography could not determine the strength of this π interaction. However, *ab initio* calculations again performed at the MP2 level for geometries and HF level for IR harmonic vibrational wavenumbers and zero-point energies were able to fill the experimental gap[63]. Three simple types of lithium compounds (LiH, LiMe and LiPh) were allowed to interact with a benzene molecule (Figure 6).

Upon coordination of the simplest model to benzene, an unexpectedly high change in the reaction enthalpy of -87.9 $kJ\,mol^{-1}$ was determined. A weak interaction like the hydrogen bonding would give about -12.6 $kJ\,mol^{-1}$. The Li–H stretching mode shifts from 1420 cm^{-1} in free LiH to 1338 cm^{-1} in coordinated LiH. These total changes of about 6% also indicate a major interaction. Correspondingly, the Li–H bond length varies from 162.4 pm to 163.3 pm. There is very little change in the bond lengths in the benzene molecule. Even the hydrogen atoms stay nearly in the molecular plane. The resulting lithium–carbon length of the adduct in C_{6v} symmetry is 252.0 pm.

The theoretical results gave in all three cases a consistent picture of the coordination of benzene to LiH, LiMe or LiPh (Figure 6)[63]. The interaction energy is about -83.7 $kJ\,mol^{-1}$ [63] unexpectedly high and suggests that the new complexes are held together with more than weak Li–benzene interactions, as suggested by the crystal structure determination[64]. When bis(benzene)chromium was used as reference compound for the bonding strength of the metal–benzene interaction, an interesting comparison came out. It was established that the formation of $Cr(C_6H_6)_2$ from a chromium atom with two molecules of benzene needs about 334.7 $kJ\,mol^{-1}$. Therefore, the bonding energy of each benzene unit to the chromium centre is 167.4 $kJ\,mol^{-1}$, which is only twice the interaction energy between lithium and benzene (83.7 $kJ\,mol^{-1}$). This high energy is due to the covalent nature of the lithium–carbon bond in the starting compound, which shows why lithium behaves like a transition metal. However, two years later, Dinnebier and coworkers determined the solid-state structure of the unsolvated Lewis base-free phenyllithium (LiC_6H_5) by high-resolution synchrotron X-ray powder diffraction and solved it by *ab initio* methods in combination with difference Fourier analysis and consecutive Rietveld refinement[65]. Solid phenyllithium was found to consist of dimeric Li_2Ph_2 molecules, which strongly interact with adjacent Li_2Ph_2 moieties, forming a polymeric, infinite-ladder structure along the crystallographic *b*-axis. In the Li_2Ph_2 units the two Li atoms and the C(*ipso*) atoms of the two phenyl rings formed an absolutely planar, four-membered ring with the two phenyl rings perpendicular to it. The bonding of the C(*ipso*) atom to the two Li atoms has been described as a three-centre, two-electron bond, where the filled sp^2 hybrid orbital of the C atom of the phenyl anion overlaps with an empty sp^2 hybrid orbital located on each Li^+ cation, respectively (Scheme 7)[65]. The third sp^2 orbital

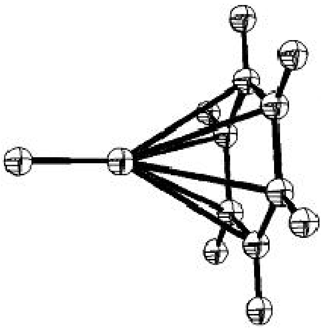

LiH: 163.3, LiC: 252.0, CC: 140.1

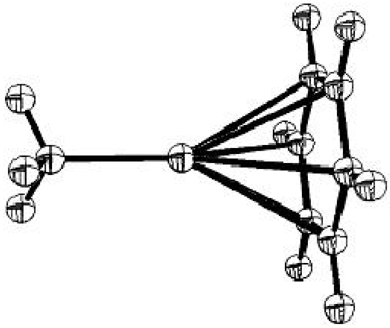

LiC (benzene): 251.7 (average)

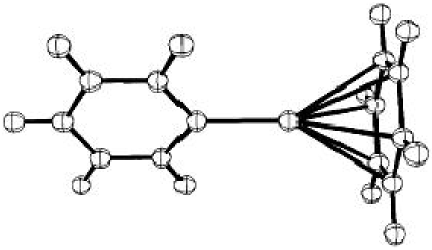

LiC (benzene): 247.0 (average)

FIGURE 6. MP2/6-31G(d,p) optimized geometries of the adducts of benzene with LiH, LiMe and LiPh. The selected bond lengths are in pm. Reprinted with permission from Reference 63

of the Li atom interacts with the lobe of a filled π-system (one of the two HOMOs of the benzene π-system) from an adjacent phenyl ring (Scheme 7)[65].

Carbonyl- and arenelithium complexes were characterised by IR spectroscopy and *ab initio* calculations for the first time. The studies underlined the ability of lithium to act like a transition metal in subcoordinated organyl compounds without having d orbitals available for bonding.

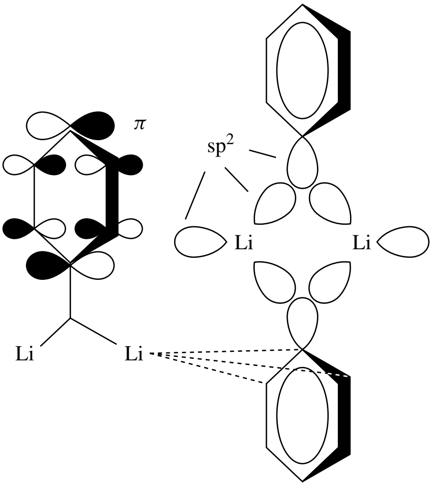

SCHEME 7

IV. OTHER ORGANOLITHIUM COMPOUNDS

A. Lithiation of Triphenyl((trimethylsilyl)imino)phosphorane, $Ph_3P{=}NSiMe_3$

Recently, we have shown that lithiation of triphenyl((trimethylsilyl)imino)phosphorane, $Ph_3P{=}NSiMe_3$, with MeLi leads to a new *ortho*-metalated species $[Li(o\text{-}C_6H_4PPh_2\text{-}NSiMe_3)]_2{\cdot}Et_2O$, which has all the requirements of an organometallic ligand capable of sidearm donation (Figure 7)[66, 67]. The deprotonated *ortho* phenyl carbon atom leads to metal–carbon σ bonds in reactions with metal halides and the $Ph_2P{=}NSiMe_3$ moiety donates an electron pair to that metal via the imine nitrogen atom. Its effectiveness as a chelating ligand was then demonstrated by reactions with zinc, copper, indium, germanium and iron halides[67, 68]. Moreover, it was found that it stabilizes diarylstannylenes and plumbylenes in their monomeric forms[69].

One of the first questions was: how are the C–Li and the formal P–N double bound affected by *ortho* phenyl ring metalation and metal coordination? Such processes are

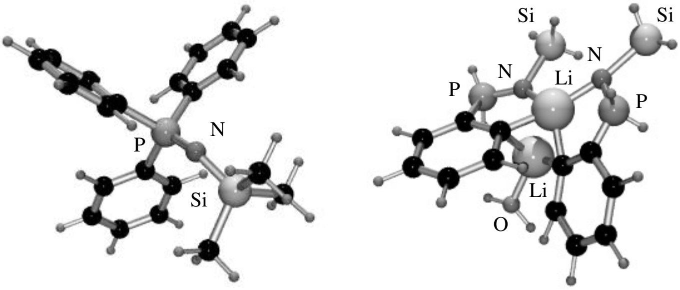

FIGURE 7. Optimized geometries of $Ph_3P{=}NSiMe_3$ and the model compound $[Li(o\text{-}C_6H_4PPh_2\text{-}NSiH_3)]_2{\cdot}H_2O$. Reprinted with permission from Reference 67. Copyright 2001 American Chemical Society

in all cases accompanied by P−N bond lengthening. This effect should be detectable in vibrational spectroscopic experiments as not all organometallic species can be obtained as single crystals. Therefore, to elucidate the coordination behaviour of [Li(*o*-$C_6H_4PPh_2NSiMe_3$)]$_2$·Et_2O in relation to the parent starting material $Ph_3P{=}NSiMe_3$, the IR and Raman spectra of the two compounds were recorded and discussed with the help of our DFT calculation results.

The geometrical parameters of $Ph_3P{=}NSiMe_3$ and the model compound [Li(*o*-$C_6H_4PPh_2NSiH_3$)]$_2$·H_2O were calculated at the BPW91/6-31G(d) and BPW91/6-31+G(d) levels of theory (Figure 7) without any symmetry restriction. In the solid state, [Li(*o*-$C_6H_4PPh_2NSiMe_3$)]$_2$·Et_2O consists of two $Ph_3P{=}NSiMe_3$ units, each deprotonated at the *ortho* position of one phenyl group. The iminophosphoranate anions bind the metal with these *ortho* carbon atoms and additionally coordinate via the imido N donor centres with a single central lithium ion. A second lithium ion is bonded to the two *ortho* ring carbon atoms and additionally coordinated to the oxygen atom of a diethyl ether molecule. The computed structural parameters for the two compounds were in good agreement with the experimental values, especially at the BPW91/6-31+G(d) level of theory. The P=N bond length in the lithium complex [156.2(2) pm, calculated 157.3(4) pm] is elongated by 2 pm compared to the parent iminophosphorane, while the P−C bond lengths do not differ significantly [180.2(2)−181.2(3) pm, calculated 181.8(3) −182.1(4) pm for [Li(*o*-$C_6H_4PPh_2NSiMe_3$)]$_2$·Et_2O and $Ph_3P{=}NSiMe_3$, respectively].

The IR and Raman spectra of the lithium complex and the starting material, in the range from 1800 to 400 cm^{-1}, are presented in Figure 8. The complete assignment is given in Table 6[67].

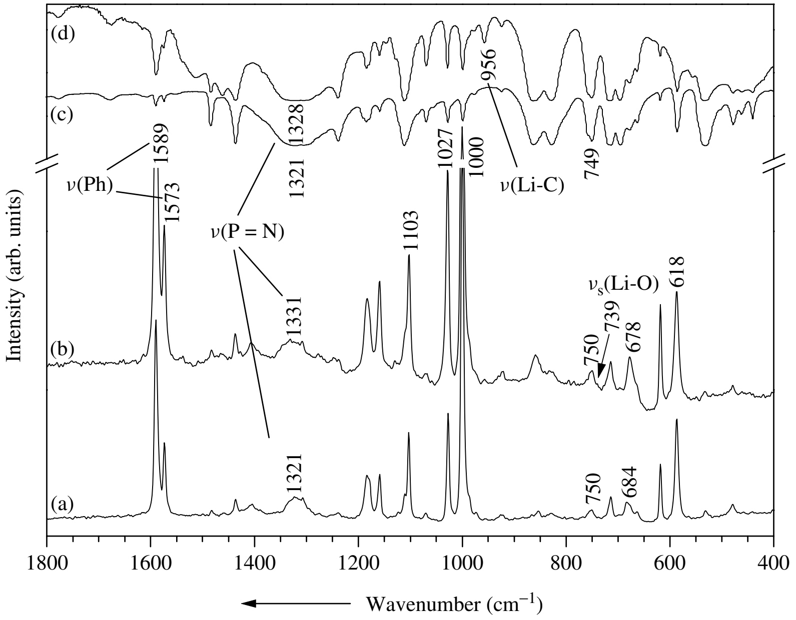

FIGURE 8. FT-Raman (at the bottom) and FT-IR (at the top) spectra of $Ph_3P{=}NSiMe_3$ (a, c) and [Li(*o*-$C_6H_4PPh_2NSiMe_3$)]$_2$·Et_2O (b, d). Reprinted with permission from Reference 67. Copyright 2001 American Chemical Society

TABLE 6. Selected experimental and calculated vibrational wavenumbers (cm^{-1}) for $Ph_3P = NSiMe_3$ and $[Li(o\text{-}C_6H_4PPh_2NSiMe_3)]_2 \cdot Et_2O$ with their tentative assignments[67]

$Ph_3P = NSiMe_3$				$[Li(o\text{-}C_6H_4PPh_2NSiMe_3)]_2 \cdot Et_2O$				Vibrational assignment[d]
Experimental		Calculated		Experimental		Calculated		
IR[c]	Raman[c]	DFT[a]	DFT[b]	IR[c]	Raman[c]	DFT[a]	DFT[b]	
1590 w	1589 vs	1623	1600	1589 w	1589 vs	1624	1614	Ph ring stretching
1575 w	1573 s	1603	1585	1576 sh	1573 s	1601	1564	
1436 s	1437 w	1457	1437	1437 m	1438 m	1463	1444	semicircle Ph ring stretching
1319 m	1322 m	1306	1328	1328 m	1331 m	1326	1332	ν(P=N)
1185 s	1184 m	1191	1190	1185 m	1182 m	1187	1193	i.p. δ(C–H)
1159 m	1158 m	1163	1165	1160 m	1159 m	1172	1178	
1113 s	1104 s	1126	1114	1112 s	1102 s	1117	1115	ν(P–Ph)
998 m	1000 vs	1008	997	998 m	1000 vs	1012	1009	Ph ring breathing
				956 w		951	952	ν(Li–C)
752 s	750 m	762	732	751 s	749 m	757	748	o.p. ω(C–H)
					739 sh			ν_{sym}(Li–O)
684 m	684 s	671	687	677 sh	678 s	675	690	$\nu_{\text{asym}}(\text{Si–C}) + \nu_{\text{sym}}(\text{Li–N})$
664 m	663 sh	662	663	663 m	663 sh	649	670	ν(Si–N)
620 m	618 m	622	612	619 m	618 m	629	598	i.p. Ph ring bending
587 s	586 s	571	568	587 s	587 s			ν_{sym}(Si–C)

[a] Calculated with BPW91/6-31G(d).

[b] Calculated with BPW91/6-31+G(d).

[c] Abbreviations: w—weak, m—medium, s—strong, vs—very strong, sh—shoulder.

[d] sym—symmetrical, asym—asymmetrical, i.p.—in-plane, o.p.—out-of-plane, ν—stretching, δ—bending, ω—wagging.

Reprinted with permission from Reference 67. Copyright 2001 American Chemical Society.

One of the most relevant features of the vibrational spectra of organometallic compounds are the metal–carbon stretching vibrations, since they are directly related to the most substantial property of the molecule, that is the M–C bond strength[70]. However, the assignment of the ν(M–C) vibrational modes is often hampered due to the presence of other bands in the same region or due to their low intensities. In our case, the lithium–carbon stretching vibration appeared only in the IR spectrum of $[Li(o\text{-}C_6H_4PPh_2NSiMe_3)]_2\cdot Et_2O$ as a weak signal at 956 cm^{-1}. The assignment of the ν(Li–C) vibration was based on the results of theoretical calculations. Significant changes in the position and relative intensities of some other bands could be observed in the Raman spectrum of the lithium complex. Thus, the band at 684 cm^{-1} (calculated 687 cm^{-1}) assigned in the spectrum of $Ph_3P{=}NSiMe_3$ to the ν_a(Si–C) vibration is shifted to lower wavenumbers by 6 cm^{-1} and the intensity is increased due to convolution of the ν_s(Li–N) vibration in the same spectral range[71]. The signal around 1100 cm^{-1} assigned to the ν(P–Ph) vibration[71] is more intense in the spectrum of $[Li(o\text{-}C_6H_4PPh_2NSiMe_3)]_2\cdot Et_2O$. The new shoulder that appeared at 739 cm^{-1} was attributed to the ν_s(Li–O) vibration of the new lithium compound[70]. In the Raman spectrum of $[Li(o\text{-}C_6H_4PPh_2NSiMe_3)]_2\cdot Et_2O$, the broad band at about 1331 cm^{-1} (calculated 1332 cm^{-1}) was assigned to the ν(P=N) stretching mode[73]. In comparison to the corresponding vibration of $Ph_3P{=}NSiMe_3$, this band is shifted to higher wavenumbers by 10 cm^{-1}, due to the N–Li coordination. The shift of the ν(P=N) vibration confirms our observation that the iminophosphorane units coordinate through the imino nitrogen atoms. The peaks, which dominate the Raman spectra of the two compounds, are due to phenyl vibrations, the most representative being assigned to the ring stretching (1573 and 1589 cm^{-1}, calculated 1585 and 1600 cm^{-1}) and ring breathing (1000 cm^{-1}, calculated 997 cm^{-1}) modes. The other characteristic motions of aromatic groups were observed in the expected spectral regions[72, 73], no differences appearing in the spectrum of $[Li(o\text{-}C_6H_4PPh_2NSiMe_3)]_2\cdot Et_2O$ compared to that of the starting material $Ph_3P{=}NSiMe_3$.

B. Lithiation of *N*,*N*′,*N*″-tris(*t*-butyl)sulphur triimide, S(NBu-*t*)$_3$

Isoelectronic replacement of the oxygen atoms in the simple p-block element oxoanions by a NR imido group is currently a flourishing area of main group chemistry[74–79]. In the polyimido sulphur anions the central sulphur atom can either adopt the oxidation state IV, as in the S-alkyliminosulphinamides[80–88] $[RS(NR')_2]^-$ and iminosulphindiamides[89] $[S(NR)_3]^{2-}$, or the oxidation state VI, as in the S-alkyldiiminosulphonamide $[RS(NR')_3]^-$ and tetraimidosulphates[90] $[S(NR)_4]^{2-}$. The anionic S^{IV} species are derived from sulphur diimides by addition of organolithium species or lithium amides to the formal S=N double bond[91]. By analogy, the S^{VI} species are derived from sulphur triimides by similar nucleophilic addition reactions[91]. However, the chemistry of sulphur triimides[92], in contrast to the chemistry of sulphur diimides, is rather unexplored[93]. One of the reasons might be the limited synthetic access to sulphur triimides. Until recently, only two reactions were known in which the sulphur triimide backbone is formed[94–96]. In our investigations of the $[S(NR)_3]^{2-}$ ligand, we found a new, simple and quantitative route to sulphur triimides[97]. Hence, the way is opened up to prepare S-alkyldiiminosulphonamide and new lithium tetraimidosulphate complexes and to explore their coordination behaviour. Consequently, dilithium tetrakis(*tert*-butyl)tetraimidosulphate $[(THF)_4Li_2(NBu\text{-}t)_4S]$ was prepared in the nucleophilic addition reaction of lithium(*tert*-butyl)amide to *N*,*N*′,*N*″-tris(*tert*-butyl)sulphur triimide in THF (equation 3)[98].

$$S(NBu\text{-}t)_3 + 2LiHNBu\text{-}t \xrightarrow{\text{THF/hexane}} [(THF)_4Li_2(NBu\text{-}t)_4S] + H_2NBu\text{-}t \qquad (3)$$

As mentioned, Raman spectroscopy is an important tool for determining structural parameters of such organolithium compounds. Unfortunately, only very few Raman spectroscopic investigations have been reported for the starting material[95, 99, 100]. These authors tentatively assigned only some of the observed bands. Therefore, at the beginning of our investigations we studied the vibrational behaviour of $S(NBu\text{-}t)_3$ using various Raman techniques, and assigned vibrational modes with assistance of the results from DFT calculations. On the basis of these results the first Raman investigation of a dilithium tetraimidosulphate complex was presented[98].

In the case of the sulphur triimide $S(NBu\text{-}t)_3$, the dispersive Raman technique applying a double monochromator and a CCD camera was employed to obtain the information from polarized measurements (solution studies) and also to obtain high-resolution spectra by low-temperature measurements. In the case of the main group metal complex, only FT-Raman studies with long-wavenumber excitation were successful, since visible-light excitation caused strong fluorescence. The FT-Raman spectra of the tetraimidosulphate residue were similar to those obtained from excitation with visible laser lines.

The DFT calculations led to a structure of C_{3h} symmetry for the model compound $S(NMe)_3$ (Figure 9 and Table 7) with 42 normal vibrations, whose irreducible representation is given by $8A'$ (Ra) $+ 18E'$ (Ra/IR) $+ 6A''$ (IR) $+ 10E''$ (Ra). The brackets indicate activities in Raman scattering and/or infrared absorption.

The sulphur triimide $S(NBu\text{-}t)_3$ can also be considered to have C_{3h} symmetry; in this case the methyl groups were treated as point masses. In contrast to the published values[95, 99, 100] in which the SN vibrations of sulphur triimides were assigned in the region around 1200 cm^{-1} to the asymmetrical and around 1150 cm^{-1} to the symmetrical mode, we located them at lower wavenumbers, i.e. in the 640–920 cm^{-1} range [$\nu_{asym}(SN_3) = 918$ cm^{-1} and $\nu_{sym}(SN_3) = 641$ cm^{-1}]. We should mention that all of the stretching modes, which are described in Table 7, are mainly due to motions of one bond, SN or CN. However, most of the vibrations are not pure vibrations with only one internal coordinate involved. This assignment is supported by the DFT calculations on $S(NMe)_3$, in which $\nu_{asym}(SN_3)(E')$ was found at 880 cm^{-1} and $\nu_{sym}(SN_3)$ at 661 cm^{-1}. Only the latter gives a strong polarized Raman band at 641 cm^{-1}. For the CN stretching modes, the Raman-active A' band was theoretically determined at 1072 cm^{-1}, whereas the experimental one was detected at 1058 cm^{-1} as a polarized band of very strong intensity. The computed E' bands (Ra/IR) at 1169/1168 cm^{-1} were attributed to the medium intensity band at 1227 cm^{-1}[98].

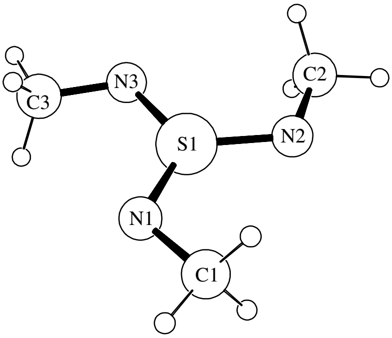

FIGURE 9. DFT-calculated geometry of $S(NMe)_3$, resulting in a molecule of C_{3h} symmetry[98]. This structure is known for $S(NBu\text{-}t)_3$, and $S(NSiMe_3)_3$ from crystal structure analyses[95, 101]. Reproduced with permission from Reference 98. Copyright 1998 Wiley-VCH

TABLE 7. Calculated wavenumbers (cm^{-1}) for the model compound $S(NMe)_3$ in comparison with the Raman measurements for $S(NBu\text{-}t)_3$ and $[(THF)_4Li_2(NBu\text{-}t)_4S]$[a] 98

$S(NMe)_3$ calculated	Vibrational assignment	$S(NBu\text{-}t)_3$ in benzene; 647.1 nm	$S(NBu\text{-}t)_3$ polycryst.; 647.1 nm	$S(NBu\text{-}t)_3$ polycryst.; 1064 nm	Vibrational assignment	$[(THF)_4Li_2(NBu\text{-}t)_4S]$ polycryst.; 1064 nm
1467 A' (Ra)	out-of-phase $\sigma(CH_3)$	1476 vw	1481 vvw, 1473 vvw	1476 w	out-of-phase $\sigma(CH_3)$	
1468, 1467 E' (Ra/IR)	out-of-phase $\sigma(CH_3)$	1453 m	1457 m, 1450 m	1449 s	out-of-phase $\sigma(CH_3)$	1452 vs (+ THF)
1463, 1462 E'' (Ra)	out-of-phase $\sigma(CH_3)$	1447 m	1446 m, 1441 w		out-of-phase $\sigma(CH_3)$	
1465 A'' (IR)						
1169, 1168 E' (Ra/IR)	$\nu(CN)$	1227 m	1230 m	1227 m	$\nu(CN)$	
1113 A' (Ra)	$\rho(CH_3)$	1216 m (p)	1217 m	1214 m	$\rho(CH_3)$ [t-Bu]	1215 s (+ THF)
1072 A' (Ra)	$\nu(CN)$	1058 vs (p)	1060 vvs	1057 vs	$\nu(CN)$	1060 w
1089, 1089 E'' (Ra)	$\rho(CH_3)$	1031 w	1036 w, 1033 w, 1030 w	1031 w	$\rho(CH_3)$ [t-Bu]	1023 w
1084 A'' (IR)						
880 E' (Ra/IR)	$\nu_{asym}(SN_3)$	918 m	924 m, 922 m, 920 m, 918 m, 916 m	918 m	$\nu_{asym}(SN_3)$	917 m
						900 s (THF)
		812 m (p)	816 m	814 m	$\nu(CC_3)$	800 s
661 A' (Ra)	$\nu_{sym}(SN_3)$	641 vs (p)	641 vs	642 vs	$\nu_{sym}(SN_3)$	534 s
504, 503 E' (Ra/IR)	i.p. $\delta(SNC)$	558 w	557 w	559 w	i.p. $\delta(SNC)$	
		446 m (p)	465 w	468 w	$\delta(CC_3)$	431 w
277 A' (Ra)	i.p. $\delta(SNC)$	287 m (p)	299 w, 278 w	293 w, 271 w	i.p. $\delta(SNC)$	276 vs (+ THF)
215, 214 E'' (Ra)	o.p. $\delta(SNC)$	253 m	255 m	254 m	o.p. $\delta(SNC)$	254 m
		193 m (p)	194 m	194 m	δ (CC_3)	164 w
144, 143 E' (Ra/IR)	i.p. $\delta(SNC)$			144 m	i.p. $\delta(SNC)$	128 w

[a] Abbreviations: w—weak, m—medium, s—strong, v—very, sh—shoulder, subscript sym—symmetrical, subscript asym—asymmetrical, i.p.—in-plane, o.p.—out-of-plane, ν—stretching, δ—bending, ω—wagging, ρ—rocking, σ—deformation.

Reproduced with permission from Reference 98. Copyright 1998 Wiley-VCH.

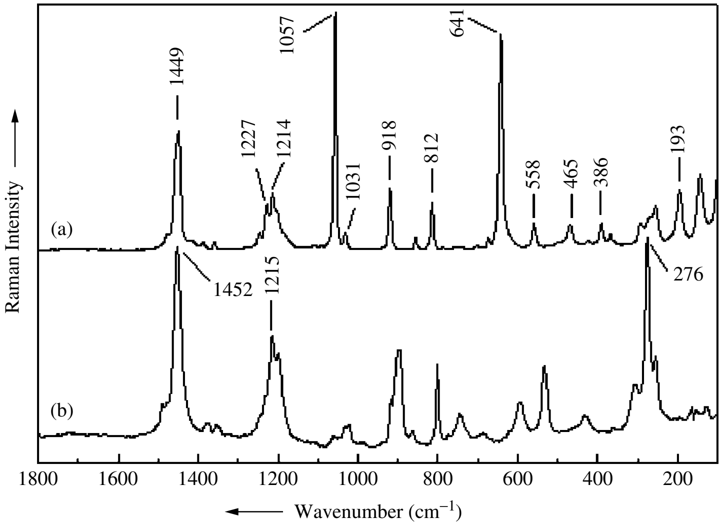

FIGURE 10. FT-Raman spectra of sulphurtriimide S(NBu-*t*)$_3$ (a) and dilithium tetraimidosulphate [(THF)$_4$Li$_2$(NBu-*t*)$_4$S] (b). Reproduced with permission from Reference 98. Copyright 1998 Wiley-VCH

The mode at 276 cm^{-1} appears in the Raman spectra of the complex with very strong intensity. It is caused by the coordinated tetrahydrofuran (THF). From this coordinated THF molecule, the high intensity of the bands at 1452 and 1215 cm^{-1} (compared with the ligand spectra) can also be rationalized (Figure 10 and Table 7)[98].

In conclusion, the Raman spectroscopic experiments and the assignment of the SN vibrations to much lower wavenumbers than previously reported suggest a mainly electrostatic contribution in the $> S^+{-}N^-$—bond of sulphur triimides and related metal complexes. The hypothesis of valence expansion at sulphur to three covalent double bonds [S(=NR$_3$)] seems no longer valid[91, 98].

V. POLYLITHIUM COMPOUNDS

A. Polylithiation of Propyne

Infrared spectroscopy is one of the few physical chemical methods which can help in determining the structure of notoriously insoluble and pyrophoric polylithium compounds such as C_3Li_4[102]. By examining the changes in the IR spectrum during the formation of C_3Li_4 by reaction of propyne with *n*-butyllithium in hexane, West and coworkers could get important information about the structure of the new polylithium compound[102, 103].

Figure 11 presents the IR spectra recorded in the most interesting region, namely 2200–1400 cm^{-1}, as a function of time and temperature after addition[102]. It is known that propyne itself does not have absorption bands between 2100 and 1600 cm^{-1}. But after addition of propyne to 4 equivalents of *n*-butyllithium in hexane, three new signals were detected at 1870, 1770 and 1675 cm^{-1}. As one can notice, the band at 1870 cm^{-1} grows weaker with time in comparison with the other two bands and disappears entirely upon brief heating[102]. Later, with longer refluxing, the peak at 1770 cm^{-1} shows a similar behaviour. The peak at 1675 cm^{-1} remains the only strong signal in this spectral

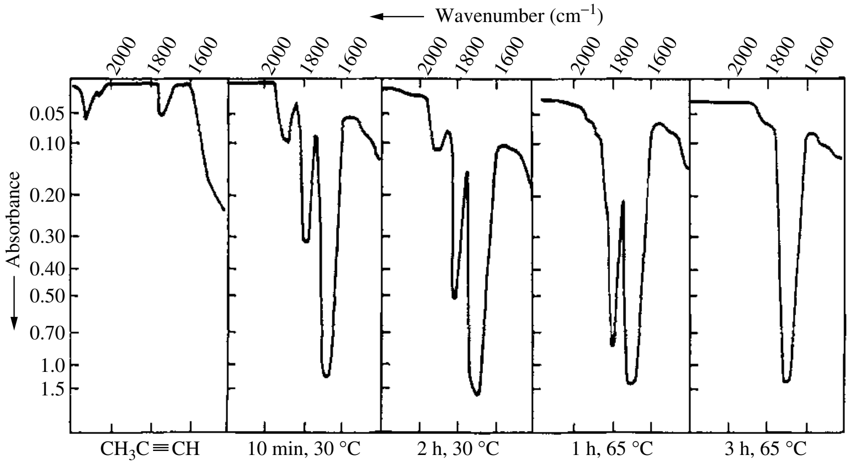

FIGURE 11. Infrared absorption in the allenic region for propyne (left) and for propyne + 4 *n*-butyllithium in hexane, as a function of time and temperature after addition. Reprinted with permission from Reference 102. Copyright 1969 American Chemical Society

range. Because $CH_3C{\equiv}CLi$ is insoluble in hexane and has a C≡C stretching motion at 2050 cm^{-1}, none of the three bands can be due to this monolithium compound. Moreover, when propyne was added to only 2 or 3 equivalents of *n*-butyllithium, the same three bands were found again in the IR spectrum, but the bands at higher wavenumbers were proportionately stronger and did not disappear on refluxing. Therefore, the three absorption peaks were attributed to three different species, namely $C_3H_2Li_2$, C_3HLi_3 and C_3Li_4.

Similar metalation studies were carried out on 1,3-bis(trimethylsilyl)propyne. The IR bands observed in the 2200–1600 cm^{-1} region of acetylenes, allenes and all the lithiated derivatives are summarized in Table 8.

As one can notice, the C≡C stretching vibrational mode of all acetylenes appears between 2190 and 2130 cm^{-1}, whereas for allenes the C=C=C asymmetrical stretching motion occurs below 2000 cm^{-1} (Table 8). Starting with propyne to lithiopropyne and then to the polylithium species, the characteristic stretching vibrational mode is lowered by 80, 180 and then by 90–100 cm^{-1} for each lithium atom, respectively (Table 8). West and Jones associated the very large change from C_3H_3Li to $C_3H_2Li_2$ with a structural change from the acetylenic to the allenic form[102]. Anyway, several years later the interpretation of the IR spectra of polylithiated terminal acetylenes was revised in terms of propargylide and allenic anions. This will be discussed later in this chapter.

Of all the lithium derivatives, only the salt-like $CH_3C{\equiv}CLi$ has absorption bands above 2000 cm^{-1}; all the others give absorption below 1900 cm^{-1} [102]. Because these modes occur at too low wavenumbers to be acetylenic, West and Jones concluded that the other lithium derivatives $C_3HLi(SiMe_3)_2$, $C_3Li_2(SiMe_3)_2$ and $C_3Li(SiMe_3)_3$ also have allenic structures[102].

B. Polylithiation of Nitriles

After the preparation of C_3Li_4, which can be formally regarded as a derivative of the linear trianion $C_3{}^{4-}$, isoelectronic with carbon dioxide, Gornowicz and West tried to fill

TABLE 8. Infrared absorption bands (cm^{-1}) in the 2200–1600 cm^{-1} region for acetylenes, allenes and some lithiated species

Compound	ν (C≡C)	ν (C=C=C)
Propyne	2130[a]	
Allene		1970[b]
Monolithio		
$CH_3C{\equiv}CLi$	2050[a]	
$PhCH_2C{\equiv}CLi$	2050[c]	
$PhC_3(SiMe_3)_2Li$	2000[c]	1850[c]
$PhC_3H(SiMe_3)Li$		1870[c]
$C_3HLi(SiMe_3)_2$		1870[a]
$C_3Li(SiMe_3)_3$		1850[a]
$CH_2{=}C{=}CHLi$		1890[d]
Dilithio		
$C_3H_2Li_2$		1870[a]
$C_3Li_2(SiMe_3)_2$		1790[a]
PhC_3HLi_2		1900[c]
$PhC_3(SiMe_3)Li_2$		1790[c]
Trilithio		
C_3HLi_3		1770[a]
PhC_3Li_3		1790[c]
$C_3(SiMe_3)Li_3$		1770[a]
Tetralithio		
C_3Li_4		1675[a]

[a] Data from Reference 102.
[b] Data from Reference 104.
[c] Data from Reference 105.
[d] Data from Reference 106.

in the gap at −3 charge in the isoelectronic series of linear species containing 16 valence electrons (the carbon dioxide structure)[107] (Table 9). So they metalated several nitriles and investigated the structure of the new polylithium compounds by IR spectroscopy[108].

The absorption bands found for the mono- and dilithiated species in the 2400–1600 cm^{-1} range are listed in Table 10. The presence of more than one peak in the mentioned spectral region for the monolithium derivatives of acetonitrile demonstrates that they exist in more than one tautomeric form (equation 4)[108].

The monolithium species, $Li(Me_3Si)_2C_2N$ and $LiMe_2C_2N$, have only one absorption at 2000 cm^{-1} (Table 10). This absorption cannot be due to a lithiated ketenimine, $R_2C{=}C{=}NLi$, as it appears at too high wavenumbers. It seems possible that these

TABLE 9. Isoelectronic species with 16 valence electrons[107, 108]

Charge	Species
+1	NO_2^+
0	CO_2, N_2O, CS_2, FCN
−1	NCO^-, NCS^-, N_3^-, CNO^-
−2	NCN^{2-}
−3	
−4	(CCC^{4-})

Reprinted with permission from Reference 108. Copyright 1971 American Chemical Society.

TABLE 10. Infrared absorption bands (cm^{-1}) in the 2400–1600 cm^{-1} region for metalated nitriles[108]

Compound	Wavenumber (cm^{-1})
LiC_2H_2N[a]	2130, 2040
LiC_2Me_2N[b]	2000
$LiC_2(Me_3Si)_2N$[c]	2000
Li_2C_2HN[d]	1820
Li_2C_2MeN[c]	1880
Li_2C_2PhN[b]	1900
$Li_2C_2(Me_3Si)N$[c]	1900

[a] Suspension in THF–hexane.
[b] Solution in hexane.
[c] Suspension in pentane or hexane.
[d] Suspension in ether.
Reprinted with permission from Reference 108. Copyright 1971 American Chemical Society.

monolithium derivatives exist in the R_2LiCCN form[108].

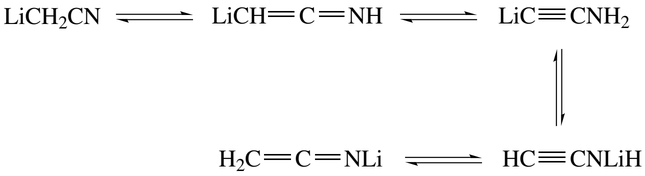

(4)

All dilithiated nitriles show one peak in the 1900–1800 cm^{-1} range. They could also occur in several tautomeric forms (equation 5).

$$RCLi_2CN \rightleftharpoons RLiC{=}C{=}NLi \rightleftharpoons RC{\equiv}CNLi_2 \qquad (5)$$

When R is hydrogen, more tautomeric forms similar to those of monometalated acetonitriles can be written[108]. These modes appear at too low wavenumbers to be acetylenic or nitrile absorptions and therefore they were attributed to ketenimine derivatives of form R(Li)C=C=NLi. For the ionic species, Gornowicz and West proposed a delocalized structure (Scheme 8)[108]. Klein and Brenner called it sesquiazacetylene in a previous study[109].

$$(RC \equiv C \equiv N)^{2-}$$

SCHEME 8

C. Polylithiation of Phenylpropynes

Mulvaney and coworkers reported a polylithiation of a non-terminal acetylene for the first time, more exactly the formation of $C_6H_5C_3Li_3$ and $C_6H_4LiC_3Li_3$ from 1-phenylpropyne and n-butyllithium in hexane[110]. Stimulated by their work, West and Gornowicz prepared and investigated new polylithium compounds from phenylpropynes and their polysilicon derivatives[105]. The structures of several of them were analysed by IR spectroscopy.

In order to determine the structures of the intermediate organolithium compounds, 1-phenylpropyne was metalated with 4 equivalents of *n*-butyllithium in refluxing cyclohexane[105]. One hour later, no absorption due to lithiated phenylpropynes was detected. The IR spectrum showed only a strong peak at 1775 cm^{-1} due to a trilithioallene, which gradually became much stronger. Apparently, the introduction of the first Li atom is much slower than subsequent lithiations, so no mono- and dilithiated species were observed in the IR spectrum.

Anyway, the same polylithium compounds can be obtained from either 1- or 3-phenylpropyne, because 1-phenylpropyne when lithiated in the methyl group immediately rearranges to give the more stable lithium acetylide, 1-lithio-3-phenylpropyne[109]. So 1-lithio-3-phenylpropyne was prepared by West and Gornowicz by adding *n*-butyllithium to 10 equivalents of 3-phenylpropyne[105]. Its IR spectrum exhibits only one weak peak in the 2200–1600 cm^{-1} range, namely at 2050 cm^{-1}. Derivatizing with trimethylchlorosilane led to the product **6** (equation 6). 3-Phenylpropyne and 2 equivalents of *n*-butyllithium gave a yellow solid with intense allenic absorption at 1900 cm^1. Derivatizing again with trimethylchlorosilane gave predominantly **7** (equation 7)[105].

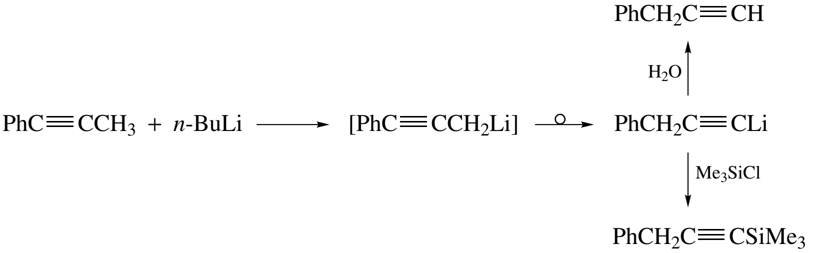

$$\begin{tikzcd}
 & & \mathrm{PhCH_2C{\equiv}CH} \\
\mathrm{PhC{\equiv}CCH_3} + n\text{-}\mathrm{BuLi} \arrow[r] & \mathrm{[PhC{\equiv}CCH_2Li]} \arrow[r, "\circ"] & \mathrm{PhCH_2C{\equiv}CLi} \arrow[u, "\mathrm{H_2O}"'] \arrow[d, "\mathrm{Me_3SiCl}"] \\
 & & \mathrm{PhCH_2C{\equiv}CSiMe_3}
\end{tikzcd} \tag{6}$$

(6)

$$\mathrm{Ph(Li)C{=}C{=}CHLi} \xrightarrow{\mathrm{Me_3SiCl}} \mathrm{Ph(Me_3Si)CHC{\equiv}CSiMe_3} \tag{7}$$

(7)

When 3-phenylpropyne was treated with 3 equivalents of *n*-butyllithium, a soluble complex of 1-phenyl-1,3-dilithioallene and *n*-butyllithium was obtained. The IR spectrum of this deep red solution shows two peaks, at 1900 and 1780 cm^{-1}. While the weak absorption at 1780 cm^{-1} due to the phenyltrilithioallene increases with time, the strong absorption at 1900 cm^{-1} gradually disappears.

The further lithiation of compounds **6** and **7** led to organolithium compounds with interesting structures and properties. While the mono- and dilithiated species of **6** shows only allenic absorptions at 1870 and 1790 cm^{-1}, the monolithiated species of **7** have both acetylenic and allenic absorptions at 2000 and 1850 cm^{-1} (Table 8). Their unchanged spectral profile suggests the existence of two isomers: $\mathrm{Ph(Me_3Si)CLiC{\equiv}CSiMe_3}$ and $\mathrm{Ph(Me_3Si)C{=}C{=}C(SiMe_3)Li}$. West and Gornowicz explained the stabilization of the acetylenic form by a combination of delocalization of charge onto the benzene ring and the strong acidifying effect on silicon[105].

The authors noticed that polylithiated phenylallenes have a vibrational behaviour similar to that of polylithiated propynes and butynes (Table 8)[105]. The monolithium compounds from terminal acetylenes were found to have acetylenic structures (2050 cm^{-1}), whereas the monolithium derivatives of non-terminal acetylenes could exist in either acetylenic (2000 cm^{-1}) or allenic (1870–1850 cm^{-1}) forms (Table 8)[105]. The polylithium compounds were found to have only allenic absorptions, significantly lowered by the lithium substitutions.

However, several years later Priester and coworkers revised the interpretation of the IR spectra of polylithiated acetylenes in terms of propargylide and allenic anions (Table 11)[111]. They divided the compounds into two categories: those that can directly form lithioacetylides (the terminal acetylenes) and those that must undergo hydrogen or alkyl shifts to form acetylides (the internal acetylenes).

While the mono- and dianions of internal acetylenes still have allenic structures, polylithiation of terminal acetylenes results in anions having a different structure, as previously reported[102, 105] (Scheme 9).

Initially monolithioacetylides, $R{-}C{\equiv}C^{-}Li^{+}$, are formed. Further lithiation results in a large bathochromic shift (180 cm^{-1}) of the characteristic absorption band, which indicates bond reorganization upon dilithiation (Scheme 10). The new structure (**8** in Scheme 9) was called propargylide, because it contains both acetylenic and propargylic lithium[111].

Priester and coworkers showed that the confusion in the previous assignments is due to the appearance at the same position of the IR absorptions of the propargylide dianion

TABLE 11. Infrared absorption bands (cm^{-1}) in the 2200–1600 cm^{-1} region for lithiated internal and terminal acetylenes in hexane[111]

Compound	Acetylides and propargylides	Allenic anions
Monolithiated		
$H_3C{-}C{\equiv}C{-}Li$[a]	2050	
$Me_2CH{-}C{\equiv}C{-}Li$	2050	
$MeCH_2{-}C{\equiv}C{-}Li$	2040	
$PhCH_2{-}C{\equiv}C{-}Li$[b]	2050	
$[Me_3SiCH{-}C{\equiv}C{-}SiMe_3]Li$[a]		1870
$[(Me_3Si)_2C{-}C{\equiv}C{-}SiMe_3]Li$[a]		1850
$[Ph(Me_3Si){-}C{-}C{\equiv}C{-}SiMe_3]Li$[b]	2000	1850
$[Ph{-}CH{-}C{\equiv}C{-}Ph]Li$[c]		1870
$[Me{-}CH{-}C{\equiv}C{-}Ph]Li$[c]		1870
Dilithiated		
$H_2C_3Li_2$[a]	1870	
$MeHC_3Li_2$	1850	
$Me_2C_3Li_2$	1850	
$PhHC_3Li_2$[b]	1900	
$[PhC{-}C{\equiv}C{-}Ph]Li_2$[c]		1790
$[Me{-}C{-}C{\equiv}C{-}Ph]Li_2$[c]		1795
$[Ph{-}C{-}C{\equiv}C{-}SiMe_3]Li_2$[b]		1790
$[Me_3Si{-}C{-}C{\equiv}C{-}SiMe_3]Li_2$[a]		1790
Trilithiated		
HC_3Li_3[a]		1750
PhC_3Li_3[b]		1780
$Me_3SiC_3Li_3$[a]		1770
MeC_3Li_3		1770
Tetralithiated		
C_3Li_4		1675

[a] Reference 102.
[b] Reference 105.
[c] Reference 112.
Reprinted with permission from Reference 111. Copyright 1976 American Chemical Society.

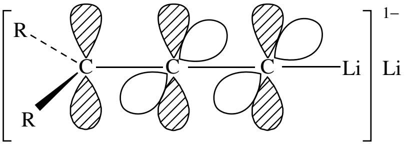

(8)

SCHEME 9

Successive lithiation of propyne vs. allene and internal acetylenes

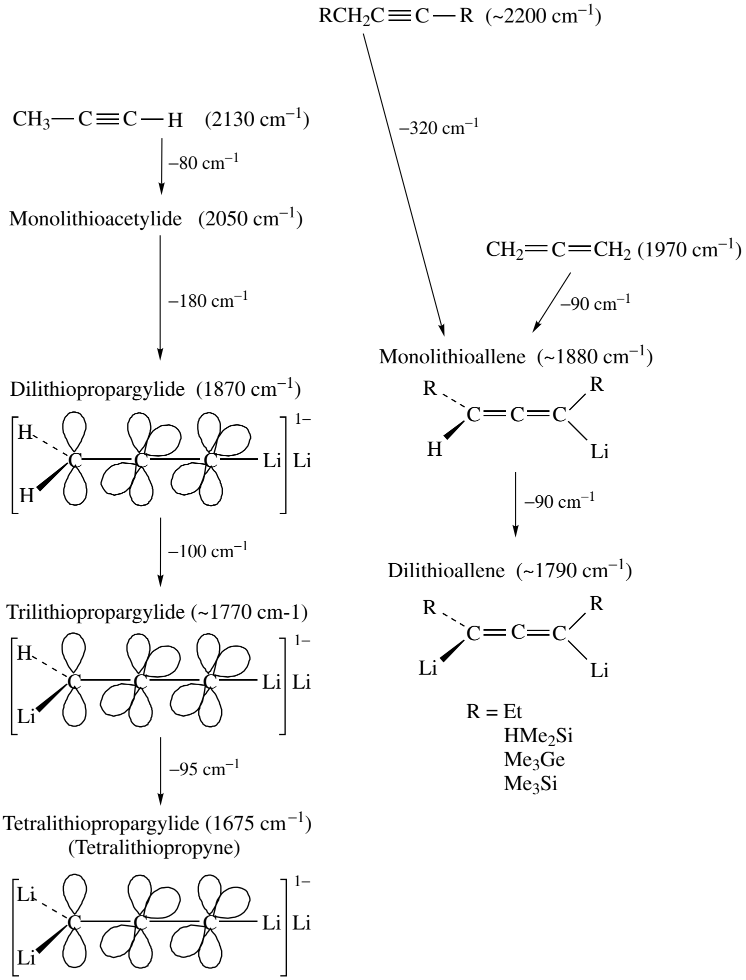

SCHEME 10

and allenic monoanion. However, since the extent of lithiation is different, these two anions must have different structures. Dilithiopropargylides have another hydrogen at the carbon atom 3 and consequently can undergo further lithiation in either an sp^2- or a p-type orbital to give trilithiopropargylide (**9**) and trilithiosesquiacetylene (**10**), respectively (Scheme 11). The resulting organolithium compounds **9** and **10** have propargylic or acetylenic structure, respectively. By coincidence, the IR absorption of trilithiated species occurs at the same wavenumber as the one of dilithiated compounds with allenic structure[111].

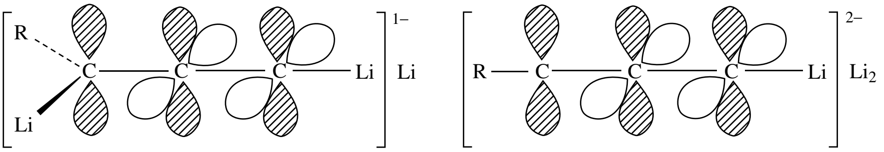

(9) **(10)**

SCHEME 11

A tetralithio derivative can be obtained only for propyne. It was described either as a tetralithiopropargylide (**11**) or a tetralithiosesquiacetylene (**12**) (Scheme 12)[111].

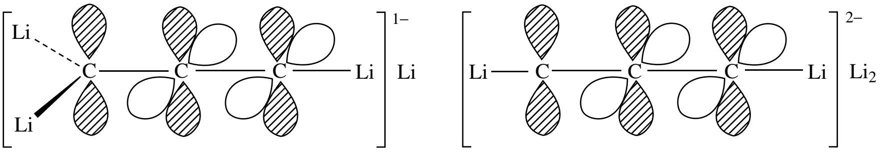

(11) **(12)**

SCHEME 12

Taking into account that allylic and vinylic hydrogen atoms have approximately the same acidity (pK_a *ca* 36), a propargyl and an allenic anion were expected to be of comparable stability. However, the acetylide anion is much more stable than an sp^2 anion. Therefore, the formation of propargylide dianions is more favoured than that of the allenic dianions. In agreement with this prediction, phenylallene *gem*-dilithiates to give the propargylide dianion rather than metalates at the benzylic position to give an allenic dianion[111,113].

As one can notice, the monolithiated allenic isomer seems to be preferred in almost all cases in hexane. However, West and Gornowicz reported that the IR spectrum of monolithio-1,3-bis(trimethylsilyl)-3-phenylpropyne exhibits two bands at 2000 and 1850 cm^{-1} and attributed them to the acetylenic and allenic forms[105]. In light of the new interpretation, Priester and coworkers ascribed the band at 2000 cm^{-1} to the propargyl anion, where both phenyl and silicon stabilized the charge at carbon atom 3[111].

The product distribution from the two types of anions is also very different. Propargylide anions derivatize to give acetylenic products exclusively (except when steric interactions favour the allenic products), while allenic anions with unhindered derivatizing agents give both allenic and acetylenic structures[105,111,114–116].

D. Polylithiation of 1,3-Pentadiyne

The reaction of 1,3-pentadiyne with excess *n*-butyllithium complexed with TMEDA led to another tetralithium compound, C_5Li_4[117]. The IR spectrum of the new perlithiated species presents a strong signal at 1800 cm^{-1}. Chwang and West attributed it to an allenic stretching mode[117], significantly lowered by the lithium substitution[102, 105]. A very weak peak was observed in the same spectral region, at about 2050 cm^{-1}. Its presence was explained by the incomplete polylithiation and formation of some monolithiated species[117]. It seems that isomerization takes place during polylithiation of 1,3-pentadiyne, as it does in lithiation of propyne and 1-phenylpropyne[102, 105, 118].

In an earlier study, Skattebol reported the synthesis of a very unstable pentatetraene, 2,6-dimethyl-2,3,4,5-heptatetraene[119]. Even though the compound was not isolated, a weak signal could be detected in its IR spectrum at 2010 cm^{-1}. The band appears at 210 cm^{-1} higher than the strong one at 1800 cm^{-1} in the IR spectrum of C_5Li_4. A similar difference of 290 cm^{-1} occurs between allene and the tetralithioallene, $Li_2C{=}C{=}CLi_2$[102].

The possible tautomeric structures of C_5Li_4 are depicted in scheme 13.

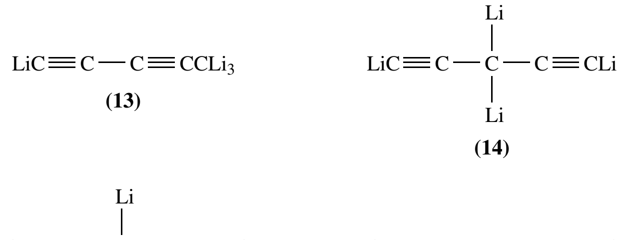

$LiC{\equiv}C{-}C{\equiv}CCLi_3$

(13)

$LiC{\equiv}C{-}C(Li)_2{-}C{\equiv}CLi$

(14)

$LiC{\equiv}C{-}C(Li){=}C{=}CLi_2$

(15)

$Li_2C{=}C{=}C{=}C{=}CLi_2$

(16)

SCHEME 13

The tautomeric forms **13–15** would be responsible for a relatively strong signal at 2050 cm^{-1}, characteristic for 1-lithioacetylenic moiety[102, 105]. Furthermore, it is hard to account for the strong and relatively broad band at 1800 cm^{-1} from either species **13** or **14**. All of the spectral features seem to indicate the tautomeric structure **16** as the most probable, with species **15** not fully excluded as a possibility. However, the simplicity of the spectral pattern indicates that one structure predominates in case of a mixture of tautomers[117].

VI. CONCLUSION

In this chapter we have presented the IR and Raman spectroscopic investigations of the most representative organolithium compounds present in the literature. It is clear now that due to major progress in Raman excitation (lasers), detection techniques (CCD cameras, FT-techniques together with modern FT-IR spectroscopies) and unambiguous signal assignment by DFT calculations, state-of-the-art vibrational spectroscopy is an excellent tool to investigate highly reactive species like lithium organics. Although the analysis of older spectra was already successful in determining the stoichiometry and the degree of aggregation of alkyllithiums, certainly the potential of the method today has improved considerably. Previous accurate signal assignment in combination with other physical investigations like X-ray structure analysis will provide even continuous on-line analysis of organolithium reaction intermediates in industrial processes or characterization of notoriously pyrophoric and insoluble polylithiums.

VII. REFERENCES

1. J. M. Chalmers and P. R. Griffiths, *Handbook of Vibrational Spectroscopy*, Vol. 1, Wiley, Chichester, 2002.
2. D. A. Long, *Raman Spectroscopy*, McGraw-Hill, 1977.
3. J. M. Hollas, *Modern Spectroscopy*, 2nd edn., Chap. 6, Wiley, Chichester, 1992.
4. A. J. Barnes and W. J. Orville, *Vibrational Spectroscopy—Modern Trends*, Elsevier, Amsterdam, 1977.
5. W. Demtröder, *Laser Spectroscopy. Basic Concepts and Instrumentation*, Springer-Verlag, Berlin, Heidelberg, 1981.
6. P. R. Bunker, *Molecular Symmetry and Spectroscopy*, Academic Press, New York, 1979.
7. H. J. Jodl, *Vibrational spectra and structure: A Series of Advances*, Vol. 13, (Ed. J. R. Durig), Elsevier, Amsterdam, 1984.
8. M. J. Almond and A. J. Downs, *Spectroscopy of Matrix Isolated Species. Advances in Spectroscopy*, Vol. 17, (Eds. R. J. H. Clark and R. E. Hester), Wiley, Chichester, 1989.
9. C. Lewis and M. S. Wrighton, *J. Am. Chem. Soc.*, **105**, 7768 (1983).
10. W. L. Andrews and G. C. Pimentel, *J. Chem. Phys.*, **44**, 2361 (1966).
11. T. L. Brown and M. T. Rogers, *J. Am. Chem. Soc.*, **79**, 1859 (1957).
12. A. N. Rodionov, D. N. Shigorin, T. V. Talalaeva and K. A. Kocheshkov, *Izv. Akad. Nauk. SSSR, Otdel. Khim. Nauk.*, 120 (1958); *Chem. Abstr.*, **52**, 38344 (1958).
13. A. N. Rodionov, D. N. Shigorin, T. V. Talalaeva and K. A. Kocheshkov, *Izv. Akad. Nauk. SSSR, Ser. Fiz.*, **22**, 1110 (1958); *Chem. Abstr.*, **53**, 4933 (1959).
14. D. N. Shigorin, *Spectrochim. Acta*, **14**, 198 (1959).
15. A. N. Rodionov, D. N. Shigorin, T. V. Talalaeva and K. A. Kocheshkov, *Dokl. Akad. Nauk. SSSR*, **123**, 113 (1958); *Chem. Abstr.*, **53**, 15041 (1959).
16. A. N. Rodionov, V. N. Vasil'eva, T. V. Talalaeva, D. N. Shigorin, E. N. Gur'yanova and K. A. Kocheshkov, *Dokl. Akad. Nauk. SSSR*, **125**, 562 (1959); *Chem. Abstr.*, **53**, 92794 (1959).
17. R. West and W. Glaze, *J. Am. Chem. Soc.*, **83**, 3580 (1961).
18. R. E. Rundle and A. I. Snow, *J. Chem. Phys.*, **18**, 1125 (1950).
19. A. I. Snow and R. E. Rundle, *Acta Crystallogr.*, **4**, 348 (1951).
20. P. H. Lewis and R. E. Rundle, *J. Chem. Phys.*, **21**, 986 (1953).
21. K. S. Pitzer and H. S. Gutowsky, *J. Am. Chem. Soc.*, **68**, 2204 (1946).
22. B. Walfort, L. Lameyer, W. Weiss, R. Herbst-Immer, R. Bertermann, J. Rocha and D. Stalke, *Chem. Eur. J.*, **7**, 1417 (2001).
23. L. J. Bellamy, *The Infrared Spectra of Complex Molecules*, 2nd edn., Chap. 2, Methuen, London, 1958.
24. G. Herzberg, *Infrared and Raman Spectra of Polyatomic Molecules*, Van Nostrand, New York, 1945, pp. 315.
25. G. Herzberg, *Infrared Spectra of Diatomic Molecules*, 2nd edn., Van Nostrand, New Jersey, 1950, pp. 75.
26. G. Wittig, F. J. Meyer and G. Lange, *Ann. Chem.*, **571**, 167 (1951).
27. Fr. Hein and H. Schramm, *Z. Phys. Chem.*, **151**, 234 (1930).
28. J. Berkowitz, D. A. Bafus and T. L. Brown, *J. Phys. Chem.*, **65**, 1380 (1961).
29. E. Weiss and E. A. C. Lucken, *J. Organometal. Chem.*, **2**, 197 (1964).
30. E. Weiss and G. Hencken, *J. Organomet. Chem.*, **21**, 265 (1970).
31. E. Weiss, T. Lambertsen, B. Schubert, J. K. Cockcroft and A. Wiedenmann, *Chem. Ber.*, **123**, 79 (1990).
32. G. E. Coates and F. Glockling, *J. Chem. Soc.*, 22 (1954).
33. M. Weiner, G. Vogel and R. West, *Inorg. Chem.*, **1**, 654 (1962).
34. T. Kottke and D. Stalke, *Angew. Chem.*, **105**, 619 (1993).
35. N. Sheppard, *Trans Faraday Soc.*, **46**, 527 (1950).
36. M. C. Tobin and A. D. Little, *J. Am. Chem. Soc.*, **75**, 1788 (1953).
37. N. Sheppard, *J. Chem. Phys.*, **16**, 690 (1948).
38. R. S. Rasmussen, *J. Chem. Phys.*, **16**, 712 (1948).

39. G. Herzberg, *Infrared and Raman Spectra*, Chap. III, Van Nostrand, Princeton, 1945.
40. R. E. Rundle and J. H. Sturdivant, *J. Am. Chem. Soc.*, **69**, 1561 (1947).
41. M. A. Weiner and R. West, *J. Am. Chem. Soc.*, **85**, 485 (1963).
42. Y. Apeloig, T. Clark, A. J. Kos, E. Jemmis and P. v. R. Schleyer, *Isr. J. Chem.*, **20**, 43 (1980).
43. A. J. Kos, E. D. Jemmis, P. v. R. Schleyer, R. Gleiter, U. Fischbach and J. Pople, *J. Am. Chem. Soc.*, **103**, 4996 (1981).
44. P. v. R. Schleyer and A. J. Kos, *J. Chem. Soc., Chem. Commun.*, 448 (1982).
45. P. v. R. Schleyer, A. J. Kos and E. Kaufmann, *J. Am. Chem. Soc.*, **105**, 7617 (1983).
46. S. M. Bachrach and A. Streitwieser, *J. Am. Chem. Soc.*, **106**, 2283 (1984).
47. L. Manceron and L. Andrews, *J. Am. Chem. Soc.*, **107**, 563 (1985).
48. L. Manceron and L. Andrews, *J. Phys. Chem.*, **90**, 4514 (1986).
49. L. Manceron, M. Hawkins and L. Andrews, *J. Phys. Chem.*, **90**, 4987 (1986).
50. A. M. Sapse and P. v. R. Schleyer, *Lithium Chemistry*, Wiley, New York, 1995.
51. N. I. Bagdanskis, M. O. Bulanin and Yu. V. Fadeev, *Opt. Spectrosc.*, **29**, 687 (1970).
52. N. I. Bagdanskis and M. O. Bulanin, *Opt. Spectrosc.*, **32**, 525 (1972).
53. E. B. Wilson, J. C. Decius and P. Cross, *Molecular Vibrations*, McGraw-Hill, New York, 1955.
54. D. Steele, *Theory of Vibrational Spectroscopy*, WB Saunders, Philadelphia, PA, 1971.
55. M. Trenary, H. F. Schaefer III and P. A. Kollman, *J. Chem. Phys.*, **68**, 4047 (1978).
56. M. Heberhold, *Metal π-Complexes*, Vol. II, Elsevier, Amsterdam, 1974.
57. J. Hiraishi, *Spectrochim. Acta, Part A*, **25**, 749 (1969).
58. M. Tacke, *Chem. Ber.*, **128**, 1051 (1995).
59. M. Tacke, P. Sparrer, R. Teuber, H.-J. Stadter and F. Schuster, *J. Mol. Struct.*, **349**, 251 (1995).
60. D. Seyferth, R. C. Hui, R. M. Weinstein and W.-L. Wang, *Nova Acta Leopold.*, **59**, 335 (1985).
61. M. Tacke, Ch. Klein, D. J. Stufkens and A. Oskam, *Z. Anorg. Allg. Chem.*, **619**, 865 (1993).
62. P. Selg, H. H. Brintzinger, R. A. Andersen and I. T. Horvath, *Angew. Chem., Int. Ed. Engl.*, **34**, 791 (1995).
63. M. Tacke, *Eur. J. Inorg. Chem.*, **5**, 537 (1998).
64. B. Schiemenz and P. P. Power, *Angew. Chem., Int. Ed. Engl.*, **35**, 2150 (1996).
65. R. E. Dinnebier, U. Behrens and F. Olbrich, *J. Am. Chem. Soc.*, **120**, 1430 (1998).
66. A. Steiner and D. Stalke, *Angew. Chem., Int. Ed. Engl.*, **34**, 1752 (1995).
67. S. Wingerter, M. Pfeiffer, T. Stey, M. Bolboacă, W. Kiefer, V. Chandrasekhar and D. Stalke, *Organometallics*, **20**, 2730 (2001).
68. S. Wingerter, H. Gornitzka, G. Bertrand and D. Stalke, *Eur. J. Inorg. Chem.*, **1**, 173 (1999).
69. S. Wingerter, H. Gornitzka, R. Bertermann, S. K. Pandey, J. Rocha and D. Stalke, *Organometallics*, **19**, 3890 (2000).
70. K. Nakamoto, *Infrared and Raman Spectra of Inorganic and Coordination Chemistry*, Part A: *Theory and Applications in Inorganic Chemistry*, 5th edn., Wiley, New York, 1997.
71. Z. K. Ismail, R. H. Hauge and J. L. Margrave, *J. Chem. Phys.*, **57**, 5137 (1972).
72. R. Pikl, F. Duschek, C. Fickert, R. Finsterer and W. Kiefer, *Vib. Spectrosc.*, **14**, 189 (1997).
73. N. B. Colthup, L. H. Daly and S. E. Wiberley, *Introduction to Infrared and Raman Spectroscopy*, Academic Press, New York, 1964, pp. 305.
74. G. M. Aspinall, M. C. Copsey, A. P. Leedham and C. A. Russell, *Coord. Chem. Rev.*, **227**, 217 (2002).
75. J. K. Brask and T. Chivers, *Angew. Chem.*, **113**, 4082 (2001).
76. J. K. Brask and T. Chivers, *Angew. Chem., Int. Ed. Engl.*, **40**, 3960 (2001).
77. D. Stalke, *Proc. Indian Acad. Sci. (Chem. Sci.)*, **112**, 155 (2000).
78. R. Fleischer and D. Stalke, *Coord. Chem. Rev.*, **176**, 431 (1998).
79. M. A. Beswick and D. S. Wright, *Coord. Chem. Rev.*, **176**, 373 (1998).
80. P. Hope and L. A. Wiles, *J. Chem. Soc.*, 5386 (1965).
81. O. J. Scherer and R. Schmitt, *J. Organomet. Chem.* **16**, 11 (1969).
82. O. J. Scherer and R. Wies, *Z. Naturforsch. B*, **25**, 1486 (1970).
83. D. Hänssgen and W. Rölle, *J. Organomet. Chem.*, **63**, 269 (1973).
84. J. Kuyper, P. C. Keijzer and K. Vrieze, *J. Organomet. Chem.*, **116**, 1 (1976).
85. F. Pauer and D. Stalke, *J. Organomet. Chem.*, **418**, 127 (1991).
86. F. Pauer, J. Rocha and D. Stalke, *J. Chem. Soc., Chem. Commun.*, 1477 (1991).

87. F. T. Edelmann, F. Knösel, F. Pauer, D. Stalke and W. Bauer, *J. Organomet. Chem.*, **438**, 1 (1992).
88. S. Freitag, W. Kolodziejski, F. Pauer and D. Stalke, *J. Chem. Soc., Dalton Trans.*, 3479 (1993).
89. R. Fleischer, S. Freitag, F. Pauer and D. Stalke, *Angew. Chem., Int. Ed. Engl.*, **35**, 204 (1996).
90. R. Fleischer, R. Rothenberger and D. Stalke, *Angew. Chem., Int. Ed. Engl.*, **36**, 1105 (1997).
91. D. Leusser, B. Walfort and D. Stalke, *Angew. Chem., Int. Ed. Engl.*, **41**, 2079 (2002).
92. D. Klamann (Ed.), *Methoden der Organischen Chemie*, *(Houben-Weyl)*, E11, Parts 1 and 2, Supplementary Volume of the 4th edn., Thieme, Stuttgart, 1985.
93. R. Mews, P. G. Watson and E. Lork, *Coord. Chem. Rev.*, **158**, 233 (1997).
94. O. Glemser and J. Wegener, *Angew. Chem., Int. Ed. Engl.*, **9**, 309 (1970).
95. O. Glemser, S. Pohl, F. M. Tesky and R. Mews, *Angew. Chem.*, **89**, 829 (1977).
96. W. Lidy, W. Sundermeyer and W. Verbeek, *Z. Anorg. Allg. Chem.*, **406**, 228 (1974).
97. R. Fleischer, S. Freitag and D. Stalke, *J. Chem. Soc., Dalton Trans.*, 193 (1998).
98. R. Fleischer, B. Walfort, A. Gbureck, P. Scholz, W. Kiefer and D. Stalke, *Chem. Eur. J.*, **4**, 2266 (1998).
99. A. Herbrechtsmeier, F. M. Schnepel and O. Glemser, *J. Mol. Struct.*, **50**, 43 (1978).
100. L. N. Markovskii, V. I. Tovstenko, V. E. Pashinnik, E. A. Mel'nichuk, A. G. Makarenko and Yu. G. Shermolovich, *Zh. Org. Khim.*, **27**, 769 (1991); *Chem. Abstr.*, **158**, 632 (1991).
101. S. Pohl, B. Krebs, U. Seyer and G. Henkel, *Chem. Ber.*, **112**, 1751 (1979).
102. R. West and P. C. Jones, *J. Am. Chem. Soc.*, **91**, 6156 (1969).
103. R. West, P. A. Carney and I. C. Mineo, *J. Am. Chem. Soc.*, **87**, 3788 (1965).
104. T. L. Jacobs and S. Singer, *J. Org. Chem.*, **17**, 475 (1952).
105. R. West and G. A. Gornowicz, *J. Am. Chem. Soc.*, **93**, 1720 (1971).
106. F. Jaffe, *J. Organomet. Chem.*, **23**, 53 (1970).
107. H. A. Bent, *J. Chem. Educ.*, **43**, 170 (1966).
108. G. A. Gornowicz and R. West, *J. Am. Chem. Soc.*, **93**, 1714 (1971).
109. J. Klein and S. Brenner, *J. Am. Chem. Soc.*, **91**, 3094 (1969).
110. J. E. Mulvaney, T. L. Folk and D. J. Newton, *J. Org. Chem.*, **32**, 1674 (1967).
111. W. Priester, R. West and T. L. Chwang, *J. Am. Chem. Soc.*, **98**, 8413 (1976).
112. J. Klein and J. Y. Becker, *J. Chem. Soc., Chem. Commun.*, 576 (1973).
113. L. Brandsma and E. Mugge, *Recl. Trav. Chim. Pays-Bas.*, **92**, 628 (1973).
114. G. Linstrumelle and D. Michelot, *J. Chem. Soc., Chem. Commun.*, 561 (1975).
115. Y. Leroux and R. Mantione, *Tetrahedron Lett.*, 591 (1971).
116. R. Mantione and Y. Leroux, *Tetrahedron Lett.*, 593 (1971).
117. T. L. Chwang and R. West, *J. Am. Chem. Soc.*, **95**, 3324 (1973).
118. J. Klein and S. Brenner, *J. Org. Chem.*, **36**, 1319 (1971).
119. L. Skattebol, *Tetrahedron Lett.*, 2175 (1965).

CHAPTER 7

Effects of structural variation on organolithium compounds

MARVIN CHARTON

Chemistry Department, School of Liberal Arts and Sciences, Pratt Institute,
Brooklyn, New York 11205, USA
Fax: 718-722-7706;   e-mail: mcharton@pratt.edu

The Chemistry of Organolithium Compounds. Edited by Z. Rappoport and I. Marek
ISBN: 0-470-84339-X

I. THE NATURE OF STRUCTURAL EFFECTS

A. Introduction

The objective of this work is to describe methods for the quantification of the effects of structural variation on measurable chemical and physical properties, chemical reactivities and biological activities of organolithium compounds.

ABBREVIATIONS

Ac	acetyl	2-Fr	2-furyl	Ph	phenyl
1-Adm	1-adamantyl	3-Fr	3-furyl	Pn	phenylene (C_6H_4)
Ak	alkyl	Hl	halogen	Pr	propyl
An	anthracenyl	Har	heteroaryl	*c*-Pr	cyclopropyl
Ar	aryl	Hx	hexyl	*i*-Pr	isopropyl
Bu	butyl	*c*-Hx	cyclohexyl	Py	pyridyl
i-Bu	*iso* butyl	Me	methyl	Pyr	pyrenyl
s-Bu	*sec* butyl	1-Nh	1-naphthyl	2-Tp	2-thienyl
t-Bu	*tert* butyl	2-Nh	2-naphthyl	3-Tp	3-thienyl
C_2	ethynylene	Oc	octyl	Tet	tetracenyl
DME	1,2-dimethoxyethane	Pe	pentyl	Vi	vinyl
DMSO	dimethyl sulfoxide	*i*-Pe	isopentyl	2-Vn	vinylene
Et	ethyl	Per	perylenyl	1-Vn	vinylidene

B. Structure–Property Quantitative Relationships (SPQR)

Structural variations in a chemical species (molecule, ion, radical, carbene, benzyne etc.) generally result in changes in some measured property of the species. The property measured may be a chemical reactivity (rate or equilibrium constant, oxidation potential etc.), a chemical property (resulting from a difference in intermolecular forces between an initial and a final state), a physical property (either of the ground state or of an excited state) or a biological activity. The change in the measured property that results from a structural variation is a structural effect. Structural effects within a set of related species can be modeled by the correlation of the measured properties with appropriate parameters using statistical methods. The resulting equation is called a structure–property quantitative relationship (SPQR). The parameters required for modeling structural effects may be obtained from physicochemical reference data sets for electrical effects[1,2] and intermolecular forces[3]; calculated from molecular geometry[4], by counts of branching at each atom of the longest chain[5,6], or by molecular mechanics calculations[7,8] in the case of steric effects, obtained from quantum chemical calculations[9], topological algorithms[10–12] and from comparative molecular field analysis (COMFA)[13]. An alternative to the use of statistical methods is the use of neural networks[14–16].

The use of physicochemical quantities generally results in pure parameters that have a direct cause and effect relationship to some property. A pure parameter is a parameter which represents a single structural effect. A composite parameter is a parameter that represents two or more structural effects. Steric parameters calculated from molecular mechanics are also pure parameters. Quantum chemical calculations can generate either pure or composite parameters, depending on the system chosen and the quantity calculated. The COMFA model involves the calculation of the interactions of fragments at the intersections of grids which form a box enclosing the species of interest. The choice of fragment determines the type of interaction. Thus, charged fragments model electrical effects, methyl groups model van der Waals interactions, OH groups model H acceptor effects, etc. Again, these represent pure parameters. Topological parameters are almost always composite parameters, as they represent a count of the number of atoms of each kind, the number of bonds of each type, the number of valence (bonding), lone pair (nonbonding) and core electrons, and the extent of branching, as well as the number of OH and NH bonds and of lone pairs on O and/or N atoms[17,18], Composite parameters can generate a predictive SPQR just as well as pure parameters[19]; they are much more difficult to interpret however, unless their composition is known.

SPQR have three functions:

1. They are predictive. Once the SPQR has been determined, the value of the property can be calculated for any chemical species for which the structural effect parameters are available. This makes possible the design of chemical species with specific chemical, physical or biological properties.
2. They are explicative. SPQR can be used to explain structural effects on a measured property. In the case of chemical reactivity, they can provide information useful in determining reaction mechanism.
3. They are archival. Information regarding structural effects on measurable properties can easily and concisely be stored in this way.

Data sets are of three types. The most frequently encountered type has the form XGY in which X is a variable substituent, Y is an active site (an atom or group of atoms responsible for the observed phenomenon) and G is a skeletal group to which X and Y are bonded. A second type has the form XY, the substituent X being directly bonded to the active site Y. In the third type, designated X_Y, the entire chemical species is both active site and variable substituent.

Structural effects are of three types: Electrical effects, steric effects and intermolecular force effects. Each of these types can be subdivided into various contributions.

II. ELECTRICAL EFFECTS

A. Introduction

It has long been known that a substituent X in an XGY system can exert an electrical effect on an active site Y. It is also well known that the electrical effect which results when X is bonded to an sp^3 hybridized carbon atom differs from that observed when X is bonded to an sp^2 or sp hybridized carbon atom. As electron delocalization is minimal in the first case, it has been chosen as the reference system. The electrical effect observed in systems of this type is a universal electrical effect which occurs in all systems. In the second type of system, a second effect (resonance effect) occurs due to delocalization which is dependent both on the inherent capacity for delocalization and on the electronic demand of the active site. In systems of the second type, the overall (total) electrical effect is assumed to be a combination of the universal and the delocalized electrical effects. Over the last sixty years much ink has been spilt and there has been a great deal of 'sound and fury signifying nothing' concerning the mode of transmission of the universal electrical effect. Two models were proposed originally by Derick[20], a through bond model (the inductive effect) and a through space model (the field effect). These proposals were developed into the classical inductive effect (CIE)[21] and the classical field effect (CFE)[22] models. As the CIE model could not account for the observed dependence of the electrical effect on path number, a modified version was introduced (the MIE model)[23]. The matter has recently been treated in some detail[24, 25]. The dependence on molecular geometry is in best agreement with a modified field effect (MFE) model[26–27].

B. Triparametric Electrical Effect Model

Electrical effects are conveniently described by the triparametric (three independent variables) LDR equation 1[2]:

$$Q_X = L\sigma_{lX} + D\sigma_{dX} + R\sigma_{eX} + h \tag{1}$$

or relationships derived from it. The parameters are described below.

σ_l is the localized (field) electrical effect parameter; it is identical to σ_I and σ_F. Though other localized electrical effect parameters such as σ_I^q have been proposed, there is no advantage to their use. The σ^* parameter and the F parameter have sometimes been used as localized electrical effect parameters; such use is generally incorrect as both of these parameters contain a small but significant delocalized effect contribution. As was noted above, the available evidence is strongly in favor of an electric field model for transmission of the localized effect.

σ_d is the intrinsic delocalized (resonance) electrical effect parameter; it represents the delocalized electrical effect in a system with no electronic demand.

σ_e is the electronic demand sensitivity parameter. It adjusts the delocalized effect of a group to meet the electronic demand of the system.

The electrical effect is characterized by two quantities derived from equation 1:

The electronic demand, η, is a property of a system or of a composite electrical effect parameter that is itself a function of both σ_d and σ_e. It is defined as R/D, where R and D are the coefficients of σ_e and σ_d, respectively.

The percent delocalized effect, P_D, is defined by equation 2:

$$P_D = \frac{100D}{L + D} \tag{2}$$

Diparametric equations[28] can be obtained from equation 1 in two ways. One alternative is to combine σ_l and σ_d to form a composite parameter σ_{CP_D} with a fixed value of P_D, resulting in the CR equation (equation 3):

$$Q_X = C\sigma_{CP_D,X} + R\sigma_{eX} + h \tag{3}$$

The other alternative is to combine σ_d and σ_e to form a composite parameter with a fixed value of η. This substituent constant is designated σ_D. The resulting LD equation is equation 4:

$$Q_X = L\sigma_{lX} + D\sigma_{DX} + h \tag{4}$$

A monoparametric equation results when a composite electrical effect parameter is obtained by combining all three pure electrical effect parameters with fixed values of both P_D and η. The Hammett substituent constants are of this type. The Hammett equation is given by equation 5:

$$Q_X = \rho\sigma_X + h \tag{5}$$

The Hammett equation traditionally combines 3-substituted and 4-substituted benzene derivatives into a single data set using the composite σ_m constants for the former and σ_p constants for the latter. This is justifiable only if ρ_3 is equal to ρ_4 ($\Delta\rho \approx 0$). We have shown that this is generally not the case[26,27], except when the geometry of XGY is comparable to that of the benzoic acids from which the σ_m and σ_p constants were defined. The Yukawa–Tsuno and related equations are based on the assumption that ρ_3 is equal to ρ_4 and are limited to applications in which this is at least approximately correct. They are briefly reviewed elsewhere[28].

C. Modified Yukawa–Tsuno Model

The Yukawa–Tsuno equation for 4-substituted benzene derivatives is approximately equivalent to the CR equation[23,24]. This observation has led to the development of a modified Yukawa–Tsuno (MYT) equation which has the form of equation 6:

$$Q_X = \rho\sigma_X + R\sigma_{eX} + h \tag{6}$$

with σ_{c50} taking the value σ_m for 3-substituted benzene derivatives and σ_{50} for 4-substituted benzene derivatives, while σ_{eX} for 3-substituted benzene derivatives is 0. The σ_{50} constants have P_D equal to 50 and η equal to zero; they are therefore equal to the sum of the σ_l and σ_d values.

If the sensitivity to electronic demand is held constant, the LDR equation reverts to the LD equation (equation 5). By means of an equation analogous to the MYT equation, the modified LD (MLD) equation (equation 7) is obtained:

$$Q_X = \rho'\sigma_X + D\sigma_{DX} + h \tag{7}$$

where σ is σ_m for 3-substituted and σ_l for 4-substituted while σ_D is 0 for 3-substituents; 3- and 4-substituted benzene derivatives can be combined into a single data set. Again, use of the MLD equation is restricted to systems for which $\Delta\rho$ is not significant.

The choice of electrical effect parameterization depends on the number of data points in the data set to be modeled. When using linear regression analysis the number of degrees of freedom, N_{DF}, is equal to the number of data points, N_{dp}, minus the number of independent variables, N_{iv}, minus one. When modeling physicochemical data N_{DF}/N_{iv} should be at least 2 and preferably 3 or more. As the experimental error in the data increases, N_{DF}/N_{iv} should also increase.

Values of electrical effect substituent constants for typical groups are presented in Tables 1–3.

TABLE 1. Electrical effect substituent constants for common substituents[a,b]

X	σ_l	σ_d	σ_e	$\sigma_{c14.3}$	$\sigma_{c16.7}$	σ_{c50}	σ_{c60}
Ak, *c*-Ak							
Me	−0.01	−0.14	−0.030	−0.03	−0.04	−0.15	−0.22
Et	−0.01	−0.12	−0.036	−0.03	−0.03	−0.13	−0.19
c-Pr	0.01	−0.17	−0.069	−0.02	−0.02	−0.16	−0.25
Pr	−0.01	−0.15	−0.036	−0.04	−0.04	−0.16	−0.24
i-Pr	0.01	−0.16	−0.040	−0.02	−0.02	−0.15	−0.22
Bu	−0.01	−0.15	−0.036	−0.04	−0.04	−0.16	−0.24
i-Bu	−0.01	−0.14	−0.036	−0.03	−0.04	−0.15	−0.22
s-Bu	−0.01	−0.14	−0.036	−0.03	−0.04	−0.15	−0.22
t-Bu	−0.01	−0.15	−0.036	−0.04	−0.04	−0.16	−0.24
Pe	−0.01	−0.14	−0.036	−0.03	−0.04	−0.15	−0.22
CH_2Bu-*t*	0.00	−0.16	−0.040	−0.03	−0.03	−0.16	−0.24
c-Hx	0.00	−0.14	−0.036	−0.02	−0.03	−0.14	−0.21
1-Adm	−0.01	−0.12	−0.060			−0.13	
CH_2Z							
CH_2Br	0.20	−0.08	−0.026	0.19	0.18	0.12	0.08
CH_2OH	0.11	−0.10	−0.025	0.09	0.09	0.01	−0.04
CH_2Cl	0.17	−0.06	−0.024	0.16	0.16	0.11	−0.08
CH_2CN	0.20	−0.01	−0.011	0.20	0.20	0.19	0.18
CH_2OMe	0.11	−0.10	−0.041	0.09	0.09	0.01	−0.04
CH_2CH_2CN	0.09	−0.11	−0.024	0.07	0.07	−0.02	−0.08
CH_2Vi	0.02	−0.16	−0.039	−0.01	−0.01	−0.14	−0.22
CH_2OEt	0.11	−0.10	−0.041	0.09	0.09	0.01	−0.04
CH_2GeMe_3	−0.02	−0.31	−0.028	−0.07	−0.08	−0.29	−0.49
CH_2SiMe_3	−0.03	−0.30	−0.029	−0.08	−0.09	−0.27	−0.48
CH_2SnMe_3	−0.03	−0.16	−0.028	−0.06	−0.06	−0.19	−0.29
CH_2-2-Tp	0.06	−0.12	−0.028	0.04	0.04	−0.06	−0.12
CH_2-2-Fr	0.05	−0.12	−0.028	0.03	0.03	−0.07	−0.13
$CH_2CH_2CO_2Et$	0.08	−0.12	−0.027	0.06	0.06	−0.04	−0.10
$CH_2CHMeCO_2Me$	0.07	−0.12	−0.027	0.05	0.05	−0.05	−0.11
CH_2NEt_2	0.03	−0.12	−0.038	0.01	0.01	−0.09	−0.15
CH_2Ph	0.03	−0.13	−0.057	0.01	0.00	−0.10	−0.17
CH_2CH_2-2-Py	0.02	−0.13	−0.03	0.00	−0.01	−0.11	−0.18
CH_2CH_2-4-Py	0.02	−0.13	−0.03	0.00	−0.01	−0.11	−0.18
CZ_3							
CF_3	0.40	0.13	−0.026	0.42	0.43	0.53	0.60
CCl_3	0.36	0.10	−0.018	0.38	0.38	0.46	0.51
$C(SiMe_3)_3$	−0.09	−0.21	−0.028	−0.13	−0.13	−0.30	−0.41
VnX							
Vi	0.11	−0.08	−0.12	0.10	0.09	0.03	−0.01
2-VnVi	0.12	−0.37	−0.12	0.06	0.05	−0.25	−0.44

TABLE 1. (*continued*)

X	σ_l	σ_d	σ_e	$\sigma_{c14.3}$	$\sigma_{c16.7}$	σ_{c50}	σ_{c60}
C_2Z							
C_2H	0.29	−0.02	−0.10	0.29	0.29	0.27	0.26
C_2Me	0.30	0.29	−0.089			0.01	
C_2-C_2H	0.39	0.04	−0.10			0.43	
Ar							
C_6F_5	0.31	0.08	−0.068	0.32	0.33	0.39	0.43
Ph	0.12	−0.12	−0.12	0.10	0.10	0.00	−0.06
PnZ							
4-$PnNMe_2$	0.09	−0.32	−0.12	0.04	0.03	−0.23	−0.39
4-$PnNEt_2$	0.08	−0.27	−0.12	0.04	0.03	−0.19	−0.34
4-PnCl	0.15	−0.01	−0.070				
4-PnMe	0.10	−0.12	−0.041				
4-PnOMe	0.11	−0.15	−0.062				
4-$PnNO_2$	0.23	−0.01	−0.045				
Har							
2-Fr	0.17	−0.18	−0.13	0.14	0.13	−0.01	−0.10
3-Fr	0.09	−0.13	−0.12	0.07	0.06	−0.04	−0.11
2-Tp	0.19	−0.20	−0.11	0.16	0.15	−0.01	−0.11
3-Tp	0.10	−0.15	−0.11	0.07	0.07	−0.05	−0.13
(CO)Z							
CHO	0.30	0.27	−0.10	0.35	0.35	0.57	0.71
CO_2H	0.30	0.17	−0.041	0.33	0.33	0.47	0.56
Ac	0.30	0.25	−0.095	0.34	0.35	0.55	0.68
CO_2Me	0.32	0.16	−0.070	0.35	0.35	0.48	0.56
CO_2Et	0.30	0.18	−0.064	0.33	0.34	0.48	0.57
$CONH_2$	0.28	0.12	−0.055				
$CONMe_2$	0.28	0.05	−0.060				
Bz	0.30	0.22	−0.11				
CN	0.57	0.12	−0.055	0.59	0.59	0.69	0.75
Si							
$SiBr_3$	0.36	0.07	0.018	0.37	0.37	0.42	0.47
$SiCl_3$	0.36	0.10	−0.017	0.38	0.38	0.46	0.51
SiF_3	0.41	0.14	−0.004	0.43	0.44	0.58	0.62
SiH_3	0	0.13	−0.038	0.02	0.03	0.13	0.20
$SiMe_3$	−0.11	0.13	−0.046	−0.09	−0.08	0.02	0.09
$SiPh_3$	−0.04	0.33	−0.055	0.02	0.03	0.29	0.46
Ge							
$GeMe_3$	−0.08	0.11	−0.050	−0.06	−0.06	0.03	0.09
$GePh_3$	−0.05	0.24	−0.053	−0.01	0.00	0.19	0.31
Sn							
$SnMe_3$	−0.09	0.12	−0.051	−0.07	−0.07	0.03	0.09
$SnPh_3$	−0.04	0.33	−0.055	0.02	0.03	0.29	0.46

(*continued overleaf*)

TABLE 1. (*continued*)

X	σ_l	σ_d	σ_e	$\sigma_{c14.3}$	$\sigma_{c16.7}$	σ_{c50}	σ_{c60}
N							
N_3	0.43	−0.27	−0.12	0.38	0.38	0.16	0.02
NH_2	0.17	−0.68	−0.13	0.06	0.03	−0.51	−0.85
NHMe	0.13	−0.67	−0.18	0.02	0.00	−0.54	−0.88
NHAc	0.28	−0.35	−0.088				
NMe_2	0.17	−0.66	−0.24	0.06	0.04	−0.49	−0.82
NEt_2	0.15	−0.65	−0.18	0.04	0.02	−0.50	−0.83
NO	0.37	0.31	−0.056	0.42	0.43	0.68	0.84
NO_2	0.67	0.18	−0.077	0.70	0.71	0.85	0.94
P							
PMe_2	0.10	−0.50	−0.27				
$POMe_2$	0.30	0.14	−0.036				
$PO(OMe)_2$	0.36	0.24	−0.036				
O							
OH	0.35	−0.57	−0.044	0.25	0.24	−0.22	−0.51
OMe	0.30	−0.55	−0.064	0.21	0.19	−0.25	−0.53
OAc	0.38	−0.24	−0.005	0.34	0.33	0.14	0.02
OEt	0.28	−0.55	−0.070	0.19	0.17	−0.27	−0.55
OPr-*i*	0.27	−0.55	−0.067	0.18	0.16	−0.28	−0.56
OBu	0.28	−0.55	−0.067	0.19	0.17	−0.27	−0.55
$OSiMe_3$	0.25	−0.44	−0.053	0.18	0.16	−0.19	−0.41
OPh	0.40	−0.51	−0.083	0.31	0.30	−0.11	−0.37
S							
SH	0.27	−0.40	−0.098	0.20	0.19	−0.13	−0.33
SMe	0.30	−0.38	−0.13	0.24	0.22	−0.08	−0.27
SAc	0.39	−0.08	−0.057			0.31	
SEt	0.26	−0.39	−0.12	0.19	0.18	−0.13	−0.33
SPh	0.31	−0.34	−0.17	0.25	0.24	−0.03	−0.20
SOMe	0.54	−0.01	−0.037			0.53	0.52
SOPh	0.51	−0.02	−0.052			0.49	0.48
SO_2Me	0.59	0.13	−0.052	0.31	0.62	0.72	0.79
SO_2Ph	0.56	0.08	−0.082	0.57	0.58	0.64	0.68
SF_5	0.59	0.04	−0.040			0.63	0.65
Se							
SeMe	0.30	−0.41	−0.096			−0.11	−0.33
Other							
H	0	0	0	0	0	0	0
Br	0.47	−0.27	−0.028	0.42	0.42	0.20	0.06
Cl	0.47	−0.28	−0.011	0.42	0.41	0.19	0.05
F	0.54	−0.48	0.041	0.46	0.44	−0.06	−0.18
I	0.40	−0.20	−0.057	0.37	0.36	−0.20	0.10

[a] Abbreviations can be found in Section I.A.

[b] For $\sigma_{\mathrm{C_pn}}$ type constants, the number after C is the value of P_D, the percentage delocalized effect.

TABLE 2. Values of σ_D for common substituents[a]

X	$\sigma_R^{\ominus}$	σ_R^{-}	σ_R^{o}	σ_R	σ_R^{+}	$\sigma_R^{\oplus}$
Ak, *c*-Ak						
Me	−0.03	−0.09	−0.16	−0.16	−0.16	−0.25
Et	−0.01	−0.07	−0.14	−0.14	−0.14	−0.28
c-Pr	0.01	*−0.08*	*−0.15*	−0.19	−0.27	−0.43
Pr				−0.16		
i-Pr	*−0.04*	−0.09	−0.16	−0.16	−0.16	−0.34
Bu				−0.16		
i-Bu				−0.16		
s-Bu				−0.16		
t-Bu	*−0.05*	−0.11	−0.18	−0.18	−0.18	−0.33
Pe				−0.16		
CH_2Bu-*t*				−0.17		
c-Hx				−0.15		
Oc				−0.16		
Vinyl						
$CH{=}CH_2$	0.45	−0.08	−0.15	−0.15	−0.15	−0.56
$CH{=}CH{-}CH{=}CH_2$	*−0.02*	*−0.23*	*−0.29*	*−0.38*	*−0.57*	*−0.91*
CH=CHPh	*0.02*	−0.23	−0.30	−0.30	−0.30	−1.01
Ethynyl						
C≡CH	0.28	0.13	−0.04	−0.04	−0.12	−0.45
C≡C−C≡CH	*0.34*	0.19	*0.02*	*0.01*	−0.17	*−0.36*
C≡CPh	*0.16*	−0.14	−0.21	−0.21	−0.21	−1.03
Aryl						
Ph	0.28	−0.04	−0.11	−0.11	−0.17	−0.69
C_6H_4Ph-4	*0.18*	*0.00*	*−0.14*	*−0.20*	*−0.36*	*−0.68*
1-Nh	*0.12*	*−0.07*	*−0.18*	*−0.26*	*−0.57*	*−0.75*
2-Nh	*0.19*	*0.01*	*−0.13*	*−0.20*	*−0.50*	*−0.67*
C_6F_5	0.28	0.20	−0.02	0.02	0.01	−0.19
PnZ						
4-PnCl	0.05	0.00	−0.07	−0.03	−0.15	−0.30
4-PnMe	0.00	−0.07	−0.12	−0.13	−0.20	−0.32
4-PnOMe		−0.01		−0.19	−0.27	
4-PnNO_2	0.29	0.04	−0.03	0.03	−0.18	−0.21
CH_2Z						
CH_2Br				−0.10		
CH_2OH				−0.07	−0.15	
CH_2Cl				−0.08		
CH_2CN				−0.04		
CH_2OMe				−0.10		
CH_2Vi				−0.14		
CH_2SiMe_3				−0.23	−0.30	
CH_2Ph				−0.13		
CZ_3						
CCl_3				0.08		
CF_3	*0.20*	0.18	0.11	0.11	0.15	0.00

(*continued overleaf*)

TABLE 2. (*continued*)

X	$\sigma_R^{\ominus}$	σ_R^-	σ_R^o	σ_R	σ_R^+	$\sigma_R^{\oplus}$
Carbonyl						
CHO	*0.57*	0.53	0.15	0.15	0.15	−0.04
Ac	0.56	0.41	0.20	0.20	0.06	−0.05
$CONH_2$	*0.28*	0.23	0.08	0.08	0.08	−0.10
CO_2Me	*0.37*	0.30	0.11	0.11	0.11	−0.12
CO_2Et	*0.37*	0.31	0.11	0.11	0.11	−0.06
CN	0.26	0.26	0.08	0.08	0.08	−0.10
N						
NH_2	*−0.30*	−0.55	−0.42	−0.80	−1.10	−1.05
NHAc	*−0.09*	−0.28	−0.25	−0.35	−0.47	−0.75
NMe_2	*0.05*	−0.30	−0.44	−0.88	−1.22	−1.38
NO_2	0.41	0.37	0.10	0.10	0.10	−0.08
N_3	*0.08*	*−0.11*	*−0.21*	−0.31	*−0.47*	*−0.67*
P						
PMe_2	*0.30*	*−0.14*	*−0.35*	*−0.55*	*−1.03*	*−1.63*
$POMe_2$	*0.24*	*0.22*	*0.08*	*0.12*	*0.14*	*0.00*
$PO(OMe)_2$	*0.34*	*0.33*	*0.15*	*0.21*	*0.25*	*0.12*
O						
OH	*−0.45*	−0.45	−0.46	−0.62	−0.64	−0.71
OMe	−0.36	−0.51	−0.44	−0.58	−0.66	−0.83
OEt	*−0.35*	−0.51	−0.44	−0.57	−0.65	−0.86
OAc	*−0.23*	−0.16	*−0.22*	−0.23	−0.26	−0.32
OPh	*−0.27*	*−0.44*	−0.42	−0.48	*−0.64*	−0.96
S						
SH	*−0.11*	*−0.29*	*−0.32*	*−0.41*	*−0.56*	*−0.81*
SMe	0.01	−0.24	−0.31	−0.38	−0.55	−0.97
SAc	*0.09*	*0.00*	−0.08	*−0.09*	*−0.13*	*−0.34*
SEt	*−0.04*	−0.10	−0.30	−0.30	*−0.59*	−0.99
SPh	*0.16*	−0.11	−0.24	−0.34	*−0.65*	−1.00
SOMe	0.13	0.05	0.00	0.00	−0.10	−0.70
SOPh	*0.03*	*0.06*	−0.07	−0.07	*−0.21*	−0.81
SO_2Me	0.18	0.35	0.11	0.11	0.11	−0.12
SO_2Ph	*0.32*	*0.22*	0.12	0.12	*−0.16*	−0.42
SF_5				0.03		
Se						
SeMe	*0.01*	*−0.23*	*−0.31*	*−0.42*	*−0.65*	*−1.02*
Other						
F	*−0.61*	−0.58	−0.44	−0.48	−0.37	*−0.25*
Cl	*−0.25*	−0.30	−0.25	−0.25	−0.21	−0.41
Br	−0.21	−0.28	−0.25	−0.25	−0.19	−0.44
I	*−0.06*	−0.18	−0.16	−0.16	−0.16	−0.57
H	0	0	0	0	0	0

[a] Values are from References 24, 25 and 27. Those in italics are estimates.

TABLE 3. Values of Hammett substituent constants

X	σ_m	σ_p^-	σ_p^o	σ_p	σ_p^+
Ak, *c*-Ak					
Me	−0.06	−0.15	−0.15	−0.17	−0.31
Et	−0.06	−0.09	−0.12	−0.15	−0.28
c-Pr	−0.08	−0.09	−0.15	−0.22	−0.46
Pr	−0.06			−0.17	
i-Pr	−0.04	*−0.12*	*−0.12*	−0.15	−0.28
t-Bu	0.00	*−0.15*	*−0.14*	−0.19	−0.26
CH_2Bu-*t*	−0.05			−0.17	
c-Hx	−0.05			−0.17	
Vinyl					
$CH{=}CH_2$	0.02	0.21	0.02	−0.05	−0.30
$CH{=}CH{-}CH{=}CH_2$	−0.08	−0.17	−0.20	−0.33	−0.76
$CH{=}CHPh$	−0.06	0.13	−0.16	−0.28	−0.68
Ethynyl					
$C{\equiv}CH$	0.24	0.50	0.26	0.21	0.05
$C{\equiv}C{-}C{\equiv}CH$	0.36	0.72	0.41	0.37	0.26
$C{\equiv}CPh$	0.26	0.39	0.11	0.12	−0.39
Aryl					
Ph	0.09	0.08	0.00	0.01	−0.51
C_6H_4Ph-4	0.06	0.11	−0.03	−0.09	−0.42
1-Nh	*−0.02*	*0.05*	*−0.07*	*−0.17*	*−0.28*
2-Nh	*0.01*	*0.13*	*−0.03*	*−0.11*	*−0.25*
CH_2Z					
CH_2Br	0.17			0.10	
CH_2OH	0.10			0.04	
CH_2Cl	0.15			0.09	
CH_2CN	0.20			0.16	
CH_2OMe	0.08			0.01	
CH_2SiMe_3	−0.11			−0.26	
CH_2Ph	−0.01			−0.10	
CX_3					
CF_3	0.46	0.74	0.52	0.53	0.61
CCl_3	0.40			0.44	
Carbonyl					
CHO	0.36	0.91	0.50	0.45	0.53
Ac	0.38	0.82	0.46	0.50	0.51
$CONH_2$	0.31	0.62	0.37	0.37	0.39
$CONMe_2$	0.31	0.62	0.37	0.37	0.39
CO_2Me	0.36	0.74	0.46	0.44	0.49
CO_2Et	0.35	0.74	0.46	0.44	0.49
Bz	0.36			0.41	
CN	0.61	1.02	0.69	0.65	0.66
N					
NH_2	−0.21	−0.51	*−0.40*	−0.63	−1.30
NHAc	0.11	0.03	0.00	−0.12	−0.46
NMe_2	−0.22	−0.35	−0.44	−0.67	−1.50
NO_2	0.74	1.29	0.82	0.77	0.79
N_3	0.27	0.38	0.20	0.08	−0.25

(*continued overleaf*)

TABLE 3. (*continued*)

X	σ_m	σ_p^-	σ_p^o	σ_p	σ_p^+
P					
PMe_2	−0.25	−0.18	−0.37	−0.61	−1.40
$POMe_2$	0.35	0.65	0.42	0.43	0.50
$PO(OMe)_2$	0.46	0.87	0.56	0.59	0.73
O					
OH	0.13	*−0.24*	−0.10	*−0.38*	*−0.61*
OMe	0.11	*−0.25*	−0.12	−0.28	−0.78
OEt	*0.07*	*−0.27*	−0.16	*−0.29*	*−0.73*
OAc	0.31	0.20	0.21	0.16	0.06
OPh	*0.23*	*−0.04*	*−0.01*	*−0.08*	*−0.57*
S					
SH	*0.07*	*−0.04*	−0.06	−0.19	*−0.58*
SMe	0.09	0.04	−0.02	−0.17	−0.60
SAc	0.34	0.50	0.33	0.28	0.18
SEt	*0.16*	*−0.01*	*−0.07*	*−0.04*	*−0.63*
SPh	*0.23*	0.18	*0.01*	*−0.15*	*−0.64*
SOMe	0.47	0.74	0.47	0.54	0.21
SOPh	*0.50*	*0.75*	*0.51*	*0.44*	*0.44*
SO_2Me	0.63	1.13	0.71	0.70	0.75
SO_2Ph	*0.62*	0.95	*0.68*	*0.68*	*0.48*
Other					
SeMe	0.05	0.03	−0.06	−0.21	−0.68
F	0.34	0.03	0.17	0.06	−0.07
Cl	0.37	0.28	0.27	0.22	0.11
Br	0.34	0.30	0.26	0.22	0.15
I	0.35	0.35	0.27	0.24	0.13
H	0	0	0	0	0

III. STERIC EFFECTS

A. Introduction

The concept of steric effects was introduced by Kehrmann[29] over a century ago. V. Meyer[30] and Sudborough and Lloyd[31] shortly thereafter presented kinetic results supporting the steric effect explanation of rate retardation in the esterification of 2-substituted and 2,6-disubstituted benzoic and 3-*cis*-substituted acrylic acids. Major early reviews of steric effects are given by Stewart[32] and Wittig[33]. Somewhat later reviews are by Wheland[34], and in a volume edited by Newman[35]. Steric effects are proximity effects that result from and are related to substituent size.

B. The Nature of Steric Effects

1. Primary steric effects

These effects are due to repulsions between electrons in valence orbitals on adjacent atoms which are not bonded to each other. They supposedly result from the interpenetration of occupied orbitals on one atom by electrons on the other, resulting in a violation of the Pauli exclusion principle. *All primary steric interactions raise the energy of the system in which they occur.* Their effect on chemical reactivity is to either decrease or increease a rate or equilibrium constant, depending on whether steric repulsions are greater in the reactant or in the product (equilibria) or transition state (rate).

2. Secondary steric effects

Secondary steric effects on chemical reactivity can result from the shielding of an active site from the attack of a reagent, from solvation, or both. They may also be due to a steric effect that determines the concentration of the reacting conformation of a chemical species. The secondary steric effect of a nonsymmetric group will also depend on its conformation.

3. Direct steric effects

These effects can occur when the active site at which a measurable phenomenon occurs is in close proximity to the substituent. Among the many skeletal groups exhibiting direct steric effects are vicinally (1,2) substituted skeletal groups such as *ortho* substituted benzenes, **1**, *cis*-substituted ethylenes, **2**, the *ortho* (1,2-, 2,1- and 2,3-) naphthalenes, **3, 4** and **5**, respectively, and *peri* (1,3) skeletal groups such as 1,8- substituted naphthalenes, **6**. Other vicinal examples are *cis*-1,2-disubstituted cyclopropanes, *cis*-2,3-disubstituted norbornanes and *cis*-2,3-disubstituted [2.2.2]-bicyclooctanes, **7, 8** and **9**, respectively. Some skeletal groups do not always show steric effects; 2,3-disubstituted five-membered ring heteroarenes such as thiophenes and selenophenes are generally free of steric effects. This is probably due to the larger XCC angle in these systems as compared with ethene and benzene systems. Geminally substituted (1,1) skeletal groups, such as disubstituted methanes, **10**, and 1,1-disubstituted ethenes, **11**, also seem to be usually free of steric effects.

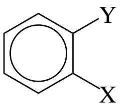

(1)

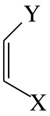

(2)

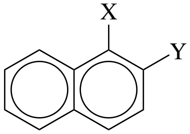

(3)

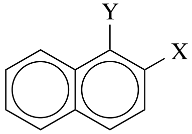

(4)

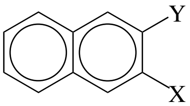

(5)

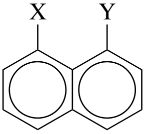

(6)

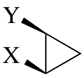

(7)

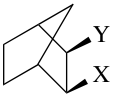

(8)

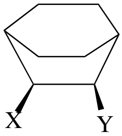

(9)

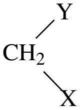

(10)

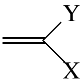

(11)

4. Indirect steric effects

These effects are observed when the steric effect of the variable substituent is relayed by a constant substituent between it and the active site, as in **12** where Y is the active site, Z is the constant substituent and X is the variable substituent. This is a type of buttressing effect.

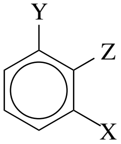

(12)

5. The directed nature of steric effects

This is easily shown by considering, for example, the ratio r of the steric parameter υ (which is defined below) for any five carbon alkyl group to that for 1-pentyl. Values of *r* are: 1-Pe, 1; 2-Pe, 1.54; 3-Pe, 2.22; CH_2Bu-*s*, 1.47; CH_2Bu-*i*, 1.00; CH_2Bu-*t*, 1.97; CMe_2Pr, 2.40; CH(*i*-Pr)Me, 1.90. All of these groups have the same volume and therefore the same bulk, but they differ in steric effect[36, 37]. In order to account for this, it is necessary to consider what happens when a nonsymmetric substituent is in contact with an active site. We consider the simple case of a spherical active site Y in contact with a nonsymmetric substituent, $CZ^LZ^MZ^S$, where the superscripts L, M and S represent the largest, the medium-sized and the smallest Z groups, respectively. The C−G bond and the Y−G bond are of comparable length. There are three possible conformations of this system (Figure 1). As all steric repulsions raise the energy of the system, the preferred conformation will be the one that results in the lowest energy increase. This is the conformation which presents the smallest face to the active site, conformation **13c**. From this observation we have the minimum steric interaction (MSI) principle which states: *a nonsymmetric substituent prefers that conformation which minimizes steric interactions*. The directed nature of steric effects results in a conclusion of vital importance: that in general *the volume of a substituent is not an acceptable measure of its steric effect*[36, 37]. There are still some who find this incomprehensible. It is nevertheless true that group volumes are not useful as steric parameters except in the case of substituents that are roughly spherical, and not even always then. Volumes are actually measures of group polarizability. In short, for a range of different substituent shapes in a data set *steric effects are not directly related to bulk, polarizability is.*

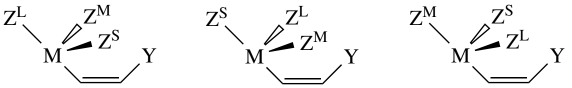

(13a) **(13b)** **(13c)**

FIGURE 1. The three possible conformations of a *cis*-1,2-disubstituted ethene having a spherical reaction site in contact with a tetrahedral substituent consisting of a central atom M bearing large (Z^L), medium (Z^M) and small (Z^S) sized groups. The energies of the conformations are **13a**, lowest, and **13c**, highest. The same types of conformation occur in other 1,2- and 1,3-disubstituted systems in which substituent and reaction site are in contact

C. The Monoparametric Model of Steric Effects

The van der Waals radii, r_V, have long been held to be an effective measure of atomic size[38]. Charton proposed the use of the van der Waals radius as a steric parameter[39] and developed a method for the calculation of group van der Waals radii for tetracoordinate symmetric top substituents MZ_3, such as the methyl and trifluoromethyl groups[40]. In later work the hydrogen atom was chosen as the reference substituent and the steric parameter υ was defined as in equation 8,

$$\upsilon_X \equiv r_{VX} - r_{VH} = r_{VX} - 1.20 \tag{8}$$

where r_{VX} and r_{VH} are the van der Waals radii of the X and H groups in Angstrom units[41].

Expressing r_V in these units is preferable to the use of picometers, because the coefficient of the steric parameter is then comparable in magnitude to the coefficients of the electrical effect parameters. Whenever possible, υ parameters are obtained directly from van der Waals radii or calculated from them. An equation has been derived which makes possible the calculation of υ values for nonsymmetric tetrahedral groups of the types $MZ_2{}^SZ^L$ and $MZ^SZ^MZ^L$ in which the Z groups are symmetric[42]. These are considered to be primary values. For the majority of substituents, however, υ parameters must be calculated from the regression equations obtained for correlations of rate constants with primary values. The values obtained in this manner are considered to be secondary υ values. All other measures of atomic size are a linear function of van der Waals radii[43]. There is therefore no reason for preferring one measure of atomic size over another. As values of υ were developed for a wide range of substituent types with central atoms including oxygen, nitrogen, sulfur and phosphorus as well as carbon, these parameters provide the widest structural range of substituents for which a measure of the steric effect is available.

1. Steric classification of substituents

Such classification is useful in understanding the way in which different types exert steric effects[44]. Substituents may be divided into three categories based on the degree of conformational dependence of their steric effects:

1. No conformational dependence (NCD). Groups of this type include monoatomic substituents such as hydrogen and the halogens, $M^a{\equiv}M^b$ substituents such ethynyl and cyano and MZ_3 groups.
2. Minimal conformational dependence (MCD). Among these groups are: (a) Nonsymmetric substituents with the structure $MH_n(lp)_{3-n}$, such as the hydroxyl and amino groups (lp is a lone pair). (b) Nonsymmetric substituents with the structure $MZ_2{}^SZ^L$, where S stands for small and L for large.
3. Strong conformational dependence (SCD). These groups have the structures: (a) $MZ_2{}^LZ^S$ and $MZ^LZ^MZ^S$, where the superscript M indicates medium. (b) Planar π-bonded groups MZ^LZ^S where M and either or both Zs are sp^2 hybridized, such as phenyl, acetyl, nitro ($X_{p\pi}$ groups). (c) Quasi-planar π-bonded groups such as dimethylamino and cyclopropyl.

The steric parameter for NCD groups can be obtained directly from van der Waals radii or calculated from them. The values for MCD groups are often obtainable from van der Waals radii, although in some cases they must be derived as secondary values from regression equations obtained by correlating rate constants with known values of the steric parameter. Steric parameters for SCD groups of the nonsymmetric type are usually obtainable only from regression equations.

2. *Planar π-bonded groups*

In the case of planar π-bonded groups, the maximum and minimum values of the steric parameter are available from the van der Waals radii (Figure 2). Both the steric effect and the delocalized electrical effect are a function of the dihedral angle when this type of group is bonded to an sp^2 hybridized carbon atom of a skeletal group[45].

D. Multiparametric Models of Steric Effects

In some cases a simple monoparametric model of the steric effect is insufficient. Examples are when the active site is itself large and nonsymmetric, or alternatively when the phenomenon studied is some form of bioactivity in which binding to a receptor determines the activity. The failure of the monoparametric model is due to the fact that a single steric parameter cannot account for the variation of the steric effect at various points in the substituent. The use of a multiparametric model of steric effects that can represent the steric effect at different segments of the substituent is required. Five multiparametric models are available: that of Verloop and coworkers[46], the simple branching model, the expanded branching model, the segmental model and the composite model. The Verloop model will not be discussed, as its assumption that the maximum perpendicular radius of a group is a useful parameter no matter where in the group it occurs is erroneous.

1. *The branching models*

The simple branching model[47] for the steric effect is given by equation 9:

$$S\psi = \sum_{i=1}^{m} a_i n_i + a_b n_b \qquad (9)$$

where $S\psi$ represents the steric effect parameterization the a_i and a_b are coefficients, n_i is the number of branches attached to the i-th atom, and n_b is the number of bonds between the first and last atoms of the group skeleton. It follows that n_b is a measure of group length. Unfortunately, it is frequently highly collinear in group polarizability, which greatly limits its utility. For saturated cyclic substituents it is necessary to determine values of n_i from an appropriate regression equation[48]. For planar π-bonded groups, n_i is taken to be 1 for each atom in the group skeleton. For other groups, n_i is obtained simply by counting branches. The model makes the assumption that all of the branches attached to a skeleton atom are equivalent. This is at best only a rough approximation. Distinguishing between branches results in an improved model called the expanded branching equation[49] (equation 10):

$$S\psi = \sum_{i=1}^{m} \sum_{j=1}^{3} a_{ij} n_{ij} + a_b n_b \qquad (10)$$

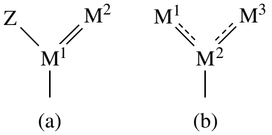

FIGURE 2. Examples of types of planar π-bonded groups. (a) Doubly bonded groups such as ZC=O, $Z^1C{=}NZ^2$, ZC=S, ZN=O, N=N, C=C etc. (b) Aryl, heteroaryl, nitro, carboxylate etc.

which allows for the difference in steric effect that results from the order of branching. This difference follows from the MSI principle. The first branch has the smallest steric effect, because a conformation in which it is rotated out of the way of the active site is preferred. In this conformation the active site is in contact with two hydrogen atoms. The preferred conformation in the case of a second branch has the larger of the two branches directed out of the way. The smaller branch and a hydrogen atom are in contact with the active site. When there are three branches, the largest will be directed out of the way and the other two will be in contact with the active site. The problem with the expanded branching method is that it requires a large number of parameters. A data set large enough to permit its use is seldom seen.

2. The segmental model[43]

This model is often the simplest and most effective of the multiparametric models. In this model each atom of the group skeleton together with the atoms attached to it constitutes a segment of the substituent. Applying the MSI principle, the segment is considered to have that conformation which presents its smallest face to the active site. The segment is assigned the υ value of the group which it most resembles. Values of the segmental steric parameters υ_i, where i designates the segment number, are given in Table 4. Numbering starts from the first atom of the group skeleton which is the atom that is attached to the rest of the system. The segmental model is given by equation 11:

$$S\psi = \sum_{i=1}^{m} S_i \upsilon_i \tag{11}$$

When only steric effects are present, equation 12 applies:

$$Q_X = S\psi_X \tag{12}$$

In the general case, electrical effects are also present and the general form of the LDRS equation (equation 13):

$$Q_X = L\sigma_{lX} + D\sigma_{dX} + R\sigma_{eX} + S\psi_X + h \tag{13}$$

is required.

3. The composite model

This model is a combination of the monoparametric υ model with the simple branching model. This method has proven useful in modelling amino acid, peptide and protein properties[50]. It is an improvement over the simple branching model and requires only one additional parameter.

E. Bond Length Difference as a Factor in Steric Effects

The steric effect exerted by some group X is a function of the lengths of the substituent-skeletal group (X—G) and active site-skeletal group (Y—G) bonds[51]. The steric parameters described above function best when they are of comparable length. In that case the contact between X and Y is that shown in Figure 3a. If the YG bond is much shorter than the XG bond the contact is as shown in Figure 3b. In that case, the distance from Y to the

TABLE 4. Steric effect parameters for common substituents[a]

X	υ	υ_1	υ_2	n_1	n_2
Ak, *c*-Ak					
Me	0.52	0.52	0	0	0
Et	0.56	0.52	0.25	1	0
Pr	0.68	0.52	0.52	1	1
i-Pr	0.78	0.78	0	2	0
Bu	0.68	0.52	0.52	1	1
i-Bu	0.98	0.52	0.78	1	2
s-Bu	1.02	0.78	0.52	2	1
t-Bu	1.24	1.24	0.52	3	0
Pe	0.68	0.52	0.52	1	1
i-Pe	0.68	0.52	0.52	1	1
c-Hx	0.87			1.5	0.74
Hx	0.73	0.52	0.52	1	1
Oc	0.68	0.52	0.52	1	1
1-Adm	1.33	1.33			
CH_2Z					
CH_2Br	0.64	0.52	0.65		
CH_2Cl	0.60	0.52	0.55		
CH_2OMe	0.63				
CH_2CH_2CN	0.68	0.52	0.52		
CH_2GeMe_3	1.53				
CH_2SiMe_3	1.46				
CH_2-2-Tp	0.70	0.52	0.57		
CH_2-2-Fr	0.70	0.52	0.57		
$CH_2CH_2CO_2Et$	0.68	0.52	0.52		
$CH_2CHMeCO_2Me$		0.52	0.78		
CH_2NEt_2		0.52	0.63		
CH_2 CH_2-2-Py	0.68	0.52	0.52		
CH_2 CH_2-4-Py	0.68	0.52	0.52		
Vn					
Vi	0.57	0.57	0.57		
2-VnVi	0.57	0.57	0.57		
2-VnPh	0.57	0.57	0.57		
Ar					
C_6F_5	0.57	0.57	0.57		
Ph	0.57	0.57	0.57		
PnZ					
4-$PnNMe_2$	0.57	0.57	0.57		
4-$PnNEt_2$	0.57	0.57	0.57		
4-PnCl	0.57	0.57	0.57		
4-PnMe	0.57	0.57	0.57		
4-PnOMe	0.57	0.57	0.57		
4-$PnNO_2$	0.57	0.57	0.57		
Har					
2-Fr	0.57	0.57	0.57		
3-Fr	0.57	0.57	0.57		
2-Tp	0.57	0.57	0.57		
3-Tp	0.57	0.57	0.57		

TABLE 4. (*continued*)

X	υ	υ_1	υ_2	n_1	n_2
Si					
$SiBr_3$	1.69	1.69	0.65		
$SiCl_3$	1.50	1.50	0.55		
SiF_3	1.01	1.01	0.27		
SiH_3	0.70	0.70	0		
$SiMe_3$	1.40	1.40	0.52		
$SiPh_3$			0.57		
Ge					
$GeMe_3$	1.44	1.44	0.52		
$GePh_3$			0.57		
Sn					
$SnMe_3$	1.55	1.55	0.52		
$SnPh_3$			0.57		
N					
NH_2	0.35	0.35			
NHAc	0.35	*0.50*	0.32		
NMe_2	0.35	0.52	0		
NO_2	0.35	0.32	0.35		
N_3	0.35	0.35	0.35		
P					
PMe_2	1.09	0.52	0		
$POMe_2$	1.39	0.52	0		
$PO(OMe)_2$	1.29	0.32	0.52		
O					
OH	0.32	0	—		
OMe	0.32	0.32	0.52		
OEt	0.36	0.32	0.52		
OAc	0.48	0.32	*0.52*		
$OSiMe_3$	0.50	0.32	1.40		
OPh	0.57	0.32	*0.57*		
S					
SH	0.60	0.60	0		
SMe	0.64	0.60	0.52		
SAc	1.09	0.60	*0.50*		
SEt	0.94	0.60	0.52		
SPh	1.00	0.60	*0.57*		
SOMe	0.76	0.74	0.52		
SOPh	1.10	0.74	*0.57*		
SO_2Me	1.13	1.03	0.52		
SO_2Ph		1.03	*0.57*		
Se					
SeMe	0.74	0.70	0.52		
Other					
H	0	0	—		
F	0.27	0.27	—		
Cl	0.55	0.55	—		
Br	0.65	0.65	—		
I	0.78	0.78	—		

[a] Abbreviations can be found in Section I.A.

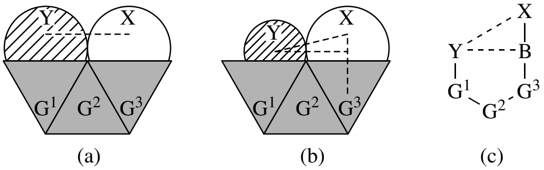

FIGURE 3. The effect of bond length on steric effects. (a) A system in which substituent X and reaction site Y have comparable X−G and Y−G bond lengths; G^1, G^2 and G^3 are atoms of the skeletal group. (b), (c) A system in which X−G and Y−G bond lengths are significantly different. Reproduced with permission from Reference 52. Copyright 1996 John Wiley & Sons, Ltd

X−G bond is less in Figure 3b than it is in Figure 3a although the XY distance in both Figures 3a and 3b is the sum of the van der Waals radii, r_{VX} and r_{VY}. The effective size of the van der Waals radius of X is reduced. Steric parameters were originally derived for systems like that in Figure 3a. In a system like 1b, corrected steric parameters are needed. An approximate value of the effective van der Waals radius of X, r^c_{VX}, can be calculated for the case in which the X−G and Y−G bonds are parallel to each other from a consideration of Figure 3c and Scheme 1, where l_{XG} and l_{YG} are the lengths of the X−G and Y−G bonds, respectively.

$$\overline{XY} = r_{VX} + r_{VY}$$

$$\overline{XB} = l_{XG} - l_{YG}$$

$$\overline{BY} = [(\overline{XY})^2 - (\overline{XB})^2]^{1/2}$$

$$\overline{BY} = [(r_{VX} + r_{VY})^2 - (l_{XG} - l_{YG})^2]^{1/2}$$

$$\overline{BY} = r_{VY} + r^c_{VX}$$

$$r^c_{VX} = [(r_{VX} + r_{VY})^2 - (l_{XG} - l_{YG})^2]^{1/2} - r_{VY}$$

SCHEME 1

Values of steric effect substituent constants for typical groups are given in Table 4.

IV. INTERMOLECULAR FORCES

A. Introduction

Inter- and intramolecular forces (imf) are of major importance in the quantitative description of structural effects on bioactivities and chemical properties. They may make a significant contribution to chemical reactivities and some physical properties as well. Common types of intermolecular forces and their parameterization are given in Table 5.[52a]

B. Parameterization of Intermolecular Forces

1. Hydrogen bonding

Two parameters are required for the description of hydrogen bonding. One is required to account for the hydrogen atom donating capacity of a substituent and another to account for its hydrogen atom accepting capacity. The simplest approach is the use of n_H, the

TABLE 5. Intermolecular forces and the quantities upon which they depend[5]

Intermolecular force[a]	Quantity
Molecule–molecule	
Hydrogen bonding (hb)	q_{MH}, q_{ME}, orbital type
Agostic bonding	
Dipole–dipole (dd)	dipole moment
Dipole–induced dipole (di)	dipole moment, polarizability
Induced dipole–induced dipole (ii)	polarizability
Charge transfer (ct)	ionization potential, electron affinity
Ion–molecule	
ion–dipole (Id)	ionic charge, dipole moment
ion–induced dipole (Ii)	ionic charge, polarizability

[a] Abbreviations are in parentheses. dd interactions are also known as Keesom interactions; di interactions are also known as Debye interactions; ii interactions are also known as London or dispersion interactions. Collectively, dd, di and ii interactions are known as van der Waals interactions. Charge transfer interactions are also known as donor–acceptor interactions.

number of OH and/or NH bonds in the substituent, and n_n, the number of lone pairs on oxygen and/or nitrogen atoms as parameters[3, 50]. The use of these parameters is based on the argument that if one of the phases involved in the phenomenon studied includes a protonic solvent, particularly water, then hydrogen bonding will be maximized. For such a system, hydrogen bond parameters defined from equilibria in highly dilute solution in an 'inert' solvent are unlikely to be a suitable model. This type of parameterization accounts only for the number of hydrogen donor and hydrogen acceptor sites in a group. It does not take into account differences in hydrogen bond energy. An improved parameterization would result from the use of the hydrogen bond energy for each type of hydrogen bond formed[52]. For each substituent, the parameter E_{hbX} would be given by equation 14:

$$E_{hbX} = \sum_{i=1}^{m} n_{hbi} E_{hbi} \tag{14}$$

where E_{hbX} is the hydrogen bonding parameter, E_{hbi} is the energy of the i-th type of hydrogen bond formed by the substituent X and n_{hbi} is the number of such hydrogen bonds. The validity of this parameterization remains untested. In any event, the site number parameterization suffers from the fact that, though it accounts for the number of hydrogen bonds formed, it does not differentiate between their energies and can therefore be only an approximation. A recent definition of a scale of hydrogen bond acceptor values from 1-octanol–water partition coefficients of substituted alkanes shows that the site number method strongly overestimates the hydrogen acceptor capability of the nitro group and seriously underestimates that of the methylsulfoxy group[52b]. It has now become apparent that there are many weak types of H donors and H acceptors that are capable of contributing significantly to the intermolecular forces which are responsible for many properties involving a change of phase. Green reported evidence many years ago for the H donor activity of CH groups, and in a more recent work Nishio, Hirota and Urezama have reviewed evidence for CH–π interactions[52c]. Much remains to be done in properly parameterizing hydrogen bonding.

2. Agostic bonding

Some time ago Brookhart and Green reviewed crystallographic, NMR and IR evidence showing a bonding interaction of the type C–H···M where M is a transition metal.

They stated that this was a three-atom two electron covalent bond, which they named an agostic bond from the Greek $\alpha\gamma o\sigma\tau\omega$, to clasp or hold to oneself. The agostic bond is characterized by:[53a]

1. Crystallographic data giving MH distances less than the sum of the van der Waals radii and some elongation of CH bond lengths.
2. NMR spectra showing chemical shifts to high field (δ is -5 to -15 ppm) and lower coupling constants [^1J(CH) is 75–100 MHz].
3. Lower IR vibrational frequencies (ν_{CH} is 2700–2300 cm^{-1}).

The agostic bond was extended to C—H$\cdots$Li interactions by Kaufmann and coworkers[53b], who regard it as a $\sigma_{\text{CH}}-n_{\text{Li}}$ interaction which induces a small polarization of the C—H bond toward the hydrogen atom, giving it an increment of negative charge. The hydrogen atom is therefore a 'hydridic' donor. These authors report that calculated energies of the agostic bond are a function of the degree of aggregation with values from -0.8 kcal mol^{-1} for the monomer of MeLi to -4.6 kcal mol^{-1} for the tetramer. The magnitude of the energy of agostic bonds in organolithium compounds is such that they are best regarded as intermolecular forces. It is tempting to regard an agostic bond as a type of hydrogen bond, but this does not seem to be the case. An ordinary hydrogen bond involves a hydrogen donor $B^{\delta-}-H^{\delta+}$ and a hydrogen acceptor, B; B:$^-$ and B are Lewis bases. The hydrogen bonded species is $B^{\delta-}-H^{\delta+}\cdots B$. The hydrogen in the donor has an increment of positive charge and is considered protic. The corresponding hydridic hydrogen bond involves a hydrogen donor $A^{\delta+}-H^{\delta-}$ and a hydrogen acceptor A, where A^+ and A are Lewis acids. The hydrogen atom in the donor has an increment of negative charge. The hydrogen bonded species is $A^{\delta+}-H^{\delta-}\cdots A$. An agostic bond in an organolithium compound is of the type $C^{\delta-}-H^{\delta-}\cdots Li^+$, where C is the charged atom of a carbanion and is therefore a Lewis base while Li^+ is a Lewis acid; the H atom has an increment of negative charge. It is conceivable that a hydrogen bond of the hydridic type could exist in LiH.

3. van der Waals interactions

These interactions (dipole–dipole, dd; dipole–induced dipole, di; and induced dipole–induced dipole, ii) are a function of dipole moment and polarizability. It has been shown that the dipole moment cannot always be replaced entirely by the use of electrical effect substituent constants as parameters[3,50]. This is because the dipole moment has no sign. Either an overall electron donor group or an overall electron acceptor group may have the same value of μ. It has also been shown that the bond moment rather than the molecular dipole moment is the parameter of choice. The dipole moments of MeX and PhX were taken as measures of the bond moments of substituents bonded to sp^3 and sp^2 hybridized carbon atoms, respectively, of a skeletal group. Application to substituents bonded to sp hybridized carbon atoms should require a set of dipole moments for substituted ethynes.

Dipole moments μ for MeX and PhX can be calculated from equations 15 and 16[27]:

$$\mu_{MeX} = 5.11(\pm 0.497)\sigma_{lX} + 1.99(\pm 0.541)\sigma_{dX} + 0.0129(\pm 0.205) \tag{15}$$

$$\mu_{PhX} = 5.47(\pm 0.150)\sigma_{lX} + 4.30(\pm 0.446)\sigma_{dX} + 6.94(\pm 1.91)\sigma_{eX} + 0.420(\pm 0.172) \tag{16}$$

The polarizability parameter used here, α, is given by equation 17:

$$\alpha \equiv \frac{MR_X - MR_H}{100} = \frac{MR_X}{100} - 0.0103 \tag{17}$$

where MR_X and MR_H are the group molar refractivities of X and H, respectively[3,50,52a]. The factor 1/100 is introduced to scale the α parameter so that its coefficients in the regression equation are roughly comparable to those obtained for the other parameters used. Many other polarizability parameters have been proposed, including parachor, group molar volumes of various kinds, van der Waals volumes and accessible surface areas, Any of these will serve as they are all highly collinear in each other[44,59]. The advantage of α is that it is easily estimated either by additivity from the values for fragments or from group molar refractivities calculated from equation 18:

$$MR_X = 0.320n_c + 0.682n_b - 0.0825n_n + 0.991 \tag{18}$$

where n_c, n_b and n_n are the number of core, bonding and nonbonding electrons, respectively, in the group X[52a].

Atomic polarizabilities P_M for atoms M may be used as polarizability parameters but they are not directly comparable to α values, thus a comparison of coefficients obtained from correlations with α are not directly comparable to those obtained with P_M. In order to obtain α values for some atoms we have first defined ΔP_M in equation 19:

$$\Delta P_M \equiv P_M - P_H \tag{19}$$

where M is the atom of interest and H is hydrogen. This is directly comparable to the definition of α in equation 11. Values of ΔP_M for the set H, F, Cl, Br, I (Table 6) were then correlated by equation 20:

$$\Delta P_M = A\alpha_M + a_o \tag{20}$$

to give the regression equation 21:

$$\Delta P_M = 31.4(\pm 0.428)\alpha - 0.0507(\pm 0.0305) \tag{21}$$

$$100r^2, 99.94; F, 5396; S_{est}, 0.0472; S^{\text{o}}, 0.0304; N_{dp}, 5.$$

Inclusion in the data set of the ΔP_M values for N, P, O, S and Se (Table 6) gave the regression equation 22:

$$\Delta P_M = 30.6(\pm 1.70)\alpha_M - 0.197(\pm 0.126) \tag{22}$$

$$100r^2, 97.26; F, 320.0; S_{est}, 0.248; S^{\text{o}}, 0.183; N_{dp}, 11.$$

Though the goodness of fit of equation 22 is decidedly poorer than that of equation 21, the values of A are not significantly different and the intercepts in both equations are not significant, furthermore, both equations are significant at the 99.9% confidence level. Values of ΔP_M for the Group 14 elements seem to lie on their own line. We have used equation 22 in the form of equation 23:

$$\alpha_M = 0.0318\Delta P_M - 0.00183 \tag{23}$$

to calculate α values for the alkali metal elements. These values are given in Table 7.

TABLE 6. ΔP_M and α values of the atoms M[a]

M, ΔP, α: H, 0, 0; F, −0.11, −0.001; Cl, 1.513, 0.0510; Br, 2.383, 0.079; I, 4.033, 0.129; O, 0.135, 0.015; S, 2.233, 0.082; Se, 3.103, 0.114; N, 0.433, 0.038; P, 2.963, 0.107; C, 1.093, 0.039; 4.633, 0.146.

[a] P_M values are from T. M. Miller, in *Handbook of Chemistry and Physics*, 67th edn., R. C. Weast, (Ed.), CRC Press, Boca Raton, 1986, pp. E66–E75.

TABLE 7. Intermolecular force substituent constants used in applications[a]

X	α	$\mu(\mathrm{sp}^2)$	$\mu(\mathrm{sp}^3)$	n_H	n_n
AK, cAK					
Me	0.046	0.37	0	0	0
Et	0.093	0.37	0	0	0
c-Pr	0.125	0.48		0	0
Pr	0.139	0.37	0	0	0
i-Pr	0.140	0.40	0	0	0
Bu	0.186	0.37	0	0	0
i-Bu	0.186		0	0	0
s-Bu	0.186		0	0	0
t-Bu	0.186	0.52	0	0	0
Pe	0.232		0	0	0
CH_2Bu-*t*	0.232		0	0	0
c-Hx	0.257		0	0	0
Hx	0.278		0	0	0
Oc	0.372		0	0	0
1-Adm	0.396		0	0	0
CH_2Z					
CH_2Br	0.124	1.87	2.069	0	0
CH_2Cl	0.095	1.83	1.895	0	0
CH_2OH	0.062	1.71	1.58	1	2
CH_2CN	0.091	3.43	3.53	0	0
CH_2OMe	0.114			0	2
CH_2CH_2CN	0.145	3.92		0	0
CH_2Vi	0.135	0.364	0.438	0	0
CH_2OEt	0.160			0	2
CH_2GeMe_3	0.300			0	0
CH_2SiMe_3	0.285	0.68		0	0
CH_2SnMe_3	0.353			0	0
CH_2-2-Tp	0.276		0.81	0	0
CH_2-2-Fr	0.215		0.65	0	2
$CH_2CH_2CO_2Et$	0.256		1.84	0	4
$CH_2CHMeCO_2Me$	0.256		1.84	0	4
CH_2NEt_2	0.278		0.612	0	1
CH_2Ph	0.290	0.22	0.37	0	0
CH_2CH_2-2-Py	0.212			0	1
CH_2CH_2-4-Py	0.212			0	1
CZ_3					
CF_3	0.040	2.86	2.321	0	0
CCl_3	0.191		1.95	0	0
$C(SiMe_3)_3$	0.760			0	0
VnX					
Vi	0.100	0.13	0.364	0	0
2-VnVi					
C_2Z					
C_2H	0.085	0.70	0.7809	1	0
C_2Me	0.131			0	0
C_2Ph	0.322	0		0	0
Ar					
C_6F_5	0.230	1.99	1.73	0	0
Ph	0.243	0	0.37	0	0

TABLE 7. (*continued*)

X	α	$\mu(sp^2)$	$\mu(sp^3)$	n_H	n_n
PnZ					
4-$PnNMe_2$	0.388		1.60	0	1
4-$PnNEt_2$	0.475		1.81	0	1
Har					
2-Fr	0.169		0.65	0	1
3-Fr	0.169		1.03	0	1
2-Tp	0.230		0.674	0	0
3-Tp	0.230		0.81	0	0
(CO)Z					
CHO	0.059	2.92	2.69	0	2
CO_2H	0.059	1.86	1.70	1	4
Ac	0.102	2.88	2.93	0	2
CO_2Me	0.118	1.92	1.706	0	4
CO_2Et	0.164	1.846	1.84	0	4
CN	0.053	4.14	3.9185	0	0
Si					
$SiBr_3$	0.338			0	0
$SiCl_3$	0.251			0	0
SiF_3	0.098			0	0
SiH_3	0.101			0	0
$SiMeBr_2$	0.305			0	0
$SiMeCl_2$	0.247			0	0
$SiMeF_2$	0.145			0	0
$SiMe_2Cl$	0.243			0	0
$SiMe_3$	0.239	0.42		0	0
$SiMe_2Et$	0.285			0	0
$SiEt_3$	0.380			0	0
$SiMe_2Ph$	0.436			0	0
$SiPh_3$	0.830			0	0
Ge					
$GeMe_3$	0.254			0	0
$GeEt_3$	0.392			0	0
$GePh_2Br$	0.681			0	0
$GePh_3$	0.845			0	0
Sn					
$SnMe_3$	0.307			0	0
$SnEt_3$	0.380			0	0
$SnPh_2Cl$	0.705			0	0
$SnPh_3$	0.898			0	0
Pb					
$PbPh_3$	0.915			0	0
N					
N_3	0.092	1.56	2.17	0	1
NH_2	0.044	1.49	1.296	2	1
NHMe	0.093	1.77	1.01	1	1
NHAc	0.139	3.75	3.71	1	3
NMe_2	0.145	1.60	0.612	0	1
NEt_2	0.232	1.81		0	1
NO	0.042	3.17		0	3
NO_2	0.063	4.28	3.56	0	4

(*continued overleaf*)

TABLE 7. (*continued*)

X	α	$\mu(sp^2)$	$\mu(sp^3)$	n_H	n_n
O					
OH	0.018	1.40	1.77	1	2
OMe	0.068	1.36	1.31	0	2
OAc	0.114	1.69	1.706	0	4
OEt	0.114	1.38	1.22	0	2
OPr-*i*	0.160			0	2
$OSiMe_3$	0.259		1.18	0	2
OBu	0.206			0	2
OPh	0.267	1.13	1.36	0	2
S					
SH	0.082	1.21	1.52	0	0
SMe	0.128	1.29	1.06	0	0
SAc	0.174			0	2
SEt	0.174			0	0
SPh	0.333	1.37	1.50	0	0
SOMe	0.127	3.98	3.96	0	2
SOPh	0.320	4.02		0	2
SO_2Me	0.125	4.73		0	4
SO_2Ph	0.322	5.00	4.73	0	4
SF_5	0.089	3.44		0	0
Se					
SeMe	0.160	1.31		0	0
Other					
H	0	0	0	0	0
Br	0.079	1.70	1.84	0	0
Cl	0.050	1.70	1.895	0	0
F	−0.001	1.66	1.8549	0	0
I	0.129	1.71	1.618	0	0

[a] Abbreviations can be found in Section I.A.

4. Charge transfer interactions

These interactions can be roughly parameterized by the indicator variables n_A and n_D, where n_A takes the value 1 when the substituent is a charge transfer acceptor and 0 when it is not, and n_D takes the value 1 when the substituent is a charge transfer donor and 0 when it is not. An alternative parameterization makes use of the first ionization potential of MeX (ip_{MeX}) as the electron donor parameter and the electron affinity of MeX as the electron acceptor parameter. Usually, the indicator variables n_A and n_D are sufficient[50, 52a]. This parameterization accounts for charge transfer interactions directly involving the substituent. If the substituent is attached to a π-bonded skeletal group, then the skeletal group is capable of charge transfer interaction the extent of which is modified by the substituent. This is accounted for by the electrical effect parameters of the substituent.

5. The intermolecular force equation

The intermolecular force (IMF) equation is a general relationship for the quantitative description of intermolecular forces. It is written as equation 24:

$$Q_X = L\sigma_{lX} + D\sigma_{dX} + R\sigma_{eX} + M\mu_X + A\alpha_X + H_1 n_{HX} \\ + H_2 n_{nX} + I i_X + B_{DX} n_{DX} + B_{AX} n_{AX} + S\psi_X + B^o \qquad (24)$$

Values of imf parameters for common substituents are given in Table 7.

V. PROPERTIES OF THE GROUP 1 ELEMENTS

A number of useful properties of the Group 1 elements (alkali metals) are given in Table 8. They include ionization potentials and electron affinities; Pauling, Allred–Rochow and Allen electronegativities; ionic, covalent and van der Waals radii; υ steric parameters and polarizabilities. It should be noted that the ionic radii, r_I, are a linear function of the molar volumes, V_M, and the α values. If they are used as parameters, they cannot distinguish between polarizability and ionic size.

A. Electrical Effect Substituent Constants for Lithium

There are two substituent constants that have been reported for Li. Knorr[54], on the basis of ^{1}H NMR coupling constants of XRC=CH$_2$ in THF and Et$_2$O, has reported σ_I^J constants for Li of −0.78 and −0.71, respectively. A value of 0.13 was reported for σ_I^J

TABLE 8. Properties of Group 1 elements

Property	Li	Na	K	Rb	Cs	Fr
$\chi_P{}^{a,b}$	0.95	0.93	0.82	0.82	0.79	0.7
$\chi_{AR}{}^{b,c}$	0.97	1.01	0.91	0.89	0.86	0.86
$\chi_{spec}{}^{d}$	0.912	0.869	0.734	0.706		
IP (kcal mol^{-1})^{b,e}	124.0	119.8	101.2	97.4	90.8	96.7
EA (kcal mol^{-1})^{b,f}	14.5	12.8	11.7	11.3	11.0	10.6
r_I(pm)^{b,g}	78	98	133	149	465	180
r_C(pm)^{b,h}	123		203		235	na
r_A(pm)^{b,i}	152	153.7	227	247.5	265.4	870?
r_V(pm)^{b,j}	189	219	253	264	278	na
υ	0.69	0.99	1.33	1.44	1.58	na
V_M(cm^3)^{b,k}	13.00	23.68	45.36	55.79	70.96	na
$P_M{}^{l}$	24.3	23.6	43.4	47.3	59.6	48.7
α	0.750	0.727	1.36	1.48	1.87	1.53

na, not available.

[a] Pauling electronegativities.

[b] From J. Emsley, *The Elements*, Oxford University Press, Oxford, 1990.

[c] Allred—Rochow electronegativities.

[d] Allen electronegativities. L. C. Allen, *J. Am. Chem. Soc.*, **111**, 9003 (1989).

[e] First ionization potentials.

[f] Electron affinities.

[g] Ionic radius.

[h] Covalent radius.

[i] Atomic radius.

[j] van der Waals radius from Reference. 43.

[k] Molar volume.

[l] From T. M. Miller, in *Handbook of Chemistry and Physics*, 67th edn., R. C. Weast (Ed.), CRC Press, Boca Raton, 1986, pp. E66–E75.

of OLi. As these parameters are only crudely related to other scales of localized (field) effect substituent constants, their significance is unclear. Angelelli and coworkers[55] have determined a value of σ_R^o equal to 0.144, from the integrated IR intensity of PhLi. In view of the very largely ionic nature of the C−Li bond, the significance of this value is also questionable. The substituent constants of ionic groups are strongly dependent on the nature of the solvent and the ionic strength of the medium.

B. Nature of the Carbon−Lithium Bond

There is now a consensus that the carbon–lithium bond is ionic[56, 57]. There is agreement, however, that a small significant covalent contribution exists.

C. Aggregation of Organolithium Compounds

Lithium compounds in general and organolithium compounds in particular exist as oligomers, with *n* ranging from two to six. The value of *n* depends on the state, the solvent if in solution and the structure. In hydrocarbon solution, unbranched lithium alkyls other than MeLi, which is tetrameric, are hexamers[57]. Branching at C1 results in a preference for tetramers. The oligomers have been accounted for by point charge (tetramer) and hard sphere (hexamer) electrostatic models[58−59]. Organolithium compounds may also exist as contact ion pairs (CIP) and solvent separated ion pairs (SSIP) in polar solvents[60−62].

VI. APPLICATIONS

We now consider the application of the methods and parameters described above to organolithium compounds.

A. Chemical Reactivities (QSRR)

1. Deprotonation

Arnett and Moe[63] have reported enthalpies of deprotonation, ΔH_{dprtn}, for 4-substituted phenols and for the alcohols XCH_2OH (sets **CR1** and **CR2**, Table 9) with $LiN(SiMe_3)_2$ in THF at 25 °C. For the phenols only electrical effects were considered. Best results were obtained with the LD equation (equation 4). The regression equation is equation 25:

$$\Delta H_{dprtn} = -6.28(\pm 0.620)\sigma_{lX} - 5.31(\pm 0.607)\sigma_d - 23.7(\pm 0.266) \qquad (25)$$

$$100R^2, 98.40; A\ 100R^2, 98.08; F, 123.1; S_{est}, 0.386; S^{\circ}, 0.167; N_{dp}, 7, r_{df/iv}, 2.0;$$
$$r_{ld}, 0.275; r_{le}, 0.540; r_{de}, 0.232; P_D, 45.8; \eta, 0; C_l, 54.2; C_d, 45.8.$$

The failure to detect a dependence on σ_e is probably due to the small size of the data set.

As only the localized electrical effect and a possible steric effect need be considered in this data set, the ΔH values for the alcohols were correlated with equation 26:

$$Q_X = L\sigma_{lX} + S\upsilon_X + h \qquad (26)$$

giving the regression equation 27:

$$Q_X = -14.5(\pm 0.484)\sigma_{lX} + 1.56(\pm 0.147)\upsilon_X - 15.9(\pm 0.118) \qquad (27)$$

$$100R^2, 99.89; A\ 100R^2, 99.84; F, 457.8; S_{est}, 0.158; S^\circ, 0.0661;$$

$$N_{dp}, 4; r_{df/iv}, 0.5; r_{lv}, 0.225; C_l, 90.3; C_d, 9.68.$$

Due to the small size of this data set no reliance can be placed on these results. We have carried out the correlation only to illustrate the method. In an earlier paper Arnett and Moe[64] reported ΔH_{dprtn} for the deprotonation of *i*-PrOH by lithium *N*-alkyl and *N*,*N*-dialkyl amides, and by lithium alkyls (sets **CR3** and **CR4**, Table 9). As the electrical effects of alkyl groups are constant within experimental error, only the number of alkyl groups, their steric effects and their polarizabilities can be variables. Values of ΔH_{dprtn} for the amides were correlated with equation 28:

$$Q_X = a_1n_1 + a_2n_2 + a_Cn_C + a_o \tag{28}$$

where n_1 is the number of N−C bonds, n_2 is the sum of the number of branches at C1 of the alkyl groups and n_C is the total number of C atoms in the amide. The regression equation is equation 29:

$$Q_X = 4.42(\pm 1.54)n_1 + 1.67(\pm 0.774)n_2 + 0.546(\pm 0.201)n_C + 10.4(\pm 1.98) \tag{29}$$

$$100R^2, 93.34; A\ 100R^2, 90.68; F, 18.70; S_{est}, 1.62; S^\circ, 0.365; N_{dp}, 8; r_{df/iv}, 1.33;$$

$$r_{12}, 0.645; r_{1C}, 0.317; r_{2C}, 0.228; C_1, 53.4; C_2, 20.2, C_C, 26.4.$$

TABLE 9. QSRR data sets

CR1. $-\Delta H_{dprtn}$ (kcal mol^{-1}), 4-C_6H_4OH + LiN$(SiMe_3)_2$. X, $-\Delta H_{dprtn}$: NO_2, 29.2; CN, 27.3; CO_2Me, 26.8; Cl, 25.1; H, 23.5; *t*-Bu, 22.9; OMe, 22.7.

CR2. $-\Delta H_{dprtn}$ (kcal mol^{-1}), XCH_2OH + LiN$(SiMe_3)_2$. X, $-\Delta H_{dprtn}$: CF_3, 20.3; Ph, 17.8; Et, 15.7; *t*-Bu, 13.9.

CR3. $-\Delta H_{dprtn}$ (kcal mol^{-1}), *i*-PrOH + LiNR^{1}R^2: R^1, R^2, $-\Delta H_{dprtn}$: *c*-Hx, *c*-Hx, 31.8; *i*-Pr, *c*-Hx, 29.6; *i*-Pr, *i*-Pr, 28.6; Et, Et, 23.4; *c*-Hx, H, 21.8; *i*-Pr, H, 21.3; *t*-Bu, H, 21.2; Oc, H, 18.9.

CR4. $-\ \Delta H_{dprtn}$ (kcal mol^{-1}), *i*-PrOH + AkLi. Ak, $-\Delta H_{dprtn}$: *t*-Bu, 56.2; *s*-Bu, 52.8; Bu, 50.0; Me, 41.6.

CR5. K_e for reaction 32, 3- or 4-XC_6H_4Br, Et_2O at 20° C. X, K$_e$: 4-Me, 0.61; 3-Me, 0.76; H, 1.00; 4-Cl, 13.2; 3-Cl, 41.2.

CR6. 10^3k_r for reaction 32 at various T (deg K). X, T, k_r: 4-Me, 288.15, 0.083; 4-Me, 293.15, 0.133; 4-Me, 298.15, 0.212; 3-Me, 288.15, 0.102; 3-Me, 293.15, 0.162; 3-Me, 298.15, 0.246; 3-Me, 303.15, 0.390; 4-Cl, 273.15, 1.44; 4-Cl, 288.15, 5.60; 4-Cl, 293.15, 7.70; 4-Cl, 298.15, 12.0; 3-Cl, 251.95, 2.55; 3-Cl, 257.4, 4.70; 265.2, 9.66; 273.2, 18.11.

CR7. K_e for reaction 32, 3- or 4-XC_6H_4Br, X, K_e: H, 1; 3-Me, 0.88; 3-CF_3, 289; 4-Me, 0.60; 4-Ph, 3.78; 4-Cl, 53.

CR8. k_r for reaction 32, 3- or 4-XC_6H_4Br. X, k_r: H, 0.59; 3-Me, 0.34; 3-CF_3, 170; 4-Me, 0.19; 4-Ph, 0.65; 4-Cl, 5.4.

CR9. log K_e for reaction 40, $M^+ArH^{-\cdot}$ ion pairs. ArH, M, Sv, log K_e: NhH, Li, Et_2O, 3.104; AnH, Li, Et_2O, 1.623; AnH, Li, THF, −6.538; AnH, Li, DME, −7.748; AnH, Na, THF, −4.796; AnH, Na, DME, −7.553; AnH, K, THF, −6.167; AnH, K, DME, −6.921; TetH, Li, Et_2O, 1.204; PyrH, Li, Et_2O, −0.569; PerH, Li, Et_2O, −0.119; Per, Li, THF, −8.699; PerH, Li, DME, −9.420; PerH, Na, −5.770, PerH, Na, −9.051; PerH, K, THF, −5.658; PerH, K, DME, −7.051; PerH, Cs, THF, −4.796; PerH, Cs, DME, −4.174.

CR10. ΔH_{rctn} (kcal mol^{-1}) for LiAk + HBr, Ak, $-\Delta H_{rctn}$: Me, 77.9; Et, 85.7; *i*-Pr, 86.9; Bu, 85.2; *s*-Bu, 90.3; *t*-Bu, 90.9.

CR11. Bond dissociation energies (kcal mol^{-1}) of AkLi. Ak, $D_{\text{Ak-Li}}$: Me, 62.0; Et, 48.0; *i*-Pr, 43.4; Bu, 48.7; *s*-Bu, 40.0; *t*-Bu, 35.9.

The ΔH_{dprtn} values for the lithium alkyls were correlated with equation 30:

$$Q_X = a_1 n_1 + a_C n_C + a_o \tag{30}$$

giving the regression equation 31:

$$Q_X = 3.10(\pm 0.171)n_1 + 1.73(\pm 0.147)n_C + 39.9(\pm 0.345) \tag{31}$$

$$100R^2, 99.95; A\ 100R^2, 98.83; F, 1001; S_{est}, 0.242; S^\circ, 0.0447; N_{dp}, 4;$$

$$r_{df/iv}, 0.5; r_{1C}, 0.775; C_1, 37.3; C_C, 62.7.$$

The excellent correlation is probably fortuitous. While the data sets are too small to permit conclusive results, it seems likely that sets **CR3** and **CR4** are a function of polarizability and steric and/or electrical effects.

2. Aryl halide–aryl lithium exchange

Batalov and Rostokin[65] have reported equilibrium and rate constants (sets **CR5** and **CR6**, Table 9) for the exchange reaction given in equation 32:

$$X^{14}C_6H_4Br + PhLi \rightleftharpoons X^{14}C_6H_4Li + PhBr \tag{32}$$

Only electrical effects should be of major importance. The equilibrium constants were correlated with the Hammett equation (equation 5). This was necessary, due to the small size of the data set which included both *meta* and *para* substituents. The application of the Hammett equation to data sets including both *meta* and *para* substituents is most successful when the geometry of the system resembles that of the benzoic acids from which the Hammett constants were obtained. That is not the case in this reaction. The regression equation is equation 33:

$$\log K_X = 3.73(\pm 0.433)\sigma_X + 0.212(\pm 0.0903) \tag{33}$$

$$100r^2, 96.11; F, 74.13; S_{est}, 0.190; S^\circ, 0.255; N_{dp}, 5; r_{df/iv}, 2.0.$$

The range of substituents studied is so limited that no reliable conclusions can be drawn other than that in the range of substituent effects studied there is a single mechanism.

As the rate constants were reported at various temperatures, they were combined into a single data set by introducing. in the correlation equation the term $T\tau$, where τ is defined by equation 34:

$$\tau \equiv \frac{100}{t} \tag{34}$$

and t is the absolute temperature. The correlation equation then becomes equation 35:

$$Q_X = \rho\sigma_X + T\tau + h \tag{35}$$

The regression equation is equation 36:

$$Q_X = 5.07(\pm 0.357)\sigma_X - 20.8(\pm 3.71)\tau + 6.84(\pm 1.28) \tag{36}$$

$$100R^2, 95.55; A\ 100R^2, 95.21; F, 129.0; S_{est}, 0.194; S^\circ, 0.236; N_{dp}, 15;$$

$$r_{df/iv}, 6.0; r_{\sigma\tau}, 0.746; C_\sigma, 42.1; C_\tau, 57.9.$$

The magnitude of ρ is in accord with a reaction at a ring C atom. Winkler and Winkler have also reported equilibrium[66] and rate[67] constants (sets **CR7** and **CR8**, Table 9). We described above a modified Yukawa–Tsuno (MYT) equation[52] (equation 6) with σ taking the value σ_m for 3-substituted benzene derivatives and σ_{50} for 4-substituted benzene derivatives, while σ_{eX} for substituents in the *meta* position is 0. For this application the appropriate value of P_D was unknown and all three pure electrical effect parameters were used for the *para* substituents; thus the MYT equation used was equation 37:

$$Q_X = L(\sigma_{lX^4}, \sigma_{mX^3}) + D\sigma_{dX^4} + R\sigma_{eX^4} + h \tag{37}$$

Correlation with equation 37 showed that the $\sigma_{c,33.3}$ constants were suitable for use with the 4-substituted compounds in correlations with equation 6. The regression equations are equation 38 for the equilibrium constants:

$$\log K_X = 4.90(\pm 0.227)\sigma_{c33.3,X} + 0.167(\pm 0.0537) \tag{38}$$

$$100r^2, 99.15; F, 464.7; S_{est}, 0.114; S^o, 0.113; N_{dp}, 6, r_{df/iv}, 4.0.$$

and equation 39 for the rate constants:

$$\log K_X = 4.73(\pm 0.669)\sigma_{c33.3,X} - 0.333(\pm 0.158) \tag{39}$$

$$100r^2, 92.58; F, 49.89; S_{est}, 0.335; S^o, 0.334; N_{dp}, 6; r_{df/iv}, 4.0.$$

The failure to observe a dependence on σ_e is almost certainly due to the small size and range of the data sets.

3. Aromatic hydrocarbon radical ion disproportionation

Szwarc and coworkers[68–72] have reported equilibrium constants for the disproportionation reaction given in equation 40:

$$2(M^+ArH^{\bullet -}) \overset{K_e}{\rightleftharpoons} 2M^+ArH^{2-} + ArH \tag{40}$$

in diethyl ether, 1,2-dimethoxyethane (DME), dioxane and tetrahydrofuran (THF) for various aromatic hydrocarbon radical ions $ArH^{\bullet -}$ with various alkali metal ions (set **CR9**, Table 9). It is necessary to parameterize the solvent effect, the variation in metal ion M^+ and the variation in $ArH^{\bullet -}$. To account for the solvent effect we have used the E_T solvent parameter. The effect of the metal ion was parameterized by its ionic radius, r_I. It seems unlikely that the $ArH^{\bullet -}$ react by a face-to-face collision as this would have to overcome electrostatic repulsion. If two ion pairs collide with the free side of the $ArH^{\bullet -}$ in one contact with the metal ion of the other, then the electron can be transferred via the metal ion from one $ArH^{\bullet -}$ to the other. (Figure 4). Then the effect of variation in $ArH^{\bullet -}$ structure should depend on the extent to which the negative charge is delocalized and the polarizability of ArH. We considered that in alternant ArH the delocalization should depend roughly on n_C, the number of C atoms in ArH. The polarizability is also a function of n_C.[71] The correlation is then given by equation 41:

$$Q = a_{Sv}E_T + a_M r_I + a_{ArH} n_C + a_o \tag{41}$$

The regression equation is equation 42:

$$\log K_{e,disp} = -2.61(\pm 0.188)E_T + 2.56(\pm 0.816)r_I + 89.0(\pm 6.83) \tag{42}$$

$$100R^2, 87.42; A\ 100R^2, 86.99; F, 97.29; S_{est}, 1.32; S^o, 0.373; N_{dp}, 31;$$

$$r_{df/iv}, 14.0; r_{ETrI}, 0.304; C_{ET}, 97.4; C_{rI}, 2.58.$$

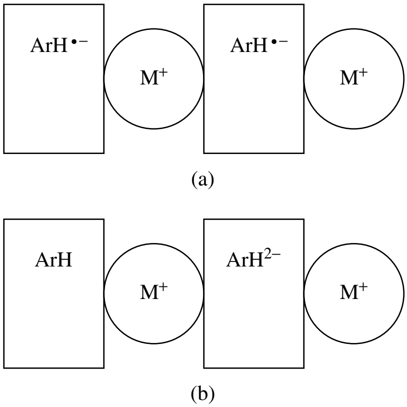

FIGURE 4. Side view of the transition state for reaction 40: (a) side view before electron transfer; (b) side view after electron transfer

The reference values used to calculate C were E_T, 37; r_I, 1. The equilibrium constant decreases with increasing solvent polarity and decreases with increasing metallic ion size. It also seems to decrease with increasing aromatic hydrocarbon size, but the descriptor n_C is ineffective. In view of the different temperatures and methods of determination of the K_e values, the goodness of fit is satisfactory. More variation in aromatic hydrocarbon structure is needed to determine its effect on K_e.

4. Other reactions

Enthalpies for the reaction of lithium alkyls with hydrogen bromide[73, 74] have been correlated with equation 28 (set **CR10**, Table 9), where n_1 and n_2 are the number of branches at the first and second C atoms of the alkyl group and n_C is the number of C atoms in the alkyl group. The regression equation is equation 43:

$$\Delta H_{Ak} = -17.0(\pm 3.13)n_1 - 9.72(\pm 6.36)n_2 - 327.8(\pm 5.96) \qquad (43)$$

$$100R^2, 91.40; A\ \ 100R^2, 89.25; F, 15.93; S_{est}, 7.34; S^{\mathrm{o}}, 0.415; N_{dp}, 6;$$

$$r_{df/iv}, 1.5; r_{n^1n^2}, 0; r_{n^1n^C}, 0.754; r_{n^1n^C}, 0.612; C_{n^1}, 63.6; C_{n^2}, 36.4.$$

There is clearly a dependence on branching at n_1 and possibly a dependence on branching at n_2 as well.

Bond dissociation enthalpies of gaseous alkyl lithiums[75] (set **CR11**, Table 9) have also been correlated with equation 28. The regression equation is equation 44:

$$D_{LiAk} = -34.5(\pm 4.85)n_1 + 244(\pm 8.63) \qquad (44)$$

$$100r^2, 92.69; F, 50.71; S_{est}, 11.4; S^{\mathrm{o}}, 0.331; N_{dp}, 6; r_{df/iv}, 4.0.$$

Branching at the first C atom accounts for the variation of the dissociation enthalpy with structure.

B. Chemical Properties (QSCR)

1. Conformation

Free energies ΔG have been reported for the rotational barriers in allyl alkali metal compounds (set **CP1**, Table 10)[76, 77]. As the only variable is the alkali metal ion, the ΔG values were correlated with equation 45:

$$\Delta G_{M^+} = a_r r_{I,M^+} + a_o \tag{45}$$

giving the regression equation 46:

$$\Delta G_{M^+} = 40.3(\pm 7.23) r_{I,M^+} + 13.0(\pm 9.04) \tag{46}$$

$$100r^2, 91.19; F, 31.04; S_{est}, 4.90; S^\circ, 0.383; N_{dp}, 5; r_{df/iv}, 1.5.$$

The rotational barrier increases with increasing ionic radius of the metal ion. We have noted above that r_I is highly linear in the polarizability parameters α and V_M and are therefore unable to determine whether this dependence is due to ionic size or ionic polarizability.

Z/E ratios have been reported for $[\text{Ak}{-}\text{CH}{-}\text{CH}{=}\text{CH}_2]^- \text{M}^+$ with M = Li, Na, K and Cs, in various solvents at various temperatures[78, 79] (set **CP2**, Table 10). These ratios are equivalent to the ratios C_Z/C_E, where C_Z and C_E are the concentrations of the *cis* and *trans* conformers, respectively. They are equal to the conformational equilibrium constants for the process depicted in equation 47:

$$Z\text{-AkCH}{=}\text{CH}{-}\text{CH}_2{}^-\text{M}^+ \rightleftharpoons E\text{-AkCH}{=}\text{CH}{-}\text{CH}_2{}^-\text{M}^+ \tag{47}$$

The three subsets in hexane at −48 °C with constant M^+ that vary in the number of branches at C1 were correlated with the simple branching equation in the form of equation 48:

$$\log(Z/E) = a_1 n_1 + a_o \tag{48}$$

giving the regression equations 49–51:

$$\log(Z/E)_{Na^+} = -0.715(\pm 0.0729) n_1 + 1.07(\pm 0.136) \tag{49}$$

$$100r^2, 97.96; F, 96.10; S_{est}, 0.163; S^\circ, 0.202; N_{dp}, 4; r_{df/iv}, 2.0.$$

$$\log(Z/E)_{K^+} = -0.841(\pm 0.166) n_1 + 1.67(\pm 0.310) \tag{50}$$

$$100r^2, 92.79; F, 25.75; S_{est}, 0.371; S^\circ, 0.380; N_{dp}, 4; r_{df/iv}, 2.0.$$

$$\log(Z/E)_{Cs^+} = -1.27(\pm 0.173) n_1 + 2.73(\pm 0.324) \tag{51}$$

$$100\text{r}^2, 96.43; \text{F}, 54.09; \text{S}_{est}, 0.387; \text{S}^\circ, 0.267; \text{N}_{dp}, 4; \text{r}_{df/iv}, 2.0.$$

while in diethyl ether at 0 °C the regression equation is equation 52:

$$\log(Z/E)_{Li^+} = -0.574(\pm 0.154) n_1 + 0.238(\pm 0.129) \tag{52}$$

$$100r^2, 97.20; F, 69.46; S_{est}, 0.154; S^\circ, 0.237; N_{dp}, 4; r_{df/iv}, 2.0.$$

Correlation of the coefficients a_1 of the four subsets with r_I gave the regression equation 53:

$$a_{1,M^+} = -0.752(\pm 0.150) r_I + 0.0414(\pm 0.185) \tag{53}$$

$$100r^2, 92.59; F, 25.01; S_{est}, 0.100; S^\circ, 0.385; N_{dp}, 4; r_{df/iv}, 2.0.$$

TABLE 10. QSCR data sets

CP1. Rotation barriers ΔG (kcal mol^{-1}) for $\text{ViCH}_2{}^{-}\text{M}^+$ at various T. M, T (deg, C), ΔG: Li,−51, 10.8; Na, 5, 11.6; K, 68, 16.9; K, 68, 17.2; Cs, 68, 18.2.

CP2. Z/E ratios of $\text{AkCH{=}CHCH}_2{}^-$ M^+ in various Solvents (Sv) at various T. Ak, M, Sv, T(°C), Z/E: Me, Li, Et_2O, 0, 2.03; Pr, Li, Et_2O, 0, 0.316; *i*-Pr, Li, Et_2O, 0, 0.163; *t*-Bu, Li, Et_2O, 0, 0.0309; Me, Li, THF, 0, 5.67; Pr, Li, THF, 0, 4.00; Me, Na, HxH, −48, 13.3; Pr, Na, HxH, −48, 1.56; *i*-Pr, Na, HxH, −48, 0.613; *t*-Bu, Na, HxH, −48, 0.0753; Pr, Na, THF, −48, 5.67; *t*-Bu, Na, THF, −48, 0.0890; Me, K, HxH, −48, 24.0; Pr, K, HxH, −48, 15.7; *i*-Pr, K, HxH, −48, 1.27; *t*-Bu, K, HxH, −48, 0.0870; Et, K, THF, 26, 6.14; *i*-Pr, K, THF, 26, 1.86; Me, Cs, HxH, −48, 99.9; Pr, Cs, HxH, −48, 10.0; *i*-Pr, Cs, HxH, −48, 1.94; *t*-Bu, Cs, HxH, −48, 0.0989; *t*-Bu, Cs, THF, 0, 0.136.

CP3. $-\Delta G_{\text{Li}^+}$, AkSH. Ak, $-\Delta G_{\text{Li}^+}$: Me, 23.2; Et, 24.1; *i*-Pr, 25.1; Pr, 25.2; *i*-Bu, 26.4; *t*-Bu, 26.6; Bu, 26.8.

CP4. $-\Delta G_{\text{Li}^+}$, Ak^1SAk^2. Ak^1, Ak^2, $-\Delta G_{\text{Li}^+}$: Me, Me, 26.1; Et, Et, 29.2; *i*-Pr, *i*-Pr, 31.7; Pr, Pr, 31.7; Bu, Bu, 33.8; *t*-Bu, *t*-Bu, 33.8; Me, Et, 27.8.

CP5. $-\Delta G_{\text{Li}^+}$, AkOH. Ak, $-\Delta G_{\text{Li}^+}$: Me, 31.2; Et, 33.1; *i*-Pr, 35.0; Pr, 34.1; *i*-Bu, 35.2; Bu, 35.6.

CP6. $-\Delta G_{\text{Li}^+}$, Ak^1OAk^2. Ak^1, Ak^2, $-\Delta G_{\text{Li}^+}$: Me, Me, 32.3; Et, Et, 36.0; *i*-Pr, *i*-Pr, 38.3; Pr, Pr, 37.5; Bu, Bu, 39.3; Me, *t*-Bu, 36.9.

CP7. $-\Delta G_{\text{Li}^+}$, XCH_2OH. X, $-\Delta G_{\text{Li}^+}$: CCl_3, 33.1; CF_3, 29.3; Ph, 38.6; *c*-Hx, 37.0; H, 31.2; Me, 33.1; Et, 34.1; Pr, 35.6; *i*-Pr, 35.2; *t*-Bu, 35.8; OMe, 45.4[a].

CP8. $-\Delta G_{\text{Li}^+}$, XCN. X, $-\Delta G_{\text{Li}^+}$: H, 28.7[a]; ClCH_2; 32.2, Et, 38.0 Pr, 38.1; Ph, 38.3; *i*-Pr, 38.5; Bu, 38.6; *t*-Bu, 39.2; MeOCH_2, 35.6; Me, 36.7; MeSCH_2, 37.0; PhCH_2, 37.8; 1-Adm, 40.9; NMe_2, 41.8; Oc, 40.3.

CP9. $-\Delta G_{\text{Li}^+}$, XMe. X, $-\Delta G_{\text{Li}^+}$: SH, 23.2[a]; SMe, 26.1[a]; NH_2, 34.1; CHO, 34.5; NHMe, 34.9; NMe_2, 34.8; OH, 31.2; Ac, 38.0; CO_2Et, 38.8; OMe, 32.3; SOMe, 43.0; CONH_2, 42.1; CO_2Me, 37.8; CN, 36.7; CONMe_2, 45.6.

CP10. ΔH_{298} for $\text{Na}^+ + \text{AkOH}$. Ak, ΔH_{298}: Me, 17.3; Et, 19.0; Pr, 19.5; *i*-Pr, 20.4; Bu, 19.7; *i*-Bu, 19.7; *s*-Bu, 20.9; *t*-Bu, 21.4.

CP11. ΔH_{298} for $\text{Na}^+ + \text{AkCl}$. Ak, ΔH_{298}: Et, 10.8; Pr, 11.6; *i*-Pr, 12.3; Bu, 12.1; *i*-Bu, 12.3; *s*-Bu, 13.0; *t*-Bu, 13.7.

CP12. ΔH_{298} for $\text{Na}^+ + \text{MeX}$. X, ΔH_{298}: H, 7.2[a], SH, 17.5[a], OH, 24.0; NH_2, 26.3; CN, 32.5; OMe, 22.2; CO_2Me, 31.8; CONH_2, 34.7; CONMe_2, 37.5; HCO, 27.5; Ac, 30.8.

CP13. log K_e for N-(4-$\text{XC}_6\text{H}_4\text{CH}_2$)monoaza-15-crown-5 + Li^+, MeCN, 25° C. X, log K_e: OMe, 4.82; H, 4.63; Cl, 4.46; CN, 4.31; NO_2, 3.70.

CP14. log K_e for N-(4-$\text{XC}_6\text{H}_4\text{CH}_2$)monaza-15-crown-5 + Na^+, MeCN, 25° C. X, log K_e: OMe, 5.74; H, 5.68; Cl, 4.70; CN, 4.52; NO_2, 3.97.

All ΔG and ΔH values are in kcal mol^{-1}.

[a] Excluded from the correlation.

This result together with the results for the subsets led to correlation of the combined subsets for Na^+, K^+ and Cs^+ with equation 54:

$$\log(Z/E) = a_1 n_1 + a_{M^+} r_{I,M^+} + a_o \tag{54}$$

The regression equation is equation 55:

$$\log(Z/E) = -0.943(\pm 0.105) n_1 + 1.23(\pm 0.428) r_{I,M^+} + 0.196(0.599) \tag{55}$$

$$100R^2, 90.83; A\ 100R^2, 89.91; F, 44.57; S_{est}, 0.406; S^{\text{o}}, 0.350; N_{dp}, 12;$$

$$r_{df/iv}, 4.5; r_{n_1 r_I}, 0; C_{n_1}, 35.2; C_{r_I}, 64.8.$$

Inclusion of the subset for $\mathrm{Li}^{+\cdot}$ gave regression equation 56:

$$\log(Z/E) = -0.851(\pm 0.0929)n_1 + 1.56(\pm 0.312)r_{I,M^+} - 0.428(0.409) \tag{56}$$

$$100R^2, 89.34; A\ 100R^2, 88.58; F, 54.49; S_{est}, 0.415; S^{\mathrm{o}}, 0.362; N_{dp}, 16;$$
$$r_{df/iv}, 6.5; r_{n_1 r_I}, 0; C_{n_1}, 43.4; C_{r_I}, 56.6.$$

As the coefficients of equation 55 are not significantly different from those of equation 56 and the goodness of fit is comparable, the inclusion of the Li^+ subset is justified. Inclusion of the data in THF gave the regression equation 57:

$$\log(Z/E) = -0.862(\pm 0.0777)n_1 + 1.31(\pm 0.263)r_{I,M^+} + 0.0703(0.321) \tag{57}$$

$$100R^2, 87.60; A\ 100R^2, 86.98; F, 67.14; S_{est}, 0.403; S^{\mathrm{o}}, 0.379; N_{dp}, 22;$$
$$r_{df/iv}, 9.5; r_{n_1 r_I}, 0.151; C_{n_1}, 39.7; C_{r_I}, 60.3.$$

The goodness of fit is poorer. The coefficients have not changed significantly. The terms in n_1 and r_I are highly significant. The conformational equilibrium in these compounds is not significantly dependent on solvent or temperature. As the data are from three different laboratories and are generally good to only two significant figures, the results are very good.

2. Metal ion affinities

In modeling metal ion affinities we have assumed that they are a function of ion–dipole and ion–induced dipole interactions. The effect of the charge on the metal ion was assumed to be a function of its magnitude and of the ionic size and/or polarizability. The charge on both of the ions studied is +1. Their size and polarizability could be represented by their ionic radius. As both of these quantities were constant throughout each data set, they did not have to be parameterized. The contribution of the organic substrate to this property will be a function of bond moment, polarizability and possibly of steric effects of the variable substituent X. The bond moment can be represented by electrical effect parameters or by the dipole moments of suitable model compounds. Polarizability can be represented by either α or, if the substituents are all alkyl groups, by n_C. In the latter case steric effects are represented by the branching parameters n_i.

Taft and coworkers[80] have reported lithium ion affinities, ΔG_{Li^+}, for various types of compounds. Values of ΔG_{Li^+} for alkyl thiols, dialkyl sulfides, alcohols and dialkyl ethers (sets **CP3**, **CP4**, **CP5** and **CP6**, Table 10) were correlated with equation 27. The regression equation for the alkyl thiols is equation 58:

$$\Delta G_{Li^+} = 1.16(\pm 0.0753)n_C + 21.9(\pm 0.240) \tag{58}$$

$$100r^2, 97.95; F, 238.5; S_{est}, 0.213; S^{\mathrm{o}}, 0.170; N_{dp}, 7; r_{df/iv}, 5.0;$$
$$r_{n_1 n_2}, 0.255; r_{n_1 n_C}, 0.607; r_{n_2 n_C}, 0.550.$$

For the dialkyl sulfides, equation 26 takes the form of equation 59:

$$Q_X = a_1 \Sigma n_1 + a_2 \Sigma n_2 + a_C \Sigma n_C + a_o \tag{59}$$

The regression equation is equation 60:

$$\Delta G_{Li^+} = 1.21(\pm 0.0651)\Sigma n_C + 24.1(\pm 0.372) \tag{60}$$

$$100r^2, 98.58; F, 347.8; S_{est}, 0.376; S^{o}, 0.141; N_{dp}, 7; r_{df/iv}, 5.0.$$

Correlation of ΔG_{Li^+} values for alkanols with equation 27 gave the regression equation 61:

$$\Delta G_{Li^+} = 1.01(\pm 0.0623)n_C + 0.846(\pm 0.152)n_1 + 30.3(\pm 0.240) \tag{61}$$

$$100R^2, 98.54; A\ 100R^2, 98.33; F, 202.7; S_{est}, 0.243; S^{o}, 0.148; N_{dp}, 9;$$

$$r_{df/iv}, 3.0; r_{n_1 n_C}, 0.349; C_{n_C}, 78.1; C_{n_1}, 21.9$$

while correlation of the values for the dialkyl ethers with equation 59 gave the regression equation 62:

$$\Delta G_{Li^+} = 0.970(\pm 0.0877)\Sigma n_C + 0.468(\pm 0.119)\Sigma n_1 + 30.6(\pm 0.399) \tag{62}$$

$$100R^2, 98.60; A\ 100R^2, 98.32; F, 141.1; S_{est}, 0.332; S^{o}, 0.156; N_{dp}, 7;$$

$$r_{df/iv}, 2.0; r_{n_1 n_C}, 0.577; C_{n_C}, 86.1; C_{n_1}, 13.9.$$

The sulfur compounds depend only on polarizability; the oxygen compounds show a small dependence on steric effects as well.

Correlation of the ΔG_{Li^+} values for XCH_2OH (set **CP7**, Table 10) with equation 63

$$Q_X = L\sigma_{lX} + A\alpha_X + h_o \tag{63}$$

gave the regression equation 64:

$$Q_X = -8.09(\pm 1.87)\sigma_{lX} + 26.0(\pm 3.43)\alpha_X + 31.6(\pm 0.565) \tag{64}$$

$$100R^2, 91.75; A\ 100R^2, 90.72; F, 38.94; S_{est}, 0.901; S^{o}, 0.343; N_{dp}, 10; r_{df/iv}, 3.5;$$

$$r_{\sigma_1\alpha}, 0.022; C_{\sigma}, 60.8; C_{\alpha}, 39.2.$$

In equation 63 the bond moment is parameterized by σ_1. The data point for OMe was excluded from the correlation due to the probable formation of a cyclic species involving the two oxygen atoms.

Correlation of the ΔG_{Li^+} values for XCN (set **CP8**, Table 10) with the LDRA equation 65:

$$Q_X = L\sigma_{lX} + D\sigma_{dX} + R\sigma_{eX} + A\alpha + h \tag{65}$$

gave, on exclusion of the value for HCN, the regression equation 66:

$$Q_X = -18.1(\pm 4.10)\sigma_{lX} - 13.2(\pm 2.05)\sigma_{dX} + 10.4(\pm 2.76)\alpha + 34.7(\pm 0.728) \tag{66}$$

$$100R^2, 85.94; A\ 100R^2, 83.38; F, 22.37; S_{est}, 1.01; S^{o}, 0.444; N_{dp}, 14; r_{df/iv}, 3.33; r_{ld}, 0.335;$$

$$r_{l\alpha}, 0.152; r_{d\alpha}, 0.122; P_D, 42.2(\pm 9.01); \eta, 0; C_l, 54.2; C_d, 39.6; C_{\alpha}, 6.21.$$

In equation 65 the bond moment is represented by σ_l, σ_d and σ_e.

Correlation of the ΔG_{Li^+} values for MeX (set **CP9**, Table 10) with equation 67:

$$Q_X = M\mu_X + A\alpha_X + h_o \tag{67}$$

gave, on exclusion of the data points for MeSH and MeSMe, the regression equation 68:

$$\Delta G_X = 2.21(\pm 0.351)\mu_X + 52.4(\pm 8.02)\alpha_X + 27.0(\pm 1.12) \tag{68}$$

$100R^2$, 90.45; A $100R^2$, 89.58; F, 47.33; S_{est}, 1.45; S^o, 0.352; N_{dp}, 15; $r_{df/iv}$, 6.0; $r_{\mu\alpha}$, 0.132; C_μ, 29.7; C_α, 70.3.

Ohanessian and coworkers[81] have collected gas-phase sodium affinities (ΔH_{298} values). Correlation of these values for alkanols and alkyl chlorides (sets **CP10** and **CP11**, Table 10) with equation 27 gave, for the alkanols, the regression equation 69:

$$\Delta H_{Na^+} = 0.456(\pm 0.0893)n_C + 0.932(\pm 0.110)n_1 + 17.0(\pm 0.228) \tag{69}$$

$100R^2$, 98.12; A $100R^2$, 97.81; F, 130.4; S_{est}, 0.204; S^o, 0.173; N_{dp}, 8; $r_{df/iv}$, 2.5; $r_{n_1 n_C}$, 0.641; C_{n_C}, 59.5; C_{n_1}, 40.5.

and equation 70 for the chlorides:

$$\Delta H_{Na^+} = 0.530(\pm 0.0358)n_C + 0.910(\pm 0.0358)n_1 + 0.210(\pm 0.0409)n_2 + 8.86(\pm 0.0643) \tag{70}$$

$100R^2$, 99.94; A $100R^2$, 99.92; F, 1768; S_{est}, 0.0314; S^o, 0.0363; N_{dp}, 7; $r_{df/iv}$, 1.0; $r_{n_1 n_2}$, 0.520; $r_{n_1 n_C}$, 0.346; $r_{n_2 n_C}$, 0.520; C_{n_C}, 58.7; C_{n_1}, 33.6; C_{n_2}, 7.75.

The excellent fit for the alkyl chlorides is probably fortuitous. The coefficients of n_C and n_1 for the alkanols and alkyl chlorides show no significant differences. Steric effects due to branching at C^2 in the chlorides are much less than those at C^1.

Correlation of the sodium affinities of MeX (set **CP12**, Table 10) with equation 67, on excluding the data point for MeSH, gave the regression equation 71:

$$\Delta H_X = 4.05(\pm 1.19)\mu_X + 63.0(\pm 26.2)\alpha_X + 13.7(\pm 2.64) \tag{71}$$

$100R^2$, 83.48; A $100R^2$, 81.42; F, 17.69; S_{est}, 3.94; S^o, 0.486; N_{dp}, 10; $r_{df/iv}$, 3.5; $r_{\mu\alpha}$, 0.520; C_μ, 39.1; C_α, 60.9.

As in the case for the lithium affinities, polarizability is the major factor. The goodness of fit is much poorer for the sodium affinities of MeX than it was for the lithium affinities. This may be due to the fact that the former were determined in several different laboratories while the latter were determined in a single laboratory.

3. Crown ether complex formation

Values of log K for the formation of N-(4-substituted benzyl)-monaza-15-crown-5, Li^+ in acetonitrile[82] (set **CP13**, Table 10) were correlated with the CR equation (equation 6) to give the regression equation 72:

$$\log K_X = -0.846(\pm 0.211)\sigma_{C_{50}} + 4.63(\pm 0.107) \tag{72}$$

$100r^2$, 84.31; F, 16.12; S_{est}, 0.195; S^o, 0.511; N_{dp}, 5; $r_{df/iv}$, 1.5.

Log K values for formation of the corresponding Na^+ complex (set **CP14**, Table 10) on correlation with the LDR equation gave the regression equation 73:

$$\log K_X = -2.24(\pm 0.506)\sigma_{lX} - 0.998(\pm 0.437)\sigma_{dX} + 5.72(\pm 0.250) \tag{73}$$

$$100R^2, 94.65; A\ 100R^2, 92.87; F, 17.69; S_{est}, 0.251; S^{\text{o}}, 0.366; N_{dp}, 5; r_{df/iv}, 1.0;$$

$$r_{\sigma_l\sigma_d}, 0.329; C_{\sigma_l}, 69.2; C_\alpha, 30.8$$

The lithium ion and sodium ion complexes show very different dependencies on electrical effects.

VII. APPENDIX GLOSSARY

This appendix is an updated and slightly modified version of one we have published elsewhere[84].

General

X:	A variable substituent.
Y:	An active site. The atom or group of atoms at which a measurable phenomenon occurs.
G:	A skeletal group to which X and Y may be attached.

Parameter: An independent variable.

Pure parameter: A parameter which represents a single effect.

Composite parameter: A parameter which represents two or more effects.

Modified composite parameter: A composite parameter whose composition has been altered by some mathematical operation.

Monoparametric equation: A relationship in which the effect of structure on a property is represented by a single, generally composite parameter. Examples are the Hammett and Taft equations.

Diparametric equation: A relationship in which the effect of structure on a property is represented by two parameters, one of which is generally composite. Examples discussed in this work include the LD, CR and MYT equations. Other examples are the Taft, Eherenson and Brownlee DSP (dual substituent parameter), Yukawa–Tsuno YT, and the Swain, Unger, Rosenquist and Swain SURS equations. The DSP equation is a special case of the LDR equation with the intercept set equal to zero. It is inconvenient to use and has no advantages. The SURS equation uses composite parameters which are of poorer quality than those used with the LDR and DSP equations. The MYT equation has all the advantages of the YT equation and gives results which are easier to interpret.

CR equation: A diparametric electrical effect model using the composite $\sigma_{Ck'}$ and pure σ_e parameters. A value of P_D is assumed and a value of η calculated.

LD equation: A diparametric electrical effect model using the pure σ_l and composite σ_D parameters. A value of P_D is calculated and a value of η assumed.

Multiparametric equation: An equation which uses three or more parameters all of which may be either pure or composite.

Electrical effect parameterization

σ_l	The localized (field) electrical effect parameter. It is identical to σ_I. Though other localized electrical effect parameters such as σ_I^q and σ_F have been proposed, there is no advantage to their use. The σ^* parameter has sometimes

been used as a localized electrical effect parameter; such use is generally incorrect. The available evidence is strongly in favor of an electric field model for transmission of the effect.

σ_d	The intrinsic delocalized (resonance) electrical effect parameter. It represents the delocalized electrical effect in a system with zero electronic demand.
σ_e	The electronic demand sensitivity parameter. It adjusts the delocalized effect of a group to meet the electronic demand of the system.
σ_D	A composite delocalized electrical effect parameter which is a function of σ_d and σ_e. Examples of σ_D constants are the σ_R^+ and σ_R^- constants. The $\sigma_{R,k}$ constants, where k designates the value of the electronic demand η, are also examples of σ_D constants.
σ_R	A composite delocalized electrical effect parameter of the σ_D type with η equal to 0.380. It is derived from 4-substituted benzoic acid pK_a values.
σ_R^o	A composite delocalized electrical effect parameter of the σ_D type with η equal to -0.376. It is derived from 4-substituted phenylacetic acid pK_a values.
σ_R^+	A composite delocalized electrical effect parameter of the σ_D type with η equal to 2.04. It is derived from rate constants for the solvolysis of 4-substituted cumyl chlorides.
$\sigma_R^\oplus$	A composite delocalized electrical effect parameter of the σ_D type with η equal to 3.31. It is derived from ionization potentials of the lowest-energy π-orbital in substituted benzenes.
$\sigma_R^\ominus$	A composite delocalized electrical effect parameter of the σ_D type with η equal to -2.98. It is derived from pK_a values of substituted nitriles.
σ_R^-	A composite delocalized electrical effect parameter of the σ_D type with η equal to -1.40. It is derived from pK_a values of substituted anilinium ions.
$\sigma_{k'/k}$	A composite parameter which is a function of σ_l, σ_d and σ_e. Its composition is determined by the values of k and k'. The Hammett σ_m and σ_p constants are of this type.
$\sigma_{Ck'}$	A composite constant that is a function of σ_l and σ_d; its composition is determined by the value of k'.
$\sigma^\blacklozenge$	An electrical effect modified composite parameter.
σ	Any electrical effect parameter.
η	The electronic demand of a system or of a composite electrical effect parameter that is a function of both σ_d and σ_e. It is represented in subscripts as k. It is a descriptor of the nature of the electrical effect. It is given by R/D, where R and D are the coefficients of σ_e and σ_d, respectively.
P_D	The percent delocalized effect. It too is a descriptor of the nature of the electrical effect. It is represented in subscripts as k'.

LDR equation: A triparametric model of the electrical effect.

P_{EA}	The percent of the $\sigma_{k'/k}$ values in a substituent matrix which exhibit an electron acceptor electrical effect.
P_{ED}	The percent of the $\sigma_{k'/k}$ values in a substituent matrix which exhibit an electron donor electrical effect.
P_0	The percent of the $\sigma_{k'/k}$ values in a substituent matrix which do not exhibit a significant electrical effect.

Steric effect parameterization

r_V	The van der Waals radius. A useful measure of group size. The internuclear distance of two nonbonded atoms in contact is equal to the sum of their van der Waals radii.
υ	A composite steric parameter based on van der Waals radii. For groups whose steric effect is at most minimally dependent on conformation, it represents the

	steric effect due to the first atom of the longest chain in the group and the branches attached to that atom. The only alternative monoparametric method for describing steric effects is that of Taft, which uses the E_S parameter. This was originally developed only for alkyl and substituted alkyl groups and for hydrogen. Hansch and Kutter[85] have estimated E_S values for other groups from the υ values using a method which in many cases disregards the MSI principle. It is best to avoid their use.
$\acute{\upsilon}$	A steric effect parameter based on van der Waals radii that has been corrected for the difference in bond length between the X−G and Y−G bonds.

Simple branching equation (SB): A topological method for describing steric effects which takes into account the order of branching by using as parameters n_i, the number of atoms other than H that are bonded to the i-th atoms of the substituent.

n_i	The number of branches on the i-th atoms of a substituent. These are the steric parameters used in the SB equation.

Expanded branching equation (XB): A topological method for describing steric effects which takes into account the order of branching by using as parameters n_{ij}, the number of j-th branching atoms bonded to the i-th atoms of the substituent.

n_{ij}	The number of j-th branches on the i-th atoms of a substituent. These are the steric parameters used in the XB model of steric effects.
n_b	The number of bonds in the longest chain of a substituent. It is a steric parameter which serves as a measure of the length of a group along the group axis.

Segmental equation: A steric effect model that separately parameterizes each segment of a substituent. It requires fewer parameters than the XB equation and is generally more effective than the SB equation.

υ_i	A steric parameter based on van der Waals radii that is a measure of the steric effect of the i-th segment of a substituent. The i-th segment consists of the i-th atom of the longest chain in the substituent and the groups attached to it. The MSI principle is assumed to apply and the segment is assigned the conformation that gives it the smallest possible steric effect.

MSI principle: The principle of minimal steric interaction, which states that the preferred conformation of a group is that which results in the smallest possible steric effect.

Intermolecular force parameterization

α	A polarizability parameter defined as the difference between the group molar refractivities for the group X and for H divided by 100. Many other polarizability parameters, such as the van der Waals volume, the group molar volume and the parachor, can be used in its place. All of these polarizability parameters are very highly linear in each other.
n_H	A hydrogen-bonding parameter which represents the lone pair acceptor (proton donor) capability of a group. It is defined as the number of OH and/or NH bonds in the group.
n_n	A hydrogen-bonding parameter which represents the lone-pair donor (proton acceptor) capability of the group. It is defined as the number of lone pairs on O and/or N atoms in the group.
i	A parameter which represents ion–dipole and ion–induced dipole interactions. It is defined as 1 for ionic groups and 0 for nonionic groups.
n_D	A charge transfer donor parameter which takes the values 1 when the substituent can act as a charge transfer donor and 0 when it cannot.
n_A	A charge transfer acceptor parameter which takes the values 1 when the substituent can act as a charge transfer acceptor and 0 when it cannot.

IMF equation: A multiparametric equation which models phenomena that are a function of the difference in intermolecular forces between an initial and a final state.

Other parameterization

τ	A parameter that accounts for the effect of temperature on the reaction velocity. It is defined as $100/T$ where T is the absolute temperature.
ϕ	A parameter that accounts for the effect of concentration of a component in a mixed solvent. It is the mole fraction of that component.
ζ	A parameter used to combine two or more data sets into a single set. It is determined by choosing a substituent present in each of the data sets to be combined and defining Q for that substituent as ζ. Thus, if the substituent chosen is Z and there are sets 1, 2 and 3 to be combined, the ζ values are Q_{Z1}, Q_{Z2} and Q_{Z3}, respectively.

Statistics

Correlation equation: An equation with which a data set is correlated by simple (one parameter) or multiple (two or more parameters) linear regression analysis.

Regression equation: The equation obtained by the correlation of a data set with a correlation equation by means of simple or multiple linear regression analysis.

N_{dp}	The number of data points in a data set.
N_{iv}	The number of independent variables.

Degrees of freedom (N_{df}): Defined as the number of data points, N_{dp}, minus the number of independent variables (parameters), (N_{iv}), plus 1. [$df = N_{dp} - (N_{iv} + 1)$.]

F statistic: A statistic which is used as a measure of the goodness of fit of a data set to a correlation equation. The larger the value of F, the better the fit. Confidence levels can be assigned by comparing the F value calculated with the values in an F table for the N_p and DF values of the data set.

$100R^2$	A statistic which represents the percent of the variance of the data accounted for by the regression equation. It is a measure of the goodness of fit. It is used when the regression has $N_{iv} \geqslant 2$. When $N_{iv} = 1$, the statistic is $100r^2$.
S_{est}	The standard error of the estimate. It is a measure of the error to be expected in predicting a value of the dependent variable from the appropriate parameter values.
S^{o}	Defined as the ratio of S_{est} to the root mean square of the data. It is a measure of the goodness of fit. The smaller the value of S^{o}, the better the fit.
$r_{df/iv}$	This is the ratio of N_{df} to N_{iv}. The reliability of the results of a correlation increases with the size of this ratio.

VIII. REFERENCES

1. M. Charton, *Prog. Phys. Org. Chem.*, **13**, 119 (1981).
2. M. Charton, *Prog. Phys. Org. Chem.*, **16**, 287 (1987).
3. M. Charton, in *Classical and 3-D QSAR in Agrochemistry and Toxicology* (Eds. C. Hansch and T. Fujita, American Chemical Society, Washington D.C., 1995, pp. 75–95.
4. M. Charton, *J. Am. Chem. Soc.*, **91**, 615 (1969).
5. M. Charton, *J. Org. Chem.*, **43**, 3995 (1978).
6. M. Charton, *J. Org. Chem.*, **44**, 903 (1979).
7. U. Burkert and N. L. Allinger, *Molecular Mechanics*, American Chemical Society, Washington D.C., 1982.
8. A. K. Rappé and C. J. Casewit, *Molecular Mechanics Across Chemistry*, Univ. Sci. Books, Saualito, CA, 1997.
9. M. R. Saunders and D. Livingstone, in *Advances in Quantitative Structure Property Relationships* (Ed. M. Charton), JAI Press, Greenwich, Conn., 1996, p. 53.
10. L. B. Kier and L. H. Hall, *Molecular Connectivity in Chemistry and Drug Research*, Vol. 1, Academic Press, New York, 1976.
11. R. E. Merrifield and H. E. Simmons, *Topological Methods in Chemistry*, Wiley-Interscience, New York, 1989.

12. A. T. Balaban (Ed.), *From Chemical Topology to Three-Dimensional Geometry*, Plenum Press, New York, 1997.
13. Y. C. Martin and Ki.-H. Kim, in *Advances in Quantitative Structure Property Relationships*, Vol. 1 (Ed. M. Charton), JAI Press, Greenwich, Conn., 1996, p. 1.
14. T. Aoyama, Y. Suzuki and H. Ichikawa, *J. Med. Chem.*, **33**, 905 (1990).
15. T. A. Andrea and H. Kalayeh, *J. Med. Chem.*, **34** 2824 (1991).
16. D. T. Manallack and D. J. Livingstone, *Methods Princ. Med. Chem.*, **3**, 293 (1995).
17. M. Charton and Bl. Charton, *Perspectives in Drug Discovery*, **3**, (2003), in press.
18. M. Charton, *Proc. 14th Eur. QSAR Conf.*, Kluwer, Amsterdam, 2003, in press.
19. M. Charton and B. I. Charton, *J. Phys. Org. Chem.*, **16** (2003), in press.
20. C. G. Derick, *J. Am. Chem. Soc.*, **33**, 1152 (1911).
21. G. K. Branch and M. Calvin, *The Theory of Organic Chemistry*, Prentice-Hall, New York, 1941, p. 211; R. W. Taft, in *Steric Effects in Organic Chemistry* (Ed. M. S. Newman), Wiley, New York, 1956, p. 556; H. B. Watson, *Modern Theories of Organic Chemistry*, Oxford University Press, Oxford, 1937, p. 40; A. E. Remick, *Electronic Interpretations of Organic Chemistry* 2nd edn., Wiley, New York, 1949, p. 93.
22. J. G. Kirkwood, *J. Chem. Phys.*, **2**, 351 (1934); J. G. Kirkwood and F. H. Westheimer, *J. Chem. Phys.*, **6**, 506 (1938); F. H. Westheimer and J. G. Kirkwood, *J. Chem. Phys.*, **6**, 513 (1938); F. H. Westheimer and M. W., Shookhoff, *J. Am. Chem. Soc.*, **61**, 555 (1939); F. H. Westheimer, *J. Am. Chem. Soc.*, **61**, 1977 (1939); J. N. Sarmousakis, *J. Chem. Phys.*, **12**, 277 (1944).
23. O. Exner and P. Fiedler, *Collect Czech. Chem. Commun.*, **45**, 1251 (1980).
24. K. Bowden and E. J. Grubbs, *Prog. Phys. Org. Chem.*, **19**, 183 (1992); K. Bowden and E. J. Grubbs, *Chem. Soc. Rev.*, **25**, 171 (1996).
25. M. Charton, *J. Phys. Org. Chem.*, **12**, 275 (1999).
26. M. Charton and B. I. Charton, *J. Chem. Soc., Perkin Trans.*, **2**, 2203 (1999).
27. M. Charton, *Collect Czech. Chem. Commun.*, **64**, 1849 (1999).
28. M. Charton and B. I. Charton, *J. Phys. Org. Chem.*, **14**, 832 (2001).
29. F. Kehrmann, *Chem. Ber*., **21**, 3315 (1888); **23**, 130 (1890); *J. prakt. chem.*, [2] **40**, 188, 257 (1889); [2] **42**, 134 (1890).
30. V. Meyer, *Chem. Ber*., **27**, 510 (1894); **28**, 1254, 2773, 3197 (1895); V. Meyer and J. J. Sudborough, *Chem. Ber*., **27**, 1580, 3146 (1894); V. Meyer and A. M. Kellas, *Z. phys. chem.*, **24**, 219 (1897).
31. J. J. Sudborough and L. L. Lloyd, *Trans. Chem. Soc.*, **73**, 81 (1898); J. J. Sudborough and L. L. Lloyd, *Trans. Chem. Soc.*, **75**, 407 (1899).
32. A. W. Stewart, *Stereochemistry*, Longmans, Green, London, 1907, pp. 314–443; 2nd edn., 1919, pp. 184–202.
33. G. Wittig, *Stereochemie*, Akademische Verlagsgesellschaft, Leipzig, 1930, pp. 333–361.
34. G. W. Wheland, *Advanced Organic Chemistry*, 3rd edn., Wiley, New York, 1960, pp. 498–54.
35. M. S. Newman (Ed.), *Steric Effects in Organic Chemistry*, Wiley, New York, 1956.
36. M. Charton, *Top. Curr. Chem*., **114**, 107 (1983).
37. M. Charton, in *Rational Approaches to the Synthesis of Pesticides* (Eds. P. S. Magee, J. J. Menn and G. K. Koan), American Chemical Society, Washington D.C., 1984, pp. 247–278.
38. L. Pauling, *The Nature of the Chemical Bond*, 3rd edn., Cornell Univ. Press, Ithaca, 1960, pp. 257–264.
39. M. Charton, *Prog. Phys. Org. Chem.*, **8**, 235 (1971).
40. M. Charton, *Prog. Phys. Org. Chem.*, **10**, 81 (1973).
41. M. Charton, *J. Am. Chem. Soc.*, **97**, 1552 (1975).
42. M. Charton and C. Sirovich, *Abstr. 27th Mid-Atlantic Regional Meeting, Am. Chem. Soc.*, New York, 1993, p. 129.
43. M. Charton, *Stud. Org. Chem.*, **42**, 629 (1992).
44. M. Charton, *Top. Curr. Chem*., **114**, 57 (1983).
45. M. Charton, *J. Org. Chem.*, **48**, 1011 (1983); M. Charton, *J. Org. Chem.*, **48**, 1016 (1983).
46. A. Verloop, W. Hoogenstraaten and J. Tipker, *Drug Design*, **7**, 165 (1976).
47. M. Charton, *J. Org. Chem.*, **43**, 3995 (1978).
48. M. Charton, in *Proceedings of the Third Congress of the Hungarian Pharmacological Society, Budapest, 1979*, Akademiaj Kiado, Budapest, 1980, pp. 211–220.

49. M. Charton, *J. Chem. Soc., Perkin Trans. 2*, 97 (1983).
50. M. Charton and B. I. Charton, *J. Theor. Biol.*, **99**, 629 (1982); M. Charton, *Prog. Phys. Org. Chem.*, **18**, 163 (1990); M. Charton, in *Trends in Medicinal Chemistry '88*, (Eds. H. van der Goot, G. Domany, L. Pallos and H. Timmerman), Elsevier, Amsterdam, 1989, pp. 89–108; M. Charton and B. I. Charton, *J. Phys. Org. Chem.*, **7**, 196 (1994).
51. M. Charton, *Adv. Mol. Struct. Res.*, **5**, 25, (1999).
52. (a) M. Charton, in *The Chemistry of Organic Germanium, Tin and Lead Compounds*, (Ed. S. Patai), Wiley, Chichester, 1996, pp. 603–664.
(b) M. Charton and B. Charton, *Abstr. Intl. Symp. Lipophilicity in Drug. Res. and Toxicol.*, Lausanne, 1995, p. O-3.
(c) R. D. Green, *Hydrogen Bonding by C–H Groups*, Wiley, New York, 1974; M. Nishio, M. Hirota and Y. Umezawa, *The CH π-Interaction. Evidence Nature and Consequences*, Wiley-VCH, New York, 1998.
53. M. Brookhart and M. L. H. Green, *J. Organomet, Chem.*, **250**, 395 (1983); P. L. A. Popelier and G. Logothetis, *J. Organomet. Chem.*, **555**, 101 (1998).
(b) E. Kaufmann, K. Raghavachari, A. E. Reed and P. v. R. Schleyer, *Organometallics*, **7**, 1597 (1988).
54. R. Knorr, *Tetrahedron*, **37**, 929 (1981).
55. J. M. Angelelli, R. T. C. Brownlee, A. R. Katritzky, R. D. Topsom and L. Yakhontov, *J. Am. Chem. Soc.*, **91**, 4500 (1969).
56. A. Streitwieser, S. M. Bachrach, A. Dorigo and P. v. R. Schleyer, in *Lithium Chemistry, A Theoretical and Experimental Overview* (Eds. A.-M. Sapse and P. v. R. Schleyer), Wiley-Interscience, New York, 1995, p. 1.
57. A.-M. Sapse, D. C. Jain and K. Raghavachari, in *Lithium Chemistry, A Theoretical and Experimental Overview*, (Eds. A.-M. Sapse and P. v. R. Schleyer), Wiley-Interscience, New York, 1995, p. 45.
58. A. Streitwieser, *J. Organomet. Chem.*, **156**, 1 (1978).
59. R. J. Busby and H. L. Steel, *J. Organomet. Chem.*, **336**, C25 (1987).
60. J. Smid, in *Ions and Ion Pairs in Organic Reactions*, Vol. 1, Wiley-Interscience, New York, 1972, p. 85.
61. M. Szwarc, A. Streitwieser and P. Mowery, in *Ions and Ion Pairs in Organic Reactions*, Vol. 2, Wiley—Interscience, New York, 1974, p. 151.
62. T. E. Hogen-Esch, *Adv. Phys. Org. Chem.*, **15**, 154 (1977).
63. E. M. Arnett and K. D. Moe, *J. Am. Chem. Soc.*, **113**, 7288 (1991).
64. E. M. Arnett and K. D. Moe, *J. Am. Chem. Soc.*,**113**, 7068 (1991).
65. A. P. Batalov and G. A. Rostokin, *J. Org. Chem. USSR, (Engl. Transl.*, **7**, 2097 (1971).
66. H. J. S. Winkler and H. Winkler, *J. Am. Chem. Soc.*, **88**, 964 (1966).
67. H. J. S. Winkler and H. Winkler, *J. Am. Chem. Soc.*, **88**, 969 (1966).
68. A. Rainis and M. Szwarc, *J. Am. Chem. Soc.*, **96**, 3008 (1974).
69. G. E. Levin, B. E. Holloway and M. Szwarc, *J. Am. Chem. Soc.*, **98**, 5706 (1976).
70. F. Jachimowicz, H. C. Wang, G. E. Levin and M. Szwarc, *J. Phys. Chem.*, **82**, 137 (1978).
71. H. C. Wang, G. E. Levin and M. Szwarc, *J. Am. Chem. Soc.*, **99**, 5056 (1977).
72. J. Pola, G. E. Levin and M. Szwarc, *J. Phys. Chem.*, **80**, 1690 (1976).
73. J. A. Martinho-Simões and J. L. Beauchamp, *Chem. Rev.*, **90**, 629 (1990).
74. J. A. Seetula, J. J. Russell and D. Gutman, *J. Am. Chem. Soc.*, **112**, 1347 (1990).
75. M. Sana, G. Leroy and C. Wilante, *Organometallics*, **10**, 264 (1991).
76. T. B. Thompson and W. T. Ford, *J. Am. Chem. Soc.*, **101**, 5459 (1979).
77. S. Brownstein, S. Bywater and D. J. Worsfield, *J. Organomet. Chem.*, **199**, 1 (1980).
78. B. A. Dolgoplosk, S. B. Golshtein and E. L. Vollershtein, *Dokl. Akad. Nauk SSSR*, **252**, 880 (1980).
79. D. H. O'Brien, C. R. Russel and A. J. Hart, *Tetrahedron Lett.*, 37 (1976).
80. R. W. Taft, F. Anvia, J.-F. Gal, S. Walsh, M. Capon, M. C. Holms, K. Hosn, G. Oloumi, R. Vasanwala and S. Yazdan, *Pure Appl. Chem.*, **62**, 17 (1990).
81. S. Hoyau, K. Norrman, T. B. McMahon and G. Ohanessian, *J. Am. Chem. Soc.*, **121**, 8864, (1999).
82. T. B. McMahon and G. Ohanessian, *Chem. Eur. J.*, **6**, 2931 (2000).

83. D. A. Gutowski, V. J. Gatto, J. Maller, L. Echegoyen and G. W. Gokel, *J. Org. Chem.*, **52**, 5172 (1987).
84. M. Charton, in *The Chemistry of Dienes and Polyenes* (Ed. Z. Rappoport), Wiley, Chichester, 1997, pp. 603–672.
85. E. Kutter and C. Hansch, *J. Med. Chem.*, **12**, 647 (1969).

CHAPTER 8

Analytical aspects of organolithium compounds

JACOB ZABICKY

Institutes for Applied Research, Ben-Gurion University of the Negev, P. O. Box 653,
Beer-Sheva 84105, Israel
Fax: +972-8-6472969; e-mail: zabicky@bgumail.bgu.ac.il

The Chemistry of Organolithium Compounds. Edited by Z. Rappoport and I. Marek
ISBN: 0-470-84339-X

I. ACRONYMS

AAS	atomic absorption spectrometry
AES	atomic emission spectrometry
COLOC	correlation spectroscopy via long-range couplings
COSY	correlation spectroscopy
CP/MAS	cross-polarization/magic-angle spinning
DFT	density functional theory
DME	1,2-dimethoxyethane
DMF	*N*,*N*-dimethylformamide
DMPU	*N*,*N*′-dimethyl-*N*,*N*′-propyleneurea
DMSO	dimethyl sulfoxide
DNMR	dynamic nuclear magnetic resonance
DOSY	diffusion-ordered NMR spectroscopy

DPFGSE	double pulsed field gradient spin echo
DSTE	double stimulated echo
EDTA	ethylenediaminetetraacetic acid
ENDOR	electron-nuclear double resonance
ESR	electron spin resonance
EXAFS	extended X-ray absorption fine structure
EXSY	exchange spectroscopy
HET-COR	heteronuclear chemical-shift correlation
HMPA	*N,N,N′,N′,N″,N″*-hexamethylphosphortriamide
HMQC	heteronuclear multiple-quantum coherence
HMTTA	*N,N,N′,N″,N‴,N‴*-hexamethyltriethylenetetraamine
HOESY	heteronuclear Overhauser enhancement spectroscopy
HRMS	high resolution mass spectra/spectroscopy
HSQC	heteronuclear single quantum correlation
ICP	inductively coupled plasma
IGAIM	individual gauges for atoms in molecules
LA	laser ablation
LiSE	lithium selective electrode
LOD	limit(s) of detection
LOQ	limit(s) of quantation
MALDI	matrix assisted desorption-ionization
MAS NMR	magic-angle spinning NMR
MQMAS NMR	multiple quantum magic-angle spinning NMR
MTHF	2-methyltetrahydrofuran
NOE	nuclear Overhauser effect
NOESY	nuclear Overhauser effect spectroscopy
OES	optical emission spectrometry
PMDTA	*N,N,N′,N″,N″*-pentamethyldiethylenetriamine
QCC	quadrupolar coupling constant
QSC	quadrupolar splitting constant
ROE	rotating-frame Overhauser effect
ROESY	rotating-frame Overhauser enhancement spectroscopy
RSD	relative standard deviation
RVS	restricted variational space
SEC	size-exclusion chromatography
THF	Tetrahydrofuran
TMEDA	*N,N,N′,N′*-tetramethylethylenediamine
TOCSY	total correlation spectroscopy
TOF	time of flight
UVV	ultraviolet-visible
XANES	X-ray absorption near edge structure
XRD	X-ray diffraction

II. INTRODUCTION

A. Scientific and Technological Significance of Organolithium Compounds

Organolithium compounds are all synthetic substances of great relevance in modern chemistry, utilized as reagents in organic synthesis and polymerization at the laboratory and industrial levels[1–8]. In Table 1 are listed lithium-containing organometallic and metallorganic compounds that can be commercially acquired. The main objectives that can be served when using these compounds in a synthesis step may be attaching either

TABLE 1. Commercially available organolithium compounds

Compound [CAS No.][a]	Properties[b]	Note
a. C−Li bond		
Methyllithium [917-54-4]	Pyrophoric solutions in THF or Et_2O, flammable non-pyrophoric solution in THF-cumene, SH2374D.	
Ethyllithium [811-49-4]	Flammable solution in hydrocarbons.	
Isopropyllithium [1888-75-1]	Flammable solution in pentane	
n-Butyllithium [109-72-8]	Pyrophoric solution in hexane, SH636A.	
s-Butyllithium [598-30-1]	Pyrophoric solution in hexane, SH636B.	
t-Butyllithium [594-19-4]	Pyrophoric solution in hexane, SH637C.	
n-Hexyllithium [21369-64-2]	Flammable solution in hexane.	
Phenyllithium [591-51-5]	Flammable solution in cyclohexane/Et_2O or in Bu_2O.	
Lithium cyclopentadienide [16733-37-4] (**1a**)	Pyrophoric solid, SH2153C, SR(2)3121A.	[c]
Lithium 1-*t*-butylcyclopentadienide [50356-03-1] (**1b**)	Pyrophoric solid.	
Lithium tetramethylcyclopentadienide [51905-34-1] (**2a**)		
Lithium pentamethylcyclopentadienide [51905-34-1] (**2b**)	Pyrophoric solid.	
2-Thienyllithium [2786-07-4] (**3**)	Flammable solution in THF.	
Lithium acetylide, ethylenediamine complex [6867-30-7]	Flammable solid, I(2)946A, SH2148C, SR(2)2705H, OJ5565000.	
Lithium phenylacetylide [4440-01-1]	Flammable solution in THF.	
b. N−Li bond		
Lithium dimethylamide [3585-33-9]	Pyrophoric solid, SH2155B, SR(2)3061E.	
Lithium diethylamide [814-43-3]	Pyrophoric solid, SH2154B, SR(2)3061G.	
Lithium diisopropylamide [4111-54-0]	Pyrophoric solid, SH2154C, SR(2)3061I.	[d]
Lithium diisopropylamide, tetrahydrofuran complex [123333-84-6]	Flammable solution in hydrocarbon, SH2155A, SR(2)3061H.	
Lithium dicyclohexylamide [4111-55-1]	Pyrophoric solid, SH2154A, SR(2)3061J	
Dilithium phthalocyanine [25510-41-2] (**4**)	λ_{max} 658 nm, SR(2)2825B.	
Lithium bis(trimethylsilyl)amide [4039-32-1]	Flammable solid, SH2150D, SR(2)2987G.	[e]
Lithium bis(dimethylethylsilyl)amide	Flammable liquid.	

TABLE 1. (*continued*)

Compound [CAS No.][a]	Properties[b]	Note
c. O—Li, S—Li bonds		
p-Toluenesulfinic acid, lithium salt [16844-27-2]	N(2)1592B, SR(2)2193B.	
Lithium acetylacetonate [18175-70-3] (**5**)		
Lithium *t*-butoxide [1907-33-1]	Flammable solid.	
Lithium ethoxide [2388-07-0]	Flammable solid.	
Lithium isopropoxide [2388-10-5]	Flammable solid, SR(2)3057A	
Lithium methoxide [845-34-9]		
Lithium phenoxide [555-24-8]	Flammable solution in THF.	
D-Lactic acid, lithium salt [598-82-3] (**6**)	$[\alpha]_D^{20} + 14.3°(c = 1, H_2O)$, I(1)548B, SR(1)625H, OJ6311000.	
Lithium acetate dihydrate [6108-17-4]	I(2)1275B, SR(1)601G.	f
Trifluoroacetic acid, lithium salt [2923-17-3]	SR(1)623B.	
2-Oxobutyric acid, lithium salt [3483-11-2]	I(1)552D, SH18D, SR(1)635M.	
Iodoacetic acid, lithium salt [65749-30-6]	N(1)853B, SR(1)621I.	
Cyclohexanebutyric acid, lithium salt [62638-00-0]	I(2)1283C.	g
Citric acid, trilithium salt hydrate [6132-04-3]	I(2)1282A, SH893B, SR(1)631K, TZ8616000.	f
Gluconic acid, lithium salt [60816-70-8] (**7**)		f
Succinic acid, lithium salt [16090-09-8]		h
Benzoic acid, lithium salt [553-54-8]	SR(3)3573M, OJ5720000.	i
Salicylic acid, lithium salt [552-38-5] (**8a**)		j
3,5-Diiodosalicylic acid, lithium salt [653-14-5] (**8b**)	SH1287D, SR(2)1885D.	
Orotic acid, lithium salt [5266-20-6] (**9**)		f
Poly(ethylene-*co*-methacrylic acid), lithium salt [27135-20-2]		
Carminic acid, lithium salt [12772-56-4] (**10**)		k
Squaric acid, dilithium salt [104332-28-7] (**11**)	N(1)709B, SH274A.	
Lithium triflate [33454-82-9]	SH2159D, SR(1)1055G.	
5-Sulfoisophthalic acid, monolithium salt [46728-75-0] (**12**)		l
n-Dodecyl sulfate, lithium salt [2044-56-6] (**13**)	SR(1)1079D.	

(*continued overleaf*)

TABLE 1. (*continued*)

Compound [CAS No.][a]	Properties[b]	Note
Lucifer Yellow CH [67769-47-5] (**14**)	$\lambda_{max}(\varepsilon)$ 280 nm(24200), 428 nm(11900) in water, I(2)955B, U427, SH2163D, SR(2)2835C.	*m*
Lucifer Yellow VS [71231-14-6] (**15**)	λ_{max} 427 nm, U429, SH2164A, SR(2)2835E.	
O-Acetylphosphoric acid, lithium potassium salt [92249-01-1]		
Lithium thiophenoxide [2973-86-6]	Flammable solution in THF.	
Lithium trimethylsilanolate [2004-14-0]	SR(2)2967B, VV7175000.	
Poly(lithium styrene-4-sulfonate) [9016-91-5]		
d. Miscellaneous		
Lithium 2-thienylcyanocuprate [112426-02-5] (**16**)	Flammable solution in THF, SH2158D.	*n*
(*S*)-Alpine hydride [100013-07-8] (**17**)	Flammable solution in THF, SH109D.	*o*
Superhydride [22560-16-3] (**18a**)	Flammable solution in THF, SH3209A.	
Superdeuteride [74540-86-6] (**18b**)	Flammable solution in THF, SH3208D.	
L-Selectride [38721-52-7] (**19a**)	Flammable solution in THF, SH2163A.	
LS-Selectride [60217-34-7] (**19b**)	Flammable solution in THF, SH2163B.	
NB-Enantride [81572-37-4] (**20**)	Flammable solution in THF, SH2523D.	*p*
Lithium 9-BBN hydride [76448-08-3] (**21**)	Flammable solution in THF.	
Lithium dimethylborohydride [84280-31-9]	Flammable solution in hydrocarbons.	
Lithium *t*-hexylborohydride [76430-48-3]	Flammable solution in THF.	
Lithium *t*-hexyllimonylborohydride [38218-68-7]	Flammable solution in THF.	
Lithium tetraphenylborate, tris-(1,2-dimethoxyethane) complex [75965-35-4]	Flammable solid, N(3)732A, SR(2)3029B.	
Lithium tri-*t*-butoxyaluminohydride [17476-04-9]	Flammable solution in THF, SH2159C, SR(2)3065B, OJ5585000.	
Lithium tri-*t*-butoxyaluminodeuteride [50306-58-6]	Flammable solid.	
Lithium tris[(3-ethyl-3-pentyl)oxy]aluminohydride [79172-99-9]	Flammable solution in THF, SH2160A.	

TABLE 1. (*continued*)

Compound [CAS No.][a]	Properties[b]	Note
Lithium tetrakis(2-methyl-8-hydroxyquinolato)boron [338949-42-1] (**22**)	λ_{max} 243 nm, photoluminescence at 470 nm.	
Lithium (1,2-ethanediolato-*O*) bis[1,2-ethanediolato(2-) *O*,*O*′]silicate [155740-37-7] (**23**)		

[a] The putative anchoring site of the Li atom need not necessarily fit the crystallographic analysis of the compound.

[b] Codes beginning with I, N and U denote FTIR spectra in Reference 10a, NMR spectra in Reference 10b and UVV spectra in Reference 11, respectively. Codes beginning with SH denote data for safe handling in Reference 12, while those beginning with SR are entries on safety regulations in Reference 13. A code of two letters followed by seven digits is a reference to a protocol in *Registry of Toxic Effects of Chemical Substances* (RTECS) of National Institute for Occupational Safety and Health/Occupational Safety and Health Administration (NIOSH/OSHA). See also Reference 14 for toxicological data.

[c] Used in the synthesis of cyclopentadienyl derivatives and metallocenes.

[d] A sterically hindered, non-nucleophilic strong base, useful for carbanion generation[15].

[e] Base for aldol coupling reactions[16], and the synthesis of lactone precursors[17] and ketones[18].

[f] Source of lithium ions in psychiatric disorders[19].

[g] Lithium standard salt in organic systems.

[h] Used in dermatological disorders[19].

[i] Diuretic and urinary disinfectant. The pharmaceutical effects mentioned in note *f* may cause complications[19].

[j] Antirheumatic agent. The pharmaceutical effects mentioned in note *f* may cause complications[19].

[k] Dyestuff[19].

[l] Monomer for synthesis of water-dispersible polyesters.

[m] Intracellular marker in biological systems. Fluorescent dye for nerve cells[20].

[n] Useful in the synthesis of other cyanocuprates[21, 22].

[o] Chiral reducing reagent for ketones[23]. Also available with (*R*)-configuration.

[p] Chiral reducing reagent for α,β-acetylenic ketones[24].

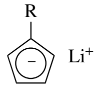

(1) **(a)** R = H
(b) R = *t*-Bu

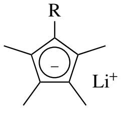

(2) **(a)** R = H
(b) R = Me

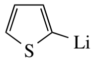

(3)

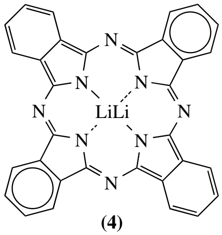

(4)

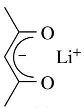

(5)

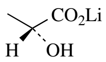

(6)

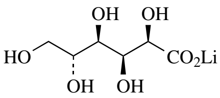

(7)

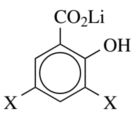

(8) **(a)** X = H
(b) X = I

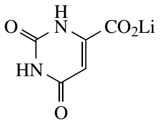

(9)

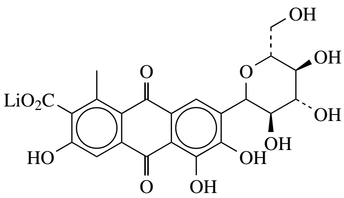

(10)

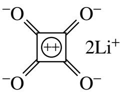

(11)

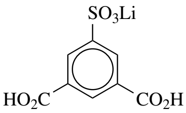

(12)

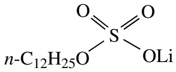

(13)

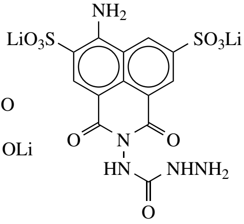

(14)

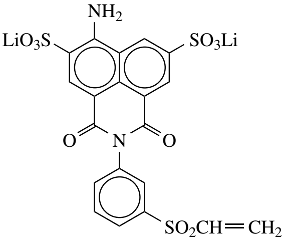

(15)

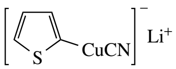

(16)

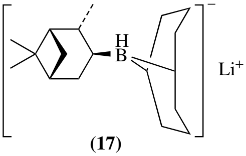

(17)

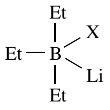

(18) **(a)** X = H
(b) X = D

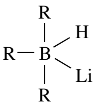

(19) **(a)** R = *s*-Bu
(b) R = *i*-PrMeCH

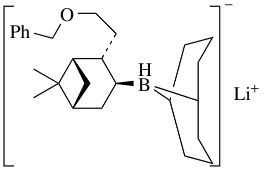

(20)

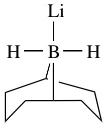

(21)

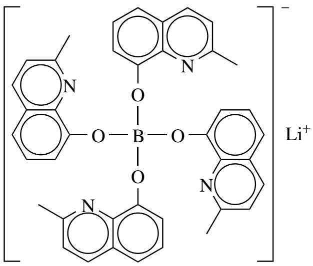

(22)

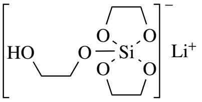

(23)

the organic group or the lithium atom to the substrate or taking advantage of the strong Lewis basicity of some of them to catalyze certain processes. Use and disposal of all organometallic (Li−C bonds) and many of the metallorganic compounds (Li−heteroatom bonds) requires special precautions, besides the usual safety measures taken when dealing with organic compounds in general[9]. Some of these compounds are pyrophoric, spontaneously igniting on exposure to air, thus affecting their transport regulations.

Working with organolithium compounds at very low temperatures frequently requires special solvents, alone or in admixture with others to achieve higher solubility, reversal of association, lowering the viscosity of the solution and forming crystalline solvates. Among the most frequently used solvents are simple alkanes, benzene and some of its alkyl derivatives like toluene and cumene, ethers such as Me_2O, Et_2O, tetrahydrofuran (THF), 2-methyltetrahydrofuran (MTHF) and 1,2-dimethoxyethane (DME), polydentate tertiary amines such as *N*,*N*,*N*′,*N*′-tetramethylethylenediamine (TMEDA), *N*,*N*,*N*′,*N*″,*N*″-pentamethyldiethylenetriamine (PMDTA) and *N*,*N*,*N*′,*N*″,*N*‴,*N*‴-hexamethyltriethylenetetraamine (HMTTA), and tertiary amides such as *N*,*N*-dimethylformamide (DMF) and *N*,*N*,*N*′, *N*′,*N*″,*N*″-hexamethylphosphortriamide (HMPA). Liquid ammonia may be used with advantage for certain organolithium compounds of lower reactivity. These solutions may themselves be flammable if the flash point of the solvent is low and even pyrophoric if the concentration of a pyrophoric solute is high.

Exposure of alkyllithium or aryllithium compounds to the atmosphere may cause degradation due to reaction with oxygen (equation 1) or air moisture (equation 2). Certain organolithium compounds are unstable at room temperature in the neat form, and require dilution; even then they should best be stored at low temperature. The instability may be the result of reactions such as the eliminations depicted in equations 3 and 4, taking place as the temperature rises[25].

$$\mathrm{RLi + O_2 \longrightarrow ROOLi \xrightarrow{RLi} 2ROLi} \tag{1}$$

$$\mathrm{RLi + H_2O \longrightarrow RH + LiOH \xrightarrow{RLi} 2RH + Li_2O} \tag{2}$$

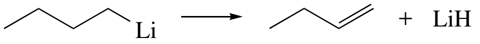

(3)

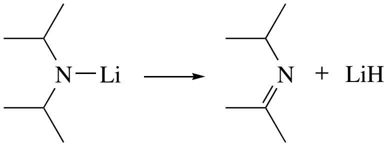

(4)

The presence of organolithium compounds in etheric solvents at temperatures above 0 °C may lead to extensive decomposition of the solvent and solute[26, 27]; a slow electron transfer side reaction of lithium naphthalene or sodium naphthalene with the THF solvent (equation 5) has been reported[28, 29]. The three isomeric forms of BuLi were shown to induce extensive decomposition of THF. The main path for this process is metallation at position 2 of THF, leading to ring opening and elimination of ethylene. An alternative path is proton abstraction at position 3, followed by ring opening. The presence of additives such as (−)-sparteine (**24**), DMPU (**25**), TMEDA and especially HMPA does not prevent decomposition but strongly affects the reaction path[27].

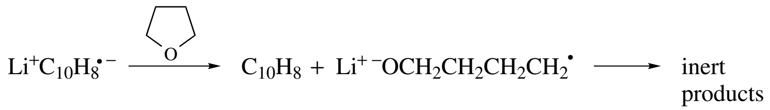

$$\mathrm{Li^+C_{10}H_8^{\bullet -} \xrightarrow{} C_{10}H_8 + Li^{+\,-}OCH_2CH_2CH_2CH_2^{\bullet} \longrightarrow \text{inert products}} \tag{5}$$

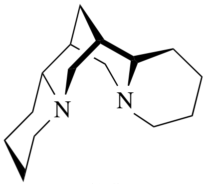

(24)

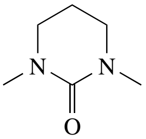

(25)

Aromatic solvents used when handling organolithium compounds, such as toluene or cumene, may undergo ring or side-chain metallation with alkyllithiums, catalyzed by certain alkoxides[30]. This reactivity of organolithium compounds usually requires working at low temperatures under an inert atmosphere of nitrogen or argon; however, if metallic lithium is used in the experiment, only argon is recommended, as nitrogen can react to give lithium nitride. The so-called Schlenk techniques are very popular for laboratory syntheses and physicochemical investigations[31,32].

B. General Considerations on the Analysis of Organolithium Compounds

Elsewhere in the *Chemistry of Functional Groups* series some remarks were presented on problems confronted in modern chemical analysis[33]. Quality control of reagents used in the laboratory and industrial processes is a condition for the success of the intended chemical reactions. The analytical methods that fulfill this aim should afford an *optimal* combination of reliability and economy. As for reliability one must choose accuracy and precision ranges that fit the nature and aims of the experiment. The economy desideratum involves multiple aspects: Short sample preparation and end analysis times, low investment in labware and instrumentation, low cost of reagents, minimal downstream operations and expenses (e.g. disposal of dangerous wastes stemming from the analysis) and, from the human point of view, a minimal training level for the application of the method and interpretation of results. Well established routine procedures for determination of the organolithium function were developed in the 1960s. Trace analysis of functional groups related to physiological, pharmacological, environmental or forensic investigations is practically devoid of relevance for many organolithium compounds in their original form, as they totally decompose on exposure to air or aqueous media, leaving only lithium ions and the derivatives of the organic residue to be analyzed for. Some research activity is shown at present in elemental analysis of lithium, by both wet and spectrometric methods. The high reactivity of most organolithium compounds makes their analysis as such rather cumbersome, requiring extreme dryness of the glassware, and, at least in part of the procedure, maintaining low temperatures and avoiding exposure to the atmosphere.

The main advances in analysis of organolithium compounds are related to their structural characterization by instrumental methods. These rely heavily on NMR spectroscopy and, when possible, on crystallographic methods, although other spectroscopic and physicochemical techniques are occasionally employed. A modern approach to the solution of complex analytical problems involves, in addition to the evidence afforded by these experimental techniques, consideration of quantum mechanical calculations for certain structures. The results of such calculations support or deny hypothetical assumptions on structural features of a molecule or possible results of a synthetic path. The following two examples illustrate these proceedings.

One investigation deals with the process depicted in equation 6 for the preparation of chiral formylated derivatives **27**, and the structure of the readily formed and relatively stable diastereoisomeric metallated intermediate **26**[34]. The first step consists of a DFT calculation using the hybrid B3LYP//PM3 method with Anders' lithium parameters[35–37]. A complete conformer search carried out for the two diastereoisomers (4*S*,6*S*) and (4*S*,6*R*) of **26** without solvent helps finding the two lowest energy conformers. Two Me_2O ligands are then introduced into each of these conformers, and their geometry is optimized to calculate the global energy minima. The energy of the (4*S*,6*R*) diastereoisomer is found to be significantly higher (by 6.1 kcal mol^{-1}), probably due to steric hindrance, because the *i*-Pr and the SMe groups are on the same side of the heterocyclic ring. Both minimum energy conformers are stabilized by the carbonyl oxygen, forming a five-membered chelate ring. The preferred (4*S*,6*S*) configuration of the organolithium compound is the one shown in equation 6 and the preferred conformation has the C—Li and S—Me bonds in antiperiplanar arrangement. This structure can be confirmed by ^{1}H and ^{13}C NMR, DPFGSE-ROE and IR spectra[34].

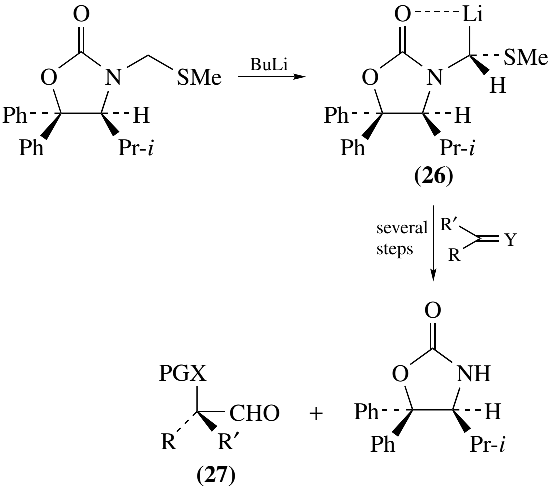

(26)

(27)

(6)

PG = protecting group or H
X = O, NH
Y = O, NR″

Another example attains the rationalization of the possible outcomes of the reaction of organolithium reagents with α,β-unsaturated fatty acids (**28**), variously substituted on the α and β positions with H, Me or Et groups. This, of course, requires excess reagent to neutralize the carboxylic proton, before other processes can take place. The main reaction paths proposed are a conjugate 1,4-addition of the organolithium compound, ultimately resulting in a β-alkylated saturated carboxylic acid, and a metallation reaction ultimately resulting in a rearrangement from α,β- to β,γ-unsaturation. Metallation is assumed to take place at the (E)-γ-position; however, in some cases replacement of a (Z)-γ-H atom is also possible. To somehow simplify the involved picture presented by the set of reagents RLi (R = Me, n-Bu, s-Bu, t-Bu, Ph) and substrates (**28**) studied in this work, three simple cases were chosen for performing semi-empirical PM3 calculations, namely 2-butenoic acid (equation 7), 2-methyl-2-butenoic acid (equation 8) and 3-methyl-2-butenoic acid (equation 9), reacting with t-BuLi. It should be pointed out that the simpler MeLi reagent cannot be considered because it fails to react, probably due to its strong tendency to form stable clusters in solution (see Section V.B.1). Taking into account the structure of the transition state complexes for the three proposed reaction paths and the corresponding activation energies, it is found that for equation 7 the activation energy of (E)-γ-metallation should be slightly higher than that of conjugate addition, this order being reversed for the transition states of equation 8. The calculations are in accordance with the observed yields of equations 7 and 8. For equation 9, the activation energies for conjugate addition and (E)-γ-metallation are quite similar to those found for the other two equations. However, the activation energy calculated for (Z)-γ-metallation is substantially lower, thus explaining the β,γ-unsaturated product and the failure to achieve alkylation of the acid[38].

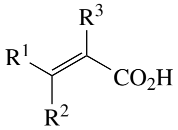

(28)

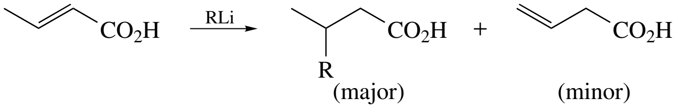

(7)

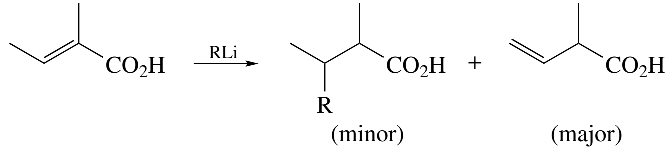

(8)

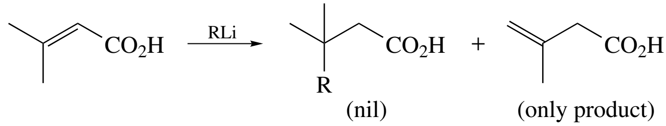

(9)

C. Scope of the Chapter

The quantitative analytical aspects of organolithium compounds are considered in two sections, dedicated to elemental analysis of lithium (Section III.A) and determination of the compounds as such (Section III.B).

For all the compounds listed in Table 1 and their analogs one may postulate bonding of the lithium atom at its anchoring site ranging from polarized covalent bonds to well defined ion pairs. Another important structural feature in the chemistry of organolithium compounds is coordination of the lithium atom with p- and π-electrons. A further bonding type is found among the complexes of atomic lithium and arene molecules, frequently considered as an ion pair between an aromatic free radical anion and a lithium cation. Lithium arene complexes are an intermediate stage in organic synthesis. Section IV deals with methods that can be considered for structural characterization. Although the inventory of spectral analysis used in organic chemistry has also been applied in the characterization of organolithium compounds, NMR techniques have been preponderant. As is frequently the case of organometallic compounds that form sufficiently large and ordered single crystals, X-ray diffraction (XRD) analysis has been applied to investigate the solid structure.

Organolithium compounds tend to associate into dimers, higher oligomers and polymers of two types: Complexes where the Li atoms are linked to each other by a chain of one or more atoms of other elements (C, N, O etc.), and complexes where the Li and other metallic atoms are close to each other, forming clusters. Section V presents examples of application of instrumental methods—mainly NMR and XRD—to structural elucidation of these associated species.

The presence of a specific organolithium compound in a synthetic process is sometimes assumed without isolation or further evidence other than having attained the expected product by a rationalized mechanism. For example, the synthesis of the alcohol depicted in equation 10 was carried out by adding the ketone to a ‘red solution’ resulting from the reaction of 2-bromopyridine with *n*-BuLi, where *ortho*-metallation of the pyridine ring is surmised and the intermediate is assumed to be quenched by the ketone reagent[39]. In the regiospecific process shown in equation 11, *n*-BuTeLi is taken to be a reactive intermediate quenched by ethanol and then further reacting with an acetylenic compound[40]. Numerous descriptions of anionic polymerization processes appear in the patent literature, where organometallic compounds serve as initiating reagents. Some examples of such proceedings are mentioned in Section VI. Many important procedural details such as temperature, solvent and reaction time are frequently omitted in the discussion, as they fall outside the scope of the chapter, while some details on the instrumental methods for reaction monitoring or product characterization are mentioned.

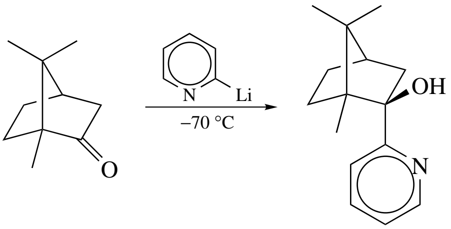

(10)

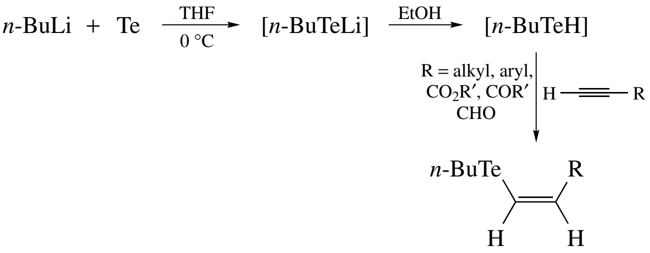

(11)

Given the capabilities of modern instrumentation, the author thinks that some effort should be invested in demonstrating the presence of certain intermediate metallized species in a reacting system. Many ‘surprises’ probably await researchers on these undertakings. This could help improving the synthetic methods, on the one hand, and deepen our understanding of organolithium compounds, on the other hand. One example of such endeavor is the in-depth investigation of the influence of association on the reactivity of butyllithium toward benzaldehyde and cyclopentadiene in THF solution, carried out by the rapid-injection NMR technique[41].

III. QUANTITATIVE ANALYSIS

A. Elemental Analysis of Lithium

1. General

When describing a new compound in the literature it is customary to report a calculated and experimental elemental analysis; however, analyses of Li in new organolithium compounds are usually omitted and only those of the ‘organic’ elements are reported.

Many methods for determination of lithium in samples of environmental, mineral, industrial and biomedical origin have been proposed, based on intensity measurements of UVV light. The sample preparation is in most cases much more complicated than what would be needed for a solution of an organolithium compound in ether or hydrocarbon solvents. In the latter instance, hydrolysis with dilute acid would usually be sufficient to cause total extraction of the Li^+ cations, followed by spectrometric absorption or emission measurements, or carrying a spectrophotometric end analysis after addition of a complexing dye and ancillaries. In some cases previous mineralization of the organic matrix would be required; for example[42], the lithium content of a polystyryllithium solution was determined by evaporating the solvent, burning off the organic matter taking care not to exceed 500 °C to avoid Li losses, dissolving the residue in acid and carrying out the end analysis spectrophotometrically using a chromophoric complexing agent. A single ion chromatography run on a high capacity cation exchange column, using an electrolytically generated methanesulfonic acid diluent, can be applied to determine down to trace levels the main cations (Li^+, Na^+, K^+, $NH_4{}^+$, Ca^{2+} and Mg^{2+}) present in drinking water, wastewater and soil extracts. Alternative methods for such analyses usually require a separate procedure for each cation or at least for the ammonium ion[43].

2. *Atomic absorption spectrometry*

A convenient method is the spectrometric determination of Li in aqueous solution by atomic absorption spectrometry (AAS), using an acetylene flame—the most common technique for this analyte. The instrument has an emission lamp containing Li, and one of the spectral lines of the emission spectrum is chosen, according to the concentration of the sample, as shown in Table 2. The solution is fed by a nebulizer into the flame and the absorption caused by the Li atoms in the sample is recorded and converted to a concentration aided by a calibration standard. Possible interference can be expected from alkali metal atoms, for example, airborne trace impurities, that ionize in the flame. These effects are canceled by adding 2000 mg of K per liter of sample matrix[44]. The method covers a wide range of concentrations, from trace analysis at about 20 μg L^{-1} to brines at about 32 g L^{-1}, as summarized in Table 2. Organic samples have to be mineralized and the inorganic residue dissolved in water. The AAS method for determination of Li in biomedical applications has been reviewed[45–49].

3. *Inductively coupled plasma emission and mass spectrometry*

An alternative to AAS is the more sensitive spectrometric determination of Li by inductively coupled plasma atomic emission spectrometry (ICP-AES) or optical emission spectrometry (ICP-OES). In Table 3 are summarized the spectral lines of the Li emission

TABLE 2. Recommended spectral lines for AAS analysis of lithium[44]

Concentration range (mg L^{-1})	Wavelength (nm)
0.02–5	670.8[a]
10–2000	323.3
200–32000	610.4

[a] The use of a sharp cutoff filter is recommended to avoid second-order interference from the Ne 335.5 nm line emitted by the lamp.

TABLE 3. Emission lines used for determination of Li by ICP-AES[50]

Wavelength (nm)	Element file
367.040	U[a]
379.472	La[a]
413.219	Ba[a]
413.256	Ba[a]
413.262	Ba[a]
460.286	Li[b]
610.364	Li[c]
670.781	Li[d]

[a] In the absence of this element, Li may also be determined at this line.

[b] The relatively large background of this line makes it suitable only for large Li concentrations.

[c] The relatively low background of this line makes it suitable for low Li concentrations.

[d] The very low background of this line makes it suitable for Li trace analysis.

spectrum that are recommended for measurements. For samples derived from organolithium compounds, probably all the lines are suitable for Li determination, with due consideration of the effects of concentration.

The most convenient form of sample for end analysis would be an aqueous solution after mineralization of the organic primary sample. However, it is possible to feed organic solutions to the instrument after certain hardware modifications and changes of the instrument operating mode; operating with organic solutions can be justified when long series of analyses have to be carried out, because of the savings in sample preparation. As in the case of AAS, a spectral line is chosen according to the analyte concentration and the presence of interfering elements (a rare occurrence with samples derived from experiments with organolithium compounds). The intensity of the emission signal is converted to a concentration with the help of calibration standards[50]. Several analytical quality aspects of ICP-OES determinations of single elements in solution were investigated for sixty-four elements. Application of the proceedings of this research turn the method into high-performance ICP-OES[51].

ICP-AES was validated for the simultaneous determination of Al, B, Ba, Be, Cd, Co, Cr, Cu, Fe, Li, Mn, Ni, Pb, Se, Sr and Zn in human serum in a clinical laboratory. The samples underwent digestion and yttrium was used as an internal standard. The LOD were as follows: 0.002–0.003 μM for Ba, Cd, Mn and Sr; 0.014–0.07 μM for Be, Co, Cr, Cu, Fe, Li, Ni, Pb and Zn and 0.2–0.9 μM for Al, B and Se. The concentrations of Al, Be and Co in human serum were found to be above the LOD, while those of Cd, Cr, Ni and Pb were below the LOQ; however, in case of acute intoxication with the latter elements the method is valid[52]. Matrix effects were evaluated for ICP-AES analysis using solution nebulization and laser ablation (LA) techniques. The main matrix-related interferences stem from elements with a low second ionization potential; however, these are drastically reduced when pure He is used as carrier gas. This points to Ar (the usual carrier) participation in the interference mechanism, probably by interacting with doubly charged species[53].

Application of ICP-MS in geology[54, 55] and the semiconductor industry[56] has been reviewed. The ^{6}Li:^{7}Li isotopic ratio of the stable lithium isotopes is an important parameter in geological[55] and chemical studies. This ratio may be determined by thermal MS or ICP-MS. LA in combination with the latter method can be applied directly on solid samples of minerals. An online monitoring method was proposed to deal with the interference caused by nonanalyte signals on the accuracy of Li determination by the ICP-MS method[57]. Recent examples follow the application of various ICP-MS modalities to analysis of biomedical and mineral samples.

A sector field ICP-MS instrument was used for determination of forty-two elements in urine after 20-fold dilution in ultrapure water containing dilute nitric acid. The concentration of most elements was above the LOD, with RSD about 10%[58]. ICP-MS was proposed for monitoring trace elements (Ba, Bi, Cd, Cu, Li, Mg, Mn, Mo, Pb, Sr, Tl and Zn) in mature breast milk. Total element concentrations in samples taken from thirty mothers in the Turin area were similar to those reported for human milk in other parts of the world[59]. Thirty-one elements were determined in wine by ICP-MS, at concentrations ranging from 0.5 μg L^{-1} to 100 mg L^{-1}, using In as internal standard. The effects of the presence of ethanol in the matrix were investigated[60]. Multicollector ICP-MS was applied for accurate and precise determination of the Li isotopic ratio in seawater and standard rocks, after carrying out a separation protocol for Li. The same protocol was proposed for efficient determination of the Li isotopic ratio in silicate rocks with low Li content, such as meteorite and the peridotites[61]. A sample preparation method was proposed to avoid matrix effects on the ICP-MS determination of Li. The method was applied to the determination of Li isotopic ratio in marine carbonate sediments containing the foraminifera *Pullenitina obliquiloculata* and *Globorotalia tumida*. Sediments of the former species were proposed as a record tracer for the changes of the Li isotopic composition in seawater through the geological ages[62]. An ICP-MS instrument was designed for continuous operation in harsh marine conditions. It was used for mapping trace elements and isotopic concentrations in seawater. A 65% depletion of Ba was discovered in a stretch of tens of kilometers off the shores of Baja California[63]. ICP-MS was applied in the determination of Al, As, Be, B, Cd, Co, Cu, Fe, Mn, Mo, Ni, Pb, Li, Rb, Se, Sr and Zn in serum and whole blood of viscachas (*Lagostomus maximus*). In the case of whole blood a digestion method was developed for the trace elements[64]. The same elements were determined in human serum. Among the advantages of ICP-MS for multi-trace element determination in serum are the short analysis time, high accuracy and precision, and low LOD. The disadvantages include a high risk of sample contamination from the environment, the relatively delicate sample handling and the high cost of the equipment[65]. A three-step analytical strategy was proposed for the analysis of sixty-seven elements in water by the ICP-MS method[66]. On the first step the major solutes are determined (Na, Mg, Si, S, Cl, K and Ca). Most elements to be analyzed on the second step are relatively abundant on the earth crust and are of widespread industrial use (B, Al, P, Cr, Fe, Mn, Ni, Cu, Zn, As, Se, Ag, Cd, Sb, Ba, Hg and Pb). The elements to be determined on the third analytical step include relatively abundant ones and extremely rare ones (Li, Be, Ti, V, Co, Ga, Ge, Br, Rb, Sr, Y, Zr, Nb, Mo, Sn, Te, I, Cs, La, Ce, Pr, Nd, Sm, Eu, Gd, Tb, Dy, Ho, Er, Tm, Yb, Lu, Hf, Ta, W, Pt, Au, Tl, Bi, Th and U). The figures of merit derived from such an analytical scheme are adequate for water quality monitoring and application of water fingerprinting to water management[66]. The lithium isotope ratio was determined in open ocean seawater, nine international rock standards and one C1 chondrite by thermal ionization MS as an alternative to other methods, such as ICP-MS and ion probe. A sample preparation technique was proposed for samples of low lithium content[67].

LA-ICP-MS was used for *in situ* determination of ultratrace elements in quartz. The analytical protocol included the following elements: Al, Ba, Be, Cr, Fe, Ge, K, Li, Mg, Mn, Pb, Rb, Sr, Th, Ti and U[68]. Application of the LA technique to heterogeneous samples usually requires preparing a homogeneous glass by fusing with lithium borate[69]. A difficulty encountered with multi-element LA-ICP-MS analysis is the absence of standards with similar matrix composition. It was proposed to use solutions for calibration coupled with an ultrasonic nebulizer[70].

4. Ultraviolet-visible spectrophotometry and colorimetry

In Table 4 are summarized some of the complexing agents that have been proposed for the UVV determination of lithium in solution.

Samples containing various alkali metals and other ions may need separation of Li before proceeding with its end analytical determination. This may be conveniently accomplished using lithium-selective sequestring agents to transfer this ion from the aqueous solution into a nonaqueous phase. The crown compounds mentioned in Table 4 accomplish the specific ion transfer; furthermore, their UVV absorption maxima undergo spectral shifts when forming the lithium complex, thus allowing Li^+ determination. Three 14-crown-4 chromogenic derivatives (**30a–c**) were synthesized and tested for their transfer capacity of Li^+ from slightly acidic or neutral aqueous solutions to 1,2-dichloroethane. 7-(2-Hydroxy-3,5-dinitrophenoxy)methyl-2,6,9,13-tetraoxatricyclo[12.4.4.0^{1,14}]-docosane (**30c**) showed good transfer capacity and 100-fold selectivity for Li^+ vs. Na^+. Transfer of the other alkali metal cations is practically nil[81]. Other chromogenic complexes of Li^+ with crown ethers[82], aza-crown ethers[83–85] and solubilized derivatives of TMC-crown formazan (**35**)[86–88] have been reported. The selectivity of 14-crown-4 derivatives for lithium ions and their potential application as ionophores for spectrophotometry, flow injection analysis, ion sensors and membrane separation was reviewed[89]. Application of macrocyclic complexing reagents to the colorimetric determination of lithium was reviewed[74].

A visual and digitalized colorimetric system for Li^+ determination was developed with operational principles similar to those of the well established pH paper. The optode is based on a thin PVC film (organic layer) applied to a paper sheet that carries the aqueous solution of the analyte at a certain pH. The organic layer contains a neutral ionophore (**36**, denoted as Σ), a cationic lipophilic dye (**37**, denoted by ΔH^+) and a lipophilic anionic additive (**38**, denoted as Λ^-) serving as counterion to the cationic dye. The color changes are based on the process depicted in equation 12, where the o and w subscripts denote the organic and aqueous phases, respectively. The analyte is extracted by the ionophore into the organic phase, forming an ion pair with the anionic additive; the latter was originally combined with the cationic dye, which becomes neutralized in the process, with a consequent change of color. Additional color effects can be obtained by incorporating a screening dye into the optode, which is an azo dye (**39b**) derived from Disperse Red 1 (**39a**). Digitalization of the color for automated measurements is based on the tristimulus principle, akin to the color perception of the eye. The linear range of the colorimetric optode for Li^+ is from 10 μM to 0.1 M. The method was validated for determination of Li^+ in saliva in the therapeutic range of 1 mM; an instrument for home use based on this colorimetric system was in development when this chapter was written[90].

$$Li^+_w + \Sigma_o + \Delta H^+\Lambda^-_o \rightleftharpoons \Sigma Li^+\Lambda^-_o + \Delta_o + H^+_w, \quad K = \frac{a_{\Sigma Li^+\Lambda^-_o}\, a_{\Delta_o}\, a_{H^+_w}}{a_{Li^+_w}\, a_{\Sigma_o}\, a_{\Delta H^+\Lambda^-_o}} \qquad (12)$$

Ion chromatography is a convenient method for simultaneous determination of alkali, alkaline earth and ammonium ion concentrations in solution. The identity of the analytes is set by the retention times and quantation is carried out by a detector. Conductivity is frequently used, after chemical suppression of the eluate, by which chloride counterions were exchanged by hydroxide. UVV spectrophotometric measurement of hydroxide ions at 200 nm was proposed as an alternative method to suppressed conductivity. Both methods

TABLE 4. Complexing dyes for spectrophotometric and colorimetric determination of the lithium cation

Compound [CAS No.]	Properties[a]	Note
1,3-Bis(8-quinolyloxy)propane derivatives (e.g., **29**)		b
Chromogenic 14-crown-4 derivatives (**30a–c**)		c
8-Hydoxyquinoline [148-24-3] (**31**)	I(2)859D, SH1960C, SR(2)2617G, VC4200000.	d
2,3,7,8,12,13,17,18-Octabromo-5,10,15,20-tetrakis(4-sulfonatophenyl)porphyrin (**32a**)	λ_{max} nm (log ε) in water, pH 7.0: 376 (4.54), 478 (5.30), 657 (4.25) and 760 (4.07).	e
Quinizarin [81-64-1] (**33**)	I(2)87A, U606, SH3024A, CB6600000.	f
Thorin I [3688-92-4] (**34**)	I(2)998D, U705, SH3340A, SR(2)2749L.	g

[a] Codes beginning with I and U denote FTIR spectra in Reference 10a and UVV spectra in Reference 11, respectively. Codes beginning with SH denote data for safety handling in Reference 12, while those beginning with SR are entries on safety regulations in Reference 13. A code of two letters followed by seven digits is a reference to a protocol in *Registry of Toxic Effects of Chemical Substances* (RTECS) of National Institute for Occupational Safety and Health/Occupational Safety and Health Administration (NIOSH/OSHA). See also Reference 14 for toxicological data.

[b] The fluorescence of compounds such as **29** significantly increases in the presence of lithium perchlorate. The increase is proportional to the lithium concentration. In MeCN the linear range is 2 to 100 μM of $LiClO_4$, while in MeOH the concentration has to be >30 mM[71].

[c] These include 14-crown-4 ethers (**30a–c**), their aza analogs and other crown compounds. The phenoxide can provide a convenient counterion for the lithium cation. Other variants may involve fluorescence and photoinduced electron transfer[72]. See text in Section III.A.3.

[d] The lithium complex can be determined colorimetrically by the greenish fluorescence emitted between 490 and 570 nm when illuminated with UV light[73]. A review appeared on the colorimetric assay of Li[74].

[e] The UVV spectrum of **32a** is pH dependent. In the presence of Li^+ ions the spectrum of **32b** shows a specific shift that allows quantation, which is carried out at 490 nm, pH ~ 13. Possible interference by traces of heavy and transition elements is masked with $[Mg{\cdot}EDTA]^{2-}$ added to the sample. The method was tested for Li^+ in seawater and deproteinized plasma[75].

[f] Determinations of Li in drugs and blood serum are carried out at 601 nm in alkaline solution[76].

[g] Originally designed for colorimetric determination of thorium in trace amounts[77]. Measurements of the lithium complex can be carried out over a wide range of wavelengths: Determination in pharmaceuticals at 468 nm, with linear range of 0.1 to 4.0 mg L^{-1} [78]; analysis of blood serum at 480 nm, after protein removal[79]; seawater can be analyzed at 482 nm in the presence of Me_2CO and at 452 nm without this additive[80].

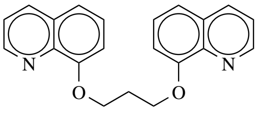

(29)

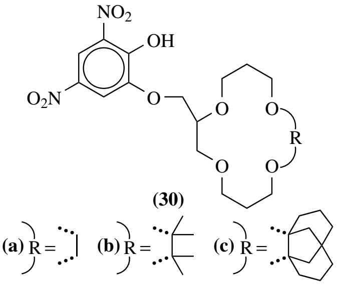

(30)

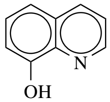

(31)

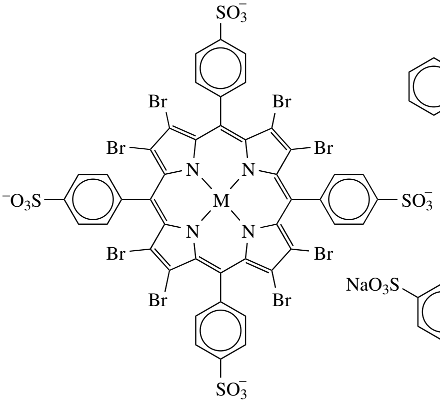

(32) **(a)** M = 2H [$H_2(OBTPPS)^{4-}$]
(b) M = Li [$Li(OBTPPS)^{5-}$]

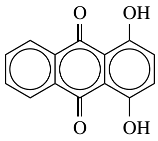

(33)

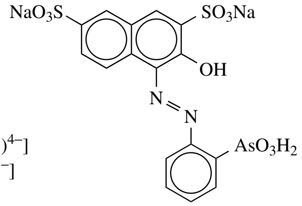

(34)

have about the same LOD for the univalent cations (1 to 6 μg L^{-1}) and spectrophotometry slightly lower ones for the bivalent cations (4 to 19 vs. 6 to 67 μg L^{-1})[91].

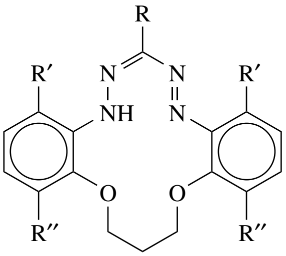

(35)

R = electron-withdrawing group
R′, R″ = H, MeO, OCH_2CO_2H,
NO_2, F, Cl, Br

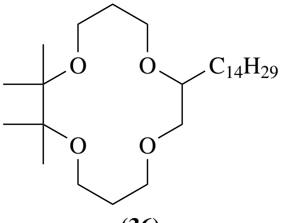

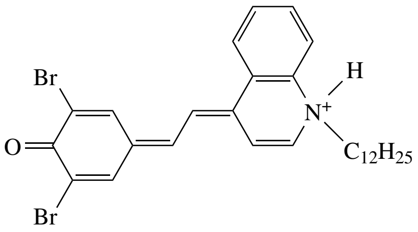

(36) **(37)**

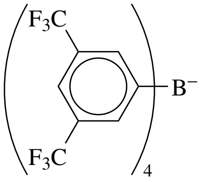

(38)

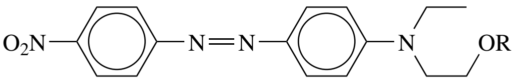

(39) **(a)** R = H
(b) R = $C_{18}H_{37}$

An instrument was proposed for measurement of Li concentration in human serum, based on the turbidimetric or nephelometric determination of the maximum rate of precipitation of a Li complex, which is related to the Li concentration in the serum. The precipitating reagent was prepared by dissolving KIO_4 and $FeCl_3$ in a KOH solution. Measurements were made every 10 s for 5 min at 550 nm. No interference was recorded for the presence of triglycerides, cholesterol, Na^+ or K^{+}[92].

5. Lithium selective electrodes

Development of lithium selective electrodes (LiSE) and their application in clinical chemistry have been amply reviewed[93–100]. Several models of lithium ion specific electrodes are commercially available. The central problems in developing such sensing devices are their dynamic range, the accuracy and precision by which the signals are correlated to the concentration of the analyte and the selectivity towards that species, especially in relation to other alkali metal cations. Additional problems of practical importance are the times of response and recovery and the durability of the electrode in the intended service.

a. Neutral ionophores in polymeric membranes. The most extensively applied working principle for LiSE consists of incorporating a neutral ionophore into a poly(vinyl chloride) membrane to accomplish complexing of Li^+ ions; sometimes specific lipophilic anionic constituents and lipophilic solvents that serve as plasticizers are also added to the membrane formulation. Among the lipophilic anionic components the tetraphenylborate (**40**) and cobalticarborane (**41**) anions have been found to effectively counterbalance the cationic charge. Lipophilicity in this case contributes to durability of the LiSE, as it reduces leaching out; anions **40c** and **40d** are more lipophilic than **40a** and **40b**[101]. The neutral ionophores usually are crown compounds, amides or combinations of these functions; however, other functional groups such as phosphine oxides and substituted 1,10-phenanthrolines have also been investigated. Specificity for Li^+ is achieved by a crowded stereochemistry that reduces the volume of the inner hole in the puckered macrocyclic compound and makes complexation with other cations thermodynamically unfavorable[94, 97, 99, 102].

Many crown compounds have been investigated as specific ionophores for Li^+, for example, dibenzo-18-crown-6 (**42**) or dicyclohexano-18-crown-6 (**43**) in conjunction with the cobalticarborane anion (**41**). The sensitivity of such combinations is higher for K^+ than for Li^+ (55 vs. 14 and 51 vs. 27 mV per M concentration decade, respectively)[101]. Other examples are the 16-crown-4 derivatives **44a–d**, for which in the best case the LiSE shows a higher than 600-fold selectivity for Li^+ vs. Na^{+}[103, 104]; compound **44a** with the THF units in *cis*-configuration has excellent selectivity for Li^+ vs. Na^+. K^+, NH_4^+, Mg^{2+} and Ca^{2+}, and the components of blood serum do not interfere with the Li^+ determination[105]; 5,5-dibenzyl-14-crown-4 (**45**) also shows good selectivity[106–108]. Placing bulky substituents

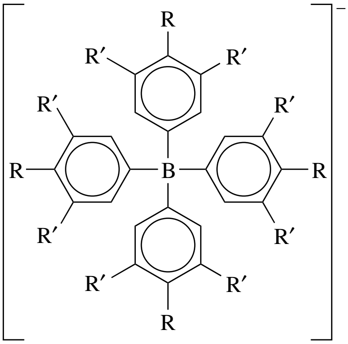

(40) **(a)** R = R′ = H
(b) R = Cl, R′ = H
(c) R = H, R′ = CF_3
(d) R = H, R′ = $C(CF_3)_2OMe$

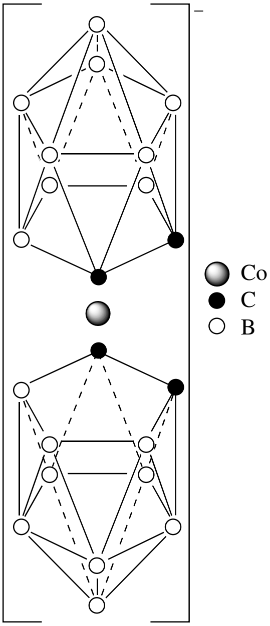

(41)

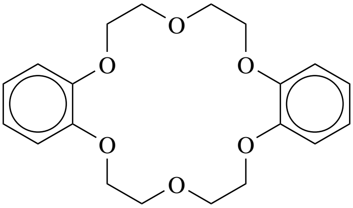

(42)

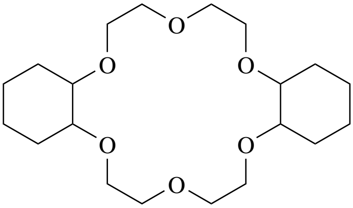

(43)

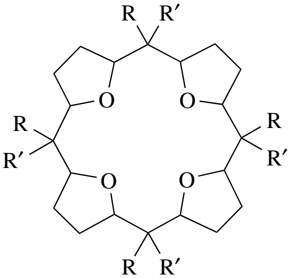

(44) **(a)** R = Me, R′ = H
(b) R = Et, R′ = H
(c) R = Me, R′ = Et
(d) R = R′ = Et

on the ethano sections of 14-crown-4 ionophores, for example compound **46**, will improve selectivity for Li^+, forming a 1:1 complex with 14-crown-4 and its derivatives, as the tendency of forming 2:1 and 3:1 adducts of the ligand with the other alkali metal ions is sterically precluded[109]. Lactonization of monensin (**47**) by condensing the groups denoted with an asterisk, followed by acylation of the hydroxyl groups yielded macrocyclic crown compounds such as **48**, that showed good Li^+ selectivity in the presence of dibenzyl ether[110].

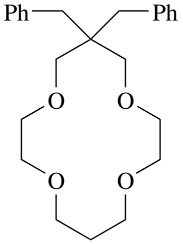

(45)

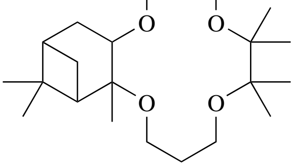

(46)

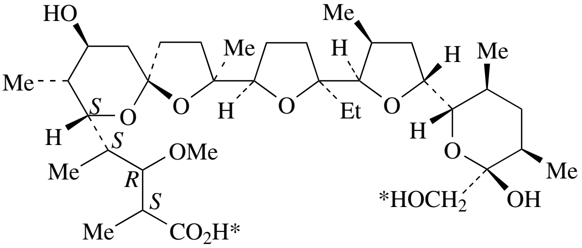

(47)

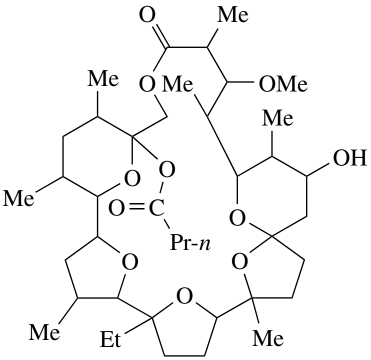

(48)

Another type of neutral complexing agents are carboxamides carrying large substituents on the N atom, such as compounds **49**[111], **50** and **51**[112–114]. Electrodes containing

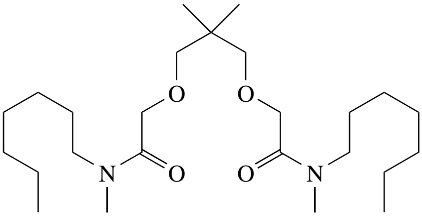

(49)

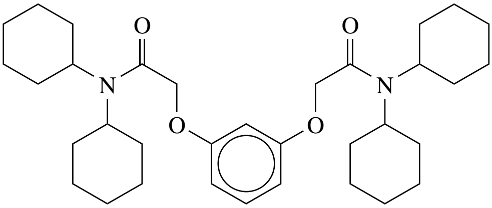

(50)

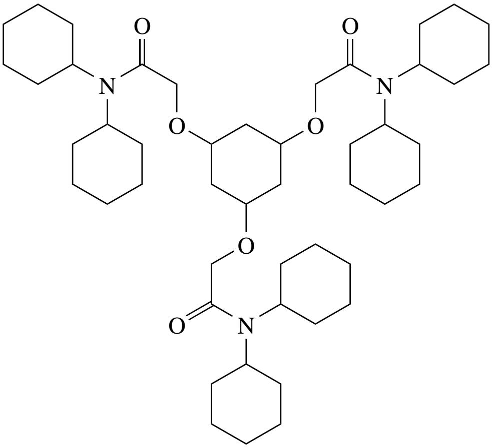

(51)

compound **51** were designed for solid contact operation. Compounds **52a–d** and **53** were investigated for their activity in LiSE. They combine the structural features of both the crown compounds and the sterically crowded diamides. Compound **53** is a variation of **52** obtained on replacing both R groups with a single tetradecamethylene chain. Membranes containing **52d** and **53** show good selectivity for Li^+ against other univalent and divalent cations, especially the latter macrocyclic compound with selectivity better than 30-fold against Na^+, several 100-fold against K^+, H^+, Ca^{2+} and NH_4^+ and better than 1000-fold against Rb^+, Cs^+, Mg^{2+}, Sr^{2+} and Ba^{2+}[115]. Derivatives of 14-crown-4 bearing two amido groups (**54a** and **54b**) show good selectivity for Li^+ vs. Na^+[116]. A LiSE based on the simpler tertiary diamide ETH 1810 (**55**) with 2-nitrophenyl octyl ether as lipophilic solvent has a higher than a thousand-fold selectivity for Li^+ over other alkali metal cations, a linear response in the range from 32 μM to 0.1 M and a detection limit of 16 μM; the Nernstenian response is 56.0 mV per decade[117].

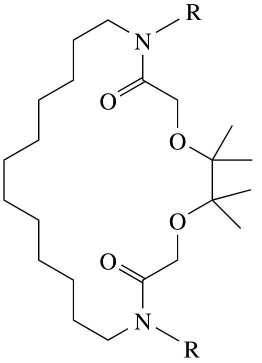

(52) **(a)** R = CH_2Ph
(b) R = $CHPh_2$
(c) R = CH_2CH_2N 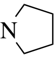
(d) R = 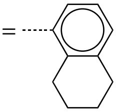

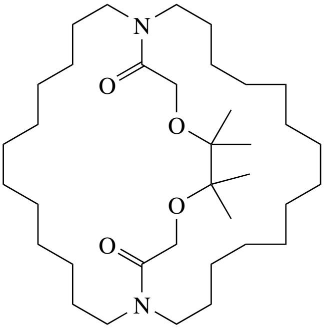

(53)

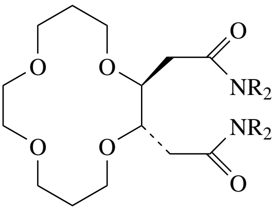

(54) **(a)** R = *s*-Bu
(b) R = *n*-Bu

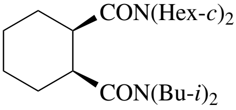

(55)

Ionophores containing the phosphine oxide group with bulky groups attached to the P atom have also been incorporated to LiSEs, for example compounds **56** and **57**[102].

1,10-Phenanthroline derivatives disubstituted at the 2,9-positions were investigated as ionophores for Li^+. Best results were obtained for 2,9-dibutyl-1,10-phenanthroline (**58**), with excellent selectivity vs. Na^+, K^+, Mg^{2+} and Ca^{2+}[118]. The importance of the plasticizer employed in the fabrication of the membrane of a LiSE was demonstrated. Thus, 1-phenoxy-2-nitrobenzene gave the best results for electrodes based on compound **58**[119]. The bridged 1,10-phenanthroline derivatives **59**, with four to seven methylene links, were investigated as neutral ionophores; the lipophilic tetrakis(4-fluorophenyl)borate anion [$(4\text{-}FC_6H_4)_4B^-$] was added to the LiSE membrane to improve its selectivity[120]. The behavior of PVC membranes containing poly(3-octylthiophene) (**60**) was investigated; the latter

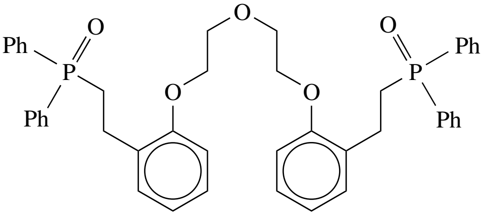

(56)

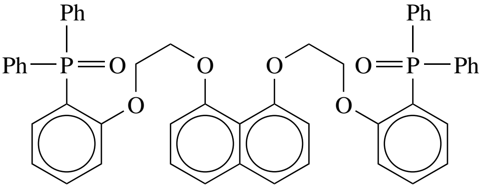

(57)

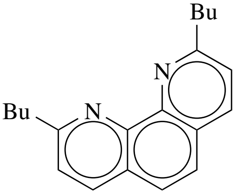

(58)

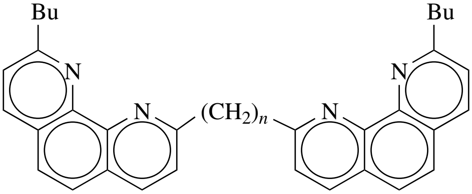

(59, $n = 4$–7**)**

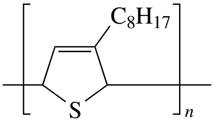

(60)

polymer is defined as a p-type semiconductor and the membrane shows a response to alkali and alkali earth ions[121, 122]. Incorporating polyaniline in a LiSE contributes to the stability of its response[114, 122, 123].

b. Electrochemical host–guest reactions. A different approach to LiSEs is based on making a membrane containing λ-MnO_2 selective for Li^+, which is used in combination with a Pt electrode in electrochemical determination by a redox reaction of the analyte[100]. The potentiometric response of a graphite-epoxy electrode containing λ-MnO_2 was investigated for the determination of Li^+. The response is log-linear over the range from 1 μM to 33 mM, with an intensity of 58.2 mV per decade, unaffected by pH in the 4–10 range; the selectivity for Li^+ is about 30-fold against Na^+ and about 100-fold against K^+, Cs^+, Mg^{2+}, Ca^{2+}, Sr^{2+} and Ba^{2+}. The response time of the electrode is less than 30 s and the lifetime more than 6 months[124].

B. Determination of Organolithium Compounds

1. General

When using alkyllithium compounds as initiating agents in anionic polymerizations it is important to have a quality assessment, because it is assumed that at the end of the initiation period each organometallic molecule will be responsible for the creation of a propagating chain, that does not undergo chain transfer or termination in the absence of oxygen or an electrophile such as the proton of methanol. This assumption on the initiation stage allows making an estimate of the degree of polymerization based on the number average. Furthermore, in some cases the presence of alkoxide and other impurities may somehow interfere with the polymerization process (see, for example, comments on methacrylate and isoprene polymerization in Section V.A.2, on superbases in Section V.A.4 and on telomerization of ethylene at the end of Section VI.B.7).

2. Titration methods

Determination methods for organolithium compounds by titration have been reviewed[125]. Alkyl and aryllithium reagents (RLi) usually contain the corresponding ROLi as an impurity. The most probable origin of this is exposure to oxygen in air, as shown in equation 1. A further degradation of organolithium may occur on exposure to moisture, as shown in equation 2, leaving a colloidal suspension of LiOH or Li_2O. Therefore, acid–base titrations of the total alkalinity generated on hydrolysis of an organolithium sample overestimates the organometallic content. Furthermore, it is frequently the case that one is interested in knowing the content of both RLi and ROLi, for any desired or undesired effects the latter species might have. A most popular procedure to overcome the pitfalls of acid–base titration consists of carrying out a double titration. The first aliquot is hydrolyzed and titrated for total basicity (RLi + ROLi + LiOH equivalents) with a standard acid solution. The second aliquot is treated with benzyl chloride, for a short time (2 min) followed by hydrolysis with water and titration with standard acid. In the second titration the organometallic compound totally reacts with benzyl chloride according to equation 13, while reaction with the other bases is much slower. The difference between the two titrations is the amount of organolithium compound in the aliquot[126]. The reagents need to be of high purity and the conditions strictly controlled to attain good reproducibility by the double titration method[127, 128]. An especially careful and tedious variation of a double titration method with benzyl chloride[129] was described for the standardization of a BuLi solution in benzene[130].

$$\text{RLi} + \text{ClCH}_2\text{Ph} \longrightarrow \text{RCH}_2\text{Ph} + \text{LiCl} \qquad (13)$$

A variant for the determination of the organolithium compounds avoiding the double titration is based on the use of diphenylacetic acid in THF solution, to which the solution of the organometallic is gradually added. The acid readily neutralizes the alkoxide and the organolithium species according to equations 14 and 15, respectively. However, only after having added one equivalent of RLi is the end point reached, where excess organolithium, acting as a strong base, causes abstraction of the benzylic proton in the diphenylacetate anion, with yellow discoloration[131]. Similar effects are observed when using 4-biphenylmethanol (**61**), 4-biphenylacetic acid (**62**) or 4-biphenylcarboxylic acid (**63**) as titrants, the latter in the presence of triphenylmethane. The preferred titrant/indicator is **61** because of its turn to orange-red, whereas **62** turns to yellow and with **63** the colorless solution becomes yellow or green before it turns to red at the end point[132].

$$\mathrm{Ph_2CHCO_2H} \xrightarrow{\mathrm{ROLi}} \mathrm{Ph_2CHCO_2^-Li^+} \qquad (14)$$

$$\mathrm{Ph_2CHCO_2H} \xrightarrow{\mathrm{RLi}} \mathrm{Ph_2CHCO_2^-Li^+} \xrightarrow{\mathrm{RLi}} \mathrm{Ph_2C^-CO_2^-2Li^+} \qquad (15)$$

$\mathrm{4\text{-}PhC_6H_4CH_2OH}$ (**61**) $\mathrm{4\text{-}PhC_6H_4CH_2CO_2H}$ (**62**) $\mathrm{4\text{-}PhC_6H_4CO_2H/Ph_3CH}$ (**63**)

Methods for direct titration based on various working principles have been proposed. Alkyllithiums and phenyllithium form colored charge transfer complexes with 1,10-phenanthroline (**64**) and 2,2′-biquinoline (**65**). These heterocyclic compounds can be used as indicators in the direct titration of the organometallics with an alcohol, according to equation 16. The end point is reached on the disappearance of discoloration[133]. The same reaction may be applied for the determination of organolithium compounds by thermometric titration with an alcohol, taking advantage of the exothermic nature of the process. The reagent is added at a fixed volumetric rate and the temperature of the sample solution is recorded as a function of time. The temperature reaches a top value and starts a descending curve. The end point is determined on linearly extrapolating the heating-up and cooling-down curves. Titration time is of the order of 1 min[134].

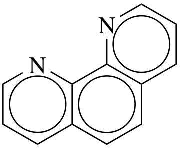

(64)

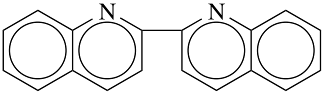

(65)

$$\mathrm{RLi + HOR' \longrightarrow RH + R'OLi} \qquad (16)$$

A known amount of benzoic acid (equation 17) or acetophenone (**66a**, equation 18) is titrated under nitrogen atmosphere, with a solution of the organolithium compound in DMSO-DME-hydrocarbon solvent, using triphenylmethane as indicator. Yellow to red end points are obtained for reaction 17 with alkyllithium compounds while with PhLi the end point is green to red-brown. When the protons of the carboxylic acid (for total basicity) or the electrophilic ketone are consumed, metallation of $\mathrm{Ph_3CH}$ takes place, and the presence of DMSO promotes a change of color at the end point[135]. High frequency titration with acetone (**66b**) may be used for the determination of organolithiums in hydrocarbon solution, based on equation 18. The titration is carried out in an oscillometer, measuring the change of capacitance of the solution as its composition changes on adding the titrant. The titration curve may undergo a gradual change of direction, passing through a maximum; however, an abrupt change of direction marks the end point[136].

$$\mathrm{RLi} + \mathrm{PhCO_2H} \longrightarrow \mathrm{RH} + \mathrm{PhCO_2Li} \qquad (17)$$

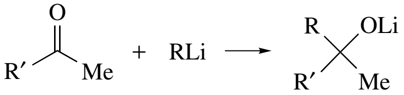

(66)

(**a**) R′ = Ph
(**b**) R′ = Me

(18)

A sample of organolithium compound solution is added to an excess of standardized iodine solution in Et_2O; the excess iodine is extracted with aqueous KI and titrated with standard thiosulfate solution. Evaluation of the organometallic compound is made according to equation 19[127]. A possible interference can be expected from the coupling reaction in equation 20. This was shown to be negligible, as demonstrated spectrofluorometrically for phenyllithium[127], whereas a low titer was found for *n*-BuLi, attributable to this side reaction[128].

$$\mathrm{RLi} + \mathrm{I_2} \longrightarrow \mathrm{RI} + \mathrm{LiI} \qquad (19)$$

$$\mathrm{RLi} + \mathrm{RI} \longrightarrow \mathrm{R_2} + \mathrm{LiI} \qquad (20)$$

An indirect oxidimetric titration method for alkyllithium compounds may be carried out, taking advantage of the fact that vanadium pentoxide causes fast and complete oxidation of alkyllithiums in solution. After the end of this reaction the reduced vanadium compounds are dissolved in sulfuric acid and titrated with Ce(IV) sulfate, using as indicator Fe(II) and 1,10-phenanthroline (**64**) sulfate. This method is inadequate for aryllithium compounds because the lithium phenoxide impurities reduce vanadium pentoxide[137].

3. Gravimetric analysis

Phenyllithium in ether solution can be directly analyzed after addition of excess triphenyltin chloride. An insoluble precipitate of tetraphenyltin is formed, filtered, washed, dried and weighed[126]. This method affords a large amplification factor for phenyllithium.

4. Gas chromatography

A method based on equation 21 may be performed, where the organic residue of an organometallic compound becomes derivatized with excess dimethylphenylchlorosilane (**67**) and determined by GC, using cumene (*i*-PrPh) as internal standard. Although lithium alkoxide impurities also react with **67**, the product appears at a different retention time. The method is also suitable for Grignard reagents[138].

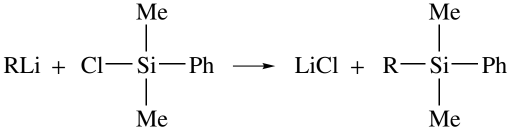

$$\mathrm{RLi} + \mathrm{Cl{-}}\underset{\mathrm{Me}}{\overset{\mathrm{Me}}{\mathrm{Si}}}\mathrm{{-}Ph} \longrightarrow \mathrm{LiCl} + \mathrm{R{-}}\underset{\mathrm{Me}}{\overset{\mathrm{Me}}{\mathrm{Si}}}\mathrm{{-}Ph} \qquad (21)$$

(67)

5. Nuclear magnetic resonance spectroscopy and magnetic titrations

Part of the NMR spectroscopy techniques mentioned in Section IV.B can be used for quantitative determination of organolithium compounds in solution.

^{1}H NMR can be used for assessment of the purity of organolithium RLi initiators. The presence of ROLi can also be determined. The dimetallated initiator 1,4-dilithio-1,1,4,4-tetraphenylbutane cannot be determined by this method due to its low solubility[128].

The progress of the reaction depicted in equation 22 may be followed by ^{1}H NMR, measuring the disappearance of $(Me_3Si)_4Si$ (δ 0.23 ppm) and MeLi (δ -2.07 ppm) reagents and the appearance of the $(Me_3Si)_3SiLi$ (δ 0.07 ppm) product. The latter crystallizes in a stable solvated form as $(Me_3Si)_3SiLi{\cdot}3THF$[139].

$$(Me_3Si)_4Si + MeLi \xrightarrow{THF} (Me_3Si)_3SiLi + Me_4Si \qquad (22)$$

Magnetic titrations are based on an operating mode different from integration of the specific peaks of the analyte. For example, they may be carried out by introducing a 500 μL aliquot of a 1 M THF solution of an alkali metal arene in an NMR tube, under controlled atmospheric and temperature conditions, adding 2 μL increments of a proton donor, and measuring the attaining downfield shift increments $\Delta\nu$ of the $\alpha{-}^1$H of THF. A plot of $\Delta\nu$ vs. the stoichiometric donor/metal arene ratio in solution shows a gradual decrease of $\Delta\nu$ until no further effect is noted for the added donor increments. The titration break point denotes the stoichiometry of the metal arene reaction with a proton. For example, lithium naphthalene titrated with methanol has the break point at 0.5, indicating a 1:2 stoichiometry, that is, it takes one proton to react with two naphthalene radical ions. Titration with n-BuNH$_2$ shows a 1:4 stoichiometry, which is in accord with the MeOH result, because one amine molecule can provide two protons. A similar technique can be applied to measure the reaction kinetics of quenching, but now the total amount of proton donor is added, $\Delta\nu_t$ values are recorded as a function of time and a plot of $\ln(\Delta\nu_t - \Delta\nu_\infty)$ vs. time shows the reaction rate behavior[140]. A magnetic titration of $Li{\cdot}C_{10}H_8$ in THF solution, carried out with t-BuCl, following the chemical shift of the THF protons as the addition of the alkyl halide proceeds, shows the break point when 0.5 moles of alkyl halide per mol of lithium naphthalene were added, pointing to a 1:2 stoichiometry for this process[141].

In an earlier work, the formation of the univalent naphthalene radical anion could be followed by measuring the magnetic susceptibility of the solution. In the presence of excess lithium, reduction of the magnetic susceptibility was indicative of the appearance of the diamagnetic naphthalene dianion. This could be reversed on addition of naphthalene to the solution. The total alkalinity of the solution includes both the monovalent and divalent anions[142]. The kinetics of naphthalene dianion formation from the singly charged radical anion in THF solution can be followed by simultaneous measurement of magnetic susceptibility and alkalinity of the solution[28, 143]. Only lithium naphthalene solutions lead to the doubly charged naphthalene anions; sodium naphthalene solutions are stable in the presence of excess sodium. However, side reactions such as equation 5 may cause loss of both magnetic susceptibility and alkalinity[28].

6. Ultraviolet-visible spectroscopy

The optical density of n-BuLi shows good linear behavior at 285 nm ($\varepsilon = 91 \pm 4$ L mol^{-1} cm^{-1}), in benzene solution, in the concentration range from 0.002 to 0.031 M. The weak absorption maximum in this region shifts slightly to a longer wavelength on increasing the concentration[128]. The kinetics of n-BuLi addition to 1,1-diphenylethylene in benzene solution (equation 23) may be followed spectrophotometrically at 428 nm, corresponding to the maximum in the absorption spectrum of the carbanion in the ion pair **68**. No analogous addition takes place with either tetraphenylethylene or 1,1,3,3-tetraphenylbut-1-ene[130].

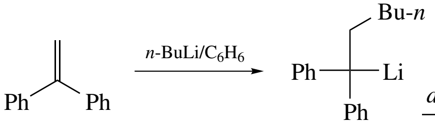

(68)

$$\frac{d[\mathbf{68}]}{dt} = k[\mathrm{Ph_2C=CH_2}][n\text{-BuLi}]^{0.18} \qquad (23)$$

The kinetics of the initiation step, involving formation of 'living' polystyrene chains (**69**) in benzene solution according to equation 24, can be followed by measuring the optical density at 335 nm, whereas the kinetics of the propagation step (growth of x) can be determined by following the disappearance of styrene at 291 nm[42]. Formation of ω-lithiopolystyrene, ω-lithiopoly(1,1-diphenylethene), ω-lithiopolyisoprene and ω-lithiopoly(1,3-butadiene) and polyisoprene was monitored by following the optical densities at wavelengths according to their specific UVV absorption spectra[144, 145].

$$n\text{-BuLi} + \mathrm{CH_2{=}CHPh} \longrightarrow n\text{-Bu}\left[\mathrm{CH_2CHPh}\right]_x\mathrm{CH_2C^{-}HPh\ Li^{+}} \qquad (24)$$

(69)

Generation of radical anions by various aromatic compounds in the presence of lithium can be ascertained by development of discoloration. Generation in THF gives a dark blue solution of lithium 1,4-di-*t*-butylbiphenyl (**70**) at 0 °C, a dark green solution of lithium 1-(dimethylamino)naphthalene (**71**) at −45 °C which decomposes at 0 °C and a dark green solution of lithium 2,6-di-*t*-butylnaphthalene (**72**) at 0 °C. Only **72** may be generated in $\mathrm{Et_2O}$ at 0 °C, in relatively low yield, as a deep purple solution[146]. Deep colored radical anion adducts of aromatic hydrocarbons with lithium, in substoichiometric concentrations, may serve as intermediate metallation agents of many types of substrates by lithium metal (see Section VI.C).

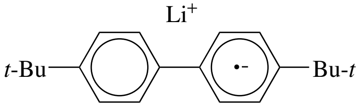

(70)

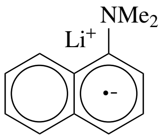

(71)

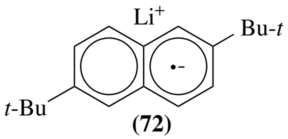

(72)

IV. CHARACTERIZATION METHODS

A. Crystallographic Methods

Application of XRD crystallographic methods for structural analysis of organic compounds is today quite a routine, though non-trivial, undertaking. However, given the high reactivity and thermal instability of many organolithium compounds, special techniques are needed to handle the sample. It might be necessary to perform the mounting of the crystal in a glove box and to flush the diffraction chamber with a dry inert gas. In some cases mounting the crystal in a capillary with some mother liquor avoids decomposition of the sample, while in other cases dipping the crystal in an oil is sufficient. Provision is made in the instruments for maintaining very low temperatures when acquiring the diffractograms of compounds that are thermally unstable at room temperature.

In this section are presented a few instances of the application of XRD crystallography for structural elucidation. Additional examples appear in Section V, dealing with association of organolithium compounds in the solid state, and in Section VI, when dealing with solid products of reactions involving organolithium intermediate stages.

The adduct formed by two lithium atoms with polycondensed aromatic hydrocarbons crystallizes with two solvating molecules of TMEDA. The structure of the crystals derived from naphthalene (**73**)[147] and anthracene (**74**)[148] was elucidated by XRD. This arrangement of the unsolvated lithium atoms, in η^6-coordination fashion on the opposite sides of two contiguous rings, was found by MNDO calculations to be the most favorable one for naphthalene, anthracene and phenanthrene (**75**)[149].

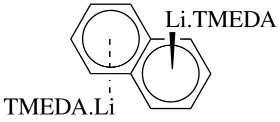

(73)

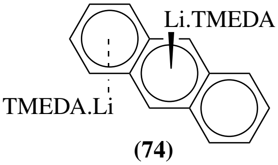

(74)

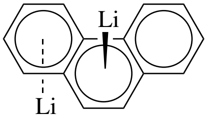

(75)

The dilithium adduct of 4,4′,5,5′-tetramethylbiphosphinine (**76**) was analyzed by XRD, after crystallization in the presence of the cryptand C(2.2.1), showing a solvent-separated ion pair structure. DFT calculations point to a preferred transoid configuration of the organic moiety, as determined crystallographically, and the natural bond order analysis points to a charge distribution in the ring of allylic nature, rather than a classical phosphide structure, in accordance with the puckered configuration of the six-membered rings[150].

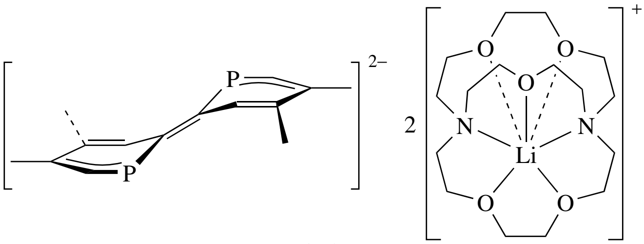

(76)

Porphyrins can be lithiated by replacement of the two N−H protons. Dialkali metal salts have been synthesized and characterized by XRD crystallography. The hole-in-the-middle of the porphyrin nucleus has sufficient room to accommodate a lithium ion, yielding a triple ion structure, as shown, for example, in formula **77**. With the larger sodium and potassium ions the atoms sit out-of-plane on both sides of the porphyrin nucleus, equally coordinated to the four N atoms[151, 152]. Similarly, XRD crystallography shows that lithium phthalocyanines consist of ion pairs variously distributed in space, including a planar anion containing a central lithium atom (**78**) and a cation that may be coordinated with various ligands, e.g. $\mathrm{Li^+\cdot 2PPh_3}$[153], n-$\mathrm{Bu_4N^+}$ and $2n$-$\mathrm{Bu_4N^+\cdot F^-\cdot 0.5H_2O}$[154].

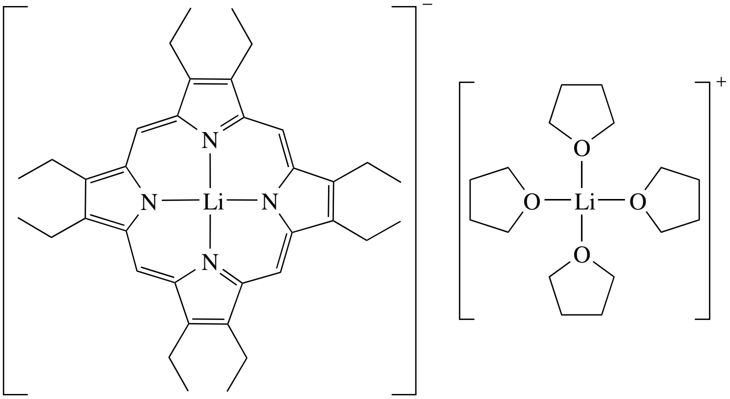

(77)

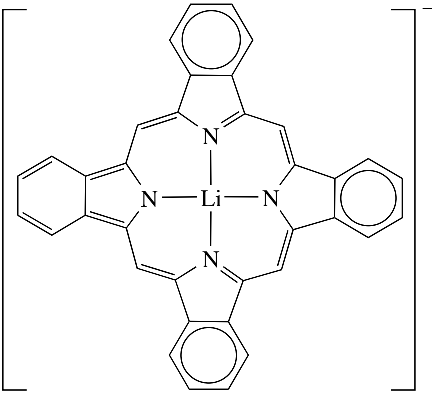

(78)

The structure of the Se insertion product of equation 25 was demonstrated by single-crystal XRD of the solvated complex (**79**·THF·TMEDA). The Li atom has tetrahedral coordination to both N atoms of TMEDA, the O atom of THF and the Se atom[155].

$$\mathrm{PhC{\equiv}CH} \xrightarrow{\mathrm{Li}} \mathrm{PhC{\equiv}CLi} \xrightarrow{\mathrm{Se}} \underset{\textbf{(79)}}{\mathrm{PhC{\equiv}CSeLi}} \qquad (25)$$

The structure of compound **80** was elucidated by XRD crystallography, where the Li atom forms part of a four-membered ring also containing C, Si and N atoms. This compound has been used for the preparation of other organometallics by transmetallation with $HgBr_2$, $AlCl_3$, $GaCl_3$ and $SnCl_4$. Excepting the organomercury compound where no coordination of the amino group with the metallic atom takes place, the four-membered ring containing the metallic heteroatom is preserved[156].

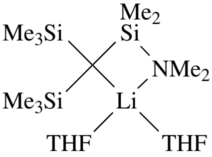

(80)

B. Nuclear Magnetic Resonance Spectroscopy

The few examples presented below in this section and the rest of the chapter point to various properties that can be investigated by NMR spectroscopy. Table 5 presents data on the atomic mass and nuclear spin of elements that are relevant to the MS and NMR spectroscopic techniques applied to organic and some organometallic compounds.

While ^{1}H and ^{13}C NMR spectra are extensively reported for the structural characterization of many organolithium compounds and their derivatives containing no lithium atoms, use of ^{6}Li and ^{7}Li NMR and their two-dimensional and solid-phase variants for direct structural characterization is more limited. Applications of NMR spectroscopy to organolithium compounds have been reviewed[158] and are amply discussed in other chapters of the present volume. An earlier review deals with the application of two-dimensional NMR and the nuclear Overhauser effect (NOE), combining ^{1}H, ^{6}Li, ^{7}Li and ^{13}C NMR, to obtain structural, mechanistic and kinetic information on the dynamic behavior of organolithium compounds in solution[159]. Some recent advances of NMR spectroscopy of organolithium compounds have been reviewed, including the isotopic fingerprint method related to ^{6}Li, one- and two-dimensional pulse experiments for homonuclear and heteronuclear spin systems, and structural aspects related to benzyllithium and formation of polylithium systems[160]. Some relevant properties of the stable isotopes of lithium are summarized in Table 5. In certain cases it is convenient to carry out NMR experiments using samples that were isotopically enriched with ^{6}Li. A review appeared on NMR spectroscopy of ^{6}Li-enriched organolithium compounds[161]. Experiments with ^{6}Li−^{15}N double labeling have been reviewed. These are useful for determination of structural, solvation and association features of lithium dialkylamides and similar species[162].

An extensive review appeared on the configurational stability of enantiomeric organolithium reagents and the transfer of the steric information in their reactions. From the point of view of the present chapter an important factor that can be evaluated is the ease by which an inversion of configuration takes place at the metallation site. It happens that ^{1}H, ^{7}Li, ^{13}C and ^{31}P NMR spectra of diastereotopic species have been central to our understanding of the epimerization mechanism depicted in equation 26, where **C** and *epi*-**C** represent the solvated complex of one chiral species and its epimer, respectively. It has been postulated that inversion of configuration at the Li attachment site takes place when a solvent-separated ion pair is formed. This leads to planarization of the carbanion, its rotation and recombination to form the C−Li bond, as shown in equation 27, where $Li^+ \cdot L_n$ is the solvated lithium cation. An alternative route for epimerization is a series of

TABLE 5. Stable isotopes frequently appearing in organic and organolithium compounds[a]

Isotope	Natural abundance (%)	Atomic mass (Da)[b]	Spin	Nuclear magnetic moment (nm)
^{1}H	99.985(1)	1.007825032	1/2+	+2.79285
^{2}H	0.015(2)	2.01401778	1+	+0.85744
^{6}Li	7.5(2)	6.0151223	1+	+0.82205
^{7}Li	92.5(2)	7.0160041	3/2−	+3.25644
^{10}B	19.2(2)	10.0129371	3+	+1.8006
^{11}B	80.1(2)	11.0093055	3/2−	+2.6886
^{12}C	98.93(8)	12.000000000	0+	0
^{13}C	1.07(8)	13.003354838	1/2+	+0.70241
^{14}N	99.632(7)	14.003074007	1+	+0.40376
^{15}N	0.368(7)	15.00010897	1/2−	−0.28319
^{16}O	99.757(16)	15.994914622	0+	0
^{17}O	0.038(1)	16.9991315	5/2+	−1.8938
^{18}O	0.205(15)	17.999160	0+	0
^{19}F	100	18.9984032	1/2+	+2.62887
^{28}Si	92.22(2)	27.97692653	0+	0
^{29}Si	4.69(1)	28.9769472	1/2+	−0.5553
^{30}Si	3.09(1)	29.97377022	0+	0
^{31}P	100	30.9737615	1/2+	+1.13160
^{32}S	94.93(31)	31.9720707	0+	0
^{33}S	0.76(2)	32.9714585	3/2+	+0.64382
^{34}S	4.29(28)	33.9678668	0+	0
^{36}S	0.02(1)	35.9670809	0+	0
^{35}Cl	75.78(4)	34.96885271	3/2+	+0.82187
^{37}Cl	24.22(4)	36.96590260	3/2+	+0.68412
^{79}Br	50.69(7)	78.918338	3/2−	+2.106400
^{81}Br	49.31(7)	80.916291	3/2−	+2.270562
^{127}I	100	126.904468	5/2+	+2.8133

[a] Effective literature cutoff for data in this table is December 2000[157].

[b] In the chemical scale the atomic mass of ^{12}C is exactly 12.000000000 Da.

jumps of the Li atom to adjacent coordination sites and its return to the opposite side of the original site (the so-called guided tour, equation 28). NMR studies include calculation of energy and entropy barriers for epimerization ($\Delta G^{\ddagger}$, $\Delta H^{\ddagger}$ and $\Delta S^{\ddagger}$) by carrying out kinetic measurements with variable temperature and estimation of structural and solvation effects[163].

$$\mathbf{C} \underset{k'}{\overset{k}{\rightleftharpoons}} epi\text{-}\mathbf{C} \tag{26}$$

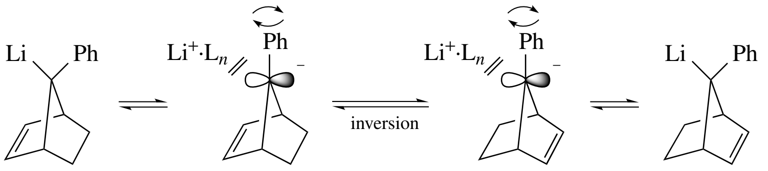

(27)

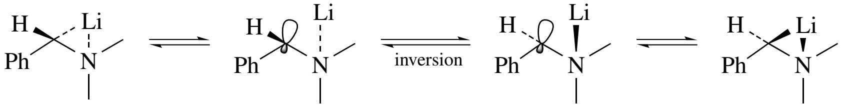

(28)

The dynamic behavior of various solid organolithium complexes with TMEDA was investigated by variable-temperature ^{13}C and ^{15}N CP/MAS and ^{7}Li MAS NMR spectroscopies. Detailed analysis of the spectra of the complexes led to proposals of various dynamic processes, such as inversion of the five-membered TMEDA-Li rings and complete rotation of the TMEDA ligands in their complex with the PhLi dimer (**81**), fast rotation of the ligands in the complex with cyclopentadienyllithium (**82**) and 180° ring flips in the complex with dilithium naphthalene (**83**)[164]. The significance of the structure of lithium naphthalene, dilithium naphthalene and their TMEDA solvation complexes, in the function of naphthalene as catalyst for lithiation reactions, was discussed[165].

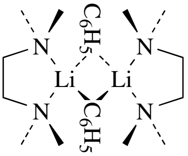

(81)

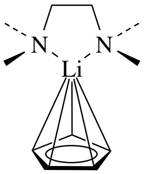

(82)

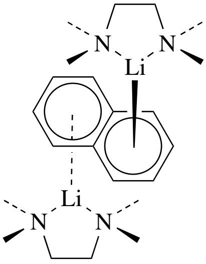

(83)

A ^{13}C NMR study in hydrocarbon solvents points to a large charge delocalization and sp^2 character at the α-carbon of compounds **84** and **85**, containing benzyl moieties, while the allylic compounds **86** and **87** have an intermediate state of hybridization at the α-carbons[166].

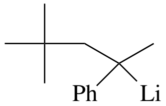

(84)

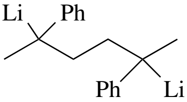

(85)

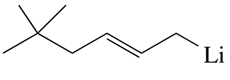

(86)

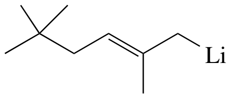

(87)

The structure of the organolithium compound **89** in solution, obtained on metallation of a cyclic aldonitrone (**88**), according to equation 29, seems to have the resonant structure (**89**), as determined by ^{13}C, ^{14}N and ^{7}Li NMR spectroscopy. Based on the spectroscopic evidence and *ab initio* calculations (MP2/6-31 + G*) on a simplified model compound (H atoms replacing the five Me groups) it was concluded that the lithium atom has partial covalent bonds to $C_{(4)}$ and the O atom (cf. **90**)[167].

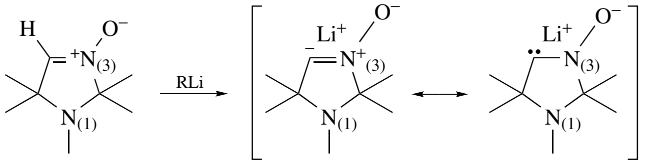

(88) **(89)** (29)

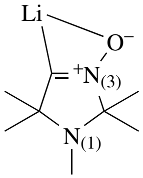

(90)

An extensive study was undertaken of the structural analysis of organolithium compounds based on the coupling constant $J(^6\text{Li}, {}^{13}\text{C})$ observed when running ^{13}C NMR spectra at low temperatures. Besides purely hydrocarbon structures many derivatives bearing halogen atoms geminal to lithium (**91–101**) were investigated, at temperatures usually below −100 °C[168].

$LiCHX_2$ **(91)**

$LiCX_3$ **(92)**

$MeCBr_2Li$ **(93)**

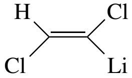

(94)

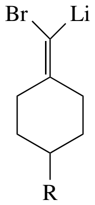

(95) **(a)** R = H
(b) R = *t*-Bu

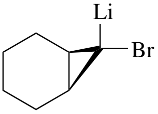

(96)

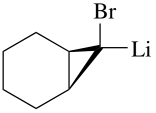

(97)

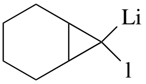

(98)

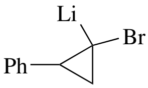

(99) **(a)** *E*
(b) *Z*

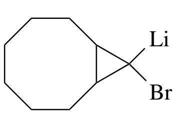

(100)

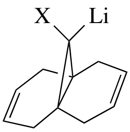

(101)

The ^{1}H and ^{13}C chemical shifts of some unsaturated species, their carbanions and the corresponding lithium complexes were calculated by the IGAIM method[169] and compared with experimental values in THF solution. Examples are the lithium salt of the allyl carbanion (**102**), the dimeric form of the latter (**103**) and the lithium salt of the bicyclo[3.2.1]octa-3,6-dienyl carbanion (**104**)[170].

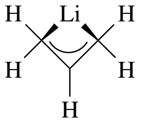

(102)

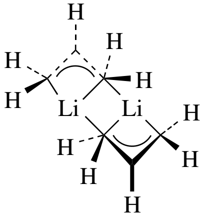

(103)

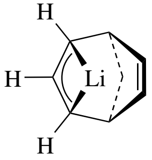

(104)

Optimization of the HMQC technique for the IS$_n$ nuclear spin system was examined, to avoid the appearance of unwanted peaks or reduce their intensity. In such spin systems I represents a metal atom of spin 1/2 or 1 and S$_n$ represents n atoms of spin 1/2 coordinated to I. The optimization method can be applied to the analysis of the ^{6}Li HMQC or HSQC spectra[171].

The quadrupolar coupling constant $\chi(^7\text{Li})$ (QCC) is a useful property for elucidation of the coordination environment of the Li atom in a compound. It can be applied to investigate whether the Li$^+$ cation is directly coordinated to the anionic site or separated from it by solvating molecules, for example, in the three solid complex systems, **105a–d, 106a–c** and **107a–c**. ^{7}Li MAS-NMR spectroscopy of all three systems of crystals complexed with two molecules of 12-crown-4 (**108**) show significantly lower $\chi(^7\text{Li})$ values ($\leqslant$30 kHz) than all the other listed complexes (>100 kHz). This may be interpreted as the complexes **105a**, **106a** and **107a** having the Li$^+$ cation sandwiched between the two crown molecules in a tetragonal-type coordination environment. The rest of the complexes can be considered as contact ion pairs[172] (for example, the structure of the solid **107c** is shown by XRD to

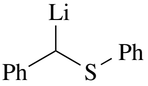

(105)

(a) complex with 2**108**
(b) complex with PMDTA
(c) complex with 3THF
(d) complex with **108**

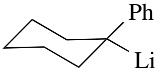

(106)

(a) complex with 2**108**
(b) complex with PMDTA
(c) complex with 3THF

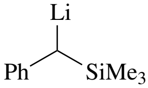

(107)

(a) complex with 2**108**
(b) complex with PMDTA
(c) complex with TMEDA

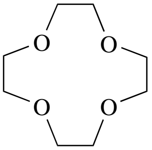

(108)

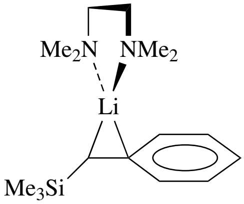

(109)

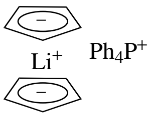

(110)

be as depicted in **109**, with the Li atom in tetrahedral coordination with both N atoms of TMEDA and to the α- and *ipso*-positions of the benzyl group[173]). A low $\chi(^7\text{Li})$ value may point to ion separation as in the cases just discussed or to a highly symmetric coordination environment of the ^{7}Li atom, even if in close contact with the counterions, as in compound **110**[174]. Other applications of $\chi(^7\text{Li})$ to structural elucidation are mentioned in Sections V.A.1–3.

Di-2-pyridylmethane can be metallated by n-BuLi in THF solution to yield compounds of peculiar structure, such as **111a**. In the presence of a ligand stronger than THF, such as 12-crown-4 (**108**), **111b** disproportionates into a lithium lithiate, with a solvent-separated ion pair structure, where the lithium cation is sandwiched between two crown molecules (**112**). The crystalline materials were characterized by XRD analysis and by ^{6}Li and ^{7}Li CPMAS/NMR spectroscopy. During the NMR analysis of compound **112** (two ^{6}Li peaks) a certain amount of a second compound appears, presumably **111** (one ^{6}Li peak), a reversed disproportionation taking place as a result of the mechanical stress exerted on **108** by the sample tube rotating at 12 kHz. The structure of the anion of **112** is very favored, allowing the synthesis of an analogous sodium lithiate crystal by carrying out the metallation reaction in the presence of a superbase containing n-BuONa[175]. The structure of compounds **111a** and **112** may be characterized by XRD crystallographic analysis[176].

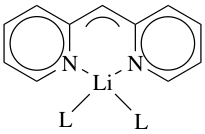

(111) **(a)** L = THF
(b) LL = 12-crown-4

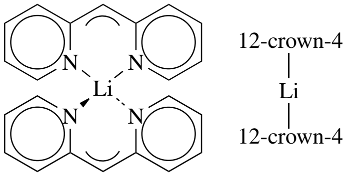

(112)

^{7}Li NOESY spectra can be used to characterize dilithium porphyrin salts such as **77** in solution. In DMSO at room temperature two bands of equal intensity are observed (-1.12 ppm/$\nu_{1/2} = 4$ Hz; -11.55 ppm/$\nu_{1/2} = 52$ Hz). These bands broaden and finally coalesce to a single peak (-6 ppm) on warming to 100 °C. The lower field signal is ascribed to a lithium ion symmetrically surrounded by solvent molecules, whereas the broader high field corresponds to a lithium ion strongly shielded by a π-electron system. At higher temperatures a fast interchange between these two sites takes place. Similar behavior is observed in acetone solution, however, over a lower temperature range. In solvents of lower polarity only one temperature-independent $^7\text{Li}\{^1\text{H}\}$ signal is detected (-12.8 ppm/THF, -16.5 ppm/TMEDA and C_6H_6), which may be interpreted as the lithium atoms being symmetrically bound to the porphyrin nucleus as depicted in **113** or **114**[152].

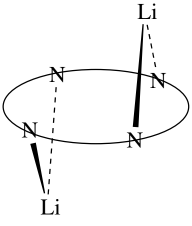

(113)

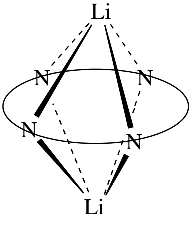

(114)

^{1}H and ^{13}C NMR spectra were applied to elucidate the electronic structure of the dianions in the dilithium arene compounds formed with anthracene, phenanthrene and 1,2,3,4-dibenzocyclooctatetraene (**115**). Although the three dianions have 16-π isoelectronic systems, the former two differ due to their charge distribution, and **115** due to the steric strain in the cyclooctane ring, interfering with a coplanar configuration[177, 178].

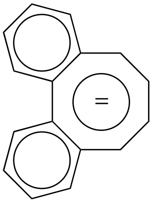

(115)

Diindeno[1,2,3,4-*defg*;1′,2′,3′,4′-*mnop*]chrysene (**116a**) can be considered as a symmetrical cap that was cut out of the fullerene C_{60} molecule. This compound and its alkylated derivative (**116b**) react with Li to yield dianions and tetraanions in solution. The standard two-dimensional NMR techniques are insufficient for the structural assignment of the spectra. A special carbon edited NOESY approach was developed for total assignment of the spectra of the neutral species and the dianion. DFT calculations aided in the assignment of the tetraanion spectra[179, 180].

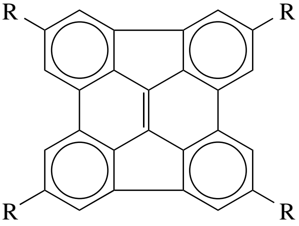

(116) **(a)** R = H
(b) R = *t*-Bu

The structure of dilithium dibenzo[*a,c*]naphthacene and its Na and K analogs (**117a–c**) was studied by ^{1}H and ^{13}C NMR spectroscopy, including long-range COSY techniques. The protons may be separated into a low-field group belonging to the phenanthrene section and a high-field group of the anthracene section. It was proposed that the negative charge is concentrated mostly on the anthracene side, while the phenanthrene side remains almost neutral[181].

The $^{3}J(^{13}C, ^{1}H)$ coupling constant value of the CH=N group of aldonitrones is taken as indicative for the feasibility of the alkoxide-catalyzed isotope exchange of the methine hydrogen by MeOD or the metallation of the methine C by *s*-BuLi. The value of this coupling constant is larger for the *E*-configuration, prevalent in cyclic aldonitrones, than for the *Z*-configuration of the open-chain aldonitrones. Stabilization of the intermediate carbanion by coordination of H or Li to the oxygen atom seems to be a condition for either reaction to take place. Thus, for example, compound **118** does not undergo D-exchange nor Li metallation, whereas for its cyclic analog (**119**) the isotopic exchange is finished after 40 hours at room temperature. The progress of this reaction can be followed by

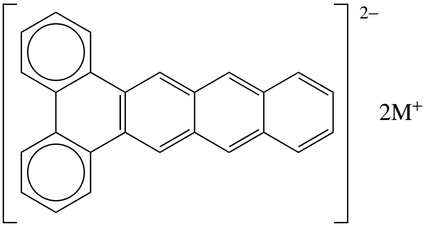

(117) **(a)** M = Li
(b) M = Na
(c) M = K

measuring the disappearance of the methine proton by ^{1}H NMR. Metallation to **120** is carried out at low temperatures ($-70\,^\circ$C) and its progress is followed by quenching with benzaldehyde to give **121**, separating the mixture by preparative TLC, and measuring the products by ^{1}H NMR[182].

^3J(C, H) = 1.5

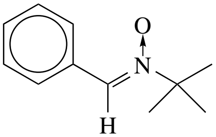

(118)

^3J(C, H) = 4.5

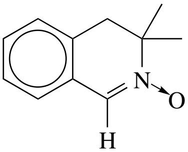

(119)

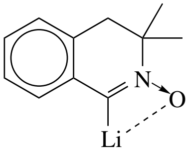

(120)

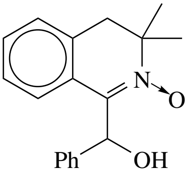

(121)

C. Miscellaneous Methods

1. Ultraviolet-visible spectroscopy

The interaction of solvents with compounds where the lithium atom is attached to an organic chromophore has been investigated by UVV spectroscopy, for compounds with organic chromophores. Two states in equilibrium can be distinguished for fluorenyl (Fl) carbanion-alkali metal cation compounds (**122**) in solution, namely a contact ion pair $\mathrm{Fl^-Li^+}$ and a solvent-separated ion pair $\mathrm{Fl^-||Li^+}$ (equation 30). The equilibrium displacement depends on the cation, solvent and temperature. A bathochromic shift is observed when in the contact-type compounds the ionic radius of the cation increases along the series from **122a** to **122d**. For the solvent-separated ion pair the absorption maximum is at $\lambda_{\max} = 373$ nm, allowing quantation of both types of species (e.g. the contact ion pairs in THF have $\lambda_{\max} = 349$, 356, 362 and 364 nm for M = Li, Na, K and Cs, respectively). Solvent separation is much influenced by the solvent polarity; for example, the lithium analog (**122a**) at room temperature appears as a contact ion pair in toluene and dioxan, whereas in THF 80% undergoes ion separation and in DME, DMSO and pyridine total ion separation takes place. For a given solvent and temperature, ion separation depends on the solvating capability of the cation; thus, for DME at 25 °C the fraction of ion separation is 100% for Li^+, 95% for Na^+, *ca* 10% for K^+ and nil for Cs^+. The tendency is for solvent separation to increase as the temperature is lowered, for example, in the case of fluorenylsodium (**122b**) the equilibrium constant K grows from 0.064 at 24.2 °C to 6.15 at −63.0 °C[183].

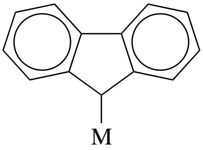

(122) **(a)** M = Li
(b) M = Na
(c) M = K
(d) M = Cs

$$\mathrm{Fl^-M^+} \xrightleftharpoons[\text{solvent}]{K} \mathrm{Fl^-\|M^+} \qquad K = [\mathrm{Fl^-\|M^+}]/[\mathrm{Fl^-M^+}] \tag{30}$$

Lithium reduces naphthalene in THF solution. The color of the solution turns first green, corresponding to a singly charged naphthalene radical anion, and finally deep purple, corresponding to a doubly charged anion (broad maximum at 550 nm). On adding a slight excess of biphenyl the solution spectrum turns into a superimposition of the spectra of singly charged naphthalene and biphenyl radical anions. Similar behavior is noted for phenanthrene, the doubly charged ion of which has a sharp absorption peak at 415 nm and a broad maximum at 580 nm; this dianion turns to a mixture of singly charged radical anions on addition of a slight excess of biphenyl[184]. The color is reversible on adding a slight excess of naphthalene. The UVV spectrum of solutions of alkali metal-arene adducts ($\mathrm{M^+A^{\bullet-}}$, $\mathrm{M^+{}_2A^{2-}}$) was measured for A = anthracene, tetracene, pentacene, biphenyl, *p*-terphenyl and *p*-quaterphenyl. A slight difference is observed between the spectra of the ion pair $\mathrm{Na^+A^{\bullet-}}$ and that of the corresponding free polycondensed arenide anion $\mathrm{A^{\bullet-}}$; for the polyphenylene chain type arenes, close but distinctive spectra are shown by $\mathrm{Na^+A^{\bullet-}}$ and $\mathrm{A^{\bullet-}}$, with the latter shifted to longer wavelengths. More tangible differences are noted for the double adducts. The $\mathrm{M^+{}_2A^{2-}}$ adducts with A = anthracene are practically undissociated ion pairs over the temperature range from −75 to 25 °C, showing two absorption bands with $\lambda_{\max}$ slightly displaced from each other in the order $\mathrm{Li} < \mathrm{Na} < \mathrm{K}$. For A = tetracene and pentacene distinctive spectra are obtained for the associated species $\mathrm{Li^+{}_2A^{2-}}$ and the dissociated anion $\mathrm{A^{2-}}$, the latter being slightly displaced to longer wavelengths[185]. The effect on the UVV spectrum observed for various solvents may be attributed to their capacity of turning the $\mathrm{M^+A^{\bullet-}}$ and $\mathrm{M^+{}_2A^{2-}}$ solutes from contact ion pairs or triple ions to solvent-separated ions[183].

The changes in structure attending the formation of alkaline metal salts of porphyrins can be followed by UVV spectroscopy. For example, on preparing the dilithium salt of octaethylporphyrin (**77**), the Soret band of the free base (398 nm) is shifted to 416 nm. Going to a higher symmetry in the salt, the four Q-bands (496, 528, 568, 622 nm) are replaced by two bands at 522 and 588 nm. Similar changes are observed for the disodium and the dipotassium analogs. Hydrolysis of the salts to the original free base can be followed spectrophotometrically[152].

2. Infrared spectroscopy

Ironpentacarbonyl reacts with organolithium compounds yielding lithium acylferrates, as shown in equation 31. The lithium atom is probably bound to the carbonyl moiety of the acyl group, as indicated by the significant shifts observed in the IR absorption peaks of the C=O group of compounds **123a** and **123b** as compared with compounds **124a** and **124b**, obtained after quenching with Me_4NBr[186].

$$\mathrm{Fe(CO)_5} \xrightarrow{\text{1. RLi/Et}_2\text{O}} \mathrm{RC(OLi)Fe(CO)_4} \xrightarrow{\text{2. Me}_4\text{NBr}} \mathrm{RCOFe(CO)_4NMe_4} \qquad (31)$$

(123) **(a)** R = Me **(124)** **(a)** R = Me
(b) R = Ph **(b)** R = Ph

A series of investigations was performed on the structure of the complexes formed by unsaturated hydrocarbons with lithium dissolved in a solid argon matrix. The structures proposed for these complexes are based on assignment of the perturbations observed in the IR spectra of the free hydrocarbons and their isotopically enriched species.

With acetylene at 15 K four different complexes can be detected, depending on the concentration of lithium and acetylene; on raising the temperature to 30 K these complexes disappear, possibly yielding associated and dismutated species. ^6Li, ^7Li, C_2H_2, C_2HD, C_2D_2 and $^{13}C_2H_2$ were used in this study. The main products are $Li{\cdot}C_2H_2$ and $Li{\cdot}2C_2H_2$. The planar structure **125** is proposed as the most probable one for the 1:1 complex, with the CC bond weakened and elongated towards ethylene values and a CCH angle of $140 \pm 10°$. The 1:2 complex is assigned a probable H-bonded structure as in **126**, with the second acetylene molecule acting as H-donor. Two minor complex products have a 2:1 stoichiometry ($2Li{\cdot}C_2H_2$). One of them is assigned structure **127**, with the C=C distance and the CCH angle approaching the values of ethylene. The second 2:1 complex is distinguished by its stability to UV-radiation[187]. The instability of the 2:1 complexes is possibly related to the findings of *ab initio* molecular dynamics calculations, that the most stable configuration of singlet $2Li{\cdot}\ C_2H_2$ is $LiH{\cdot}HC_2Li$, namely lithium acetylide in association with lithium hydride[188].

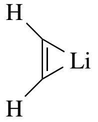

(125)

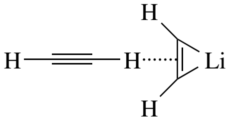

(126)

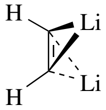

(127)

Lithium atoms form two types of complexes with benzene molecules dissolved in solid argon, namely $Li{\cdot}C_6H_6$ and $Li{\cdot}2C_6H_6$. Assignment of the perturbations observed in the IR spectrum of free benzene and its deuteriated analog in the presence of Li atoms leads to the conclusion that the lithium atom sits on the C_{6v} axis of the benzene ring of the 1:1 complex and on the common axis for the two rings of the 1:2 complex. No analogous complexes are observed for Na[189]. The adducts formed by Li and phenylacetylene or styrene vapors, trapped in a matrix of solid argon, were analyzed by IR spectrophotometry, observing the perturbations on the IR spectra of the free hydrocarbons and their deuteriated analogs caused by the presence of Li in the system. It may be concluded that there are complexes where the lithium atom is coordinated to the π-system of the side chain and others where coordination takes place with the π-system of the phenyl group, the latter being the most stable. The former type can be transformed to the latter by photochemical activation. A third type of complex is observed, where the Li atom is sandwiched between two phenylacetylene molecules, coordinated to the phenyl groups[190].

Various adducts may be identified by IR spectroscopy of Li and ethylene in a frozen argon matrix, using ^{6}Li, ^{7}Li, C_2H_4, $^{13}C_2H_4$, CH_2CD_2 and C_2D_4. Bonding of Li to the π-electrons of ethylene causes the HCH planes to form dihedral angles with the CC bond (**128**). This puckering effect is the strongest for the Li$\cdot nC_2H_4$ complex when $n = 1$ and is weakened along the series $n = 2$, 3. Two structures (**129** and **130**) are concomitant with the experimental result for the Li$\cdot 2C_2H_4$ complex, with D_{2h} and D_{2d} symmetry, respectively. For the Li$\cdot 3C_2H_4$ complex two structures (**131** and **132**) with D_{3h} symmetry may be proposed. As for the 2Li$\cdot C_2H_4$ complex, structure **133** with C_{2v} symmetry is found to best fit the spectra[191].

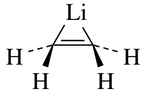

(128)

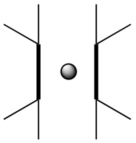

(129)

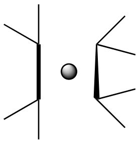

(130)

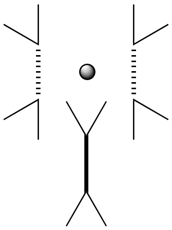

(131)

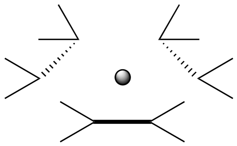

(132)

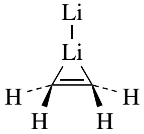

(133)

3. Electron spin resonance

Naphthalene is reduced by alkali metals in solvents such as THF or liquid ammonia, yielding mono- and dinegative anions. The singly charged anion is paramagnetic, with the extra electron residing in a π-LUMO of naphthalene. The doubly charged one is diamagnetic[192–194]. Lithium naphthalene (Li$\cdot C_{10}H_8$) has ion pair structure and the anion is also a free radical. This was demonstrated by ESR spectroscopy. At 20 °C the anion spectrum presents two splitting sets, related to two groups of four equivalent H atoms ($a_\alpha^H = 4.83$ gauss and $a_\beta^H = 1.82$ gauss). Superimposed on this is a quartet hyperfine splitting due to contact ion pair formation with $^7Li^+$ (spin 3/2, $a = 0.39 \pm 0.02$ gauss). However, the magnitude of the latter value is strongly dependent on temperature and solvent, due to the solvation capacity of the cation, interfering with contact ion pair formation. Investigation of lithium naphthalene should be carried out on fresh solutions because the solute gradually decomposes by reaction with the solvent[194–196]. The adducts of alkali metals with anthracene and azulene (**134**) show in their ESR spectra hyperfine splitting constants with the various H atoms that point to perturbations dependent on the metal, solvent and temperature. This variability can be attributed in part to ion pair formation[197].

The structures of the radical anion of dibenzo[*a,c*]naphthacene (**135**) and the corresponding radical cation were investigated by ESR and proton-ENDOR spectroscopies[181].

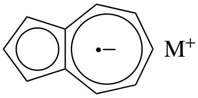

(134) **(a)** M = Li
(b) M = Na
(c) M = K

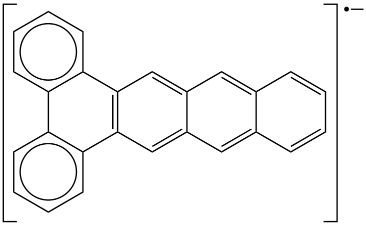

(135)

4. Mass spectrometry

A low pressure, a gaseous stream of benzene or variously substituted chlorobenzenes was exposed to lithium vapor and the resulting products were condensed on a cold finger filled with liquid N_2. The accumulated condensate of each run was quenched with deuterium oxide and the organic mixture was analyzed by GC, and the analysis was confirmed by high resolution MS. The identified deuteriated species may be assumed to be derived from the corresponding organolithium compounds. For example, 65% of benzene reacts yielding the following major products: C_2Li_2, C_2Li_4, C_2Li_6, C_3Li_4, C_3Li_6, C_3Li_8 and less than 1% of PhLi, as the main representative of a series of minor metallated benzenes[198].

5. Electrochemical methods

Cyclic voltammetry and second-harmonic AC voltammetry can be applied to determine the electrochemical oxidation potentials of $PhCH_2Li$, allyllithium and t-BuC≡CCH_2Li in THF-HMPA solution, and the values used to make an estimate of the pK_a of the corresponding hydrocarbons. Electrochemical measurements for Ph_2CHLi and cyclopentadienyllithium allow making estimates of the bond dissociation energy of Ph_2CH_2 and the pK_a of cyclopentadiene, respectively, whereas the electrochemical behavior of MeLi, n-BuLi, PhLi and vinyllithium does not allow making useful estimates other than the lower limits to the pK_a of the corresponding hydrocarbons[199].

The electrical conductivity of the fluorenylmetal compounds **122a, 122b** and **122d** in THF solution may be measured at temperatures in the −70 to 25 °C range in order to investigate the thermodynamics of their dissociation[200]. The electrical conductivity of the dilithium salt of octaethylporphyrin (**77**) varies according to the solvent; thus, in acetone and acetonitrile conductivities indicate the presence of a 1:1 electrolyte, while in THF the solution is practically nonconducting, pointing to a strongly bound ion-pair structure. This is in accordance with ^{7}Li NMR evidence, interpreted as the ion pair being solvent separated in polar solvents such as acetone or DMSO and of the contact type for less polar solvents like THF and TMEDA[152].

The molar conductance of MTHF solutions of alkali metal-arene adducts ($M^+A^{\bullet-}$, $M^+{}_2A^{2-}$) was measured for A = anthracene, tetracene, pentacene, biphenyl, p-terphenyl and *p,p*-quaterphenyl. In the case of adducts $M^+A^{\bullet-}$, at a given temperature from −75 to 25 °C, the conductivity slightly increases with the size of the organic molecule, for both the polycondensed and the chain arene series. The effect of temperature is different for each of the metals: Conductivity is relatively the lowest for M = K, showing a slight decrease with temperature over the range, for M = Na conductivity passes through a maximum at mid-range becoming the highest of all there and for M = Li the conductivity shows an almost linear increase from the lowest value at −75 °C to the highest value at room temperature. The conductivity of adducts ${M^+}_2A^{2-}$ (A = polycondensed hydrocarbon) is significantly lower than for adducts $M^+A^{\bullet-}$, with that of ${Li^+}_2A^{2-}$ being slightly higher than the other two and all show nil to weak variation with temperature. The conductivity behavior may be interpreted in terms of the presence in solution of nonconducting ion pairs and free metal cations and arenide anions[185]. The adducts of alkali metals with A = anthracene in THF solution precipitate at −70 °C, with composition $Li_2A \cdot 4THF$, $Na_2A \cdot 3THF$ and $K_2A \cdot 2.6THF$. On thermal treatment in vacuum of these compounds the solvating THF evaporates, leaving Li_2A, Na_2A and K_2A, respectively. The specific conductivity of these solids is pressure dependent and larger for Na_2A than for Li_2A[201].

6. Calorimetry

The relative basicity of eighteen organolithium compounds was studied by calorimetric measurements of the compounds dissolved in hexane–Et_2O (9:1 by volume) interacting with isopropyl alcohol. The order of exothermicity is shown in equation 32[202].

$$R{-}Li > R_2N{-}Li > RNH{-}Li > RO{-}Li \tag{32}$$

V. ASSOCIATION

A. Monomers, Dimers, . . . , Polymers

1. General

Various methods have been applied, singly or in combination, to determine the degree of association of organolithium compounds in solution, including kinetic measurements, differential vapor-pressure, cryoscopy, ebulliometry and osmometry. Among the NMR methods direct observation of the spectra and determination of certain functions such as quadrupolar coupling and splitting constants (QCC, QSC) have been applied, both for evaluation of association equilibria in solution and for structural characterization of the associated species. An empirical correlation ($J = 17$ Hz/n) was proposed for estimation of the association number n of ^{6}Li-enriched compounds in solution, based on measurement of the coupling constant $^1J(^{13}C{-}^6Li)$[203]. For the solid state, XRD structural analysis is a direct solution of the problem; however, MAS NMR solid-state techniques may be useful in cases where no suitable crystals are available for XRD.

The importance of solvation in establishing the degree of aggregation of organolithium species cannot be overemphasized. Determination of the state of aggregation of organolithium compounds in solution is usually a difficult task, complicated by a plethora of possible structures in dynamic equilibrium. In such cases theoretical calculations may be helpful to focus attention on certain species that one may try to sort out from a complex scene of experimental evidence. MNDO calculations were carried out to determine the enthalpy of formation of monomeric (**136**), cyclic dimeric (**137**), open-chain dimeric (**138**) and triple ion species (**139**), derived from lithium *N,N*-dialkylamides solvated to various degrees with water, dimethyl ether, THF, phosphortriamide and HMPA. Except for one minor irregularity, predicting an energetically favorable open-chain dimer doubly solvated with HMPA (**138b**·2HMPA) as compared to the cyclic analog (**137b**·2HMPA), calculations are in accord with experimental observations derived from ^{6}Li, ^{15}N and ^{31}P NMR spectra of **136a–c** in solutions containing THF and HMPA[204].

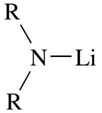

(136) **(a)** R = Me

(b) R = *i*-Pr

(c) RR = 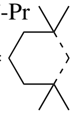

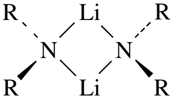

(137)

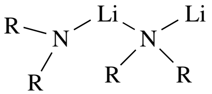

(138)

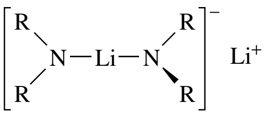

(139)

The association number of Li amides, such as $LiN(SiMe_3)_2$, organolithium compounds bound at the α-position to S or Se atoms, such as $LiCH_2SePh$, and various transition metal complexes was determined at 0 °C in THF or at −35 °C in Et_2O, by differential vapor-pressure osmometry. The method allows handling compounds sensitive to autooxidation, moisture and temperature[205].

Fractional kinetic orders of homogenous reactions in solution may point to association of a particular reagent. The kinetics of the initiation step of styrene polymerization in the presence of *n*-BuLi (equation 33) is in accordance with the assumption that this organolithium compound in a nonbonding solvent forms aggregates of six molecules on the average[42].

$$\frac{d[\mathrm{BuLi}]}{dt} = -k_1[n\text{-BuLi}]^{1/6}[\mathrm{PhCH=CH_2}] \tag{33}$$

2. Compounds with C–Li bonds

Cryoscopy and ^{13}C NMR spectroscopy may be applied to determine the state of association of organolithium compounds in solution. *t*-BuLi is dimeric in Et_2O and monomeric in THF solutions. Other organolithium compounds that remain monomeric in THF solvent are *s*-butyllithium, phenyllithium, mesityllithium (**140a**) and supermesityllithium (**140b**). Isobutyllithium in THF at −108 °C is in equilibrium, with the monomeric and dimeric species present in 88:12 molar ratio; for dilute PhLi in THF at −103 °C the ratio becomes 35:65. Addition of PMDTA to the solution turns all dimeric species into monomers. The C–Li bond has a strongly ionic character and the magnitude of the C–Li coupling constants depends mainly on the state of association of the organolithium compound[206]. On the basis of cryoscopic determinations, *t*-BuLi was assumed to form a yellow-orange complex with naphthalene of formula 2*t*-BuLi·$2C_{10}H_8$ (MW 360 ± 14) in hydrocarbon solution[207]; however, the same results were interpreted more recently as corresponding to the complex 4*t*-BuLi·$C_{10}H_8$ (MW 384)[141]. From differential vapor-pressure and kinetic measurements it may be concluded that MeLi and *n*-BuLi are tetrameric in Et_2O or THF at 25 °C, allyllithium is monomeric, vinyllithium trimeric or tetrameric and PhLi dimeric[208].

A study was carried out applying ^{6}Li and ^{13}C NMR spectroscopies, on the behavior of ^{6}Li-enriched BuLi and PhLi (RLi) in toluene solution, in the presence of chelating diamines **141–143** and (−)sparteine (**24**), denoted by L. Dimeric complexes 2RLi·2L

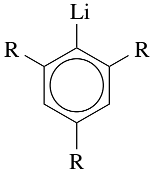

(140) **(a)** R = Me
(b) R = *t*-Bu

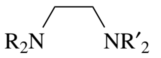

(141) **(a)** R = R′ = Me (TMEDA)
(b) R = R′ = Et
(c) $R^2 = R'_2 = (CH_2)_5$

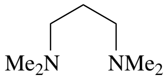

(142)

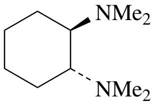

(143)

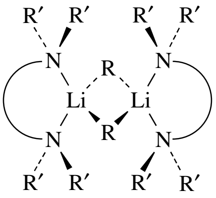

(144)

(**144**) are formed in each case. In the presence of a mixture of two diamines (L and L′) the homosolvated (2RLi·2L and 2RLi·2L′) and the heterosolvated species (2RLi·L·L′) are formed, and the relative free energy of solvation can be estimated for the competing diamines. For certain pairs the heterosolvated species is highly stable, pointing to correlated solvation. The rates of reaction of RLi in the presence of TMEDA can be determined by IR spectrophotometry for the 1,2-addition to imine **145** (equation 34) and for α-metallation of imine **147** (equation 35), following the disappearance of the substrates. The mechanism proposed for both reactions involves a monomeric solvated molecule of RLi, as depicted by intermediates **146** and **148**, respectively[209]. XRD crystallographic analysis shows that the Li atoms in the solid dimeric complex 2PhLi·2TMEDA have contacts with the *ipso* positions of the other phenyl groups[210]. BuLi in THF solution consists of solvated dimer and tetramer species in equilibrium. On raising the temperature, equilibrium is displaced towards the tetramer. The presence of Li alkoxide in solution leads to formation of mixed alkyllithium–lithium alkoxide species containing up to three alkoxide ligands. This study was carried out by ^{1}H and ^{7}Li NMR spectroscopies[211].

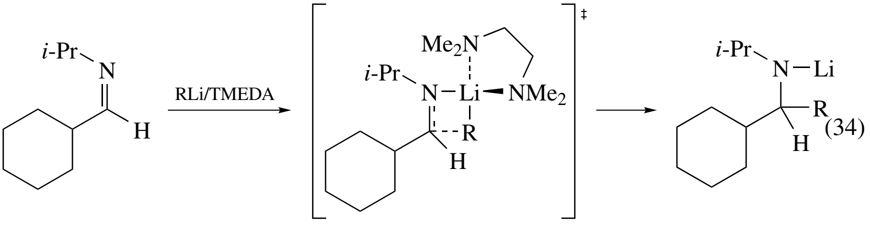

(34)

(145) **(146)**

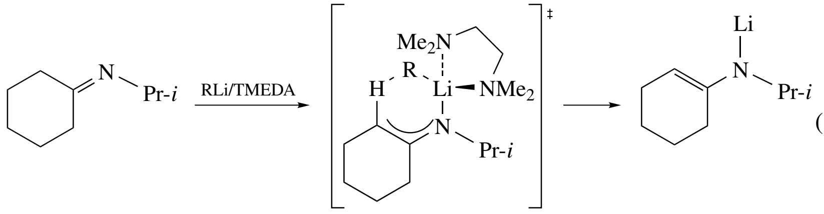

(35)

(147) **(148)**

A ^{6}Li, ^{13}C and ^{15}N NMR study reveals that at low temperatures 2-lithio-*N*-methylpyrrolidine is dimeric, for example, having the homochiral *(S,S)* configuration **149**, whereas 2-lithio-*N*-methylpiperidine and its 4-*t*-butyl derivative are monomeric, for example, having the *(R)* configuration (**150a,b**). It can also be observed that these anomers are chirally stable at low temperatures. Reacting these compounds with electrophiles such as aldehydes or ketones leads to conservation of configuration at the Li-bearing carbon. Furthermore, reacting with electrophiles such as alkyl halides usually leads to inversion of configuration. However, in compound **150b**, where the bulky *t*-Bu group maintains the Li atom fixed in a pseudoequatorial conformation, no inversion of configuration can take place[212].

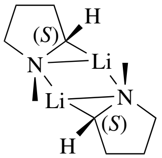

(149)

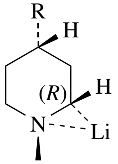

(150) (**a**) R = H
(**b**) R = *t*-Bu

Methyl α-lithioisobutyrate (**151**) in THF solution, in the concentration range between 0.05 and 2.0 M, below *ca* −70 °C, appears as a mixture of the dimer and the tetramer, as shown by two distinct chemical shifts in the ^{7}Li NMR spectrum[213]. A study involving ^{7}Li and ^{13}C NMR spectra, conducted at low temperatures on THF solutions of **151** in the presence of LiCl, points to formation of mixed dimeric **151**·LiCl and mixed trimeric **151**·2LiCl complexes over a large temperature range. The possible mixed tetrameric complex **151**·3LiCl, observed below −55 °C, dissociates into **151**·2LiCl and free LiCl at higher temperatures. The behavior of **151** is taken as a model for the effect of the presence of LiCl on the dispersity of poly(methyl methacrylate), as the salt may affect the modes of aggregation of the living polymer (**152a**)[214]. An investigation was carried out using ^{1}H, ^{6}Li, ^{7}Li and ^{13}C NMR spectra, in both homonuclear (COESY, NOESY, ROESY) and heteronuclear (HET-COR, COLOC, HOESY) variants. These were applied to determine the degree of self-association of lithium 2-(2-methoxyethoxy)ethoxide (**153**) in solution, and the formation of mixed aggregates of this alkoxide with di-*t*-butyl 2-lithio-2,4,4-trimethylglutarate (**154**). Such complexation behavior may be used as a model to aid understanding how the association of living polymer **152b** with **153** may affect the polymerization process[215]. The effect of the presence of LiCl on such polymerization was also investigated by the same methods[216]. It should be pointed out that MNDO calculations were carried out to discern energetically favored associated species that could not be differentiated by spectral methods alone[215,216].

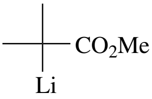

(151)

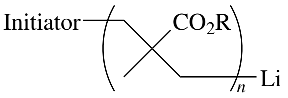

(152) **(a)** R = Me
(b) R = *t*-Bu

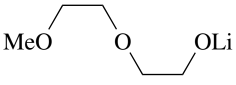

(153)

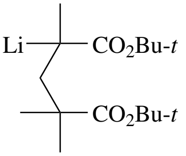

(154)

Complexes $(Me_3Si)_2CHLi{\cdot}TMEDA$ and $(Me_3Si)_2CHLi{\cdot}PMDTA$ are shown to be monomeric by ebullioscopy, and the latter also by XRD crystallography. The short C−Li distance (213 pm) points to the covalent nature of this bond[217].

The degree of association of organolithium compounds depends strongly on the solvent. Some of these compounds are very soluble in liquid ammonia and resist ammonolysis. The degree of association (n) in such solutions can be investigated by cryoscopy. The value of n measured at a certain molal concentration (m) is given for the following compounds as (n/m): 2-Phenylethynyllithium (**155**, $1.56 \pm 0.14/0.1500$) at the given concentration is present about 56% as a dimer and about 44% as a monomer; this compound is mainly a dimer in THF solution, whereas in the solid state it is either a dimer or a polymer of tetrameric units. Lithium cyclopentadienide (**1a**, $1.40 \pm 0.13/0.1533$) is mostly monomeric in liquid ammonia, with some extent of dimerization; NMR studies of CpLi in polar solvents point to a contact ion pair structure and XRD of some derivatives point to a preferred η^5-coordination (**156**). Various possible structures can be suggested for the dimeric species: a solvated complex with mixed η^2-η^3-coordination (**157**), or, keeping in mind the preferred η^5-coordination, formation of unsolvated (**158**) or solvated (**159**) lithiocene anions, in combination with a Li^+ cation solvated with ammonia. The structure of a possible trimer has been suggested as the combination of one of these anions with the complex cation **160**[218].

$PhC{\equiv}CLi$

(155)

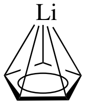

(156)

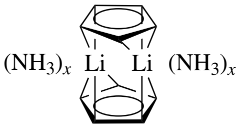

(157)

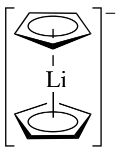

(158)

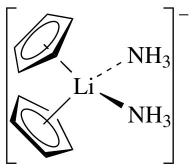

(159)

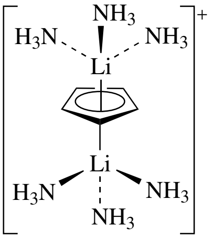

(160)

The ^{7}Li quadrupolar coupling constant (QCC), $\chi(^7\text{Li}) = e^2Qq/h$, where Q is the quadrupole moment, q the field gradient at the nucleus, e the elementary charge and h the Planck constant, can be determined from ^{7}Li solid-state NMR spectra, and bears useful correlations to structural features of the compound, such as the association state of the molecules and the coordination of Li to neighboring atoms. A correlation exists between the C−Li−C angle as determined by XRD crystallography and the ^{7}Li QCC value, as shown for compounds **161–166**. Such behavior of the ^{7}Li QCC may be useful for discerning structural details in cases where no suitable crystals are available for XRD analysis[219]. *Ab initio* (HF/6-31-G*) and DFT (B3LYP/6-31 + G*) calculations were carried out for theoretical justification of the formation of monomeric, dimeric and tetrameric complexes of aryllithiums, and the participation of TMEDA in these processes[220].

106°/156 kHz

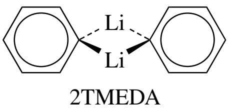

(161)

114°/264 kHz

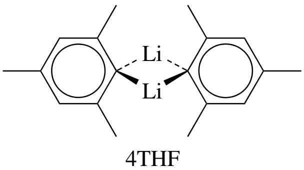

(162)

118°/252 kHz

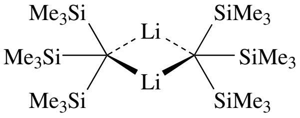

(163)

143°/334 kHz

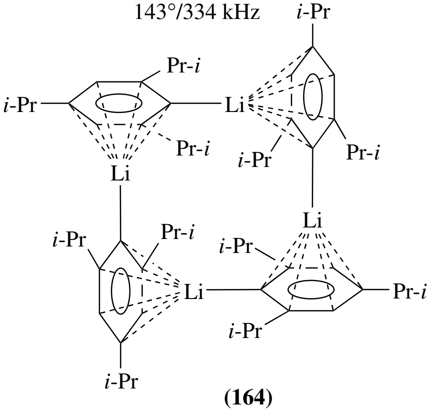

(164)

174°/460 kHz

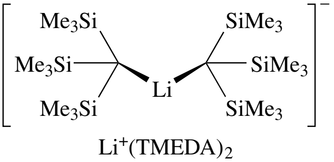

(165)

180°/478 kHz

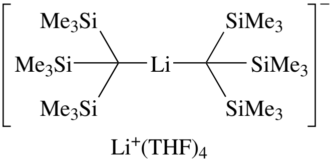

(166)

Similarly to compound **164**, sterically crowded aryllithium compounds such as **167** crystallize with the lithium atoms η^6-coordinated to aromatic rings. Compound **167b** crystallizes as a dimer, with the lithium atoms coordinated to one of the phenyl substituents of the paired molecule (**168**). A further example of this type of coordination is compound **169**, that crystallizes with a benzene molecule. The structure of these crystals was determined by XRD. No evidence for the presence of η^6-coordination is found for compounds **167** in solution from ^{1}H and ^{13}C NMR spectra, probably due to solvation of Li by etheric solvents being stronger than its coordination to π-systems[221]. Crystallographic analysis of complex **170** shows that it is monomeric. Coordination of the lithium atom of **170** is rather meager, as it shows close contacts only with the central C atom, the O atom of THF and a rather weak contact with the *ipso* position of one of the phenyl groups[222].

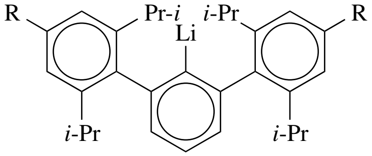

(167) **(a)** R = H
(b) R = *i*-Pr

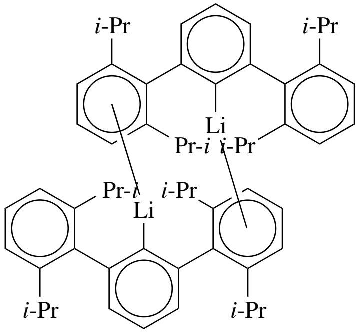

(168)

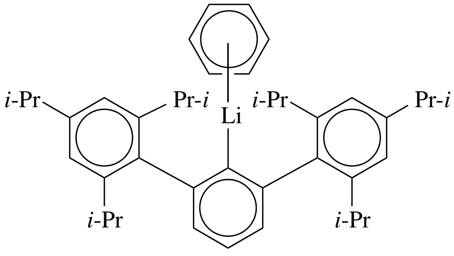

(169)

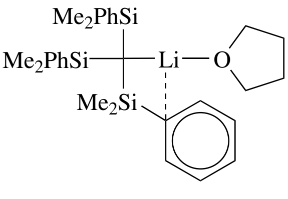

(170)

A function closely related to QCC is the ^{7}Li quadrupolar splitting constant (QSC), defined as QSC $= (1 + \eta^2/3)^{1/2}\chi(^7\text{Li})$, where η is the asymmetry parameter. The ^{7}Li QSC values can be estimated from the ^{7}Li and ^{13}C(*para*) spin–lattice relaxation times. The QSC values are correlated with the effects of structure, solvent and temperature on association in solution for aryllithium compounds (**155, 171, 172**). Conclusions can be drawn about the structure of the associated species in cases where no supporting XRD evidence is available[223].

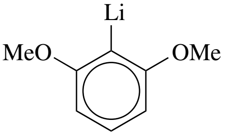

(171)

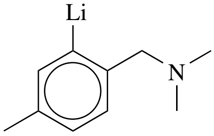

(172)

1-(Dimethylamino)naphthalene becomes metallated by *n*-BuLi at the 8-position. The product is oligomeric (**173**) in hydrocarbon solution; however, in the presence of moderately binding solvents such as diethyl ether, it turns into a dimer (**174**), as shown in the equilibrium depicted in equation 36. This equilibrium is strongly temperature-dependent starting at the nearly pure ether-solvated dimer at −90 °C to the pure oligomer at 0 °C, and mixtures thereof at intermediate temperatures. The structure of the aggregates can be characterized by ^{1}H, ^{13}C and ^{7}Li NMR spectra. Crystals of **174** can be analyzed by XRD. The dimer shows a pair of Li atoms bound to the same pair of C atoms on two naphthalene molecules, to the amino groups and to a pair of Et_2O molecules[224].

A change of the heteroatom in the following tridentate lithium compounds may induce totally different modes of association in the solid phase: $(MeOMe_2Si)_3CLi$ crystallizes as independent dimeric units (**175**) whereas the analogous $(Me_2NMe_2Si)_3CLi$ crystallizes as a linear polycarbanion structure (**176**)[225].

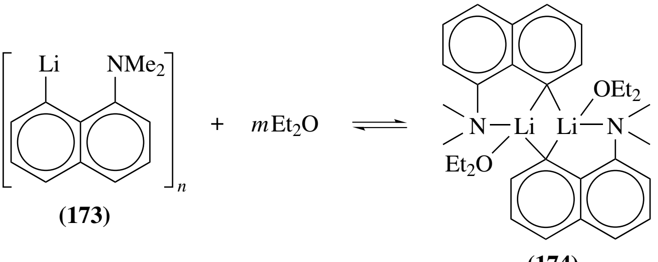

(173)

(174)

(36)

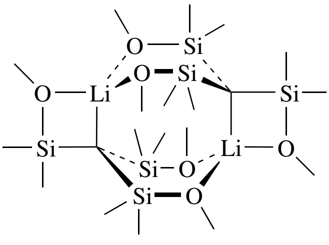

(175)

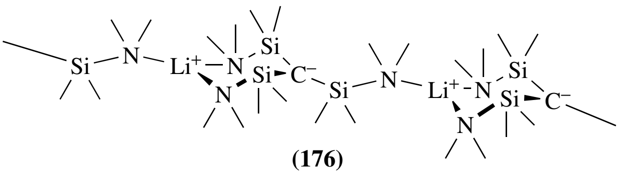

(176)

The degree of aggregation in solution of α-lithiocarboxylic esters was determined by vapor-phase osmometry. Ethyl α-lithioisobutyrate (**177**), for example, shows an average degree of aggregation of 6.6 in benzene solution, that diminishes to 3.5 in THF solution. Adding equivalent amounts of *t*-BuOLi to the solution reduces the degree of aggregation to 2.8 and 1.8 in benzene and THF, respectively. Consideration of the effect that introduction of Li in the α-position has on the IR absorption bands related to the carboxylic ester function led to the conclusion that association takes place mainly through coordination of carbonyl groups, as illustrated for a dimer (**178**) of **177**[226].

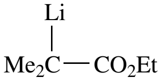

(177)

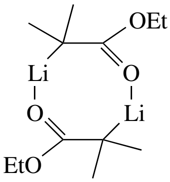

(178)

^{7}Li NMR association studies carried out on living polyisoprenes in hydrocarbon solution show upfield chemical shift displacements on increasing the degree of Li association. Monofunctional polyisoprenyllithium shows an equilibrium between dimeric (δ 0.02 ppm) and tetrameric (δ -0.10 ppm) associated species[227]. The dilithio compound **179** serves as initiator for isoprene polymerization, as shown in equation 37. The α, ω-dilithio living polymer (**180**, the tacticity not assured) presents two groups of bands, one similar to that of the monofunctional polymer, and a weaker upfield one with resonances at $\delta-1.64$, -1.85 and -1.92 ppm. These peaks may be tentatively assigned to tetrameric associations involving cyclic and linear aggregates, thus changing the chemical environment of the Li atoms. Addition of THF to the solution suppresses the higher order association, leaving mainly the dimer signal and a minute signal at $\delta-0.37$. Addition of Me_2SiCl_2 to the dilithio polymer solution replaces the upfield bands by one at $\delta-1.63$ ppm, attributed to association of LiCl with living polymer chains[228].

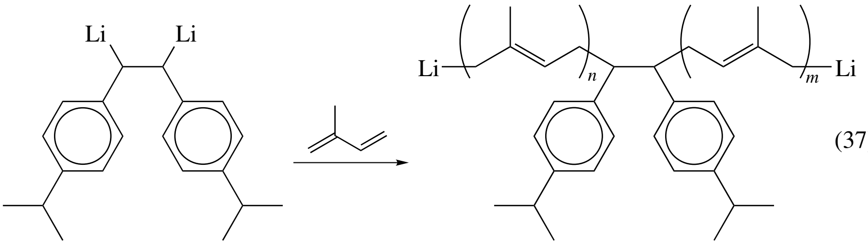

(179) **(180)**

(37)

3. Compounds with N−Li bonds

Monomeric crystalline organolithium compounds containing N−Li bonds are rather scarce. Such is the product of excess phenyl-2-pyridylamine reacting with n-BuLi in HMPA (**181**), as shown by XRD analysis[229]. A solid dimeric form (**182**) was obtained and characterized crystallographically, from excess phenyl-2-pyridylamine reacting with n-BuLi, containing the original amine acting as solvating agent[230]. An interesting feature of these complexes is the presence of H-bonding between the solvating and the metallated amino groups, possibly causing an agostic H−Li interaction. In the analogous dimeric species **183**, formation of the internal hydrogen bonds and H−Li contacts, involving the secondary amino groups of the solvating molecules, are probably precluded by the bulk of the trimethylsilyl groups, as shown by the XRD crystallographic analysis[231].

Aggregation of lithium dialkylamides in noncoordinating solvents and in the presence of varying concentrations of ligands was investigated using NMR techniques. Thus, to a solution Pr_2NLi enriched with ^{6}Li and ^{15}N dissolved in hydrocarbon solvent various amounts of a solvating agent, S (**184–187**), are added to attain various degrees of solvation. The

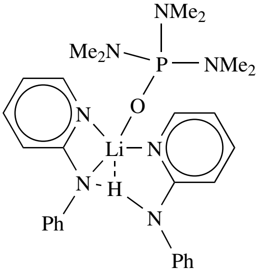

(181)

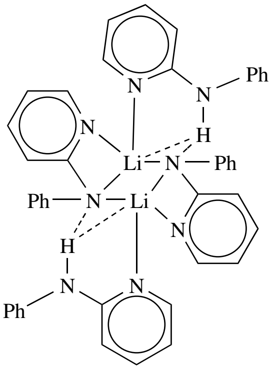

(182)

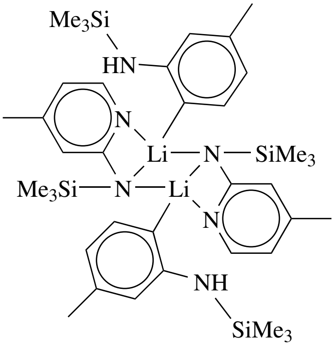

(183)

(184)

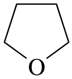

(185)

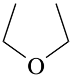

(186)

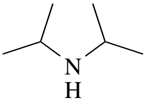

(187)

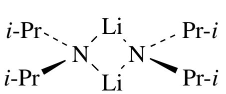

(188)

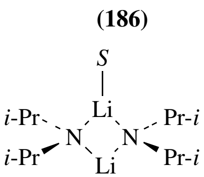

(189)

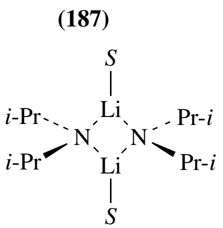

(190)

possible degrees of association and solvation are depicted for the dimer (**188–190**) and the trimer (**191–194**). The picture presented by ^{6}Li {^{15}N} NMR spectra of the solvates with oxirane **(184)** is the clearest: A nearly unresolved peak of the oligomers **188** and **191** appears in the absence of a solvating agent. On adding 0.25 equivalents of **184**, the unsolvated peak persists together with peaks ascribed to the partially solvated species **189, 192** and **193**. On increasing **184** to 0.5 equivalents only small amounts of unsolvated species persist, and some disolvated dimer (**190**) appears. At 0.75 equivalents of oxirane nearly all consists of disolvated species **190** and **193**, with a small amount of **189** still remaining. On adding 1 equivalent of solvating species only **190** is present in solution. A two-dimensional ^{6}Li,^{15}N HMQC spectrum was also performed, based on $^{6}\mathrm{Li}\{^{15}\mathrm{N}\}$, and $^{15}\mathrm{N}\{^{1}\mathrm{H}^{6},\mathrm{Li}\}$ decoupling. Analogous species are formed on solvation with **185** and **186**; however, in no case is formation of the trisolvated trimer (**194**) noted. Diisopropylamine (**187**) is a rather ineffective solvating agent[232]. The degrees of oligomerization and solvation seem to depend on the steric demands of the groups attached to the N atom. For example, if $\mathrm{Me_3Si}$ in placed instead of *i*-Pr, only a partially solvated dimer and the unsolvated trimer are formed; on the other hand, adding substoichiometric amounts of etheric ligands to $\mathrm{Et_2NLi}$ leads to formation of ladder-like oligomers such as **195**[233, 234].

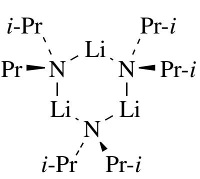

(191)

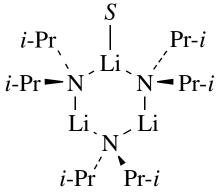

(192)

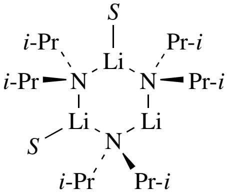

(193)

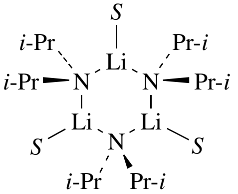

(194)

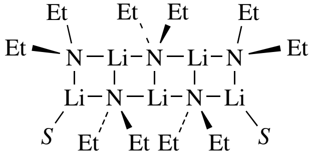

(195)

A solid-state investigation was carried out using ^{6}Li, ^{7}Li, ^{13}C and ^{15}N MAS and CP/MAS NMR spectroscopy techniques, including DNMR, the main objective of which was correlation of QCC and QSC values with the structure of lithium amides, crystallizing in various forms of association: Cyclic dimeric species, such as lithium diisopropylamide solvated by THF (**196**) and lithium bis(trimethylsilyl)amide solvated by $\mathrm{Et_2O}$ (**197**), a cyclic trimer, such as lithium bis(trimethylsilyl)amide (**198**), a cyclic tetramer such as 1-lithio-2,2,6,6-tetramethylpiperidine (**199**), a ladder tetramer such as 1-lithiopyrrolidine solvated by TMEDA (**200**), a cyclic ladder hexamer, such as 1-lithioazacycloheptane (**201**), and a helix polymer, such as lithium diisopropylamide (**202**). A solid of unknown structure, derived from pyrrolidine and lithium, was assigned a polymeric ladder structure (**203**) based on its $\chi(^{7}\mathrm{Li})$ value, which is correlated to the N−Li−N angle[235].

A study of the state of association of the functionalized organolithium compounds **204a–d** was carried out by multinuclear (^{1}H, ^{6}Li, ^{7}Li, ^{13}C, ^{15}N and ^{31}P) NMR spectroscopy, using ^{6}Li- and ^{15}N-enriched species. Spectral evidence, supported in part by XRD crystallographic evidence, points to compounds **204a–c** being dimerically associated in etheric solutions in three different forms (**205–207**). The interconversion among these three

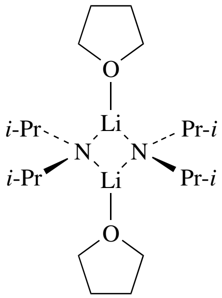

(196)

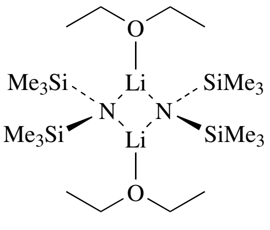

(197)

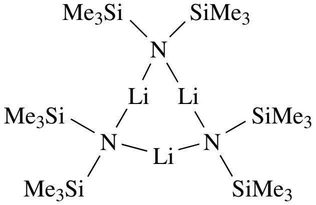

(198)

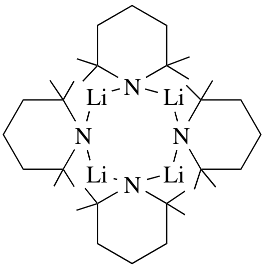

(199)

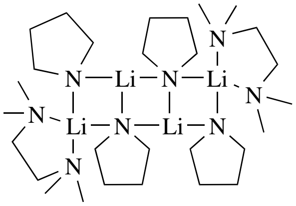

(200)

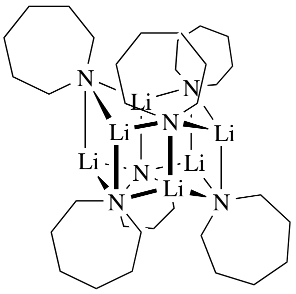

(201)

isomeric forms was investigated by DNMR. Addition of strongly solvating solvents such as TMEDA or PMDTA does not disrupt the association; however, HMPA partially does.

Compound **204d** appears to be strongly chelated but no dimeric species are formed; however, dimerization into a lithium lithiate (**208**) is induced on adding HMPA to the solution. The *o*-methoxy groups contribute to the stabilization of the complex[236].

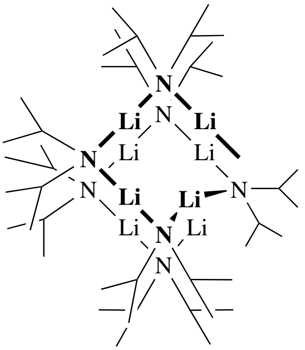

(202)

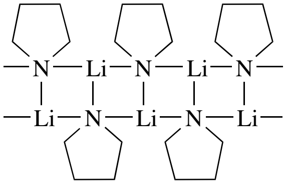

(203)

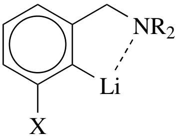

(204) **(a)** X = H, $R_2 = Me_2$
(b) X = H, $R_2 = Et_2$
(c) X = H, R_2 = Me, *i*-Pr
(d) X = OMe, $R_2 = Me_2$

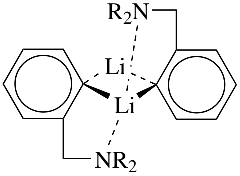

(205)

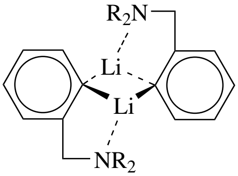

(206)

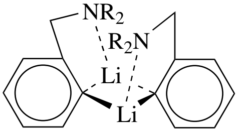

(207)

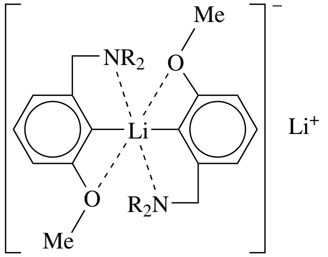

(208)

A variable-temperature ^{6}Li, ^{13}C, ^{15}N NMR spectroscopy study was carried out on the ligand structure and association behavior of [^{6}Li, ^{15}N]-enriched lithium bis(trimethylsilyl)-amide in hydrocarbon solution. The system behaves as shown, for example, in equation 38, with the solute adopting a dimeric form (**209**), which turns to the monomeric **210** on adding a ligand such as the bidentate TMEDA. With excess TMEDA the 3-coordinated Li may become 4-coordinated by η^1-bonding to an additional TMEDA molecule. On addition of THF to the solution the dimeric form **209** persists in solvated form (**211**). Adding TMEDA to the solution containing THF leaves **211** unchanged. At very low temperatures two Me signals can be distinguished for the N−Me groups of **210**, due to puckering of the five-membered ring, giving rise to two conformers; on raising the temperature these signals coalesce. DNMR line shape analysis allows the estimation of $\Delta H^{\circ\ddagger} = 7.5 \pm 0.3$ kcal mol^{-1} for the conformer interconversion. The behavior of **209** was also studied in the presence of other ligands of various types (diamino, such as **24, 141b,c, 142, 143**, its *cis*-isomer and **212**); triamino, such as PMTTA and **213**; tetraamino, such as HMTTA; diether, such as DME and **214**; open-chain polyether (**215**), crown ether, such as **108, 216** and **217**; mixed amino-ether, **218–220** and the cryptand C[2.1.1] (**221**)[237].

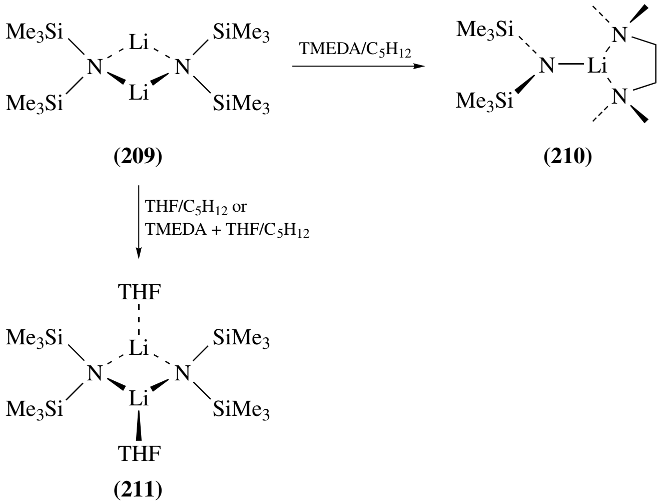

(38)

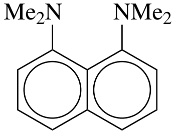

(212)

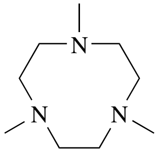

(213)

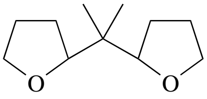

(214)

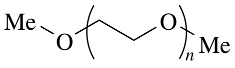

(215)

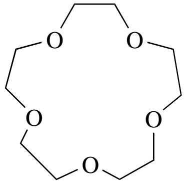

(216)

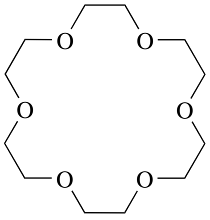

(217)

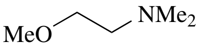

(218)

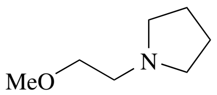

(219)

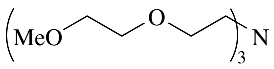

(220)

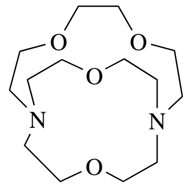

(221)

The ligand structure in these solvation complexes varies over a wide range of coordination modes, depending on the ligand and its stoichiometric relation to the lithium amide. Thus, solvated monomers and dimers can be observed with one or more solvating molecules coordinated to lithium. An interesting case of insolubilization by gradual addition of a solvating solvent is shown for DME in equation 39. Starting with the dimer (**209**) solution an equilibrium with a dimerized dimer (**222**) is established towards a DME:Li = 1:4 stoichiometry; on increasing the DME:Li ratio dimer oligomerization takes place, and towards a 1:2 ratio precipitation takes place, presumably due to dimer telomerization to **223**; further addition of DME towards a 1:1 ratio brings about resolubilization of disolvated dimer units (**224**); finally, with a large excess of DME an equilibrium is established with the solvated monomeric units (**225**)[237].

Triple ion species (**226**) are formed from the dimer (**209**) in the presence of compounds **108, 216, 217, 220** and **221**. The crown ether ligands (**108, 216, 217**) may yield uni- (**226a**) and dicoordinated (**226b**) lithium species, the latter presumably involving a Li^+ cation sandwiched between two ligand molecules. The ether-amine (**220**) and the cryptand (**221**) ligands totally surround the cation. The latter two cases and the complexes **226b** can be considered as solvent-separated ion pairs. Oligomers with point group C_{nh} ($n = 2, \ldots$) symmetry can be distinguished on applying the inverse-detected ^{15}N zero-quantum NMR technique, ^{6}Li$-^{15}$N resonance correlations by single frequency ^{15}N decoupling or ^{6}Li$-^{15}$N HMQC spectroscopy[237].

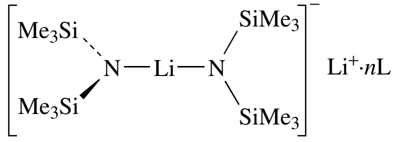

(226) **(a)** $n = 1$
(b) $n = 2$

A stable triple ion species of a different nature can be isolated as crystalline solid (**227**) on reacting pentafluorophenyl iodide with pentafluorophenyllithium (equation 40). XRD

(39)

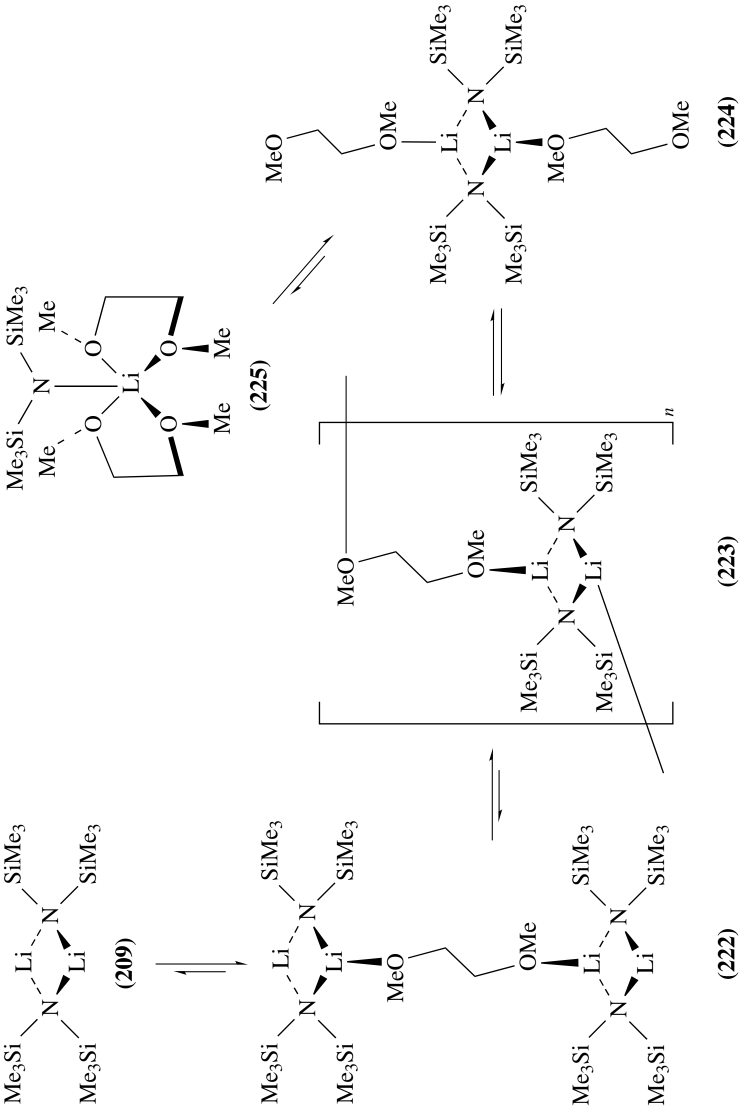

(209) **(222)** **(223)** **(224)** **(225)**

analysis of adduct **227** shows the ring planes at nearly right angles to each other and a very long, nearly linear C−I−C bond arrangement[238].

$$C_6F_5{-}Li + I{-}C_6F_5 \xrightarrow{TMEDA} [C_6F_5{-}I{-}C_6F_5]^- \ Li^+\cdot 2TMEDA \qquad (40)$$

(227)

Bis(trimethylsilyl)methyllithium undergoes a double 1,2-addition to the CN group of aromatic nitriles as shown in equation 41, to yield a lithium α, β-diketiminate, that crystallizes in dimeric form (**228**). XRD crystallographic analysis shows that the two diketiminato ligands lie on different planes and that the Li atoms are not coplanar with them[239]. Similar processes take place with organolithium reagents bearing 2-pyridyl or 2-quinolyl groups on the carbanion, as shown, for example, in equation 42, leading to monomeric (**229**) or dimeric (**230**) adducts, depending on the stoichiometric ratio of benzonitrile[240].

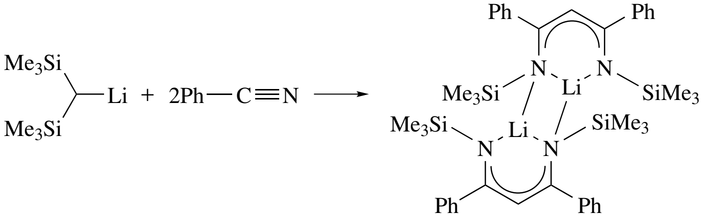

(228)

(41)

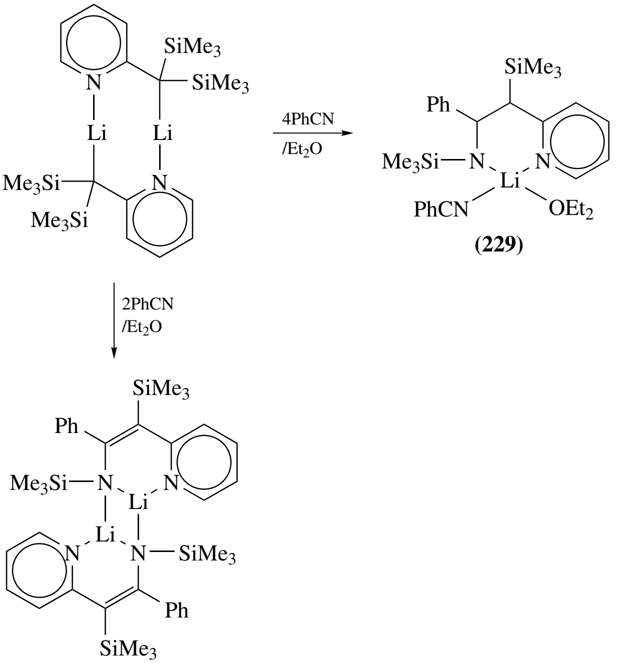

(229)

(230)

(42)

Metallation of malonaldehyde bis(phenylimine) hydrochloride with two equivalents of *n*-BuLi, in the presence of HMPA, yields lithium *N*,*N*′-diphenyl-β-diketiminate. The product crystallizes as a dimer complex with the Li atoms coordinated to the O atoms of a pair of HMPA molecules (**231**), as shown by XRD crystallography. The dimeric complex exists also in solution, as attested by ^{1}H, ^{31}P{^{1}H}, ^{7}Li and ^{13}C NMR spectroscopies[241].

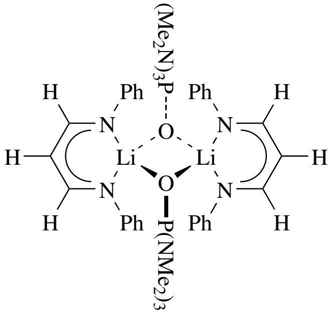

(231)

N,*N*′-Diphenylbenzamidine undergoes metallation in toluene, the crystalline precipitate (**232**) is probably polymeric and contains solvating toluene (average 0.7 mol per Li atom). The lithium imidinate solid produced in the presence of HMPA is dimeric (**233**) whereas the solids obtained in the presence of bidentate and tridentate ligands (e.g. TMEDA and PMDTA) are monomeric (**234** and **235**). The products were characterized by ^{1}H NMR spectra and XRD crystallography, except for **232**, for which no crystals suitable for XRD could be prepared[242].

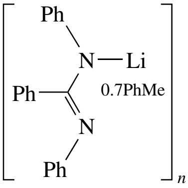

(232)

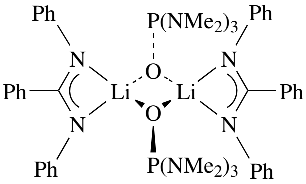

(233)

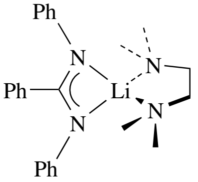

(234)

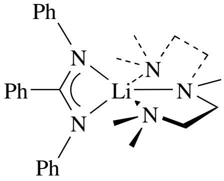

(235)

The reaction depicted in equation 43 between a nitrile and a lithium amide takes place as a 1,2-addition to the cyano group. The product crystallizes as a dimer (**236**) in which the lithium atoms are solvated by nitrile molecules and differently bonded to the amidine moieties, as shown by XRD analysis. Low-temperature ^{1}H NMR spectrum in solution points to uniform chemical environments for both the aryl groups and for the Me−Si groups, and to rapid rearrangement of the Li−N coordination structures. Acidolysis of the dimer in solution yields the corresponding amidine (**237**)[243]. The crystal structure of the THF-solvated analog of **236** shows dissimilar N−Li bond lengths for the two Li atoms in the dimer[244]. A trimer species (**238**) crystallizes from hexane, where one of the lithium atoms is bound to four amidine N atoms and a fifth N atom belonging to benzonitrile; the other two Li atoms are bound only to three amidine N atoms[245].

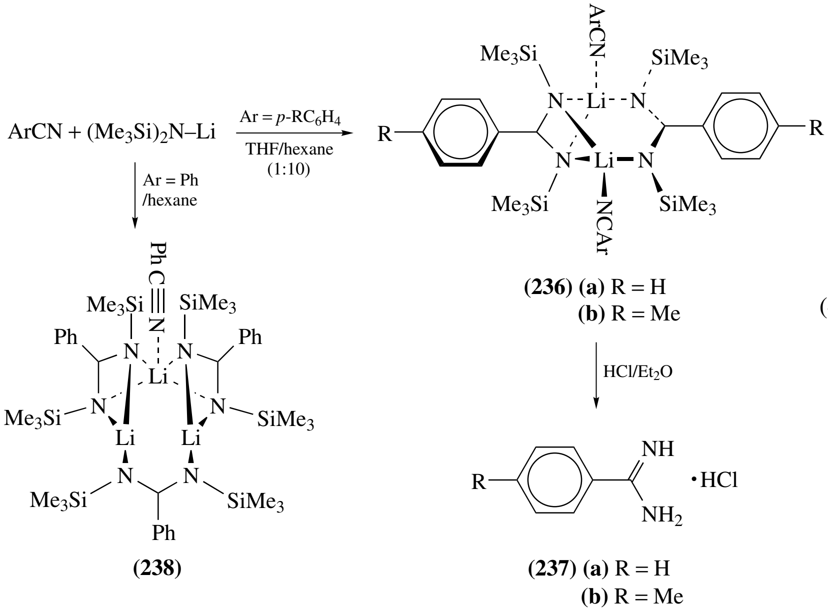

(238)

(236) (**a**) R = H
(**b**) R = Me

(237) (**a**) R = H
(**b**) R = Me

(43)

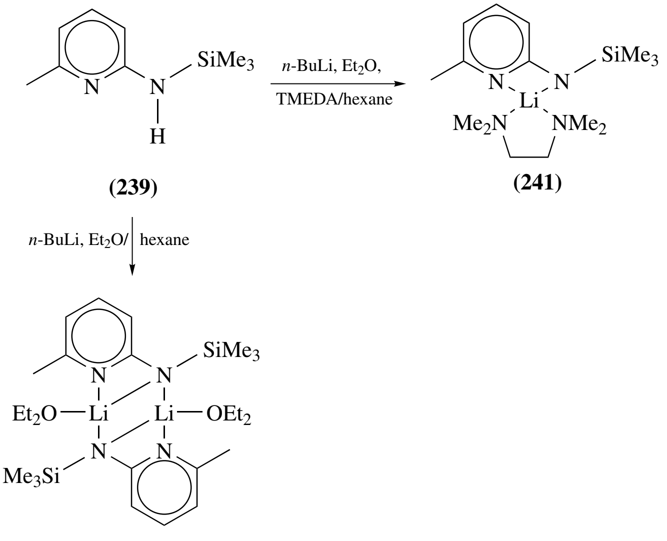

(239)

(241)

(240)

(44)

The 2-aminopyridine proton of **239** is sufficiently acidic to participate in the *N*-metallation reactions depicted in equation 44. The process yields crystals of dimeric structure (**240**); however, in the presence of a strongly binding ligand such as TMEDA the precipitate is monomeric (**241**). The quinoline derivative **242** shows a similar behavior. A 5:2 mixture of **239** and the primary amine **243** undergoes metallation with seven *n*-BuLi equivalents to yield a crystalline complex [7Li·5**239**·2**243**($-7H^+$)], where every amino group has lost one proton and every lithium atom has a different chemical environment. The structure of the crystalline products was determined by XRD analysis[246].

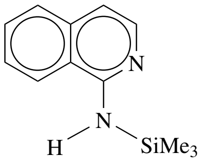

(242)

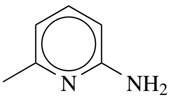

(243)

Interesting reactions take place in benzene solution at 20 °C between *s*-triazine (**244**) and lithium amides and carbides, as depicted in equations 45–47, leading to ring opening and rearrangement crystalline products, such as **245–248**, which were analyzed by single-crystal XRD. The crystalline reaction product of equation 45 is trimeric. Cryoscopic measurements of **245** in benzene solution show an average association number of 2.6, indicating that the trimeric structure of the crystalline state is also largely prevalent in solution. ^{7}Li{^{1}H} NMR spectra point to the presence of two types of Li atoms, in 2:1 ratio. Addition of strongly binding solvents such as TMEDA or PMDTA does not affect this trimer. The stability of the trinuclear structure of **245** is further supported by the MS spectrum showing a parent peak at *m/z* 503, corresponding to the $Li_3L_2^+$ ion, where L is the organic residue of the complex. The stability of the association complexes derived from carbylamides is lower. For example, product **246** undergoes a structural change to **247** when it is recrystallized in the presence of the tridentate solvent PMDTA. A complex equilibrium exists between various isomers of **248** in solution; thus, variable-temperature ^{7}Li NMR experiments show many peaks of variable strength at −90 °C, which gradually coalesce to one peak on raising the temperature to 15 °C; the ^{1}H NMR of this solution at −60 °C shows twelve peaks for the SiMe protons, pointing to the existence of six isomers[247].

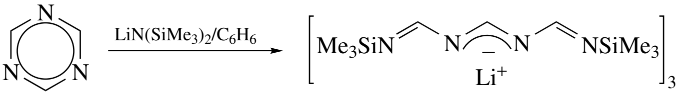

(244) **(245)**

(45)

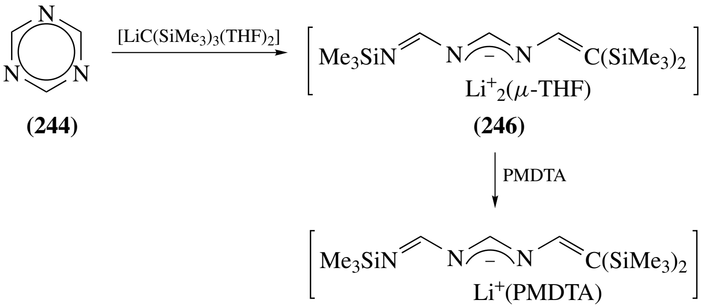

(244) **(246)**

(46)

(247)

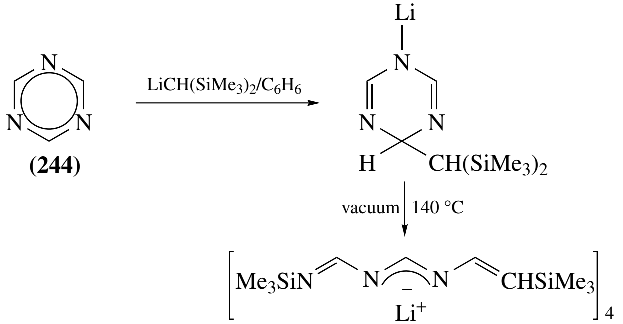

(244)

(248)

(47)

The ^{7}Li QSC values may be correlated with the effects of structure, solvent and temperature on association in solution for arylamides such as lithium indolide (**249**) and lithium *N*-alkylanilides (**250a–c**)^{226}.

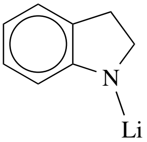

(249)

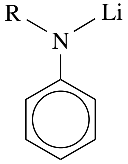

(250) (**a**) R = Me
(**b**) R = *i*-Pr
(**c**) R = *t*-Bu

Dimethylzinc reacts with *N*-2-pyridylaniline to yield the corresponding zincamide (**251**), which undergoes transmetallation with butyllithium to yield a lithium zincate (**252a** and **252b**), as shown in equation 48. Compound **252a** undergoes oxidation at the Zn nucleus with gaseous O_2 bubbled into a solution in toluene, with the butyl group turning into butoxide, as shown in equation 49. The oxidation product dimerizes and crystallizes in either of two forms, depending on the nature of the cosolvent: A unidentate coordinating solvent such as THF yields isolated dimer units $[(2\text{-PyPhN})_2\text{ZnOBu-}n\text{-Li}\cdot\text{THF}]_2$ (**253**), whereas the solvated crystals obtained in the presence of a bidentate cosolvent such as DME are linear polymers of the dimeric units $\{[(2\text{-PyPhN})_2\text{ZnOBu-}n\text{-Li}]_2\cdot\text{DME}\}_\infty$ (**254**). Characterization of compounds **251–254** was carried out by XRD. Supporting information was obtained from ^{1}H and ^{13}C NMR spectra. The ^{1}H spectrum of **252a** shows a 2:1 ratio between 2-pyridyl and *n*-butyl groups. Cross-peaks appear in the NOESY between the α-methylene and the aromatic signals, pointing to a heterobimetallate complex in C_6D_6 solution; furthermore, NOESY shows that the complex can adopt various geometries, and COSY points to one of them as dominant (α-methylene with δ 1.75 and 29.7 for ^{1}H and ^{13}C NMR, respectively). Two types of 2-pyridyl groups can be distinguished in the crystalline state of the oxidized product **253**, namely an *endo* and *exo* configuration. The ^{13}C NMR spectrum of **253** in hydrocarbon solvent shows double peaks of aromatic signals, pointing to preservation of the configuration prevalent in the crystal. ^{1}H NMR spectroscopy shows that compounds **253** and **254** have the same dimeric structure in hydrocarbon solution[248].

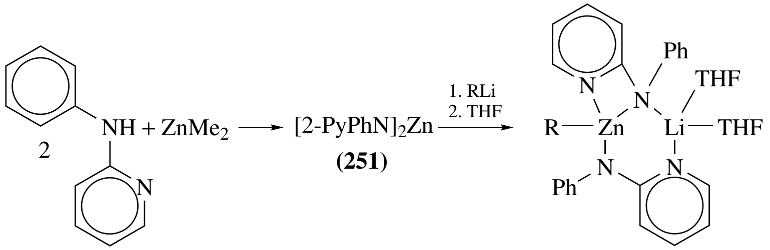

(48)

(252) **(a)** R = *n*-Bu
(b) R = *t*-Bu

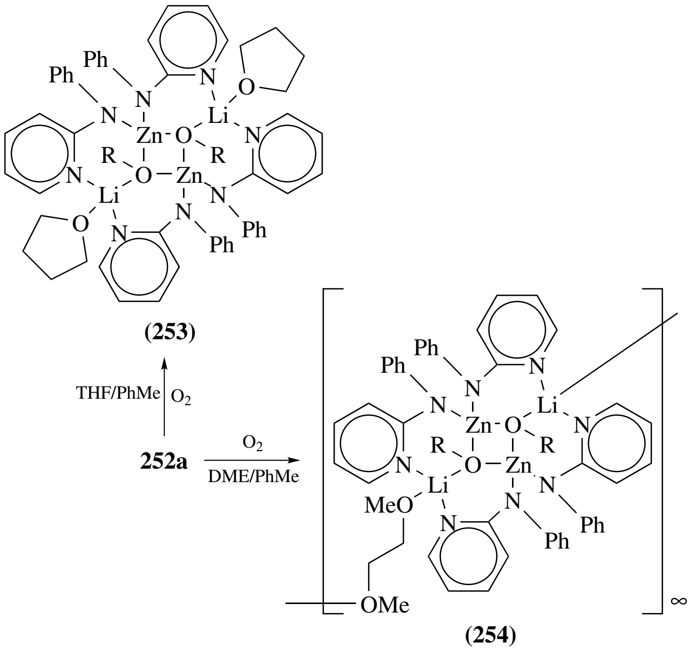

(49)

4. Compounds with O–Li bonds

The solubility of normal lithium alkoxides in hydrocarbon solvents is much lower than that of the branched ones. This can be attributed to formation of insoluble associated species in the case of the normal alkoxides. The solubility of lithium dialkylamides is lower than that of the analogous alkoxides[249].

The following n/m values were obtained for the degrees of association n at molal concentration m, measured in ammonia by cryoscopy. Lithium phenolate (**255a**, 2.21 ± 0.20/0.1530) is nearly dimeric in ammonia, while in pyridine and dioxolane it is tetrameric, as shown by vapor pressure and NMR measurements. The 2,6-dimethyl homologue (**255b**) is mainly dimeric both in dioxan solution and as a solid solvated by THF. Lithium thiophenolate (PhSLi, 1.32 ± 0.12/0.0708) is mostly monomeric in liquid ammonia. Lithium acetophenone enolate (**256**, 2.18 ± 0.20/0.0708) is dimeric in liquid ammonia[218]. Lithium enolates solvated by THF are tetrameric in the solid state, as determined by XRD analysis, while in THF solution association varies from dimers to tetramers. The ^{7}Li QSC values are correlated with the effects of structure, solvent and temperature on association in solution of lithium phenolates (**255a** and **255b**) and aromatic lithium enolates (**256a, 256b** and **257**)[223].

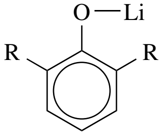

(255) **(a)** R = H
(b) R = Me

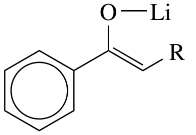

(256) **(a)** R = H
(b) R = Me

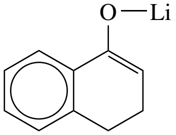

(257)

The term *superbase* applies to the complexes formed when an alkyllithium compound and an alkali metal alkoxide are present together in solution. These combinations show increased nucleophilic reactivity, hence their name, and have been applied in organic synthesis and anionic polymerization[250]. A linear increase of the solubility of *n*-BuOLi in *n*-heptane, from *ca* 1% to *ca* 9%, is observed on changing the concentration of *n*-BuLi from 0 to *ca* 1.1 M[249]. The complex $[n\text{-BuLi}\cdot t\text{-BuOLi}\}_4$ was analyzed by XRD, revealing two sets of four Li atoms. In one set the Li atom has contacts with two α-C atoms and one β-C atom of *n*-Bu groups, one O atom and one of the H atoms on the β-C atom. The second set of Li atoms is characterized by two contacts with O atoms and one contact to an α-C atom of an *n*-Bu group, leaving the fourth coordination empty. Such structure may be related to the increased reactivity of superbases in solution[251]. Superbases including chiral alcoholates are important reagents to induce asymmetric syntheses and to initiate asymmetric anionic polymerizations. *n*-BuLi in hexane solution produces in the presence of lithium anisylfencholate (**258a**) a 1:3 complex precipitate, with a central Li_4O_3C distorted cubic core (**259**), where the C atom belongs to the butyl group and the O atoms are the alkoxide moieties; furthermore, the three O atoms of the methoxy groups are coordinated to Li vertices of the cube. When the anisyl group carries a Me_3Si substituent (**258b**) a 2:1 complex precipitates, with a central $Li_4O_2C_2$ distorted cubic core (**260**). In this complex the two Li atoms that are not coordinated to methoxy groups show agostic interactions with the β-C atoms of the butyl groups, with Li−H contacts as close as 218 and 225 pm. In formulas **259** and **260** the arcs represent the organic residue of compounds **258a** and **258b**, respectively. The structure of these complexes was elucidated by XRD crystallographic analysis[252].

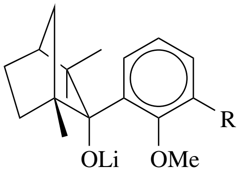

(258) **(a)** R = H
(b) R = SiMe3

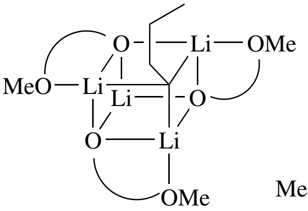

(259)

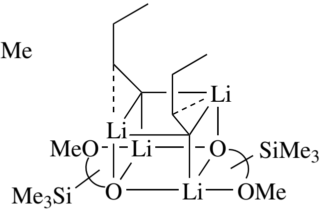

(260)

N,N,N′-Trimethylethylenediamine undergoes metallation and subsequent 1,2-addition to variously substituted benzaldehydes, as shown in equation 50. The lithium alcoholate products precipitate as tetrameric aggregates (**261a–c**) with a central Li_4O_4 distorted cubic core, as shown by XRD crystallographic analysis. In the case of benzaldehyde (R=H) none of the four N atoms of the NMe_2 groups have contacts with the Li atoms at the vertices of the cube (**262**), whereas in the two other cases such contacts exist with concomitant weakening of some Li−O contacts; however, these effects are distributed in different fashion in both products. The behavior of the products **261a–c** in solution was investigated by variable-temperature ^{1}H and ^{7}Li NMR, HMQC and ^{1}H DPFGSE NOE techniques. The corresponding tetramers (**262**) are preserved in solution but dissociation sets in on dilution, possibly leading to ladder- and cyclic-type oligomers, down to the free metallated diamine and the aromatic aldehydes[253].

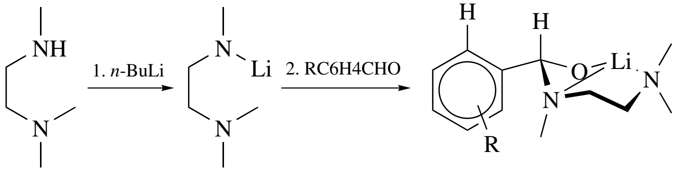

(50)

(261) (**a**) R = H
(**b**) R = 2-OMe
(**c**) R = 4-OMe

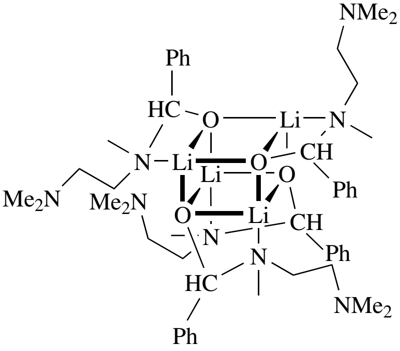

(262)

The process depicted in equation 51 affords several associated products that crystallize in different forms, depending on the conditions. The structure of these products was elucidated by ^{1}H NMR spectroscopy and single-crystal XRD. The Al atom of methylaluminium bis(2,6-di-*t*-butyl-4-methylphenoxide) (**263**) has planar trigonal coordination. This compound can crystallize with THF (**263**·THF) and other ligands. Transmetallation between **263** and organolithium compounds R'Li takes place, leading to the formation of the lithium phenolate **264**, that crystallizes as a solvated dimer [**264**·THF]$_2$. The Li atom of crystalline **265** has a pseudo-distorted octahedral coordination, due to four very short Li···HC agostic interactions with nearby methyl groups. Also, the Li−O distance in compound **265** is exceptionally short[254]. Other examples of compounds with reported agostic interactions for Li are $[\mathrm{Li}(\mu_3\text{-Me})_2\mathrm{BMe}_2]_\infty$[255, 256], $[(\mathrm{Me_3Si})_2\mathrm{NLi}]_2$[257] and *anti*-$[(\mathrm{Et_2O})\mathrm{Li}]_2[(t\text{-Bu})_6\mathrm{Al_6O_6Me_2}]$[258].

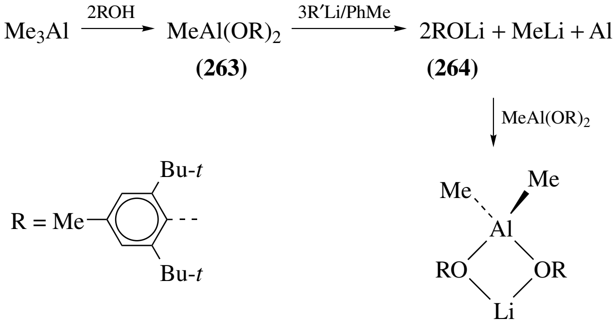

(263) **(264)** **(265)**

(51)

5. Miscellaneous Li bonds

The salts **266–268** form solid dimers solvated with THF. The association into dimers is preserved in solution. They can be characterized in solution by ^{1}H, ^{7}Li and ^{13}C NMR spectroscopies and in the solid state by ^{6}Li MAS NMR, ^{13}C CP/MAS NMR and two-dimensional ^{7}Li MAS NMR spectroscopies and XRD crystallography[259].

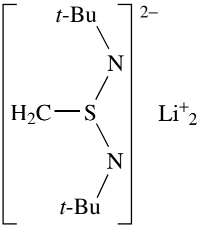

(266)

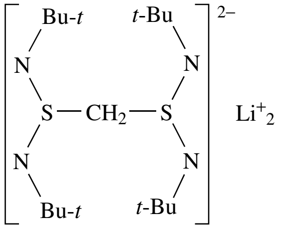

(267)

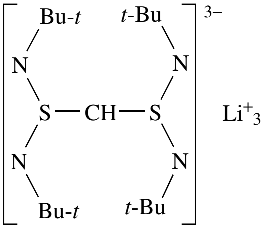

(268)

The organolithium compound **269** yields a lithium monoalkylcuprate according to equation 52. The product crystallizes in monomeric (**270**) and dimeric (**271**) forms, depending on the crystallization procedure. The Na analog of **271** can also be prepared. The K analog product of equation 52 crystallizes as a cubic cage tetramer, with no solvent molecules and N and K atoms alternatively placed on the vertices of the cube. Characterization of these compounds can be carried out by ^{1}H, ^{13}C and ^{29}Si NMR and IR spectroscopies and by single-crystal XRD. No dialkylcuprates analogous to $[\{(Me_3Si)_3C\}_2Cu]^{-}Li^{+}$ are formed[260]. Synthesis involving lithium dialkylcuprates was reviewed[261]. The structure of the higher order cyanocuprate obtained from CuCN + 2BuLi was investigated by X-ray absorption near edge structure (XANES) and extended X-ray absorption fine structure (EXAFS) spectroscopies. In contrast to the cyanocuprate formed by CuCN + BuLi, the CN ions of CuCN + 2BuLi are found to be removed from the Cu atoms. *Ab initio* calculations are in accord with these findings, showing that in the most stable structure the cyanide is associated with the alkyl groups bound to the Cu atoms[262].

$$(Me_2PhSi)_3CLi \;+\; Cu(I)CN \longrightarrow (Me_2PhSi)_3CCu(CN)Li \qquad (52)$$

(269)

$(Me_2PhSi)_3CCu(CN)Li \cdot 3THF$

(270)

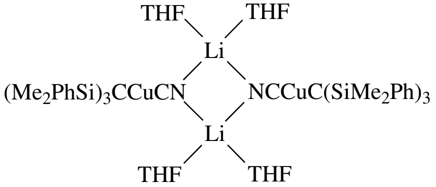

(271)

The silylene **272**, a thermally stable carbene analog, undergoes an intercalation reaction with silicolithium or carbolithium compounds (equation 53). The mechanism probably involves donor–acceptor intermediates (**273**) that rearrange to the silanolithium compounds **274**. The products were characterized by various methods: ^1H, ^7Li, $^{13}C\{^1H\}$ and $^{29}Si\{^1H\}$ NMR spectroscopies (variable-temperature ^{29}Si spectra of **274a** point to dissociation of the Si−Li bond in solution); electron impact MS (the M−Li·nL peak is either the parent peak or a strong one for all the products) and single-crystal XRD (the Si to Li distance is quite large as compared to the distance of Si to the other bonded atoms). It may be anticipated that the lithium compounds **274a–d** would be good transfer agents for the silylene to other metals[263].

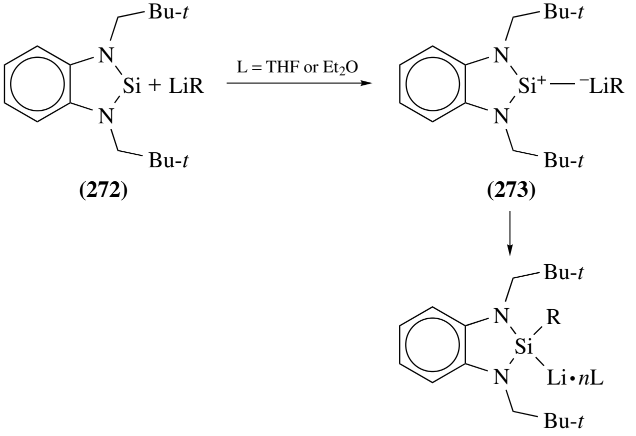

(272) **(273)**

(53)

(274) **(a)** R = $Si(SiMe_3)_3$, nL = 2THF
(b) R = Me, nL = $2Et_2O$
(c) R = t-Bu, nL = 3THF
(d) R = $CH(SiMe_3)_2$, nL = Et_2O

Organolithium compounds of structure **275** can been applied as transfer agents for transition metal ions, for example, as shown in equation 54 for scandium(III) with tetrahedral coordination (**276**). The structure of these complexes, elucidated by XRD crystallography, shows the transition metals forming part of an anionic entity, paired to solvated lithium cations. Further structural information can be obtained from ^1H, ^{13}C and ^{11}B NMR spectroscopies[264].

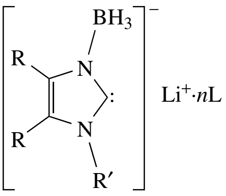

(275) **(a)** R = R′ = Me
(b) R = H, R′ = Me
(c) R = H, R′ = *n*-Bu
(d) RR = HC = CH, R′ = Me

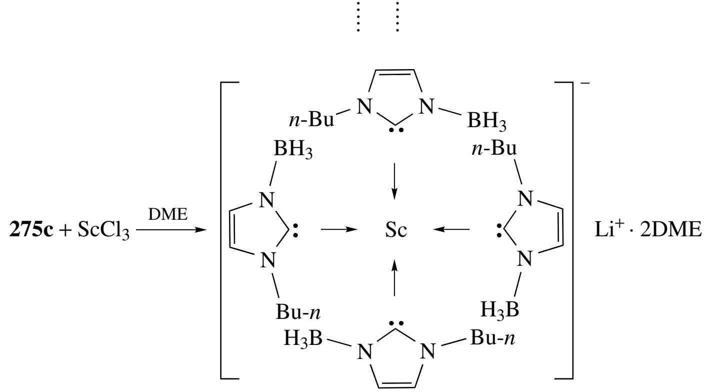

(54)

(276)

The functionalized tertiary phosphine **277** undergoes, in the presence of THF, specific metallation at a benzylic site (**278**), according to equation 55, but not at the other probable sites denoted by an asterisk. Let two molecules of monomer **278** be designed as *A*Li and *B*Li, respectively. An asymmetric dimer *AB*$\mathrm{Li_2}$ (**279**) crystallizes from the solution bearing asymmetric centers on both P atoms and one of the benzylic positions of each monomeric unit. Crystallographic analysis by XRD shows that the absolute configuration of **279** is *RRSS*. One of the Li atoms has close contact with a benzylic C, the adjacent *ipso*- and *ortho*-positions of ligand *A* and the P and one of the N atoms of ligand *B*; the other Li atom has contacts with a benzylic and *ipso*-carbons on ligand *B* and P and one of the N atoms on ligand *A*. Multielement NMR spectra of the product in toluene solution point to the preservation at low temperatures of most of the structural features of the dimeric solid; however, some internal rearrangements yield a C_2 symmetry with only one P and one Li environment. On the other hand, four distinct signals are shown for the Me protons, pointing to slow inversion at the $\mathrm{NMe_2}$ groups. On raising the temperature the Me signals coalesce in pairs. Interesting behavior is observed for the variable-temperature ^{7}Li and ^{31}P{^{1}H} NMR spectra. At low temperature the ^{7}Li signal is a doublet (δ 0.93) and the ^{31}P signal a 1:1:1:1 quartet, ($\delta - 47.6$), with $^{1}J(^{31}\mathrm{P}{-}^{7}\mathrm{Li}) = 63.2$ Hz, pointing to individual P–Li units. On raising the temperature the bands do not turn to singlets, as would normally be expected, but to a 1:2:1 triplet and a 1:2:3:4:3:2:1 septet, respectively. Formation of a $\mathrm{P_2Li_2}$ unit in the dimer is precluded for several reasons, and therefore the observed splitting is attributed to time averaging given by $[^{1}J(^{31}\mathrm{P}{-}^{7}\mathrm{Li}) + {}^{n}J(^{31}\mathrm{P}{-}^{7}\mathrm{Li})]/2 = (63.2 + 0)/2 = 31.6$ Hz ($n > 3$)[265]. Equation 56 shows that in petroleum ether metallation of **277** with *n*-BuLi takes place at the *P*-Me site to give **280**, leading to the formation of a tetramer (**281**).

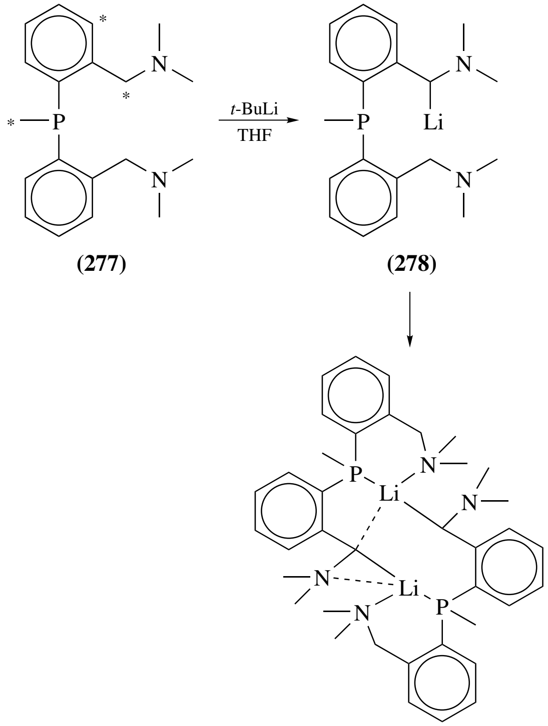

(277) **(278)** **(279)**

(55)

Thermal treatment of the dimeric species **279** brings about a rearrangement to tetramer **281** (equation 56). The structure of **281** can be characterized by ^{1}H, ^{13}C{^{1}H}, ^{31}P{^{1}H} and ^{7}Li NMR spectroscopies. Recrystallization of **281** from toluene yields solvated crystals of formula **281**·3PhMe, which show a core 12-membered macrocycle of C, P and Li atoms according to XRD crystallography[266, 267].

The reaction of *N*,*N*′-diphenylbenzamidine (**282** = AmH) with Me_2Zn and *t*-BuLi followed by oxidation yields different lithium zincate derivatives, depending on the solvent composition (equation 57). The products were crystallized and their structure was analyzed by single-crystal XRD. These are cage-like structures, each one with its peculiar coordination mode for the added oxygen atoms. In compound **283** the O atoms are in tetrahedral coordination with Me, Li and two Zn atoms. In compound **284** the only oxygen atom is in distorted octahedral coordination with the four Li and the two Zn atoms; regarding two of the Li atoms and the Zn, their placement is disordered. Compound **285** is a polymeric string of cubic cages with oxygen atoms in tetrahedral coordination[268].

The η-lithium complex **286** undergoes an equilibrium dimerization in solution, as shown in equation 58. This can be followed by ^{1}H NMR spectroscopy, with the appearance of the peak for the N−H bonds in **287**. Boiling a solution of **286** brings about formation of **287** crystals. The structure of the monomeric and dimeric forms was determined by XRD crystallography. Transmetallation of the Li atoms leads to the formation of a variety of Ni, Co and Ru complexes[269].

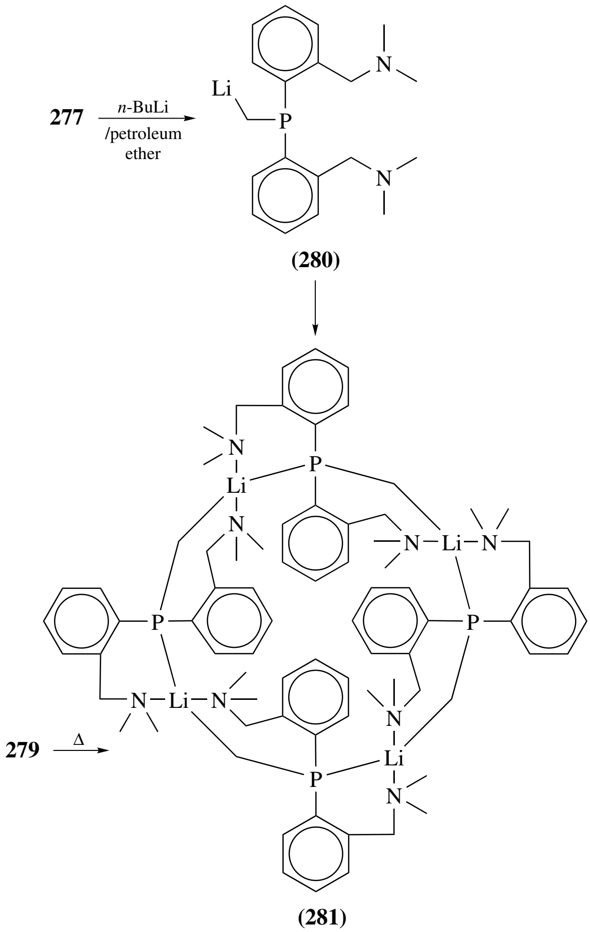
277
n-BuLi
/petroleum ether
Li
P
N
N
(280)
279
Δ
P
Li
N
(281)

(56)

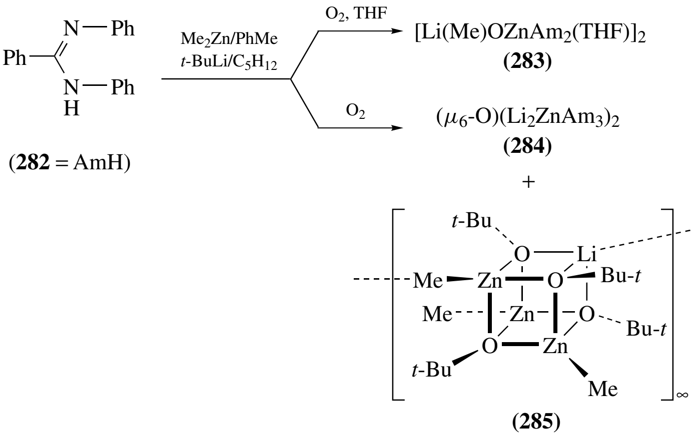
Ph
N—Ph
N—Ph
H
(282 = AmH)
Me2Zn/PhMe
t-BuLi/C5H12
O2, THF
[Li(Me)OZnAm2(THF)]2
(283)
O2
(μ6-O)(Li2ZnAm3)2
(284)
+
t-Bu
O
Li
Me
Zn
Bu-t
Zn
(285)

(57)

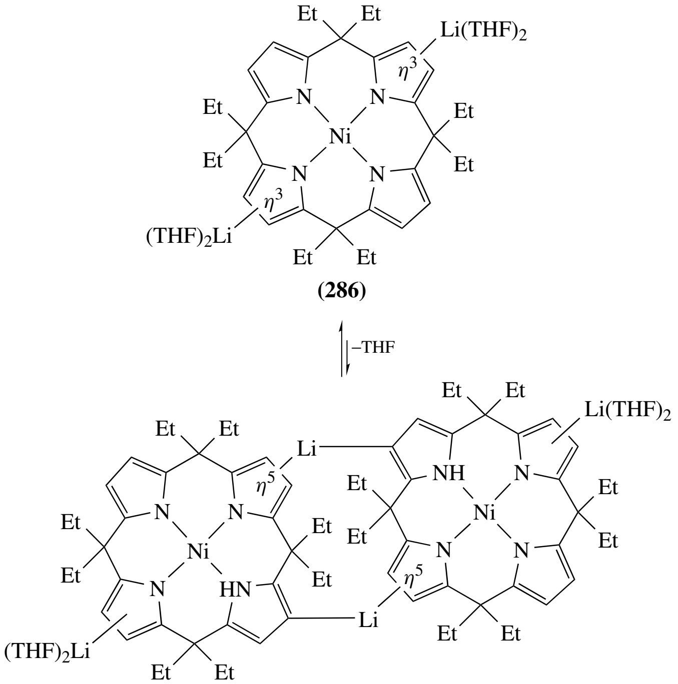

(286)

(287)

(58)

B. Clusters of Metallic Atoms

1. Simple organolithium species

Organolithium compounds tend to form clusters of lithium atoms[270, 271] and crystallize preserving the associates, with solvent molecules frequently being included in the crystal. Clusters of two (**288**) or three (**289**) Li atoms (shaded circles) are rare, for example, (t-BuLi$\cdot$Et$_2$O)$_2$, (t-BuLi$\cdot$TMEDA)$_2$ and MeLi$_3$S(NBu-t)$_3\cdot$3THF. In the latter complex the Me group is coordinated to all three Li atoms of the triangular cluster. PhLi forms a crystalline dimer of structure **144**, where the Li atoms at a distance of 249.0 pm from each other may be considered as a cluster of two Li atoms[210]. The crystalline trimeric species **238** may be taken as an example of a loose cluster of three Li atoms, with interatomic distances of 277.0, 262.1 and 256.2 pm[245]. The most frequent associations of organolithium compounds are into tetrahedral clusters (**290a–c**) of four Li atoms and octahedral ones (**291a–e**) of six Li atoms.

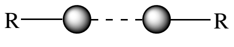

(288)

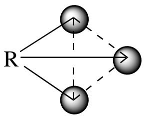

(289)

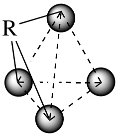

(290) **(a)** R = Me
(b) R = Et
(c) R = *t*-Bu

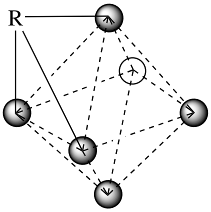

(291) **(a)** R = *i*-Pr
(b) R = *n*-Bu
(c) R = *c*-Hex
(d) R = *i*-Pr_2CHCH_2
(e) R = Me_3SiCH_2

The structure of solid organolithium compounds was elucidated by single-crystal XRD analysis. Coordination between the α-carbon of the R group and Li is usually with a triangular face of the Li cluster, as shown for simplicity for one R group only in **290** and **291**. However, a long-range interaction with a vertex Li atom of a neighboring cluster is also important, as was shown by XRD for the d_3-Me analog of **290a**. This was further confirmed by ^{7}Li MAS NMR, yielding two signals of 3:1 ratio, the first one for the Li_3 triangular face and the second one for the vertex. On the other hand, ^{13}C MAS NMR could not resolve the two signals, yielding a single broad band[271]. Early CNDO/2 calculations pointed to charge delocalization and diminution of polarity of the C−Li bond in RLi compounds (R = Me, Et, vinyl) in the series monomer > dimer > tetramer, and consequent decrease of nucleophilicity of the compound[272]. More recently, a theoretical quantitative analysis of the intramolecular forces leading to associate formation in organolithium species was carried out using the RVS decomposition scheme. The electrostatic contribution to the stabilization of the complex overcompensates the instability introduced by distortion of the associating species[273].

XRD analysis of $(n\text{-BuLi})_6$ (**291b**) reveals that the cluster of six Li atoms has an approximate D_{3d} symmetry (trigonal antiprismatic), with the six *n*-Bu groups placed around the axis of rotation. Each Li atom is coordinated to four Li atoms, one α-C and one β-C atom; the conformation of the six *n*-Bu groups is such that the α-C atom is coordinated to the three Li atoms of a face of the distorted octahedron and the β-C atom to one of them only[274].

Indirect evidence for the aggregation into hexamers of *n*-BuLi in benzene is obtained from the rate of formation of adduct **68** in equation 23[130]. The state of association of *n*-BuLi in various solvents and the rate of interconversion of the oligomers can be examined by NMR spectroscopy[41, 275]. The α-CH_2 ^{1}H NMR peaks at −84 °C point to formation of dimeric and tetrameric associates, while 2D-TOCSY experiments allow assignment of all the butyl group resonances. Also ^{7}Li spectra show both oligomers, while ^{7}Li EXSY experiments point to a slow Li interchange between associates. Diffusion-ordered NMR spectroscopy (DOSY) with ^{1}H and ^{7}Li detection can also be applied for these purposes, using a DSTE sequence with longitudinal eddy current delay to suppress the effects of convection currents. The integrated resonances are used to calculate diffusion coefficients and relative diffusion coefficients of the associates. The results of these measurements are in excellent accord with those obtained for the solvates $(n\text{-BuLi})_2\cdot 4THF$ and $(n\text{-BuLi})_4\cdot 4THF$ on applying the Stokes–Einstein equation ($D = k_BT/6\pi\eta r$), where D is the diffusion coefficient, k_B the Boltzmann constant, T the absolute temperature, η the viscosity and r the radius of the diffusing molecule. The viscosity of the neat solvent can be taken from the literature[200] and the radius may be calculated from the molecular volume according to published XRD structures[276, 277] or from PM3-optimized structures[275] using Anders' parameters for Li[36]. The $(n\text{-BuLi})_4$ complex in THF solution shows Li$-\beta$-H interaction, as revealed by the -^{1}H, ^{6}Li-^{4}H HOESY spectrum, with the n-Bu group in the energetically most favorable conformation[278].

When bidentate solvents are present, the clusters may crystallize forming linear polymers by linking clusters together, as in complexes **292–295**. This further diminishes solubility and reactivity of the alkyllithium compound, making the unassociated RLi species the most probable reactive form in synthetic processes. MeLi dissolved in diethoxymethane shows at room temperature a single ^{7}Li NMR peak, that resolves into four distinct peaks at −80 °C, pointing to temperature-dependent monomer/oligomer/polymer equilibria[271].

$[(\text{MeLi})_4{\cdot}2\text{Me}_2\text{NCH}_2\text{NMe}_2]_\infty$ **(292)**

$[(n\text{-BuLi})_4{\cdot}\text{Me}_2\text{NCH}_2\text{NMe}_2]_\infty$ **(293)**

$[(n\text{-BuLi})_4{\cdot}\text{MeOCH}_2\text{OMe}]_\infty$ **(294)**

$[(\text{MeLi})_4{\cdot}1.5\text{MeOCH}_2\text{OMe}]_\infty$ **(295)**

Two approaches were reported for disruption of the tendency of MeLi to form the tetrahedral clusters, thus increasing its reactivity in organic synthesis. One was producing the **295** polymer, which has an ice-like crystalline structure, with micropores of diameter 0.72 nm, that are full with the solvent, thus helping solubilization of non-associated units. The other approach is by disturbing the quadruple coordination of the methide groups in the $(\text{MeLi})_4$ cluster. This can be done by adding certain lithium salts that form new types of complexes; for example, according to equation 59, after adding lithium sulfide in the presence of tri-t-butylamine, the methide group is coordinated only as in **289** while the long-range coordination with the vertex of a neighboring cluster is absent, as was shown by single-crystal XRD. The ^{6}Li and ^{7}Li MAS NMR spectra of **296** show two peaks in 2:1 ratio, pointing to a structure where the methide ion is closer and equidistant to one pair of Li atoms than to the third one[271].

$$(\text{MeLi})_4 + 2[\text{Li}_2\text{S}\{\text{N(Bu-}t)_3\}_2 \xrightarrow{\text{THF}} \underset{\textbf{(296)}}{4[\text{MeLi}_3\text{S}\{\text{N(Bu-}t)_3\}\text{THF})_3]} \qquad (59)$$

The equilibria depicted in equations 60a–e take place simultaneously in a solution containing an alkyllithium and a lithium halide. The LiX species appearing in equation 60b can also participate in association equilibria on its own, of which only equation 60f is shown. A variable-temperature ^{1}H and ^{7}Li NMR investigation was carried out on the behavior of MeLi solutions in Et_2O in the presence of LiBr and LiI, the interpretation of which takes into account the prevailing **290a** cluster structure. At low temperature four species can be distinguished in the presence of LiBr, namely Li_4Me_4, $\text{Li}_4\text{Me}_3\text{Br}$, $\text{Li}_4\text{Me}_2\text{Br}_2$, and equilibrium 60f with X = Br. In the case of LiI only the $\text{Li}_4\text{Me}_3\text{I}$ cluster can be assigned[279].

$$\text{Li}_4\text{R}_3\text{X} \rightleftharpoons \text{Li}_2\text{RX} + \text{Li}_2\text{R}_2 \qquad (60a)$$

$$\text{Li}_2\text{RX} \rightleftharpoons \text{LiR} + \text{LiX} \qquad (60b)$$

$$\text{Li}_4\text{R}_3\text{X} + \text{LiX} \rightleftharpoons \text{Li}_4\text{R}_2\text{X}_2 + \text{LiR} \qquad (60c)$$

$$Li_2R_2 \rightleftharpoons 2LiR \quad (60d)$$

$$2Li_2R_2 \rightleftharpoons Li_4R_4 \quad (60e)$$

$$2Li_2X_2 \rightleftharpoons Li_4X_4 \quad (60f)$$

2. Functionalized organolithium species

A planar arrangement (**297**) for a cluster of four Li atoms, consisting of two equilateral triangles, is found by XRD for the solid complex **298**. Each Li atom is coordinated to methylene groups of both types (from *n*-BuLi and the metallated carbosilane) and to N and O atoms of the substituent in the carbosilane. Further characterization of the solid **298** can be made by ^6Li and ^{13}C CP/MAS NMR spectroscopies, and in solution by ^1H, ^7Li, ^{13}C and ^{29}Si NMR spectroscopies. The combination of both organolithium compounds in **298** is found to form a more effective reagent than each of them alone[280].

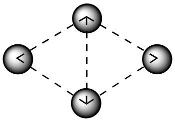

(297)

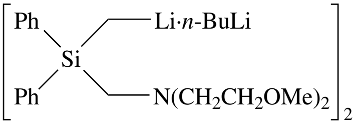

(298)

3. Heterometallic species

n-BuLi brings about ring metallation of the sodium amide **299**, as shown in equation 61. The product crystallizes in the presence of TMEDA to yield a tetramer (**300**·TMEDA)$_4$ of complicated structure that was elucidated by XRD. The four Li atoms form a planar cluster nearly as in **297**. Two of the aromatic molecules are nearly coplanar with the cluster and have the metallated C atoms bound each to two Li and two Na atoms; the other two organic molecules are arranged nearly perpendicularly, above and below the lithium cluster plane, with the metallated C atoms bound each to three Li and one Na atom. Each one of the four N atoms of these organic molecules has contacts with one Li and one Na atom. Finally, each one of the sodium atoms is solvated by one bidentate TMEDA molecule[281].

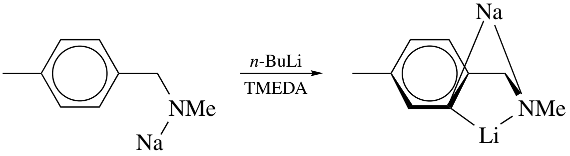

(299) **(300)** (61)

The cluster [NiMe$_4$·Li$_2$·THF]$_2$ (**301**) is obtained on treating certain Ni complexes with excess MeLi. Recrystallization of **301** from THF leads to the formation of [NiMe$_4$·Li$_2$·THF$_2$]$_2$ (**302**). The Ni atoms have square planar coordination. The Li atoms are stabilized mainly by agostic Li−H interactions with four neighboring Me groups, as confirmed by the Li−H distances and the Li−H−C bond angles obtained from XRD analysis. The composition of these compounds was established by elemental analysis: Ni by EDTA titration using murexide (**303**) as indicator, and Li by AAS. No CH analysis was attempted due to the highly pyrophoric behavior of the compounds. Structural

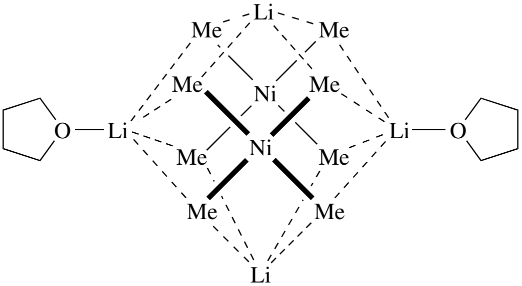

(301)

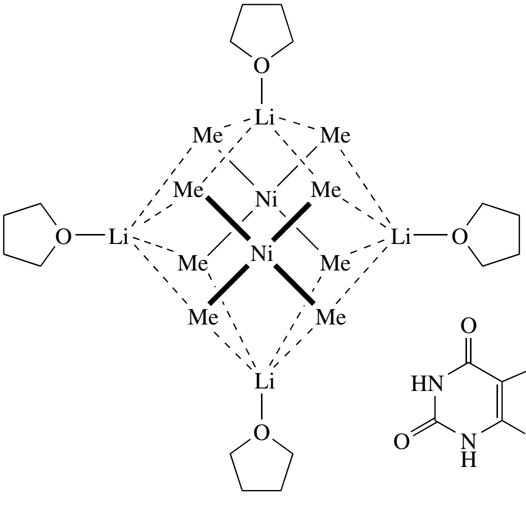

(302)

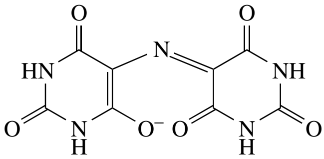

(303)

characterization was done by single-crystal XRD, and confirmed by ^{1}H, ^{13}C and ^{7}Li NMR spectroscopies[282].

VI. ANALYSIS BY INFERENCE AFTER QUENCHING

A. General

In the present section are shown examples, far from exhaustive, of reactions involving organolithium compounds as intermediate stages, the attendance of which was only assumed, as no effort was made to demonstrate their presence. The products of such reactions may be considered as the result of derivatizing procedures used in the analysis of organic functional groups. For example, the mass spectrometric analysis mentioned in Section IV.C.4 led to the conclusion that the deuteriated species, obtained after treatment with deuterium oxide, stemmed from organolithium compounds where each deuterium atom replaced a lithium atom. The usual procedure is to start with a commercial organolithium compound solution, in a suitable solvent (hydrocarbon or etheric), at very low temperature, blanketed by argon, using carefully dried glassware, reagents and ancillary chemicals (the so-called Schlenk techniques[31, 32] are frequently applied), adding a substrate for metallation and possibly a cosolvent (e.g. TMEDA) and an asymmetric induction agent, for example (−)-sparteine (**24**), adding a quenching electrophile, and letting the solution reach a certain temperature at which the desired reaction proceeds for several minutes or hours or days. This may be followed if necessary by a final quenching, product separation and product identification or characterization, as the case might require. The electrophiles used in the final workup of a synthesis might be either alkyl halides (e.g. the reaction with MeI of metallized aniline derivatives, or the functionalization of a living polymer, mentioned at the beginning of Section VI.B.2) or a proton or a deuteron, stemming from water, an alcohol or their deuteriated analogs. An important variation of this sequence is preparing *in situ* an organolithium compound for metallation of the substrate, for example Li powder in the presence of substoichiometric amounts of an aromatic compound form a lithium arene (e.g. naphthalene yields $\mathrm{Li{\cdot}C_{10}H_8}$) that serves as reducing/metallating agent (see Section VI.C).

Various topics related to the production of metallated intermediates or their quenching to final products have been reviewed:

a) Processes involving the lithium–halogen exchange reaction in aliphatic substrates (equation 62) have been examined from the mechanistic and synthetic points of view. The presence of unsaturation in the R′ group may bring about cyclization of the substrate[283].

$$\mathrm{R{-}Li} + \mathrm{R'{-}X} \rightleftharpoons \mathrm{R{-}X} + \mathrm{R'{-}Li} \tag{62}$$

b) The reactions of aryl halides with alkyllithiums (equation 63) have been examined from the mechanistic and synthetic points of view. Various reaction paths have been distinguished, depending on the nature of the aryl and alkyl groups and the processing conditions[284].

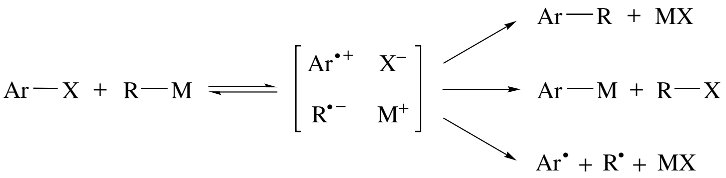

$$\mathrm{Ar{-}X} + \mathrm{R{-}M} \rightleftharpoons \begin{bmatrix} \mathrm{Ar}^{\bullet +} & \mathrm{X}^{-} \\ \mathrm{R}^{\bullet -} & \mathrm{M}^{+} \end{bmatrix} \begin{array}{l} \nearrow \mathrm{Ar{-}R} + \mathrm{MX} \\ \longrightarrow \mathrm{Ar{-}M} + \mathrm{R{-}X} \\ \searrow \mathrm{Ar}^{\bullet} + \mathrm{R}^{\bullet} + \mathrm{MX} \end{array} \tag{63}$$

c) Lateral and directed *ortho*-metallation of aromatic compounds are important steps in many synthetic paths. An interesting case is shown in equation 64, where the products depend on the stoichiometric amounts of the quenching reagent (MeI). When using

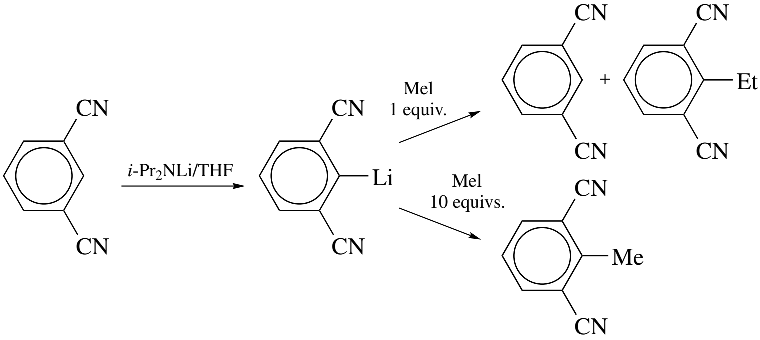

(64)

1 equivalent of MeI the intermediate aryl lithium causes lateral metallation of the intermediate toluene product, leading to a final ethylbenzene product, whereas in the presence of a large excess of MeI a fast quenching consumes the aryllithium intermediate in a straightforward manner[285].

d) Certain aromatic compounds carry the so-called directed metallation groups, capable to induce introduction of a lithium atom at an *ortho*-position, or at a definite remote position. The review deals with combining directed *ortho* or remote metallation with cross-coupling reactions. In equation 65 one of the general synthetic strategies involving these concepts is shown, where the rings represent aromatic of heteroaromatic nuclei, X are directed metallation groups, RM are metallizing agents and Y are leaving groups[286].

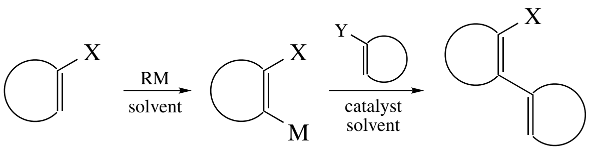

(65)

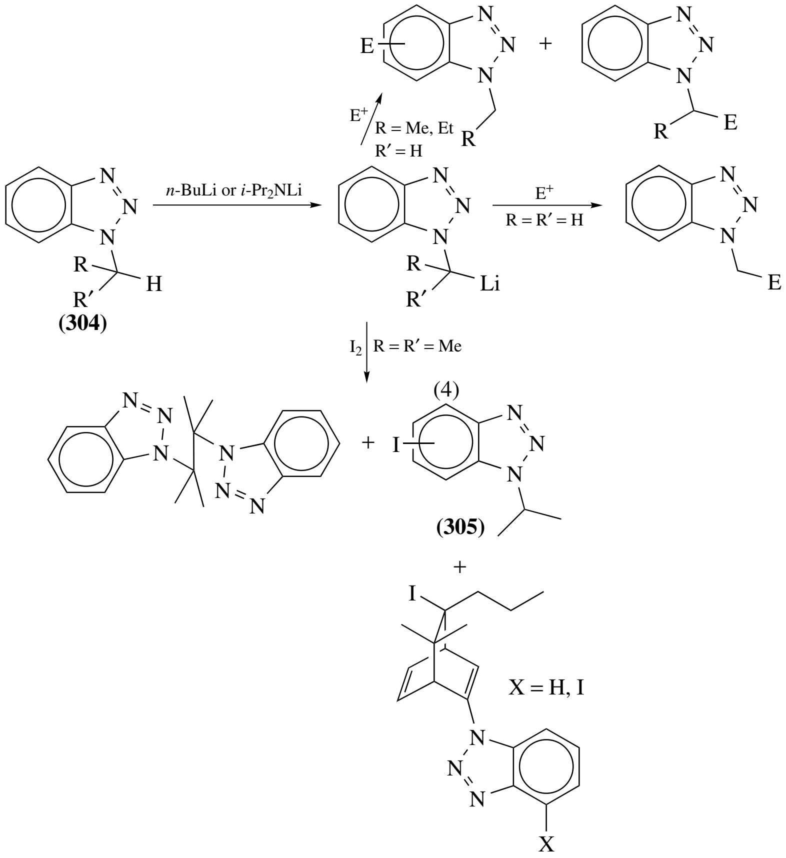

(304)

(305)

(66)

e) The synthetic methods mediated by N-alkylbenzotriazole (**304**) metallated on the α-position may afford various advantages in organic synthesis, such as better control of the reaction path, increased stereochemical selectivity and the possibility of working at higher temperatures. In equation 66 are shown the first steps of various synthetic paths, depending on the alkyl group, the electrophile and the reaction conditions[287]. Of the iodination products, only the 4-iodo isomer of **305** was isolated in moderate amounts, all the rest of the products being obtained in minor to trace yields[288].

f) Organolithium compounds afford viable starting materials for the synthesis of fluoro compounds, on quenching with various fluorinating agents, such as fluorine, perchloryl fluoride ($FClO_3$), *N*-fluorosulfonamides and *N*-fluorosulfonimides. The latter two classes of reagents are easier to handle and allow in some cases stereochemical control of the fluorination, as shown in equation 67[289].

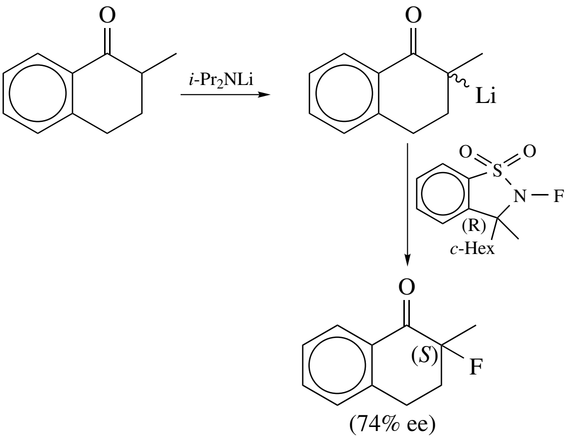

(67)

g) The stability, reactivity and selectivity of organoalkali metals, and in particular organolithium compounds, can be modified by addition of various alkoxides[290].

h) The formation of *O*- and *N*-heterocyclic compounds from unsaturated organolithium intermediates was reviewed[291].

B. Reagents Containing C−Li Bonds

Various commercially available compounds containing C−Li bonds are listed in Table 1. The alkyllithium and aryllithium species listed there are usually very reactive. These compounds serve to prepare *in situ* other intermediate reagents. These proceedings may afford various advantages in organic synthesis, such as better control of the reaction path, increased stereochemical selectivity and the possibility of working at higher temperatures.

1. Transmetallation

Transmetallation with organolithium reagents is applied to convert stable organometallic compounds to more reactive intermediates that undergo some desired transformations. The organotin compound **306** in the presence of BuLi is converted to (+)-pseudoheliotridane (**309**) of 94% *ee*, according to equation 68. The process is assumed to include a transmetallation step to intermediate **307** and then cyclization by stereospecific 1,2-addition to the double bond, yielding intermediate **308**. The product was characterized by its optical rotation, MS (showing the molecular peak), ^1H and ^{13}C NMR spectra and some properties of the picrate derivative. The enantiomeric excess can be determined with the aid of the solvating agent (R)-(−)-2,2,2-trifluoro-1-(9-anthryl)ethanol (**310**) that shifts upfield the Me doublet of the free base (**309**) and splits it into two doublets[292, 293].

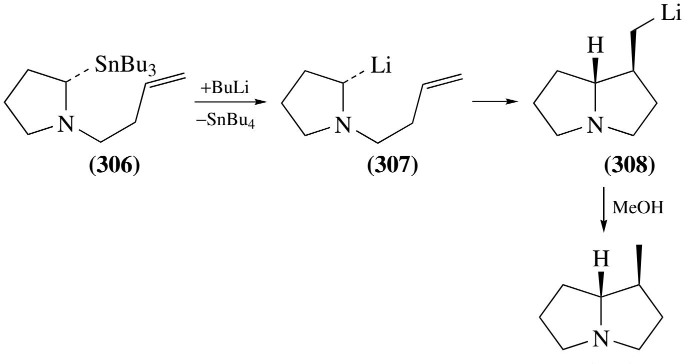

(306) **(307)** **(308)** **(309)**

(68)

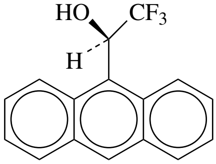

(310)

Dialkoxymethyllithium compounds, for example 2-lithio-1,3-dioxan (**311**), are generated *in situ* as shown in equation 69, either by reductive lithiation of a phenyl thioether with a lithium arene or by transmetallation of the corresponding trialkylstannyl compound. Subsequent quenching with electrophiles leads to the usual alkylated or functionalized species[294].

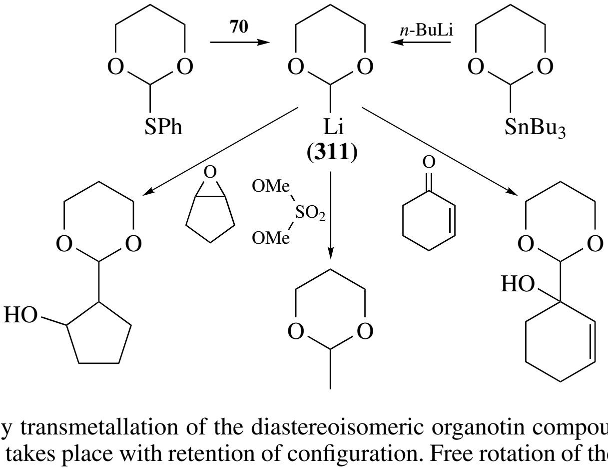

(311)

(69)

Lithiation by transmetallation of the diastereoisomeric organotin compounds according to equation 70 takes place with retention of configuration. Free rotation of the carboxamide group is sterically precluded, thus providing a second chiral center in addition to the metallation site. The main evidence for the structure of the organolithium products stems from the ^{1}H NMR spectrum taken at −40 °C and from analysis of the products after quenching[295].

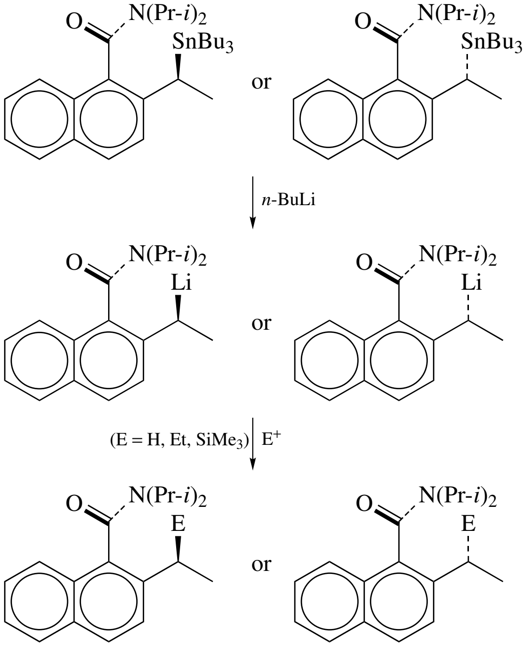

(70)

Transmetallation reactions are important in synthetic applications; however, their steric course is unclear in many cases. The major course of reaction depicted in equation 71, for the sterically defined and stable α-carbamoyloxy organolithium compounds, can be predicted to preserve configuration, as happens for Li/Sn, Li/Mg and Li/Ce transmetallations of **312a**[296]; on the other hand, the benzyl derivative **312b** seems to be configurationally unstable and total racemization takes place on stannation[297]. The racemic benzyl analog **312b** undergoes asymmetric induction in the presence of (−)-sparteine (**24**) to yield a stannylated product enriched with the *S* enantiomer. Further confirmation of configurational retention can be attained on treating the transmetallated compound with an organic electrophile, e.g. an aldehyde (equation 71), and examining the configurational purity of the product[296].

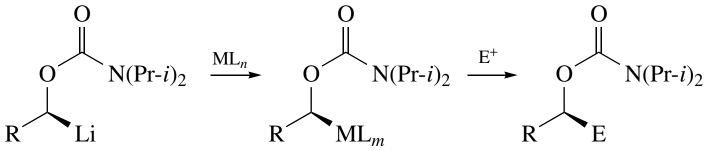

(71)

(312) **(a)** R = $PhCH_2CH_2$
(b) R = Ph

Variously substituted γ-metallated 2-*n*-propylnaphthalenes (**313a**), or their corresponding oxa (**313b**) and aza (**313c**) analogs, undergo transmetallation with alkyllithium, and the lithium intermediate undergoes cyclization with attendant dearomatization. The process is stereoselectively finished by treatment with an electrophile, as illustrated in equation 72 for a particular case of **313b**, namely compound **314**. For both electrophiles listed, configuration **315** is the preferred one over configuration **316** by a factor greater than 25. Structural characterization of the products was performed by ^1H and ^{13}C NMR and FTIR spectroscopies, and chemical ionization MS[298].

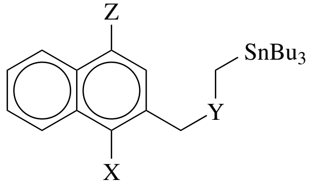

(313) **(a)** Y = CH_2
(b) Y = O
(c) Y = NR

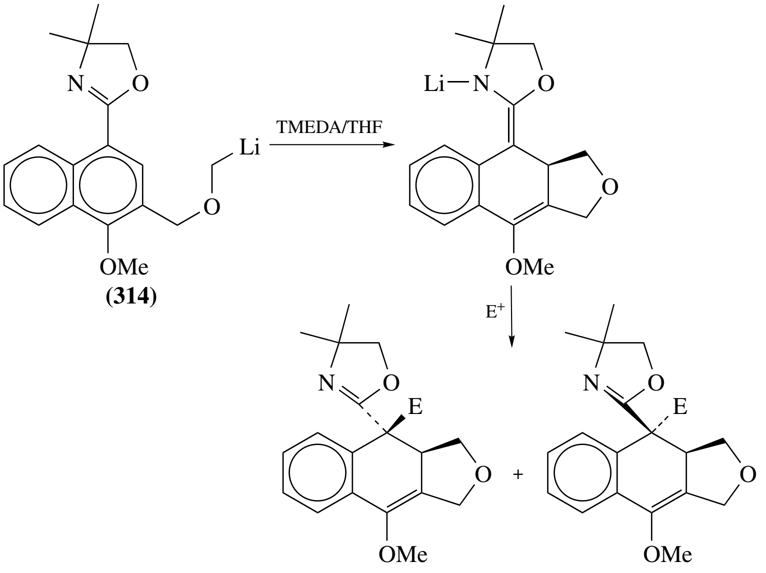

(314) **(315)** **(316)**

(72)

(a) E = H (from H_2O)
(b) E = Me (from MeI)

Phenylketene thiotelluroacetals (e.g. **317**) undergo regioselective transmetallation. Quenching the organolithium intermediate with DMF leads to the formation of an aldehyde with (*E*)-configuration, whereas the other tested electrophiles lead to the formation of a (*Z*)-product, as shown in equation 73. The products can be purified by column chromatography and characterized by ^1H and ^{13}C NMR, MS and IR spectra[299].

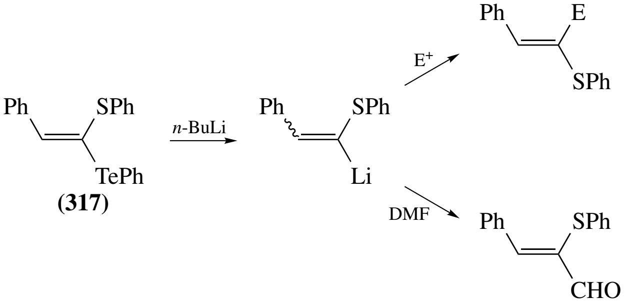

(317)

(73)

Organolithium compounds undergo transmetallation with lithium 2-thienylcyanocuprate (**16**, Table 1) leading to the so-called higher-order lithium cuprates. These intermediates react as the original organolithium compounds but in a more controlled manner. Equations 74–76 illustrate three different modes of quenching higher-order lithium cyanocuprates[21, 22].

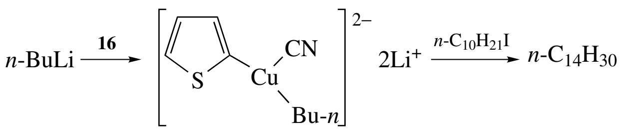

(74)

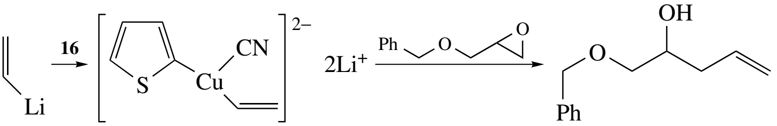

(75)

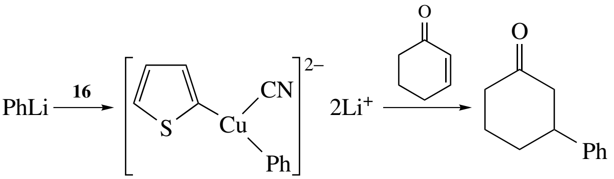

(76)

2. Halide displacement

Quenching organolithium intermediates with an alkyl or aryl halide frequently serves as a finishing step of a synthetic path, as illustrated in the following two paragraphs for some substituted anilines (**318a–c**) and a living polymer (equation 77). In most cases it may be assumed that such processes take place on nucleophilic displacement of the halide by a carbanion. A more complex mechanism has to be assumed, on the other hand, for displacement of halide functional groups by Li, when simple organolithium compounds react with halogenated substrates, leading to metallation of the substrates. These surmised intermediate organolithium compounds may be useful for the initial step of a synthetic path. See also Section VI.C.2.

The site and extent of metallation of organolithium compounds can be determined by adding an alkyl iodide, typically MeI, to a solution of the organometallic compound and, after a few hours, extracting the products and analyzing the mixture. This method can be applied to investigate the site of the metallation reaction of the three isomers of *N*,*N*-dimethyl(methylthio)aniline (**318a–c**) under various conditions, using *n*-BuLi, *t*-BuLi and the superbase resulting from a mixture of *n*-BuLi and *t*-BuOLi. At a certain stage the reaction mixture is brought to room temperature, MeI is added and the mixture is left for 12 h. The mixture is poured into water, acidified, extracted with ether and analyzed by GC-MS. The *p*-isomer (**318c**), for example, is shown to undergo under certain conditions single metallation at either of the ring positions giving **319** and **320**, and at the position α to the S atom giving **321**. Double metallation also takes place at two ring positions giving **322** and at the position α to the S atom and one of the ring sites giving **323** and **324**[300].

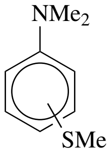

(318) (**a**) *o*-
(**b**) *m*-
(**c**) *p*-

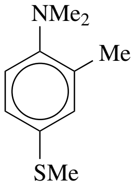

(319)

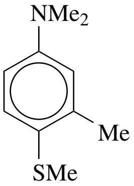

(320)

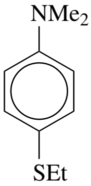

(321)

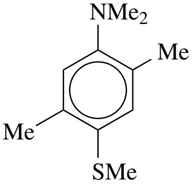

(322)

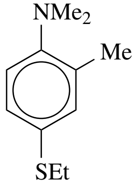

(323)

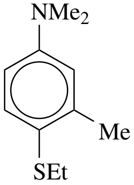

(324)

The living polymers polystyryllithium and polyisopropenyllithium can be functionalized with 3-(dimethylamino)propyl chloride in benzene solution (equation 77). The presence of LiCl increases the functionalization yields. The products were analyzed by size exclusion chromatography and titration of the amino end groups[301].

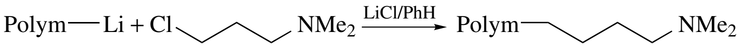

(77)

The synthesis of thiophenol **326** according to equation 78 is assumed to proceed via an intermediate organolithium compound **325**. There is a warning against trying to purify intermediate **325** and similar metallated compounds due to a danger of explosion[302].

Heavily substituted 1,4-diiodo-1,3-butadienes undergo metallation by replacement of the iodine atoms. The dilithio intermediates (**327**) give good yields of the corresponding cyclopentadienones when quenched with carbon dioxide, as shown in equation 79[303]. Quenching intermediates **327** with carbon disulfide does not yield the analogous thiones, but proceeds as in equation 80, by one or more of three different paths, involving intermediates **328–330**. The first two lead to thiophenes and dithio-δ-lactones, respectively, whereas the presence of **330** can be demonstrated on quenching with MeI[304].

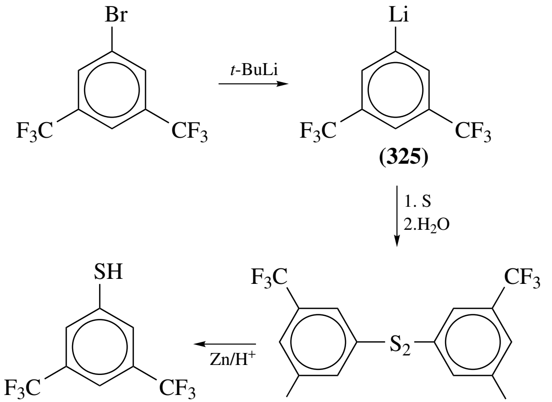

(325)

(326)

(78)

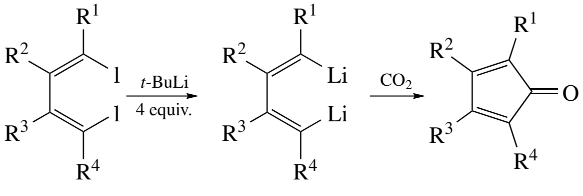

(327)

(79)

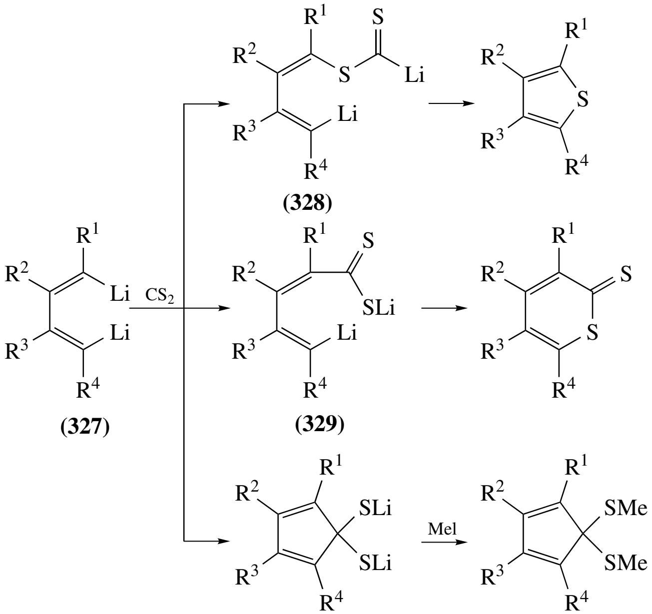

(328)

(327)

(329)

(330)

(80)

Various organolithium intermediates may be postulated for the synthesis of functionalized indoles and other heterocyclic compounds, from substituted *N*-allylanilines (**331a–c**) or the cyclic analog **332**, on treatment with *t*-BuLi. For example, in equation 81 intermediate **333**, derived from **331a**, was quenched with deuterium oxide. Participation of benzyne metallated intermediates, such as **334**, derived from **332**, is surmised in equation 82 and other processes. The products of equations 81 and 82 can be characterized by ^{1}H and ^{13}C NMR spectra[305].

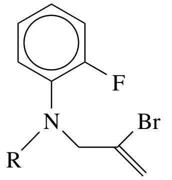

(331) (**a**) R = Me
(**b**) R = allyl
(**c**) R = CH2CH=CHCH3

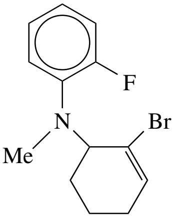

(332)

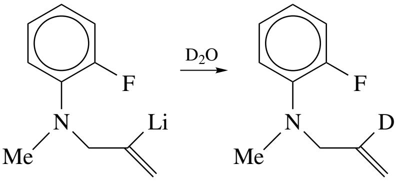

(333)

(81)

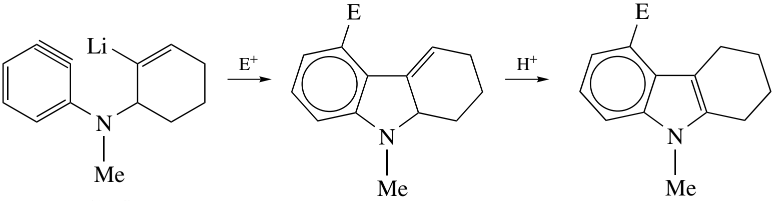

(334)

(82)

The synthetic scheme for functionalized indolines shown in equation 83 assumes formation of a doubly metallated intermediate (**335**), derived from *N*,*N*-diallyl-2,6-dibromo-*p*-toluidine, that may be quenched to the dehalogenated toluidine **336**, or may undergo cyclization to **337**. Quenching of **337** with trimethylchlorosilane in the presence of TMEDA leads to formation of indoline derivatives **338** and **339**. Apparently a second cyclization of intermediate **337** to compound **340** is hard to accomplish[306].

The configurational stability of organolithium compounds with the Li atom at an α-position to an amino group was discussed[307]. Reactions of organolithium compounds in the presence of the asymmetric alkaloid (−)-sparteine (**24**) can be highly enantioselective, as is the case of the cyclization depicted in equation 84, involving an olefinic group. The enantiomeric purity of the product can be established by HPLC, using a chiral special-purpose column and polarimetry[308].

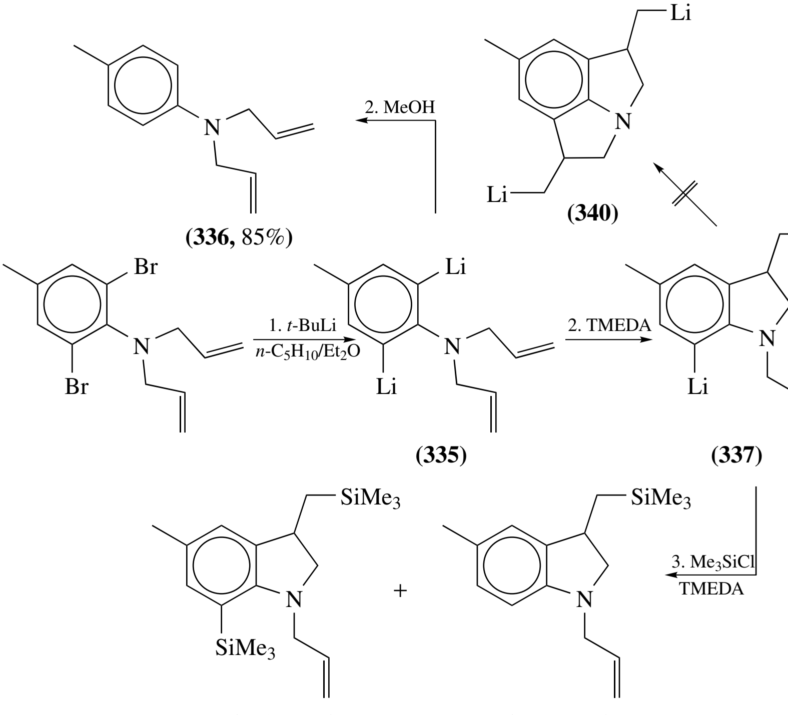

(**336,** 85%) (**340**) (**335**) (**337**) (83)

(**338,** 64%) (**339,** 20%)

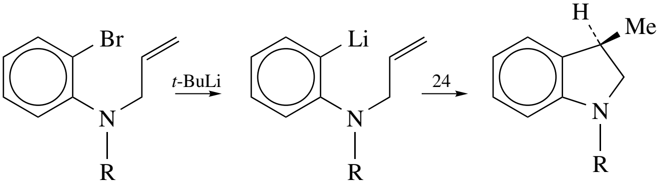

(84)

A multiple sequence of metallation and rearrangement reactions can be proposed (equation 85) for (dichloromethyl)tris(trimethylsilyl)silane (**341**) reacting with various organolithium compounds (**342a–e**). A reaction takes place, involving three equivalents of the simpler alkyllithium and aryllithium compounds (**342a–d**), leading to double alkylation or arylation products **343a–d**, whereas only two equivalents of the functionalized aryllithium compound **342e** are consumed, leading to the formation of a stabilized silene product (**344**). The structure of the products may be characterized by ^{1}H, ^{13}C and ^{29}Si NMR spectra and MS; XRD crystallographic analysis confirmed the structure of compound **344**[309].

A multiple-step scheme is presented in equation 86 for the metallation of organic halides containing group 14 elements (**345a–c**) with various organolithium compounds (**346d–f**). The process is assumed to proceed via unsaturated intermediates (**347a–c**), which may undergo a subsequent metallation to a lithiated intermediate **348**, a dimerization reaction to a heterocyclic cyclobutane **349** or scavenging by various agents, e.g.

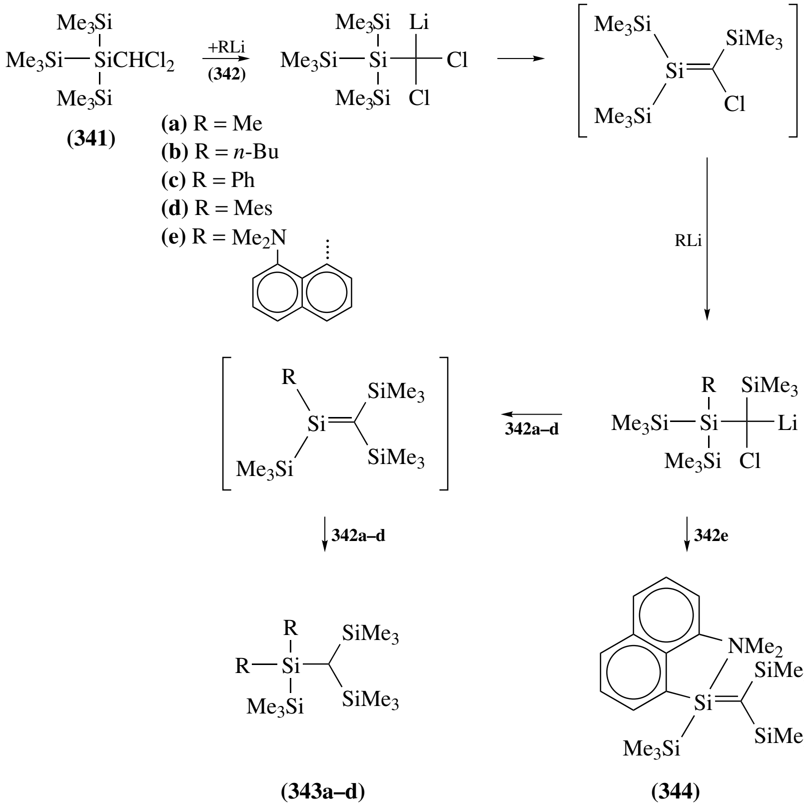
Me3Si
Me3Si—SiCHCl2
Me3Si
(341)
+RLi
(342)
(a) R = Me
(b) R = n-Bu
(c) R = Ph
(d) R = Mes
(e) R = Me2N
Me3Si Li
Me3Si—Si—Cl
Me3Si Cl
Me3Si
SiMe3
Si
Cl
Me3Si
RLi
R SiMe3
Me3Si—Si—Li
Me3Si Cl
342a–d
R
SiMe3
Si
SiMe3
Me3Si
342a–d
342e
R
R—Si
Me3Si
SiMe3
SiMe3
(343a–d)
NMe2
SiMe3
Si
SiMe3
Me3Si
(344)

(85)

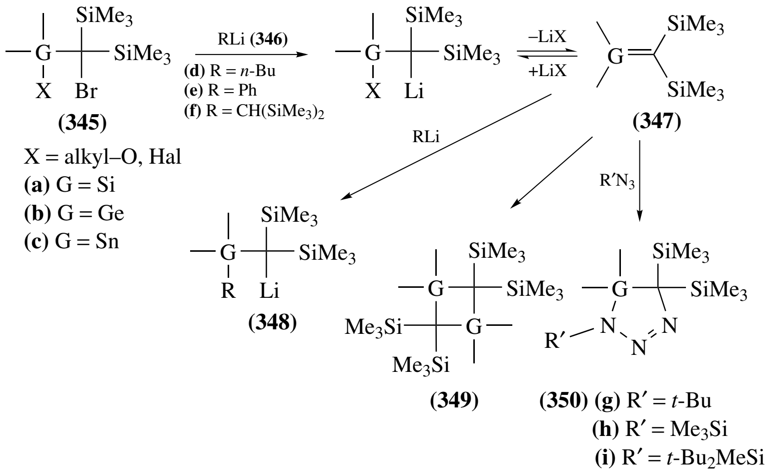
SiMe3
G
SiMe3
X Br
(345)
X = alkyl–O, Hal
(a) G = Si
(b) G = Ge
(c) G = Sn
RLi (346)
(d) R = n-Bu
(e) R = Ph
(f) R = CH(SiMe3)2
SiMe3
G
SiMe3
X Li
–LiX
+LiX
G
SiMe3
SiMe3
(347)
RLi
R′N3
SiMe3
G
SiMe3
R Li
(348)
SiMe3
G
SiMe3
Me3Si
G
Me3Si
(349)
SiMe3
G
SiMe3
R′
N
N
N
(350) (g) R′ = t-Bu
(h) R′ = Me3Si
(i) R′ = t-Bu2MeSi

(86)

alkyl azides to **350g–i**, butadiene, 2,3-dimethylbutadiene etc. The relative rates of the latter competing processes can be measured under various conditions, following the development of the products by ^{1}H NMR analysis[310].

Various alternative reaction paths may be discerned for the oligomerization via lithio derivatives of cubane depicted in equations 87 and 88. 1-Phenyl-4-lithiocubane (**351**) undergoes a double decomposition equilibrium process in the presence of 1,4-diiodocubane (**352**), leading to the formation of **353** (the precursor of **351**) and iodo(lithio)cubane (**354**). The latter organolithium compound undergoes an elimination reaction to attain the cubane-1,4-diyl singlet (**355**). Oligomerization takes place by intercalation of **355** in cubyllithium species such as **351** or **356**. Oligomerization stops when cubyllithium species react with 1,4-diiodocubane (**352**), producing rod-like molecules (**357**) of various lengths. The extent of oligomerization is limited by the low solubility of **352** in Et_2O and the stoichiometric ratio **351**:**352**; for example, for a 4:1 ratio the recovered yields of oligomer (*n*) based on **351** are 66%(2), 12%(3), 0%(4), while for a 1:1 ratio the yields are 38%(2), 24%(3), 6%(4). The oligomeric products **357** can be separated by column chromatography and characterized by ^{1}H and ^{13}C NMR and MS spectra and by single-crystal XRD crystallography[311].

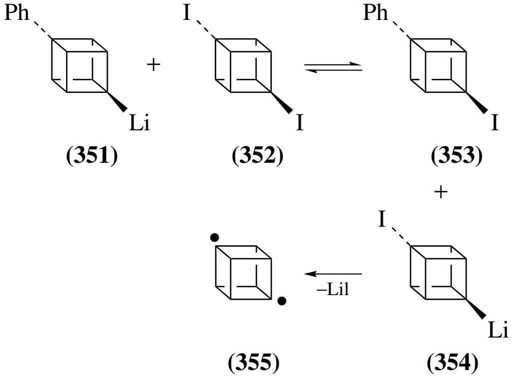

(87)

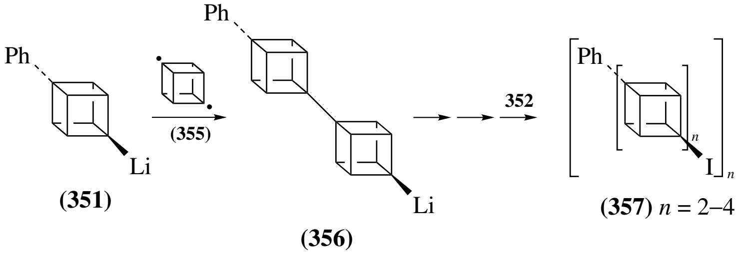

(88)

The intermediate organolithium compound **358** shown in equation 89 is sufficiently stable at low temperature to be determined by ^{19}F NMR spectroscopy. Its presence can also be deduced after quenching with an electrophile, separating and purifying the product **359** and characterizing its structure by physical methods, including IR, ^{1}H and ^{19}F NMR spectroscopies and MS[312].

The dendritic lithiocarbosilane intermediates **360a** and **360b** are obtained by treating the corresponding bromocarbosilanes with *n*-BuLi. They can be functionalized by reaction with various electrophiles and subsequently characterized[313].

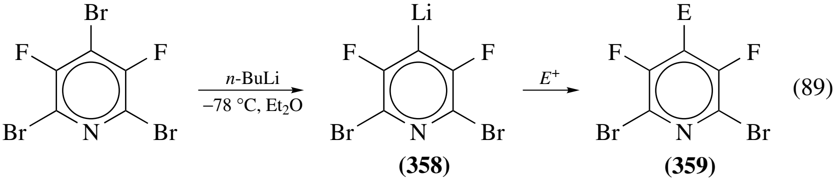

(358) **(359)**

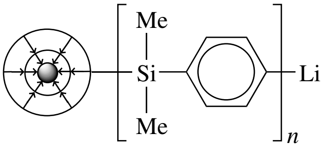

(360) **(a)** $n = 6$
(b) $n = 12$

3. Addition to carbon–carbon double bonds

The reaction of C—Li reagents with carbon–carbon double bonds has great technological relevance because it is the basis of the anionic polymerization processes. This reaction also affords convenient synthetic routes to cyclic compounds, when internal addition to an olefinic double bond present in the metallated molecule takes place (e.g. equations 68, 83 and 84).

In cinnamyl alcohol (**361**) the alkyl groups are inserted at the β-position relative to the phenyl ring. If the reaction is carried out in the presence of (−)-sparteine (**24**) the (*S*)-enantiomer **362** is obtained. In fact, one may proceed with a selective diastereoisomeric synthesis by adding more alkyllithium. However, this reagent acts now as a metallating agent at the benzylic position, leading to intermediate **363**, which may be subsequently quenched with many reagents. In equation 90 quenching is done with diphenyl disulfide, to yield the corresponding diastereoisomeric product **364**. If the starting olefinic double bond has (*Z*)-configuration, for example, the *cis* form of cinnamyl alcohol (**365**), the anomeric configurations **366–368** are obtained, namely the alkylating step affords the (*R*)-configuration product and so forth for the diastereoisomer. For equations 90 and 91 to proceed stereospecifically nonbonding solvents such as hexane or cumene are needed and bonding solvents such as Et_2O or THF should be avoided[314].

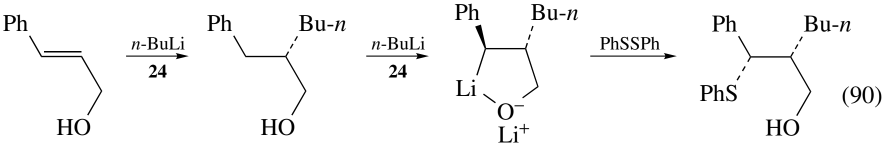

(361) **(362)** **(363)** **(364)**

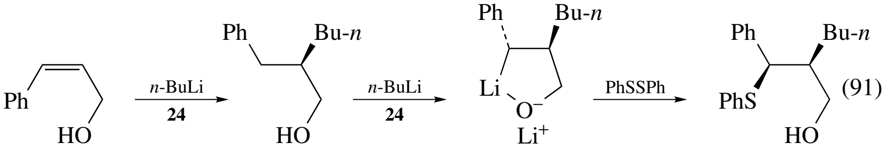

(365) **(366)** **(367)** **(368)**

Styrene and its functional derivatives undergo 1,2-addition reactions with organolithium compounds in Et_2O (equation 92), under conditions where polymerization can be avoided; after quenching with methanol the products are separated by column chromatography and identified by the usual spectroscopic methods. The relative reactivity shown by the various reagents is presented in equation 93. At −78 °C the reaction proceeds with good yield for $X = o$-MeO but not for $X = p$-MeO; however, the latter isomer becomes reactive on raising the temperature to −40 °C. *o*-Allyloxy and *o*-benzyloxy substituents undergo an alkyl transfer rearrangement if the reaction mixture is left to warm up to room temperature (rt) before quenching with MeOH, as shown in equation 94; the rearrangement does not affect the configuration of the migrating group. The nature of the R group affects only slightly the yields of this rearrangement; when the *o*-substituent bears an alcohol function an additional equivalent of RLi reagent has to be added[315].

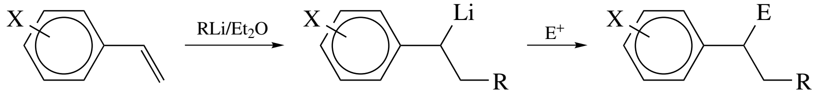

(92)

$$t\text{-alkyl},\ s\text{-alkyl} > n\text{-alkyl} \gg \text{methyl, alkenyl, phenyl} \qquad (93)$$

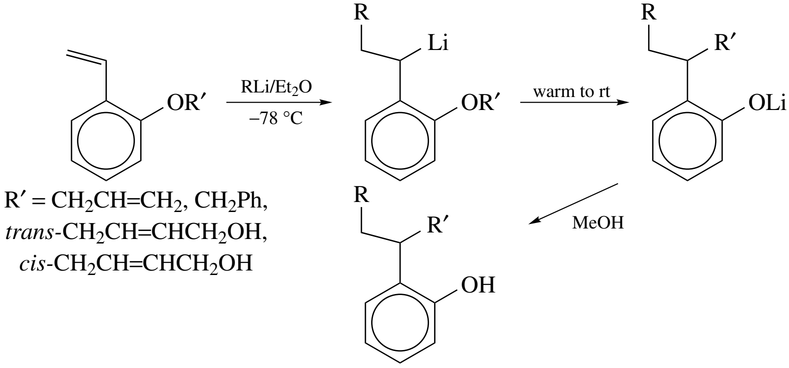

R′ = $CH_2CH{=}CH_2$, CH_2Ph,
trans-$CH_2CH{=}CHCH_2OH$,
cis-$CH_2CH{=}CHCH_2OH$

(94)

Equation 95 depicts two examples of synthesis of chiral metallocenes, involving lithiation of 6-(dimethylamino)fulvene (**369**) with various aryllithium compounds, in the presence of (−)-sparteine (**24**). The intermediate organolithium compounds (**370a–d**) react in one case with iron(II) acetylacetonate and lithium pentamethylcyclopentadienide (**2b**, Table 1) to yield the ferrocenes **371a–d**; the enantiomeric purity of these products is of the order of 99%, except for **371a**, which is slightly lower. In the other case, intermediates **370a–d** react with the rhodium(I) chloride complex with norbornadiene [$RhCl\cdot C_7H_8$] to yield hybrid rhodium metallocenes (**372a–d**) of good enantiomeric quality. Characterization of the products can be carried out by LC on a chiral column, and by ^1H and ^{13}C NMR spectra[316].

The kinetics of addition of *s*-BuLi to *m*-divinylbenzene (equation 96) was investigated by quantitative GC of samples quenched with protons. The final product at −23 °C is the diadduct derived from **374** in quantitative yield. The effects of a Lewis base (Et_3N) and a Lewis acid (Et_2Zn) on the reaction were also studied. The reactivity of the substrate is reduced in the presence of Et_2Zn, and the reaction does not proceed beyond the monoadduct **373**. At −79 °C, in the presence of Et_3N, the divinylbenzene totally disappears to yield 6% of **373** and 94% of **374**. Pure **374** is an initiating agent for butadiene polymerization of a predictable molecular weight and narrow molecular weight distribution[317].

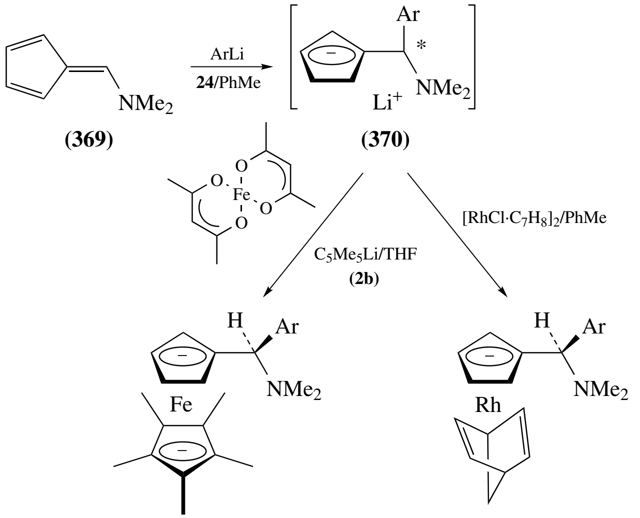

(95)

(371) **(a)** Ar = Ph
(b) Ar = o-MeC$_6$H$_4$
(c) Ar = o-MeOC$_6$H$_4$
(d) Ar = α-C$_{10}$H$_7$

(372) **(a)** Ar = Ph
(b) Ar = o-MeC$_6$H$_4$
(c) Ar = o-MeOC$_6$H$_4$
(d) Ar = α-C$_{10}$H$_7$

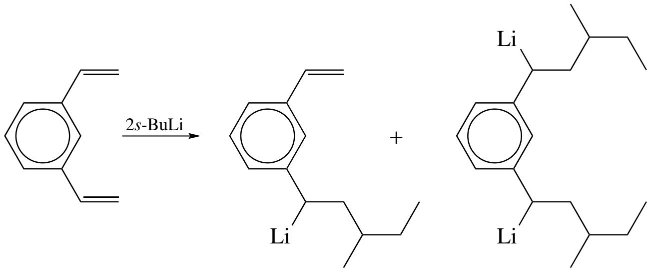

(96)

(373) **(374)**

The consecutive addition reactions of s-BuLi to 1,4-divinylbenzene according to equation 97 can be followed, after quenching with methanol, by GC, ^{1}H NMR and MS of the products. The main product is the diadduct **376**; however, a slow addition side reaction (equation 98) takes place between the monoadduct **375** and the diadduct, leading to the

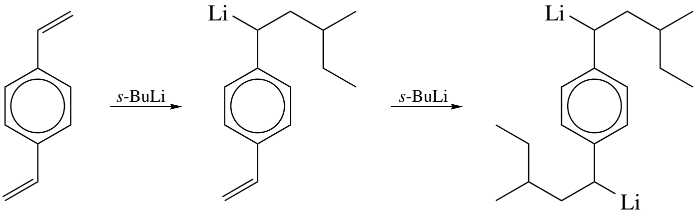

(97)

(375) **(376)**

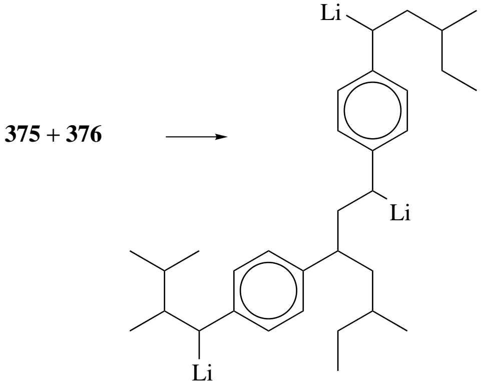

(377)

(98)

formation of the trilithio compound **377**. The diadduct serves as initiator in the anionic polymerization of 1,3-butadiene[318,319].

t-BuLi and naphthalene form a stable yellow-orange complex in pentane solution; however, on adding one equivalent of THF a series of reactions take place that are summarized in equation 99. This results in single substitution reactions to yield metallated (**378a**) and alkylated (**378b**) naphthalene, and 1,4- and 1,2-additions to yield dearomatized products (**379a–c**) that are both metallated and alkylated. A detailed study of the mechanism of the processes taking place in this system was carried out and compared with the alkylation taking place with *t*-BuCl and lithium naphthalene (equations 123–125 in Section VI.C.2). The products can be analyzed by a combination of GC, GC/MS and NMR techniques[141].

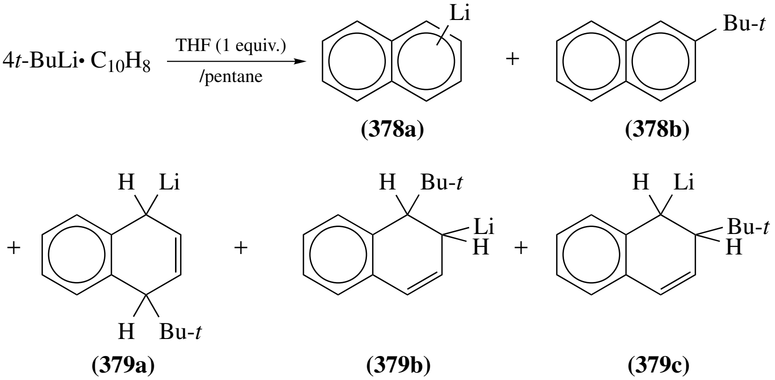

(378a) **(378b)** **(379a)** **(379b)** **(379c)**

(99)

4. Addition to carbonyl compounds and their imino derivatives

Quenching organolithium compounds with aldehydes and ketones is a frequently used route for attaining secondary and tertiary alcohols. Quenching with imines or similar compounds leads to functionalization with the corresponding variants of the amino group. Such reaction can be carried out at the end of long synthetic paths, just before the final quenching with protons.

The reaction depicted in equation 100, involving a dithiane organolithium reagent (**380**) and an α,β-unsaturated carbonyl compound, takes place exclusively by the 1,2-addition route in THF solvent, leading to adduct **381**. The course of reaction may be changed on adding HMPA; for example, addition of 2 equivalents of HMPA affords more than 95% of adduct **382**, by a 1,4-addition mechanism. The reaction is regiospecific in the presence of four equivalents of HMPA. Molecules of **380a** in THF solution are shown to be monomeric by cryoscopic measurements[320], and those of **380b** may also be presumed to be so, as branching usually interferes with oligomerization of organolithium species. The degree of evolution of various solvation species of reagents **380** can be followed on gradual addition of HMPA to the THF solution, up to four equivalents, using ^{6}Li, ^{7}Li and ^{31}P NMR spectra[321]. The course of equation 100 much depends on the presence of certain additives. For example, when the reaction of **380a** takes place with no additives or in the presence of the chiral urea derivatives (*S*,*S*)-**383** or (*R*,*R*)-**384**, the main product is **381** (1,2-addition); this points to the additives probably being unable to coordinate with the moieties involved in the transition state. On the other hand, the preferred course of reaction leads to **382** (1,4-addition) in the presence of HMPA or the less crowded urea derivatives DMPU (**25**) or (*S*,*S*)-**385**. No enantioselectivity is induced by any of the chiral additives employed. Product characterization can be performed by LC on a chiral column and ^{1}H and ^{13}C NMR spectroscopies[322].

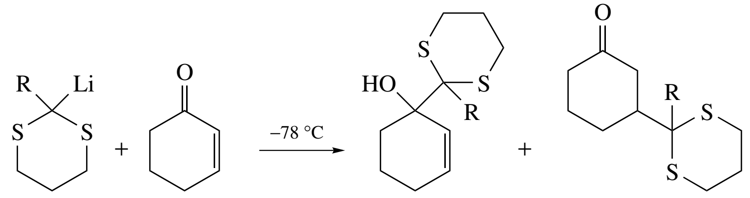

(380) **(a)** R = H
(b) R = Me

(381)

(382)

(100)

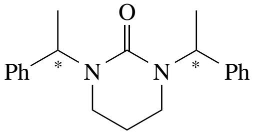

(383)

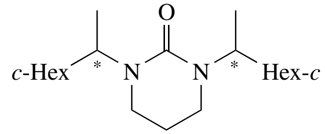

(384)

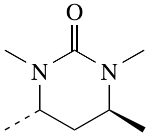

(385)

α-Alkylation of ketones can be accomplished by metallation of the corresponding ketoxime followed by quenching with an alkyl halide, as illustrated in equation 101. The last step in this process is a cyclization catalyzed by sulfuric acid[323].

Conjugated dienes can be prepared from certain ketones via their trisylhydrazones (**386**) by the Shapiro reaction (equation 102). This involves a reductive metallation to a vinyllithium intermediate, transmetallation, for example, with Cu(I) iodide, and oxidative coupling[324].

Quenching polystyryllithium and polybutadienyllithiums with *N*-benzylidenemethylamine (PhCH=NMe) in benzene solution leads to amine-functionalized polymers (equation 103), that can be characterized by SEC, TLC, acid–base titration and ^{1}H and ^{13}C NMR spectroscopies. The end groups are monomeric. Gradual addition of Et_2O reduces the yields. This is attributed to increased reactivity of the alkyllithium residues in the polymer, bringing about a concurrent metallation reaction of the imine reagent (e.g. equation 101)[325].

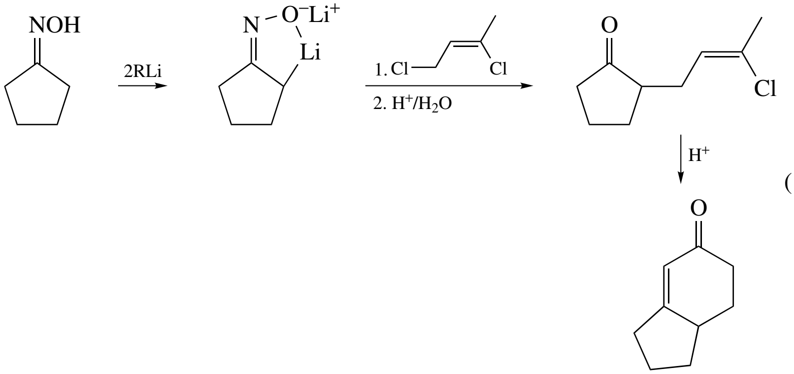

(101)

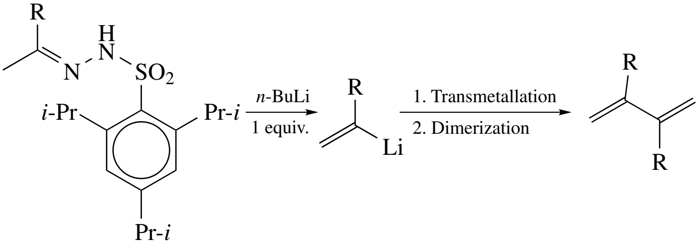

(102)

(386) **(a)** R = n-C_7H_{15}
(b) R = c-Hex

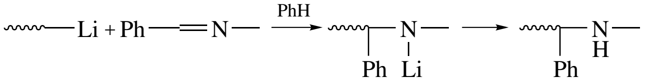

(103)

Compound **388** is an acylating agent for electron-deficient alkenes, in a Michael addition process. It is formed by treating molybdenum hexacarbonyl with an organolithium compound, followed by quenching the intermediate **387** with boron trifluoride (equation 104). The structure of **388** (R = Ph) can be elucidated by ^{13}C NMR spectroscopy[326]. Other examples of enantioselective and diastereoselective Michael-type additions involving lithium-containing intermediates in the presence of chiral additives can be found elsewhere in the literature[327].

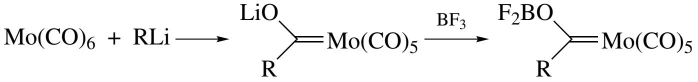

(104)

(387) **(388)**

5. Directed ortho-substitution

Metallation of variously substituted benzanilides (**389**), followed by treatment with an electrophile, lead to the formation of 2-aryl-3-hydroxyisoindol-1-ones (**391**), as shown in equation 105. The intermediate organolithium compound (**390**) closes a five-membered ring on reacting with electrophilic methyl benzoates (**392a** and **392b**), *N*,*N*-dimethyl-4-pyridinecarboxamide (**393**) or DMF (source for $R^5 = H$). Products **391** can be characterized by ^1H NMR[328].

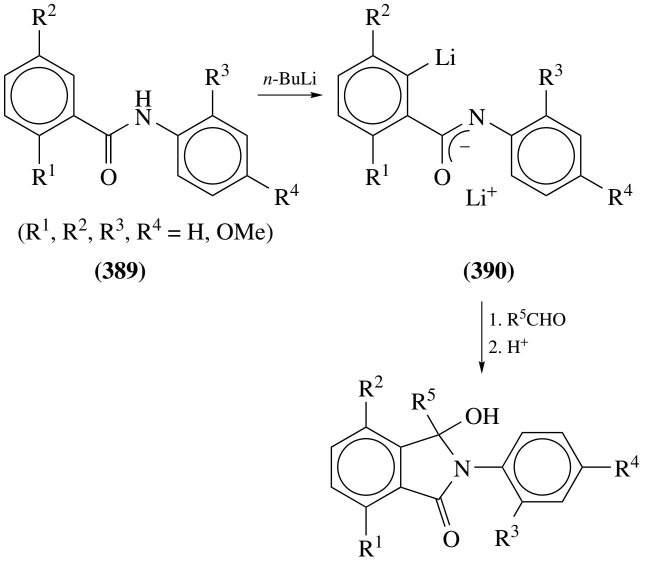

(R^1, R^2, R^3, R^4 = H, OMe)

(389)

(390)

(105)

(R^5 = Ph, 4-ClC_6H_4, 4-Py, H)

(391)

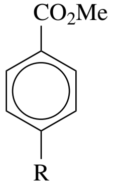

(392) **(a)** R = H
(b) R = Cl

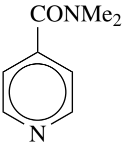

(393)

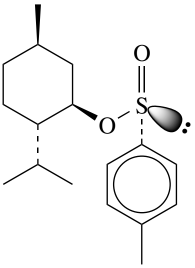

(394)

Enantioselective synthesis of atropoisomeric species can be achieved by asymmetric induction with (1*R*,2*S*,5*R*)-(−)-menthyl (S_S)-*p*-toluenesulfinate (**394**). This is illustrated, for example, in equation 106, depicting a first metallation followed by sulfoxide formation that traps the bulky diisopropylamino group of the carboxamide and the *p*-tolyl group of the sulfoxide in an antiperiplanar configuration. Furthermore, asymmetric induction by **394** leaves the amide in (*R*)-configuration. The second metallation step preserves the configuration of the carboxamido group, and the final atropoisomer is attained on treatment with a bulky electrophile. The reaction products can be characterized by LC, polarimetry, IR and ^1H NMR spectroscopies and single-crystal XRD crystallographic analysis[329].

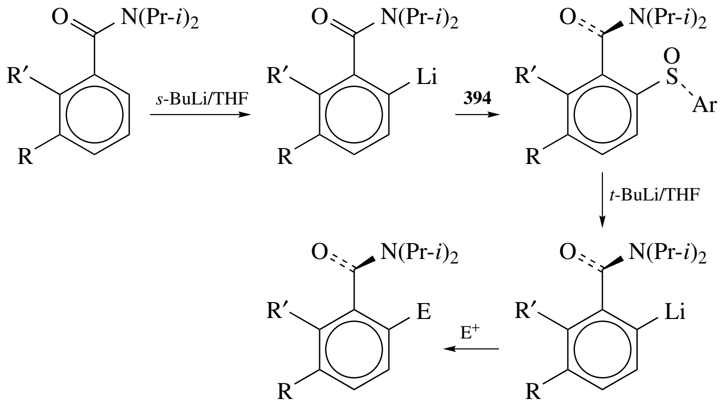

(106)

Lithiation of the sterically hindered amide **395** leads to an equilibrium mixture of α- and *o*-metallated species, as shown in equation 107. This can be demonstrated by the usual methods of analysis of the products **396** and **397**, obtained after quenching with an electrophile. The relative amounts of these products depend on the electrophile and mode of operation; for example, the ratio is larger than 10:1 in favor of **397** for E = Me_3Si, whereas for E = Me it is 2:1 in favor of **396**, which increases to 10:1 when addition of MeI

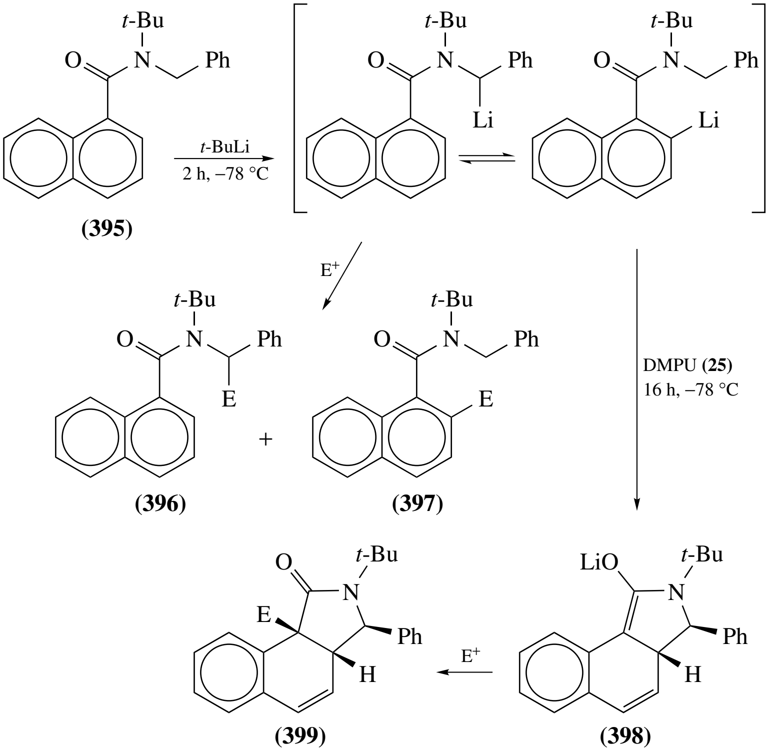

(107)

is made shortly after adding DMPU (**25**). The metallated species undergoes stereospecific dearomatization and cyclization to intermediate **398**, and finally stereospecific quenching to product **399**[330, 331].

6. Reaction with tertiary amides

Tertiary amides bearing epoxide and other labile moieties can be converted to the corresponding ketones (**400a** and **400b**) in good yields, by treatment with alkyl- or aryllithiums followed by the usual quenching with a proton (equation 108). Furthermore, if the quenching is done with a peracid the amide is transformed to an ester (**401**, equation 109). Both processes leave the epoxy function unscathed[332].

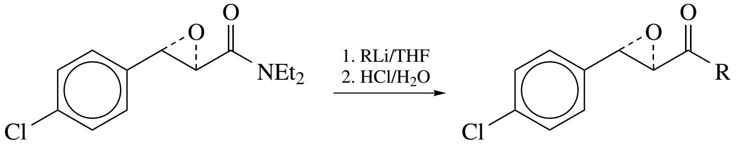

(108)

(400) **(a)** R = Me
(b) R = Ph

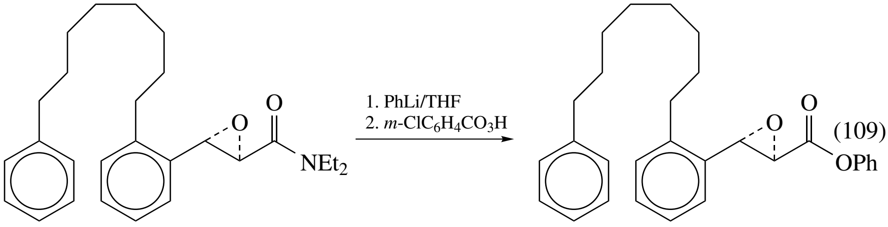

(109)

(401)

7. Metallation at allylic and benzylic positions

Prochiral N-Boc-N-arylcinnamylamine (**402**) undergoes a stereospecific metallation at the allylic position. In the presence of (−)-sparteine (**24**), a complex crystallizes which is shown by XRD analysis to have the absolute configuration **403**, where the Li atom is η^3-bonded to the propene carbanion and coordinated to the O atom of the amido group; the molecule of the alkaloid is represented by two N atoms joined by an arc. It may be assumed that this configuration is kept also in solution, as demonstrated by highly stereoselective reactions taking place at the benzylic position marked with an asterisk on **403** (equation 110). Benzyl bromide undergoes nucleophilic substitution by approaching the carbanion from underneath, resulting in an inversion of configuration (product **404**), whereas reactions with β-nitrostyrene, cyclohexanone or 5,6-dihydro-2H-pyran-2-one preserve the configuration in their respective products **405**, **406** and **407**. This is probably due to formation of intermediate 1,2- and 1,4-addition products. Determination of the enantiomeric and diastereoisomeric purities can be carried out by preparative LC using a chiral stationary phase, followed by ^{1}H and ^{13}C NMR spectroscopies and HRMS[333–336]. The configurational stability of carbamate-stabilized organolithium species is enhanced by steric restriction; carbamate stabilization seems to be more efficient than the stabilization attained by Boc-amino groups[337].

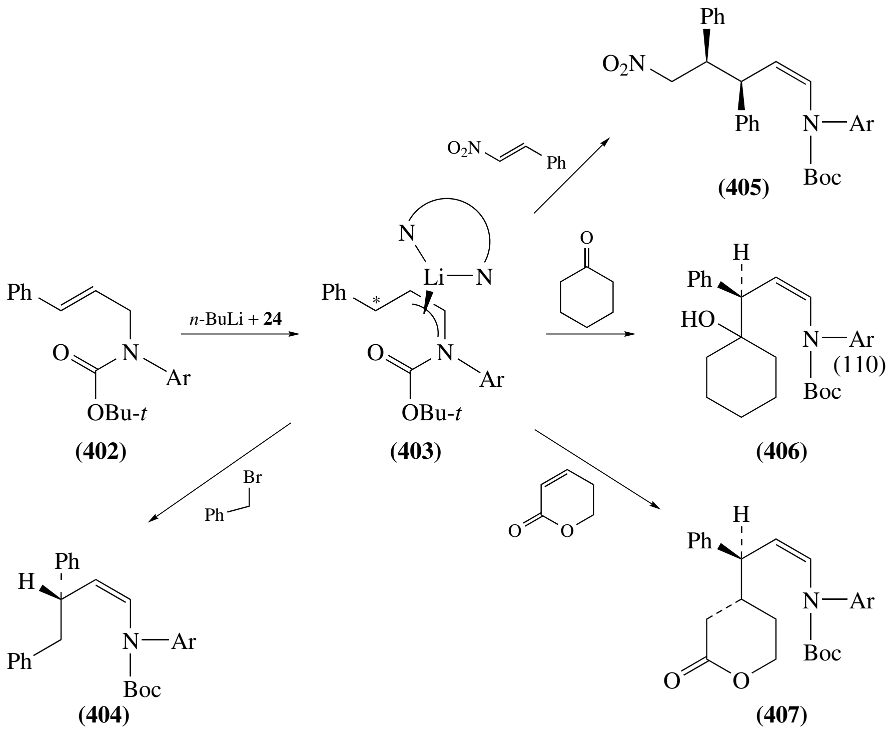

(110)

Methylbenzenes undergo metallation at benzylic positions in the presence of certain alkoxides. Quenching with ethylene leads to formation of 3-pentylbenzenes, as shown for mesitylene in equation 111. The quenching reaction seems to be limited by steric effects on two accounts: No replacement of the third benzylic H atom takes place, and only methyl groups with an adjacent empty position on the benzene ring undergo double alkylation. Thus, durene, pentamethylbenzene and hexamethylbenzene yield under the same conditions compounds **408a**, **408b** and **408c**, respectively. The presence of the alkoxides precludes telomerization of ethylene[338a].

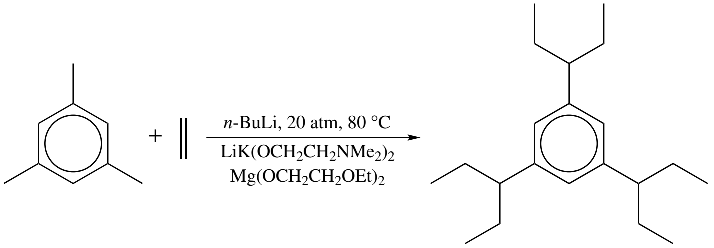

(111)

A study of methods for controlling the grafting sites of polystyrene polymers may serve as an example for the quantitative and structural analysis of the site of lithiation. Trimethylsilyl chloride serves as the quenching agent owing to the low incidence of side reactions besides metal replacement. Thus, on varying the conditions of metallation of low molecular weight polystyrene (**409**) and poly(4-methylstyrene) (**410**), aromatic and

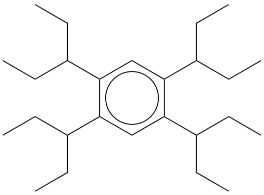

(408a)

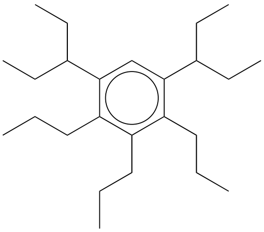

(408b)

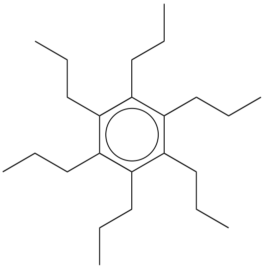

(408c)

aliphatic substitution can be distinguished by ^{1}H NMR of the $SiMe_3$ group. However, ^{29}Si NMR may also be used for more detailed analysis of the various sites[38b].

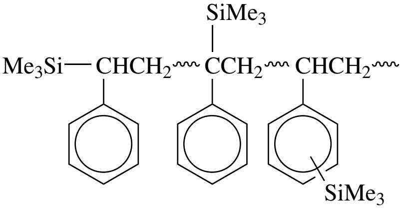

(409)

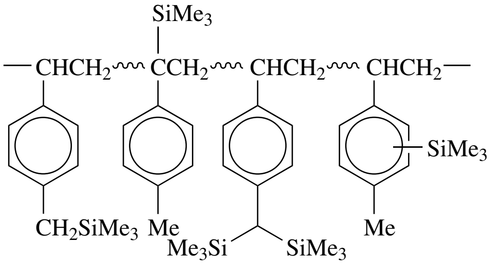

(410)

8. Cleavage of C−O bonds

Reactions of organolithium species with epoxides, yielding secondary alcohols, are shown in equations 69 and 75 (Section VI.B.1).

On quenching polystyryllithium with excess ethylene oxide, the question arises whether this leads to formation of oligomeric end chains derived from the quenching reagent. When using ^{13}C-enriched ethylene oxide, the absence of ^{13}C NMR peaks at $\delta = 69-70$ and 72−73 ppm, corresponding to $OCH_2CH_2OCH_2CH_2OH$ end chains, points to formation of monomeric end groups only. This can be confirmed by MALDI-TOF MS, where only peaks corresponding to CH_2CH_2OH and C_4H_9 (stemming from the initiation reagent) are detected. A small peak (*ca* 3%) corresponding to a dimeric end chain appears in the MS when using a tenfold excess of ethylene oxide[339].

Carbolithium compounds of moderate reactivity open the O−C bond of cyclic sulfate esters or cyclic sulfamidates to produce new C−C links, as shown, for example, in equation 112 for a chiral cyclic sulfamidinate and 2-lithio-1,3-dithiane (**380a**). More reactive organolithium species, such as *n*-BuLi and PhLi, yield mixtures of products, probably due to attack on the S atom of the sulfonamido group too[340].

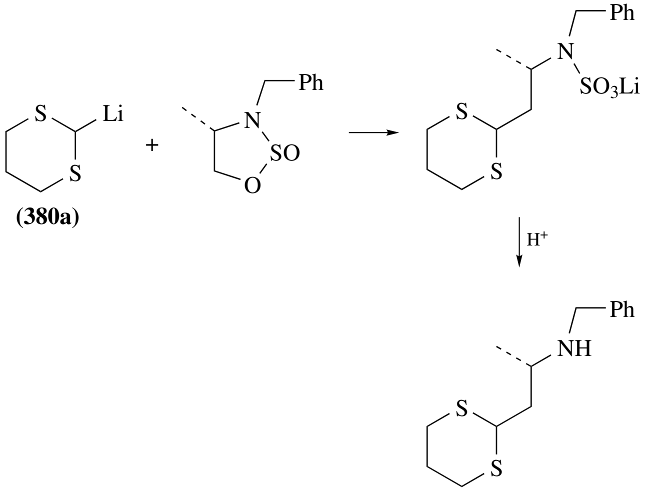

(112)

C. Metallation with Lithium Arenes

Various effective synthetic routes can be based on metallation of organic substrates with lithium arenes, obtained *in situ* from metallic lithium and an arene present in substoichiometric amounts. Immediate quenching of the lithiated intermediates may be considered as a reduction reaction of the original substrate. Otherwise, further functionalization may be attained when using diverse electrophiles. Various examples of such processes follow (see also equation 69 in section VI.B.1).

1. Scission of cyclic ethers and thioethers

Opening 2,3-benzocyclic ethers with lithium arenes may break either or both C−O bonds, by the so-called dealkylation or dearylation processes, leading to different products after quenching with protons. For example, 2,3-benzofuran undergoes only the dealkylation opening shown in equation 113, leading to formation of 2-vinylphenol. The *Z*-configuration of the metallated intermediate can be surmised from the configuration of the products after quenching with electrophiles other than protons. When 2,3-benzo-4*H*-chromene (**411**) is subjected to the same lithiation treatment, both dearylation and dealkylation openings take place (equation 114), leading to formation of 3-phenylpropanal and 2-allylphenol, respectively, in 2:1 molar ratio[341].

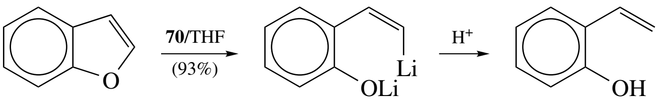

(113)

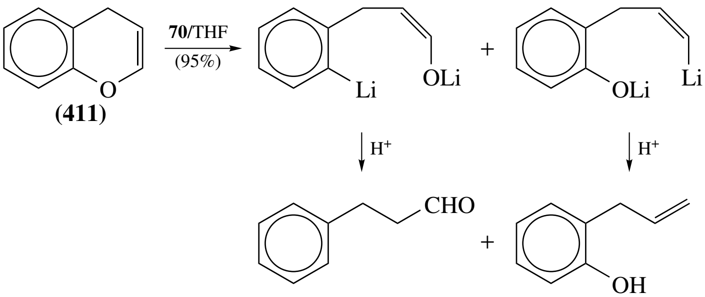

(114)

Functionalized organolithium intermediates **412–417**, can be used as synthones for addition to various substrates containing the C=C–C=O moiety or for dimerization via the C–Li bonds, all catalyzed by Cu(I) and Cu(II) salts[342, 343]. They may also be exposed to various electrophiles; for example, intermediate **412** reacts with carbon dioxide as shown in equation 115, to yield a lactone (**418**) as the only product after workup[344].

Other synthetic routes may be proposed, involving intermediates **413** and **414**, as depicted in equations 116 and 117, respectively. These intermediate stages are obtained on metallation by lithium catalyzed by substoichiometric amounts of 1,4-di-*t*-butylbiphenyl, probably via the radical anion adduct formed by this arene with lithium (**70**). The process involves additional metallated intermediates obtained on treatment with zinc bromide, treatment with electrophiles such as aryl or vinyl bromides catalyzed by Pd(II) and final quenching by protons[345, 346]. The course of reaction after adding $ZnBr_2$ or other Lewis acids and quenching with α,β-unsaturated ketones (e.g. 2-cyclopentenone) or esters (e.g. methyl 2-butenoate) has been investigated[347]. Intermediates resulting from the scission of cyclic ethers (**419**) undergo cross-coupling with α,β-unsaturated aldehydes, ketones or esters (**420** and others such as 2-cyclopentenone and 2-cyclohexenone), in the presence of 2 equivalents of a Cu(I) salt (CuI and HMPA or DMPU or the complex $Cu(I)Br{\cdot}SMe_2$, equation 118). When the process is conducted in the presence of a Cu(II) salt ($CuCl_2$), the only product is a dimer of **419**. The final quenching is done in either case with an aqueous solution of ammonium chloride. The products can be characterized by the usual IR, ^{1}H and ^{13}C NMR and MS spectroscopies[348].

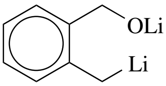

(412)

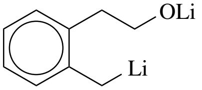

(413)

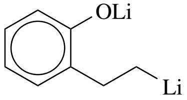

(414)

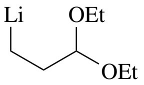

(415)

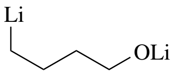

(416)

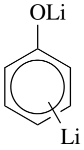

(417) **(a)** *m*-Li
(b) *p*-Li

(115)

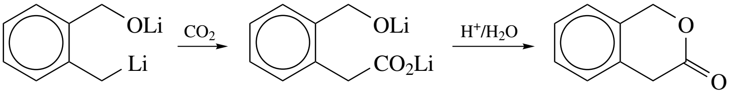

(412) **(418)**

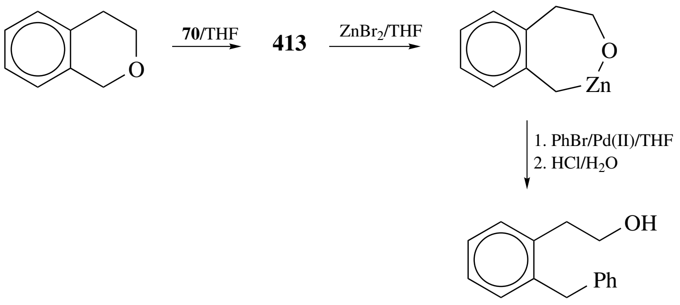

(116)

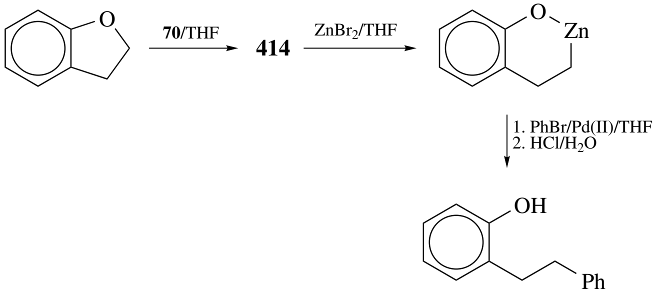

(117)

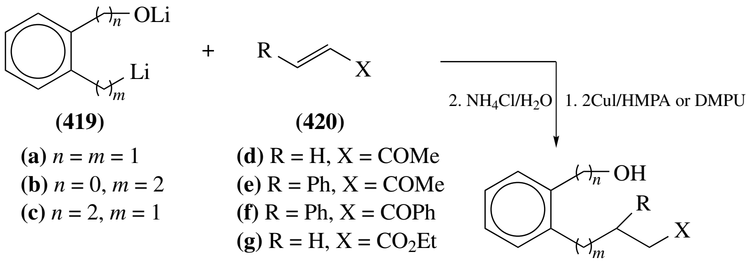

(419)

(**a**) $n = m = 1$
(**b**) $n = 0$, $m = 2$
(**c**) $n = 2$, $m = 1$

(420)

(**d**) R = H, X = COMe
(**e**) R = Ph, X = COMe
(**f**) R = Ph, X = COPh
(**g**) R = H, X = CO_2Et

(118)

A linear phenylene–ethylene copolymer is obtained by a Wurtz-type condensation of 1,2-dibromoethane and 1,4-dibromobenzene. A cross-linked variation can be obtained on addition of 1,3,5-tribromobenzene to the reaction mixture. Equation 119 illustrates the reductive scission of a cyclic ether, catalyzed by such polymers in the presence of lithium, followed by quenching with cyclohexanone[349].

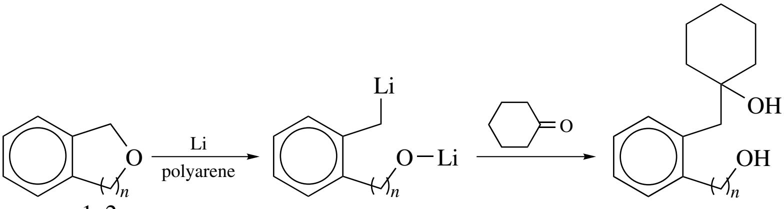

$n = 1, 2$

(119)

Epoxide (**421a**) and oxetane (**421b**) rings are opened by a suspension of Li in the presence of catalytic amounts of 1,4-di-*t*-butylbiphenyl, as shown in equation 120. The solutions, presumably containing an intermediate organolithium compound, can be treated with an electrophile E, such as water, deuterium oxide, benzaldehyde, acetone or cyclohexanone. After workup, the products **422** are isolated and their structure can be determined by the usual spectroscopic and crystallographic methods[350].

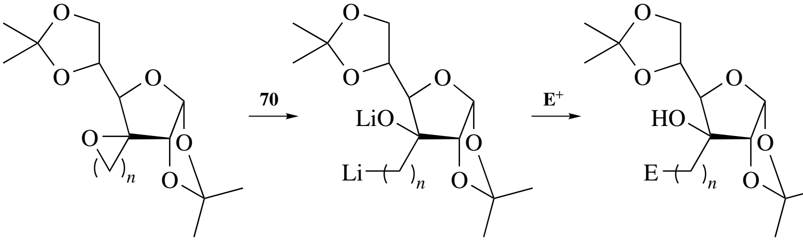

(120)

(421) **(a)** $n = 1$
(b) $n = 2$

(422)

Metallation of substrates containing the oxazolidine ring (**423**) affords more stable organolithium intermediates (**424**), probably due to coordination of the *C*-Li to the alkoxide group. Equation 121 illustrates quenching with $PhCH_2Cl$, BuBr or BuI, leading to good stereoselectivity (**425:426** ratio $\geqslant$ 93:7). Quenching with the less bulky protons or deuterons gives poor stereoselectivity, or with the less reactive BuCl gives poor yields and stereoselectivity, as analyzed by ^1H NMR and GC-MS methods[351].

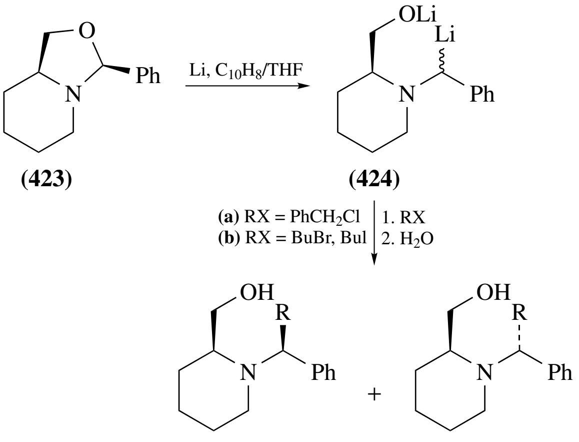

(423) **(424)**

(121)

(425) **(426)**

Metallation of 4-hetero-substituted dibenzothiins (**427**) with lithium, catalyzed by 4,4′-di-*t*-butylbiphenyl (equation 122), breaks one of the C−S bonds. Quenching with carbonyl compounds leads to the corresponding thiophenols (**428**) that may be cyclized to the homologous seven-membered heterocycles (**429**). The products can be characterized by IR, ^1H and ^{13}C NMR spectroscopies and MS[352].

2. Metallation of halides

A detailed analysis of the reaction mechanism of *t*-BuCl with lithium naphthalene in THF solution raises some interesting points. Although the overall stoichiometry of the

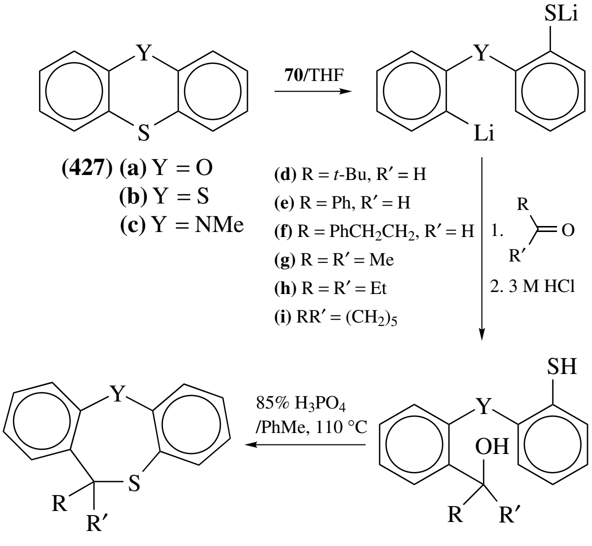

(427) **(a)** Y = O
(b) Y = S
(c) Y = NMe

(d) R = *t*-Bu, R′ = H
(e) R = Ph, R′ = H
(f) R = $PhCH_2CH_2$, R′ = H
(g) R = R′ = Me
(h) R = R′ = Et
(i) RR′ = $(CH_2)_5$

(122)

(429) **(428)**

reaction is 1:2, according to magnetic titration (see Section III.B.5), various products are obtained, including metallation of the alkyl group (pivalic acid results on quenching with CO_2) and alkyldihydronaphthyl carbanions (possibly as a result of the reaction scheme depicted in equations 123–125). The mechanism of this system may be compared to that of the reaction of *t*-BuLi with naphthalene (equation 99). The products can be analyzed by a combination of GC, GC-MS and NMR techniques[141].

$$R{-}X + C_{10}H_8^{\cdot -} \longrightarrow R^{\cdot} + X^- + C_{10}H_8 \qquad (123)$$

$$R^{\cdot} + C_{10}H_8^{\cdot -} \longrightarrow RC_{10}H_8^- \qquad (124)$$

$$R^{\cdot} + C_{10}H_8^{\cdot -} \longrightarrow R^- + C_{10}H_8 \qquad (125)$$

Chlorocyclohexenes (**430a** and **430b**) undergo metallation with Li in the presence of substoichiometric quantities of naphthalene, as shown in equation 126. The organolithium intermediate reacts with electrophiles such as water, aldehydes and ketones to form products (**431a** and **431b**) in good yields. Diastereoselectivity is high in some cases; for example, acetophenone yields on reaction with **430a** a secondary alcohol with diastereoisomeric ratio (R^*, R^*):(R^*, S^*) = 4:1 and *N*-benzylideneaniline yields a secondary amine with (R^*, R^*):(R^*, S^*) = 1:9[353].

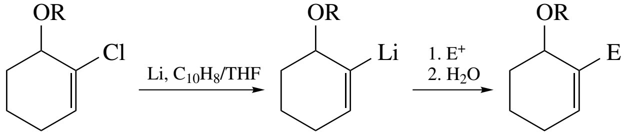

(126)

(430) **(a)** R = Me
(b) R = OCH_2OEt

(431)

Organic compounds possessing a 6-chloro-1-hexene open-chain partial structure may undergo two possible arene-catalyzed lithiation processes, depending on the temperature at which metallation takes place. This enables synthetic routes to two different skeletal systems. At low temperatures the usual halogen-for-lithium exchange takes place at the 6-position, leading to the open-chain derivatives, as illustrated in equation 127 for quenching with 3-pentanone. When metallation is carried out at a higher temperature, a 2,6-cyclization takes place with metallation at the 1-position, leading to cyclopentane derivatives, as shown in equation 128 for the same quenching reagent. A mechanism was proposed for the processes (equation 129) involving two single electron transfers from the lithium arene radical anion to the organic substrate. On the first electron transfer a reduction takes place to a free radical that may undergo cyclization when working at the higher temperatures; the second electron transfer produces the carbanion to which the Li$^+$ cation becomes anchored[354].

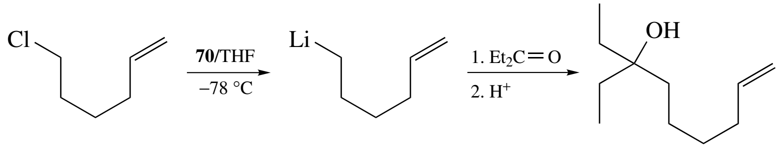

(127)

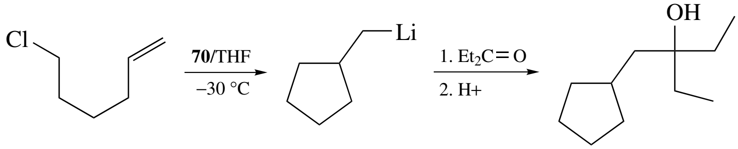

(128)

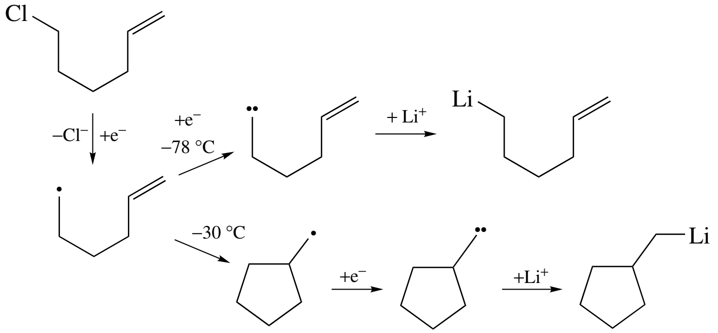

(129)

Two different reactions involving organolithium reagents are depicted in equation 130. The first one is a straightforward combination with an allyl bromide to produce a homoallyl thioether (**432**). The second one involves *in situ* generation of the radical anion lithium 1-(dimethylamino)naphthalene (**71**), a reductive metallation of **432** to a homoallyllithium intermediate and addition to α,4-dimethylstyrene to yield still another organolithium intermediate (**433**). Instead of this being the initiation of a living polymerization, in the given environment **433** undergoes cyclization to the sesquiterpene (±)-cuparene (**434**)[146].

The same polymeric arenes that served as metallation catalysts in equation 119 can also be used for silylation in Barbier-type reactions (equation 131). The polymer is presumably converted to a lithium arene adduct that activates metallic lithium for metallation of the halogenated substrates, before addition of an electrophile to achieve the synthetic goal. Equations 132–135 illustrate some of the cases investigated. The products can be characterized by the usual spectroscopic methods[349].

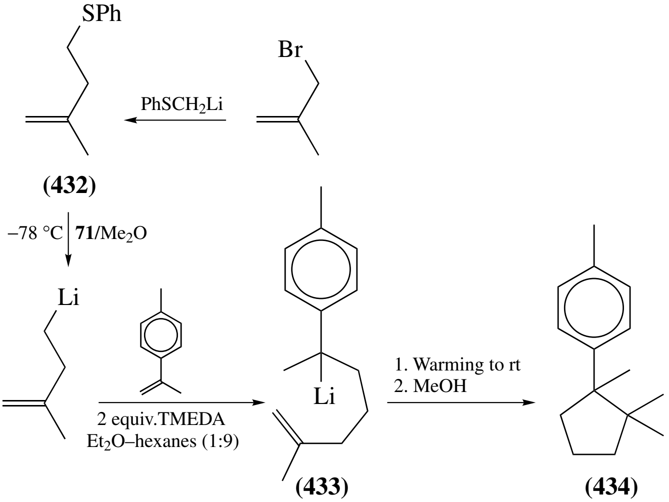

(130)

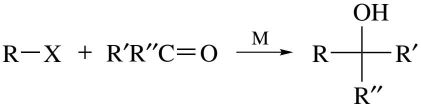

$$R{-}X \ + \ R'R''C{=}O \xrightarrow{M} R{-}\overset{OH}{\underset{R''}{C}}{-}R'$$

M = Li, Mg, Sm(II), Zn
R = alkyl, aryl, vinyl, allyl
X = Cl, Br, I

(131)

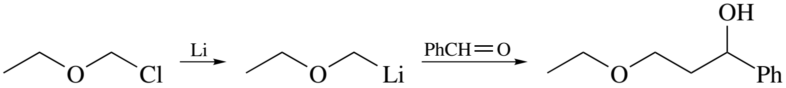

(132)

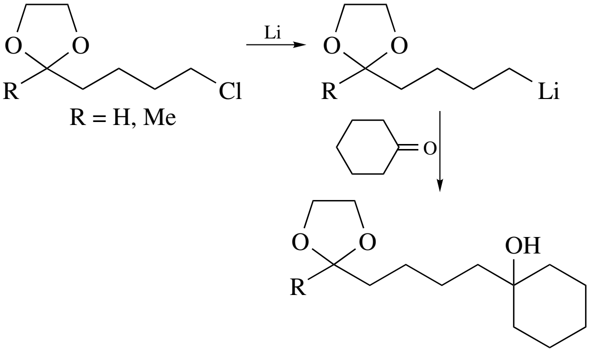

(133)

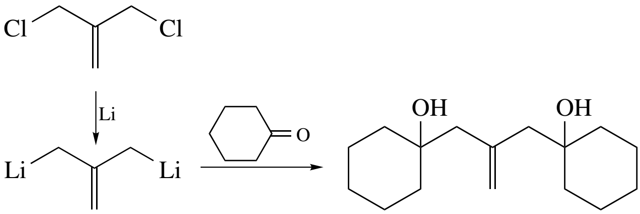

(134)

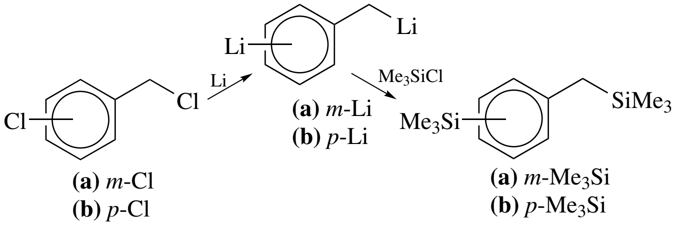

(135)

Polystyrene functionalized with chloromethyl groups (**435**) can be metallated with lithium powder in the presence of 4,4′-di-*t*-butylbiphenyl (**70**) and quenched with water or deuterium oxide, yielding the corresponding methylated polystyrenes (**436a** and **436b**). When quenching with trimethylsilyl chloride and various aldehydes (butanal, benzaldehyde) or ketones (3-pentanone, cyclohexanone), best results are obtained by carrying out the metallation in the presence of the electrophile, followed by a final quenching with MeOH (Barbier conditions, equation 136)[355].

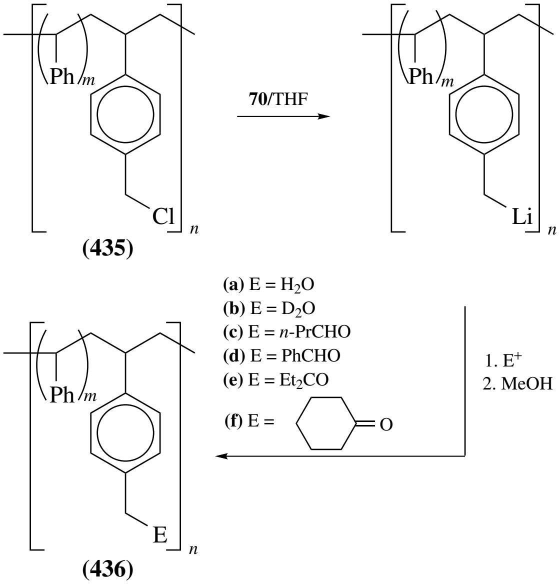

(136)

3. Metallation of diphenylacetylene

Dimerization of diphenylacetylene in the presence of lithium is of historic significance. Formation of organolithium intermediates according to the first step of equation 137 was proposed, though not directly demonstrated. The 1,2,3,4-tetraphenyl-1,3-butadiene dimer was obtained on quenching with dry ethanol the ‘red granular solid’ that precipitated from the reaction mixture[356]. It should be pointed out that this work was carried out at room temperature and without provision for an inert atmosphere; the good yield of dimer obtained was probably due to the relatively small amount of oxygen that was present in the closed reaction flask. The presence of the same dianionic intermediate **437** can be inferred for the course of the cyclization reaction depicted in equation 137, where selenium atoms become intercalated similarly to equation 25 (Section IV.A). Strict control of reaction conditions, including reaction time, is necessary in view of the competing cyclization of **438** into a naphthyl moiety. The structure of tetraphenylselenophene (**438**) can be elucidated from IR and ^{1}H NMR spectra and single-crystal XRD analysis[155].

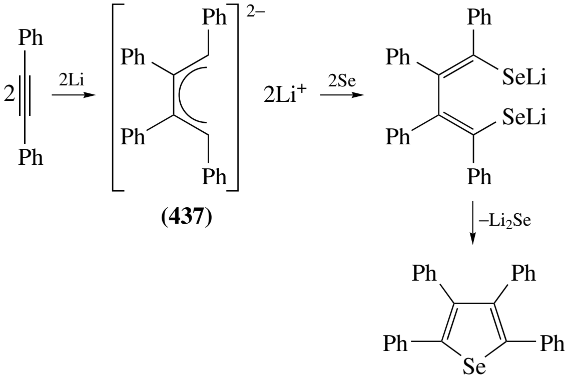

(437)

(438)

(137)

4. Metallation of acetic acid

Among the varied applications of lithium naphthalene in organic synthesis[7] the reaction with carboxylic acids to yield β-hydroxycarboxylic acids after quenching with a ketone is presented in equation 138. A controlled process is operative when the carboxylic acid is slowly added to a solution of the reagent, presumably leading to the formation of a carbanion in the α-position. Quenching with (+)-camphor (**439**) and (−)-fenchone (**442**) is the first stage of a multistep synthesis of chiral amino alcohols **441** and **444**, respectively (equations 139 and 140). It should be noted that the intermediate β-hydroxycarboxylic acids **440** and **443** have different configurations at the β-site, as a result of steric interaction between methyl groups of the terpene and the bulky CH_2CO_2H group. Characterization of compounds **440, 441, 443** and **444** can be carried out by IR, ^{1}H and ^{13}C NMR spectra, and polarimetry. Compounds **441** and **444** are effective catalysts for certain asymmetric syntheses involving diethylzinc[357–359].

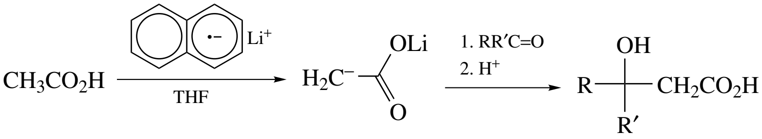

(138)

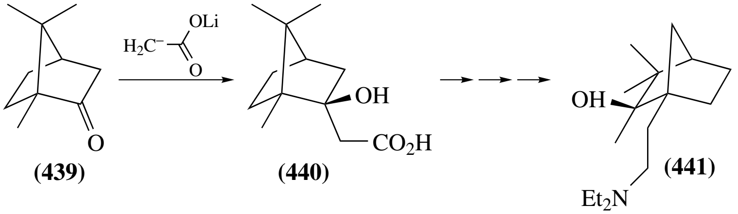

(439) **(440)** **(441)**

(139)

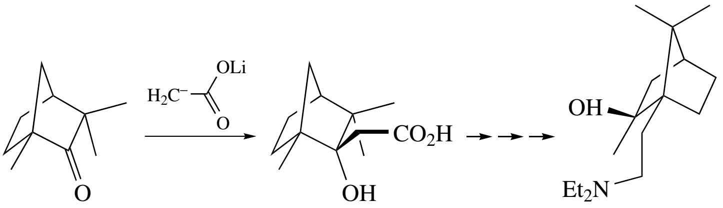

(442) **(443)** **(444)** (140)

D. Reagents Containing Si−Li Bonds

A sila-Peterson type reaction (equation 141) can be applied in the synthesis of stable silenes (**446**), using sterically crowded silyllithium reagents. The process involves addition of a sterically crowded silyllithium (**445**) to a carbonyl compound and elimination of a silanolate residue. This is illustrated by products **447a** and **447b**, derived from adamantanone, after elimination of $R^3OLi = Me_3SiOLi$. The presence of the *t*-Bu groups in **445b** and **445c** has a stabilizing effect relative to **445a**. The presence of the double bond in products **447** can be demonstrated by ^{29}Si NMR and UVV spectroscopies and XRD crystallography[360]. When the reaction is carried out with a 2:1 stoichiometric ratio (equation 142), using aldehydes such as formaldehyde, 4-phenyl-3-butenal and various benzaldehydes (**448a–f**), or ketones such as acetone, 3-methyl-2-butanone, acetophenone and benzophenone, the silene undergoes an addition reaction leading to an intermediate (**450**) that may undergo rearrangement of a Me_3Si group, to give **452**. Quenching **450** or **452** with protons or trimethylsilyl groups leads to very crowded silanes (**451, 453** and **453′**). Characterization of these products can be carried out by IR, ^1H and ^{29}Si NMR spectroscopies, MS and XRD crystallography[361]. Similar processes were described in equation 85 (Section VI.B.2).

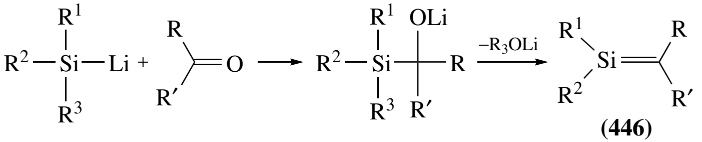

(446) (141)

(445) **(a)** $R^1 = R^2 = R^3 = SiMe_3$

(b) $R^1 = SiMe_2Bu\text{-}t$, $R^2 = R^3 = SiMe_3$

(c) $R^1 = R^2 = SiMe_2Bu\text{-}t$, $R^3 = SiMe_3$

E. Reagents Containing N−Li Bonds

Metallation with lithium amides may be more convenient than with carbolithium compounds. In certain cases the lithium amide reagent introduces functionalization.

Based on the course of the enolization in similar reactions, it is expected that addition of the nonnucleophilic strong base lithium diisopropylamide would help directing the enolization of the cyclopentanones **454**. Indeed, $i\text{-}Pr_2NLi$ promotes increased yields of the kinetically controlled product **455** in relation to the thermodynamically controlled **456**, as depicted in equation 143, where the yield ratio **456/455** attained for various R substituent groups is shown. To explain the unexpected values obtained for R substituents containing an unsubstituted phenyl group or a phenyl group bearing electron-donating groups, formation of an intermediate π-complex between the aromatic moiety and the

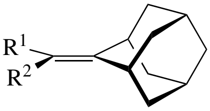

(447) **(a)** $R^1 = R^2 = SiMe_3$
(b) $R^1 = SiMe_2Bu\text{-}i$, $R^2 = SiMe_3$

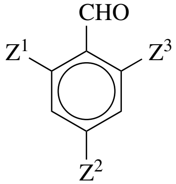

(448) **(a)** $Z^1 = Z^2 = Z^3 = H$
(b) $Z^1 = OMe$, $Z^2 = Z^3 = H$
(c) $Z^1 = Z^2 = Z^3 = Me$
(d) $Z^1 = Z^2 = Z^3 = i\text{-Pr}$
(e) $Z^2 = NMe_2$, $Z^1 = Z^3 = H$
(f) $Z^1 = Z^2 = Z^3 = OMe$

Li^+ cation (**457**) may be postulated. The effect of the aryl substituents is diminished in DME and increased in Et_2O solvents, corresponding to increased and diminished solvation of the cation concurrent with π-complex formation, in further support of the proposed explanation. The structure of the products can be elucidated by ^1H NMR spectroscopy[362].

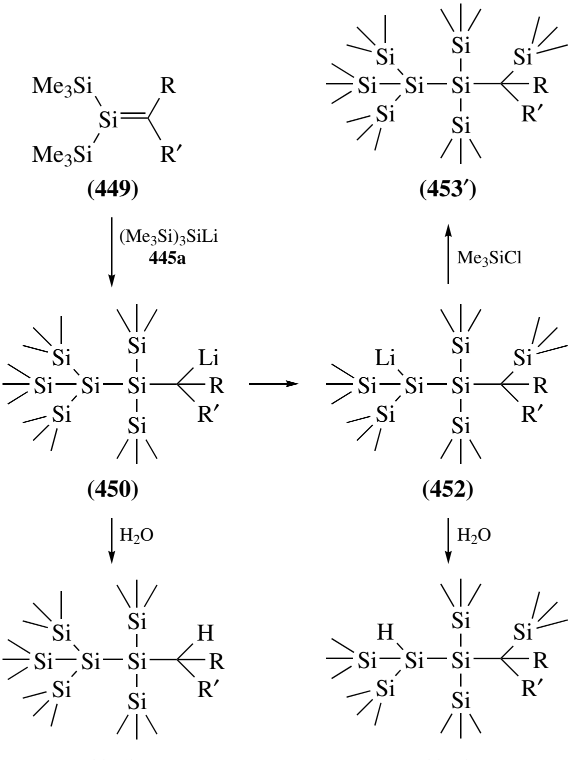

(142)

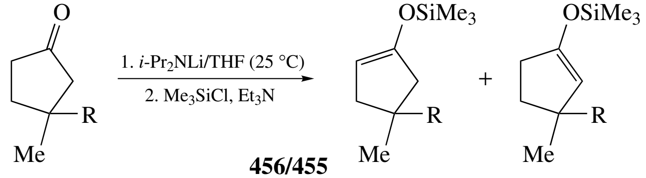

(455) **(456)** (143)

	456/455
(454) **(a)** R = Ph	3.3
(b) R = 4-MeC_6H_4	4.3
(c) R = 4-$MeOC_6H_4$	7.4
(d) R = 4-$O_2NC_6H_4$	0.9
(e) R = $PhCH_2$	6.1
(f) R = n-Bu	0.3

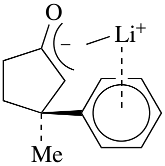

(457)

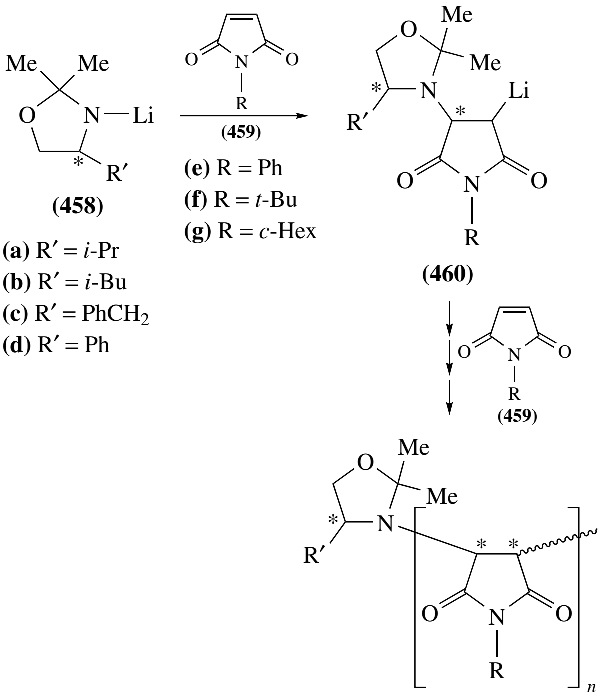

(458)

(a) R′ = i-Pr
(b) R′ = i-Bu
(c) R′ = $PhCH_2$
(d) R′ = Ph

(459)

(e) R = Ph
(f) R = t-Bu
(g) R = c-Hex

(460)

(461) (144)

Equation 144 depicts the polymerization of achiral N-substituted maleimides (**459**) initiated by variously substituted chiral oxazolidines (**458**) that underwent metallation with n-BuLi. The polymer product obtained after treatment of **461** with acidified methanol is optically active, due in part to the incorporation of the chiral residue of the initiator (**460**), as demonstrated by ^{1}H NMR spectroscopy, and in part to asymmetric induction in the main chain. The polymerization steps have to proceed by *trans*-addition to the double bond of monomer **459**, due to steric hindrance on *cis*-addition. The configuration of the products of successive addition steps may be *threo*-diisotactic, resulting in enantiomeric excess of either the (S,S) or the (R,R) configuration and optical activity, or *threo*-disyndiotactic, leading to a balanced number of S and R centers and no optical activity contribution from the main chain. Some of the polymers show a strong optical activity as a result of the induced isotactic structure, as demonstrated by ^{13}C NMR spectra. Additional evidence for the contribution of asymmetric induction in the main chain is obtained from experiments where fluorenyllithium (**122a**) is also used as initiating agent; the polymer containing a fluorenyl group instead of the oxazolidine moiety still shows optical activity. The chiral properties can be analyzed by polarimetry and circular dichroism[363].

VII. REFERENCES

1. A.-M. Sapse and P. v. R. Schleyer (Eds.), *Lithium Chemistry: A Theoretical and Experimental Overview*, Wiley, New York, 1995.
2. F. Totter, *East. Pharm.*, **38**, 49 (1995).
3. G. Fuelling, *Spec. Chem.*, **15**, 118 (1995).
4. G. Fuelling, *Spec. Chem.*, **15**, 161 (1995).
5. H. L. Hsieh and R. P. Quirk, *Anionic Polymerization*, Dekker, New York, 1996.
6. R. K. Dieter, *Lithium Link*, [fall] 1 (1999); http://www.fmclithium.com
7. S. Watanabe, *Recent Res. Devel. Oil Chem.*, **5**, 51 (2001).
8. M. Schlosser, in *Organometallics in Synthesis. A Manual*, 2nd edn. (Ed. M. Schlosser), Wiley, Chichester, 2002, p. 1.
9. J. A. Schwindeman, C. J. Woltermann and R. J. Letchford, *Chem. Health Safety*, **9**, 6 (2002).
10. (a) C. J. Pouchert, *The Aldrich Library of FT-IR Spectra*, Aldrich Chemical, Milwaukee, WI, 1997.
    (b) C. J. Pouchert, *The Aldrich Library of NMR Spectra*, 2nd edn., Aldrich Chemical, Milwaukee, WI, 1983.
11. F. J. Green, *The Sigma-Aldrich Handbook of Stains, Dyes and Indicators*, Aldrich Chemical, Milwaukee, WI, 1990.
12. R. E. Lenga (Ed.), *The Sigma-Aldrich Library of Chemical Safety Data*, 2nd edn., Aldrich Chemical, Milwaukee, WI, 1988.
13. R. E. Lenga and K. L. Votoupal (Eds.), *The Sigma-Aldrich Library of Regulatory and Safety Data*, Aldrich Chemical, Milwaukee, WI, 1992.
14. N. I. Sax, *Dangerous Properties of Industrial Materials*, 6th edn., Van Nostrand Reinhold, New York, 1984.
15. Anonymous, *Aldrichim. Acta*, **17**, 80 (1984).
16. M. Hirama, T. Noda, S. Takeishi and S. Itô, *Bull. Chem. Soc. Jpn.*, **61**, 2645 (1988).
17. S. K. Taylor, J. A. Fried, Y. N. Grasal, A. E. Marolewski, E. A. Pelton, T.-J. Poel, D. S. Rezanka and M. R. Whittaker, *J. Org. Chem*., **58**, 7304 (1993).
18. B. Ye, L.-X. Qiao, Y.-B. Zhang and Y.-L. Wu, *Tetrahedron*, **50**, 9061 (1994).
19. J. E. F. Reynolds (Ed.), *Martindale—The Extra Pharmacopoeia*, 13th edn., The Pharmaceutical Press, London, 1993.
20. W. W. Stewart, *Nature*, **292**, 17 (1981).
21. B. H. Lipshutz, M. Koerner and D. A. Parker, *Tetrahedron Lett.*, **28**, 945 (1987).
22. B. H. Lipshutz, *Synthesis*, 325 (1987).
23. S. Krishnamurthy, F. Vogel and H. C. Brown, *J. Org. Chem.*, **42**, 2534 (1977).
24. M. M. Midland and A. Kazubski, *J. Org. Chem.*, **47**, 2495 (1982).
25. F. Totter and P. Rittmayer, in Reference 1, p. 171.

26. P. Stanetty and M. D. Mihovilovic, *J. Org. Chem.*, **62**, 1514 (1997).
27. J. Clayden and S. A. Yasin, *New J. Chem.*, **26**, 191 (2002).
28. G. Henrici-Olivé and S. Olivé, *Z. Phys. Chem.*, **43**, 334 (1964).
29. K. H. J. Bushow and G. J. Hoijtink, *J. Chem. Phys.*, **40**, 2501 (1964).
30. N. Nugay, T. Nugay, R. Jerome and Ph. Teyssie, *J. Mol. Catal. A*, **179**, 59 (2002).
31. W. Schlenk and A. Thal, *Chem. Ber.*, **46**, 2840 (1913).
32. D. F. Shriver and M. A. Drezdon (Eds.), *The Manipulation of Air-Sensitive Compounds*, 2nd edn., Wiley, New York, 1986.
33. J. Zabicky, in *The Chemistry of Phenols* (Ed. Z. Rappoport), Chap. 13, Wiley, Chichester, 2003.
34. C. Gaul, P. I. Arvidsson, W. Bauer, R. E. Gawley and D. Seebach, *Chem. Eur. J.*, **7**, 4117 (2001).
35. J. J. P. Stewart, *J. Comput. Chem.*, **10**, 209 (1989).
36. E. Anders, R. Koch and P. Freunscht, *J. Comput. Chem.*, **14**, 1301 (1993).
37. A. Abbotto, A. Streitwieser and P. v. R. Schleyer, *J. Am. Chem. Soc.*, **119**, 11255 (1997).
38. M. J. Aurell, L. R. Domingo, R. Mestres, E. Muñoz and R. J. Zaragozá, *Tetrahedron*, **55**, 815 (1999).
39. F. E. Kühn, A. M. Santos, A. D. Lopes, I. S. Gonçalves, J. E. Rodriguez-Borges, M. Pillinger and C. C. Romão, *J. Organomet. Chem*., **621**, 207 (2001).
40. R. E. Barrientos-Astigarraga, P. Castelani, J. V. Comasseto, H. V. Formiga, N. C. da Silva, C. Y. Sumida and M. L. Vieira, *J. Organomet. Chem.*, **623**, 43 (2001).
41. J. F. McGarrity, C. A. Ogle, Z. Brich and H.-R. Loosli, *J. Am. Chem. Soc.*, **107**, 1810 (1985).
42. D. J. Worsfold and S. Bywater, *Can. J. Chem.*, **38**, 1891 (1960).
43. D. H. Thomas, M. Rey and P. E. Jackson, *J. Chromatogr. A*, **956**, 181 (2002).
44. *Flame Atomic Absorption Spectrometry—Analytical Methods*, Varian Publication No. 85–100 009-00, Varian Australia, Mulgrave, 1989, p. 35.
45. G. D. Christian, *Anal. Chem.*, **41**, 24A (1969).
46. O. Oster and W. Prellwitz, *Fortschr. Atomspektrom. Spurenanal.*, **2**, 185 (1986); *Chem. Abstr.*, **106**, 81110 (1987).
47. A. Tada and H. Zenda, *Rinsho Kensa*, **32**, 1473 (1988); *Chem. Abstr.*, **110**, 127879 (1989).
48. J. Quiñonero, C. Mongay and M. de la Guardia, *Ann. Chim. (Rome*), **79**, 311 (1989).
49. N. Janz, *Mta Spektrum*, **16**, 359 (2001).
50. *ICP Emission Spectrometry—Optima 3000 Wavelength Tables*, operating manual, Vol. 3, The Perkin-Elmer Corporation, 1993, p. 52.
51. M. L. Salit, G. C. Turk, A. P. Lindstrom, T. A. Butler, C. M. Beck II and B. Norman, *Anal. Chem.*, **73**, 4821 (2001).
52. R. Rahil-Khazen, H. Henriksen, B. J. Bolann and R. J. Ulvik, *Scand. J. Clin. Lab. Invest.*, **60**, 677 (2000).
53. G. C.-Y. Chan, W.-T. Chan, X. Mao and R. E. Russo, *Spectrochim. Acta B*, **56**, 77 (2001).
54. W. I. Ridley, *Trends Geochem.*, **1**, 1 (2000).
55. K.-D. Zhao and S.-Y. Jiang, *Gaoxiao Dizhi Xuebao*, **7**, 390 (2001); *Chem. Abstr.*, **136**, 250331 (2002).
56. D. Potter, A. Walsh, E. McCurdy and R. C. Hutton, *Anal. Sci.*, **7**, 467 (1991).
57. H. Ying, M. Antler, J. W. Tromp and E. D. Salin, *Spectrochim. Acta B*, **57**, 277 (2002).
58. I. Rodushkin and F. Odman, *J. Trace Elements Med. Biol.*, **14**, 241 (2001).
59. E. Coni, B. Bocca, B. Galoppi, A. Alimonti and S. Caroli, *Microchem. J.*, **67**, 187 (2000).
60. M. M. Castineira, R. Brandt, A. von Bohlen and N. Jakubowski, *Fresenius J. Anal. Chem.*, **370**, 553 (2001).
61. Y. Nishio and S. Nakai, *Anal. Chim. Acta*, **456**, 271 (2002).
62. J. Kosler, M. Kucera and P. Sylvester, *Chem. Geol.*, **181**, 169 (2001).
63. A. M. Volpe, B. K. Esser and G. M. Bianchini, *J. Anal. At. Spectrom.*, **16**, 801 (2001).
64. R. Forrer, C. Wenker, K. Gautschi and H. Lutz, *Biol. Trace Element Res.*, **81**, 47 (2001).
65. R. Forrer, K. Gautschi and H. Lutz, *Biol. Trace Element Res.*, **80**, 77 (2001).
66. J. L. Fernández-Turiel, J. F. Llorens, F. López-Vera, C. Gómez-Artola, I. Morell and D. Gimeno, *Fresenius J. Anal. Chem.*, **368**, 601 (2000).
67. R. H. James and M. R. Palmer, *Chem. Geol.*, **166**, 319 (2000).
68. B. Flem, R. B. Larsen, A. Grimstvedt and J. Mansfeld, *Chem. Geol.*, **182**, 237 (2002).

69. C. Pickhardt, I. B. Brenner, J. S. Becker and H. J. Dietze, *Fresenius J. Anal. Chem.*, **368**, 79 (2000).
70. C. Pickhardt, J. S. Becker and H. J. Dietze, *Fresenius J. Anal. Chem.*, **368**, 173 (2000).
71. K. Hiratani, *Analyst (London)*, **113**, 1065 (1988).
72. T. Gunnlaugsson, B. Bichel and C. Nolan, *Tetrahedron Lett.*, **43**, 4989 (2002).
73. M. H. Fletcher and J. Parks, *Anal. Chem.*, **23**, 478 (1951).
74. B. P. Czech, A. Kumar and E. Chapoteau, *Lithium*, **5**, 11 (1994).
75. M. Tabata, J. Nishimoto and T. Kusano, *Talanta*, **46**, 703 (1998).
76. L. Gámiz Gracia, L. Cuadros Rodríguez and M. Román Ceba, *Talanta*, **44**, 75 (1997).
77. P. F. Thomason, M. A. Perry and W. M. Bierly, *Anal. Chem.*, **21**, 1239 (1949).
78. A. González-Portal, A. López-Rodríguez and C. Baluja-Santos, *Anal. Lett.*, **28**, 2191 (1995).
79. J. K. Trautman, V. P. Y. Gadzekpo and G. D. Christian, *Talanta*, **30**, 587 (1983).
80. K. Uesugi and T. Murakami, *Bunseki Kagaku*, **15**, 482 (1966); *Chem. Abstr.*, **65**, 72190 (1966).
81. Y. Shibutani, H. Sakamoto, K. Hayano and T. Shono, *Anal. Chim. Acta*, **375**, 81 (1998).
82. K. Kimura, M. Tanaka, S. Iketani and T. Shono, *J. Org. Chem.*, **52**, 836 (1987).
83. K. Sasaki and G. Pacey, *Anal. Chim. Acta*, **174**, 141 (1985).
84. K. Wilcox and G. E. Pacey, *Anal. Chim. Acta*, **245**, 235 (1991).
85. K. Wilcox and G. E. Pacey, *Talanta*, **38**, 1315 (1991).
86. C. I. Lin and M. Pirio, U.S. Patent. 4742010, 3 May 1988.
87. A. S. Attiyat, Y. A. Ibrahim and G. D. Christian, *Microchem. J.*, **37**, 114 (1988).
88. G. D. Christian, *Lithium*, **1**, 181 (1990).
89. K. Kimura, *Trends Org. Chem.*, **4**, 203 (1993).
90. E. Hirayama, T. Sugiyama, H. Isamoto and K. Suzuki, *Anal. Chem.*, **72**, 465 (2000).
91. P. Pastore, A. Boaretto, I. Lavagnini and A. Diop, *J. Chromatogr.*, **591**, 219 (1992).
92. R. Fleming, U.S. Patent. 4766080, 23 Aug. 1988.
93. G. J. Moody, *J. Biomed. Eng.*, **7**, 183 (1985).
94. V. P. Y. Gadzekpo, G. J. Moody and J. D. R. Thomas, *Port. Electrochim. Acta*, **4**, 5 (1986).
95. V. P. Y. Gadzekpo, G. J. Moody, J. D. R. Thomas and G. D. Christian, *Ion-Sel. Electrode Rev.*, **8**, 173 (1986).
96. K. Kina, *Bunseki*, 642 (1987); *Chem. Abstr.*, **108**, 642 (1988).
97. H. Sakamoto, *Bunseki*, 468 (1992); *Chem. Abstr.*, **117**, 123502 (1992).
98. G. D. Christian, *J. Pharm. Biomed. Anal.*, **14**, 899 (1996).
99. K. Kobiro, *Coord. Chem. Rev.*, **148**, 135 (1996).
100. H. Kanoh, Q. Feng and K. Ooi, *Nippon Ion Kokan Gakkaishi*, **8**, 166 (1997); *Chem. Abstr.*, **128**, 94486 (1998).
101. M. Krondak, R. Volf and V. Kral, *Collect. Czech. Chem. Commun.*, **66**, 1659 (2001).
102. O. M. Petrukhin, E. V. Shipulo, S. A. Krylova, S. L. Rogatinskaya, A. F. Zhukov, S. Wilke, H. Mueller, E. N. Tsvetkov, V. E. Baulin et al., *Zh. Anal. Khim.*, **49**, 1299 (1994); *Chem. Abstr.*, **122**, 329252 (1995).
103. J. S. Kim, *Anal. Sci. Technol.*, **5**, 33 (1992).
104. S. O. Jung, S. S. Park, B. G. Kim and J. S. Kim, *Bull. Kor. Chem. Soc.*, **16**, 197 (1995); *Chem. Abstr.*, **122**, 260110 (1995).
105. Y. R. Kang, K. M. Lee, H. Nam, G. S. Cha, S. O. Jung and J. S. Kim, *Analyst*, **122**, 1445 (1997).
106. H. Sakamoto, T. Miura, M. Tanaka and T. Shono, *Bunseki Kagaku*, **39**, 779 (1990); *Chem. Abstr.*, **114**, 177410 (1991).
107. S. Sawada, T. Osakai and M. Senda, *Anal Sci.*, **11**, 733 (1995).
108. S. Sawada, H. Torii, T. Osakai and T. Kimoto, *Anal. Chem.*, **70**, 4286 (1998).
109. K. Suzuki, H. Yamada, K. Sato, K. Watanabe, H. Hisamoto, Y. Tobe and K. Kobiro, *Anal. Chem.*, **65**, 3404 (1993).
110. K. Tohda, K. Suzuki, N. Kosuge, K. Watanabe, H. Nagashima, H. Inoue and T. Shirai, *Anal. Chem.*, **62**, 936 (1990).
111. G. I. Shumilova, *Russ. J. Electrochem.*, **32**, 193 (1997).
112. M. Bochenska and M. Gdaniec, *J. Inclusion Phenomena Mol. Recognition Chem.*, **20**, 53 (1994).
113. M. Bochenska, *J. Mol. Struct.*, **450**, 107 (1998).

114. A. L. Grekovich, N. N. Markuzina, K. N. Mikhelson, M. Bochenska and A. Lewenstam, *Electroanalysis*, **14**, 551 (2002).
115. Z. Hruška and J. Petránek, *Collect. Czech. Chem. Commun.*, **56**, 2154 (1991).
116. R. Kataky, P. E. Nicholson, D. Parker and A. K. Covington, *Analyst*, **116**, 135 (1991).
117. J. Zhong, J. Li, M. Liu, Y. Bai, X. Yang, D. Xiao and K. Wang, *Huaxue Chuanganqi*, **20**, 12 (2000); *Chem. Abstr.*, **134**, 231180 (2001).
118. H. Sugihara, T. Okada and K. Hiratani, *Anal. Sci.*, **9**, 593 (1993).
119. T. Okada, H. Sugihara and K. Hiratani, *Analyst*, **120**, 2381 (1995).
120. L.-X. Sun, T. Okada, J.-P. Collin and H. Sugihara, *Anal. Chim. Acta*, **329**, 57 (1996).
121. J. Bobacka, A. Lewenstam and A. Ivaska, *Talanta*, **40**, 1437 (1993).
122. J. Bobacka, T. Lindfors, M. McCarrick, A. Ivaska and A. Lewenstam, *Anal. Chem.*, **67**, 3819 (1995).
123. T. Lindfors, P. Sjoberg, J. Bobacka, A. Lewenstam and A. Ivaska, *Anal. Chim. Acta*, **385**, 163 (1999).
124. M. Fernado de S. Teixeira, O. Fatibello-Filho, L. C. Ferracin, R. C. Rocha-Filho and N. Bocchi, *Sensors Actuators*, **B67**, 96 (2000).
125. C. W. Kamienski, *Lithium Link*, (4), 1 (1994); http://www.fmclithium.com
126. H. Gilman and F. K. Cartledge, *J. Organomet. Chem.*, **2**, 447 (1964).
127. A. K. Clifford and R. R. Olsen, *Anal. Chem.*, **32**, 544 (1960).
128. P. J. Reed and J. R. Urwin, *J. Organometal. Chem.*, **39**, 1 (1972).
129. H. Gilman and A. H. Haubein, *J. Am. Chem. Soc.*, **66**, 1515 (1944).
130. A. G. Evans and D. B. George, *J. Chem. Soc.*, 4653 (1961).
131. W. G. Kofron and L. M. Baclawski, *J. Org. Chem.*, **41**, 1879 (1976).
132. E. Juaristi, A. Matínez-Richa, A. García-Rivera and J. S. Cruz-Sánchez, *J. Org. Chem*., **48**, 2603 (1983).
133. S. C. Watson and J. F. Eastham, *J. Organomet. Chem.*, **9**, 165 (1967).
134. W. L. Everson, *Anal. Chem.*, **36**, 854 (1964).
135. R. L. Eppley and J. A. Dixon, *J. Organomet. Chem*., **8**, 176 (1967).
136. S. C. Watson and J. F. Eastham, *Anal. Chem.*, **39**, 171 (1967).
137. P. F. Collins, C. W. Kamienski, D. L. Esmay and R. B. Ellestad, *Anal. Chem.*, **33**, 468 (1961).
138. H. O. House and W. L. Respess, *J. Organomet. Chem.*, **4**, 95 (1965).
139. B. Gutekunst and A. G. Brook, *J. Organomet. Chem.*, **225**, 1 (1982).
140. C. G. Screttas, G. I. Ioannou and M. Micha-Screttas, *J. Org. Chem.*, **51**, 511 (1996).
141. C. G. Screttas, M. Micha-Screttas and B. R. Steele, *J. Organomet. Chem.*, **536–537**, 149 (1997); *J. Organomet. Chem.*, **556**, 243 (1998).
142. G. Henrici-Olivé and S. Olivé, *Z. Phys. Chem.*, **43**, 327 (1964).
143. G. Henrici-Olivé and S. Olivé, *Z. Phys. Chem.*, **43**, 340 (1964).
144. R. P. Quirk, K. Han and Y. Lee, *Polym. Int.*, **48**, 99 (1999).
145. R. P. Quirk and J. Kuang, *J. Polym. Sci., A*, **37**, 1143 (1999).
146. T. Cohen, T. Kreethadumrongdat, X. Liu and V. Kulkarni, *J. Am. Chem. Soc.*, **123**, 3478 (2001).
147. J. J. Brooks, W. E. Rhine and G. D. J. Stucky, *J. Am. Chem. Soc.*, **94**, 7346 (1972).
148. W. E. Rhine and G. D. J. Stucky, *J. Am. Chem. Soc*., **97**, 2079 (1975).
149. A. Sygula, K. Lipkowitz and P. W. Rabideau, *J. Am. Chem. Soc*., **109**, 6602 (1987).
150. P. Rosa, N. Mézailles, L. Ricard, F. Mathey and P. Le Floch, *Angew. Chem., Int. Ed.*, **40**, 4476 (2001).
151. J. Arnold, *Chem. Commun.*, 976 (1990).
152. J. Arnold, D. Y. Dawson and C. G. Hoffman, *J. Am. Chem. Soc.*, **115**, 2707 (1993).
153. A. Aßmann, A. Franken and H. Homborg, *Z. Anorg. Allg. Chem.*, **621**, 1715 (1995).
154. B. Latte, B. Aßmann and H. Homborg, *Z. Anorg. Allg. Chem.*, **623**, 1281 (1997).
155. M. A. Beswick, C. N. Harmer, P. R. Raithby, L. Steiner, M. Tombul and D. S. Wright, *J. Organomet. Chem.*, **573**, 267 (1999).
156. S. S. Al-Juaid, C. Eaborn, S. N. El-Hamruni, P. B. Hitchcock and J. D. Smith, *Organometallics*, **18**, 45 (1999).
157. N. E. Holden, in *CRC Handbook of Chemistry and Physics*, 82nd edn. (Ed. D. R. Lide), CRC Press, Boca Raton, 2001, pp. **11**-50 ff.
158. H. Günther, in *Advanced Applications of NMR to Organometallic Chemistry* (Eds. M. Gielen, R. Willen and B. Wrackmeyer), Wiley, Chichester, 1996.

159. H. Günther, D. Moskau, P. Bast and D. Schmalz, *Angew. Chem.*, **99**, 1242 (1987).
160. H. Günther, *J. Braz. Chem. Soc.*, **10**, 241 (1999).
161. R. D. Thomas, *Isot. Phys. Biomed. Sci.*, **2**(*Isot. Appl. NMR Stud.*), 367 (1991).
162. D. B. Collum, *Acc. Chem. Res.*, **26**, 227 (1993).
163. A. Basu and S. Thayumanavan, *Angew. Chem., Int. Ed.*, **41**, 716 (2002).
164. W. Baumann, Y. Oprunenko and H. Günther, *Z. Naturforsch.*, **50a**, 429 (1995).
165. M. Yus, R. P. Herrera and A. Guijarro, *Chem. Eur. J.*, **8**, 2574 (2002).
166. S. Bywater, P. Lachance and D. J. Worsfold, *J. Phys. Chem.*, **79**, 2148 (1975).
167. M. A. Voinov, G. E. Salnikov, A. M. Genaev, V. I. Mamatyuk, M. M. Shakirov and I. A. Grigor'ev, *Magn. Reson. Chem.*, **39**, 681 (2001).
168. D. Seebach, R. Hässig and J. Gabriel, *Helv. Chim. Acta*, **66**, 308 (1983).
169. T. A. Keith and R. F. W. Bader, *Chem. Phys. Lett.*, **194**, 1 (1992).
170. H. Werstiuk and J. Ma, *Can. J. Chem.*, **74**, 875 (1996).
171. B. Xiang, M. D. Winemiller, T. F. Briggs, D. J. Fuller and D. B. Collum, *Magn. Reson. Chem.*, **39**, 137 (2001).
172. M. Kühnen, H. Günther, J.-P. Amoureux and C. Fernandéz, *Magn. Reson. Chem.*, **40**, 24 (2002).
173. W. Zarges, M. Marsch, K. Harms, W. Koch, G. Frenking and G. Boche, *Chem. Ber.*, **124**, 543 (1991).
174. D. Johnels, A. Boman and U. Edlund, *Magn. Reson. Chem.*, **36**, S151 (1998).
175. H. Gornitzka and D. Stalke, *Angew. Chem., Int. Ed. Engl.*, **33**, 693 (1994).
176. H. Gornitzka and D. Stalke, *Organometallics* **13**, 4398 (1994).
177. K. Müllen, *Helv. Chim. Acta*, **59**, 1357 (1976).
178. K. Müllen, *Helv. Chim. Acta*, **61**, 1296 (1978).
179. R. Shenhar, R. Beust, R. E. Hoffman, I. Willner, H. E. Bronstein, L. T. Scott and M. Rabinovitz, *J. Org. Chem.*, **66**, 6004 (2001).
180. R. Shenhar, R. Beust, S. Hagen, H. E. Bronstein, I. Willner, L. T. Scott and M. Rabinovitz, *J. Chem. Soc., Perkin Trans. 2*, 449 (2002).
181. Y. Cohen, Y. Fraenkel, M. Rabinovitz, P. Felder and F. Gerson, *Helv. Chim. Acta*, **73**, 2048 (1990).
182. M. A. Voinov and I. A. Grigor'ev, *Russ. Chem. Bull., Int. Ed.*, **51**, 297 (2002).
183. T. E. Hogen-Esch and J. Smid, *J. Am. Chem. Soc.*, **88**, 307 (1966).
184. J. Smid, *J. Am. Chem. Soc.*, **87**, 655 (1965).
185. K. H. J. Buschow, J. Dieleman and G. J. Hoijtink, *J. Chem. Phys.*, **42**, 1993 (1965).
186. E. O. Fischer and V. Kiener, *J. Organometal. Chem.*, **23**, 215 (1970).
187. L. Manceron and L. Andrews, *J. Am. Chem. Soc.*, **107**, 563 (1985).
188. U. Röthlisberger and M. L. Klein, *J. Am. Chem. Soc.*, **117**, 42 (1995).
189. L. Manceron and L. Andrews, *J. Am. Chem. Soc.*, **110**, 3840 (1988).
190. L. Manceron and L. Andrews, *J. Phys. Chem.*, **92**, 2150 (1988).
191. L. Manceron and L. Andrews, *J. Phys. Chem.*, **90**, 4514 (1986).
192. D. E. Paul, D. Lipkin and S. I. Weissman, *J. Am. Chem. Soc.*, **78**, 116 (1956).
193. G. Henrici-Olivé and S. Olivé, *Z. Phys. Chem.*, **43**, 145 (1964).
194. W. H. Bruning, G. Henrici-Olivé and S. Olivé, *Z. Phys. Chem.*, **47**, 340 (1966).
195. P. B. Ayscough and F. P. Sargent, *J. Chem. Soc. (B)*, 900 (1966).
196. N. M. Atherton, *Chem. Commun.*, 254 (1966).
197. A. H. Reddoch, *J. Chem. Phys.*, **43**, 225 (1965).
198. L. A. Shimp, C. Chung and R. J. Lagow, *Inorg. Chim. Acta*, **29**, 77 (1978).
199. B. Jaun, J. Schwarz and R. Breslow, *J. Am. Chem. Soc.*, **102**, 5741 (1980).
200. T. E. Hogen-Esch and J. Smid, *J. Am. Chem. Soc.*, **88**, 318 (1966).
201. K. Lühder and H. Füllbier, *Acta Phys. Slovaca*, **38**, 311 (1988); *Chem. Abstr.*, **111**, 153880 (1989).
202. E. M. Arnett and K. D. Moe, *J. Am. Chem. Soc.*, **113**, 7068 (1991).
203. W. Bauer, in Reference 1, p. 125.
204. F. E. Romesberg and D. B. Collum, *J. Am. Chem. Soc.*, **114**, 2112 (1992).
205. K. R. Dress, T. Rolle, A. Wenzel, G. Bosherz, N. Frommknecht, E. Merkel and W. Sauer, *Z. Phys. Chem. (Muenchen)*, **215**, 77 (2001).
206. W. Bauer, W. R. Winchester and P. v. R. Schleyer, *Organometallics*, **6**, 2371 (1987).
207. R. L. Eppley and J. A. Dixon, *J. Am. Chem. Soc.*, **90**, 1606 (1968).

208. P. West and R. Waak, *J. Am. Chem. Soc.*, **89**, 4395 (1967).
209. J. L. Rutherford, D. Hoffmann and D. B. Collum, *J. Am. Chem. Soc.*, **124**, 264 (2002).
210. D. Thoennes and E. Weiss, *Chem. Ber.*, **111**, 3157 (1978).
211. J. F. McGarrity and C. A. Ogle, *J. Am. Chem. Soc.*, **107**, 1805 (1985).
212. E. Low and R. E. Gawley, *J. Am. Chem. Soc.*, **122**, 9562 (2000).
213. J. S. Wang, R. Jérôme, R. Warin and Ph. Teyssié, *Macromolecules*, **26**, 1402 (1993).
214. J. S. Wang, R. Warin, R. Jérôme and Ph. Teyssié, *Macromolecules*, **26**, 6776 (1993).
215. C. Zune, P. Dubois, R. Jérôme, J. Křiž, J. Dybal, L. Lochmann, M. Janata, P. Vlãek, T. M. Werkhoven and J. Lugtenburg, *Macromolecules*, **31**, 2731 (1998).
216. C. Zune, P. Dubois, R. Jérôme, J. Křiž, J. Dybal, L. Lochmann, M. Janata, P. Vlãek, T. M. Werkhoven and J. Lugtenburg, *Macromolecules*, **31**, 2744 (1998).
217. M. P. Lappert, L. M. Engelhardt, C. L. Raston and A. H. White, *Chem. Commun.*, 1323 (1982).
218. R. den Besten, S. Harder and L. Brandsma, *J. Organomet. Chem.*, **385**, 153 (1990).
219. A. Pepels, H. Günther, J.-P. Amoureux and C. Fernandéz, *J. Am. Chem. Soc.*, **122**, 9858 (2000).
220. J. M. Saá, *Helv. Chim. Acta*, **85**, 814 (2002).
221. B. Schiemenz and P. P. Power, *Angew. Chem., Int. Ed. Engl.*, **35**, 2150 (1996).
222. C. Eaborn, P. B. Hitchcock, J. D. Smith and A. C. Sullivan, *Chem. Commun.*, 1390 (1983).
223. L. M. Jackman, L. M. Scarmoutzos and C. W. DeBrosse, *J. Am. Chem. Soc.*, **109**, 5355 (1987).
224. J. T. B. H. Jastrzebski, G. van Koten, K. Goubitz, C. Arlen and M. Pfeffer, *J. Organomet. Chem.*, **246**, C75 (1983).
225. A. Farook, C. Eaborn, P. B. Hitchcock and J. D. Smith, *Chem. Commun.*, 741 (1996).
226. V. Halaška and L. Lochmann, *Collect. Czech. Chem. Commun.*, **38**, 1780 (1973).
227. A. El Madani, J. Belleney, J.-C. Favier, P. Hémery and P. Sigwalt, *Polym. Int.*, **31**, 169 (1993).
228. J.-M. Boutillier, J.-C. Favier, P. Hémery and P. Sigwalt, *Polymer*, **37**, 5197 (1996)
229. D. Barr, W. Clegg, R. E. Mulvey and R. Snaith, *Chem. Commun.*, 469 (1984).
230. M. Polamo and M. Leskelä, *J. Chem. Soc., Dalton Trans.*, 4345 (1996).
231. R. Kempe, A. Spannenberg and S. Brenner, *Z. Kristallogr.*, **211**, 567 (1996).
232. J. L. Rutherford and D. B. Collum, *J. Am. Chem. Soc.*, **123**, 199 (2001).
233. D. B. Collum, *Acc. Chem. Res.*, **26**, 227 (1993).
234. B. L. Lucht and D. B. Collum, *Acc. Chem. Res.*, **32**, 1035 (1999).
235. M. Hartung, H. Günther, J.-P. Amoureux and C. Fernandéz, *Magn. Reson. Chem.*, **36**, S61 (1998).
236. H. J. Reich, W. S. Goldenberg, B. Ö. Gudmundsson, A. W. Sanders, K. J. Kulicke, K. Simon and I. A. Guzei, *J. Am. Chem. Soc.*, **123**, 8067 (2001).
237. B. L. Lucht, M. P. Bernstein, J. F. Remenar and D. B. Collum, *J. Am. Chem. Soc.*, **118**, 10707 (1996).
238. W. B. Farnham and J. C. Calabrese, *J. Am. Chem. Soc.*, **108**, 2449 (1986).
239. P. B. Hitchcock, M. F. Lappert and D.-S. Liu, *Chem. Commun.*, 1699 (1994).
240. B.-J. Deelman, M. F. Lappert, H.-K. Lee, T. C. W. Mak, W.-P. Leung and P.-R. Wei, *Organometallics*, **16**, 1247 (1997).
241. F. S. Mair, D. Scully, A. J. Edwards, P. R. Raithby and R. Snaith, *Polyhedron*, **14**, 2397 (1995).
242. J. Barker, D. Barr, N. D. R. Barnett, W. Clegg, I. Craig-Hine, M. G. Davidson, R. P. Davies, S. M. Hodgson, J. A. K. Howard, M. Kilner, C. W. Lehmann, I. Lopez-Solera, R. E. Mulvey, P. R. Raithby and R. Snaith, *J. Chem. Soc., Dalton Trans.*, 951 (1997).
243. M. S. Eisen and M. Kapon, *J. Chem. Soc., Dalton Trans.*, 3507 (1994).
244. D. Stalke, M. Wedler and F. T. Edelmann, *J. Organomet. Chem.*, **431**, C1 (1992).
245. T. Gebauer, K. Dehnicke, H. Goessmann and D. Fenske, *Z. Naturforsch.*, **49b**, 1444 (1994).
246. L. M. Engelhardt, G. E. Jacobsen, P. C. Junk, C. L. Raston, B. W. Skelton and A. H. White, *J. Chem Soc., Dalton Trans.*, 1011 (1988).
247. W. M. Boesveld, P. B. Hitchcock and M. F. Lappert, *J. Chem. Soc., Dalton Trans.*, 4041 (1999).
248. S. R. Boss, R. Haigh, D. J. Linton and A. E. H. Wheatley, *J. Chem. Soc., Dalton Trans.*, 3129 (2002).

249. C. W. Kamienski and D. H. Lewis, *J. Org. Chem.*, **30**, 3498 (1965).
250. L. Lochmann, *Eur. J. Inorg. Chem.*, 1115 (2000).
251. M. Marsch, K. Harms, L. Lochmann and G. Boche, *Angew. Chem., Int. Ed. Engl.*, **29**, 308 (1990).
252. B. Goldfuss, M. Steigelmann and F. Rominger, *Angew. Chem., Int. Ed.*, **39**, 4133 (2000).
253. D. R. Armstrong, J. E. Davies, R. P. Davies, P. R. Raithby, R. Snaith and A. E. H. Wheatley, *New J. Chem.*, 35 (1999).
254. W. Clegg, E. Lamb, S. T. Liddle, R. Snaith and A. E. H. Wheatley, *J. Organomet. Chem.*, **573**, 305 (1999).
255. W. E. Rhine, G. Stucky and S. W. Peterson, *J. Am. Chem. Soc.*, **97**, 6401 (1975).
256. P. B. Hitchcock, J. A. K. Howard, M. F. Lappert, W.-P. Leung and S. A. Mason, *J. Chem. Soc., Chem. Commun.*, 847 (1990).
257. I. Hemme, B. Tecklenburg, M. Noltmeyer and U. Klingebiel, *Chem. Ber.*, **128**, 351 (1995).
258. C. J. Harlan, S. G. Bott and A. R. Barron, *J. Am. Chem. Soc.*, **117**, 6465 (1995).
259. B. Walfort, R. Bertermann and D. Stalke, *Chem. Eur. J.*, **7**, 1424 (2001).
260. C. Eaborn, M. S. Hill, P. B. Hitchcock and J. D. Smith, *Organometallics*, **19**, 5780 (2000).
261. P. Wipf and J.-K. Peter, *Chem. Rev.*, **99**, 1469 (1999).
262. T. L. Stemmler, T. M. Barnhart, J. E. Penner-Hahn, C. E. Tucker, P. Knochel, M. Boehme and G. Frenking, *J. Am. Chem. Soc.*, **117**, 12489 (1995).
263. X. Cai, B. Gehrhus, P. B. Hitchcock, M. F. Lappert and J. C. Slootweg, *J. Organomet. Chem.*, **643–644**, 272 (2002).
264. A. Wacker, C. G. Yan, G. Kaltenpoth, A. Ginsberg, A. M. Arif, R. D. Ernst, H. Pritzkow and W. Siebert, *J. Organomet. Chem.*, **641**, 195 (2002).
265. W. Clegg, K. Izod, W. McFarlane and P. O'Shaughnessy, *Organometallics*, **18**, 3950 (1999).
266. K. Izod, P. O'Shaughnessy, W. Clegg and S. T. Liddle, *Organometallics*, **20**, 648 (2001).
267. K. Izod, P. O'Shaughnessy and W. Clegg, *Organometallics*, **21**, 641 (2002).
268. A. D. Bond, D. J. Linton, P. Schooler and A. E. H. Wheatley, *J. Chem. Soc., Dalton Trans.*, 3173 (2001).
269. L. Bonomo, E. Solari, M. Latronico, R. Scopelliti and C. Floriani, *Chem. Eur. J.*, **5**, 2040 (1999).
270. E. Weiss, *Angew. Chem, Int. Ed. Engl.*, **32**, 1501 (1993).
271. B. Walfort, L. Lameyer, W. Weiss, R. Herbst-Irmer, R. Bertermann, J. Rocha and D. Stalke, *Chem. Eur. J.*, **7**, 1417 (2001).
272. G. R. Peyton and W. H. Glaze, *Theor. Chim. Acta*, **13**, 259 (1969).
273. C. Fressigne, J. Maddaluno and C. Giessner-Prettre, *J. Chem. Soc., Perkin Trans. 2*, 2197 (1999).
274. T. Kottke and D. Stalke, *Angew. Chem., Int. Ed. Engl.*, **32**, 580 (1993).
275. I. Keresztes and P. G. Williard, *J. Am. Chem. Soc.*, **122**, 10228 (2000).
276. M. A. Nichols and P. G. Williard, *J. Am. Chem. Soc.*, **115**, 1568 (1993).
277. N. D. R. Barnett, R. E. Mulvey, W. Clegg and P. A. O'Neil, *J. Am. Chem. Soc.*, **115**, 3 (1993).
278. W. Bauer, T. Clark and P. v. R. Schleyer, *J. Am. Chem. Soc.*, **109**, 970 (1987).
279. D. P. Novak and T. L. Brown, *J. Am. Chem. Soc.*, **94**, 3793 (1972).
280. C. Strohmann and B. C. Abele, *Organometallics*, **19**, 4173 (2000).
281. S. Harder, M. Lutz and T. Kremer, *Organometallics*, **14**, 2133 (1995).
282. D. Walther, M. Stollenz and H. Görls, *Organometallics*, **20**, 4221 (2001).
283. W. F. Bailey, *Lithium Link*, [spring] 1 (1994); http://www.fmclithium.com
284. D. W. Slocum, *Lithium Link*, [winter] 1 (1993); http://www.fmclithium.com
285. T. Rathman, *Lithium Link*, [spring] 1 (1992); http://www.fmclithium.com
286. V. Snieckus and A. Larkin, *Lithium Link*, [winter] 1 (2000); http://www.fmclithium.com
287. A. R. Katritzky, D. O. Tymoshenko and M. Qi, *Lithium Link*, [spring] 2 (2002); http://www.fmclithium.com
288. A. R. Katritzky, D. C. Oniciu, L. Crdyuk and I. Ghiviriga, *J. Org. Chem.*, **60**, 1244 (1995).
289. A. J. Poss, *Lithium Link*, [summer] 3 (2002); http://www.fmclithium.com
290. C. G. Screttas and B. R. Steele, *Appl. Organometal Chem.*, **14**, 653 (2000).
291. M. J. Mealy and W. F. Bailey, *J. Organomet. Chem.*, **646**, 59 (2002).
292. I. Coldham, R. Hufton and D. J. Snowden, *J. Am. Chem. Soc.*, **118**, 5322 (1996).
293. N. J. Ashweek, I. Coldham, D. J. Snowden and G. P. Vennall, *Chem. Eur. J.*, **8**, 195 (2002).

294. C. S. Shiner, T. Tsunoda, B. A. Goodman, S. Ingham, S.-H. Lee and P. E. Vorndam, *J. Am. Chem. Soc.*, **111**, 1381 (1989).
295. J. Clayden, M. Helliwell, J. H. Pink and N. Westlund, *J. Am. Chem. Soc.*, **123**, 12449 (2001).
296. K. Tomooka, H. Shimizu and T. Nakai, *J. Organomet. Chem.*, **624**, 364 (2001).
297. T. Hoppe and T. Hense, *Angew. Chem., Int. Ed. Engl.*, **36**, 5531 (1997).
298. J. Clayden and M. N. Kenworthy, *Org. Lett.*, **4**, 787 (2002).
299. C. C. Silveira, G. Perin, A. L. Braga, M. J. Dabdoub and R. G. Jacob, *Tetrahedron*, **55**, 7421 (1999).
300. M. G. Cabiddu, S. Cabiddu, E. Cadoni, R. Cannas, S. De Montis, C. Fattuoni and S. Melis, *J. Organomet. Chem.*, **620**, 263 (2001).
301. R. P. Quirk and Y. Lee, *J. Polym. Sci. A*, **38**, 145 (2000).
302. H. J. Reich and W. H. Sikorski, *J. Org. Chem.*, **64**, 14 (1999).
303. Z. Xi and Q. Song, *J. Org. Chem.*, **65**, 9157 (2000).
304. J. Chen, Q. Song and Z. Xi, *Tetrahedron Lett.*, **43**, 3533 (2002).
305. J. Barluenga, F. J. Fañanás, R. Sanz and Y. Fernández, *Chem. Eur. J.*, **8**, 2036 (2002).
306. W. F. Bailey and X.-L. Jiang, *J. Org. Chem.*, **61**, 2596 (1996).
307. R. A. Gawley and Q. Zhang, *Tetrahedron*, **50**, 6077 (1994).
308. W. F. Bailey and M. J. Mealy, *J. Am. Chem. Soc.*, **122**, 6787 (2000).
309. M. Mickoleit, K. Schmohl, R. Kempe and H. Oehme, *Angew. Chem., Int. Ed.*, **39**, 1610 (2000).
310. N. Wiberg, T. Passler and S. Wagner, *J. Organomet. Chem.*, **598**, 304 (2000).
311. P. E. Eaton, K. Pramod, T. Emrick and R. Gilardi, *J. Am. Chem. Soc.*, **121**, 4111 (1999).
312. H. Benmansour, R. D. Chambers, G. Sandford, G. McGowan, S. Dahaoui, D. S. Yufit and J. A. K. Howard, *J. Fluorine Chem.*, **112**, 349 (2001).
313. P. Wijkens, J. T. B. H. Jastrzebski, P. A. Van der Schaaf, R. Kolly, A. Hafner and G. Van Koten, *Org. Lett.*, **2**, 1621 (2000).
314. S. Norsikian, I. Marek, S. Klein, J. F. Poisson and J. F. Normant, *Chem. Eur. J.*, **5**, 2055 (1999).
315. X. Wei, P. Johnson and R. J. K. Taylor, *J. Chem. Soc., Perkin Trans. 1*, 1109 (2000).
316. T. Suzuka, M. Masamichi and T. Hayashi, *J. Org. Chem.*, **67**, 3355 (2002).
317. R. D. Sanderson, A. H. A. Roediger and G. J. Summers, *Polym. Int.*, **35**, 263 (1994).
318. R. D. Sanderson, G. Costa, G. J. Summers and C. A. Summers, *Polymer*, **40**, 5429 (1999).
319. Y. S. Yu, P. Dubois, R. Jérôme and P. Teyssié, *Macromolecules*, **29**, 1753 (1996).
320. W. Bauer and D. Seebach, *Helv. Chim. Acta.*, **67**, 1972 (1984).
321. W. H. Sikorski and H. Reich, *J. Am. Chem. Soc.*, **123**, 6527 (2001).
322. E. Juaristi, M. Hernández-Rodríguez, H. López-Ruiz, J. Aviña, O. Muñoz-Muñiz, M. Hayakawa and D. Seebach, *Helv. Chim. Acta*, **85**, 1999 (2002).
323. W. G. Kofron and M.-K. Yeh, *J. Org. Chem.*, **41**, 439 (1976).
324. M. S. Addie and R. J. K. Taylor, *ARKIVOC*, **1**, 660 (2000); online computer file http://www.arkat.org/arkat/journal/Issue5/ms0064/ms0064.pdf
325. R. P. Quirk, T.-H. Cheong and T. Yoo, *Macromol. Chem. Phys.*, **203**, 1178 (2002).
326. J. Barluenga, F. Rodríguez and F. J. Fañanás, *Chem. Eur. J.*, **6**, 1930 (2000).
327. M. D. Curtis and P. Beak, *J. Org. Chem.*, **64**, 2996 (1999).
328. J. Epsztajn, A. Jóźwiak, P. Kołuda, I. Sadokierska and I. D. Wilkowska, *Tetrahedron*, **56**, 4837 (2000).
329. J. Clayden, D. Mitjans and L. H. Youssef, *J. Am. Chem. Soc.*, **124**, 5266 (2002).
330. A. Ahmed, J. Clayden and M. Rowley, *Chem. Commun.*, 297 (1998).
331. A. Ahmed, J. Clayden and M. Rowley, *Tetrahedron Lett.*, **39**, 6103 (1998).
332. V. K. Aggarwal, G. Hynd, W. Picoul and J.-L. Vasse, *J. Am. Chem. Soc.*, **124**, 9964 (2002).
333. D. J. Pippel, G. A. Weisenburger, S. W. Wilson and P. Beak, *Angew. Chem., Int. Ed.*, **37**, 2522 (1998).
334. S. H. Lim, M. D. Curtis and P. Beak, *Org. Lett.*, **3**, 711 (2001).
335. S. H. Lim and P. Beak, *Org. Lett.*, **4**, 2657 (2002).
336. T. A. Johnson, M. D. Curtis and P. Beak, *Org. Lett.*, **4**, 2747 (2002).
337. K. M. Bertini and P. Beak, *J. Am. Chem. Soc.*, **123**, 315 (2001).
338. (a) C. G. Screttas and B. R. Steele, *J. Am. Chem. Soc.*, **122**, 2391 (2000).
    (b) M. Janata, L. Lochmann, J. Brus and P. Vlček, *Macromolecules*, **34**, 1593 (2001).

339. R. P. Quirk, R. T. Mathers, J.-J. Ma, C. Wesdemiotis and M. A. Arnould, *Macromol. Symp.*, **183**, 17 (2002).
340. M. K. Pound, D. L. Davies, M. Pilkington, M. M. de Pina Vaz Sousa and J. D. Wallis, *Tetrahedron Lett.*, **43**, 1915 (2002).
341. M. Yus, F. Foubelo, F. V. Fernández and A. Bachki, *Tetrahedron*, **58**, 4907 (2002).
342. I. M. Pastor and M. Yus, *Tetrahedron*, **57**, 2365 (2001).
343. I. M. Pastor and M. Yus, *Tetrahedron*, **57**, 2371 (2001).
344. J. Almena, F. Foubelo and M. Yus, *Tetrahedron*, **51**, 3351 (1995).
345. M. Yus and J. Gomis, *Tetrahedron Lett.*, **42**, 5721 (2001).
346. M. Yus and J. Gomis, *Eur. J. Org. Chem.*, 1989 (2002).
347. M. Yus, I. M. Pastor and J. Gomis, *Tetrahedreon*, **57**, 5799 (2001).
348. I. M. Pastor and M. Yus, *Tetrahedron Lett.*, **41**, 1589 (2000).
349. M. Yus, I. Gómez and C. Candela, *Tetrahedron*, **58**, 6207 (2002).
350. T. Soler, A. Bachki, L. R. Falvello, F. Foubelo and M. Yus, *Tetrahedron: Asymmetry*, **11**, 493 (2000).
351. U. Azzena, L. Pilo and E. Piras, *Tetrahedron Lett.*, **42**, 129 (2001).
352. M. Yus, F. Foubelo and J. V. Ferrández, *Chem. Lett.*, 726 (2002).
353. M. Yus, D. J. Ramón and I. Gómez, *Tetrahedron*, **58**, 5163 (2002).
354. M. Yus, R. Ortiz and F. F. Huerta, *Tetrahedron Lett.*, **43**, 2957 (2002).
355. M. Yus, C. Gómez and P. Candela, *Tetrahedron Lett.*, **42**, 3977 (2001).
356. L. I. Smith and H. H. Hoehn, *J. Am. Chem. Soc.*, **63**, 1184 (1941).
357. N. Hanyu, T. Aoki, T. Mino, M. Sakamoto and T. Fujita, *Tetrahedron Lett.*, **41**, 4587 (2000).
358. N. Hanyu, T. Aoki, T. Mino, M. Sakamoto and T. Fujita, *Tetrahedron: Asymmetry*, **11**, 2971 (2000).
359. N. Hanyu, T. Aoki, T. Mino, M. Sakamoto and T. Fujita, *Tetrahedron: Asymmetry*, **11**, 4127 (2000).
360. Y. Apeloig, M. Bendikov, M. Yusefovich, M. Nakash and D. Bravo-Zhivotovskii, *J. Am. Chem. Soc.*, **118**, 12228 (1996).
361. K. Sternberg, H. Reinke and H. Oehme, *Z. Anorg. Allg. Chem.*, **625**, 467 (1999).
362. G. H. Posner and C. M. Lentz, *Tetrahedron Lett.*, 3211 (1977).
363. T. Oishi, K. Onimura, K. Tanaka, W. Horimoto and H. Tsutsumi, *J. Polym. Sci. A*, **37**, 473 (1999).

CHAPTER 9

The preparation of organolithium reagents and intermediates

FRÉDÉRIC LEROUX

Laboratoire de stéréochimie, Université Louis Pasteur (ECPM), 25 rue Becquerel, F-67087 Strasbourg, France
Fax: +33-3-9024-2742; e-mail: lerouxf@ecpm.u-strasbg.fr

MANFRED SCHLOSSER

Institute of Molecular and Biological Chemistry, Swiss Federal Institute of Technology, CH-1015 Lausanne, Switzerland
Fax: +41-21-693-9365; e-mail: manfred.schlosser@epfl.ch

and

ELINOR ZOHAR and ILAN MAREK

Department of Chemistry and Institute of Catalysis, Science and Technology, Technion — Israel Institute of Technology, Technion City, 32000 Haifa, Israel
Fax: +972-4-829-3709; e-mail: chilanm@tx.technion.ac.il

The Chemistry of Organolithium Compounds. Edited by Z. Rappoport and I. Marek

ISBN: 0-470-84339-X

I. INTRODUCTION

To attach a metal to an organic entity, one has to displace an already present substituent Z (Table 1)[1a]. Five classes of leaving groups may be considered: halogens (X = Cl, Br, I), chalcogens (Y = O, S, Se, Te), metalloids (Q = Hg, Sn), carbon (in particular triarylmethyl units) and hydrogen. The source of the metal can be either the element (M) itself or a metal derivative (M−R), in general a commercial organometallic reagent or a metal salt. In the first case, the metal undergoes a reductive insertion into the C−Z (C−X, X−Y, C−Q, C−C or C−H) bond and the displaced substituent Z is expelled as a nucleofugal group. Alternatively, a permutational interconversion may be performed whereby the displaced substituent Z is transferred as an electrofugal group to the organic part (R) of the reagent.

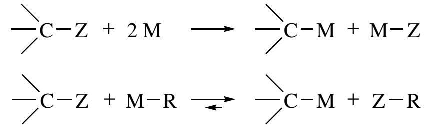

TABLE 1. A survey of the standard methods applied to the preparation of organometallic compounds: three crosses mean ‘generally applicable’, two ‘restricted, though important scope of applicability’ and one ‘narrow scope’

Reductive insertion	Z (leaving group)	Permutational interconversion
⊕⊕⊕	X (halogen)	⊕⊕⊕
⊕⊕	Y (chalcogen)	⊕
⊕⊕	Q (metalloid)	⊕⊕
⊕	C (carbon)	⊕
⊕	H (hydrogen)	⊕⊕⊕

What makes the permutation approach so attractive is the ease of execution and the mild reaction conditions. A possible drawback is its moderate exothermicity which may prevent the interconversion to go to completion but rather to stop as soon as an equilibrium composition is attained. Moreover, to rely on an organometallic exchange reagent merely defers the problem. Ultimately, the genesis of any organometallic compound can be traced back to the elemental metal.

For reasons of space only the most important methods for the generation of organometallic reagents and intermediates can be covered in this Chapter. This holds for the reductive insertion of lithium into organic halides (Section II), the permutational interconversion of organic halides with organolithiums (Section III) and the permutational interconversion of hydrocarbons with organolithiums (‘metalation’, Section IV). In addition, three special methods will be featured, the Brook isomerization (Section V), the Shapiro reaction (Section VI) and the sulfoxide/alkyllithium interconversion (Section VII). These topics have been neglected for a long while, but begin to find now the attention they deserve because of their unexploited potential. Readers who seek information about other prominent methods such as the reductive ether cleavage[1b] or the selenium/lithium[1c] and tin/lithium[1d] permutations are referred to a recently edited Handbook[1].

II. REDUCTIVE METAL INSERTION INTO CARBON–HALOGEN BONDS

Standard reagents such as methyllithium, ethyllithium, butyllithium, hexyllithium, isopropyllithium, *sec*-butyllithium, *tert*-butyllithium and phenyllithium are nowadays commercially available, even in various solvents and concentrations[2]. However, in general it is less expensive to make such reagents themselves rather than to purchase them. References to the preparation of primary alkyllithiums (Table 2), secondary or tertiary alkyllithiums (Table 3), 1-alkenyllithiums (Table 4) and aryllithiums without or with hetero-substituents (Tables 5 and 6) have been compiled below.

TABLE 2. Primary alkyllithiums Li–R (including neopentylic ones) by metal insertion into halides R–X: yields as determined by titration[1e] or after trapping with an electrophile *El*–X′

Li–R	X	*Sv*[a]	Product	*El*–X′	Reference
Li–CH_3	Cl, Br, I	DEE	*ca* 80%	titration	3, 4
Li–C_2H_5	Cl, Br	PET	50%	titration	5–9
Li–C_3H_7	Cl	PET	*ca* 80%	titration	5, 10
Li–C_4H_9	Cl, Br	PET	*ca* 95%	[b]	11, 12
Li–C_6H_{13}	Cl	DEE	⩾90%	titration	13
Li–C_8H_{17}	Cl	THF	94%	H_2O	14
Li–$C_{12}H_{25}$	Cl	DEE	77%	titration	15, 16
Li–$CH_2C(CH_3)_3$	Cl	PET; DEE	71%	$[(H_3C)_2CH]_2CO$	17, 18
Li–$CH_2Si(CH_3)_3$	Cl	PET; DEE	90%	isol. by sublim.	19

[a] Solvent *Sv*: PET = petroleum ether (pentanes, hexanes, heptanes), DEE = diethyl ether, THF = tetrahydrofuran.
[b] Various electrophiles.

TABLE 3. Secondary and tertiary alkyllithiums Li–R: yields of trapping products as a function of the precursor halide X and the electrophile *El*–X′ used

Li–R	X	*Sv*[a]	Product	*El*–X′	Reference
Li–$CH(CH_3)_2$	Br	PET	45%	titration	5
Li–$CH(CH_3)C_2H_5$	Cl	PET	50%	titration	20
Li–$C(CH_3)_3$	Cl	PET	62%	CO_2	21
			89%	titration	22–24
Li–$CH(CH_2)_2$[b]	Br	DEE	88%	$SnCl_4$	25
Li–$CH(CH_2)_5$[c]	Cl	DEE	70%	$GeCl_4$	26
Li–C_7H_{11}[d]	Cl	PET	51%	CO_2	27
Li–$C_{10}H_{15}$[e]	Cl	PET	82%	D_2O	28

[a] Solvent *Sv* : PET = petroleum ether (pentanes, hexanes, heptanes), DEE = diethyl ether.

[b] 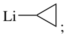 ; [c]  ; [d] 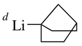 ; [e] 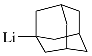 .

TABLE 4. 1-Alkenyllithiums Li–R: yields of trapping products as a function of the precursor halide X and the electrophile *El*–X′ (common temperature range: +25 °C to +50 °C)

Li–R	X	*Sv*[a]	Product	*El*–X′	Reference
Li–$CH{=}CH_2$	Cl	THF	70–80%	[b]	23, 29, 30
Li–$CH{=}C(CH_3)_2$	Br	DEE	30%	H_5C_6CHO	31, 32
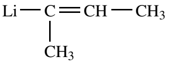 Li–$C(CH_3){=}CH$–CH_3	Br	DEE	75%	$H_3CCOOC_2H_5$	33
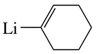	Cl	DEE	40%	H_5C_6CHO	31, 32

[a] Solvent *Sv*: DEE = diethyl ether, THF = tetrahydrofuran.
[b] Various electrophiles *El*–X′.

TABLE 5. Aryllithiums Li−R lacking hetero-substituents by metal insertion into haloarenes, the reactions being generally conducted in diethyl ether and in the temperature range of 0 °C to +40 °C (refluxing ether)

Li−R	X[a]	Product	*El*−X′ [b]	Reference
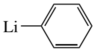	Cl, Br[c]	*ca* 85%	CO_2	34–38
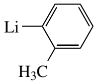	Br	93%	Titration	39
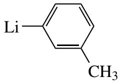	Br	86%	Titration	39
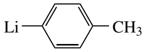	Br	95%	Titration	34–37, 39
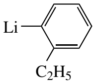	I	50%	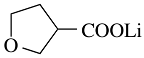	40
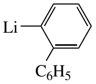	Br, I	*ca* 75%	CO_2	41, 42
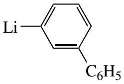	Br	72%	Titration	41
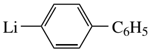	Br	87%	Titration	41, 43
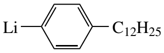	Br	75%	Titration	44
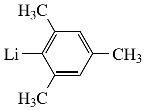	Br Br	85% 44%	CO_2 Titration	45, 46
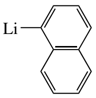	Br	80%	Titration	39
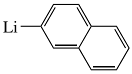	Br	81%	$SiCl_4$	39, 47

[a] X = Halogen in the starting material, being displaced by metal.
[b] The concentration of the organometallic solution prepared was determined either by the titration[1e] of an aliquot or by isolation of the product formed upon the trapping of an aliquot using an electrophilic reagent *El*−X′.
[c] In diethyl ether or tetrahydrofuran.

TABLE 6. Aryllithiums Li−R carrying amino and alkoxy substituents prepared in diethyl ether by metal insertion into the corresponding bromoarene

Li−R	Product	*El*−X′ [a]	Reference
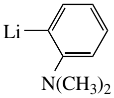	0%	$(H_5C_6)_3PbCl$	48
	58%	$(H_5C_6)_3SiCl$	49, 50
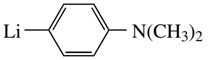	65%	CO_2	22, 51
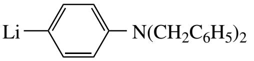	22%	$R'COOC_2H_5$ [b]	52
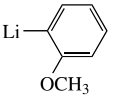	85%	titration	53
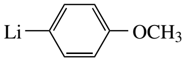	66%	titration	53

[a] *El*−X′ = electrophilic trapping reagent.

[b] 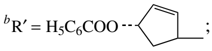 ; then oxidation with CrO_3.

Whenever possible, alkyllithiums should be prepared from chloroalkanes in paraffinic media for reasons of economy. As a 1930 landmark study has revealed, both bromoalkanes and iodoalkanes react rapidly with butyllithium in benzene and extremely rapidly in diethyl ether (Table 7) producing butane, 1-butene, 2-butene, octane and possibly also methylcyclopropane.

TABLE 7. Butyllithium in the presence of butyl chloride, bromide and iodide (0.50 M initial concentrations): half-lives $\tau_{1/2}$ (in hours) as a function of the solvent benzene (BNZ) or diethyl ether (DEE) at ambient temperature[54]

$H_9C_4{-}X + LiC_4H_9$	$\tau_{1/2}^{BNZ}$ (in hours)	$\tau_{1/2}^{DEE}$ (in hours)
X = I	3	<0.1
X = Br	40	0.5
X = Cl	>100	40

When the halogen in the precursor is exceptionally mobile as an anion, even chloro compounds may give poor yields due to extensive self-destruction. For example, chloromethyl methyl ether can be expediently converted into methoxymethyllithium only if sodium/lithium alloy is used and a carefully elaborated protocol is meticulously followed[55]. In the case of 7-chloronorbornadiene, the lithium/4,4′-di-*tert*-butylbiphenyl 'radical anion' has to be employed[56, 57] to further reduce the contact time between 7-norbornadienyllithium and its labile precursor. Many reductive metal insertions into carbon−halogen bonds require the presence of electron carriers such as 4,4′-di-*tert*-butylbiphenyl, naphthalene or anthracene. The *in situ* generation of 'radical anions' from sub-stoichiometric amounts of suitable arenes is highlighted in Chapter 11.

III. PERMUTATIONAL HALOGEN/METAL INTERCONVERSIONS

When treated with butyllithium in diethyl ether at −50 °C, bromobenzene undergoes the permutational exchange of the halogen against the metal only slowly, but rapidly at 0 °C. The transformation is complete after a few seconds if conducted in tetrahydrofuran at −75 °C. Iodobenzene reacts instantaneously in any case.

In contrast to the bromo and iodo analogs, organic chloro compounds are relatively inert toward organolithium reagents. There are only a few classes of chlorinated substrates, notably *gem*-dichlorocyclopropanes[58], 1,1-dichloro-1-alkenes[59, 60] and doubly vicinal oligochlorobenzenes (1,2,3-trichlorobenzene[61, 62], 1,2,3,4-tetrachlorobenzene[61, 62], hexachlorobenzene[63] etc.) that are capable of sustaining the halogen/lithium permutation mode.

How well an organolithium reagent fares as an exchange component depends on its basicity. Thus, *tert*-butyllithium outperforms *sec*-butyllithium, which in turn is superior to butyllithium. Methyllithium is the least reactive alkyllithium but still surpasses phenyllithium, at least at low concentrations, i.e. the order is:

$$\mathrm{Li{-}C(CH_3)_3 > Li{-}CH(CH_3)C_2H_5 > Li{-}CH_2C_3H_7 > Li{-}CH_3 \gtrsim Li{-}C_6H_5}$$

To make neopentyllithium or any other alkyllithium from the corresponding iodoalkane, *tert*-butyllithium is the best, if not the only choice (Tables 8 and 9). Besides its reactivity,

TABLE 8. Primary aliphatic organolithiums Li−R by halogen/metal permutation between haloalkanes X−R and *tert*-butyllithium in diethyl ether at −75 °C

Li−R	X[a]	Product	*El*−X′ [b]	Reference
Li−CH$_3$[c]	Br	64%	titration	64−66
Li−C$_4$H$_9$	I	91%	H$_9$C$_4$CH=O	67
Li−C$_8$H$_{17}$	I	93%	H$_3$CCOCH$_3$	67
Li−C$_{10}$H$_{15}$[d, e]	I	66%	CO$_2$	68
Li−CH$_2$− 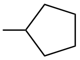	I	91%	CO$_2$	67
Li−(CH$_2$)$_2$C$_6$H$_5$	I	91%	CO$_2$	67−69
Li−CH$_2$C(CH$_3$)$_3$	I	89%	H$_7$C$_3$CH=O	67
Li−(CH$_2$)$_2$CH=CH$_2$	I	88%	ClSn(CH$_3$)$_3$	69
Li−(CH$_2$)$_3$CH=CH$_2$	I	87%	CO$_2$	70
Li−(CH$_2$)$_2$C≡C−C$_4$H$_9$	I	80%	ClSn(CH$_3$)$_3$	69
Li−(CH$_2$)$_4$C≡C−C$_6$H$_5$	I	87%	D$_2$O	71

[a] X = halogen displaced by the metal.
[b] *El*−X′ = electrophilic trapping reagent.
[c] Using butyllithium rather than *tert*-butyllithium.
[d] C$_{10}$H$_{15}$ = 2-adamantyl.
[e] At −45 °C rather than −75 °C.

TABLE 9. Cyclopropyl- and other cycloalkyllithiums Li—R by halogen/metal permutation between haloalkanes X—R and reagents Li—R′ in diethyl ether (DEE)

Li—R	Li—R′	X[a]	*T*[b]	Product	*El*—X′[c]	Reference
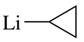 [d]	$LiCH(CH_3)_3$	Br	−75 °C	91%	$(H_5C_6)_2CO$	72, 73
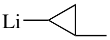	$LiCH(CH_3)_2$	Br	0 °C	15%	CO_2	74
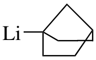	$LiC(CH_3)_3$	I	−60 °C	60–90%	H_5C_6CHO	75
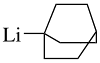	$LiC(CH_3)_3$	I	−70 °C	60–90%	H_5C_6CHO	75
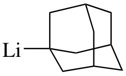	$LiC(CH_3)_3$	I	−70 °C	*ca* 70%	H_5C_6CHO	76
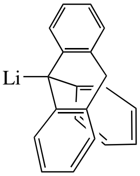	LiC_4H_9	Br	+25 °C	41%	CO_2	77, 78

[a] X = halogen which is displaced by the metal.
[b] Exchange and trapping temperature.
[c] *El*—X′ = electrophilic trapping reagent.
[d] In tetrahydrofuran (THF) rather than DEE.

it offers another distinct advantage. It reacts with its own exchange products, 2-bromo-2-methylpropane (*tert*-butyl bromide) or 2-iodo-2-methylpropane (*tert*-butyl iodide) rapidly, even at −75 °C, with elimination of lithium halide. In this way, any equilibrium can be rigorously and irreversibly shifted to one side. This explains why *tert*-butyllithium can be used to generate 1-adamantyllithium **2**, equally a tertiary alkyllithium, from 1-iodoadamantane **1** (equation 1)[76].

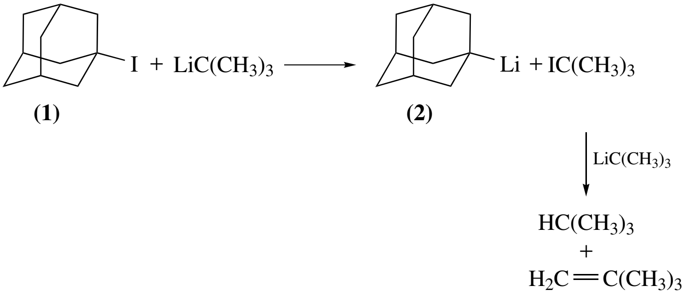

(1)

Alkoxy groups or halogen atoms at the α- or β-position of open-chain or cyclic alkyllithiums diminish the basicity of such species and hence facilitate the halogen/metal permutation. Other than *tert*-butyllithium, also *sec*-butyllithium or butyllithium, even methyllithium, or phenyllithium, can now be employed (Tables 10 and 11).

TABLE 10. α-Fluoro-, α-chloro-, α-bromo- and α-iodoalkyllithiums Li−R by halogen/metal permutation using organometallic reagents Li−R′

Li−R	Li−R′	X[a]	*T*	Product	*El*−X′ [b]	Reference
$Li{-}CH_2C$	LiC_4H_9	I	−75 °C	88%	H_5C_6CHO[c]	79−82
$Li{-}CH_2I$	LiC_4H_9	I	−75 °C	89%	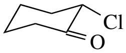 [d]	83
$Li{-}CH(CH_3)Cl$	$LiCH(CH_3)C_2H_5$	Br	−115 °C	63%	H_5C_6CHO	84
$Li{-}CH(CH_3)Br$	$LiCH(CH_3)C_2H_5$	Br	−115 °C	59%	H_5C_6CHO	84
$Li{-}C(CH_3)_2Br$	$LiCH(CH_3)C_2H_5$	Br	−115 °C	41%	H_5C_6CHO	84
$Li{-}C(C_6H_5)_2Cl$	LiC_4H_9	Cl	−100 °C	75%	CO_2	85
$Li{-}CBr_2CH_3$	LiC_4H_9	Br	−100 °C	—	[e]	60
$Li{-}C_2F_5$	$LiCH_3$[c, f]	I	−75 °C	88%	H_5C_2CHO	86
$Li{-}C_3F_7$	$LiCH_3$[c, f]	I	−40 °C	54%	$(H_5C_6)_2CO$	87, 88
$Li{-}C_7F_{15}$	LiC_4H_9[f]	I	−90 °C	38%	CO_2	89
$Li{-}CF(CF_3)_2$	$LiCH_3$[c, f]	I	−75 °C	53%	H_5C_6CHO	90
$Li{-}CCl_3$	LiC_4H_9	Cl	−100 °C	76%	CO_2	85,91
$Li{-}CBr_3$	LiC_6H_5[g]	Br	−110 °C	91%	CO_2	60, 92

[a] X = halogen being displaced.
[b] *El*−X′ = electrophilic trapping reagent.
[c] Halogen/metal exchange performed in the presence (*in situ*) of the electrophile.
[d] The isolated product emanated from a subsequent reaction.
[e] Detected by NMR.
[f] Diethyl ether (DEE) rather than THF as the solvent.
[g] Or butyllithium.

Being less basic than the saturated analogs, vinyllithium as all other acyclic or cyclic 1-alkenyllithiums can be prepared from iodo or bromo and sometimes even chloro precursors using butyllithium or *tert*-butyllithium (Tables 12 and 13). Hetero-substituents such as dialkylamino, alkoxy and silyloxy groups or halogen atoms again accelerate the exchange process considerably (Table 14). This holds for *O*-lithiated hydroxy or carboxy functions as well (Table 15).

Bromo- and iodoarenes are the oldest and most typical substrates for permutational halogen/metal interconversions. Butyllithium is routinely used for this purpose (Table 16). Hetero-substituents such as dialkylamino or bis(trialkylsilyl)amino, cyano or nitro (Table 17), alkoxy and 2-tetrahydropyranyloxy (Table 18), lithiooxy or lithiooxycarbonyl (Table 19) and fluoro or trifluoromethyl (Table 20) and chloro, bromo or iodo (Table 21) are well tolerated.

Bromopyridines and bromoquinolines smoothly undergo a halogen/metal interconversion when treated at low temperatures with butyllithium in diethyl ether or tetrahydrofuran (Table 22). Additional hetero-substituents such as dialkylamino and alkoxy groups or halogen atoms may be present in the substrate. 2,5-Dibromopyridine gives rise to a solvent-controlled optional site selectivity. When the exchange is accomplished in tetrahydrofuran, the nitrogen-remote halogen at the 5-position is displaced[221] whereas the reaction occurs in toluene at the site adjacent to the nitrogen atom[220]. Not only pentabromopyridine[227] but also pentachloropyridine[224−226] are subject to a butyllithium-promoted rapid interconversion at the 4-position.

TABLE 11. α- or β-Alkoxy- and α-halocyclopropyllithiums Li−R by halogen/metal permutation between bromocyclopropanes and organolithium reagents Li−R′ followed by trapping with electrophiles *El*−X′

Li−R	Li−R′	*Sν*[a]	*T*	Product	*El*−X′ [b]	Reference
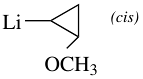	$LiC(CH_3)_3$	DEE	−75 °C	92%	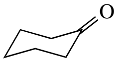	93
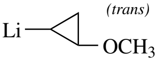	$LiC(CH_3)_3$	DEE	−75 °C	85%	$H_{13}C_6CHO$	93
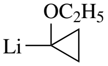	$LiC(CH_3)_3$	DEE	−75 °C	81%	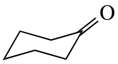 [c]	94
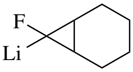	LiC_4H_9	THF	−135 °C	9%	H_2O	95
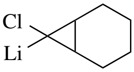	LiC_4H_9	THF	−110 °C	64%	Br_2	58, 95
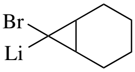	LiC_4H_9	THF	−100 °C	39%	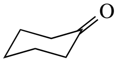	96–99
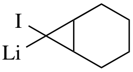 [d]	LiC_4H_9	THF	−80 °C	—	[e]	92
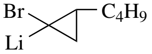	LiC_4H_9	THF	−100 °C	70%	$(H_3C)_2CO$	100
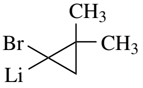	LiC_4H_9	THF	−100 °C	60%	$(H_3C)_2CO$	100, 101
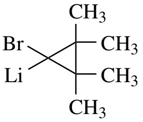	LiC_4H_9	THF	−100 °C	80%	H_9C_4CHO	100
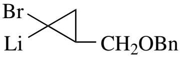 [f]	LiC_4H_9	DEE	−95 °C	83%	HOC_2H_5	102–104
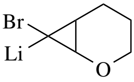	$LiCH_3$	DEE	−80 °C	88%	CO_2	105
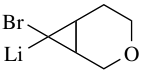	$LiCH_3$	DEE	−80 °C	65%	CO_2	105

[a] Solvent (*Sν*): DEE = diethyl ether, THF = tetrahydrofuran.
[b] *El*−X′ = electrophilic trapping reagent.
[c] Product isolated after subsequent transformation.
[d] 7,7-Diiodonorcarane as the starting material.
[e] Detected by NMR.
[f] $Bn = CH_2C_6H_5$.

TABLE 12. 1-Alkenyllithiums Li–R by halogen/metal permutation

Li–R	X[a]	Li–R′	*Sv*[b]	*T*	Product	*El*–X′ [c]	Reference
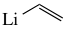	Br	$LiC(CH_3)_3$	THF	−115 °C	74%	$(SC_6H_5)_2$	106, 107
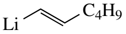	I	$LiC(CH_3)_3$	PET	+25 °C	71%	H_5C_6CHO	106, 107
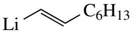	I	LiC_4H_9[d]	PET	+25 °C	71%	H_5C_6CHO	106, 108
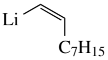	I	LiC_4H_9[e]	DEE	−50 °C	91%	H_3CCHO	109
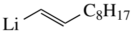	I	$LiC(CH_3)_3$	PET	+25 °C	74%	H_5C_6CHO	110
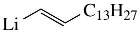	I	$LiC(CH_3)_3$	PET	+25 °C	77%	H_5C_6CHO	110
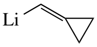	Br	$LiC(CH_3)_3$	DEE	−80 °C	24%	c-$(H_2C)_5CO$	111
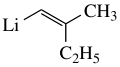	I	LiC_4H_9[e]	DEE	−50 °C	91%	$(H_5C_2)_2CO$	109

[a] X = halogen displaced by the metal.
[b] Solvent (*Sv*): PET = petroleum ether (pentanes, hexanes, heptanes), DEE = diethyl ether, THF = tetrahydrofuran.
[c] *El*–X′ = electrophilic trapping reagent.
[d] Or $LiC(CH_3)_3$.
[e] Or LiC_2H_5.

TABLE 13. 1-Cycloalkenyllithium compounds Li–R by halogen/metal permutation

Li–R	X[a]	Li–R′	*Sv*[b]	*T*	Product	*El*–X′ [c]	Reference
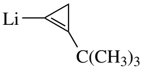	Cl[d]	$LiCH_3$	DEE	+25 °C	72%	CO_2	112
	Br[d]	$LiCH_3$	DEE	+25 °C	78%	CO_2	113
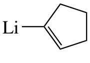	Br	$LiC(CH_3)_3$	THF	−75 °C	73%	I_2	106
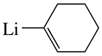	Br	$LiC(CH_3)_3$	THF	−75 °C	52%	[e]	106
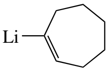	Br	$LiC(CH_3)_3$	THF	−75 °C	93%	$ClSi(CH_3)_3$	106
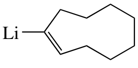	Br	$LiC(CH_3)_3$	THF	−75 °C	83%	$(SCH_3)_2$	114
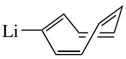	Br	LiC_4H_9	THF	−60 °C	7%[f]	$FClO_3$	115, 116

[a] X = halogen displaced by the metal.
[b] Solvent (*Sv*): DEE = diethyl ether, THF = tetrahydrofuran.
[c] *El*–X′ = electrophilic trapping reagent.
[d] Prepared *in situ* from trihalocyclopropanes.
[e] Bis(trimethylsilyl)peroxide.
[f] 59% with CO_2.

TABLE 14. Hetero (β-amino, β- or γ-alkoxy, β- or γ-silyloxy, α- or β-halo) substituted 1-alkenyllithiums Li–R by halogen/metal permutation

Li–R	X[a]	Li–R′[b]	*Sv*[c]	*T*	Product	*El*–X′[d]	Reference
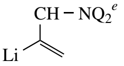	Br	LIT	DEE	−80 °C	82%	H_5C_6NCO	117
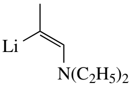	Br	LIT	THF	−70 °C	100%	$(H_3C)_2NCHO$	118, 119
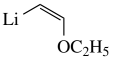	Br	LIC	THF	−75 °C	75%	H_5C_6CHO	120–122
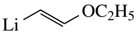	Br	LIC	THF	−75 °C	75%	$(H_5C_6)_2CO$	121
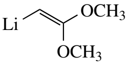	Br	LIC	THF	−75 °C	67%	$(H_3C)_3SiCl$	121, 123
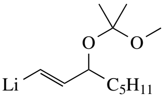	I	LIC	PET	−70 °C	90%	D_2O	124
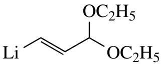	Br	LIT	THF	−120 °C	93%	H_5C_6CHO	125
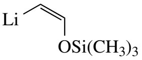	Br	LIT	DEE	−70 °C	97%	β-ionone	126
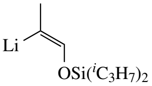	I	LIT	DEE	−75 °C	70%	CO_2	127
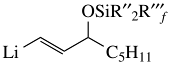	I	LIT	PET	[g]	[g]	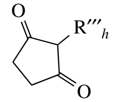	128, 129
Li—CF═CH$_2$	Br	LIC	DEE	−75 °C	25%	$(H_2C)_5CO$	130
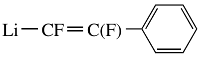	Cl	LIC	DEE	−110 °C	90%	H_2O	131
Li—CF═CF$_2$	Cl	LIC	THF	−135 °C	82%	$(H_2C)_5CO$[i]	132
	Cl	LIT	DEE	−60 °C	90%	$(H_2C)_5CO$[i]	133, 134
	Br	LIM	DEE	−75 °C	66%	$(H_2C)_5CO$[i]	135
Li—C(CF$_3$)═CH$_2$	Br	LIC	DEE	−85 °C	51%	$H_5C_6COCH_3$	136
Li—CCl═CF$_2$	Br	LIC	THF	−110 °C	92%	CO_2	137

[a] X = halogen in the precursor.

[b] Exchange reagent Li–R′: LIT = $LiC(CH_3)_3$, LIC = LiC_4H_9, LIM = $LiCH_3$.

[c] Solvent (*Sv*): PET = petroleum ether; DEE = diethyl ether, THF = tetrahydrofuran.

[d] *El*–X′ = electrophilic trapping reagent.

[e] NQ_2 = 2, 2, 5, 5-tetramethyl-1-aza-2,5-disilolanyl.

[f] SiR''_2R''' = $Si(CH_3)_2C(CH_3)_3$.

[g] Not specified.

[h] R‴ = *cis*-CH_2–CH = CH–$(CH_2)_3$–$COOCH_3$.

[i] $(H_2C)_5CO$ = Cyclohexanone; product isolated after acid hydrolysis as an α,β-unsaturated carbonyl compound.

TABLE 15. 1-Alkenyllithiums Li–R carrying lithiooxy or lithiooxycarbonyl groups (at the γ or β position, respectively): generation by halogen/metal permutation using exchange reagents Li–R′ in diethyl ether or, with respect to the first and last two entries, in tetrahydrofuran

Li–R	X[a]	Li–R′	*T*[b]	Product	*El*–X′[c]	Reference
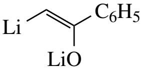	Br[d]	$LiC(CH_3)_3$	0 °C	88%	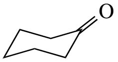	138
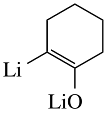	Br[d]	$LiC(CH_3)_3$	0 °C	64%	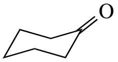	138
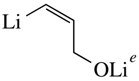 [e]	Br, I	$LiC(CH_3)_3$[f]	−75 °C	55%	H_5C_6CHO	139
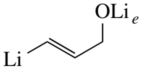 [e]	Br, I	$LiC(CH_3)_3$	−75 °C	57%	H_5C_6CHO	139
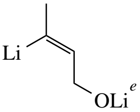 [e]	Br, I	$LiC(CH_3)_3$[f]	−75 °C	28%	H_5C_6CHO	139, 140
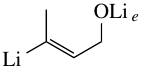 [e]	Br, I	$LiC(CH_3)_3$	−75 °C	65%	$(H_3C)_3CCHO$	139
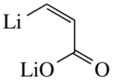	Br	LiC_4H_9	−100 °C	38%	H_5C_6CHO[g]	141
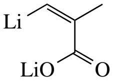	Br	LiC_4H_9	−100 °C	61%	H_5C_6CHO[g]	141
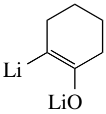	Br	LiC_4H_9	−100 °C	47%	H_5C_6CHO[g]	138

[a] X = halogen displaced by the metal.

[b] If the temperature at *T* which the organometallic intermediate was generated varied, only the highest one is given.

[c] *El*–X′ = electrophile used to trap the organometallic intermediate.

[d] First the lithium β-bromoenolate was generated from the corresponding α-bromoketone using 2.0 equiv. of $LiCH_3$.

[e] Similar results were obtained with *O*-*tert*-butyldimethylsilyl protected 1-alkenyl bromides as the precursors.

[f] Or *sec*-butyllithium.

[g] Isolated as the lactone.

TABLE 16. Heteroatom-free aryllithiums Li—R by halogen/metal permutation between bromo- or iodoarenes and butyllithium

Li—R	X[a]	$S\nu$[b]	T	Product	El—X′ [c]	Reference
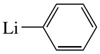	Br, I	PET[d]	[e]	65%	CO_2	142–145
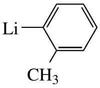	Br	DEE	+50 °C	84%	CO_2	142, 143
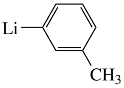	Br	DEE	+50 °C	65%	CO_2	142, 143
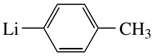	Br	PET	+25 °C	86%	CO_2	142, 143
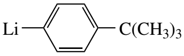	I	DEE	−70 °C	76%	CO_2	146
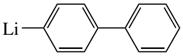	Br	DEE	+25 °C	62%	CO_2	142–145, 147
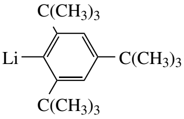	Br	DEE	−75 °C	60%	Cl_3SiBr	148, 149
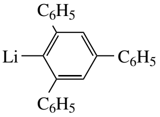	Br	DEE	+25 °C	87%	crystallized	150
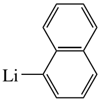	Br	DEE	+25 °C	97%	CO_2	151, 153
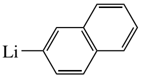	Br	DEE	+25 °C	77%	CO_2	151
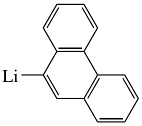 [f]	Br	DEE	+40 °C	51%	CO_2	154
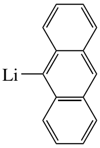	Br	PET	+25 °C	72%	CO_2	155

[a] X = halogen displaced by the metal.

[b] Solvent ($S\nu$): PET = petroleum ether, DEE = diethyl ether.

[c] El—X′ = electrophilic trapping reagent.

[d] Or in benzene or in diethyl ether.

[e] In DEE in the range of −75 °C to +40 °C (reflux), in pure hydrocarbon media at +25 °C.

[f] In the presence of *N,N,N′,N′*-tetramethylethylenediamine (TMEDA).

TABLE 17. Amino-, cyano- and nitro-substituted aryllithiums Li–R by halogen/metal permutation using butyllithium or phenyllithium

Li–R	Li–R′[a]	*Sν*[b]	*T*	Product	*El*–X′[c]	Reference
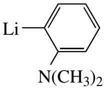	LiC_4H_9	THF	−75 °C	83%	$(H_5C_6)_2CO$	156
	LiC_4H_9	DEE	+49 °C	32%	CO_2	157
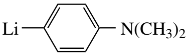	LiC_4H_9	DEE	+40 °C	56%	CO_2	157, 158
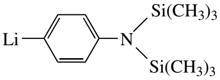	LiC_4H_9	DEE	0 °C	80%	$(H_5C_6)_2CO$	159
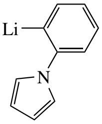	LiC_4H_9	THF	−80 °C	75%	H_5C_6CHO	160
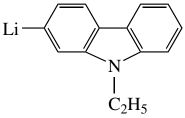	LiC_4H_9	DEE	+40 °C	71%	CO_2	161
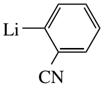	LiC_4H_9	THF	−100 °C	72%	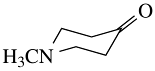	162
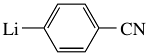	LiC_4H_9	DEE	−70 °C	17%	CO_2	163
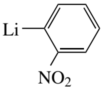	LiC_4H_9	THF	−100 °C	97%	CO_2	164
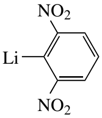	LiC_6H_5	THF	−100 °C	61%	CO_2	164
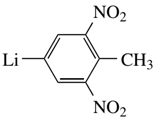	LiC_6H_5	THF	−100 °C	41%	CO_2	164
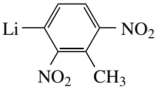	LiC_6H_5	THF	−100 °C	82%	CO_2	164

[a] Li–R′ = organometallic exchange reagent.
[b] Solvent (*Sν*): DEE = diethyl ether, THF = tetrahydrofuran.
[c] *El*–X′ = electrophilic trapping reagent.

TABLE 18. Alkoxy- and acetal-substituted aryllithiums Li−R by halogen/metal permutation between bromo- or iodoarenes and butyllithium

Li−R	X[a]	$S\nu$[b]	T	Product	El−X′[c]	Reference
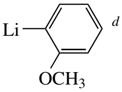	Br, I	DEE	+25 °C	90%	$(H_5C_6)_2CO$	165–167
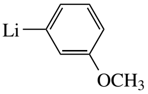	Br	THF[d]	−75 °C	52%	CO_2	168, 169
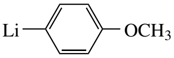	Br, I	BNZ	+25 °C	82%	CO_2	142–144
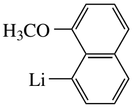	Br	PET	+25 °C	[e]	D_2O	170
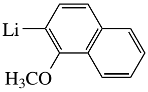	Br	THF	−75°	[e]	D_2O	170
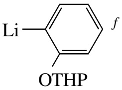	Br	THF	−75 °C	80%	[g]	171
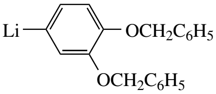	Br, I	DEE	−75 °C	42%	[h]	172
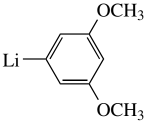	Br	THF	−75 °C	52%	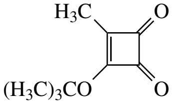	173, 174
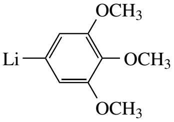	Br	THF	−75 °C	38%	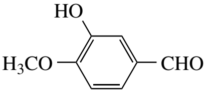	175
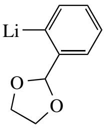	Br	THF	−75 °C	75%	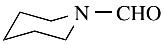	176

[a] X = halogen displaced by the metal.

[b] Solvent ($S\nu$): PET = petroleum ether; DEE = diethyl ether, THF = tetrahydrofuran, BNZ = benzene.

[c] El−X′ = electrophilic trapping reagent.

[d] Or using phenyllithium in DEE at +25 °C.

[e] Not specified.

[f] OTHP = (2-tetrahydropyranyl)oxy.

[g] 1-p-Anisyl-3-phenyl-2-butanone.

[h] *N*-Benzyl-6-aza-2-bicyclo[2.2.2]octanone.

TABLE 19. Lithiooxy-substituted aryllithiums Li–R by halogen/metal permutation between butyllithium and *O*-lithiated bromophenols, bromobenzyl alcohols, bromo-2-phenethyl alcohols and bromobenzoic acids

Li–R[a]	*Sv*[b]	*T*	Product	*El*–X′[c]	Reference
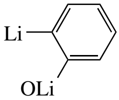	DEE	+25 °C	67%	CO_2	177–181
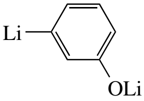 [d]	THF	0 °C	61%	[e]	182
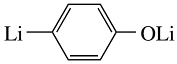	DEE,THF	+25 °C	75%	CO_2	177–181
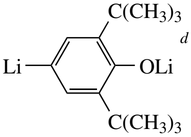 [d]	THF	0 °C	61%	H_5C_6CN	183
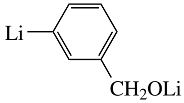	DEE	+25 °C	32%	CO_2	162
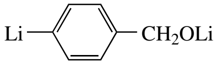	DEE	+25 °C	18%	CO_2	162
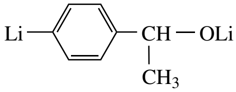	DEE	+25 °C	45%	CO_2	162
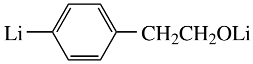	DEE	+25 °C	52%	CO_2	162
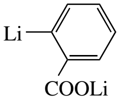	DEE	−75 °C	35%	CO_2	161, 177–181
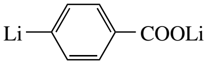	DEE	−75 °C	62%	CO_2	166, 177–181, 184

[a] OLi by deprotonation of OH prior to the halogen/metal permutation.

[b] Solvent (*Sv*): DEE = diethyl ether, THF = tetrahydrofuran.

[c] *El*–X′ = electrophilic trapping reagent.

[d] Using *tert*-butyllithium rather than butyllithium.

[e] (1) SO_2, (2) HO_3SONH_2.

TABLE 20. Fluoro- and trifluoromethyl-substituted arylithium Li−R by halogen/metal permutation between bromoarenes and butyllithium

Li−R	*Sv*[a]	*T*	Product	*El*−X′ [b]	Reference
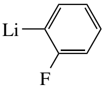	DEE	−70 °C	84%	$(H_5C_6)_2CO$	185
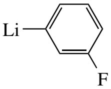	DEE	−40 °C	65%	CO_2	186
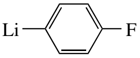	BNZ	+25 °C	50%	CO_2	144
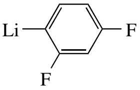	DEE	−75 °C	83%	CO_2	187, 188
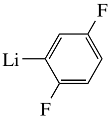	DEE	−75 °C	77%	CO_2	189
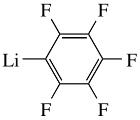	DEE	−75 °C	51%	H_2O	190, 191
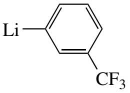	DEE	+25 °C	61%	CO_2	192
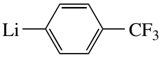	DEE	−50 °C	64%	CO_2	193
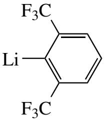	DEE	0 °C	48%	$Cl_2C = CF_2$	194
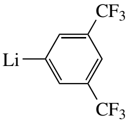	DEE	−75 °C	94%	CO_2	195
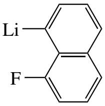	DEE	−70 °C	78%	$R'_4As^+I^-$ [c]	196

[a] Solvent (*Sν*): DEE = diethyl ether, BNZ = benzene.
[b] *El*−X′ = trapping electrophile.
[c] R'_2 = 4,4-Dimethyl-2,2′-biphenyldiyl.

TABLE 21. Chloro-, bromo- and iodo-substituted aryllithiums Li–R by halogen/metal permutation between bromoarenes and butyllithium in diethyl ether

Li–R	T	Product	El–X′ [a]	Reference
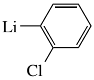	−90 °C	93%	CO_2	197
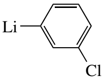 [b]	+25 °C	42%	CO_2	142, 143, 184
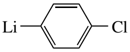 [b]	+25 °C	90%	CO_2	142–144
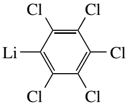 [c]	−10 °C	71%	$(H_5C_6)_2CO$	198, 199
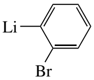	−100 °C	38%	CO_2	142, 143, 200
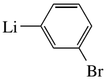	+35 °C	44%	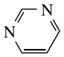 [d]	201–202
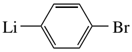	+25 °C	90%	CO_2	144, 203, 204
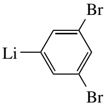	−75 °C	93%	$F_7C_3COOC_2H_5$	205
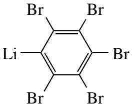	−15 °C	16%	CO_2	122
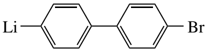	+25 °C	67%	H_2O	142, 143
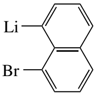	−70 °C	30%	$R'_4P^+I^-$ [e]	196
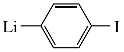 [f]	+25 °C	80%	$(H_5C_2)_3GeBr$	206

[a] El–X′ = electrophilic trapping reagent.

[b] Also from the corresponding iodoarenes and also in benzene rather than diethyl ether.

[c] From hexachlorobenzene.

[d] Nucleophilic addition of 3-bromophenyllithium to the 4-position of pyrimidine followed by the elimination of lithium hydride.

[e] R'_2 = 4,4′-dimethyl-2,2′-biphenyldiyl.

[f] From 1,4-diiodobenzene.

TABLE 22. Pyridyl- and quinolyllithiums Li–R by halogen/metal permutation using butyllithium as the exchange reagent

Li–R	X[a]	*Sv*[b]	*T*	Product	*El*–X′ [c]	Reference
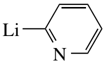	Br	DEE	−15 °C	69%	H_5C_6CHO	207–209
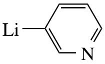	Br	DEE	−35 °C	62%	CO_2	207–212
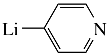	Br	DEE	−75 °C	55%	$(H_5C_6)_2CO$	211–213
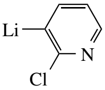	Br	THF	−60 °C	80%	H_3CI	214
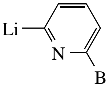	Br	DEE	−40 °C	82%	$H_3CCON(CH_3)_2$	215–219
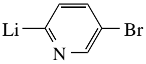	Br	TOL	−75 °C	79%	$(H_3C)_2CO$	220
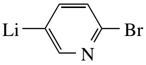	Br	THF	−100 °C	85%	D_2SO_4	221
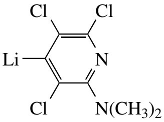	Cl	DEE	−35 °C	84%	H_2O	222
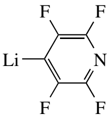	I	DEE	−35 °C	65%	CO_2	223
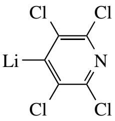	Cl	DEE	−75 °C	29%	CO_2	224–226
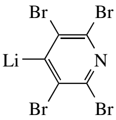	Br	DEE	−75 °C	16%	CO_2	227
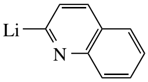	Br, I	DEE	−50 °C	50%	$(H_5C_6)_2CO$	228, 229
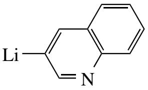	Br	DEE	−45 °C	48%	CO_2	184, 207–213

[a] X = halogen displaced by the metal.
[b] Solvent (*Sv*): DEE = diethyl ether, THF = tetrahydrofuran, TOL = toluene.
[c] *El*–X′ = electrophilic trapping reagent.

Numerous examples of halogen/metal permutations involving five-membered nitrogen heterocycles such as pyrroles, indoles, pyrazoles and imidazoles (Table 23) or five-membered chalcogen heterocycles such as furans, thiophenes, benzothiophenes and selenoles (Table 24) are known. If two or more competing halogens are available in a given substrate, they can be sequentially replaced, first by lithium and subsequently by a suitable electrophile *El*, starting at the intrinsically most acidic position and ending with the least acidic one. Thus, 5,7-dibromo-2,3-dihydro-1-benzofuran **3** reacts first at the 7-position[259] and 1-(benzyloxy)methyl-2,4,5-triiodoimidazole **4**[260] or its tribromo analog[261] exchanges with butyllithium first the halogen at the 2-position and next the halogen at the 5-position (equation 2).

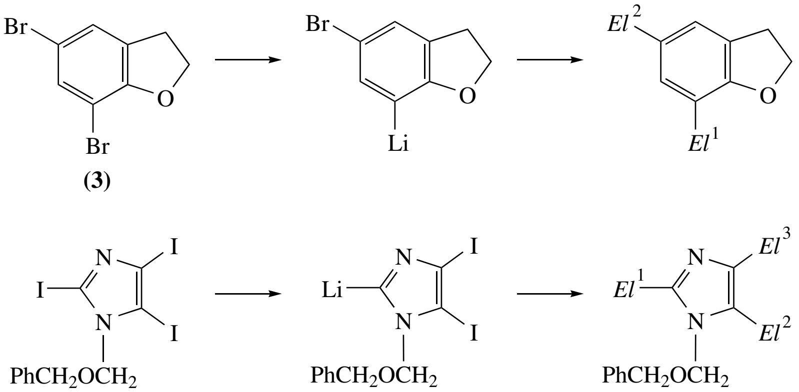

(3)

(4)

(2)

Regioselectivity in the exchange of formally equal halogens can be found also outside the heterocyclic series. Inductive effects appear to be the controlling factor. For example, 3,3′,5-tribromodibenzyl ether (1,3-dibromo-5-[(3-bromophenylmethoxy)methyl]benzene; **5**) is exclusively converted into 3-bromo-5-[(3-bromophenylmethoxy)methyl]benzoic acid (equation 3) when treated consecutively with butyllithium in tetrahydrofuran[262] at −75 °C and dry ice.

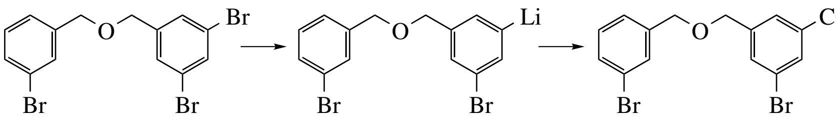

(5)

(3)

Stereoselectivity is encountered when 1,1-dibromoalkenes **6**[96, 102–104, 263–265] or *gem*-dibromocyclopropanes **7**[102–104, 266, 267] are submitted to a halogen/metal permutation (equation 4). In the initial stages of the reaction the sterically less hindered *exo*-oriented halogen is replaced preferentially. However, due to the reversibility of the permutational process, an equilibration sets in showing the *endo*-Li-isomers to be the thermodynamically strongly favored species (equation 4).

TABLE 23. Pyrryl-, indolyl-, pyrazolyl- and imidazolyllithiums Li−R by halogen/metal permutation between a five-membered bromoheterocycle and butyllithium in an ethereal solvent

Li−R	Sv[a]	T	Product	El−X′ [b]	Reference
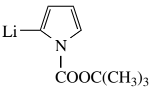	THF	−75 °C	83%	$(H_3C)_3SiCl$	230
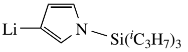	THF	−75 °C	88%	CO_2	231, 232
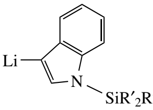 [c, d]	THF	−75 °C	94%	$(H_3C)_3SnCl$	233–235
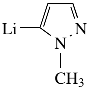 [d]	DEE	−100 °C	77%	CO_2	236
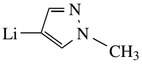	DEE	−30 °C	74%	$(H_5C_6)_2CO$	237
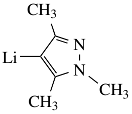	DEE	−30 °C	81%	CO_2	237
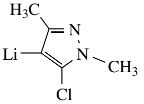	DEE	+25 °C	97%	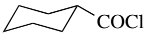	238
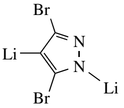	DEE	−30 °C	80%	CO_2	237
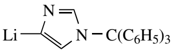 [e]	THF	−75 °C	51%[f]	$(H_3C)_2NCHO$	239
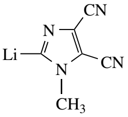	THF	−100 °C	42%	CO_2	240
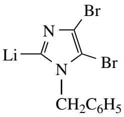	DEE	−75 °C	54%[g]	$(H_3CS)_2$	241–243

[a] Solvent (*Sv*): DEE = diethyl ether, THF = tetrahydrofuran; in case of mixtures (containing, *e.g.*, petroleum ether) only the most polar component is indicated.
[b] *El*−X′ = trapping electrophile.
[c] $SiR'_2R'' = Si(CH_3)_2C(CH_3)_3$.
[d] *tert*-Butyllithium instead of butyllithium.
[e] 4-Iodo-1-triphenylmethylimidazole as the starting material.
[f] Plus 7% 2-isomer.
[g] Plus 14% 5-isomer.

TABLE 24. Furyl-, thienyl-, benzothienyl- and selenophenyllithiums Li–R by halogen/metal permutation between haloheterocycles and butyllithium in diethyl ether

Li–R	X[a]	*T*	Product	*El*–X′ [b]	Reference
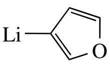	Br	−70 °C	63%	$(H_9C_4O)_3B/H_2O$	244–248
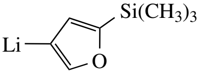	Br [c]	−70 °C	78%	$H_5C_6N(CH_3)CHO$	249
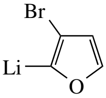	Br	−45 °C	49%	$H_3CCON(CH_3)_2$	246–248
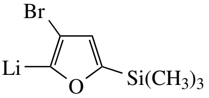	Br	−80 °C	65%	H_2O	249
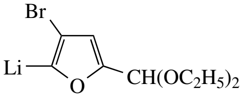	Br	−45 °C	61%	$(H_9C_4O)_3B/H_2O$	246–248, 250
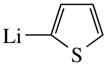	I	+25 °C	58%	CO_2	251
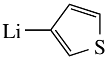	I	−70 °C	78%	CO_2	252, 253
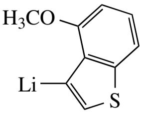	Br	−75 °C	51%	$(H_3C)_2NCHO$	254
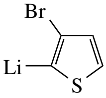	Br	−70 °C	90%	CO_2	253
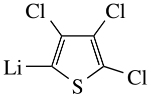	Cl	0 °C	69%	CO_2	255, 256
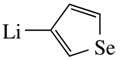	Br[d]	+40 °C	65%	CO_2	257
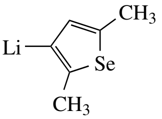	I[e]	−100 °C	51%	CO_2	258

[a] X = halogen in the precursor.
[b] *El*–X′ = electrophilic trapping reagent.
[c] Using *sec*-butyllithium instead of butyllithium.
[d] Using phenyllithium instead of butyllithium.
[e] Using ethyllithium instead of butyllithium.

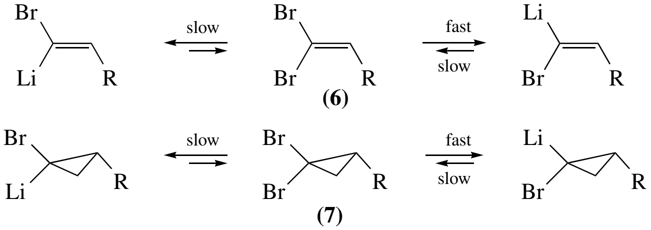

(4)

IV. PERMUTATIONAL HYDROGEN/METAL INTERCONVERSIONS ('METALATIONS')

Acid/base reactions in aqueous medium, even if just isoenergetic rather than exoenergetic (for example, the proton transfer from a hydronium ion to a water molecule), are generally diffusion-controlled processes. The analogous reaction between a paraffinic hydrocarbon, say methane, and the conjugate base, methanide (methyl anion), could only be accomplished in the gas phase. If the experiments were attempted in a condensed phase, only alkanes or cycloalkanes would be sufficiently inert toward the alkylmetal which would replace the inaccessible alkanide ion. Due to the extremely low polarity of the medium, alkylmetals would not only persist as contact species or, in other words, prove unable to dissociate into ions but, worse, they would even form oligomeric or polymeric clusters, so-called aggregates. Thus, they can attain a reactive, deprotonation-triggering state only after having undergone an energy-expensive structural reorganization. The claimed hydrogen/metal permutation between butylpotassium and pentane, hexane and cyclohexane[268] has never been experimentally verified, not to speak of having been applied to practical preparative work.

Standard organolithium reagents such as butyllithium, *sec*-butyllithium or *tert*-butyllithium deprotonate rapidly, if not instantaneously, the relatively acidic hydrocarbons of the 1,4-diene, diarylmethane, triarylmethane, fluorene, indene and cyclopentadiene families and all terminal acetylenes (1-alkynes) as well. Butyllithium alone is ineffective toward toluene but its coordination complex with *N*,*N*,*N*′,*N*′-tetramethylethylenediamine does produce benzyllithium in high yield when heated to 80 °C[269]. To introduce metal into less reactive hydrocarbons one has either to rely on neighboring group-assistance or to employ so-called superbases.

A. The Superbase Approach

The 'LIC-KOR' reagent consisting of stoichiometrically equal amounts of butyllithium ('LIC') and potassium *tert*-butoxide ('KOR') was conceived in Heidelberg and optimized in a trial-and-error effort[270, 271]. The fundamental idea was simple. To activate butyllithium optimally by deaggregation and carbon–metal bond polarization, a ligand was required that would surpass as an electron donor any crown ether but not suffer from the drawback of the latter, i.e. its proneness to β-elimination. Whereas pinacolates and other *vic*-diolates[272] proved too labile to be generally useful, potassium *tert*-butoxide or any other bulky, hence relatively soluble, potassium or cesium alkoxide was found to serve the purpose[273].

Later, in Lausanne, further mixed metal reagents were tested. LIC-KOR confirmed its role as a faithful 'workhorse'[271] in numerous situations, e.g. the metalation of 2- or 4-fluoroanisole[274] and 2- or 4-fluoro-1-(methoxymethoxy)benzene[275]. The mixture of methyllithium and potassium *tert*-butoxide ('LIM-KOR') gives optimum results if congested positions are targeted[276], whereas the mixture of *tert*-butyllithium and potassium *tert*-butoxide ('LIT-KOR') shows a perfect discrimination between sterically hindered and freely accessible positions[277]. The mixture of butyllithium and sodium *tert*-butoxide ('LIC-NAOR') outperformed all other reagents in the metalation of norbornene, norbornadiene and cycloheptatriene[278]. The yields of the metalation by the different reagents of these substrates are shown below.

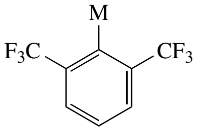

LIM-KOR (M = Li, K)
92% [CO$_2$][276]

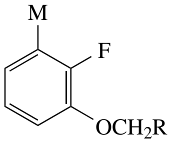

LIC-KOR (M = Li, K)
R = H : 50% [CO$_2$][274]
R = OCH$_3$: 84% [CO$_2$][275]

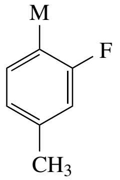

LIT-KOR (M = Li, K)
84% [CO$_2$][277]

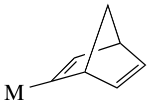

LIC-NAOR (M = Li, Na) :
92% [ClSi(CH$_3$)$_3$][278]

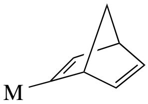

LIC-NAOR (M = Li, Na) :
88% [ClSi(CH$_3$)$_3$][278]

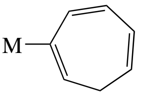

LIC-NAOR (M = Li, Na) :
57% [ClSi(CH$_3$)$_3$][278]

Even before the term 'superbase' was coined[273, 279], there existed already a tacit understanding about where to place the bar of qualification for this label. The crucial benchmark chosen was to metalate benzene rapidly in high yield and at ambient temperature. The above-mentioned mixed metal reagents and the pentylsodium/potassium *tert*-butoxide ('NAC-KOR') mixture as well (metalation of norcarane[280], nortricyclane[281, 282], camphene[282, 283], bicyclo[2.2.2]octene[280] and 6-bicyclo[3.2.0]heptene[278, 284] in 30, 60, 71 and 66% yield of trapping products) pass this test without problems. Other combinations fail to attack benzene to any significant extent. This is, for example, the case with TMEDA-activated butyllithium ('LIC-TMEDA'), the butyllithium/lithium 2-(dimethylamino)ethoxide blend ('LIC-LIDMAE', 'Caubère's base'[285]) or with the complexes lithium diisopropylamide/potassium *tert*-butoxide ('LIDA-KOR', 'Margot–Mordini mix')[286–288] and lithium 2,2,6,6-tetramethylpiperidide/potassium *tert*-butoxide/*N*,*N*,*N*′,*N*′,*N*′-pentamethyldiethylenetriamine ('LITMP-KOR-PMDTA', 'Faigl mix')[289].

Ailing reactivity as a base must not necessarily be a handicap. The LIC-KOR mixture is of course immensely more powerful than butyllithium alone. This offers the possibility to functionalize whole families of otherwise inert hydrocarbons[290, 291]. What should not be overlooked, however, is the fact that the chemical potential of the so-called superbase is attenuated when compared to butylpotassium. The latter reagent is instantaneously destroyed when brought in contact with tetrahydrofuran even at temperatures below −100 °C. In contrast, the LIC-KOR mixture survives in the same solvent almost indefinitely at −75 °C and can be exposed to −50 °C at least for a while[292]. Thus, a manifold of aromatic, benzylic and allylic organometallic intermediates can be generated in an ethereal medium under particularly mild and hence optimally selective conditions. The symbiotic action of two different metals obviously suppresses erratic side reactions without diminishing too much the deprotonation power of the superbasic reagent. Although its detailed structure remains unknown, there can be no doubt about a progressive change in its composition regardless of whether or not a substrate is present or, in other words, a chemical transformation occurs simultaneously. Potassium *tert*-butoxide exists in tetrahydrofuran mainly as a tetramer and in hexanes as a virtually insoluble polymer. However, at the end of a LIC-KOR promoted metalation of a hydrocarbon, the oxygen atoms are mostly, yet by far not exclusively, associated with lithium (the exceptional strength of the O−Li bond being the obvious driving force) whereas the heavier alkali metal is mainly found attached to the carbon backbone. The enhanced metal mobility in allylic or benzylic structures makes it even possible to isolate pure potassium species after the specific removal of lithium *tert*-butoxide by extraction with hot benzene or toluene[293].

B. Neighboring Group Assistance to Metalations

As pointed out above, neither methane nor its higher homologs (ethane, propane, hexane) can be effectively metalated. The introduction of a hetero-substituent changes this outset profoundly. Second-row and third-row elements (such as silicon, phosphorus and sulfur) will not be considered in this context as they are known to acidify hydrocarbons strongly due to d-orbital resonance (or polarization) effects. But also the first-row elements nitrogen, oxygen and fluorine can distinctly facilitate the deprotonation of paraffinic hydrocarbons.

The metalation of trimethylamine[294] with butyllithium, *N*-methylpiperidine[295] with *sec*-butyllithium in the presence of potassium *tert*-butoxide and *N*,*N*,*N*′,*N*′-tetramethylethylenediamine[296, 297] (TMEDA), all exclusively at methyl groups, have been reported. The yields were moderate but increased substantially with *N*,*N*,*N*′,*N*″,*N*″-pentamethylethylenetriamine[297] (PMDTA, **8**) as the substrate which underwent a deprotonation both at the terminal and inner methyl groups in varying, stoichiometry-dependent ratios. Ring strain combined with dipole-activation enabled the smooth lithiation of an α-methylene group in *N*-(*tert*-butoxycarbonyl)pyrrolidine **9**[298] providing again excellent yields of trapping products (equation 5).

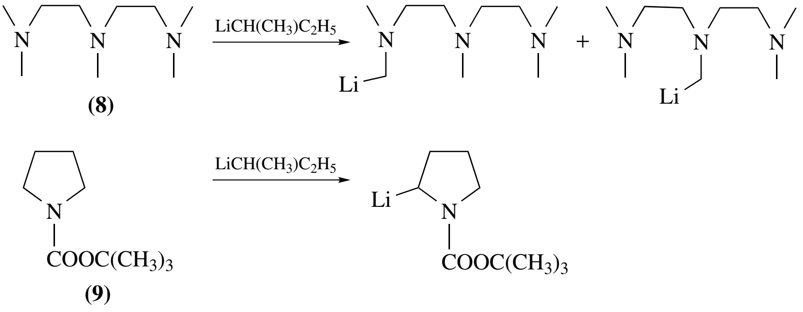

(8)

(9)

(5)

No reproducible metalation of a saturated, open-chain or cyclic ether with butyllithium, *sec*-butyllithium or *tert*-butyllithium has been described so far[292]. The intermediates generated by the treatment of dimethyl ether or *tert*-butyl methyl ether with potassium *tert*-butoxide activated butyllithium or *sec*-butyllithium gave trapping products in only poor yields (3–30%), far below the yields (75–95%) achieved with butylpotassium[292]. Due to ring strain acidification, oxiranes undergo the hydrogen/metal permutation quite readily when treated, for example, with *sec*-butyllithium and a diamine ligand such as *N*,*N*-dibutyl-3,7-diazabicyclo[3.3.1]nonane or sparteine at −90 °C. However, the resulting

C-lithiated intermediates isomerize through ring-opening if not being trapped *in situ*[299] or stabilized by an α-trialkylsilyl- or α-triarylsilyl substituent (as in **10**, equation 6)[300–302].

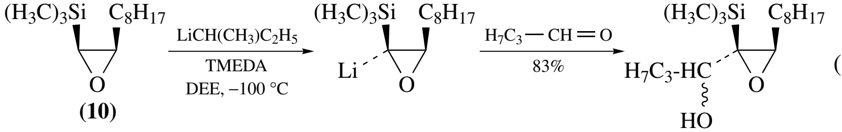

(6)

Fluoromethane would presumably tend to react by an S_N2 process rather than by deprotonation, whatever the base used. On the other hand, potassium *tert*-butoxide[303] and fluoride[304] suffice already to set free the trifluoromethyl anion from trifluoromethane (fluoroform). Being extremely fragile, the trifluoromethanide must be trapped *in situ*, for example by addition to *N,N*-dimethylformamide.

The three-membered carbocycle being activated by ring strain, cyclopropane and congeners are metalated, if sluggishly, by alkylsodiums when activated or not by potassium *tert*-butoxide[1f] (see also Section IV.A). Hetero-substituted cyclopropanes react much more readily. Thus, *sec*-butyllithium in the presence of TMEDA metalates cleanly the cyclopropyl 2,4,6-tris(isopropyl)benzoate[305]. *N*-*tert*-Butoxycarbonyl-2-methylaziridine **11** and congeners can be selectively substituted at the 3-position by treating them consecutively with *sec*-butyllithium and the appropriate electrophile[306]. The *tert*-butyl-*N*-ethyl-*N*-cyclopropylcarbamate **12** is lithiated in the three-membered ring, again at a nitrogen-adjacent position[306]. In contrast, the *N*-BOC protected 4-azaspiro[2.5]octane **13** is attacked exclusively at the three-membered ring, in other words at a β-position with respect to the nitrogen atom rather than at the α-methylene group of the six-membered ring[307] (equation 7).

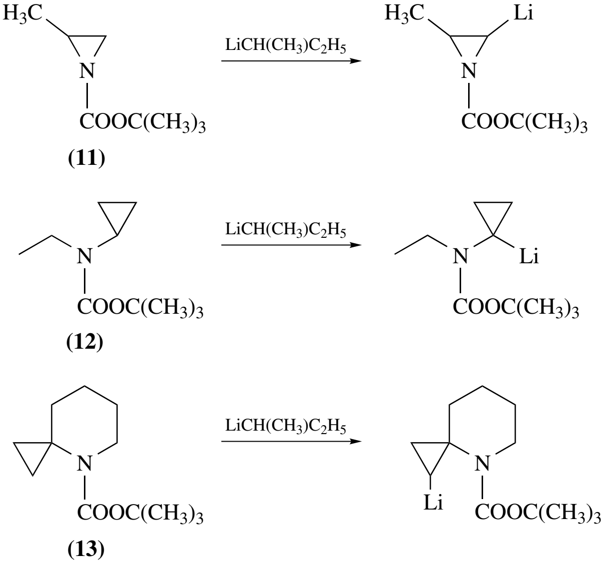

(7)

An olefinic double bond can be conceived as a two-membered ring[308]. The specific geometry at the unsaturated centers makes the latter prone to deprotonation. Nevertheless, superbasic reagents are required for the metalation of heteroatom-free alkenes (see Section

IV.B), the only exception being the remarkably acidic cyclopropenes which do react with alkyllithiums alone[309, 310].

The attachment of nitrogen, oxygen or fluorine substituents at the double bond activates the olefinic positions sufficiently to make them undergo rapid hydrogen/metal permutation when treated with alkyllithiums. Thus, 1-vinylbenzotriazole **14a** and both 1-propenylbenzotriazoles **14b,c** are readily deprotonated by butyllithium at the olefinic α-position[311]. The two 2-propenylbenzotriazoles act in the same way[311]. Unexpectedly, *tert*-butyllithium promotes the proton abstraction from the β-position of chelating enamines, regardless whether the α-position is vacant, as in N-1-heptenyl-*N,N′,N′*-trimethyl-1,2-ethanediamine **15**, or occupied, as in N-1-cyclohexenyl-*N,N′,N′*-trimethyl-1,2-ethanediamine **16**[312]. N-Lithioamido groups can mediate the metalation of terminal olefinic sites even if the functionality is placed at a remote γ-position. This is illustrated by N-(*tert*-butyl)allylamine **17**[313] and N-(trimethylsilyl)allylamine **18**[314] as typical substrates (equation 8).

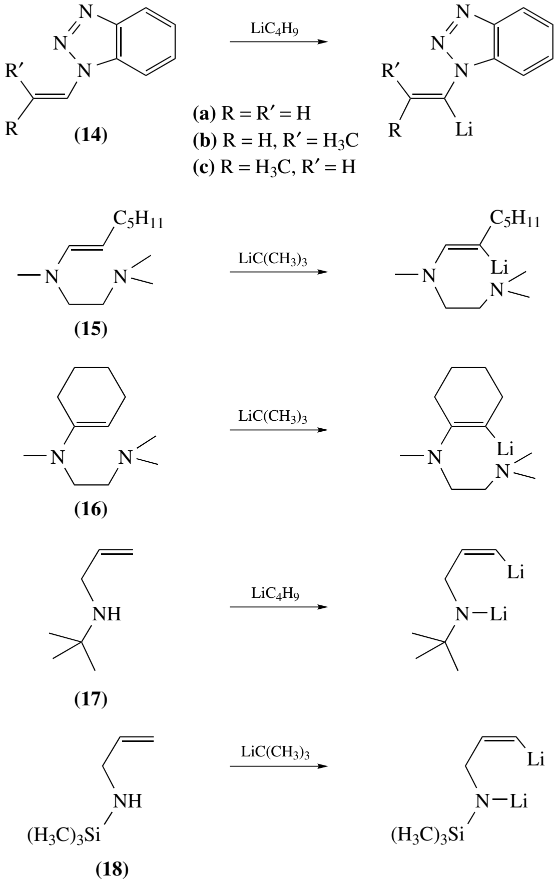

(14)

(**a**) $R = R' = H$
(**b**) $R = H, R' = H_3C$
(**c**) $R = H_3C, R' = H$

(15)

(16)

(17)

(18)

(8)

Ethyl vinyl ether **19a**[315–317] and methyl vinyl ether[318] **19b** are metalated by *tert*-butyllithium at the oxygen-adjacent methine site. β-Alkyl groups retard the reaction substantially. Thus, 1-methoxy-2-methyl-2-propene was found to be inert toward all alkyllithiums, activated or not. However, 1-methoxymethoxy-2-methyl-2-propene **20**, just as the corresponding tetrahydropyranyloxy derivative too, reacts smoothly with *sec*-butyllithium at the olefinic α-position[319]. If no α-position is accessible as is the case with 1-methoxymethoxy-1-phenylethylene **21**[320], the β-position may be attacked. 1-Ethoxy-2-bicyclo[2.2.1]oct-2-enyllithium, which owes its chemical stability to the Bredt rule, can be easily generated by treatment of the bridgehead ether **22** with *tert*-butyllithium[321]. The neighboring group assistance provided by the alkoxy substituent located in a β'-position with respect to the double bond becomes evident when one compares this substrate with 2-bicyclo[2.2.2]octene itself, which is completely inert toward ordinary alkyllithium and reacts only with superbases[280]. Finally, metal can be introduced in the terminal olefinic position of linalool **23** or other 1,1-dialkylated allyl alcohols using butyllithium in hexanes and in the presence of TMEDA[322, 323]. This is another one of the rare examples where a γ-positioned hetero-substituent exerts control over the outcome of a metalation reaction (equation 9).

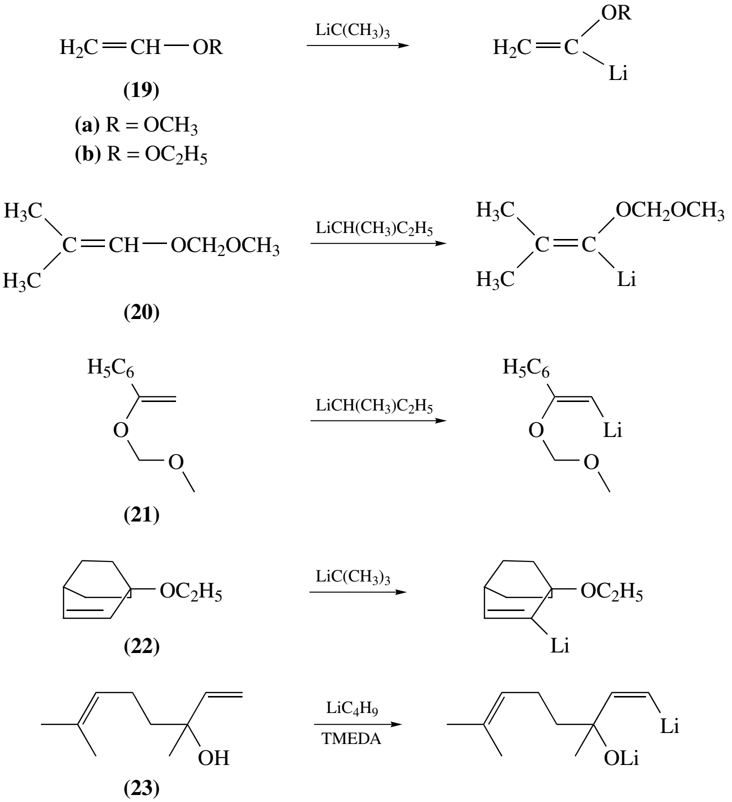

(19)

(**a**) $R = OCH_3$
(**b**) $R = OC_2H_5$

(20)

(21)

(22)

(23)

(9)

The metalation of fluoroethylene (vinyl fluoride) has not yet been reported although trifluoroethylene **24**[324, 325], (*E*)-α,β-difluorostyrene **25**[326] and both (*Z*)- and (*E*)-isomers of 1,2-difluoro-1-alkenes (**26**, *cis* isomer shown)[326, 327] undergo smooth metalation at the α-position. Proton abstraction from β-positions occurs with *gem*-difluoroethylene[324, 325, 328] and 1,1,3,3,3-pentafluoropropene[329] (equation 10).

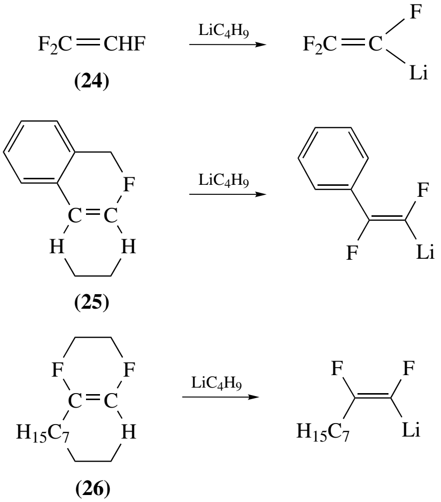

(10)

When moving from methane or other simple (cyclo)alkanes through cyclopropanes to alkenes, a progressive increase in acidity and reactivity was recognized. Both cyclopropanes and alkenes are deprotonated by alkylsodiums or superbases. The possibility of π-cloud polarization[330] makes benzene (and derivatives thereof) even more reactive. If employed in excess, it is metalated by the LIC-KOR mixture in the course of minutes if not seconds. No hydrogen/metal permutation can be accomplished with pyridine, as the nucleophilic addition of the organometallic reagent to the imine entity is the predominant process[331]. However, hetero-substituted pyridines or quinolines can be smoothly metalated. Furans, thiophenes, pyrroles and other five-membered heterocycles contain the electronegative element already incorporated in a slightly strained ring. This ensures particularly fast and complete deprotonation of the α-positions. The proton mobility again increases in the direction of the arrows shown in the scheme below.

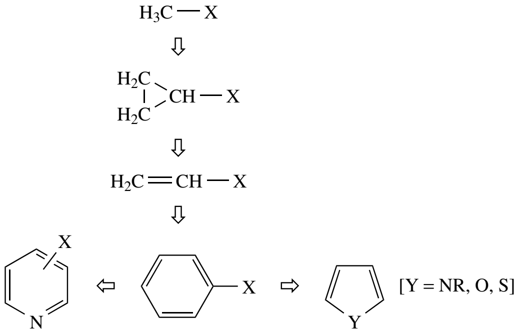

The neighboring group-assisted metalation of arenes and heterocycles is an area too vast to be included into this Chapter. Major aspects have been summarized in Chapter 10 of this book and a comprehensive, though still not exhaustive treatment of this theme can be found in a recent monograph[1g].

V. THE BROOK ISOMERIZATION

The Brook isomerization is the migration of a silyl group from a carbon atom to an oxygen anion as illustrated in its simplest [1,2] form (e.g. **27** to **28** in equation 11)[332].

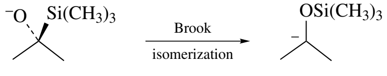

(27) **(28)**

(11)

The isomerization is driven forward by the increased thermodynamic stability of the silyl ether product relative to the alcohol starting material due to the formation of a Si−O bond in place of a Si−C bond[333]. Investigations revealed that all types of silyl carbinols rearrange, often fairly readily, when treated with small amounts of active metals, organometallic reagents or bases[332]. This isomerization has been extensively studied mechanistically by Brook and shown to proceed intramolecularly via a mechanism involving a hypervalent pentacoordinate silicon species with retention of configuration at silicon and inversion of configuration at carbon[334]. In accord with that mechanistic hypothesis, substrates having substituents on carbon that help delocalize negative charge, e.g. aryl or vinyl, accelerate the rate of the isomerization. The counterpart of this isomerization, the retro-Brook (or silyl Wittig or West) isomerization, namely the transfer of silicon from oxygen to carbon (**28** into **27**), has also been observed and synthetically used[335].

In this section, we will concentrate on the chemistry of the Brook isomerization mediated by organolithium compounds and on their unusual routes to potentially useful carbanions.

A. Anionic [1,2] Brook Isomerization

A general approach is to generate silyl alkoxides by addition of suitable organometallic reagents (RLi) to silyl ketones such as acyl silanes. If either one of the alkyl groups (from the acylsilane **29** or from the alkyllithium **30**) contains a α-leaving group, the carbanion **32**, coming from the [1,2] Brook isomerization of **31**, can undergo a β-elimination to form a silyl enol ether **33** (equation 12)[336].

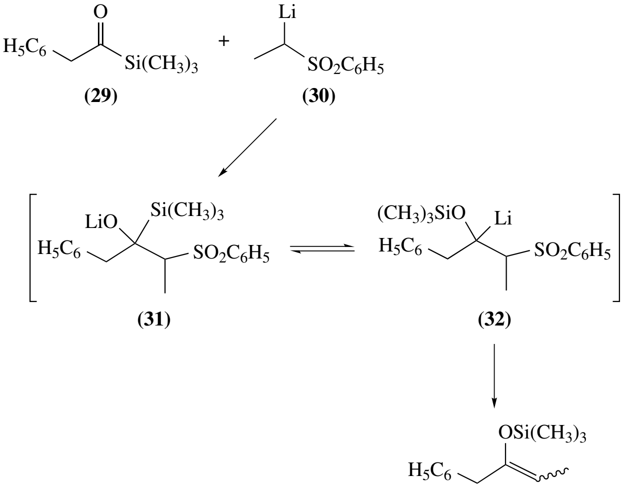

(29) **(30)** **(31)** **(32)** **(33)**

(12)

The importance of this approach to **33** lies in the fact that enolization of 1-phenyl-2-butanone does not give pure **33** under kinetic or thermodynamic conditions. Moreover, if the acylsilane possesses a stereogenic center in the α-position, the addition occurs according to the Felkin–Anh mode[337].

If the addition involves an alkynyllithium such as **34**, the first-formed alkoxide intermediate **35** isomerizes into the propargylic-allenic lithium reagent. Reactions with electrophiles lead to either **36a** or the allenol silyl ethers **36b** (equation 13)[338].

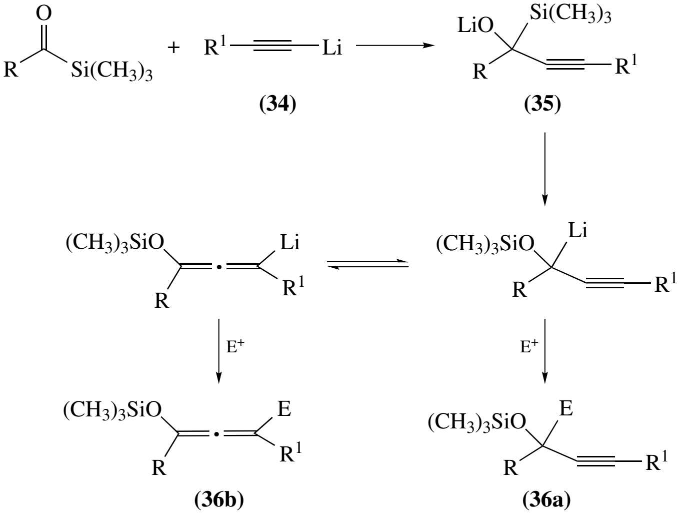

(13)

$E^+ = CH_3I, CH_3CH_2I, CH_3SSCH_3, CH_2{=}CH{-}CH_2Br$

$E = CH_3, CH_3CH_2, CH_3S, CH_2{=}CH{-}CH_2$

By using this strategy, intramolecular alkylations to unusual enol ethers **37** are easily accessible (equation 14)[338].

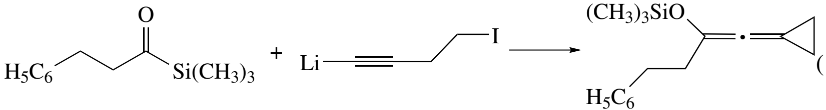

(14)

(37)

Allenyl silyl ethers **40** have also been prepared by the reaction of 2-lithiofurans **38** with acylsilanes **39** via the Brook isomerization (equation 15)[339].

Even the starting acylsilane **39** can be easily prepared via a Brook isomerization by the reaction of silylmethyllithium **41** with carbon monoxide[340]. Initially, the reaction gives the corresponding unstable acyllithium **42** which underwent the Brook isomerization affording the stable lithium enolate (equation 16).

If the alkenyllithium **43** is used as organolithium compound with **39**, siloxyallyllithium reagents **44** are formed[341]. As example, the isomerization of the silyl(allyl)alkoxides **44** gives the corresponding lithio-(Z)-silyl enol ethers **45** which react with various electrophiles to give **46** (equation 17)[342].

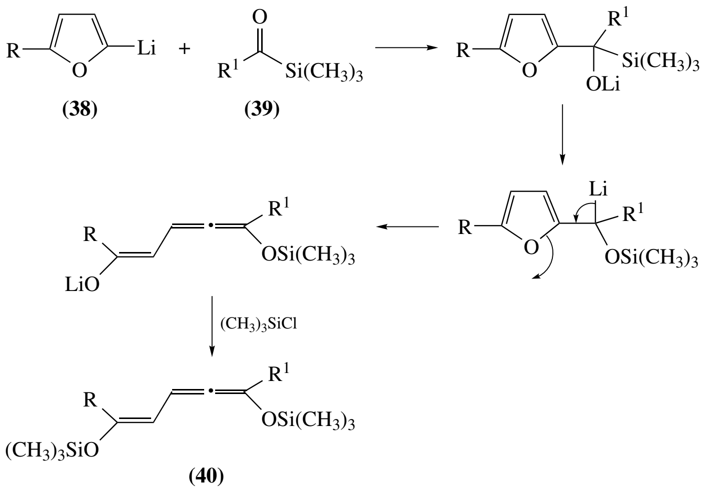

(15)

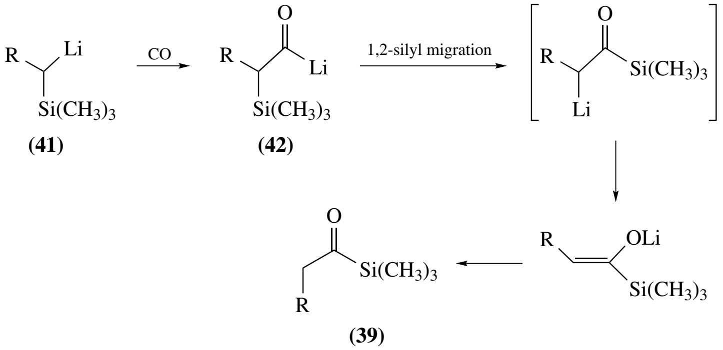

(16)

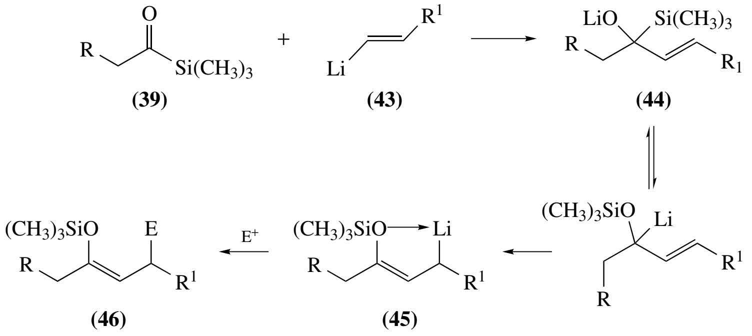

(17)

E^+ = HCl, CH_3OD
E = H, D

This strategy was very recently used for the total synthesis of δ-Araneosene[343]. In the first step of the synthesis, methyl *tert*-butyldimethylsilyl ketone **47** was treated with 2-propenyllithium **48** in ether and then with 2-isopropylallyl bromide **49** in THF to give the (Z)-enol silyl ether **50** in 82% yield. The sequence of reactions that leads to **50** includes (1) carbonyl addition of **48**, (2) Brook isomerization and (3) allylation of the resulting allylic lithium reagent (equation 18)[344].

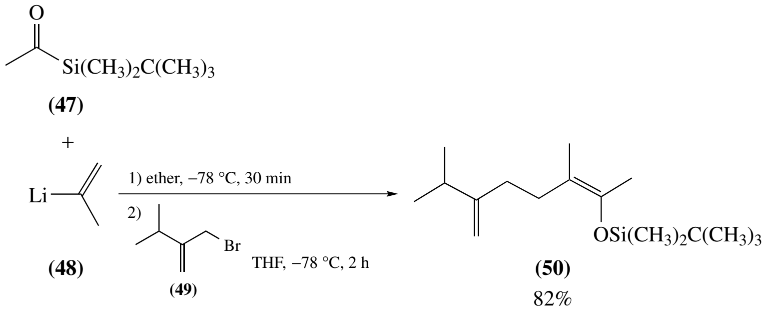

(18)

Ketone enolate **51** could also serve as a two-carbon component in [3 + 2] annulation when reacted with β-heteroatom-substituted α,β-unsaturated acylsilane **52**[345]. For instance, the enolate of 3-methyl-2-butanone **51** (R = i-Pr) reacts with [β-(trimethylsilyl)acryloyl]trialkylsilane (**52**, X = $SiMe_3$) at low temperature to give the corresponding cyclopentanol **53** as single isomer (equation 19). Reactions of benzoylsilanes and crotylsilanes with lithium enolates afford the cyclopropane diol derivatives[346].

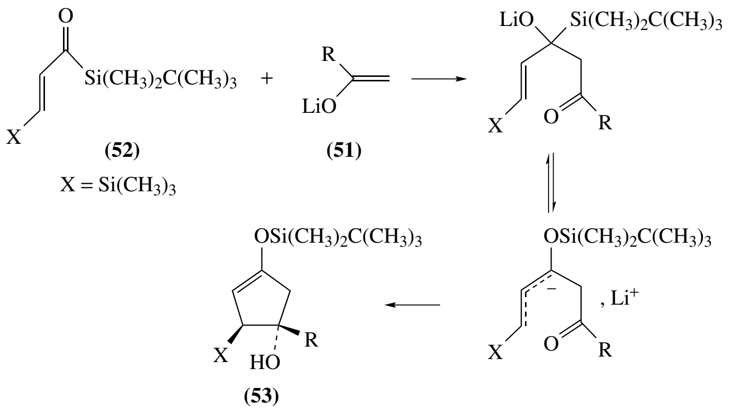

(19)

Similarly, the [3 + 4] annulation of the E- and Z-isomers of β-hetero-substituted acryloylsilanes **52** with lithium enolates of α,β-unsaturated methyl ketones **54** gave stereospecifically the *cis*-6,7-cyclopentyl-5-trimethylsilyl-3-cycloheptenone **55** (equation 20)[347]. The stereospecificity in the annulation was explained by an anionic oxy-Cope isomerization of the 1,2-divinylcyclopropanediol intermediate **56**, which was generated through the Brook isomerization of the initial 1,2-adduct (equation 20).

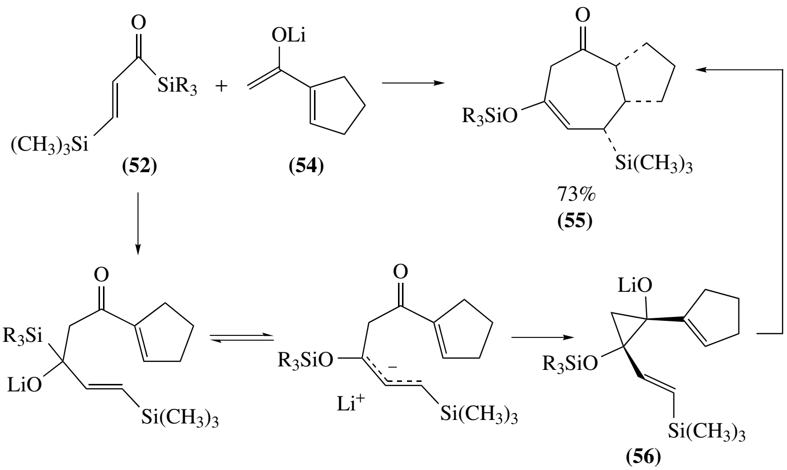

(20)

Metalloaldimines **57** bearing a silicon linked to a carbon can be alkylated with a range of carbon electrophiles. When **57** is treated with an aldehyde, the resulting adduct **58** undergoes the Brook isomerization providing a new lithioaldimine intermediate **59**. Reaction of this lithioaldimine with electrophiles such as chlorotrimethylsilane provides a new imidoylsilane **60** in 62% yield (equation 21)[348].

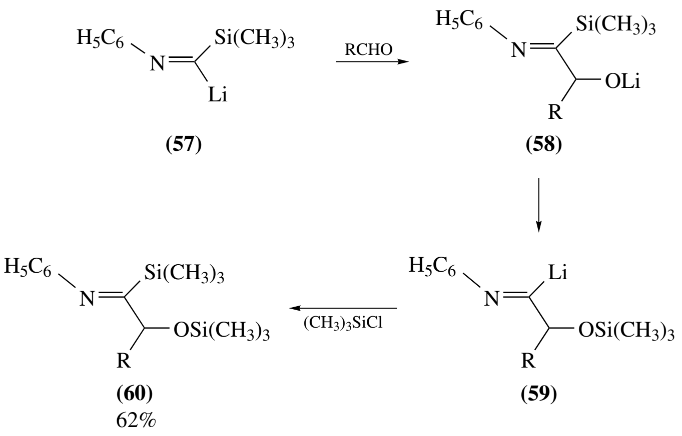

(21)

In contrast to 1,2-migrations between C and O, there are few reports on the Brook isomerization of α-silylamine (aza-Brook isomerization). The reaction of (α-silylallyl)amine **61** with n-C_4H_9Li in THF at low temperature followed by the addition of HMPA and CH_3I gives the methylated product **62** in quantitative yield. These results indicate that an aza-Brook isomerization occurs, i.e. the silyl group of **61** migrates from carbon to nitrogen and the lithium salt of an allyl anion **63** is produced (equation 22)[349].

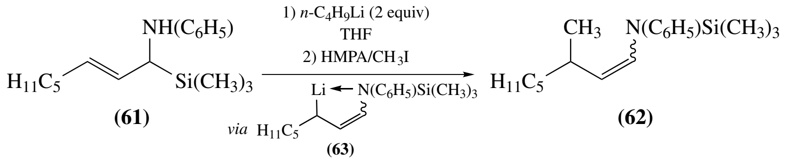

(22)

B. Anionic [1,3] Brook Isomerization

1,3-Isomerization of silicon from carbon to alkoxide is rare since olefin formation via 1,2-elimination of β-silyloxy is rapid (known as the Peterson olefination, equation 23)[350].

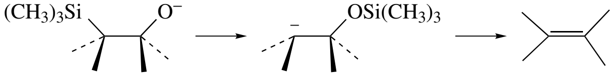

(23)

Thus, only few reports were disclosed for the [1,3] Brook isomerization; Utimoto, Oshima and coworkers have reported that the treatment of *tert*-butyldimethyl(dibromomethyl)silane **64** with LDA followed by the addition of an excess of benzaldehyde lead to the 1,3-diol monosilyl ether **66** via the intermediacy of lithium carbenoid **65** (equation 24)[351]. The rate of isomerization was dependent on the solvent used and HMPA was found to be the best solvent[352].

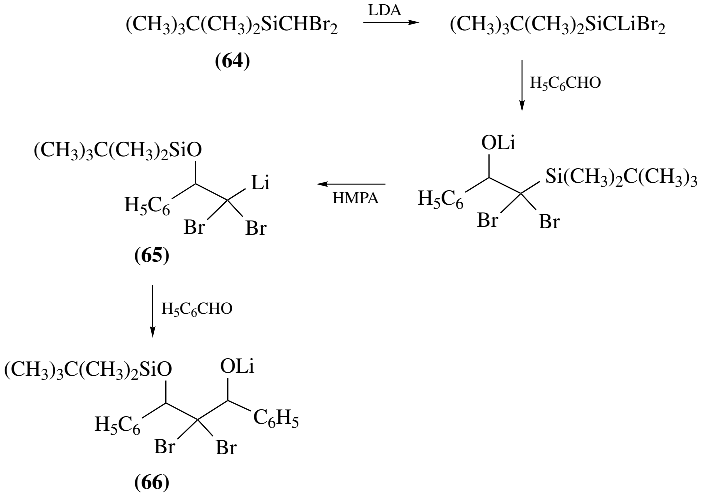

(24)

C. Anionic [1,4] Brook Isomerization

When a solution of lithium enolate **68**, prepared by the addition of *N*,*N*-dimethyl-2-trimethylsilylacetamide **67** to a THF solution of LDA, is treated with an equivalent amount of propylene oxide **69**, a single product **71** is obtained in 75% yield (equation 25)[353]. This result is rationalized by assuming an initial addition of **68** at the less substituted side of the epoxide, followed by the first observed 1,4-migration of silicon from carbon to oxygen (**70** to **71**).

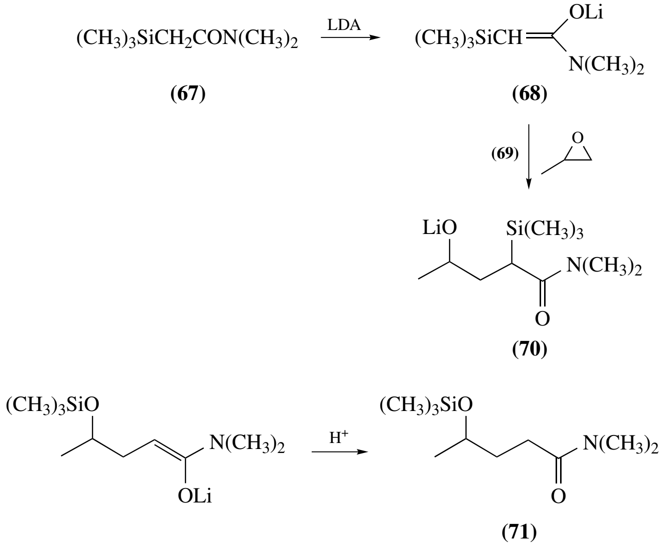

(25)

This isomerization was used in the heteroconjugate addition to the acyclic system. Therefore, the substituted olefin **72**, in which the double bond is conjugated with both sulfone and silicon atoms, undergoes a diastereoselective addition of CH_3Li[354]. The resulting lithium alcoholate is quantitatively converted into the silyl ether dianion **73** and the addition of deuterium oxide afforded the functionalized product **74** in excellent yield (equation 26)[355].

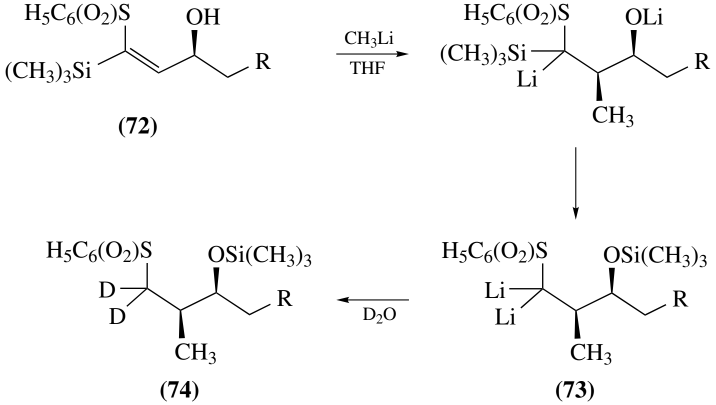

(26)

$R = CH_2C_6H_5, (CH_2)_3OCH_2OCH_3$

Enantiopure **77** was easily prepared by treatment of 2-trimethylsilyl-1,3-dithiane **75** and chiral epoxides **76** in a sequential addition in the presence of a crown ether. In this sequence, a monosilylated 1,5-diol **77** is obtained, allowing a discrimination of the two hydroxy groups formed (equation 27)[356].

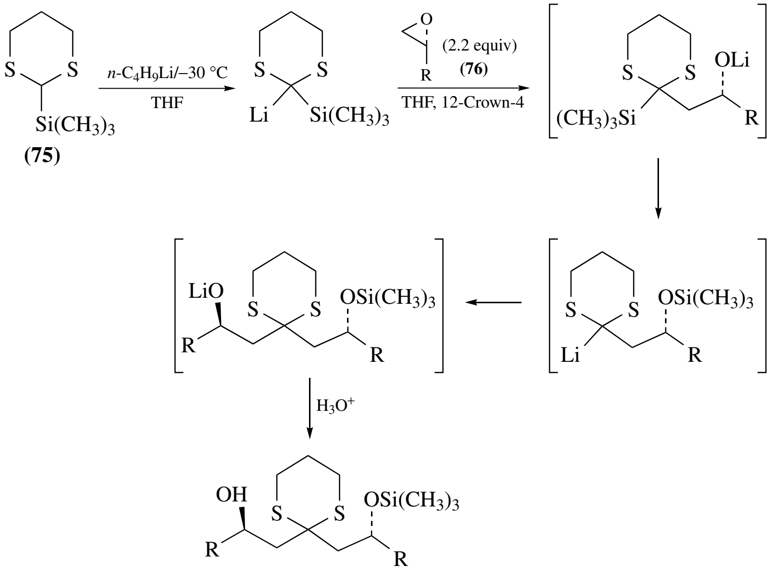

(27)

(77)

R = CH_3, C_6H_5

However, this process requires a reaction time of 2 days and is inapplicable to unsymmetrical couplings (two different epoxides). As the study described in equation 24 revealed a dramatic solvent effect on similar Brook isomerizations in the adduct of lithio dihalo(trialkylsilyl)methanes with epoxides (isomerization did not occur following metalation and initial alkylation in THF but proceeded readily upon addition of HMPA), the effect of HMPA for promoting the Brook isomerization was studied once the first alkylation was complete (equation 28)[357].

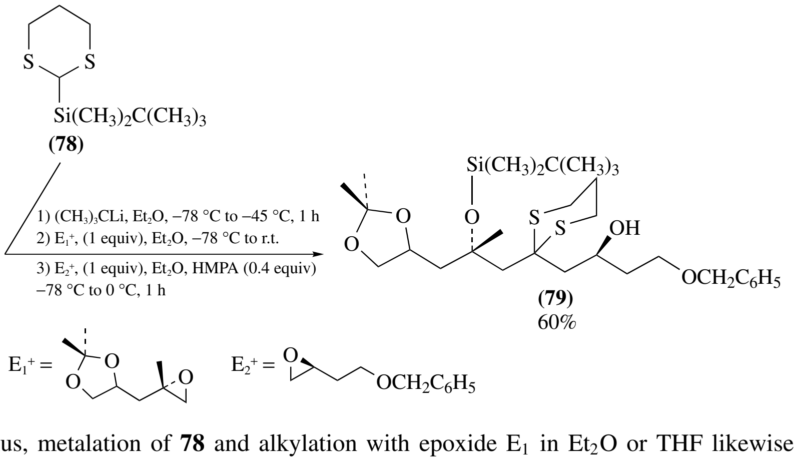

(28)

Thus, metalation of **78** and alkylation with epoxide E_1 in Et_2O or THF likewise furnished the unrearranged carbinols exclusively. Then, addition of HMPA or DMPU induced the 1,4-Brook isomerization (equation 28) and addition of a second epoxide leads to **79** in 60% yield. Then, the introduction of two different electrophiles is now successful and scalemic epoxides are particularly well suited to this process, because the configurations of the resulting carbinols stereocenters are predetermined, circumventing the formation and separation of unwanted diastereomers.

Assembling a five-component coupling product in a single operation further extended this methodology. Following alkylation of dithiane **78** with epoxide (−)**79** (2.6 equivalent each) to generate the unrearranged alkoxy dithiane **80**, sequential addition of HMPA and (−)-epichlorohydrin **81** (1 equivalent) furnished the bis(silyloxy dithiane) carbinols (+)**82** in 66% yield (equation 29)[357].

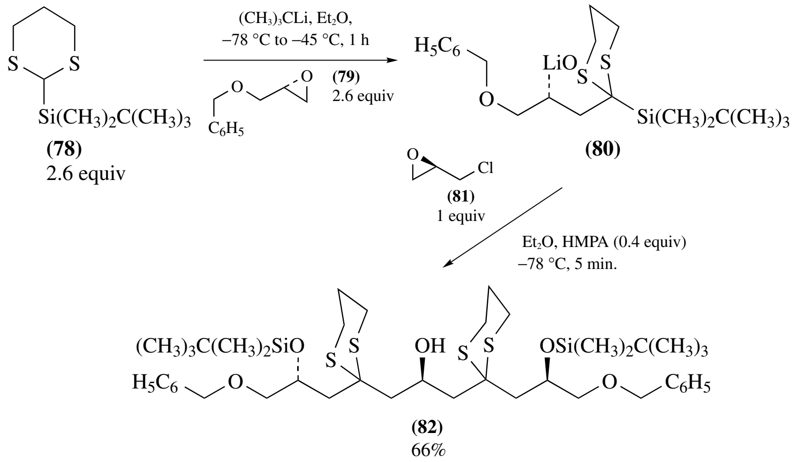

(29)

Finally, addition of the carbanions derived from **83** to non-enolizable aldehydes is a facile process. Aryl and tertiary alkyl aldehydes gave trimethylsilyl allyl ethers **85** by a [1,4]-Brook isomerization (equation 30)[358]. The stereochemistry of the intermediate alkoxides **84** dramatically influences the reaction conditions required[359].

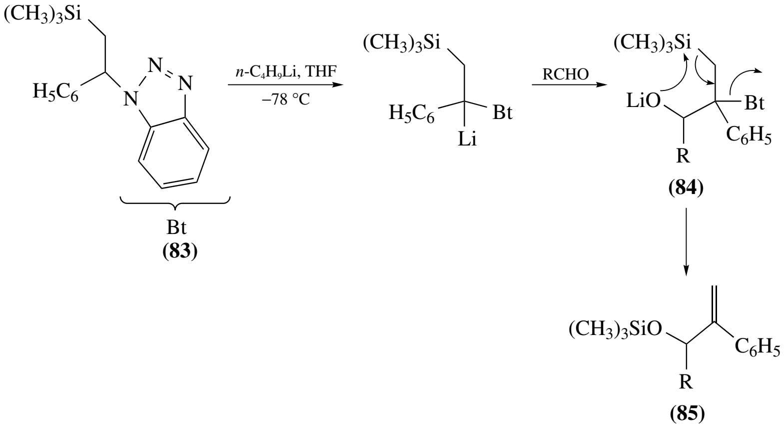

(30)

VI. THE SHAPIRO REACTION

The Shapiro reaction occurs when a tosylhydrazone **86**, easily prepared from a ketone and tosylhydrazine, is treated with 2 equivalents of an ethereal solution of *n*-butyllithium **87**, resulting first in the removal of the N−H proton to give the anion **88** and then of a one proton from the less-substituted α position to give the dianion **89**. Elimination of lithium *p*-toluenesulfinate in the rate-limiting step gives the lithium alkenyldiazenide **90**, which suffers loss of nitrogen to afford the alkenyllithium **91** (equation 31)[360, 361].

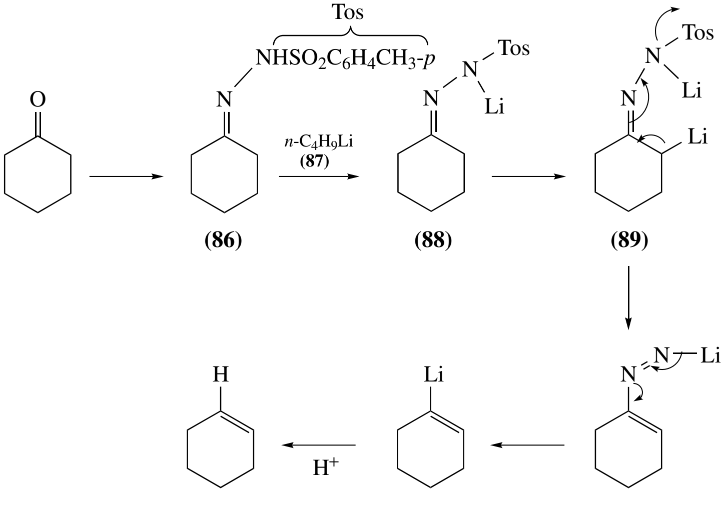

(86) **(88)** **(89)** **(92)** **(91)** **(90)**

(31)

Unfortunately, the vinyl anion undergoes protonation under these reaction conditions and leads to the simple alkene **92** as the major product. It has been suggested that the proton source is actually the tosylhydrazone monoanion **88**[362], and that the basicity of **91** is strong enough to abstract an α proton from the unreacted tosylhydrazone monoanion **88** or even from **89** by *ortho*-metalation of the tosyl ring. Thus, in order to avoid this protonation in the reaction, an excess of base (>3 equivalents) was required to obtain good conversion into alkenyl derivatives.

Moreover, a deuterium quenching study has shown that quantitative formation of the dianion **89** occurs at −78 °C, but if the reaction mixture is allowed to warm to 0 °C, the excess of *n*-butyllithium quantitatively *ortho*-metalates the ring to give a trianion before the vinyl anion is formed in a significant amount[363]. The trianion then decomposes to the vinyl anion, which is stable under these conditions and can be trapped by electrophiles. The use of only 2 equivalents of alkyllithium leaves the ring unmetalated and vulnerable to further reactions. Thus, the requirement for an excess of base stems from the need to *premetalate* the tosyl ring, as in the formation of **93**, thus removing the acidic *ortho*-hydrogen before it can protonate the alkyllithium product (equation 32).

In order to use only a stoichiometric amount of alkyllithiums, a modified sulfonylhydrazone leaving group containing no acidic *ortho* protons was required, such as 2,4,6-triisopropylbenzenesulfonyl (Trisyl **94**) (equation 33).

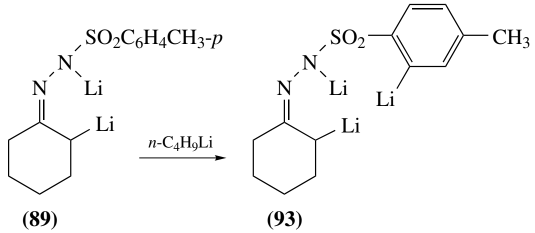

(32)

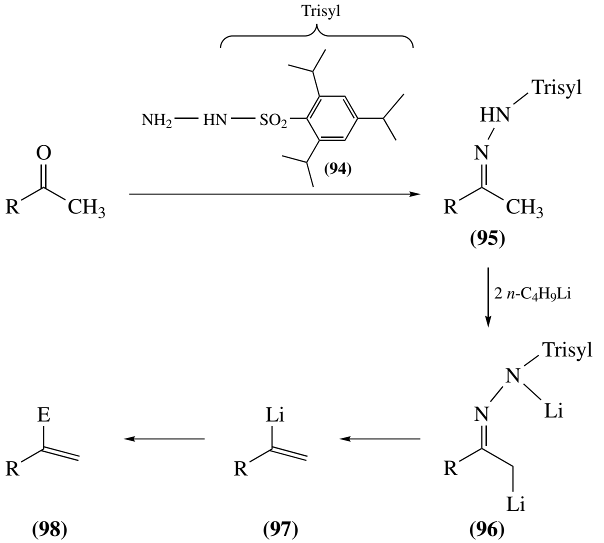

(33)

As a result, trisylhydrazones **95** allow the use of just 2 equivalents of alkyllithium, and thus only a single equivalent of electrophile (E) is needed to trap the resultant vinyllithium **97** to form the functionalized alkene **98**. Moreover, trisylhydrazone dianions **96** undergo the elimination reaction much faster than do those derived from tosylhydrazones. This rate enhancement allows the use of even more acidic solvents, such as tetrahydrofuran.

A. Regioselectivity

Arenesulfonylhydrazones exist as mixtures of E- and Z-isomers. The ratio is dependent upon the size of the groups attached to the azomethine carbon, but the E isomer is the major isomer[364] (i.e. **99** and **100**, equation 34). Then, for these unsymmetrically substituted species, deprotonation of the monoanion occurs at the less-substituted α position ($RCH_3 > R_2CH_2 > R_3CH$) to give the corresponding less-substituted vinyllithium products **101** and **102** (in a ratio usually >50:1) (equation 34)[362].

On the other hand, differential substitution adjacent to equivalently substituted α positions does not afford a good regiochemical control (compare **103** and **104**, equation 35)[365, 366].

It is also possible to generate the more highly substituted vinyllithium regioisomer in some cases by using an *in situ* alkylation step (see Section VI.C for further functionalization).

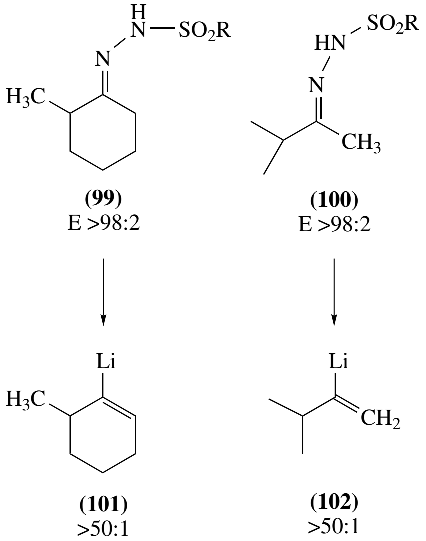

(99) E >98:2

(100) E >98:2

(101) >50:1

(102) >50:1

(34)

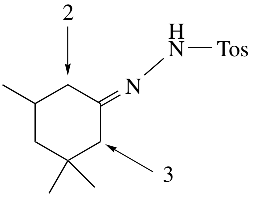

(103)

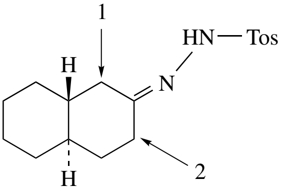

(104)

(35)

B. Stereoselectivity

The issue of stereoselectivity of the vinyllithium formed from acyclic arylhydrazones has also been addressed. For symmetrical linear-chain ketone derivatives such as **105**, the *E*-vinyllithium **106** is the exclusive product (equation 36)$^{362, 367-372}$.

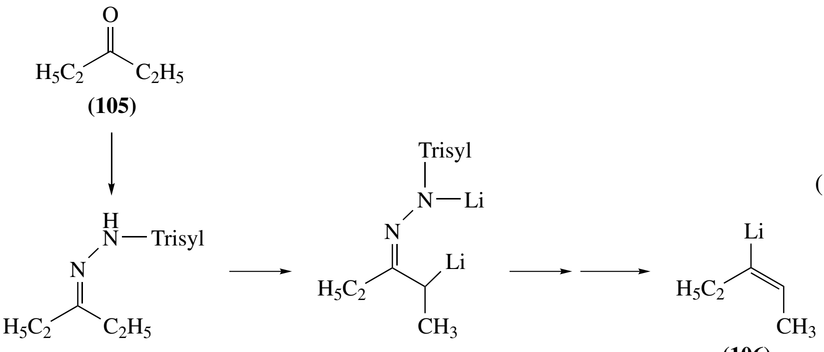

(105)

(106)

(36)

These results are consistent with a *syn* deprotonation of the hydrazone monoanion conformer, in which the α-alkyl group R is *anti* to the hydrazone moiety (a lower steric interaction in **107** than in **108**) during the formation of the dianion (equation 37)[373].

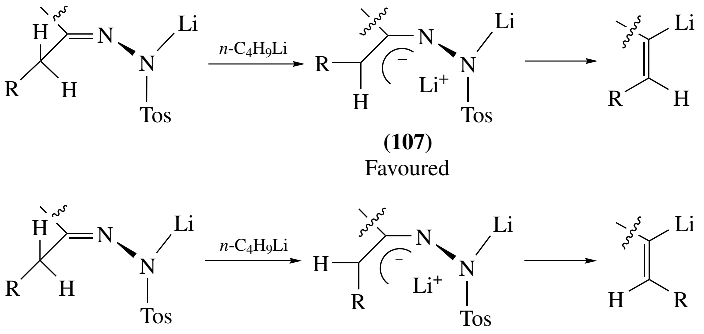

(107)
Favoured

(108)
Disfavoured

(37)

When medium and large ring ketones are also treated with ArSO$_2$NH$-$NH$_2$ and then with n-C$_4$H$_9$Li, the *E* isomer is also the predominant form (equation 38)[374].

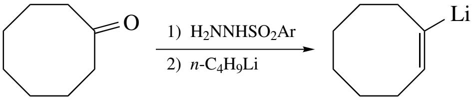

(38)

C. Further Functionalization

The *syn*-directed deprotonation of arylhydrazones can be used to reverse the normal preference of the less-substituted vinyllithium. By employing a one-flask dianion alkylation procedure, the formation of an almost exclusive stereoisomer of acyclic vinyllithiums

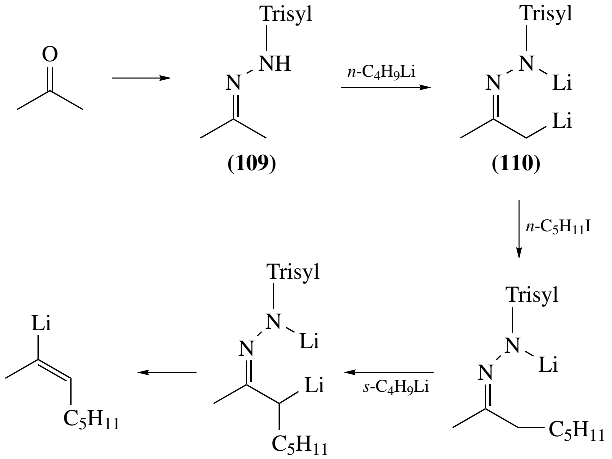

(109) **(110)**

(113) **(112)** **(111)**

(39)

could be achieved that would be impossible to prepare selectively by the direct reaction. Less than 2% of the less-substituted regioisomer is produced. As example, acetone trisylhydrazone **109** can be converted into the corresponding dianion **110**, followed by alkylation into **111** at low temperature with a primary alkyl iodide. This functionalized monoanion is regiochemically stable at that temperature and, upon the addition of one more equivalent of alkyllithium base such as *s*-C_4H_9Li, it undergoes an exclusive *syn* deprotonation at the more highly-substituted α-position to give a dianion **112**, which now can rearrange into **113** by simply warming the reaction mixture (equation 39)[373].

This sequence reverses completely the regioselectivity observed for the direct reaction of 2-octanone trisylhydrazone **114** (equation 40). Indeed, only the isomer **115** is obtained.

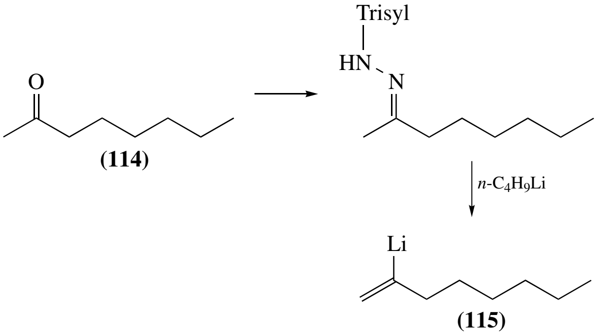

(40)

D. The Catalytic Shapiro Reaction

As described previously, the Shapiro reaction requires stoichiometric amounts of base to generate the alkyllithium reagents. An efficient catalytic method of the Shapiro reaction, which showed excellent regio- and stereo-selectivity, has also been reported. Indeed, the combination of ketone phenyl aziridinylhydrazones **116** and a catalytic amount of lithium amides leads to the corresponding alkene **117** in good overall yield (equation 41)[375].

A regioselective deprotonation with amide base by preferential abstraction of the α-methylene hydrogen *syn* to the phenylaziridyl moiety in **116** and subsequent decomposition of the resulting monoanion furnishes, with extrusion of styrene and nitrogen, the alkyllithium **118**. After abstraction of the amine proton, the *cis*-alkene **117** is formed with regeneration of the lithium amide base for further use in the catalytic cycle.

E. Application of the Shapiro Reaction

The Shapiro reaction provides a convenient, easy and straightforward method to convert ketones into a plethora of olefinic substances in high yields. Many of these vinyllithium derivatives are useful for further synthetic manipulations. No attempt is made in this chapter to cover all the applications of the Shapiro reaction and only few representative examples will be described. A variety of polyolefins such as **119**, used for cation olefin cyclization, can be stereospecifically formed in a concise and modular approach in a single step from the components shown in equation 42 via the Shapiro reaction[376].

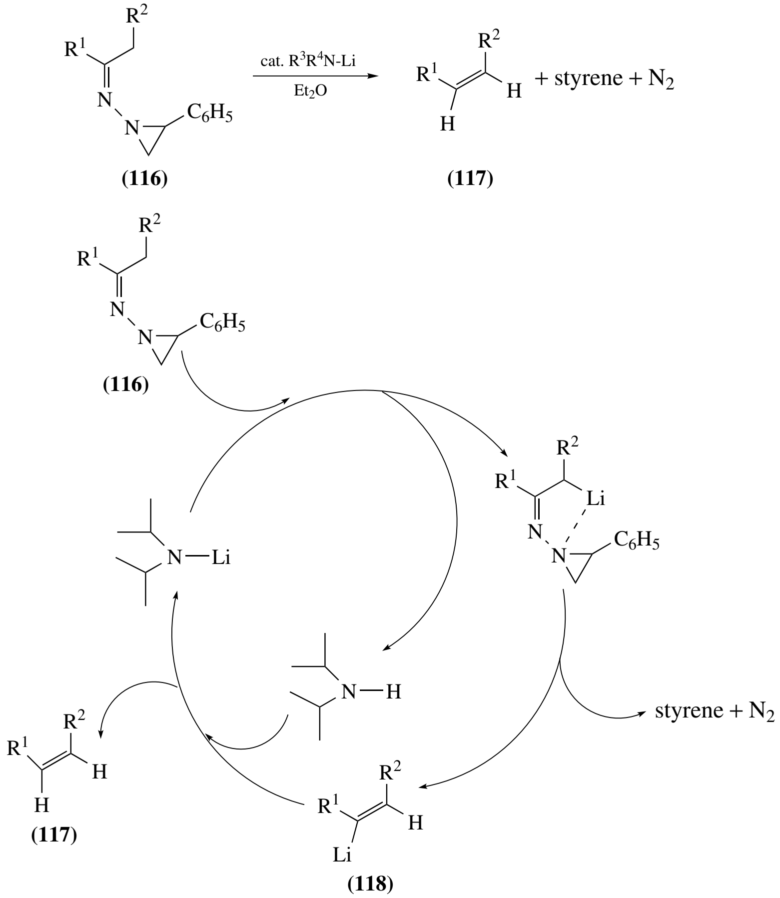

(41)

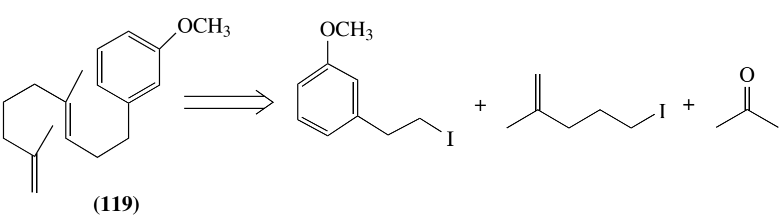

(42)

The sequence of steps involved in the present route to trisubstituted olefins is described in equation 43. Double deprotonation of acetone 2,4,6-triisopropylbenzenesulfonylhydrazone **109**, first at nitrogen and then at the α-methyl that is *syn* to the N-trisyl group, followed by coupling with an alkyl halide at $-65\,^{\circ}$C produces the unsymmetrical hydrazone intermediate **120**. At low temperature **120** is configurationally stable and the N-trisyl group remains *syn* to the alkylated carbon. Subsequent deprotonation with TMEDA and n-C_4H_9Li occurs at the α-carbon *syn* to the N-trisyl group to give **121**.

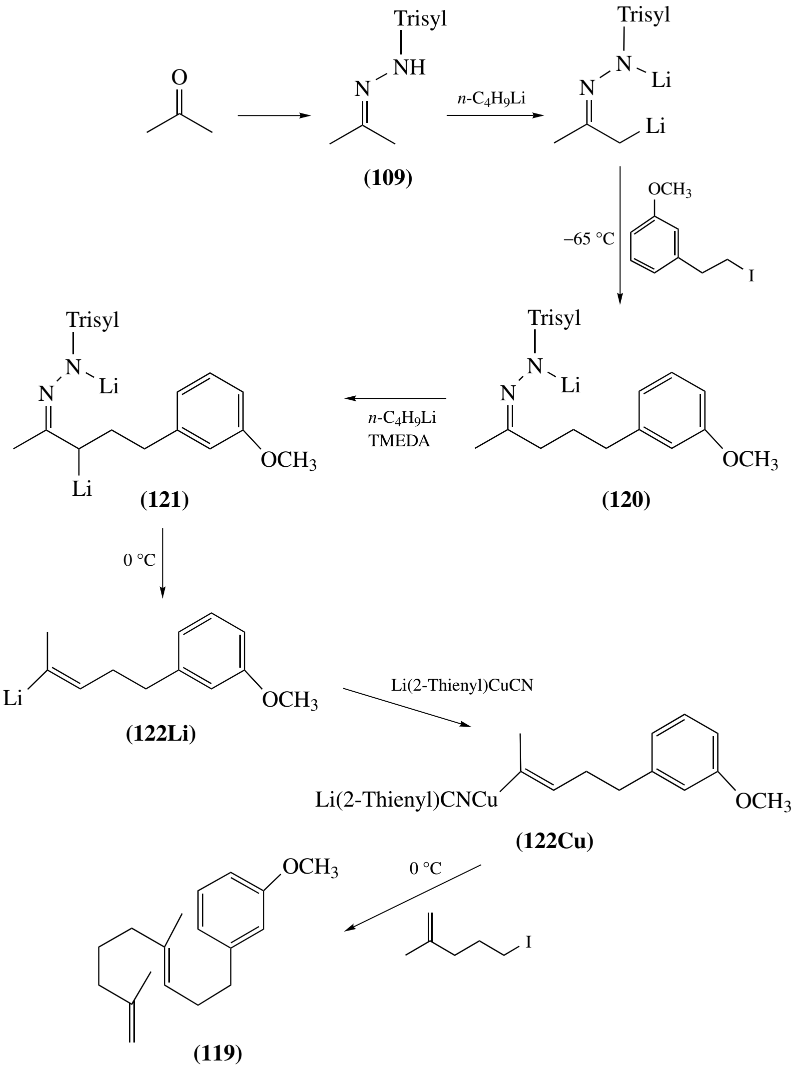

(43)

Warming of the resulting dianion **121** to 0 °C for several minutes effects extrusion of N_2 and formation of Z-vinyllithium reagent **122Li**. Conversion of the vinyllithium reagent **122Li** to the mixed cuprate **122Cu** with lithium 2-thienylcyanocuprate and coupling at 0 °C with a second electrophile produces the trisubstituted olefin **119** in a single-pot operation.

The use of the trisylhydrazone **124** of 2-butanone **123** in the coupling process provides access to products containing an ethyl-substituted olefin **126**. The starting unsymmetrical hydrazone **124** undergoes deprotonation and alkylation at the terminal α-carbon leading to a single metallated olefinic product **125Li** (equation 44). The electrophilic component 2,3-dibromopropene leads to **126**, which can be further elaborated via subsequent reactions.

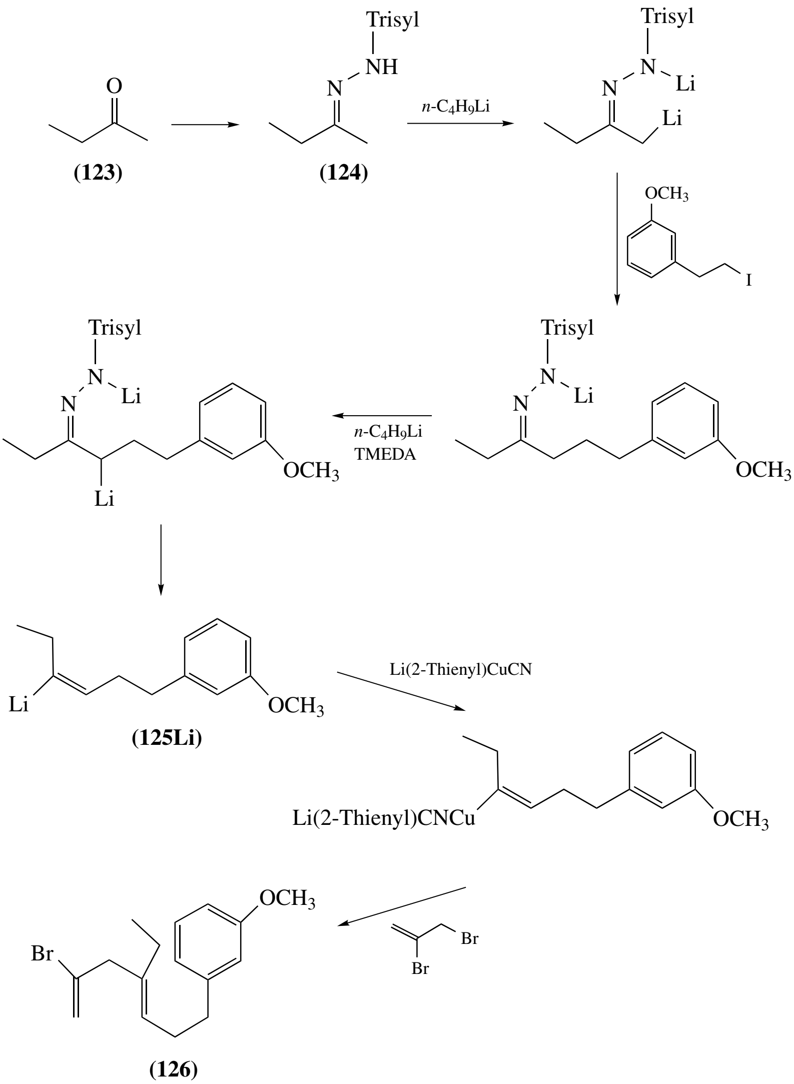

(123) **(124)** **(125Li)** **(126)**

(44)

An elegant application of the catalytic Shapiro reaction has been found in the synthesis of the natural product **129** (equation 45), a component of the sex pheromone of the summer fruit tortrix moth (*Adoxophyes orana*)[377].

The selective lithiation of 2-hexanone phenylaziridinyl-(*E*)-hydrazone **127** with LDA and subsequent alkylation with 8-(*tert*-butyldimethylsilyloxy)octyl bromide gave (*Z*)-hydrazone **128** in 65% yield. Its LDA-catalyzed selective decomposition followed by hydrolysis of the silyl ether yielded (*Z*)-9-tetradecen-1-ol, which was acetylated to afford the target compound **129** in 80% yield with a complete regioselectivity and a *cis*/*trans* ratio of 99.6/0.4.

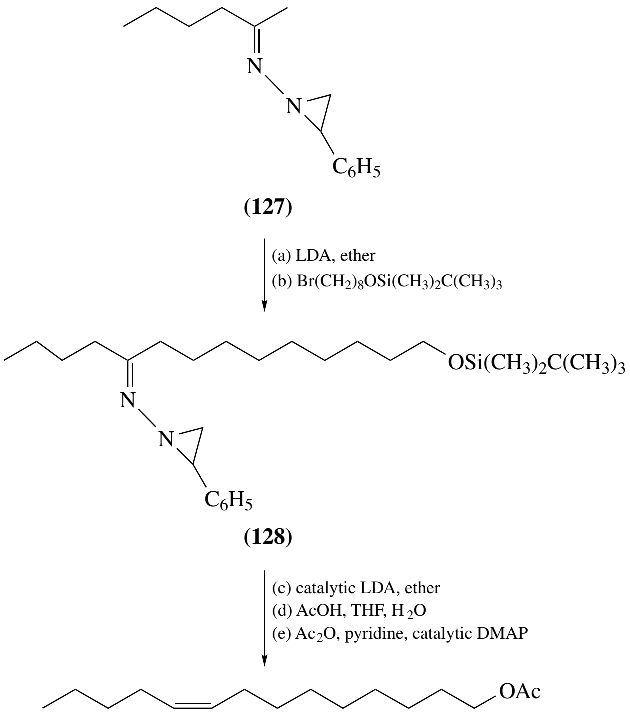

(127)

(128)

(129)

(45)

VII. THE SULFOXIDE/LITHIUM DISPLACEMENT

The reaction of sulfinyloxirane **130** with n-C_4H_9Li takes place at the sulfinyl group to afford the desulfinated epoxide **133** in good yield[378]. This reaction proceeds at −100 °C with concomitant formation of phenyl n-butyl sulfoxide **132**. Thus, oxiranyllithium **131** picks up the acidic proton of the *in situ* formed **132** to generate the reduce epoxide **133** (equation 46)[379].

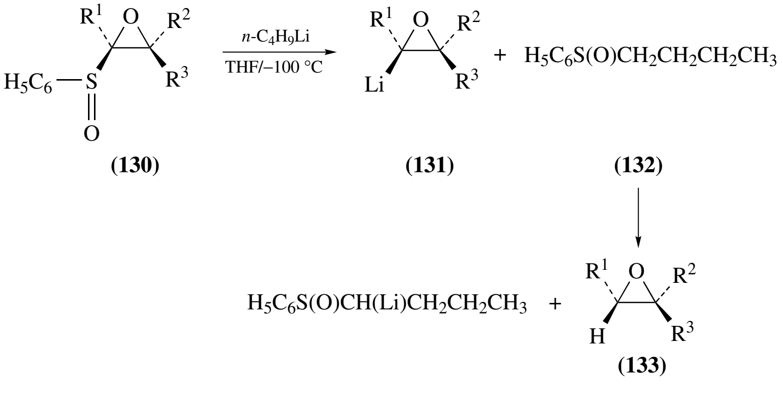

(130) **(131)** **(132)**

(46)

(133)

The reaction is stereospecific and the configuration of the carbon bearing the sulfinyl group is retained. Therefore, isomeric sulfinyloxiranes **134** and **135** gives epoxides **136** and **137** respectively on treatment with n-C_4H_9Li at $-100\,°C$ (equation 47)[380]. However, the reaction temperature as well as the amounts of butyllithium are critical for the success of this reaction[381].

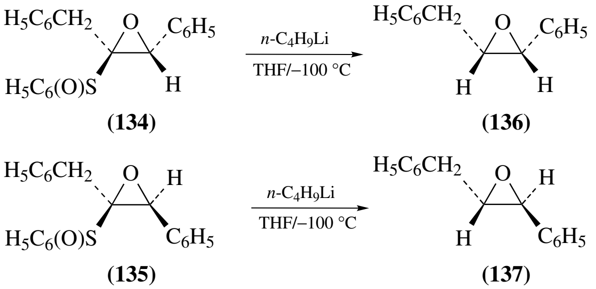

(47)

This procedure was extended to a method for asymmetric synthesis of optically active epoxides starting from optically active sulfoxides[382]. As the oxiranyllithium **131** reacts with the acidic hydrogen of the n-butyl aryl sulfoxide, the introduction of electrophiles to the reaction mixture was problematic. Therefore, the reaction was performed by addition of 1 equivalent of t-C_4H_9Li at $-100\,°C$ to **130** and the sulfoxide–lithium exchange reaction was found to be extremely rapid (within a few seconds at this temperature). Moreover, as t-butyl aryl sulfoxide **138** has now no more acidic hydrogen, the addition of several electrophiles leads to functionalized epoxides **139** (equation 48)[383].

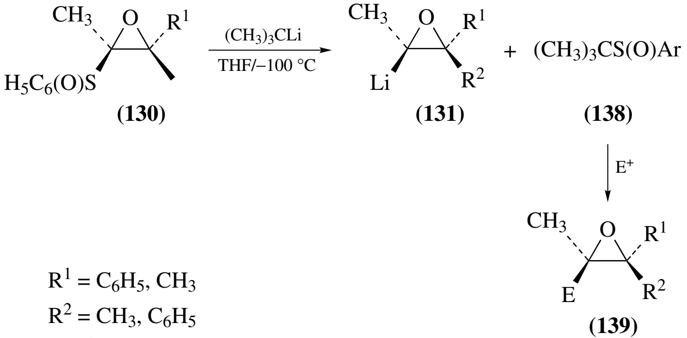

(48)

$R^1 = C_6H_5, CH_3$

$R^2 = CH_3, C_6H_5$

$R^1R^2 = (CH_2)_4$

$E^+ = C_2H_5CHO, CH_3COCH_3, (CH_3)_3SiCl, C_2H_5OCOCl, (CH_3)_2NCOCl$

Several alkylmetals[384] including alkyllithium derivatives react also with sulfinylaziridine **140** to give the aziridinyllithium **141** via a stereospecific desulfinylation at low temperature[385]. The corresponding aziridinyllithium **141** generated is stable at low temperature, such as $-30\,°C$, and can react with a large variety of electrophiles such as aldehydes, ketones and chloroformates, to give functionalized aziridines (equation 49)[386].

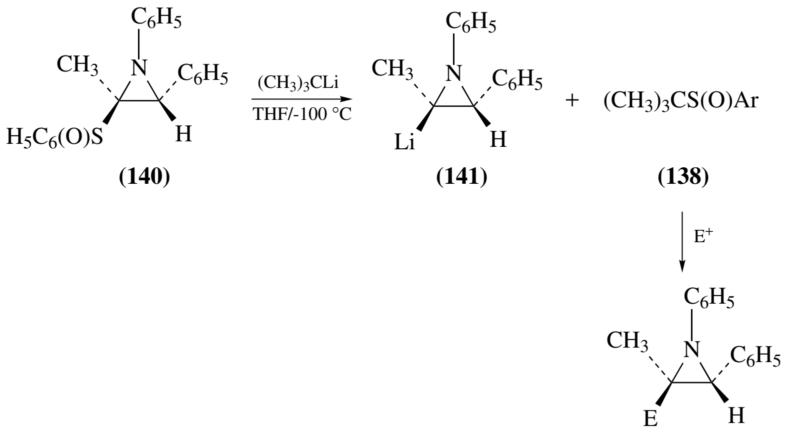

(140) **(141)** **(138)**

(49)

$E^+ = C_2H_5CHO, CH_3COCH_3, C_2H_5COOCl, (C_2H_5O)_2POCl$

The sulfoxide–lithium exchange reaction of alkenyl sulfoxides **142** possessing leaving groups in a β-position was also developed[387] and it has been found that the reaction gives good yields of the corresponding allenes **143** (equation 50)[388].

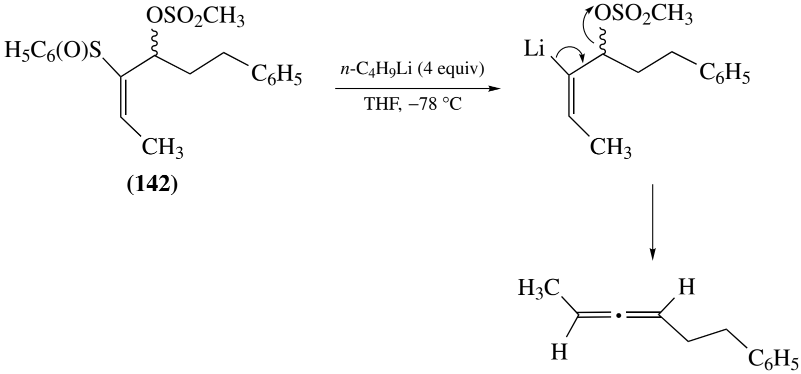

(142)

(143)
89%

(50)

α-Sulfinyl ketones having two alkyl groups on the α-carbon (such as **145**) can be easily prepared from the isopropyl p-tolyl sulfoxide **144** (or cyclohexyl p-tolyl sulfoxide **146**). Then, the resulting enol triflate **147** was prepared by reaction of **145** with LDA followed by the addition of $PhNTf_2$ in the presence of HMPA as a cosolvent. Once all the starting material was consumed, excess n-C_4H_9Li was added to promote the sulfoxide–lithium exchange, which gives after β-elimination the corresponding trisubstituted allene **148** (or **149**) in moderate yield (equation 51)[387].

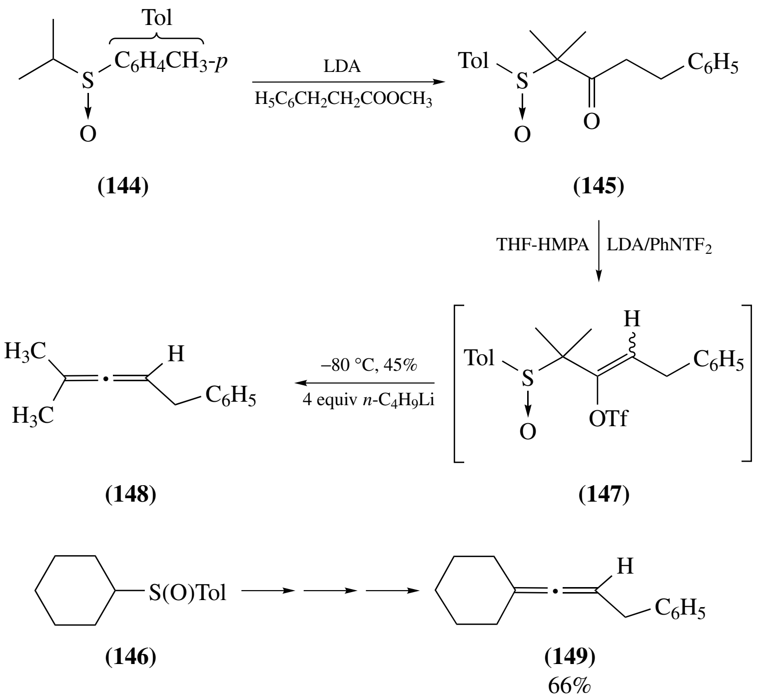

(144) **(145)** **(147)** **(148)** **(146)** **(149)**

(51)

The same methodology was successfully applied for the preparation of alkynes **152** and alkenes[389] **153** from α-sulfinyl ketones **150** and β-mesyloxy sulfoxides **151**, respectively (equation 52).

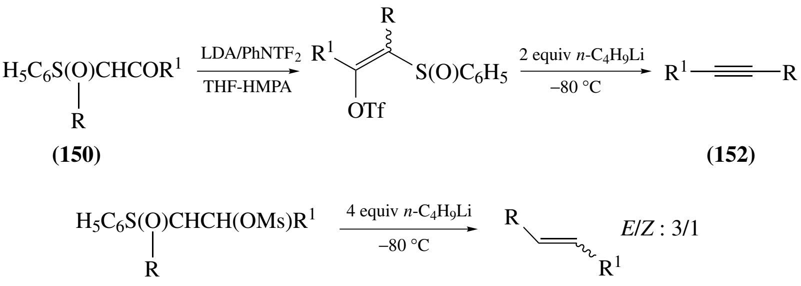

(150) **(152)** (52)

(151) **(153)**

Finally, the addition of the carbanion of 1-chloroalkyl p-tolyl sulfoxides **154** to carbonyl compounds gave the adducts **155**, which were treated with alkyllithium such as t-C_4H_9Li to afford the one-carbon homologated carbonyls compounds **158**, from their lithium enolate forms **157**, having an alkyl group at the α-position, via the carbenoid β-alkoxides **156** (equation 53)[390].

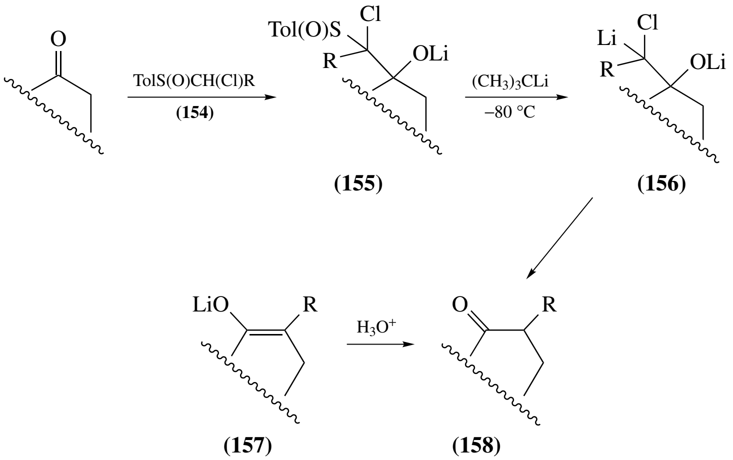

(53)

VIII. ACKNOWLEDGMENTS

The Lausanne authors are indebted to the Swiss National Science Foundation, Bern (grant 20-63′584-00). The Israeli authors thank the Israel Science Foundation administered by the Israel Academy of Sciences and Humanities (79/01-1) and the Fund for the Promotion of Research at the Technion.

IX. REFERENCES

1. M. Schlosser, in *Organometallics in Synthesis: A Manual* (Ed. M. Schlosser), 2nd edn., Wiley, Chichester, 2002: (a) p. 85, (b) pp. 138–148, (c) pp. 150–155, (d) pp. 159–171, (e) pp. 295–297, (f) p. 250, (g) pp. 185–284 and Tables 80–144.
2. F. Totter and P. Rittmeyer, in *Organometallics in Synthesis: A Manual* (Ed. M. Schlosser), 1st edn., Wiley, Chichester, 1994, pp. 167–194.
3. K. Ziegler, K. Nagel and M. Patheiger, *Z. Anorg. Allg. Chem.*, **282**, 345 (1955).
4. U. Schöllkopf, in *Houben-Weyl: Methoden der organischen Chemie* (Ed. E. Müller), Vol. 13/1, Thieme, Stuttgart, 1970, pp. 87–253.
5. H. Gilman, F. W. Moore and O. Baine, *J. Am. Chem. Soc.*, **63**, 2479 (1941).
6. R. M. Anker and A. H. Cook, *J. Am. Chem. Soc.*, **63**, 323 (1941).
7. P. Karrer and J. Benz, *Helv. Chim. Acta*, **31**, 1048, (1948).
8. C. N. Eid and J. P. Konopelski, *Tetrahedron*, **47**, 975 (1991).
9. Y.-J. Kim, M. P. Bernstein, A. S. Galiano Roth, F. E. Romesberg, P. G. Williard, D. J. Fuller, A. T. Harrison and D. B. Collum, *J. Org. Chem.*, **56**, 4435 (1991).
10. J.-L. Luche and J.-C. Damiano, *J. Am. Chem. Soc.*, **102**, 7926 (1980).
11. H. Gilman, J. A. Beel, C. G. Brannen, M. W. Bullock, G. E. Dunn and L. S. Miller, *J. Am. Chem. Soc.*, **71**, 1499 (1949).
12. D. Bryce-Smith and E. E. Turner, *J. Chem. Soc.*, 861 (1953).
13. J. A. Schwindeman, R. C. Morrison, B. T. Dover, J. F. Engel, C. W. Kamienski, R. W. Hall and D. E. Sutton, US-Patent 5,332,533 (to FMC Corp. filed on 6 July, 1993, issued on 26 July, 1994); *Chem. Abstr.*, **121**, 231044 (1994).
14. P. K. Freeman and L. L. Hutchingson, *J. Org. Chem.*, **45**, 1924 (1980).
15. R. N. Meals, *J. Org. Chem.*, **9**, 211 (1944).
16. R. Damico, *J. Org. Chem.*, **29**, 1971 (1964).
17. H. D. Zook, J. March and D. F. Smith, *J. Am. Chem. Soc.*, **81**, 1617 (1959).
18. B.-H. Chang, H.-S. Tung and C. H. Brubaker, *Inorg. Chim. Acta*, **51**, 143 (1981).

19. C. Tessier-Youngs and O. T. Beachley, *Inorg. Synth.*, **24**, 95 (1986).
20. W. H. Glaze, J. Lin and E. G. Felton, *J. Org. Chem.*, **30**, 1258 (1965).
21. S. V. Puntambeker and E. A. Zoellner, *Org. Synth., Coll. Vol.*, **1**, 524 (1941).
22. G. W. Kamienski and D. L. Esmay, *J. Org. Chem.*, **25**, 1807 (1960).
23. W. N. Smith, *J. Organomet. Chem.*, **82**, 1 (1974).
24. G. Giancaspro and G. Sleiter, *J. Prakt. Chem.*, **321**, 876 (1979).
25. D. Seyferth and H. M. Cohen, *J. Organomet. Chem.*, **1**, 15 (1963).
26. O. H. Johnson and W. H. Nebergall, *J. Am. Chem. Soc.*, **71**, 1720 (1949).
27. R. L. Bixler and C. Niemann, *J. Org. Chem.*, **23**, 742 (1958).
28. G. Molle, P. Bauer and J. E. Dubois, *J. Org. Chem.*, **48**, 2975 (1983).
29. H. Gilman and T. S. Soddy, *J. Org. Chem.*, **22**, 565 (1957).
30. R. Waack and M. A. Doran, *J. Org. Chem.*, **32**, 3396 (1967).
31. E. A. Braude and C. J. Timmons, *J. Chem. Soc.*, 2207 (1950).
32. E. A. Braude and J. A. Coles, *J. Chem. Soc.*, 2012 and 2014 (1950).
33. R. S. Threlkel, J. E. Bercraw, P. F. Seidler, J. M. Stryker and R. D. Bergman, *Org. Synth., Coll. Vol.*, **8**, 505 (1993).
34. G. Wittig, *Angew. Chem.*, **53**, 241 (1940).
35. G. Wittig, *Angew. Chem.*, **62**, 391 (1949).
36. H. Gilman and J. W. Morton, *Org. React.*, **8**, 286 (1954).
37. H. Gilman and B. J. Gaj, *J. Org. Chem.*, **22**, 1165 (1957).
38. U. Schöllkopf, in *Houben-Weyl: Methoden der organischen Chemie* (Ed. E. Müller), Vol. 13/1, Thieme, Stuttgart, 1970, p. 147.
39. H. Gilman, E. A. Zoellner and W. M. Selby, *J. Am. Chem. Soc.*, **54**, 1957 (1932).
40. V. Boekelheide and G. C. Morrison, *J. Am. Chem. Soc.*, **80**, 3905 (1958).
41. H. Gilman and G. C. Gainer, *J. Am. Chem. Soc.*, **69**, 877 (1947).
42. G. Wittig and D. Hellwinkel, *Chem. Ber.*, **97**, 784 (1964).
43. H. Gilman and G. E. Dunn, *J. Am. Chem. Soc.*, **73**, 5078 (1951).
44. W. E. Truce and J. F. Lyons, *J. Am. Chem. Soc.*, **73**, 126 (1951).
45. R. C. Fuson, W. C. Hammann and P. R. Jones, *J. Am. Chem. Soc.*, **79**, 928 (1957).
46. H. Gilman and R. D. Nelson, *J. Am. Chem. Soc.*, **70**, 3316 (1948).
47. H. Gilman and C. G. Brannen, *J. Am. Chem. Soc.*, **72**, 4280 (1950).
48. H. Gilman and C. G. Stuckwisch, *J. Am. Chem. Soc.*, **72**, 4553 (1950).
49. H. Gilman and H. W. Melvin, *J. Am. Chem. Soc.*, **72**, 995 (1950).
50. H. Gilman and L. Summers, *J. Am. Chem. Soc.*, **72**, 2767 (1950).
51. D. F. Taber, R. P. Meagley and D. Supplee, *J. Chem. Educ.*, **73**, 259 (1996).
52. J. B. Wright and E. S. Gutsell, *J. Am. Chem. Soc.*, **81**, 5193 (1959).
53. H. Gilman, H. A. Pacevitz and O. Baine, *J. Am. Chem. Soc.*, **62**, 1514 (1940).
54. K. Ziegler and H. Colonius, *Justus Liebigs Ann. Chem.*, **479**, 136 (1930).
55. U. Schöllkopf, H. Küppers, H. J. Traencker and W. Pitteroff, *Justus Liebigs Ann. Chem.*, **704**, 120 (1967).
56. J. Stapersma and G. W. Klumpp, *Tetrahedron*, **37**, 187 (1981).
57. J. Stapersma, P. Kuipers and G. W. Klumpp, *Recl. Trav. Chim. Pays-Bas*, **101**, 213 (1982).
58. G. Köbrich and W. Goyert, *Tetrahedron*, **24**, 4327 (1968).
59. D. Seyferth and R. L. Lambert, *J. Organomet. Chem.*, **54**, 123 (1973).
60. D. Seebach, R. Haessig and J. Gabriel, *Helv. Chim. Acta*, **66**, 308 (1983).
61. I. Haiduc and H. Gilman, *J. Organomet. Chem.*, **12**, 394 (1968).
62. M. Schlosser, E. Marzi, F. Cottet, H. H. Büker and N. M. M. Nibbering, *Chem. Eur. J.*, **7**, 3511, spec. Footnotes to Table 6 (2001).
63. M. D. Rausch, F. E. Tibbetts and H. B. Gordon, *J. Organomet. Chem.*, **5**, 493 (1966).
64. T. L. Brown and M. T. Rogers, *J. Am. Chem. Soc.*, **79**, 1859 (1957).
65. D. J. Aberhart and L. J. Lin, *J. Chem. Soc., Perkin Trans. 1*, 2320 (1974).
66. R. J. Parry, A. E. Mizusawa, I. C. Chiu, M. V. Naidu and M. Ricciardone, *J. Am. Chem. Soc.*, **107**, 2512 (1985).
67. W. F. Bailey and E. R. Punzalan, *J. Org. Chem.*, **55**, 5404 (1990).
68. J. H. Wieringa, H. Wynberg and J. Strating, *Synth. Commun.*, **1**, 7 (1971).
69. E. Negishi, D. R. Swanson and C. J. Rousset, *J. Org. Chem.*, **55**, 5406 (1990).
70. W. F. Bailey, T. T. Nurmi, J. J. Patricia and W. Wang, *J. Am. Chem. Soc.*, **109**, 2442 (1987).
71. W. F. Bailey, T. V. Ovaska and T. K. Leipert, *Tetrahedron Lett.*, **30**, 3901 (1989).

72. H. M. Walborsky and C. Zimmermann, *J. Am. Chem. Soc.*, **114**, 4996 (1992).
73. T. Rausis and M. Schlosser, unpublished results (1999).
74. D. E. Applequist and A. H. Peterson, *J. Am. Chem. Soc.*, **83**, 862 (1961).
75. P. T. Lansbury and J. D. Sidler, *Tetrahedron Lett.*, 691 (1965).
76. P. T. Lansbury and J. D. Sidler, *J. Chem. Soc., Chem. Commun.*, 373 (1965).
77. U. Schöllkopf and G. Wittig, *Tetrahedron*, **3**, 91 (1958).
78. G. Wittig and W. Tochtermann, *Justus Liebigs Ann. Chem.*, **660**, 23 (1962).
79. G. Köbrich and R. H. Fischer, *Tetrahedron*, **24**, 4343 (1968).
80. K. M. Sadhu and D. S. Matteson, *Tetrahedron Lett.*, **27**, 795 (1986).
81. D. S. Matteson, *Tetrahedron*, **54**, 10555 (1998).
82. D. S. Matteson, *J. Organomet. Chem.*, **581**, 51 (1999).
83. J. M. Concellón, L. Llavona and P. L. Bernard, *Tetrahedron*, **51**, 5573 (1995).
84. R. Tarhouni, B. Kirschleger and J. Villieras, *J. Organomet. Chem.*, **272**, C1 (1984).
85. D. F. Hoeg, D. I. Lusk and A. L. Crunbliss, *J. Am. Chem. Soc.*, **87**, 4147 (1965).
86. P. G. Gassman and N. J. O'Reilly, *J. Org. Chem.*, **52**, 2481 (1987).
87. O. R. Pierce, E. T. McBee and G. F. Judd, *J. Am. Chem. Soc.*, **76**, 474 (1954).
88. J. J. Lagowski, *Quart. Rev.*, **13**, 23, pp. 233–264, spec. 238–239 (1959).
89. P. Johncock, *J. Organomet. Chem.*, **19**, 257 (1969).
90. R. D. Chambers, W. K. R. Musgrave and J. Savory, *J. Chem. Soc.*, 1993 (1962).
91. G. Köbrich, *Angew. Chem.*, **79**, 15 (1967); *Angew. Chem., Int. Ed. Engl.*, **6**, 41 (1967).
92. R. H. Fischer and G. Köbrich, *Chem. Ber.*, **101**, 3230 (1968).
93. E. J. Corey and P. Ulrich, *Tetrahedron Lett.*, 3685 (1975).
94. R. C. Gadwood, M. C. Rubino, S. C. Nagarajan and S. T. Michel, *J. Org. Chem.*, **50**, 3255 (1985).
95. T. Ishihara, K. Hayashi, T. Ando and H. Yamanaka, *J. Org. Chem.*, **40**, 3264 (1975).
96. D. Seyferth, R. L. Lambert and M. Massol, *J. Organomet. Chem.*, **88**, 255 (1975).
97. H. J. Loozen, W. M. M. Robben and H. M. Buck, *Recl. Trav. Chim. Pays-Bas*, **95**, 245 (1976).
98. H. J. J. Loozen, W. A. Castenmiller, E. J. M. Buter and H. M. Buck, *J. Org. Chem.*, **41**, 2965 (1976).
99. A. Oku, T. Harada, Y. Homoto and M. Iwamoto, *J. Chem. Soc., Chem. Commun.*, 1490 (1988).
100. M. Braun, R. Dammann and D. Seebach, *Chem. Ber.*, **108**, 2368 (1975).
101. A. Schmidt and G. Köbrich, *Tetrahedron Lett.*, 2561 (1974).
102. K. Kitani, T. Hiyama and H. Nozaki, *Bull. Chem. Soc. Jpn.*, **50**, 3288 (1977).
103. K. Kitani, T. Hiyama and H. Nozaki, *J. Am. Chem. Soc.*, **97**, 949 (1975).
104. K. Kitani, H. Yamamoto, T. Hiyama and H. Nozaki, *Bull. Chem. Soc. Jpn.*, **50**, 2158 (1977).
105. K. G. Taylor, W. E. Hobbs and M. Saquet, *J. Org. Chem.*, **36**, 369 (1971).
106. H. Neumann and D. Seebach, *Chem. Ber.*, **111**, 2785 (1978).
107. M. Rottländer, L. Boymond, G. Cahiez and P. Knochel, *J. Org. Chem.*, **64**, 1080 (1999).
108. T. Yokoo, H. Shinokubo, K. Oshima and K. Utimoto, *Synlett*, 645 (1994).
109. G. Cahiez, D. Bernard and J. F. Normant, *Synthesis*, 245 (1976).
110. M. A. Peterson and R. Polt, *Synth. Commun.*, **22**, 477 (1992).
111. M. Bertrand, G. Leandri and A. Meou, *Tetrahedron Lett.*, 1841 (1979).
112. M. S. Baird, H. H. Hussain and W. Nethercott, *J. Chem. Soc., Perkin Trans. 1*, 1845 (1986).
113. M. S. Baird and B. Grehan, *J. Chem. Soc., Perkin Trans. 1*, 1547 (1993).
114. D. Seebach and H. Neumann, *Chem. Ber.*, **107**, 847 (1974).
115. A. C. Cope, M. Burg and S. W. Fenton, *J. Am. Chem. Soc.*, **74**, 173 (1952).
116. D. E. Gwynn, G. M. Whitesides and J. D. Roberts, *J. Am. Chem. Soc.*, **87**, 2862 (1965).
117. J. Barluenga, R.-M. Canteli and J. Flórez, *J. Org. Chem.*, **59**, 1586 (1994).
118. L. Duhamel and J. M. Poirier, *Bull. Soc. Chim. Fr.*, 297 (1982).
119. L. Duhamel, J. M. Poirier and N. Tedga, *J. Chem. Res. (S)*, 222 (1983).
120. K. S. Y. Lau and M. Schlosser, *J. Org. Chem.*, **43**, 1595 (1978).
121. M. Schlosser and H.-x. Wei, *Tetrahedron*, **53**, 1735 (1997).
122. H.-x. Wei and M. Schlosser, *Chem. Eur. J.*, **4**, 1738 (1998).
123. H.-x. Wei and M. Schlosser, *Tetrahedron Lett.*, **37**, 2771 (1996).
124. A. F. Kluge, K. G. Untch and J. H. Fried, *J. Am. Chem. Soc.*, **94**, 7827, 9256 (1972).
125. A. I. Meyers and R. F. Spohn, *J. Org. Chem.*, **50**, 4872 (1985).

126. L. Duhamel, P. Duhamel and J. P. Lecouve, *J. Chem. Res. (S)*, 34 (1986).
127. A. Ashimori, M. Takaharu, L. E. Overman and D. J. Poon, *J. Org. Chem.*, **58**, 6949 (1993).
128. E. J. Corey and D. J. Beames, *J. Am. Chem. Soc.*, **94**, 7210 (1972).
129. E. J. Corey and H. S. Sachdev, *J. Am. Chem. Soc.*, **95**, 8483 (1973).
130. F. G. Drakesmith, R. D. Richardson, O. J. Stewart and P. Tarrant, *J. Org. Chem.*, **33**, 286 (1968).
131. J. F. Normant, *J. Organomet. Chem.*, **400**, 19 (1990).
132. J. F. Normant, J. P. Foulon, D. Masure, R. Sauvêtre and J. Villieras, *Synthesis*, 122 (1975).
133. N. G. Rondan, K. N. Houk, P. Beak, W. J. Zajdel, J. Chandrasekhar and P. v. R. Schleyer, *J. Org. Chem.*, **46**, 4108 (1981).
134. R. D. Bach, M. L. Braden and G. J. Wolber, *J. Org. Chem.*, **48**, 1509 (1983).
135. P. Tarrant, P. Johncock and J. Savory, *J. Org. Chem.*, **28**, 839 (1963).
136. F. G. Drakesmith, O. J. Stewart and P. Tarrant, *J. Org. Chem.*, **33**, 280 (1968).
137. G. Köbrich and K. Flory, *Chem. Ber.*, **99**, 1773 (1966).
138. C. J. Kowalski and K. W. Fields, *J. Am. Chem. Soc.*, **104**, 1777 (1982).
139. H.-x. Wei and M. Schlosser, manuscript in preparation.
140. M. Schlosser and E. Hammer, *Helv. Chim. Acta*, **57**, 276 (1974).
141. D. Caine and A. S. Frobese, *Tetrahedron Lett.*, 5167 (1978).
142. H. Gilman, W. Langham and F. W. Moore, *J. Am. Chem. Soc.*, **62**, 2327 (1940).
143. H. Gilman and R. G. Jones, *J. Am. Chem. Soc.*, **63**, 1443 (1941).
144. M. Schlosser and V. Ladenberger, *J. Organomet. Chem.*, **8**, 193 (1967).
145. W. J. Trepka and R. J. Sonnenfeld, *J. Organomet. Chem.*, **16**, 317 (1969).
146. G. Wittig, H. Braun and H. Cristau, *Justus Liebigs Ann. Chem.*, **751**, 17 (1971).
147. M. Schlosser and T. Kadibelban, unpublished results (1964).
148. E. E. Betts and L. R. C. Barclay, *Can. J. Chem.*, **33**, 1768 (1955).
149. H. Weiss and H. Oehme, *Z. Anorg. Allg. Chem.*, **572**, 186 (1989).
150. M. M. Olmstead and P. P. Power, *J. Organomet. Chem.*, **408**, 1 (1991).
151. H. Gilman and F. W. Moore, *J. Am. Chem. Soc.*, **62**, 1843 (1940).
152. H. Gilman, F. W. Moore and O. Baine, *J. Am. Chem. Soc.*, **63**, 2479 (1941).
153. X.-h. Wang, G.-f. Zhong, L. Garamszegi and M. Schlosser, unpublished results (1993).
154. H. Gilman and T. H. Cook, *J. Am. Chem. Soc.*, **62**, 2813 (1940).
155. W. Neugebauer, T. Clark and P. v. R. Schleyer, *Chem. Ber.*, **116**, 3283 (1983).
156. A. Ginanneschi and M. Schlosser, unpublished results (1999).
157. H. Gilman and I. Banner, *J. Am. Chem. Soc.*, **62**, 344 (1940).
158. A. G. Giumanini and G. Lercker, *J. Org. Chem.*, **35**, 3756 (1970).
159. D. R. M. Walton, *J. Chem. Soc.*, 1706 (1966).
160. M. E. K. Cartoon and G. W. H. Cheesman, *J. Organomet. Chem.*, **212**, 1 (1981).
161. H. Gilman and S. J. Spatz, *J. Am. Chem. Soc.*, **63**, 1553 (1941).
162. W. E. Parham, E. C. Egberg, Y. A. Sayed, R. W. Thraikill, G. E. Keyser, M. Neu, W. C. Montgomery and L. D. Jones, *J. Org. Chem.*, **41**, 2628 (1976).
163. H. Gilman and D. S. Melstrom, *J. Am. Chem. Soc.*, **70**, 4177 (1948).
164. G. Köbrich and P. Buck, *Chem. Ber.*, **103**, 1412 (1970); P. Buck and G. Köbrich, *Chem. Ber.*, **103**, 1420 (1970).
165. G. Wittig and G. Fuhrmann, *Chem. Ber.*, **73**, 1197 (1940); W. H. Glaze and A. C. Ranade, *J. Org. Chem.*, **36**, 3331 (1971).
166. L. S. Liebeskind and J. Zhang, *J. Org. Chem.*, **56**, 6379 (1991).
167. S. Harder, J. Boersma, L. Brandsma, G. P. M. van Mier and J. A. Kanters, *J. Organomet. Chem.*, **364**, 1 (1989).
168. J. A. Ladd and J. Parker, *J. Chem. Soc., Dalton Trans.*, 930 (1972).
169. J. A. Dodge and A. R. Chamberlin, *Tetrahedron Lett.*, **29**, 4827 (1988).
170. G. W. Klumpp and M. J. Sinnige, *Tetrahedron Lett.*, **27**, 2247 (1986).
171. A. B. Foster, M. Jarman, O.-T. Leung, R. McCague, G. Leclerq and N. Devleeschouwer, *J. Med. Chem.*, **28**, 1491 (1985).
172. S.-J. Law, J. M. Morgan, L. W. Masten, R. F. Borne, G. W. Arana, N. S. Kula and R. J. Baldessarini, *J. Med. Chem.*, **25**, 213 (1982).
173. L. Lamza, *J. Prakt. Chem.*, **25**, 294 (1964).
174. K. Lee, P. Turnbull and H. W. Moore, *J. Org. Chem.*, **60**, 461 (1995).
175. Z. Getahun, L. Jurd, P. S. Chu, C. M. Lin and E. Hamel, *J. Med. Chem.*, **35**, 1058 (1992).

176. G. D. Hartman, W. Halczenko and B. T. Phillips, *J. Org. Chem.*, **50**, 2423, 2427 (1985).
177. H. Gilman, C. E. Arntzen and F. J. Webb, *J. Org. Chem.*, **10**, 374 (1945).
178. H. Gilman and C. E. Arntzen, *J. Am. Chem. Soc.*, **69**, 1537 (1947).
179. J. J. Talley, *Synthesis*, 845 (1983).
180. J. J. Talley and I. A. Evans, *J. Org. Chem.*, **49**, 5267 (1984).
181. J. Heinicke, R. Kadyrov, M. K. Kindermann, M. Koesting and P. G. Jones, *Chem. Ber.*, **129**, 1547 (1996).
182. H. G. Selnick, M. L. Bourgeois, J. W. Butcher and E. M. Radzilowski, *Tetrahedron Lett.*, **34**, 2043 (1993).
183. H. Kurato, T. Tanaka, T. Sauchi, T. Kawase and M. Oda, *Chem. Lett.*, 947 (1997).
184. W. Davidsohn, B. R. Laliberté, C. M. Goddard and M. C. Henry, *J. Organomet. Chem.*, **36**, 283 (1972).
185. H. Gilman and R. D. Gorsich, *J. Am. Chem. Soc.*, **77**, 3919 (1955).
186. H. Gilman, R. D. Gorsich and B. J. Gai, *J. Org. Chem.*, **27**, 1023 (1962).
187. A. J. Bridges, W. C. Patt and T. M. Stickney, *J. Org. Chem.*, **55**, 773 (1990).
188. P. L. Coe, A. J. Waring and T. D. Yarwood, *J. Chem. Soc., Perkin Trans. 1*, 2729 (1995).
189. H. H. Ong, J. A. Profitt, V. B. Anderson, H. Kruse, J. C. Wilker and H. M. Geyer, *J. Med. Chem.*, **24**, 74 (1981).
190. P. L. Coe, R. Stephens and J. C. Tatlow, *J. Chem. Soc.*, 3227 (1962).
191. D. E. Fenton, *J. Organomet. Chem.*, **2**, 437 (1964).
192. H. Gilman and L. A. Woods, *J. Am. Chem. Soc.*, **66**, 1981 (1944).
193. Y. Yu, J. Sun and J. Chen, *J. Organomet. Chem.*, **533**, 13 (1997).
194. P. Aeberli and W. J. Houlihan, *J. Organomet. Chem.*, **67**, 321 (1974).
195. J. Porwisiak and M. Schlosser, *Chem. Ber.*, **129**, 233 (1996).
196. D. Hellwinkel, W. Lindner and H. J. Wilfinger, *Chem. Ber.*, **107**, 1428 (1974).
197. H. Gilman and B. J. Gaj, *J. Org. Chem.*, **22**, 447 (1957); V. Franzen and H.-I. Joschek, *Justus Liebigs Ann. Chem.*, **703**, 90 (1967).
198. M. D. Rausch, F. E. Tibbetts and H. B. Gordon, *J. Organomet. Chem.*, **5**, 493 (1966).
199. G. A. Moser, E. O. Fischer and M. D. Rausch, *J. Organomet. Chem.*, **27**, 379 (1971).
200. H. Gilman, L. S. Chen, G. J. Chen and C. Tamborski, *J. Organomet. Chem.*, **193**, 283 (1980).
201. B. Muke and T. Kauffmann, *Chem. Ber.*, **113**, 2739 (1980).
202. H. R. Roger and J. Houk, *J. Am. Chem. Soc.*, **104**, 522 (1982).
203. L. S. Chen, G. J. Chen and C. Tamborski, *J. Organomet. Chem.*, **251**, 139 (1983).
204. G. J. Chen and C. Tamborski, *J. Organomet. Chem.*, **251**, 149 (1983).
205. L. S. Chen, G. J. Chen and C. Tamborski, *J. Organomet. Chem.*, **215**, 281 (1981).
206. C. Eaborn and K. C. Pande, *J. Chem. Soc.*, 3200 (1960).
207. H. Gilman and S. M. Spatz, *J. Org. Chem.*, **16**, 1485 (1951).
208. J. P. Wibaut, A. P. de Jonge, H. G. P. van der Voort and P. P. H. L. Otto, *Recl. Trav. Chim. Pays-Bas*, **70**, 1054 (1951).
209. H. Malmberg and M. Nilsson, *Tetrahedron*, **42**, 3981 (1986).
210. H. E. French and K. Sears, *J. Am. Chem. Soc.*, **73**, 469 (1951).
211. A. Murray, W. W. Foreman and W. Langham, *J. Am. Chem. Soc.*, **70**, 1037 (1948).
212. A. Murray and W. Langham, *J. Am. Chem. Soc.*, **72**, 6289 (1950).
213. J. P. Wibaut and L. G. Heeringa, *Recl. Trav. Chim. Pays-Bas*, **74**, 1003 (1955).
214. M. Mallet and G. Quéguiner, *Tetrahedron*, **35**, 1625 (1979).
215. J. E. Parks, B. E. Wagner and R. H. Holm, *J. Organomet. Chem.*, **56**, 53 (1973).
216. K. Utimoto, N. Sakai and H. Nozaki, *J. Am. Chem. Soc.*, **96**, 5601 (1974).
217. K. Utimoto, S. N. Akai and H. Nozaki, *Tetrahedron Lett.*, **32**, 769 (1976).
218. D.-W. Cai, D. L. Hughes and T. R. Verhoeven, *Tetrahedron Lett.*, **37**, 2537 (1996).
219. M. A. Peterson and J. R. Mitchell, *J. Org. Chem.*, **62**, 8237 (1997).
220. X. Wang, P. Rabbat, P. O'Shea, R. Tillyer, E. J. J. Grabowski and P. J. Reider, *Tetrahedron Lett.*, **41**, 4335 (2000).
221. W. E. Parham and R. M. Piccirilli, *J. Org. Chem.*, **42**, 257 (1977).
222. D. J. Berry, B. J. Wakefield and J. D. Cook, *J. Chem. Soc. [C]*, 1227 (1971).
223. R. E. Banks, R. N. Haszeldine, E. Phillips and I. N. Young, *J. Chem. Soc. [C]*, 2091 (1967).
224. J. D. Cook, B. J. Wakefield and C. J. Clayton, *J. Chem. Soc., Chem. Commun.*, 150 (1967).
225. S. S. Dua and H. Gilman, *J. Organomet. Chem.*, **12**, 299 (1968).
226. J. D. Cook and B. J. Wakefield, *J. Organomet. Chem.*, **13**, 15 (1968).

227. D. J. Berry and B. J. Wakefield, *J. Chem. Soc. [C]*, 2342 (1969).
228. H. Gilman and T. S. Soddy, *J. Org. Chem.*, **22**, 565 (1957).
229. R. Waack and M. A. Doran, *J. Org. Chem.*, **32**, 3396 (1967).
230. W. Chen, E. K. Stephenson, M. P. Cava and Y. A. Jackson, *Org. Synth.*, **70**, 151 (1992).
231. J. M. Muchowski and R. Naef, *Helv. Chim. Acta*, **67**, 1168 (1984).
232. A. P. Kozikowski and X.-m. Cheng, *J. Org. Chem.*, **49**, 3239 (1984).
233. M. Amat, S. Halida, S. Sathyanarayana and J. Bosch, *J. Org. Chem.*, **59**, 10 (1994).
234. M. Amat, S. Halida and J. Bosch, *Tetrahedron Lett.*, **35**, 793 (1994).
235. M. Amat, S. Halida, S. Sathyanarayana and J. Bosch, *Org. Synth.*, **74**, 248 (1997).
236. J. W. Pavlik and E. M. Kurzweil, *J. Heterocycl. Chem.*, **29**, 1357 (1992).
237. R. Hüttel and M. E. Schön, *Justus Liebigs Ann. Chem.*, **625**, 55 (1959).
238. D. E. Butler and H. A. DeWald, *J. Org. Chem.*, **36**, 2542 (1971).
239. K. L. Kirk, *J. Heterocycl. Chem.*, **22**, 57 (1985).
240. P. G. Apen and P. G. Rasmussen, *J. Heterocycl. Chem.*, **29**, 1091 (1992).
241. B. Iddon, A. K. Petersen, J. Becher and N. J. Christensen, *J. Chem. Soc., Perkin Trans. 1*, 1475 (1995).
242. B. Iddon and N. Khan, *J. Chem. Soc., Perkin Trans. 1*, 735 (1982).
243. B. Iddon and N. Khan, *J. Chem. Soc., Perkin Trans. 1*, 1445 (1987).
244. S. Gronowitz and G. Sörlin, *Acta Chem. Scand.*, **15**, 1419 (1961).
245. Y. Fukuyama, T. Miwa and T. Tokoroyama, *Synthesis*, 443 (1974).
246. D. Florentin, B. P. Roques and M. C. Fournie-Zaluski, *Bull. Soc. Chim. Fr.*, 1999 (1976).
247. M. C. Zaluski, M. Robba and M. Bonhomme, *Bull. Soc. Chim. Fr.*, 1838 (1970).
248. R. Sornay, J. M. Meunier and P. Fournari, *Bull. Soc. Chim. Fr.*, 990 (1971).
249. P. Bury, G. Hareau, P. Kocieński and D. Dhanak, *Tetrahedron*, **50**, 8793 (1994).
250. Z. N. Nazarova, B. A. Tertov and Y. A. Gabaraeva, *Khim. Geterotsikl. Soedin.*, 746 (1967); *Chem. Abstr.*, **68**, 13021m (1968).
251. E. Campaigne and W. O. Foye, *J. Am. Chem. Soc.*, **70**, 3941 (1948).
252. S.-O Lawesson, *Arkiv Kemi*, **11**, 387 (1957); *Chem. Abstr.*, **52**, 1136f (1958).
253. P. Moses and S. Gronowitz, *Arkiv Kemi*, **18**, 119 (1961); *Chem. Abstr.*, **56**, 10173c (1962).
254. E. Campaigne and R. B. Rogers, *J. Heterocycl. Chem.*, **10**, 963 (1973).
255. I. Haiduc and H. Gilman, *Rev. Roum. Chem.*, **16**, 305 (1971); *Chem. Abstr.*, **75**, 36230n (1971).
256. M. D. Rausch, T. R. Criswell and A. K. Ignatowicz, *J. Organomet. Chem.*, **13**, 419 (1968).
257. Y. K. Yurev, N. K. Sadovaya and E. A. Grekova, *Zh. Obshch. Khim.*, **34**, 847 (1964); *Chem. Abstr.*, **60**, 15817d (1964).
258. S. Gronowitz and T. Freyd, *Acta Chim. Scand.*, **24**, 2656 (1970).
259. R. A. Murphy, H. F. Kung, M.-P. Kung and J. Billings, *J. Med. Chem.*, **27**, 171 (1990).
260. P. Groziak and L. Wei, *J. Org. Chem.*, **57**, 3776 (1992).
261. B. H. Lipshutz and W. Hagen, *Tetrahedron Lett.*, **33**, 5865 (1992).
262. F. Leroux, unpublished results (2002).
263. H. Mahler and M. Braun, *Chem. Ber.*, **124**, 1379 (1991).
264. M. Braun and K. Opdenbusch, *Justus Liebigs Ann. Chem.*, 141 (1997).
265. D. Granjean and P. Pale, *Tetrahedron Lett.*, **34**, 1155 (1993).
266. M. Mühlebach, M. Neuenschwander and P. Engel, *Helv. Chim. Acta*, **76**, 2089 (1993).
267. D. Seyferth and R. L. Lambert, *J. Organomet. Chem.*, **88**, 287 (1975).
268. R. A. Finnegan, *Tetrahedron Lett.*, 429 (1963).
269. G. G. Eberhardt and W. A. Butte, *J. Org. Chem.*, **29**, 2928 (1964); G. G. Eberhardt, *J. Organomet. Chem. Rev.*, **1**, 491 (1966).
270. M. Schlosser, *J. Organomet. Chem.*, **8**, 9 (1967).
271. M. Schlosser, *Modern Synth. Meth.*, **6**, 227 (1992).
272. M. Schlosser and P. Weiß, *Synthesis*, 257 (1970).
273. M. Schlosser and S. Strunk, *Tetrahedron Lett.*, **25**, 741 (1984).
274. G. Katsoulos, S. Takagishi and M. Schlosser, *Synlett*, 731 (1991).
275. E. Marzi, F. Mongin, A. Spitaleri and M. Schlosser, *Eur. J. Org. Chem.*, 2911 (2001).
276. M. Schlosser, F. Mongin, J. Porwisiak, W. Dmowski, H. H. Büker and N. M. M. Nibbering, *Chem. Eur. J.*, **4**, 1279 (1998).
277. M. Schlosser and H. Geneste, *Chem. Eur. J.*, **4**, 1969 (1998).
278. M. Stähle, R. Lehmann, J. Kramař and M. Schlosser, *Chimia*, **39**, 229 (1985).
279. M. Schlosser, *Pure Appl. Chem.*, **60**, 1627 (1988).

280. M. Schlosser, J. Hartmann, M. Stähle, J. Kramař, A. Walde and A. Mordini, *Chimia*, **40**, 306 (1986).
281. R. A. Finnegan and R. S. McNees, *J. Org. Chem.*, **29**, 3234 3241 (1964).
282. J. Hartmann and M. Schlosser, *Helv. Chim. Acta*, **59**, 453 (1976).
283. L. Garamszegi and M. Schlosser, *Chem. Ber.*, **130**, 77 (1997).
284. J. Kramař, Doctoral Dissertation, Université de Lausanne, 1978, pp. 20–30.
285. P. Gros, Y. Fort and P. Caubère, *J. Chem. Soc., Perkin Trans. 1*, 1685 (1998).
286. A. Mordini, E. Ben Rayana, C. Margot and M. Schlosser, *Tetrahedron*, **46**, 2401 (1990).
287. C. Margot, M. Rizzolio and M. Schlosser, *Tetrahedron*, **46**, 2411 (1990).
288. C. Margot, Q. Wang and M. Schlosser, *Tetrahedron*, **46**, 2425 (1990).
289. F. Faigl, E. Marzi and M. Schlosser, *Chem. Eur. J.*, **6**, 771 (2000).
290. E. Baston, Q. Wang and M. Schlosser, *Tetrahedron Lett.*, **41**, 667 (2000).
291. E. Baston, R. Maggi, K. Friedrich and M. Schlosser, *Eur. J. Org. Chem.*, 3985 (2001).
292. R. Lehmann and M. Schlosser, *Tetrahedron Lett.*, **25**, 745 (1984).
293. M. Schlosser and J. Hartmann, *Angew. Chem.*, **85**, 544 (1973); *Angew. Chem., Int. Ed. Engl.*, **12**, 508 (1973).
294. D. J. Peterson and H. R. Hays, *J. Org. Chem.*, **30**, 1939 (1965).
295. H. Ahlbrecht and H. Dollinger, *Tetrahedron Lett.*, **25**, 1353 (1984).
296. D. J. Peterson, *J. Organomet. Chem.*, **21**, P63 (1970).
297. M. Schakel, M. P. Aarnts and G. W. Klumpp, *Recl. Trav. Chim. Pays-Bas*, **109**, 305 (1990).
298. S. T. Kerrick and P. Beak, *J. Am. Chem. Soc.*, **113**, 9708 (1991).
299. D. M. Hodgson and S. L. M. Norsikian, *Org. Lett.*, **3**, 461 (2001).
300. J. J. Eisch and J. E. Galle, *J. Am. Chem. Soc.*, **98**, 4646 (1976).
301. G. A. Molander and K. Mautner, *J. Org. Chem.*, **54**, 4042 (1989).
302. N. S. Mani and C. A. Townsend, *J. Org. Chem.*, **62**, 636 (1997).
303. B. Folleas, I. Marek, J.-F. Normant and L. Saint-Jalmes, *Tetrahedron Lett.*, **39**, 2973 (1998).
304. S. Large, N. Roques and B. R. Langlois, *J. Org. Chem.*, **65**, 8848 (2000).
305. R. C. Gadwood, M. C. Rubino, S. C. Nagarajan and S. T. Michel, *J. Org. Chem.*, **50**, 3255 (1985).
306. P. Beak, S.-D. Wu, E. K. Yum and Y. M. Jun, *J. Org. Chem.*, **59**, 276 (1994).
307. Y. S. Park and P. Beak, *Tetrahedron*, **52**, 12333 (1996).
308. L. Pauling, Kekule Lecture, London, 15 Sept, 1958; *The Nature of the Chemical Bond*, 3rd edn., Cornell University Press, Ithaca, 1960, pp. 136–142, Sepc. 138.
309. C. Dumont and M. Vidal, *Bull. Soc. Chim. Fr.*, 2301 (1973).
310. G. L. Closs, in *Advances Alicyclic Chemistry*, (Eds. H. Hart and G. I. Karabatsos), Vol. 1, Academic Press, New York, 1966, p. 102.
311. A. R. Katritzky, J.-q. Li and N. Malhotra, *Justus Liebigs Ann. Chem.*, 843 (1992).
312. G. Stork, C. S. Shiner, C.-W. Cheng and R. L. Polt, *J. Am. Chem. Soc.*, **108**, 304 (1986).
313. D. Hänssgen and E. Odenhausen, *Chem. Ber.*, **112**, 2389 (1979).
314. J. Schulze, R. Boese and G. Schmid, *Chem. Ber.*, **114**, 1297 (1981).
315. U. Schöllkopf and P. Hänßle, *Justus Liebigs Ann. Chem.*, **763**, 208 (1972).
316. E. M. Dexheimer and L. Spialter, *J. Organomet. Chem.*, **107**, 229 (1976).
317. I. Hoppe and U. Schöllkopf, *Justus Liebigs Ann. Chem.*, 1474 (1980).
318. J. E. Baldwin, G. A. Höfle and O. W. Lever, *J. Am. Chem. Soc.*, **96**, 7125 (1974).
319. J. Hartmann, M. Stähle and M. Schlosser, *Synthesis*, 888 (1974).
320. P. G. McDougal, J. C. Rico and D. VanDerveer, *J. Org. Chem.*, **51**, 4492 (1986).
321. K. J. H. Kruithof, R. F. Schmitz and G. W. Klumpp, *Recl. Trav. Chim. Pays-Bas*, **104**, 1 (1985).
322. T. Cuvigny, M. Julia and C. Rolando, *J. Chem. Soc., Chem. Commun.*, 8 (1984).
323. T. Cuvigny, M. Julia and C. Rolando, *Tetrahedron Lett.*, **28**, 2587 (1987).
324. F. G. Drakesmith, R. D. Richardson, O. J. Stewart and P. Tarrant, *J. Org. Chem.*, **33**, 286 (1968).
325. F. G. Drakesmith, O. J. Stewart and P. Tarrant, *J. Org. Chem.*, **33**, 472 (1968).
326. P. A. Morken, H.-Y. Lu, A. Nakamura and D. J. Burton, *Tetrahedron Lett.*, **32**, 4271 (1991).
327. D. J. Burton, T. D. Spawn, P. L. Heinze, A. R. Bailey and S. Shin-ya, *J. Fluorine Chem.*, **44**, 167 (1989).
328. T. Taguchi, T. Morikawa, O. Kitagawa, T. Mishima and Y. Kobayashi, *Chem. Pharm. Bull.*, **33**, 5137 (1985).

329. P. A. Morken, H.-Y. Lu, A. Nakamura and D. J. Burton, *Tetrahedron Lett.*, **32**, 4271 (1991).
330. E. Castagnetti and M. Schlosser, *Chem. Eur. J.*, **8**, 799 (2000).
331. K. Ziegler and H. Zeiser, *Ber. Dtsch. Chem. Ges.*, **63**, 1847 (1930).
332. A. G. Brook, *Acc. Chem. Res.*, **7**, 77 (1974).
333. Z. Rappoport and Y. Apeloig (Eds.), *The Chemistry of Organic Silicon Compounds*, Vol. 2 Parts 1–3, Wiley, Chichester, 1998.
334. A. G. Brook and J. D. Pascoe, *J. Am. Chem. Soc.*, **93**, 6224 (1971).
335. For a good review, see R. West, in *Advances in Organometallic Chemistry* (Eds F. G. A. Stone and R. West), Vol. 16, Academic Press, New York, 1977, p. 1.
336. H. J. Reich, J. J. Rusek and R. E. Olson, *J. Am. Chem. Soc.*, **101**, 2225 (1979).
337. H. J. Reich, R. C. Holtan and C. Bolm, *J. Am. Chem. Soc.*, **112**, 5609 (1990).
338. H. J. Reich, R. E. Olson and M. C. Clark, *J. Am. Chem. Soc.*, **102**, 1423 (1980).
339. I. Kuwajima, K. Matsumoto and T. Inoue, *Chem. Lett.*, 1239 (1979).
340. S. Murai, I. Ryu, J. Iriguchi and N. Sonoda, *J. Am. Chem. Soc.*, **106**, 2440 (1984).
341. I. Kuwajima and M. Kato, *J. Chem. Soc., Chem. Commun.*, 708 (1979).
342. I. Kuwajima, M. Kato and A. Mori, *Tetrahedron Lett.*, **21**, 2745 (1980).
343. T. Hu and E. J. Corey, *Org. Lett.*, **4**, 2441 (2002).
344. S. Lin and E. J. Corey, *J. Am. Chem. Soc.*, **118**, 8765 (1996).
345. K. Takeda, M. Fujisawa, T. Makino, E. Yodhii and K. Yamaguchi, *J. Am. Chem. Soc.*, **115**, 9351 (1993).
346. K. Takeda, J. Nakatani, H. Nakamura, K. Sako, E. Yoshii and K. Yamaguchi, *Synlett*, 841 (1993).
347. K. Takeda, A. Nakajima, M. Takeda, Y. Okamoto, T. Sato, E. Yoshii, T. Koizumi and M. Shiro, *J. Am. Chem. Soc.*, **120**, 4947 (1998).
348. Y. Ito, T. Matsuura and M. Murakami, *J. Am. Chem. Soc.*, **109**, 7888 (1987).
349. T. Honda and M. Mori, *J. Org. Chem.*, **61**, 1196 (1996).
350. P. F. Hudrlik and A. M. Hudrlik, in *Advances in Silicon Chemistry*, Vol. 2, JAI Press, Greenwich, C.T., 1993, p. 1.
351. H. Shinokubo, K. Miura, K. Oshima and K. Utimoto, *Tetrahedron Lett.*, **34**, 1951 (1993).
352. H. Shinokubo, K. Miura, K. Oshima and K. Utimoto, *Tetrahedron*, **52**, 503 (1996).
353. R. P. Woodbury and M. W. Rathke, *J. Org. Chem.*, **43**, 1947 (1978).
354. M. Isobe, M. Kitamura and T. Goto, *Tetrahedron Lett.*, 3465 (1979).
355. M. Isobe, M. Kitamura and T. Goto, *Tetrahedron Lett.*, **21**, 4727 (1980).
356. L. F. Tietze, H. Geissler, J. A. Gewert and U. Jakobi, *Synlett*, 511 (1994).
357. A. B. Smith III and A. M. Boldi, *J. Am. Chem. Soc.*, **119**, 6925 (1997).
358. A. R. Katrizky and D. Toader, *J. Am. Chem. Soc.*, **119**, 9321 (1997).
359. A. R. Katrizky, D. Toader and X. Wang, *J. Org. Chem.*, **63**, 9978 (1998).
360. R. H. Shapiro, *Org. React.*, **23**, 405 (1976).
361. A. R. Chamberlin and S. H. Bloom, *Org. React.*, **39**, 1, (1990).
362. R. H. Shapiro and E. C. Hornaman, *J. Org. Chem.*, **39**, 2302 (1974).
363. A. R. Chamberlin, J. E. Stemke and F. T. Bond, *J. Org. Chem.*, **43**, 147 (1978).
364. C. A. Bunnell and P. L. Fuchs, *J. Org. Chem.*, **42**, 2614 (1977).
365. P. C. Traas, H. Boelens and H. J. Tokken, *Tetrahedron Lett.*, 2287 (1976).
366. T. K. Jones and S. E. Denmark, *Helv. Chim. Acta.*, **66**, 2377 (1983).
367. R. T. Taylor, C. R. Degenhart, W. P. Melega and L. A. Paquette, *Tetrahedron Lett.*, 159 (1977).
368. L. A. Paquette, E. E. Fristad, D. S. Dime and T. R. Bailey, *J. Org. Chem.*, **45**, 3071 (1980).
369. D. G. Mislankar and S. D. Darling, *Tetrahedron Lett.*, **22**, 4619 (1981).
370. B. Cazes, E. Guillet, S. Julia and O. Ruel, *J. Organomet. Chem.*, **177**, 67 (1979).
371. A. S. Kende and L. N. Jungheim, *Tetrahedron Lett.*, **21**, 3849 (1980).
372. T. H. Chan, M. Baldassarre and D. Massuda, *Synthesis*, 801 (1976).
373. A. R. Chamberlin and F. T. Bond, *Synthesis*, 44 (1977).
374. R. G. Daniel and L. A. Paquette, *Organometallics*, **1**, 1449 (1982).
375. K. Maruoka, M. Oishi and H. Yamamoto, *J. Am. Chem. Soc.*, **118**, 2289 (1996).
376. E. J. Corey, J. Lee and B. E. Roberts, *Tetrahedron Lett.*, **38**, 8915 (1997).
377. A. K. Minks and S. Voerman, *Entomol. Exp. Appl.*, **16**, 541 (1973).
378. T. Satoh, Y. Kaneko and K. Yamakawa, *Tetrahedron Lett.*, **27**, 2379 (1986).
379. T. Satoh and K. Yamakawa, *Synlett*, 455 (1992).

380. T. Satoh, *Chem. Rev.*, **96**, 3303 (1996).
381. T. Satoh, Y. Kanedo and K. Yamakawa, *Bull. Chem. Soc. Jpn.*, **59**, 2463 (1986).
382. T. Satoh, T. Oohara, Y. Ueda and K. Yamakawa, *J. Org. Chem.*, **54**, 3130 (1989).
383. T. Satoh and K. Horiguchi, *Tetrahedron Lett.*, **36**, 8235 (1995).
384. T. Satoh, T. Oohara and K. Yamakawa, *Tetrahedron Lett.*, **29**, 4093 (1988).
385. T. Satoh, M. Ozawa, K. Takano and M. Kudo, *Tetrahedron Lett.*, **39**, 2345 (1998).
386. T. Satoh, M. Ozawa, K. Takano, T. Chyouma and A. Okawa, *Tetrahedron*, **56**, 4415 (2000).
387. T. Satoh, N. Itoh, S. Watanabe, H. Koide, H. Matsuno, K. Matsuda and K. Yamakawa, *Tetrahedron*, **51**, 9327 (1995).
388. T. Satoh, N. Hanaki, Y. Kuramochi, Y. Inoue, K. Hosaya and K. Sakai, *Tetrahedron*, **58**, 2533 (2002).
389. T. Satoh, N. Yamada and T. Asano, *Tetrahedron Lett.*, **39**, 6935 (1998).
390. T. Satoh, N. Itoh, K. Gengyo and K. Yamakawa, *Tetrahedron Lett.*, **33**, 7543 (1992).

CHAPTER 10

Directed metallation of aromatic compounds

JONATHAN CLAYDEN

Department of Chemistry, University of Manchester, Oxford Road,
Manchester M13 9PL, UK
Fax: +44 161 275 4939; e-mail: j.p.clayden@man.ac.uk

The Chemistry of Organolithium Compounds. Edited by Z. Rappoport and I. Marek
ISBN: 0-470-84339-X

I. ORTHOLITHIATION OF CARBOCYCLIC AROMATIC COMPOUNDS

A. Introduction: Mechanism

Ortholithiation—the directed metallation of an aromatic ring adjacent to a heteroatom-containing functional group—has arguably overtaken classical electrophilic aromatic substitution as the principal means of making regiospecifically substituted aromatic rings. Landmarks in the development of ortholithiation since the first metallations of anisole by Gilman[1] and by Wittig[2] have included the publication of the extensive and seminal review in the area by Gschwend and Rodriguez[3], and more recently the introduction and development of amide and oxazoline-based directing groups by Beak[4], Meyers[5] and Snieckus[6,7]. Detailed reviews[3,7,8] of the area have been published.

Ortholithiations typically involve the deprotonation of a substituted aromatic ring by an organolithium—usually *n*-, *s*- or *t*-butyllithium or (for more electron-deficient aromatic rings) LDA or LiTMP. Given that benzene is some ten orders of magnitude more acidic than butane, thermodynamics pose no barrier to the removal of any proton attached to an aromatic ring by butyllithium. However, the kinetics of most such reactions impede their usefulness: *n*-butyllithium deprotonates benzene in hexane negligibly after 3 h at room temperature[8,9]. The problem is that the reaction of hexameric *n*-BuLi (its structure in hydrocarbons)[10] is extremely slow, and only after a lithium-coordinating reagent such as THF or TMEDA has broken up the BuLi aggregates can lithiation proceed at a reasonable rate. Addition of TMEDA to a BuLi/benzene/hydrocarbon mixture is sufficient to do this—the less aggregated BuLi–TMEDA complexes deprotonate benzene at room temperature almost quantitatively (Scheme 1)[9].

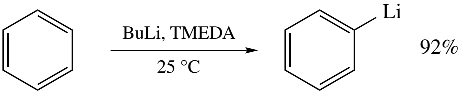

SCHEME 1

Ortholithiation is considered to work by providing the alkyllithium with a point of coordination, increasing reactivity specifically in the locality of the coordination site (typically a basic heteroatom) of the substrate, and hence directing the regioselectivity[11]. Although there is evidence that this is not the case with weaker ortholithiation directors (see below), it can generally be assumed that for a strong director coordination between substrate and the alkyllithium, perhaps entailing deaggregation of the alkyllithium, marks the first step towards lithiation, whether ortholithiation or not. IR and kinetic studies[12–14] have shown, for example, that a substrate–alkyllithium complex is formed en route to lithiation in benzylic positions α to nitrogen substituents such as amides, and the functional groups involved in these α-lithiations are essentially the same as those which direct ortholithiation. It seems reasonable to suppose that ortholithiation, forming the more basic phenyl anion, is even more in need of assistance than the benzylic α-lithiation.

Given that BuLi–TMEDA will deprotonate benzene[9], a similar coordination of BuLi *with the substrate* should be sufficient to allow the deprotonation of substituted aromatics. And indeed, amine **1**, whose aromatic protons are no more acidic than those of benzene, is deprotonated rapidly (much faster than benzene)[15,16] and regioselectively (at the 2-position, closest to the directing group) (Scheme 2)[17].

Attempts to use intermolecular and intramolecular kinetic isotope effects (KIE's) to identify a complexation step during ortholithiation have so far been inconclusive. Both intramolecular and intermolecular KIE's for the deprotonation of **2** and **3** by *s*-BuLi

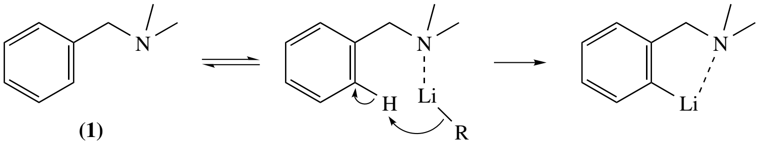

SCHEME 2

at −78 °C have values too high to measure, perhaps because complexation is fast and reversible but deprotonation is slow (Scheme 3)[18].

Stratakis[19] showed that a similar situation exists for the deprotonation of anisole by BuLi in Et_2O or TMEDA. The kinetic isotope effects are much lower, but give no evidence regarding the existence of an anisole−BuLi complex prior to deprotonation.

Detailed NMR and theoretical studies have identified and characterized a number of the complexes along the proposed reaction pathways for anisole, 1,2-dimethoxybenzene and *N*,*N*-dimethylaniline[20,21]. For example, anisole deaggregates the BuLi hexamer to form a tetrameric BuLi−anisole complex **4**. Adding TMEDA displaces the anisole from the tetramer and breaks it down further to give a BuLi−TMEDA dimer **5**, which deprotonates anisole at >0 °C yielding **6** (Scheme 4).

It has usually been assumed that the lithiation step involves loss of TMEDA and re-formation of a BuLi−anisole complex prior to the deprotonation itself. However, the kinetics of the deprotonation step are inconsistent with this proposition: both TMEDA molecules remain part of the complex during the deprotonation[22], which may therefore involve no O−Li coordination and be directed purely by the acidifying effect on nearby protons of the σ-electron-withdrawing MeO substituent[23].

Acidity is evidently the only factor directing lithiation when coordination to the heteroatom is electronically or geometrically impossible. For example, fluorobenzene is slowly lithiated by BuLi−TMEDA at −50 °C, despite the unlikelihood of a strong F−Li complex forming (in contrast with anisole, no PhF−BuLi complex is discernible by NMR[20]).

As far as synthetic utility goes, it is clear that rings bearing electron-withdrawing substituents which acidify nearby protons (by an inductive effect) are usually (not always) lithiated much more rapidly than those which acidify nearby protons only weakly or not at all. Although steric effects are undoubtedly involved as well, the differing regioselectivities in the series of peri- and ortholithiations of 1-substituted naphthalenes **7** shown in Table 1[24,25] serve to illustrate the increasing importance of acidity as substituents become more inductively withdrawing. While a group X directing lithiation by coordination can promote lithiation at either the *ortho* or the *peri* position of **7**, a group whose directing effect derives mainly from its ability to acidify nearby protons can direct lithiation only to the *ortho* position (Scheme 5). A study[26] of 1-methoxynaphthalene (**7**, X = OMe) showed that the ortholithiated product is obtained with *n*-BuLi under kinetic control (a kinetic isotope effect is observed) while with *t*-BuLi the perilithiated product is obtained under thermodynamic control (with no kinetic isotope effect).

The aminoalkyl substituted compound analogous to **1** (entry 1) is lithiated solely in the *peri* position, presumably because this is a purely coordination-driven lithiation, and the geometry for perilithiation by the amine-complexed BuLi is more favourable than the geometry for ortholithiation. The same is true for other amino-substituted naphthalenes (entries 2–4). With alkyl groups themselves bearing electron-withdrawing substituents, ortholithiation begins to make an appearance (entries 5 and 6). Acidity seems to become more important when the naphthalene bears the more inductively withdrawing oxygen substituents (entries 7–10)—they give either peri- or ortholithiation (or both) depending

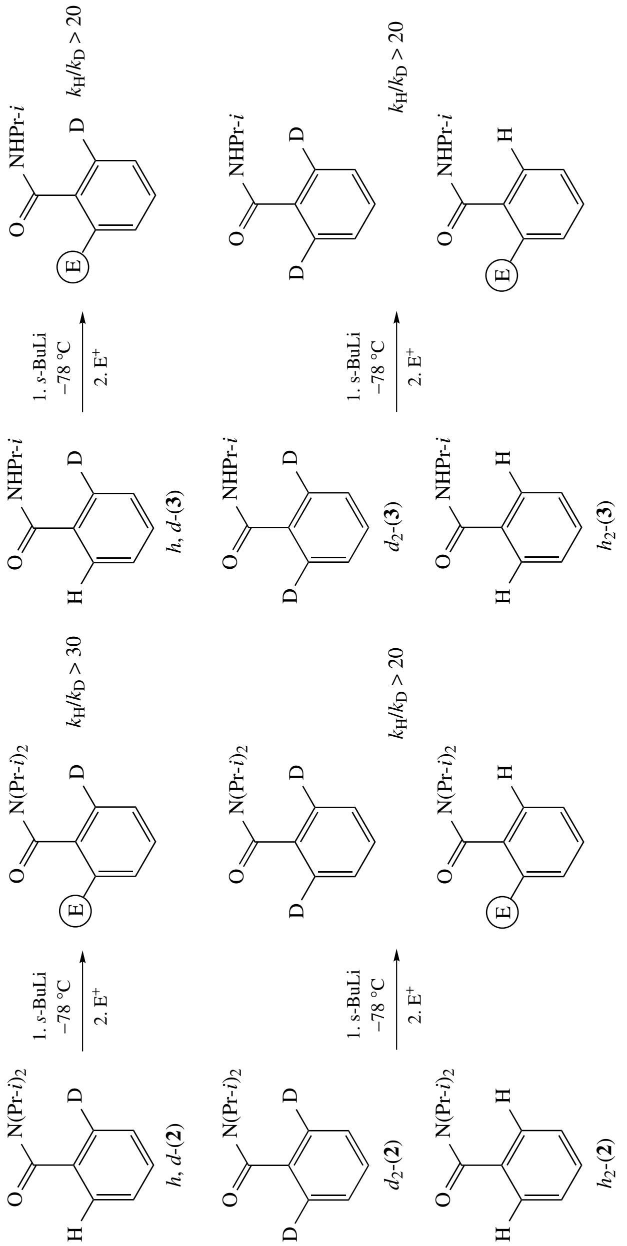
h, d-(2)
d2-(2)
h2-(2)
1. s-BuLi
−78 °C
2. E+
kH/kD > 30
kH/kD > 20
h, d-(3)
d2-(3)
h2-(3)
kH/kD > 20
kH/kD > 20

SCHEME 3

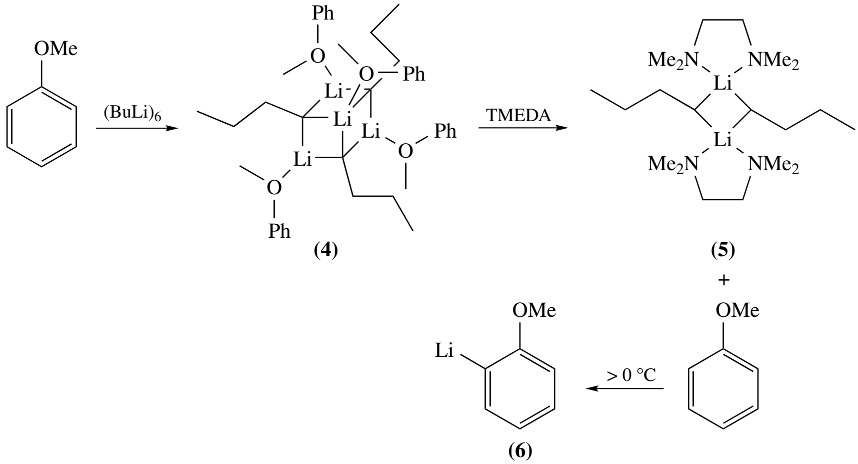

SCHEME 4

TABLE 1. Ortho- and perilithiation of 1-substituted naphthalenes[24]

Entry^{Ref}	X	Conditions	E$^+$	Yield *peri*-**8**	Yield *ortho*-**8**
1^{27}	CH_2NMe_2	BuLi, Et_2O, hexane, 20 °C	Ph_2CO	58 (91)[a]	0 (9)[a]
2^{28}	NH_2	BuLi x 3, Et_2O, Δ	CO_2	20	0
$3^{29,30}$	NLiR	*t*-BuLi, Et_2O, 20 °C	D_2O	(100)[a]	(0)[a]
$4^{31,32}$	NMe_2	BuLi, Et_2O, 20 °C	DMF	76	0
5^{33}	$CH(NEt_2)OLi$	BuLi, PhH, Δ	DMF	32	2
6^{33}	$CH(OMe)_2$	*t*-BuLi, Et_2O	MeI	27	13
7^{34}	OH	*t*-BuLi, TMEDA, 20 °C	various	(100)[a]	(0)[a]
8^{35}	OH	*n*-BuLi, THP, 50 °C	Me_2S_2	50	19
$9^{26,36}$	OMe	*t*-BuLi, cyclohexane, 20 °C	CO_2	35	0
10^{26}	OMe	*n*-BuLi, TMEDA, 20 °C	CO_2	0	59
11^{37}	OMOM	*n*-BuLi, TMEDA	RCHO	0	73
12^{7}	$OCONR_2$	*s*-BuLi, TMEDA, THF, −78 °C	MeI	0	90
$13^{24,38}$	$CONR_2$	*s*-BuLi, TMEDA, THF, −78 °C	various	0	76–93
14^{39}	SONHBu-*t*	BuLi, THF, 25 °C	CO_2	14	0
15^{40}	SO_2Bu-*t*	BuLi, −70 °C	CO_2	0	47

[a] Ratio in crude product.

on conditions. More strongly withdrawing and coordinating acetal (entry 11) and carbamate (entry 12) groups give even higher levels of ortholithiation, as does the strongly electron-withdrawing amide substituent (entry 13). For these last two or three entries, the geometry for coordination to a *peri*-lithium atom may also be very unfavourable. Interestingly, secondary sulphonamides (entry 14) also direct lithiation to the *peri*-position, perhaps by equilibration to the thermodynamic product via proton exchange with the starting material. The sulphone (entry 15), on the other hand, directs *ortho*.

The relative importance of coordination and acidity can furthermore depend on the base employed in the lithiation. Once coordinated to a basic solvent (TMEDA or THF, for example) alkyllithiums become less Lewis-acidic: they have a somewhat decreased tendency to be directed by coordination and acidity can become the dominant factor.

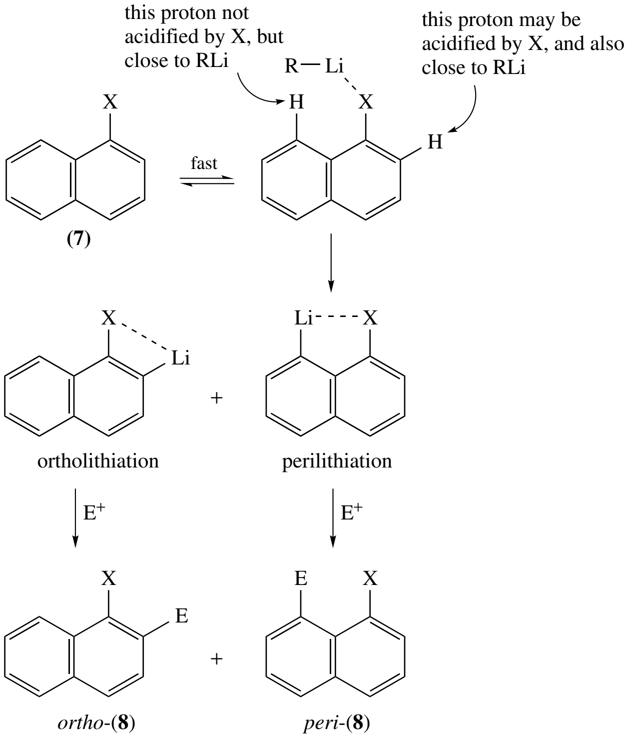

SCHEME 5

Deprotonation of **9** and **10** illustrates this effect: in the absence of TMEDA, deprotonation occurs *ortho* to the more Lewis-basic amino group, while in the presence of TMEDA, the deprotonation occurs *ortho* to the more electronegative, and therefore more acidifying, MeO group (Scheme 6)[41].

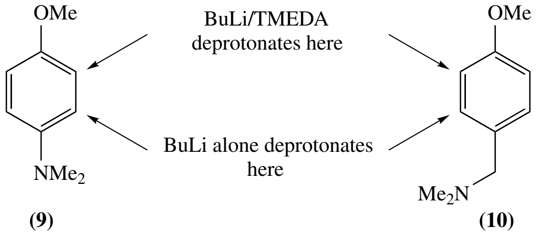

SCHEME 6

Coordination to strongly *ortho*-directing groups is responsible for the regiochemistry of some other reactions which do not involve ortholithiation. For example, while the electron-withdrawing nature of the oxazoline would be expected to direct the addition of the organolithium nucleophile to benzyne **11** towards the *meta* position, the major product that arises is the result of addition at the *ortho* position to give **12** (Scheme 7)[42].

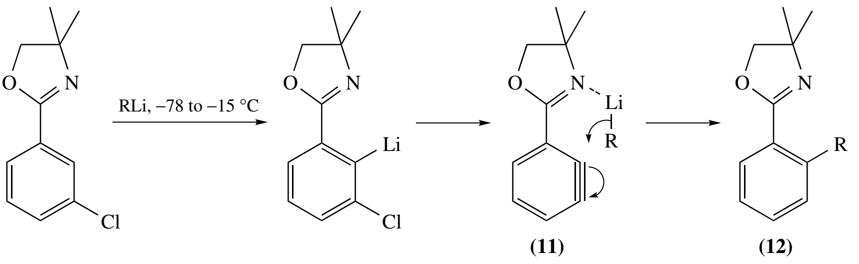

(11) **(12)**

SCHEME 7

By and large, the correlation between ring acidity and the rate of deprotonation is relatively loose: under the kinetically controlled conditions usually used for an ortholithiation reaction it is difficult to quantify 'acidity'. Fraser and coworkers have published a quantified scale of acidifying effect for a range of functional groups by measuring the extent of lithiation by lithium tetramethylpiperidide **13** (LiTMP) (p$K_a = 37.8$) using NMR spectroscopy (Scheme 8)[43]. The results are shown in Table 2. There is a moderately good correlation between pK_a and the *peri*- vs. *ortho*-directing ability summarised in Table 1. With lithium amide bases, lithiation becomes reversible and a pK_a scale of acidity is useful for determining lithiation regioselectivity.

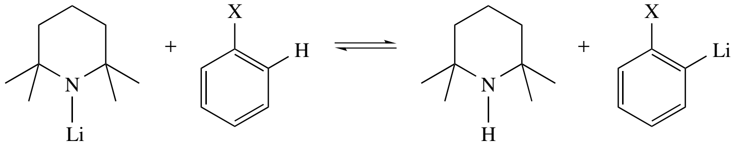

(13)

SCHEME 8

To summarize, ortholithiation is a reaction with two steps (complex-formation and deprotonation) in which two features (rate and regioselectivity of lithiation) are controlled by two factors (coordination between organolithium and a heteroatom and acidity of the proton to be removed). In some cases, some of these points are less important (acidity, for example, or the coordination step). The best directing groups tend to have a mixture of the basic properties required for good coordination to lithium and the acidic properties required for rapid and efficient deprotonation.

B. Classes of Directing Group

As far as their simple ability to direct metallation goes, functional groups may broadly be placed in the sequence shown in Scheme 9. Several studies of relative directing ability have been carried out[4, 41, 44–48], sometimes with conflicting results (though these may often be ascribed to differences in conditions, or whether the competition was inter- or intramolecular), and these studies are taken into account here. Also in the scheme is a guide to the conditions typically required for lithiation of a certain functional group. This is a picture painted with a broad brush, and is not intended to provide detailed information, but aims to give a general impression of the approach required for each class of functional group.

The most powerful classes, for several reasons, comprise carboxylic acid and carbonate-derived functions containing both nitrogen and oxygen: secondary and tertiary amides[7],

TABLE 2. pK_a and ortholithiation[43]

Entry	X	pK_a
1	CH_2NMe_2	$>40.3^a$
2	NHCOBu-*t*	$>40.3^a$
3	NMe_2	$>40.3^a$
4	OLi	$>40.3^a$
5	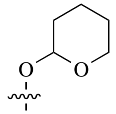	40.0
6	OMe	39.0
7	OPh	38.5
8	SO_2NEt_2	38.2
9	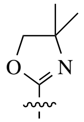	38.1
10	CN	38.1
11	CON(Pr-*i*)$_2$	37.8
12	$OCONEt_2$	37.2

[a]Not lithiated by LiTMP.

oxazolines[5,49] and carbamates[7]. We have grouped these functional groups into the 'N + O class'. Their importance stems firstly from their 'amphoteric' nature: they are all functional groups which have a highly basic heteroatom (the oxygen atom in the carbonyl group of an amide is among the most basic of neutral oxygen atoms in organic chemistry) and many are strongly electron-withdrawing groups which acidify the protons of the ring. Secondly, they are functional groups which are transformable to useful targets. They do nonetheless have a drawback: they all contain an electrophilic carbonyl group (or equivalent) which may itself suffer attack by the lithiating agent. Typically, therefore, they need to be highly sterically encumbered to prevent this, and this may make their subsequent removal or transformation difficult. Steric hindrance is avoidable if the functional group can be deactivated by deprotonation, and such amide and carbamate anions (and in fact many other anionic functional groups) are surprisingly powerful directors, considering they have little power to lower the acidity of the ring protons.

Sulphones and sulphonamides—the 'S + O class'—are similarly powerful directors[47], and do not suffer electrophilic attack at sulphur (though they occasionally suffer nucleophilic attack on the aromatic ring)[40,50] but are less useful because of their more limited synthetic applications[50,51]. Aryl *t*-butylsulphoxides are also powerful *ortho*-directors[52], but less hindered diaryl sulphoxides are susceptible to attack by organolithiums at sulphur[53].

Less powerful with regard to directing ability (they are less basic and less acidifying) but of high synthetic value are functional groups containing oxygen only (ethers, acetals, carboxylates... the 'O class') and nitrogen only (amines, imines, nitriles... the 'N class'). They typically direct lithiation more slowly or at higher temperatures, but in many cases have the advantage that they cannot be attacked by the organolithium reagent. No special structural features are therefore necessary and, for example, the simple methyl ethers of MOM acetals occurring in normal synthetic routes or even target molecules may be used as lithiation substrates. The most powerful members of the N class are those which can use a nitrogen lone pair to coordinate to the organolithium—in other words, those other than the anilines. In the O-class, the best directors are by contrast those in which the

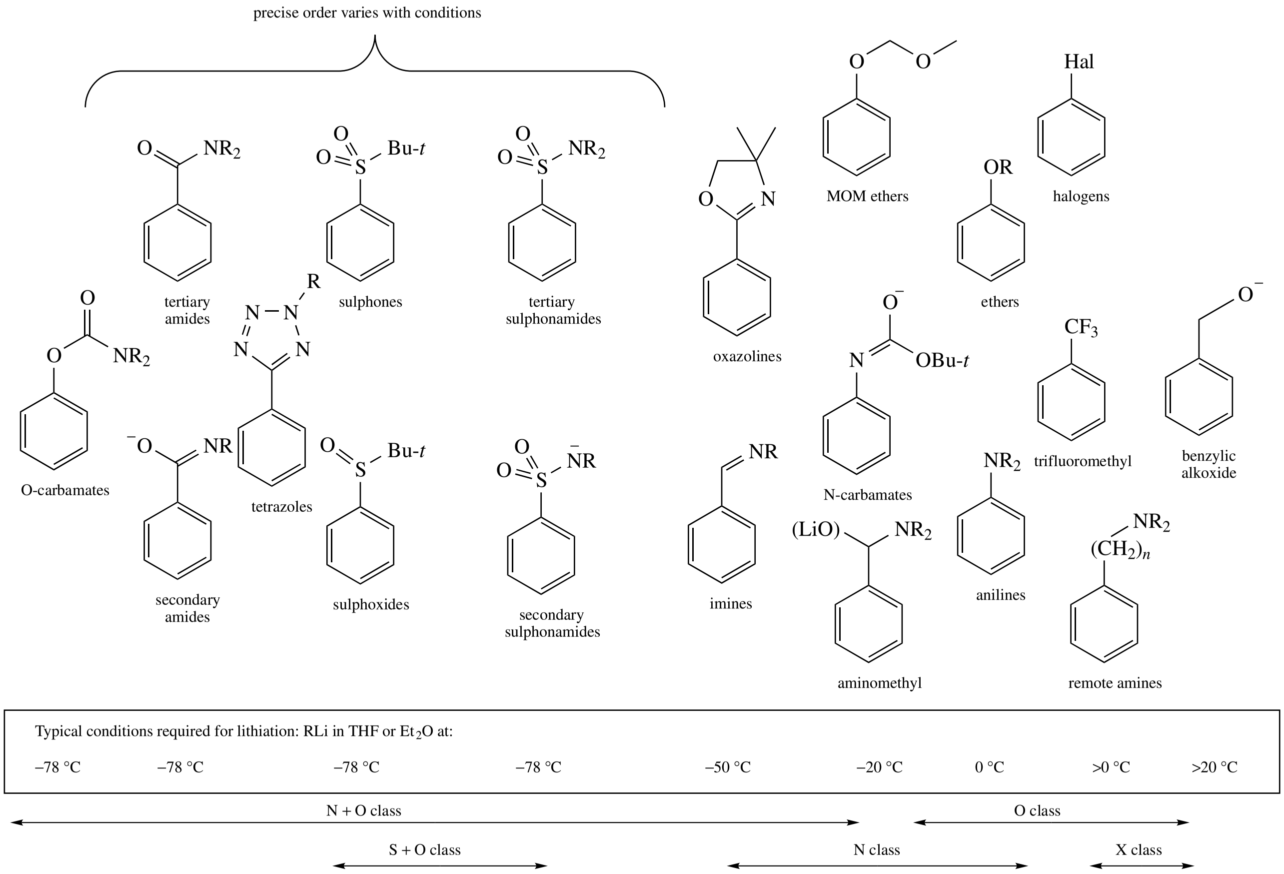
precise order varies with conditions
tertiary amides
sulphones
tertiary sulphonamides
oxazolines
MOM ethers
ethers
halogens
O-carbamates
tetrazoles
N-carbamates
trifluoromethyl
benzylic alkoxide
secondary amides
sulphoxides
secondary sulphonamides
imines
aminomethyl
anilines
remote amines
Typical conditions required for lithiation: RLi in THF or Et$_2$O at:
−78 °C
−78 °C
−78 °C
−78 °C
−50 °C
−20 °C
0 °C
>0 °C
>20 °C
N + O class
O class
S + O class
N class
X class

SCHEME 9

oxygen is attached to the ring, inductively acidifying nearby protons, and those which carry a second oxygen atom (an acetal, for example) for lithium coordination.

The halogens, the ‘X class’, are gaining importance as lithiation directors, particularly for the lithiation of heteroaromatics. Halogens direct by an inductive, acidifying effect alone, and work best when there are additional factors favouring deprotonation—if the aromatic ring is an electron-deficient heterocycle, for example. Halogens are susceptible to attack by organolithiums, and ortholithiated haloarenes are prone to elimination to give benzynes, so conditions must be carefully controlled: typically these directing groups are used in conjunction not with organolithiums but with LDA.

It is interesting to note the surprising fact that even a lithio substituent activates an aromatic ring towards lithiation: the deprotonation of phenyllithium is easier than the deprotonation of benzene[54]. More remote lithium substituents also have a directing effect, presumably mediated by a complexed TMEDA molecule: bromine–lithium exchange of **14** with excess BuLi in TMEDA gives an organolithium **15** which is deprotonated regioselectively on the ring *cis* to the first lithio substituent to give **16** (Scheme 10)[55].

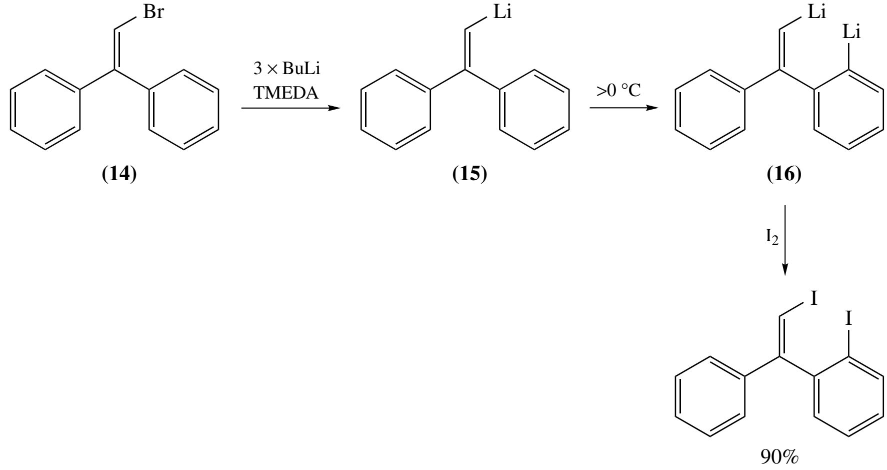

SCHEME 10

Double ortholithiation (to give a dilithiated ring) is usually feasible when two separate directing groups are involved, but using one group to direct simultaneously to both *ortho* positions usually fails[56]. Simultaneous triple lithiation has never been achieved even with three separate groups[56].

1. N + O class

a. Secondary and tertiary amides. Hauser and coworkers reported in 1973[57] that *N*,*N*-diethylbenzamide **17** is attacked at the carbonyl group by *n*-BuLi to give aryl ketone **18**. However, by using the hindered, non-nucleophilic base LiTMP Beak and coworkers were able to avoid attack at C=O and to ortholithiate **17**[58]. The product **19** immediately attacks another molecule of starting material (a recurring problem in $-CONEt_2$ ortholithiation chemistry) to yield 2-benzoyl benzamide **20** (Scheme 11). A similar reaction occurs with the diethylamide and *s*-BuLi, but not if TMEDA is added[59]—presumably the starting material’s own deprotonation then outpaces its attack by other newly ortholithiated molecules. For this reason, the addition of TMEDA is essential for the lithiation of diethyl amides in THF. *N*,*N*-Diisopropyl amides **21**, on the other hand, are almost completely resistant to attack at C=O, and can be ortholithiated without difficulty with *s*-BuLi, *t*-BuLi or even *n*-BuLi in the presence or absence of TMEDA. For practicality's sake, the most appropriate conditions with $-\mathrm{CONPr}\text{-}i_2$ amides are *s*-BuLi or *n*-BuLi in THF at $-78\,^{\circ}\mathrm{C}$ (no TMEDA required)[38].

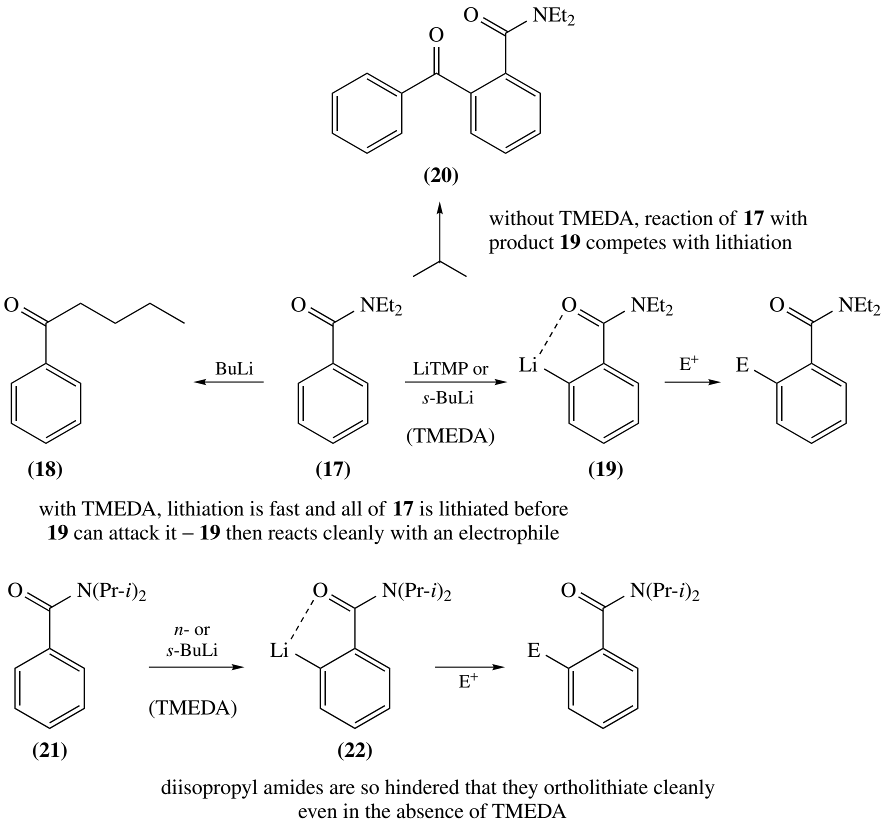

without TMEDA, reaction of **17** with product **19** competes with lithiation

with TMEDA, lithiation is fast and all of **17** is lithiated before **19** can attack it – **19** then reacts cleanly with an electrophile

diisopropyl amides are so hindered that they ortholithiate cleanly even in the absence of TMEDA

SCHEME 11

The ortholithiated products **19** and **22** will then react with a wide range of electrophiles: the only reported important exceptions are enolisable aldehydes and allylic halides. Products requiring these electrophiles are best made by first transmetallating the organolithium to a Grignard reagent with $\mathrm{MgCl_2}$[7] or copper salts[60].

N,*N*-Dimethyl amides are susceptible to attack at C=O, but can be successfully ortholithiated if kept cold. Keck and coworkers used successive ortholithiations of **23** in a route towards pancratistatin (Scheme 12)[61]. (Park and Danishefsky's similar route using *N*,*N*-diethylamides[62] suffered from difficulties removing the amide group.)

In more heavily substituted amides, the amide group is forced to lie perpendicular to the aromatic ring[38, 63]—even in **21** the amide and the ring are not coplanar[64]. Clearly this poses greater difficulties for ortholithiation, and Beak and coworkers have shown that the

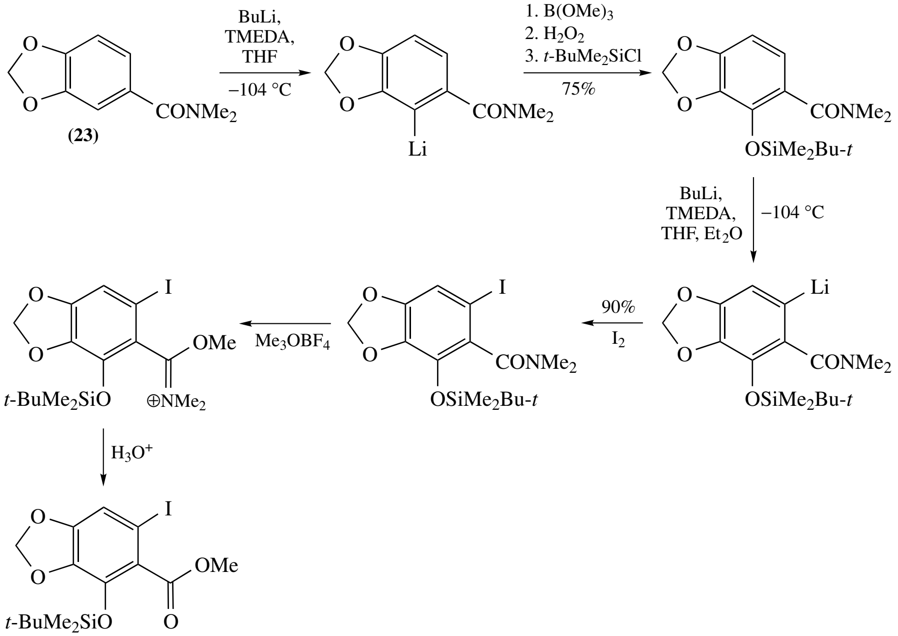

SCHEME 12

rate of lithiation is dependent on the angle between the amide plane and the plane of the ring[64]. With ring and amide perpendicular, a single lithium atom would be unable to bridge between O and C, and X-ray crystal structures of **22** and **25**[65] (Scheme 13) show that in fact ortholithiation of **21** and **24** gives organolithiums which are (at least in the solid state) bridged dimers, with one lithium atom more or less in the plane of the amide and the other more or less in the plane of the ring.

For the same reason that they resist attack at C=O by alkyllithiums, tertiary amides can be extremely difficult to hydrolyse—almost impossible in the case of $-\text{CONPr-}i_2$, and even $-\text{CONEt}_2$ amides are stable to 6 M HCl for 72 h. For reactions in which an amide is not required in the product, it is preferable to use $-\text{CONEt}_2$ and to remove the amide from the product by reduction, as in Scheme 14 (note the cooperative effect of the amide and methoxy group in the first step)[66]. Hydrolysis can also be achieved via an imidate (see Scheme 12).

Removal of the amide function is much easier if the reaction is intramolecular, and $-\text{CONEt}_2$ amides (sometimes even $-\text{CONPr-}i_2$ amides) may be converted to lactones, lactams and other heterocycles in this way[25,67]. Addition of an aldehyde or ketone as an electrophile generates a hydroxyl group (in some cases, atroposelectively, as it happens[38,68]—though this is usually irrelevant to the stereochemistry of the product) which cyclizes to give a lactone via a benzylic cation in acid. This reaction has found wide use in the synthesis of polycyclic aromatics, particularly alkaloids.

Lactonization of alcohols derived by organometallic addition to 2-formyl amides, lactol formation from 2-formyl amides themselves[7] and lactam formation from their nitrogen counterparts[69] are also useful synthetically.

Rather than fighting against the lack of electrophilicity at the amide carbonyl group, it can be more fruitful to exploit its electron-rich nature in cyclizations onto carbocations.

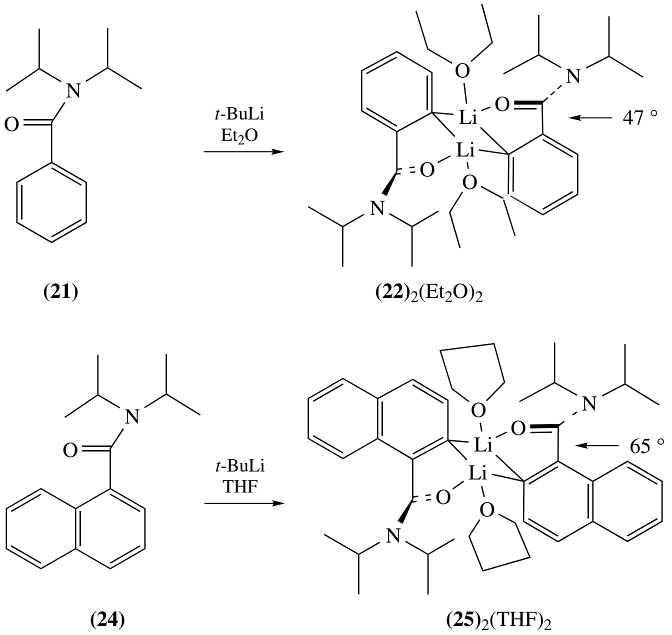

(21) **(22)**$_2$(Et$_2$O)$_2$

(24) **(25)**$_2$(THF)$_2$

SCHEME 13

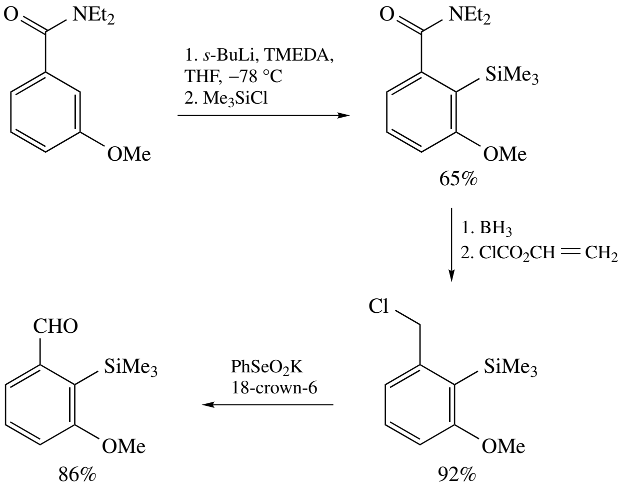

SCHEME 14

For example, the allyl-substituted amide **26** cyclizes to the 6-membered lactone **27** in refluxing 6M HCl (Scheme 15)[70].

Although there is no shortage of applications for the lithiation of diethylamides, their potential would clearly be widened if the limitations of the amides' reactivity could be

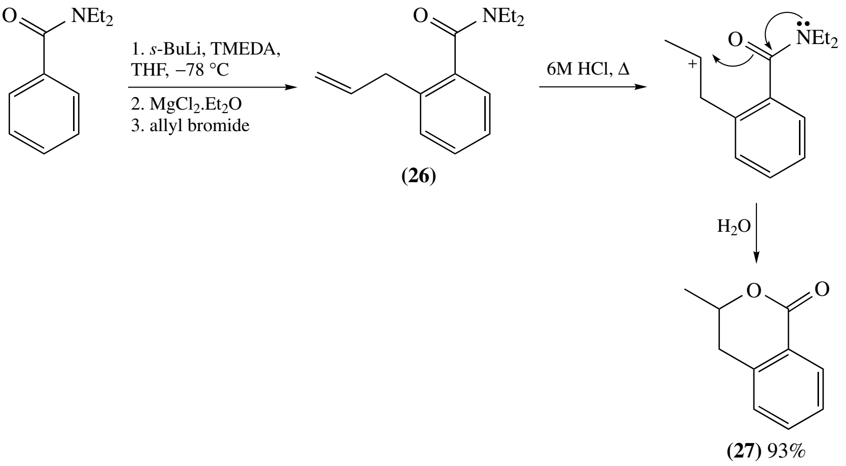

SCHEME 15

overcome. Alternative *N*-substituents have been devised with the aim of increasing the number of transformations available at the amide group. Clearly, the *N*-substituents must be highly resistant to strong base, but can be sensitive to acid or fluoride. One solution is to replace the methyl groups of one isopropyl with silyl groups, as in **28**[71]. After functionalization, fluoride treatment gives **29** which is then much more easily hydrolysed or reduced (Scheme 16).

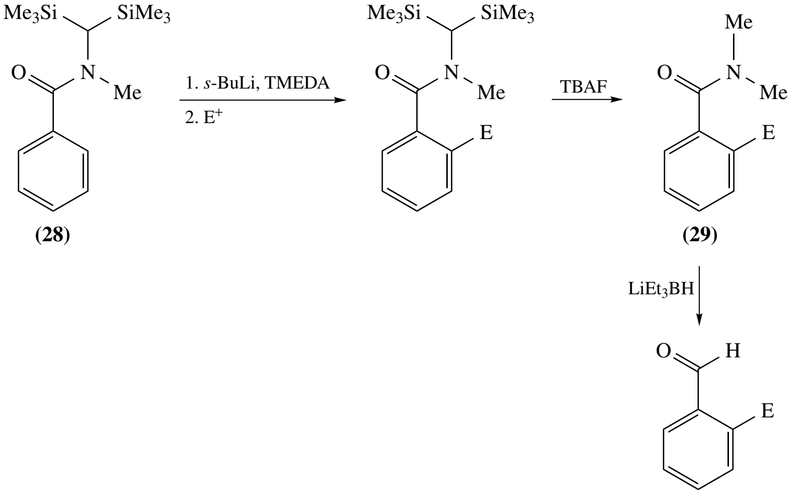

SCHEME 16

More practical from the point of view of starting material availability is the use of the *N*-*t*-butyl-*N*-methyl amides **30**, whose *t*-butyl group may be removed with acid (Scheme 17)[72]. De-*t*-butylation of amides can be capricious however, though it seems much more successful with acyclic than cyclic amides.

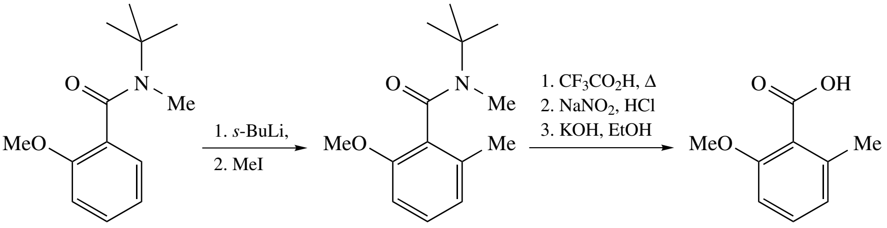

(30)

SCHEME 17

We have introduced an amide based on the acid-sensitive oxazolidine employed by Hintze and Hoppe[73] to make base-resistant, acid-labile alkylcarbamates. Our aim was to retain a high degree of steric hindrance around the nitrogen atom for purposes of stereoselectivity. The amides based on **31** seem to have many of the properties of *N*,*N*-diisopropylamides, but are readily hydrolysed by treatment with $MeSO_3H$ for 5 min in refluxing MeOH (Scheme 18)[74]. One disadvantage of these acyl oxazolidines is their existence as a mixture of slowly interconverting conformers (sometimes separable geometrical isomers) which complicates their characterization by NMR.

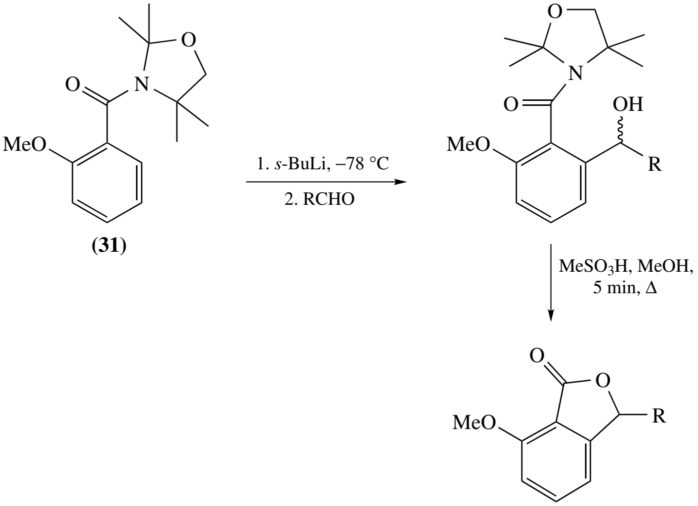

(31)

SCHEME 18

Other more readily cleavable tertiary amides include **32**[75] and **33**[76].

Secondary amides (but not primary amides, which resist ortholithiation under all conditions) are ortholithiated with two equivalents of organolithium—the first-formed amide anion (**34**) prevents nucleophilic attack by the second equivalent of organolithium[77]. Many anionic groups are surprisingly powerful directors of ortholithiation, given that the acidity of the ring protons can hardly be enhanced by the presence of a negatively charged heteroatom. Any loss of acidity must be more than outweighed by the highly favourable complexation of the organolithium to this charged intermediate. Reaction of **35** with

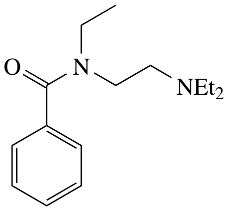

(32)

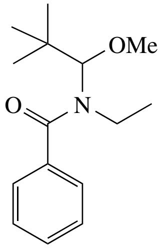

(33)

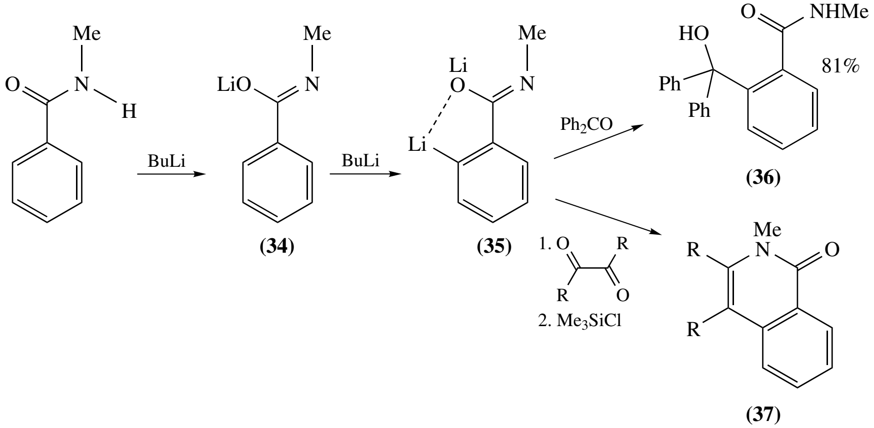

SCHEME 19

simple electrophiles leads to *ortho*-substituted amides **36**; with diketones, isoquinolones **37** are formed (Scheme 19)[78].

Secondary amides have the advantage over tertiary amides that they are relatively easy to remove. It is quite difficult to stop the addition products from aldehydes, ketones, amides, epoxides and nitriles cyclizing directly to give a variety of lactone derivatives (by attack of OH on the secondary amide) or lactam derivatives (by attack of the secondary amide on the new electrophilic centre)[3]. Thioamides behave similarly[79].

Secondary amides **38** based on cumylamine[80] or dialkylhydrazines[81,82] are particularly useful. The cumyl protecting group is removed by E1 elimination in strong acid to form **39** or by formation of a nitrile **40** (Scheme 20), while hydrazines can be cleaved oxidatively.

Attachment to a solid support via a secondary amide linkage allows ortholithiations to be carried out in the solid phase. After a reaction with an aldehyde or ketone, refluxing in toluene returns the amino-substituted polymer **41** (Scheme 21)[83].

Secondary and tertiary amides are particularly effective for directing the metallation of heterocycles[7,82,84–91]. Lithiation α to the heteroatom can be a competing reaction with the 5-membered heterocycles[88]. Lithiation of furan-2-carboxamides **42** can lead to ring cleavage to give **44**[80], though the intermediate **43** is stable with a chelating amide group[91]. Thiophene-2-carboxamides lithiate preferentially α to sulphur. Lithiation in the 3-position is achieved by double deprotonation to give **46** or by silyl protection: **47** gives **48** (Scheme 22)[7]. The strategy of silyl protection is discussed in more detail in Section VII.

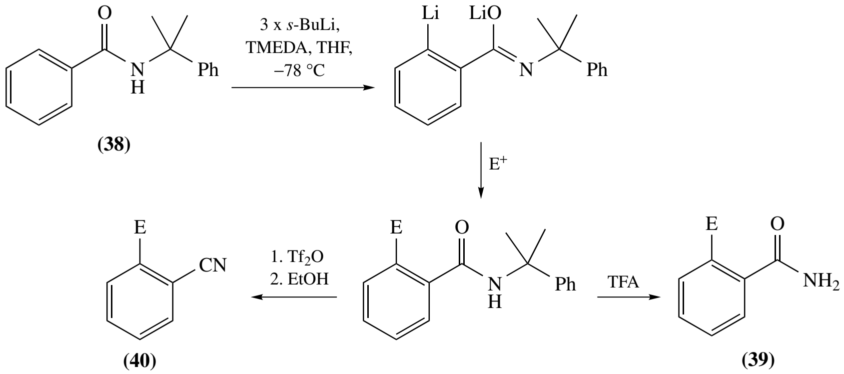

SCHEME 20

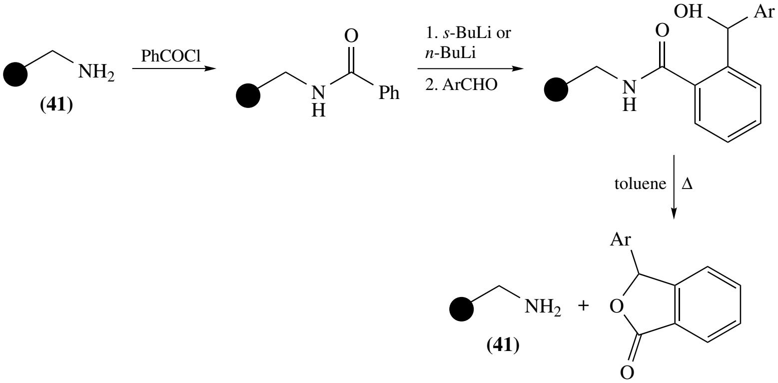

SCHEME 21

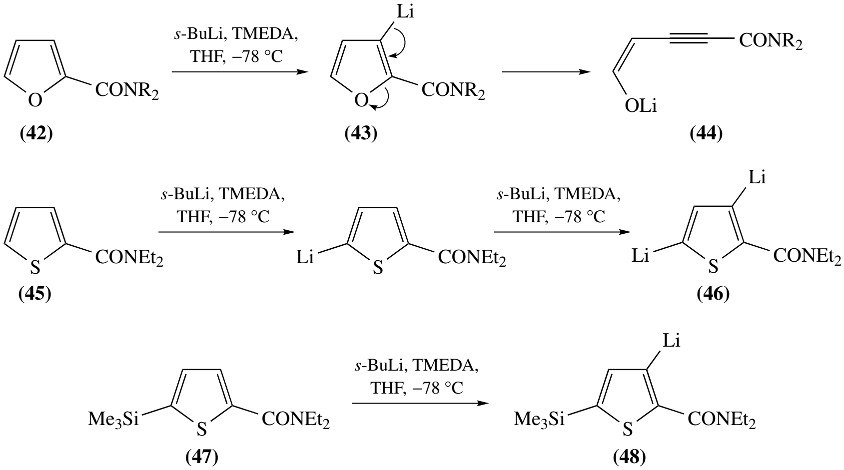

SCHEME 22

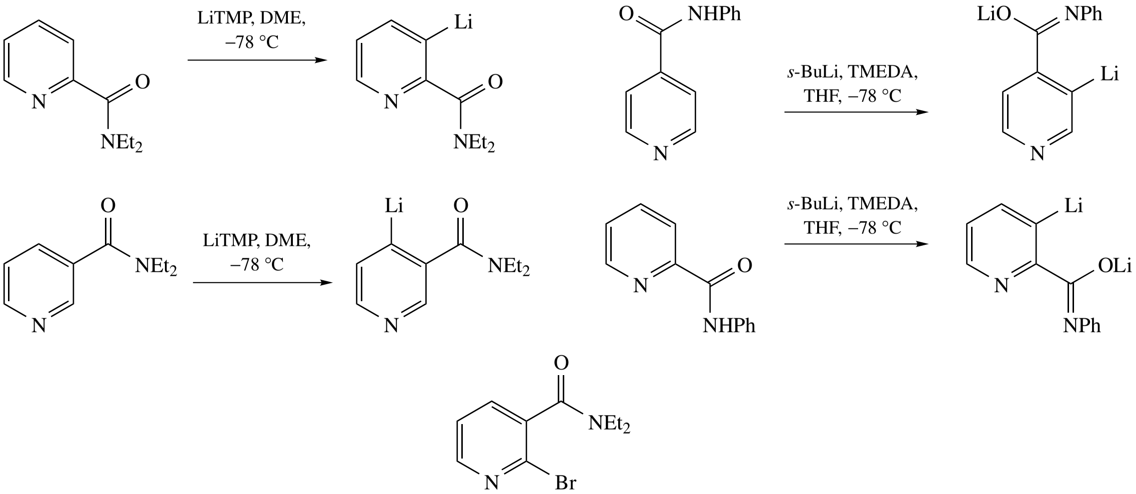
LiTMP, DME, −78 °C
LiTMP, DME, −78 °C
s-BuLi, TMEDA, THF, −78 °C
s-BuLi, TMEDA, THF, −78 °C
NEt$_2$
O
Li
NHPh
LiO
NPh
OLi
N
Br

(49)

SCHEME 23

Pyridines bearing secondary amides may be lithiated with *n*-BuLi at −78 °C; with tertiary amides the optimum conditions are LiTMP, DME, 5–15 min (Scheme 23)[92]. Lithiated tertiary amidopyridines react well with carbonyl electrophiles but poorly with alkylating agents. Lithiation of the bromopyridine **49** with LDA is a key step in the synthesis of eupoluramine[93].

Scheme 24 shows the synthesis of a quinone by a second lithiation α to the sulphur of a thiophene[94].

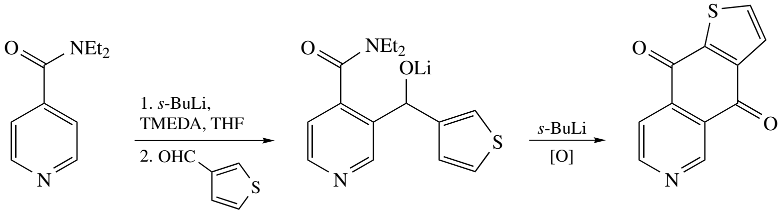

SCHEME 24

To summarize: the amides are most suitable for the formation, by ortholithiation, of condensed heterocycles and polycyclic aromatics (in which subsequent rings are formed by intramolecular attack on the amide group). In other cases the removal of the amide group may be problematic, though if carboxylic acids, aldehydes or hydroxymethyl-substituted compounds are required, alternative amide substituents may be used.

b. α-Amino alkoxides. N,*N*-Dimethylbenzamides can be used as lithiation directors even under conditions that lead to alkyllithium attack at the carbonyl group to give ketones. The tetrahedral intermediate in this sequence **50** is a good director of lithiation (note its similarity to a deprotonated secondary amide) and an excess of organolithium intercepts this intermediate and ortholithiates it to give **51**. The overall synthetic result is effectively that of an ortholithiation-directing ketone or aldehyde (Scheme 25).

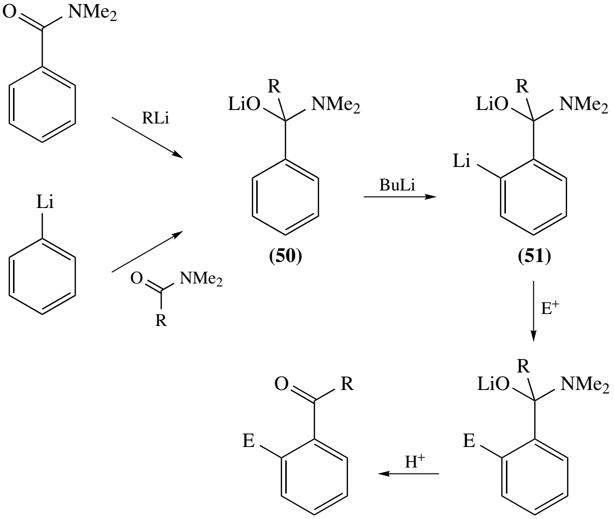

SCHEME 25

The same intermediate **50** is formed when an aryllithium attacks dimethylformamide *en route* to an aldehyde. Intercepting this intermediate can provide a useful way of synthesizing *ortho*-substituted aromatic aldehydes such as **52** (Scheme 26)[95].

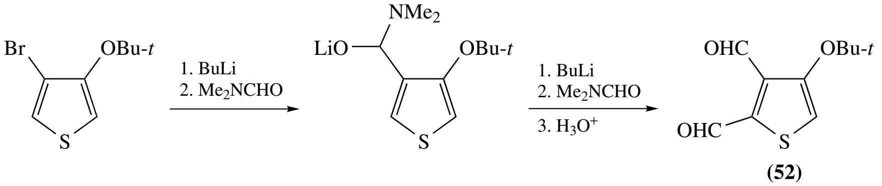

SCHEME 26

Addition of a lithiated secondary amine to an aldehyde both protects the aldehyde from attack by RLi and turns it into an ortholithiation directing group. The best lithioamines for this purpose are *N*-lithio-*N*-methylpiperazine **53**, *N*-lithio-*N*,*N*,*N*′-trimethylethylenediamine **56** and *N*-lithio-*N*,*O*-dimethylhydroxylamine **58**[96], which optimize the opportunity for coordination of BuLi to the intermediate alkoxide (**54**) (Scheme 27)[33,97,98].

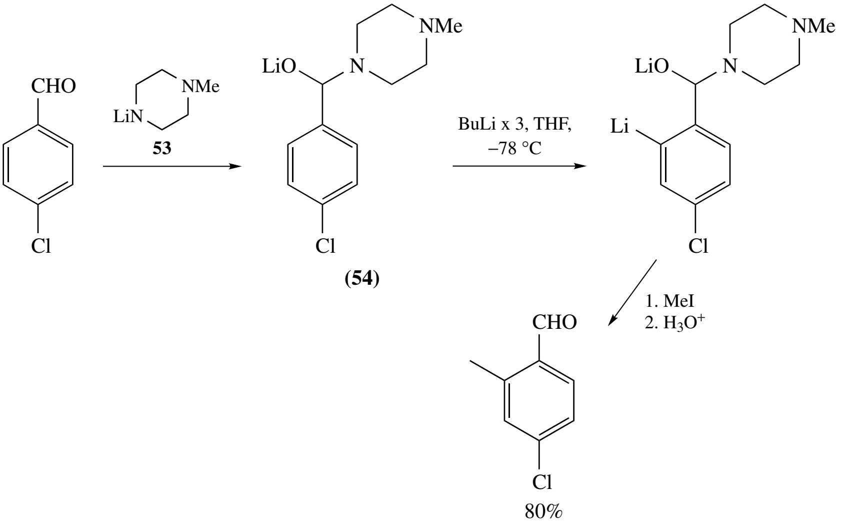

SCHEME 27

The more conformationally flexible lithioamine **56** derived from *N*,*N*,*N*′-trimethylethylenediamine enhances the directing group ability of the aminoalkoxide: while both **53** and **56** can be used for the protection of **55** during the lithiation step, **56** leads to a directing group stronger than OMe, while **55** leads to a directing group weaker than OMe (Scheme 28)[99]. Protection of **57** by **58** leads to lithiation α to oxygen.

c. Oxazolines. Aryl oxazolines exhibit resistance to nucleophilic attack and can be lithiated with *n*-BuLi. A range of methods are available for activation of the oxazoline group of the products to allow constructive conversion to other functional groups[5,49]. A sequence of

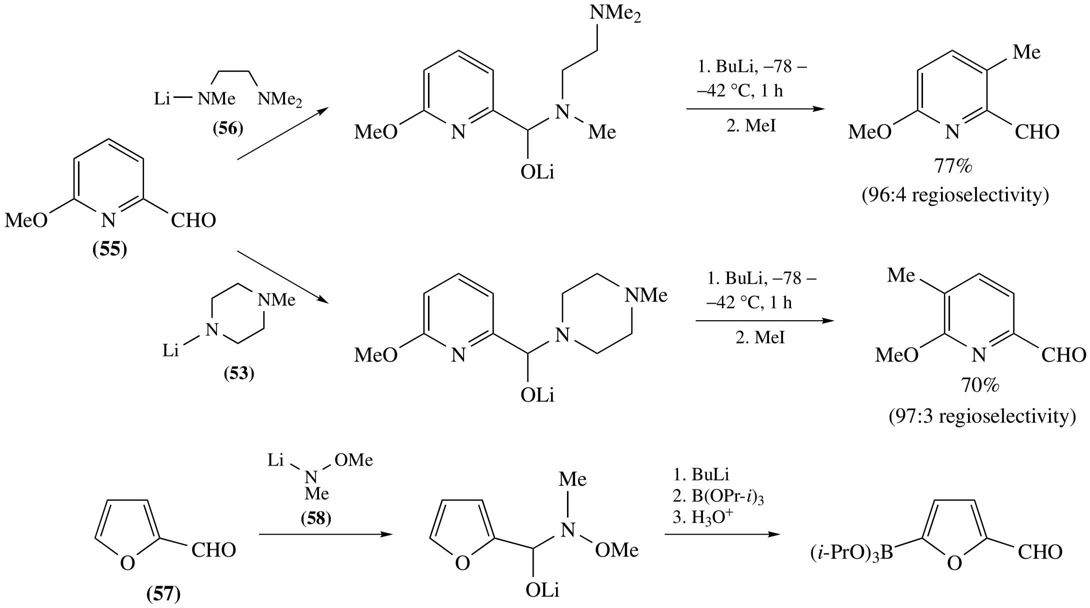
Li — NMe NMe$_2$
(56)
MeO
N
CHO
(55)
Li
N
NMe
(53)
MeO
N
N
Me
NMe$_2$
OLi
MeO
N
N
NMe
OLi
1. BuLi, −78 –
−42 °C, 1 h
2. MeI
MeO
N
CHO
Me
77%
(96:4 regioselectivity)
Me
MeO
N
CHO
70%
(97:3 regioselectivity)
O
CHO
(57)
Li
N
OMe
Me
(58)
O
Me
N
OMe
OLi
1. BuLi
2. B(OPr-i)$_3$
3. H_3O^+
(i-PrO)$_3$B
O
CHO

SCHEME 28

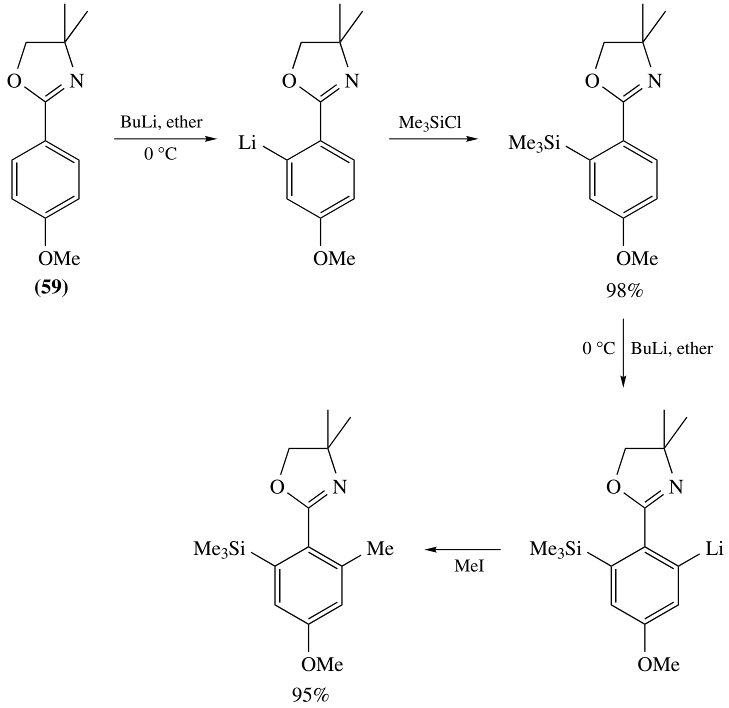

SCHEME 29

simple lithiations of **59** illustrates the potential of this method at the start of this synthesis of a precursor to a steroid (Scheme 29)[100].

The cooperative effect of MeO and the oxazoline directs the lithiation of **60** in this synthesis of a lipoxygenase inhibitor AC-5-1 **61** (Scheme 30)[101].

Ortholithiated oxazoline **62** is best transmetallated to its magnesium analogue before reaction with aldehydes. As with the equivalent amide reaction, treatment with 4.5 M HCl then cyclizes the products to lactones (Scheme 31)[102].

d. O-Carbamates. The *O*-aryl *N*,*N*-diethyl carbamates **63** are the most readily lithiated of the oxygen-based metallation directing groups, and have chemistry which is closely associated with that of tertiary amides[7]. Like the amides, they are hard to hydrolyse, requiring vigorous basic conditions[103]. Hydrolysis is easier with nearby functional groups, which must play an assisting role; alternatively, the carbamates may be reduced to phenols by $LiAlH_4$ (Scheme 32).

N,*N*-Diisopropylcarbamates generally offer little advantage over their *N*,*N*-diethyl analogues, and their removal is even more difficult. *O*-Aryl *N*-cumyl carbamates do, however, offer some advantages, and can be hydrolysed to phenols under acid conditions[80].

N,*N*-Dimethylcarbamates are unstable once ortholithiated, and rearrange rapidly by a carbamoyl transfer mechanism known as the 'anionic *ortho*-Fries rearrangement'[7]. With *N*,*N*-diethylcarbamates, this rearrangement can be controlled: the ortholithiated carbamate **64** is stable at −78 °C but, on warming to room temperature, rearranges to give a 2-hydroxybenzamide **65** (Scheme 33)[103].

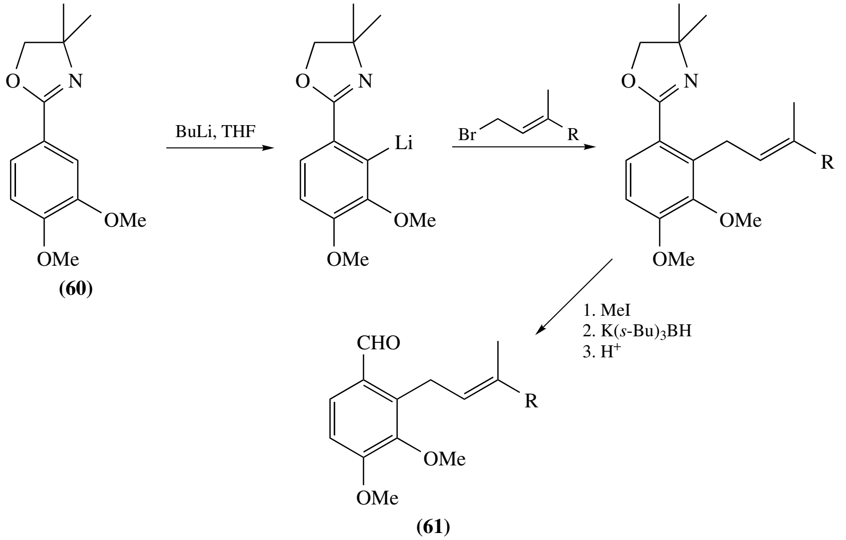

SCHEME 30

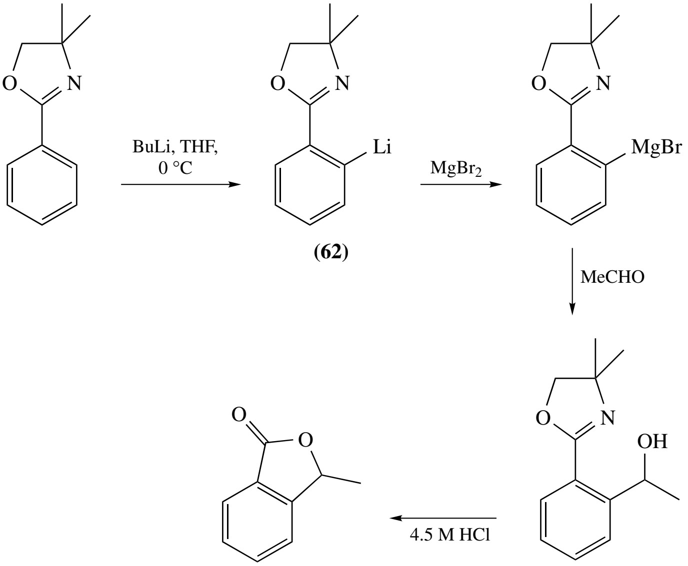

SCHEME 31

This chemistry can be very powerful, since the amide product itself offers further possibilities for functionalization by lithiation. The synthesis of the natural product ochratoxin A illustrates this point. Ochratoxins A **66** and B **67** (Scheme 34) are metabolites of *Aspergillus ochraceus* and *Penicillium viridicatum* whose presence in agricultural products

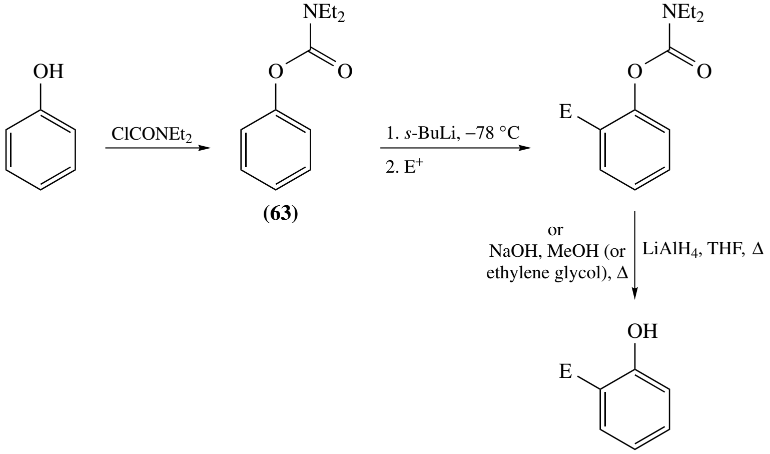

SCHEME 32

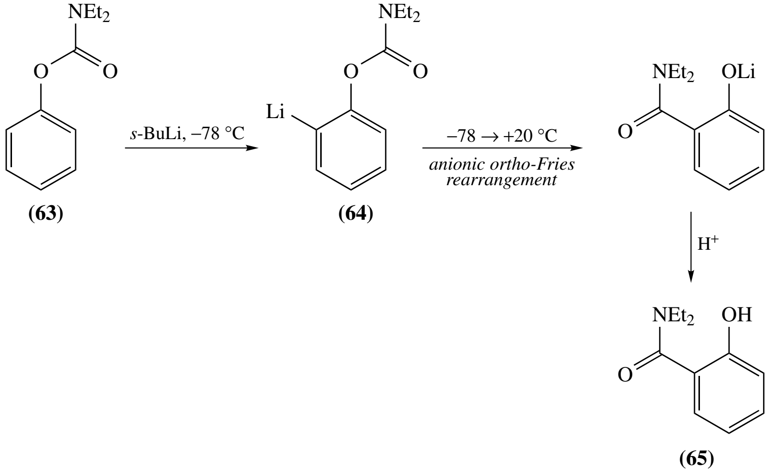

SCHEME 33

poses a health hazard to both animals and humans. Snieckus' synthesis (Scheme 35)[104] uses a series of directed ortholithiations to control the 1,2,3,4,(5)-polysubstitution pattern, introducing the two carbonyl substituents (an amide and a lactone) as tertiary amides to capitalize on their powerful lithiation chemistry (Scheme 34).

The starting point for the metallation sequence leading to ochratoxin B was *p*-chlorophenol, whose directing power was first maximized by conversion to the carbamate **68**. Ortholithiation and reaction with *N*,*N*-diethylcarbamoyl chloride gave the amide **69**. The second *ortho* carbonyl substituent was then introduced simply by allowing the lithiated carbamate **70** to undergo an anionic *ortho*-Fries rearrangement to the bis-amide **71**. The phenol was protected as its methyl ether **72**.

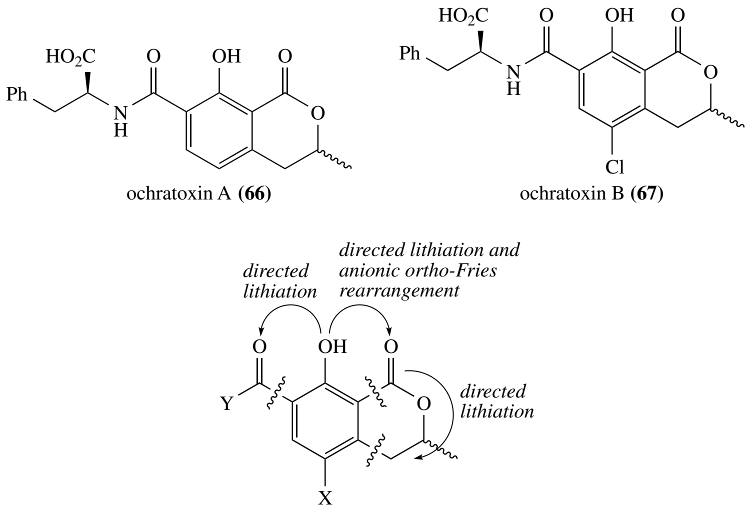
ochratoxin A (**66**)

ochratoxin B (**67**)

SCHEME 34

The alkyl substituent *meta* to the methoxy substituent was easily introduced into the symmetrical diamide **72** by yet another ortholithiation. Allyl electrophiles react poorly with aryllithiums, so the ortholithiated amide **73** was first transmetallated to the Grignard reagent before allylation with allyl bromide to give **74**.

A combined lactonization and deprotection to give **75** was achieved by refluxing **74** in 6N HCl. Peptide coupling with phenylalanine affords a mixture of diastereoisomers of the target compound **67**.

An anionic *ortho*-Fries rearrangement has been used to make BINOL derivatives[105].

e. Anilides and N-aryl carbamates. Anilines are poor directors of lithiation[106]: the nitrogen's lone pair is less basic than an amine's, and the nitrogen has a weaker acidifying effect than a corresponding oxygen substituent. *N*,*N*-Dimethylaniline can nonetheless be lithiated by BuLi in refluxing hexane[107, 108], and the lithiation of *N*,*N*-dialkylanilines is made more efficient by the addition of TMEDA[109].

By far the best solution to the problem of lithiating an amino-substituted aromatic ring is to acylate an aniline to give a pivalanilide **76**[110] or an *N*-Boc carbamate **79**[111]. Two equivalents of base (BuLi) deprotonate first the nitrogen and then cleanly ortholithiate the anion to give **78** (Scheme 36). As with the secondary amides described above, the lack of acidifying effect in the intermediate anion (which this time *is* conjugated with the ring) is more than outweighed by the powerful lithium-coordinating ability of the anionic intermediate **77**.

With *N*-Boc anilides **79**, the best conditions for lithiation are *t*-BuLi (2.2 equivalents) in Et_2O at $-10\,^{\circ}C$ (Scheme 37).

Amides of aminopyridines have also been widely used to direct lithiation, and are most effective when lithiated with BuLi in the absence of TMEDA (Scheme 38)[84]. The lithiation of **80** can be used as a key step in the synthesis of naphthyridines and other condensed polycyclic heterocycles[112].

Ortholithiation of thioanilides **81** has been used to construct benzothiazole rings **83** via the benzyne **82** (Scheme 39)[113].

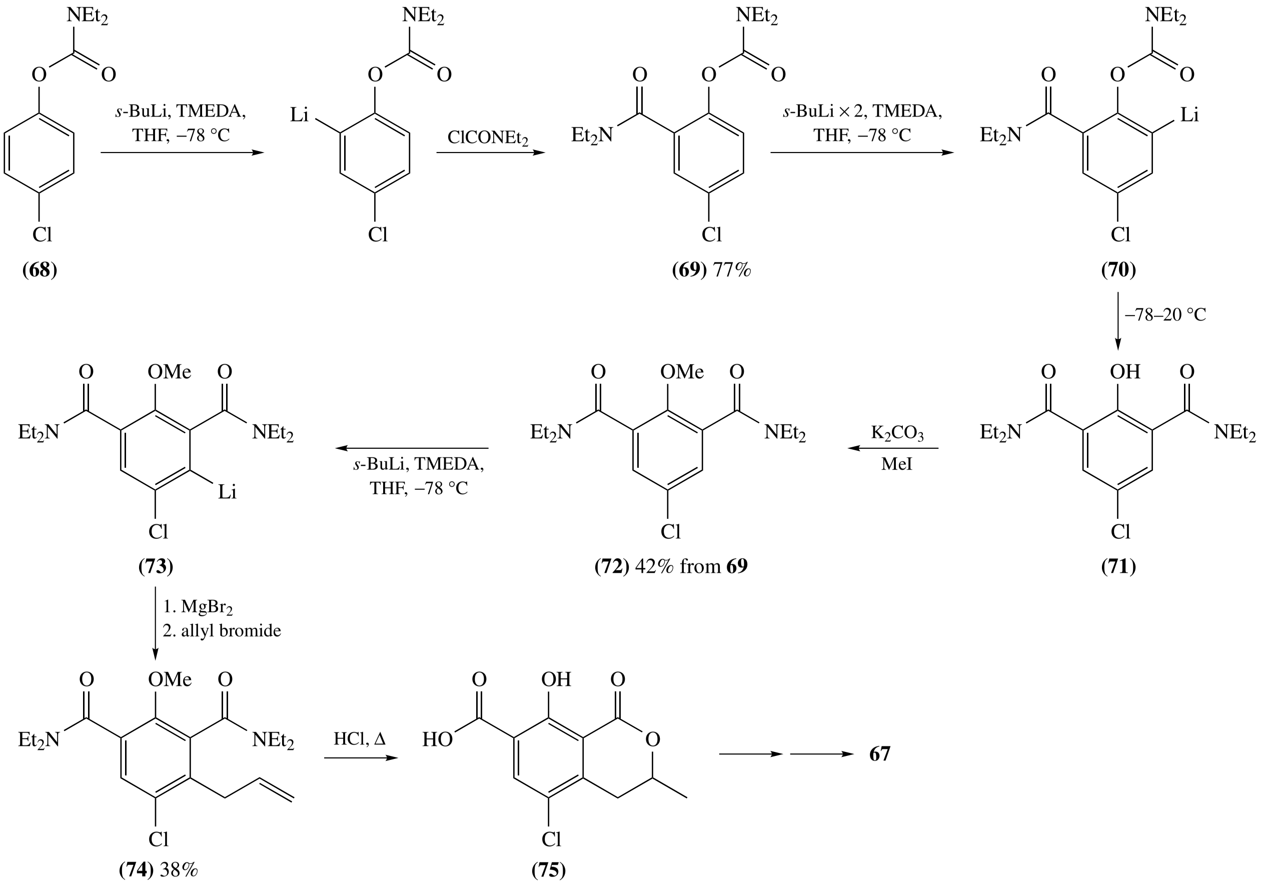
NEt2
O
O
Cl
(68)
s-BuLi, TMEDA,
THF, −78 °C
Li
ClCONEt2
Et2N
(69) 77%
s-BuLi × 2, TMEDA,
THF, −78 °C
(70)
−78–20 °C
OH
(71)
K2CO3
MeI
OMe
(72) 42% from 69
s-BuLi, TMEDA,
THF, −78 °C
(73)
1. MgBr2
2. allyl bromide
(74) 38%
HCl, Δ
HO
(75)
67

SCHEME 35

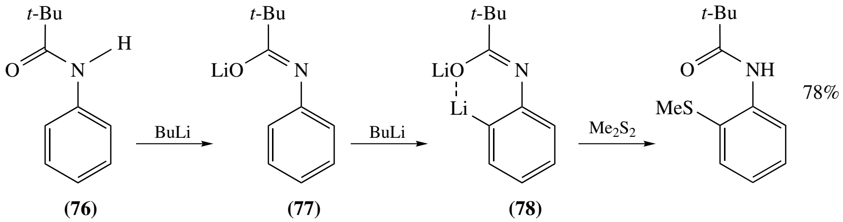

SCHEME 36

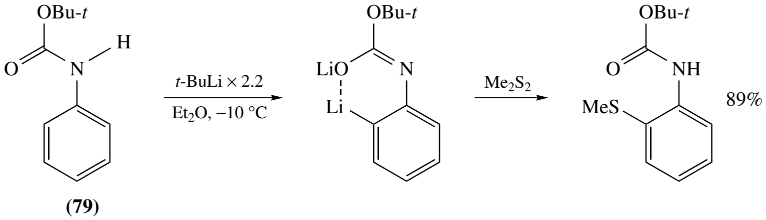

SCHEME 37

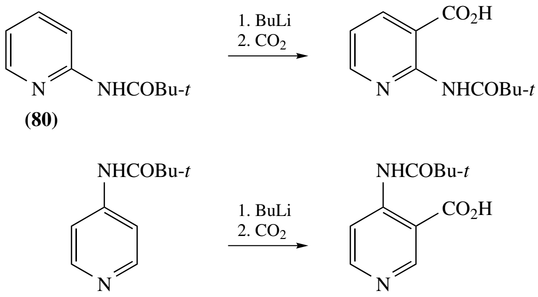

SCHEME 38

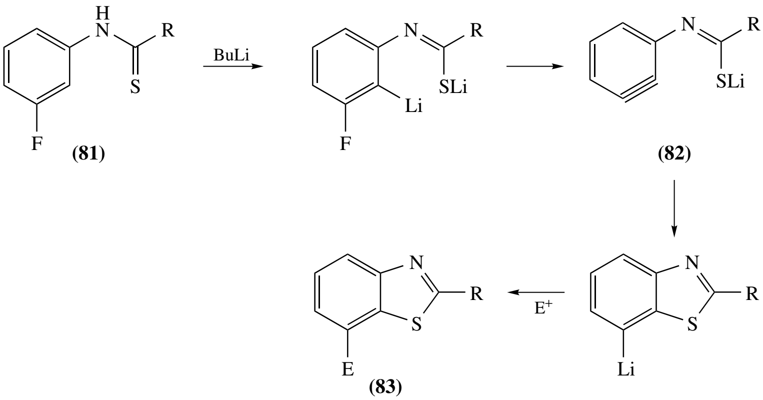

SCHEME 39

Ureas of anilines **84** can also be lithiated[114, 115]. The products are generally very hard to cleave, but quenching the intermediate organolithiums **85** with carbon monoxide generates acyllithiums **86** which cyclize to give isatins **87** (Scheme 40)[116].

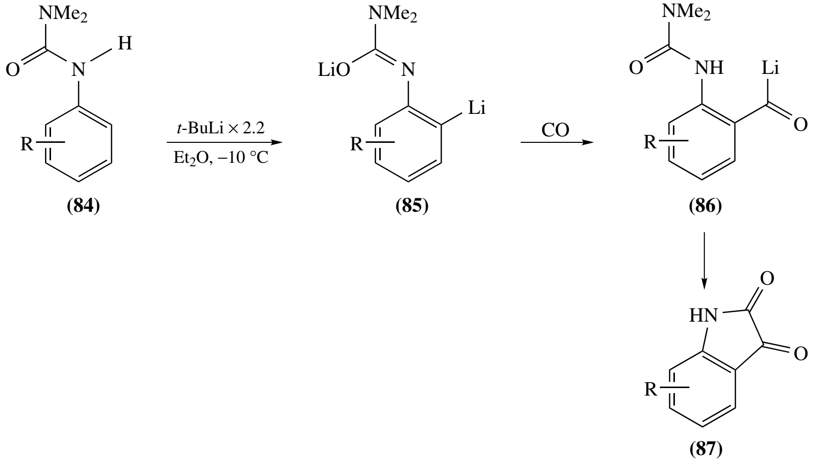

SCHEME 40

f. Tetrazoles. Both *N*-unsubstituted and *N*-substituted tetrazoles are efficient orthodirectors—the tetrazole group in **88**, for example, is a more powerful director than the secondary amide (Scheme 41)[48].

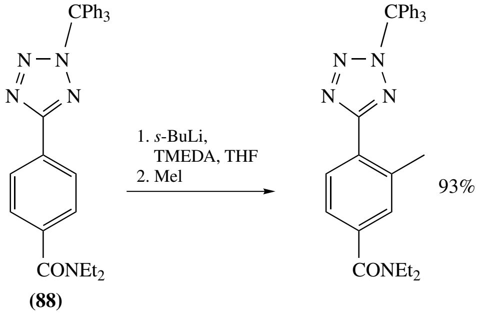

SCHEME 41

2. S + O class

Sulphides are weak orthodirectors (Scheme 42), and the lithiation of thioanisole **89** with BuLi leads to a mixture of α- and ortholithiated compounds **90** and **91**[117]. The ortholithiated compound forms about one third of the kinetic product mixture, but slow isomerization to the α-lithiated sulphide follows. The isomerization is much faster (and therefore the yield of α-lithiated sulphide much higher) if BuLi is used in the presence of DABCO[118]. With two equivalents of BuLi, clean *ortho* + α double lithiation occurs, giving **92**: the SCH_2Li group is itself an *ortho*-director[119], though a weaker one than

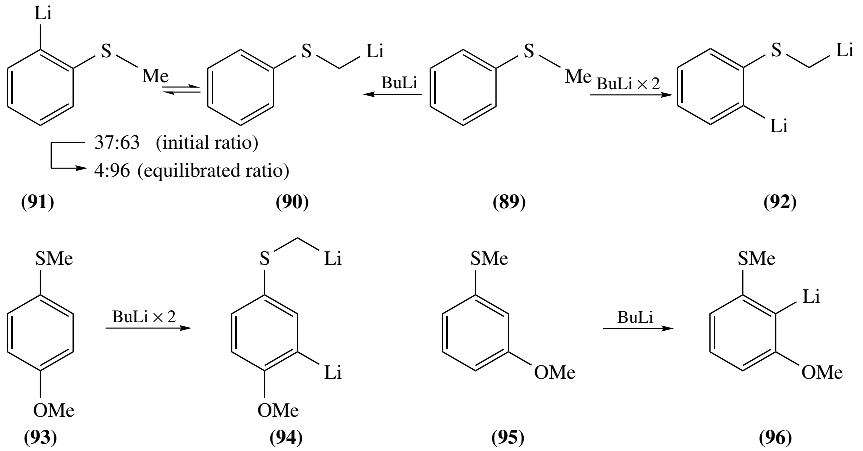

SCHEME 42

OMe, since doubly lithiated **93** has the regiochemistry **94**[120]. A methylthio substituent in conjunction with a methoxy substituent directs to their mutual *ortho* position (**95** → **96**).

Ethyl phenyl sulphide is lithiated mainly in the *ortho* position, but with significant amounts of *meta* and *para* lithiation and substitution products. Superbases, on the other hand, prefer to deprotonate alkylthio benzenes at benzylic or α-positions, rather than on the ring[121, 122].

Diaryl sulphides are lithiated *ortho* to sulphur, but less efficiently than diaryl ethers: dibenzothiophene **97**, for example, lithiates to give **98** and hence **99**. Highlighting preferential lithiation at the more acidic positions *ortho* to O, **100** gives **101** rather than **102** (Scheme 43)[8].

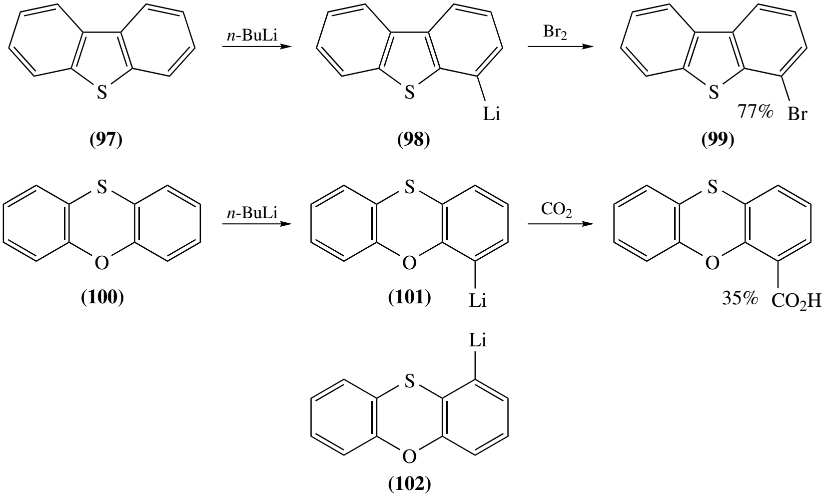

SCHEME 43

In sulphoxides, sulphur's weak acidifying effect is enhanced, and the oxygen atom introduces a powerful coordination effect: in contrast with sulphides, sulphoxides are very powerful directors of both ortholithiation and α-lithiation. Ortholithiation is possible with aryl sulphoxides lacking an α-proton, but since sulphoxides suffer from the disadvantage of being electrophilic at sulphur, diaryl sulphoxides must be lithiated with lithium amide bases rather than alkyllithiums. Pyridyl sulphoxides **103** are ortholithiated by LDA, and have the added feature that the sulphinyl group can subsequently be displaced by Grignard reagents, leading, for example, to the bipyridyl **104** (Scheme 44)[123]. When the electrophile is an aldehyde, the chiral sulphoxide can control up to 7:1 stereoselectivity at the new stereogenic centre[124].

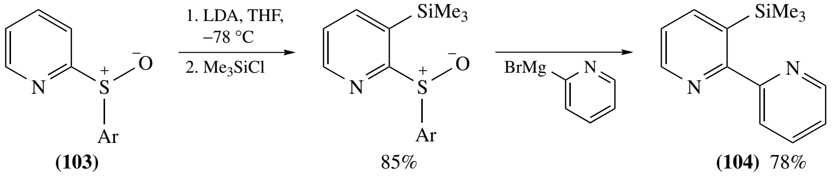

(103) **(104)**

SCHEME 44

Sulphoxide removal using sulphoxide–lithium exchange is also effective[125]. It was employed in tandem with a sulphoxide-directed stereoselective ortholithiation of the ferrocene **105**[126, 127] in the synthesis of the phosphine ligand **106** (Scheme 45)[128]. Ferrocene lithiation is discussed further in Section III.

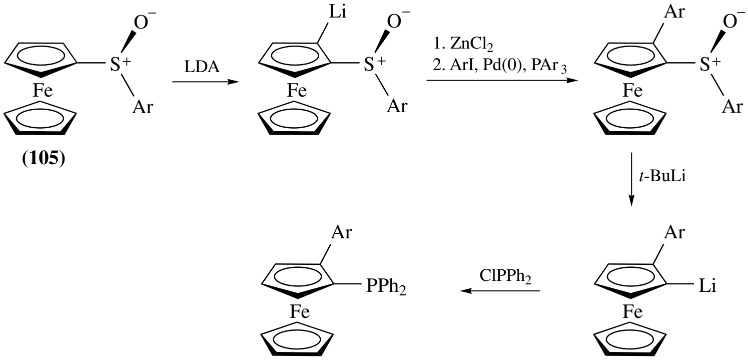

(105) **(106)**

SCHEME 45

Aryl t-butylsulphoxides are sufficiently hindered for attack at sulphur to be less of a problem[52]. The chiral sulphoxide offers no control over the new stereogenic centre in the reaction of **107** to give **108** (Scheme 46).

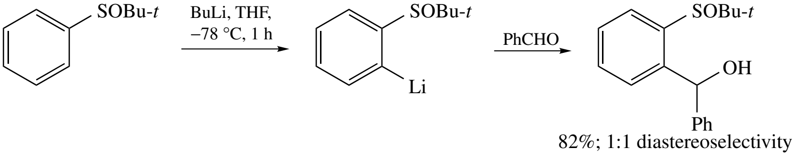

(107) **(108)**

SCHEME 46

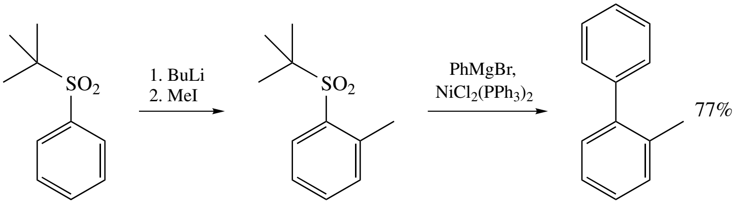

SCHEME 47

Sulphones are similar in some ways: even more acidifying, and with a powerful ability to coordinate, but less likely to be attacked at S. As with sulphoxides, lithiation α to S competes, and ortholithiation is useful only with sulphones lacking α-protons[47]. After lithiation, the removal of sulphones can sometimes be accomplished by transition metal-catalysed reduction or substitution (Scheme 47)[51, 50].

Even sulphonate esters **109** are powerful directing groups, competing well with tertiary amides. No substitution accompanies ortholithiation of ethyl or isopropyl benzenesulphonate by BuLi. Hydrolysis and chlorination of the products **110** gives functionalized sulphonyl chlorides **111** (Scheme 48)[129].

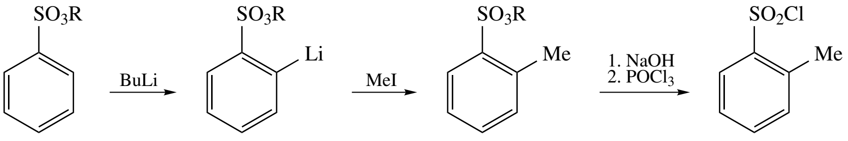

(109) **(110)** 95% **(111)**

SCHEME 48

Secondary and tertiary sulphonamides are among the most powerful *ortho*-directing groups known[130, 131]. There is no danger of attack at S, and *N*,*N*-dimethylsulphonamides **112** may be lithiated with *n*-BuLi alone[132]. Secondary *N*-*t*-butyl sulphonamides **113** are particularly useful because the *t*-butyl group is readily removed in polyphosphoric acid. Carbonation of **114** and cyclization in acid give the saccharin analogues **115** (Scheme 49)[39].

Naphthyl sulphones **116** are susceptible to nucleophilic attack at the 2-position of the naphthalene ring by the alkyllithiums[40]; secondary sulphonamides **117**, on the other hand, undergo perilithiation with alkyllithiums (Scheme 50)[39].

N-Aryl sulphonamides have not been investigated in detail, but 'anion translocation' from the *S*-substituted ring to the *N*-substituted ring takes place in diaryl sulphonamides **118**, ultimately leading to the rearrangement shown in Scheme 51[133, 134].

The ortholithiation of benzenesulphinamides **119** is of use in the regioselective synthesis of *meta*-substituted compounds **120**: the sulphinamide group is used to set up two *ortho* relationships and then removed reductively (Scheme 52)[135]. The same concept has been explored with other sulphur-containing *ortho*-directors[47, 50].

Phosphine oxides are similar: excellent *ortho*-directors which have seen only limited use so far. The iodide **123**, for example—a precursor of a new class of bisphosphine ligands—can be made by cooperatively-directed ortholithiation of the phosphine oxide **122**, itself derived by halogen–metal exchange from **121** (Scheme 53)[136].

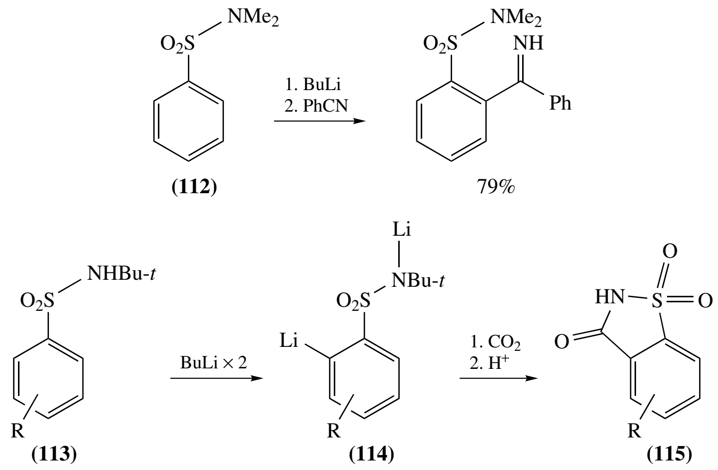

SCHEME 49

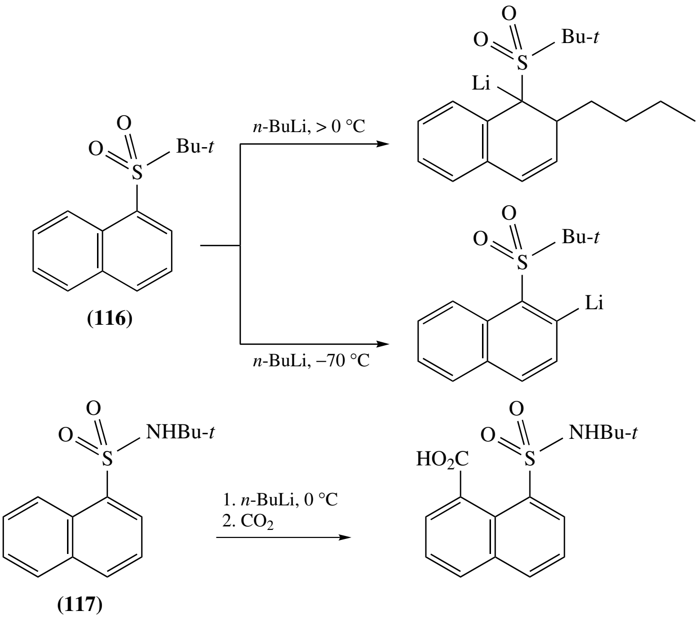

SCHEME 50

3. N class

a. Aminomethyl groups. Dimethylaminomethyl groups are among the most powerful of the non-acidifying functional groups with regard to directing ability, and reliably direct ortholithiation with *n*-BuLi[17, 137, 138]. Other dialkylaminomethyl (e.g. **124**)[3], and even monoalkylaminoalkyl groups (e.g. **125**, R $\neq$ H), which are doubly deprotonated by

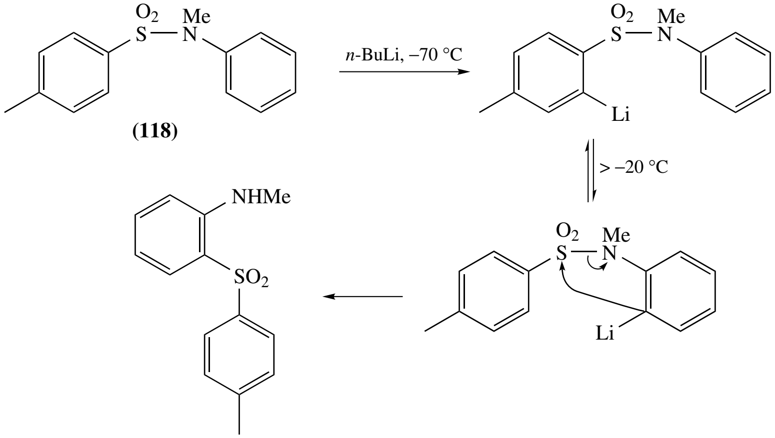

SCHEME 51

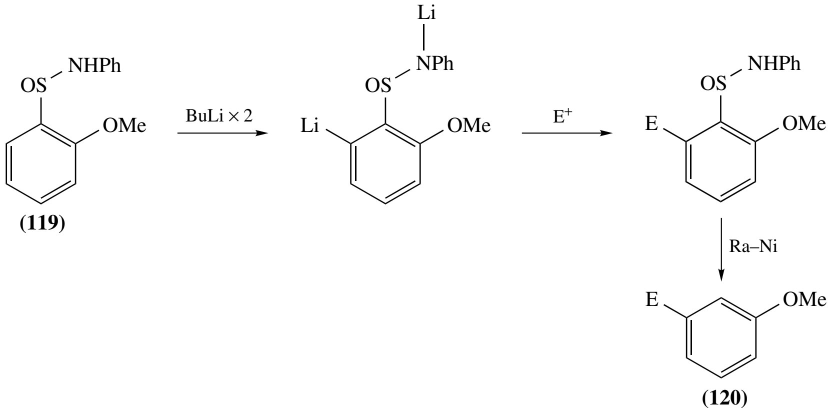

SCHEME 52

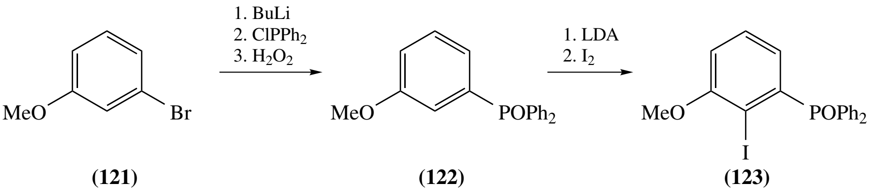

SCHEME 53

BuLi–TMEDA[139], are similarly powerful directors (Scheme 54). By contrast, the related amides, carbamates and ureas (**125**, R = COAr, $CONR_2$, CO_2R) usually undergo benzylic α-lithiation (see Section II.B). The bias can be shifted towards ortholithiation by additional electron-withdrawing substituents on the ring[140].

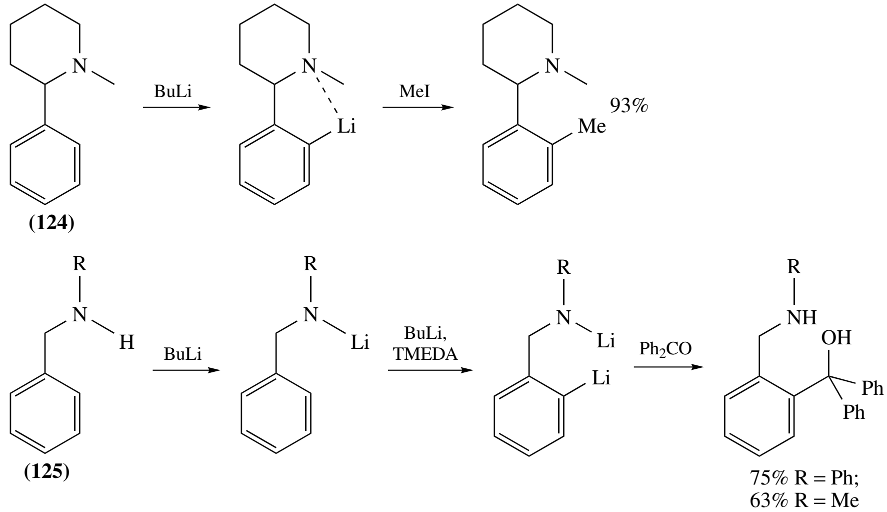

SCHEME 54

Groups bearing amino substituents even further from the aromatic ring are very weak *ortho*-directors[3].

b. Anilines and isocyanides. Anilines are poor directors of lithiation because the delocalization of the lone pair into the ring, which lessens the nitrogen's coordinating ability, is not counterbalanced by an increase in acidity of the ring protons (N is not sufficiently electronegative). However, the theme emerging in the N + O class—that anionic substituents are suprisingly good lithiation directors—is echoed by the lithium salts of anilines. The neutral heterocycle **126** gains a weak acidifying effect from both N and from S, and lithiates poorly *ortho* to both (Scheme 55). In the anion **128** derived from heterocycle **127**, the negative charge is delocalized around the rings, and the nitrogen now bears a lone pair perpendicular to the π-system. Even though the entire system must have lessened acidity, ortholithiation is much more efficient because of coordination to this lone pair[141].

Isocyanides are converted, on addition of t-BuLi at the electrophilic carbon atom, to lithioimines—another class of anionic, nitrogen-containing functions which turn out to have good *ortho*-directing ability[142]. The electrophile reacts at both lithium-bearing centres of **129** (Scheme 56).

Amino-substituted naphthalenes are readily perilithiated (Scheme 57)[143–145].

c. Imines, nitriles, hydrazones and nitrogen heterocycles. The powerful ability of trigonal (sp^2) nitrogen to coordinate to lithium[146] means compounds of general structure **130** may be ortholithiated, provided addition to C=N can be avoided.

It is just about possible to ortholithiate imines, but in nearly all cases, the side reaction of nucleophilic attack at C=N is at least as important. Ortholithiation can overcome this side-reaction if it is assisted by an additional directing group (Scheme 58)[147,148].

Hydrazones may also direct lithiation, and are particularly effective after deprotonation to an azaenolate **131** (Scheme 59)[3].

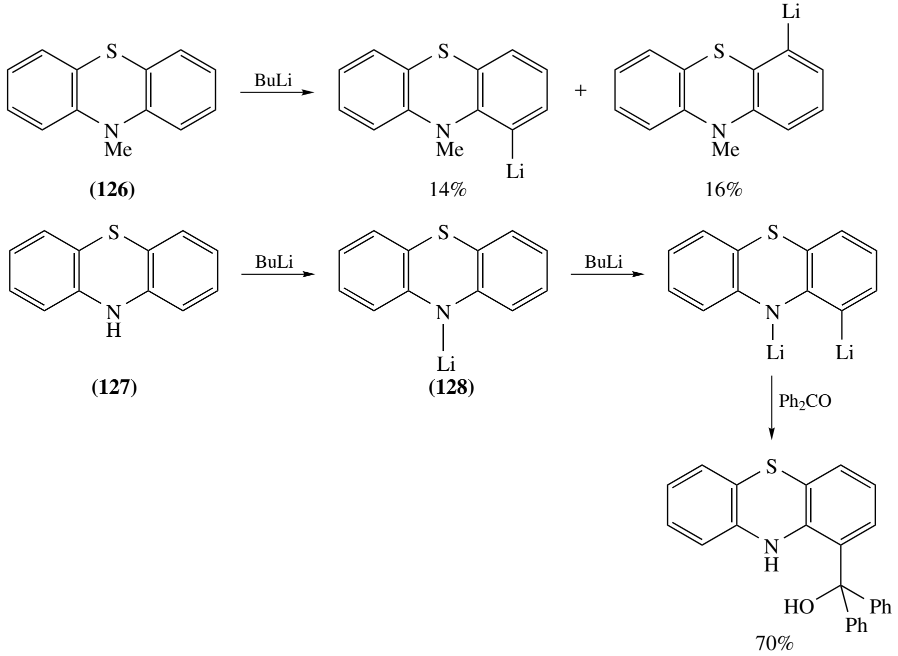

SCHEME 55

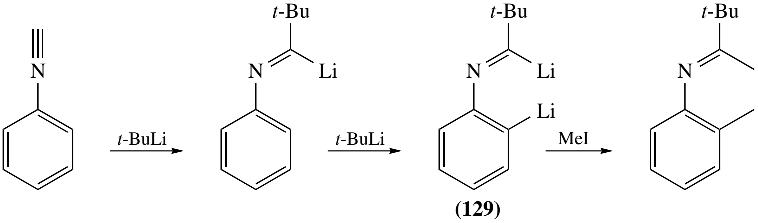

SCHEME 56

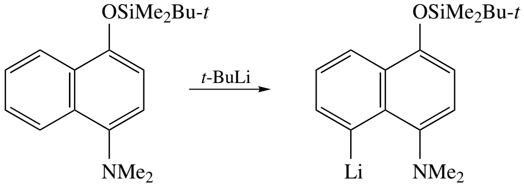

SCHEME 57

Nitriles will direct lithiation with non-nucleophilic bases such as LiTMP, particularly in conjuction with another nitrile group[149]. The nitriles presumably act by an acidifying effect alone—no intramolecular N–Li coordination is possible in the intermediate (Scheme 60).

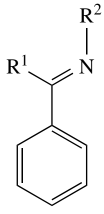

R^1 = H, alkyl, aryl
R^2 = NR_2, alkyl, aryl
or R^1, R^2 = completion of heteroaromatic ring

(130)

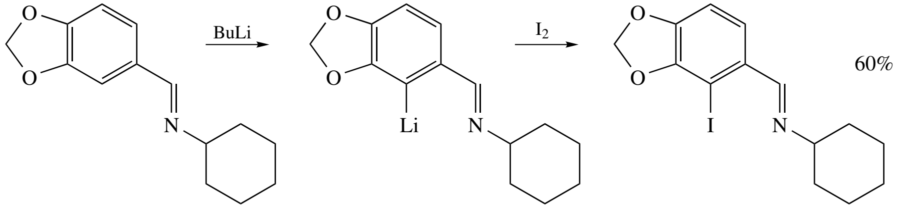

SCHEME 58

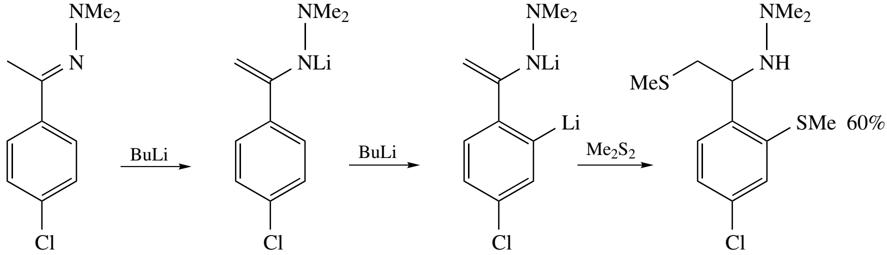

(131)

SCHEME 59

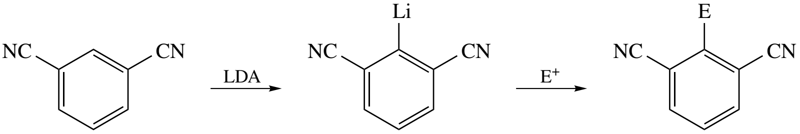

SCHEME 60

No heterocycle containing a C=N bond is as powerful a director as the oxazolines or tetrazoles described above, but their imidazoline analogues **132** direct well if deprotonated to the amidine equivalent **133** of a secondary amide anion (Scheme 61)[3]. Pyrazoles **134** also direct lithiation, but need protecting with a bulky *N*-substituent to prevent nucleophilic attack by the base (Scheme 62)[3].

Pyridines are yet more susceptible to nucleophilic attack, but may just about direct lithiation if ring addition can be avoided. Organolithium **135** is unstable and slowly isomerizes to **136** (Scheme 63)[3].

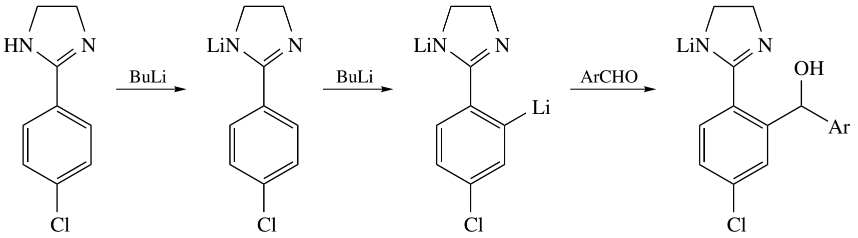

(132) **(133)**

SCHEME 61

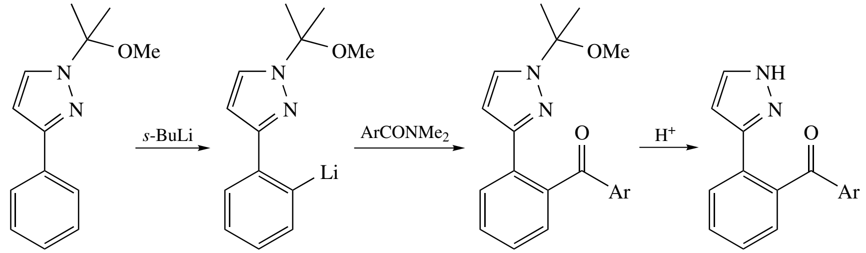

(134)

SCHEME 62

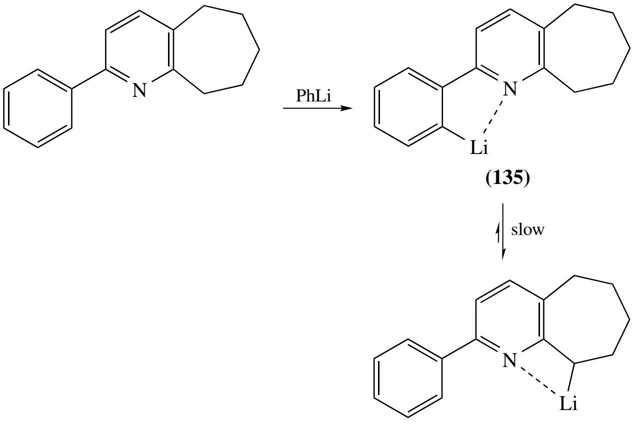

(135)

(136)

SCHEME 63

4. O class

a. Ethers and alkoxides. Alkyl aryl ethers have a long history in lithiation reactions, and there are detailed reports on the mechanism (see Section I.A) and relative efficiency[41] of the lithiation of anisole and its derivatives. Methyl aryl ethers are often lithiated in Et_2O, but THF can be just as effective. The stabilization afforded to an ortholithiated anisole relative to a *para*-lithiated anisole can be judged from their relative heats of protonation by *s*-BuOH (Scheme 64)[150].

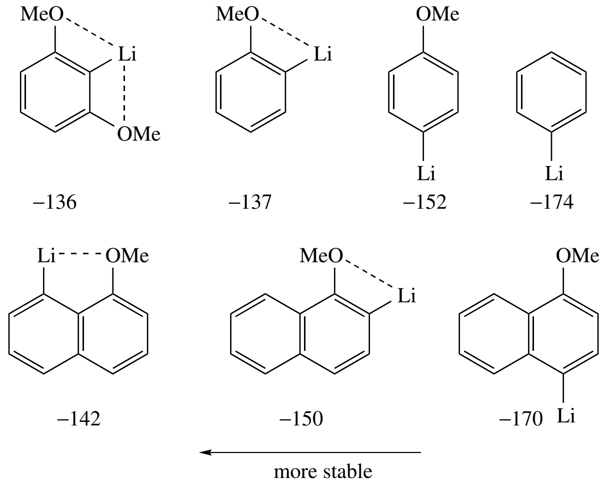

SCHEME 64

Particularly powerful synthetically is the ability of two *meta*-disposed methoxy groups jointly to direct lithiation to the position between them[151, 152]. Lithiation and carboxylation of 1,3-dimethoxybenzene, for example, is a key step in the synthesis of methicillin (Scheme 65)[153].

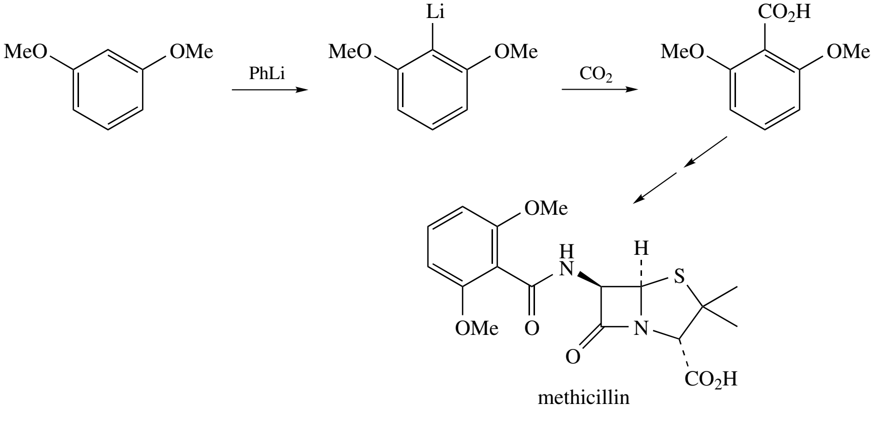

SCHEME 65

1,3,5-Trimethoxybenzene **137** can be lithiated twice (but not three times) by excess BuLi (Scheme 66)[154].

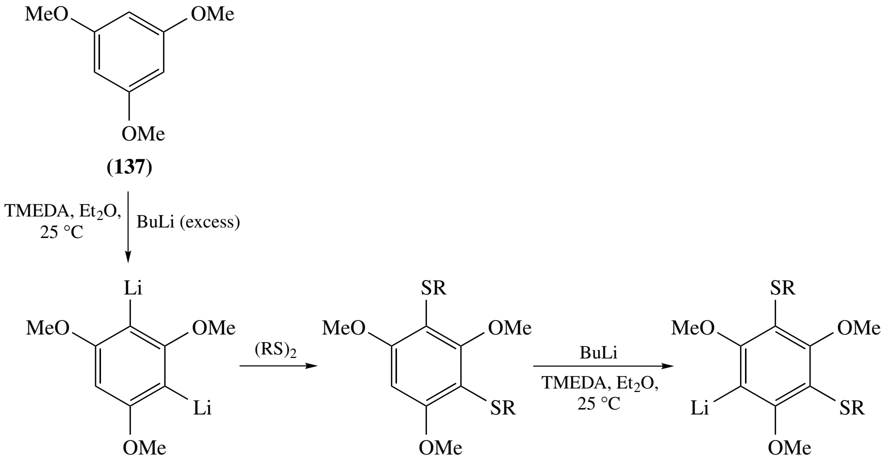

(137)

SCHEME 66

A single methoxy group alone is a relatively weak director, but their small size means methoxy groups are extremely good at biasing lithiation to the position in between themselves and another, better director, leading to 1,2,3-trisubstituted aromatics.

1-Methoxynaphthalenes may be lithiated in their *ortho* or *peri* positions according to conditions (see Table 1 in Section I.A). 1,4-Dimethoxynaphthalene, for example, perilithiates cleanly with *t*-BuLi (Scheme 67)[26, 145].

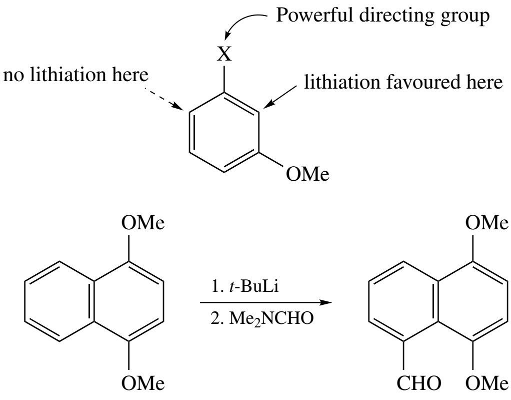

(138)

SCHEME 67

Other alkyl aryl ethers lithiate cleanly—for instance, benzoxepine **139**[155]. Lithiation of a fluoroacetal forms the first step in a route to the drug fludioxinil (Scheme 68).

The lithiation of phenols protected as acetals—methoxymethyl acetals like **140** in particular—is especially valuable: the second oxygen supplies a powerful coordination component to their directing effect (Scheme 69)[156, 157]. The regioselective lithiation of **141** was used in the synthesis of the pterocarpans 4′-deoxycabenegrins A-I.

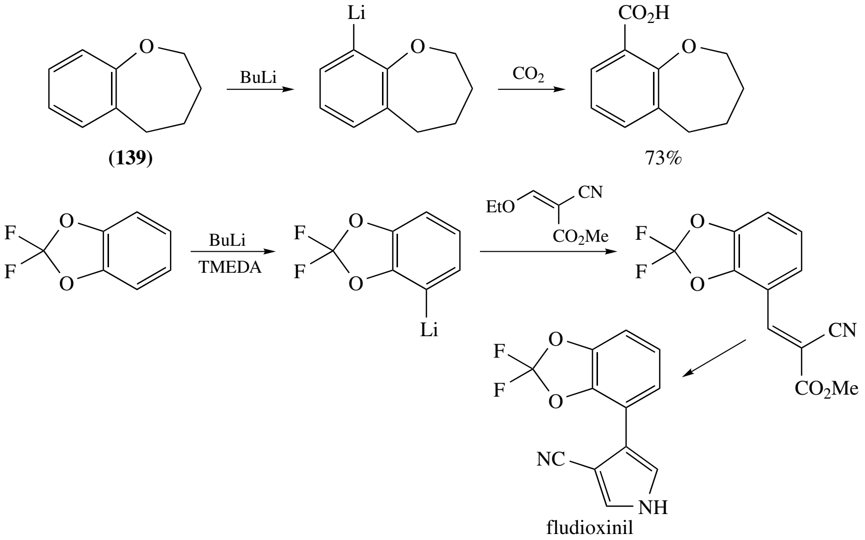

SCHEME 68

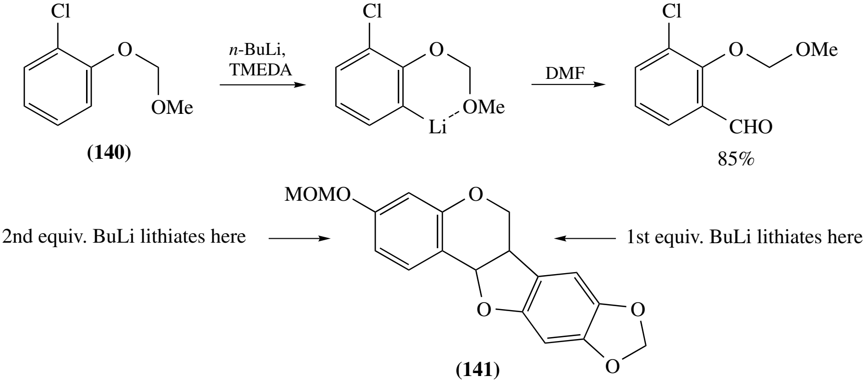

SCHEME 69

The reactions in Scheme 70[158, 159] illustrate the fact that −MOM acetals lie between −OMe and −OCON(Pr-*i*)$_2$ groups in their directing ability. Orthogonal deprotection conditions (acid for MOM, base for the carbamate) makes MOM and OCON(Pr-*i*)$_2$ a useful pair of directors for the regioselective synthesis of substituted phenols and aryl ethers.

A note of warning: both MOM acetals and methyl ethers *ortho* to electron-withdrawing groups—particularly oxazolines, aldehydes, imines and amides—are susceptible to nucleophilic aromatic substitution reactions involving loss of the alkoxy substituent[5, 82, 160].

Aryl ethers are less powerful directing groups than alkyl ethers: **142** gives only **143**[161]. Diaryl ethers can usually be lithiated on one (the more acidic) or both rings, according to the amount of alkyllithium employed. Diphenyl ether **144** will give, for example, silaxanthene **145** on quench with a dichlorosilane (Scheme 71).

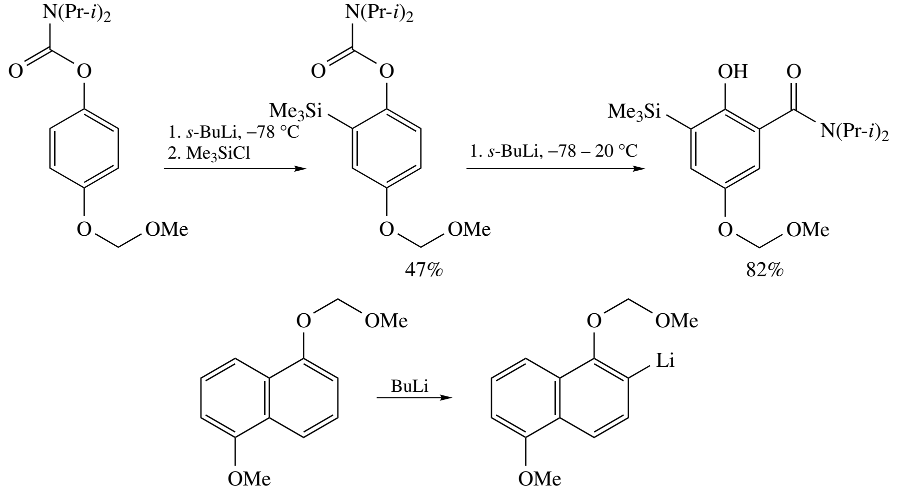

SCHEME 70

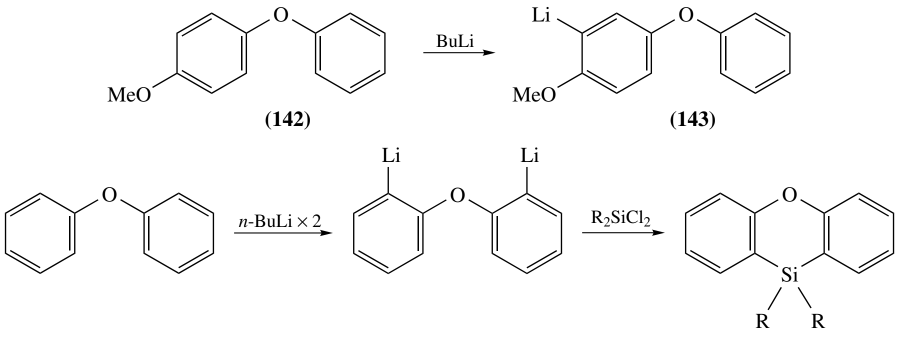

(142) **(143)** **(144)** **(145)**

SCHEME 71

Double lithiation of the xanthene derivative **146**[162] is the key step in an important synthesis of the ligand xantphos **147**[163, 164]. Benzofuran **148** is also doubly lithiated by excess BuLi/TMEDA (Scheme 72)[165, 166].

Unlike benzylic amines, benzylic ethers undergo benzylic lithiation and 1,2-Wittig rearrangement too readily to be directors of lithiation[167]. In the absence of benzylic protons, ortholithiation of **149** can occur, for example to give **150**, which undergoes a curious addition to a second phenyl ring, ultimately eliminating methoxide to give 9-phenylfluorenyllithium **151** (Scheme 73)[168].

Free phenols (as their phenoxides) have a weak, and synthetically useless, directing effect[34, 35, 169], but the alkoxides of benzylic alcohols can be useful as lithiation directors (see below)[8, 170], especially when assisted by a second director (Scheme 74)[171].

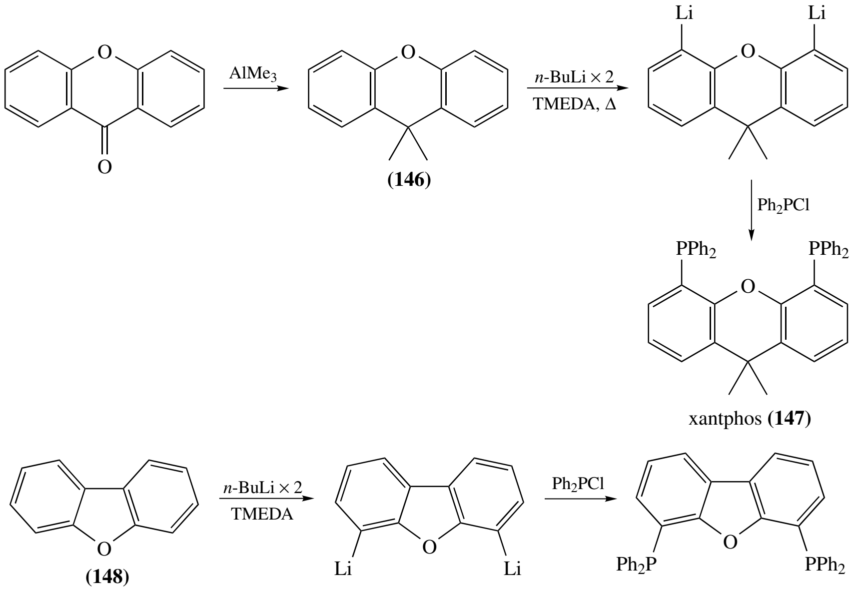

SCHEME 72

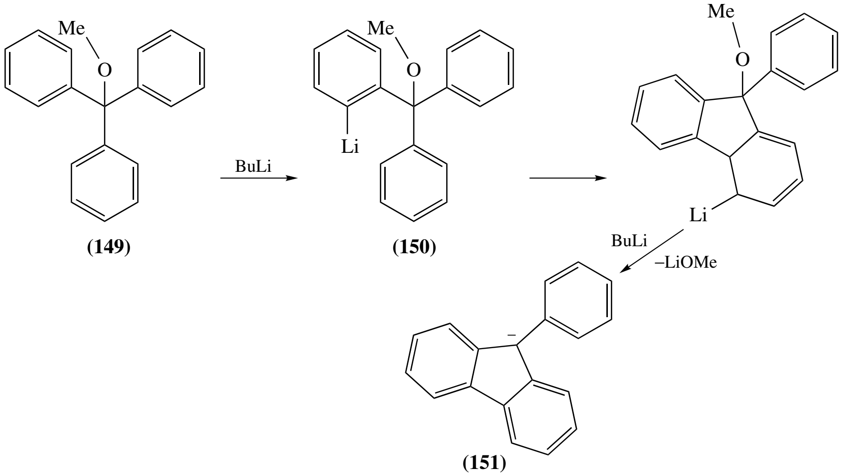

SCHEME 73

b. Ketones, esters and carboxylates. Lithium amides (LiTMP) can give good yields of products resulting from ortholithiation of both ketones and lithium carboxylates. Benzophenone **152**, for example, with LiTMP gives a good yield of the ortholithiation–dimerisation product **152** (Scheme 75)[4]. In general, however, ketones and aldehydes are best lithiated by the method developed by Comins described in Section I.B.1.b.

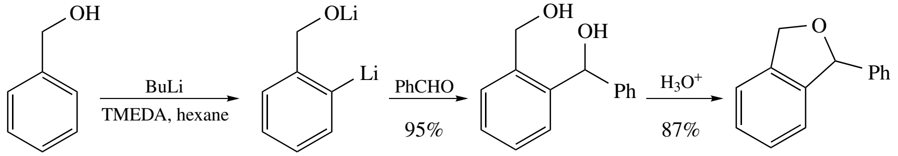

SCHEME 74

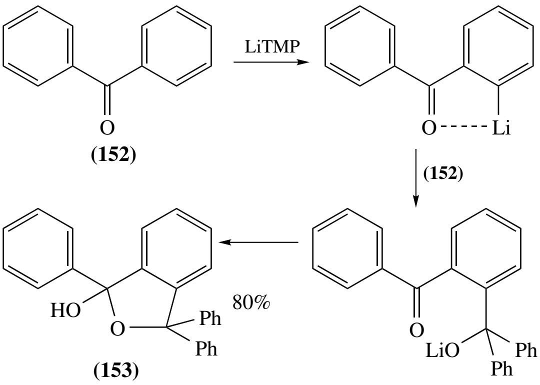

SCHEME 75

The lithiation of lithium carboxylates was believed to be impossible by Gschwend and Rodriguez[3] because of competing attack at C=O by an organolithium. Carboxylates are insufficiently strong orthodirectors to be lithiated by LDA but, provided temperatures are kept low, BuLi lithiation without nucleophilic addition is possible. Treatment of **154** with 2.2 equivalents of BuLi at −90 °C in the presence of TMEDA leads to good yields of ortholithiated product **155** (Scheme 76)[172, 173]. In terms of their directing power, $-\mathrm{CO_2Li}$ is weaker than those in the N + O class, but among the strongest of the O class[174].

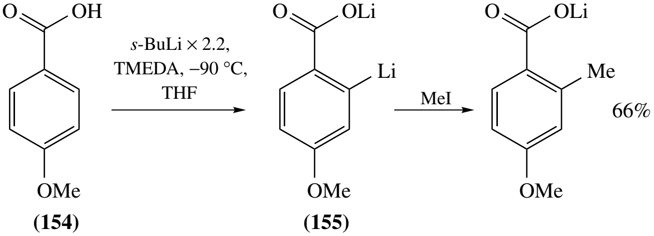

SCHEME 76

In the pyridine- and quinolinecarboxylic acid series, the greater acidity of the ring protons means that LDA or LiTMP can be used for metallation; all three pyridinecarboxylic acids **156–158** are lithiated in good yield (Scheme 77)[175].

The thiophenecarboxylic acid **159** is lithiated *ortho* to the carboxylate group by BuLi[87], but α to the ring sulphur by LDA[176]—presumably a case of regioselectivity determined

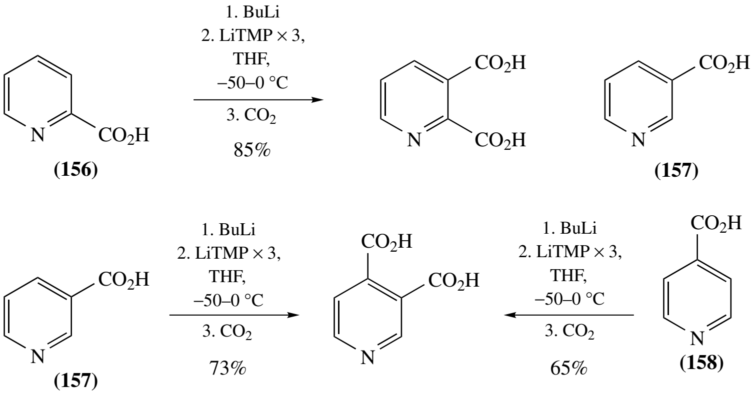

SCHEME 77

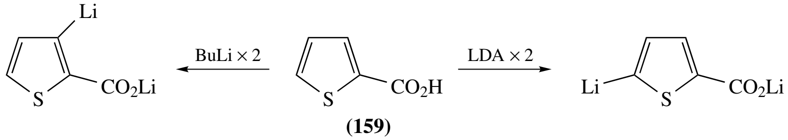

SCHEME 78

kinetically (with BuLi—better coordination to O than S) or thermodynamically (with LDA—acidification of positions α to S) (Scheme 78).

Even esters can be ortholithiated, provided the electrophile is present *in situ* during the lithiation. Neopentyl ester **160** gives, on treatment with LDA in the presence of triisopropylborate, the boron derivative **161**, which can be deprotected and used in Suzuki coupling reactions (Scheme 79)[177]. Less hindered esters can also be successfully ortholithiated in the presence of a boron electrophile (Scheme 80)[178].

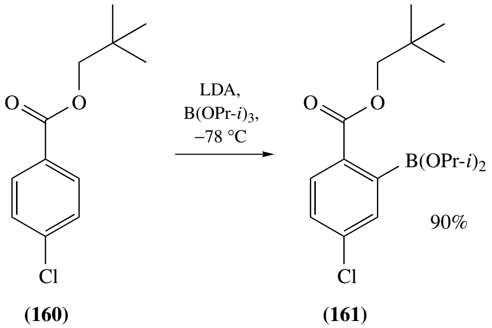

SCHEME 79

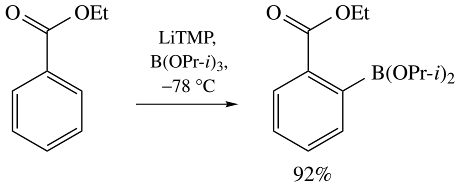

SCHEME 80

5. X class

Fluorine acidifies[179] an *ortho* proton rather more than chlorine or bromine, whose weak directing effects are more or less comparable[180]. Deprotonation of fluorobenzene is feasible in THF, and at temperatures below −50 °C the lithiated species **162** is stable and does not collapse to a benzyne (Scheme 81)[54, 181].

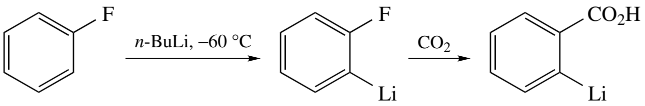

(162) 60%

SCHEME 81

The trifluoromethyl group behaves in a similar way[152], but it is now clear that deprotonation of sites *ortho* to such acidifying but non-coordinating and non-electrophilic substituents is best carried out with BuLi−KOBu-*t* superbases (see Section VI). A combination of BuLi metallation and superbase metallation of fluoroarenes has been used in the synthesis of components **163** and **164** for fluorinated liquid crystals (Scheme 82)[182].

Chlorobenzene is lithiated more slowly[180] and cannot be lithiated completely at temperatures where benzyne formation is slow[3]. With 1,2,3,4-tetrachlorobenzene **165**, MeLi leads to ortholithiation; *t*-BuLi, on the other hand, leads to halogen−metal exchange (Scheme 83)[183].

Successful lithiation of aryl halides—carbocyclic or heterocyclic—with alkyllithiums is, however, the exception rather than the rule. The instability of ortholithiated carbocyclic aryl halides towards benzyne formation is always a limiting feature of their use, and aryl bromides and iodides undergo halogen−metal exchange in preference to deprotonation. Lithium amide bases avoid the second of these problems, but work well only with aryl halides benefitting from some additional acidifying feature. Chlorobenzene and bromobenzene can be lithiated with moderate yield and selectivity by LDA or LiTMP at −75 or −100 °C[180].

Meyers and coworkers have exploited both the lithiation-directing and benzyne-forming abilities of a chloro substituent to form the benzyne **167** from oxazoline **166** (Scheme 84). Excess organolithium adds regioselectively to the 2-position of the benzyne (probably directed by coordination to the oxazoline) to give **168**[184, 185].

C. Stereoselective Ortholithiation

Stereochemistry is rarely an issue in ortholithiation reactions unless the directing group is chiral and a prochiral electrophile is used which gives rise to a new stereogenic centre. Most attempts to use metallation-directing groups containing stereogenic

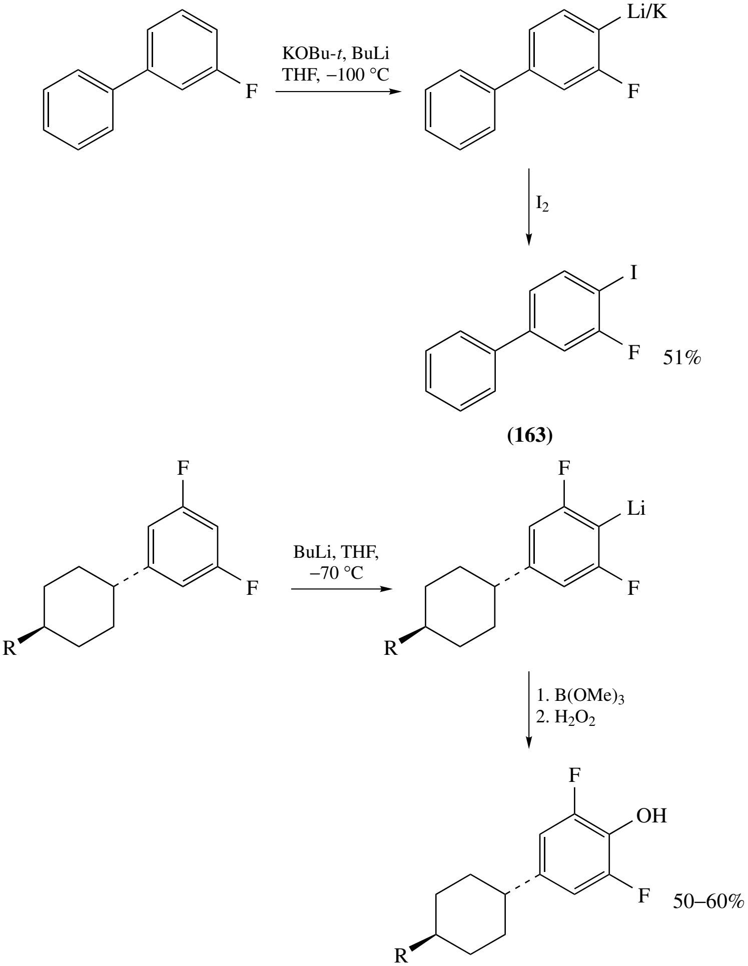

(163)

(164)

SCHEME 82

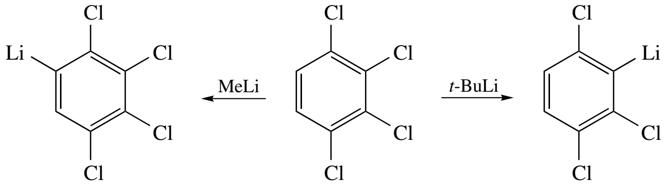

(165)

SCHEME 83

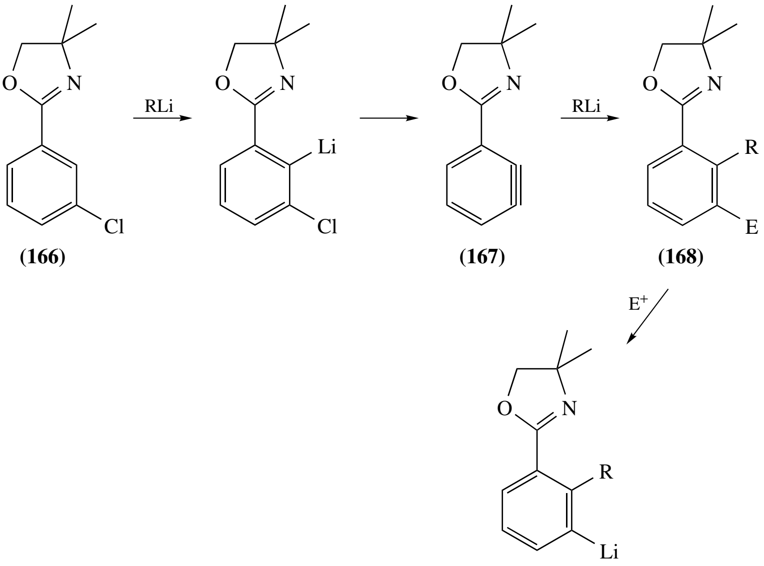

(166) (167) (168)

SCHEME 84

centres have failed to give any useful level of stereoselectivity—for example, lithiated arylsulphoxides[52] and lithiated chiral amides[46] and hydrazines[81] all add to benzaldehyde to give close to 1:1 mixtures of diastereoisomers. In the heterocyclic and ferrocenyl series, by contrast, additions of ortholithiated sulphoxides to aldehydes can lead to good levels of stereoselectivity (see Sections II and III). Asymmetric lithiation of prochiral ferrocenes or arenechromium tricarbonyl complexes with chiral bases is also effective (see Section III).

In aromatic compounds bearing two rotationally restricted amide groups, diastereoisomeric atropisomers can arise because of the relative orientation of the amides. Ortholithiation can therefore lead to diastereoselectivity if the ortholithiation forms one of the two diastereoisomers selectively. A simple case is **169**, whose double lithiation–ethylation leads only to the C_2-symmetric diamide **170**, indicating the probable preferred conformation of the starting material (Scheme 85)[162].

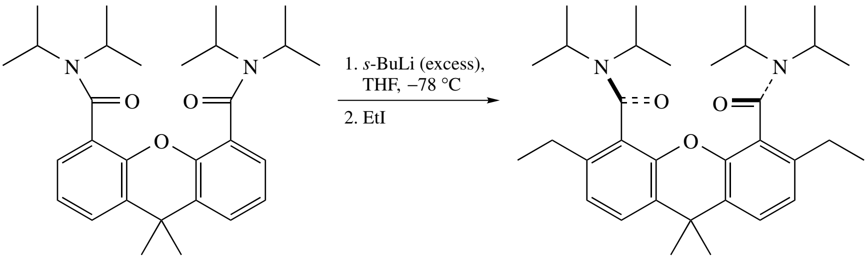

(169) (170)

SCHEME 85

The biphenyl diamide **171** also displays diastereoselectivity in its ortholithiation–electrophilic quench, giving the C_2-symmetric, chiral diastereoisomer of the diamide **172**[186].

Heating the product converts it mainly to the more stable achiral, centrosymmetric diamide **173** (Scheme 86)[162].

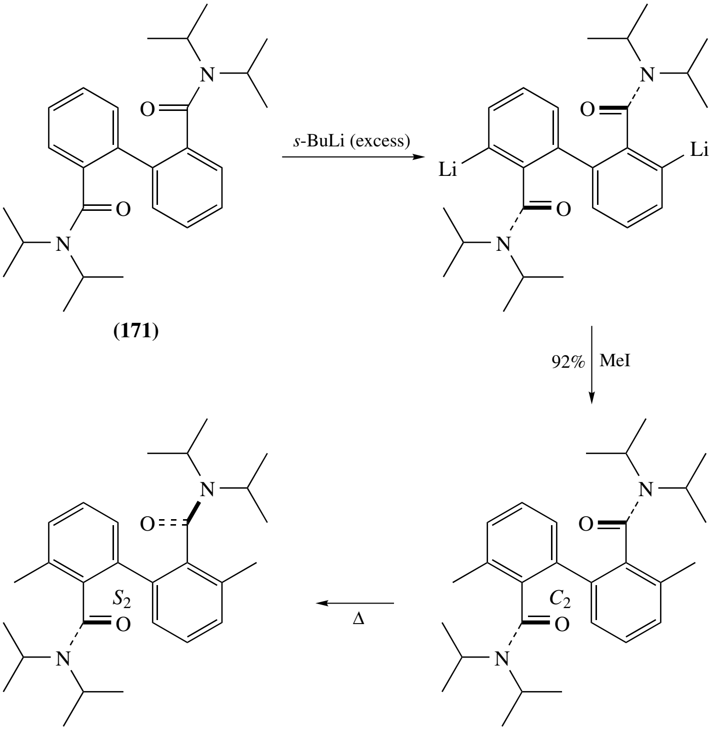

(171)

(173)

(172)

SCHEME 86

II. ORTHOLITHIATION OF AROMATIC HETEROCYCLES

A. Electron-deficient Heterocycles

Electron-deficient six-membered aromatic heterocycles are distinctly more acidic than their carbocyclic analogues, and not only are LDA and other lithium amides capable of deprotonating them in good yield[84], but they are in many cases also a necessity since alkyllithiums prefer addition to the electron-deficient ring over deprotonation. Even when heterocycles can be successfully lithiated, the addition of the organolithium product to remaining starting material may itself pose a problem—as in the attempted lithiation of pyridine with LDA at −70 °C, which gives a 50% yield of bipyridine **175** via **174** (Scheme 87)[187].

Lithiation of pyridine itself (and quinoline) is best carried out using a combination of BuLi and the lithiated amino alcohol LiDMAE **176** (Scheme 88)[188].

Bipyridines can be lithiated with LiTMP (if only in moderate yield), with one nitrogen atom directing the lithiation of the other ring (Scheme 89)[189]. Both 2,2′- and 2,4-bipyridines **177** and **178** can be lithiated in this way.

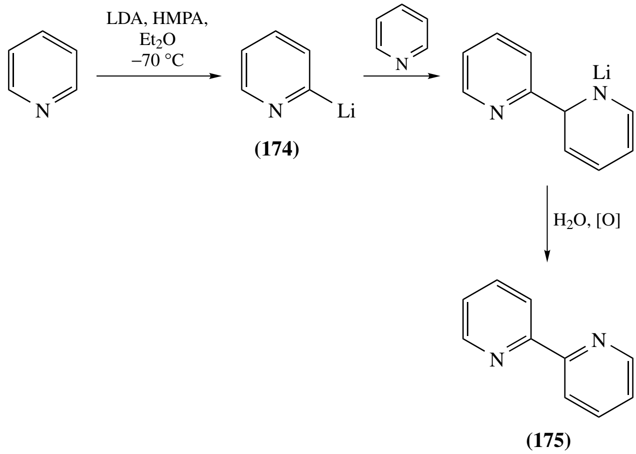

SCHEME 87

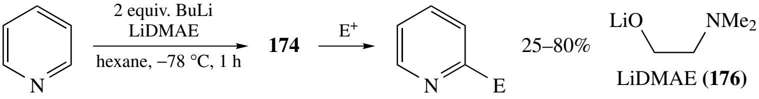

SCHEME 88

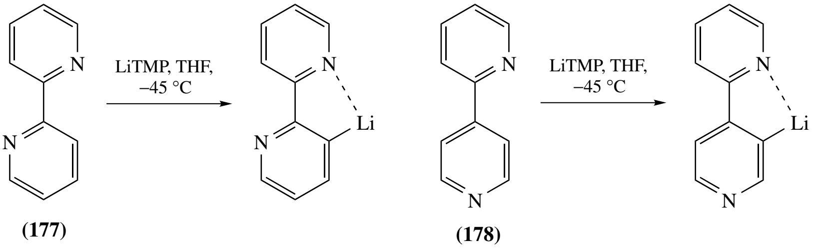

SCHEME 89

Halogen substituents are of course easy to introduce to heteroaromatic rings, and they also enhance the acidity of the ring protons. *n*-BuLi will, for example, lithiate the tetrafluoropyridine **179** at −60 °C in ether[190, 191], but with pyridine itself it leads to addition/reoxidation products[192]. Addition to the ring is the major product with 2-fluoropyridine **180**, though some metallation can be detected; selectivity in favour of metallation is complete with LDA in THF at −75 °C[193, 194] or with phenyllithium and catalytic *i*-Pr_2NH at −50 °C (Scheme 90)[195]. Similar results are obtained with quinolines[196].

With even more electrophilic heterocycles, addition of the lithiated species to the starting material can become a problem—for example, LDA will lithiate pyrimidine **181** at −10 °C, but the product, after work up, is the biaryl **182** resulting from ortholithiation and readdition (Scheme 91). By lithiating in the presence of benzaldehyde, a moderate yield of the alcohol **183** is obtainable[197]. Strategies for the lithiation of pyrimidines and other very electrophilic heterocycles are discussed below[198].

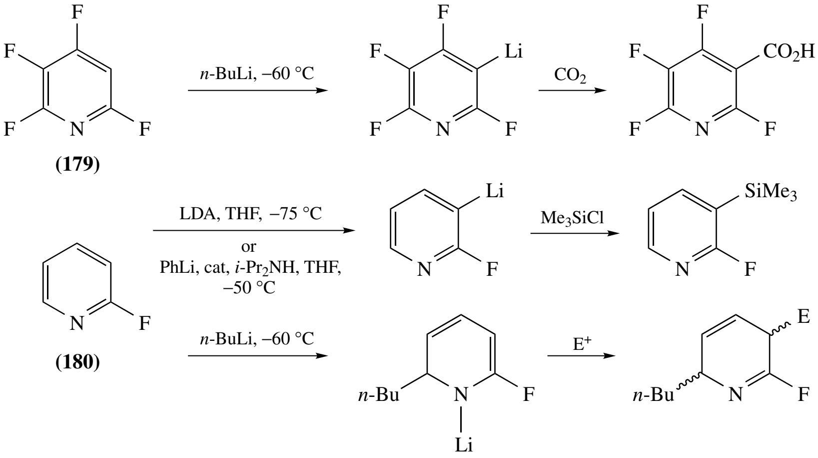

SCHEME 90

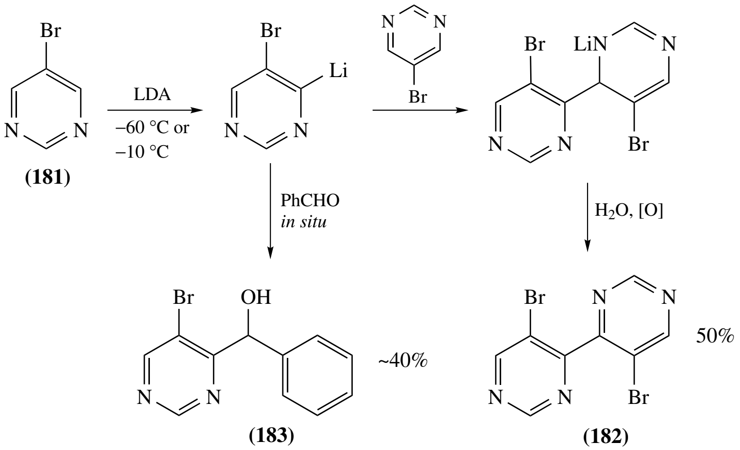

SCHEME 91

Because lithiation with lithium amides leads to the thermodynamically favoured product, regioselectivity in the lithiation of electron-deficient heterocycles is often determined more by anion stability than by the rate of deprotonation—in other words, the coordination aspect of lithiation may take second place to the acidifying effect of the substituents[199]. This has an important consequence for the regiochemistry of lithiation, because while the nitrogen lone pair of pyridine may on occasions act as a directing group by coordinating to Li, it also has a destabilizing effect on an anion formed at the adjacent carbon because of repulsion between the lone pair and the C−Li bond. The relative stabilities of organolithiums at the 4-, 3- and 2-positions on a pyridine ring are indicated by the relative acidities of the protons, 700:72:1 (Scheme 92)[200].

Overall, the most stable pyridinyllithiums are those bearing Li at the 3- or 4-positions; 2-pyridinyllithiums may on occasion be formed faster, but given a proton source they

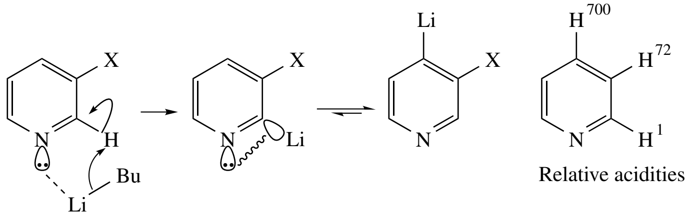

SCHEME 92

will readily isomerize to 4-pyridinyllithiums. The deprotonation of 3-fluoropyridine **184** at the 4-position with Schlosser's BuLi–KOBu-*t* ('LiC-KOR') superbase[201] illustrates this (Scheme 93)[202]. In contrast, BuLi–TMEDA in Et_2O leads mainly to 2-lithiation. BuLi–TMEDA in THF, on the other hand, gives 4-metallation, showing how closely balanced these two factors are.

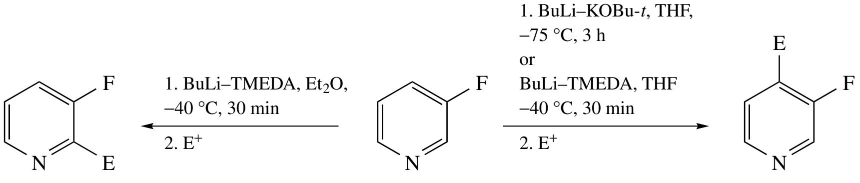

(184)

SCHEME 93

With 3-trifluoromethylpyridine **185**, BuLi in ether also lithiates cleanly at the 2-position (Scheme 94)[203].

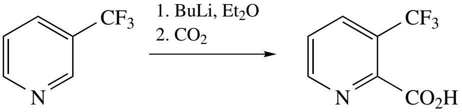

(185)

SCHEME 94

Blocking either the 2- or 4-position allows lithiation at the other: LDA or BuLi can be used to 4-lithiate the 2-blocked 3-fluoropyridines **186**[204], **187**[205] and **188** (Scheme 95)[206, 207], and BuLi 2-lithiates the 4-blocked 3-fluoropyridine **189**[204, 208, 209]. Note the selectivity for removal of the acidified pyridine protons in **188** and **189** over the coordination-activated ones adjacent to the pivalanilide group. A double *ortho*-directing effect ensures 4-lithiation of **190**[210].

Fluoropyridines form valuable starting materials for a range of disubstituted pyridines because, after lithiation, nucleophilic substitution of fluoride[194] (sometimes via the *N*-oxide) can be used to introduce, say, N or O substituents as in **191** and **192** (Scheme 96). Subsequent annelations can allow complex polycyclic heteroaromatics to be constructed[84].

Chloropyridines behave largely similarly to fluoropyridines: they are lithiated by LDA (or in some cases BuLi, though addition to the pyridine ring may pose problems)[84, 199]. 3-Chloropyridines such as **193** are readily 4-lithiated[211, 212], and 2-chloropyridines **194**–**196**

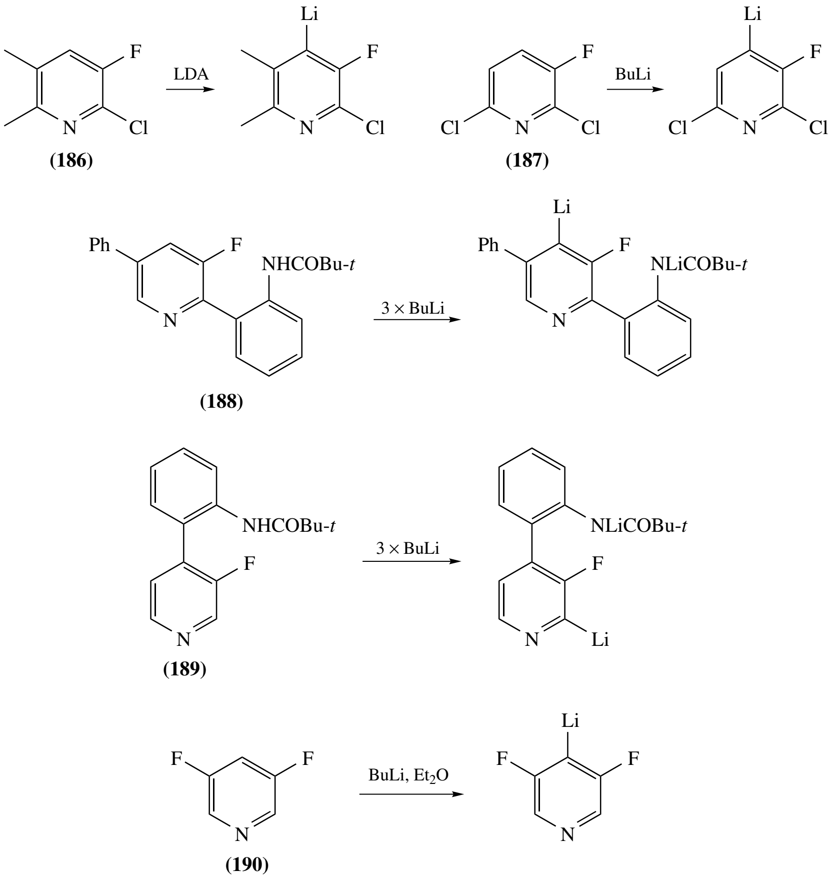

(186) **(187)** **(188)** **(189)** **(190)**

SCHEME 95

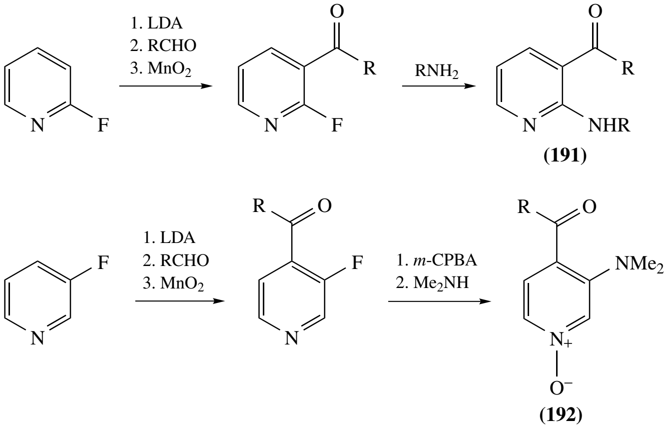

(191) **(192)**

SCHEME 96

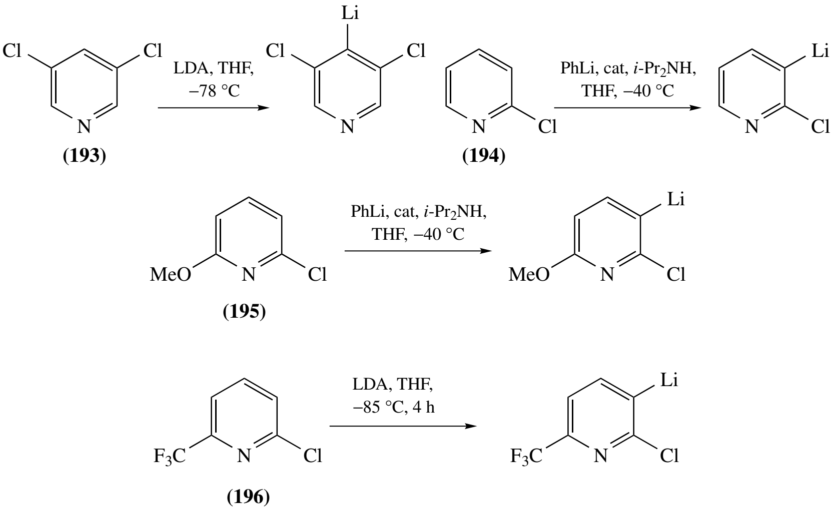

SCHEME 97

can be 3-lithiated with LDA or PhLi/cat. i-Pr$_2$NH (Scheme 97)[179, 195, 213]. Chloropyridines **195** and **196** are lithiated *ortho* to Cl rather than CF$_3$ or even the usually more strongly directing MeO.

Since chlorine is less electronegative than fluorine, the role of the inherent relative acidities of the positions on the pyridine ring becomes more important in chloropyridine lithiations[214]. Not surprisingly, **197** is lithiated cleanly in the 4-position rather than the less acidic 3-position (Scheme 98)[215]. When **198** is lithiated with BuLi, the preference for 4-lithiation wins out even though the intermediate lithium lacks an adjacent acidifying Cl atom. By contrast, LDA lithiation of this compound under thermodynamic control gives the expected regioselectivity[213]. A similar effect is observed in the lithiation of **196** with BuLi and with LDA[179].

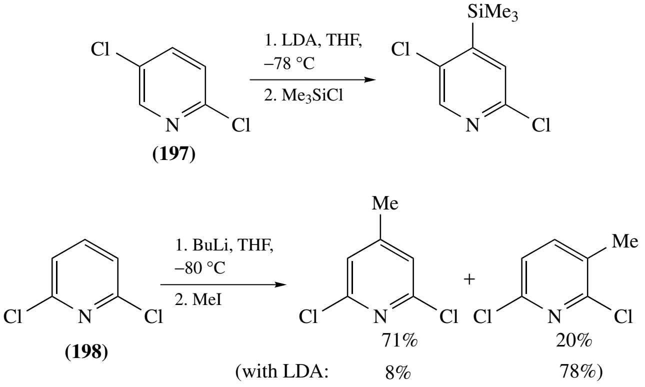

SCHEME 98

2-Bromopyridine **199** can be 3-lithiated with LDA, but this too appears to be a thermodynamic effect: *in situ* quench of the first-formed mixture of organolithiums from **199** shows some 4-lithiation even with LDA (Scheme 99)[216, 217].

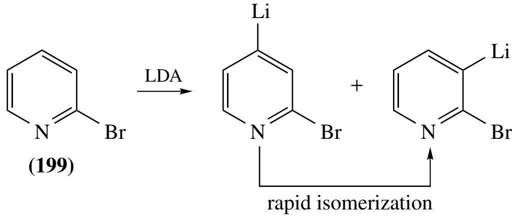

SCHEME 99

4-Bromopyridines **200**[218] and 3,5-dibromopyridines **201**[219] lithiate quite normally with LDA, as does 3-bromopyridine **202** provided the temperature is kept below −78 °C (Scheme 100)[220]. At −100 °C, or with *in situ* Me_3SiCl, evidence that the 2-lithiopyridine **204** is an intermediate in the formation of **203** can be obtained[216, 217].

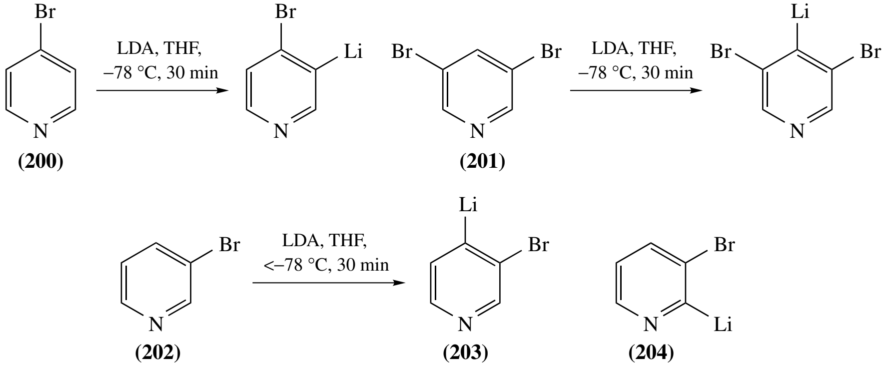

SCHEME 100

Lithiation of 3-bromopyridine at higher temperatures leads to a mixture of products of which the major (**209**) has the bromine at the 4-position and is clearly formed by rearrangement of **205** to **208** via halogen–metal exchange, probably through formation of a catalytic amount of 3,4-dibromopyridine **207** (Scheme 101)[221].

Halogen–metal exchange processes can also isomerize a less stable 2-lithiopyridine to a more stable 4-lithiopyridine. In some cases, this leads to complex mixtures of regioisomers[84]. However, these rearrangements (known as 'halogen-dance' reactions) can be put to good use in the synthesis of unusual substitution patterns of bromo and iodopyridines[222]. For example, kinetic lithiation of **210** takes place at C-2, but rapid isomerization by reversible iodine–lithium exchange ensues, and products are isolated resulting from electrophilic quench of **211** (Scheme 102)[222].

Metallation of simple iodopyridines fails[220], but iodopyridines containing additional halogens metallate and rearrange to place the lithium between the two directing groups, as shown in Scheme 103[222].

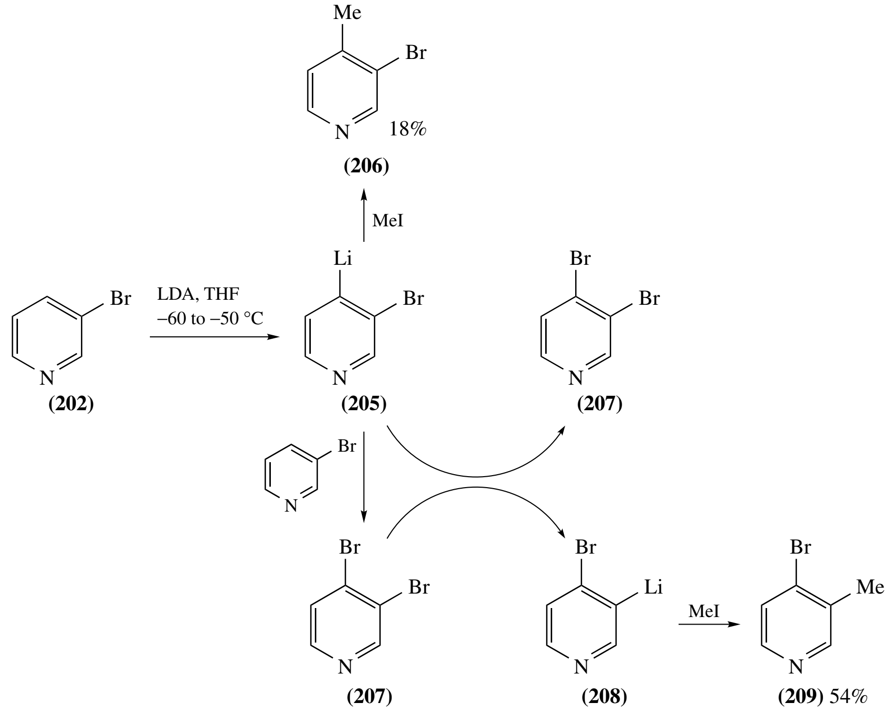

SCHEME 101

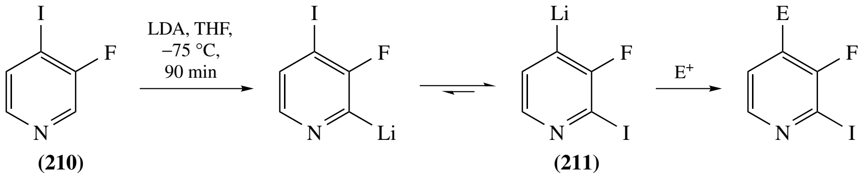

SCHEME 102

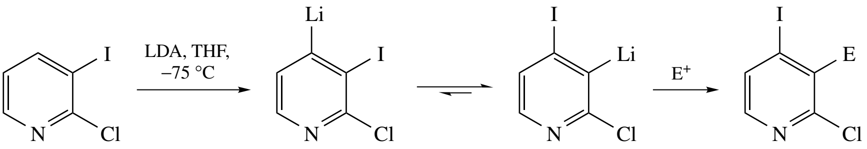

SCHEME 103

2-Fluoro-3-iodopyridine **212** was used by Comins and Saha as the starting material in a synthesis of mappicine[223]. The first-formed organolithium **213** rearranges to **214** and a quench gives **215**. Iodine–lithium exchange allows introduction of the C-4 hydroxypropyl substituent of **216** (Scheme 104).

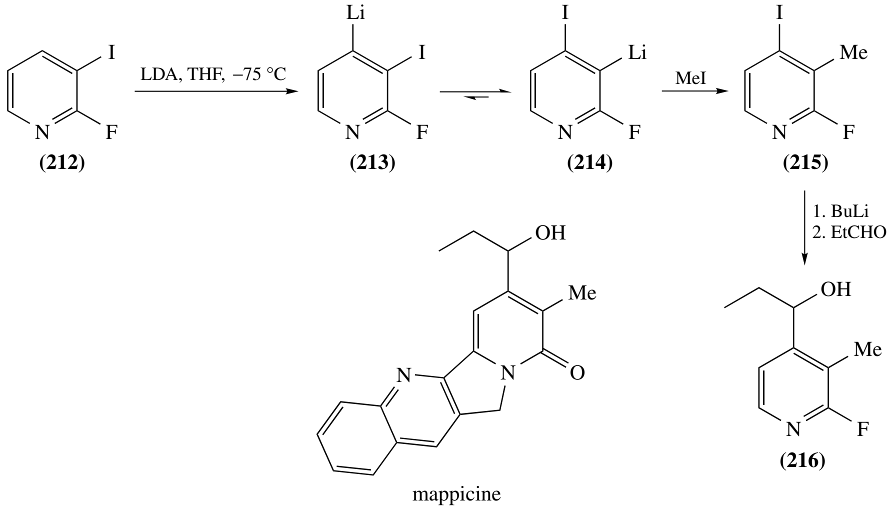

SCHEME 104

Iodopyridines bearing other lithium-stabilizing groups behave similarly[224], and in the case of the amide **217** the intermediate 4-lithio species **218** was detectable by *in situ* silylation (Scheme 105)[225].

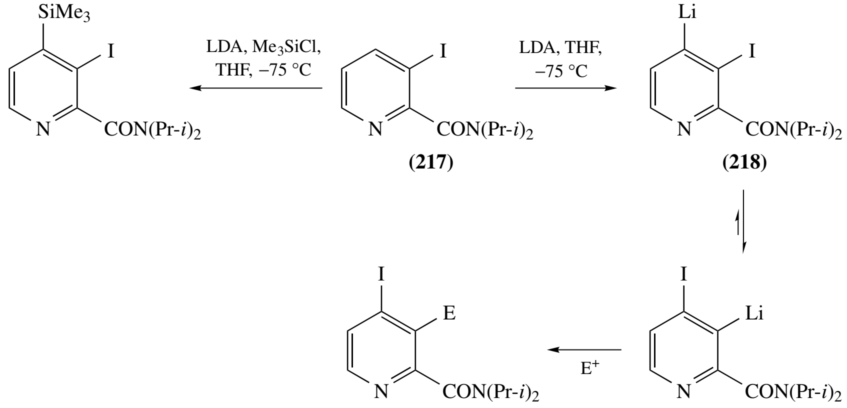

SCHEME 105

A similar bromine–lithium exchange mediated isomerization of 2-lithiopyridine **219** (Scheme 106)[226] was used in a synthesis of atpenin B (see below)[227].

Methoxypyridines are much more resistant than halopyridines to addition to the heterocyclic ring and they may be lithiated with alkyllithiums[228, 229]. They generally show unremarkable selectivities (Scheme 107)[230]: in the case of **221** the 2-lithio species—presumably the kinetic product—is preferred, and a similar reaction was used in the synthesis of the natural product UK-2A[231]. The lithiation of **220** with PhLi was a key step in the synthesis of caerulomycin C[226].

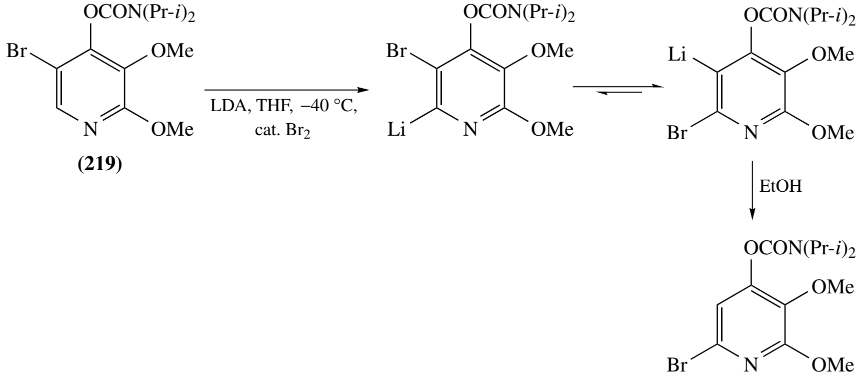

(219)

SCHEME 106

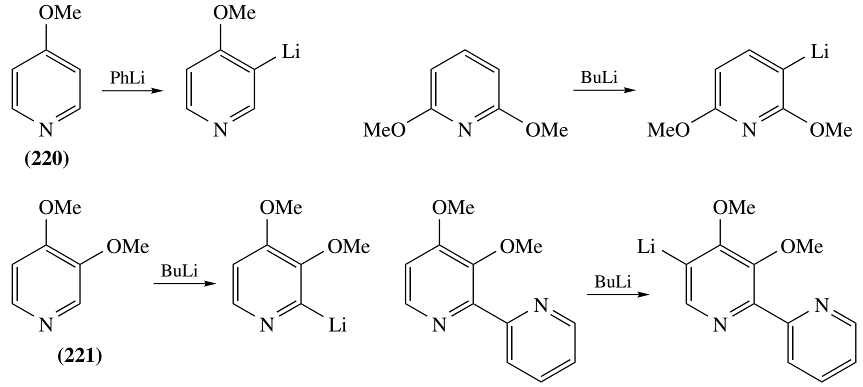

(220)

(221)

SCHEME 107

The delicate balance between 2- and 4-lithiation of 3-substituted pyridines is again illustrated clearly by the way that MeLi lithiates **222** at C-4, while BuLi–TMEDA lithiates it at C-2 (Scheme 108)[84]. More strongly coordinating directing groups (such as OMOM) direct even more strongly to C-4 because they rely less on coordination to the nitrogen atom[84]. Base-dependent selectivities are evident when OR and Cl are in competition as directing groups on a pyridine ring[199, 232, 233].

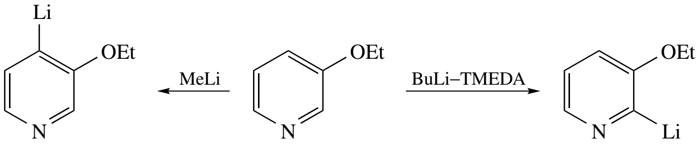

(222)

SCHEME 108

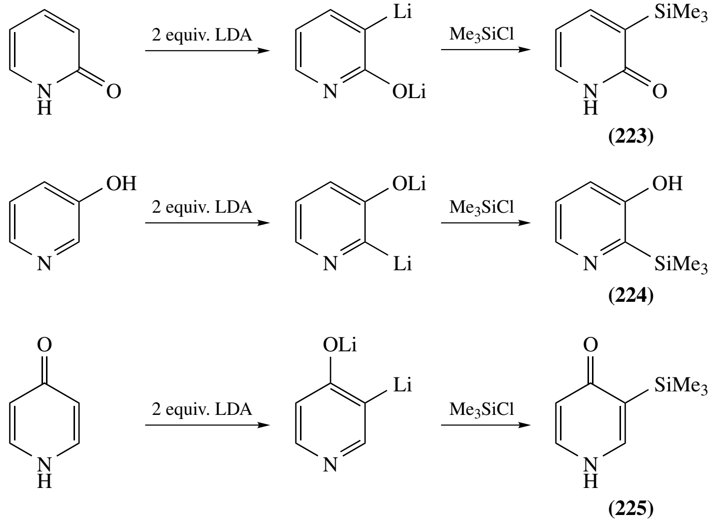

(223)

(224)

(225)

SCHEME 109

On deprotonation, pyridones and quinolones carry an oxyanion substituent which turns out to be a good director of lithiation. Two equivalents of LDA lead to the compounds **223–225** (Scheme 109)[217].

2-Quinolones behave similarly, and unlike quinolines are not attacked by BuLi at the ring[234]. *N*-Substituted pyridones and quinolones are lithiated, sometimes on the *N*-substituent, sometimes *ortho* to N and sometimes *ortho* to O[199]. By way of example, the 4-pyridone **226** lithiates α to N in the ring, while in the 2-pyridone **227** the combined lateral directing effect of the O and the α-directing effect of N lead to lithiation on the side chain (Scheme 110)[235].

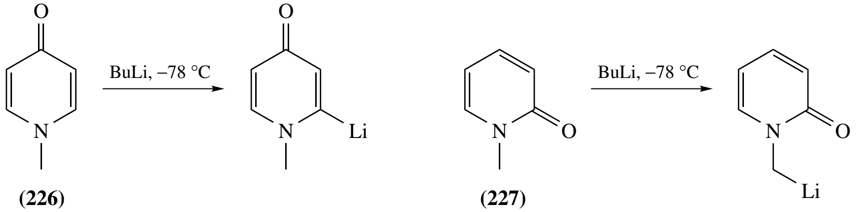

(226)

(227)

SCHEME 110

Closely related are the pyridine-*N*-oxides, which are readily lithiated in the 2-position[84, 236], even in examples such as **228** where there is a powerful competing directing group (Scheme 111)[237]. Lithiation of the bipyridine-*N*-oxide **229** was used in a synthesis of the caerulomycins and collismycins[238].

N-Activation by BF_3 to form complex **230** can be used to promote ortholithiation of pyridine itself[239, 240], though not quinoline and isoquinoline (Scheme 112). Temporary formation of a pyridine–hexafluoroacetone adduct **231** achieves the same result[241].

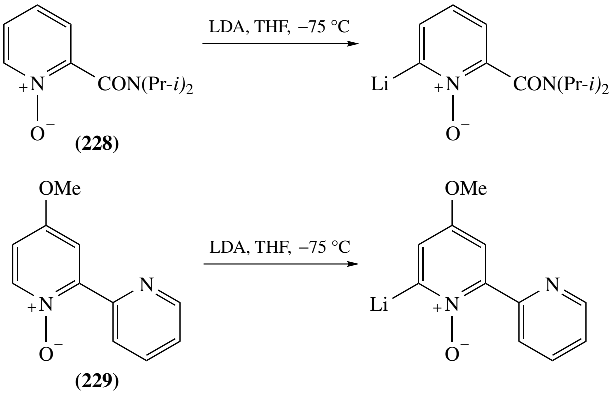

SCHEME 111

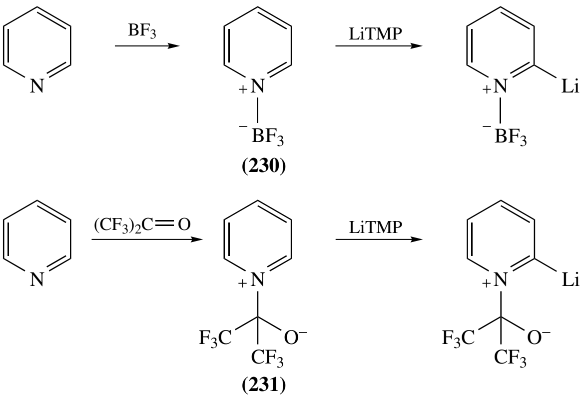

SCHEME 112

Complexation of pyridine by chromium tricarbonyl also facilitates removal of the ring protons[242].

More powerful directing groups such as those based on amides and sulphonamides are successful with pyridines as with carboxylic rings, and will not be discussed separately. The enhanced acidity of pyridine ring protons makes the simple carboxylate substituent an ideal director of lithiation in pyridine systems[175]. The pyridinecarboxylic acids **232**–**234** are deprotonated with BuLi and then lithiated with an excess of LiTMP: all the substitution patterns are lithiated; nicotinic acid **233** is lithiated in the 4-position (Scheme 113). The method provides a valuable way of introducing substituents into the picolinic, nicotinic and isonicotinic acid series.

Quinolinecarboxylic acids **235** and **236** are also deprotonated with LiTMP (Scheme 114)[243].

Another directing group whose value and effectiveness is greatly enhanced in the pyridine series is the α-aminoalkoxide group derived by addition of a lithioamine to an aldehyde[97] (see Section I.B.1.b). Aldehyde **237** was converted to **238**, and thence to an intermediate **239** in the synthesis of the alkaloid maxonine, by this method (Scheme 115)[244].

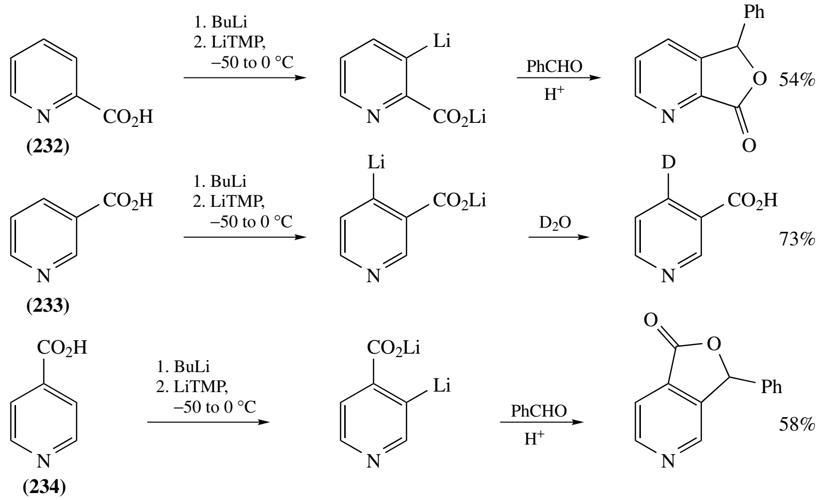

SCHEME 113

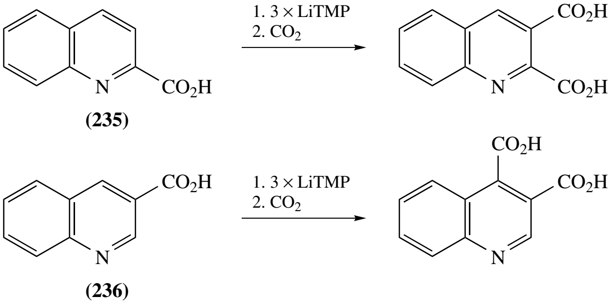

SCHEME 114

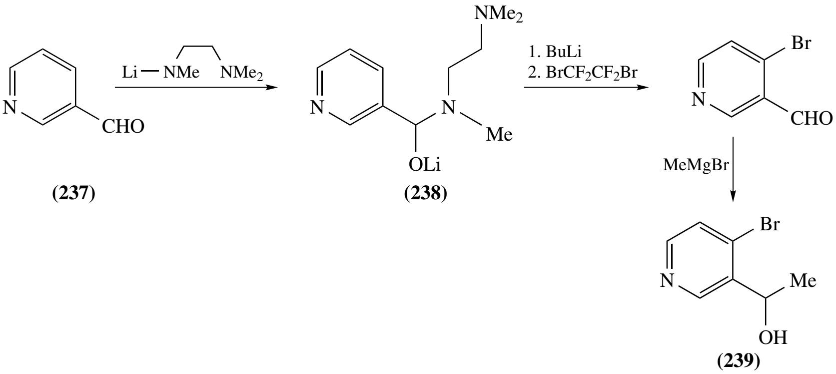

SCHEME 115

Halogenated *quinolines* very often undergo nucleophilic addition with BuLi, so must be lithiated with LDA or LiTMP[84, 199]. The regioselectivity of their reactions parallels that of the pyridines, and similar halogen migrations are observed (Scheme 116)[245, 246].

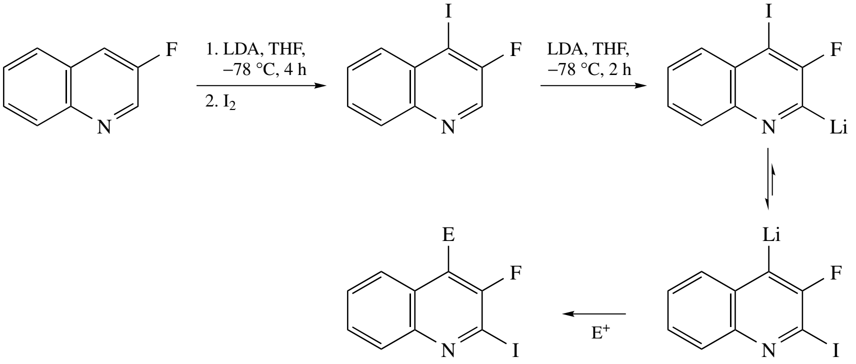

SCHEME 116

Fluoropyrimidines[247, 248] and fluoropyrazines[249] must also be metallated with LDA or LiTMP to avoid ring addition. Replacing F with CF_3 also allows metallation, but side-reactions are more of a problem (Scheme 117).

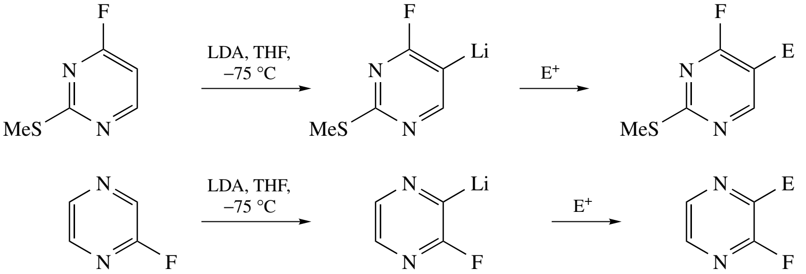

SCHEME 117

Certain chloropyrimidines can be metallated even with BuLi[247, 198], and the metallation of methoxy- and chloropyrazines[250] is useful in the synthesis of flavouring compounds[251] (Scheme 118) and the antiarrhythmic agent arglecin (Scheme 119)[252].

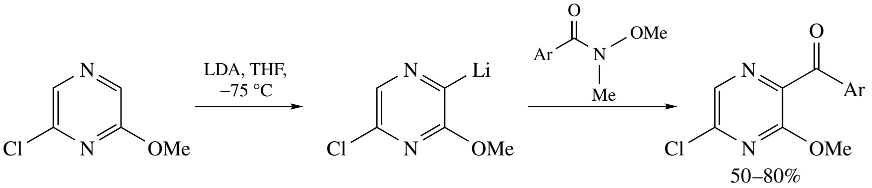

SCHEME 118

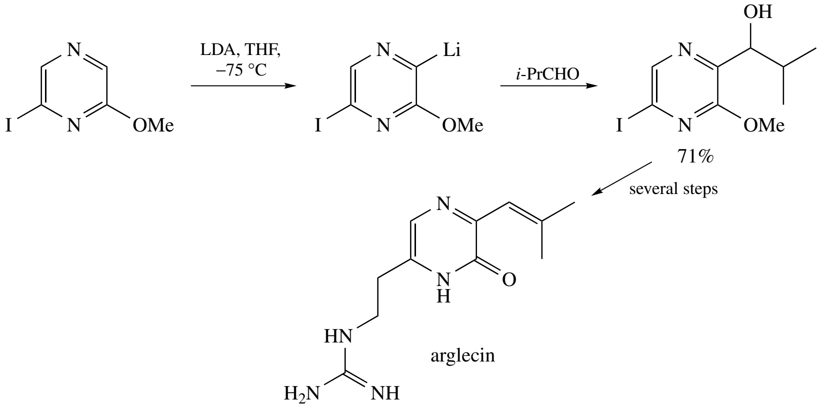

SCHEME 119

The protons of pyrimidines, pyrazines and pyridazines are relatively acidic[198] even without halogen activation, and the three simple heterocycles **240**–**242** have been lithiated (with varying success) with LiTMP (Scheme 120)[253].

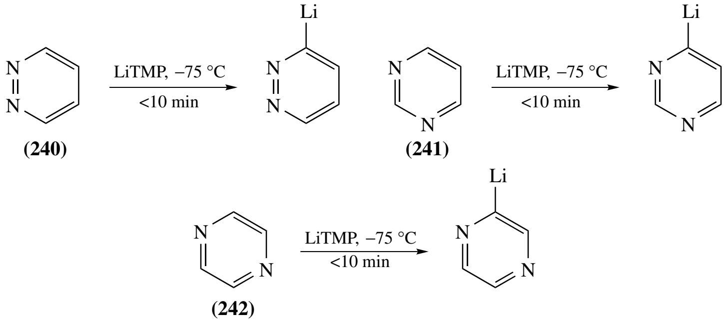

SCHEME 120

This acidity means that even iodopyrimidines and iodopyrazines may be lithiated because hindered, non-nucleophilic lithium amide bases will deprotonate them. For example, the base **244**, which is easily made by BuLi attack on the imine, deprotonates **243** α to N rather than *ortho* to I[254], and the lithiation of **245** with LiTMP is also successful (Scheme 121)[254].

Comparing the ortholithiation of **243** with the ortholithiation of the methoxypyrimidine **246**—the key step in a synthesis of an analogue **247** of bacimethrin[255]—contrasts the directing effects of I and MeO. This substitution pattern reacts well[256], as does the symmetrical **248** (Scheme 122)[257].

Methoxypyrazines **249** and **250** are lithiated with LiTMP as shown in the two syntheses in Scheme 123[258], the first being part of a route to kelfizine and sulphalene[257].

The lithiation of methoxypyridazines (which, for **251**, works even with BuLi) has been used to develop new routes to heterocyclic biaryls such as **252** (Scheme 124)[259]. In the pyridazine series MeO turns out to be a stronger director than Cl, as expected[252]. It also

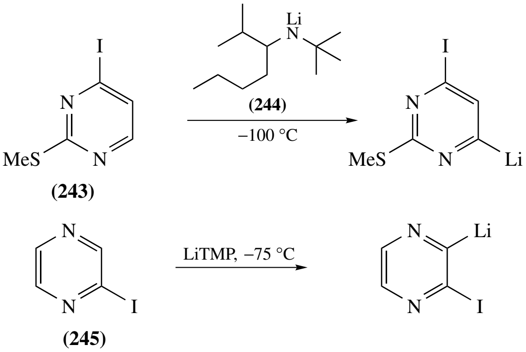

SCHEME 121

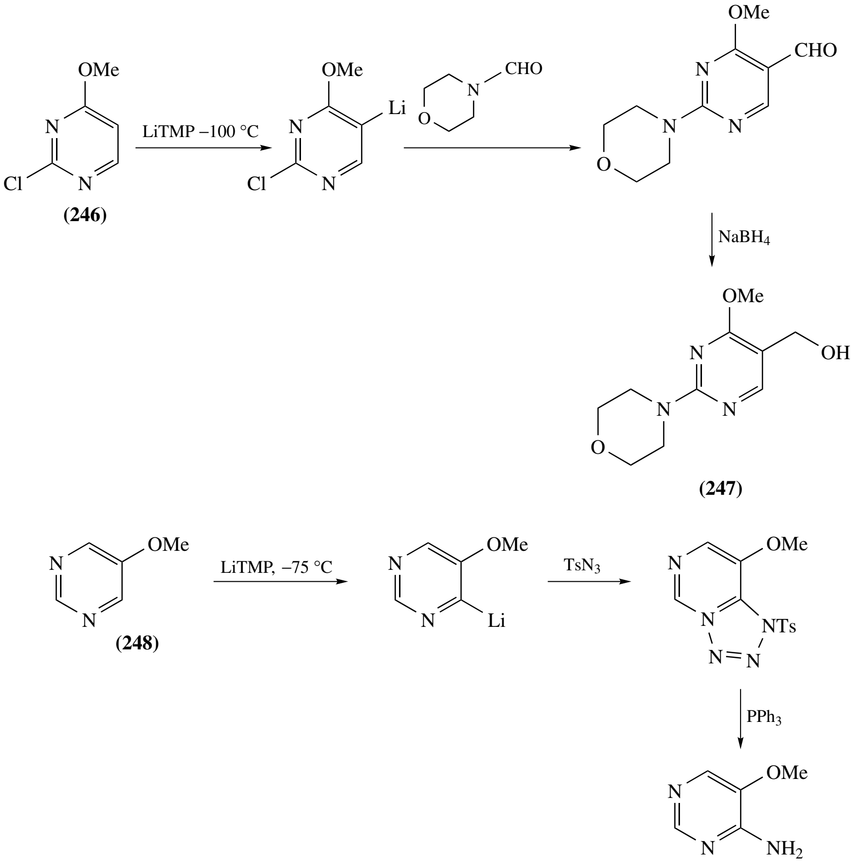

SCHEME 122

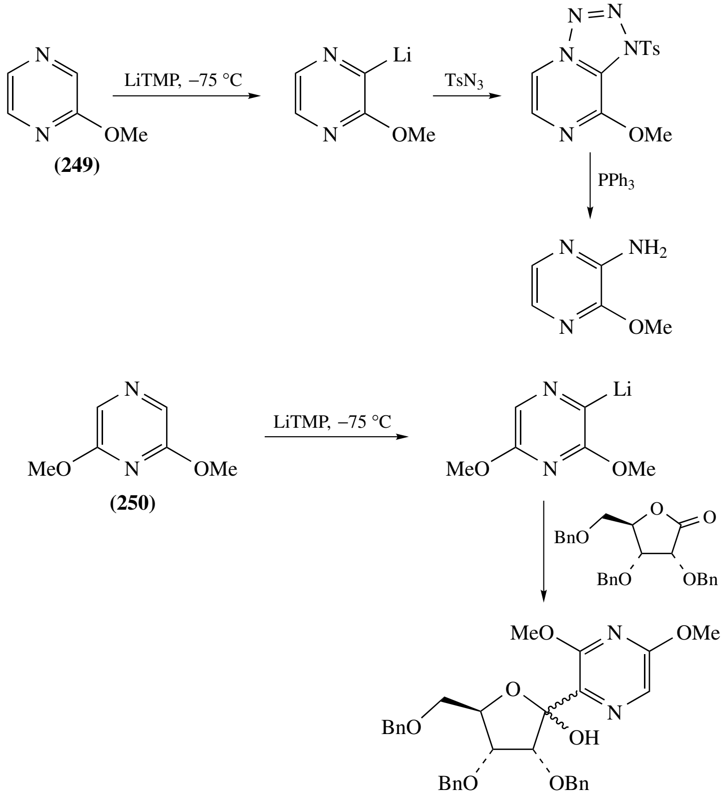

(249)

(250)

SCHEME 123

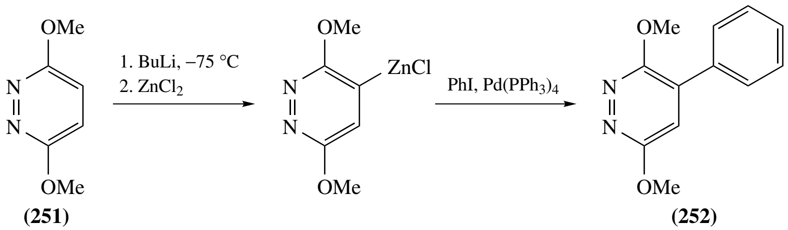

(251)

(252)

SCHEME 124

out-directs an alkylsulphanyl (RS) substituent, but sulphinyl and sulphonyl groups direct more strongly than MeO[260].

The usually very powerfully *ortho*-directing groups such as secondary carboxamide surprisingly do not always lead to ortholithiation on pyrazine and pyridazine rings: lithiation of **253** and **254**, for example, takes place principally (at least kinetically) at the '*meta*' and '*para*' positions (Scheme 125)[261, 262].

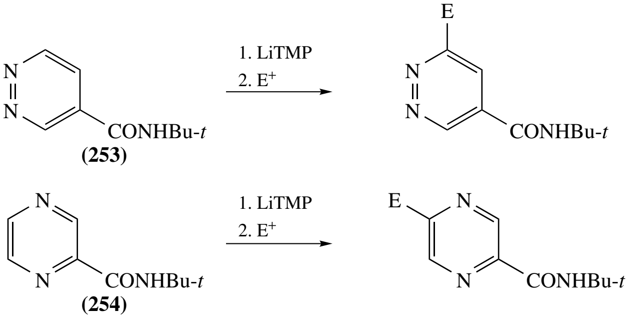

SCHEME 125

An excellent example of the application of pyridine lithiation is the synthesis of the fully substituted pyridine atpenin B **255**, an antibiotic produced by *Penicillium*. Its first synthesis[227], in 1994, was achieved by a series of directed metallations (Scheme 126) which started with 2-chloropyridine **256** and introduced the substituents stepwise around the ring. 2-Chloropyridine can be lithiated (*ortho*-directed by the chlorine) by either LDA or by PhLi, and the organolithium **257** was oxidized to **258** with trimethylborate and then peracetic acid. *O*-Methylation and substitution of chloride by methoxide gave 2,3-dimethoxypyridine **259** (Scheme 127).

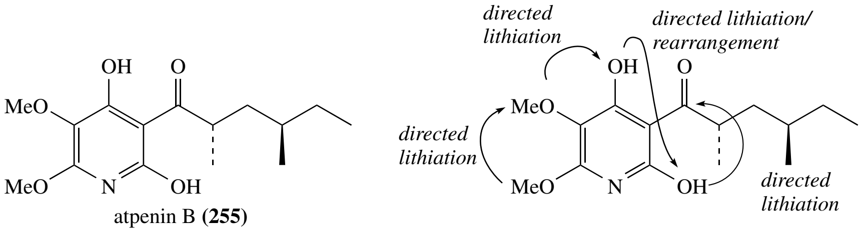

SCHEME 126

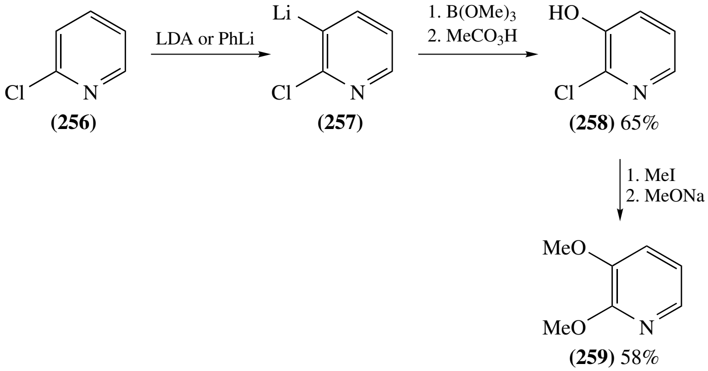

SCHEME 127

The second metallation in the sequence, which transformed **259** into **261**, required excess *n*-BuLi (a common characteristic of the lithiation of molecules bearing more than one directing group). Oxidation of the organolithium **260**, as before, gave 4-pyridone **261**. The new oxygen substituent of **261** has itself to act as a directing group, and for this reason **261** was converted to the carbamate **262** (Scheme 128).

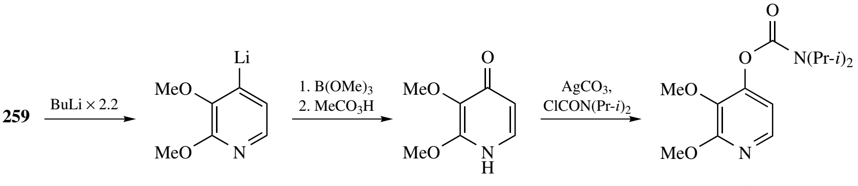

(260) **(261)** 64% **(262)** 71%

SCHEME 128

Lithiation gave **263**, which was brominated with cyanogen bromide to yield the 5-bromopyridine **264**. In fact, the next substituent to be introduced must be the hydroxyl group at C-6, in order to reserve the introduction of the acyl group at C5 until the end of the sequence. Treatment of the C-5 brominated **264** with LDA in the presence of catalytic bromine sets up an equilibrium between **265** and **266** (a 'halogen-dance') in which **266** (with the lithium *ortho* to the carbamate) predominates. Hydrolysis gives the C-6 brominated **267**. Regioselectivity is then correct for a bromine–lithium exchange of **267** to give **268** and oxidation again using the boronate–peracetic acid method yields **269** (Scheme 129).

O-Protection of this 2-pyridone was followed by lithiation to give **271** with BuLi and *i*-Pr$_2$NH followed by reaction with a diastereoisomeric mixture of the aldehyde **272**. Oxidation gave a diastereoisomeric mixture of the ketones **273** whose deprotection yields a stereoisomeric mixture of **255**.

B. Electron-rich Heterocycles

In many ways, the electron-rich five-membered aromatic heterocycles behave very much like carbocyclic aromatic compounds when it comes to lithiation. Lithiation α to O or S of furan and thiophene is straightforward (Scheme 130)[263–265]. The usual selection of *ortho*-directing groups allows lithiation at other positions[7, 82, 84–91, 266], and some examples were given in Section I.B. Furan-2-carboxylic acid **274** can be lithiated at either the 3- or the 5-position[267, 87].

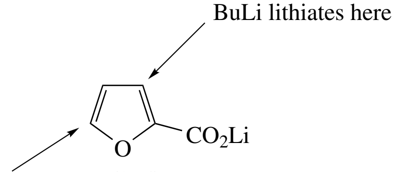

(274)

Pyrroles are lithiated at the 2-position whether or not the *N*-protecting group has the ability to coordinate (Scheme 131)[268–273]. 3-Lithiopyrroles are best obtained by halogen–metal exchange on 3-bromo-*N*-TIPS pyrrole **275** (Scheme 132)[274].

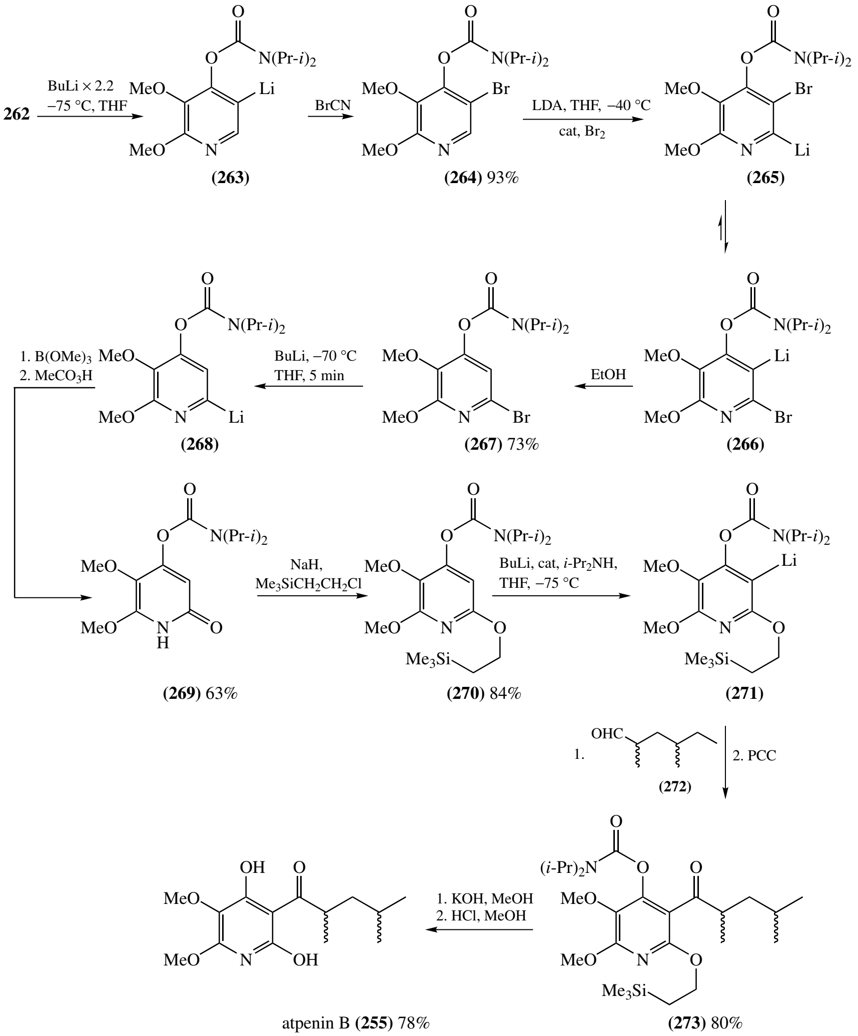

SCHEME 129

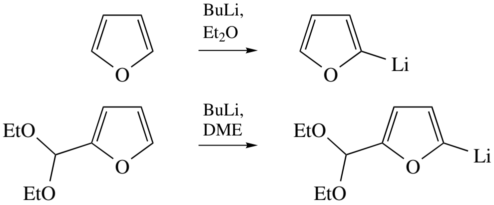

SCHEME 130

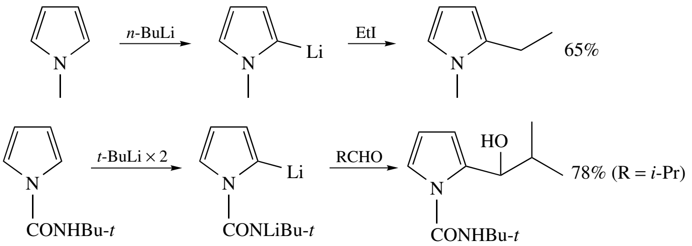

SCHEME 131

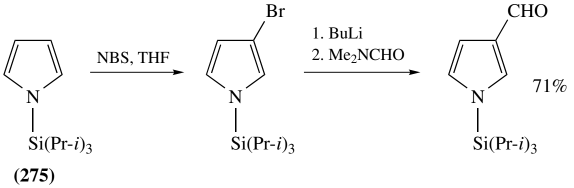

(275)

SCHEME 132

Interestingly, indoles are lithiated at either the 2- or the 3-position, depending on protection at N[275, 276]. For 2-lithiation, probably the best technique is *in situ* protection of nitrogen by CO_2. The lithiocarbamate group of **276** acts as a good *ortho*-director (Scheme 133)[277]. With more bulky, non-coordinating *N*-protecting groups such as triisopropylsilyl (**277**), lithiation occurs at C-3[278].

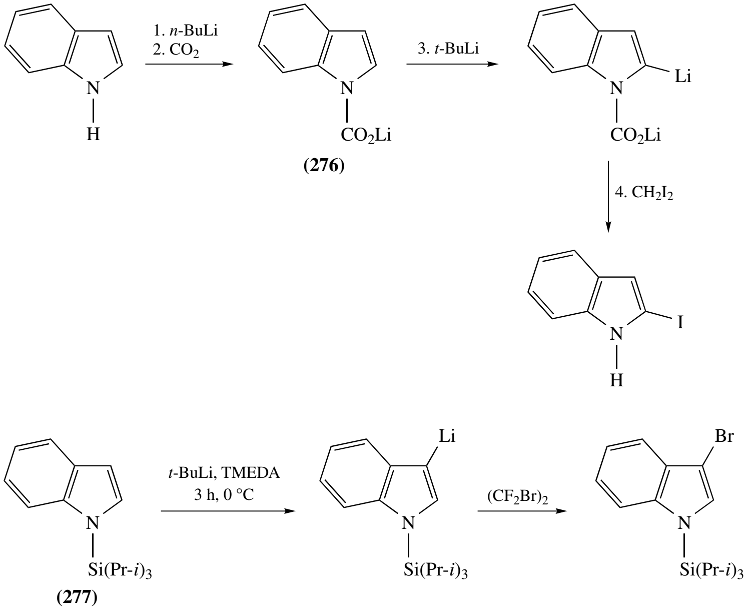

SCHEME 133

III. LITHIATION OF METAL–ARENE COMPLEXES

By coordinating to arenes, transition metals can facilitate ring lithiation by decreasing the electron density in the ring and acidifying the ring protons. We shall consider briefly the two most important metal–arene complexes in this regard—arenechromium tricarbonyls and ferrocenes.

A. Ferrocenes

Ferrocene is best deprotonated by *t*-BuLi/*t*-BuOK in THF at 0 °C[279], since BuLi alone will not lithiate ferrocene in the absence of TMEDA and leads to multiple lithiation in the presence of TMEDA. In the example in Scheme 134[128], a sulphur electrophile and a Kagan–Sharpless epoxidation lead to the enantiomerically pure sulphinyl ferrocene **278**. The sulphinyl group directs stereoselective ortholithiation (see Section I.B.2), allowing the formation of products such as **279**. Nucleophilic attack at sulphur is avoided by using triisopropylphenyllithium for this lithiation.

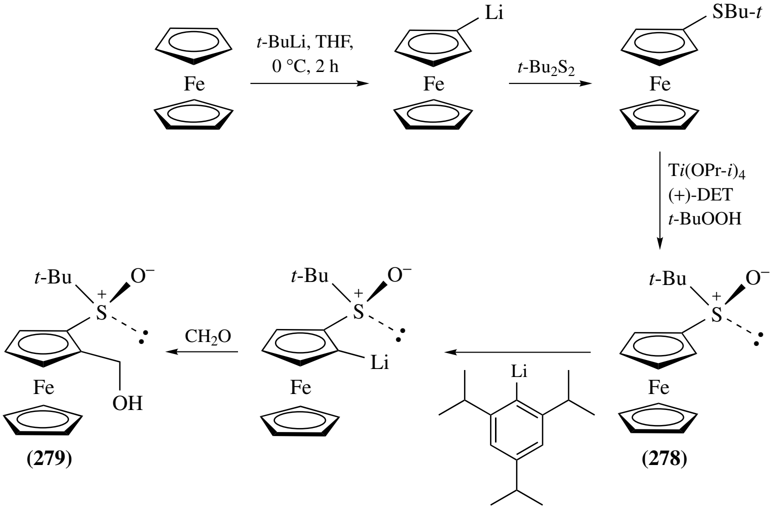

SCHEME 134

Chiral ferrocenes form a class of powerful and useful chiral ligands, and a number of methods are available for their enantioselective synthesis. The introduction of a second substituent via directed metallation[280] is a simple and powerful way to make disubstituted ferrocenes with planar chirality from simple, achiral monosubstituted ferrocenes[281]. Chiral 1,2-disubstituted ferrocenes **280** for this reason are much more readily available than chiral 1,3-disubstituted ferrocenes **281**. Control of absolute planar stereochemistry during the lithiation of a monosubstituted ferrocene **282** may be achieved either by reagent control (using a chiral base to remove selectively only one of two enantiotopic protons H^A and H^B of **282** with a simple achiral substituent R) or by substrate control (starting with a ferrocene **282** lacking planar chirality but bearing a chiral substituent R, which directs a base towards removal of only one of two diastereotopic protons H^A and H^B).

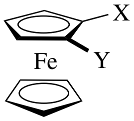

(280)
chiral 1,2-disubstituted ferrocene

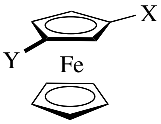

(281)
chiral 1,3-disubstituted ferrocene

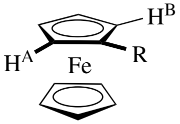

(282)

1. Diastereoselective lithiation of chiral ferrocenes

Nozaki pioneered the investigation of both routes to enantiomerically pure ferrocenes in the late 1960's[282], and after one early example of a diastereoselective acylation[283], most early attempts to control planar chirality made use of ferrocenes bearing chiral and enantiomerically pure aminoalkyl substituents. The amino groups could readily be made by reductive amination or substitution; they also facilitated both resolution and lithiation, acting as metallation directing groups[280]. Many ferrocenes used as chiral ligands (such as PPFA **283** and BPPFA **284**) retain these aminoalkyl substituents, and others (such as Josiphos **285** or Xyliphos **286**) carry groups derived from them by simple substitution chemistry[284]. More recently, in the interests of versatility, fully removable auxiliaries have been used to direct diastereoselective lithiation, including those based on oxazolines, hydrazones, acetals and sulphoxides, each of which is discussed below.

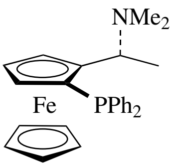

(283) = PPFA

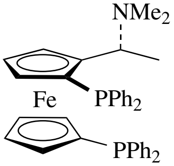

(284) = BPPFA

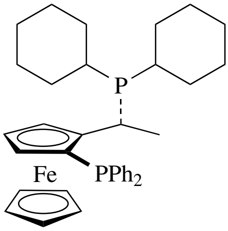

Josiphos **(285)**

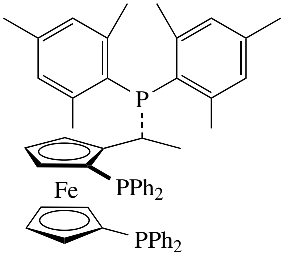

Xyliphos **(286)**

a. Lithiation directed by aminoalkyl groups. In 1969, Nozaki and coworkers published the first diastereoselective lithiation of a ferrocene **287** (Scheme 135)[282]. Ugi and coworkers improved[285] upon these reactions by shifting the stereocontrolling influence closer to the ring[286, 287]. His lithiation of **288**, which achieved 96:4 diastereoselectivity over the new chiral plane, is under kinetic control, and is governed by the relative favourability of

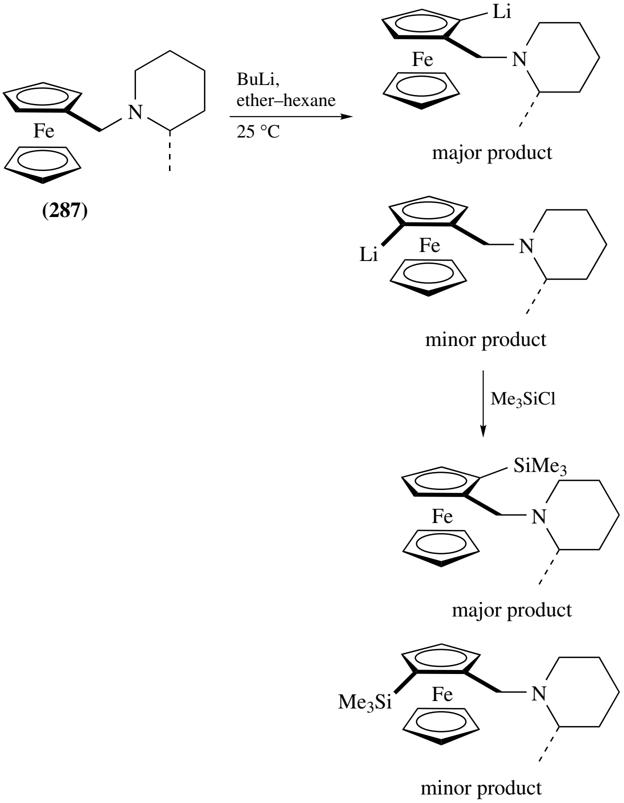

SCHEME 135

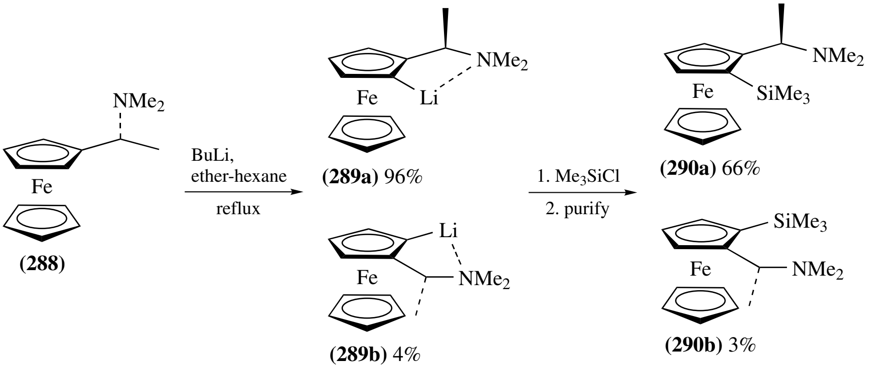

SCHEME 136

the transition state leading to **289a**, which keeps the α-methyl group clear of the lower portion of the ferrocene sandwich (Scheme 136).

The stereochemistry of the organolithium **290a**, obtained almost diastereoisomerically pure, was proved by an X-ray crystal structure of its anisaldehyde adduct. **289a** reacts with a range of electrophiles, including, importantly, $ClPPh_2$, which generates the ligand PPFA **283** after removal of a small amount of the minor diastereoisomer by recrystallization[288]. Addition of a second equivalent of alkyllithium can be used to form a 'dianion', allowing a one-pot double functionalization—reaction of **293** (R = Me), for example, gives the ligand BPPFA **284** (Scheme 137)[288–293].

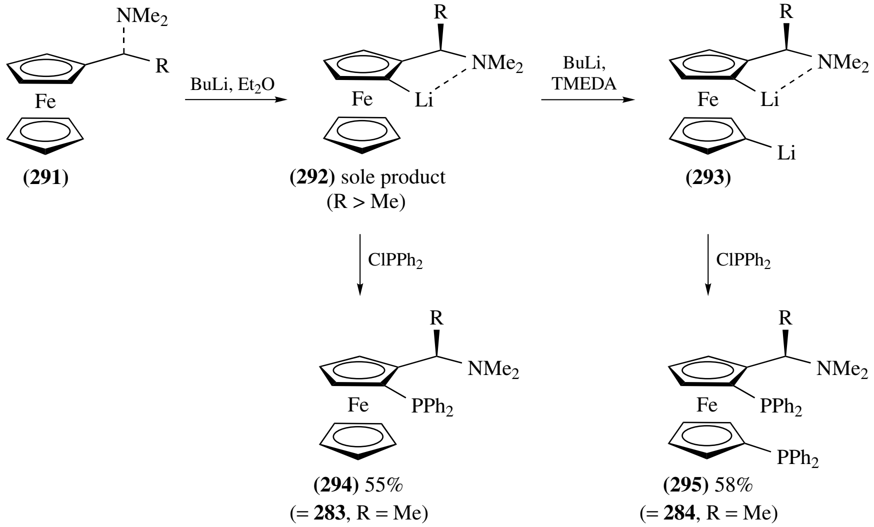

SCHEME 137

Despite the resolution which was required to produce the enantiomerically pure starting materials (which fortunately is highly efficient—recrystallization of the mother liquors allows isolation of both enantiomers)[294], Ugi's lithiation provided the basis for a rapid growth in the use of enantiomerically pure, planar chiral ferrocenes which has continued since. Several reviews[284] have covered applications of enantiomerically pure ferrocenes as chiral ligands, which until the 1990's were all made using Ugi's method[295].

The diastereoselectivity of Ugi's lithiation can be improved upon by replacing the methyl group α to nitrogen by isopropyl[296]. Complete (>99:1) selectivity is observed in the lithiation of **291** (R = i-Pr). Attempts to lithiate compounds **291** with even bigger α-substituents (and avoid the need for a resolution in the synthesis of the enantiomerically pure starting material) failed.

The resolution required for the synthesis of **288** or **291** can be avoided by making them by asymmetric reduction[297] or by asymmetric alkylation of an aldehyde[298]. The amines **291** (R = Et or n-Bu) formed in this way are lithiated with diastereoselectivity similar to, or greater than, that achieved with **288**. α-Ethyl and α-butylphosphines **294** incidentally may show even higher selectivity than the more widely used α-methylphosphine ligand PPFA **283**.

b. Lithiation directed by acetals. Although much mileage has been made out of ligands which retain the stereogenic centre of the aminoalkyl side-chain in compounds derived from **289a** and **292**, more versatile methods based on removable auxiliaries are clearly desirable. The first of these to be reported was Kagan's use of the acetal **297**[299], made by condensing aldehyde **296** with a malic acid-derived triol followed by O-methylation (Scheme 138). Lithiation of **297** with *t*-BuLi in hexane–ether at −78 °C (higher temperatures yield lower selectivities, though completion of the deprotonation at 25 °C is necessary for good yields) gives organolithium **298** with complete diastereoselectivity, probably via a transition state involving chelation of Li by the OMe group[299, 300]. The reaction of this organolithium with electrophiles yields products such as **299** with >99:1 diastereoselectivity and in 80–90% yield. Acid hydrolysis allows clean removal of the diol auxiliary, allowing the synthesis of versatile formylferrocenes such as **300** of ee $\geqslant 95\%$ with planar chirality only.

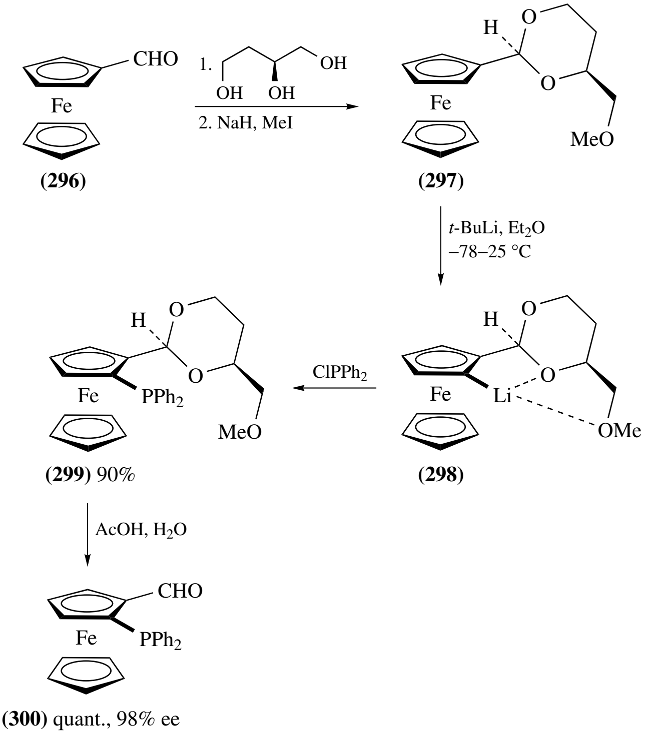

SCHEME 138

Attempts to make C_2-symmetric ferrocenes by double lithiation of a bis-acetal met with only limited success[301]. A second lithiation of the ferrocenylacetal **298** leads to functionalization of the lower ring of the ferrocene, in contrast with the second adjacent lithiation of the oxazolines described below. This can be used to advantage if, for example, the first-formed aldehyde **301** is protected *in situ* by addition of the lithiopiperazine **53**[302], directing *t*-BuLi to the lower ring (Scheme 139)[303]. The same strategy can be used to introduce further functionalization to products related to **302**. For example, silane **303**, produced in enantiomerically pure form by the method of Scheme 138, may be converted to the ferrocenophane **304** by lithiopiperazine protection, lithiation and functionalization (Scheme 140)[303].

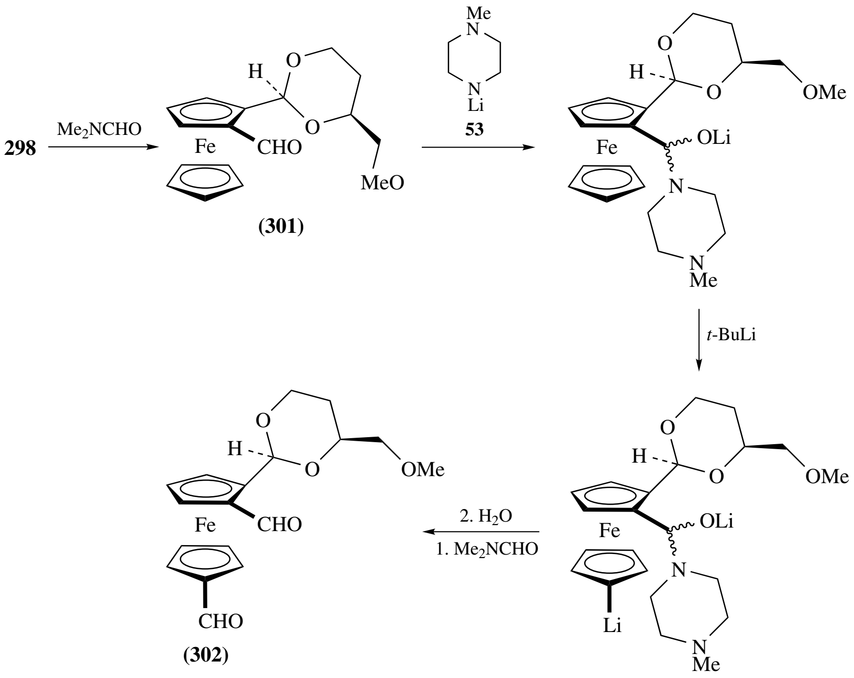

SCHEME 139

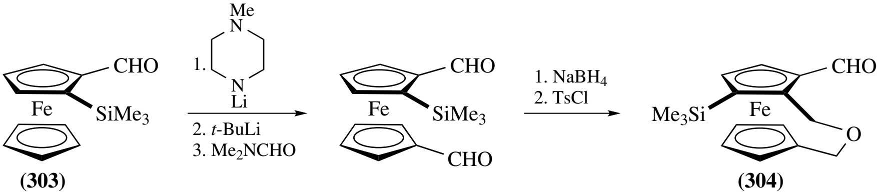

SCHEME 140

c. Lithiation directed by oxazolines. Early in 1995, the groups of Richards[304], Uemura[305] and Sammakia[306] simultaneously published results showing that chiral oxazolines attached to aromatic rings are capable of directing diastereoselective lithiation. The best conditions for the diastereoselective lithiation of **305**, derived from either valine or *tert*-leucine, are *s*-BuLi in TMEDA–hexane at −78 °C. Organolithium **306** is formed with a diastereoselectivity of $>500:1$[307], and electrophilic quench gives a single diastereoisomer of the silane **307** (Scheme 141). Similar results have been obtained with related oxazolines bearing a further chiral substituent[308].

Lithiation of the conformationally constrained ferrocenyloxazoline **308** (Scheme 142) provided useful information about the mechanism by which lithiation of **305** achieves diastereoselectivity[309]. The product **310** must have arisen from an organolithium **309** in which the oxazoline nitrogen coordinates to the lithium (Scheme 142). It is likely that

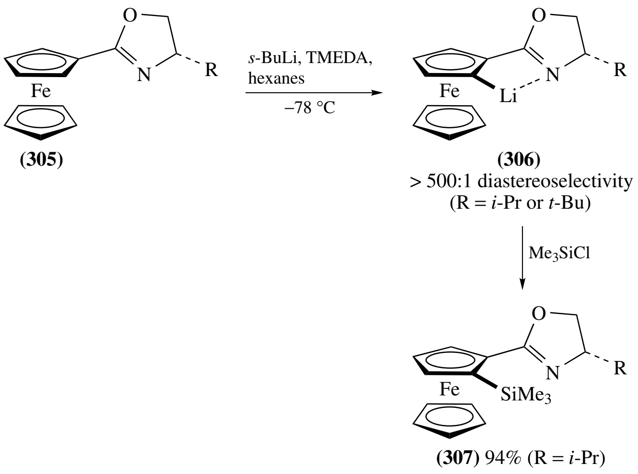

SCHEME 141

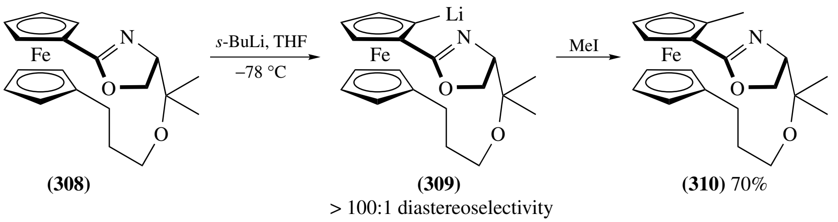

SCHEME 142

stereoselectivity in the lithiation of **305** results from a similar intermediate **306**, in which the oxazoline R group surprisingly points towards the ferrocene nucleus. Presumably, while this is not the ground state of the starting material, lithiation in this conformation is faster since the organolithium's approach is unhindered.

Although oxazolines can be used as auxiliaries and later removed[306, 310], they have also been retained in target molecules which have then been used as ligands for a variety of asymmetric transformations. Ferrocenes carrying oxazoline and phosphine coordination sites[304, 305, 311–313], oxazoline and amine coordination sites[314], and ferrocene bis-oxazolines[315–317] have been synthesized by the method of Scheme 141.

A ferrocenyloxazoline with only one adjacent position available for deprotonation will lithiate at that position irrespective of stereochemistry. This means that the same oxazoline can be used to form ferrocenes with either sense of planar chirality. The synthesis of the diastereoisomeric ligands **311** and **313** illustrates the strategy (Scheme 143), which is now commonly used with other substrates to control planar chirality by lithiation (see below). Ferrocene **311** is available by lithiation of **305** directly, but diastereoselective silylation followed by a second lithiation (best carried out *in situ* in a single pot) gives the diastereoisomeric phosphine **313** after deprotection by protodesilylation[304, 311, 313].

Double lithiation of bisoxazoline **314** is possible with either *s*-BuLi[317] or *t*-BuLi[315], and each base gives different planar diastereoselectivity. Double lithiation with *s*-BuLi, quenching the dianion with $ClPPh_2$, leads to the C_2-symmetric bisphosphine **315** as the

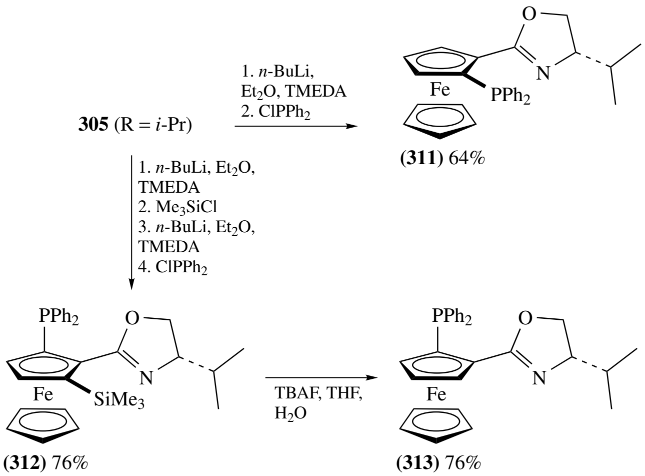

SCHEME 143

major product (Scheme 144). With *t*-BuLi, the diastereoisomeric bisphosphine **316** is isolated as the sole product.

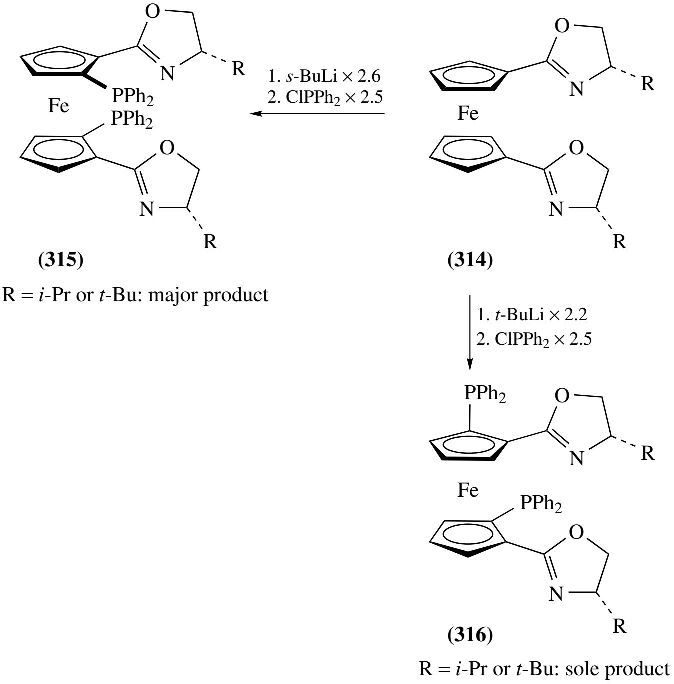

SCHEME 144

Bis-oxazoline ligands can also be produced by oxidative coupling of the copper derivative of diastereoisomerically pure **306** (Scheme 145)[316]. Further lithiations of the product **317**, which was produced as single diastereoisomer, occur (as in Scheme 143) at the second site adjacent to the oxazoline, giving, for example, **318**, despite the (presumably) less favourable stereochemistry of the lithiation step. Bisoxazolines **318** direct the asymmetric copper-catalysed cyclopropanation of styrene using diazoacetate.

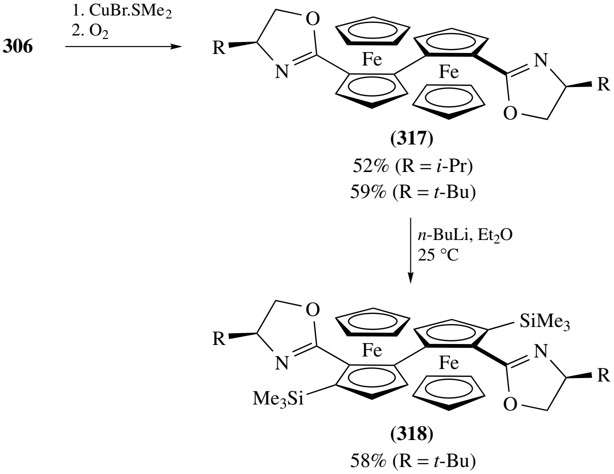

SCHEME 145

In removing the oxazoline auxiliary from the products, Richards and coworkers have demonstrated the use of the diastereoselective ferrocenyloxazoline lithiation in the synthesis of conformationally constrained amino acid derivatives (Scheme 146)[310]. Amination of **305** was achieved by nitration, reducing to the amino group after removal of the oxazoline under standard conditions. Using the trick of silylating the more reactive diastereotopic site, it was possible to make either enantiomer of **321** from the same oxazoline starting material.

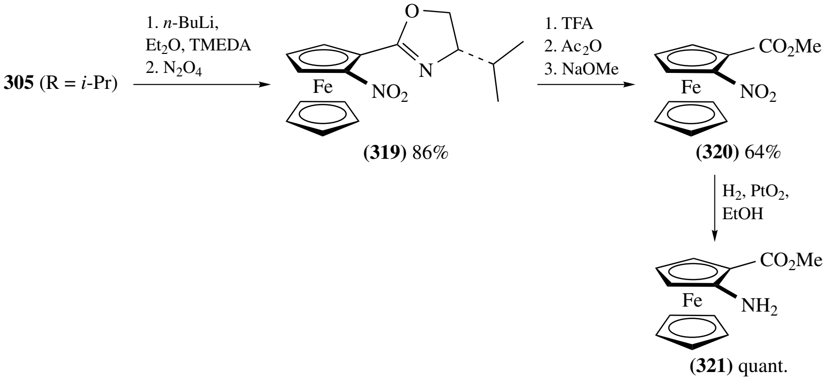

SCHEME 146

d. Lithiation directed by other diamine and aminoalcohol derivatives. A number of alternatives to oxazolines based on other diamine or amino alcohol derivatives have been proposed, and in several cases good control over planar stereoselectivity can be achieved. The earliest results, published before any work on ferrocenyloxazolines, drew on Nozaki and coworkers' early studies[282, 318] on stereoselective lithiation of aminomethylferrocenes, and made use of the proline-derived amino ether **323** (Scheme 147)[319]. Substitution of **322** gave **324**, whose lithiation proceeded with 93:7 stereoselectivity with *n*-BuLi in ether at −78 °C and with 99:1 stereoselectivity with *s*-BuLi in ether at −78 °C. Reaction of the mixture of **325a** and **325b** with ClPPh$_2$ gave **326** after purification; the enantiomer is available by silylation, re-lithiation, phosphination and deprotection in the manner of Scheme 143. Removal of the prolinol auxiliary is achieved by acetylation and hydrolysis to **327**[320].

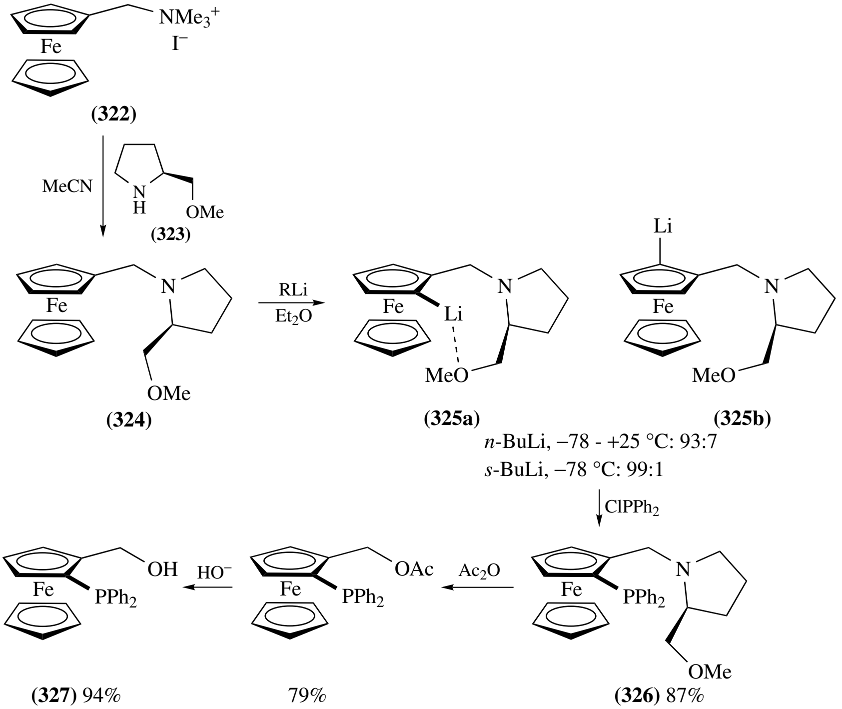

SCHEME 147

The same proline-derived ring system features in Enders' RAMP and SAMP ((*R*)- and (*S*)-1-amino-2-methoxymethylpyrrolidine) chiral hydrazone auxiliaries, and Enders and coworkers[321–324] have shown that RAMP and SAMP hydrazones derived from acylferrocenes will direct the diastereoselective lithiation of the ferrocene ring (Scheme 148). For example, treating benzoyl ferrocene **328** with (*S*)-*N*-amino-*O*-methylprolinol **329** generates **330** after silica-catalysed equilibration to the more stable *E* hydrazone[321]. Lithiation of **330** gives organolithium **331** selectively: after electrophilic quench, products **332** were obtained in 80–95% yield and with <2% of a minor diastereoisomer. Removal of the auxiliary is achieved by oxidative or reductive means.

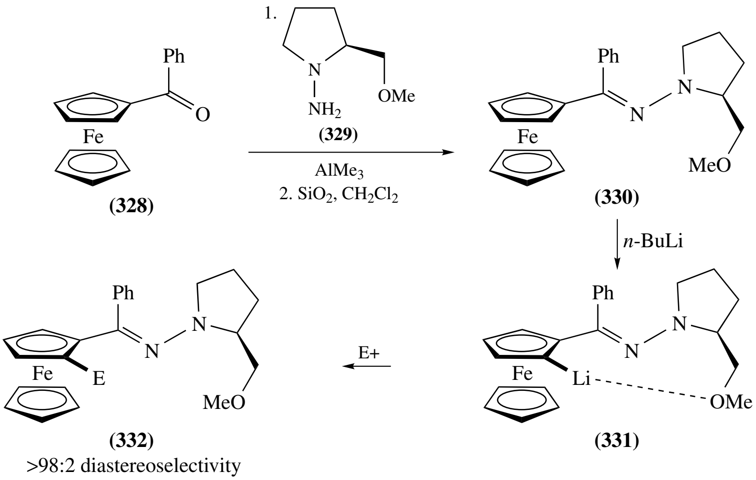

SCHEME 148

Similar chemistry is possible starting from hydrazones bearing acidic α protons: an initial diastereoselective enolization and electrophilic functionalization of the hydrazone can be followed by derivatization which is stereoselective in the planar sense[322, 323].

An acyclic methoxyamine, *O*-methylephedrine **333**, plays a similar role in the diastereoselective lithiation of **334**. Substitution with **335** gives **336** from **322**, and lithiation of **334** typically gives products **335** with >90:10 diastereoselectivity (Scheme 149)[325]. Auxiliary removal is possible by quaternization and substitution with dimethylamine (giving **336**) or other nucleophiles, producing potential ligands with planar chirality only. Usefully, the products formed by this method are enantiomeric with those formed by most other auxiliary methods when the more readily available enantiomers of the starting materials are used.

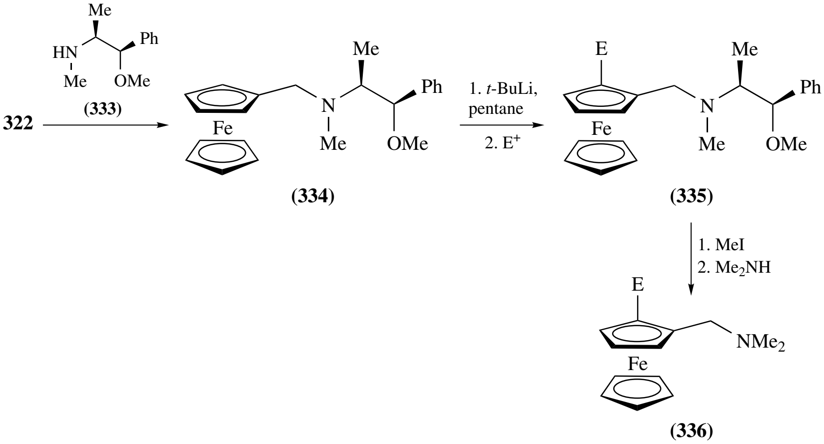

SCHEME 149

Aminomethylferrocene **338**, this time without further methoxy substituents, also lithiates diastereoselectively (Scheme 150)[326, 327], and similar results may be obtained with simple chiral pyrrolidines[328]. Treatment of **322** with the binaphthylamine **337** yields **338**. Lithiation generates a 9:1 mixture of diastereoisomeric organolithiums, which give the phosphine **339** (Scheme 150)[326, 327] Attempts to obtain reversed planar diastereoselectivity by using silylation to block the more reactive lithiation site failed.

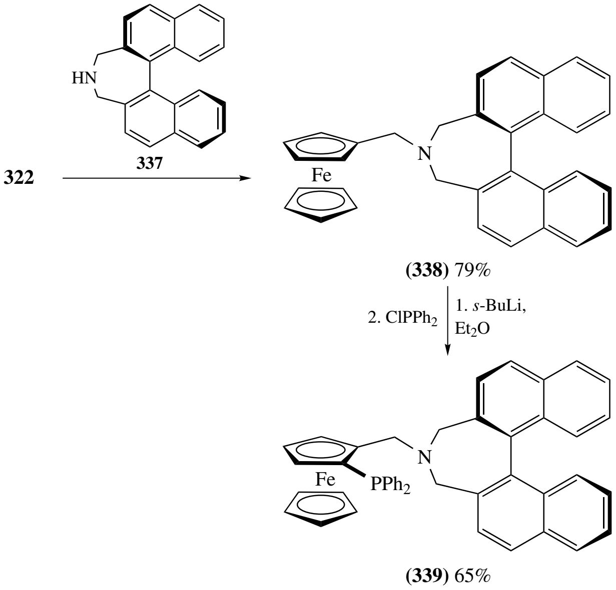

SCHEME 150

Some success has been achieved by a method which bridges the gap between the use of a chiral base and the use of an auxiliary to functionalize ferrocenes stereoselectively. Double protection of the dialdehyde **340** by addition of the chiral amine **341**, and lithiation with *t*-BuLi, gives a mixture of lithiated species which lead to **342** and **343**, in proportions dependent on the amount of *t*-BuLi employed (Scheme 151). Though the yields of each are not high, both products **342** and **343** are obtained in very high enantiomeric excess[303].

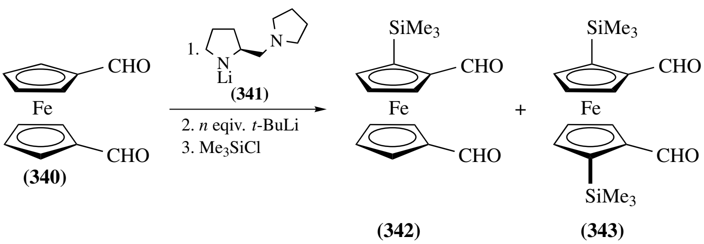

$n = 1.5$ 29% yield, 96% ee
$n = 3$ 28% yield, >99% ee

SCHEME 151

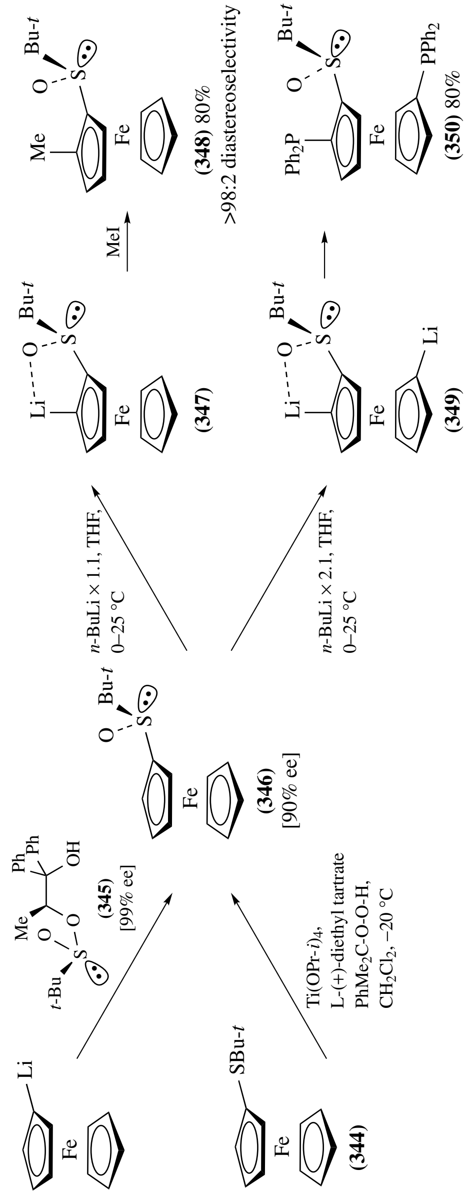
Li
Fe
SBu-t
Fe
(344)
t-Bu
S
O
O
Me
Ph
Ph
OH
(345)
[99% ee]
Ti(OPr-i)4,
L-(+)-diethyl tartrate
PhMe2C-O-O-H,
CH2Cl2, −20 °C
O
S
Bu-t
Fe
(346)
[90% ee]
n-BuLi × 1.1, THF,
0–25 °C
n-BuLi × 2.1, THF,
0–25 °C
Li
O
S
Bu-t
Fe
(347)
Li
O
S
Bu-t
Fe
Li
(349)
MeI
Me
O
S
Bu-t
Fe
(348) 80%
>98:2 diastereoselectivity
Ph2P
O
S
Bu-t
Fe
PPh2
(350) 80%

SCHEME 152

e. Lithiation directed by sulphoxides and sulphoximines. Probably most versatile of all the auxiliary methods for asymmetric functionalization of ferrocenes are based upon sulphoxides. First reported by Kagan and coworkers in 1993[329], the strategy (Scheme 152) entails the formation of a ferrocenylsulphoxide in enantiomerically pure form and its diastereoselective lithiation. For example, the *t*-butylferrocenylsulphoxide **346** may be formed either with full enantiomeric purity by stereospecific substitution of the sulphite **345** or in 90% ee by Sharpless–Kagan oxidation of the sulphide **344**. Treatment of the sulphoxide **346** with *n*-BuLi at 0 °C leads to diastereoselective lithiation, giving **347** with >98:2 selectivity, and subsequent addition of electrophiles, such as MeI, produces diastereoisomer **348** as the major product[329–331]. Evidence from the crystal structure of the product suggests that the lithiation is directed by the orientation of the sulphoxide oxygen with the *t*-butyl group pointing away from the ferrocene nucleus. The stereochemistry of the reaction is under kinetic control—higher temperatures lead to some erosion of stereoselectivity[330]. A second lithiation of **346** functionalizes the second Cp ring and can give, via **349**, the diphosphine **350**[329]. The planar chiral ferrocenyl *t*-butylsulphoxides have been used as chiral auxiliaries[330] and as chiral ligands[331].

Similar deprotonations are possible using the *p*-tolylsulphoxide **351** made by substitution of menthyl toluenesulphinate (Scheme 153)[330, 332]. This substitution is prone to loss of stereospecificity, since the product is able to undergo inversion by further reaction with another molecule of lithioferrocene, though careful control of conditions[332] ensures fully invertive substitution. The ability of the sulphur to undergo electrophilic attack enhances the value of the tolylsulphoxides by allowing them to undergo subsequent substitution reactions by sulphoxide lithium exchange. Lithiation (with LDA, to avoid nucleophilic substitution at sulphur) and quench of **351** gives products **352**. Treatment with *t*-BuLi then generates an organolithium **353** which reacts quite generally with electrophiles. The sequence shown in Scheme 153 therefore allows a ferrocene **354** to be elaborated enantioselectively with any pair of groups which can be introduced by successive electrophilic attack. Among the molecules produced in this way are the interesting planar chiral bisphosphines **355, 356**[333] and **357**[334], which direct a number of catalytic transformations with moderate to good enantioselectivity.

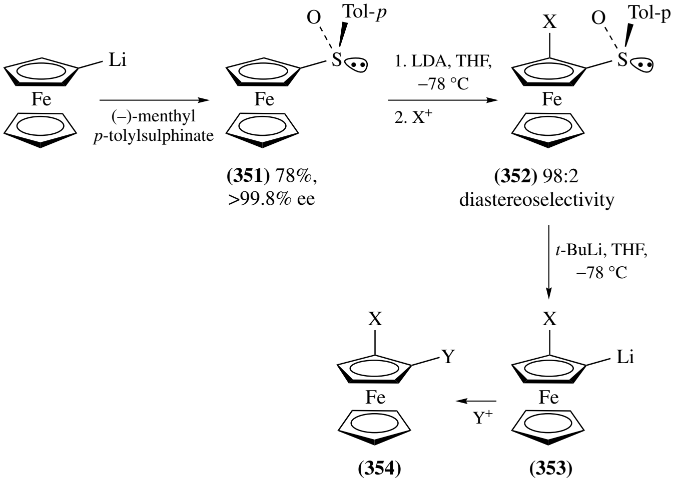

SCHEME 153

Sulphoximinoferrocenes[335] and ferrocenyl sulphonates[336] can also be lithiated diastereoselectively, with the sulphoximine oxygen atom of **358** directing the deprotonation.

2. Enantioselective lithiation of achiral ferrocenes

a. Chiral lithium amide bases. The diastereoselective lithiation of **351** shows that ferrocenes bearing electron-withdrawing directors of lithiation are sufficiently acidic to allow deprotonation with lithium amide bases. By replacing LDA with a chiral lithium amide, enantioselectivity can be achieved in some cases. The phosphine oxide **359**, for example, is silylated in 54% ee by treatment with *N*-lithio bis(α-methylbenzyl)amine **360** in the presence of Me_3SiCl (Scheme 154)[337].

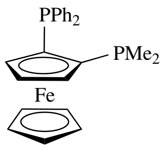

(355)

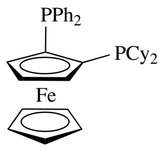

(356)

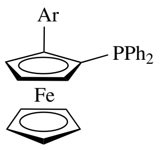

(357)

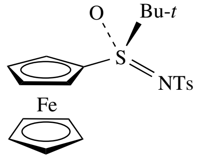

(358)

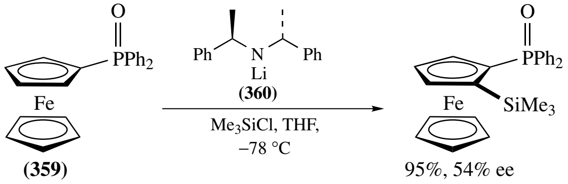

SCHEME 154

b. Alkyllithium–(−)-sparteine complexes. More generally successful, however, has been the use of alkyllithium/chiral tertiary amine (and, in particular, *s*-BuLi–(−)-sparteine) combinations[338]. One of the very first examples of asymmetric lithiation involved ferrocene: Nozaki and coworkers'[282, 318] (−)-sparteine-promoted functionalization of isopropylferrocene with moderate asymmetric induction. For useful results in this area, however, a lithiation-directing group is required. A breakthrough came when Snieckus lithiated the amide **361** with *n*-BuLi in the presence of (−)-sparteine **362** at −78 °C in Et_2O: reaction of the organolithium **363** with electrophiles generated products **364** in generally excellent yield and up to 99% ee (Scheme 155)[339, 340]. Further lithiation of **364** led to substitution on the lower, unfunctionalized ring.

Lithiation of the dicarboxamide **365** is similarly diastereoselective, and after two successive *n*-BuLi–(−)-sparteine lithiations C_2-symmetric products such as **367** can be made with high ee (Scheme 156)[341, 342]. Attempted double lithiation of **365** in one pot fails with *n*-BuLi; with *s*-BuLi–(−)-sparteine the major product is the *meso* isomer of **367**[342]. The amidophosphine **366** has been used as a chiral ligand for Pd chemistry; the amides can be reduced to amino groups with BH_3:THF[339].

Contemporaneously with Snieckus, Uemura and coworkers[343] showed that ferrocene **369** bearing an aminomethyl group may also be lithiated enantioselectively by alkyllithiums to give **370**: in these cases, better results are obtained with the C_2-symmetric amine **368** than with (−)-sparteine (Scheme 157).

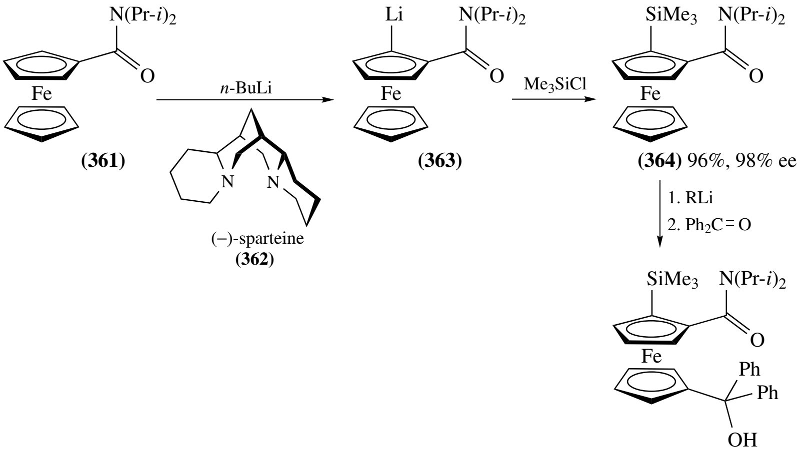

SCHEME 155

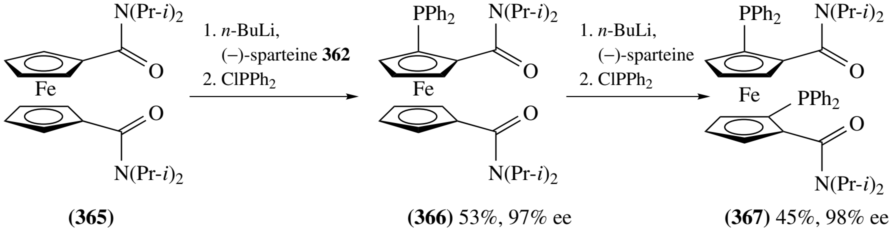

SCHEME 156

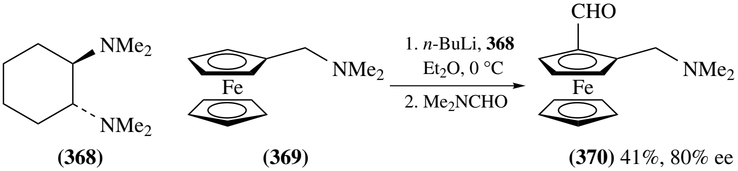

SCHEME 157

B. Chromium–Arene Complexes[344]

Benzenechromium tricarbonyl **371** is deprotonated by BuLi in Et$_2$O–THF at −40 °C in a reaction that needs careful control for good yields[345]. The product **372** can be silylated to give **373** in 60% yield (Scheme 158). Toluenechromium tricarbonyl lithiates non-regioselectively on the ring (but at the benzylic position with Na or K bases). Excess base can lead to polylithiation[346].

Anisolechromium tricarbonyl, however, is lithiated cleanly *ortho* to the methoxy group, giving products such as **374**[347, 348]. Coordination of **375** to Cr(CO)$_3$ changes the regioselectivity from the expective cooperatively directed **376** to **377** (Scheme 159).

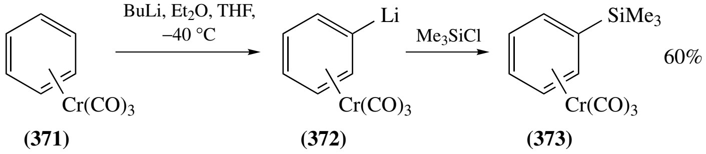

SCHEME 158

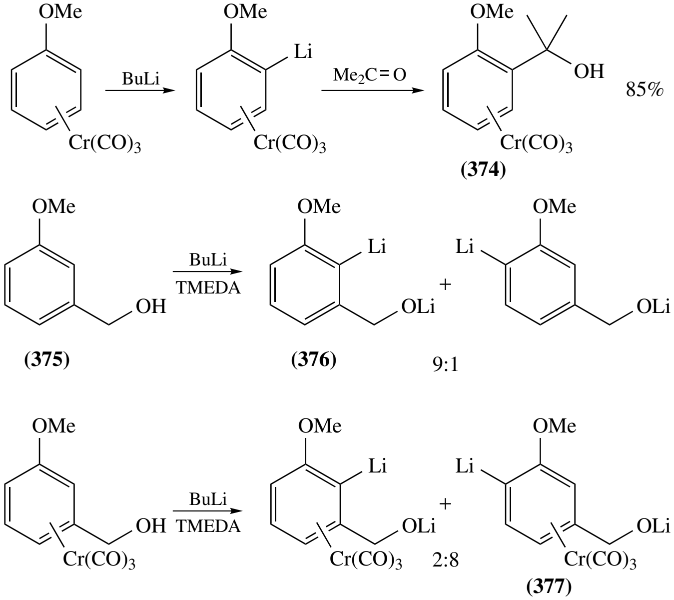

SCHEME 159

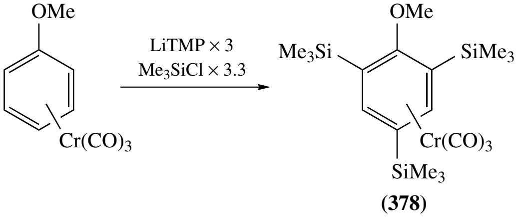

SCHEME 160

Multiple lithiation of anisolechromium tricarbonyl is easy to achieve: three equivalents of LiTMP give **378** (Scheme 160)[346].

Unlike the ferrocenes, the arene complexes of chromium, in particular the arenechromiumtricarbonyls, have seen much less use in asymmetric catalysis. This is beginning to change, however[349], and a number of synthetic transformations of arenechromiumtricarbonyls owe their existence to the formation of planar chiral chromium complexes by asymmetric lithiation processes[350]. The relative importance of substrate-controlled chiral auxiliary methods and reagent-controlled chiral base methods in the synthesis of planar chiral arenechromiumtricarbonyls is essentially the inverse of the situation with ferrocenes: the chiral lithium amide base chemistry is much more well developed with the chromium compounds because of the greater acidity of the arene protons relative to the Cp protons of ferrocene, making them removable even by LDA[351]. We shall deal with the use of auxiliaries to direct planar stereoselective lithiation before moving on to chiral base methods.

1. Diastereoselective lithiation of chiral arenechromium tricarbonyl complexes

a. Chiral alkoxy, aminoethyl and sulphinyl substituents. Early examples of diastereoselective lithiation of arenechromium tricarbonyls involved arenes bearing chiral amino substituents, following the precedent of Ugi's ferrocene chemistry. Lithiation of **379** with *t*-BuLi (*n*-BuLi is less selective) gives organolithium **380**, which may be quenched with electrophiles to give single diastereoisomers of products such as the methylated **381** in high yield (Scheme 161)[352–356]. Lithiation proceeds when the methyl group can lie *anti* to the chromium in the chelated intermediate. Additions of **380** to aldehydes proceed with diastereoselectivity at the new hydroxyl-bearing centre; either diastereoisomer of the products **383a** and **383b** can be formed by choosing between this reaction and an alternative diastereoselective nucleophilic addition to aldehyde **382**. Interestingly, decomplexation and recomplexation provides a third diastereoisomer **383c**. Similar chemistry is possible using ephedrine-derived arenechromium tricarbonyls[357].

As a chiral auxiliary, the aminoethyl group is a poor candidate as it is hard to remove. Davies and Hume demonstrated that removable chiral alkoxy groups will direct diastereoselective lithiation provided LDA is used as the base[358] (alkyllithiums lead to substitution reactions with chromium-complexed ethers)[355]. Chromium-promoted substitution of **384** with **385** gives **386**, whose treatment with LDA gives **387** completely regio- and stereoselectively (Scheme 162). Quenching with DMF yields the aldehyde **388**. This aldehyde reacts diastereoselectively with PhMgBr, and decomplexation and Birch reduction of the auxiliary yields the otherwise difficult to obtain diol **390a**. The enantiomer **390b** is available by acylation of **387** to give **391** followed by reduction to **389b** and deprotection.

Some headway has been made using sulphoxides to direct the lithiation of arenechromium tricarbonyls in the manner of Kagan's work with ferrocenes[359, 360]. Diastereoselectivities in the lithiation-quench of **392** are excellent, though yields are poor with most electrophiles. Diastereoselectivity reverses on double lithiation, because the last-formed anionic site in **394** is the most reactive (Scheme 163).

b. Chiral acetals and aminals. In 1991, Green and coworkers showed that slow addition of *n*-BuLi to a solution of the tartrate-derived acetal **395** leads to diastereoselective lithiation and hence allows formation of the complexes **397** (Scheme 164)[361, 362]. Similar acetals **398** and **399** (R = H) performed much less successfully. Formation of the organolithium **396** required an excess of alkyllithium base, and its stereoselectivity appeared to be under thermodynamic control arising from equilibration of various lithiated species[362]. Unfortunately, removal of the auxiliary from **397** and its analogues proved problematic.

The malic acid-derived auxiliary which gives good results in the ferrocene series also looks promising among the chromium complexes, and the six-membered acetal of **400** is much more easily hydrolysed than the tartrate-derived acetals of Scheme 164[363, 364]. Lithiation and bromination of **400** gives, after hydrolysis of the acetal, the complex **401** in 90% ee, increasing to >99% after recrystallization (Scheme 165). **401** is an intermediate in a formal synthesis of (−)-steganone (Scheme 182, Section III.B.2.b).

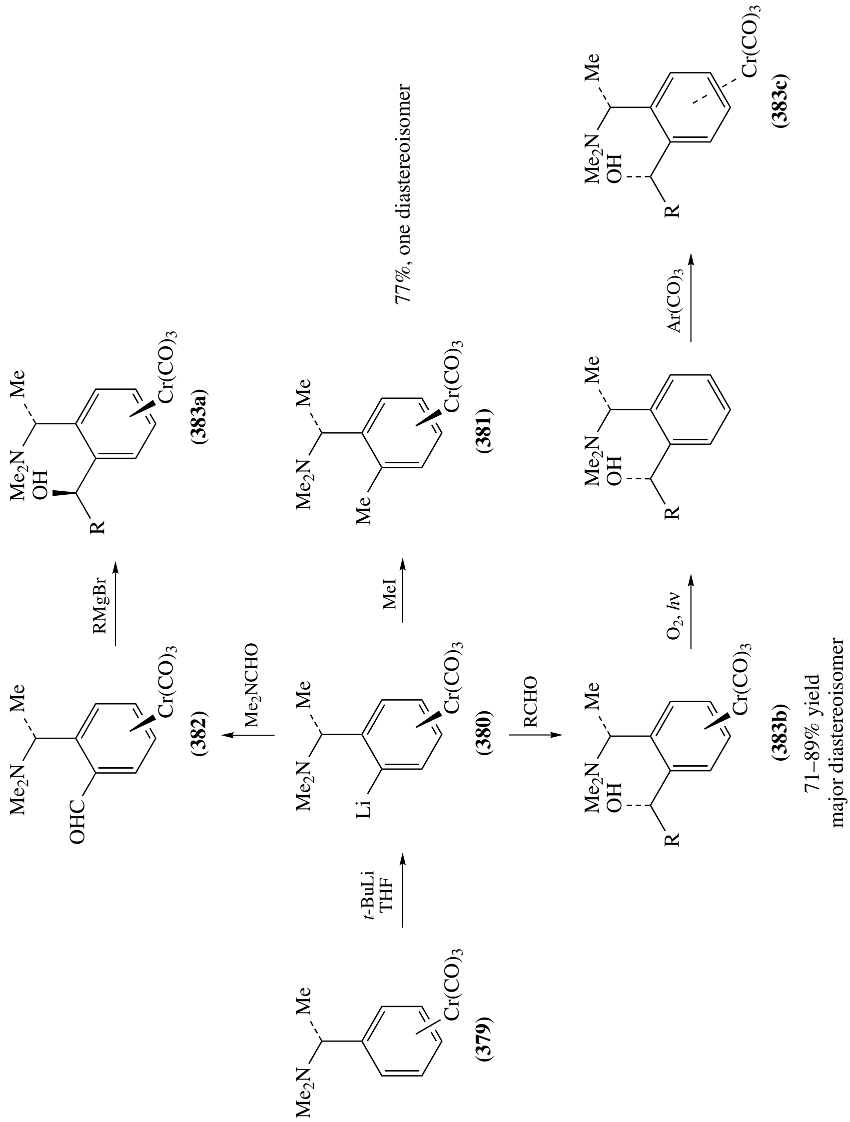
Me2N
Me
Cr(CO)3
(379)
t-BuLi
THF
Li
(380)
Me2NCHO
OHC
(382)
RMgBr
R
OH
(383a)
MeI
(381)
77%, one diastereoisomer
RCHO
(383b)
71–89% yield
major diastereoisomer
O2, hν
Ar(CO)3
(383c)

SCHEME 161

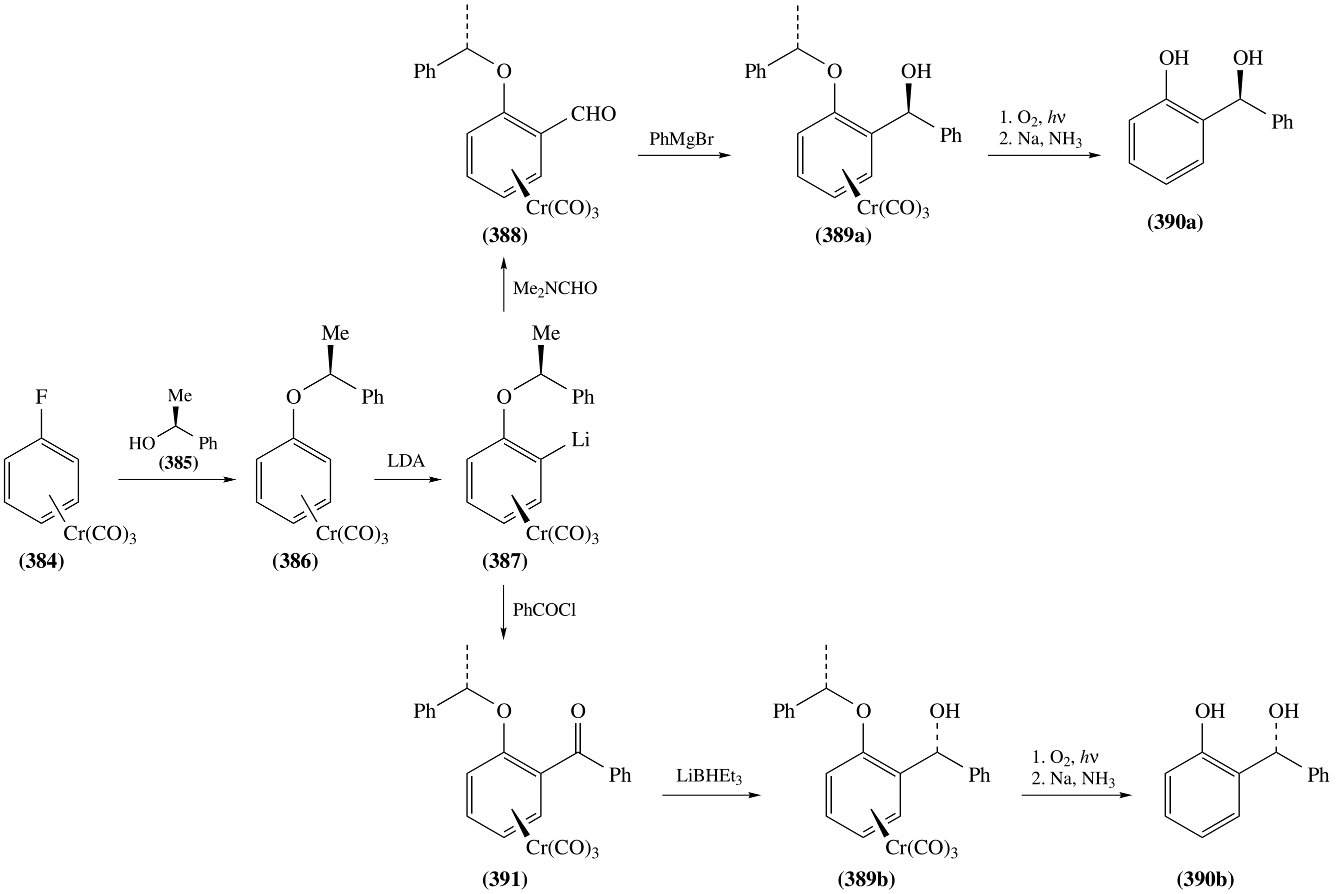
(384)
(385)
(386)
LDA
(387)
Me2NCHO
(388)
PhMgBr
(389a)
1. O2, hν
2. Na, NH3
(390a)
PhCOCl
(391)
LiBHEt3
(389b)
1. O2, hν
2. Na, NH3
(390b)

SCHEME 162

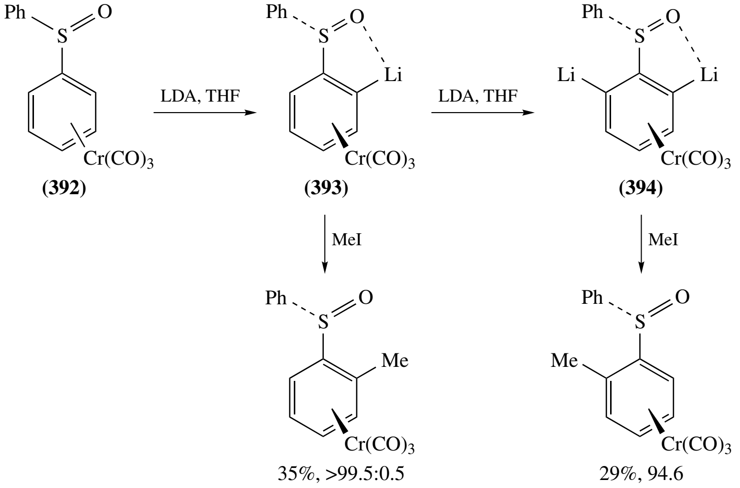

SCHEME 163

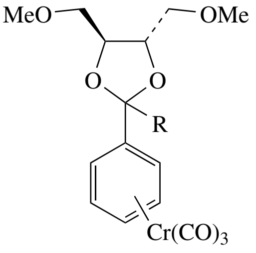

(398)

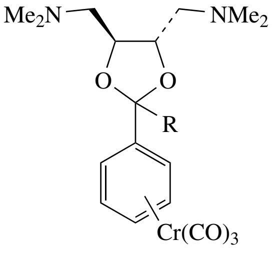

(399)

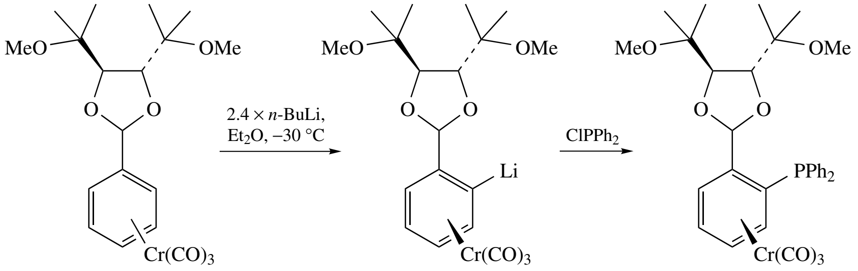

SCHEME 164

Among derivatives of acetophenone, the acetal **399** (R = Me) performs the best[365]. Lithiation with *t*-BuLi in THF and electrophilic quench gives **402a** in 60–85% yield and with about 95:5 diastereoselectivity (Scheme 166). Switching to Et_2O as the solvent leads to a precipitate which reacts with completely reversed diastereoselectivity, giving **402b**.

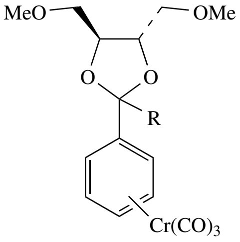

(398)

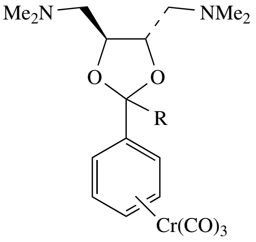

(399)

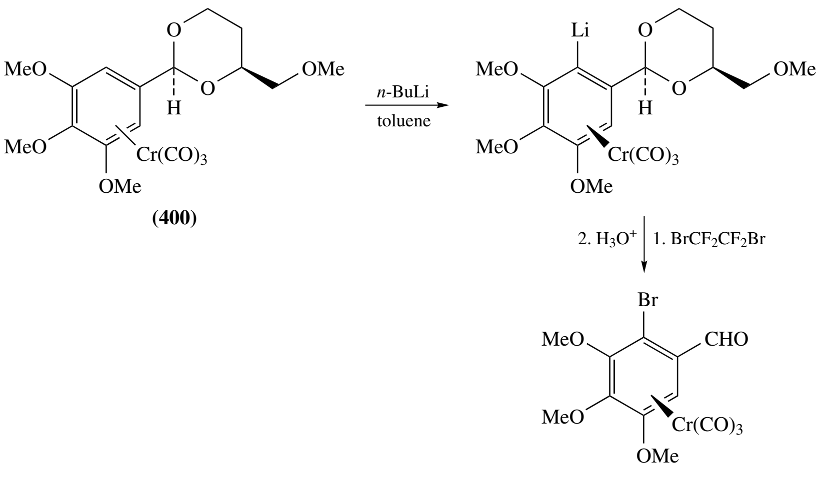

(400) **(401)**

SCHEME 165

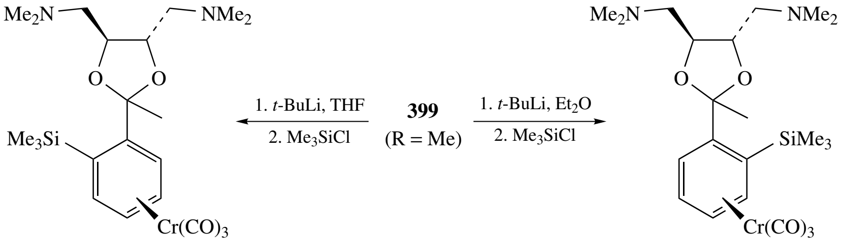

(402a) **(402b)**

SCHEME 166

The problem of auxiliary removal is overcome when acetals are replaced with the much more labile aminals, formed by reaction of benzaldehydechromium tricarbonyl **403** with diamines, and readily cleaved with mild acid. The best choice of diamine is **404**, because the aminal **405** lithiates with good to excellent regioselectivity in the *ortho* position (Scheme 167): the same could not be said for diamines lacking further lithium-coordinating side-chains[366]. Treatment of **405** with three equivalents of *n*-BuLi in

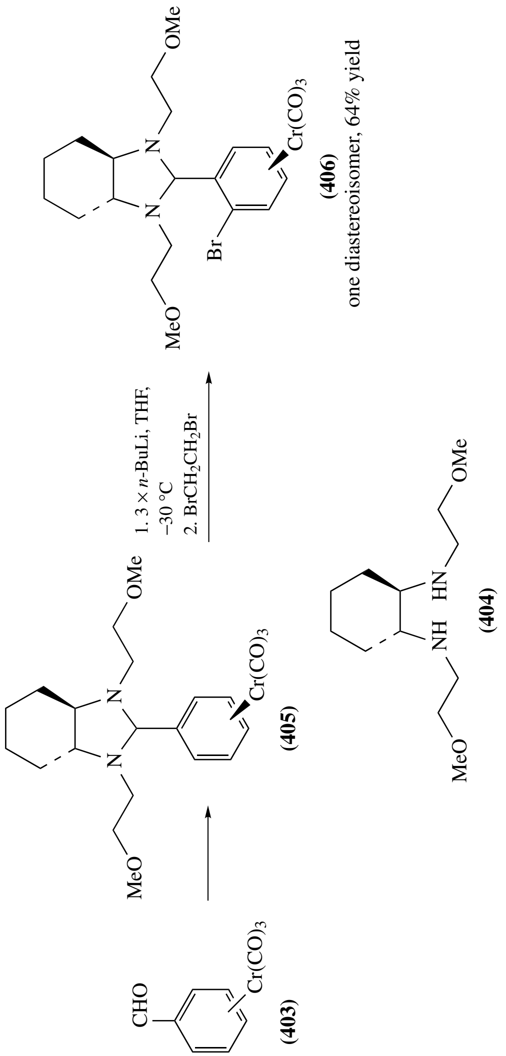
CHO
Cr(CO)$_3$
(403)
MeO
OMe
N
N
Cr(CO)$_3$
(405)
NH
HN
MeO
OMe
(404)
1. 3 × n-BuLi, THF, −30 °C
2. BrCH$_2$CH$_2$Br
MeO
OMe
N
N
Br
Cr(CO)$_3$
(406)
one diastereoisomer, 64% yield

SCHEME 167

THF at −30 °C followed by electrophilic quench with 1,2-dibromoethane, for example, yields the product **406** with no trace of its diastereoisomer (>99.5:0.5 selectivity) in 64% isolated yield.

Even greater ease of deprotection is achieved with the *in situ* protection strategy for the lithiation of aldehydes developed by Comins[302]. Alexakis and coworkers showed that a lithiodiamine **407** related to **404** achieved *in situ* protection of benzaldehyde chromium tricarbonyl at the same time as directing regio- and stereoselective lithiation (Scheme 168)[366]. Treatment of **403** with a slight excess of the lithium amide followed by three equivalents of *n*-BuLi and then the electrophile (Me_3SiCl) gave, after work-up, the product **409** in 72% ee and 68% yield. NMR examination of the intermediate **408** suggests that stereoselectivity is controlled by diastereoselective formation of the new α-aminoalkoxide centre.

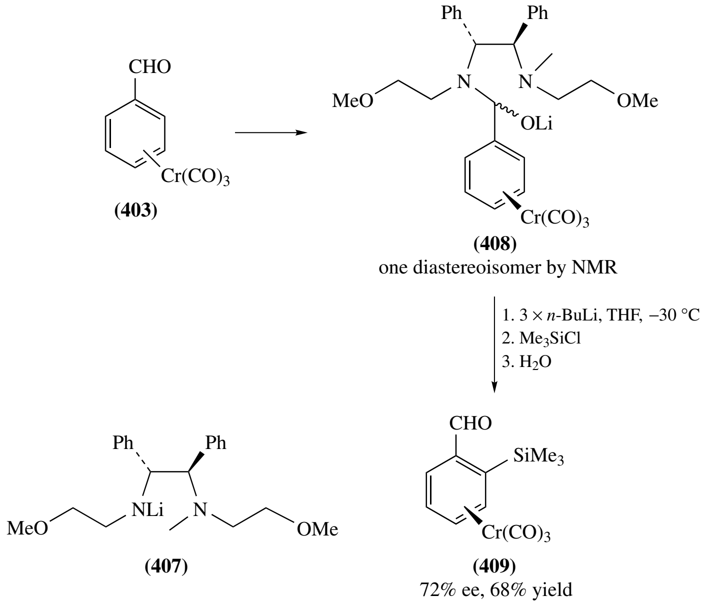

SCHEME 168

2. Enantioselective lithiation of achiral arene–chromium complexes

a. Chiral lithium amide bases. Arenechromium tricarbonyls are considerably more acidic than ferrocenes. Complexation to $Cr(CO)_3$ allows even electron-rich rings such as anisole to be deprotonated by lithium amides[350]. In 1994, Simpkins and coworkers showed that chiral lithium amides[367] could be used to achieve this transformation enantioselectively[368]. Anisole complex **410** was treated with the chiral base **360** in the presence of Me_3SiCl, giving the silane **411** in 83% yield and 84% ee accompanied by small amounts of a doubly silylated by-product (Scheme 169). Other related deprotonations were less successful, either in terms of yield (**412** gives silylated product of 84% ee but only in 36% yield, with benzylic deprotonation being a problem) or ee (**413–415** give varying amounts of product in <50% ee).

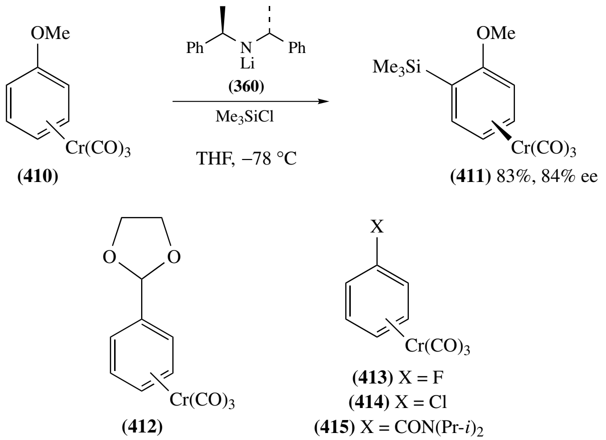

SCHEME 169

Early attempts to vary the electrophile or to use an 'external quench'—i.e. to add the electrophile after lithiation was complete—were unsuccessful. However, further studies[369, 370] on this reaction produced some intriguing and valuable insights into its mechanism and allowed some of these problems to be solved. It became clear that racemization of the lithiated intermediate **417** by proton exchange with the amine **418** was the process which had previously destroyed enantioselectivity when electrophiles were added after completion of the lithiation. For example, an authentic sample of **417** could be formed by a second lithiation-quench of **411**, desilylating with TBAF, and then submitting the product to tin–lithium exchange (Scheme 170). **417** turned out to be fully configurationally stable in the absence of **418**, but configurationally labile in its presence. The lithiation of **410** turns out to be much faster in the presence of LiCl, and this acceleration is sufficient to allow complete metallation before significant racemization has occurred, and therefore to extend the range of electrophiles which can be used with **417** (for example, benzaldehyde successfully gives **419**). Preferred conditions for the metallation are shown in Scheme 171. Other bases failed to improve the enantioselectivity[371].

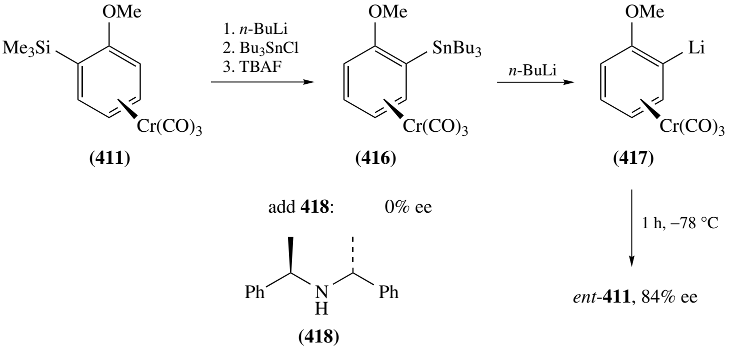

SCHEME 170

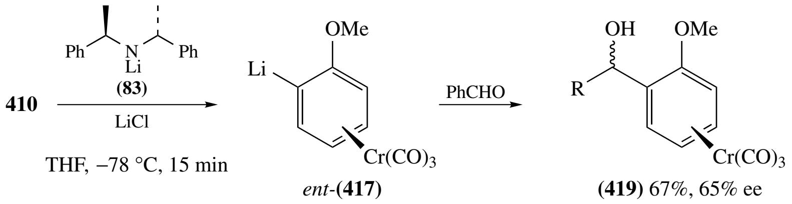

SCHEME 171

The enantioselective lithiation of anisolechromium tricarbonyl was used by Schmalz and Schellhaas in a route towards the natural product (+)-ptilocaulin[372, 373]. *In situ* lithiation and silylation of **410** with *ent*-**360** gave *ent*-**411** in an optimized 91% ee (reaction carried out at $-100\,^{\circ}$C over 10 min, see Scheme 169). A second, substrate-directed lithiation with BuLi alone, formation of the copper derivative and a quench with crotyl bromide gave **420**. The planar chirality and reactivity of the chromium complex was then exploited in a nucleophilic addition of dithiane, which generated ptilocaulin precursor **421** (Scheme 172). The stereochemistry of compound **421** has also been used to direct dearomatizing additions, yielding other classes of enones[374].

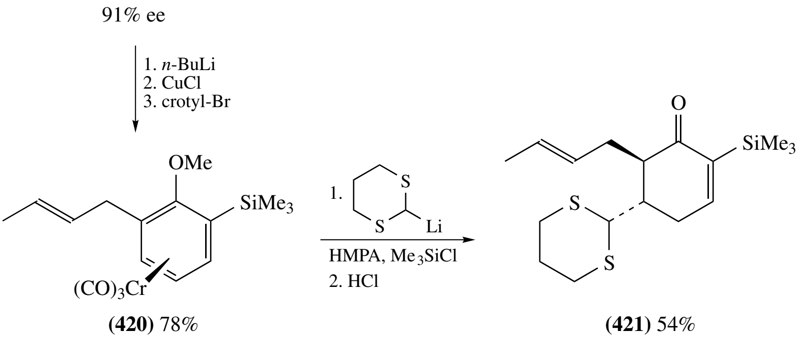

SCHEME 172

1,2-Dimethoxybenzene derivatives may be silylated under similar conditions, sometimes with higher enantioselectivity (see Scheme 184)[375]. Enantioselective lithiation of complex **422** does not require such careful control of conditions. Treatment of **422** with chiral bases **360** or **425** leads to an organolithium **423** which may be quenched with a range of electrophiles to yield products **424** in excellent yield and with ee's in the range 65–75%, recrystallizable to >90% (Scheme 173)[376, 377]. The intermediate **423**, on warming, undergoes rearrangement to a phenoxide trapped as **426**, but in only 54% ee due to concurrent racemization. The application of other bases to this deprotonation has also been studied[371].

This reaction has been used in the synthesis of some phosphine ligands: **424** (E = Br) of 62% ee was recrystallized to provide material of 95–97% ee. Suzuki coupling gave biarylchromium complexes **427**, and the chromium's electron-withdrawing ability was exploited to turn the carbamate into a leaving group: addition of Ph_2PLi gave **428** (Scheme 174)[378].

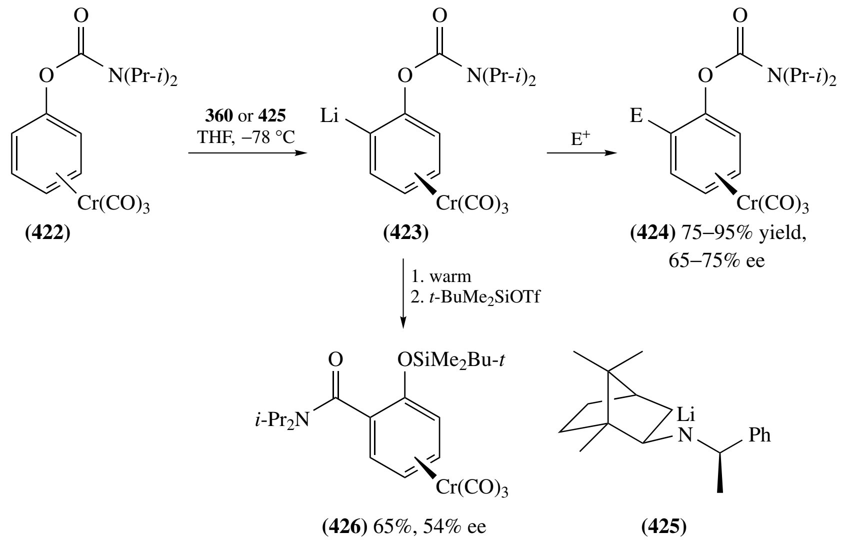

SCHEME 173

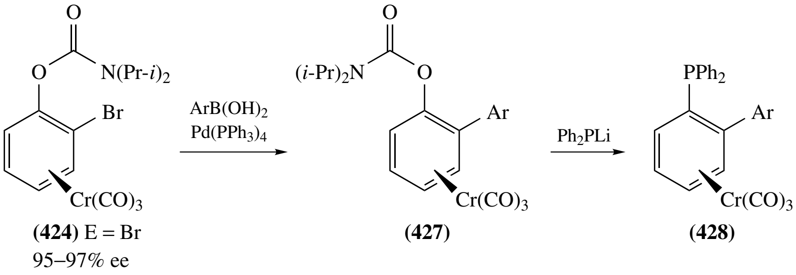

SCHEME 174

The chromium tricarbonyl complex **429** of triphenylphosphine oxide is lithiated and silylated (*in situ* quench) by **360** and Me_3SiCl to give **430** (X = Si) in 90% yield and 73% ee (Scheme 175)[379, 380]. Interestingly, the sense of asymmetric induction is reversed from the anisole result. With two equivalents of chiral base, bis-silyl compounds **432** could be formed.

Adding electrophiles 'externally' (after complete lithiation) failed, and in order to make potential ligands based upon the arenechromium skeleton, it was necessary to use Bu_3SnCl in an internal quench procedure. Reduction of **430** (X = Sn) yielded a phosphine without decomplexation, and tin–lithium exchange can lead to a variety of products **431** in about 70% ee.

Alkoxyalkyl-substituted arenechromium complexes have been lithiated enantioselectively in the benzylic position without control over planar chirality[381, 382], and the tendency for lithium amides to lithiate at a benzylic position rather than on the ring itself poses a problem with some substrates. In the lithiation of **433**, an element of planar stereochemistry is introduced during a benzylic lithiation (Scheme 176)[370, 383]. Exploiting

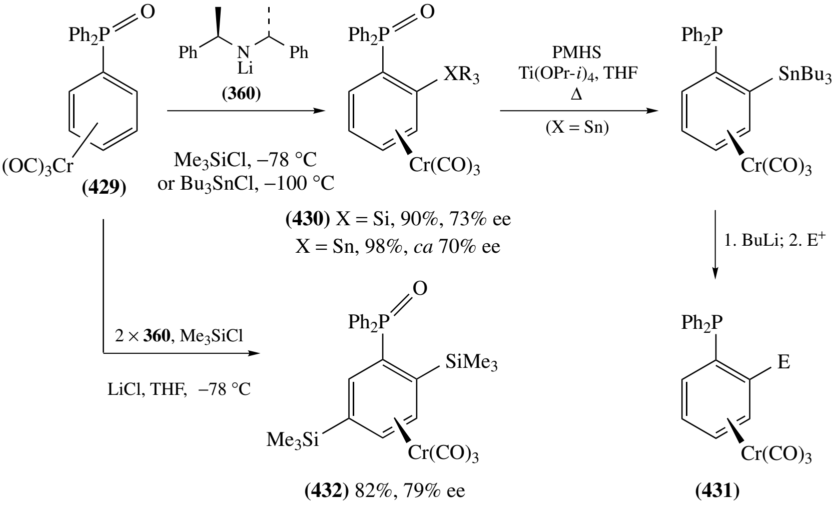

SCHEME 175

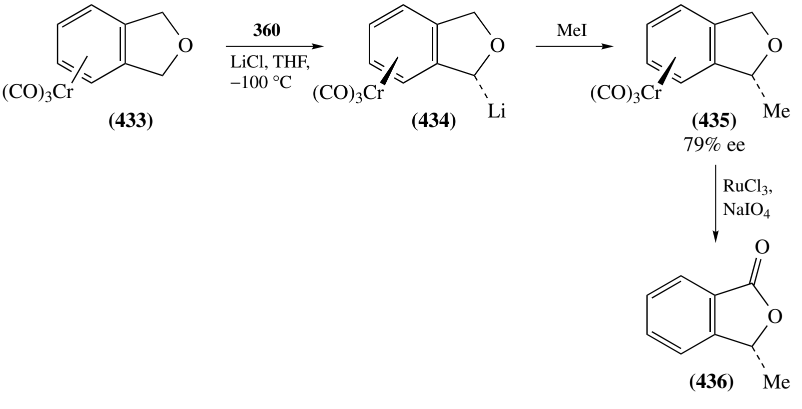

SCHEME 176

the accelerating effect of added LiCl on such lithiations, treatment of **433** with **360** and LiCl followed by MeI gave the ether **435** in 79% ee. Oxidative decomplexation yields known lactone **436**.

The chiral base **360** turns out not to be the best choice for enantioselective lithiation of the sulphur analogue **437** (Scheme 177): the bis-lithium amide **438** in the presence of LiCl at −100 °C gives better yields and enantioselectivity[380, 384]. The base **438** often turns out to be a good choice as an alternative to **360** for reactions that fail to give good enantioselectivity[382].

Attempts to deprotonate the benzaldehyde derivative **412** enantioselectively met with some success (see Scheme 169), but the reaction is complicated by benzylic lithiation[371, 376]. Better results are obtained with the benzaldimine **441**, which is lithiated by **360** with good enantioselectivity and whose product is easily hydrolysed to the aldehyde **442** (Scheme 178).

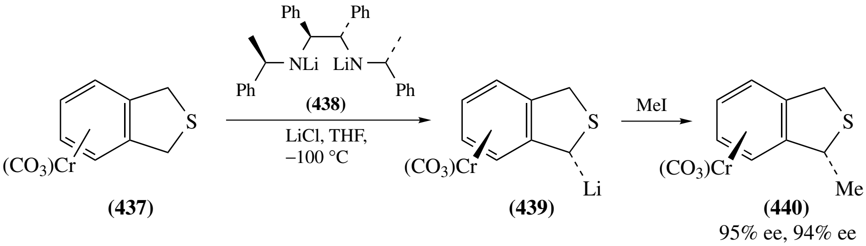

SCHEME 177

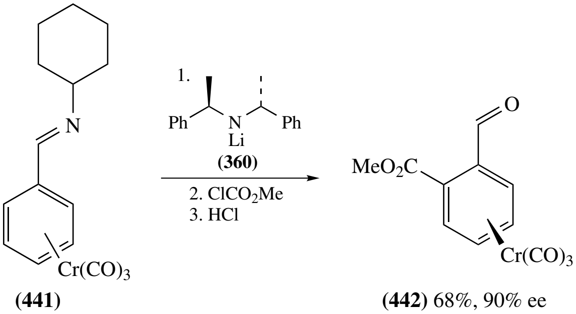

SCHEME 178

b. Chiral alkyllithium–diamine complexes. An alternative approach to the asymmetric synthesis of arenechromium tricarbonyls is to use achiral alkyllithiums in the presence of a chiral ligand—the diamine (−)-sparteine **362**, for example. In a study of the relative efficiencies of a range of diamines, Uemura and coworkers showed that the best ligand for introducing enantioselectivity into the lithiation of **443** and **446** was the diamine **444**[385]. (−)-Sparteine **362** performed relatively poorly with **443** (Scheme 179) but **444** gave **445** in 75% el.

By careful optimization, Widdowson and coworkers were able to show that methoxymethyl ethers of phenols are better substrates for alkyllithium–diamine controlled enantioselective deprotonation, and (−)-sparteine **362** is then also the best ligand among those surveyed: the BuLi–(−)-sparteine complex deprotonates **447** to give, after electrophilic quench, compounds such as **449** in 58% yield and 92% ee (Scheme 180)[386]. Deprotonation of the anisole complex **410** (see Scheme 169) under these conditions gave products of opposite absolute stereochemistry with poor ee.

A problem with (−)-sparteine **362** is its lack of availability in both enantiomeric forms. Reversed selectivity in the generation of planar chirality has been achieved by second lithiations (see Schemes 163 and 171) and a remarkable modification of this strategy works with arenechromium tricarbonyls. By using excess BuLi (sometimes *t*-BuLi is required) in the presence of sparteine **362**, a doubly lithiated species **450** may be formed from **448**[387]. The formation of the doubly lithiated species may be confirmed by double deuteriation with excess D_2O. However, other electrophiles react selectively only once and give products of opposite absolute stereochemistry from those formed after monolithiation, if in rather low yield. Presumably, the first lithiation, which is directed by (−)-sparteine, produce an organolithium **448** whose complexation with (−)-sparteine remains favourable. The second lithiation must produce a less stable organolithium—one which cannot form a

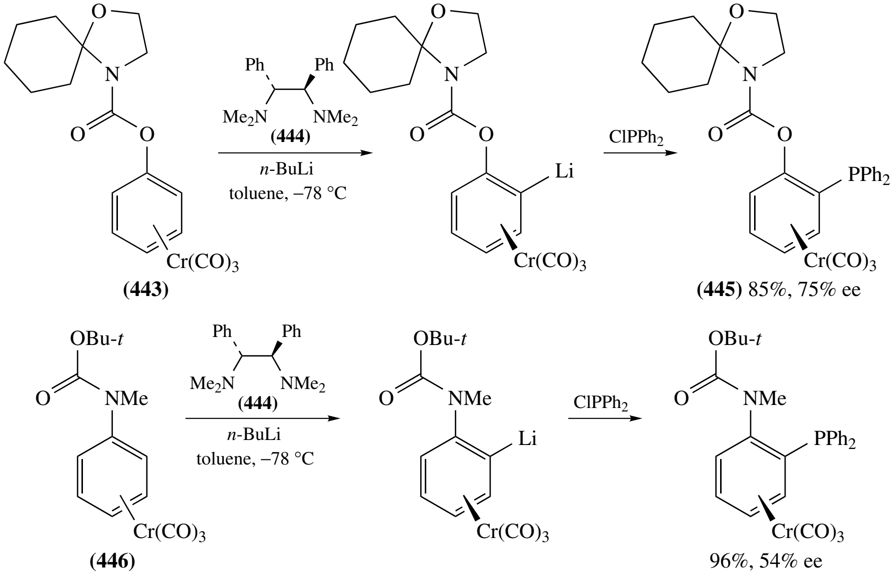

SCHEME 179

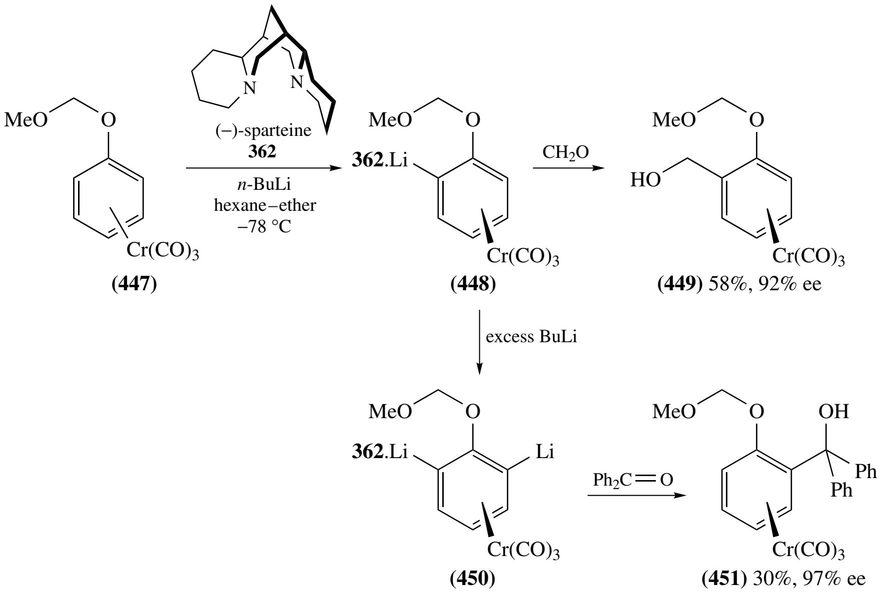

SCHEME 180

stabilizing complex with (−)-sparteine. This second formed 'anion' is the first to react, and monofunctionalization achieved the required reversal of stereochemistry (Scheme 180).

Siwek and Green have deprotonated arenechromium tricarbonyls bearing acidic benzylic protons with chiral bases in which the organolithium itself is chiral. Menthyllithium **452** (R = H) performed variably in terms of ee, but 8-phenylmenthyllithium **452** (R = Ph) gave good yields and ee's (in the opposite enantiomeric series from **452** (R = H)) in the deprotonation of **412** (Scheme 181)[388]. Unlike most chiral bases, **452** (R = Ph) gives better results in THF than in ether.

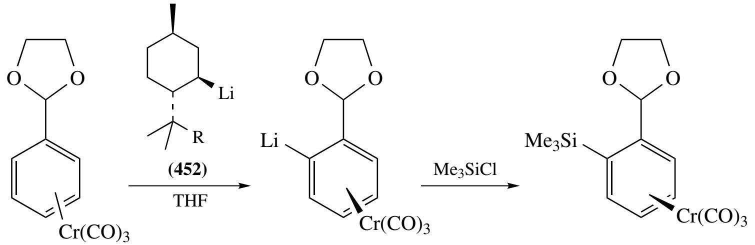

(412)

R = Ph: 77%, 80% ee
R = H: 85%, −30% ee (−70% ee in Et_2O–THF)

SCHEME 181

A valuable application of chiral arenechromium complexes has been in the synthesis of enantiomerically pure biaryls. Kawikawa and Uemura pioneered the atroposelective Suzuki coupling of planar chiral haloarenechromium tricarbonyls with areneboronic acids to yield biarylchromium tricarbonyls with defined planar and axial chirality[389]. A valuable feature of these reactions is that the major atropisomer about the new aryl–aryl bond generated in the coupling is typically the one bearing the larger group *syn* to chromium. This also turns out to be thermodynamically the less stable of the two atropisomers, so thermal equilibration allows the axial stereochemistry of the product to be inverted, and choice of conditions allows either atropisomer to be formed[390]. Schemes 182 and 183 show this method in action in the synthesis of two biaryl natural products, (−)-steganone **455**[363] and *O*,*O*′-dimethylkorupensamine A **462**[391, 392]. In the first, an acetal auxiliary is used to direct the diastereoselective lithiation and bromination, yielding **401** (see Scheme 165). Coupling with boronic acid **453** in refluxing methanol yields the thermodynamically more stable of two relatively easily interconverted atropisomeric biaryls. Further steps convert the axial chirality of **454** into the axially chiral natural product **455**.

The protected diol side-chain of **456** is introduced by asymmetric dihydroxylation and directs diastereoselectivity in the formation of **457** and **458** by lithiation. The most acidic position of **456**, between the two methoxy groups, is first protected by silylation. Suzuki coupling of **459** with the boronic acid **460** gives the kinetic product **461**—the more severe hindrance to bond rotation in this compound does not allow equilibration to the more stable atropisomer of the biaryl under the conditions of the reaction.

Couplings can also be carried out by simple nucleophilic substitution reactions of arenechromium tricarbonyls[393]. For example, in the synthesis of biaryl **469**, asymmetric lithiation of **463** using *in situ* silylation provides the complex **466** via **464** and **465**. Nucleophilic substitution by the tolyl Grignard **467** yields **468** as a single atropisomer in 68% yield, and decomplexation gives the biaryl **469** in 92% yield (Scheme 184).

Wilhelm and Widdowson have exploited the asymmetric deprotonation of **470** in a synthesis of a protected version **478** of the biaryl component of vancomycin, actinoidinic acid (Scheme 185)[394, 395]. One of the rings derives from an arenechromium tricarbonyl with stereochemistry controlled by asymmetric lithiation. The most readily lithiated position of **470**, between the two methoxy groups, first needed blocking. Enantioselective

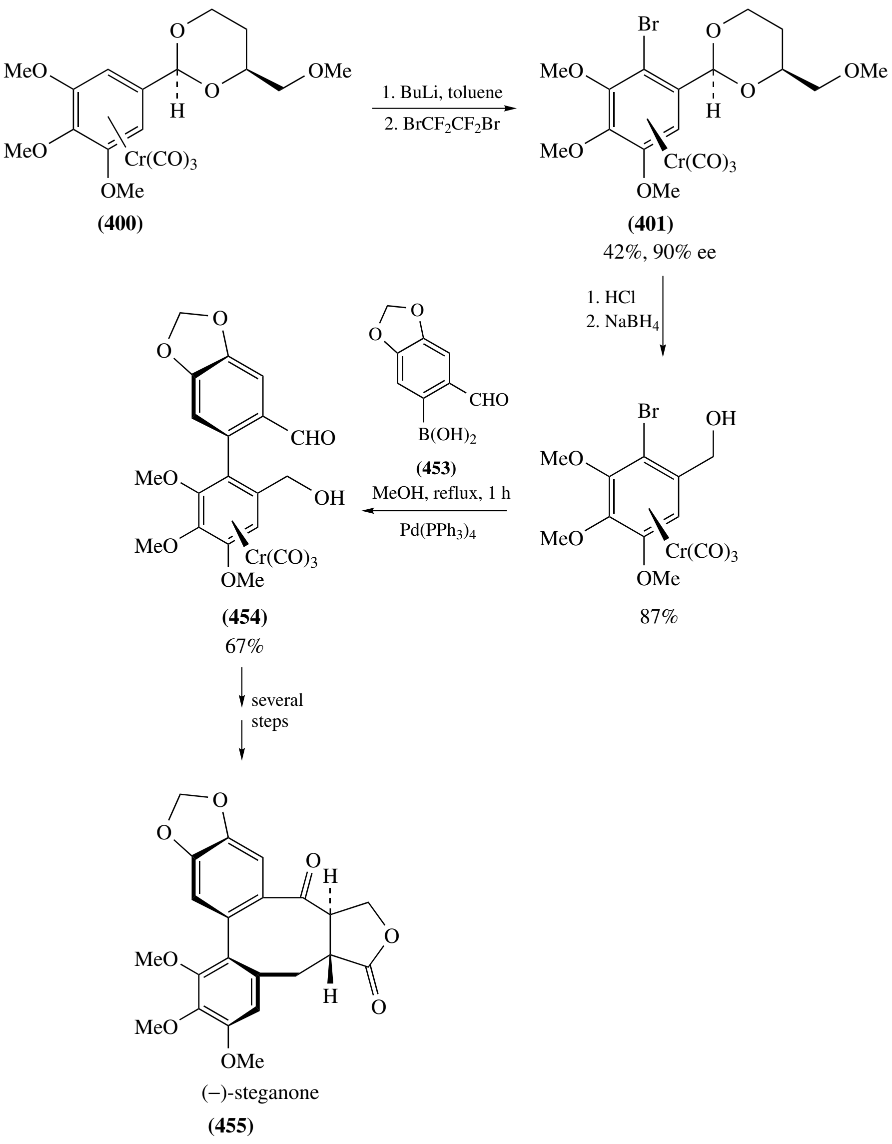

SCHEME 182

lithiation and chlorination of **471** gave **473** (TMEDA was needed to displace sparteine from **472** and restore reactivity towards a poor electrophile). Suzuki coupling of **474** with the boronic acid **475** transfers planar to axial stereochemistry and gives a single axial stereoisomer **476**. Deprotection of the aldehyde lowers the barrier to Ar−Ar rotation and allows relaxation to the thermodynamically preferred stereoisomer **477**.

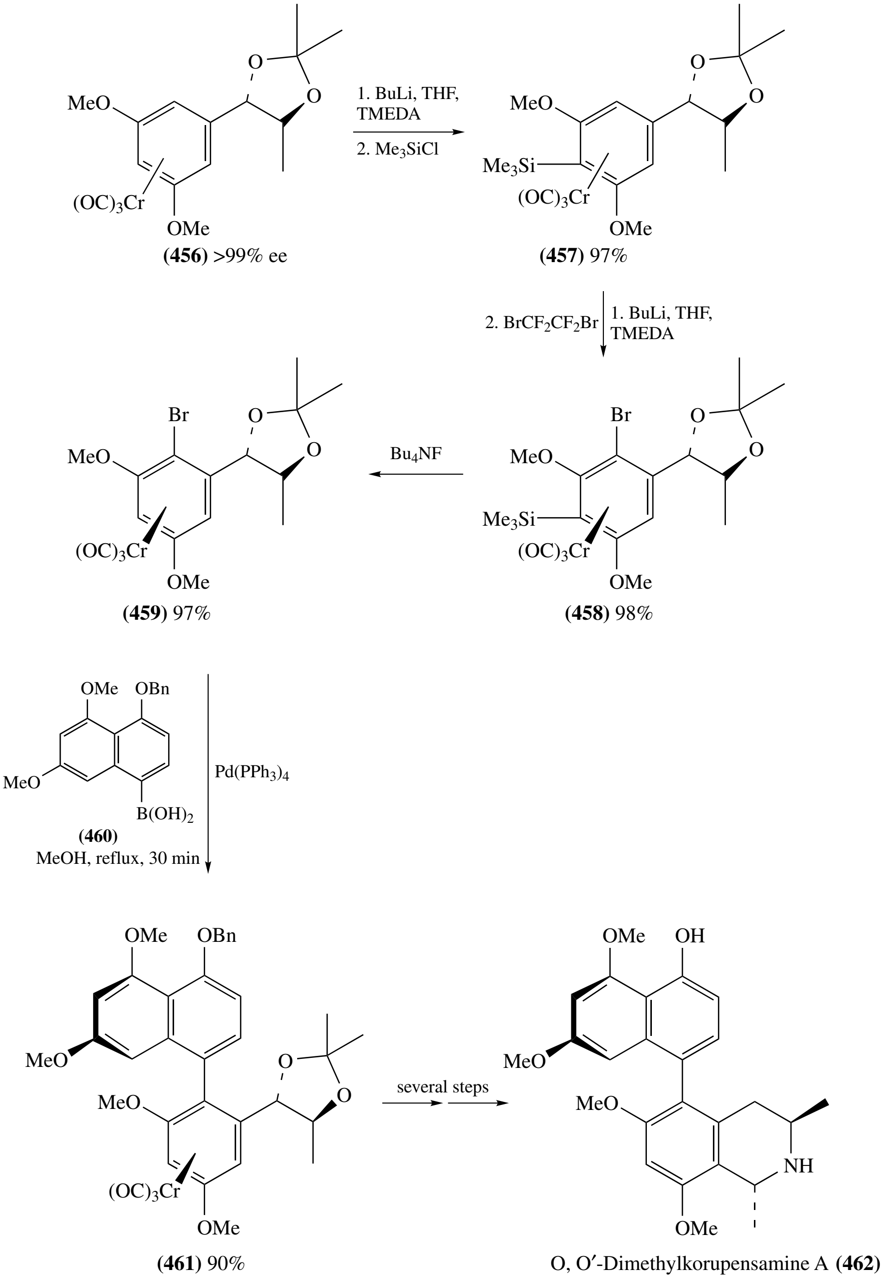
MeO
(OC)$_3$Cr
OMe
O
O
(456) >99% ee
1. BuLi, THF, TMEDA
2. Me$_3$SiCl
Me$_3$Si
(457) 97%
1. BuLi, THF, TMEDA
2. BrCF$_2$CF$_2$Br
Br
(458) 98%
Bu$_4$NF
(459) 97%
OMe OBn
B(OH)$_2$
(460)
MeOH, reflux, 30 min
Pd(PPh$_3$)$_4$
(461) 90%
several steps
OH
NH
O, O′-Dimethylkorupensamine A (462)

SCHEME 183

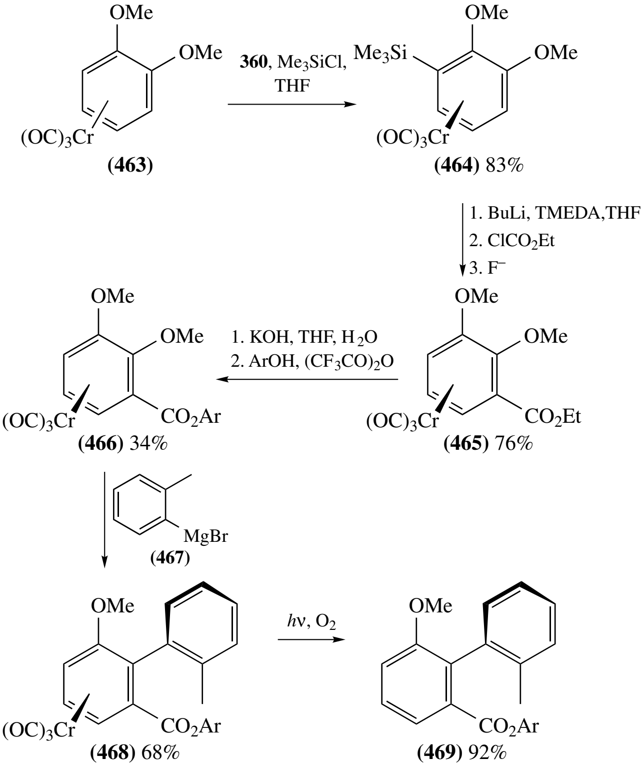

SCHEME 184

IV. LATERAL LITHIATION

Lateral lithiation is the lithiation of the benzylic position alkyl groups which are themselves *ortho* to a directing group[396]. A general scheme for a lateral lithiation directed by a group G is shown in Scheme 186.

The organolithium deriving from a lateral lithiation is benzylic, and therefore often of significantly greater thermodynamic stability than the equivalent ortholithiated species. In general, ortho- and lateral lithiation strategies have developed in parallel with one another, and since the starting materials for a lateral lithiation may often be made by ortholithiation there are many links between the two classes of reaction.

A. Mechanism and Regioselectivity

Benzylic lithiation requires an activating group if it is to be an efficient and synthetically valuable process. Both the ability to coordinate and the ability to acidify are important in a lateral lithiation-directing group, and most of the classes of directing group which will promote ortholithiation will also promote lateral lithiation. However, it is important to note one fundamental difference. In ortholithiation, acidifying groups must operate by an inductive effect since the C−Li bond is in the plane of the aromatic ring. For lateral

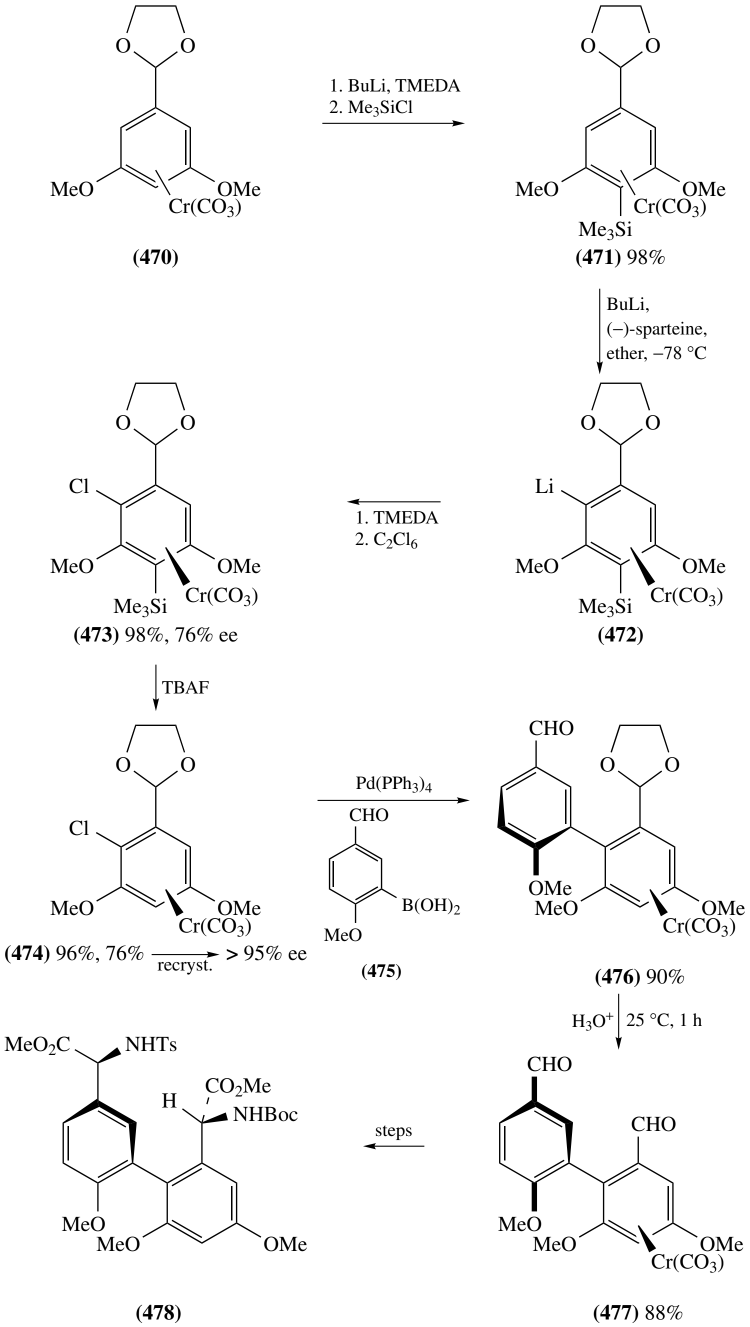
MeO
OMe
Cr(CO3)
(470)
1. BuLi, TMEDA
2. Me3SiCl
MeO
OMe
Cr(CO3)
Me3Si
(471) 98%
BuLi,
(−)-sparteine,
ether, −78 °C
Li
MeO
OMe
Me3Si
Cr(CO3)
(472)
1. TMEDA
2. C2Cl6
Cl
MeO
OMe
Me3Si
Cr(CO3)
(473) 98%, 76% ee
TBAF
Cl
MeO
OMe
Cr(CO3)
(474) 96%, 76% → recryst. > 95% ee
Pd(PPh3)4
CHO
B(OH)2
MeO
(475)
CHO
OMe
MeO
OMe
Cr(CO3)
(476) 90%
H3O+ 25 °C, 1 h
CHO
CHO
MeO
MeO
OMe
Cr(CO3)
(477) 88%
steps
MeO2C
NHTs
H
CO2Me
NHBoc
MeO
MeO
OMe
(478)

SCHEME 185

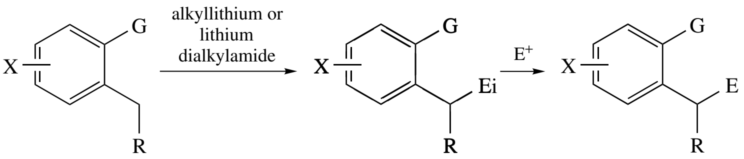

SCHEME 186

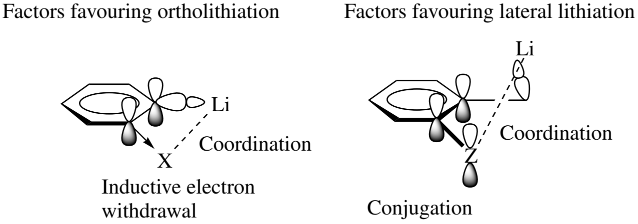

SCHEME 187

lithiation, the benzylic C−Li bond means that acidifying groups work best by conjugation (Scheme 187).

Toluene itself can be lithiated by *n*-BuLi−TMEDA at or above room temperature, and deprotonation occurs almost exclusively at the methyl group—about 10% ring metallation (mainly in the *meta* position) is observed with *n*-BuLi−TMEDA (Scheme 188)[397, 398]. At lower temperatures deprotonation is very slow[399], and the best conditions for achieving the metallation of toluene are the Lochmann−Schlosser superbases (see Section VI)[400].

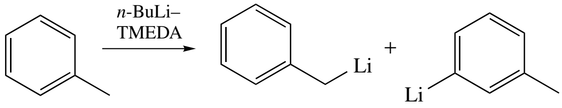

SCHEME 188

By contrast, the lithiation of **479** with *n*-BuLi, which is assisted by coordination to the NMe_2 group, is faster, reaching completion in less than 6 h at 25 °C, and completely regioselective[401, 402]. The mesitylmethyl amine **480** is lithiated only at the methyl group *ortho* to the aminomethyl substituent (Scheme 189).

The dimethylaminomethyl group must operate solely by coordination to Li, and it is assumed, as for ortholithiation, that the deprotonation takes place after the initial equilibrium formation of a BuLi−amine complex.

Similar is the lateral lithiation of amide **481**[57], which is presumably assisted both by coordination of the amide to the lithium and by conjugation of the aromatic ring with the amide. Both **481** and **484** may be lithiated with LDA[4], suggesting that conjugation is more important than coordination in stabilizing the benzylic organolithiums with such electron-withdrawing groups. Given LDA's tendency to deprotonate its substrates reversibly, the formation of **485** is probably a result of thermodynamic control (though the methyl group may nonetheless be the site of kinetic lithiation with LDA): kinetically controlled lithiation with *s*-BuLi−TMEDA gives the ortholithiated **483** (Scheme 190)[4]. As noted before, coordination to lithium is a less important factor in LDA-promoted deprotonation, though it does ensure that mesitamides such as **486** are deprotonated only at the 2-methyl group[403].

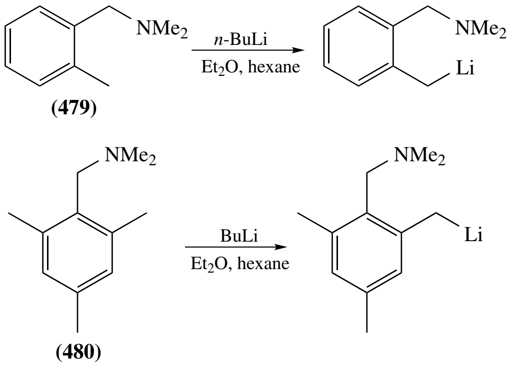

SCHEME 189

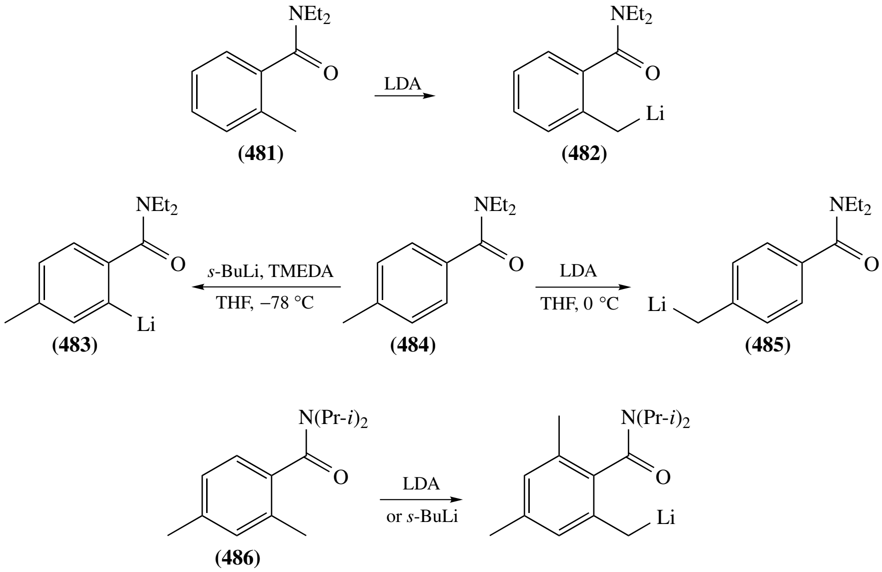

SCHEME 190

Organolithium **482** has been represented by the extended enolate structure **487** (Scheme 191), though the chirality of some analogues of **482** argues in favour of the localized structure **482**[404].

B. Classes of Directing Group

1. Secondary and tertiary amides

Resistance of the deprotonated amide to attack by alkyllithium means that two equivalents of BuLi, even at 0 °C, will give the dilithiated **488** in good yield, and various electrophiles can be used to introduce benzylic functionality (Scheme 192)[405].

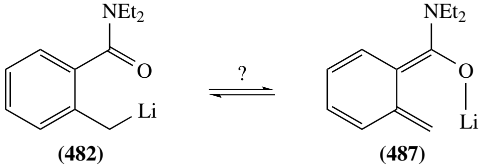

SCHEME 191

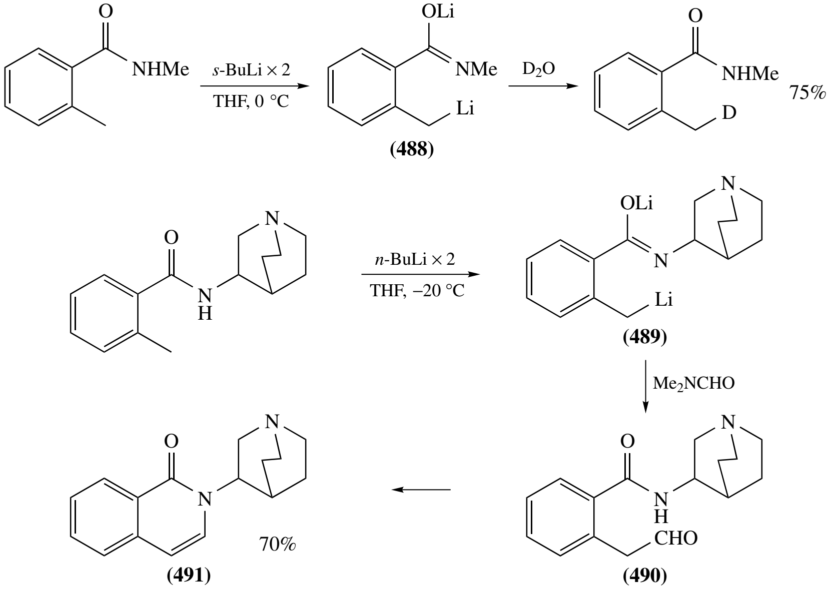

SCHEME 192

In the case of **489**, the product **490** cyclizes to the isoquinolone **491**, and the amide substituent is a required part of the target molecule[406]. However, it frequently occurs that the amide substituent is not required in the final product, and the acid-sensitive alkenyl substituent of **492** has been used as a solution to the problem of cleaving a C−N bond in the product (Scheme 193)[407, 408]. Weinreb-type amides **493** can also be laterally lithiated, and the methoxy group removed from **494** by $TiCl_4$[409]. Hydrazones similarly can be laterally lithiated and oxidatively deprotected[82].

Laterally lithiated *tertiary* amides are more prone to self-condensation than the anions of secondary amides, so they are best lithiated at low temperature (−78 °C). *N*,*N*-Dimethyl, diethyl (**495**) and diisopropyl amides have all been laterally lithiated with alkyllithiums or LDA, but, as discussed in Section I.B.1.a, these functional groups are resistant to manipulation other than by intramolecular attack[410]. Clark has used the addition of a laterally lithiated tertiary amide **496** to an imine to generate an amino-amide **497** product whose cyclization to lactams such as **498** is a useful (if rather low-yielding) way of building up isoquinoline portions of alkaloid structures (Scheme 194)[411]. The addition of laterally lithiated amines to imines needs careful control as it may be reversible at higher temperatures[412].

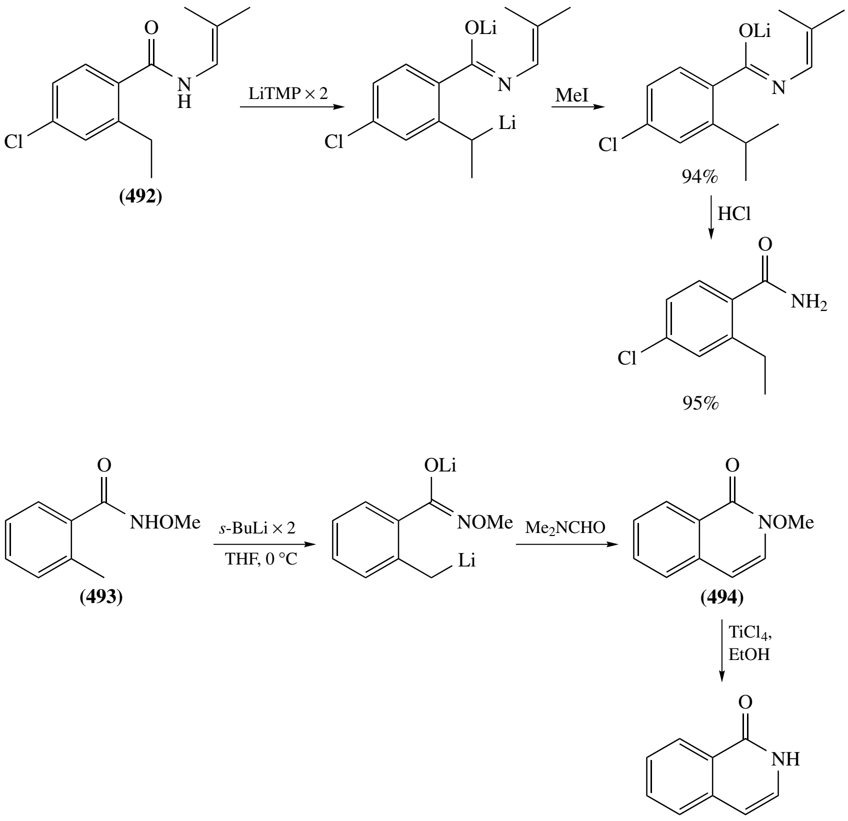

SCHEME 193

Under certain conditions, the cyclization to lactam **499** occurs spontaneously, eliminating one equivalent of lithium diethylamide, which goes on to deprotonate the benzylic position a second time to yield **500** and then **501**[411].

These reactions have been used in the synthesis of alkaloids such as corydalic acid methyl ester **502** (Scheme 195). Isolated from *Corydalis incisa*, **502** is derived from a proposed biosynthetic intermediate in the route to the tetrahydroprotoberberine alkaloids. The 1,2,3,4-tetrasubstituted ring of **502** demands control by an ortholithiation strategy, and the synthetic route proposed by Clark and Jahangir[413] employs a lateral lithiation of **503** and addition to an imine as the key disconnection at the centre of the molecule.

The amide **504** may be made by ortholithiation of benzodioxolane **505**, though a higher-yielding preparation starts from 1,2-dihydroxybenzoic acid **506**. Ortholithiation of **504**, directed by the tertiary amide group, is straightforward, and gives the alkylated amide **503** (Scheme 196).

The directing effect of the amide group can then be used a second time in the lateral lithiation of **503** to give an organolithium **507** which adds to the imine **508** in a stereoselective manner, probably under thermodynamic control (imine additions of laterally lithiated amides appear to be reversible). Warming the reaction mixture to room temperature leads to a mixture of **509** and some of the (ultimately required) cyclized product

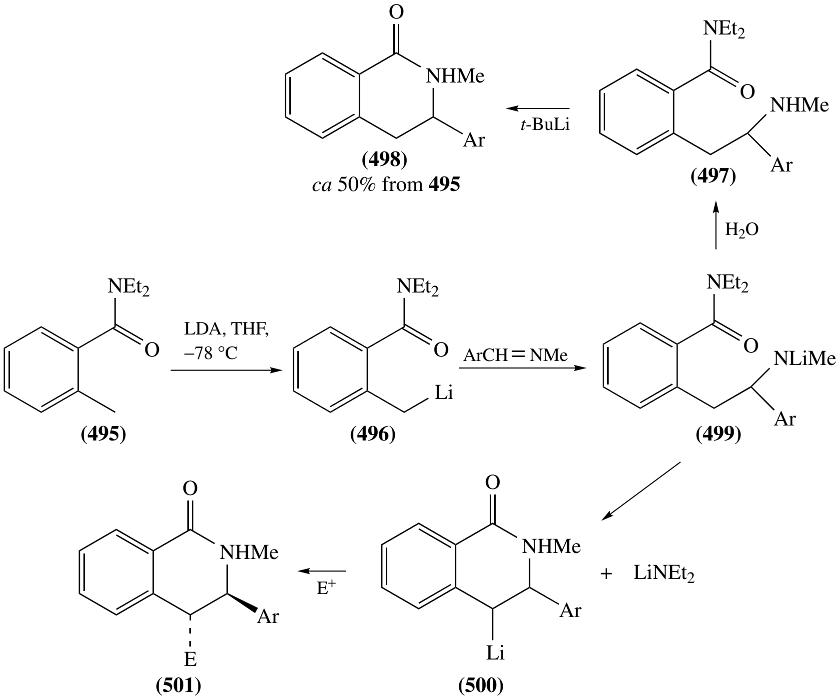

SCHEME 194

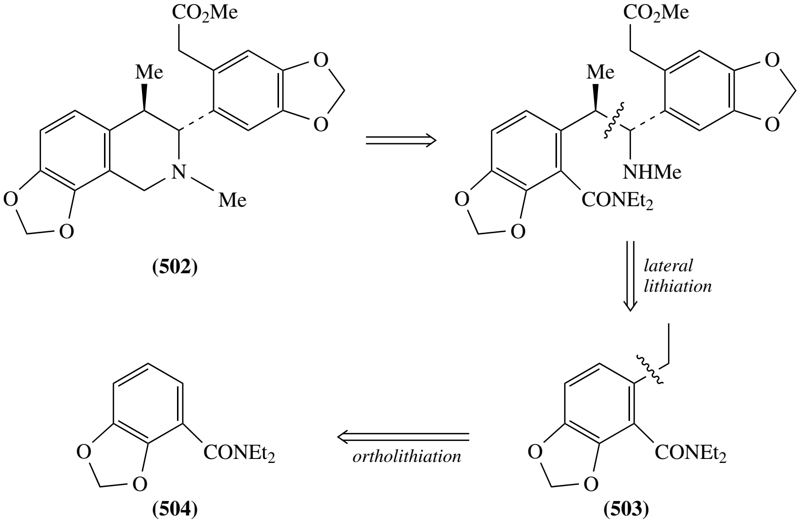

SCHEME 195

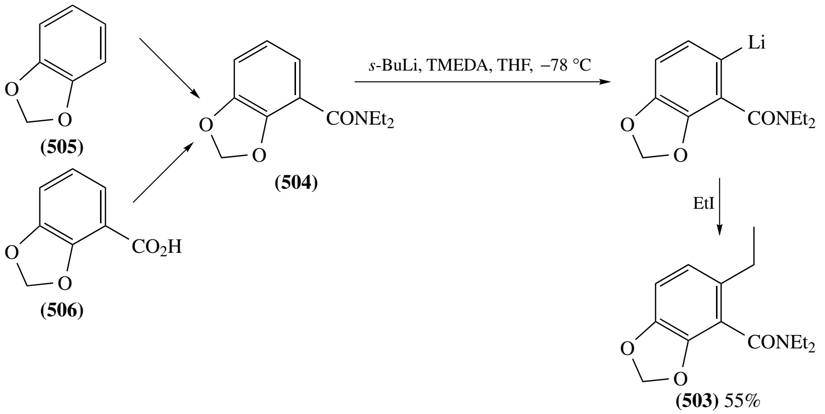

SCHEME 196

510. The uncyclized product could readily be cyclized to **510** by treatment with *t*-BuLi at −30 °C (Scheme 197).

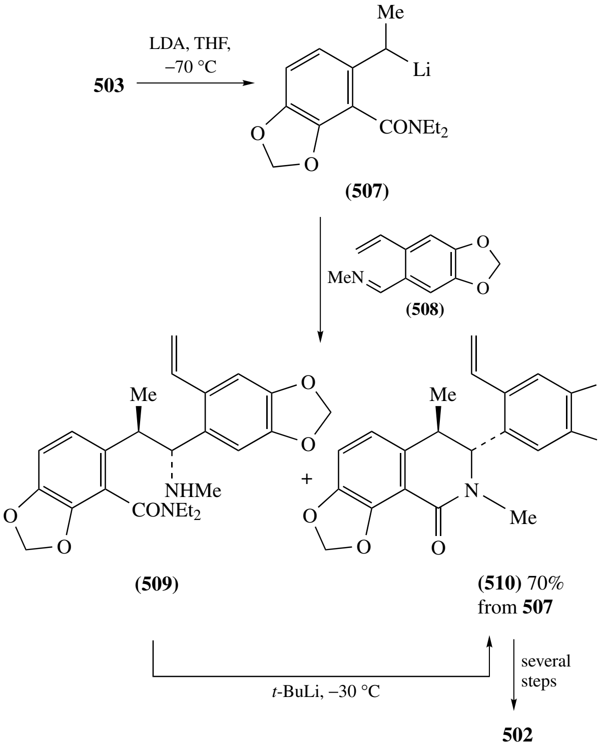

SCHEME 197

Conversion to the target molecule **502** was achieved by oxidation ($TlNO_3$ then $KMnO_4$) of the vinyl group and reduction of the lactam.

The labile tertiary amide groups described in Section I.B.1.a are also applicable to lateral lithiations[72]; the piperazine-based amide **511** has been used to direct lateral lithiation before being methylated and cleaved to the acid **512** (Scheme 198)[414].

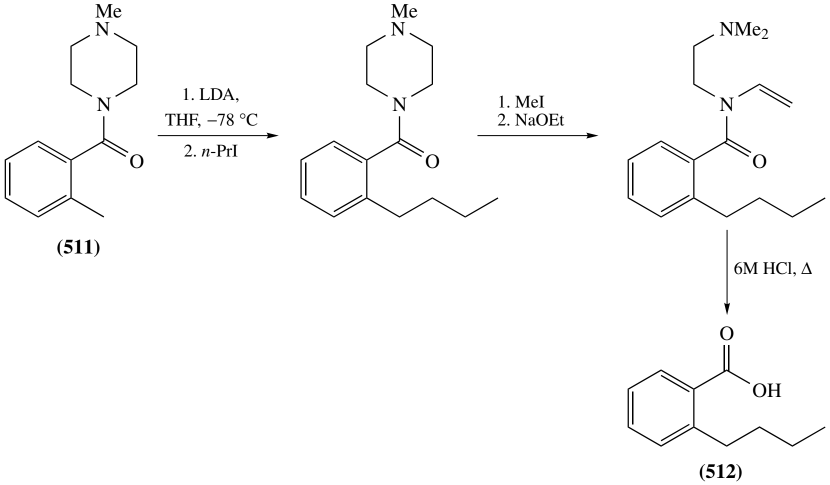

SCHEME 198

2. Nitriles

Lateral lithiation of nitriles can be achieved—and self-condensation avoided—if LiTMP is used in THF at −78 °C (Scheme 199)[415].

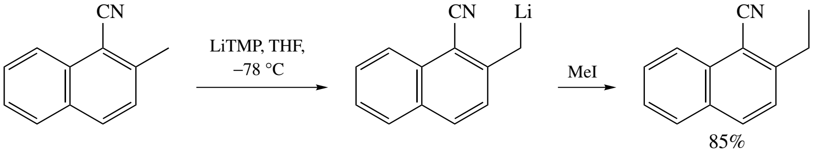

SCHEME 199

3. Oxazolines, imidazolines and tetrazoles

Oxazolines[416], imidazolines[417] and tetrazoles[418] can all be laterally lithiated. Oxazolines have been used in this regard rather less than for ortholithiation (Scheme 200).

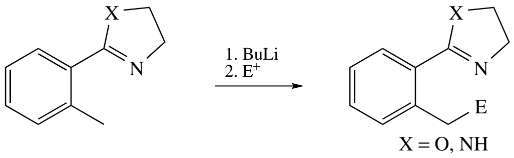

SCHEME 200

4. Carboxylates

2-Methylbenzoic acid **513** can be laterally lithiated with two equivalents of lithium amide base (LDA[419] or LiTMP[420]) or alkyllithium[421, 422], provided the temperature is kept low to avoid addition to the carbonyl group (Scheme 201). It is usually preferable to carry out the lithiation using alkyllithiums[421], since with lithium amides the subsequent reaction of **514** with electrophiles is disrupted by the presence of the amine by-product (diisopropylamine, for example)[421, 423]. The dilithio species **514** is stable in THF even at room temperature, and (as with the amide **483**) since LDA will also dilithiate **515** stabilization presumably comes principally from conjugation with the carboxylate.

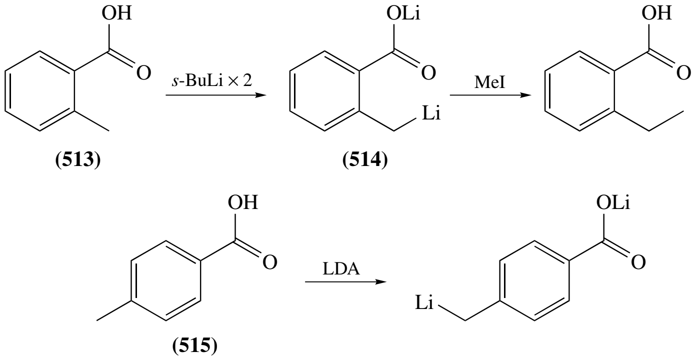

SCHEME 201

5. Carboxylic esters

The greater acidity of lateral protons means that LDA is more than basic enough to remove them and hence many more electrophilic directing groups can be used for lateral lithiation than ortholithiation. Methyl 2-methylbenzoate **516** is deprotonated at −78 °C by LDA, but as soon as the product organolithium forms it adds to unreacted starting material to give products **517** (Scheme 202)[424].

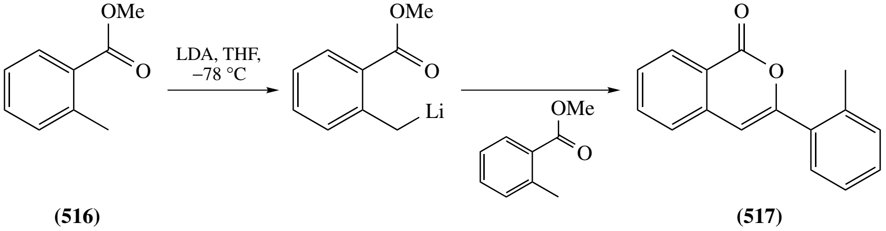

SCHEME 202

This addition reaction is much slower with 2,6-disubstituted esters (and phenoxides), and organolithiums **518** and **520** can be formed and reacted with external electrophiles to give compounds such as **519** and **521** (Scheme 203)[424,425]. An asymmetric version of this reaction has been developed[426,427].

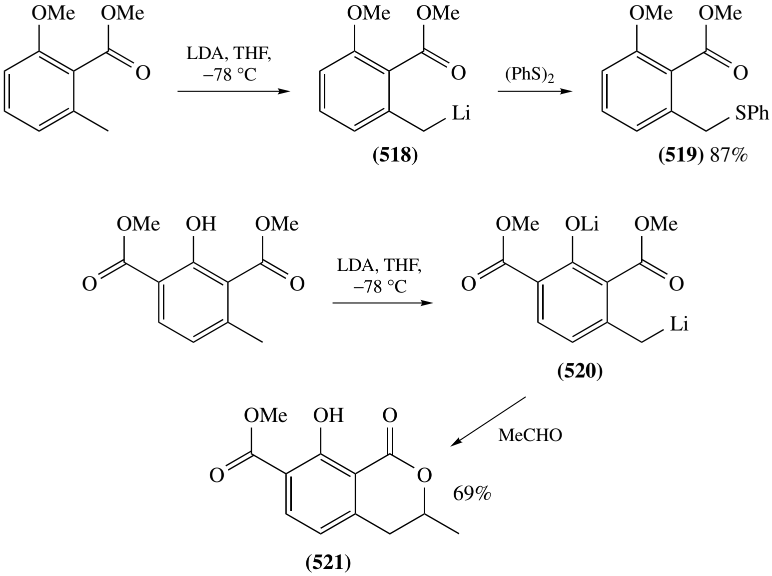

SCHEME 203

6. Ketones

Ketones may direct lateral lithiation even if the ketone itself is enolized: enolates appear to have moderate lateral-directing ability. Mesityl ketone **522**, for example, yields **523** after silylation—BuLi is successful here because of the extreme steric hindrance around the carbonyl group (Scheme 204)[428]. The lithium enolate can equally well be made from less hindered ketones by starting with a silyl enol ether[428].

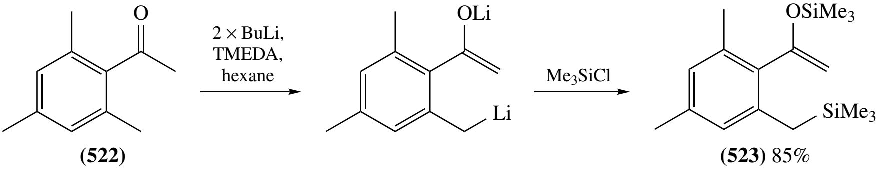

SCHEME 204

When the ketone cannot be enolized, lateral lithiation appears to be very easy; **524** is lithiated by LDA at −78 °C (Scheme 205)[429].

7. Aldehydes protected as α-amino alkoxides

Temporary protection of an aldehyde by addition of a lithium amide can be used to facilitate lateral lithiation by *n*-BuLi. The best lithium amide for this purpose is **56**: interestingly, lithium piperidide **53** promotes *ortho*-, rather than lateral, lithiation of **525** (Scheme 206)[430], while **56** yields **526**.

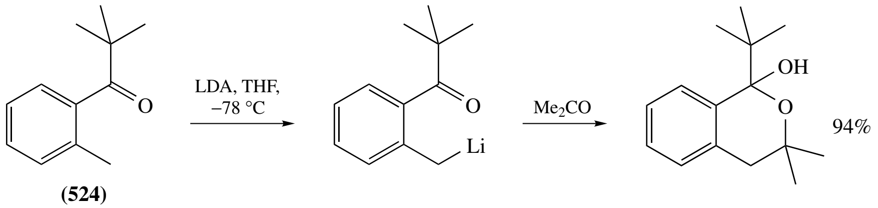

SCHEME 205

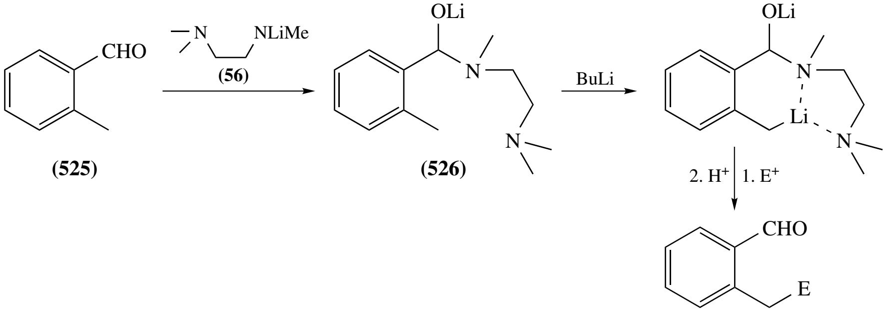

SCHEME 206

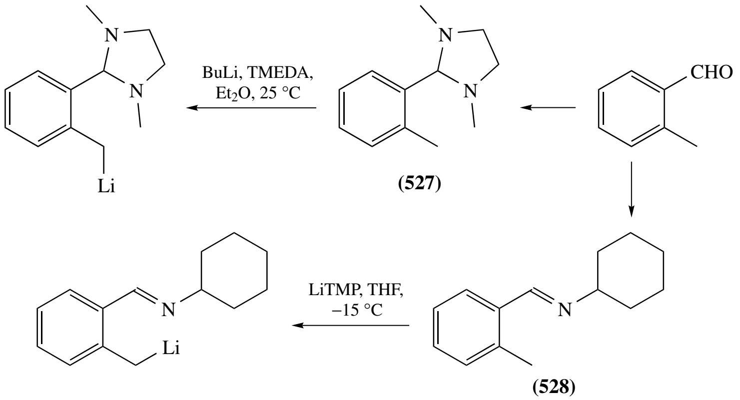

SCHEME 207

Aldehydes can also be laterally lithiated if protected as imidazolidines (**527**)[431] or as imines (**528**)[432]. With imines, LiTMP must be used to prevent nucleophilic addition to C=N (Scheme 207).

8. Alcohols and phenols (cresols) and their derivatives

2-Methylbenzyl alcohol **529** can just about be lithiated by treatment with BuLi in Et_2O at room temperature, but the activation of the methyl group is very weak[433]. Lateral lithiation of cresol **530** is even harder to achieve, and the superbase conditions required

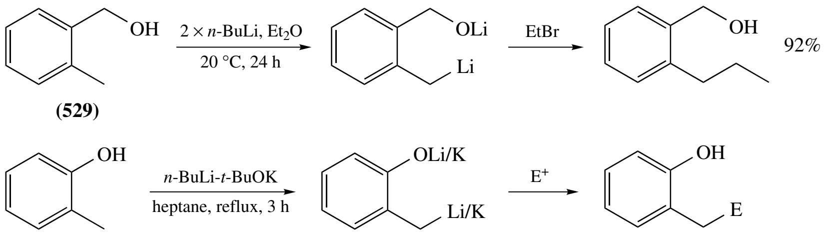

(529)

(530)

SCHEME 208

are similar to those used to deprotonate toluene (Scheme 208)[434]. The coordinating effect of the oxyanion is overpowered by electron-donation into the ring.

The deactivating effect of a phenoxide oxyanion is removed in the ether series, but in cases such as **531** where ortholithiation can compete with lateral lithiation, mixtures of products are frequently obtained[435]. The MOM acetal **532** is fully *ortho*-selective in its reaction with *t*-BuLi (Scheme 209)[436,437].

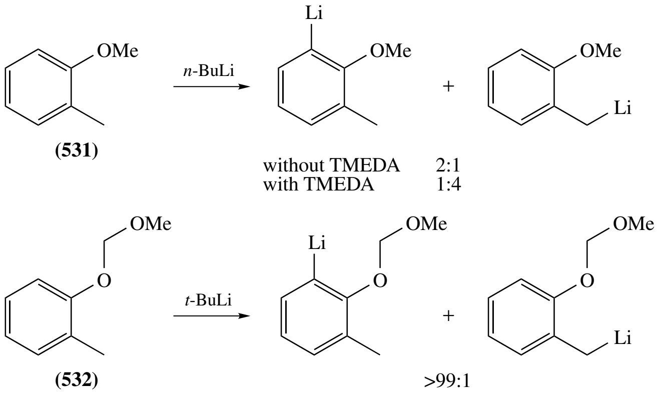

(531)

(532)

SCHEME 209

The prospects for lateral lithiation are slightly improved if ortholithiation is blocked, though even then yields are moderate at best (Scheme 210).

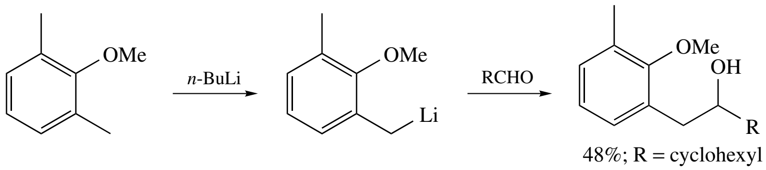

SCHEME 210

Better for the lateral lithiation of phenols are the *N*,*N*-dialkylcarbamate derivatives **533**. These may be lithiated with LDA, allowing complete selectivity for the lateral position, presumably because this is the thermodynamic product[103]. With *s*-BuLi, ortholithiation is

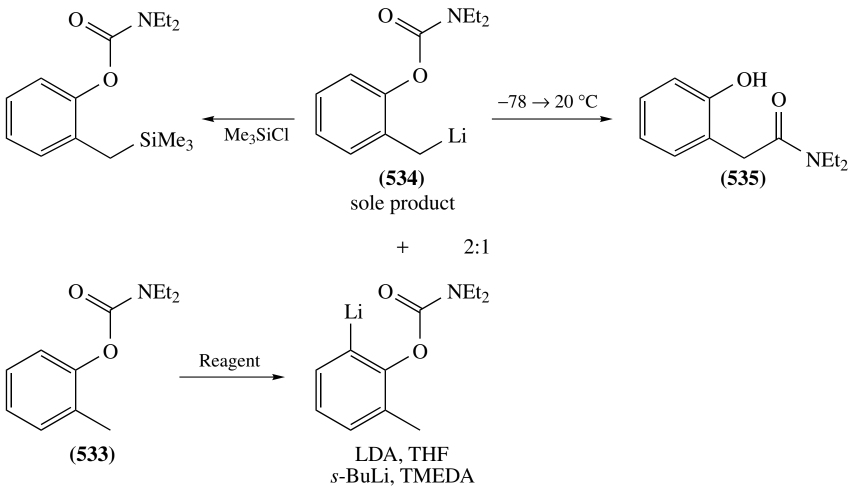

SCHEME 211

the predominant reaction pathway. If the lateral organolithium **534** is warmed to room temperature, an acyl transfer from O to C takes place, analogous to the anionic *ortho*-Fries (see Section I.B.1.d), giving amide **535** (Scheme 211)[396].

The best phenol-derived lateral director of all appears to be the diaminophosphoryl group. Lithiation of **536** at −105 °C with *s*-BuLi gives a highly reactive organolithium which adds to electrophiles even at −90 °C (Scheme 212)[438].

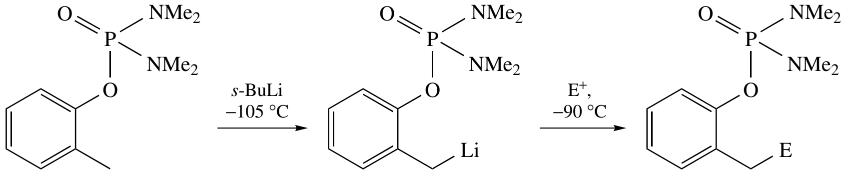
(536)

SCHEME 212

9. Sulphur-based functional groups

The problem of lithiation regioselectivity is particularly acute with arylsulphides since sulphur can promote α, lateral and ortholithiation to a broadly similar degree. Lithiating **537** in ether, for example, gives a 20:10:1 ratio of the α, lateral and orthofunctionalized products **538, 539** and **540**[439]. If **537** is deprotonated twice, a good yield of the dilithio species **541**, and hence the doubly quenched compounds **542**, results (Scheme 213)[440]. The SCH_2Li group is clearly having some directing effect in this reaction, since no second deprotonation occurs if the methyl group is in the *meta* or *para* position.

α-Lithiation is suppressed in aryl isopropylsulphides, but now ortholithiation wins out over lateral lithiation unless there are no deprotonatable *ortho* positions[439].

Sulphoxides direct lateral lithiation in a reaction which is also highly stereoselective[441]. In common with other electrophiles, $ClCO_2Et$ produces as a single diastereoisomer of **544**

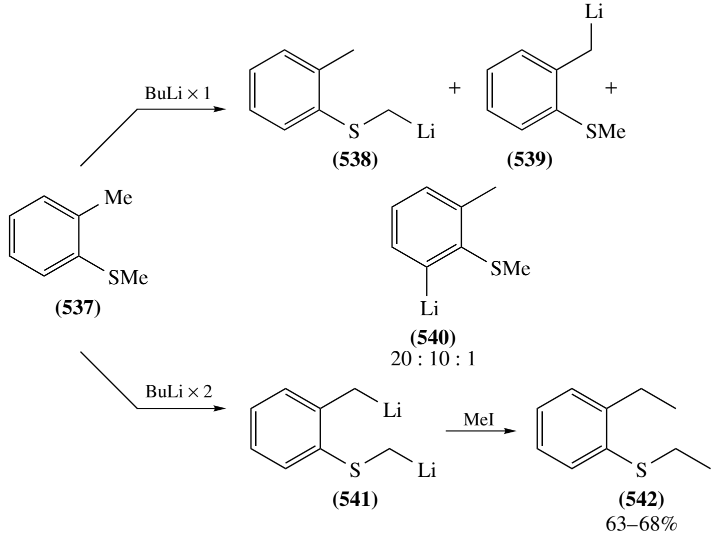

SCHEME 213

from **543**, and Raney nickel can be used to remove the sulphinyl group from the product, making this a very versatile method for asymmetric functionalization of a benzyl group (Scheme 214).

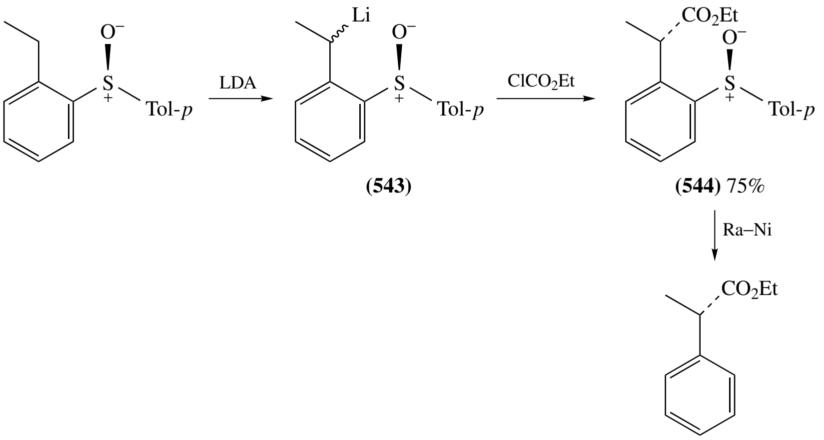

SCHEME 214

Remarkably, ethyl *o*-tolylsulphonate **545** can be laterally lithiated by BuLi at −78 °C (Scheme 215)[442]. With the methyl ester, the expected substitution at the methyl group takes place. The *p*-substituted analogue also undergoes lithiation of the methyl group, suggesting that the sulphonate group acts substantially by conjugation.

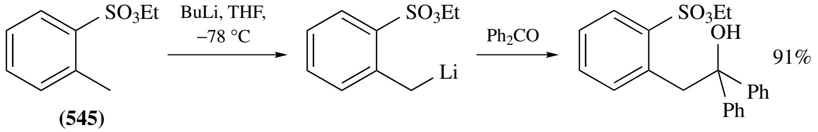

(545)

SCHEME 215

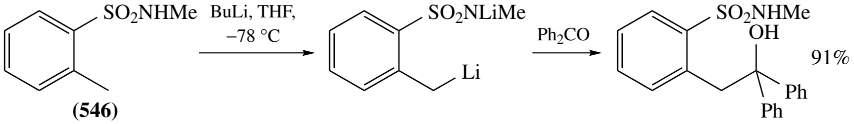

(546)

SCHEME 216

By contrast, while the *o*-methyl sulphonamide **546** can be laterally lithiated, its *p*-methyl isomer undergoes ortholithiation rather than benzylic lithiation (Scheme 216)[443–445].

10. Aniline and aminoalkylbenzene derivatives

N,*N*-Dimethyl-*o*-toluidine **547** is reluctantly lithiated with *n*-BuLi−TMEDA at 25 °C; ortholithiation occurs to some extent in the reaction but the yield of laterally functionalized product is maximized after 3 h (Scheme 217)[109]. Without TMEDA, the extent of ortholithiation is increased.

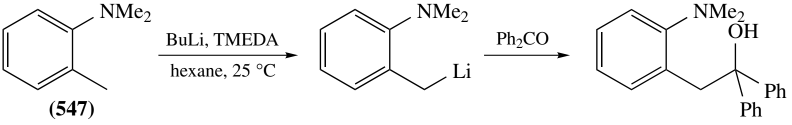

(547) **(548)**

SCHEME 217

Much more versatile than the simple anilines are their anilide derivatives. Pivalanilides, benzanilides and other non[110,446] (or scarcely[447]) enolizable amides **549** are laterally lithiated on treatment with two equivalents of BuLi, and may be quenched with electrophiles to give **551**. In the absence of an electrophile, the organolithiums **550** cyclize to indoles **552** (Scheme 218).

A similar cyclization can result from lithiation of an isonitrile; lithiation of **553** requires two equivalents of LDA and the organolithium **554** can either be trapped with other electrophiles at low temperature or warmed to give an indole **555** (Scheme 219)[448,449]. It is quite clear that isonitriles activate purely by conjugation, and indeed they promote deprotonation of methyl groups *para* to an isonitrile just as well as *ortho*. The ease with which isonitriles can be made from formamides suggests that these methods could be rather more widely used than they are.

The carbamates **549** (R = OBu-*t*) behave similarly, though they must be lithiated with *s*-BuLi to avoid addition to the carbonyl group[450]. It is possible simply to use a lithium carbamate to protect an amino group during a lateral lithiation: an initial deprotonation and carbonation generates the lithium carbamate **556**, which is then deprotonated twice more by *t*-BuLi (Scheme 220). After electrophilic quench, acid hydrolysis of the carbamic

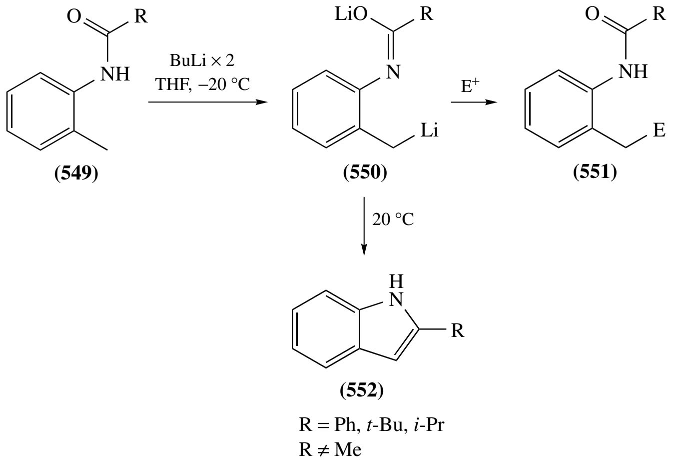

SCHEME 218

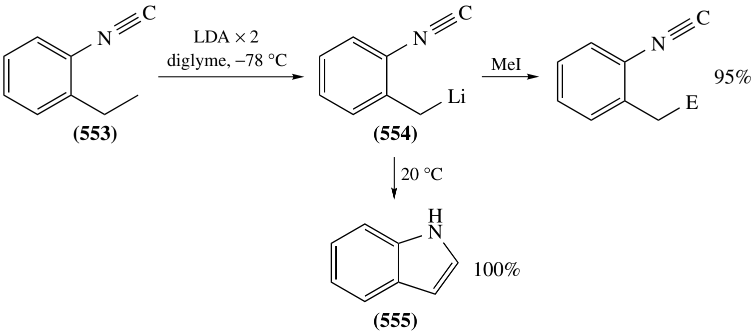

SCHEME 219

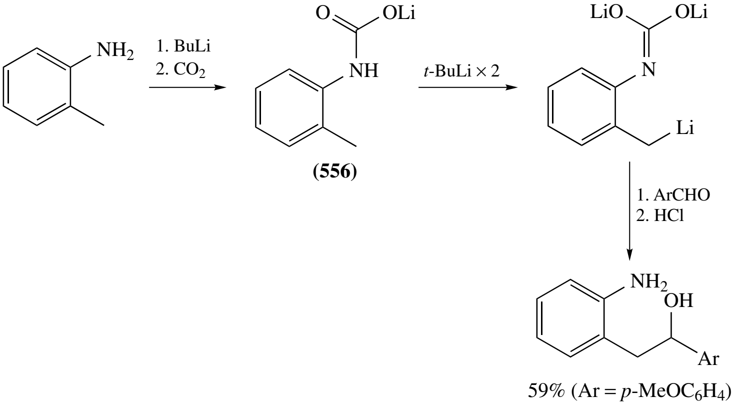

SCHEME 220

acid returns the unprotected aniline[451,452]. An alternative *in situ* protection sequence relies on temporary trimethylsilylation of the aniline[453].

Amines in the benzylic position, and their carbamate derivatives, promote lateral lithiation through coordination to Li, and lack the disadvantage that their ArNHR isomers have of attenuated acidity due to the nitrogen lone pair. As described above, simple benzylamines are readily lithiated—more so than the equivalent anilines[17,402]; their carbamate derivatives such as **557** also lithiate well in the lateral position (Scheme 221)[408] (in the absence of a 2-methyl group, benzylic lithiation α to nitrogen is the major pathway[454]). As the amino group is moved further and further from the aromatic ring, benzylic lithiation of the aminoalkyl chain becomes a more and more important side reaction[455].

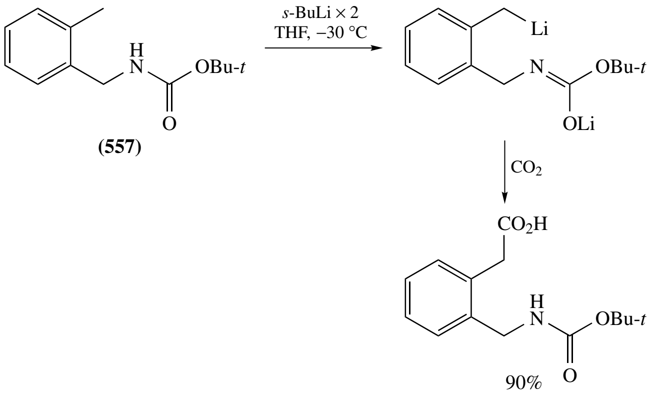

SCHEME 221

11. Halogens

2-Fluorotoluene can be deprotonated in the benzylic position by the superbases, but the halogen appears to offer little activation to the process. 2-Trifluoromethyltoluene is more readily deprotonated, but decomposes by elimination of fluoride even at $-100\,^{\circ}\mathrm{C}$[396].

12. Lateral lithiation of heterocycles[268]

Alkyl groups attached to electron-deficient heterocyclic rings can usually be lithiated even in the absence of a directing group. The pK_a values of methyl groups attached to some representative heterocycles are shown in Scheme 222[456].

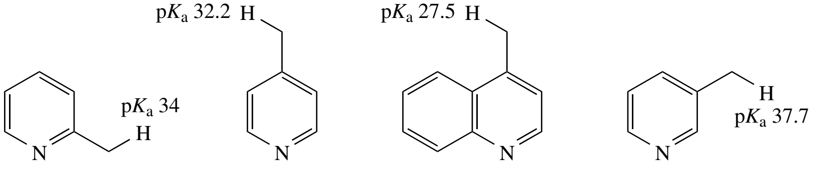

SCHEME 222

Those of 2- and 4-substituted pyridines fall about half-way between those of toluene (*ca* 40) and of a ketone (*ca* 20)—the organolithiums have significant 'azaenolate' character (as shown in **558** and **559**). A representative reaction is the synthesis of **560**[457]. Lithiation of 2-methylpyridine to give **560** has also been used in the synthesis of the anti-angina drug perhexiline (Scheme 223)[153].

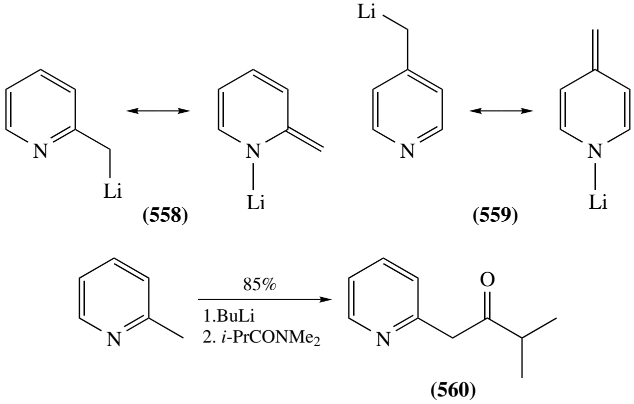

(558) **(559)**

(560)

SCHEME 223

The pK_a of 3-methylpyridine, whose anion cannot be delocalized onto N, is closer to that of toluene, and deprotonation gives only low yields with most bases. However, with a combination of BuLi and lithiodimethylaminoethanol (LiDMAE) deprotonation is quantitative but yields products **561** arising from apparent lithiation α to N (Scheme 224)[458]! Trying to force lateral lithiation of pyridines is generally doomed to failure, as ring lithiation or nucleophilic addition usually takes place first[396].

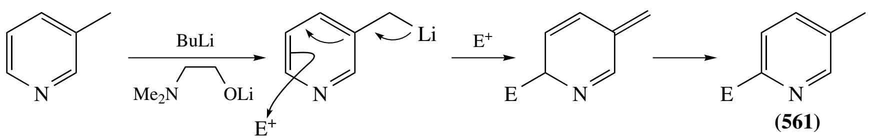

(561)

SCHEME 224

Electron-rich heterocycles, such as pyrrole and furan, bear more resemblance to carbocyclic rings: their side chains are much less acidic, and undergo lateral lithiation much less readily. Without a second directing group, methyl groups only at the 2-position of furan, pyrrole or thiophene may be deprotonated.

Even with directing groups, lateral lithiations of furans and thiophenes especially are beset by uncertainty over regiocontrol[396]. The best lateral lithiations of electron-rich heterocycles are those of 2-alkyl indoles and pyrroles where the directing group is carried by the ring nitrogen atom and where there is no question of regioselectivity[459]. A remarkable example is shown in Scheme 225: the indole **562** is temporarily protected as its lithium carbamate, and the carbamate group is powerful enough to direct two successive lithiations of the methyl group, giving **563**[459].

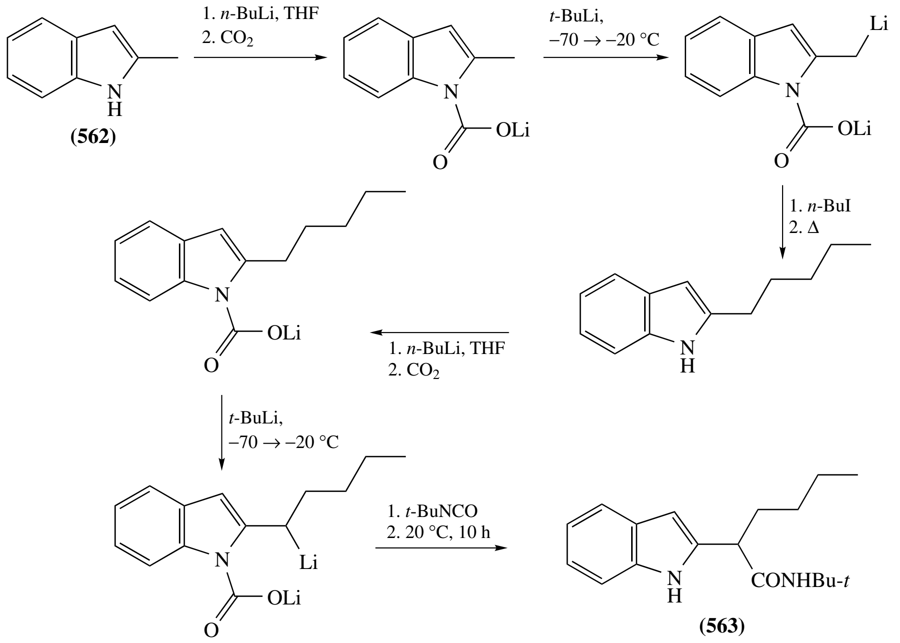

SCHEME 225

The usual directing groups such as secondary amides will also successfully direct lateral lithiation at the 2-methyl group of a pyrrole (Scheme 226)[406].

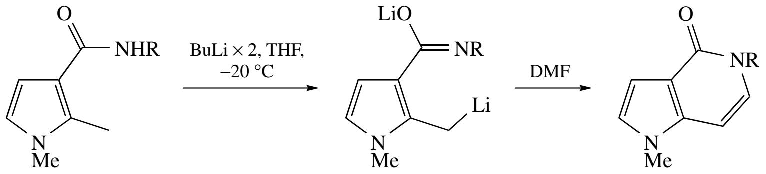

SCHEME 226

The reduced electrophilicity of indole-3-carboxylic esters (they are vinylogous carbamates) means that they are much more versatile directors of lateral lithiation than the comparable benzoates, as illustrated by the synthesis of **564** (Scheme 227)[460].

Pyrroles and indoles have one further unique mode of lateral lithiation—deprotonation of an *N*-methyl group (also an α lithiation). The reaction works particularly well with an aldehyde director, temporarily protected as the α-amino alkoxide **565** (Scheme 228)[90,461].

With furans and thiophenes, ring lithiation α to the heteroatom is usually the preferred process. The only lateral directing group studied to any extent for furans and thiophenes is the lithium carboxylate group, and **566** and **567** are the only two compounds in this class to undergo lateral lithiation reliably. With the 2-position blocked (**568**), thiophene still lithiates at the 2-methyl group rather than the one lateral to CO_2Li to give **569** (Scheme 229)[396].

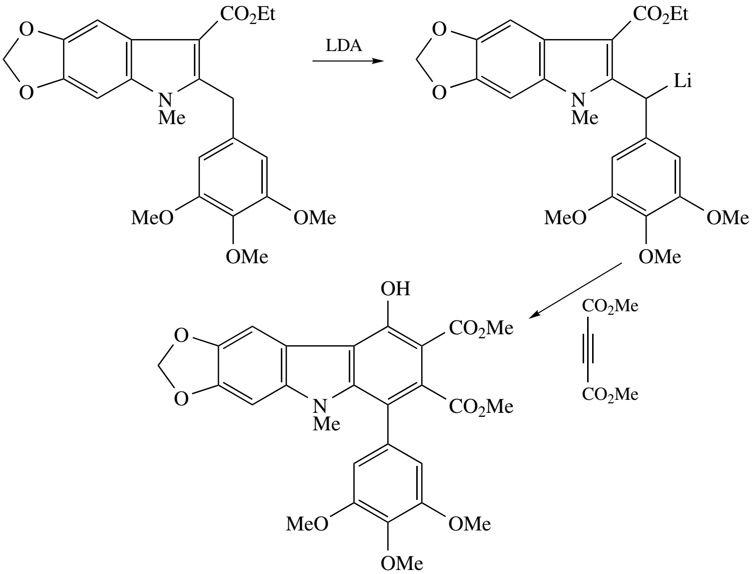

(564)

SCHEME 227

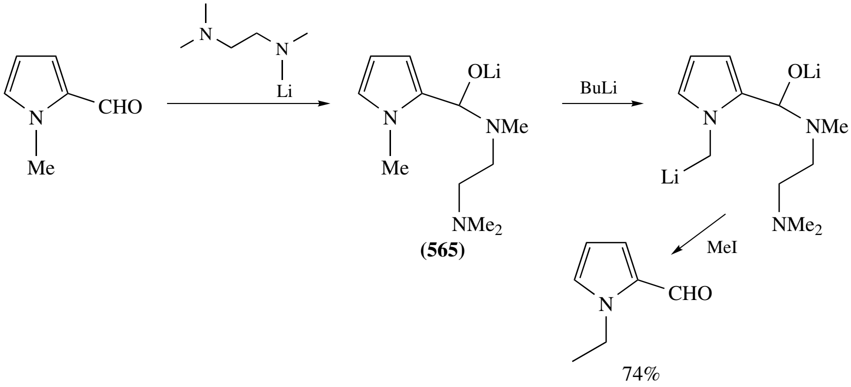

(565)

SCHEME 228

C. Stereoselective Lateral Lithiation

1. Diastereoselectivity

Most benzylic organolithiums, unless they bear an α heteroatom, are configurationally unstable over a period of seconds or more[462], so any stereoselectivity in lateral lithiation is rarely detectable. However, as implied above, the lateral lithiation of tertiary 1-naphthamides **570** is stereoselective, and yields a single diastereoisomeric atropisomer of the organolithium **571**[463-465]. Both diastereoisomers of **571** were characterized by

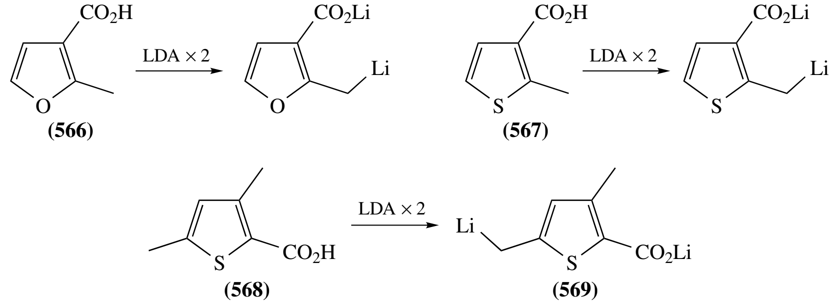

SCHEME 229

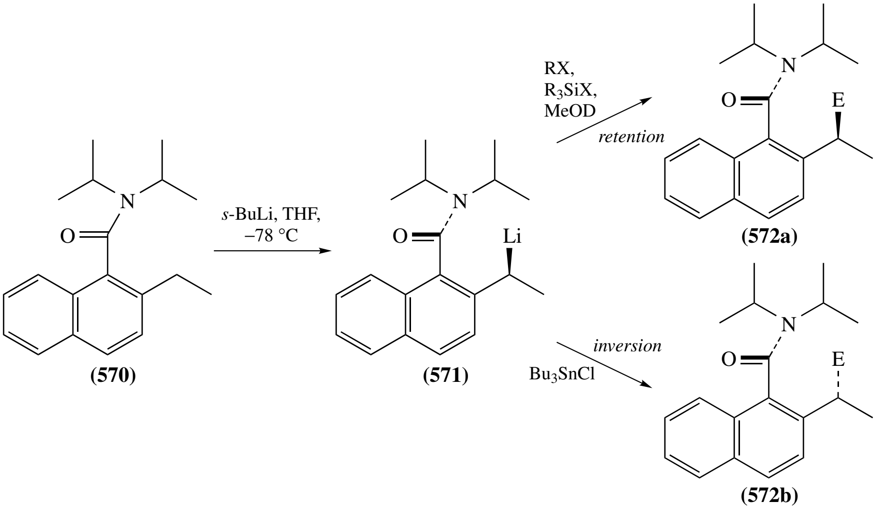

SCHEME 230

NMR. These organolithiums react with most electrophiles to give **572a** with retention of stereochemistry, but with trialkyltin halides to give **572b** with inversion (Scheme 230).

By carrying out a subsequent ortholithiation at low temperature, it was possible to show that tertiary benzamides also react atroposelectively in laterally lithiation–electrophilic quench sequences[463]. Either atropisomer **575** or **578** could be made starting from **573** or **576** (Scheme 231).

The double lateral lithiation–silylation of **579** allows the construction of remote stereogenic centres of **580** in a single step (Scheme 232)[162].

2. Enantioselectivity

Enantioselective reactions of laterally lithiated amides and anilides have been reported by Beak and coworkers[466] but these are properly asymmetric transformations in which stereoselectivity arises subsequent to the lateral lithiation step: they are not enantioselective lithiations.

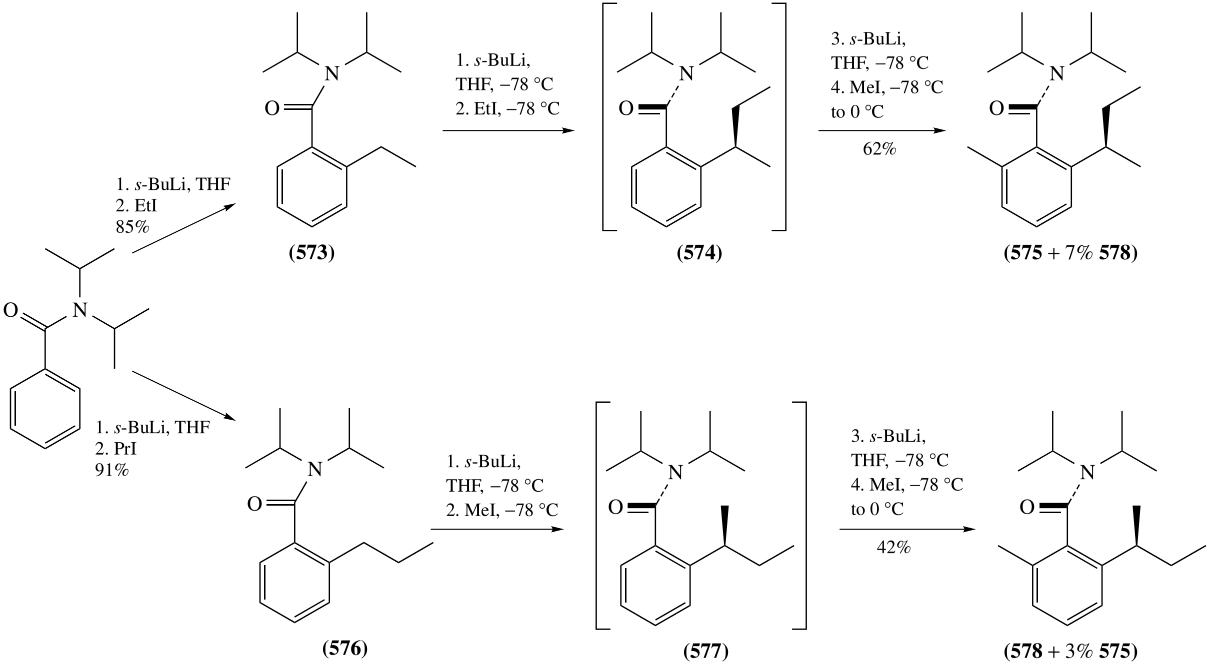
1. s-BuLi, THF
2. EtI
85%
(573)
1. s-BuLi,
THF, −78 °C
2. EtI, −78 °C
(574)
3. s-BuLi,
THF, −78 °C
4. MeI, −78 °C
to 0 °C
62%
(575 + 7% 578)
1. s-BuLi, THF
2. PrI
91%
(576)
1. s-BuLi,
THF, −78 °C
2. MeI, −78 °C
(577)
3. s-BuLi,
THF, −78 °C
4. MeI, −78 °C
to 0 °C
42%
(578 + 3% 575)

SCHEME 231

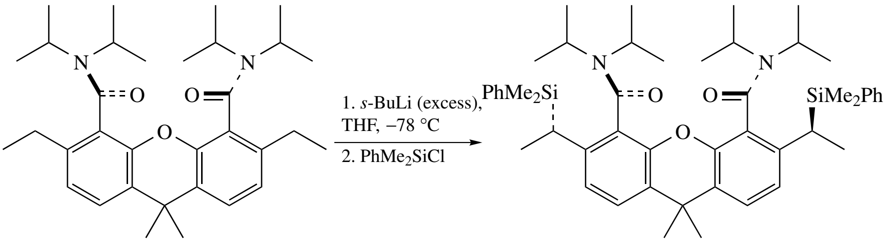

(579) **(580)** 60%

SCHEME 232

Stereoselective deprotonation of compound **581** is possible (Scheme 233), but the yields and enantioselectivities obtained are poorer than for the chromium-complexed analogues (see below). With an internal electrophilic quench it was possible to form the axially chiral benzamide **582** in 89% ee using lithium amide **360**[467].

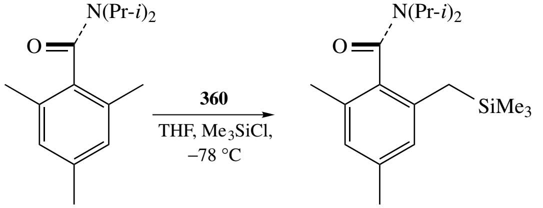

(581) **(582)** 55%, 89% ee

SCHEME 233

Enantioselective lateral lithiation of chromium-complexed amides was reported by Uemura and coworkers, who showed that the achiral complexes **583, 587, 591** and **595** are deprotonated enantioselectively to give **584**, **588** and **592** by treatment with chiral lithium amide bases (Scheme 234 and 235)[468–470]. The stereogenic C−C and C−N axes in these compounds are orientated such that the larger NR_2 and acyl groups respectively are directed away from the chromium. A range of chiral lithium amides such as **390** or **597** was investigated, and by careful selection it was possible to obtain products **585, 589, 593** and **596** with excellent yield and enantioselectivity. Decomplexation returns atropisomers with no loss of absolute stereochemistry, though products such as **586** racemize slowly on standing. Even with the same base, the anilides **587** and amides **583** give products in opposite enantiomeric series. The diethyl substituted anilide **595** could be functionalized enantio- and diastereoselectively to yield such products as **596** with control over chiral plane, axis and centre (Scheme 235).

While not strictly a directed metallation, an important early example of enantioselective lithiation in a benzylic position was the lithiation of the achiral biaryl **598** using *n*-BuLi-(−)-sparteine. The product **599** of unknown configuration was obtained in moderate ee (Scheme 236)[471].

V. REMOTE LITHIATION, AND β-LITHIATION OF NON-AROMATIC COMPOUNDS

A number of reactions have close similarities to *ortho*- and lateral lithiation, even if they do not fall under the more rigid definition of the terms[150]. For example, vinylic

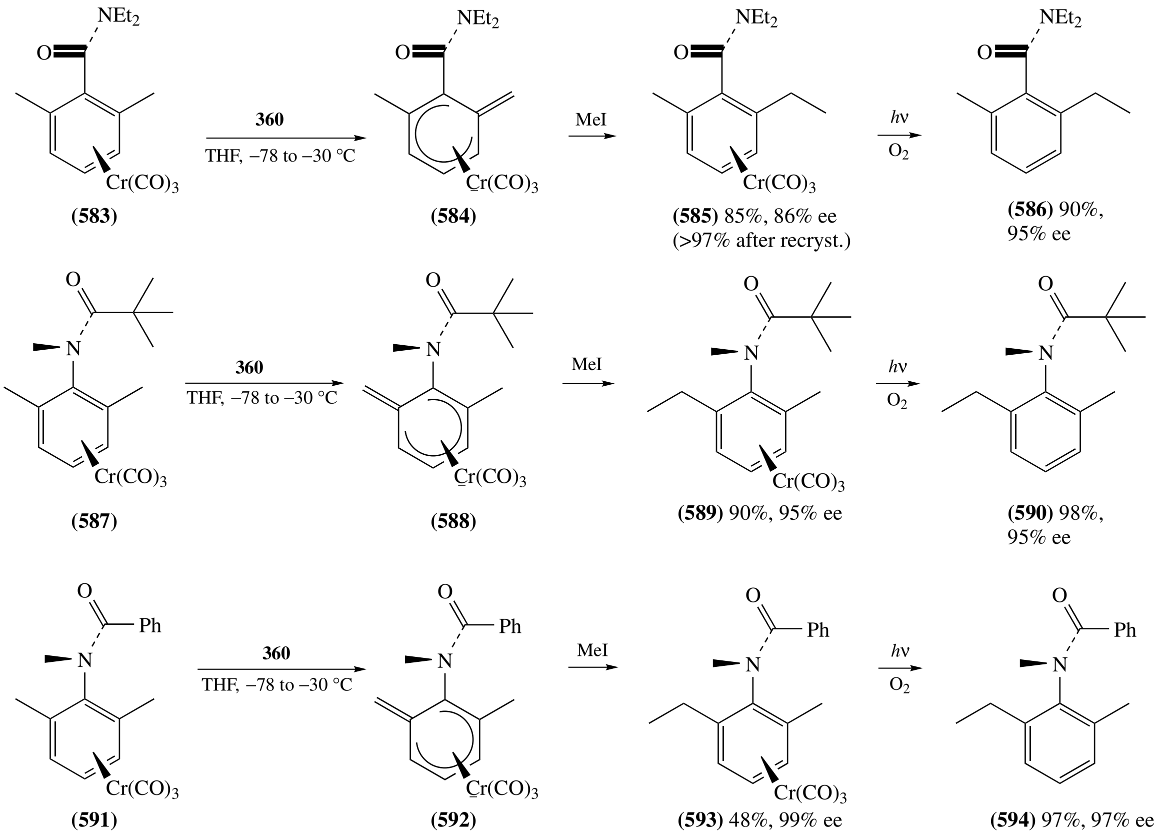
NEt$_2$
O
Cr(CO)$_3$
(583)
360
THF, −78 to −30 °C
(584)
MeI
(585) 85%, 86% ee
(>97% after recryst.)
$h\nu$
O$_2$
(586) 90%,
95% ee
N
O
(587)
(588)
(589) 90%, 95% ee
(590) 98%,
95% ee
Ph
(591)
(592)
(593) 48%, 99% ee
(594) 97%, 97% ee

SCHEME 234

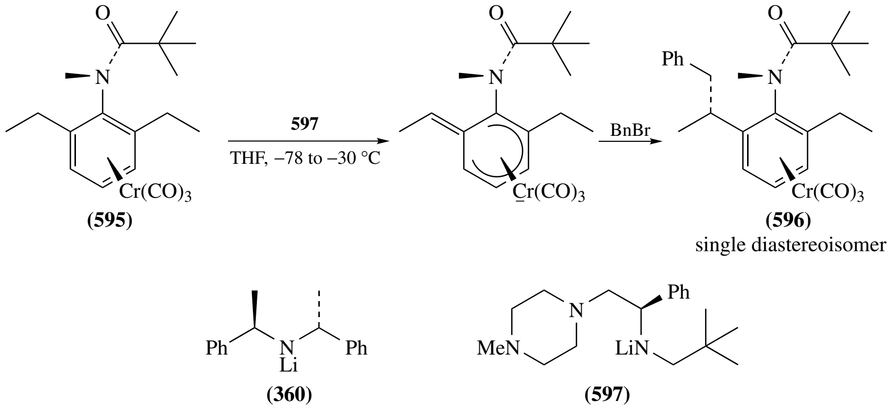

(595) **(596)** single diastereoisomer

(360) **(597)**

SCHEME 235

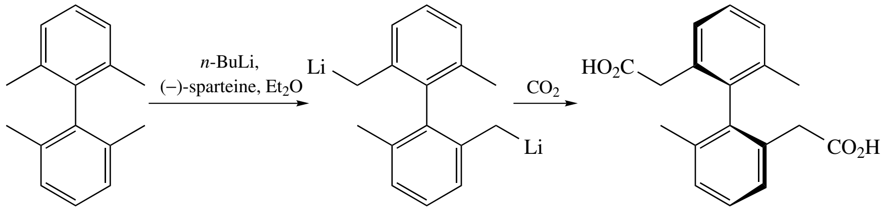

(598)

(599) 80 % yield; 40 % ee; (absolute configuration unknown)

SCHEME 236

protons with nearby directing groups can frequently be lithiated readily. Some examples are shown—**600–604** are all lithiated as though the double bond were part of an aromatic ring (Scheme 237)[150]. The importance of coordination in these reactions is shown by **604**, which lithiates at the more acidic position α to S if HMPA is added to disrupt Li−O interactions. Other similar lithiations are known in the cyclopropyl and cyclobutyl series[150].

Tertiary amides can direct vinylic lithiations in the manner of ortholithiations as shown by the example of **605** and **606**[472,473]. Even methyl groups can be lithiated given an appropriate director and base: **607** forms the cyclopropane **609** on treatment with **608** in refluxing heptane (Scheme 238)[474].

In aromatic compounds, potent but frustrated (their *ortho* positions blocked) directing groups may lead to lithiations at positions other than *ortho*. For example, when the carbamate **610** is treated with LDA in refluxing THF, lithiation occurs at a remote position (not *peri*, note) and an anionic Fries rearrangement ensues to give **611** (see Section I.B.1.d). Lactonization gives **612** (Scheme 239)[475].

Carbamate **613** under the same conditions also undergoes remote lithiation and a remote anionic Fries rearrangement, and then the product amide **614** proceeds to direct a remote benzylic lithiation, even though it has a free *ortho* position. Finally, the benzylic organolithium **615** cyclizes onto the amide to form **616**—all in one pot (Scheme 240)[476].

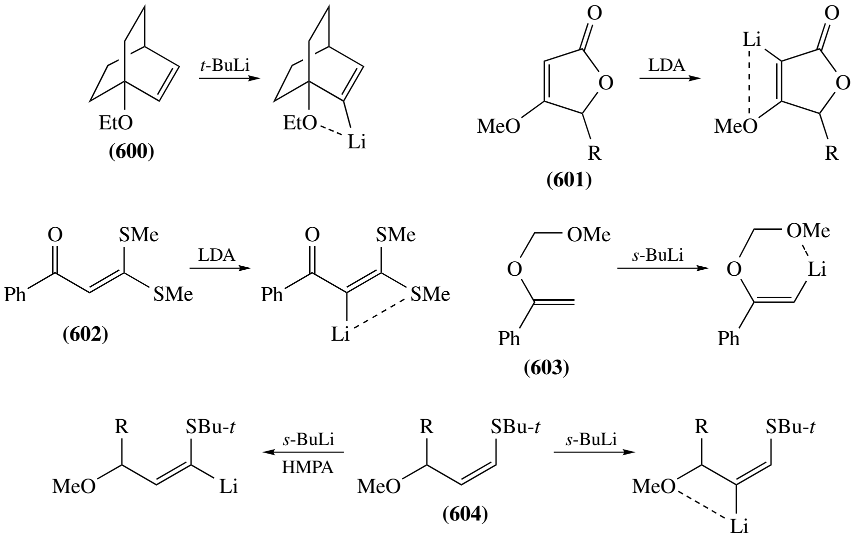

SCHEME 237

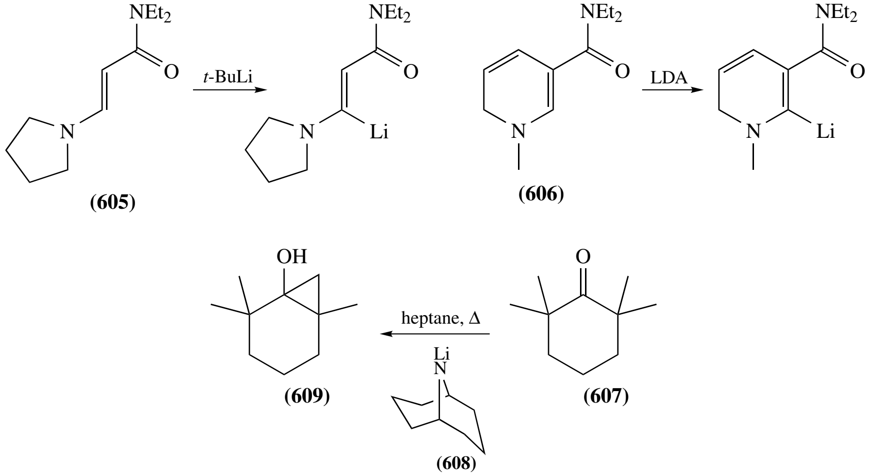

SCHEME 238

VI. SUPERBASES[477]

The combination of an alkyllithium with a metal alkoxide provides a marked increase in the basicity of the organolithium[400, 478, 479]. The most widely used of these 'superbases' is the one obtained from BuLi and KOBu-*t*, known as 'LiCKOR' (Li−C + KOR)[201]. The exact nature of the products obtained by superbase deprotonations—whether they are organolithiums, organopotassiums, or a mixture of both—is debatable, as is the precise nature of the superbase itself. For example, while prolonged mixing of alkyllithium and

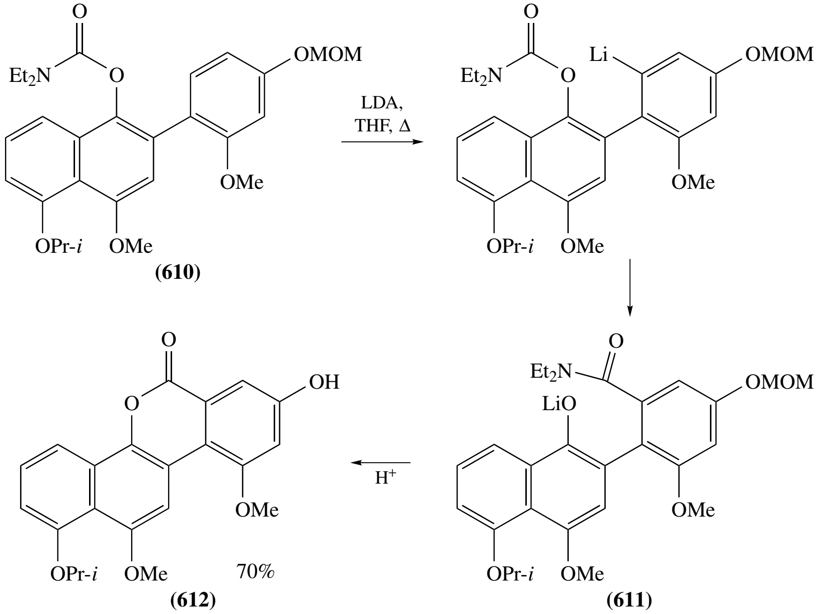

SCHEME 239

KOBu-*t* in hexane gives a precipitate of butylpotassium[478,480,481], the reactivity of a slurry of BuLi−KOBu-*t* does not match that of BuK[482]. Simplistically, superbases can be considered to be organolithiums solvated by very electron-donating ligands (much more so than THF or TMEDA). As synthetic tools they provide a useful top end to the armoury of bases for regioselective functionalization by deprotonation.

The violence of superbasic slurries towards functionalized organic molecules means that they are at their most effective with simple hydrocarbons; they also tolerate ethers and fluoro substituents. LiCKOR will deprotonate allylic, benzylic, vinylic, aromatic and cyclopropane C−H bonds with no additional assistance. From benzene, for example, it forms a mixture of mono and dimetallated compounds **617** and **618** (Scheme 241)[483]. ('Li/K' indicates metallation with a structurally ill-defined mixture of lithium and potassium.)

Typically, superbases care little for coordination effects, and simply remove the most acidic proton on offer; this provides useful alternative selectivities in the lithiation of aromatic rings, for example. With groups that direct principally by acidification, orthometallation occurs, and treatment with BuLi−KOBu-*t* is the most efficient way of orthofunctionalizing fluorobenzene or trifluoromethylbenzene (Scheme 241)[484].

BuLi−KOBu-*t* metallates *ortho* to powerfully electron-withdrawing and acidifying fluoro even if much stronger directors (by the usual considerations) are present, such as methoxy (**619, 620**) or anilide (**621**) groups (Scheme 242)[485].

Flurbiprofen **622** (Froben®, Cebutid®) is a non-steroidal anti-inflammatory whose structure makes it an ideal target for synthesis using a combination of the powerful deprotonating ability of the superbases and the weakly directing effects of a fluoro or an aryl substituent (Scheme 243)[486].

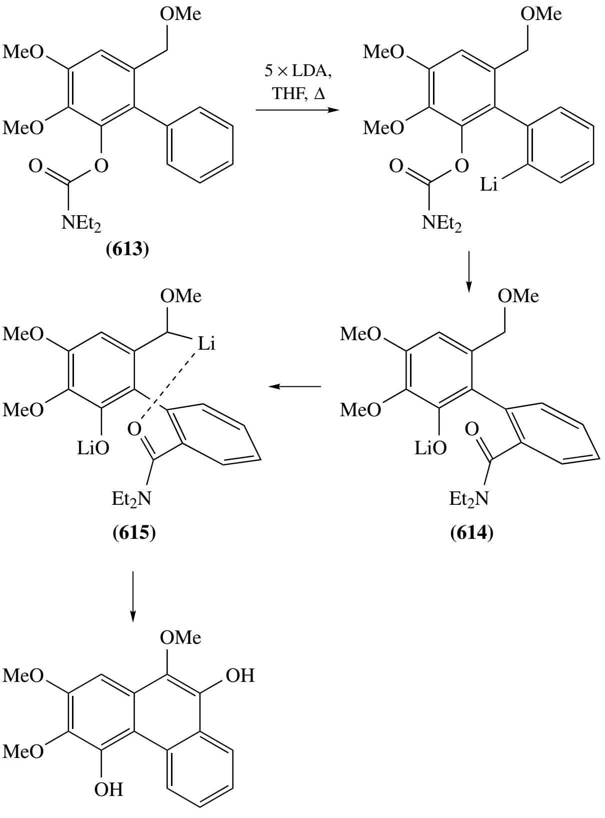

(613) **(614)** **(615)** **(616)**

SCHEME 240

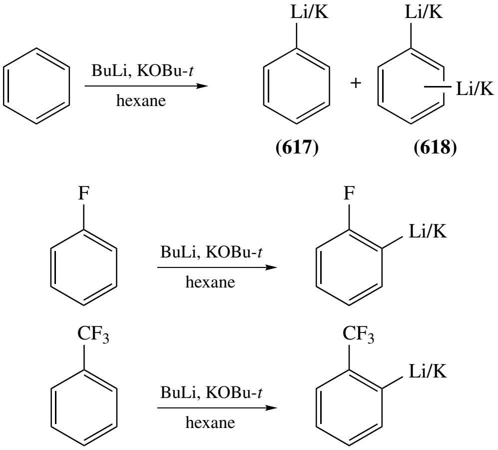

(617) **(618)**

SCHEME 241

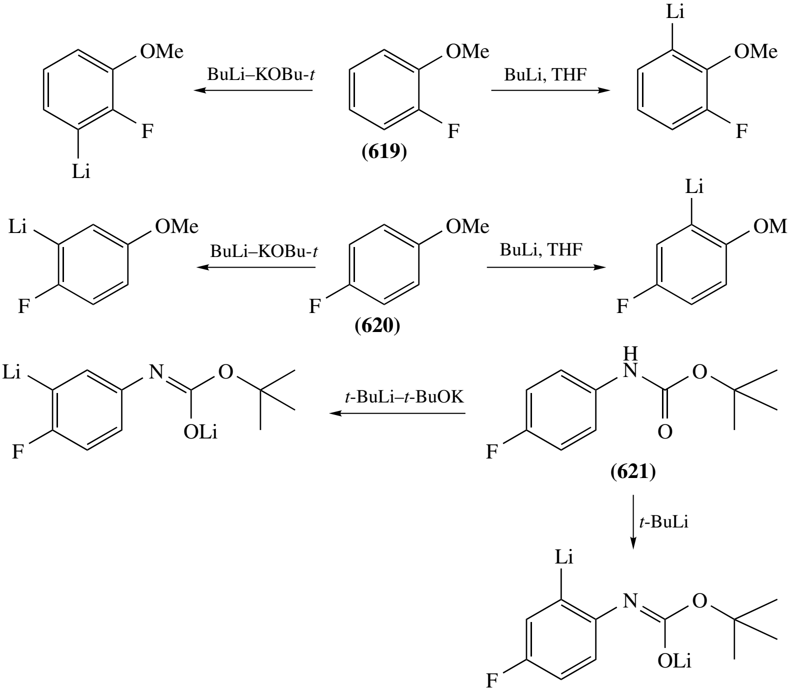

SCHEME 242

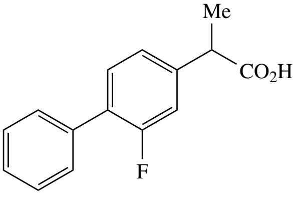

flurbiprofen **(622)**

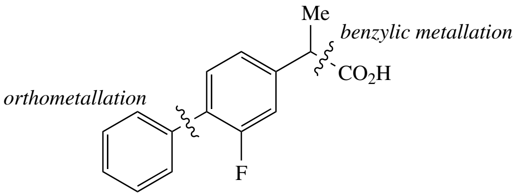

SCHEME 243

Deprotonation of 3-fluorotoluene **623** with *n*-BuLi−KOBu-*t* or, better, *t*-BuLi−KOBu-*t* follows the selectivity expected with these superbases and leads to metallation at the least hindered position *ortho* to the fluoro substituent. Trapping the metallated intermediate **624** with dimethylfluoroboronate gave, after hydrolysis, a boronic acid whose Suzuki arylation provided the biaryl **625**. These four steps may be carried out in a single pot, giving **625** in 79% overall yield from **623** (Scheme 244).

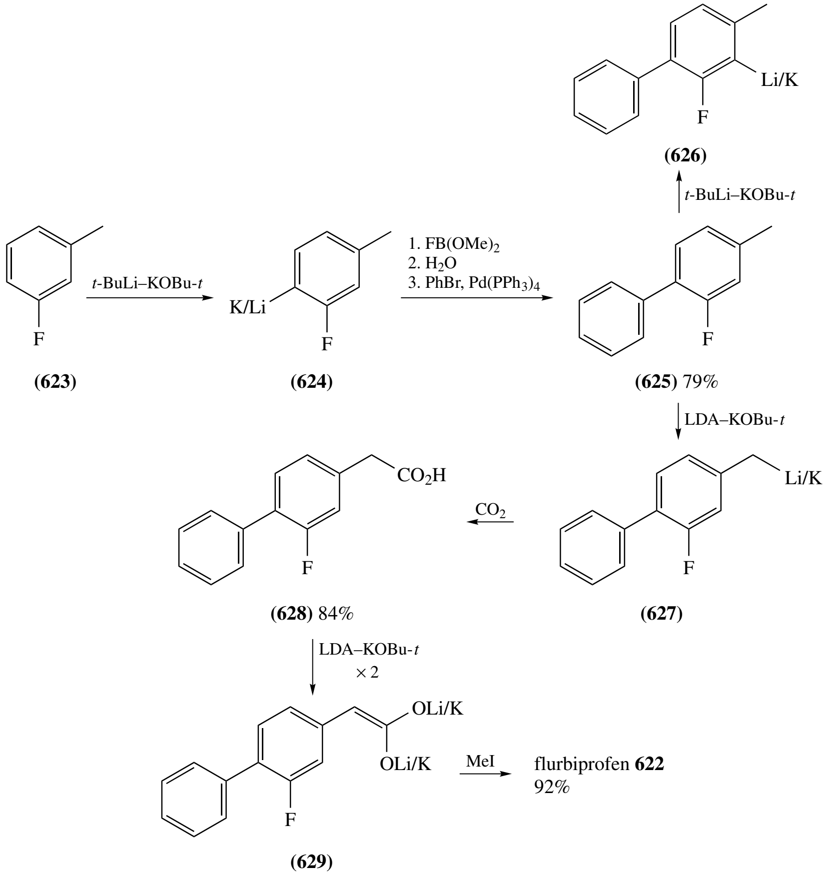

SCHEME 244

While metallation of **625** with a LiCKOR reagent such as BuLi−KOBu-*t* again leads to orthometallation and **626**, reversible metallation of **625** by LDA-KOBu-*t* generates the more stable benzylically metallated species **627**. Carboxylation and alkylation (2 equiv. LDA-KOBu-*t* then MeI) of **627** gives flurbiprofen **622**.

Similar chemistry been used by Faigl and Schlosser in an elegant and simple synthesis of ibuprofen **632** using only superbase chemistry (Scheme 245)[487]. Starting with *para*-xylene **630**, two successive metallations and alkylations give **631**, which is once more metallated at the less hindered benzylic site and carbonated to give ibuprofen **632**.

Other superbases based on LDA + BuLi[201], LDA + KOBu-*t*[201] and BuLi + lithiodimethylamino ethanol (LiDMAE)[458, 488] are also widely used.

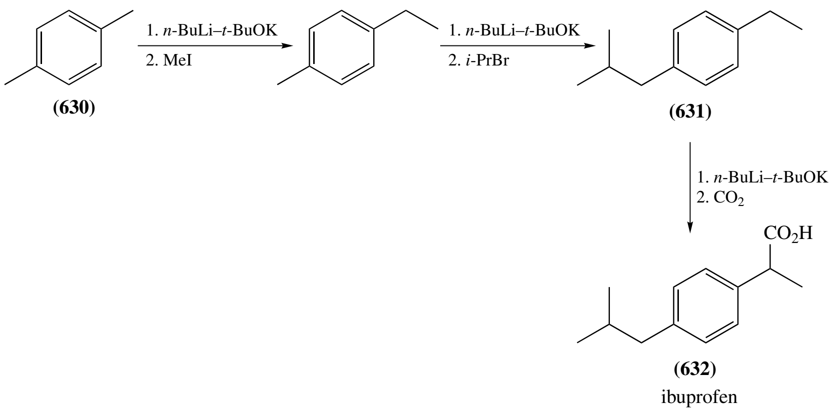

(630) **(631)** **(632)**

SCHEME 245

VII. COOPERATION, COMPETITION AND REGIOSELECTIVITY

Numerous studies of the relative abilities of different ortholithiation directors to control regioselectivity have been published, and these are summarized in Section I.B. While Scheme 9 aims to place *ortho*-directors into an approximate order of potency, these studies show quite clearly that relative directing power depends on a variety of factors and varies from compound to compound.

What is clearer is that, if two lithiation-directing groups are placed *meta* to one another, lithiation nearly always occurs between them. The only exceptions are when the resulting polysubstituted arene ring would be exceptionally hindered; lithiation then takes place *ortho* to the better of the two directing groups. For example, lithiation of **633** gives **634** by lithiation at the 5- rather than the 2-position (Scheme 246)[489].

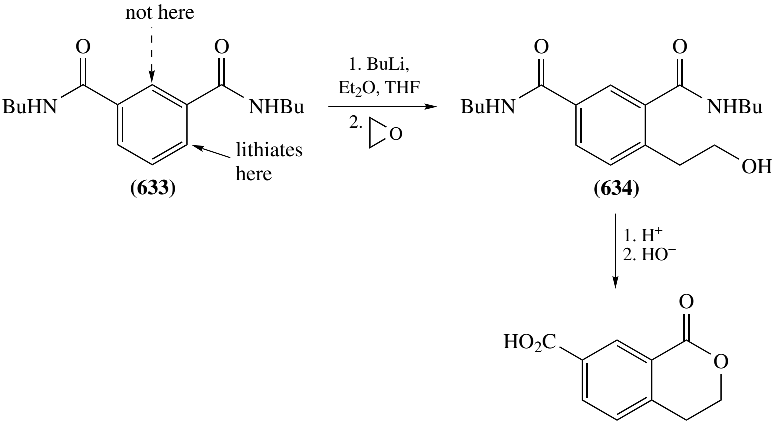

(633) **(634)**

SCHEME 246

Lithiation between two directing groups which would lead to a 1,2,3,4-tetrasubstituted ring is usually difficult[490]. For example, **635** undergoes kinetic lithiation at a site (**636**)

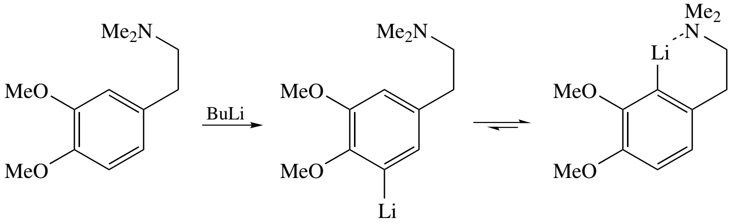

(635) **(636)** **(637)**

SCHEME 247

which avoids the formation of a 1,2,3,4-tetrasubstituted ring. Only on standing does isomerization to the thermodynamically more stable **637** occur (Scheme 247)[491].

A. Kinetic and Thermodynamic Control

Change of regioselectivity with time is a feature of a number of lithiations where the site which is deprotonated fastest does not give the most stable possible organolithium. Dibenzothiophene **638** provides a nice example. Double lithiation occurs initially *ortho* to the sulphur atom to give **639**, but on heating, an isomerization takes place to give the organolithium **640**, perhaps because of beneficial chelation of the two adjacent lithium atoms by TMEDA[492]. Similarly, BuLi at 0 °C ortholithiates the sulphonate **641**, but at 25 °C deprotonation occurs at the *para* methyl group where the benzylic anion can gain conjugation with the sulphonate (Scheme 248)[130].

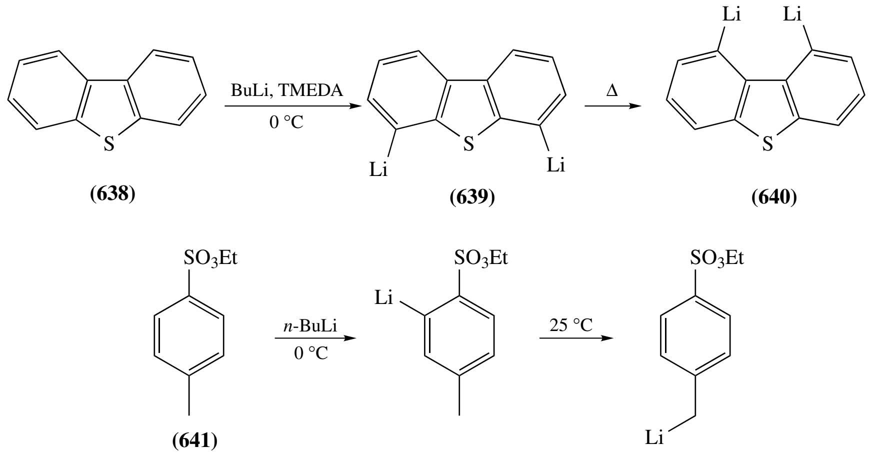

(638) **(639)** **(640)**

(641)

SCHEME 248

Formation of the most stable organolithium is much faster when a lithium amide is used as the base, since re-deprotonation of the amine by-product provides a mechanism for ‘anion translocation’ from one site to another. Several examples were discussed in Sections I, II and IV: the lithiations of **642** and of **643** with BuLi and with LDA illustrate the point well (Scheme 249).

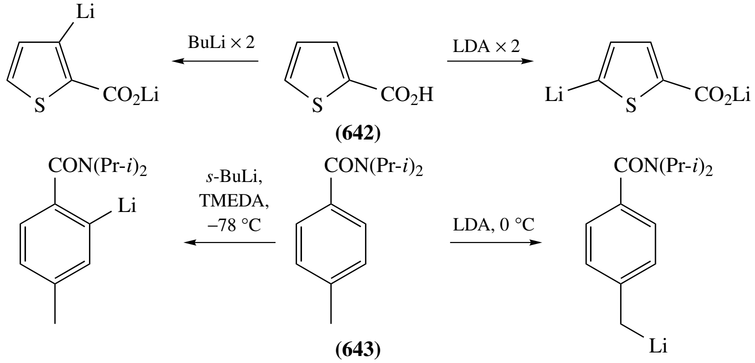

SCHEME 249

Organolithiums formed from lithium amide bases are presumably formed with a secondary amine ligand bound to lithium, and it is frequently noted that intramolecular coordination to a basic heteroatom is less important for their stability. The presence of donor ligands such as TMEDA[41] or PMDTA[278] can bias lithiation selectivity in favour of a more acidic site rather than a more readily coordinated site. The ethoxyvinyllithium (EVL)–HMPA combination, discovered by Shimano and Meyers[493,494], demonstrates unusual regioselectivities more similar to those typically of the superbases (Section VI). For example, it selectively deprotonates *ortho* to OMe rather than *ortho* to an amide **644** or oxazoline **645**, and chooses to deprotonate **646** *para* rather than *ortho* to the oxazoline (Scheme 250). Once the benefits of coordination to a heteroatom have been removed (lithium-bearing HMPA ligands are already well supplied with electron density) EVL–HMPA presumably prefers to deprotonate the site that is (a) next to the most inductively withdrawing group and (b) the least hindered.

There are reports that other HMPA–organolithium complexes have a dramatic effect on lithiation regioselectivity away from coordination-favoured sites[495].

The superbases are similar in that they avoid hindered positions next to coordinating groups, and prefer to deprotonate *ortho* to small, powerfully inductively withdrawing OMe, or even at benzylic positions. Superbases prefer to deprotonate both **647** and **648** *ortho* to OMe rather than the usually more powerfully directing anilide group (Scheme 251)[496].

Steric hindrance controls a three-way divergence of regioselectivity in the metallation of **649**[497]. *n*-BuLi lithiates *ortho* to OMe at the site where coordination to the secondary amide can also be achieved. *t*-BuLi prefers to lithiate at the less hindered benzylic site, still presumably benefitting from amide coordination. The superbase, on the other hand, cares nothing for coordination to the amide and metallates at the less hindered site *ortho* to OMe (Scheme 252). Selectivity in the lithiation of the indole **650** can also be controlled by the choice of base[276]. In this case, the TMEDA complex appears to lithiate where coordination to the C=O group can be achieved while the superbase chooses the thermodynamically most acidic site α to nitrogen. The coordinatively saturated PMDTA complex would also favour the more acidic site but for its steric hindrance: it puts up with second best and lithiates to form an organolithium stabilized by hyperconjugation.

Other additives can have unexpected effects on regioselectivity: one equivalent of water, for example, changes the completely unselective lithiation of **651** into a synthetically useful reaction (Scheme 253)[498].

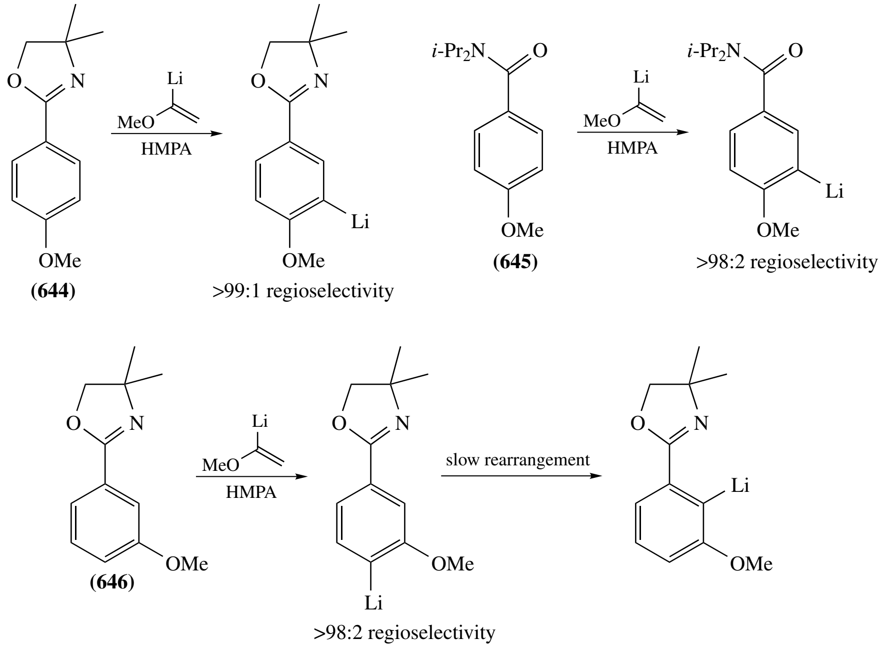

SCHEME 250

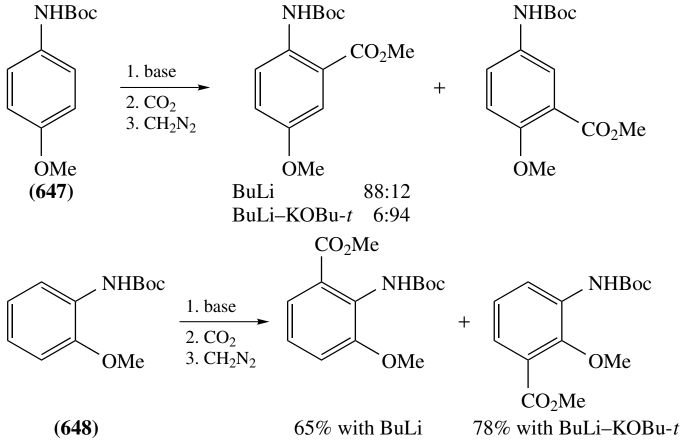

SCHEME 251

Coordination to more than one heteroatom may turn off an otherwise favourable lithiation by preventing the organolithium reagent from approaching the substrate sufficiently closely. For example, the oxazoline **652** is not lithiated by BuLi even under forcing conditions, presumably because coordination to both N and O prevents approach of BuLi to the *ortho* position (Scheme 254)[499].

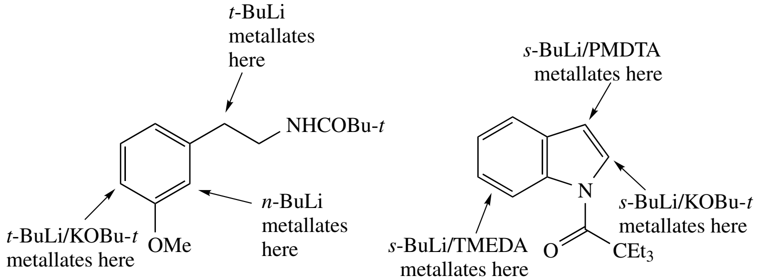

(649) **(650)**

SCHEME 252

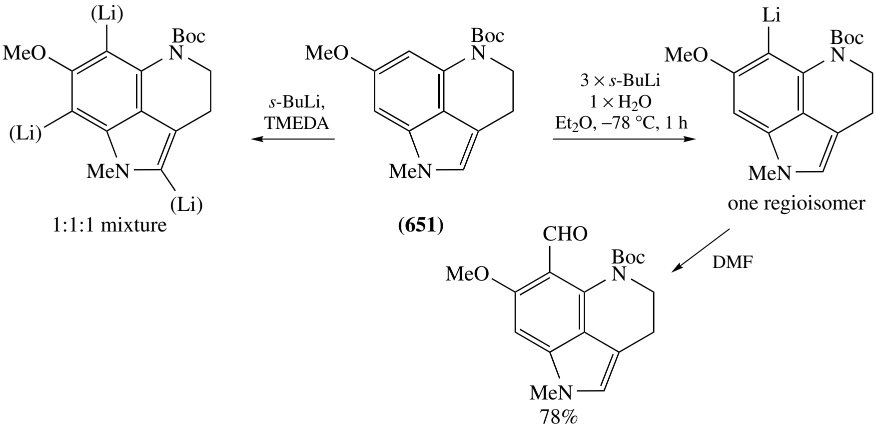

(651)

SCHEME 253

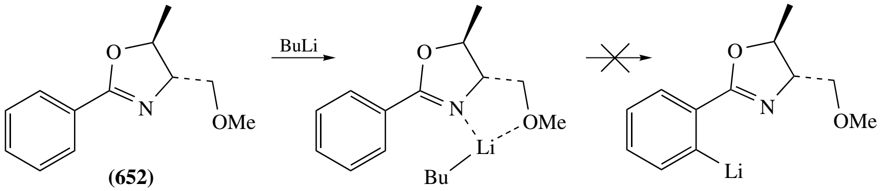

(652)

SCHEME 254

There are a number of other reports of difficulties in ortholithiation when further coordination sites are present: molecules containing more than one strong coordinating substituent frequently require numerous equivalents of alkyllithium for lithiation[162].

The competition between ortholithiation and alternative reactivity—α- or lateral lithiation for example, or halogen–metal exchange—has been quantified in only a few cases, and where such issues of chemoselectivity arise they are mentioned in the sections on these topics.

B. Ortholithiation vs. Halogen–Metal Exchange

Provided the target organolithium is not too basic, ortholithiation can be favoured by using a more stable organolithium (PhLi for example[490], or its more hindered congeners **653**[128]) or a lithium amide base. The possibilities for altering chemo- or regioselectivity with a change in base are well illustrated by the series of reactions of bromothiophenes and bromofurans **654–657** in Scheme 255[500].

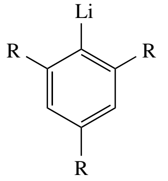

(653) R = Me or *i*-Pr

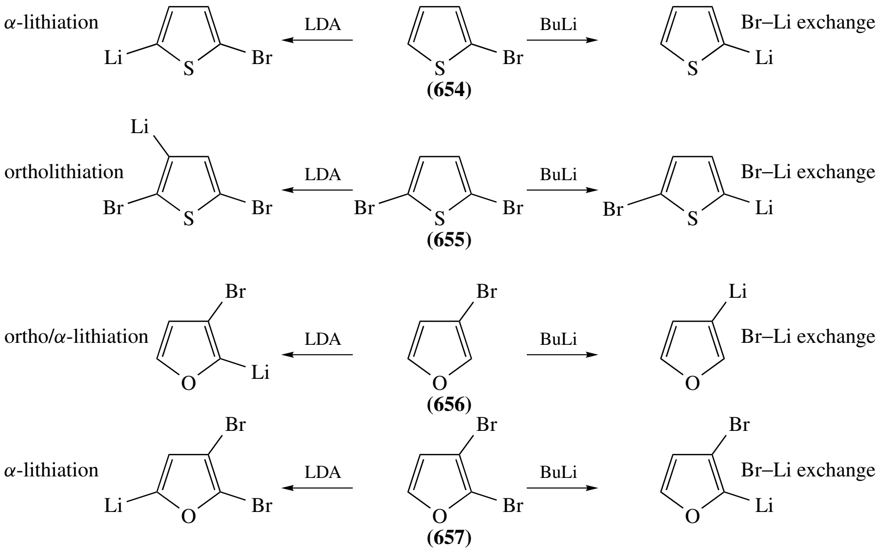

SCHEME 255

C. Ortholithiation vs. Benzylic or Lateral Lithiation

Usually, ortholithiated species are more basic than benzylically lithiated species, and lithium amide bases favour formation of the latter. Alkyllithiums give a better chance of achieving *ortho*-selectivity. The factors controlling *ortho* vs. lateral lithiation in tertiary amides have been studied in detail (Scheme 256)[501], and show that increased substitution at an *ortho*-alkyl group disfavours lateral lithiation—*ortho*-isopropyl groups (**660**) cannot be lithiated and only **661** is formed. Increasing substitution at the *meta* position, which restricts the ability of the alkyl group to adopt a conformation suitable for deprotonation, also disfavours lateral lithiation. **658**, for example, gives only **659** with *s*-BuLi, while **662** gives a mixture of **663** and **664**. LDA gives only **663** from **662**.

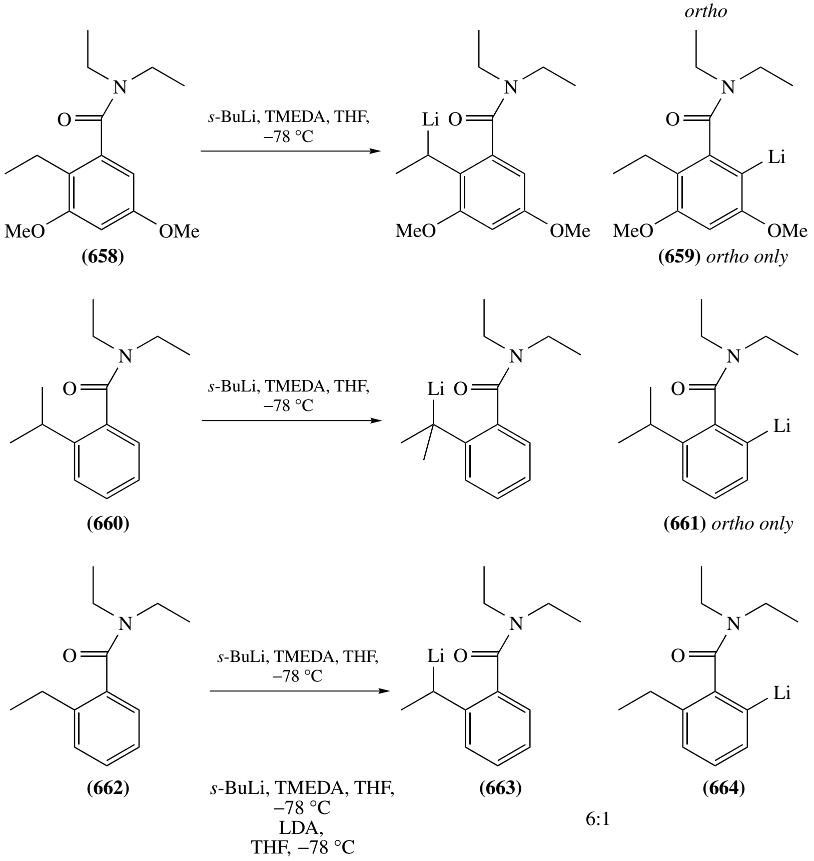

SCHEME 256

For cases where the regioselectivity of lithiation cannot be biased in the required direction, silylation can be used to block acidic sites while further lithiations are carried out. The blocking silyl group is later readily removed with fluoride[502]. This method was used to avoid a competing lateral lithiation in the synthesis of the aldehyde **665** (Scheme 257)[503].

Silicon protection is also commonly used to direct lithiation chemistry in five-membered heterocycles. For example, oxazoles[504], thiazoles[505] and *N*-alkylimidazoles[506, 507] lithiate preferentially at C-2, where the inductive effect of the heteroatoms is greatest. If C-2 is blocked, lithiation occurs at C-5, where there is no adjacent lone pair to destabilize the organolithium. Functionalization of these heterocycles at C-5 can therefore be achieved by first silylating C-2, reacting at C-5 and then removing the silyl group. The synthesis of **666** illustrates this sort of sequence (Scheme 258)[508].

A less well developed, but potentially less intrusive alternative is to block acidic sites with deuterium and to use the kinetic isotope effect to prevent lithiation[509, 510]. If the substrate can be polylithiated, the use of dianions (with the last-formed anion being likely to be the most reactive) may give the required selectivity.

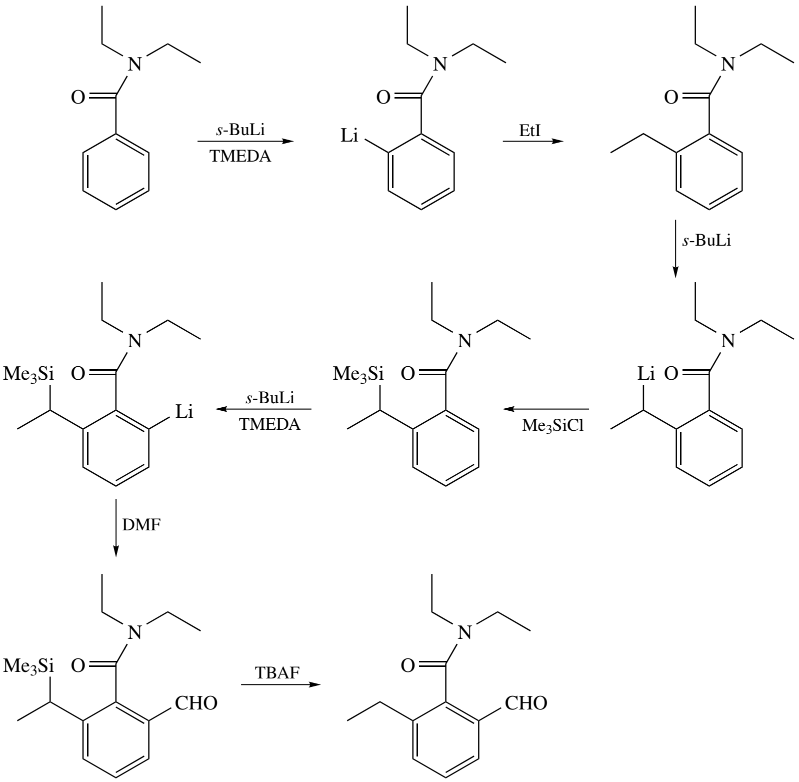

(665)

SCHEME 257

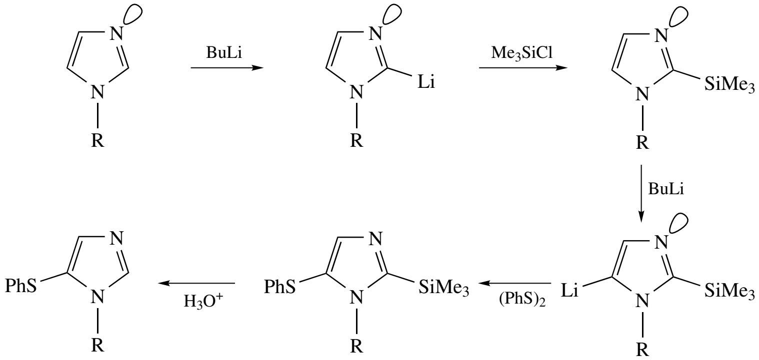

(666)

SCHEME 258

VIII. REFERENCES

1. H. Gilman and R. L. Bebb, *J. Am. Chem. Soc.*, **61**, 109 (1939).
2. G. Wittig and G. Fuhrman, *Chem. Ber.*, **73**, 1197 (1940).
3. H. W. Gschwend and H. R. Rodriguez, *Org. React.*, **26**, 1 (1979).
4. P. Beak and R. A. Brown, *J. Org. Chem.*, **47**, 34 (1982).
5. T. G. Gant and A. I. Meyers, *Tetrahedron*, **50**, 2297 (1994).
6. P. Beak and V. Snieckus, *Acc. Chem. Res.*, **15**, 306 (1982).
7. V. Snieckus, *Chem. Rev.*, **90**, 879 (1990).
8. H. Gilman and J. W. Morton, *Org. React.*, **8**, 258 (1954).
9. M. D. Rausch and D. J. Ciappenelli, *J. Organomet. Chem.*, **10**, 127 (1967).
10. H. L. Lewis and T. L. Brown, *J. Am. Chem. Soc.*, **92**, 4664 (1970).
11. J. D. Roberts and D. Y. Curtin, *J. Am. Chem. Soc.*, **68**, 1658 (1946).
12. M. Al-Aseer, P. Beak, D. Hay, D. J. Kempf, S. Mills and S. G. Smith, *J. Am. Chem. Soc.*, **105**, 2080 (1983).
13. D. R. Hay, Z. Song, S. G. Smith and P. Beak, *J. Am. Chem. Soc.*, **110**, 8145 (1988).
14. A. I. Meyers and D. I. Dickman, *J. Am. Chem. Soc.*, **109**, 1263 (1987).
15. A. I. Shatenshtein, *Tetrahedron*, **18**, 95 (1962).
16. R. Huisgen, W. Mack, K. Herbig, N. Ott and E. Anneser, *Chem. Ber.*, **93**, 412 (1960).
17. F. N. Jones, M. F. Zinn and C. R. Hauser, *J. Org. Chem.*, **28**, 663 (1963).
18. D. R. Anderson, N. C. Faibish and P. Beak, *J. Am. Chem. Soc.*, **121**, 7553 (1999).
19. M. Stratakis, *J. Org. Chem.*, **62**, 3024 (1997).
20. W. Bauer and P. v. R. Schleyer, *J. Am. Chem. Soc.*, **111**, 7191 (1989).
21. N. J. R. van Eikema Hommes and P. v. R. Schleyer, *Tetrahedron*, **50**, 5903 (1994).
22. R. A. Rennels, A. S. Maliakal and D. B. Collum, *J. Am. Chem. Soc.*, **120**, 421 (1998).
23. S. T. Chadwick, R. A. Rennels, J. L. Rutherford and D. B. Collum, *J. Am. Chem. Soc.*, **122**, 8640 (2000).
24. J. Clayden, C. S. Frampton, C. McCarthy and N. Westlund, *Tetrahedron*, **55**, 14161 (1999).
25. N. S. Narasimhan and R. S. Mali, *Synthesis*, 957 (1983).
26. J. Betz and W. Bauer, *J. Am. Chem. Soc.*, **124**, 8699 (2002).
27. R. L. Gay and C. R. Hauser, *J. Am. Chem. Soc.*, **89**, 2297 (1967).
28. C. Eaborn, P. Golborn and R. Taylor, *J. Organomet. Chem.*, **10**, 171 (1967).
29. J. Barluenga, R. González, F. J. Fañanás, M. Yus and F. Foubelo, *J. Chem. Soc., Perkin Trans. 1*, 1069 (1994).
30. N. S. Narasimhan and A. C. Ranade, *Indian J. Chem.*, **7**, 538 (1969).
31. A. J. Kirby and J. M. Percy, *Tetrahedron*, **44**, 6903 (1988).
32. C. Kiefl and A. Mannschreck, *Synthesis*, 1033 (1995).
33. D. L. Comins and J. D. Brown, *J. Org. Chem.*, **49**, 1078 (1984).
34. J. M. Saá., J. Morey, A. Frontera and P. M. Deyá, *J. Am. Chem. Soc.*, **117**, 1105 (1995).
35. G. Coll, J. Morey, A. Costa and J. M. Saá, *J. Org. Chem.*, **53**, 5345 (1988).
36. D. A. Shirley and C. F. Cheng, *J. Organomet. Chem.*, **20**, 251 (1969).
37. T. Kawikawa and I. Kubo, *Synthesis*, 431 (1986).
38. P. Bowles, J. Clayden, M. Helliwell, C. McCarthy, M. Tomkinson and N. Westlund, *J. Chem. Soc., Perkin Trans. 1*, 2607 (1997).
39. J. G. Lombardino, *J. Org. Chem.*, **36**, 1843 (1971).
40. F. M. Stoyanovich, R. G. Karpenko and Y. L. Gol'dfarb, *Tetrahedron*, **27**, 433 (1971).
41. D. W. Slocum and C. A. Jennings, *J. Org. Chem.*, **41**, 3653 (1976).
42. A. I. Meyers and P. D. Pansegrau, *Tetrahedron Lett.*, **24**, 4935 (1983).
43. R. R. Fraser, M. Bresse and T. S. Mansour, *J. Am. Chem. Soc.*, **105**, 7790 (1983).
44. A. I. Meyers and K. Lutomski, *J. Org. Chem.*, **44**, 4464 (1979).
45. P. Beak and R. A. Brown, *J. Org. Chem.*, **44**, 4463 (1979).
46. P. Beak, A. Tse, J. Hawkins, C.-W. Chen and S. Mills, *Tetrahedron*, **39**, 1983 (1983).
47. M. Iwao, T. Iihama, K. K. Mahalanabis, H. Perrier and V. Snieckus, *J. Org. Chem.*, **54**, 24 (1989).
48. P. Rhonnstad and D. Wensbo, *Tetrahedron Lett.*, **43**, 3137 (2002).
49. M. Reuman and A. I. Meyers, *Tetrahedron*, **41**, 837 (1985).
50. J. Clayden, J. J. A. Cooney and M. Julia, *J. Chem. Soc., Perkin Trans. 1*, 7 (1995).
51. J. Clayden and M. Julia, *J. Chem. Soc., Chem. Commun.*, 1682 (1993).

52. C. Quesnelle, T. Iihama, T. Aubert, H. Perrier and V. Snieckus, *Tetrahedron Lett.*, **33**, 2625 (1992).
53. J. P. Lockard, C. W. Schroeck and C. R. Johnson, *Synthesis*, 485 (1973).
54. L. G. M Schlosser and F. Leroux, *J. Am. Chem. Soc.*, **123**, 3822 (2001).
55. S. F. Koreev and D. F. Kantmann, *Synthesis*, 487 (2002).
56. R. J. Mills, R. F. Horvath, M. P. Sibi and V. Snieckus, *Tetrahedron Lett.*, **26**, 1145 (1985).
57. R. E. Ludt, T. S. Griffiths, K. N. McGrath and C. R. Hauser, *J. Org. Chem.*, **38**, 1668 (1973).
58. P. Beak, G. R. Brubaker and R. Farney, *J. Am. Chem. Soc.*, **98**, 3621 (1976).
59. P. Beak and R. A. Brown, *J. Org. Chem.*, **42**, 1823 (1977).
60. R. Casas, C. Cavé and J. d'Angelo, *Tetrahedron Lett.*, **36**, 1039 (1995).
61. G. E. Keck, T. T. Wager and J. F. D. Rodriguez, *J. Am. Chem. Soc.*, **121**, 5176 (1999).
62. T. K. Park and S. J. Danishefsky, *Tetrahedron Lett.*, **36**, 195 (1995).
63. A. D. Bond, J. Clayden and A. E. H. Wheatley, *Acta Crystallogr., Sect. E*, **57**, 291 (2001).
64. P. Beak, S. T. Kerrick and D. J. Gallagher, *J. Am. Chem. Soc.*, **115**, 10628 (1993).
65. J. Clayden, R. P. Davies, M. A. Hendy, R. Snaith and A. E. H. Wheatley, *Angew. Chem., Int. Ed.*, **40**, 1238 (2001).
66. M. P. Sibi, K. Shankaran, W. R. Hahn, B. I. Alo and V. Snieckus, *Tetrahedron Lett.*, **28**, 2933 (1987).
67. M. A. Brimble and S. H. Chan, *Aust. J. Chem.*, **51**, 275 (1998).
68. P. Bowles, J. Clayden and M. Tomkinson, *Tetrahedron Lett.*, **36**, 9219 (1995).
69. J. Clayden, N. Westlund and F. X. Wilson, *Tetrahedron Lett.*, **40**, 3329 (1999).
70. M. P. Sibi, M. A. J. Miah and V. Snieckus, *J. Org. Chem.*, **49**, 737 (1984).
71. J.-C. Cuevas, P. Patil and V. Snieckus, *Tetrahedron Lett.*, **30**, 5841 (1989).
72. D. B. Reitz and S. M. Massey, *J. Org. Chem.*, **55**, 1375 (1990).
73. F. Hintze and D. Hoppe, *Synthesis*, 1216 (1992).
74. M. Anstiss, J. Clayden, A. Grube and L. H. Youssef, *Synlett*, 290 (2002).
75. D. L. Comins and J. D. Brown, *J. Org. Chem.*, **51**, 3566 (1986).
76. D. P. Phillion and D. M. Walker, *J. Org. Chem.*, **60**, 8417 (1995).
77. W. H. Puterbaugh and C. R. Hauser, *J. Org. Chem.*, **29**, 853 (1964).
78. A. S. Kiselyov, *Tetrahedron Lett.*, **36**, 493 (1995).
79. J. J. Fitt and H. W. Gschwend, *J. Org. Chem.*, **41**, 4029 (1976).
80. C. Metallinos, S. Nerdinger and V. Snieckus, *Org. Lett.*, **1**, 1183 (1999).
81. S. A. Pratt, M. P. Goble, M. J. Mulvaney and P. G. M. Wuts, *Tetrahedron Lett.*, **41**, 3559 (2000).
82. S. W. McCombie, S.-I. Lin and S. F. Vice, *Tetrahedron Lett.*, **40**, 8767 (1999).
83. P. Garibay, P. H. Toy, T. Hoeg-Jensen and K. D. Janda, *Synlett*, 1478 (1999).
84. G. Quéguiner, F. Marsais, V. Snieckus and J. Epsztajn, *Adv. Heterocycl. Chem.*, **52**, 187 (1991).
85. L. D. Vecchia and I. Vlattas, *J. Org. Chem.*, **42**, 2649 (1977).
86. D. J. Chadwick, M. V. McKnight and R. Ngochindo, *J. Chem. Soc., Perkin Trans. 1*, 1343 (1982).
87. A. J. Carpenter and D. J. Chadwick, *Tetrahedron Lett.*, **26**, 1777 (1985).
88. A. J. Carpenter and D. J. Chadwick, *J. Org. Chem.*, **50**, 4362 (1985).
89. E. G. Doast and V. Snieckus, *Tetrahedron Lett.*, **26**, 1149 (1985).
90. D. L. Comins and M. O. Killpack, *J. Org. Chem.*, **52**, 104 (1987).
91. T. J. Donohoe, J.-B. Guillermin, A. A. Calabrese and D. S. Walter, *Tetrahedron Lett.*, **42**, 5841 (2001).
92. M. Iwao and T. Kuraishi, *Tetrahedron Lett.*, **24**, 2649 (1983).
93. X. Wang and V. Snieckus, *Tetrahedron Lett.*, **32**, 4883 (1991).
94. M. Watanabe and V. Snieckus, *J. Am. Chem. Soc.*, **102**, 1457 (1980).
95. C. Paulmier, J. Morel, D. Semard and P. Pastour, *Bull. Soc. Chim. Fr.*, 2434 (1973).
96. F. Roschangar, J. C. Brown, B. F. Cooley, M. J. Sharp and R. T. Matsuoka, *Tetrahedron*, **58**, 1657 (2002).
97. D. L. Comins, *Synlett*, 615 (1992).
98. D. L. Comins, J. D. Brown and N. B. Mantlo, *Tetrahedron Lett.*, **23**, 3979 (1982).
99. D. L. Comins and M. O. Killpack, *J. Org. Chem.*, **55**, 69 (1990).
100. H. Butenschon, M. Winkler and K. P. C. Vollhardt, *J. Chem. Soc., Chem. Commun.*, 388 (1986).

101. J. Nakano, K. Uchida and Y. Fujimoto, *Heterocycles*, **29**, 427 (1989).
102. C. A. Boulet and G. A. Poulton, *Heterocycles*, **28**, 405 (1989).
103. M. P. Sibi and V. Snieckus, *J. Org. Chem.*, **48**, 1935 (1983).
104. M. P. Sibi, S. Chattopadhyay, J. W. Dankwardt and V. Snieckus, *J. Am. Chem. Soc.*, **107**, 6312 (1985).
105. A. Cunningham, M. R. Dennis and S. Woodward, *J. Chem. Soc., Perkin Trans. 1*, 4422 (2000).
106. J. Sisko and S. M. Weinreb, *Synth. Commun.*, 1035 (1988).
107. A. P. Lepley, W. A. Khan, A. B. Giumanini and A. G. Giumanini, *J. Org. Chem.*, **31**, 2047 (1966).
108. D. W. Slocum, G. Bock and C. A. Jennings, *Tetrahedron Lett.*, 3443 (1970).
109. R. E. Ludt, G. P. Crowther and C. R. Hauser, *J. Org. Chem.*, **35**, 1288 (1970).
110. W. Fuhrer and H. W. Gschwend, *J. Org. Chem.*, **44**, 1133 (1979).
111. P. Stanetty, H. Koller and M. Mihovilovic, *J. Org. Chem.*, **57**, 6833 (1992).
112. J. A. Turner, *J. Org. Chem.*, **48**, 3401 (1983).
113. P. Stanetty and B. Krumpak, *J. Org. Chem.*, **61**, 5130 (1996).
114. K. Smith, G. A. El-Hiti and A. P. Shukla, *J. Chem. Soc., Perkin Trans. 1*, 2305 (1999).
115. J.-P. Meigh, M. Álvarez and J. A. Joule, *J. Chem. Soc., Perkin Trans. 1*, 2012 (2001).
116. K. Smith, G. A. El-Hiti and A. C. Hawes, *Synlett*, 945 (1999).
117. D. A. Shirley and B. J. Reeves, *J. Organomet. Chem.*, **16**, 1 (1969).
118. E. J. Corey and D. Seebach, *J. Org. Chem.*, **31**, 4097 (1966).
119. S. Cabiddu, C. Floris and S. Melis, *Tetrahedron Lett.*, **27**, 4625 (1986).
120. S. Cabiddu, C. Fattuoni, C. Floris, G. Gelli, S. Melis and F. Sotgiu, *Tetrahedron*, **46**, 861 (1990).
121. S. Cabiddu, C. Fattuoni, C. Floris, G. Gelli and S. Melis, *Tetrahedron*, **49**, 4965 (1993).
122. S. Cabiddu, C. Fattuoni, C. Floris, S. Melis and A. Serci, *Tetrahedron*, **50**, 6037 (1994).
123. N. Furukawa, T. Shibutani and H. Fujihara, *Tetrahedron Lett.*, **30**, 7091 (1989).
124. T. Shibutani, H. Fujihara and N. Furukawa, *Tetrahedron Lett.*, **32**, 2943 (1991).
125. G. Argouarch, O. Samuel, O. Riant, J.-C. Daran and H. B. Kagan, *Eur. J. Org. Chem.*, 2893 (2000).
126. O. Riant, G. Argouarch, D. Guillaneux, O. Samuel and H. B. Kagan, *J. Org. Chem.*, **63**, 3511 (1998).
127. D. H. Hua, N. M. Lagneau, Y. Chen, P. M. Robben, G. Clapham and P. D. Robinson, *J. Org. Chem.*, **61**, 4508 (1996).
128. H. L. Pedersen and M. Johanssen, *J. Chem. Soc., Chem. Commun.*, 2517 (1999).
129. L. A. Spangler, *Tetrahedron Lett.*, **37**, 3639 (1996).
130. S. L. MacNeil, O. B. Familoni and V. Snieckus, *J. Org. Chem.*, **66**, 3662 (2001).
131. O. B. Familoni, *Synlett*, 1181 (2002).
132. H. Watanabe, R. A. Schwarz, C. R. Hauser, J. Lewis and D. W. Slocum, *Can. J. Chem.*, **47**, 1543 (1969).
133. S. J. Shafer and W. D. Closson, *J. Org. Chem.*, **40**, 889 (1975).
134. D. Hellwinkel and M. Supp, *Tetrahedron Lett.*, 1499 (1975).
135. A. R. Katritzky and P. Lue, *J. Org. Chem.*, **55**, 74 (1990).
136. R. Schmid, J. Foricher, M. Cereghetti and P. Schönholzer, *Helv. Chim. Acta*, **74**, 370 (1991).
137. F. N. Jones, R. Vaulx and C. R. Hauser, *J. Org. Chem.*, **28**, 3461 (1963).
138. K. P. Klein and C. R. Hauser, *J. Org. Chem.*, **32**, 1479 (1967).
139. R. E. Ludt and C. R. Hauser, *J. Org. Chem.*, **36**, 1607 (1971).
140. G. Simig and M. Schlosser, *Tetrahedron Lett.*, **29**, 4277 (1988).
141. G. Cauquil, A. Casadevall and E. Casadevall, *Bull. Soc. Chim. Fr.*, 1049 (1960).
142. H. M. Walborsky and P. Ronman, *J. Org. Chem.*, **43**, 731 (1978).
143. A. J. Kirby and J. M. Percy, *Tetrahedron*, **44**, 6903 (1988).
144. R. A. Barnes and L. J. Nehmsmann, *J. Org. Chem.*, **27**, 1939 (1962).
145. G. Kraus and J. Kim, *J. Org. Chem.*, **67**, 2358 (2002).
146. M. I. Bruce, *Angew. Chem., Int. Ed. Engl.*, **16**, 73 (1977).
147. F. E. Ziegler and K. W. Fowler, *J. Org. Chem.*, **41**, 1564 (1976).
148. L. A. Flippin and J. M. Muchowski, *J. Org. Chem.*, **58**, 2631 (1993).
149. T. D. Krizan and J. C. Martin, *J. Org. Chem.*, **47**, 2681 (1982).
150. G. W. Klumpp, *Recl. Trav. Chim. Pays-Bas*, **105**, 1 (1986).

151. D. A. Shirley and J. P. Hendrix, *J. Organomet. Chem.*, **11**, 217 (1968).
152. D. A. Shirley, J. R. Johnson and J. P. Hendrix, *J. Organomet. Chem.*, **11**, 209 (1968).
153. F. Totter and P. Rittmeyer, in *Organometallics in Synthesis* (Ed. M. Schlosser), Wiley, New York, 1994, pp. 167–194.
154. S. Cabiddu, L. Contini, C. Fattuoni, C. Floris and G. Gelli, *Tetrahedron*, **47**, 9279 (1991).
155. H. Christensen, *Synth. Commun.*, **4**, 1 (1974).
156. H. Christensen, *Synth. Commun.*, **5**, 65 (1975).
157. R. Stern, J. English and H. G. Cassidy, *J. Am. Chem. Soc.*, **79**, 5797 (1957).
158. J. Clayden, M. Helliwell, C. McCarthy and N. Westlund, *J. Chem. Soc., Perkin Trans. 1*, 3232 (2000).
159. T. Kamikawa and I. Kubo, *Synthesis*, 431 (1986).
160. M. Pocci, V. Bertini, F. Lucchesini, A. de Munno, N. Picci, F. Iemma and S. Alfei, *Tetrahedron Lett.*, **42**, 1351 (2001).
161. W. Langham, R. Q. Brewster and H. Gilman, *J. Am. Chem. Soc.*, **63**, 545 (1941).
162. J. Clayden, M. N. Kenworthy, L. H. Youssef and M. Helliwell, *Tetrahedron Lett.*, **41**, 5171 (2000).
163. S. Hillebrand, J. Bruckmann, C. Krüger and M. W. Haenel, *Tetrahedron Lett.*, **36**, 75 (1995).
164. K. McWilliams and J. W. Kelly, *J. Org. Chem.*, **61**, 7408 (1996).
165. M. W. Haenel, D. Jakubik, E. Rothenberger and G. Schroth, *Chem. Ber.*, **124**, 1705 (1991).
166. F. Jean, O. Melnyk and A. Tartar, *Tetrahedron Lett.*, **36**, 7657 (1995).
167. U. Schöllkopf, *Angew. Chem., Int. Ed. Engl.*, **18**, 763 (1979).
168. H. Gilman, W. J. Meikle and J. W. Morton, *J. Am. Chem. Soc.*, **74**, 6282 (1952).
169. L. Santucci and H. Gilman, *J. Am. Chem. Soc.*, **80**, 4537 (1958).
170. N. Meyer and D. Seebach, *Angew. Chem., Int. Ed. Engl.*, **17**, 522 (1978).
171. M. Uemura, S. Tokuyama and T. Sakan, *Chem. Lett.*, 1195 (1975).
172. J. Mortier, J. Moyroud, B. Bennetau and P. A. Cain, *J. Org. Chem.*, **59**, 4042 (1994).
173. B. Bennetau, J. Mortier, J. Moyroud and J.-L. Guesnet, *J. Chem. Soc., Perkin Trans. 1*, 1265 (1995).
174. G. Ameline, M. Vaultier and J. Mortier, *Tetrahedron Lett.*, **37**, 8175 (1996).
175. F. Mongin, F. Trécourt and G. Quéguiner, *Tetrahedron Lett.*, **40**, 5483 (1999).
176. D. W. Knight and A. P. Nott, *J. Chem. Soc., Perkin Trans. 1*, 1125 (1983).
177. S. Caron and J. M. Hawkins, *J. Org. Chem.*, **63**, 2054 (1998).
178. J. Kristensen, M. Lysén, P. Pedsø and M. Begtrup, *Org. Lett.*, **3**, 1435 (2001).
179. F. Mongin, A. Tognini, F. Cottet and M. Schlosser, *Tetrahedron Lett.*, **39**, 1749 (1998).
180. F. Mongin and M. Schlosser, *Tetrahedron Lett.*, **38**, 1559 (1997).
181. H. Gilman and T. S. Soddy, *J. Org. Chem.*, **22**, 1715 (1957).
182. P. Kirsch and M. Bremer, *Angew. Chem., Int. Ed.*, **39**, 4217 (2000).
183. I. Haiduc and H. Gilman, *Chem. Ind. (London)*, 1278 (1968).
184. A. I. Meyers and P. D. Pansegrau, *J. Chem. Soc., Chem. Commun.*, 690 (1985).
185. P. D. Pansegrau, W. F. Rieker and A. I. Meyers, *J. Am. Chem. Soc.*, **110**, 7178 (1988).
186. J. Clayden, A. Lund and L. H. Youssef, *Org. Lett.*, **3**, 4133 (2001).
187. A. J. Clarke, S. McNamara and O. Meth-Cohn, *Tetrahedron Lett.*, 2373 (1974).
188. P. Gros, Y. Fort and P. Caubère, *J. Chem. Soc., Perkin Trans. 1*, 3597 (1997).
189. J. A. Zoltewicz and C. D. Dill, *Tetrahedron*, **52**, 14469 (1996).
190. R. D. Chambers, F. G. Drakesmith and W. K. R. Musgrave, *J. Chem. Soc.*, 5045 (1965).
191. R. D. Chambers, C. A. Heaton and W. K. R. Musgrave, *J. Chem. Soc., C*, 1700 (1969).
192. R. F. Francis, C. D. Crews and B. S. Scott, *J. Org. Chem.*, **43**, 3227 (1978).
193. F. Marsais, P. Granger and G. Quéguiner, *J. Org. Chem.*, **46**, 4494 (1981).
194. T. Güngör, F. Marsais and G. Quéguiner, *J. Organomet. Chem.*, **215**, 139 (1981).
195. M. Mallet, *J. Organomet. Chem.*, **406**, 49 (1991).
196. F. Marsais, E. Bouley and G. Quéguiner, *J. Organomet. Chem.*, **171**, 273 (1979).
197. T. J. Kress, *J. Org. Chem.*, **44**, 2081 (1979).
198. A. Turck, N. Plé, F. Mongin and G. Quéguiner, *Tetrahedron*, **57**, 4489 (2001).
199. F. Mongin and G. Quéguiner, *Tetrahedron*, **57**, 4059 (2001).
200. F. Marsais and G. Quéguiner, *Tetrahedron*, **39**, 2009 (1983).
201. M. Schlosser, *Mod. Synth. Methods*, **6**, 227 (1992).
202. G.-Q. Shi, S. Takagishi and M. Schlosser, *Tetrahedron*, **50**, 1129 (1994).
203. J. Porwisiak and W. Dmowski, *Tetrahedron*, **50**, 12259 (1994).

204. P. Rocca, F. Marsais, A. Godard and G. Quéguiner, *Tetrahedron*, **49**, 3325 (1993).
205. P. Remuzon, D. Bouzard and J.-P. Jacquet, *Heterocycles*, **36**, 431 (1993).
206. E. Arzel, P. Rocca, F. Marsais, A. Godard and G. Quéguiner, *J. Heterocycl. Chem.*, **34**, 1205 (1997).
207. E. Arzel, P. Rocca, F. Marsais, A. Godard and G. Quéguiner, *Heterocycles*, **50**, 215 (1999).
208. P. Rocca, F. Marsais, A. Godard and G. Quéguiner, *Tetrahedron*, **35**, 2003 (1994).
209. P. Rocca, F. Marsais, A. Godard, G. Quéguiner, L. Adams and B. Alo, *J. Heterocycl. Chem.*, **32**, 1171 (1995).
210. R. D. Chambers, C. W. Hall, J. Hutchinson and R. W. Millar, *J. Chem. Soc., Perkin Trans. 1*, 1705 (1998).
211. Y. Ito, K. Kunimoto, S. Miyachi and T. Kako, *Tetrahedron*, **32**, 4007 (1991).
212. V. Bertini, F. Lucchesini, M. Pocci and A. De Munno, *Heterocycles*, **41**, 675 (1995).
213. R. Radinov, C. Chanev and H. Haimova, *J. Org. Chem.*, **56**, 4793 (1991).
214. E. Marzi, A. Bigi and M. Schlosser, *Eur. J. Org. Chem.*, 1371 (2001).
215. C. W. Murtiashaw, R. Breitenbach, S. W. Goldstein, S. L. Pezzullo, G. J. Quallich and R. Sarges, *J. Org. Chem.*, **57**, 1930 (1992).
216. G. Karig, J. A. Spencer and T. Gallagher, *Org. Lett.*, **3**, 835 (2001).
217. F. Effenberger and W. Daub, *Chem. Ber.*, **124**, 2119 (1991).
218. A. Numata, Y. Kondo and T. Sakamoto, *Synthesis*, 306 (1999).
219. Y. G. Gu and E. K. Bayburt, *Tetrahedron Lett.*, **37**, 2565 (1996).
220. G. W. Gribble and M. G. Saulnier, *Heterocycles*, **35**, 151 (1993).
221. M. Mallet and G. Quéguiner, *Tetrahedron*, **38**, 3035 (1982).
222. P. Rocca, C. Cochennec, F. Marsais, L. Thomas-dit-Dumont, A. Godard and G. Quéguiner, *J. Org. Chem.*, **58**, 7832 (1993).
223. D. L. Comins and J. K. Saha, *J. Org. Chem.*, **61**, 9623 (1996).
224. C. Cochennec, P. Rocca, F. Marsais, A. Godard and G. Quéguiner, *Synthesis*, 321 (1995).
225. T. Sammakia and T. B. Hurley, *J. Org. Chem.*, **64**, 4652 (1999).
226. F. Trécourt, B. Gervais, M. Mallet and G. Quéguiner, *J. Org. Chem.*, **61**, 1673 (1996).
227. F. Trécourt, M. Mallet, O. Mongin and G. Quéguiner, *J. Org. Chem.*, **59**, 6173 (1994).
228. F. G. Fang, S. Xie and M. W. Lowery, *J. Org. Chem.*, **59**, 6142 (1994).
229. H. Muratake, M. Tonegawa and M. Natsume, *Chem. Pharm. Bull.*, **46**, 400 (1998).
230. D. L. Comins, S. P. Joseph and R. R. Goehring, *J. Am. Chem. Soc.*, **116**, 4719 (1994).
231. M. Shimano, T. Shibata and N. Kamei, *Tetrahedron Lett.*, **39**, 4363 (1998).
232. D. L. Comins, M. F. Baevsky and H. Hong, *J. Am. Chem. Soc.*, **114**, 10971 (1992).
233. K. E. Henegar, S. W. Ashford, T. A. Baughman, J. C. Sih and R.-L. Gu, *J. Org. Chem.*, **62**, 6588 (1997).
234. O. Martin, E. de la Cuesta and C. Avendaño, *Tetrahedron*, **51**, 7547 (1995).
235. P. Patel and J. A. Joule, *J. Chem. Soc., Chem. Commun.*, 1021 (1985).
236. P. Beak and D. B. Reitz, *Chem. Rev.*, **78**, 275 (1978).
237. O. Mongin, P. Rocca, L. Thomas-dit-Dumont, F. Trécourt, F. Marsais, A. Godard and G. Quéguiner, *J. Chem. Soc., Perkin Trans. 1*, 2503 (1995).
238. F. Trécourt, B. Gervais, O. Mongin, C. Le Gal, F. Mongin and G. Quéguiner, *J. Org. Chem.*, **63**, 2892 (1998).
239. S. V. Kessar and P. Singh, *Chem. Rev.*, **97**, 721 (1997).
240. E. Vedejs and X. Chen, *J. Am. Chem. Soc.*, **118**, 1809 (1996).
241. S. L. Taylor, D. Y. Lee and J. C. Martin, *J. Org. Chem.*, **48**, 4156 (1983).
242. S. G. Davies and M. R. Shipton, *J. Chem. Soc., Perkin Trans. 1*, 501 (1991).
243. A.-S. Rebstock, F. Mongin, F. Trécourt and G. Quéguiner, *Tetrahedron Lett.*, **43**, 767 (2002).
244. T. R. Kelly, W. Xu and J. Sundaresan, *Tetrahedron Lett.*, **34**, 6173 (1993).
245. E. Arzel, P. Rocca, F. Marsais, A. Godard and G. Quéguiner, *Tetrahedron Lett.*, **39**, 6465 (1998).
246. E. Arzel, P. Rocca, F. Marsais, A. Godard and G. Quéguiner, *Tetrahedron*, **55**, 12149 (1999).
247. A. Turck, N. Plé and G. Quéguiner, *Heterocycles*, **37**, 2149 (1994).
248. N. Plé, A. Turck, A. Heynderickx and G. Quéguiner, *J. Heterocycl. Chem.*, **31**, 1311 (1994).
249. N. Plé, A. Turck, A. Heynderickx and G. Quéguiner, *Tetrahedron*, **54**, 4899 (1998).
250. A. Turck, D. Trohay, L. Mojovic, N. Plé and G. Quéguiner, *J. Organomet. Chem.*, **412**, 301 (1991).
251. J. S. Ward and L. Merritt, *J. Heterocyclic Chem.*, **28**, 765 (1991).

252. A. Turck, N. Plé, D. Dognon, C. Harmoy and G. Quéguiner, *J. Heterocycl. Chem.*, **31**, 1449 (1994).
253. N. Plé, A. Turck, K. Couture and G. Quéguiner, *J. Org. Chem.*, **60**, 3781 (1995).
254. N. Plé, A. Turck, A. Heynderickx and G. Quéguiner, *Tetrahedron*, **54**, 9701 (1998).
255. N. Plé, A. Turck, F. Bardin and G. Quéguiner, *J. Heterocycl. Chem.*, **29**, 467 (1992).
256. J. J. Lee and S. H. Cho, *Bull. Korean Chem. Soc.*, **17**, 868 (1996).
257. N. Plé, A. Turck, K. Couture and G. Quéguiner, *Synthesis*, 838 (1996).
258. W. Liu, J. A. Walker, J. J. Chen, D. S. Wise and B. L. Townend, *Tetrahedron Lett.*, **37**, 5325 (1996).
259. A. Turck, N. Plé, A. Leprêtre-Gauquère and G. Quéguiner, *Heterocycles*, **49**, 205 (1998).
260. A. Turck, N. Plé, P. Pollet, L. Mojovic, J. Duflos and G. Quéguiner, *J. Heterocycl. Chem.*, **34**, 621 (1997).
261. A. Turck, N. Plé, L. Mojovic, B. Ndzi, G. Quéguiner, N. Haider, H. Schuller and G. Heinisch, *J. Heterocycl. Chem.*, **32**, 841 (1995).
262. A. Turck, N. Plé, D. Trohay, B. Ndzi and G. Quéguiner, *J. Heterocycl. Chem.*, **29**, 699 (1992).
263. H. Gilman and F. Breur, *J. Am. Chem. Soc.*, **56**, 1123 (1934).
264. D. A. Shirley and M. D. Cameron, *J. Am. Chem. Soc.*, **72**, 2788 (1950).
265. M. S. McClure, F. Roschnagar, S. J. Hodson, A. Miller and M. H. Osterhout, *Synthesis*, 1681 (2001).
266. T. Grimaldi, M. Romero and M. D. Pujol, *Synlett*, 1788 (2000).
267. D. W. Knight and A. P. Knott, *J. Chem. Soc., Perkin Trans. 1*, 1125 (1981).
268. J. A. Joule, K. Mills and G. F. Smith, *Heterocyclic Chemistry*, Third edn., Chapman and Hall, London, 1995.
269. I. Hasan, E. R. Marineli, L. C. C. Lin, F. W. Fowler and A. B. Levy, *J. Org. Chem.*, **46**, 957 (1981).
270. A. R. Katritzky, K. Akutagawa and A. R. Jones, *Synth. Commun.*, **18**, 1151 (1988).
271. M. P. Edwards, A. M. Doherty and S. V. Ley, *Tetrahedron*, **47**, 3723 (1986).
272. M. Gharpure, A. Stoller, F. Bellamy, G. Firnan and V. Snieckus, *Synthesis*, 1079 (1991).
273. T. Sotoyama, S. Hara and A. Suzuki, *Bull. Chem. Soc. Jpn.*, **52**, 1865 (1979).
274. J. M. Muchowski and R. Naef, *Helv. Chim. Acta*, **67**, 1168 (1984).
275. G. W. Rewcastle and A. R. Katritzky, *Adv. Heterocycl. Chem.*, **56**, 172 (1993).
276. T. Fukuda, Y. Mine and M. Iwao, *Tetrahedron*, **57**, 975 (2001).
277. A. R. Katritzky and K. Akutagawa, *Tetrahedron Lett.*, **26**, 5935 (1985).
278. M. Matsuzono, T. Fukuda and M. Iwao, *Tetrahedron Lett.*, **42**, 7621 (2001).
279. R. Sander and U. T. Mueller-Westerhoff, *J. Organomet. Chem.*, **512**, 219 (1996).
280. H. W. Gschwend and H. R. Rodriguez, *Org. React.*, **26**, 1 (1979).
281. D. W. Slocum, B. W. Rockett and C. R. Hauser, *J. Am. Chem. Soc.*, **87**, 1241 (1965).
282. T. Aratani, T. Gonda and H. Nozaki, *Tetrahedron Lett.*, 2265 (1969).
283. H. Falk and K. Schlögl, *Monatsh. Chem.*, **96**, 1065 (1965).
284. C. J. Richards and A. J. Locke, *Tetrahedron: Asymmetry*, **9**, 2377 (1998).
285. G. Gokel, P. Hoffmann, H. Kleimann, H. Klusacek, D. Marquarding and I. Ugi, *Tetrahedron Lett.*, 1771 (1970).
286. D. Marquarding, H. Klusacek, G. Gokel, P. Hoffmann and I. Ugi, *J. Am. Chem. Soc.*, **92**, 5389 (1970).
287. L. F. Battelle, R. Bau, G. Gokel, R. T. Okayawa and I. K. Ugi, *J. Am. Chem. Soc.*, **95**, 482 (1973).
288. T. Hayashi, T. Mise, M. Fukushima, M. Kagotani, N. Nagashima, Y. Hamada, A. Matsumoto, S. Kawakami, M. Konishi and K. Yamamoto, *Bull. Chem. Soc. Jpn.*, **53**, 1138 (1980).
289. T. D. Appleton, W. R. Cullen, J. V. Evans, T.-J. Kim and J. Trotter, *J. Organomet. Chem.*, **279**, 5 (1985).
290. T. Hayashi and A. Yamazaki, *J. Organomet. Chem.*, **413**, 295 (1991).
291. S. D. Pastor, *Tetrahedron*, **44**, 2883 (1988).
292. A. A. Naiini, C.-K. Lai, D. L. Ward and C. H. Brubaker, *J. Organomet. Chem.*, **390**, 73 (1990).
293. I. R. Butler, W. R. Cullen and S. J. Rettig, *Can. J. Chem.*, **65**, 1452 (1987).
294. G. Gokel and I. Ugi, *J. Chem. Educ.*, **49**, 294 (1972).
295. L. Beyer, R. Richter and O. Seidelmann, *J. Organomet. Chem.*, **561**, 199 (1998).
296. N. Deus, D. Robles and R. Herrmann, *J. Organomet. Chem.*, **386**, 253 (1990).

297. D. M. David, L. A. P. Kane-Maguire and S. G. Pyne, *Chem. Commun.*, 888 (1990).
298. A. Ohno, M. Yamane, T. Hayashi, N. Oguni and M. Hayashi, *Tetrahedron: Asymmetry*, **6**, 2495 (1995).
299. O. Riant, O. Samuel and H. B. Kagan, *J. Am. Chem. Soc.*, **115**, 5835 (1993).
300. O. Riant, O. Samuel, T. Flessner, S. Taudien and H. B. Kagan, *J. Org. Chem.*, **62**, 6733 (1997).
301. G. Iftime, J.-C. Daran, E. Manoury and G. G. A. Balavoine, *J. Organomet. Chem.*, **565**, 115 (1998).
302. D. L. Comins, *Synlett*, 615 (1992).
303. G. G. A. Balavoine, J.-C. Daran, G. Iftime, E. Manoury and C. Moreau-Bossuet, *J. Organomet. Chem.*, **567**, 191 (1998).
304. C. J. Richards, T. Damalidis, D. E. Hibbs and M. B. Hursthouse, *Synlett*, 74 (1995).
305. Y. Nishibayashi and M. Uemura, *Synlett*, 79 (1995).
306. T. Sammakia, H. Latham and D. R. Schaad, *J. Org. Chem.*, **60**, 10 (1995).
307. T. Sammakia and H. A. Latham, *J. Org. Chem.*, **60**, 6002 (1995).
308. E. Manoury, J. S. Fossey, H. Ait-Haddou, J.-C. Daran and G. G. A. Balavoine, *Organometallics*, **19**, 3836 (2000).
309. T. Sammakia and H. A. Latham, *J. Org. Chem.*, **61**, 1629 (1996).
310. R. Salter, T. E. Pickett and C. J. Richards, *Tetrahedron: Asymmetry*, **9**, 4239 (1998).
311. C. J. Richards and A. W. Mulvaney, *Tetrahedron: Asymmetry*, **7**, 1419 (1996).
312. Y. Nishibayashi, K. Segawa, Y. Arikawa, K. Ohe, M. Hidai and S. Uemura, *J. Organomet. Chem.*, **545**, 381 (1997).
313. K. H. Ahn, C.-W. Cho, H.-H. Baek, J. Park and S. Lee, *J. Org. Chem.*, **61**, 4937 (1996).
314. R. Sebesta, S. Toma and M. Salisova, *Eur. J. Org. Chem.*, 692 (2002).
315. J. Park, S. Lee, K. H. Ahn and C.-W. Cho, *Tetrahedron Lett.*, **36**, 7263 (1995).
316. S.-G. Kim, C.-W. Cho and K. H. Ahn, *Tetrahedron: Asymmetry*, **8**, 1023 (1997).
317. W. Zhang, Y. Adachi, T. Hirao and I. Ikeda, *Tetrahedron: Asymmetry*, **7**, 451 (1996).
318. T. Aratani, T. Gonda and H. Nozaki, *Tetrahedron*, **26**, 5453 (1970).
319. C. Ganter and T. Wagner, *Chem. Ber.*, **128**, 1157 (1995).
320. L. Xiao, K. Mereiter, W. Weissensteiner and M. Widhalm, *Synthesis*, 1354 (1999).
321. D. Enders, R. Peters, R. Lochtman and J. Runsink, *Synlett*, 1462 (1997).
322. D. Enders, R. Peters, R. Lochtman and G. Raabe, *Angew. Chem., Int. Ed.*, **38**, 2421 (1999).
323. D. Enders, R. Peters, R. Lochtman, G. Raabe, J. Runsink and J. W. Bats, *Eur. J. Org. Chem.*, 3399 (2000).
324. D. Enders and T. Klumpen, *J. Organomet. Chem.*, **637**, 698 (2001).
325. L. Xiao, R. Kitzler and W. Weissensteiner, *J. Org. Chem.*, **66**, 8912 (2001).
326. M. Widhalm, K. Mereiter and M. Bourghida, *Tetrahedron: Asymmetry*, **9**, 2983 (1998).
327. M. Widhalm, U. Nettekoven and K. Mereiter, *Tetrahedron: Asymmetry*, **10**, 4369 (1999).
328. A. Farrell, R. Goddard and P. J. Guiry, *J. Org. Chem.*, **67**, 4209 (2002).
329. F. Rebière, O. Riant, L. Ricard and H. B. Kagan, *Angew. Chem., Int. Ed. Engl.*, **32**, 568 (1993).
330. N. M. Lagneau, Y. Chen, P. M. Robben, H.-S. Sin, K. Takasu, J.-S. Chan, P. D. Robinson and D. H. Hua, *Tetrahedron*, **54**, 7301 (1998).
331. J. Priego, O. G. Mancheño, S. Cabrera and J. C. Carretero, *J. Org. Chem.*, **67**, 1346 (2002).
332. O. Riant, G. Argouarch, D. Guillaneux, O. Samuel and H. B. Kagan, *J. Org. Chem.*, **63**, 3511 (1998).
333. G. Argouarch, O. Samuel, O. Riant, J.-C. Daran and H. B. Kagan, *Eur. J. Org. Chem.*, 2893 (2000).
334. H. L. Pedersen and M. Johanssen, *Chem. Commun.*, **40**, 2517 (1999).
335. C. Bolm, M. Kesselgruber, K. Muñiz and G. Raabe, *Organometallics*, **19**, 1648 (2000).
336. C. Metallinos and V. Snieckus, *Org. Lett.*, **4**, 1935 (2002).
337. D. A. Price and N. S. Simpkins, *Tetrahedron Lett.*, **36**, 6135 (1995).
338. D. Hoppe and T. Hense, *Angew. Chem., Int. Ed. Engl.*, **36**, 2282 (1997).
339. M. Tsukazaki, M. Tinkl, A. Roglans, B. J. Chapell, N. J. Taylor and V. Snieckus, *J. Am. Chem. Soc.*, **118**, 685 (1996).
340. B. F. Bonini, M. Comes-Franchini, M. Fochi, G. Mazzanti, A. Ricci, A. Alberti, D. Macciantelli, M. Marcaccio and S. Roffia, *Eur. J. Org. Chem.*, 543 (2002).
341. R. S. Laufer, U. Veith, N. J. Taylor and V. Snieckus, *Org. Lett.*, **2**, 629 (2000).

342. H. Jendralla and E. Paulus, *Synlett*, 471 (1997).
343. Y. Nishibayashi, Y. Arikawa, K. Ohe and S. Uemura, *J. Org. Chem.*, **61**, 1172 (1996).
344. S. G. Davies, *Organotransition Metal Chemistry: Application to Organic Synthesis*, Pergamon, Oxford, 1982.
345. M. D. Rausch and R. E. Gloth, *J. Organomet. Chem.*, **153**, 59 (1978).
346. S. E. Gibson (née Thomas), J. W. Stead and S. Sur, *J. Chem. Soc., Perkin Trans. 1*, 636 (2001).
347. M. F. Semmelhack, J. Bisaha and J. Czarny, *J. Am. Chem. Soc.*, **101**, 768 (1979).
348. R. S. Card and W. S. Trahanovsky, *J. Org. Chem.*, **45**, 2560 (1980).
349. C. Bolm and K. Muniz, *Chem. Soc. Rev.*, **28**, 51 (1999).
350. A. Berger, J. P. Djukic and C. Michon, *Coord. Chem. Rev.*, **225**, 215 (2002).
351. J. P. Gilday, J. T. Negri and D. A. Widdowson, *Tetrahedron*, **45**, 605 (1989).
352. J. Blagg, S. G. Davies, C. L. Goodfellow and K. H. Sutton, *J. Chem. Soc., Perkin Trans. 1*, 1805 (1987).
353. S. G. Davies and C. L. Goodfellow, *J. Organomet. Chem.*, **370**, C5 (1987).
354. J. A. Heppert, J. Aubé., M. E. Thomas-Miller, M. L. Milligan and F. Takusagawa, *Organometallics*, **7**, 2581 (1988).
355. J. A. Heppert, J. Aubé., M. E. Thomas-Miller, M. L. Milligan and F. Takusagawa, *Organometallics*, **9**, 727 (1990).
356. M. Uemura, R. Miyake, K. Nakayama, M. Shiro and Y. Hayashi, *J. Org. Chem.*, **58**, 1238 (1993).
357. S. J. Coote, S. G. Davies, C. L. Goodfellow, K. H. Sutton, D. Middlemiss and A. Naylor, *Tetrahedron: Asymmetry*, **1**, 817 (1990).
358. S. G. Davies and W. E. Hume, *Chem. Commun.*, 251 (1995).
359. S. G. Davies, T. Loveridge and J. M. Clough, *Chem. Commun.*, 817 (1995).
360. S. G. Davies, T. Loveridge, M. F. C. C. Teixeira and J. M. Clough, *J. Chem. Soc., Perkin Trans. 1*, 3405 (1999).
361. Y. Kondo, J. R. Green and J. Ho, *J. Org. Chem.*, **56**, 7199 (1991).
362. Y. Kondo, J. R. Green and J. Ho, *J. Org. Chem.*, **58**, 6182 (1993).
363. M. Uemura, A. Daimon and Y. Hayashi, *Chem. Commun.*, 1943 (1995).
364. T. Watanabe, M. Shakadou and M. Uemura, *Inorg. Chim. Acta*, **296**, 80 (1999).
365. J. Aubé, J. A. Heppert, M. L. Milligan, M. J. Smith and P. Zenk, *J. Org. Chem.*, **57**, 3563 (1992).
366. A. Alexakis, T. Kanger, P. Mangeney, F. Rose-Munch, A. Perrotey and E. Rose, *Tetrahedron: Asymmetry*, **6**, 47 (1995).
367. S. E. Gibson and E. G. Reddington, *Chem. Commun.*, 989 (2000).
368. D. A. Price, N. S. Simpkins, A. M. MacLeod and A. P. Watt, *J. Org. Chem.*, **59**, 1961 (1994).
369. D. A. Price, N. S. Simpkins, A. M. MacLeod and A. P. Watt, *Tetrahedron Lett.*, **35**, 6159 (1994).
370. R. A. Ewin, A. M. MacLeod, D. A. Price, N. S. Simpkins and A. P. Watt, *J. Chem., Soc. Perkin Trans. 1*, 401 (1997).
371. S. Pache, C. Botuha, R. Franz, E. P. Kündig and J. Einhorn, *Helv. Chim. Acta*, **83**, 2436 (2000).
372. H.-G. Schmalz and K. Schellhaas, *Angew. Chem., Int. Ed. Engl.*, **35**, 2146 (1996).
373. K. Schellhaas, H.-G. Schmalz and J. W. Bats, *Chem. Eur. J.*, **4**, 57 (1998).
374. A. Quattropani, G. Anderson, G. Bernardinelli and E. P. Kündig, *J. Am. Chem. Soc.*, **119**, 4773 (1997).
375. H.-G. Schmalz and K. Schellhaas, *Tetrahedron Lett.*, **36**, 5515 (1995).
376. E. P. Kündig and A. Quattropani, *Tetrahedron Lett.*, **35**, 3497 (1994).
377. A. Quattropani, G. Bernardinelli and E. P. Kündig, *Helv. Chim. Acta*, **82**, 90 (1999).
378. S. Nelson and M. A. Hilfiker, *Org. Lett.*, **1**, 1379 (1999).
379. A. Ariffin, A. J. Blake, W.-S. Li and N. S. Simpkins, *Synlett*, 1453 (1997).
380. A. Ariffin, A. J. Blake, R. A. Ewin, W.-S. Li and N. Simpkins, *J. Chem. Soc., Perkin Trans. 1*, 3177 (1999).
381. E. L. M. Courton, S. E. Gibson (née Thomas), M. J. Schneider and M. H. Smith, *Chem. Commun.*, 839 (1996).
382. S. E. Gibson (née Thomas), P. O' Brien, E. Rahimian and M. H. Smith, *J. Chem. Soc., Perkin Trans. 1*, 909 (1999).

383. R. A. Ewin and N. S. Simpkins, *Synlett*, 317 (1996).
384. A. Ariffin, A. J. Blake, R. A. Ewin and N. S. Simpkins, *Tetrahedron: Asymmetry*, **9**, 2563 (1998).
385. M. Uemura, Y. Hayashi and Y. Hayashi, *Tetrahedron: Asymmetry*, **5**, 1427 (1994).
386. R. Wilhelm, I. K. Sebhat, A. J. P. White, D. J. Williams and D. A. Widdowson, *Tetrahedron: Asymmetry*, **11**, 5003 (2000).
387. Y.-L. Tang, D. A. Widdowson and R. Wilhelm, *Synlett*, 1632 (2001).
388. M. J. Siwek and J. R. Green, *Chem. Commun.*, 2359 (1999).
389. K. Kamikawa and M. Uemura, *Synlett*, 938 (2000).
390. T. Watanabe, K. Kamikawa and M. Uemura, *Tetrahedron Lett.*, **36**, 6695 (1995).
391. T. Watanabe and M. Uemura, *Chem. Commun.*, 871 (1998).
392. K. Kamikawa, A. Watanabe, A. Daimon and M. Uemura, *Tetrahedron*, **56**, 2325 (2000).
393. K. Kamikawa and M. Uemura, *Tetrahedron Lett.*, **37**, 6359 (1996).
394. R. Wilhelm and D. A. Widdowson, *Org. Lett.*, **3**, 3079 (2001).
395. Y. L. Tan, A. J. P. White, D. A. Widdowson, R. Wilhelm and D. J. Williams, *J. Chem. Soc., Perkin Trans. 1*, 3269 (2001).
396. R. D. Clark and A. Jahangir, *Org. React.*, **47**, 1 (1995).
397. C. D. Broaddus, *J. Am. Chem. Soc.*, **88**, 4174 (1966).
398. C. D. Broaddus, *J. Org. Chem.*, **35**, 10 (1970).
399. H. Gilman and B. J. Gaj, *J. Org. Chem.*, **28**, 1725 (1963).
400. L. Lochmann and J. Petranek, *Tetrahedron Lett.*, **32**, 1482 (1991).
401. F. N. Jones, M. F. Zinn and C. R. Hauser, *J. Org. Chem.*, **28**, 663 (1963).
402. R. L. Vaulx, F. N. Jones and C. R. Hauser, *J. Org. Chem.*, **29**, 1387 (1964).
403. J. Clayden, M. Darbyshire, J. H. Pink, N. Westlund and F. X. Wilson, *Tetrahedron Lett.*, **38**, 8587 (1997).
404. J. Clayden and L. H. Youssef, unpublished work.
405. C.-L. Mao and C. R. Hauser, *J. Org. Chem.*, **35**, 3704 (1970).
406. R. D. Clark, A. B. Miller, J. Berger, D. B. Repke, K. K. Weinhardt, B. A. Kowalczyk, R. M. Eglen, D. W. Bonhaus, C. H. Lee, A. D. Michel, W. L. Smith and E. H. F. Wong, *J. Med. Chem.*, **36**, 2645 (1993).
407. L. E. Fisher, J. M. Muchowski and R. D. Clark, *J. Org. Chem.*, **57**, 2700 (1992).
408. R. D. Clark, Jahangir and J. A. Langston, *Can. J. Chem.*, **72**, 23 (1994).
409. L. E. Fisher, J. M. Caroon, Jahangir, S. R. Stavler, S. Lundberg and J. M. Muchowski, *J. Org. Chem.*, **58**, 3643 (1993).
410. M. Watanabe, M. Sahara, M. Kubo, S. Furukawa, R. J. Billedeau and V. Snieckus, *J. Org. Chem.*, **49**, 742 (1984).
411. R. D. Clark and Jahangir, *J. Org. Chem.*, **52**, 5378 (1987).
412. J. Clayden, N. Westlund and F. X. Wilson, *Tetrahedron Lett.*, **40**, 3331 (1999).
413. R. D. Clark and Jahangir, *J. Org. Chem.*, **54**, 1174 (1989).
414. D. L. Comins and J. D. Brown, *J. Org. Chem.*, **51**, 3566 (1986).
415. R. R. Fraser and S. Savard, *Can. J. Chem.*, **64**, 621 (1991).
416. H. W. Gschwend and A. Hamdan, *J. Org. Chem.*, **40**, 2008 (1975).
417. W. J. Houlihan and V. A. Parriano, *J. Org. Chem.*, **47**, 5177 (1982).
418. L. A. Flippin, *Tetrahedron Lett.*, **32**, 6857 (1991).
419. P. L. Creger, *J. Am. Chem. Soc.*, **92**, 1396 (1970).
420. R. C. Thompson and J. Kallmerten, *J. Org. Chem.*, **55**, 6076 (1990).
421. J. L. Belletire and E. G. Spletzer, *Synth. Commun.*, **16**, 575 (1986).
422. A. G. Schultz and N. J. Green, *J. Am. Chem. Soc.*, **113**, 4931 (1991).
423. P. E. Pfeffer, L. S. Silbert and J. M. Chirinkoi, *J. Org. Chem.*, **37**, 451 (1970).
424. F. M. Hauser, R. P. Rhee, S. Prasanna, S. M. Weinreb and J. H. Dodd, *Synthesis*, 72 (1980).
425. G. A. Kraus, *J. Org. Chem.*, **46**, 201 (1981).
426. A. C. Regan and J. Staunton, *J. Chem. Soc., Chem. Commun.*, 764 (1983).
427. A. C. Regan and J. Staunton, *J. Chem. Soc., Chem. Commun.*, 520 (1987).
428. J. Klein and A. Medlik-Balan, *J. Org. Chem.*, **41**, 3307 (1976).
429. K. Kobayashi, A. Konishi, Y. Kanno and H. Suginome, *J. Chem. Soc., Perkin Trans. 1*, 111 (1993).
430. D. L. Comins and J. D. Brown, *J. Org. Chem.*, **49**, 1078 (1984).
431. T. D. Harris and G. P. Roth, *J. Org. Chem.*, **44**, 2004 (1979).

432. L. A. Flippin, J. M. Muchowski and D. S. Carter, *J. Org. Chem.*, **58**, 2463 (1993).
433. M. Braun and E. Ringer, *Tetrahedron Lett.*, **24**, 1233 (1983).
434. R. B. Bates and T. J. Siahaan, *J. Org. Chem.*, **51**, 1432 (1986).
435. T. E. Harmon and D. A. Shirley, *J. Org. Chem.*, **39**, 3164 (1974).
436. M. R. Winkle and R. C. Ronald, *J. Org. Chem.*, **47**, 2101 (1982).
437. R. C. Ronald and M. R. Winkle, *Tetrahedron*, **39**, 2031 (1983).
438. M. Watanabe, M. Date, K. Kawanishi, T. Hori and S. Furukawa, *Chem. Pharm. Bull.*, **39**, 41 (1991).
439. S. Cabiddu, S. Melis, P. P. Piras and F. Sotgiu, *J. Organomet. Chem.*, **178**, 291 (1979).
440. S. Cabiddu, C. Floris, G. Gelli and S. Melis, *J. Organomet. Chem.*, **366**, 1 (1989).
441. J. L. García Ruano, M. C. Carreño, M. A. Toledo, J. M. Aguirre, M. T. Aranda and J. Fischer, *Angew. Chem., Int. Ed.*, **39**, 2736 (2000).
442. B. I. Alo, O. B. Familoni, F. Marsais and G. Quéguiner, *J. Chem. Soc., Perkin Trans. 1*, 1611 (1990).
443. H. Watanabe and C. R. Hauser, *J. Org. Chem.*, **33**, 4278 (1968).
444. H. Watanabe, C.-L. Mao, I. T. Barnish and C. R. Hauser, *J. Org. Chem.*, **34**, 919 (1969).
445. H. Watanabe, R. L. Gay and C. R. Hauser, *J. Org. Chem.*, **33**, 900 (1968).
446. W. J. Houlihan, V. A. Parrino and Y. Uike, *J. Org. Chem.*, **46**, 4511 (1981).
447. G. Spadoni, B. Stankov, A. Duranti, G. Biella, V. Lucini, A. Salvatori and F. Fraschini, *J. Med. Chem.*, **36**, 4069 (1993).
448. Y. Ito, K. Kobayashi and T. Saegusa, *J. Am. Chem. Soc.*, **99**, 3532 (1977).
449. Y. Ito, K. Kobayashi, N. Seko and T. Saegusa, *Bull. Chem. Soc. Jpn.*, **57**, 73 (1984).
450. R. D. Clark, J. M. Muchowski, L. E. Fisher, L. A. Flippin, D. B. Repke and M. Souchet, *Synthesis*, 871 (1991).
451. A. R. Katritzky, M. Black and W.-Q. Fan, *J. Org. Chem.*, **56**, 5045 (1991).
452. A. R. Katritzky, W.-Q. Fan, K. Akutagawa and J. Wang, *Heterocycles*, **30**, 407 (1990).
453. A. B. Smith, J. N. Haseltine and M. Visnick, *Tetrahedron*, **45**, 2431 (1989).
454. A. M. Kanazawa, A. Correa, J.-N. Denis, J.-M. Luche and A. E. Greene, *J. Org. Chem.*, **58**, 255 (1993).
455. R. D. Clark and Jahangir, *Tetrahedron*, **49**, 1351 (1993).
456. R. R. Fraser, T. S. Mansour and S. Savard, *J. Org. Chem.*, **50**, 3232 (1985).
457. H. Hamana and T. Sugasawa, *Chem. Lett.*, 1591 (1984).
458. J. Mathieu, P. Gros and Y. Fort, *J. Chem. Soc., Chem. Commun.*, 951 (1999).
459. A. R. Katritzky and K. Akutagawa, *J. Am. Chem. Soc.*, **108**, 6808 (1986).
460. R. S. Mali and P. G. Jagtap, *Tetrahedron Lett.*, **33**, 1655 (1992).
461. D. L. Comins and M. O. Killpack, *Tetrahedron Lett.*, **30**, 4337 (1989).
462. J. Clayden, *Organolithiums: Selectivity for Synthesis*, Pergamon, Oxford, 2002.
463. J. Clayden and J. H. Pink, *Tetrahedron Lett.*, **38**, 2561 (1997).
464. J. Clayden and J. H. Pink, *Tetrahedron Lett.*, **38**, 2565 (1997).
465. J. Clayden, M. Helliwell, J. H. Pink and N. Westlund, *J. Am. Chem. Soc.*, **123**, 12449 (2001).
466. S. Thayumanavan, A. Basu and P. Beak, *J. Am. Chem. Soc.*, **119**, 8209 (1997).
467. J. Clayden, P. Johnson and J. H. Pink, *J. Chem. Soc., Perkin Trans. 1*, 371 (2001).
468. T. Hata, H. Koide, N. Taniguchi and M. Uemura, *Org. Lett.*, **2**, 1907 (2000).
469. T. Hata, H. Koide and M. Uemura, *Synlett*, 1145 (2000).
470. H. Koide, T. Hata and M. Uemura, *J. Org. Chem.*, **67**, 1929 (2002).
471. L. M. Engelhardt, W.-P. Leung, C. L. Raston, G. Salem, P. Twiss and A. H. White, *J. Chem. Soc., Dalton Trans.*, 2403 (1988).
472. R. R. Schmidt and J. Talbiersky, *Angew. Chem., Int. Ed. Engl.*, **15**, 171 (1976).
473. R. R. Schmidt and G. Berger, *Chem. Ber.*, **109**, 2936 (1976).
474. C. S. Shiner, A. H. Berks and A. M. Fisher, *J. Am. Chem. Soc.*, **110**, 957 (1988).
475. C. A. James and V. Snieckus, *Tetrahedron Lett.*, **38**, 8149 (1997).
476. X. Wang and V. Snieckus, *Tetrahedron Lett.*, **32**, 4829 (1991).
477. M. Schlosser, *Pure Appl. Chem.*, **60**, 1627 (1988).
478. L. Lochmann, J. Pospísil and D. Lím, *Tetrahedron Lett.*, 257 (1966).
479. M. Schlosser, *J. Organomet. Chem.*, **8**, 9 (1967).
480. L. Lochmann and J. Trekoval, *J. Organomet. Chem.*, **99**, 329 (1975).
481. L. Lochmann and D. Lím, *J. Organomet. Chem.*, **28**, 153 (1971).
482. J. Hartmann and M. Schlosser, *Helv. Chim. Acta*, **59**, 453 (1976).

483. M. Schlosser, J. H. Choi and S. Takagishi, *Tetrahedron*, **46**, 5633 (1990).
484. M. Schlosser, G. Katsoulos and S. Takagishi, *Synlett*, 747 (1990).
485. G. Katsoulos, S. Takagishi and M. Schlosser, *Synlett*, 731 (1991).
486. M. Schlosser, *Chem. Eur. J.*, **4**, 1969 (1998).
487. F. Faigl and M. Schlosser, *Tetrahedron Lett.*, **32**, 3369 (1991).
488. P. Gros, Y. Fort and P. Caubère, *J. Chem. Soc., Perkin Trans. 1*, 3071 (1997).
489. B. H. Bhida and N. S. Narasimhan, *Chem. Ind. (London)*, 75 (1974).
490. K. Wamada, Y. Yazawa, D. Uemura, M. Toda and Y. Hirata, *Tetrahedron*, **25**, 1969 (1969).
491. C. D. Liang, *Tetrahedron Lett.*, **27**, 1971 (1986).
492. M. W. Haenel, A. Fieseler, D. Jakubik, B. Gabor, R. Goddard and C. Krüger, *Tetrahedron Lett.*, **34**, 2107 (1993).
493. M. Shimano and A. I. Meyers, *J. Am. Chem. Soc.*, **116**, 10815 (1994).
494. M. Shimano and A. I. Meyers, *Tetrahedron Lett.*, **38**, 5415 (1997).
495. A. Ahmed and J. Clayden, unpublished results.
496. R. Massi and M. Schlosser, *J. Org. Chem.*, **61**, 5430 (1996).
497. G. Simig and M. Schlosser, *Tetrahedron Lett.*, **32**, 1963 (1991).
498. Y. Moro-oka, S. Iwakiri, T. Fukuda and M. Iwao, *Tetrahedron Lett.*, **41**, 5225 (2000).
499. A. I. Meyers, W. F. Ricker and L. M. Fuentes, *J. Am. Chem. Soc.*, **105**, 2082 (1983).
500. G. M. Davies and P. S. Davies, *Tetrahedron Lett.*, **33**, 3507 (1972).
501. J. J. Court and D. J. Hlasta, *Tetrahedron Lett.*, **37**, 1335 (1996).
502. R. J. Mills, N. J. Taylor and V. Snieckus, *J. Org. Chem.*, **54**, 4372 (1989).
503. J. Clayden and L. W. Lai, *Tetrahedron Lett.*, **42**, 3163 (2001).
504. J. C. Hodges, W. C. Patt and C. J. Conolly, *J. Org. Chem.*, **56**, 449 (1991).
505. A. Dondoni, G. Fantin, M. Fagagnolo, M. Medici and P. Pedrini, *J. Org. Chem.*, **53**, 1748 (1988).
506. B. Iddon, *Heterocycles*, **23**, 417 (1985).
507. S. Ohta, M. Matsukawa, N. Ohashi and K. Nagayama, *Synthesis*, 78 (1990).
508. G. Shapiro and B. Gomez-Lor, *Heterocycles*, **41**, 215 (1995).
509. A. Ahmed, J. Clayden and M. Rowley, *Tetrahedron Lett.*, **39**, 6103 (1998).
510. J. Clayden, J. H. Pink, N. Westlund and F. X. Wilson, *Tetrahedron Lett.*, **39**, 8377 (1998).

CHAPTER **11**

Arene-catalyzed lithiation

MIGUEL YUS

Departamento de Química Orgánica, Facultad de Ciencias, Universidad de Alicante,
Apdo. 99, 03080 Alicante, Spain
Fax: 34 965 903 549; e-mail: yus@ua.es

The Chemistry of Organolithium Compounds. Edited by Z. Rappoport and I. Marek
ISBN: 0-470-84339-X

I. INTRODUCTION

The use of metals in synthetic organic chemistry has become a general tool for the construction of complex organic molecules. In fact, nowadays it is unimaginable to carry out a synthetic sequence without employing a metal in some of the corresponding steps. A problem associated with the use of metals in organic reactions is that in many cases (i.e. low reactivity of the metal or very mild reaction conditions), they should be activated to get reactive species[1−3]. General methods for activating metals include:

(1) *Alkali metal reductions of metallic salts* using an arene as electron carrier, lithium being the most used metallic component (Rieke method)[4,5]. Although not belonging to this group of metals, magnesium-anthracene has found some applications in the activation of other metals[6].

(2) *Ultrasound activation of metals*. Since its discovery as an activation technique some fifty years ago[7], sonication has been demonstrated to be of general use for the depassivation of different metals[8]. In this case, the activation consists in cleaning the surface of the metal, making possible better contact between the reagents. Probably the most important applications of ultrasonic irradiation are the direct preparation of organometallic reagents and different metal-assisted reactions, for instance in aqueous media[9−15].

(3) *Other procedures*, involving metal vapors[16], electrochemical activation[17], as well as alloys[18], colloids[18] and metal-graphite[19] are of less general use, requiring in some cases sophisticated equipment.

In the case of the activation of lithium, probably the most useful methodology involves the use of an arene, naphthalene and 4,4′-di-*tert*-butylbiphenyl (DTBB) being the most commonly used[20]. This procedure employs a stoichiometric amount of the arene and THF as solvent, so a dark-colored solution of the corresponding metal-arene (also called metal arenide) is easily prepared[21]. The resulting paramagnetic solution, which contains the corresponding arene radical-anion, is very effective and can be used for the generation of very unstable organolithium reagents under very mild reaction conditions. For instance, different functionalized organolithium compounds can be prepared at low temperature, mainly by halogen−lithium exchange[22−25]. However, this methodology (the use of a lithioarene) has some problems like the removal of a big amount of the arene at the end of the reaction, and the existence of undesirable by-processes resulting from the reaction of the arene radical-anion with the electrophile, used in the reaction after the lithiation process. For these reasons, in the last few years a catalytic version of the mentioned arene-promoted lithiation has been developed, which uses a substoichiometric ('catalytic') amount (<10%) of the corresponding arene. The mixture, which is far more reactive than the solution of the corresponding lithio-arene, allows one to perform new reactions in a very efficient manner, most of them not being able to be carried out using other activation methods including the stoichiometric version of this reaction. In this chapter, the scope and applications in synthetic organic chemistry of arene-catalyzed lithiation will be explored, paying special attention to new and selective reactions[26–29].

II. MECHANISTIC ASPECTS

Since different reactivity is observed for both the stoichiometric and the catalytic version of the arene-promoted lithiation, different species should be involved in the electron-transfer process from the metal to the organic substrate. It has been well-established that in the case of the stoichiometric version an arene-radical anion [lithium naphthalenide ($LiC_{10}H_8$) or lithium di-*tert*-butylbiphenylide (LiDTBB) for using naphthalene or 4,4′-di-*tert*-butylbiphenyl (DTBB) as arenes, respectively] is responsible for the reduction of the substrate, for instance for the transformation of an alkyl halide into an alkyllithium[30, 31]. For the catalytic process, using naphthalene as the arene, an arene-dianion **2** has been proposed[32, 33], which is formed by overreduction of the corresponding radical-anion **1** (Scheme 1). Actually, the dianionic species **2** has been prepared by a completely different approach, namely by double deprotonation of 1,4-dihydronaphthalene, and its X-ray structure determined as its complex with two molecules of *N*,*N*,*N*′,*N*′-tetramethylethylenediamine (TMEDA)[34].

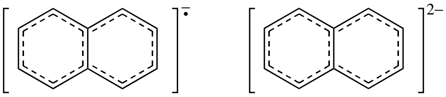

(1) **(2)**

SCHEME 1

Concerning the reactivity of the dianion **2** compared to that of the radical-anion **1**, the first one behaves as a typical lithiating agent toward alkyl chlorides displaying an outer-sphere electron transfer reactivity profile: no significant kinetic differences are found in the reaction of dianion **2** (as well as the radical-anion **1**) with primary, secondary, tertiary and phenyl chlorides. On the other hand, a notable difference has been found in the reactivity of both species with several substrates and solvents[35].

The participation of dianion **2** in naphthalene-catalyzed lithiation of a general substrate RX is shown in Scheme 2: once the radical-anion **1** is initially formed, the presence of an excess of lithium makes possible the generation of the dianion **2**, which can transfer one electron to the substrate regenerating the radical-anion. A final electron transfer of a new electron to the radical $R^{\bullet}$ generates, generally in a rapid process, the real intermediate organolithium RLi. The trapping of this intermediate with an electrophile would lead to the formation of the desired products, usually generating a new carbon–carbon bond (for carbon electrophiles) and in many cases a new functional group (i.e. with carbonyl compounds), as usually occurs in the chemistry of organolithium compounds[36–40].

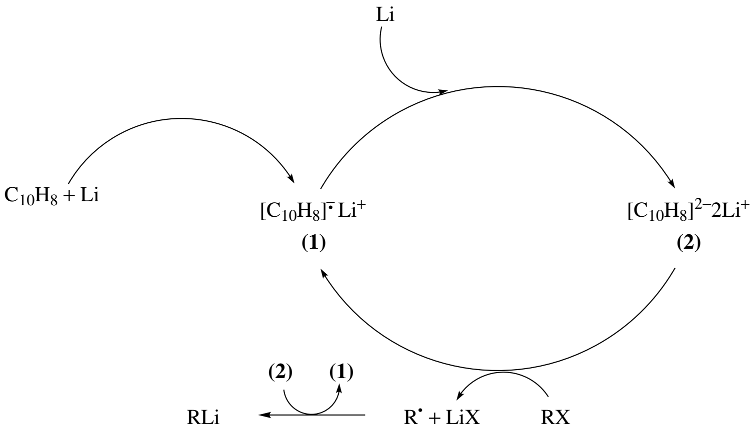

SCHEME 2

III. ORGANOLITHIUMS BY HALOGEN–LITHIUM EXCHANGE

The use of substoichiometric amounts of an arene (naphthalene or biphenyl) was first studied in the reaction of bromobenzene and benzaldehyde with sodium[41, 42], under Barbier-type reaction conditions[43, 44]. The possibility of using a substoichiometric amount of DTBB in the lithiation of alkyl chlorides was anticipated more than twenty years ago[45]. However, this methodology has been used in few cases. For instance, cumyl chloride **3** and adamantanone (**4**) reacted with lithium and a catalytic amount (1–3%) of DTBB to yield the expected alcohol **5** (Scheme 3)[46].

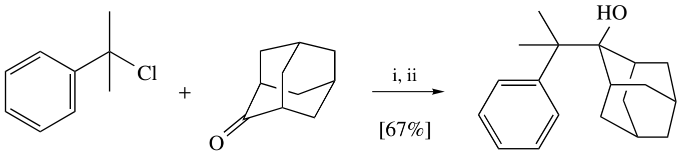

(3) **(4)** **(5)**

SCHEME 3. Reagents: (i) Li, DTBB (1–3%), THF, 0 °C; (ii) $NH_4Cl–H_2O$

Using 10% of DTBB as electron carrier, 2,5-disubstituted chlorocyclopentanes **6** were lithiated, the corresponding organolithium intermediates having being employed for the preparation of boronic esters **7**, after reaction with triethyl borate and the corresponding 1,3-diol (Scheme 4)[47].

The intramolecular carbolithiation of 6-lithio-1-hexene (**9**) was studied after lithiation of 6-chloro-1-hexene (**8**) in the presence of a catalytic amount of DTBB (5%). At −78 °C the corresponding organolithium compound **9** is stable, giving the expected products **10** by reaction with different electrophiles. However, when the lithiation step was carried out at −30 °C a cyclization reaction took place, so that a new organolithium intermediate **11** was formed, which reacted with the same electrophiles to give cyclic products **12** (Scheme 5)[48].

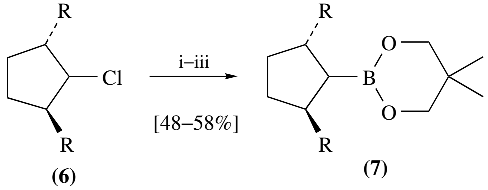

[R = Me, Ph]

SCHEME 4. Reagents: (i) Li, DTBB (10%), THF, −78 °C; (ii) $B(OEt)_3$, −78 to 25 °C; (iii) $HOCH_2CMe_2CH_2OH$, THF, 25 °C

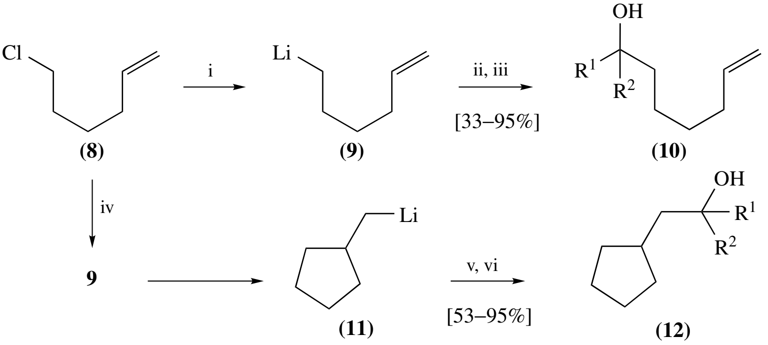

[R^1 = H, Me, Et; R^2 = Et, *t*-Bu, Ph; $R^1R^2 = (CH_2)_5$]

SCHEME 5. Reagents: (i) Li, DTBB (5%), THF, −78 °C; (ii) E = *t*-BuCHO, PhCHO, Et_2CO, *c*-$(CH_2)_5CO$, PhCOMe, −78 °C; (iii) H_2O, −78 to 20 °C; (iv) Li, DTBB (5%), THF, −30 °C; (v) E = *t*-BuCHO, PhCHO, Et_2CO, *c*-$(CH_2)_5CO$, PhCOMe, −30 °C; (vi) H_2O, −30 to 20 °C

Although the lithiation of chlorobenzene did not occur in THF at −78 °C after 4 h, the addition of a catalytic amount of naphthalene (3%) allows this transformation after 45 min under the same reaction conditions[49].

The *in situ* generation of an alkyllithium reagent, from an alkyl chloride **13** and lithium in the presence of a catalytic amount of naphthalene (10%), and its reaction with carboxylic acids **14** allowed a general preparation of ketones **15** in a one-pot procedure (Scheme 6)[50].

$$\underset{\textbf{(13)}}{R^1Cl} \quad + \quad \underset{\textbf{(14)}}{R^2CO_2H} \quad \xrightarrow[\text{[15–75\%]}]{\text{i, ii}} \quad \underset{\textbf{(15)}}{R^1COR^2}$$

[R^1 = Bu, *s*-Bu, *t*-Bu, $Me_2C{=}CH$, Ph
R^2 = *c*-C_3H_5, Pr, $Me_2C{=}CH$, (*E,E*)-$MeCH{=}CHCH{=}CH$, Ph, (*E*)-$PhCH{=}CH$]

SCHEME 6. Reagents: (i) Li, $C_{10}H_8$ (10%), THF, 0 °C; (ii) H_2O

Finally, the lithiation of a soluble chloromethylated polystyrene **16** (prepared by AIBN-induced copolymerization of styrene and 4-chloromethylstyrene in a 3:1 molar ratio) with lithium and a catalytic amount of DTBB (10%) in THF at −78 °C gave the expected

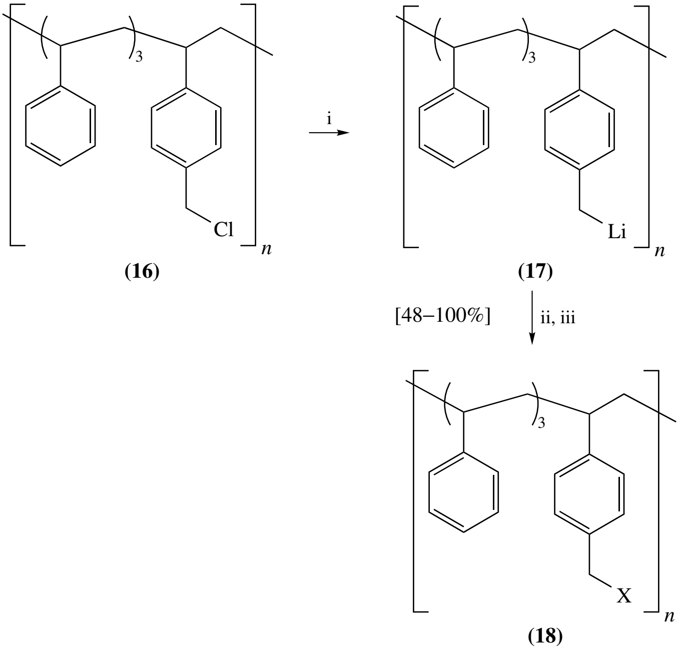

[X = H, D, *t*-BuCHOH, PhCHOH, Et_2COH, *c*-$(CH_2)_5COH$, Me_3Si]

SCHEME 7. Reagents: (i) Li, DTBB (10%), THF, −78 °C; (ii) E = H_2O, D_2O, *t*-BuCHO, PhCHO, Et_2CO, *c*-$(CH_2)_5CO$, Me_3SiCl, −78 °C; (iii) H_2O, −78 to 20 °C

lithiated polymer **17**, which by reaction with different electrophiles afforded the expected functionalized polymers **18** (Scheme 7)[51].

IV. ORGANOLITHIUMS FROM ACYCLIC NONHALOGENATED MATERIALS

Although organolithium compounds are commonly prepared by a halogen (iodine, bromine or chlorine)–lithium exchange[36–40], other methodologies involving different starting materials could be of synthetic interest[52].

A. Carbon–Carbon Bond Cleavage

As expected, only few examples involving carbon–carbon bond cleavage have been described in the literature. Namely, only nitriles and *N*-methoxycarboxamides undergo a reductive carbon–carbon bond cleavage by lithiation under arene-catalyzed conditions.

1. Nitriles

Aliphatic and aromatic nitriles **19** were decyanated with lithium and a catalytic amount (5%) of DTBB in the presence of different carbonyl compounds as electrophiles

$$\underset{\mathbf{(19)}}{\mathrm{RCN}} \xrightarrow[\text{[21–63\%]}]{\text{i, ii}} \underset{\mathbf{(20)}}{\mathrm{RX}}$$

$$\left[\begin{array}{l} \mathrm{R} = \mathrm{Me},\ c\text{-}\mathrm{C_3H_5},\ \mathrm{Ph},\ \mathrm{PhCH_2} \\ \mathrm{X} = i\text{-}\mathrm{PrCHOH},\ n\text{-}\mathrm{C_7H_{15}CHOH},\ \mathrm{Me_2COH},\ \mathrm{Et_2COH},\ c\text{-}\mathrm{(CH_2)_5COH},\ \mathrm{Ph_2COH},\ \mathrm{Me_3Si} \end{array}\right]$$

SCHEME 8. Reagents: (i) Li, DTBB (5%), E = *i*-PrCHO, *n*-$C_7H_{15}CHO$, Me_2CO, Et_2CO, *c*-$(CH_2)_5$ CO, Ph_2CO, Me_3SiCl, THF, −30 or −78 °C; (ii) H_2O, −30 or −70 to 20 °C

(Barbier-type reaction conditions[43,44]) in THF at −30 °C (−78 °C for phenylacetonitrile) yielding, after hydrolysis, the expected compounds **20** (Scheme 8)[53].

2. Carboxamides

An interesting and unprecedented reaction took place when several *N*-methoxyamides **21** were treated with lithium and DTBB (10%) under THF reflux, so after hydrolysis the corresponding alkanes **22** with one less carbon atom were obtained (Scheme 9)[54]. The mechanism for this decarbamoylation process is not known.

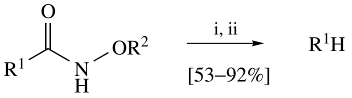

(21) **(22)**

$$\left[\begin{array}{l} \mathrm{R^1} = n\text{-}\mathrm{C_{10}H_{21}},\ \mathrm{EtCHPh},\ 1\text{-adamantyl},\ 4\text{-}\mathrm{MeC_6H_4} \\ \mathrm{R^2} = \mathrm{Me},\ \mathrm{Ph},\ \mathrm{PhCH_2} \end{array}\right]$$

SCHEME 9. Reagents: (i) Li, DTBB (10%), THF reflux; (ii) H_2O

B. Carbon–Fluorine Bond Cleavage

From the lithium chemistry point of view, the carbon–fluorine bond cannot be considered as a carbon–halogen bond because alkyl or aryl fluorides are not adequate starting materials in lithiation processes, due to the fact that this bond is the strongest that carbon can form[55]. On the other hand, a possible reductive defluorination process could be important from an environmental point of view due to the difficult degradation of fluoro derivatives in nature[56,57].

The reaction of different aryl fluorides **23** with lithium and a catalytic amount of naphthalene (7%) in THF at −30 °C afforded a solution of the corresponding aryllithiums **24**, which after treatment with an electrophile (E) and final hydrolysis gave the expected substituted arenes **25** (Scheme 10)[58,59].

$$\underset{\mathbf{(23)}}{\mathrm{ArF}} \xrightarrow{\text{i}} \underset{\mathbf{(24)}}{\mathrm{ArLi}} \xrightarrow[\text{[31–72\%]}]{\text{ii, iii}} \underset{\mathbf{(25)}}{\mathrm{ArX}}$$

$$\left[\begin{array}{l} \mathrm{Ar} = \mathrm{Ph},\ 2\text{-}\mathrm{MeC_6H_4},\ 4\text{-}\mathrm{MeC_6H_4},\ 4\text{-}\mathrm{MeOC_6H_4},\ 4\text{-}\mathrm{FC_6H_4} \\ \mathrm{X} = i\text{-}\mathrm{PrCHOH},\ \mathrm{PhCHOH},\ \mathrm{Et_2COH},\ c\text{-}\mathrm{(CH_2)_5COH},\ \mathrm{PhC(OH)Me},\ \mathrm{Me_3Si} \end{array}\right]$$

SCHEME 10. Reagents: (i) Li, $C_{10}H_8$ (7%), THF, −30 °C; (ii) E = *i*-PrCHO, PhCHO, Et_2CO, *c*-$(CH_2)_5CO$, PhCOMe, Me_3SiCl, −30 to 0 °C; (iii) H_2O

The naphthalene-catalyzed lithiation of aromatic fluoro compounds has been extended to allylic and benzylic substrates. Thus, differently substituted benzylic (**26**) or geranyl fluorides (**27**) reacted with lithium and naphthalene (8%) in the presence of different electrophiles in THF at −30 to 0 °C giving, after hydrolysis, the expected compounds **28** and **29**, respectively (Scheme 11)[60]. One interesting feature when geranyl fluoride (**27**) was used as starting material, is that whereas with chlorotrimethylsilane only **29**$\boldsymbol{\alpha}$ was obtained resulting from a α-attack, the same reaction with carbonyl compounds gave **29**$\boldsymbol{\gamma}$ exclusively from the attack at the γ-position. The reaction shown in Scheme 11 has interest because the same process using other halides, mainly chlorides or bromides, gives almost exclusively formation of Wurtz-type products[36–40].

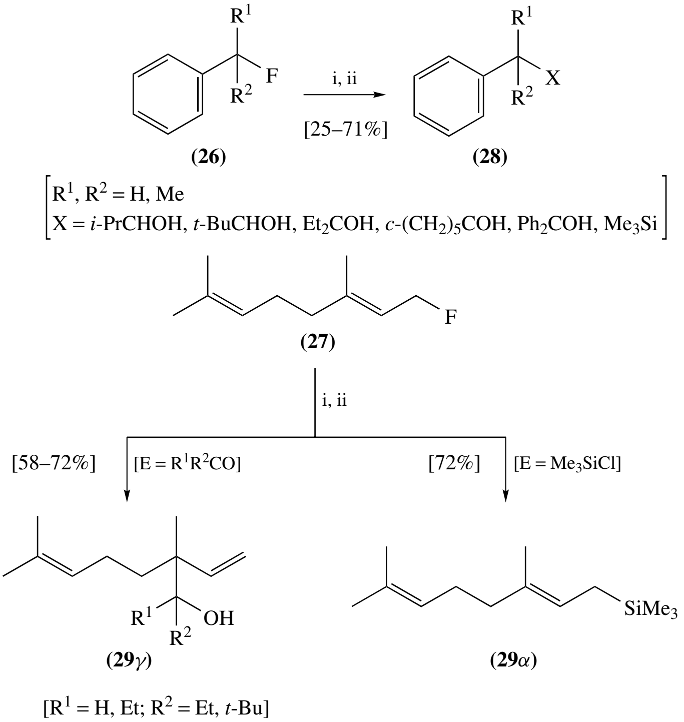

[R^1, R^2 = H, Me
X = i-PrCHOH, t-BuCHOH, Et_2COH, c-$(CH_2)_5COH$, Ph_2COH, Me_3Si]

[R^1 = H, Et; R^2 = Et, t-Bu]

SCHEME 11. Reagents: (i) Li, $C_{10}H_8$ (8%), E = i-PrCHO, t-BuCHO, Et_2CO, c-$(CH_2)_5CO$, Ph_2CO, Me_3SiCl, −30 to 0 °C; (ii) H_2O

C. Carbon–Oxygen Bond Cleavage

Apart from the carbon–halogen bond, the carbon–oxygen one is rather active toward the reductive cleavage due to its polarity, so different types of compounds bearing a carbon–oxygen bond are able to undergo this reaction.

1. Alcohols and their O-silylated derivatives

Allylic and benzylic alcohols (**30** and **31**, respectively) were deprotonated with n-butyllithium at 0 °C followed by lithiation with lithium and DTBB (5%) to give a solution of the corresponding organolithium compound (**32** and **33**, respectively), which after successive treatment with electrophiles and final hydrolysis gave the expected products **34** and **35**, respectively (Scheme 12)[61].

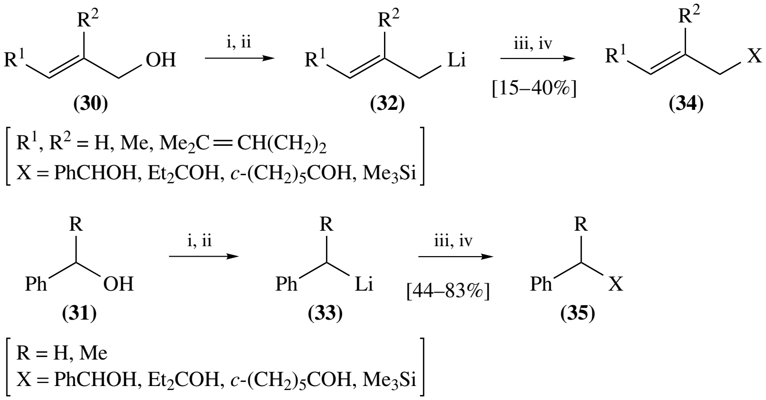

R^1, R^2 = H, Me, $Me_2C{=}CH(CH_2)_2$
X = PhCHOH, Et_2COH, c-$(CH_2)_5COH$, Me_3Si

R = H, Me
X = PhCHOH, Et_2COH, c-$(CH_2)_5COH$, Me_3Si

SCHEME 12. Reagents: (i) *n*-BuLi, THF, 0 °C; (ii) Li, DTBB (5%), 20 °C; (iii) E = PhCHO, Et_2CO, c-$(CH_2)_5CO$, Me_3SiCl, −30 to 20 °C; (iv) H_2O

When the corresponding allylic or benzylic *O*-silyl alcohols **36** and **37** were lithiated at room temperature, it was necessary to work under Barbier-type conditions in order to avoid the decomposition of the *in situ* generated organolithium intermediates (**32** and **33**, respectively). Thus, using these starting materials, **34** and **35** were respectively obtained (Scheme 13)[61]. Also, in the case of geraniol or its *O*-silyl derivatives the same regiochemistry as for geranyl fluoride (**27**) was observed.

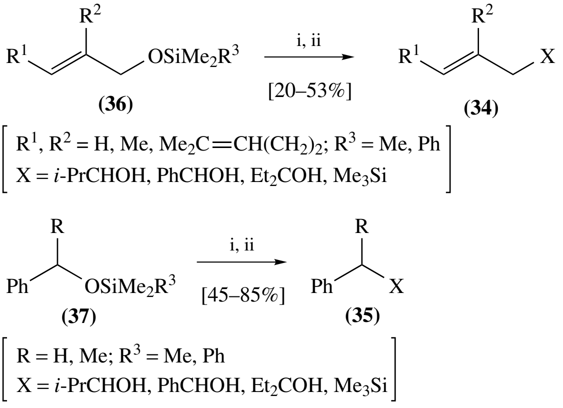

R^1, R^2 = H, Me, $Me_2C{=}CH(CH_2)_2$; R^3 = Me, Ph
X = i-PrCHOH, PhCHOH, Et_2COH, Me_3Si

R = H, Me; R^3 = Me, Ph
X = i-PrCHOH, PhCHOH, Et_2COH, Me_3Si

SCHEME 13. Reagents: (i) Li, DTBB (5%), E = *i*-PrCHO, PhCHO, Et_2CO, c-$(CH_2)_5CO$, Me_3SiCl, 20 °C; (ii) H_2O

The chemistry shown in Scheme 13 has been applied to the synthesis of 5-substituted resorcinols, interesting naturally occurring compounds, which possess a wide variety of biological activity including fungicidal and bactericidal properties[62]. Starting from the protected material **38**, naphthalene-catalyzed lithiation in the presence of adequate aldehydes gave the homobenzylic alcohols **39**. Subsequent dehydroxylation (through the corresponding mesylates for alkyl derivatives or directly by catalytic hydrogenation in the case of the phenyl compound) afforded compounds **40**, which after final deprotection gave products **41–43**. Among them are olivetol (**41**), grevillol (**42**) and dihydropinosilvine (**43**) (Scheme 14)[63].

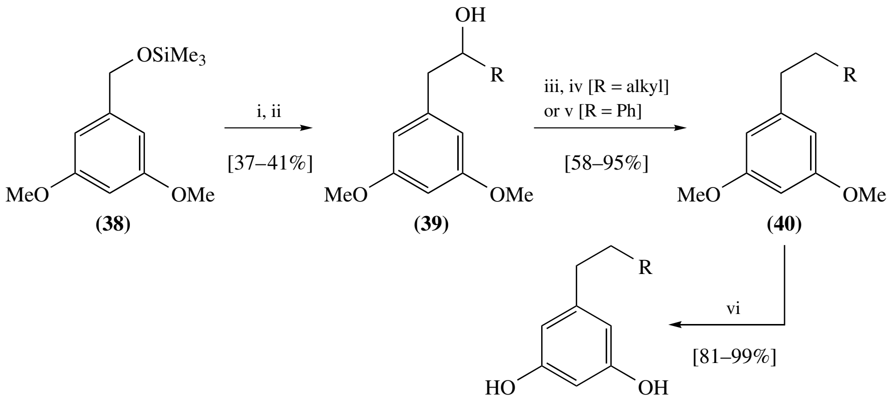

(**41**) R = *n*-Pr : olivetol
(**42**) R = *n*-$C_{11}H_{23}$: grevillol
(**43**) R = Ph : dihydropinosilvine

SCHEME 14. Reagents: (i) Li, $C_{10}H_8$ (4%), RCHO, THF, −30 or 0 °C; (ii) H_2O; (iii) MsCl, Et_3N, 0 °C; (iv) NaI, Zn, glyme; (v) H_2, Pd-C, MeOH–H_2O; (vi) HBr, HOAc reflux

When the dehydration of **39** was carried out (H_3PO_4 or DMSO under reflux) instead of its dehydroxylation, a different class of stilbene derivatives, such as pinosilvine **44**, resveratrol **45** or piceatannol **46**, were easily obtained[63]. From these compounds, resveratrol has shown very potent anticancer properties *in vivo*, this activity being proven in rats[64].

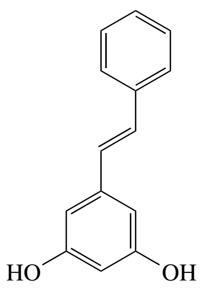

(**44**) pinosilvine

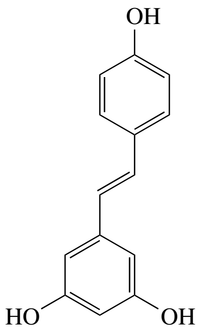

(**45**) resveratrol

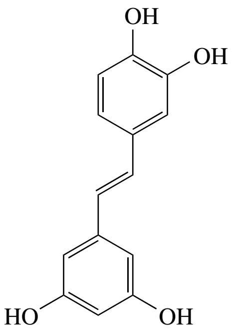

(**46**) piceatannol

2. Ethers

It is well known in the literature that one of the best procedures to prepare allyllithium is the lithiation of allyl phenyl ethers[65]. This reaction can be easily induced when 'a pinch of biphenyl was introduced' at the beginning of the process[66].

For primary alkyl phenyl ethers **47**, their lithiation under catalytic conditions (DTBB, 5%) in THF at room temperature gave the expected alkyllithiums, which by reaction with carbonyl compounds afforded, after hydrolysis, the expected alcohols **48** (Scheme 15)[67]. In this case, only the O$-$C$_{\text{alkyl}}$ bond cleavage was observed[58]. On the other hand, the reaction shown in Scheme 15 failed for secondary (R = *i*-Pr) or tertiary (R = *t*-Bu) starting materials.

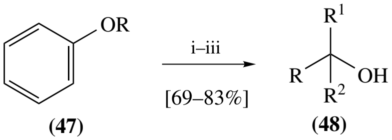

[R = Me, Et
R^1 = H, Me; R^2 = Ph]

SCHEME 15. Reagents: (i) Li, DTBB (5%), THF, 20 °C; (ii) R^1R^2CO = PhCHO, PhCOMe, −40 to 0 °C; (iii) H_2O

Allylic and benzylic ethers can also be cleaved using an arene-catalyzed lithiation, so the corresponding organolithium intermediates could be generated. Thus, different benzylic ethers **49** were lithiated using a catalytic amount of naphthalene (5%) to yield the expected intermediates **50**, which after reaction with electrophiles and final hydrolysis gave products **51** (Scheme 16)[68].

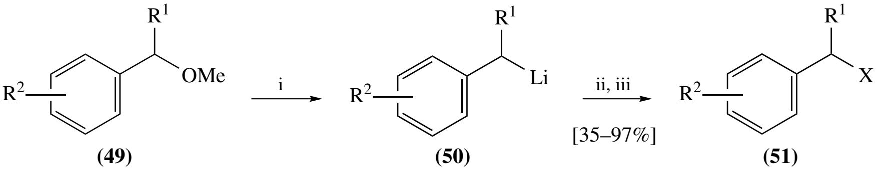

[R^1 = H, Me; R^2 = 4-Me, 2-MeO, 3-MeO, 4-MeO, 4-F, 4-Me_2N, 3, 5-$(MeO)_2$
X = D, Me, *t*-BuCHOH, PhCHOH]

SCHEME 16. Reagents: (i) Li, $C_{10}H_8$ (5%), THF, −78 to −10 °C; (ii) E = D_2O, MeI, *t*-BuCHO, PhCHO; (iii) H_2O

A similar process can be efficiently used for the deallylation or debenzylation of the corresponding ethers **52** and **53**, just using water as the quenching reagent after the lithiation process. Some examples giving alcohols or phenols **54** are included in Scheme 17[69].

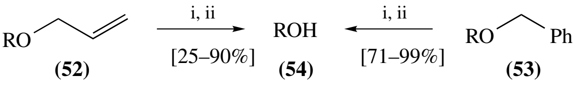

[R = geranyl, menthyl, *n*-$C_{22}H_{45}$, Ph]

SCHEME 17. Reagents: (i) Li, $C_{10}H_8$ (4%), THF, −78 to 20 °C; (ii) H_2O

3. Carboxylates and carbonates

Nonenolizable benzylic carboxylates, such as pivalates **55**, were lithiated in the presence of a catalytic amount of naphthalene (10%) and the electrophile, to yield, after hydrolysis, the expected products **20**. The application of the same reaction to different allylic or benzylic carbonates **56** yielded the same type of products **20** (Scheme 18)[70].

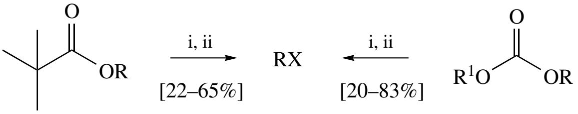

(55) **(20)** **(56)**

R = $CH_2CH{=}CH_2$, geranyl, $PhCH_2$, PhCHMe
R^1 = *t*-Bu, $CH_2CH{=}CH_2$, $PhCH_2$, PhCHMe
X = *i*-PrCHOH, *t*-BuCHOH, PhCHOH, Me_2COH, Et_2COH, *c*-$(CH_2)_5COH$, Ph_2COH, Me_3Si

SCHEME 18. Reagents: (i) Li, $C_{10}H_8$ (10%), E = *i*-PrCHO, *t*-BuCHO, PhCHO, Me_2CO, Et_2CO, *c*-$(CH_2)_5CO$, Ph_2CO, Me_3SiCl, THF, −78 to 20 °C; (ii) H_2O

4. Carbamates

N,*N*-Diisopropyl *O*-benzylic carbamates **57** gave after naphthalene-catalyzed (10%) lithiation, as described in Scheme 18 (Barbier conditions), and final hydrolysis the corresponding products **20** containing the benzylic moiety (Scheme 19)[70].

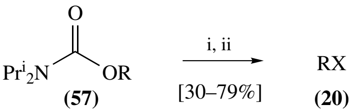

(57) **(20)**

R = $PhCH_2$, PhCHMe
X = *t*-BuCHOH, Et_2COH

SCHEME 19. Reagents: (i) Li, $C_{10}H_8$ (10%), E = *t*-BuCHO, Et_2CO, THF, −78 or −30 °C; (ii) H_2O, −78 or −30 to 20 °C

5. Mesylates

Allylic, methallylic and benzylic mesylates **58** are adequate starting materials to generate the corresponding organolithium intermediates by an arene-catalyzed (4%) lithiation. The reaction can be carried out either under Barbier-type reaction conditions at 0 °C or in a two-step process, performing the lithiation at −78 °C followed by reaction with the electrophile at temperatures ranging from −78 to 20 °C, to furnish **20** (Scheme 20)[71]. This process is of interest, since it represents an indirect way of transforming allylic and benzylic alcohols (precursors of the starting mesylates) into the corresponding organolithium compounds.

6. Triflates

As shown in the last section, the arene-catalyzed lithiation of mesylates has the limitation that it only proceeds for allylic and benzylic substrates. This drawback has been

$$\mathrm{ROSO_2Me} \xrightarrow[\text{or iv, iii}]{\text{i–iii}} \mathrm{RX}$$

(58) [21–80%] **(20)**

$$\left[\begin{array}{l} \mathrm{R = CH_2CH{=}CH_2, CH_2C(Me){=}CH_2, PhCH_2} \\ \mathrm{X = \mathit{i}\text{-}PrCHOH, PhCHOH, Et_2COH, \mathit{c}\text{-}(CH_2)_5COH, Ph_2COH, PhCH_2S} \end{array}\right]$$

SCHEME 20. Reagents: (i) Li, $C_{10}H_8$ (4%), THF, −78 °C; (ii) E = *i*-PrCHO, PhCHO, Et_2CO, *c*-$(CH_2)_5CO$, Ph_2CO, $(PhCH_2S)_2$, −78 to 20 °C; (iii) H_2O; (iv) Li, $C_{10}H_8$ (4%), E = *i*-PrCHO, PhCHO, Et_2CO, *c*-$(CH_2)_5CO$, Ph_2CO, $(PhCH_2S)_2$, THF, 0 °C

overcome using triflates. Thus, aliphatic triflates **59** were lithiated using a catalytic amount of naphthalene (4%) in the presence of different electrophiles at temperatures ranging between −78 and 0 °C to give, after hydrolysis, the expected products **20** (Scheme 21)^{72}. Also in this case, this methodology represents an indirect way for transforming alcohols into alkyllithium intermediates through the corresponding triflates.

$$\mathrm{ROSO_2CF_3} \xrightarrow{\text{i, ii}} \mathrm{RX}$$

(59) [15–91%] **(20)**

$$\left[\begin{array}{l} \mathrm{R = Me, Et, MeC{\equiv}C(CH_2)_2, \mathit{n}\text{-}C_6H_{13}} \\ \mathrm{X = \mathit{t}\text{-}BuCHOH, PhCHOH, 4\text{-}MeOC_6H_4CHOH, \mathit{n}\text{-}C_7H_{15}CHOH, \mathit{c}\text{-}(CH_2)_5COH,} \\ \mathrm{(\mathit{c}\text{-}C_3H_5)_2COH, PhC(OH)Me, 4\text{-}MeC_6H_4C(OH)Ph, PhCHNHPh, \mathit{n}\text{-}C_8H_{17}CO} \end{array}\right]$$

SCHEME 21. Reagents: (i) Li, $C_{10}H_8$ (4%), E = *t*-BuCHO, PhCHO, 4-$MeOC_6H_4CHO$, *n*-C_7H_{15}-CHO, *c*-$(CH_2)_5CO$, (*c*-$C_3H_5)_2CO$, PhCOMe, 4-MeC_6H_4COPh, PhCH=NPh, *n*-$C_8H_{17}CON(CH_2)_4$-*c*, THF, −78 to 0 °C; (ii) H_2O

7. Sulfates

Another possibility of transforming indirectly alcohols into alkyllithium compounds consists in using the corresponding sulfates. Alkyl sulfates **60** were lithiated using naphthalene (4%) as the electron carrier catalyst in THF at −78 °C yielding two equivalents of the corresponding alkyllithium **61**. Further addition of an electrophile at −78 to 0 °C led to the formation, after hydrolysis, of the final products **20** (Scheme 22)^{73,74}.

$$\mathrm{(RO)_2SO_2} \xrightarrow{\text{i}} \mathrm{2\,RLi} \xrightarrow{\text{ii, iii}} \mathrm{2\,RX}$$

(60) **(61)** [15–99%] **(20)**

$$\left[\begin{array}{l} \mathrm{R = Me, Et, \mathit{i}\text{-}Pr, Bu, \mathit{n}\text{-}C_6H_{13}CHMe} \\ \mathrm{X = \mathit{i}\text{-}PrCHOH, PhCHOH, Et_2COH, PrC(OH)Me, \mathit{c}\text{-}(CH_2)_5COH, Ph_2COH, PhCH_2S} \end{array}\right]$$

SCHEME 22. Reagents: (i) Li, $C_{10}H_8$ (4%), THF, −78 °C; (ii) E = *i*-PrCHO, PhCHO, Et_2CO, PrCOMe, *c*-$(CH_2)_5CO$, Ph_2CO, $(PhCH_2S)_2$, −78 to 20 °C; (iii) H_2O

When the reaction shown in Scheme 22 was applied to cyclic 1,2- or 1,3-sulfates, instead of the corresponding 1,2- or 1,3-dilithio compounds, olefins or cyclopropanes were obtained through the corresponding β- or γ-elimination processes, respectively. Actually, the second reaction has been used to prepare substituted cyclopropanes **64** in a

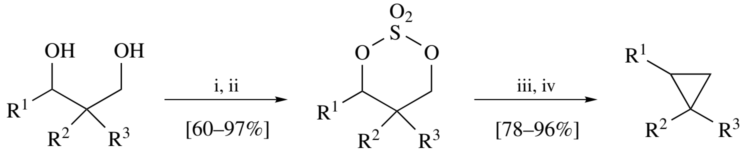

(62) **(63)** **(64)**

[R^1, R^2, R^3 = H, Me, Et, $PhCH_2$, R^1R^2, R^2R^3 = *c*-$(CH_2)_4$]

SCHEME 23. Reagents: (i) $SOCl_2$, CCl_4 reflux; (ii) $NaIO_4$, $RuCl_3$ (0.1%), MeCN–H_2O, 0 to 20 °C; (iii) Li, DTBB (5%), THF, 0 °C; (iv) H_2O

two-step process starting from 1,3-diols **62**, via the cyclic sulfates **63** and through a final DTBB-catalyzed (5%) lithiation (Scheme 23)[75].

8. Phosphates

Alkyl or allyl phosphates **65** were lithiated using DTBB (5%) as catalyst in the presence of an electrophile. The *in situ* generated organolithium reagent reacted with the electrophilic reagent giving, after hydrolysis, the expected products **20** (Scheme 24)[76]. The reaction has the drawback that only one alkyl group is transferred to the electrophile, except in the case of the allyl derivative in which three groups are involved in the process. In addition, for mixed phosphates it was found that the preference of forming the corresponding organolithium intermediate follows the series: allyl = benzyl > primary alkyl ≫ secondary alkyl. The reaction is highly chemoselective.

$$\underset{\textbf{(65)}}{(RO)_3PO} \xrightarrow[\text{[31–90\%]}]{\text{i, ii}} \underset{\textbf{(20)}}{RX}$$

$$\left[\begin{array}{l} R = Et,\ CH_2CH{=}CH_2,\ i\text{-}Pr,\ Bu,\ Ph \\ X = PhCHOH,\ Et_2COH,\ PhC(OH)Et,\ Me_3Si,\ PhMe_2Si \end{array}\right]$$

SCHEME 24. Reagents: (i) Li, DTBB (5%), E = PhCHO, Et_2CO, PhCOEt, Me_3SiCl, $PhMe_2SiCl$, THF, −30 °C; (ii) H_2O, −30 to 20 °C

D. Carbon–Nitrogen Bond Cleavage

Except in two isolated cases, in which *N*,*N*-dimethylaniline was transformed into *N*-methylaniline[58] and *N*-(diphenylmethyl)benzotriazole gave a mixture of products[77] (using biphenyl or DTBB as the electron carrier, respectively), the reductive carbon–nitrogen bond cleavage has always been applied to amides and their derivatives.

1. Carboxamides

The naphthalene-catalyzed (10%) lithiation of *N*-allylic or *N*-benzylic pivalamides **66** in the presence of an electrophile at −78 or 0 °C, respectively, gave, after hydrolysis, the expected products **20** (Scheme 25)[70].

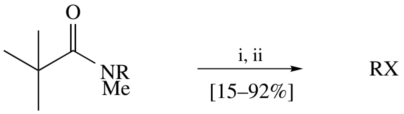

(66) **(20)**

$\left[\begin{array}{l} R = CH_2CH{=}CH_2,\ PhCH_2,\ PhCHMe \\ X = Et_2COH,\ c\text{-}(CH_2)_5COH,\ Me_3Si \end{array}\right]$

SCHEME 25. Reagents: (i) Li, $C_{10}H_8$ (10%), E = Et_2CO, c-$(CH_2)_5CO$, Me_3SiCl, THF, −78 or 0 °C; (ii) H_2O, −78 or 0 to 20 °C

The reaction shown in Scheme 25 has been successfully used to deprotect *N*-benzylic carboxamides using water as the quenching reagent, after the naphthalene-catalyzed lithiation[69].

2. Triflamides

An alternative to the use of pivalamides **66** is the lithiation of triflamides **67** catalyzed by naphthalene (4%) in the presence of different electrophiles at temperatures ranging between −78 and 0 °C, so after hydrolysis the expected products **20** were isolated (Scheme 26)[72].

$$\underset{\textbf{(67)}}{CF_3SO_2NRR^1} \xrightarrow[\text{[25–94\%]}]{\text{i, ii}} \underset{\textbf{(20)}}{RX}$$

$\left[\begin{array}{l} R = CH_2CH{=}CH_2,\ PhCH_2 \\ R^1 = Me,\ CH_2CH{=}CH_2 \\ X = i\text{-}PrCHOH,\ PhCHOH,\ Et_2COH,\ c\text{-}(CH_2)_5COH \end{array}\right]$

SCHEME 26. Reagents: (i) Li, $C_{10}H_8$ (4%), E = i-PrCHO, PhCHO, Et_2CO, c-$(CH_2)_5CO$, THF, −78 to 0 °C; (ii) H_2O

3. Carbamates

O-tert-Butyl *N*-benzyl carbamates **68** are adequate precursors to generate *in situ* the corresponding benzylic organolithium compounds, which by reaction with the electrophile present in the reaction medium gave, after final hydrolysis, the expected products **35** (Scheme 27)[70].

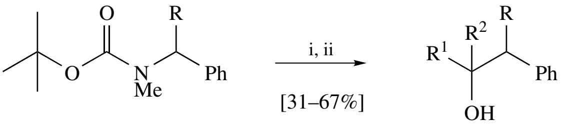

(68) **(35)**

$\left[\begin{array}{l} R = H,\ Me \\ R^1,\ R^2 = H,\ Et,\ t\text{-}Bu \end{array}\right]$

SCHEME 27. Reagents: (i) Li, $C_{10}H_8$ (10%), E = t-BuCHO, Et_2CO, THF, −78 or −30 °C; (ii) H_2O, −78 or −30 to 20 °C

4. Ureas

The application of the naphthalene-catalyzed (10%) lithiation to benzylic ureas **69** under Barbier-type conditions in THF at −78 or −30 °C led to the formation of the expected products **35**, after hydrolysis (Scheme 28)[70].

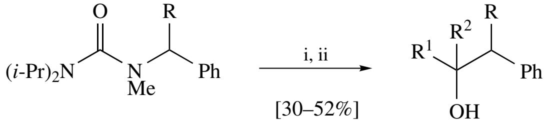

(69) **(35)**

$\left[\begin{array}{l}R = H, Me \\ R^1, R^2 = H, Et, t\text{-}Bu\end{array}\right]$

SCHEME 28. Reagents: (i) Li, $C_{10}H_8$ (10%), E = t-BuCHO, Et_2CO, THF, −78 or −30 °C; (ii) H_2O, −78 or −30 to 20 °C

E. Carbon–Sulfur Bond Cleavage

Although the most important reaction of reductive carbon–sulfur bond cleavage involves alkyl phenyl thioethers, arene-catalyzed lithiation has also been studied using other sulfur-containing compounds, such as thiols, disulfides, sulfoxides and sulfones.

1. Thiols

Benzyl thiol **70** was deprotonated using *n*-butyllithium in THF at room temperature, lithiated with DTBB (5%) at 0 °C to give the benzyllithium **71** and then treated with electrophiles at temperatures ranging between −30 and 0 °C. Final hydrolysis afforded the expected products **72** (Scheme 29)[78]. The reaction applied to allyl mercaptan failed, giving an intractable mixture of products.

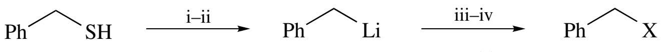

(70) **(71)** **(72)**

[X = t-BuCHOH, PhCHOH, Et_2COH, c-$(CH_2)_5COH$, Me_3Si]

SCHEME 29. Reagents: (i) *n*-BuLi, THF, 20 °C; (ii) Li, DTBB (5%), THF, 0 °C; (iii) E = t-BuCHO, PhCHO, Et_2CO, c-$(CH_2)_5CO$, Me_3SiCl, THF, −30 to 0 °C; (iv) H_2O

2. Thioethers

The classical preparation of alkyllithium compounds by reductive cleavage of alkyl phenyl sulfides with lithium naphthalene (stoichiometric version)[79,80] was also carried out with the same electron carrier but under catalytic conditions (1–8%)[81]. When secondary alkyl phenyl sulfides **73** were allowed to react with lithium and a catalytic amount of naphthalene (8%) in THF at −40 °C, secondary alkyllithium intermediates **74** were formed, which finally reacted successively with carbon dioxide and water, giving the expected carboxylic acids **75** (Scheme 30)[80].

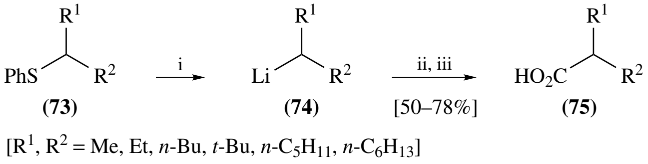

SCHEME 30. Reagents: (i) Li, $C_{10}H_8$ (8%), THF, −40 °C; (ii) CO_2, Et_2O, −78 to 20 °C; (iii) H_2O

The generation of an alkyllithium mediated by an arene-catalyzed PhS/Li exchange has been applied to thioethers **76**[82] and **77**[83] using naphthalene and DTBB, respectively, as the electron-transfer catalyst and used in the preparation of polyols.

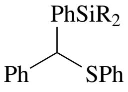

(76)

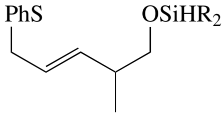

(77)

3. Disulfides

Digeranyl and dibenzyl disulfides **78** were lithiated under DTBB catalysis (5%) in THF at 0 °C to yield to the corresponding organolithium compounds. Reaction with electrophiles at −30 to 0 °C and final hydrolysis afforded the expected products **20** (Scheme 31)[78].

$$\underset{\textbf{(78)}}{\mathrm{RSSR}} \xrightarrow[\text{[23–48\%]}]{\text{i–iii}} \underset{\textbf{(20)}}{\mathrm{RX}}$$

$$\left[\begin{array}{l}\mathrm{R = geranyl,\ PhCH_2}\\ \mathrm{X = \mathit{t}\text{-}BuCHOH,\ Et_2COH,\ Me_3Si}\end{array}\right]$$

SCHEME 31. Reagents: (i) Li, DTBB (5%), THF, 0 °C; (ii) E = t-BuCHO, Et_2CO, Me_3SiCl, −30 to 0 °C; (iii) H_2O

4. Sulfoxides

Phenyl sulfoxides **79** were lithiated in the presence of a catalytic amount of naphthalene or DTBB (5–8%) and an electrophile at −78 (naphthalene) or 0 °C (DTBB) to room temperature, to give, after hydrolysis, the expected products **20** (Scheme 32)[84].

$$\underset{\textbf{(79)}}{\mathrm{PhSOR}} \xrightarrow[\text{[14–58\%]}]{\text{i, ii}} \underset{\textbf{(20)}}{\mathrm{RX}}$$

$$\left[\begin{array}{l}\mathrm{R = Me,\ \mathit{i}\text{-}Pr,\ CH_2CH{=}CH_2,\ PhCH_2}\\ \mathrm{X = \mathit{i}\text{-}PrCHOH,\ PhCHOH,\ Et_2COH,\ Ph_2COH}\end{array}\right]$$

SCHEME 32. Reagents: (i) Li, $C_{10}H_8$ or DTBB (5–8%), E = i-PrCHO, PhCHO, Et_2CO, Ph_2CO, THF, −78 or 0 to 20 °C; (ii) H_2O

5. Sulfones

The naphthalene-catalyzed (8%) lithiation of phenyl sulfones **80** under Barbier conditions in THF at temperatures ranging between −78 and 20 °C led, after hydrolysis, to the formation of the corresponding products **20** (Scheme 33)[84, 85].

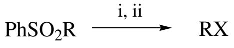

$$PhSO_2R \xrightarrow[\text{[17–61\%]}]{\text{i, ii}} RX$$

(80) **(20)**

R = Et, *i*-Pr, $CH_2CH{=}CH_2$, $PhCH_2$
X = *i*-PrCHOH, PhCHOH, Et_2COH, *c*-$(CH_2)_5COH$, Me_3Si

SCHEME 33. Reagents: (i) Li, $C_{10}H_8$ (8%), E = *i*-PrCHO, PhCHO, Et_2CO, *c*-$(CH_2)_5CO$, Me_3SiCl, THF, −78 to 20 °C; (ii) H_2O

When the reaction shown in Scheme 33 was applied to sulfolene (**81**), instead of generating a possible dilithium intermediate, unexpected cyclic vinyl sulfinates **82** were the only reaction products isolated with low yields (Scheme 34)[84].

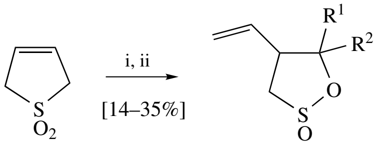

(81) **(82)**

[R^1, R^2 = H, Me, Et, *i*-Pr; R^1R^2 = $(CH_2)_4$, $(CH_2)_5$]

SCHEME 34. Reagents: (i) Li, $C_{10}H_8$ (8%), R^1R^2CO = *i*-PrCHO, Me_2CO, Et_2CO, *c*-$(CH_2)_4CO$, *c*-$(CH_2)_5CO$, THF, −78 to 20 °C; (ii) H_2O

F. Oxygen–Nitrogen Bond Cleavage

The application of arene-catalyzed lithiation to cleave an oxygen–nitrogen bond has only been used with carboxamides and nitrones.

1. Carboxamides

Different alkyl or aryl *N*-methoxy or *N*-phenoxy carboxamides **83** were subjected to the dealkoxylation or dephenoxylation with lithium and a catalytic amount of DTBB (10%) giving, after hydrolysis, the corresponding amides **84** (Scheme 35)[54].

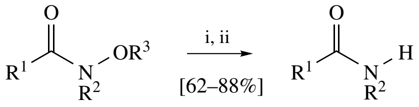

(83) **(84)**

R^1 = *i*-Bu, EtCHPh, 1-adamantyl, 4-MeC_6H_4, *n*-$C_{10}H_{21}$
R^2 = H, Me; R^3 = Me, Ph

SCHEME 35. Reagents: (i) Li, DTBB (10%), THF, 20 °C; (ii) H_2O

2. Nitrones

Treatment of nitrones **85** with lithium and DTBB (10%) in THF at room temperature yielded, after hydrolysis, the corresponding imines **86** (Scheme 36)[86].

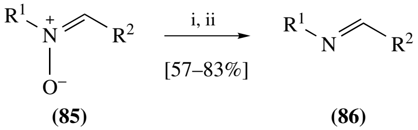

[R^1, R^2 = Pr, *i*-Pr, Bu, *t*-Bu, *n*-C_8H_{17}, Ph; R^1R^2 = $(CH_2)_4$]

SCHEME 36. Reagents: (i) Li, DTBB (10%), THF, 20 °C; (ii) H_2O

G. Nitrogen–Nitrogen Bond Cleavage

The only example of nitrogen–nitrogen bond cleavage promoted by lithium and a catalytic amount of DTBB (10%) in THF at room temperature was performed with alkyl and aryl azides **87**. After hydrolysis, the corresponding primary amides **88** were isolated (Scheme 37)[54].

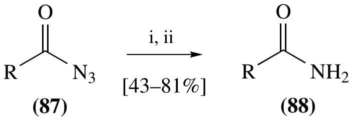

[R = *c*-C_6H_{11}, 1-adamantyl, 4-MeC_6H_4, 4-$MeOC_6H_4$]

SCHEME 37. Reagents: (i) Li, DTBB (10%), THF, 20 °C; (ii) H_2O

H. Nitrogen–Sulfur Bond Cleavage

A wide variety of differently substituted sulfonamides **89** were very easily desulfonylated using lithium and a catalytic amount (4%) of naphthalene in THF at temperatures ranging between −78 °C to room temperature. After hydrolysis, the expected products **90** were isolated (Scheme 38)[69].

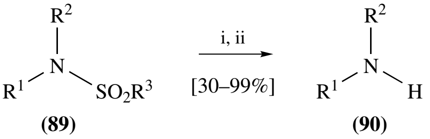

[R^1, R^2 = H, Me, *i*-Pr, *t*-Bu, *n*-C_8H_{17}, *n*-C_6H_{13}CHMe, $PhCH_2$, 2,6-$Me_2C_6H_3$, *t*-BuOCO
R^3 = Me, 4-MeC_6H_4]

SCHEME 38. Reagents: (i) Li, $C_{10}H_8$ (4%), THF, −78 to 20 °C; (ii) H_2O

The methodology shown in Scheme 38 was applied successfully to the desulfonylation of several sulfonamides[87, 88].

V. FUNCTIONALIZED ORGANOLITHIUM COMPOUNDS BY HALOGEN–LITHIUM OR SULFUR–LITHIUM EXCHANGE

Functionalized organolithium compounds[22–25] are interesting intermediates in synthetic organic chemistry because, in their reaction with electrophilic reagents, a transfer of the functionality occurs in only one chemical step, affording polyfunctionalized molecules. In this section, different functionalized organolithium compounds prepared by arene-catalyzed lithiation will be considered, being classified according to the relative position (α, β, ...) of the heteroatom present in the functional moiety and the lithium atom. Actually, this classification correlates perfectly with the nomenclature introduced by Seebach[89] in the development of the umpolung concept: d^n-reagents involving α- (d^1), β- (d^2), γ- (d^3), ... and ω-reagents (d^n).

A. α-Functionalized Organolithiums

In this type of intermediates (d^1-reagents), an oxygen or nitrogen atom uses to be at the α-position respect to the metal. They will be classified here according to this consideration.

1. Acyllithiums

Acyl anions[90] having umpolung reactivity[89] are able to transfer the acyl functionality to electrophiles, so making possible the preparation of functionalized carbonyl compounds in a direct manner.

The naphthalene-catalyzed (3%) lithiation of carbamoyl or thiocarbamoyl chlorides **91** in the presence of carbonyl compounds or imines as electrophiles in THF at temperatures ranging between −78 to 20 °C led to the expected functionalized amides or thioamides **92** after hydrolysis (Scheme 39)[91, 92].

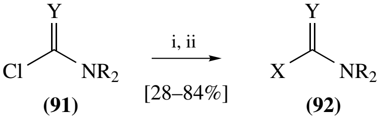

(91) **(92)**

Y = O, S; R = Me, $CH_2CH{=}CH_2$, *i*-Pr
X = EtCHOH, *i*-PrCHOH, BuCHOH, *i*-BuCHOH, *t*-BuCHOH, PhCHOH, 4-$MeOC_6H_4$CHOH, Me_2COH, *c*-$(CH_2)_5$COH, *i*-BuC(OH)Me, PhC(OH)Me, PhCHNHPh

SCHEME 39. Reagents: (i) Li, $C_{10}H_8$ (3%), E = EtCHO, *i*-PrCHO, BuCHO, *i*-BuCHO, *t*-BuCHO, PhCHO, 4-$MeOC_6H_4$CHO, Me_2CO, *c*-$(CH_2)_5$CO, *i*-BuCOMe, PhCOMe, PhCH=NPh, THF, −78 to 20 °C; (ii) H_2O

The reaction shown in Scheme 39 was also performed starting from a chiral carbamoyl chloride (**91**, Y = O) derived from (*R*)-*N*-methyl-*N*-(1-phenylethyl)amine, in order to study the possible asymmetric induction using prochiral carbonyl compounds. Thus, with pivalaldehyde or benzaldehyde the mixture of diastereomers obtained was *ca* 1:1. This behavior was also observed with other chiral functionalized organolithium compounds[22–25].

Another type of acyllithium synthons was generated *in situ* from chloroimines. The naphthalene-catalyzed (4%) lithiation of chloroimines **93** in THF at −78 °C was followed by filtration of the excess of lithium, being then treated with an electrophile and finally hydrolyzed, to yield functionalized imines **94** (Scheme 40)[93, 94].

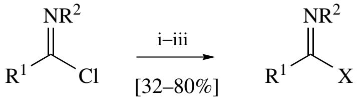

(93) **(94)**

R^1 = t-Bu, n-C_6H_{13}, c-C_6H_{11}
R^2 = n-C_8H_{17}, 2,6-$Me_2C_6H_3$
X = i-PrCHOH, t-BuCHOH, n-C_5H_{11}CHOH, PhCHOH, Et_2COH,
c-$(CH_2)_5$COH, CO_2Et, CSOMe, n-C_7H_{15}CO, 1/2$[CH_2O(CH_2)_2OCO]_2$

SCHEME 40. Reagents: (i) Li, $C_{10}H_8$ (4%), THF, −78 °C, then filtration; (ii) E = i-PrCHO, t-BuCHO, n-C_5H_{11}CHO, PhCHO, Et_2CO, c-$(CH_2)_5$CO, EtOCOCl, MeOCSCl, n-C_7H_{15}CON-(Me)OMe, $[CH_2O(CH_2)_2OCOCl]_2$, −78 to 20 °C; (iii) H_2O

When the excess of lithium was not filtered off, an over-reduction took place giving functionalized amines **95** in moderated yields (10–45%)[94].

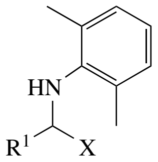

(95)

R^1 = t-Bu, c-C_6H_{11}
X = t-BuCHOH, PhCHOH, Et_2COH, c-$(CH_2)_5$COH,
PhC(OH)Me, CO_2Et, menthyloxycarbonyl

Finally, products **94** can be easily transformed into the corresponding functionalized ketones **96** (by hydrolysis with 2 M HCl in THF at 20 °C) or 1,2-aminoalcohols **97** (by reduction of hydroxyimines **94** with LiAlH$_4$ in THF at 20 °C) in 31–95% or 70–90%, respectively.

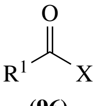

(96)

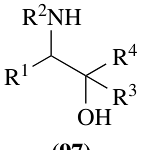

(97)

R^1 = t-Bu
X = i-PrCHOH, t-BuCHOH, PhCHOH,
n-C_7H_{15}, c-$(CH_2)_5$COH

R^1 = t-Bu, c-C_6H_{11}
R^2 = n-C_8H_{17}, 2, 6-$Me_2C_6H_3$
R^3, R^4 = H, i-Pr, t-Bu, n-C_5H_{11}, Ph

2. Oxygenated intermediates

These compounds, also called 'carbenoids' for their tendency to decompose via an α-elimination into carbenes, have been prepared by a chlorine–lithium or sulfur–lithium exchange catalyzed by an arene.

Chloromethyl ethyl ether **98** was lithiated in the presence of a catalytic amount of DTBB (5%) and an electrophile in THF at 0 °C, to give after hydrolysis the expected functionalized ethers **99** (Scheme 41)[95, 96]. Alternatively, the same process can be carried out in a two-step reaction, but performing the lithiation at −90 °C in order to avoid the decomposition of α-ethoxymethyllithium **100** followed by the introduction of the electrophile.

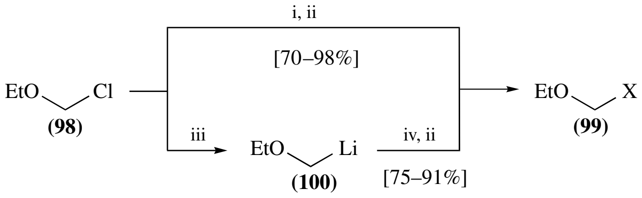

[X = BuCHOH, *t*-BuCHOH, PhCHOH, *i*-Pr$_2$COH, *t*-Bu$_2$COH, *c*-(CH$_2$)$_4$COH, *c*-(CH$_2$)$_3$CH=CHC(OH), PhC(OH)Me, PhMe$_2$Si, CO$_2$H, PhCO, *c*-C$_6$H$_{11}$NCO, PhCHNHPh]

SCHEME 41. Reagents: (i) Li, DTBB (5%), E = BuCHO, *t*-BuCHO, PhCHO, *i*-Pr$_2$CO, *t*-Bu$_2$CO, *c*-(CH$_2$)$_4$CO, 2-cyclohexenone, PhCOMe, THF, 0 °C; (ii) H$_2$O; (iii) Li, DTBB (5%), THF, −90 °C; (iv) E = BuCHO, *c*-(CH$_2$)$_4$CO, PhCOMe, PhMe$_2$SiCl, CO$_2$, PhCN, PhCONMe$_2$, *c*-C$_6$H$_{11}$NCO, PhCH=NPh, −90 or −90 to −60 °C

Chiral lithiomethyl ethers **101–103** were submitted to the same protocols indicated in Scheme 41 in order to study both the enantiomerically pure compounds (EPC) synthesis[97] using non-prochiral electrophiles, and the possible asymmetric induction with prochiral ones. As described for **91**, Y = O (Scheme 39), no asymmetric induction was detected[98].

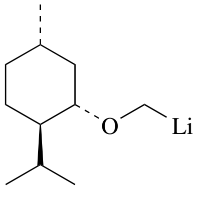

(101)

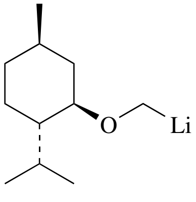

(102)

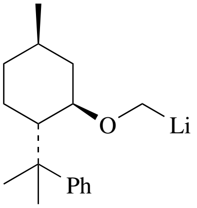

(103)

α-Oxygenated organolithium compounds can also be derived from *O*-chloroalkyl carbamates. The lithiation of chlorocarbamates **104** promoted by a catalytic amount of DTBB (2.5%) and under Barbier conditions (in the presence of the corresponding electrophile) in THF at temperatures ranging between −78 and −60 °C gave, after hydrolysis with water, the expected products **105** (Scheme 42)[99, 100]. The reaction has to be performed under Barbier conditions in order to avoid the decomposition of the intermediates **106**, in spite of their possible stabilization by the so-called CIPE (complex induced proximity effect)[101], which postulates a strong stabilization by intramolecular chelation of the lithium atom.

Easy hydrolysis of hydroxycarbamates of type **105** (resulting from the use of carbonyl compounds as electrophiles) with lithium hydroxide gave diols of type **107** in 81–96% yield.

A different route to α-functionalized organolithium compounds is the naphthalene-catalyzed sulfur–lithium exchange. This reaction was applied to study the configurational

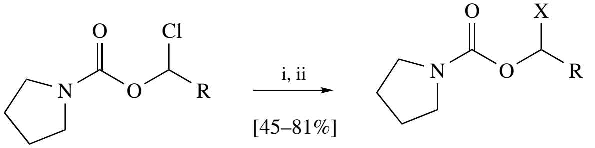

(104) **(105)**

$\left[\begin{array}{l} R = H, Me, c\text{-}C_6H_{11} \\ X = i\text{-BuCHOH}, t\text{-BuCHOH}, PhCHOH, Et_2COH, c\text{-}(CH_2)_5COH, \\ PhC(OH)Me, Ph_2COH, Me_3Si \end{array}\right]$

SCHEME 42. Reagents: (i) Li, DTBB (2.5%), E = *i*-BuCHO, *t*-BuCHO, PhCHO, Et_2CO, *c*-$(CH_2)_5$ CO, PhCOMe, Ph_2CO, Me_3SiCl, THF, −78 or −78 to −60 °C; (ii) H_2O

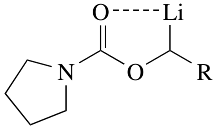

(106)

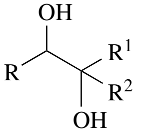

(107)

$\left[\begin{array}{l} R = H, Me, c\text{-}C_6H_{11};\ R^1 = H, Et, Ph \\ R^2 = Me, Et, i\text{-Bu}, t\text{-Bu}, Ph;\ R^1R^2 = (CH_2)_5 \end{array}\right]$

stability of the corresponding intermediates derived from protected 1,3-diols **108**. Their lithiation using a catalytic amount of naphthalene (5%) at −78 °C yielded, after reaction with acetone, the *trans*-product **109**, whereas on allowing the temperature to rise to −20 °C an inversion in the configuration took place to afford the *cis*-product **110** (Scheme 43)[102].

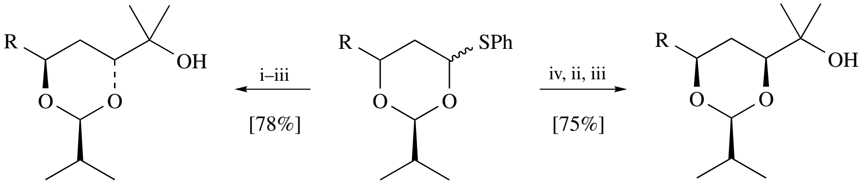

(109) **(108)** **(110)**

[R = *n*-C_6H_{13}]

SCHEME 43. Reagents: (i) Li, $C_{10}H_8$ (5%), THF, −78 °C; (ii) Me_2CO, −78 to 20 °C; (iii) H_2O; (iv) Li, $C_{10}H_8$ (5%), THF, −78 to −20 °C

It seems that the kinetically most stable intermediate organolithium **111**, initially formed, is configurationally unstable and then transformed into the thermodynamically more stable intermediate **112**.

3. Nitrogenated intermediates

The transformation **93** → **94** (Scheme 40) could also be considered in this section, an alternative to this reaction being the arene-catalyzed lithiation of chloro enamines.

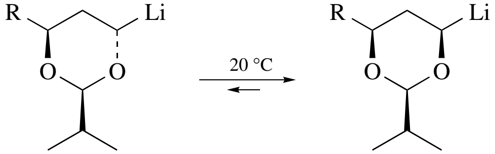

(111) **(112)**

Thus, chloro enamines **113**, either under Barbier-type reaction conditions (−40 °C) or in a two-step process (lithiation at −90 °C and S_E reaction at −90 to −40 °C), were lithiated with DTBB (5%) and finally hydrolyzed, after condensation with different electrophiles, giving the expected functionalized enamines **114** (Scheme 44)[103].

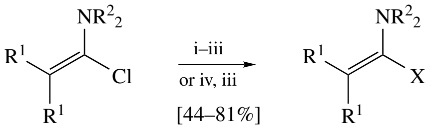

(113) **(114)**

$R^1 = R^2 = Me$; $R^1R^1 = R^2R^2 = (CH_2)_4$
X = D, Me_3Si, *t*-BuCHOH, *n*-C_5H_{11}CHOH, PhCHOH,
PhC(OH)CH=CHPh, CO_2H, *c*-C_6H_{11}NCO

SCHEME 44. Reagents: (i) Li, DTBB (5%), THF, −90 °C; (ii) E = D_2O, Me_3SiCl, PhCOCH=CHPh, CO_2, *c*-C_6H_{11}NCO, −90 to −40 °C; (iii) H_2O, −40 to 20 °C; (iv) Li, DTBB (5%), E = *t*-BuCHO, *n*-C_5H_{11}CHO, PhCHO, THF, −40 °C

Compounds **114** were easily hydrolyzed (2 M HCl) giving the expected products **115** in 27−55% yield.

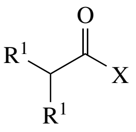

(115)

$R^1 = Me$; $R^1R^1 = (CH_2)_4$
X = *t*-BuCHOH, *n*-C_5H_{11}CHOH, PhCHOH,
PhC(OH)CH=CHPh, CO_2H, *c*-C_6H_{11}NCO

α-Aminated methyllithiums were prepared *in situ* by a DTBB-catalyzed lithiation starting from *N*-chloromethyl carbamates of type **116**. It was also necessary in this case to use the Barbier-type conditions, and then, after final hydrolysis, products **117** were isolated (Scheme 45)[104, 105].

Products **117** derived from carbonyl compounds (E = R^1R^2CO) were easily transformed into the corresponding aminoalcohols **118** under either basic (3 M NaOH) or acidic (HCl, AcOH) conditions.

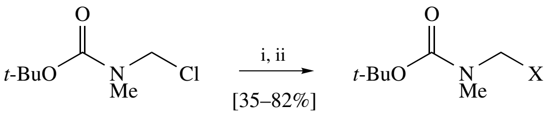

(116) **(117)**

[X = *i*-BuCHOH, *t*-BuCHOH, PhCHOH, 4-$MeOC_6H_4CHOH$, *c*-$(CH_2)_4COH$,
PrC(OH)Me, Et_2COH, $MeC(OH)(CH_2)_2CH{=}CH_2$, PhC(OH)Me, BuC(OH)Ph, Ph_2COH]

SCHEME 45. Reagents: (i) Li, DTBB (2.5%), E = *i*-BuCHO, *t*-BuCHO, PhCHO, 4-$MeOC_6H_4CHO$, *c*-$(CH_2)_4CO$, PrCOMe, Et_2CO, $MeCO(CH_2)_2CH{=}CH_2$, PhCOMe, BuCOPh, Ph_2CO, THF, −78 °C; (ii) H_2O, −78 to 20 °C

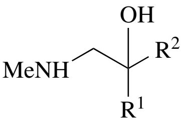

(118)

[R^1, R^2 = H, Me, Et, Pr, $(CH_2)_2CH{=}CH_2$, Bu, *i*-Bu, *t*-Bu, Ph, 4-$MeOC_6H_4$
R^1 R^2 = $(CH_2)_4$]

A different approach to α-aminated organolithium compounds implies a carbon−oxygen bond cleavage promoted by lithium and a catalytic amount of naphthalene (5%). Following this methodology and working in a two-step process in THF at −20 °C, aminoethers **119** gave the corresponding intermediates **120** which, after successive condensation with an electrophile and final hydrolysis with water, afforded the expected products **121** (Scheme 46)[106].

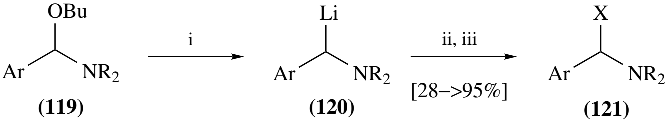

(119) **(120)** **(121)**

[R = Me; RR = $(CH_2)_5$; Ar = Ph, 2-$MeOC_6H_4$
X = H, D, $PhCH_2$, *i*-Pr, Bu, *t*-BuCHOH, Me_2COH]

SCHEME 46. Reagents: (i) Li, $C_{10}H_8$ (5%), THF, −20 °C; (ii) E = H_2O, D_2O, $PhCH_2Cl$, *i*-PrBr, BuBr, *t*-BuCHO, Me_2CO, −20 °C; (iii) H_2O, −20 to 20 °C

The above-mentioned preparation of organolithium compounds by reductive cleavage of phenyl sulfones through an arene-catalyzed lithiation (Section IV.E.5) has been applied to the generation of α-aminated organolithiums. Tosylmethyl amines, amides and urethanes **122** undergo lithiation in the presence of naphthalene (4%) and an electrophile in THF at temperatures ranging between −78 and 0 °C to give, after hydrolysis with water, the expected products **123** (Scheme 47)[107, 108].

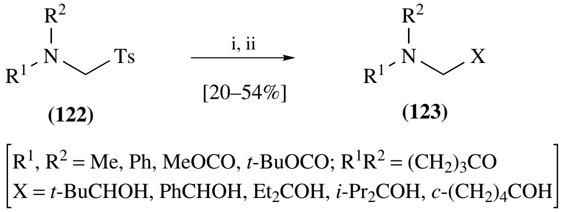

SCHEME 47. Reagents: (i) Li, $C_{10}H_8$ (4%), E = t-BuCHO, PhCHO, Et_2CO, i-Pr_2CO, c-$(CH_2)_4CO$, c-$(CH_2)_5CO$, PhCOMe, Me_3SiCl, THF, −78 to 0 °C; (ii) H_2O

4. Ferrocenyl intermediates

An interesting reaction, which demonstrates that both sulfur−lithium exchange and the further electrophilic substitution reaction (S_E) proceed with retention of configuration, took place on a chiral ferrocenyl derivative. The starting material **124** was lithiated with naphthalene (*ca* 12%) as the electron carrier catalyst in THF at low temperatures (−100 to −78 °C) to give the organolithium intermediate **125** (considered here because the ferrocenyl functionality is at the α-position with regard to the lithium atom). **125** was reacted *in situ* in Barbier-type reaction conditions with acetone or 3-pentanone to give, after methanolysis, the chiral ferrocenyl alcohols **126** with both high diastereo- (up to >96% de) and enantioselectivity (up to 95% ee) (Scheme 48)[109].

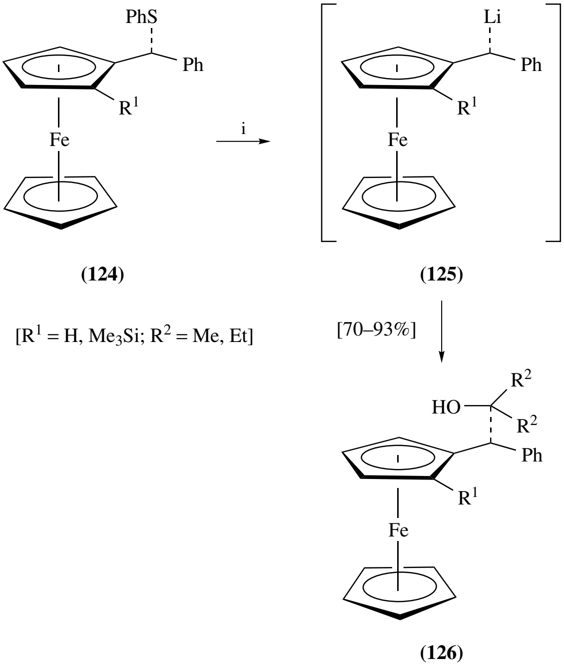

SCHEME 48. Reagents: (i) Li, $C_{10}H_8$ (12%), E = Me_2CO, Et_2CO, THF, −100 or −78 °C, then MeOH, −100 or −78 to 20 °C

B. β-Functionalized Organolithiums

There are many examples of β-amido and β-oxido functionalized organolithium compounds, which were prepared mainly using the stoichiometric version of the arene-promoted lithiation[22–24]. In this section, the preparation of the same type of intermediates by halogen–or sulfur–lithium exchange will be considered, using the catalytic version of the mentioned lithiation.

1. Oxygenated intermediates

Deprotonation of a chlorohydrin followed by chlorine–lithium exchange using the arene-catalyzed lithiation methodology allows the generation of β-oxido functionalized organolithium compounds. The application of this strategy to 1-chloro-2-propanol (**127**) using naphthalene (2%) in THF at −78 °C led to the corresponding intermediate **128**, which by reaction with isobutanal gave, after hydrolysis, the expected diol **129** (Scheme 49)[81]. This chemistry has been applied to prepare the so-called branched-chain functionalized sugars, as exemplified with the chlorohydrin derivative **130**, which after deprotonation with *n*-butyllithium was lithiated under DTBB-catalysis (5%) and reacted with electrophiles giving, after hydrolysis, the corresponding functionalized protected sugars **132** through the β-functionalized intermediate **131** (Scheme 49)[110].

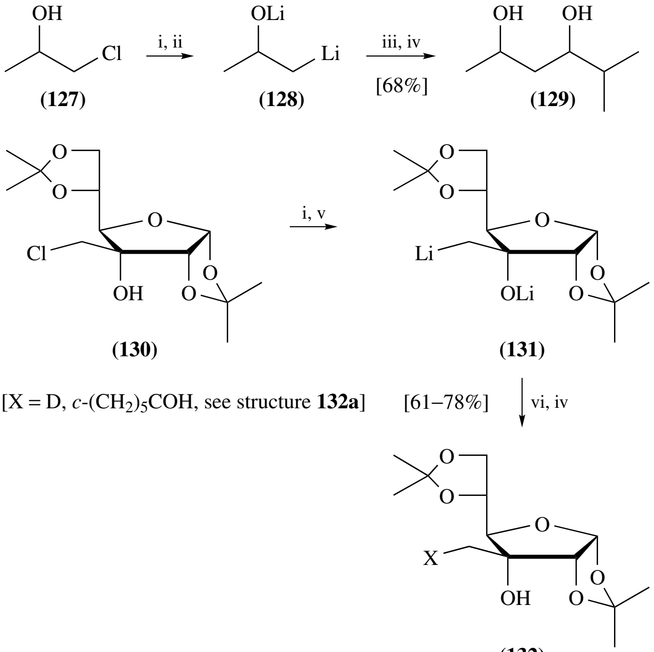

SCHEME 49. Reagents: (i) BuLi, THF, −78 °C; (ii) Li, $C_{10}H_8$ (2%), THF, −78 °C; (iii) *i*-PrCHO, −78 to 20 °C; (iv) H_2O; (v) Li, DTBB (5%), THF, −78 °C; (vi) E = D_2O, *c*-$(CH_2)_5CO$, ketone **133**, −78 to 0 °C

Among **132**, a methylene-bridged disaccharide **132a** was obtained when the intermediate **131** was allowed to react with ketone **133** (precursor of the starting chlorohydrin **130**).

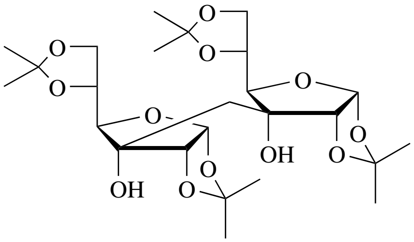

(132a)

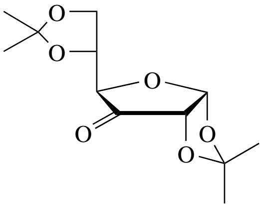

(133)

β-Oxido functionalized organolithium compounds of type **128** or **131** are also accessible by sulfur–lithium exchange using the arene-catalyzed lithiation technology. β-Hydroxyalkyl thioethers **134** reacted successively with *n*-butyllithium and lithium containing a catalytic amount of DTBB (5%), both in THF at −78 °C, to form intermediates **135**, which in a second step were allowed to react with different electrophiles to yield, after final hydrolysis, the expected functionalized alcohols **136** (Scheme 50)[111, 112].

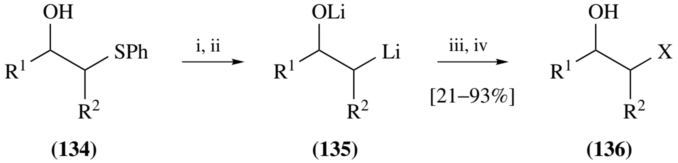

R^1, R^2 = H, Ph, *n*-C_6H_{13}; R^1R^2 = $(CH_2)_4$
X = D, *t*-BuCHOH, PhCHOH, Me_2COH, *c*-$(CH_2)_5COH$

SCHEME 50. Reagents: (i) BuLi, THF, −78 °C; (ii) Li, DTBB (5%), THF, −78 °C; (iii) E = D_2O, *t*-BuCHO, PhCHO, Me_2CO, *c*-$(CH_2)_5CO$, −78 to 20 °C; (iv) H_2O

The preparation of β-oxygenated organolithium compounds having a neutral functionality at the β-position is problematic, due to the very easy decomposition of these compounds through a β-elimination process. However, in special cases, for instance when the double bond has to be formed giving an allene in a five- or six-membered ring, it is possible to prepare such intermediates by an arene-catalyzed lithiation. Reaction of unsaturated chloroethers **137** with lithium and naphthalene (4%) in THF at −78 °C led to the formation of intermediate **138** which, instead of suffering a β-elimination process, reacted with different electrophiles at the same temperature to give, after final hydrolysis with water, the expected compounds **139** (Scheme 51)[113].

A similar situation takes place when an unsaturated chlorinated ketal is used as starting material. When the β-chloro unsaturated ketal **140** (R = H) was submitted to a DTBB-catalyzed (5%) lithiation in THF at −78 °C, the corresponding lithium intermediate **141** was generated, which after reaction with different electrophiles at the same temperature gave, after hydrolysis, the expected products **142** (Scheme 52)[114].

The use of a chiral starting material (**140**, R = Me) and a prochiral electrophile, such as pivalaldehyde, gave a *ca* 1:1 mixture of diastereomers. On the other hand, careful hydrolysis of compounds **142** (aqueous oxalic acid, silica gel) afforded the corresponding functionalized α, β-unsaturated cyclohexenones **143** in >95% yield.

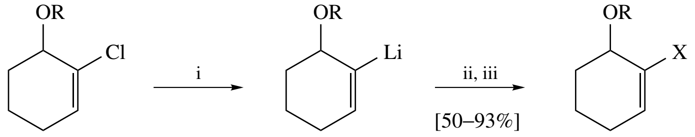

(137) **(138)** **(139)**

R = Me, $EtOCH_2O$
X = H, *t*-BuCHOH, PhCHOH, Et_2COH, *c*-$(CH_2)_4COH$, *c*-$(CH_2)_5COH$,
PhC(OH)Me, PhCHNHPh

SCHEME 51. Reagents: (i) Li, $C_{10}H_8$ (4%), THF, −78 °C; (ii) E = H_2O, *t*-BuCHO, PhCHO, Et_2CO, and *c*-$(CH_2)_4CO$, *c*-$(CH_2)_5CO$, PhCOMe, PhCH=NPh, −78 °C; (iii) H_2O, −78 to 20 °C

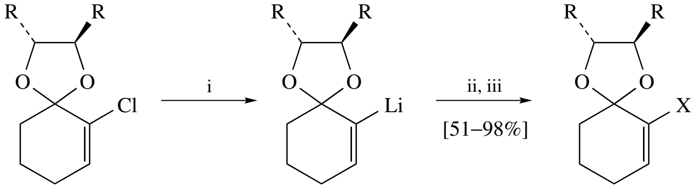

(140) **(141)** **(142)**

R = H, Me
X = *t*-BuCHOH, Me_2COH, *c*-$(CH_2)_4COH$, Me_3Si

SCHEME 52. Reagents: (i) Li, DTBB (5%), THF, −78 °C; (ii) E = *t*-BuCHO, Me_2CO, *c*-$(CH_2)_4CO$, Me_3SiCl, −78 °C; (iii) H_2O, −78 to 20 °C

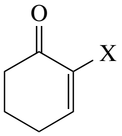

(143)

[X = *t*-BuCHOH, Me_2COH, *c*-$(CH_2)_4COH$]

Using a similar strategy, the chloro ketene ketal **144** was lithiated with a catalytic amount of DTBB (10%) in THF at −20 °C to give the corresponding intermediate **145**, which by reaction with carbonyl compounds and final hydrolysis gave different compounds depending on the reaction conditions: whereas under basic conditions hydroxy esters **147** were obtained, by acidic work-up unsaturated esters **148** were the isolated products, in both cases through intermediates **146** (Scheme 53)[115]. This methodology has been used to prepare precursors of vitamin A employing β-cyclocitral as electrophile.

Another type of sp^2-hybridized β-oxido functionalized organolithium compounds has been easily prepared from chloroacetic acid (**149**). After a double deprotonation with lithium diisopropylamide in THF at −78 °C, a DTBB catalyzed (5%) lithiation in the presence of different carbonyl compounds as electrophiles at the same temperature followed by final hydrolysis afforded the expected β-hydroxy acids **151**. The corresponding intermediate **150** was probably involved in the process (Scheme 54)[116].

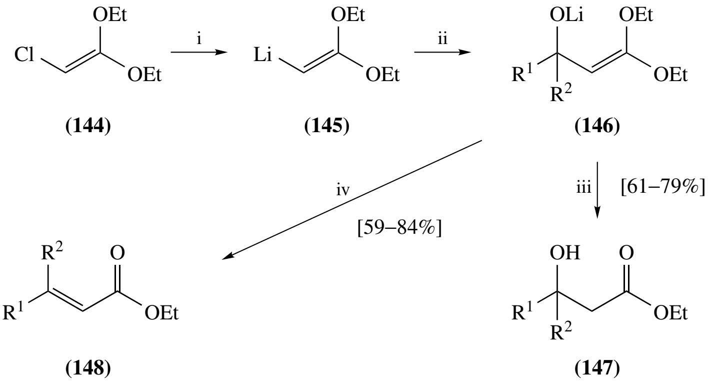

[R^1, R^2 = H, Me, *i*-Bu, Ph
$R^1R^2 = (CH_2)_4$, $(CH_2)_5$,$(CH_2)_2CH{=}CHCOH$,
$(CH_2)_3CH{=}CHCOH$, $[Me_2C(CH_2)_3CMe{=}C]CH{=}CHC(OH)Me$]

SCHEME 53. Reagents: (i) Li, DTBB (10%), THF, −20 °C; (ii) R^1R^2CO = *i*-BuCHO, PhCHO, PhCOMe, and *c*-$(CH_2)_4CO$, *c*-$(CH_2)_5CO$, cyclopentenone, cyclohexenone, *β*-ionone, −20 °C; (iii) H_2O, −20 to 20 °C; (iv) 1 M HCl

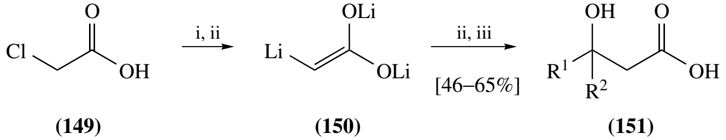

[R^1, R^2 = H, Me, Et, *t*-Bu, Ph; $R^1R^2 = (CH_2)_5$]

SCHEME 54. Reagents: (i) 2 LDA, THF, −78 °C; (ii) Li, DTBB (5%), R^1R^2CO = *t*-BuCHO, PhCHO, Et_2CO, *c*-$(CH_2)_5CO$, PhCOMe, −78 °C; (iii) H_2O, −78 to 20 °C

A naphthalene-catalyzed (<10%) lithiation of *α*,*α*-dibromo esters **152** in THF at −78 °C was used to generate ester dianions **153**, which by warming at 0 °C gave lithium ynolates **154**. These intermediates were trapped by carbonyl compounds, for instance benzophenone, to give, after final hydrolysis with water, *α*,*β*-unsaturated acids **155** (Scheme 55)[117, 118].

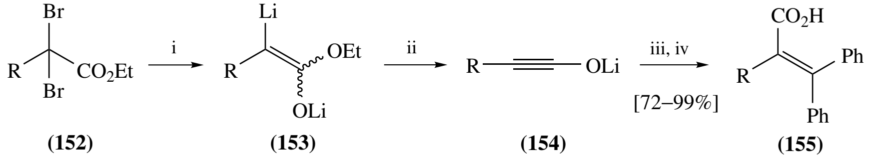

[R = Me, *i*-Pr, Bu, *t*-Bu, Ph, $Ph(CH_2)_2$]

SCHEME 55. Reagents: (i) Li, $C_{10}H_8$ (<10%), THF, −78 °C; (ii) −78 to 0 °C; (iii) Ph_2CO, 20 °C; (iv) H_2O

2. Nitrogenated intermediates

Chiral chloramines **156** (or their enantiomers *ent*-**156**) cannot be lithiated under catalytic conditions because the amide moiety does not survive this potent reductive mixture. In this case, the stoichiometric version should be employed[119, 120].

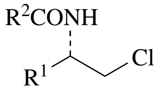

(156)

[R^1, R^2 = Et, *i*-Pr, Ph]

However, either for aliphatic or aromatic amines, the corresponding β-phenylthio derivatives are adequate precursors in order to generate β-amido organolithium intermediates. Starting materials **157** were successively treated with *n*-butyllithium and lithium in the presence of a catalytic amount of DTBB (15%) in THF at −78 °C giving the expected functionalized organolithium intermediates **158**, which reacted with different electrophiles to afford, after hydrolysis, the corresponding products **159** (Scheme 56)[111, 112].

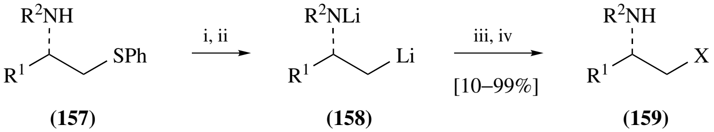

R^1, R^2 = H, *i*-Pr, Ph
X = D, *t*-BuCHOH, PhCHOH, Me_2COH, *c*-$(CH_2)_5COH$

SCHEME 56. Reagents: (i) *n*-BuLi, THF, −78 °C; (ii) Li, DTBB (5%), THF, −78 °C; (iii) E = D_2O, *t*-BuCHO, PhCHO, Me_2CO, *c*-$(CH_2)_5CO$, −78 to 20 °C; (iv) H_2O

C. γ-Functionalized Organolithiums

γ-Functionalized organolithium intermediates (d^3-reagents) are appropriate reagents to introduce functionalized three-carbon atoms into electrophiles. They can be easily prepared by an arene-catalyzed lithiation and can bear an oxygen-, nitrogen- or sulfur-containing functionality.

1. Oxygenated intermediates

The γ-chloro alcohol **160** was lithiated, after deprotonation with a *n*-butyllithium in THF at −78 °C, using lithium and a catalytic amount of naphthalene (1%) at the same temperature to give the corresponding intermediate **161**, which was quenched with water, yielding 1-phenylpropanol (**162**) (Scheme 57)[81].

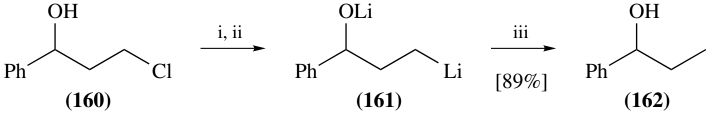

SCHEME 57. Reagents: (i) *n*-BuLi, THF −78 °C; (ii) Li, $C_{10}H_8$ (1%), THF, −78 °C; (iii) H_2O, −78 to 20 °C

Functionalized methallyl chlorides containing an ether functionality **163** were lithiated using catalytic conditions with naphthalene (8%) in the presence of a carbonyl compound as electrophile, to give different reaction products depending on the nature of the group attached to the oxygen: whereas the *n*-butyl derivative kept this group in the final product **164**, in the case of the benzyl derivative a deprotection occurred[69] giving functionalized allyl alcohols **165** (Scheme 58)[121].

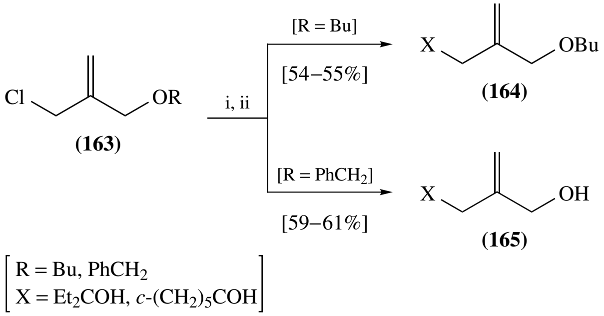

SCHEME 58. Reagents: (i) Li, $C_{10}H_8$ (8%), E = Et_2CO, *c*-$(CH_2)_5CO$, THF, −78 °C; (ii) H_2O, −78 to 20 °C

sp^2-Hydridized γ-phenoxy functionalized organolithium intermediates were generated *in situ* through an arene-catalyzed lithiation. Thus, the chlorinated allyl ether **166** was lithiated in the presence of DTBB (5%) and an electrophile in THF at −78 °C giving, after hydrolysis with water, the corresponding functionalized ethers **167** (Scheme 59). An interesting feature of this reaction is that the geometry of the starting material is not kept in the final diastereomeric ratio, which depends strongly on the electrophile used giving the (Z)-diastereomer as the major one (1.5:1 to 1:0)[122].

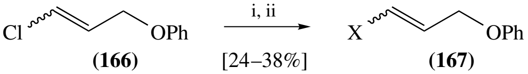

[X = *i*-PrCHOH, *t*-BuCHOH, Et$_2$COH, *c*-(CH$_2$)$_5$COH]

SCHEME 59. Reagents: (i) Li, DTBB (5%), E = *i*-PrCHO, *t*-BuCHO, Et_2CO, *c*-$(CH_2)_5CO$, THF, −78 °C; (ii) H_2O, −78 to 20 °C

γ-Functionalized organolithium compounds having a non-anionic functionality are far more stable than the corresponding β-functionalized ones. This fact reflects that the γ-elimination is not as easy as the β-elimination. When the chlorinated ketals **168** were lithiated with lithium, a catalytic amount of naphthalene (4%) in the presence or not of an electrophile in THF at −78 °C gave, after hydrolysis, the expected products **170** through the corresponding lithiated intermediate **169** (Scheme 60)[123]. In this case, this intermediate is able to transfer a protected diol functionality to the electrophile.

Acyclic and cyclic sp^2-hybridized ketal-containing γ-functionalized organolithium compounds can be generated using an arene-catalyzed lithiation at low temperature. In the case of acyclic precursors **171** (R^2 = H) it was necessary to lower the temperature to −90 °C in the lithiation step under DTBB catalysis (4%) in order to avoid decomposition of intermediates **172**. Final electrophilic substitution reaction of these intermediates with electrophiles occurred with retention of configuration at temperatures ranging between

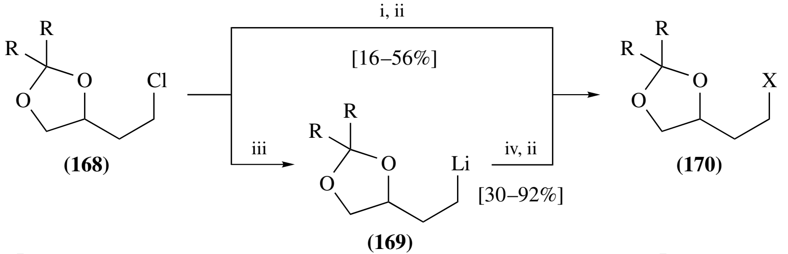

$R = Me; RR = (CH_2)_5$
$X = i\text{-PrCHOH}, t\text{-BuCHOH}, PhCHOH, Me_2COH, Et_2COH, PrC(OH)Me, c\text{-}(CH_2)_5COH, PhC(OH)Me, Me_3Si$

SCHEME 60. Reagents: (i) Li, DTBB (5%), E = *i*-PrCHO, *t*-BuCHO, PhCHO, PrCOMe, *c*-$(CH_2)_5$CO, THF, −78 °C; (ii) H_2O, −78 to 20 °C; (iii) Li, DTBB (4%), THF, −78 °C; (iv) E = *i*-PrCHO, *t*-BuCHO, PhCHO, Me_2CO, Et_2CO, PrCOMe, *c*-$(CH_2)_5$CO, PhCOMe, Me_3SiCl, −78 °C

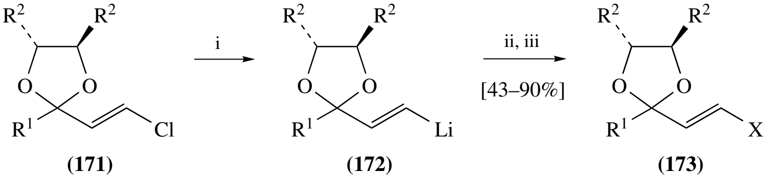

$R^1 = Pr, i\text{-Pr}; R^2 = H, Me$
$X = H, D, t\text{-BuCHOH}, PhCHOH, Me_2COH, c\text{-}(CH_2)_4COH, PhC(OH)Me$

SCHEME 61. Reagents: (i) Li, DTBB (4%), THF, −90 °C; (ii) E = H_2O, D_2O, *t*-BuCHO, PhCHO, Me_2CO, *c*-$(CH_2)_4$CO, PhCOMe, −90 to −60 °C; (iii) H_2O, −60 to 20 °C

−90 and −60 °C giving, after hydrolysis, the *trans*-products **173** (Scheme 61)[114]. The use of chiral precursors **171** (R^2 = Me) yielded a *ca* 1:1 mixture of diastereomers when a prochiral carbonyl compound (pivalaldehyde or benzaldehyde) was used as electrophile.

Careful hydrolysis of compounds **173** (aqueous oxalic acid, silica gel) yielded the corresponding functionalized α,β-unsaturated ketones **174** in >95% yield.

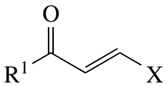

(174)

$R^1 = Pr, i\text{-Pr}$
$X = t\text{-BuCHOH}, PhCHOH, Me_2COH, c\text{-}(CH_2)_4COH, PhC(OH)Me$

The lithiation of γ-chloro acetal **175** with lithium and a catalytic amount of naphthalene (4%) allowed the preparation of the intermediate **176**, which can be considered as a masked lithium homoenolate[124], and was used for the preparation of the hydroxy ketone **179** through the hydroxy acetal **177** and dithiane **178** using known chemistry (Scheme 62)[125].

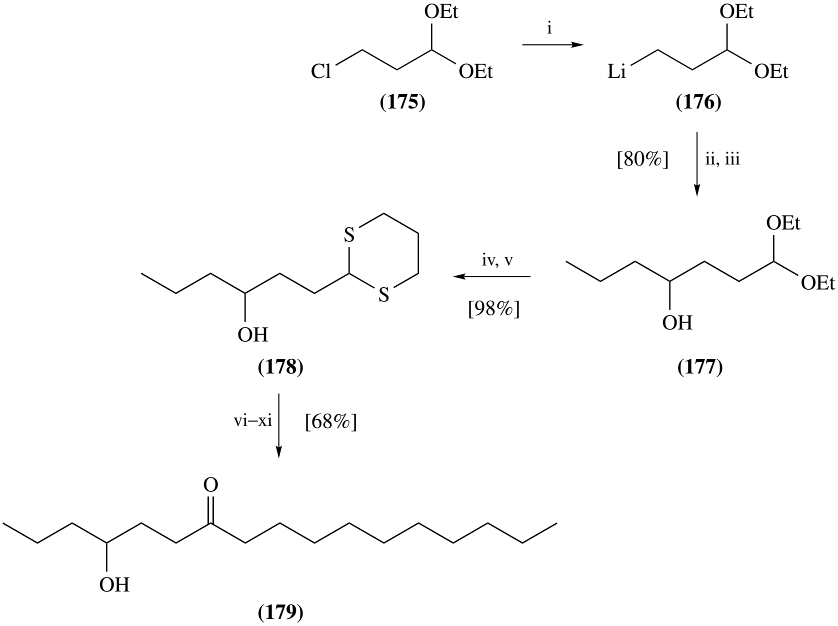

SCHEME 62. Reagents: (i) Li, $C_{10}H_8$ (4%), THF, −78 °C; (ii) PrCHO, −78 °C; (iii) H_2O, −78 to 20 °C; (iv) $HS(CH_2)_3SH$, $BF_3{\cdot}OEt_2$, $CHCl_3$, 0 to 20 °C; (v) $NaHCO_3$–H_2O; (vi) dihydropyran, PTSA cat., CH_2Cl_2; (vii) BuLi, THF, 20 °C; (viii) $Me(CH_2)_9I$, −78 to 20 °C; (ix) H_2O; (x) MeI, Me_2CO-H_2O reflux; (xi) 3 M HCl, THF

Compound **179** was isolated from the roots of *Chiococca alba* and shows important biological activity[126].

A completely different approach to lithium homoenolate synthons uses a carbon–oxygen bond cleavage. Lithiation of acrolein diethyl acetal **180** with lithium and a catalytic amount of DTBB (2.5%) in the presence of different carbonyl compounds in THF at 0 °C gave, after final hydrolysis, the corresponding γ-products **181** in different diastereomeric ratios (Z/E: 3/1 to 20/1) (Scheme 63)[127].

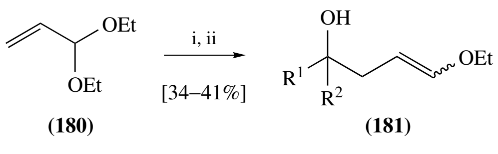

[R^1, R^2 = H, Et, *i*-Pr, *t*-Bu; $R^1R^2 = (CH_2)_5$]

SCHEME 63. Reagents: (i) Li, DTBB (2.5%), E = *t*-BuCHO, Et_2CO, *i*-Pr_2CO, *c*-$(CH_2)_5CO$, THF, 0 °C; (ii) H_2O

The same protocol shown in Scheme 63 was also applied to the cyclopentenone ketal **182**, which gave the expected compounds **183** after final deprotection under acidic conditions (2 M HCl) in 33–40% yield. This acidic deprotection applied to products **181** gave

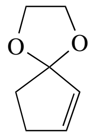

(182)

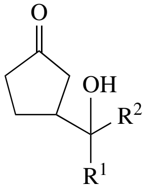

(183)

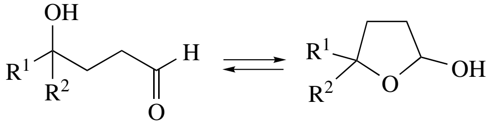

(184) **(185)**

[R^1, R^2 = H, Me, Et, *i*-Pr, *t*-Bu; $R^1R^2 = (CH_2)_5$]

the expected hydroxy aldehydes **184**, which are in equilibrium with the corresponding lactols **185**[127].

Lithium homoenolates derived from carboxylic acids were generated from the corresponding β-chloro acids by means of an arene-catalyzed lithiation. Chloro acids **186** were deprotonated with *n*-butyllithium and lithiated *in situ* with lithium and a catalytic amount of DTBB (5%) in the presence of different carbonyl compounds to yield, after hydrolysis, the expected hydroxy acids (**187**). Since the purification of these products is difficult, they were cyclized without isolation upon treatment with *p*-toluenesulfonic acid (PTSA) under benzene reflux, into substituted γ-lactones **188** (Scheme 64)[116].

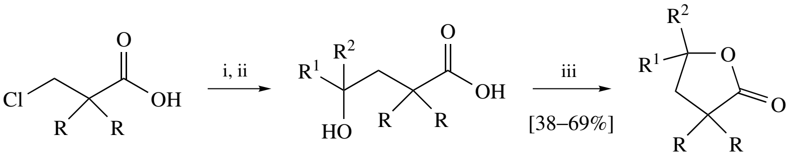

(186) **(187)** **(188)**

R = H, Me
R^1, R^2 = H, Me, Et, *t*-Bu, Ph; $R^1R^2 = (CH_2)_5$

SCHEME 64. Reagents: (i) BuLi, Li, DTBB (5%), E = *t*-BuCHO, PhCHO, Et_2CO, *c*-$(CH_2)_5CO$, PhCOMe, THF, −78 °C; (ii) H_2O, −78 to 20 °C; (iii) PTSA (10%), PhH reflux

2. Nitrogenated intermediates

sp^3-Hybridized organolithium compounds having a nitrogen-containing functionality at the γ-position were prepared by naphthalene-catalyzed (8%) lithiation of chloramines **189** in the presence of different carbonyl compounds in THF at −78 °C, so functionalized unsaturated amines **190** were isolated, after hydrolysis (Scheme 65)[121]. It is noteworthy that in this case no debenzylation took place, which was the case for the corresponding oxygenated systems (see Scheme 58).

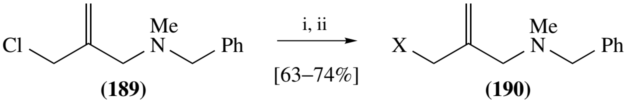

(189) **(190)**

[X = Et_2COH, *c*-$(CH_2)_5COH$]

SCHEME 65. Reagents: (i) Li, $C_{10}H_8$ (8%), E = Et_2CO, $(CH_2)_5CO$, THF, −78 °C; (ii) H_2O, −78 to 20 °C

By a DTBB-catalyzed (5%) lithiation of chlorinated unsaturated amines **191** in the presence of a carbonyl compound as electrophile, the final hydrolysis afforded **192** as a Z/E mixture of diastereomers (Scheme 66)[122]. In this process, the corresponding sp^2-hybridized functionalized organolithium intermediate is probably involved.

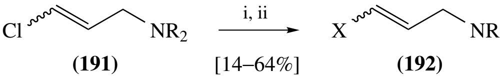

(191) **(192)**

R = $CH_2CH{=}CH_2$; RR = $(CH_2CH_2)_2O$
X = *i*-PrCHOH, *t*-BuCHOH, *c*-$(CH_2)_5COH$

SCHEME 66. Reagents: (i) Li, DTBB (5%), E = *i*-PrCHO, *t*-BuCHO, *c*-$(CH_2)_5CO$, THF, −78 °C; (ii) H_2O

A reasonable alternative to the chlorine–lithium exchange, as a methodology to prepare γ-functionalized organolithium compounds, is the arene-catalyzed lithiation of phenylsulfides bearing a nitrogen-containing functionality at the γ-position. This is the case of aminothioethers **193**, which after deprotonation with *n*-butyllithium in THF at −78 °C, and lithiation using lithium and a catalytic amount of DTBB (5%), gave the expected intermediates **194**. Treatment of these γ-functionalized organolithium compounds with several carbonyl compounds yielded, after hydrolysis, the expected functionalized amines **195** (Scheme 67). By this methodology intermediates **194** having an ionized primary amine (R^2 = H) are accessible, which could not be prepared by chlorine–lithium exchange.

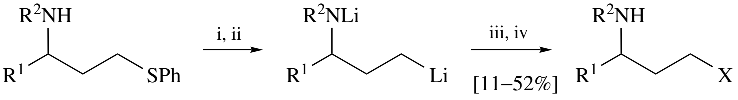

(193) **(194)** **(195)**

R^1, R^2 = H, Me, *i*-Pr
X = *t*-BuCHOH, PhCHOH, Me_2COH, Et_2COH, *c*-$(CH_2)_4COH$, *c*-$(CH_2)_5COH$

SCHEME 67. Reagents: (i) *n*-BuLi, THF, −78 °C; (ii) Li, DTBB (5%), THF, −78 °C; (iii) E = *t*-BuCHO, PhCHO, Me_2CO, Et_2CO, and *c*-$(CH_2)_4CO$, *c*-$(CH_2)_5CO$, −78 to 20 °C; (iv) H_2O

A particular case for the generation of a γ-substituted organolithium compound, derived from an imine, was used for the synthesis of 2-substituted pyrrolidines. DTBB-catalyzed (5%) lithiation of γ-chloro imines **196** yielded, after hydrolysis, 2-substituted pyrrolidines **198**, including nornicotine (R^1 = H, R^2 = 3-pyridyl). The corresponding γ-nitrogenated organolithium intermediate **197** was probably involved (Scheme 68)[128].

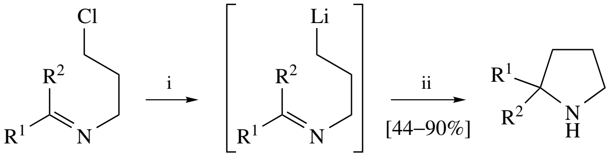

(196) **(197)** **(198)**

[R^1, R^2 = H, Me, c-C_6H_{11}, aryl, 3-pyridyl]

SCHEME 68. Reagents: (i) Li, DTBB (5%), THF, −78 to 20 °C; (ii) H_2O

3. Sulfurated intermediates

3-Lithioalkyl thioethers are interesting, since they should decompose by intra- or intermolecular deprotonation of the more acidic hydrogen at the α-position with respect to the sulfur atom. However, the lithiation of chloro or bromo thioethers **199** using naphthalene or DTBB as an electron-carrier catalyst (2–5%) allowed the generation of the corresponding lithiated intermediate **200** which, either under Barbier-type conditions (room temperature) or in a two-step process (−78 to 20 °C, through intermediate **200**), react with different electrophiles giving, after hydrolysis, the final functionalized thioethers **201** (Scheme 69)[129].

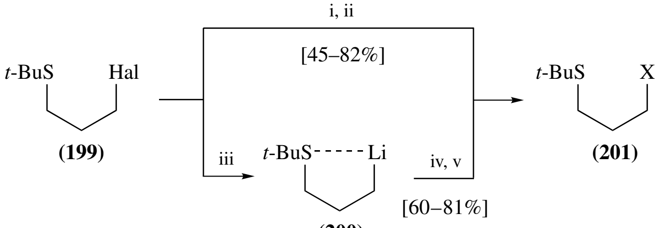

(199) **(200)** **(201)**

Hal = Cl, Br
X = H, D, MeS, CO_2H, t-BuCHOH, PhCHOH, Me_2COH, c-$(CH_2)_5COH$, c-$C_3H_5C(OH)Ph$, Me_3Si

SCHEME 69. Reagents: (i) Li, DTBB (2.5%), E = t-BuCHO, PhCHO, Me_2CO, c-$(CH_2)_5CO$, c-C_3H_7COPh, Me_3SiCl, THF, 20 °C; (ii) H_2O; (iii) Li, $C_{10}H_8$ (2.5%), THF, −78 °C; (iv) E = H_2O, D_2O, Me_2S_2, CO_2, −78 to 20 °C

Interestingly, compounds **201** can be easily detertbutylated to give the corresponding thiols **202** upon treatment with mercury(II) acetate in trifluoroacetic acid followed by reaction with hydrogen sulfide in 54–79% yield[130].

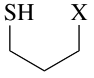

(202)

Naphthalene-catalyzed (5%) lithiation of the chlorinated thioether **203** in the presence of pivalaldehyde gave, after hydrolysis, the product **204** in which, together with the

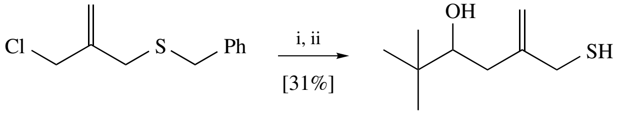

(203) **(204)**

SCHEME 70. Reagents: (i) Li, $C_{10}H_8$ (8%), *t*-BuCHO, THF, −78 °C; (ii) H_2O, −78 to 20 °C

expected tandem chlorine–lithium exchange and S_E reaction, a debenzylation occurred (Scheme 70)[121].

D. δ-Functionalized Organolithiums

Naphthalene-catalyzed (5%) lithiation of the diiodinated ketal **205** afforded directly the cyclobutane derivative **206**, a δ-iodinated organolithium compound probably being involved (Scheme 71)[131]. In this case, a δ-elimination of lithium iodide is preferred to a γ- or δ-elimination of lithium alkoxide.

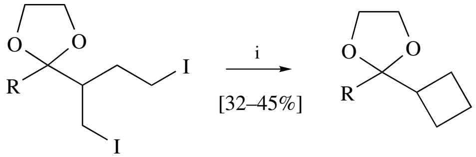

(205) **(206)**

[R = Me, Et]

SCHEME 71. Reagent: (i) Li, $C_{10}H_8$ (5%), THF, 0 °C

δ-Functionalized organolithium compounds **207** and **208** were generated by sulfur–lithium exchange starting from the corresponding phenylthioethers by a DTBB-catalyzed (19%) lithiation in THF at −78 °C, and were used in the key step for the synthesis of interesting heterocyclic compounds, such as dihydropyrroloisoquinolones[132].

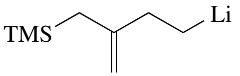

(207)

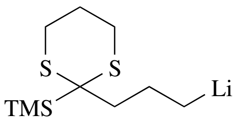

(208)

In the case of unsaturated chloramines **209**, the DTBB-catalyzed lithiation had to be carried out in the presence of the electrophile in THF at −78 °C in order to avoid decomposition of the corresponding functionalized organolithium intermediate through elimination reactions. Final hydrolysis yielded a mixture (variable ratios: 11.5/1 to 1/19 depending on the electrophile) of the α- and γ-products **210** (Scheme 72)[133].

δ-Functionalized propargylic organolithium compounds are probably involved in the transformation of chlorinated ethers or amines **211** into polyfunctionalized products **212**, which were achieved through a DTBB-catalyzed lithiation under Barbier-type reaction conditions (Scheme 73)[134]. The reaction failed for the corresponding thioethers (Y =

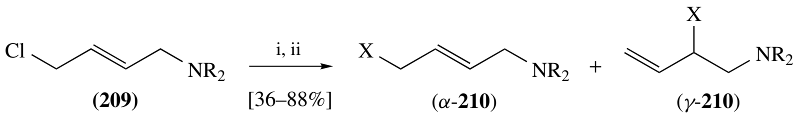

(209) (*α*-**210**) (*γ*-**210**)

[R = $CH_2CH{=}CH_2$, $PhCH_2$; RR = $(CH_2CH_2)_2O$
X = *t*-BuCHOH, PhCHOH, Me_2COH, *c*-$(CH_2)_5COH$, (*c*-$C_3H_5)_2COH$, Me_3Si]

SCHEME 72. Reagent: (i) Li, DTBB (5%), E = *t*-BuCHO, PhCHO, Me_2CO, *c*-$(CH_2)_5CO$, (*c*-$C_3H_5)_2$ CO, Me_3SiCl, THF, −78 °C; (ii) H_2O, −78 to 20 °C

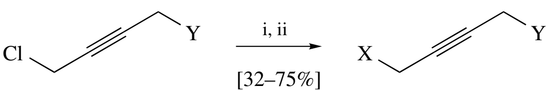

(211) **(212)**

[Y = OTHP, $N(CH_2CH_2)_2O$, $N(CH_2CH{=}CH_2)_2$
X = *i*-PrCHOH, *t*-BuCHOH, PhCHOH, Me_2COH,
c-$(CH_2)_5COH$, (*c*-$C_3H_5)_2COH$, Me_3Si]

SCHEME 73. Reagents: (i) Li, DTBB (5%), E = *i*-PrCHO, *t*-BuCHO, PhCHO, Me_2CO, *c*-$(CH_2)_5CO$, (*c*-$C_3H_5)_2CO$, Me_3SiCl, THF, −78 °C; (ii) H_2O, −78 to 20 °C

t-BuS) because a mixture of products was obtained resulting from a chlorine–lithium and sulfur–lithium exchange.

A special class of *δ*-functionalized organolithium compounds are the so-called masked lithium bis-homoenolates, which are useful reagents in order to introduce a four-carbon atom fragment bearing a carbonyl group, in the reaction with electrophiles. The arene-catalyzed lithiation of chloro ketals **213** using naphthalene (1%), biphenyl (1%) or DTBB (1%) as the electron-carrier agents in THF at −78 °C led to the generation of the corresponding intermediates **214**, which by reaction with cyclohexanone at −78 to 20 °C led to the formation of the expected functionalized dioxolanes **215**, after hydrolysis (Scheme 74)[81].

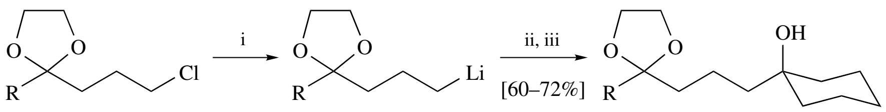

(213) **(214)** **(215)**

[R = H, Me]

SCHEME 74. Reagents: (i) Li, $C_{10}H_8$, Ph_2 or DTBB (1%), THF, −78 °C; (ii) E = *c*-$(CH_2)_5CO$, −78 to 20 °C; (iii) H_2O

An interesting application of intermediates **214** is their reaction with protected *α*-hydroxy ketones **216** as electrophilic reagents. After final hydrolysis under acidic conditions (2 M HCl), the corresponding substituted 6,8-dioxabicyclo[3.2.1]-octanes **217** were obtained[135]. Among them, frontalin (R = R^1 = Me, R^2 = R^3 = H) and brevicomins (R = Me, R^1 = H, R^2 or R^3 = Et) are particularly important because they are beetle

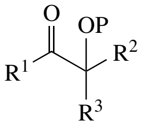

(216)

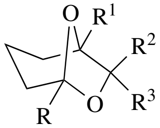

(217)

[R^1, R^2, R^3 = H, Me, Et
P = Li, Me_3Si, $PhCH_2$]

aggregation pheromones[136, 137], which can be used in racemic form to protect ecologically coniferous forests[138].

ω-Chloro orthoesters **218** or **219** were lithiated using a catalytic amount of DTBB (5%) as the electron carrier and in the presence of the corresponding electrophile, so after controlled hydrolysis with phosphate buffer and final deprotection with methanol and a catalytic amount of PTSA, functionalized esters **220** were obtained (Scheme 75)[139].

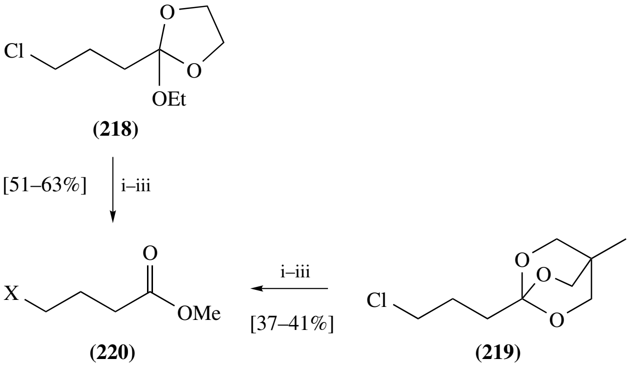

[X = *t*-BuCHOH, PhCHOH, Et_2COH, *c*-$(CH_2)_5COH$, PhC(OH)Me, PhCHNHPh, Me_3Si]

SCHEME 75. Reagents: (i) Li, DTBB (5%), E = *t*-BuCHO, PhCHO, Et_2CO, *c*-$(CH_2)_5CO$, PhCOMe, PhCH=NPh, Me_3SiCl, THF, −78 °C; (ii) phosphate buffer, −78 to 20 °C; (iii) MeOH, PTSA cat.

E. ε-Functionalized and Higher-range Functionalized Organolithiums

ε-Chlorinated ketals **221** were lithiated using a catalytic amount (8%) of naphthalene in THF at −78 °C to generate the corresponding masked lithium δ-enolates **222**, which upon treatment with different electrophiles in THF at temperatures ranging between −78 and 20 °C, and final hydrolysis with water, afforded protected functionalized ketals **223** (Scheme 76). The application of this methodology to the chlorinated dithiane **224**, under the same reaction conditions, gave the intermediate **225** and finally products **226** (Scheme 76)[81, 140, 141].

ε-Functionalized organolithium compounds, having a protected carboxylic acid functionality, can also be considered as masked lithium tris-homoenolates and were prepared by DTBB-catalyzed (5%) lithiation of the corresponding ω-chlorinated materials. For instance, compound **227** in THF at −78 °C leads to the expected organolithium intermediate **228**, which reacts with a series of electrophiles present in the reaction medium

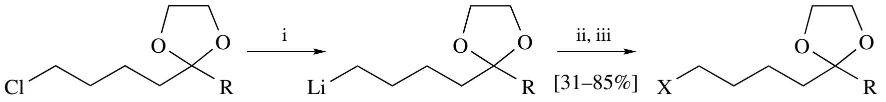

(221) **(222)** **(223)**

R = H, Et, Ph
X = H, D, $PhCH_2S$, *i*-PrCHOH, PhCHOH, Et_2COH, PhC(OH)Me,
c-$(CH_2)_5COH$, HCO, PrCO, PhCO, EtOCO, PhCHNHPh

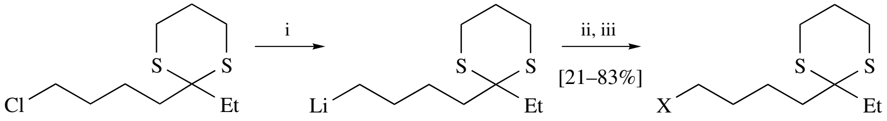

(224) **(225)** **(226)**

[X = H, D, *i*-PrCHOH, *t*-BuCHOH, PhCHOH, *c*-$(CH_2)_5COH$]

SCHEME 76. Reagents: (i) Li, $C_{10}H_8$ (8%), THF, −78 °C; (ii) E = H_2O, D_2O, $(PhCH_2S)_2$, *i*-Pr CHO, *t*-BuCHO, PhCHO, Et_2CO, PhCOMe, *c*-$(CH_2)_5CO$, $HCONMe_2$, $PrCON(CH_2)_4$-*c*, $PhCON(CH_2)_4$-*c*, PhCN, EtOCOCl, PhCH=NPh, −78 to 20 °C; (iii) H_2O

(Barbier-type reaction conditions) to yield, after hydrolysis with phosphate buffer and final esterification with methanol under PTSA catalysis, the corresponding functionalized methyl esters **229** (Scheme 77)[139].

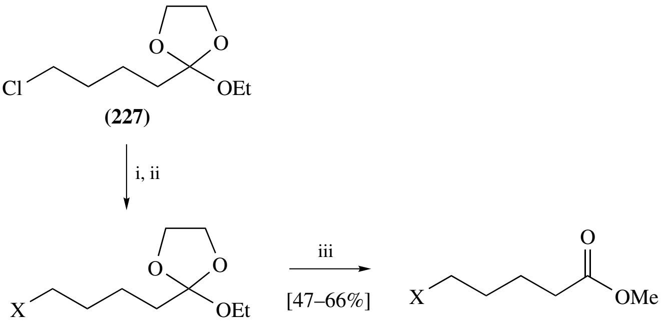

(228) **(229)**

[X = *t*-BuCHOH, PhCHOH, Et_2COH, *c*-$(CH_2)_5COH$, PhC(OH)Me, PhCHNHPh, Me_3Si]

SCHEME 77. Reagents: (i) Li, DTBB (5%), E = *t*-BuCHO, PhCHO, Et_2CO, *c*-$(CH_2)_5CO$, PhCOMe, PhCH=NPh, Me_3SiCl, THF, −78 °C; (ii) phosphate buffer, −78 to 20 °C; (iii) MeOH, PTSA cat., 20 °C

The lithiation of the *ω*-chloro acetal **230** using a catalytic amount of naphthalene (4%) in THF at −78 °C gave the corresponding masked *ω*-lithio enolate **231**, which reacted with different electrophiles at −78 °C to room temperature yielding, after hydrolysis with water, the expected functionalized acetals **232** (Scheme 78)[125].

Hydrolysis of compounds **232** with 2 M HCl gave the corresponding functionalized aldehydes **233** in practically quantitative yields (>95%). Among them, keto aldehyde **234**

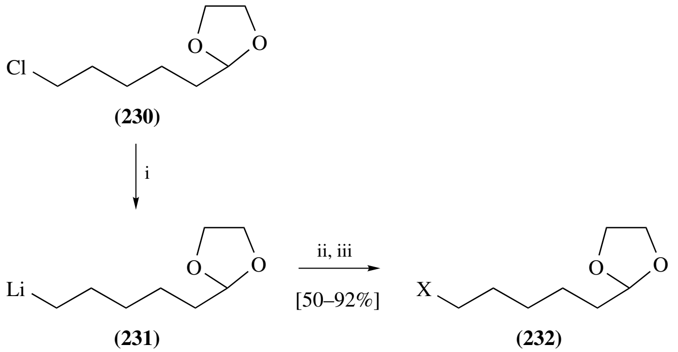

(230) **(231)** **(232)**

[X = H, *t*-BuCHOH, PhCHOH, Et_2COH, *c*-$(CH_2)_5COH$, *n*-$C_6H_{13}CO$, *n*-$C_7H_{15}CO$]

SCHEME 78. Reagents: (i) Li, $C_{10}H_8$ (4%), THF, −78 °C; (ii) E = H_2O, *t*-BuCHO, PhCHO, Et_2CO, *c*-$(CH_2)_5CO$, $Me(CH_2)_nCON(OMe)Me$ ($n = 5, 6$), −78 to 20 °C; (iii) H_2O

(resulting from the use of Weinreb amides as electrophiles) is an interesting example, since it can lead to the hydroxy ketones **235** by *in situ* treatment with *n*-butyltitanium triisopropoxide in 42–66% yield. Actually, **235** with $n = 6$ is a natural compound isolated from the roots of Rubiaceae family plants[142].

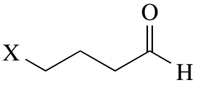

(233)

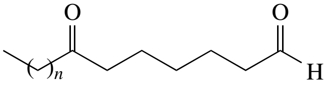

(234) [$n = 5, 6$]

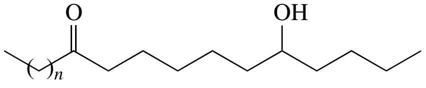

(235) [$n = 5, 6$]

F. Aromatic and Heteroaromatic Organolithiums

In this section, functionalized aryl and heteroaryl compounds prepared by arene-catalyzed lithiation will be considered.

1. Aromatic intermediates

The naphthalene-catalyzed (3–12%) lithiation of deprotonated chloro phenols and anilides **236** performed with *n*-butyllithium in THF at 0 or −78 °C, respectively, gave the corresponding functionalized aryllithium intermediates **237** which, by reaction with electrophiles and final hydrolysis, yielded the corresponding polyfunctionalized molecules **238** (Scheme 79)[49].

The preparation of functionalized aryllithium compounds bearing an oxygen- or sulfur-containing functionality in a benzylic position is also possible by arene-catalyzed lithiation. When chlorinated materials **239** were deprotonated (for Y = OH, SH) with *n*-butyllithium in THF at −78 °C and then lithiated using DTBB as the catalyst at the same temperature,

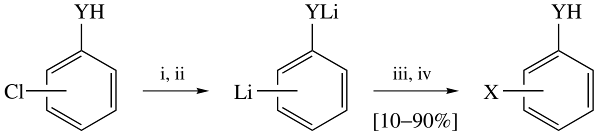

(236) **(237)** **(238)**

Y = O, *t*-BuCON, EtOCON
X = *i*-PrCHOH, *t*-BuCHOH, Et_2COH, *c*-$(CH_2)_5COH$, PhCO

SCHEME 79. Reagents: (i) BuLi, THF, 0 °C; (ii) Li, $C_{10}H_8$ (3–12%), 0 (for Y = O) or −78 °C (for Y = RCON); (iii) E = *i*-PrCHO, *t*-BuCHO, Et_2CO, *c*-$(CH_2)_5CO$, PhCN, 0 or −78 to 20 °C; (iv) H_2O

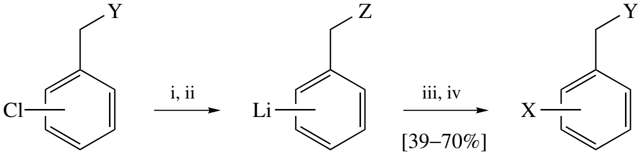

(239) **(240)** **(241)**

Y = OH, SH, NMe_2, $N(CH_2CH{=}CH_2)_2$
Z = OLi, SLi, NR_2
X = *i*-PrCHOH, *t*-BuCHOH, Et_2COH, *c*-$(CH_2)_5COH$, PhC(OH)Me, Me_3Si

SCHEME 80. Reagents: (i) BuLi, THF, −78 °C (only for Y = OH, SH); (ii) Li, DTBB (2.5%), −78 °C; (iii) E = *i*-PrCHO, *t*-BuCHO, Et_2CO, *c*-$(CH_2)_5CO$, PhCOMe, Me_3SiCl, −78 °C; (iv) H_2O, −78 to 20 °C

the corresponding functionalized aryllithium intermediates **240** were formed. Their further electrophilic substitution reaction followed by final hydrolysis afforded the expected products **241** (Scheme 80)[143].

A special case of functionalized aryllithium reagents appears when the corresponding aryl group bears a ketal moiety at the benzylic position due to the lability of the benzylic carbon–oxygen bonds. However, working under Barbier-type conditions and using naphthalene (10%) as the electron carrier catalyst, the reaction of chlorinated materials **242** afforded, after hydrolysis with water, the corresponding polyfunctionalized products **243** (Scheme 81)[144].

2. Heteroaromatic intermediates

Lithiation of heteroaromatic compounds, especially nitrogen-containing systems, is an important methodology, because the lithiated intermediates can be easily functionalized in a regioselective manner by reaction with electrophiles. This process can be performed by deprotonation only at the *ortho* position of the heteroatom, but obviously the reaction is not possible at other positions[145].

The reaction of the three chloro pyridines **244** with lithium in the presence of a catalytic amount of naphthalene (4%) and different electrophiles in THF at −78 °C gave, after hydrolysis, the expected functionalized pyridines **245** (Scheme 82)[146].

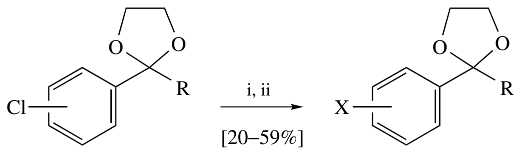

(242) **(243)**

[R = H, Me
X = *t*-BuCHOH, *c*-$(CH_2)_5$COH, PhC(OH)Me]

SCHEME 81. Reagents: (i) Li, $C_{10}H_8$ (10%), E = *t*-BuCHO, Et_2CO, *c*-$(CH_2)_5$CO, PhCOMe, THF, −78 °C; (ii) H_2O, −78 to 20 °C

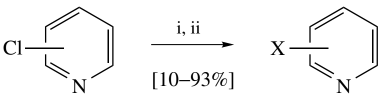

(244) **(245)**

[X = PrCHOH, *t*-BuCHOH, PhCHOH, Et_2COH, PhC(OH)Me, $(n\text{-}C_5H_{11})_2$COH,
PhCH=CHC(OH)Me, PhCHNHPh, *n*-C_6H_{13}CO, PhCO, *i*-PrO_2CNNHCO_2Pr-*i*]

SCHEME 82. Reagents: (i) Li, $C_{10}H_8$ (4%), E = PrCHO, *t*-BuCHO, PhCHO, Et_2CO, PhCOMe, $(n\text{-}C_5H_{11})_2$CO, PhCH=CHCOMe, PhCH=NPh, Me$(CH_2)_5$CON$(CH_2)_4$-*c*, PhCN, *i*-PrO_2CN = NCO_2Pr-*i*, THF, −78 °C; (ii) H_2O, −78 to 20 °C

The reaction shown in Scheme 82 was also applied to the heterocycles **246–250**, so that the corresponding chlorine–lithium exchange was carried out under the same reaction conditions (Barbier-type) yielding the expected final products in a regioselective manner, in which the electrophilic fragments occupy the position of the chlorine atoms in the starting material. Interestingly, when the reaction products obtained from compound **249** were treated with 45% HBr in glacial acetic acid, the corresponding functionalized uracils **251** were obtained in 32–90% yield[146].

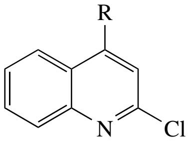

(246)

[R = H, Me]

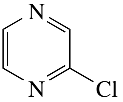

(247)

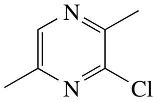

(248)

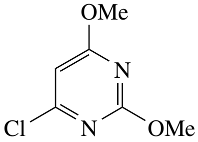

(249)

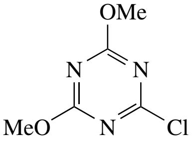

(250)

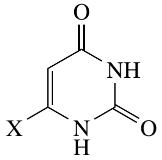

(251)

[X = *t*-BuCHOH, Et_2COH, *i*-PrC(OH)Me]

VI. RING OPENING OF HETEROCYCLES

The reductive ring opening of heterocycles by using arene-catalyzed lithiation represents a versatile and useful methodology in order to prepare functionalized organolithium compounds, which are interesting intermediates for the synthesis of polyfunctionalized organic molecules[147]. This section will be organized according to the size of the ring.

A. Three-membered Rings

The ring opening of three-membered rings, namely epoxides and aziridines, is a useful way to generate oxygen- and nitrogen-containing β-functionalized organolithium compounds.

1. Epoxides

The ring opening of epoxides, which can also be performed by using the stoichiometric version of the arene-promoted lithiation[148], was carried out generally using a catalytic amount of DTBB and chiral epoxides. Thus, treatment of compounds **252** with lithium and DTBB (5%) in THF at −78 °C led to the formation of chiral β-oxido functionalized organolithium compounds **253**, which by reaction with non-prochiral electrophiles gave, after hydrolysis, enantiomerically pure functionalized alcohols **254** (Scheme 83)[149, 150]. The reaction is regioselective, giving exclusively the most stable primary organolithium intermediates **253**, without enantioracemization along the process.

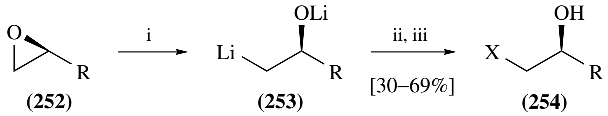

R = Me, MOMOCH$_2$
X = H, D, *t*-BuCHOH, PhCHO, *c*-(CH$_2$)$_5$COH, PhC(OH)Me, CO$_2$H

SCHEME 83. Reagents: (i) Li, DTBB (5%), THF, −78 °C; (ii) E = H$_2$O, D$_2$O, *t*-BuCHO, PhCHO, *c*-(CH$_2$)$_5$CO, PhCOMe, CO$_2$, −78 °C; (iii) H$_2$O, −78 to 20 °C

Starting from different chiral epoxides, such as **255** or **256**, and following the same protocol as for the epoxide **252**, the expected primary organolithium intermediates **257** and **258** were generated, and then the final compounds **259** and **260**, respectively, by reaction with different electrophiles and final hydrolysis in 69–80% and 70–90%, respectively.

For all the chiral intermediates above mentioned (**253, 257** and **258**) the reaction with prochiral electrophiles (aldehydes or differently substituted ketones) gave a *ca* 1:1 mixture of diastereomers so, as occurred in other chiral functionalized organolithium compounds, the asymmetric induction is practically non-existent.

A useful application of the chemistry shown in Scheme 83 is the synthesis of branched-chain functionalized carbohydrates. For this purpose two epoxides **261** and **262** derived from D-glucose and **263** derived from D-fructose were prepared following reported methodologies, and were submitted to a DTBB-catalyzed lithiation as described above in Scheme 83. The expected intermediates **264–266** and final products **267–269** were prepared in a regio- and stereoselective manner in 15–95% yield[110, 151]. Also here, the use of a prochiral electrophile gave equimolecular amounts of both diastereomers.

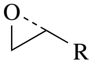

(255)

[R = *i*-Pr, MOMOCH$_2$]

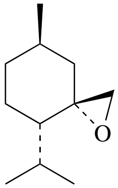

(256)

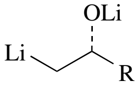

(257)

[R = *i*-Pr, MOMOCH$_2$]

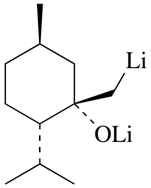

(258)

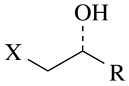

(259)

R = *i*-Pr, MOMOCH$_2$
X = *t*-BuCHOH, PhCHOH, *c*-(CH$_2$)$_5$COH, CO$_2$H

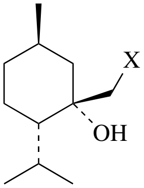

(260)

[X = H, D, CO$_2$]

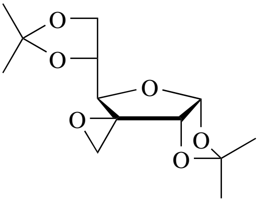

(261)

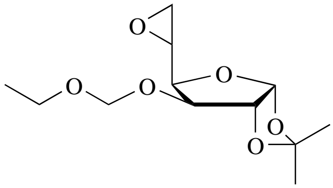

(262)

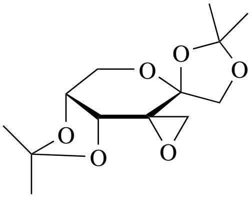

(263)

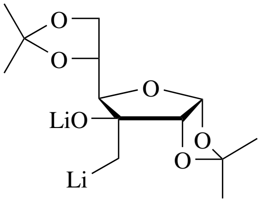

(264)

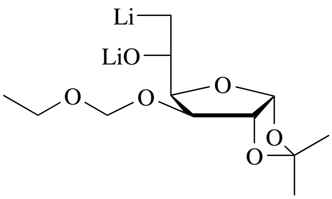

(265)

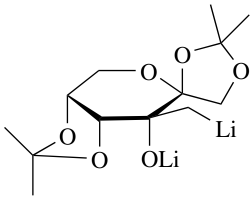

(266)

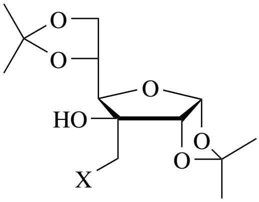

(267)

[X = H, D, Me_3Si, PhCHOH, Me_2COH, *c*-$(CH_2)_5COH$]

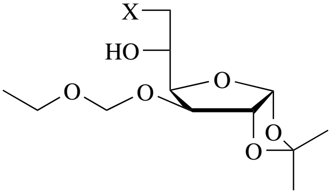

(268)

[X = H, D, PhCHOH, Me_2COH, *c*-$(CH_2)_5COH$, CO_2H]

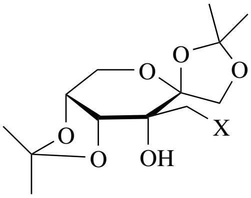

(269)

[X = H, D, PhCHOH, Et_2COH, *c*-$(CH_2)_5COH$]

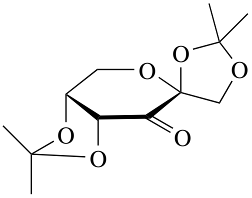

(270)

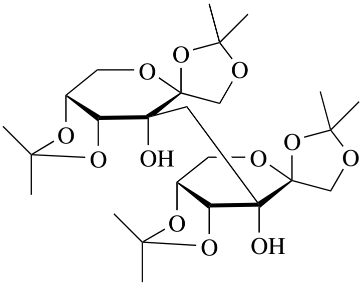

(271)

On the other hand, when intermediate **266** reacted with the ketone **270** (precursor of epoxide **263**), a methylene-bridged disaccharide **271** was the only reaction product isolated in low yield (15%), due to difficulties in its purification by column chromatography.

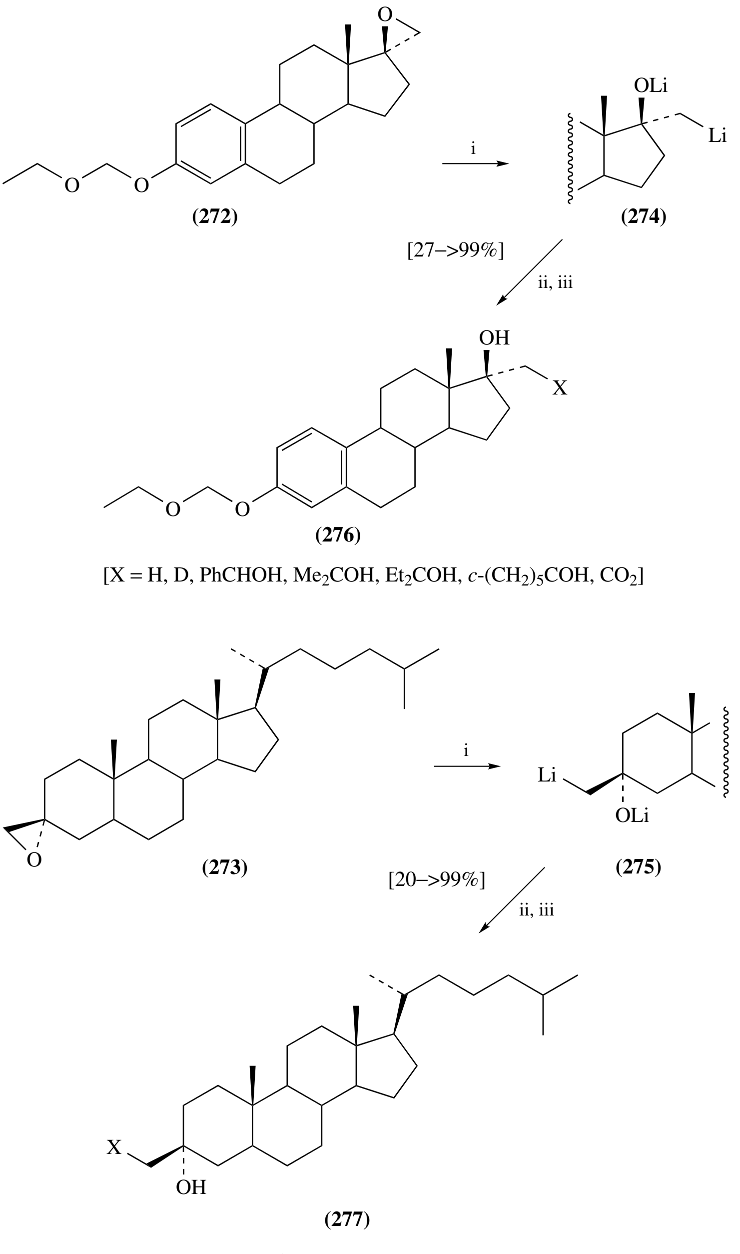

(272) **(274)** **(276)** **(273)** **(275)** **(277)**

[27–>99%]

[X = H, D, PhCHOH, Me_2COH, Et_2COH, *c*-$(CH_2)_5COH$, CO_2]

[20–>99%]

[X = H, D, PhCHOH, Et_2COH, *c*-$(CH_2)_5COH$]

SCHEME 84. Reagents: (i) Li, DTBB (7%), THF, −78 °C; (ii) E = H_2O, D_2O, PhCHO, Me_2CO, Et_2CO, *c*-$(CH_2)_5CO$, −78 °C; (iii) H_2O, −78 to 20 °C

Concerning steroids, although their physical and chemical properties are rather predictable due to their rigid structures, small changes in the structure can cause extensive changes in their biological activity[152]. For these reasons, two epoxides **272** and **273**, derived from estrone and cholestanone, respectively, were prepared in order to study their DTBB-catalyzed lithiation. After lithiation using a catalytic amount of DTBB (7%) in THF at −78 °C, the expected primary β-oxido functionalized organolithium compounds **274** and **275** were, respectively, obtained. Further reaction with different electrophiles at −78 °C, and final hydrolysis with water, afforded the expected functionalized steroids **276** and **277**, respectively (Scheme 84)[153, 154].

When intermediate **274** reacted with ketones **133** (from D-glucose) or **270** (from D-fructose), mixed steroid–sugar compounds **278** and **279** were, respectively, obtained in low yields (10–16%). In addition, the use of protected estrone **280** (precursor of the epoxide **272**) as electrophile allows the preparation of the dimeric steroid **281** in 26% yield. The low yields obtained for compounds **278, 279** and **281** are due to extensive decomposition during their column chromatographic purification.

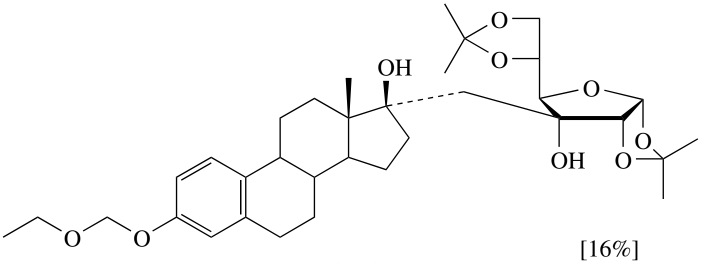

(278)

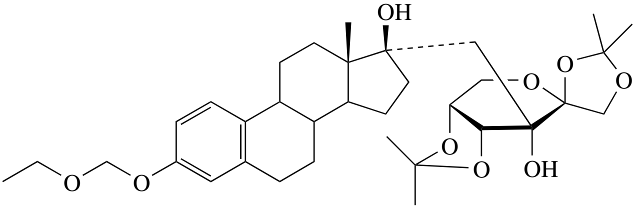

(279)

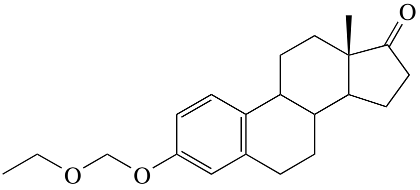

(280)

An interesting case of different regiochemistry in the ring opening of an epoxide using a substoichiometric amount (60%) of naphthalene in the lithiation process was observed with epoxides **282**. After the naphthalene-promoted lithiation process the most unstable

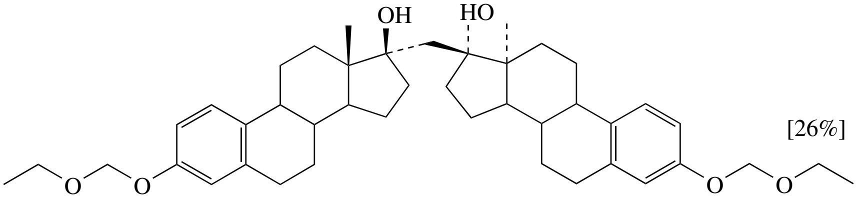

(281)

tertiary organolithium intermediates **283** were obtained (instead of the most stable primary ones), which undergo a β-elimination giving a Z/E-mixture of allyl alcohols **284**, the Z-one being the major component (Scheme 85)[155]. The formation of the most substituted intermediate **283** can be explained by the coordination of the lithium atom by the benzotriazole group (CIPE).

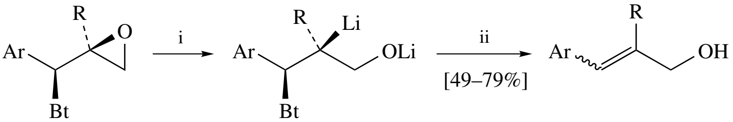

(282) **(283)** **(284)**

R = Me, *i*-Bu, Ph, 3-MeC$_6$H$_4$, 2, 5-Me$_2$C$_6$H$_3$
Ar = Ph, 3-MeC$_6$H$_4$, 3-MeOC$_6$H$_4$, 3-PhOC$_6$H$_4$, 2-Py, 3-Py, 6-Me-2-Py
Bt = benzotriazole

SCHEME 85. Reagents: (i) Li, C$_{10}$H$_8$ (60%), THF, 20 °C; (ii) H$_2$O

2. Aziridines

Aziridines **285** and **286** bearing a phenyl group somewhere in the ring, which cannot be opened using lithium–arene (the stoichiometric version of the arene-promoted lithiation), undergo a naphthalene-catalyzed (5%) lithiation in THF at −78 °C to give the expected intermediates **287** (primary) and **288** (benzylic), respectively. Further reaction of these β-functionalized organolithium compounds with an electrophile at temperatures ranging between −78 °C and room temperature led, after hydrolysis, to the formation of products **289** and **290**, respectively, in a regioselective manner (Scheme 86)[35, 156].

The application of the methodology shown in Scheme 86 to (Z) and (E) chiral aziridines **291** and **292** gave a surprising result: independently of the configuration of the starting aziridine, after the tandem lithiation-S$_E$ reaction, the same series of enantiomerically pure functionalized amines **295** were obtained. A possible explanation for this strange behavior can be found considering that the rather rigid structure of the intermediates [due to the coordination of the heteroatom with the lithium atom (CIPE: complex induced proximity effect)] **293** and **294** provokes an inversion in the configuration of the most congested intermediate [from the (Z)-aziridine] in favor of the less congested one [from (E)-aziridine], so finally the same compounds **295** arose from the same intermediate **294** (Scheme 87)[35, 156].

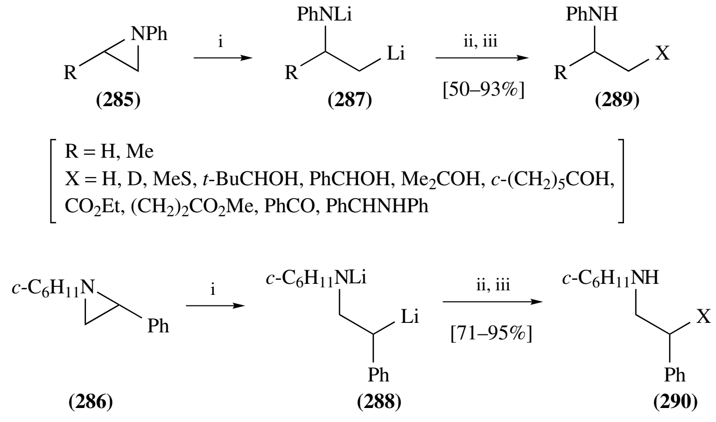

R = H, Me
X = H, D, MeS, t-BuCHOH, PhCHOH, Me_2COH, c-$(CH_2)_5COH$, CO_2Et, $(CH_2)_2CO_2Me$, PhCO, PhCHNHPh

[X = H, D, Me, $CH_2{=}CHCH_2$]

SCHEME 86. Reagents: (i) Li, $C_{10}H_8$ (5%), THF, −78 °C; (ii) E = H_2O, D_2O, Me_2S_2, t-BuCHO, PhCHO, Me_2CO, c-$(CH_2)_5CO$, $(EtO)_2CO$, $CH_2{=}CHCO_2Me$, $PhCON(CH_2)_4$-c, PhCH=NPh, MeI, $CH_2{=}CHCH_2Br$, −78 to 20 °C; (iii) H_2O

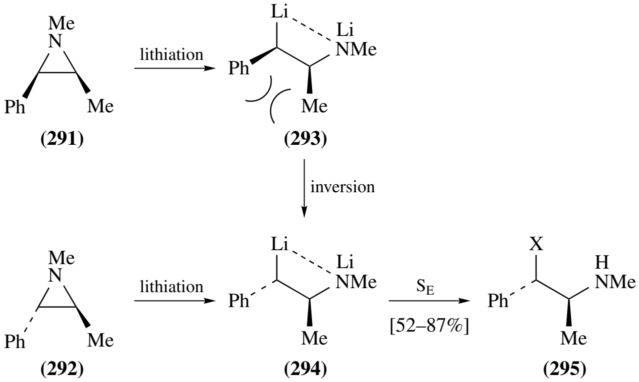

[X = H, D, $CH_2{=}CHCH_2$, Me_2COH, $(c$-$C_3H_5)_2COH$]

SCHEME 87

B. Four-membered Rings

d^3-Reagents containing oxygen, nitrogen and sulfur heteroatoms at the γ-position with respect to the metal are accessible through arene-catalyzed lithiation from the corresponding saturated heterocycles.

1. Oxetanes

3,3-Dimethyloxetane (**296**) was opened for the first time by using lithium and a catalytic (20%) amount of DTBB in THF at 0 °C to give the corresponding γ-oxido functionalized alkyllithium **297**, which by reaction with crotonaldehyde underwent 1,2-addition affording

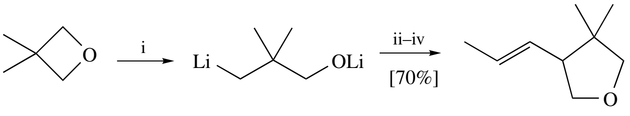

(296) **(297)** **(298)**

SCHEME 88. Reagents: (i) Li, DTBB (20%), THF, 0 °C; (ii) (*E*)-MeCH=CHCHO; (iii) H_2O; (iv) PTSA, CH_2Cl_2, 25 °C

an unsaturated diol. Final cyclization promoted by PTSA in dichloromethane at room temperature yielded the corresponding substituted tetrahydrofuran **298** (Scheme 88)[157].

The same process shown in Scheme 88 starting from different 2-substituted oxetanes and using biphenyl as the electron-carrier catalyst under THF reflux has been used to prepare regioselectively substituted primary alcohols[158]. On the other hand, the combination of a DTBB-catalyzed (*ca* 20%) lithiation with triethylaluminium in THF at −78 °C has been used for the transformation of strained oxetanes to substituted di- and triquinanes through a rearrangement process[159]. An example is given in Scheme 89 for the transformation of oxetane **299** into the product **302** through radicals **300** and **301**.

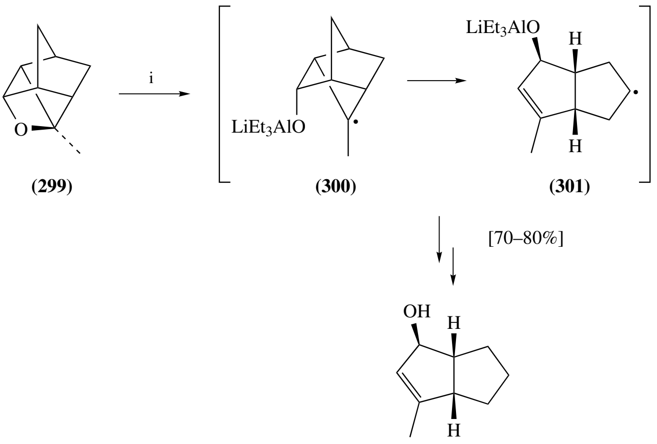

(299) **(300)** **(301)** **(302)**

SCHEME 89. Reagents: (i) Li, DTBB (20%), Et_3Al, THF, −78 °C

A chiral version of the above-mentioned ring opening of oxetanes has been applied to chiral oxetanes. An example is shown in Scheme 90 starting from oxetane **303**, which after DTBB-catalyzed (5%) lithiation in THF at 0 °C gave the γ-functionalized organolithium intermediate **304**, which by treatment with different electrophiles and final hydrolysis with water yielded the corresponding products **305** (Scheme 90)[160].

Other chiral oxetanes used to generate chiral γ-oxido functionalized organolithium intermediates are **306–309**, which gave the expected enantiopure products by reaction with non-prochiral electrophiles[110, 160]. In all cases, when prochiral electrophilic reagents were used, a mixture of the corresponding diastereomers was obtained in variable proportions depending on the electrophile, which could be easily separated by column chromatography.

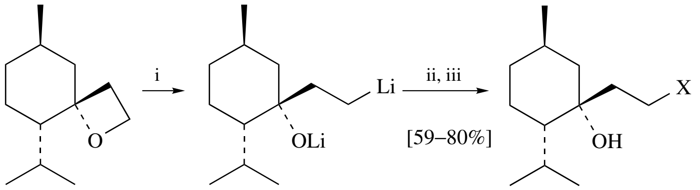

(303) **(304)** **(305)**

[X = H, D, CO_2H, *t*-BuCHOH, PhCHOH, Me_2COH, *c*-$(CH_2)_5COH$]

SCHEME 90. Reagents: (i) Li, DTBB (5%), THF, 0 °C; (ii) E = H_2O, D_2O, CO_2, *t*-BuCHO, PhCHO, Me_2CO, *c*-$(CH_2)_5CO$, −78 °C; (iii) H_2O, −78 to 20 °C

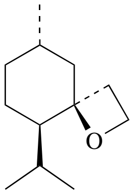

(306)

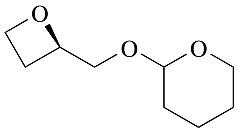

(307)

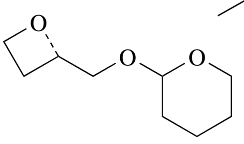

(308)

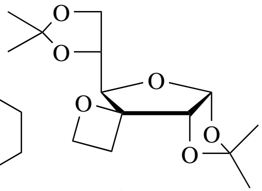

(309)

Vinyl oxetane **310** was opened with lithium and a catalytic amount (*ca* 7%) of DTBB in THF at −78 to 0 °C to give the intermediate **311**, which reacted with electrophiles at −78 °C yielding, after hydrolysis, the corresponding products **312** (Scheme 91)[161]. As shown, the electrophile reacted with the more reactive enolate moiety of the intermediate **311** instead at the benzylic position.

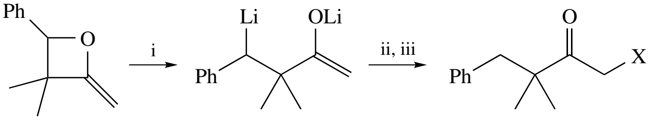

(310) **(311)** **(312)**

[X = H, Me, MeCHOH, *t*-BuCHOH, *c*-$(CH_2)_5COH$, Me_3Si]

SCHEME 91. Reagents: (i) Li, DTBB (7%), THF, −78 to 20 °C; (ii) H_2O, MeI, MeCHO, *t*-BuCHO, *c*-$(CH_2)_5CO$, Me_3SiCl, −78 °C; (iii) H_2O, −78 to 20 °C

An unexpected result was obtained when DTBB-catalyzed lithiation was applied to the vinyl-oxetane **313**[162]. After work-up, lactone **314** was isolated, the process being explained by an elimination reaction via a radical pathway more than by reduction of the benzyl radical into the anion. Thus, this hypothetical intermediate reacted with the lithium enolate of acetaldehyde, generated *in situ* by reductive decomposition of THF[163] (Scheme 92).

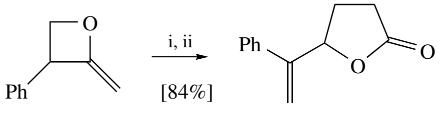

(313) **(314)**

SCHEME 92. Reagents: (i) Li, DTBB (5%), THF, −78 to 0 °C; (ii) H_2O

2. Azetidines

Treatment of *N*-phenylazetidine **315** with lithium and a catalytic amount of DTBB (5%) in THF at −15 °C led to a solution of the corresponding γ-functionalized organolithium intermediate **316**, which by reaction with different electrophiles at temperatures ranging between −78 and 20 °C, and final hydrolysis, afforded the expected functionalized amines **317**. The same reaction using azetidine **318** yielded products **320**, functionalized at the benzylic position, intermediates **319** being involved in the process (Scheme 93)[164].

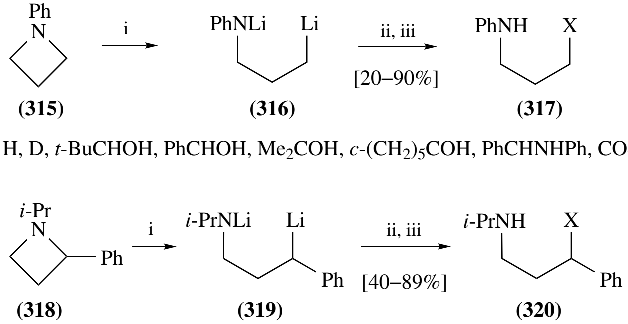

[X = H, D, *t*-BuCHOH, PhCHOH, Me_2COH, *c*-$(CH_2)_5COH$, PhCHNHPh, CO_2H]

[X = H, D, PhCHOH, Me_2COH, $CH_2{=}CHCH_2$]

SCHEME 93. Reagents: (i) Li, DTBB (5%), THF, −15 °C; (ii) E = H_2O, D_2O, *t*-BuCHO, PhCHO, Me_2CO, *c*-$(CH_2)_5CO$, PhCH=NPh, CO_2, −78 to 20 °C; (iii) H_2O

3. Thietanes

2-Phenylthietane (**321**) was opened with lithium and a catalytic amount of DTBB (5%) in THF at −78 °C to generate the most stable benzylic intermediate **322** which, by reacting with an electrophile at the same temperature followed by hydrolysis with water, gave functionalized thiols **323** (Scheme 94)[165]. When carbon dioxide was used as electrophilic reagent, 2-phenyl γ-thiolactone was directly obtained.

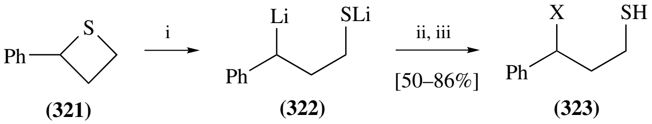

[X = D, *t*-BuCHOH, Et_2COH, CO_2H]

SCHEME 94. Reagents: (i) Li, DTBB (5%), THF, −78 °C; (ii) E = D_2O, *t*-BuCHO, Et_2CO, CO_2, −78 °C; (iii) H_2O, −78 to 20 °C

C. Five-membered Rings

The ring opening of five-membered rings allows one of the easiest entries to δ-functionalized organolithium intermediates (d^4-reagents).

1. Oxygen-containing heterocycles

Tetrahydrofuran itself can be opened using either the stoichiometric[166] or the catalytic[167] version of arene-promoted lithiation, but both cases need the activation by boron trifluoride. The catalytic reaction was performed by treating the solvent THF **324** with the complex boron trifluoride-etherate and a catalytic amount (4%) of naphthalene. The intermediate **325** was formed. Further reaction with carbonyl compounds and final hydrolysis yielded the expected 1,5-diols **326** (Scheme 95), which could be easily cyclized to the corresponding substituted tetrahydropyrans under acidic conditions (concentrated HCl).

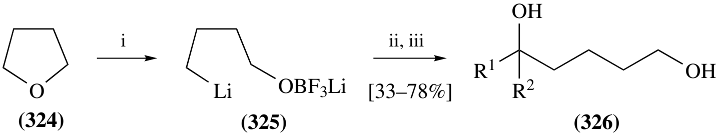

[R^1, R^2 = H, Me, Et, *i*-Pr, Bu, *t*-Bu, Ph]

SCHEME 95. Reagents: (i) $BF_3 \cdot OEt_2$, Li, $C_{10}H_8$ (4%), THF, −78 °C; (ii) R^1R^2CO = *i*-PrCHO, BuCHO, *t*-BuCHO, PhCHO, MeCOBu-*t*, MeCOPh, Et_2CO, −78 to 20 °C; (iii) H_2O

2,3-Dihydrobenzofuran (**327**) reacted with lithium and a catalytic amount (5%) of DTBB in THF at 0 °C to give mainly or exclusively the corresponding intermediate **328**, which by treatment with an electrophile at the same temperature and final hydrolysis yielded functionalized phenols **329** (Scheme 96)[67, 168].

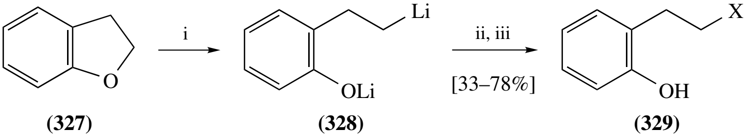

[X = H, *t*-BuCHOH, PhCHOH, $PhCH_2CHOH$, $Ph(CH_2)_2CHOH$, 2-furylCHOH, Me_2COH, Et_2COH, *c*-$(CH_2)_4COH$, *c*-$(CH_2)_5COH$, *c*-$(CH_2)_7COH$]

SCHEME 96. Reagents: (i) Li, DTBB (5%), THF, 0 °C; (ii) E = H_2O, *t*-BuCHO, PhCHO, $PhCH_2CHO$, $Ph(CH_2)_2CHO$, furfural, Me_2CO, Et_2CO, *c*-$(CH_2)_4CO$, *c*-$(CH_2)_5CO$, *c*-$(CH_2)_7CO$, (−)-menthone, −78 °C; (iii) H_2O, −78 to 20 °C

The naphthalene-catalyzed (2.5%) lithiation of phthalan **330**[169] (or its substituted derivatives[170, 171]) in THF at room temperature allowed the preparation of the functionalized benzyllithium intermediate **331**, which reacted with electrophiles at −78 °C to give, after hydrolysis, the corresponding functionalized benzyl alcohols **332** (Scheme 97). When carbon dioxide was used as the electrophilic reagent, the corresponding δ-lactone was directly obtained[169]. When carbonyl compounds were used as electrophiles, the cyclization of the resulting products **332** under acidic conditions (85% H_3PO_4) allows the synthesis of substituted isochromans.

The chemistry described in Scheme 97 has been applied to the synthesis of 4-arylisochroman-3-acetic acids[172], interesting precursors of benzo[*c*]pyran antibiotics[173].

Special cases concerning the reactivity of intermediate **331** with electrophiles involve the use of *N*-silylimine or epoxides. In the first case, aminoalcohol **333** was prepared, which was easily cyclized (thionyl chloride followed by basic treatment) to the corresponding substituted tetrahydroisoquinoline **334** (Scheme 98)[174].

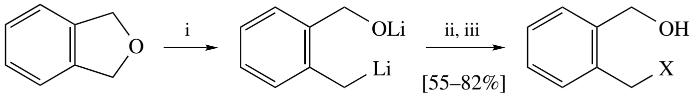

(330) **(331)** **(332)**

[X = D, CO_2H, *t*-BuCHOH, PhCHOH, Et_2COH, *c*-$(CH_2)_5COH$, PhC(OH)Me]

SCHEME 97. Reagents: (i) Li, DTBB (2.5%), THF, 20 °C; (ii) E = D_2O, CO_2, *t*-BuCHO, PhCHO, Et_2CO, *c*-$(CH_2)_5CO$, PhCOMe, −78 °C; (iii) H_2O, −78 to 20 °C

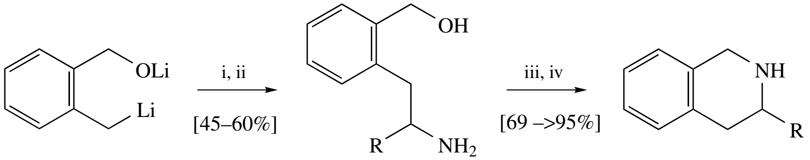

(331) **(333)** **(334)**

[R = *t*-Bu, Ph, 2-furyl]

SCHEME 98. Reagents: (i) RCH=NSiMe$_3$, −45 to 20 °C; (ii) H_2O; (iii) Cl_2SO, $CHCl_3$, 50 °C; (iv) NaOH

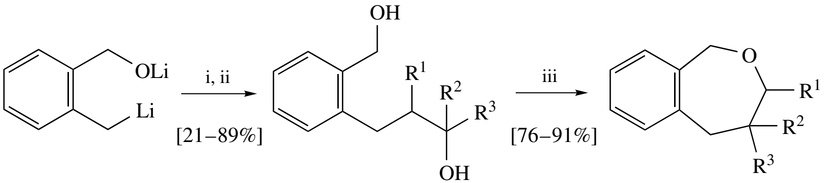

(331) **(335)** **(336)**

[R^1, R^2, R^3 = H, Me, *n*-C_6H_{13}, Ph; R^1R^2 = $(CH_2)_4$; R^2R^3 = $(CH_2)_7$]

SCHEME 99. Reagents: (i) $R^1CH(O)CR^2R^3$, THF, 0 °C; (ii) H_2O; (iii) $BF_3{\cdot}OEt_2$, CH_2Cl_2, −30 to 20 °C

By using epoxides as electrophiles, diols **335** were isolated and easily cyclized by treatment with boron trifluoride into the corresponding substituted tetrahydrobenzoxepines **336** (Scheme 99)[175].

Intermediate **331** was used in the reaction with ketone-derived sugars **133** (from D-glucose) or **270** (from D-fructose) and with the protected estrone **280** so that, after hydrolysis, diols **337–339**[110, 154] were obtained in 25–80% yield. Further cyclization of these diols under Mitsunobu-type reaction conditions (PPh_3, DIAD, benzene reflux) gave the mixed heterocyclic sugars **340** and **341**[110], and the steroid derivative **342**[154], respectively, in 45–50% yield.

In order to modulate the reactivity of intermediate **331**, it was transformed into its copper derivative by treatment with copper(I) bromide or iodide in THF at −78 °C, and then was allowed to react with α,β-unsaturated carbonyl compounds (to give compounds **343** resulting from a conjugated addition), acyl chlorides (to give ketones **344**) and copper(II) chloride (to dimerize giving compounds **345**) (Scheme 100)[176, 177].

Actually, the conjugate addition of intermediate **331** to α,β-unsaturated carbonyl compounds can be promoted not only by copper(I) salts but also with other Lewis acids, such

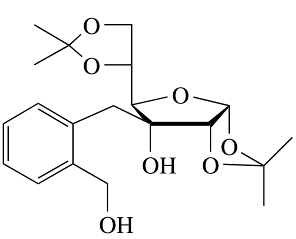

(337)

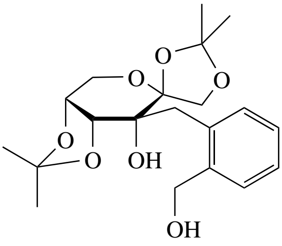

(338)

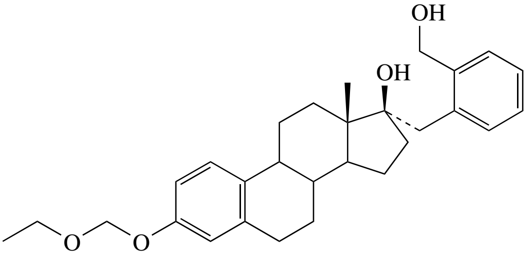

(339)

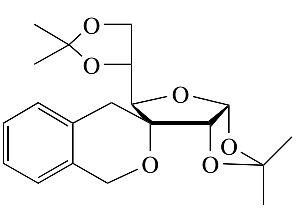

(340)

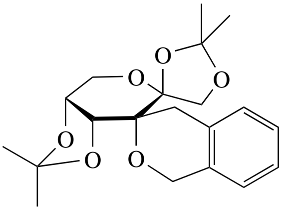

(341)

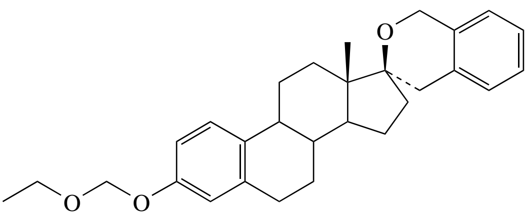

(342)

as zinc dihalides (chloride, bromide or iodide), aluminum trichloride, iron trichloride or boron trifluoride in THF at −78 °C. In all cases 1,4-addition is predominant (up to 79%) compared to the corresponding 1,2-addition ($<30\%$) using α,β-unsaturated ketones or esters[178].

Concerning the lithium–zinc transmetallation from intermediate **331**, it has been used (THF, room temperature) to perform a palladium-catalyzed Negishi cross-coupling reaction with aryl bromides[179, 180] and a S_N2' regioselective allylation in the presence of copper cyanide[181]. **346** and **347** were, respectively, obtained (Scheme 101).

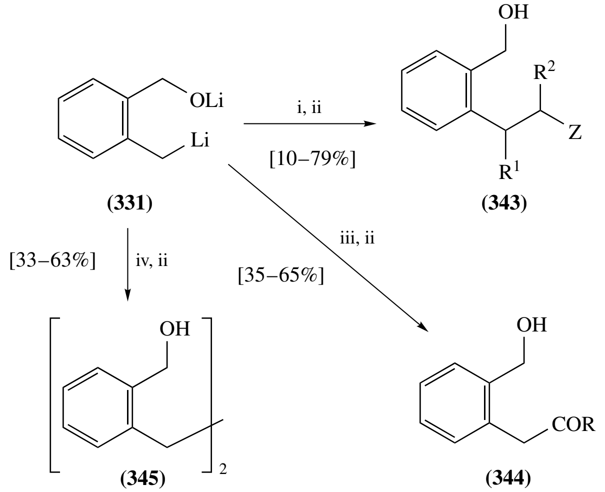

R = *t*-Bu, Ph; R^1, R^2 = H, Me, Ph
Z = COMe, COPh, CO_2Me, CO_2Et; R^1Z = $(CH_2)_2CO$, $(CH_2)_3CO$

SCHEME 100. Reagents: (i) CuX (X = Br, I), $R^1CH{=}C(R^2)Z$ (Z = COR, CO_2R), THF, −78 °C; (ii) NH_4Cl–H_2O, −78 to 20 °C; (iii) CuX, RCOCl (R = *t*-Bu, Ph), THF, −78 °C; (iv) $CuCl_2$, THF, −78 °C

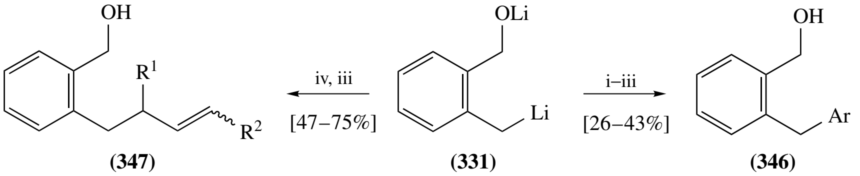

Ar = Ph, 4-*t*-BuC_6H_4, 4-MeOC_6H_4
R^1, R^2 = H, Me, Ph, CH_2Br

SCHEME 101. Reagents: (i) $ZnBr_2$, THF, −20 °C; (ii) ArBr, $Pd(PPh_3)_4$ or $Pd(PPh_3)_2(OAc)_2$ (5%), THF, 65 °C; (iii) HCl–H_2O; (iv) $ZnBr_2$, CuCN, $R^1CH{=}CHCH(R^2)X$ (X = Cl, Br), THF, −78 or 25 °C

In a different study, intermediate **331** was transformed into its titanium derivative (by treatment with triisopropoxytitanium chloride) in order to discriminate between carbonyl compounds[182]. It was found that this reagent reacted preferentially or exclusively with aldehydes in the presence of ketones (which were recovered unaltered) or with aliphatic aldehydes in the presence of aromatic ones[183].

Concerning 2,3-benzofuran (**348**), its DTBB-catalyzed (5%) lithiation in THF at 0 °C gave the intermediate **349** having a (*Z*)-configuration, which reacted with electrophiles and was finally hydrolyzed to afford (*Z*)-products **350** (Scheme 102)[184]. Cyclization of compounds **350**, resulting from the reaction with carbonyl compounds, under acidic conditions (85% H_3PO_4, under toluene reflux or zinc chloride in 1,2-dichloroethane at room temperature), yielded substituted 2-*H*-chromenes including desoxycordiachromene.

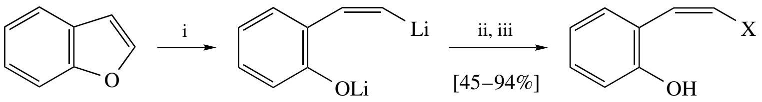

(348) **(349)** **(350)**

[X = D, *t*-BuCHOH, PhCHOH, $Ph(CH_2)_2CHOH$, Me_2COH, PrC(OH)Me, PhC(OH)Me, *c*-$(CH_2)_4COH$]

SCHEME 102. Reagents: (i) Li, DTBB (5%), THF, 0 °C; (ii) E = H_2O, D_2O, *t*-BuCHO, PhCHO, $Ph(CH_2)_2CHO$, Me_2CO, PrCOMe, PhCOMe, *c*-$(CH_2)_4CO$, −78 °C; (iii) H_2O, −78 to 20 °C

2. Nitrogen-containing heterocycles

2-Phenyl-*N*-isopropylpyrrolidine (**351**) was opened with lithium and a catalytic amount (4.5%) of DTBB in THF at room temperature to give the most stable benzylic intermediate **352**, which after tandem electrophilic substitution reaction at −78 °C and final hydrolysis afforded the expected functionalized amines **353** (Scheme 103)[185].

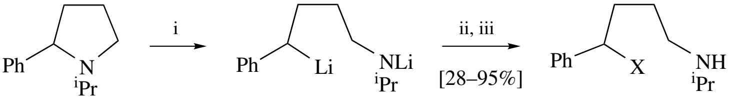

(351) **(352)** **(353)**

[X = H, D, Me, *t*-BuCHOH, PhCHOH, Me_2COH, *c*-$(CH_2)_4COH$, *c*-$(CH_2)_5COH$, CO_2H]

SCHEME 103. Reagents: (i) Li, DTBB (4.5%), THF, 20 °C; (ii) E = H_2O, D_2O, MeI, *t*-BuCHO, PhCHO, Me_2CO, *c*-$(CH_2)_4CO$, *c*-$(CH_2)_5CO$, CO_2, −78 °C; (iii) H_2O, −78 to 20 °C

The same reaction applied to the pyrrolidine **354** gave a mixture of both α- and γ-products (**356** and **357**, respectively), which were formed from the corresponding delocalized allyllithium intermediate **355**[185] in 34–85% yield.

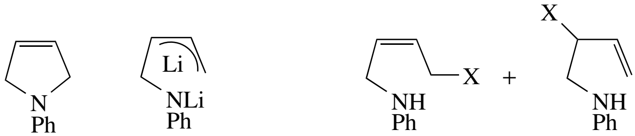

(354) **(355)** **(356)** **(357)**

[X = H, D, *t*-BuCHOH, Me_2COH, *c*-$(CH_2)_4COH$, *c*-$(CH_2)_5COH$, CO_2H]

N-Phenylisoindoline (**358**) was submitted to DTBB-catalyzed (4.5%) lithiation in THF at room temperature to give the corresponding benzylic organolithium intermediate **359**. Successive reaction of this compound with an electrophile and water gave the expected products **360** (Scheme 104)[185].

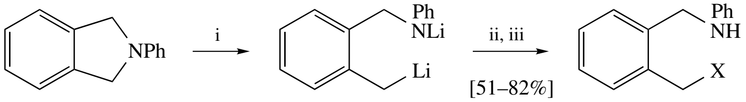

(358) **(359)** **(360)**

[X = H, D, *i*-PrCHOH, *t*-BuCHOH, PhCHOH, Me_2COH, PhC(OH)Me]

SCHEME 104. Reagents: (i) Li, DTBB (4.5%), THF, 20 °C; (ii) E = H_2O, D_2O, *i*-PrCHO, *t*-BuCHO, PhCHO, Me_2CO, PhCOMe, −78 °C; (iii) H_2O, −78 to 20 °C

3. Sulfur-containing heterocycles

When 2-phenyltetrahydrothiophene (**361**) was treated with lithium and a catalytic amount of DTBB (5%) in THF at −78 °C, the corresponding intermediate **362** was generated which, by further electrophilic substitution reaction at the same temperature and final hydrolysis, gave the expected functionalized thiols **363** (Scheme 105)[165].

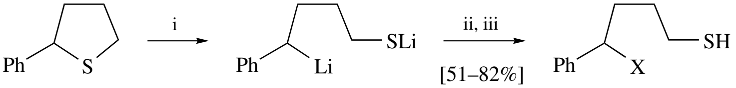

(361) **(362)** **(363)**

[X = D, *t*-BuCHOH, Me_2COH, Et_2COH, *c*-$(CH_2)_4COH$, CO_2H]

SCHEME 105. Reagents: (i) Li, DTBB (5%), THF, −78 °C; (ii) E = D_2O, *t*-BuCHO, Me_2CO, Et_2CO, *c*-$(CH_2)_4CO$, CO_2, −78 °C; (iii) H_2O, −78 to 20 °C

Thiophthalan (**364**) gave a similar reactivity to phthalan (**330**). Thus, its lithiation using a catalytic amount of DTBB (5%) as the electron carrier in THF at −78 °C gave the intermediate **365**, able to react with different electrophiles to yield, after hydrolysis, the corresponding functionalized thiols **366** (Scheme 106)[186].

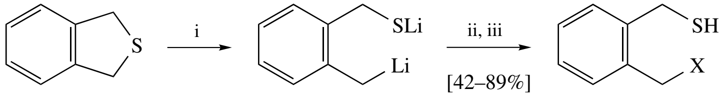

(364) **(365)** **(366)**

[X = H, D, *i*-PrCHOH, *t*-BuCHOH, PhCHOH, *c*-$(CH_2)_4COH$, PhC(OH)Me]

SCHEME 106. Reagents: (i) Li, DTBB (5%), −78 °C; (ii) E = H_2O, D_2O, *i*-PrCHO, *t*-BuCHO, PhCHO, *c*-$(CH_2)_4CO$, PhCOMe, −78 °C; (iii) H_2O, −78 to 20 °C

The use of carbon dioxide as electrophile afforded directly the thiolactone **367** in 72% yield. Finally, compounds **366**, derived from the use of a carbonyl compound as electrophile, were easily cyclized under acidic conditions (85% H_3PO_4, toluene reflux) to yield the corresponding thioisochromans **368**[186] in 85–97% yield.

D. Six-membered Rings

Six-membered heterocycles are more resistant to an arene catalyzed lithiation than the corresponding five-membered ones. For instance, tetrahydropyran can not be cleaved under the reaction condition employed to open tetrahydrofuran (activation by BF_3)[166, 167].

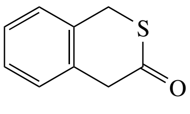

(367)

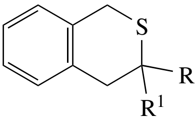

(368)

R^1, R^2 = H, Me, *i*-Pr, *t*-Bu, Ph
$R^1R^2 = (CH_2)_4$

1. Oxygen-containing heterocycles

Chroman (**369**) was lithiated under DTBB-catalyzed (5%) conditions in THF at 0 to 25 °C giving, after treatment with an electrophile at −78 °C and final hydrolysis with water, mainly or exclusively compounds **372**. The unexpected formation of these products can be explained by an initial cleavage of the phenyl–oxygen bond (compare to 2,3-dihydrobenzofuran[67, 168], in which the alkyl–oxygen bond was broken) giving the intermediate **370**, followed by an intramolecular deprotonation into the new benzylic intermediate **371**. The second γ-functionalized organolithium compound **371** is strongly stabilized by intermolecular coordination (CIPE: complex induced proximity effect) (Scheme 107)[168].

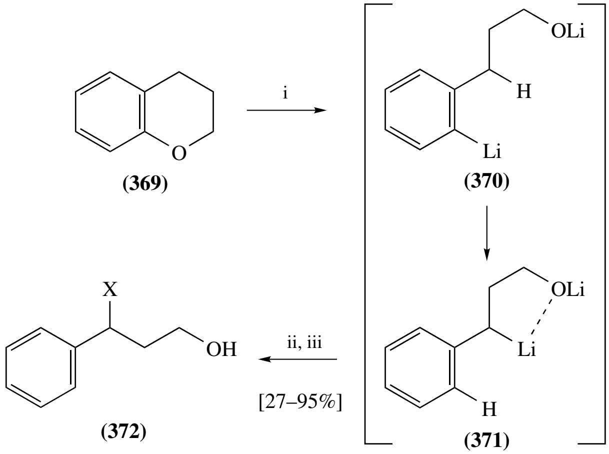

(369) **(370)** **(371)** **(372)**

X = H, *t*-BuCHOH, PhCHOH, 2-furylCHOH,
Me_2COH, $(n\text{-}C_5H_{11})_2COH$, $c\text{-}(CH_2)_5COH$, Ph_2COH

SCHEME 107. Reagents: (i) Li, DTBB (5%), THF, 0 to 20 °C; (ii) E = H_2O, *t*-BuCHO, PhCHO, furfural, Me_2CO, $[Me(CH_2)_4]_2CO$, $c\text{-}(CH_2)_5CO$, (−)-menthone, Ph_2CO, −78 °C; (iii) H_2O, −78 to 20 °C

The ring opening of isochroman (**373**) by means of lithium and DTBB (2.5%) in THF at room temperature gave the benzylic intermediate **374**, which by reaction with an electrophile at temperatures ranging between −78 and 20 °C yielded, after hydrolysis, the expected products **375** (Scheme 108)[187].

When carbon dioxide was used as electrophile, the seven-membered lactone **376** was isolated after treatment of the initially formed hydroxy acid (**375** with X = CO_2H) with

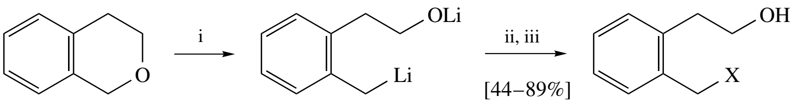

(373) **(374)** **(375)**

[X = H, D, CO_2H, EtCHOH, *i*-PrCHOH, *i*-BuCHOH, *t*-BuCHOH, PhCHOH, Me_2COH, Et_2COH, *c*-$(CH_2)_5COH$, PhC(OH)Me]

SCHEME 108. Reagents: (i) Li, DTBB (2.5%), THF, 20 °C; (ii) E = H_2O, D_2O, CO_2, EtCHO, *i*-PrCHO, *i*-BuCHO, *t*-BuCHO, PhCHO, Me_2CO, Et_2CO, *c*-$(CH_2)_4CO$, *c*-$(CH_2)_5CO$, PhCOMe, −78 to 20 °C; (iii) H_2O

a catalytic amount of PTSA under toluene reflux in 75% yield. On the other hand, compounds **375** resulting from the reaction of intermediate **374** with benzaldehyde or ketones were easily cyclized to the corresponding oxepanes **377** under acidic conditions (85% H_3PO_4 under toluene reflux) in 67–79% yield. For aliphatic aldehydes, this acidic treatment afforded different products coming from an isomerization of the initially formed carbenium ion.

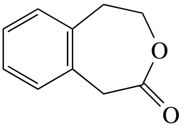

(376)

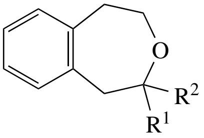

(377)

As was described for phthalan **330**, the intermediate **374** has also been used for the EPC synthesis of branched-chain sugars **378** and **379**[110] and the steroid **380**[154] in 15–70% yield, employing ketones **133** and **270**, as well as **280**, respectively.

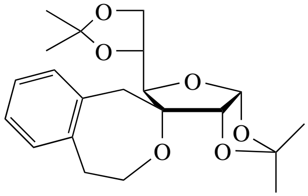

(378)

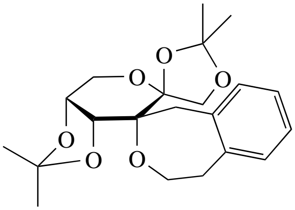

(379)

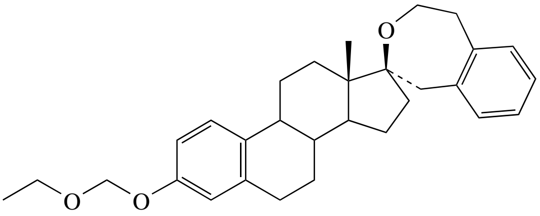

(380)

Also in the case of intermediate **374**, a lithium–copper transmetallation with a copper(I) halide (bromide or chloride) allowed one to carry out the conjugate addition [to electrophilic olefins $R^1CH = CH_2Z$ ($Z = COR, CO_2R$) giving compounds **381** in 31–76% yield], the acylation (with acyl chlorides yielding ketones **382** in 35–65% yield) and dimerization [using copper(II) chloride as the additive, to give compound **383** in 59% yield] processes[176, 177].

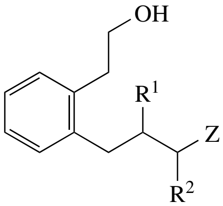

(381)

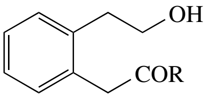

(382)

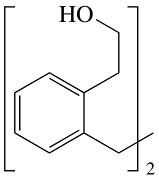

(383)

R^1, R^2 = H, Me, Ph
Z = COMe, COPh, CO_2Me, CO_2Et
$R^1Z = (CH_2)_2CO, (CH_2)_3CO$

[R = *t*-Bu, Ph]

When the metallic additive to the intermediate **374** was zinc dihalide (or another Lewis acid, such as aluminum trichloride, iron trichloride or boron trifluoride), a conjugate addition to electrophilic olefins affords **381**[178]. In the case of the lithium–zinc transmetallation, a palladium-catalyzed Negishi cross-coupling reaction with aryl bromides or iodides allowed the preparation of arylated compounds **384**[179, 180] in 26–77% yield. In addition, a S_N2' allylation of the mentioned zinc intermediates with reagents of type $R^1CH{=}CHCH(R^2)X$ (X = chlorine, bromine) gave the corresponding compounds **385** in 52–68% yield[181].

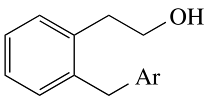

(384)

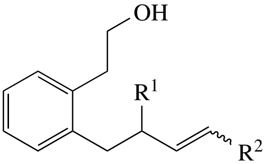

(385)

Ar = Ph, 4-FC_6H_4, 4-$CF_3C_6H_4$, 4-$MeOC_6H_4$,
4-$Me_2NC_6H_4$, 4-$MeCOC_6H_4$, 4-NCC_6H_4,
4-$EtO_2CC_6H_4$, 1-naphthyl, 4-Py, 2-thienyl, 3-furyl

[R^1, R^2 = H, Me, Ph, CH_2Br]

Lithium–titanium transmetallation of intermediate **374** made possible the chemoselective discrimination between aldehydes and ketones, reacting mainly or exclusively with the first type of carbonyl compounds, as observed for the phthalan-derived intermediate **331**[183].

Concerning the arene-catalyzed lithiation of 4-*H*-chromene **386**, the process is not of synthetic interest as compared to the same process applied to 2,3-benzofuran **348** because both alkyl–and aryl–oxygen cleavage took place using DTBB (5%) as the electron-carrier catalyst in THF at temperatures ranging between 0 and 25 °C. These intermediates **387** and **388** were obtained (2:1 molar ratio) as was proven after hydrolysis with water: a mixture of products **389** and **390** were isolated in the mentioned ratio (Scheme 109)[168].

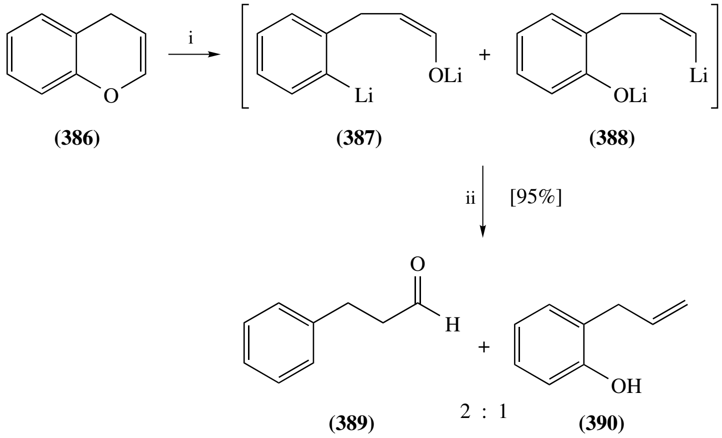

SCHEME 109. Reagents: (i) Li, DTBB (5%), THF, 0 to 20 °C; (ii) H_2O, −78 to 20 °C

2. Nitrogen-containing heterocycles

The reductive ring opening of six-membered nitrogen-containing heterocycles was studied with *N*-phenyltetrahydroisoquinoline (**391**). Its lithiation with lithium and a catalytic amount of DTBB (4.5%) afforded the benzylic intermediate **392**, which was allowed to react with electrophiles giving, after hydrolysis, functionalized amines **393** (Scheme 110)[185]. It is noteworthy that in the reaction with carbon dioxide, instead of the corresponding lactam, amino acid **393** with X = CO_2H was exclusively isolated.

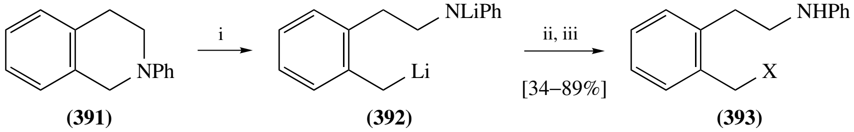

[X = H, D, *i*-BuCHOH, PhCHOH, Me_2COH, PrC(OH)Me, *c*-$(CH_2)_4COH$, CO_2H]

SCHEME 110. Reagents: (i) Li, DTBB (4.5%), THF, 20 °C; (ii) E = H_2O, D_2O, *t*-BuCHO, PhCHO, Me_2CO, PrCOMe, *c*-$(CH_2)_4CO$, CO_2, −78 °C; (iii) H_2O, −78 to 20 °C

When the reaction shown in Scheme 110 was applied to *N*-methyltetrahydroisoquinoline (**394**), compounds **398** were unexpectedly obtained. An explanation involving intermediates **395–397** has been postulated (Scheme 111)[185].

3. Sulfur-containing heterocycles

The α-phenyl substituted six-membered sulfur-containing material **399** was reductively cleaved using DTBB (5%) as the arene catalyst in THF at −78 °C. The resulting intermediate **400** was then reacted with an electrophile followed by hydrolysis, yielding functionalized thiols **401** (Scheme 112)[165].

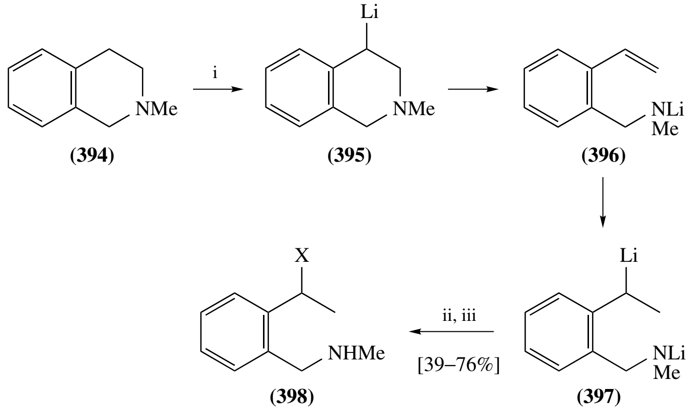

[X = H, D, $CH_2{=}CHCH_2$, c-$(CH_2)_4COH$]

SCHEME 111. Reagents: (i) Li, DTBB (4.5%), THF, 20 °C; (ii) E = H_2O, D_2O, $BrCH_2CH{=}CH_2$, c-$(CH_2)_4CO$, −78 °C; (iii) H_2O, −78 to 20 °C

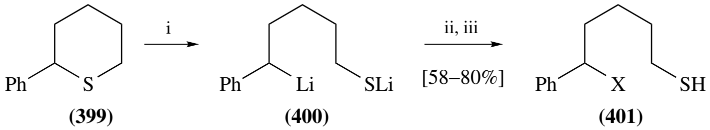

[X = D, t-BuCHOH, Me_2COH, Et_2COH, c-$(CH_2)_4COH$, Me_3Si, CO_2H]

SCHEME 112. Reagents: (i) Li, DTBB (5%), THF, −78 °C; (ii) E = D_2O, t-BuCHO, Me_2CO, Et_2CO, c-$(CH_2)_4CO$, Me_3SiCl, CO_2, −78 °C; (iii) H_2O, −78 to 20 °C

Finally, the ring opening of substituted thioisocromans (**402**) with lithium and a catalytic amount of DTBB (5%) in THF at −78 °C gave the expected benzylic intermediates **403** which, after reaction with electrophiles at the same temperature and final hydrolysis with water, yielded functionalized thiols **404** (Scheme 113)[186].

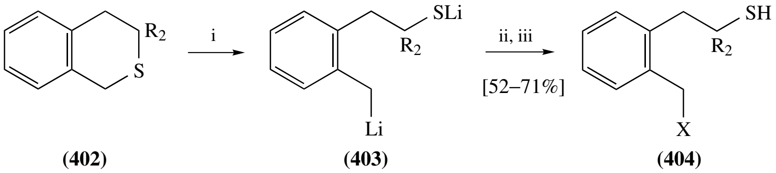

[R = H, Me]

[X = D, t-BuCHOH, Me_2COH, c-$(CH_2)_4COH$, CO_2H]

SCHEME 113. Reagents: (i) Li, DTBB (5%), THF, −78 °C; (ii) E = D_2O, t-BuCHO, Me_2CO, c-$(CH_2)_4CO$, CO_2, −78 °C; (iii) H_2O, −78 to 20 °C

In the case of using carbon dioxide as the electrophile, seven-membered ring lactones were obtained, the reaction being exemplified with compound **405** (67% yield). On the other hand, for carbonyl compound derivatives of type **404**, their cyclization under acidic conditions (85% H_3PO_4, toluene reflux) gave the corresponding cyclic thioethers **406** in 76–90% yield[186].

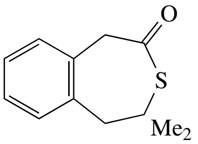

(405)

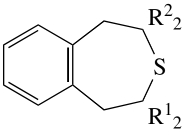

(406)

[R^1, R^2 = H, Me; R^{1}R^1 = $(CH_2)_4$]

E. Seven-membered Rings

Dibenzo oxygen-, nitrogen- and sulfur-containing seven-membered ring derivatives **407** were submitted to a naphthalene (10%) or DTBB (5%) catalyzed lithiation in THF at different temperatures (−15 to 20 °C for Y = O, 0 °C for Y = NMe and −78 °C for Y = S) giving the corresponding intermediates **408**. These functionalized organolithium compounds reacted with electrophiles giving, after hydrolysis, the expected functionalized products **409** (Scheme 114)[188, 189].

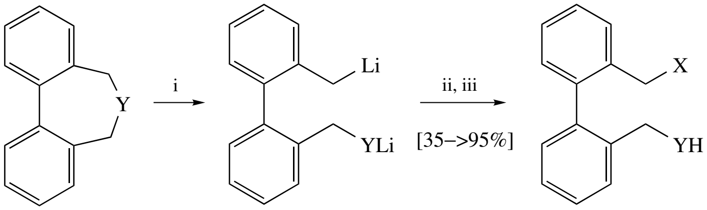

(407) **(408)** **(409)**

Y = O, NMe, S
X = H, D, *i*-PrCHOH, BuCHOH, *t*-BuCHOH, PhCHOH, $Ph(CH_2)_2CHOH$,
Me_2COH, $(n\text{-}C_5H_{11})_2COH$, *c*-$(CH_2)_5COH$, *c*-$(CH_2)_7COH$, Me_3Si

SCHEME 114. Reagents: (i) Li, $C_{10}H_8$ (10% for Y = O, NMe) or DTBB (5% for Y = S), THF, for temperature, see text; (ii) E = H_2O, D_2O, *i*-PrBr, BuBr, *t*-BuCHO, PhCHO, $Ph(CH_2)_2CHO$, Me_2CO, $[Me(CH_2)_4]_2CO$, *c*-$(CH_2)_5CO$, *c*-$(CH_2)_7CO$, (−)-menthone, Me_3SiCl; (iii) H_2O

F. Heterocycles Containing Two Heteroatoms

The presence of two equal or different heteroatoms in the heterocyclic compound to be opened reductively makes this chemistry different than that of heterocycles containing only one heteroatom.

1. Five-membered rings

2-Substituted 2-phenyl 1,3-dioxolanes **410** reacted with lithium and a catalytic amount of naphthalene (4%) in THF at −40 °C to yield intermediates **411** and products **412**, after successive electrophilic substitution reaction at the same temperature and final hydrolysis (Scheme 115)[190].

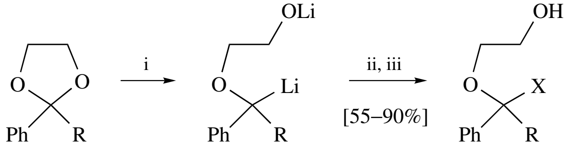

(410) **(411)** **(412)**

$R = H, Me$
$X = H, D, Me_2COH, Et_2COH, c\text{-}(CH_2)_4COH, c\text{-}(CH_2)_5COH$

SCHEME 115. Reagents: (i) Li, $C_{10}H_8$ (4%), THF, −40 °C; (ii) E = H_2O, D_2O, Me_2CO, Et_2CO, c-$(CH_2)_4CO$, c-$(CH_2)_5CO$, −40 °C; (iii) H_2O, −40 to 20 °C

The ring opening of aryl-substituted heterocycles **413** containing oxygen and nitrogen as heteroatoms was carried out with lithium and a catalytic amount of naphthalene (10%) in THF at −20 °C to give intermediates **414** in which the cleavage of the more polar carbon−oxygen bond took place exclusively. Their reaction with electrophiles gave, after hydrolysis, the expected compounds **415** (Scheme 116)[105, 191].

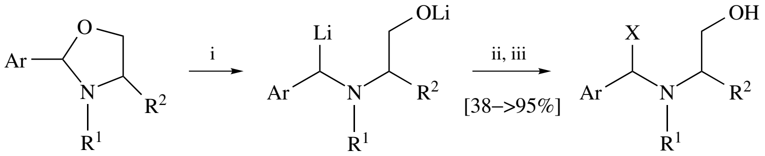

(413) **(414)** **(415)**

$Ar = Ph, 2,3\text{-}(MeO)_2C_6H_3, 4\text{-}Me_2NC_6H_4$
$R^1 = Me; R^1R^2 = (CH_2)_4$
$X = H, D, Me, Et, Bu, n\text{-}C_6H_{13}, i\text{-}PrCHOH, Me_2COH, c\text{-}(CH_2)_5COH$

SCHEME 116. Reagents: (i) Li, $C_{10}H_8$ (10%), THF, −20 °C; (ii) E = H_2O, D_2O, MeI, EtBr, BuBr, n-$C_6H_{13}Br$, i-PrCHO, Me_2CO, c-$(CH_2)_5CO$; (iii) H_2O

2. Six-membered rings

1,3-Dioxanes can be opened by an arene-catalyzed lithiation only if the carbon−oxygen bond to be cleaved occupies an allylic or benzylic position. This is the case of the vinyldioxane **416**, which reacted with lithium and a catalytic amount of DTBB in THF at 0 °C, and the allylic intermediate **417** generated reacted at the γ-position with tridecyl iodide to yield the compound **418**, used in the synthesis of plasmenyl-type lipids (Scheme 117)[192].

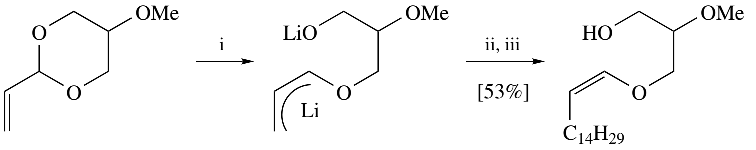

(416) **(417)** **(418)**

SCHEME 117. Reagents: (i) Li, DTBB (cat.), THF, 0 °C; (ii) $C_{13}H_{27}I$, 0 °C; (iii) H_2O

The corresponding benzylic reductive cleavage was carried out using aryl-substituted 1,3-dioxanes **419**, lithium and a catalytic amount of naphthalene (10%) in THF at temperatures ranging from −78 to −40 °C. The obtained benzylic intermediates **420** were then treated with different electrophiles giving, after hydrolysis, the corresponding products **421** (Scheme 118)[193, 194].

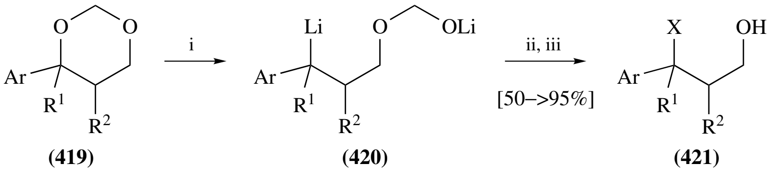

(419) **(420)** **(421)**

Ar = Ph, 4-MeOC$_6$H$_4$
R^1, R^2 = H, Me, Bu, Ph
X = H, D, *i*-Pr, Bu, *n*-C$_6$H$_{13}$, PhCH$_2$, *i*-PrCHOH, Me$_2$COH, Me$_3$Si, CO$_2$H

SCHEME 118. Reagents: (i) Li, C$_{10}$H$_8$ (10%), THF, −78 to −40 °C; (ii) E = H$_2$O, D$_2$O, MeOD, *i*-PrBr, BuBr, *n*-C$_6$H$_{13}$Br, PhCH$_2$Cl, *i*-PrCHO, Me$_2$CO, Me$_3$SiCl, CO$_2$, −60 to −40 °C; (iii) H$_2$O, −60 or −40 to 20 °C

Another type of heterocycle containing two heteroatoms susceptible of being cleaved reductively are 1,3-dioxanes or 1,3-oxathianes **422**. They were treated with lithium and a catalytic amount of DTBB (4.5%) in THF at room temperature (Y = O) or at −78 °C (Y = S) to yield, after hydrolysis with water, functionalized homobenzylic alcohols **425** (Scheme 119)[195]. The participation of intermediates **423** and **424** has been postulated in order to explain the obtained results.

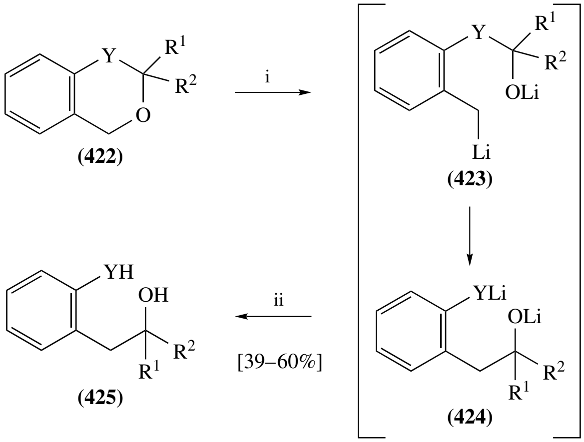

(422) **(423)** **(424)** **(425)**

Y = O, S
R^1, R^2 = H, Me, *i*-Pr, *i*-Bu, *t*-Bu, Ph(CH$_2$)$_2$; R^{1}R^2 = (CH$_2$)$_5$

SCHEME 119. Reagents: (i) Li, DTBB (4.5%), THF, 20 °C; (ii) H$_2$O

The ring opening of phenoxathiin (Y = O), phenothiazine (Y = NMe) or thianthrene (Y = S) **426** using lithium and a catalytic amount of DTBB (7.5%) in THF at −78

(Y = O) or −90 °C (Y = NMe, S) gave the corresponding intermediates **427** resulting from a carbon−sulfur cleavage. Further reaction of these functionalized organolithium compounds with different electrophiles at the same temperature, followed by hydrolysis with water, yielded products **428** (Scheme 120)[196].

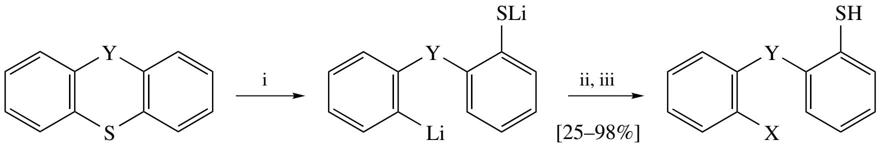

(426) **(427)** **(428)**

Y = O, NMe, S
X = H, D, *t*-BuCHOH, PhCHOH, $Ph(CH_2)_2CHOH$, Me_2COH, Et_2COH, *c*-$(CH_2)_5COH$

SCHEME 120. Reagents: (i) Li, DTBB (7.5%), THF, −90 or −78 °C; (ii) E = H_2O, D_2O, *t*-BuCHO, PhCHO, $Ph(CH_2)_2CHO$, Me_2CO, Et_2CO, *c*-$(CH_2)_5CO$, −78 °C; (iii) H_2O, −78 to 20 °C

From a heterocyclic point of view, **428** derived from the reaction with carbonyl compounds are of interest, since their cyclization under acidic conditions (85% H_3PO_4, toluene reflux) gave the seven-membered ring derivatives **429** in 74−97% yield.

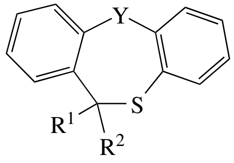

(429)

[Y = O, S; R^1, R^2 = H, Et, *t*-Bu, Ph]

VII. POLYLITHIUM SYNTHONS

The use of polylithium synthons[197] in synthetic organic chemistry presents the advantage of making possible the simultaneous introduction of various electrophilic fragments in the reaction with electrophiles, in such a way that polyfunctionalized molecules can be directly prepared.

A. *gem*-Polylithium Synthons

The reaction of dichloromethane (or its dideuterio derivative) (**430**) with lithium and a catalytic amount of DTBB (5%) in the presence of a carbonyl compound as electrophile in THF at −40 °C led, after final hydrolysis with water, to the corresponding 1,3-diols **431** (Scheme 121)[198, 199].

The Barbier-type reaction shown in Scheme 121 was also applied to the dichlorinated materials **432−434**, as well as trichloroalkanes **435** and even tetrachloromethane **436**. In every case, all chlorine atoms were replaced by electrophilic fragments, so the starting material behaved as polylithium synthons. Actually, the whole process takes place probably by successive tandem lithiation-S_E reactions until consumption of all chlorine atoms

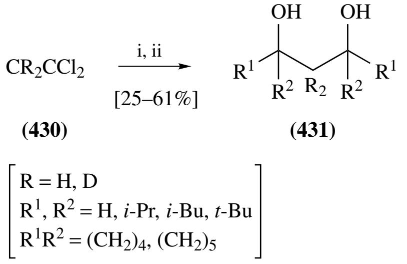

(430) **(431)**

R = H, D
R^1, R^2 = H, *i*-Pr, *i*-Bu, *t*-Bu
$R^1R^2 = (CH_2)_4, (CH_2)_5$

SCHEME 121. Reagents: (i) Li, DTBB (5%), R^1R^2CO = *i*-PrCHO, *i*-BuCHO, *t*-BuCHO, *c*-$(CH_2)_4CO$, *c*-$(CH_2)_5CO$, THF, −40 °C; (ii) H_2O, −40 to 20 °C

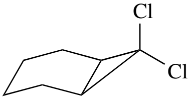

(432)

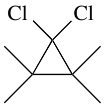

(433)

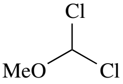

(434)

$RCCl_3$ **(435)**

CCl_4 **(436)**

[R = H, D, Me, Ph]

(51–98%). As an example, carbon tetrachloride (**436**) gave tetrakis(trimethylsilyl)methane by reaction with chlorotrimethylsilane in 80% isolated yield.

When 2,2-diphenyl-1,3-dioxolane (**410**, R = Ph) was lithiated with lithium and a catalytic amount of naphthalene (4%) in THF at −40 °C (see Section VI.F.1) and then reacted with an aldehyde as electrophile, intermediates **437** were generated. The further lithiation of these compounds at the same temperature cleaved the second benzylic carbon–oxygen bond giving new organolithium intermediates **438**, and a second electrophile could be introduced to give **439**, after hydrolysis. In these products, two different electrophilic fragments have been incorporated, so the starting material behaves as the 1,1-diphenylmethane dianion synthon (Scheme 122)[190].

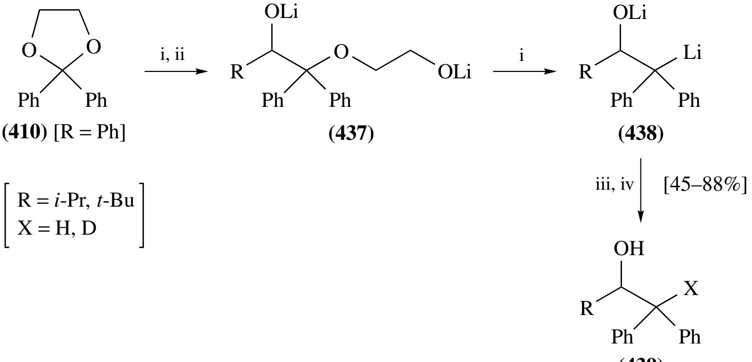

(410) [R = Ph] **(437)** **(438)** **(439)**

R = *i*-Pr, *t*-Bu
X = H, D

SCHEME 122. Reagents: (i) Li, $C_{10}H_8$ (4%), THF, −40 °C; (ii) RCHO = *i*-PrCHO, *t*-BuCHO, −40 °C; (iii) E = H_2O, D_2O, −40 °C; (iv) H_2O, −40 to 20 °C

A different approach to 1,1-dilithium synthons takes advantage of both the activation of a sulfur atom at the *α*-position and a sulfur–lithium exchange, so making it possible to discriminate between both carbon–lithium bonds in a *gem*-dilithiated synthon. When phenyl vinyl sulfide (**440**) was deprotonated with *n*-butyllithium in THF and TMEDA at −78 °C and then reacted with a carbonyl compound, a thioether alkoxide **441** was formed. Treatment of this alkoxide with lithium and a catalytic amount of DTBB (5%) gave a new intermediate **442**, which was trapped with a second carbonyl compound giving, after hydrolysis, unsaturated 1,3-diols **443** with different substituents at both sides of the molecule (Scheme 123)[200, 201].

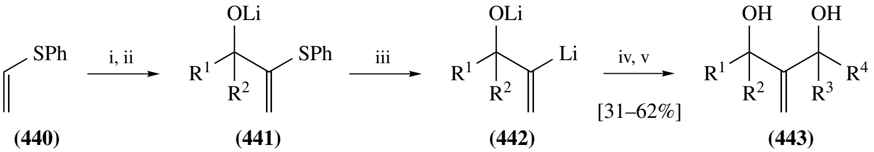

[R^1, R^2, R^3, R^4 = H, Me, *t*-Bu, Ph; R^1R^2, R^3R^4 = $(CH_2)_5$]

SCHEME 123. Reagents: (i) BuLi, TMEDA, THF, −78 °C; (ii) R^1R^2CO = *t*-BuCHO, PhCHO, *c*-$(CH_2)_5CO$, −78 °C; (iii) Li, DTBB (5%), −78 °C; (iv) R^3R^4CO = Me_2CO, *c*-$(CH_2)_5CO$, −78 °C; (v) H_2O, −78 to 20 °C

The same protocol shown in Scheme 123 was used with cyclopropyl phenyl thioether, so cyclopropylic 1,3-diols **444** were obtained in 31–53% yield[201].

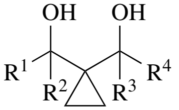

(444)

[R^1, R^2, R^3, R^4 = H, Me, *t*-Bu, *n*-C_5H_{11}, Ph
R^1R^2, R^3R^4 = $(CH_2)_5$, $(CH_2)_7$]

A slightly different reaction was carried out starting from di(phenylthio)methane (**445**). In this case, after deprotonation and reaction with a carbonyl compound under the reaction conditions mentioned above (Scheme 123), intermediates **446** were generated. Further sulfur–lithium exchange catalyzed by DTBB (5%) followed by a reaction with a second carbonyl compound gave dialkoxides **447**, which were chemically characterized after hydrolysis as mercapto diols **448** (Scheme 124)[201, 202]. However, a third lithiation of intermediate **447** by DTBB-catalyzed (5%) lithiation gave the very unstable species **449**, which could not be reacted with electrophiles, because they decomposed by a β-elimination reaction giving a *ca* 1:1 mixture of allyl alcohols **450**. This result is not interesting from a synthetic point of view, but acidic treatment of this mixture with 6 M HCl gave practically quantitative yields of the corresponding substituted 1,3-dienes.

B. 1,2-Dilithium Synthons

The generation of 1,2-dilithioalkanes by a double chlorine–lithio exchange is not possible, because after the first lithiation the chloro–lithio intermediate suffers spontaneously β-elimination, even at temperatures as low as −100 °C[203]. However, when one of the two chlorine atoms is attached to a sp^2-hybridized carbon atom, as

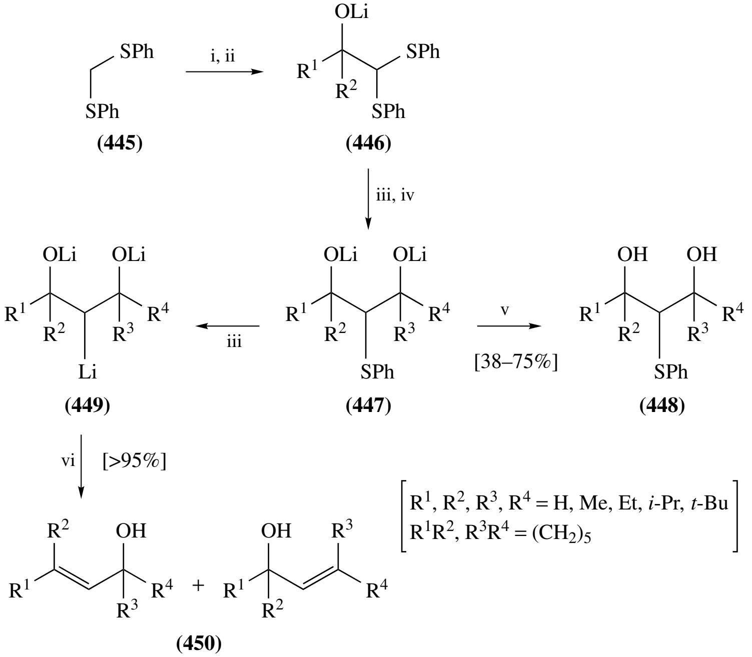

SCHEME 124. Reagents: (i) BuLi, THF, 0 °C; (ii) $R^1R^2CO = t$-BuCHO, Me_2CO, Et_2CO, c-$(CH_2)_5CO$, −40 °C; (iii) Li, DTBB (5%), −78 °C; (iv) $R^3R^4CO = i$-PrCHO, t-BuCHO, Me_2CO, Et_2CO, c-$(CH_2)_5CO$, −78 °C; (v) H_2O, −78 to 20 °C; (vi) −78 to 20 °C, then H_2O

in 2,3-dichloropropene (**451**), its lithiation in the presence of a catalytic amount of DTBB (5%) and the corresponding carbonyl compound as the electrophile in THF at 0 °C gave, after hydrolysis with water, the corresponding unsaturated 1,4-diols **452** (Scheme 125)[204, 205].

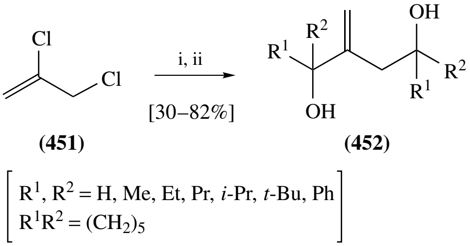

SCHEME 125. Reagents: (i) Li, DTBB (5%), E = i-PrCHO, t-BuCHO, PhCHO, PrCOMe, Et_2CO, c-$(CH_2)_5CO$, PhCOEt, THF, 0 °C; (ii) H_2O

Cyclization of **452** under acidic conditions (3 M HCl) gave substituted methylene tetrahydrofurans **453** in 50–97% yield.

A completely different reaction to give 1,2-dilithio synthons was performed by double lithiation of thianthrene **426** (Y = S) under catalytic conditions. Thus, after the first lithiation with lithium and DTBB (4%) in THF at −90 °C, the corresponding intermediate (of

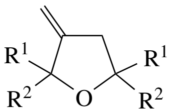

(453)

[R^1, R^2 = H, Me, Et, Pr, Ph
$R^1R^2 = (CH_2)_4, (CH_2)_5$]

type **427** with Y = S; see Section VI.F.2) was allowed to react with a carbonyl compound R^1R^2CO, to give **454**. Then, by raising the temperature to −78 °C, the second sulfur–lithium exchange takes place to give **455**, which reacts *in situ* with a second carbonyl compound R^3R^4CO to give after hydrolysis the substituted diols **456** (Scheme 126)[206].

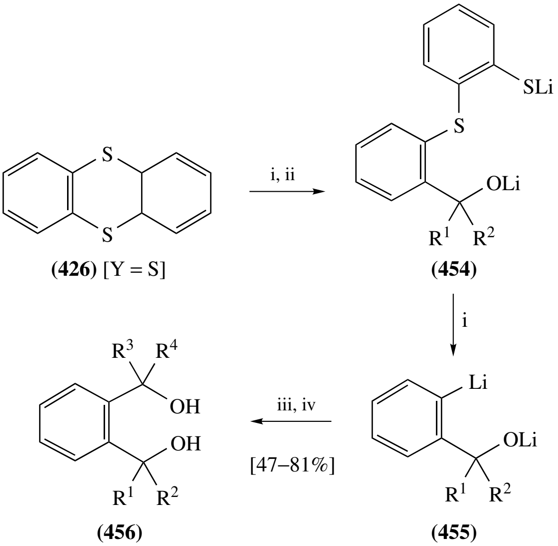

[R^1, R^2, R^3, R^4 = H, Me, Et, *t*-Bu, Ph, $Ph(CH_2)_2$
$R^1R^2, R^3R^4 = (CH_2)_5$]

SCHEME 126. Reagents: (i) Li, DTBB (4%), THF, −90 °C; (ii) R^1R^2CO = *t*-BuCHO, Me_2CO, Et_2CO, *c*-$(CH_2)_5CO$, −90 °C; (iii) R^3R^4CO = *t*-BuCHO, PhCHO, $Ph(CH_2)_2CHO$, Me_2CO, Et_2CO, *c*-$(CH_2)_5CO$, −90 to −78 °C; (iv) H_2O, −78 to 20 °C

When carbon dioxide was used as the second electrophile, the acidic work-up (3 M HCl) afforded directly the corresponding lactones **457** in 55–58% yield. On the other hand, diols **456** were easily cyclized under acidic conditions (85% H_3PO_4, toluene reflux) to give quantitatively the corresponding substituted phthalans **458**.

C. 1,3-Dilithium Synthons

The naphthalene-catalyzed (6%) lithiation of 3-chloro-2-chloromethylpropene **459** in the presence of different carbonyl compounds as electrophiles in THF at temperatures

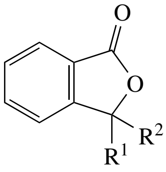

(457)

[R^1, R^2 = H, Me, Ph]

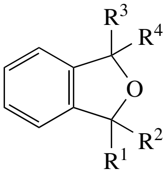

(458)

[R^1, R^2, R^3, R^4 = Me, Et, $Ph(CH_2)_2$
R^1R^2, R^3R^4 = $(CH_2)_5$]

ranging between −78 and 20 °C led, after hydrolysis, to the formation of unsaturated 1,5-diols **460** (Scheme 127)[207,208]. When this process was performed in the absence of the electrophile (two-step reaction) the only reaction product isolated was 1,4-dimethylenecyclohexane, resulting from the dimerization of the monolithiated intermediate initially generated.

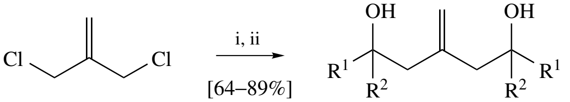

(459) **(460)**

[R^1, R^2 = H, Me, Et, c-C_3H_5, i-Pr, Ph
R^1R^2 = $(CH_2)_4$, $(CH_2)_5$, $(CH_2)_7$]

SCHEME 127. Reagents: (i) Li, $C_{10}H_8$ (6%), R^1R^2CO = i-PrCHO, PhCHO, Me_2CO, Et_2CO, $(c\text{-}C_3H_5)_2CO$, $i\text{-}Pr_2CO$, $c\text{-}(CH_2)_4CO$, $c\text{-}(CH_2)_5CO$, $c\text{-}(CH_2)_7CO$, THF, −78 to 20 °C; (ii) H_2O

Also in this case, diols **460** can be cyclized under acidic conditions: whereas with 6 M HCl the *exo*-heterocycles **461** were the main products (25–81% yield), using 12 M HCl an isomerization occurred giving mainly the *endo*-compounds **462** in 39–84% yield.

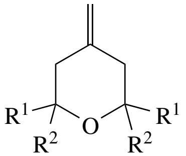

(461)

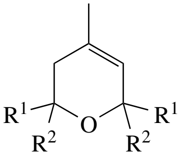

(462)

[R^1, R^2 = Et, c-C_3H_5, i-Pr; R^1 R^2 = $(CH_2)_4$, $(CH_2)_5$, $(CH_2)_7$]

An interesting application of unsaturated diols **460** is the preparation of substituted perhydrofurofurans **463**, a heterobicyclic core, present in families of naturally occurring products, such as aflatoxines[209]. Hydroboration of diols **460** with BH_3 in THF at 0 °C

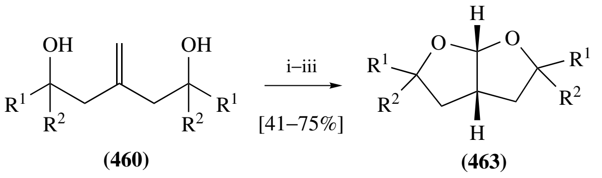

$R^1, R^2 = H, Me, Et, i\text{-}Pr, t\text{-}Bu, c\text{-}C_6H_{11}, Ph$
$R^1R^2 = (CH_2)_5, (CH_2)_2O(CH_2)_2$

SCHEME 128. Reagents: (i) $BH_3{\cdot}THF$, 0 °C; (ii) H_2O_2, 3 M NaOH, 0 °C; (iii) $(Ph_3P)_3RuCl$, PhH, 0 °C (for $R^2 = H$) or PCC, CH_2Cl_2, 0 °C

followed by oxidation with H_2O_2 in 3 M NaOH yielded the corresponding primary alcohols. Further oxidation with the complex $(Ph_3P)_3RuCl$ or PCC, depending on the nature of the groups R^1 and R^2, gave directly perhydrofurofurans **463** (Scheme 128)[210, 211].

Perhydrofurofurans bearing different groups at both sides of the molecule were prepared from the corresponding differently substituted diols. The preparation of these diols was performed starting from the chloroether **464** taking advantage of the different reactivity of both carbon–chloride and carbon–oxygen bonds toward the arene-catalyzed lithiation. Thus, treatment of chloroether **464** with lithium and naphthalene (2.5%) in the presence of different electrophiles in THF at −78 °C allowed the selective replacement of the chlorine atom by electrophiles. After warming at −30 °C a second lithiation took place at the carbon–oxygen bond, and thus a second (different) electrophile was added at −30 to 0 °C to give, after hydrolysis, the expected diols **465** (Scheme 129)[211, 212].

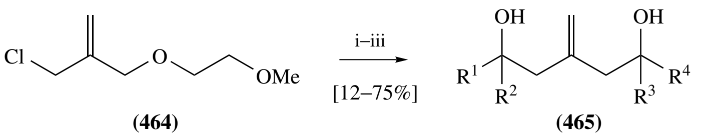

$R^1, R^2, R^3, R^4 = H, Me, Et, t\text{-}Bu, Ph$
$R^1R^2, R^3R^4 = (CH_2)_4, (CH_2)_5, (CH_2)_2O(CH_2)_2$

SCHEME 129. Ragents: (i) Li, $C_{10}H_8$ (2.5%), $R^1R^2CO = t\text{-}BuCHO$, Et_2CO, $c\text{-}(CH_2)_5CO$, $O(CH_2CH_2)_2CO$, PhCOMe, THF, −78 to −30 °C; (ii) $R^3R^4CO = t\text{-}BuCHO$, Me_2CO, Et_2CO, $t\text{-}Bu_2CO$, $c\text{-}(CH_2)_4CO$, $c\text{-}(CH_2)_5CO$, t-BuCOMe, THF, −30 to 20 °C; (iii) H_2O

Diols **465** were easily transformed into perhydrofurofurans **466** following the same methodology described above for diols **460**.

The reactivity of **464** was also used to prepare perhydrofuropyrans with the same methodology as shown in Scheme 129, but with an epoxide as second electrophile. Diols **467** were obtained in 35–68% yield which, after hydroboration and oxidation reactions (as shown in Scheme 128), gave perhydrofuropyrans **468** in 57–64% yield[213]. This heterocyclic unit is present in many natural products, azadirachtins being probably the most important ones[214].

A different cyclization reaction of **460**, by treatment with iodine and silver oxide, gave 1,6-dioxaspiro[3.4]octanes **469** (Scheme 130)[215]. This heterocyclic core present in a series of sesquiterpenic lactones has interesting biological activity and is isolated as secondary metabolites from species of the *Compositae* family[216].

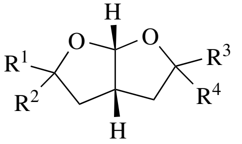

(466)

[R^1, R^2, R^3, R^4 = H, Me, Et, *t*-Bu, Ph
R^1R^2, R^3R^4 = $(CH_2)_4$, $(CH_2)_5$, $(CH_2)_2O(CH_2)_2$]

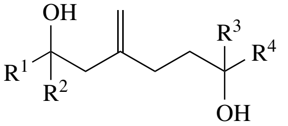

(467)

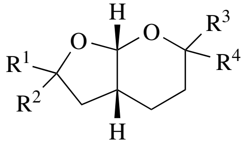

(468)

[R^1, R^2, R^3, R^4 = H, Me, Et, *n*-C_5H_{11}, *n*-C_6H_{13}, Ph
R^1R^2, R^3R^4 = $(CH_2)_4$, $(CH_2)_5$]

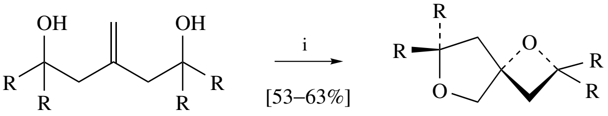

(460) [$R^1 = R^2 = R$] **(469)**

[R = Et; RR = $(CH_2)_4$, $(CH_2)_5$, $(CH_2)_2O(CH_2)_2$]

SCHEME 130. Reagents: (i) I_2, Ag_2O, dioxane–H_2O, 20 °C

A different type of 1,3-dilithium synthon was prepared from 1,3-dichloropropene (**470**), by lithiation in the presence of a catalytic amount of DTBB (5%) and a carbonyl compound in THF at 0 °C. After hydrolysis, a (Z/E)-mixture of diastereomers **471** was isolated (Scheme 131)[217].

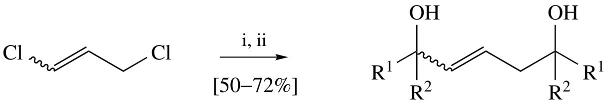

(470) **(471)**

[R^1, R^2 = H, Me, Et, *t*-Bu; R^1R^2 = $(CH_2)_4$, $(CH_2)_5$]

SCHEME 131. Reagents: (i) Li, DTBB (5%), R^1R^2CO = *t*-BuCHO, Me_2CO, Et_2CO, *c*-$(CH_2)_4CO$, *c*-$(CH_2)_5CO$, THF, 0 °C; (ii) H_2O

The different reactivity of both carbon–chlorine and carbon–oxygen bonds toward arene-catalyzed lithiation (see Scheme 129) was applied to 3-chloropropyl phenyl ether

472 in order to introduce two different carbonyl compounds as electrophiles in the molecule. After DTBB-catalyzed (5%) lithiation in THF at −78 °C, the first carbonyl compound R^1R^2CO was added to **473** to give **474**. Then, the temperature was allowed to rise to 20 °C and the second lithiation took place giving the new intermediate **475**, which after reaction with the second carbonyl compound R^3R^4CO at −78 °C, and final hydrolysis, gave differently substituted diols **476** (Scheme 132)[218, 219].

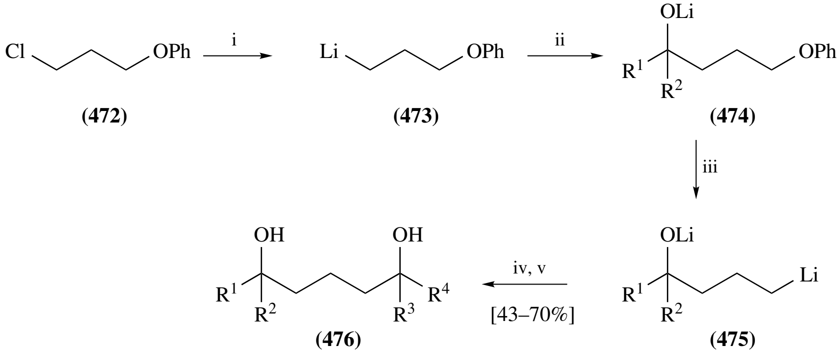

[R^1, R^2, R^3, R^4 = H, Me, Pr, *t*-Bu, Ph; R^1R^2, R^3R^4 = $(CH_2)_5$]

SCHEME 132. Reagents: (i) Li, DTBB (5%), THF, −78 °C; (ii) R^1R^2CO = *t*-BuCHO, Me_2CO, *c*-$(CH_2)_5CO$, (−)-menthone; (iii) −78 to 20 °C; (iv) R^3R^4CO = *t*-BuCHO, PhCHO, Me_2CO, PrCOMe, *c*-$(CH_2)_5CO$, (−)-menthone, −78 °C; (v) H_2O, −78 to 20 °C

The sulfur–lithium exchange catalyzed by an arene (DTBB, 3.5%) generates in THF at −78 °C, the 1,3-dilithium synthons, namely the 1,3-(phenylmercapto)propane **477**, which is then treated with a carbonyl compound R^1R^2CO at the same temperature. After final hydrolysis 1,5-diols **478** were obtained (Scheme 133)[220].

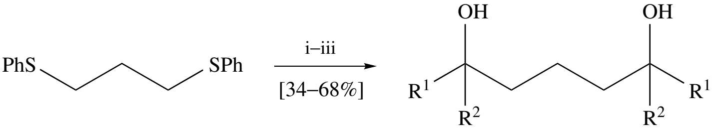

(477) **(478)**

[R^1, R^2 = H, Et, *t*-Bu, Ph, $PhCH_2$; R^1R^2 = $(CH_2)_5$, $(CH_2)_7$]

SCHEME 133. Reagents: (i) Li, DTBB (3.5%), THF, −78 °C; (ii) R^1R^2CO = *t*-BuCHO, PhCHO, $PhCH_2CHO$, Et_2CO, *c*-$(CH_2)_5CO$, *c*-$(CH_2)_7CO$, (−)-menthone, Ph_2CO, −78 °C; (iii) H_2O, −78 to 20 °C

Also in this case, the use of the chloro thioether **479** allowed the introduction of two different electrophiles in a sequential process. Using lithium naphthalene (the stoichiometric version of the arene-promoted lithiation) in THF at −78 °C, only a chlorine–lithium exchange occurred, so the first electrophile R^1R^2CO was introduced (−78 to −50 °C). Then the second lithiation (sulfur–lithium exchange) takes place under catalytic conditions (naphthalene) and the second electrophile R^3R^4CO was introduced. After final hydrolysis, differently substituted 1,5-diols **476** were isolated (Scheme 134)[220].

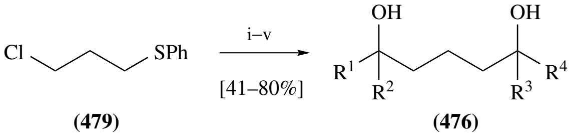

R^1, R^2, R^3, R^4 = H, Me, *t*-Bu, *n*-C_5H_{13}, Ph
R^1R^2 = $(CH_2)_5$, $(CH_2)_7$

SCHEME 134. Reagents: (i) $LiC_{10}H_8$, THF, −78 °C; (ii) R^1R^2CO = Me_2CO, *c*-$(CH_2)_5CO$, *c*-$(CH_2)_7CO$, (−)-menthone, $[Me(CH_2)_4]_2CO$, −78 to −50 °C; (iii) Li, −50 °C; (iv) R^3R^4CO = *t*-BuCHO, PhCHO, −50 °C; (v) H_2O, −50 to 20 °C

D. 1,4-Dilithium Synthons

DTBB-catalyzed (5%) lithiation of any of the dichlorobutenes **480–482** in the presence of an electrophile in THF at 0 °C gave, after hydrolysis, the same isomeric mixture of 1,2- and 1,4-products (**483** and **484**, respectively), independently of the structure of the starting material (Scheme 135)[221]. Unexpectedly, the (*Z*)-isomer was the major one for products **484**. The result obtained in this reaction indicates that the mechanistic pathway should be the same in the three cases.

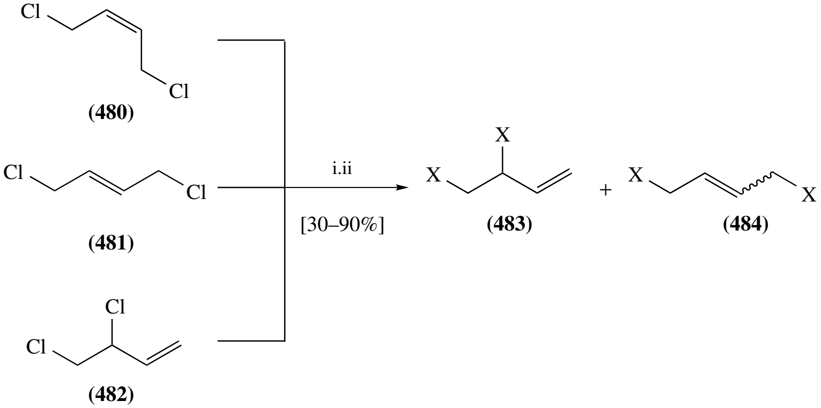

[X = *t*-BuCHOH, *c*-$(CH_2)_4COH$, Me_3Si]

SCHEME 135. Reagents: (i) Li, DTBB (5%), E = *t*-BuCHO, *c*-$(CH_2)_4CO$, Me_3SiCl, THF, 0 °C; (ii) H_2O

The dipropargylic dichloride **485** was lithiated in the presence of a catalytic amount of DTBB (2.5%) and an electrophile in THF at −40 °C giving, after hydrolysis with water, the corresponding functionalized alkynes **486** (Scheme 136)[222].

DTBB-catalyzed (2.5%) lithiation of phthalan (**330**) (see also Section VI.C.1) was performed in a sequential fashion. After the first lithiation at room temperature the first electrophile was reacted at −78 °C, giving **487** as intermediates. After allowing the temperature to rise to 20 °C, a second lithiation took place giving the new intermediates **488**, which finally were treated with a second electrophile giving, after hydrolysis, the difunctionalized products **489** (Scheme 137)[169].

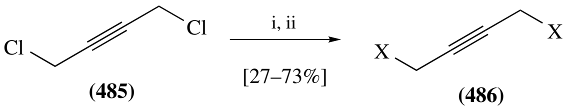

[X = t-BuCHOH, Me_2COH, c-$(CH_2)_4COH$, c-$(CH_2)_5COH$, c-$(CH_2)_7COH$, Me_3Si]

SCHEME 136. Reagents: (i) Li, DTBB (2.5%), E = t-BuCHO, Me_2CO, c-$(CH_2)_2CO$, c-$(CH_2)_2CO$, c-$(CH_2)_2CO$, Me_3SiCl, THF, −40 °C; (ii) H_2O, −40 to 20 °C

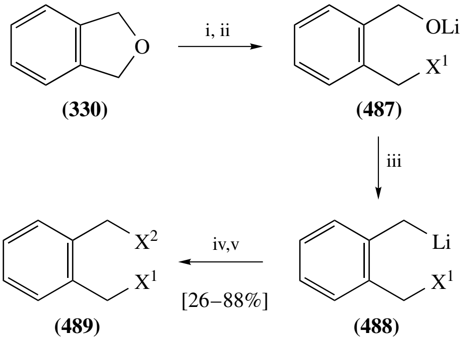

X^1 = EtCHOH, i-PrCHOH, t-BuCHOH, Me_2COH, Et_2COH, c-$(CH_2)_4COH$, c-$(CH_2)_5COH$, PhCHNHPh
X^2 = H, D, CO_2H, EtCHOH, t-BuCHOH, PhCHOH, Et_2COH, c-$(CH_2)_5COH$

SCHEME 137. Reagents: (i) Li, DTBB (2.5%), THF, 20 °C; (ii) E^1 = EtCHO, i-PrCHO, t-BuCHO, Me_2CO, Et_2CO, c-$(CH_2)_2CO$, c-$(CH_2)_2CO$, PhCH=NPh, −78 °C; (iii) Li, DTBB (2.5%), −78 to 20 °C; (iv) E^2 = H_2O, D_2O, CO_2, EtCHO, t-BuCHO, PhCHO, Et_2CO, c-$(CH_2)_2CO$, −78 °C; (v) H_2O, −78 to 20 °C

When a carbonyl compound and CO_2 were successively added as the two electrophiles, the resulting hydroxy-acid was easily cyclized to give the corresponding lactones **490** in 73–87% yield. On the other hand, when two carbonyl compounds were used, the obtained diols of type **489** were cyclized to the corresponding oxepanes **491** in 52–96% yield with 85% H_3PO_4 under toluene reflux.

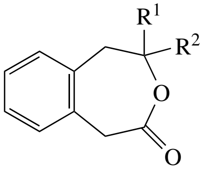

(490)

[R^1, R^2 = H, Et, i-Pr, t-Bu]

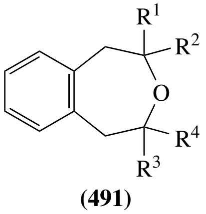

(491)

R^1, R^2, R^3, R^4 = H, Me, Et, t-Bu
R^1R^2, R^3R^4 = $(CH_2)_4$, $(CH_2)_5$

Following the same sequential methodology showed in Scheme 132 for 3-chloropropyl phenyl ether (**472**), 4-chlorobutyl phenyl ether (**492**) was transformed into the corresponding differently substituted 1,6-diols **493** in 36–68% yield.

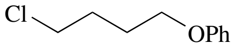

(492)

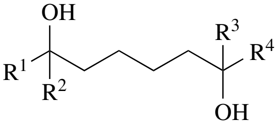

(493)

$\left[\begin{array}{l} R^1, R^2, R^3, R^4 = \text{H, Me, } t\text{-Bu} \\ R^1R^2, R^3R^4 = (CH_2)_5 \end{array}\right]$

E. Other 1,*n*-Dilithium Synthons

Starting from different dichlorinated acetylenes **485, 494** and **495**, and using dichlorodimethylsilane or dichlorodimethylgermane as electrophiles, the corresponding macrocyclic diynes **496–498** were obtained via a biphenyl-catalyzed (*ca* 20%) lithiation in THF at −20 °C (Scheme 138)[223].

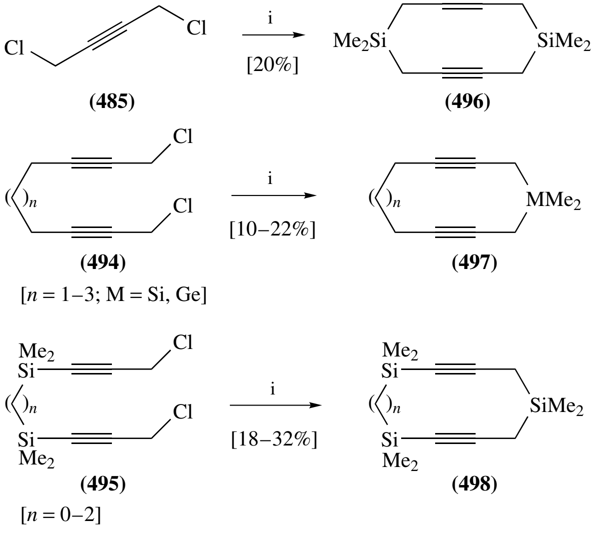

SCHEME 138. Reagents: (i) Li, Ph_2 (20%), Me_2MCl_2 (M = Si, Ge), THF, −20 °C

Working with a dichlorinated disilane[224] or dichlorophosphines[225] as electrophiles, **499** and **500** were prepared in low yields from dichlorinated acetylenes **485** and **494** and using a biphenyl-catalyzed (*ca* 20%) lithiation (Scheme 139)[224, 225].

On the other hand, treatment of **494** with lithium and a catalytic amount of biphenyl gave the corresponding macrocycles of **501** in 10–20% yield by lithium chloride elimination[226, 227].

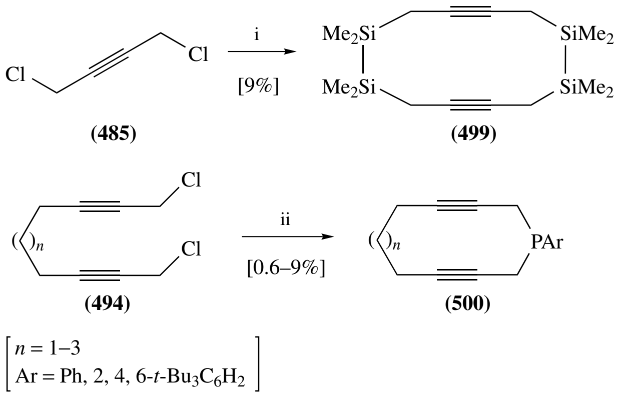

$n = 1–3$
Ar = Ph, 2, 4, 6-t-$Bu_3C_6H_2$

SCHEME 139. Reagents: (i) Li, Ph_2 (20%), $(Me_2ClSi)_2$, THF, −20 °C; (ii) Li, Ph_2 (20%), $ArPCl_2$, THF, −20 °C

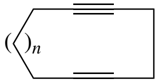

(501)

[n = 1-3]

Dichlorobenzenes **502** were lithiated in the presence of a catalytic amount of naphthalene (3%) in THF at −78 °C, being then successively treated with two electrophiles, so difunctionalized benzenes **503** were obtained (Scheme 140)[49].

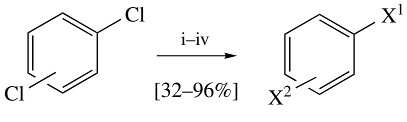

(502) **(503)**

X^1 = t-BuCHOH, c-$(CH_2)_5COH$
X^2 = H, D, Et_2COH

SCHEME 140. Reagents: (i) Li, $C_{10}H_8$ (3%), THF, −78 °C; (ii) E^1 = t-BuCHO, c-$(CH_2)_2CO$, −78 °C; (iii) E^2 = H_2O, D_2O, Et_2CO, −78 to 20 °C; (iv) H_2O

In the case of chlorobenzyl chlorides **504**, the same process had to be performed under Barbier-type reaction conditions. These dichlorinated materials **504** were lithiated with DTBB in a catalytic amount (4%) in the presence of different electrophiles to give, after final hydrolysis with water, the corresponding difunctionalized products **505** (Scheme 141)[143, 228].

The same situation occurred with dibenzylic dichlorides **506** which, undergoing the same process described in Scheme 141, gave the expected products **507** in 30–88% yield[229].

This chemistry was also applied to dichlorinated material **508** and **509** was obtained in 45–85% yield, in which the same electrophilic fragments occupy finally the places of the chlorine atom in the starting material[230].

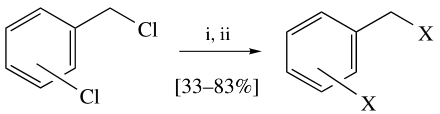

(504) **(505)**

$\left[\begin{array}{l}X = i\text{-PrCHOH, } t\text{-BuCHOH, Et}_2\text{COH,}\\ c\text{-(CH}_2)_5\text{COH, PhC(OH)Me, Me}_3\text{Si}\end{array}\right]$

SCHEME 141. Reagents: (i) Li, DTBB (4%), E = *i*-PrCHO, *t*-BuCHO, Et_2CO, *c*-$(CH_2)_2CO$, PhCOMe, Me_3SiCl, THF, −50 °C; (ii) H_2O, −50 to 20 °C

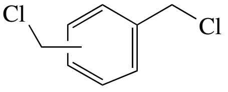

(506)

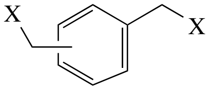

(507)

$\left[\begin{array}{l}X = i\text{-PrCHOH, } t\text{-BuCHOH, PhCHOH,}\\ c\text{-(CH}_2)_5\text{COH, PhC(OH)Me, Me}_3\text{Si}\end{array}\right]$

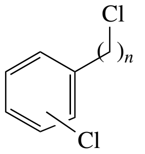

(508)

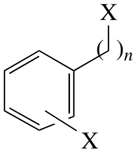

(509)

$\left[\begin{array}{l}n = 2, 3\\ X = t\text{-BuCHOH, PhCHOH, Me}_2\text{COH,}\\ \text{Et}_2\text{COH, } c\text{-(CH}_2)_5\text{COH, PhC(OH)Me}\end{array}\right]$

The only way to introduce two different electrophilic fragments in compounds such as **508** is to have a starting material with different halogens. This is the case with **510**, which could be lithiated (bromide–lithium exchange) with *t*-butyllithium in THF at −100 °C giving intermediates **511**, which reacted with a carbonyl compound R^1R^2CO and, after naphthalene-catalyzed lithiation, gave the new functionalized organolithium intermediate **512**. Final reaction with 3-pentanone followed by hydrolysis yielded mixed products **513** (Scheme 142)[230].

Finally, dilithium synthons can be generated by double sulfur–lithium exchange starting from 2,7-dihydrobenzothiopin **407** (Y = S). Thus, after the first DTBB-catalyzed ring opening and reaction with a carbonyl compound electrophile (see Section VI. E), a second lithiation took place giving a new intermediate of the type **514** which, after reaction with a second electrophile, gave after hydrolysis **515** in 35–46% yield, in which two different electrophilic fragments have been introduced[189].

VIII. ACTIVATION OF OTHER METALS

As indicated in Section I, one of the most commonly used methodologies to activate different metals is the use of a metallic salt and a solution of an equimolecular amount

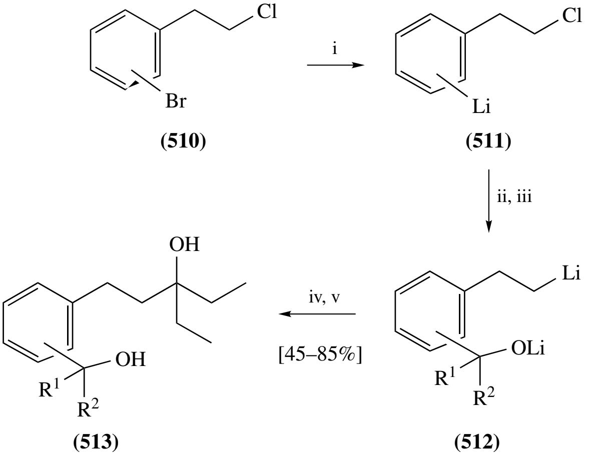

[R^1, R^2 = H, Ph; R^1R^2 = $(CH_2)_5$]

SCHEME 142. Reagents: (i) *t*-BuLi, THF, −100 °C; (ii) R^1R^2CO = PhCHO, *c*-$(CH_2)_2CO$, −100 °C; (iii) Li, $C_{10}H_8$ (8%), THF, −78 °C; (iv) Et_2CO, −78 to 20 °C; (v) H_2O

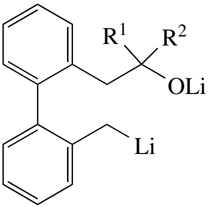

(514)

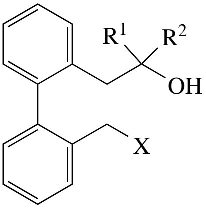

(515)

[R^1, R^2 = Me; R^1R^2 = $(CH_2)_5$
X = Me_2COH, Et_2COH, *c*-$(CH_2)_5COH$, CO_2Et]

of an electropositive metal and an arene[3–5]. As a typical combination, the so-called lithium–naphthalene (or lithium naphthalenide) in THF is a very useful and versatile mixture to perform the activation of different metals. However, only in few cases has a substoichiometric amount of the arene been used in the mentioned reaction.

A. Activated Zinc

Zinc was effectively activated from zinc chloride using lithium and a catalytic amount (10%) of naphthalene in order to prepare secondary or tertiary alkylzinc bromides **517** (starting from the corresponding alkyl bromides **516**). These reagents react with acyl chlorides[231] or α,β-unsaturated ketones[232] to give the expected ketones **15** and **518** (Scheme 143).

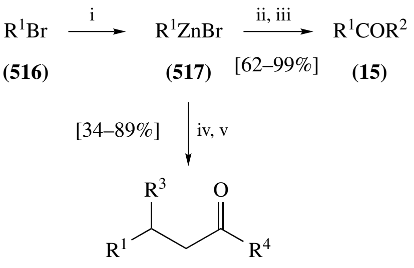

(518)

R^1 = *s*-Bu, *t*-Bu, Et_2CMe, $EtCMe_2$, *c*-C_5H_5, *c*-C_6H_{11}, $MeCHCH_2CO_2Me$, 1-adamantyl
R^2 = Ph, $(CH_2)_4Cl$
R^3, R^4 = H, Me; R^3R^4 = $(CH_2)_3$, $CH_2CHMeCH(CO_2Et)$

SCHEME 143. Reagents: (i) activated Zn [$ZnCl_2$, Li, naphthalene (10%), THF], THF reflux; (ii) CuCN, LiBr, R^2COCl, THF −45 to 20 °C; (iii) 3 M HCl; (iv) R^3 CH=CH-COR^4, BF_3, TMSCl, pentane, −30 °C; (v) $NH_4Cl{-}H_2O$

B. Activated Manganese

Different primary, secondary aryl or heteroaryl manganese bromides **519** were prepared by reaction of activated manganese [prepared form manganese dichloride, lithium and a catalytic amount (15%) of 2-phenylpyridine as electron carrier, in THF] with the corresponding brominated compounds **516**. These intermediates react with different electrophiles in THF at 0 °C with or without copper chloride, to yield the corresponding products **20** (Scheme 144)[233].

$$\underset{\textbf{(516)}\ [R^1 = R]}{\mathrm{RBr}} \xrightarrow{\text{i}} \underset{\textbf{(519)}}{\mathrm{RMnBr}} \xrightarrow[\text{[56–93\%]}]{\text{ii, iii}} \underset{\textbf{(20)}}{\mathrm{RX}}$$

R = Bu, *c*-C_6C_{11}, *n*-C_7H_{15}, $PhCH_2$, 3-ClC_6H_4
X = *n*-C_7H_{15}, *n*-$C_6H_{13}CH{=}CH$, BuCHOH, Me_2CCH_2CHO,
c-$CH(CH_2)_3COCH_2$, $MeCHCH_2CO_2Et$, BuCO, PhCO

SCHEME 144. Reagents: (i) activated Mn [$MnCl_2{\cdot}LiCl$, Li, 2-PhPy (15%), THF], THF, 0 °C; (ii) E = *n*-$C_7H_{15}Br$, *n*-$C_7H_{15}I$, *n*-$C_6H_{13}CH = CHI$, BuCHO, $Me_2C{=}CHCHO$, cyclohexenone, $MeCH{=}CHCO_2Et$, BuCOCl, PhCOCl, CuCl, −10 °C; (iii) 3 M HCl

C. Activated Nickel

A very different case is the activation of dehydrated nickel(II) dichloride, with lithium and a catalytic amount of naphthalene, because it represents a new methodology useful for the reduction of different organic functional groups. Thus, olefins **520** were hydrogenated with nickel(II) chloride dihydrate, lithium and a catalytic amount of naphthalene (17%) in THF at room temperature to give the expected alkanes **521** (Scheme 145)[234, 235]. One interesting feature is that the use of a nickel salt containing deuterium oxide instead of water allowed the preparation of dideuterated alkanes **522**, the source of deuterium being in this

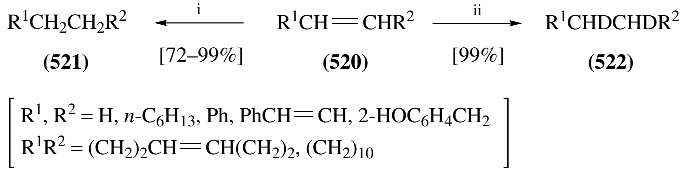

SCHEME 145. Reagents: (i) $NiCl_2{\cdot}2H_2O$, Li, $C_{10}H_8$ (17%), THF; (ii) $NiCl_2{\cdot}2D_2O$, Li, $C_{10}H_8$ (17%), THF

case the cheapest that one can imagine. On the other hand, for isolated dienes, adjusting the stoichiometry of the nickel salt promotes the mono or dihydrogenation reaction.

Concerning the possible reaction mechanism, the activated lithium can both reduce the nickel(II) salt to give nickel(0) and react with the crystallization water present in the metallic salt to produce molecular hydrogen. However, no gas evolution was observed in the reaction, so the hydrogen initially formed was probably adsorbed on the surface of the active nickel to perform like 'hydrogenation without hydrogen' in the sense that no external source of molecular hydrogen was employed.

In the case of alkynes **523**, mono- or dihydrogenation could be achieved depending on the stoichiometry used, giving the corresponding alkenes **520** or alkanes **521**, working under the same reaction conditions as shown in Scheme 145. Also in this case, perdeuteriation was performed using the deuterium oxide version of the process affording labelled products **524** (Scheme 146)[236].

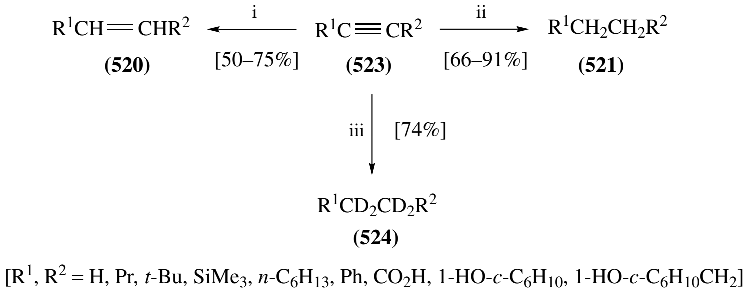

SCHEME 146. Reagents: (i) $NiCl_2{\cdot}2H_2O$, Li, $C_{10}H_8$ (8%), THF; (ii) 2 $NiCl_2{\cdot}2H_2O$, Li, $C_{10}H_8$ (8%), THF; (iii) 2 $NiCl_2{\cdot}2D_2O$, Li, $C_{10}H_8$ (8%), THF

Concerning the stereochemistry of the olefins in the semireduction reaction, different results were obtained depending on the structure of the starting alkanes, so the corresponding mechanism is not clear.

The reduction of all types of halogenated compounds **20** (aliphatic or aromatic chlorides, bromides and iodides)[237] or alkyl sulfonates (mesylates or triflates)[238] gave the corresponding alkanes **22** or deuterioalkanes **525**, applying the above-mentioned methodology but using DTBB as the arene electron carrier (Scheme 147). Enol triflates can also be hydro- or deuterio-desulfonylated, giving the corresponding olefins or deuteriolefins. However, the application of this methodology to aryl triflates gave moderate to poor yields.

One interesting application of the use of the $NiCl_2{\cdot}2H_2O$/Li/arene combination was the Birch-type reaction using different arene or heterocycles[238], in the second case DTBB (10%) being used as the corresponding electron transfer agent. Some examples (including the

$$\underset{(\mathbf{22})}{\text{R-H}} \xleftarrow[\text{[43–99\%]}]{\text{i}} \underset{(\mathbf{20})}{\text{R-X}} \xrightarrow[\text{[70–99\%]}]{\text{ii}} \underset{(\mathbf{525})}{\text{R-D}}$$

X = Cl, Br, I, $MeSO_3$, CF_3SO_3
R = n-$C_{10}H_{21}$, n-$C_{12}H_{25}$, n-$C_{16}H_{33}$, $Ph(CH_2)_2$, Ph_3C,
$PhCH_2CHMe$, menthyl, 4-MeC_6H_4, 4-PhC_6H_4, 4-HOC_6H_4,
4-$MeOC_6H_4$, 4-$H_2NC_6H_4$, 4-$HOCH_2C_6H_4$

SCHEME 147. Reagents: (i) $NiCl_2{\cdot}2H_2O$, Li, DTBB (5–10%), THF; (ii) $NiCl_2{\cdot}2D_2O$, Li, DTBB (5–10%), THF

precursors) are **526** (80%, from naphthalene), **527** (58%, from 1,4-dimethylnaphthalene), **528** (45%, from α-naphthol), **529** (82%, from β-naphthylamine), **530** and **531** (94–98%, from anthracene), **532** (75%, from quinoline) and **533** (73%, from acridine).

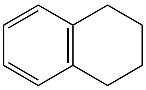

(526)

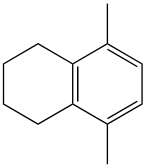

(527)

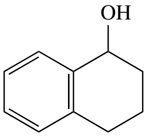

(528)

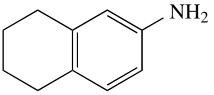

(529)

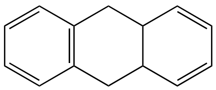

(530)

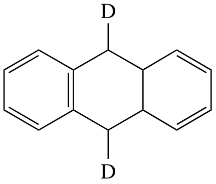

(531)

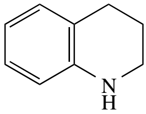

(532)

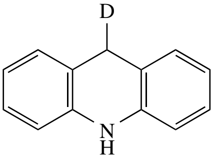

(533)

The reduction of different aliphatic or aromatic aldehydes or ketones **15** was easily achieved using the combination of dihydrated nickel(II) chloride, lithium and a catalytic amount of naphthalene (16%) or DTBB (8%) in THF, yielding the corresponding alcohols without (**534**) or with (**535**) deuterium labelling in 57–86% yield. For imines **536**, the same process afforded the corresponding amines **537** or deuterio amines **538** in 54–>95% yield[239].

Another type of compound, which can be reduced using the above-described methodology, are nitrones **539**. Depending on the nickel salt used (containing water or deuterium oxide), amines **540** or deuterio amines **541** were obtained in 41–80% yield[86].

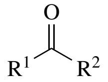

(15)

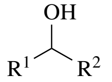

(534)

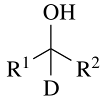

(535)

$R^1, R^2 = H, Me, Et, i\text{-Bu}, Ph, PhCH{=}CH$
$R^1R^2 = (CH_2)_5, (CH_2)_3CH{=}CH, CH_2CMe_2CH_2CMe{=}CH$

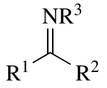

(536)

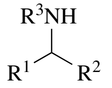

(537)

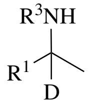

(538)

$R^1, R^2 = H, Me, Pr, i\text{-Pr}, n\text{-}C_5H_{11}, Ph$
$R^3 = Bu, t\text{-Bu}, c\text{-}C_6H_{11}, Ph, PhCH_2$

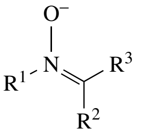

(539)

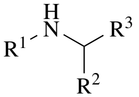

(540)

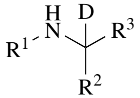

(541)

$R^1, R^2, R^3 = H, Me, Pr, i\text{-Pr}, Bu, t\text{-Bu}, n\text{-}C_7H_{15}, n\text{-}C_8H_{17}, Ph$
$R^1R^2 = (CH_2)_4$

Aromatic hydrazines **542**, azo compounds **543** or azoxy compounds **544** were reduced using the $NiCl_2{\cdot}2H_2O$/Li/DTBB (10%) combination in THF at room temperature to yield the corresponding aromatic amines **545** in 57–88% yield[240].

Finally, a very simple way to deoxygenate aliphatic or aromatic amine *N*-oxides involved the same $NiCl_2{\cdot}2H_2O$/Li/DTBB (10%) combination, so, for instance, compounds **546–550** are examples of this reaction in 66–80% yield[240].

When the nickel salt does not contain any crystallization water, its arene-catalyzed lithiation gave a very active nickel(0), which can be used as a catalyst for hydrogenation processes with molecular hydrogen at room temperature and one atmosphere[241]. Thus, alkenes, alkynes, carbonyl compounds and their imine derivatives, halogenated compounds, aromatic and heteroaromatic derivatives, as well as other nitrogen-containing materials, such as hydrazines, azoxy compounds or amine *N*-oxides, were hydrogenated to give the corresponding reduced compounds, the same as the products obtained using the above-mentioned methodology with the corresponding dihydrated nickel salt.

IX. OTHER METHODOLOGIES

Not included in the former sections are methodologies involving arene-catalyzed lithiation that are based on deprotonation reactions, carbon–carbon bond cleavage, addition processes as well as the preparation of lithium telluride.

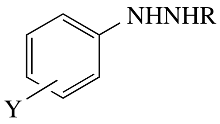

(542)

Y = H, 4-*i*-Pr, 4-MeO
R = H, Ph

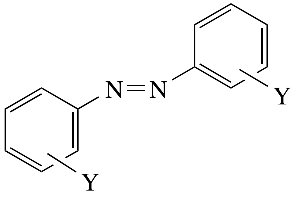

(543)

[Y = H, 2-HO, 2-MeO, 4-MeO]

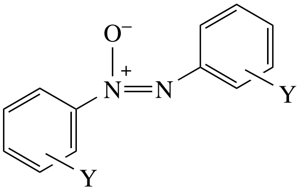

(544)

[Y = H, 4-MeO]

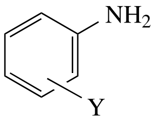

(545)

[Y = H, 4-*i*-Pr, 2-HO, 2-MeO, 4-MeO]

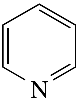

(546)

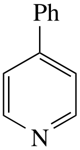

(547)

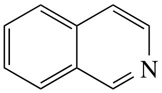

(548)

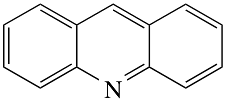

(549)

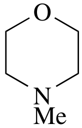

(550)

A. Deprotonation Reactions

Different heterocycles, such as furan, 2,3-dihydrofuran, *N*-methylpyrrole, thiophene, *N*-methylindol or 5-methyl-1,3-triazole, were deprotonated at the α-position with lithium and a catalytic amount of naphthalene or anthracene (1–7%) in THF at room temperature to give, after trapping with methyl iodide, the corresponding methylated products in 56–93%[242].

B. Carbon–Carbon Bond Cleavage Reactions

Apart from the reactions included in Section IV.A, other processes, including reductive carbon–carbon cleavage with less synthetic importance, will be considered.

Whereas 1,1,1-triphenylethane **551** gave only 2% of triphenylacetic acid **552** after treatment with lithium and a substoichiometric amount (50%) of biphenyl, followed by carbonation and acidic hydrolysis, the same process carried out starting from 1,1,1,2-tetraphenyl ethane **553** or 1,1,2,2-tetraphenylethane **554** gave tri- **552** or diphenylacetic acid **555**, respectively, with excellent yields (Scheme 148)[58].

$$\underset{\mathbf{(551)}}{Ph_3CCH_3} \xrightarrow[{[2\%]}]{\text{i–iii}} \underset{\mathbf{(552)}}{Ph_3CCO_2H}$$

$$\underset{\mathbf{(553)}}{Ph_3CCH_2Ph} \xrightarrow[{[93\%]}]{\text{i–iii}} \mathbf{552}$$

$$\underset{\mathbf{(554)}}{Ph_2CHCHPh_2} \xrightarrow[{[83\%]}]{\text{i–iii}} \underset{\mathbf{(555)}}{Ph_2CHCO_2H}$$

SCHEME 148. Reagents: (i) Li, Ph_2 (50%), THF, 25–66 °C; (ii) CO_2, −75 °C; (iii) H_2O–HCl

The addition of lithium to dicyclopropylacetylene (**556**) catalyzed by biphenyl (3%) in THF at −30 °C provoked a carbon–carbon bond cleavage in one of the cyclopropyl rings giving a delocalized dianion **557**, which by reaction with dimethyl sulfate at −78 °C gave the alkene **558** (Scheme 149)[243].

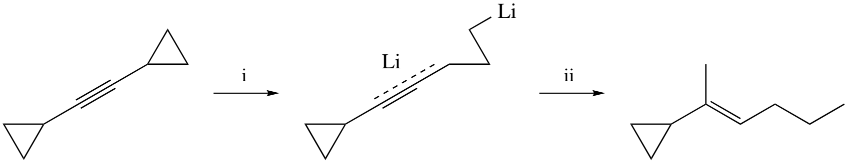

(556) **(557)** **(558)**

SCHEME 149. Reagents: (i) Li, Ph_2 (3%), THF, −30 °C; (ii) Me_2SO_4, −78 °C

C. Addition Reactions

According to the type of unsaturated bond to be lithiated, carbon–carbon, carbon–oxygen and carbon–nitrogen bonds will be considered.

1. Carbon–carbon double bonds

Lithium homoenolates **560** were generated by lithiation of enones **559** with lithium and a catalytic amount of naphthalene (4%) in the presence of different carbonyl compounds as electrophiles and a Lewis acid (LiCl, $TiCl_4$, $SnBu_4$, $SnCl_4$, BF_3) in THF at

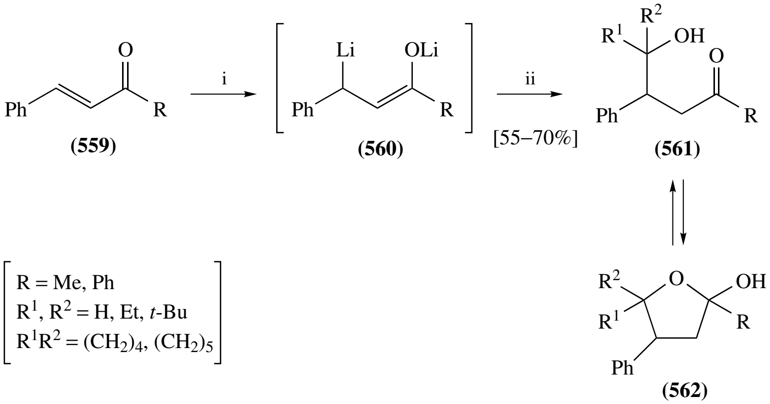

R = Me, Ph
R^1, R^2 = H, Et, *t*-Bu
R^1R^2 = $(CH_2)_4$, $(CH_2)_5$

SCHEME 150. Reagents: (i) Li,$C_{10}H_8$ (4%), R^1R^2CO = *t*-BuCHO, Et_2CO, *c*-$(CH_2)_2CO$, *c*-$(CH_2)_2$ CO, Lewis acid (LiCl, $TiCl_4$, $SnBu_4$, $SnCl_4$, BF_3), THF, −78 to 0 °C; (ii) H_2O

temperatures ranging between −78 and 0 °C. So after final hydrolysis with water, hydroxyketones **561** were obtained, which are in equilibrium with the corresponding lactols **562** (Scheme 150)[244].

Compounds **561/562** were transformed into substituted tetrahydrofurans **563** in 23–51% yield by reaction with silicon-containing nucleophiles in the presence of BF_3[245]. On the other hand, application of the methodology shown in Scheme 150 to α,β-unsaturated esters yielded directly the corresponding γ-lactones **564** in 37–86% yield.

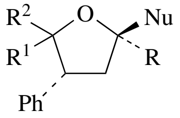

(563)

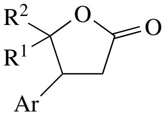

(564)

Nu = H, CN, $CH_2CH{=}CH_2$
R, R^1, R^2 = H, Me, Et, *t*-Bu, Ph
R^1R^2 = $(CH_2)_4$, $(CH_2)_5$

R^1, R^2 = H, Et, *t*-Bu
R^1R^2 = $(CH_2)_4$, $(CH_2)_5$
Ar = Ph, 4-MeC_6H_4, 3,4-$(CH_2O)_2C_6H_3$

Benzamides **565** without any substituent at the *para* position reacted with lithium and a catalytic amount of naphthalene under Barbier-type reaction conditions (in the presence of a carbonyl compound) in THF at −78 °C to give, after hydrolysis, the corresponding dearomatized products **566** (Scheme 151). When **567** was used as starting material with a 4-*tert*-butyl group in *p*-position, and using 3-pentanone as electrophile and under the same reaction conditions, the *trans*-product **568** was the only one isolated[246].

2. Carbon–oxygen double bonds

Aromatic ketones **569**, benzylic alcohols **570** and **571** as well as alkyl aryl ethers **572** reacted with lithium under ultrasonic irradiation in the presence of catalytic amounts of DTBB (2%) in THF to give, after alkylation with an alkyl iodide at 0 °C and final

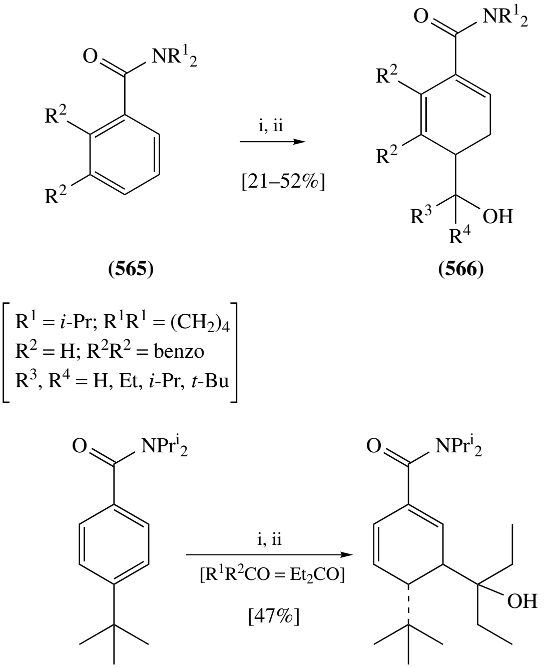

SCHEME 151. Reagents: (i) Li, $C_{10}H_8$ (4%), $R^1R^2CO = t\text{-BuCHO}, Et_2CO, (i\text{-Pr})_2CO$, THF, −78 °C, (ii) H_2O, −78 to 20 °C

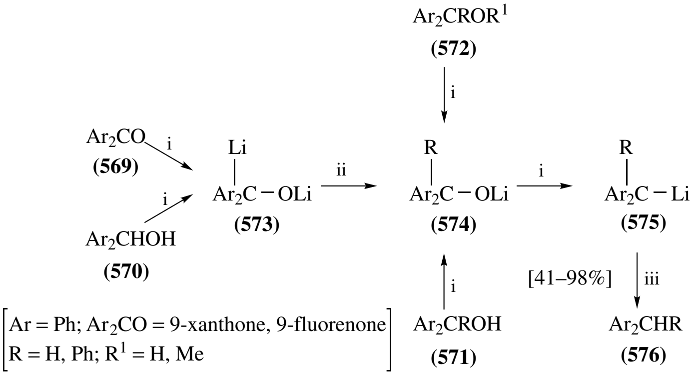

SCHEME 152. Reagents: (i) Li, DTBB (2%), THF; (ii) RI = MeI, EtI, 0 °C; (iii) $NH_4Cl–H_2O$

hydrolysis with aqueous NH_4Cl, the corresponding hydrocarbons **576** (Scheme 152). Organolithium intermediates **573–575** are probably involved in the process[247].

The reactivity of **573** has been extended to the use of carbonyl compounds as electrophiles, so 1,2-diols **577** were prepared by lithiation of phenones **569** with lithium and a catalytic amount of naphthalene (8%) in THF at −30 °C. After further treatment with carbonyl compounds and final hydrolysis, diols **577** were isolated in 13–96% yield[248].

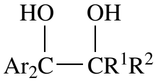

$$Ar_2\overset{\displaystyle HO}{\overset{|}{C}}—\overset{\displaystyle OH}{\overset{|}{C}}R^1R^2$$

(577)

$$\left[\begin{array}{l} Ar = Ph, 2\text{-}MeC_6H_4, 3\text{-}MeC_6H_4 \\ 4\text{-}MeC_6H_4, 4\text{-}MeOC_6H_4, 2,4\text{-}Me_2C_6H_3 \\ R^1, R^2 = H, i\text{-}Pr, Ph; R^1R^2 = (CH_2)_5 \end{array}\right]$$

When the same lithiation process indicated in Scheme 152 was applied to aliphatic esters **578**, the corresponding ketones **580** were mainly isolated after acidic work-up (Scheme 153). ^{1}H NMR studies show that the corresponding β-ketoesters **579** are intermediates in the process[249].

$$\underset{\textbf{(578)}}{RCH_2CO_2R^1} \xrightarrow{\text{i}} \underset{\textbf{(579)}}{\left[RCH_2COCHRCO_2R^1\right]} \xrightarrow[\text{[48–82\%]}]{\text{i, ii}} \underset{\textbf{(580)}}{(RCH_2)_2CO}$$

[R = n-C_6H_{13}, Ph, n-$C_{10}H_{21}$; R^1 = Me, Et]

SCHEME 153. Reagents: (i) Li, DTBB (4–5%); (ii) NH_4Cl–H_2O

For aromatic esters **581** or their corresponding acids **582**, the reaction shown in Scheme 153 gave mainly dibenzylic products **583** or aromatic 1,2-diketones **584**, respectively, in 49–85% yield[250, 251].

$ArCO_2R$	$ArCO_2H$	$ArCH_2CH_2Ar$	$ArCOCOAr$
(581)	**(582)**	**(583)**	**(584)**

$$\left[\begin{array}{l} Ar = Ph, 2\text{-}MeC_6H_4, 3\text{-}MeC_6H_4, 4\text{-}MeC_6H_4, 4\text{-}t\text{-}BuC_6H_4 \\ R = Me, Et, PhCH_2, Li, Na \end{array}\right]$$

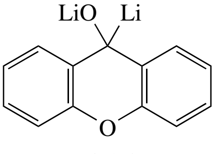

(585)

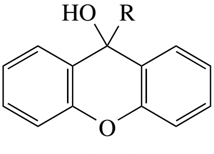

(586)

[R = Me, Pr, t-Bu, $PhCH_2$, tropylium]

From a mechanistic point of view, 9-substituted xanthenols **586** (prepared from the dianion of xanthen-9-one **585** *in situ* generated by a DTBB-catalyzed lithiation in THF, and different alkyl halides in 31–93% yield) are of interest due to rearrangements, which occurred under acidic conditions[252–254].

3. Carbon–nitrogen double bonds

Phenone imines **587** were lithiated with lithium and a catalytic amount of naphthalene (8%) in the presence of different carbonyl compounds as electrophiles in THF at temperatures ranging between −78 and room temperature, giving, after hydrolysis with water, the corresponding 1,2-aminoalcohols **588** (Scheme 154)[255].

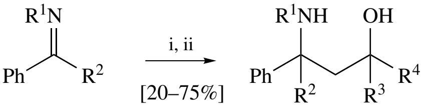

(587) **(588)**

R^1 = Me, c-C_6H_{11}, Ph
R^2 = H, Me, Ph
R^3, R^4 = H, Me, Et, i-Pr, Ph; $R^1R^2 = (CH_2)_4$, $(CH_2)_5$

SCHEME 154. Reagents: (i) Li, $C_{10}H_8$ (8%), R^3R^4CO = i-PrCHO, PhCHO, Me_2CO, Et_2CO, c-$(CH_2)_2CO$, c-$(CH_2)_2CO$, THF, −78 to 20 °C; (ii) H_2O

4. Heterocycles

High diastereoselectivity (ds >10:1) has been achieved when the substituted pyrrole **589** was reacted with lithium and a catalytic amount (8%) of naphthalene in THF at −78 °C, being methylated with methyl iodide; hence *trans*-product **590** was obtained (Scheme 155)[256].

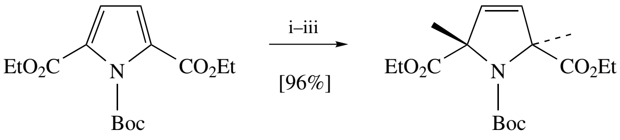

(589) **(590)**

SCHEME 155. Reagents: (i) Li, $C_{10}H_8$ (8%), THF, −78 °C; (ii) MeI, −78 to 20 °C

In the case of the monoester **591**, the same reaction as shown in Scheme 155, but using benzoyl chloride as electrophile, yielded the corresponding acylated ester **592**[257, 258].

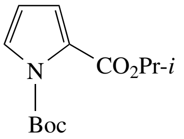

(591)

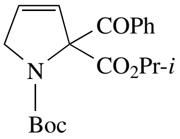

(592)

D. Lithium Telluride

Lithium telluride (Li_2Te) was prepared from elemental tellurium and lithium in the presence of a catalytic amount of naphthalene in THF at room temperature, and then used for the preparation of tellurophenes[259].

X. THE POLYMER-SUPPORTED VERSION

A further advance in arene-promoted lithiation would be to use a polymer-supported arene as the electron-carrier agent, because through this methodology the polymer could be easily separated at the end of the lithiation and eventually re-used. A stoichiometric version of this reaction using a polymer **593** has been reported[260,261].

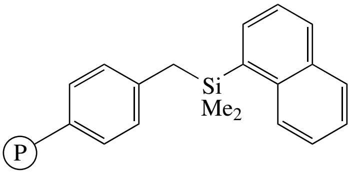

(593)

The corresponding catalytic version of this reaction was performed using either naphthalene- or biphenyl-supported polymers **594** or **595**, respectively, which were prepared by cross-coupling copolymerization of 2-vinylnaphthalene or 4-vinylbiphenyl with vinylbenzene and divinylbenzene promoted by AIBN in THF and polyvinyl alcohol[262, 263]. These polymers have been used as catalysts (10%) in lithiation reactions involving either chlorinated functionalized compounds or dichlorinated materials in THF at −78 °C and were re-used up to ten times without loss of activity, which is comparable to the use of the corresponding soluble arenes.

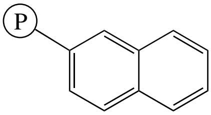

(594)

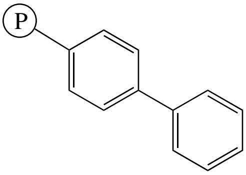

(595)

Another two polymers, which have been used for the same type of arene-catalyzed lithiation reactions, are compounds **596** and **597**, which were prepared by ring-opening metathesis polymerization (ROMP) starting from the corresponding aryl norbonenes **598**[263].

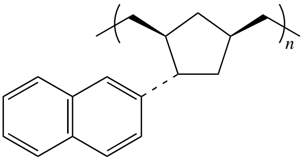

(596)

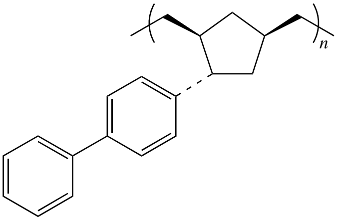

(597)

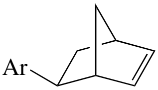

(598)

Also, linear or cross-linked polyphenylene of type **599** worked efficiently as catalyst in lithiation processes from functionalized chlorinated materials, dichlorinated compounds and benzofused cyclic ethers, with lithium powder in THF at −78 °C to room temperature. Yields are similar to those obtained in solution[265].

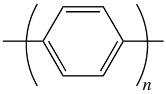

(599)

Finally, polymer **594** has been used as an arene-catalyst to activate nickel from nickel(II) chloride and lithium, in order to perform hydrogenation of different organic substrates such as alkenes, alkynes, carbonyl compounds and their imines, alkyl and aryl halides (chlorides, bromides and iodides), aromatic and heteroaromatic compounds as well as nitrogen-containing systems such as hydrazines, azoxy compounds or *N*-amino oxides, giving comparable results to those obtained in the corresponding reaction in solution[266].

XI. CONCLUSIONS

In this chapter the scope of arene-catalyzed lithiation has been reported, paying special attention to the application of this process in synthetic organic chemistry. Apart from the advantages of this methodology compared to the stoichiometric version (derived from the easy work-up, having a small amount of the arene to be removed), the main characteristic aspect of the catalytic version is that it is far more reactive than the stoichiometric one, so enabling one to perform new reactions not achievable using other types of activated lithium. This fact is probably a consequence of an involvement of an arene dianion as electron carrier, being more potent as reducing agent than the corresponding radical anion, which is the accepted acting reductive agent in the stoichiometric version of arene-promoted lithiation. Finally, in many cases, for very unstable species (i.e. dilithium synthons), the lithiation has to be carried out in the presence of the electrophile (Barbier-type reaction conditions) in order to avoid decomposition of the different lithiated intermediates involved in the process. Besides the generation of a wide range of organolithium compounds bearing or not a functional group or polylithium synthons, this methodology is useful to activate other metals, especially nickel, being also possible in all cases to be used as an arene-supported version of the catalytic process.

XII. ACKNOWLEDGMENTS

I thank our current Spanish Ministerio de Ciencia y Tecnología for continuous financial support. I also thank my lovely daughter Eva for her help in the preparation of the manuscript.

XIII. REFERENCES

1. P. Cintas, *Activated Metals in Organic Synthesis*, CRC Press, Boca Raton, 1993.
2. A. Fürstner (Ed.), *Active Metals*, VCH, Weinheim, 1995.
3. A. Guijarro, C. Gómez and M. Yus, *Trends Org. Chem.*, **8**, 65 (2000).
4. R. D. Rieke, M. S. Sell, W. R. Klein, T. Chen, J. D. Brown and M. V. Hanson, in Reference 2, pp. 1–59.
5. R. D. Rieke, *Science*, **246**, 1260 (1989).
6. L. E. Aleandri and B. Bogdanovic, in Reference 2, pp. 299–338.
7. P. Renaud, *Bull. Soc. Chim. Fr.*, 1044 (1950).
8. J.-L. Luche and P. Cintas, in Reference 2, pp. 135–190.
9. T. J. Mason (Ed.), *Advances in Sonochemistry*, JAI Press, Greenwhich, 1993.
10. K. S. Suslick (Ed.), *Ultrasond, its Chemical, Physical, and Biological Effects*, VCH, Weinheim, 1988.

11. C. Einhorn, J. Einhorn and J. L. Luche, *Synthesis*, 787 (1989).
12. S. Yu, R. Goldberg, E. Sturkovich and E. Lukevics, *Appl. Organomet. Chem*., **2**, 215 (1988).
13. G. J. Price (Ed.), *Current Trends in Sonochemistry*, Royal Society of Chemistry, London, 1992.
14. T. J. Mason, *Practical Sonochemistry*, Ellis Horwood, Chichester, 1991.
15. T. J. Mason and J. P. Lorimer, *Sonochemistry. Theory, Applications and Uses of Ultrasound in Chemistry*, Ellis Horwood, Chichester, 1988.
16. K. J. Klabunde and G. Cárdenas-Trivino, in Reference 2, pp. 237–278.
17. M. T. Reetz, W. Helbig and S. A. Quaiser, in Reference 2, pp. 279–297.
18. H. Bönemann and W. Brijoux, in Reference 2, pp. 339–379.
19. A. Fürstner, in Reference 2, pp. 381–446.
20. N. L. Holy, *Chem. Rev*., **74**, 243 (1974).
21. P. K. Freeman and L. L. Hutchinson, *Tetrahedron Lett*., 1849 (1976).
22. C. Nájera and M. Yus, *Trends Org. Chem*., **2**, 155 (1991).
23. C. Nájera and M. Yus, *Recent Res. Devel. Org. Chem*., **1**, 67 (1997).
24. C. Nájera and M. Yus, *Curr. Org. Chem*., in press.
25. A. Boudier, L. O. Bromm, M. Lotz and P. Knochel, *Angew. Chem., Int. Ed*., **39**, 4414 (2000).
26. M. Yus, *Chem. Soc. Rev*., **25**, 155 (1996).
27. D. J. Ramón and M. Yus, *Eur. J. Org. Chem*., 225 (2000).
28. M. Yus, *Synlett*, 1197 (2001).
29. M. Yus and D. J. Ramón, *Latv. J. Chem*., 79 (2002).
30. C. G. Screttas, *J. Chem. Soc., Chem. Commun*., 752 (1972).
31. H. E. Zieger, I. Augres and L. Maresca, *J. Am. Chem. Soc*., **95**, 8201 (1973).
32. M. Yus, R. P. Herrera and A. Guijarro, *Tetrahedron Lett*., **42**, 3455 (2001).
33. M. Yus, R. P. Herrera and A. Guijarro, *Chem. Eur. J*., **8**, 2574 (2002).
34. J. J. Brooks, W. Rhine and G. D. Stucky, *J. Am. Chem. Soc*., **94**, 7346 (1972).
35. J. Almena, F. Foubelo and M. Yus, *J. Org. Chem*., **59**, 3210 (1994).
36. B. J. Wakefield, *Organolithium Methods*, Academic Press, New York, 1988.
37. A. M. Sapse and P. v. R. Schleyer (Eds.), *Lithium Chemistry: A Theoretical and Experimental Overview*, Wiley, Chichester, 1995.
38. R. Bartsab, C. Doost and U. Klingebiel, in *Synthetic Methods of Organometallic and Inorganic Chemistry*, W. Herrmann (Ed.), Thieme Verlag, Stuttgart, 1996, pp. 1–23.
39. M. Gray, M. Tinkel and V. Snieckus, in *Comprehensive Organometallic Chemistry II* (Eds. E. W. Abel, F. G. A. Stone, G. Wilkinson and A. McKillop), Vol. 11, Pergamon Press, Oxford, 1995, pp. 1–92.
40. J. Clayden, *Organolithiums: Selectivity for Synthesis*, Pergamon Press, Oxford, 2002.
41. P. J. Pearce, D. H. Richards and N. F. Scilly, *J. Chem. Soc., Perkin Trans. 1*, 1655 (1972).
42. T. van den Ancker and M. J. Hodson, *J. Chem. Soc., Perkin Trans. 1*, 2869 (1999).
43. C. Blomberg, *The Barbier Reaction and Related Processes*, Springer, Berlin, 1993.
44. F. Alonso and M. Yus, *Recent Res. Dev. Org. Chem*., **1**, 397 (1997).
45. P. K. Freeman and L. L. Hutchinson, *J. Org. Chem*., **45**, 1924 (1980).
46. H. Choi, A. A. Pinkerton and J. L. Fry, *J. Chem. Soc., Chem. Commun*., 225 (1987).
47. C.-D. Graf and P. Knochel, *Tetrahedron*, **55**, 8801 (1999).
48. M. Yus, R. Ortiz and F. F. Huerta, *Tetrahedron Lett*., **43**, 2957 (2002).
49. A. Guijarro, D. J. Ramón and M. Yus, *Tetrahedron*, **49**, 469 (1993).
50. F. Alonso, E. Lorenzo and M. Yus, *J. Org. Chem*., **61**, 5058 (1996).
51. M. Yus, C. Gómez and P. Candela, *Tetrahedron Lett*., **42**, 3977 (2001).
52. D. Guijarro and M. Yus, *Recent Res. Dev. Org. Chem*., **2**, 713 (1998).
53. D. Guijarro and M. Yus, *Tetrahedron*, **50**, 3447 (1994).
54. M. Yus, G. Radivoy and F. Alonso, *Synthesis*, 914 (2001).
55. M. Hudlicky, *Chemistry of Organic Fluorine Compounds*, Prentice Hall, Englewood Cliffs, 1992, p. 175.
56. R. E. Banks, B. E. Smart and J. C. Tatlow (Eds.), *Organofluorine Chemistry: Principles and Commercial Applications*, Plenum Press, New York, 1994.
57. M. Hudlicky and A. E. Pavlath (Eds.), *Chemistry of Organic Fluorine Compounds II. A Critical Review*, ACS, New York, 1995.
58. J. J. Eisch, *J. Org. Chem*., **28**, 707 (1963).
59. D. Guijarro and M. Yus, *Tetrahedron*, **56**, 1135 (2000).

60. D. Guijarro and M. Yus, *J. Organomet. Chem*., **624**, 53 (2001).
61. E. Alonso, D. Guijarro and M. Yus, *Tetrahedron*, **51**, 11457 (1995).
62. B. A. Lindemberg and M. Massin, *J. Physiol. (Paris)*, **49**, 285 (1957).
63. E. Alonso, D. J. Ramón and M. Yus, *J. Org. Chem*., **62**, 417 (1997).
64. M. Jang, L. Cai, G. O. Udeani, K. V. Slowing, C. F. Thomas, C. W. Beecher, H. H. Fong, N. R. Farnsworth, A. D. Kinghorn, R. G. Mehta, R. C. Moon and J. M. Pezzuto, *Science*, **275**, 218 (1997).
65. J. J. Eisch, *Organomet. Synth*., **2**, 91 (1981).
66. J. J. Eisch and A. M. Jacobs, *J. Org. Chem*., **28**, 2145 (1963).
67. A. Bachki, F. Foubelo and M. Yus, *Tetrahedron Lett*., **39**, 7759 (1998).
68. U. Azzena, S. Carta, G. Melloni and A. Sechi, *Tetrahedron*, **53**, 16205 (1997).
69. E. Alonso, D. J. Ramón and M. Yus, *Tetrahedron*, **53**, 14355 (1997).
70. E. Alonso, D. Guijarro, P. Martínez, D. J. Ramón and M. Yus, *Tetrahedron*, **55**, 11027 (1999).
71. D. Guijarro, B. Mancheño and M. Yus, *Tetrahedron*, **48**, 4593 (1992).
72. E. Alonso, D. J. Ramón and M. Yus, *Tetrahedron*, **52**, 14341 (1996).
73. D. Guijarro, B. Mancheño and M. Yus, *Tetrahedron Lett*., **33**, 5597 (1992).
74. D. Guijarro, G. Guillena, B. Mancheño and M. Yus, *Tetrahedron*, **50**, 3427 (1994).
75. D. Guijarro and M. Yus, *Tetrahedron*, **51**, 11445 (1995).
76. D. Guijarro, B. Mancheño and M. Yus, *Tetrahedron*, **50**, 8551 (1994).
77. A. R. Katritzky and M. Qi, *J. Org. Chem*., **62**, 4116 (1997).
78. P. Martínez, unpublished results.
79. C. G. Screttas and M. Micha-Screttas, *J. Org. Chem*., **43**, 1064 (1978); **44**, 713 (1979).
80. T. Cohen and M. Bhupathy, *Acc. Chem. Res*., **22**, 152 (1989)
81. M. Yus and D. J. Ramón, *J. Chem. Soc., Chem. Commun.*, 398 (1991).
82. E. J. Corey and Z. Chen, *Tetrahedron Lett*., **35**, 8731 (1994).
83. K. Tanino, N. Yoshitani, F. Moriyama and I. Kuwajima, *J. Org. Chem*., **62**, 4206 (1997).
84. E. Alonso, D. Guijarro and M. Yus, *Tetrahedron*, **51**, 2699 (1995).
85. D. Guijarro and M. Yus, *Tetrahedron Lett*., **35**, 2965 (1994).
86. G. Radivoy, F. Alonso and M. Yus, *Synthesis*, 427 (2001).
87. D. A. Alonso and P. G. Andersson, *J. Org. Chem*., **63**, 9455 (1998).
88. C. E. Neipp, J. M. Humphrey and S. F. Martin, *J. Org. Chem*., **66**, 531 (2001).
89. D. Seebach, *Angew. Chem., Int. Ed. Engl*., **18**, 239 (1979).
90. C. Nájera and M. Yus, *Org. Prep. Proced. Int*., **27**, 383 (1995).
91. D. J. Ramón and M. Yus, *Tetrahedron Lett*., **34**, 7115 (1993).
92. D. J. Ramón and M. Yus, *Tetrahedron*, **52**, 13739 (1996).
93. E. Alonso, D. J. Ramón and M. Yus, *Tetrahedron Lett*., **38**, 8903 (1997).
94. E. Alonso, D. J. Ramón and M. Yus, *Tetrahedron*, **54**, 12007 (1998).
95. A. Guijarro and M. Yus, *Tetrahedron Lett*., **34**, 3487 (1993).
96. A. Guijarro, B. Mancheño, J. Ortiz and M. Yus, *Tetrahedron*, **52**, 1643 (1996).
97. D. Seebach and E. Hungerbühler, in *Modern Synthetic Methods*, R. Scheffold (Ed.), Salle-Sauerländer-Verlag, Frankfurt, 1980.
98. J. Ortiz, A. Guijarro and M. Yus, *An. Quim. Int. Ed*., **93**, 44 (1997).
99. A. Guijarro and M. Yus, *Tetrahedron Lett*., **37**, 5593 (1996).
100. J. Ortiz, A. Guijarro and M. Yus, *Eur. J. Org. Chem*., 3005 (1999).
101. P. Beak and A. I. Meyers, *Acc. Chem. Res*., **19**, 356 (1986).
102. S. D. Rychnovsky and D. J. Skalitzky, *J. Org. Chem*., **57**, 4336 (1992).
103. M. Yus, J. Ortiz and C. Nájera, *ARKIVOC*, 38 (2002).
104. A. Guijarro, J. Ortiz and M. Yus, *Tetrahedron Lett*., **37**, 5597 (1996).
105. J. Ortiz, A. Guijarro and M. Yus, *Tetrahedron*, **55**, 4831 (1999).
106. U. Azzena, L. Pilo and E. Piras, *Tetrahedron*, **56**, 3775 (2000).
107. D. A. Alonso, E. Alonso, C. Nájera and M. Yus, *Synlett*, 491 (1997).
108. D. A. Alonso, E. Alonso, C. Nájera, D. J. Ramón and M. Yus, *Tetrahedron*, **53**, 4835 (1997).
109. T. Ireland, J. J. Almena Perea and P. Knochel, *Angew. Chem., Int. Ed*., **38**, 1457 (1999).
110. T. Soler, A. Bachki, L. R. Falvello and M. Yus, *Tetrahedron: Asymmetry*, **11**, 493 (2000).
111. F. Foubelo, A. Gutierrez and M. Yus, *Tetrahedron Lett*., **38**, 4837 (1997).
112. F. Foubelo, A. Gutierrez and M. Yus, *Synthesis*, 503 (1999).
113. M. Yus, D. J. Ramón and I. Gómez, *Tetrahedron*, **58**, 5163 (2002).
114. A. Bachki, F. Foubelo and M. Yus, *Tetrahedron*, **53**, 4921 (1997).

115. M. S.-Fodil, H. Ferreira, J. Gralak and L. Duhamel, *Tetrahedron Lett*., **39**, 8975 (1998).
116. I. M. Pastor and M. Yus, *Tetrahedron Lett*., **41**, 5335 (2000).
117. M. Shindo, R. Koretsune, W. Yokota, K. Itoh and K. Shishido, *Tetrahedron Lett*., **42**, 8357 (2001).
118. M. Shindo, K. Matsumoto, S. Mori and K. Shishido, *J. Am. Chem. Soc*., **124**, 6840 (2002).
119. F. Foubelo and M. Yus, *Tetrahedron Lett*., **35**, 4831 (1994).
120. F. Foubelo and M. Yus, *Tetrahedron: Asymmetry*, **7**, 2911 (1996).
121. D. J. Ramón and M. Yus, *Tetrahedron*, **49**, 10103 (1993).
122. C. Gómez, F. F. Huerta and M. Yus, *Tetrahedron*, **54**, 6177 (1998).
123. F. F. Huerta, C. Gómez and M. Yus, *Tetrahedron*, **52**, 8333 (1996).
124. I. Kuwajima and E. Nakamura, in *Comprehensive Organic Synthesis*, (Eds. B. Trost, I. Fleming and C. H. Heathcock), Pergamon Press, Oxford, 1991, pp. 441–473.
125. E. Alonso, D. J. Ramón and M. Yus, *An. Quim. Int. Ed*., **94**, 56 (1998).
126. M. A. Abd El-Hafiz, B. Weniger, J. C. Quirino and R. Anson, *Phytochemistry*, **30**, 2029 (1991).
127. J. F. Gil, D. J. Ramón and M. Yus, *Tetrahedron*, **50**, 3437 (1994).
128. M. Yus, T. Soler and F. Foubelo, *J. Org. Chem*., **66**, 6207 (2001).
129. J. Almena, F. Foubelo and M. Yus, *Tetrahedron*, **51**, 11883 (1995).
130. O. Nishimura, C. Kitada and M. Fujino, *Chem. Pharm. Bull*., **26**, 1576 (1978).
131. K. Ramig, Y. Dong and S. D. Van Arnum, *Tetrahedron Lett*., **37**, 443 (1996).
132. I. Manteca, B. Etxarri, A. Ardeo, S. Arrasate, I. Osante, N. Sotomayor and E. Lete, *Tetrahedron*, **54**, 12361 (1998).
133. F. F. Huerta, C. Gómez and M. Yus, *Tetrahedron*, **52**, 13243 (1996).
134. C. Gómez, F. F. Huerta, I. M. Pastor and M. Yus, *Tetrahedron*, **53**, 17201 (1997).
135. M. Yus and D. J. Ramón, *J. Org. Chem*., **57**, 750 (1992).
136. J. H. Borden, in *Comprehensive Insect Physiology, Biochemistry and Pharmacology*, (Eds. G. A. Kerkut and L. I. Gilberts), Vol. 9, Pergamon Press, Oxford, 1985, p. 257.
137. T. L. Payne, N. A. Andryszak, H. Wieser, E. A. Dixon, N. Ibrahim and J. Coers, *J. Chem. Ecol*., **14**, 1217 (1988).
138. A. C. Oehlschlager and B. D. Johnston, *J. Org. Chem*., **52**, 940 (1987).
139. I. M. Pastor and M. Yus, *Tetrahedron Lett*., **42**, 1029 (2001).
140. J. F. Gil, D. J. Ramón and M. Yus, *Tetrahedron*, **49**, 4923 (1993).
141. J. F. Gil, D. J. Ramón and M. Yus, *Tetrahedron*, **50**, 7307 (1994).
142. R. Ballini, G. Bosica and G. Rafaiani, *Helv. Chim. Acta*, **78**, 879 (1995).
143. C. Gómez, F. F. Huerta and M. Yus, *Tetrahedron*, **54**, 1853 (1998).
144. F. F. Huerta, C. Gómez and M. Yus, *Tetrahedron*, **55**, 4043 (1999).
145. G. Quéguiner, F. Marsais, V. Snieckus and J. Epsztajn, *Adv. Heterocycl. Chem*., **52**, 186 (1991).
146. I. Gómez, E. Alonso, D. J. Ramón and M. Yus, *Tetrahedron*, **56**, 4043 (2000).
147. M. Yus and F. Foubelo, *Rev. Heteroatom Chem*., **17**, 73 (1997).
148. E. Bartmann, *Angew. Chem., Int. Ed. Engl*., **25**, 653 (1986).
149. A. Bachki, F. Foubelo and M. Yus, *Tetrahedron: Asymmetry*, **6**, 1907 (1995).
150. A. Bachki, F. Foubelo and M. Yus, *Tetrahedron: Asymmetry*, **7**, 2997 (1996).
151. T. Soler, A. Bachki, L. R. Falvello, F. Foubelo and M. Yus, *Tetrahedron: Asymmetry*, **9**, 3939 (1998).
152. R. F. Witzmann, *Steroids-Key to Life*, Van Nostrum Reinhold, New York, 1981.
153. L. R. Falvello, F. Foubelo, T. Soler and M. Yus, *Tetrahedron: Asymmetry*, **11**, 2063 (2000).
154. M. Yus, T. Soler and F. Foubelo, *Tetrahedron: Asymmetry*, **12**, 801 (2001).
155. Y. H. Kang, C. J. Lee and K. Kim, *J. Org. Chem*., **66**, 2149 (2001).
156. J. Almena, F. Foubelo and M. Yus, *Tetrahedron Lett*., **34**, 1649 (1993).
157. B. Mudryk and T. Cohen, *J. Org. Chem*., **54**, 5657 (1989).
158. K. Rama and M. A. Pasha, *Tetrahedron Lett*., **41**, 1073 (2000).
159. C. A. Dvorak, C. Dufour, S. Iwasa and V. H. Rawal, *J. Org. Chem*., **63**, 5302 (1998).
160. A. Bachki, L. R. Falvello, F. Foubelo and M. Yus, *Tetrahedron: Asymmetry*, **8**, 2633 (1997).
161. M. Hashemzadeh and A. R. Howell, *Tetrahedron Lett*., **41**, 1855 (2000).
162. M. Hashemzadeh and A. R. Howell, *Tetrahedron Lett*., **41**, 1859 (2000).
163. R. B. Bates, L. M. Kroposki and D. E. Potter, *J. Org. Chem*., **37**, 560 (1972).
164. J. Almena, F. Foubelo and M. Yus, *Tetrahedron*, **50**, 5775 (1994).

165. J. Almena, F. Foubelo and M. Yus, *Tetrahedron*, **53**, 5563 (1997).
166. B. Mudryk and T. Cohen, *J. Am. Chem. Soc*., **113**, 1866 (1991).
167. D. J. Ramón and M. Yus, *Tetrahedron*, **48**, 3585 (1992).
168. M. Yus, F. Foubelo, J. V. Ferrández and A. Bachki, *Tetrahedron*, **58**, 4907 (2002).
169. J. Almena, F. Foubelo and M. Yus, *Tetrahedron*, **51**, 3351 (1995).
170. U. Azzena, S. Dermartis, M. G. Fiori, G. Melloni and L. Pisano, *Tetrahedron Lett*., **36**, 8123 (1995).
171. U. Azzena, S. Demartis and G. Melloni, *J. Org. Chem*., **61**, 4913 (1996).
172. A. Bieniek, J. Epsztajn, J. A. Kowalska and Z. Malinowski, *Tetrahedron Lett*., **42**, 9293 (2001).
173. M. Tsukamoto, S. Nakajima, K. Murooka, M. Naito, H. Suzuki, M. Hirayama, K. Hirano, K. Kojiri, and H. Suda, *J. Antibiot*., **53**, 687 (2000).
174. F. Foubelo, C. Gómez, A. Gutierrez and M. Yus, *J. Heterocycl. Chem*., **37**, 1061 (2000).
175. M. Yus, T. Soler and F. Foubelo, *Tetrahedron*, **58**, 7009 (2002).
176. I. M. Pastor and M. Yus, *Tetrahedron Lett*., **41**, 1589 (2000).
177. I. M. Pastor and M. Yus, *Tetrahedron*, **57**, 2371 (2001).
178. M. Yus, I. M. Pastor and J. Gomis, *Tetrahedron*, **57**, 5799 (2001).
179. M. Yus and J. Gomis, *Tetrahedron Lett*., **42**, 5721 (2001).
180. M. Yus and J. Gomis, *Eur. J. Org. Chem*., 1989 (2002).
181. J. Gomis, unpublished results.
182. M. T. Reetz, *Organotitanium Reagents in Organic Synthesis*, Springer-Verlag, Berlin, 1986.
183. I. M. Pastor and M. Yus, *Tetrahedron*, **57**, 2365 (2001).
184. M. Yus, F. Foubelo and J. V. Ferrández, *Eur. J. Org. Chem*., 2809 (2001).
185. J. Almena, F. Foubelo and M. Yus, *Tetrahedron*, **52**, 8545 (1996).
186. J. Almena, F. Foubelo and M. Yus, *J. Org. Chem*., **61**, 1859 (1996).
187. J. Almena, F. Foubelo and M. Yus, *Tetrahedron*, **51**, 3365 (1995).
188. U. Azzena, S. Demartis, L. Pilo and E. Piras, *Tetrahedron*, **56**, 8375 (2000).
189. M. Yus and F. Foubelo, *Tetrahedron Lett*., **42**, 2469 (2001).
190. J. F. Gil, D. J. Ramón and M. Yus, *Tetrahedron*, **49**, 9535 (1993).
191. U. Azenna, *J. Chem. Soc., Perkin Trans. 1*, 360 (2002).
192. J. Shin, M. M. Qualls, J. A. Boomer, J. Robarge and D. H. Thompson, *J. Am. Chem. Soc*., **123**, 508 (2001).
193. U. Azenna and L. Pilo, *Synthesis*, 664 (1999).
194. M. A. Arrica, U. Azenna, L. Pilo and E. Piras, *Tetrahedron Lett*., **43**, 5137 (2002).
195. P. K. Choudhury, J. Almena, F. Foubelo and M. Yus, *Tetrahedron*, **53**, 17373 (1997).
196. M. Yus, F. Foubelo and J. V. Ferrández, *Chem. Lett*., 726 (2002).
197. F. Foubelo and M. Yus, *Trends Org. Chem*., **7**, 1 (1998).
198. A. Guijarro and M. Yus, *Tetrahedron Lett*., **35**, 253 (1994).
199. A. Guijarro and M. Yus, *Tetrahedron*, **52**, 1797 (1996).
200. F. Foubelo, A. Gutierrez and M. Yus, *Tetrahedron Lett*., **40**, 8173 (1999).
201. M. Yus, A. Gutierrez and F. Foubelo, *Tetrahedron*, **57**, 4411 (2001).
202. F. Foubelo, A. Gutierrez and M. Yus, *Tetrahedron Lett*., **40**, 8177 (1999).
203. M. Schlosser and V. Ladenberger, *Angew. Chem., Int. Ed. Engl*., **5**, 519 (1966).
204. A. Guijarro and M. Yus, *Tetrahedron Lett*., **34**, 2011 (1993).
205. F. F. Huerta, C. Gómez, A. Guijarro and M. Yus, *Tetrahedron*, **51**, 3375 (1995).
206. M. Yus, F. Foubelo and J. V. Ferrández, *Tetrahedron Lett*., **43**, 7205 (2002).
207. D. J. Ramón and M. Yus, *Tetrahedron Lett*., **33**, 2217 (1992).
208. C. Gómez, D. J. Ramón and M. Yus, *Tetrahedron*, **49**, 4117 (1993).
209. C. A. Towsen and R. E. Minto, Chap. 1.17 in *Comprehensive Natural Products Chemistry* (Eds. D. Barton, K. Nakanishi, D. Meth-Cohn and V. Sankawa), Vol. 1, Elsevier, Amsterdam, 1999.
210. F. Alonso, E. Lorenzo and M. Yus, *Tetrahedron Lett*., **38**, 2187 (1997).
211. E. Lorenzo, F. Alonso and M. Yus, *Tetrahedron*, **56**, 1745 (2000).
212. F. Alonso, E. Lorenzo and M. Yus, *Tetrahedron Lett.*, **39**, 3303 (1998).
213. E. Lorenzo, F. Alonso and M. Yus, *Tetrahedron Lett*., **41**, 1661 (2000).
214. J. Ishihara, Y. Tamamoto, N. Kanoh and A. Murai, *Tetrahedron Lett*., **40**, 4387 (1999).
215. F. Alonso, L. R. Falvello, P. E. Fanwick, E. Lorenzo and M. Yus, *Synthesis*, 949 (2000).

216. I. G. Collado, F. A. Macias, G. M. Massanet, J. M. Molinillo and F. R. Luis, *J. Org. Chem*., **52**, 3323 (1987).
217. A. Guijarro and M. Yus, *Tetrahedron*, **50**, 13269 (1994).
218. F. Foubelo and M. Yus, *Tetrahedron Lett*., **40**, 743 (1999).
219. F. Foubelo, S. A. Saleh and M. Yus, *J. Org. Chem*., **65**, 3478 (2000).
220. F. Foubelo and M. Yus, *Tetrahedron Lett*., **41**, 5047 (2000).
221. A. Guijarro and M. Yus, *Tetrahedron*, **50**, 7857 (1994).
222. A. Guijarro and M. Yus, *Tetrahedron*, **51**, 231 (1995).
223. R. Gleiter, G. Haberhauer, H. Irngartinger, T. Oeser and F. Rominger, *Organometallics*, **18**, 3615 (1999).
224. G. Haberhauer, R. Gleiter, H. Irngartinger, T. Oeser and F. Rominger, *J. Chem. Soc., Perkin Trans. 2*, 2093 (1999).
225. R. Popp, R. Gleiter and F. Rominger, *Tetrahedron Lett*, **41**, 4075 (2000).
226. G. Haberhauer, R. Roers and R. Gleiter, *Tetrahedron Lett*., **38**, 8679 (1997).
227. G. Haberhauer, F. Rominger and R. Gleiter, *J. Chem. Soc., Perkin Trans. 2*, 947 (1999).
228. C. Gómez, F. F. Huerta and M. Yus, *Tetrahedron Lett*., **38**, 687 (1997).
229. C. Gómez, F. F. Huerta and M. Yus, *Tetrahedron*, **53**, 13897 (1997).
230. M. Yus, D. J. Ramón and I. Gómez, *J. Organomet. Chem.*, **663**, 21 (2002).
231. M. V. Hanson, J. D. Brown, R. D. Rieke and Q. J. Niu, *Tetrahedron Lett*., **35**, 7205 (1994).
232. M. V. Hanson and R. D. Rieke, *J. Am. Chem. Soc*., **117**, 10775 (1995).
233. G. Cahiez, A. Martín and T. Delacroix, *Tetrahedron Lett.*, **40**, 6407 (1999).
234. F. Alonso and M. Yus, *Tetrahedron Lett*., **37**, 6925 (1996).
235. F. Alonso and M. Yus, *J. Chem. Educ*., **78**, 1517 (2001).
236. F. Alonso and M. Yus, *Tetrahedron Lett*., **38**, 149 (1997).
237. F. Alonso, G. Radivoy and M. Yus, *Tetrahedron*, **55**, 4441 (1999).
238. G. Radivoy, F. Alonso and M. Yus, *Tetrahedron*, **55**, 14479 (1999).
239. F. Alonso and M. Yus, *Tetrahedron*, **54**, 1921 (1998).
240. F. Alonso, G. Radivoy and M. Yus, *Tetrahedron*, **56**, 8673 (2000).
241. F. Alonso and M. Yus, *Adv. Synth. Catal*., **343**, 188 (2001).
242. U. Lischka, D. Rittmayer and U. Wietelmann, German Patent DE 19849197 (2000); *Chem. Abstr*., **132**, 137554 (2000).
243. A. Maerker and U. Girreser, *Angew. Chem., Int. Ed. Engl*., **29**, 667 (1990).
244. E. Alonso, D. J. Ramón and M. Yus, *Tetrahedron*, **53**, 2641 (1997).
245. A. Schmitt and H.-U. Reissig, *Synlett*, 40 (1990).
246. E. Alonso, D. J. Ramón and M. Yus, *Tetrahedron*, **54**, 13629 (1998).
247. R. Karaman, D. T. Kohlman and J. L. Fry, *Tetrahedron Lett*., **31**, 6155 (1990).
248. D. Guijarro, B. Mancheño and M. Yus, *Tetrahedron*, **49**, 1327 (1993).
249. R. Karaman and J. L. Fry, *Tetrahedron Lett*., **30**, 4935 (1989).
250. R. Karaman and J. L. Fry, *Tetrahedron Lett*., **30**, 4931 (1989).
251. R. Karaman and J. L. Fry, *Tetrahedron Lett*., **30**, 6267 (1989).
252. R. Karaman, I. T. Badejo and J. L. Fry, *J. Am. Chem. Soc*., **111**, 6450 (1989).
253. I. T. Badejo, R. Karaman, N. W. I. Lee, E. C. Lutz, M. T. Mamanta and J. L. Fry, *J. Chem. Soc., Chem. Commun*., 566 (1989).
254. I. T. Badejo, R. Karaman and J. L. Fry, *J. Org. Chem*., **54**, 4591 (1989).
255. D. Guijarro and M. Yus, *Tetrahedron*, **49**, 4761 (1993).
256. T. J. Donohoe, R. R. Harji and R. P. C. Causins, *Tetrahedron Lett*., **41**, 1327 (2000).
257. T. J. Donohoe, R. R. Harji and R. P. C. Causins, *Tetrahedron Lett*., **41**, 1331 (2000).
258. T. J. Donohoe and D. House, *J. Org. Chem*., **67**, 5015 (2002).
259. M. Katkevics, S. Yamaguchi, A. Toshimitsu and K. Tamao, *Organometallics*, **17**, 5796 (1998).
260. T. R. van den Ancker, G. R. Hanson, F.-C. Lee and C. L. Raston, *Chem. Commun*., 125 (1997).
261. T. R. van den Ancker and C. L. Raston, *J. Organomet. Chem*., **550**, 283 (1998).
262. C. Gómez, S. Ruiz and M. Yus, *Tetrahedron Lett*., **39**, 1397 (1998).
263. C. Gómez, S. Ruiz and M. Yus, *Tetrahedron*, **55**, 7017 (1999).
264. T. Arnauld, A. G. M. Barret and B. T. Hopkins, *Tetrahedron Lett*., **43**, 1081 (2002).
265. M. Yus, C. Gómez and P. Candela, *Tetrahedron*, **58**, 6207 (2002).
266. P. Candela, unpublished results.

CHAPTER **12**

Rearrangements of organolithium compounds

KATSUHIKO TOMOOKA

Department of Applied Chemistry, Tokyo Institute of Technology, Meguro-ku, Tokyo 152-8552, Japan
Fax: +81-3-5734-3931; e-mail: ktomooka@apc.titech.ac.jp

The Chemistry of Organolithium Compounds. Edited by Z. Rappoport and I. Marek
ISBN: 0-470-84339-X

I. INTRODUCTION

This chapter mainly concerns common rearrangements of organolithium compounds which are synthetically valuable in terms of a C−C bond or C−heteroatom bond formation.

Allylic, propargylic and benzylic protons adjacent to a suitable heteroatom such as oxygen, nitrogen or sulfur are sufficiently acidic to give good yields of carbanion upon treatment with a strong base such as alkyllithium and lithium amide reagents. In certain systems, the α-heterocarbanion acts as a migration terminus in a rearrangement. These α-heterocarbanion rearrangements are classified by the types of cleaving and forming bonds and also by their positions (Table 1). The driving force for these rearrangements is the transfer of a formal negative charge from the less electronegative carbon to the more electronegative heteroatom. This chapter will deal with a small range of common rearrangements in which an organolithium is the starting material. The rearrangements which generate organolithiums, such as the Shapiro reaction and Brook rearrangement, are not covered.

II. REARRANGEMENTS OF ORGANOLITHIUMS

A. [1,2]-Wittig Rearrangement and Related Reactions (O−C → C−C)[1]

The first example of a 1,2-alkyl migration from oxygen to carbanion in the reactions of benzylic ethers with phenyllithium was reported by Wittig and Löhmann in 1942[2]. Since then, the general name 'Wittig rearrangement' has been given to this type of carbanion rearrangement of ethers or acetals which involves a 1,2-alkyl shift onto an α-oxycarbanion terminus (equation 1). The synthetic application of the [1,2]-Wittig rearrangement is limited. However, it is a potentially useful carbon−carbon bond-forming reaction.

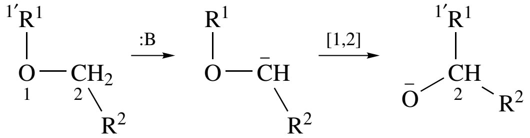

(1)

1. Mechanistic aspects

Several mechanisms had been proposed for the [1,2]-Wittig rearrangement, including (i) a concerted process taking place through a pentacoordinate transition state, (ii) a

TABLE 1. Rearrangements of organolithium compounds

Transformation		
$O{-}C \longrightarrow C{-}C$	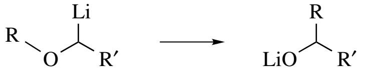	[1,2]-Wittig rearrangement
	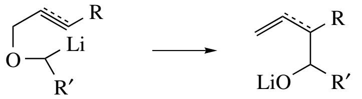	[2,3]-Wittig rearrangement
	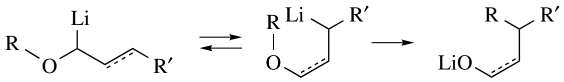	[1,4]-Wittig rearrangement
$N{-}C \longrightarrow C{-}C$	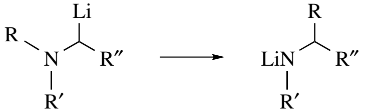	Aza-[1,2]-Wittig rearrangement
	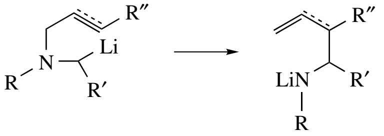	Aza-[2,3]-Wittig rearrangement
$S{-}C \longrightarrow C{-}C$	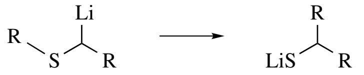	Thia-[1,2]-Wittig rearrangement
	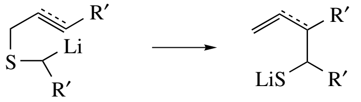	Thia-[2,3]-Wittig rearrangement
$O{-}Si \longrightarrow C{-}Si$	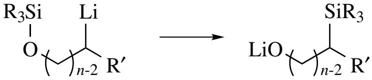	[1,*n*]-Retro-Brook rearrangement
$O{-}P \longrightarrow C{-}P$	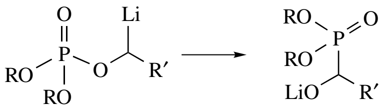	Phosphate-phosphonate rearrangement

two-step dissociative process involving the formation of R^{1-} and $O{=}CHR^2$ followed by recombination of the two fragments (heterolytic dissociation mechanism), and (iii) a two-step process involving the formation of a pair of radicals and subsequent recombination (homolytic dissociation mechanism)[1]. It is now well recognized that among them, the radical cleavage-recombination mechanism best accommodates the experimental findings (equation 2)[3]. Thus, the [1,2]-Wittig rearrangement is now classified as a special class of intramolecular radical processes.

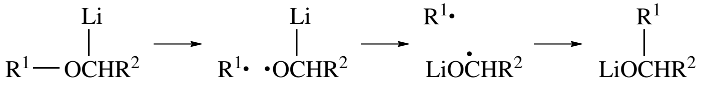

$$R^1{-}O\overset{\overset{Li}{|}}{C}HR^2 \longrightarrow R^1\cdot\ \cdot O\overset{\overset{Li}{|}}{C}HR^2 \longrightarrow LiO\overset{R^1\cdot}{\dot{C}}HR^2 \longrightarrow LiO\overset{\overset{R^1}{|}}{C}HR^2 \tag{2}$$

On the other hand, recent *ab initio* calculations have shown that the [1,2]-Wittig rearrangement preferentially proceeds via the heterolytic dissociation in gas phase[4]. One might speculate that the solvent could generate a situation different from the transition state obtained computationally.

Generally speaking, the scope and limitation of the [1,2]-Wittig rearrangement is determined principally by the migratory aptitude of the R^1 group and the reactivity of the carbanion terminus dictated by the nature of the R^2 group. The migratory aptitude of the R^1 group increases in the following order: *prim*− < *sec*− < *tert*-alkyl < benzyl. This order is roughly consistent with the stability order of the corresponding radicals ($R^1\bullet$) involved[1a]. Best results from the [1,2]-Wittig rearrangement are obtained when the migrating group R^1 and the organolithium substituent R^2 are radical stabilizing groups[1a, 5–7]. For example, benzyloxymethyllithium **1** (R = H) does not undergo [1,2]-rearrangement[6], although its ethyl homologue **2** ($R = C_2H_5$) does (90%)[5]. In other words, rather stable carbanions that can be generated by direct deprotonation undergo the Wittig rearrangement in most cases, while the rearrangement involving a relatively unstable carbanion terminus requires a migrating group such as benzyl, of which the radical species is substantially stabilized. Chart 1 summarizes the scope and limitations of the [1,2]-Wittig rearrangement in terms of the radical stabilities of the migrating group and terminus.

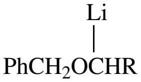

$$PhCH_2O\overset{\overset{Li}{|}}{C}HR$$

(1) R = H

(2) $R = C_2H_5$

		Organolithium substituent (R^2)			
		H	*n*-alkyl	vinyl	Ph
Migrating group (R^1)	Me	×	×	×	×
	Et	×	×	○	○
	i-Pr	×	×	○	○
	Bn	×	○	○	○

[a] ○, good combination; ×, bad combination.

CHART 1. Scope and limitation of the [1,2]-Wittig rearrangement[a]

One of the most important side reactions often observed with the [1,2]-Wittig rearrangement is the α,β'-elimination (equation 3)[8]. In fact, treatment of benzyl ether **3** with *n*-BuLi afforded predominantly the elimination product **4** (equation 4)[9].

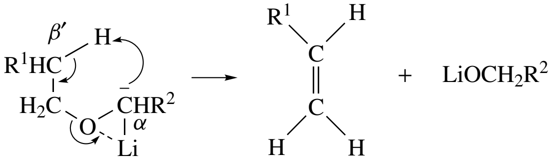

(3)

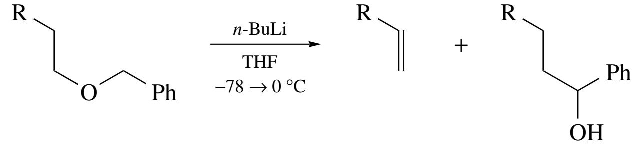

(4)

(3) R = $TBSO(CH_2)_8$ **(4)** 90% [1,2]-product 0%

An interesting problem of the periselectivity arises in the rearrangement involving an α-oxyallylic carbanion as the terminus. In this particular case, the [1,4]-shift may compete with the [1,2]-Wittig rearrangement (see Section II.C). For example, the rearrangement of **5** affords a mixture of the [1,4]-product **6** and the [1,2]-product **7** (equation 5)[10].

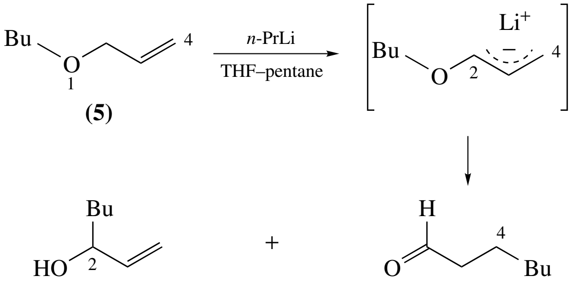

(5)

(5)

(7) 23%
[1,2]-product

(6) 29%
[1,4]-product

2. Stereochemical aspects

There are two aspects to the stereospecificity of the [1,2]-Wittig rearrangement: the steric course (inversion vs. retention) at the migrating carbon atom and at the Li-bearing carbanion center (equation 6).

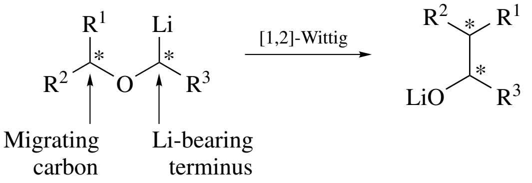

(6)

Schöllkopf and colleagues have reported that the rearrangement of the enantiopure forms of α-chiral alkyl benzyl ethers **8** followed by oxidation affords ketone **9** of the predominantly retained configuration at the migrating carbon in 20% ee (R = H) and 80% ee (R = Ph) (equation 7)[11].

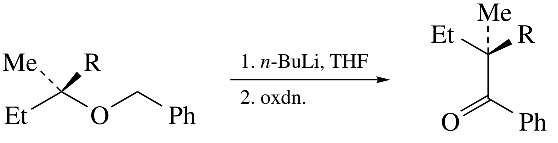

(8) **(9)**

(7)

R = H: 60% retention
R = Ph: 90% retention

These findings prove that the rearrangements proceed predominantly with retention of configuration at the migrating carbon, the degree depending critically on the nature of the migrating group. The steric course at the Li-bearing center has been investigated by several groups. Verner and Cohen have presented evidence for inversion of configuration at the Li-bearing terminus in the desulfurizative lithiation-induced rearrangement of the sterically biased cyclic system **10** to **11** (equation 8)[12]. Hoffmann and Brückner have also reported that the deselenative lithiation-induced rearrangement of O, Se-ketal **12** to **13** proceeds with complete inversion of configuration at the Li-bearing terminus (equation 9)[7, 13]. The steric course in an acyclic system has been investigated in the destannylative lithiation-induced rearrangement of enantiomerically defined α-oxy stannane[5, 14]. The reaction of (R)-**14** (88% ee) with n-BuLi was found to afford 90% of the [1,2]-Wittig product (R)-**15** in 42% ee[14]. Since the Sn/Li exchange involved is well established to occur with complete retention of configuration[15], this outcome reveals that the rearrangement proceeds with 74% inversion of configuration at the Li-bearing terminus. This means that the radical recombination occurs within a 'cage' after the initially formed O-radical might be converted to the C-radical of the predominantly inverted configuration (equation 10). It is interesting to note that the inversion stereochemistry of the present 1,2-alkyl shift is in contrast to the retention of configuration observed for the 1,2-silyl shift in the [1,2]-retro Brook rearrangement (Section II.F).

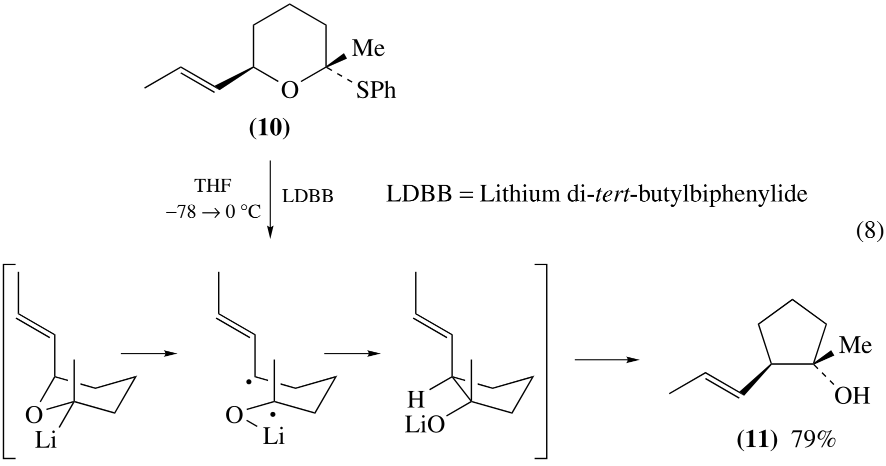

(10)

LDBB = Lithium di-*tert*-butylbiphenylide

(8)

(11) 79%

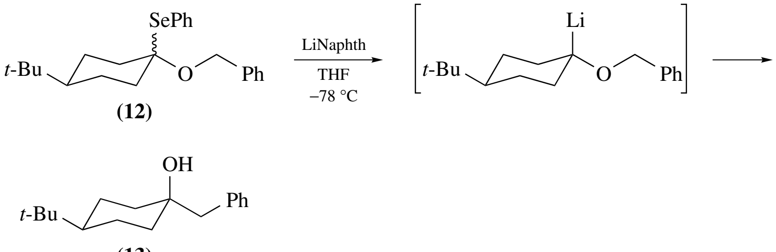

(12)

(13)

(9)

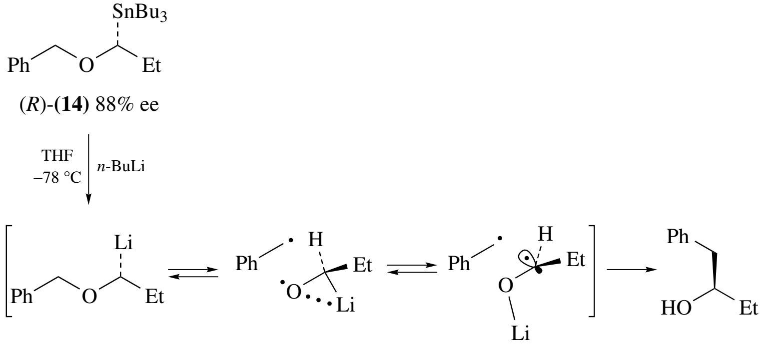

(R)-(14) 88% ee

O-radical

C-radical

(R)-(15) 42% ee

(10)

3. Stereocontrol

a. Diastereocontrol. Schreiber and Goulet have reported that the rearrangement of **16** proceeds with a high diastereofacial selectivity to afford the 1,3-*syn*-diol monoether **17** as the major product, although the yield is quite low[16]. The *syn* diols were obtained in 14–32% yield with 90–95% diastereoselectivity along with the [1,4]-rearrangement product **18**. The *syn* selectivity is explainable by a transition state model in which ether oxygen coordinates to the lithium counterion of the acrolein ketyl (equation 11).

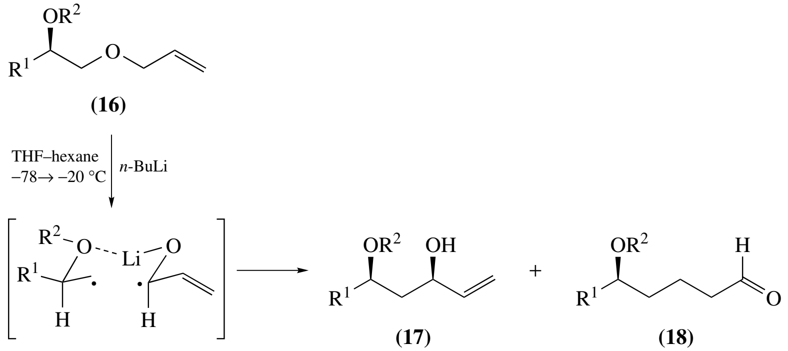

(16)

(17)

(18)

14–32% dr = 90–95%

(11)

On the other hand, a double asymmetric version where both radical fragments are chiral has been investigated (equation 12)[5]. The stereochemistry of the rearrangement products **20a** and **20b** is not the result of chelation control, but is determined by the stereochemistry of the lithium-bearing terminus. The significant difference in the stereospecificity of **19a** and **19b** reveals that a substantial level of mutal recognition of the radical enantiomers takes place during the recombination process.

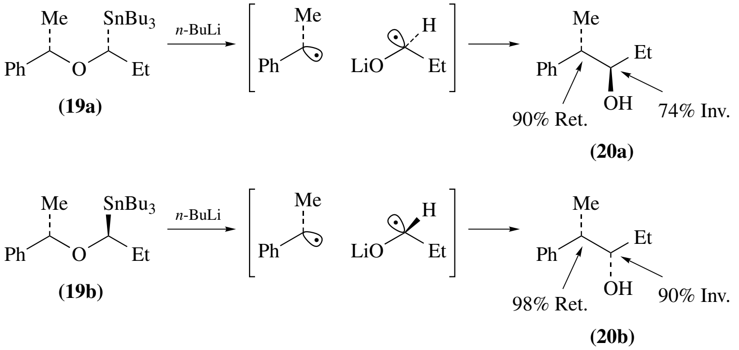

(12)

As an extention of these studies, Maleczka and Geng have investigated a chelation effect in the diastereoselective [1,2]-Wittig rearrangement where a lithium-bearing terminus is enantiomerically defined[17].

b. Enantiocontrol. In 1983, Mazaleyrat and Welvart reported the kinetic resolution of racemic binaphthyl ether, which involves the enantioselective variant of [1,2]-Wittig rearrangement (equation 13)[18]. The reaction of binaphthyl ether *rac*-**21**, which displays atropisomerism, with *n*-BuLi and a chial coordinating agent, i.e. (−)-sparteine (**24**), gave the rearrangement product (+)-(*S*)-**22** and pentahelicene (+)-(*P*)-**23**, along with the recovered ether (*R*)-**21** as an enantioenriched form (28% ee). This result reveals that the (*S*)-**21** rearranges faster than its (*R*)-isomer in the presence of (−)-**24**.

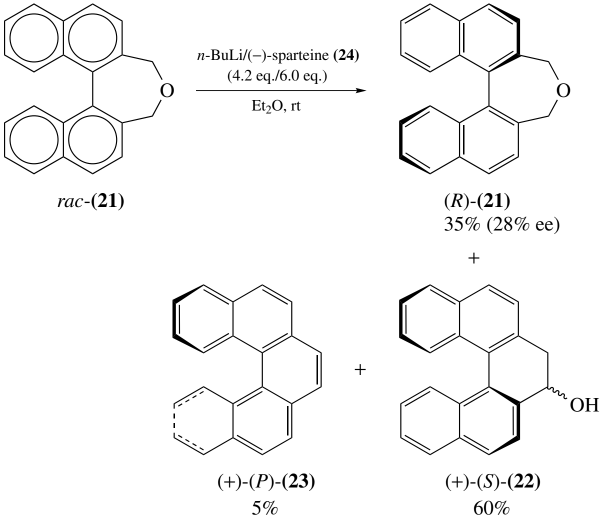

(13)

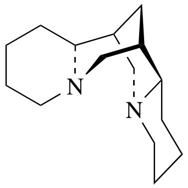

(24)

Recently, a more versatile enantioselective variant was accomplished by use of the chiral bis(oxazoline) **27** as a chiral coordinating agent[19]. For example, a rearrangement of dibenzyl ether **25** using the premixed complex *t*-BuLi (2.0 equivalents)/(*S*,*S*)-**27** (1.0 equivalents) in ether at −78 °C afforded 94% yield of alcohol (*S*)-**26** in 62% ee. Furthermore, an 'asymmetric catalytic version' of this rearrangement has been developed (equation 14). This protocol provides the tertiary alcohol **29** with a relatively high % ee from *rac*-**28** (equation 15).

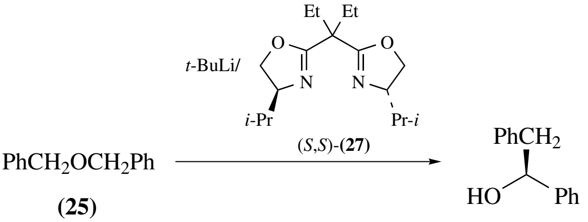

(25)

(*S*)-**(26)**

(14)

t-BuLi (2 eq.)/(*S*,*S*)-**(27)** (1 eq.) 94% (62% ee)

t-BuLi (2 eq.)/(*S*,*S*)-**(27)** (0.1 eq.) 86% (60% ee)

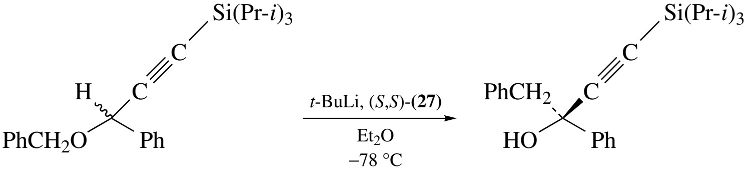

rac-**(28)**

(29) 65% (65% ee)

(15)

4. Synthetic applications

1,3-Polyols synthesis: A two-directional application of chelation-controlled [1,2]-Wittig rearrangement has been used to prepare the all *syn* polyol **31** from **30** (equation 16)[20].

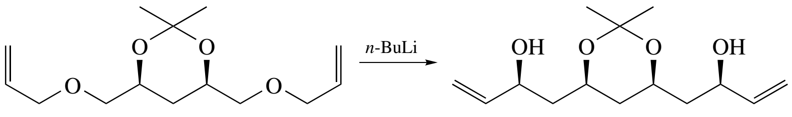

(30)

(31) 14% (dr = >10 : 1)

(16)

Medium sized carbocycle synthesis: Ring contracting [1,2]-Wittig rearrangement: Yadav and Ravishankar have demonstrated that the Wittig rearrangement of the cyclic substrate **32** is useful for the construction of the taxane skeleton **33**, albeit in low yield (equation 17)[21].

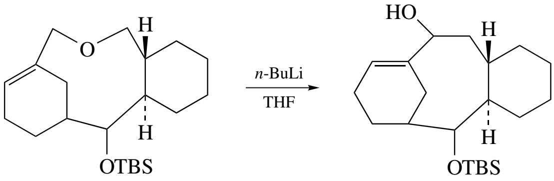

(32) **(33)** 40%

(17)

C-Glycoside synthesis (Acetal [1,2]-Wittig rearrangement): Recently, a novel variant of [1,2]-Wittig rearrangement has been developed by the author's group and involves an acetal C−O bond cleavage instead of ether bond cleavage (equation 18)[22, 23]. The rearrangement of *O*-glycosides (cyclic acetals) proceeds with efficient stereocontrol over both the anomeric center and the side-chain chiral center to give a novel class of the stereodefined *C*-glycosides. The stereoselective synthesis of *C*-glycosides using this protocol is summarized in Table 2. This acetal [1,2]-Wittig protocol was efficiently utilized as a key step of a total synthesis of zaragozic acid A (**36**) from **34** via **35** (equation 19)[24].

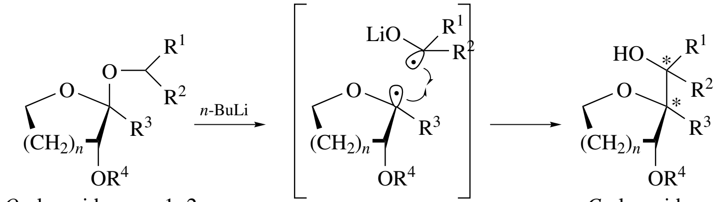

O-glycoside $n = 1–2$ *C*-glycoside

(18)

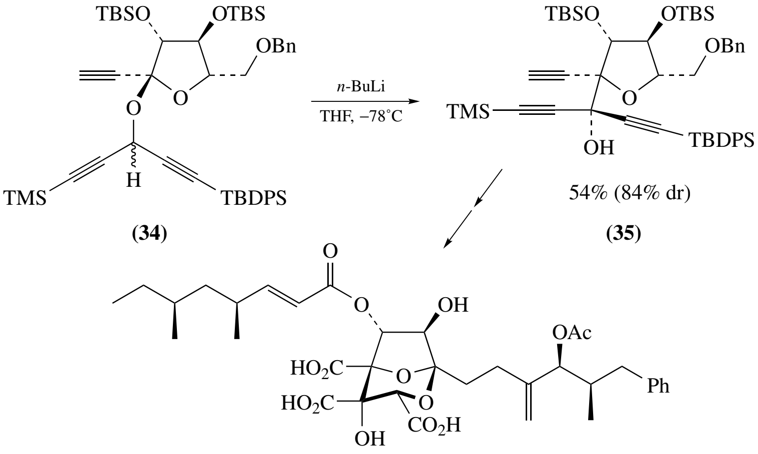

(34)

54% (84% dr)

(35)

(19)

Zaragozic acid A

(36)

TABLE 2. The acetal [1,2]-Wittig rearrangement

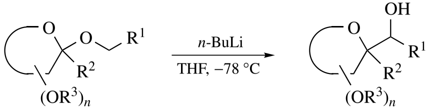

Substrate	Product	Yield(%) (% dr)	Substrate	Product	Yield(%) (% dr)
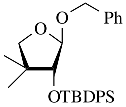	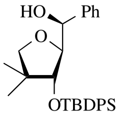	67 (>98% dr)	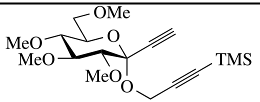	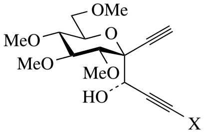	71 (>98% dr) X = TMS, H
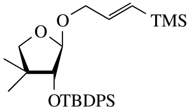	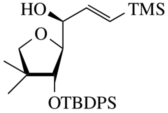	60 (>98% dr)	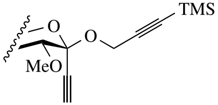	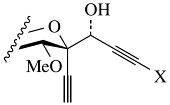	71 (87% dr) X = TMS, H
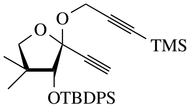	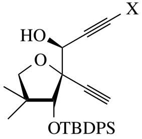	81 (96% dr) X = TMS, H	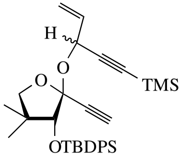	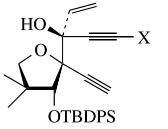	72 (>98% dr) X = TMS, H
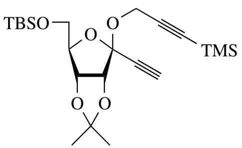	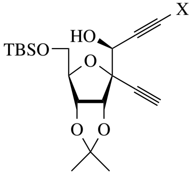	90 (90% dr) X = TMS, H	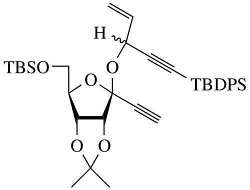	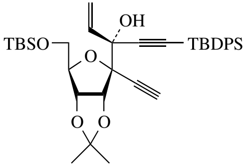	77 (82% dr)

The acetal [1,2]-Wittig rearrangement protocol is also applicable to the synthesis of medium-sized cyclic ethers. For example, a reaction of the 9-membered cyclic acetal **37** with lithium piperidide provides the 8-membered ring ether **38** in good yield along with high diastereoselectivity (equation 20)[25].

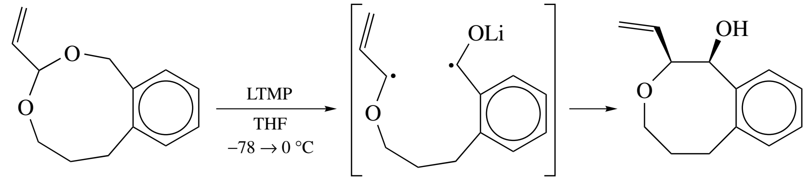

(37) **(38)** 77% (92% dr)

LTMP = Lithium 2,2,6,6-tetramethylpiperidide (20)

Recently, Gärtner and colleagues have reported the [1,2]-Wittig rearrangement of camphor-derived acetal **39** to **40** (equation 21)[26].

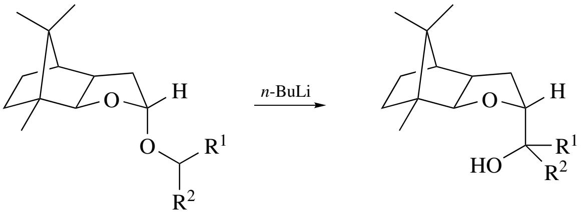

(39) **(40)** (21)

Aldol derivative synthesis: Kitagawa and Taguchi group have shown a rearrangement of α-alkoxycarboxamides **41** which proceeds with a high level of retention at the migrating center to give optically active β-hydroxycarboxamides **42** (equation 22)[27].

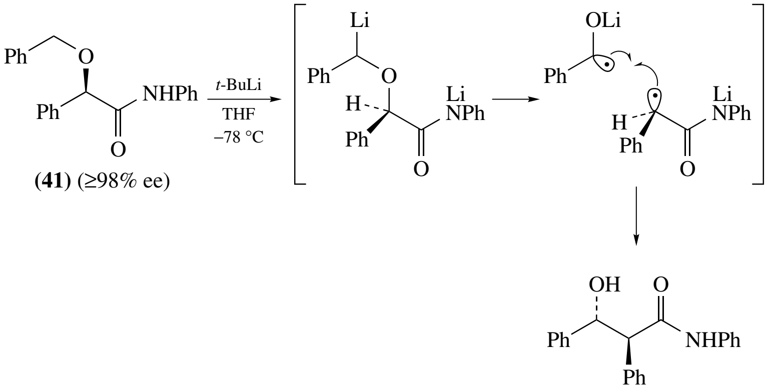

(41) (≥98% ee)

(22)

(42) 69%
(94% ee, *anti* : *syn* = 99 : 1)

Miscellaneous: The treatment of allyl 1-bromo-2-naphthyl ether **43** with *t*-BuLi affords benzyl alcohol **44** via a sequential reaction consisting of bromine–lithium exchange, and anion translocation, followed by a [1,2]-Wittig rearrangement (equation 23)[28].

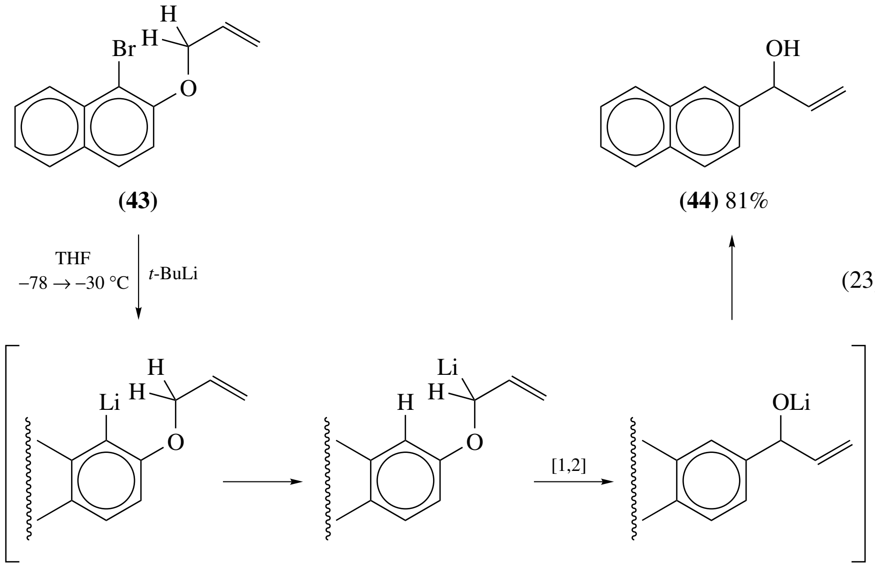

(43)

(44) 81%

(23)

Diastereoselective rearrangement of binaphthol-derived ether **45** to **46** (equation 24) has been developed by Kiyooka and colleagues for the stereoselective functionalization of binaphthol[29].

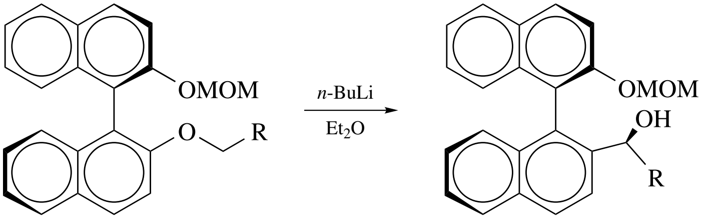

(24)

(45) R = Ph, CH═CH$_2$, etc.

(46) 39–57%
single dr

5. Related reactions

The 1,2-shift of an sp^2-carbon such as in CH═CHR, C(═NOR)H and C(═O)NR$_2$ onto the α-oxycarbanion which is formally related to the [1,2]-Wittig rearrangement, has been reported (equation 25)[30–33].

(25)

$X = CH_2, CR^1{}_2$; Y = Alk, H[30]
$X = NOR^2$; Y = Alk, Ar, H[31]
X = O; $Y = NR^3{}_2$[32]

Rautenstrauch and colleagues have shown the rearrangement of vinyl ethers **47** to **48** (equation 26) and proposed an ionic dissociation–recombination pathway as the mechanism[30].

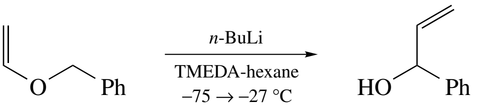

(26)

(47) **(48)** 89%

As an application of this class of rearrangement, Naito's group reported a synthesis of cytoxazone (**50**) from **49** based on the imino [1,2]-Wittig rearrangement (equation 27)[31].

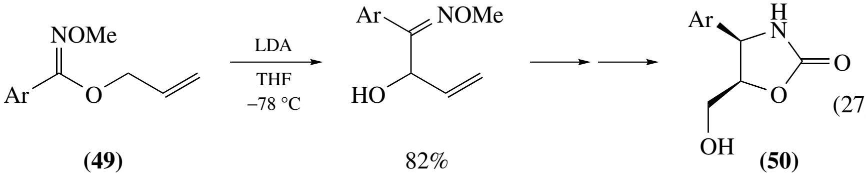

(27)

(49) 82% **(50)**

Ar = p-$MeOC_6H_4$

The enantioselective version of carbamoyl migration was accomplished by use of chiral coordinating agent protocol[33]. The reaction of carbamate **51** with pre-mixed *s*-BuLi/(−)-sparteine (**24**) gave the (*R*)-α-hydroxyamide **52** in 46% yield with 96% ee (equation 28). This stereochemical outcome reveals that the 1,2-carbamoyl migration occurs with complete retention of configuration at the α-oxycarbanion. The steric course of the 1,2-carbamoyl migration is in an opposite sense to that of the [1,2]-Wittig rearrangement (predominantly inversion), and the different stereochemical outcome was explained by the addition–elimination pathway in which intramolecular addition of the α-oxycarbanion to the carbamoyl-carbonyl occurs in completely stereoretentive fashion.

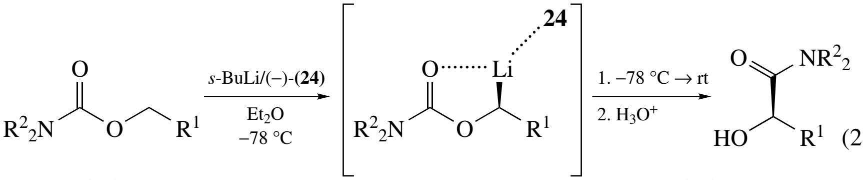

(28)

(51) (*R*)-**(52)** 46% (96% ee)

$R^1 = CH_2CH_2Ph$
R^2 = *i*-Pr

As a special class of a [1,2]-Wittig rearrangement, a 1,2-carbanion rearrangement involving an enolate as a migration terminus has been reported. Curtin's group has shown the potassium enolate rearrangements of α-alkoxy ketone and ester[34]. Recently, potassium or lithium enolate variants of a similar rearrangement have been investigated by Paquette's group[35] and Bonnet-Delpon's group[36]. For example, the lithium enolate of α-benzyloxy β-lactam **53** undergoes [1,2]-rearrangement which provides the α-benzylated α-hydroxy β-lactam **54** in moderate yield (equation 29)[36].

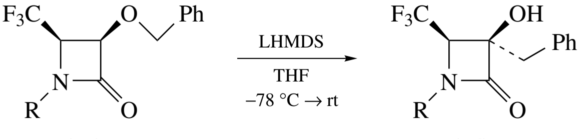

(29)

(53) **(54)** 63%

Azzena and colleagues have shown the [1,2]-Wittig-type rearrangement of aromatic acetals **55** induced by reductive electron transfer with lithium to give **56** (equation 30)[37], which was originally discovered by Schlenk and Bergmann in 1928 (with sodium)[38].

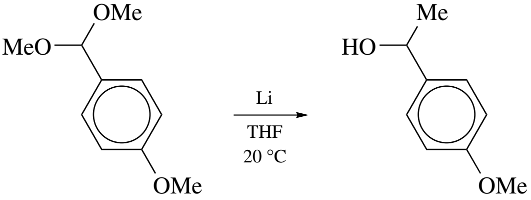

(30)

(55) **(56)** 78%

B. [2,3]-Wittig Rearrangement (O−C → C−C)

The [2,3]-Wittig rearrangement is a special class of [2,3]-sigmatropic rearrangements which involves an α-oxycarbanion as the migration terminus to afford a variety of homoallylic alcohols or allenic alcohols (equation 31). The regiospecific carbon−carbon bond formations with allylic transposition of the oxygen function as well as the stereoselective formation of vicinal chiral centers via the [2,3]-Wittig rearrangement enjoy widespread application in many facets of stereoselective synthesis[1b, 39].

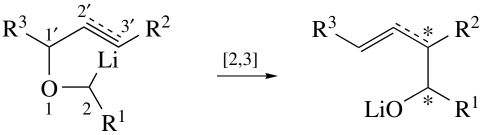

(31)

The first example of a [2,3]-Wittig rearrangement is the reaction of allyl fluorenyl ether **57** which was prepared in 1960 in the context of mechanistic studies on the [1,2]-Wittig rearrangement and gave the rearranged **58** and **59**[40]. The mechanisms of the [1,2]-Wittig and [2,3]-Wittig rearrangement are quite different. The [1,2]-Wittig rearrangement proceeds via a radical dissociation−recombination mechanism (Section II.A), while the [2,3]-Wittig rearrangement is a concerted reaction that proceeds through a six-electron, 5-membered envelope-like transition state in a suprafacial fashion (Figure 1).

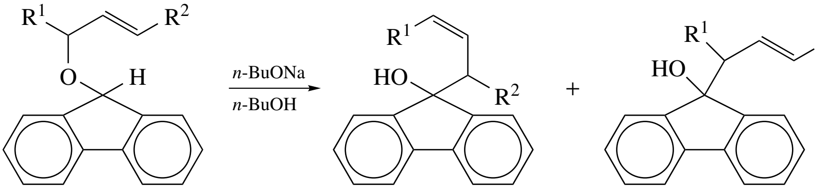

(32)

[2,3]-product [1,2]-product

(57) **(58)** **(59)**

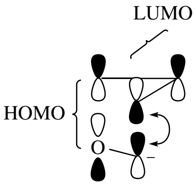

FIGURE 1. The transition state for the [2,3]-Wittig rearrangement

It is now recognized that among the proposed 'folded envelope' transition state conformations **A**–**C**[41–43], the 'Rautenstrauch model' (**A**) best accommodates the experimental findings and *ab initio* calculation[44] (Figure 2).

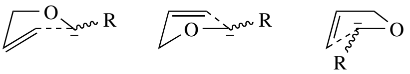

(**A**) (**B**) (**C**)

FIGURE 2

Theoretically, it is thus evident that the smaller the energy gap between the HOMO (carbanion) and the LUMO (allyl, alkynyl), the more readily the rearrangement occurs. This means roughly that the less stable the carbanion involved, the faster the rearrangement. The synthetic utility is determined principally by the availability of methods for generating the oxycarbanions. The serious side reaction often observed with the [2,3]-Wittig rearrangement is the [1,2]-Wittig rearrangement. For example, treatment of ether **60** with *n*-BuLi gives mainly the [2,3]-Wittig product **61**, with the proportion of [1,2]-Wittig product **62** increasing at a higher temperature (equation 33). In case of some cyclic systems, in which formation of an envelope-like transition state is difficult, the [1,2]-product is formed predominantly.

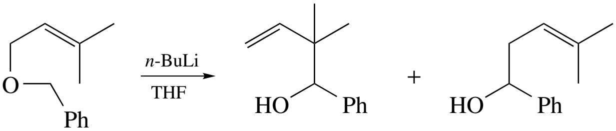

(33)

[2,3]-product [1,2]-product

(60) **(61)** **(62)**

Various aspects of the [2,3]-Wittig rearrangement have been well-reviewed in the literature[1b, 39]. Therefore, this section deals only with the enantioselective variants of the [2,3]-Wittig rearrangement which recently progressed dramatically. The enantioselective version of the rearrangement should involve an enantioselective generation of the chiral migration terminus from an achiral substrate with a chiral base. It can be categorized into two classes, according to the type of chiral base employed.

1. Enantiocontrol using chiral lithium amide

The pioneering work on enantioselective [2,3]-Wittig rearrangement was carried out by Marshall and Lebreton in the ring-contracting rearrangement of a 13-membered cyclic ether using lithium bis(1-phenylethyl) amide (**63**) as a chiral base (equation 34)[45]. Upon treatment with a (*S*,*S*)-**63** (3 equivalents) in THF at −70 to −15 °C, ether **64** afforded the enantioenriched [2,3]-product **65** in 82% yield with 69% ee. The reaction was applied in the synthesis of (+)-aristolactone (**66**).

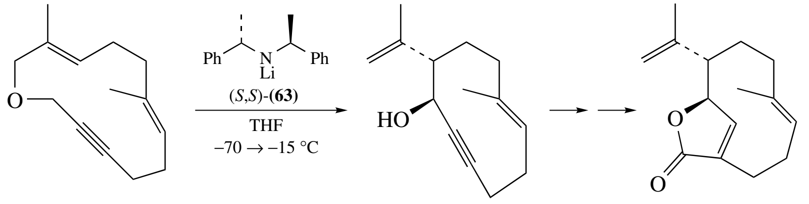

(34)

(64)

(*S*,*S*)-**(65)**
82% (69% ee)

(+)-aristolactone **(66)**

However, a similar rearrangement of the related 9- and 17-membered substrates **67** and **69** with amide **63** provided lower ee values (25 and 33% ee in the products **68** and **70**, respectively) (equations 35 and 36)[45, 46]. Accordingly, the level of enantioselection appears to depend critically upon the chiral environment provided by the cyclic framework of the substrate. In fact, no appreciable level of enantioselectivity was observed in the rearrangement of acyclic substrate **71** to **72** with amide **63** (equation 37).

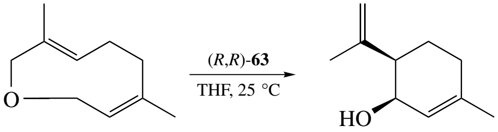

(35)

(67)

(*R*,*R*)-**68**
52%
(>95% dr, 25% ee)

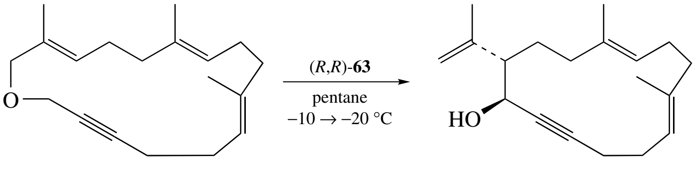

(36)

(69)

(70)
23%
(60% dr, 33% ee)

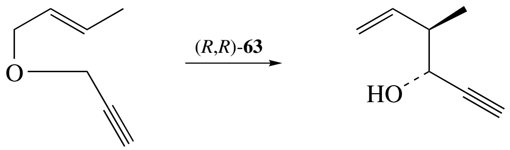

(71) **(72)**

68~70%

(>95% dr, 0% ee)

(37)

A transition state model proposed by Marshall[45] for the rearrangement is shown in Scheme 1. The chiral amide **63** coordinates either one of the two enantiotopic propargylic protons in the chair-like conformation (Scheme 1). Complex **I** should be of lower energy as it lacks the unfavorable 1,4-phenyl/alkyne interactions present in complex **II**, thus the pro-*S* proton was removed predominantly. This rationale suggests that the enantioselectivity is predominantly determined at the lithiation step.

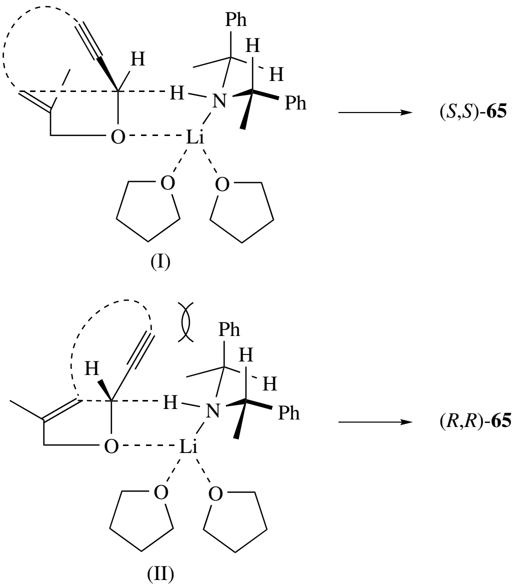

SCHEME 1

A high level of enantioselectivity in an acyclic system has been reported in the rearrangement of tricarbonylchromium(0) complexes of allyl benzyl ethers using chiral lithium amide base **73** (equation 38)[47]. Upon treatment with 1.1 equivalents of lithium amide **73** and 1 equivalent of LiCl at −78 to −50 °C, ether **74** afforded the rearrangement product (*R*)-**75** in 80% yield with 96% ee. The effect of substituents on the chemical yields and enantioselectivity of the [2,3]-Wittig rearrangement was also studied (see Table 3).

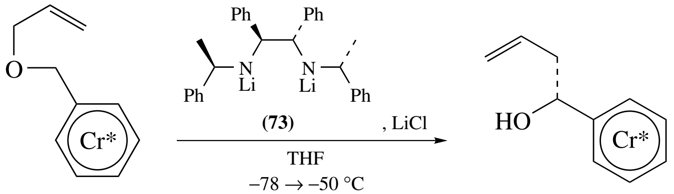

(74) (*R*)-**(75)** (38)

Cr* = Cr(CO)$_3$ 80% (96% ee)

2. Enantiocontrol using alkyl lithium-chiral coordinating agent complex

Recently, a number of successful results have been reported for the enantioselective [2,3]-Wittig rearrangement induced by the combined use of achiral (or racemic) alkyllithium and chiral non-racemic coordinating agent including sparteine, isosparteine, norpseudoephedrine, bis(oxazoline) etc. The first example of alkyllithium and (−)-sparteine (**24**) or (−)-α-isosparteine (**76**)-mediated rearrangement was reported by Kang's group[48]. The rearrangement of (Z)-**77** induced by *s*-BuLi/(−)-isosparteine (**76**) provides the [2,3]-products *syn*-**78** in 71% ee and *anti*-**78** in 46% ee, whereas the use of (−)-sparteine (**24**) shows poor enantioselectivity (12% and 2% ee, respectively) (equation 39).

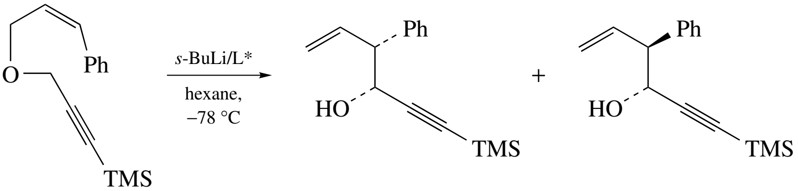

(77) *syn*-**(78)** *anti*-**(78)**

		syn-**(78)**	*anti*-**(78)**
L* = (−)-**(76)**	dr 74:26	71% ee	46% ee
L* = (−)-**(24)**	dr 38:62	12% ee	2% ee

(39)

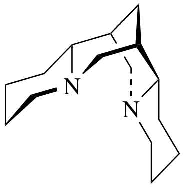

(−)-**(76)**

This protocol was applied to the rearrangement of *o*-allyloxymethylbenzamide **79** to **80** (equation 40)[49], crotyl 2-furfuryl ether (equation 41)[50], allylbenzothiazole ether (equation 42)[51] and α-propargyloxyacetic acid (equation 43)[52]. Moreover, an 'asymmetric catalytic version' of the rearrangement has been reported[49]. The reaction of **79** with 2.2 equivalents of *s*-BuLi in the presence of 0.2 equivalent of (−)-**24** gave the [2,3]-product **80** in 48% ee, whereas a rearrangement using 2.2 equivalents of (−)-**24** provided the alcohol **80** in 60% ee (equation 40). A similar rearrangement of a racemic α-deuteriated ether **79**-*d* was found to afford 60% yield of **80**-*d* (>98% D-content) with significantly decreased enantioselectivity (35% ee) (equation 44). This result suggests that the enantioselectivity is predominantly determined at the lithiation step.

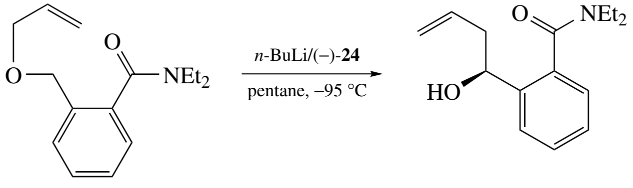

(79) (*S*)-**(80)**

(2.2 eq./2.2 eq.) 83% (60% ee)

(2.2 eq./0.2 eq.) 44% (48% ee)

(40)

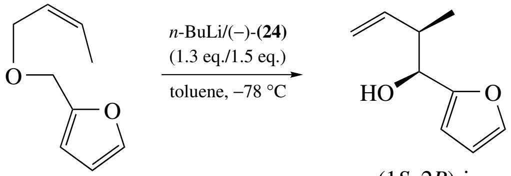

syn-(1*S*, 2*R*)-isomer

37% (42% ee)

(41)

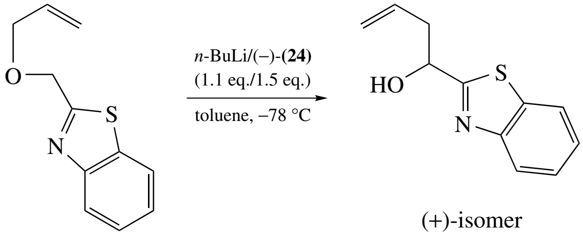

(+)-isomer

90% (46% ee)

(42)

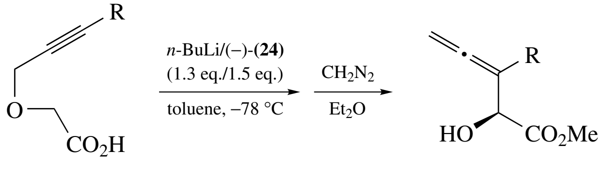

R = *n*-C_7H_{15}

(*S*)-isomer

35% (48% ee)

(43)

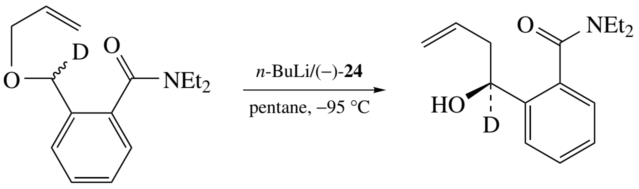

rac-**(79)**-*d*

(*S*)-**(80)**-*d*
60%, >98% D
(35% ee)

(44)

Norpseudoephedrine-derived amino ether **81** was also used as a chiral coordinating agent for the enantioselective [2,3]-Wittig rearrangement[53]. The rearrangement of propargyl ether **82** induced by *n*-BuLi/**81** provided allenyl alcohol (*S*)-**83** in 62% ee (equation 45). In contrast, a similar reaction with (−)-**24** provided only 9% ee of (*S*)-**83**.

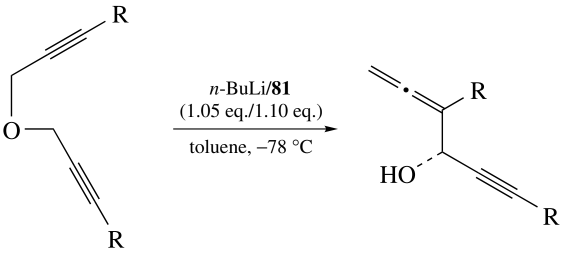

(82) R = *c*-Hex

(*S*)-**(83)**
51% (62% ee)

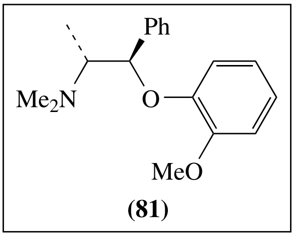

(81)

(45)

Chiral bis(oxazoline) **27** is an effective chiral coordinating agent for enantiocontrol in the [2,3]-Wittig rearrangement. The rearrangement of (Z)-crotyl benzyl ether **84** with *t*-BuLi/(*S*,*S*)-**27** (1.5 equivalents each) in hexane provided [2,3]-shift product (1*R*,2*S*)-**85** in 40% ee (equation 46)[54]. The feasibility of the asymmetric catalytic version was also examined. In this case, the rearrangement with 20 mol% of **27** in ether was found to provide the same level of enantioselectivity (34% ee).

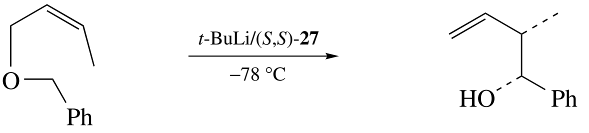

rac-**(84)**

syn-(1*R*, 2*S*)-**(85)**

(46)

(1.5 eq./1.5 eq.), hexane	89% *syn* (40% ee)
(1.5 eq./1.5 eq.), ether	89% *syn* (34% ee)
(1.5 eq./0.2 eq.), ether	89% *syn* (34% ee)

A similar rearrangement of a racemic α-deuteriated ether **84**-*d* afforded 70% yield of **85**-*d* (98% D-content) with significantly decreased enantioselectivity (14% ee) (equation 47). This result suggests that the enantioselectivity may be determined substantially at the lithiation step, since the enantioselectivity should be the same as observed with the non-deuteriated substrate, if determined at the post-lithiation step.

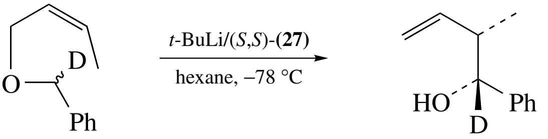

(47)

(84)-*d*

syn-(1*R*, 2*S*)-**(85)**
70%, 98% D
(86% *syn*, 14% ee)

It is noteworthy that the rearrangement of crotyl propargyl ether **86** with *t*-BuLi/(*S*,*S*)-**27** at −95 °C carried out in pentane provided [2,3]-shift product **87** in high enantiopurity (89% ee, 47% yield) with high (>95%) *anti*-selectivity (equation 48).

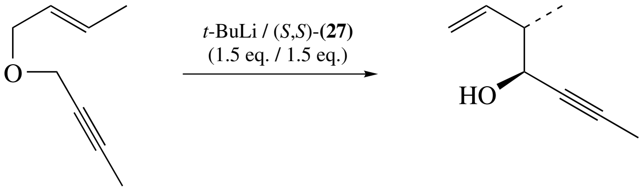

(48)

(86)

anti-(3*S*, 4*S*)-**(87)**

hexane, −78 °C	90% (93% *anti*, 75% ee)
pentane, −95 °C	47% (>95% *anti*, 89% ee)

3. Tabular survey of enantioselective [2,3]-Wittig rearrangements

The enantioselective [2,3]-Wittig rearrangements are grouped according to the structure of substrate in Table 3.

C. [1,4]-Wittig Rearrangement (O−C → C−C)

The Wittig rearrangement of allyl alkyl ethers has been shown to lead to aldehydes or ketones arising from 1,4-migration of alkyl group (equation 49)[1b]. As a pioneering work, Felkin and Tambute have reported that carbanion rearrangement of alkyl allyl ether **5** affords aldehyde **6** ([1,4]-Wittig product) in about 30% yield along with [1,2]-products (Section II.A., equation 5)[10].

TABLE 3. Enantioselective [2,3]-Wittig rearrangements

Migration terminus	Substrate	Reagent, conditions	Product(s) yield (%), stereopurity		Reference
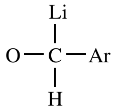 $O-C(Li)(H)-Ar$	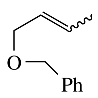		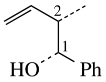 (1*R*, 2*S*)	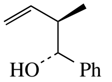 (1*R*, 2*R*)	
	(*E*)	*n*-BuLi/**81**, toluene, −78 °C	31 (16% ee)	17 (12% ee)	53
	(*Z*)	*n*-BuLi/**81**, toluene, −78 °C	45 (64% ee)	5 (80% ee)	53
	(*Z*)	*t*-BuLi/**27**, hexane, −78 °C	89 (40% ee)	11 (–)	54
	(*Z*)	*t*-BuLi/**27** *cat.*, ether, −78 °C	89 (34% ee)	11 (–)	54
	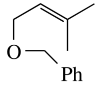		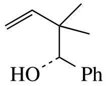		
		n-BuLi/**81**, toluene, −78 °C	68 (40% ee)		53
		n-BuLi/**24**, toluene, −78 °C	70 (19% ee)		52
	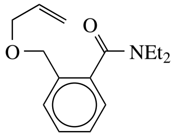		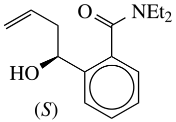 (*S*)		
		n-BuLi/**24**, pentane, −78 °C	65 (44% ee)		49
		n-BuLi/**24**, pentane, −95 °C	83 (60% ee)		49
		n-BuLi/**24** *cat.* pentane, −95 °C	44 (48% ee)		59

(*continued overleaf*)

TABLE 3. (*continued*)

Migration terminus	Substrate	Reagent, conditions	Product(s) yield (%), stereopurity	Reference
	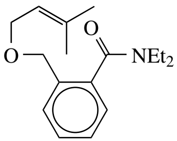	n-BuLi/**24**, pentane, −95 °C	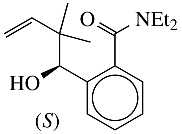 (S) 71 (62% ee)	49
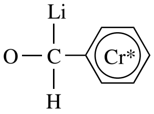 Cr* = Cr(CO)$_3$	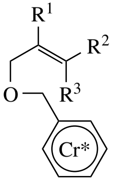 $R^1 = R^2 = R^3 = H$	**73**, LiCl, THF, −78 → 50 °C	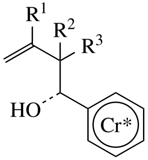 80 (96% ee)	47
	$R^1 = H, R^2 = R^3 = Me$		82 (84% ee)	47
	$R^1 = Me, R^2 = R^3 = H$		33 (91% ee)	47
	$R^1 = R^3 = H, R^2 = Me$		82 (95% *syn*, 96% ee)	47
	$R^1 = R^2 = H, R^3 = Me$		24 (50% *syn*, 90% ee)	47
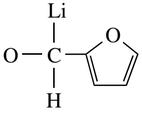	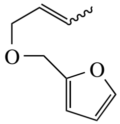 (Z)	s-BuLi/**24**, pentane, −78 °C	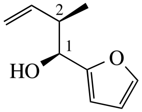 (1S, 2R) 36 (98% *syn*, 28% ee)	50
	(E)	n-BuLi/**24**, toluene, −78 °C	37 (98% *syn*, 42% ee)	50

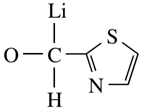	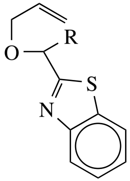		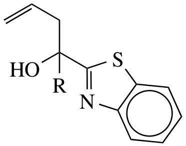	
	R = H R = Ph	*n*-BuLi/**24**, toluene, −78 °C	90 (46% *ee*) 79 (50% *ee*)	51 51
	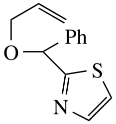		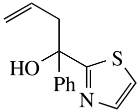	
		n-BuLi/**24**, toluene, −78 °C	90 (44% ee)	51
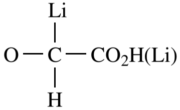	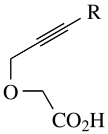		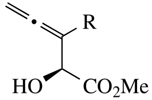	
	R = n-C_7H_{15}	*n*-BuLi/**24**, toluene, −78 °C	35 (48% ee)	52
	R = i-Bu		36 (40% ee)	52
	R = i-Pr		44 (42% ee)	52

(*continued overleaf*)

TABLE 3. (*continued*)

Migration terminus	Substrate	Reagent, conditions	Product(s) yield (%), stereopurity	Reference
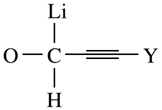 $\mathrm{O{-}C(Li)(H){-}C{\equiv}C{-}Y}$	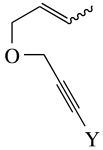		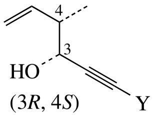 (3*R*, 4*S*) 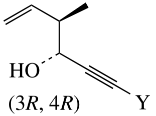 (3*R*, 4*R*)	
	(*E*), Y = TMS	*s*-BuLi/**24**, hexane, −78 °C	dr = 82:18 [16% ee (3*R*, 4*S*)] [11% ee (3*R*, 4*R*)]	48
		s-BuLi/**76**, hexane, −78 °C	dr = 77:23 [29% ee (3*R*, 4*S*)] [31% ee (3*R*, 4*R*)]	48
		t-BuLi/**27**, hexane, −78 °C	dr = 80:20 [32% ee (3*S*, 4*R*)] [−]	54
	(*Z*), Y = TMS	*s*-BuLi/**24**, hexane, −78 °C	dr = 92:8 [24% ee (3*R*, 4*S*)] [−]	48
		s-BuLi/**76**, hexane, −78 °C	dr = 100:0 [42% ee (3*R*, 4*S*)] [−]	48
		t-BuLi/**27**, hexane, −78 °C	dr = 95:5 [45% ee (3*S*, 4*R*)] [−]	54
	(*E*), Y = Me	*t*-BuLi/**27**, hexane, −78 °C	dr = 7:93 [−] [75% ee (3*S*, 4*S*)]	54
		t-BuLi/**27**, hexane, −95 °C	dr =< 5 :> 95 [−] [89% ee (3*S*, 4*S*)]	54
		s-BuLi/**24**, hexane, −78 °C	dr = 32:68 [−] [2% ee (3*R*, 4*S*)]	54
	(*Z*), Y = Me	*t*-BuLi/**27**, hexane, −78 °C	dr = 94:6 [39% ee (3*S*, 4*R*)] [−]	54

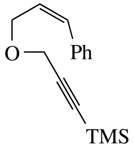		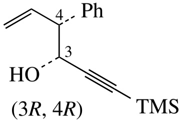	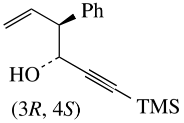	
	s-BuLi/**24**, hexane, −78 °C	dr = 38:62 [12% ee (3*R*, 4*R*)]	[2% ee (3*R*, 4*S*)]	48
	s-BuLi/**76**, hexane, −78 °C	dr = 74:26 [71% ee (3*R*, 4*R*)]	[2% ee (3*R*, 4*R*)]	48
	t-BuLi/**27**, hexane, −78 °C	dr = 45:55 [12% ee (3*S*, 4*S*)]	[2% ee (3*S*, 4*R*)]	54
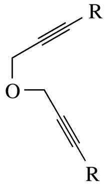 R = *c*-hex		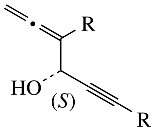		
	n-BuLi/**81**, toluene, −78 °C	51 (62% ee)		53
	n-BuLi/**24**, toluene, −78 °C	23 (9% ee)		53
	t-BuLi/**27**, pentane, −78 °C	44 [67% ee (*R*)]		54

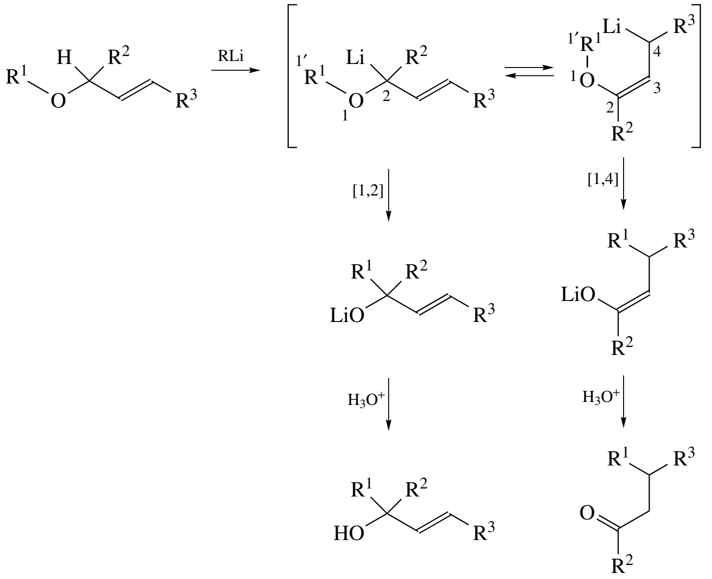

(49)

1. Mechanistic and stereochemical aspects

According to the Woodward–Hoffmann rules, a concerted process of [1,4]-Wittig rearrangement is allowed by symmetry, though it should only be possible from the *cisoid* (horse-shoe) conformation (path a in equation 50). Indeed, Rautenstrauch reported a highly [1,4]-selective carbanion rearrangement in a dihyropyran system **88** to **89** and **90** which should proceed via *cisoid* conformation (equation 51)[55]. However, on the other hand, cyclic allylic ether **91**, which cannot adopt the *cisoid* conformation, affords appreciable amounts of the [1,4]-product **92** (equation 52)[10, 56]. This result suggests that the rearrangement can proceed via a non-concerted radical process also (path b in equation 50)[56].

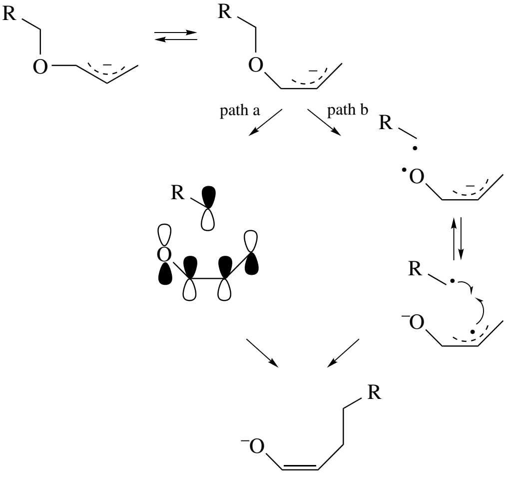

(50)

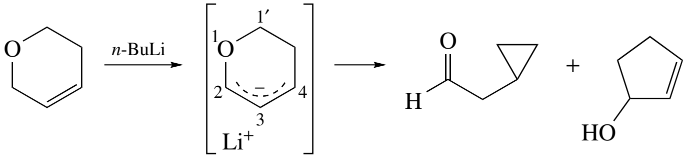

(88) **(89)** 57% [1,4]-product **(90)** 0% [1,2]-product (51)

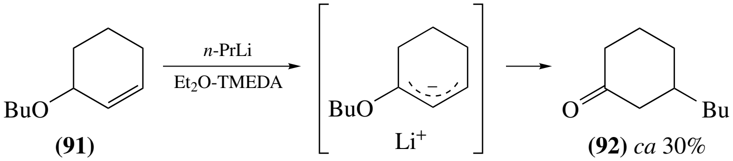

(91) **(92)** *ca* 30% [1,4]-product (52)

The steric course of the [1,4]-Wittig rearrangement at the migrating carbon has been investigated. Felkin and colleagues have shown that the rearrangement of the enantiopure forms of α-phenethyl allyl ether (*S*)-**93** followed by reductions affords [1,4]-Wittig rearrangement product (*S*)-**94** of the predominantly retained configuration at the migrating carbon in 69% ee along with [1,2]-rearrangement product **95** (74% ee, 67% ee) and [2,3]-product **96** (>90% ee) (equation 53)[56]. This result proves that the [1,4]-rearrangements proceed predominantly (not completely) with retention of configuration at the migrating carbon and the extent of racemization is similar for the [1,4]- and [1,2]-rearrangement. This result also suggests that [1,4]-Wittig rearrangement is occurring via the non-concerted radical mechanism (equation 54).

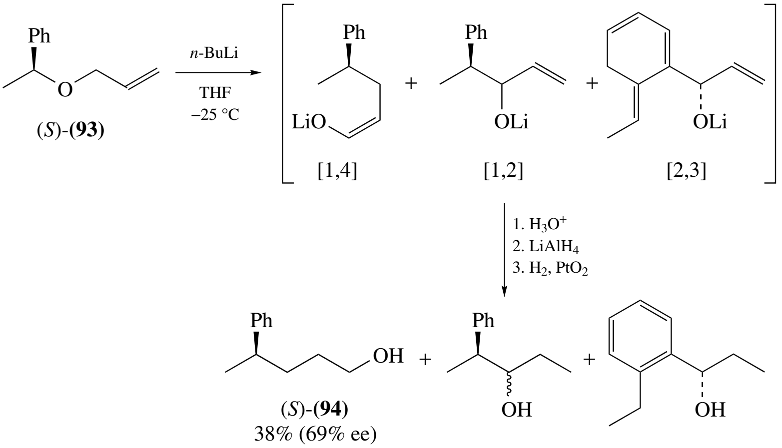

(*S*)-(**93**)

(*S*)-(**94**)
38% (69% ee)

(95)
22%
(*syn* / *anti* = 56 : 44)
(*syn* 74% ee
anti 67% ee)

(96)
9% (>90% ee)

(53)

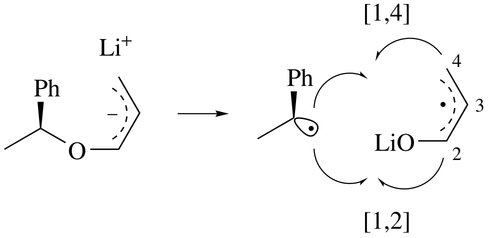

(54)

The steric course at the Li-bearing center has been investigated using an enantiomerically enriched ethynylvinylmethanol-derived system. A reaction of ether **97** (78% ee) with *n*-BuLi gave [1,4]-product ketone **98** only in the racemic form (equation 55)[57]. This lack of stereospecificity is partly due to racemization of the α-oxyalkyllithium and partly due to the [1,4]-rearrangement pathway.

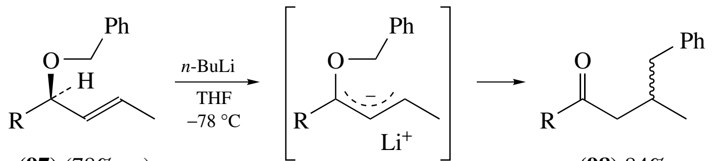

(55)

(97) (78% ee)
R = TBS−C≡C−

(98) 84%

2. Synthetic applications and stereocontrol

The [1,4]-Wittig rearrangement is potentially useful not only for the carbon−carbon bond formation but also for enolate formation. However, synthetic applications have been rather limited, because of the low yields and restricted range of substrates. Schlosser's group have developed a practical approach to aldehydes based on a [1,4]-rearrangement/enolate trapping sequence. In contrast, standard aqueous workup gave poor yield of aldehyde. This protocol was employed as the key step in a synthesis of pheromone (**102**) from **99** via **100** and **101** (equation 56)[58].

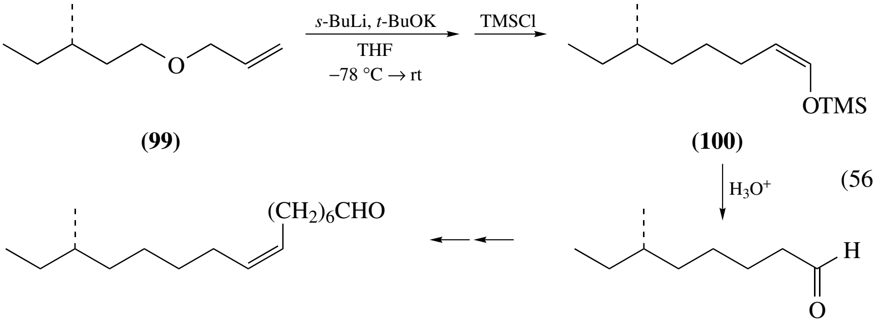

(56)

(99) **(100)** **(102)** **(101)** 64%

Recently, a novel and synthetically useful rearrangement system has been developed by the author's group[23, 57]. The key to its success is the choice of an ethynylvinylmethanol-derived migration terminus which provides the corresponding ketone enolates (equation 57).

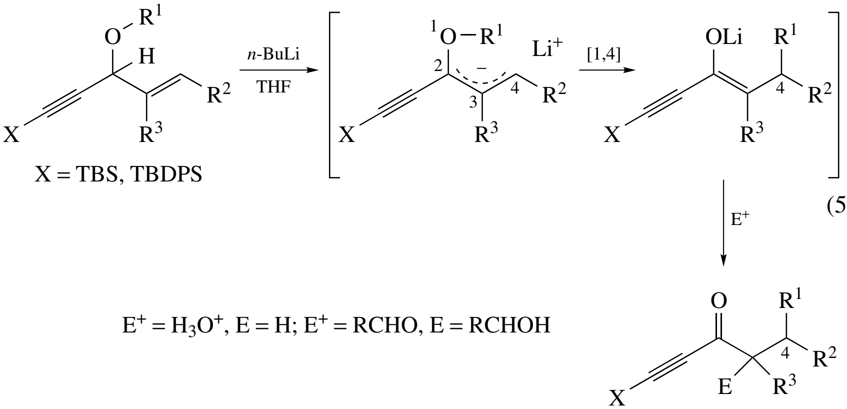

E$^+$ = H$_3$O$^+$, E = H; E$^+$ = RCHO, E = RCHOH

(57)

This [1,4]-Wittig rearrangement system is applicable to the sequential [1,4]-rearrangement/aldol reaction which provides β-hydroxy ketones with moderate diastereoselectivity (Table 4).

The first enantioselective version was also accomplished with this class of substrates. For example, the rearrangement of ether *rac*-**103** with *t*-BuLi/bis(oxazoline) **27** afforded ketones **104a** and **104b** in 48%–50% ee (equation 58)[59].

TABLE 4. [1,4]-Wittig rearrangement of propargyl ether systems

Substrate	Electrophile	Product	Yield (%) (% dr)
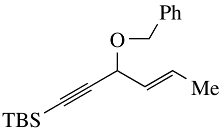	H$_3$O$^+$	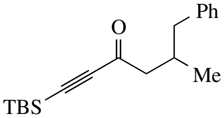	81
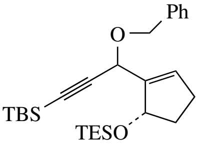	HCHO	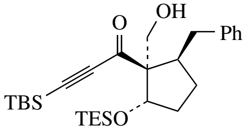	75 (88% dr)
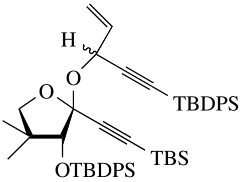	HCHO	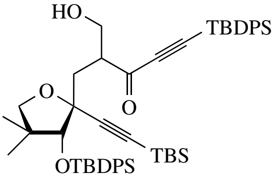	60 (60% dr)

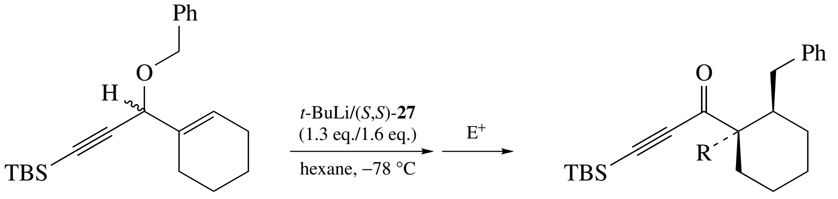

(103)

$E^+ = H_3O^+$ **(104a)** (R = H) (58)

67% (63% dr, 48% ee)

$E^+ = HCHO$ **(104b)** (R = CH_2OH)

50% (69% dr, 50% ee)

Taylor and colleagues have shown the sequential carbolithiation/[1,4]-Wittig rearrangement of styryl ethers **105** (e.g., **105a**) which provide appropriately functionalized 2-alkylphenol **106** (e.g., **106a**) in good yield[60]. In this reaction, the alkenyl transfer occurs with retention of configuration (equations 59 and 60).

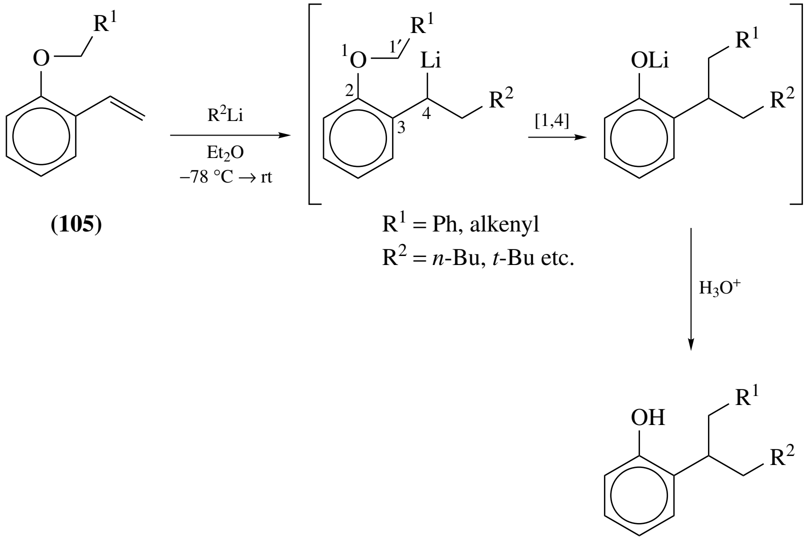

(105)

R^1 = Ph, alkenyl
R^2 = n-Bu, t-Bu etc.

(59)

(106) 70–80%

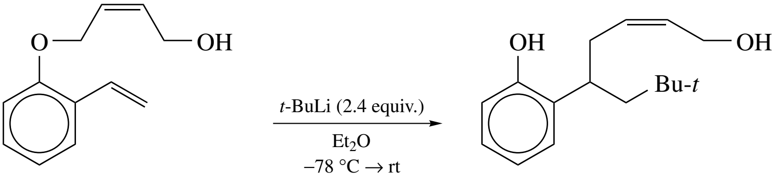

(60)

(105a) **(106b)** 67%

3. Related reactions

As a unique [1,4]-Wittig rearrangement, the transformation of 3-iodoalkyl vinyl ether **107** to the 4-alken-1-ol **108** has been reported by Bailey's group (equation 61, Table 5)[61]. The rearrangement is undoubtedly mediated by a regiospecific 5-*exo*-trig ring closure.

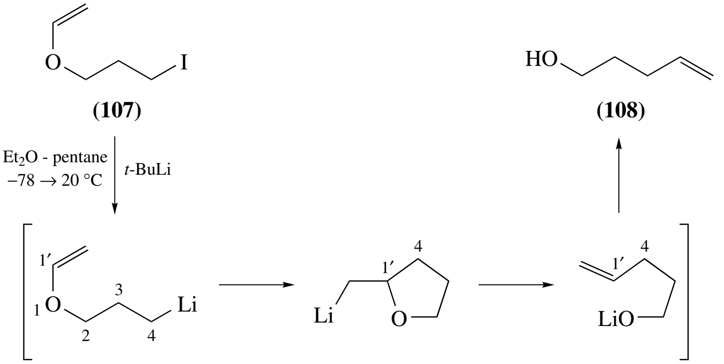

(107) **(108)**

(61)

TABLE 5. Rearrangements of 4-oxa-5-hexenyl lithiums

Substrates	Product	Yield (%)
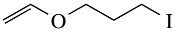	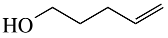	93
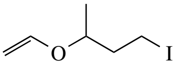	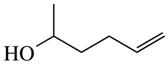	94
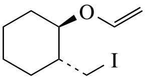	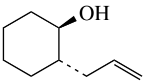	95
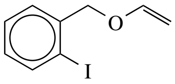	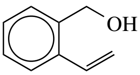	95

D. Aza-Wittig Rearrangement (N−C → C−C)

The nitrogen analogue of the Wittig rearrangement is an isomerization of α-metalated tertiary amines to skeletally rearranged metal amides, which yield secondary amines[1b, 62]. In general, the aza-Wittig rearrangement is less facile than the corresponding original (oxa-) Wittig rearrangement; However, it is a potentially useful reaction in terms of synthesis of various kinds of nitrogen-containing compounds. Similarly to the original Wittig rearrangement, the problem of competition of the [1,2]- and [2,3]-shift arises in the rearrangement of the allyl amine system (equation 62).

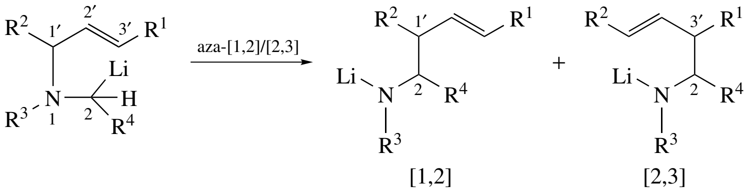

(62)

1. General aspects

Perhaps the first example of the aza-Wittig rearrangement is the reaction of *N*,*N*-diphenylbenzylamine **109**, which was reported by Eisch and Kovacs in 1971[63]. The reaction of amine **109** with *n*-BuLi at 25 °C for 1 h followed by quenching with D_2O gave only α-deuteriated product **110**. However, when the reaction mixture was allowed to stand at 25 °C for prolonged reaction time, [1,2]-rearrangement product **111** was obtained in 75% yield (equation 63). In contrast, similar reaction of the cyclic analogue **112** provides no rearrangement product **114**, not even after 72 h, and **113** with the unrearranged skeleton was obtained on deuteriation (equation 64).

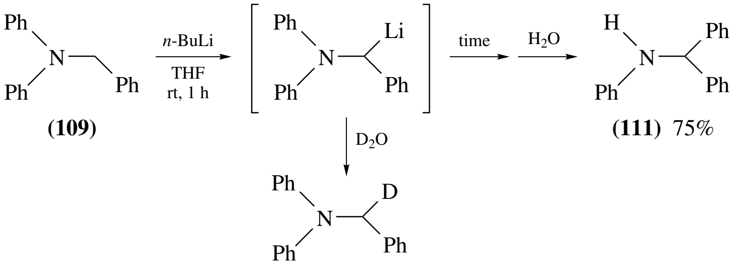

(109) **(111)** 75% **(110)** 90%

(63)

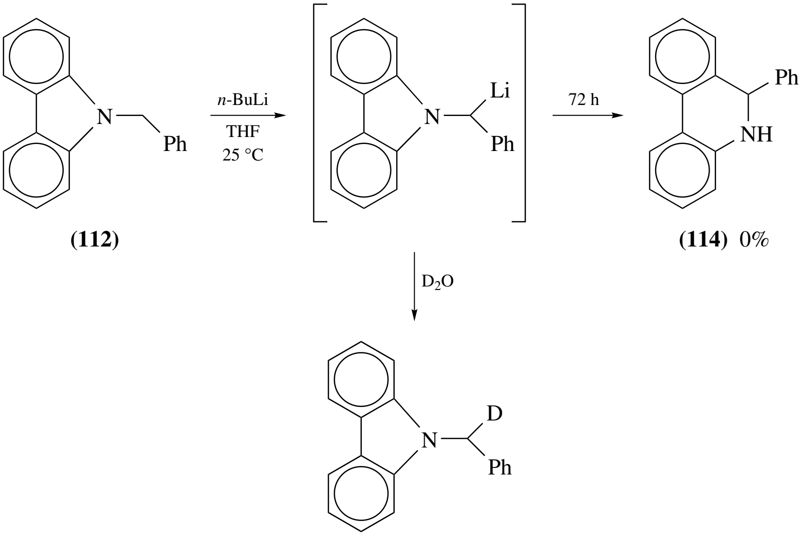

(112) **(114)** 0% **(113)** 90%

(64)

Reetz and Schinzer have examined the [2,3]-rearrangement of *N*-allyl-*N*-(9-fluorenyl)-methylamine **115** to **116** (equation 65)[64]. The α-amino lithiation can occur with *n*-BuLi at rt, but rearrangement requires heating for several hours in refluxing THF, which is in sharp contrast to the high reactivity of the oxy-analogue **57a** which rearranges to **58b** in 95% (equation 66)[65].

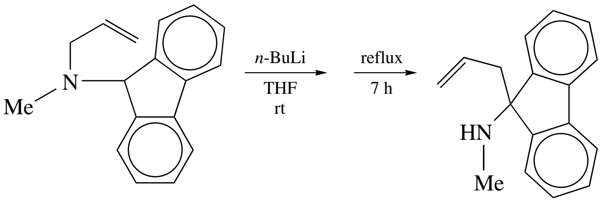

(115) **(116)** 44%

(65)

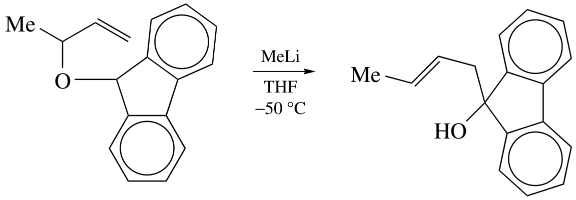

(57a) **(58b)** 95%

(66)

In general, the aza-Wittig rearrangement proceeds considerably more slowly than the corresponding original Wittig rearrangement. It was pointed out that this difference might be due to the stability of the rearrangement product (R_2N^- Li^+ vs. RO^- Li^+). To prepare the migration terminus of the aza-Wittig rearrangement (α-amino carbanion), not only the deprotonation methods (*vide supra*) but also tin–lithium transmetalation ($SnBu_3 \rightarrow Li$), and reductive lithiation of *S*,*N*-acetal (SPh → Li) methods were developed by Coldham's and Broka's groups, respectively[68, 70]. Other examples for comparison between aza- and oxa-systems are shown in equations 67–69.

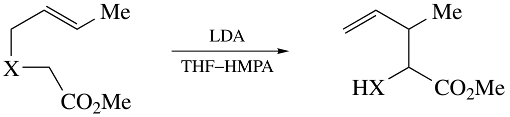

(67)

X = NMe	0%[66]
X = O	60%[67]

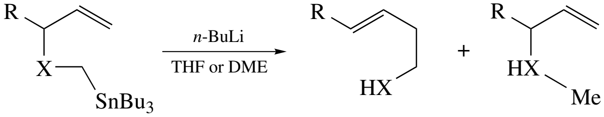

(68)

X = NBn, R = H	12%	48%[68]
X = O, R = n-C_7H_{15}	>95%	<5%[69]

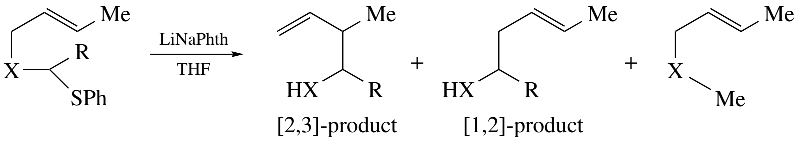

(69)

X = N-C_7H_{15}-n, R = H	—	13%	53%[66]
X = O, R = n-C_9H_{19}	67%	—	—[70]

To enhance the reactivity of the aza-Wittig rearrangement, several contrivances have been developed. Durst's group developed the small-ring assisted aza-Wittig rearrangement in 1972[71]. The reaction of N-benzyl β-lactam **117** with LDA (THF, $-78\,^\circ$C) provides the aza-[2,3]-Wittig rearrangement product **118** in quantative yield (equation 70), while the corresponding acyclic system **119** did not undergo any rearrangement to **120** at room temperature (equation 71). These results have been ascribed to the relief of small-ring strain in going from a 4- to a 7-membered ring.

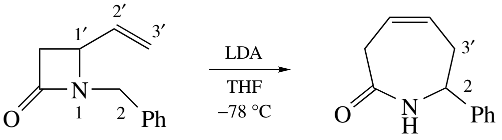

(117) **(118)** quant.

(70)

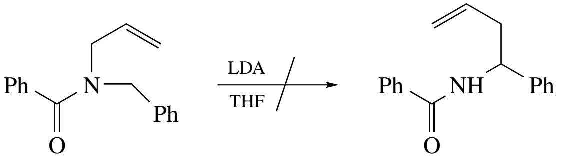

(119) **(120)**

(71)

As a different type of small-ring assisted aza-Wittig rearrangement, Åhman and Somfai reported the rearrangement of vinylaziridines[72]. For example, treatment of **121** with LDA (THF, $-78\,^\circ$C) led to the corresponding [2,3]-Wittig product, substituted tetrahydropyridine **122**, with high diastereoselectivity in 93% yield, by a rapid rearrangement within less than five minutes (equation 72).

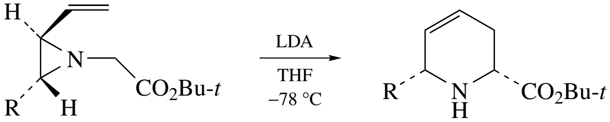

R = BnOCH$_2$

(121) **(122)** 93%

(72)

Recently, practically useful acyclic aza-[2,3]-Wittig rearrangement has been developed by Anderson and colleagues[73]. The key to success is the introduction of a t-butoxycarbonyl group (Boc) on nitrogen, which facilitates the lithiation at the α-nitrogen position and stabilizes the nitrogen anion formed from the rearrangement. For example, a reaction of Boc-protected homoallylic amine **123a** with n-BuLi (Et_2O–HMPA, $-78 \rightarrow -40\,^\circ$C) provides the *syn* and *anti* [2,3]-rearrangement products **124a** in 82% yield. Furthermore, they found that the introduction of a bulky trialkylsilyl group on the allyl part increases the diastereoselectivity and reactivity of the rearrangement **123b** → **124b** due to the electronic and steric effect (equation 73). The *anti*-selectivity is explainable by the 5-membered cyclic transition state model similar to that for the oxy-[2,3]-Wittig rearrangement (equation 74). More recently, Manabe reported another example of acyclic aza-[2,3]-rearrangement in which phosphoramide acts as the anion stabilizing group instead of the Boc group[74].

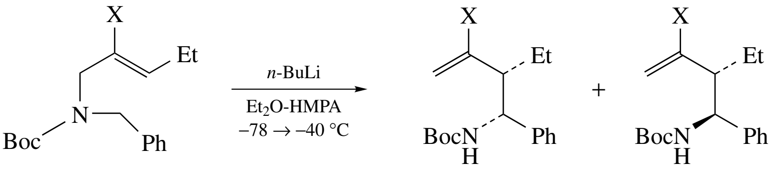

(73)

(123) *syn*-**(124)** *anti*-**(124)**

(a) X = H 82% (*syn*:*anti* = 3:2)

(b) X = $SiMe_3$ 92% (*syn*:*anti* = 1:18)

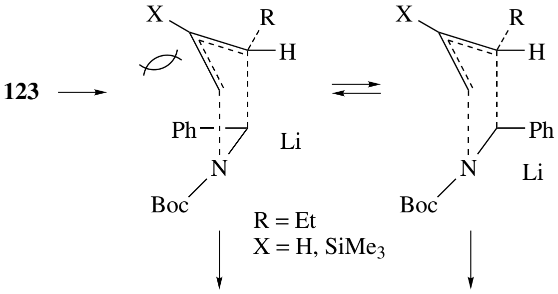

(74)

syn-**124** *anti*-**124**

As a similar transformation of aza-[2,3]-Wittig rearrangement, a [2,3]-Stevens rearrangement to **126** of the *N*-silylated ylide derived from *N*-crotylglycine ester (**125**) was reported (equation 75)[66].

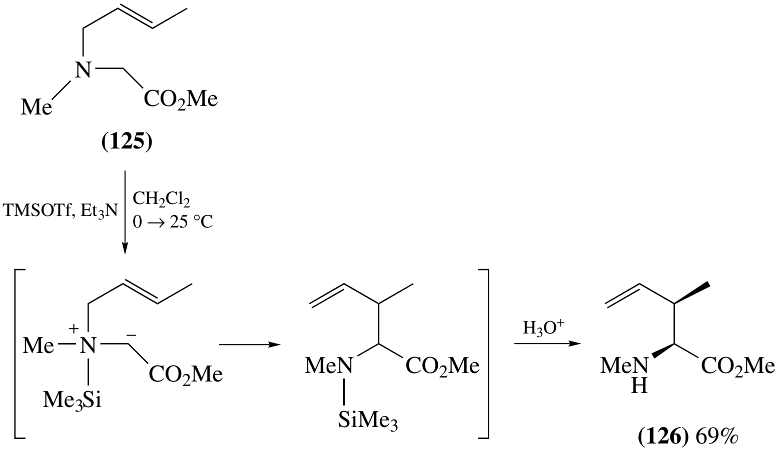

(125)

(75)

(126) 69%

(*syn*: *anti* = 4 : 1)

2. Mechanistic and stereochemical aspects

It is generally accepted that the aza-[1,2]-Wittig rearrangement proceeds via a radical dissociation–recombination mechanism, whereas the aza-[2,3]-rearrangement proceeds via a concerted mechanism. On the other hand, recent *ab initio* calculations have shown that the aza-[2,3]-Wittig rearrangement preferentially proceeds via the homolytic dissociation route in the gas phase[75]. One might speculate that the solvent is responsible for the difference.

The steric course at the Li-bearing center of aza-Wittig rearrangement has been investigated by using enantio-enriched α-aminoorganolithiums. Gawley and colleagues have presented evidence for predominant inversion of configuration at the Li-bearing terminus in the destannylative lithiation-induced rearrangement of a cyclic amine system[76]. A reaction of (*S*)-*N*-allyl-2-(tributylstannyl)pyrrolidine (**127a**) (94% ee) with *n*-BuLi (THF-TMEDA, 13 °C, 4 h) provides enantio-enriched [2,3]-rearrangement product (*S*)-**128a** in 64% yield with 48% ee. This lack of stereospecificity is partly due to racemization of the α-aminoorganolithium and partly due to competitive [1,2]- and [2,3]-rearrangement pathways. Steric influences are important in the rearrangement, as shown by the reaction of the trisubstituted allyl amine **127b**, which afforded nearly racemic product **128b** in low yield (equation 76).

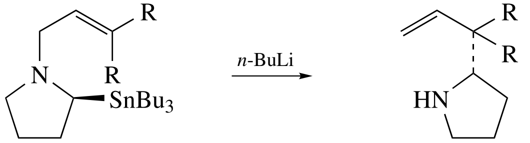

(76)

(*S*)-**(127a)** R = H (94% ee)
(*S*)-**(127b)** R = Me (94% ee)

(*S*)-**(128a)** 64% (48% ee)
(*S*)-**(128b)** 32% (8% ee)

In a similar way, the steric course for an acyclic system has been investigated in the destannylative lithiation-induced rearrangement of enantiomerically defined α-amino stannane[77]. The reaction of *N*,*N*-diallylaminostannane (*R*)-**129** with *n*-BuLi (THF, $-78 \rightarrow 0$°C) afforded the inversion product (*R*)-**130** ([2,3]- and/or [1,2]-rearrangement product) in 50% yield with 48% ee (equation 77). To clarify the steric course of aza-[1,2]- and [2,3]-Wittig rearrangement separately, an *N*-propargyl system was also studied[78]. Reaction of *N*,*N*-dipropargyl aminostannane (*R*)-**131** afforded the [1,2]-product (*R*)-**132** in 62% ee and the [2,3]-product (*R*)-**133** in 66% ee (equation 78). This result clearly indicates that both the aza-[1,2]- and [2,3]-Wittig rearrangement of *N*-propargyl systems proceed predominantly via inversion at a Li-bearing terminus.

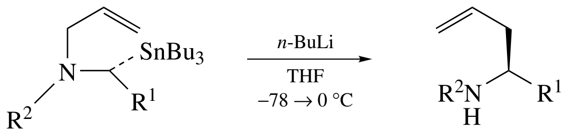

(77)

(*R*)-**(129)** (>95% ee)

(*R*)-**(130)** 50% (48% ee)

$R^1 = PhCH_2CH_2$
$R^2 = CH_2{=}CHCH_2$

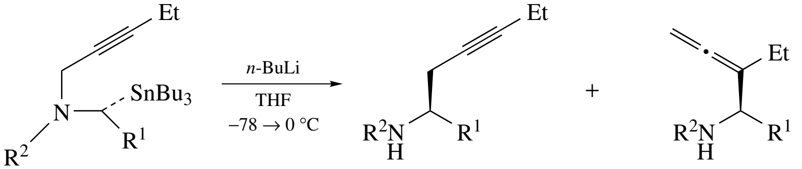

(78)

(*R*)-**(131)** (>95% ee) (*R*)-**(132)** 10% (62% ee) [1,2]-product (*R*)-**(133)** 36% (66% ee) [2,3]-product

$R^1 = PhC_2H_5$
$R^2 = EtC{\equiv}CCH_2$

3. Synthetic applications

Somfai's group has demonstrated that the aza-[2,3]-Wittig rearrangement of the vinylaziridines **134** to **135** is useful for the stereoselective construction of the indolizidine alkaloids **136**[72b, c].

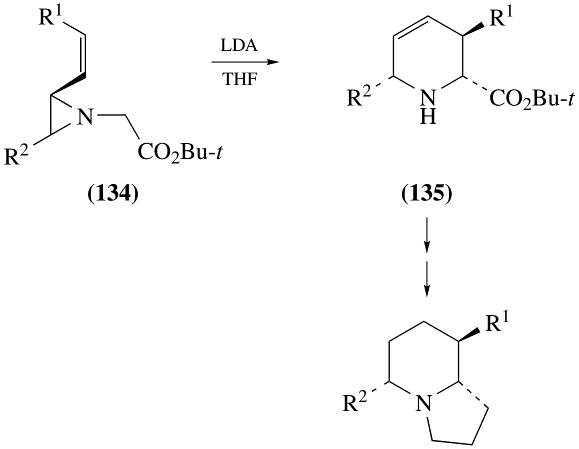

(134) **(135)**

(79)

Indolizidine 209D **(136a)** : $R^1 = H$, $R^2 = C_6H_{13}$ [72b]
Indolizidine 209B **(136b)** : $R^1 = Me$, $R^2 = C_5H_{11}$ [72c]

4. Tabular survey of aza-Wittig rearrangement

Aza-Wittig rearrangements are grouped according to substrate structure in Table 6.

E. Thia-Wittig Rearrangement (S—C → C—C)

The sulfur analogue of the Wittig rearrangement is an isomerization of α-metalated sulfides to skeletally rearranged metal thiolates, which yield thiols (equation 80).

TABLE 6. Aza-Wittig rearrangements

Preparation of migration terminus	Substrate	Reagent conditions	Product(s), yield (%)	Reference
H → Li	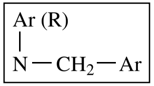 $\boxed{\overset{\text{Ar (R)}}{\overset{\vert}{\text{N}}}-\text{CH}_2-\text{Ar}}$			
	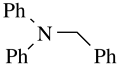	*n*-BuLi, THF 25 °C	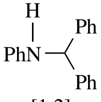 [1,2] >75	63
	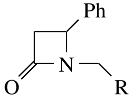 R = Ph R = $CH_2 = CH$	LDA, THF −78 °C	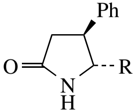 [1,2] 93 97	71
	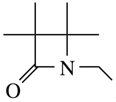	LDA, THF −78 °C	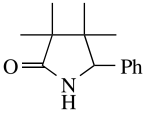 [1,2] 45 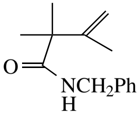 45	71

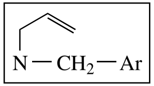

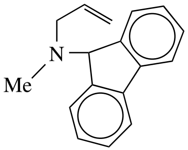	*n*-BuLi, THF reflux	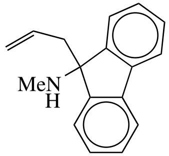 [1,2] and/or [2,3] 44	64
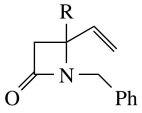 R = H R = Me	LDA, THF −78 °C	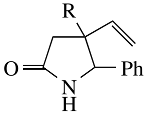 [1,2] – 36 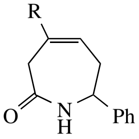 [2,3] quant 54	71 71
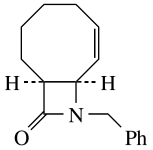	LDA, THF −78 °C	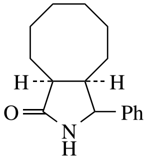 [1,2] >90	71

(continued overleaf)

TABLE 6. (*continued*)

Preparation of migration terminus	Substrate	Reagent conditions	Product(s) yield (%)	Reference
	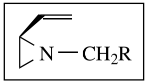			
	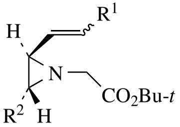	LDA, THF −78 °C	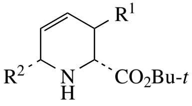 [2,3]	
	$R^1 = H, R^2 = Me$		99	72e
	$R^1 = H, R^2 = BnOCH_2$		93	72a
	$R^1 = H, R^2 = C_6H_{13}$		98	72a
	$R^1 = H, R^2 = t$-Bu		95 ($R^1 = \beta$-Me)	72a
	$R^1 = (Z)$-Me, $R^2 = t$-Bu		92 ($R^1 = \alpha$-Me)	72a
	$R^1 = (E)$-Me, $R^2 = t$-Bu		92 ($R^1 = \beta$-Me)	72a
	$R^1 = (Z)$-Me, $R^2 = C_5H_{11}$		97	72c
	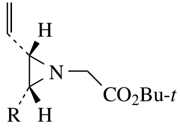 R = $BnOCH_2$	LDA, THF −78 °C	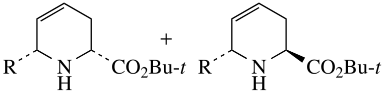 [2,3] 60 + [2,3] 33	72a
	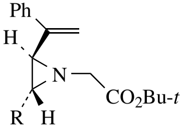	LDA, THF −78 °C	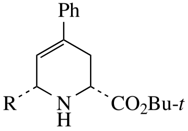 [2,3]	79
	R = Me		57	
	R = *n*-Bu		55	
	R = *i*-Pr		66	

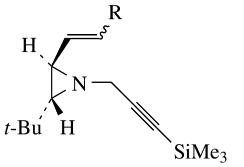	s-BuLi, THF −78 °C	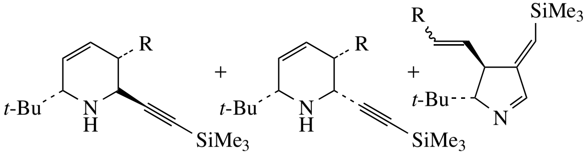 [2,3]	[2,3]		
R = H		29	19	16	72d
R = Me (E : Z = 3.2 : 1)		25	12	12	72d
R = Me (Z)		–	–	30	72d
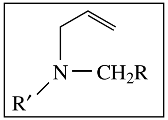					
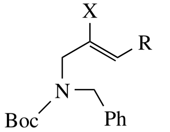		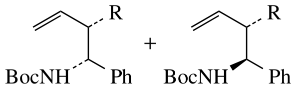 syn-[2,3] + $anti$-[2,3]			
X = H, R = Me	n-BuLi, Et$_2$O-HMPA, −78 → −40 °C, 14 h	82 (3 : 2)			73a
X = H, R = Et	”	69 (1 : 1)			73b
X = H, R = i-Pr	”	54 (4 : 3)			73b
X = SiMe$_3$, R = Me	”	88 (1 : >20)			73b
X = SiMe$_3$, R = Et	”	92 (1 : 18)			73b
X = SiMe$_3$, R = i-Pr	”	94 (1 : 11)			73b
X = SiPhMe$_2$, R = Me	n-BuLi, THF, −78 °C, 14 h	81 (0 : 100)			73c
X = SnBu$_3$, R = Me	n-BuLi, THF-HMPA, −78 → −40 °C, 20 h	71 (<5 : >95)			73d

(*continued overleaf*)

TABLE 6. (*continued*)

Preparation of migration terminus	Substrate	Reagent conditions	Product(s) yield (%)	Reference
	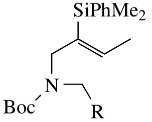		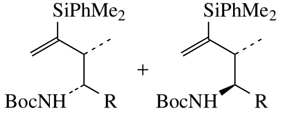 *syn*-[2,3] + *anti*-[2,3]	
	R = CO_2Me	LDA, THF-HMPA, −78 → −40 °C, 14 h	70 (1 : >20)	73f
	R = $CONMe_2$	LDA, THF-HMPA, −78 → −40 °C, 3 h,	70 (1 : >20)	73f
		KH, 18-C-6	94 (1 : >20)	73g
	R = Oxazoline	*n*-BuLi, THF-HMPA, −78 → −40 °C, 14 h	70 (1 : >20)	73f
	R = CN	LDA, THF-HMPA, −78 → −40 °C, 14 h	67 (1 : 3)	73f
	R = $C{\equiv}CSiMe_3$	”	77 (1 : 10)	73f
	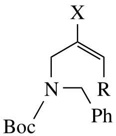		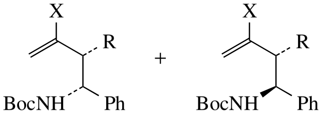 *syn*-[2,3] + *anti*-[2,3]	
	X = H, R = Me	*n*-BuLi, THF-HMPA, −78 → −40 °C, 14 h	0 −	73a
	X = $SiMe_3$, R = Et	”	62 (3 : 1)	73e
	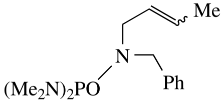	*n*-BuLi, THF, 0 °C, 2 h	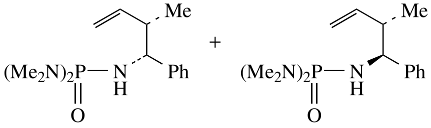 *syn*-[2,3] + *anti*-[2,3]	
	(*E*)-isomer		90 (1 : 1)	74
	(*Z*)-isomer		90 (1 : 1)	74

SAr → Li	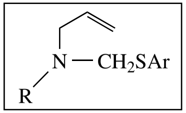			
	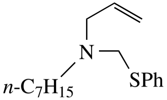	LiNaphth, THF, 0 °C, 2 h	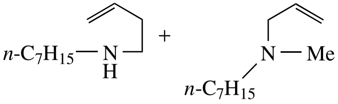 [1,2] and / or [2,3] 76 (4 : 1)	70
	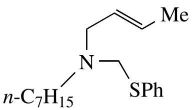	”	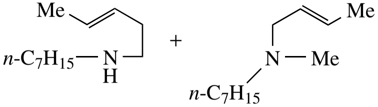 [1,2] 66 (1 : 4)	66
SnR$_3$ → Li	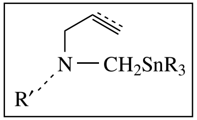			
	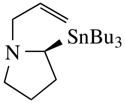 (94% ee)	n-BuLi, THF-HMPA, 13 °C, 4 h	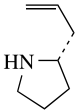 [1,2] and / or [2,3] 64 (48% ee)	76

(continued overleaf)

TABLE 6. (*continued*)

Preparation of migration terminus	Substrate	Reagent conditions	Product(s) yield (%)	Reference
	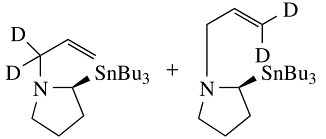 (7 : 1)	*n*-BuLi, THF-HMPA, 13 °C, 4 h	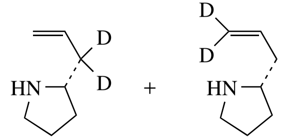 [1, 2] from major isomer [2, 3] from major isomer (4.3 : 1)	76
	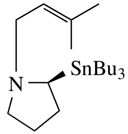 (94% ee)	*n*-BuLi, THF-HMPA, 13 °C, 4 h	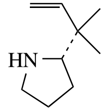 [2,3] 32 (8% ee)	76
	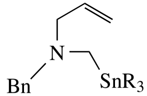		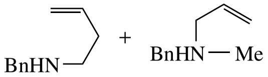 [1,2] and / or [2,3]	68
	R = Bu	*n*-BuLi, THF −78 °C → rt	65 (17 : 83)	
	R = Me	MeLi, THF −78 °C → rt	61 (75 : 25)	
	R = Me	MeLi, toluene −78 °C → rt	80 (30 : 70)	

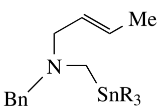	MeLi, DME	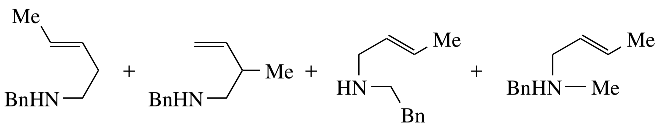 allyl - [1,2] [2,3] benzyl [1,2] 62 (10 : 0 : 43 : 47)	68
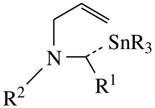 (>95% ee)	n-BuLi, THF $-78 \rightarrow 0\,^{\circ}\mathrm{C}$	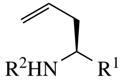 [1,2] and / or [2,3] 50 (48% ee)	77
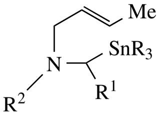 $R^1 = PhCH_2$, $R^2 = CH_2{=}CH{-}CH_2$	n-BuLi, THF $-78 \rightarrow 0\,^{\circ}\mathrm{C}$	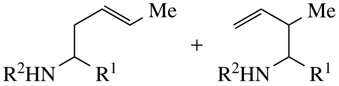 [1,2] [2,3] 34 45	77
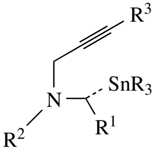 (>95% ee) $R^1 = PhCH_2$, $R^2 = R^3{-}C{\equiv}CCH_2$ $R^3 = H$ $R^3 = Me$ $R^3 = Et$	n-BuLi, THF $-78 \rightarrow 0\,^{\circ}\mathrm{C}$	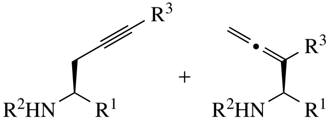 [1,2] [2,3] 75(0%*ee*) - - 25(48%*ee*) 10(62%*ee*) 36(66%*ee*)	78

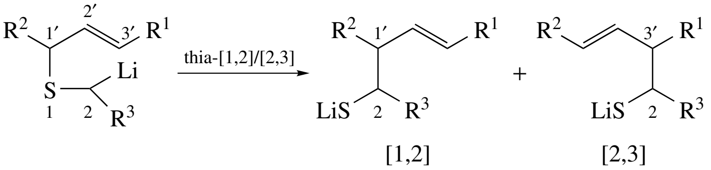

(80)

1. General aspects

The pioneering work on thia-[2,3]-Wittig rearrangement was reported by Rautenstrauch in 1971[80]. The reaction of allyl sulfides **137** with *n*-BuLi at −30 °C for 1.5–4 h gave homoallyl sulfide or thiol **138** ([2,3]-product) exclusively (equation 81). In contrast, a similar reaction of vinyl sulfide **139** gave no [1,2]-rearrangement product **141** albeit α-thio-carbanion was generated as shown by its methylation to **140** (equation 82)[30].

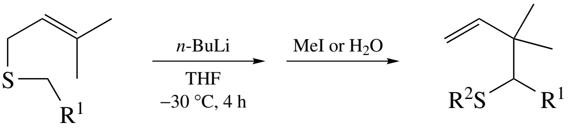

(81)

(137a) $R^1 = Ph$
(137b) $R^1 = CH{=}CMe_2$

(138a) $R^2 = Me$ quant.
(138b) $R^2 = H$ quant.

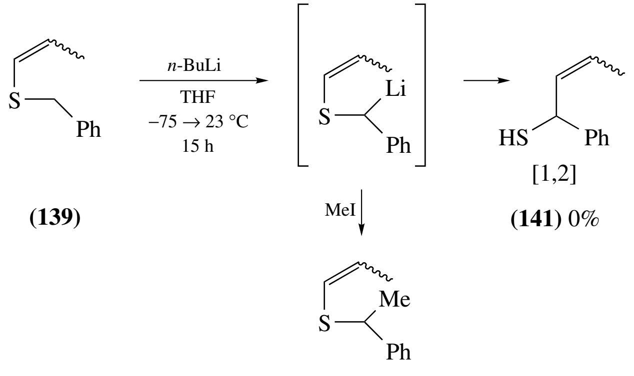

(139)

(141) 0%

(140) 40%

(82)

The most popular method for generation of α-thio-carbanion (migration terminus) is direct lithiation (deprotonation) with alkyllithium or lithium amide. These deprotonation methods are widely applicable to various substrates, not only benzyl or allyl sulfides[80], but also dithioacetals **142** which form **143** (equation 83)[81], and a phosphonate substituted system **144** which gives **145** (equation 84)[82].

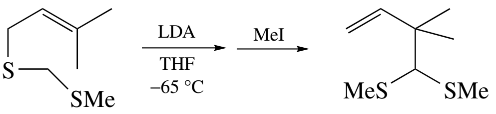

(142)

(143) 92%

(83)

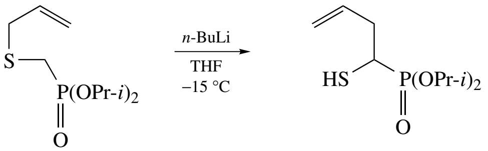

(144) **(145)** quant. (84)

On the other hand, transmetalation methods such as the tin–lithium exchange protocol or reductive lithiations of *S*,*S*-acetals were also developed by Emde and Brückner[83]. They have shown the significant difference in the stereoselectivity between the Sn → Li exchange and SAr → Li exchange protocols (Table 7).

TABLE 7. Thia-[2,3]-Wittig rearrangements of stannylated precursors and *S*,*S*-acetals[83]

Substrate	Reagent, conditions[a]	Product(s) yield (%)
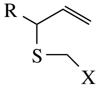		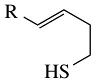
$R = p\text{-MeOC}_6\text{H}_4\text{C}_2\text{H}_4$		
X = SnBu$_3$	A	88 ($E : Z = 1 : 1$)
X = SPh	B	88 ($E : Z = 4 : 1$)
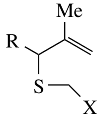		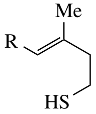
R = 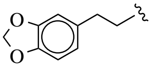		
X = SnBu$_3$	A	91 ($E : Z = 1 : 4$)
X = SPh	B	96 ($E : Z = 4 : 1$)
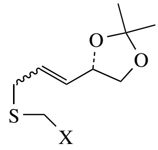		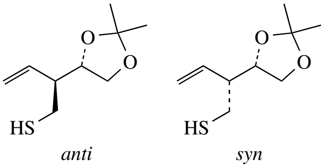
E-isomer		
X = SnBu$_3$	A	68 (*anti* : *syn* = 94 : 6)
X = SPh	B	66 (*anti* : *syn* = 54 : 46)
X = SnBu$_3$	A	83 (*anti* : *syn* = 98 : 2)
X = SPh	B	49 (*anti* : *syn* = 35 : 65)
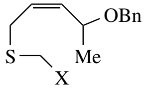		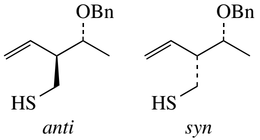
X = SnBu$_3$	A	90 (*anti* : *syn* = 96 : 4)
X = SPh	B	75 (*anti* : *syn* = 74 : 26)

[a] A: *n*-BuLi, THF, −78 °C; B: LiNaphth, THF, −78 °C.

2. Stereochemical aspects

The steric course of thia-Wittig rearrangement at the Li-bearing center has been investigated by Brückner and colleagues[84]. They have presented evidence for inversion of configuration at the Li-bearing terminus in the destannylative lithiation-induced rearrangement of diastereomerically defined **146** to **147** (equation 85). In this study, they have found that the benzyl sulfide **148** also turned out to be a precursor for thia-[2,3]-Wittig rearrangement to **149** rather than [1,2]-rearrangement, albeit with poor diastereoselectivity (equation 86).

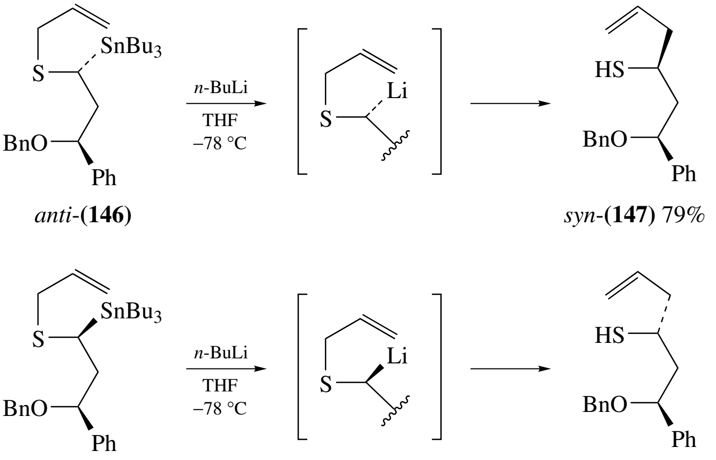

anti-**(146)** *syn*-**(147)** 79%

syn-**(146)** *anti*-**(147)** 89%

(85)

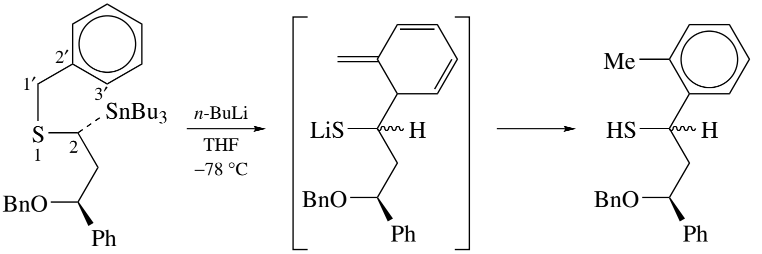

(148) **(149)**

69% (*syn*:*anti* = 71:29)

(86)

3. Synthetic applications

Snider and colleagues have developed the sequential ene reaction/thia-[2,3]-Wittig reaction which provide appropriately functionalized product **152** at allylic position on simple alkene **150** in two steps involving intermediate **151** (equation 87)[85]. Thia-[2,3]-Wittig rearrangement was often utilized as a key step of natural product synthesis. Masaki and colleagues have demonstrated that the potassium enolate thia-[2,3]-rearrangement of allyl sulfide **153** to **154** is useful for the synthesis of terpenoid diol component **155** of the pheromonal secretion of the queen butterfly (equation 88)[86].

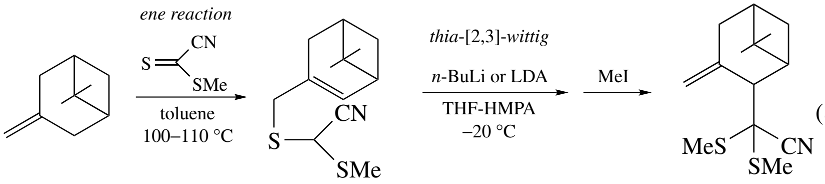

(150) **(151)** 83% **(152)** 72% (87)

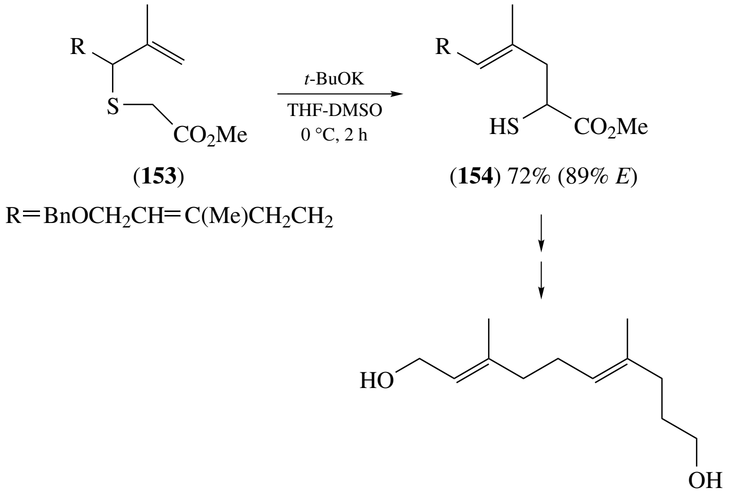

(**153**) (**154**) 72% (89% *E*)

R=BnOCH$_2$CH=C(Me)CH$_2$CH$_2$

(**155**) (88)

Recently, the asymmetric thia-[2,3]-Wittig rearrangement using di-(*l*)-menthyl phosphonate **156** as the chiral auxiliary to **157** has been developed by Masson and colleagues (equation 89)[82b].

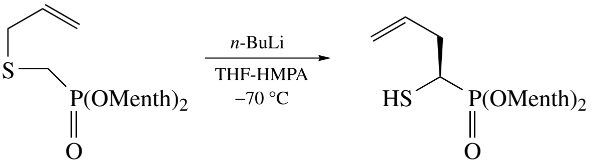

(**156**) (**157**) quant. (88% de) (89)

F. Retro-Brook Rearrangement (O−Si → C−Si)

The reverse process of a Brook rearrangement, the *O*- to *C*-trialkylsilyl group shift from a silyl ether to a carbanion terminus (equation 90), is well-known and has been intensively studied[87–89]. This rearrangement is sometimes referred to as the silyl-Wittig rearrangement. Numerous examples of [1,*n*]-retro-Brook rearrangement ($n = 2–6$) have been reported so far, and these are generally considered to proceed intramolecularly via pentacoordinate silicon-containing intermediates.

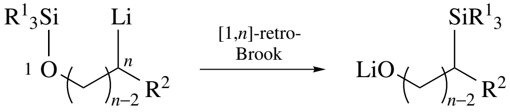

(90)

The first example of a retro-Brook rearrangement **158** → **159** was discovered by West and colleagues for the [1,3]-variant (equation 91)[90]. Subsequently, the [1,2]-variant **160** → **161** was reported by the same group (equation 92)[91, 92]. The rearrangement is much faster than the corresponding Wittig rearrangement.

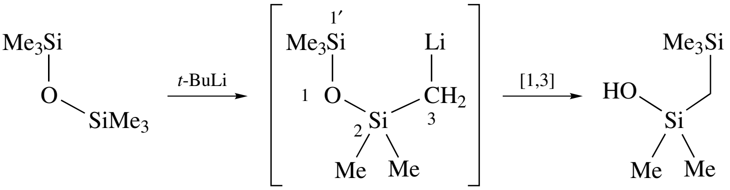

(91)

(**158**) (**159**) 30%

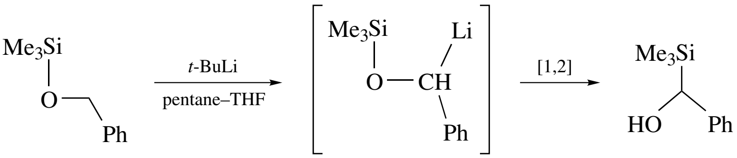

(92)

(**160**) (**161**) 95%

1. *[1,2]-Retro-Brook rearrangement*

a. Mechanistic aspects. The intramolecularity of the rearrangement is demonstrated by the cross-over experiment conducted by West's group[91a]. A reaction of mixed ethers **160** and **162** gave only non cross-products **161** and **163** (equation 93).

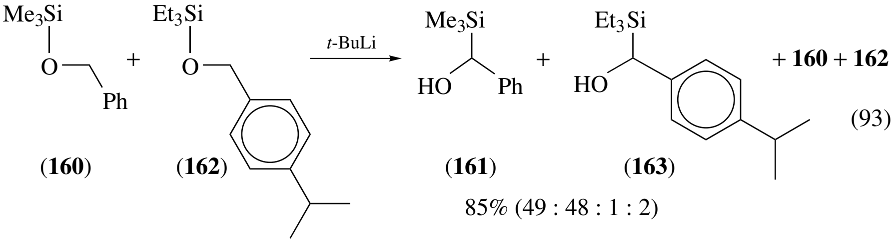

(93)

(**160**) (**162**) (**161**) (**163**)

85% (49 : 48 : 1 : 2)

Linderman and Ghannam have shown that the reaction of **164** to give **165** proceeds without cyclopropane ring opening (**166** was not formed), which shows that no radicals intervene in this rearrangement (equation 94), in contrast with the [1,2]-Wittig rearrangement[93]. Wright and West have proposed pentacoordinated silicon as a reasonable intermediate for the [1,2]-retro-Brook rearrangement (equation 95)[92].

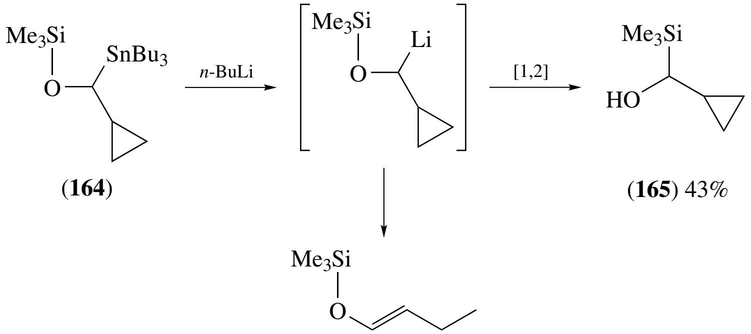

(**164**) (**165**) 43% (94)

(**166**) ~0%

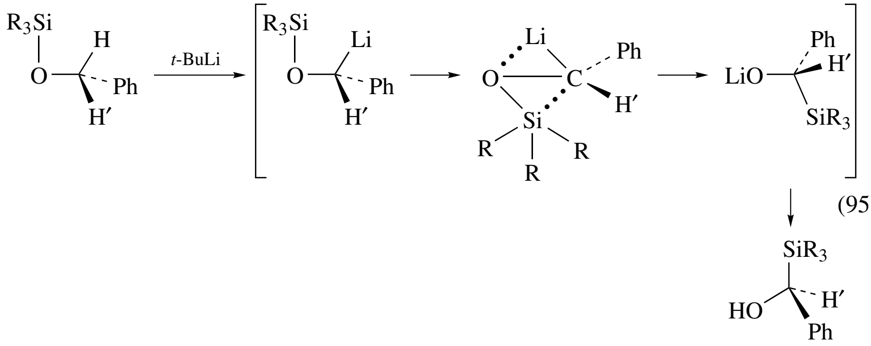

(95)

b. Stereochemical aspects. Similarly to the [1,2]-Wittig rearrangement, there are two aspects of the stereospecificity of the [1,2]-retro-Brook rearrangement: the steric course (inversion vs. retention) at the Li-bearing carbanion center and at the migrating silicon atom. Wright and West elucidated the steric course at the carbanion center of retro-[1,2]-Brook rearrangement in which the trialkyl silyl group of **167** migrates to a lithiated benzylic carbon to give **168** (equation 96)[92]. This rearrangement exhibits complete inversion of configuration. Quite differently, the rearrangement of **169** involving a simple aliphatic carbanion instead of a benzylic one gives **170** with a predominant retention of configuration (equation 97)[93b].

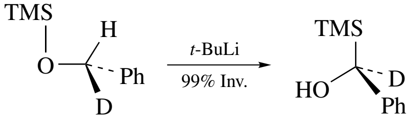

(96)

(*S*)-(**167**) (*S*)-(**168**)

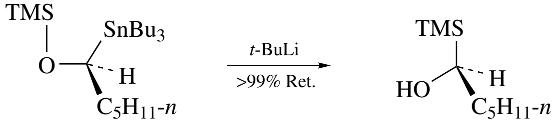

(97)

(*S*)-(**169**) (98% ee) (*S*)-(**170**) (97% ee)

To gain insight into the reaction mechanisms of these rearrangements, X-ray crystallography analysis of diphenyl(trimethylsilyloxy)methyllithium·3THF was performed by Boche's group[94] and *ab initio* calculations were conducted by several groups[4a, 95]. Wang and Dolg have shown that the alkyl-substituted system favors the retention transition state, while the vinyl-substituted one (a model for benzyl anion) with its delocalizing ability dramatically reduces the relative energies of the inversion transition state[95]. They also proposed that the migration of the silyl group retains the configuration at the silicon center.

c. Synthetic applications. Still and Macdonald have suggested that the allylic anion derived from allyloxysilane can undergo [1,2]-retro-Brook rearrangement[96]. Hosomi, Hashimoto and Sakurai have developed a practical rearrangement of allyloxysilanes and demonstrated the utility of the rearrangement products as homoenolate anion equivalents (equation 98)[97].

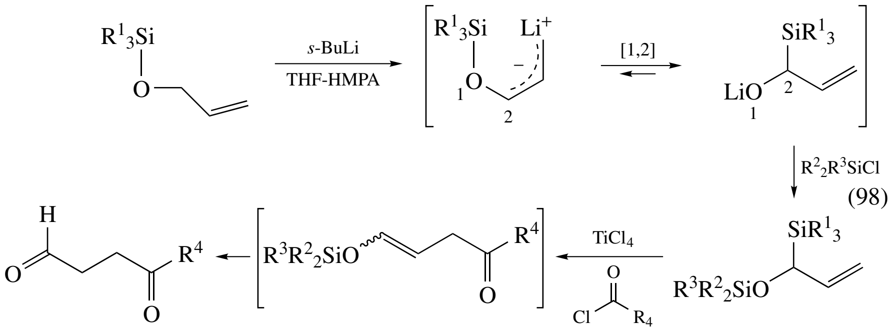

(98)

Verlhac and colleagues have shown the destannylative lithiation-induced [1,2]-retro-Brook rearrangement of siloxyvinyltins (equation 99)[105]. This rearrangement provides the corresponding acylsilanes (equation 99).

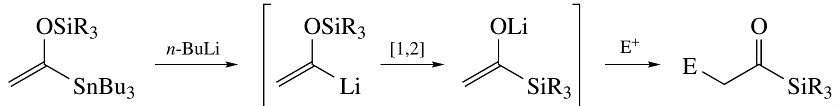

(99)

$E^+ = R^1X$, $E = R^1$; $E^+ = R^2CHO$, $E = R^2CHOH$; $E^+ = R^3COX$, $E = R^3CO$

Representative examples of [1,2]-retro-Brook rearrangements are summarized in Table 8.

2. *[1,3]-Retro-Brook rearrangement*

Retro-Brook rearrangement of the [1,3]-variant will readily take place in sp^3 and sp^2 carbanion systems. Kuwajima and Takeda[108] and Corey and Rücker[109] have developed the [1,3]-retro-Brook rearrangement of silyl enol ether anions which provide α-silyl ketones (equation 100 and 101).

TABLE 8. [1,2]-Retro-Brook rearrangements

Migration terminus, preparation	Substrate	Reagent, condition/ electrophile	Product(s) (yield %)	Reference
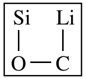				
H → Li	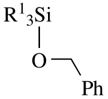		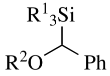	
	$R^1 = Et$	t-BuLi, pentane, rt /H_3O^+	$R^2 = H$ (96)	91a,b
	$R^1 = Me$	t-BuLi, pentane-TMEDA, −23 °C/TMSCl	$R^2 = TMS$ (60)	91a,b
	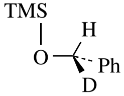	t-BuLi, THF, −78 → −50 °C /H_3O^+	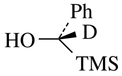 (73)	92
$SnBu_3$ → Li	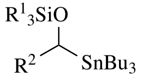	n-BuLi, THF, −78 °C /H_3O^+	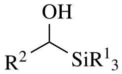	
	$R^1 = Me, R^2 = n\text{-}C_7H_{15}$		(67)	93b
	$R^1 = Me, R^2 = BnCH_2CH_2$		(56)	93b
	$R^1 = Me, R^2 = c\text{-Hex}$		(57)	93b
	$R^1 = Me, R^2 = t\text{-Bu}$		(49)	93b
	$R^1 = Me, R^2 = Ph$		(65)	93b
	$R^1 = Et, R^2 = n\text{-}C_7H_{15}$		(63)	93b
	$R^1 = Et, R^2 = Ph$		(60)	93b

(continued overleaf)

TABLE 8. (*continued*)

Migration terminus, preparation	Substrate	Reagent, condition/ electrophile	Product(s) (yield %)	Reference
	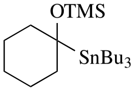	n-BuLi, THF, −78 °C /H_3O^+	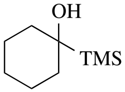 (50)	93b
	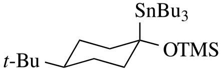	n-BuLi, THF, −78 °C /H_3O^+	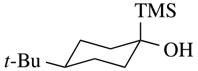 (20)	93b
	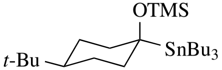	n-BuLi, THF, −78 °C /H_3O^+	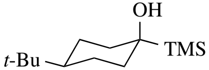 (40)	93b
	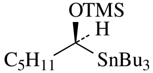	n-BuLi, THF, −78 °C /H_3O^+	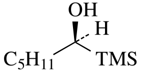 (91)	93b
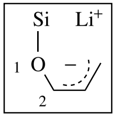				
H → Li	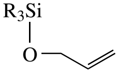	s-BuLi, THF, /H_3O^+	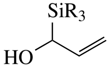 –	(96)
	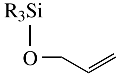 R = Me R = Et	s-BuLi, THF-HMPA, /TMSCl	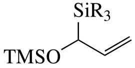 R = Me (80) R = Et (72) R = Et (92)	97 97 98

	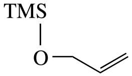	*t*-BuLi, pentane, −25 °C, 2 hr /H_3O^+/oxidn.	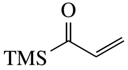 (66–68)	99a
		n-BuLi, THF, −78 °C, 1.25 hr /H_3O^+/oxidn.	(64–79)	99b
	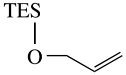	*t*-BuLi, THF-HMPA, −78 °C /TMSCl	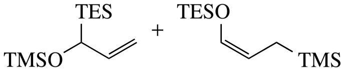 (50) (50)	100
	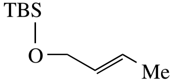	*s*-BuLi, THF-TMEDA, −45 °C /AcOH, THF, −78 °C	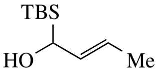 (66)	101
	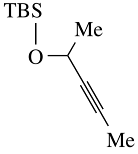	*n*-BuLi, THF, −45 °C /AcOH, −78 °C	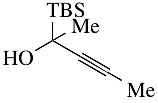 (86)	102
$SnMe_3$ → Li	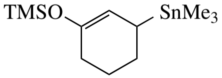	*n*-BuLi, THF	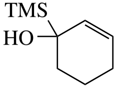	103
SPh → Li	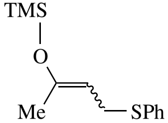	LDMAN, THF, −78 °C or −45 °C /H_3O^+ LDMAN = Lithium 1-(dimethylamino)naphthalene	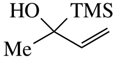 (79)	104

(*continued overleaf*)

TABLE 8. (*continued*)

Migration terminus, preparation	Substrate	Reagent, condition/ electrophile	Product(s) (yield %)	Reference
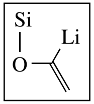				
$SnBu_3$ → Li	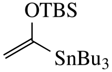	n-BuLi, THF, −78 °C /TMSCl	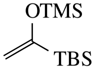 (73)	105
	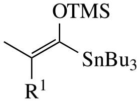	n-BuLi, THF, −78 °C /R^2Br	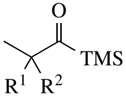	
	$R^1 = H, R^2 = (CH_3)_2C{=}CHCH_2$		(48)	105
	$R^1 = Me, R^2 = PhCH{=}CHCH_2$		(60)	105
SPh → Na	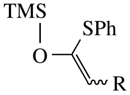	Na, TMSCl, benzene, reflux	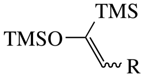 (82–94)	106, 107

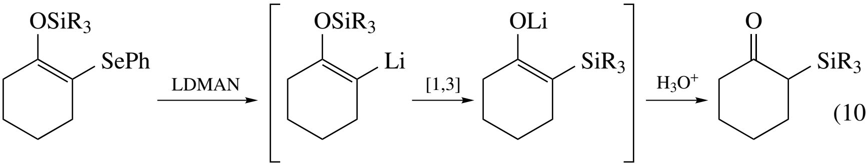

(100)

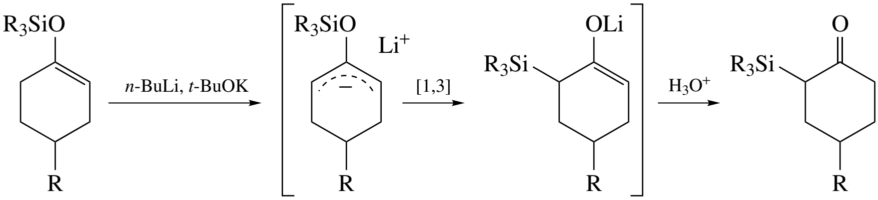

(101)

[1,3]-Retro-Brook rearrangement of aromatic systems has been developed by Simchen and Pfletschinger (equation 102)[110].

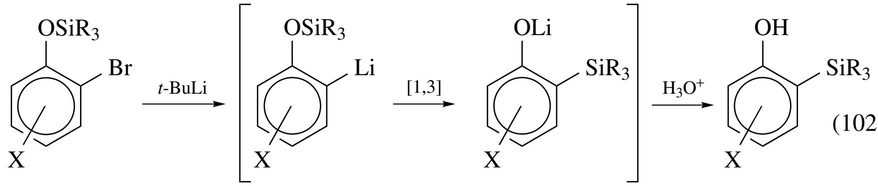

(102)

Representative examples of [1,3]-retro-Brook rearrangement are summarized in Table 9.

3. [1,4]-Retro-Brook rearrangement

[1,4]-Retro-Brook rearrangement is relatively common and enjoys widespread application in many facets of organic synthesis. For example, vinylsilane synthesis from allyloxysilane (equation 103)[119], allylsilane synthesis (equation 104)[120], and lithium enolate formation from silyl enol ether (equation 105)[121] were reported.

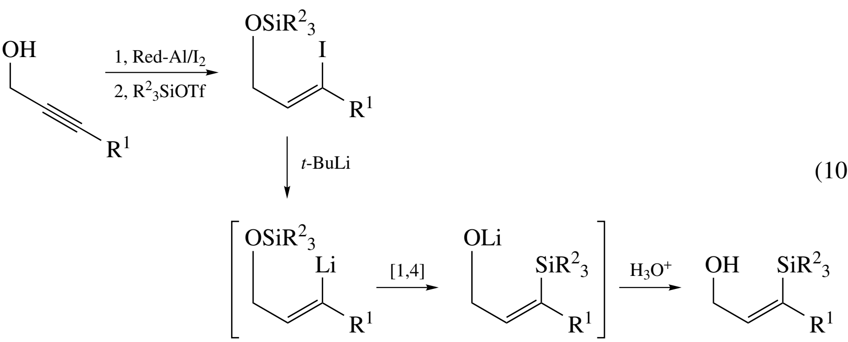

(103)

TABLE 9. [1,3]-Retro-Brook rearrangements

Migration terminus, preparation	Substrate	Reagent, condition/ electrophile	Product(s) (yield %)	Reference
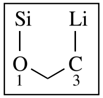				
H → Li	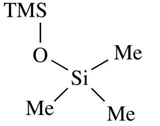	t-BuLi, pentane-TMEDA $/H_3O^+$	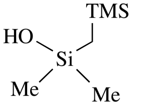 (30)	90a,b
SPh → Li	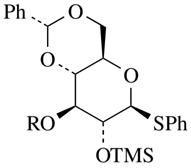 R = TMS R = Bn	LiNaphth, THF, −78 °C	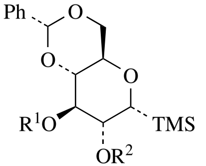 + 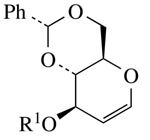 $R^1 = H, R^2 =$ TMS (61) $R^1 =$ TMS (12) $R^1 = Bn, R^2 = H$ (40) $R^1 = Bn$ (58)	111 111
Carbolithiation	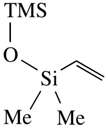	t-BuLi, Et_2O, −95 °C $/H_3O^+$	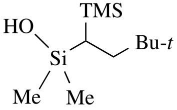 + 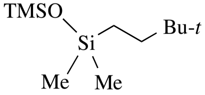 (23) (77)	

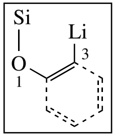

H → Li	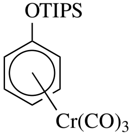	t-BuLi, THF, −78 °C /MeI, H_3O^+	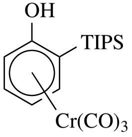 (3)	113
	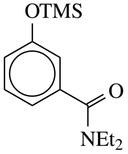	s-BuLi, THF-TMEDA, −78 °C /H_2O	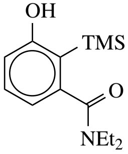 (62)	114
	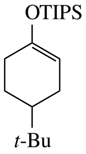	n-BuLi, t-BuOK, hexane, rt /H_3O^+	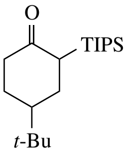 (98) dr = 5 : 1	114

(*continued overleaf*)

TABLE 9. (*continued*)

Migration terminus, preparation	Substrate	Reagent, condition/ electrophile	Product(s) (yield %)	Reference
X → Li	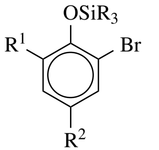	t-BuLi, THF, −30 °C /aq. NH_4Cl	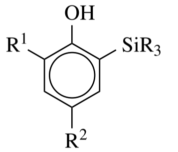	
	R = Me, $R^1 = R^2 = H$		(76)	110
	R = Et, $R^1 = R^2 = H$		(97)	110
	$R = R^2 = Me$, $R^1 = H$		(93)	110
	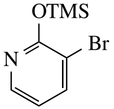	t-BuLi, THF, 25 °C /aq. NH_4Cl	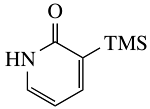 (62)	110
	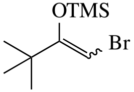	n-BuLi, −78 °C /aq. NH_4Cl	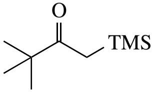 (68)	115
	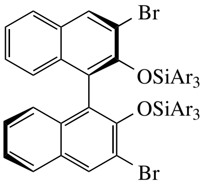 Ar = Ph, 3,5-xylyl	t-BuLi, THF /H_3O^+	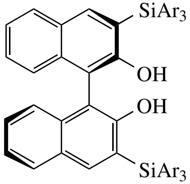 (80–95)	116

	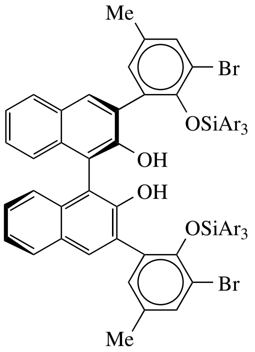 Ar = *o*-tolyl	*t*-BuLi, THF /H_3O^+	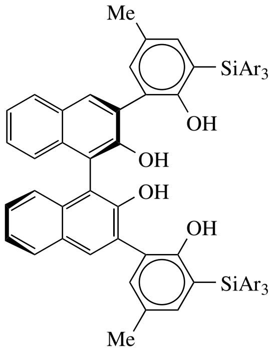 (68–84)	117
	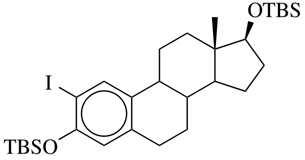	*n*-BuLi, THF, −78 °C /H_3O^+	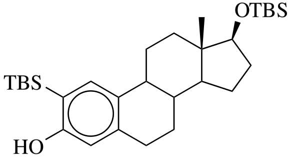 (54.7)	118
SePh → Li	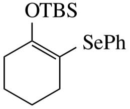	LDMAN, THF, −50 °C /H_3O^+	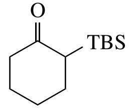 (85)	108

LDMAN = Lithium 1-(dimethylamino)naphthalene

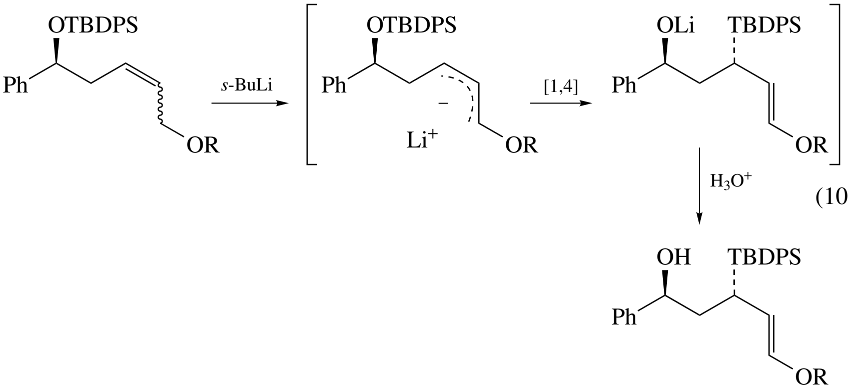

(104)

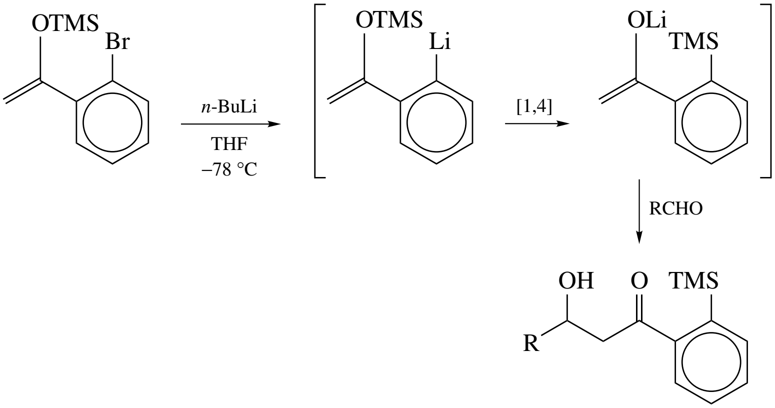

(105)

The [1,4]-rearrangement of the allyloxysilane system is a potentially useful method for allylsilane synthesis (equation 106). However, in general, a [1,2]-rearrangement may occur predominantly in this system (see Section II.F.1). To this end, the author's group recently found that the rearrangement of **171** in the presence of excess amount of HMPA provides the [1,4]-retro-Brook rearrangement product **172** in excellent yield (equation 107)[122].

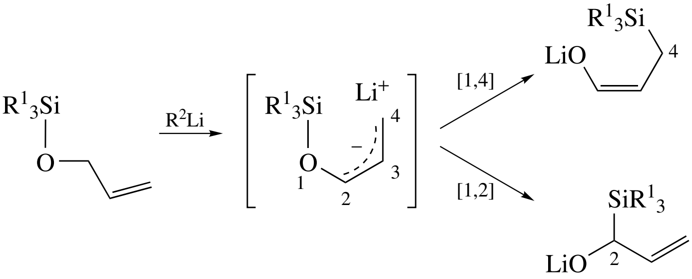

(106)

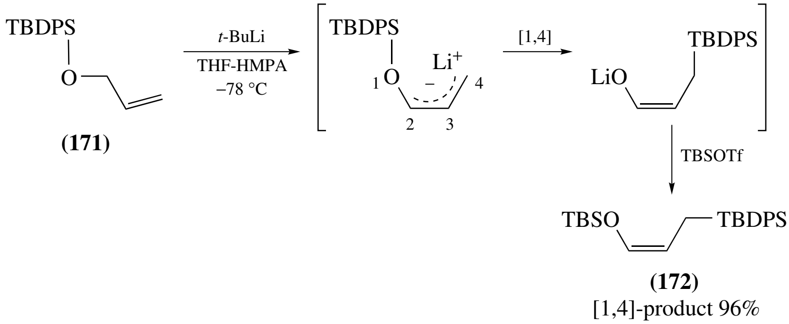

(171)

(172)

[1,4]-product 96%

(107)

The steric course at the Li-bearing center has been investigated by Lautens' group[123] and by Hoffmann and Brückner[124], independently. They have presented evidence for retention of configuration at the Li-bearing terminus in the retro-[1,4]-Brook rearrangement of aliphatic carbanion systems **174** and **176** (equations 108 and 109). On the other hand, the steric course at the migrating silicon atom was elucidated by the author's group by use of the optically active siloxane **177** (equation 110)[122]. A reaction of (*S*)-**177** (97% ee) with *t*-BuLi followed by trapping with optically active sultam derivative afforded (*R*)-**178** (97% ee at silicon) in 66%. This result proves that the rearrangement proceeds completely with retention of configuration at the migrating silicon.

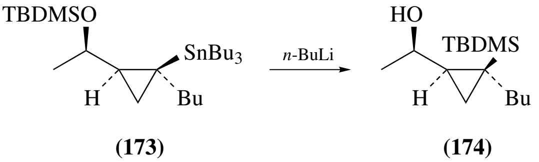

(173) **(174)**

(108)

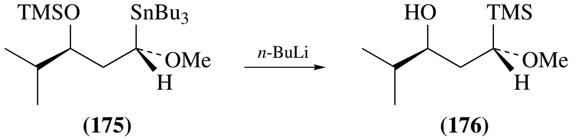

(175) **(176)**

(109)

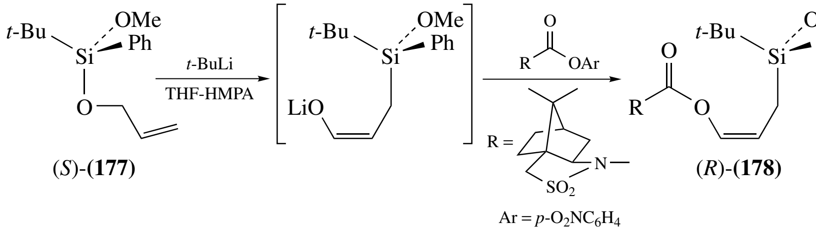

(*S*)-**(177)** (*R*)-**(178)**

(110)

The enantioselective version of a retro-[1,4]-Brook rearrangement was accomplished as the subsequent reaction of enantioselective cyclocarbolithiation by Hoppe and colleagues (equation 111)[125]. The cyclization precursor **179** was treated with *s*-BuLi/(−)-sparteine (**24**) in ether, providing the cyclized and silyl-rearranged product (*R*,*R*,*R*)-**180** in 58% yield as a single stereoisomer.

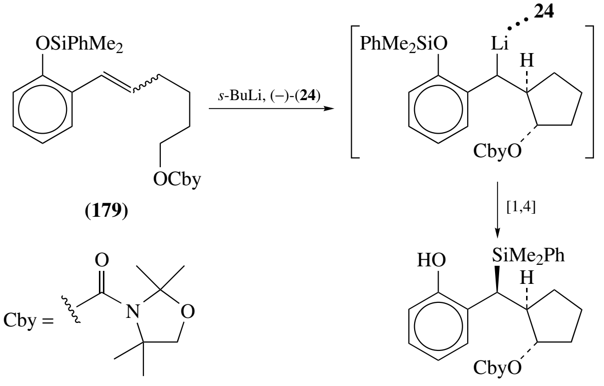

(*R*, *R*, *R*)-(**180**)
58% (>99% dr, >98% ee)

(111)

Representative examples of [1,4]-retro-Brook rearrangements are summarized in Table 10.

4. [1,5]- and [1,6]-Retro-Brook rearrangement

Jung and Nichols have reported a tandem [1,2]-Brook/[1,6]-retro-Brook rearrangement of a 1-(trimethylsilyl)-2,4-pentadien-1-ol anion to the aldehyde **181** (equation 112)[149]. Representative examples of [1,5]- and [1,6]-retro-Brook rearrangements are summarized in Table 11.

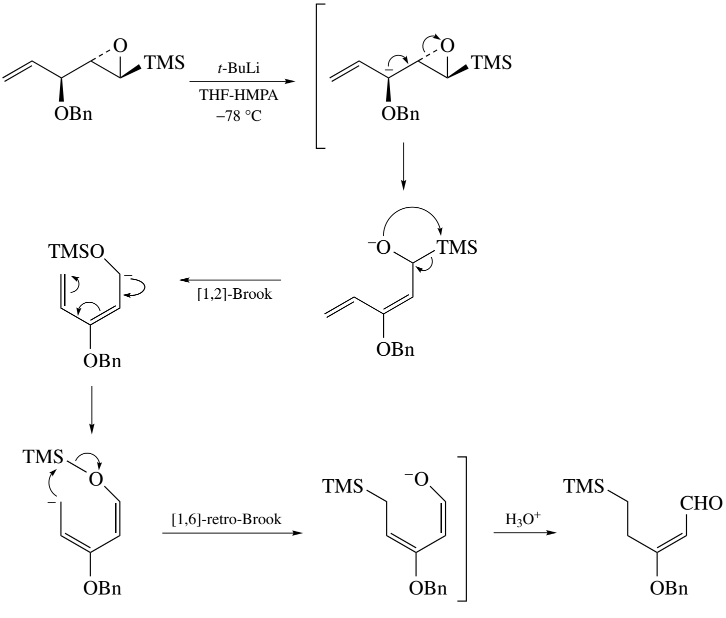

(**181**) 40%

(112)

TABLE 10. [1,4]-Retro-Brook rearrangements

Migration terminus, preparation	Substrate	Reagent, condition/ electrophile	Product(s) (yield %)	Reference
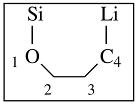				
H → Li	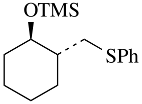	t-BuLi, THF-HMPA, $-15\,^{\circ}$C /H_3O^+	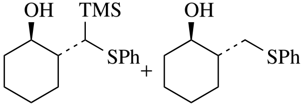 1.2 : 1	126
	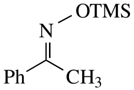	LDA, $-30\,^{\circ}$C /H_3O^+	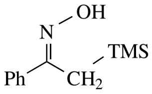 (95)	127
	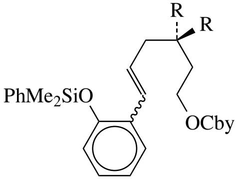	s-BuLi, (−)-sparteine (**24**), Et_2O, $-78 \rightarrow -40\,^{\circ}$C /MeOH	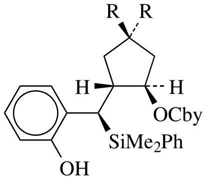 >96% ee, >98%dr	
	R = H		(60)	124
	R = Me		(47)	124
X → Li	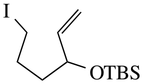	t-BuLi, Et_2O-TMEDA-pentane, $-78 \rightarrow 0\,^{\circ}$C /$H_3O^+$	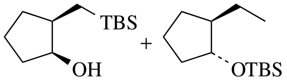 (60) (15)	128

(*continued overleaf*)

TABLE 10. (*continued*)

Migration terminus, preparation	Substrate	Reagent, condition/ electrophile	Product(s) (yield %)	Reference
SPh → Li	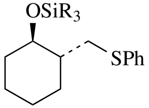 R = Me R = *i*-Pr	LDBB, THF, −78 °C /H$_3$O$^+$ LDBB = Lithium di-*t*-butylbiphenylide	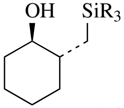 R = Me (73) R = *i*-Pr (85)	 126 126
	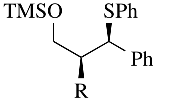 R = Me(64% *syn*) R = Bn(98% *syn*)	LDBB, THF, −78 °C /aq. NaHCO$_3$	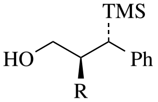 R = Me (94) > 98% *anti* R = Bn (95) > 99% *anti*	129, 130
	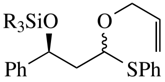 *syn*/*anti* = 1/1 R$_3$Si = TMS R$_3$Si = TES R$_3$Si = TBDPS	LiNaphth, THF, −78 °C /aq. NH$_4$Cl	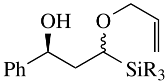 (81) 64% *anti* (61) 56% *anti* (77) 50% *anti*	 131 131 131
SnBu$_3$ → Li	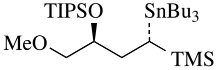	MeLi, THF, −78 °C → rt /MeI	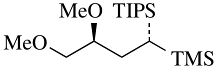 (66) dr = 3 : 1	122
	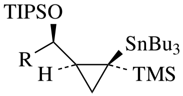 R = Me R = *n*-Pr	MeLi, THF, 0 °C /H$_3$O$^+$	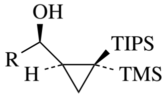 R = Me (75) R = *n*-Pr (91)	 122 122

	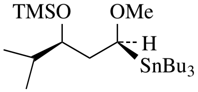	n-BuLi, THF, −78 °C /aq. NH_4Cl	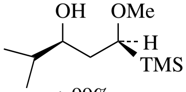 >99% *syn* (82)	123
	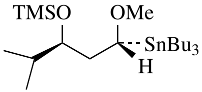	n-BuLi, THF, −78 °C /aq. NH_4Cl	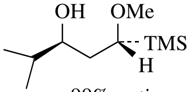 >99% *anti* (78)	123
SePh → Li	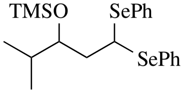	n-BuLi, Et_2O, −78 → >40 °C /H_3O^+	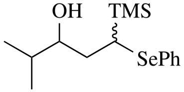 (61) 66% dr	132
SeMe → Li	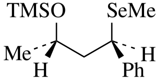	n-BuLi, THF, −78 °C /MeOH	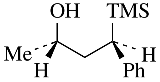 (86) 26% de	133
	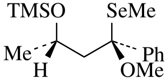		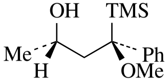 (57) 76% de	133

(*continued overleaf*)

TABLE 10. (*continued*)

Migration terminus, preparation	Substrate	Reagent, condition/ electrophile	Product(s) (yield %)	Reference
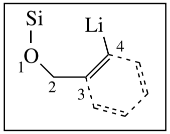				
H → Li	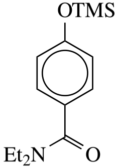	s-BuLi, THF-TMEDA, −78 → 0 °C /H_3O^+	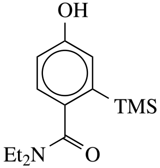 (78)	114
	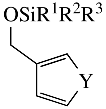 Y = O $R^1 = R^2 = Ph$ $R^3 = t\text{-Bu}$ Y = S $R^1 = R^2 = R^3 = i\text{-Pr}$	n-BuLi, THF-HMPA, −20 °C /H_3O^+	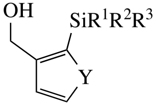 (87) (89)	134 134
X → Li	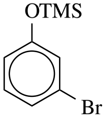	t-BuLi, THF, −30 °C /aq. NH_4Cl	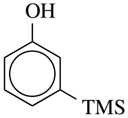 (80)	110

	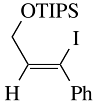	t-BuLi, THF, −78 → 23 °C /H_3O^+	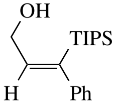 (80)	118
	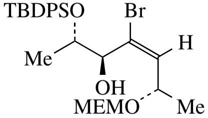	t-BuLi, Et_2O, −78 → 20 °C /H_3O^+	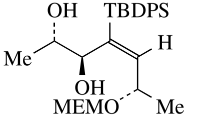 (>51)	135
	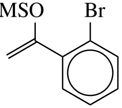	n-BuLi, THF, −78 °C /PhCHO	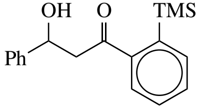 (74)	120
$SnBu_3$ → Li	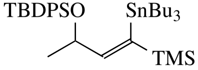	MeLi, THF, −40 °C /H_3O^+	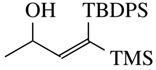 (92)	122
	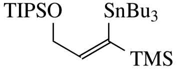	MeLi, THF, 0 °C /aq. NH_4Cl	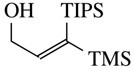 (98)	136

(*continued overleaf*)

TABLE 10. (*continued*)

Migration terminus, preparation	Substrate	Reagent, condition/ electrophile	Product(s) (yield %)	Reference
	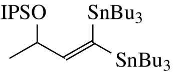	MeLi, THF, 0 °C /aq. NH_4Cl	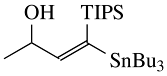 (40)	136
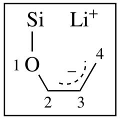 H → Li	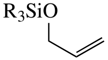 R = Me, Et	*s*-BuLi, THF-HMPA, −78 → −10 °C /TMSCl	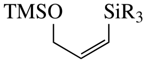 (−)	137
	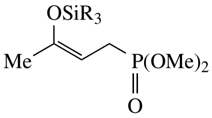 R = Me, Et	*n*-BuLi, THF, −65 °C	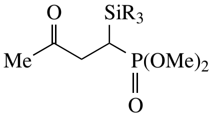 (−)	138
	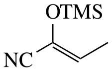	LDA, THF, −78 °C /Me_2HSiCl	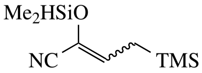 (61)	139
	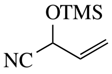	LDA, THF, −78 → 25 °C /TMSCl	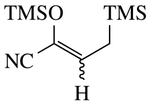 (−)	140

	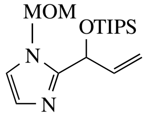	*n*-BuLi, THF-TMEDA, > −90 °C	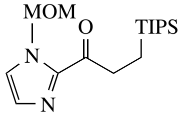 (−)	141
H → Li	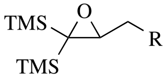	LDA	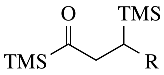 (71)	142
	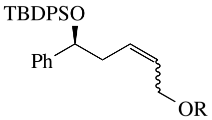 R = Me, MON	*s*-BuLi, THF, −78 °C $/H_3O^+$	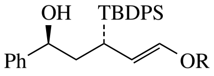 major dr (79–84)	143
SPh → Li	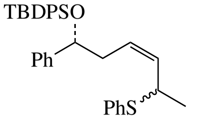 5 : 1 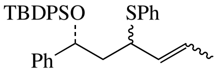	LiNaphth, THF, −78 °C /aq. NH_4Cl	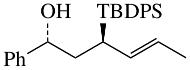 + 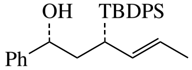 *anti*, *trans* *syn*, *trans* (91) 93 : 7	144
SPh → K	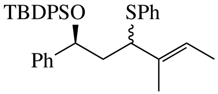	KNaphth, THF, −78 °C $/H_3O^+$	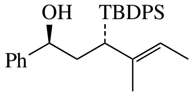 + 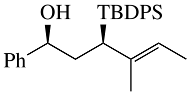 (98) 96 : 4	119, 145

(*continued overleaf*)

TABLE 10. (*continued*)

Migration terminus, preparation	Substrate	Reagent, condition/ electrophile	Product(s) (yield %)	Reference
$SAr_3 \rightarrow Li$	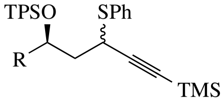	LiNaphth, THF $/H_3O^+$	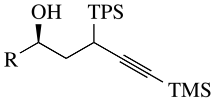	
	R = Me		(79) 81% *anti*	146
	R = *t*-Bu		(56) 87% *syn*	146
$SnBu_3 \rightarrow Li$	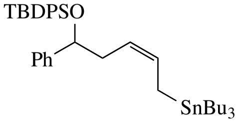	*n*-BuLi, THF, −78 °C $/H_3O^+$	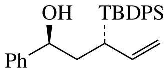 (69) 95% *anti*	147
	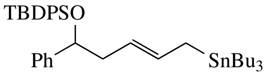	*n*-BuLi, THF, −78 °C $/H_3O^+$	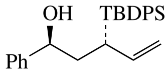 (67) 97% *anti*	147
Brook rearrangement	 $R = C_7H_{15}$, $R^1 = t$-Bu	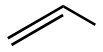Li, THF, −78 °C→rt $/ H_3O^+$	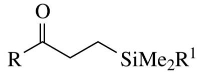 (88)	148

TABLE 11. [1,5]- and [1,6]-Retro-Brook rearrangements

Migration terminus, preparation	Substrate	Reagent, condition/ electrophile	Product(s) (yield %)	Reference
[1,5]				
X → Li	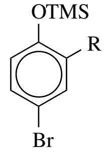	t-BuLi, THF, 25 °C /aq. NH_4Cl	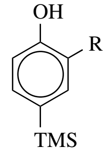	
	R = H		(85)	110
	R = Me		(80)	110
	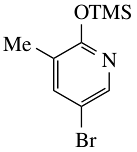	t-BuLi, THF, 25 °C /aq. NH_4Cl	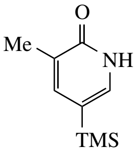 (98)	110
SPh → Li	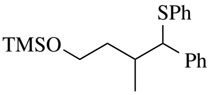	LDBB, THF, −78 °C /aq. $NaHCO_3$ LDBB = Lithium di-t-butyl biphenylide	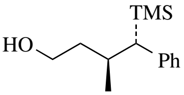 (88)	129, 130
[1,6]				
H → Li	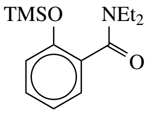	s-BuLi, TMEDA, THF, −78 °C/H_3O^+	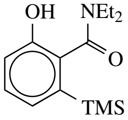 (68)	114
H → Li	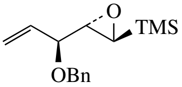	t-BuLi, THF-HMPA, (25 : 1), −78 °C /aq. HCl	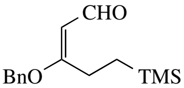 (40)	149
X → Li	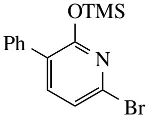	t-BuLi, THF, 25 °C /aq. NH_4Cl	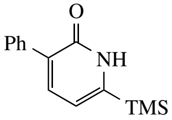 (69)	110

5. Related reactions

The sulfur analogue of retro-Brook rearrangement is reported by Wright and West[150]. Furthermore, silyl groups will migrate from carbon to the adjacent carbanion center[89]. The driving force for these rearrangements is the formation of a more stable carbanion. Representative examples are shown in equations 113 and 114[151, 152].

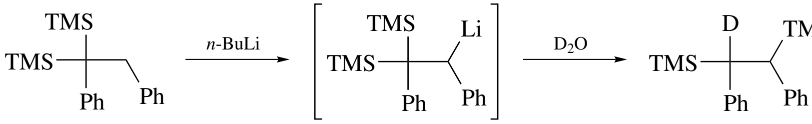

(113)

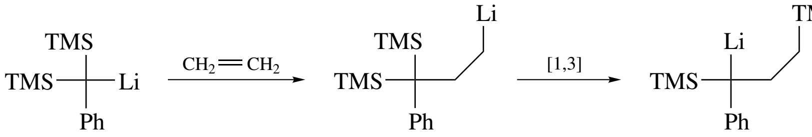

(114)

G. Miscellaneous

1. Phosphate–phosphonate rearrangement (O–P → C–P)

Phosphate-derived α-oxycarbanions can rearrange into α-hydroxy phosphonates. This class of rearrangement is known to proceed with retention of configuration at the carbanion terminus[153]. The enantioselective version of this rearrangement has been developed using a chiral lithium amide as a base (equation 115)[154]. The reaction of benzyl dimethyl phosphate **182** with amide (*R*,*R*)-**63** in THF gave the hydroxy phosphonate (*S*)-**183** in 30% in enantioenriched form (52% ee).

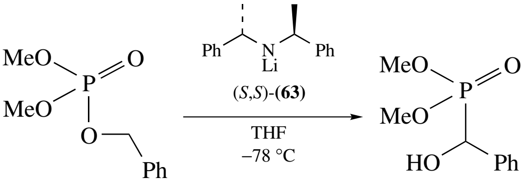

(115)

(182) (*R*)-**(183)** 30% (52% ee)

2. Lithiated epoxide rearrangement

α-Lithiated epoxides **184** can undergo various C–H insertions and 1,2-hydride shifts as well as cyclopropanations via an α-lithiooxy carbene generated by α-ring opening. These rearrangements have been well-reviewed in the literature[155].

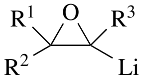

(184)

III. REFERENCES

1. (a) U. Schöllkopf, *Angew. Chem., Int. Ed. Engl.*, **9**, 763 (1970).
   (b) J. A. Marshall, in *Comprehensive Organic Synthesis* (Eds. B. M. Trost and I. Fleming), Vol. 3, Pergamon Press, Oxford, 1991, p. 975.
   (c) K. Tomooka, H. Yamamoto and T. Nakai, *Liebigs Ann. / Recueil*, 1275 (1997).
   (d) K. Tomooka and T. Nakai, *J. Synth. Org. Chem. Jpn.*, **54**, 1000 (1996).
2. G. Wittig and L. Löhmann, *Justus Liebigs Ann. Chem.*, **550**, 260 (1942).

3. (a) P. T. Lansbury, V. A. Pattison, J. D. Sidler and J. B. Bieber, *J. Am. Chem. Soc.*, **88**, 78 (1966).
   (b) H. Schäfer, U. Schöllkopf and D. Walter, *Tetrahedron Lett.*, 2809 (1968).
   (c) J. F. Garst and C. D. Smith, *J. Am. Chem. Soc.*, **98**, 1526 (1976).
4. (a) P. Antoniotti and G. Tonachini, *J. Org. Chem.*, **58**, 3622 (1993).
   (b) J. C. Sheldon, M. S. Taylor, J. H. Bowie, S. Dua, C. S. B. Chia and P. C. H. Eichinger, *J. Chem. Soc., Perkin Trans.* 2, 333 (1999).
5. K. Tomooka, T. Igarashi and T. Nakai, *Tetrahedron*, **50**, 5927 (1994).
6. W. C. Still, *J. Am. Chem. Soc.*, **100**, 1481 (1978).
7. R. Hoffmann, T. Rückert and R. Brückner, *Tetrahedron Lett.*, **34**, 297 (1993).
8. A. Maercker, *Angew. Chem., Int. Ed. Engl.*, **26**, 972 (1987).
9. M. Matsushita, Y. Nagaoka, H. Hioki, Y. Fukuyama and M. Kodama, *Chem. Lett.*, 1039 (1996).
10. H. Felkin and A. Tambuté, *Tetrahedron Lett.*, 821 (1969).
11. (a) U. Schöllkopf and W. Fabian, *Justus Liebigs Ann. Chem.*, **642**, 1 (1961).
    (b) U. Schöllkopf and H. Schäfer, *Justus Liebigs Ann. Chem.*, **663**, 22 (1963).
12. E. J. Verner and T. Cohen, *J. Am. Chem. Soc.*, **114**, 375 (1992).
13. R. Hoffmann and R. Brückner, *Chem. Ber.*, **125**, 1957 (1992).
14. K. Tomooka, T. Igarashi and T. Nakai, *Tetrahedron Lett.*, **34**, 8139 (1993).
15. (a) W. C. Still and C. Sreekumar, *J. Am. Chem. Soc.*, **102**, 1201 (1980).
    (b) J. S. Sawyer, A. Kucerovy, T. L. Macdonald and G. J. McGarvey, *J. Am. Chem. Soc.*, **110**, 842 (1988).
16. S. L. Schreiber and M. T. Goulet, *Tetrahedron Lett.*, **28**, 1043 (1987).
17. R. E. Maleczka and F. Geng, *J. Am. Chem. Soc.*, **120**, 8551 (1998).
18. J. P. Mazaleyrat and Z. Welvart, *Nouv. J. Chim.*, **7**, 491 (1983).
19. (a) K. Tomooka, K. Yamamoto and T. Nakai, *Angew. Chem., Int. Ed.*, **38**, 3741 (1999).
    (b) K. Tomooka, *J. Synth. Org. Chem. Jpn.*, **59**, 322 (2001).
20. S. L. Schreiber, M. T. Goulet and G. Schulte, *J. Am. Chem. Soc.*, **109**, 4718 (1987).
21. J. S. Yadav and R. Ravishankar, *Tetrahedron Lett.*, **32**, 2629 (1991).
22. K. Tomooka, H. Yamamoto and T. Nakai, *J. Am. Chem. Soc.*, **118**, 3317 (1996).
23. K. Tomooka, H. Yamamoto and T. Nakai, *Angew. Chem., Int. Ed.*, **39**, 4500 (2000).
24. (a) K. Tomooka, M. Kikuchi, K. Igawa, P.-H. Keong and T. Nakai, *Tetrahedron Lett.*, **40**, 1917 (1999).
    (b) K. Tomooka, M. Kikuchi, K. Igawa, M. Suzuki, P. -H. Keong and T. Nakai, *Angew. Chem., Int. Ed.*, **39**, 4503 (2000).
25. K. Tomooka, Y. Kadomoto and K. Takahashi, to appear.
26. (a) P. Gärtner, M. F. Letschnig, M. Knollmüller and H. Völlenkle, *Tetrahedron: Asymmetry*, **10**, 4811 (1999).
    (b) P. Gärtner, M. F. Letschnig, M. Knollmüller and K. Mereiter, *Tetrahedron: Asymmetry*, **11**, 1003 (2000).
27. O. Kitagawa, S. Momose, Y. Yamada, M. Shiro and T. Taguchi, *Tetrahedron Lett.*, **42**, 4865 (2001).
28. J. Barluenga, F. J. Fananas, R. Sanz, C. Marcos and M. Trabada, *Org. Lett.*, **4**, 1587 (2002).
29. S. Kiyooka, T. Tsutsui and T. Kira, *Tetrahedron Lett.*, **37**, 8903 (1996).
30. V. Rautenstrauch, G. Büchi and H. Wuest, *J. Am. Chem. Soc.*, **96**, 2576 (1974).
31. (a) O. Miyata, T. Koizumi, I. Ninomiya and T. Naito, *J. Org. Chem.*, **61**, 9078 (1996).
    (b) O. Miyata, H. Asai and T. Naito, *Synlett*, 1915 (1999).
32. (a) D. Hoppe, *Angew. Chem., Int. Ed. Engl.*, **23**, 932 (1984).
    (b) P. Zhang and R. E. Gawley, *J. Org. Chem.*, **58**, 3223 (1993).
    (c) S. Superchi, N. Sotomayor, G. Miao, B. Joseph, M. G. Campbell and V. Snieckus, *Tetrahedron Lett.*, **37**, 6061 (1996).
33. K. Tomooka, H. Shimizu, T. Inoue, H. Shibata and T. Nakai, *Chem. Lett.*, 759 (1999).
34. (a) D. Y. Curtin and S. Leskowitz, *J. Am. Chem. Soc.*, **73**, 2633 (1951).
    (b) D. Y. Curtin and W. R. Proops, *J. Am. Chem. Soc.*, **76**, 494 (1954).
35. L. A. Paquette and Q. Zeng, *Tetrahedron Lett.*, **40**, 3823 (1999).
36. A. Garbi, L. Allain, F. Chorki, M. Ourévitch, B. Crousse, D. Bonnet-Delpon, T. Nakai and J. -P. Bégue, *Org. Lett.*, **3**, 2529 (2001).
37. U. Azzena, T. Denurra, G. Melloni and A. M. Piroddi, *J. Org. Chem.*, **55**, 5532 (1990).

38. W. Schlenk and E. Bergmann, *Justus Liebigs Ann. Chem.*, **464**, 1 (1928).
39. (a) R. W. Hoffmann, *Angew. Chem., Int. Ed. Engl.*, **18**, 563 (1979).
    (b) T. Nakai and K. Mikami, *Chem. Rev.*, **86**, 885 (1986).
    (c) R. Brückner, in *Comprehensive Organic Synthesis* (Eds. B. M. Trost and I. Fleming), Vol. 6, Pergamon Press, Oxford, 1991, p. 873.
    (d) R. Brückner, *Kontakte (Darmstadt)*, **2**, 3 (1991).
    (e) R. Brückner, *Kontakte (Darmstadt)*, **3**, 3 (1991).
    (f) T. Nakai and K. Mikami, *Org. React.*, **46**, 105 (1994).
    (g) T. Nakai and K. Tomooka, *Pure Appl. Chem.*, **69**, 595 (1997).
40. J. Cast, T. S. Stevens and J. Holmes, *J. Chem. Soc.*, 3521 (1960).
41. V. Rautenstrauch, *J. Chem. Soc., Chem. Commun.*, 4 (1970).
42. B. M. Trost and L. S. Melvin, *Sulfur Ylides,* Chap. 7, Academic Press, New York, 1975.
43. K. Mikami, Y. Kimura, N. Kishi and T. Nakai, *J. Org. Chem.*, **48**, 279 (1983).
44. Y.-D. Wu, K. N. Houk and J. A. Marshall, *J. Org. Chem.*, **55**, 1421 (1990).
45. (a) J. A. Marshall and J. Lebreton, *Tetrahedron Lett.*, **28**, 3323 (1987).
    (b) J. A. Marshall and J. Lebreton, *J. Org. Chem.*, **53**, 4108 (1988).
46. J. A. Marshall and J. Lebreton, *J. Am. Chem. Soc.*, **110**, 2925 (1988).
47. S. E. Gibson, P. Ham and G. R. Jefferson, *Chem. Commun.*, 123 (1998).
48. J. Kang, W. O. Cho, H. G. Cho and H. J. Oh, *Bull. Korean. Chem. Soc.*, **15**, 732 (1994).
49. (a) T. Kawasaki and T. Kimachi, *Synlett*, 1429 (1998).
    (b) T. Kawasaki and T. Kimachi, *Tetrahedron*, **55**, 6847 (1999).
50. M. Tsubuki, T. Kamata, M. Nakatani, K. Yamazaki, T. Matsui and T. Honda, *Tetrahedron: Asymmetry*, **11**, 4725 (2000).
51. V. Capriati, S. Florio, G. Ingrosso, C. Granito and L. Troisi, *Eur. J. Org. Chem.*, 478 (2002).
52. S. Manabe, *Chem. Pharm. Bull.*, **46**, 335 (1998).
53. S. Manabe, *Chem. Commun.*, 737 (1997).
54. (a) K. Tomooka, N. Komine and T. Nakai, *Tetrahedron Lett.*, **39**, 5513 (1998).
    (b) K. Tomooka, N. Komine and T. Nakai, *Chirality*, **12**, 505 (2000).
55. V. Rautenstrauch, *Helv. Chim. Acta*, **55**, 594 (1972).
56. (a) H. Felkin and C. Frajerman, *Tetrahedron Lett.*, 3485 (1977).
    (b) R. Briére, M. Chérest, H. Felkin and C. Frajerman, *Tetrahedron Lett.*, 3489 (1977).
57. K. Tomooka and Y. Tanabe, to appear.
58. M. Schlosser and S. Strunk, *Tetrahedron*, **45**, 2649 (1989).
59. K. Tomooka, Y. Tanabe, K. Endou, M. Kikuchi and N. Seki, to appear.
60. (a) X. Wei and R. J. K. Taylor, *Tetrahedron Lett.*, **37**, 4209 (1996).
    (b) X. Wei, P. Johnson and R. J. K. Taylor, *J. Chem. Soc., Perkin Trans. 1*, 1109 (2000).
61. W. F. Bailey and L. M. Zarcone, *Tetrahedron Lett.*, **32**, 4425 (1991).
62. C. Vogel, *Synthesis*, 497 (1997).
63. J. J. Eisch and G. A. Kovacs, *J. Organomet. Chem.*, **30**, C97 (1971).
64. M. T. Reetz and D. Schnizer, *Tetrahedron Lett.*, 3485 (1975).
65. U. Schöllkopf and K. Fellenberger, *Justus Liebigs Ann. Chem.*, **698**, 80 (1966).
66. Y. Murata and T, Nakai, *Chem. Lett.*, 2069 (1990).
67. (a) T. Nakai, K. Mikami, S. Taya, Y. Kimura and T. Mimura, *Tetrahedron Lett.*, **22**, 69 (1981).
    (b) O. Takahashi, T. Saka, K. Mikami and T. Nakai, *Chem. Lett.*, 1599 (1986).
68. I. Coldham, *J. Chem. Soc., Perkin Trans. 1*, 1275 (1993).
69. W. C. Still and A. Mitra, *J. Am. Chem. Soc.*, **100**, 1927 (1978).
70. C. A. Broka and T. Shen, *J. Am. Chem. Soc.*, **111**, 2981 (1989).
71. T. Durst, R. Van den Elzen and J. LeBelle, *J. Am. Chem. Soc.*, **94**, 9261 (1972).
72. (a) J. Åhman and P. Somfai, *J. Am. Chem. Soc.*, **116**, 9781 (1994).
    (b) J. Åhman and P. Somfai, *Tetrahedron Lett.*, **36**, 303 (1995).
    (c) J. Åhman and P. Somfai, *Tetrahedron*, **51**, 9747 (1995).
    (d) J. Åhman and P. Somfai, *Tetrahedron Lett.*, **37**, 2495 (1996).
    (e) P. Somfai, T. Jarevång, U. M. Lindström and A. Svensson, *Acta Chem. Scand.*, **51**, 1024 (1997).
    (f) U. M. Lindström and P. Somfai, *Chem. Eur. J.*, **7**, 94 (2001).
73. (a) J. C. Anderson, D. C. Siddons, S. C. Smith and M. E. Swarbrick, *J. Chem. Soc., Chem. Commun.*, 1835 (1995).

(b) J. C. Anderson, D. C. Siddons, S. C. Smith and M. E. Swarbrick, *J. Org. Chem.*, **61**, 4820 (1996).

(c) J. C. Anderson, S. C. Smith and M. E. Swarbrick, *J. Chem. Soc., Perkin Trans. 1*, 1517 (1997).

(d) J. C. Anderson and C. A. Roberts, *Tetrahedron Lett.*, **39**, 159 (1998).

(e) J. C. Anderson, P. Dupau, D. C. Siddons, S. C. Smith and M. E. Swarbrick, *Tetrahedron Lett.*, **39**, 2649 (1998).

(f) J. C. Anderson, A. Flaherty and M. E. Swarbrick, *J. Org. Chem.*, **65**, 9152 (2000).

(g) J. C. Anderson and A. Flaherty, *J. Chem. Soc., Perkin Trans. 1*, 267 (2001).

74. S. Manabe, *Tetrahedron Lett.*, **38**, 2491 (1997).
75. F. Haeffner, K. N. Houk, S. M. Schulze and J. K. Lee, *J. Org. Chem.*, **68**, 2310 (2003).
76. R. E. Gawley, Q. Zhang and S. Campagna, *J. Am. Chem. Soc.*, **117**, 11817 (1995).
77. T. Tomoyasu, K. Tomooka and T. Nakai, *Tetrahedron Lett.*, **44**, 6121 (2003).
78. T. Tomoyasu and K. Tomooka, to appear.
79. I. Coldham, A. J. Collis, R. J. Mould and R. E. Rathmell, *Tetrahedron Lett.*, **36**, 3557 (1995).
80. V. Rautenstrauch, *Helv. Chim. Acta.*, **54**, 739 (1971).
81. C. Huyuh and S. Julia, *Synth. Commun.*, **7**, 103 (1977).
82. (a) H. Makomo, S. Masson and M. Saquet, *Tetrahedron Lett.*, **34**, 7257 (1993).
    (b) M. Gulea, P. Marchand, M. Saquet, S. Masson and N. Collignon, *Phosphorus, Sulfur, Silicon*, **153–154**, 327 (1999).
83. H. v. d. Emde and R. Brückner, *Tetrahedron Lett.*, **33**, 7323 (1992).
84. (a) K. Brickmann and R. Brückner, *Chem. Ber.*, **126**, 1227 (1993).
    (b) K. Brickmann, F. Hambloch, E. Spolaore and R. Brückner, *Chem. Ber.*, **127**, 1949 (1994).
85. B. B. Snider, N. J. Hrib and L. Fuzesi, *J. Am. Chem. Soc.*, **98**, 7115 (1976).
86. Y. Masaki, K. Sakuma and K. Kaji, *Chem. Lett.*, 1061 (1980).
87. A. G. Brook and A. R. Bassindale, in *Rearrangements in Ground and Excited States*, Vol. 2 (Ed. P. de Mayo), Academic Press, New York, 1980, p. 149.
88. M. A. Brook, *Silicon in Organic, Organometallic, and Polymer Chemistry*, Wiley, New York, 2000.
89. R. West, in *Advances in Organometallic Chemistry*, Vol. 16 (Eds. F. G. A. Stone and R. West), Academic Press, New York, 1977, p. 1.
90. (a) G. A. Gornowicz and R. West, *J. Am. Chem. Soc.*, **90**, 4478 (1968).
    (b) R. West and G. A. Gornowicz, *J. Organomet. Chem.*, **28**, 25 (1971).
91. (a) R. West, R. Lowe, H. F. Stewart and A. Wright, *J. Am. Chem. Soc.*, **93**, 282 (1971).
    (b) A. Wright and R. West, *J. Am. Chem. Soc.*, **96**, 3214 (1974).
92. A. Wright and R. West, *J. Am. Chem. Soc.*, **96**, 3222 (1974).
93. (a) R. J. Linderman and A. Ghannam, *J. Org. Chem.*, **53**, 2878 (1988).
    (b) R. J. Linderman and A. Ghannam, *J. Am. Chem. Soc.*, **112**, 2392 (1990).
94. G. Boche, A. Opel, M. Marsch, K. Harms, F. Haller, J. C. W. Lohrenz, C. Thümmler and W. Koch, *Chem. Ber.*, **125**, 2265 (1992).
95. Y. Wang and M. Dolg, *Tetrahedron*, **55**, 12751 (1999).
96. W. C. Still and T. L. Macdonald, *J. Am. Chem. Soc.*, **96**, 5561 (1974).
97. A. Hosomi, H. Hashimoto and H. Sakurai, *J. Org. Chem.*, **43**, 2551 (1978).
98. A. Hosomi, H, Hashimoto and H. Sakurai, *J. Organomet. Chem.*, **175**, 1 (1979).
99. (a) R. L. Danheiser, D. M. Fink, K. Okano, Y.-M. Tsai and S. W. Szczepanski, *Org. Synth.*, **66**, 14 (1987).
    (b) R. L. Danheiser, D. M. Fink, K. Okano, Y.-M. Tsai and S. W. Szczepanski, *J. Org. Chem.*, **50**, 5393 (1985).
100. P. W. K. Lau and T. H. Chan, *J. Organomet. Chem.*, **179**, 24 (1979).
101. R. E. Ireland and M. D. Varney, *J. Am. Chem. Soc.*, **106**, 3668 (1984).
102. K. Sakaguchi, M. Fujita, H. Suzuki, M. Higashino and Y. Ohfune, *Tetrahedron Lett.*, **41**, 6589 (2000).
103. W. C. Still and A. Mitra, *Tetrahedron Lett.*, 2659 (1978).
104. T. Cohen and J. R. Matz, *J. Am. Chem. Soc.*, **102**, 6900 (1980).
105. J. -B. Verlhac, H. Kwon and M. Pereyre, *J. Organomet. Chem.*, **437**, 13 (1992).
106. I. Kuwajima, M. Kato and T. Sato, *J. Chem. Soc., Chem. Commun.*, 478 (1978).
107. I. Kuwajima, A. Mori and M. Kato, *Bull. Chem. Soc. Jpn.*, **53**, 2634 (1980).
108. I. Kuwajima and R. Takeda, *Tetrahedron Lett.*, **22**, 2381 (1981).

109. E. J. Corey and C. Rücker, *Tetrahedron Lett.*, **25**, 4345 (1984).
110. G. Simchen and J. Pfletschinger, *Angew. Chem., Int. Ed. Engl.*, **15**, 428 (1976).
111. V. Pedretti, A. Veyriéres and P. Sinaÿ, *Tetrahedron*, **46**, 77 (1990).
112. H. A. Firgo and W. P. Weber, *Organometallics*, **1**, 649 (1982).
113. N. F. Masters and D. A. Widdowson, *J. Chem. Soc., Chem. Commun.*, 955 (1983).
114. R. J. Billedeau, M. P. Sibi and V. Snieckus, *Tetrahedron Lett.*, **24**, 4515 (1983).
115. P. Sampson and D. F. Wiemer, *J. Chem. Soc., Chem. Commun.*, 1746 (1985).
116. K. Maruoka, T. Itoh, T. Shirasaka and H. Yamamoto, *J. Am. Chem. Soc.*, **110**, 310 (1988).
117. K. Maruoka, N. Murase and H. Yamamoto, *J. Org. Chem.*, **58**, 2938 (1993).
118. H. -M. He, P. E. Fanwick, K. Wood and M. Cushman, *J. Org. Chem.*, **60**, 5905 (1995).
119. K. D. Kim and P. A. Magriotis, *Tetrahedron Lett.*, **31**, 6137 (1990).
120. C. Gibson, T. Buck, M. Noltemeyer and R. Brückner, *Tetrahedron Lett.*, **38**, 2933 (1997).
121. B. M. Comanita, S. Woo and A. G. Fallis, *Tetrahedron Lett.*, **40**, 5283 (1999).
122. A. Nakazaki and K. Tomooka, to appear.
123. M. Lautens, P. H. M. Delanghe, J. B. Goh and C. H. Zhang, *J. Org. Chem.*, **57**, 3270 (1992).
124. R. Hoffmann and R. Brückner, *Chem. Ber.*, **125**, 2731 (1992).
125. S. H. Kleinfeld, E. Wegelius and D. Hoppe, *Helv. Chim. Acta*, **82**, 2413 (1999).
126. C. Rücker, *Tetrahedron Lett.*, **25**, 4349 (1984).
127. J. Mora and A. Costa, *Tetrahedron Lett.*, **25**, 3493 (1984).
128. X.-L. Jiang and W. F. Bailey, *Organometallics*, **14**, 5704 (1995).
129. S. Marumoto and I. Kuwajima, *Chem. Lett.*, 1421 (1992).
130. S. Marumoto and I. Kuwajima, *J. Am. Chem. Soc.*, **115**, 9021 (1993).
131. R. Hoffmann and R. Brückner, *Chem. Ber.*, **125**, 1471 (1992).
132. R. W. Hoffmann and M. Bewersdorf, *Tetrahedron Lett.*, **31**, 67 (1990).
133. J. Bousbaa, F. Ooms and A. Krief, *Tetrahedron Lett.*, **38**, 7625 (1997).
134. E. J. Bures and B. A. Keay, *Tetrahedron Lett.*, **28**, 5965 (1987).
135. M. Braun and H. Mahler, *Justus Liebigs Ann. Chem.*, 29 (1995).
136. M. Lautens, P. H. M. Delanghe, J. B. Goh and C. H. Zhang, *J. Org. Chem.*, **60**, 4213 (1995).
137. W. C. Still, *J. Org. Chem.*, **41**, 3063 (1976).
138. D. A. Evans, J. M. Takacs and K. M. Hurst, *J. Am. Chem. Soc.*, **101**, 371 (1979).
139. S. Hünig and M. Öller, *Chem. Ber.*, **113**, 3803 (1980).
140. U. Hertenstein, S. Hünig, H. Reichelt and R. Schaller, *Chem. Ber.*, **115**, 261 (1982).
141. D. H. Davies, N. A. Haire, J. Hall and E. H. Smith, *Tetrahedron*, **48**, 7839 (1992).
142. D. M. Hodgson and P. J. Comina, *Tetrahedron Lett.*, **37**, 5613 (1996).
143. D. Goeppel and R. Brückner, *Tetrahedron Lett.*, **38**, 2937 (1997).
144. K. Behrens, B. O. Kneisel, M. Noltemeyer and R. Brückner, *Justus Liebigs Ann. Chem.*, 385 (1995).
145. C. Gibson, T. Buck, M. Walker and R. Brückner, *Synlett*, 201 (1998).
146. F. Sammtleben, M. Noltemeyer and R. Brückner, *Tetrahedron Lett.*, **38**, 3893 (1997).
147. E. Winter and R. Brückner, *Synlett*, 1049 (1994).
148. J. Enda and I. Kuwajima, *J. Am. Chem. Soc.*, **107**, 5495 (1985).
149. M. E. Jung and C. J. Nichols, *J. Org. Chem.*, **61**, 9065 (1996).
150. A. Wright and R. West, *J. Am. Chem. Soc.*, **96**, 3222 (1974).
151. J. J. Eisch and M.-R. Tsai, *J. Am. Chem. Soc.*, **95**, 4065 (1973).
152. J. J. Eisch and M.-R. Tsai, *J. Organomet. Chem.*, **225**, 5 (1982).
153. F. Hammerschmidt and H. Völlenkle, *Justus Liebigs Ann. Chem.*, 2053 (1986).
154. (a) F. Hammerschmidt and A. Hanninger, *Chem. Ber.*, **128**, 823 (1995).
(b) F. Hammerschmidt and S. Schmidt, *Phosphorus, Sulfur, Silicon*, **174**, 101 (2001).
155. (a) Y. Mori, *J. Synth. Org. Chem. Jpn.*, **55**, 176 (1999).
(b) D. M. Hodgson and E. Gras, *Synthesis*, 1625 (2002).
(c) D. M. Hodgson, K. Tomooka and E. Gras, *Top. Organomet. Chem.* **5**, 217 (2003).

CHAPTER 13

Lithium carbenoids

MANFRED BRAUN

Institut für Organische Chemie und Makromolekulare Chemie, Universität Düsseldorf, D-40225 Düsseldorf, Germany
Fax: +49-211-81-15079; e-mail: braunm@uni-duesseldorf.de

I. INTRODUCTION

Organometallic compounds containing a lithium atom and an electronegative element at the same carbon atom have been termed ‘carbenoids’, thus taking their carbene-like chemical behavior into account[1]. Thermal lability is typical of lithium carbenoids, the chemistry of which has been disclosed by the seminal work of Köbrich[2, 3]. Another feature of lithium carbenoids is an ambiphilic behavior, which originates from the coexistence of an electron-donating and an electron-withdrawing substituent at the carbon center. As a consequence, lithium carbenoids have been shown to have nucleophilic as well as electrophilic reactivity[4–7]. In recent years, structure determinations[8–16] and spectroscopic investigations[7, 16–21] combined with theoretical calculations[7, 16, 22–29] have brought an insight into the ‘chameleon-like’ character of these organometallic compounds. On the other hand, synthetic chemistry takes more and more advantage of the high reactivity and selectivity of lithium carbenoids, which developed into useful reagents for carbon–carbon bond formations[30–34]. In this chapter, a discussion of the reactivity and an

The Chemistry of Organolithium Compounds. Edited by Z. Rappoport and I. Marek
ISBN: 0-470-84339-X

overview on recent structure investigations are presented. Emphasis, however, is given to the application of lithium carbenoids in organic synthesis. For this purpose, the different methods for the generation of lithium carbenoids are presented first. In the following part, dealing with reactions of lithium carbenoids, carbenoid typical reactions are treated first, followed by an overview on conversions that are based on the carbanion typical reactivity. As the reactivity of these species depends significantly on the heteroatom bound to the carbenoid center, the different paragraphs are ordered according to different types of α-hetero substituents. Another influence on the reactivity comes from the hybridization of the α-carbon atom, so that a subdivision dealing with alkyl, including cycloalkyl, and vinylidene carbenoids has been introduced.

II. GENERAL REACTIVITY AND STRUCTURE INVESTIGATIONS

The particular substitution pattern of lithium carbenoids, the fact that both an electropositive metal and an electronegative substituent X are bound to the same carbon atom, causes the ambiphilic character of this species. The 'chameleon-like' reactivity becomes evident from the resonance formulas of the carbenoid **1b** (equation 1): Whereas the carbanionic character is expressed by the resonance formula **1a**, the electrophilic character is represented by **1c**. In an analogous way, the reactivity of vinylidene carbenoids **2b** is expressed by the mesomeric structures **2a** and **2c**.

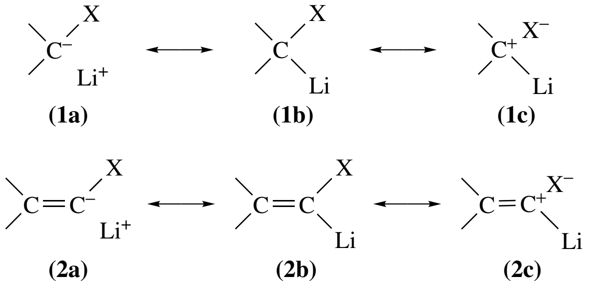

(1)

It should be pointed out that the large majority of organolithium compounds do not exhibit electrophilic reactivity. Thus, the term 'lithium carbenoids' should be restricted to those organometallic compounds that have both electrophilic and nucleophilic character. On the other hand, reagents that behave just like carbanions (according to mesomeric formulas **1a** and **2a**) should be considered as α-hetero-substituted organolithium compounds[32]. The different reactivities are illustrated by the following typical reactions of vinylidene carbenoids. A large number of reactions with electrophiles demonstrates the anionic character (expressed by **1a** and **2a**) of lithium carbenoids, and often served as a first proof of the formation of the organolithium compound (equation 2, reaction a). The carbanionic character has been shown for lithium carbenoids with different α-substituents, but it is the typical reactivity, when sulfur or nitrogen serves as α-heteroatom. The particular value of such α-hetero-substituted organolithium compounds results from the fact that they can serve as reagents for umpolung of the reactivity[35, 36].

The electrophilic reactivity of lithium carbenoids (reaction b) becomes evident from their reaction with alkyl lithium compounds. A, probably metal-supported, nucleophilic substitution occurs, and the leaving group X is replaced by the alkyl group R^3 with inversion of the configuration[21, 37, 38]. This reaction, typical of metal carbenoids, is not restricted to the vinylidene substitution pattern, but occurs in alkyl and cycloalkyl lithium carbenoids as well[39, 40]. With respect to the α-heteroatom X, the carbenoid character is

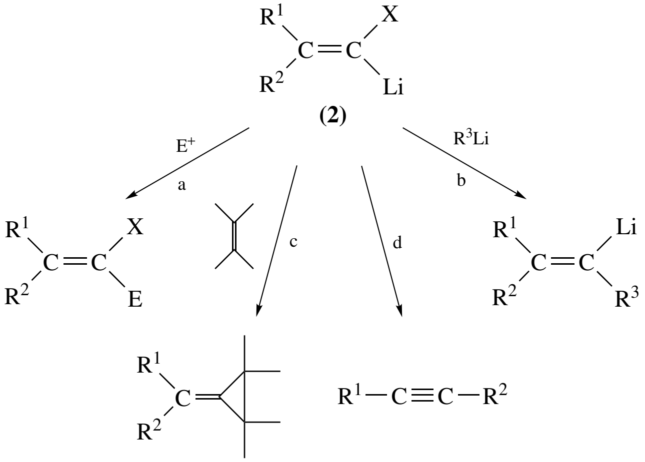

(2)

most pronounced in the halogen-substituted derivatives, but it has also been observed in α-lithiated ethers.

Another feature of carbenoid-type reactivity is the cyclopropanation (reaction c). Again, this reaction does not only take place in vinylidene but also in alkyl carbenoids[30]. On the other hand, the intramolecular shift of a β-aryl, cyclopropyl or hydrogen substituent, known as the Fritsch–Buttenberg–Wiechell rearrangement, is a typical reaction of α-lithiated vinyl halides (reaction d)[2,3]. A particular carbenoid-like reaction occurring in α-halo-α-lithiocyclopropanes is the formation of allenes and simultaneous liberation of the corresponding lithium halide (equation 3)[41–44].

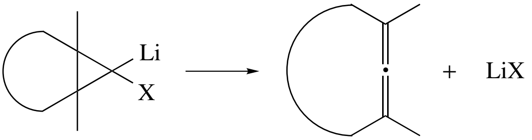

(3)

In order to obtain a better understanding of the ambivalent character of lithium carbenoids, various attempts at structure determinations were made. However, these studies were impeded by the thermal lability, in particular in case of α-halo-α-lithio compounds, most of which are not stable above −90 °C. Nevertheless, new insight into the structure and reactivity of lithium carbenoids came in recent years from improved calculations[7,16,22–29], NMR techniques[17–21] and finally X-ray structure analyses[7–16], which were performed under capricious conditions. Köbrich had already assumed that in α-chloro- and α-bromo-substituted lithioalkenes the C−Li bond has a larger s content and, as a consequence, the C−X bond has a higher p-content compared to the non-lithiated compounds[2,3]. Thus, an elongated C−X bond is expected. This conclusion has been confirmed by theoretical calculations which show, for example, that in $LiCH_2F$ the C−F bond is elongated compared to CH_3F (Scheme 1)[16].

Although *ab initio* calculations predict different non-classical structures of various lithium carbenoids, there is a general tendency that shows a relatively high positive charge at the carbenoid carbon center, thus correlating with the resonance formulas **1c** and **2c**[16] (equation 1). The cationic character, highlighted by these mesomeric structures, has been confirmed convincingly by ^{13}C-NMR investigations performed by Seebach and coworkers[17–20]. They discovered that the α-carbon atom in different types of halogen

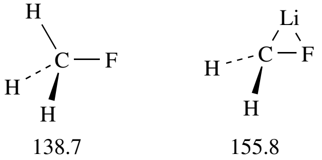

SCHEME 1. Calculated C−F bond lengths in pm in CH_3F and CH_2FLi

lithium carbenoids is strongly shifted to lower field in comparison to the carbon atom in non-lithiated compounds. Downfield shifts of $\Delta\delta = 40$ to 280 have been observed (Scheme 2)[19]. Usually, the formation of 'carbanions' by lithiation of alkanes has the opposite effect: small upfield shifts are observed in lithiated alkanes ($\Delta\delta \approx 15$), except for alkenyl lithium compounds, which show a small downfield shift[45].

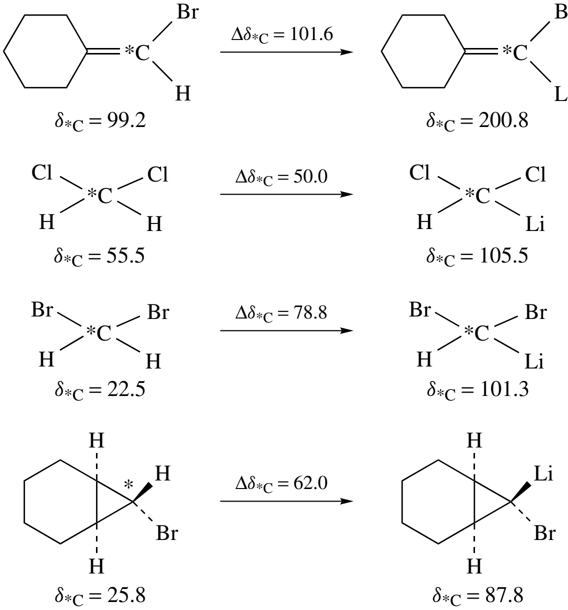

SCHEME 2. Typical downfield shifts in ^{13}C-NMR spectra of lithium carbenoids

The deshielding of the ^{13}C resonance in lithium carbenoids is explained by the polarization of the elongated C−X bond and shows that the carbocationic structures **1c** and **2c** have to be taken into account. The postulated high s character of the C−Li bond is also confirmed by the NMR-spectroscopic investigations insofar as enhanced ^{13}C−^{6}Li coupling constants have been observed in lithium carbenoids[19]. Thus, the effect of the metalation that leads to the formation of lithium carbenoids can be summarized as follows (Scheme 3)[16].

The hypothesis of a particular hybridization of the carbon center in lithium carbenoids has been confirmed by recent X-ray structure analyses performed by Boche and coworkers. To date, the crystal structures of two chloro-substituted and several oxygen-substituted

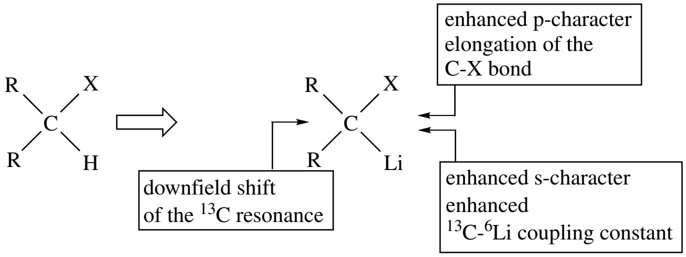

SCHEME 3. Features of lithium carbenoids and their effect on the NMR data

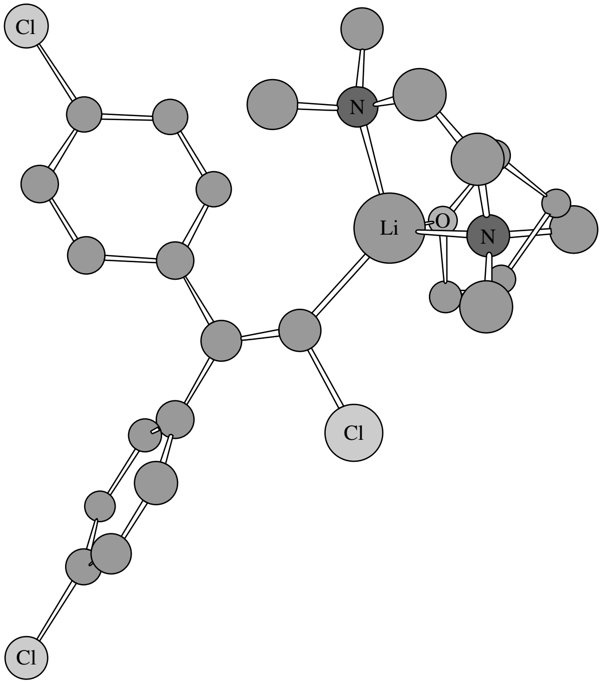

FIGURE 1. Crystal structure of **3**. Reproduced by permission of VCH, Weinheim from Reference 8

lithium carbenoids have been determined. In the crystal structure of 1-chloro-2,2-bis(4-chlorophenyl)-1-lithioethene·TMEDA·2 THF (**3**) (Scheme 4), the first structure of a lithium carbenoid (Figure 1)[8], the bond between the carbenoid carbon and the chloro atom is significantly elongated (by 12 pm) with respect to the non-lithiated alkene. Further remarkable features of this structure are the Cl1−C1−C2 angle of 112.6(5)°, which is smaller than the 120° angle at sp^2-hybridized carbon atoms, and the Li1−C1−C2 angle, which is distinctly larger [137.1(6)°]. Thus, the postulate of the enhanced p-character of the carbon−halogen bond and the enhanced s-character of the carbon−lithium bond is confirmed by the crystal structure (Scheme 4 and Figure 1). The predictions of calculations, which postulate a carbon−halogen bond bridged by the lithium, are not confirmed. This contradiction is easily explained by the fact that the calculations did not consider a solvation of the lithium, whereas in the crystal structure the lithium is solvated by TMEDA and THF. The second THF molecule is located on a free lattice position and is not coordinated to the lithium. The crystal structure of the Grignard compound **4** disclosed significant similarity to that of the lithium carbenoid **3**. Thus, the C−Br bond in the magnesium carbenoid **4** is 10 pm longer than in the corresponding vinyl bromide (Scheme 4)[9].

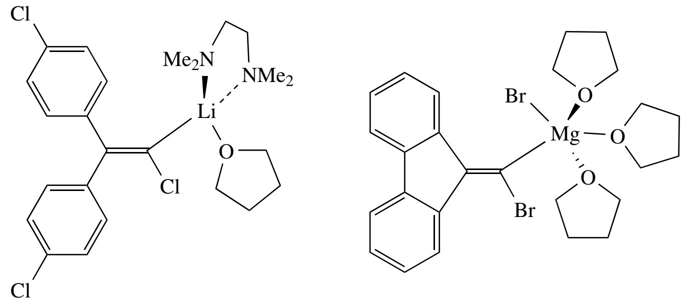

(3) **(4)**

SCHEME 4. Structures of lithium carbenoid **3** and the magnesium carbenoid **4**

Halogen−lithium carbenoids of a tetragonal alkyl carbon atom are less stable than the corresponding vinylidene carbenoids. Nevertheless, a crystal structure of dichloromethyllithium-pyridine (**5**) could be obtained (Scheme 5, Figure 2)[10]. The lithium atom obtains a tetracoordination by using three pyridine molecules as ligands. Here again, the carbenoid character becomes evident from the fact that the C−Cl bonds in **5** are elongated by approximately 10 pm compared to dichloromethane. Furthermore, the sum of the bond angles of Cl1−C1−Cl2, Cl1−C1−H1 and Cl2−C1−H1 amounting to 308° is significantly lower than the corresponding value expected for a tetragon, 328.5°. This also indicates a higher p-character of the C−Cl bonds.

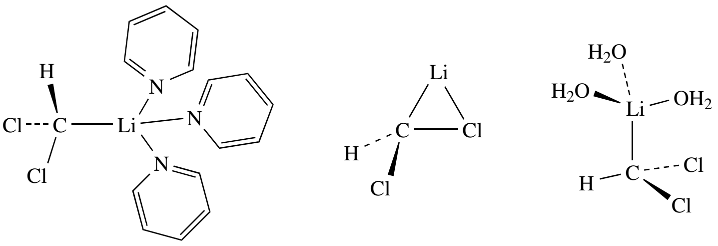

(5) **(6)** **(7)**

SCHEME 5. Structure of dichloromethyllithium: X-ray structure analysis of $LiCHCl_2$·3 pyridine (**5**), calculated structure of $LiCHCl_2$ (**6**), calculated structure of $LiCHCl_2$·$3H_2O$ (**7**)

At a glance, the result of the X-ray structure analysis of **5** contradicts theoretical calculations that predict the bridged structure **6** to be the most stable alternative of Cl_2CHLi. However, calculations of the trihydrate of Cl_2CHLi result in the structure **7** wherein the lithium is solvated by three water molecules[10]. The similarity between the calculated trihydrate **7** and the tris(pyridine) coordinated structure **5** is obvious.

To date, the crystal structures of several α-lithiated ethers have been determined[11−15]. Despite the aggregation, i.e. polymers, dimers or monomers, depending on the solvation,

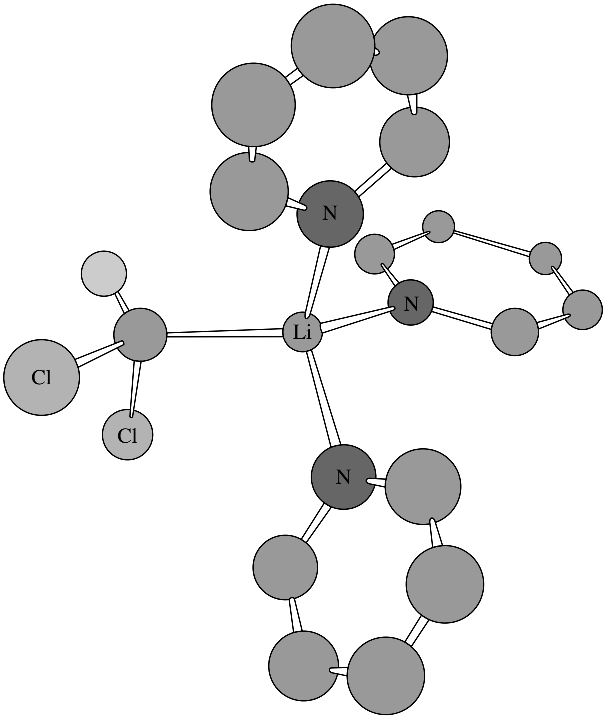

FIGURE 2. Crystal structure of **5**. Reproduced by permission of VCH, Weinheim from Reference 8

their results confirm substantial predictions of theoretical calculations of $LiCH_2OH$[16]. An essential feature becoming evident from theoretical calculations and X-ray structure analysis is a significant elongation of the C−O bonds by 7–10 pm compared to the corresponding non-lithiated compounds, which clearly underlines the carbenoid character of α-lithiated ethers. A structure, typical of an α-oxygen-substituted vinylidene carbenoid is represented by the lithiated benzofuran **8**[12] which, in the crystalline state, dimerized along the C−Li bond (Scheme 6). In addition, lithium bridges the carbon and oxygen atoms and obtains a fourth coordination by binding to one solvent molecule (*i*-Pr_2O). Compared to the average bond length in benzofuranes, amounting to 138.5 pm, the corresponding C (lithiated)−O bond in **8** is elongated to 147.0 pm. This carbenoid-typical elongation of the carbon−heteroatom bond in lithiated benzofurans corresponds to their electrophilic reactivity, to be discussed in Section III.B.1. Carbamate-protected alcohols are easily metalated due to a dipole stabilization to give a class of α-oxygen-substituted lithium carbenoids that are frequently used for synthetic purposes. A crystal structure of a representative compound, the (−)-sparteine-complexed carbamoyloxy-3-trimethylsilylallyllithium **9** (Scheme 6 and Figure 3)[14], also shows a carbenoid-typical C−O bond elongation (147.6 pm). The compound is monomeric, which is easily explained by the fact that the lithium atom is satisfied by coordination to the carbamoyl oxygen atom (dipole stabilization) and complexation to the bidentate sparteine ligand. The carbenoid carbon is pyramidal.

Numerous structures of α-lithiated amines, amides, carbamates as well as α-lithiated thioethers, sulfoxides, sulfones and sulfonamides have been determined. Although a slight

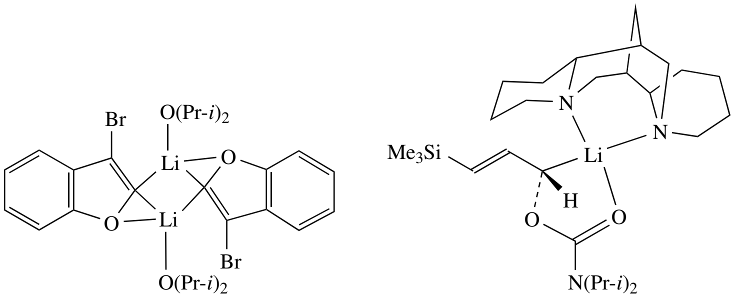

(8) **(9)**

SCHEME 6. Crystal structures of α-oxygen-substituted lithium carbenoids: lithiated benzofuran **8** and carbamate **9**

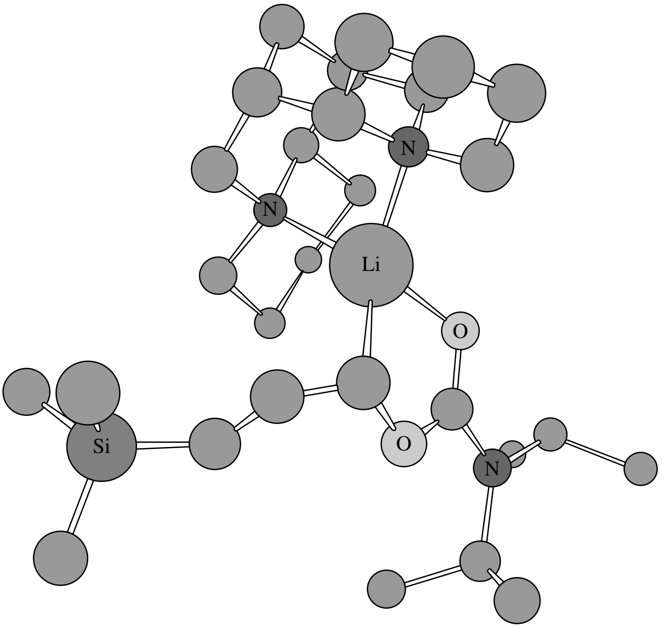

FIGURE 3. Crystal structure of **9**. Reproduced by permission of VCH, Weinheim from Reference 14

carbon–heteroatom bond elongation has been observed in several of these structures, the carbenoid-typical electrophilic reactivity does not occur in that type of compound. They are rather 'carbanions' with broad versatility and synthetic utility.

The question of configurational stability has been investigated first for vinylidene carbenoids and, more recently, for alkylcarbenoids. Vinyl anions are usually considered to be configurationally stable[46–50]; the calculated inversion barrier of the ethenyl anion **10** (R = H) is about 35 kcal mol^{-1} (equation 4)[46]. Concerning lithioalkenes, this configurational stability has been confirmed experimentally for α-hydrogen, α-alkyl and α-aryl substituted derivatives[51–61]. The inversion of vinylidene lithium carbenoids was already investigated by Köbrich and coworkers who found out that Z-**11**, obtained at $-110\,^\circ$C, partially isomerizes to the more stable E-**11** upon warming to $-85\,^\circ$C (equation 5)[37]. As a matter of fact, inversion of the configuration of 1-halo-1-lithioalkenes has to compete with the thermal decomposition of these labile compounds. On the other hand, the kinetically favored isomer of 1-halo-1-lithioalkenes can be obtained at low temperatures and used for carbon−carbon bond formations without any E/Z-isomerization, in particular when the substitution pattern allows an intramolecular coordination on the lithium atom (equation 6) by a suitable donor atom Y in **12** (equation 6).

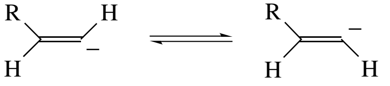

Z-(**10**) E-(**10**)

(4)

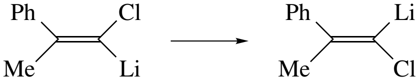

Z-(**11**) E-(**11**)

(5)

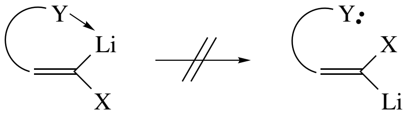

Z-(**12**) E-(**12**)

(6)

Y = OMe, OMEM, OTHP

Metalated vinyl ethers are configurational stable up to $-20\,^\circ$C in tetrahydrofuran. ^{1}H-NMR measurements of 1-ethoxy-1-lithioethene·TMEDA did not show any coalescence of the signals for the vinyl protons until the onset of decomposition. Thus, there is no evidence of inversion in this case[62]. Similar configurational stability is displayed by α-lithiated thioethers in tetrahydrofuran: no inversion occurs up to $0\,^\circ$C. On the contrary, deprotonated vinyl sulfoxides and sulfones are configurationally less stable[63].

Lithium carbenoids at an alkyl carbon atom are thermally and configurationally even much more labile than the corresponding vinylic compounds. Nevertheless, efforts have been made to obtain configurationally stable alkyllithium carbenoids or, in other words, to find out the frontiers of that stability[64–84]. In contrast to the corresponding vinylidene carbenoids, the alkyl derivatives have a remarkable feature insofar as the carbenoid carbon atom becomes a stereogenic center when suitably substituted (equation 7). Thus, an inversion of the carbenoid center emerges as racemization or, if the residue in **13** contains a stereogenic unit, as epimerization. With respect to the application in stereoselective syntheses, configurationally stable organolithium compounds are highly valuable. In this context, the relevant time scale of the configurational stability is defined by their generation and subsequent reactions with electrophiles.

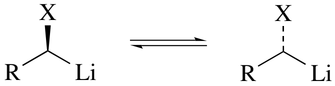

S-(**13**) R-(**13**)

(7)

X = halogen, OR, OCONR$'_2$ etc.

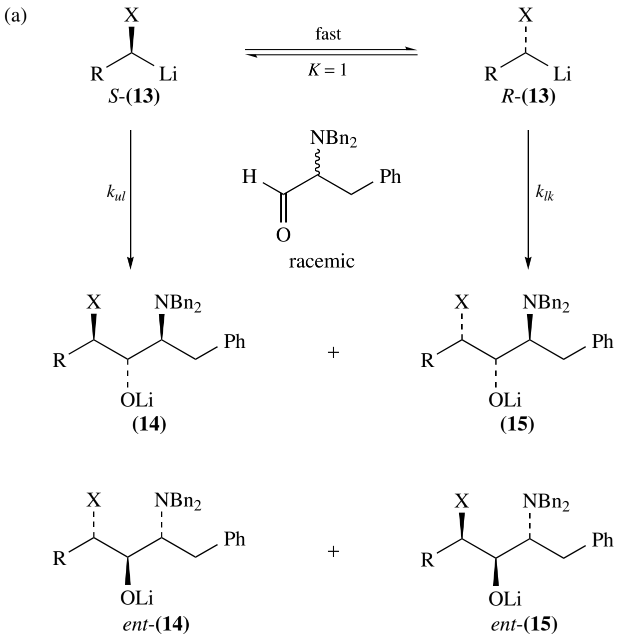

ratio (**14** + *ent*-**14**):(**15** + *ent*-**15**) = k_{ul}:k_{lk}
14 and **15**: racemic compounds

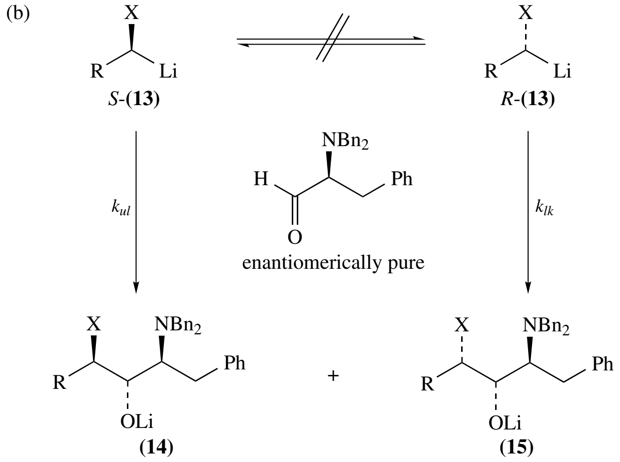

ratio **14**:**15** = 50:50
14 and **15**: enantiomerically pure compounds

SCHEME 7. Test of the configurational stability of alkyl lithium carbenoids: (a) fast equilibrium between enantiomeric lithium carbenoids; (b) configurational stable lithium carbenoid **13**

A test for the configurational stability of chiral organometallic compounds like carbenoids **13** has been developed by Hoffmann's group[67]. It is based on kinetic resolution, can be carried out on a racemic organolithium compound **13** and consists of a set of two reactions (Scheme 7). First, the racemic lithium carbenoid **13** is allowed to react with the racemate of a chiral aldehyde, preferably an O-protected lactaldehyde or an 2-(*N*,*N*-dibenzylamino)alkanal. The ratio of the products **14** and **15** reflects the degree of the kinetic resolution k_{ul}/k_{lk}. In order to obtain relevant information, this value has to be sufficiently different from 1; preferably, it should amount to 1.5 to 3.0. In a second experiment, the racemic lithium carbenoid **13** is allowed to react with the enantiomerically pure aldehyde. If the same diastereomeric ratio of the products **14** and **15** results as in the first experiment, the carbenoid **13** has proven itself to be configurationally labile (relative to the time scale, defined above). This result means that, in a typical Curtin–Hammett case, the enantiomers of the carbenoid **13** are in a fast equilibrium so that the diastereoselectivity in the addition to the aldehyde depends only on the difference $\Delta\Delta G^{\neq}$ in the activation energies of the diastereotopic transition states (*lk* and *ul* addition). If, on the other hand, the diastereomeric ratio in the second experiment approaches or is equal to 50:50, one has to conclude that the organometallic species is configurationally stable on the time scale defined above. Thus, the ratio of the products **14** and **15** corresponds exactly to the ratio of enantiomeric starting materials *S*-**13** and *R*-**13**, which is 50:50 because a racemic mixture of the lithium carbenoid has been chosen to start with.

The application of this test to racemic 1-bromo-1-lithiopentane **13** (R = *n*-Bu, X = Br), generated by bromine-lithium exchange reaction from 1,1-dibromopentane, shows that this carbenoid is configurational stable at −110 °C in the sense that its reaction with 2-(*N*,*N*-dibenzyl)aminopropanal is faster than inversion of the configuration[68]. As a probe, a second stereogenic center can be incorporated into the lithium carbenoid, as in the case of **16** generated by tin–lithium exchange. The subsequent reaction with acetone leads to the epoxide **17** in 99% diastereomeric purity (equation 8).

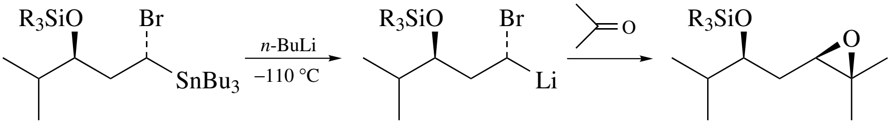

(16) **(17)** (8)

At a glance, this result shows that the carbenoid **16** is configurationally stable at −110 °C. When, however, the same carbenoid **16** has been generated by means of a bromine–lithium exchange, partial epimerization leading to **18** occurs (equation 9)[66].

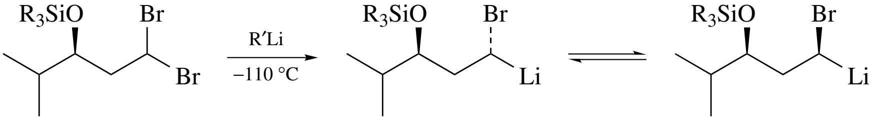

(16) **(18)** (9)

Enantiomerically pure α-lithiated ethers have been prepared from stannanes and turned out to react with electrophiles under retention. The configurational stability of the lithium carbenoid **19** has been deduced from equation 10[74, 85, 86]. Lithiated benzyl methyl ether, chelated by a chiral bis(oxazoline) ligand, proved itself to be configurationally stable as well[87, 88].

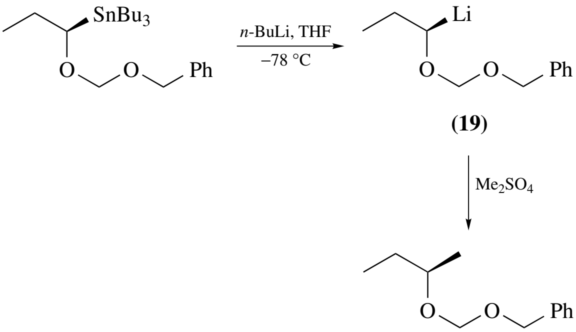

(10)

Configurational stability has also been confirmed for various metalated carbamates by Hoppe and coworkers[33]. Remarkably, carbamate-protected alcohols such as **20** are deprotonated enantioselectively, when treated with *s*-butyllithium in the presence of (−)-sparteine. The lithium carbenoids like **21** (R = alkyl) thus generated turn out to retain their configuration (equation 11)[83]. Similar results have been obtained for α-lithiated amines and carbamate protected amines[89−91]. As a rule, dipole stabilization of the organolithium compounds in general also enhances the configurational stability of α-oxygen-substituted lithium carbenoids.

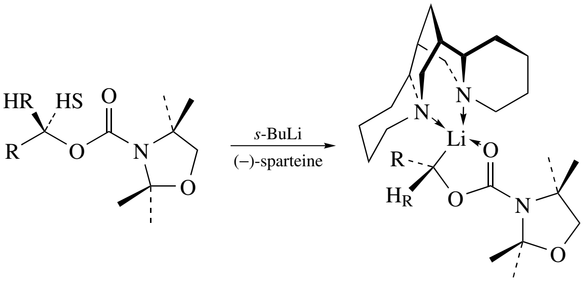

(11)

(20) **(21)**

α-Lithiated sulfides (X = SPh, equation 7) and selenides **13** (X = SePh, equation 7), versatile reagents in organic synthesis, have been found to be configurationally more labile[92]. Novel mechanisms for the racemization processes have been postulated for α-lithiated sulfides and selenides[93, 94]. With regard to the pronounced ‘anionic’ and ‘non-carbenoid’ character of these organolithium compounds, a detailed discussion is not given here. The different aspects of the configurational stability of chiral organolithium reagents have been reviewed recently[34].

III. LITHIUM CARBENOIDS AS REACTIVE INTERMEDIATES IN SYNTHESIS

A. Generation of Lithium Carbenoids

1. Halogen as α-heteroatom

Generally, α-heteroatom-substituted alkyl and vinyl lithium compounds are generated in solution under inert conditions at appropriate low temperatures and allowed to react further without isolation. The acidity of monohalogen-substituted alkanes is usually not high enough to permit the generation of α-lithio-α-halogen alkanes by deprotonation.

Thus, the halogen–lithium exchange reaction, the so-called Wittig–Gilman reaction, is the method of choice to prepare this type of lithium carbenoid (equation 12). For this purpose, geminal dibromoalkanes are treated with alkyllithium reagents[32, 95]. In mixed dihaloalkanes, the heavier halogen is exchanged, as shown in equations 13[96–99] and 14[100]. The halogen–lithium exchange also opens easy access to 1-halo-1-lithiocyclopropanes (equation 15)[101].

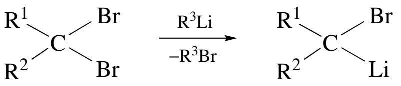

(12)

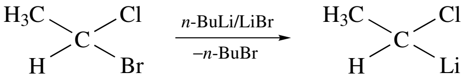

(13)

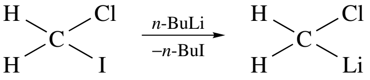

(14)

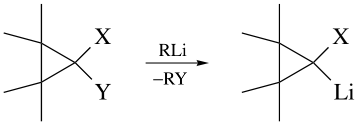

(15)

X = F, Cl, Br, I
Y = Cl, Br, I

In the latter reaction, remarkable examples of diastereoselectivity have been reported. Thus, the treatment of 7,7-dibromonorcarane **22** with *n*-butyllithium leads to *exo*-7-bromo-*endo*-7-lithiobicyclo[4.1.0]heptane **23** exclusively, as shown by carboxylation (Scheme 8). It turns out that a slight excess of dibromonorcarane **22** relative to butyllithium is prerequisite to that high degree of stereoselectivity. The result is explained as follows: the *exo*-bromine atom in **22** is exchanged first in a kinetically controlled reaction so that the *endo*-bromo-*exo*-lithio-isomer **24** is formed. In a second step, an equilibration occurs by means of another bromine–lithium exchange, which takes place between **24** and the dibromonorcarane **22** (still present because used in excess). Thus, the thermodynamically

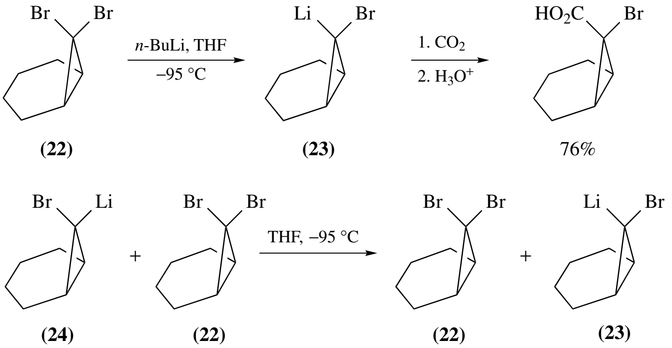

SCHEME 8. Diastereoselective bromine–lithium exchange reaction in dibromonorcarane **22**

favored lithium carbenoid **23** results, even at −95 °C (Scheme 8)[102]. Steric repulsion of the *endo*-bromine atom in **24** is assumed to be the driving force, since it can be avoided in **23**.

Chelation is another driving force that provides diastereoselective bromine–lithium exchange reactions to give cyclopropyl carbenoids. Thus, the *exo*-bromine atom in dibromocyclopropane **25** is exchanged exclusively due to the methoxy substituent, which encourages the lithium to occupy the *cis* orientation (equation 16)[103, 104]. Several representative examples of cyclopropyl bromo lithium carbenoids obtained by bromine–lithium exchange reactions are given in Table 1.

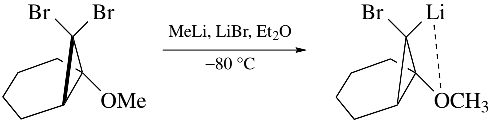

(25)

(16)

TABLE 1. Representative examples of α-halo-α-lithiocyclopropanes generated by bromine–lithium exchange; see also Reference 19

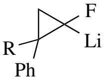 R = H, Me Reference 105	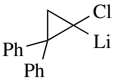 Reference 106	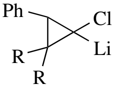 R = Ph, cyclopropyl Reference 106
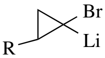 R = C_5H_{11}, $CH{=}CH_2$, Ph, CH_2OCH_2Ph, OEt, SPh Reference 40,102,106,107–109	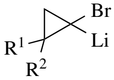 $R^1 = R^2 =$ Me, C_6H_{13} $R^1 =$ Me, $R^2 = CO_2Bu$-*t* $R^1R^2 = (CH_2)_5$ Reference 102,110–113	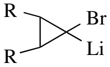 R = Me, C_6H_{13}, Ph Reference 102,112,119
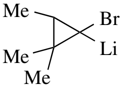 Reference 110	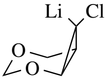 Reference 104	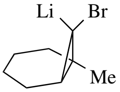 Reference 114
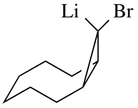 Reference 115	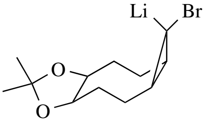 Reference 116	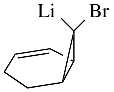 Reference 117
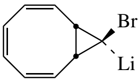 Reference 115	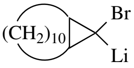 Reference 114	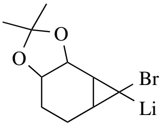 Reference 118

An alternative access to alkyl bromo lithio carbenoids is provided by the tin–lithium exchange reaction, as shown in equation 8[66, 74]. When the carbenoid carbon atom is substituted by electron-withdrawing groups like carboxylic ester or keto groups, the carbenoid character is no longer maintained. On the contrary, these species are rather halogen-substituted enolates **26** than carbenoids. They are usually obtained by deprotonation, the typical protocol for the generation of enolates (equation 17)[120–142]. Analogously, this holds for azaenolates like **27**–**29**[143–146].

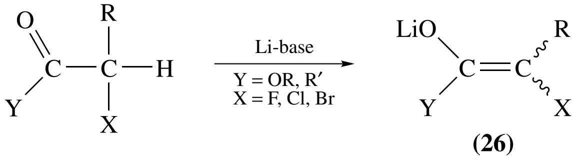

(26)

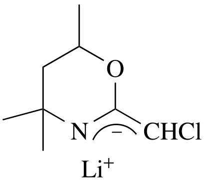

(27)

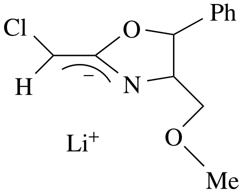

(28)

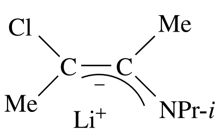

(29)

(17)

Due to the acidifying effect of a second halogen atom, dihalo-substituted lithium carbenoids **30** can be obtained by deprotonation of geminal dihaloalkanes, the most frequently applied method for the generation of lithium carbenoids with this substitution pattern[147, 148]. Representative examples of α-dihalo-substituted lithioalkanes are given in Table 2. Alternatively, the halogen–lithium exchange of trihaloalkanes also leads to the carbenoids **30** (equation 18)[19, 149].

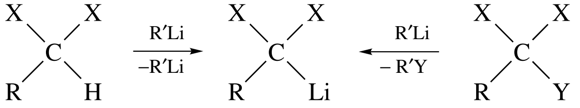

X = Cl, Br, I **(30)** X = F, Cl, Br, I; Y = Br, I (18)

Various mixed α-halo-lithioalkanes **31** with an additional OR, SR, SOR, SO_2R, $P(O)(OR)_2$ substituent in the α-position are available by deprotonation and, in some cases, by halogen–lithium exchange (equation 19)[32]. Both methods are also suitable for the generation of halo lithio methanes **32** (equation 20)[19, 32, 165].

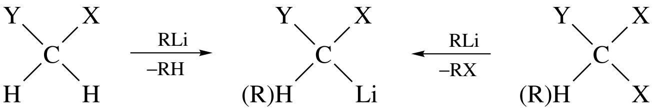

(19)

X = F, Cl, Br; **(31)** X = Cl; Y = $P(O)(OR')_2$

Y = OR′, SR′, SOR′, SO_2R', $P(O)(OR')_2$

TABLE 2. Representative examples of 1, 1-dihalo-1-lithioalkanes generated by deprotonation (method A) or halogen–lithium exchange (method B) or metal–lithium exchange (method C)

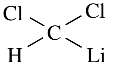 method A[150,151] method B[19]	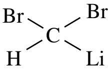 method A[152] method B[19]	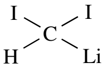 method A[153]	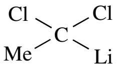 method A[154]
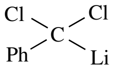 method A[155]	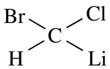 method A[156]	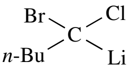 method A[156]	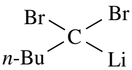 method A[152]
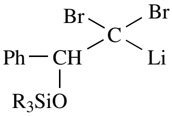 method A[157]	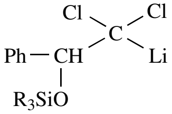 method A[154]	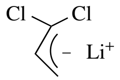 method B[158] method C[158]	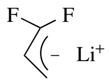 method A[159] method C[160]
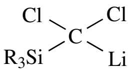 method A[152,161,162]	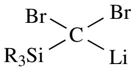 method A[152] method B[163]	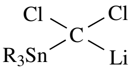 method C[164]	

In 1-halo-1-alkenes, the acidity of the vinylic hydrogen atom is enhanced compared to the correspondingly substituted alkanes due to the higher s proportion of the C—H bond in alkenes[166]. As a consequence, 1-halo-1-alkenes **33** react with *n*-, *s*- or *t*-butyllithium in tetrahydrofuran or diethyl ether at −100 °C to give fluoro-, chloro- and bromo-substituted 1-lithioalkenes **34** (equation 21). In vinyl fluorides and vinyl chlorides, the deprotonation is much faster than the halogen-lithium exchange, which can, however, occur in bromoalkenes. Vinyllithium compounds **36**, available from vinyl fluorides **35** by lithium-2,2,6,6-tetramethylpiperidine-induced deprotonation, have been found to be configurationally stable up to −78 °C (equation 22)[167–173]. In order to generate the labile butadienyl carbenoid **37**, the metalation (hydrogen–lithium exchange) has been performed in the 'Trapp mixture', the solvent mixture of tetrahydrofuran, diethyl ether and pentane that has a low freezing point (equation 23)[174, 175].

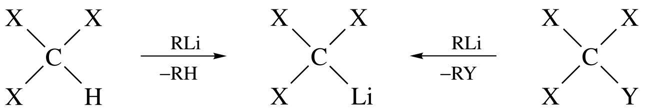

X = F, Cl, Br, I **(32)** X = F, Cl, Br, I; Y = Br, I

(20)

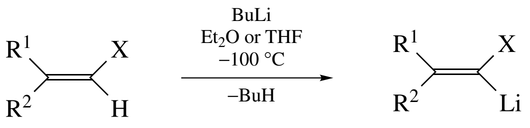

(33) X = F, Cl, Br **(34)**

(21)

The most important method, however, for generating α-halo-substituted vinylidene carbenoids is the halogen–lithium exchange in dihaloalkenes (equation 24). The reaction is usually performed using *n*-, *s*-, or *t*-butyllithium, whereas metallic lithium is applied only occasionally. Numerous examples[176–188], some of which are shown in Table 3, demonstrate the efficiency of the method.

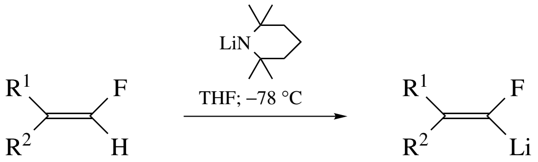

Z-(**35**) $R^1 = CF_3$; $R^2 = Ph$

E-(**35**) $R^1 = Ph$; $R^2 = CF_3$

(36)

(22)

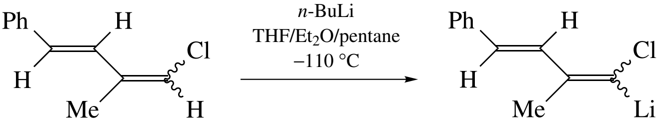

(37)

(23)

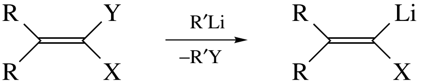

(24)

The rate of the halogen–lithium exchange increases when going from chlorine to iodine, as outlined above for the alkyl halogen–lithium carbenoids. As a consequence, only the bromine atom is replaced in 1-chloro-1-bromo- and 1-bromo-1-fluoroalkenes when they are treated with butyllithium[38, 176, 177, 189]. Remarkably, the bromine–lithium exchange is so fast that it can compete with the addition of butyllithium to a keto group: in the reaction of the dibromoalkene **38** with *n*-butyllithium, bromine–lithium exchange occurs, and the lithium carbenoid **39** thus generated undergoes either a nucleophilic addition to the keto group or an elimination yielding the alkyne (equation 25)[190].

When 1,1-dichloro- and 1,1-dibromoalkenes with different β-substituents ($R^1 \neq R^2$) are submitted to a halogen–lithium exchange, the problem of stereoselectivity arises. The substituents R^1 and R^2 may differ in their steric demand and in their ability to chelate the lithium atom. For the former case, there is a tendency in the sense that the bulky group seems to favor lithiation in the Z position[184, 186, 191], as illustrated by equation 26[186].

The influence that a possible chelation has on the stereochemistry of the bromine–lithium exchange in dibromoalkenes was first studied in the chiral MEM (methoxyethoxymethyl) ether **40**. When this compound is treated with 1.2 equivalents of *n*-butyllithium in tetrahydrofuran, the acids *E*- and *Z*-**42** are obtained in a ratio of 32:68 after carboxylation. Obviously, a kinetically favored substitution of the more easily accessible *trans* bromine atom occurs. When, however, slightly less than one equivalent (0.95–0.98 equiv) of *n*-butyllithium is slowly added to a solution of **40** in diethyl ether at −105 °C, the *E*-configurated carbenoid **41** forms almost exclusively, and the carboxylic acids *E*- and *Z*-**42** are obtained after reaction with dry ice in a ratio of over 99:1 (Scheme 9)[192, 193].

TABLE 3. 1-Halo-1-lithio-1-alkenes generated by halogen–lithium exchange

1, 1-Dihalogen-1-alkene	Lithiation reagent	1-Halo-1-lithio-1-alkene	Reference
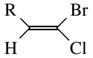 $R = C_4H_9$, CMe_3, C_6H_{13}, cyclohexyl, 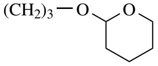	*t*-BuLi	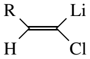	176
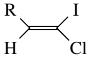 $R = C_4H_9$, CMe_3, C_6H_{13}, cyclohexyl	*t*-BuLi	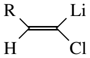	176
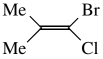	*n*-BuLi	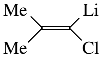	177
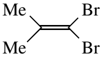	*n*-BuLi	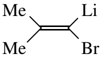	178
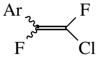 Ar = Ph 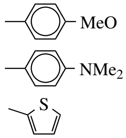	*n*-BuLi or *i*-BuLi or *t*-BuLi	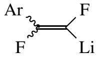	179, 180
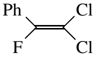	*n*-BuLi	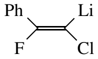	181
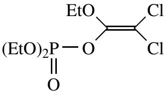	*n*-BuLi	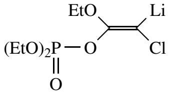	182
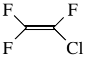	*n*-BuLi	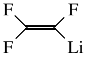	183
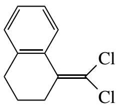	*n*-BuLi	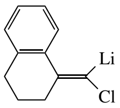	184, 185
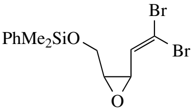	MeLi	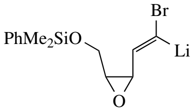	186
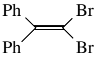	*n*-BuLi	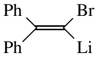	187
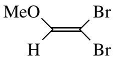	*n*-BuLi	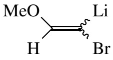 $E:Z = 3:2$	188

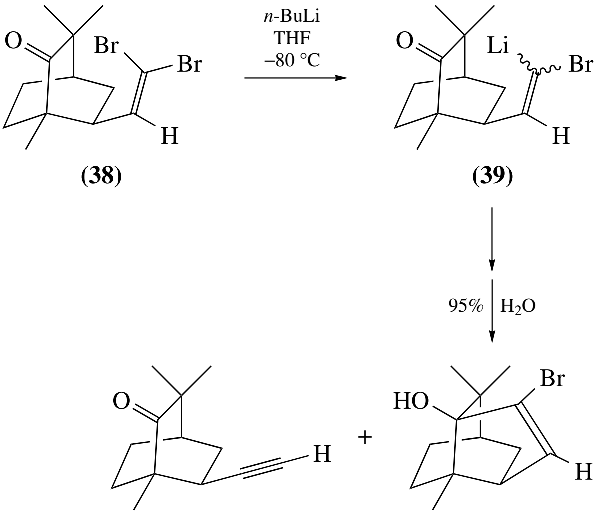

(38) **(39)**

(25)

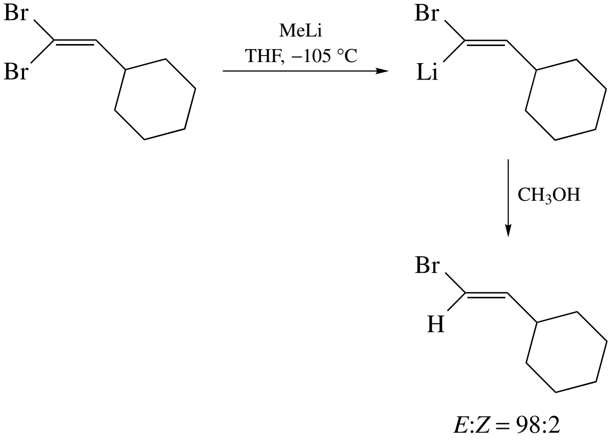

(26)

The highly stereoselective bromine–lithium exchange in the ether **40** can be explained in a similar way to that in which it has been rationalized for dibromonorcarane (see Scheme 8)[102]. Thus, an equilibrium is postulated which involves the diastereomeric carbenoids E- and Z-**41** as well as the dibromoalkene **40**. Thus, Z-**41** formed in the kinetically controlled reaction can undergo another bromine–lithium exchange with **40** so that finally E-**41** results exclusively in a thermodynamically controlled reaction. The higher stability of E-**41** compared to Z-**41** may have two reasons: the lower space requirement of the lithium versus the bromine atom and, particularly, the intramolecular complexation of the lithium atom by the MEM group. A similar thermodynamic reaction control has been observed in the methyl ether **43**, which yields the E-isomer of **44** predominantly, although with a lower degree of selectivity (equation 27)[185].

Recently, two more stereoselective cases of bromine–lithium exchange reactions have been observed. Both the glyceraldehyde-derived bromoalkene **45** and lactaldehyde-derived **47** yield the E-configurated lithium carbenoids **46** and **48**, respectively, when treated with *n*-butyllithium in diethyl ether. The *E*:*Z* ratio amounts to 95:5 in both cases. It remains to find out if this selectivity is caused by the steric effect or chelation (equation 28)[194, 195].

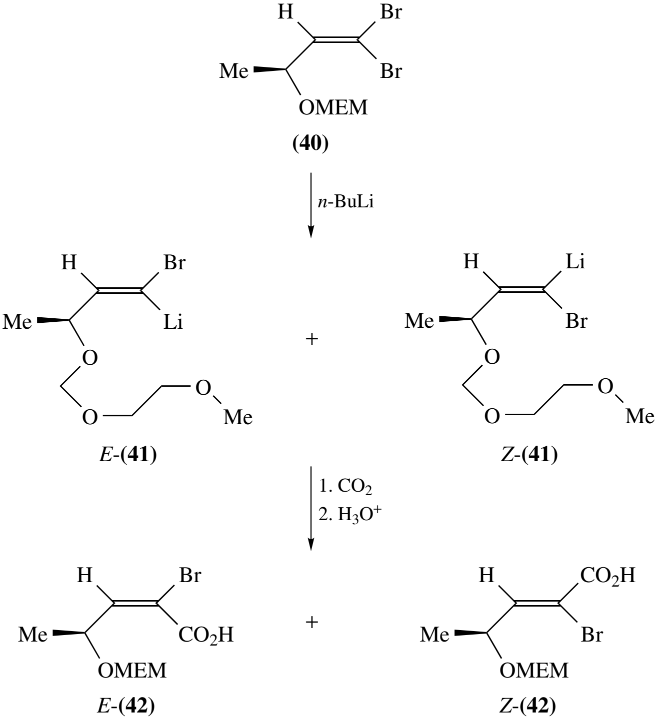

	E-**42**:*Z*-**42**
1.2 *n*-BuLi, THF	32:68
0.95 *n*-BuLi, Et_2O	>99:1

SCHEME 9

The tin–lithium exchange reaction does not play an important role for the generation of 1-halo-1-lithioalkenes. Whereas in α-bromoalkylstannanes tin–lithium exchange occurs upon treatment with *n*-butyllithium[66], the bromine rather than the tin is replaced against lithium, when α-bromovinylstannanes are allowed to react with *n*-butyllithium[196].

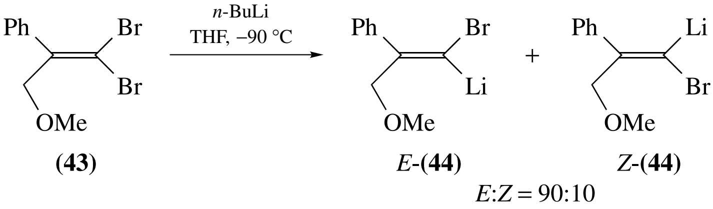

(27)

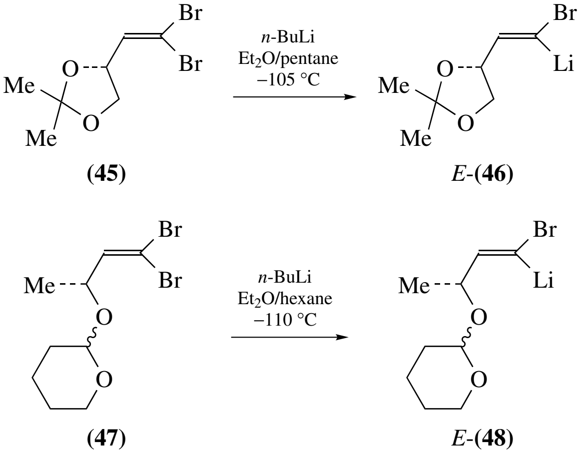

(28)

2. Oxygen as α-heteroatom

α-Lithiated ethers have been generated *in situ* since the first half of the last century in the context of the Wittig rearrangement[197–200]. Compared to an alkyllithium compound HCR_2Li, there is only a slight stabilization in the corresponding lithiated ether $R'OCR_2Li$ by 5–6 kcal mol^{-1}, according to low-temperature ^{1}H-NMR exchange experiments. Thus, Scheme 10 shows order of stability of alkyl- and alkoxyalkyllithium compounds (decreasing stability) that has been postulated[201].

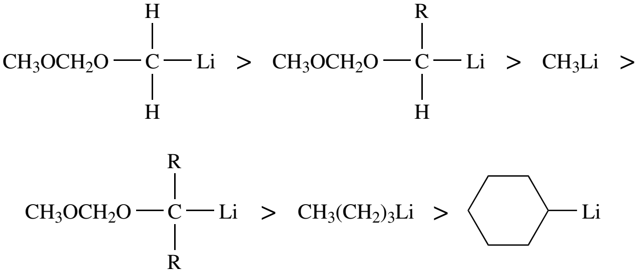

SCHEME 10. Decreasing stability of alkyl- and alkoxyalkyllithium compounds

In general, however, particularly strong bases are required in order to bring about the deprotonation of alkyl ethers. Thus, the metalation of *t*-butyl methyl ether[202] has been reported to be feasible by means of the Lochmann–Schlosser base[203, 204] (equation 29); α-lithiated tetrahydrofuran, however, undergoes a fragmentation to give ethene and lithium ethenoate[205].

$$\mathrm{Me_3C{-}O{-}CH_3} \xrightarrow[-78\ ^\circ\mathrm{C}]{s\text{-BuLi/KOCMe}_3} \mathrm{Me_3C{-}O{-}CH_2M} \qquad (29)$$

As a consequence, the quantitative generation of α-oxygen-substituted alkyllithium compounds by metalation of ethers will be efficient only if the carbon acids are carrying electron-withdrawing substituents in either the α-position (equation 30) or if they contain anion-stabilizing groups in the α'-position (equation 31). Among the former, relatively acidic substrates, there are not only benzyl and allyl ethers but also α-oxygen-substituted nitriles, lactones, lactams, amides, carboxylic esters and carboxylates[206–224]. As the corresponding lithium compounds are typical enolate 'anions', they do not display any carbenoid character and are therefore not discussed here in detail. Among the α-oxygen-substituted alkyllithium compounds with an electron-withdrawing group in the α'-position the lithiated, dipole-stabilized esters **49**[225–228] and carbamates **50**[33, 83, 84, 229, 230] are accessible by deprotonation (equations 32 and 33).

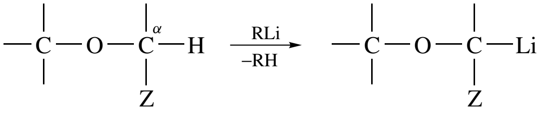

(30)

Z = aryl, vinyl, CN, CO_2R, $CONR_2$, CO_2Li

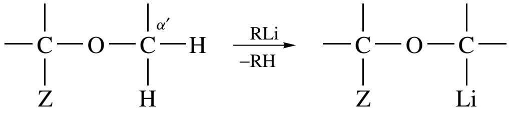

(31)

Z = aryl, vinyl, CN, CO_2R, $CONR_2$, CO_2Li

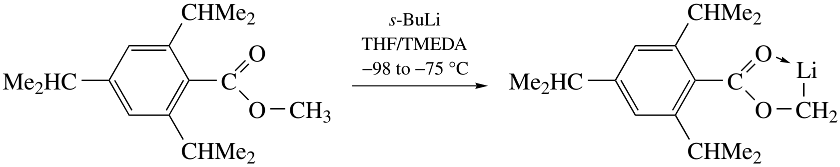

(49) (32)

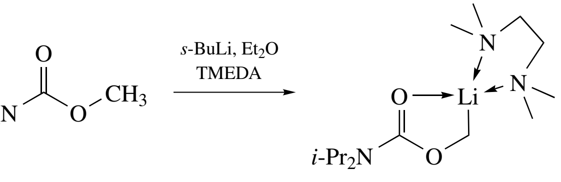

(50) (33)

Whereas the halogen–lithium exchange is of limited importance for the generation of α-lithiated ethers, the reductive lithiation of O/S-acetals has been applied more frequently, the versatility being enhanced by remarkable diastereoselective variants. Thus, a single diastereomer of the lithium carbenoid **52** results from the diastereomeric mixture **51** (equation 34)[70, 71]. Representative examples of α-lithiated ethers generated by this method and their reactions with electrophiles are given in Table 4.

The tin–lithium exchange is of particular interest for the generation of configurationally stable, non-racemic α-lithiated alkyl ethers[74] **19** (equation 10). The metal–metal exchange has been found to occur under retention of the configuration. Examples of this method

TABLE 4. Representative examples of α-lithiated alkyl ethers, generated by reductive lithiation of α-phenylthio and α-phenylsulfonyl ethers, and reactions with electrophiles

α-Lithiated alkyl ether	Electrophile and/or work-up conditions	Product(s) Yield	Reference
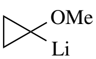 a) c)	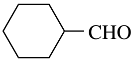	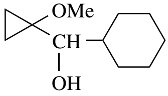 90%	231
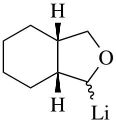 a) c)	PhCHO	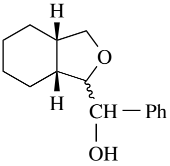 56%	70
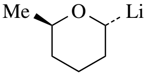 a) c)	PhCHO	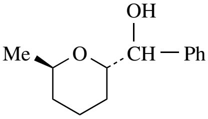 56%	70
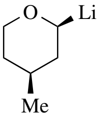 a) d)	MeCOMe	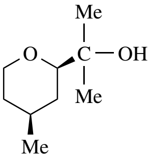 55%	72, 73
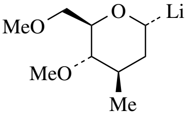 a) d)	MeCOMe	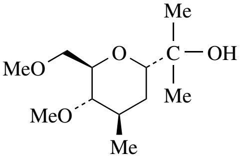 81%	72, 73
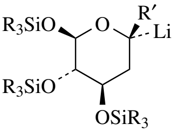 b) e)	MeOH	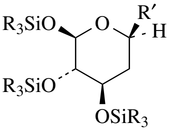 43–80%	76–78
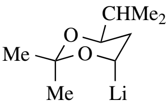 a) d), −78 °C	MeCOMe	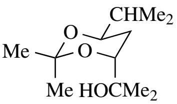 54%	72, 73

(*continued overleaf*)

TABLE 4. (*continued*)

α-Lithiated alkyl ether	Electrophile and/or work-up conditions	Product(s) Yield	Reference
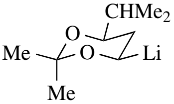 a) d), −20 °C	MeCOMe	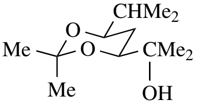 78%	72, 73
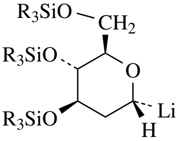 b) e)	PhCHO	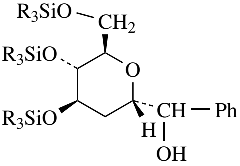 66%	76–78

a) Precursor: α-phenylthioether; b) precursor: α-phenylsulfonyl ether. Metalating agents: c) lithium-(1-dimethylaminonaphthalenide); d) lithium-4,4′-di-*t*-butyl-biphenylide; e) lithium-naphthalenide.

are given in Table 5. α-Lithiated silyl ethers have been found to undergo a reverse Brook rearrangement[233], whereas α-allyloxy-α-lithio alkanes are suitable starting materials of a [2,3]-Wittig rearrangement[234, 235].

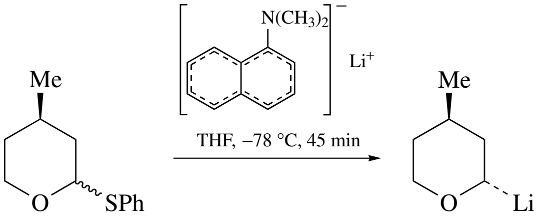

(51) **(52)** (34)

The tin–lithium exchange is also suitable for the generation of α-lithiated oxiranes **53**[245–247]. Due to the enhanced acidity of a carbon atom incorporated into a three-membered ring, the metalation of epoxides by treatment with various alkyllithium reagents of lithium amide bases also permits one to obtain carbenoids **53** *in situ* (equation 35)[248–250].

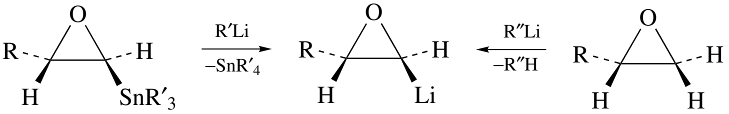

(53) (35)

Enhanced acidity also characterizes the sp^2-carbon bonded hydrogen compared to the sp^3 one[251]. As a consequence, alkyl vinyl ethers are more acidic than dialkyl ether and thus can be deprotonated more easily. 1-Ethoxy-1-lithioethene **54**[252–254] was first generated by Schöllkopf and Hänssle[252]. The hydrogen–lithium exchange in ethyl vinyl ether

TABLE 5. Representative examples of α-lithiated ethers, generated by tin–lithium exchange, and reactions with electrophiles

α-Lithiated alkyl ether	Electrophile and/or work-up conditions	Product(s) Yield	Reference
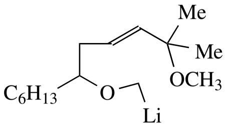	0 °C	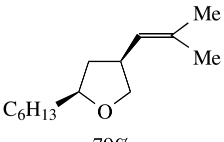 79% + 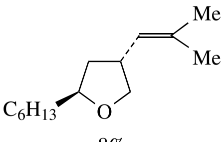 8%	236
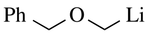	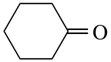	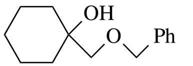 98%	232
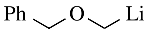	1. CuBr/Me_2S 2. 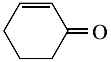	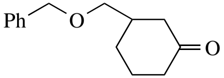 95%	237
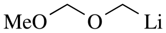	Ph-$CH_2COC_2H_5$	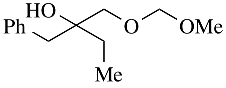 96%	238
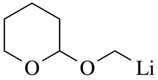	1. CuBr/Me_2S 2. 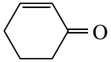	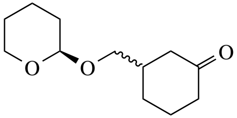 67%	237

(*continued overleaf*)

TABLE 5. (*continued*)

α-Lithiated alkyl ether	Electrophile and/or work-up conditions	Product(s) Yield	Reference
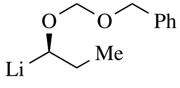 90% *ee*	$(MeO)_2SO_2$	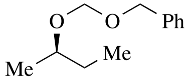 90% *ee*	85
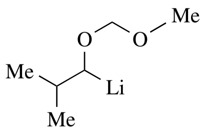	1. CuCN 2. 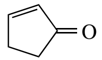 3. Me_3SiCl 4. Et_3N 5. $TiCl_4$, CH_2Cl_2	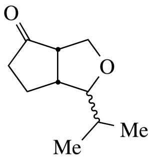 82%	239–241
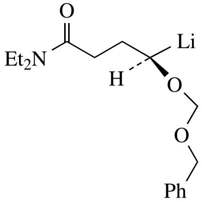	—	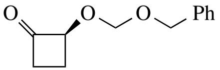 70%	242
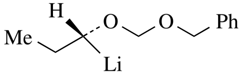	1. CO_2 2. H_3O^+	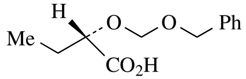 99%, 95–98% *ee*	81

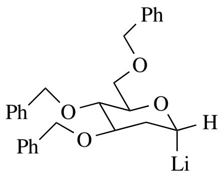	1. CuBr/Me$_2$S 2. 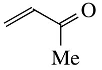	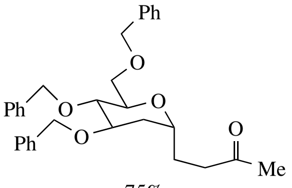 75%	237
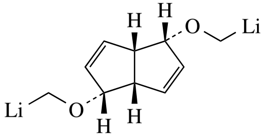	H$^+$	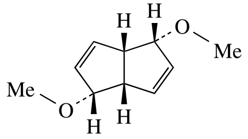	243
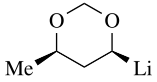	1. CuI, TMEDA 2. 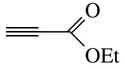	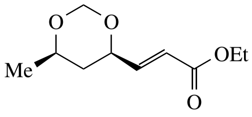 92%	244
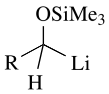	1. a) 2. H$^+$	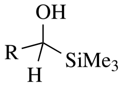 45–68%	233
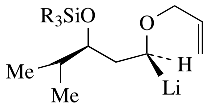	1. b) 2. H$^+$	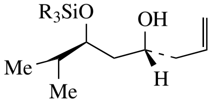 67%	234

---

a) Retro-Brook rearrangement; b) [2,3]-Wittig rearrangement.

was achieved by treatment with *t*-butyllithium in pentane in the presence of the cosolvent TMEDA (equation 36). *t*-Butyllithium in tetrahydrofuran[255] or tetrahydropyran[256] as well as a mixture of potassium *t*-butoxide and butyllithium[257] also bring about the deprotonation of alkyl vinyl ethers. A series of lithiated vinyl ethers have been generated according to this or similar procedures[258–279]. Typical examples of lithiated alkyl vinyl ethers and esters generated by deprotonation and their reactions with electrophiles are given in Table 6. Concerning thermal stability, lithiated alkyl vinyl ethers are less sensitive than 1-halo-1-lithioalkenes. The β-difluoro-substituted vinyllithium compounds **55a**[280–285], **55b**[286–289] and **55c**[287–291] can be generated directly from the corresponding derivative of trifluoroethanol by treatment with two equivalents of lithium diisopropylamide (equation 37).

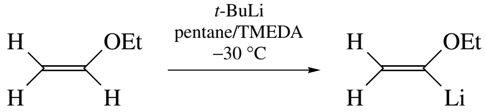

(54)

(36)

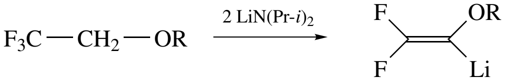

(55a) R = SO_2Tol-*p*
(55b) R = $CONEt_2$
(55c) R = $CH_2OCH_2CH_2OCH_3$

(37)

In view of the fact that alkyl vinyl ethers are that easily metalated, the generation of lithiated vinyl ethers by halogen–lithium[303, 304] or tin–lithium[305–307] exchange is seldom applied. Nevertheless, 1-lithio-1-methoxyethene **56** can be generated in this way (equations 38 and 39).

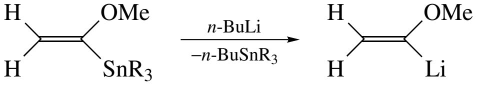

(56)

(38)

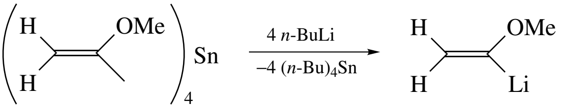

(56)

(39)

Whereas carbenoid character is definitely present in metalated alkyl vinyl ethers, lithiated alkyl and aryl vinyl sulfides and thioesters, which are easily available by hydrogen–lithium exchange, do not display carbenoid-typical reactions[16]. They rather behave like nucleophilic reagents, so that their discussion is beyond the scope of this overview despite their utility in synthesis[31, 32]. The same applies to various derivatives of enamines, deprotonated in the vinylic α-nitrogen position[31, 308, 309].

TABLE 6. Representative examples of α-lithiated vinyl ethers, generated by deprotonation, and reactions with electrophiles

α-Lithiated vinyl ether	Electrophile and/or work-up conditions	Product Yield	Reference
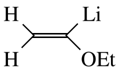	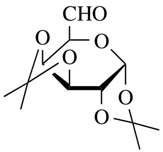	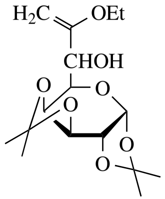 67% (1:1 diasteromeric mixture)	253
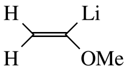	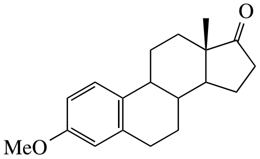	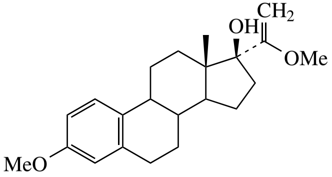 83%	292
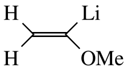	1. 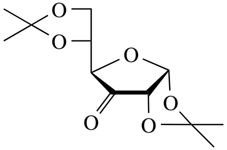 2. HCl, H_2O, dioxane	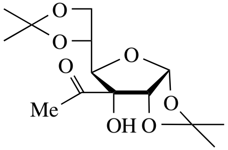 37%	293

(*continued overleaf*)

TABLE 6. (*continued*)

α-Lithiated vinyl ether	Electrophile and/or work-up conditions	Product Yield	Reference
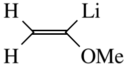	1. 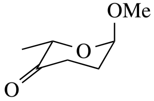 2. HCl, H_2O, dioxane	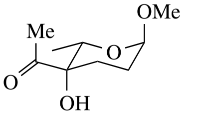 46%	294
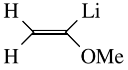	1. 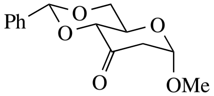 2. HCl, H_2O, dioxane	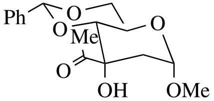 79%	294
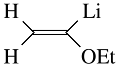	1. Bu_3SnCl 2. H_3O^+ 3. *R*-BINAL-H 4. $PhCH_2OCH_2Cl$, *i*-Pr_2NEt	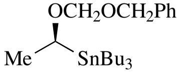 90% *ee*	295
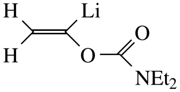	1. $ZnBr_2$ 2. $[PdC_{12}(dppf)]^a$ (cat.) 3. 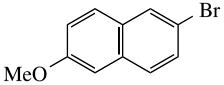	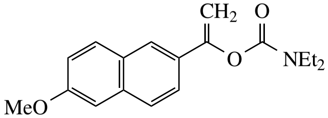 88%	279

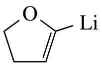	Me_2SiHCl	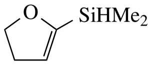 50%	259
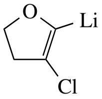	1. CuI 2. 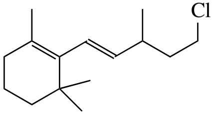 3. 2 MeLi	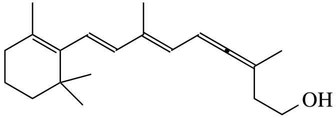 55%	296
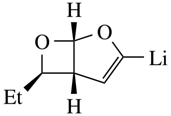	Me_3C-CHO	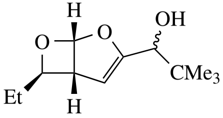 72% (1:1 diastereomeric mixture)	297
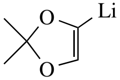	$ClCO_2Me$	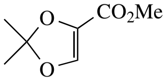 72%	298

(*continued overleaf*)

TABLE 6. (*continued*)

α-Lithiated vinyl ether	Electrophile and/or work-up conditions	Product Yield	Reference
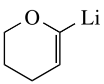	1. Me_3Al 2. 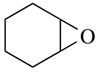 3. $BF_3 \cdot OEt_2$	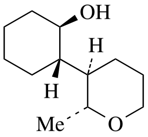 78%	267
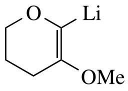	1. $I(CH_2)_3OCH_2Ph$ 2. Me_3SiCl, NaI, MeCN 3. H_2, Pd/C 4. MeOH, H^+	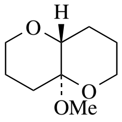 41%	299
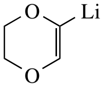	1. CuCN, LiCl 2. 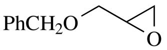 $BF_3 \cdot OEt_2$ 3. 3-chloroperbenzoic acid 4. TsOH, MeOH 5. Ag_2CO_3, celite	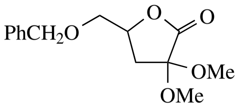 60%	274
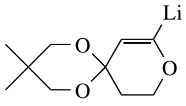	1. 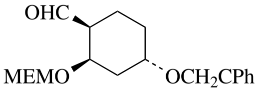 2. H_3O^+ 3. Swern oxidation	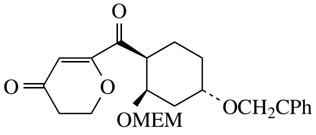 71%	300

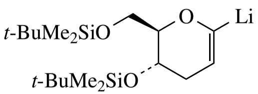	CH_3I	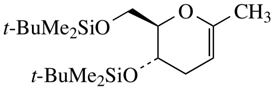 86%	301
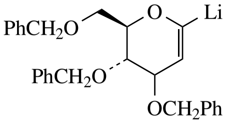	PhCHO	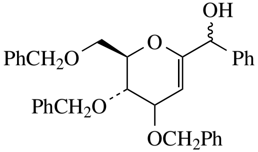 89% (1:1 diastereomeric mixture)[b]	301
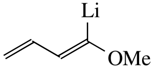	Me_2SiHCl	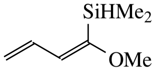 77%	302
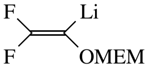	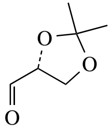	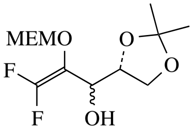 26% (6:4 diasteromeric mixture)	291

---

[a] dppf = bis(diphenylphosphanyl)ferrocene.
[b] Synthesized by tin−lithium exchange.

B. Reactions of Lithium Carbenoids

1. Reactions typical of carbenoids

Only the α-halo- and the α-oxygen-substituted alkyl- and alkenyllithium compounds undergo reactions which are typical of carbenoids. The cyclopropanation reaction of α-halo-substituted alkyl lithium carbenoids, reviewed recently[310], has been demonstrated to proceed directly from the organometallic compound and does not involve the free carbene[1, 311, 312]. Concerning carbenoid-typical reactions of 1-halo-1-lithiocyclopropanes, the rearrangement to the corresponding allene is the most important one for synthetic purposes, a topic that has been reviewed recently in this series[44]. The electrophilic character of 1-halo-1-lithiocyclopropanes is shown by the reaction of 1,1-dibromocyclopropanes **57** with an excess of *n*-butyllithium: The carbenoid **58** formed initially reacts as an electrophilic species, whereby the bromine atom of the carbenoid is replaced by the nucleophilic butyl residue to give the cyclopropyllithium compound **59** (equation 40)[39, 40].

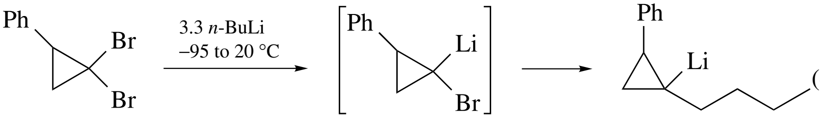

(40)

(57) **(58)** **(59)**

The stereochemical outcome of that nucleophilic substitution has been studied by using non-racemic chlorocyclopropane *R*-**60** (87.5% ee)[38]. When treated with 2 equivalents of *n*-butyllithium, among other components, two major products result after workup: diphenylbutylcyclopropane *S*-**64** is obtained in 20% yield and with 51% inversion of configuration, and the alkyne *S*-**67** is formed in 50% yield and with 90% inversion of configuration. Both products result from a carbenoid **61** which is generated under retention by deprotonation of *R*-**60**. The formation of the non-racemic products *S*-**64** and *S*-**67** is rationalized based on a 'metal-assisted ionization', as outlined in Scheme 11. As a result of a part dissociation of the chloride anion supported by the lithium atom, the carbenoid *R*-**61** acquires a cyclopropyl cation character *R*-**62**, still retaining its configuration due to the permanent coordination of lithium to chloride. Thus nucleophilic addition of butyllithium occurring under inversion leads the cyclopropyllithium compound *S*-**63** which gives *S*-**64** upon protonation. A cyclopropylcarbenoid **62**, on the other hand, can readily undergo a ring opening to give the diphenylallene **65** under simultaneous formation of lithium chloride. Diphenylallene, a smaller part of which is indeed found among the mixture of products (5%), reacts readily with *n*-butyllithium by deprotonation to give the corresponding allenyl lithium, in metallotropic equilibrium with its propargylic isomer **66**. Now, another nucleophilic reagent is available in the reaction mixture and adds to the electrophilic carbenoid *R*-**62**, again under inversion of configuration, to yield the final product **67** upon protonation.

A similar type of substitution, which clearly shows the electrophilic character, occurs in vinylidene carbenoids. In an early example of this reaction, Köbrich and Ansari[37] observed that the alkene **70** results when the *E*-configurated vinyl lithium compound **68** is treated with an excess of butyllithium and the lithioalkene **69** formed thereby is protonated (equation 41). Obviously, the nucleophilic attack of the butyl residue on the carbenoid takes place with inversion of the configuration.

The axially chiral vinyl chloride **71** (as well as the corresponding bromide) served to study in detail the stereochemical outcome of the nucleophilic substitution in vinylidene

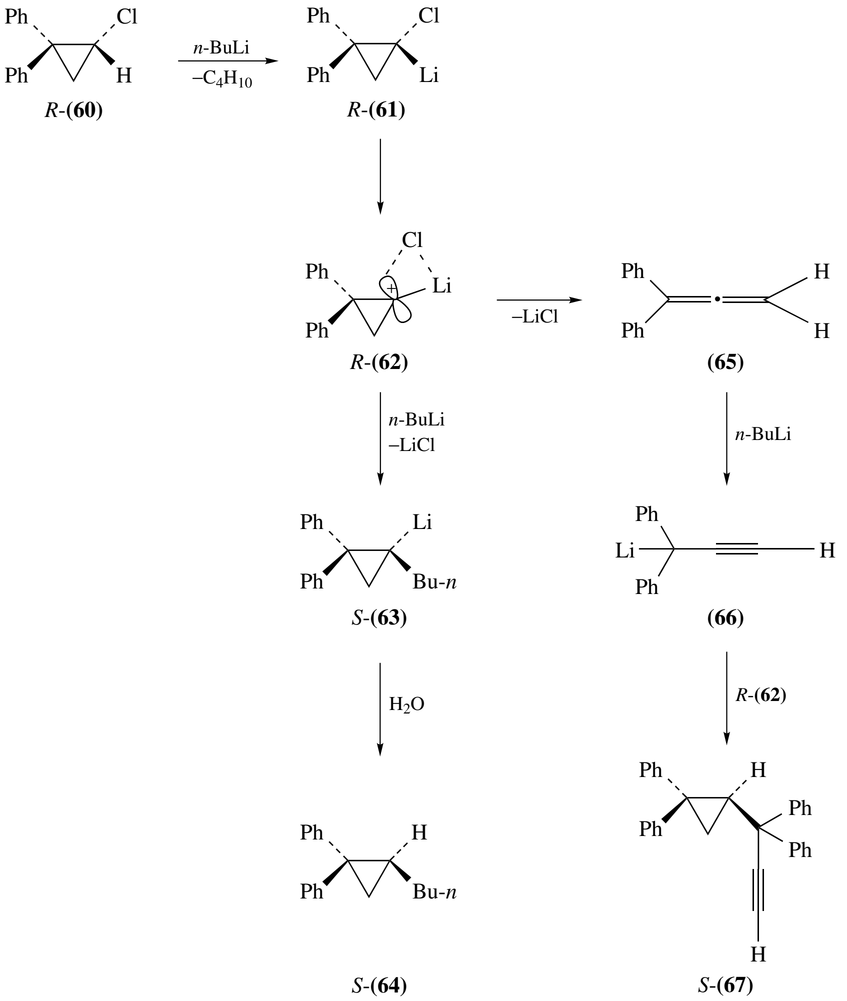

SCHEME 11. Electrophilic character of cyclopropyl carbenoids: Reaction of 2,2-diphenylcyclopropane with *n*-butyllithium (2 equivalents)

carbenoids[38]. When treated with *t*-butyllithium, metalation of **71** occurs under retention. The resulting carbenoid **72** reacts further with *t*-butyllithium to give the substitution product **73** that is trapped by deuteriolysis to give the alkene **74**.

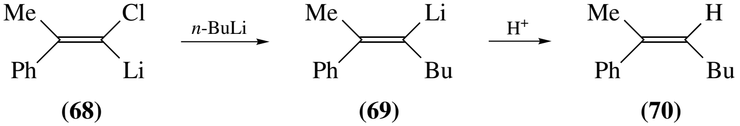

(41)

The sequence started from enantiomerically pure vinyl chloride *S*-**71** and yielded the *R*-configurated alkene **74**, however in an enantiomeric excess of only 39% (equation 42).

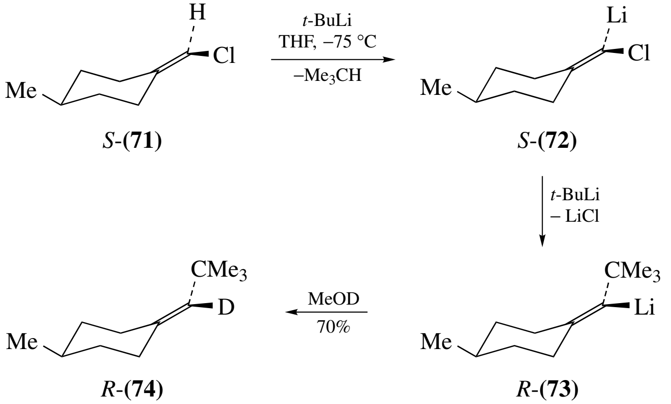

(42)

The mechanism outlined in Scheme 12 can explain the nucleophilic substitution at the vinylidene carbenoid **72**[38, 313]. At a temperature that is typical for a particular carbenoid, a loosening of the carbon−halogen bond takes place. This process is supported by the lithium atom ('metal-assisted ionization'), which remains bonded to the carbon atom. In the course of this step, rehybridization occurs and the positive charge is localized in the p-orbital of the intimate ion pair **75**. The lithium atom is assumed to be collinear with the double bond. Nevertheless, the chiral information of the carbenoid **72** is preserved in the intimate ion pair **75** due to the chlorine atom, which occupies one of the enantiotopic faces. The nucleophile (*t*-butyllithium in the present case) attacks the face of the intermediate **75** that is away from the chloride, so that an inversion of the configuration results in *R*-**73**

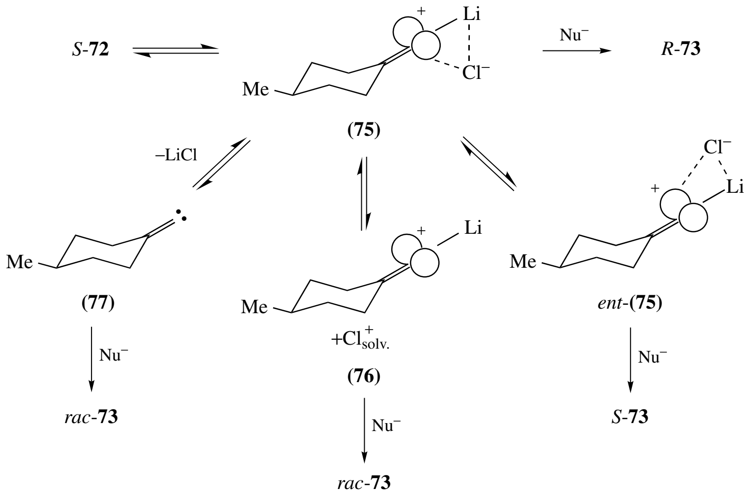

SCHEME 12. Nucleophilic substitution at the chiral vinylidene carbenoid *S*-**72**

as determined after deuteriolysis of *R*-**73** to the product *R*-**74**. Several reasons could be responsible for the partial racemization of the final product **74**. Thus, a separation of cation and anion by the solvent could occur, so that the chiral information is lost in **76**, or the free achiral carbene **77** could form by a completed α-elimination. Both intermediates would form racemic **73**. Finally, the partial racemization can be rationalized by a migration of the chlorine atom associated with the lithium to the enantiotopic face. This partly occurring process would lead from **75** to *ent*-**75** so that the inverted lithium compound *S*-**73** would result. The intimate ion pair **75** postulated in this rationale is very well compatible with the ^{13}C-NMR studies of Seebach and coworkers[19]. Although the linearity of the C=C−Li moiety assumed in **75** is not confirmed by the X-ray structure analysis of a vinylidene carbenoid by Boche and coworkers (see Figure 1; scheme 4), at least the beginning rehybridization is already indicated in this structure[8]. There is also evidence for a complex that is supposed to be formed between the vinylidene carbenoid (e.g. **72**) and the alkyllithium reagent, the so-called quasi-dianion complex ('QUADAC')[314].

The nucleophilic attack of *t*-butyllithium on lithium vinylidene carbenoids has also been used for synthetic purposes in as far as the reaction permits to generate sterically hindered alkenes. Thus, treatment of the dibromoalkene **78** generated from adamantanone with an excess of *t*-butyllithium results in the formation of the alkene **79** that contains three bulky substituents at the double bond (equation 43)[315]. In an analogous way, a *t*-butyl residue is introduced into chloroenamine **80** (equation 44)[316].

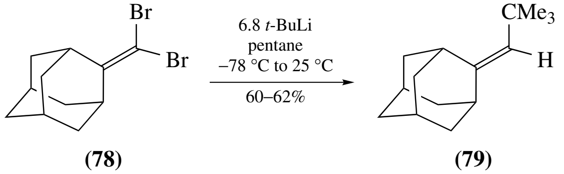

(43)

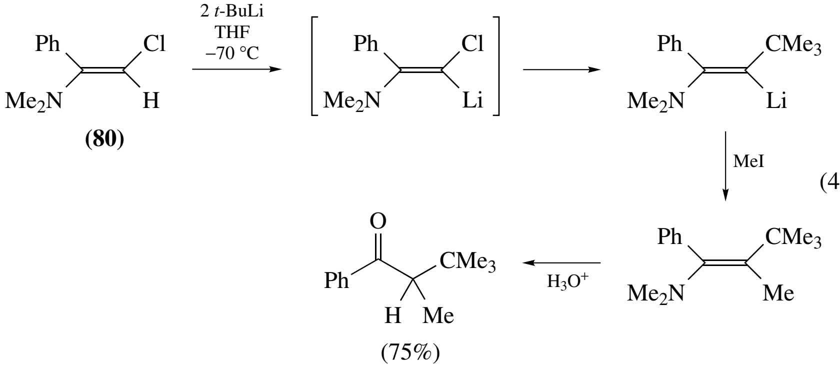

(44)

A reaction typical of vinylidene carbenoids is a rearrangement that was independently observed at the end of the 19th century by Fritsch, Buttenberg and Wiechell[317–319]. Long before α-halo vinyl anions were recognized as intermediates, these authors reported that tolanes **81** arise from the treatment of 2,2-diaryl-1-haloethenes with sodium alkoxide (equation 45). This rearrangement, which takes place in an intramolecular manner, also occurs in 1-halo-1-lithioalkenes **82** provided that at least one of the two β-substituents is an aryl, alkenyl or cyclopropyl group. If there are two substituents in the β-position that are suitable migrating groups, the one in the *trans* position with respect to the halogen atom migrates exclusively (equation 46)[320, 321].

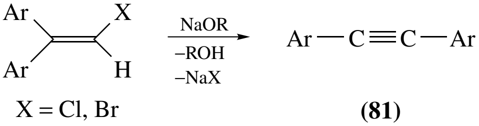

(45)

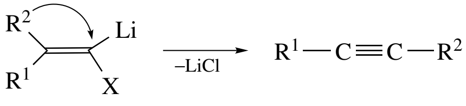

(82)

(46)

This stereochemical outcome of the Fritsch–Buttenberg–Wiechell rearrangement is well compatible with the crystal structure of the carbenoid **3** (Figure 1, Scheme 4)[8]. The aryl moiety *trans* to the vinylic chlorine atom is bent towards C1 (C1–C2–C9 116.5°). Thus, migration of the *trans*-aryl group with simultaneous liberation of lithium chloride becomes evident. The free vinylidene carbene can be ruled out as the intermediate.

When 1-bromo- and 1-chloro-1-lithioalkenes have a hydrogen substituent in the β-position, they undergo a hydride shift that is analogous to the Fritsch–Buttenberg–Wiechell rearrangement. The hydride shift taking place at temperatures above −70 °C is frequently used to transform aldehydes into alkynes **84** with homologation. To this purpose, the aldehydes are first converted into dibromoalkenes **83** by carbonyl olefination. Subsequent bromine–lithium exchange and hydride shift of the carbenoid lead to the alkyne **84**[322–333]. If an excess of the alkyllithium reagent (e.g. *n*-butyllithium) is used, the alkyne **84** is deprotonated *in situ* so that it can be submitted to a reaction with an electrophile immediately (Scheme 13)[331]. In a similar way, the preparation of 1-propynyllithium from 1-chloro- and 1-bromo-1-propene starts with an α-metalation and subsequent hydride shift of the corresponding carbenoid[334, 335].

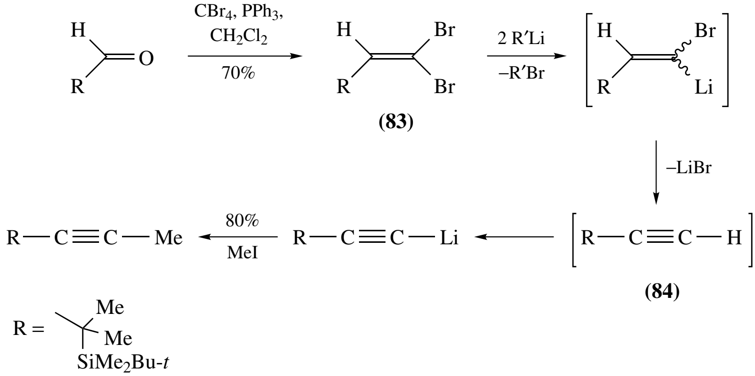

SCHEME 13. Conversion of aldehydes into alkynes under homologation. Application of hydride shifts in vinylidene carbenoids

The carbenoid character of 1-halo-1-lithioalkenes becomes also evident from C−H insertions and cyclopropanations, examples of which are given in equations 47 and 48, respectively[336, 337].

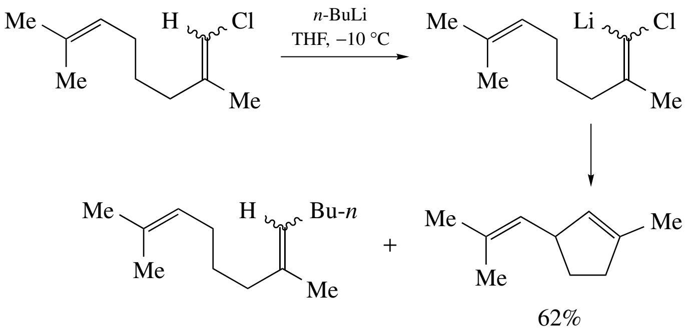

(47)

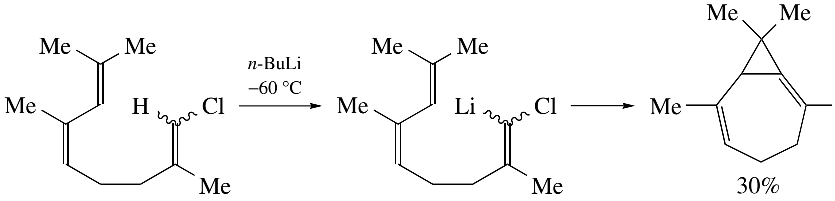

(48)

Reactivity typical of carbenoids is distinctly displayed by α-oxygen-substituted alkyl- and alkenyl-lithium compounds. The carbenoid character is particularly pronounced in the absence of groups at the carbenoid center that are either anion stabilizing or lithium chelating. Thus α-lithiated alkyl ethers, vinyl ethers and epoxides have the suitable substitution pattern to display carbenoid reactivity. Although not recognized as a carbenoid, the electrophilic character of an α-lithiated ether was first detected as early as in the nineteen-thirties by Lüttringhaus and von Sääf and confirmed later in the course of studies on the Wittig rearrangement[197, 198]. Thus, treatment of benzyl phenyl ether with an excess of phenyllithium yielded diphenylmethane and phenol after protonation, easily rationalized now as a nucleophilic substitution at the carbenoid **85** (equation 49). Later on, the carbenoid character of **85** was confirmed by a cyclopropanation reaction, which occurs in the presence of alkenes[338].

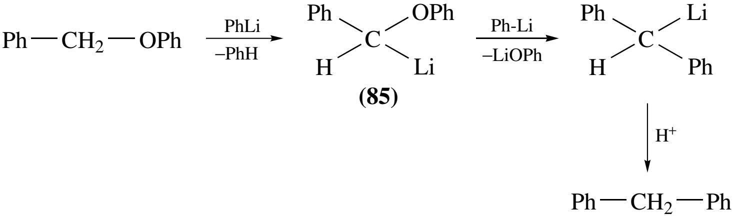

(49)

Similar results were obtained when the reaction of dimethyl ether with n-hexyllithium was studied by Ziegler and Gellert. Thus, the carbenoid **86** formed initially reacted with n-hexyllithium to give n-heptyllithium **87**, which in turn reacted with **86** to give n-octyllithium **88** and so on (equation 50)[339]. Although the chemistry of α-lithiated alkyl ethers has been investigated systematically, their carbenoid-like reactivity is only of limited synthetic value.

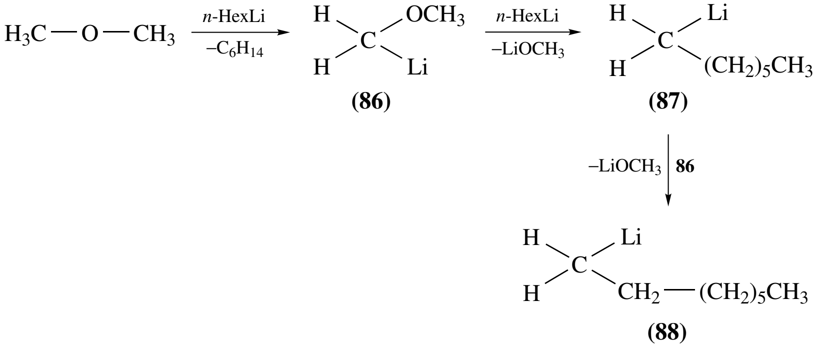

(50)

On the contrary, α-lithiated epoxides have found wide application in syntheses[340]. The existence of this type of intermediate as well as its carbenoid character became obvious from a transannular reaction of cyclooctene oxide **89** observed by Cope and coworkers[341]. Thus, deuterium-labeling studies revealed that the lithiated epoxide **90** is formed upon treatment of the oxirane **89** with bases like lithium diethylamide. Then, a transannular C−H insertion occurs and the bicyclic carbinol **92** forms after protonation (equation 51). This result can be interpreted as a C−H insertion reaction of the lithium carbenoid **90** itself. On the other hand, this transformation could proceed via the α-alkoxy carbene **91**. In both cases, the release of strain due to the opening of the oxirane ring is a significant driving force of the reaction.

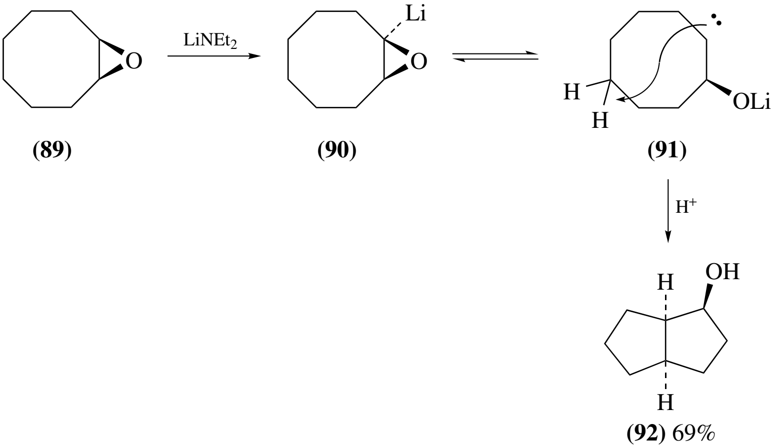

(51)

The reaction became particularly interesting for synthetic purposes when enantioselective variants were elaborated[33, 342]. Thus, the deprotonation of *meso*-epoxides like **89** converts an achiral compound into a chiral one, the carbenoid **90**. If the lithiation has been carried out with a differentiation of the enantiotopic protons, the subsequent transannular

C—H insertion reaction occurs in a stereoselective manner. Various attempts based on chiral lithium amide bases gave only moderate enantioselectivities. More efficiently, the reaction is carried out by means of *s*-butyl- or *iso*-propyl-lithium in the presence of (—)-sparteine; under these conditions, the bicyclic alcohol **92** was obtained in 74% yield and 83% ee. This concept has been extended to various *meso*-epoxides, an example of which is shown in equation 52[343].

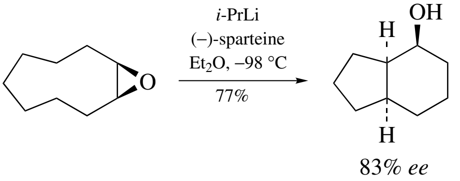

(52)

Another carbenoid-typical reaction of α-lithiated epoxides is the 1,2-hydrogen shift, illustrated in Scheme 14. Two mechanistic pathways offer an explanation for the formation of the lithium enolate **94**: First, the route via the α-ring opening of the epoxide followed by an 1,2-hydride shift in the carbene **93**, and second, the electrocyclic ring opening of an oxiranyl anion **95** to an enolate 'anion' **94**. Both mechanisms are in accordance with different experimental data[344, 345].

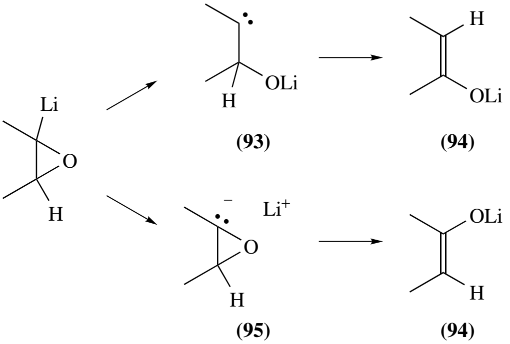

SCHEME 14. Ring opening of α-lithiated epoxides; formation of lithium enolates

Here again, stereoselective variants have been elaborated. The ring opening of the *meso*-epoxide **96** may illustrate the enantioselective version of the reaction. When treated with *s*-butyllithium in the presence of (—)-sparteine, the chiral ketone **97** forms in 71% ee, the chemical yield being rather modest (equation 53)[346]. α-Isosparteine, a diastereomer of sparteine, turned out to be somewhat more efficient with regard to this conversion (40% yield, 87% ee). An α-lithiooxycarbene intermediate (of type **93**) might also be responsible for an intramolecular cyclopropanation which occurs when the oxirane **98** is treated with phenyllithium. The formation of the final product **101** is plausibly explained by a ring opening of the strained bicyclobutane derivative **100**, the intermediate that results from the intramolecular cyclopropanation step (equation 54)[347, 348]. In a way that is typical for transformations which are based on the carbenoid character of α-hetero-substituted alkyllithium compounds, the reaction is performed at relatively high temperatures, whereby no attempt is made to quench the α-lithiated epoxide **99**.

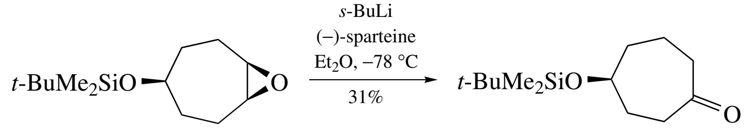

(96) **(97)**
71% *ee*

(53)

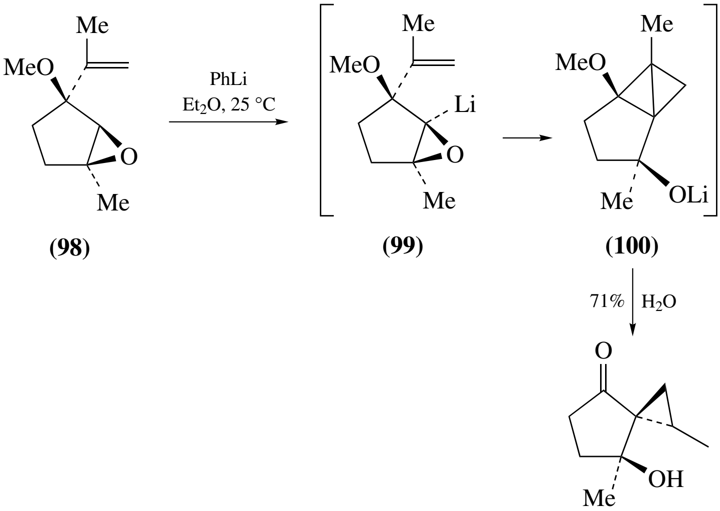

(98) **(99)** **(100)** **(101)**

(54)

Finally, a reaction that clearly shows the electrophilic carbenoid-type character of α-lithiated epoxides is the 'reductive alkylation' discovered by Crandall and Apparu. The transformation is illustrated by the treatment of *t*-butyl ethylene oxide with *t*-butyllithium to yield *E*-di-*t*-butylethene (equation 55). The overall reaction results in a conversion of an oxirane into an alkene under simultaneous substitution of an α-hydrogen atom by the alkyllithium reagent[249, 250, 349].

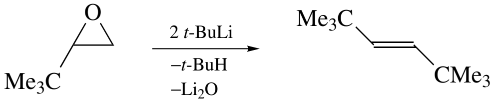

(55)

The proposed mechanism of this reaction is based on the nucleophilic attack of the alkyllithium compound at the carbenoid carbon atom or at the α-lithiooxy carbene. The dilithium compound **102** gives the alkene **103** by the loss of lithium oxide (equation 56). When an alkoxy residue, which is a better leaving group than Li_2O, is offered in the α-position of the corresponding dilithium compound, the elimination of lithium alkoxide takes place instead of lithium oxide. This is illustrated by the reaction of epoxide **104** that delivers the allylic alcohol **105** upon treatment with *n*-butyllithium (equation 57)[350]. The reaction has been applied successfully to more functionalized epoxides[351].

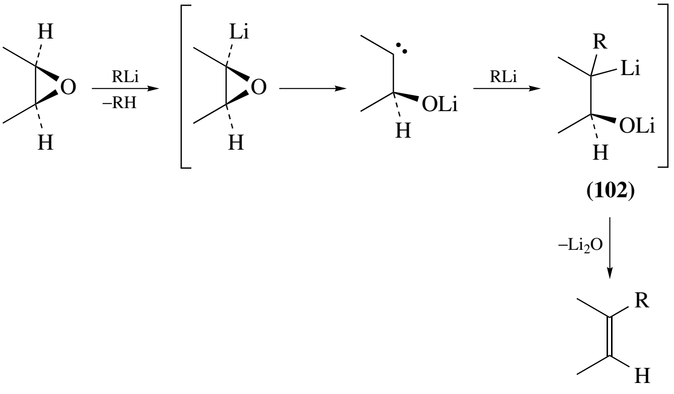

(102)

(103)

(56)

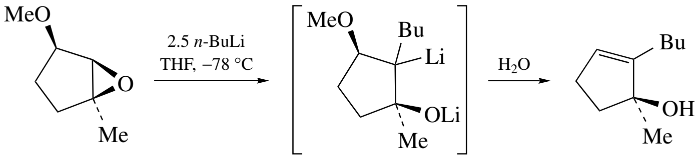

(104) **(105)**

(57)

There is also evidence for a carbenoid character in lithiated acetals[352], lithiated thioacetals[353] and tris(phenylthio)methyllithium[354]. Reactivity typical of carbenoids is also displayed by α-lithiated vinyl ethers. The electrophilic nature of α-lithiated cyclic unsaturated ethers, in particular dihydrofuran **106** and dihydropyran **108** which are readily available by deprotonation, becomes evident from the reaction with alkyllithium compounds: In a nucleophilic substitution, the alkyl group R is introduced under complete inversion of configuration at the carbenoid center to give the ring-opened products **107** and **109**. After protonation, they serve as useful intermediates in natural product synthesis (equation 58)[261, 355]. The yield in this reaction can be improved substantially, when the ring opening is catalyzed by CuCN. An analogous conversion is observed when lithiated benzofuran **110** is treated with different alkyl- and aryllithium reagents (equation 59)[21].

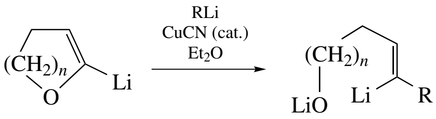

(106) $n = 1$
(108) $n = 2$

(107) $n = 1$
(109) $n = 2$

(58)

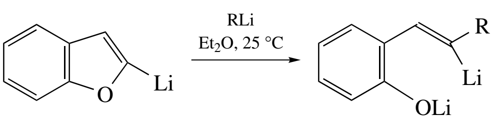

(110)

(59)

A final carbenoid-type reactivity of α-oxygen-substituted vinylidene carbenoids has been reported for the carbamate **111**. When warmed up to temperatures higher than −40 °C, a Fritsch–Buttenberg–Wiechell rearrangement takes place to give the alkyne **112** (equation 60). Below that temperature, the lithium compound **111** maintains its nucleophilic reactivity[355].

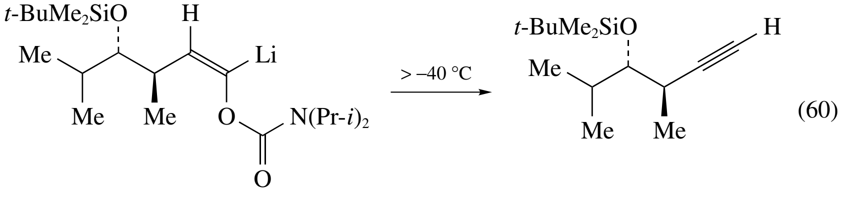

(111) **(112)**

The question whether a particular α-halogen- or α-oxygen-substituted organolithium compound reacts as a 'carbanion' or as a 'carbenoid' depends basically on two parameters: first, on the particular substituent pattern (e.g. additional anion stabilizing groups, chelating effects, ring strain), and second, on the temperature. In general, nucleophilic reactivity is displayed at lower temperatures. When the temperature is raised, loosening of the LiX or LiOR group starts, and the carbenoid character predominates. The answer to the question, at which temperature the 'carbanion' becomes a 'carbenoid', depends individually on the particular α-hetero-substituted alkyl or alkenyllithium compound.

2. Reactions typical of carbanions

The broadest applicability and versatility of α-hetero-substituted alkyl- and vinyllithium compounds is based on their carbanionic character for the following reasons. First, they can react with a large variety of electrophiles; second, they are inherent 'umpoled reagents' due to their particular substitution; and finally, stereoselective variants of their reactions with electrophiles have been elaborated more recently. In case of α-halogen- and α-oxygen-substituted alkyl- and alkenyl-lithium reagents, it becomes necessary to suppress the carbenoid reactivity. This is, in most cases, easily accomplished by maintaining appropriately low temperatures. It is not aimed to list the reactions of these alkyl-lithium compounds with standard electrophiles, a subject which has been treated in several overviews[6, 31, 32]. Instead, synthetically important conversions of α-halogen- and α-oxygen-substituted alkyl- and alkenyl-lithium compounds as well as their consecutive transformations will be presented here.

A conversion typical of α-halo-α-lithioalkanes is the formation of epoxides that results from their reaction with aldehydes or ketones. As illustrated in equation 61, the bromolithium carbenoid is usually generated by halogen–lithium exchange. The intermediate lithium alkoxide **113** undergoes an *in situ* ring closure to give the oxirane **114**[356].

As shown in equation 8, the reaction is also feasible with configurationally stable α-bromo-α-lithioalkanes[66]. When α-bromo-α-lithiocyclopropanes are allowed to react with ketones, an analogous conversion occurs. Thus oxaspiropentanes like **116** are obtained from dibromonorcarane **22**. Although highly strained, the epoxide **116** results from the intramolecular substitution in the intermediate alkoxide **115** with liberation of lithium bromide. One can take advantage of the inherent ring strain of oxaspiropentanes **116** which undergo a smooth ring enlargement to yield cyclobutanones **117** (equation 62)[110, 356].

This type of cyclobutanone annelation is feasible with various dibromocyclopropanes. When diaryl ketones are used as electrophiles, the oxaspiropentane–cyclobutanone rearrangement occurs spontaneously, so that the cyclobutanone is obtained directly (equation 63)[110, 357]. When 1-bromo-1-lithiocyclopropanes are allowed to react with aldehydes, the formation of cyclopropyl ketones results[110].

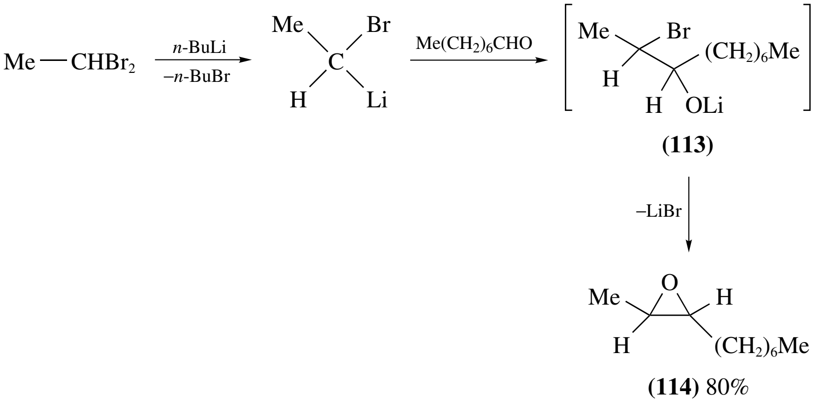

(61)

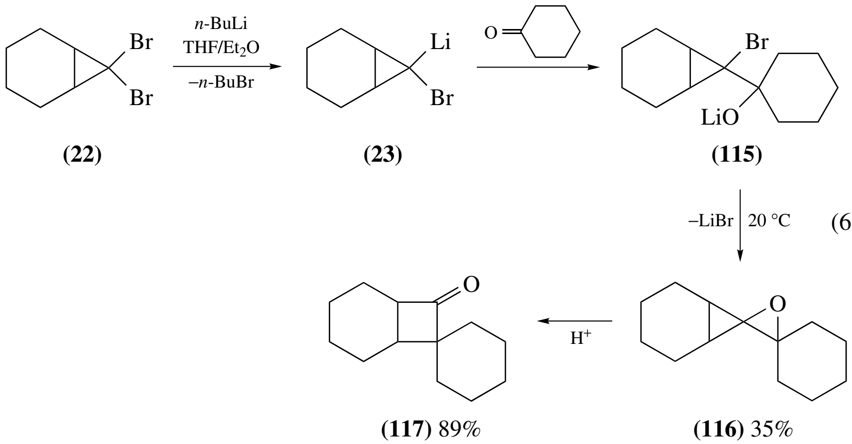

(62)

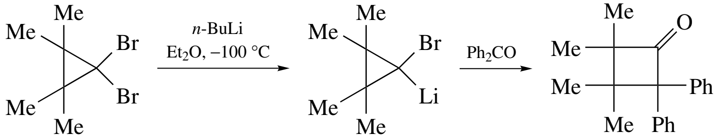

(63)

α-Halo-α-lithioalkanes **118** carrying one or more substituents Y in α-position undergo epoxide formations as well, when reacted with aldehydes or ketones. In case of a carboalkoxy group as substituent Y, a variant of Darzens glycidic ester condensation occurs[120–124], whereby the organolithium compound **118** corresponds to a 'preformed enolate'[358]. Epoxide formation also occurs when the substituent Y in **118** equals

SiR_3[359–363] or SR[364–366] (equation 64).

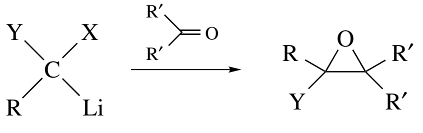

(118)

(64)

X = Cl, Br
Y = CO_2R'', SiR″, SR″

Sequential nucleophilic and electrophilic reactivity of a bromo lithio carbenoid is a feature of the transformation that permits a ring enlargement of cyclic ketones (Scheme 15)[367, 368]. Thus, nucleophilic addition of dibromo lithio methane, which has been generated by deprotonation of dibromomethane, to cyclododecanone **119** leads to the

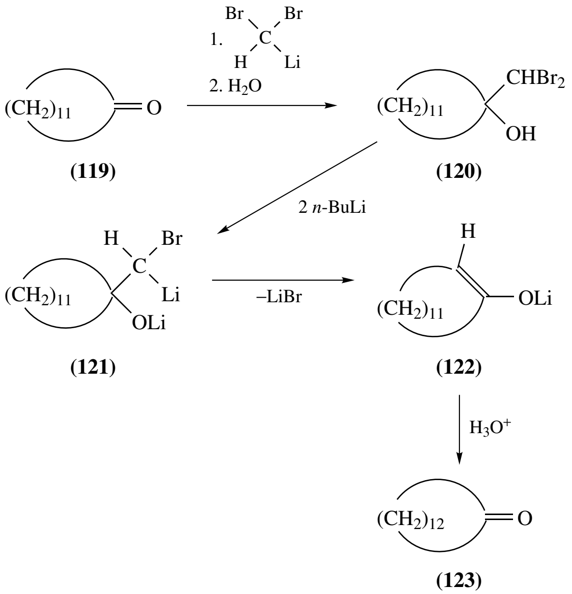

SCHEME 15. Sequential nucleophilic and carbenoid-type reactivity of α-bromo-α-lithioalkanes. Ring enlargement of cycloalkanones

carbinol **120**. When treated with two equivalents of *n*-butyllithium, both O-deprotonation and bromine–lithium exchange occur in the alcohol **120** so that the carbenoid **121** is generated. Loss of lithium bromide, which demonstrates the carbenoid character of **121**, and carbon migration give the enolate **122** that finally yields the homologated ring-enlarged ketone **123**[367].

An annulation protocol has been elaborated that uses lithiated 3,3-dichloropropene **124** generated *in situ* by deprotonation as a key intermediate. When added to a cycloalkanone, the homoallylic alcohol **125** forms upon aqueous workup. Its subsequent treatment with trifluoroacetic acid brings about elimination of water and dissociation of a chloride anion.

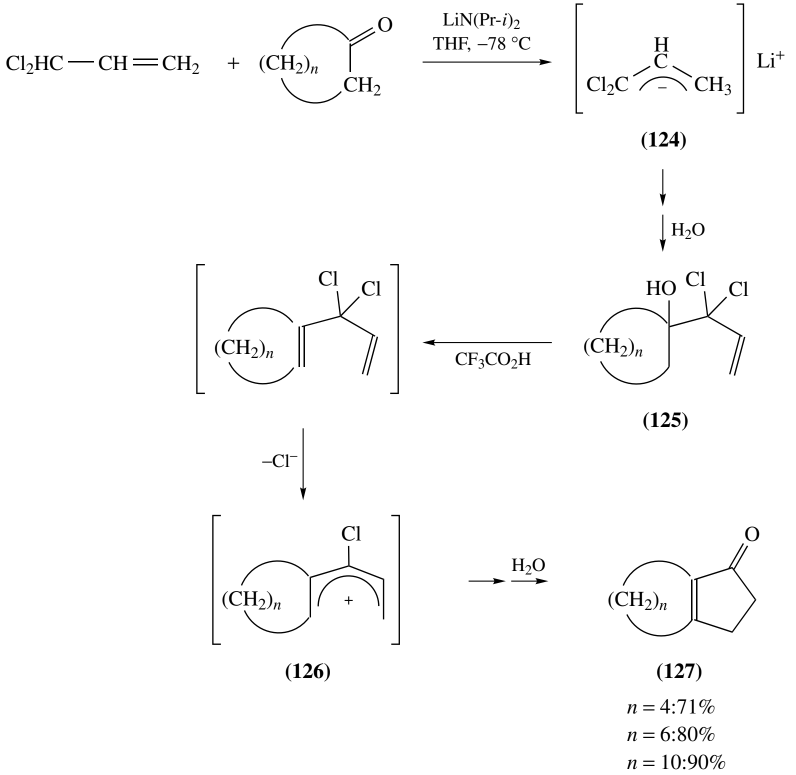

SCHEME 16. Ring annulation of cycloalkanones due to lithiated 3,3-dichloropropene

The pentadienyl cation **126** thus formed undergoes an electrocyclic ring closure that leads, after hydrolysis, to the annulated ketone **127** (Scheme 16)[369].

Although the trihalolithiomethanes seem to be predestined to deliver the corresponding dihalocarbenes by spontaneous α-elimination, they have been shown to be stable at temperatures below $-100\,^{\circ}\mathrm{C}$ so that they could be characterized by NMR spectroscopy[19]. Furthermore, their nucleophilic reactivity has been demonstrated by the addition to ketones. Herein, the *in situ* generation of trichloro- and tribromo-lithio-methane **128** and **129** provides a convenient protocol (equation 65)[153].

Among the various mixed trihetereo-substituted methyllithium compounds, the substitution pattern of the phosphonates **130** and **132** opens the possibility of a carbonyl alkenylation. Thus, the reaction of **130** and **132** with aldehydes or ketones leads to the formation of dichloro- and dibromoalkenes **131** and **133**, respectively (equations 66 and 67)[327,370].

A carbonyl alkenylation protocol that is based on 1-bromo-1-lithioalkenes and leads to allenes has been elaborated as well. Thus, bromine–lithium exchange in dibromoalkenes like **134** and addition of the vinylidene carbenoid **135** thus formed to benzaldehyhde yields the allylic alcohol **136a**. After conversion of the hydroxy residue into a leaving group, giving **136b**, a second bromine–lithium exchange induces an elimination of lithium trimethylsiloxide and affords the allene **137** (equation 68)[4].

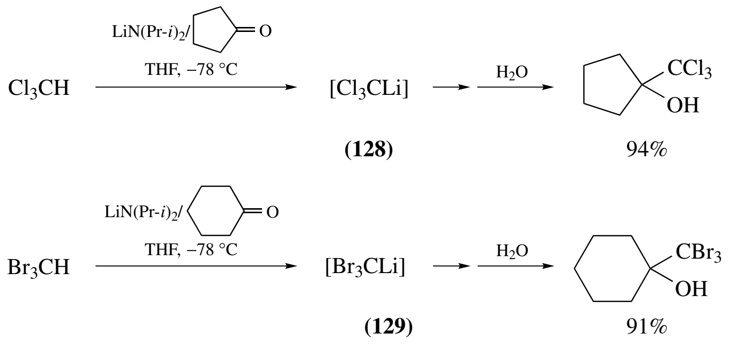
LiN(Pr-i)$_2$/
O
THF, −78 °C
Cl_3CH
[Cl_3CLi]
H_2O
CCl_3
OH
(128)
94%
LiN(Pr-i)$_2$/
O
THF, −78 °C
Br_3CH
[Br_3CLi]
H_2O
CBr_3
OH
(129)
91%

(65)

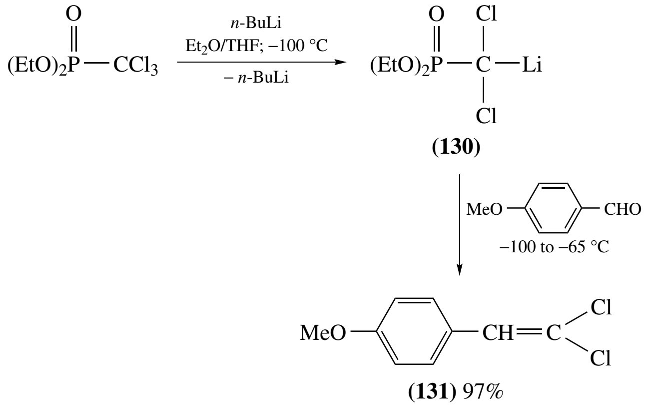
O
(EtO)$_2$P—CCl_3
n-BuLi
Et_2O/THF; −100 °C
− n-BuLi
O
Cl
(EtO)$_2$P—C—Li
Cl
(130)
MeO
CHO
−100 to −65 °C
MeO
CH=C
Cl
Cl
(131) 97%

(66)

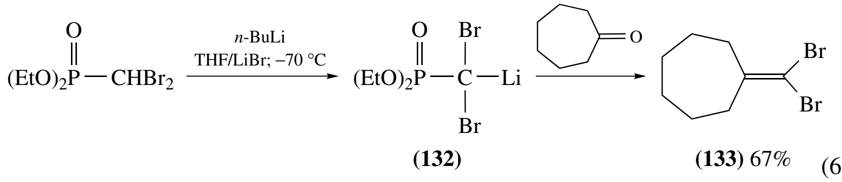
O
(EtO)$_2$P—$CHBr_2$
n-BuLi
THF/LiBr; −70 °C
O
Br
(EtO)$_2$P—C—Li
Br
O
Br
Br
(132)
(133) 67%

(67)

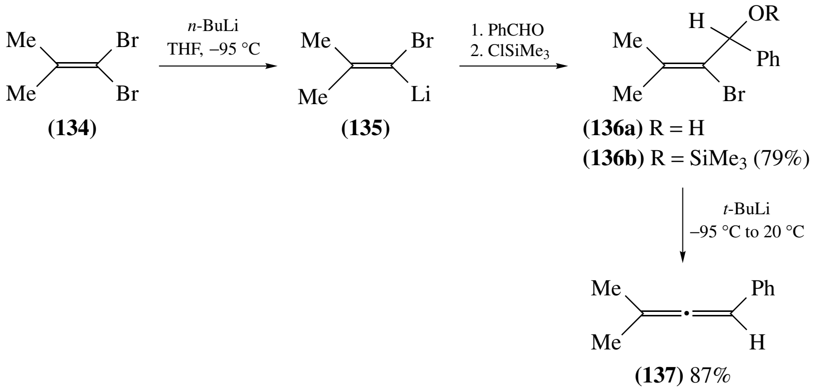
Me
Br
Me
Br
(134)
n-BuLi
THF, −95 °C
Me
Br
Me
Li
(135)
1. PhCHO
2. $ClSiMe_3$
H
OR
Me
Ph
Me
Br
(136a) R = H
(136b) R = $SiMe_3$ (79%)
t-BuLi
−95 °C to 20 °C
Me
Ph
Me
H
(137) 87%

(68)

The lithiated trifluoroethene **138**, which is available by deprotonation or chlorine–lithium exchange, opens a possibility for a carbonylalkenylation in as much as ketones are converted into α-fluoro-substituted acrylic acid derivatives **141**. Thus, the carbenoid **138** acting again as a nucleophilic reagent adds to ketones, to give the carbinols **139** which rearrange into the acyl fluorides **140** upon treatment with sulfuric acid. The reactive acyl fluorides **140** can be converted into various acrylic acid derivatives **141** (equation 69)[167, 169, 371].

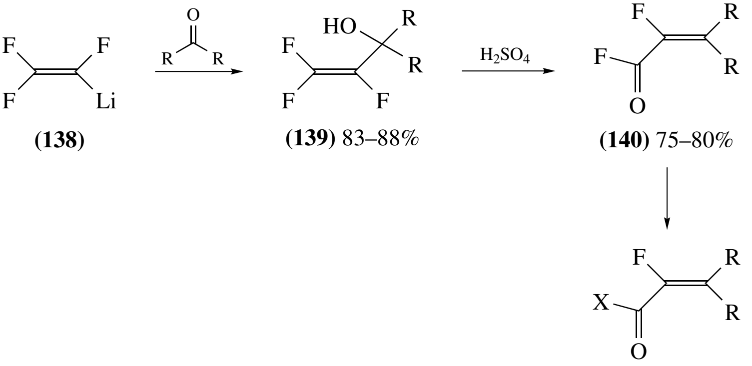

(138) **(139)** 83–88% **(140)** 75–80%

(141) X = OH, OEt, NEt_2

(69)

Being aware of the fact that a hetero-substituted carbon–carbon double bond is convertible into a carbonyl group, one can use α-hetero-substituted lithio-alkenes **2** as nucleophilic acylation reagents **142** and **143**, which display the 'umpoled' d^1 reactivity, provided that the carbanionic character is effective. Depending on the hetero-substituent X, the conversion of the vinyl moiety into a carbonyl group can be effected either by hydrolysis or by ozonolysis. The former procedure has been applied preferentially in the case of lithiated vinyl ethers, whereas the latter has been used in particular for cleavage of the double bond in such products that result from the reaction of lithiated vinyl bromides with electrophiles (Scheme 17).

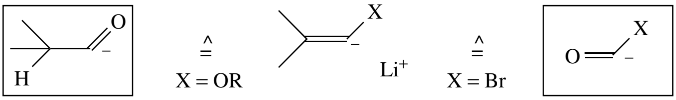

(142) **(2a)** **(143)**

SCHEME 17. α-Hetero-substituted lithioalkenes as reagents for carbonyl umpolung

A new stereocenter is formed when a synthon **143** with umpoled carbonyl reactivity (d^1 reactivity) is introduced into aldehydes or imines. The enantioselective variant of this type of reaction was a longstanding problem in asymmetric synthesis. The very large majority of α-hetero-substituted carbanions which serve as equivalents for synthons like **142** and **143** lead to racemic products with aldehydes or imines. However, enantiomerically pure acylions and α-hydroxy carboxylic acids or aldehydes (**144** and *ent*-**144**, respectively) as well as α-amino acids and aldehydes (**145** and *ent*-**145**) are accessible either by using chiral d^1 reagents or by reacting the components in the presence of chiral additives (Scheme 18).

It turned out that the requirements of such a chiral d^1 reagent are fulfilled by the 1-bromo-1-lithio-1-alkenes *S*- and *R*-**41**, which are available from the corresponding enantiomer of lactate[192, 193]. When added to aldehydes or imines, significant diastereoselectivity will be displayed only by the *E*-diastereomer **41**. Thus, the selective exchange of the bromine atom in the *Z*-position of the dibromoalkene **40**, outlined in Scheme 9, is prerequisite to the efficiency of this concept.

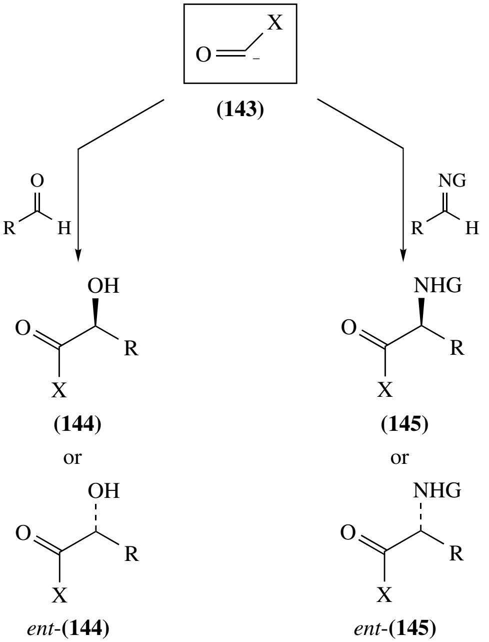

SCHEME 18. Route to enantiomerically pure α-hydroxy and α-amino-carbonyl compounds by addition of chiral d^1 synthons **143** to aldehydes and imines. X = H, OH; G = protecting group

The dibromoalkene *S*-**40** can be prepared from *S*-ethyl lactate by introduction of the MEM (methoxyethoxymethyl) protecting group, reduction to the *O*-protected lactaldehyde and Corey–Fuchs carbonyl olefination (Scheme 19). The *R*-enantiomer of **40** is available analogously from *R*-isobutyl lactate and serves as the reagent in the enantiomeric series. The lithium carbenoid *S*-**41** is generated from *S*-**40** by treatment with *n*-butyllithium in diethyl ether and reacted with aliphatic and aromatic aldehydes in tetrahydrofuran. High diastereoselectivities are reached, as shown in Scheme 19[193].

The *S*-configurated nucleophilic reagent **41** preferentially adds to the aldehyde from the *Re* face (*ul* topicity), and the predominant or almost exclusive formation of the diastereomers **146** results (Scheme 20). The reaction of *S*-**41** with enantiomerically pure *S*-configurated aldehydes leads to the products **146c–e** in high diastereoselectivity as well, thus suggesting the assumption of a matched pair in this combination of enantiomerically pure starting materials (see below)[372–375].

When the bromoalkenes **146**, which are obtained in 88 to over 98% *de*, are submitted to another bromine–lithium exchange, the dilithium compound **148** is generated. This reaction takes place under complete retention of the configuration, as proven by the protonation that yields the *Z*-alkenes **149**[193]. A debromination protocol that is based on a free

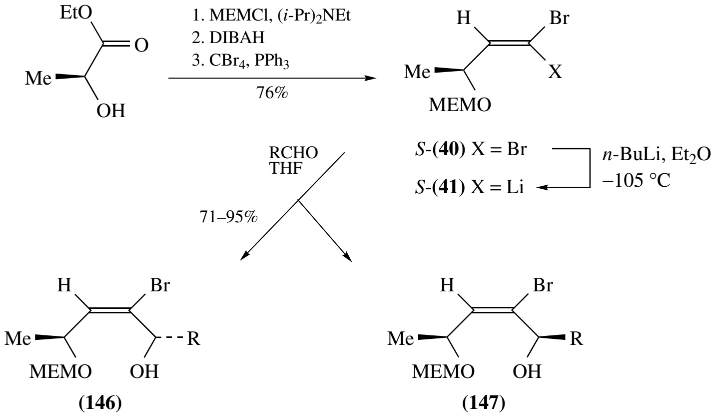

	R	**146:147**	**146 + 147**
a	Me$_2$CH	94:6	87%
b	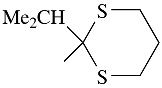	99:1	71%
c	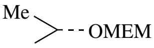	95:5	92%
d	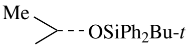	98:2	76%
e		96:4	95%
f	Ph	>99:<1	93%
g	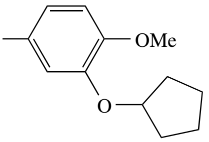	>99:<1	92%

SCHEME 19. Preparation of dibromoalkene **40** and stereoselective addition of bromolithioalkene **41** to aldehydes. Thex = Me$_2$CHCMe$_2$

radical mechanism leads to E-alkenes **150**: they are formed exclusively upon treatment of bromoalkenes **146** with n-Bu$_3$SnH in the presence of azobisisobutyronitrile[376]. This stereodivergent behavior of the bromoalkene **146** is easily explained by the configurational stability of vinyl anions on one hand and the configurational instability of vinyl radicals on the other[377–380]. The latter pathway leads to the formation of the thermodynamically favored E-isomer **150**.

The alkenes **149** and **150** are easily cleaved by ozonolysis either directly or after protection of the hydroxy group. Depending on the workup conditions of the ozonolysis, either diols **151** or O-protected aldehydes **152** can be obtained. The C_2 symmetric ketone **153** (dr: 75:25) is available from another addition of the dilithium reagent **148** (R = Ph)

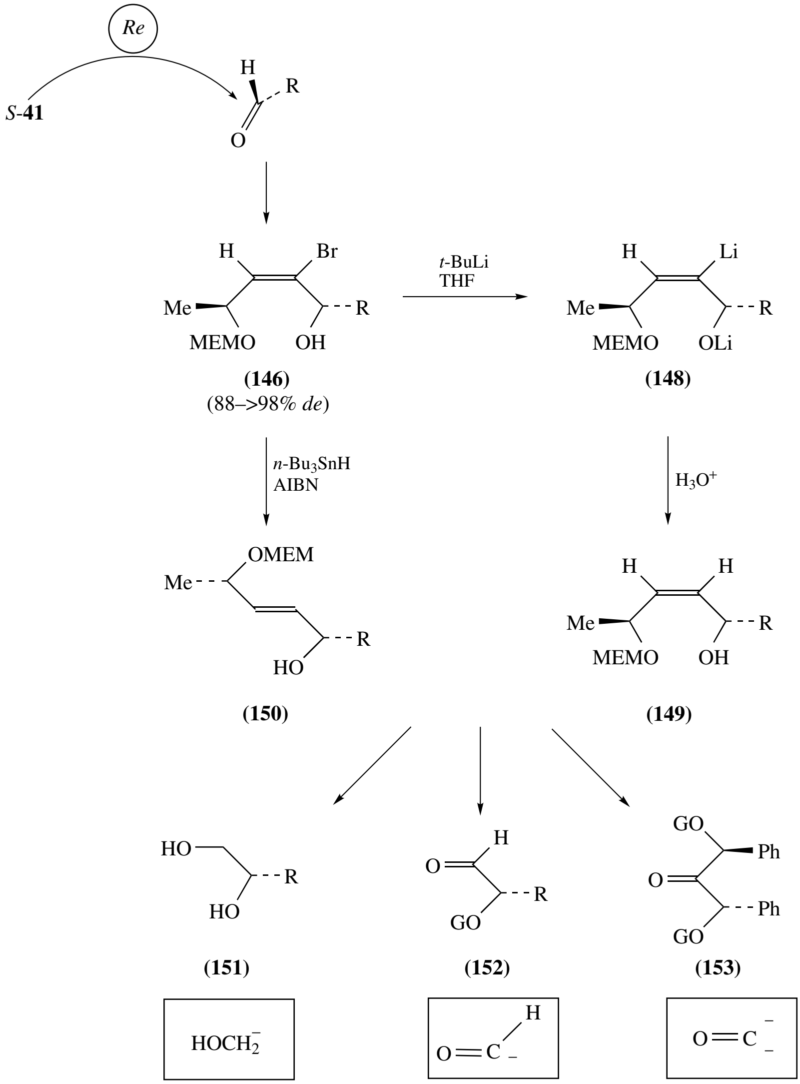

SCHEME 20. Debromination of bromoalkenes **146**. Synthesis of diols **151**, O-protected α-alkoxy aldehydes **152** and α,α'-dialkoxyketones **153**; G = protecting group

to benzaldehyde[381]. Thus, the method permits one to introduce the synthons given in Scheme 20 into aldehydes in an enantioselective way.

Aside from aldehydes, imines can be considered to be suitable substrates for the addition of reagents with umpoled carbonyl reactivity because useful building blocks and important compounds like α-amino acid and aldehydes will result from this conversion (Scheme 21)[382]. The *S*-configurated carbenoid **41** has been found to add to mesitylenesulfonylimines **154**, available from the corresponding aldehydes with predominant attack

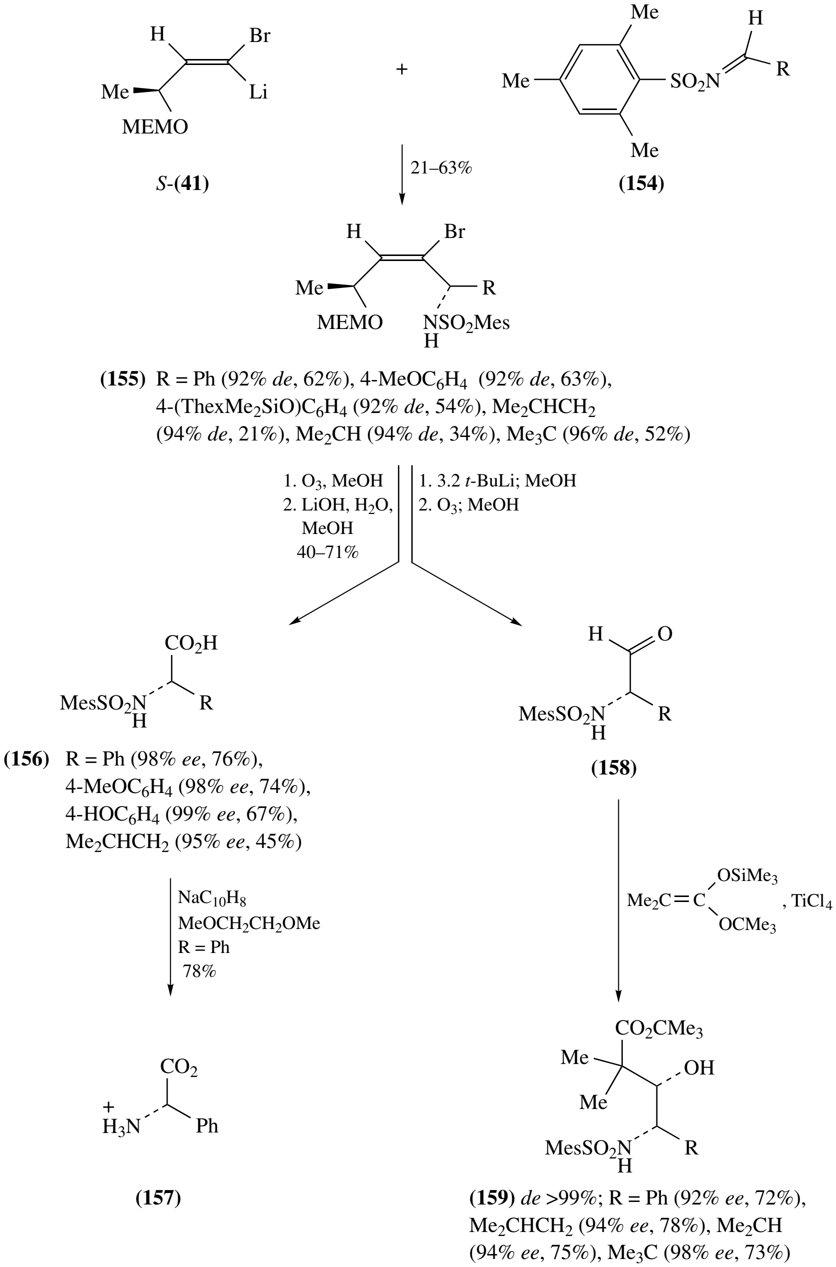

S-(**41**) + (**154**)

(**155**) R = Ph (92% *de*, 62%), 4-$MeOC_6H_4$ (92% *de*, 63%), 4-$(ThexMe_2SiO)C_6H_4$ (92% *de*, 54%), Me_2CHCH_2 (94% *de*, 21%), Me_2CH (94% *de*, 34%), Me_3C (96% *de*, 52%)

(**156**) R = Ph (98% *ee*, 76%), 4-$MeOC_6H_4$ (98% *ee*, 74%), 4-HOC_6H_4 (99% *ee*, 67%), Me_2CHCH_2 (95% *ee*, 45%)

(**158**)

(**157**)

(**159**) *de* >99%; R = Ph (92% *ee*, 72%), Me_2CHCH_2 (94% *ee*, 78%), Me_2CH (94% *ee*, 75%), Me_3C (98% *ee*, 73%)

SCHEME 21. Synthesis of N-protected α-amino acids and aldehydes by stereoselective addition of bromolithioalkene *S*-**41** to sulfonylimines. Mukaiyama aldol reaction of α-aminoaldehydes on the *Re* face. Thus, bromoalkenes **155** are obtained with high diastereoselectivity. When submitted to an ozonolysis in methanol, the methyl esters are formed directly and their saponification leads to α-N-mesitylsulfonylcarboxylic acids **156**. As shown with the example of the transformation into phenylglycine (S-**157**), the mesitylsulfonyl protecting group can be removed by means of sodium in ammonia or sodium naphthalenide. As shown in the case of aldehyde adducts **158**, the substitution of bromine versus hydrogen is feasible by bromine–lithium exchange followed by protonation, so that allylamines are formed from bromoalkenes **155**. The subsequent ozonolysis yield α-sulfonylamino aldehydes **158**, which are configurationally labile but nevertheless can be isolated and used in further reactions. In order to demonstrate the synthetic potential, the aldehydes **158** have been submitted to Mukaiyama aldol reaction with the silyl ketene acetal of t-butyl isobutyrate in the presence of $TiCl_4$. Very high diastereoselectivities in the sense of chelate control are reached in this reaction that yields diastereomerically pure β-hydroxy-γ-amino carboxylic esters **159** in 92 to 98% *ee*.

The highly diastereoselective addition of the chiral bromo lithioalkene S-**41** to chiral aldehydes, outlined in Scheme 19, raises the question whether enantiomerically pure aldehydes and ketones will display any 'substrate induced stereoselectivity' when reacted with achiral 1-bromo-1-lithio alkenes. Therefore, the addition of an achiral vinylidene carbenoid to a series of enantiomerically pure α-alkoxy-substituted aldehydes has been studied. When this type of carbonyl compound is allowed to react with polar organometallic compounds, diastereomeric alcohols *syn*-**160** and *anti*-**161** result. In general, polar organometallic compounds like alkyllithium or Grignard reagents (R″M) (Scheme 22) react with α-alkoxy aldehydes or ketones whose carbonyl compound is not incorporated into a ring in the sense of 'chelate control'[383], a result which is rationalized by Cram's cyclic model[384–387]. The alternative stereochemical outcome, the 'non-chelate control'[383] leading to the diastereomeric carbinol, is usually explained by the Felkin–Anh model[388,389]. It is less frequently observed when alkyllithium or Grignard compounds are added to α-alkoxy aldehydes (Scheme 22)[390].

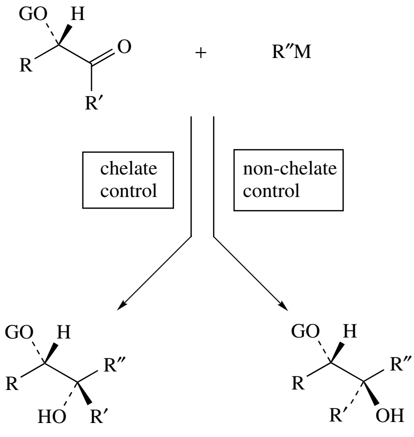

syn-(**160**) *anti*-(**161**)

SCHEME 22. Stereochemical outcome of the addition of polar organometallic compounds R″M to α-alkoxy aldehydes and ketones (G = protecting group)

A remarkable feature of vinylidene lithium carbenoids carrying a bromine atom and an alkoxy residue as an α-substituent is the distinct preference for a non-chelate control when reacted with α-alkoxy aldehydes. Thus, the addition of 1-bromo-1-lithio-2-methyl-1-propene **164**, generated by bromine–lithium exchange from dibromoalkene **163**, to O-protected lactaldehydes **162a–c** leads to the formation of *anti*-carbinols **165** predominantly, as a result of Felkin–Anh selectivity (Scheme 23)[372, 374]. The high *anti:syn* ratio of **165:166** is particularly remarkable in the case of the products resulting from MEM-protected lactaldehyde **162a**, because it seems to be predestined[391] to direct the attack of the nucleophilic reagent **164** in the sense of a chelate control. When silyl-protected lactaldehydes **162b, c** are used as substrates, the selectivity in favor of the non-chelate-controlled products **165b, c** is even enhanced (Scheme 23). The following transformation serves to illustrate that the lithium carbenoid **164** functions as a umpoled formyl d^1 synthon: The silyl ether **165b** is converted into the alkene **167** by another bromine–lithium exchange and subsequent protonation. Desilylation to the diol, protection of both hydroxy groups as MEM ethers and ozonolysis give the α,β-dialkoxyaldehyde **168** in 94% diastereomeric excess (*de*) and greater than 99% *ee*[372, 374]. The bromoalkene **165c**, submitted to a similar protocol, served as an enantiomerically pure building block for a synthesis of L-digitoxose. When, on the other hand, the sequence is performed in the enantiomeric series, which means starting from O-protected R-lactaldehyde *ent*-**162**, enantiomeric D-digitoxose is obtained[378].

The reaction of α-oxygen-substituted alkyllithium compounds with electrophiles permits various synthetically useful transformations due to the fact that these reagents are configurationally stable, at least to such a degree that they can be obtained in enantiomeric and/or diastereomeric purity under the conditions that they are generated and allowed to react with electrophiles. This concept has already been outlined in equation 10, where the non-racemic lithium carbenoid **19** has been shown to react with electrophiles (dimethyl sulfate) under retention of configuration. In a similar way, α-lithiated cyclic ethers that are generated by reductive metalation, as shown in equation 34, serve as a source of substituted tetrahydropyrans and tetrahydrofurans in high diastereomeric purity. Representative examples of reactions of lithiated ethers generated either by reductive metalation or by tin–lithium exchange are given in Tables 4 and 5. In most cases, where a determination of the stereochemical outcome is possible, the result has been retention.

The highly selective abstraction of one of the enantiotopic protons in carbamates due to the presence of (−)-sparteine during the metalation step, outlined in equation 11, proved itself to be a particularly fruitful concept in the context of chiral economy: Thus the protocol permits one to convert a prochiral substrate into a non-racemic product in remarkable enantioselectivity. Usually, metalated carbamates like **21** generated by this method react with electrophiles under retention of configuration (equation 70). In the metalation step, mediated by (−)-sparteine, the pro-S proton is removed predominantly, and reaction products **169** are obtained in >95% *ee* as a rule (equation 70)[83, 392].

When the protocol is applied to allylcarbamates **170**, the deprotonation in the presence of (−)-sparteine does not occur with kinetic preference. Indeed, a dynamic resolution by crystallization takes place. The epimeric allyllithium compounds **171** and **172** are equilibrating, whereby one of them crystallizes predominantly. Under optimized conditions, when n-butyllithium is used for the deprotonation and cyclohexane serves as a cosolvent, the preference of the diastereomer **172** leads to substitution products in 90–94% *ee*[393–395]. An enantioselective homoaldol reaction has been developed based on this protocol: Transmetalation of the organolithium into the titanium compound occurring under inversion of the configuration (**172** → **173**) and subsequent addition to aldehydes leads to

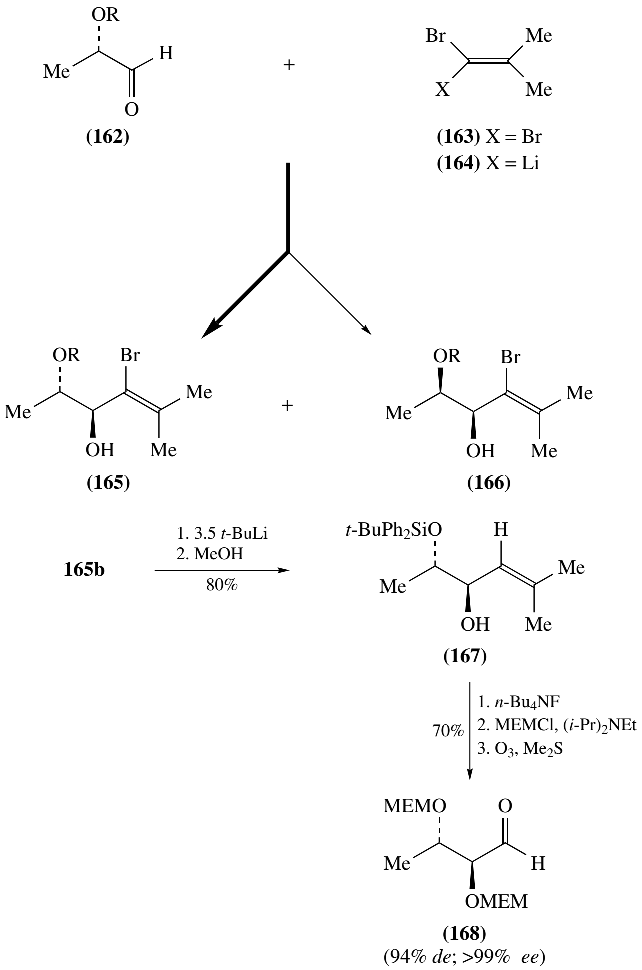

	R	**165**:**166**	**165** + **166**
a	MEM	92:8	92%
b	t-BuPh$_2$Si	>97:<3	84%
c	ThexMe$_2$Si	95:5	93%

SCHEME 23. Non-chelate controlled addition of 1-bromo-1-lithioalkene **164** to *O*-protected lactaldehydes **162**. Introduction of an umpoled formyl d^1 synthon $^-$CHO

homoallylic alcohols **174**. Finally, a two-step procedure leads to γ-lactones **175**, which result in 84–92% *ee* (Scheme 24)[394].

The (−)-sparteine-induced enantioselective deprotonation and subsequent alkylation and hydroxyalkylation has been extended to *O*-benzylcarbamates and cinnamylcarbamate.

Although the generation of the corresponding α-nitrogen-substituted compound can be achieved in general in a highly enantioselective manner, a complication can result from the observation that the stereochemical outcome of the reaction with electrophiles (i.e. retention or inversion) depends on the nature of the electrophile and is not always uniform. The chemistry of lithiated carbamates has been reviewed in a comprehensive manner[33].

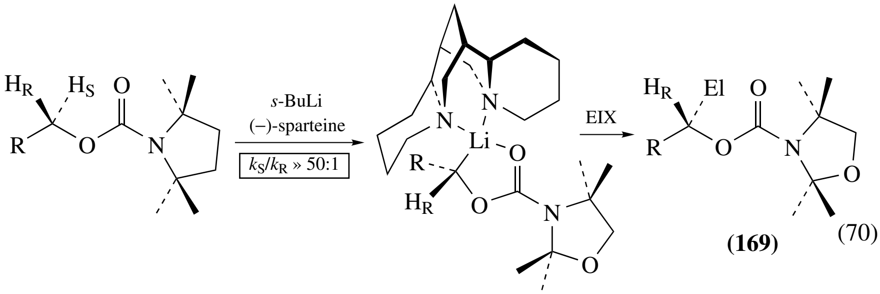

(21)

(169)

(70)

R: Me, $(CH_3)_2CH$, $CH_3(CH_2)_6$, $PhCH_2CH_2$, ferrocenyl-CH_2, $CH_3(CH_2)_{11}$

ElX: CO_2 (then: CH_2N_2), Me_3SnCl, PhCHO, $H_2C{=}CHCH_2Br$, PhCOCl, Me_3SiCl, Ph_2PCl

El: CO_2Me, Me_3Sn, PhCHOH, $H_2C{=}CHCH_2$, Ph_2CO, Me_3Si, Ph_2P

The role that metalated carbamates play in synthesis is pointed out in equation 71: As they can be considered as protected alcohols, they serve as equivalents of alkanol d^1 synthons **176**. Starting from prochiral carbinols, an alkylation is feasible in a highly enantioselective manner.

The metalation of vinyl ethers, the reaction of α-lithiated vinyl ethers obtained thereby with electrophiles and the subsequent hydrolysis represent a simple and efficient method for carbonyl umpolung. Thus, lithiated methyl vinyl ether **56** and ethyl vinyl ether **54**, available by deprotonation with *t*- or *n*-butyllithium, readily react with aldehydes, ketones and alkyl halides. When the enol ether moiety of the adducts formed in this way is submitted to an acid hydrolysis, methyl ketones are obtained as shown in equations 72[396] and 73[255]. Thus, the lithiated ethers **56** and **54** function as an acetaldehyde d^1 synthon **177**. The reactivity of α-metalated vinyl ethers has been reviewed recently[397].

The introduction of umpoled synthons **177** into aldehydes or prochiral ketones leads to the formation of a new stereogenic center. In contrast to the pendant of α-bromo-α-lithio alkenes, an efficient chiral α-lithiated vinyl ether has not been developed so far. Nevertheless, substantial diastereoselectivity is observed in the addition of lithiated vinyl ethers to several chiral carbonyl compounds, in particular cyclic ketones. In these cases, stereocontrol is exhibited by the chirality of the aldehyde or ketone in the sense of 'substrate-induced'[398] stereoselectivity. This is illustrated by the reaction of 1-methoxy-1-lithio ethene **56** with estrone methyl ether, which is attacked by the nucleophilic carbenoid exclusively from the α-face[399]—the typical stereochemical outcome of the nucleophilic addition to 17-ketosteroids[400]. Representative examples of various acyclic and cyclic α-lithiated vinyl ethers, generated by deprotonation, and their reactions with electrophiles are given in Table 6.

The range of applications of lithiated vinyl ethers like **54** and **56** is distinctly enhanced by transmetalation. Thus, cuprate **178** derived of 1-ethoxy-1-lithioethene **54** undergoes

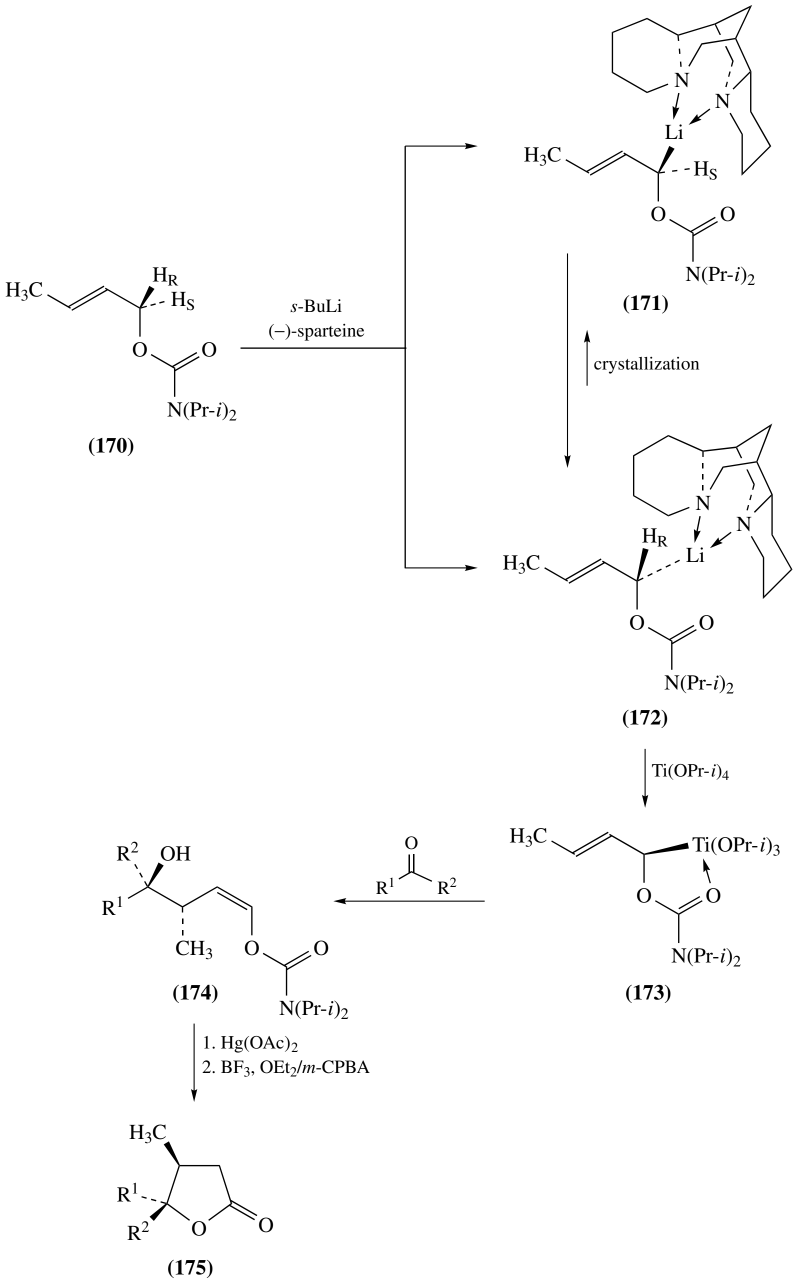

SCHEME 24. (−)-Sparteine-induced deprotonation of allyl carbamate **170**. Dynamic resolution by crystallization and enantioselective homoaldol reaction

1,4-additions when reacted with enones (equation 74)[401, 402] whereas the zinc reagent **179** can be coupled with vinyl or aryl iodides under palladium catalysis (equation 75)[403, 404]. Further examples of transition-metal-mediated coupling reactions are given in Table 6.

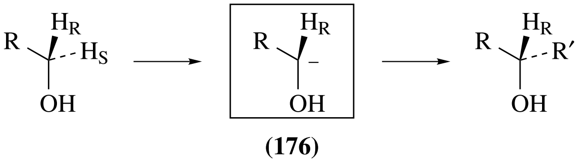

(71)

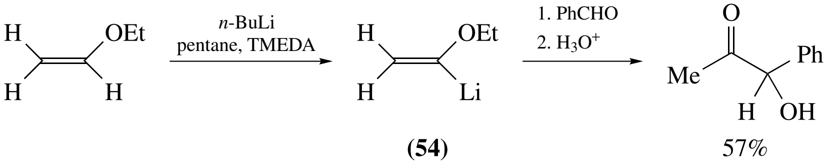

(72)

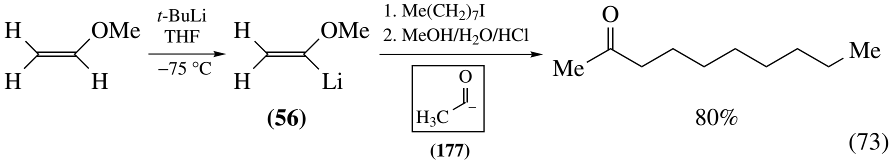

(73)

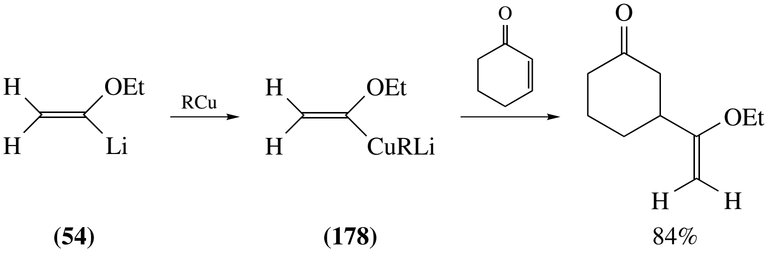

(74)

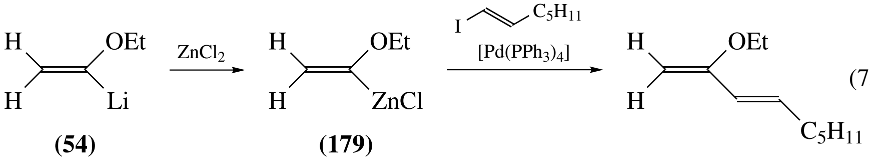

(75)

An intramolecular alkyl group transfer occurs upon warming up solutions of the ate-complex **180** generated by transmetalation of 1-lithio-1-methoxyethene **56** (equation 76)[405, 406]. Tungsten and chromium carbene complexes **181** and **182**, respectively, have been isolated from 1-lithio-1,2-dimethoxyethene (equation 77)[304].

1-Lithio-1-methoxyallene **183**[407, 408], readily accessible by deprotonation of methoxyallene with *n*-butyllithium in diethyl ether, turned out to be a versatile C-3 building block[409–411]. It adds to aldehydes and ketones giving hydroxyalkylated allenes **184**, which undergo a ring-closure reaction under basic conditions. Thus, 3-methoxy-2,5-dihydrofurans **185** are obtained. Subsequent acid hydrolysis leads to the formation of dihydro-3(2*H*)-

furanones **186** (equation 78)[408, 412–414]. Thus, lithiated methoxyallene **183** functions as an equivalent of the umpoled d^1 synthon **187**.

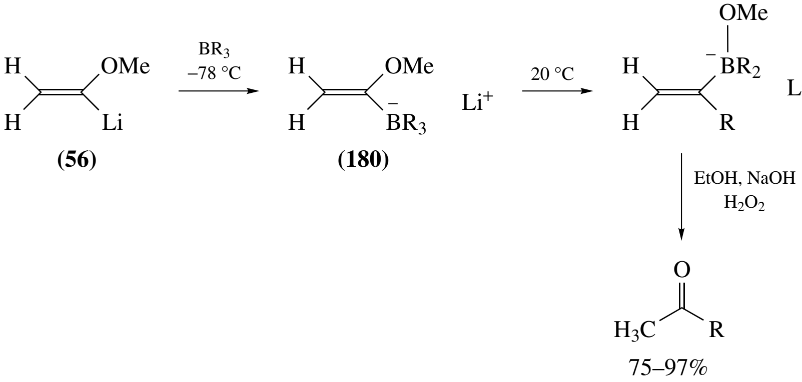

(76)

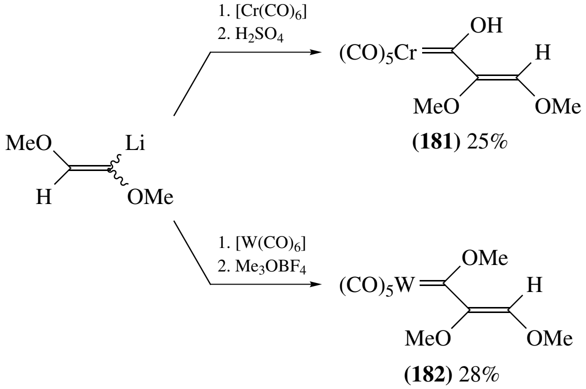

(77)

A stereochemical behavior similar to that of the 1-bromo-1-lithio alkene **164** with regard to chiral aldehydes is shown by the lithiated methoxyallene **183**. When added to *N*,*N*-dibenzylated α-aminoaldehydes **188**, it reacts with non-chelate control so that *anti*-carbinols **189** are obtained predominantly. Diastereomeric ratios of **189:190** range from 80:20 to 95:5. As outlined above, the hydroxyalkylated allenes **189/190** can be converted into furanones **191/192** upon treatment with potassium *t*-butoxide and subsequent acid hydrolysis[410]. When, on the other hand, the adducts of **183** to the aldehydes **193** are submitted to an ozonolysis, *N*-protected α-hydroxy-β-amino esters **194/195** result (Scheme 25)[415].

When, instead of aldehydes, *N*-tosyl imine **196** is used as an electrophile in a reaction with lithiated methoxyallene **183**, allenyl imines **197** result. As shown in Scheme 26, they can be converted into pyrrole derivatives **198** and **199**[416].

A different type of heterocyclic compound, 1,2-oxazines **201**, are accessible from the addition of 1-lithio-1-methoxyallene **183** to isopropylidene glyceraldehyde-derived nitrone **200**. The predominant formation of the *syn*-configurated product **201** (*syn:anti* $\geqslant$ 98:2) results. Nevertheless, the stereochemical outcome can be reversed by a precomplexation of the nitrone **200** with diethyl aluminum chloride (equation 79)[417].

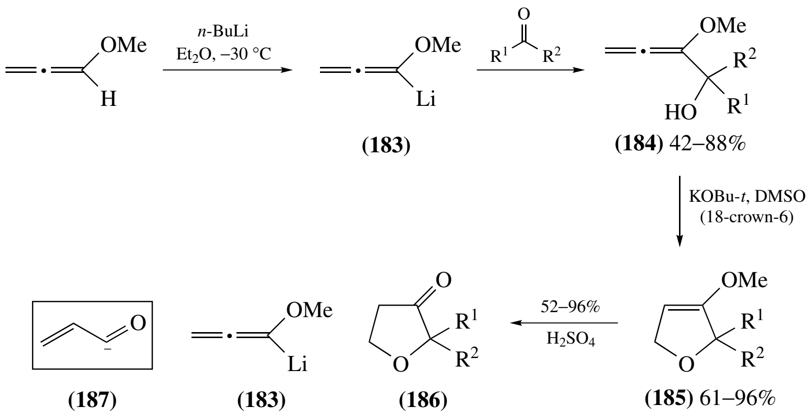

(78)

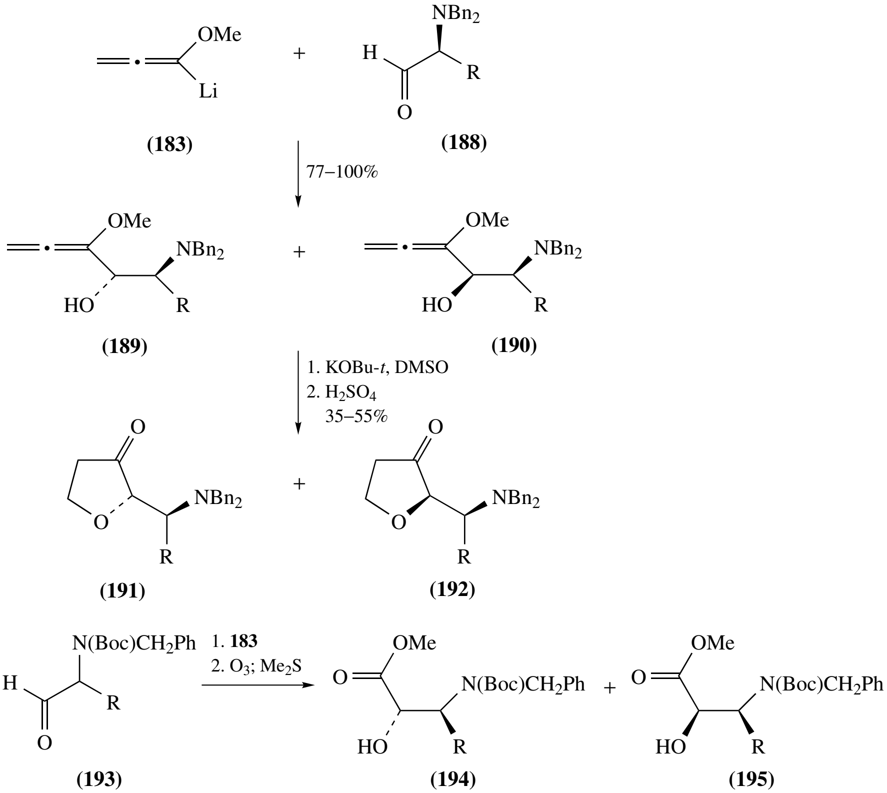

SCHEME 25. Addition of lithiated methoxyallene **183** to *N*-protected α-aminoaldehydes **188**. R = Me, $PhCH_2$, Me_2CHCH_2

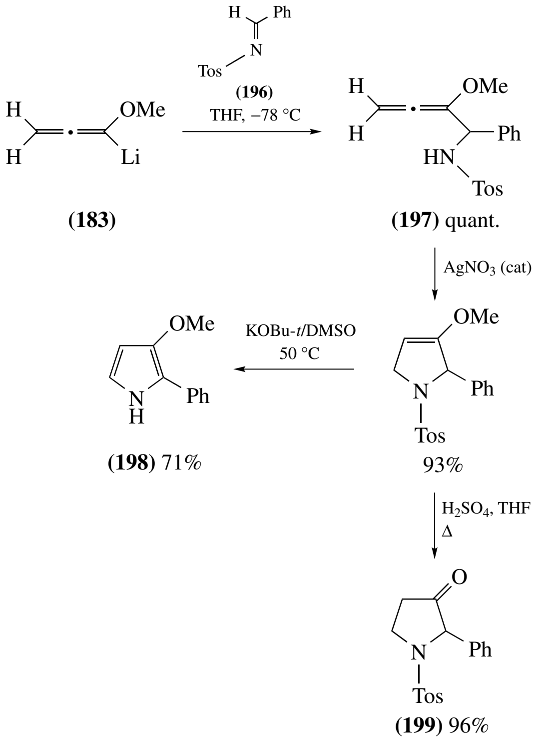

SCHEME 26. Addition of lithiated methoxyallene **183** to tosylimine **196**. Synthesis of pyrrole derivatives

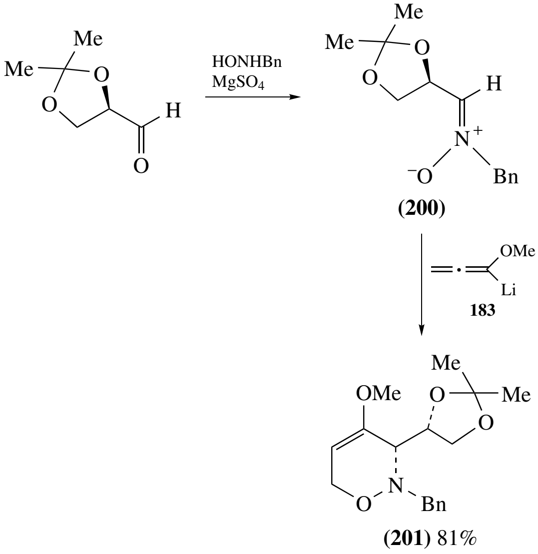

(79)

More recently, lithiated allenes with chiral α-alkoxy groups have been generated and added to aldehydes[418,419] as well as to a tosylimine[411,420] with substantial diastereoselectivity.

IV. CONCLUSIONS

The chemistry of lithium carbenoids, organolithium compounds with an electronegative heteroatom in the α-position, has been developed in two respects during the last two decades. First, the ambiphilic character of these partly short-lived and mostly thermally sensitive compounds is well understood today, due to structure determinations, spectroscopic investigations and theoretical calculations. Second, many of the lithium carbenoids, formerly considered as exotic species, have developed into useful reagents that proved to be particularly fruitful in stereoselective syntheses.

V. ACKNOWLEDGMENTS

The author would like to thank the Fonds der Chemischen Industrie and the Deutsche Forschungsgemeinschaft for financial support. He is also grateful to Dr. Hellmut Mahler, Dr. Kersten Opdenbusch, Dr. Claudia Unger, Dr. Jaykumar Rahematpura, Dipl.-Chem. Jörg Moritz and Dipl.-Chem. Andreas Hohmann for their dedicated work.

VI. REFERENCES

1. G. L. Closs and R. A. Moss, *J. Am. Chem. Soc.*, **86**, 4042 (1964).
2. G. Köbrich, *Angew. Chem., Int. Ed. Engl.*, **6**, 41 (1967).
3. G. Köbrich, *Angew. Chem., Int. Ed. Engl.*, **11**, 473 (1972).
4. H. Siegel, *Top. Curr. Chem.*, **106**, 55 (1982).
5. A. Maercker, *Angew. Chem., Int. Ed. Engl.*, **32**, 1023 (1993).
6. M. Braun, *Angew. Chem., Int. Ed. Engl.*, **37**, 430 (1998).
7. G. Boche and J. C. W. Lohrenz, *Chem. Rev.*, **101**, 697 (2001) and references cited therein.
8. G. Boche, M. Marsch, A. Müller and K. Harms, *Angew. Chem., Int. Ed. Engl.*, **32**, 1032 (1993).
9. G. Boche, K. Harms, M. Marsch and A. Müller, *J. Chem. Soc., Chem. Commun.*, 1393 (1994).
10. A. Müller, M. Marsch, K. Harms, J. C. W. Lohrenz and G. Boche, *Angew. Chem., Int. Ed. Engl.*, **35**, 1518 (1996).
11. K. Sorger, W. Bauer, P. v. R. Schleyer and D. Stalke, *Angew. Chem., Int. Ed. Engl.*, **34**, 1594 (1995).
12. G. Boche, F. Bosold, P. Zulauf, M. Marsch, K. Harms and J. Lohrenz, *Angew. Chem., Int. Ed. Engl.*, **30**, 1455 (1991).
13. S. Harder, J. Boersma, L. Brandsma, J. A. Kanters, W. Bauer, R. Pi, P. v. R. Schleyer, H. Schöllhorn and U. Thewalt, *Organometallics*, **8**, 1688 (1989).
14. M. Marsch, K. Harms, O. Zschage, D. Hoppe and G. Boche, *Angew. Chem., Int. Ed. Engl.*, **30**, 321 (1991).
15. G. Boche, A. Opel, M. Marsch, K. Harms, F. Haller, J. Lohrenz, C. Thümmler and W. Koch, *Chem. Ber.*, **125**, 2265 (1992).
16. For a review on the structure of lithiated amines and lithiated ethers, see: G. Boche, J. C. W. Lohrenz and A. Opel, in *Lithium Chemistry: A Theoretical and Experimental Overview* (Eds. A.-M. Sapse and P. v. R. Schleyer), Chap. 7, Wiley, New York, 1995, pp. 195–226.
17. D. Seebach, H. Siegel, K. Müllen and K. Hiltbrunner, *Angew. Chem., Int. Ed. Engl.*, **18**, 784 (1979).
18. H. Siegel, K. Hiltbrunner and D. Seebach, *Angew. Chem., Int. Ed. Engl.*, **18**, 785 (1979).
19. D. Seebach, H. Siegel, J. Gabriel and R. Hässig, *Helv. Chim. Acta*, **66**, 308 (1983).
20. D. Seebach, J. Gabriel and R. Hässig, *Helv. Chim. Acta*, **67**, 1083 (1984).
21. G. Boche, F. Bosold, J. C. W. Lohrenz, A. Opel and P. Zulauf, *Chem. Ber.*, **126**, 1873 (1993).

22. T. Clark and P. v. R. Schleyer, *J. Chem. Soc., Chem. Commun.*, 883 (1979).
23. T. Clark and P. v. R. Schleyer, *Tetrahedron Lett.*, 4963 (1979).
24. T. Clark and P. v. R. Schleyer, *J. Am. Chem. Soc.*, **101**, 7747 (1979).
25. C. Rhode, T. Clark, E. Kaufmann and P. v. R. Schleyer, *J. Chem. Soc., Chem. Commun.*, 882 (1982).
26. P. v. R. Schleyer, T. Clark, A. J. Kos, G. W. Spitznagel, C. Rohde, D. Arad, K. N. Houk and N. G. Rondan, *J. Am. Chem. Soc.*, **106**, 6467 (1984).
27. C. Lambert, P. v. R. Schleyer and E. U. Würthwein, *J. Org. Chem.*, **58**, 6377 (1993).
28. B. Wang and C. Deng, *Chem. Phys. Lett.*, **147**, 99 (1988); **161**, 388 (1989).
29. H. Qiu and C. Deng, *Chem. Phys. Lett.*, **249**, 279 (1996).
30. M. Regitz (Ed.), *Houben-Weyl, Methoden der Organischen Chemie*, E19b, Vols 1 and 2, Thieme, Stuttgart, 1989.
31. M. Braun, in *Houben-Weyl, Methoden der Organischen Chemie*, E19d (Ed. M. Hanack), Thieme, Stuttgart, 1993, pp. 278–368.
32. M. Braun, in *Houben-Weyl, Methoden der Organischen Chemie*, E19d (Ed. M. Hanack), Thieme, Stuttgart, 1993, pp. 853–1138.
33. D. Hoppe and T. Hense, *Angew. Chem., Int. Ed. Engl.*, **36**, 2282 (1997).
34. A. Basu and S. Thayumanavan, *Angew. Chem., Int. Ed.*, **41**, 716 (2002).
35. D. Seebach, *Angew. Chem., Int. Ed. Engl.*, **18**, 239 (1979).
36. T. A. Hase, *Umpoled Synthons*, Wiley, New York, 1987.
37. G. Köbrich and F. Ansari, *Chem. Ber.*, **100**, 2011 (1967).
38. M. Topolski, M. Duraisamy, J. Rachon, J. Gawronski, K. Gawronska, V. Goedken and H. M. Walborsky, *J. Org. Chem.*, **58**, 546 (1993).
39. T. Hiyama, A. Kanakura, Y. Yamamoto and H. Nozaki, *Tetrahedron Lett.*, 3047 (1978).
40. K. Kitatani, H. Yamamoto, T. Hiyama and H. Nozaki, *Bull. Chem. Soc. Jpn.*, **50**, 2158 (1977).
41. W. von E. Doering and P. M. La Flamme, *Tetrahedron*, **2**, 75 (1958).
42. H. Hopf, in *The Chemistry of Ketenes, Allenes and Related Compounds* (Ed. S. Patai), Wiley, New York, 1980, pp. 779–901.
43. H. F. Schuster and G. M. Coppola, *Allenes in Organic Synthesis*, Wiley, New York, 1984.
44. H.-U. Reissig, in *The Chemistry of the Cyclopropyl Group* (Ed. Z. Rappoport), Chap. 8, Wiley, New York, 1987, pp. 410–412.
45. For an explanation, see Reference 19 and J. E. Williams, Jr. and A. Streitwieser, Jr., *J. Am. Chem. Soc.*, **97**, 2634 (1975).
46. P. Caramella and K. N. Houk, *Tetrahedron Lett.*, **22**, 819 (1981).
47. S. I. Miller and W. G. Lee, *J. Am. Chem. Soc.*, **81**, 6313 (1959).
48. Y. Apeloig, P. v. R. Schleyer, J. S. Binkley and J. A. Pople, *J. Am. Chem. Soc.*, **98**, 4332 (1976).
49. W. D. Laidig and H. F. Schaefer III, *J. Am. Chem. Soc.*, **101**, 7184 (1979).
50. S. Nagase and K. Morokuma, *J. Am. Chem. Soc.*, **100**, 1666 (1978).
51. D. Y. Curtin and J. W. Crump, *J. Am. Chem. Soc.*, **80**, 1922 (1958).
52. D. Y. Curtin and W. J. Koehl, Jr., *J. Am. Chem. Soc.*, **84**, 1967 (1962).
53. D. Seyferth and L. G. Vaughan, *J. Organomet. Chem.*, **1**, 201 (1963).
54. D. Seyferth and L. G. Vaughan, *J. Am. Chem. Soc.*, **86**, 883 (1964).
55. R. W. M. ten Hoedt, G. van Koten and J. G. Noltes, *J. Organomet. Chem.*, **161**, C13 (1978); **170**, 131 (1979).
56. H. M. Walborsky and R. B. Banks, *Bull. Soc. Chim. Belg.*, **89**, 849 (1980) and references cited therein.
57. R. Knorr and E. Lattke, *Tetrahedron Lett.*, 3969 (1977).
58. E. Lattke and R. Knorr, *Chem. Ber.*, **114**, 1600 (1981).
59. R. Knorr and E. Lattke, *Chem. Ber.*, **114**, 2116 (1981).
60. R. Knorr, E. Lattke and E. Räpple, *Chem. Ber.*, **114**, 1581 (1981).
61. R. Knorr, E. Lattke, F. Ruf and H.-U. Reissig, *Chem. Ber.*, **114**, 1592 (1981).
62. R. Knorr and T. von Roman, *Angew. Chem., Int. Ed. Engl.*, **23**, 366 (1984).
63. R. R. Schmidt, H. Speer and B. Schmid, *Tetrahedron Lett.*, 4277 (1979).
64. R. W. Hoffmann and M. Julius, *Liebigs Ann. Chem.*, 811 (1991).
65. R. W. Hoffmann, M. Bewersdorf, M. Krüger, W. Mikolaiski and R. Stürmer, *Chem. Ber.*, **124**, 1243 (1991).
66. R. W. Hoffmann and M. Bewersdorf, *Chem. Ber.*, **124**, 1259 (1991).

67. R. Hirsch and R. W. Hoffmann, *Chem. Ber.*, **125**, 975 (1992).
68. R. W. Hoffmann, M. Julius, F. Chemla, T. Ruland and G. Frenzen, *Tetrahedron*, **50**, 6049 (1994).
69. M. Shimizu, Y. Takebe, M. Kuroboshi and T. Hiyama, *Tetrahedron Lett.*, **37**, 7387 (1996).
70. T. Cohen and M. T. Lin, *J. Am. Chem. Soc.*, **106**, 1130 (1984).
71. E. J. Verner and T. Cohen, *J. Am. Chem. Soc.*, **114**, 375 (1992); *J. Org. Chem.*, **57**, 1072 (1992).
72. S. D. Rychnovsky and D. E. Mickus, *Tetrahedron Lett.*, **30**, 3011 (1989).
73. S. D. Rychnovsky and D. J. Skalitzky, *J. Org. Chem.*, **57**, 4336 (1992).
74. W. C. Still and C. Sreekumar, *J. Am. Chem. Soc.*, **102**, 1201 (1980).
75. J. S. Sawyer, T. L. Macdonald and G. J. McGarvey, *J. Am. Chem. Soc.*, **106**, 3376 (1984).
76. J.-M. Beau and P. Sinay, *Tetrahedron Lett.*, **26**, 6185 (1985).
77. J.-M. Beau and P. Sinay, *Tetrahedron Lett.*, **26**, 6189 (1985).
78. J.-M. Beau and P. Sinay, *Tetrahedron Lett.*, **26**, 6193(1985).
79. P. Lesimple, J.-M. Beau and P. Sinay, *J. Chem. Soc., Chem. Commun*., 894 (1985).
80. J. M. Chong and E. K. Mar, *Tetrahedron Lett.*, **31**, 1981 (1990).
81. P. C.-M. Chan and J. M. Chong, *Tetrahedron Lett.*, **31**, 1985 (1990).
82. O. Zschage, J.-R. Schwark and D. Hoppe, *Angew. Chem., Int. Ed. Engl.*, **29**, 296 (1990).
83. D. Hoppe, F. Hintze and P. Tebben, *Angew. Chem., Int. Ed. Engl.*, **29**, 1422 (1990).
84. D. Hoppe, A. Carstens and T. Krämer, *Angew. Chem., Int. Ed. Engl.*, **29**, 1424 (1990).
85. P. C.-M. Chan and J. M. Chong, *J. Org. Chem.*, **53**, 5584 (1988).
86. K. Tomooka, T. Igarashi and T. Nakai, *Tetrahedron Lett.*, **35**, 1913 (1994).
87. K. Tomooka, L.-F. Wang, N. Komine and T. Nakai, *Tetrahedron Lett.*, **40**, 6813 (1999).
88. N. Komine, L. F. Wang, K. Tomooka and T. Nakai, *Tetrahedron Lett.*, **40**, 6809 (1999).
89. P. Beak, S. T. Kerrick, S. Wu and J. Chu, *J. Am. Chem. Soc.*, **116**, 3231 (1994).
90. N. C. Fabish, Y. S. Park, S. Lee and P. Beak, *J. Am. Chem. Soc.*, **119**, 11561 (1997).
91. K. M. Bertini Gross and P. Beak, *J. Am. Chem. Soc.*, **123**, 315 (2001) and references cited therein.
92. R. W. Hoffmann, T. Rühl and J. Harbach, *Liebigs. Ann. Chem.*, 725 (1992).
93. T. Ruland, R. Dress and R. W. Hoffmann, *Angew. Chem., Int. Ed. Engl.*, **32**, 1467 (1993).
94. H. Reich and R. J. Dykstra, *Angew. Chem., Int. Ed. Engl.*, **32**, 1469 (1993).
95. U. Schöllkopf, in *Houben-Weyl, Methoden der Organischen Chemie*, 13/1 (Ed. E. Müller), Thieme, Stuttgart, 1970, pp 134–162.
96. G. Köbrich and R. H. Fischer, *Tetrahedron*, **24**, 4343 (1968).
97. T. Tarhouni, B. Kirschleger, M. Rambaud and J. Villieras, *Tetrahedron Lett.*, **25**, 835 (1984).
98. J. Villieras, R. Tarhouni, B. Kirschleger and M. Rambaud, *Bull. Soc. Chim. Fr.*, 825 (1985).
99. J. Villieras, B. Kirschleger, R. Tarhouni and M. Rambaud, *Bull. Soc. Chim. Fr.*, 470 (1986).
100. J. Barluenga, L. Llavona, P. J. Bernad and J. M. Concellón, *Tetrahedron Lett.*, **34**, 3173 (1993).
101. U. Schöllkopf, in *Houben-Weyl, Methoden der Organischen Chemie*, 13/1 (Ed. E. Müller), Thieme, Stuttgart, 1970, pp 201–205.
102. D. Seyferth, R. L. Lambert and M. Massol, *J. Organomet. Chem.*, **88**, 255 (1975).
103. K. G. Taylor, W. E. Hobbs, M. S. Clark and J. Chaney, *J. Org. Chem.*, **37**, 2436 (1972).
104. K. G. Taylor and J. Chaney, *J. Am. Chem. Soc.*, **98**, 4158 (1976).
105. C. Müller, F. Stier and P. Weyerstahl, *Chem. Ber.*, **110**, 124 (1977).
106. V. Sander and P. Weyerstahl, *Chem. Ber.*, **111**, 3879 (1978).
107. J. P. Marino and L. J. Browne, *Tetrahedron Lett.*, 3241 (1976).
108. K. Kitatani, T. Hiyama and H. Nozaki, *J. Am. Chem. Soc.*, **97**, 949 (1975).
109. A. Weber, R. Galli, G. Sabbioni, U. Stämpfli, S. Walter and M. Neuenschwander, *Helv. Chim. Acta*, **72**, 41 (1989).
110. M. Braun, R. Dammann and D. Seebach, *Chem. Ber.*, **108**, 2368 (1975).
111. A. Schmidt and G. Köbrich, *Tetrahedron Lett.*, 2561 (1974).
112. H. Saimoto, K. Nishio, H. Yamamoto, M. Shinoda, T. Hiyama and H. Nozaki, *Bull. Chem. Soc. Jpn.*, **56**, 3093 (1983).
113. A. Schmidt, G. Köbrich and R. W. Hoffmann, *Chem. Ber.*, **124**, 1253 (1991).
114. M. Braun and D. Seebach, *Chem. Ber.*, **109**, 669 (1976).
115. H. J. J. Loozen, W. A. Castenmüller, E. J. M. Buter and H. M. Buck, *J. Org. Chem.*, **41**, 2965 (1976).

116. H. J. J. Loozen, W. M. M. Robben and H. M. Buck, *Recl. Trav. Chim. Pay-Bas*, **95**, 245 (1976).
117. P. M. Warner and R. D. Herold, *J. Org. Chem*., **48**, 5411 (1983).
118. M. B. Banwell, G. L. Gravatt, J. S. Buckleton, G. R. Clark and C. E. F. Ricard, *J. Chem. Soc., Chem. Commun*., 865 (1989).
119. M. A. Fox, C.-C. Chen and K. A. Campbell, *J. Org. Chem*., **48**, 321 (1983).
120. M. S. Newman and B. J. Magerlein, *Org. React.*, **5**, 413 (1949).
121. M. Ballester, *Chem. Rev*., **55**, 283 (1955).
122. H. O. House, *Modern Synthetic Reactions*, 2nd edn., W. A. Benjamin, Inc., Menlo Park, 1972, pp. 666–671.
123. J. D. Morrison and H. S. Mosher, *Asymmetric Organic Reactions*, ACS, Washington, 1976, pp. 152–154.
124. H. Pielartzik, B. Irmisch-Pielartzik and T. Eicher, in *Houben Weyl, Methoden der Organischen Chemie*, E 5/1 (Ed. S. Falbe), Thieme, Stuttgart, 1985, pp. 707–708.
125. R. F. Borch, *Tetrahedron Lett*., 3761 (1972).
126. J. Villieras, D. Pyan, Y. Anguelova and J.-F. Normant, *J. Organomet. Chem*., **42**, C5 (1972).
127. H. Normant, *J. Organomet. Chem*., **100**, 189 (1975).
128. G. Kyriakakou, M. C. Roux-Schmitt and J. Seyden-Penne, *Tetrahedron*, **31**, 1883 (1975).
129. C. R. Johnson and T. R. Bade, *Synthesis*, 285 (1982).
130. C. R. Johnson and T. R. Bade, *J. Org. Chem.*, **47**, 1205 (1982).
131. J. T. Welch and S. Eswarakrishnan, *J. Chem. Soc., Chem. Commun*., 186 (1985).
132. J. T. Welch, K. Seper, S. Eswarakrishnan and J. Samartino, *J. Org. Chem*., **49**, 4720 (1984).
133. J. T. Welch and S. Eswarakrishnan, *J. Org. Chem*., **50**, 5403 (1985).
134. K. Araki, J. A. Wichtowski and J. T. Welch, *Tetrahedron Lett*., **32**, 5461 (1991).
135. J. T. Welch, J. S. Plummer and T.-S. Chou, *J. Org. Chem.*, **56**, 353 (1991).
136. C.-P. Qian and T. Nakai, *Tetrahedron Lett*., **31**, 7043 (1990).
137. C.-P. Qian and T. Nakai, *J. Am. Chem. Soc*., **112**, 4602 (1990).
138. J. Villieras, P. Perriot, M. Bourgain and J.-F. Normant, *Synthesis*, 533 (1975).
139. R. Nouri-Bimorghi, *Bull. Soc. Chem. Fr.*, 1876 (1975).
140. J. Villieras, P. Perriot, M. Bourgain and J.-F. Normant, *J. Organomet. Chem*., **102**, 129 (1975).
141. J. Villieras, J. R. Disnar and J.-F. Normant, *J. Organomet. Chem*., **81**, 281 (1974).
142. F. DiNino, T. R. Beattie and B. G. Christensen, *J. Org. Chem*., **42**, 2960 (1977).
143. G. R. Malone and A. I. Meyers, *J. Org. Chem*., **39**, 618 (1974).
144. A. I. Meyers, G. Knaus and J. M. Kendall, *Tetrahedron Lett*., 3495 (1974).
145. P. Sulmon, N. De Kimpe, N. Schamp, J.-P. Declercq and B. Tinant, *J. Org. Chem*., **53**, 4457 (1988).
146. L. Duhamel and J.-Y. Valnot, *Tetrahedron Lett.*, 3319 (1979).
147. G. Köbrich and H. R. Merkle, *Chem. Ber*., **99**, 1782 (1966).
148. U. Schöllkopf, in *Houben Weyl, Methoden der Organischen Chemie*, 13/1 (Ed. E. Müller), Thieme, Stuttgart, 1970, pp. 112–113.
149. J. Villieras, P. Perriot and J. F. Normant, *Synthesis*, 968 (1979).
150. J. Villieras, P. Perriot and J. F. Normant, *Synthesis*, 502 (1979).
151. K. Sato, K. Suzuki, M. Ueda, M. Katayama and Y. Kajihara, *Chem. Lett*., 1469 (1991).
152. J. Villieras, C. Baquet and J. F. Normant, *Bull. Soc. Chim. Fr*., 1797 (1975).
153. H. Taguchi, H. Yamamoto and H. Nozaki, *J. Am. Chem. Soc*., **96**, 3010 (1974); *Bull. Chem. Soc. Jpn*., **50**, 1588 (1977).
154. J. Villieras, P. Perriot and J. F. Normant, *Bull. Soc. Chim. Fr*., 765 (1977).
155. D. F. Hoeg, D. I. Lusk and A. L. Crumbliss, *J. Am. Chem. Soc*., **87**, 4147 (1965).
156. J. Villieras and M. Rambaud, *C. R. Acad. Sci. Paris, Sér. C*, **290**, 295 (1980).
157. H. Shinokubo, K. Miura, K. Oshima and K. Utimoto, *Tetrahedron Lett*., **34**, 1951 (1993).
158. D. Seyferth, G. J. Murphy and R. A. Woodruff, *J. Am. Chem. Soc*., **96**, 5011 (1974); *J. Organomet. Chem.*, **66**, C29 (1974); *J. Organomet. Chem*., **141**, 71 (1977).
159. D. Seyferth and K. R. Wursthorn, *J. Organomet. Chem*., **182**, 455 (1979).
160. D. Seyferth, R. M. Simon, D. J. Sepelak and H. R. Klein, *J. Am. Chem. Soc*., **105**, 4634 (1983).
161. D. Seyferth, E. M. Hanson and F. M. Armbrecht, Jr., *J. Organomet. Chem*., **23**, 361 (1970).
162. G. L. Larson and O. Rosario, *J. Organomet. Chem*., **168**, 13 (1979).
163. D. Seyferth, R. L. Lambert, Jr. and E. M. Hanson, *J. Organomet. Chem*., **24**, 647 (1970).

164. D. Seyferth, F. M. Armbrecht, Jr. and E. M. Hanson, *J. Organomet. Chem*., **10**, 25 (1967).
165. U. Schöllkopf, in *Houben Weyl, Methoden der Organischen Chemie*, 13/1 (Ed. E. Müller), Thieme, Stuttgart, 1970, pp. 196–204.
166. C. Lambert and P. v. R. Schleyer, in *Houben-Weyl, Methoden der Organischen Chemie*, E 19d. (Ed. M. Hanack), Thieme, Stuttgart, 1993, pp. 15–19.
167. J.-F. Normant, J. P. Foulon, D. Masure, R. Sauvêtre and J. Villieras, *Synthesis*, 122 (1975).
168. C. Chuit, R. Sauvêtre, D. Masure, M. Baudry, J.-F. Normant and J. Villieras, *J. Chem. Res. (S)*, 104 (1977); *J. Chem. Res. (M)*, 1147 (1977).
169. R. Sauvêtre, D. Masure, C. Chuit and J. F. Normant, *Synthesis*, 128 (1978).
170. J. L. Hahnfeld, D. J. Burton, *Tetrahedron Lett*., 773 (1975); see also P. Tarrant, R. W. Whitfiled, Jr. and R. H. Summerville, *J. Fluorine Chem.*, **1**, 31 (1971/72).
171. A. Pelter, J. Kvicala and D. E. Parry, *J. Chem. Soc., Perkin Trans 1*, 2681 (1995).
172. K. H. Dötz and J. Glänzer, *J. Chem. Soc., Chem. Commun*., 1036 (1993).
173. J. Burdon, P. L. Coe, I. B. Haslock and R. L. Powell, *Chem. Commun.*, 49 (1996).
174. H. Fienemann and G. Köbrich, *Chem. Ber*., **107**, 2797 (1974).
175. G. Köbrich, B. Kolb, A. Mannschreck and R. A. Misra, *Chem. Ber.*, **106**, 1601 (1973).
176. G. Zweifel, W. Lewis and H. P. On, *J. Am. Chem. Soc*., **101**, 5101 (1979).
177. R. F. Cunico and Y. K. Han, *J. Organomet. Chem*., **162**, 1 (1978).
178. D. Seyferth and D. Dagani, *J. Organomet. Chem*., **104**, 145 (1976).
179. S. Martin, R. Sauvêtre and J. F. Normant, *Tetrahedron Lett*., **23**, 4329 (1982).
180. L. M. Yagupol'skii, M. M. Kremlev, Y. A. Fialkov, V. A. Khranovskii and V. M. Yurchenko, *Zh. Org. Khim*., **13**, 1561 (1977); *Chem. Abstr*., **87**, 151788 (1977).
181. D. Masure, R. Sauvêtre, J. F. Normant and J. Villieras, *Synthesis*, 761 (1976).
182. F. Karrenbrock and H. J. Schäfer, *Tetrahedron Lett.*, 2913 (1979).
183. J. F. Normant, J. P. Foulon, D. Masure, R. Sauvêtre and J. Villieras, *Synthesis*, 122 (1975).
184. A. Oku, T. Harada, K. Hattori, Y. Nozaki and Y. Yamaura, *J. Org. Chem*., **53**, 3089 (1988).
185. T. Harada, T. Katsuhira and A. Oku, *J. Org. Chem*., **57**, 5805 (1992).
186. D. Grandjean and P. Pale, *Tetrahedron Lett*., **34**, 1155 (1993).
187. M. Iyoda, H. Otani, M. Oda, Y. Kai, Y. Baba and N. Kasai, *J. Am. Chem. Soc*., **108**, 5371 (1986).
188. R. H. Smithers, *J. Org. Chem*., **48**, 2095 (1983).
189. A. Pelter, J. Kvicala and D. E. Parry, *J. Chem. Soc., Perkin Trans. 1*, 2681 (1995).
190. H. Monti and P. Charles, *Synlett*, 193 (1995).
191. J. Barluenga, M. A. Rodríguez, P. J. Campos and G. Asensio, *J. Am. Chem. Soc*., **110**, 5567 (1988).
192. H. Mahler and M. Braun, *Tetrahedron Lett*., **28**, 5145 (1987).
193. H. Mahler and M. Braun, *Chem. Ber*., **124**, 1379 (1991).
194. M. Braun, J. Rahematpura, C. Bühne and T. C. Paulitz, *Synlett*, 1070 (2000).
195. M. Braun and A. Hohmann, unpublished.
196. R. K. Boeckman, Jr., J. E. Starrett, Jr., D. G. Nickell and P. E. Sum, *J. Am. Chem. Soc*., **108**, 5549 (1986).
197. A. Lüttringhaus and G. von Sääf, *Angew. Chem*., **51**, 915 (1938).
198. G. Wittig and L. Löhmann, *Justus Liebigs Ann. Chem*., **550**, 260 (1942).
199. U. Schöllkopf, in *Houben-Weyl, Methoden der Organischen Chemie* (Ed. E. Müller), 13/1, Thieme, Stuttgart, 1970, pp. 228–230.
200. T. Nakai and K. Mikami, *Chem. Rev*., **86**, 855 (1986).
201. J. S. Sawyer, A. Kucerovy, T. L. Macdonald and G. J. McGarvey, *J. Am. Chem. Soc*., **110**, 842 (1988).
202. E. J. Corey and T. M. Eckrich, *Tetrahedron Lett*., **24**, 3165 (1983).
203. L. Lochmann, J. Pospisil and D. Lim, *Tetrahedron Lett*., 257 (1966).
204. M. Schlosser, *J. Organomet. Chem*., **8**, 9 (1967).
205. R. Lehmann and M. Schlosser, *Tetrahedron Lett*., **25**, 745 (1984).
206. G. Stork and L. Maldonado, *J. Am. Chem. Soc*., **93**, 5286 (1971); **96**, 5272 (1974).
207. K. Deuchert, U. Hertenstein and S. Hünig, *Synthesis*, 777 (1973).
208. G. Wehner and S. Hünig, *Synthesis*, **180**, 391 (1975).
209. U. Hertenstein, S. Hünig and M. Öller, *Synthesis*, 416 (1976).
210. S. Arseniyadis, K. Kyler and D. S. Watt, *Org. React*., **31**, 1 (1984).
211. R. Naef and D. Seebach, *Justus Liebigs Ann. Chem*., 1930 (1983).

212. D. Seebach, A. R. Sting and M. Hoffmann, *Angew. Chem., Int. Ed. Engl.*, **35**, 2708 (1996).
213. J. W. Ludwig, M. Newcomb and D. E. Bergbreiter, *Tetrahedron Lett*., **27**, 2731 (1986).
214. A. Zask, *J. Org. Chem*., **57**, 4558 (1992).
215. J. d'Angelo, O. Pagés, J. Maddaluno, F. Dumas and G. Revial, *Tetrahedron Lett*., **24**, 5869 (1983).
216. W. Ladner, *Chem. Ber*., **116**, 3413 (1983).
217. I. Ojima, Y. H. Park, C. M. Sun, T. Brigaud and M. Zhao, *Tetrahedron Lett*., **33**, 5737 (1992).
218. W. Adam and L. A. Arias-Encarnacion, *Synthesis*, 388 (1979).
219. W. Adam and H.-H. Fick, *J. Org. Chem*., **43**, 772, 4574 (1978).
220. M. Newcomb and D. E. Bergbreiter, *J. Org. Chem*., **43**, 3963 (1978).
221. M. Braun, in *Houben-Weyl, Methoden der Organischen Chemie*, E21b (Eds. G. Helmchen, R. W. Hoffmann, J. Mulzer and E. Schaumann), Thieme, Stuttgart, 1995, pp. 1624–1666.
222. T. Kaneko, D. L. Turner, M. Newcomb and D. E. Bergbreiter, *Tetrahedron Lett*., 103 (1979).
223. T. M. Harris, C. M. Harris, P. C. Kuzma, J. Y.-C. Lee, S. Mahalingam and S. G. Gilbreath, *J. Am. Chem. Soc*., **110**, 6186 (1988).
224. S. G. Davies, C. L. Goodfellow and K. H. Sutton, *Tetrahedron: Asymmetry*, **3**, 1303 (1993).
225. P. Beak and B. G. McKinnie, *J. Am. Chem. Soc*., **99**, 5213 (1977).
226. P. Beak, M. Baillargeon and L. C. Carter, *J. Org. Chem*., **43**, 4255 (1978).
227. P. Beak and D. B. Reitz, *Chem. Rev*., **78**, 275 (1978).
228. R. Schlecker, D. Seebach and W. Lubosch, *Helv. Chim. Acta*, **43**, 4255 (1978).
229. P. Zhang and R. E. Gawley, *J. Org. Chem*., **58**, 3223 (1993).
230. P. Sommerfeld and D. Hoppe, *Synlett*, 746 (1992).
231. T. Cohen and J. R. Matz, *J. Am. Chem. Soc*., **102**, 6900 (1980).
232. W. C. Still, *J. Am. Chem. Soc*., **100**, 1481 (1978).
233. R. J. Linderman and A. Ghannam, *J. Org. Chem*., **53**, 2878 (1988).
234. R. Hoffmann and R. Brückner, *Angew. Chem., Int. Ed. Engl*., **31**, 647 (1992).
235. K. Tomooka, T. Igarashi, M. Watanabe and T. Nakai, *Tetrahedron Lett*., **33**, 5795 (1992).
236. C. A. Broka and T. Shen, *J. Am. Chem. Soc*., **111**, 2981 (1989).
237. D. K. Hutchinson and P. L. Fuchs, *J. Am. Chem. Soc*., **107**, 4930 (1987).
238. C. R. Johnson and J. R. Medich, *J. Org. Chem*., **53**, 4131 (1988).
239. R. J. Linderman and A. Godfrey, *J. Am. Chem. Soc*., **110**, 6249 (1988); *Tetrahedron Lett*., **27**, 4553 (1986).
240. R. J. Linderman, A. Godfrey and K. Horne, *Tetrahedron Lett*., **28**, 3911 (1987).
241. D. S. Matteson, P. A. Tripathy, A. Sarkar and K. M. Sadhu, *J. Am. Chem. Soc*., **111**, 4399 (1989).
242. G. J. McGarvey and M. Kimura, *J. Org. Chem*., **50**, 4655 (1985).
243. D. G. Farnum and T. Monego, *Tetrahedron Lett*., **24**, 1361 (1983).
244. R. J. Linderman and B. D. Griedel, *J. Org. Chem*., **56**, 5491 (1991).
245. J. J. Eisch and J. E. Galle, *J. Organomet. Chem*., **341**, 293 (1988).
246. J. A. Soderquist and C. Lopez, *Tetrahedron Lett*., **32**, 6305 (1991).
247. P. Lohse, H. Loner, P. Acklin, F. Steinfeld and A. Pfaltz, *Tetrahedron Lett*., **32**, 615 (1991).
248. J. K. Crandall and L. H. C. Lin, *J. Am. Chem. Soc*., **89**, 4526 (1967).
249. J. K. Crandall and M. Apparu, *Org. React*., **29**, 345 (1983).
250. J. J. Eisch and J. E. Galle, *J. Org. Chem*., **55**, 4825 (1990).
251. C. Lambert and P. v. R. Schleyer, in *Houben-Weyl, Methoden der Organischen Chemie*, E19d (Ed. M. Hanack), Thieme, Stuttgart, 1993, p. 15–19.
252. U. Schöllkopf and P. Hänssle, *Justus Liebigs Ann. Chem*., **763**, 208 (1972).
253. I. Hoppe and U. Schöllkopf, *Justus Liebigs Ann. Chem*., 1474 (1980).
254. F. T. Oakes and J. F. Sebastian, *J. Org. Chem*., **45**, 4959 (1980).
255. J. E. Baldwin, G. A. Höfle and O. W. Lever, Jr., *J. Am. Chem. Soc*., **96**, 7125 (1974).
256. M. Shimano and A. I. Meyers, *Tetrahedron Lett*., **35**, 7727 (1994).
257. L. Brandsma and H. Verkruijsse, *Preparative Polar Organometallic Chemistry 1*, Springer, Berlin, 1987, pp. 83–88.
258. R. K. Boeckman, Jr. and K. J. Bruza, *Tetrahedron Lett*., 4187 (1977); *Tetrahedron*, **37**, 3997 (1981).
259. E. Lukevics, V. Gevorgyan, Y. Goldberg, J. Popelis, M. Gavars, A. Gaukhman and M. Shimanska, *Heterocycles*, **22**, 987 (1984).
260. B. L. Groh, G. R. Magrum and T. J. Barton, *J. Am. Chem. Soc*., **109**, 7568 (1987).

261. P. Kocienski, S. Wadman and K. Cooper, *J. Am. Chem. Soc.*, **111**, 2363 (1989).
262. M. Schlosser, B. Schaub, B. Spahic and G. Sleiter, *Helv. Chim. Acta*, **56**, 2166 (1973).
263. B. Schaub and M. Schlosser, *Helv. Chim. Acta*, **58**, 556 (1975).
264. M. Stocks, P. Kocienski and D. K. Donald, *Tetrahedron Lett.*, **31**, 1637 (1990).
265. A. Lebouc, J. Delaunay and O. Riobé, *Synthesis*, 610 (1979).
266. T. Cohen and M. Bhupathy, *Tetrahedron Lett.*, **24**, 4163 (1983).
267. A. Alexakis, J. Hanaizi, D. Jachiet, J.-F. Normant and L. Toupet, *Tetrahedron Lett.*, **31**, 1271 (1990).
268. S. V. Ley, R. Leslie, P. D. Tiffin and M. Woods, *Tetrahedron Lett.*, **33**, 4767 (1992).
269. R. W. Saylor and J. F. Sebastian, *Synth. Commun.*, **12**, 579 (1982).
270. M. Fétizon, I. Hanna and J. Rens, *Tetrahedron Lett.*, **26**, 3453 (1985).
271. M. Fétizon, P. Goulaouic and I. Hanna, *Tetrahedron Lett.*, **26**, 4925 (1985).
272. M. Fétizon, P. Goulaouic, I. Hanna and T. Prangé, *J. Org. Chem.*, **53**, 5672 (1988).
273. V. Blanchot, M. Fétizon and I. Hanna, *Synthesis*, 755 (1990).
274. V. Blanchot-Courtois and I. Hanna, *Tetrahedron Lett.*, **33**, 8087 (1992).
275. N. Ruiz, M. D. Pujol, G. Guillaumet and G. Goudert, *Tetrahedron Lett.*, **33**, 2965 (1992).
276. S. Sengupta and V. Snieckus, *J. Org. Chem.*, **55**, 5680 (1990).
277. P. Kocienski and N. J. Dixon, *Synlett*, 52 (1989).
278. M. Tsukazaki and V. Snieckus, *Tetrahedron Lett.*, **34**, 411 (1993).
279. S. Superchi, N. Sotomayor, G. Miao, B. Joseph and V. Snieckus, *Tetrahedron Lett.*, **37**, 6057 (1996).
280. K. Tanaka, T. Nakai and N. Ishikawa, *Tetrahedron Lett.*, 4890 (1978).
281. J. Ichikawa, T. Sonoda and H. Kobayashi, *Tetrahedron Lett.*, **30**, 1641 (1989).
282. J. Ichikawa, T. Sonoda and H. Kobayashi, *Tetrahedron Lett.*, **30**, 5437 (1989).
283. J. Ichikawa, S. Hamada, T. Sonoda and H. Kobayashi, *Tetrahedron Lett.*, **33**, 337 (1992).
284. J. Ichikawa, T. Minami, T. Sonoda and H. Kobayashi, *Tetrahedron Lett.*, **33**, 3779 (1992).
285. J. Ichikawa, C. Ikeura and T. Minami, *Synlett*, 739 (1992).
286. A. J. Bennett, J. M. Percy and M. H. Rock, *Synlett*, 483 (1992).
287. J. Lee, M. Tsukazaki and V. Snieckus, *Tetrahedron Lett.*, **34**, 415 (1993).
288. P. J. Crowley, J. A. Howarth, W. M. Owton, J. M. Percy and K. Stansfield, *Tetrahedron Lett.*, **37**, 5975 (1996).
289. P. J. Crowley, J. M. Percy and K. Stansfield, *Tetrahedron Lett.*, **37**, 8233 (1996).
290. J. M. Percy, *Tetrahedron Lett.*, **31**, 3931 (1990).
291. S. T. Patel, J. M. Percy and R. D. Wilkes, *Tetrahedron*, **51**, 9201 (1995).
292. J. E. Baldwin, O. W. Lever, Jr. and N. R. Tzodikov, *J. Org. Chem.*, **41**, 2312 (1976).
293. J. S. Brimacombe and A. M. Mather, *J. Chem. Soc., Perkin Trans. 1*, 269 (1980).
294. J. S. Brimacombe, R. Hanna, A. M. Mather and T. J. R. Weakley, *J. Chem. Soc., Perkin Trans. 1*, 273 (1980).
295. R. S. Coleman and E. B. Grant, *J. Am. Chem. Soc.*, **117**, 10889 (1995).
296. R. Ruzziconi and M. Schlosser, *Angew. Chem., Int. Ed. Engl.*, **21**, 855 (1982).
297. S. L. Schreiber and J. A. Porco, Jr., *J. Org. Chem.*, **54**, 4721 (1989).
298. F. M. Atta, R. Betz, B. Schmid and R. R. Schmidt, *Chem. Ber.*, **119**, 472 (1986).
299. P. Cox, M. F. Mahon, K. C. Molloy, S. Lister and T. Gallagher, *Tetrahedron Lett.*, **29**, 1993 (1988).
300. A. B. Smith III and M. Fukui, *J. Am. Chem. Soc.*, **109**, 1269 (1987).
301. P. Lesimple, J.-M. Beau, G. Jaurand and P. Sinay, *Tetrahedron Lett.*, **27**, 6201 (1986).
302. J. A. Soderquist and A. Hassner, *J. Org. Chem.*, **45**, 541 (1980).
303. C. N. Skold, *Synth. Commun.*, **6**, 116 (1976).
304. K. H. Dötz, W. Kuhn and A. Thewalt, *Chem. Ber.*, **118**, 1126 (1985).
305. J. A. Soderquist and G. J.-H. Hsu, *Organometallics*, **1**, 830 (1982).
306. J. A. Soderquist and I. Rivera, *Tetrahedron Lett.*, **30**, 3919 (1989).
307. P. Kocienski, S. Jarowicki and S. Marczak, *Synthesis*, 1191 (1991).
308. T. Kawase, S.-I. Fujino and M. Oda, *Tetrahedron Lett.*, **31**, 545 (1990).
309. J. E. Baldwin and J. C. Bottaro, *J. Chem. Soc., Chem. Commun.*, 1121 (1981).
310. K.-P. Zeller and H. Gugel, in *Houben-Weyl, Methoden der Organischen Chemie*, E19b (Eds. M. Regitz and B. Giese), Thieme, Stuttgart, 1989, pp. 179–211.
311. H. C. Stiasny and R. W. Hoffmann, *Chem. Eur. J.*, **1**, 619 (1995) and references cited therein.
312. A. Hirai, M. Nakamura and E. Nakamura, *Chem. Lett.*, 927 (1998).

313. M. Topolski and H. M. Walborsky, *J. Org. Chem*., **59**, 5506 (1994).
314. A. Maercker, in *Lithium Chemistry: A Theoretical and Experimental Overview* (Eds. A.-M. Sapse and P. v. R. Schleyer), Chap. 11, Wiley, New York, 1995, pp. 477–577 and references cited therein.
315. G. Olah and A. Wu, *Synthesis*, 885 (1990).
316. L. Duhamel and J. M. Poirier, *J. Org. Chem*., **44**, 3585 (1979).
317. P. Fritsch, *Justus Liebigs Ann. Chem*., **279**, 319 (1894).
318. W. P. Buttenberg, *Justus Liebigs Ann. Chem*., **279**, 324 (1894).
319. H. Wiechell, *Justus Liebigs Ann. Chem*., **279**, 337 (1894).
320. A. A. Bothner-By, *J. Am. Chem. Soc*., **77**, 3293 (1955).
321. D. Y. Curtin, W. E. Flynn and R. F. Nystrom, *J. Am. Chem. Soc*., **80**, 4599 (1958).
322. F. Ramirez, N. B. Desai and N. McKelvie, *J. Am. Chem. Soc*., **84**, 1745 (1962).
323. E. J. Corey and P. L. Fuchs, *Tetrahedron Lett*., 3769 (1972).
324. H. J. Bestmann and H. Frey, *Liebigs Ann. Chem*., 2061 (1980).
325. M. C. McIntosh and S. M. Weinreb, *J. Org. Chem*., **58**, 4823 (1993).
326. D. Grandjean, P. Pale and J. Chuche, *Tetrahedron Lett*., **35**, 3529 (1994).
327. J. Villieras, P. Perriot and J. F. Normant, *Synthesis*, 458 (1975).
328. W. G. Salmond, M. C. Sobala and K. D. Maisto, *Tetrahedron Lett*., 1237 (1977).
329. W. G. Salmond, *Tetrahedron Lett*., 1239 (1977).
330. A. Hosomi, M. Inaba and H. Sakurai, *Tetrahedron Lett*., **24**, 4727 (1983).
331. L. F. Tietze, T. Neumann, M. Kajino and M. Pretor, *Synthesis*, 1003 (1995).
332. M. T. Reetz, T. J. Strack, J. Kanand and R. Goddard, *J. Chem. Soc., Chem. Commun*., 733 (1996).
333. E. Mainetti, L. Fensterbank and M. Malacria, *Synlett*, 923 (2002).
334. D. J. Nelson, *J. Org. Chem*., **49**, 2059 (1984).
335. J. Suffert and D. Toussaint, *J. Org. Chem*., **60**, 3550 (1995).
336. R. H. Fischer, M. Baumann and G. Köbrich, *Tetrahedron Lett*., 1207 (1974).
337. M. Baumann and G. Köbrich, *Tetrahedron Lett*., 1217 (1974).
338. U. Schöllkopf and M. Eisert, *Justus Liebigs Ann. Chem*., **664**, 76 (1963).
339. K. Ziegler and H.-G. Gellert, *Justus Liebigs Ann. Chem*., **567**, 185 (1950).
340. For a review, see: D. M. Hodgson and E. Gras, *Synthesis*, 1625 (2002).
341. A. C. Cope, G. A. Berchtold, P. E. Peterson and S. H. Sharman, *J. Am. Chem. Soc*., **82**, 6370 (1960).
342. R. K. Boeckman, Jr., *Tetrahedron Lett*., 4281 (1977).
343. D. M. Hodgson and G. P. Lee, *J. Chem. Soc., Chem. Commun*., 1015 (1996).
344. R. W. Thies and R. H. Chiarello, *J. Org. Chem*., **44**, 1342 (1979).
345. A. Yanagisawa, K. Yasue and H. Yamamoto, *J. Chem. Soc., Chem. Commun*., 2103 (1994).
346. D. M. Hodgson, L. A. Robinson and M. L. Jones, *Tetrahedron Lett*., **40**, 8637 (1999).
347. C. Agami, L. Dechoux, E. Doris and C. Mioskowski, *Tetrahedron Lett*., **38**, 4071 (1997).
348. L. Dechoux, C. Agami, E. Doris and C. Mioskowski, *Eur. J. Org. Chem*., 4107 (2001).
349. E. Doris, L. Dechoux and C. Mioskowski, *Synlett*, 337 (1998).
350. L. Dechoux, E. Doris and C. Mioskowski, *J. Chem. Soc., Chem. Commun*., 549 (1996).
351. D. M. Hodgson, M. A. H. Stent and F.-X. Wilson, *Org. Lett*., **3**, 3401 (2001); *Synthesis*, 1445 (2002).
352. C. S. Shiner, T. Tsunoda, B. A. Goodman, S. Ingham, S. Lee and P. E. Vorndam, *J. Am. Chem. Soc*., **111**, 1381 (1989).
353. T. Cohen, D. Ouellette, K. Pushpanandu, A. Senaratne and L.-C. Yu, *Tetrahedron Lett*., **22**, 3377 (1981).
354. M. Nitsche, D. Seebach and A. K. Beck, *Chem. Ber.*, **111**, 3644 (1978).
355. P. Kocienski and C. Barber, *Pure Appl. Chem*., **62**, 1933 (1990).
356. G. Cainelli, A. Umani Ronchi, F. Bertini, P. Grasselli and G. Zubiani, *Tetrahedron*, **27**, 6109 (1971).
357. M. Braun and D. Seebach, *Angew. Chem., Int. Ed. Engl*., **13**, 277 (1974).
358. C. H. Heathcock, in *Modern Synthetic Methods 1992*, VHCH, Basel; VCH, Weinheim, 1992, pp. 1–102.
359. C. Burford, F. Cooke, E. Ehlinger and P. Magnus, *J. Am. Chem. Soc*., **99**, 4536 (1977).
360. C. Burford, F. Cooke, G. Roy and P. Magnus, *Tetrahedron*, **39**, 867 (1983).
361. D. S. Matteson and D. Majumdar, *J. Organomet. Chem*., **184**, C 41 (1980).

362. F. Cooke and D. Magnus, *J. Chem. Soc., Chem. Commun.*, 513 (1977).
363. F. Cooke, G. Roy and D. Magnus, *Organometallics*, **1**, 893 (1982).
364. D. T. Tavares and R. E. Estep, *Tetrahedron Lett.*, 1229 (1973).
365. T. Satoh, T. Sato, T. Oohara and K. Yamakawa, *J. Org. Chem.*, **54**, 3973 (1989).
366. T. Satoh, T. Oohara and K. Yamakawa, *Tetrahedron Lett.*, **29**, 2851 (1988).
367. H. Taguchi, H. Yamamoto and H. Nozaki, *J. Am. Chem. Soc.*, **96**, 6510 (1974); *Bull. Chem. Soc. Jpn.*, **50**, 1592 (1977).
368. C. J. Kowalski, M. S. Haque and K. W. Fields, *J. Am. Chem. Soc.*, **107**, 1429 (1985).
369. T. Hiyama, M. Shinoda and H. Nozaki, *Tetrahedron Lett.*, 771 (1978).
370. P. Savignac and P. Coutrot, *Synthesis*, 197 (1976).
371. C. Chuit, R. Sauvêtre, D. Masure, M. Baudry, J. F. Normant and J. Villieras, *J. Chem. Res. (S)*, 104 (1977); *J. Chem. Res. (M)*, 1147 (1977).
372. M. Braun and H. Mahler, *Angew. Chem., Int. Ed. Engl.*, **28**, 896 (1989).
373. M. Braun and H. Mahler, *Synlett*, 587 (1990).
374. M. Braun and H. Mahler, *Liebigs Ann. Chem.*, 29 (1995).
375. M. Braun and J. Moritz, *Synlett*, 750 (1991).
376. M. Braun, C. Unger and K. Opdenbusch, *Eur. J. Org. Chem.*, 2389 (1998).
377. H. G. Kuivila, *Synthesis*, 499 (1970); *Adv. Organomet. Chem.*, **1**, 47 (1964).
378. W. P. Neumann, *Synthesis*, 665 (1987).
379. M. Pereyre, J.-P. Quintard and A. Rahm, *Tin in Organic Synthesis*, Butterworths, London, 1987, p. 35.
380. J. O. Metzger, in *Houben-Weyl, Methoden der Organischen Chemie*, E19a (Eds. M. Regitz and B. Giese), Thieme, Stuttgart, 1989, p. 166.
381. M. Braun and J. Moritz, *Chem. Ber.*, 1215 (1989).
382. M. Braun and K. Opdenbusch, *Angew. Chem., Int. Ed. Engl.*, **32**, 578 (1993); *Liebigs Ann./Recueil*, 141 (1997).
383. M. T. Reetz, *Angew. Chem., Int. Ed. Engl.*, **23**, 556 (1984); *Acc. Chem. Res.* **26**, 462 (1993).
384. D. J. Cram and F. A. Abd Elhafez, *J. Am. Chem. Soc.*, **74**, 5828 (1952).
385. D. J. Cram and D. R. Wilson, *J. Am. Chem. Soc.*, **85**, 1245 (1963).
386. E. L. Eliel, in *Asymmetric Synthesis*, Vol. 2, Part A (Ed. J. D. Morrison), Academic Press, New York, 1983, p. 125.
387. J. Mulzer, H.-J. Altenbach, M. Braun, K. Krohn and H.-U. Reissig, *Organic Synthesis Highlights*, VCH, Weinheim, 1991, p. 3.
388. M. Chérest, H. Felkin and N. Prudent, *Tetrahedron Lett.*, 2199 (1968).
389. N. T. Anh, *Top. Curr. Chem.*, **88**, 145 (1980).
390. R. M. Devant and H.-E. Radunz, in *Houben-Weyl, Methoden der Organischen Chemie*, E21a (Eds. G. Helmchen, R. W. Hoffmann, J. Mulzer and E. Schaumann), Thieme, Stuttgart, 1995, pp. 1151–1334.
391. W. C. Still and J. H. McDonald III, *Tetrahedron Lett.*, **21**, 1031 (1980).
392. F. Hintze and D. Hoppe, *Synthesis*, 1216 (1992).
393. D. Hoppe and O. Zschage, *Angew. Chem., Int. Ed. Engl.*, **28**, 67 (1989).
394. O. Zschage and D. Hoppe, *Tetrahedron*, **48**, 5657 (1992).
395. H. Paulsen, C. Graeve and D. Hoppe, *Synthesis*, 141 (1996).
396. U. Schöllkopf, in *Houben-Weyl, Methoden der Organischen Chemie*, 13/1 (Ed. E. Müller), Thieme, Stuttgart, 1970, p. 116.
397. R. W. Friesen, *J. Chem. Soc., Perkin Trans. 1*, 1969 (2001).
398. G. Helmchen, in *Houben-Weyl, Methoden der Organischen Chemie* E21a (Eds. G. Helmchen, R. W. Hoffmann, J. Mulzer and E. Schaumann), Thieme, Stuttgart, 1995, pp. 1–74.
399. M. Iwao and T. Kuraishi, *Tetrahedron Lett.*, **26**, 6213 (1985).
400. G. Habermehl and P. Hammann, *Naturstoffchemie*, Chap. 2, Springer, Berlin 1992.
401. R. K. Boeckman, Jr., K. J. Bruza, J. E. Baldwin and O. W. Lever, *J. Chem. Soc., Chem. Commun.*, 519 (1975).
402. R. K. Boeckman, Jr. and K. J. Bruza, *J. Org. Chem.*, **44**, 4781 (1979).
403. E. Negishi and F.-T. Luo, *J. Org. Chem.*, **48**, 1560 (1983).
404. C. E. Russell and L. S. Hegedus, *J. Am. Chem. Soc.*, **105**, 943 (1983).
405. A. B. Levy and S. J. Schwartz, *Tetrahedron Lett.*, 2201 (1976).
406. A. B. Levy, S. J. Schwartz, N. Wilson and B. Christic, *J. Organomet. Chem.*, **156**, 123 (1978).
407. S. Hoff, L. Brandsma and J. F. Arens, *Recl. Trav. Chim. Pays-Bas*, **87**, 916, 1197 (1968).

408. S. Hoff, L. Brandsma and J. F. Arens, *Recl. Trav. Chim. Pays-Bas*, **88**, 609 (1969).
409. R. Zimmer, *Synthesis*, 165 (1993).
410. R. Zimmer and F. A. Kahn, *J. Prakt. Chem*., **338**, 92 (1996).
411. H.-U. Reissig, W. Schade, M. Okala Amombo, R. Pulz and A. Hausherr, *Pure Appl. Chem*., **74**, 167 (2002).
412. S. Hormuth and H.-U. Reissig, *Synlett*, 179 (1991).
413. D. Gange and P. Magnus, *J. Am. Chem. Soc*., **100**, 7746 (1978).
414. S. Hormuth and H.-U. Reissig, *J. Org. Chem*., **59**, 67 (1994).
415. S. Hormuth, H.-U. Reissig and D. Dorsch, *Liebigs Ann. Chem*., 121 (1994).
416. M. Okala Amombo, A. Hausherr and H.-U. Reissig, *Synlett*, 1871 (1999).
417. W. Schade and H.-U. Reissig, *Synlett*, 632 (1999).
418. P. Rochet, J.-M. Vatèle and J. Goré, *Synlett*, 105 (1993).
419. J.-P. Surivet, J. Goré and J.-M. Vatèle, *Tetrahedron Lett.*, **37**, 371 (1996).
420. A. Hausherr, B. Orschel, S. Scherer and H.-U. Reissig, *Synthesis*, 1377 (2001).

CHAPTER **14**

Addition of organolithium reagents to double bonds

HIROSHI YAMATAKA

Institute of Scientific and Industrial Research, Osaka University, Ibaraki, Osaka 567–0047, Japan
Fax: +81-6-6879-8469; e-mail: yamataka@sanken.osaka-u.ac.jp

and

K. YAMADA and K. TOMIOKA

Graduate School of Pharmaceutical Sciences, Kyoto University, Yoshida, Sakyo-ku, Kyoto 606–8501, Japan
Fax: +81-75-753-4604; e-mail: yamak@pharm.kyoto-u.ac.jp and tomioka@pharm.kyoto-u.ac.jp

---

The Chemistry of Organolithium Compounds. Edited by Z. Rappoport and I. Marek
ISBN: 0-470-84339-X

I. INTRODUCTION

Organolithium reagents are among the most versatile reagents in synthetic organic chemistry. The mechanism of the addition reaction of the reagents to double bonds has been studied extensively in order to understand the reaction in detail and to design more effective and sophisticated reagents. In this chapter, mechanism and synthetic applications, in particular asymmetric reactions, of organolithium reagents with double bonds are described. Mechanistically, two points are important in understanding the reaction. First, the static structure of organolithium reagents in solution and the identity of the reacting species. Although a simple alkyl lithium reagent, abbreviated as RLi, is usually written as if it is a monomer, RLi is known to exist as aggregates in solution. What types of aggregate each RLi forms in solvents and whether RLi reacts as an aggregate or dissociates to a monomer before the reaction with the electrophile are the important issues in mechanistic investigation. Second, RLi may react with carbon−oxygen double bonds in two ways: direct nucleophilic attack of formal R anion on the carbonyl function or initial electron transfer (ET) from RLi to the carbonyl compound followed by a radical coupling process. These two mechanistic points in the RLi reaction are discussed by comparing the reaction of RLi with that of RMgX, the Grignard reaction. In the field of synthetic chemistry, enantioselective construction of organic compounds is one of the areas studied most eagerly by organic chemists because of the growing demand for enanantiomerically pure molecules (e.g. pharmaceuticals). Alkenes having an electron-withdrawing group are electrophilic and undergo addition with nucleophiles. The addition, referred to as a conjugate addition or a 1,4-addition, initially gives a β-substituted stabilized carbanion, which is then trapped by an electrophile (equation 1). Because conjugate addition can simultaneously form two bonds and two (or more in some cases) stereogenic centers, enantioselective conjugate addition is one of the most powerful synthetic methods[1]. Chiral copper catalysts have been used with organolithiums or Grignard reagents in enantioselective conjugate addition[1]. Recently, organozinc reagents with a copper catalyst[2] and arylboronic acids with a rhodium catalyst[3] were successfully utilized in enantioselective conjugate addition. Organolithium reagents are highly reactive species, thus the development of asymmetric conjugate addition with organolithium is challenging. This chapter provides an overview of recent progress in asymmetric conjugate addition of organolithium compounds controlled by an external chiral ligand[4]. Finally, diastereofacial discriminating asymmetric addition controlled by a chiral auxiliary is also briefly described.

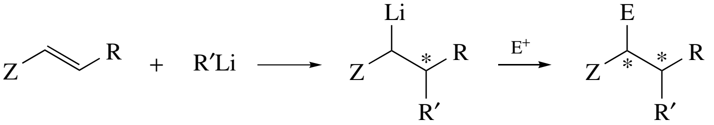

(1)

Z = electron-withdrawing group

E^+ = electrophile

II. RLi AGGREGATION AND KINETICS

A. RLi Aggregation

The state of aggregation of RLi in various solvents has been investigated by a variety of methods. In 1967, West and Waack used a differential vapor pressure technique to study solution colligative properties of RLi[5]. Deviations from ideality indicated that in THF at 25 °C, MeLi and BuLi are tetrameric, PhLi dimeric and benzyllithium monomeric. MeLi was also suggested to be tetrameric in diethyl ether.

Much later in 1984, Jackman and Scarmoutzos confirmed by NMR study that PhLi is indeed dimeric in THF at room temperature as well as at −120 °C, although it is tetrameric in cyclohexane/diethyl ether as in the solid state[6]. In dilute diethyl ether solution, however, tetrameric and dimeric structures coexist for PhLi.

McGarrity and Ogle examined the aggregation of BuLi in THF by using ^1H and ^7Li NMR spectroscopy and determined that BuLi exists as a tetramer in equilibrium with a dimer in THF. Activation and equilibrium parameters were measured for the tetramer–dimer equilibrium (equation 2). No evidence was obtained for a monomer at concentrations of BuLi down to 0.1 mM[7].

$$(\mathrm{BuLi})_4 \cdot 4\mathrm{THF} + 4\mathrm{THF} \rightleftharpoons 2((\mathrm{BuLi})_2 \cdot 4\mathrm{THF}) \qquad (2)$$

$$\Delta H^\circ = -(6.3 \pm 0.4)\ \mathrm{kJ\,mol^{-1}}, \quad \Delta S^\circ = -(58 \pm 2)\ \mathrm{J\,mol^{-1}\,K^{-1}}$$

$$\Delta H^{\neq} = -(41 \pm 2)\ \mathrm{kJ\,mol^{-1}}, \quad \Delta S^{\neq} = -(30 \pm 10)\ \mathrm{J\,mol^{-1}\,K^{-1}}$$

Recent NMR study suggested that PhLi exists as a mixture of tetramer and dimer in diethyl ether and that the addition of a stoichiometric amount of a coordinating solvent such as THF, dioxolane, DME or TMEDA induces complete conversion of the mixture to dimeric solvates[8]. In a THF solution PhLi exists as a mixture of dimer and monomer. It was noted that the addition of 12-crown-4 or HMPA increases the reactivity and decreases the selectivity of PhLi in THF.

B. RLi Kinetics

Measurement of rate constants provides information not only on the rate process but on the reactant state as well. The first kinetic study on the addition of RLi to ketones goes back to 1950, when Swain and Kent reported the results of kinetic experiments for the addition reaction of RLi and RMgX with ketone[9]. In these studies, a flow method was used to measure the reactivity of these fast reactions. The reaction was carried out by rapidly mixing a diethyl ether solution of PhLi and a toluene solution of 4,4′-bis(dimethylamino)benzophenone, and the reaction showed 2nd order kinetics, 1st order for each substrate, as could be expected[9]. Analogous reaction of PrMgBr with diisopropyl ketone gave more complex results, which suggested kinetics with 1st order in the ketone and 2nd order in RMgX[10]. The results were rationalized by a mechanism in which the ketone and RMgX formed a 1:1 complex that was attacked by another molecule of RMgX. Thus, different behavior of RLi and RMgX was already noted.

An example of obtaining information on the state of aggregation of RLi in solution from kinetic study was presented by Waack and coworkers, who measured rate constants of the reactions of various RLi with 1,1-diphenylethene at variable RLi concentrations by a UV method[11, 12]. Since 1,1-diphenylethene is not highly reactive and the reaction takes *ca* one hour in THF at 22 °C, the rate constant can easily be determined. The measured rate constants and kinetic orders were listed in Table 1. First-order kinetic behaviors can result from the reagent being monomeric. Alternatively, an aggregated species may be predominant in solution and is responsible for product formation. A previous report of benzyllithium being monomeric in THF[5] favored the former interpretation for this reagent. Fractional reaction order observed for MeLi, BuLi, PhLi and vinyl-Li could be interpreted by a mechanism in which a reactive species, presumably the monomer, exists in a minor amount in equilibrium with unreactive aggregates[13].

Similar fractional reaction orders with respect to RLi reagents were reported for metalation of triphenylmethane in THF at 22 °C when using an excess of RLi[14]. The kinetic orders were the same as in the additions to $Ph_2C{=}CH_2$, i.e. 1/4th for MeLi, BuLi, vinyl-Li, 0.6th for PhLi and 1st for allyl-Li and benzyl-Li. Again, the results were consistent with the colligative measurements of the aggregation state of these RLi reagents; BuLi is tetrameric in diethyl ether and MeLi is tetrameric in THF and in diethyl ether[5]. The fact that the kinetic order varies with the reagent indicated that the effective reactivity order also varies with the reagent concentration; e.g. the reactivity order is benzyl-Li > allyl-Li > BuLi > PhLi > vinyl-Li > MeLi at 0.1 M, and benzyl-Li > BuLi > allyl-Li > vinyl-Li > PhLi > MeLi at 0.01 M.

Later, Smith and coworkers succeeded in measuring rate constants of the reaction of MeLi with a carbonyl compound at various reagent concentrations with a stopped-flow/rapid scan spectroscopic method, and demonstrated that the reaction also exhibited a fractional kinetic order[15]. Thus, the reaction of 2,4-dimethyl-4′-methylmercaptobenzophenone with MeLi in diethyl ether at 25 °C showed one-fourth order in MeLi in the concentration range of MeLi between 3.9 mM and 480 mM (Figure 1). The rate constant was $200 \pm 7\ M^{1/4}\ s^{-1}$. Under these conditions, the monomer was considered the reactive species that exists in equilibrium with the tetramer. Addition of LiBr or LiI depressed the reaction rate but did not change the kinetic order. The same

TABLE 1. Kinetic parameters for addition of organolithium reagents to 1,1-diphenylethene in THF at 22 °C[12]

RLi	Reaction order	Rate constant[a]
MeLi	0.24 ± 0.03	0.12
PhLi	0.66 ± 0.04	0.25
vinyl-Li	0.34 ± 0.1	0.11
BuLi	(*ca* 0.4)[b]	470
Allyl-Li	(*ca* 1)[b]	110
Benzyl-Li	1.1 ± 0.2	3000

[a] $l^{1/n}\ mol^{-1/n}\ s^{-1} (\times 10^2)$.

[b] The number of points is too small to give reliable values.

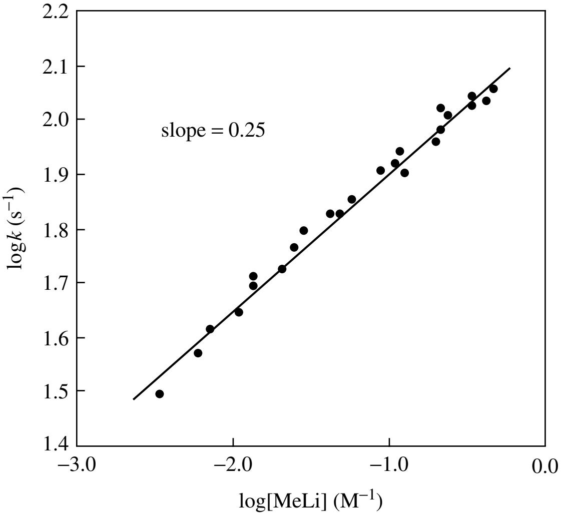

FIGURE 1. Log k vs. log [MeLi] plot for the reaction of 2,4-dimethyl-4′-methylmercaptobenzophenone with MeLi in diethyl ether at 25 °C

kinetic order observed for different substrates (electrophiles) strongly suggests that the fractional order is not due to a specific interaction between the reagent and the substrate, but due to the state of the reagent in solution.

The reaction of BuLi with 4-methylmercaptoacetophenone in benzene was examined in detail with IR and UV stopped-flow spectrophotometric techniques[16]. The UV spectrum showed that after mixing (*ca* 1 ms) of the ketone with BuLi, the $\pi-\pi^*$ absorption of the ketone was broadened and shifted toward a longer wavelength, although such a spectrum change was not clear in the IR. A similar absorbance shift in the spectrum was reported in both UV and IR in reactions of ketones with MeMgBr[17]. In these cases, the long-wavelength absorbance was attributed to a complex between the Grignard reagent and the ketones. The rate of the BuLi addition increased rapidly with the increase of the BuLi concentration in a low concentration range and reached a constant maximum at high BuLi concentration. This nonlinear response of the rate to the reagent concentration could be interpreted in two ways: one is a mechanism, where monomer is the reactive species that exists in equilibrium with higher aggregates, as in the case of MeLi in diethyl ether, or by the other mechanism, in which the reaction proceeds in a two-step process of an initial complex formation and the conversion of the complex to the product. The mechanism of the reaction in benzene has not yet been fully studied.

Fractional reaction orders with respect to BuLi (0.25–0.33) in the reactions with electrophiles repeatedly reported in the literature were attributed to monomer/tetramer equilibrium[12, 14, 16, 18, 19]. Holm measured the rate of the reaction of BuLi with solvent molecules (i.e. diethyl ether, THF) by UV at 240 nm (diethyl ether) and 270 nm (THF)[20]. These reactions have an advantage in that a wide range of the reagent concentration can be examined, free from a side reaction with the solvent, since the reaction with the solvent itself is the reaction studied here. The reaction order with respect to BuLi in THF was found to be 0.3 above 0.1 M and increased up to 1.0 when the concentration was reduced below 10^{-2} M. On the other hand, it was claimed to be 0.33 over the concentration range of 0.1 mM to 2.0 M for the reaction with diethyl ether, although the logarithmic plot in diethyl ether was not a straight line but apparently curved downward, showing the reaction order changes from 0.25 to 0.5 on decreasing the BuLi concentration[20].

As described above, the NMR study by McGarrity and Ogle revealed that BuLi in THF exists as an equilibrium mixture of the dimer and the tetramer with no evidence for the monomer at concentration down to 0.1 mM[7]. The results, however, apparently disagreed with the report by Holm, who demonstrated that the reaction order with respect to BuLi in the reaction with THF was 0.3 above 0.1 M and increased up to 1.0 when the concentration of BuLi was reduced below 10^{-2} M[20]. Holm concluded that the true reacting species is the monomer, which exists as a minor component in the monomer–aggregate equilibrium at a high reagent concentration.

If the monomer is the true reacting species and the reaction of the monomer with an electrophile is fast enough compared to the monomer–aggregate equilibrium, then the rate should be independent of the electrophile concentration. This was indeed found for the reaction of BuLi with methyl trifluoroacetate in diethyl ether; the reaction was extremely fast (18.5 s^{-1} at −28 °C) and was 0th order with respect to the ester concentration[18]. Reaction of benzonitrile with BuLi in diethyl ether was slower, but the rate increased with increasing the benzonitrile concentration and reached a maximum value similar to that (7×10^{-3} s^{-1} at −82 °C) with methyl trifluoroacetate and the reaction order approached 0. Thus, the rate-determining step for the reaction of benzonitrile changed with its concentration.

Kinetics of the reaction of *sec*-BuLi and BuLi with substituted phenyl *sec*-butyl ketones in cyclohexane was studied by stopped-flow IR spectroscopy at 25 °C[21]. Immediately after mixing (3 ms) of RLi and the ketones, a new C=O absorption appeared at a wavenumber lower by about 10 cm^{-1}. The equilibrium constants could be determined and found to depend on the substituent on the phenyl ring of the ketone (Table 2). The Hammett plot gave the ρ value of -0.86 ± 0.05. Thus, an electron-withdrawing substituent makes smaller both the equilibrium constant and the shift of the C=O wavenumber. The rate was measured under excess BuLi concentration conditions. For a ketone with an electron-withdrawing substituent the rate increased with the BuLi concentration and leveled off at a high concentration range, whereas the rate for a ketone with an electron-donating substituent showed a maximum when plotted against the BuLi concentration. The results were interpreted by assuming two reaction pathways: (1) a complex formation between the ketone and the reagent aggregate, followed by the product formation, and (2) a direct product formation from the ketone and the BuLi monomer. For a ketone with an electron-donating substituent, as the reagent concentration increases the fraction of the path through the ketone–aggregate complex increases much more rapidly than the monomeric path. Since the monomer is more reactive than the aggregate, the overall rate decreases with the increase in the BuLi concentration. For a ketone with an electron-withdrawing substituent, on the other hand, the reaction with the more reactive monomer predominates, since the

TABLE 2. IR carbonyl wavenumber shifts[a] and equilibrium constants for the reactions of *sec*-BuLi with substituted phenyl *sec*-butyl ketones in cyclohexane at 25 °C[21]

Substituent	$\Delta\nu_{CO}(cm^{-1})$	$K(M^{-1})$
p-C_6H_5O	−13	49 ± 5
H	−11	37 ± 3
p-Cl	−11	29 ± 4
m-CF_3	−9	26 ± 3

[a] A shift of carbonyl wavenumber of the ketone upon mixing with *sec*-BuLi, $\Delta\nu_{CO} \pm 2$ cm^{-1}.

equilibrium constant for the complex formation is small and therefore a saturation plot was obtained.

A rapid-injection NMR study for the reaction of BuLi with benzaldehyde in THF suggested that both the BuLi dimer and the tetramer are the reacting species and the dimer is 10 times more reactive than the tetramer in THF at −85 °C[22]. In the initial stage, the reaction of the dimer was faster than its generation from the tetramer. If benzaldehyde was injected into a large excess of BuLi pre-equilibrated in THF at −85 °C, benzaldehyde was no longer present after 50 ms. The reaction was too rapid to follow with the NMR technique. However, if BuLi in toluene was injected into benzaldehyde in THF, it could be seen that the tetramer reacted directly with benzaldehyde faster than its dissociation to the dimer, and the dimer reacts 10 times faster than the tetramer. Aggregation with LiOBu increased the reactivity of BuLi[22].

Finally, Nudelman and coworkers examined the effects of temperature, reagent concentration, reaction time, a radical trap, light and solvent on the formation of radical byproduct, in the reaction of PhLi with *E*-cinnamaldehyde. It was claimed that the PhLi dimer is the reacting species with the aldehyde and that the reaction is initiated by an ET from the PhLi dimer to the cinnamaldehyde. MO calculations at the MNDO level of theory were claimed to be consistent with the participation of a dimer species[23].

C. Comparison with RMgX — Aggregation and Kinetics

Kinetic study of the reactions of RLi and RMgX has been carried out in a similar manner, but in fact the studies of RMgX were ahead of those of RLi since reactions of RLi are more vigorous and difficult to control. The mechanisms of the Grignard and RLi reactions are similar in some way but yet somewhat different.

As in the case of RLi, a 1:1 complex formation between the carbonyl function and RMgX was considered to be an important step of the Grignard reaction[10, 24, 25]. For the reaction of MeMgBr and 2,4-dimethyl-4′-methylmercaptobenzophenone in diethyl ether Smith and coworkers detected a new band in the UV, which was ascribed to the C=O⋅⋅RMgX complex[26]. The rates of decrease of the absorbance of the two bands, 315 nm for the free ketone and 355 nm for the complex, were followed by a stopped-flow technique. It was found that the absorbance decreased with time at the same rate, showing that there was an equilibrium between the two species. Under the conditions that the concentration of the ketone was much lower (10^{-4} M) than that of the Grignard reagent (0.01–0.4 M) the pseudo-first-order rate constant did not follow a linear dependence on the reagent concentration but exhibited a saturation curve. The logarithmic plot is not linear as shown in Figure 2, which differs from the case of MeLi, and a linear regression gave an apparent slope of 0.65. The nonlinear plot was analyzed with a reaction scheme $\text{Ketone} + \text{MeMgBr} \rightleftharpoons \text{Complex} \rightarrow \text{Product}$. Fitting numerical parameters, equilibrium and rate constants, reproduced the observation. A similar nonlinear dependence was observed for the reaction of MeMgBr with 4-methylmercaptoacetophenone. On the other hand, the pseudo-first-order rate constant for the reaction of benzophenone showed a linear dependence on the Grignard reagent concentration, in sharp contrast to the curved dependence for the 2,4-dimethyl-4′-methylmercaptobenzophenone and 4-methylmercaptoacetophenone reactions, suggesting that the reaction with benzophenone was free from complication due to the complex formation equilibrium.

Similar kinetic behavior was observed for the reaction of 4-methylmercaptoacetophenone with Me_2Mg in diethyl ether[27]. Two absorption maxima at 308 nm (free ketone) and 337 nm (complex) showed saturation kinetics, which fitted with the scheme $\text{Ketone} + Me_2Mg \rightleftharpoons \text{Complex} \rightarrow \text{Product}$. From a linear plot of $1/k$ vs. $1/[Me_2Mg]$, k_2 and K were calculated where k_2 is the rate constant of the second step and k is the equilibrium constant of the first step.

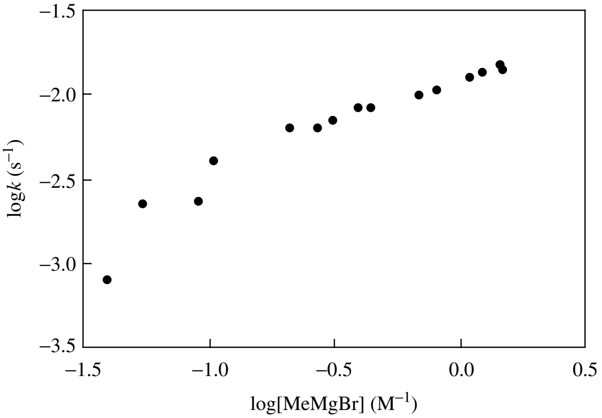

FIGURE 2. Log *k* vs. log [MeMgBr] plot for the reaction of 2,4-dimethyl-4′-methylmercaptobenzophenone with MeMgBr in diethyl ether at 25 °C

Kinetic study of the reaction of cyclopentyl-MgBr + 4-methylmercaptoacetophenone by using stopped-flow UV and IR spectroscopies also showed that the rate constant was in the range of 2–6 s^{-1} in diethyl ether at 25 °C, and the rate was first order in RMgX at low concentration (*ca* 0.1 M) and 0th order at high concentrations (0.3–0.8 M)[17]. The results were interpreted by the mechanism which involved pre-equilibrium of complex formation and conversion of the complex to the product.

Ashby and coworkers measured the rate of the reaction of MeMgBr with benzophenone in diethyl ether by a UV method under the conditions that the concentration of MeMgBr was lower than 1.52×10^{-2} M and the concentration ratio of the reagent to ketone was 25–150[28]. At the low MeMgBr concentration, which is low enough for the reagent to exist as a monomer but is still sufficiently larger than that of the ketone, the rate was functionally dependent on the reagent concentration. It was proposed that the results support Swain's suggestion that the ketone and the Grignard reagent form a complex, which by the attack of another molecule of the reagent gives product (equation 3). However, the data did not fit with either Smith's mechanism (equation 4), where the complex gives product without the attack by another reagent, or a simple dimer mechanism, Ketone + $(RMgX)_2 \rightarrow$ Product.

$$\text{Ketone} + \text{RMgX} \rightleftharpoons \text{complex} \xrightarrow{\text{RMgX}} \text{Product} \qquad (3)$$

$$\text{Ketone} + \text{RMgX} \rightleftharpoons \text{complex} \longrightarrow \text{Product} \qquad (4)$$

The kinetics of the Grignard reaction was recognized to be much more complex than originally considered because of several factors: the Schlenk equilibrium produces many reacting species, a metal impurity induces an ET process, and the primary product, ROMgX, contributes to the reaction[29].

III. Li ENOLATE AGGREGATION AND KINETICS

A. Li Enolate Aggregation

Lithium enolates are the most studied lithium reagents because of their importance in synthetic chemistry. As in the cases of other lithium reagents, the state of aggregation has been an important topic for these reagents[30,31]. For the enolates of ketones such as pinacolone and isobutyrophenone, the tetrameric structure has been indicated in THF[32–36]. Lithium pinacolone enolate in hydrocarbon solvent is hexameric[36,37].

Lithium enolate of *p*-phenylisobutyrophenone exists as a mixture of monomer and tetramer in dilute THF with $K_{1,4} = 5.0 \times 10^8$ M^{-3}[32]. On the other hand, it was shown to be a tetramer in methyl *tert*-butyl ether (MTBE)[38], whereas it is a monomer in DME. The results are consistent with the idea that the monomer is preferred in more coordinating solvents and that the coordination ability of the ether solvents is in the order DME > THF > MTBE[39]. Jackman and Szeverenyi concluded from NMR study that at higher concentration the lithium enolate of isobutyrophenone in DME is a mixture of a tetramer and a lower aggregate that they considered to be the dimer[34]. The lithium enolate of 2-phenyl-α-tetralone is present as a monomer/dimer equilibrium in THF with $K_{1,2} = 1930$ M^{-1}[32].

B. Li Enolate Kinetics

Streitwieser and coworkers recently reported that the lithium enolate of *p*-(phenylsulfonyl)isobutyrophenone exists as a monomer–dimer mixture in THF, with the equilibrium constant $K = (5.0 \pm 0.1) \times 10^4$ M^{-1}[40]. The rate of the reaction of the enolate with *p-tert*-butylbenzyl bromide was measured spectrophotometrically at the enolate concentration range of 7×10^{-4} to 5×10^{-3} M, where the percentage of the monomer was 4.5 to 11%. The logarithmic plot of the rate vs the enolate concentration was linear with a slope of 0.50 ± 0.04, indicating that the reacting species is the monomer that exists as a minor component in the equilibrium with the dimer.

They later reported that the lithium enolate of *p*-phenylisobutyrophenone in THF exists mainly as a tetramer and the monomer/tetramer equilibrium constant is $K_{1,4} = 5.0 \times 10^8$ M^{-3}[32]. Thus, the predominant aggregate is tetramer in this case and dimer in the case above. Temperature effect measurements revealed that the aggregation is an entropy-driven process. Alkylation rates of the enolate with *p-tert*-butylbenzyl bromide were measured in THF with various formal enolate concentrations that corresponded to the equilibrium aggregation numbers of 1.6 to 3.6. The kinetics followed rate laws with apparent reaction order of 0.50 (lower concentration) to 0.30 (higher concentration) in the formal enolate concentration. Thus, the reaction order varied with the formal enolate concentration, but it was first order in the monomer concentration. It was clear that the reactive species was the monomer, even when the tetramer dominated the equilibrium[32]. The reactivity study indicated that under synthetic conditions of several tenths molar, alkylation occurs dominantly via the monomer. On the other hand, although the monomer of a lithium enolate is much more reactive (*ca* 1000) than the aggregates in alkylation reactions[32,36], for acylation of ester the reactivity difference was found to be surprisingly small (*ca* 10), and hence aggregates are important for acylation under the normal synthetic conditions where the concentration of enolates is high[41]. The small reactivity difference in acylation reactions is apparently due to the possibility that both oxygens in the ester can coordinate to Li cations in the aggregate transition state (TS; dimer TS), making the TS with the aggregate stable[38,41,42]. Such stabilization does not exist in the monomer TS.

Lithiation of 2-biphenylcyclohexanone gave two enolate species in THF: one an unconjugated secondary enolate and the other a conjugated tertiary enolate. The former exists dominantly as the tetramer and the latter as a monomer–dimer mixture. In both cases the monomer reacts faster than the aggregates with alkylating substrates[43].

Reactivities of lithium pinacolone enolate with various ketones were determined by competition experiments in diethyl ether at −78 °C. For a series of substrates, $MeCOCH_2X$ and $PhCOCH_2X$, $\rho_I(X) = 6.62$ and 7.61, indicating a large electronic field effect[44].

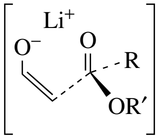

monomer TS

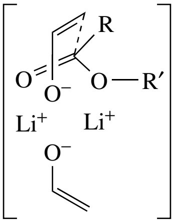

dimer TS

IV. MECHANISM AND REACTION PATHWAYS

A. ET vs. Polar Addition Pathway

The addition of RLi and other nucleophiles to carbonyl functions in general proceeds via one of the two possible reaction pathways, polar addition (PL) and electron transfer (ET)–radical coupling (RC) sequence (equation 5). Current reaction design for the synthetic purpose of additions of common nucleophiles to aldehydes and ketones is mostly based on the polar mechanism, but apparently the ET process is involved in some reactions of, for example, Grignard reagents[45–49]. Mechanistically there are three possible variations: the PL pathway, the ET rate-determining ET-RC route and the RC rate-determining ET-RC route.

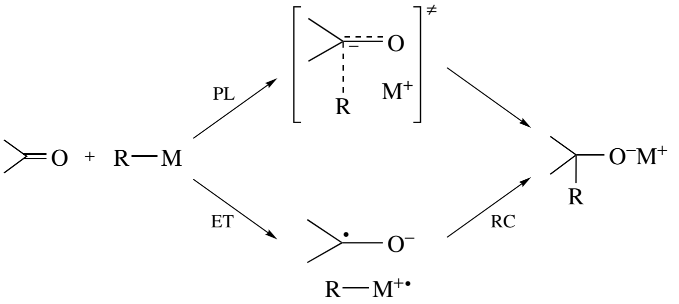

(5)

Distinction between PL and ET mechanisms is not straightforward. Various experimental methods have been used so far to demonstrate the ET process, including spectroscopic detection of radical intermediates[46, 47, 50–54], detection of products indicative of radical intermediates[51–53, 55–58], and measurement of secondary deuterium[59, 60] and carbonyl carbon kinetic isotope effects (KIEs)[49, 60–65]. The combination of several experimental methods, including KIE, substituent effect and probe experiments, was shown to be useful in distinguishing the ET process from the PL process for the addition reactions of the Grignard[49, 63, 64] and other organometallic reagents[66].

B. Spectroscopic Evidence

1. Reaction of R_2CuLi

In 1966, House and coworkers observed that the reaction of MeLi or MeMgBr with *trans*-3-penten-2-one (*trans* enone) in diethyl ether gave the 1,2-addition product, whereas the addition of copper salts changed the product to predominantly (MeMgBr) or exclusively (MeLi) 1,4-adduct[67]. A copper reagent, like $Li^+Me_2Cu^-$, was presumed, which preferably gave the 1,4-adduct. It was also noted that although fluorenone reacted very rapidly with MeMgBr to give the 1,2-adduct, it yielded a deep green solution as soon as it was mixed with the copper reagent. The ESR spectrum was consistent with the formation of the radical ion pair of the ketone with the Li cation. Hydrolysis of the reaction mixture gave fluorenone, the 1,2-adduct and pinacol. Later, the reaction of lithium dimethylcuprate (Me_2CuLi) with benzophenone was examined in detail[51]. A mixture of benzophenone and Me_2CuLi in diethyl ether at −70 °C gave a red-colored solution ($\lambda_{max} = 422$ nm). The ESR, Raman and NMR spectra of the solution indicated that the red color arose from a charge-transfer absorption and that the species responsible for the color was present only at low concentration. When this solution was warmed up to 0 °C, the color of the solution changed to blue ($\lambda_{max} = 600$ nm), due to the formation of benzophenone ketyl. Upon hydrolysis (after 30 min), the solution gave the 1,2-adduct (80%) and recovered benzophenone (20%).

Competition experiment in which a limited amount (0.9 molar equiv) of Me_2CuLi was allowed to react with a mixture of PhCOPh and an enone, $Me_2C{=}CHCHO$, was carried out. In spite of the fact that both substrates have similar reduction potential, the reaction of Me_2CuLi with the enone was at least 15 times as rapid as addition to PhCOPh. The results indicated that the rate of ET was not the sole controlling factor of the reactivity of these reactions. It was suggested that the recombination step to give the 1,2-adduct was too slow to allow appreciable concentration of the ketyl to accumulate in the reaction mixture[51].

2. Reaction of Li enolate

It has clearly been shown that although lithium enolates of various ketones exist predominantly as aggregates, the reacting species is the monomer. Then what is the mechanism of the addition reaction of these enolates with ketones and aldehydes? Ashby and Argyropoulos reported that the reaction of the lithium enolate of pinacolone with benzophenone and *o*-methylbenzophenone gave ESR active species; the rate of decay of the intermediate of *o*-methylbenzophenone (1.4×10^{-6} s^{-1}) agreed with the rate of formation of the adduct[68]. A radical chain mechanism was eliminated since no effect of light, *p*-dinitrobenzene or dicyclohexylphosphine was detected; free ketyl did not go outside of the solvent cage. It was concluded that ET from the enolate to ketones was involved in the reaction, although the ET step could be a blind alley in the overall reaction scheme, as the authors noticed.

Arnett and coworkers later examined the reaction of lithium pinacolone enolate with substituted benzaldehydes in THF at 25 °C. The determination of the heat of reaction indicated that the Hammett ρ value for the process is 3.37[69]. Although the aldol reaction was instantaneous in THF at 25 °C, the reaction with *o*- or *p*-methylbenzaldehyde could be followed using a rapid injection NMR method in methylcyclohexane solvent at −80 °C. Application of Eberson's criterion[70] based on the Marcus equation, which relates the free energy of ET determined electrochemically and the free energy of activation determined by kinetics, revealed that the barriers for the ET mechanism should be unacceptably high. They concluded that the reaction proceeds via the polar mechanism[69, 71]. Consistent with the polar mechanism, cyclizable probe experiments were negative[71]. The mechanistic discrepancy between the reactions of benzaldehyde and benzophenone was later solved by carbon kinetic isotope effect study (*vide infra*)[72].

C. Radical Probe Experiment

Judging from their reduction potentials, ET should be a feasible process between Me_2CuLi and alkyl aryl ketones or enones. In order to detect the occurrence of ET, House and coworkers carried out reactions of a series of ketones and analyzed the products to see whether any intramolecular rearrangement indicative of radical anion intermediates had occurred[52, 73]. Cyclopropyl enone (**1**) only gave the 'expected' 1,4-adduct with Me_2CuLi and the 1,2-adduct with MeLi in diethyl ether with no evidence for the formation of the ring-opened product **2**[73]. The reactions of cyclopropyl phenyl ketones (**3**) with Me_2CuLi gave the 1,2-adduct as a major product with a small mount of ring-opened product **4**. The facts that **3a** gave more ring-opened product than **3b** or **3c** and that the products **4b** and **4c** were derived from addition of a methyl group to the unsubstituted cyclopropane carbon suggested that the ring-opened products were not derived from an anion radical intermediate but from direct nucleophilic attack of the cuprate on the cyclopropane ring[52]. On the other hand, bicyclic cyclopropyl enones (**5** and **6**) gave ring-opened compounds as a major product[53, 74]. The results for **5** or **6** were taken as evidence for the occurrence of ET during the reactions. Furthermore, the α-bromoketone, $PhCOCMe_2Br$, gave the reduced ketone, $PhCOCHMe_2$, as a major product (77%) in the reaction with Me_2CuLi in diethyl ether, presumably through the anion radical intermediate[52].

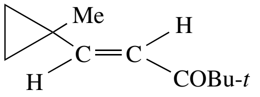

(1)

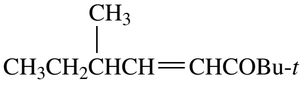

$$CH_3CH_2\overset{CH_3}{\overset{|}{C}}HCH{=}CHCOBu\text{-}t$$

(2)

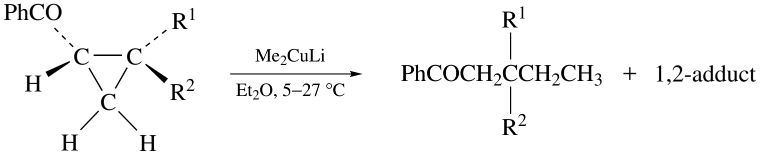

(3a) $R^1 = R^2 = H$
(3b) $R^1 = R^2 = Me$
(3c) $R^1 = H$; $R^2 = Ph$

(4a) $R^1 = R^2 = H$ (3.5% yield)
(4b) $R^1 = R^2 = Me$ (0.6%)
(4c) $R^1 = H$; $R^2 = Ph$ (0.9%)

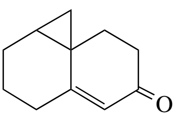

(5)

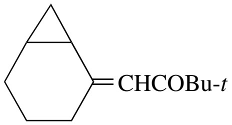

(6)

Later, Tanko and coworkers analyzed the structural effects on the rates of ring opening of cyclopropyl radicals and radical anions[75, 76]. It was demonstrated that aryl cyclopropyl ketyl anion, with only H or R on the cyclopropyl ring, underwent reversible ring opening, and dimerized in a second-order fashion. Thus, these species cannot be reliable probes for ET processes[75]. The ketyl with Ph on the cyclopropyl ring decays with rate-determining ring opening, and thus this can be a compound for detecting ET. Structural effects on the rate of ring opening of the carbon radical, R(or Ph)-$C^{\bullet}$(X)-Pr-*c* (or *c*-Bu), were examined. For R = alkyl, the neutral radical (X = H) was more stable than the radical anion

($X = O^-$), whereas for $R = Ph$, the lifetime of the radical anion was longer. Delocalization of the anion contributes to the stability of the radical ion.

Cyclizable[77], chiral[78] and dehalogenation[63, 66c] probe compounds have been successfully used to detect the occurrence of ET during the addition reactions of Grignard and other reagents. However, no such probe experiment has been examined for lithium reagents.

D. Enone Isomerization Probe

One of the most successful probe compounds for detecting the intermediacy of ketyl in the nucleophilic addition reactions of ketones is 2,2,6,6-tetramethylhept-4-en-3-one (**7**)[55, 79]. Here, isomerization of the starting *Z*-enone (**Z-7**) to *E*-enone (***E*-7**) upon mixing with a reagent is taken as an indication of the occurrence of ET from the reagent to the enone. Since **Z-7** has more negative reduction potential (−2.28V vs. SCE) than benzaldehyde (−1.84V) and benzophenone (−1.82V)[80], a positive response in the enone-isomerization experiment then indicates the possible occurrence of ET to the aromatic aldehyde and ketone. House[79] and Ashby[55] and their coworkers used this probe for the reactions of various organometallic reagents, and found the distribution of the products **8–10** as listed in Table 3. It is clear that the reactions can be classified into two groups. First, no isomerization either in the product or in the recovered reactant was induced by the addition of the organometallic reagent, and second, isomerization was detected in both the recovered enone and the product. MeLi and allyl-MgCl belong to the first group, for which the reaction did not produce the ketyl intermediate or the lifetime of the intermediate was too short to be detected. Me_2CuLi, *t*-BuLi, MeMgBr and *t*-BuMgCl belong to the second category, for which the reactions were considered to form the ketyl intermediate of sufficient lifetime.

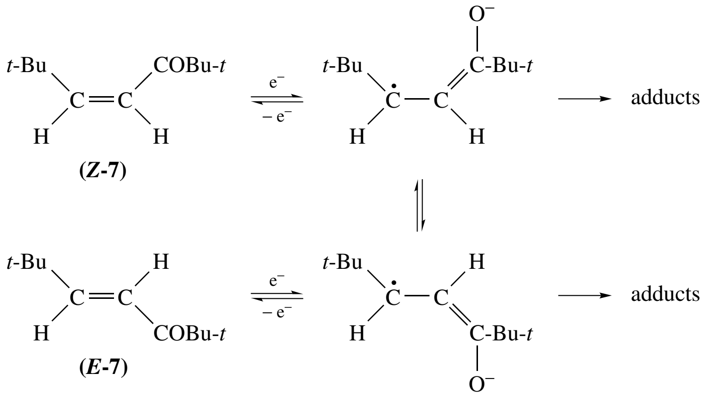

E. Carbon Kinetic Isotope Effect

The size of heavy atom KIEs is usually considered to be normal (larger than unity) when the total bonding at the labeled atom is decreasing in the TS and inverse (less than unity) when the bonding is increasing. This is true of course, but an equally or even more important factor that determines the size of a primary KIE is the dynamic character of the TS; the KIE is larger if the labeled atom is involved to a greater extent in the reaction-coordinate motion[81]. The importance of the reaction-coordinate contribution has been well

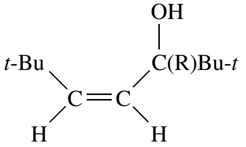

(*Z*-8)

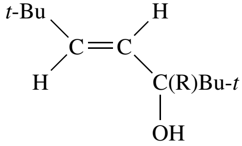

(*E*-8)

$t\text{-Bu-}\overset{\displaystyle \text{R}}{\overset{|}{\text{C}}}\text{HCH}_2\text{COBu-}t$

(9)

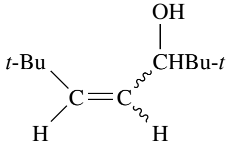

(10)

TABLE 3. Products from the reactions of organometallic reagents with *Z*-**7**[a]

R-Metal	Temp (°C)	Time (min)	*Z*-**7**	*E*-**7**	*Z*-**8**	*E*-**8**	**9**	**10**	Reference
MeLi	22–25	120	71	0	28	0	0	0	79
Me_2CuLi	0	90	1	69	0	0	23	0	79
MeLi	rt[b]		99	1	99	1	0	0	55
Me_2CuLi	rt[b]		0	100	0	0	100	0	55
t-BuLi	rt[b]		63	37	86	7	7	1	55
MeMgBr	rt[b]		85	15	40	19	0	0	55
t-BuMgCl	rt[b]		4	96	3	25	12	60	55
Allyl-MgCl	rt[b]		99	1	99	1	0	0	55

[a] All yields in Reference 79 are based on the amount of starting enone employed. Yields in Reference 55 are normalized in the recovered enone and in the product.

[b] Room temperature.

demonstrated for primary carbon KIEs[82–84]. Thus, a carbonyl carbon KIE of considerable magnitude would be expected if the reaction proceeds via the polar mechanism or if the rate-determining step is the RC step in the ET-RC route, since the motion of the labeled carbon is directly involved in the reaction coordinate in these cases. In contrast, the KIE would be much smaller for the rate-determining ET mechanism since there is no contribution from the reaction-coordinate motion.

Yamataka and coworkers determined carbonyl carbon KIEs for the reactions of various organolithium reagents with benzophenone and benzaldehyde[64, 65, 72]. The results are summarized in Table 4 together with those for the Grignard reaction[49]. Table 4 also lists the Hammett ρ values for these reactions determined by competition experiments. It can be seen that there are clear differences in the KIE values between RLi and RMgX. For most of the Grignard reagents carbonyl carbon KIEs of considerable magnitude were observed, which indicated that the C−C bond-forming step is rate-determining for these reagents. Since evidence from spectroscopic measurements and probe experiments described above indicated the occurrence of ET in the Grignard reaction, it was concluded that the reactions of these Grignard reagents with the aromatic aldehyde or ketone proceed via the ET-RC route and that the RC step is rate-determining. A similar mechanism could be assigned to the reaction of Me_2CuLi by the same reasoning. In contrast, most of the RLi reagents

TABLE 4. Carbonyl carbon-14 KIEs, substituent effects and enone isomerization for the reactions of organolithium and magnesium reagents with benzophenone[a]

Reagent/solvent	Carbonyl ^{14}C KIE	Hammett ρ value	Enone isomerization	Rate-determining step	Reference
$MeLi/Et_2O$	1.000 ± 0.002	0.23 ± 0.09	No	ET	65
$MeLi/Et_2O^b$	1.023 ± 0.004			RC	65
PhLi/*c*-Hex-Et_2O	1.003 ± 0.001	0.19 ± 0.08	nd	ET	64
PhLi/*c*-Hex-Et_2O^c	0.998 ± 0.003	0.13 ± 0.07	nd	ET	64
$CH_2{=}CHCH_2Li/Et_2O$	0.994 ± 0.003	0.21 ± 0.09	nd	ET	64
$LiCh_2SPh/THF^c$	0.999 ± 0.003	0.07 ± 0.06	nd	ET	72b
$LiCH_2CN/THF$	0.995 ± 0.003	0.14 ± 0.07	No	ET	72b
$CH_2{=}C(OLi)Bu\text{-}t/THF^c$	1.039 ± 0.009	1.16 ± 0.31	No	PL	72a
Me_2CuLi/Et_2O	1.030 ± 0.005	1.96 ± 0.12	Yes	RC	65
$MeMgI/Et_2O$	1.056 ± 0.002	0.54 ± 0.16	nd	RC	49a
$MeMgBr/Et_2O$	1.050 ± 0.011	nd	Yes	RC	49a
$MeMgBr/THF$	1.056 ± 0.004	0.90 ± 0.11	nd	RC	49a
$PhMgBr/Et_2O$	1.056 ± 0.004	0.59 ± 0.10	nd	RC	49a
o-MeC_6H_4MgBr/THF	1.060 ± 0.014	nd	nd	RC	49a
$CH_2{=}CHCH_2MgBr/Et_2O$	0.999 ± 0.003	-0.02 ± 0.09	nd	ET	49a
$CH_3CH{=}CHCH_2MgBr/Et_2O$	0.999 ± 0.002	0.01 ± 0.03	nd	ET	49a
$CH_2{=}C(OMgBr)CBu\text{-}t/Et_2O^c$	1.044 ± 0.008	1.16 ± 0.31	No	PL	49b

[a] At 0 °C. nd: not determined.
[b] With 2,4,6-trimethylbenzophenone.
[c] With benzaldehyde.

gave carbon KIE of unity, indicating there is little or no bonding change at the carbonyl carbon in the rate-determining TS. These results were reasonably interpreted by a mechanism involving an ET-RC route with a rate-determining ET step. The failure of detecting enone isomerization with these reagents was ascribed to a short lifetime of the ketyl intermediate. One of the origins of the mechanistic difference between RMgX and RLi can be the different stability of the ketyl intermediate. Recent *ab initio* MO calculations suggested that the MeLi radical anion is much more unstable than the MeMgCl radical anion, and hence the ketyl intermediate generated in RLi reactions should decompose much faster than that in RMgX reactions[85].

It is interesting to note that a significant carbon KIE was observed for the reaction of MeLi with 2,4,6-trimethylbenzophenone. Clearly C−C bond formation is involved in the rate-determining step of the reaction of 2,4,6-trimethylbenzophenone. The result was rationalized by the shift of the rate-determining step from ET for benzophenone to RC for 2,4,6-trimethylbenzophenone because the RC step became slower for the more hindered ketone. Negligible KIE for allylic Grignard reagents suggested that the mechanism for those reagents was similar to those for RLi, namely rate-determining ET, probably due to an enhanced RC step for the allylic reagents since they can generate more stable six-membered TS geometry in the RC step. It was concluded that the reactions of Li and Mg enolates with benzaldehyde proceed via the PL pathway based on the KIE and an enone-isomerization experiment. The conclusion supported the previous mechanistic assignment by Arnett and coworkers for the reaction of benzaldehyde[69, 71]. The reaction of the lithium enolate with benzophenone is much slower than with benzaldehyde, and the ET mechanism is still possible for the reaction with benzophenone as suggested by Ashby and Argyropoulos[68].

A considerable magnitude of Hammett ρ value is reasonably expected for the polar mechanism. A significant substituent effect would also be observed for the rate-determining

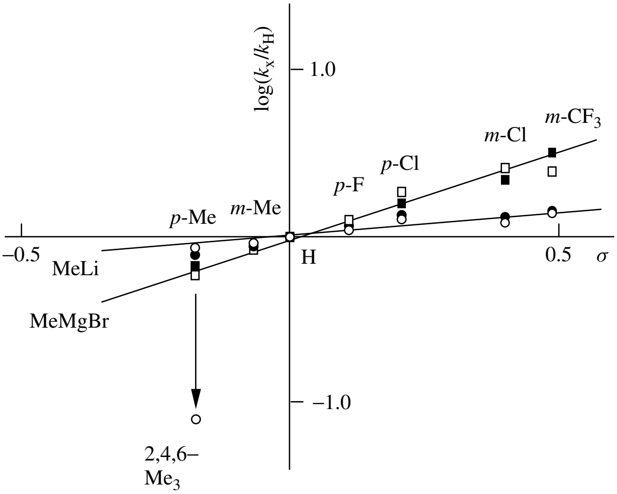

FIGURE 3. Hammett plots for the reactions of substituted benzophenones with MeLi (circles) and MeMgBr (squares) at 0 °C. Open points are based on competition experiments and filled points on direct rate measurements

RC mechanism because this mechanism involves ET pre-equilibrium, for which the Hammett ρ value is large[86]. Thus, the PL and the rate-determining RC mechanism would show similar kinetic behavior. On the other hand, the magnitude of the ρ value for the rate-determining ET mechanism was not easily predictable. The observed small ρ values for the ET process were rationalized in terms of a predominant contribution of solvent reorganization in the activation process of the charge-separation-type ET process[65]. The magnitude of the Hammett ρ value was found to vary with the change in the reaction mechanism in a manner similar to that of the KIE. Figure 3 illustrates an example of the Hammett plots[49, 65, 87]. Here the results of two reagents (MeLi and MeMgBr) are shown, for each of which reactivities were measured by competition experiment (open points) and direct kinetic study with a stopped-flow technique (filled points). All reactions were carried out at 0 °C in Et$_2$O except for the competition experiment with MeLi, for which the solvent was THF. It can be seen that the competition experiments and the direct rate measurements gave essentially the same results. The difference in the substituent effect for the lithium and the magnesium reagent is apparent. The downward deviation of 2,4,6-trimethylbenzophenone from the correlation plot for the reactions of MeLi with substituted benzophenones is consistent with the rate-determining shift for this compound mentioned above. The deduced mechanisms of these lithium and magnesium reactions are listed in Table 4.

F. Deuterium Kinetic Isotope Effects

α-Deuterium and carbon-13 KIEs of RLi and RMgX reagents were measured for the reactions with benzophenone and 2-octanone by competition experiments[60, 88]. As shown in Table 5, the α-deuterium KIE of RLi is normal whereas it is slightly inverse for RMgX. It was claimed that the reaction mechanism for RLi is ET since electron detachment from RLi makes the C−H(D) bond weaker. In contrast, the mechanism for the RMgX reaction was deduced to be polar because the C−C bond formation at the polar TS makes vibrations

TABLE 5. KIEs of RLi and RMgX in reactions with benzophenone and 2-octanone in diethyl ether at 20 °C[60]

Labeled reagent	KIE (benzophenone)	KIE (2-octanone)
$CD_3Li + LiI$	1.136 ± 0.007	1.096 ± 0.002
$CH_3CD_2Li + LiBr$	1.104 ± 0.019	1.087 ± 0.012
CD_3MgI	0.960 ± 0.001	0.977 ± 0.005
CH_3CD_2MgBr	0.991[a]	0.965[a]
$^{13}CH_3Li + LiI$	1.020 ± 0.009	1.015 ± 0.006
$CH_3{}^{13}CH_2Li$	1.025 ± 0.020	1.026 ± 0.009
$^{13}CH_3MgI$	1.023 ± 0.002	1.026 ± 0.007
$CH_3{}^{13}CH_2MgBr$	1.027 ± 0.012	1.024 ± 0.007

[a] The experimental error was not reported.

at the C−H(D) bond stiffer, although the observed inverse D KIEs are also consistent with the ET-RC mechanism with a rate-determining RC step. The observed clear difference in the D KIEs of RLi and RMgX is interesting, but the interpretation of the results may not be straightforward because isotopic partitioning in the monomer–aggregate equilibrium influences the magnitudes of KIEs. Furthermore, possible formation of mixed aggregates (e.g. $(CD_3Li)_2(CH_3Li)_2$ tetramer) may deteriorate the observed KIEs because isotope enrichment in the monomer species may be different from that in the total reagent due to a possible IE on the monomer–aggregate equilibrium. It was claimed that carbon KIE of the reagents provided no obvious indication of the mechanisms of their reactions with ketones[60].

α-D KIEs of benzaldehyde were measured for the reactions with various RLi and RMgX reagents in diethyl ether at −78 °C and the results are listed in Table 6[59]. The basic idea in the use of the α-D KIE of benzaldehyde as a mechanistic criterion was that the ET process should give normal D KIE whereas the PL mechanism should yield inverse KIE. However, it should be noted again that the KIE values do not allow one to distinguish the PL mechanism from the ET-RC mechanism with the rate-determining RC step. The observed D KIEs were somewhat puzzling. The normal KIEs observed for allyl-Li and allyl-MgBr were taken as evidence for the ET process, consistent with the

TABLE 6. α-D KIE for additions of RLi and RMgX to PhCHO/PhCDO[59]

Reagent	k_H/k_D[a]
MeLi (0.1 M)	0.87
MeLi (0.01 M)	0.88
PhLi (0.1 M)	0.95
BuLi	0.99
t-BuLi[b]	0.99
Allyl-Li	1.095
MeMgBr (0.1 M)	0.95
MeMgBr (0.01 M)	0.87
PhMgBr	1.00
Allyl-MgBr (0.1 M)	1.04
Allyl-MgBr (0.01 M)	1.04

[a] In Et_2O at −78 °C unless otherwise noted. Average deviation is ±0.03.

[b] In pentane.

mechanistic assignment based on carbonyl carbon KIEs[49,65]. In contrast, both MeLi and MeMgBr gave similar inverse isotope effects, which imply that in both cases the C−C bond formation is involved in the rate-determining step, disagreeing with the carbon KIE results. Qualitative differences in the KIEs observed for MeLi and BuLi and for MeMgBr and PhMgBr were also difficult to reconcile.

V. PRODUCT SELECTIVITY — ADDITION vs. REDUCTION

Reactions of RMgX and RLi with carbonyl compounds give the reduction product when the reagents have a β-hydrogen, in addition to the normal 1,2-addition product. The product distributions for RLi and RMgX reactions were different. It is a general trend that more addition product is formed with RLi, whereas more reduction is observed with RMgX[89,90], although the product ratio in the Grignard reactions is diverse[10,91–94]. It was recognized that more addition product was formed at higher Grignard reagent concentrations for the reaction of MeCOEt + i-PrMgBr in diethyl ether, which is consistent with the mechanism that the addition reaction proceeds via the attack of a second molecule of the Grignard reagent on the initially formed ketone–reagent complex[92].

A systematic study on the addition vs. reduction product ratio for the reactions of benzophenone with BuLi and BuMgBr in diethyl ether revealed interesting trends[95]. In Table 7 are shown the addition/reduction ratio in these reactions of substituted benzophenone with BuLi and BuMgBr. Table 8 shows the effect of concentration on the product ratio. It was found that the product distribution was highly dependent on the substituents and the reagent concentration in the BuMgBr reaction whereas it was essentially independent of the substituents and the reagent concentration in the BuLi reaction. The results suggested that in the Grignard reaction the reduction took place as a unimolecular decomposition of the ketone–Grignard reagent complex, while the addition occurred in higher order molecularity, as proposed previously[10,47,92]. The insensitivity of the product ratio in the BuLi reaction to the substituent and the concentration could not be rationalized with the polar mechanism, and suggested that both products were formed by unimolecular decomposition of the ketyl intermediate. The addition product was probably not formed directly

TABLE 7. Addition/reduction product ratio in the reactions of substituted benzophenones with BuLi and BuMgBr[95]

	Addition/Reduction[a]	
Substituent	BuMgBr	BuLi
o,p-Me$_2$	2/98	65/35
p-MeO	62/38	77/23
p-Me	40/60	73/27
m-Me	39/61	72/28
o-Me	6/94	71/29
H	33/67	73/27
p-F	32/68	71/29
p-Cl	10/90	73/27
o-Cl	4/96	67/33
m-CF$_3$	13/87	72/28
o-CF$_3$	3/97	77/23

[a] In diethyl ether at 0 °C with 0.67 M ketone and 0.14 M BuMgBr, or 0.08 M ketone and 0.12 M BuLi.

TABLE 8. Effect of concentration on the addition/reduction ratio in the reactions of X-substituted benzophenones[95]

	Addition/Reduction[a, b]			
X	0.170,0.083	0.140,0.067	0.095,0.047	0.058,0.031
H	37/63	26/74	24/76	18/82
p-Me	40/60	38/62	32/68	29/71
	Addition/Reduction[a, c]			
X	0.190,0.095	0.170,0.086	0.140,0.071	0.062,0.034
H	67/33	65/35	65/35	65/35
p-Me	68/32	67/33	67/33	67/33

[a] In diethyl ether at 0 °C.

[b] BuMgBr (M), $XC_6H_4COC_6H_5$ (M).

[c] BuLi, $XC_6H_4COC_6H_5$ (M).

from the intermediate but via a stepwise process with a transient Bu radical species, because the product ratio was independent of the steric effect of the *ortho* substituent.

VI. THEORETICAL CALCULATIONS

The first *ab initio* MO calculation of the reaction between MeLi and $H_2C{=}O$ was carried out mostly at the HF/3-21G level of theory[96]. The comparison of the reaction profiles for the monomer and dimer species revealed that the first complex formation was less exothermic and the barrier for the addition step was lower for the dimer reaction, but the overall barrier height was similar for the two systems. The overall reaction was more exothermic for the dimer reaction.

Reactivities of the MeLi dimer with formaldehyde and acetaldehyde were examined by MO calculations at the $MP2/6\text{-}31 + G^*//HF/6\text{-}31 + G^*$ level of theory[97]. The reaction scheme assumed that the MeLi dimer–aldehyde complex gave an 'open dimer' intermediate before forming six-membered addition TS. The calculation may be more relevant to other organometallic reagents than MeLi, since the accumulated experimental facts suggested that the MeLi monomer is the true reacting species even though it is a minor component in the monomer–aggregate equilibrium. Complexes and TSs were also optimized for the MeLi monomer and dimer reagents with H_2CO and MeCHO at HF, DFT, MP2 with various basis sets[98]. The addition reaction of MeLi to cyclohexanone is known to occur preferentially via equatorial attack, whereas BH_3 addition favors axial attack[99, 100]. The origin of these different π-facial selectivities has been analyzed by *ab initio* MO calculations at $MP2/6\text{-}31G^*//HF/6\text{-}31G^*$[101].

In spite of these studies the real contribution from theoretical calculations to the reactions of RLi must wait for the development of more sophisticated theoretical methods, which make it possible to describe both aggregation phenomena in solution and ET processes since these are key features of the reaction of RLi reagents[102].

VII. DIASTEREOFACE DISCRIMINATING ADDITION TO ACCEPTORS HAVING A CHIRAL AUXILIARY

In 1975 Meyers and coworkers, having studied reactions of lithiated chiral oxazolines with various electrophiles, applied the chiral oxazoline method to conjugate addition of organolithium reagents[103]. The diastereoselective asymmetric addition of various organolithiums to chiral alkenyloxazolines **11** gave, after direct hydrolysis with aqueous sulfuric acid, β-substituted alkanoic acids **12** with high enantiomeric purity (equation 6)[104].

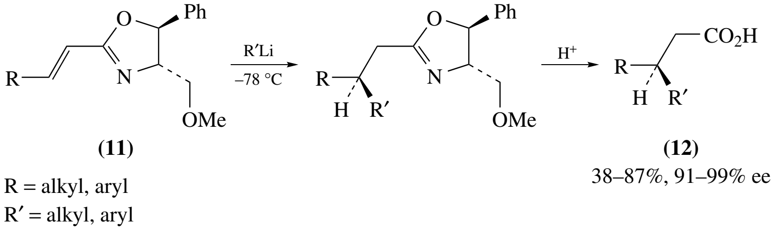

(11)

R = alkyl, aryl
R′ = alkyl, aryl

(12)

38–87%, 91–99% ee

(6)

The methodology was extended to an asymmetric introduction of substituents to a naphthalene ring. When chiral naphthyloxazolines **13** were used as substrates, di- or trisubstituted dihydronaphthalenes **15** were obtained in high diastereomeric ratio (dr) after the treatment of intermediate azaenolate **14** with an electrophile (equation 7)[105]. Analogous reactions with a chiral naphthaldehyde imine were also reported[106].

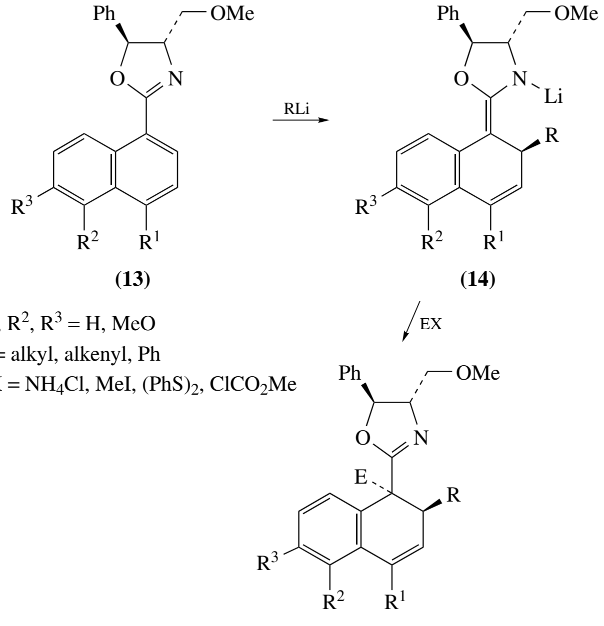

(13)

(14)

R^1, R^2, R^3 = H, MeO
R = alkyl, alkenyl, Ph
EX = NH_4Cl, MeI, $(PhS)_2$, $ClCO_2Me$

(15)

E = H, Me, PhS, MeO_2C
50–99%, dr 65:35–97:3

(7)

The highly selective addition was rationalized by a chelation control as shown in equation 8. Tetracoordinate organolithium can form complexes **16a** and **16b** with the chiral oxazoline. The addition, which can be viewed as a suprafacial 1,5-sigmatropic rearrangement, proceeds from **16b** where the C−Li bond is parallel to the π-orbital of the naphthalene ring. The attack of an electrophile on the azaenolate **17** formed by the addition occurs from the more accessible opposite side to that from which the addition of the organolithium occurred.

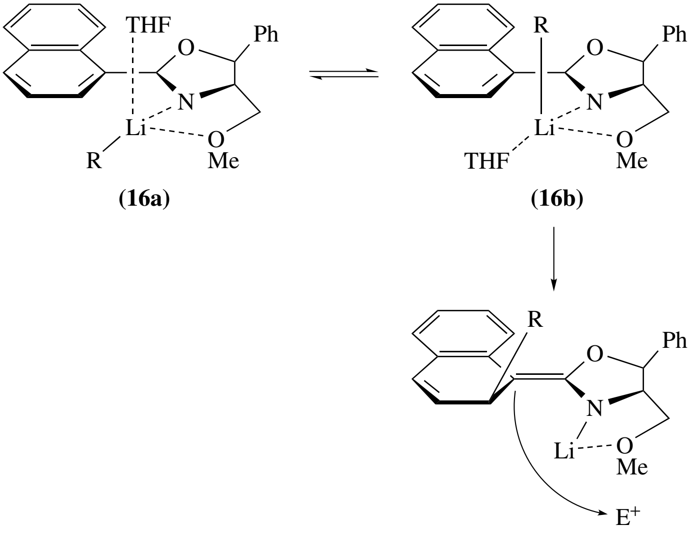

(16a) **(16b)**

(17)

(8)

Chiral β,β-diarylpropionic acid moieties are often found in compounds showing biological activities, such as antiarrhythmics[107, 108], vasodilators[107, 109], antidepressives[107, 110], antihistamines[107] and controllers of cerebral insufficiency[111]. In the course of synthetic studies of chiral β,β-diarylpropionic acid derivatives, Merck researchers developed stereoselective conjugate addition of aryllithium reagents to the α,β-unsaturated *tert*-butyl esters **18** bearing a chiral imidazolidine or oxazolidine auxiliary at the *ortho* position of an aryl group. The addition furnished chiral β,β-diarylpropionic acid derivatives **19** with up to 97% ee after acidic hydrolysis (equation 9)[112].

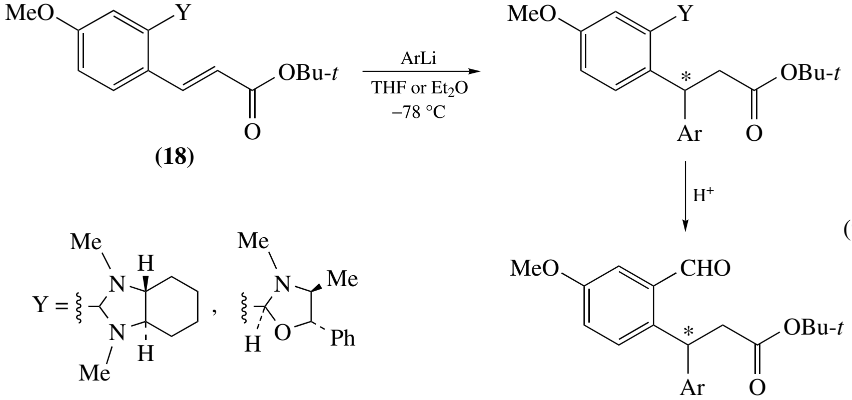

(18)

(9)

(19)
55–95%, 71–97% ee

VIII. REACTIONS MEDIATED BY AN EXTERNAL CHIRAL LIGAND

A. Basic Concept

In ether solvents, organolithium reagents exist as dimers or tetramers, which are highly reactive species and usually react with electrophiles without further activation. In nonpolar solvents such as toluene or hexane, organolithiums are less reactive because more aggregated oligomers, mainly hexamers, are formed. Addition of an external ligand to the solution of organolithium in a nonpolar solvent causes deaggregation of the oligomers to monomers or dimers, and therefore increases the nucleophilicity of the reagents. The other success in asymmetric conjugate addition of organolithium compounds is based on the use of an external chiral ligand to activate and asymmetrize organolithium reagents at the same time.

B. Early Works

In 1979, during studies on chiral solvents and complexing reagents, Seebach and coworkers developed multidentate chiral ligand **21** from tartaric acid (equation 10). In the presence of chiral ligand **21**, the conjugate addition of butyllithium to nitroalkene **20** yielded adduct **23** with 58% ee[113]. A dilute solution in pentane was advantageous. The use of ligand **22** with a decreased number of coordination sites gave a less satisfactory result (28% ee), probably due to the lower complexing ability. This work showed the validity of the basic concept above and encouraged the development of new efficient chiral ligands.

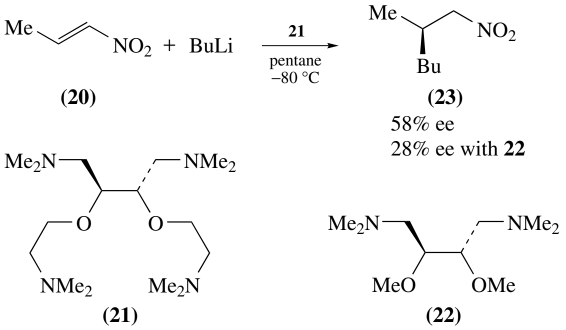

(20) **(23)** 58% ee, 28% ee with **22** **(21)** **(22)**

(10)

Tridentate chiral amino diether ligand **26** was reported to be designed and prepared from phenylalanine by Tomioka and coworkers in 1985 (equation 11). Lithiated phenyldithiane **25**, generated from the corresponding dithioacetal, underwent addition to α,β-unsaturated ester **24** in the presence of **26**, providing adduct **27** with 67% ee[114] after work up. The

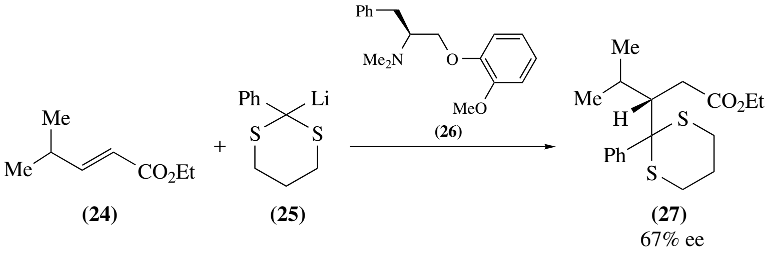

(24) **(25)** **(27)** 67% ee

(11)

steric bulk of **25** prevented its addition to the carbonyl carbon, and only the conjugate addition took place. Ligand **26** was later found to be effective for asymmetric addition of organolithiums to imines[115].

The C_2 symmetric chiral diether **28**[116] and the naturally occurring chiral diamine, (−)-sparteine (**29**), have been the most successful external chiral ligands for asymmetric conjugate addition of organolithium reagents. The rest of this review highlights organolithium addition, which is mediated or sometimes catalyzed by **28** or **29**.

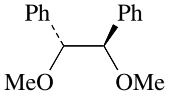

(28)

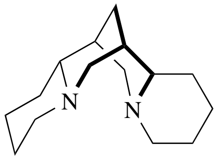

(–)-sparteine **(29)**

C. Reactions with a C_2 Symmetric Chiral Diether Ligand

1. Addition to α,β-unsaturated esters

Conjugate addition of organolithium reagents to α,β-unsaturated esters proceeded with high enantioselectivity by the mediation of chiral ligands **28** or **29** (Table 9, entries 1–12). Linear (entries 1–4), cyclic (entries 5–8) and also naphthalenecarboxylic acid esters (entries 9–12) are good acceptors for the addition. Undesirable 1,2-addition was avoided by the use of bulky 2,6-di-*tert*-butyl-4-methoxyphenyl (BHA) esters[117]. In the addition reactions to α,β-unsaturated BHA esters, ligands **28** and **29** are complementary to each other. Thus, diether **28** is the ligand of choice for the addition of sp^2 organolithiums, such as vinyl- and aryllithium (entries 3 and 4), while diamine **28** is effective with sp^3 alkyllithiums (entries 1 and 2). Conjugate addition to a *tert*-butyl ester was also reported (equation 12)[118]. With chiral ligand **28**, addition of aryllithium to α,β-unsaturated *tert*-butyl ester **30** gave the corresponding adduct **31** in good yield and enantiomeric excess. The substituent at the 2-position of the phenyl group of the α,β-unsaturated ester was required to obtain adducts in high selectivity.

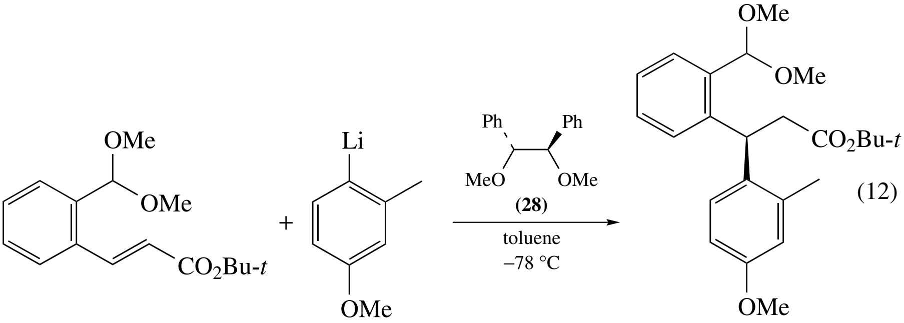

(12)

(30) **(31)**

90%, 88% ee

TABLE 9. Asymmetric conjugate addition of organolithium reagents to α,β-unsaturated esters and imines in the presence of chiral diether ligand **28** or (−)-sparteine (**29**)[a]

Entry	Substrate	RLi	Ligand (eq)[b]	Product		% Yield	% ee	Reference
1	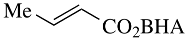	BuLi	**28**(1.4)	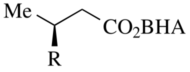	R = Bu	80	85	119
2		BuLi	**29**(1.4)		R = Bu	73(95)[c]	96(85)[c]	119
3		PhLi	**28**(1.1)		R = Ph	62	84	119
4		PhLi	**29**(1.4)		R = Ph	89	42	119
5	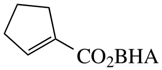	BuLi	**29**(1.4)	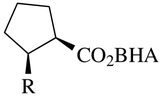	R = Bu	78/8[d]	95	119
6		PhLi	**28**(1.1)		R = Ph	97/2[d]	93	119
7	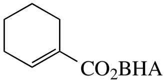	BuLi	**29**(1.4)	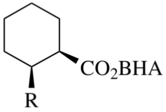	R = Bu	87/2[d]	94	119
8		PhLi	**28**(1.1)		R = Ph	83/1[d]	92	119
9	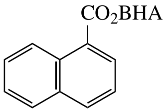	PhLi	**28**(1.1)	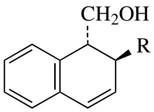 [e]	R = Ph	80(76)[c]	84(75)[c]	120
10		1-Naph-Li	**28**(1.1)		R = 1-Naph	82	91	120
11	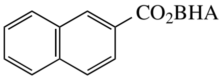	PhLi	**28**(1.1)	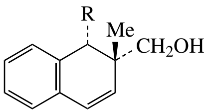 [f]	R = Ph	54(78)[c]	90(70)[c]	120
12		1-Naph-Li	**28**(1.1)		R = 1-Naph	40	95	120
13	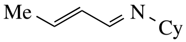	PhLi	**28**(1.1)	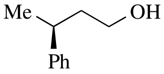 [g]		48	99	121

14	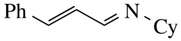	BuLi	**28**(1.1)	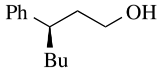 [g]		40	82	121
15	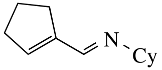	PhLi	**28**(1.4)	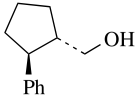 [g]		59	98	121
16	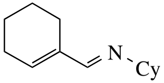	PhLi	**28**(1.4)	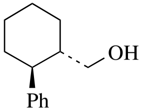 [g]		61	96	121
17 18	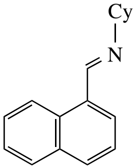	BuLi PhLi	**28**(1.1) **28**(1.1)	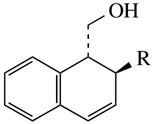 [g]	R = Bu R = Ph	80 82	91 94	121 121
19	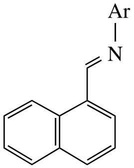	PhLi	**28**(1.1)	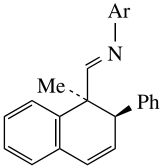 [h]		97	93	122

(*continued overleaf*)

TABLE 9. (*continued*)

Entry	Substrate	RLi	Ligand (eq)^{b}	Product	% Yield	% ee	Reference
20	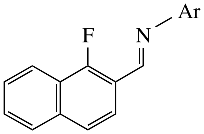	1-Naph-Li	**28**(1.1)	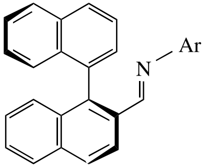	99 (97)^{c}	90 (82)^{c}	123
21	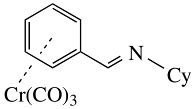	MeLi	*ent*-**28**(2)	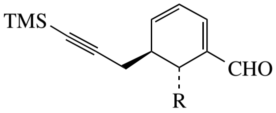 ^{i} R = Me	62	91	124
22		PhLi	*ent*-**28**(2)	R = Ph	64	93	124

[a] Conducted in toluene. BHA = 2,6-di-*tert*-butyl-4-methoxyphenyl; Naph = naphthyl; Cy = cyclohexyl; Ar = 2,6-diisopropylphenyl; *ent* = enantio.

[b] Molar equivalents to the amounts of organolithium.

[c] Numbers in parentheses are results with the catalytic amount (0.03–0.3 eq to organolithium) of the ligands.

[d] *cis/trans*.

[e] Obtained after reductive cleavage of the BHA group and following reduction of the resulting aldehyde.

[f] Obtained after reductive cleavage of the BHA group, treatment with methyl iodide and reduction of the resulting aldehyde.

[g] Obtained after hydrolysis and reduction.

[h] Obtained after treatment with methyl iodide.

[i] Obtained after treatment with 3-trimethylsilylprop-2-ynyl bromide.

2. Addition to α,β-unsaturated imines

α,β-Unsaturated imines are also applicable as an acceptor (Table 9, entries 13–22). As well as acyclic (entries 13 and 14) and cyclic imines (entries 15 and 16), imines bearing naphthalene ring (entries 17–20) or tricarbonylchromium complex of benzene ring (entries 21 and 22) undergo addition to organolithium reagents in the presence of chiral ether **28**, giving the corresponding alcohols with high enantiomeric excess after hydrolysis and reduction. In entry 20, the central chirality, initially formed at the 1-position of the naphthalene ring of the imine in the addition step, was efficiently transferred to the axial chirality of the product binaphthyl through the elimination of fluoride ion. The use of 2,6-diisopropylphenyl group instead of cyclohexyl increased the selectivity in the addition. It is important to use lithium bromide-free naphthyllithium, prepared from naphthylpropyltellurium and butyllithium, to realize high enantioselectivity in this reaction. The use of a catalytic amount of the chiral ligands is sufficient in some cases (entries 2, 9, 11 and 20) where regeneration of the complex between the organolithium and the chiral ligand from the product–chiral ligand complex through ligand exchange proceeds rapidly enough. This shows much higher reactivity of the monomeric organolithium–ligand complex than that of ligand-free oligomeric species.

The sense of the enantiofacial selection was predictable from the model complex of organolithium, imine and chiral diether **28**, where the migrating C–Li bond is parallel to the π-system of the α,β-unsaturated imine (Figure 4). From the favored complex the R group of the organolithium reagent is transferred to the less hindered face of the double bond of the unsaturated imine.

A substituent on the imine nitrogen affects the addition mode of the organolithium reagent, i.e. whether 1,2- or 1,4-addition occurs. On changing the substituent from cyclohexyl where the addition is nearly exclusively 1,4 to p-anisyl, the 1,2-addition to the C=N bond becomes predominant (equation 13). This switch of the selectivity is mainly ascribable to the relative magnitude of the LUMO coefficient on the two possible reaction sites[122, 125]. N-Alkylimine, which favors 1,4-addition, has a larger LUMO coefficient at the β-position of the imine than that at the imine carbon. The reverse is the case with N-arylimine, which favors 1,2-addition. Imine bearing a 2,6-diisopropylphenyl group, however, favors 1,4-addition (Table 9, entries 19 and 20). Due to the bulky substituents at the 2- and 6-position, the most stable conformer of the imine has a dihedral angle between the C=N plane and the phenyl ring plane of almost 90°[122], where the two isopropyl groups cover both sides of the C=N double bond. Moreover, this conformation forbids the π-system of the aryl group to overlap with that of the α,β-unsaturated imine

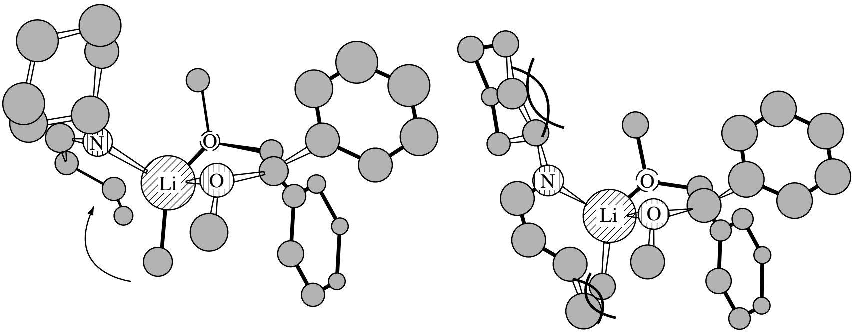

FIGURE 4. Chem3D view of the complex of methyllithium, crotonaldehyde imine and chiral diether **28**. The favorable complex (left) and the unfavorable one (right)

moiety, resulting in *N*-alkylimine-like LUMO of the imine. Both steric hindrance by the isopropyl group and the LUMO effect cooperate in directing the 1,4-selective addition.

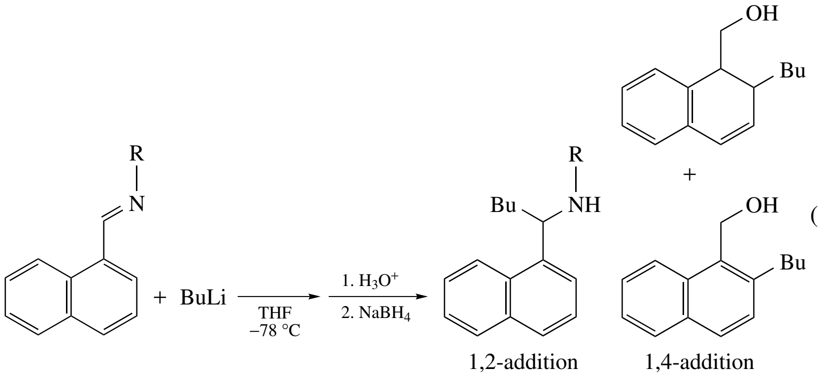

(13)

	1,2-addition	1,4-addition
R = cyclohexyl	<1%	83%
R = 4-$MeOC_6H_4$	79%	6%

D. Reactions with the Chiral Diamine Ligand (−)-Sparteine

1. Asymmetric deprotonation with (−)-sparteine

(−)-Sparteine (**29**) is an excellent chiral ligand for the asymmetric conjugate addition of lithiated *N*-Boc-allylic and benzylic amines. *N*-Boc-allylic and benzylic amines **32** and **33** are asymmetrically deprotonated by butyllithium in the presence of **29**, giving chiral organolithium–ligand complexes **34** and **35**, respectively (equation 14)[126–128], which are then applied for the addition reactions. The complexation of the organolithium reagent with **29** prevents the inversion at the carbanionic chiral center at −78 °C. The structure of **35** including absolute configuration was unambiguously established by X-ray crystallography[129], while that of **34** was deduced from the stereochemical outcome of the reactions.

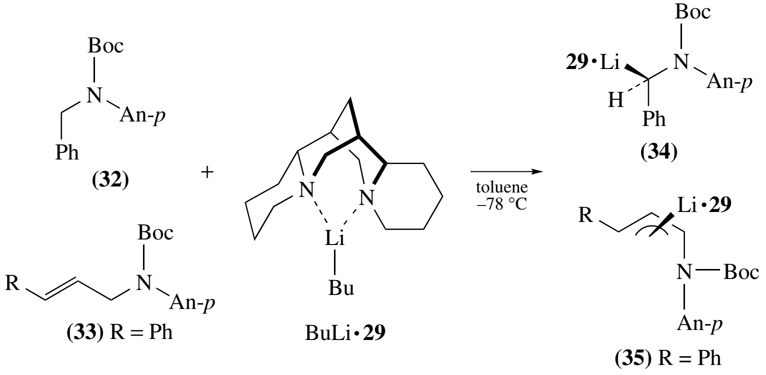

(14)

2. Addition to electrophilically activated alkenes

Asymmetric conjugate addition to a variety of electrophilic alkenes using chiral organolithium–ligand complexes are summarized in Table 10. The complexes **34** and **35** prefer

TABLE 10. Asymmetric conjugate addition of *N*-Boc-aminobenzylic and allylic organolithiums in the presence of (−)-sparteine (**29**)[a]

Entry	Acceptor		Organo-Li	Product	% Yield	% ee	Reference
1[b]	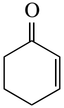		**34**	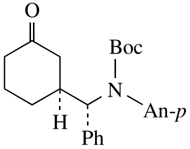	82	92	131
2[b] 3[b]	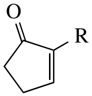	R = H R = Me	**34** **34**	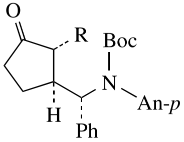	86 75/6[c]	92 90[d]	131 131
4[b]	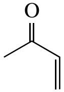		**34**	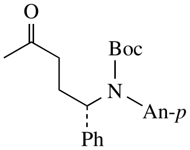	63	94	131
5[b]	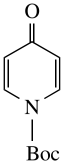		**35**	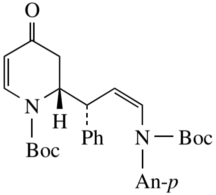	74/6[c]	80[d]	132

(*continued overleaf*)

TABLE 10. (*continued*)

Entry	Acceptor	Organo-Li	Product	% Yield	% ee	Reference
6[b]	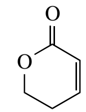	**35**	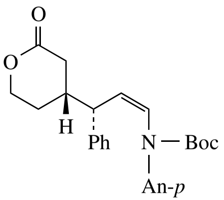	76/9[c]	92[d]	132
7[b]	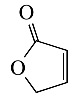	**35**	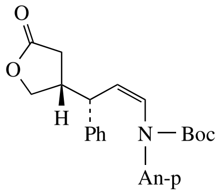	71	94	132
8[b]	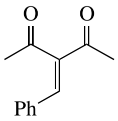	**34**	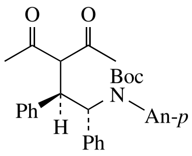	90	90	133
9[b]	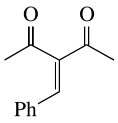	**35**	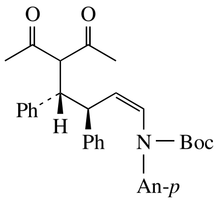	78	92	133

10	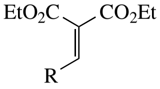	R = Me	**34**	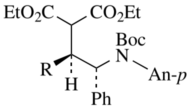	74/8[c]	94/86[c]	133
11		R = Ph	**34**		72	92	133
12		R = Me	**35**	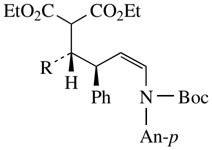	74/19[c]	96[d]	133
13		R = Ph	**35**		81/5[c]	96[d]	133
14	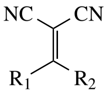	R^1 = Cy R^2 = H	**35**	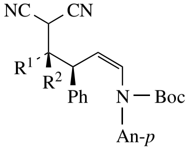	53/27[c]	88/90[c]	133
15		R^1 = Ph R^2 = Me	**35**		76/19[c]	86/76[c]	133
16		R^1 = Ph R^2 = Me	**34**	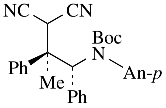	84/7[c]	90[d]	133
17	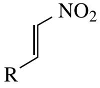	R = Me	**34**	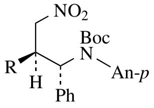	86/9[c]	>98[d]	134
18		R = *i*-Pr	**34**		89/1[c]	94[d]	134
19		R = Ph	**34**		86/7[c]	>98[d]	134
20		R = Ph[e]	**34**		55/26[c]	92[d]	134
21		R = OTIPS	**34**		63/9[c]	76[d]	134
22	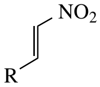	R = *i*-Bu	**35**	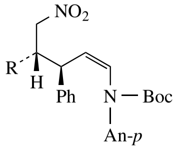	72/1[c]	>94[d]	134
23		R = Ph	**35**		85/5[c]	88[d]	134

(*continued overleaf*)

TABLE 10. (*continued*)

Entry	Acceptor	Organo-Li	Product	% Yield	% ee	Reference
24	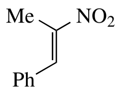	**34**	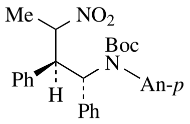	43/29[c]	76[d]	134
25		**35**	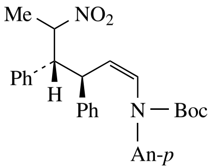	36/32[c]	> 98[d]	134
26	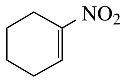	**34**	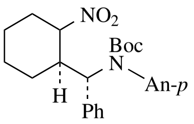	52/25[c]	96/90[c]	134
27		**35**	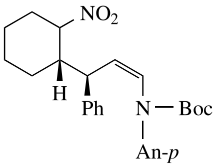	55/10[c]	> 98[d]	134

[a] Conducted in toluene. Boc = *tert*-butoxycarbonyl; Cy = cyclohexyl; TIPS = triisopropylsilyl.
[b] In the presence of trimethylsilyl chloride.
[c] Major diastereomer/minor diastereomer.
[d] For major diastereomer.
[e] (*Z*)-β-Nitrostyrene was used.

1,4-addition to 1,2-addition with α,β-unsaturated carbonyl compounds. Conjugate addition to cyclic (entries 1–3) and acyclic enones (entry 4) took place with high selectivity. A heterocyclic enone (entry 5) and α,β-unsaturated lactones (entries 6 and 7) were also applicable, giving the corresponding adducts with good enantiomeric excess. Doubly activated tri- and tetrasubstituted alkenes are acceptors compatible with the reaction (entries 8–16). In the reactions with enones and α,β-unsaturated lactones (entries 1–9), trimethylsilyl chloride prevents side reactions and significantly improves the yields. Nitroalkenes are also good substrates for the addition. In addition to alkyl- (entries 17, 18, and 22) and aryl-substituted nitroalkenes (entries 19, 20 and 23), a nitroalkene-containing oxygen functionality was also applicable (entry 21). (*E*)-β-Nitrostyrene gave the product in a better selectivity than the (*Z*)-isomer (entries 19 and 20). The addition with trisubstituted acyclic (entries 24 and 25) and cyclic nitroalkene (entries 26 and 27) proceeded with good enantioselectivity as well. It is noteworthy that enantiofacial selection in both organolithiums and alkenes are controlled in these reactions, forming contiguous two stereocenters with high diastereo- and enantioselectivities. The epimers of chiral organolithium–ligand complexes **34** and **35** are available through a stannylation–lithiation sequence (equation 15), which provides accessibility to the enantiomers of the products[130].

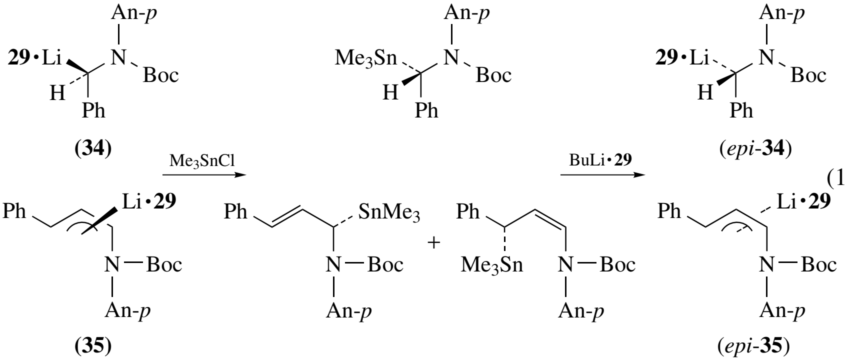

(15)

The enantioselective addition of the amino organolithium reagents consists of two stereo-controlled reactions, the asymmetric deprotonation (equation 14) and the following addition to electrophiles. The stereochemical course of the addition depends on the electrophile E. In the cases where heterocyclic enone or α,β-unsaturated lactones are the electrophiles (entries 5–7), the addition proceeds with retention of configuration. In contrast, with the other electrophiles in Table 10 and trimethyltin chloride in equation 15, the addition proceeds with inversion of configuration. In the addition which proceeds with retention of configuration, a pre-complexation between the electrophiles and lithium may be involved (equation 16).

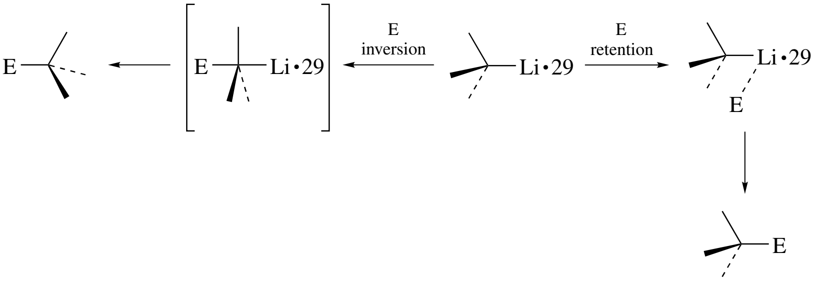

(16)

IX. APPLICATION TO ASYMMETRIC SYNTHESES OF BIOLOGICALLY ACTIVE COMPOUNDS

A. Dihydrexidine

The external chiral ligand-controlled asymmetric conjugate addition technology was applied to asymmetric syntheses of biologically significant compounds. A dopamine D1 full agonist, dihydrexidine **39**, which is a potential anti-Parkinson's disease agent[135], was synthesized with the asymmetric conjugate addition of phenyllithium to α,β-unsaturated ester **36** being a key step (equation 17)[136]. The key step, conjugate addition in the presence of the enantiomer of chiral diether ligand **28**, provided adduct **37** in good enantiomeric excess. The adduct was converted to optically pure amine **38** through enantioenrichment by recrystallization and Curtius rearrangement-type transformation. Pictet–Spengler-type cyclization completed the skeleton construction.

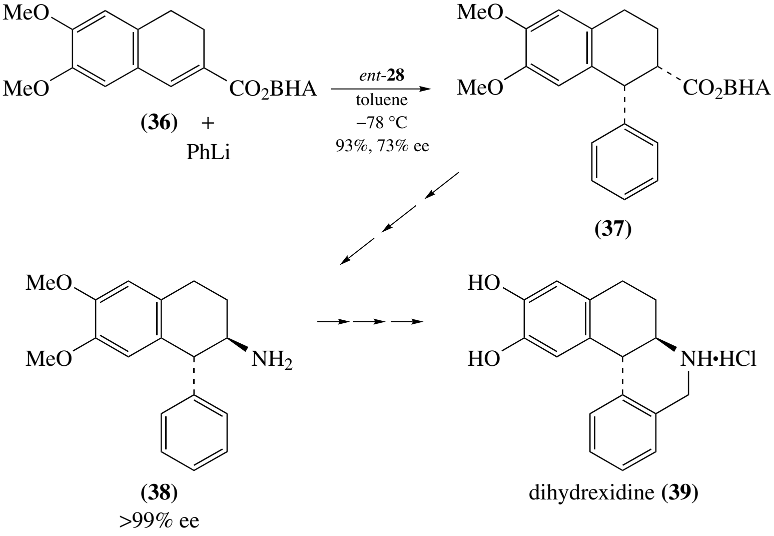

(17)

BHA = 2,6-di-*tert*-butyl-4-methoxyphenyl

B. Paroxetine

A selective serotonin reuptake inhibitor, paroxetine (**44**), was synthesized using an asymmetric deprotonation-conjugate addition sequence mediated by (−)-sparteine (**29**) (equation 18)[134a]. The addition of the chiral organolithium–ligand complex generated from the allylic amine **40** to nitroalkene **41** gave nitro enamine **42** with high enantiomeric excess. Mesylate **43** derived from **42** was cyclized to construct a piperidine ring, affording paroxetine (**44**) after introduction of the aryl ether and cleavage of the Boc group.

X. CONCLUSION

Physical organic experiments have shown that simple organolithium reagents exist as aggregates in solution and react with aromatic aldehydes and ketones as a monomer. In most cases, the reactions are initiated by ET, as in Grignard reactions, although

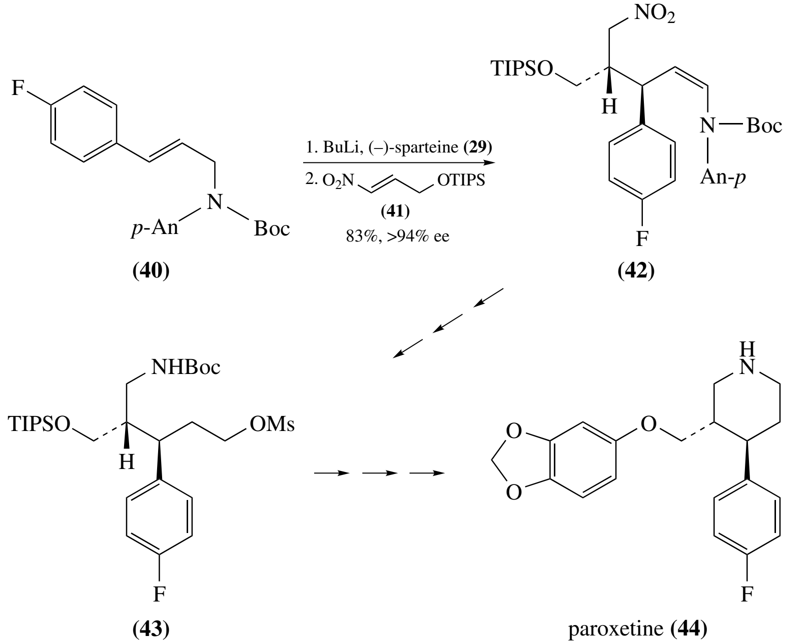

(18)

the mechanistic details are different for lithium and magnesium reagents. Asymmetric conjugate addition of organolithium reagents has been extensively developed in the last decade, and moreover, several examples of a catalytic version have appeared. Although transition-metal-catalyzed asymmetric conjugate addition has recently become conspicuous, asymmetric addition with organolithium reagents is still attractive not only because it is challenging to control very reactive reagents, but also because high reactivity of the reagents make possible extremely fast reactions.

XI. REFERENCES

1. P. Perlmutter, *Conjugate Addition Reactions in Organic Synthesis*, *Tetrahedron Organic Chemistry Series* Vol. 9, Pergamon Press, Oxford, 1992; B. E. Rossiter and N. M. Swingle, *Chem. Rev.*, **92**, 771 (1992); J. Leonard, E. Díez-Barra and S. Merino, *Eur. J. Org. Chem.*, 2051 (1998); M. P. Sibi and S. Manyem, *Tetrahedron*, **56**, 8033 (2000); N. Krause and A. Hoffmann-Röder, *Synthesis*, 171 (2001); K. Tomioka and Y. Nagaoka, in *Comprehensive Asymmetric Catalysis* (Eds. E. N. Jacobsen, A. Pfaltz and H. Yamamoto), Vol. III, Chap. 31.1, Springer, Berlin, 1999; K. Tomioka, in *Modern Carbonyl Chemistry* (Ed. J. Otera), Chap. 12, Wiley-VCH, Weinheim, 2000.
2. A. Alexakis, C. Benhaim, S. Rosset and M. Humam, *J. Am. Chem. Soc.*, **124**, 5262 (2002); C. A. Luchaco-Cullis and A. H. Hoveyda, *J. Am. Chem. Soc.*, **124**, 8192 (2002) and references cited therein.
3. T. Hayashi, M. Sakai and N. Miyaura, *J. Am. Chem. Soc.*, **120**, 5579 (1998); M. Kuriyama and K. Tomioka, *Tetrahedron Lett.*, **42**, 921 (2001); M. Kuriyama, K. Nagai, K. Yamada, Y. Miwa, T. Taga and K. Tomioka, *J. Am. Chem. Soc.*, **124**, 8932 (2002).
4. K. Tomioka, *Synthesis*, 541 (1990).
5. P. West and R. Waack, *J. Am. Chem. Soc.*, **89**, 4395 (1967).
6. L. M. Jackman and L. M. Scarmoutzos, *J. Am. Chem. Soc.*, **106**, 4627 (1984).

7. J. F. McGarrity and C. A. Ogle, *J. Am. Chem. Soc.*, **107**, 1805 (1985).
8. H. J. Reich, D. P. Green, M. A. Medina, W. S. Goldberg, B. Ö. Gudmundsson, R. R. Dykstra and N. H. Phillips, *J. Am. Chem. Soc.*, **120**, 7201 (1998).
9. C. G. Swain and L. Kent, *J. Am. Chem. Soc.*, **72**, 518 (1950).
10. C. G. Swain and H. B. Boyles, *J. Am. Chem. Soc.*, **73**, 870 (1951).
11. R. Waack, P. West and M. A. Doran, *Chem. Ind. (London)*, 1035 (1966).
12. R. Waack and M. A. Doran, *J. Am. Chem. Soc.*, **91**, 2456 (1969).
13. A. G. Evans and D. George, *J. Chem. Soc.*, 4653 (1961); R. A. Castling, A. G. Evans and N. H. Rees, *J. Chem. Soc.*, 519 (1966); W. Bywater and D. J. Worsfold, *J. Organometal. Chem.*, **10**, 1 (1967); D. Wosfold and W. Bywater, *Can. J. Chem.*, **38**, 189 (1960); A. G. Evans and N. H. Rees, *J. Chem. Soc.*, 6039 (1963); A. G. Evans, C. Gore and N. H. Rees, *J. Chem. Soc.*, 5110 (1965).
14. P. West, R. Waack and J. I. Purmort, *J. Am. Chem. Soc.*, **92**, 840 (1970).
15. S. G. Smith, L. F. Charbonneau, D. P. Novak and T. L. Brown, *J. Am. Chem. Soc.*, **94**, 7059 (1972).
16. L. F. Charbonneau and S. G. Smith, *J. Org. Chem.*, **41**, 808 (1976).
17. S. E. Rudolph, L. F. Charbonneau and S. G. Smith, *J. Am. Chem. Soc.*, **95**, 7083 (1973).
18. T. Holm, *Acta Chem. Scand.*, **23**, 1829 (1969).
19. R. Waack and P. West, *J. Organomet. Chem.*, **5**, 188 (1966).
20. T. Holm, *Acta Chem. Scand.*, **B32**, 162 (1978).
21. M. A. Al-Aseer and S. G. Smith, *J. Org. Chem.*, **49**, 2608 (1984).
22. J. F. McGarrity, C. A. Ogle, Z. Brich and H.-R. Loosli, *J. Am. Chem. Soc.*, **107**, 1810 (1985).
23. N. S. Nudelman, H. G. Schuls and G. V. García, *J. Phys. Org. Chem.*, **11**, 722 (1998).
24. M. Anteunis, *J. Org. Chem.*, **26**, 4214 (1961).
25. T. Holm, *Acta Chem. Scand.*, **19**, 1819 (1965); **20**, 1139 (1966); **21**, 2753 (1967); **23**, 579 (1969).
26. S. G. Smith, *Tetrahedron Lett.*, 409 (1963); S. G. Smith and G. Su, *J. Am. Chem. Soc.*, **86**, 2750 (1964), **88**, 3995 (1966); J. Billet and S. G. Smith, *J. Am. Chem. Soc.*, **90**, 4108 (1968).
27. S. G. Smith and J. Billet, *J. Am. Chem. Soc.*, **89**, 6948 (1967).
28. E. C. Ashby, R. Duke and H. M. Neumann, *J. Am. Chem. Soc.*, **89**, 1964 (1967).
29. E. C. Ashby, J. Laemmle and H. M. Neumann, *J. Am. Chem. Soc.*, **93**, 4601 (1971); E. C. Ashby, J. Laemmle and H. M. Neumann, *J. Am. Chem. Soc.*, **94**, 5421 (1972).
30. L. M. Jackman and B. C. Lange, *Tetrahedron*, **33**, 2737 (1977).
31. D. Seebach, R. Amsturz and J. D. Dunitz, *Helv. Chem. Acta*, **64**, 2622 (1981).
32. A. Abbotto, S. S.-W. Leung, A. Streitwieser and K. V. Kilway, *J. Am. Chem. Soc.*, **120**, 10807 (1998).
33. L. M. Jackman and R. C. Haddon, *J. Am. Chem. Soc.*, **95**, 3687 (1973).
34. L. M. Jackman and N. M. Szeverenyi, *J. Am. Chem. Soc.*, **99**, 4954 (1977).
35. P. G. Willard and J. M. Salvino, *Tetrahedron Lett.*, **26**, 3931 (1985).
36. D. Seebach, *Angew. Chem., Int. Ed. Engl.*, **27**, 1624 (1988).
37. E. M. Arnett, F. J. Ficher, M. A. Nichols and A. A. Ribeiro, *J. Am. Chem. Soc.*, **111**, 748 (1989).
38. A. Streitwieser, E. Juaristi, Y.-J. Kim and J. K. Pugh, *Org. Lett.*, **2**, 3739 (2000).
39. D. B. Collum, *Acc. Chem. Res.*, **25**, 448 (1992); **26**, 227 (1993); B. L. Lucht and D. B. Collum, *Acc. Chem. Res.*, **32**, 1035 (1999).
40. F. Abu-Hasanayn, M. Stratakis and A. Streitwieser, *J. Org. Chem.*, **60**, 4688 (1995).
41. S. S.-W. Leung and A. Streitwieser, *J. Am. Chem. Soc.*, **120**, 10557 (1998).
42. A. Streitwieser, S. S.-W. Leung and Y.-J. Kim, *Org. Lett.*, **1**, 145 (1999).
43. A. Streitwieser and D. Z.-R. Wang, *J. Am. Chem. Soc.*, **121**, 6213 (1999).
44. G. Das and E. R. Thornton, *J. Am. Chem. Soc.*, **115**, 1302 (1993).
45. E. C. Ashby and J. R. Bowers, Jr., *J. Am. Chem. Soc.*, **103**, 2242 (1981).
46. E. C. Ashby and A. B. Goel, *J. Am. Chem. Soc.*, **103**, 4983 (1981).
47. K. Maruyama and T. Katagiri, *J. Am. Chem. Soc.*, **108**, 6263 (1986).
48. T. Holm and I. Crossland, *Acta Chem. Scand.*, **25**, 59 (1971).
49. (a) H. Yamataka, T. Matsuyama and T. Hanafusa, *J. Am. Chem. Soc.*, **111**, 4912 (1989).
    (b) H. Yamataka, M. Shimizu and M. Mishima, *Bull. Chem. Soc. Jpn.*, **75**, 127 (2002).
50. Y. Zhang, B. Wenderoth, W.-Y. Su and E. C. Ashby, *J. Organomet. Chem.*, **292**, 29 (1985).
51. H. O. House and C.-Y. Chun, *J. Org. Chem.*, **41**, 3083 (1976).

52. H. O. House, A. V. Prabbu, J. M. Wilkins and L. F. Lee, *J. Org. Chem.*, **41**, 3067 (1976).
53. H. O. House and K. A. J. Snoble, *J. Org. Chem.*, **41**, 3076 (1976).
54. K. Maruyama and T. Katagiri, *J. Phys. Org. Chem.*, **1**, 21 (1988).
55. E. C. Ashby and T. L. Wiesemann, *J. Am. Chem. Soc.*, **100**, 3101 (1978).
56. E. C. Ashby, J. Bowers and R. Depriest, *Tetrahedron Lett.*, **21**, 3541 (1980).
57. M. Newcomb and D. P. Curran, *Acc. Chem. Res.*, **21**, 206 (1988).
58. M. Newcomb, T. R. Verick and S.-Y. Choi, *J. Org. Chem.*, **57**, 373 (1992).
59. J. J. Gajewski, W. Bocian, N. J. Harris, L. P. Olson and J. P. Gajewski, *J. Am. Chem. Soc.*, **121**, 326 (1999).
60. T. Holm, *Acta Chem. Scand.*, **48**, 362 (1994).
61. T. Holm, *J. Am. Chem. Soc.*, **115**, 916 (1993).
62. H. Yamataka, T. Matsuyama and T. Hanafusa, *Chem. Lett.*, 647 (1987); T. Matsuyama, H. Yamataka and T. Hanafusa, *Chem. Lett.*, 1367 (1988).
63. H. Yamataka, K. Yamaguchi, T. Takatsuka and T. Hanafusa, *Bull. Chem. Soc. Jpn.*, **65**, 1157 (1989).
64. H. Yamataka, Y. Kawafuji, K. Nagareda, N. Miyano and T. Hanafusa, *J. Org. Chem.*, **54**, 4706 (1989).
65. H. Yamataka, N. Fujimura, Y. Kawafuji and T. Hanafusa, *J. Am. Chem. Soc.*, **109**, 4305 (1987).
66. (a) H. Yamataka, K. Nagareda, Y. Takai, M. Sawada and T. Hanafusa, *J. Org. Chem.*, **53**, 3877 (1988).
    (b) H. Yamataka, K. Nagareda, K. Ando and T. Hanafusa, *J. Org. Chem.*, **57**, 2865 (1992).
    (c) H. Yamataka, K. Ando, T. Takatsuka and T. Hanafusa, *Chem. Lett.*, 1531 (1992).
    (d) H. Yamataka, K. Nagareda, T. Takatsuka, K. Ando, T. Hanafusa and S. Nagase, *J. Am. Chem. Soc.*, **115**, 8570 (1993).
67. H. O. House, W. L. Respess and G. M. Whitesides, *J. Org. Chem.*, **31**, 3128 (1966).
68. E. C. Ashby and J. N. Argyropoulos, *J. Org. Chem.*, **51**, 472 (1986).
69. E. M. Arnett and C. A. Palmer, *J. Am. Chem. Soc.*, **112**, 7354 (1990).
70. L. Eberson, *Electron Transfer Reactions in Organic Chemistry*, Springer-Verlag, New York, 1987; L. Eberson, *Adv. Phys. Org. Chem.*, **18**, 79 (1982).
71. C. A. Palmer, C. A. Ogle and E. M. Arnett, *J. Am. Chem. Soc.*, **114**, 5619 (1992).
72. (a) H. Yamataka, D. Sasaki, Y. Kuwatani, M. Mishima and Y. Tsuno, *J. Am. Chem. Soc.* **119**, 9975 (1997).
    (b) H. Yamataka, D. Sasaki, Y. Kuwatani, M. Mishima, M. Shimizu and Y. Tsuno, *J. Org. Chem.*, **66**, 2131 (2001).
73. H. O. House and P. D. Weeks, *J. Am. Chem. Soc.*, **97**, 2778 (1975).
74. J. M. Marshall and R. A. Ruden, *J. Org. Chem.*, **37**, 659 (1972).
75. J. M. Tanko and R. E. Rumright, *J. Am. Chem. Soc.*, **112**, 5362 (1990).
76. J. M. Tanko and J. P. Phillips, *J. Am. Chem. Soc.*, **121**, 6078 (1999).
77. E. C. Ashby and J. S. Bowers, Jr., *J. Am. Chem. Soc.*, **99**, 8504 (1977).
78. R. W. Hoffmann and B. Hölzer, *Chem. Commun.*, 491 (2001).
79. H. O. House and P. D. Weeks, *J. Am. Chem. Soc.*, **97**, 2770 (1975).
80. H. Yamataka, K. Nagareda, T. Hanafusa and S. Nagase, *Tetrahedron Lett.*, **30**, 7187 (1989).
81. L. Melander and W. H. Saunders, Jr., *Reaction Rates of Isotopic Molecules*, Wiley-Interscience, New York, 1980.
82. H. Yamataka and T. Ando, *J. Phys. Chem.*, **85**, 2281 (1981).
83. H. Yamataka, S. Tamura, T. Hanafusa and T. Ando, *J. Am. Chem. Soc.*, **107**, 5429 (1985).
84. L. B. Sims and D. E. Lewis, in *Isotopes in Organic Chemistry* (Eds. E. Buncel and C. C. Lee), Vol. VI, Chap. 4, Elsevier, Amsterdam, 1984.
85. T. Kudo and H. Yamataka, unpublished results.
86. P. Zuman, O. Exner, R. F. Rekker and W. Nauta, *Collect. Czech. Chem. Commun.*, **33**, 3213 (1968).
87. M. Shimizu and H. Yamataka, unpublished results.
88. T. Holm, *J. Organomet. Chem.*, **506**, 37 (1996).
89. F. Huet and G. Emptoz, *J. Organometal. Chem.*, **101**, 139 (1975).
90. H. Nakamura, H. Yamamoto and H. Nozaki, *Chem. Lett.*, 1167 (1972).
91. M. J. Anteunis and R. D'Hollander, *Tetrahedron Lett.*, 1275 (1962).
92. J. Miller, G. Gregoriou and H. S. Mosher, *J. Am. Chem. Soc.*, **83**, 3966 (1961).

93. D. Cowan and J. Mosher, *J. Org. Chem.*, **27**, 1 (1962).
94. K. Maruyama and T. Katagiri, *J. Phys. Org. Chem.*, **2**, 205 (1989).
95. H. Yamataka, N. Miyano and T. Hanafusa, *J. Org. Chem.*, **56**, 2573 (1991).
96. E. Kaufmann and P. v. R. Schleyer, *J. Am. Chem. Soc.*, **107**, 5560 (1985).
97. M. Nakamura, E. Nakamura, N. Koga and K. Morokuma, *J. Am. Chem. Soc.*, **115**, 11016 (1993).
98. C. Fressigné, J. Maddaluno, A. Marquez and C. G. Prettre, *J. Org. Chem.*, **65**, 8899 (2000).
99. E. C. Ashby and J. T. Laemmle, *Chem. Rev.*, **75**, 521 (1975); E. C. Ashby and S. A. Noding, *J. Org. Chem.*, **44**, 4371 (1979).
100. H. C. Brown and V. Varma, *J. Am. Chem. Soc.*, **88**, 2871 (1966).
101. H. Yamataka, *J. Phys. Org. Chem.*, **8**, 445 (1995).
102. H. Yamataka and M. Aida, *Bull. Chem. Soc. Jpn.*, **75**, 2555 (2002).
103. A. I. Meyers and K. A. Lutomski, in *Asymmetric Synthesis* (Ed. J. D. Morrison), Vol. 3, Part B, Academic Press, Orlando, Florida, 1984.
104. A. I. Meyers and C. E. Whitten, *J. Am. Chem. Soc.*, **97**, 6266 (1975); A. I. Meyers, R. K. Smith and C. E. Whitten, *J. Org. Chem.*, **44**, 2250 (1979).
105. B. A. Barner and A. I. Meyers, *J. Am. Chem. Soc.*, **106**, 1865 (1984); A. I. Meyers and D. Hoyer, *Tetrahedron Lett.*, **25**, 3667 (1984); A. I. Meyers, G. P. Roth, D. Hoyer, B. A. Barner and D. Laucher, *J. Am. Chem. Soc.*, **110**, 4611 (1988); G. P. Roth, C. D. Rithner and A. I. Meyers, *Tetrahedron*, **45**, 6949 (1989); A. J. Robichaud and A. I. Meyers, *J. Org. Chem.*, **56**, 2607 (1991).
106. A. I. Meyers, J. D. Brown and D. Laucher, *Tetrahedron Lett.*, **28**, 5283 (1987).
107. A. L. Mueller, S. T. Moe, M. F. Balandrin, E. G. Delmar, B. C. Vanwagenen, L. D. Artman, R. M. Barmore and D. L. Smith, WO Patent 96/40097, June 5, 1995.
108. R. E. Johnson and C. A. Busacca, US Patent 5,098,901, March 24, 1991.
109. R. Mannhold, P. L. Caldirola, G. J. Bijloo and H. Timmerman, *Eur. J. Med. Chem.*, **28**, 727 (1993).
110. R. F. Maisey, G. Jones, A. R. Somerville and B. A. Whittle, *J. Med. Chem.*, **14**, 161 (1971); E. J. Corey and T. G. Gant, *Tetrahedron Lett.*, **35**, 5373 (1994).
111. W. Aschwanden, R. Imhof, R. Jakob-Roete and E. Kyburz, US Patent 5,017,608, May 21, 1991.
112. L. F. Frey, R. D. Tillyer, A.-S. Caille, D. M. Tschaen, U.-H. Dolling, E. J. J. Grabowski and P. J. Reider, *J. Org. Chem.*, **63**, 3120 (1998).
113. W. Langer and D. Seebach, *Helv. Chim. Acta*, **62**, 1710 (1979); D. Seebach, G. Crass, E. M. Wilka, D. Hilvert and E. Brunner, *Helv. Chim. Acta*, **62**, 2695 (1979).
114. K. Tomioka, M. Sudani, Y. Shinmi and K. Koga, *Chem. Lett.*, 329 (1985).
115. I. Inoue, M. Shindo, K. Koga and K. Tomioka, *Tetrahedron*, **50**, 4429 (1994).
116. M. Nakajima, K. Tomioka, Y. Iitaka and K. Koga, *Tetrahedron*, **49**, 10793 (1993); B. H. Mckee, D. G. Gilheany and K. B. Sharpless, *Org. Synth.*, **70**, 47 (1992).
117. M. P. Cooke Jr, *J. Org. Chem.*, **51**, 1637 (1986).
118. F. Xu, R. D. Tillyer, D. M. Tschaen, E. J. J. Grabowski and P. J. Reider, *Tetrahedron: Asymmetry*, **9**, 1651 (1998).
119. Y. Asano, A. Iida and K. Tomioka, *Tetrahedron Lett.*, **38**, 8973 (1997); Y. Asano, A. Iida and K. Tomioka, *Chem. Pharm. Bull.*, **46**, 184 (1998).
120. K. Tomioka, M. Shindo and K. Koga, *Tetrahedron Lett.*, **34**, 681 (1993); M. Shindo, K. Koga, Y. Asano and K. Tomioka, *Tetrahedron*, **55**, 4955 (1999).
121. K. Tomioka, M. Shindo and K. Koga, *J. Am. Chem. Soc.*, **111**, 8266 (1989); M. Shindo, K. Koga and K. Tomioka, *J. Org. Chem.*, **63**, 9351 (1998).
122. K. Tomioka, Y. Shioya, Y. Nagaoka and K. Yamada, *J. Org. Chem.*, **66**, 7051 (2001).
123. M. Shindo, K. Koga and K. Tomioka, *J. Am. Chem. Soc.*, **114**, 8732 (1992).
124. D. Amurrio, K. Khan and E. P. Kündig, *J. Org. Chem.*, **61**, 2258 (1996).
125. K. Tomioka, T. Okamoto, M. Kanai and H. Yamataka, *Tetrahedron Lett.*, **35**, 1891 (1994).
126. N. C. Faibish, Y. S. Park, S. Lee and P. Beak, *J. Am. Chem. Soc.*, **119**, 11561 (1997) and references cited therein.
127. G. A. Weisenburger, N. C. Faibish, D. J. Pippel and P. Beak, *J. Am. Chem. Soc.*, **121**, 9522 (1999); D. J. Pippel, G. A. Weisenburger, N. C. Faibish and P. Beak, *J. Am. Chem. Soc.*, **123**, 4919 (2001) and references cited therein.

128. P. Beak, A. Basu, D. J. Gallagher, Y. S. Park and S. Thayumanavan, *Acc. Chem. Res.*, **29**, 552 (1996); D. Hoppe and T. Hense, *Angew. Chem., Int. Ed. Engl.*, **36**, 2283 (1997).
129. D. J. Pippel, G. A. Weisenburger, S. R. Wilson and P. Beak, *Angew. Chem., Int. Ed.*, **37**, 2522 (1998).
130. Y. S. Park, M. L. Boys and P. Beak, *J. Am. Chem. Soc.*, **118**, 3757 (1996); G. A. Weisenburger and P. Beak, *J. Am. Chem. Soc.*, **118**, 12218 (1996).
131. Y. S. Park, G. A. Weisenburger and P. Beak, *J. Am. Chem. Soc.*, **119**, 10537 (1997).
132. S. H. Lim, M. D. Curtis and P. Beak, *Org. Lett.*, **3**, 711 (2001).
133. M. D. Curtis and P. Beak, *J. Org. Chem.*, **64**, 2996 (1999).
134. (a) T. A. Johnson, M. D. Curtis and P. Beak, *J. Am. Chem. Soc.*, **123**, 1004 (2001).
(b) T. A. Johnson, D. O. Jang, B. W. Slafer, M. D. Curtis and P. Beak, *J. Am. Chem. Soc.*, **124**, 11689 (2002).
135. W. K. Brewster, D. E. Nichols, R. M. Riggs, D. M. Mottola, T. W. Lovenberg, M. H. Lewis and R. B. Mailman, *J. Med. Chem.*, **33**, 1756 (1990).
136. Y. Asano, M. Yamashita, K. Nagai, M. Kuriyama, K. Yamada and K. Tomioka, *Tetrahedron Lett.*, **42**, 8493 (2001).

CHAPTER **15**

Polylithium organic compounds: Syntheses and selected molecular structures

CARSTEN STROHMANN and DANIEL SCHILDBACH

Institut für Anorganische Chemie, Universität Würzburg, Am Hubland,
D-97074 Würzburg, Germany
Fax: +49 931 888 4605; e-mail: mail@carsten-strohmann.de

I. INTRODUCTION

Lithium organic compounds are widely used in preparative organic and inorganic chemistry. Despite the high polarity of the lithium–carbon bond, which makes these molecules act as strong nucleophiles or bases, monolithiated compounds are mostly soluble in polar (ethers) as well as in non-polar solvents (hydrocarbons). In contrast to that, polylithiated systems are polyfunctional carbon nucleophiles and mostly soluble in polar solvents only—sometimes even insoluble. Thus, to avoid incomplete metalation reactions caused by precipitating partialy lithiated intermediates, working in ethers is almost inevitable when synthesizing polylithium compounds. Since side reactions like the deprotonation and/or the decomposition of the polar solvent molecules increase at higher temperatures, the ideal polylithiation reaction is a fast homogeneous reaction at low temperatures. Different methods of activation or increasing solubility have been developed and the method of synthesis to be used

---

The Chemistry of Organolithium Compounds. Edited by Z. Rappoport and I. Marek
ISBN: 0-470-84339-X

often depends on the nature of the chosen precursor molecule. Established methods of synthesis are at the same time the body of this chapter:

(i) Deprotonation
(ii) Halide–Lithium Exchange
(iii) Metal–Lithium Exchange
(iv) Reductive Cleavage of Carbon–Sulphur Bonds
(v) Addition/Single-Electron Transfer

The subject of this chapter is to present recent polylithium organic compounds[1] that have been reported since the publication of the well-known review articles of Maercker and Theis[2, 3]. The main topics are the syntheses and the molecular structures of these compounds. The displayed structural formulas, in many cases, can only represent the reactivity of the corresponding polylithium compound, since the structures of the species in solution or the solid state are unknown. In other cases, where the solid-state structure was determined by structural analysis or NMR studies were performed, either the Lewis formula is to represent the 'true' structure of the molecule or the *Schakal-Plot*[4] of the structural analysis will be presented. The variety of compounds chosen was limited to reports, where experiments clearly indicate the successful synthesis of a polylithiated compound and at least a structural formula of the compound was shown by the authors. Furthermore, experiments that include the generation and the trapping of polylithiated compounds were not considered, where a successive lithiation-substitution sequence instead of multiple lithiation followed by multiple substitution could not be excluded. Reactions of this type, which are mostly arene-catalysed reductions, have been summarized in review articles[5–7]. Such transformations have a large synthetic potential, but the main goal is not the synthesis of polylithiated molecules.

II. METHODS OF SYNTHESIS

A. Deprotonation

The synthesis of polylithiated compounds by hydrogen–lithium exchange can face difficulties due to the kinetic hindrance of cascading deprotonation steps. Therefore, highly acidic C−H bonds or C−H-activating groups (side-arm donation) are required. Compounds of this type sometimes are generated by a first lithiation step, using a method different from deprotonation. This simultaneous activation of the systems (especially in larger aggregates) allows an introduction of further lithium centres by deprotonation (see the end of this subsection).

Moreover, in deprotonation reactions with common alkyllithium bases (e.g. butyllithium), no side-products are formed, that increase the solubility of the polylithium compound. Also, product mixtures are only rarely observed with this method. Thus, the resulting polylithium compound can be isolated or crystallized more easily. This is why—in addition to Section II. E—only this section presents many visualizations of successful X-ray structural analyses of polylithiated compounds.

Dilithiated diamine **2** was synthesized by Karsch by a two-fold metalation of *N,N,N′,N′*-tetramethylmethylenediamine (TMMDA) (**1**)[8]. The reaction was effected in *n*-pentane at low temperatures, yielding the poorly soluble *N,N′*-bis(lithiomethyl)-*N,N′*-dimethylmethylenediamine (**2**) (Scheme 1). Due to its low solubility in toluene or THF, the highly pyrophoric compound was characterized by derivatization with several electrophiles, mainly chlorosilanes. Obviously, the addition of coordinating additives, such as TMEDA, DME (dimethoxyethane) or THF, does not enhance the solubility of the dilithium compound. Interestingly, as the author comments, TMEDA is only monolithiated in modest yields by alkyllithium bases.

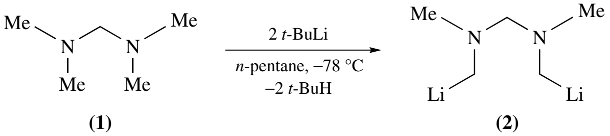

SCHEME 1

3,3′-Dimethyl-2,2′-bipyridine (**3**) can be monolithiated or dilithiated at its methyl groups in the presence of TMEDA, depending on the molar amount of *n*-butyllithium used (Scheme 2)[9]. By trapping reactions with chlorotrimethylsilane and a close observation of colours, it was found that the monolithiation of **3** occurs readily at −78 °C, while the second lithiation step affords elevated temperatures of around −60 °C. The dilithiated bipyridine **4** was trapped by reaction with two equivalents of chlorotrimethylsilane to give bis(trimethylsilyl) derivative **5**, which was again dilithiated by reaction with two further equivalents of *n*-butyllithium. The dilithium compound **6** could be obtained as single crystals by Leung and coworkers and its molecular structure in the solid state was determined (Figure 1).

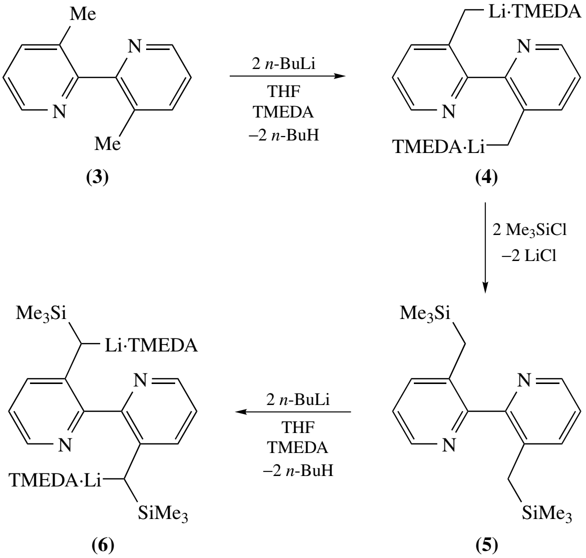

SCHEME 2

The dilithiated bis(phosphane) **8**, with a methylene group bridging both phosphorous(V) centres, was independently synthesized by Cavell and coworkers[10] as well as by Ong and Stephan[11]. Interestingly, both geminal hydrogen atoms of the methylene group could be abstracted by deprotonation in one reaction step. The (trimethylsilyl)imino substituted bis(phosphane) **7** was reacted with two equivalents of phenyllithium (or methyllithium) in toluene to yield the geminal dilithiated compound **8** as single crystals (Scheme 3). The dimeric molecular structure in the crystal was determined, showing the interesting structural motif of an Li_4-square, capped by the two metalated carbon centres on both sides (Figure 2). The same compound, generated by reaction with two equivalents of methyllithium in benzene, was independently reported by Ong and Stephan together with the X-ray crystal structure.

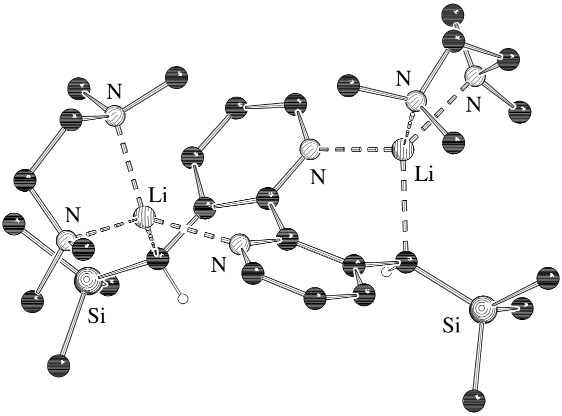

FIGURE 1. Molecular structure of **6** in the solid state

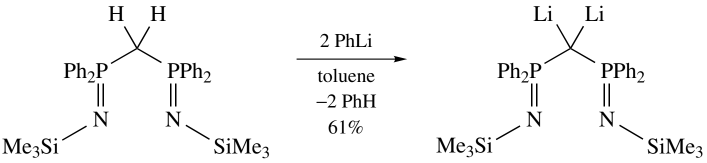

(7) **(8)**

SCHEME 3

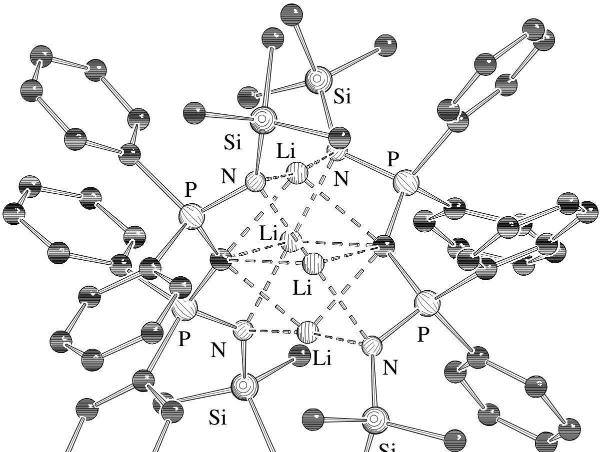

FIGURE 2. Molecular structure of **8** in the solid state

Another geminal dilithiated compound could be obtained in the group of J. F. K. Müller and coworkers[12, 13]. When (trimethylsilylmethyl)phosphonic ester **9** is reacted with two equivalents of *n*-butyllithium in hexane in the presence of TMEDA, both methylene hydrogen atoms are abstracted to give the dilithiated phophonate **10** (Scheme 4). The molecular structure of the compound was determined by single-crystal X-ray structural analysis, revealing a hexameric cluster of six dilithiated phosphonates and two molecules of lithium dimethylamide, the latter resulting from the decomposition of metalated TMEDA (Figure 3).

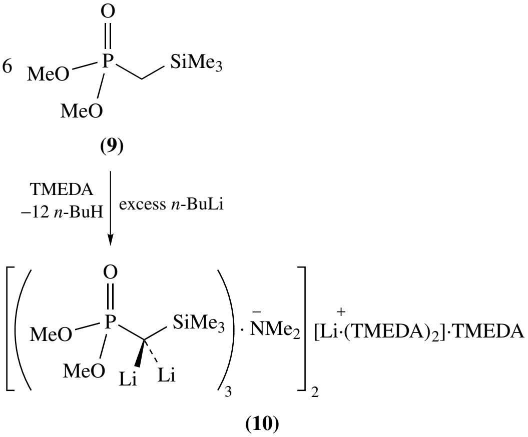

SCHEME 4

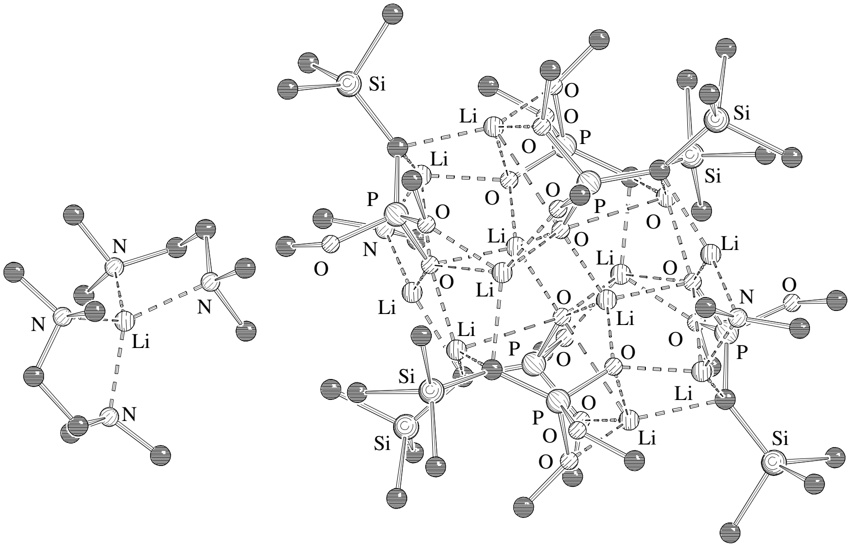

FIGURE 3. Molecular structure of **10** in the solid state

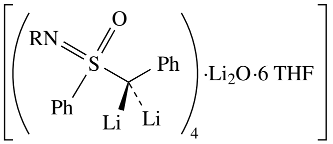

(11a) R = H
(11b) R = Me

FIGURE 4. Lewis formula of **11**

The related geminal dilithiated compound **11** was generated by the same group by reaction of a substituted sulphoximine with 2.5 equivalents of *n*-butyllithium in THF (Figure 4)[12, 14]. Also in this case, the crystal structure of the dilithium compound could be cleared up by X-ray structural analysis (Figure 5).

Substituted dilithiated 2-butenes of type **13** were generated by a two-fold deprotonation, starting from disubstituted 2-butenes **12** using *n*-butyllithium in the presence of TMEDA (Scheme 5)[15]. Both systems described by Raston and coworkers carry trimethylsilyl substituents in 1,4-positions in order to increase the acidity of the starting compounds on the one hand as well as the stability of the dilithium compounds on the other (polarizability effects). Intensive NMR studies on the structure of the dilithiated butenes in solution were performed by the authors.

The THF adduct of dilithio-1,4-bis(trimethylsilyl)-2-butene (**14**) (Figure 6), which was prepared by the same method as the compounds of type **13** (a reduction of the corresponding 1,3-butadiene with metallic lithium, as described in Section II. E, can be an

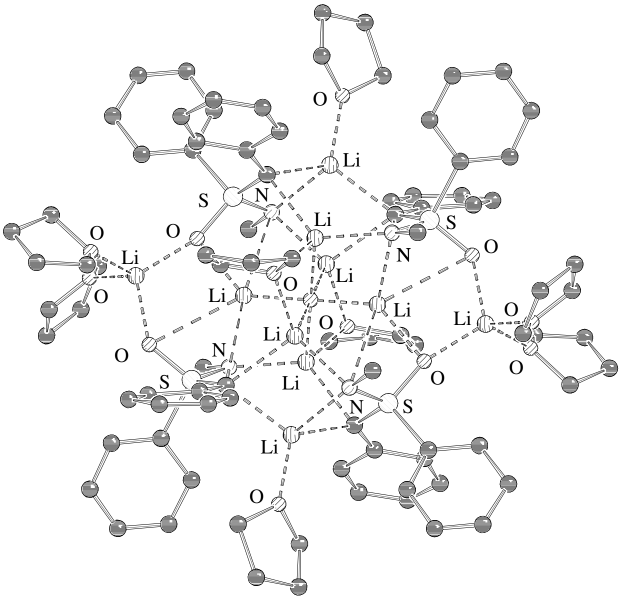

FIGURE 5. Molecular structure of **11b** in the solid state

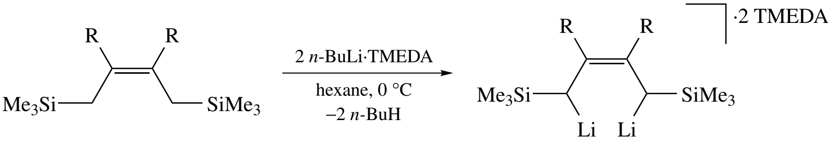

(12a) R = H
(12b) R = Me

(13a) R = H
(13b) R = Me

SCHEME 5

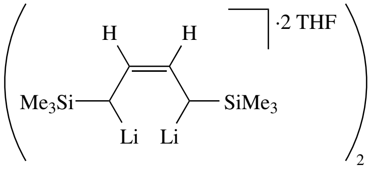

(14)

FIGURE 6. Lewis formula of **14**

alternative pathway to this compound), was studied in the solid state by X-ray structural analysis[16]. The molecular structure reveals a dimer, consisting of two dilithiated butenes in Z-configuration (Figure 7). (The reaction of a 1,2,3-butatriene with excess lithium metal yields a similar, but monomeric molecular structure in E-configuration, see Section II. E).

Bailey and coworkers were able to synthesize mono- and dilithiated phosphonioylides by the reaction of the phosphonium salt **15** with two or three equivalents of n-butyllithium[17]. In both cases, the ylidic precursor **16** is generated by reaction with one equivalent of the base. By the addition of a further one or two equivalents of the base, the monolithiated compound **17** or the dilithiated compound **18** is formed, respectively (Scheme 6). The results were confirmed by NMR studies and trapping experiments.

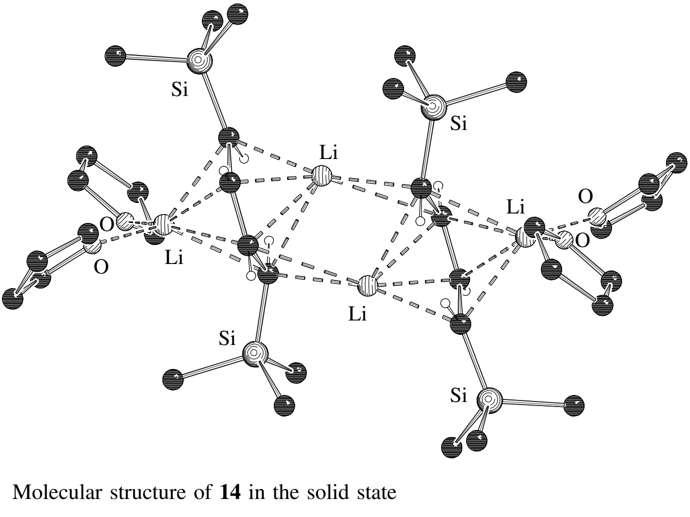

FIGURE 7. Molecular structure of **14** in the solid state

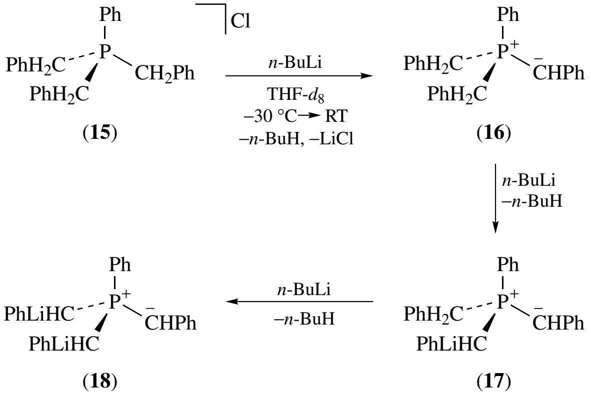

SCHEME 6

In the group of Izod, the tris(phosphane oxide) **19** was 1,2-dilithiated by the reaction with two equivalents of *n*-butyllithium in THF at room temperature (Scheme 7)[18]. The similarity of the structural formula of compound **20** (Lewis formula) to 1,2-dilithium compounds found by Sekiguchi and coworkers (see Section II. E), where two lithium centres are bridging a C_2 unit, is not maintained in the solid state. The X-ray structural analysis reveals a centrosymmetric dimer containing no carbon-lithium contacts (Figure 8).

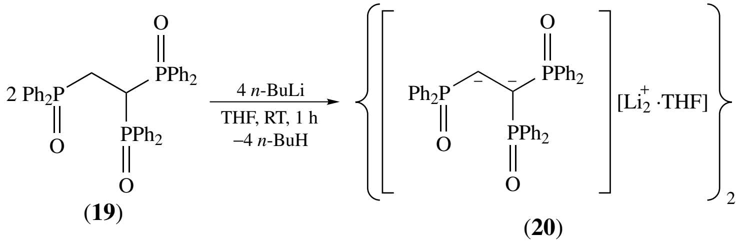

SCHEME 7

A hexameric 1,3-dilithiated benzylsilane could be synthesized in our group, using a two-step strategy[19]. While in non-polar solvents the metalation of **21** occurs at one of the methyl groups, deprotonation in the presence of polar coordinating molecules takes place at the benzyl group quantitatively. The formation of compound **22** without the coordination of solvent molecules (like THF) to the lithium centre required this (lithiophenylmethyl)silane to be synthesized in a non-polar solvent. Thus, metalation with *t*-butyllithium at the benzyl position in toluene could be achieved by using a two-fold excess of **21** (the presence of the non-metalated starting material has the same effect on the regioselectivity as THF, but **21** does not form an adduct with the desired monolithiated compound **22**). Further lithiation of **22** with a second equivalent of the base yielded the 1,3-dilithiated compound **23** (Scheme 8), which reveals a hexameric molecular structure in the solid state (Figure 9).

A two-fold lithiation of diphenyl ether (**24**) and diphenyl thioether was achieved by Schleyer and coworkers[20] as well as by Ogle and coworkers[21]. The reaction with two

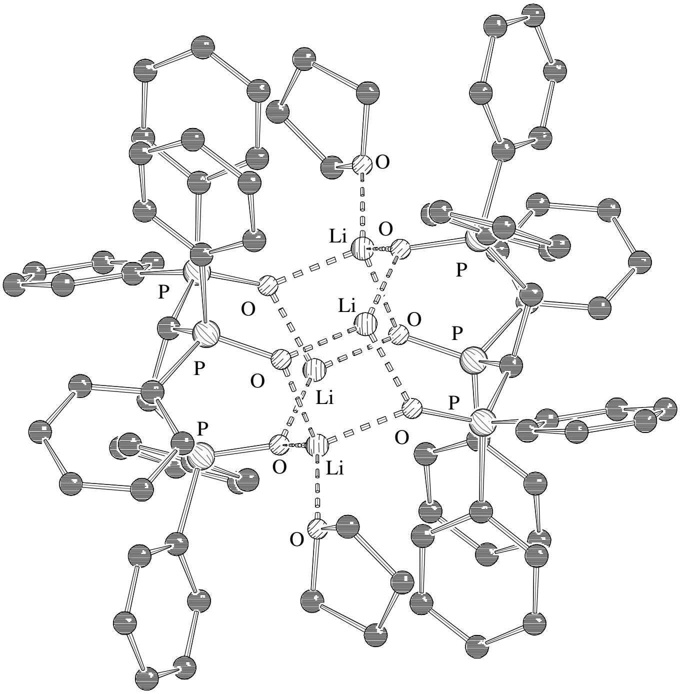

FIGURE 8. Molecular structure of **20** in the solid state

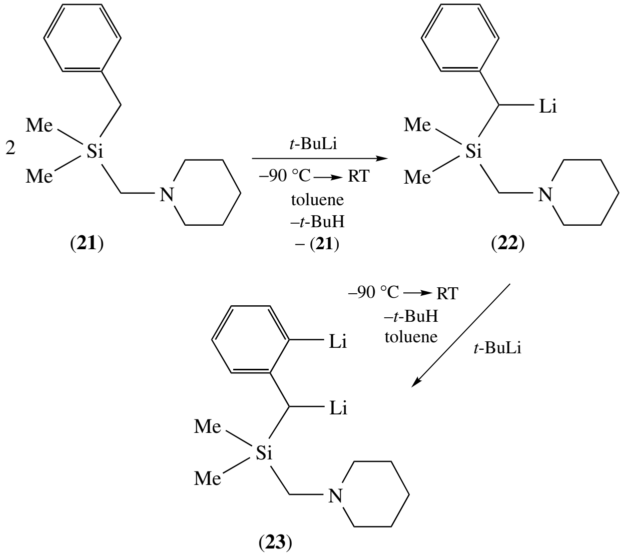

SCHEME 8

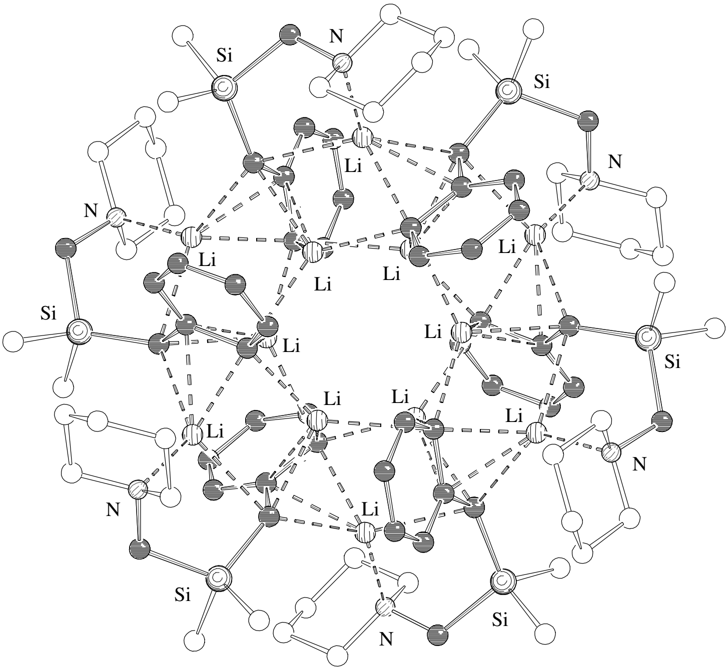

FIGURE 9. Molecular structure of **23** in the solid state

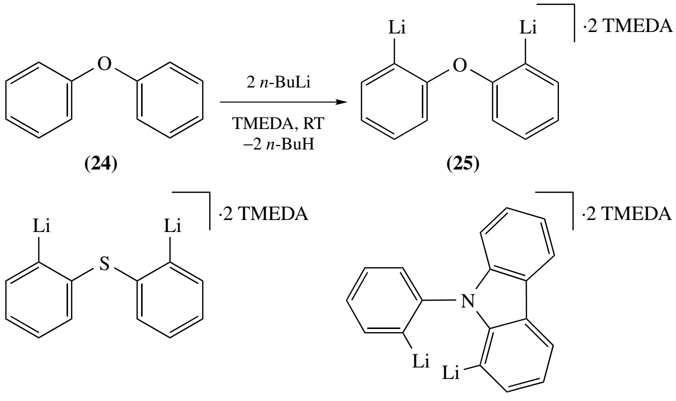

SCHEME 9

equivalents of *n*-butyllithium in the presence of TMEDA was effected at room temperature to give *o*,*o*′-bis(lithiophenyl) ether (**25**) from **24** and *o*,*o*′-bis(lithiophenyl) thioether (**26**) as TMEDA adducts[20]. Also, the TMEDA adduct of the dilithiated *N*-phenylcarbazole **27** was synthesized (Scheme 9). All three compounds were studied by theoretical and

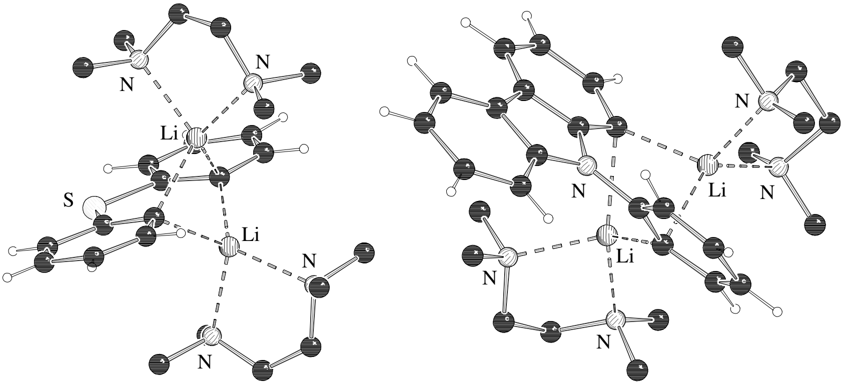

FIGURE 10. Molecular structures of **26** and **27** in the solid state

X-ray structural methods. As examples for the three related crystal structures, molecular structures of compounds **26** and **27** are shown (Figure 10).

A related dilithiated compound, bis[(2-lithio)-3-thienyl] thioether (**29**), was obtained by the same method at 0 °C from bis(3-thienyl) thioether (**28**) (Scheme 10)[22].

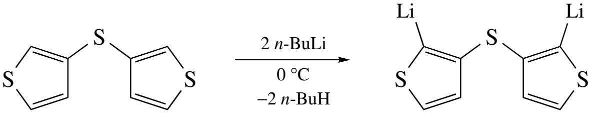

(28) **(29)**

SCHEME 10

The 3-thienyl substituted silane **30** was trilithiated by Nakayama and coworkers, when reacted with a three-fold excess of *n*-butyllithium (Scheme 11)[23]. Target molecule **31** can also be obtained by bromine-lithium exchange, but with a reduced yield.

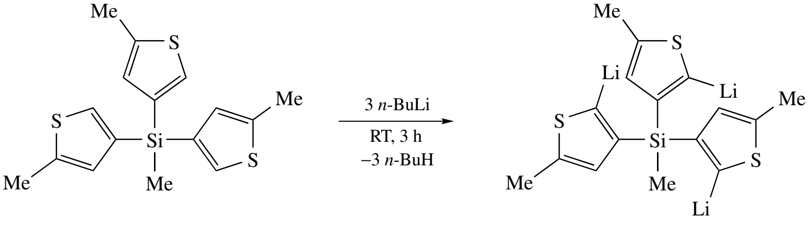

(30) **(31)**

SCHEME 11

In the group of van Koten, dilithiated precursors for the peripheral functionalization of carbosilane dendrimers were generated by deprotonation of compounds **32**, **34a** and **34b** using *t*-butyllithium[24]. The reaction was effected in *n*-pentane at room temperature, using the appropriate amount of the alkyllithium base. Dilithiated compounds **33**, **35a** and **35b** were almost quantitatively obtained, the *para* positions of the aromatic ring systems activated by one or two (dimethylamino)methyl groups (pre-coordination of the base at the pincer ligand systems) (Schemes 12 and 13). In the case of compound **35a** ($n = 2$), the molecular structure in the solid state could be investigated by X-ray structural analysis (Figure 11).

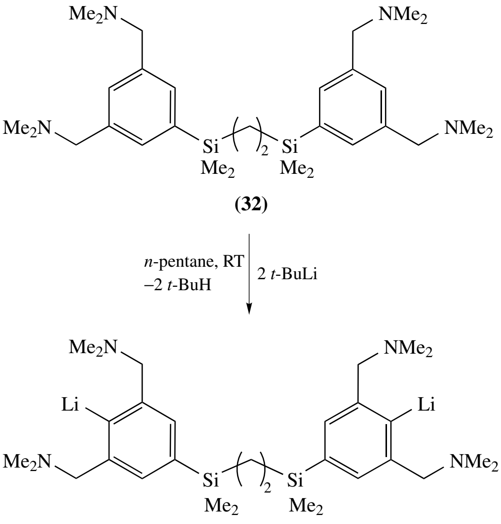

(32)

(33)

SCHEME 12

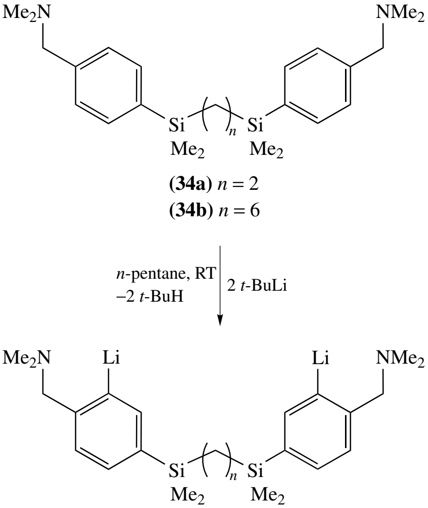

(34a) $n = 2$
(34b) $n = 6$

(35a) $n = 2$
(35b) $n = 6$

SCHEME 13

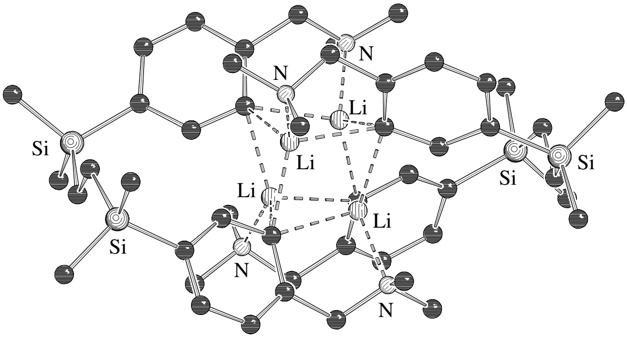

FIGURE 11. Molecular structure of **35a** in the solid state

By the same method, the authors were able to synthesize dendrimers of the generations zero and one, bearing the *para* lithiated pincer ligands in their periphery[24]. Compounds containing four and twelve lithium centres could be obtained cleanly and in almost quantitative yield (as an example, dodecalithiated carbosilane dendrimer **36** is shown in Figure 12).

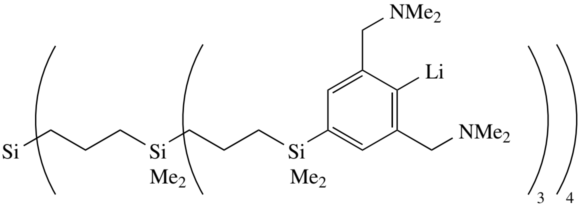

(36)

FIGURE 12

The reaction of 1,4-bis(trimethylsilyl)-2,5,7-cyclooctatriene (**37**) with two equivalents of *n*-butyllithium in a mixture of hexane and 1,2-dimethoxyethane (DME) gives the dilithiated species **38** in a yield of 78% (Scheme 14)[25]. The compound could be isolated by Edelmann and coworkers as single crystals and thus the molecular structure in the solid state could be determined. It reveals an almost planar eight-membered ring which is capped by two lithium–DME units in a η^3-manner from both sides of the ring plane.

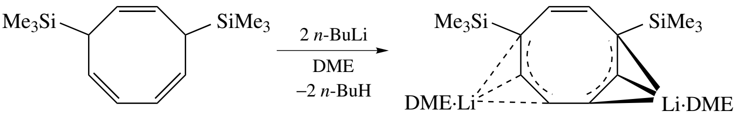

(37) **(38)**

SCHEME 14

In order to synthesize substituted bis(indenyl)methanes, Nifant'ev and coworkers generated several aromatic dilithiated compounds with two metalated cyclopentadienyl rings each[26], like dilithium compound **40** from bis(indenyl)methane **39**. By reaction with alkyl halides or chlorogermanes, variously substituted systems like type **41a**, **41b** or **42** were obtained in varying yields (Scheme 15).

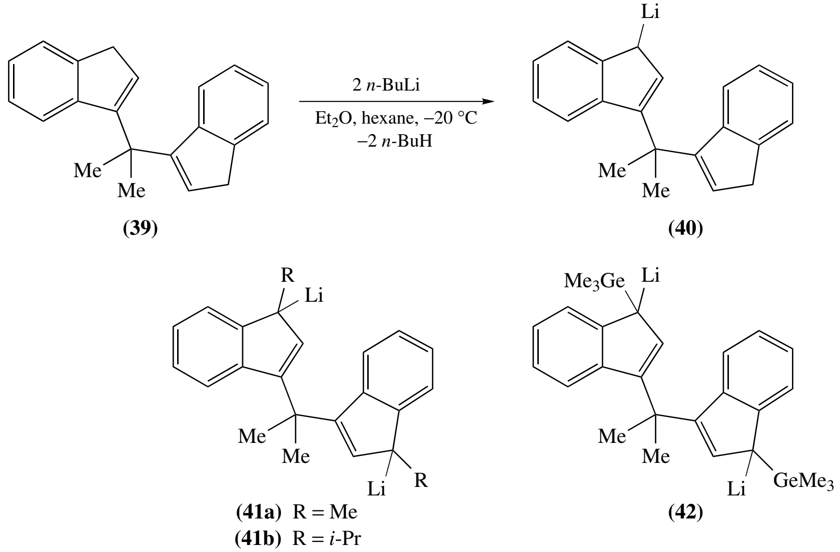

SCHEME 15

As evidence that a monolithiated compound can form an equilibrium with the corresponding dilithiated compound involved, the group of Linti and coworkers crystallographically examined 9,9-dilithiofluorene (**45**)[27]. The molecule is formed when 9-lithiofluorene (**44**) is dissolved in a THF/benzene mixture by an intermolecular deprotonation yielding **45** and fluorene (**43**). In spite of the poor solubility of compound **45**, which does not allow a characterization by NMR methods, the equilibrium is still on the side of the monolithiated compound (Scheme 16). The crystal structure of compound **45** has been reported and reveals a coordination polymer in the solid state (Figure 13).

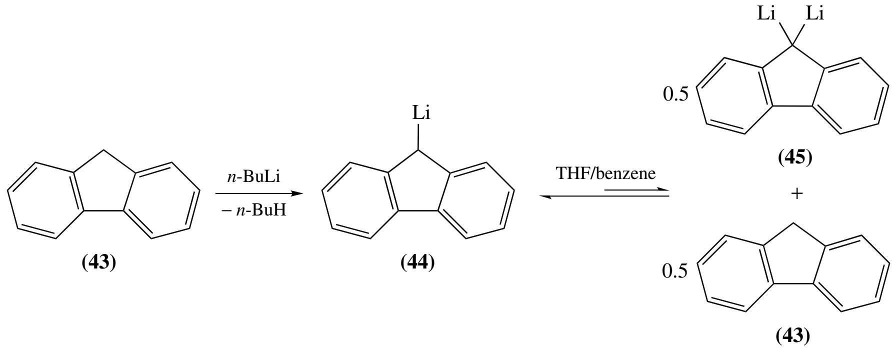

SCHEME 16

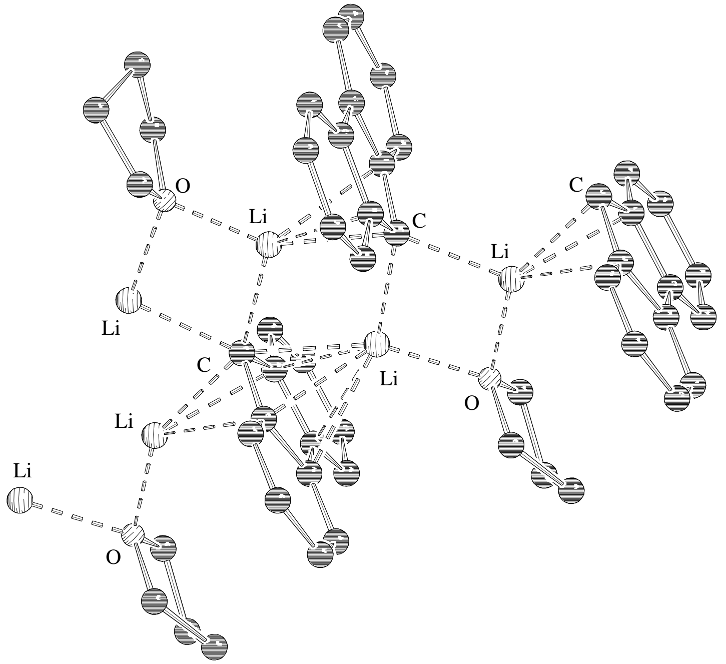

FIGURE 13. Molecular structure of **45** (cut-out of coordination polymer) in the solid state

Korneev and Kaufmann successfully lithiated 2-bromo-1,1-diphenylethylene (**46**) by bromide–lithium exchange to form 2-lithio-1,1-diphenylethylene[28] (**47**). A second lithiation could be effected in four hours at room temperature by deprotonation of the aromatic ring with *n*-butyllithium in the presence of TMEDA (Scheme 17). Like in the synthesis of compound **23**, the first lithiation activates the *ortho*-hydrogen atom of the *Z*-phenyl substituent to give 1,4-dilithium compound **48**. In total, three equivalents of the alkyllithium base are required; the third equivalent is consumed in the trapping reaction of *n*-bromobutane with generation of octane.

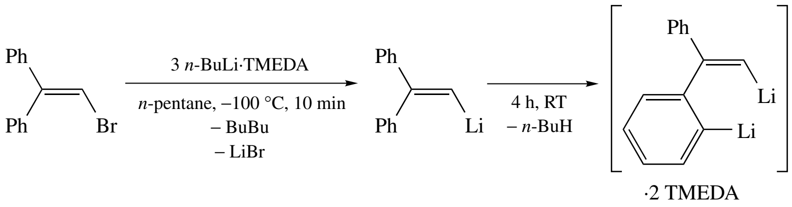

(46) **(47)** **(48)**

SCHEME 17

In the first step, when **49** was treated with two equivalents of *n*-butyllithium in a mixture of *n*-pentane and diethyl ether, the dilithiated dibenzylphosphane **50** was obtained as reported by G. Müller and coworkers[29]. The additional introduction of two more equivalents of the alkyllithium base to **50** gave quadruply lithiated dibenzylphosphane **51** in a yield of 50% (Scheme 18). Moreover, this compound could be investigated in the solid state by single-crystal X-ray structural analysis, revealing a dimer via a central bridging four-membered lithium rectangle (Figure 14).

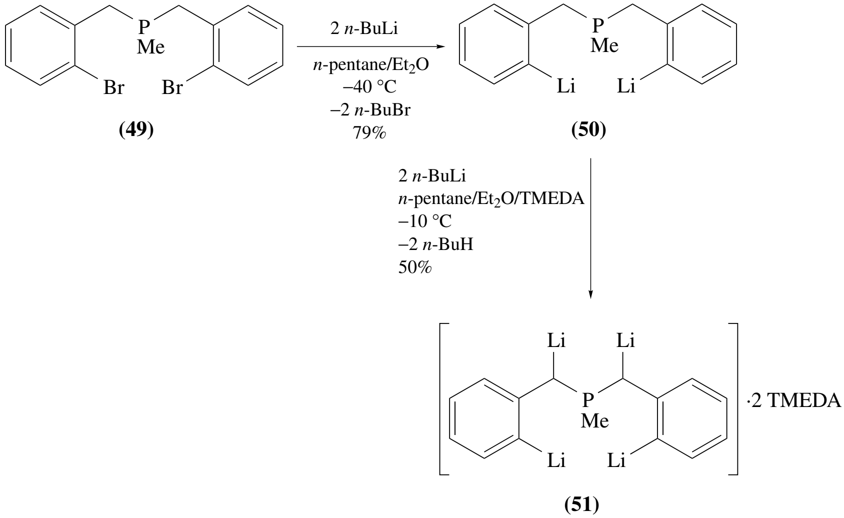

SCHEME 18

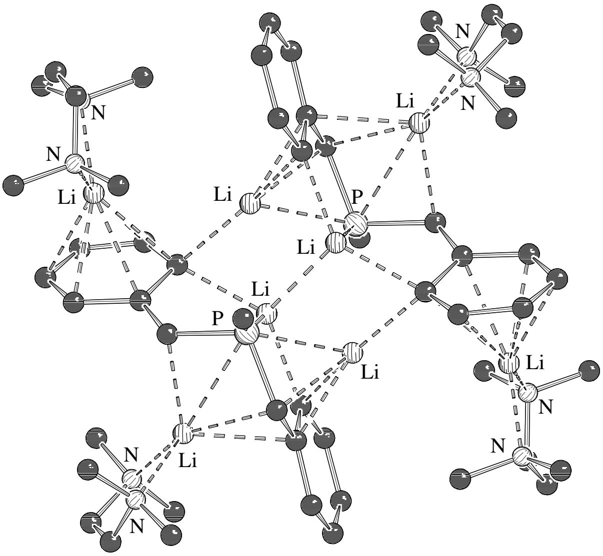

FIGURE 14. Molecular structure of **51** in the solid state

In the same group, Feustel and G. Müller have observed an interesting reaction between two equivalents of the tris(phosphinomethyl)methanol **52** and five equivalents of *n*-butyllithium[30]. Formally, the elimination of lithium oxide leads to the formation of a mixed aggregate of the lithium alkoxide **53** and the dilithiated trimethylenemethane dianion **54** in the solid state (Scheme 19, Figure 15). The mechanism of the formal elimination of lithium oxide, which could also be part of a further mixed aggregate, has not been cleared up yet.

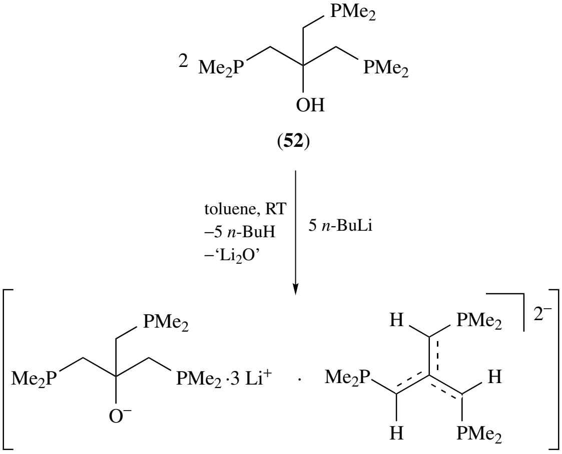

(**52**)

(**53**) (**54**)

SCHEME 19

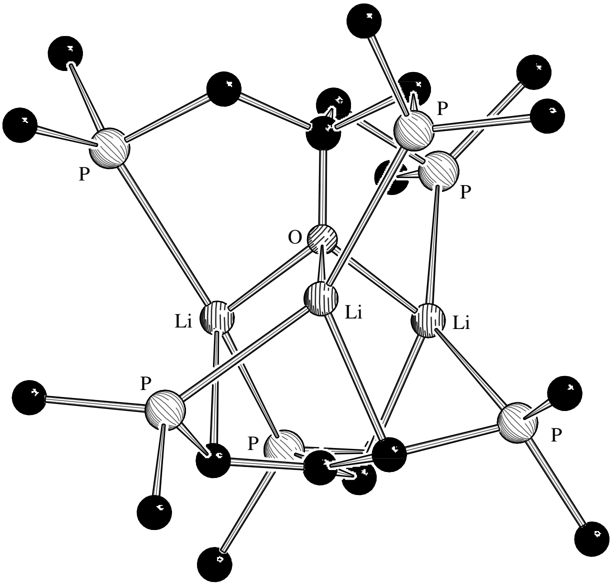

FIGURE 15. Molecular structure of **53**. **54** in the solid state

By the monolithiation of acetylene (**55**), Mortier and coworkers observed the disproportionation of lithioacetylene (**56**) into 1,2-dilithioacetylene (**57**) and acetylene (**55**) (Scheme 20)[31]. By trapping reactions of monolithiated **56**, which is obtained by reaction of acetylene and *n*-butyllithium in THF at −78 °C, with several electrophiles in yields up to 98%, it could be shown that the reaction gives monolithioacetylene (**56**) at these temperatures. At elevated temperatures of around 0 °C, the compound disproportionates into the non-metalated **55** and the dimetalated compound **57**, which precipitates. Due to the poor solubility of the dilithium compound and the reversibility of the disproportionation, trapping reactions of the reaction mixture at 0 °C only yield monosubstituted trapping products.

$$\underset{\textbf{(55)}}{HC{\equiv}CH} \xrightarrow[\substack{-78\ ^\circ C \\ -n\text{-BuH}}]{n\text{-BuLi}} \underset{\textbf{(56)}}{HC{\equiv}CLi} \xrightleftharpoons[0\ ^\circ C]{} \underset{\textbf{(57)}}{LiC{\equiv}CLi} + \underset{\textbf{(55)}}{HC{\equiv}CH}$$

SCHEME 20

B. Halide–Lithium Exchange

The halide–lithium exchange reaction is the classical route towards monolithiated alkyls (many commercially available and/or industrially synthesized lithium alkyls are obtained by this method). Since side-reactions (especially elimination reactions) are very common for lithiated alkyl halides (lithium centres separated by one, two or three carbon centres), this method is almost exclusively suitable for polylithium compounds with lithium centres separated by four or more carbon centres. Only a few examples have been reported, where the halide–lithium exchange has been performed with metallic lithium or lithium *p*,*p*′-di-*t*-butylbiphenylide (LiDBB, see Section II. D) respectively, where the formation of the corresponding lithium halide is the driving force of the reaction. The bigger part of lithium–halide exchanges has been effected using butyllithiums. Although a thermodynamically controlled equilibrium is responsible for the product ratio in this case, the equilibrium is far on the side of the products, when aryl bromides are used.

Brandsma and coworkers were able to show that *meta*- (**59a**) and *para*-dilithiated benzene (**59b**) are accessible via iodine–lithium exchange, using *n*-butyllithium[32]. Therefore, 1,3- and 1,4-diiodobenzene (**58a** and **58b**) respectively were reacted with two equivalents of *n*-butyllithium in diethyl ether at low temperatures (Scheme 21). The polylithiation was confirmed by trapping reactions with dimethyl disulphide. The same reactions, starting from the corresponding dibromobenzenes, had led only to monolithiated benzenes.

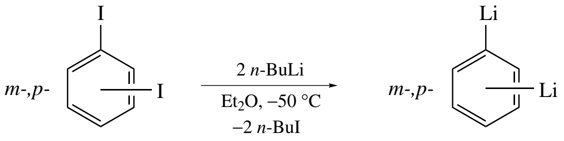

(**58a**) *m*-$C_6H_4I_2$
(**58b**) *p*-$C_6H_4I_2$

(**59a**) *m*-$C_6H_4Li_2$
(**59b**) *p*-$C_6H_4Li_2$

SCHEME 21

1,3,5-Trilithiated benzene (**65**) was synthesized by Rot and Bickelhaupt, starting from 1,3,5-tribromobenzene (**60**)[33]. While the approach of using *t*-butyllithium resulted only in the formation of a mixture of mono- or dilithiated products **61**–**64** (even with the addition of TMEDA), the halide–lithium exchange using LiDBB could be successfully applied (Scheme 22). Tribromobenzene (**60**) was reacted with seven equivalents of LiDBB in diethyl ether at low temperatures, yielding as the main product 1,3,5-trilithiobenzene (**65**) (yields between 21 and 79%) besides 1,3-dilithio- (**61**) and monolithiobenzene (**66**). The results were confirmed by trapping reactions with various electrophiles, mainly 1,2-diiodoethane.

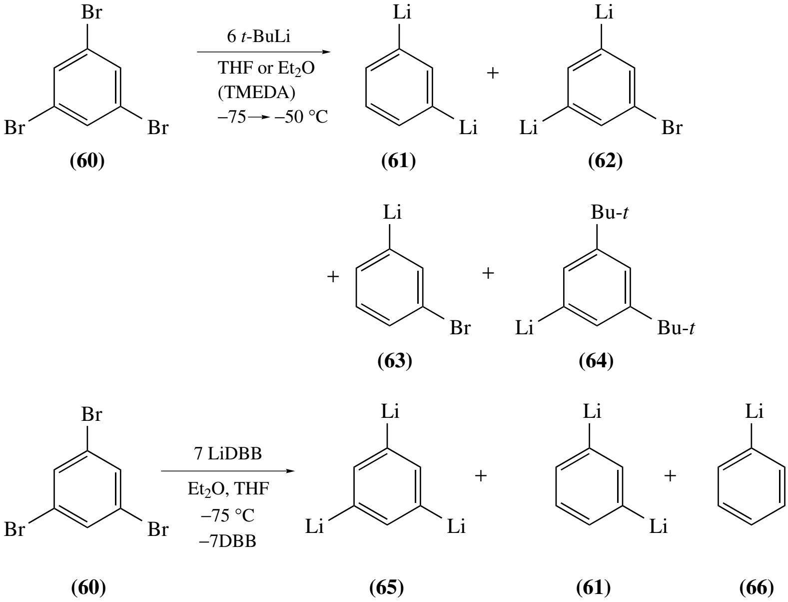

SCHEME 22

Considering the results of Brandsma[32] and Bickelhaupt[33], the synthesis of hexalithiobenzene (**68**) by Lagow and coworkers seems remarkable[34]. The group reported on the synthesis of this highly metalated compound, starting from hexachlorobenzene (**67**). At very low temperatures, the chlorobenzene was reacted with a large excess of *t*-butyllithium in the presence of 1,4-dioxane (Scheme 23). The main trapping product, hexadeuteriobenzene, was characterized using mass spectrometry and NMR methods.

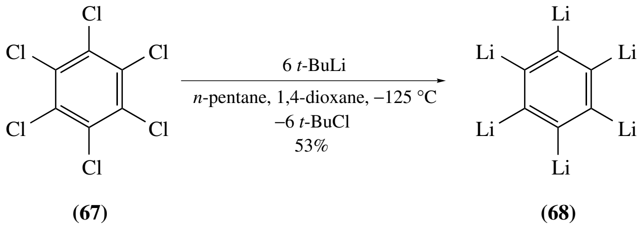

SCHEME 23

The possible molecular structure of compound **68** was investigated thoroughly by Xie and Schaefer[35] and by Smith[36] using quantum-chemical methods.

In order to functionalize the periphery of dendrimers of the type **69**, van Koten and coworkers developed a strategy to cleanly obtain 4-lithioaryl substituted carbosilane dendrimers of the dendrimer generations zero ($n = 4$, **70a**) and one ($n = 12$, **70b**) (Scheme 24)[37]. The bromide–lithium exchange using *n*-butyllithium was successfully applied and the quantitative lithiation confirmed by hydrolysis or by conversion into functionalized dendrimers by reaction with various electrophiles.

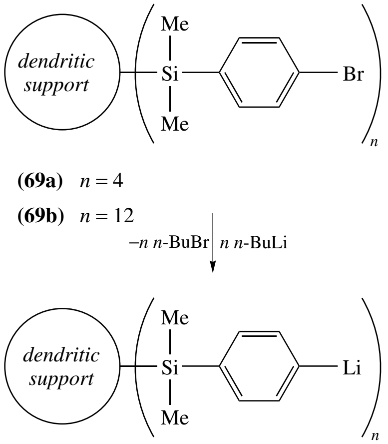

(69a) $n = 4$
(69b) $n = 12$

(70a) $n = 4$
(70b) $n = 12$

SCHEME 24

Van Koten and coworkers also applied this strategy to obtain intramolecularly stabilized 1,4-dilithiated pincer ligands of the type **72**[38]. 1,4-Dilithio-2,3,5,6-tetrakis(dimethylamino)benzene (**72**) was generated by the reaction of the corresponding dibromo compound **71** with two equivalents of *n*-butyllithium in THF at low temperatures (Scheme 25).

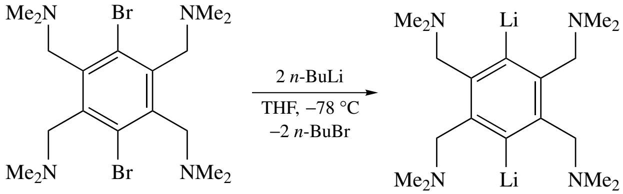

(**71**) (**72**)

SCHEME 25

By a two-fold bromine–lithium exchange on 1,2-bis(2-bromo-3,5-di-*t*-butylphenyl)ethane (**73**), Yoshifuji and coworkers were able to generate 1,6-dilithium compound **74**[39]. The reaction was carried out using *n*-butyllithium in THF at −78 °C (Scheme 26).

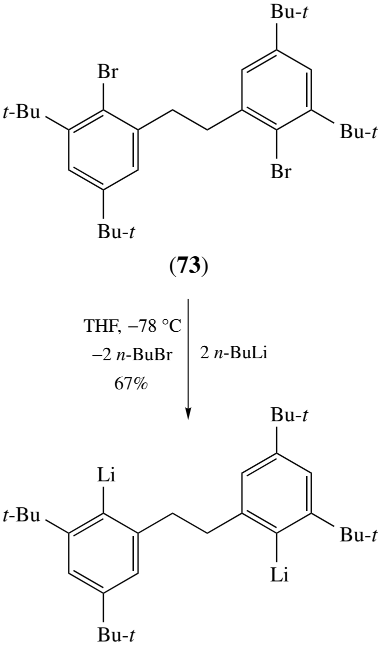

(**73**)

(**74**)

SCHEME 26

Tris(4-lithiophenyl)methane (**76**), a 1,9,9′-trilithiated compound, was obtained by Oda and coworkers[40]. The starting tribromo compound **75** reacts with three equivalents of *n*-butyllithium in THF at low temperatures. Trapping reactions with various electrophiles resulted in yields between 59 and 90% (Scheme 27).

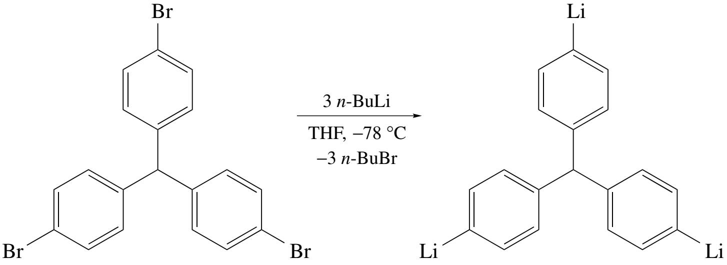

(**75**) (**76**)

SCHEME 27

The heterocyclic 2,5-dilithio-3,4-di-(*t*-butyl)thiophene (**78**) could be generated by Nakayama and coworkers, starting from the corresponding 2,5-dibromo compound **77**[41]. The bromide–lithium exchange reaction was effected using two equivalents of

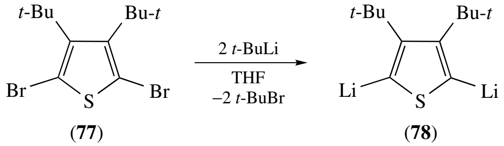

SCHEME 28

t-butyllithium in THF (Scheme 28). The dilithiation was confirmed by reaction with various chlorosilanes.

The comparable unsubstituted 2,5-dilithiothiophene (**80**) was synthesized from 2,5-dibromothiophene (**79**) by Ritter and Nöftle based on the same synthetic route, using *n*-butyllithium (Scheme 29)[42].

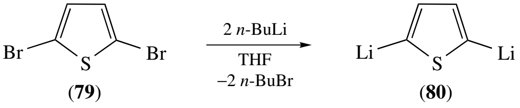

SCHEME 29

When hexachloro-1,3-butadiene (**81**) is reacted with four equivalents of *n*-butyllithium in diethyl ether, a series of lithiation and elimination reactions gives 1,4-dilithio-1,3-butadiyne (**82**) in good yields (Scheme 30). Ijadi-Maghsoodi and Barton verified this by derivatization with various chlorosilanes in yields up to 94%[43].

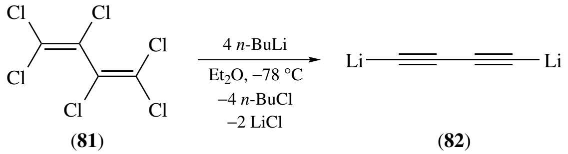

SCHEME 30

The geminal dihalogenated cyclopropane derivatives **83a** and **83b** were lithiated by Vlaar and Klumpp[44]. 7,7-Dichloro- (**83a**) and 7,7-dibromonorcarane (**83b**) were reacted with four equivalents of LiDBB in diethyl ether and several reaction conditions were examined by the authors such as reaction temperatures, the influence of different coordinating additives as well as various methods (Scheme 31). The achieved maximum yield for the geminal dilithium compound **84** was 55% (from **83b**). Side-products, like the 1,2-dilithioethane derivative **85**, the dilithiated dicyclohexylacetylene **86** or 1,3-dilithium compound **87**, were observed in different quantities, sensitively depending on the reaction conditions. Also, carbenoid intermediates were formed as verified by trapping reactions (deuteriolysis).

The bromide–lithium exchange of 1,1-dibromo-2,2-diphenylethylene (**88**) was thoroughly examined by Maercker and coworkers[45]. It could be shown that the number of side-products drastically decreases when LiDBB instead of metallic lithium is used as lithiation agent. The reaction was performed in THF at low temperatures by addition of the solution of the geminal dibrominated alkene to the solution of LiDBB (Scheme 32). By this method, 1,1-dilithio-2,2-diphenylethylene (**89**) could be obtained in 36% yield together with the 1,4-dilithium compound **48** and monolithiated **47** (51 and 2%, respectively). The yields were determined after trapping the reaction mixture with dimethyl sulphate.

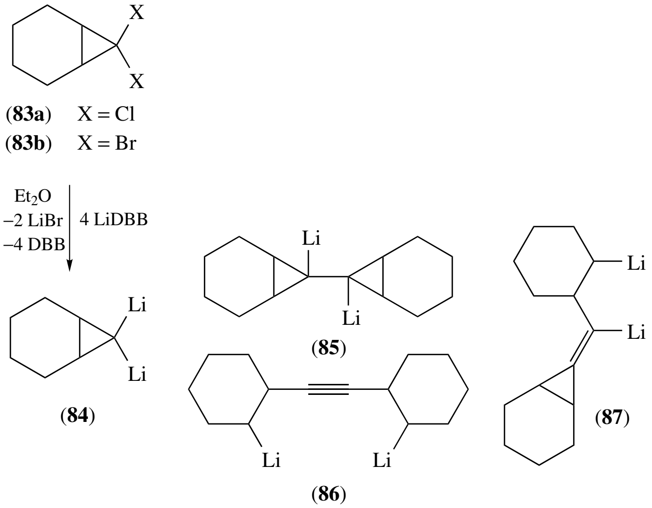

SCHEME 31

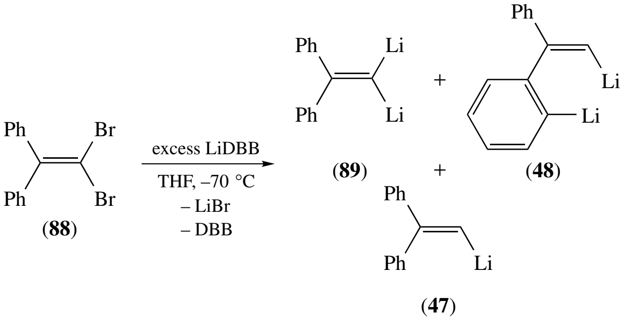

SCHEME 32

The aggregation behaviour and the structure in solution of two closely related dilithium compounds **90** and **91** (Figure 16) was studied by Günther, Maercker and coworkers, using one- and two-dimensional NMR techniques (^{1}H, ^{13}C, ^{6}Li)[46]. While in diethyl ether, both compounds exist as a dimer, the dimeric structure is partly broken up in THF or by the addition of TMEDA. Also, activation barriers and thermodynamic parameters of aggregate exchanges were determined by temperature-dependent NMR studies.

Three different di- and trilithiated phenylmethanes **93**, **95** and **97** were generated by Baran Jr. and Lagow[47]. Dichlorodiphenylmethane (**92**), dichlorophenylmethane (**94**) and trichlorophenylmethane (**96**) were reacted with the appropriate amount of *t*-butyllithium in THF at very low temperatures. Except for dilithiodiphenylmethane (**93**), the observed yields were very low, verified by deuteriolysis of the lithiated compounds (Scheme 33).

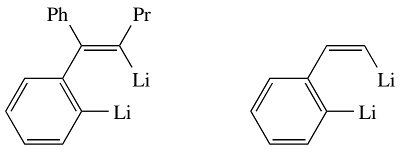

(90) **(91)**

FIGURE 16. Lewis formulas of **90** and **91**

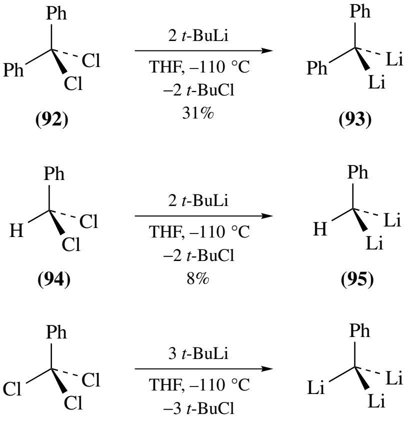

(92) **(93)** **(94)** **(95)** **(96)** **(97)**

SCHEME 33

C. Metal–Lithium Exchange

Metal–lithium exchange has been used in metathesis reactions to generate polylithiated alkyl groups. As starting compounds, polyorganotellurium and polyorganomercury compounds, as well as polyorganotin and organocobalt compounds can be found. Usually, these compounds react with several equivalents of alkyllithium in ethers to give the corresponding alkylmetal derivatives. Especially in the case of the fast tellurium–lithium- and mercury–lithium exchange reactions, thermodynamically controlled equilibria are observed. The metalation reaction therefore usually stops at the level of the thermodynamically most stable compounds. This can, but must not be the desired polylithium compound, as the following examples will demonstrate.

In our group, the tin–lithium exchange has been used to synthesize the doubly lithiated dimethyl sulphane **99** by the reaction of bis(tributylstannomethyl)sulphane (**98**) with two equivalents of *n*-butyllithium in diethyl ether[48]. Two equivalents of tetrabutylstannane are cleaved off in this reaction (Scheme 34).

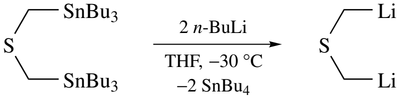

(98) **(99)**

SCHEME 34

On the contrary, when bis(tributylstannomethyl)silane **100** is reacted with two equivalents of *n*-butyllithium in diethyl ether, only monolithiated compound **102** is formed[49]. The doubly lithiated compound **101** is not accessible by this method (Scheme 35).

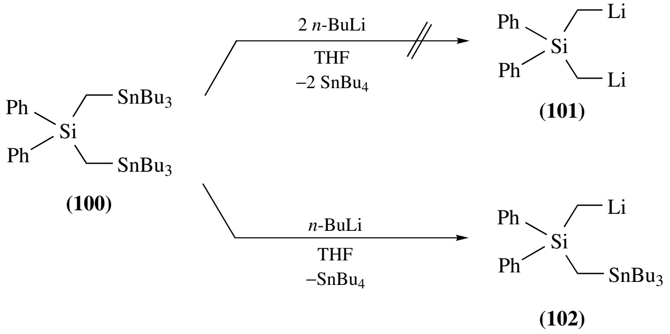

(100) **(101)** **(102)**

SCHEME 35

Also by tin−lithium exchange, Ashe and coworkers were able to generate 2,5-dilithio-1,5-hexadiene (**104**), a divinyllithium compound[50]. The reaction, starting from 2,5-bis(trimethylstanno)-1,5-hexadiene (**103**), is believed to proceed via the dimeric pentacoordinated lithium stannate **105** (Scheme 36).

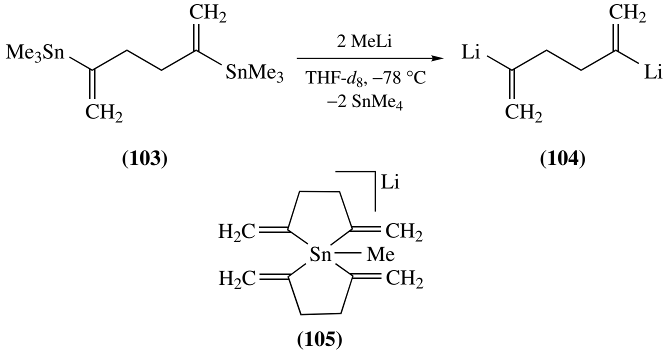

(103) **(104)** **(105)**

SCHEME 36

The formation of doubly lithiated bis(lithiomethyl)acetylene (**107**) is accompanied by the formation of 2,3-dilithio-1,3-butadiene (**108**), when starting from bis(trimethylstannomethyl)acetylene (**106**)[51]. As reported by Reich and coworkers, the molar ratio X of the two compounds depends on the applied temperature protocol (ratio determined by trapping reactions with chlorotrimethylsilane) (Scheme 37).

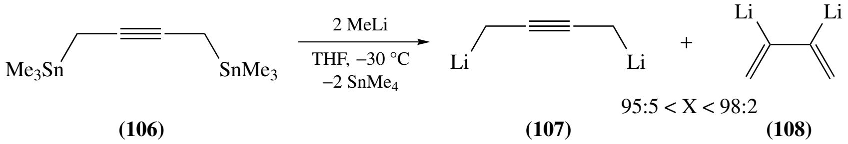

(106) **(107)** **(108)**

SCHEME 37

Butadiene **108** is formed as the only reaction product, when bis-2,3-(trimethylstanno)-1,3-butadiene (**109**) is used as starting material (Scheme 38)[51].

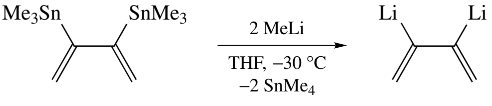

(109) **(108)**

SCHEME 38

De Meijere, Stalke and coworkers were able to generate dilithiated **111**, where the tricyclic non-metalated form can be considered as a subunit of the smallest possible fullerene C_{20}[52]. By a two-fold tin–lithium exchange of the bis(trimethylstanno) derivative **110** with methyllithium, the dilithium compound **111** was cleanly obtained (Scheme 39); its solid-state structure could be clarified by means of X-ray crystallography.

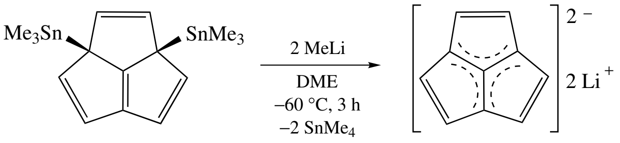

(110) **(111)**

SCHEME 39

Bis(lithiomethyl) sulphane (**99**) is also accessible by tellurium–lithium exchange reaction, when reacting bis(butyltelluriomethyl) sulphane (**112**) with two equivalents of *n*-butyllithium in diethyl ether[48]. Two equivalents of dibutyltellurium are cleaved off in this reaction (Scheme 40).

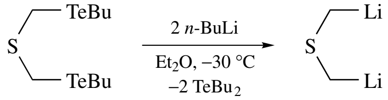

(112) **(99)**

SCHEME 40

The analogous oxygen compound, bis(lithiomethyl) ether (**114**), can also be synthesized by this method[49]. When bis(butyltelluriomethyl) ether (**113**) is treated with *n*-butyllithium under the same conditions, compound **114** can be generated in one step. In contrast to the sulphide **99**, the doubly lithiated ether **114** undergoes a rearrangement at temperatures above −50 °C, resulting in the formation of lithium 2-lithioethoxide (**115**) (Scheme 41).

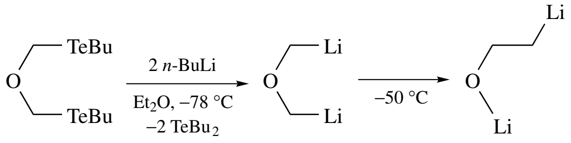

(113) **(114)** **(115)**

SCHEME 41

In contrast to tin–lithium exchange, doubly lithiated bis(lithiomethyl)silanes **117a** and **101** with methyl or phenyl substituents at the silicon centre are accessible from bis(telluriomethyl)silanes **116a,b** by a two-fold tellurium–lithium exchange (Scheme 42)[49].

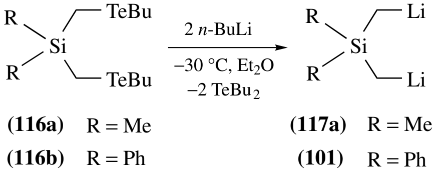

SCHEME 42

Due to the formation of phenyllithium, the reaction of bis(phenyltelluriomethyl)silane **118** with n-butyllithium does not lead to the doubly lithiated compound **117a**, but to the bis(butyltelluriomethyl)silane **119** and phenyllithium (Scheme 43)[49].

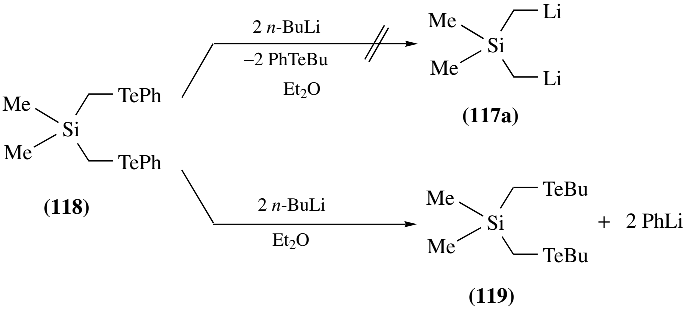

SCHEME 43

Tellurium–lithium exchange in cyclic systems, like the telluranaphthalene **120**, has been demonstrated by Sashida[53]. The possibility of a two-fold tellurium–carbon bond cleavage introduces a route to doubly lithiated compounds. When compound **120** is treated with an excess of n-butyllithium in THF, the lithiated lithium tellurate **121** is formed, which is interconverting to the doubly lithiated compound **122** (Scheme 44, verified by deuteriolysis).

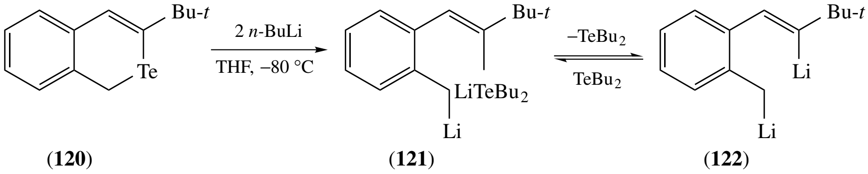

SCHEME 44

For the lithiation reactions of the closely related compound **123** with n-butyllithium, a significant solvent effect was observed by Maercker and coworkers[54]. While a two-fold lithiation process by tellurium–lithium exchange takes place in hexane, yielding highly pyrophoric **91**, only α-deprotonation occurs when the reaction is effected in THF, yielding the monolithiated tellurole **124** (Scheme 45).

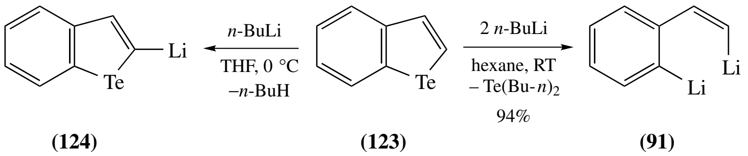

SCHEME 45

By the analogous reaction, the doubly lithiated sulphur substituted vinyllithium compound **126** was generated by Brandsma, Maercker and coworkers, starting from telluracycle **125**[55]. An interesting pathway to functionalized heteroatom-substituted polylithium compounds has been introduced by this method (Scheme 46).

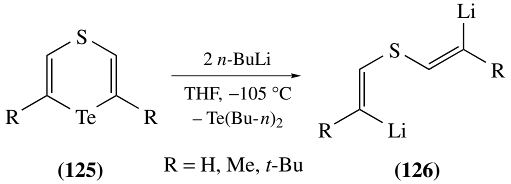

SCHEME 46

Variously substituted siloles of type **129** could be synthesized by Tamao and coworkers by the reaction of 1,4-diaryl-1,4-dilithio-1,3-butadienes of type **128** with chlorosilanes[56]. The 1,1′-spirobisilole **130** was accessible by reaction of the diphenyl substituted dilithium compound **128a** with tetramethoxysilane (Scheme 47). All of the dilithium compounds **128a**–**e** were obtained by reaction of 2,5-diaryltellurophenes **127a**–**e** with *s*-butyllithium in diethyl ether.

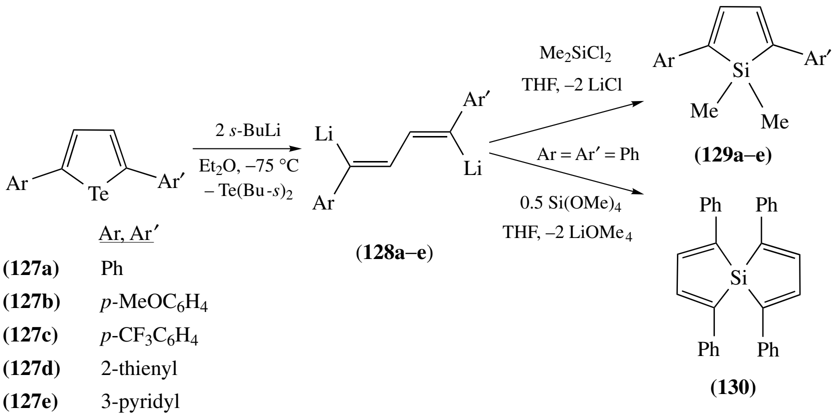

SCHEME 47

The dilithiated vinyllithium compound 1,2-dilithioethylene (**132**) was synthesized by Maercker and coworkers, using the mercury–lithium exchange reaction[57]. Bis(chloromercurio)ethylene (**131**) was reacted with four equivalents of *t*-butyllithium in THF. While by the first two equivalents of the alkyllithium compound, the intermediate bis(*t*-butylmercurio)ethylene is formed, the remaining two equivalents effect the mercury–carbon bond cleavage under formation of the dilithiated product **132** (Scheme 48).

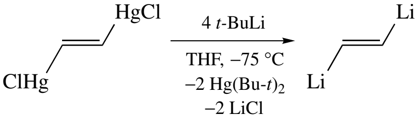

(**131**) (**132**)

SCHEME 48

The interesting sandwich compounds pentamethylpentalithioruthenocene (**135**) and decalithioruthenocene (**134**) could be obtained by effecting the same type of reaction, starting from the corresponding (acetoxymercurio)ruthenocenes[58, 59], like compound **133** (Scheme 49). The polylithium compounds were characterized by trapping reactions using water, iodomethane or bromine by Bretschneider-Hurley and Winter. An overview for this class of compounds is given in a review article[60].

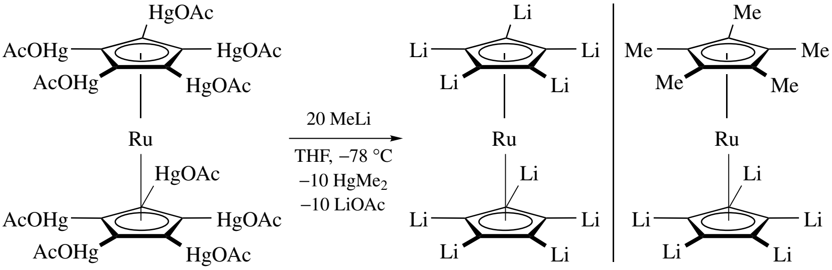

(**133**) (**134**) (**135**)

SCHEME 49

By cobalt–lithium exchange, the group of Sekiguchi and coworkers generated several dilithium salts of variously substituted cyclobutadiene dianions[61]. By the reaction of the functionalized acetylenes (e.g. compound **137**) with CpCo(CO)$_2$ (**136**), the corresponding cobalt sandwich complexes, related to compound **138**, were obtained (Scheme 50). These can be interconverted into the dilithium salts of the accordant cyclobutadiene dianions (e.g. dilithium compound **139**) by reaction with metallic lithium in THF. Bicyclic as well as tricyclic (e.g. dilithium compound **141**, starting from cobalt complex **140**) silyl substituted systems were generated (Scheme 51)[62].

By the choice of substituents at the acetylene precursor, symmetrical as well as asymmetrical cyclobutadiene dianions **142a–c** in *cis* and *trans* form could be obtained (Scheme 52)[63, 64].

A first structural characterization of a cyclobutadiene dianion was performed by Boche and coworkers, who generated the dilithium salt of the 1,2-diphenylbenzocyclobutadiene dianion (**143**) (by deprotonation with *n*-butyllithium in the presence of TMEDA) (Figure 17)[65–68]. Nevertheless, the molecular structure of **143** resembles more the structures of dilithiated alkenes, synthesized by reaction of the corresponding alkynes with metallic lithium. In that class of compounds, carbon–carbon bonds, capped by two lithium centres, are the structural motif (see Section II. E).

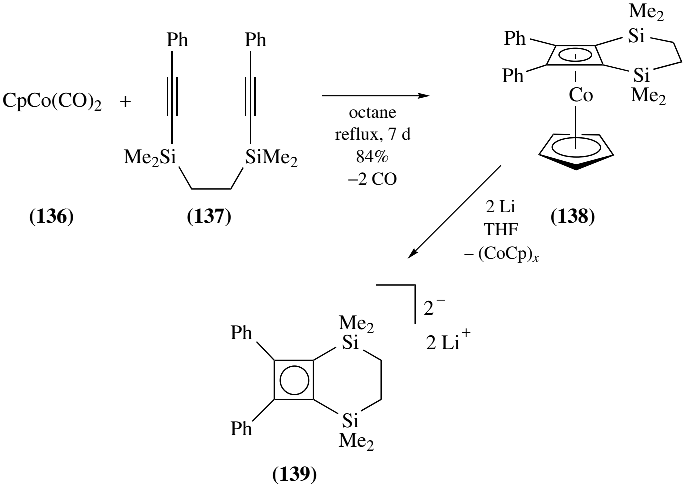

SCHEME 50

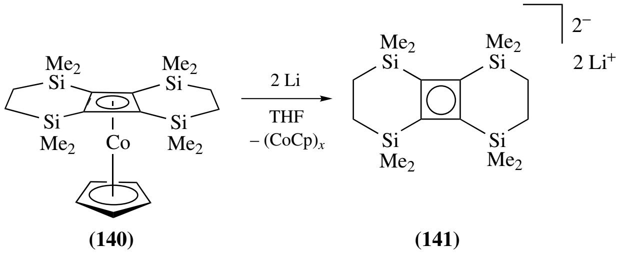

SCHEME 51

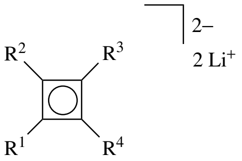

$R^1 = R^2 = R^3 = R^4 = SiMe_3$ (**142a**)
$R^1 = R^2 = Ph$; $R^3 = R^4 = SiMe_3$ (**142b**)
$R^1 = R^3 = Ph$; $R^2 = R^4 = SiMe_3$ (**142c**)

SCHEME 52

By means of X-ray crystallography, NMR studies and quantum-chemical studies, an insight into the problem of aromaticity of the tetrakis(trimethylsilyl)cyclobutadiene dianion **142a** of Sekiguchi could be gained (Figure 18)[69]. The cyclic dianion, which should be aromatic due to Hückel's Rule, shows non-alternating C−C bond distances in the solid

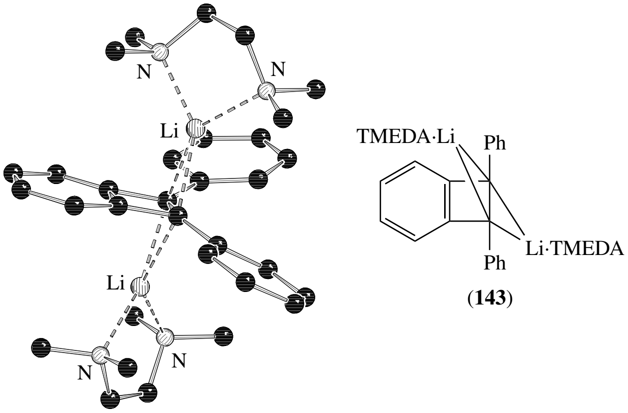

(**143**)

FIGURE 17. Molecular structure of **143** in the solid state and Lewis formula

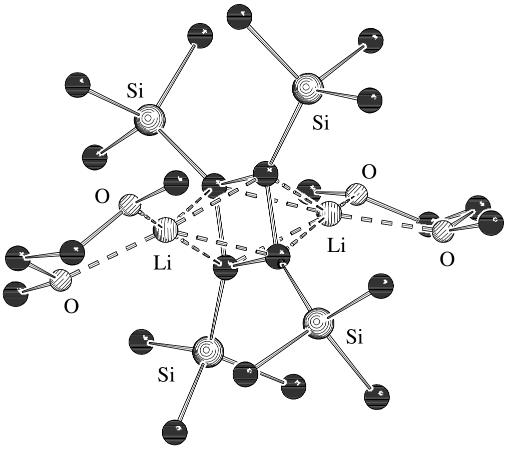

FIGURE 18. Molecular structure of **142a** in the solid state

state and a planar four-membered ring that misses the D_{4h} symmetry marginally (predicted by theoretical methods). Due to the highly shielded ^{6}Li chemical shift in the NMR experiment, a diatropic ring current can be assumed supporting an aromatic character of the cyclobutadiene dianion system.

Furthermore, the molecular structure of **142a** with two lithium centres capping the four-membered ring is a basis for corresponding NICS calculations (Nucleus Independent Chemical Shift, quantum-chemical tool for probing the aromaticity), that had been performed by Schleyer and coworkers before the discovery of the experimental molecular structure in the solid state[70]. These quantum-chemical studies had predicted aromaticity for the tetramethyl- and tetrakis(*t*-butyl)cyclobutadiene dianion dilithium salt, but no planar C_4 ring system for both compounds. Furthermore, geometric parameters and NMR chemical shift values were investigated.

D. Reductive Cleavage of Carbon–Sulphur Bonds

In many cases, the synthesis of polylithium organic compounds by successive deprotonation reactions is difficult; the second deprotonation step is often kinetically hindered. In exchange reactions (halide–lithium, metal–lithium), the thermodynamic equilibrium sometimes can prevent the formation of the desired polylithium compound. To circumvent these problems, ether cleavage reactions (reductive carbon–sulphur bond cleavage) have successfully been applied to generate polylithiated compounds. While heterogeneous reactions with lithium metal are becoming too slow at low temperatures, lithium naphthalenide ($LiC_{10}H_8$, **144a**) and especially lithium *p*,*p*′-di-*t*-butylbiphenylide (LiDBB, **145**) (Figure 19) can be used homogeneously in THF solution even at −78 °C. The possibility of preparing $LiC_{10}H_8$ (**144a**) in THF solution even at room temperature must be emphasized as a major advantage of this reagent, since LiDBB (**145**) decomposes at temperatures above 0 °C. In a recent article by Yus and coworkers, the importance of a catalytic addition of DBB to polylithiation reactions with metallic lithium has been stressed[71]. This has become even more important for $LiC_{10}H_8$ (**144a**), since a large excess of lithium might produce the $Li_2C_{10}H_8$ dianion (**144b**), which has a higher reduction potential[72].

Since only very few examples for the synthesis of polylithium compounds by a reductive cleavage of carbon–sulphur bonds had been reported before, all examples for this method of synthesis will be presented.

Screttas and Micha-Screttas synthesized various dilithiated alkyls by the method of reductive sulphur–carbon bond cleavage with metallic lithium. The example of compound **147** shows that thioethers **146** are cleaved selectively in the presence of ether functionalities (Scheme 53)[73].

By the same method, compounds **148**, **149** and **150a–e** were generated, all bearing phenyl substituents in α-position to the lithiated carbon centre (Figure 20)[74].

For selective reactions at low temperatures (e.g. −78 °C), the addition of DBB to the reaction mixture becomes necessary, to form the soluble LiDBB radical anion (**145**). Heterogeneous reactions, like lithium in THF, are too slow at these temperatures. The

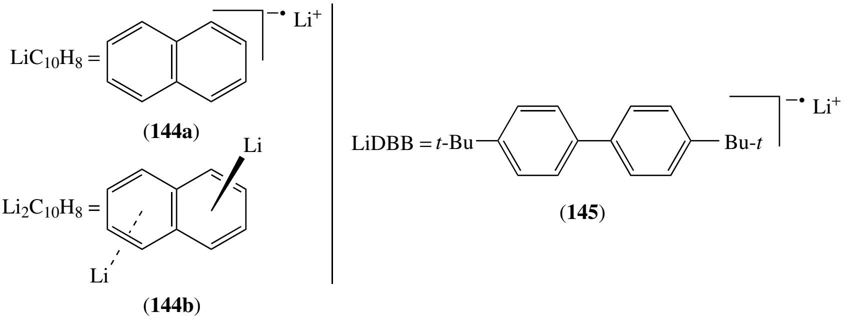

FIGURE 19. Lewis formulas of **144a**, **144b** and **145**

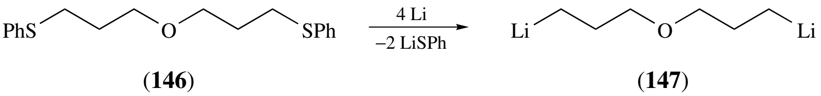

SCHEME 53

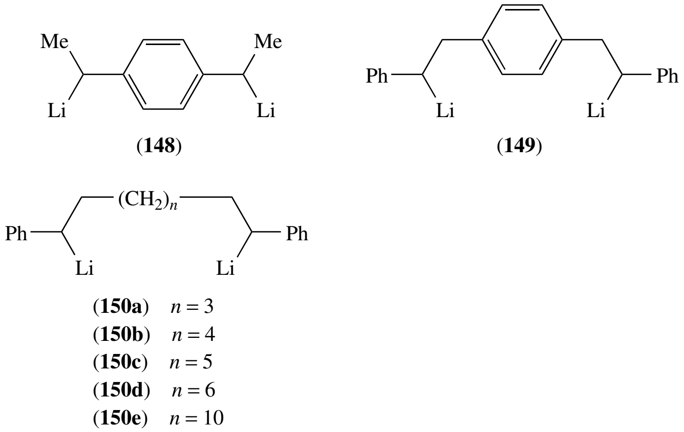

(**148**) (**149**)

(**150a**) $n = 3$
(**150b**) $n = 4$
(**150c**) $n = 5$
(**150d**) $n = 6$
(**150e**) $n = 10$

FIGURE 20. Lewis formulas of **148**, **149** and **150a–e**

following example of Rücker and coworkers shows the formation of the triply lithiated trimethoxycyclohexane derivative **152**, starting from 1,3,5-trimethoxy-2,4,6-tris(phenylthiomethyl) cyclohexane (**151**) (Scheme 54)^{75}.

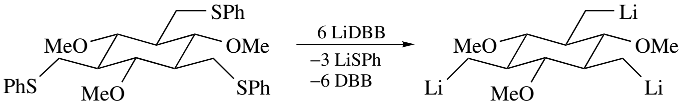

(**151**) (**152**)

SCHEME 54

By the synthesis of doubly α-lithiated organosilane **154a** and organogermane **154b** from the corresponding starting compounds **153a** and **153b**, Akkerman and Bickelhaupt made use of the stabilizing effect of large polarizable heteroatoms, like silicon or germanium, in α-position to metalated carbon centres (Scheme 55)^{76}.

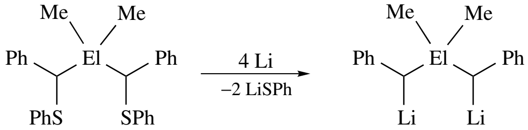

El = Si (**153a**), Ge (**153b**) El = Si (**154a**), Ge (**154b**)

SCHEME 55

Polymetalated systems of this type without phenyl substitution at the lithiated carbon centre are only accessible when solutions of $LiC_{10}H_8$ (**144a**) or LiDBB (**145**) in THF instead of a suspension of metallic lithium in THF are reacted with bis(phenylthiomethyl)silanes of type **155**. In our group, variously substituted bis(lithiomethyl)silanes **117a**, **156b–e** and **101** were synthesized by reductive cleavage of the carbon–sulphur bond with $LiC_{10}H_8$

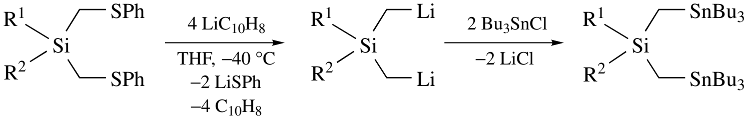

(155a)	$R^1 = R^2 = Me$	**(117a)**	**(157a)**
(155b)	$R^1 = Me, R^2 = Et$	**(156b)**	**(157b)**
(155c)	$R^1 = Me, R^2 = Vinyl$	**(156c)**	**(157c)**
(155d)	$R^1 = Me, R^2 = Ph$	**(156d)**	**(157d)**
(155e)	$R^1 = R^2 = Et$	**(156e)**	**(157e)**
(155f)	$R^1 = R^2 = Ph$	**(101)**	**(100)**

SCHEME 56

(**144a**) (Scheme 56)[77,78]. By the reaction of the dilithium compounds with chlorostannanes, bis(tributylstannomethyl)silanes **157a–e** and **100** were generated, which can serve as precursors for the tin–lithium exchange reaction (Section II. C).

As a particular example, reactions of diphenylbis(phenylthiomethyl)silane (**155f**) are shown. While the reaction of **155f** with four equivalents of $LiC_{10}H_8$ at −40 °C yields the dimetalated bis(lithiomethyl)diphenylsilane (**101**), a selective monolithiation (compound **158**) can be achieved by using only two equivalents of the electron transfer reagent at −60 °C. A side reaction of the monolithiated silane **158** is observed, when the reaction temperature rises above −30 °C, giving [lithio(phenylthio)methyl]methyldiphenylsilane (**159**) (Scheme 57). This problem, also observed for other (phenylthiomethyl)element systems, can mostly be avoided by an exact control of the reaction temperature[77].

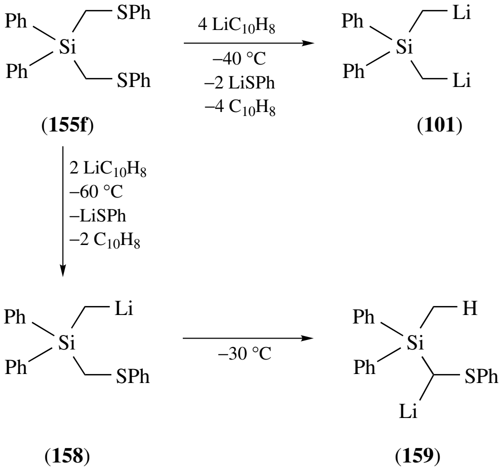

SCHEME 57

Moreover, it could be shown that the monolithiated intermediate **158** is formed during the synthesis of dilithiated **101** and that the trapping products, like bis(tributylstannomethyl)silanes **157a–e** and **100**, are not formed by a repeated monometalation/trapping sequence (examples, generated by such repeated monometalation/trapping sequences which can be regarded as polyanion synthons, will not be listed in detail).

By prior substitution at the α-carbon centre (deprotonation, followed by silylation), also asymmetrically functionalized bis(lithiomethyl)silanes like compound **161** are accessible from their substituted parent compounds (e.g. compound **160**). This selective reaction sequence is based on the possibility of deprotonating bis(phenylthiomethyl)silane **155f** with *n*-butyllithium without attacking the thioether groups (Scheme 58)[83].

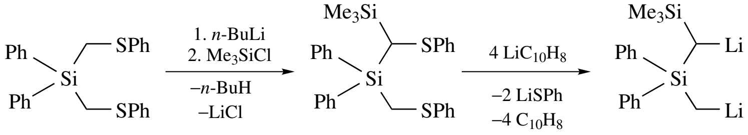

(155f) **(160)** **(161)**

SCHEME 58

Tris- and tetrakis(lithiomethyl)silanes are accessible by using LiDBB as an electron transfer reagent[79, 80]. Variously substituted tris(phenylthiomethyl)silanes **162a–d** and tetrakis(phenylthiomethyl)silane (**164**) can be turned into the triply and quadruply lithiated organosilanes **163a–d** and **165** by reaction with LiDBB at −40 °C. Di-, tetra and hexalithiated organosilanes **166–168** as well as dilithiated disilanes (e.g. compound **169**) can be obtained using this method (Scheme 59).

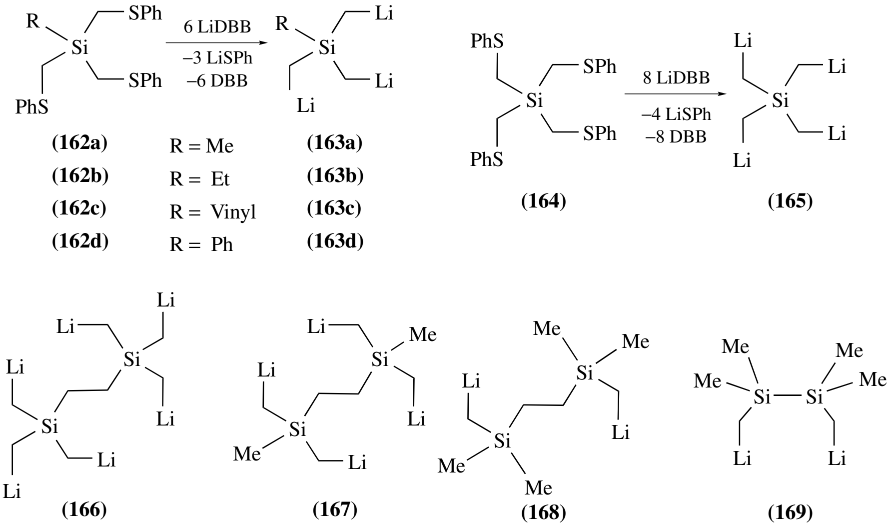

(162a) R = Me **(163a)**
(162b) R = Et **(163b)**
(162c) R = Vinyl **(163c)**
(162d) R = Ph **(163d)**

(164) **(165)**

(166) **(167)** **(168)** **(169)**

SCHEME 59

By extension and application of this method, which our group is using for the preparation of silacycles[77–79], polysilacage molecules have been synthesized by Shimizu and coworkers[81], using the polylithium compounds **170–172** as building blocks (Figure 21)[82].

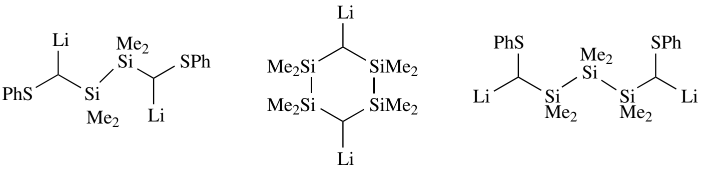

(170) **(171)** **(172)**

FIGURE 21. Lewis formulas of **170–172**

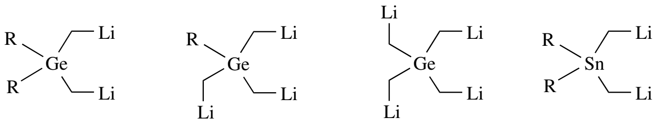

(173a) R = Me
(173b) R = Et
(173c) R = Ph

(174a) R = Me
(174b) R = Et
(174c) R = Ph

(175)

(176a) R = Me
(176b) R = *n*-Bu

FIGURE 22. Lewis formulas of **173a–c**, **174a–c**, **175**, **176a** and **176b**

Except for silanes, other heteroatom substituted systems have been used to stabilize multiply lithiated centres, e.g. (phenylthiomethyl)germanes **173a–c, 174a–c** and **175**, -stannanes **176a** and **176b** (Figure 22), -amines and (phenylthiomethyl)phosphanes[49, 83].

When organylbis(phenylthiomethyl)amines **177a–e**, prepared by a Mannich-type reaction by mixing thiophenol, formaldehyde and the corresponding amine, are treated with $LiC_{10}H_8$ (**144a**), the corresponding 1,3-dilithiated organylbis(lithiomethyl)amines **179a–e** are formed. As a side-reaction, the generation of substituted piperazines of type **178** is observed (Scheme 60). The yields depend on the steric demand of the substituents R and on the rate of the metalation reaction. Thus, control of the reaction temperature is essential, which is demonstrated by the yields of the trapping products **180a–e** (Table in Scheme 60)[84].

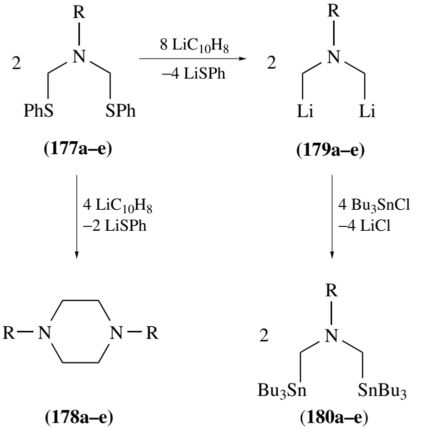

R	−78 °C	−50 °C	
Me	90%	50%	**(180a)**
Et	75%	60%	**(180b)**
Ph	60%	85%	**(180c)**
i-Pr	50%	95%	**(180d)**
t-Bu	–	40%	**(180e)**

SCHEME 60

By the same Mannich-type reaction, *N*,*N*′-bis(phenylthiomethyl)piperazine (**182**) can be synthesized from piperazine (**181**), which is converted into *N*,*N*′-bis(lithiomethyl)piperazine (**183**) by the use of $LiC_{10}H_8$ (**144a**) in THF (Scheme 61)[85].

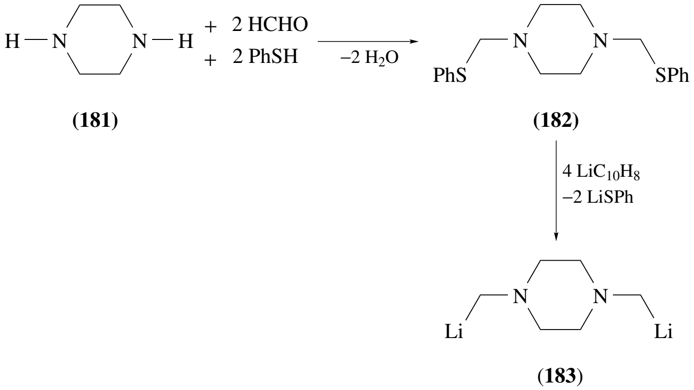

SCHEME 61

By this method, open-chain 1,6- (**186a** and **186b**) and 1,7-dilithiated (**187**) amines were prepared using $LiC_{10}H_8$ (**144a**) or lithium as reducing agent with the corresponding bifunctional bis(phenylthiomethylamino)alkanes **185** as precursors (starting materials **185** also easily obtained by Mannich-type reaction) (Scheme 62)[86].

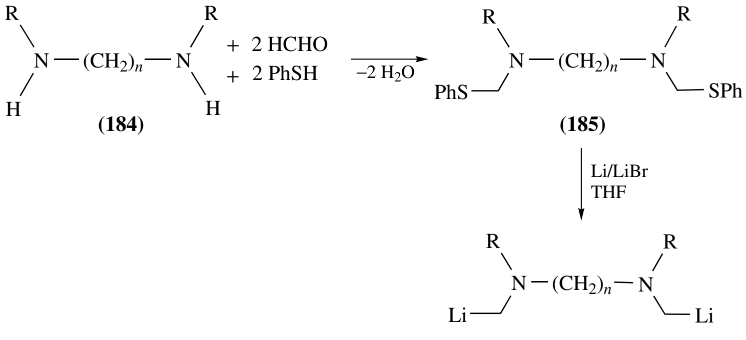

(186a) $n = 2$, R = Me
(186b) $n = 2$, R = Ph
(187) $n = 3$, R = Et

SCHEME 62

By the reaction of lithiated thioanisole with primary dichlorophosphanes, organylbis(phenylthiomethyl)phosphanes **188a** and **188b** can be prepared. By reductive cleavage of the carbon–sulphur bonds, the corresponding organylbis(lithiomethyl)phosphanes **189a**

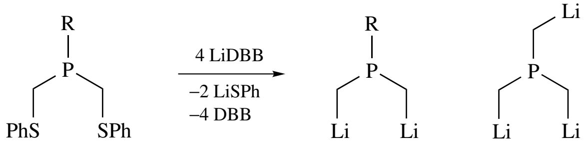

(188a) R = *t*-Bu **(189a)** **(190)**

(188b) R = Ph **(189b)**

SCHEME 63

and **189b** were obtained. Even the triply lithiated tris(lithiomethyl)phosphane **190** was synthesized applying this universal method (Scheme 63)[87].

E. Addition/Single-Electron Transfer

The transformations described in this chapter include mostly heterogeneous reactions at the surface of metallic lithium. Processes of this type can become too slow on a preparative scale at low temperatures. This is why either they have to be carried out at elevated temperatures (possible decomposition reactions) or an activation (e.g. ultrasound) of the lithium metal is necessary. In spite of the relatively high reaction temperatures, very selective reactions are observed, when this method is applied to the presented systems. Thus, in addition to Section II. A (Deprotonation), this section contains many visualisations of X-ray structural analyses.

A particular class of polylithium compounds, remarkably large and structurally well examined, has been introduced and stimulated by the early works of Walczak and Stucky[88]: These are doubly lithium bridged carbon–carbon bonds, activated by phenyl or silyl substitution. 1,2-Diphenylethane (**191**) was deprotonated, using *n*-butyllithium in the presence of TMEDA or PMDTA (Scheme 64). The crystal structures of compounds **192a** and **192b** have been described: as the typical structural motif, the central carbon–carbon bond is bridged by two lithium-ligand units from both sides of the plane of the *trans*-stilbene-like planar carbon backbone.

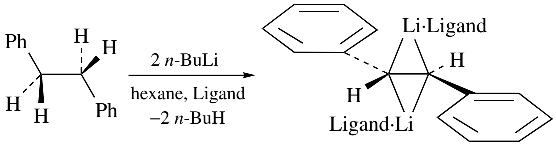

(191) **(192a)** Ligand = TMEDA

(192b) Ligand = PMDTA

SCHEME 64

A number of compounds with the similar structural motif of the two bridging lithium centres was prepared by Sekiguchi and coworkers by single-electron transfer reaction[89]. Instead of phenyl substituents, the group uses the silyl substitution for activation and stabilization of the metalated carbon centres. All of the obtained polylithium compounds were characterized in the solid state (some of these examples are presented in the following figures). Moreover, the metalation reaction was effected by reducing carbon–carbon multiple bonds with metallic lithium. In the case of tetrakis(trimethylsilyl)ethylene (**193**),

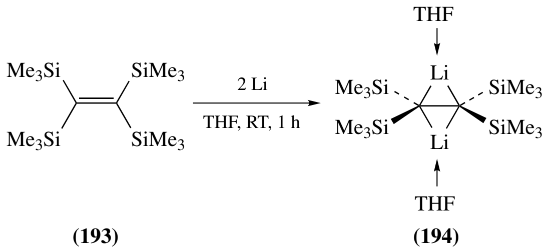

(193) **(194)**

SCHEME 65

the reaction with an excess of lithium metal at room temperature in THF affords the dilithiated compound **194** (Scheme 65), whose solid-state structure was determined[89].

By the same method, the asymmetrical compounds **196a** and **196b** (from alkenes **195a** and **195b**), the related dilithiated compounds of tetrakis(dimethylsilyl)ethylene (**197**) and the tetrasilabicyclopentylidene **198** were accessible (Scheme 66)[90–93]. The results of the X-ray structural analyses are shown (Figures 23 and 24).

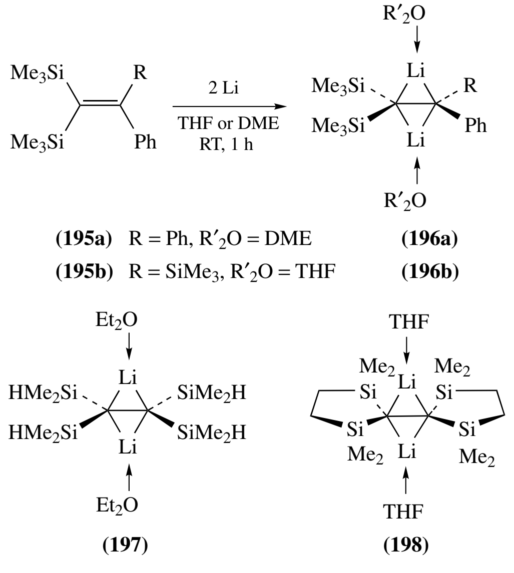

(195a) $R = Ph, R'_2O = DME$ **(196a)**

(195b) $R = SiMe_3, R'_2O = THF$ **(196b)**

(197) **(198)**

SCHEME 66

The structural motif of a doubly lithium bridged carbon–carbon bond was also extended to double bonds embedded in ring systems by Sekiguchi and coworkers[94]. The reaction of bicyclic compound **199** with an excess of metallic lithium afforded dilithium compound **200**, the reduced double bond bridged by two lithium complex fragments (Scheme 67). The related symmetrical tricyclic compounds **202a** and **202b** could be generated from tricyclic **201** bearing varying substituents at the four terminal silicon centres (Scheme 68).

The reaction of larger extended π-systems **203** and **205** with excess lithium metal yields di- and tetralithiated compounds **204** and **206** (Schemes 69 and 70) with extraordinary solid-state molecular structures, where the lithium centres no longer exactly bridge the

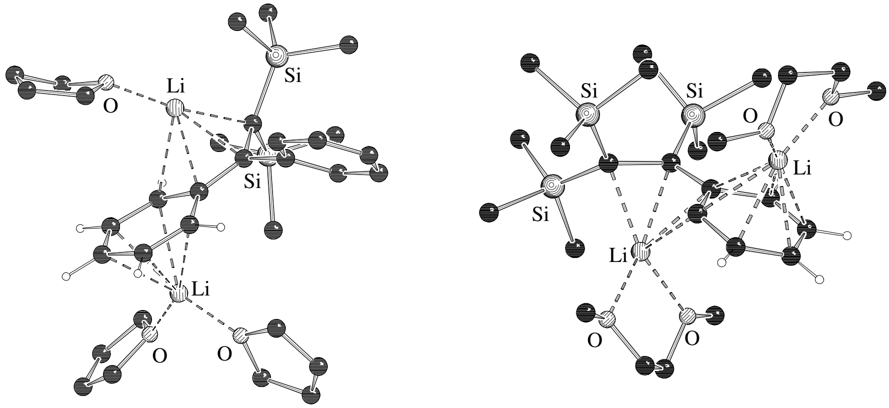

FIGURE 23. Molecular structures of **196a** and **196b** in the solid state

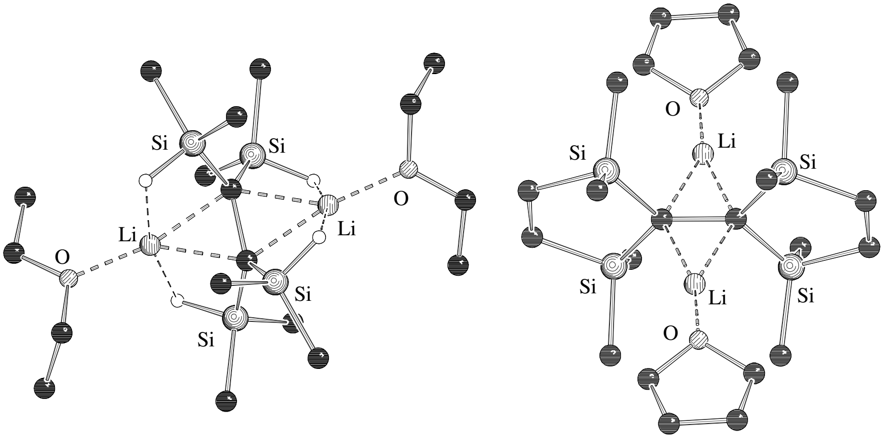

FIGURE 24. Molecular structures of **197** and **198** in the solid state

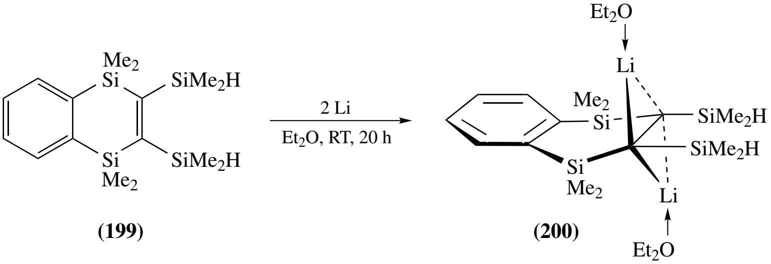

SCHEME 67

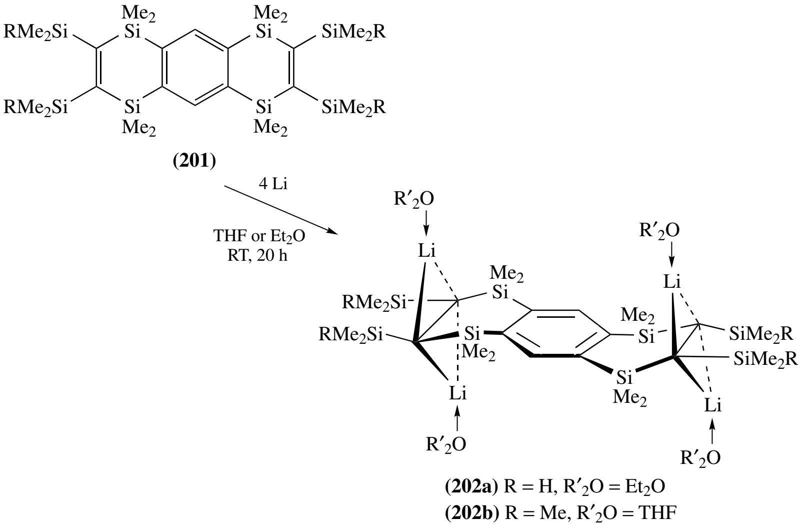

(201)

(202a) R = H, R′$_2$O = Et$_2$O
(202b) R = Me, R′$_2$O = THF

SCHEME 68

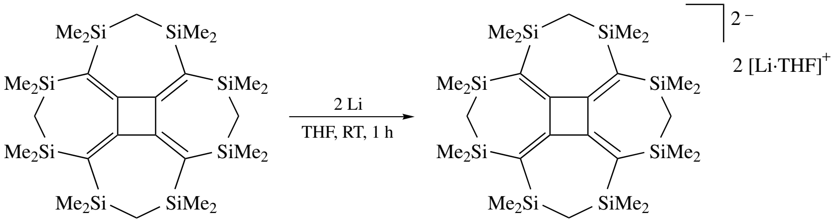

(203) **(204)**

SCHEME 69

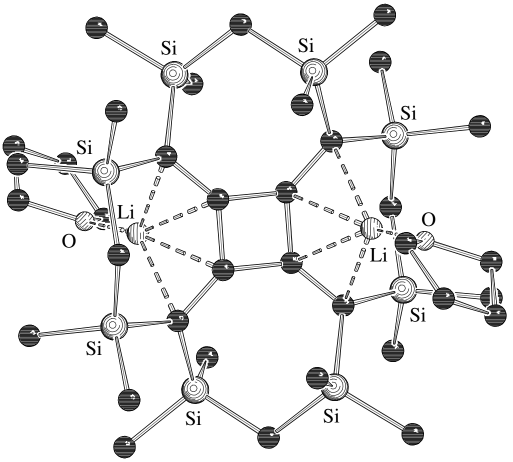

FIGURE 25. Molecular structure of **204** in the solid state

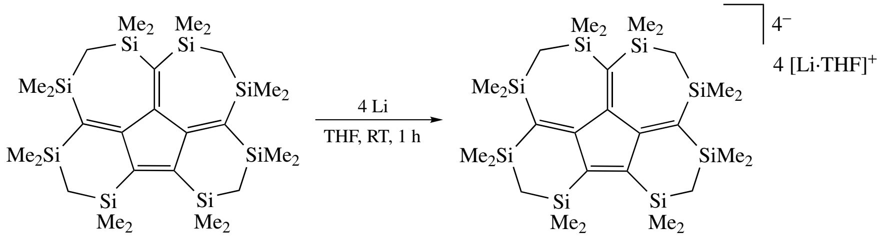

(205) **(206)**

SCHEME 70

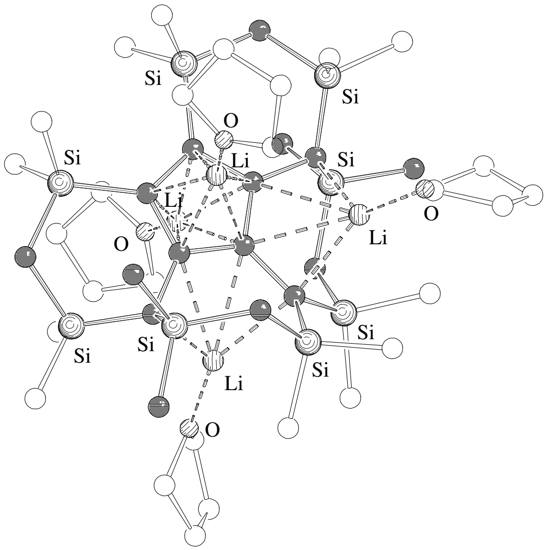

FIGURE 26. Molecular structure of **206** in the solid state

corresponding carbon–carbon bonds (e.g. the capping lithium centre in the molecular structure of compound **206**) (Figures 25 and 26)[95–97].

The closely related dilithiated compound **208**, also with a central four-membered ring, was obtained from starting compound **207** in DME (Scheme 71). The molecule represents the first bis(allyl)dianion system consisting of six carbon atoms involving eight π electrons (6C-8π). The crystal structure of **208** was reported[98].

Dilithium compound **210**, obtained from the lithiation of hexasilylfulvene **209** in THF at room temperature (Scheme 72), represents the first X-ray structural analysis of a dilithiated fulvene derivative. In the solid state, one lithium centre is capping the central five-membered ring, while the second lithium centre is located at the exocyclic carbon atom of the fulvene unit (Figure 27)[99].

The reaction of 1,2,3-butatriene **211** with excess lithium metal affords dilithiated compound **212** with the central carbon–carbon bond bridged by the two lithium centres (Scheme 73). In the solid state, the C_4 unit is bent, rather than linear, due to the

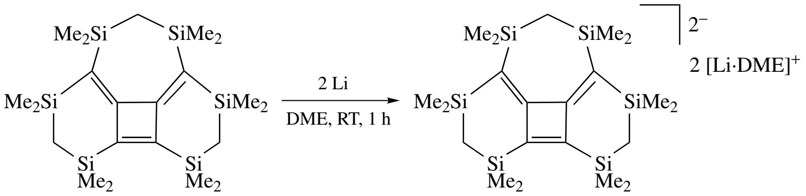

(207) **(208)**

SCHEME 71

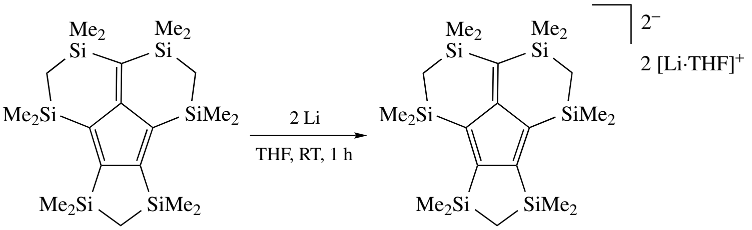

(209) **(210)**

SCHEME 72

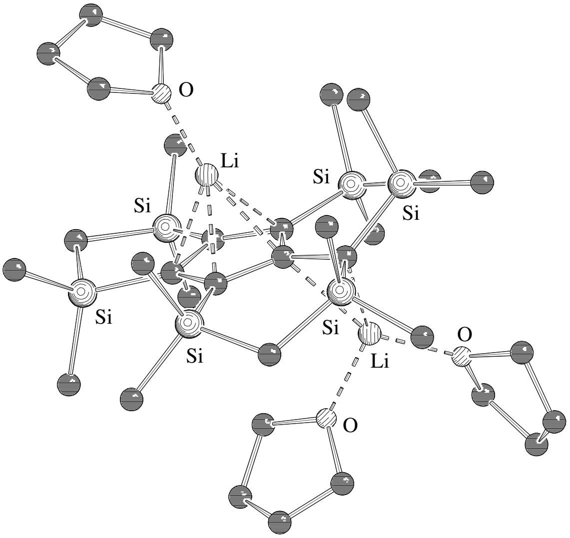

FIGURE 27. Molecular structure of **210** in the solid state

coordination of the lithium centres (Figure 28). When compound **212** is exposed to reduced pressure, crystallization from hexane yields the dimeric form of the compound **213** with only two molecules of THF coordinating two of the four lithium centres (Scheme 73, Figure 28)[100].

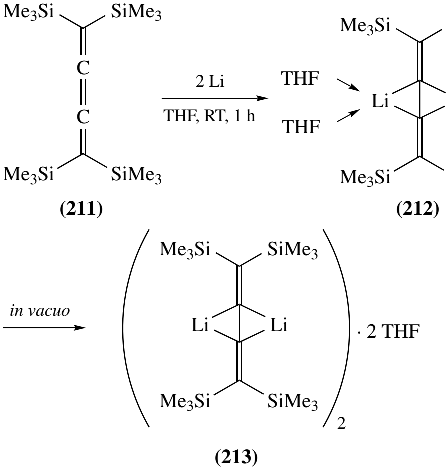

SCHEME 73

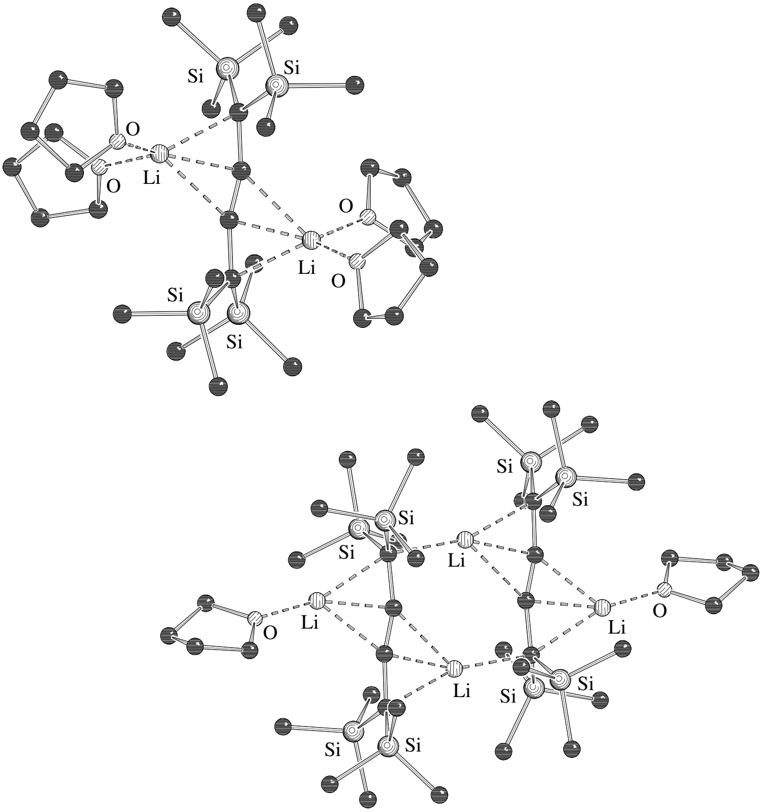

FIGURE 28. Molecular structures of **212** (top) and **213** (bottom) in the solid state

In contrast to the experiments of Sekiguchi, 1,2-dilithiated butadienes of type **215**, obtained from 1,2,3-butatrienes **214a** and **214b**, undergo a lithiotropy by the formation of 1,3-dilithiated butadienes of type **217** (Scheme 74). Maercker and coworkers were able to show by mechanistic investigations that this specific sort of rearrangement is an intermolecular process. The intermediary formed 1,4-dilithiated compounds of type **216**, and also the 1,2- and 1,3-dilithium compounds were characterized by trapping reactions with D_2O. The synthetic potential of the mixed vinyllithium–allyllithium intermediate of type **216** was furthermore proven by the synthesis of functionalized 2,5-dihydrosiloles in reactions with dichlorosilanes[101].

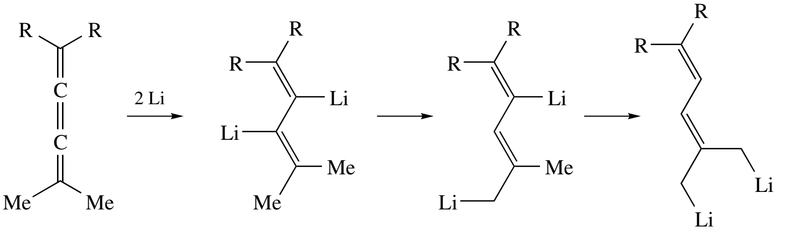

(214a) R = Me

(214b) RR = $-(CH_2)_5-$

(215a) **(215b)** **(216a)** **(216b)** **(217a)** **(217b)**

SCHEME 74

Asymmetrically substituted butatrienes **218a–c** also react readily with lithium metal, although the risk of the formation of product mixtures is higher. Upon substitution reactions with various electrophiles, 3,4-disubstituted 1,2-butadienes, 2,3-disubstituted 1,3-butadienes or 1,4-disubstituted 2-butynes are obtained, the product ratio depending on the electrophile used. Under certain reaction conditions, the formal direct substitution products of dilithium compounds **219a–c** and **220a–c** could be obtained quantitatively. Substitution products of **221a–c** could be enriched up to 80% yield, while formal derivatives of **222a–c** were almost not observed. Thus, an equilibrium, involving these dilithium compounds, is assumed by the authors (Scheme 75)[102].

The reaction between asymmetrical alkyl substituted allenes of type **223** and metallic lithium has also been investigated by the group of Maercker (Scheme 76). Generally, these allenes require more elevated reaction temperatures than the related tetraphenyl substituted compounds, even when a mixture of lithium and sodium is applied as the reducing agent. Moreover, polar solvents must be used for the metalation reaction, although side reactions (mostly deprotonation reactions) are increasingly observed in these types of solvents (Et_2O, THF). The regioselectivity of substitution reactions with various electrophiles was investigated[103].

Various diboriodilithiomethanes of type **225** were synthesized by Berndt and coworkers, adding different aryllithium compounds to the boron–carbon bonds of compounds **224a–e** (Scheme 77)[104]. The dilithium compounds have been characterized in the solid state by X-ray structural analysis. **225a–e** adopt the structure of a 1,3-diborataallene system, where lithium–diethyl ether units are bridging the twisted B-C-B axis from both sides.

In the group of Sekiguchi, the dilithiated derivatives of tetrakis- and hexakis(trimethylsilyl)benzene **226** and **228** in Schemes 78 and 79, respectively, have been synthesized by the reaction of the parent compounds with an excess of metallic lithium in coordinating solvents at room temperature. Both molecular structures in the solid state were cleared up by X-ray structural analysis (Figures 29 and 30)[105].

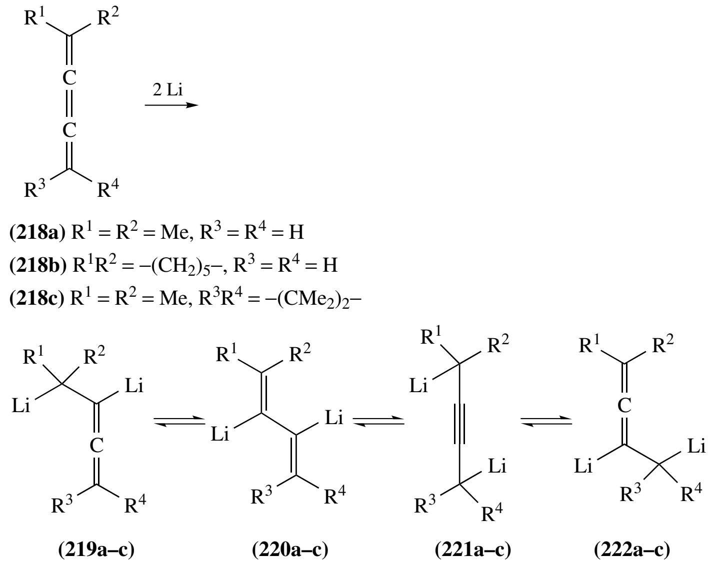

(218a) $R^1 = R^2 = Me, R^3 = R^4 = H$
(218b) $R^1R^2 = -(CH_2)_5-, R^3 = R^4 = H$
(218c) $R^1 = R^2 = Me, R^3R^4 = -(CMe_2)_2-$

(219a–c) **(220a–c)** **(221a–c)** **(222a–c)**

SCHEME 75

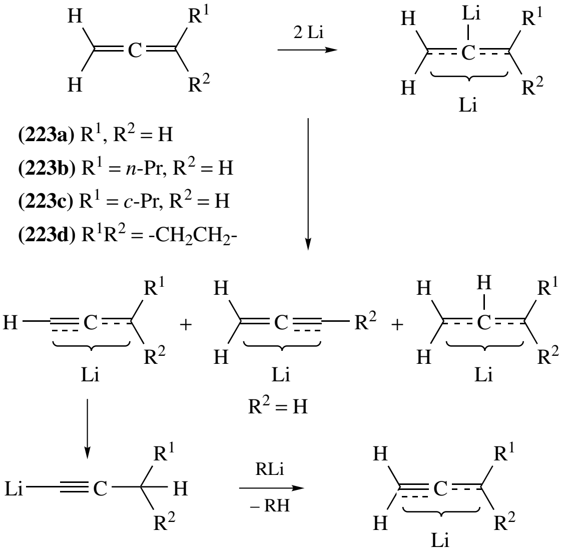

(223a) $R^1, R^2 = H$
(223b) $R^1 = n\text{-}Pr, R^2 = H$
(223c) $R^1 = c\text{-}Pr, R^2 = H$
(223d) $R^1R^2 = -CH_2CH_2-$

SCHEME 76

Unexpectedly, the molecular structures of **227** and **229** are not similar. While tetrasilylated dilithium compound **227** is capped by the two lithium centres from both sides of the ring plane (Figure 29), hexasilylated dilithium compound **229** is capped by its two lithium centres from one side of the ring (Figure 30)[106]. Moreover, the phenyl ring of

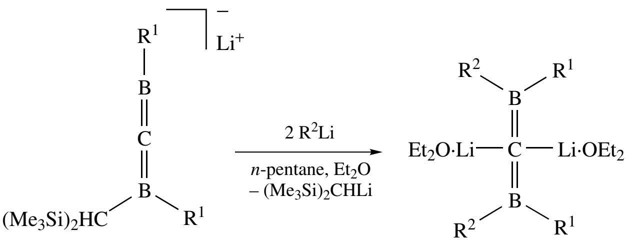

(225a–e)

(224a) $R^1 = R^2 =$ mesityl

(224b) $R^1 = R^2 =$ duryl

(224c) $R^1 = R^2 =$ 2,6-dimethyl-4-*t*-butylphenyl

(224d) $R^1 =$ duryl, $R^2 =$ 2,4,5-trimethylphenyl

(224e) $R^1 =$ mesityl, $R^2 =$ *t*-butyl

SCHEME 77

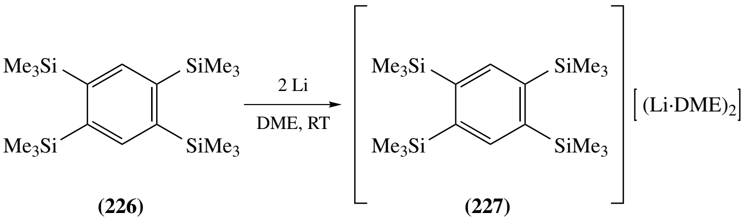

(226) **(227)**

SCHEME 78

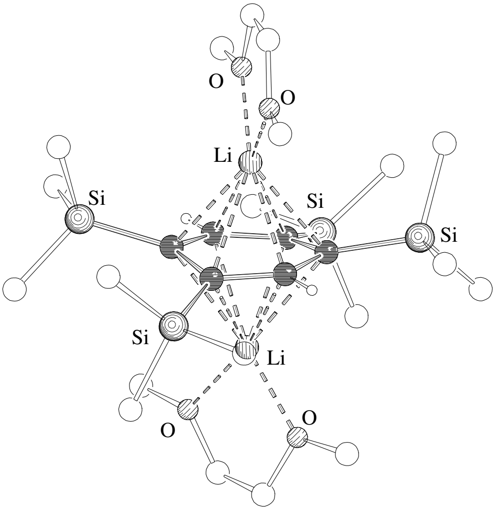

FIGURE 29. Molecular structure of **227** in the solid state

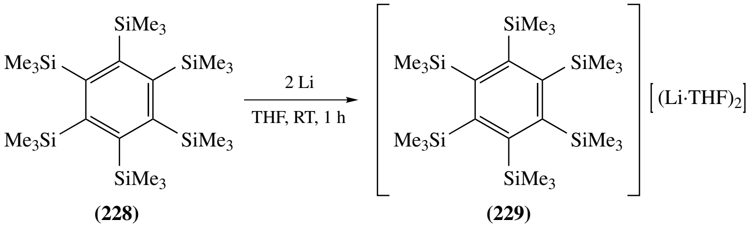

SCHEME 79

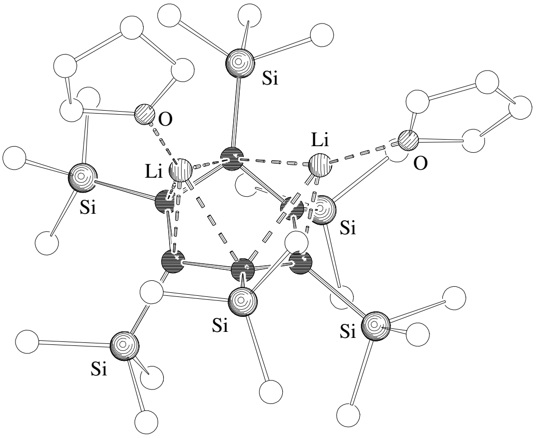

FIGURE 30. Molecular structure of **229** in the solid state

compound **229** is no longer planar, showing a boat conformation. A theoretical investigation of this structural difference between compounds **227** and **229** was reported by Sygula and Rabideau[107].

A molecular structure, similar to that of hexasilylated benzene derivative **229**, was obtained from tetracyclic hexasilylbenzene **230** by Kira, Sakurai and coworkers, where the six silicon centres are incorporated in three five-membered ring systems (Scheme 80)[108]. In dimetalated compound **231**, two lithium centres, coordinated by a quinuclidine ligand each, are capping the phenyl ring plane from both sides in the solid state. Moreover, it could be found that compound **231** has a thermally accessible triplet state, investigated by temperature-dependent ESR spectroscopy[109].

A planar molecular structure in the solid state was observed for dilithiated dibenzo[*a*, *e*]cyclooctatetraene by Rabideau and coworkers. Dilithiated **233** is formed in THF by the reaction of compound **232** with an excess of metallic lithium at room temperature (Scheme 81). In the solid state, two lithium-TMEDA units are capping both sides of the central eight-membered ring plane[110].

In the solid-state structure of dilithiated fluoranthene (**235**), generated from **234** in dimethoxyethane at room temperature by Bock and coworkers (Scheme 82), lithium–DME units are capping the naphthalene moiety from both sides of the plane alternatingly (compound **235** forms a coordination polymer in the solid state). The metallic lithium, used for the reaction, was activated by ultrasonic irradiation. Moreover, several structures of related polysodium compounds were also characterized in the solid state[111].

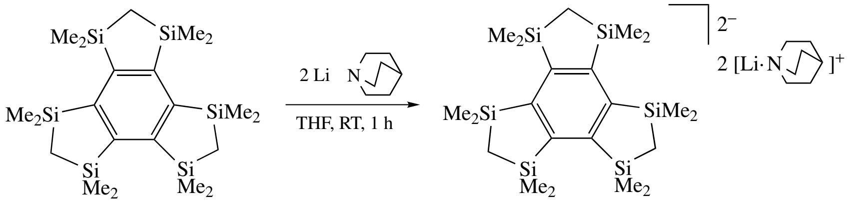

(230) **(231)**

SCHEME 80

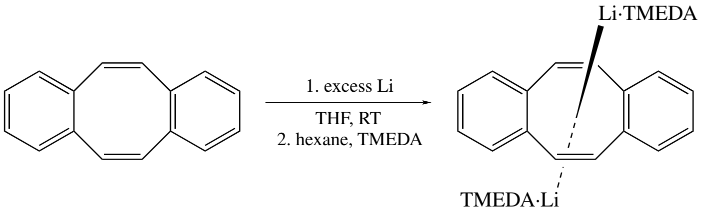

(232) **(233)**

SCHEME 81

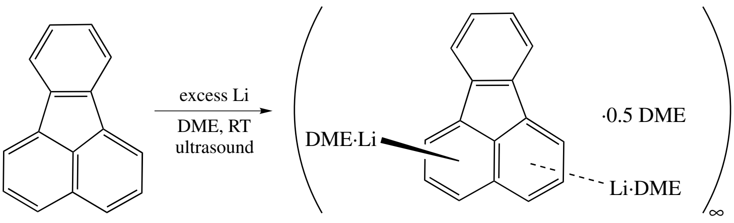

(234) **(235)**

SCHEME 82

The solution structure of the dilithium compound **237**, generated by treating *trans*-1,2-diphenyl-1,2-bis(trimethylsilyl)ethylene (**236**) with excess lithium metal in THF (Scheme 83), was studied by 1D and 2D NMR techniques in the group of Fürstner[112]. As a conclusion, the dilithium compound **237** adopts a C_2-symmetric twisted *trans*-arrangement with two bridging lithium centres in solution, underlining the various X-ray structural studies in the solid state by Sekiguchi and coworkers.

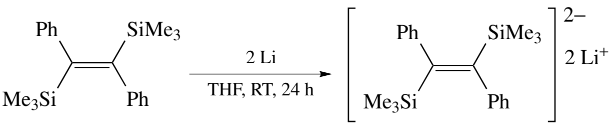

(236) **(237)**

SCHEME 83

The mechanism of the well-known reduction of diphenylacetylene (**238**) with metallic lithium was investigated by Maercker and coworkers. The reaction of **238** with lithium in THF at low temperatures leads to *cis*-1,2-dilithiostilbene (**239**), while the reduction with metallic sodium generates *trans*-1,2-disodiostilbene (**240**) (verified by trapping reactions with methanol and UV/Vis spectroscopy). When a metathesis reaction is effected, using two equivalents of lithium chloride, followed by the trapping reaction of compound **241**, only *cis*-stilbene is formed. Thus, the solution structures of the two dimetalated compounds **239** and **240** must be profoundly different and *cis*-1,2-dilithiostilbene (**239**) must be the thermodynamically favoured isomer in solution (Scheme 84)[113].

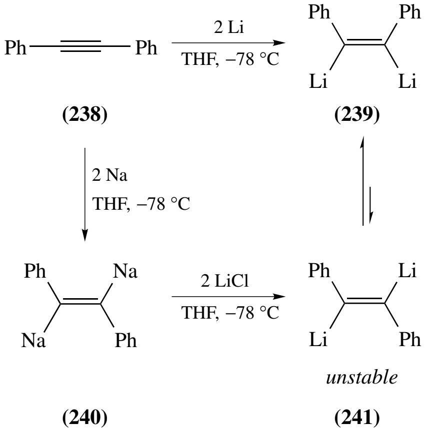

SCHEME 84

When alkenes like **242a**–**d** are treated with metallic lithium, not only the reduction leading to doubly lithium bridged compounds of type **243** can occur, but also addition reactions under the formation of 1,4-dilithiobutanes of type **244**[114]. The impact of various substituents on this well-known phenomenon and further reaction steps was examined intensively by Maercker and coworkers (Scheme 85). On this basis, an insight into the mechanisms of controlling these highly sensitive reactions can be gained.

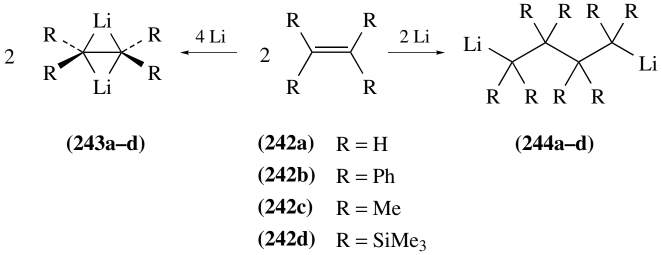

SCHEME 85

The reduction of the bis(phenylethynyl)silanes **245a**–**f** into a two-fold radical anion, followed by an *intra*molecular carbon–carbon coupling reaction, was introduced by Tamao and coworkers to generate variously substituted 2,5-dilithio-3,4-diphenylsiloles of type

246 (Scheme 86). For the high selectivity and a good yield in this reaction, it is important to slowly add the silane to a large excess of $LiC_{10}H_8$ (**144a**) (four molar amounts) in THF. The 2,5-dilithiosiloles were 'trapped' with manifold electrophiles to form a series of functionalized 3,4-diphenylsiloles[115–117].

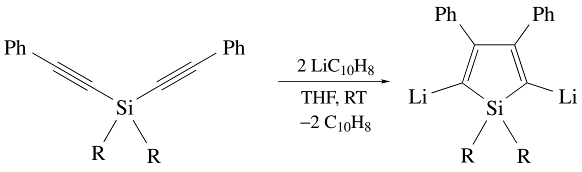

(246a–f)

(245a) R = Me
(245b) R =Et
(245c) R = *i*-Pr
(245d) R = Hex
(245e) R = Ph
(245f) R = NEt_2

SCHEME 86

The *inter*molecular coupling of two lithium diphenylacetylide radical anions to give 1,4-dilithio-1,2,3,4-tetraphenylbutadiene (**247**) has been reported by Braye and coworkers (Scheme 87)[118]. Pauer and Power were able to clear up the solid-state structure of this well-known dilithium compound, confirming an *S-cis* conformation of **247** in the crystal[119]. Two lithium–DME units are capping the C_4 moiety, which is not fully planar, from both sides (Figure 31). A similar structure of the corresponding TMEDA adduct has been reported by Schleyer[120].

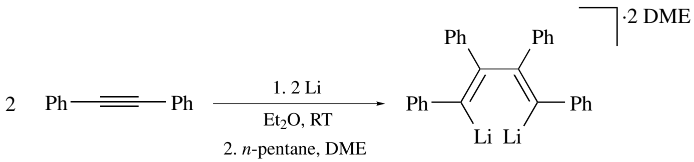

(238) **(247)**

SCHEME 87

The reduction of 1,1-bis(diphenylphosphanyl) ethylene (**248**) with an excess of metallic lithium, activated by ultrasonic irradiation, leads to C–C coupling under the formation of a 1,1,4,4-tetrakis(diphenylphosphanyl)butane (**249**) (Scheme 88)[121]. Surprisingly, the lithium centres in the resulting dilithium compound do not form any lithium–carbon contacts, being coordinated by two diphenylphosphanyl groups and two THF molecules each. With this structural motif, the molecular structure is similar to the one of tris(phosphaneoxide) **20** (Section II. A), also obtained by Izod and coworkers upon deprotonation[18].

The reaction of hexaphenylbenzene (**250**) with an excess of metallic lithium, activated by ultrasonic irradiation, was effected by Bock and coworkers[122]. The reaction is carried out at room temperature and is accompanied by the release of hydrogen gas, caused by the formation of two additional C–C bonds (Scheme 89). The resulting dilithium

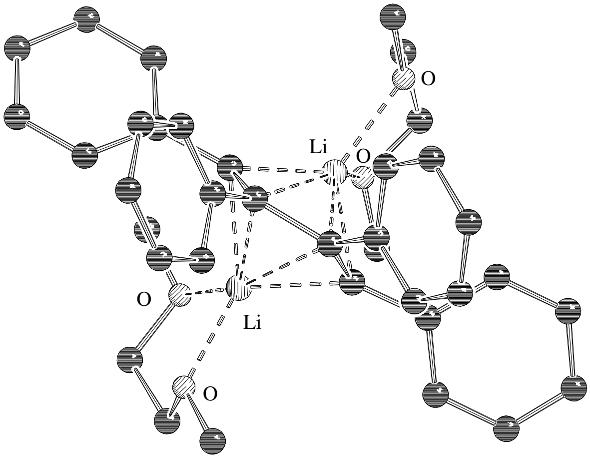

FIGURE 31. Molecular structure of **247** in the solid state

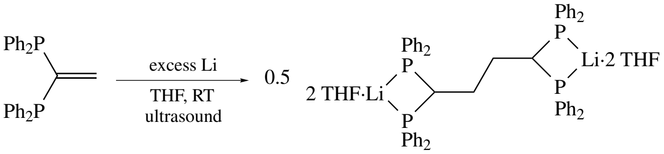

(248) **(249)**

SCHEME 88

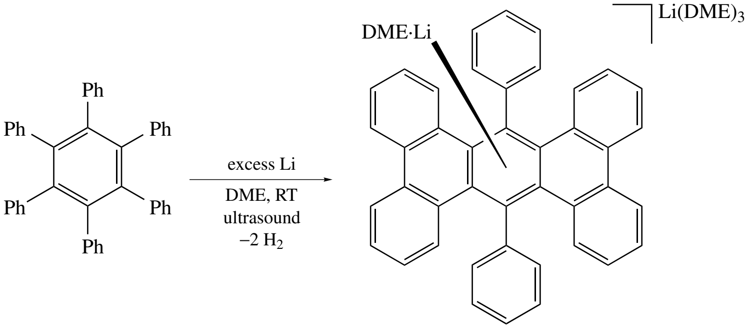

(250) **(251)**

SCHEME 89

9,10-diphenyltetrabenz[*a*,*c*,*h*,*j*]anthracenide (**251**) was studied thoroughly in the solid state by X-ray structural methods, showing one lithium–DME unit capping the central six-membered ring, while a Li(DME)$_3$ unit forms a solvent-separated counter ion. Mechanistic investigations were supported by quantum-chemical methods.

III. CONCLUSION

The review of the literature on the chemistry of polylithium organic compounds has proven the manifold synthetic applications of these systems in preparative organic and inorganic chemistry. Moreover, an insight into the mechanisms of formation and transformation of polylithiated alkyls has been successfully gained by the effort to isolate the obtained compounds and therefore by an increasing number of reported solid-state structural analyses. Obviously, the methods and skills of handling these highly reactive compounds have greatly improved during the past ten years.

It has been observed that respectable advances have been achieved in the fields of all the five basic synthetic methods treated in this chapter. Thus, it is hoped that new polylithium organic compounds, and especially suitable synthetic applications, will be developed in the future, accompanied by a deeper understanding of the mechanisms of formation and interconversion.

IV. REFERENCES

1. The basis for the collection of the literature of this chapter was an inquiry in *Chemical Abstracts (CA)*® and the *Cambridge Structural Database (CSD)*®, August 2002.
2. A. Maercker and M. Theis, *Top. Curr. Chem.*, **1**, 138 (1987).
3. A. Maercker, in *Lithium Chemistry, A Theoretical and Experimental Overview* (Eds. A.-M. Sapse and P. v. R. Schleyer), Chap. 11, Wiley, Chichester, 1995, p. 477.
4. E. Keller, *SCHAKAL99, A Computer Program for the Graphic Representation of Molecular and Crystallographic Models*, University of Freiburg (Germany), 1999.
5. F. Foubelo and M. Yus, *Trends Org. Chem.*, **7**, 1 (1998).
6. M. Yus, *Chem. Soc. Rev.*, **25**, 155 (1996).
7. D. J. Ramon and M. Yus, *Eur. J. Org. Chem.*, 225 (2000).
8. H. H. Karsch, *Chem. Ber.*, **129**, 483 (1996).
9. W.-P. Leung, K. S. M. Poon, T. C. W. Mak and Z.-Y. Zhang, *Organometallics*, **15**, 3262 (1996).
10. A. Kasani, R. P. Kamalesh Babu, R. McDonald and R. G. Cavell, *Angew. Chem., Int. Ed.*, **38**, 1483 (1999).
11. C. M. Ong and D. W. Stephan, *J. Am. Chem. Soc.*, **121**, 2939 (1999).
12. J. F. K. Müller, *Eur. J. Inorg. Chem.*, 789 (2000).
13. J. F. K. Müller, M. Neuburger and B. Spingler, *Angew. Chem., Int. Ed.*, **38**, 92 (1999).
14. J. F. K. Müller, M. Neuburger and B. Spingler, *Angew. Chem., Int. Ed.*, **38**, 3549 (1999).
15. L. D. Field, M. G. Gardiner, C. H. L. Kennard, B. A. Messerle and C. L. Raston, *Organometallics*, **10**, 3167 (1991).
16. M. G. Gardiner, C. L. Raston, F. G. N. Cloke and P. B. Hitchcock, *Organometallics*, **14**, 1339 (1995).
17. P. J. Bailey, T. Barrett and S. Parsons, *J. Organomet. Chem.*, **625**, 236 (2001).
18. K. Izod, W. McFarlane and W. Clegg, *Chem. Commun.*, 2532 (2002).
19. C. Strohmann, K. Lehmen, A. Ludwig and D. Schildbach, *Organometallics*, **20**, 4138 (2001).
20. M. Kranz, H. Dietrich, W. Mahdi, G. Müller, F. Hampel, T. Clark, R. Hacker, W. Neugebauer, A. J. Kos and P. v. R. Schleyer, *J. Am. Chem. Soc.*, **115**, 4698 (1993).
21. V. B. Birman, A. Chopra and C. A. Ogle, *Tetrahedron Lett.*, **37**, 5073 (1996).
22. S. Fauré, B. Valentin, J. Rouzaud, H. Gornitzka, A. Castel and P. Rivière, *Inorg. Chim. Acta*, **305**, 46 (2000).
23. A. Ishii, T. Tsuchiya, J. Nakayama and M. Hoshino, *Tetrahedron Lett.*, **34**, 2347 (1993).
24. A. W. Kleij, H. Kleijn, J. T. B. H. Jastrzebski, W. J. J. Smeets, A. L. Spek and G. van Koten, *Organometallics*, **18**, 268 (1999).
25. P. Poremba, H.-G. Schmidt, M. Noltemeyer and F. T. Edelmann, *Organometallics*, **17**, 986 (1998).
26. I. E. Nifant'ev, P. V. Ivchenko, L. G. Kuzmina, Y. N. Luzikov, A. A. Sitnikov and O. E. Sizan, *Synthesis*, 469 (1997).
27. G. Linti, A. Rodig and H. Pritzkow, *Angew. Chem., Int. Ed.*, **41**, 4503 (2002).

28. S. M. Korneev and D. E. Kaufmann, *Synthesis*, 491 (2002).
29. M. Winkler, M. Lutz and G. Müller, *Angew. Chem., Int. Ed. Engl.*, **33**, 2279 (1994).
30. A. Feustel and G. Müller, *Chem. Commun.*, 1024 (2001).
31. J. Mortier, M. Vaultier, F. Carreaux and J.-M. Douin, *J. Org. Chem.*, **63**, 3515 (1998).
32. M. Fossatelli, R. den Besten, H. D. Verkruijsse and L. Brandsma, *Recl. Trav. Chim. Pays-Bas*, **113**, 527 (1994).
33. N. Rot and F. Bickelhaupt, *Organometallics*, **16**, 5027 (1997).
34. J. R. Baran Jr., C. Hendrickson, D. A. Laude Jr. and R. J. Lagow, *J. Org. Chem.*, **57**, 3759 (1992).
35. Y. Xie and H. F. Schaefer III, *Chem. Phys. Lett.*, **179**, 563 (1991).
36. B. J. Smith, *Chem. Phys. Lett.*, **207**, 403 (1993).
37. P. Wijkens, J. T. B. H. Jastrzebski, P. A. Van der Schaaf, R. Kolly, A. Hafner and G. van Koten, *Org. Lett.*, **2**, 1621 (2000).
38. P. Steenwinkel, J. T. B. H. Jastrzebski, B.-J. Deelman, D. M. Grove, H. Kooijman, N. Veldman, W. J. J. Smeets, A. L. Spek and G. van Koten, *Organometallics*, **16**, 5486 (1997).
39. M. Yoshifuji, N. Shinohara and K. Toyota, *Tetrahedron Lett.*, **37**, 7815 (1996).
40. M. Oda, T. Kawase and C. Wei, *Pure Appl. Chem.*, **68**, 267 (1996).
41. J. Nakayama, T. Yu, Y. Sugihara, A. Ishii and S. Kumakura, *Heterocycles*, **45**, 1267 (1997).
42. S. K. Ritter and R. E. Nöftle, *Chem. Mater.*, **4**, 872 (1992).
43. S. Ijadi-Maghsoodi and T. Barton, *Macromolecules*, **23**, 4485 (1990).
44. C. P. Vlaar and G. W. Klumpp, *Angew. Chem., Int. Ed. Engl.*, **32**, 574 (1993).
45. A. Maercker, B. Bos and M. T. Hajgholipour, *J. Organomet. Chem.*, **566**, 143 (1998).
46. H. Günther, O. Eppers, H. Hausmann, D. Hüls, H.-E. Mons, K.-D. Klein and A. Maercker, *Helv. Chim. Acta*, **78**, 1913 (1995).
47. J. R. Baran Jr. and R. J. Lagow, *J. Am. Chem. Soc.*, **112**, 9415 (1990).
48. C. Strohmann, *Angew. Chem., Int. Ed. Engl.*, **35**, 528 (1996).
49. C. Strohmann, Habilitation Thesis, University of Saarbrücken (Germany), 1995.
50. A. J. Ashe, III, L. L. Lohr and S. M. Al-Taweel, *Organometallics*, **10**, 2424 (1991).
51. H. J. Reich, I. L. Reich, K. E. Yelm, J. E. Holladay and D. Gschneidner, *J. Am. Chem. Soc.*, **115**, 6625 (1993).
52. R. Haag, R. Fleischer, D. Stalke and A. de Meijere, *Angew. Chem., Int. Ed. Engl.*, **34**, 1492 (1995).
53. H. Sashida, *Synthesis*, 1866 (1999).
54. A. Maercker, H. Bodenstedt and L. Brandsma, *Angew. Chem., Int. Ed. Engl.*, **31**, 1339 (1992).
55. H. J. M. Schoufs, A. Maercker and L. Brandsma, *J. Organomet. Chem.*, **441**, 1 (1992).
56. M. Katkevics, S. Yamaguchi, A. Toshimitsu and K. Tamao, *Organometallics*, **17**, 5796 (1998).
57. A. Maercker, T. Graule and W. Demuth, *Angew. Chem., Int. Ed. Engl.*, **26**, 1032 (1987).
58. A. Bretschneider-Hurley and C. H. Winter, *J. Am. Chem. Soc.*, **116**, 6468 (1994).
59. K. N. Seneviratne, A. Bretschneider-Hurley and C. H. Winter, *J. Am. Chem. Soc.*, **118**, 5506 (1996).
60. C. H. Winter, K. N. Seneviratne and A. Bretschneider-Hurley, *Comments Inorg. Chem.*, **19**, 1 (1996).
61. T. Matsuo, T. Mizue and A. Sekiguchi, *Chem. Lett.*, 896 (2000).
62. A. Sekiguchi, M. Tanaka, T. Matsuo and H. Watanabe, *Angew. Chem., Int. Ed.*, **40**, 1675 (2001).
63. A. Sekiguchi, T. Matsuo and M. Tanaka, *Organometallics*, **21**, 1072 (2002).
64. K. Ishii, N. Kobayashi, T. Matsuo, M. Tanaka and A. Sekiguchi, *J. Am. Chem. Soc.*, **123**, 5356 (2001).
65. G. Boche, H. Etzrodt, M. Marsch and W. Thiel, *Angew. Chem., Int. Ed. Engl.*, **21**, 132 (1982).
66. G. Boche, H. Etzrodt, M. Marsch and W. Thiel, *Angew. Chem., Int. Ed. Engl.*, **21**, 133 (1982).
67. G. Boche, H. Etzrodt, W. Massa and G. Baum, *Angew. Chem., Int. Ed. Engl.*, **24**, 863 (1985).
68. P. J. Garratt and R. Zahler, *J. Am. Chem. Soc.*, **100**, 7753 (1978).
69. A. Sekiguchi, T. Matsuo and H. Watanabe, *J. Am. Chem. Soc.*, **122**, 5652 (2000).
70. M. Balci, M. L. McKee and P. v. R. Schleyer, *J. Phys. Chem. A*, **104**, 1246 (2000).
71. M. Yus, P. Martinez and D. Guijarro, *Tetrahedron*, **57**, 10119 (2001).

72. M. Yus, R. P. Herrera and A. Guijarro, *Chem. Eur. J.*, **8**, 2574 (2002).
73. C. G. Screttas and M. Micha-Screttas, *J. Org. Chem.*, **43**, 1064 (1978).
74. C. G. Screttas and M. Micha-Screttas, *J. Org. Chem.*, **44**, 713 (1979).
75. C. Rücker, *J. Organomet. Chem.*, **310**, 135 (1986).
76. O. S. Akkerman and F. Bickelhaupt, *J. Organomet. Chem.*, **338**, 159 (1988).
77. C. Strohmann, S. Lüdtke and E. Wack, *Chem. Ber.*, **129**, 799 (1996).
78. C. Strohmann and S. Lüdtke, in *Organosilicon Chemistry II: From Molecules to Materials* (Eds. N. Auner and J. Weis), Wiley-VCH, Weinheim, 1996, p. 499.
79. C. Strohmann, S. Lüdtke and O. Ulbrich, *Organometallics*, **19**, 4223 (2000).
80. C. Strohmann, F. Pillong, E. Wack, S. Lüdtke and O. Ulbrich, unpublished results.
81. M. Shimizu, T. Hiyama, T. Matsubara and T. Yamabe, *J. Organomet. Chem.*, **611**, 12 (2000).
82. After this chapter had been finished, Moss and coworkers reported on the synthesis of highly lithiated carbosilane dendrimers: R. Meijboom, A. T. Hutton and J. R. Moss, *Organometallics*, **22**, 1811 (2003).
83. C. Strohmann and E. Wack, in *Organosilicon Chemistry III: From Molecules to Materials* (Eds. N. Auner and J. Weis), Wiley-VCH, Weinheim, 1998, p. 217.
84. C. Strohmann and J. Frenzel, unpublished results.
85. C. Strohmann and B. C. Abele, *Angew. Chem., Int. Ed. Engl.*, **35**, 2378 (1996).
86. A. R. Katritzky, M. Qi and D. Feng, *J. Org. Chem.*, **63**, 6712 (1998).
87. C. Strohmann and O. Ulbrich, unpublished results.
88. M. Walczak and G. Stucky, *J. Am. Chem. Soc.*, **98**, 5531 (1976).
89. A. Sekiguchi, T. Nakanishi, C. Kabuto and H. Sakurai, *J. Am. Chem. Soc.*, **111**, 3748 (1989).
90. A. Sekiguchi, M. Ichinohe, T. Nakanishi, C. Kabuto and H. Sakurai, *Bull. Chem. Soc. Jpn.*, **68**, 3215 (1995).
91. A. Sekiguchi, M. Ichinohe, M. Takahashi, C. Kabuto and H. Sakurai, *Angew. Chem., Int. Ed. Engl.*, **36**, 1533 (1997).
92. A. Sekiguchi, M. Ichinohe, C. Kabuto and H. Sakurai, *Organometallics*, **14**, 1092 (1995).
93. A. Sekiguchi, M. Ichinohe, C. Kabuto and H. Sakurai, *Bull. Chem. Soc. Jpn.*, **68**, 2981 (1995).
94. T. Matsuo, H. Watanabe and A. Sekiguchi, *Bull. Chem. Soc. Jpn.*, **73**, 1461 (2000).
95. A. Sekiguchi, T. Matsuo and H. Sakurai, *Angew. Chem., Int. Ed.*, **37**, 1662 (1998).
96. A. Sekiguchi, T. Matsuo and C. Kabuto, *Angew. Chem., Int. Ed. Engl.*, **36**, 2462 (1997).
97. A. Sekiguchi, T. Matsuo and R. Akaba, *Bull. Chem. Soc. Jpn.*, **71**, 41 (1998).
98. A. Sekiguchi, T. Matsuo, K. Ebata and H. Sakurai, *Chem. Lett.*, 1133 (1996).
99. T. Matsuo, A. Sekiguchi, M. Ichinohe, K. Ebata and H. Sakurai, *Organometallics*, **17**, 3143 (1998).
100. T. Matsuo, M. Tanaka and A. Sekiguchi, *Chem. Commun.*, 503 (2001).
101. A. Maercker, H. Wunderlich and U. Girreser, *Eur. J. Org. Chem.*, 793 (1998).
102. A. Maercker, H. Wunderlich and U. Girreser, *Tetrahedron*, **52**, 6149 (1996).
103. A. Maercker, A. Tatai, B. Grebe and U. Girreser, *J. Organomet. Chem.*, **642**, 1 (2002).
104. Y. Sahin, M. Hartmann, G. Geiseler, D. Schweikart, C. Balzereit, G. Frenking, W. Massa and A. Berndt, *Angew. Chem., Int. Ed.*, **40**, 2662 (2001).
105. A. Sekiguchi, K. Ebata, C. Kabuto and H. Sakurai, *J. Am. Chem. Soc.*, **113**, 7081 (1991).
106. A. Sekiguchi, K. Ebata, C. Kabuto and H. Sakurai, *J. Am. Chem. Soc.*, **113**, 1464 (1991).
107. A. Sygula and P. W. Rabideau, *J. Am. Chem. Soc.*, **113**, 7797 (1991).
108. K. Ebata, W. Setaka, T. Inoue, C. Kabuto, M. Kira and H. Sakurai, *J. Am. Chem. Soc.*, **120**, 1335 (1998).
109. W. Setaka, K. Ebata, H. Sakurai and M. Kira, *J. Am. Chem. Soc.*, **122**, 7781 (2000).
110. A. Sygula, F. R. Fronczek and P. W. Rabideau, *J. Organomet. Chem.*, **526**, 389 (1996).
111. H. Bock, C. Arad and C. Näther, *J. Organomet. Chem.*, **520**, 1 (1996).
112. A. Fürstner, G. Seidel, H.-E. Mons and R. Mynott, *Eur. J. Inorg. Chem.*, 1771 (1998).
113. A. Maercker, M. Kemmer, H. C. Wang, D.-H. Dong and M. Szwarc, *Angew. Chem., Int. Ed.*, **37**, 2136 (1998).
114. A. Maercker, K. Reider and U. Girreser, *Eur. J. Org. Chem.*, 1455 (1998).
115. S. Yamaguchi and K. Tamao, *J. Chem. Soc., Dalton Trans.*, **116**, 3693 (1998).
116. S. Yamaguchi, R.-Z. Jin, K. Tamao and M. Shiro, *Organometallics*, **16**, 2230 (1997).

117. K. Tamao, S. Yamaguchi and M. Shiro, *J. Am. Chem. Soc.*, **116**, 11715 (1994).
118. E. H. Braye, W. Hubel and I. Caplier, *J. Am. Chem. Soc.*, **83**, 4406 (1961).
119. F. Pauer and P. P. Power, *J. Organomet. Chem.*, **474**, 27 (1994).
120. P. v. R. Schleyer, unpublished results.
121. W. Clegg, K. Izod, W. McFarlane and P. O'Shaughnessy, *Organometallics*, **17**, 5231 (1998).
122. H. Bock, Z. Havlas, K. Gharagozloo-Hubmann and M. Sievert, *Angew. Chem., Int. Ed.*, **38**, 2240 (1999).

CHAPTER 16

α-Amino-organolithium compounds

ROBERT E. GAWLEY*

Department of Chemistry, University of Miami, Coral Gables, FL 33124, USA
e-mail: bgawley@uark.edu

and

IAIN COLDHAM

School of Chemistry, University of Exeter, Stocker Road, Exeter EX4 4QD, UK
e-mail: i.coldham@exeter.ac.uk

---

* *Current address*: Department of Chemistry and Biochemistry, University of Arkansas, Fayetteville, AR 72701, USA.

The Chemistry of Organolithium Compounds. Edited by Z. Rappoport and I. Marek
ISBN: 0-470-84339-X

I. INTRODUCTION TO α-AMINO-ORGANOLITHIUM COMPOUNDS

α-Amino-organolithium compounds are an extremely important subclass of organolithium compounds due to the prevalence of nitrogen-containing compounds in natural products and in biologically active molecules, as well as the extraordinary versatility of these species as synthetic tools. This review describes the formation and reactions of organolithium compounds that have a nitrogen atom attached at the α position. The focus is on sp^3-hybridized organolithium compounds, rather than compounds such as lithiated enamines or aromatic heterocycles. The review is divided into five sections: (1) the so-called unstabilized (or non-stabilized) organolithium compounds (in which there is no dipole or mesomeric stabilization), (2) dipole-stabilized organolithium compounds, (3) dipole-stabilized organolithium compounds that have an additional heteroatom on the metal-bearing carbon atom, (4) mesomerically stabilized organolithium compounds (by virtue of being allylic or benzylic) and (5) organolithium compounds that are both dipole and mesomerically stabilized. The rationale for this subdivision is based on general trends in the dynamic and chemical properties of the organolithium compounds. Among the properties that can vary are the method of synthesis (including the kinetic barrier to deprotonation), the configurational stability and susceptibility to single electron transfer, the reactivity toward various electrophiles (including other metals) and the propensity toward reactions such as cyclization, cycloaddition and sigmatropic rearrangement.

There are three fundamentally different ways to prepare α-amino-organolithium compounds (Scheme 1). One is by proton abstraction (path a), a second is by exchange of another metal, such as tin (path b), and a third is by reductive lithiation of, for example, a sulfide (path c). Each of these routes has advantages and disadvantages, such that the strategies complement each other well. For example, deprotonation can sometimes be accomplished enantioselectively using a chiral base, to produce an enantiomerically enriched organolithium compound that is useful in asymmetric synthesis. Some organolithium compounds are not accessible by direct proton removal due to a prohibitively high kinetic barrier or an unwanted regiochemical preference. In such cases, reductive lithiation or tin–lithium exchanges can give direct access to the desired organolithium compound. Since tin–lithium exchange is stereospecific in these compounds, enantiomerically enriched organostannanes provide access to enantiomerically enriched organolithium compounds.

The carbanionic carbon of α-amino-organolithium compounds is often tetrahedral and the carbon–lithium ion pair is sometimes tight enough that $^1J\,^6\text{Li}-^{13}\text{C}$ couplings can be observed in NMR spectra. If the lithium-bearing carbon is secondary, it is stereogenic. If one stereoisomer predominates over the other, this fact can be used to advantage in asymmetric synthesis. The predominance may be because of a diastereomeric bias

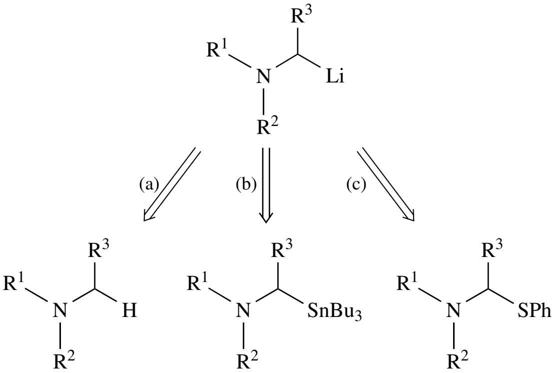

SCHEME 1

in a configurationally labile system, or because of a stereoselective deprotonation or transmetalation in a configurationally stable system. It is most convenient to draw the carbon–lithium bond as covalent.

α-Amino-organolithium compounds are versatile reagents that can react with a wide variety of electrophiles to give products of bimolecular electrophilic substitution (S_E2) in excellent yield, although the reactivity and yield depend on structural features such as allylic or benzylic stabilization and the substituents on the nitrogen atom. Suitable electrophiles include alkyl halides, trialkylsilyl and trialkylstannyl halides, aldehydes, ketones, carbonic acid derivatives (CO_2, chloroformates etc.) and Michael acceptors. Moreover, transmetalation from lithium to magnesium or a transition metal may afford species with reactivity profiles that complement those of the organolithium. Additionally, α-amino-organolithium compounds can undergo stereoselective rearrangements and anionic cyclizations to give a variety of elaborate products. This field has been reviewed a number of times since the early 1970s.[1-23]

Stereochemistry is a recurring theme in this field, so it is appropriate to lay the groundwork for what follows with a brief discussion of the dynamics of chiral organolithium compounds. Two issues dominate the chemistry of stereoselective reactions of α-amino-organolithium compounds having a stereogenic lithium-bearing carbon atom: configurational stability and the steric course of the reaction. These two issues will be discussed in general terms before proceeding to the examples in the following sections. Readers are also directed to the review in this volume by Hoppe (Chapter 17).

The question of configurational stability of any carbanion, whether the counterion is lithium or another metal, is *relative*: the answer depends on the time scale under consideration. One must also consider whether the two organolithium stereoisomers are enantiomeric or diastereomeric. For enantiomers (Figure 1a), equilibration results in a racemate; in an achiral environment, the equilibrium constant between the two enantiomers is unity ($K = 1$; $\Delta G^\circ = 0$). In such instances, configurational stability can only be observed if a single enantiomer is produced selectively *and* if the kinetic barrier to inversion is *relatively* high ($\Delta G^\ddagger \gg 0$) when compared to some reference time scale such as an electrophilic substitution reaction or a time interval. In the presence of a chiral ligand (L*) such as (−)-sparteine, the chiral ligand renders the organolithium complexes diastereomeric. For diastereomers, the two stereoisomers are not isoenergetic ($\Delta G^\circ \neq 0$). In such cases, configurational stability may be observed for kinetic reasons (Figure 1b, $\Delta G^\ddagger$ large), or because equilibration produces a predominance of one epimer (Figure 1c,

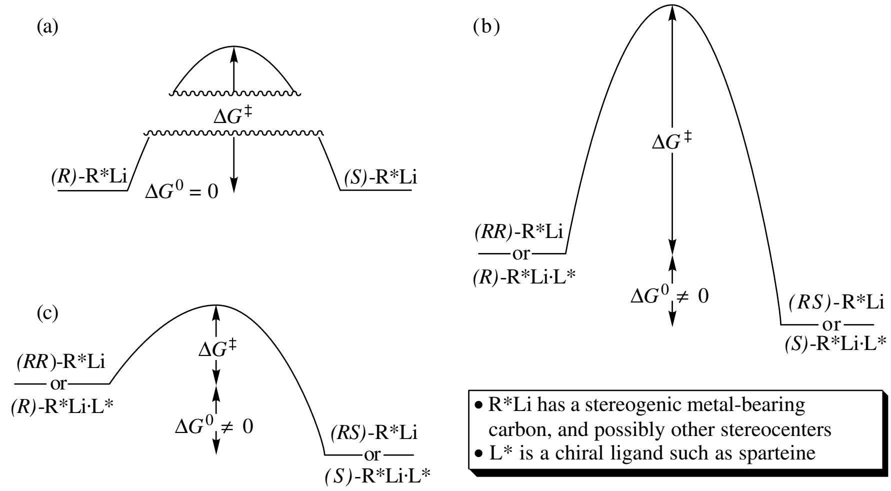

FIGURE 1

$\Delta G^{\ddagger}$ small); this situation may arise from a chiral ligand external to the carbanion, or because there are additional stereocenters in the carbanion.

Superimposed on these analyses is the additional factor of the *relative* rate of carbanion inversion *vs.* further reactions such as electrophilic substitution. For diastereomeric organolithium complexes, there are two limiting pathways for electrophilic substitution, as shown in Figure 2. If inversion of the organolithium is slow relative to the rate of substitution, the population of the two organolithium stereoisomers may determine the product ratio (Figure 2a). If the electrophilic quench is stereospecific (which cannot be assumed, *vide infra*), the product ratio will reflect the ratio of the organolithium stereoisomers. In some cases, it is possible to equilibrate a pair of organolithium diastereomers by raising the temperature to a point where equilibrium is reached; if the temperature is then lowered such that the rate of inversion is *relatively* slow, then ΔG° determines the (now static) population of the two epimers. In the specific case of organolithium *enantiomers* that are rendered diastereomeric by virtue of an external chiral ligand (e.g., (R)-R*Li · L*), such a process may be termed a dynamic thermodynamic resolution.[12, 21, 24]

Figure 2b shows the other extreme, whereby the rate of epimerization is fast relative to the rate of substitution. In this case, Curtin–Hammett kinetics apply, and the product ratio is determined by $\Delta\Delta G^{\ddagger}$[25]. In the specific case of organolithium *enantiomers* that are rendered diastereomeric by virtue of an external chiral ligand, such a process may be termed a dynamic kinetic resolution.[12, 24, 26–28] Both of these processes are also known by the more general term 'asymmetric transformation'.[29] One should be careful to restrict the term 'resolution' to a separation (either physical or dynamic) of *enantiomers*. An asymmetric transformation may also afford dynamic separation of equilibrating *diastereomers*, but such a process is not a resolution.[30]

The steric course of electrophilic substitution reactions can only be evaluated if the organolithium is configurationally stable and if the configuration is known. There are two limiting mechanisms for bimolecular electrophilic substitutions, polar and radical (Scheme 2). The latter can occur when an electrophile oxidizes the carbanion by single electron transfer (SET); subsequent radical coupling gives substitution products (Scheme 2). The steric course of such radical couplings is random. For polar processes,

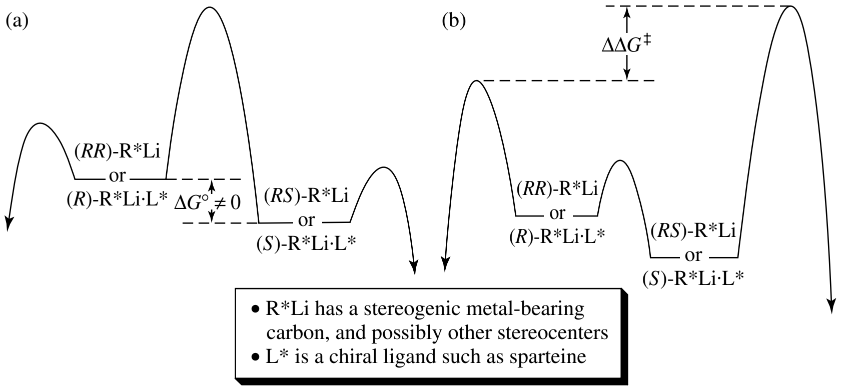

FIGURE 2

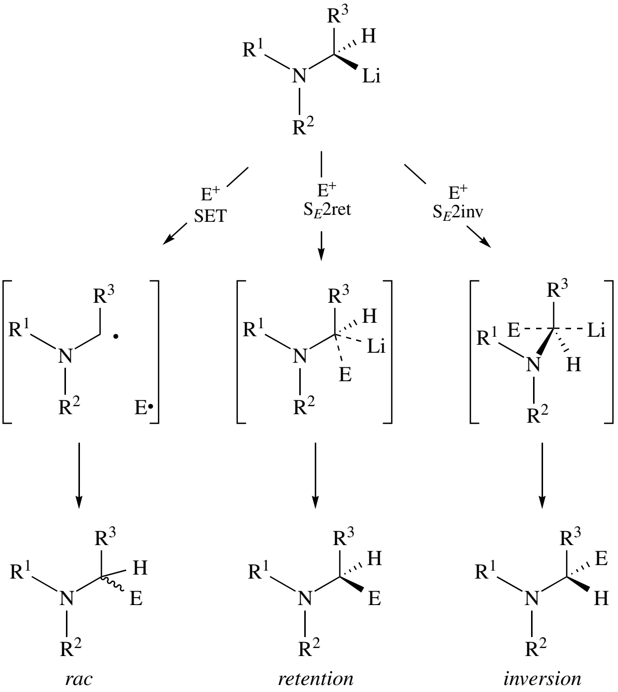

SCHEME 2

both retentive and invertive pathways are allowed by orbital symmetry,[31,32] and are referred to as S_E2ret and S_E2inv.[33] Both pathways have been reported, sometimes in competition with each other (Scheme 2).[34] Analysis of the mechanism of an electrophilic substitution of an organolithium compound must therefore begin with an evaluation of the configurational stability of the organolithium species, including consideration of the relative rates of epimerization and electrophilic substitution, and conclude with the steric course of the reaction with an electrophile.

II. UNSTABILIZED α-AMINO-ORGANOLITHIUM COMPOUNDS

A. Synthesis and Configurational Stability

'Unstabilized' α-amino-organolithium species are tertiary amines that are lithiated α to the nitrogen atom. The term 'unstabilized' is used to indicate that the nitrogen atom is not acylated, and that there is no dipole stabilization; neither is there any mesomeric stabilization of the carbanionic lone pair. These species were first made by deprotonation,[35, 36] but they remained largely inaccessible until the early 1970s, when Peterson showed that they could be formed easily by tin–lithium exchange.[37–39] Reduction of a thiophenyl ether (*S*,*N* acetal) has also been used to generate unstabilized α-amino-organolithiums, though less frequently.[40–42]

For many years, tin–lithium exchange has been used in the preparation of unstabilized primary[37–39,43] and secondary α-amino-organolithiums.[10, 34, 44–47] Tin–lithium exchange is preferable to deprotonation[35, 36] because it circumvents a kinetic barrier and permits lithiation at a specific site. Nevertheless, the reaction is not quite general. Several failures have been reported in the literature,[41, 48–51] and one wonders how many more failures have been found but not reported. Figure 3 shows how very subtle structural differences can affect the success or failure of this reaction. Chong and coworkers showed in 1993[48] that Peterson's original example from 1970,[37] when modified with a substituent on the metal-bearing carbon atom, fails (compare Figure 3a,f). Tsunoda showed that enclosing the nitrogen atom in a pyrrolidine ring (Figure 3g) also fails if the secondary metal-bearing carbon atom is acyclic.[41] Interestingly, the thiophenyl analog of this stannane (substitute $-$SPh for $-SnBu_3$ in Figure 3g) can be reduced to the organolithium.[41] Chong and coworkers found that simple modification to include a proximal heteroatom (Figure 3b) restores transmetalation reactivity to secondary acyclic systems.[48] Parenthetically, replacement of an alkyl group on the nitrogen atom with a carbonyl also facilitates transmetalation to a dipole-stabilized organolithium species (see Section III.C). In 1993, Gawley and coworkers found that if the metal is attached to the pyrrolidine ring then transmetalation occurs easily,[44, 52] and it was later found by Gawley and Coldham and their coworkers that *N*-allyl and *N*-alkenyl groups transmetalate as well (Figure 3c).[52, 53]

In THF, the tin–lithium exchange reaction proceeds via an ate complex formed by addition of BuLi to the tetraalkyltin (Figure 3, inset).[54] One view[55] of failures to transmetalate is that the ate complex is not formed due to steric effects caused by bulky groups on tin. Switching from butyl to methyl is supposed to alleviate the problem. However, Pearson and coworkers showed that substitution of trimethylstannyl for tributylstannyl was no help in cases such as those in Figure 3f,g, since treatment of the trimethylstannane shown in Figure 3h with excess butyllithium exchanged the methyls for butyls but failed to produce any α-amino-organolithium.[49] Vedejs and Kendall showed that the stannane in Figure 3f can be transmetalated slowly, with an excess of BuLi, after first complexing the nitrogen atom to BH_3.[56]

In 2000, Chambournier and Gawley reported the failure of a conformationally locked 2-(tributylstannyl)piperidine to transmetalate: when the 2-(tributylstannyl) moiety of a 4-*tert*-butylpiperidine is equatorial, Sn/Li exchange is facile, but when the 2-tributylstannyl group is axial, transmetalation fails (compare Figure 3d,i).[47] In other words, in these conformationally rigid piperidines, there appears to be a configurational requirement for transmetalation: the nitrogen atom lone pair has to be synclinal to the adjacent carbon–tin bond for transmetalation to succeed.

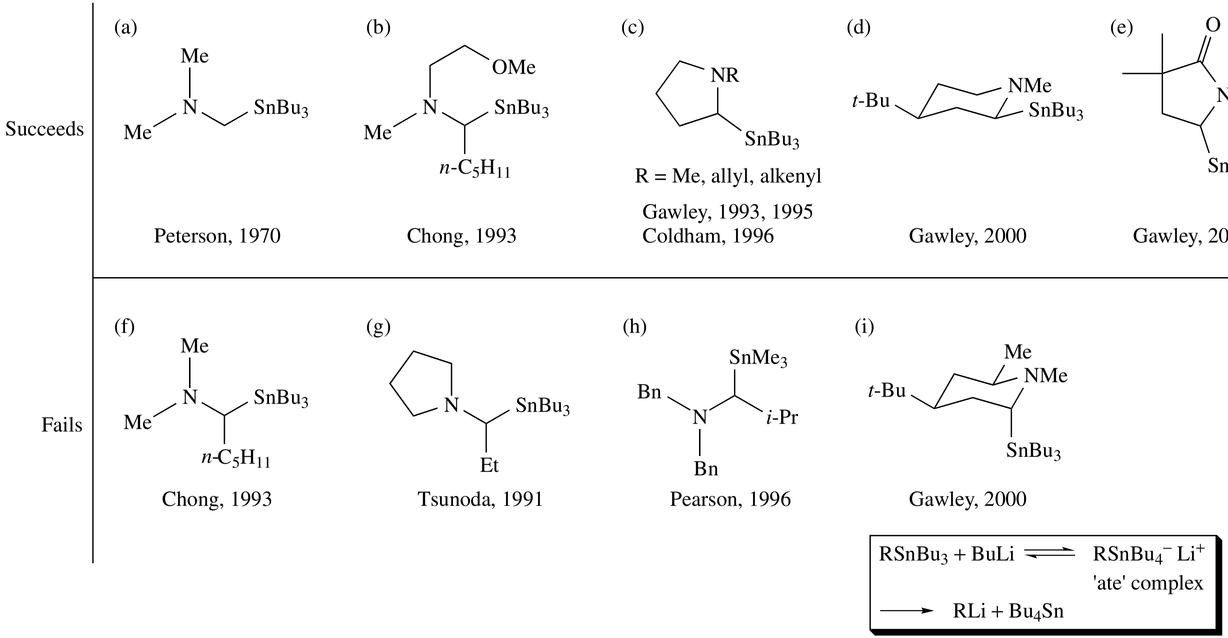
Succeeds
Fails
(a)
Peterson, 1970
(b)
Chong, 1993
(c)
R = Me, allyl, alkenyl
Gawley, 1993, 1995
Coldham, 1996
(d)
Gawley, 2000
(e)
Gawley, 2000
(f)
Chong, 1993
(g)
Tsunoda, 1991
(h)
Pearson, 1996
(i)
Gawley, 2000
RSnBu3 + BuLi ⇌ RSnBu4− Li+
'ate' complex
→ RLi + Bu4Sn

FIGURE 3

One hypothesis is that the alkyl group that is eliminated from the tin *ate* complex (Figure 3, inset) will be the most stable 'carbanion'.[55] To explain one of the failures of the α-lithiated pyrrolidines to transmetalate, Evanseck and coworkers used computational methods to show that the heat of formation of two constitutional isomers of lithio *N*-ethylpyrrolidine differ by 2.51 kcal mol^{-1}, with the ring metalated compound being more stable (Figure 4a).[49] This difference in stability is apparently enough to prevent loss of the α-amino-organolithium from the tin *ate* complex when the carbanionic carbon is not in a ring. Note that Figure 4a shows the lithium atom bridged across the carbon and nitrogen atoms. There is considerable theoretical and structural evidence of lithium bridging in many unstabilized α-amino-organolithium compounds.[57–61] However, we will only draw a nitrogen bridge when it is known to exist *and* when it is relevant to our discussion. Complexation of the nitrogen atom of either *N*-ethylpyrrolidine or *N*-ethylpiperidine with BF_3 and deprotonation with *sec*-BuLi/*t*-BuOK results in metalation on the ring (Figure 4b), indicating a kinetic preference for removal of a ring proton in an ylid.[13, 62]

The kinetics of tin–lithium transmetalation have not been studied extensively for the compounds where it is successful, but some trends in variability of rate have been noted. The times specified for transmetalation of α-amino(tributyl)stannanes are summarized in Figure 5. Peterson's original examples were transmetalated in hexane at 0 °C in a few minutes (Figure 5a). When the nitrogen atom had one or two aryl groups (e.g. Figure 5b), a small amount of THF was necessary to achieve transmetalation.[38] For 2-(tributylstannyl)pyrrolidines, the conditions depend on the nitrogen substituent. The *N*-methyl compounds (Figure 5c) transmetalate in a few seconds in THF at −78 °C. In ether at that temperature, the transmetalation is sluggish, but is accelerated by TMEDA.[10] The same compounds transmetalate at room temperature in hexane, but only very slowly. The product is an amorphous (pyrophoric and hygroscopic) white powder. For a 5-(tributylstannyl)-2-pyrrolidinone (Figure 5d), transmetalation in THF·TMEDA takes 30 min at −50 °C.[63] *N*-Isobutyl-2-(tributylstannyl)-pyrrolidine (Figure 5e) takes an hour to transmetalate in 4:1 hexane/ether at room temperature.[64] The *N*-methoxyethyl analog (Figure 5f) transmetalates in seconds at 0 °C in 4:1 hexane/ether. *N*-Allyl, *N*-butenyl and *N*-pentenyl compounds (Figure 5g) transmetalate readily in THF at −78 °C, but at rates similar to the *N*-alkyl compounds in 4:1 hexane/ether.[43, 52, 53, 65, 66] Thus, although the *N*-methoxyethyl substituent accelerates the transmetalation in hexane/ether, the double bond does not have a similar effect.

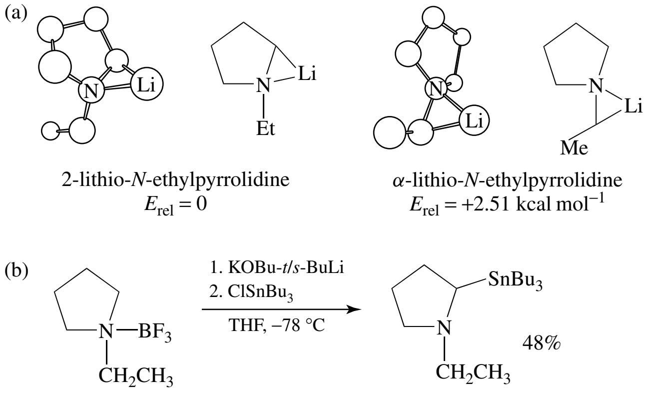

2-lithio-*N*-ethylpyrrolidine $E_{rel} = 0$

α-lithio-*N*-ethylpyrrolidine $E_{rel} = +2.51$ kcal mol^{-1}

FIGURE 4

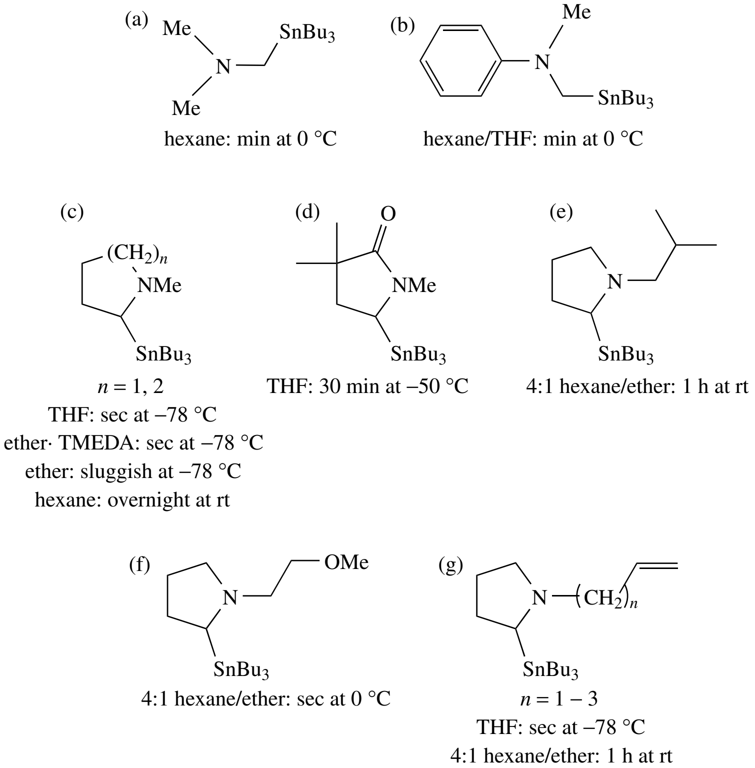

(a) hexane: min at 0 °C

(b) hexane/THF: min at 0 °C

(c) $n = 1, 2$
THF: sec at −78 °C
ether· TMEDA: sec at −78 °C
ether: sluggish at −78 °C
hexane: overnight at rt

(d) THF: 30 min at −50 °C

(e) 4:1 hexane/ether: 1 h at rt

(f) 4:1 hexane/ether: sec at 0 °C

(g) $n = 1 - 3$
THF: sec at −78 °C
4:1 hexane/ether: 1 h at rt

FIGURE 5. Relative case of transmetalation

There have been only a few studies on the configurational stability of unstabilized α-amino-organolithiums. In 1993, Vedejs and Moss reported that a 2-lithioaziridine (Figure 6a) was configurationally stable for 15 minutes at −60 °C, with brief warming to −10 °C.[67] The same year, Burchat, Chong and Park reported that an acyclic organolithium (Figure 6b) had to be cooled to −95 °C in THF to prevent racemization.[48] As reported by Gawley and Zhang, cyclic α-amino-organolithiums (Figure 6c–e) exhibit extraordinary configurational stability.[10, 44] The N-methylpyrrolidines and piperidines illustrated in Figure 6c were studied extensively, and the methoxyethylpyrrolidine in Figure 6d was compared to the acyclic organolithium of Figure 6b.[10] In addition to the indicated upper limit where racemization is very slow, studies of the N-methylpyrrolidine turned up an interesting effect of TMEDA: in the absence of TMEDA (THF solvent), chemical decomposition is faster than racemization. TMEDA seems to be more necessary for chemical stability than for configurational stability.

2-Lithio-N-methylpiperidines and -pyrrolidines are chemically and configurationally stable for at least 45 min at −40 °C in THF/TMEDA. Structural studies in THF showed that the piperidine is a bridged monomer in both racemic and enantiopure form, whereas the pyrrolidine is a homochiral dimer in both enantiopure and racemic forms.[61] The difference in aggregation state does not appreciably affect the temperatures at which racemization is avoided. These N-methyl heterocycles are considerably more robust than the

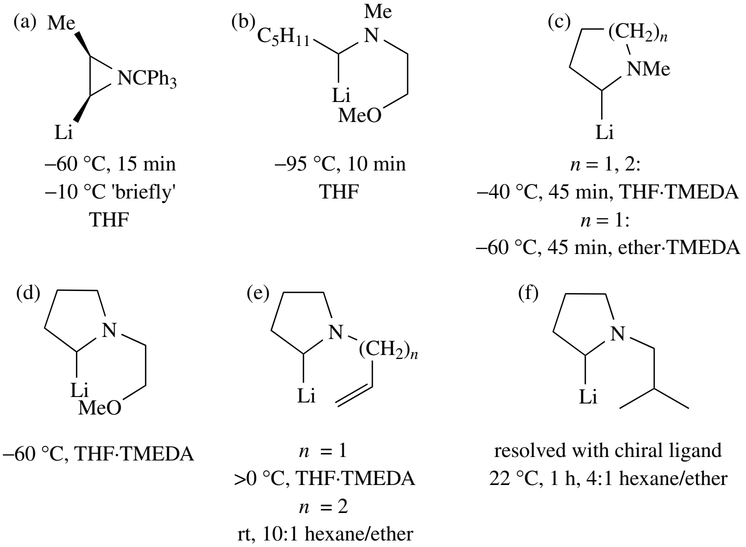

(a) −60 °C, 15 min
−10 °C 'briefly'
THF

(b) −95 °C, 10 min
THF

(c) $n = 1, 2$:
−40 °C, 45 min, THF·TMEDA
$n = 1$:
−60 °C, 45 min, ether·TMEDA

(d) −60 °C, THF·TMEDA

(e) $n = 1$
>0 °C, THF·TMEDA
$n = 2$
rt, 10:1 hexane/ether

(f) resolved with chiral ligand
22 °C, 1 h, 4:1 hexane/ether

FIGURE 6. Relative configurational stabilities

acyclic methoxyethyl compound in Figure 6b. Much of the added configurational stability is due to the ring, as shown by comparison with the methoxyethylpyrrolidine in Figure 6d. Interestingly, this compound is chemically *destabilized* by the presence of TMEDA, in contrast to the *N*-methyl compounds (Figure 6c).[10] An allyl or homoallyl group on the nitrogen atom also appears to stabilize the configuration (Figure 6e). For example, the *N*-allyl compound of 97:3 er (Figure 6e, $n = 1$) undergoes [1,2]- and [2,3]-rearrangements over 4 h at 13 °C in THF (see section below on rearrangements); electrophilic quench before complete conversion afforded unrearranged products of electrophilic substitution in 82:18 er.[52] Anionic cyclization of analogous compounds (see Section D on cyclizations) show that racemization may compete with cyclization, depending on the ring size, and the anionic terminating group.[53, 68] It is also interesting to note that the *N*-methoxyethyl substituent accelerates both transmetalation from the stannane *and* racemization, relative to the *N*-alkyl and *N*-alkenyl pyrrolidines. 2-Lithio-*N*-alkylpyrolidines (Figure 6f) are chemically stable but configurationally unstable at room temperature in hexane/ether.[64]

B. Electrophilic Substitution

1. Lithium on a carbon that is not in a ring

Although there is a kinetic barrier to the direct deprotonation of tertiary amines,[35, 69] Ahlbrecht and Dollinger showed in 1984 that the Schlosser superbase, *sec*-BuLi/*t*-BuOK, can deprotonate *N*-methylpiperidine selectively on the methyl group (Scheme 3).[69] This superbase probably yields an α-amino-organopotassium species (and *t*-BuOLi), but treatment with LiBr effects transmetalation to the more nucleophilic, and less basic, α-amino-organolithium species. Electrophilic quench with several aldehydes and ketones gives substitution products in good yields as typified by the example in Scheme 3.[69] Similarly,

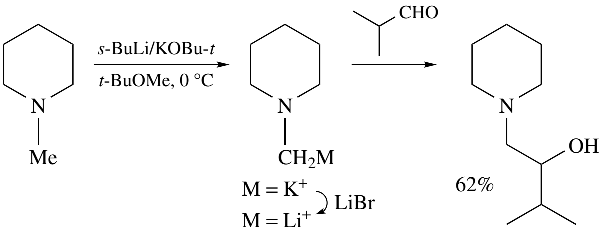

SCHEME 3

TMEDA can be deprotonated on a methyl group, but the only reaction reported was with the electrophile trimethylstannyl chloride.[70]

In 1991, Kessar and coworkers demonstrated that the kinetic barrier could be lowered by complexing the tertiary amine with BF_3, such that s-BuLi is able to deprotonate the ammonium compound, which can be added to aldehydes and ketones as shown by the example in Scheme 4a.[71, 72] Note the selectivity of deprotonation over vinyl and allyl sites. A limitation of this methodology is that the ylide intermediate does not react well with alkyl halide electrophiles. To get around this, a sequence that begins with the stannylation and decomplexation shown in Scheme 4b was developed. The stannane can be isolated in 94% yield (Scheme 4b) and subsequently subjected to tin–lithium exchange[37–39] to afford an unstabilized lithiomethylpiperidine that is a very good nucleophile. However, isolation of the stannane is not necessary and a procedure was devised in which the amine is activated with BF_3, deprotonated, stannylated, decomplexed from BF_3 with CsF, transmetalated back to lithium and alkylated, *all in one pot* (Scheme 4c).[62]

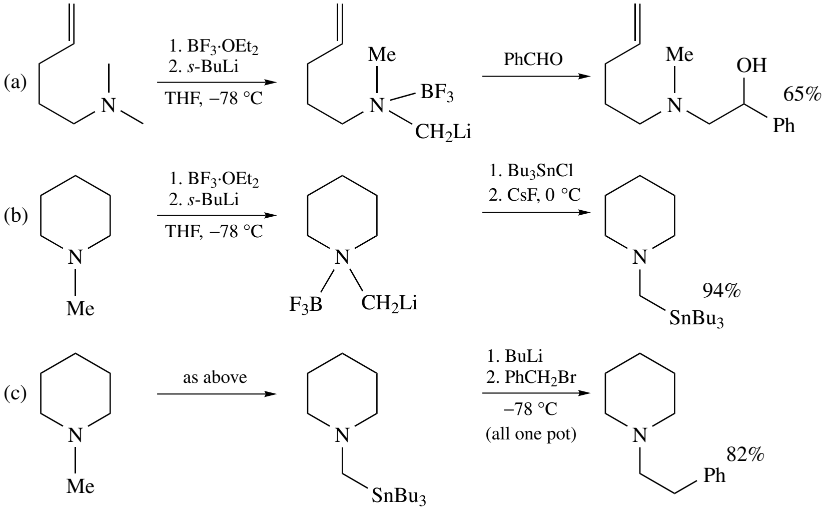

SCHEME 4

Generation of an α-amino-organolithium by tin–lithium exchange was first introduced by Peterson in 1970,[37–39] who showed that these compounds add well to aldehydes, but

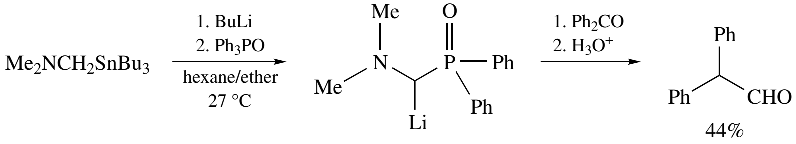

SCHEME 5

who also showed that they could be used to make Horner–Wittig type reagents by reaction with triphenylphosphine oxide, as shown in Scheme 5.[38]

Other methods of generating acyclic α-amino-organolithiums include reduction of α-amino sulfides (*S*,*N* acetals)[40, 41, 73] and benzotriazoles.[74, 75]

2. Lithium on a ring carbon

Although *N*-methyl piperidine is deprotonated on the methyl group by the Schlosser superbase, after activation with BF_3 (Scheme 4), *N*-ethyl piperidine and pyrrolidine are deprotonated on the ring.[13, 62] The reaction has not been well developed, but applications to the deprotonation and alkylation of quinuclidine and DABCO have been evaluated for a number of aldehyde, ketone and ester electrophiles (the cation bound to carbon is probably potassium).[72] The more acidic aziridine ring can be activated with BH_3 and deprotonated with *s*-BuLi (Scheme 6).[56] In the illustrated example, deprotonation occurs primarily *cis* to the boron atom, due to a combination of steric and electrostatic effects. In particular, the N–B bond is slightly longer than the exocyclic N–C bond so that the BH_3 moiety is more tolerant of eclipsing interactions with the BuLi base; moreover, electrostatic attraction between the formally negative boron atom and the lithium cation are suggested to stabilize the transition state for *syn*-lithiation.

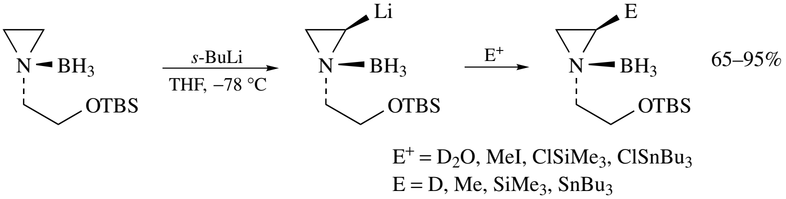

SCHEME 6

Lithiated aziridines are also available by tin–lithium exchange and by reduction of an aziridinyl sulfoxide. These species are configurationally stable, and react well with nonenolizable carbonyl electrophiles. The first example of a tin–lithium exchange to generate an α-amino-organolithium at a secondary position is shown in Scheme 7a, reported by Vedejs and Moss in 1993.[67] Addition of the lithiated aziridine to benzaldehyde gives a mixture of diastereomers. In 1998, Satoh and coworkers showed that an aziridinyl sulfoxide can be reduced by *t*-BuLi or RMgX/*t*-BuLi mixtures, as shown by the example in Scheme 7b.[76, 77] Again, these compounds give good yields only if the carbonyl electrophile is not enolizable.

Alkylation of pyrrolidine and piperidine heterocycles was investigated extensively by Gawley and coworkers.[10, 34, 44, 45, 66] The initial evaluation of 2-lithio-*N*-methylpiperidine and 2-lithio-*N*-methylpyrrolidine as nucleophiles was conducted on racemic material, but

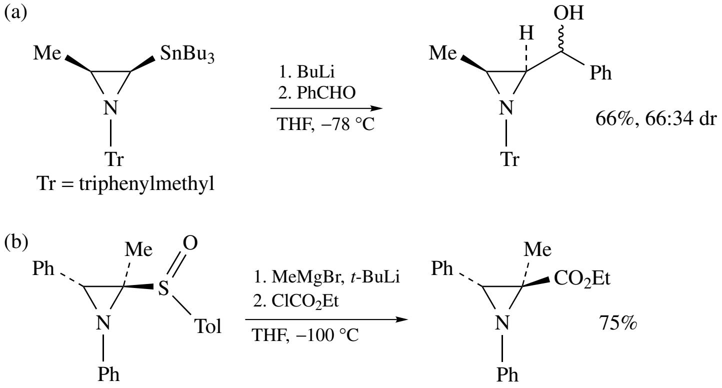

SCHEME 7

no differences in product yield or reactivity were observed between the racemic and nonracemic organolithiums (*vide infra*). The racemic stannanes are conveniently prepared from the *N*-Boc heterocycle by stannylation according to Beak's method (*vide infra*, Scheme 28)[45, 78, 79] followed by reduction with DIBAL.[45] After transmetalation (BuLi, THF/TMEDA, −78 °C, 15 min), the organolithiums were allowed to react with a variety of electrophiles. The results of these evaluations are summarized in Scheme 8. These data are notable because of the uniformly high yields of coupling products, virtually independent of the electrophile. With primary alkyl halides, coupling products are obtained in excellent yields in both the pyrrolidine and piperidine series. By adding an extra equivalent of butyllithium before the electrophile, *ω*-hydroxy alkyl halides can be used as electrophiles without protecting the hydroxyl group. 2-Lithio-*N*-methylpiperidine also reacts equally well with carbon dioxide, methyl chloroformate and dimethyl carbonate, but 2-lithio-*N*-methylpyrrolidine only reacts with carbon dioxide; the reaction with methyl chloroformate and dimethyl carbonate did not afford the anticipated proline ester. Other carbonyl electrophiles work equally well with both the piperidines and pyrrolidines. Examples tested include pivaloyl chloride, cyclohexanone, acetone and benzophenone. Benzaldehyde affords good yield of adducts as a mixture of *u* and *l* diastereomers.

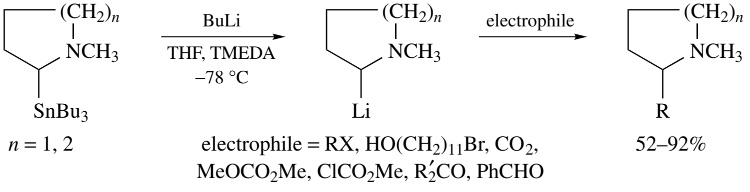

SCHEME 8

These organolithiums were also available in nonracemic form, which allowed the evaluation of the steric course of these reactions. Scheme 9 summarizes the steric course for pyrrolidines, and Scheme 10 for piperidines. In the discussion that follows, it is assumed that the transmetalation from tin to lithium takes place with retention of configuration at

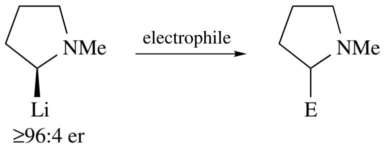

RETENTION:	*INVERSION:*	*RACEMIZATION:*
CO_2 (82%, ≥96:4 er)	$Ph(CH_2)_3Br$ (80%, 75.5:24.5 er)	$PhCH_2Br$ (60%)
t-BuCOCl (55%, 91:19 er)	$Br(CH_2)_{11}OLi$ (52%, er not det.)	$BrCH_2CO_2$*t*-Bu (77%)
acetone (85%, 97.5:2.5 er)	hexenyl bromide (61%, 73:27 er)	Ph_2CO (72%)
cyclohexanone (86%, 97.5:2.5 er)		
PhCHO (75%, 1:1 dr, each 94:5:5.5 er)		

SCHEME 9

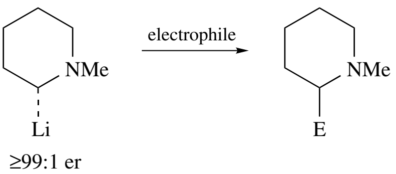

RETENTION:	*INVERSION:*	*RACEMIZATION:*
$ClSnBu_3$ (81%, >99:1 er)	$Br(CH_2)_{11}$ OLi (78%, 95:5 er)	$PhCH_2Br$ (91%)
CO_2 (82%, >99:1 er)	$Ph(CH_2)_3Br$ (76%, >99:1 er)	$BrCH_2CO_2Bu$-*t* (75%)
$MeOCO_2Me$ (84%, >99:1 er)		Ph_2CO (70%; mixture of 1, 2- and 1, 6-addition products
$ClCO_2Me$ (76%, >99:1 er)		
t-BuCOCl (85%, >99:1 er)		
acetone (70%, 97.5:2.5 er)		
cyclohexanone (79%, >99:1 er)		
C_6H_5CHO (74%, 1:1 dr, each 96:4 er)		

SCHEME 10

carbon. As discussed above (cf. Figure 6), these lithiated heterocycles exhibit extraordinary configurational stability, showing no detectable racemization after 75 min at −80 °C in ether or THF.[10]

Comparison of the configuration of the stannane with the products of reaction reveals that primary alkyl halides that are not benzylic or α to a carbonyl react with inversion at the lithium-bearing carbon atom. In the piperidine series, the best data are for the 3-phenylpropyl compound, which was shown to be $\geqslant$99:1 er. In the pyrrolidine series, the er of the analogous compound indicates 21–22% retention and 78–79% inversion of configuration. Activated alkyl halides such as benzyl bromide and *tert*-butyl bromoacetate afford racemic adducts. In both the pyrrolidine and piperidine series, most carbonyl electrophiles (i.e. carbon dioxide, dimethyl carbonate, methyl chloroformate, pivaloyl chloride, cyclohexanone, acetone and benzaldehyde) react with virtually complete retention of configuration at the lithium-bearing carbon atom. The only exceptions are benzophenone, which affords racemic adduct, and pivaloyl chloride, which shows some inversion. The inversion observed with pivaloyl chloride may be due to partial racemization of the ketone product during work-up.

The three limiting possibilities for aliphatic electrophilic substitution are shown in Scheme 11.[33] If substitution takes place via a polar mechanism, substitution with net retention or net inversion are possible, and both are allowed. Single electron transfer (SET) is also possible, whereby the electrophile oxidizes the anion to a radical. Bimolecular coupling of such radicals is stereorandom, and products are racemic. An extensive mechanistic investigation revealed that the completely racemic products obtained by reaction of lithiopyrrolidines and lithiopiperidines with activated alkyl halides and with benzophenone are produced by an SET mechanism.[34] The reactions with carbonyl electrophiles showing 100% retention are polar, as are the invertive alkylations with alkyl halides. The diminished selectivity obtained in the alkylations of lithiopyrrolidines is *not* due to a contribution from SET, but from competing S_E2inv and S_E2ret mechanisms.[34]

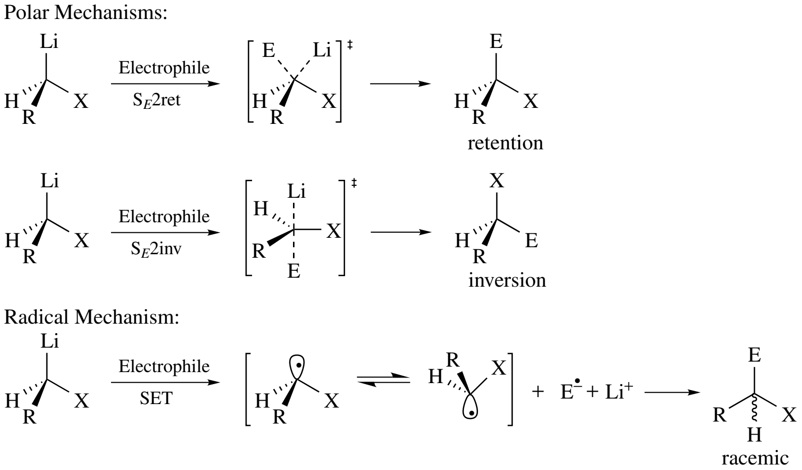

SCHEME 11

Several transmetalations were investigated for these compounds, and the results varied according to ring size in some cases.[45] The reaction of 2-lithio-*N*-methylpiperidine with tributyltin chloride occurs with 100% retention. Transmetalation of 2-lithio-*N*-methylpyrrolidine with zinc chloride afforded a species that failed to react with benzaldehyde, cyclohexanone or pivaloyl chloride. Treatment with magnesium chloride afforded a species that failed to react with either CO_2 or cyclohexanone. The *R* lithiopiperidine, after treatment with magnesium chloride at −78 °C in THF, was treated with pivaloyl chloride to afford *R* ketone (net inversion) in 56% yield and 86.5:13.5 er (Scheme 12a). Since the piperidinostannane was $\geqslant$99:1 er, this indicates approximately 87% inversion and 13% retention of configuration (some racemization could have occurred during work-up). In contrast, the *S* lithiopyrrolidine afforded *R* ketone (net retention) in 75% yield and 81:19 er after similar treatment (Scheme 12b). Since the pyrrolidinostannane had an er of 97:3, this indicates approximately 83% retention and 17% inversion. Assuming that the reaction of the Grignard species with the acid chloride is retentive in both ring systems, the reaction of lithiated heterocycles with magnesium chloride occurs with predominant retention in the pyrrolidine series and inversion in the piperidine series.

This chemistry would be even more useful if it was not restricted to *N*-methyl heterocycles. From the standpoint of synthetic flexibility, *N*-allyl heterocycles may be more

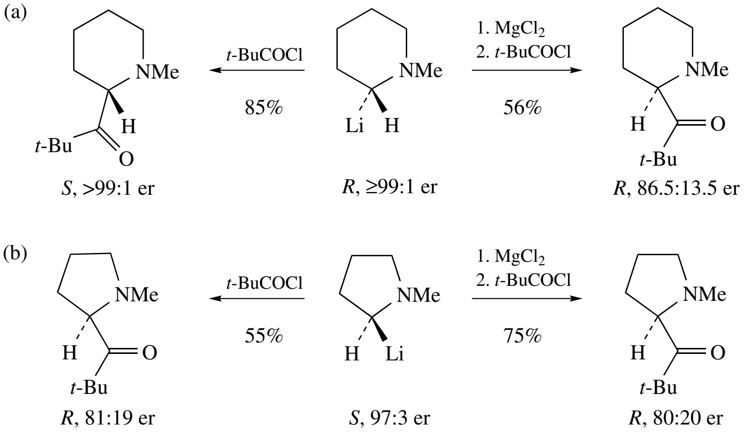

SCHEME 12

desirable educts, since the allyl group can be removed, and the heterocycle further elaborated to fused bicyclics, etc. To date, only pyrrolidines have been examined, which were chosen because they could easily be made in enantio-enriched form.

S-*N*-Allyl-2-(tributylstannyl)pyrrolidine can be prepared by removing the Boc group of *S*-*N*-Boc-2-tributylstannylpyrrolidine (96:4–97:3 er[80, 81]) with either B-bromocatechol borane or trimethylsilyl iodide. Alkylation with allyl bromide affords *S*-*N*-allyl-2-(tributylstannyl)pyrrolidine, in 50–55% overall yield after flash chromatography on neutralized silica.[66] This compound is thermally labile, but can be stored in a freezer under an inert atmosphere for several days. The *N*-allylpyrrolidinyl stannane can be transmetalated using butyllithium in THF/TMEDA at −80 °C in a few minutes. Quenching the organolithium with a carbon dioxide stream and reducing the crude *N*-allylproline with LAH afforded *N*-allylprolinol in 57% yield (after flash chromatography) as a colorless oil having 93.5:6.5 er (Scheme 13). Thus, the reaction of the lithiated *N*-allylpyrrolidine with carbon dioxide occurred with at least 96% retention of configuration. Since the enantiomeric ratios of both starting material and product were determined by rotation, it is likely that the stereoselectivity is 100%, analogous to the carboxylations of the *N*-methyl compounds (the enantiomeric ratios of which were determined by Mosher analysis).

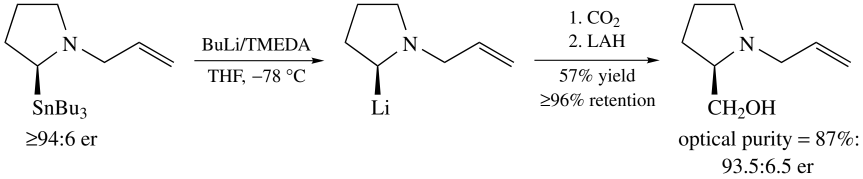

SCHEME 13

Similarly, a number of other electrophiles were tested, and the results are shown in Scheme 14. In all cases, the products of alkylation were formed in excellent yields. Comparison of the absolute configuration and enantiomer purity of the various products with that of the stannane reveal that the trends observed in the *N*-methyl series (Scheme 9) are largely followed: carbon dioxide adds with retention of configuration, while most primary

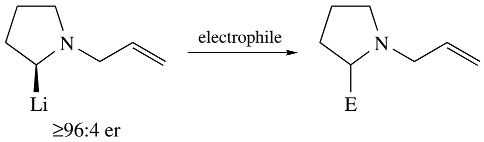

RETENTION:	INVERSION:
CO_2 (57%, 93.5:6.5 er)	$Ph(CH_2)_3Br$ (87%, 88:12 er)
$PhCH_2Br$ (76%, 76:24 er)	*n*-PrBr (68%, 89:11 er)
PhCHO (90%, 1:1 dr; er not det.)	*n*-heptyl bromide (75%, 89:11 er)
1-Naphthoyl chloride (75%, 55:45 er)	hexenyl bromide (65%, er not det.)

SCHEME 14

alkyl halides react with about 90% inversion of configuration. The 90% stereoselectivity for reactions with alkyl halides is significantly higher than that observed with 2-lithio-*N*-methylpyrrolidines, which were only about 78% selective (also showing inversion).[45] The result using benzyl bromide as electrophile was surprising. In the *N*-methyl series (Scheme 9), the product of benzylation was racemic, but here a 76:24 ratio of enantiomers was found. Even more surprising is that this alkyl halide reacted with about 78% *retention* of configuration, making it the only alkyl halide (so far found) that reacts with these lithioheterocycles predominantly with retention! Replacement of the Boc group in *N*-Boc-2-tributylstannyl pyrrolidine with an allyl group, followed by tin–lithium exchange, affords an α-amino-organolithium species that reacts with either retention or inversion of configuration, depending on the electrophile. Since the allyl group may be removed by transition metal catalysis, this two-step sequence may find use in applications where direct alkylation of the Boc-pyrrolidine is inefficient, or when the opposite enantiomer is desired.

In summary (Scheme 15), 2-lithiopiperidines and 2-lithiopyrrolidines appear to be very versatile nucleophiles for the elaboration of these heterocyclic systems, affording a variety of 2-substituted heterocycles in excellent yields. The stereoselectivity of the reaction is near 100% in the piperidine series with most carbonyl electrophiles (retention of configuration) and alkyl halides (inversion of configuration). In the pyrrolidine series, the selectivity is also near 100% with carbonyl electrophiles (retention), but less selective (inversion predominates) with alkyl halides (less problematic with *N*-allylpyrrolidines).

The steric course of reactions of lithiopiperidines having a *tert*-butyl substituent that locks the ring has been investigated briefly.[47] As shown in Scheme 16, the results are consistent with expectations based on the foregoing. With the lithium atom in an equatorial configuration on the rigid ring, only electrophilic substitutions that occur with retention should be favored, since only from an axial position can an invertive substitution occur. In the event, carbonyl electrophiles, which react with retention in unsubstituted piperidines, work well, while electrophiles that typically react with inversion or racemization do not. In the latter case, side products hint at the intervention of SET/radical processes.[47]

The study of retention, inversion or racemization on electrophilic quench of chiral organolithium species is crucial to an understanding of the reactivity of such species. The ability to prepare enantioenriched α-amino-organolithium species that are configurationally stable allows this study and hence the formation of enantioenriched substituted amine products. An alternative method for the formation of enantioenriched products by electrophilic substitution uses configurationally unstable α-amino-organolithium species in the presence of a chiral ligand. Unstabilized α-amino-organolithium species such as *N*-alkyl-2-lithiopyrrolidines, although configurationally stable at low temperature, undergo racemization at room temperature in nonpolar solvents such as hexane–ether. Addition of a chiral ligand can therefore promote dynamic resolution. Coldham and coworkers have

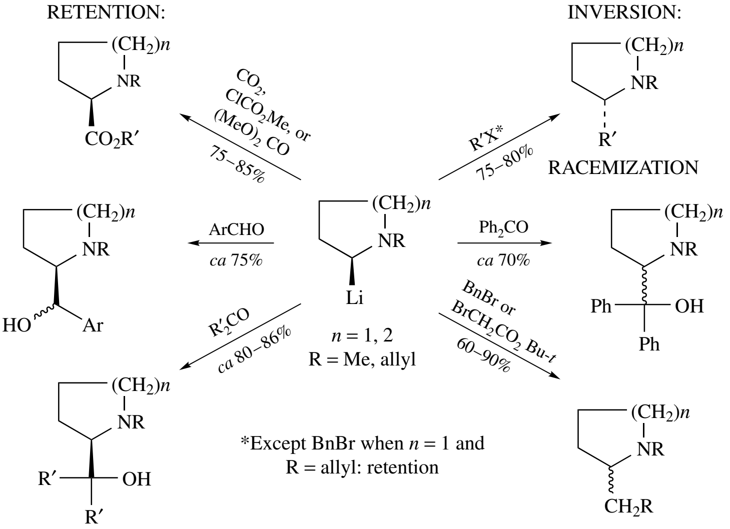

SCHEME 15

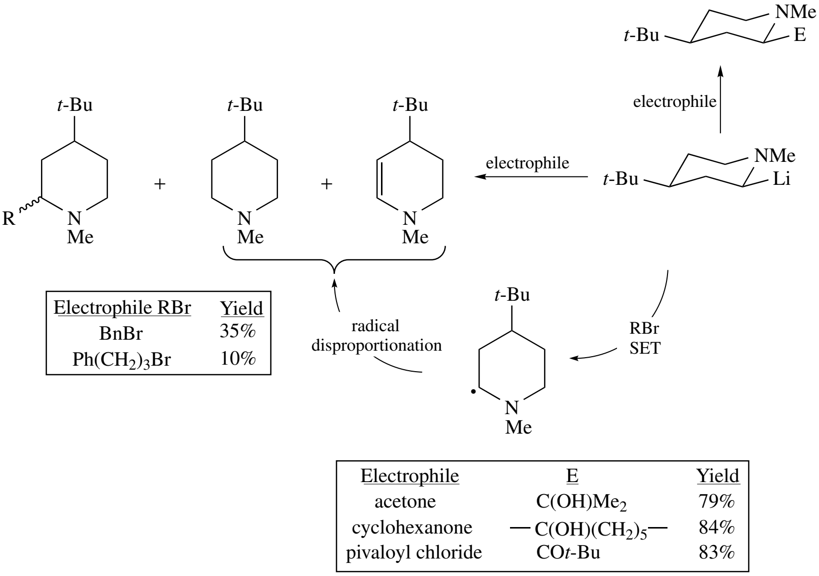

Electrophile RBr	Yield
BnBr	35%
$Ph(CH_2)_3Br$	10%

Electrophile	E	Yield
acetone	$C(OH)Me_2$	79%
cyclohexanone	$—C(OH)(CH_2)_5—$	84%
pivaloyl chloride	CO*t*-Bu	83%

SCHEME 16

recently achieved success in this approach using racemic *N*-isobutyl-2-lithiopyrrolidine, which undergoes dynamic thermodynamic resolution in the presence of (−)-sparteine or lithiated 1-(1-methyl-2-pyrrolidinylmethyl)pyrrolidine-2-methanol, to give high yields of optically active 2-substituted *N*-isobutylpyrrolidines (Scheme 17).[64]

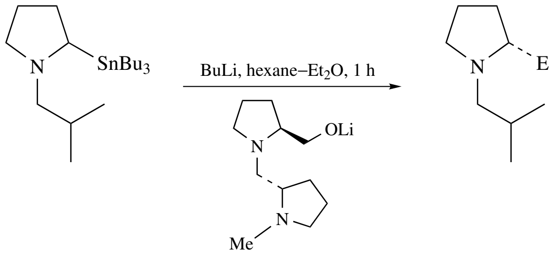

then E^+ $E^+ = PhNCO, Me_2CO, p\text{-}MeOC_6H_4CHO, Me_2SO_4, TMSCl, Bu_3SnCl$

$E = CONHPh, C(OH)Me_2, CH(OH)\text{-}p\text{-}MeOC_6H_4, Me, SiMe_3, SnBu_3$

54–75% er >95:5

SCHEME 17

C. Sigmatropic Rearrangements

The [2,3]-sigmatropic (Wittig) rearrangement of allylic ethers has been the subject of considerable interest over the past fifty years,[82–87] and synthetic applications have increased since Still and Mitra showed[88] that the rearrangement may be initiated by tin–lithium exchange of an α-alkoxy stannane. This observation was important for the synthesis of enantio-pure compounds because of the configurational stability of the intermediate α-alkoxyorganolithiums. Three independent studies, published virtually simultaneously, showed that the reaction is stereospecific, and proceeds with inversion of configuration at the lithium-bearing carbon atom.[89–91]

The analogous reaction involving α-amino carbanions is less common among unstabilized carbanions. Usually, the carbanionic carbon is stabilized by a double bond, an aromatic ring or a carbonyl group. When they occur, [2,3]-rearrangements are driven by relief of ring strain,[92–96] Lewis acid activation[97] or activation by a second heteroatom such as silicon or tin.[98–101]

A single example of an aza-Wittig rearrangement of an unstabilized α-amino-organolithium, induced by reductive lithiation of an *S*,*N* acetal, was reported by Broka and Shen in 1989.[40] In 1993, Coldham reported two examples of aza-[1,2]-Wittig rearrangements initiated by tin–lithium exchange, and which proceed by a radical mechanism.[102] In 1993, Vedejs and Moss reported the [1,2]-rearrangement of *N*-trityl-2-lithioaziridine shown in Scheme 18.[67] The authors suggest that the most likely mechanism involves the caged radical pair shown. The reason for the stereoselectivity of the rearrangement may be due to two factors: the bulky trityl group would be more stable *trans* to the R group, and the lithium atom may be bridged to the nitrogen atom in the anion, placing the trityl on the opposite side of the ring in the first place.

Gawley and coworkers reported a study of the steric course of the aza-Wittig rearrangement in an enantio-enriched pyrrolidine ring system.[52] Specifically (Scheme 19), *N*-allyl-2-lithiopyrrolidine rearranges at 13 °C (4 hours) with 76% inversion and 24% retention of configuration. Isotope labeling experiments showed that the reaction proceeded by competing [1,2] and [2,3] pathways.

Nitrogen ylides are also known to undergo [1,2]- (Stevens) and [2,3]-rearrangements.[103] The Stevens rearrangement occurs through a mechanism that involves homolytic cleavage

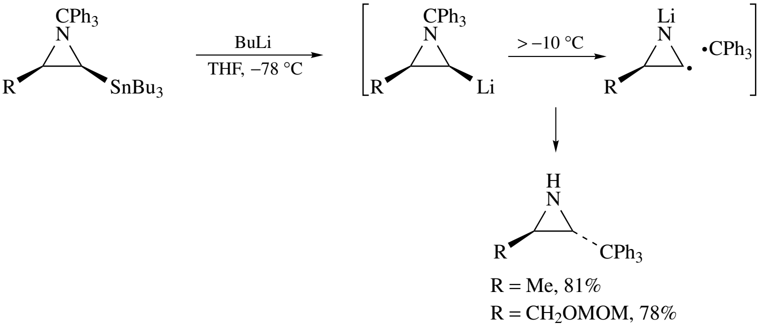

SCHEME 18

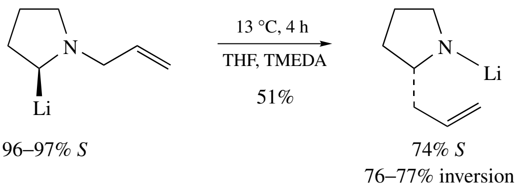

SCHEME 19

to a radical pair and recombination in a solvent cage. It proceeds with retention of configuration at both migrating atoms.[104] Since the leaving group in a concerted ylide rearrangement is a neutral amine instead of an amide anion, the ylide rearrangement is more facile and occurs at lower temperatures.[105–110] Gawley and coworkers established the steric course of the ylide rearrangement in 1995.[52] As illustrated in Scheme 20a, the rearrangement is stereospecific, proceeding with 100% inversion (within the error limits of the analysis). This stereospecific rearrangement deserves further investigation and development. One such possibility is shown in Scheme 20b: quaternization of an *N*-methyl heterocycle with allyl bromide and rearrangement.[52]

In summary, [2,3]-sigmatropic rearrangements of lithio α-amino anions and ylides occur with inversion of configuration at the metal-bearing carbon atom. For anions, [1,2] and [2,3] mechanisms compete in the aza-Wittig rearrangement. The rearrangement of unstabilized nitrogen ylides is an extremely facile reaction that, since it is stereospecific, may have considerable synthetic potential.

D. Cyclizations

The synthesis of oxygen- and nitrogen-containing heterocyclic compounds by anionic cyclization of unsaturated organolithium compounds has been reviewed recently.[111] Broka and Shen reported the first intramolecular reaction of an unstabilized α-amino-organolithium compound using reductive lithiation of an *N*,*S*-acetal derived from a homoallylic secondary amine (Scheme 21).[40] Just one example was reported; treatment with lithium naphthalenide gave the pyrrolidine product, predominantly as the *cis* isomer.

A more popular method for the generation and cyclization of unstabilized α-amino-organolithium compounds uses tin–lithium exchange, and has been explored extensively by Coldham and others. A variety of solvent systems can be employed, although the use

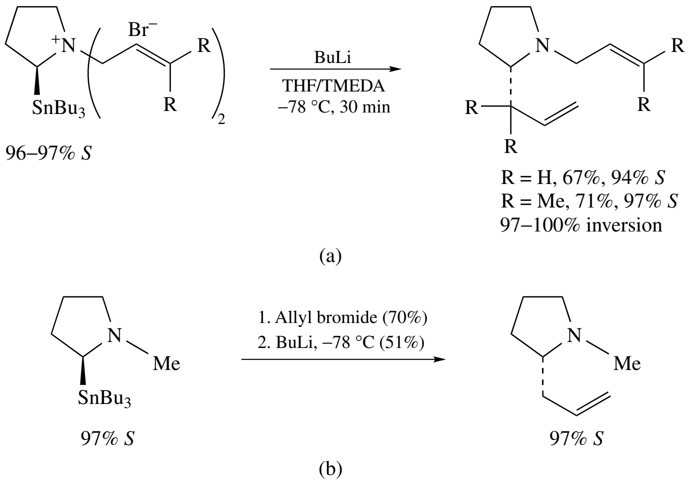

SCHEME 20

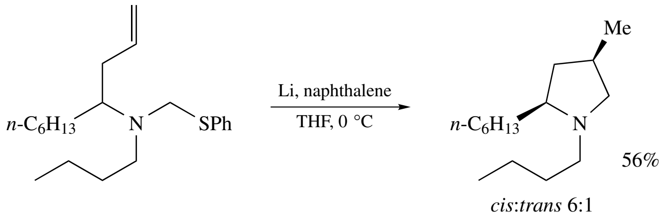

SCHEME 21

of the nonpolar solvent hexane, with a little Et_2O to promote transmetalation, is normally preferable, as this allows the subsequent quench of the product organolithium compound with an electrophile (avoiding competing proton abstraction, as obtained using THF). Two examples from Coldham and coworkers, toward simple pyrrolidines and bridged bicyclic amines, are illustrated in Scheme 22.[112, 113] Such cyclization reactions are thought to proceed by coordination of the lithium atom with the alkene π-bond, as shown by the transition states in both reactions. After cyclization, the organolithium can be quenched with a number of electrophiles in moderate to excellent yields. Interestingly, the latter example is successful using either the *cis* or the *trans* pyrrolidinyl stannane. Since the starting material is a 1:1 mixture of stereoisomers, and since the products are (sometimes) obtained in higher than 50% yield, it follows that epimerization of the *trans* organolithium compound to the *cis* isomer probably occurs prior to cyclization. Reactions that are sluggish often benefit from the presence of the additive TMEDA.

The availability of enantioenriched 2-tributylstannylpyrrolidines[80, 81] can be used to advantage in these reactions. Conversion to a substrate suitable for cyclization allows, after transmetalation, the determination of the stereoselectivity on intramolecular carbolithiation. Treatment of the enantioenriched stannane shown in Scheme 23 with butyllithium resulted in the formation of the pyrrolizidine alkaloid pseudoheliotridane.[53] The product was formed as a single diastereomer and with no loss of optical purity, occurring with overall retention of configuration at the carbanion center. Related cyclization reactions

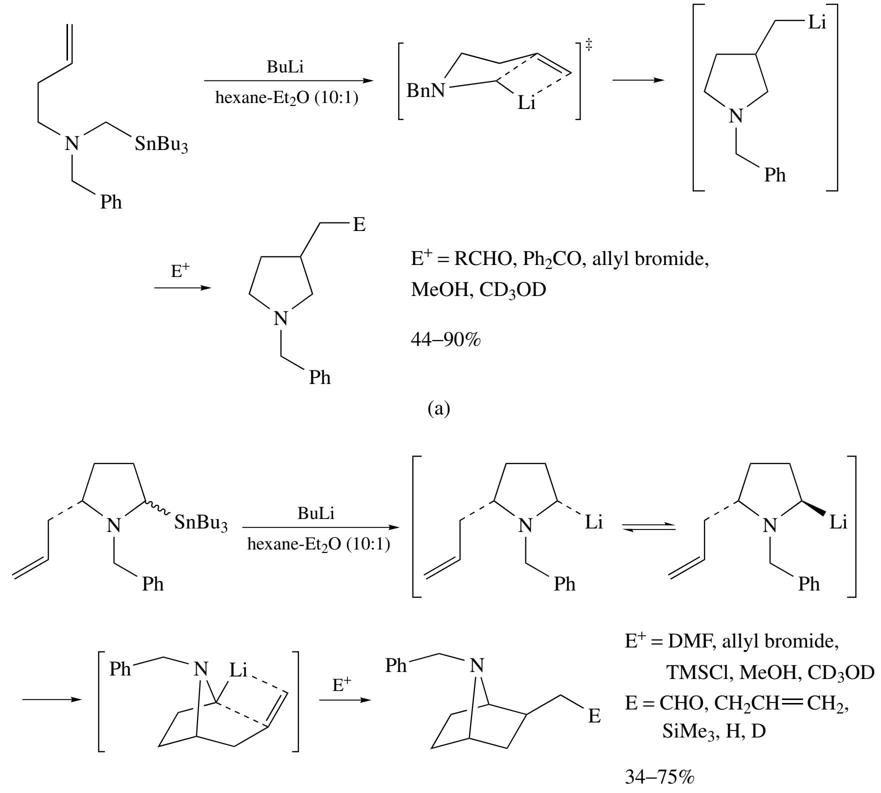

E$^+$ = RCHO, Ph$_2$CO, allyl bromide, MeOH, CD$_3$OD

44–90%

(a)

E$^+$ = DMF, allyl bromide, TMSCl, MeOH, CD$_3$OD
E = CHO, CH$_2$CH=CH$_2$, SiMe$_3$, H, D

34–75%

(b)

SCHEME 22

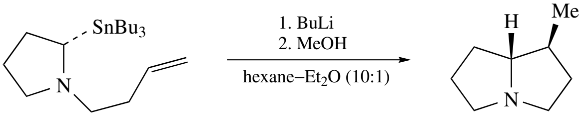

er 97:3

90% er 97:3

SCHEME 23

to the corresponding indolizidine ring system (6-membered ring formation) and to the azabicyclo[3.2.0]heptane ring system (4-membered ring formation) occur with competing racemization.[114] For cyclization to the indolizidine ring system, kinetic studies have allowed the determination of the rate of cyclization and racemization and it has been found that a terminal phenylthio group enhances the rate of cyclization.

The electrophile for the cyclization reaction of an α-amino-organolithium compound is not restricted to a terminal (or phenylthio-substituted) alkene and examples have been reported using carboxylic amides, alkynes and allylic ethers.[115, 116] For example, Lautens and Kumanovic reported that treatment of the bicyclic stannane shown in Scheme 24 with methyllithium gave the fused ring product shown, formed by tandem cyclization and alkoxide elimination (Scheme 24).[116]

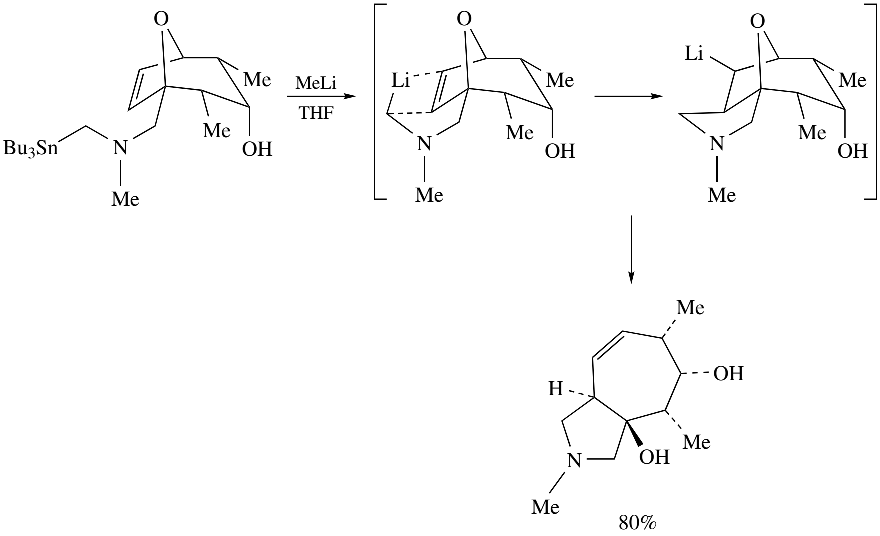

SCHEME 24

Recently, some examples of the dearomatizing cyclization of unstabilized α-amino-organolithium compounds have been reported. For example, Clayden and Kenworthy showed that cyclization onto an oxazoline-activated naphthalene ring gives a lithium azaenolate. Note the high diastereoselectivity of the subsequent electrophilic quench, which places the electrophile *cis* to the carbon–carbon bond formed in the cyclization step (Scheme 25).[117]

Vedejs and Little showed that cyclization onto an indole ring can be used in a route to the ring system of the biologically active mitomycin antibiotics (Scheme 26).[118] In this example, the deuterium serves the purpose of a removable blocking group that discourages competitive deprotonation at C-2 of the indole.

III. DIPOLE-STABILIZED α-AMINO-ORGANOLITHIUM COMPOUNDS

α-Amino-organolithium compounds in which the nitrogen atom is part of a functional group such as an amide are said to be dipole-stabilized.[2] The delocalization of the nitrogen atom's lone pair into the amide carbonyl (or similar functional group) gives a dipolar resonance form with a positively charged nitrogen atom adjacent to the carbanionic carbon atom (Figure 7a), hence the term 'dipole-stabilized'. One might infer from this rationale that structural features such as a shortening of the amide carbonyl–nitrogen bond might ensue, but this is not the case, as shown by X-ray crystal structural analysis.[58,119,120] Theoretical[121–124] and chemical studies[63,123] suggest that chelation of the lithium atom (Figure 7b) provides most of the stabilization, as also evidenced by the structural studies.[58,119]

One of the most important features of dipole-stabilized α-amino-organolithium compounds is the fact that the carbon–lithium bond is in the nodal plane of the π orbitals

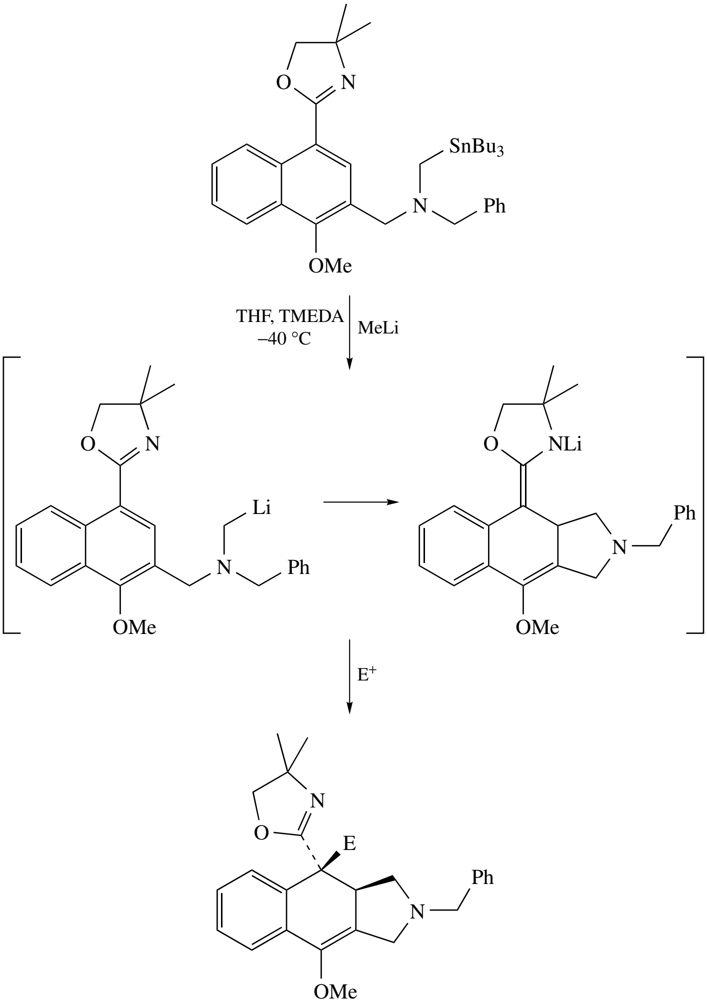

E^+ = allyl bromide, MeI, PhCHO, NH_4Cl
E = $CH_2CH{=}CH_2$, Me, CH(OH)Ph, H
57–80% dr > 96:4

SCHEME 25

of the carbonyl group.[121–125] This preference is observable in substitution reactions of rigid piperidine derivatives and in the X-ray structures mentioned above,[58, 119, 120] and stands in contrast to the lithiation and electrophilic substitution of *N*-nitrosamines. As shown in Scheme 27, nitrosamine **1** is lithiated to give an anion that adds benzaldehyde in the axial position,[126] whereas lithiation of amide **2** and addition of benzaldehyde gives the equatorially substituted product,[121, 127] thereby providing the less stable diastereomer (destabilized due to $A^{1,3}$ allylic strain[128]).

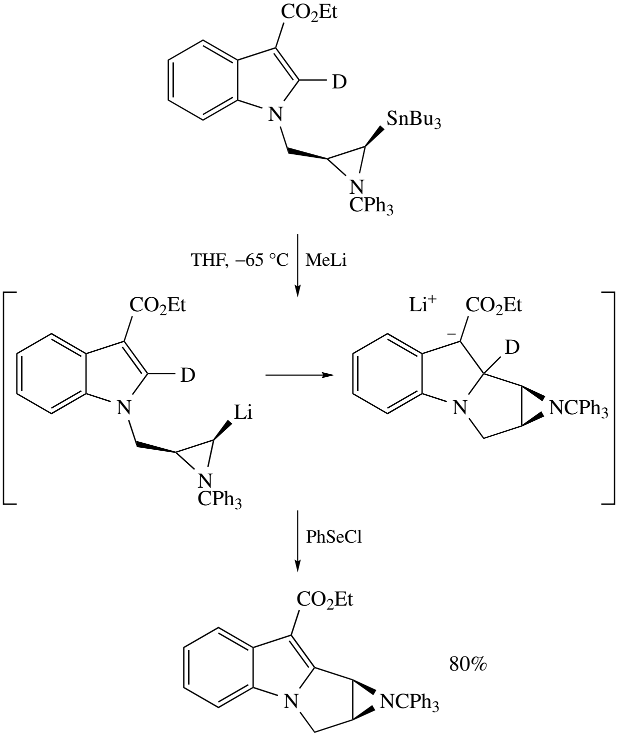

SCHEME 26

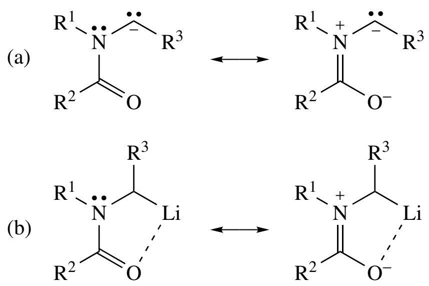

FIGURE 7

A. Deprotonation and Electrophilic Substitution

Removal of a proton α to a nitrogen atom is promoted after derivatization of a secondary amine with an activating group. This group serves two purposes: to deliver the organolithium base to the α-proton by precomplexation with the amide or other directing group,$^{129-135}$ and to stabilize the resultant organolithium by chelation. Electrophilic substitution of dipole-stabilized organolithium compounds with carbonyl electrophiles is

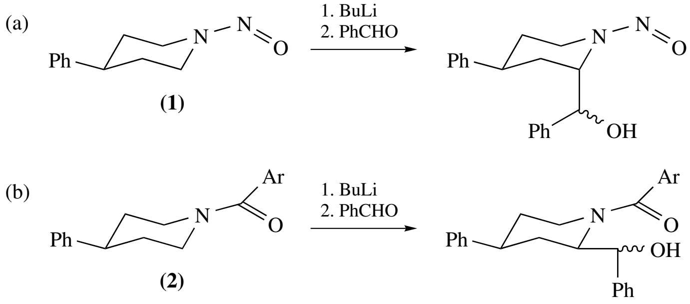

SCHEME 27

efficient, but reaction with most alkyl halides is a poor reaction because of the tendency of the reactants to undergo single electron transfer processes. Transmetalation with copper or palladium salts can afford α-amino-organometallics with considerable utility. Following evaluation of a large number of activating groups, two have emerged as having the greatest utility: amidines and carbamates. The properties of these two activating groups vary in terms of diastereoselectivity when another stereocenter is present.[79, 136, 137] The regiochemistry of deprotonation of carbamates has been examined.[138] After formation of a dipole-stabilized organolithium, transmetalation from lithium to copper affords a reagent that couples with a variety of electrophiles, including allenes, propargyl halides, enones, and aryl and vinyl iodides and triflates.[139–142] The copper reagent is very sensitive to impurities in reagents used in the process.[143, 144] This section describes dipole-stabilized α-amino-organolithium compounds. For such compounds that also have mesomeric stabilization, see Section VI.

Formamidines are made by condensation of a secondary amine, such as pyrrolidine, piperidine or perhydroazepine, with dimethyl *tert*-butylformamidine. The formamidine may be deprotonated using *sec*-butyllithium. Quenching of the organolithium with alkyl halides does not proceed well, affording low yields of coupled products as well as byproducts that suggest radical disproportionation resulting from single electron transfer oxidation of the carbanion by the electrophile. After coupling via the cuprate (Scheme 28), the formamidine may be removed by saponification or hydrazinolysis. This method has been used to alkylate a bridgehead position α to a nitrogen atom.[145]

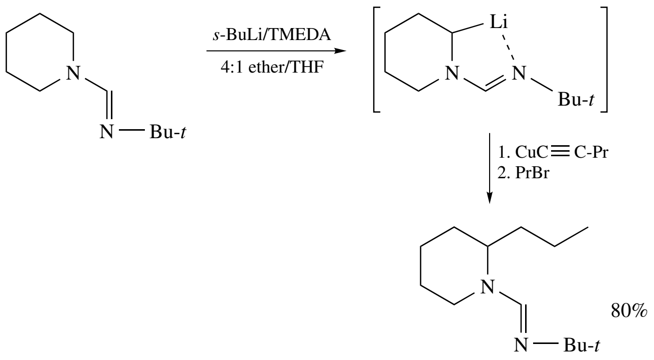

SCHEME 28

A versatile activating group for the removal of α-protons that are not benzylic is the carbamate *tert*-butoxycarbonyl, or *t*-Boc group, developed for this purpose by Beak and Lee in 1989.[78] Its utility derives from the fact that the Boc group is easy to attach to a secondary amine, and easy to remove after a deprotonation/alkylation sequence. Moreover, stannylation affords α-amino-organostannanes that are themselves useful precursors of α-amino-organolithium compounds (Scheme 29) (see Section II). In a chiral pyrrolidine system, it has been shown that both deprotonation (H → Li) and methylation (Li → Me) occur with retention of configuration.[146]

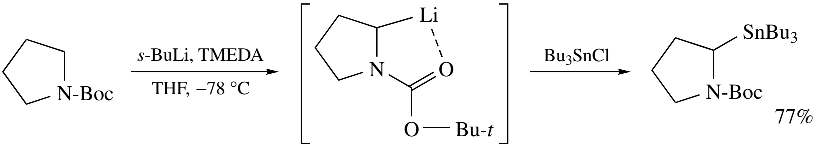

SCHEME 29

The *N*-Boc group also activates secondary acyclic amines toward deprotonation, and unsymmetrical amines may be deprotonated regioselectively in some instances. For example, selective deprotonation of a methyl proton over a methylene can be expected, as shown by the example in Scheme 30a.[147] Similarly, regioselective removal of a cyclopropyl proton occurs in preference to a methylene, as shown in Scheme 30b.[148]

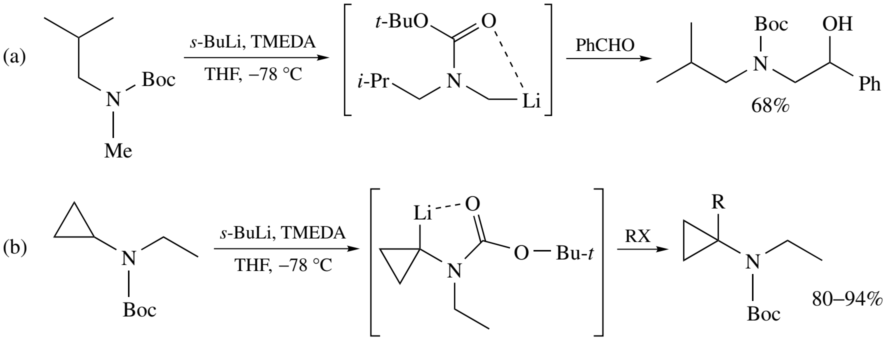

RX = CH_3I, $BrCH_2CH{=}CH_2$, $ClCO_2CH_3$

SCHEME 30

The preferential removal of a cyclopropyl proton via carbamate activation can be used in a tandem lithiation/ring contraction/lithiation/electrophilic substitution sequence, as shown in Scheme 31.[148] There are several interesting and noteworthy features of this sequence. Following the first lithiation, the ring contraction to the cyclopropylpyrrolidine must have occurred with inversion of configuration at the lithiated carbon atom through the transition state shown. In contrast, the intermolecular reaction of lithiated *N*-Boc saturated heterocycles with alkyl halides is a typically low-yielding reaction. It is possible that a preferred mode of alkylation for these organolithium compounds is invertive electrophilic substitution ($S_E2$inv). When inversion is impossible, as it would be in an intermolecular reaction of an alkyl halide with an equatorial carbon−lithium bond, it may be that low yields in intermolecular substitutions are partly due to intervention of other reaction manifolds

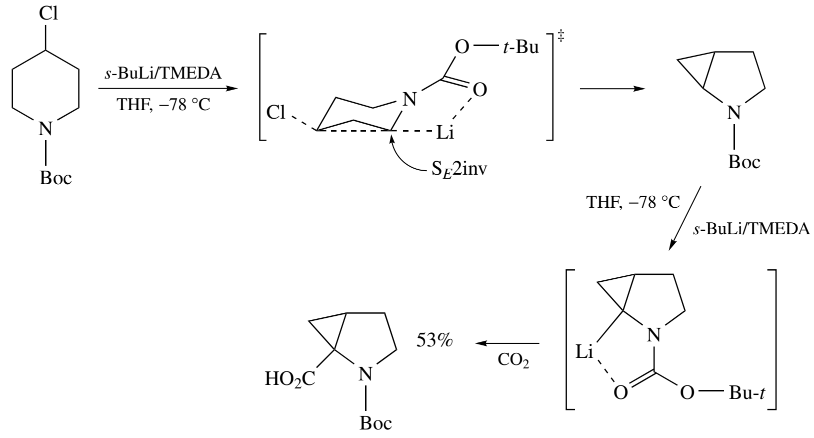

SCHEME 31

such as SET. This is certainly the case in *N*-alkyl α-amino-organolithium compounds (see Section II).[47] The product of ring contraction, the cyclopropylpyrrolidine intermediate, could, in principle, be deprotonated on either the methylene or cyclopropyl methine, but the trend evidenced in the preceding example (Scheme 30b) is followed here.

Use of aryl, vinyl and alkynyl iodides as electrophiles is possible using Pd^0 catalysis.[140] Dieter and Li have evaluated the reaction between *N*-Boc-pyrrolidine and *N*-Boc-piperidine with several aryl and heteroaryl iodides, 1- and 2-iodo-1-hexene, and 1-iodohexyne. The yields range from about 10–80%, with typical yields in the 40–60% range (Scheme 32).

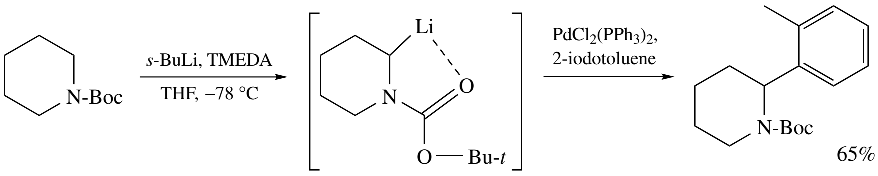

SCHEME 32

B. Asymmetric Deprotonation and Electrophilic Substitution

One of the most important developments in the area of α-amino-organolithium chemistry was Beak and coworkers' discovery,[80, 81] following earlier reports from Hoppe in α-alkoxy systems,[149] that (−)-sparteine mediates the asymmetric deprotonation of *N*-Boc-pyrrolidine (and later indoline[150]) by *s*-BuLi in high enantiomeric purity. The *s*-BuLi is complexed by the (−)-sparteine to make a chiral base[151] that removes one of a pair of enantiotopic hydrogen atoms in a rate-determining lithiation.[132, 134, 135] So far, (−)-sparteine is the only commercially available chiral ligand suitable for this reaction,[152] which incidentally fails to deprotonate *N*-Boc-piperidine as efficiently as pyrrolidine.[153] The intermediate dipole-stabilized organolithium is configurationally stable, and adds to benzophenone with retention of configuration (Scheme 33). O'Brien and coworkers have

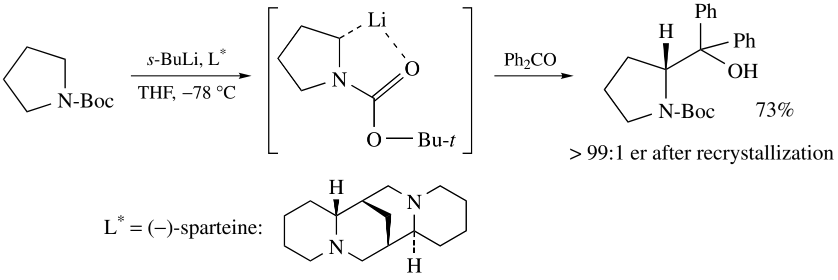

SCHEME 33

reported a new ligand that selectively produces the opposite organolithium enantiomer in this deprotonation.[154]

The small number of electrophiles that react well with *N*-Boc-2-lithiopyrrolidine limits applications of the asymmetric deprotonation of *N*-Boc-pyrrolidine. In a significant development, Dieter and coworkers have shown that transmetalation of the enantioenriched 2-lithiopyrrolidine with CuCN·2LiCl forms a cuprate that reacts enantioselectively with vinyl and allenyl iodides (Scheme 34).[155] Enantioselectivities in the 90–95% range were achieved, although the reaction is very sensitive to reagent purity.[144, 155]

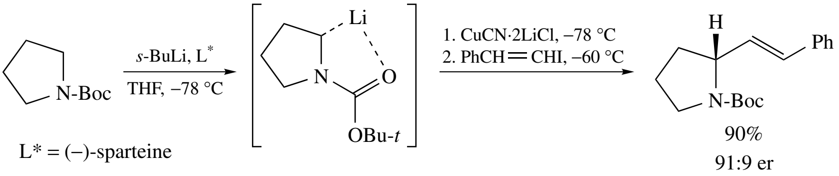

SCHEME 34

Coldham and coworkers have shown that the asymmetric deprotonation protocol can be used to regioselectively alkylate the 5-position of imidazolidines (Scheme 35).[156] The process is used as part of a sequence that results in asymmetric alkylation of 1,2-diamines with high stereoselectivity. The yields are limited, in this case, by the barrier to rotation around the carbamate C−N bond. Thus, only the amide rotamer having the carbonyl group *syn* to C-5 of the heterocycle is deprotonated. There are several examples in this review where this limitation is possible; whether it is a factor or not may depend on the temperature at which amide bond rotation occurs versus the stability of the organolithium compound. In this case, the barrier to amide bond rotation was determined as 16.6 kcal mol^{-1} at 60 °C.

C. Transmetalation and Electrophilic Substitution

As indicated in Section III.B, deprotonation of a carbamate affords a dipole-stabilized α-amino-organolithium that can be transmetalated with copper salts to form cuprates, thereby expanding the versatility of the organolithium. Suitable electrophiles include enones, alkenyl, alkynyl, allenyl and dienyl carboxylic acid derivatives, nitriles and sulfoxides.[141] Dieter and coworkers have shown that the same process can be accomplished via transmetalation of a stannane (Scheme 36).[141, 142, 144] The procedure is particularly

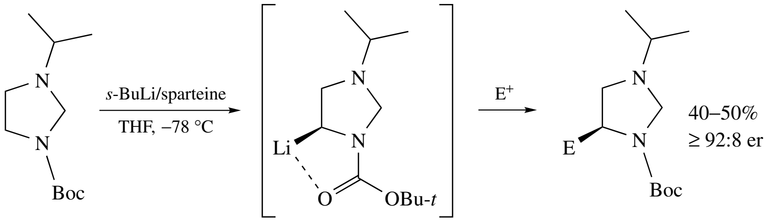

$E^+ = Bu_3SnCl$,
Me_3SiCl, $Ph_2MeSiCl$,
$Ph_2C{=}O$, MeI
$E = Bu_3Sn$, Me_3Si, Ph_2MeSi,
$C(OH)Ph_2$, Me

SCHEME 35

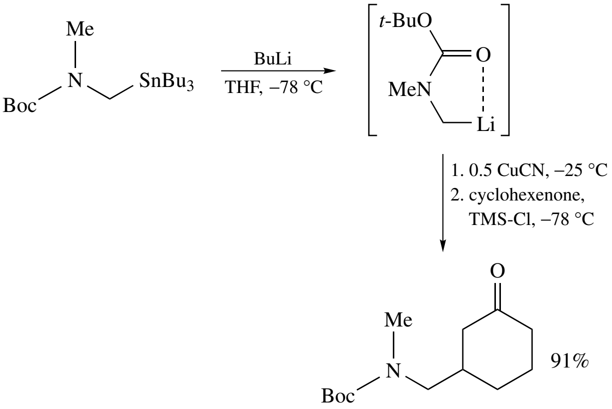

SCHEME 36

useful when direct deprotonation using *s*-BuLi·TMEDA or *s*-BuLi·sparteine gives significantly lower yields.[142]

Scheme 37a illustrates a carbamate substrate that has three possible sites for deprotonation: the benzylic sites α to either nitrogen or oxygen and the methylene attached to nitrogen. Of these three, the site least likely to deprotonate is the latter. Scheme 37b shows that this organolithium, inaccessible by deprotonation, can be made readily by tin–lithium exchange.[157] The derived organolithium compound can be added to electrophiles such as cyclohexanone in good yields.

In 1991, Pearson and coworkers showed that transmetalation of epimeric organostannanes affords a mixture of organolithium compounds that equilibrate, in a few minutes, to the same thermodynamic mixture of organolithium diastereomers (Scheme 38a).[158, 159] In this case, the use of an organostannane serves two purposes. First, it provides access, under mild conditions, to an organolithium that would be difficult to form by deprotonation. Second, since the tin–lithium exchange occurs stereospecifically, and since the same mixture of organolithium epimers is obtained, the steric course is under thermodynamic control. More recently, Nakai and coworkers have shown that a similar organolithium

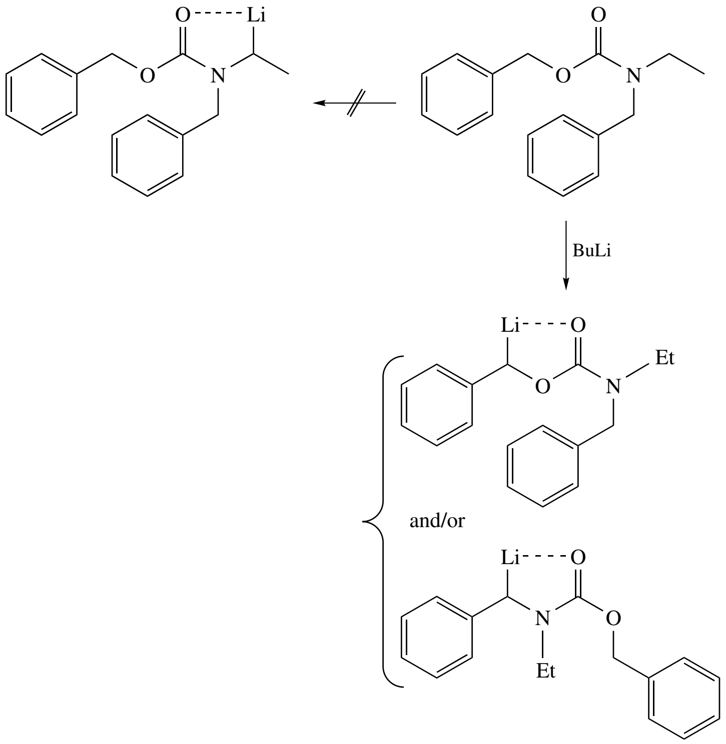

SCHEME 37a

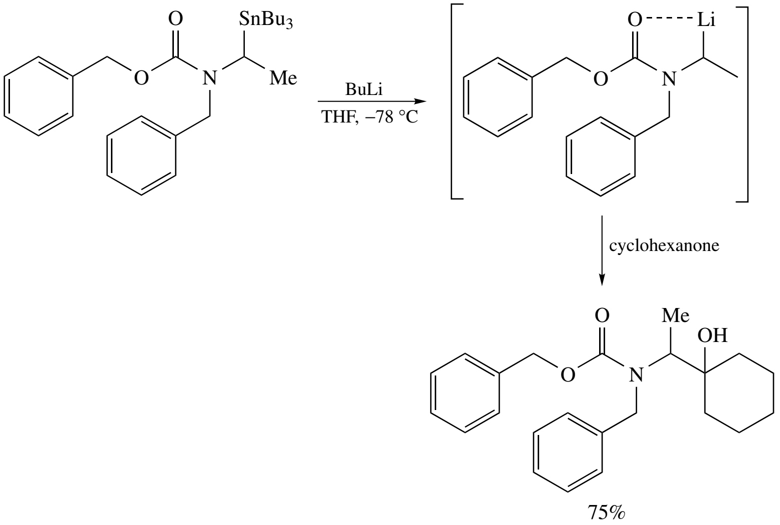

SCHEME 37b

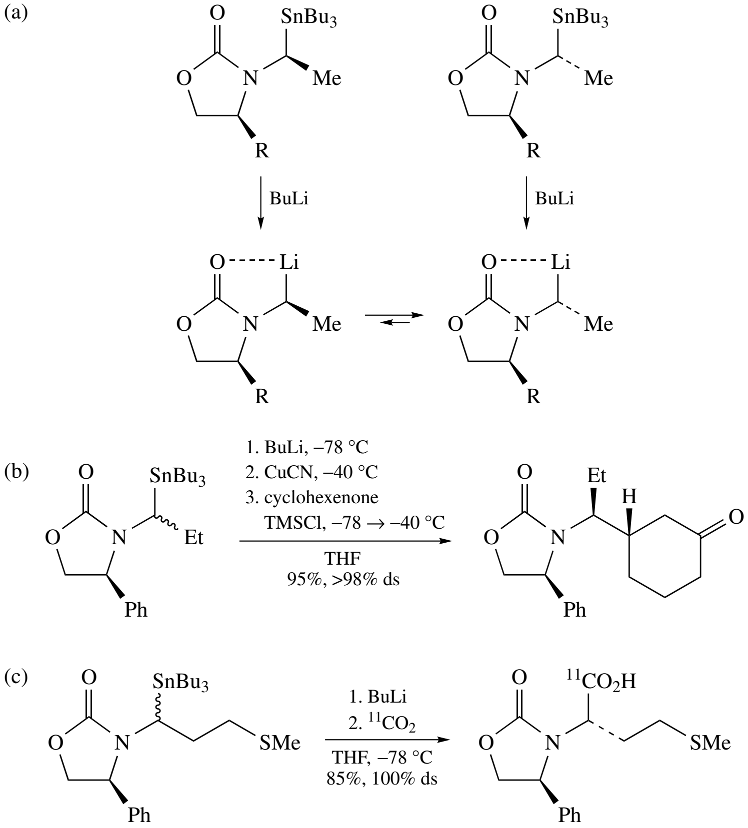

SCHEME 38

compound can be transmetalated to a cuprate that adds with a high degree of stereoselectivity to cyclohexenone (Scheme 38b).[160] An interesting application of this methodology is the synthesis of short-lived ^{11}C isotopes of α-amino acids, as exemplified by the synthesis of methionine, leucine, alanine and homocysteine.[161, 162] The synthesis shown in Scheme 38c can be executed in less than 15 min, and subsequent reductive removal of the oxazolidinone affords L-methionine in 85% yield. The total time for the process, from the stage of bubbling in $^{11}CO_2$, is 35–40 min.

IV. DIPOLE- *AND* HETEROATOM-STABILIZED α-AMINO-ORGANOLITHIUM COMPOUNDS

To provide some subdivision of the large category of dipole-stabilized organolithium compounds, this section deals with those examples in which a second heteroatom (in addition to the *N*-carbonyl group) is present in the substrate.

Katritzky and coworkers showed that the benzotriazole group can be used to activate the α-position toward deprotonation. Treatment of *N*-Boc-*N*-(benzotriazol-1-ylmethyl)-3-chloropropylamine with *n*-butyllithium in toluene at −78 °C gives *N*-Boc-2-benzotriazolylpyrrolidine in reasonable yield (Scheme 39). This is a useful starting material for preparing 2-substituted-*N*-Boc-pyrrolidines by addition of organometallic reagents.[163]

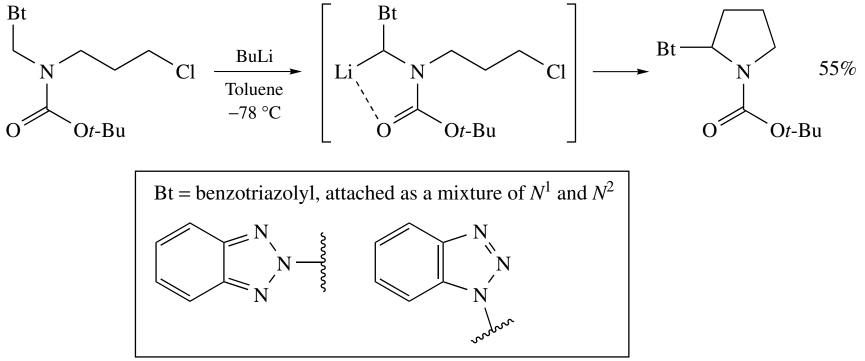

SCHEME 39

Asymmetric deprotonation of the achiral oxazolidine *N*-Boc-4,4-dimethyl-1,3-oxazolidine with *s*-BuLi·(−)-sparteine affords a lithium derivative that adds unselectively to aldehydes. However, the transmetalation from lithium to magnesium, and addition of the resulting Grignard to benzaldehyde occurs with 90% diastereoselectivity and 93% enantioselectivity.[164] The authors speculate that deprotonation and lithiation occur stereoselectively to give the *R* organolithium compound, and subsequent transmetalation and addition to benzaldehyde proceed with retention (Scheme 40).

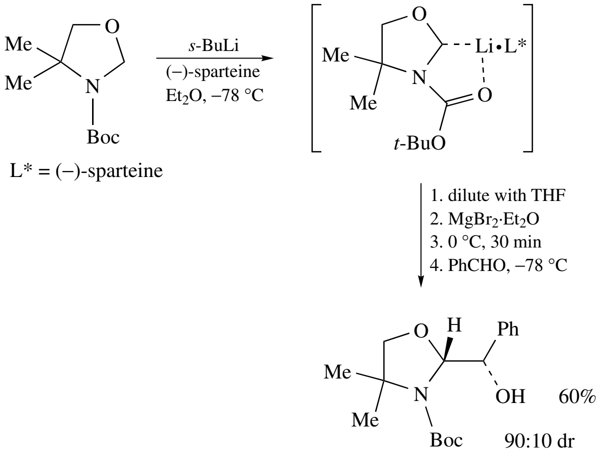

SCHEME 40

Gaul and Seebach showed that lithiated methylthiomethyl-substituted chiral oxazolidinones react with aldehydes, ketones, imines and chalcones (Scheme 41). In this case, the oxazolidinone is derived from diphenylvalinol. The products, with two new asymmetric centers, are formed in good yield and excellent diastereoselectivity.[165] A detailed mechanistic study of this and related systems, using computational methods, IR and NMR spectroscopy, established that the solution structure of the organolithium is as shown.[166] The features influencing this structure include the expected coordination of the lithium atom to the carbonyl oxygen atom, a stereoelectronically enforced antiperiplanar torsion around the Li−C−S−C bond, and the *S* configuration at the lithiated carbon atom so as to orient the SMe away from the isopropyl group. With the configuration of the carbanionic carbon established, it became obvious that the electrophilic substitution had taken place with retention of configuration. The steric course can be rationalized by postulating the complex shown in the inset, in which the carbonyl *Re* face is exposed to the carbanionic carbon.

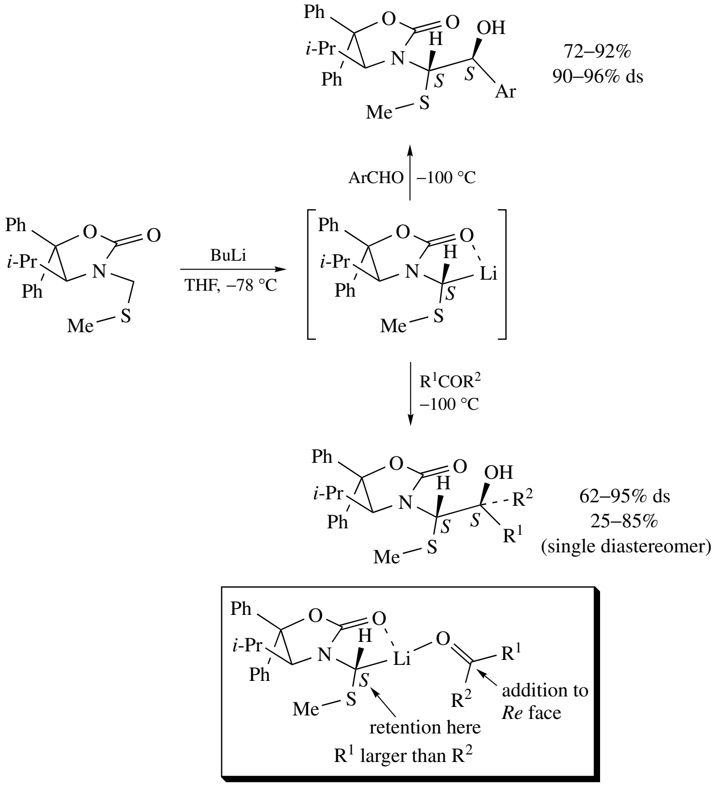

SCHEME 41

The utility of *S*-phenyl camphor-derived oxazolidinones as chiral formyl anion synthons has been demonstrated by Gawley and coworkers (Scheme 42). Deprotonation yields a dipole-stabilized organolithium intermediate and the absolute configuration of the lithium-bearing carbon is presumed to be *R*. Additions to benzaldehyde and cyclohexane carboxaldehyde are 86% and 76% diastereoselective, respectively, but recrystallization affords a single diastereomer in the yields shown. Addition is postulated to proceed via the pre-complex shown in the inset, in which the aldehyde is coordinated to the *R* epimer

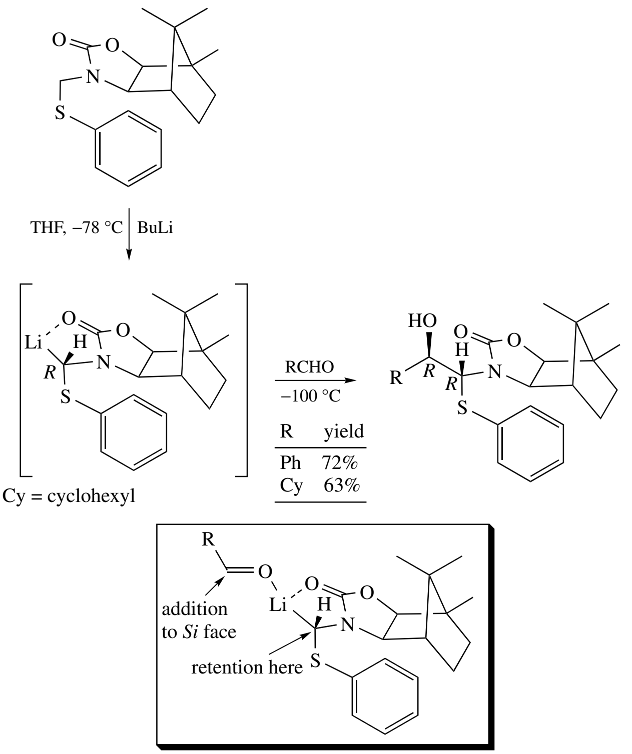

SCHEME 42

of the organolithium, presenting the *Si* face of the aldehyde to the lithiated carbon. These adducts can be hydrolyzed to enantiopure α-hydroxy aldehydes in good yields.[167]

V. MESOMERICALLY STABILIZED α-AMINO-ORGANOLITHIUM COMPOUNDS

Two structural types are covered in this product subclass: lithiated allylic or benzylic amines, and 2-azaallyl anions. Allylic or benzylic amines that are lithiated α to the nitrogen atom enjoy varying degrees of resonance stabilization of the negative charge, and the position of the lithium atom is not always obvious. For example, the solution structure of α-lithio *N*,*N*-dimethylbenzyl amine shows a dynamic equilibrium between η^1 and η^3 bonding, with the position of the equilibrium variable with temperature. At higher temperature, η^3 predominates, but at lower temperature, η^1 predominates.[168] The crystal structure of the same species is a heterochiral dimer with η^1 binding of lithium,[58] but the solid state NMR shows η^3 binding, apparently because it is less soluble and precipitates first.[169] Scheme 43 shows the two structural types, and also illustrates dative bonding from the nitrogen to the lithium atom. Bridging of the lithium atom between the carbon and nitrogen atoms is apparent in the η^1 species in the X-ray structure.[58] The lithiated benzylic amines, which react at the α position, will be arbitrarily drawn as η^1 species, whereas allyl systems will be drawn as delocalized anions having a proximal lithium ion whose position is not specified.

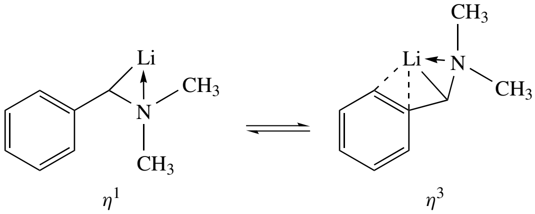

SCHEME 43

If the mesomeric stabilization is provided by a double bond, the lithiated species is a homoenolate synthon, as shown in Scheme 44a. Reaction with an electrophile typically occurs at the γ-position, yielding an enamine, which can then be hydrolyzed to a carbonyl compound. An important application of this approach is to incorporate a chiral auxiliary into the nitrogen substituents so as to effect an asymmetric synthesis.[19] 2-Azaallyl anions (Scheme 44b), which are generated by tin–lithium exchange, can be useful reagents for inter- and intramolecular cycloaddition reactions.[170–172]

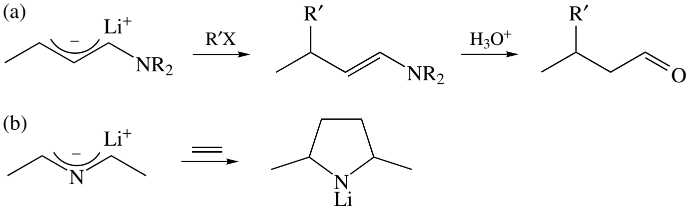

SCHEME 44

A. Deprotonation and Electrophilic Substitution

When the α-amino-organolithium compound is mesomerically stabilized but not dipole-stabilized (contrast with those that are both in Section VI), then the kinetic barrier to deprotonation may limit their synthesis by this method. Deprotonation is only effective if there is stabilization by an aromatic ring in addition to a double bond. Neither a benzene ring alone nor a double bond alone are normally sufficient. Therefore, many applications begin by generating the organolithium by tin–lithium exchange. It is possible to lower the barrier to deprotonation by quaternizing the nitrogen atom by alkylation or by Lewis acid complexation. Deprotonation then gives a nitrogen ylide.

Ahlbrecht and coworkers showed that the stereoselective alkylation of *N*-cinnamyl (*S*)-2-methoxymethylpyrrolidine (*S*MP), followed by hydrolysis, affords enantiomerically enriched 3-substituted phenylpropionaldehydes, as shown in Scheme 45.[173] This method is analogous to the asymmetric alkylation of *S*AMP/*R*AMP hydrazones,[174] as the anions are isoelectronic. The mechanisms of asymmetric induction for the two systems are probably similar. For the lithio cinnamyl amine, methylation can be optimized up to 97.5% ds. Most of the procedures in this paper include potassium *tert*-butoxide, so the cation in these examples may be potassium. Under these conditions, methyl, primary and secondary alkyl iodides typically afford the products with selectivities in the 90–93% ds range.[173]

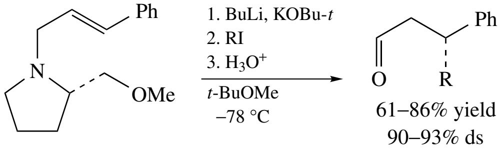

R = Me, Et, Bu, hexyl, allyl *i*-Pr, cyclohexyl

SCHEME 45

B. Transmetalation and Electrophilic Substitution

Ahlbrecht and coworkers showed that tin–lithium exchange can be used to lithiate enamines of 2-methoxymethylpyrrolidine, as shown in Scheme 46. A 50:50 mixture of diastereomers is transmetalated, and the resultant organolithium(s) alkylated to give, after enamine hydrolysis, a $\geqslant$98:2 ratio of ketone enantiomers.[175] In this system, the low barrier to inversion allows equilibration to a single organolithium species, which alkylates by an S_E2inv mechanism.

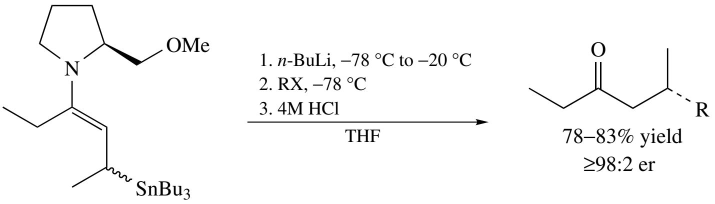

R = Et, Pr, heptyl, allyl, benzyl, *i*-Pr, *t*-Bu, TMS, cyclohexyl

SCHEME 46

C. Transmetalation and Cycloaddition

2-Azaallyl anions are readily available by tin–lithium exchange. Pearson and coworkers have shown that cycloaddition with alkenes and alkynes gives pyrrolidines and pyrrolines in good yield. Intermolecular cycloadditions with unsymmetrical alkenes are not always regioselective, although intramolecular cycloadditions are commonly highly selective. The examples shown in Scheme 47a and 47b show how triarylpyrrolidines can be assembled by this method. The example in Scheme 47c is an interesting example that illustrates the selectivity of an alkene over an alkyne, and that (presumably) steric influences can enhance regioselectivity.[170] Intramolecular variants of this method have been shown to be useful in alkaloid synthesis.[172]

VI. DIPOLE- *AND* MESOMERICALLY STABILIZED α-AMINO-ORGANOLITHIUM COMPOUNDS

A. Deprotonation and Electrophilic Substitution

α-Amino-organolithium compounds that are dipole- and mesomerically stabilized can often be formed readily by proton abstraction with an alkyllithium base. For example, Beak and coworkers showed that *N*-Boc-(3-pyridyl)methyl-4-chlorobutylamine can be converted to *N*-Boc nornicotine (Scheme 48). The benzylic hydrogen atom is deprotonated

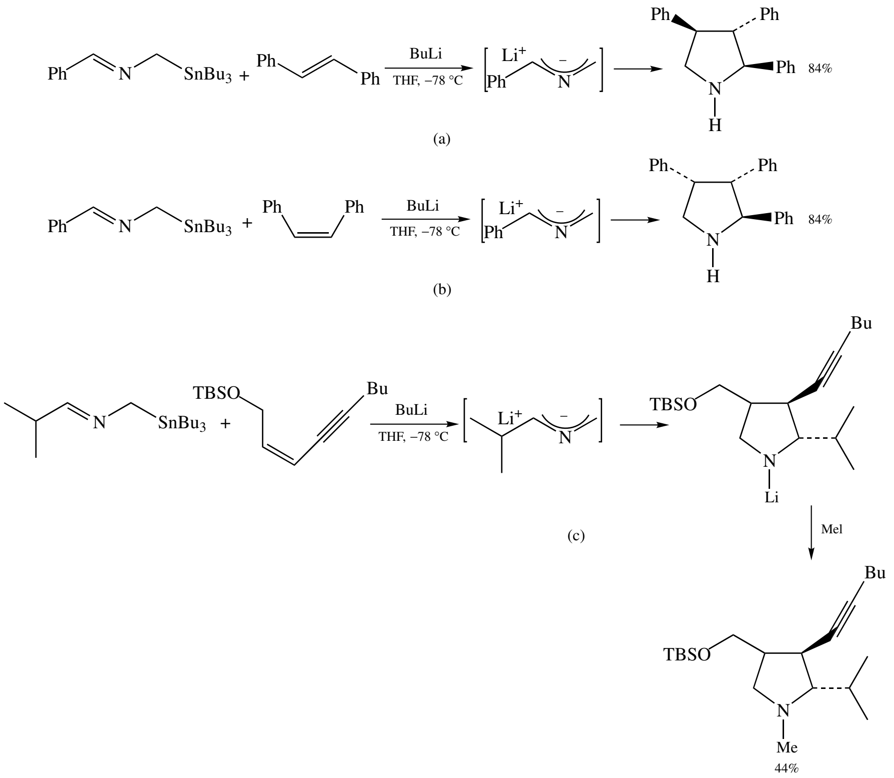

SCHEME 47

selectively and is followed by spontaneous cyclization.[148] Meyers and Marra showed that similar schemes are possible with the formamidine activating group.[176]

Greene and coworkers showed that deprotonation of *N*-Boc-*N*-benzylamine with a threefold excess of *s*-BuLi and twofold excess of TMEDA yields a dilithiated species which adds in a 1,2-fashion to acrolein in 49% yield. The *syn:anti* diastereomer ratio is 86:14 (Scheme 49).[177] The racemic mixture of diastereomers can be protected, oxidized and resolved to yield the enantiomerically pure (⩾99%) acid shown in 46% overall yield. This molecule is a precursor to the side chain of Taxol®.

Resek and Beak showed that addition of lithium dianions of *N*-allyl-*N*-Boc amines to benzaldehyde results in a 50:50 mixture of α- and γ-addition products in 30% overall yield. However, when the dianion is first treated with 1.1 equivalents of $ZnCl_2$, the resulting organozinc reagent reacts with aldehydes and ketones in the α-position regioselectively, with little or no interference from deprotonation (Scheme 50). With aldehydes, diastereoselectivity improves moderately with increasing steric bulk of the aldehyde. The relative configuration was assigned for benzaldehyde, which adds with increased selectivity at lower temperature.[178]

Lithiated tetrahydroisoquinoline pivalamides add to aldehydes with poor diastereoselectivity. However, Seebach and coworkers found that transmetalation to a Grignard

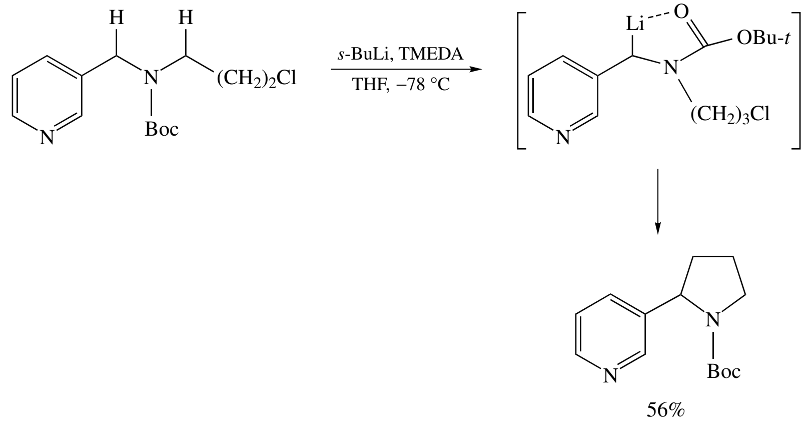

SCHEME 48

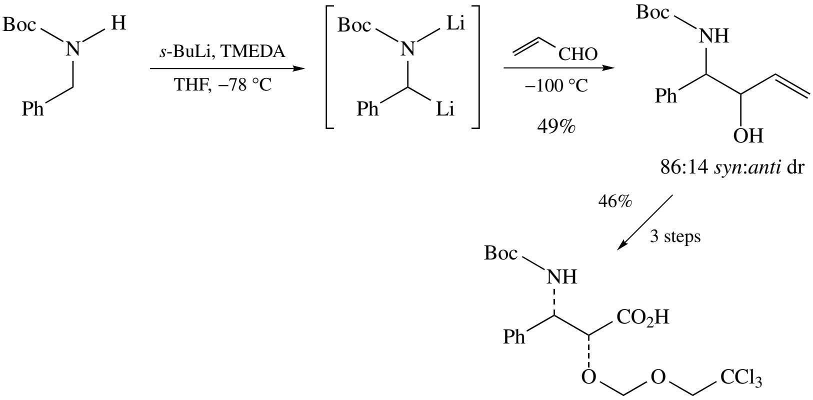

SCHEME 49

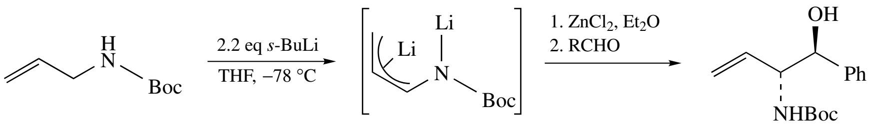

R′	Yield (%)	Temp (°C)	dr
Ph	70	−78	85:15
Ph	77	−98	94:6
Ph	70	−120	97:3

SCHEME 50

reagent with magnesium bromide yields a species that reacts with aldehydes with excellent diastereoselectivity and good yields (Scheme 51). In this way two asymmetric centers are formed selectively and simultaneously. The methodology has been applied to a variety of racemic phthalide alkaloids.[119, 179–181] The reason for the difference in stereoselectivity between the lithium and magnesium compounds appears to be the tendency of the former to undergo single electron transfer reactions.[182]

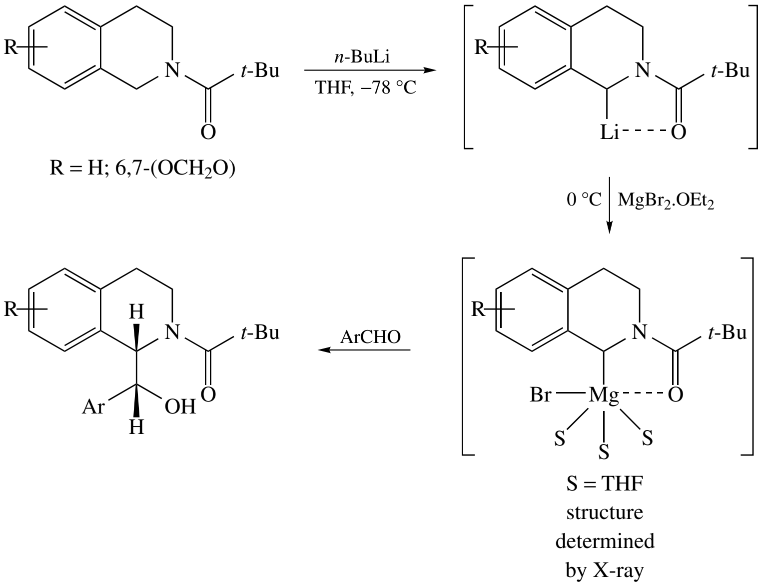

SCHEME 51

The organolithium compounds, formed by deprotonation of *N*-benzylic-*N*-Boc *p*-anisole carbamates, react with imines to yield *trans*-4,5-disubstituted 1,3-imidazolin-2-ones in good yield and excellent stereoselectivity (Scheme 52).[183] Benzaldehydes gave poor stereoselectivity, and the use of imines as electrophiles is critical. The stereoselectivity can be explained by the transition states shown, in which the aryl and R substituents on the 4-membered ring are *trans* to one another.

B. Deprotonation and Rearrangement

Regioselective deprotonation of *N*-benzyl-*N*-Boc-2-(trimethylsilyl)crotylamine occurs at the benzylic position. Anderson and coworkers demonstrated that the resultant organolithium undergoes a highly selective aza-[2,3]-Wittig rearrangement when warmed to −40 °C (Scheme 53).[99] This is an improvement of previous work which used the non-silylated *N*-benzyl-*N*-crotylamine to demonstrate the first exclusively acyclic aza-[2,3]-Wittig rearrangement without evidence of the competitive aza-[1,2]-Wittig rearrangement.[98] The silyl group is thought to activate the rearrangement by stabilizing a build-up of negative charge at C-2 of the allyl group and to provide the steric bulk to favor the orientation in which the TMS is opposite to the phenyl group in the 5-membered transition state.

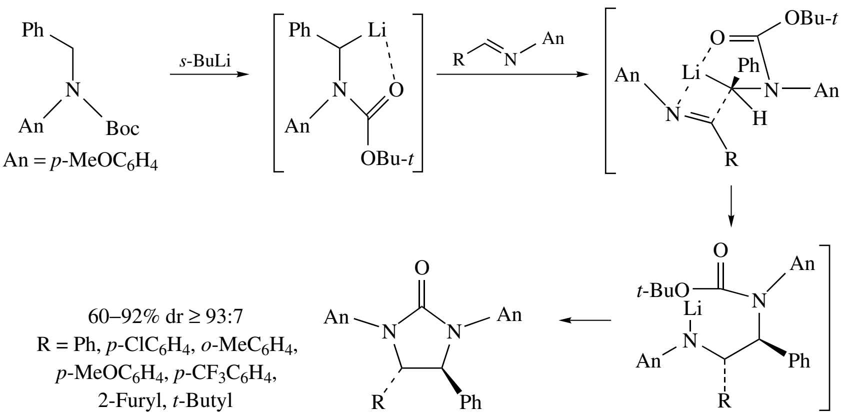

SCHEME 52

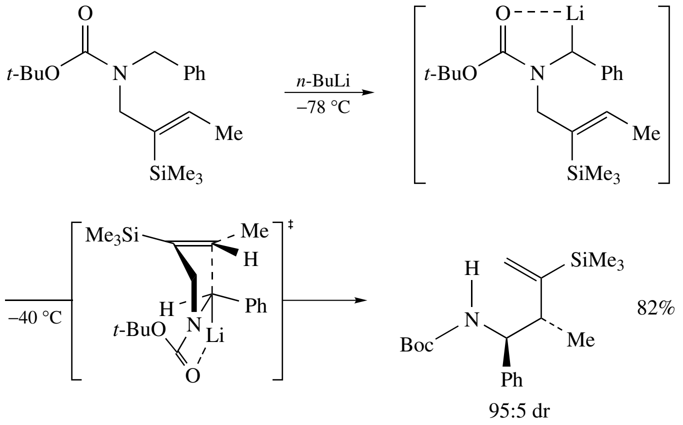

SCHEME 53

C. Deprotonation of Chiral Substrates and Electrophilic Substitution

Alkylation of benzylic amines can be made stereoselective if the benzylic nitrogen atom is incorporated into a chiral oxazoline ring, as shown by Gawley and coworkers and illustrated in Scheme 54. The authors suggested that the proximity of the metalation site to the center of chirality was responsible for the high selectivity. It is likely that the organolithium species is, at least predominantly, the single diastereomer shown, in which the lithium atom is chelated by the carbonyl oxygen atom, and in which the aryl group is oriented away from the isopropyl group. This explanation is consistent with observations made later, in related systems.[159, 166] The initial alkylation products are often crystalline. A 3-step sequence of hydrolysis, oxidative cleavage and hydrolysis liberates the benzylic amines. In some cases, the er of the amine was slightly lower than the dr of the alkylation product, indicating some possible racemization, probably in the oxidative cleavage step.[184]

Deprotonation of chiral formamidines of 6,7-dimethoxy- and 6,7-methylenedioxytetrahydroisoquinolines, followed by alkylation affords 1-substituted tetrahydroisoquinolyl

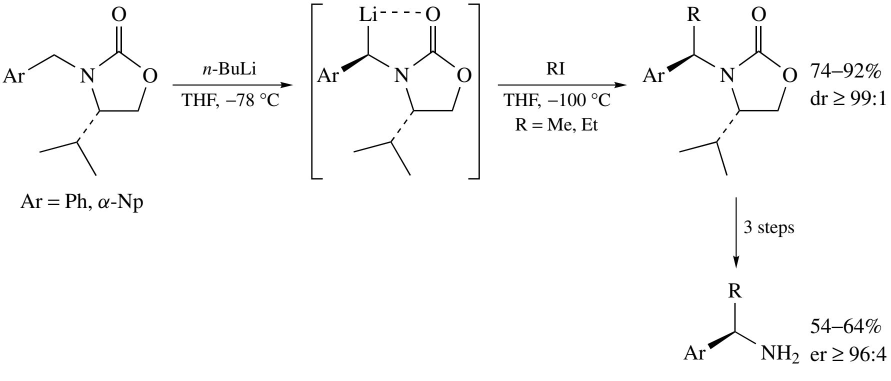

SCHEME 54

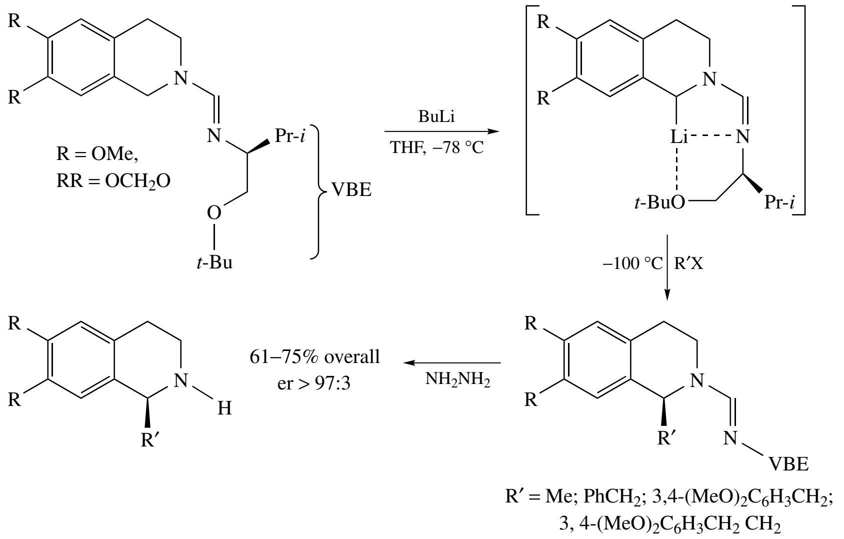

SCHEME 55

formamidines in excellent yield, and ⩾98:2 dr in most cases, as developed in the Meyers group. Hydrazinolysis effects deprotection to yield the 1-substituted tetrahydroisoquinolines in good yield and excellent enantiomeric ratio (Scheme 55).[185, 186] Application of this methodology provides intermediates leading to the alkaloids (−)-norcoralydine and (+)-homolaudanosine, (+)-octeine, (+)-reticulene, (+)-glaucine, (+)-homoglaucine and the protoberberine ring system.[187, 188] The synthesis of the chiral auxiliary and an asymmetric alkylation are *Organic Syntheses* preparations.[189, 190]

Reaction of butyllithium with VBE tetrahydroisoquinolyl formamidine proceeds as shown in Scheme 56.[191] The lack of a kinetic isotope effect in deuteriated substrates revealed that the slow step in the sequence is the complexation of the BuLi with the formamidine, followed by selective removal of the α proton as shown.[191] A rationale for this selectivity is that the butyl group is oriented *trans* to the isopropyl of the 5-membered

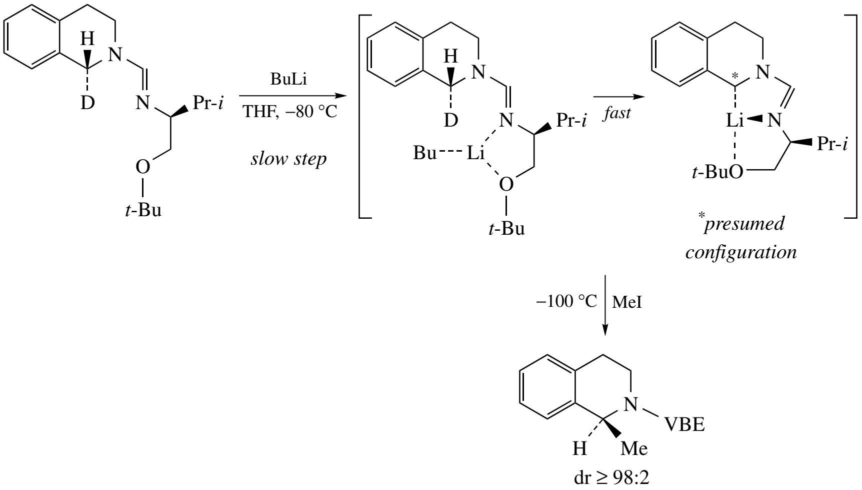

SCHEME 56

chelate ring, placing it proximal to the α hydrogen atom. Although this benzylic anion probably has an inherently low barrier to inversion,[192, 193] it is believed to be configurationally stable, and to have the configuration shown, due to the bias imposed by the chiral auxiliary.[191] Alkylation with methyl iodide gives the configuration shown, which implies invertive alkylation. Interestingly, a second deprotonation and alkylation sequence occurs with overall retention in a deprotonation–electrophilic substitution sequence.[194]

Tetrahydrocarboline formamidines can be deprotonated after the indole nitrogen atom is protected with an appropriate group. Use of methoxymethyl (MEM) worked well and a variety of electrophiles were added to the lithium species in good yield. The MEM and formamidine groups are easily removed.[195, 196] By using the chiral VBE formamidine auxiliary and with the indole nitrogen atom protected, a variety of indole alkaloids can be made in high enantiomeric purity. This is demonstrated for (−)-yohimbone in Scheme 57.[197–199]

Gawley and coworkers showed that oxazolines can be used in place of formamidines for asymmetric alkylations of tetrahydroisoquinolines.[200, 201] A number of substituted oxazolines were evaluated as chiral auxiliaries, and one derived from valinol was found to be optimal.[201] Interestingly, the same enantiomer of valinol[202] affords the opposite enantiomers of the substituted tetrahydroisoquinoline when incorporated into formamidine or oxazoline auxiliaries. An example is shown in Scheme 58, as applied to a synthesis of laudanosine and the morphinan 9-*R*-*O*-methylflavinantine.[203]

The mechanism of this sequence is enlightening when contrasted with the mechanism of the formamidine auxiliary (Scheme 56). Scheme 59a illustrates the results of some deprotonation–alkylation experiments on deuteriated diastereomers.[201, 204] Two features of the product of these experiments were examined: the diastereomer ratio and the percent deuterium incorporation. The deuterium incorporation in the product reveals that there is a preference for removal of the β-proton. When deuterium is in the β-position, this selectivity is opposed by the isotope effect, and the product has about half the original deuterium remaining. When deuterium is in the α-position, the selectivity for the β-proton (imposed by the chiral auxiliary) and the isotope effect act in concert, and virtually all the

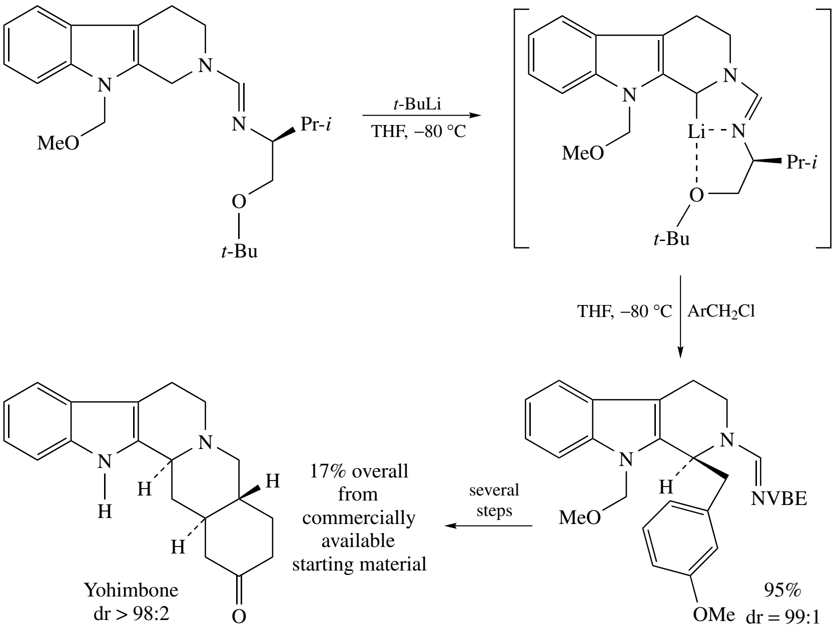

SCHEME 57

deuterium is retained. Interestingly, the diastereoselectivity of the entire sequence is independent of the stereoselectivity of the deprotonation. The rationale for the stereoselective removal of the β-proton is that a prior coordination of the lithium atom to the oxazoline nitrogen atom occurs, with the butyl group oriented *anti* to the isopropyl group, and in the vicinity of the β-proton, as shown in Scheme 59b. NMR studies of the equilibrating organolithium diastereomers placed an upper limit of about 8.2 kcal mol^{-1} on the barrier to inversion.[193] This example shows how the stereoselectivity of each step of a two-step sequence can be deconvoluted to determine the steric course of each. Even though the deprotonation step is stereoselective, it is irrelevant to the steric course of the overall reaction, which is determined by Curtin–Hammett kinetics.

Addition of an aldehyde as the electrophile allows hydroxyalkylation (Scheme 51) of the tetrahydroisoquinoline ring system and this can be rendered enantioselective by using an oxazoline as the chiral auxiliary.[205, 206] Addition of the lithium derivative is stereorandom, producing all four possible stereoisomers via a SET mechanism.[182] However, transmetalation to a magnesium salt allowed the formation of a mixture of only two diastereomers.[193, 205, 207, 208] Zhang and Gawley evaluated a number of oxazoline auxiliaries, and the optimal one, based on a camphor ring system, is illustrated in Scheme 60.[206] This auxiliary affords about 80% diastereoselectivity for a number of examples, and has the advantage that many of the addition products are highly crystalline and can be purifed without chromatography. The effect of temperature on selectivity was evaluated, and it is interesting that the optimal temperature is about −65 °C. Either higher or lower temperatures produced lower selectivities. Dynamic NMR studies of a magnesiated species revealed a dynamic process with a coalescence temperature of −65 °C. Probably, optimal selectivity is achieved at a temperature where the rate of epimerization of the carbanion versus the rate of addition to the carbonyl are best matched.[193] After removal of the chiral

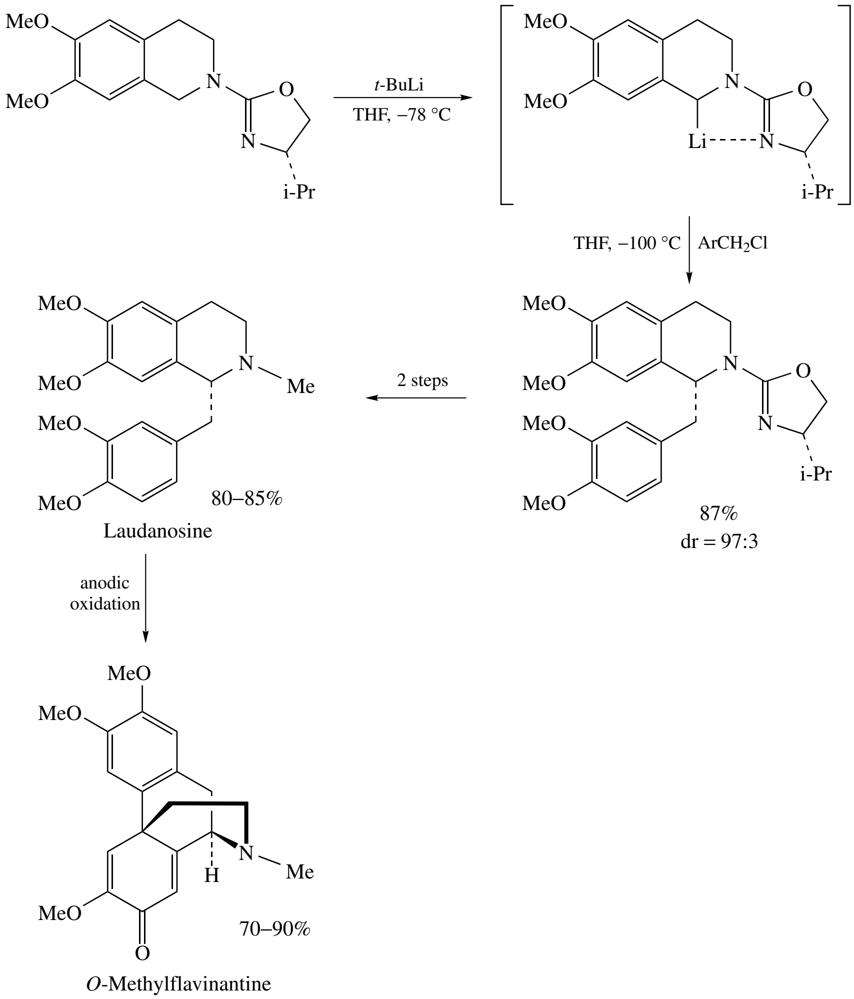

SCHEME 58

auxiliary, the products can be converted to a variety of phthalide isoquinoline alkaloids, such as corlumine.[193, 205, 207]

Isoindole is an interesting precursor for successive alkylations at the α- and α'-positions because both are benzylic. Oxazoline[209] and formamidine[210] auxiliaries have been used to accomplish the α,α'-dialkylation to give a C_2-symmetric amine. The C_2-symmetric amine products are envisioned as possible tools for a variety of asymmetric processes. The diastereoselectivity of the second alkylation is enhanced by the presence of the stereocenter formed in the first alkylation (Scheme 61).[209] Several other electrophiles were evaluated with the formamidine auxiliary.[210]

Another type of C_2-symmetric amine is available by the α,α'-dialkylation of 1,1'-binapazepines. As shown in Scheme 62a, sequential alkylation of a *tert*-butylformamidine

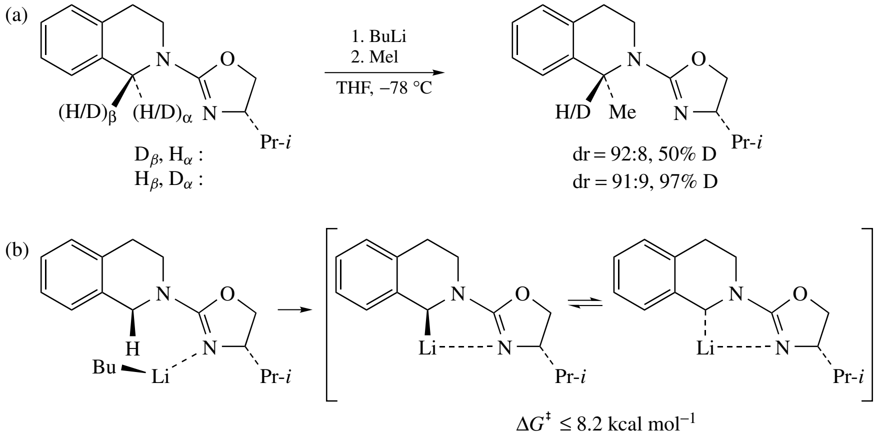

SCHEME 59

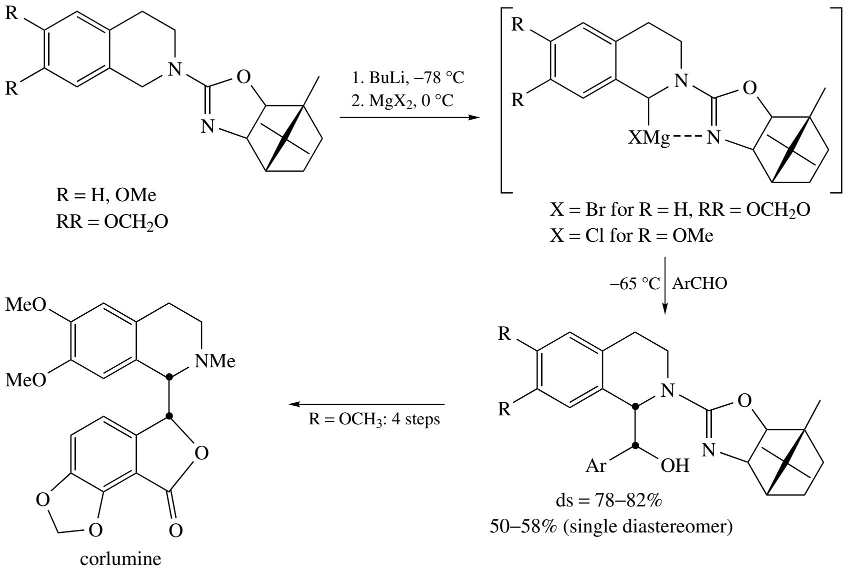

SCHEME 60

gives the *S*,*S*-dimethyl product of the *P*-binapazepine. As shown in Scheme 62b, the *R*,*R*-dimethyl product is available using a chiral formamidine auxiliary (compare Scheme 55).[211]

D. Deprotonation of Achiral Substrates with a Chiral Base and Electrophilic Substitution

As discussed previously, the chiral alkaloid (−)-sparteine (Scheme 33) forms a bidentate complex with compounds such as butyllithium, and this chiral base can distinguish

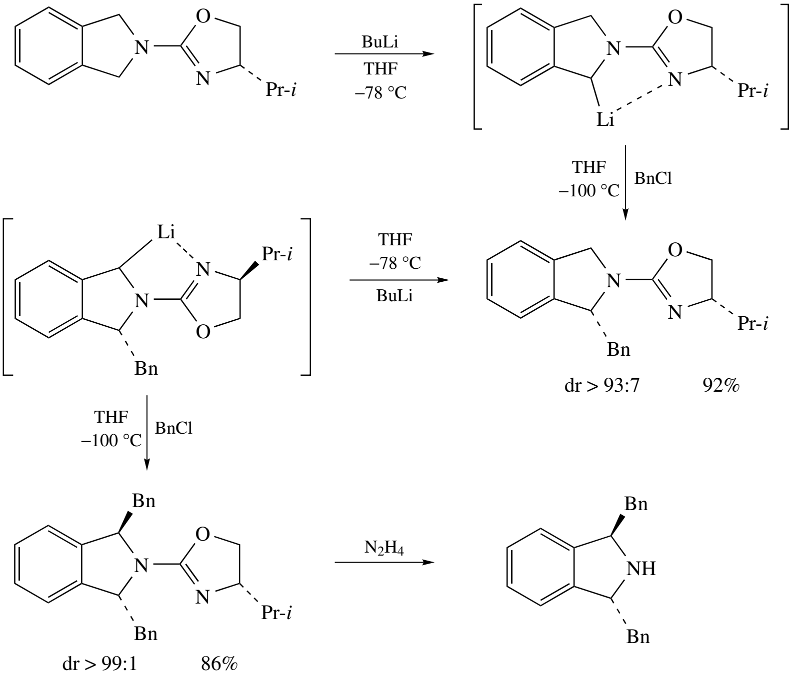

SCHEME 61

enantiotopic protons, as it does in the enantioselective deprotonation of *N*-Boc pyrrolidine to generate a configurationally stable organolithium species. However, because the systems discussed in this section are benzylic or allylic, they are likely to have a low inherent barrier to inversion at the carbanionic carbon. Nevertheless, the (−)-sparteine often remains coordinated to the lithium atom, such that the epimeric carbanions are rendered diastereomeric by the (−)-sparteine. Often, these complexes possess configurational stability due to this diastereomeric bias, either on a laboratory time scale, or in comparison with their rate of reaction. The introduction in Section I discusses the factors that must be considered in evaluating these systems.

The chiral base *s*-BuLi/(−)-sparteine enantioselectively deprotonates the benzylic position of *N*-Boc-3-chloropropyl carbamates, which then cyclize to yield 2-substituted pyrrolidines with enantiomeric ratios greater than 90:10 (Scheme 63).[212] Beak and coworkers showed that enantioselectivity is achieved through an asymmetric deprotonation to give an enantioenriched organolithium intermediate, which undergoes cyclization faster than epimerization.

Beak's group also showed that the chiral base complex *n*-BuLi·(−)-sparteine may be used to lithiate *N*-benzyl-*N*-Boc anisidines. By quenching with an appropriate electrophile, α-, β- and γ-amino acids are available, usually with enantiomeric ratios greater than 90:10.[213] The *p*-methoxyphenyl group can be removed by ceric ammonium nitrate in good yield, to afford the corresponding *N*-Boc amines. The deprotonation is stereoselective and gives the *R* organolithium·(−)-sparteine complex shown in Scheme 64, which is configurationally stable in the presence of the (−)-sparteine ligand. Electrophilic substitution of lithium by carbon dioxide, 4-bromo-2-methyl-2-butene, carbomethoxymethyl

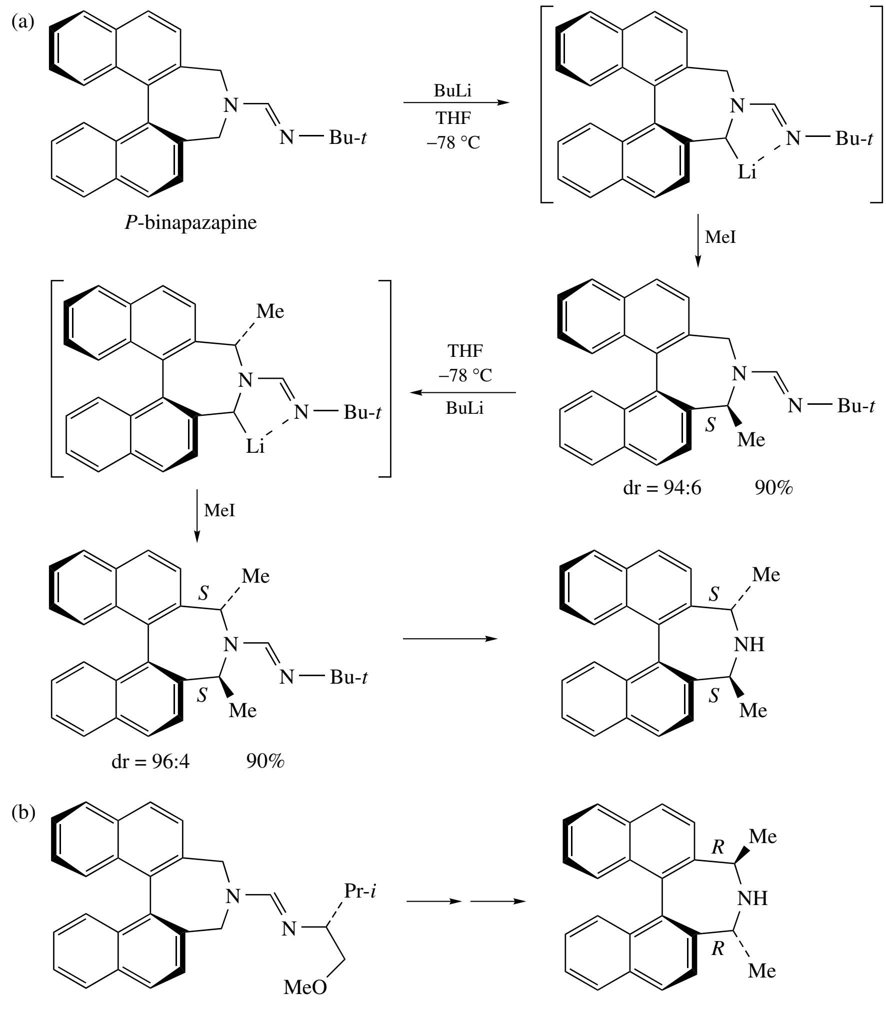

SCHEME 62

trifluoromethanesulfonate, trimethyltin chloride or acrolein (1,4-addition) proceeds with inversion of configuration ($S_E2$inv). In contrast, substitution with methyl chloroformate or methyl bromoacetate proceeds with retention of configuration ($S_E2$ret). Functional group manipulation of the products of electrophilic substitution affords either enantiomer of β-lactams from a single organolithium epimer.[214]

The ligand chosen to complex *n*-BuLi affects not only the configuration of the carbanion but also the regioselectivity of the addition to α,β-unsaturated ketones (Scheme 65). Depending on the chelating diamine, the ratio of 1,2- *vs*. 1,4-addition can range from 95:5 to 6:94. With (−)-sparteine, 1,4-addition to enones predominates when TMSCl is present. Diastereoselectivity in the formation of the two new stereocenters is >99:1, and enantioselectivity is >96%. Subsequent alkylation, in one pot, is also possible.[215]

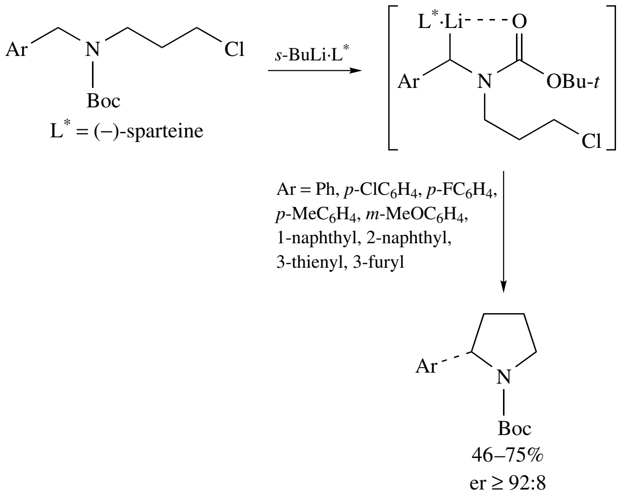

SCHEME 63

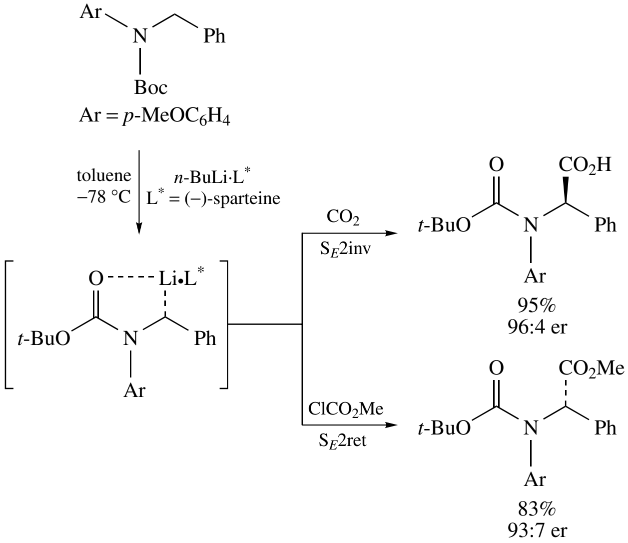

SCHEME 64

Deprotonation of *N*-cinnamyl anisidines gives rise to a η^3 coordinated organolithium compound that has been characterized crystallographically.[216] Taking advantage of the steric course of successive transmetalations (electrophilic substitutions), either of two diastereomeric organolithium complexes can be formed selectively. Thus, direct deprotonation with *n*-BuLi·(−)-sparteine gives the epimer having the *R* configuration at the carbon atom attached to the nitrogen atom. Stannylation of this species occurs with inversion of configuration to afford a mixture of α- and γ-stannanes, both having the

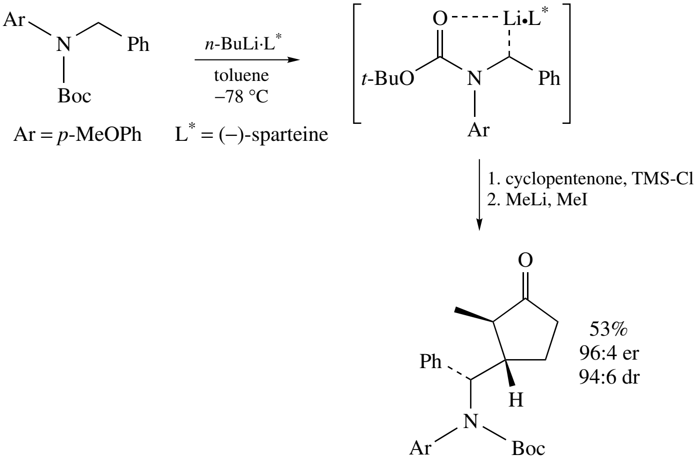

SCHEME 65

S configuration (the original assignment of *R* configurations of these stannanes[217] was subsequently revised[216]). A second metal exchange of the α-amino-organostannane with *n*-BuLi (this time Sn back to Li!) occurs with retention of configuration to give the $S\eta^3$-organolithium compound, as shown in Scheme 66.

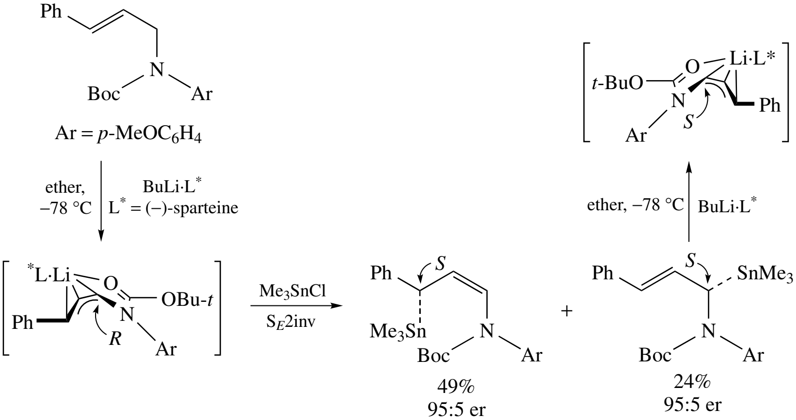

SCHEME 66

The η^3 α-amino-organolithium species shown in Scheme 66 react with several different electrophiles at the γ-position relative to the nitrogen atom. With benzyl bromide, electrophilic substitution is invertive, but with enones and ketones, it is retentive (Scheme 67). Reversal of steric course between CO_2 ($S_E2$inv) and $ClCO_2Me$ ($S_E2$ret) is also observed in this system (compare Scheme 64). Hydrolysis of the enamine products affords β-substituted aldehydes that can be further elaborated.[214, 216, 218]

The aldehyde homoenolate synthons discussed above do not add to aldehydes with a high degree of stereoselectivity. However, transmetalation to aluminum or titanium

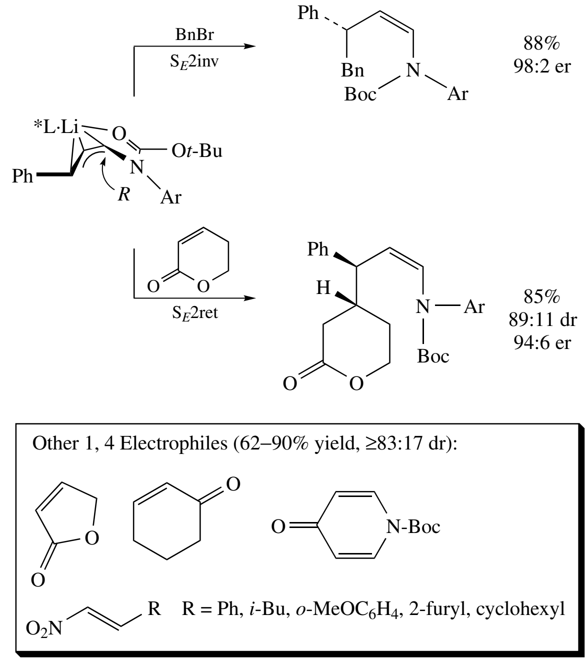

SCHEME 67

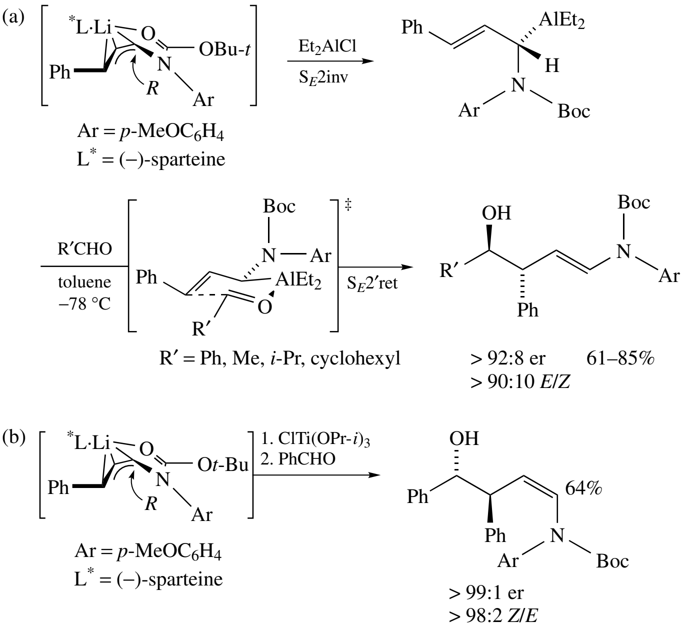

SCHEME 68

complexes provides an entry to *anti* homoaldol products with excellent enantio- and diastereoselectivities (Scheme 68a and b).[219] Beak and coworkers postulate a Zimmerman–Traxler-like transition state to account for the relative configuration of the major product. The E/Z geometric isomers of the product from the aluminum transmetalation sequence have opposite configurations at their two stereocenters. In order to maintain the high enantiomeric purity of the aldehyde hydrolysis product, the E and Z geometric isomers must be separated. Both the absolute configuration and the double bond geometry obtained by transmetalation with $ClTi(OPr\text{-}i)_3$ are opposite to that obtained with Et_2AlCl.

VII. ACKNOWLEDGMENTS

REG is grateful to the National Institutes of Health (GM 56271) and IC is grateful to the EPSRC and the Leverhulme Trust (UK) for financial support of their work in α-amino-organolithium chemistry. We are both grateful to the US National Science Foundation and the Leverhulme Trust (UK) for supporting this collaboration.

VIII. REFERENCES

1. D. J. Peterson, *Organomet. Rev. A*, **7**, 295 (1972).
2. P. Beak and D. B. Reitz, *Chem. Rev*., **78**, 275 (1978).
3. A. Krief, *Tetrahedron*, **36**, 2531 (1980).
4. P. Beak, W. J. Zajdel and D. B. Reitz, *Chem. Rev*., **84**, 471 (1984).
5. A. I. Meyers, *Aldrichimica Acta*, **18**, 59 (1985).
6. R. E. Gawley and K. Rein, in *Comprehensive Organic Synthesis. Selectivity, Strategy, and Efficiency in Modern Organic Chemistry* (Eds. B. M. Trost and I. Fleming), Vol. 1, Pergamon, Oxford, 1991, p. 459.
7. R. E. Gawley and K. Rein, in *Comprehensive Organic Synthesis. Selectivity, Strategy, and Efficiency in Modern Organic Chemistry* (Eds. B. M. Trost and I. Fleming), Vol. 3, Pergamon, Oxford, 1991, p. 65.
8. T. K. Highsmith and A. I. Meyers, in *Advances in Heterocyclic Natural Product Synthesis* (Ed. W. H. Pearson), Vol. 1, JAI, Greenwich, CT, 1991, p. 95.
9. A. I. Meyers, *Tetrahedron*, **48**, 2589 (1992).
10. R. E. Gawley and Q. Zhang, *Tetrahedron*, **50**, 6077 (1994).
11. D. Hoppe, F. Hintze, P. Tebben, M. Paetow, H. Ahrens, J. Schwerdtfeger, P. Sommerfeld, J. Haller, W. Guarnieri, S. Kolczewski, T. Hense and I. Hoppe, *Pure Appl. Chem*., **66**, 1479 (1994).
12. P. Beak, A. Basu, D. J. Gallagher, Y. S. Park and S. Thayumanavan, *Acc. Chem. Res*., **29**, 552 (1996).
13. S. V. Kessar and P. Singh, *Chem. Rev*., **97**, 721 (1997).
14. D. Hoppe and T. Hense, *Angew. Chem., Int. Ed. Engl*., **36**, 2283 (1997).
15. R. E. Gawley, *Curr. Org. Chem*., **1**, 71 (1997).
16. R. E. Gawley, in *Advances in Asymmetric Synthesis* (Ed. A. Hassner), Vol. 3, JAI, Greenwich, CT, 1998, p. 77.
17. A. R. Katritzky and M. Qi, *Tetrahedron*, **54**, 2647 (1998).
18. M. R. Edben and N. S. Simpkins, *Tetrahedron*, **54**, 12923 (1998).
19. H. Ahlbrecht and U. Beyer, *Synthesis*, 365 (1999).
20. A. R. Katritzky, M. Piffl, H. Lang and E. Anders, *Chem. Rev*., **99**, 665 (1999).
21. P. Beak, D. R. Anderson, M. D. Curtis, J. M. Laumer, D. J. Pippel and G. A. Weisenburger, *Acc. Chem. Res*., **33**, 715 (2000).
22. A. Basu and S. Thayumanavan, *Angew. Chem., Int. Ed.*, **41**, 716 (2002).
23. R. E. Gawley, S. O'Connor and R. Klein, in *Science of Synthesis* (Ed. V. Snieckus), Vol. 8, Wiley, Chichester, 2003, in press.
24. S. Caddick and K. Jenkins, *Chem. Soc. Rev*., **25**, 447 (1996).
25. J. I. Seeman, *Chem. Rev*., **83**, 83 (1983).

26. H. B. Kagan and J. C. Fiaud, in *Topics in Stereochemistry* (Eds. E. L. Eliel and S. H. Wilen), Vol. 18, Interscience, New York, 1988, p. 249.
27. R. Noyori, M. Tokunaga and M. Kitamura, *Bull. Chem. Soc. Jpn*., **68**, 36 (1995).
28. R. S. Ward, *Tetrahedron: Asymmetry*, **6**, 1475 (1995).
29. M. M. Harris, in *Progress in Stereochemistry* (Eds. W. Klyne and P. B. D. de la Mare), Butterworths, London, 1958, p. 157.
30. J. Jacques, A. Colbert and S. H. Wilen, *Enantiomers, Racemates and Resolutions*, Wiley-Interscience, New York, 1981.
31. R. G. Pearson, *Acc. Chem. Res*., **4**, 152 (1971).
32. D. A. Slack and M. C. Baird, *J. Am. Chem. Soc*., **98**, 5539 (1976).
33. R. E. Gawley, *Tetrahedron Lett*., **40**, 4297 (1999).
34. R. E. Gawley, E. Low, Q. Zhang and R. Harris, *J. Am. Chem. Soc*., **122**, 3344 (2000).
35. D. J. Peterson and H. R. Hays, *J. Org. Chem*., **30**, 1939 (1965).
36. A. R. Lepley and W. A. Khan, *J. Org. Chem*., **31**, 2061 (1966).
37. D. J. Peterson, *J. Organomet. Chem*., **21**, P63 (1970).
38. D. J. Peterson, *J. Am. Chem. Soc*., **93**, 4027 (1971).
39. D. J. Peterson and J. F. Ward, *J. Organomet. Chem*., **66**, 209 (1974).
40. C. A. Broka and T. Shen, *J. Am. Chem. Soc*., **111**, 2981 (1989).
41. T. Tsunoda, K. Fujiwara, Y. Yamamoto and S. Itô, *Tetrahedron Lett*., **32**, 1975 (1991).
42. I. Coldham, S. Holman and M. S. Lang-Anderson, *J. Chem. Soc., Perkin Trans. 1*, 1481 (1997).
43. I. Coldham, R. Hufton and R. E. Rathmell, *Tetrahedron Lett*., **38**, 7617 (1997).
44. R. E. Gawley and Q. Zhang, *J. Am. Chem. Soc*., **115**, 7515 (1993).
45. R. E. Gawley and Q. Zhang, *J. Org. Chem*., **60**, 5763 (1995).
46. R. E. Gawley, E. Low and G. Chambournier, *Org. Lett*., **1**, 653 (1999).
47. G. Chambournier and R. E. Gawley, *Org. Lett*., **2**, 1561 (2000).
48. A. F. Burchat, J. M. Chong and S. B. Park, *Tetrahedron Lett*., **34**, 51 (1993).
49. R. E. Gawley, J. D. Evanseck, W. H. Pearson and E. P. Stevens, in *ECHET96. Electronic Conference on Heterocyclic Chemistry* (Eds. H. Rzepa and J. Snyder), Royal Society of Chemistry, London, 1997 (CD-ROM), www.ch.ic.ac.uk/ectoc/echet96.
50. L. Colombo, M. Di Giacomo, G. Brusotti and G. Delogu, *Tetrahedron Lett*., **35**, 2063 (1994).
51. L. Colombo, M. Di Giacomo, G. Brusotti and E. Milano, *Tetrahedron Lett*., **36**, 2863 (1995).
52. R. E. Gawley, Q. Zhang and S. Campagna, *J. Am. Chem. Soc*., **117**, 11817 (1995).
53. I. Coldham, R. Hufton and D. J. Snowden, *J. Am. Chem. Soc*., **118**, 5322 (1996).
54. H. J. Reich, J. P. Borst, M. B. Coplein and N. H. Phillips, *J. Am. Chem. Soc*., **114**, 6577 (1992).
55. J. S. Sawyer, A. Kucerovy, T. L. Macdonald and G. J. McGarvey, *J. Am. Chem. Soc*., **110**, 842 (1988).
56. E. Vedejs and J. T. Kendall, *J. Am. Chem. Soc*., **119**, 6941 (1997).
57. P. v. R. Schleyer, T. Clark, A. J. Kos, G. W. Spitznagel, C. Rohde, D. Arad, K. N. Houk and N. G. Rondan, *J. Am. Chem. Soc*., **106**, 6467 (1984).
58. G. Boche, M. Marsch, J. Harbach, K. Harms, B. Ledig, F. Schubert, J. C. W. Lohrenz and H. Ahlbrecht, *Chem. Ber*., **126**, 1887 (1993).
59. F. Becke, F. W. Heinemann, T. Rüffer, P. Wiegeleben, R. Boese, D. Bläser and D. Steinborn, *J. Organomet. Chem*., **548**, 205 (1997).
60. C. Bruhn, F. Becke and D. Steinborn, *Organometallics*, **17**, 2124 (1998).
61. E. Low and R. E. Gawley, *J. Am. Chem. Soc*., **122**, 9562 (2000).
62. S. V. Kessar, P. Singh, K. N. Singh and S. K. Singh, *Synlett*, 517 (2001).
63. D. Iula and R. E. Gawley, *J. Org. Chem*., **65**, 6196 (2000).
64. I. Coldham, S. Dufour, T. F. N. Haxell, S. Howard and G. P. Vennall, *Angew. Chem., Int. Ed.*, **41**, 3887 (2002).
65. I. Coldham, J.-C. Fernàndez and D. J. Snowden, *Tetrahedron Lett*., **40**, 1819 (1999).
66. R. E. Gawley and S. Campagna, in *ECHET96. Electronic Conference on Heterocyclic Chemistry* (Eds. H. Rzepa and J. Snyder), Royal Society of Chemistry, London, 1997 (CD-ROM), www.ch.ic.ac.uk/ectoc/echet96.
67. E. Vedejs and W. O. Moss, *J. Am. Chem. Soc*., **115**, 1607 (1993).
68. I. Coldham and G. P. Vennall, *Chem. Commun*., 1569 (2000).
69. H. Ahlbrecht and H. Dollinger, *Tetrahedron Lett*., **25**, 1353 (1984).

70. F. H. Köhler, N. B. Herktorn and J. Blümel, *Chem. Ber*., **120**, 2081 (1987).
71. S. V. Kessar, P. Singh, R. Vohra, N. P. Kaur and K. N. Singh, *J. Chem. Soc., Chem. Commun*., 568 (1991).
72. S. V. Kessar, P. Singh, K. N. Singh and S. K. Singh, *Chem. Commun*., 1927 (1999).
73. C. Strohmann and B. C. Abele, *Angew. Chem., Int. Ed. Engl*., **35**, 2378 (1996).
74. A. R. Katritzky, M. Qi and D. Feng, *J. Org. Chem*., **63**, 6712 (1998).
75. A. R. Katritzky, M. Qi, D. Feng and D. A. Nichols, *J. Org. Chem*., **62**, 4121 (1997).
76. T. Satoh, M. Ozawa, K. Takano, T. Chyouma and A. Okawa, *Tetrahedron*, **56**, 4415 (2000).
77. T. Satoh, M. Ozawa, K. Takano and M. Kudo, *Tetrahedron Lett*., **39**, 2345 (1998).
78. P. Beak and W.-K. Lee, *Tetrahedron Lett*., **30**, 1197 (1989).
79. P. Beak and W. K. Lee, *J. Org. Chem*., **58**, 1109 (1993).
80. S. T. Kerrick and P. Beak, *J. Am. Chem. Soc*., **113**, 9708 (1991).
81. P. Beak, S. T. Kerrick, S. Wu and J. Chu, *J. Am. Chem. Soc*., **116**, 3231 (1994).
82. R. Hoffmann, *Angew. Chem., Int. Ed. Engl*., **18**, 563 (1979).
83. R. K. Hill, in *Asymmetric Synthesis* (Ed. J. D. Morrison), Vol. 3, Academic Press, Orlando, 1984, p. 503.
84. T. Nakai and K. Mikami, *Chem. Rev*., **86**, 885 (1986).
85. K. Mikami and T. Nakai, *Synthesis*, 594 (1991).
86. J. A. Marshall, in *Comprehensive Organic Synthesis. Selectivity, Strategy, and Efficiency in Modern Organic Chemistry* (Eds. B. M. Trost and I. Fleming), Vol. 3, Pergamon, Oxford, 1991, p. 975.
87. R. Brückner, in *Comprehensive Organic Synthesis. Selectivity, Strategy, and Efficiency in Modern Organic Chemistry* (Eds. B. M. Trost and I. Fleming), Pergamon, Oxford, 1991, Vol. 6, p. 873.
88. W. C. Still and A. Mitra, *J. Am. Chem. Soc*., **100**, 1927 (1978).
89. E. J. Verner and T. Cohen, *J. Am. Chem. Soc*., **114**, 375 (1992).
90. R. Hoffmann and R. Brückner, *Angew. Chem., Int. Ed. Engl*., **31**, 647 (1992).
91. K. Tomooka, T. Igarashi, M. Watanabe and T. Nakai, *Tetrahedron Lett*., **33**, 5795 (1992).
92. T. Durst, V. D. Elzen and M. LeBelle, *J. Am. Chem. Soc*., **94**, 9261 (1972).
93. J. Åhman and P. Somfai, *J. Am. Chem. Soc*., **116**, 9781 (1994).
94. J. Åhman and P. Somfai, *Tetrahedron Lett*., **36**, 303 (1995).
95. I. Coldham, A. J. Collis, R. J. Mould and R. E. Rathmell, *J. Chem. Soc., Perkin Trans. 1*, 2739 (1995).
96. J. Åhman, T. Jarevång and P. Somfai, *J. Org. Chem*., **61**, 8148 (1996).
97. I. Coldham, M. L. Middleton and P. L. Taylor, *J. Chem. Soc., Perkin Trans. 1*, 2817 (1998).
98. J. C. Anderson, D. C. Siddons, S. C. Smith and M. E. Swarbrick, *J. Chem. Soc., Chem. Commun*., 1835 (1995).
99. J. C. Anderson, D. C. Siddons, S. C. Smith and M. E. Swarbrick, *J. Org. Chem*., **61**, 4820 (1996).
100. J. C. Anderson, A. Flaherty and M. E. Swarbrick, *J. Org. Chem*., **65**, 9152 (2000).
101. J. C. Anderson, S. C. Smith and M. E. Swarbrick, *J. Chem. Soc., Perkin Trans. 1*, 1517 (1997).
102. I. Coldham, *J. Chem. Soc., Perkin Trans. 1*, 1275 (1993).
103. I. Markó, in *Comprehensive Organic Synthesis. Selectivity, Strategy and Efficiency in Modern Organic Chemistry* (Eds. B. M. Trost and I. Fleming), Vol. 3, Pergamon, Oxford, 1991, p. 913.
104. W. D. Ollis, M. Rey and I. O. Sutherland, *J. Chem. Soc., Perkin Trans. 1*, 1009 (1983).
105. K. Honda, S. Inoue and K. Sato, *J. Am. Chem. Soc*., **112**, 1999 (1990).
106. J. S. Clark and P. B. Hodgson, *Tetrahedron Lett*., **36**, 2519 (1995).
107. E. Vedejs and G. R. Martinez, *J. Am. Chem. Soc*., **101**, 6452 (1979).
108. E. Vedejs, J. P. Hagen, B. L. Roach and K. L. Spear, *J. Org. Chem*., **43**, 1185 (1978).
109. E. Vedejs and N. Lee, *J. Am. Chem. Soc*., **117**, 891 (1995).
110. S. V. Kessar, P. Singh, K. N. Singh, V. K. Kaul and G. Kumar, *Tetrahedron Lett*., **36**, 8481 (1995).
111. M. J. Mealy and W. F. Bailey, *J. Organomet. Chem*., **646**, 59 (2002).
112. I. Coldham and R. Hufton, *Tetrahedron*, **52**, 12541 (1996).
113. I. Coldham, J. Fernandéz, K. N. Price and D. J. Snowden, *J. Org. Chem*., **65**, 3788 (2000).
114. N. J. Ashweek, I. Coldham, D. J. Snowden and G. P. Vennall, *Chem. Eur. J*., **8**, 195 (2002).

115. I. Coldham, M. M. S. Lang-Anderson, R. E. Rathmell and D. J. Snowden, *Tetrahedron Lett*., **38**, 7621 (1997).
116. M. Lautens and S. Kumanovic, *J. Am. Chem. Soc*., **117**, 1954 (1995).
117. J. Clayden and M. N. Kenworthy, *Org. Lett*., **4**, 787 (2002).
118. E. Vedejs and J. Little, *J. Am. Chem. Soc*., **124**, 748 (2002).
119. D. Seebach, J. Hansen, P. Seiler and J. M. Gromek, *J. Organomet. Chem*., **285**, 1 (1985).
120. M. Marsch, K. Harms, O. Zschage, D. Hoppe and G. Boche, *Angew. Chem., Int. Ed. Engl*., **30**, 321 (1991).
121. N. G. Rondan, K. N. Houk, P. Beak, W. J. Zajdel, J. Chandrasekhar and P. v. R. Schleyer, *J. Org. Chem*., **46**, 4108 (1981).
122. R. D. Bach, M. L. Braden and G. J. Wolber, *J. Org. Chem*., **48**, 1509 (1983).
123. A. R. Katritzky, R. Murugan, H. Luce, M. Zerner and G. P. Ford, *J. Chem. Soc., Perkin Trans. 2*, 1695 (1987).
124. L. J. Bartolotti and R. E. Gawley, *J. Org. Chem*., **54**, 2980 (1989).
125. K. B. Wiberg and W. F. Bailey, *J. Org. Chem*., **67**, 5365 (2002).
126. R. R. Fraser, T. B. Grindley and S. Passannanti, *Can. J. Chem*., **53**, 2473 (1975).
127. D. Seebach, W. Wykypiel, W. Lubosch and H. O. Kalinowski, *Helv. Chim. Acta*, **61**, 3100 (1978).
128. R. W. Hoffmann, *Chem. Rev*., **89**, 1841 (1989).
129. M. Al-Aseer, P. Beak, D. Hay, D. J. Kempf, S. Mills and S. G. Smith, *J. Am. Chem. Soc*., **105**, 2080 (1983).
130. A. I. Meyers, W. F. Rieker and L. M. Fuentes, *J. Am. Chem. Soc*., **105**, 2082 (1983).
131. P. Beak and A. I. Meyers, *Acc. Chem. Res*., **19**, 356 (1986).
132. D. J. Gallagher and P. Beak, *J. Org. Chem*., **60**, 7092 (1995).
133. D. J. Pippel, G. A. Weisenburger, N. C. Faibish and P. Beak, *J. Am. Chem. Soc*., **123**, 4919 (2001).
134. K. B. Wiberg and W. F. Bailey, *Angew. Chem., Int. Ed.*, **39**, 2127 (2000).
135. K. B. Wiberg and W. F. Bailey, *J. Am. Chem. Soc*., **123**, 8231 (2001).
136. T. T. Shawe and A. I. Meyers, *J. Org. Chem*., **56**, 2751 (1991).
137. A. I. Meyers and G. Milot, *J. Am. Chem. Soc*., **115**, 6652 (1993).
138. K. M. Bertini Gross and P. Beak, *J. Am. Chem. Soc*., **123**, 315 (2001).
139. A. I. Meyers, P. D. Edwards, W. F. Rieker and T. R. Bailey, *J. Am. Chem. Soc*., **106**, 3270 (1984).
140. R. K. Dieter and S. Li, *J. Org. Chem*., **62**, 7726 (1997).
141. R. K. Dieter, K. Lu and S. E. Velu, *J. Org. Chem*., **65**, 8715 (2000).
142. R. K. Dieter, C. W. Alexander and L. E. Nice, *Tetrahedron*, **56**, 2767 (2000).
143. R. K. Dieter, J. W. Dieter, C. W. Alexander and N. S. Bhinderwala, *J. Org. Chem*., **61**, 2930 (1996).
144. R. K. Dieter, C. M. Topping and L. E. Nice, *J. Org. Chem*., **66**, 2302 (2001).
145. J. A. Monn and K. C. Rice, *Tetrahedron Lett*., **30**, 911 (1989).
146. M. E. Kopach and A. I. Meyers, *J. Org. Chem*., **61**, 6764 (1996).
147. V. Snieckus, M. Roger-Evans, P. Beak, W. K. Lee, E. K. Yum and J. Freskos, *Tetrahedron Lett*., **35**, 4067 (1994).
148. P. Beak, S. Wu, E. Kyun Yum and Y. Moo Jun, *J. Org. Chem*., **59**, 276 (1994).
149. D. Hoppe, F. Hintze and P. Tebben, *Angew. Chem., Int. Ed. Engl*., **29**, 1422 (1990).
150. K. M. Bertini Gross, Y. M. Jun and P. Beak, *J. Org. Chem*., **62**, 7679 (1997).
151. D. J. Gallagher, S. T. Kerrick and P. Beak, *J. Am. Chem. Soc*., **114**, 5872 (1992).
152. D. J. Gallagher, S. Wu, N. A. Nikolic and P. Beak, *J. Org. Chem*., **60**, 8148 (1995).
153. W. F. Bailey, P. Beak, S. T. Kerrick, S. Ma and K. B. Wiberg, *J. Am. Chem. Soc*., **124**, 1889 (2002).
154. M. J. Dearden, C. R. Firkin, J.-P. R. Hermet and P. O'Brien, *J. Am. Chem. Soc*., **124**, 11870 (2002).
155. R. K. Dieter, C. M. Topping, K. R. Chandupatla and K. Lu, *J. Am. Chem. Soc*., **123**, 5132 (2001).
156. I. Coldham, R. C. B. Copley, T. F. N. Haxell and S. Howard, *Org. Lett*., **3**, 3799 (2001).
157. W. H. Pearson and A. C. Lindbeck, *J. Org. Chem*., **54**, 5651 (1989).
158. W. H. Pearson, A. C. Lindbeck and J. W. Kampf, *J. Am. Chem. Soc*., **115**, 2622 (1993).
159. W. H. Pearson and A. C. Lindbeck, *J. Am. Chem. Soc*., **113**, 8546 (1991).

160. T. Tomoyasu, K. Tomooka and T. Nakai, *Tetrahedron Lett*., **41**, 345 (2000).
161. F. Jeanjean, G. Fournet, D. Le Bars and J. Goré, *Eur. J. Org. Chem*., 1297 (2000).
162. F. Jeanjean, N. Pérol, J. Goré and G. Fournet, *Tetrahedron Lett*., **38**, 7547 (1997).
163. A. R. Katritzky, Z. Luo and Y. Fang, *Tetrahedron Lett*., **41**, 9691 (2000).
164. N. Kise, T. Urai and J. Yoshida, *Tetrahedron: Asymmetry*, **9**, 3125 (1998).
165. C. Gaul and D. Seebach, *Org. Lett*., **2**, 1501 (2000).
166. C. Gaul, P. I. Arvidsson, W. Bauer, R. E. Gawley and D. Seebach, *Chem. Eur. J*., **7**, 4117 (2001).
167. R. E. Gawley, S. A. Campagna, M. Santiago and T. Ren, *Tetrahedron: Asymmetry*, **13**, 29 (2002).
168. H. Ahlbrecht, J. Harbach, T. Hauck and H.-O. Kalinowski, *Chem. Ber*., **125**, 1753 (1992).
169. H. Ahlbrecht, J. Harbach, H.-O. Kalinowski, A. Lang and G. Maier, *Chem. Ber./Recueil*, **130**, 683 (1997).
170. W. H. Pearson, D. P. Szura and M. J. Postich, *J. Am. Chem. Soc*., **114**, 1329 (1992).
171. W. H. Pearson and E. P. Stevens, *J. Org. Chem*., **63**, 9812 (1998).
172. W. H. Pearson and F. E. Lovering, *J. Org. Chem*., **63**, 3607 (1998).
173. H. Ahlbrecht, D. Enders, L. Santowski and G. Zimmerman, *Chem. Ber*., **122**, 1995 (1989).
174. A. Job, C. F. Janek, W. Bettray, R. Peters and D. Enders, *Tetrahedron*, **58**, 2253 (2002).
175. H. Ahlbrecht, R. Schmidt and U. Beyer, *Eur. J. Org. Chem*., 1371 (1998).
176. A. I. Meyers and J. M. Marra, *Tetrahedron Lett*., **26**, 5863 (1985).
177. A. M. Kanazawa, A. Correa, J.-N. Denis, M.-J. Luche and A. E. Greene, *J. Org. Chem*., **58**, 255 (1993).
178. J. E. Resek and P. Beak, *Tetrahedron Lett*., **34**, 3043 (1993).
179. D. Seebach and M. A. Syfrig, *Angew. Chem., Int. Ed. Engl*., **23**, 248 (1984).
180. D. Seebach, I. M. P. Huber and M. A. Syfrig, *Helv. Chim. Acta*, **70**, 1357 (1987).
181. I. M. P. Huber and D. Seebach, *Helv. Chim. Acta*, **70**, 1944 (1987).
182. K. S. Rein, Z.-H. Chen, P. T. Perumal, L. Echegoyen and R. E. Gawley, *Tetrahedron Lett*., **32**, 1941 (1991).
183. N. Kise, K. Kashiwagi, M. Watanabe and J.-I. Yoshida, *J. Org. Chem*., **61**, 428 (1996).
184. R. E. Gawley, K. Rein and S. Chemburkar, *J. Org. Chem*., **54**, 3002 (1989).
185. A. I. Meyers, M. Boes and D. A. Dickman, *Angew. Chem., Int. Ed. Engl*., **23**, 458 (1984).
186. A. I. Meyers, D. A. Dickman and M. Boes, *Tetrahedron*, **43**, 5095 (1987).
187. A. I. Meyers and J. Guiles, *Heterocycles*, **28**, 295 (1989).
188. M. A. Matulenko and A. I. Meyers, *J. Org. Chem*., **61**, 573 (1996).
189. A. I. Meyers, M. Boes and D. A. Dickman, *Organic Syntheses*, **Coll. Vol. VIII**, 573 (1993).
190. D. A. Dickman, M. Boes and A. I. Meyers, *Organic Syntheses*, **Coll. Vol. VIII**, 204 (1993).
191. A. I. Meyers and D. A. Dickman, *J. Am. Chem. Soc*., **109**, 1263 (1987).
192. A. I. Meyers, J. Guiles, J. S. Warmus and M. A. Gonzalez, *Tetrahedron Lett*., **32**, 5505 (1991).
193. R. E. Gawley and P. Zhang, *J. Org. Chem*., **61**, 8103 (1996).
194. A. I. Meyers, J. S. Warmus, M. A. Gonzalez, J. Guiles and A. Akahane, *Tetrahedron Lett*., **32**, 5509 (1991).
195. A. I. Meyers and S. Hellring, *J. Org. Chem*., **47**, 2229 (1982).
196. A. I. Meyers and M. F. Loewe, *Tetrahedron Lett*., **25**, 2641 (1984).
197. M. F. Loewe and A. I. Meyers, *Tetrahedron Lett*., **26**, 3291 (1985).
198. A. I. Meyers, T. Sohda and M. F. Loewe, *J. Org. Chem*., **51**, 3108 (1986).
199. A. I. Meyers, D. B. Miller and F. H. White, *J. Am. Chem. Soc*., **110**, 4778 (1988).
200. R. E. Gawley, G. Hart, M. Goicoechea-Pappas and A. L. Smith, *J. Org. Chem*., **51**, 3076 (1986).
201. K. Rein, M. Goicoechea-Pappas, T. V. Anklekar, G. C. Hart, G. A. Smith and R. E. Gawley, *J. Am. Chem. Soc*., **111**, 2211 (1989).
202. D. A. Dickman, A. I. Meyers, G. A. Smith and R. E. Gawley, *Organic Syntheses*, **Coll. Vol. VII**, 530 (1990).
203. R. E. Gawley and G. A. Smith, *Tetrahedron Lett*., **29**, 301 (1988).
204. R. E. Gawley, *J. Am. Chem. Soc*., **109**, 1265 (1987).
205. K. S. Rein and R. E. Gawley, *Tetrahedron Lett*., **31**, 3711 (1990).
206. P. Zhang and R. E. Gawley, *Tetrahedron Lett*., **33**, 2945 (1992).
207. K. S. Rein and R. E. Gawley, *J. Org. Chem*., **56**, 1564 (1991).

208. K. S. Rein and R. E. Gawley, *J. Org. Chem*., **56**, 839 (1991).
209. R. E. Gawley, S. R. Chemburkar, A. L. Smith and T. V. Anklekar, *J. Org. Chem*., **53**, 5381 (1988).
210. A. I. Meyers and B. Santiago, *Tetrahedron Lett*., **36**, 5877 (1995).
211. A. I. Meyers and T. H. Nguyen, *Tetrahedron Lett*., **36**, 5873 (1995).
212. S. Wu, S. Lee and P. Beak, *J. Am. Chem. Soc*., **118**, 715 (1996).
213. Y. S. Park and P. Beak, *J. Org. Chem*., **62**, 1574 (1997).
214. B. J. Kim, Y. S. Park and P. Beak, *J. Org. Chem*., **64**, 1705 (1999).
215. Y. S. Park, G. A. Weisenburger and P. Beak, *J. Am. Chem. Soc*., **119**, 10537 (1997).
216. D. J. Pippel, G. A. Weisenburger, S. R. Wilson and P. Beak, *Angew. Chem., Int. Ed. Engl*., **37**, 2522 (1998).
217. G. A. Weisenburger and P. Beak, *J. Am. Chem. Soc*., **118**, 12218 (1996).
218. S. H. Kim, M. D. Curtis and P. Beak, *Org. Lett*., **3**, 711 (2001).
219. M. C. Whisler, L. Vaillancourt and P. Beak, *Org. Lett*., **2**, 2655 (2000).

CHAPTER 17

Asymmetric deprotonation with alkyllithium–(−)-sparteine

DIETER HOPPE and GUIDO CHRISTOPH

Organisch-Chemisches Institut der Westfälischen Wilhelms-Universität Münster,
Correnstr. 40, D-48149 Münster, Germany
Fax: +49-251-83-36531; e-mail: dhoppe@uni-muenster.de

The Chemistry of Organolithium Compounds. Edited by Z. Rappoport and I. Marek
ISBN: 0-470-84339-X

I. INTRODUCTION

A. Chiral Organolithium Compounds

1. General features

Highly enantioenriched organolithium compounds were first described in 1980 by Still and Sreekumar. They cleaved the optically active stannane **1** by means of *n*-BuLi and trapped the resulting (*R*)-1-(benzyloxymethoxy)propyllithium (**2**) with dimethyl sulfate to form the benzyloxymethyl (BOM) ether of (*R*)-2-butanol (**3**)[1]. Both reaction steps proceed with strict stereoretention; configurational stability of intermediate **2** was found below $-40\,^\circ$C (equation 1). Configurational stability at low temperatures is a general feature of α-oxy-substituted sp^3-hybridized lithium compounds. According to calculations by von Ragué Schleyer, Houk and coworkers and by Boche and coworkers, these adopt a C-Li-O-bridged structure in the ground state which increases the activation energy of the inversion process[2]. This strategy required the resolution of *rac*-**1**.

A much more efficient procedure consists in the deprotonation of prochiral substrates **4** by chiral base **5** (equation 2). The removal of the enantiotopic protons in **4** proceeds through diastereotopic transition states having different energies $\Delta G^{\neq}$ and thus yielding the diastereomeric carbanions **6** and *epi*-**6** in unequal amounts (equation 2).

Providing the deprotonation reaction is kinetically controlled, meaning the intermediates **6** and *epi*-**6** do not interconvert (path A), the enantiomeric ratio **7**/*epi*-**7** (e.r.) of the trapping products reflects the ratio k_S/k_R. This is exactly true, if the deprotonation is irreversible and if the reactions of both epimers are complete and stereospecific and proceed with identical yields. (−)-Sparteine **11** proved to be a powerful ligand for the chiral modification of lithium bases[3–6]. Unfortunately, configurational stability of lithium carbanions is rarely given. The first recorded attempt was the asymmetric deprotonation of ethylbenzene (**8**), which has been described by Nozaki and coworkers (equation 3)[7].

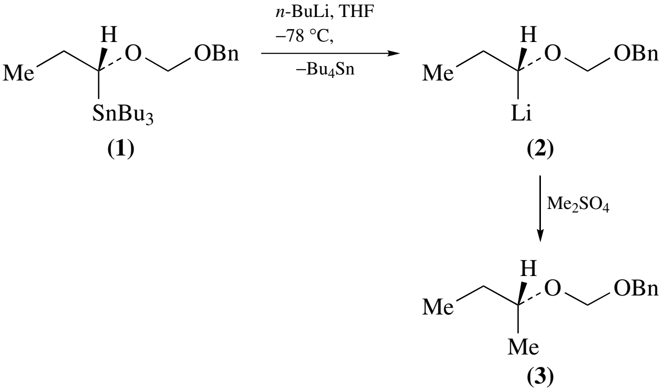

(1)

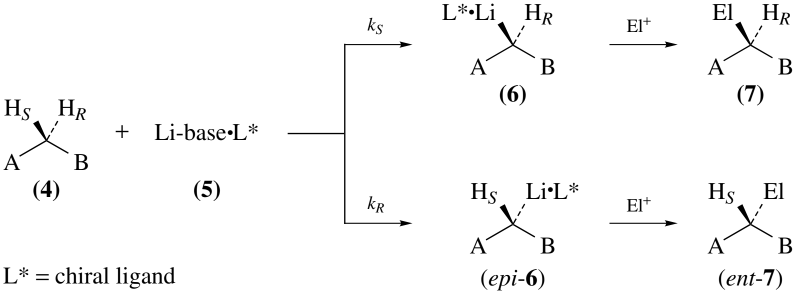

(2)

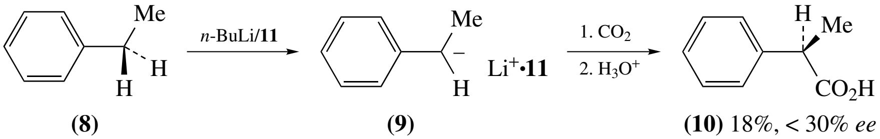

(3)

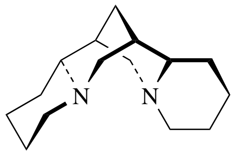

(11)

2-Phenylpropionic acid (**10**) was obtained in low yield and low enantiomeric purity. Although not necessarily detrimental, here configurational instability of the intermediate lithium carbanion pairs **9**/*epi*-**9** is the major reason for the insufficient result. This issue will be examined more closely in Section III.A.

The first successful examples for asymmetric deprotonation by alkyllithium/(−)-sparteine (**11**) utilizing *O*-allyl and *O*-alkyl carbamates were published in 1989–1990 by Hoppe and coworkers[8–10]. Later, in 1991, Kerrick and Beak contributed the application of this method to *N*-Boc-pyrrolidine[11] (Sections II.D.1).

Early investigations on organometallic (−)-sparteine complexes concern the nucleophilic addition of lithium[7], magnesium[12] and zinc complexes[13, 14] onto carbonyl compounds, utilization in polymerization[15, 16] and also NMR spectroscopic investigations[17, 18].

2. Sparteine and analogues

(−)-Sparteine (**11**) is extracted from broom (*Cytisus scoparius*) on a technical scale and supplied as free base or the sulphate pentahydrate[5]. The oily liquid is best stored in the refrigerator in the dark and frequently distilled over calcium hydride before use. Due to the low solubility of the free base and of the sulphate in water, recovery from aqueous suspensions is a facile operation.

The enantiomer (+)-sparteine (*ent*-**11**), although occurring naturally in *Sophora pachycarpa*[19], is not commercially available. It can be prepared in a gram scale from racemic lupanine extracted from cheap bitter lupine seed (from *Lupinus albus*) by resolution with 10-camphorsulphonic acid and subsequent reductive deoxygenation[20]. A multi-step total synthesis of *ent*-**11** has recently been developed by Aubé and coworkers[21]. Most remarkably, compound (+)-**12** serves as a powerful substitute for *ent*-**11**[22]; it is obtained within three steps from (−)-cytisine **13**, extracted from gold rain (*Laburnum anagyroides*) seed[23].

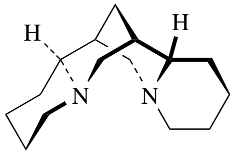

(−)-Sparteine **(11)**

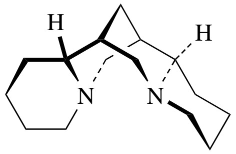

(+)-Sparteine (*ent*-**11**)

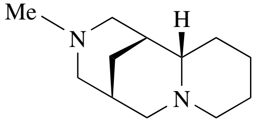

(+)-Sparteine surrogate **(12)**

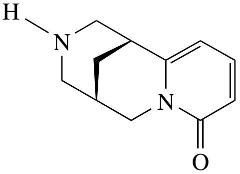

(−)-Cytisine **(13)**

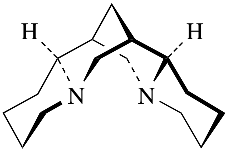

(−)-α-Isosparteine **(14)**

The sparteines are not C_2-symmetric; there is evidence that just this feature seems to be important for their ability to support the deprotonation of very weak carbon acids (see Section II.A.2). (−)-α-Isosparteine (**14**), the C_2-symmetric epimer of **11**, can be prepared by $AlCl_3$-mediated isomerization of **11**[24].

3. General aspects of stereoselection

The simplest case in which the relative rates of deprotonation determine the enantiomeric ratio of product is only given when the intermediate carbanionic species are configurationally stable under the reaction conditions. If the diastereomers **6** and *epi*-**6** interconvert, two borderline situations are possible[25]: when **6** and *epi*-**6** have been allowed to equilibrate and the rates of substitution by the electrophile (El^+) k_1, k_2 are much larger than the rates of epimerization k_{epi}, k_{-epi}, the enantiomeric product ratio **7**/*ent*-**7** is equal to the ratio of intermediates **6**/*epi*-**6** (path B); this situation is often called '*thermodynamic resolution*' (equation 4).

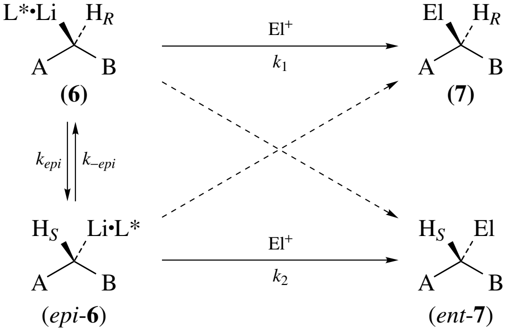

(4)

If k_{epi}, k_{-epi} are much larger than the rates k_1, k_2 of substitution, the enantiomeric ratio **7**/*epi*-**7** is similar to k_1/k_2 (path C, '*dynamic kinetic resolution*')[26]. Both mechanisms are performing when the rates of the two steps are similar. Since rates and equilibrium are temperature-dependent, enhancement of stereoselectivities can be achieved by sophisticated protocols (see Section III.E). The equilibrium **6**/*epi*-**6** is determined by the difference of free energy $\Delta\Delta G$. This effective energy difference is enlarged if it can be coupled with a '*second order transformation*'[27] such as the selective crystallization of one diastereomer ('*dynamic thermodynamic resolution*'). In fact, this applies to the first successful (−)-sparteine-mediated deprotonation[8, 28] (Section IV.C.1).

The direction of stereospecificity[25] depends on the carbanionic species and the electrophile, including its leaving group. sp^3-Hybridized carbanionic centres adjacent to oxy and amino groups, which are not connected to −M substituents, generally add all external electrophiles in a suprafacial manner with retention of configuration. The lithium ion pairs of benzylic, allylic and propargylic carbanions, which are considerably flattened due to resonance, have a high tendency for antarafacial processes, resulting in stereoinversion or *anti*-S_E' substitution. Suprafacial processes are often found for those electrophiles, which strongly interact with the cation in the substitution step (Brønsted acids, aldehydes). A similar pattern is found for chiral α-thioalkyllithium derivatives (Section II.E). Since mesomerically stabilized organolithium compounds more readily form separated ion pairs and thus have a higher tendency to equilibrate, and their stereochemical course of substitution is less predictable, these are treated separately.

II. NON-MESOMERICALLY STABILIZED ORGANOLITHIUM COMPOUNDS

A. Acidification by Dipole Stabilization

Deprotonation is the most convenient manner for the generation of alkyllithium derivatives. However, most of the potential precursors have insufficient acidity. Notable exceptions are those substrates which lead to dipole-stabilized carbanions[29], among them *O*-alkyl *N*,*N*-dialkylcarbamates **15**[10] and *N*-Boc-(cyclo)alkylamines **18**[30] (equation 5). A

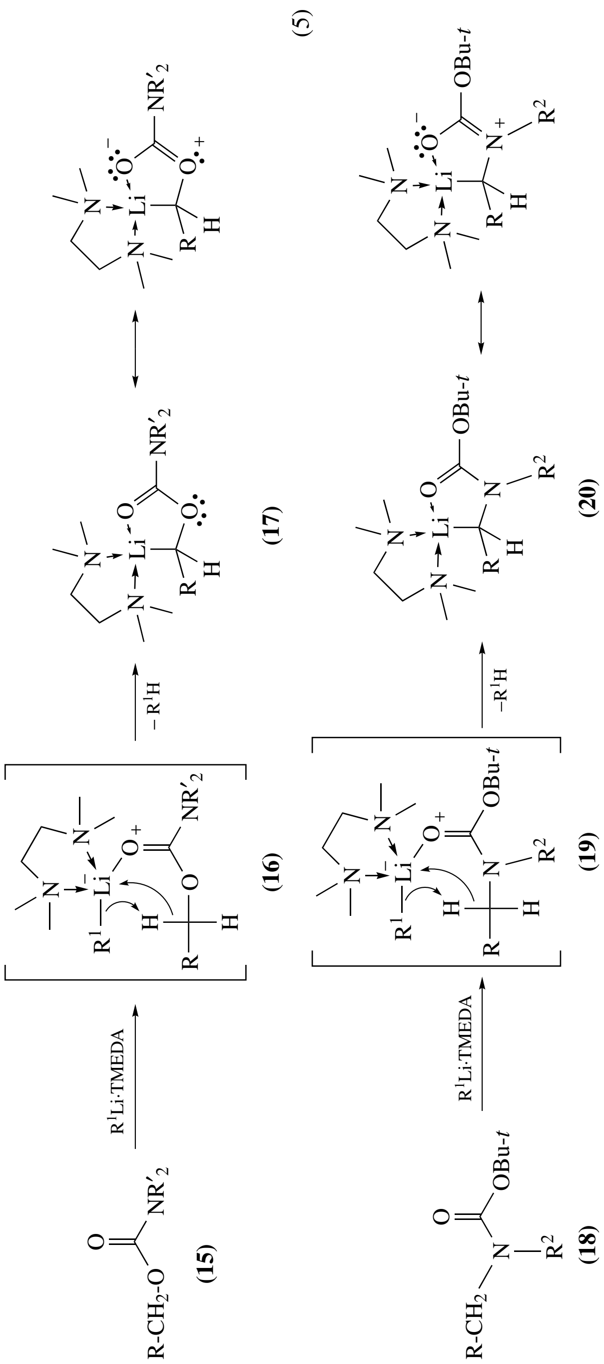

(5)

(15) (16) (17) (18) (19) (20)

rapid deprotonation is achieved by treatment with *s*-BuLi/TMEDA in unpolar solvents such as THF, diethyl ether, toluene or pentane at low temperature.

The chelate formation in lithium complexes **17** or **20** contributes to stabilization. Enhancement of kinetic acidity arises from the formation of pre-complexes **16** and **19**, respectively. Here, already a dipole is induced and, in addition, proton exchange can proceed intramolecularly via a five- or six-membered ring. Despite these favourable features, the acidity of alkyl carbamates **15** is lower than those of the 1-proton in butane: *n*-BuLi does not lead to deprotonation. In order to suppress carbonyl attack, a branched amino residue NR'_2 such as diisopropylamino (in *Cb*) or 2,2,4,4-tetramethyl-1,3-oxazolidin-3-yl (in *Cby*) is essential[31]. A study on the carbenoid nature of compounds **17** was undertaken by Boche and coworkers[32].

B. Asymmetric Deprotonation Adjacent to Oxygen

1. Non-stereogenic alkyl carbamates

The highly ordered transition states of the deprotonation reactions offer a good chance for an efficient differentiation between stereoheterotopic groups in alkyl carbamates by chiral bases[4, 33]. The complex formed from *s*-BuLi/(−)-sparteine (**11**)[34] proved to be the most efficient base for asymmetric deprotonation at −78 °C. With substrates **21**, having no further strongly complexing groups in the vicinity, usually the selection in favour of the *pro-S*-proton in complex **22** to form the epimer **23** is greater than 97:3, and occasionally ratios of 99:1[35, 36] have been recorded (equation 6). **23** does not equilibrate below −40 °C with its diastereomer *epi*-**23** and both can be trapped by electrophiles with strict stereoretention to yield the enantiomeric products **24**/*ent*-**24** with e.r. > 97:3 (> 94% *ee*). Suitable solvents are toluene, diethyl ether or pentane; THF causes displacement of the chiral ligand.

Scheme 1 gives an impression of the scope of the reaction. Short (in **25**) or long (**26, 27**) or α-branched alkyl chains (**28**) do not disturb the selectivity. However, the double-branched *tert*-butyl residue in **29** completely suppresses the (−)-sparteine-mediated deprotonation[37]. Non-conjugated double bonds[38, 39] (**30, 31a**), γ-phenyl[4, 40] (**32a**) or ferrocenyl[41] residues (**34a**) do not give rise to a selectivity change. The strongly directing power of the carbamoyloxy group is best seen in a deprotonation experiment with the 3-(2-methoxyphenyl)propyl carbamate **33a**[4, 42]: Although the compound holds further—in a thermodynamic sense—more acidic positions at the aryl ring and in the benzylic position, it is exclusively deprotonated adjacent to the carbamate group. β- and γ-dibenzylamino groups in compounds **35a**[43–45] or **36a**[46] do not compete severely with sparteine for complexation. The same is true for γ-carbamoyloxy groups in dicarbamates **37a** and **38a**, although these support non-stereoselective deprotonation in the absence of (−)-sparteine or TMEDA[47]. Even remote complexing stereogenic assemblies such as those found in the (*S*)-glutamic acid-derived dicarbamate **40a** do not alter the selectivities of deprotonation[48]. The safest way to protect ω-hydroxyalkyl carbamates is the introduction of the *O*-TBS group, such as in **39a**[49].

Electrophiles, which lead to high yields, are methyl iodide, trialkyltin- and trialkylsilyl chlorides, diphenylphosphinyl chloride, acid chlorides, aldehydes and carbon dioxide. Remarkably, though highly acidic ketones are formed on acylation, no deprotonation or racemization by excess of carbanionic species occurs. Other alkyl halides than methyl iodide react very sluggishly with low yields. Benzylic and allylic halides lead to partial racemization[4], presumably due to single-electron transfer (SET) in the alkylation step. As very recently found by Papillon and Taylor, racemization of **42** can be suppressed by copper–zinc–lithium exchange before alkylation[36] to **43** via the Knochel cuprates (equation 7)[50].

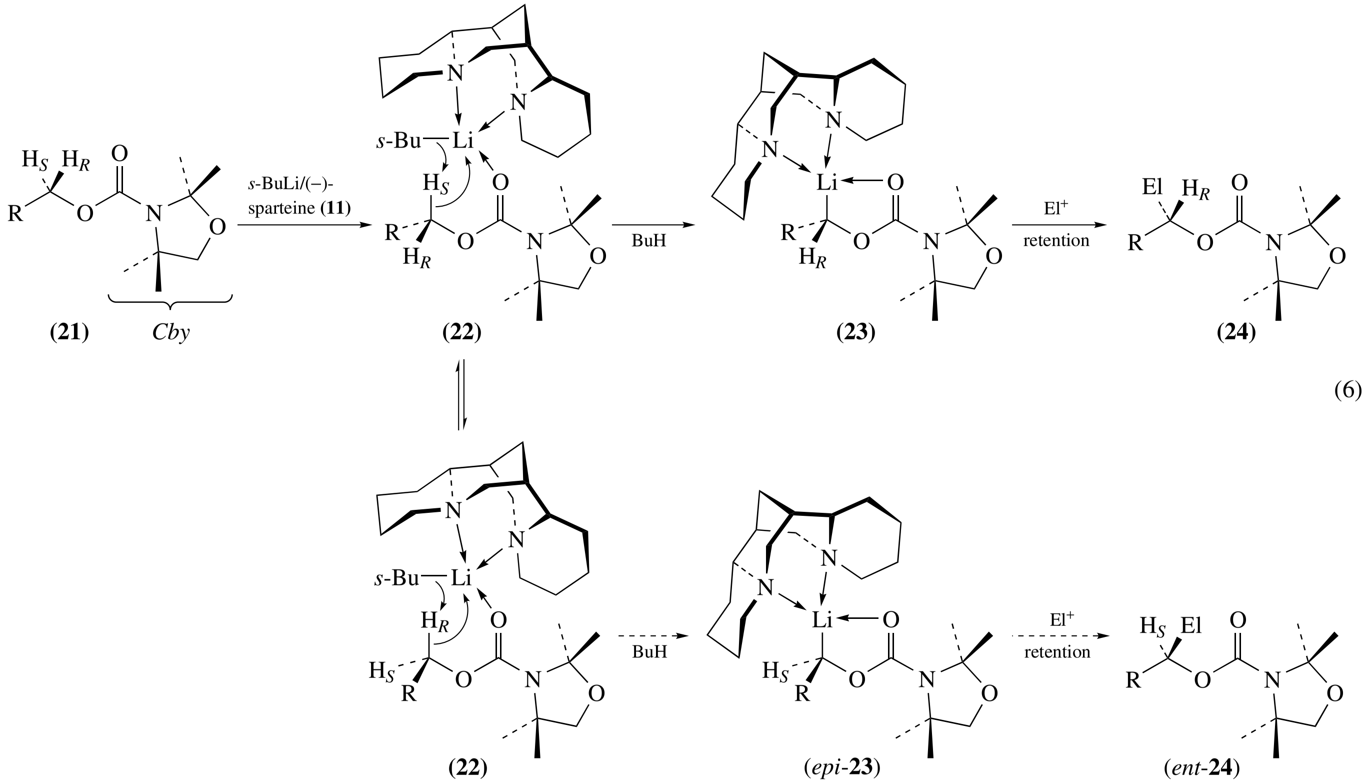
(21)
Cby
s-BuLi/(−)-sparteine (11)
(22)
BuH
(23)
El+
retention
(24)
(22)
BuH
(epi-23)
El+
retention
(ent-24)

(6)

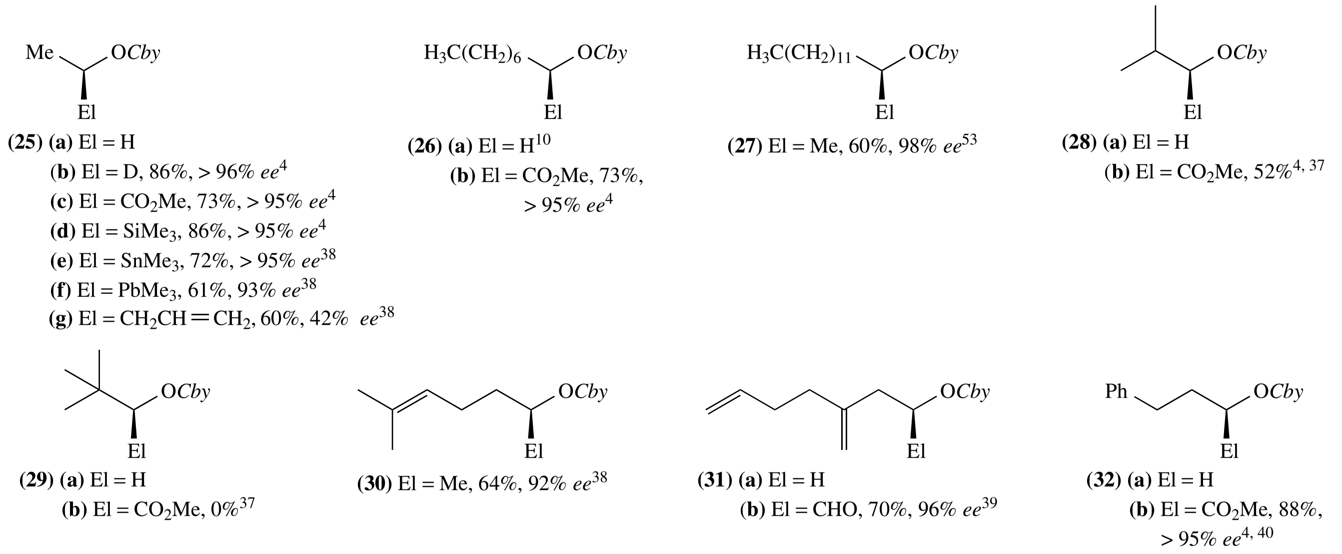

(25) **(a)** El = H
(b) El = D, 86%, > 96% *ee*[4]
(c) El = CO_2Me, 73%, > 95% *ee*[4]
(d) El = $SiMe_3$, 86%, > 95% *ee*[4]
(e) El = $SnMe_3$, 72%, > 95% *ee*[38]
(f) El = $PbMe_3$, 61%, 93% *ee*[38]
(g) El = $CH_2CH{=}CH_2$, 60%, 42% *ee*[38]

(26) **(a)** El = H[10]
(b) El = CO_2Me, 73%, > 95% *ee*[4]

(27) El = Me, 60%, 98% *ee*[53]

(28) **(a)** El = H
(b) El = CO_2Me, 52%[4, 37]

(29) **(a)** El = H
(b) El = CO_2Me, 0%[37]

(30) El = Me, 64%, 92% *ee*[38]

(31) **(a)** El = H
(b) El = CHO, 70%, 96% *ee*[39]

(32) **(a)** El = H
(b) El = CO_2Me, 88%, > 95% *ee*[4, 40]

SCHEME 1

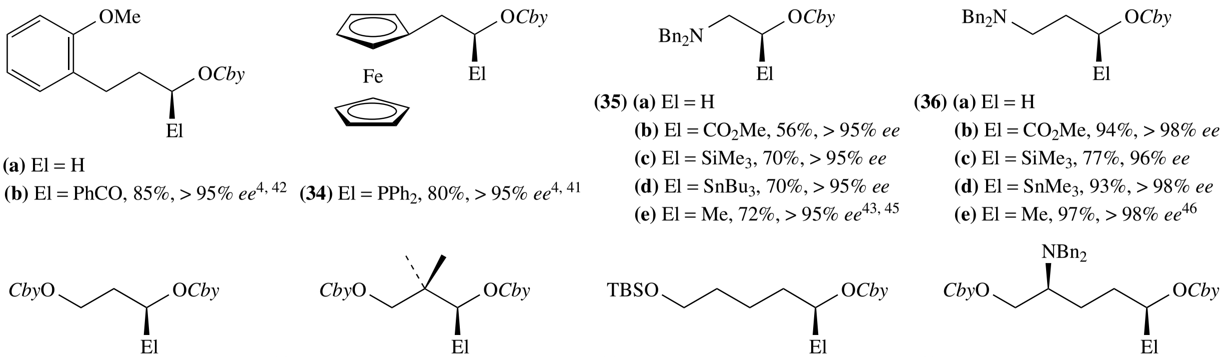

(33) **(a)** El = H
(b) El = PhCO, 85%, > 95% *ee*[4, 42]

(34) El = PPh$_2$, 80%, > 95% *ee*[4, 41]

(35) **(a)** El = H
(b) El = CO$_2$Me, 56%, > 95% *ee*
(c) El = SiMe$_3$, 70%, > 95% *ee*
(d) El = SnBu$_3$, 70%, > 95% *ee*
(e) El = Me, 72%, > 95% *ee*[43, 45]

(36) **(a)** El = H
(b) El = CO$_2$Me, 94%, > 98% *ee*
(c) El = SiMe$_3$, 77%, 96% *ee*
(d) El = SnMe$_3$, 93%, > 98% *ee*
(e) El = Me, 97%, > 98% *ee*[46]

(37) **(a)** El = H
(b) El = Me, 85%, > 95% *ee*[47]

(38) **(a)** El = H
(b) El = CO$_2$Me, 80%, > 95% *ee*[47]

(39) **(a)** El = H
(b) El = SnBu$_3$, 85%, > 95% *ee*[49]

(40) **(a)** El = H
(b) El = CO$_2$Me, 85%, d.r. > 98:2[43, 48]

SCHEME 1. (*continued*)

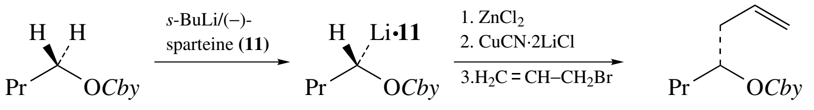

(7)

(41) **(42)** **(43)** 83%, > 99% *ee*

Generally, metal exchange in these carbamates proceeds with retention[51].

Lithiated alkyl carbamates [e.g. **44** from **32a** (*Cb* for *Cby*)] decompose above −40 °C with migration of the carbamoyl group to produce α-hydroxy carboxamides **45** (equation 8)[52].

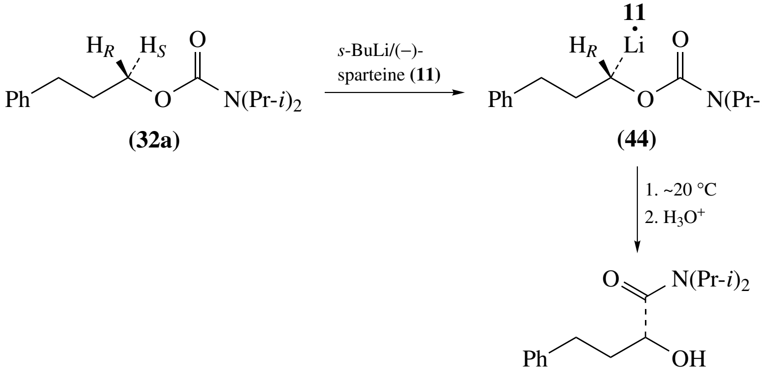

(8)

(45) 46%, 96% *ee*

We prefer the 2,2,4,4-tetramethyl-1,3-oxazolidin-3-yl group (*Cby*)[53] over the *N*,*N*-diisopropylcarbamoyl group (*Cb*)[54] for the activation of alkanols, since the group is easily removed (equation 9): The amino acetal moiety in carbamates **24** is cleaved under moderate acidic conditions; the basic hydrolysis of the intermediate hydroxy urethane **46** to liberate the alcohol **47** is obviously facilitated by neighbouring group participation of the hydroxy group. We originally applied a cyclohexanespirooxazolidine group[10], but its ^{1}H NMR-spectroscopic properties are less appealing.

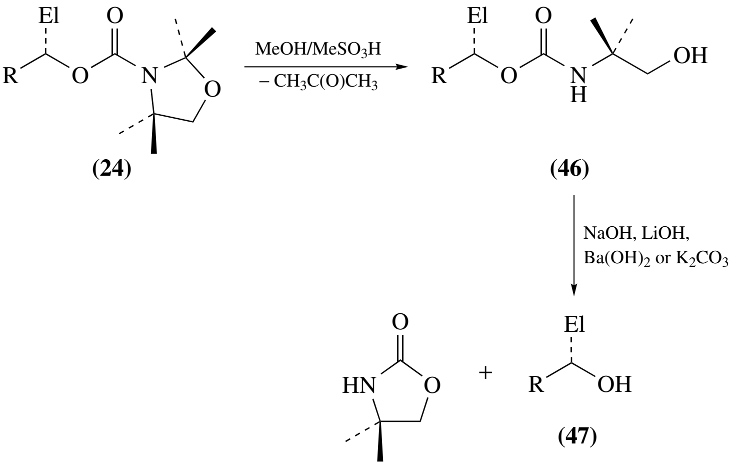

(9)

2. Mechanism of the alkyl carbamate deprotonation

The asymmetric (−)-sparteine-mediated deprotonation of alkyl carbamates was unprecedented until discovered in 1990[10]. For the first time, protected 1-alkanols could be transformed generally to the corresponding carbanionic species by a simple deprotonation protocol. Moreover, an efficient differentiation between enantiotopic protons in the substrate took place and the extent of stereoselection could be 'stored' in a chiral ion pair, bearing the chiral information at the carbanionic centre.

An extraordinarily high kinetic isotope effect (> 70) was found for the chiral (*S*)-α-deuterioethyl carbamate **48** (equation 10)[35]. **48** is deprotonated by *s*-BuLi/(−)-sparteine (**11**) very slowly and, after silylation, the expected product (*R*)-**49** is formed only in traces. On the other hand, the deprotonation of (*S*)-**48** (98% *ee*) by means of *s*-BuLi/TMEDA and subsequent silylation yielded the α-D-silane (*S*)-**25d** with $> 96\%$ *ee* and 98.2% deuteriation. To the best of our knowledge, this reaction represents the first examples of an efficient asymmetric synthesis, based solely on isotope effects. We have also already used the introduction of D in order to protect the most acidic H against deprotonation[55, 56]. A kinetic isotope effect of $k_{\mathrm{H}}/k_{\mathrm{D}} > 70$ is calculated from these experimental data; evidence supports the fact that the proton to be removed and the entering electrophile occupy the same stereotopic position. The high kinetic isotope effect is a hint for a highly ordered transition state in the deprotonation step. Obviously, an intermediate **22** (equation 6) is formed from the carbamate, *s*-BuLi and (−)-sparteine. Now, in the favoured transition state, the *pro-S*-H shifts preferentially onto the alkanide carbon atom in a four-membered transition state. Haller and Hoppe calculated by less advanced theoretical methods (MOPAC/PM3) the transition states of lowest energy[4, 57] for the deprotonation of the ethyl carbamate, using achiral isopropyllithium as the base. The calculated energy difference for the two diastereomorphic pathways of 0.2 kcal mol^{-1} is much too low; it should be around 2 kcal mol^{-1} (conducted from the experimental selectivities). As pointed out in Section I.A.2, (−)-sparteine (**11**) is not C_2-symmetric. This is a most important feature, since the reaction centre finds a niche below the *cis*-annulated 'wing' of (−)-sparteine.

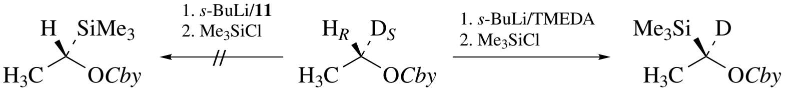

(10)

(25d) (*S*)-**(48)** (*R*)-**(49)**

$> 96\%$ *ee*, 98.2% D

The unsymmetrical structure of (−)-sparteine creates an additional stereogenic centre at the lithium cation. As a consequence, two diastereotopic transition states for the interaction of isopropyllithium/(−)-sparteine (**11**) have to be taken into consideration.

E.-U. Würthwein and D. Hoppe calculated the relative energies of the corresponding transition states of deprotonation by the B3LYP/6-31G* method[58]. The relative (gas phase) energies are marked in brackets: Li_R, *pro-S*-H (0.00 kcal mol^{-1}); Li_R, *pro-R*-H (2.71 kcal mol^{-1}); Li_S, *pro-S*-H (3.76 kcal mol^{-1}); Li_S, *pro-R*-H (4.36 kcal mol^{-1}). The Li_R-transition states have lower energies than the Li_S-transition states, with Li_R, *pro-S*-H being favoured by 2.71 kcal mol^{-1}. This value matches well with the observed data ($\geqslant$2 kcal mol^{-1}). The assumption that monomeric complexes are the intermediates is supported by the solid-state characterization of a monomeric (−)-sparteine–lithium compound (Section IV.C.1). For similar calculations for *N*-Boc-pyrrolidines, see Section IV.D.2.

In (−)-sparteine-mediated deprotonation and electrophilic substitution reactions, the minor enantiomer is close to the limits of exact determination. Therefore, the influence of the alkyl residue on selectivity was investigated for less efficient (*R*,*R*)-1,2-bis(dimethylamino)cyclohexane/*s*-BuLi (equation 11)[37]. On the base of the isolated corresponding methyl carboxylates **25c**/*ent*-**25c**, **28b**/*ent*-**28b** or **29b**/*ent*-**29b**, the ethyl carbamate **25a** provides a very low e.r. (63:37). It increases with increasing steric bulk of the residue R (77:23 for the isobutyl derivative **28a** and 89.5:10.5 for the neopentyl carbamate **29a**). The observed selectivities match well with the high-level quantum-chemical calculations for the differences in the energy of activation of both diastereomorphic pathways via **50** and *epi*-**50**, respectively, (0.37 kcal mol^{-1} for **25a**, 1.23 kcal mol^{-1} for **29a**)[37]. Further calculations revealed that, besides the bulk of the residue R, the size of the base and the carbamate group contribute significantly to the enhancement of the energy difference[37].

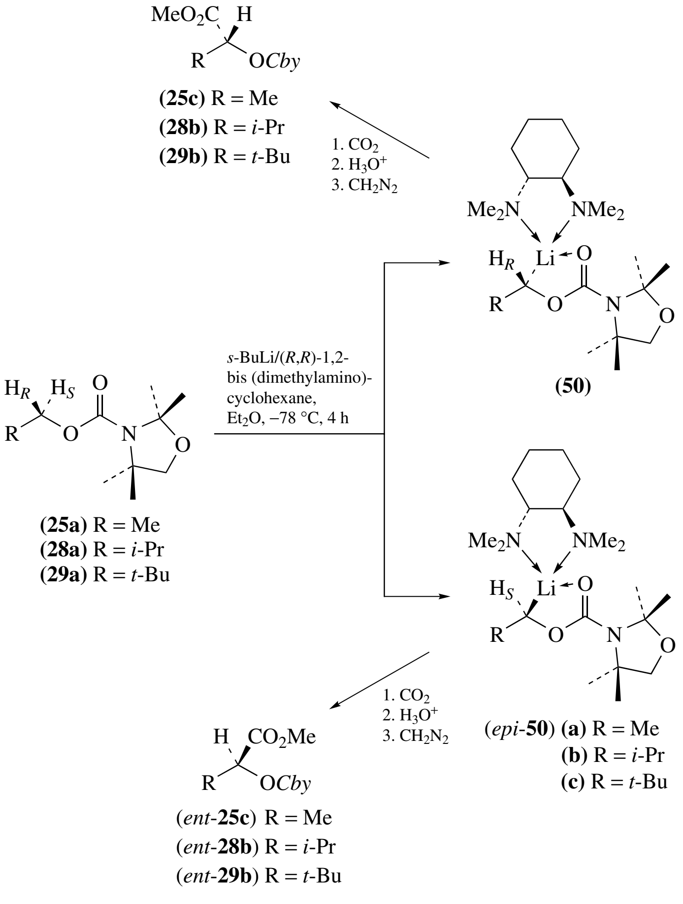

(11)

TABLE 1. Data for the reactions in equation 11

Starting material	Product	Yield (%)	e.r. (*ee*)	ΔH_{calc} (kcal mol^{-1})
25a	**25c**/*ent*-**25c**	81	63:37 (26%)	0.37
28a	**28b**/*ent*-**28b**	96	77:23 (54%)	—
29a	**29b**/*ent*-**29b**	42	89.5:10.5 (79%)	1.23

Since the (−)-sparteine reagent does not support the deprotonation of the neopentyl carbamate **29a** (1.5 equivalents of *s*-BuLi, diethyl ether, 5 h at −78 °C) it becomes evident that *trans*-1,2-bis(dimethylamino)cyclohexane, which is available in both enantiomers[59], is the chiral additive of choice for bulky alkyl carbamates. (−)-α-Isosparteine (**14**), which holds two *trans*-fused piperidine rings, does not support the deprotonation of alkyl carbamates at all[37].

3. Intramolecular reactions of metallated alkyl carbamates

O→*C* migrations of the carbamoyl group occasionally have been observed[52,60]. 2-Substituted, lithiated 1,3-dicarbamates have a high tendency to undergo 1,3-cycloelimination with formation of cyclopropyl carbamates[35]. On the attempt of silylating the lithio-sparteine complex **51**, the (*S*)-configured cyclopropane **52** was obtained with > 95% *ee* (equation 12)[35,61]. Obviously, traces of lithium chloride serve as catalyst to activate the leaving group, but also zinc chloride turned out to be effective. Deprotonation (*s*-BuLi/TMEDA) of **52** and methoxycarbonylation lead to the optically active ester **53**

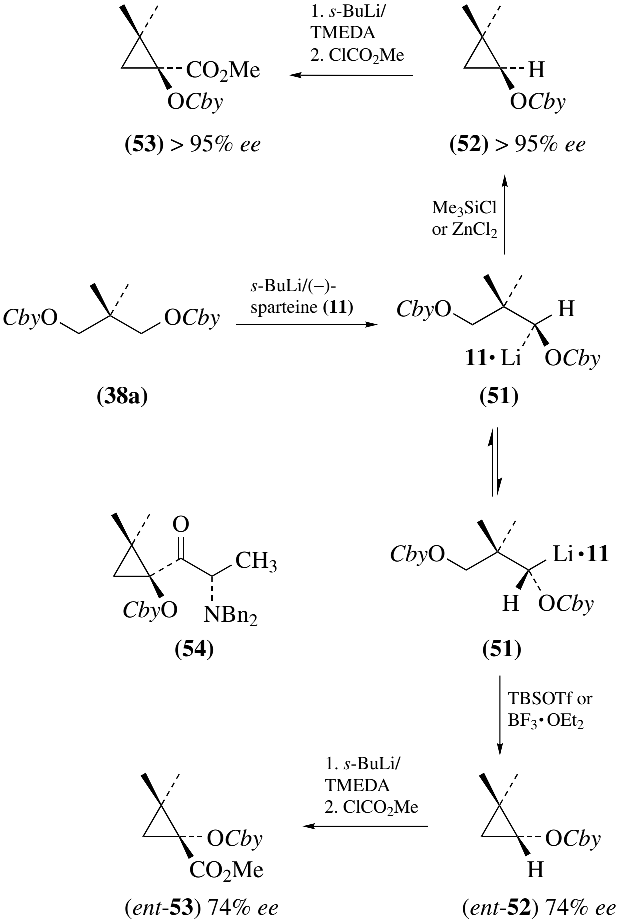

(12)

via the configurationally stable 1-lithiocyclopropyl carbamate. The absolute configuration was proven on the stage of the amino ketone **54**; thus the expected stereoretention at the carbanionic centre took place in the cycloalkylation step. Based on isotope-labelling studies, inversion was recorded adjacent to the nucleofugic leaving group[35]. Surprisingly, when applying stronger Lewis acids, such as boron trifluoride etherate or silyl triflates, the opposite enantiomer *ent*-**52** was obtained with 74% *ee* (equation 12). This is, to the best of our knowledge, the only case where inversion was recorded for a lithiated alkyl carbamate. The stereochemical course may be caused by cyclization from a W-conformation[364], resulting in inversion at both termini. Cyclopropane formation from intermediate γ-lithioalkyl carbamates occurred occasionally[62–64].

The asymmetric deprotonation can be advantageously coupled with intramolecular cyclocarbolithiations[65]. (*E*)- and (*Z*)-6-phenylhex-5-enyl carbamates **55** are lithiated by *s*-BuLi/(−)-sparteine adjacent to the carbamoyloxy group (equation 13). The intermediates

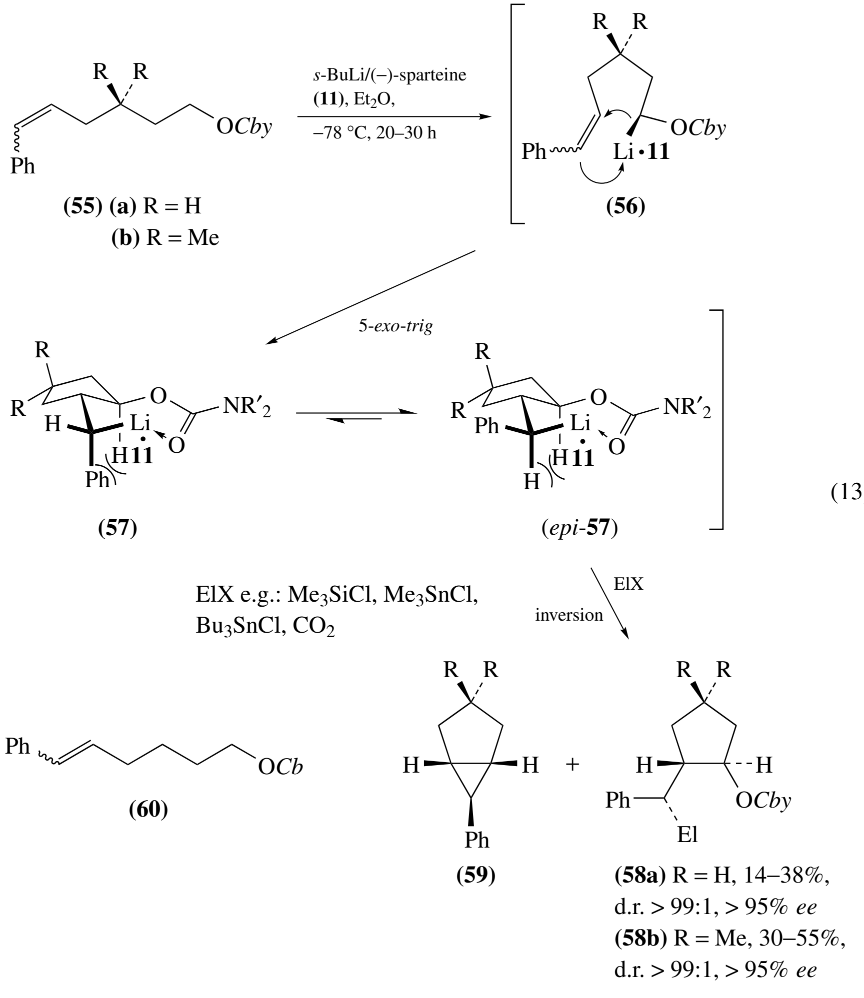

(13)

56 undergo a *syn*-5-*exo*-*trig* ring closure to form the equilibrating α-(cyclopentyl)benzyllithium compounds **57**/*epi*-**57**[62, 64], which are trapped by electrophiles, leading with high preference to the diastereomers **58**. Unfortunately, an 1,3-cycloelimination competes and yields the *meso*-bicyclo[3.1.0]hexane **59**. The extent of cyclopropane depends on the complexing diamine; in the presence of TMEDA, up to 93% of **59** were obtained.

The same cyclocarbolithiation reaction, using the corresponding *N*,*N*-diisopropylcarbamate **60** and applying a five-fold excess of the chiral base, has been reported by Nakai and coworkers[63]. Starting with the racemic 4-TBSO-hexenyl carbamate *rac*-**61**, a diastereomer resolution takes place: The 1,3-*cis*-compound **62a** remains stable until trapped by protonation (40% of **63**, d.r. = 95:5), but from **62b** the enantiomerically and diastereomerically pure bicyclo[3.1.0]hexane **64** (38%, > 95% *ee*) results (equation 14)[63].

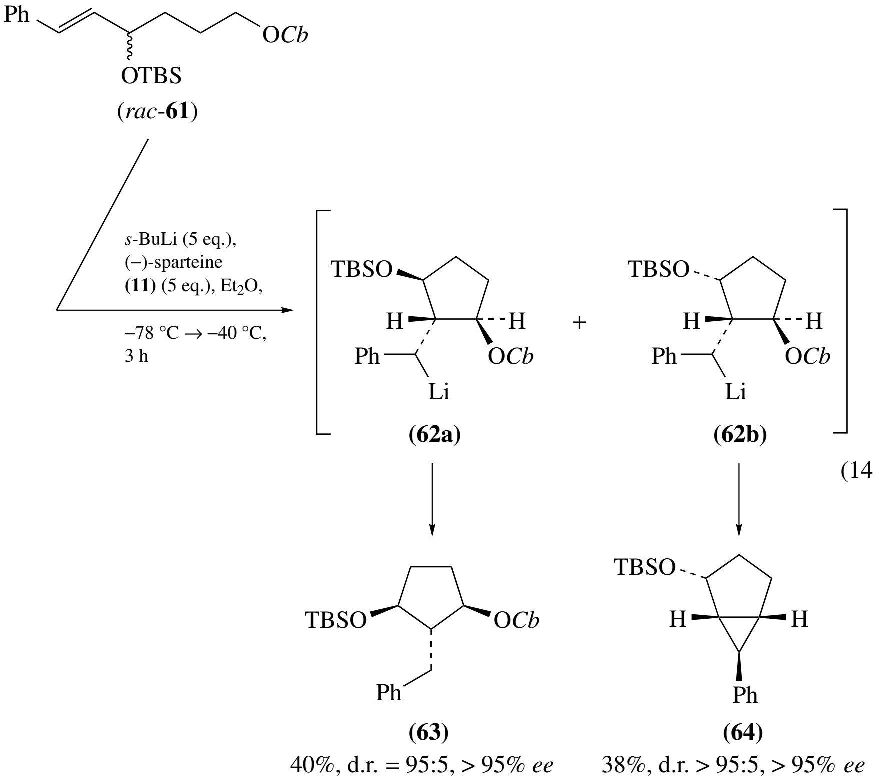

(14)

The cyclopropanation can be suppressed by making possible a [1,4]-*retro*-Brook rearrangement at the stage of the carbanionic intermediate. From the 2-(dimethylphenylsiloxy)-6-phenylhexenyl carbamate **65**, the diastereomerically pure (α-silylbenzyl)cyclopentane **66** (58%) and few (9%) of cyclopropane **67** were formed (equation 15)[66]. Due to the intramolecular delivery of the silyl group, the opposite stereochemistry at the stereocentre in the side chain results; decarbamoylation, followed by Tamao–Fleming oxidation, gave the pure triol **68**. For a stereochemical study of [1,4]-*retro*-Brook rearrangement to the benzylic position, see elsewhere[67].

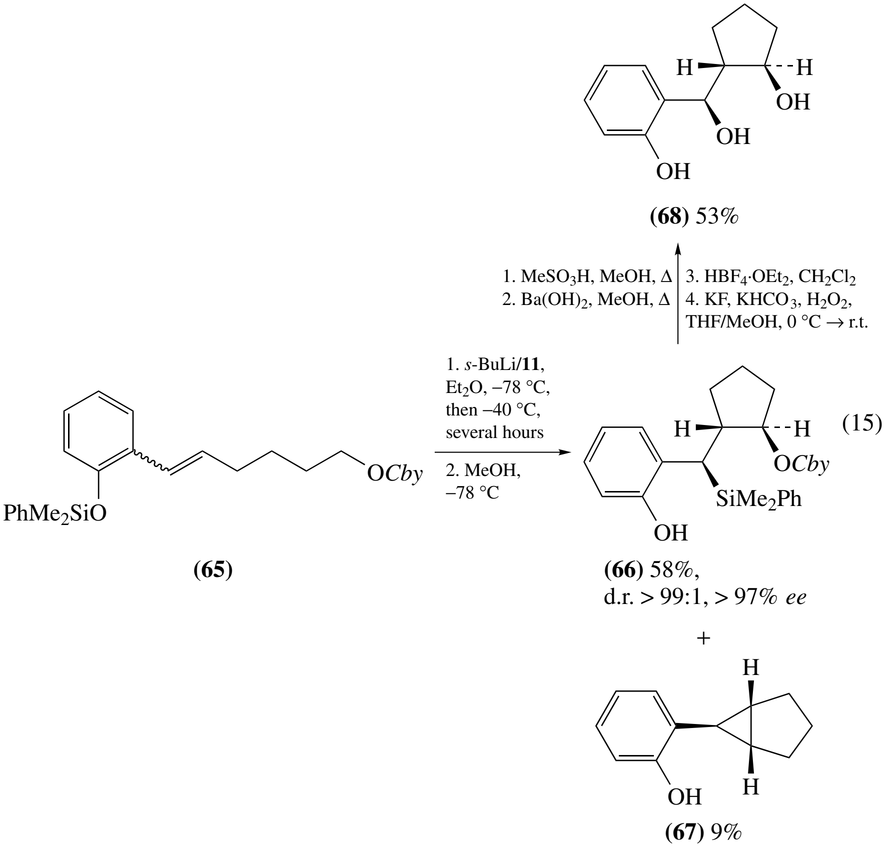

(68) 53%

(65)

(66) 58%, d.r. > 99:1, > 97% *ee*

(67) 9%

(15)

Smooth cyclization requires a carbanion-stabilizing substituent in the 6-position of the precursor. Some examples are listed in equation 16. A stereogenic centre in the 4-position does not influence the steric course of the asymmetric deprotonation. Thus, starting from the (*S*)-4-(*N*,*N*-dibenzylamino)alkenyl carbamate **69**, the enantiomerically and diastereomerically pure *trans,trans*-trisubstituted cyclopentane **70** was obtained[64] whereas the racemic 4-oxyalkynyl carbamate *rac*-**71** furnished a 1:1 mixture of both epimers **72** and **73** (equation 16)[68, 69]. It is evident from these results that the 1-*pro*-*S*-H is abstracted with high selectivity and the addition step proceeds as a *syn* addition with retention at the carbanionic centre. Even the diene **74** was cleanly deprotonated adjacent to the carbamoyloxy group; the cyclocarbolithiation leads to a stereo-homogeneous allyl anion **75**, which on protonation furnishes two isomers **76** and **77**[70]. Similarly to both previous examples, the bulky (+)-M-substituent prevents a competing deprotonation in 4-position.

If further acidic C−H bonds in the molecule cause problems, the ‘tin-trick’ can be applied. The asymmetric deprotonation of a bifunctional carbamate (**39a**) is accomplished at an early stage and the masked carbanionic centre carried through the synthesis as a stannyl group. For instance, the (*S*)-5-silyloxy-1-tributylstannyl-pentyl carbamate **39b** (> 95% *ee*) was produced by the usual means and converted by standard steps via the aldehyde **78** into the allyl chloride **79** (equation 17)[49]. Lithiodestannylation of **79** by *n*-BuLi proceeds faster than reductive lithiation in the allylic position to form the lithiocarbamate **80**,

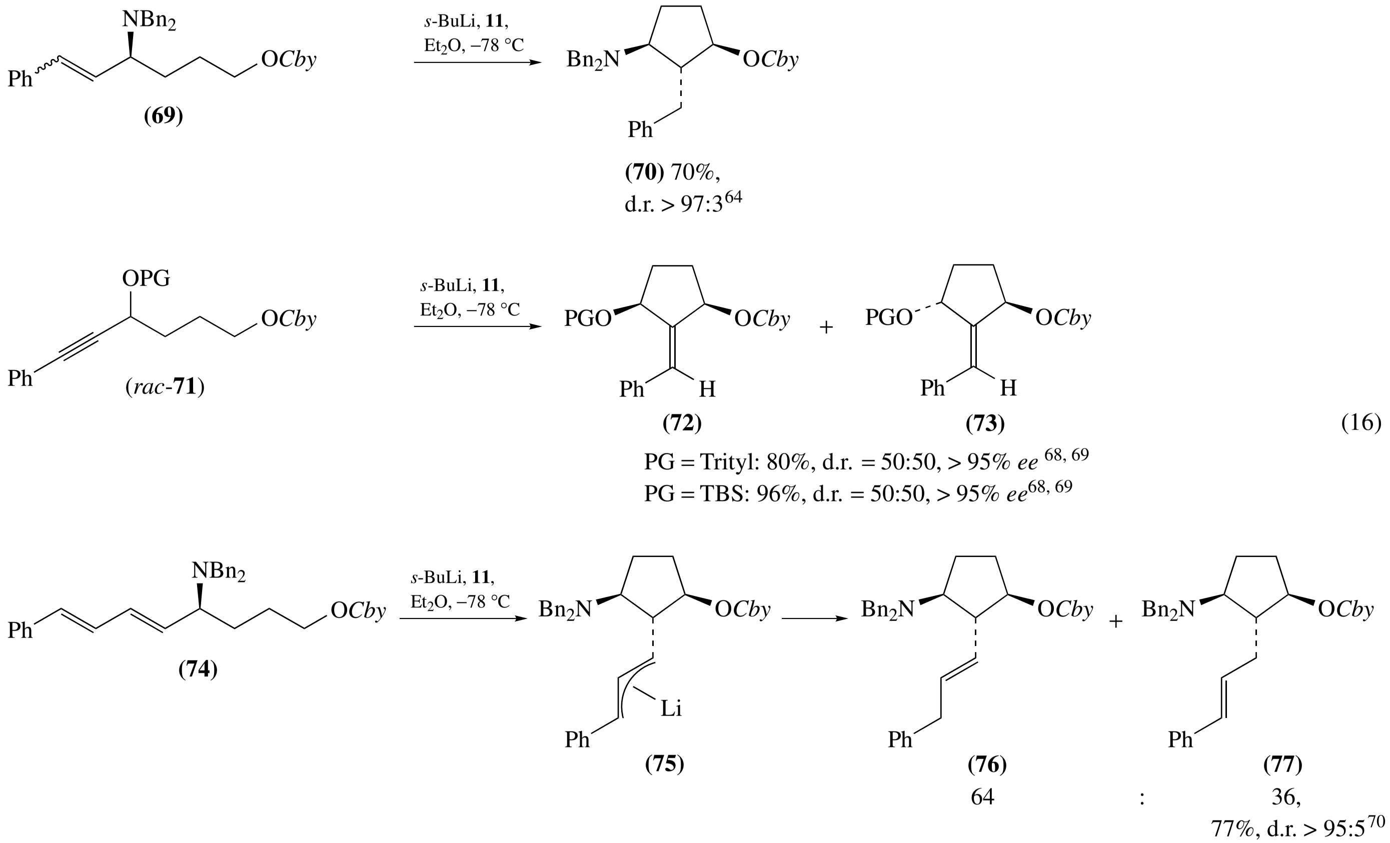

(16)

PG = Trityl: 80%, d.r. = 50:50, > 95% *ee* [68, 69]
PG = TBS: 96%, d.r. = 50:50, > 95% *ee*[68, 69]

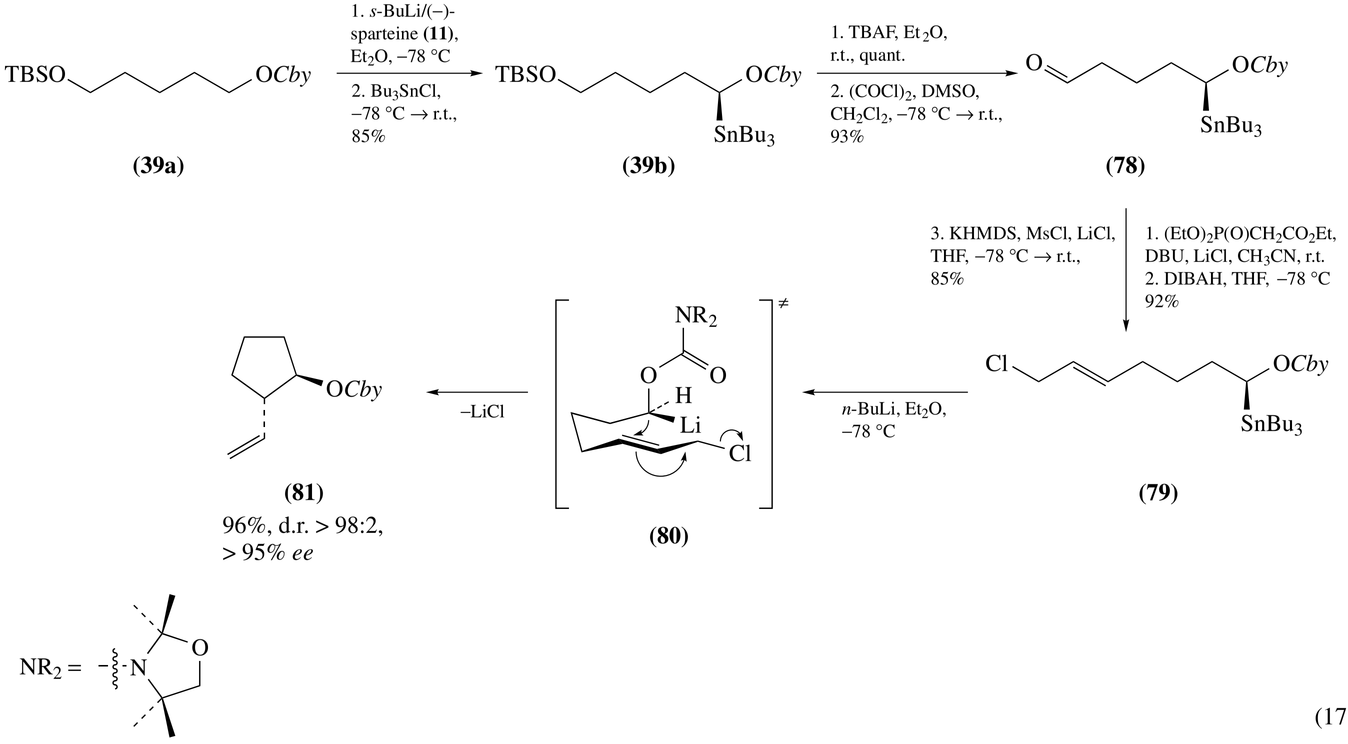
TBSO
OCby
(39a)
1. s-BuLi/(−)-sparteine (11), Et2O, −78 °C
2. Bu3SnCl, −78 °C → r.t., 85%
TBSO
OCby
SnBu3
(39b)
1. TBAF, Et2O, r.t., quant.
2. (COCl)2, DMSO, CH2Cl2, −78 °C → r.t., 93%
O
OCby
SnBu3
(78)
1. (EtO)2P(O)CH2CO2Et, DBU, LiCl, CH3CN, r.t.
2. DIBAH, THF, −78 °C 92%
3. KHMDS, MsCl, LiCl, THF, −78 °C → r.t., 85%
Cl
OCby
SnBu3
(79)
n-BuLi, Et2O, −78 °C
NR2
O
O
H
Li
Cl
≠
(80)
−LiCl
OCby
(81)
96%, d.r. > 98:2, > 95% ee
NR2 =
N
O

(17)

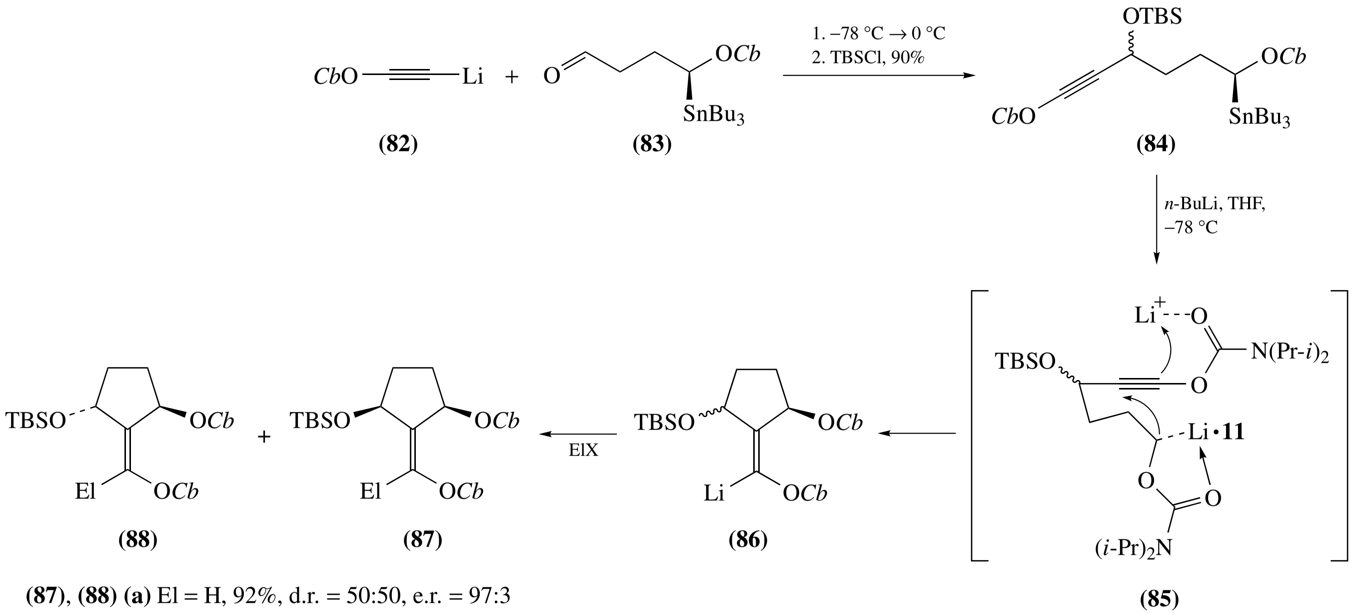

(87), **(88)** **(a)** El = H, 92%, d.r. = 50:50, e.r. = 97:3
(b) El = $SiMe_3$, 91%
(c) El = Me, 90%

(18)

which undergoes an intramolecular S_N'-reaction with formation of the *trans*-(1*R*,2*S*)-2-vinylcyclopentyl carbamate **81**. The principle could be applied to the synthesis of several five-membered carbo- and heterocycles[49].

An interesting chain elongation of 4-oxo-1-tributylstannylbutyl carbamate **83** by ethynyl *N*,*N*-diisopropyl carbamate (**82**) to the dicarbamate **84** and the subsequent intramolecular carbolithiation to form the alkenyllithium **86** has been reported very recently (equation 18)[71]. **86** was trapped by electrophiles to yield—as expected—both epimers **87** and **88** in essentially equal amounts. From an X-ray analysis of a derivative, the shown absolute configuration and the (*E*)-stereochemistry at the double bond was concluded. Thus, the attack at the triple bond here took place in the *anti* fashion, which is quite unusual. We suggest that a lithium cation in **85**, captured by the second carbamoyl group, catalyses the *anti* addition[71].

4. Kinetic resolutions and desymmetrization reactions

If the carbamate already contains a stereogenic centre, the internal chiral induction will either oppose or enforce the external induction exerted by the chiral base[72]. In the (*S*)-*N*,*N*-dibenzylphenylalaninol carbamate **89** (equation 19), *s*-BuLi/TMEDA removes preferently the *pro-R*-H to form the (2*S*,1*R*)-configured lithium compound **90a** besides few **91a**, ratio 90:10. However, when *s*-BuLi/(−)-sparteine (**11**) is applied, due to its high preference for *pro-S*-protons, the ratio **90b/91b** is inverted (10:90)[45]. The intermediates had been applied to the synthesis of several dipeptide isostere spacers[73].

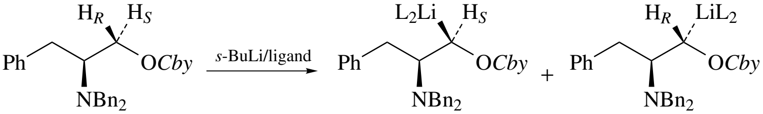

(89) **(90)** **(91)** (19)

(90), **(91)** **(a)** L_2 = TMEDA : 90 : 10
(b) L_2 = (−)-sparteine : 10 : 90

(*S*)-2-Aminoalkyl carbamates bearing a β-branched carbon chain, such as the (*S*)-valinol derivative (Me_2CH for $PhCH_2$ in **89**), are not deprotonated at all under (−)-sparteine conditions[45]. This represents an ideal situation for a kinetic resolution during the deprotonation reactions. As can be seen in equation 20, there is only one favoured reaction course [the doubly matched case (*R*)-**92**] among the four possibilities: removal of the *pro-S*-H in (*R*)-**92** to give the lithium compound (1*S*,2*R*)-**93**, which can be trapped by electrophiles to produce the highly enantiomerically and diastereomerically enriched stereoisomer **94**. Compound **96** is formed (via **95**) only in small amount. The major amount of (*S*)-**92** remains unchanged. Kinetic resolution of the cyclopropylalaninol derivative *rac*-**92a**, followed by carboxylation or acylation of **93**, turned out to be successful although the conditions were not optimized[74].

Efficient kinetic resolution was also observed during the deprotonation of the carbamates *rac*-**97** and *rac*-**100**. Equation 21 shows the preferred products [(2*R*)-**98** and (2*S*)-**101**] obtained from the racemates with recovery of the enantiomerically enriched starting materials (*S*)-**97** and (2*R*)-**100**[57, 75]. Diastereomer (2*S*)-**99** arises in low yield but high *ee*. Even simple PM3 calculations reflect the experimentally recorded (opposite) diastereoselectivities well[57].

s-BuLi/(−)-sparteine (**11**) has a high capability for the differentiation between enantiotopic groups. The 1,3-dicarbamate **102** bears two enantiotopic carbon branches each holding a set of two diastereotopic protons (equation 22). The chiral base can remove H_S in the *pro-S* branch or H_S in the *pro-R* branch. The selectivity in the formation of lithium compounds **103** and **104** is determined by the internal chiral induction. Trapping these

(20)

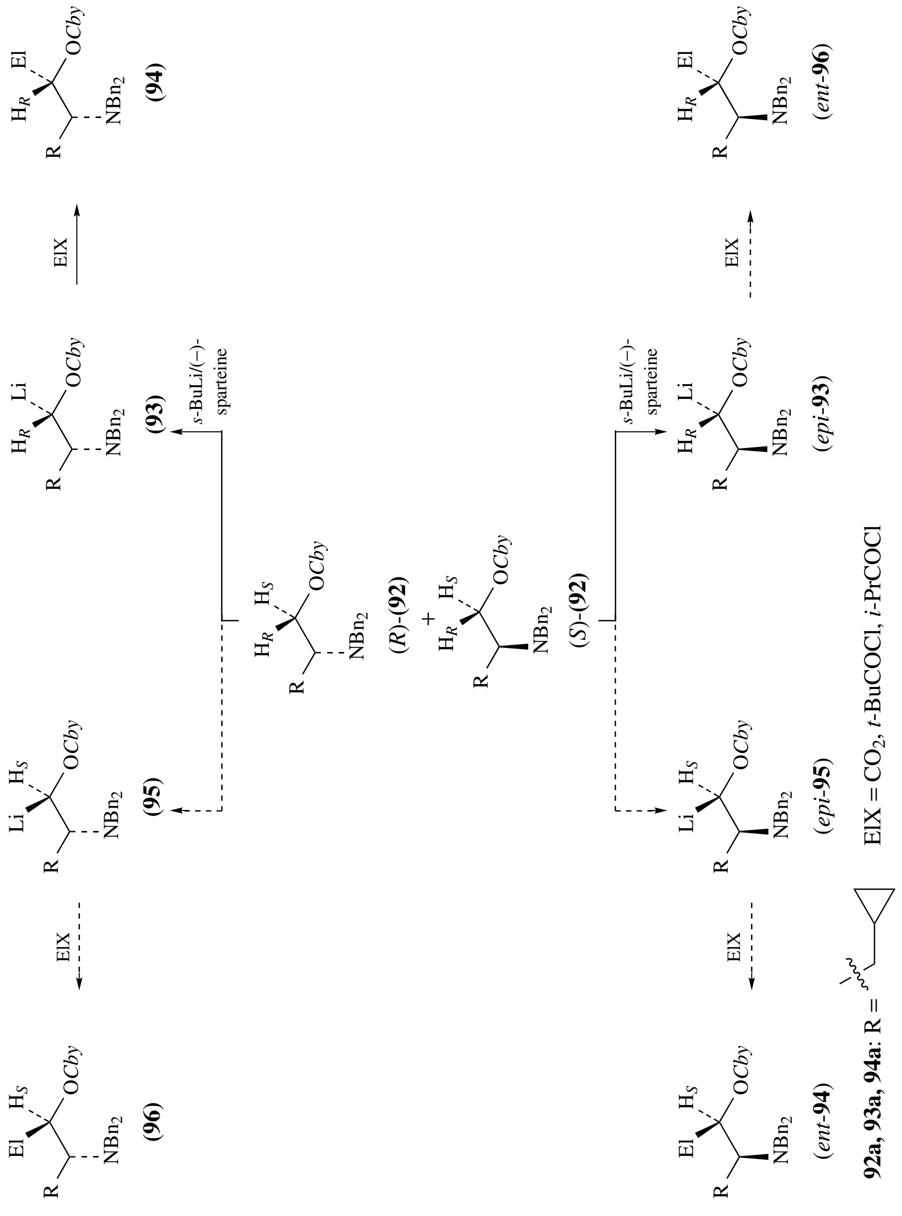

ElX = CO_2, *t*-BuCOCl, *i*-PrCOCl

92a, 93a, 94a: R =

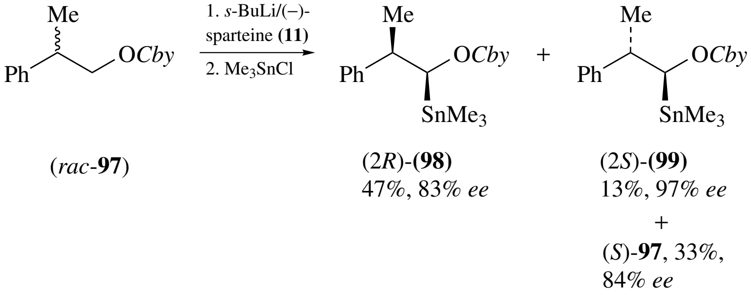

(21)

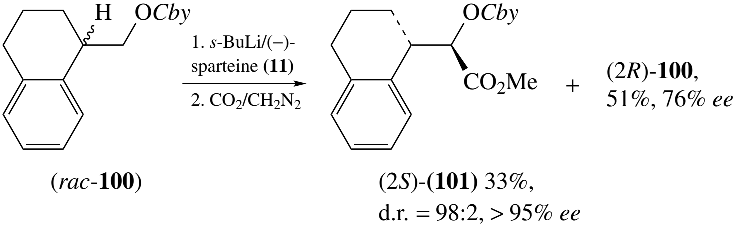

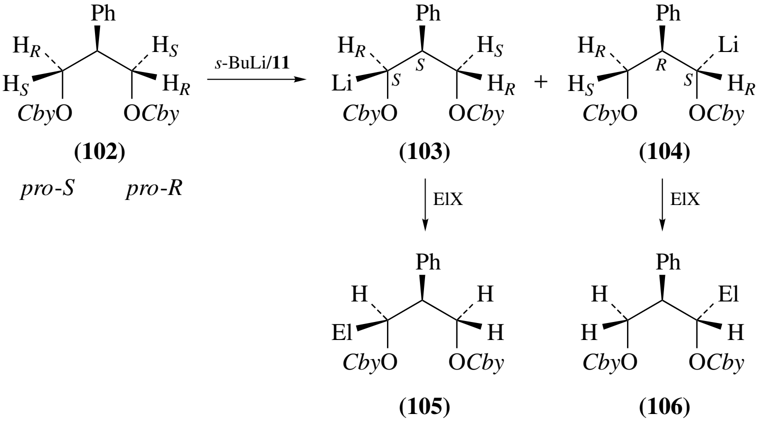

(22)

(105), (106) **(a)** ElX = Me_3SnCl, 65%, d.r. = 90:10, > 95% *ee*

(b) ElX = $Me_3CC(O)Cl$, 78%, d.r. = 83:17

with trimethyltin chloride yielded the diastereomers **105a** and **106a** in a ratio of 90:10, each with > 95% *ee*[76]. 2,2-Dimethylpropanoyl chloride furnished the ketones **105b** and **106b** in a ratio of 83:17. On the first view, the d.r. values in both reactions should be equal, since the substitution proceeds with strict stereoretention. However, different yields were obtained and point to a kinetic resolution between the diastereomeric lithium compounds. It can be concluded that **103** is the more reactive one.

Kinetic resolution is also very efficient in the *meso*-1,4-dicarbamate **107** (equation 23)[60]. Here the proton H_S in the *pro-R* branch turned out to be more reactive towards *s*-BuLi/(−)-sparteine (**11**), and the lithium compound **108** is formed in large excess besides a trace of **110** leading to **111**. Adding electrophiles leads to the major products **109** with high diastereomeric and enantiomeric ratios. The stereoselectivity is low when allyl and benzyl bromide are used, presumably due to the participation of SET mechanisms.

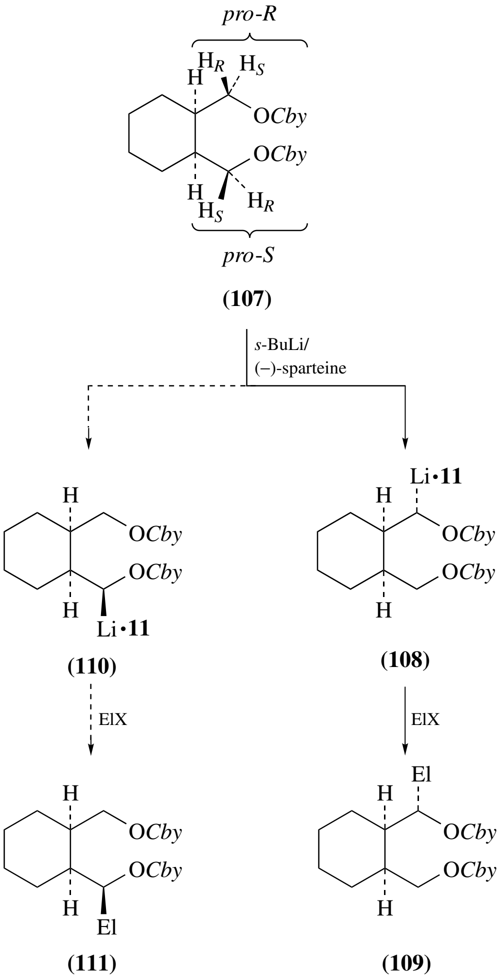

(23)

(109) **(a)** ElX = Me_3SnCl, 65%, d.r. = 98:2, > 95% *ee*
(b) ElX = CO_2/CH_2N_2, 63%, d.r. = 96:4, > 95% *ee*
(c) ElX = MeI, 70%, d.r. = 95:5, > 95% *ee*

The products **109** are versatile precursors for bicyclic tetrahydro-2-furanones and -furans[60]. The tributylstannane *rac*-**109d** undergoes a kinetic resolution of medium efficiency when it is treated with MeLi/(−)-sparteine (equation 24)[60]. The substitution products **109b** and the less reactive enantiomer *ent*-**109d** are obtained with medium enantioselectivity.

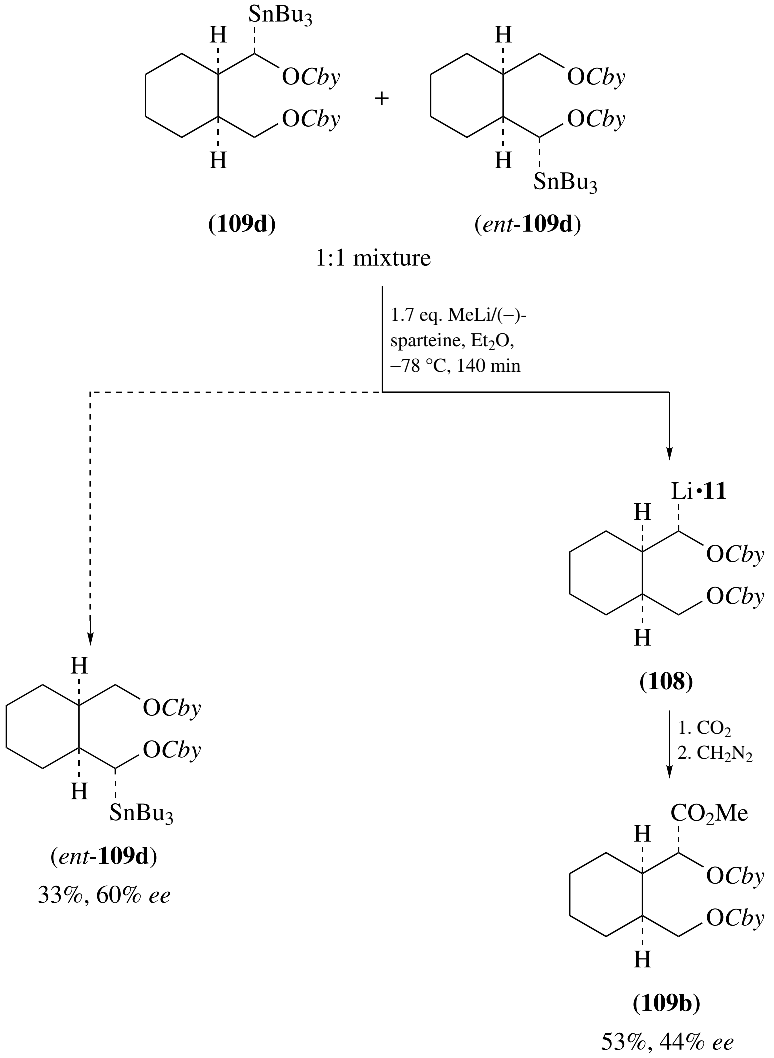

(109d) (*ent*-**109d**)
1:1 mixture

(108)

(109b)
53%, 44% *ee*

(*ent*-**109d**)
33%, 60% *ee*

(24)

An efficient kinetic resolution was also observed during the (−)-sparteine-mediated deprotonation of the piperidin-2-ylmethyl carbamate *rac*-**112** (equation 25)[77]. By treatment of *rac*-**112** with *s*-BuLi/(−)-sparteine (**11**), the *pro-S* proton in (*R*)-**112** is removed preferentially to form the lithium compound **113**, which undergoes intramolecular cyclocarbolithiation, and the indolizidinyl-benzyllithium intermediate **114** was trapped with several electrophiles. The mismatched combination in the deprotonation of (*S*)-**112**, leading to *epi*-**113**, does not significantly contribute to product formation. Under optimized conditions [0.75 equivalents of *s*-BuLi, 0.8 equivalents of (−)-sparteine, 22 h at −78 °C in diethyl ether] the indolizidine **115** was isolated with 34% yield (based on *rac*-**112**), d.r. = 98:2, e.r. = 97:3; optically active (*S*)-**112** was recovered (46%, 63% *ee*).

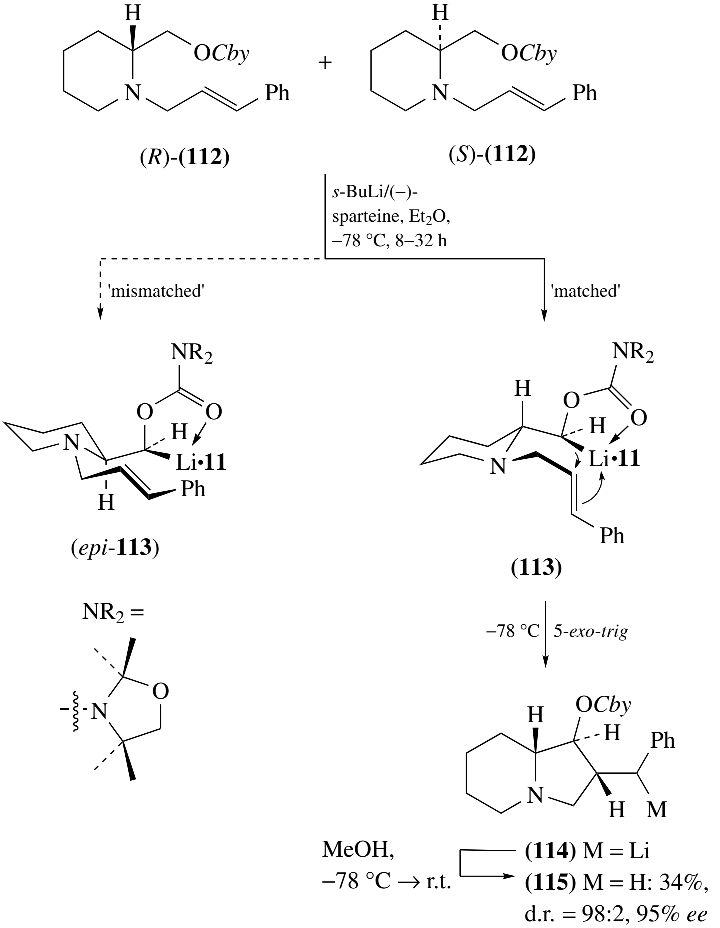

(25)

Kinetic resolution between diastereomeric (−)-sparteine–lithium complexes may also occur on a later step of a reaction sequence[78]. Almost no stereodifferentiation between the enantiomers (*R*)- and (*S*)-**116** takes place in the deprotonation of *rac*-**116**; (*S*,*S*)-**117** and (*R*,*S*)-**117** are formed in essentially equal amounts (equation 26)[78]. Only (*R*,*S*)-**117** undergoes a cyclocarbolithiation, presumably furnishing the benzyllithium derivative **118** (which is expected to be configurationally labile at the carbanionic centre). External electrophiles (HOMe, DOMe, EtI, Bu_3SnCl) approach from the least hindered *exo*-face and yield the substituted benzobicyclo[3.3.0]octenes **119**; (*S*)-**116** is recovered after aqueous workup. To some extent, intramolecular cycloalkylation of the anion **118** occurs to give the tricyclic cyclopropane **120**[78].

A safe prediction if the substrate-inherent asymmetric or the (−)-sparteine-induced induction determines the stereoselection is yet not possible, but quantum-chemical calculations are in progress. Small structural changes have large influence. Scheme 2 shows some striking examples[43, 44, 48, 55, 56, 79]; the proton being removed preferentially with *s*-BuLi/(−)-sparteine (**11**) in diethyl ether is circled. Changes in ring size (**121** versus **122**) or in chain length (**40a** versus **123**) can result in preference for substrate control.

(26)

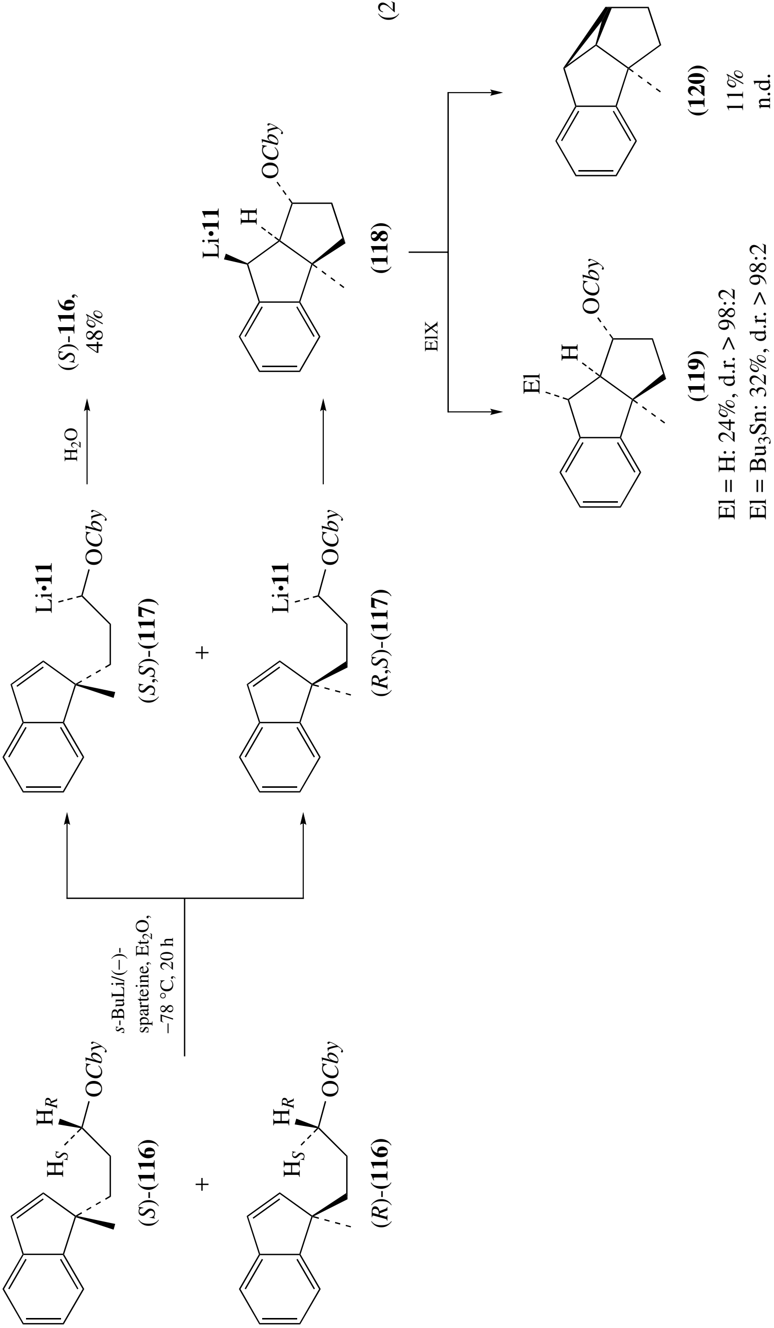
(S)-(116)
+
(R)-(116)
H_S
H_R
OCby
s-BuLi/(−)-sparteine, Et_2O, −78 °C, 20 h
Li•11
OCby
(S,S)-(117)
+
(R,S)-(117)
H_2O
(S)-116, 48%
Li•11
H
OCby
(118)
ElX
El
H
OCby
(119)
El = H: 24%, d.r. > 98:2
El = Bu_3Sn: 32%, d.r. > 98:2
(120)
11%
n.d.

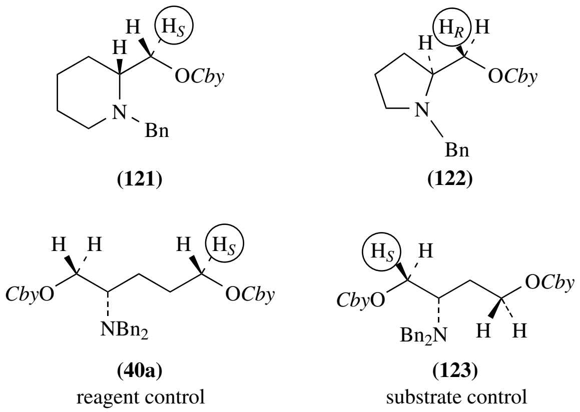
(121) **(122)**

(40a) reagent control

(123) substrate control

SCHEME 2

C. Desymmetrization of *meso*-Epoxides and Related Compounds

Cyclic epoxides such as **124** can react in two ways with strong bases: (a) via abstraction of a β-proton to form allylic alcoholates **125** or (b) by deprotonation at the epoxide carbon atom forming the intermediate **126** and, after electrophilic substitution, the epoxides **128**. If there is a suitable C−H bond in the vicinity of the C−Li moiety, intramolecular carbenoid insertion reactions to **127** may take place (equation 27)[80–82].

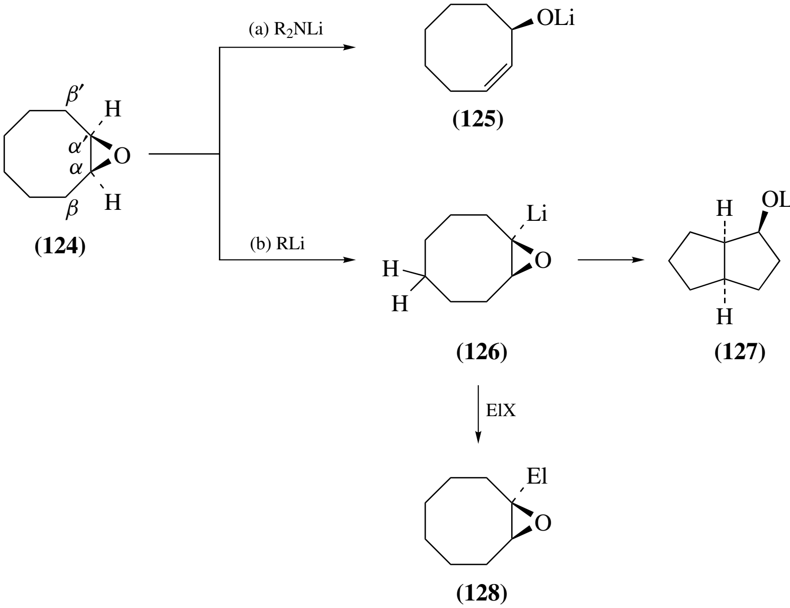
(124) **(125)** **(126)** **(127)** **(128)**

(27)

When applying chiral lithium amides, considerable enantioselectivities have been achieved due to a differentiation between the enantiotopic β- and β'-positions; the many examples are outside of the scope of this chapter[83]. Hodgson and coworkers accomplished a selection between the enantiotopic α- and α'-methine protons in *meso*-epoxides by utilization of *s*-BuLi or *i*-PrLi/(−)-sparteine (**11**) or (−)-α-isosparteine (**14**) (equation 28)[83–85]. The conditions have been optimized for the example of *cis*-cyclooctene oxide (**124**) (equation 28). *i*-PrLi/(−)-α-isosparteine (**14**) gave the best results. It is surprising that substoichiometric amounts, such as 0.01 equivalents of **14**, gave good enantioselectivities[85] of the formed products **129**/*ent*-**129**.

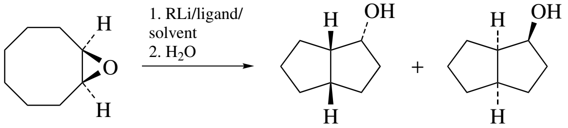

(124) **(129)** (*ent*-**129**) (28)

TABLE 2. Data related to the products of equation 28

Ligand	RLi	Ratio ligand:RLi:epoxide	Temperature	Yield (%) **129**	Enantiomeric ratio (e.r.)
11	*s*-BuLi	1.45:1.4:1	−78 °C	81	85:15
11	*i*-PrLi	1.45:1.4:1	−78 °C	75	89:11
11	*i*-PrLi	1.45:1.4:1	−98 °C	74	92:8
14	*i*-PrLi	1.45:1.4:1	−78 °C	92	91:9
11	*i*-PrLi	0.2:1.4:1	−98 °C	62	87:13
11	*i*-PrLi	0.01:1.4:1	−98 °C	63	65:35
14	*i*-PrLi	0.2:1.4:1	−98 °C	86	92:8
14	*i*-PrLi	0.01:1.4:1	−98 °C	71	85:15

The desymmetrization works also well with higher substituted *meso*-epoxides such as *endo*-norbornene oxide (**130**)[86], *cis*-5,6- and 4,7-difunctionalized cyclooctene oxides **132** and **134**, giving the alcohols **131, 133** and **135**, respectively; but for the diastereomer **136**, the rearrangement to form the allylic alcohol **138** beside **137** cannot be completely suppressed (equation 29; best results are given)[87].

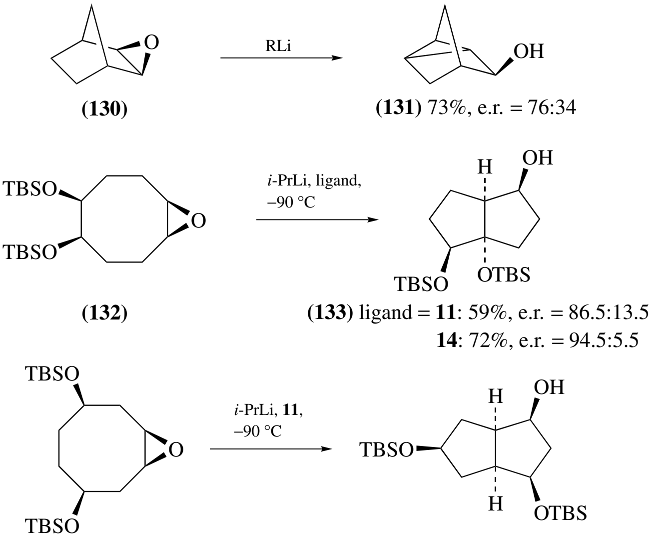

(130) **(131)** 73%, e.r. = 76:34

(132) **(133)** ligand = **11**: 59%, e.r. = 86.5:13.5
14: 72%, e.r. = 94.5:5.5 (29)

(134) **(135)** 70%, e.r. = 92:8

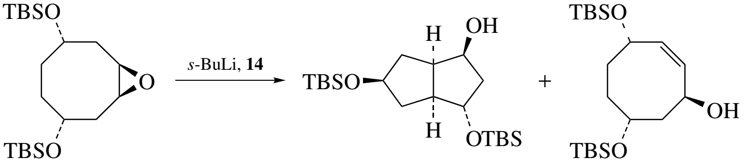

(136) **(137)** 56%, e.r. = 92:8 **(138)** 10%, e.r. = 80:20

(29 *continued*)

1,5-Cyclooctadiene-1-epoxide (**139**) rearranges on treatment with *s*-BuLi/(−)-sparteine (**11**) at −90 °C to form (*R*)-2,5-cyclooctadien-1-ol (**140**), but when boron trifluoride is added, a carbenoid insertion produces the bicyclo[5.1.0]octa-5-en-2-ol **141** with 71% *ee* (equation 30)[88]. Further examples are found elsewhere[89].

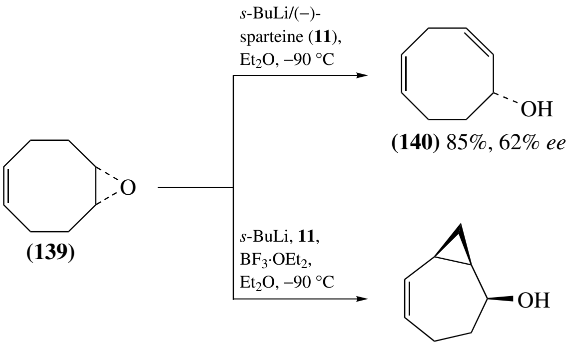

(139)

(140) 85%, 62% *ee*

(141) 75%, 71% *ee*

(30)

Astonishingly enough, enantioenriched lithiated cyclooctene oxides **142**, originating from (−)-sparteine-mediated lithiation of **124** by *s*-BuLi/(−)-sparteine (**11**), could be trapped by external electrophiles, resulting in substituted epoxides **143** (equation 31)[90, 91]. Again, the use of *i*-PrLi furnished better enantioselectivities (approx. 90:10). Lithiated epoxides, derived from tetrahydrofurans and *N*-Boc-pyrrolidines, undergo an interesting elimination reaction[92].

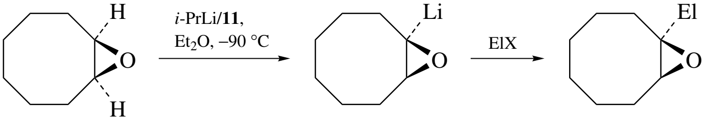

(124) **(142)** **(143)** (31)

(143) **(a)** El = Me$_3$Si: 72%, e.r. = 87:13
(b) El = Bu$_3$Sn: 60%, e.r. = 90:10
(c) El = EtCH(OH): 74%, e.r. = 88:12
(d) El = EtOCO: 58%, e.r. = 90:10

Meso-epoxides, nucleophilic ring-opening reactions by aryllithium/(−)-sparteine (**11**) have been realized by Alexakis and coworkers with very good differentiation between the enantiotopic positions[93]. Eliminative desymmetrization reactions of *meso*-oxacycles such as **144** or **147**, which are triggered by an enantiotopos-differentiating deprotonation reaction by alkyllithium/(−)-sparteine (**11**), had been reported previously by Lautens and coworkers (equation 32)[94–96]. The initially formed lithiated 2,5-dihydrofurans such as **145** rearrange in a stereoselective manner and form highly substituted seven-membered ring compounds (**146, 148**) with good *ee* values.

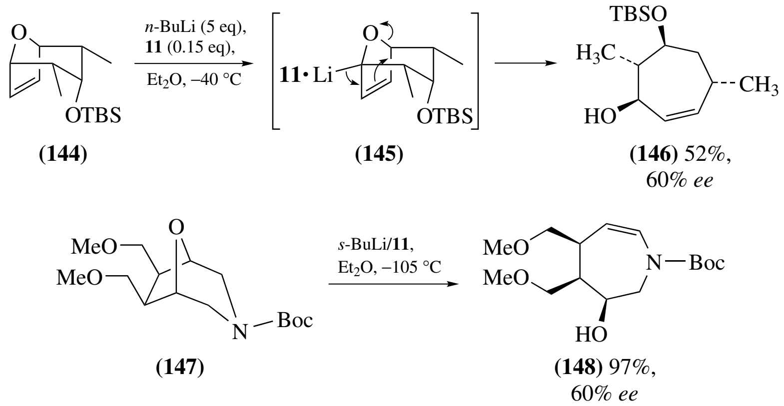

(144) **(145)** **(146)** 52%, 60% *ee*

(147) **(148)** 97%, 60% *ee*

(32)

D. Asymmetric Lithiation Adjacent to Nitrogen

1. *N-Boc-Azacycles*

As Beak and coworkers have established several years ago, *N*-*tert*-butoxycarbonylamines are sufficiently acidic to be deprotonated adjacent to the nitrogen atom[97]. When applying *s*-BuLi/(−)-sparteine (**11**) to *N*-Boc-pyrrolidine, asymmetric deprotonation (**149**), one *pro*-*S*-H is removed with high selectivity, furnishing the configurationally stable 2-lithio derivative **150** which was trapped with several electrophiles to form the optically active substitution products **151** (equation 33)[3,4,11,35,98]. A prescription in '*Organic Syntheses*' is available for the compound **151d**[99]. **150** adds with retention of the configuration to bicyclic imines[100].

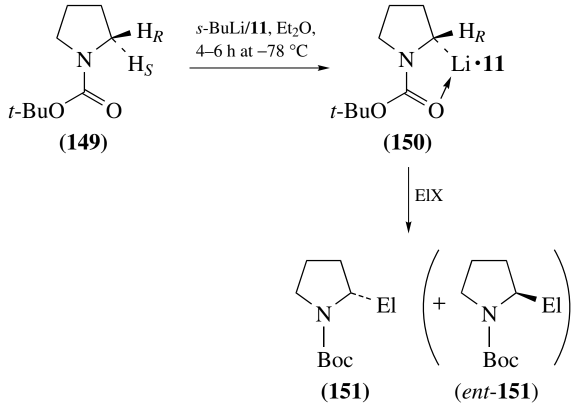

(149) **(150)**

(151) (*ent*-**151**)

(33)

(151) **(a)** El = Me_3Si: 87%, e.r. = 98:2
(b) El = Me: 88%, e.r. = 97:3
(c) El = Bu_3Sn: 83%, e.r. = 98:2
(d) El = $Ph_2C(OH)$: 75%, e.r. = 95:5

All evidence points to a kinetically controlled differentiation between enantiotopic protons, leading to a configurationally stable intermediate **150**[98], which is stereospecifically substituted with retention of the configuration. Experiments with the deuteriated substrate **149-D** (D for H at N-CH_2 in **149**) and the results of kinetic studies support this assumption[98]. The ligand (−)-sparteine (**11**) in **150** contributes to enhanced configurational stability; this can be concluded from the lithiodestannylation experiment shown in equation 34.

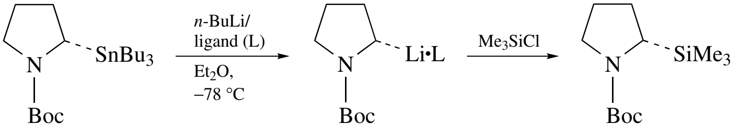

(151c) 96% *ee* **(151a)**

(34)

L = none: 15%, e.r. = 96.5:3.5
L = TMEDA: 36%, e.r. = 87:13

A synthesis of optically active trihydroxyindolizidines, developed by Majewski and coworkers, is based on the lithiated pyrrolidine[101]. A second asymmetric lithiation/substitution in the 5-position is possible, but the yields are usually not high. The problem lies in the slow interconversion of the pre-complexes (*E*)- and (*Z*)-**152** (equation 35)[25, 98]; directed lithiation is only possible in (*E*)-**152**.

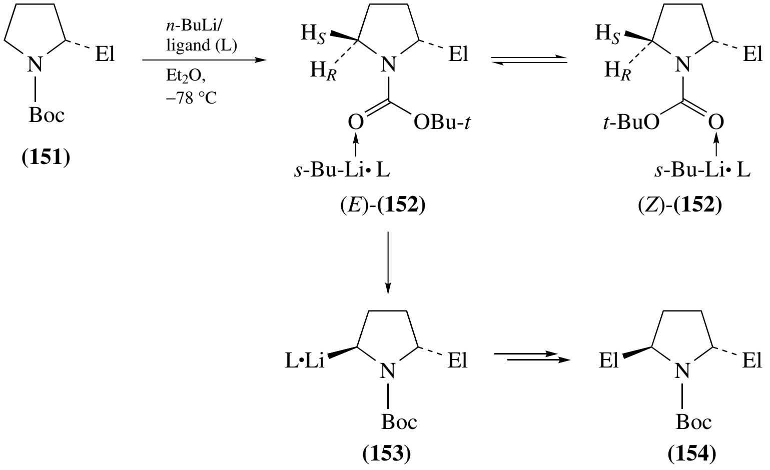

(151) (*E*)-**(152)** (*Z*)-**(152)** **(153)** **(154)**

(35)

Many chiral bidentate ligands and their ability for supporting the asymmetric deprotonation of **149** have been investigated[102, 103]; however, sparteine remained unbeaten. (−)-α-Isosparteine (**14**) does not support this deprotonation.

Wiberg and Bailey undertook extensive quantum-chemical investigations on the stereodifferentiating step of the deprotonation of **149** by *i*-PrLi/(−)-sparteine (**11**) on a high level[104–106] including conformational studies of the components[107]. The free energy of activation $\Delta\Delta G^{\neq}$ for the intramolecular abstraction of *pro-S*-α-proton in the pre-complex was found to be 3.2 kcal mol^{-1} lower than for abstraction of the *pro-R*-H[106]. The origin of the energy differences mainly arises from steric effects. The stannane **151c** has been converted to non-Boc-containing chiral 2-lithiopyrrolidines such as **155**[108], **156**[109],

157[110] and **158**[111] and the cuprate reagents which retain their chiral information[112]. Surprisingly, the lithium compound **155** was reported by Gawley and Zhang to react with alkyl halides under stereoinversion[108]. Coldham and coworkers undertook very interesting cyclocarbolithiation studies with similar compounds[109, 110, 113, 114].

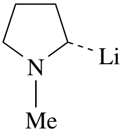

(155)

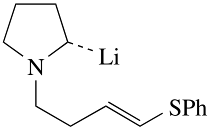

(156)

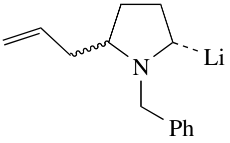

(157)

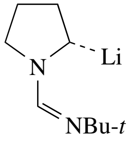

(158)

The deprotonation of *N*-Boc-piperidine (**159**), giving substituted piperidines such as **160**, proceeds with much lower efficiency (equation 36)[115, 116]. The main side reaction is the attack of *s*-BuLi at the Boc-group. The observation of slower and less selective lithiation is supported by quantum-chemical studies[115].

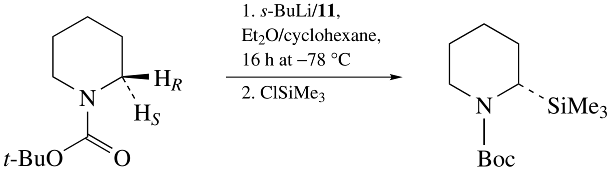

(159) **(160)**

8%, e.r. = 87:13

(36)

N-Boc-4-tosyloxypiperidine (**161**) undergoes, upon (−)-sparteine-mediated deprotonation, cycloalkylation to form via the lithium compound **162** the 1-azabicyclo[3.1.0]hexane **163**. **163** is subsequently deprotonated at the bridged-head carbon atom and lithium compound **164** is trapped by silylation; the yield of **165** and the e.r. are low (equation 37)[115, 117].

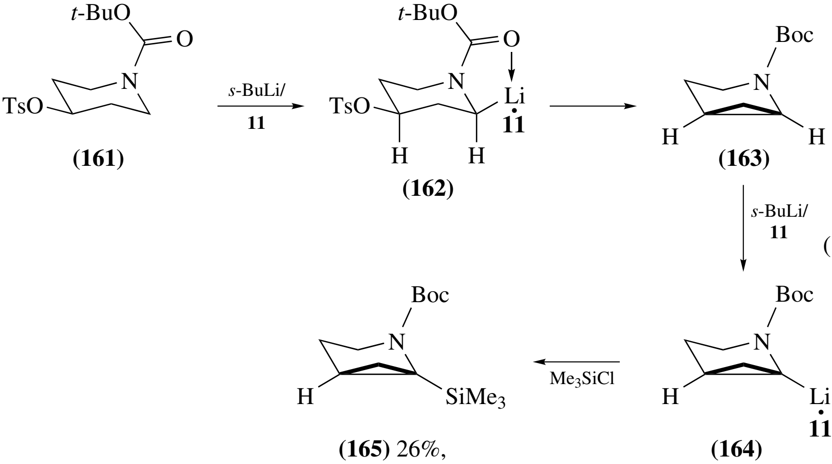

(161) **(162)** **(163)** **(164)**

(165) 26%,
e.r. = 75:25

(37)

Bertini-Gross and Beak demonstrated in a broad study that conformationally restricted bicyclic carbamates undergo rapid diastereoselective deprotonation with *s*-BuLi/TMEDA[118]. The proton closest to the carbonyl group is preferentially removed. Competition experiments gave information about the relative rates of deprotonation. Scheme 3 summarizes some second-order competitive efficiencies.

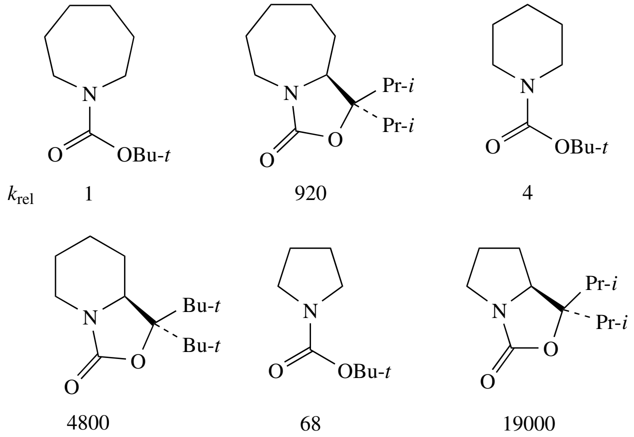

SCHEME 3

N-Boc-indoline **166** is deprotonated by *s*-BuLi/TMEDA (Et_2O, −78 °C) preferentially in the 7-position to form the stannane **168** via the corresponding aryllithium compound[119, 120]. However, when the deprotonation is performed in the presence of (−)-sparteine in cumene, substitution in the 2-position is observed, to yield the stannane (*S*)-**167** with e.r. = 99:1 (equation 38)[121]. The change in regioselectivity is mainly caused by the bulky ligand **11**, since with *N*,*N*′-dibutylbispidine (**169**) the same regioselectivity (producing *rac*-**167**) is found.

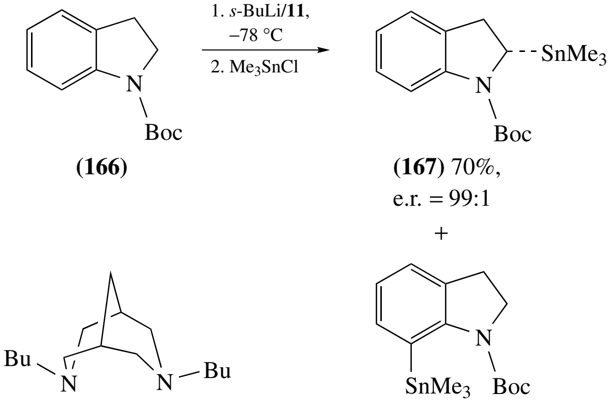

(166) **(167)** 70%, e.r. = 99:1 + **(168)** 3% (38)

(169)

Enantioenriched open-chain *N*-Boc-1-lithioalkylamines **172** have been generated by Chong and Park from the appropriate enantioenriched (1-hydroxyalkyl)stannanes **170** via the Mitsunobu reaction and transmetallation of the intermediate stannane **171** (equation 39)[122].

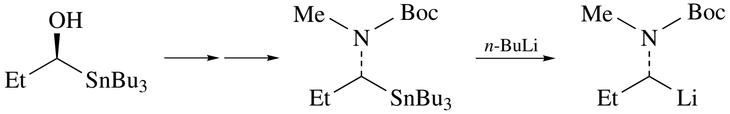

(170) **(171)** **(172)** (39)

2. Further N-Boc-heterocycles with two heteroatoms

The *N*-Boc-1,3-oxazolidine **173** was deprotonated at the 2-position by *s*-BuLi/(−)-sparteine (**11**) and added to benzaldehyde to yield a *syn*/*anti* mixture of hydroxybenzyl derivatives **174** with good enantiomeric ratios (equation 40)[123]. The *syn*/*anti*-ratio is improved by magnesium–lithium exchange. The major enantiomers arise from the substitution of the *pro-S*-H in **173**.

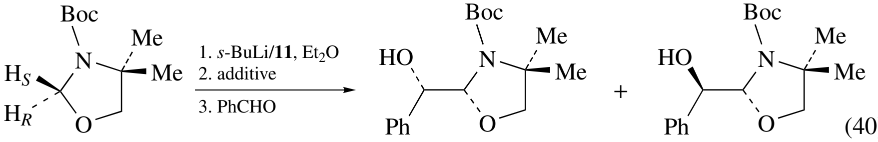

(173) (*syn*-**174**) (*anti*-**174**) (40)

additive = none: 71%, *syn*/*anti* = 46(90% *ee*):54(88% *ee*)
additive = $MgBr_2$: 67%, *syn*/*anti* = 90(86% *ee*):10(83% *ee*)

N-Boc-*N*′-isopropylimidazolidine (**175**) is deprotonated by the (−)-sparteine method and alkylated to form imidazolidines **176** (equation 41)[124]. The yields remain below 50%, since only a part of **175** exists in the shown conformation, which is required for the directed deprotonation. At low temperature, the interconversion between the *s-trans*- and *s-cis*-conformation is too slow. Ring cleavage furnishes synthetically useful chiral 1,2-diamines **177**.

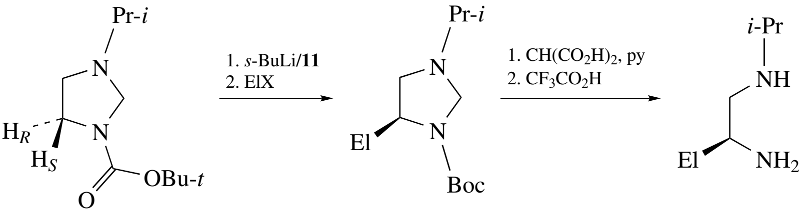

(41)

(175)

(176) (**a**) ElX = Me_3SiCl, 40%, e.r. = 93:7
(**b**) ElX = MeI, 44%, e.r. = 92:8

(177) (**a**) 76%
(**b**) 81%

E. Asymmetric Deprotonation Adjacent to S, Se, and P

Only few configurationally stable, enantioenriched α-thioalkyllithium compounds are known today (**178**[125], **179**[126], **181**[128, 129]); Scheme 4 includes also those which are mesomerically stabilized (**180**[127], **182**[130, 131], **183**[132]). No example of a preparation by efficient (−)-sparteine-mediated deprotonation has been published.

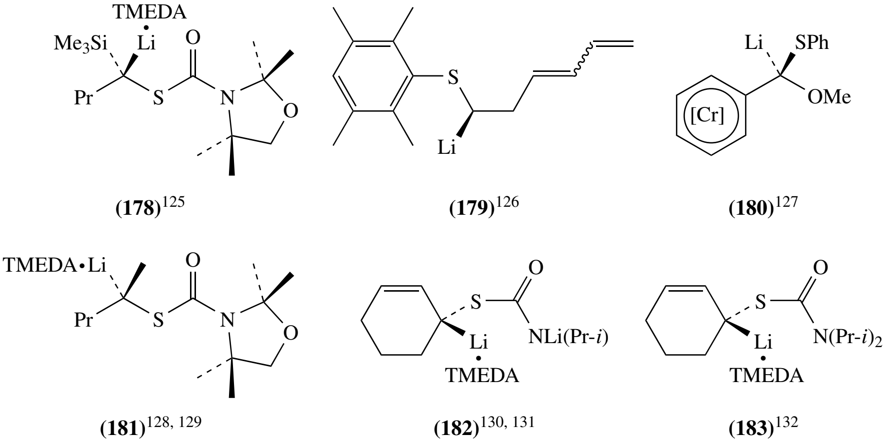

(178)[125] **(179)**[126] **(180)**[127]

(181)[128, 129] **(182)**[130, 131] **(183)**[132]

SCHEME 4

S-Alkyl *N*,*N*-dialkylmonothiocarbamates have sufficient kinetic acidity for being deprotonated by means of alkyllithium[125]. When applying *s*-BuLi/(−)-sparteine (**11**) to the *S*-butyl derivative **184** and trapping the lithium intermediates **185** and *epi*-**185** by electrophiles, the products **186** and *ent*-**186** are formed with low enantiomeric excesses (equation 42)[125]. Control experiments revealed that not only the rapid interconversion of **185** and *epi*-**185** is the problem, but also the degree of stereodifferentiation in the deprotonation step is low[125].

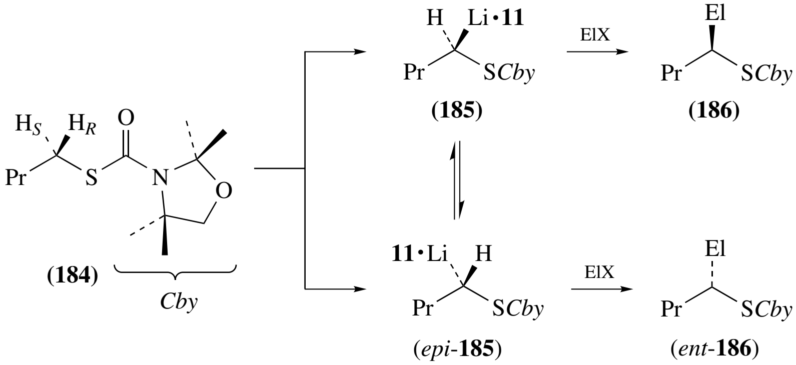

(42)

El = Me_3Si: 92%, **186**:*ent*-**186** = 63:37
El = CO_2Me: 91%, **186**:*ent*-**186** = 63.5:36.5

The (−)-sparteine-mediated double deprotonation of 3-arylthio-*N*-methylpropanamides **187** to dilithiated arylsulphides **188**, followed by aldehyde addition, also provided low, strongly varying enantiomeric excesses of the resulting products **189** (equation 43)[133].

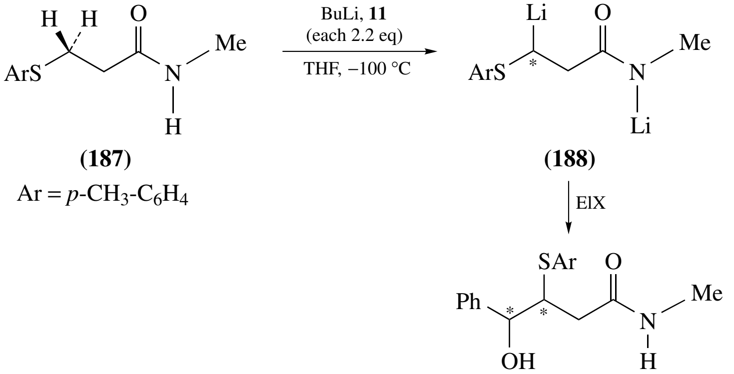

(187)
Ar = p-CH_3-C_6H_4

(188)

(189)

(43)

(189a) ElX = PhCHO, 82%,
anti/*syn* = 95:5, 30% *ee*

Mainly from the work of R. W. Hoffmann and coworkers[134] and H. J. Reich and coworkers[135, 136], evidence has accumulated that in many cases not the inversion of the carbanionic centre but the torsion around the C-S or C-Se bond is the rate-determining step of racemization. Maximal n-σ^* overlap of the carbanionic centre with the adjacent C-S or C-Se bond requires an antiperiplanar arrangement[25]. Consequently, bulky substituents such as 2,3,5,6-tetramethylphenyl at S or Se raise the inversion barrier significantly[137]. The ratio of the 1-phenylselanylalkyllithium compounds **191a** and **191b** derived from diselenides **190a,b** in diethyl ether solution at −70 °C in the presence of bidentate ligands (L_2 = **11**, **192**) has been investigated by NMR spectroscopy (equation 44)[138, 139].

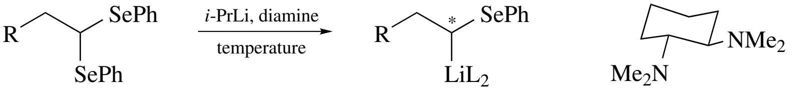

(190) **(a)** R = *n*-Pr
(b) R = *i*-Pr

(191) **(a)** R = *n*-Pr
(b) R = *i*-Pr

(192)

(44)

L_2 = (−)-sparteine (**11**), −70 °C, R = *n*-Pr: d.r. = 60:40
L_2 = diamine **192**, −80 °C, R = *i*-Pr: d.r. = 72:28
L_2 = diamine **192**, −100 °C, R = *i*-Pr: d.r. = 90:10

As the last example in equation 44 demonstrates, synthetically interesting enantioenrichments can be achieved from configurationally labile 1-phenylselanylalkyllithium compounds[140]. It has been shown that the e.r. in aldehyde addition roughly corresponds with the d.r., and it has been concluded that the interconversion of diastereomers is slower than the addition step[140].

The application of the Hoffmann test[141–143] confirms configurational stability of these lithium compounds on the microscopic scale at low temperature, indicating that rather thermodynamic than dynamic kinetic resolution is operating at the reaction conditions[143].

The barrier of epimerization in α-lithiated sulphones, according to Gais, is increased by electron-withdrawing substituents, such as in trifluoromethylsulphones[144, 145].

α-Lithiated alkyldiphenylphosphine oxides, such as **193**, were found to be configurationally labile at the carbanionic centre even at −78 °C[146], and application of the sparteine method was not successful[147]. Early attempts to furnish asymmetric lithiation by *n*-BuLi/(−)-sparteine (**11**) in aryldimethylphosphine oxides **194**, which would create the stereogenic centre at phosphorous, gave only low *ee*[148].

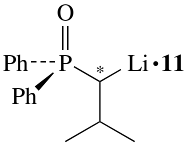

(193)

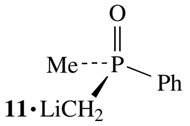

(194)

The breakthrough was achieved by D. A. Evans and coworkers[149], who demonstrated that aryldimethylphosphine-borane complexes **195** are easily deprotonated by *s*-BuLi/(−)-sparteine (**11**), furnishing efficient enantiotopic selection between the methyl groups (equation 45). The intermediate lithium compound **196** was added to benzophenone (to give alcohols **197**) or oxidatively coupled to furnish bisphosphines **198** with high *ee*. The major amount of the minor diastereomer *epi*-**196** is removed as separable *meso*-**198**.

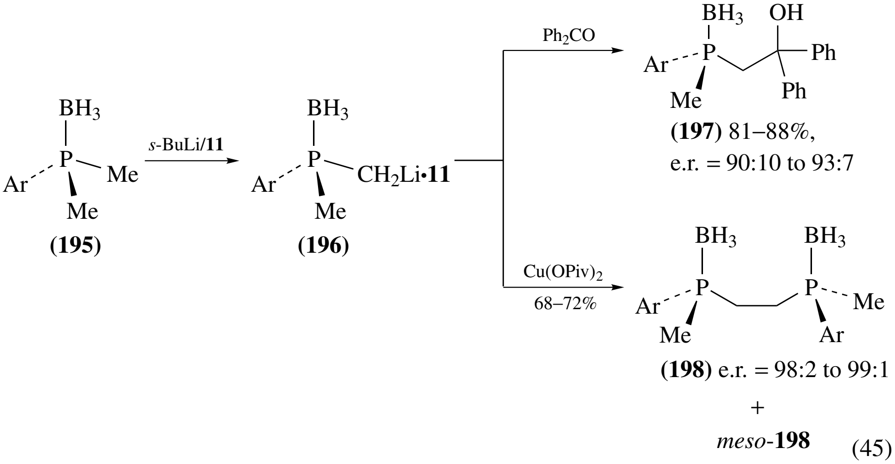

(45)

Similarly, the alkyl analogues (alkyl for Ar) of **198** were prepared by Imamoto and coworkers and used as efficient catalysts for asymmetric rhodium-catalysed hydrogenation[150]. Bulky chiral diphosphines could be constructed on the base of this enantioselective deprotonation[151].

The principle has been successfully applied to the differentiation between enantiotopic methylene groups in 1-phenylphospholane- and 1-phenylphosphorinane–borane complexes (**199, 200**) by Kobayashi and coworkers (equation 46)[152]. The conditions for optimized yields, diastereomeric and enantiomeric ratios of appropriate 2-carboxylic acids **201** or **202** were carefully worked out. For the deprotonation of **199**, the application of each 1.0 equivalent of the reagents at 25 °C gave the best results, whereas the synthesis of **202** proceeded best at −78 °C.

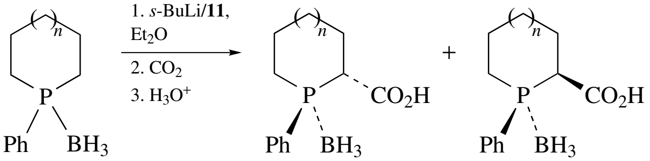

(199) $n = 0$

(200) $n = 1$

(201) $n = 0$, 55%, d.r. = 4:1, e.r. = 96:4

(202) $n = 1$, 79%, d.r. = 7.4:1, e.r. = 88:12

(46)

An efficient resolution of the racemic lithium *tert*-butylphosphine-borane complex **203** during deprotonation by *n*-BuLi/(−)-sparteine (**11**) and alkylation was reported by Livinghouse and Wolfe (equation 47)[153]. One of the epimers **204**/*epi*-**204** on warming to 0 °C crystallizes during a dynamic thermodynamic resolution, and reaction with alkyl halides furnishes the alkylation products **205** with high *ee* values. Applying dihalides, essentially enantiomerically pure diphosphines such as **206**, besides few of the *meso*-diastereomer, were obtained. Borane is removed by treatment with diethylamine to yield the free tertiary phosphines **207**.

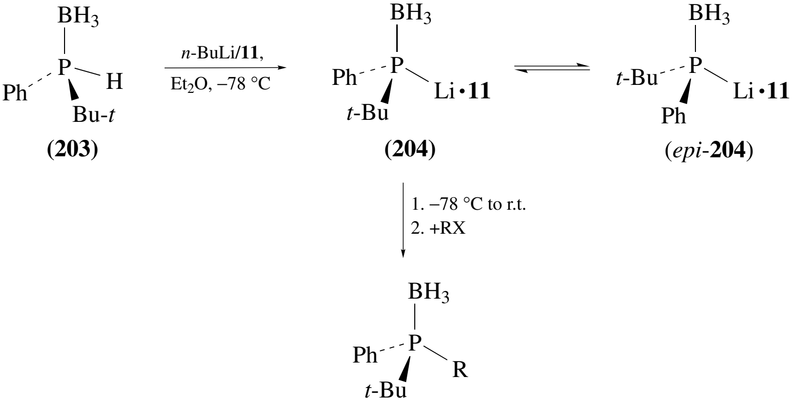

(203) **(204)** (*epi*-**204**)

(205)

R = Me: 88%, 93% *ee*

(47)

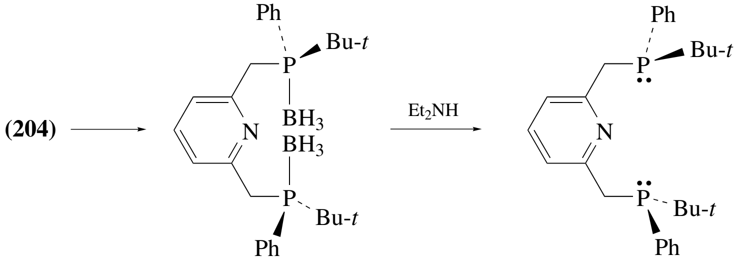

(206) 71%, d.r. = 92:8,
e.r. > 99.5:0.5

(207) 85–90%,
e.r. > 91:9 to 97.5:2.5

Highly enantiomerically enriched lithium phosphides of type **204** were also prepared by oxidation of the lithium compounds **196** and oxidative degradation of the hydroxymethyl group[154] or reductive cleavage of the benzophenone adducts[155].

III. (−)-SPARTEINE-INDUCED LITHIATION WITH FORMATION OF BENZYL-TYPE ORGANOLITHIUMS

A. General Remarks

Benzylic compounds have—compared to the corresponding methyl derivatives—a higher thermodynamic acidity by 10 to 15 pK_a units[156]. Mesomeric stabilization requires a considerable flattening of the carbanionic centre towards sp^2 hybridization (the sum of bond angles is 360° for sp^2 and 328° for sp^3). However, we should be aware that even if the carbanionic framework would be completely planar, the ion pair **209** is a planar-chiral species. For epimerization, the cation has to migrate from one face to the other one (equation 48). Due to a more facile flipping of the carbanionic centre and an easier formation of solvent-separated ion pairs, most of chiral benzyllithium compounds **208**/*ent*-**208** racemize with great ease.

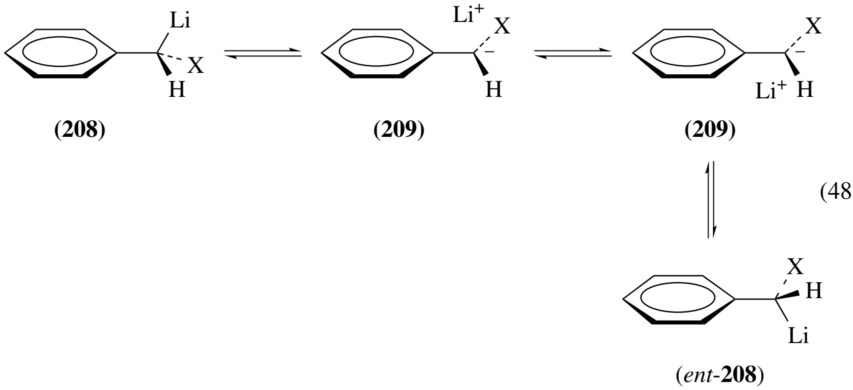

(48)

Boche and coworkers obtained an X-ray crystal structure analysis of (S)-α-(methylpivaloylamino)-benzyllithium•(−)-sparteine **210**[157]. It exists even in the solid as the monomer. The sum of bond angles is 341°, which is a typical value for solvated benzyllithium derivatives. Thus, a trend towards substitution with inversion is observed.

The (−)-sparteine-complex of 1-(2-pyridyl)-1-(trimethylsilyl)methyllithium is monomeric and shows, according to an X-ray analysis, an almost planar methine group[158]. The lithium cation is placed in a η^3-fashion above the plane of the azaallyl anion moiety.

Only few types of benzyllithium compounds being configurationally stable in solution at −78 °C are known: lithium−TMEDA complexes of secondary *O*-benzyl *N*,*N*-dialkyl carbamates, such as **211**[159] or the 2,4,6-triisopropylbenzoate **212**[160, 161], of secondary *N*-aryl-*N*-Boc-benzylamines (**213**) and the dilithio-(−)-sparteine derivative **214**[162].

Compound **211** and several related compounds are readily accessible by stereospecific deprotonation of the appropriate optically active carbamic esters with *s*-BuLi/TMEDA[159, 163]. Much of the knowledge about the stereochemical course of substitution in benzyllithium derivatives was obtained from experiments with these compounds. Only the reaction with proton acids, aliphatic aldehydes, ketones or esters as electrophiles proceed with retention; for alkyl, silyl and stannyl halides, acid chlorides,

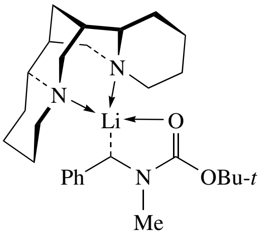

(210)

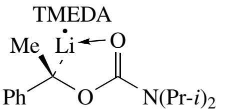

(211)

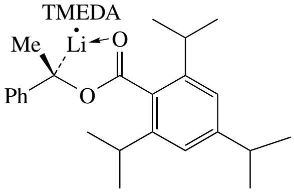

(212)

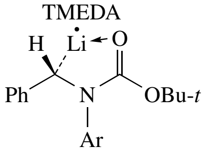

(213)

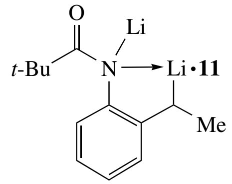

(214)

carbon dioxide, carbon disulphide and alkyl isocyanates, inversion was recorded[4, 6, 25, 159]. The sequence stannylation/lithiodestannylation via the stannane **215** allowed for the clean inversion in the benzyllithium **211** to *epi*-**211** (equation 49)[159, 164].

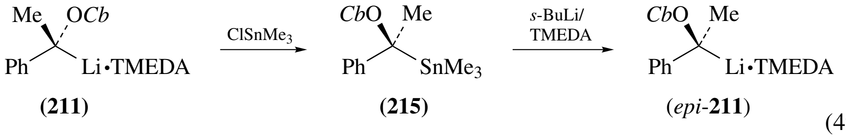

(49)

If a (cyclic) benzyllithium is forced by ring strain to a higher degree of pyramidalization, the tendency for stereoretention is enhanced. The lithiated indanyl carbamate **217** derived from **216** reacts with most electrophiles under retention of configuration to the substitution products **218** (equation 50)[165]. Inversion of the configuration to form *ent*-**218** is only observed with chloro-stannanes. Similar results were found by Hammerschmidt and coworkers for the stannylation of the triisopropylbenzoate **219**[161]. From these investigations, the absolute configuration of a tin derivative was elucidated by X-ray crystal structure analysis[161].

These results were recorded for the TMEDA complexes, but there is little doubt that the sparteine complexes exhibit similar reactivity, presumably with a further shift towards inversion.

A new, readily cleavable carbamate protecting group, the *N*-[2-(*tert*-butyldiphenylsiloxy)ethyl]-*N*-isopropylcarbamoyl group (*Cbse*) (in **220**), which is suitable for the deprotection of sensitive tertiary benzylic carbamates, was developed during these studies (equation 51)[166]. The cleavage of this protecting group to form the tertiary benzylic alcohols **221** is accomplished under mild basic conditions, which is in contrast to the harsh acidic conditions required for the *Cb* group.

During the investigations by Beak and coworkers, further knowledge on the stereospecifity was assembled[25]. All together, the prediction of the sense of stereospecifity in a new case may be difficult, since structural features, the electrophile and its leaving group play together.

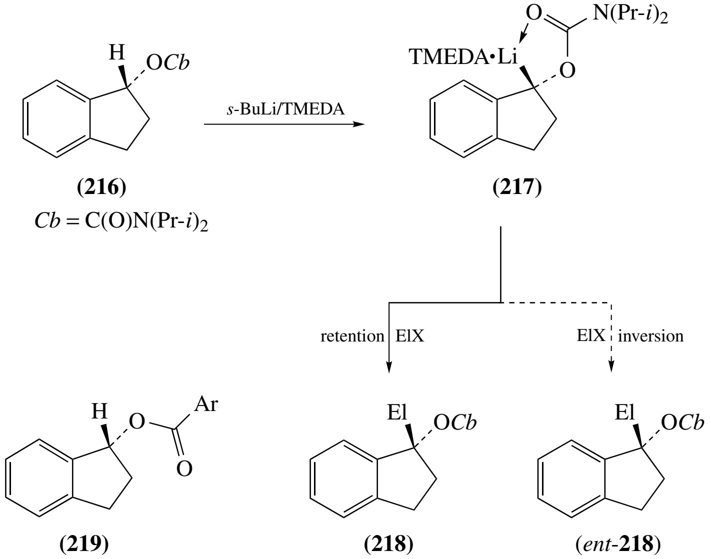

(216) $Cb = C(O)N(Pr\text{-}i)_2$

(217)

(219) $Ar = 2,4,6\text{-}(i\text{-}Pr)_3C_6H_2$

(218)

(*ent*-**218**)

(50)

$ElX = HOMe$: 92%, e.r. > 97:3
$= MeOCOCl$: 85%, e.r. > 97:3
$= CO_2$: 82%, e.r. > 97:3
$= CS_2$: 80%, e.r. = 99:1
$= Me_3SiCl$: 46%, e.r. = 96:4
$= Bu_3SnCl$: 81%, e.r. < 10:90

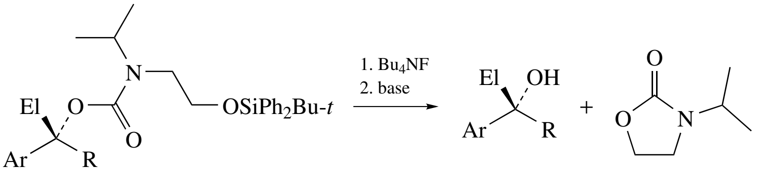

(220) **(221)**

(51)

B. Lithiation Adjacent to Oxygen

1. Lithiation of benzylic carbamates

The TMEDA complex of α-lithiobenzyl N,N-diisopropylcarbamate was found to be configurationally stable on the microscopical scale in the Hoffmann test[167]. The (−)-sparteine complex **222** has moderate configurational stability on the macroscopic scale, which could not been brought to useful selectivities in substitution reactions[4, 168]. As was reported by Lete and coworkers, the lithium complexes of type **222**, obtained by (−)-sparteine-mediated deprotonation of primary benzyl *N*,*N*-diisopropyl carbamates, add to *N*-(4-methoxybenzylidene)imine with high diastereoselectivity and with medium enantioselectivity[169].

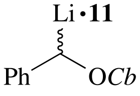

(222)

2. Lithiation of benzylic ethers

The deprotonation of benzyl methyl ether (**223**) by alkyllithium in the presence of (−)-sparteine (**11**) and trapping of the carbanionic intermediates afforded no enantioenrichment[170]. However, excellent results were found by Nakai and coworkers when the deprotonation was carried out with *t*-BuLi and the bisoxazoline **224** (equation 52)[170]. Control experiments revealed that the intermediate complexes **225** are configurationally labile, and the experimental evidence points to a dynamic thermodynamic resolution as the major influence; one epimer **225** or *epi*-**225** must dominate. However, the reaction of **225** with different aldehydes resulted in strongly varying e.r. values of the resulting alcohols **227**[171]. On the other hand, the carboxylation with carbon dioxide furnished the corresponding acid **226** with excellent yield and enantioselectivity. One must conclude that also a dynamic kinetic resolution via interconversion of **225** and *epi*-**225** contributes significantly. Unfortunately, it is not recorded whether a precipitation was observed after deprotonation, which could enhance the actual energy difference. Similarly, an asymmetric lithiation substitution of isochroman (**228**) and phthalan (**229**) was achieved[172].

The (−)-sparteine-mediated deprotonation of *o*-(allylmethoxy)benzamides (**230)** in the benzylic position lead to a [2,3]-Wittig rearrangement of the carbanionic intermediate (**231**) to yield the secondary allyl carbinol **232** of unknown configuration with 60% *ee* (equation 53)[173]. Enantiomeric excesses between 28% and 43% were observed in the (−)-sparteine-mediated lithiation and subsequent [2,3]-Wittig rearrangement of (*E*)- and (*Z*)-crotyl 2-furfuryl ethers[174]. Enantiopure secondary 2-alkenyl ethers are deprotonated (*t*-BuLi/THF) and rearranged with complete chirality transfer[174]. The [2,3]-Wittig rearrangement of few (benzothiazol-2-yl)methyl 2-propenyl ethers under 'sparteine conditions' afforded roughly 50% *ee*[175].

Although slightly outside the scope of this review, an interesting case of stereoselection should be presented here. It has been observed by Gibson (née Thomas) and coworkers during the deprotonation of tricarbonylchromium complexes of benzyl alkyl ethers by means of the chiral bis(lithiumamide) base **234** (equation 54)[127, 176]. The base removes the benzylic *pro*-*R*-H atom in **233** from the most reactive conformation to form the planary chiral intermediate **235**. The attack of the electrophile forming **236** proceeds exclusively from the upper face in **235**, because the bulky chromium moiety shields the lower face. Simpkins and coworkers extended the method to the enantioselective substitution of the chromium complexes of 1,3-dihydroisobenzofurans[177, 178].

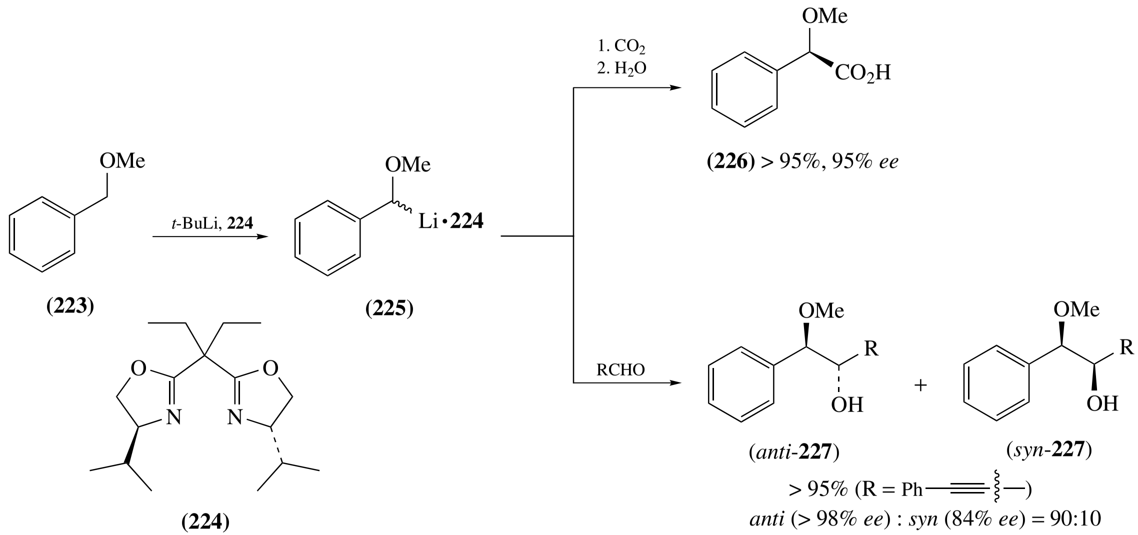

(223) **(225)** **(224)**

(226) > 95%, 95% *ee*

(*anti*-**227**) (*syn*-**227**)

> 95% (R = Ph—≡—)

anti (> 98% *ee*) : *syn* (84% *ee*) = 90:10

(52)

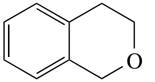

(228)

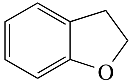

(229)

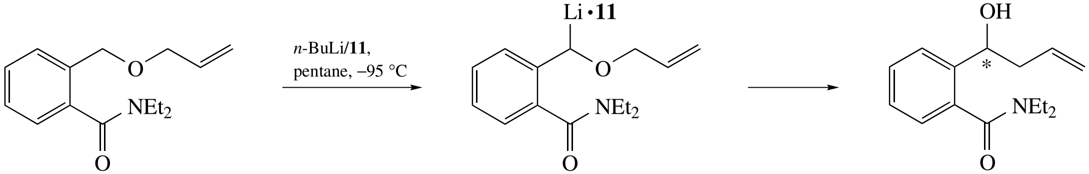

(230) **(231)**

(232) 83%,
e.r. = 80:20

(53)

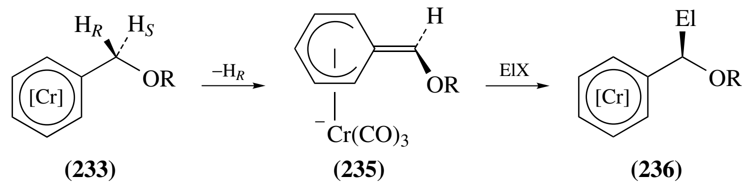

(54)

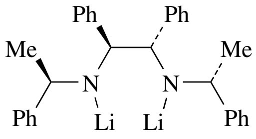

(234)

R = Me, ElX = $(PhS)_2$,
86%, e.r. = 98.5:1.5
R = $PhCH_2$, ElX = MeI,
89%, e.r. > 99.5:0.5

C. Lithiation Adjacent to Nitrogen

N-Boc-benzylamines are readily deprotonated by alkyllithium/TMEDA[97]. Schlosser and Limat investigated the deprotonation of *N*-Boc-*N*-methylbenzylamine (**237**) by *s*-BuLi/(−)-sparteine (**11**) (equation 55)[179].

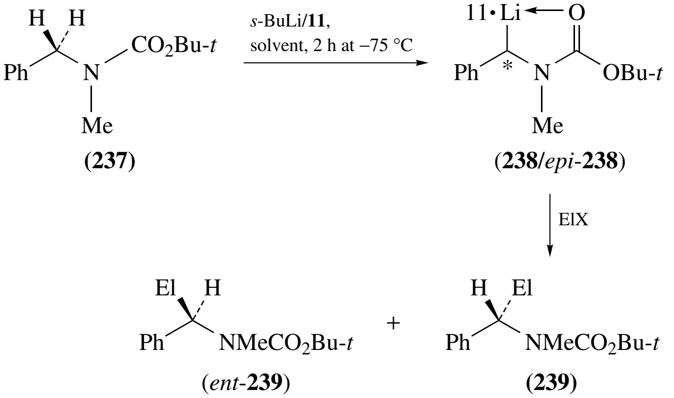

(237) (**238**/*epi*-**238**)

(55)

(*ent*-**239**) **(239)**

Trapping the mixture of **238**/*epi*-**238**, produced in hexane or Et_2O, with various electrophiles gave the enantiomers **239** with good enantiomeric excesses. However, in THF, where a precipitate was observed, the opposite enantiomers *ent*-**239** were formed. Since the ion pairs **238**/*epi*-**238** proved to be configurationally unstable under the reaction conditions, it is quite likely that the crystallization step furnished the enrichment. Using 1,2-dimethoxyethane (DME) as the solvent, completely racemic products were formed,

TABLE 3. Table to equation 55. Enantiomeric ratios **239**/*ent*-**239**

239/*ent*-**239**	ElX	Hexane	Et_2O	THF
a	CO_2	90.5:9.5	83.5:16.5	7.5:92.5
b	CS_2	69:31	75.5:24.5	13:87
c	MeI	87.5:12.5	81:19	10:90
d	$(MeO)_2SO_2$	77.5:22.5	76.5:23.5	16:84

indicating that DME displaces (−)-sparteine (**11**). The reviewer concludes that the enantiomers **239** arise from (*R*)-**238** and vice versa. Voyer and coworkers independently reported the synthesis of (−)-phenylsarcosine via the carboxylation of a derivative of **237**[180] and the deprotonation in the presence of (−)-sparteine (**11**) and silyl migration of the appropriate *N*-trimethylsilyl and *N*-triisopropylsilyl derivative (R^3Si for Me in **238**)[181].

Beak and coworkers accomplished the asymmetric deprotonation of several *N*-Boc-*N*-(3-chloropropyl)arylmethylamines (**240**) with enantiomeric excesses up to 98:2 (equation 56)[182]. The intermediate lithium compound **241** cyclizes to form pyrrolidines **242** in good yields and enantioselectivities. The rapid intramolecular substitution step conserves the originally achieved high kinetic differentiation in the deprotonation step.

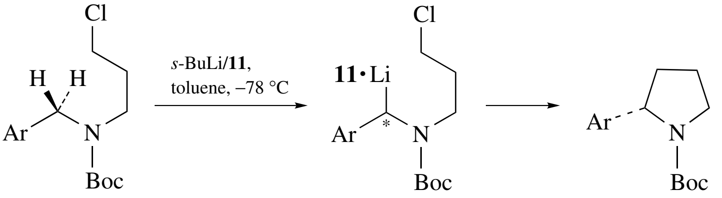

(240) **(241)** **(242)** (56)

Ar = Ph: 72%, e.r. = 98:2

Beak and coworkers found the (−)-sparteine-complex of *N*-Boc-*N*-(*p*-methoxyphenyl)benzyllithium **244**, obtained from **243** by deprotonation with *n*-BuLi/(−)-sparteine (**11**) in toluene, to be configurationally stable (equation 57)[183, 184]. On trapping **244** with different electrophiles, the substitution products **245** are formed with high *ee*. Efficient addition reactions with imines and aldehydes have also been reported. The *p*-methoxyphenyl residue is conveniently removed by treatment with cerium ammonium nitrate (CAN).

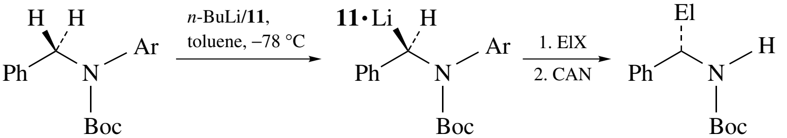

(243) **(244)** **(245)** (57)

Ar = 4-MeOC_6H_4

(a) ElX = MeOTf, 81%, e.r. = 97:3
(b) = BnOTf, 73%, e.r. = 98:2
(c) = AllOTf, 69%, e.r. = 97:3

The methylation product **245a**, on deprotonation with *n*-BuLi/TMEDA, provides the configurationally stable anion (*S*)-**246**, which was allylated with inversion of the configuration to yield (*R*)-**247** with 97% *ee* (equation 58)[183]. The enantiomer (*R*)-**247** is available via the tin compound **245d**, which is cleaved with *n*-BuLi/**11** with retention of the configuration to *epi*-**244**, followed by the same sequence of alkylation steps[183].

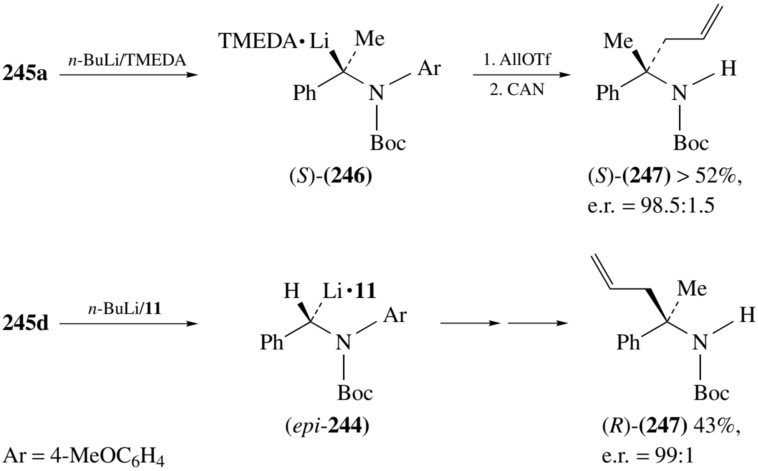

(58)

Chain elongation of **244** (or *epi*-**244**) to (*R*)- or (*S*)-α-, β- and γ-amino acids by carbon dioxide, 3-methylbut-2-enyl bromide, followed by oxidative cleavage of the C−C double bond, or 1,4-addition onto acrolein (followed by oxidation), respectively, proceeds smoothly and with high enantiomeric excesses[185].

The enantioselective deprotonation of the borane complex **248** of *N*-methylisoindoline was investigated by Simpkins and coworkers (equation 59)[186, 187]. Deprotonation with *s*-BuLi/(−)-sparteine (**11**) in diethyl ether at −78 °C for 1 h, followed by quenching with chlorotrimethylsilane, yielded the silanes **251**, *ent*-**252, 252**, *ent*-**251** in a ratio of 86.3:0.4:6.3:7.0[186]; after destroying the chiral centre at nitrogen by treatment of the whole mixture with triethylamine, an e.r. **253**/*ent*-**253** of 86.7:13.3 is expected.

The diastereomers **251**/*ent*-**251** and **252**/*ent*-**252** could be separated and were decomplexed separately. From the fraction of **251**/*ent*-**251, 253** was obtained with 85% *ee* (e.r. = 92.5 : 7.5), and the fraction of **252**/*ent*-**252** yielded *ent*-**253** with 88% *ee* (e.r. = 6:94). A similar situation results from the reaction with tributyltin chloride or alkylation reagents, but the diastereomeric ratio is strongly dependent on the electrophile. The following conclusion is drawn from these and further experiments: The enantiomeric ratio is determined by a selection of the chiral base between the diastereotopic methylene groups, since the benzylic carbanionic centres are labile, whereas the diastereomeric ratio results from the relative rate of the electrophile approach *syn* or *anti* with respect to the *N*-methyl group. One question remains—why are opposite d.r. values formed in the alkylation by methyl iodide and ethyl iodide[186]?

D. Asymmetric Deprotonation Adjacent to Sulphur

α-Thio-substituted organolithium compounds have a very limited configurational stability (see Section II.E). As Toru and coworkers found, this is also true for α-phenylthiobenzyllithium (*rac*-**254**) (equation 60)[188, 189]. However, in the presence of the bis(oxazoline) **255** in toluene or cumene as solvent, trapping the reaction mixture with aldehydes or ketones, the adducts **256** have been isolated with 87 to 99% *ee*. Other electrophiles or the application of (−)-sparteine (**11**) gave lower *ee* values. All experimental evidence, which was supported by quantum-chemical calculations, attributes the origin to a dynamic kinetic resolution between the rapidly equilibrating ion pairs **254•255**.

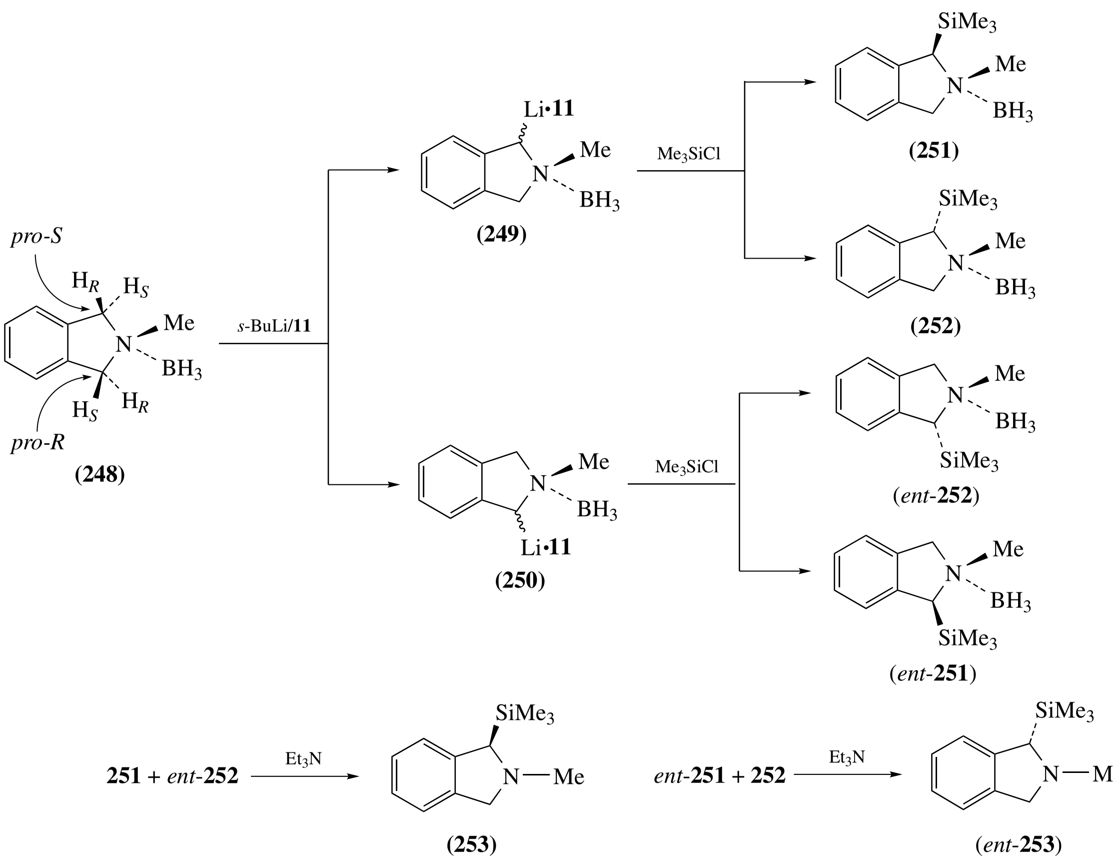
pro-S
pro-R
H$_R$
H$_S$
Me
N
BH$_3$
(248)
s-BuLi/11
Li•11
(249)
(250)
Me$_3$SiCl
SiMe$_3$
(251)
(252)
(ent-252)
(ent-251)
251 + ent-252
ent-251 + 252
Et$_3$N
(253)
(ent-253)

(59)

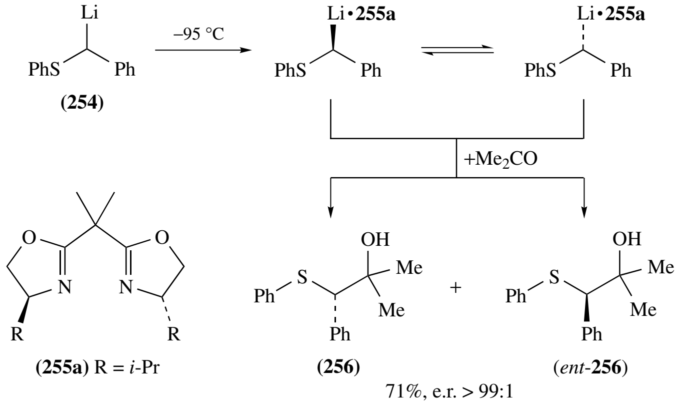

(60)

The closely related α-(pyrid-2-ylthio)benzyllithium (**257**) has a higher configurational stability, and equilibration with the chiral ligand prior to the substitution step is required[189], indicating that a dynamic thermodynamic resolution is important (equation 61). Depending on the method of calculation, (R)-**257•255b** was found to be by 1.42 to 1.92 kcal mol^{-1} more stable than (S)-**257•255b**[189].

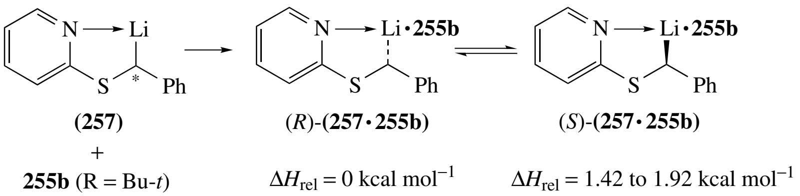

(61)

An interesting result, contributed by Gibson (nee Thomas) and coworkers, should be added[190]: The tricarbonylchromium complexes **258** are readily deprotonated by the chiral bis(lithium amide) **234** and alkylated to provide highly enantioenriched alkylation products **260** (equation 62). The decisive intermediate **259** presumably is formed by abstraction of the *pro-S* proton and is attacked from above. Related work has been published by Ewin and Simpkins[177].

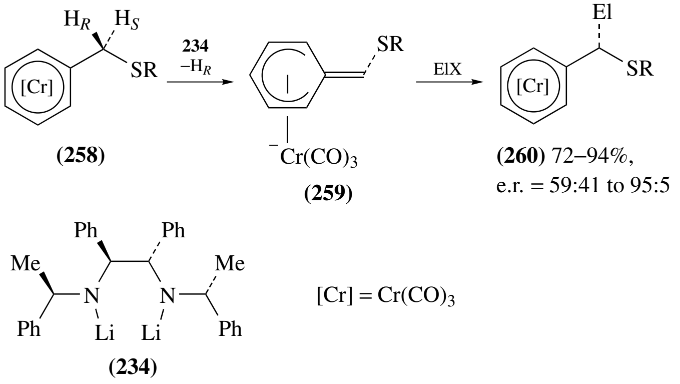

(62)

E. Deprotonation at Non-heteroatom Substituted Benzylic Positions

If no complexing substituents are in the vicinity, the deprotonation at benzylic methyl groups is a rather slow reaction. The first recorded attempt of (−)-sparteine-mediated lithiation by Nozaki and coworkers[191] has already been mentioned in Section I.A.1. Raston and coworkers obtained by dilithiation of 2,2′,6,6′-tetramethylbiphenyl followed by bismethylation one of the atropoisomers of 2,2′-diethyl-6,6′-dimethylbiphenyl with 40% *ee*[192].

Dilithiation of *N*-methyl-3-phenylpropaneamide (**261**) and subsequent addition of a slight excess of (−)-sparteine (**11**) form a mixture of epimeric ion pairs **262**/*epi*-**262**, which is substituted by electrophiles to give the β-substitution products **263** with good *ee* values (equation 63)[193–196]. The intermediates are not configurationally stable, but at low temperature one epimer **262** or *epi*-**262** dominates due to the higher thermodynamic stability. Consequently, Beak and coworkers propose on the basis of a detailed mechanistic investigation the pathway of dynamic thermodynamic resolution[196].

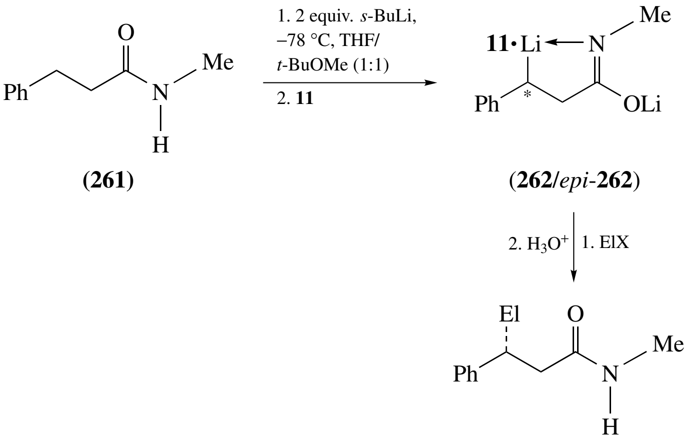

(261)

(**262**/*epi*-**262**)

(63)

(263) **(a)** ElX = Me_3SiCl, 86%, 94% *ee*
(b) ElX = MeI, 84%, 78% *ee*
(c) ElX = PhCHO, 63%, 65% *ee*

N-(2-Phenylethyl)isobutyramide (**264**) is dilithiated by means of *s*-BuLi/(−)-sparteine (**11**) to form the benzyllithium derivative **265** (equation 64)[197]. The reaction with different electrophiles (Me_3SiCl, Bu_3SnCl, alkyl halides, cyclohexanone, benzaldehyde) provides the (*S*)-enantiomers of the phenylethylamides **266** with good excesses. Beak and coworkers propose a dynamic thermodynamic resolution as the origin; albeit not all of the mechanistic studies with different electrophiles are completely consistent.

An interesting stereochemical situation was found for the lithium-(−)-sparteine complex derived from *o*-ethyl-*N*,*N*-diisopropylcarboxamide **267** (equation 65)[194, 198, 199]. Control experiments, involving lithiodestannylation experiments and the Hoffmann test, led to the conclusion that **268**/*epi*-**268** are configurationally unstable at −78 °C and the e.r. in **269** is determined by a dynamic kinetic resolution of the rapidly interconverting intermediates[199]. It is noteworthy that the configuration is inverted by using tosylates[199].

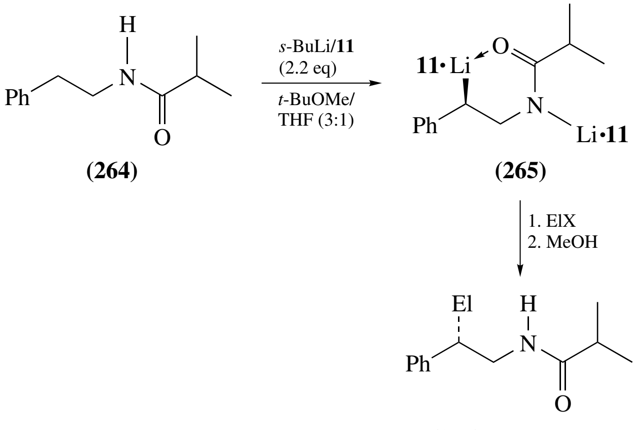

(264) (265)

(266) 68–90%,
e.r. = 72:28 to 91:9

(64)

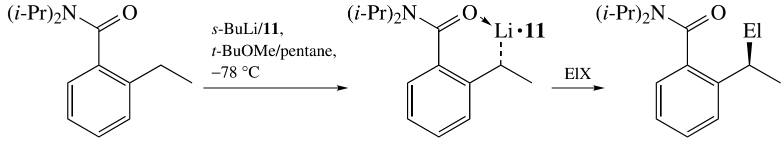

(267) (268/*epi*-268) (269)

(65)

TABLE 4. Data for the reactions in equation 65

Entry	Solvent	ElX	Yield **269** (%)	e.r.
1	*t*-BuOMe/pentane	Me_3SiCl	79	96:4
2	Pentane	Bu_3SnCl	78	94:6
3	*t*-BuOMe/pentane	$PhCH_2Cl$	52	84:16
4	Pentane	Allyl-Cl	89	96:4
5	Pentane	Allyl-OTos	46	6:94
6	*t*-BuOMe/pentane	C_4H_9I	71	64:36
7	Pentane	C_4H_9Cl	95	90:10
8	Pentane	C_4H_9-OTos	52	1:99

The authors assume that the halides react with stereoinversion, whereas the tosylates prefer suprafacial attack due to binding interaction with the lithium ion in the transition state[199]. A comparable dependence of the stereochemical course from the leaving group has been observed in other stereodefined benzyllithiums, too[200]. The addition of **268** to *N*-methyl-benzylideneimine proceeds with only low yield[201].

Starting from 2-ethyl-5,*N*-dimethyl-*N*-octylbenzamide (**270**), formal syntheses of both enantiomers of curcuphenols were developed (equation 66)[202]. The sequence of deprotonation and substitution afforded the amide **271** with 80% *ee*. **271** was transformed in a few further steps into the curcuphenols **272**.

The double deprotonation of *o*-ethyl-*N*-pivaloylaniline (**273**) leads to intermediates **274** being configurationally stable at −78 °C (equation 67)[198]. With most electrophiles,

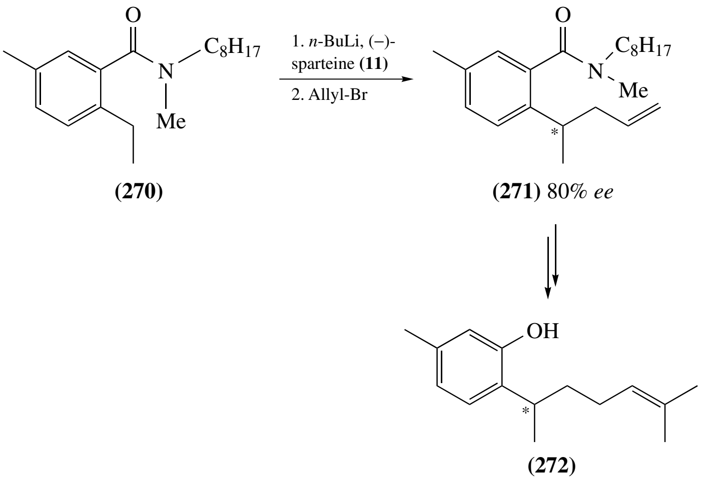

(66)

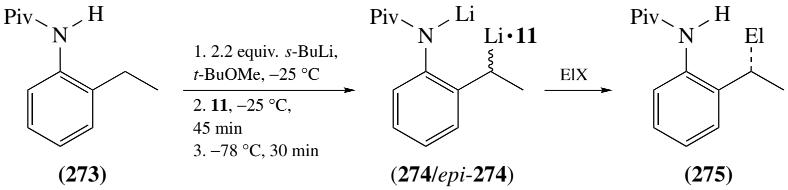

Piv = C(=O)-Bu-*t*

(67)

TABLE 5. Data related to the products of equation 67

Entry	ElX	Yield **275** (%)	e.r.
1	Me_3SiCl	72	95:5
2	Me_3SnCl	77	83:17
3	Allyl-Cl	78	88:12
4	Allyl-OTos	53	86:14
5	BnBr	56	90:10
6	Cyclohexanone	80	89:11

the substitution products **275** are formed with roughly 70 to 80% *ee*[199]. The chiral information is introduced after the deprotonation step at −25 °C. After addition of (−)-sparteine (**11**) an equilibrium takes place; the equilibrium is frozen at −78 °C. Thus, a dynamic thermodynamic resolution is the major origin of the observed enantioselectivity. It can be improved by a so-called warm-cool protocol by adding the electrophile in smaller portions and allowing the remaining intermediate **274**/*epi*-**274** again to equilibrate at −25 °C before bringing the reaction to completion[162, 198].

Racemic, cyclic and open-chain 1,2-diarylalkanes have been deprotonated under the regime of the sparteine protocol[203, 204]. *N*-Methyl-4-phenyl-1,2,3,4-tetrahydroisoquinoline (**276**) was deprotonated by *s*-BuLi/(−)-sparteine (**11**) and the intermediates **277** were quenched by MeOD. When performing the reaction in diethyl ether, (*R*)-**278** was isolated with high *ee* values, up to 88% (equation 68)[203].

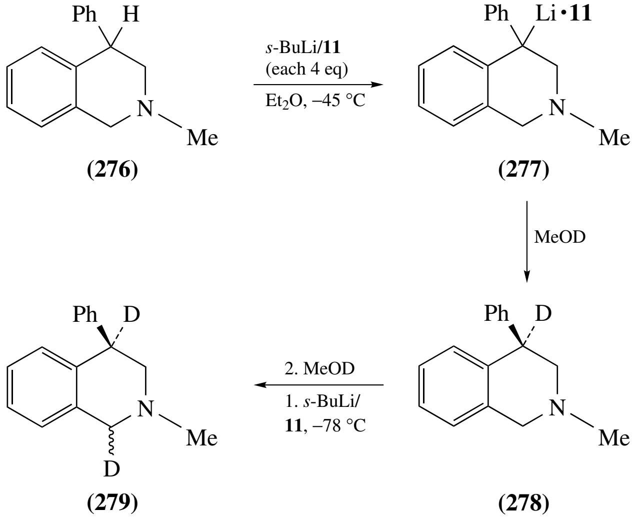

(68)

Repeated deprotonation of **278** removed due to a high H/D kinetic isotope effect the 1-proton, forming the dideuterio compound **279** with low diastereoselectivity[203]. It is quite likely that a dynamic thermodynamic resolution is the origin. Intermediate **277** is configurationally labile, enabling an equilibration of the diastereomeric ion pairs **277** and *epi*-**277**. Similar studies were undertaken with 1-phenyl-1-pyrid-2-ylethane (**280**) and 1-(4-chlorophenyl)-1-(pyrid-2-yl)-3-(dimethylamino)propane (**281**) (50% *ee*)[204]. An improvement of the achieved enantiomeric excesses resulted when external chiral proton sources, such as **282** or **283**, were applied (84% *ee* for **280** with **283** and 75% *ee* for **281**).

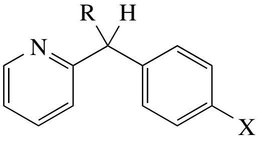

(280) R = Me, X = H

(281) R = $CH_2CH_2NMe_2$, X = Cl

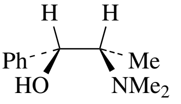

(282)

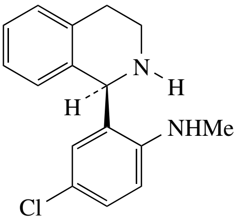

(283)

The asymmetric deprotonation of 1-(benzothiazol-2-yl)-1-chloroethane followed by carbonyl addition served as a tool for the enantioselective synthesis of chlorohydrins and oxiranes[205].

IV. ALLYLLITHIUM–(−)-SPARTEINE COMPLEXES

A. General Aspects

Allylic compounds have acidities similar to those of the corresponding benzylic analogues[206]. Due to the mesomeric stabilization, the carbanionic centre is considerably but not completely flattened. As a result, configurational stability is decreased and antarafacial reactions with electrophiles are easily feasible. In addition, further complications arise from the competition of α- and γ-substitution (S_E- and S'_E-substitution). Moreover, in an unsymmetrically 1,3-disubstituted η^1-allylmetal, up to eight regio- and torsion isomers **284a**–**284h** may be in equilibrium, even if assuming that the 'cation' performs exclusively suprafacial 1,3-migrations (equation 69)[207]. If the system prefers η^3-complexation, the number of isomers is reduced to four (**285a**–**285d**). These are equivalent to the transition states of suprafacial 1,3-migrations of the cation (equation 69).

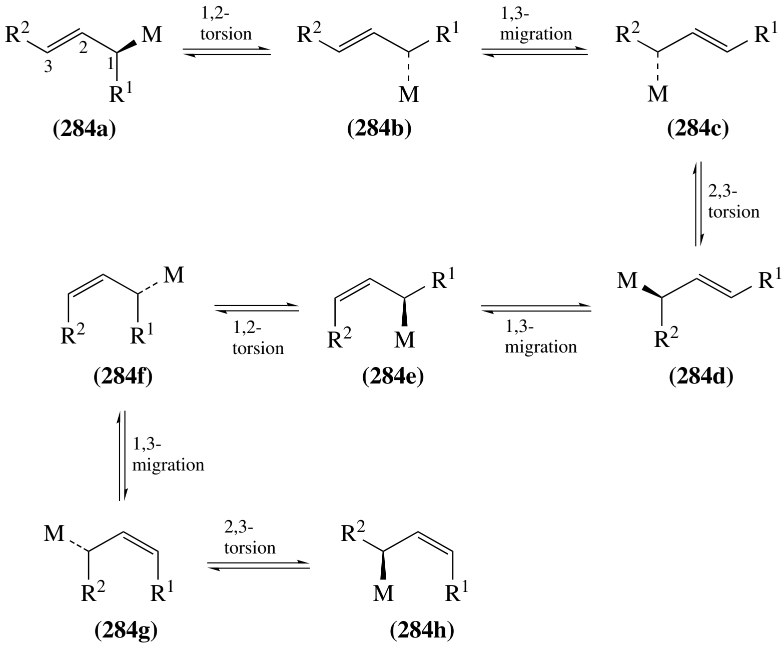

(69)

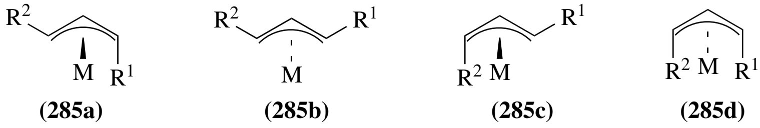

Each of these isomers **284** can be attacked by electrophiles through four different pathways ($S_E$ret, $S_E$inv, *syn*-S'_E, *anti*-S'_E). This is demonstrated in equation 70 only for the torsion isomers **284a** and **284b**, already giving rise to six different products (**286, 287, 288** and the corresponding enantiomers). In view of the difficulties it is quite surprising that synthetically useful, highly selective chiral reagents could be developed on the base of allyllithium reagents.

The most important chemical means for solving these problems were:

(a) Introduction of a strongly complexing substituent X such as *N*,*N*-dialkylcarbamoyloxy by Hoppe and coworkers[208,209] and *N*-(alkoxycarbonyl)amino groups by Beak and coworkers[30,97] ties up the lithium cation closely onto the 1-position, thus enhancing the torsion barrier of the 2,3-bond.

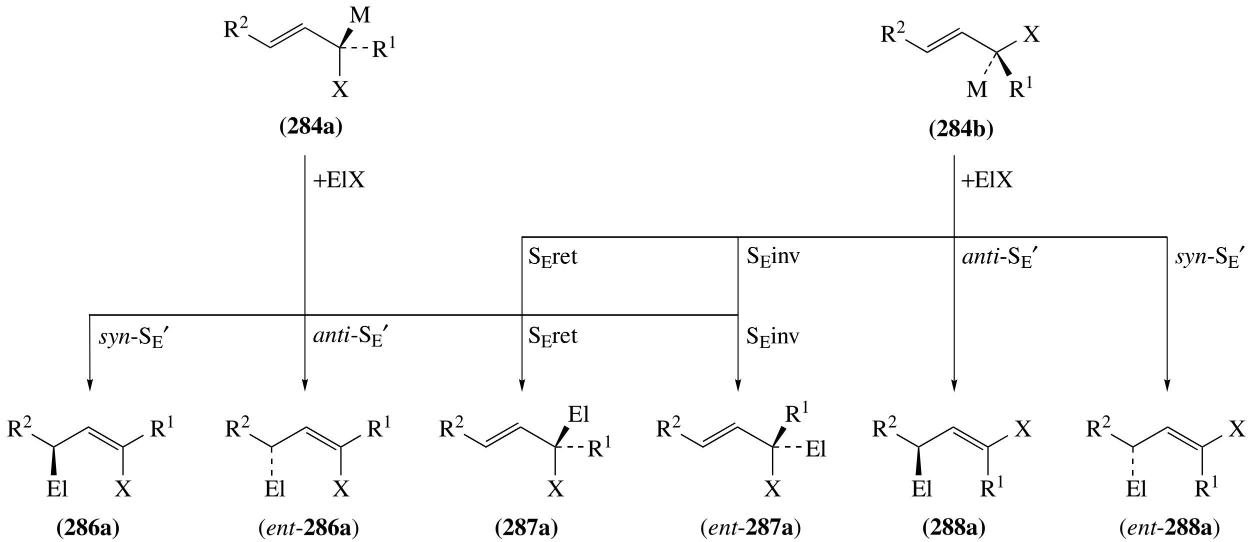
(284a)
+ElX
(284b)
+ElX
$S_E$ret
$S_E$inv
anti-S_E'
syn-S_E'
syn-S_E'
anti-S_E'
$S_E$ret
$S_E$inv
(286a)
(ent-286a)
(287a)
(ent-287a)
(288a)
(ent-288a)

(70)

(b) Exchange of lithium for a covalently bound metal residue (X_3Ti^{210}, $R_2Al^{211,212}$) before the reaction with an electrophile.

B. Non-functionalized Allyllithium–(−)-Sparteine Complexes

3-Methyl- and 3-butyl-3*H*-indene (**289a, 289b**) are smoothly deprotonated in the presence of (−)-sparteine (**11**) by *n*-BuLi in ethereal solution (equation 71)[213]. A precipitate is formed on prolonged stirring, consisting in the stereohomogeneous lithium–(−)-sparteine complexes **290a** and **290b**, respectively. In solution, these are in equilibrium with the diastereomers **291a** and **291b**. An X-ray crystal structure 1-butylinilene-lithium/(−)-sparteine analysis could be obtained from **290b**[213]. **290b** exists as η^3-complex in which the lithium cation binds one equivalent of sparteine as bidentate ligand. The distances C(1)–Li (243.2 pm) and C(3)–Li (233.4 pm) are quite different in **290b**. Since (−)-sparteine is not a C_2-symmetric ligand, a stereogenic but kinetically mobile centre is created at the lithium cation.

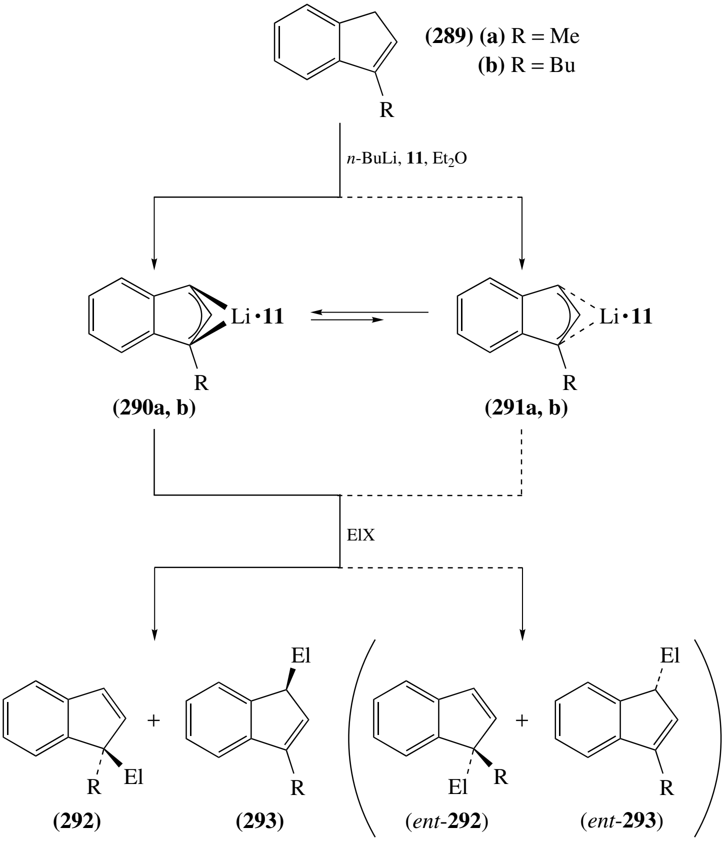

(71)

Reactions of the formed slurries of **290a** and **290b** with aldehydes, ketones or acid chlorides proceed highly stereoselectively to produce the substitution products **292** and **293** with > 95% *ee*[213]. Their absolute configurations were elucidated by the combination of X-ray analyses[214] and chemical correlation of the products, revealing that the η^3-complex is 'opened' with retention of configuration. Small and reactive electrophiles (such as

TABLE 6. Data related to equation 71

Entry	R	ElX	Yield (%)	Ratio **292/293**	e.r.
1	Me	MeOC(O)Cl	64	$>$ 97:3	$>$ 97:3
2	Me	MeC(O)Cl	63	$>$ 97:3	$>$ 97:3
3	Bu	PhC(O)Cl	79	$>$ 97:3	$>$ 97:3
4	Me	t-BuCHO	55	$<$ 3:97	n.d.
5	Me	Me_2CO	36	31:69	$>$ 97:3

methyl chloroformate, acetyl chloride, benzoyl chloride) attack with high selectivity the weaker C(1)–Li bond to form the sterically more encumbered products **292**, whereas bulkier electrophiles (acetone, 2,2-dimethylpropanal) are introduced to the 3-position with formation of the isomers **293**. Alkyl and silyl chlorides failed to react. When the electrophiles were added before the crystallization was complete, much lower *ee* values were achieved. Obviously, the major amount of the configurationally labile, epimeric lithium compounds is converted into the $(1S)$-diastereomer **290** by equilibration and selective crystallization. This '*asymmetric transformation of the second order*'[27] is sometimes assigned as a '*dynamic thermodynamic resolution*'[25]. The sparteine complexes **290** are quite labile: on addition of THF to the solution of **290a**, the η^1-3-methylindenyllithium–$(THF)_3$ complex (**294**) is formed and was characterized by X-ray analysis[213].

Surprisingly, the unsubstituted indenyllithium–(−)-sparteine **289c** ($R = H$) in many cases leads to similarly high enantioselectivities[41]. The stereoselection here is considered to occur by kinetic resolution at constitutionally identical but diastereotopic positions 1 and 3. Unfortunately, the absolute configuration of the addition products could not be determined due to its facile racemization.

The exact nature of the epimerization is still not known. NMR studies are hampered by line broadening and multiplication due to frozen rotations in the N,N-diisopropylcarbamoyl group at the required low temperatures. Some indications were gained by a ^1H NMR investigation of the temperature dependence of the kinetics in the epimerization of the (−)-sparteine and (−)-α-isosparteine complexes derived from 1-lithioinden-1-yl carbamates **295** and **296**, carried out in cooperation with G. Fraenkel (equation 72, Table 7)[215]. These complexes are chemically stable above 0 °C, and interpretable spectra were obtained.

The epimerization process in diethyl ether-d_{10} as the solvent follows first order or pseudo-first order kinetics. The (−)-α-isosparteine complexes **296a** and **296b** show much lower barriers than the corresponding (−)-sparteine complexes. A 2-methyl group (**295b** and **296b**) enhances $\Delta H^{\neq}$ significantly. Surprisingly, the entropies of activation are negative, indicating that an addition step (of the solvent?) might be rate determining. Since (−)-sparteine (**11**) is not C_2-symmetric, an additional stereogenic centre arises at Li in complexes **295**/*epi*-**295**, giving rise to a set of four diastereomers. However, no hints were found for the participation of two additional diastereomers. Possibly, these are markedly higher in energy and epimerization at the lithium cation is a very facile process.

meso-1,3-Diphenylallyllithium–(−)-sparteine (**297**) was obtained in crystalline form (equation 73) and was subjected to X-ray analysis[216]. The stereochemical situation is similar to those in indenyllithium–(−)-sparteine (**290**). The η^3-bound carbanionic moiety has two constitutionally identical nucleophilic positions [C(1) and C(3)], which are diastereotopic, and thus the bond lengths C(1)–Li (245.8 pm) and C(3)–Li (221.3 pm) differ significantly. C(1) and C(3) are completely planarized, as a result of the good resonance stabilization in the carbanion. Electrophiles such as acetone and trimethylsilyl chloride achieve only a marginal differentiation, and products **298** are obtained with very low enantiomeric excesses (0–22% *ee*).

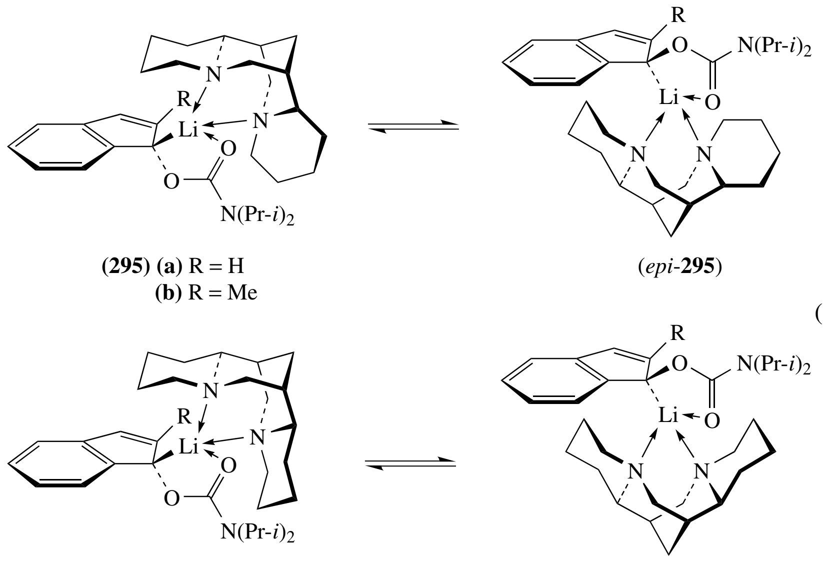

(295) **(a)** R = H
(b) R = Me

(*epi*-**295**)

(72)

(296) **(a)** R = H
(b) R = Me

(*epi*-**296**)

TABLE 7. Activation parameters for epimerization of lithiated sparteine and α-isosparteine complexed indenes (complexes **295** and **296**)

Compound	d.r.[a]	$\Delta H^{\neq}$ (kcal mol^{-1})	$\Delta S^{\neq}$ (kcal mol^{-1} K^{-1})
295a	55:45	13.5	−8
295b	60:40	> 25	—[b]
296a	—[c]	< 5	—[b]
296b	18:82	8.0–8.5	−25.1

[a] Isomer appearing at lower field at left.

[b] Line shape analysis not possible.

[c] The diastereomeric ratio could not be determined due to fast epimerization.

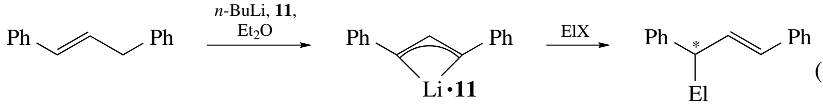

(297)

(298) 0–22% *ee*

(73)

C. 1-(*N*,*N*-Dialkylcarbamoyloxy)-2-alkenyllithium–(−)-Sparteine Complexes

1. Preparation and structure

As was found in 1980 by Hoppe and coworkers, a *N*,*N*-diisopropylcarbamoyloxy group in allylic position not only facilitates the deprotonation reaction by n-BuLi/TMEDA, but also enhances the chemical stability of the lithium compounds[54, 208, 209, 217]. Moreover, it was demonstrated in 1986 that lithiation of optically active, secondary allyl carbamates **299** give rise to unprecedented, configurationally stable lithium compounds **300** (equation 74)[218, 219]. The enantiomerically pure 1-methylated precursors, such as **299b**, are easily accessible by Wittig olefination of (*R*)- or (*S*)-*O*-carbamoyl lactaldehydes[220].

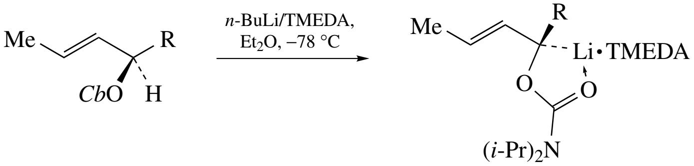

(*R*)-(**299**) (**a**) R = *i*-Bu
(**b**) R = Me

(*S*)-(**300**)

(74)

When the racemic carbamate **299b** is deprotonated by 0.5 equivalents of *n*-BuLi/(−)-sparteine (**11**), an efficient kinetic resolution takes place to produce the lithium compound (*S*)-**300b** (80–82% *ee*) and leaving (*R*)-**299b** (80% *ee*) behind (equation 75)[9, 219, 221–223].

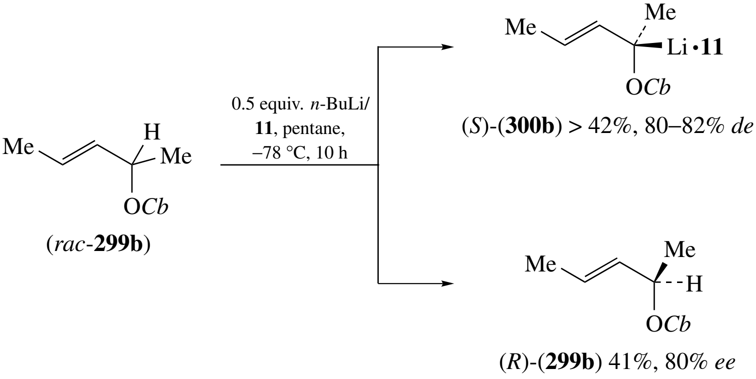

(*rac*-**299b**)

(*S*)-(**300b**) > 42%, 80–82% *de*

(*R*)-(**299b**) 41%, 80% *ee*

(75)

The lithium–(−)-sparteine complexes, derived from primary 2-alkenyl carbamates, are usually configurationally labile even at −78 °C. During the investigation of the (*E*)-crotyl carbamate **301**, the (−)-sparteine complex (*S*)-**302** crystallized in a dynamic thermodynamic resolution process (equation 76) and stereospecific substitutions could be performed with the slurry[8, 224, 225]. An incorrect assignment of the configuration of the lithium intermediate occurred in the first publication[8]. An optimized procedure has been published[28].

An X-ray crystal structure analysis was obtained from the 3-(trimethylsilyl)-allyllithium–(−)-sparteine complex (*S*)-**302b**[226]. It reveals the monomeric structure of these allyllithium compounds and a η^1-coordination of the allylic anion to the lithium cation. The latter is tetracoordinated and takes advantage of the chelating oxo group. The fixation of the lithium at the α-carbon atom is supposed to be the origin of the high regioselectivity of several substitution reactions.

A couple of 2-alkenyl carbamates have been deprotonated by *n*-BuLi/(−)-sparteine (**11**) (toluene, −78 °C) in the presence of an excess of trimethylsilyl chloride. The *ee* values in the silane, formed *in situ* with inversion of the configuration, demonstrate the

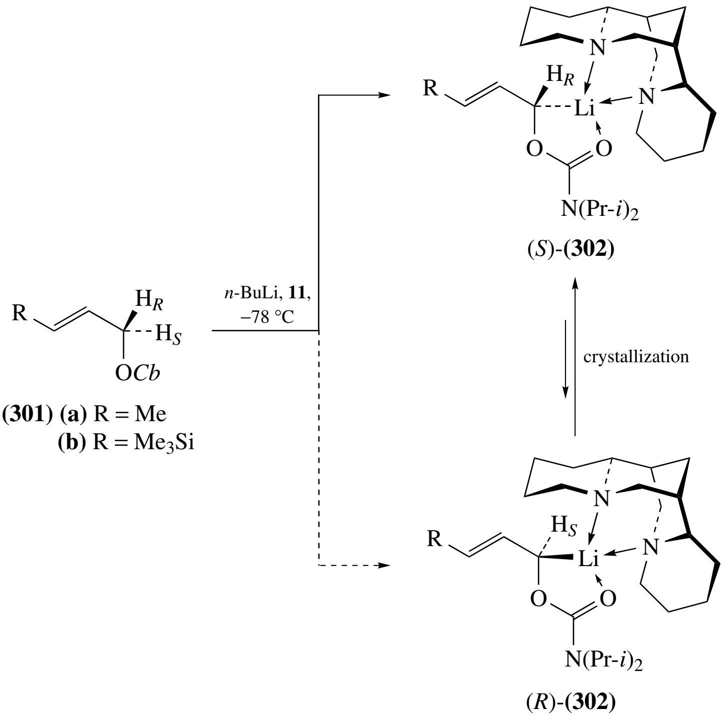

(301) **(a)** R = Me
(b) R = Me_3Si

(*S*)-**(302)**

(*R*)-**(302)**

(76)

minimum value of kinetically controlled enantiofacial selectivity achieved in the deprotonation experiment with the achiral precursor (H for Me_3Si). The *pro-S*-H is abstracted more rapidly. Some examples (**303a**-**303f**) are collected in Scheme 5.

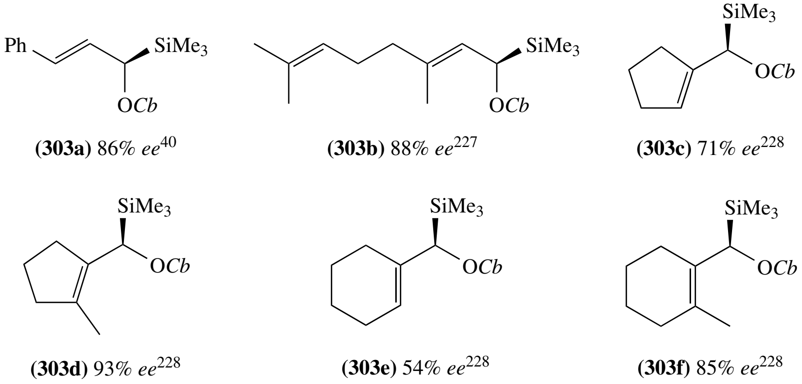

(303a) 86% *ee*[40]

(303b) 88% *ee*[227]

(303c) 71% *ee*[228]

(303d) 93% *ee*[228]

(303e) 54% *ee*[228]

(303f) 85% *ee*[228]

SCHEME 5

Usually, the enantiomeric ratios decrease on prolonged reaction times to approach the thermodynamically determined ratios of diastereomers. Notable exceptions are the lithium–(−)-sparteine derivatives of (2-methyl-1-cycloalkenyl)methyl carbamates *ent*-**303d** and *ent*-**303f** (Li•**11** for Me_3Si), which turned out to be configurationally stable under the reaction conditions[228]. The cinnamyl carbamate *ent*-**303a** (Li • **11** for Me_3Si) epimerizes to a 90:10 ratio in favour of the (*R*)-epimer[40]. High enantiomeric excesses can be conserved if a reactive electrophilic moiety is attached to the allylic carbamates in order to promote a rapid intramolecular reaction (see Section IV.C.3)[229].

The geometry of the 2,3-double bond in alkyl-substituted 2-alkenyl carbamates is usually retained during the lithiation; however, the (*Z*)-3-silyl-substituted lithium–TMEDA compound **305** derived from the allyl carbamate **304** undergoes a rapid and complete (*Z*) → (*E*) torsion, forming the TMEDA complex (*E*)-**306** (equation 77)[209, 230, 231]. This is also true for (−)-sparteine complexes, although a possible large difference in the rates has not yet been investigated more closely[226].

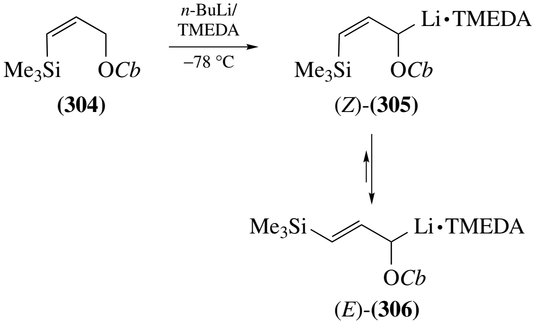

(304) (*Z*)-**(305)** (*E*)-**(306)**

(77)

Another very useful approach to essentially enantiopure, 1-aryl-substituted 1-lithio-2-alkenyl carbamates has been found very recently[232, 233]. It constitutes the (−)-sparteine-mediated γ-deprotonation of (*Z*)-1-aryl-1-alkenyl carbamates **307** by *n*-BuLi/(−)-sparteine (**11**) (equation 78). The configuration of the lithium intermediate **308** has not yet been elucidated without any doubt. Most of the arguments count for its (1*S*,3*E*)-configuration. The majority of electrophiles attack the γ-position with high regioselectivity to form the adducts (*S*)-**309** with > 95% *ee*. The method avoids kinetic resolution, since an achiral precursor is subjected to enantiotopos differentiation. A chiral auxiliary-controlled approach to generate chiral lithioalkenyl carbamates is also available[234].

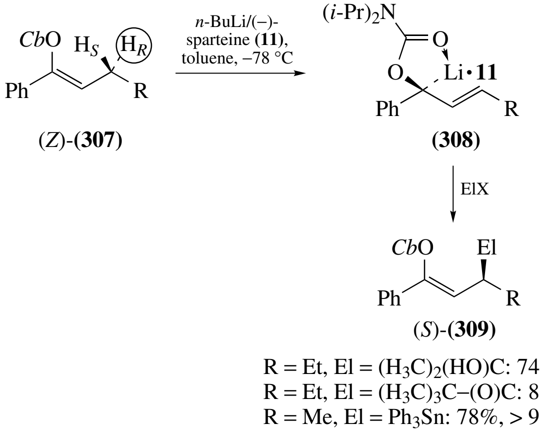

(*Z*)-**(307)** **(308)** (*S*)-**(309)**

(78)

R = Et, El = $(H_3C)_2(HO)C$: 74%, > 95% *ee*[232]
R = Et, El = $(H_3C)_3C{-}(O)C$: 83%, > 95% *ee*[232]
R = Me, El = Ph_3Sn: 78%, > 95% *ee*[233]

2. Lithiated allyl carbamates stereochemistry of electrophilic substitution

Contrary to lithiated alkyl carbamates, which hold a pyramidalized sp^3-hybridized carbanionic centre and thus generally react with electrophiles under retention of configuration (see Section II.B.1), lithiated (*E*)-allyl carbamates **310** have a high tendency for antarafacial reactions, which seem to be enforced by the bulky sparteine as the lithium ligand (equation 79). Fortunately, in these reactions, the *N*,*N*-diisopropylcarbamoyloxy group prefers the *endo*-position to lead to the α-product **311** (inversion) and to the γ-product (*Z*)-**312** [sometimes besides small amounts of (*E*)-*ent*-**312**)].

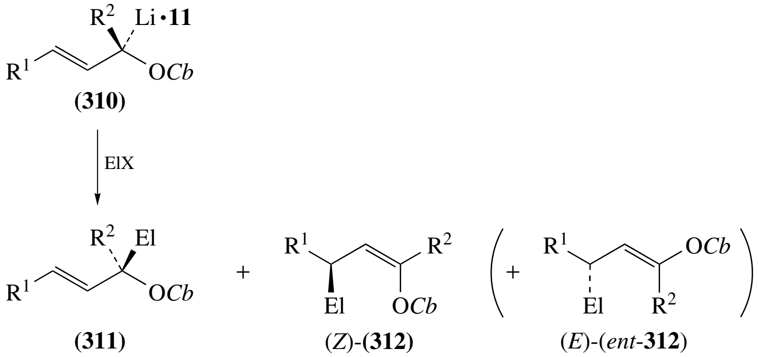

(79)

The most important reaction, the homoaldol reaction of the titanium derivatives, proceeds as an efficient *syn*-S$'_E$ process and will be discussed separately (see Section IV.C.5). Reactions with further electrophiles will be presented very briefly. The silylation of primary substrates **302** by different chlorotriorganosilanes proceeds with good α-selectivity and with inversion of the configuration[40, 228, 229, 235].

The regioselectivity in the reaction of enantioenriched lithioallyl carbamates with chlorotributyl- or chlorotrimethyltin depends largely on the substitution pattern of the alkenyl residue. Those derived from primary 2-alkenyl carbamates **302** provide exclusively or with large excess the 1-substitution products **313** with inversion of the configuration (equation 80)[28, 40, 228, 235]. No (*E*)-*ent*-**314** was observed.

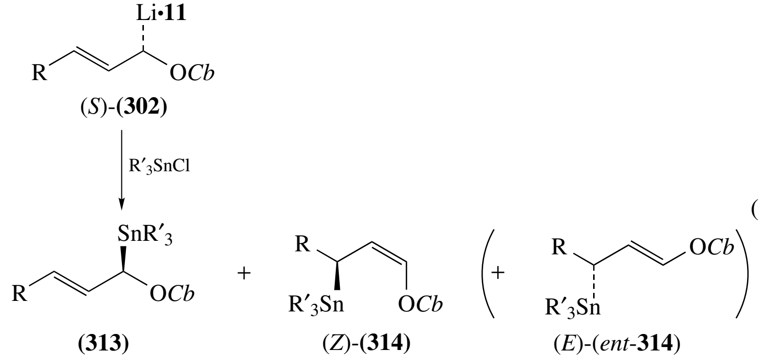

(80)

	(313)	(Z)-(314)
R = Me, R′ = Bu:	58%, 90% *ee*	22%, 82% *ee*
R = Me, R′ = Me:	21%, 82% *ee*	48%, 82% *ee*

TABLE 8. Data related to equation 80

Entry	R	R′	Yield (*ee*) **313** (%)	Yield (*ee*) (*Z*)-**314** (%)	Yield (*E*)-*ent*-**314** (%)	Reference
1	Me	Me	58 (90)	22 (82)	—	28
2	Me	Bu	21 (82)	48 (82)	—	28
3	Ph	Me	71 (80)	—	—	40
4	Ph	Bu	85[a]	—	—	40

[a] The enantiomeric ratio could not be determined.

Complete α-regioselectivity for (*S*)-**302** and overall retention of the configuration is achieved by intermediate titanium exchange (equation 81)[28].

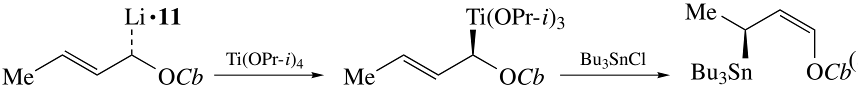

(*S*)-**(302a)** **(315)** (*ent*-**314**) 80%, 95% *ee* (81)

The stannylation of (2*S*,3*E*)-2-(*N*,*N*-diisopropylcarbamoyloxy)-3-penten-2-yllithium–(−)-sparteine [(*E*)-**300b**] takes place with complete γ-regioselectivity, leading to an *E*/*Z*-diastereomeric mixture of (*R*,*Z*)- and (*S*,*E*)-**315** (equation 82)[219, 221].

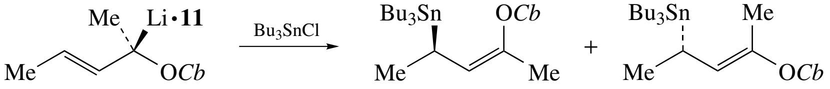

(*S*, *E*)-**(300b)** (*R*, *Z*)-**(315)** (*S*, *E*)-**(315)**

96%, 87 : 13 (82)

The appropriate enantioenriched lithium–TMEDA complexes derived from **300b** or its (*Z*)-isomer (*Z*)-**300b** exhibit an increased γ-regioselectivity[221].

Although these allylic stannanes are rather resistant to uncatalysed or Lewis acid-catalysed carbonyl addition[236], they are valuable, shelf-stable homoenolate reagents (see Section IV.C.5), which are activated by Lewis acids or lithiodestannylation. Titanium tetrachloride converts the allylstannanes stereospecifically with inversion into very reactive intermediates (equation 83)[28, 219, 221]. Both isomers, (*R*,*Z*)- and (*S*,*E*)-**315**, are transformed in a stereoconvergent process to the same unstable intermediate (*S*,*E*)-**316**. Since it decomposes rapidly, the trichlorotitanate has to be generated in the presence of a reactive aldehyde or ketone.

The lithium–titanium exchange in the allyllithium–sparteine complexes **317** by tetraisopropoxytitanium (TIPT) or chloro-triisopropoxytitanium, resulting in titanates **318**, proceeds with strict stereoinversion (equation 84)[237]. We assume that—contrary to the lithium–TMEDA complexes—the lithium–(−)-sparteine complexes are weaker Lewis acids and are no longer capable of binding the TIPT in the transition state of the exchange reaction.

Less extended investigations have been carried out for the stereochemistry of further substitution reactions, which mostly proceed with lower regioselectivities: α-carboxylation (inversion)[222]; reaction with methyl chloroformate in the α-position (inversion)[222]; α-acylation by 2,2-dimethylpropanoyl chloride (inversion)[40]; γ-methylation by methyl iodide (*anti*-S_E') and methyl triflate (*syn*-S_E')[40]; intramolecular reactions with allyl chlorides (α, inversion or γ, *anti*-S_E'; see Section IV.C.3).

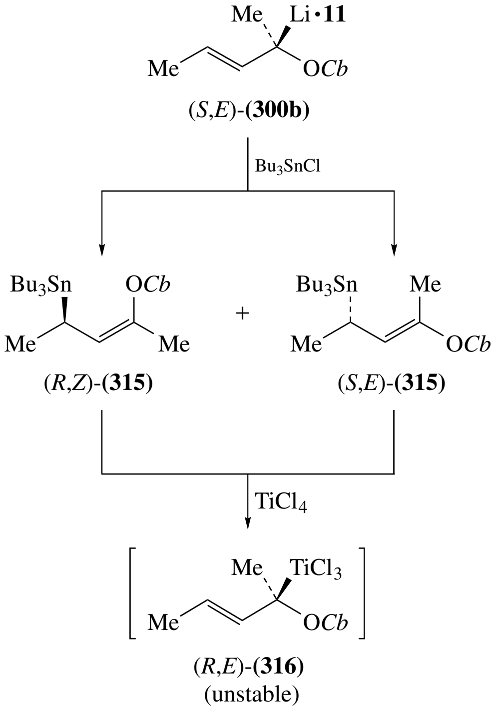

(83)

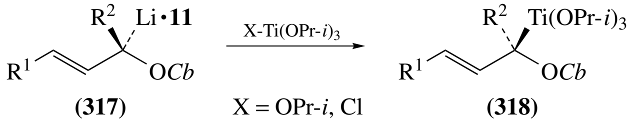

(84)

In conclusion concerning these results, we assume that stereoretention or *syn*-S'_E processes take place in allyllithium compounds only when a strong interaction of the cation and the electrophile is operating.

3. Intramolecular cycloallylation

Allylic chloride survives the (−)-sparteine-mediated deprotonation of allylic carbamates by *n*-BuLi. When the (*E*,*E*)-9-chloro-2,7-nonadienyl carbamate (*E*,*E*)-**319** was treated with two equivalents of *n*-BuLi/(−)-sparteine (**11**) at −90 °C in toluene, the *cis*-divinylcyclopentane **321** was formed with an enantiomeric ratio of 90:10 (equation 85)[229]. The epimerization to form (*R*)-**320** (which leads to *ent*-**321**) is much slower than the cycloalkylation step under the reaction conditions. **321** was converted in few steps into (+)-(3*R*,4*R*)-dihydromultifiden[229, 235].

The isomer (*Z*,*Z*)-**319** furnished under identical conditions, surprisingly, the (1*S*,2*Z*,7*Z*)-cyclonona-2,7-dienyl carbamate **323** with 88% *ee*, which could be converted to the free alcohol **324** (equation 86)[238]. The stereochemical outcome implies inversion of the configuration at the carbanionic centre in (*S*)-**322**. The method could also be successfully applied to 5-oxy-substituted dienes[238].

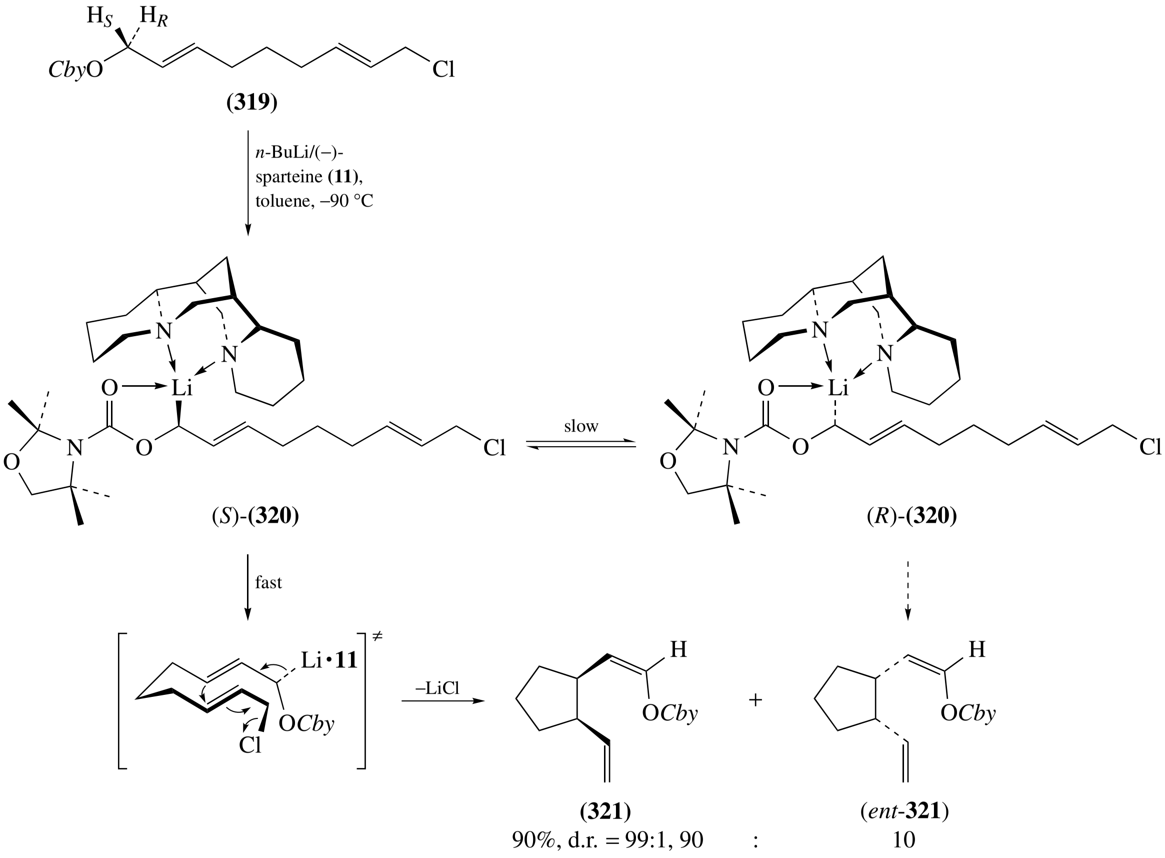
H$_S$
H$_R$
CbyO
Cl
(319)
n-BuLi/(−)-
sparteine (11),
toluene, −90 °C
N
N
O
Li
O
N
O
Cl
(S)-(320)
slow
N
N
O
Li
O
N
O
Cl
(R)-(320)
fast
Li·11
OCby
Cl
≠
−LiCl
H
OCby
+
H
OCby
(321)
90%, d.r. = 99:1, 90
:
(ent-321)
10

(85)

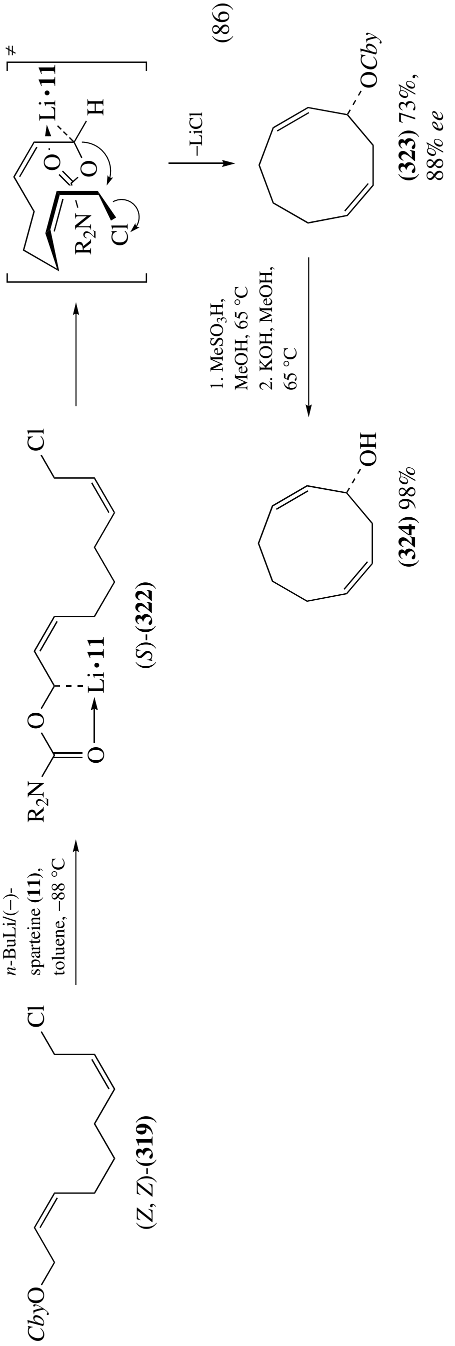

(86)

(Z, Z)-**(319)**

(*S*)-**(322)**

(323) 73%, 88% *ee*

(324) 98%

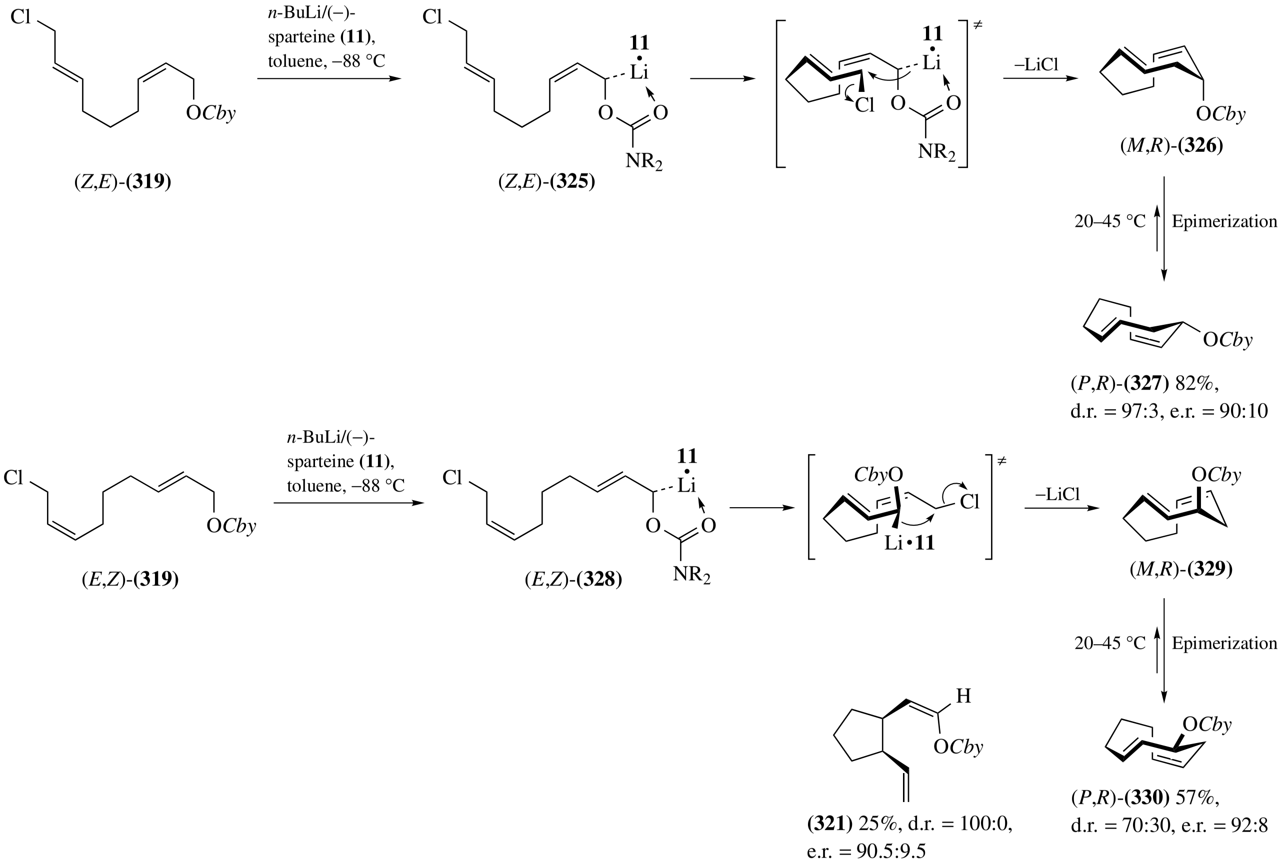
(Z,E)-(319)
n-BuLi/(−)-sparteine (11), toluene, −88 °C
(Z,E)-(325)
11
Li
O
NR2
Cl
≠
−LiCl
(M,R)-(326)
OCby
20–45 °C
Epimerization
(P,R)-(327) 82%, d.r. = 97:3, e.r. = 90:10
(E,Z)-(319)
(E,Z)-(328)
CbyO
Li•11
(M,R)-(329)
(P,R)-(330) 57%, d.r. = 70:30, e.r. = 92:8
H
(321) 25%, d.r. = 100:0, e.r. = 90.5:9.5

(87)

The remaining geometrical isomers (2*Z*,7*E*)- and (2*E*,7*Z*)-**319**[239, 240] lead to planar-chiral (*E*,*Z*)-cyclononadienes (*M*,*R*)-**326** (80% *ee*) and (*M*,*R*)-**329** via the corresponding lithium species (*Z*,*E*)-**325** and (*E*,*Z*)-**328**, respectively; some divinylcyclopentane **321** is formed from (*E*,*Z*)-**319** (equation 87). Both cyclononadienes come to equilibrium with the corresponding epimers (*P*,*R*)-**327** or (*P*,*R*)-**330** above 20 °C by inversion of the chiral plane.

The S_N'-cyclization is also suitable for the construction of enantioenriched heterocycles as demonstrated by the synthesis of the divinylpyrrolidine **333** (90% *ee*) from the dialkenylamine **331** (equation 88)[241]. The absolute configuration (3*R*,4*R*) (elucidated by anomalous X-ray diffraction) again results from stereoinversion at the metal-bearing C(1) atom in (*S*)-**332** during the formation of the five-membered ring by S_N'-substitution.

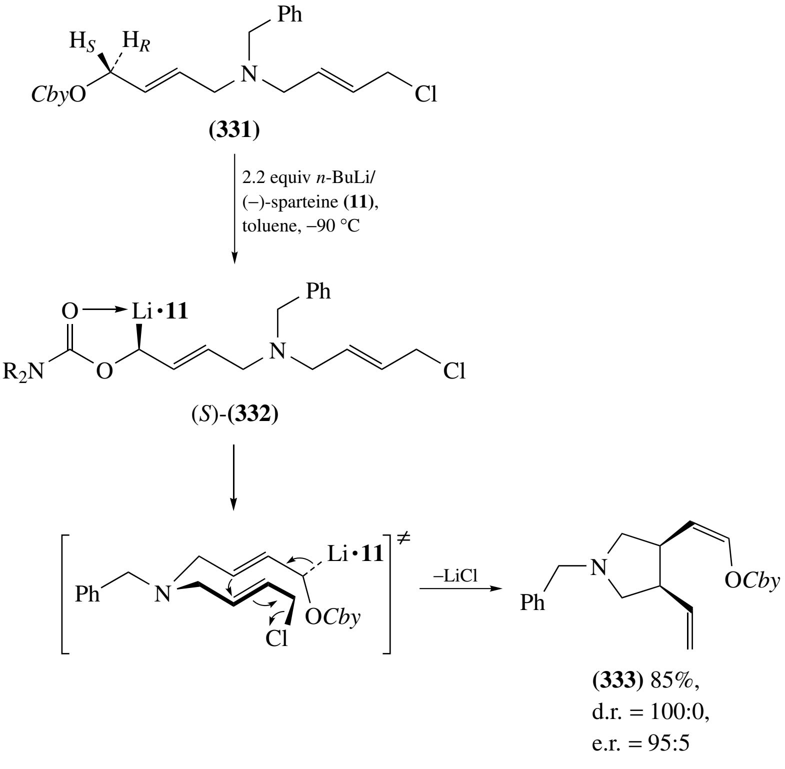

(88)

4. Diastereoselective homoaldol reaction

As was worked out with the racemic reagents, titanated (*E*)-2-alkenyl carbamates *rac*-**334** and *rac*-**335** undergo a highly diastereoselective addition to aldehydes via a Zimmerman–Traxler transition state[242] (equation 89)[208, 210, 243]. The yields are high and the diastereomeric ratios for the racemic (*Z*)-*anti*-diastereomer *rac*-**336** usually exceed 97:3. Since enol carbamates of 4-hydroxyalkanals (or *γ*-hydroxyalkanones) are produced by formation of the C(3)–C(4) bond, we named the process '*homoaldol reaction*'[4, 225, 244–246].

The titanium reagents are configurationally stable and react from the 1-*endo*-conformation with a high degree of *syn*-1,3-chirality transfer. As a result, the reaction

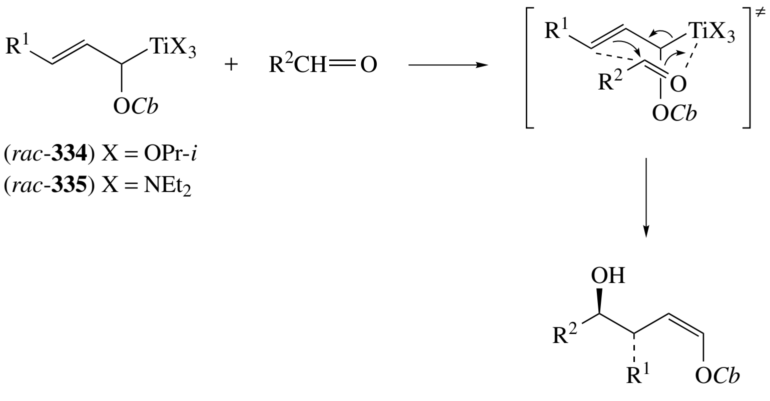

(*rac*-**334**) X = OPr-*i*
(*rac*-**335**) X = NEt_2

(89)

(*rac*-**336**)

of both enantiomers in the racemate with enantiopure 2-hetero-substituted aldehydes **337** furnish two diastereomers **338** and **339**, which differ in the absolute configuration of the newly created stereocentres (equation 90).

The enantiopure diastereomers **338** (4,5-*syn*) and **339** (4,5-*anti*) have a different capability for performing intramolecular hydrogen bonding and are therefore easily separated by silica gel chromatography.

Various racemic titanium-homoenolate reagents have been successfully applied to *O*-protected (*R*)- and (*S*)-lactaldehydes (X = OPG)[141, 247, 248], (*S*)-2-(*N*,*N*-dibenzylamino)alkanols (X = NBn_2)[231] and (*S*)-2-(*N*-Boc-amino)- and *N*-*Cb*O-alkanols[249]. Both diastereotopic pathways **A** and **B** (equation 90) are different in their energy, consisting in a '*matched*' and '*mismatched pair*'[72], and thus proceed with different reaction rate. Therefore, such a reaction was taken as one of the first examples for the Hoffmann test on configurational stability of carbanionic species[141, 250].

It has been demonstrated by Pancrazi, Ardisson and coworkers that an efficient kinetic resolution takes place when an excess (2 equivalents) of the racemic titanated alkenyl carbamate *rac*-**334a** (R^1 = Me) is allowed to react with the enantiopure ω-hydroxyaldehyde **341** or alternatively the corresponding γ-lactol **340**, since the mismatched pair contributes to a lower extent to the product ratio (equation 91)[251]. Under best conditions, the ratio of the enantiomerically pure diastereomers 3,4-*anti*-4,5-*syn* (**342**) and 3,4-*anti*-4,5-*anti* (**343**) is close to 14:1. Surprisingly, approximately 9% of the *syn,syn*-diastereomer **344** resulted when the starting (*E*)-crotyl carbamate was contaminated by the (*Z*)-isomer. The reasons which apply here are unknown. Extra base has to be used in order to neutralize the free hydroxy group. The pure *anti,anti*-product **345** was obtained with 85% yield from the reaction of the ω-oxy-substituted titanate *rac*-**334b** and lactol **340**. **345** is an intermediate in the asymmetric synthesis of tylosine[251].

5. Homoaldol reaction with enantioenriched 1-metallo-2-alkenyl carbamates

When employing enantioenriched 1-titano-2-alkenyl carbamates **334** in carbonyl addition, the selectivity depends on the enantiomeric purity that was achieved in its preparation (see Section IV.C.1). The (*E*)-crotyl derivative (*R*)-**334a** has been employed several times (equation 92)[224, 252, 253]. The optically active homoaldol products **346** are easily converted into γ-lactones **347** by four different pathways, which require an oxidation step (see Section IV.C.6). Applications in target synthesis include the natural products (+)-quercus

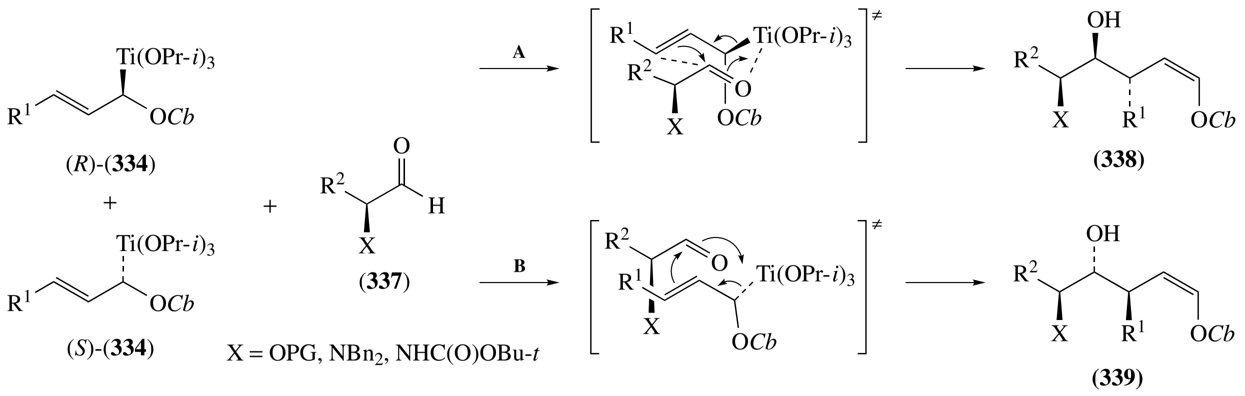

(*R*)-(**334**) + (*S*)-(**334**) + (**337**)

X = OPG, NBn$_2$, NHC(O)OBu-*t*

(**338**)

(**339**)

(90)

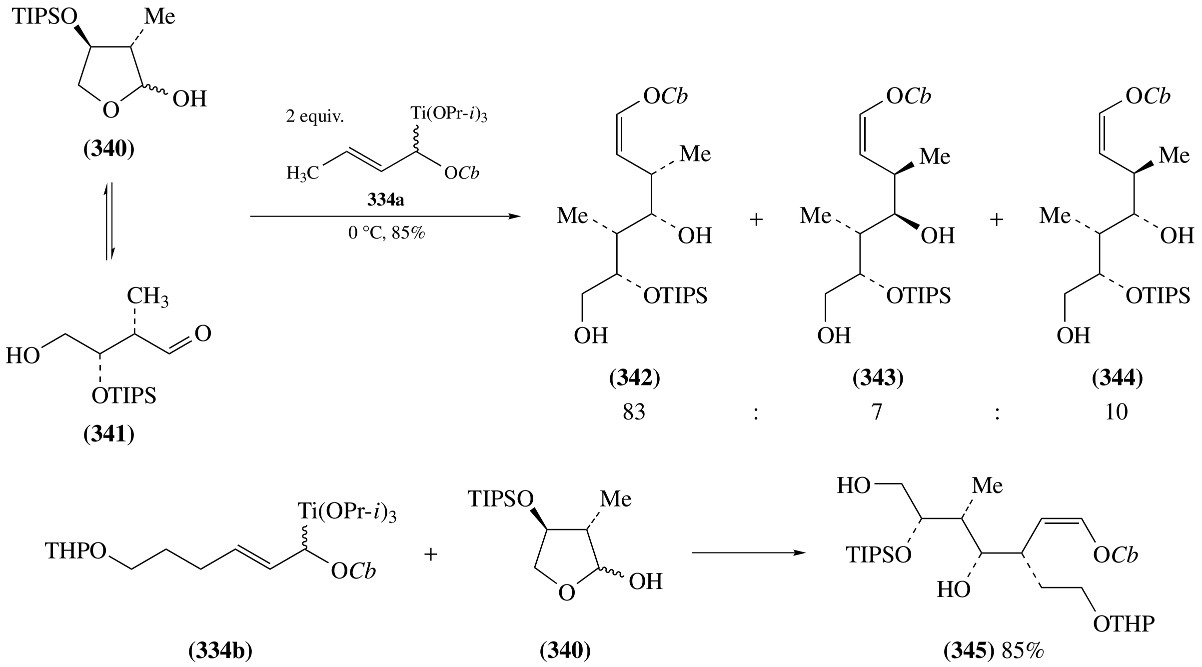
TIPSO
Me
OH
O
(340)
CH3
O
HO
OTIPS
(341)
2 equiv.
Ti(OPr-i)3
H3C
OCb
334a
0 °C, 85%
OCb
Me
Me
OH
OTIPS
OH
(342)
83
+
:
(343)
7
+
:
(344)
10
THPO
Ti(OPr-i)3
OCb
(334b)
+
(340)
HO
TIPSO
(345) 85%
OTHP

(91)

lactone (**347c**) and (+)-eldanolide (**347e**)[253]. The reagent **334a** has also been applied in total syntheses of more complicated natural products: dihydroavermectin B_{1b} by Julia and coworkers[256], tylonolide[251] and *rac*-tylonolide[257] by Ardisson, Pancrazi and coworkers, and jaspamide[258] and herboxidiene[259] by Kocienski and coworkers.

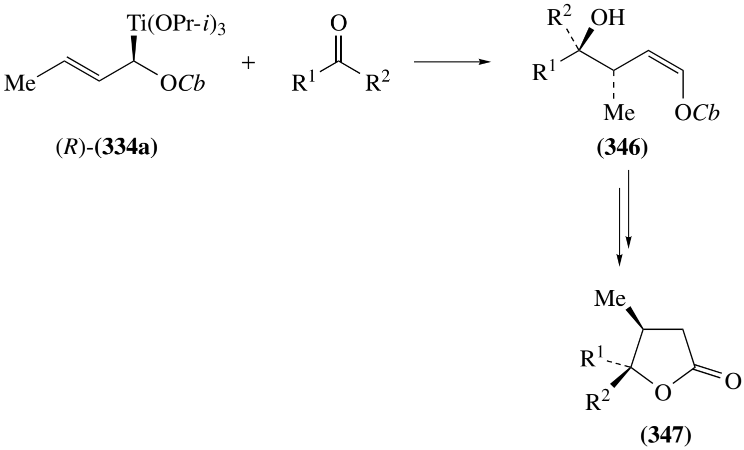

(92)

TABLE 9. Data related to equation 92

346	R^1	R^2	Yield (%)	*ee* (%)	Yield **347** (%)	Reference
a	$(CH_3)_2CH$	H	90	90[a]	89	224
b	CH_3	H	95	80[a]	—	224
c	$CH_3(CH_2)_3$	H	93	84[a]	90	224
d	CH_3CH_2	H	90	—[b]	—	254, 255
e	$(CH_3)_2C{=}CHCH_2$	H	62	92	75	253
f	$H_2C{=}CCH_3$	H	78	86[a]	—	252
g	$H_2C{=}C{-}CH(CH_3)_2$	H	81	90	—	252
h	CH_3	CH_3	92	82	—	224

[a] Non-optimized preparation of **334a**.
[b] Racemic.

Some alkenyl carbamates leading to configurationally labile lithium intermediates could be subjected to asymmetric homoaldol reaction with less efficiency (Scheme 6); these reactions have not been optimized yet[224, 226].

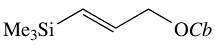

(**301b**)[225]

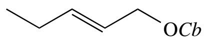

(**301c**)[225]

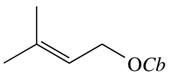

(**348**)[225,227]

SCHEME 6

The titanium compounds, derived from the configurationally stable lithium–(−)-sparteine complexes **349a,b** prepared from primary allyl carbamates, undergo lithium–titanium exchange with chlorotriisopropoxytitanium to form the allyltitanates

350[228]. These add to aldehydes providing the homoaldol products **351** with high stereoselectivity following the expected stereochemical course, as could be elucidated by several X-ray crystal structure analyses under anomalous dispersion (equation 93). It is currently unknown why the yields are relatively low (21–35%), since we could not detect side products besides traces of starting material. The corresponding lithium–TMEDA complexes, after titanation, deliver good yields (71–79%). The homoaldol products are easily converted to enantioenriched bicyclic γ-lactones of type **352**[260].

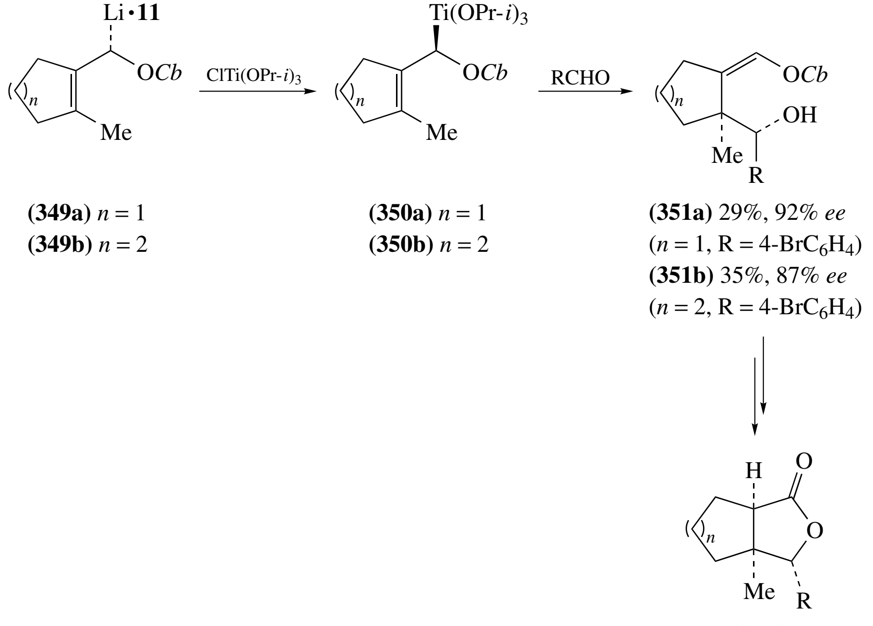

(349a) $n = 1$
(349b) $n = 2$

(350a) $n = 1$
(350b) $n = 2$

(351a) 29%, 92% *ee*
($n = 1$, R = 4-BrC_6H_4)
(351b) 35%, 87% *ee*
($n = 2$, R = 4-BrC_6H_4)

(352) (93)

Enantioenriched 3-(trialkylstannyl)alkenyl carbamates are accessible from the lithium compound (*S*)-**302a** in both enantiomeric forms[28]. These can be kept for several days in the refrigerator. Metal exchange with titanium tetrachloride in the presence of an aldehyde or ketone generates the highly reactive α-trichlorotitanium intermediate **353**, leading to homoaldol adducts **354** or *ent*-**354**, respectively. From the configuration of these adducts it is concluded that the metal exchange proceeds as an *anti*-S'_E process, followed by the usual *syn* carbonyl addition via a Zimmerman–Traxler transition state, accompanied by a high degree of chirality transfer (equation 94). The stereochemical course is in agreement with results of Marshall and coworkers[261, 262] and previous results, achieved with 1-substituted derivatives[219].

6. Synthetic transformations and applications of 4-hydroxy-1-alkenyl carbamates

The vinyl carbamates of type **355**, although being enol esters, are very stable under acidic or basic conditions and can be handled, similar to usual alkenes, without problems[208]. Quite a number of synthetically useful transformations have been developed over the years. Five aspects can be addressed selectively by suitable reagents:

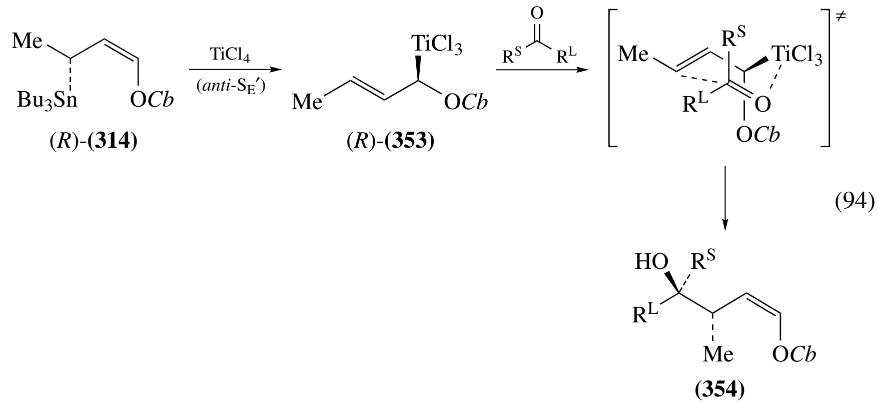

TABLE 10. Data related to equation 94

Product (**354**)	Starting material (% *ee*)	R^L	R^S	Yield (%)	*ee* (%)	Reference
a	(*R*)-**314a** (90)	$(CH_3)_2CH$	H	91	88	28
ent-**354a**	(*S*)-**314a** (82)	$(CH_3)_2CH$	H	82	82	28
a	(*R*)-**314b** (96)	$(CH_3)_2CH$	H	96	96	28
b	(*R*)-**314b** (80)	$(CH_3)_3C$	CH_3	80	74	28
c	(*R*)-**314b** (94)	$EtO_2C(CH_2)_3$	CH_3	84	94	28
d	(*R*)-**314b** (94)	$EtO_2C(CH_2)_3$	CH_3	91[a]	94	28

[a] Isolated as its corresponding lactone.

(a) the enolic double bond,
(b) the C=O group of the carbamoyl moiety,
(c) the 4-hydroxy group,
(d) the highly acidic H(1),
(e) the whole carbamoyl group by vinylic substitution.

Several of the reactions mentioned in this chapter proved to be successful for diastereomerically pure but racemic substrates **355**. No reason is seen why racemization or epimerization should occur and therefore application to optically active substrates is possible without expecting difficulties. Of course, one must take into account sensitive functional groups, eventually being present in the residues R^1 and R^2.

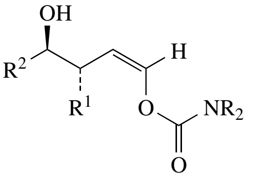

(355)

C(1) in **355** is in the oxidation state of an aldehyde or a ketone in 1-alkylated products. The necessary solvolytic attack of the enol carbamate double bond requires substoichiometric amounts of a catalyst such as mercuric acetate or palladium chloride and one equivalent of acid (e.g. methanesulphonic acid) for binding the liberated diisopropylamine.

If the 4-hydroxy group is free, then when using methanol as solvent, anomeric lactol ethers **356** are formed with high yields (equation 95). Oxidation by the Grieco method[263] leads to γ-substituted γ-lactones **357** (equation 95)[209, 224, 231, 243, 249, 260].

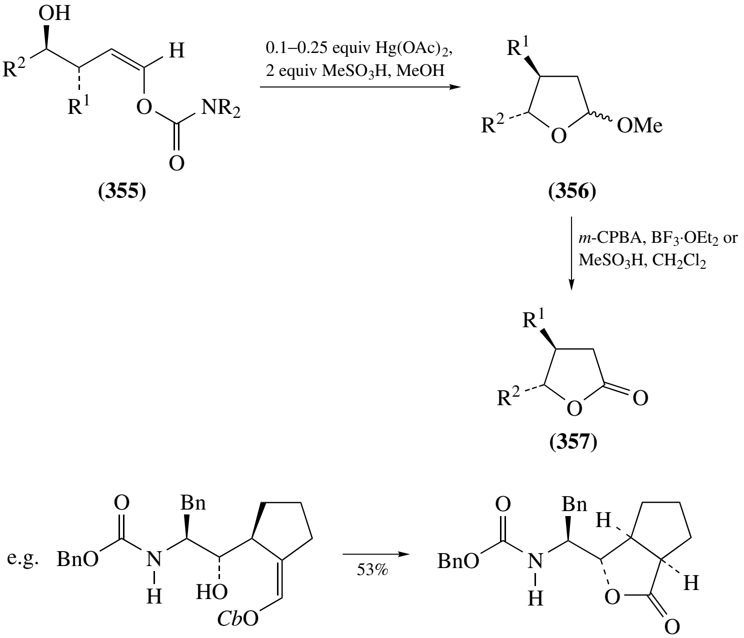

(355) **(356)** **(357)**

(95)

Another approach for the deprotection of highly functionalized enol carbamates is based on hydroboration (equation 96)[231, 249].

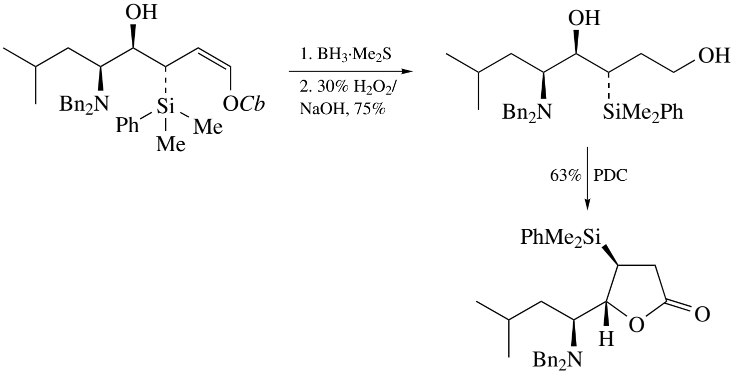

(96)

If Lewis acid-sensitive double bonds are located in the residues R^1 or R^2, an indirect oxidation of the vinylic hydrogen via lithiation/sulphenylation turns out to be a good solution[253, 264] and it was applied during the final steps of (+)-eldanolide (**358**) synthesis (equation 97)[253].

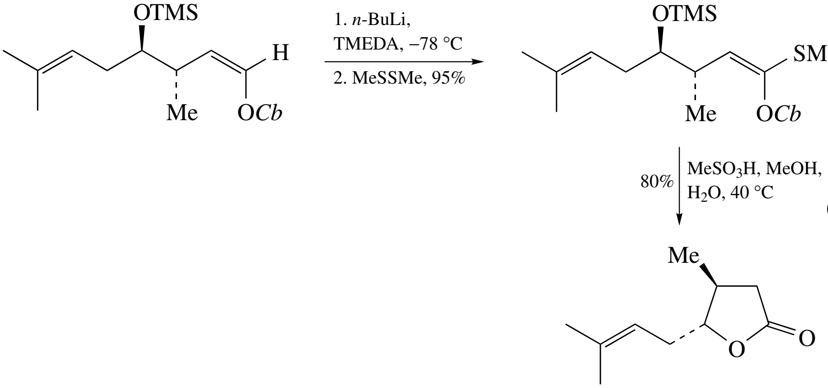

(97)

(358)

According to results published by Férézou and coworkers, the N,N-diisopropylcarbamoyl group of homoaldol adducts can be directly attacked by ‘slim’ nucleophiles such as lithium ethynylide or excess methyllithium (equation 98)[265]. The TIPS ether **359** was treated with three equivalents of methyllithium to yield [via the (Z)-enolate **360**] the aldehyde **361**. Trapping of **360** by TBSCl gives rise to the synthetically valuable (Z)-silyl enol ether **362**.

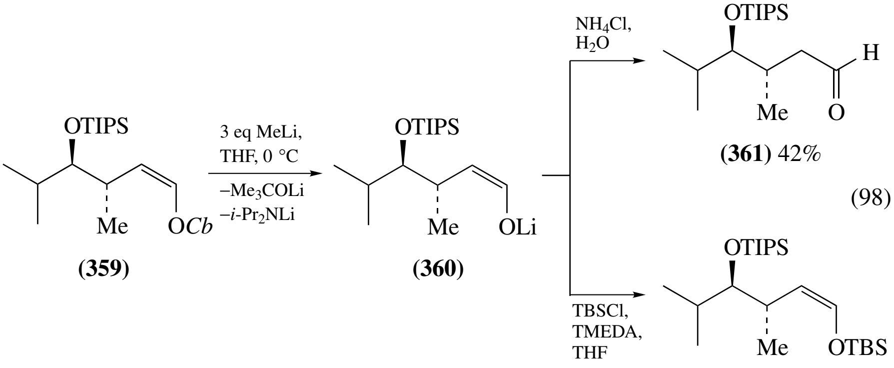

(359) **(360)** **(361)** 42% **(362)** 84%

(98)

(Z)-*anti*-4-Hydroxy-1-alkenyl carbamates **363**, when subjected to substrate-directed, vanadyl-catalysed epoxidation[266–268], lead to diastereomerically pure epoxides of type **364** (equation 99)[247, 252, 269]. These epoxides are highly reactive in the presence of Lewis or Brønsted acids to form β-hydroxylactol ethers **366**; in some cases the intermediate lactol carbamates **365** could be isolated[247]. However, most epoxides **364** survive purification by silica gel chromatography[247]. The asymmetric homoaldol reaction, coupled with directed epoxidation, and solvolysis rapidly leads to high stereochemical complexity. Some examples are collected in equation 99. The furanosides **368** and **370**, readily available from (R)-O-benzyl lactaldehyde[247] via the corresponding enol carbamates **367** and **369**, respectively, have been employed in a short synthesis of the key intermediates of the Kinoshita rifamycin S synthesis[270, 271]. 1,5-Dienyl carbamates such as **371**, obtained from 2-substituted enals, provide a facile access to branched carbohydrate analogues[252].

(99)

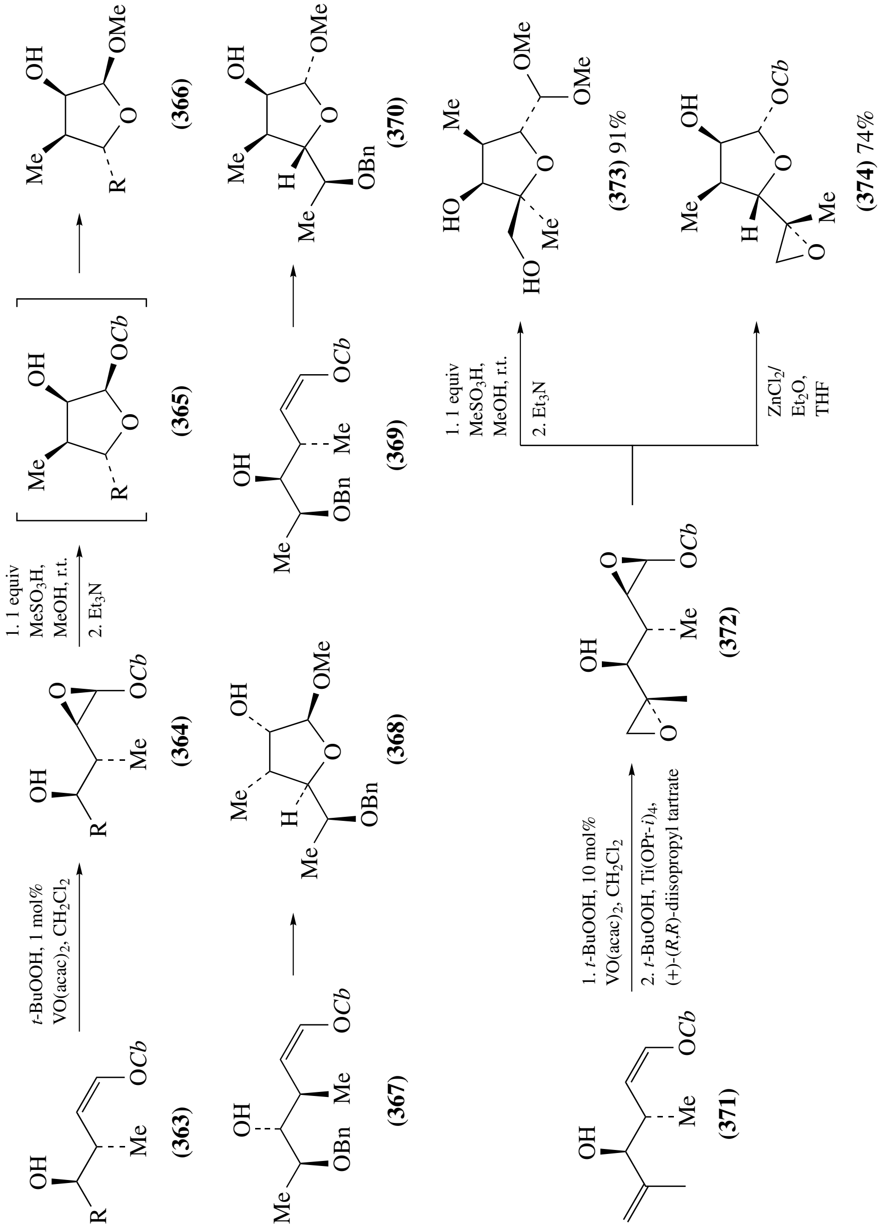

(363)
t-BuOOH, 1 mol%
VO(acac)$_2$, CH$_2$Cl$_2$
(364)
1. 1 equiv
MeSO$_3$H,
MeOH, r.t.
2. Et$_3$N
(365)
(366)
(367)
(368)
(369)
(370)
(371)
1. t-BuOOH, 10 mol%
VO(acac)$_2$, CH$_2$Cl$_2$
2. t-BuOOH, Ti(OPr-i)$_4$,
(+)-(R,R)-diisopropyl tartrate
(372)
1. 1 equiv
MeSO$_3$H,
MeOH, r.t.
2. Et$_3$N
ZnCl$_2$/
Et$_2$O,
THF
(373) 91%
(374) 74%

Epoxidation of the 1,2-double bond is followed by highly diastereoselective attack at the 5,6-double bond; both oxirane rings in **372** can be opened separately under controlled conditions, forming the tetrasubstituted tetrahydrofurans **373** and **374** with very good overall yields[252].

Strong nucleophiles applied under basic conditions attack epoxides **364a** at C(2) with inversion of the configuration, leading to *trans,trans*-2,3,4-trisubstituted γ-lactols **375**, which are easily oxidized to the corresponding γ-lactones **376** (equation 100)[269].

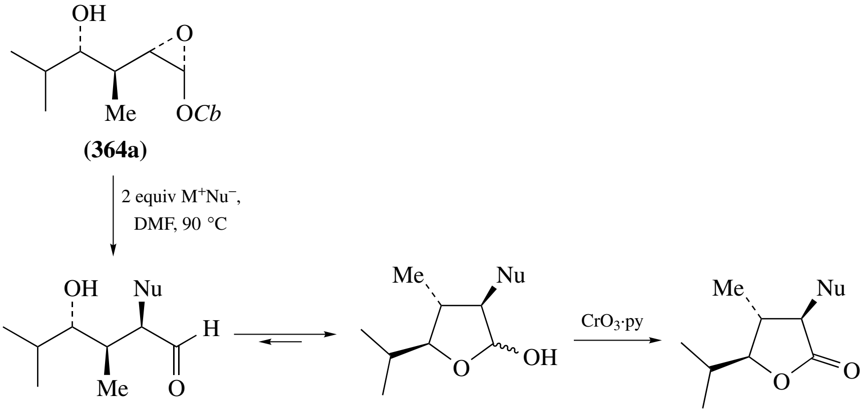

(364a)

(375) **(a)** Nu = OAc, 71%
(b) Nu = OPh, 64%
(c) Nu = N_3, 63%
(d) Nu = SPh, 89%

(376)

(100)

The enol carbamates **377** can be regarded as weak enolate reagents. This type of reactivity is released by reactions with aldehydes, ketones or the corresponding acetals under boron trifluoride catalysis (equation 101)[272]. Stereochemically homogeneous, tri- or tetra-substituted 3-tetrahydrofuran-3-carbaldehydes or -ketones **379** or **378** are isolated in high yields. Presumably, the (*E*)-oxonium ions **380** are formed via the attack at the free hydroxy group and subsequently undergo intramolecular Mukaiyama-type reactions to form the cations **381**, which are hydrolysed to give the carbonyl compounds **379**. For cyclization, the intermediate **380** adopts the particular conformation, which avoids 1,3-allylic strain[273]; this turns out to be a powerful tool for controlling the diastereoselectivity. Some examples are collected in equation 101. The 8-oxo derivatives **382** undergo an intramolecular version to form 8-oxabicyclo[3.2.1]octanes **383**[274].

According to equation 102, stereochemically homogeneous 3-carbonyl-substituted tetrahydrofurans are constructed in a brick-box system by sequential homoaldol and aldol reaction. The metallated allyl carbamate serves as an equivalent for the chiral dianion **A**, which accepts two different aldehydes **B** and **C** in a highly controlled manner[272].

In comparison to other vinylic compounds[275], the vinyl proton in 1-alkenyl carbamates, deprotonation has a very high kinetic acidity[276–279]. After protection of the 4-hydroxy group in the homoaldol products by silylation, deprotonation (*n*-BuLi, TMEDA, diethyl ether or THF) of enol carbamate **384** is complete at −78 °C (equation 103), and the resulting vinyllithium **385** can be kept at this temperature without decomposition for several hours. Stannylation[276], silylation[278], methoxycarbonylation (with methyl chloroformate)[278]

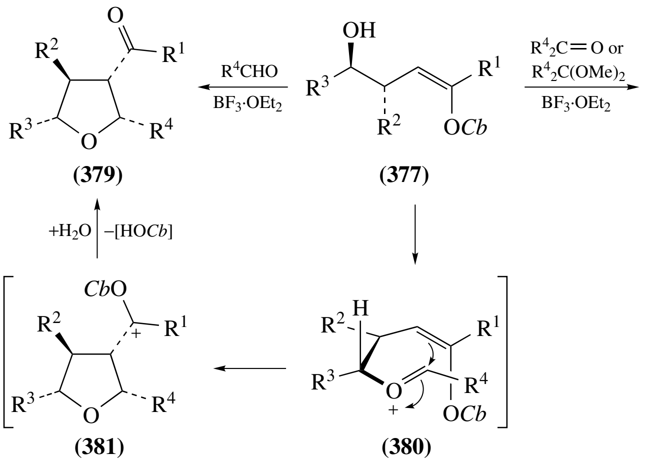

(379) (377) (378)

(381) (380)

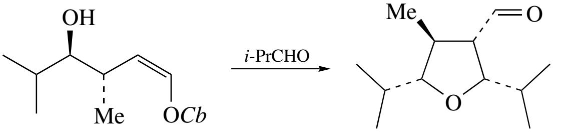

(377a) (379a)

(101)

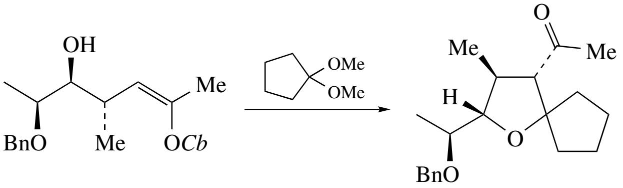

(377b) (378a)

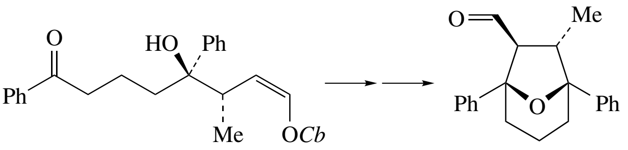

(382) (383)

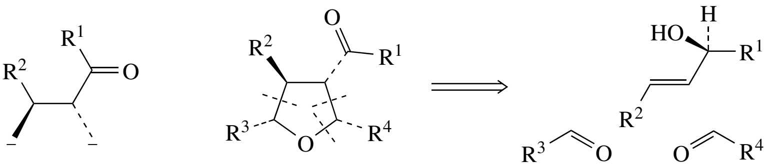

A (379) B C

(102)

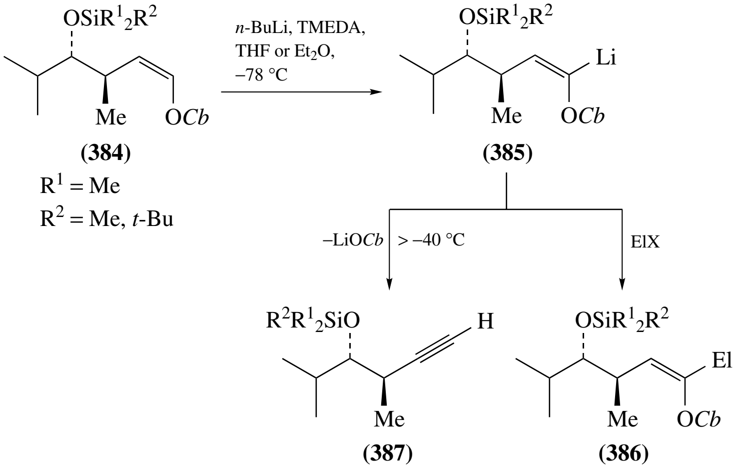

TABLE 11. Data related to equation 103

386	R^1	R^2	El	Yield (%)	Reference
a	Me	*t*-Bu	Me_3Sn	95	276
b	Me	*t*-Bu	$CH_3CH_2CH_2$	56	276
c	Me	Me	Me_3Si	93	278
d	Me	Me	CO_2Me	66	278

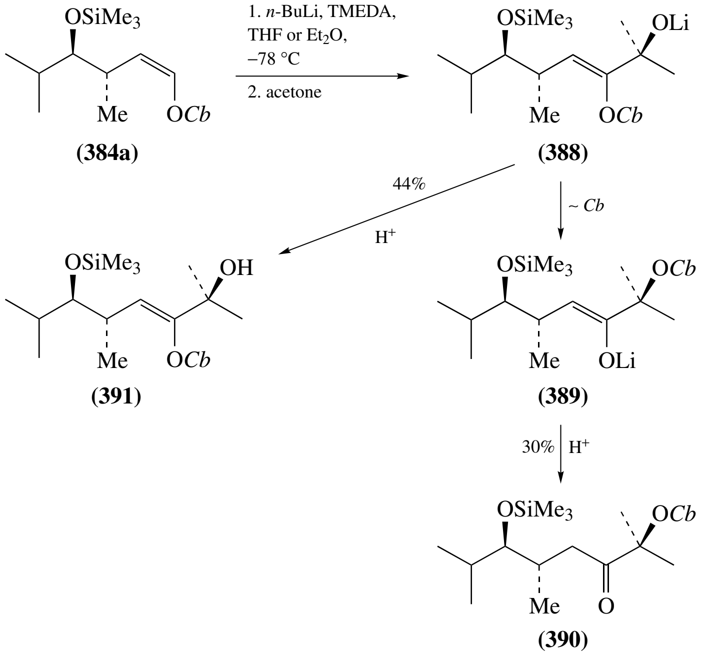

(103)

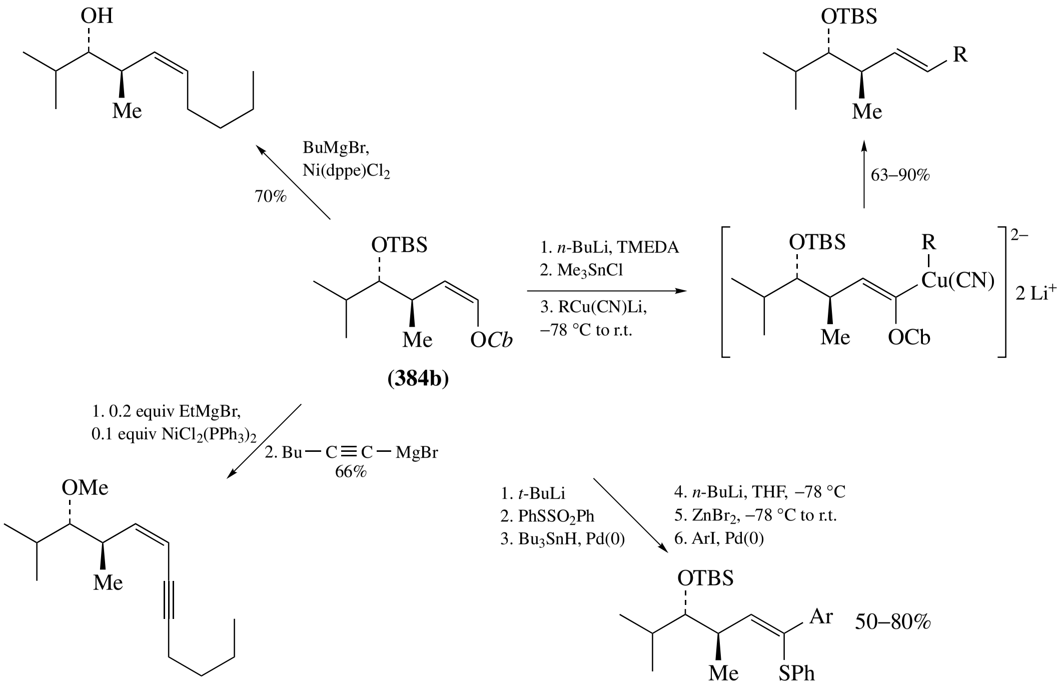
OH
Me
BuMgBr,
Ni(dppe)Cl$_2$
70%
OTBS
Me
63–90%
OTBS
Me
OCb
1. n-BuLi, TMEDA
2. Me$_3$SnCl
3. RCu(CN)Li,
−78 °C to r.t.
OTBS
R
Cu(CN)
Me
OCb
2–
2 Li$^+$
1. 0.2 equiv EtMgBr,
0.1 equiv NiCl$_2$(PPh$_3$)$_2$
2. Bu—C≡C—MgBr
66%
OMe
Me
1. t-BuLi
2. PhSSO$_2$Ph
3. Bu$_3$SnH, Pd(0)
4. n-BuLi, THF, −78 °C
5. ZnBr$_2$, −78 °C to r.t.
6. ArI, Pd(0)
OTBS
Ar
Me
SPh
50–80%

(384b)

(104)

and alkylation (with propyl iodide/HMPA)[276] to form the carbamates **386** proceed without difficulties. Addition of aldehydes or ketones furnishes the alcoholates, such as **388**, which rearrange with migration of the carbamoyl group to give lithium enolates **389**; after aqueous workup, mixtures of alkenols **391** and ketones **390** are obtained[278]. Similar acyl migrations have been observed for simpler substrates by Snieckus and Sengupta[277]. When warming these vinyllithiums of type **385** to temperatures above −40 °C, a Fritsch–Buttenberg–Wiechell rearrangement, which includes the α-elimination of lithium carbamate and the migration of the vinylic hydrogen, provides 1-alkynes **387**[276].

A couple of further useful reactions, involving organometallic reagents, have been developed—mainly by Kocienski and coworkers—for converting 4-hydroxy-1-alkenyl carbamates into various alkenes (equation 104)[276, 280–283]. For each reaction type, only one example is depicted.

These reactions involve metallate rearrangements[280], migratory insertion and transition metal-catalysed vinylic substitution reactions. They also perform well in applications in natural product synthesis[254, 255, 259, 282]. Many useful synthetic possibilities arise from application of ring-closing olefin metathesis (RCM) to unsaturated homoaldol products and their derivatives by means of the Grubbs catalyst **394**[284–286]. Equation 105 presents some examples[287].

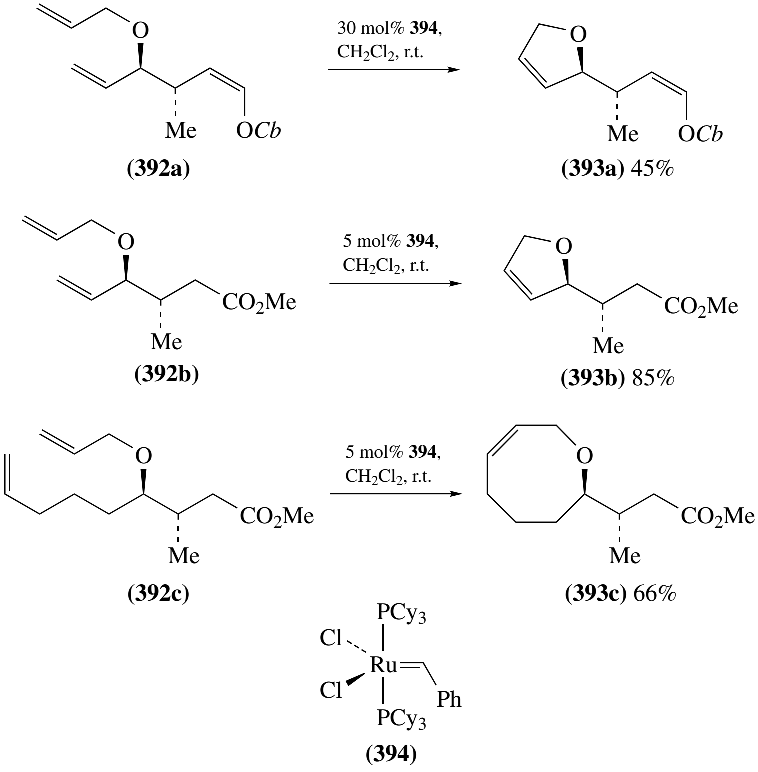

(105)

The N,N-diisopropylcarbamoyl group interferes with the catalyst, as seen in the transformation of the allylic ether **392a** into the dihydrofuran **393a**; high amounts of **394** are required. The metathesis reaction to similar oxacycles **393b** and **393c** proceeds more smoothly when the vinyl carbamate has been converted into the corresponding esters **392b** and **392c**, respectively.

D. Lithiated *N*-Boc-Allylamines

1. Enantioenriched 2-substituted pyrrolidines

The asymmetric lithiation/substitution of *N*-Boc-*N*-(3-chloropropyl)-2-alkenylamines **395** by *n*-BuLi/(−)-sparteine (**11**) provides (*S*)-*N*-Boc-2-(alken-1-yl)pyrrolidines **397** via the allyllithium–sparteine complexes **396** (equation 106)[182, 288]. Similarly, the piperidine corresponding to **397** was obtained from the *N*-(4-chlorobutyl)amine. Intramolecular epoxide openings gave rise to enantioenriched pyrrolidinols[288]. Beak and coworkers conclude from further experiments that an asymmetric deprotonation takes place, but it is followed by a rapid epimerization; a kinetic resolution in favour of the observed stereoisomer concludes the cyclization step.

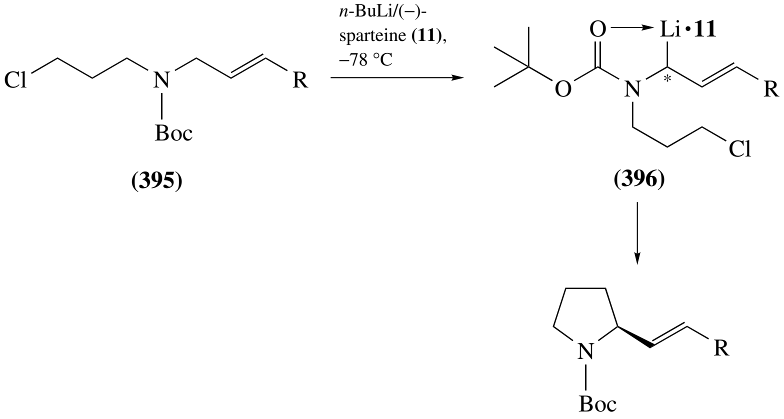

(106)

(397) **(a)** R = H: 93%, e.r. = 83:17
(b) R = Ph: 85%, e.r. = 90:10

2. N-Boc-N-(4-methoxyphenyl)-2-alkenyllithium derivatives

(*E*)-*N*-Boc-*N*-(4-methoxyphenyl)cinnamylamine **398a** was deprotonated by Beak and coworkers with *n*-BuLi/(−)-sparteine (**11**) and the resulting lithium intermediates **399** furnished upon alkylation or silylation highly enantioenriched γ-substitution products **400** (equation 107)[289]. The substitution from both conformers 1-*endo*- and 1-*exo*-**399** proceeds with clean stereoinversion, but retention is observed for trimethylsilyl triflate. An X-ray crystal structure analysis of **399** could be obtained[290], giving evidence for the absolute configuration [*R* at C(1)] and for a η^3-complexation of the lithium cation in the solid state.

A conscientious investigation of the stereochemical features was undertaken, including ^{6}Li and ^{13}C NMR studies of the lithium intermediates[291]. The epimeric ratio is kinetically controlled in the deprotonation step by a high preference for the 1-*pro*-*R*-H in **398a**, and the stereocentre is configurationally stable at −78 °C. The ratio of 1-*endo*-**399** and its epimer (Li behind the plane) was found to be 96:4. The interconversion of the *E*/*Z*-isomers 1-*endo*-**399** and 1-*exo*-**399** at −78 °C is slower than the rate of alkylation with

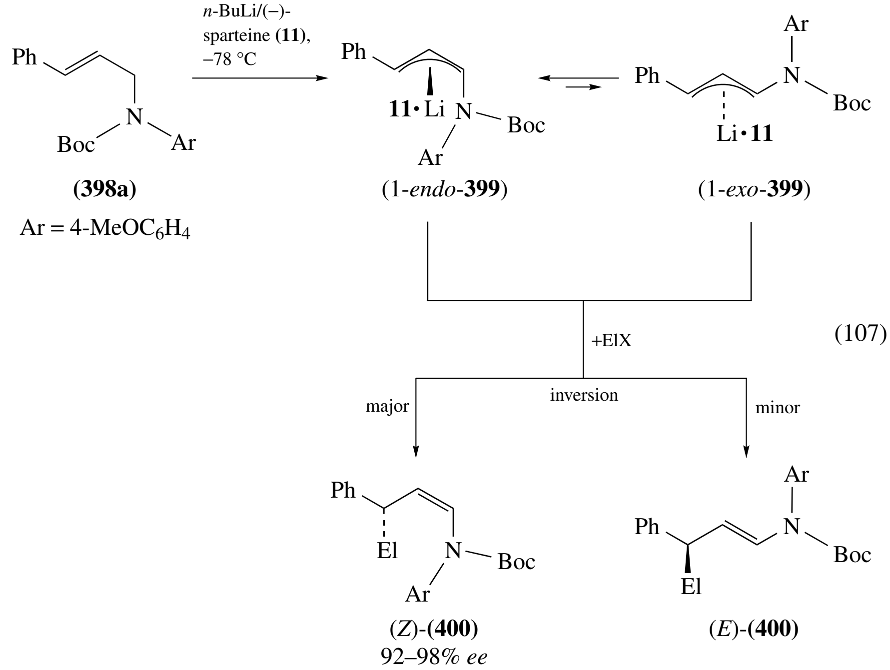

(107)

methyl iodide[291], but at approximately −25 °C the major trapping product is (*E*)-**400**, arising from the more reactive lithium intermediate 1-*exo*-**399**[291]; a more detailed discussion is given elsewhere[25]. Stannylation proceeds with stereoinversion and lithiodestannylation occurs with retention, thus permitting the transformation of the lithium compounds into their epimers *epi*-**399**[291]. A couple of reactions such as acylation with methyl chloroformate, addition to cyclohexanone and Michael additions to α,β-unsaturated carbonyl compounds[292] take stereoretentive pathways[289, 291].

High enantiomeric excesses are also obtained by applying these reactions to (*E*)-*N*-Boc-*N*-(4-methoxyphenyl)-3-cyclohexylallylamine, lithiation **401** (equation 108)[289, 293]. NMR and also kinetic investigations reveal that in **402** the lithium cation is bound in a η^1-manner to the allyl moiety; as a result the barrier for the torsion around the C(1)−C(2) bond is very low. **402** is configurationally stable with respect to the stereogenic centre at low temperature. A high kinetic H/D isotope effect of **401** in the deprotonation is consistent with the breaking of the C−H(D) bond to be the rate-determining step, which proceeds by pseudo-first order. Kinetic experiments under IR observation lead to the conclusion that a complex is formed from *n*-BuLi/(−)-sparteine (**11**) prior to deprotonation and the substrate. Kinetic evidence led to the assumption that the formation of an 'unproductive' pre-complex competes. One may speculate that of the two geometrical isomers *trans*-**404** and *cis*-**404**, an intramolecular proton shift is possible only in *trans*-**404** (equation 109).

3. Synthetic applications of lithiated N-Boc-allylamines

Lithium−metal exchange in the lithium−(−)-sparteine complexes **399** or **402**, respectively, by diethylaluminium chloride or triisopropoxytitanium chloride proceeds with inversion providing useful reagents for enantioselective homoaldol reactions

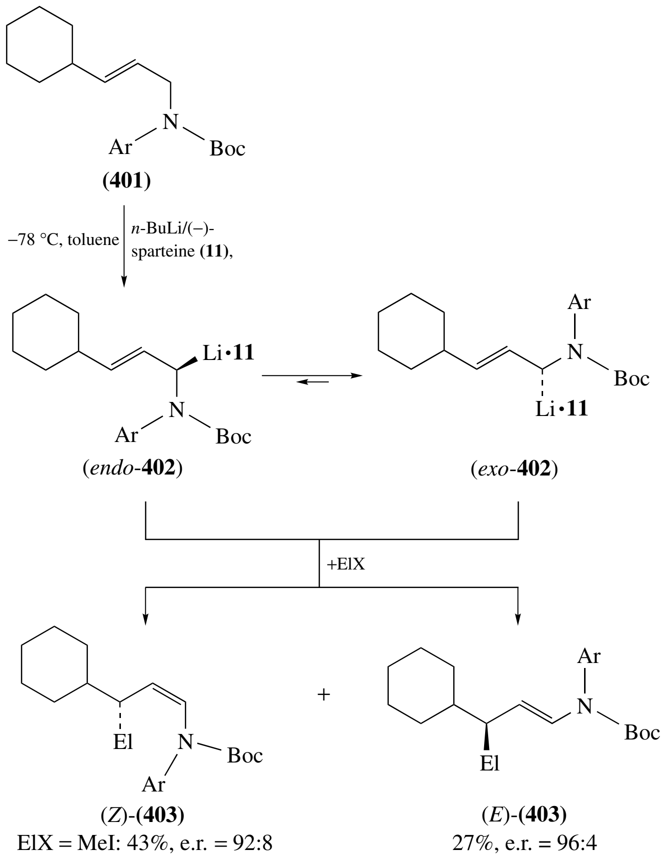

(108)

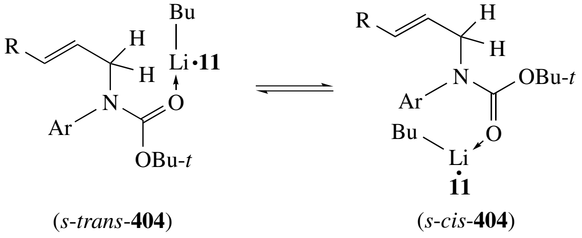

(109)

(equation 110)[212]. Since the aluminium derivative **405** leads to the (*E*)-diastereomers **406**, the absolute configuration is opposite to those of the adducts **408** produced by the titanium method via the titanates **407**. The enantiomer *ent*-**408** was obtained as major product when tetraisopropoxytitanium is used for the metal exchange. The authors assume stereoretention in the latter transmetallation, but it has not been excluded that the metal exchange might not take place; the lithium compound **402** might be the actual reacting species (with *syn* addition). A related observation had been made in the attempt of metal exchange by means of tetraisopropoxytitanium in lithium–(−)-sparteine complexes of 3-alkyl-3*H*-indenes[213] and 2-methylcyclohexene-2-yl *N*,*N*-diisopropylcarbamate[294].

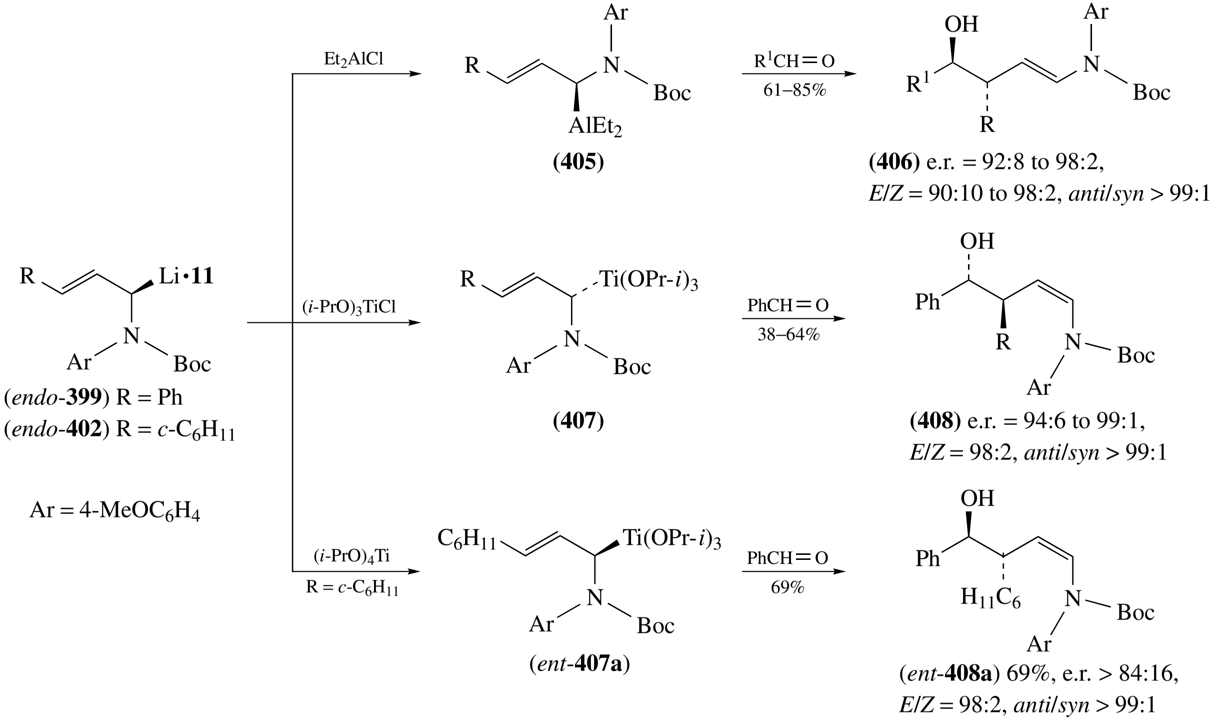
(endo-399) R = Ph
(endo-402) R = c-C6H11
Ar = 4-MeOC6H4
Li•11
Et2AlCl
(i-PrO)3TiCl
(i-PrO)4Ti
R = c-C6H11
(405)
(407)
(ent-407a)
R1CH=O
61–85%
PhCH=O
38–64%
PhCH=O
69%
(406) e.r. = 92:8 to 98:2,
E/Z = 90:10 to 98:2, anti/syn > 99:1
(408) e.r. = 94:6 to 99:1,
E/Z = 98:2, anti/syn > 99:1
(ent-408a) 69%, e.r. > 84:16,
E/Z = 98:2, anti/syn > 99:1

(110)

The (−)-sparteine–lithium compounds **409** undergo a facile conjugate addition to 1-nitroalkenes **410** with high enantio- and diastereoselectivity (equation 111)[289, 295, 296]. The (1*Z*)-3,4-*syn*-diastereomers **411** are produced. A manifold of synthetically useful transformations of nitroenamines **411** has been worked out. Equation 112 presents a few of them utilizing the diphenyl derivatives **411a**[295, 296]. The enantiomers *ent*-**412**–*ent*-**416** are available via inversion of **409** by stannylation/lithiodestannylation with slightly decreased overall selectivities[296].

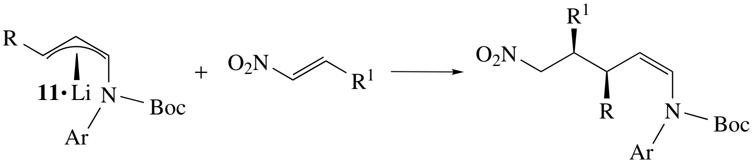

(111)

(409) **(a)** R = Ph
(b) R = 2-furyl
(c) R = Me

(410)

(411) 73–90%,
d.r. = 84:16 to 98:2,
e.r. = 96:4 to > 97:3

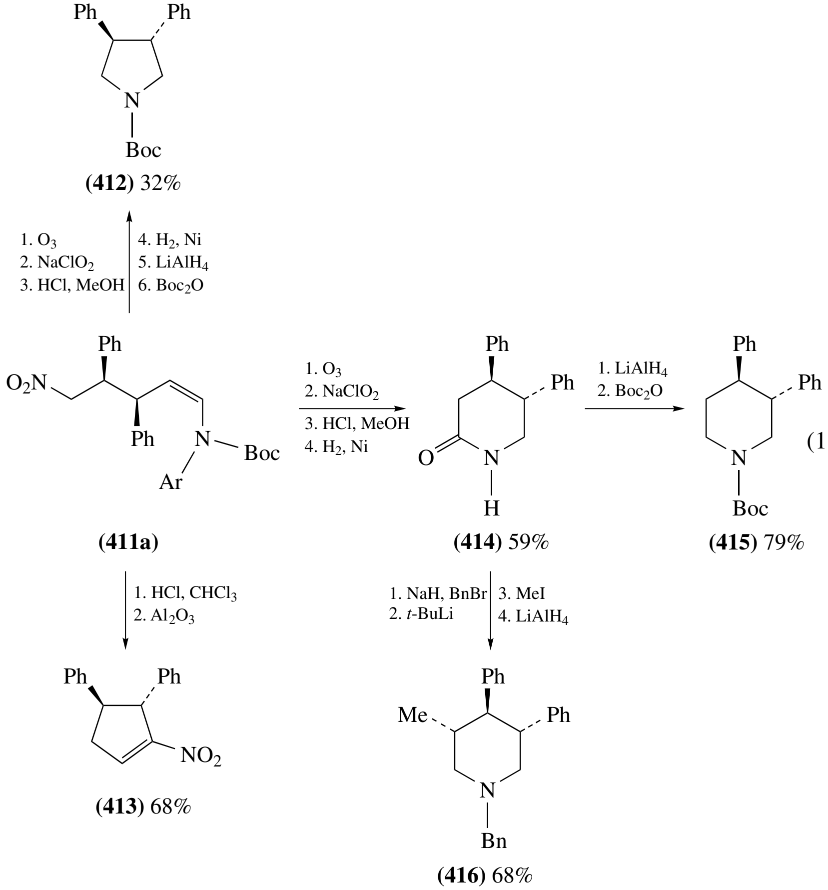

(112)

When the chiral lithium compound **409a** is reacted with racemic α,β-unsaturated lactones *rac*-**417**, an efficient kinetic resolution of the substrate takes place during the Michael addition to form essentially stereohomogeneous γ-lactones **418** (equation 113)[297]. The reaction with six-membered alkenolides of type *rac*-**419** takes the identical stereochemical course, although the diastereoselectivity is decreased[297]. Beak and Lim propose a high energetic difference in the competing transition structures **420** and **421** as the origin for the enantiomer differentiation. In **420**, derived from (*R*)-**417**, the steric interactions between the phenyl group and the residue R are minimized[297].

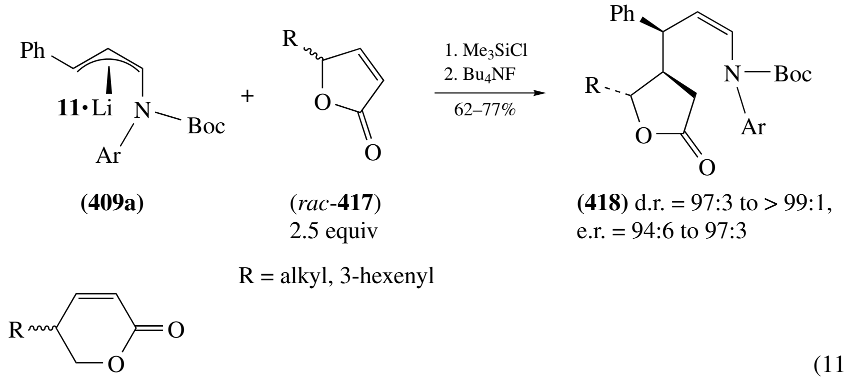

(409a) (*rac*-**417**) 2.5 equiv **(418)** d.r. = 97:3 to > 99:1, e.r. = 94:6 to 97:3

R = alkyl, 3-hexenyl

(*rac*-**419**)

(113)

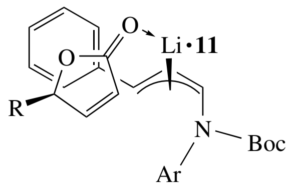

(420)

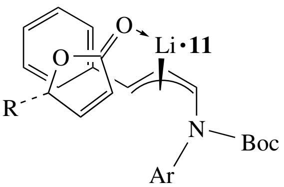

(421)

V. LITHIUM–(–)-SPARTEINE COMPLEXES OF 2-ALKYNYL CARBAMATES

2-Alkynyl *N*,*N*-diisopropylcarbamates **422** are smoothly deprotonated by *n*-BuLi/TMEDA (equation 114)[298, 299]. It was shown by NMR studies, carried out by Reich and Holladay, that the propargylic structure **423** dominates the ground state[300]. After lithium–titanium exchange, the intermediate alkynyl-triisopropoxytitanates *rac*-**424** add to aldehydes with high regio- and diastereoselectivity to form the allenyl carbinols *rac*-**425**[298, 299]. Some interesting elimination and rearrangement reactions of the alcohols **425** have been developed[301–303].

A certain configurational stability of an intermediate lithiated primary 2-alkynyl alkenyl ether was recorded by Marshall and Lebreton[304] during a [2,3]-Wittig rearrangement. Transient enantioenriched 1-lithio-1-alkoxyalkynides have been generated via lithiodestannylation by Nakai and coworkers for enantioselective Wittig rearrangements[305]. However, even the lithium–TMEDA complex, prepared by deprotonation of the optically active secondary alkynyl carbamate **426a**, underwent rapid racemization when kept at −78 °C[306].

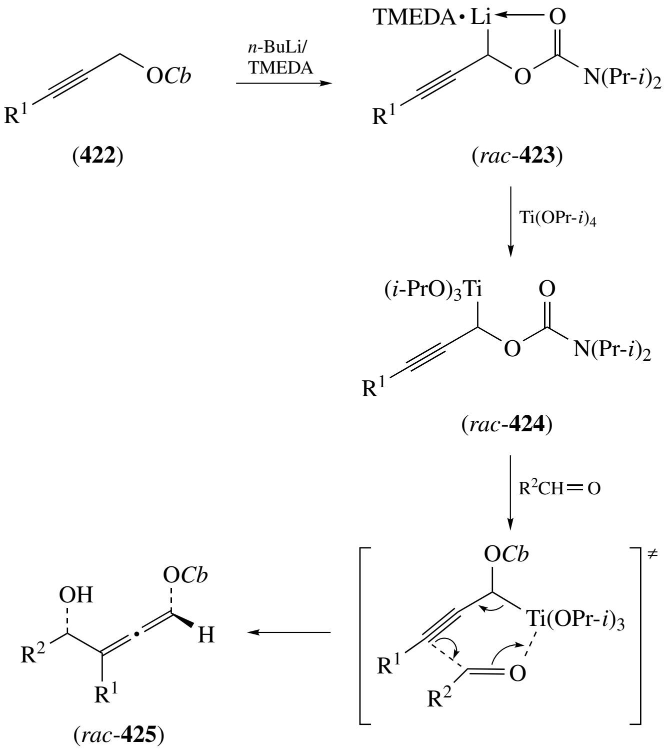

(114)

Increasing the steric bulk in the 3-position led to dramatic enhancement of the configurational stability; for the *tert*-butyl derivative **426c**, a complete chirality transfer occurred[307]. Some epimerization took place with the 3-cyclohexylalkynyl carbamate[307].

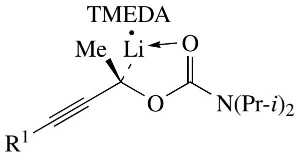

(426) **(a)** $R^1 = Me$
(b) $R^1 = c\text{-}C_6H_{11}$
(c) $R^1 = C(CH_3)_3$

The deprotonation of (achiral) primary 2-alkynyl carbamates **422** by the sparteine method leads to complexes **427**, which are not configurationally stable in solution (diethyl ether, toluene, pentane) even at −78 °C (equation 115)[308]. For intermediates (*S*)-**427a** and (*S*)-**427b**, conditions could be found for the dynamic thermodynamic resolution by preferential crystallization of one of the diastereomers. (*S*)-**427a,b** are transmetallated by rapid addition of triisopropoxytitanium chloride from the solid state in the slurry with complete inversion of the configuration; subsequent addition of an aldehyde leads to the highly enantioenriched, diastereomerically pure allenyl carbinols **430** with greater than 93% *ee*[308].

Protonation of the titanium intermediates (*S*)-**428a,b** furnishes the enantioenriched allenyl carbamates (*M*)-**429a,b** (80%, 84% *ee*, and 86%, 88% *ee*, respectively)[308].

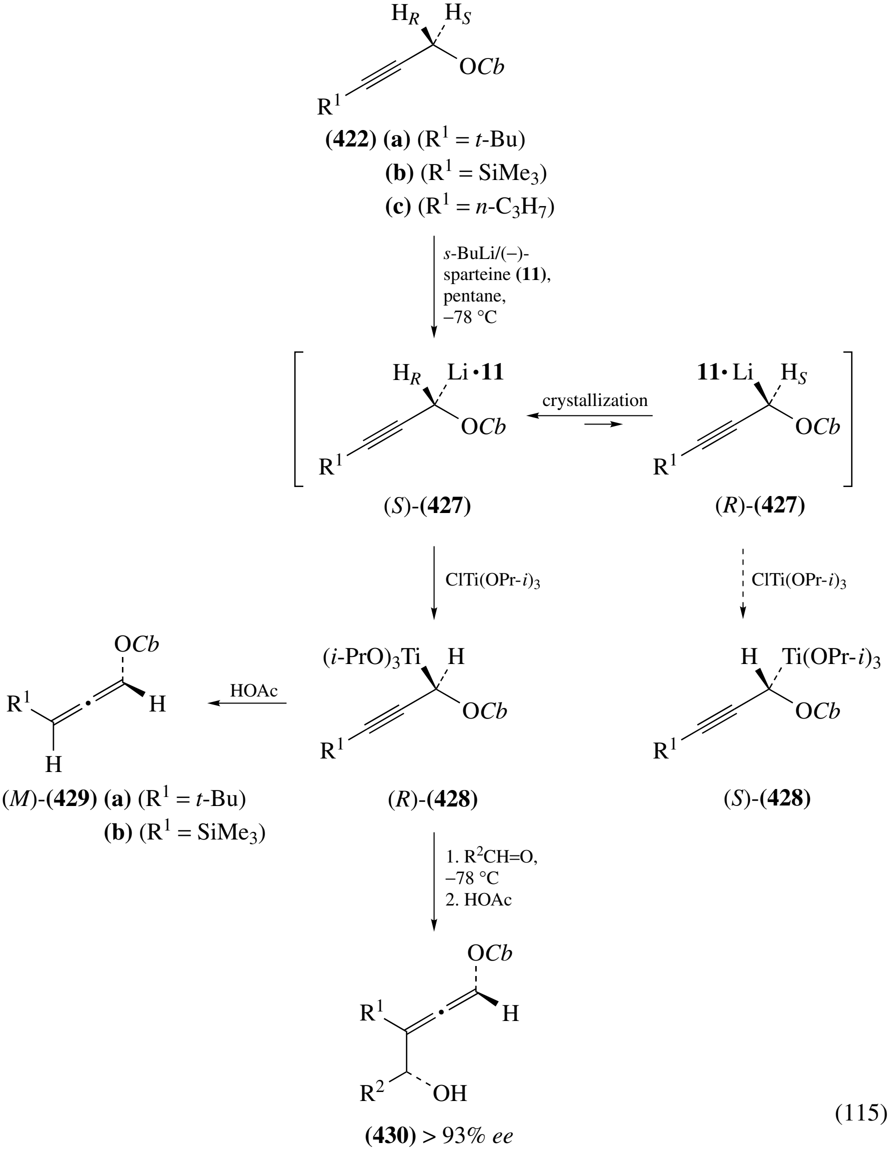

(115)

The allenyl carbamate (*M*)-**429a** is smoothly deprotonated by means of *s*-BuLi/TMEDA leading to axially chiral, configurationally stable 1-lithioallene (*M*)-**431a**[308, 309]. This was trapped by trialkylstannylation or acylation with complete stereoretention. Addition to (*E*)-α,β-enones yields diastereomeric lithium alcoholates **432**, which rearrange with migration of the carbamoyl group to form reactive transient lithium allenolates, with **433** bearing an allylic leaving group (equation 116)[309]. The stereospecific cyclization of **433** leads to enantioenriched, highly substituted alkylidene cyclopentenones **434** and **435**[309].

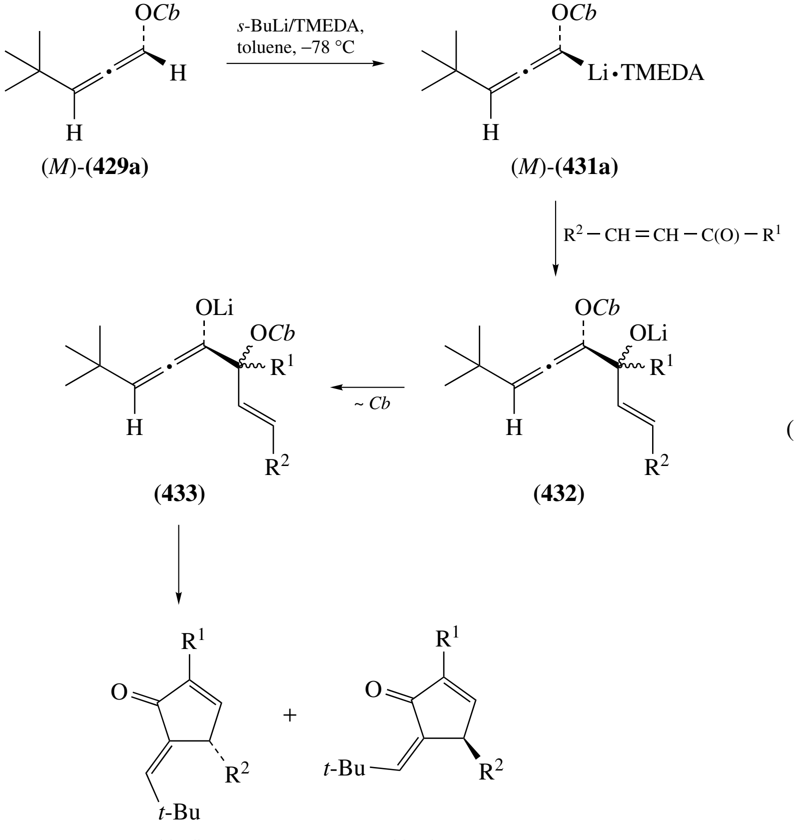

(*M*)-(**429a**) (*M*)-(**431a**) (**433**) (**432**) (**434**) (**435**)

(116)

VI. AXIAL-CHIRAL AND PLANAR-CHIRAL LITHIUM–(−)-SPARTEINE COMPLEXES

Early attempts at introducing axial chirality to allenes (via carbene rearrangement)[310, 311] or to biaryls [through (−)-sparteine-mediated deprotonation of 2,2′,6,6′-tetramethylbiphenyl][192] proved less successful.

A kinetic resolution by enantiodifferentiating deprotonation of atropoisomeric[312] 1-naphthalenecarboxamides *rac*-**436** by means of *s*-BuLi/(−)-sparteine (**11**) was reported by Thayumanavan, Beak and Curran (equation 117)[313]. Compound (*S*)-**437** racemizes essentially completely during 8 d at room temperature. The stereoselectivity is achieved in the deprotonation step, as was demonstrated by control experiments.

N,*N*-Diisopropyl-*o*-ethylbenzamide **267** reacts with *s*-BuLi/(−)-sparteine (**11**) preferently from one of the atropoisomeric conformations under lateral deprotonation and leads to the enantiomerically enriched silane **438** (equation 118)[314]. At 20 °C, a rapid equilibration of the diastereomers **438** and **439** takes place by torsion of the carboxamide group.

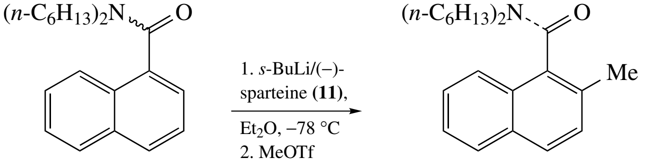

(*rac*-**436**) (*S*)-(**437**)
25%, 55% *ee*

(117)

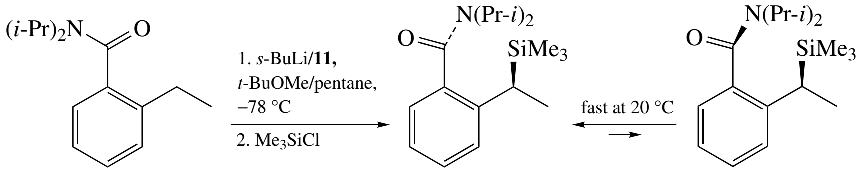

(**267**) (**438**) (**439**)
90%, 69% *ee*

(118)

The oxidative coupling of 1,1′-dilithiobiaryls in the presence of (−)-sparteine (**11**) yielded optically active tetra-*o*-phenylenes with up to 59% *ee*[315].

Achiral *N*,*N*-diisopropyl-ferrocenecarboxamide (**440**) was deprotonated by Snieckus and coworkers by *n*-BuLi/(−)-sparteine (**11**) (equation 119)[316]. The base discriminates well between the enantiotopic protons H(2) and H(5) in the substituted ring to form the diastereomer **441** with high selectivity. Trapping the intermediate with a couple of different electrophiles afforded the substitution products **442a-d** with 85 to 99% *ee*[317, 318].

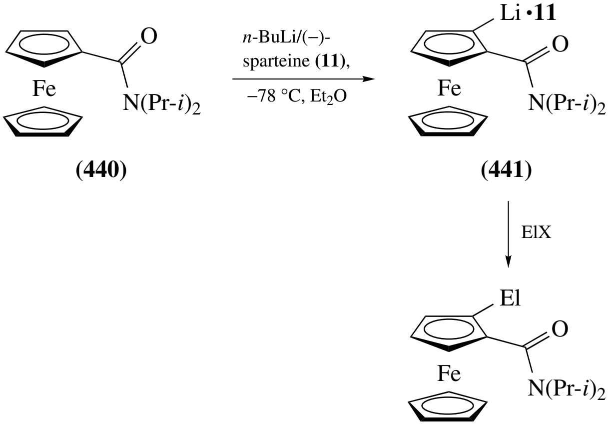

(**440**) (**441**)

(119)

(**442**) (**a**) ElX = Me_3SiCl, 96%, 98% *ee*
(**b**) ElX = I_2, 85%, 96% *ee*
(**c**) ElX = Ph_2PCl, 82%, 90% *ee*
(**d**) ElX = $B(OMe)_3$, 89%, 85% *ee*

The dicarboxamide **443** could be sequentially lithiated and substituted twice under similar conditions and was reacted with several electrophiles[319]. The sequence is shown in equation 120 for the synthesis of the bis(diphenylphosphine) **445**. Only a little *meso*-**445** is formed, removing most of the minor enantiomer of **445**. The phosphines **444, 445** and *meso*-**445** had been prepared earlier by Jendralla and Paulus applying the Snieckus method, and had been tested in enantioselective Pd-catalysed reactions[320].

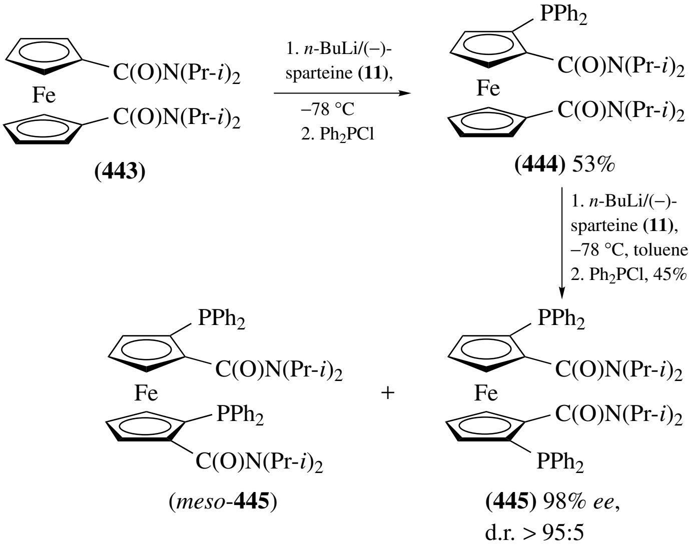

(120)

The isopropoxysulphonyl group is a more powerful directing group than the *N*,*N*-diisopropylcarbamoyl group in lithiation reactions[321, 322]. However, in (−)-sparteine-mediated deprotonations of the isopropyl ferrocenesulphonate **446a** under several conditions, only low enantioselectivities were achieved (equation 121)[323]. Applying the (1*R*,2*S*,5*R*)-menthyl sulphonate, the enantiomeric ratios **447b**/*ent*-**447b** increased to 90:10 due to a matched pair situation by double asymmetric induction.

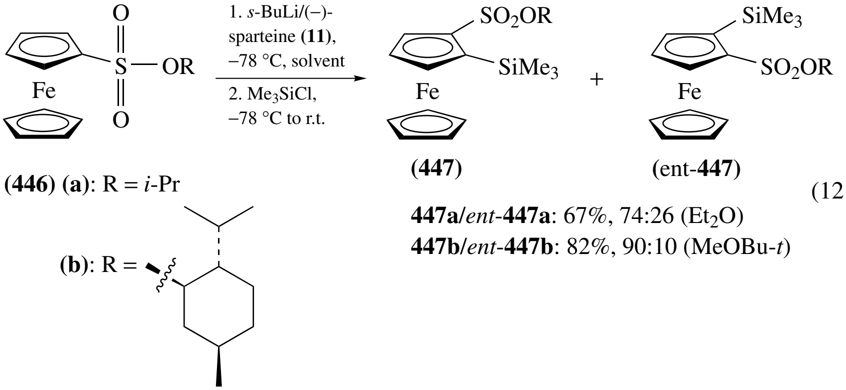

(121)

According to Widdowson, [(methoxymethoxy)benzene]tricarbonylchromium (**448**) was deprotonated with enantiotopos differentiation by *n*-BuLi/(−)-sparteine (**11**), and the lithium intermediate **449** was trapped by various electrophiles to give the products **451** with *ee* values up to 97% (equation 122)[324–326]. Surprisingly, opposite enantiomers are formed when stoichiometric or excess amounts of base are applied. The authors presume that in the dilithium intermediate **450** the C−Li bond (in the rear) has a higher reactivity than the other one (pointed to the front). The deprotonation procedure was also applied to a couple of 1,4-disubstituted chromium complexes[324, 326].

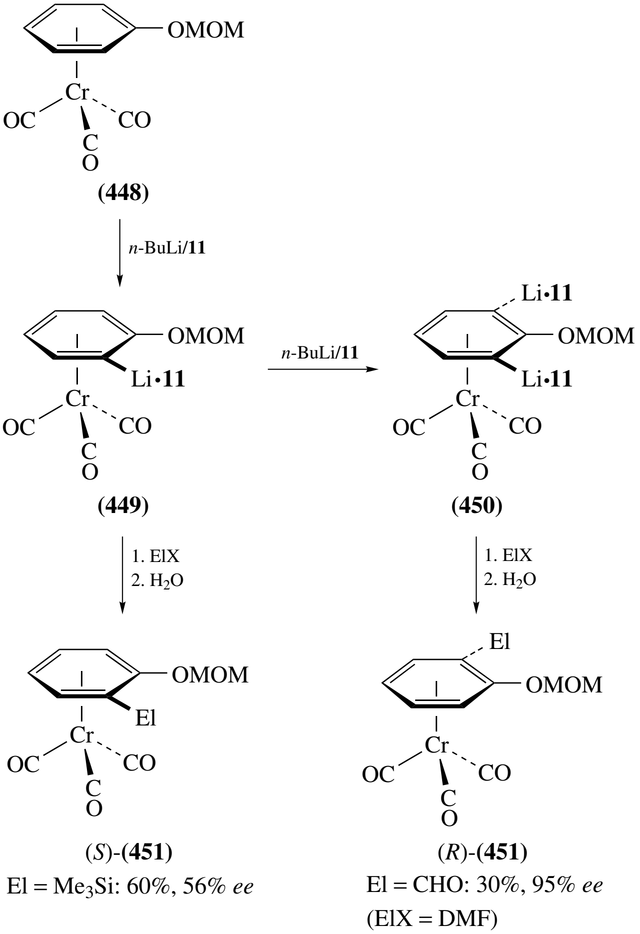

(122)

VII. ENANTIOSELECTIVE ADDITION OF ACHIRAL CARBANIONIC COMPOUNDS IN THE PRESENCE OF (−)-SPARTEINE

A. Enantioselective Addition to C=O and C=N Bonds

The aim in the previous sections was to generate chiral carbanions with enantiomeric excess by the interaction of (−)-sparteine (**11**) during the deprotonation. The addition of the complexes **452** formed with achiral RLi, bearing enantiomerically enriched ligands at the lithium cation, onto aldehydes lead to diastereomeric alcoholates **453** and *epi*-**453** via transition states of unequal energy, finally forming the alcohols **454** and *ent*-**454** with different rates (equation 123). This topic is outside the general scope and can be reviewed only very briefly.

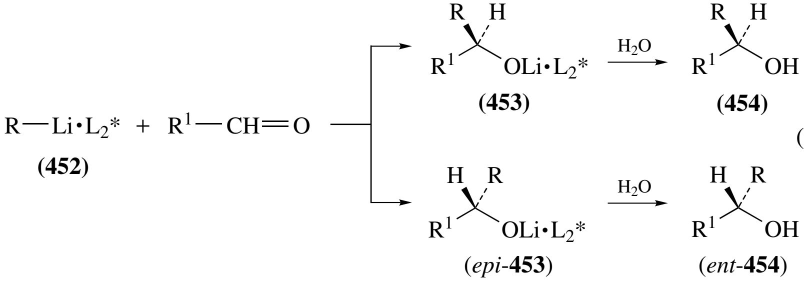

(123)

A great number of chiral bidentate nitrogen and oxygen ligands, which served well with other cations than lithium, are known[327–334]. Only very limited success was achieved with organolithium compounds in the classical examples of addition reactions onto aldehydes[7, 12, 335–337].

(−)-Sparteine (**11**) catalyses efficiently the addition of organolithiums onto *N*-(*p*-methoxyphenyl)imines **455** (equation 124)[338]. Even substoichiometric amounts (e.g. 0.2 equiv.) of **11** gave good enantioenrichment. Alternatively, bis(oxazoline) ligands serve well[338].

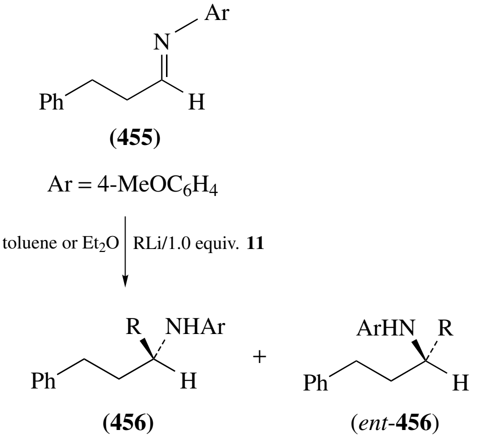

(124)

R = Me, 71%, e.r. = 86:14 (toluene, −78 °C)
R = Bu, 90%, e.r. = 95.5:4.5 (Et_2O, −94 °C)
R = Bu, 91%, e.r. = 89.5:10.5 (Et_2O, −78 °C, 0.2 equiv. of **11**)

Several further publications report on the (−)-sparteine-mediated addition of alkyl- or aryllithium onto imines[339–341] or the C=N bond of isoquinolines[342–344]. Usually, the achieved enantiomeric excesses are low and, sometimes, other chiral ligands serve better. As reported by Müller and coworkers, the nucleophilic substitution of arenecarbaldehyde dialkyl acetals by *o*-substituted aryllithium reagents is an alternative[345, 346].

B. Enantioselective Addition to Carbon–Carbon Multiple Bonds

The addition of alkyllithium–(−)-sparteine complexes to C=C bonds can lead to chiral carbanions and may be an interesting alternative to deprotonation.

Organolithium–(−)-sparteine complexes have been used to initiate the anionic polymerization of acrylates and styrenes[347].

In order to avoid polymerization and to achieve better stereocontrol by quasi-intramolecular addition, a carbanion-stabilizing group and a complexing substituent for capturing alkyllithium/(−)-sparteine in the substrate are useful. This carbolithiation protocol was realized with great success by Marek, Normant and coworkers (equation 125)[65, 348, 349]. Addition of *n*-BuLi/(−)-sparteine (**11**) onto the lithium alcoholate derived from (*E*)-cinnamyl alcohol (**457**) in cumene at 0 °C afforded the addition product with 82% yield and 80% *ee*.

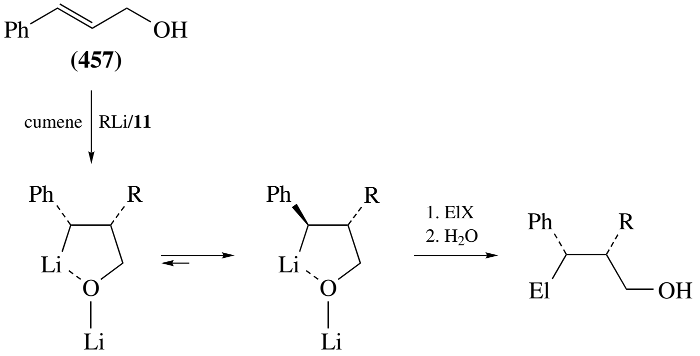

(457) **(458)** (*epi*-**458**) **(459)**

(125)

(459) **(a)** R = Bu, ElX = H_3O^+, 82%, e.r. = 90:10
(b) R = Bu, ElX = $(PhS)_2$, 61%, e.r. = 91.5:8.5
(c) R = Et, ElX = H_3O^+, 68%, e.r. = 92.5:7.5

Since carbolithiations usually proceed as *syn* additions, **458** is expected to be formed first. Due to the configurationally labile benzylic centre it epimerizes to the *trans*-substituted chelate complex *epi*-**458**. The substitution of *epi*-**458** is assumed to occur with inversion at the benzylic centre. Sterically more demanding reagents (*t*-BuLi) or the well-stabilized benzyllithium do not add. The reaction works with the same efficiency when other complexing cinnamyl derivatives, such as ethers and primary, secondary, or tertiary amines, are used as substrates[348]. A substoichiometric amount (5 mol%) of (−)-sparteine (**11**) serves equally well. The appropriate (*Z*)-cinnamyl derivatives give rise to *ent*-**459**, since the opposite enantiotopic face of the double bond is attacked[348, 349].

Mixed (*E*)-cinnamyl acetals **460** undergo the enantioselective carbolithiation readily in the presence of stoichiometric or catalytic amounts, as low as 1 mol%, of (−)-sparteine (**11**) (equation 126)[349, 350]. When quenching the reaction mixture of **461, 462** below −50 °C with MeOH/HCl, the alcohols **463** are obtained with good yields and excellent *ee* values. However, upon warming to 20 °C, a 1,3-cycloelimination from conformation **462** gives rise to the formation of optically active *trans*-cyclopropanes **464**[349, 350].

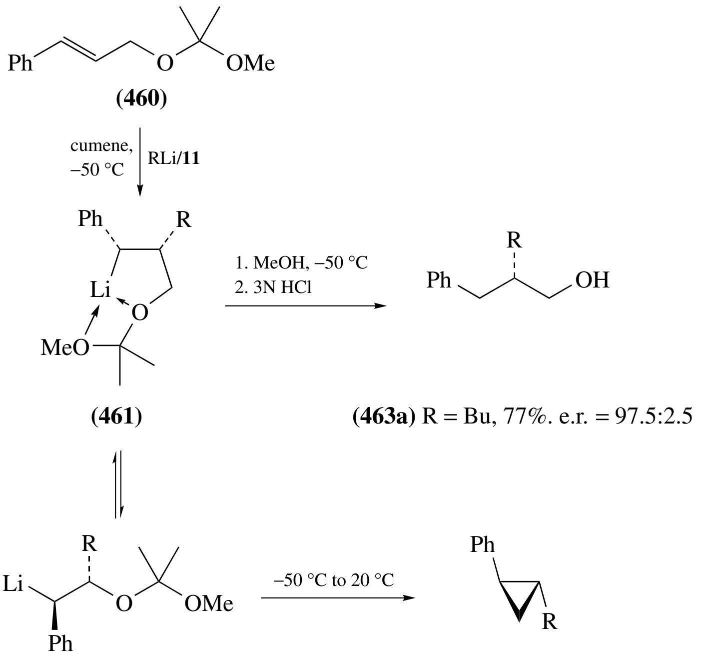

(460)

(461) **(463a)** R = Bu, 77%. e.r. = 97.5:2.5

(462) **(464a)** R = Bu, 60%. e.r. = 97.5:2.5

(126)

Surprisingly, non-heteroatom-substituted (*E*)-styrenes react similarly without posing difficulties (equation 127). From (*E*)-1-phenyl-1-propene (**465**), with hexyllithium the addition product **466** was obtained in good yield and enantiomeric ratio[351]. The (*Z*)-olefins react very sluggishly and remain unchanged in the reaction mixture[351].

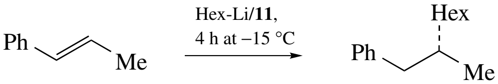

(465) **(466)** 86%, e.r. = 92:8

(127)

Cinnamate salts and cinnamic amides react with low regioselectivity to yield mixtures of the 2- and 3-alkylated products[352, 353]. *ortho*-Substituted aryllithium–(−)-sparteine complexes **468** add with good enantiofacial discrimination to *ortho*-substituted *tert*-butyl cinnamates **467** to give **469** (equation 128)[354]. The chiral additive (*R*,*R*)-1,2-dimethoxy-1,2-diphenylethane in some cases gave improved *ee* values.

Occasionally, very good enantioselectivities were achieved in the (−)-sparteine-mediated carbolithiation of 6-dimethylaminofulvene (**470**) by *ortho*-substituted aryllithiums **471** (equation 129)[355]. Here, (−)-sparteine (**11**) turned out the best chiral additive. The lithium cyclopentadienides **472** were converted to the corresponding Rh(I)–norbornadiene complexes **473**.

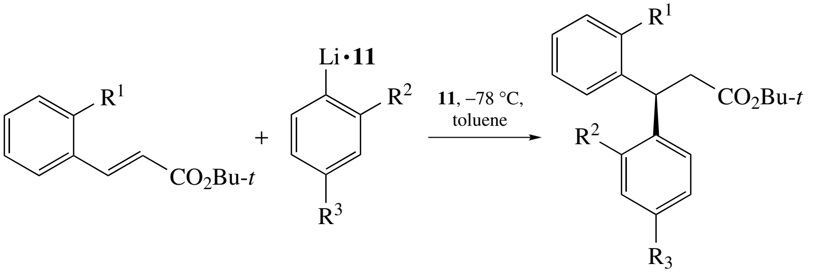

(128)

(467) **(468)** **(469)** **(a)** $R^1 = CH(OMe)_2$, $R^2 = Me$, $R^3 = OMe$ 91%, 68% *ee*

(b) $R^1 = Ph$, $R^2 = CH_2Ph$, $R^3 = H$ 91%, 74% *ee*

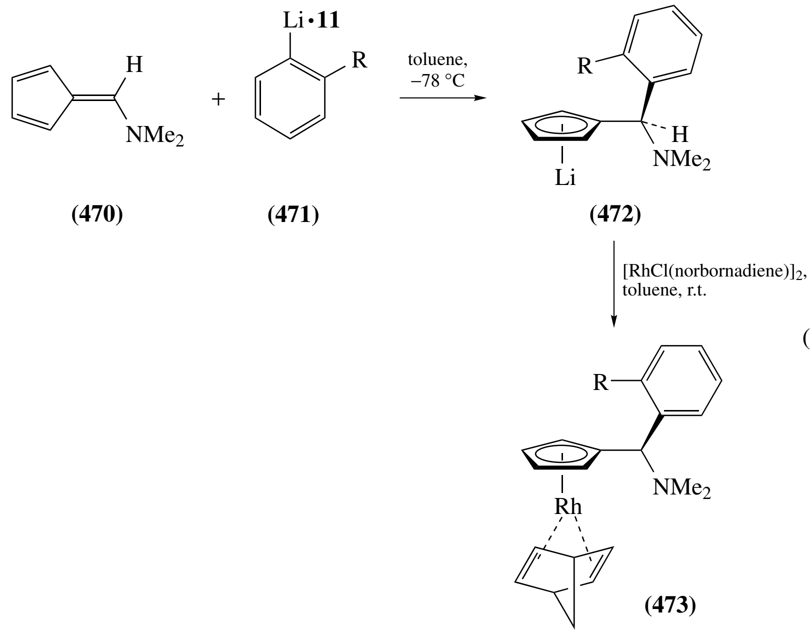

(470) **(471)** **(472)**

(129)

(473)

R = Me: 92%, 91% *ee*

ω-Substituted 2,4-alkadien-1-ols such as **474** add the alkyllithium/(−)-sparteine complex preferentially to the 2-position to form via the alkoxide the corresponding allyllithium intermediates **475**[356]. Protic workup leads to a mixture of E/Z-alkenols **476** and **477**; on catalytic hydrogenation the β-branched alcohols **478** are isolated (equation 130).

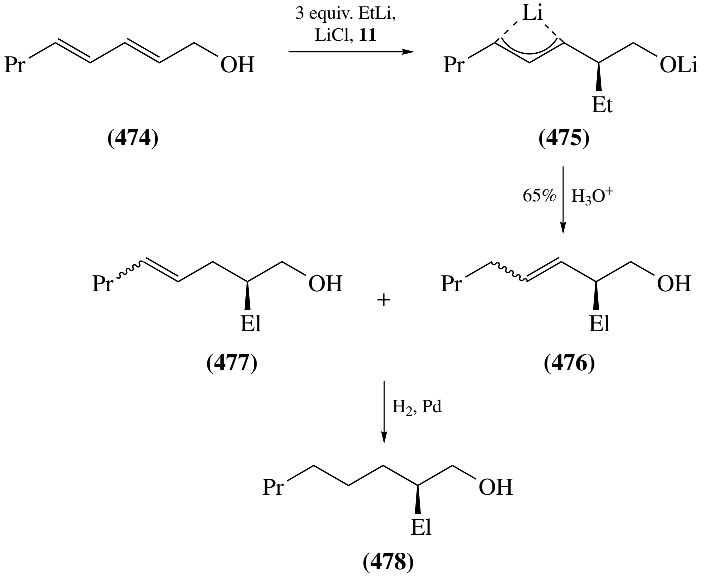

El = Et: 71%, e.r. = 87:13

(130)

By application of the corresponding dienyl acetals **479** (*n*-BuLi and 0.1 equiv. of **11**), enantioenriched *trans*-1-alkenyl-2-alkylcyclopropanes **481** are formed by 1,3-cycloelimination of the allylic intermediate **480** (equation 131)[357].

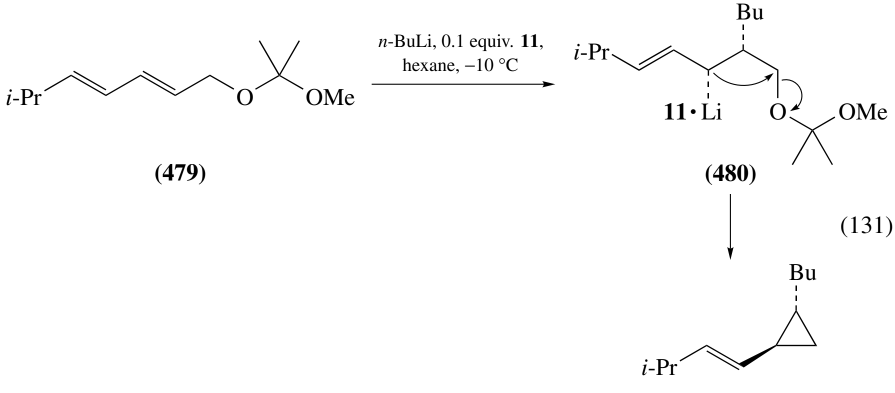

(131)

(481) 60%,
e.r. = 77:23

The carbolithiation of the oxazoline-substituted (tricarbonylchromium)benzene **482** in the presence of (−)-sparteine (**11**) proceeds with medium enantioselectivity (equation 132)[358]. The cyclohexadienyllithium derivative **483** is alkylated by propargyl bromide from the opposite diastereotopic face to yield the trisubstituted 1,3-cyclohexadiene **484**. The application of (*S*,*S*)-1,2-dimethoxy-1,2-diphenylethane (**485**) furnished better enantiomeric excesses (marked in equation 132 in parentheses)[358].

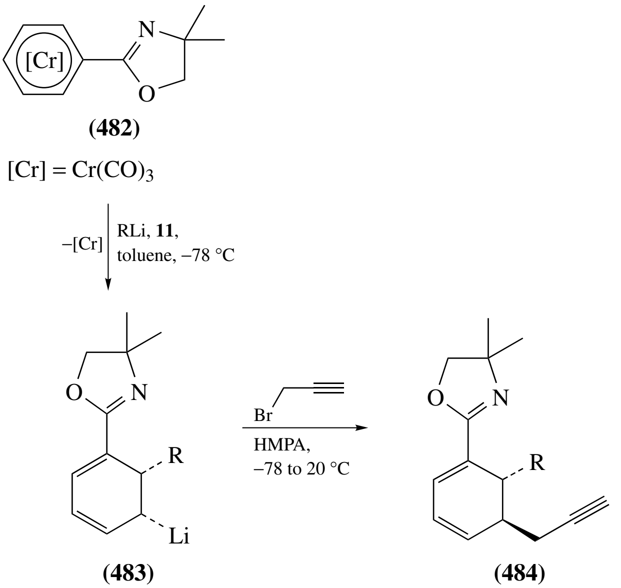

(132)

R = Ph: 72%, e.r. = 77:23 (96.5:3.5)
R = Vinyl: 87%, e.r. = 67:33 (93.5:6.5)
R = Me: 70%, e.r. = 73.5:26.5 (93.5:6.5)
R = Bu: 65%, e.r. = 68:32 (82.5:17.5)

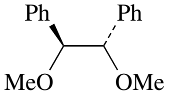

(485)

The carbolithiation of styryl carbamates such as **486** by alkyllithium/(−)-sparteine (**11**) leads to configurationally stable benzyllithium compounds **487**, which have been further substituted by electrophiles (equation 133)[359, 360]. However, only low enantioselectivities could be achieved with (−)-sparteine (**11**) (e.r. = 70:30) or (−)-α-isosparteine (**14**) (e.r. $\leqslant$ 75:25)[359].

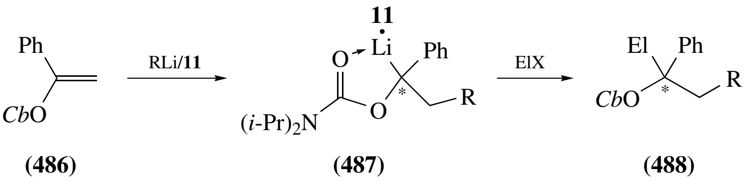

(133)

Surprisingly high *ee* values have been independently recorded by Bailey and Mealy[361] and Sanz Gil and Groth[362] for the cyclocarbolithiation of 2-lithio-*N*-(2-alkenyl)anilines in the presence of (−)-sparteine (**11**) to form 1,3-disubstituted indolines

492 (equation 134)[361]. The lithium compound **490**, formed by halogen–lithium exchange from the bromide **489**, undergoes a 5-*exo-trig* cyclization, accompanied by high facial selection at the double bond to give **491**. Further, less enantioselective cyclizations are described elsewhere[361].

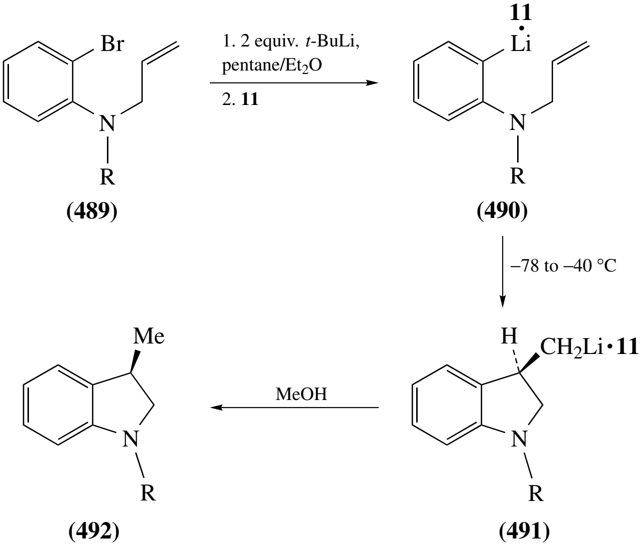

(489) **(490)** **(491)** **(492)**

R = Allyl: 69%, e.r. = 93:7

(134)

Sanz Gil and Groth applied several substituted *N*-allyl-*N*-benzyl-2-bromobenzenes **493** for a similar reaction sequence and trapped the lithiomethyl intermediates **494** by hydrolysis (El = H) or by bromination with 1,2-dibromoethane (El = Br) giving **495** (equation 135)[362].

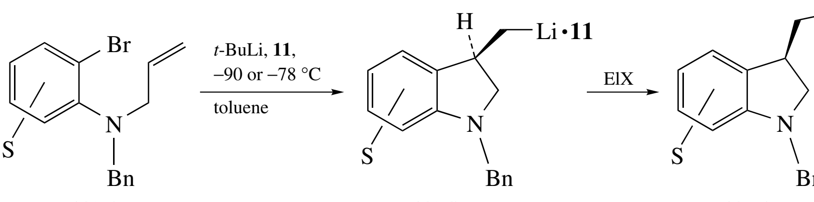

(493) **(494)** **(495)**

(135)

TABLE 12. Data on the reaction of equation 135

Compound	Substituent S	Temperature	El	Yield	e.r.
495a	H	−90 °C	Br	70%	92.5:7.5
495b	4-BnO	−78 °C	H	80%	93.5:6.5
495c	4-F	−90 °C	H	80%	95:5

An elegant asymmetric synthesis of *trans*-1-(2-hydroxyaryl)-2-trimethylsilylcyclopropanes **497** of unknown absolute configuration from 2-bromoaryl ethers **496**, involving a (−)-sparteine-mediated lithium–bromine exchange, has been developed by Barluenga and coworkers (equation 136)[363].

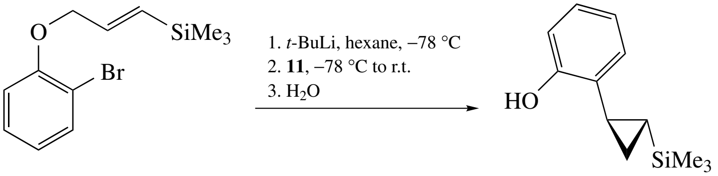

(496) **(497)** 52%, 78% *ee* (136)

VIII. REFERENCES

1. W. C. Still and C. Sreekumar, *J. Am. Chem. Soc.*, **102**, 1201 (1980); V. J. Jephcote, A. J. Pratt and E. J. Thomas, *J. Chem. Soc., Perkin Trans. 1*, 1529 (1989).
2. P. v. Ragué Schleyer, T. Clark, A. J. Kos, G. W. Spitznagel, C. Rohde, D. Arad, K. N. Houk and N. G. Rondan, *J. Am. Chem. Soc.*, **106**, 6467 (1984); G. Boche, A. Opel, M. Marsch, K. Harms, F. Haller and J. C. W. Lohrenz, *Chem. Ber.*, **126**, 2265 (1993).
3. Review: P. Beak, A. Basu, D. J. Gallagher, Y. S. Park and S. Thayumanavan, *Acc. Chem. Res.*, **29**, 552 (1996).
4. Review: D. Hoppe and T. Hense, *Angew. Chem.*, **109**, 2376 (1997); *Angew. Chem., Int. Ed. Engl.*, **36**, 2282 (1997).
5. Review: D. Hoppe, (−)-Sparteine, in *Encyclopedia of Reagents for Organic Synthesis* (Ed. L. A. Paquette), Vol. 7, Wiley, Chichester, 1995, pp. 4662–4664.
6. Review: D. Hoppe, F. Marr and M. Brüggemann, 'α-Chiral α-oxy-substituted lithium carbanions', in *Advances in Organometallic Chemistry* (Ed. D. M. Hodgson), Springer-Verlag, Heidelberg, 2003, in press.
7. H. Nozaki, T. Aratani, T. Toraya and R. Noyori, *Tetrahedron*, **27**, 905 (1971).
8. D. Hoppe and O. Zschage, *Angew. Chem.*, **101**, 67 (1989); *Angew. Chem., Int. Ed. Engl.*, **28**, 69 (1989).
9. O. Zschage, J.-R. Schwark and D. Hoppe, *Angew. Chem.*, **102**, 336 (1990); *Angew. Chem., Int. Ed. Engl.*, **29**, 296 (1990).
10. D. Hoppe, F. Hintze and P. Tebben, *Angew. Chem.*, **102**, 1457 (1990); *Angew. Chem., Int. Ed. Engl.*, **29**, 1422 (1990).
11. S. T. Kerrick and P. Beak, *J. Am. Chem. Soc.*, **113**, 9708 (1991).
12. H. Nozaki, T. Aratani and T. Toraya, *Tetrahedron Lett.*, 4097 (1968).
13. M. Guetté, J. Capillon and J.-P. Guetté, *Tetrahedron*, **29**, 3659 (1973).
14. M. M. Hansen, P. A. Bartlett and C. H. Heathcock, *Organometallics*, **6**, 2069 (1987).
15. Y. Okamoto, K. Suzuki, T. Kitayama, H. Yuki, H. Kageyama, K. Miki, N. Tanaka and N. Kasai, *J. Am. Chem. Soc.*, **104**, 4618 (1982).
16. G. Wulff, R. Sczepan and A. Steigel, *Tetrahedron Lett.*, **27**, 1991 (1986).
17. G. Fraenkel, B. Appleman and G. Ray, *J. Am. Chem. Soc.*, **96**, 5113 (1974).
18. G. Fraenkel, C. Cottrell, J. Ray and J. Russell, *Chem. Commun.*, 273 (1971).
19. A. Orechoff, M. Rabinowitch and R. Kolowanowa, *Ber. Dtsch. Chem. Ges.*, **66**, 621 (1933).
20. T. Ebner, M. Eichelbaum, P. Fischer and C. O. Meese, *Arch. Pharm.*, **322**, 399 (1989).
21. B. T. Smith, J. A. Wendt and J. Aubé, *Org. Lett.*, **4**, 2577 (2002).
22. M. J. Dearden, C. R. Firkin, J.-P. R. Nermet and P. O'Brien, *J. Am. Chem. Soc.*, **124**, 11870 (2002).
23. E. Marrière, J. Roudon, V. Tadino and M.-C. Lasne, *Org. Lett.*, **2**, 1121 (2000).
24. F. Galinovsky, P. Knoth and W. Fischer, *Monatsh. Chem.*, **86**, 1014 (1955).
25. Review: A. Basu and S. Thayumanavan, *Angew. Chem.*, **114**, 740 (2002); *Angew. Chem., Int. Ed.*, **41**, 716 (2002).
26. Review: S. Caddick and K. Jenkins, *Chem. Soc. Rev.*, 447 (1996).
27. M. M. Harris, *Prog. Stereochem.*, **2**, 157 (1958).
28. H. Paulsen, C. Graeve and D. Hoppe, *Synthesis*, 141 (1996).

29. P. Beak and D. B. Reitz, *Chem. Rev.*, **78**, 275 (1978).
30. P. Beak and W. K. Lee, *Tetrahedron Lett.*, **30**, 1197 (1989).
31. Y. B. Xiang, K. Snow and M. Belley, *J. Org. Chem.*, **58**, 993 (1993).
32. G. Boche, F. Bosold, J. C. W. Lohrenz, A. Opel and P. Zulauf, *Chem. Ber.*, **126**, 1873 (1993).
33. Review: D. Hoppe, F. Hintze, P. Tebben, M. Paetow, H. Ahrens, J. Schwerdtfeger, P. Sommerfeld, J. Haller, W. Guarnieri, S. Kolczewski, T. Hense and I. Hoppe, *Pure Appl. Chem.*, **66**, 1479 (1994).
34. D. J. Gallagher, S. T. Kerrick and P. Beak, *J. Am. Chem. Soc.*, **114**, 5872 (1992).
35. D. Hoppe, M. Paetow and F. Hintze, *Angew. Chem.*, **105**, 430 (1993); *Angew. Chem., Int. Ed. Engl.*, **32**, 394 (1993).
36. J. P. N. Papillon and R. J. K. Taylor, *Org. Lett.*, **4**, 119 (2002).
37. E.-U. Würthwein, K. Behrens and D. Hoppe, *Chem. Eur. J.*, **5**, 3459 (1999).
38. F. Hintze, Dissertation, Universität Kiel, 1993.
39. M. Menges and R. Brückner, *Eur. J. Org. Chem.*, 1023 (1998).
40. K. Behrens, R. Fröhlich, O. Meyer and D. Hoppe, *Eur. J. Org. Chem.*, 2397 (1998).
41. I. Hoppe and D. Hoppe, unpublished results.
42. C. Boie, Dissertation, Universität Münster, 1996.
43. J. Schwerdtfeger and D. Hoppe, *Angew. Chem.*, **104**, 1547 (1992); *Angew. Chem., Int. Ed. Engl.*, **31**, 1505 (1992).
44. B. Weber, J. Schwerdtfeger, R. Fröhlich, A. Göhrt and D. Hoppe, *Synthesis*, 1915 (1999).
45. J. Schwerdtfeger, S. Kolczewski, B. Weber, R. Fröhlich and D. Hoppe, *Synthesis*, 1573 (1999).
46. P. Sommerfeld and D. Hoppe, *Synlett*, 764 (1992).
47. M. T. Reetz, F. Kayser and K. Harms, *Tetrahedron Lett.*, **33**, 3452 (1992).
48. W. Guarnieri, M. Grehl and D. Hoppe, *Angew. Chem.*, **106**, 1815 (1994); *Angew. Chem., Int. Ed. Engl.*, **33**, 1734 (1994).
49. G. Christoph and D. Hoppe, *Org. Lett.*, **4**, 2189 (2002); G. Christoph, Dissertation, Universität Münster, 2002.
50. P. Knochel, J. J. A. Perea and P. Jones, *Tetrahedron*, **54**, 8275 (1998).
51. K. Tomooka, H. Shimizu and T. Nakai, *J. Organomet. Chem.*, **624**, 364 (2001).
52. K. Tomooka, H. Shimizu, T. Inoue, H. Shibata and T. Nakai, *Chem. Lett.*, 759 (1999).
53. F. Hintze and D. Hoppe, *Synthesis*, 1216 (1992).
54. D. Hoppe, R. Hanko, A. Brönneke and F. Lichtenberg, *Angew. Chem.*, **93**, 1106 (1981); *Angew. Chem., Int. Ed. Engl.*, **20**, 1024 (1981).
55. H. Helmke and D. Hoppe, *Synlett*, 978 (1995).
56. W. Guarnieri, M. Sendzik, R. Fröhlich and D. Hoppe, *Synthesis*, 1274 (1998).
57. J. Haller, T. Hense and D. Hoppe, *Justus Liebigs Ann. Chem.*, 489 (1996).
58. E.-U. Würthwein and D. Hoppe, unpublished results.
59. J. F. Larrow, E. N. Jacobsen, Y. Gao, Y. Hong, X. Nie and C. M. Zepp, *J. Org. Chem.*, **59**, 1939 (1994).
60. J. van Bebber, H. Ahrens, R. Fröhlich and D. Hoppe, *Chem. Eur. J.*, **5**, 1905 (1999).
61. M. Paetow, M. Kotthaus, M. Grehl, R. Fröhlich and D. Hoppe, *Synlett*, 1034 (1994).
62. M. J. Woltering, R. Fröhlich and D. Hoppe, *Angew. Chem.*, **109**, 1805 (1997); *Angew. Chem., Int. Ed. Engl.*, **36**, 1764 (1997).
63. K. Tomooka, N. Komine, T. Sasaki, H. Shimizu and T. Nakai, *Tetrahedron Lett.*, **39**, 9715 (1998).
64. D. Hoppe, M. J. Woltering, M. Oestreich and R. Fröhlich, *Helv. Chim. Acta*, **82**, 1860 (1999).
65. Review: I. Marek, *J. Chem. Soc., Perkin Trans. 1*, 535 (1999).
66. S. H. Kleinfeld, E. Wegelius and D. Hoppe, *Helv. Chim. Acta*, **82**, 2413 (1999).
67. J. Bousbaa, F. Doms and A. Krief, *Tetrahedron Lett.*, **38**, 7625 (1997).
68. M. Oestreich, R. Fröhlich and D. Hoppe, *Tetrahedron Lett.*, **39**, 1745 (1998).
69. M. Oestreich, R. Fröhlich and D. Hoppe, *J. Org. Chem.*, **64**, 8616 (1999).
70. M. Oestreich and D. Hoppe, *Tetrahedron Lett.*, **40**, 1881 (1999).
71. G. Gralla, B. Wibbeling and D. Hoppe, *Org. Lett.*, **4**, 2193 (2002).
72. Review: S. Masamune, W. Choy, J. S. Petersen and L. R. Sita, *Angew. Chem.*, **97**, 1 (1985); *Angew. Chem., Int. Ed. Engl.*, **24**, 1 (1985).
73. B. Weber, S. Kolczewski, R. Fröhlich and D. Hoppe, *Synthesis*, 1593 (1999).
74. T. Hense and D. Hoppe, *Synthesis*, 1394 (1997).

75. J. Haller, T. Hense and D. Hoppe, *Synlett*, 726 (1993).
76. M. Kotthaus, Dissertation, Universität Münster, 1997.
77. M. J. Woltering, R. Fröhlich, B. Wibbeling and D. Hoppe, *Synlett*, 797 (1998).
78. H. Laqua, R. Fröhlich, B. Wibbeling and D. Hoppe, *J. Organomet. Chem.*, **624**, 96 (2001).
79. M. Sendzik, W. Guarnieri and D. Hoppe, *Synthesis*, 1287 (1998).
80. J. K. Crandall, *J. Org. Chem.*, **29**, 2830 (1964).
81. J. K. Whitesell and P. D. White, *Synthesis*, 602 (1975).
82. R. K. Boeckman, Jr., *Tetrahedron Lett.*, 4281 (1977).
83. Review: D. M. Hodgson, A. R. Gibbs and G. P. Lee, *Tetrahedron*, **52**, 14361 (1996).
84. D. M. Hodgson and G. P. Lee, *J. Chem. Soc., Chem. Commun.*, 1015 (1996).
85. D. M. Hodgson, G. P. Lee, R. E. Marriott, A. J. Thompson, R. Wisedale and J. Witherington, *J. Chem. Soc., Perkin Trans. 1*, 2151 (1998).
86. D. M. Hodgson and R. Wisedale, *Tetrahedron: Asymmetry*, **7**, 1275 (1996).
87. D. M. Hodgson and I. D. Cameron, *Org. Lett.*, **3**, 441 (2001).
88. A. Alexakis, E. Vrancken and P. Mangeney, *J. Chem. Soc., Perkin Trans. 1*, 3354 (2000).
89. D. M. Hodgson and L. A. Robinson, *Chem. Commun.*, 309 (1999).
90. D. M. Hodgson and E. Gras, *Angew. Chem.*, **114**, 2482 (2002); *Angew. Chem., Int. Ed.*, **41**, 2376 (2002).
91. D. M. Hodgson, I. D. Cameron, M. Christlieb, R. Green, G. P. Lee and L. A. Robinson, *J. Chem. Soc., Perkin Trans. 1*, 2161 (2001).
92. D. M. Hodgson, C. R. Maxwell, T. J. Miles, E. Paruch, M. A. H. Stent, J. R. Matthews, F. X. Wilson and J. Witherington, *Angew. Chem.*, **114**, 4489 (2002); *Angew. Chem., Int. Ed.*, **41**, 4313 (2002).
93. A. Alexakis, E. Vrancken and P. Mangeney, *Synlett*, 1165 (1998).
94. M. Lautens, C. Gajda and P. Chiu, *J. Chem. Soc., Chem. Commun.*, 1193 (1993).
95. M. Lautens, E. Fillion and M. Sampat, *J. Org. Chem.*, **62**, 7080 (1997).
96. Review: P. Chiu and M. Lautens, *Top. Curr. Chem.*, **190**, 1 (1997).
97. Review: P. Beak, W. J. Zajdel and D. B. Reitz, *Chem. Rev.*, **84**, 471 (1984).
98. P. Beak, S. T. Kerrick, S. Wu and J. Chu, *J. Am. Chem. Soc.*, **116**, 3231 (1994).
99. N. A. Nikolic and P. Beak, *Org. Synth.*, **74**, 23 (1997).
100. N. Graf v. Keyserlingk and J. Martens, *Eur. J. Org. Chem.*, 301 (2002).
101. M. Majewski, J. Shao, K. Nelson, P. Nowak and N. M. Irvine, *Tetrahedron Lett.*, **39**, 6787 (1998).
102. D. J. Gallagher, S. Wu, N. A. Nikolic and P. Beak, *J. Org. Chem.*, **60**, 8148 (1995).
103. X. Li, L. B. Schenkel and M. C. Kozlowski, *Org. Lett.*, **2**, 875 (2000).
104. K. B. Wiberg and W. F. Bailey, *Angew. Chem.*, **112**, 2211 (2000); *Angew. Chem., Int. Ed.*, **39**, 2127 (2000).
105. K. B. Wiberg and W. F. Bailey, *J. Mol. Struct.*, **556**, 239 (2000).
106. K. B. Wiberg and W. F. Bailey, *J. Am. Chem. Soc.*, **123**, 8231 (2001).
107. K. B. Wiberg and W. F. Bailey, *Tetrahedron Lett.*, **41**, 9365 (2000).
108. R. E. Gawley and Q. Zhang, *J. Org. Chem.*, **60**, 5763 (1995).
109. I. Coldham and G. P. Vennall, *Chem. Commun.*, 1569 (2000).
110. I. Coldham, J.-C. Fernàndez and D. J. Snowden, *Tetrahedron Lett.*, **40**, 1819 (1999).
111. T. R. Elworthy and A. I. Meyers, *Tetrahedron*, **50**, 6089 (1994).
112. R. K. Dieter, C. M. Topping, K. R. Chadupatla and K. Lu, *J. Am. Chem. Soc.*, **123**, 5132 (2001).
113. N. J. Ashweek, I. Coldham, D. J. Snowden and G. Vennall, *Chem. Eur. J.*, **8**, 195 (2002).
114. I. Coldham, R. Hufton and R. E. Rathmell, *Tetrahedron Lett.*, **38**, 7617 (1997).
115. W. F. Bailey, P. Beak, S. T. Kerrick, S. Ma and K. B. Wiberg, *J. Am. Chem. Soc.*, **124**, 1889 (2002).
116. P. Beak and W. K. Lee, *J. Org. Chem.*, **58**, 1109 (1993).
117. Y. S. Park and P. Beak, *Tetrahedron*, **52**, 12333 (1996).
118. K. M. Bertini-Gross and P. Beak, *J. Am. Chem. Soc.*, **123**, 315 (2001).
119. A. I. Meyers and G. Milot, *J. Org. Chem.*, **58**, 6538 (1993).
120. M. Iwao and T. Kuraishi, *Heterocycles*, **34**, 1031 (1992).
121. K. M. Bertini-Gross, Y. M. Jun and P. Beak, *J. Org. Chem.*, **62**, 7679 (1997).
122. J. M. Chong and S. B. Park, *J. Org. Chem.*, **57**, 2220 (1992).
123. N. Kise, T. Urai and J.-I. Yoshida, *Tetrahedron: Asymmetry*, **9**, 3125 (1998).

124. I. Coldham, R. C. B. Copley, T. F. N. Haxell and S. Howard, *Org. Lett.*, **3**, 3799 (2001).
125. B. Kaiser and D. Hoppe, *Angew. Chem.*, **107**, 344 (1995); *Angew. Chem., Int. Ed. Engl.*, **34**, 323 (1995).
126. R. W. Hoffmann and R. Koberstein, *J. Chem. Soc., Perkin Trans. 2*, 595 (2000).
127. S. E. Gibson (née Thomas), P. C. V. Potter and M. H. Smith, *Chem. Commun.*, 2757 (1996).
128. D. Hoppe, B. Kaiser, O. Stratmann and R. Fröhlich, *Angew. Chem.*, **109**, 2872 (1997); *Angew. Chem., Int. Ed. Engl.*, **36**, 2784 (1997).
129. O. Stratmann, B. Kaiser, R. Fröhlich, O. Meyer and D. Hoppe, *Chem. Eur. J.*, **7**, 423 (2001).
130. F. Marr, R. Fröhlich and D. Hoppe, *Org. Lett.*, **1**, 2081 (1999).
131. F. Marr, R. Fröhlich, B. Wibbeling, C. Diedrich and D. Hoppe, *Eur. J. Org. Chem.*, 2970 (2002).
132. F. Marr and D. Hoppe, *Org. Lett.*, **4**, 4217 (2002).
133. T. Shinozuka, Y. Kikori, M. Asaoka and H. Takei, *J. Chem. Soc., Perkin Trans. 1*, 119 (1996).
134. T. Ruhland, R. Dress and R. W. Hoffmann, *Angew. Chem.*, **105**, 1487 (1993); *Angew. Chem., Int. Ed. Engl.*, **32**, 1467 (1993).
135. H. J. Reich and R. R. Dykstra, *Angew. Chem.*, **105**, 1489 (1993); *Angew. Chem., Int. Ed. Engl.*, **32**, 1469 (1993).
136. H. J. Reich and K. J. Kulicke, *J. Am. Chem. Soc.*, **117**, 6621 (1995).
137. R. W. Hoffmann, R. K. Dress, T. Ruhland and A. Wenzel, *Chem. Ber.*, **128**, 861 (1995).
138. W. Klute, R. Dress and R. W. Hoffmann, *J. Chem. Soc., Perkin Trans. 2*, 1409 (1993).
139. R. W. Hoffmann, W. Klute, R. K. Dress and A. Wenzel, *J. Chem. Soc., Perkin Trans. 2*, 1721 (1995).
140. R. W. Hoffmann and W. Klute, *Chem. Eur. J.*, **2**, 694 (1996).
141. R. W. Hoffmann, J. Lanz, R. Metternich, G. Tarara and D. Hoppe, *Angew. Chem.*, **99**, 1196 (1987); *Angew. Chem., Int. Ed. Engl.*, **26**, 1145 (1987).
142. T. Kauffmann, H. Kieper and H. Pieper, *Chem. Ber.*, **125**, 899 (1992).
143. R. W. Hoffmann, M. Julius, F. Chemla, T. Ruhland and G. Frenzen, *Tetrahedron*, **50**, 6049 (1994).
144. H.-J. Gais, G. Hellmann, H. Günther, F. Lopez, H. J. Lindner and S. Braun, *Angew. Chem.*, **101**, 1061 (1989); *Angew. Chem., Int. Ed. Engl.*, **28**, 1025 (1989).
145. H.-J. Gais and G. Hellmann, *J. Am. Chem. Soc.*, **114**, 4439 (1992).
146. P. O'Brien and S. Warren, *Tetrahedron Lett.*, **36**, 8473 (1995).
147. P. O'Brien and S. Warren, *Synlett*, 579 (1996).
148. L. T. Byrne, L. M. Engelhardt, G. E. Jacobsen, W.-P. Leung, R. I. Papasergio, C. L. Raston, B. W. Skelton, P. Twiss and A. H. White, *J. Chem. Soc., Dalton Trans.*, 105 (1989).
149. R. A. Muci, K. R. Campos and D. A. Evans, *J. Am. Chem. Soc.*, **117**, 9075 (1995).
150. T. Imamoto, J. Watanabe, Y. Wada, H. Matsuda, H. Yamada, H. Tsuruta, S. Matsukawa and K. Yamaguchi, *J. Am. Chem. Soc.*, **120**, 1635 (1998).
151. F. Maienza, F. Spindler, M. Thommen, B. Pugit, C. Malan and A. Mezzetti, *J. Org. Chem.*, **67**, 5339 (2002).
152. S. Kobayashi, N. Shiraishi, W.-L. Lam and K. Matanabe, *Tetrahedron Lett.*, **42**, 7303 (2001).
153. B. Wolfe and T. Livinghouse, *J. Am. Chem. Soc.*, **120**, 5116 (1998).
154. K. Nagata, S. Matsukawa and T. Imamoto, *J. Org. Chem.*, **65**, 4185 (2000).
155. B. Wolfe and T. Livinghouse, *J. Org. Chem.*, **66**, 1514 (2001).
156. K. Matsumoto, N. Suzuki and H. Ohta, *Tetrahedron Lett.*, **31**, 7163 (1990).
157. G. Boche, M. Marsch, J. Harbach, K. Harms, B. Ledig, F. Schubert, J. C. W. Lohrenz and H. Ahlbrecht, *Chem. Ber.*, **126**, 1887 (1993).
158. R. I. Papasergio, B. W. Skelton, P. Twiss, A. H. White and C. L. Raston, *J. Chem. Soc., Dalton Trans.*, 1161 (1990).
159. A. Carstens and D. Hoppe, *Tetrahedron*, **50**, 6097 (1994).
160. F. Hammerschmidt and A. Hanninger, *Chem. Ber.*, **128**, 1069 (1995).
161. F. Hammerschmidt, A. Hanninger, B. Peric, H. Völlenkle and A. Werner, *Eur. J. Org. Chem.*, 3511 (1999).
162. A. Basu and P. Beak, *J. Am. Chem. Soc.*, **118**, 1575 (1996).
163. D. Hoppe, A. Carstens and T. Krämer, *Angew. Chem.*, **102**, 1455 (1990); *Angew. Chem., Int. Ed. Engl.*, **29**, 1424 (1990).
164. W. H. Pearson and A. C. Lindbeck, *J. Org. Chem.*, **54**, 5651 (1989).
165. C. Derwing, H. Frank and D. Hoppe, *Eur. J. Org. Chem.*, 3519 (1999).

166. C. Derwing and D. Hoppe, *Synthesis*, 149 (1996).
167. R. W. Hoffmann, T. Rühl and J. Harbach, *Justus Liebigs Ann. Chem.*, 725 (1992).
168. S. Retzow, Dissertation, Universität Kiel, 1993.
169. S. Arrasate, E. Lete and N. Sotomayor, *Tetrahedron: Asymmetry*, **13**, 311 (2002).
170. N. Komine, L.-F. Wang, K. Tomooka and T. Nakai, *Tetrahedron Lett.*, **40**, 6809 (1999).
171. K. Tomooka, L.-F. Wang, N. Komine and T. Nakai, *Tetrahedron Lett.*, **40**, 6813 (1999).
172. K. Tomooka, L.-F. Wang, F. Okazaki and T. Nakai, *Tetrahedron Lett.*, **41**, 6121 (2000).
173. T. Kawasaki and T. Kimachi, *Synlett*, 1429 (1998).
174. M. Tsubuki, T. Kamata, M. Nakatani, K. Yamazaki, T. Matsui and T. Honda, *Tetrahedron: Asymmetry*, **11**, 4725 (2000).
175. V. Capriati, S. Florio, G. Ingrosso, C. Granito and L. Troisi, *Eur. J. Org. Chem.*, 478 (2002).
176. E. L. Cowston, S. E. Gibson (née Thomas), M. J. Schneider and M. H. Smith, *J. Chem. Soc., Chem. Commun.*, 839 (1996).
177. R. A. Ewin and N. S. Simpkins, *Synlett*, 317 (1996).
178. R. A. Ewin, A. M. MacLeod, D. A. Price, N. S. Simpkins and A. P. Watt, *J. Chem. Soc., Perkin Trans. 1*, 401 (1997).
179. M. Schlosser and D. Limat, *J. Am. Chem. Soc.*, **117**, 12342 (1995).
180. N. Voyer and J. Roby, *Tetrahedron Lett.*, **36**, 6627 (1995).
181. C. Barberis and N. Voyer, *Tetrahedron Lett.*, **39**, 6807 (1998).
182. S. Wu, S. Lee and P. Beak, *J. Am. Chem. Soc.*, **118**, 715 (1996).
183. Y. S. Park, M. L. Boys and P. Beak, *J. Am. Chem. Soc.*, **118**, 3757 (1996).
184. N. C. Faibish, Y. S. Park, S. Lee and P. Beak, *J. Am. Chem. Soc.*, **119**, 11561 (1997).
185. Y. S. Park and P. Beak, *J. Org. Chem.*, **62**, 1574 (1997).
186. A. Ariffin, A. J. Blake, M. R. Ebden, W.-S. Li, N. S. Simpkins and D. N. A. Fox, *J. Chem. Soc., Perkin Trans. 1*, 2439 (1999).
187. M. R. Ebden, N. S. Simpkins and D. N. A. Fox, *Tetrahedron*, **54**, 12923 (1998).
188. S. Nakamura, R. Nakagawa, Y. Watanabe and T. Toru, *Angew. Chem.*, **112**, 361 (2000); *Angew. Chem., Int. Ed.*, **39**, 353 (2000).
189. S. Nakamura, R. Nakagawa, Y. Watanabe and T. Toru, *J. Am. Chem. Soc.*, **122**, 11340 (2000).
190. S. E. Gibson (née Thomas), P. Ham, G. R. Jefferson and M. H. Smith, *J. Chem. Soc., Perkin Trans. 1*, 2161 (1997).
191. N. Nozaki, T. Aratani, T. Toraya and R. Noyori, *Tetrahedron*, **27**, 905 (1971).
192. L. M. Engelhardt, W.-P. Leung, C. L. Raston, G. Salem, P. Twiss and A. H. White, *J. Chem. Soc., Dalton Trans.*, 2403 (1988).
193. P. Beak and H. Du, *J. Am. Chem. Soc.*, **115**, 2516 (1993).
194. S. Thayumanavan, S. Lee, C. Liao and P. Beak, *J. Am. Chem. Soc.*, **116**, 9755 (1994).
195. G. P. Lutz, H. Du, D. J. Gallagher and P. Beak, *J. Org. Chem.*, **61**, 4542 (1996).
196. D. J. Gallagher, H. Du, S. A. Long and P. Beak, *J. Am. Chem. Soc.*, **118**, 11391 (1996).
197. J. M. Laumer, D. D. Kim and P. Beak, *J. Org. Chem.*, **67**, 6797 (2002).
198. A. Basu, D. J. Gallagher and P. Beak, *J. Org. Chem.*, **61**, 5718 (1996).
199. S. Thayumanavan, A. Basu and P. Beak, *J. Am. Chem. Soc.*, **119**, 8209 (1997).
200. A. L. Costa, M. G. Piazza, E. Tagliavini, C. Trombini and A. Umani-Ronchi, *J. Am. Chem. Soc.*, **115**, 7001 (1993).
201. V. Derdau and V. Snieckus, *J. Org. Chem.*, **66**, 1992 (2001).
202. T. Kimachi and Y. Takemoto, *J. Org. Chem.*, **66**, 2700 (2001).
203. L. Prat, L. Mojovic, V. Levacher, G. Dupas, G. Quéguiner and J. Bourguignon, *Tetrahedron: Asymmetry*, **9**, 2509 (1998).
204. L. Prat, G. Dupas, G. Quéguiner, J. Bourguignon and V. Levacher, *Tetrahedron Lett.*, **42**, 4515 (2001).
205. S. Florio, V. Capriati and V. Russo, *Tetrahedron Lett.*, **38**, 5843 (1997).
206. Review: C. Lambert and P. v. R. Schleyer, 'Carbanionen-Polare Organometall-Verbindungen', in *Houben-Weyl, Carbanionen* (Ed. M. Hanack), Vol. E 19d, Thieme-Verlag, Stuttgart, 1993, pp. 1–106.
207. Review: M. Schlosser, *Mod. Synth. Methods*, **6**, 227 (1992).
208. Review: D. Hoppe, *Angew. Chem.*, **96**, 930 (1984); *Angew. Chem., Int. Ed. Engl.*, **23**, 932 (1984).
209. D. Hoppe, R. Hanko, A. Brönneke, F. Lichtenberg and E. van Hülsen, *Chem. Ber.*, **118**, 2822 (1985).

210. R. Hanko and D. Hoppe, *Angew. Chem.*, **94**, 378 (1982); *Angew. Chem., Int. Ed. Engl.*, **21**, 372 (1982).
211. D. Hoppe and F. Lichtenberg, *Angew. Chem.*, **96**, 241 (1984); *Angew. Chem., Int. Ed. Engl.*, **23**, 239 (1984).
212. M. C. Whisler, L. Vaillancourt and P. Beak, *Org. Lett.*, **2**, 2655 (2000).
213. I. Hoppe, M. Marsch, K. Harms, G. Boche and D. Hoppe, *Angew. Chem.*, **107**, 2328 (1995); *Angew. Chem., Int. Ed. Engl.*, **34**, 2158 (1995).
214. I. Hoppe, D. Hoppe, M. Marsch, K. Harms and G. Boche, *Z. Kristallographie*, **211**, 331 (1996).
215. T. Heinl, S. Retzow, D. Hoppe, G. Fraenkel and A. Chow, *Chem. Eur. J.*, **5**, 3464 (1999).
216. F. Marr, R. Fröhlich and D. Hoppe, *Tetrahedron: Asymmetry*, **13**, 2587 (2002).
217. D. Hoppe, R. Hanko and A. Brönneke, *Angew. Chem.*, **92**, 637 (1980); *Angew. Chem., Int. Ed. Engl.*, **19**, 625 (1980).
218. D. Hoppe and T. Krämer, *Angew. Chem.*, **98**, 171 (1986); *Angew. Chem., Int. Ed. Engl.*, **25**, 160 (1986).
219. O. Zschage, J.-R. Schwark, T. Krämer and D. Hoppe, *Tetrahedron*, **48**, 8377 (1992).
220. J.-R. Schwark and D. Hoppe, *Synthesis*, 291 (1990).
221. T. Krämer, J.-R. Schwark and D. Hoppe, *Tetrahedron Lett.*, **30**, 7037 (1989).
222. O. Zschage and D. Hoppe, *Tetrahedron*, **48**, 8389 (1992).
223. Review: H. Kunz and H. Waldmann, *Chemtracts—Org. Chem.*, **3**, 421 (1990).
224. O. Zschage and D. Hoppe, *Tetrahedron*, **48**, 5657 (1992).
225. Review: D. Hoppe, '(E)-1-(N,N-Diisopropylcarbamoyloxy)crotyllithium' in *Encyclopedia of Reagents for Organic Synthesis* (Ed. L. A. Paquette), Vol. 2, Wiley, Chichester, 1995, pp. 1927–1929.
226. M. Marsch, K. Harms, O. Zschage, D. Hoppe and G. Boche, *Angew. Chem.*, **103**, 338 (1991); *Angew. Chem., Int. Ed. Engl.*, **30**, 321 (1991).
227. W. Zeng and D. Hoppe, unpublished results.
228. M. Özlügedik, J. Kristensen, B. Wibbeling, R. Fröhlich and D. Hoppe, *Eur. J. Org. Chem.*, 414 (2002).
229. A. Deiters and D. Hoppe, *Angew. Chem.*, **111**, 529 (1999); *Angew. Chem., Int. Ed.*, **38**, 546 (1999).
230. E. van Hülsen and D. Hoppe, *Tetrahedron Lett.*, **26**, 411 (1985).
231. F. Rehders and D. Hoppe, *Synthesis*, 859 (1992).
232. M. Seppi, Dissertation, Universität Münster, 2001.
233. R. Kalkofen, intended Dissertation, Universität Münster.
234. D. Heimbach and D. Hoppe, *Synlett*, 950 (2000).
235. A. Deiters and D. Hoppe, *J. Org. Chem.*, **66**, 2842 (2001).
236. Review: Y. Nishigaichi, A. Takuwa, Y. Naruta and K. Maruyama, *Tetrahedron*, **49**, 7395 (1993).
237. T. Krämer and D. Hoppe, *Tetrahedron Lett.*, **28**, 5149 (1987).
238. A. Deiters, R. Fröhlich and D. Hoppe, *Angew. Chem.*, **112**, 2189 (2000); *Angew. Chem., Int. Ed.*, **39**, 2105 (2000).
239. A. Deiters, C. Mück-Lichtenfeld, R. Fröhlich and D. Hoppe, *Org. Lett.*, **2**, 2415 (2000).
240. A. Deiters, C. Mück-Lichtenfeld, R. Fröhlich and D. Hoppe, *Chem. Eur. J.*, **8**, 1833 (2002).
241. A. Deiters, B. Wibbeling and D. Hoppe, *Adv. Synth. Catal.*, **343**, 181 (2001).
242. H. E. Zimmerman and M. D. Traxler, *J. Am. Chem. Soc.*, **79**, 1920 (1957).
243. D. Hoppe and A. Brönneke, *Tetrahedron Lett.*, **24**, 1687 (1983).
244. Review: D. Hoppe and O. Zschage, 'Chiral metallated carbamates: Tools for new strategies in asymmetric synthesis', in *Organic Synthesis via Organometallics* (Eds. K. H. Dötz and R. W. Hoffmann), Vieweg, Braunschweig, 1990, pp. 267–284.
245. Review: D. Hoppe, 'Formation of C−C bonds by addition of allyl-type organometallic compounds to carbonyl compounds', in *Houben-Weyl, Allyltitanium and Allylzirconium Reagents* (Eds. G. Helmchen, R. W. Hoffmann, J. Mulzer and E. Schaumann), Vol. E 21b, Thieme-Verlag, Stuttgart, 1995, pp. 1551–1583.
246. Review: H. Ahlbrecht and U. Beyer, *Synthesis*, 365 (1999).
247. D. Hoppe, G. Tarara and M. Wilckens, *Synthesis*, 83 (1989).
248. D. Hoppe, G. Tarara, M. Wilckens, P. G. Jones, D. Schmidt and J. C. Stezowski, *Angew. Chem.*, **99**, 1079 (1987); *Angew. Chem., Int. Ed. Engl.*, **26**, 1034 (1987).

249. R. Hanko, K. Rabe, R. Dally and D. Hoppe, *Angew. Chem.*, **103**, 1725 (1991); *Angew. Chem., Int. Ed. Engl.*, **30**, 1690 (1991).
250. R. Hirsch and R. W. Hoffmann, *Chem. Ber.*, **125**, 975 (1992).
251. I. Berque, P. Le Ménez, P. Razon, A. Pancrazi, J. Ardisson and J.-D. Brion, *Synlett*, 1135 (1998).
252. B. Peschke, J. Lüßmann, M. Dyrbusch and D. Hoppe, *Chem. Ber.*, **117**, 1421 (1992).
253. H. Paulsen and D. Hoppe, *Tetrahedron*, **48**, 5667 (1992).
254. P. Le Ménez, V. Fargeas, J. Poisson, J. Ardisson, J.-Y. Lallemand and A. Pancrazi, *Tetrahedron Lett.*, **35**, 7767 (1994).
255. P. Le Ménez, I. Berque, V. Fargeas, J. Ardisson and A. Pancrazi, *Synlett*, 998 (1994).
256. J. P. Férézou, M. Julia, R. Khourzom, Y. Li, A. Pancrazi and P. Robert, *Synlett*, 611 (1991).
257. P. Le Ménez, V. Fargeas, I. Berque, J. Poisson, J. Ardisson, J.-Y. Lallemand and A. Pancrazi, *J. Org. Chem.*, **60**, 3592 (1995).
258. P. Ashworth, B. Broadbelt, P. Jankowski, A. Pimm and P. Kocienski, *Synthesis*, 199 (1995).
259. N. D. Smith, P. J. Kocienski and S. D. A. Street, *Synthesis*, 652 (1996).
260. M. Özlügedik, J. Kristensen, R. Fröhlich and D. Hoppe, *Synthesis*, manuscript submitted.
261. Review: J. A. Marshall, *Chem. Rev.*, **96**, 31 (1996).
262. J. A. Marshall, *Chemtracts, Org. Chem.*, **11**, 697 (1998).
263. P. A. Grieco, T. Oguri and Y. Yokoyama, *Tetrahedron Lett.*, 419 (1978).
264. M. Putala, *Enantiomer*, **4**, 243 (1999).
265. D. Madec, V. Henrion and J.-P. Férézou, *Tetrahedron Lett.*, **40**, 8103 (1999).
266. K. B. Sharpless and T. R. Verhoeven, *Aldrichimica Acta*, **12**, 63 (1979).
267. B. E. Rossiter, T. R. Verhoeven and K. B. Sharpless, *Tetrahedron Lett.*, 4733 (1979).
268. E. D. Mihelich, *Tetrahedron Lett.*, 4729 (1979).
269. J. Lüßmann, D. Hoppe, P. G. Jones, C. Fittschen and G. M. Sheldrick, *Tetrahedron Lett.*, **31**, 3595 (1986).
270. G. Tarara and D. Hoppe, *Synthesis*, 89 (1989).
271. M. Nakata, K. Toshima, T. Kai and M. Kinoshita, *Bull. Chem. Soc. Jpn.*, **58**, 3457 (1985); and previous publications.
272. D. Hoppe, T. Krämer, C. Freire Erdbrügger and E. Egert, *Tetrahedron Lett.*, **30**, 1233 (1989).
273. R. W. Hoffmann, *Chem. Rev.*, **89**, 1841 (1989).
274. H. Paulsen, C. Graeve, R. Fröhlich and D. Hoppe, *Synthesis*, 145 (1996).
275. Review: M. Braun, *Angew. Chem.*, **110**, 445 (1998); *Angew. Chem., Int. Ed.*, **37**, 430 (1998).
276. Review: P. Kocienski and N. J. Dixon, *Synlett*, 52 (1989).
277. S. Sengupta and V. Snieckus, *J. Org. Chem.*, **55**, 5680 (1990).
278. B. Peschke, Dissertation, Universität Kiel, 1991.
279. J. A. Howarth, W. M. Owton and J. M. Percy, *Synlett*, 503 (1994).
280. P. Kocienski and C. Barber, *Pure Appl. Chem.*, **62**, 1933 (1990).
281. A. Pimm, P. Kocienski and S. D. A. Street, *Synlett*, 886 (1992).
282. G. Hareau-Vittini and P. J. Kocienski, *Synlett*, 893 (1995).
283. D. Madec, S. Pujol, V. Henryon and J. P. Férézou, *Synlett*, 435 (1995).
284. M. S. Sanford, J. A. Love and R. H. Grubbs, *J. Am. Chem. Soc.*, **123**, 6543 (2001).
285. Review: R. H. Grubbs, S. J. Miller and G. C. Fu, *Acc. Chem. Res.*, **28**, 446 (1995).
286. Review: M. Schuster and S. Blechert, *Angew. Chem.*, **109**, 2124 (1997); *Angew. Chem., Int. Ed. Engl.*, **36**, 2036 (1997).
287. K. R. K. Prasad and D. Hoppe, *Synlett*, 1067 (2000).
288. C. Serino, N. Stehle, Y. S. Park, S. Florio and P. Beak, *J. Org. Chem.*, **64**, 1160 (1999).
289. G. A. Weisenburger and P. Beak, *J. Am. Chem. Soc.*, **118**, 12218 (1996).
290. D. J. Pippel, G. A. Weisenburger, S. R. Wilson and P. Beak, *Angew. Chem.*, **110**, 2600 (1998); *Angew. Chem., Int. Ed.*, **37**, 2522 (1998).
291. G. A. Weisenburger, N. C. Faibish, D. J. Pippel and P. Beak, *J. Am. Chem. Soc.*, **121**, 9522 (1999).
292. Y. S. Park, G. A. Weisenburger and P. Beak, *J. Am. Chem. Soc.*, **119**, 10537 (1997).
293. D. J. Pippel, G. A. Weisenburger, N. C. Faibish and P. Beak, *J. Am. Chem. Soc.*, **123**, 4919 (2001).
294. M. Özlügedik, Dissertation, Universität Münster, 2001.
295. T. A. Johnson, M. D. Curtis and P. Beak, *Org. Lett.*, **4**, 2747 (2002).

296. T. A. Johnson, D. O. Jang, B. W. Slafer, M. D. Curtis and P. Beak, *J. Am. Chem. Soc.*, **124**, 11689 (2002).
297. S. H. Lim and P. Beak, *Org. Lett.*, **4**, 2657 (2002).
298. D. Hoppe and C. Riemenschneider, *Angew. Chem.*, **95**, 64 (1983); *Angew. Chem., Int. Ed. Engl.*, **22**, 54 (1983).
299. D. Hoppe, C. Gonschorrek, D. Schmidt and E. Egert, *Tetrahedron*, **43**, 2457 (1987).
300. H. J. Reich and J. E. Holladay, *J. Am. Chem. Soc.*, **117**, 8470 (1995).
301. D. Hoppe and C. Gonschorrek, *Tetrahedron Lett.*, **28**, 785 (1987).
302. E. Egert, H. Beck, D. Schmidt, C. Gonschorrek and D. Hoppe, *Tetrahedron Lett.*, **28**, 789 (1987).
303. D. Hoppe, C. Gonschorrek, E. Egert and D. Schmidt, *Angew. Chem.*, **97**, 706 (1985); *Angew. Chem., Int. Ed. Engl.*, **24**, 700 (1985).
304. J. A. Marshall and J. Lebreton, *Tetrahedron Lett.*, **28**, 3323 (1987).
305. K. Tomooka, N. Komine and T. Nakai, *Synlett*, 1045 (1997).
306. S. Dreller, M. Dyrbusch and D. Hoppe, *Synlett*, 397 (1991).
307. Z.-F. Xie, *Tetrahedron: Asymmetry*, **2**, 733 (1991).
308. C. Schultz-Fademrecht, B. Wibbeling, R. Fröhlich and D. Hoppe, *Org. Lett.*, **3**, 1221 (2001).
309. C. Schultz-Fademrecht, M. A. Tius, S. Grimme, B. Wibbeling and D. Hoppe, *Angew. Chem.*, **115**, 1610 (2002); *Angew. Chem., Int. Ed.*, **41**, 1532 (2002).
310. T. Aratani, T. Gonda and H. Nozaki, *Tetrahedron Lett.*, 2265 (1969).
311. T. Aratani, T. Gonda and H. Nozaki, *Tetrahedron*, **26**, 5453 (1970).
312. J. Clayden, *Synlett*, 810 (1998).
313. S. Thayumanavan, P. Beak and D. P. Curran, *Tetrahedron Lett.*, **37**, 2899 (1996).
314. J. Clayden, P. Johnson, J. H. Pink and M. Helliwell, *J. Org. Chem.*, **65**, 7033 (2000).
315. A. Rajca, H. Wang, P. Bolshov and S. Rajca, *Tetrahedron*, **57**, 3725 (2001).
316. M. Tsukazaki, M. Tinkl, A. Roglans, B. J. Chapell, N. J. Taylor and V. Snieckus, *J. Am. Chem. Soc.*, **118**, 685 (1996).
317. Review: A. Togni, *Angew. Chem.*, **108**, 1581 (1996); *Angew. Chem., Int. Ed. Engl.*, **35**, 1475 (1996).
318. Review: S. Borman, *Chem. Eng. News*, **74**, 38 (1996).
319. R. S. Laufer, U. Veith, N. J. Taylor and V. Snieckus, *Org. Lett.*, **2**, 629 (2000).
320. H. Jendralla and E. Paulus, *Synlett*, 471 (1997).
321. J. N. Bonfiglio, *J. Org. Chem.*, **51**, 2833 (1986).
322. L. A. Spangler, *Tetrahedron Lett.*, **37**, 3639 (1996).
323. C. Metallinos and V. Snieckus, *Org. Lett.*, **4**, 1935 (2002).
324. Y.-L. Tan, A. J. P. White, D. A. Widdowson, R. Wilhelm and D. J. Williams, *J. Chem. Soc., Perkin Trans. 1*, 3269 (2001).
325. Y.-L. Tan, D. A. Widdowson and R. Wilhelm, *Synlett*, 1632 (2001).
326. R. Wilhelm, I. K. Sebhat, A. J. P. White, D. J. Williams and D. A. Widdowson, *Tetrahedron: Asymmetry*, **11**, 5003 (2000).
327. Review: K. Tomioka, *Synthesis*, 541 (1990).
328. R. Noyori and M. Kitamura, *Angew. Chem.*, **103**, 34 (1991); *Angew. Chem., Int. Ed. Engl.*, **30**, 49 (1991).
329. Review: H.-U. Blaser, *Chem. Rev.*, **92**, 935 (1992).
330. Review: A. Togni and L. M. Venanzi, *Angew. Chem.*, **106**, 517 (1994); *Angew. Chem., Int. Ed. Engl.*, **33**, 497 (1994).
331. Review: J. M. Brown, 'Formation of C−C bonds by alkylation using chiral additives', in *Houben-Weyl, Stereoselective Synthesis* (Eds. G. Helmchen, R. W. Hoffmann, J. Mulzer and E. Schaumann), Vol. E 21a, Thieme-Verlag, Stuttgart, 1995, pp. 1119–1126.
332. Y. L. Bennani and S. Hanessian, *Chem. Rev.*, **97**, 3161 (1997).
333. D. Lucet, T. Le Gall and C. Mioskowski, *Angew. Chem.*, **110**, 2724 (1998); *Angew. Chem., Int. Ed.*, **37**, 2580 (1998).
334. D. Seebach, A. K. Beck and A. Heckel, *Angew. Chem.*, **113**, 96 (2001); *Angew. Chem., Int. Ed.*, **40**, 92 (2001).
335. D. Seebach, H. Dörr, B. Bastani and V. Ehrig, *Angew. Chem.*, **81**, 1002 (1969); *Angew. Chem., Int. Ed. Engl.*, **8**, 982 (1969).
336. N. Kunieda and M. Kinoshita, *Phosphorous Sulfur*, **10**, 383 (1981).
337. J.-P. Mazaleyrat and D. J. Cram, *J. Am. Chem. Soc.*, **103**, 4585 (1981).

338. S. E. Denmark, N. Nakajima and O. J.-C. Nicaise, *J. Am. Chem. Soc.*, **116**, 8797 (1994).
339. M. Nakajima, K. Tomioka and K. Koga, *Tetrahedron*, **49**, 9751 (1993).
340. S. Arrasate, E, Lete and N. Sotomayor, *Tetrahedron: Asymmetry*, **12**, 2077 (2001).
341. D. Krishnamurthy, Z. Han, S. A. Wald and C. H. Senanayake, *Tetrahedron Lett.*, **43**, 2331 (2002); C. A. Gittins (née Jones) and N. North, *Tetrahedron: Asymmetry*, **8**, 3789 (1997).
342. D. Taniyama, M. Hasegawa and K. Tomioka, *Tetrahedron: Asymmetry*, **10**, 221 (1999).
343. M. Chrzanowska and J. Sokolowska, *Tetrahedron: Asymmetry*, **12**, 1435 (2001).
344. A. Alexakis and F. Amiot, *Tetrahedron: Asymmetry*, **13**, 2117 (2002).
345. P. Müller, P. Nury and G. Bernardinelli, *Eur. J. Org. Chem.*, 4137 (2001).
346. P. Müller and P. Nury, *Org. Lett.*, **2**, 2845 (2000).
347. Review: Y. Okamoto and T. Nakano, *Chem. Rev.*, **94**, 349 (1994).
348. S. Klein, I. Marek, J.-F. Poisson and J. F. Normant, *J. Am. Chem. Soc.*, **117**, 8853 (1995).
349. S. Norsikian, I. Marek, S. Klein, J. F. Poisson and J. F. Normant, *Chem. Eur. J.*, **5**, 2055 (1999).
350. S. Norsikian, I. Marek, J.-F. Poisson and J. F. Normant, *J. Org. Chem.*, **62**, 4898 (1997).
351. S. Norsikian, I. Marek and J. F. Normant, *Tetrahedron Lett.*, **38**, 7523 (1997).
352. N. Bremand, I. Marek and J. F. Normant, *Tetrahedron Lett.*, **40**, 3379 (1999).
353. N. Bremand, I. Marek and J. F. Normant, *Tetrahedron Lett.*, **40**, 3383 (1999).
354. F. Xu, R. D. Tillyer, D. M. Tschaen, E. J. J. Grabowski and P. J. Reider, *Tetrahedron: Asymmetry*, **9**, 1651 (1998).
355. T. Suzuka, M. Ogasawara and T. Hayashi, *J. Org. Chem.*, **67**, 3355 (2002).
356. S. Norsikian, M. Baudry and J. F. Normant, *Tetrahedron Lett.*, **41**, 6575 (2000).
357. S. Majumdar, A. de Meijere and I. Marek, *Synlett*, 423 (2002).
358. D. Amurrio, K. Khan and E. P. Kündig, *J. Org. Chem.*, **61**, 2258 (1996).
359. J. G. Peters, M. Seppi, R. Fröhlich, B. Wibbeling and D. Hoppe, *Synthesis*, 381 (2002).
360. S. Superchi, N. Sotomayor, G. Miao, B. Joseph, M. G. Campbell and V. Snieckus, *Tetrahedron Lett.*, **37**, 6061 (1996).
361. W. F. Bailey and M. J. Mealy, *J. Am. Chem. Soc.*, **122**, 6787 (2000).
362. G. Sanz Gil and U. M. Groth, *J. Am. Chem. Soc.*, **122**, 6789 (2000).
363. J. Barluenga, F. J. Fananás, R. Sanz and C. Marcos, *Org. Lett.*, **4**, 2225 (2002).
364. A. Krief and M. Hobe, *Tetrahedron Lett.*, **33**, 6529 (1992).

CHAPTER 18

Reactivity of oxiranes with organolithium reagents

FABRICE CHEMLA and EMMANUEL VRANCKEN

Laboratoire de Chimie Organique, Université Pierre et Marie Curie, Tour 44-45 2ème étage, Bte 183, 4 Place Jussieu, F-75252 Paris Cedex 05, France
Fax: (+) 33 1 44 27 75 67; e-mail: fchemla@ccr.jussieu.fr, vrancken@ccr.jussieu.fr

---

The Chemistry of Organolithium Compounds. Edited by Z. Rappoport and I. Marek
ISBN: 0-470-84339-X

I. GENERAL INTRODUCTION

Organolithiums behave as very versatile reagents, acting as nucleophiles or bases depending on their nature, the structure of the oxiranes or the experimental conditions. When they act as nucleophiles, an S_N2-type process furnishes the corresponding α-substituted alcohols **1**. As bases, they can abstract a proton either from a carbon adjacent to the epoxide ring (β-deprotonation) to provide allylic alcohols **2** or directly on the heterocyclic ring (α-deprotonation), leading to the transient carbenoid species **3** (Scheme 1).

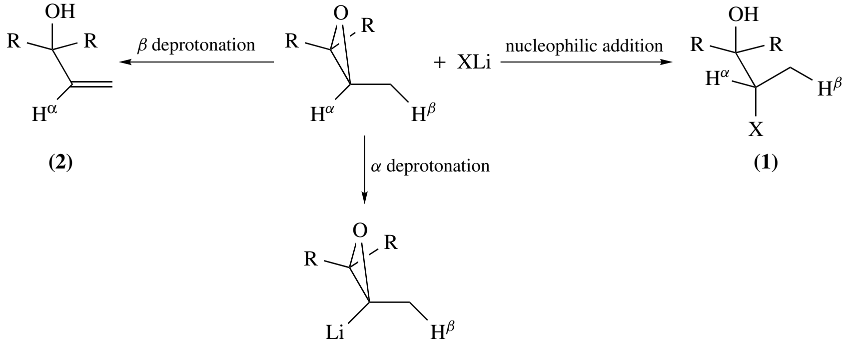

SCHEME 1

An early illustration of this ambiguous behavior was provided by Letsinger and coworkers[1] in 1952 who wanted to prepare alkyl cyclohexanols by addition of n-butyllithium to cyclohexene oxide. Only 7% of the desired butyl cyclohexanol **4** was isolated from the reaction mixture; the major product was the allylic alcohol **5** (35%) along with traces of ketone **6** probably stemming from the rearrangement of an oxiranyl anion intermediate (Scheme 2).

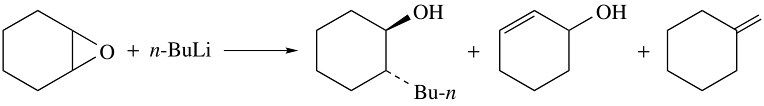

(**4**) 7% (**5**) 35% (**6**) traces

SCHEME 2

As in most cases, the organolithium reagent behaves as a base rather than a nucleophile, and the product distribution reflects the three competitive modes of reactivity toward oxiranes, i.e. nucleophilic addition, β- and α-deprotonation (Scheme 1).

Nucleophilic addition is generally observed as the principal mode of action for poorly basic organolithium reagents or activated epoxides. This reaction will be described in detail in Section IV.

The stereochemistry of the β-deprotonation reaction (also called β-elimination) in relatively nonpolar solvents using lithium amides has been established to be *syn* to the oxirane by kinetic and deuterium-labeling experiments[2–4]. A crucial point is the ambivalent behavior of the lithium cation: its coordination to the oxygen both activates the C—O bond and directs the base close to the β-proton. By this 'push-pull' effect, the abstraction ability of the β-proton is enhanced. The regio- and stereoselectivity of the elimination is thus rationalized by a two-step process, involving the formation of a 1:1 base–epoxide complex **7** (step I) that subsequently undergoes a concerted six-center rearrangement **8** to allylic lithium alcoholate **9** (step II), as depicted in Scheme 3.

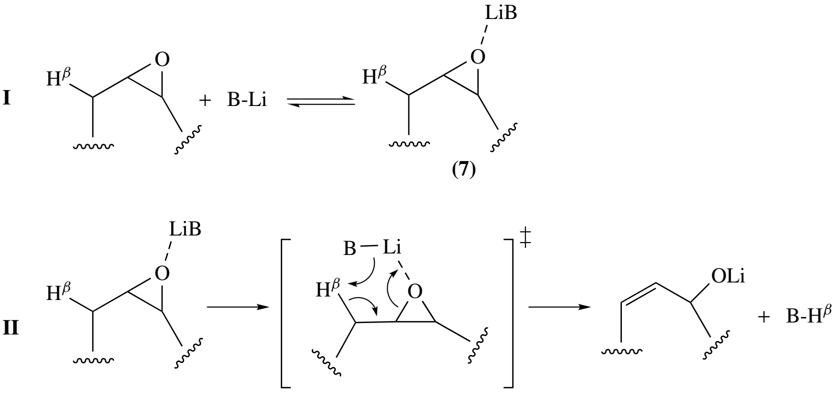

(**7**) (**8**) (**9**)

SCHEME 3

Competitive with β-deprotonation, α-deprotonation furnishes the carbenoid-type oxiranyl anion species **10**. In selected cases anion formation has been established to be a reversible process by deuterium-labeling experiments[4,5]. As opposed to β-deprotonation which gives only allylic alcohols, α-deprotonation can give rise to a variety of products as summarized in Scheme 4. This behavior will be further discussed in Section V. Some of these products, such as bicyclic alcohols **11** or functionalized alkenes **12**, as well as oxiranes **14** (arising from trapping with an electrophile) and lithium enolates **15** and **16** are characteristic of an oxiranyl anion intermediate. On the other hand, the generation of allylic alcohols **13** may arise from either α- or β-deprotonation and is more ambiguous mechanistically.

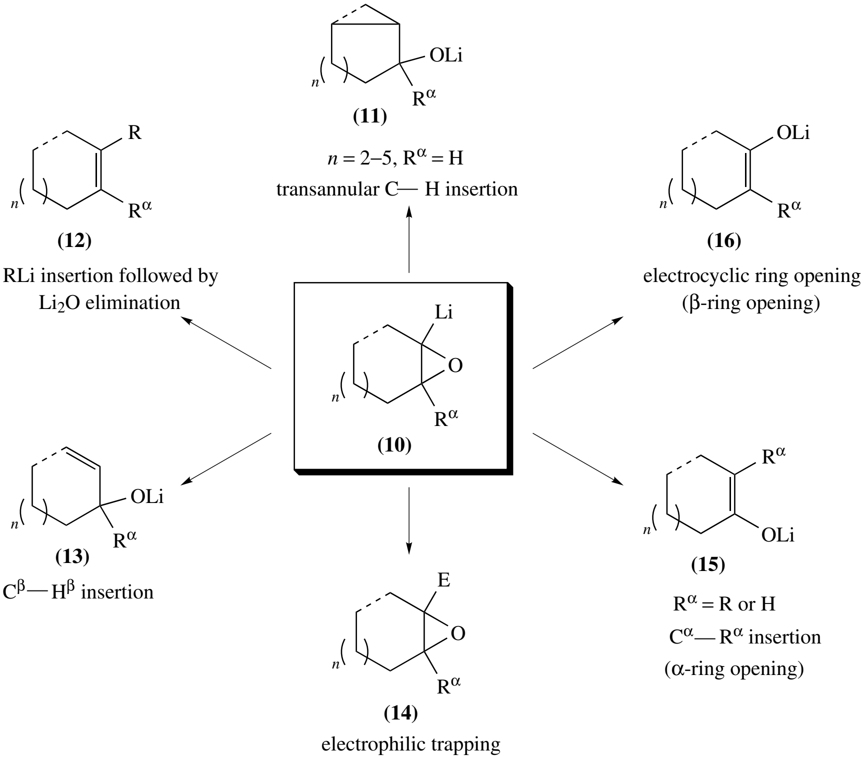

SCHEME 4

Owing to the growing interest in enantioselective base-promoted isomerization of oxiranes to allylic alcohols, a knowledge of this mechanism is necessary to design appropriate chiral bases. Moreover, the development of new methodologies to prepare highly functionalized products from oxiranes with substantial regio-, diastereo- and even enantioselective control is of current interest. It is thus of great importance to understand the factors influencing the competition between α- and β-deprotonation. This aspect will be discussed in the following section.

II. α-/β-DEPROTONATION

The β-deprotonation reaction was initially considered as the normal mode of oxirane isomerization in basic media with α-deprotonation appearing as an alternative pathway when the principal process was slowed. Recent studies based on kinetic studies, calculations and labeling experiments, along with advances in the determination of the organolithium aggregation state have challenged this point of view, showing these two processes as really competitive. Several factors influence the chemoselectivity of the deprotonation, such as the structure of the oxirane, experimental conditions (solvent, temperature) and the nature of the lithium base.

A. Structure of the Oxirane

As seen above, β-deprotonation implies a six-center transition state. Recent computational studies show an important variation of the H^{β}—C—C—O dihedral angle from reactant to transition state[6]. Thus, the ground state geometry of the oxirane cannot be used to predict its reactivity. However, for structural reasons, some oxiranes cannot adopt a suitable conformation for β-deprotonation and furnish exclusively α-deprotonation products. This concept is well illustrated by the norbornene oxide **17**, which gives exclusively the transannular 1,3 insertion product **18** in the presence of lithium amide (Scheme 5)[7].

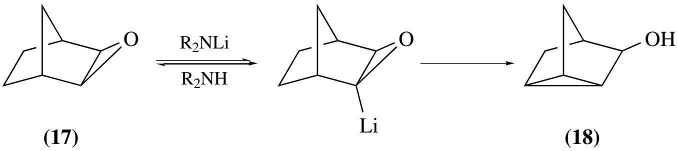

(17) **(18)**

SCHEME 5

More generally, the acidity of the α-proton is closely related to the geometry of the oxirane. As shown by deuterium-labeling experiments, the rearrangement of simple linear oxiranes into allylic alcohols induced by organolithium species proceeds through a β-elimination pathway. For example, treatment of deuteriated *cis*- or *trans*-epoxides **19** and **20** with lithium diethylamide gives in both cases the *trans*-allylic alcohol **21** without loss of the deuterium label, demonstrating that ring-proton abstraction by base is not occurring (Scheme 6)[8].

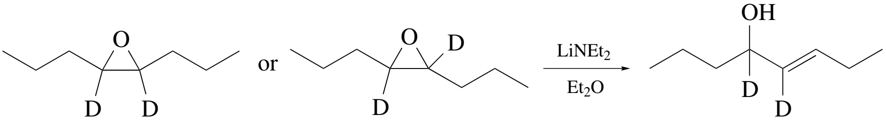

(19) **(20)** **(21)**

SCHEME 6

Nevertheless, whereas the base-promoted isomerization of simple linear oxiranes and cyclohexene oxide occurs via a β-deprotonation mechanism, recent deuterium-labeling experiments demonstrate that the LDA-mediated rearrangement of cyclopentene oxide in nonpolar solvents furnishes the corresponding cyclopentenol through an α-deprotonation route (Scheme 7)[4, 6].

To explain this unusual reactivity, further calculations on α-anion stabilities and strain energies have been made (Table 1)[6].

It appears that oxiranes known to give predominantly α-deprotonation in basic media (cyclopentene, cyclooctene and *exo*-norbornene oxide) are also the more strained (Table 1; entries 3, 6, 7). On the other hand, oxiranes that give mainly β-deprotonation (butene, cyclohexene oxide) have lower strain energies and higher α-anion stabilities (Table 1;

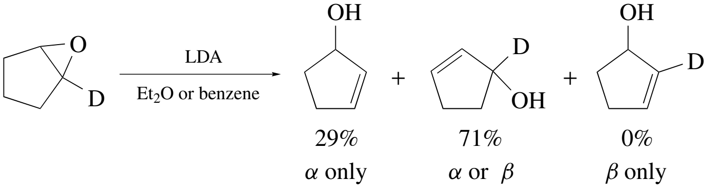

SCHEME 7

TABLE 1. Strain and α-anion energies (in kcal mol^{-1}) of various oxiranes

Entry	Oxirane	Strain energies	α-Anion energies
1	Propene oxide	23.3	—
2	1,2-Dimethyloxirane	—	18.7
3	Cyclopentene oxide	28.7	13.5
4	Cyclohexene oxide	26.6	17.5
5	Cycloheptene oxide	29.6	—
6	Cyclooctene oxide	30.4	—
7	*exo*-Norbornene oxide	46.0	—

entries 2, 4). Moreover, calculations on α-anion structures show a greater pyramidalization for cyclopentene oxide than for cyclohexene or butene oxide. Thus, an increase in oxirane strain stabilizes the anion in an orbital having more s-character and consequently increases the α-proton acidity of the corresponding oxirane.

However, the strain of the oxirane is not the only determining factor in the α/β competition, as illustrated by *cis*-substituted cyclopentene oxides of type **22** which are known to give β-deprotonation with lithium amides in nonpolar solvents (Scheme 8)[9].

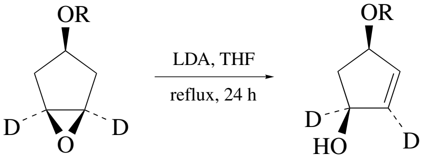

(22)

SCHEME 8

In this particular case, remote control by the heteroatom of the substituent is invoked to explain the regioselectivity of the elimination. Complexation of lithium with both oxygens fixes the basic carbon atom close to the β-proton[9]. A similar model is proposed to rationalize the reversal to regiospecific α-deprotonation proximate to the hydroxyl group for oxiranes of type **23**, the basic site now being close to the α-proton (Scheme 9)[10–12].

B. Influence of the Base/Temperature Effects

The structure of the base will also have a significant impact on the α/β competition, particularly for cycloalkene oxides. One of the most intriguing examples of this effect was reported by Whitesell and White in 1975. They found that the reaction of LDA with

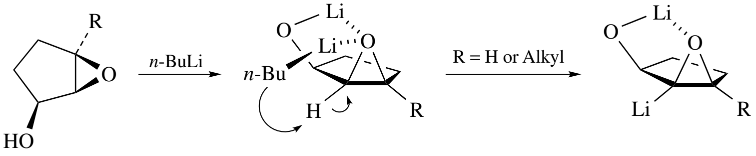

(23)

SCHEME 9

cyclooctene oxide **24** in ether gives almost exclusively the bicyclic alcohol **25**, the product of base-promoted transannular cyclization. Conversely, the use of LDEA (lithium diethylamide) under the same conditions affords predominantly the β-deprotonation product **26** (Scheme 10)[13].

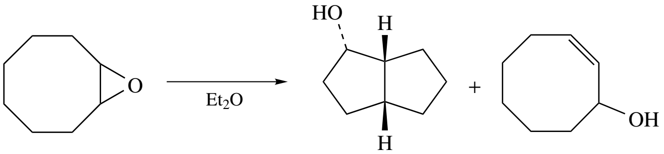

(24) **(25)** **(26)**

	(25)		(26)
$LiN(C_3H_7\text{-}i)_2$	98	:	2
$LiN(C_2H_5)_2$	20	:	80

SCHEME 10

Without consideration of the state of aggregation, this result could be rationalized by considering the isomeric aggregates **27** and **28** arising from the complexation of the lithium cation to the oxygen (Scheme 11)[5]. The required conformation for the β-deprotonation process induces a deformation of the ring chain. A severe steric hindrance with the base thus appears in the *syn* complex **27**, which can only be formed with sterically small bases. For larger ones the *anti* complex **28** is favored. In such a complex, the base is held in close proximity to the α-proton, inducing α-deprotonation. Consequently, the bulkiness of the lithium base could have a dramatic effect on the equilibrium and thus control the balance between the two modes of reaction[14]. An increase in the size of the base could thus turn the cycloalkene oxide isomerization toward oxirane ring-metalation.

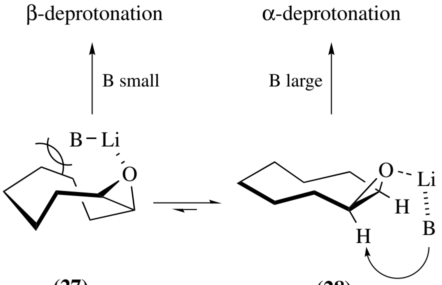

(27)
syn complex

(28)
anti complex

SCHEME 11

The temperature also has a dramatic effect on the α/β competition. It has been noted[15] that low temperature favors α-deprotonation, whereas β-deprotonation is favored by higher temperatures (Scheme 12).

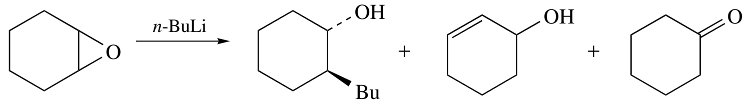

Ether/hexane −78 °C to rt	0	/	34	/	66
Ether/pentane reflux	16	/	84	/	0

SCHEME 12

Since lithium amides (unlike alkylithiums) are unreactive toward most oxiranes at low temperature, they are widely used for β-deprotonation reaction around room temperature whereas (bulky) alkyllithium bases are generally employed to generate oxiranyl anions at low temperature (−78 °C).

C. Solvent Effects/Aggregation State

Relatively little work has been recorded concerning the state of aggregation in the transition state for either α- or β-deprotonation. The structure of the transition state will, however, have a significant impact on the α/β competition. Although little information has been reported so far about organolithium reagents, the lithium amide case has been more studied, essentially because this class of compounds represents the key access to enantioselective transformations. ^{6}Li and ^{15}N NMR experiments in coordinating solvents (THF, TMEDA etc.) show that lithium dialkylamides exist almost exclusively as dimers of type **29** (Figure 1)[16].

Based on this feature, aggregation states of transition-state structures for base-promoted isomerization of oxiranes have been established by kinetic studies of LDA-mediated isomerizations of selected oxiranes in nonpolar media in the presence of variable concentrations of coordinating solvents (ligands)[17]. Results reported provide the idealized rate law $v = k[\text{ligand}]^{-1}[\text{base}]^{1}[\text{oxirane}]$ for α-deprotonation and $v = k[\text{ligand}]^{0}[\text{base}]^{1/2}[\text{oxirane}]$

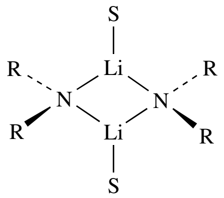

(29)

S = solvent

FIGURE 1

for β-deprotonation. The following models have been deduced for the two types of deprotonation:

α-deprotonation

$$(\text{base})_2(\text{ligand})_2 + \text{oxirane} \rightleftharpoons (\text{base})_2(\text{ligand})(\text{oxirane}) + \text{ligand}$$

$$(\text{base})_2(\text{ligand})(\text{oxirane}) \longrightarrow \text{product}$$

β-deprotonation

$$1/2\ (\text{base})_2(\text{ligand})_2 + \text{oxirane} \rightleftharpoons (\text{base})(\text{ligand})(\text{oxirane})$$

$$(\text{base})(\text{ligand})(\text{oxirane}) \longrightarrow \text{product}$$

As shown by these equations, the different deprotonation pathways differ in their transition-state structures: a 2/1 base–oxirane trimer of type **30** for α-deprotonation, compared with a 1/1 base–oxirane dimer of type **31** for β-deprotonation (Scheme 13). Similar results have been reported for the β-deprotonation of cyclohexene oxide by proline-derivated amides[18].

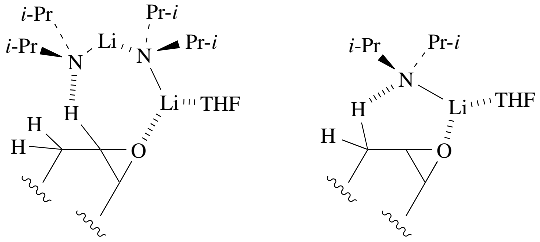

(30) **(31)**

SCHEME 13

In light of these kinetic studies, a decrease in the concentration of the ligand is predicted to favor the α-deprotonation pathway. On the contrary, further studies show that the α/β deprotonation ratio is independent of this concentration. This observation, associated with deuterium-labeling studies, suggests the involvement of the α-deprotonation in the formation of the allylic alcohols at low concentration of ligand[17]. Conversely, the presence of highly coordinating solvents such as HMPA, which break up ion pairs, suppresses both α-deprotonation and nucleophilic addition (Scheme 14)[19–22].

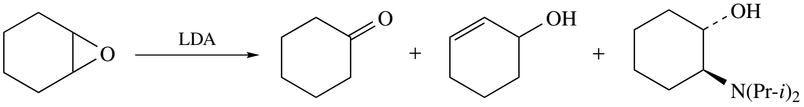

Et_2O	33%	38%	28%
HMPA	0%	100%	0%

SCHEME 14

As shown in this scheme, the presence of HMPA during the reaction of LDA with cyclohexene oxide yields exclusively the β-deprotonation product. This rearrangement is

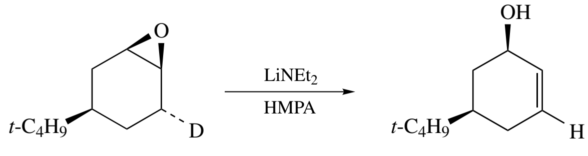

(32) **(33)**

SCHEME 15

known to occur via *anti* elimination under such conditions, as demonstrated by Morgan and Gronert in the example shown in Scheme 15[6].

The treatment of the deuteriated *cis* oxirane **32** by LDA in HMPA yields exclusively the nondeuteriated alcohol **33**. Indeed, complexation of the lithium cation by HMPA prevents the formation of the six-center transition state. The isomerization thus follows a more common E2 process, i.e. *anti* β-elimination.

In conclusion, the regioselectivity of the deprotonation (α/β competition) is related not only to the structure of the oxirane but also to the experimental conditions (nature of the base, solvent, temperature etc.). Thus, prediction must take into account all of these parameters and evaluate their relative importance.

III. β-DEPROTONATION

A. Regio- and Stereoselectivity of the β-Deprotonation

The following section is a summary of the review of Crandall and Apparu published in 1983[5]. Only the general trends of the nonenantioselective β-deprotonation of oxirane will be developed and some recent developments in this area reported.

The complexation of the base with the oxirane in nonpolar solvents drives the β-deprotonation to occur from the *syn* face (see above), but also influences its regio- and stereochemistry. During the aggregation step, two conformational structures can be formed depending on which lone pair of the oxygen is used as the donor site. The relative stabilities of these complexes are largely influenced by nonbonded interactions between the base and the *syn* substituents on the epoxide (Scheme 16).

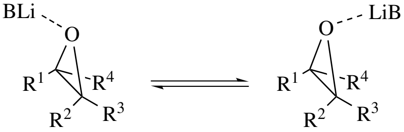

SCHEME 16

For example, *cis*-disubstituted oxiranes ($R^1 = R^2 =$ alkyl; $R^3 = R^4 =$ H) will favor the complex fixing the base *syn* to the less hindered hydrogens. For *trans*-disubstituted or trisubstituted oxiranes, the equilibrium between the two possible complexes is reflected by the relative importance of steric interaction of the base with the different substituents. This model is very useful for rationalizing the regioselectivity of numerous α- and β-deprotonation reactions[5,14–25]. Isomerizations of linear epoxides are particularly revealing[2]. As depicted in Scheme 17, the formation of the more stable complex drives the base to

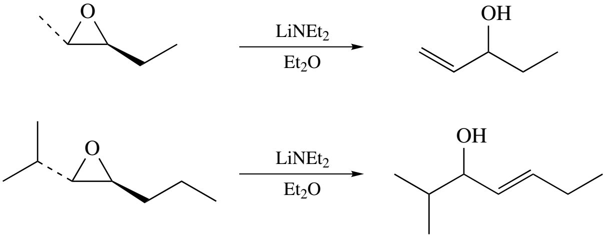

SCHEME 17

remove preferentially a proton on the less hindered β-carbon ($CH_3 > CH_2 > CH$). A rate factor of at least 100 has been reported between these different carbon centers[20, 26].

In the same way, proton removal from the least hindered CH_3 group of trisubstituted epoxides is usually anticipated (Scheme 18, equation 1)[5, 27]. With the same degree of substitution, deprotonation occurs randomly, affording a mixture of isomers (Scheme 18, equation 2)[2].

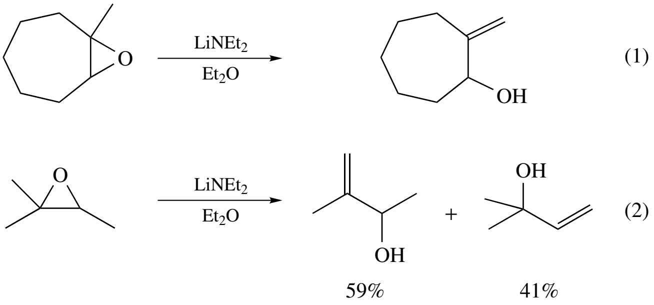

SCHEME 18

In conclusion, the ability to abstract the β-proton is correlated to its degree of substitution. However, substituents other than simple alkyl groups may modify this facility of proton removal and influence the course of the β-elimination. As anticipated, the presence on the adjacent carbon of the epoxide of an allylic or benzylic group results in a dramatic enhancement of the β-elimination rate and modifies its regioselectivity[28, 29]. As shown in Scheme 19, the rearrangement of the phenyl-substituted epoxide **34** is complete within a few minutes, whereas several hours are required in the case of the corresponding alkyl-substituted epoxide **35**.

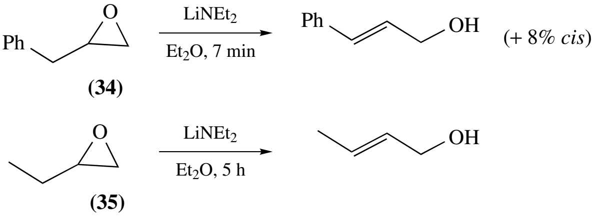

SCHEME 19

The presence of β-unsaturation normally leads to the formation of the corresponding conjugated system. The usual order of reactivity of a β proton is thus: benzylic, allylic > CH_3 > CH_2 > CH. However, this preference can be offset by additional substitution at the more activated position; competition between the β-elimination modes leads to a mixture of regio-isomers[29] as shown in Scheme 20.

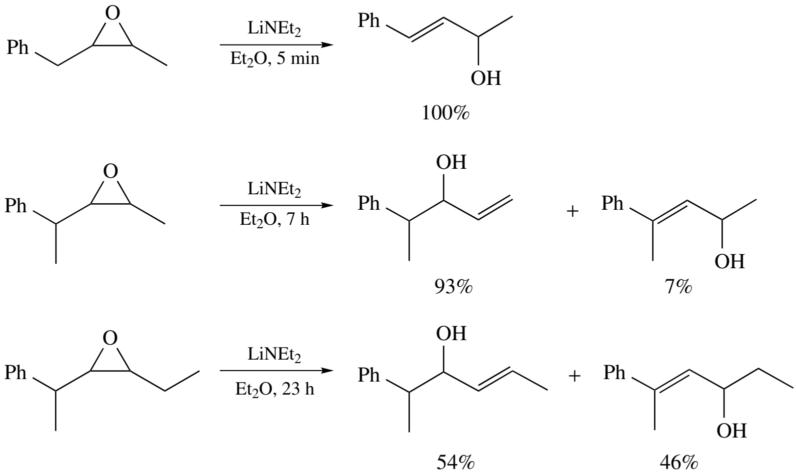

SCHEME 20

Another important point deals with selectivity in the abstraction of β-protons on equally substituted carbons. In a *syn*-periplanar transition state as described above, the minimization of energy concept implies proton abstraction with a maximum of orbital overlap and a minimum of molecular deformation. Consequently, conformations possessing the more acute dihedral angles for bonds H_β—C—C—O will be favored (Scheme 21)[5].

As depicted in Scheme 21, the *trans*-substituted epoxide **36** reacts cleanly with the base to afford almost exclusively the regio-isomer **38** (97%), the minor regio-isomer **37** being slightly observed (3%). This selectivity is consistent with the previous model, considering that in the half-chair conformation of lowest energy the *syn* pseudo-axial hydrogen is abstracted preferentially to the *syn* pseudo-equatorial hydrogen. The same arguments are used to explain the regioselectivity in the rearrangement of *trans*-2-decalene oxide **39**[2], leading to the allylic alcohols **40** and **41** in a 98/2 ratio. In the same way, spiroepoxide **42** reacts cleanly with the base to give exclusively the allylic alcohol product **43**, no trace of the regio-isomer **44** being detected (Scheme 22)[23, 30, 31].

The isomerization of epoxides affords mainly E-olefins, in moderate to high selectivity[8,32–34], as illustrated in Scheme 6 (see above) according to which both *cis*- and *trans*-disubstituted epoxides give the E allylic alcohol product. This tendency in E-selectivity can be rationalized by considering the nonbonded interactions involving the side-chains R existing for both *cis* and *trans* isomer and favoring the transition state **46** over **45**, affording E-**47** as the major product rather than the Z-**47** isomer (Scheme 23)[28].

In selected cases, an improvement of the yield and selectivity has been reported by using an equimolar mixture of lithium diisopropylamide and potassium *tert*-butoxide[35, 36]. Similarly to the model seen above, an eight-membered cyclic transition state of type **48** or **49** including the two organometallic species was invoked, as shown in Figure 2[37].

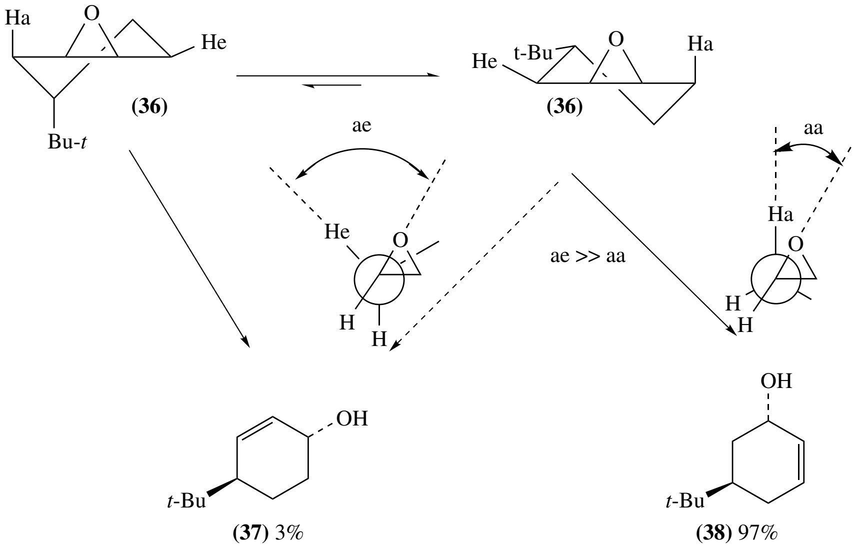

SCHEME 21

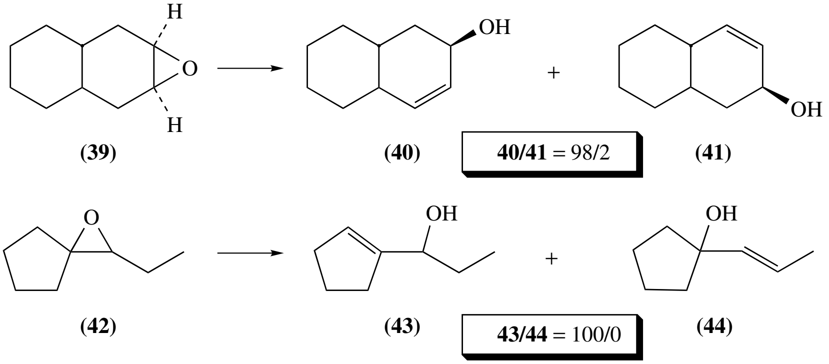

SCHEME 22

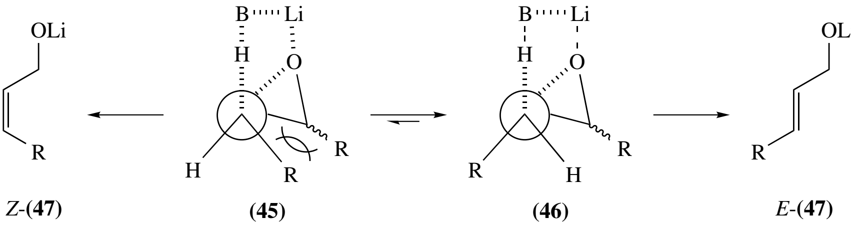

SCHEME 23

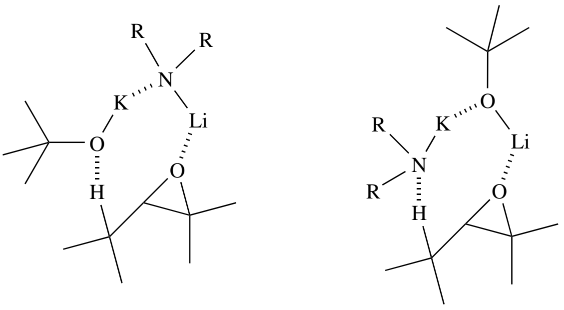

(48) **(49)**

FIGURE 2

B. Enantioselective Access to Allylic Alcohols via Asymmetric Rearrangement

The growing interest in enantioselective isomerization of *meso* oxiranes to allylic alcohols arises from the ready availability of starting materials and the synthetic value of the homochiral products. First applied to simple *meso* cycloalkene oxides, this methodology has been successfully extended to functionalized *meso* oxiranes, and even to the kinetic resolution of racemic oxiranes, demonstrating its potential in accessing highly advanced synthons.

The enantioselective base-promoted rearrangement of oxiranes was achieved by Whitesell and Felman in 1980[38]. Various homochiral lithium amides were used for the isomerization of cyclohexene oxide with an enantiomeric excess (ee) up to 36% with the employment of **50** in refluxing THF (Scheme 24).

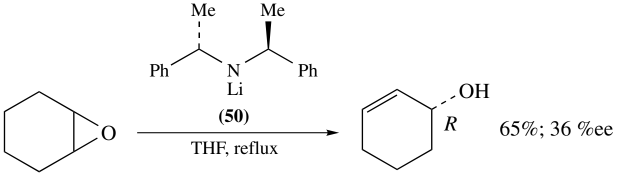

SCHEME 24

As for any desymmetrization of *meso* compounds, enantioselectivity comes from the ability of a homochiral base to distinguish between two enantiotopic protons, in this particular case, to discriminate between the two pseudo-axial protons of the rapidly equilibrating enantiomeric half-chair conformations **51** and **52** (Scheme 25).

Although modest, the results obtained with nonracemic lithium dialkylamides demonstrated the feasibility of such enantioselective transformations and important work has been undertaken from this date to improve both the yield and the ee values as well as developing a catalytic process. With this objective, both the use of homochiral lithium amide (HCLA) bases and organolithium–homochiral ligand complexes have been explored. This field has been extensively reviewed[39–44] and the following section presents a selection of the most outstanding results and recent developments.

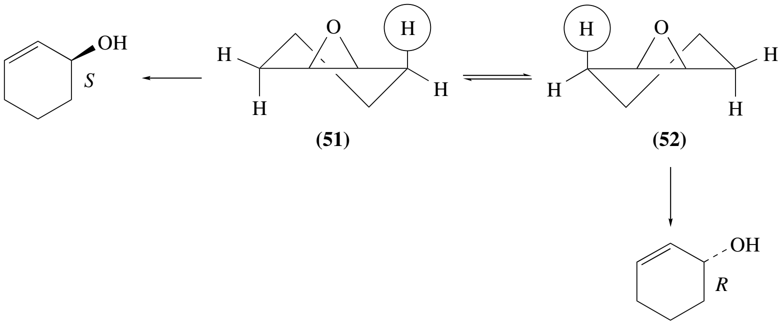

SCHEME 25

1. Homochiral lithium amides (HCLA)

Numerous HCLA have been developed and used for the enantioselective isomerization of oxiranes to allylic alcohols and, in most cases, their efficiency strongly depends on the structure of the oxirane. The HCLA species can be divided into two groups: monolithiated vicinal diamines or ether-amines and dilithiated diamines or amido-alcoholates.

a. Monolithiated diamines and ether-amines. i. Stoichiometric processes. Asami first reasoned that the presence of a vicinal heteroatom in the base, such as a tertiary nitrogen, should generate, through an internal chelation, a structurally rigid complex that would induce a more ordered transition state and consequently improve the enantioselectivity. Indeed, the employment of the proline-derived base **53** for the isomerization of the model substrate cyclohexene oxide has resulted in a significant enhancement in the levels of asymmetric induction (Scheme 26)[45].

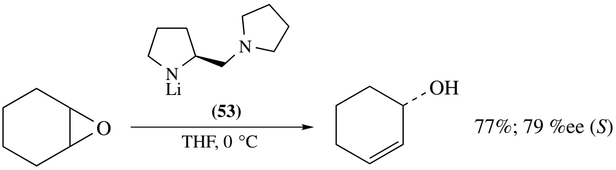

SCHEME 26

Based on this concept, a large variety of HCLA bases incorporating a vicinal heteroatom (tertiary amine, ether) has been tested for this transformation. These are of two types: the proline type, which can be considered as a conformationally restricted *cis*-fused 5-membered ring bicyclic structure (type A), and the norephedrine- or phenylglycine-type, leading to a more flexible, substituted 5-membered ring structure (type B) (Figure 3).

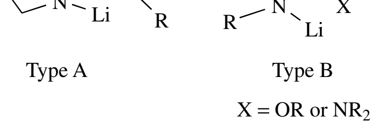

X = OR or NR_2

FIGURE 3

Table 2 reports a selection of these two types of HCLA, used in stoichiometric amount, in the isomerization of cyclohexene oxide into the corresponding allylic alcohol.

As shown in Table 2, HCLA bases of type A are still among the best reagents for this transformation. Obviously, the configuration of the proline moiety determines the sense

TABLE 2. Stoichiometric asymmetric rearrangement of cyclohexene oxide using HCLA **54** to **59**

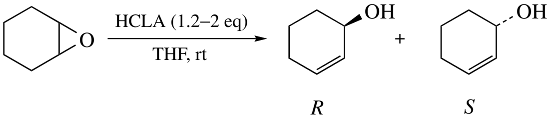

Entry	HCLA		Yield (%)	ee (%)
	Type A :			
1	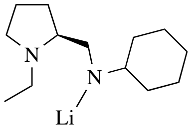	**54**	80	78 (*R*)[a][46]
2	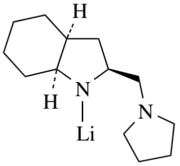	**55**	86	89 (*S*)[47]
3[b]	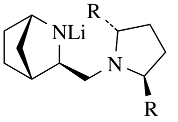	R = H: **56a**	87	97 (*R*)[c][48, 49]
		R = Me: **56b**	80	99 (*R*)[c][50]
	Type B :			
4	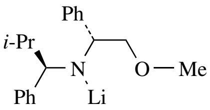	**57**	—	74 (*R*)[51]
5	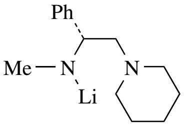	**58**	60	80 (*S*)[52–56]
6	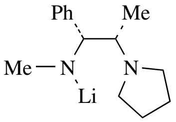	**59**	96	93 (*S*)[57, 58]

[a] In the presence of 1.65 eq HMPA.
[b] Reaction performed at 0 °C.
[c] In the presence of 10 eq DBU.

of the enantioselection. Indeed, in all cases (*S*)-proline analogues **53** (Scheme 26) and **55** (entry 2) provide (*S*)-cyclohexenol, whereas the (*R*)-analogue **56a**, obtained in seven steps from (*S*)-phenylethylamine[48, 59], gives the opposite enantiomer (entry 3). Interestingly, a reversal of selectivity is observed with HCLA (*S*)-**54** where the lithium amide is located on the extracyclic nitrogen (entry 1). Moreover, a slight improvement of selectivity is obtained by judicious substitution of both pyrrolidinyl and lithium pyrrolidide cycles, as illustrated by HCLA **56b** which promotes the conversion of cyclohexene oxide into (*R*)-cyclohexenol in 99% ee (entry 3), to date the highest level of enantioselectivity for this rearrangement. Nevertheless, design of more readily accessible bases is still of current interest. With this aim in view, HCLA bases **57–59** have been investigated in the same reaction, and promising results in terms of reactivity (up to 96% yield) and stereocontrol (ee up to 93%) have been reported (entries 4 to 6). A comparison of **58** and **59** shows the beneficial effect of an adjacent stereogenic center on the stereoselectivity. Furthermore, the observed stereocontrol obtained with these two bases in a similar study performed on the bis-substituted cyclohexene oxide **60** (Table 3) strongly suggests that the sense of induction is controlled by the benzylic stereogenic center α to the lithium amide group[58, 60].

The origin of the enantiodiscrimination appears to be strongly dependent on the structure of the HCLA employed. For HCLA bases of type A (**53** to **56**), stereoselectivity has been empirically deduced to arise [in the transition state (TS)] from the difference of energy between the two diastereoisomeric 1/1 HCLA/oxirane complexes **TS1** and **TS2** (Scheme 27). Indeed, the steric repulsions between cyclohexene oxide and the pyrrolidinyl substituents in **TS 1** favor **TS 2**, as proposed by Asami in 1990 for enantioselective rearrangement of cyclohexene oxide by HCLA **53** (Scheme 26)[61].

The existence of such complexes has been confirmed by kinetic experiments, multidimensional and multinuclear (^{6}Li, ^{1}H) NMR, and the beneficial effect of substitutions at the lithium pyrrolidide ring outlined[62, 63]. Nevertheless, recent computational studies

TABLE 3. Evaluation of HCLA **58, 59** and **61** in the asymmetric rearrangement of oxirane **60**

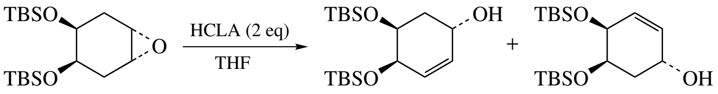

(60) (1*S*, 4*R*, 5*S*) (1*R*, 4*S*, 5*R*)

Entry	HCLA (type B)		Yield (%)	ee (%)
1	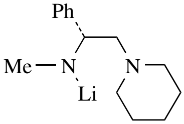	(*R*)-**58**	71	76 (1*S*, 4*R*, 5*S*)
2	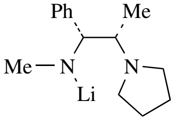	(1*R*, 2*S*)-**59**	93	>95 (1*S*, 4*R*, 5*S*)
3	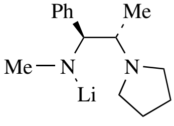	(1*S*, 2*S*)-**61**	97	86 (1*R*, 4*S*, 5*R*)

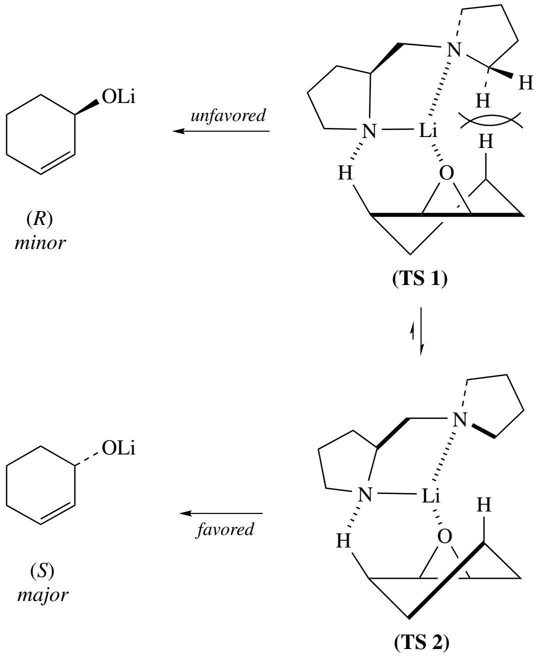

SCHEME 27

have demonstrated that in addition to the steric interactions shown in Scheme 28, the solvation of the complex has a dramatic influence on the stereoselectivity[64].

In contrast, it has been suggested that for HCLA bases of type B, the stereodifferentiation proceeds via a complex composed of a lithium amide dimer and one molecule of oxirane. Indeed, these bases are known to aggregate in solution to C_2 symmetric homodimers of type **62**, as shown by multinuclear (^{13}C, ^{6}Li, ^{15}N) NMR for HCLA **57** (Figure 4)[51].

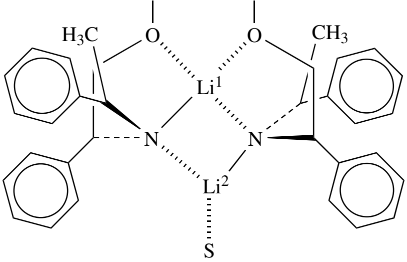

(62)

S = solvent

FIGURE 4

The stereodetermining step has been postulated to occur during the exchange between the molecule of solvent (S) bonded to the tricoordinated Li^2 of **62** (Figure 4) and the oxirane in one of the two possible conformations **51** and **52** (Scheme 28). A new complex is thus obtained in which the conformation of the oxirane is fixed. Then a fast depolymerization followed by the β-deprotonation step gives the allylic alcohol. Thus, as opposed to type A HCLA bases, the stereodiscrimination could occur prior to the β-deprotonation (**TS**), during the formation of an initial complex, also called initial state (**IS**, Scheme 28)[51, 65, 66].

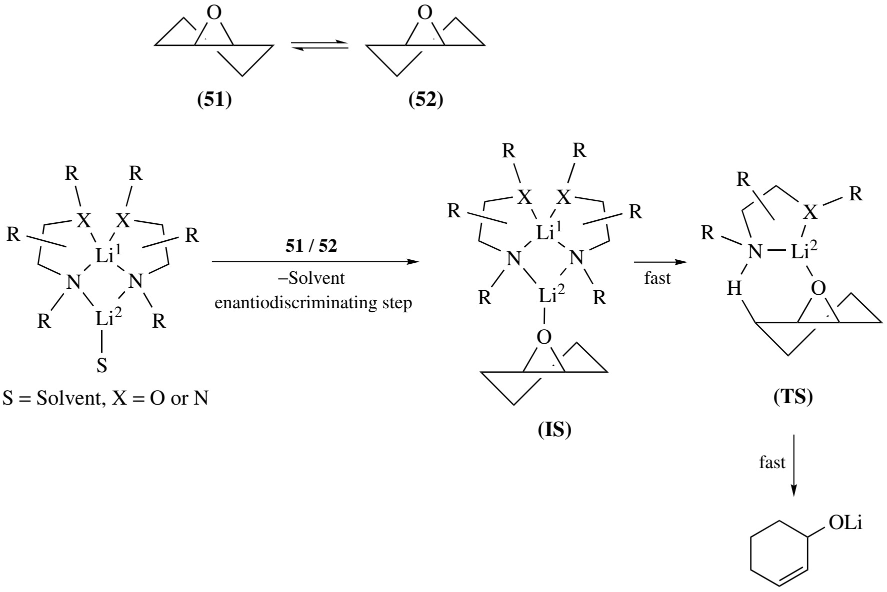

SCHEME 28

To conclude, the models proposed below are in good agreement with the empirical data and allow a first approach to an efficient rational design of homochiral bases. However, they only take the major NMR or X-ray observable solution HCLA complexes into consideration: minor aggregates involving allylic alcoholate or protonated amine products, that might be reactive and contribute to the product formation, are ignored[63, 67].

ii. Catalytic processes. Catalytic processes are based upon the regeneration in situ of the HCLA base used in sub-stoichiometric quantity from its protonated form (HCLA-H) by a stoichiometric amount of an achiral base (co-base). To ensure good stereocontrol, the co-base must regenerate the HCLA base significantly faster than it deprotonates the oxirane ($k_A > k_C$) (Figure 5)[43].

The first example of such a process was reported in 1994 by Asami, who noticed that LDA was less reactive than HCLA **53** toward oxirane and thus proposed its use as a co-base in a catalytic cycle[68]. Based upon this seminal result, the system has been extended to other HCLAs and various co-bases have been tested[47, 48, 68–75]. Selected results for the asymmetric rearrangement of cyclohexene oxide mediated by sub-stoichiometric quantities of HCLA are collected in Table 4.

In most cases, the use of LDA as the co-base results in a significant decrease of the stereoselectivity (compare Table 4, entries 1, 6, 9 with Scheme 26 and Table 2, entries 5, 6).

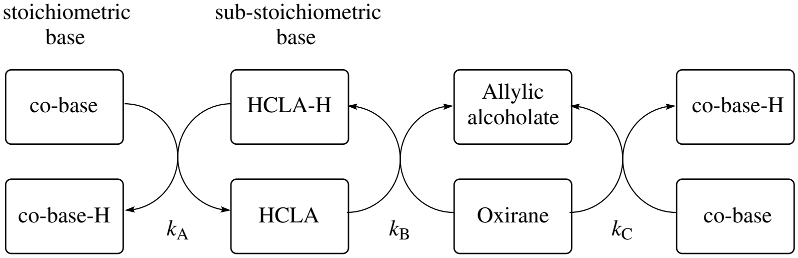

FIGURE 5

TABLE 4. Influence of various co-bases and additives

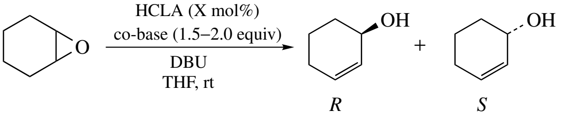

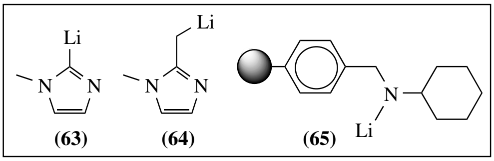

(63) **(64)** **(65)**

Entry	HCLA (mol%)	co-base (n equiv.)	Additive (n equiv)	Reaction time (h)	Yield (%)	ee (%)
1	**53** (20)	LDA (2.0)	none	12	63	68 (*S*)[73]
2	**53** (20)	LDA (1.0)	DBU (6.0)	12	71	75 (*S*)[68]
3	**53** (6)	LDA (1.14)	DBU (6.0)	—	61	59 (*S*)[68]
4	**53** (20)	**62** (2.0)	none	28	84	76 (*S*)[73]
5	**53** (20)	**63** (2.0)	none	8	78	80 (*S*)[73]
6	**58** (20)	LDA (2.0)	none	32	86	19 (*S*)[73]
7	**58** (20)	**62** (2.0)	none	69	58	73 (*S*)[73]
8	**58** (20)	**63** (2.0)	none	42	65	73 (*S*)[73]
9	**59** (20)	LDA (2.0)	none	32	90	22 (*S*)[73]
10	**59** (20)	**62**(2.0)	none	198	96	93 (*S*)[73]
11	**59** (20)	**63** (2.0)	none	13	96	93 (*S*)[73]
12	**55** (20)	LDA (1.8)	none	18	95 (89)[a]	88 (94)[a](*S*)[47]
13	**55** (5)	LDA (1.95)	none	42	51[a]	81[a] (*S*)[47]
14	**55** (20)	LDA (1.8)	DBU (2.0)	6	68	78 (*S*)[47]
15	**55** (5)	**65** (1.45)	none	36	91	92(*S*)[74]
16	**56** (5)	LDA (1.5)	DBU (5.0)	6	95[a]	99[a] (*R*)[48]

[a] Reaction performed at 0 °C

As shown in Table 4, there is a relationship between the LDA/HCLA ratio and the ee observed, an increase in this ratio inducing a decrease in selectivity (entry 2 vs. 3, 12 vs. 13).

These results, together with the observation that a slow addition of LDA can improve the enantioselectivity in selected cases[70], strongly suggest a competitive, nonstereoselective deprotonation by this co-base. Interestingly, using a large excess of DBU with HCLA **53** improves the selectivity (entry 1 vs. 2). Nevertheless, this effect is not general, as illustrated in the case of HCLA **55** (entry 13 vs. 14). Thus, in order to ensure that product is formed exclusively through reaction with the substoichiometric chiral base, other co-bases with a lower kinetic basicity but a comparable thermodynamic basicity to LDA were required.

Since the rate of proton transfer between highly electronegative atoms (such as nitrogen) and a carbon is usually faster than the one between two carbons, C−Li nonreactive bulky bases have been investigated[70–73]. It has been found that bases **63** and **64** exhibit the same basicity as LDA in THF but are unreactive toward oxiranes. Therefore, they have been tested as co-bases in the catalytic process. As expected, the use of **63** with HCLA **53** results in an increase of the ee as compared to the result obtained with LDA in the same conditions (entry 4 vs. 3). A further improvement is noted with **64** leading to a better ee than the corresponding stoichiometric reaction and an acceleration of the reaction (entry 5). Similar results are reported for HCLA **58** and **59** with **63** and **64**, the enantioselectivities being, in both cases, identical to the stoichiometric reactions. Again, acceleration of the reaction is noted with co-base **64** compared to **63** (entries 7, 8, 10, 11)[71–73]. It has been shown, by multinuclear (^{6}Li, ^{15}N) NMR spectroscopy, that the addition of **63** or **64** to a THF solution of the homodimer of HCLA **59** resulted in the formation of more stable mixed dimers of type **66** (Scheme 29)[71,72]. Therefore, the catalytic rearrangement mediated by HCLA **59** with **63** or **64** is suspected to occur via this heterodimer **66** whose complexation with the oxirane could be the rate-limiting transition state (see above, enantiodiscrimination for HCLA of type B)[73].

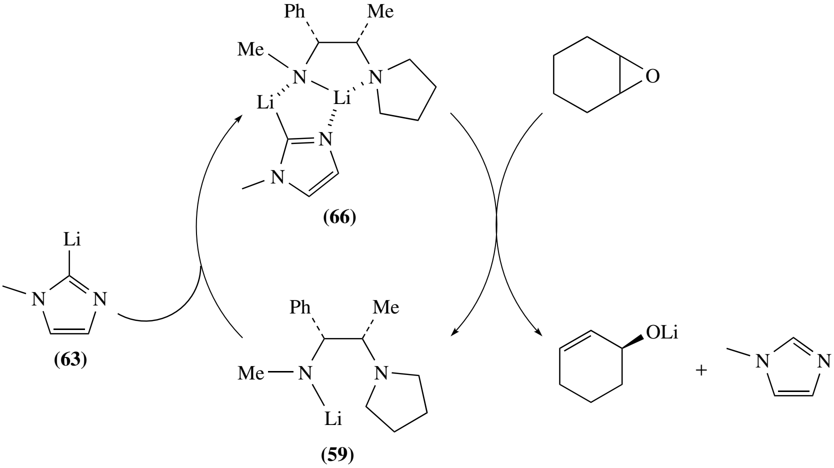

SCHEME 29

The catalytic system has been successfully extended to polymer-bound lithium amide co-bases of type **65** (see Table 4) which, like C−Li bases of type **63** and **64**, are efficient regenerating agents of HCLA and poorly reactive toward oxiranes. For instance, the isomerization of cyclohexene oxide by 0.05 equiv of HCLA **55** in the presence of 1.45 equiv of **65** affords (*S*)-cyclohexenol in 92% ee (entry 15). It is of interest to note that, similarly to co-bases **63** and **64**, the use of **65** leads to an increase of selectivity compared to the stoichiometric reaction at room temperature (Table 2, entry 2)[74,75].

Finally, HCLA bases **56a** and **56b** prove to be the most efficient reagents with only 5% of **56b** being sufficient to obtain an excellent yield and an almost perfect 99% ee in the asymmetric rearrangement of cyclohexene oxide (entry 16). These bases have been successfully applied to a wide range of oxiranes, making them the most general in scope among the known lithium amides (Table 5)[48,76].

iii. Role of additive. There are some reports in the literature of the beneficial effect of powerful donor solvents such as DBU on the reactivity and enantioselectivity of HCLA-mediated oxirane rearrangements for both stoichiometric and catalytic processes. However, this effect is not general (see above) and the role of such additives is still unclear. In one study, the influence of the concentration of DBU on the relationship between the ee's of catalyst and the product for the enantioselective isomerization of cyclohexene oxide mediated by substoichiometric amount of HCLA **56a** (20 mol%) in the presence of LDA (2 equiv) has been investigated[48]. At high DBU concentration (6 equiv), the enantiomeric

TABLE 5. Catalytic asymmetric rearrangement of oxiranes mediated by HCLA **56a** and **56b**

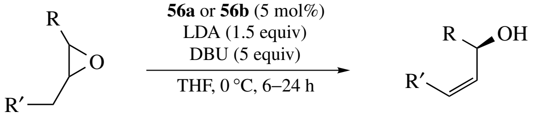

		56b		**56a**	
Entry	Oxirane	Yield (%)	ee (%)	Yield (%)	ee (%)
1	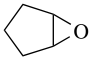	81	96 (*R*)[a]	67	49 (*R*)[a,b]
2	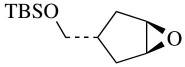	—	—	42	95 (*R*)
3	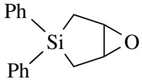	—	—	72	91 (*R*)
4	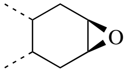	94	98 (*R*)	95	94 (*R*)
5	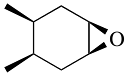	85	99 (*R*)	95	97 (*R*)
6	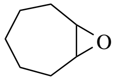	93	>99 (*R*)	89	96 (*R*)
7	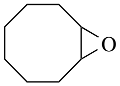	—	—	81	78 (*R*)
8	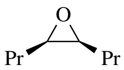	80	91 (*R*)	82	66 (*R*)

[a] Reaction performed at rt.
[b] 15 mol% catalyst.

purity of the product matches that of the catalyst, whereas at lower concentrations a pronounced negative nonlinear correlation is observed. It has been suggested that in such cases, the additive can act as a dissociating agent, generating highly enantioselective, monomeric catalyst species by inhibiting the formation of less reactive, unselective aggregates. Additionally, it has been independently demonstrated by NMR studies that under such experimental conditions DBU is partially deprotonated by LDA to give lithiated DBU **67**[77–79], which could be involved in the enantioselective process. Accordingly, the reaction mixture of the catalytic process would thus be composed of HCLA, **67** and DBU in excess. Moreover, multinuclear NMR studies of isotopically labeled HCLA **59** and **67** have shown the formation of a mixed dimer **68** (Figure 6) similar to those obtained with co-bases **63** and **64** (see above, Scheme 29).

Further investigations revealed that the efficiency of this complex for the enantioselective isomerization of cyclohexene oxide under conditions similar to the catalytic process (mixture of HCLA **59, 67** and DBU) is close to that of the presumed HCLA **59** homodimer (Table 6, entries 1 and 2). These experiments also confirmed the dramatic influence of DBU on both enantioselectivity and rate (entry 3)[73].

It is of interest to note that not only do the rate and enantioselectivity of the reaction increase with the concentration of the additive but also with its polarity, comparable results being obtained with DBU, DBN (1,5-diazabicyclo[4.3.0]non-5-ene) or HMPA, as illustrated in Table 7 for the use of HCLA **56a**[48].

Entry 6 is particularly interesting. Indeed, it has been shown by deuterium labeling experiments that the presence in the reaction mixture of a strong donor solvent such as HMPA induces a change in the stereoselectivity of the β-elimination, from *syn* to *anti* (see above, Section II.C.). Therefore, both the increase in rate and the enantioselectivity

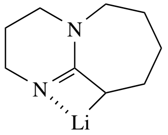

(67)

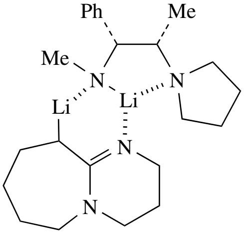

(68)

FIGURE 6

TABLE 6. Role of DBU on the enantioselectivity and the rate of the allylic alcohol formation

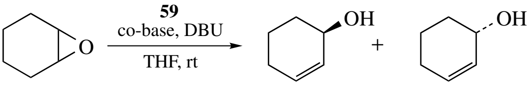

Entry	**59** (n equiv)	Co-base (n equiv)	DBU (n equiv)	Reaction time (h)	Yield (%)	ee (%)
1	1	none	none	25	95	93 (*S*)
2	0.2	DBU-Li (2)	5	60	88	94 (*S*)
3	0.2	DBU-Li (2)	none	240	57	89 (*S*)

TABLE 7. Influence of additives on enantioselectivity

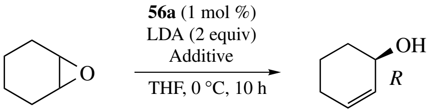

Entry	Additive (n equiv)	Yield (%)	ee (%)
1	none	40	44
2	TMEDA (5)	67	40
3	DBU (5)	92	78
4	DBU (10)	85	81
5	DBN (5)	81	67
6	HMPA (5)	80	69

of the elimination, induced by such additives, could possibly result from a change of mechanism[6].

b. Dilithiated bases. Lithium amide–potassium alkoxide mixed base systems have been found to be particularly efficient in oxirane isomerization reactions with rate and selectivity being considerably enhanced compared to lithium amide used alone. It has been suggested that the formation of a transition state of type **48** or **49** (see Figure 2, Section III.A), in which the complexation of the lithium to the oxygen fixes the potassium amide or alkoxide close to the β-proton, could create a strong push-pull effect and thus accelerate the reaction. These results have prompted several research groups to test dilithiated bases as analog in an enantioselective version.

The first study was performed by Milne and Murphy, who found that the rearrangement of substituted cyclopentene oxide **69** into **70** by a stoichiometric amount of the dilithiated homochiral base **71** derived from norephedrine occurred in excellent yield and good ee (Scheme 30)[80, 81].

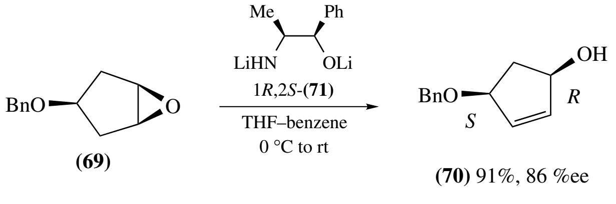

SCHEME 30

This result and the availability of homochiral base **71** in both enantiomeric forms has made this procedure particularly interesting. It has then been successfully applied to the rearrangement of unprotected oxirane **72a** into **73a**, with excellent stereoselectivity (95% ee; Scheme 31)[82, 83].

It is interesting to note that no reaction is observed with oxirane **72a** if the hydroxyl group is protected. Moreover, whereas deuterium labeling experiments indicate a clean β-deprotonation process for both oxiranes **69** and **72a**, the same enantiomer of base **71** furnishes the corresponding allylic alcohols **70** and **73a** with the opposite absolute configurations (Scheme 30 vs. 31). The same studies on vicinal disubstituted analogues **72b,c** showed that both the sense and the level of enantioselectivity are unchanged, which

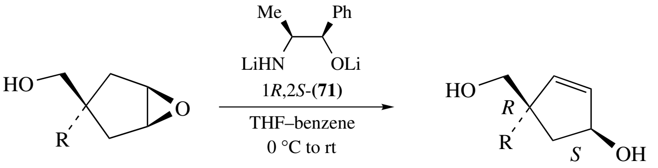

(72a) R = H
(72b) R = Me
(72c) R = Bu

(73a) R = H 66%, 95 %ee
(73b) R = Me 63%, 99 %ee
(73c) R = Bu 67%, 96 %ee

SCHEME 31

indicates that the presence of alkyl groups has no effect on the stereochemical outcome of the reaction. A *syn* process is thus still involved (Scheme 31)[9, 84].

Bis-lithium diamides, which are known to exhibit a higher basicity than the corresponding mono-lithium amides and thus are expected to be more reactive toward oxiranes, have also been investigated[69, 85]. In order to reduce the multiplicity of transition states, C_2 symmetric homochiral lithium diamides derived from readily accessible homochiral diamines have been chosen. The effect of chelating properties and the steric bulk of nitrogen substituents has been studied. Similarly to mono-lithiated amides, homochiral base **74** (see Table 8) with nitrogen substituents bearing chelating atoms gave the best results. Various oxiranes have been tested in stoichiometric and catalytic conditions, as summarized in Table 8.

While homochiral base **74** promotes asymmetric deprotonation of various oxiranes with an interesting level of enantioselectivity, it appears surprisingly unreactive, as illustrated

TABLE 8. Asymmetric rearrangement of various oxiranes using base **74**

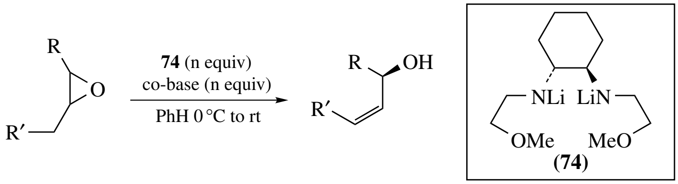

Entry	Oxiranes	**74** (n equiv)	Co-base (n equiv)	Reaction time (h)	Yield (%)	ee (%)
1	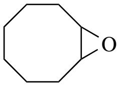	1.5	—	44	49	87 (*R*)
2		1.5	—	21	68	76 (*R*)[a]
3	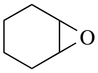	0.2	LDA (1.5)	22	66	32 (*R*)
4		0.2	*n*-BuLi (1.0)	48	47	67 (*R*)
5		0.2	MeLi (1.0)	68	56	67 (*R*)
6	TBSO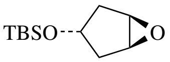	0.2	MeLi (1.5)	24	50	75 (*R*)[b]

[a] Reaction performed in THF.
[b] Reaction performed in ether.

by the long reaction times and the moderate yields observed in the stoichiometric version (entries 1 and 2). Owing to this lack of reactivity, the use of LDA as a co-base in the catalytic version induced a dramatic decrease in the selectivity (entry 3). In this case, the nonselective pathway become highly competitive. The use of less reactive C−Li bases restores the selectivity (entries 4 to 6), as observed for monolithiated bases (see Section III.B.1.a).

2. RLi:homochiral ligand complexes

The RLi:homochiral ligand complexes are seldom used for the base-promoted isomerization of oxiranes into allylic alcohols because their poor chemoselectivity lead to complex mixtures of products. As examples, the treatment of cyclohexene oxide by a 1:1 *s*-BuLi/(−)-sparteine mixture in ether at low temperature provides a mixture of three different products arising respectively from β-deprotonation (**75**), α-deprotonation (**76**) and nucleophilic addition (**77**) (Scheme 32)[86]. When exposed to similar conditions, the disubstituted cyclooctene oxide **78** affords a nearly 1:1 mixture of α- and β-deprotonation products (**79** and **80**) with moderate ee (Scheme 32, entry 1). Further studies have demonstrated that the α/β ratio depends strongly on the type of ligand used (Scheme 32, entry 1 vs. entry 2)[87, 88].

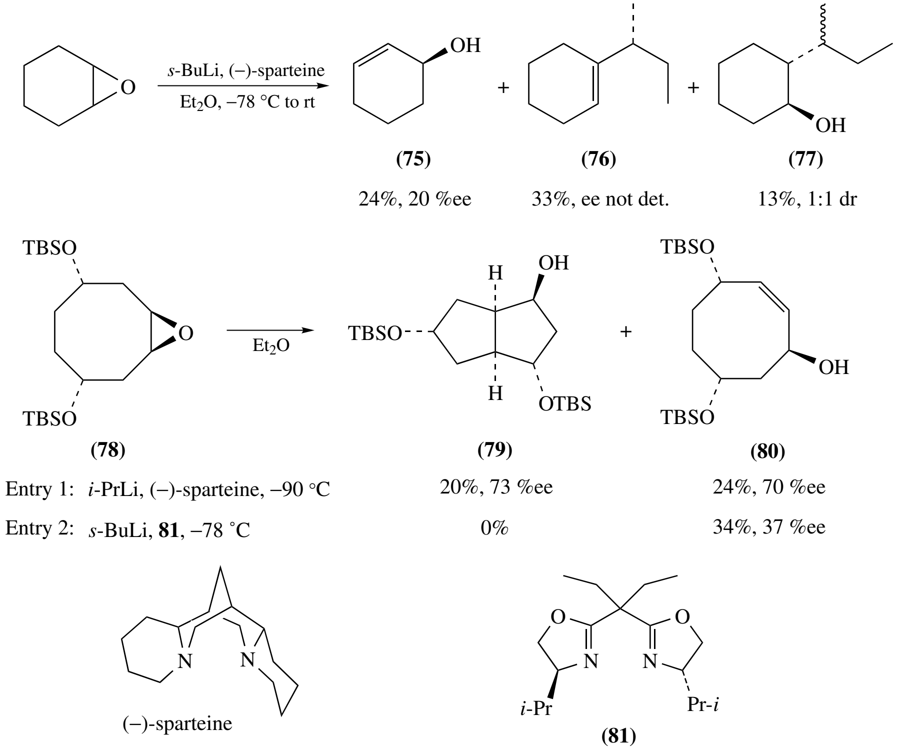

SCHEME 32

Two examples using *s*-BuLi/(−)-sparteine mixture as base have been reported to promote effective allylic alcohols formation in moderate ee for the spiro epoxide **82**[89] and cyclooctadiene oxide **83**[90] (Scheme 33). In the last case, such regioselectivity could be explained by the relatively flat conformation of the medium-sized oxirane which favors the *syn* base–oxirane complex (see Section II.A).

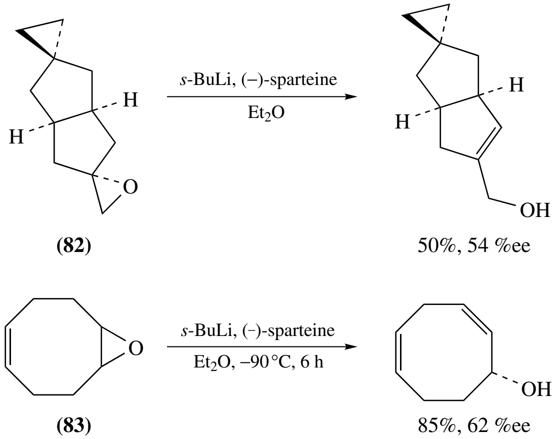

SCHEME 33

3. Kinetic resolution

By contrast with the enantioselective deprotonation of *meso* oxiranes, there is only a limited number of reports on the kinetic resolution of unsymmetrically substituted oxiranes. This reaction involves the preferential recognition of one of the two enantiomers of a racemic mixture by a chiral reagent to provide both the starting material and the product in enantioenriched form[91–93]. Several HCLA bases developed for enantioselective deprotonation have been tested as chiral reagent in stoichiometric or catalytic amount for the kinetic resolution of cyclic and linear oxiranes.

The stoichiometric approach has been successfully used as the key step for the synthesis of biologically active compounds, to obtain enantioenriched allylic alcohols, as illustrated by the synthesis of conduritols derivatives **84**[94] or the aggregation pheromone of the Douglas-fir beetle **85**[95], as well as enantioenriched oxiranes, intermediates for the synthesis of (−)-isomenthone **86**[96] (Scheme 34).

With regard to the general behavior of oxiranes, studies on kinetic resolution of alkyl[97] or alkoxy[98] substituted linear oxiranes mediated by 0.5 to 0.75 equivalent of HCLA base **53** have shown better enantiomeric discrimination for *cis* (Table 9, entries 1 and 4) rather than *trans* or terminal oxiranes (Table 9, entries 2, 3 and 5).

The stereoselectivity can be rationalized by considering nonbonding interactions between R^2 and the pyrrolidinyl substituents in **TS 3**, which favor **TS 4** (Figure 7). Therefore, a decrease of the selectivity is observed for terminal or *trans* substituted oxiranes where R^2 is a hydrogen.

It is interesting to note that such model, which is in good agreement with the enantio- and diastereoselectivity observed, is consistent with the model proposed for the enantioselective rearrangement of *meso* oxiranes mediated by this base (see Section III.B.1.a).

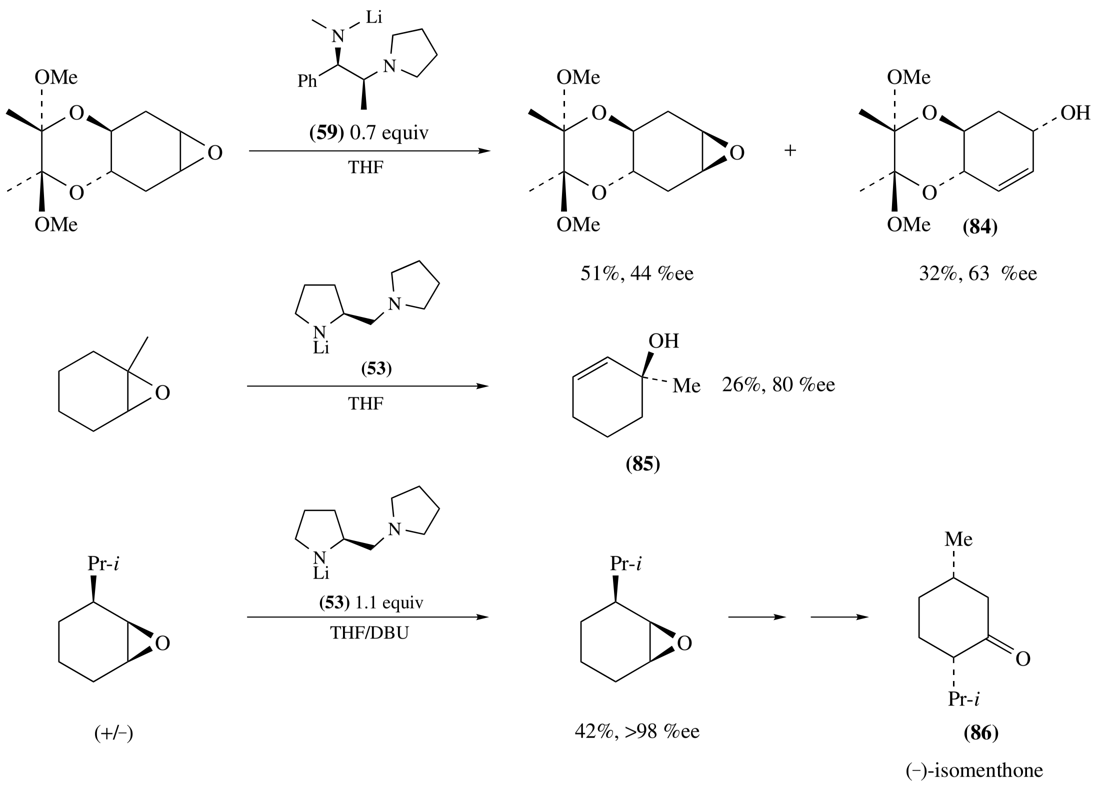
OMe
O
O
OMe
O
Li
N
Ph
N
(59) 0.7 equiv
THF
OMe
O
O
OMe
O
+
OMe
O
O
OMe
OH
(84)
51%, 44 %ee
32%, 63 %ee
O
N
Li
N
(53)
THF
OH
Me
26%, 80 %ee
(85)
Pr-i
O
(+/–)
N
Li
N
(53) 1.1 equiv
THF/DBU
Pr-i
O
42%, >98 %ee
Me
O
Pr-i
(86)
(–)-isomenthone

SCHEME 34

TABLE 9. Kinetic resolution of racemic oxiranes using HCLA **53**

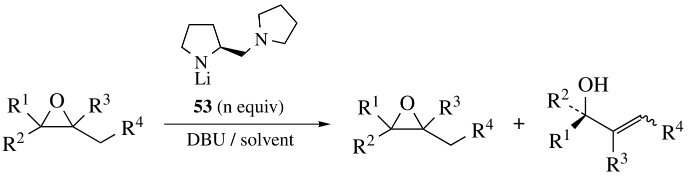

Entry	Oxirane	53 (n equiv)	Solvent	Recovered oxirane		Allylic alcohol	
				Yield (%)[a]	ee (%)	Yield (%)[a]	ee (%)
1	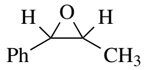	0.75	THF	31	95 (1*S*, 2*R*)	60	35 (*R*)
2	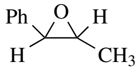	0.75	THF	27	45 (1*S*, 2*S*)	63	15 (*S*)
3	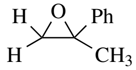	0.75	THF	11	39 (*R*)	69	—
4	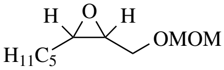	0.5	benzene	—	—	25 (*Z*/*E*: 2/98)	*E*: 43 (*S*)
5	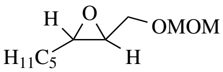	0.5	benzene	—	—	25 (*Z*/*E*: 45/55)	E: 30 (*S*) *Z*: 45 (*R*)

[a] Isolated yield.

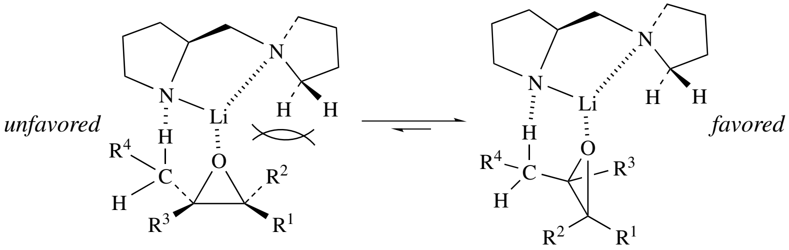

(TS 3) **(TS 4)**

FIGURE 7

As for enantioselective deprotonation, the best results are obtained with HCLA bases of type **56** which can be employed as catalyst (10 mol%) in the presence of excess amounts of LDA (2 equivalents)[49, 99]. In such conditions, high levels of selectivity are reached with linear and cyclic oxiranes. The general study undertaken with this base toward cyclic oxiranes has shown the beneficial influence of bulky substituents branched directly on the oxirane ring (Table 10, entries 3, 5 and 6) or on the 3-position (Table 10,

TABLE 10. Kinetic resolution of racemic oxiranes using HCLA **56a**

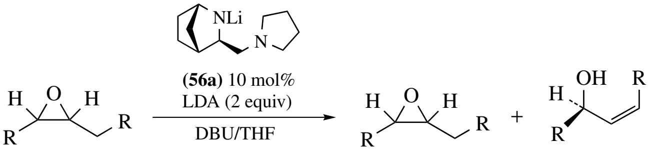

			Recovered oxirane		Allylic alcohol		
Entry	Oxiranes	% conversion	Yield (%)^a	ee (%)		Yield (%)^a	ee (%)
1	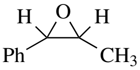	55	45	94	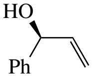	35	84 (*R*)
2	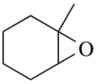	52	38	87	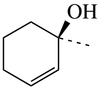	40	94 (*R*)
3	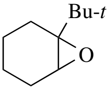	58	36	99	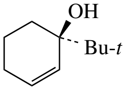	40	99 (*R*)
4	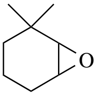	52	47	99	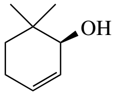	43	94 (*S*)
5	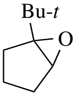	42	50	nd	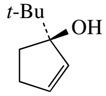	34	79 (*R*)
6	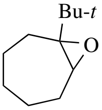	47	48	nd	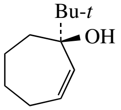	40	90 (*R*)
7	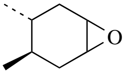	50	nd	nd	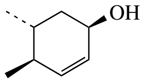	nd	40

^{a}isolated yield.

entry 4). On the contrary, the enantioselectivity drops dramatically when the substituents are more remote from the oxirane ring (Table 10, entry 7). With regard to the size of the ring, the selectivity decreases dramatically from 6 to 5 or 7 member ring oxiranes (Table 10, entry 3 vs. entries 5 and 6), as observed for enantioselective deprotonation (see Section III.B.1.a).

IV. OXIRANE RING OPENING BY ORGANOLITHIUM REAGENTS

The oxirane ring opening reaction with organolithium reagents is an important reaction as it gives direct access to β-hydroxyalkylated products. This reaction has been reviewed[100–103] several times, and only general trends will be described here.

The mechanism of the ring opening reaction is considered to involve cationic assistance through complexation of the lithium ion to the oxygen atom (Scheme 35, the oxirane substituents have been omitted for clarity). These considerations explain how the addition of strongly cation-solvating agents such as glymes, crown ethers or cryptands[104, 105] or HMPA[19] decreases the reaction rate or totally inhibits the ring opening reaction. This cationic assistance has been supported by *ab initio* calculations[106]. From the point of view of the regioselectivity, in the absence of any activation by a functional group, the less hindered carbon atom of the oxirane ring is preferentially attacked. Concerning the stereoselectivity of the reaction, ring opening occurs clearly with inversion of the configuration at the attacked carbon center. This preference has been attributed to a strong repulsive electrostatic interaction between the nucleophile and the oxirane oxygen on which a negative charge is developing[107], or to the precocity of the transition state in the inversion pathway compared to the one with retention[106].

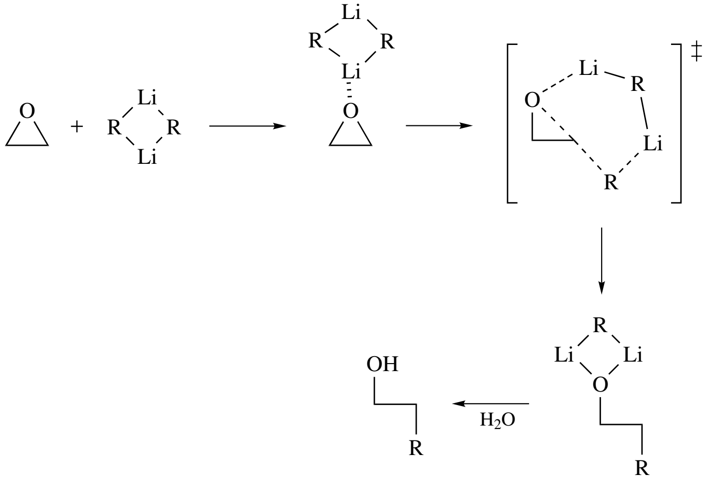

SCHEME 35

From the practical piont of view however, due to other favorable possible pathways (α- or β-deprotonation) as depicted above, it is interesting to differentiate between simple organolithium reagents, which show a high basicity, and stabilized organolithium reagents, with a lower basicity, but also a moderate nucleophilicity. In many cases, activation of the reaction can be obtained by the addition of a strong Lewis acid.

A. Epoxide Ring Opening with Nonstabilized Organolithium Reagents

Early work[1, 108] has shown that the reaction of simple organolithium reagents with oxiranes lead mainly to products from α- or β-deprotonation and not from the desired ring opening reaction. However, some reactions of methyllithium[109], allyllithium[19], aryllithiums[110], and vinyllithium/potassium reagents[111] with oxiranes are reported (Scheme 36).

Intramolecular reactions from organolithium reagents (Scheme 37) have also been reported. The organolithium reagent is produced through iodine–lithium exchange[112], through a carbometalation reaction[105] or by deprotonation at a position activated by an aryl,

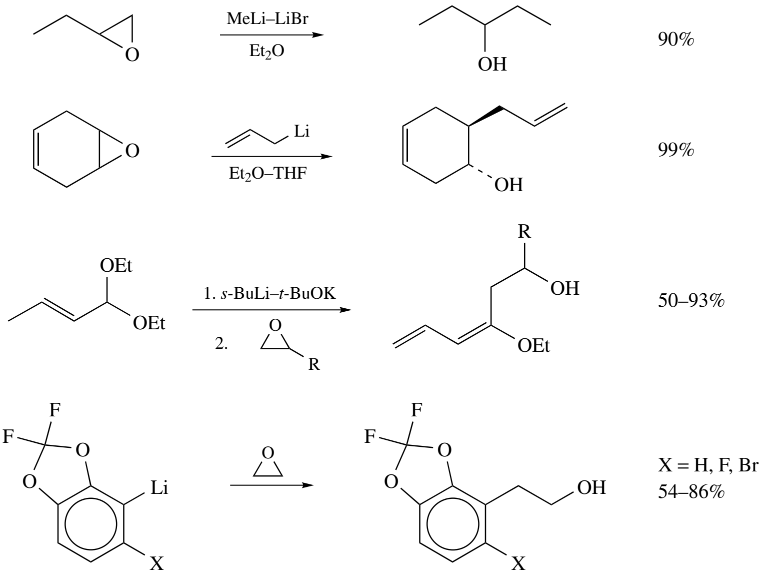

SCHEME 36

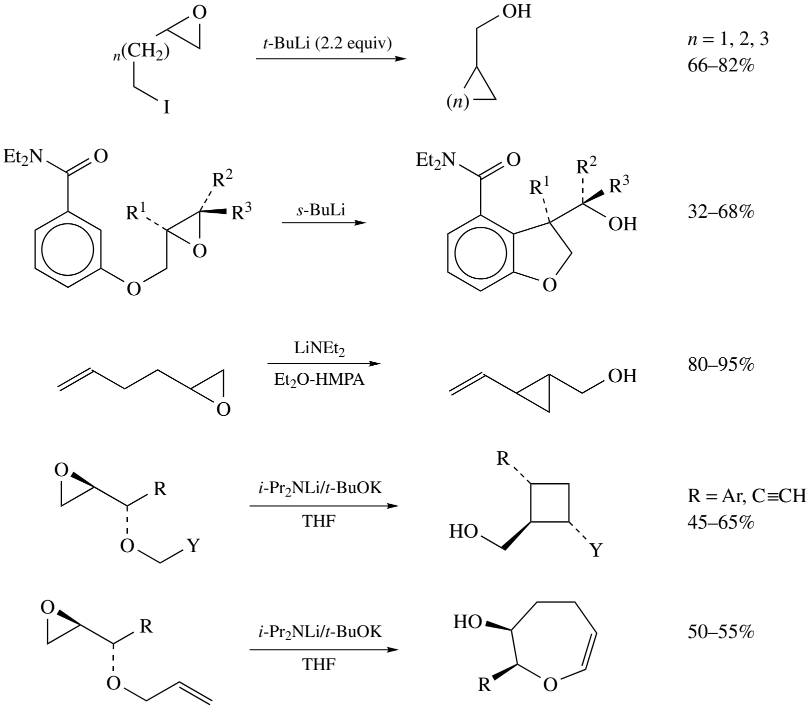

SCHEME 37

a vinyl or an alkynyl group. Deprotonation can also be favored by a complex induced proximity effect[113]. The deprotonation agent can be a lithium amide[114] or an alkyllithium[115,116], or a mixed lithium/potassium amide[117–121]. In the first two cases HMPA is often necessary to achieve the deprotonation, and to inhibit the ring opening reaction. By contrast, mixed lithium/potassium amides can be used in THF without any cosolvent. Some representative examples are depicted in Scheme 37.

The regioselectivity of vinyloxiranes is interesting. Indeed, the ring opening of 3,4-epoxy-1-butene **87**[109,122] and 3,4-epoxycyclohexene **88**[123] with organolithium reagents affords a mixture of the three possible regioisomers (Scheme 38). By contrast, the reaction of 3,4-epoxycyclooctene **89** with allyllithium gives only one regioisomer[19] (from the S_N2 ring opening at the allylic center), whereas the reaction of isoprene oxide **90** and vinylepoxysilane **91** with organolithium reagents yields only S_N2' ring opening products[124–126].

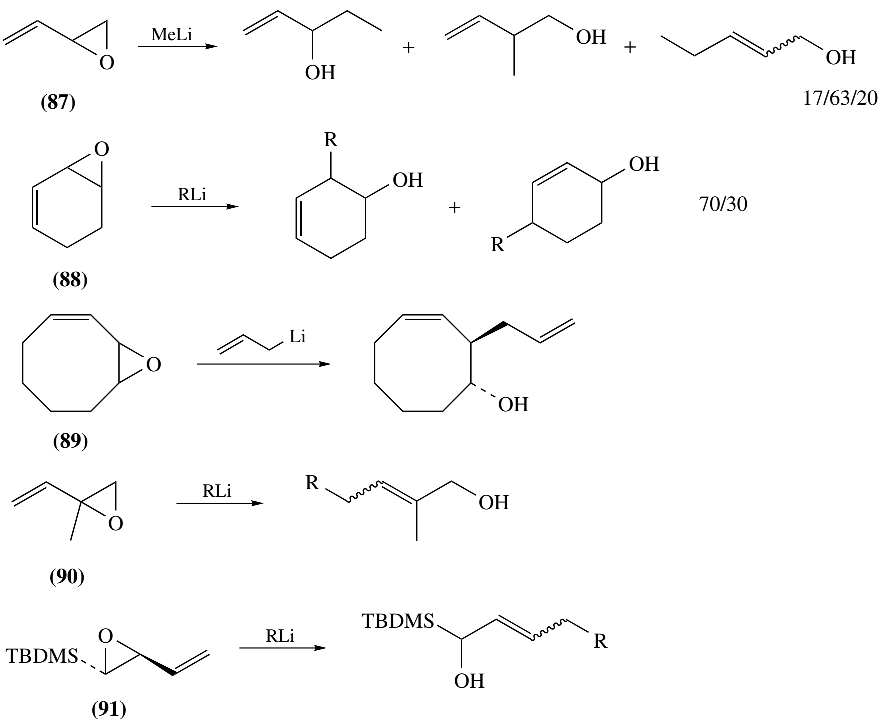

SCHEME 38

However, the more general method for the oxirane ring opening reaction with organolithium reagents is to activate the reaction at low temperature with a strong Lewis acid such as BF_3•Et_2O[127]. This method, originally applied[128] in the case of alkynyllithium reagents (see Section IV.B.2), has been examined by low temperature NMR studies[127] and the reaction of the organolithium reagent on the complex oxirane–BF_3 has been evidenced (Scheme 39). The transmetalation of the organolithium reagent to fluoroborates is a slow reaction at the commonly used temperatures and produces species which are not reactive with oxiranes at these temperatures.

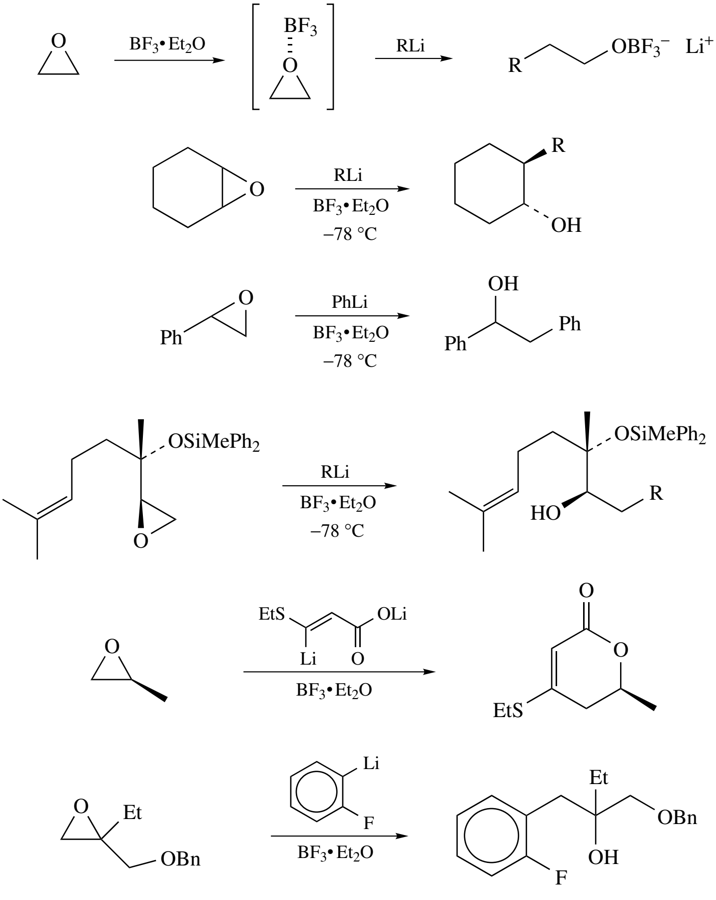

SCHEME 39

The reaction occurs quickly at low temperature, with inversion of configuration at the attacked carbon center. The oxirane is reacting usually at the less hindered site. This reaction has found widespread use in organic synthesis[129–131], particularly in the case of stabilized organolithium and alkynyllithium species (see Section IV.B.2). In the intramolecular versions, the presence of BF_3 has been reported to modify the regioselectivity[112]. Other Lewis acids such as organolanthanids[132] or $LiClO_4$[133] have also been used to a lesser extent.

The effect of the BF_3 activation on the regioselectivity of the ring opening of vinylic and acetylenic oxiranes is dramatic, as in these conditions the reaction occurs exclusively on the allylic[134] or the propargylic[135–137] position, and still with inversion (Scheme 40). This excellent regioselectivity allows the direct stereospecific preparation of homoallylic and homopropargylic alcohols in excellent yields. In the case of acetylenic oxiranes, a remarkable difference in the reactivity of *cis* and *trans* oxiranes has been evidenced, the former being more reactive.

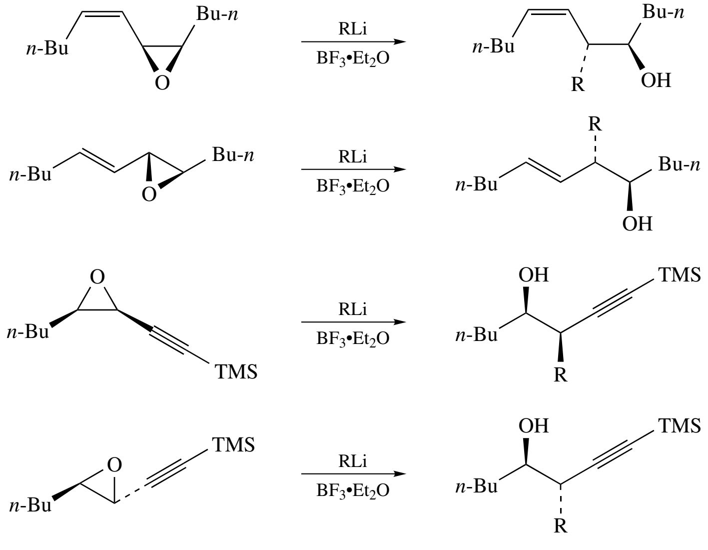

SCHEME 40

B. Oxirane Ring Opening with Low Basicity Organolithium Reagents

With low basicity organolithium reagents (stabilized organolithium reagents or alkynyllithium reagents), the problem of α- or β-deprotonation vs. ring opening is limited or avoided. However, these anions generally present a lower nucleophilicity than nonstabilized organolithium reagents, and then the ring opening reaction has often to be helped by raising the temperatures or by adding a stronger Lewis acid such as BF_3•Et_2O or a polar cosolvent such as HMPA.

1. Sulfur stabilized organolithium reagents

Metalated dithianes react very slowly with oxiranes[138–140]. When anions are short-lived and/or the oxiranes are relatively poor electrophiles (for example, 2,3-disubstituted), the reaction is capricious[141]. The reaction is greatly accelerated by the addition of BF_3•Et_2O[142] or, more frequently, of a polar cosolvent such as HMPA[141, 143] or DMPU[144]. This coupling reaction has been applied in the total synthesis of natural products[145]. The effect of the HMPA addition is ambiguous, as, for example, it increases the rate of the reaction of the lithiated dithiane **92** but decreases the reaction rate of lithiated dithiane **93** (Scheme 41). This effect has recently been explained[146] in terms of *contact ion pairs* (CIP) and *separated ion pairs* (SIP). HMPA can enhance the nucleophilicity of carbanions by separating the ion pair, but has also a pernicious effect on the ring opening by increasing the complexation of the lithium cation and then lowering its Lewis acidity and its complexation to the oxygen atom of the oxirane. The lithiated dithiane **92** is present mainly as CIP in THF, and the addition of at least two equivalents of HMPA enhances the ion pair separation. By contrast, the lithiated dithiane **93** is already present as a SIP in THF and then the addition of HMPA decreases the ring opening rate. The lithiated dithiane **94** shows an intermediate behavior. The regioselectivity in the ring opening of vinyloxiranes by lithiated dithianes such as **92** and analogues has been examined[147]. Unencumbered lithiated dithianes such as

92, 92a and **92b** undergo a purely S_N2 reaction whereas sterically encumbered dithianes such as **92c, 92d** and **92e** lead preferentially or only to S_N2' additions. Furthermore, these S_N2' additions have been shown to follow stereospecifically a pure *syn* pathway.

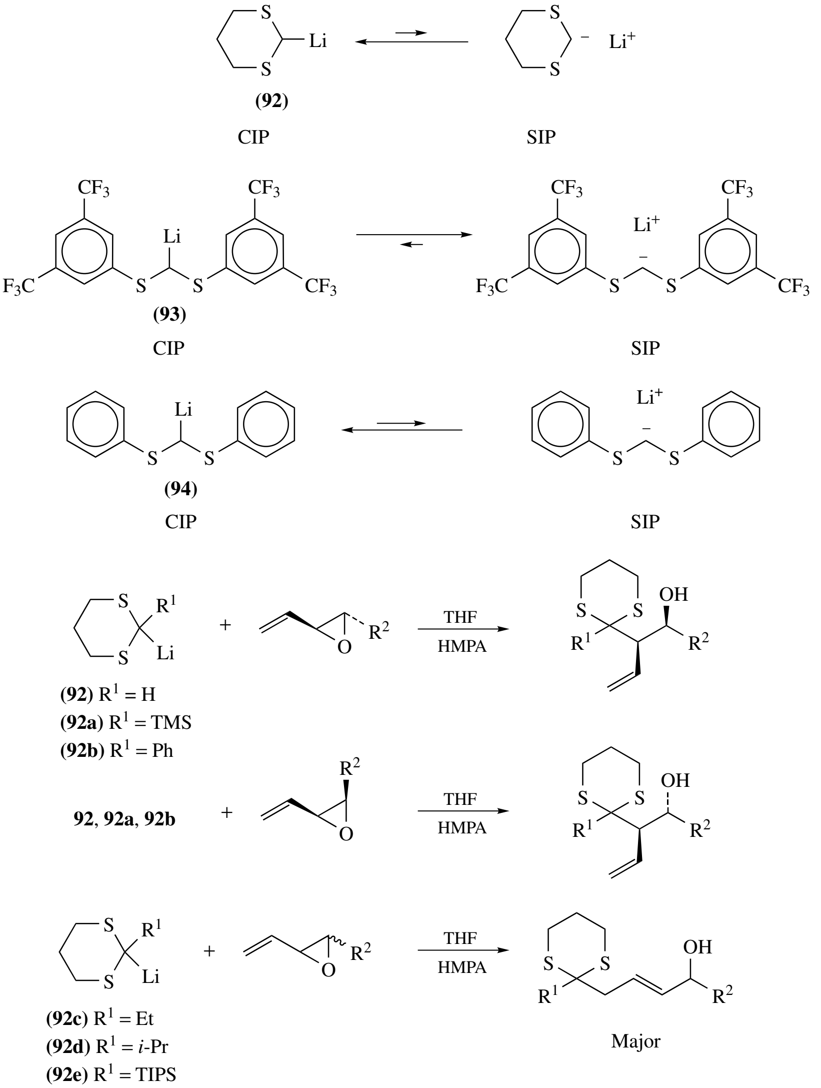

SCHEME 41

Sulfonyl carbanions react readily with oxiranes, usually on the less hindered site[148, 149]. With 2,3-disubstituted oxiranes, harsher conditions have to be used[150]; the addition of HMPA[149, 151, 152] and/or $BF_3{\bullet}Et_2O$[153, 154] can enhance the rate and the yield of the reaction, as in the case of lithiated dithianes. The reaction has been widely employed in organic synthesis[155, 156], including intramolecular cyclizations[157–164] and total synthesis[165]. In the case of α-oxy sulfones, the reaction has been applied in the synthesis of spiroketals[166, 167], including the total synthesis of milbemycin β_1[168]. Several examples are depicted in Scheme 42.

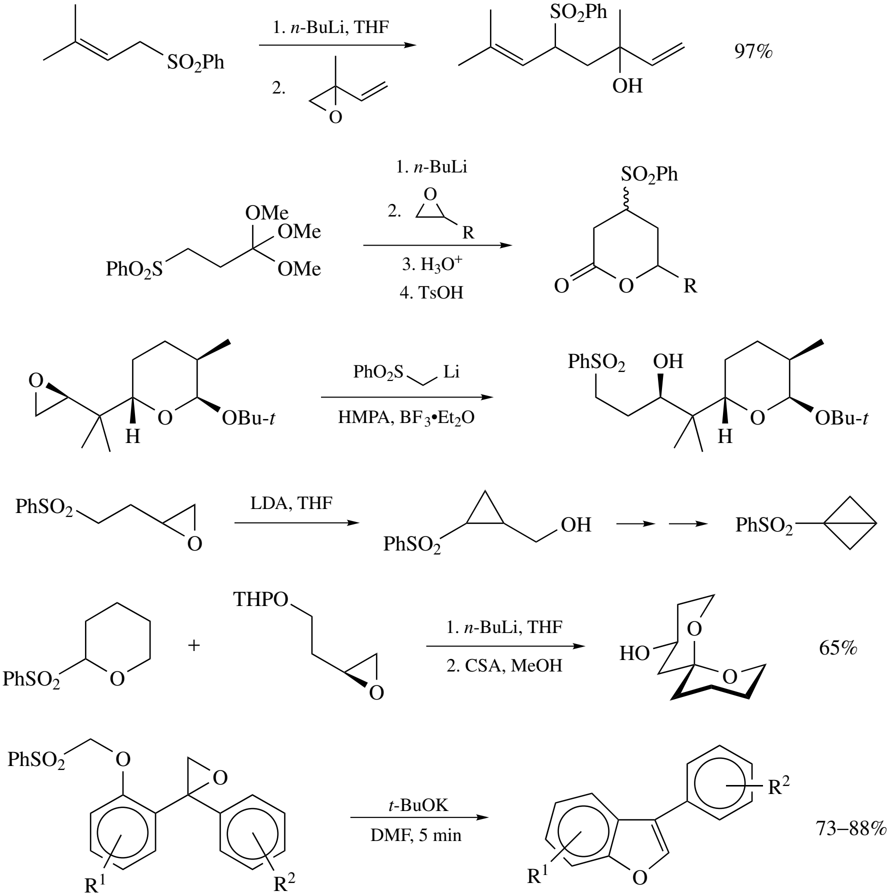

SCHEME 42

Some reports concerning the reaction of lithiated thioallylethers with oxiranes have been published. A slow reaction was observed[151] with a terminal oxirane. However, with cyclopentadiene oxide, the reaction occured smoothly[169] with an excellent regioselectivity in favor of the S_N2 displacement in the allylic position. Other examples involving sulfur, selenium and silicon stabilized organolithium reagents have been reported[103].

2. Alkynyllithiums

The oxirane ring opening reaction with alkynyllithiums is of considerable synthetic value, as stereodefined homopropargylic alcohols can be obtained. The lithium acetylide•

ethylenediamine complex reacts smoothly with oxiranes in DMSO[170–174]. The dianion of propiolic acid has been shown to react with oxiranes in the presence of HMPA[175]. For other alkynyllithiums, the best methodology is the use of an activation with BF_3•Et_2O[128]. Numerous examples, including total synthesis, have been reported[176–184]. Ring opening takes place stereospecifically with inversion at the attacked carbon center[185], and this attack generally occurs at the less hindered position. The reaction conditions are compatible with functional groups such as halogens, acetals or esters. Other Lewis acids such as Me_3Ga[186, 187], Me_3Al[188] or $LiClO_4$[189] have been employed.

The regioselectivity in the ring opening of substituted epoxyalcohols **95** is interesting. When the alcohol moiety is unprotected, the ring opening reaction occurs[190] on the oxirane formed by the Payne rearrangement (Scheme 43). On the other hand, in the case of **96**, where the alcohol moiety is protected, the ring opening occurs regioselectively on the carbon γ to the alcohol[191]. The regioselectivity with the compound **97** is much lower. Analogous substrates **98**, where the oxirane is terminal, react only at the less hindered terminus[179, 180, 182].

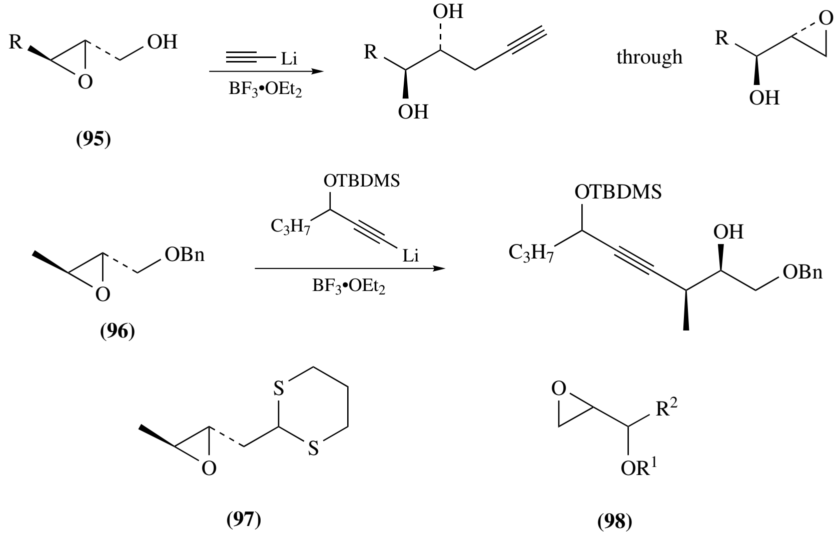

(95) **(96)** **(97)** **(98)**

SCHEME 43

3. Lithium enolates and related compounds

The reactivity of oxiranes with lithium enolates and related compounds has been widely explored and reviewed[103, 192, 193]. Dianions derived from carboxylic acids react readily with oxiranes, but the reaction can be slowed by steric hindrance[192]. The reaction of oxiranes with dianions of acetoacetates is greatly accelerated by the addition of BF_3•Et_2O[194]. Oxiranes react readily with lithium salts derived from nitriles[195–198], malonates and analogues[103], lithiated oxazolines[199, 200] and lithio enamines[201–203].

Lithium enolates derived from esters react poorly with oxiranes[193]. To circumvent this lack of reactivity, the use of malonates or sulfur-containing dianions[204–206] has been developed (Scheme 44). Lithium enolates of ketones do not react directly with oxiranes, presumably due to their low nucleophilicity and moderate thermal stability. However,

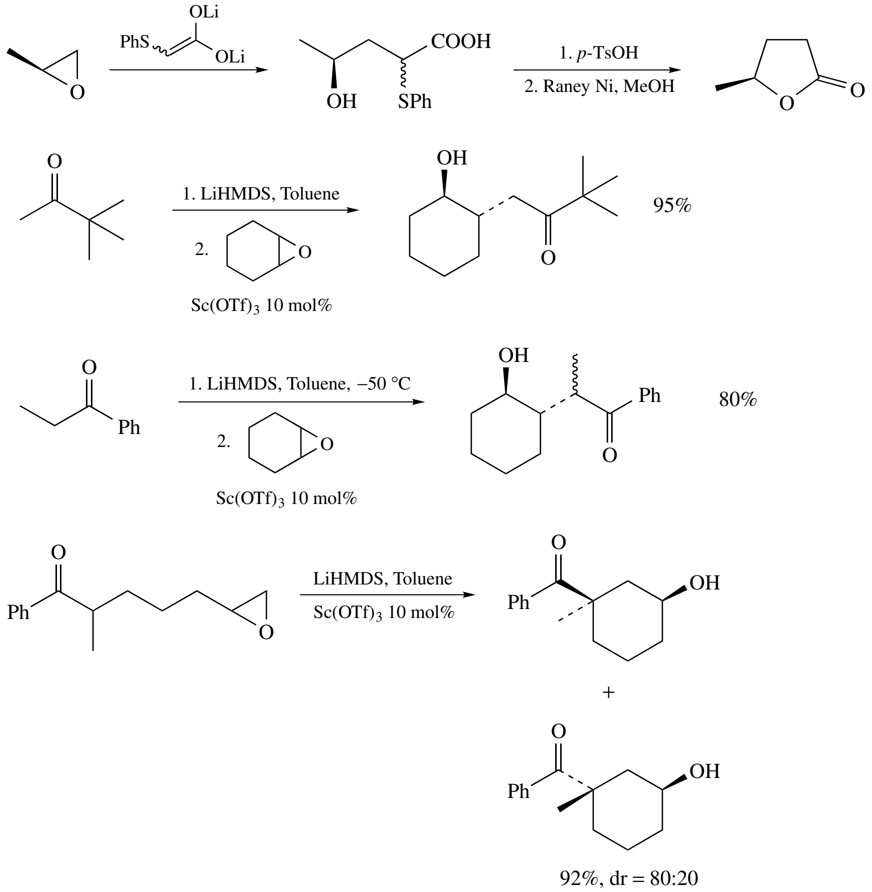

SCHEME 44

activation of the oxirane by Me$_3$Al[207], LiClO$_4$[208], Y(OTf)$_3$[209] and, better, Sc(OTf)$_3$[210–212] has proven to be efficient (Scheme 44).

By contrast, lithium enolates derived from tertiary amides do react with oxiranes[193, 213, 214]. The diastereoselectivity in the reaction of simple amide enolates with terminal oxiranes has been addressed and found to be low[215] (Scheme 45). The chiral bicyclic amide enolate **99** reacts with a good diastereoselectivity with ethylene oxide[216]. The reaction of the chiral amide enolate **100** with the chiral oxiranes **101** and **102** occurs with a good diastereoselectivity (in the matched case[217]); interestingly, the stereochemical course is opposite to the one observed with alkyl iodides. The same reversal is found in the reaction of the amide enolate **103**[218]. By contrast, this reversal in diastereoselectivity compared to alkyl iodides was not found in the reaction of the lithium enolate **104** with the chiral oxiranes **105**[219] and **106**[220]. It should be noted that a strong matched/mismatched effect occurs for enolates **100** and **103** with chiral oxiranes, and excellent diastereoselectivities can be achieved.

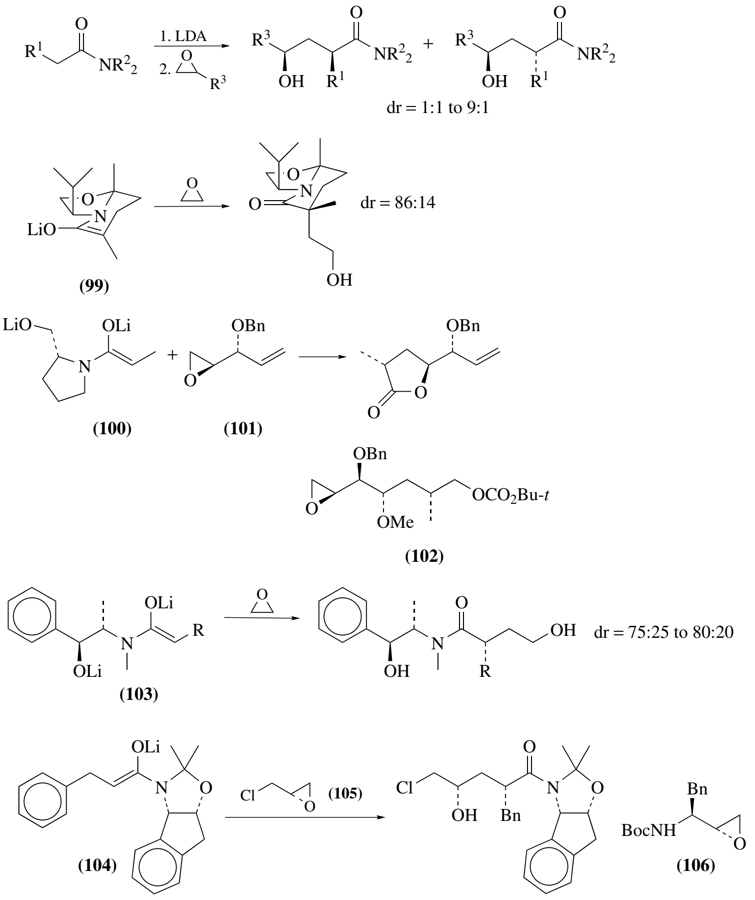

SCHEME 45

C. Enantioselective Nucleophilic Opening of Symmetrical Oxiranes by C−Li Reagents

A number of methodologies utilizing asymmetric catalytic systems has been successfully developed for the enantioselective opening of *meso* oxiranes by noncarbon nucleophiles such as halide ions, azide ion, cyanide ion and alkylamines[221]. By contrast, there are few reports of efficient processes using organometallic reagents (RMgX, R_2CuLi, R_3Al, RZnX etc.) for such a reaction. The best results have been obtained with organolithium compounds, and methods using a stoichiometric or catalytic amount of an external homochiral ligand have been developed.

1. Stoichiometric processes

The first significant advance in the field of enantioselective nucleophilic opening of oxiranes was achieved in 1996 by using an organolithium/homochiral ether combination in the presence of BF_3. Several organolithium reagents have been employed to give the

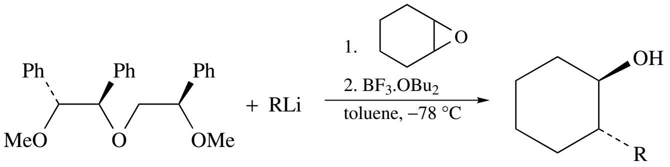

R = n-Bu : 68%, 26 %ee

PhC≡C : 93%, 22 %ee

Ph : 90%, 47 %ee

SCHEME 46

corresponding *trans*-substituted cyclohexanols in excellent yield with ee's up to 47% (Scheme 46)[222, 223].

Stronger Lewis bases such as (−)-sparteine can be used as homochiral ligand. However, an important effect of the nature of the organolithium species on the enantioselectivity is then observed. A significant ee is obtained only with aryllithium reagents. Among them, *ortho*-substituted aryllithiums give the best results, and particularly 1-naphthyllithium. Its addition to 5- to 7-membered cyclic oxiranes affords the corresponding products in moderate to good ee's (Scheme 47)[224].

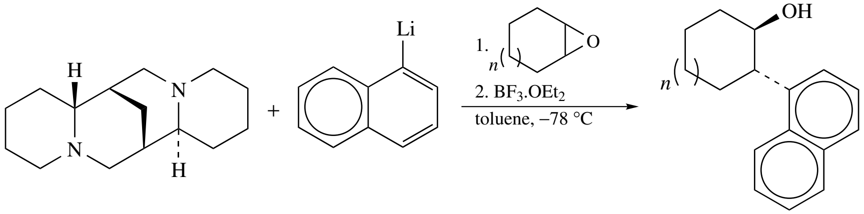

n = 0 : 78%, 53 %ee

1 : 87%, 87 %ee

2 : 71%, 52 %ee

SCHEME 47

2. Catalytic processes

The only known example of such a catalytic process was reported in 1998 for enantioselective arylation of both linear and small ring *cis* oxiranes. The oxirane is added to a precomplexed mixture of phenylithium (1.6 equivalents) and a homochiral Schiff base of type **107** or **108** (5 mol%) to afford the (S,R) ring opening product in moderate to excellent yield with ee's up to 90% (Scheme 48)[225].

The use of a catalytic amount of the homochiral ligand is here allowed by the poor reactivity of aryllithium reagents toward oxiranes, the reaction being supposed to occur through the more reactive organolithium/Schiff base complex **109**, as depicted in Scheme 49.

V. SYNTHESIS AND REACTIVITY OF LITHIOOXIRANES

Lithiooxirane intermediates were envisioned for the first time in 1951 by Cope[226] to explain the rearrangement of cyclooctatetraene oxide in the presence of organolithium

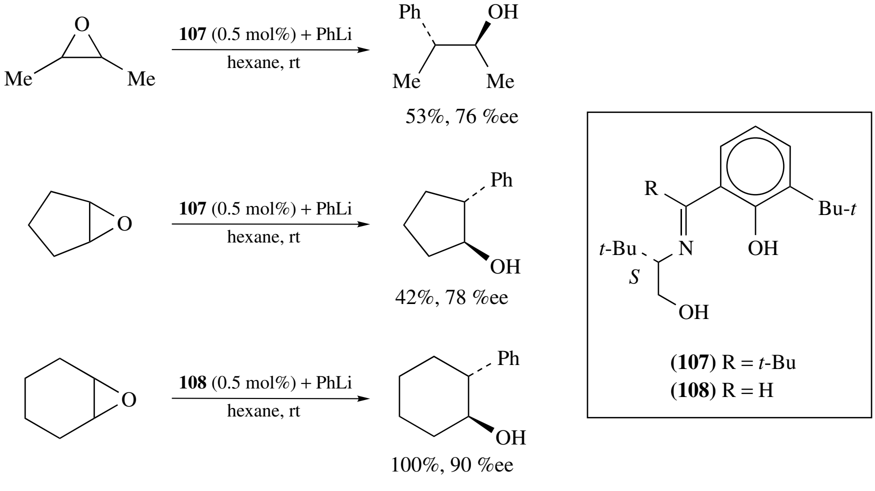

SCHEME 48

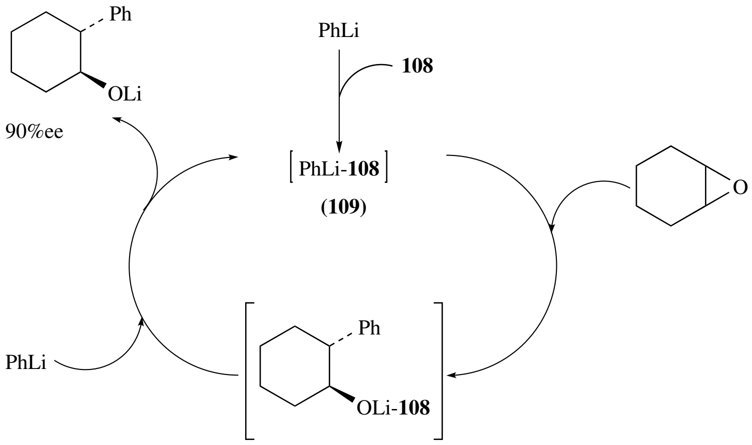

SCHEME 49

reagents; however, the first direct evidence of such a species through deuteriolysis was only reported in 1974[227]. These very reactive and unstable species show a highly versatile chemistry, which raised interest over the past years. Their preparation and reactivity has been reviewed several times[5, 25, 41, 228–231] and just general trends and recent results will be summarized here.

Lithiooxiranes can be classified into two general groups (Scheme 50): *nonstabilized lithiooxiranes* (**110**) and *stabilized lithiooxiranes* (**111**).

Their chemical behavior appears to be very different. Nonstabilized lithiooxiranes generally show a highly marked carbenoidic character and reactivity. They behave mostly as electrophiles and generally react through hydrogen or carbon migration[232, 233] as well as insertion into carbon–metal, carbon–carbon or carbon–hydrogen bonds. Relatively

(110)
R = H, alkyl

(111)
G = SiR_3, SO_2R, $P(O)(OR)_2$, CO_2R, CN, Ar, Vinyl, Alkynyl, Heterocycle

SCHEME 50

few examples of reactions with electrophiles have been reported. In contrast, when the carbanionic moieties are stabilized by an adjacent electron-withdrawing group, their thermal stability and reactivity as nucleophiles are enhanced, although the electrophilic behavior still remains. Silyl, sulfonyl, phosphinyl, trifluoromethyl, imino, oxazolinyl, alkoxycarbonyl and cyano groups induce stabilization as well as unsaturated organyl groups such as aromatic, vinyl and alkynyl moieties.

A. Generation and Reactivity of Nonstabilized Lithiooxiranes

1. Preparation of nonstabilized lithiooxiranes and reactions with external electrophiles

Nonstabilized lithiooxiranes can be prepared by the reaction of strong bases such as alkylithium reagents or lithium amides. However, as already discussed in a preceding section (Section II), the competition between α- and β-deprotonation has to be adressed, and the issue of this competition is highly dependent on the structure of the starting oxirane as well as on the nature of the base used. These lithiooxiranes are very reactive species. In order to prevent their decomposition, they can be stabilized by a diamine ligand. Further stabilization can be obtained by a remote functionality.

Terminal oxiranes have recently[234] been deprotonated by *s*-BuLi at −90 °C in the presence of various diamine ligands. The resulting lithiooxirane could be trapped by TMSCl to give *trans* epoxysilanes in good yields (Scheme 51).

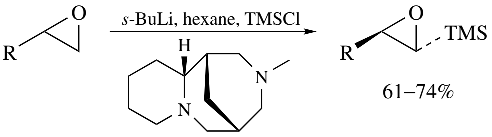

SCHEME 51

In the case of medium-size cyclic oxiranes[235], in the presence of diamine ligands, the decomposition of the oxiranyllithium intermediate can be prevented at low temperature and the lithium species can be trapped by various electrophiles (Scheme 52). The use of (−)-sparteine **112** has led to the corresponding functionalized oxiranes in good ee's.

The lithiooxirane can also be stabilized by a remote functionality in the molecule. The deprotonation of the two isomeric terminal oxiranes **113** and **114** (Scheme 53) affords the two remote carbonyl stabilized lithiooxiranes **115** and **116** which, due to this stabilization, could be trapped by various electrophiles. Deprotonation occurs stereoselectively *cis* to the ester moiety. The reaction with aldehydes gives the corresponding epoxylactones in good yields and excellent stereoselectivities[236].

Another example of remote stabilization has been reported very recently. The formation of the lithiooxirane **118** from the chlorohydrin **117** was reported[237], as well as its

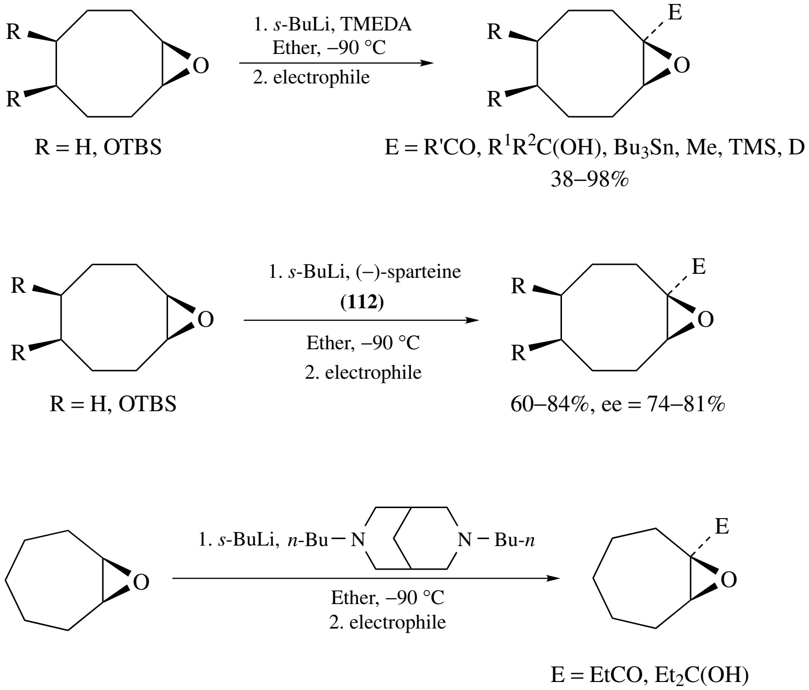

SCHEME 52

reactions with boronate reagents. The formation of **118** could be explained (Scheme 54) by the formation of an α-chlorooxirane and its transformation into **118** with n-BuLi (see Section V.B.7 for the specific reactivity of α-chloro lithiooxiranes). This lithiooxirane could be trapped by various boronate reagents to afford stereoselectively substituted trifluoromethyl olefins after 1,2-metallate rearrangement with ring opening of the oxiranyl moiety and subsequent stereospecific β-elimination processes. The relative stability and the stereochemistry of this lithiooxirane **118** was attributed to a remote stabilization by the adjacent trifluoromethyl group, through an intramolecular Li−F interaction.

A different preparation of lithiooxiranes is by the exchange reaction of an epoxy stannane or an epoxy sulfoxide with organolithium reagents. Lithiooxiranes have been prepared through tin−lithium exchange by n-BuLi in the presence of TMEDA[238]. This diamine ligand is necessary not to make the exchange easier, but, as mentioned before, to stabilize the lithiooxirane which undergoes a reductive dimerization in its absence (Scheme 55). It should be noted that retention of configuration was observed, establishing the configurational stability of these lithiooxiranes at −90 °C.

The stereospecific desulfinylation of sulfinyloxiranes has been widely reported and used in stereo- and enantioselective synthesis[239–241]. When the reaction is performed at low temperature with an excess of t-BuLi, the resulting lithiooxirane can be trapped[242, 243] by various electrophiles including carbonyl compounds, chloroformates and chlorocarbamates as well as TMSCl (Scheme 56). Here again, retention of configuration was observed at −100 °C.

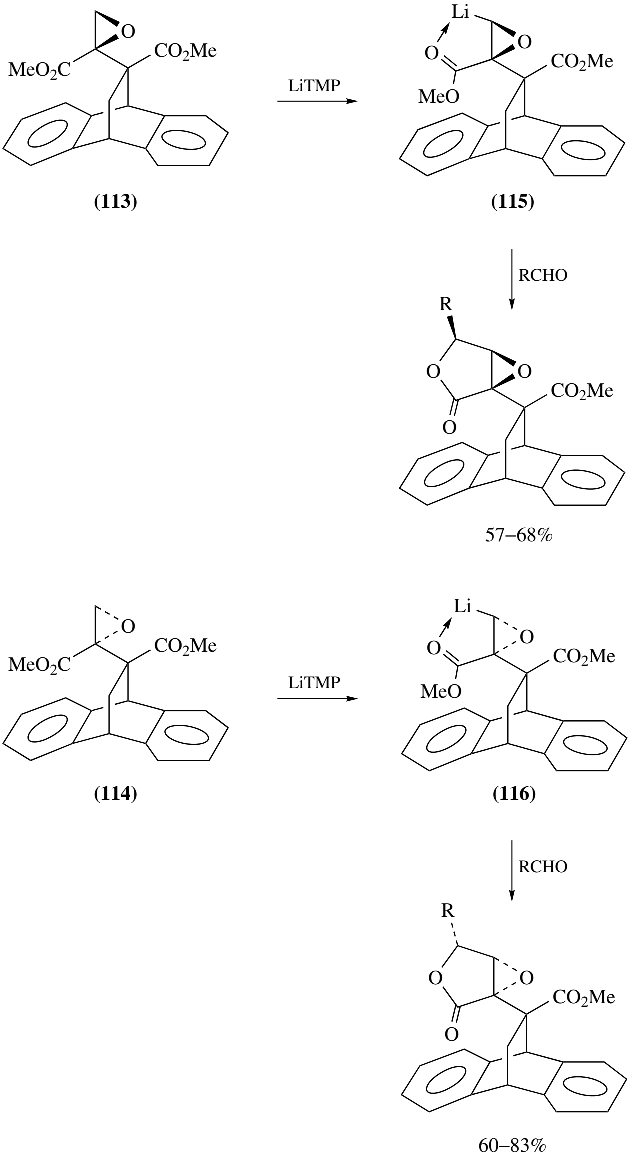

SCHEME 53

2. Electrophilic reactions of lithiooxiranes

Various electrophilic reactions of lithiooxiranes are possible, depending on the reaction conditions and particularly on the structure of the starting oxirane. These reactions can be tentatively classified into three types:

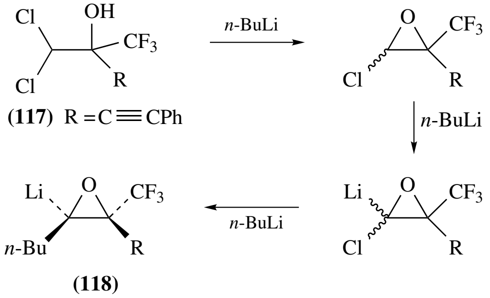

SCHEME 54

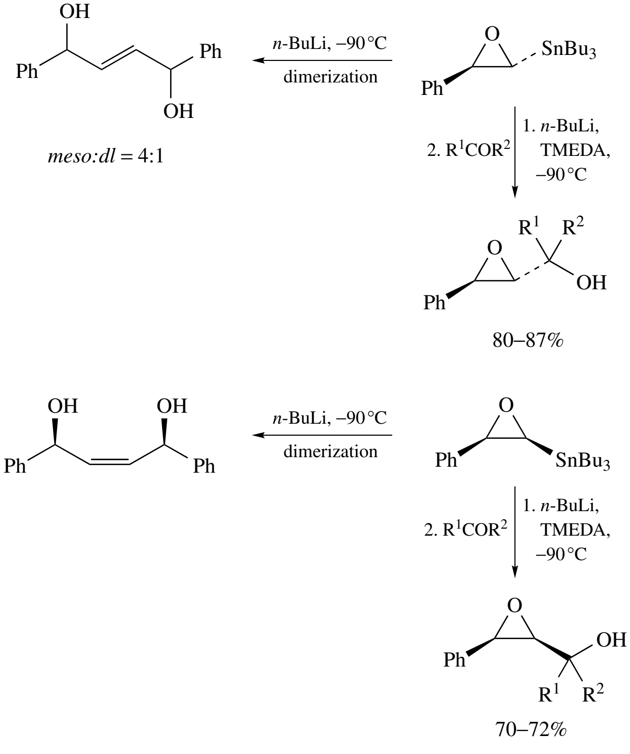

SCHEME 55

(i) Electrocyclic α-ring opening and 1,2 shifts. The rearrangement of lithiooxiranes into lithium enolates can follow two possible different pathways (Scheme 57). Starting from the same lithiooxirane **119,** electrocyclic α-ring opening (path a) can occur to give the corresponding enolate **120**, and, upon hydrolysis, the ketone **121**. The isomeric ketone **123** can be obtained through enolate **122** which arises from a 1,2-H shift in **119** (path b); in this reaction the hydrogen involved is located on the oxirane moiety. Another hydrogen

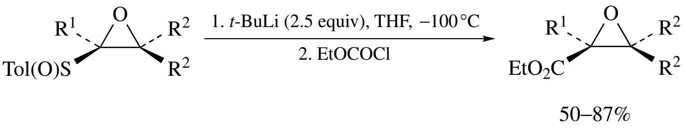

SCHEME 56

can also effect a 1,2-H shift from the other side of the oxirane (path c); by this pathway the allylic alcohol **124** is obtained. The choice between these three different pathways will be highly dependent of the structure of the starting oxirane.

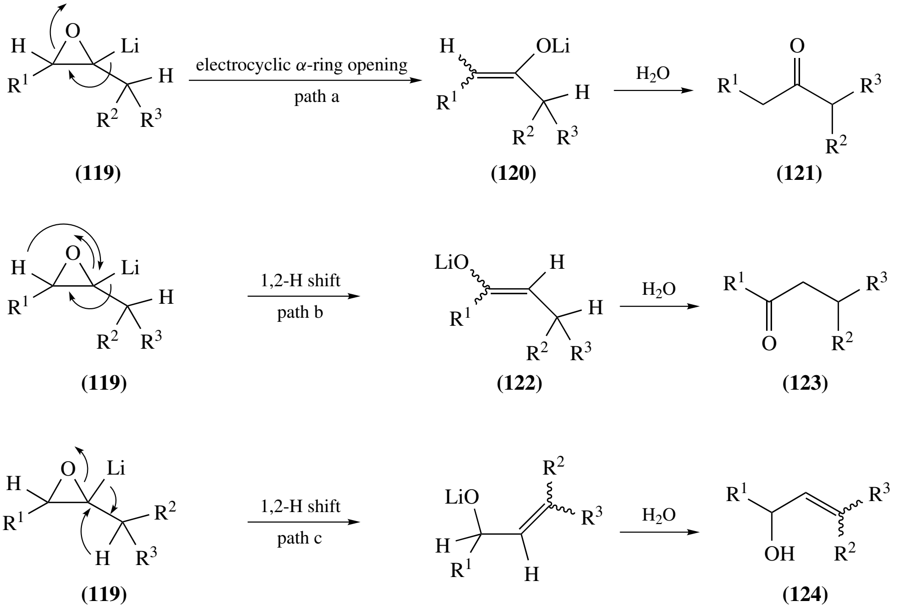

SCHEME 57

When both positions α to the C−Li bond of the lithiooxirane have no hydrogen to shift, a 1,2-alkyl shift (Scheme 58) can occur. This rearrangement has been observed recently in the case of oxiranes **125** derived from cyclopentenols. This 1,2-alkyl shift can occur on both sides of the lithiooxirane (Scheme 58, paths a and b). The resulting lithium enolate then undergoes a β-elimination process of Li_2O, leading to diversely substituted cyclopentenones **126** and **127**.

(ii) Transannular insertions. These insertion reactions of the carbenoid intermediate into C−H bonds (Scheme 59) have been widely exemplified for cyclic oxiranes **128** to give the bicyclic alcohols **129**. Medium-size oxiranes are particularly concerned by this reaction.

(iii) Reactions with electron-rich functionalities (organolithium reagents and double bonds). In many cases, when the deprotonation step is conducted with an alkyllithium compound, the intramolecular processes depicted above can be circumvented by another reaction, namely the intermolecular alkylative insertion into C−Li bonds (Scheme 60, path a). The resulting substituted β-lithio lithium alkoxide undergoes Li_2O elimination to

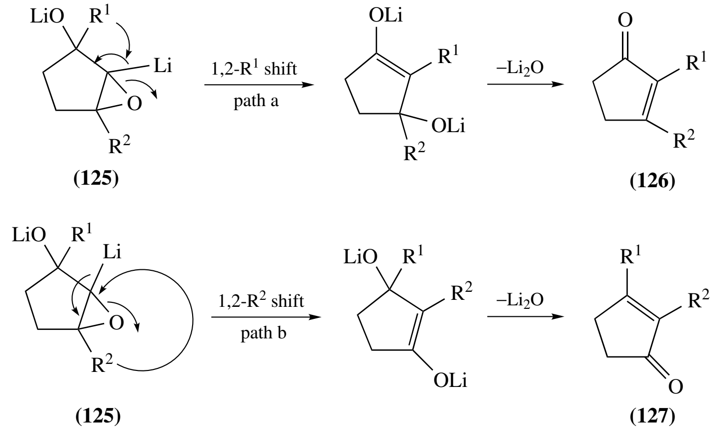

SCHEME 58

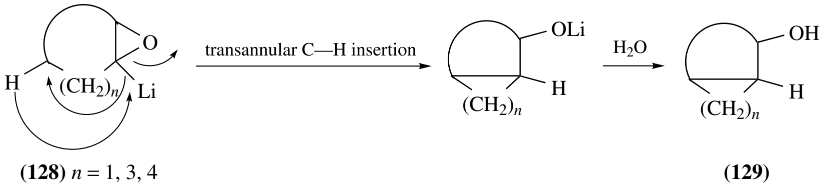

SCHEME 59

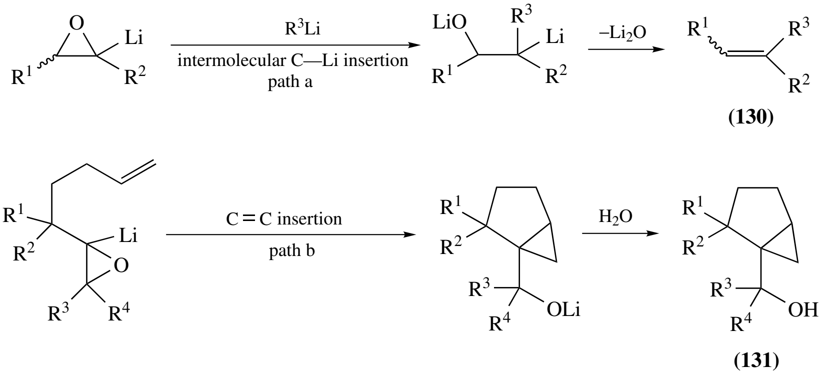

SCHEME 60

alkene **130**. On the other hand, formation of fused cyclopropanes **131** can occur through intramolecular cyclopropanation onto a double bond on the right position (path b).

Here again, all these reactions have been widely reviewed[5, 25, 41, 228, 231] and just general trends will be discussed here, with a special focus on the mechanisms. These mechanisms can involve a carbenoid rearrangement or a free carbene rearrangement. The question of the carbenoid or carbene intermediacy has been largely addressed and, in most cases, the carbenoid itself (lithiooxirane) and not the carbene has been shown to be the real reacting species. However, in some reactions, the carbenoid intermediacy has not been fully established, and true free carbenes could be involved.

a. Electrocyclic α-ring opening and 1,2 shifts. Rearrangements of lithiooxiranes into ketones can follow two distinct mechanistic pathways: electrocyclic α-ring opening (path a in Scheme 57) or 1,2-H shift (path b in Scheme 57). The choice between these two possible mechanisms is highly dependent on the reaction conditions as well as on the structure of the starting oxirane. The question of the pathway followed (α-ring opening or 1,2-H shift) in the ketone formation has been little addressed. The problem is complicated by the known[2, 20, 28, 244] ability of primarily formed allylic lithium alcoholates (through a β-elimination process) to undergo a base-induced isomerization into lithium enolates. However, in other examples, these lithium enolates have been shown to be the primary products formed directly through a rearrangement of an α-lithiooxirane[14, 15].

Early examples involving triaryloxiranes **132** show[245] that the electrocyclic α-ring opening is a possible pathway, as depicted in Scheme 61. Regioselective deprotonation of benzocyclooctene oxide **133** leads to the ketone **134** through electrocyclic α-ring opening (along with a noticeable amount of transannular rearrangement product)[26]. The base-induced rearrangement of terminal oxiranes into aldehydes[246] has been shown to involve electrocyclic α-ring opening through experiments with labeled oxiranes **135** and **136** (Scheme 61).

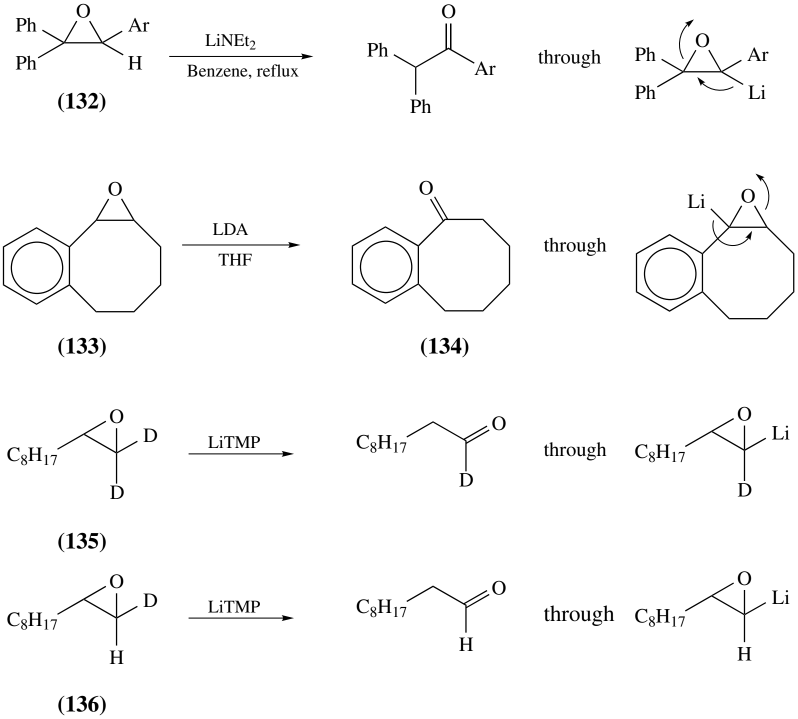

(132)

(133) **(134)**

(135)

(136)

SCHEME 61

In contrast, a 1,2-H shift mechanism for different types of oxiranes has also been reported. For example, the regioselective deprotonation of benzocycloheptene oxide **137** gives the ketone **138** (Scheme 62)[247]. This result strongly contrasts with the rearrangement of **133** into **134** in Scheme 61. Similarly, the rearrangement of the *cis,cis*-diene monoepoxide **139** gives a mixture of ketones arising from a 1,2-H shift in the oxiranyllithium intermediate and a partial subsequent double-bond migration upon hydrolysis[29]. The rearrangement of *trans* β-methylstyrene oxide **140** gives a mixture of three products: the allylic alcohol **141** and the two ketones **142** and **143**[28]. The latter arises from the 1,2-H shift from the benzylic α-lithiooxirane, whereas the former is produced by a

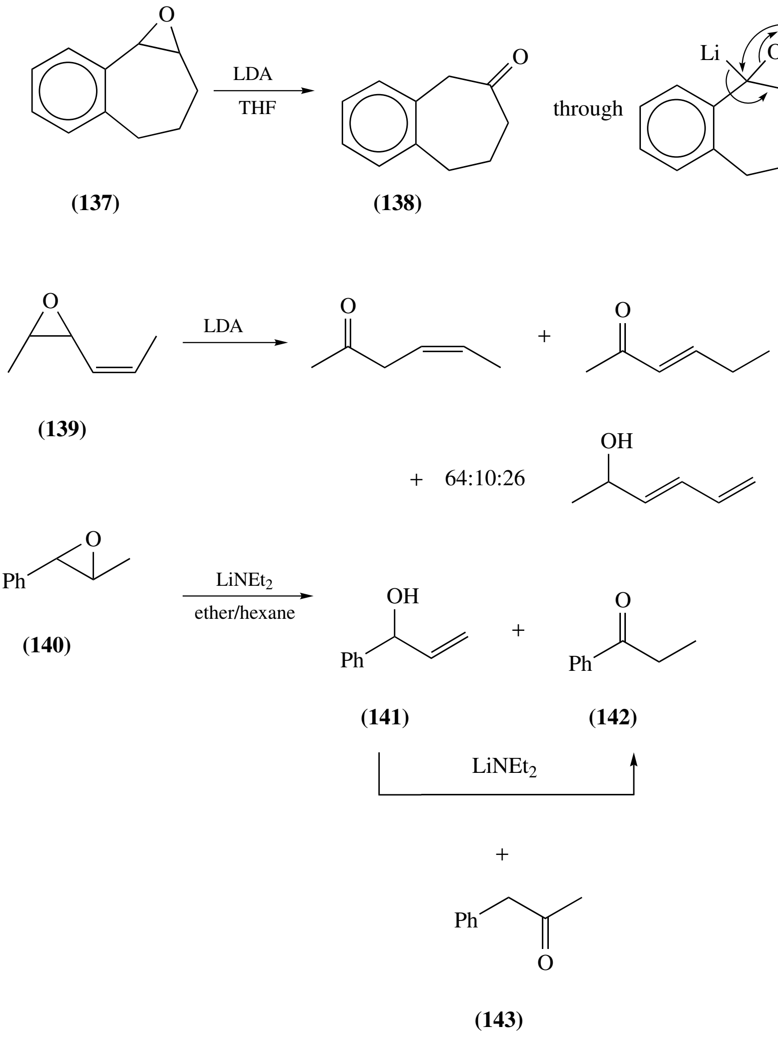

SCHEME 62

base-induced isomerization from the allylic alcoholate corresponding to **141**. Interestingly, the rearrangement of *cis* β-methylstyrene oxide is much slower and gives mainly the ketone **142** from isomerization of **141**.

The deprotonation of *meso* oxiranes **144** and **145** by the system alkyllithium/diamine leads to the enantiomeric ketones (*S*)- and (*R*)-**146** (Scheme 63)[248]. Due to the general propensity of these systems to achieve deprotonation at the *R* carbon of the oxirane ring, it was then concluded that this rearrangement follows exclusively a 1,2-H shift.

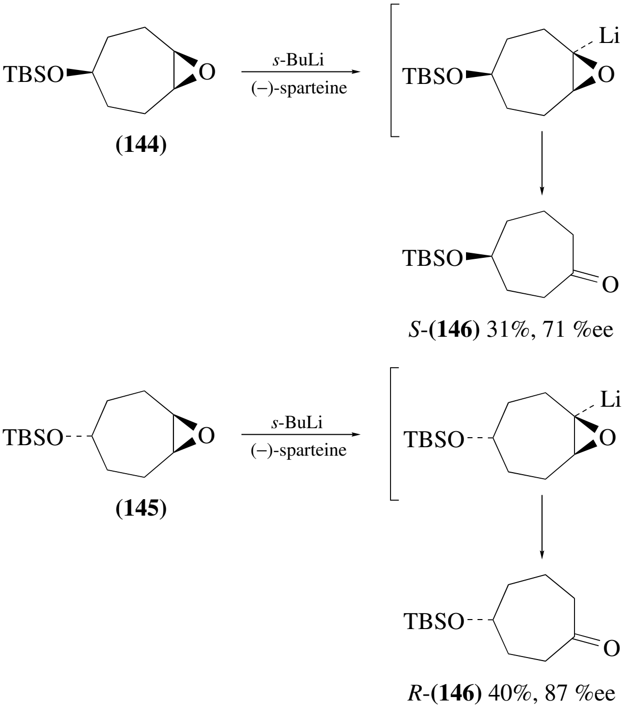

SCHEME 63

The enantioselective formation of bicyclic ketones through enantioselective deprotonation of the bicyclooxiranes **147, 148** and **149** (Scheme 64) by homochiral lithium amides (such as **50**) and subsequent rearrangement have also been reported with moderate enantiomeric excesses and yields[86, 249].

It should be noted that whereas *endo* norbornene oxide **148**, when reacting with lithium amides, gives mainly the corresponding ketone, the isomeric *exo* norbornene oxide **17** gives mainly[7] the transannular insertion product (see Section V.A.2.b). In the same way, when oxirane **150** or **36**[5] react with LDA or $LiNEt_2$, the transannular insertion product is obtained, whereas for the reaction of **149** with the chiral lithium amide **50**, the rearrangement product is obtained predominantly. This shows that the behavior of lithiooxiranes is highly dependent on the structure of the starting oxirane, as well as on the nature of the base. For example, the use of a lithium amide–lithium alcoholate mixture instead of lithium amide alone enhances the deprotonation rate[250], and then the subsequent rearrangements.

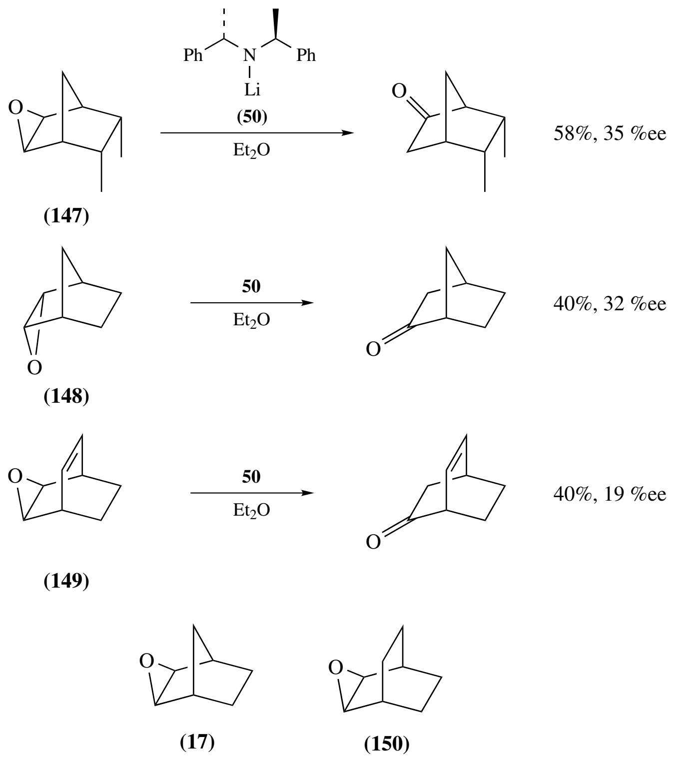

SCHEME 64

It has been shown recently (see Section II.A) that the base induced rearrangement of cyclopentene oxide into 3-cyclopentenol **151** follows an α-deprotonation pathway. The allylic alcohol is obtained through a 1,2-H shift (Scheme 65). The product distribution in the rearrangement of lithiated cyclopentene oxide has been compared[251] to the product distributions obtained through the thermal or photolytic decomposition of the two cyclopentenol azirines **152** and **153** through the corresponding carbenes **154** and **155**. Whereas no cyclopentanone is formed from the lithiooxirane, this represents the main product from the rearrangement of carbenes. Calculations indicate that the rearrangement from carbene **154** to cyclopentanone is favored over the rearrangement to cyclopentenol by 6.4 kcal mol^{-1}. From **155**, this value is higher (7.1 kcal mol^{-1}). These values indicate that the 1,2-H shift rearrangement occurs mainly from the carbenoid itself (lithiooxirane) and *not* from the alkoxy carbene **155**.

Concerning the possible rearrangement of the lithiooxirane into the alkoxy carbene **155**, calculations have also shown that the activation energies of the 1,2-H shifts (to cyclopentanone enolate or cyclopentenol) are extremely high (at least 23 kcal mol^{-1}) from **155**, whereas they are much lower (between -0.4 kcal mol^{-1} and 8.8 kcal mol^{-1}) from carbene **154**. This is explained by a strong intramolecular stabilization of the carbene by the alcoholate moiety, as depicted in Scheme 66. This stabilization could signify that the formation of a carbene from the carbenoid is a disfavored process, and that the carbenoid itself is involved in the rearrangement reaction.

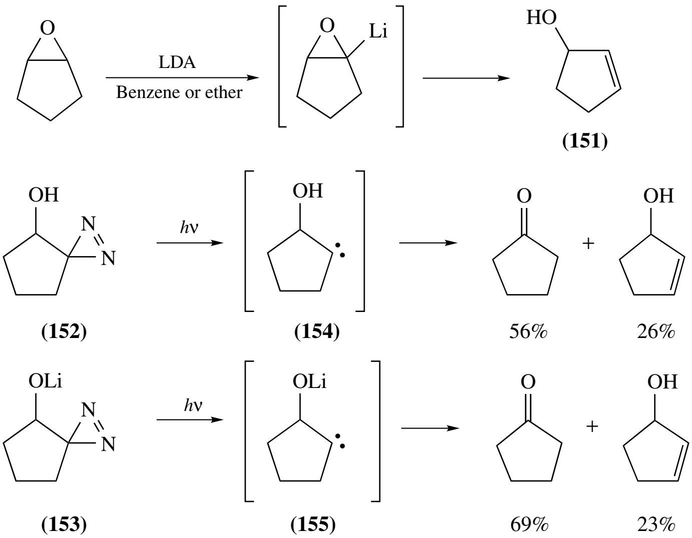

SCHEME 65

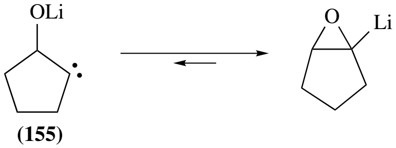

SCHEME 66

Recently, interesting examples have been reported of 1,2-alkyl shift (paths a and b in Scheme 58) in the rearrangement of substituted cyclopentenol and -hexenol oxides[10, 11, 230]. These examples are limited to oxiranes with no hydrogen α to the oxiranyl ring. Starting from the same disubstituted cyclopentenol **125**, R^1 migration leads to the lithium enolate **125a** which could be quenched by TMSCl. The treatment of the reaction mixture in mild acidic aqueous medium leads to the cyclopentenone **126** after elimination of Li_2O (Scheme 67). On the other hand, R^2 migration yields the isomeric cyclopentenone **127** after elimination of Li_2O. The relative migratory aptitude of various alkyl substituents has been determined and follows the general order: hydride > methyl > *n*-butyl > aryl > *t*-butyl. The presence of the lithium alkoxide moiety α to the oxirane ring is important, as the same reaction, when performed on similar substrates but bearing a methoxy group in place of the alkoxide group, leads mainly to intra- or intermolecular insertions (see Sections V.A.2.b and V.A.2.c).

It is noteworthy that the ratio between the two possible migrations is also dependent on the starting oxirane. The rearrangement starting from oxirane **156** gives the two ketones **157** and **158** in a 50:50 ratio (Scheme 67), whereas the rearrangement starting from the oxirane **159** yields to **157** and **158** in a 10:90 ratio. This provides good evidence of the carbenoid nature of the reacting species (**160** and **161),** as the corresponding carbenic species **162** should be symmetrical and should not show any selectivity in the cyclopentenone formation. The reaction has been extended to six-membered oxiranes, but acyclic substrates react exclusively through a classical β-elimination pathway.

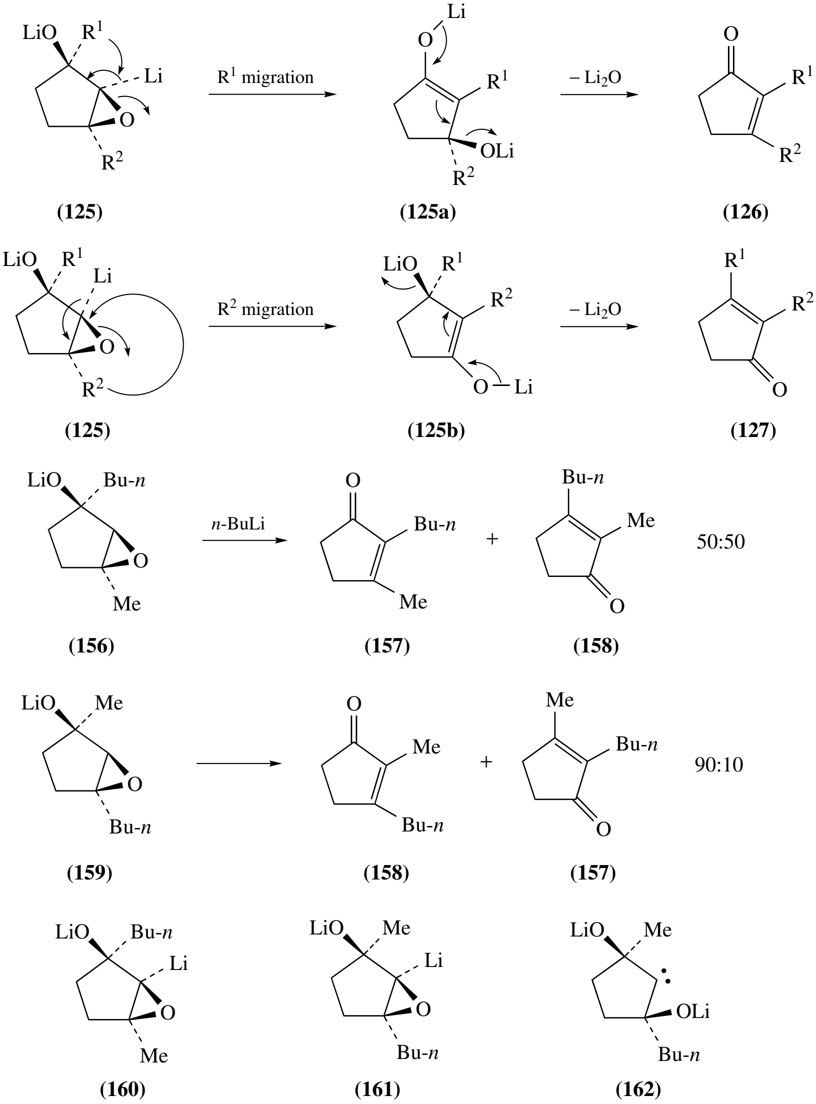

SCHEME 67

b. Intramolecular insertions into C—H bonds. The intramolecular insertion of lithiated oxiranes into C—H bonds has been initially observed for medium-size oxiranes (seven- to ten-membered rings), as cyclooctene oxides **24** and **163**[252] (Scheme 68), or cyclodecene oxides **164** and **165**[253]. The predominance of this pathway over other possible pathways has been attributed to conformational properties of the lithiooxirane intermediate[5, 26]; for the same reason, this predominance can be precluded for substituted medium-size oxiranes[244]. This reaction is also widely observed in the case of bicyclic oxiranes where

Bredt's rule and the blocked conformation (see Section II.A) precludes the allylic alcohol formation, such as norbornene oxide **17**[254, 255]. However, it has been very seldom reported in the case of linear oxiranes[256]. The intermediacy of a true carbenoid species has been established by the stereospecific formation of *exo* or *endo* bicyclic alcohols starting from the isomeric *cis* or *trans* oxiranes, and has been explained[5] in terms of 'backside' insertion; however, this stereoselectivity is not observed in some cases. Here again, this stereospecificity implies that the lithiooxirane intermediate retains its stereochemistry before and during the insertion process.

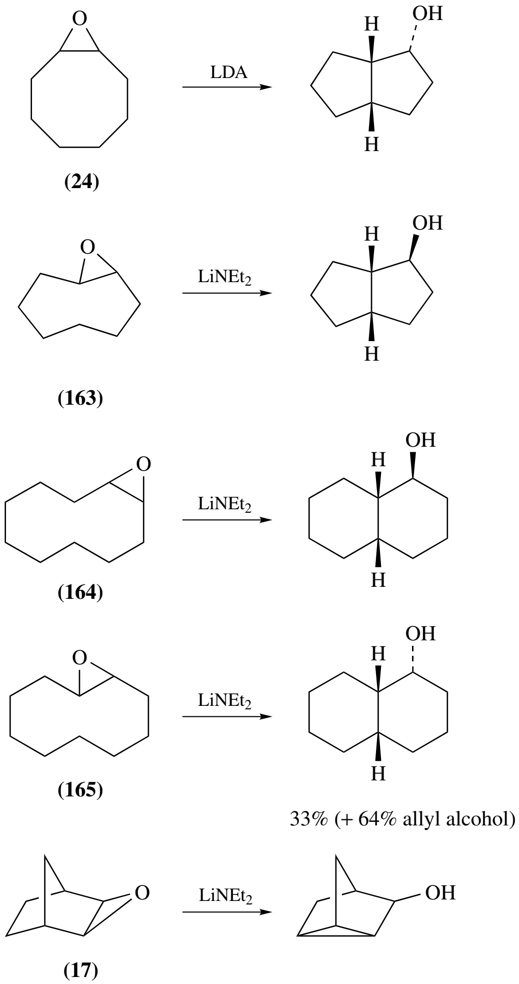

SCHEME 68

In the case of cyclooctene oxide **24**, the nature of the base used has a direct influence on the competition between α- and β-deprotonation, as already discussed in Section II.

1,5 and 1,6 C−H insertions are the most common rearrangements described in the literature. However, some examples of 1,3 C−H insertions, already depicted above in the case of norbornene oxides, are reported in other series[5]. For example (Scheme 69), 1-epoxy-5-cyclooctene **83** rearranges in the presence of HMPA into the bicyclo [5.1.0] octanol **166** through 1,3 C−H insertion[21]. It should be noted that 1-epoxy-3-cyclooctene **167** leads to the bicyclo [3.3.0] octenol **168** through 1,5 C−H insertion[20]; of course, assuming that deprotonation occurs on the more acidic allylic position, there is no longer any possibility of 1,3 C−H insertion. Other examples of 1,3 C−H insertions in the cyclopentene oxide series have been reported[257], as for compounds **169**. These compounds, when treated with organolithium compounds, lead to a mixture of the two compounds **170** (through intramolecular 1,3 C−H insertion) and **171** (through intermolecular C−Li insertion). Interestingly, the competition between these two processes was found to be dependent on the solvent polarity, although mixtures were generally obtained.

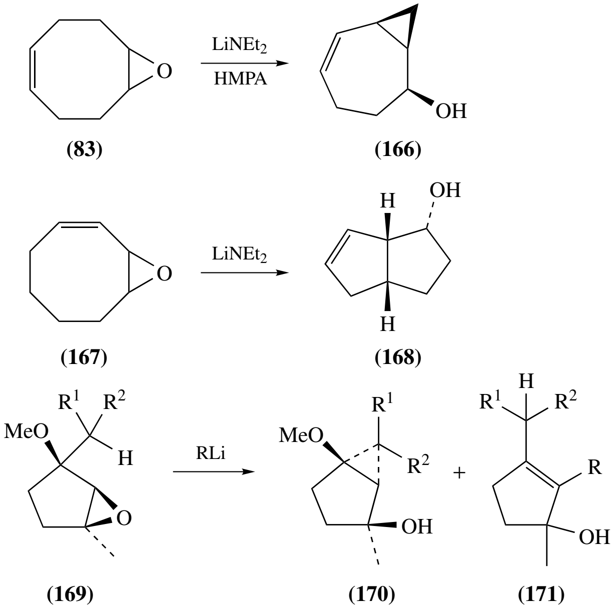

SCHEME 69

The accelerating influence of an external Lewis acid is very important on the alkylative ring opening of oxiranes (see Section IV), but also on the rate of the rearrangement reactions. For example, the rearrangement of **167** into **168** must be conducted[20] in refluxing ether when using lithium diethylamide as a base (Scheme 69). By contrast, in the presence of BF_3, the reaction takes place within 10 min at −78 °C[90]. This accelerating effect can be interpreted in terms of a stronger carbenoidic character of the lithiooxirane intermediate. However, the stereoselectivity of the reaction is still excellent, as even in the presence of BF_3 the reaction of cyclooctene oxide leads to the bicyclic alcohol as only one diastereomer.

The presence of BF_3 in the reaction can also have an effect on the α- vs. β-deprotonation regioselectivity. The oxirane **83** (Scheme 70), when treated with the mixture *s*-BuLi/(−)-sparteine, leads to the cyclooctadiene alcohol **172** (through a β-deprotonation process[258]), whereas in the same conditions but in the presence of BF_3 the bicyclic compound **166** is obtained (through an α-deprotonation process). Presumably, the high yield in the rearranged product **166** can be interpreted by the higher acidity of the oxiranyl protons in the presence of BF_3, or by an enhanced carbenoidic character of the lithiooxirane intermediate, or both. Interestingly, in all these reactions, the presence of BF_3 is compatible with the diamine ligand.

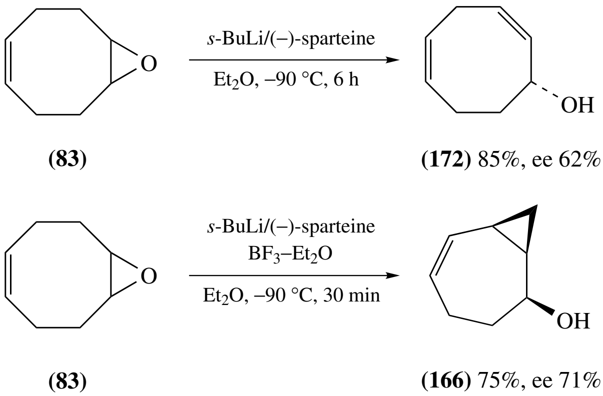

(83) **(172)** 85%, ee 62%

(83) **(166)** 75%, ee 71%

SCHEME 70

The enantioselective version of the intramolecular C−H insertion has been extensively studied[231]. The key step is the enantioselective deprotonation of *meso* oxiranes, as already depicted above (see Section II.A.1). The resulting enantioenriched lithiooxirane can be trapped by electrophiles, but by raising the temperature it undergoes the C−H insertion reaction to yield the enantioenriched bicyclic alcohols. The best results have been obtained by using a combination of an alkyllithium (*i*-PrLi or *s*-BuLi) with a chiral diamine, generally (−)-sparteine **112** (Scheme 71). In some cases, (−)-α-*iso*sparteine **173** give better results. Due to the fact that both **112** and **173** exist as only one naturally occurring enantiomer, some other diamine ligands have been developed. Among them, the bisoxazoline **174**[259] and very recently the diamine **175** derived from (−)-cytisine[260] have been shown to be efficient surrogates of (+)-sparteine. Several representative examples[86–88, 90,259–262] are listed in Scheme 71, and an other has been already depicted in Scheme 70.

An interesting related rearrangement reaction has been reported[87, 263]. This rearrangement involves (Scheme 72) the intramolecular nucleophilic attack of a nitrogen atom on the electrophilic lithiooxirane formed through deprotonation. The resulting nitrogen ylide undergoes a Stevens-type rearrangement to give an indolizidine in a moderate yield and a good ee.

c. Intermolecular C−Li insertions. Lithiooxiranes can react as electrophiles with organolithium reagents in an intermolecular fashion. This reaction is of course

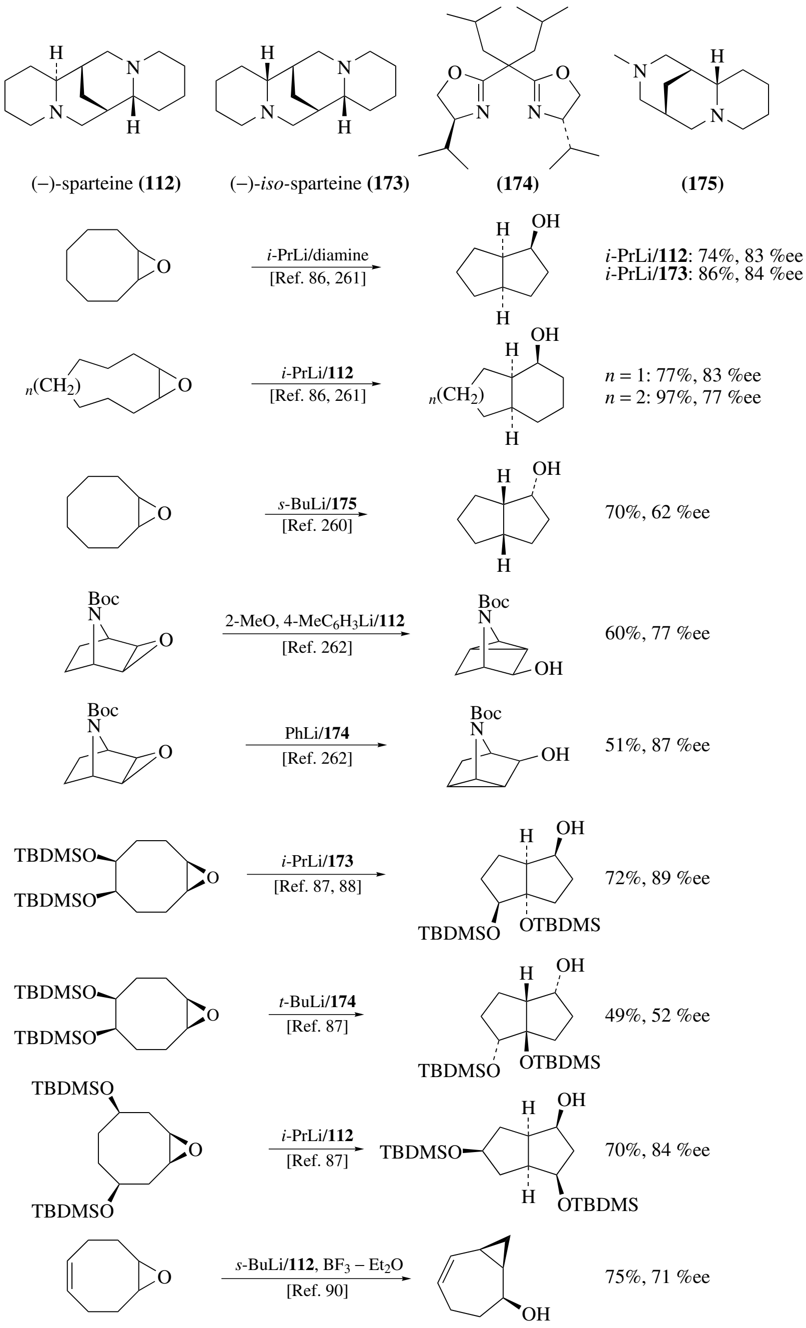
H
N
N
H
(−)-sparteine (112)
H
N
N
H
(−)-*iso*-sparteine (173)
O
N
N
O
(174)
N
H
N
(175)
O
i-PrLi/diamine
[Ref. 86, 261]
H
OH
H
i-PrLi/112: 74%, 83 %ee
i-PrLi/173: 86%, 84 %ee
$_n$(CH$_2$)
O
i-PrLi/112
[Ref. 86, 261]
H
OH
$_n$(CH$_2$)
H
n = 1: 77%, 83 %ee
n = 2: 97%, 77 %ee
O
s-BuLi/175
[Ref. 260]
H
OH
H
70%, 62 %ee
Boc
N
O
2-MeO, 4-MeC$_6$H$_3$Li/112
[Ref. 262]
Boc
N
OH
60%, 77 %ee
Boc
N
O
PhLi/174
[Ref. 262]
Boc
N
OH
51%, 87 %ee
TBDMSO
TBDMSO
O
i-PrLi/173
[Ref. 87, 88]
H
OH
TBDMSO
OTBDMS
72%, 89 %ee
TBDMSO
TBDMSO
O
t-BuLi/174
[Ref. 87]
H
OH
TBDMSO
OTBDMS
49%, 52 %ee
TBDMSO
O
TBDMSO
i-PrLi/112
[Ref. 87]
H
OH
TBDMSO
H
OTBDMS
70%, 84 %ee
O
s-BuLi/112, BF$_3$ – Et$_2$O
[Ref. 90]
OH
75%, 71 %ee

SCHEME 71

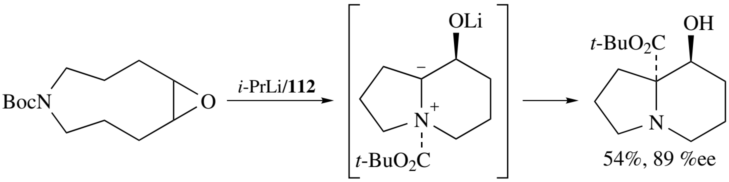

SCHEME 72

limited to cyclopentene or cyclohexene oxide-type oxiranes (as medium-size cyclic lithiooxiranes undergoes mainly transannular C−H insertions), but is also efficient with linear oxiranes. Actually, as the base is the organolithium itself and not a lithium amide, the β-deprotonation reaction leading to allylic alcohols is generally avoided or limited (see Section II.B). The substituted organolithium reagent formed by the C−Li insertion undergoes generally a β-elimination reaction of Li_2O with the lithium alcoholate[230, 256, 264–267], but other β-elimination processes[257, 268–270] are reported (Scheme 73).

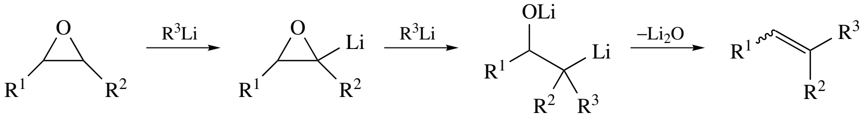

SCHEME 73

Although early works have reported variable yields and substrate dependence, a marked tendency to stereospecificity has been noticed. For example, the reaction of the *trans* epoxysilane **176** (Scheme 74) with lithium reagents results, after Si−Li exchange, electrophilic trapping of the resulting lithiooxirane by RLi and Li_2O elimination, in the stereoselective formation of an (*E*) alkene in good yield[271].

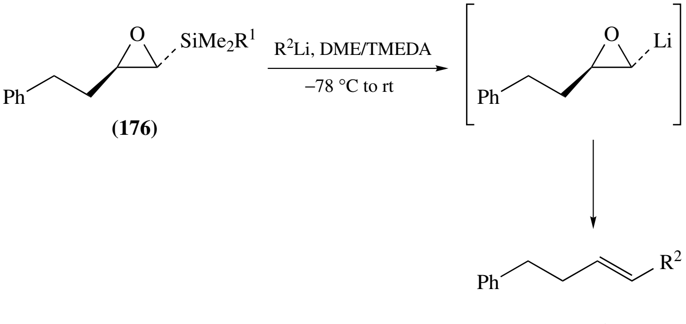

(176)

SCHEME 74

More recently[267], the stereochemical course of the reaction with linear oxiranes has been fully examined and high stereospecificity has been evidenced. Several representative examples are depicted below in Scheme 75.

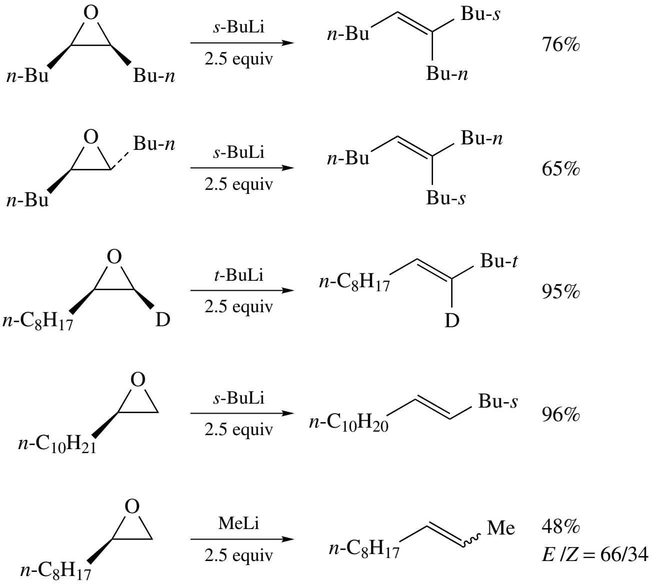

SCHEME 75

The results are consistent with an *anti* substitution reaction, followed by a *syn* Li_2O elimination process. Alternatively, a *syn* substitution reaction followed by an *anti* Li_2O elimination process can also be envisioned (Scheme 76). These results imply again that the initially formed lithiooxirane retains its configurational integrity on the time scale of the reaction, and that the insertion step is stereospecific. In the case of terminal oxiranes, a high tendency in the deprotonation of the unsubstituted carbon of the oxirane was noted, but the stereoselectivity in the deprotonation reaction was variable, depending on the steric demand of the starting organolithium reagent.

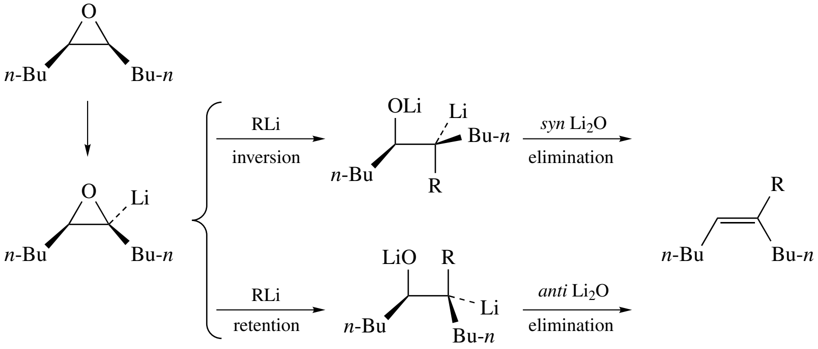

SCHEME 76

The β-elimination of Li_2O can be prevented if a better leaving group (generally an ether moiety) is present in a β-position to the organolithium reagent formed through the insertion (substitution) process. A substituted allyl alcohol is then obtained starting from an allyl ether oxide (Scheme 77). It should be noted that when the methoxy group in **177a** or **177b** is replaced by a hydroxy group, the reaction follows a totally different pathway (1,2-alkyl shift, see Section V.A.2.a, or Payne rearrangement).

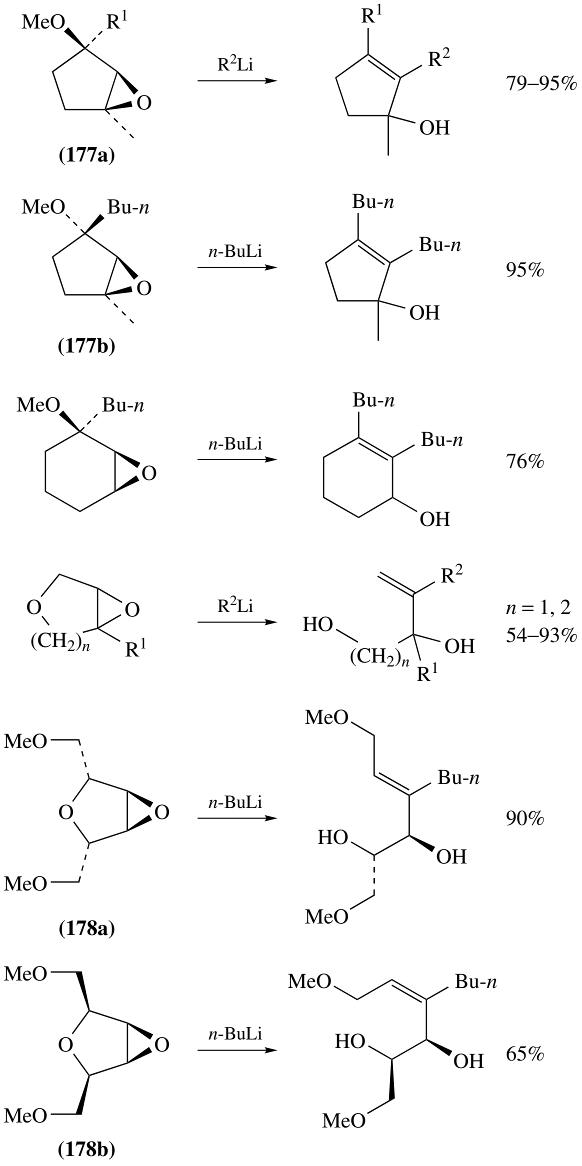

SCHEME 77

Although the observed stereospecificity in the reaction of **178a** and **178b** was given[269] as a proof of a mechanism involving a C—Li insertion with inversion followed by an *anti* β-elimination process, the identical behavior of compounds **177a** and **177b** shows[268] that the β-elimination process after the insertion can follow indifferently both *syn* and *anti* pathways. It then seems difficult to conclude unequivocally about the stereochemical course of the C—Li insertion. However, this step is more likely a reaction with inversion, by analogy with similar 1,2-metallate rearrangements on other carbenoids[272–275]. Application of these processes in the case of *meso* oxiranes, in the presence of chiral ligands as sparteine **112** or bisoxazoline **174**, has recently[276] been reported, leading to substituted allylic alcohols in moderate to good ee's.

d. Cyclopropanations. The lithiooxiranes can react, in some cases, intramolecularly with a double bond in the proper position to afford[10,277,278] fused cyclopropanes (Scheme 78). This reaction occurs stereospecifically and the stereochemical information of the double bond is retained, thus again establishing the full carbenoidic character[279] of the lithiooxirane in this reaction. In the case of oxiranes **179** derived from 3-methoxy cyclopentene, the resulting tricyclo[4.1.0.0.1.5]heptanols **180** can be obtained. These highly strained compounds are very unstable (although one could be isolated and fully characterized) and rearrange readily and stereospecifically to spiro[2.4]heptan-4-ones **181**.

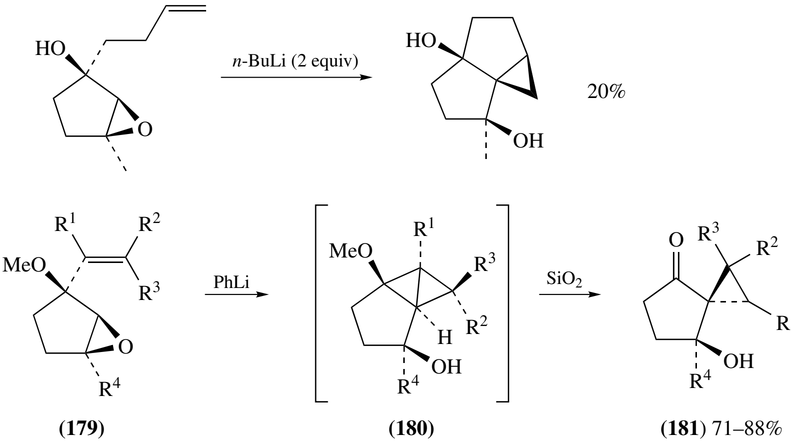

SCHEME 78

B. Generation and Reactivity of Stabilized Lithiooxiranes

Compared to nonstabilized lithiooxiranes, the chemistry of stabilized lithiooxiranes is much simpler, as the presence of an electron-withdrawing group greatly diminishes the electrophilic character of the lithiooxirane. These species behave then as common lithium nucleophiles and react readily with various electrophiles, although in certain cases some electrophilic character still remains. Their thermal stability is enhanced and depends on the nature of the electron-withdrawing group. As mentioned above, several stabilizing groups have been used. The chemistry of epoxysilanes[280,281] and epoxysulfones[229,282] has been largely studied and reviewed, but other lithiooxiranes stabilized by unsaturated groups (aromatic and heteroaromatic, alkenyl and alkynyl groups), carbonyl groups and analogues (ketone, ester, nitrile, imine and oxazolidine groups) as well as the trifluoromethyl group and chlorine have been studied and reported. The generation and reactivity of these stabilized lithiooxiranes will be discussed here briefly. The special case of α-chlorooxiranes will be discussed separately.

1. Silicon-stabilized lithiooxiranes

The deprotonation of epoxysilanes and subsequent trapping of the resulting lithiooxirane by various electrophiles was first achieved at the end of the 1970's[265, 283, 284]. The configurational stability at −78 °C of the lithiooxirane derived from **182** has been shown[265] (Scheme 79). However, the analogous lithiooxirane derived from **183** has been found[285] to be configurationally unstable at the same temperature, presumably due to the remote substitution. By contrast, at lower temperature, the configurational stability of lithiooxiranes stabilized by a TMS group (lithiooxiranes derived from epoxysilanes **184** and **185**) was shown[24, 280], as well as the configurational stability of lithiooxirane derived from the vinylic epoxysilane **186**[126] or from the strained epoxysilane **187**, which has been used in a synthetic approach to spatol[286]. Configurational instability was noticed only for one epoxysilane (**188**). It should be noted that at low temperature, the deprotonation rate is highly dependent on the stereochemistry of the starting epoxysilane. When *cis* epoxysilanes can be deprotonated at −116 °C within 10 min, the corresponding *trans* epoxysilanes require 4 h at the same temperature to achieve completion of the deprotonation. In some cases, it was reported that the *cis* epoxysilane is readily deprotonated, whereas the *trans* epoxysilane undergoes ring opening[126] or Si−Li exchange[271]. This was explained[24, 280] by the higher steric hindrance in the initially formed epoxysilane−alkyllithium complex in the *trans* case before the deprotonation step (Scheme 79, see also Section III.A).

These lithiooxiranes can be trapped by various electrophiles with retention of the configuration. The addition to aldehydes occurs with a low diastereoselectivity[24, 280, 126] [but this can be enhanced by adding $ClTi(OPr\text{-}i)_3$]. The reaction with enones occurs in a 1,2 fashion only. Intramolecular 1,4-silicon shift has also been reported[287]. The reaction of the enantiomerically pure TMS-stabilized lithiooxirane **189** (Scheme 80) with an aldehyde has been used in a total synthesis of (+)-cerulenine[288]. It must be noted that protodesilylation using TBAF (tetrabutylammonium fluoride)[289] occurs with conservation of the oxirane stereochemistry.

Only one example of electrophilic behavior of silicon-stabilized lithiooxiranes is reported. Intermolecular C−Li insertion followed by Li_2O elimination occurs by raising the temperature[271], and (*E*) vinylsilanes are obtained stereoselectively (Scheme 80). Reaction of lithiooxiranes with aluminum[285], zirconium[290] and silicon[291−293] reagents leads to the corresponding ate complexes, which undergo 1,2-metallate rearrangements.

2. Sulfur-stabilized lithiooxiranes

Since the end of the 1980's, fundamental studies[294−298] as well as synthetic applications[229,299−308] have shown that the carbanion derived from the deprotonation of an epoxysulfone reacts with retention of configuration, regardless of the initial stereochemistry of the epoxysulfone. The carbanion derived from an (*E*)-epoxysulfone is reasonably configurationally stable at −95 °C. By contrast, the carbanion derived from a (*Z*)-epoxysulfone is much less configurationally stable, beginning to isomerize within 3 min[297] at −100 °C to the more stable (*E*)-isomer (Scheme 81). However, carrying out the deprotonation at −100 °C under Barbier conditions circumvents this isomerization and degradation[297, 300].

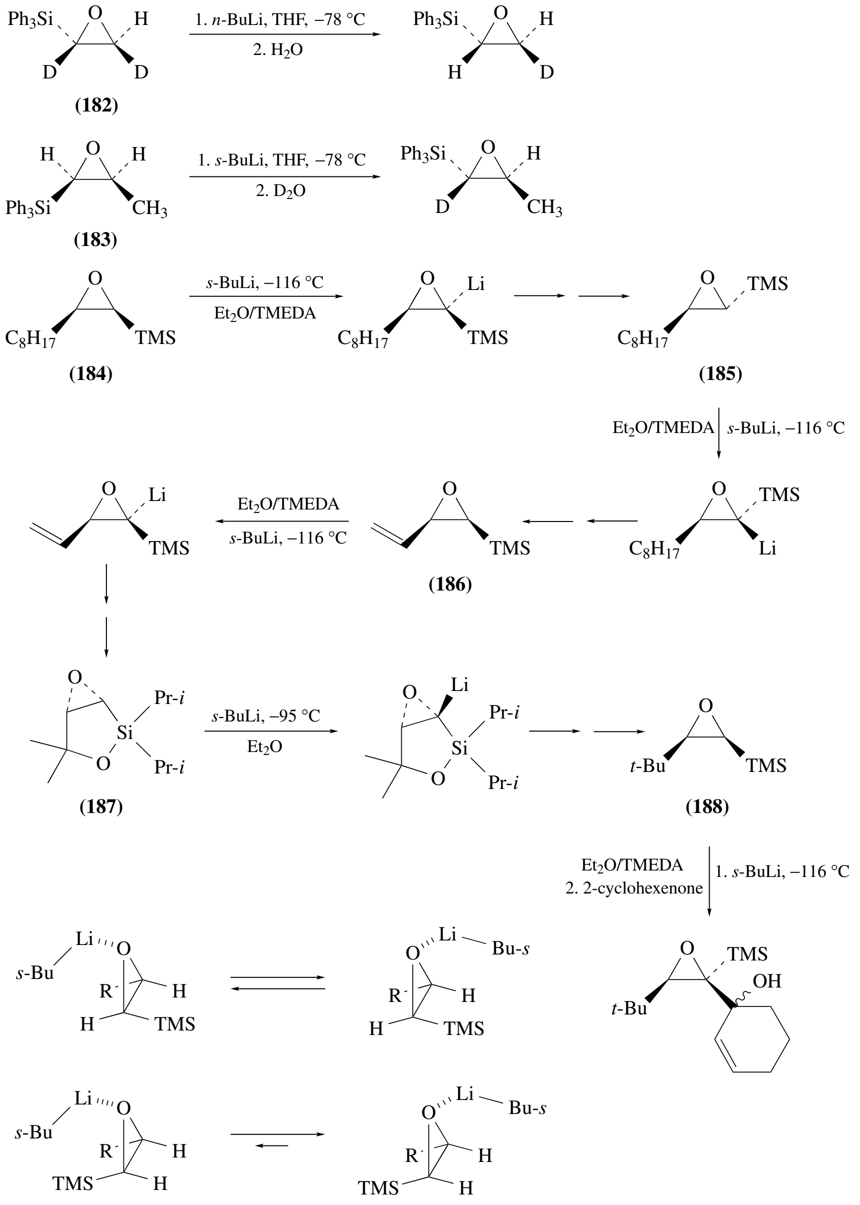

SCHEME 79

Treatment of sulfoximinooxiranes with MeOLi in MeOD results in H−D exchange with retention of configuration. However, all attempts to achieve deprotonation of these sulfoximinooxiranes using the same conditions as sulfonyloxiranes lead only to decomposition products[309] (Scheme 81).

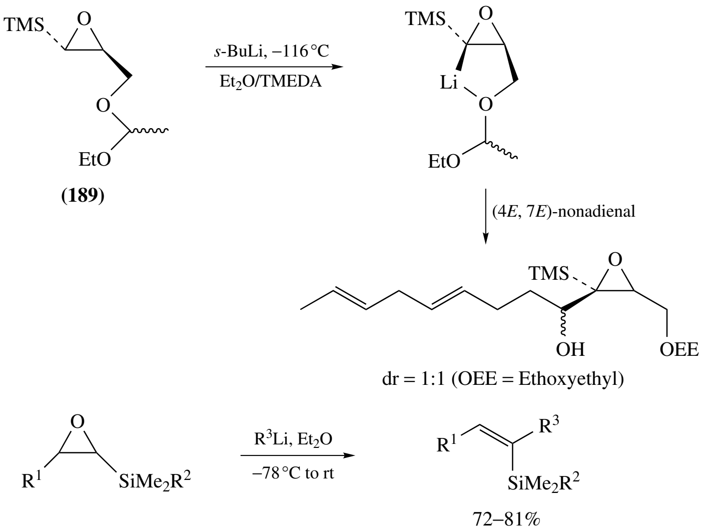

SCHEME 80

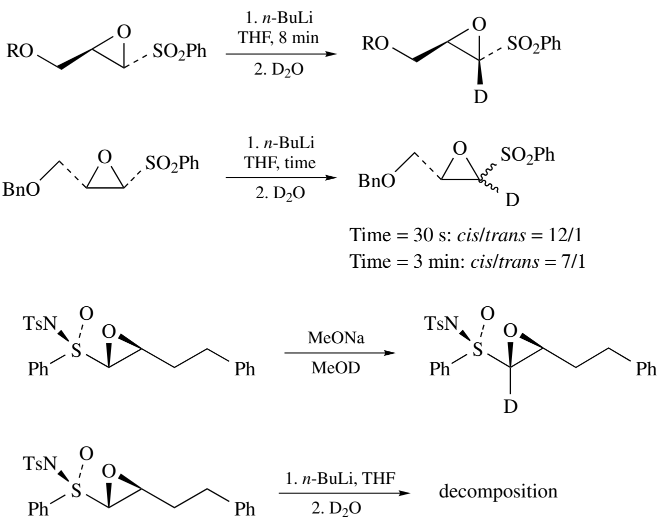

SCHEME 81

3. Alkenyl-, alkynyl-, aryl- and heteroaromatic-stabilized lithiooxiranes

Oxiranes bearing an alkenyl or an aryl moiety as stabilizing group can be deprotonated by *s*-BuLi[310] or *t*-BuLi[311] in the presence of TMEDA. In the case of an alkynyl moiety, *n*-BuLi/TMEDA is sufficient[312] for achieving the deprotonation, and in the case of a benzothiazolyl[313] or benzotriazolyl[314] moiety, *n*-BuLi or LDA can be used. The corresponding lithiooxiranes (Scheme 82) have been quenched with various electrophiles

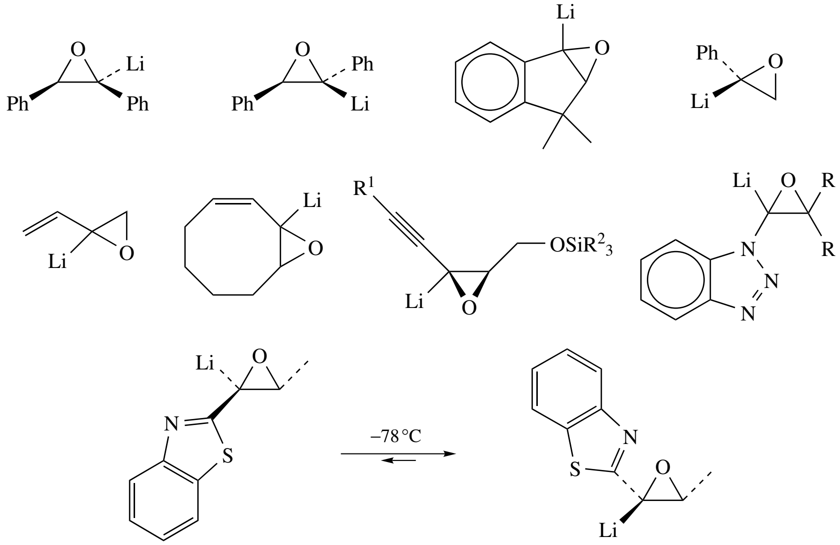

SCHEME 82

such as Me$_3$SnCl, amides, CO$_2$, TMSCl, carbonyl compounds and alkyl halides. Reactions with aldehydes or imines occur generally with low stereoselectivity. In the case of chalcone epoxides, deprotonation with LDA or LiTMP occurs preferentially[315] at the aryl-substituted terminus. Further remote stabilization of aryl-stabilized lithiooxiranes by an oxazoline moiety has also been reported[316], and these anions have been used in a straightforward synthesis of α,β-epoxy-γ-butyrolactones. The configurational stability of the anions has been evidenced at $-95\,^{\circ}$C for aryl-stabilized lithiooxiranes[310] and at $-80\,^{\circ}$C for alkynyl-stabilized lithiooxiranes[312] by deprotonation of enantiomerically pure substrates and subsequent quench with electrophiles. Enantioselective deprotonation of *cis* stilbene oxide in the presence of (−)-sparteine with TMSCl as internal electrophile affords[41] the corresponding epoxysilane in low ee (30%). By contrast, benzothiazolyl-stabilized lithiooxiranes show[313] low configurational stability, leading to the *cis* lithiooxirane at $-78\,^{\circ}$C.

In contrast to the examples reported above, some other aryl- and vinyl-stabilized lithiooxiranes show[311] a strong electrophilic behavior and undergo rearrangement reactions (Scheme 83, see also Section V.A.2.a for other examples). Lithiated styrene oxide has been engaged in 1,2-metallate rearrangement with zirconacycles[290].

Recently[314], a benzotriazolyl-stabilized lithiooxirane has been reported to undergo electrocyclic rearrangement at $-78\,^{\circ}$C to afford diphenylketene through a lithium enolate.

4. Carbonyl-stabilized lithiooxiranes and related compounds

Attempts[311] at deprotonation of epoxyketone **190** with LDA or *n*-BuLi at $-95\,^{\circ}$C result only in reduction or addition to the carbonyl moiety. By contrast, deprotonation of the epoxy imine **191** leads to the aziridine **192** through[317] a stereoselective dimerization/aza-Darzens/β-deprotonation process (Scheme 84). No example of reaction of this lithiooxirane with other electrophiles is reported.

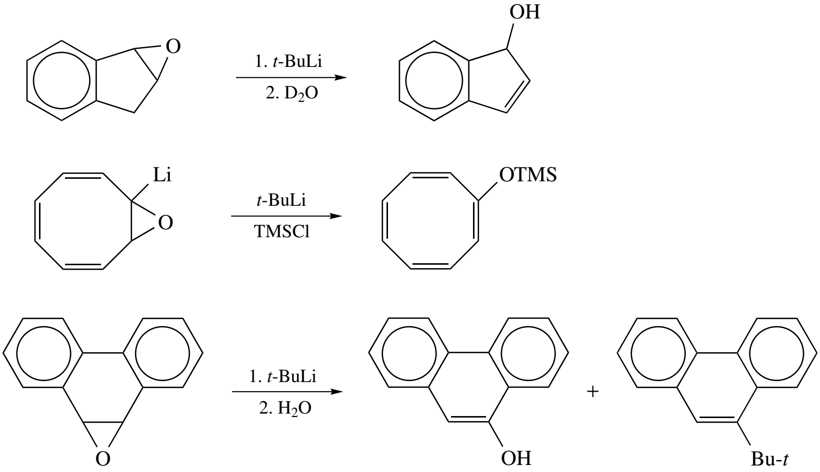

SCHEME 83

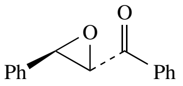

(190)

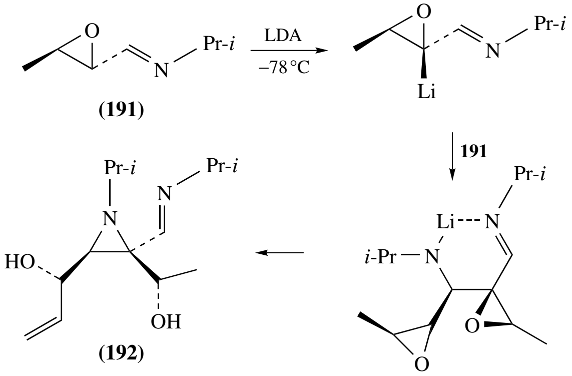

(191)

(192)

SCHEME 84

5. Carbalkoxy-stabilized lithiooxiranes and related compounds

Lithiooxiranes stabilized by a carbethoxy[311] or a cyano[290, 311, 318] group can be readily prepared by deprotonation by LDA at −80 °C and quenched with various electrophiles. The lithiooxirane **193** (Scheme 85) is configurationally stable at this temperature, whereas α-cyano lithiooxiranes show[318] a limited configurational stability. These α-cyano lithiooxiranes have been engaged in 1,2-metallate rearrangements with zirconium compounds. By contrast, deprotonation of the epoxylactone **194** was achieved[319] only in the presence of

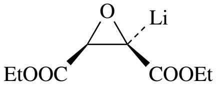

(193)

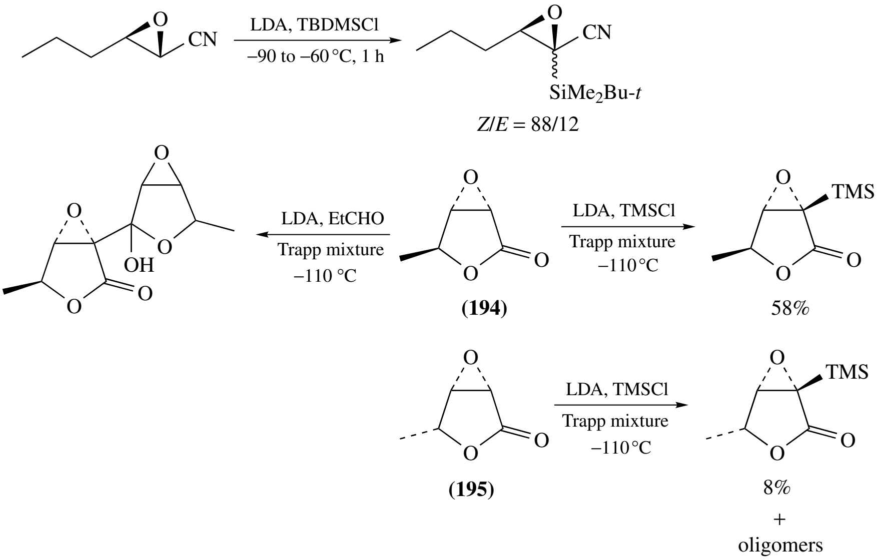

SCHEME 85. (Trapp mixture is a mixture of THF, ether and pentane which freezes at <110 °C)

TMSCl as internal electrophile. Otherwise, only dimerization was observed. The diastereomeric epoxy lactone **195** undergoes mainly oligomerization under the same conditions.

Oxazolinyloxiranes can be readily deprotonated by *s*-BuLi in the presence of TMEDA at −100 °C to afford oxazolinyl-stabilized lithiooxiranes[320–323] (Scheme 86). These species can be quenched by various electrophiles, the reaction with aldehydes showing a low or no diastereoselectivity. Deprotonation of *cis* oxiranes occurs faster than that of *trans* oxiranes, and the corresponding *cis*-lithiooxiranes are more reactive toward electrophiles than their *trans* counterparts[323]. *Trans*-oxazolinyl lithiooxiranes are configurationally stable at −100 °C for hours, whereas their *cis* counterparts show a high tendency to isomerize to the presumably more stable *trans* diastereomer within few minutes[321, 323]. However, they can react with some electrophiles with a good diastereoselectivity under Barbier conditions[323]. Deprotonation of enantiopure oxazolinyl oxiranes and reactions with electrophiles affords tetrasubstituted oxiranes in good yields[323].

Upon warming, these oxazolinyl-stabilized lithiooxiranes undergo an electrocyclic α-ring opening to give α-oxo-2-oxazolines after hydrolysis[322] (Scheme 87). However, all attempts to quench the presumed oxazolidine enolate intermediates through reaction with electrophiles failed.

6. Trifluoromethyl-stabilized lithiooxiranes

A very recent example is reported[324] of the deprotonation of (*S*)-2,3-epoxy-1,1,1-trifluoropropane **196** with *n*-BuLi in THF at −100 °C (Scheme 88). The resulting lithiooxirane is configurationally stable at this temperature and reacts with various electrophiles.

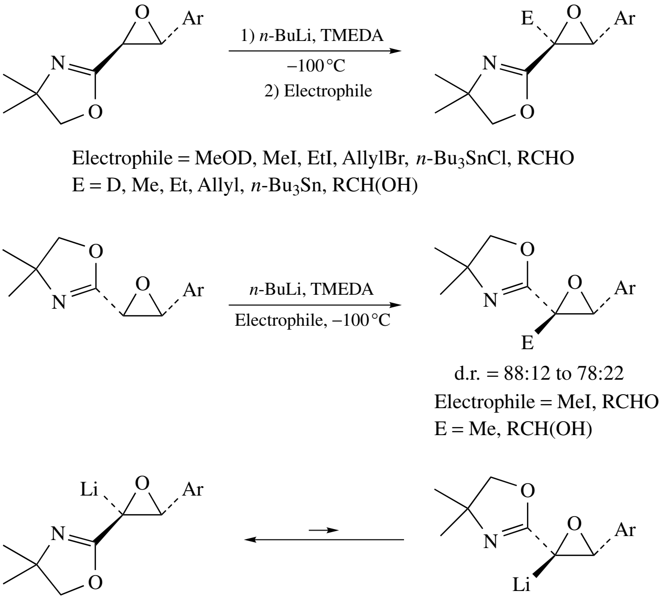

Electrophile = MeOD, MeI, EtI, AllylBr, n-Bu_3SnCl, RCHO
E = D, Me, Et, Allyl, n-Bu_3Sn, RCH(OH)

d.r. = 88:12 to 78:22
Electrophile = MeI, RCHO
E = Me, RCH(OH)

SCHEME 86

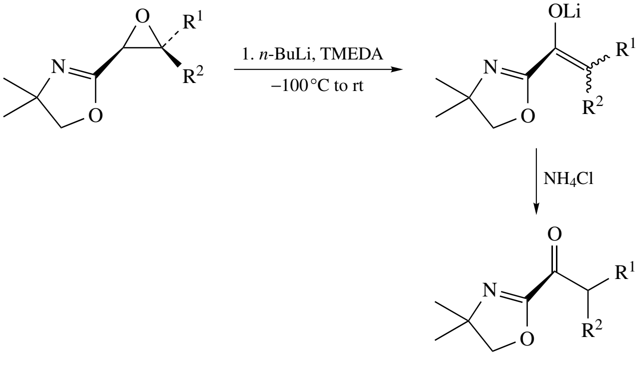

30–80%

SCHEME 87

Reaction with aldehydes gives trifluoromethylated epoxy alcohols with good diastereoselectivities (around 80:20); however, the relative stereochemistry of the products is not reported.

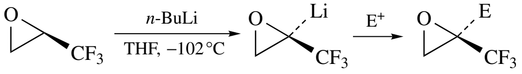

(196) 70–99%

SCHEME 88

7. Halogen-stabilized lithiooxiranes

Some examples[5,237,325,326] are reported for the deprotonation of halogeno oxiranes by organolithium reagents. The resulting α-halogeno lithiooxiranes have never been evidenced directly, but are involved (Scheme 89) in substitution reactions with the organolithium reagent used for the deprotonation reaction to give substituted lithiooxiranes. Actually, this methodology historically gave the first[227] direct evidence for a lithiooxirane compound through deuteriolysis.

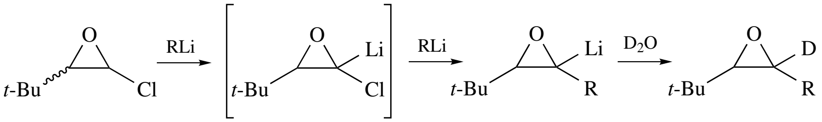

SCHEME 89

Recently, the same behavior has been observed starting from α,α-dichloro trifluoroalcohols (see Section V.A.1, Scheme 54). It is noteworthy that this type of starting material is also involved in the one-carbon homologation methodologies[327] described by the groups of Normant[328,329] and Nozaki[330,331] (Scheme 90). These reactions, attributed to a β-oxido carbenoid intermediate, could also be attributed to an α-halogeno lithiooxirane, which could then undergo alkyl migration (and not intermolecular insertion into a C−Li bond as in Scheme 89) to give the lithium enolate observed at the end of the reaction. This alternative mechanistic hypothesis had been proposed[332,333] in the early work on this one-carbon homologation reaction.

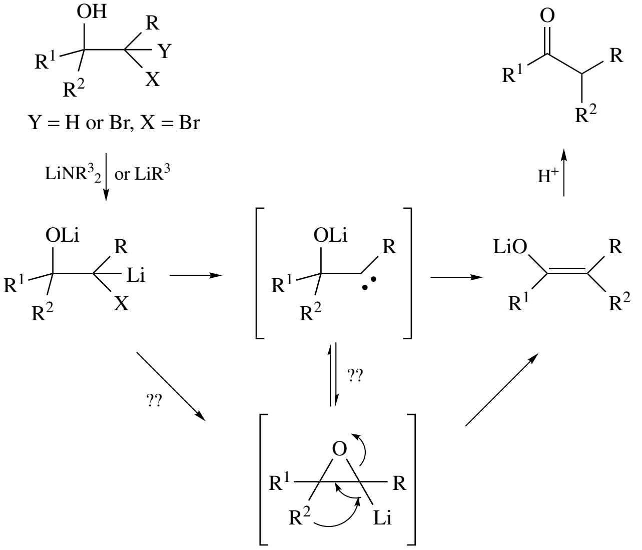

SCHEME 90

VI. GENERAL CONCLUSION

Oxiranes behave as very versatile compounds when exposed to organolithium reagents. Various reactions can be observed, depending on the structure of the oxirane, the nature of the organolithium reagent and the reaction conditions. The three main reaction pathways (i.e. β-deprotonation to allylic alcohols, α-deprotonation to lithiooxiranes and ring opening reaction) can be observed, and it is sometimes difficult to anticipate the reactivity of a system. Moreover, lithiooxiranes themselves show a very interesting, but somewhat complicated ambident reactivity. Owing to their carbenoidic character, they behave as electrophiles and/or nucleophiles. We hope that this chapter will help the reader determine the best conditions in which to obtain a particular reactivity.

VII. ACKNOWLEDGMENTS

Many thanks are due to Prof. J. K. Crandall and Dr. P. Mangeney for helpful discussions and comments.

VIII. REFERENCES

1. R. L. Letsinger, J. G. Traynham and E. Bobko, *J. Am. Chem. Soc.*, **74**, 399 (1952).
2. B. Rickborn and R. P. Thummel, *J. Org. Chem.*, **34**, 3583 (1969).
3. R. P. Thummel and B. Rickborn, *J. Am. Chem. Soc.*, **92**, 2064 (1970).
4. K. M. Morgan and J. J. Gajewski, *J. Org. Chem.*, **61**, 820 (1996).
5. J. K. Crandall and M. Apparu, *Organic Reactions*, **29**, 345 (1983).
6. K. M. Morgan and S. Gronert, *J. Org. Chem.*, **65**, 1461 (2000).
7. J. K. Crandall, *J. Org. Chem.*, **29**, 2830 (1964).
8. A. C. Cope and J. K. Heeren, *J. Am. Chem. Soc.*, **87**, 3125 (1965).
9. D. M. Hodgson, A. R. Gibbs and M. G. B. Drew, *J. Chem. Soc., Perkin Trans. 1*, 3579 (1999).
10. E. Doris, L. Dechoux and C. Mioskowski, *J. Am. Chem. Soc.*, **117**, 12700 (1995).
11. E. Doris, L. Dechoux and C. Mioskowski, *Synlett*, 3808 (1998).
12. P. Perlmutter, *Conjugate Addition Reactions in Organic Synthesis*, Pergamon Press, Oxford, 1992.
13. J. K. Whitesell and P. D. White, *Synthesis*, 602 (1975).
14. C. L. Kissel and B. Rickborn, *J. Org. Chem.*, **37**, 2060 (1972).
15. R. K. Boeckman Jr, *Tetrahedron Lett.*, 4281 (1977).
16. D. B. Collum, *Acc. Chem. Res.*, **26**, 227 (1993) and references cited therein.
17. A. Ramirez and D. B. Collum, *J. Am. Chem. Soc.*, **121**, 11114 (1999).
18. R. I. Olsson and P. Ahlberg, *Tetrahedron: Asymmetry*, **10**, 3991 (1999).
19. M. Apparu and M. Barelle, *Bull. Soc. Chim. Fr.*, 947 (1977).
20. M. Apparu and M. Barelle, *Tetrahedron*, **34**, 1541 (1978).
21. M. Apparu and M. Barelle, *Tetrahedron*, **34**, 1691 (1978).
22. M. Apparu and M. Barelle, *Tetrahedron*, **34**, 1817 (1978).
23. B. M. Trost and M. J. Bogdanowicz, *J. Am. Chem. Soc.*, **95**, 5311 (1973).
24. G. A. Molander and K. Mautner, *J. Org. Chem.*, **54**, 4042 (1989).
25. E. Doris, L. Dechoux and C. Mioskowski, *Synlett*, 337 (1998).
26. J. K. Crandall and L. H. Chang, *J. Org. Chem.*, **32**, 435 (1967).
27. E. E. van Tamelen and J. P. McCormick, *J. Am. Chem. Soc.*, **92**, 737 (1970).
28. R. P. Thummel and B. Rickborn, *J. Org. Chem.*, **37**, 3919 (1972).
29. R. P. Thummel and B. Rickborn, *J. Org. Chem.*, **37**, 4250 (1972).
30. B. M. Trost and S. Kurozumi, *Tetrahedron Lett.*, 1929 (1974).
31. R. P. Thummel and B. Rickborn, *J. Org. Chem.*, **36**, 1365 (1971).
32. L. I. Zakharkin, *Izv. Akad. Nauk SSSR, Otd. Khim. Nauk*, 2245 (1961); *Chem. Abstr.*, **57**, 11040 (1962).
33. H. Nozaki, T. Mori and R. Noyori, *Tetrahedron*, **22**, 1207 (1966).
34. A. Mordini, S. Pecchi, G. Capozzi, A. Capperucci, A. Degl'Innocenti, G. Reginato and A. Ricci, *J. Org. Chem.*, **59**, 4784 (1994).
35. C. Margot and M. Schlosser, *Tetrahedron Lett.*, **26**, 1035 (1985).
36. A. Mordini, in *Comprehensive Organometallic Chemistry II*, (Eds. E. W. Abel, F. G. A. Stone and G. Wilkinson), Vol. 11, Pergamon, Oxford, 1995, p. 93.

37. A. Mordini, E. Ben Rayana, C. Margot and M. Schlosser, *Tetrahedron*, **46**, 2401 (1990).
38. J. K. Whitesell and S. W. Felman, *J. Org. Chem.*, **45**, 755 (1980).
39. P. J. Cox and N. S. Simpkins, *Tetrahedron: Asymmetry*, **2**, 1 (1991).
40. M. Asami, *J. Synth. Org. Chem. Jpn.*, **54**, 188 (1996).
41. D. M. Hodgson, A. R. Gibbs and G. P. Lee, *Tetrahedron*, **52**, 14361 (1996).
42. P. O'Brien, *J. Chem. Soc., Perkin Trans. 1*, 1439 (1998).
43. J. Eames, *Eur. J. Org. Chem.*, 393 (2002).
44. A. Magnus, S. K. Bertilsson and P. G. Andersson, *Chem. Soc. Rev.*, **31**, 223 (2002).
45. M. Asami, *Chem. Lett.*, 829 (1984).
46. M. Asami and H. Kirihara, *Chem. Lett.*, 389 (1987).
47. M. Asami, T. Suga, K. Honda and S. Inoue, *Tetrahedron Lett.*, **38**, 6425 (1997).
48. M. J. Södergren and P. G. Andersson, *J. Am. Chem. Soc.*, **120**, 10760 (1998).
49. J. Södergren, S. K. Bertilsson and P. G. Andersson, *J. Am. Chem. Soc.*, **122**, 6610 (2000).
50. S. K. Bertilsson, J. Södergren and P. G. Andersson, *J. Org. Chem.*, **67**, 1567 (2002).
51. G. Hilmersson, P. I. Arvidsson, Ö. Davidsson and M. Håkansson, *Organometallics*, **16**, 3352 (1997).
52. D. Bhuniya and V. K. Singh, *Synth. Commun.*, **24**, 375 (1994).
53. D. Bhuniya and V. K. Singh, *Synth. Commun.*, **24**, 1475 (1994).
54. D. Bhuniya, A. Datta Gupta and V. K. Singh, *Tetrahedron Lett.*, **36**, 2847 (1995).
55. D. Bhuniya, A. Datta Gupta and V. K. Singh, *J. Org. Chem.*, **61**, 6108 (1996).
56. P. Saravanan, A. Bisai, S. Bakhtaraman, M. Chandrasekhar and V. K. Singh, *Tetrahedron*, **58**, 4693 (2002).
57. D. Pettersen, M. Amedjkouh, S. O. Nilsson Lill, K. Dahlén and P. Ahlberg, *J. Chem. Soc., Perkin Trans. 2*, 1654 (2001).
58. B. Colman, S. E. de Sousa, P. O'Brien, T. D. Towers and W. Watson, *Tetrahedron: Asymmetry*, **10**, 4175 (1999).
59. D. Guijarro, P. Pinho and P. G. Andersson, *J. Org. Chem.*, **63**, 2530 (1998).
60. S. E. de Sousa, P. O'Brien and C. D. Pilgram, *Tetrahedron*, **58**, 4643 (2002).
61. M. Asami, *Bull. Chem. Soc. Jpn.*, **63**, 721 (1990).
62. A. Z.-Q. Khan, R. W. de Groot, P. I. Arvidsson and Ö. Davidsson, *Tetrahedron: Asymmetry*, **9**, 1223 (1998).
63. R. I. Olsson and P. Ahlberg, *Tetrahedron: Asymmetry*, **10**, 3991 (1999).
64. S. O. Nilsson Lill, P. I. Arvidsson and P. Ahlberg, *Tetrahedron: Asymmetry*, **10**, 265 (1999).
65. G. Hilmersson and Ö. Davidsson, *J. Org. Chem.*, **60**, 7660 (1995).
66. G. Hilmersson, P. I. Arvidsson, Ö. Davidsson and M. Håkansson, *J. Am. Chem. Soc.*, **120**, 8143 (1998).
67. P. I. Arvidsson, G. Hilmersson and P. Ahlberg, *J. Am. Chem. Soc.*, **121**, 1883 (1999).
68. M. Asami, T. Ishizaki and S. Inoue, *Tetrahedron: Asymmetry*, **5**, 793 (1994).
69. J. P. Tierney, A. Alexakis and P. Mangeney, *Tetrahedron: Asymmetry*, **8**, 1019 (1997).
70. S. K. Bertilsson and P. G. Andersson, *Tetrahedron*, **58**, 4665 (2002).
71. S. O. Nilsson Lill, D. Pettersen, M. Amedjkouh and P. Ahlberg, *J. Chem. Soc., Perkin Trans. 1*, 3054 (2001).
72. M. Amedjkouh, D. Pettersen, S. O. Nilsson Lill, Ö. Davidsson and P. Ahlberg, *Chem. Eur. J.*, **7**, 4368 (2001).
73. D. Pettersen, M. Amedjkouh and P. Ahlberg, *Tetrahedron*, **58**, 4669 (2002).
74. M. Asami and A. Seki, *Chem. Lett.*, 160 (2002).
75. A. Seki and M. Asami, *Tetrahedron*, **58**, 4655 (2002).
76. D. Liu and S. A. Kozmin, *Angew. Chem., Int. Ed.*, **40**, 4757 (2001).
77. N. Matsumura, T. Ohba and S. Yoneda, *Chem. Lett.*, 317 (1983).
78. N. Matsumura, H. Nishiguchi, M. Okada and S. Yoneda, *Heterocycles*, 885 (1985).
79. D. Pettersen, M. Amedjkouh, S. O. Nilsson Lill and P. Ahlberg, *J. Chem. Soc., Perkin Trans. 2*, 1397 (2002).
80. D. Milne and P. J. Murphy, *J. Chem. Soc., Chem. Commun.*, 884 (1993); Corrigendum: *J. Chem. Soc., Chem. Commun.*, 675 (1994).
81. P. C. Brooks, D. J. Milne, P. J. Murphy and B. Spolaore, *Tetrahedron*, **58**, 4675 (2002).
82. D. M. Hodgson, J. Whiterington and B. A. Moloney, *Tetrahedron: Asymmetry*, **5**, 337 (1994).
83. D. M. Hodgson, J. Whiterington and B. A. Moloney, *J. Chem. Soc., Perkin Trans. 1*, 3373 (1994).

84. D. M. Hodgson and A. R. Gibbs, *Tetrahedron: Asymmetry*, **7**, 407 (1996).
85. E. Vrancken, Thèse de doctorat de l'Université Paris VI, 2000, pp. 46–60.
86. D. M. Hodgson, G. P. Lee, R. E. Marriott, A. J. Thompson, R. Wisedale and J. Witherington, *J. Chem. Soc., Perkin Trans. 1*, 2151 (1998).
87. D. M. Hodgson, I. D. Cameron, M. Christlieb, R. Green, G. P. Lee and L. A. Robinson, *J. Chem. Soc., Perkin Trans. 1*, 2161 (2001).
88. D. M. Hodgson and I. D. Cameron, *Org. Lett.*, **3**, 441 (2001).
89. J. Leonard, L. Bennet and A. Mahmood, *Tetrahedron Lett.*, **40**, 3965 (1999).
90. A. Alexakis, E. Vrancken and P. Mangeney, *J. Chem. Soc., Perkin Trans. 1*, 3354 (2000).
91. V. Schurig and F. Betschinger, *Chem. Rev.*, **92**, 873 (1992).
92. H. B. Kagan and J. C. Fiaud, *Topics in Stereochemistry* (Eds E. L. Eliel and J. C. Fiaud), Vol. 18, Wiley, New York, 1988, pp. 249–230.
93. H. B. Kagan, *Tetrahedron*, **57**, 2449 (2001).
94. A. Kee, P. O'Brien, C. D. Pilgram and S. T. Watson, *Chem. Commun.*, 1521 (2000).
95. K. Mori, B. G. Hazra, R. J. Pfeiffer, A. K. Gupta and B. S. Lindgren, *Tetrahedron*, **43**, 2249 (1987).
96. M. Asami, S. Sato, K. Honda and S. Inoue, *Heterocycles*, **52**, 1029 (2000).
97. M. Asami and N. Kanemaki, *Tetrahedron Lett.*, **30**, 2125 (1989).
98. A. Bigi, A. Mordini, A. Thurner, F. Faigl, G. Poli and L. Tõke, *Tetrahedron: Asymmetry*, **9**, 2293 (1998).
99. A. Gayet, S. Bertilsson and P. G. Andersson, *Org. Lett.*, **4**, 3777 (2002).
100. R. E. Parker and N. S. Issacs, *Chem. Rev.*, **59**, 737 (1959).
101. S. Patai (Ed.), *The Chemistry of the Ether Linkage*, Wiley, New York, 1967.
102. M. Bartok and K. L. Lang, in *The Chemistry of Ethers, Crown Ethers, Hydroxyl Groups and their Sulfur Analogues*, Part I, Supplement E, (Ed. S. Patai), Wiley, New York, 1980, pp. 609–682.
103. J. Gorzynski Smith, *Synthesis*, 629 (1984).
104. C. J. Chang, R. F. Kiesel and T. E. Hogen-Esch, *J. Am. Chem. Soc.*, **95**, 8446 (1973).
105. R. Herges and H. Neumann, *Angew. Chem., Int. Ed. Engl.*, **33**, 993 (1994).
106. S. Harder, J. H. van Lenthe, N. R. J. van Eikema Hommes and P. v. R. Schleyer, *J. Am. Chem. Soc.*, **116**, 2508 (1994).
107. H. Fujimoto, I. Hataue, N. Koga and T. Yamasaki, *Tetrahedron Lett.*, **25**, 5339 (1984).
108. J. K. Heeren, T. C. Flood and R. H. Cunningham, *J. Organomet. Chem.*, **9**, P18 (1967).
109. R. W. Herr and C. R. Johnson, *J. Am. Chem. Soc.*, **92**, 4979 (1970).
110. E. Castagnetti and M. Schlosser, *Eur. J. Org. Chem.*, 691 (2001).
111. A. Deagostino, C. Prandi and P. Venturello, *Tetrahedron*, **52**, 1433 (1996).
112. M. P. Cooke Jr and I. N. Houpis, *Tetrahedron Lett.*, **26**, 3643 (1985).
113. K. Shankaran and V. Snieckus, *J. Org. Chem.*, **49**, 5022 (1984).
114. M. Apparu and M. Barelle, *Tetrahedron*, **34**, 1691 (1978).
115. Y. Ichikawa, S. Niitsuma, K. Kato and T. Takita, *J. Chem. Soc., Chem. Commun.*, 625 (1988).
116. C. W. Bird and N. Hormozi, *Tetrahedron Lett.*, **31**, 3501 (1990).
117. A. Mordini, S. Bindi, S. Pecchi, A. Degl'Innocenti, G. Reginato and A. Serci, *J. Org. Chem.*, **61**, 4374 (1996).
118. A. Mordini, S. Bindi, S. Pecchi, A. Capperucci, A. Degl'Innocenti and G. Reginato, *J. Org. Chem.*, **61**, 4466 (1996).
119. A. Thurner, F. Faigl, A. Mordini, A. Bigi, G. Reginato and L. Töke, *Tetrahedron*, **54**, 11597 (1998).
120. A. Thurner, F. Faigl, L. Töke, A. Mordini, M. Valacchi, G. Reginato and G. Czira, *Tetrahedron*, **57**, 9173 (2001).
121. A. Mordini, S. Bindi, A. Capperucci, D. Nistri, G. Reginato and M. Valacchi, *J. Org. Chem.*, **66**, 3201 (2001).
122. C. B. Rose and S. K. Taylor, *J. Org. Chem.*, **39**, 578 (1974).
123. D. M. Wieland and C. R. Johnson, *J. Am. Chem. Soc.*, **93**, 3046 (1971).
124. G. C. M. Aithie and J. A. Miller, *Tetrahedron Lett.*, 4419 (1975).
125. M. Tamura and G. Suzukamo, *Tetrahedron Lett.*, **22**, 577 (1981).
126. J.-C. Marié, C. Courillon and M. Malacria, *Synlett*, 553 (2002).
127. M. J. Eis, J. E. Wrobel and B. Ganem, *J. Am. Chem. Soc.*, **106**, 3693 (1984).
128. M. Yamaguchi and I. Hirao, *Tetrahedron Lett.*, **24**, 391 (1983).

129. G. W. Gribble and D. A. Johnson, *Tetrahedron Lett.*, **28**, 5259 (1987).
130. N. C. Barua and R. R. Schmidt, *Synthesis*, 1067 (1986).
131. K. Couture, V. Gouverneur and C. Mioskowski, *Bioorg. Med. Chem. Lett.*, **9**, 3023 (1999).
132. I. Mukerji, A. Wayda, G. Dabbagh and S. H. Bertz, *Angew. Chem., Int. Ed. Engl.*, **25**, 760 (1986).
133. J. C. Saddler and P. L. Fuchs, *J. Am. Chem. Soc.*, **103**, 2112 (1981).
134. A. Alexakis, E. Vrancken, P. Mangeney and F. Chemla, *J. Chem. Soc., Perkin Trans. 1*, 3352 (2000).
135. N. Bernard, F. Chemla and J. Normant, *Tetrahedron Lett.*, **39**, 6715 (1998).
136. F. Chemla, N. Bernard and J. Normant, *Eur. J. Org. Chem.*, 2067 (1999).
137. F. Chemla and F. Ferreira, *Curr. Org. Chem.*, **6**, 539 (2002).
138. D. Seebach and E. J. Corey, *J. Org. Chem.*, **40**, 231 (1975).
139. B. T. Gröbel and D. Seebach, *Synthesis*, 357 (1977).
140. M. Bénéchie and F. Khuong-Huu, *Synlett*, 267 (1992).
141. M. Ide and M. Nakata, *Bull. Chem. Soc. Jpn.*, **72**, 2491 (1999).
142. J. M. Fang and M. Y. Chen, *Tetrahedron Lett.*, **29**, 5939 (1988).
143. A. B. Smith III and S. A. Lodise, *Org. Lett.*, **1**, 1249 (1999).
144. R. E. Doolittle, *Org. Prep. Proced. Int.*, **12**, 1 (1980).
145. A. B. Smith III, S. M. Condon and J. A. McCauley, *Acc. Chem. Res.*, **31**, 35 (1998).
146. H. J. Reich, A. W. Sanders, A. T. Fiedler and M. J. Bevan, *J. Am. Chem. Soc.*, **124**, 13386 (2002).
147. A. B. Smith III, S. M. Pitram, M. J. Gaunt and S. A. Kozmin, *J. Am. Chem. Soc.*, **124**, 14516 (2002).
148. M. Julia and D. Uguen, *Bull. Soc. Chim. Fr.*, 513 (1976).
149. J. C. Carretero and L. Ghosez, *Tetrahedron Lett.*, **29**, 2059 (1988).
150. S. O. Nwaukwa, S. Lee and P. M. Keehn, *Synth. Commun.*, **16**, 309 (1986).
151. J. A. Marshall and R. C. Andrews, *J. Org. Chem.*, **50**, 1602 (1985).
152. D. Craig and A. M. Smith, *Tetrahedron Lett.*, **31**, 2631 (1990).
153. T. Nakata, K. Saito and T. Oishi, *Tetrahedron Lett.*, **27**, 6345 (1986).
154. B. Achmatowicz, S. Marczak and L. Wicha, *J. Chem. Soc., Chem. Commun.*, 1226 (1987).
155. N. S. Simpkins, *Sulphones in Organic Synthesis*, Pergamon Press, Oxford, 1993, pp. 118–123.
156. F. Chemla, *J. Chem. Soc., Perkin Trans. 1*, 275 (2002).
157. B. Corbel, J. M. Decesare and T. Durst, *Can. J. Chem.*, **56**, 505 (1978).
158. V. Cere, C. Paolucci, S. Pollicino, E. Sandri and A. Fava, *J. Org. Chem.*, **56**, 4513 (1991).
159. J. M. Decesare, B. Corbel, T. Durst and J. F. Blount, *Can. J. Chem.*, **59**, 1415 (1981).
160. F. Benedetti, S. Fabrissin, T. Gianferrara and A. Risaliti, *J. Chem. Soc., Chem. Commun.*, 406 (1987).
161. Y. Gaoni, *J. Org. Chem.*, **47**, 2564 (1982).
162. T. Satoh, Y. Kawase and K. Yamakawa, *J. Org. Chem.*, **55**, 3962 (1990).
163. D. Tanner, H. H. Mig and M. Bergdahl, *Tetrahedron Lett.*, **29**, 6493 (1988).
164. K. C. Nicolaou, S. A. Snyder, A. Bigot and J. A. Pfefferkorn, *Angew. Chem., Int Ed.*, **39**, 1093 (2000).
165. S. Hanessian, N. G. Cooke, B. DeHoff and Y. Sakito, *J. Am. Chem. Soc.*, **112**, 5276 (1990).
166. D. Diez-Martin, P. Grice, H. C. Kolb, S. V. Ley and A. Madin, *Tetrahedron Lett.*, **31**, 3445 (1990).
167. C. Greck, P. Grice, S. V. Ley and A. Wonnacott, *Tetrahedron Lett.*, **27**, 5277 (1986).
168. S. V. Ley, N. J. Anthony, A. Armstrong, M. G. Brasca, T. Clarke, D. Culshaw, C. Greck, P. Grice, A. J. Jones, B. Lygo, A. Madin, R. N. Sheppard, A. M. Z. Slawin and D. J. Willians, *Tetrahedron*, **45**, 7161 (1989).
169. R. H. Bradbury and K. A. M. Walker, *J. Org. Chem.*, **48**, 1741 (1983).
170. E. Casadevall, J. C. Jallageas, L. Mion, M. Mion and P. Moreau, *C. R. Acad. Sci., Ser. C*, **265**, 839 (1967).
171. M. Hanack, E. Kunzmann and W. Schumacher, *Synthesis*, 26 (1978).
172. R. G. Carlson and D. E. Henton, *J. Chem. Soc., Chem. Commun.*, 674 (1969).
173. P. H. Buist and R. A. Adeney, *J. Org. Chem.*, **56**, 3449 (1991).
174. S. Tanimoto, S. Jo and T. Sugimoto, *Synthesis*, 53 (1981).
175. R. M. Carlson and A. R. Oyler, *Tetrahedron Lett.*, 2615 (1974).
176. M. Yamaguchi, Y. Nobayashi and I. Hirao, *Tetrahedron Lett.*, **24**, 5121 (1983).

177. M. Yamaguchi, Y. Nobayashi and I. Hirao, *Tetrahedron*, **40**, 4261 (1984).
178. S. Hatakeyama, K. Sakurai, K. Saijo and A. D. S. Takano, *Tetrahedron Lett.*, **26**, 1333 (1985).
179. D. Askin, C. Angst and S. J. Danishefsky, *J. Org. Chem.*, **50**, 5005 (1985).
180. J. Morris and D. G. Wishka, *Tetrahedron Lett.*, **27**, 803 (1986).
181. R. M. Soll and S. P. Seitz, *Tetrahedron Lett.*, **28**, 5457 (1987).
182. T. W. Bell and J. A. Ciaccio, *Tetrahedron Lett.*, **29**, 865 (1988).
183. D. W. C. MacMillan and L. E. Overman, *J. Am. Chem. Soc.*, **117**, 10391 (1995).
184. C. Semeyn, R. H. Blaauw, H. Hiemstra and W. N. Speckamp, *J. Org. Chem.*, **62**, 3426 (1997).
185. For a counter example, see: A. J. Briggs and K. A. M. Walker, *J. Org. Chem.*, **55**, 2962 (1990).
186. K. Utimoto, C. Lambert, Y. Fukuda, H. Shiragami and H. Nozaki, *Tetrahedron Lett.*, **25**, 5423 (1984).
187. T. Ooi, J. Morikawa, H. Ichikawa and K. Maruoka, *Tetrahedron Lett.*, **40**, 5881 (1999).
188. T. Ooi, N. Kagoshima, H. Ichikawa and K. Maruoka, *J. Am. Chem. Soc.*, **121**, 3328 (1999).
189. M. Chini, P. Crotti, L. Favero and F. Macchia, *Tetrahedron Lett.*, **32**, 6617 (1991).
190. M. Yamaguchi and I. Hirao, *J. Chem. Soc., Chem. Commun.*, 202 (1984).
191. T. Skrydstrup, M. Bénéchie and F. Khuong-Huu, *Tetrahedron Lett.*, **31**, 7145 (1990).
192. N. Petragnani and M. Yonashiro, *Synthesis*, 521 (1982).
193. S. K. Taylor, *Tetrahedron*, **56**, 1149 (2000).
194. M. Yamaguchi and I. Hirao, *Chem. Lett.*, 337 (1985).
195. J. F. Le Borgne, T. Cuvigny, M. Larchevèque and H. Normant, *Synthesis*, 238 (1976).
196. S. Murata and I. Matsuda, *Synthesis*, 221 (1978).
197. I. Matsuda, S. S. Murata and Y. Ishii, *J. Chem. Soc., Perkin Trans. 1*, 26 (1979).
198. S. K. Taylor, D. De Young, L. J. Simons, J. R. Vyvyan, M. A. Wemple and N. K. Wood, *Synth. Commun.*, **28**, 1691 (1998).
199. A. I. Meyers and E. D. Mihelich, *J. Org. Chem.*, **40**, 1187 (1975).
200. A. I. Meyers, Y. Yamamoto and E. D. Mihelich, *J. Org. Chem.*, **45**, 2792 (1980).
201. M. Larchevèque, G. Valette, T. Cuvigny and H. Normant, *Synthesis*, 256 (1975).
202. E. J. Corey and D. Enders, *Tetrahedron Lett.*, 11 (1976).
203. J. F. Le Borgne, *J. Organomet. Chem.*, **122**, 139 (1976).
204. J. D. White and J. C. Amedio Jr, *J. Org. Chem.*, **54**, 736 (1989).
205. J. D. White, G. N. Reddy and G. O. Spesard, *J. Am. Chem. Soc.*, **110**, 124 (1988).
206. J. D. White, T. C. Somers and G. N. Reddy, *J. Org. Chem.*, **57**, 4991 (1992).
207. S. L. Schreiber, *J. Am. Chem. Soc.*, **102**, 6163 (1980).
208. M. Chini, P. Crotti, L. Favero and M. Pineschi, *Tetrahedron Lett.*, **32**, 7583 (1991).
209. P. Crotti, V. Di Bussolo, L. Favero, F. Macchia and M. Pineschi, *Tetrahedron Lett.*, **35**, 6537 (1994).
210. P. Crotti, V. Di Bussolo, L. Favero and M. Pineschi, *J. Org. Chem.*, **61**, 9548 (1996).
211. P. Crotti, V. Di Bussolo, L. Favero, F. Minutolo and M. Pineschi, *Tetrahedron: Asymmetry*, **7**, 1347 (1996).
212. P. Crotti, V. Di Bussolo, L. Favero, F. Macchia, M. Pineschi and E. Napolitano, *Tetrahedron*, **55**, 5853 (1999).
213. P. Hullot, T. Cuvigny, M. Larchevèque and H. Normant, *Can. J. Chem.*, **55**, 266 (1977).
214. R. P. Woodbury and M. W. Rathke, *J. Org. Chem.*, **42**, 1688 (1977).
215. F. Sauriol-Lord and T. B. Grindley, *J. Org. Chem.*, **46**, 2831 (1981).
216. A. I. Meyers, R. Hanreich and K. T. Wanner, *J. Am. Chem. Soc.*, **107**, 7776 (1985).
217. D. Askin, R. P. Volante, K. M. Ryan, R. A. Reamer and I. Shinkai, *Tetrahedron Lett.*, **29**, 4245 (1988).
218. A. G. Myers and L. McKinstry, *J. Org. Chem.*, **61**, 2428 (1996).
219. D. Askin, K. K. Eng, K. Rossen, R. M. Purick, K. M. Wells, R. P. Volante and P. J. Reider, *Tetrahedron Lett.*, **35**, 673 (1994).
220. D. Askin, M. A. Wallace, J. P. Vacca, R. A. Reamer, R. P. Volante and I. Shinkai, *J. Org. Chem.*, **57**, 2771 (1992).
221. For a comprehensive review see: M. C. Willis, *J. Chem. Soc. Perkin Trans. 1*, 1765 (1999).
222. M. Mizuno, M. Kanai, A. Iida and K. Tomioka, *Tetrahedron: Asymmetry*, **7**, 2483 (1996).
223. M. Mizuno, M. Kanai, A. Iida and K. Tomioka, *Tetrahedron*, **53**, 10699 (1997).
224. A. Alexakis, E. Vrancken and P. Mangeney, *Synlett*, 1165 (1998).
225. N. Oguni, Y. Miyagi and K. Itoh, *Tetrahedron Lett.*, **39**, 9023 (1998).
226. A. C. Cope and B. D. Tiffany, *J. Am. Chem. Soc.*, **73**, 4158 (1951).

227. H. Molines, J.-M. Normant and C. Wakselman, *Tetrahedron Lett.*, 951 (1974).
228. T. Satoh, *Chem. Rev.*, **96**, 3303 (1996).
229. Y. Mori, *Rev. Heteroatom Chem.*, **17**, 183 (1997).
230. E. Doris, L. Dechoux and C. Mioskowski, *Synlett*, 337 (1998).
231. D. M. Hodgson and E. Gras, *Synthesis*, 1625 (2002).
232. H. F. Schaefer III, *Acc. Chem. Res.*, **12**, 288 (1979).
233. A. Nickon, *Acc. Chem. Res.*, **26**, 84 (1993).
234. D. M. Hodgson and S. L. M Norsikian, *Org. Lett.*, **3**, 461 (2001).
235. D. M. Hodgson and E. Gras, *Angew. Chem., Int. Ed.*, **41**, 2376 (2002).
236. J. Lertvorachon, Y. Thebtaranonth, T. Thongpangchang and P. Thongyoo, *J. Org. Chem.*, **66**, 4692 (2001).
237. M. Shimizu, T. Fujimoto, H. Minezaki, T. Hata and T. Hiyama, *J. Am. Chem. Soc.*, **123**, 6947 (2001).
238. P. Lohse, H. Loner, P. Acklin, F. Sternfeld and A. Pfaltz, *Tetrahedron Lett.*, **32**, 615 (1991).
239. T. Satoh, Y. Kaneko and K. Yamakawa, *Tetrahedron Lett.*, **27**, 2379 (1986).
240. T. Satoh, T. Oohara and K. Yamakawa, *Tetrahedron Lett.*, **29**, 2851 (1988).
241. T. Satoh, T. Oohara, Y. Ueda and K. Yamakawa, *J. Org. Chem.*, **54**, 3130 (1989).
242. T. Satoh and K. Horiguchi, *Tetrahedron Lett.*, **36**, 8235 (1995).
243. T. Satoh, S. Kobayashi, S. Nakanishi, K. Horiguchi and S. Irisa, *Tetrahedron*, **55**, 2515 (1999).
244. J. K. Crandall and L. H. C. Lin, *J. Org. Chem.*, **33**, 2375 (1968).
245. A. C. Cope, P. A. Trumbull and E. Trumbull, *J. Am. Chem. Soc.*, **80**, 2844 (1958).
246. A. Yaganisawa, K. Yasue and H. Yamamoto, *J. Chem. Soc., Chem. Commun.*, 2103 (1994).
247. R. W. Thies and R. H. Chiarello, *J. Org. Chem.*, **44**, 1342 (1979).
248. D. M. Hodgson, L. A. Robinson and M. L. Jones, *Tetrahedron Lett.*, **40**, 8637 (1999).
249. D. M. Hodgson and R. E. Marriott, *Tetrahedron: Asymmetry*, **8**, 519 (1997).
250. P. Saranavan, A. Datta Gupta, D. Bhuniya and V. K. Singh, *Tetrahedron*, **53**, 1855 (1997).
251. K. M. Morgan, M. J. O'Connor, J. L. Humphrey and K. E. Buschman, *J. Org. Chem.*, **66**, 1600 (2001).
252. A. C. Cope, H. H. Lee and H. E. Petree, *J. Am. Chem. Soc.*, **80**, 2849 (1958).
253. A. C. Cope, M. Brown and H. H. Lee, *J. Am. Chem. Soc.*, **80**, 2855 (1958).
254. J. K. Crandall, *J. Org. Chem.*, **29**, 2830 (1964).
255. J. K. Crandall, L. C. Crawley, D. B. Banks and L. C. Lin, *J. Org. Chem.*, **36**, 510 (1971).
256. J. K. Crandall and L. H. C. Lin, *J. Am. Chem. Soc.*, **89**, 4526 (1967).
257. L. Dechoux, C. Agami, E. Doris and C. Mioskowski, *J. Org. Chem.*, **64**, 9279 (1999).
258. J. K. Crandall and L.-H. Chang, *J. Org. Chem.*, **32**, 532 (1967).
259. D. M. Hodgson and G. P. Lee, *Tetrahedron: Asymmetry*, **8**, 2303 (1997).
260. M. J. Dearden, C. R. Firkin, J.-P. R. Hermet and P. O'Brien, *J. Am. Chem. Soc.*, **124**, 11870 (2002).
261. D. M. Hodgson and G. P. Lee, *J. Chem. Soc., Chem. Commun.*, 1015 (1996).
262. D. M. Hodgson, C. R. Maxwell and I. R. Matthews, *Tetrahedron: Asymmetry*, **10**, 1847 (1999).
263. D. M. Hodgson and L. A. Robinson, *J. Chem. Soc., Chem. Commun.*, 309 (1999).
264. J. K. Crandall and L. H. C. Lin, *J. Am. Chem. Soc.*, **89**, 4527 (1967).
265. J. J. Eisch and J. E. Galle, *J. Am. Chem. Soc.*, **98**, 4646 (1976).
266. A. R. Lepley, W. G. Khan, A. B. Giumanini and A. G. Giumanini, *J. Org. Chem.*, **31**, 2047 (1966).
267. E. Doris, L. Dechoux and C. Mioskowski, *Tetrahedron Lett.*, **35**, 7943 (1994).
268. L. Dechoux, E. Doris and C. Mioskowski, *J. Chem. Soc., Chem. Commun.*, 549 (1996).
269. D. M. Hodgson, M. A. H. Stent and F. X. Wilson, *Org. Lett.*, **3**, 3401 (2001).
270. D. M. Hodgson, M. A. H. Stent and F. X. Wilson, *Synthesis*, 1445 (2002).
271. Y. Ukaji, A. Yoshida and T. Fujisawa, *Chem. Lett.*, 157 (1990).
272. T. Harada, T. Katsuhira, K. Hattori and A. Oku, *J. Org. Chem.*, **58**, 2958 (1993).
273. P. Kocienski and C. Barber, *Pure Appl. Chem.*, **62**, 1933 (1990).
274. G. Boche and J. C. W. Lohrenz, *Chem. Rev.*, **101**, 697 (2001).
275. I. Marek, *Tetrahedron*, **58**, 9463 (2002).
276. D. M. Hodgson, C. R. Maxwell, T. J. Miles, E. Paruch, M. A. H. Stent, I. R. Matthews, F. X. Wilson and J. Witherington, *Angew. Chem., Int. Ed.*, **41**, 4313 (2002).
277. C. Agami, L. Dechoux, E. Doris and C. Mioskowski, *Tetrahedron Lett.*, **38**, 4071 (1997).

278. L. Dechoux, C. Agami, E. Doris and C. Mioskowski, *Eur. J. Org. Chem.*, 4107 (2001).
279. R. W. Hoffmann and H. C. Stiasny, *Chem. Eur. J.*, **1**, 619 (1995).
280. G. A. Molander and K. Mautner, *Pure Appl. Chem.*, **62**, 707 (1990).
281. P. F. Hudrlik and A. M. Hudrlik, in *Advances in Silicon Chemistry*, Volume 2 (Ed. G. L. Larson), JAI Press, Greenwich, 1993, pp. 1–89.
282. F. Chemla, *J. Chem. Soc., Perkin Trans. 1*, 275 (2002).
283. J. J. Eisch and J. E. Galle, *J. Organomet. Chem.*, **121**, C10 (1976).
284. C. Burford, F. Cooke, G. Roy and P. Magnus, *Tetrahedron*, **39**, 867 (1983).
285. M. Taniguchi, K. Oshima and K. Utimoto, *Tetrahedron Lett.*, **32**, 2783 (1991).
286. K. K. Murthi and R. G. Salomon, *Tetrahedron Lett.*, **35**, 517 (1994).
287. M. Lautens, P. H. M. Delanghe, J. B. Goh and C. H. Zhang, *J. Org. Chem.*, **60**, 4213 (1995).
288. N. S. Mani and C. A. Townsend, *J. Org. Chem.*, **62**, 636 (1997).
289. T. H. Chan, P. W. K. Lau and M. P. Li, *Tetrahedron Lett.*, 2667 (1976).
290. A. N. Kasatkin and R. J. Whitby, *Tetrahedron Lett.*, **41**, 5275 (2000).
291. K. Takeyama, K. Oshima and K. Utimoto, *Tetrahedron Lett.*, **31**, 6055 (1990).
292. K. Takeyama, K. Oshima and K. Utimoto, *Tetrahedron Lett.*, **31**, 6059 (1990).
293. K. Matsumoto, K. Miura, K. Oshima and K. Utimoto, *Tetrahedron Lett.*, **32**, 6383 (1991).
294. J. J. Eisch and J. E. Galle, *J. Organomet. Chem.*, **341**, 293 (1988).
295. M. Ashwell and R. F. W. Jackson, *J. Chem. Soc., Perkin Trans. 1*, 835 (1989).
296. M. Ashwell and R. F. W. Jackson, *J. Chem. Soc., Chem. Commun.*, 645 (1988).
297. M. Ashwell, W. Clegg and R. F. W. Jackson, *J. Chem. Soc., Perkin Trans. 1*, 897 (1991).
298. S. F. C. Dunn and R. F. W. Jackson, *J. Chem. Soc., Perkin Trans. 1*, 2863 (1992).
299. Y. Mori, T. Sawada and H. Furukawa, *Tetrahedron Lett.*, **40**, 731 (1999).
300. Y. Mori, K. Yaegashi, K. Iwase, Y. Yamamori and H. Furukawa, *Tetrahedron Lett.*, **37**, 2605 (1996).
301. Y. Mori, K. Yaegashi, K. Iwase, Y. Yamamori and H. Furukawa, *Tetrahedron Lett.*, **37**, 6959 (1996).
302. Y. Mori, K. Yaegashi and H. Furukawa, *Tetrahedron*, **53**, 12917 (1997).
303. Y. Mori, K. Yaegashi and H. Furukawa, *J. Am. Chem. Soc.*, **118**, 8158 (1996).
304. Y. Mori, K. Yaegashi and H. Furukawa, *J. Am. Chem. Soc.*, **119**, 4557 (1997).
305. Y. Mori, *Chem. Eur. J.*, **3**, 849 (1997).
306. Y. Mori, K. Yaegashi and H. Furukawa, *J. Org. Chem.*, **63**, 6200 (1998).
307. Y. Mori, K. Yaegashi and H. Furukawa, *Tetrahedron Lett.*, **40**, 7239 (1999).
308. Y. Mori, H. Furuta, T. Takase, S. Mitsuoka and H. Furukawa, *Tetrahedron Lett.*, **40**, 8019 (1999).
309. P. L. Bailey, W. Clegg, R. F. W. Jackson and O. Meth-Cohn, *J. Chem. Soc., Perkin Trans. 1*, 343 (1993).
310. V. Capriati, S. Florio, R. Luisi and A. Salomone, *Org. Lett.*, **4**, 2445 (2002).
311. J. J. Eisch and J. E. Galle, *J. Org. Chem.*, **55**, 4835 (1990).
312. D. Grandjean, P. Pale and J. Chuche, *Tetrahedron: Asymmetry*, **4**, 1991 (1993).
313. S. Florio, G. Ingrosso, L. Troisi and V. Lucchini, *Tetrahedron Lett.*, **34**, 1363 (1993).
314. A. R. Katritzky, K. Manju and P. J. Steel, *J. Org. Chem.*, **68**, 407 (2003).
315. A. Baramee, J. Clardy, P. Kongsaeree, S. Rajviroongit, C. Suteerachanon, C. Thebtaranonth and Y. Thebtaranonth, *J. Chem. Soc., Chem. Commun.*, 1511 (1996).
316. V. Capriati, L. Degennaro, R. Favia, S. Florio and R. Luisi, *Org. Lett.*, **4**, 1551 (2002).
317. D. Alickmann, R. Fröhlich and E.-U. Würthwein, *Org. Lett.*, **3**, 1527 (2001).
318. A. N. Kasatkin and R. J. Whitby, *Tetrahedron Lett.*, **41**, 6201 (2000).
319. K. Kuramochi, S. Nagata, H. Itaya, K. Takao and S. Kobayashi, *Tetrahedron Lett.*, **40**, 7371 (1999).
320. S. Florio, V. Capriati and S. Di Martino, *Tetrahedron Lett.*, **39**, 5639 (1998).
321. S. Florio, V. Capriati, S. Di Martino and A. Abbotto, *Eur. J. Org. Chem.*, 409 (1999).
322. V. Capriati, S. Florio, R. Luisi, V. Russo and A. Salomone, *Tetrahedron Lett.*, **41**, 8835 (2000).
323. A. Abbotto, V. Capriati, L. Degennaro, S. Florio, R. Luisi, M. Pierrot and A. Salomone, *J. Org. Chem.*, **66**, 3049 (2001).
324. Y. Yamauchi, T. Katagiri and K. Uneyama, *Org. Lett.*, **4**, 173 (2002).
325. G. Köbrich, W. Werner and J. Grosser, *Chem. Ber.*, **106**, 2620 (1973).
326. G. Köbrich and W. Werner, *Tetrahedron Lett.*, 2181 (1969).

327. P. M. Wovkulich, in *Comprehensive Organic Synthesis* (Eds. B. M. Trost and I. Fleming), Vol. 1, Pergamon Press, Oxford, 1991, pp. 873–877.
328. J. Villiéras, C. Bacquet and J. F. Normant, *J. Organomet. Chem.*, **40**, C1 (1972).
329. J. Villiéras, C. Bacquet and J. F. Normant, *J. Organomet. Chem.*, **97**, 325 (1975).
330. H. Taguchi, H. Yamamoto and H. Nozaki, *Tetrahedron Lett.*, 4661 (1972).
331. H. Taguchi, H. Yamamoto and H. Nozaki, *Bull. Chem. Soc. Jpn.*, **50**, 1592 (1977).
332. G. Köbrich and J. Grosser, *Chem. Ber.*, **106**, 2626 (1973).
333. G. Köbrich and J. Grosser, *Tetrahedron Lett.*, 4117 (1972).

Author Index

The Chemistry of Organolithium Compounds. Edited by Z. Rappoport and I. Marek
ISBN: 0-470-84339-X

With kind thanks to K. Raven for compilation of this index.

Subject Index

Entries are in letter-by-letter alphabetical order ignoring spaces and punctuation marks. Page numbers in *italic* refer to Figures and Tables not included in the relevant page ranges.

The Chemistry of Organolithium Compounds. Edited by Z. Rappoport and I. Marek
© 2004 John Wiley & Sons, Ltd. ISBN: 0-470-84339-X

With thanks to C. Barlow for creation of this index.